SERIES IN
MATERNAL-FETAL
MEDICINE

# Fetal Cardiology

## Embryology, Genetics, Physiology, Echocardiographic Evaluation, Diagnosis, and Perinatal Management of Cardiac Diseases

## THIRD EDITION

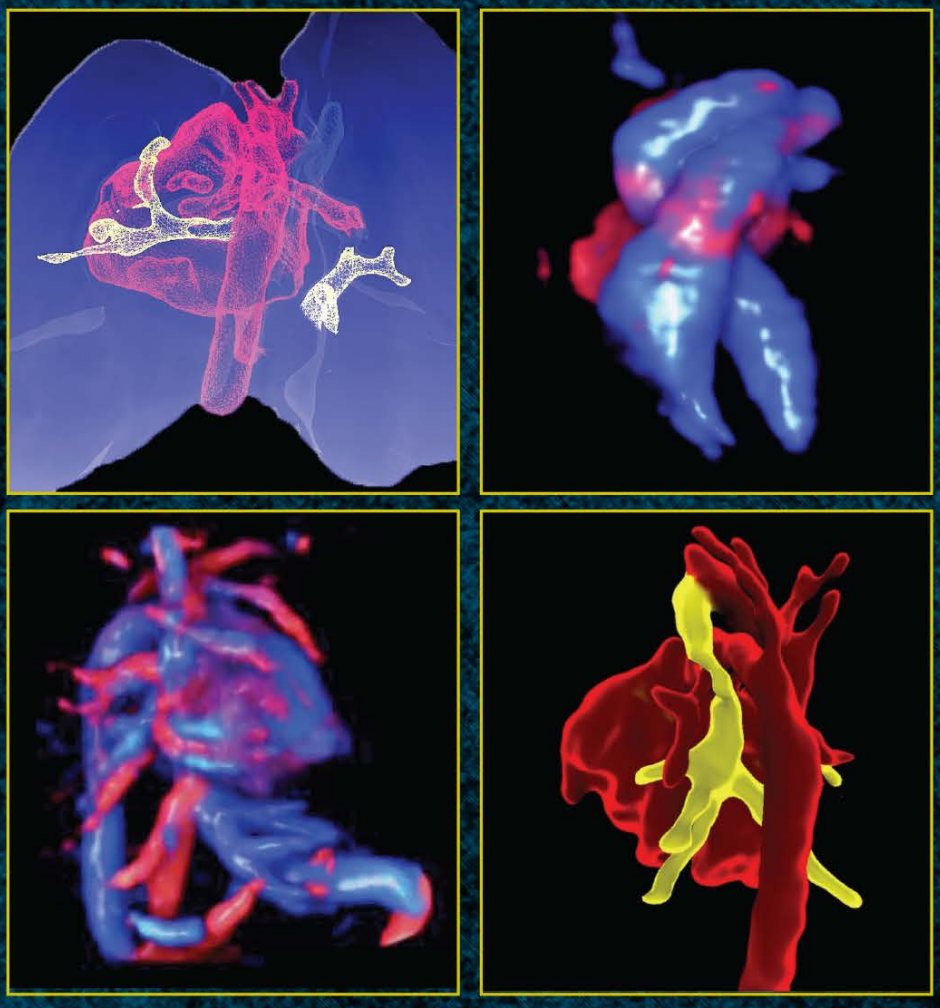

Edited by
**Simcha Yagel, Norman H. Silverman, and Ulrich Gembruch**

WITH VITALSOURCE® EBOOK

CRC Press
Taylor & Francis Group

# Fetal Cardiology

# SERIES IN MATERNAL-FETAL MEDICINE

## About the Series

Published in association with the *Journal of Maternal Fetal and Neonatal Medicine*, the series in *Maternal Fetal Medicine* keeps readers up to date with the latest clinical therapies to improve the health of pregnant patients and ensure a successful birth. Each volume in the series is prepared separately and typically focuses on a topical theme. Volumes are published on an occasional basis, depending on the emergence of new developments.

**Fetal Cardiology: Embryology, Genetics, Physiology, Echocardiographic Evaluation, Diagnosis and Perinatal Management of Cardiac Diseases**
Simcha Yagel, Norman H. Silverman, Ulrich Gembruch

**Stillbirth: Understanding and Management**
Fabio Facchinetti, Gustaaf Dekker, Dante Baronciani, George Saade

**Neurology and Pregnancy: Clinical Management**
Michael S. Marsh, Lina Nashef, Peter Brex

**Recurrent Pregnancy Loss: Causes, Controversies, and Treatment, Second Edition**
Howard J. A. Carp

**Textbook of Diabetes and Pregnancy, Third Edition**
Moshe Hod, Lois G. Jovanovic, Gian Carlo Di Renzo, Alberto De Leiva, Oded Langer

**Cesarean Delivery: A Comprehensive Illustrated Practical Guide**
Gian Carlo Di Renzo, Antonio Malvasi

**Obstetric Evidence Based Guidelines, Third Edition**
Vincenzo Berghella

**Maternal-Fetal Evidence Based Guidelines, Third Edition**
Vincenzo Berghella

**Maternal-Fetal and Obstetric Evidence Based Guidelines, Two Volume Set, Third Edition**
Vincenzo Berghella

**The Long-Term Impact of Medical Complications in Pregnancy: A Window into Maternal and Fetal Future Health**
Eyal Sheiner

**Operative Obstetrics, Fourth Edition**
Joseph J. Apuzzio, Anthony M. Vintzileos, Vincenzo Berghella, Jesus R. Alvarez-Perez

**Placenta Accreta Syndrome**
Robert M. Silver

For more information about this series please visit:
https://www.crcpress.com/Series-in-Maternal-Fetal-Medicine/book-series/CRCSERMATFET

# Fetal Cardiology

## Embryology, Genetics, Physiology, Echocardiographic Evaluation, Diagnosis, and Perinatal Management of Cardiac Diseases

Third Edition

Edited by

Simcha Yagel
Magda and Richard Hoffman Center for Human Placenta Research
Division of Obstetrics and Gynecology
Hadassah-Hebrew University Medical Center
Jerusalem, Israel

Norman H. Silverman
Division of Pediatric Cardiology
Lucile Packard Children's Hospital
Stanford University Medical Center
Palo Alto, California, USA

Ulrich Gembruch
Department of Obstetrics and Prenatal Medicine
University Bonn Medical School
Bonn, Germany

Associate Editor

Sarah Margalyt Cohen
Department of Obstetrics and Gynecology
Hadassah-Hebrew University Medical Center
Mount Scopus
Jerusalem, Israel

CRC Press
Taylor & Francis Group
Boca Raton London New York

CRC Press is an imprint of the
Taylor & Francis Group, an **informa** business

CRC Press
Taylor & Francis Group
6000 Broken Sound Parkway NW, Suite 300
Boca Raton, FL 33487-2742



Printed on acid-free paper

International Standard Book Number-13: 978-1-4987-7176-4 (Pack- Hardback and eBook)



**Library of Congress Cataloging-in-Publication Data**

Names: Yagel, Simcha, editor. | Silverman, Norman H., editor. | Gembruch, Ulrich, editor.
Title: Fetal cardiology : embryology, genetics, physiology, echocardiographic evaluation, diagnosis, and perinatal management of cardiac diseases / edited by Simcha Yagel, Norman H. Silverman and Ulrich Gembruch.
Other titles: Series in maternal-fetal medicine.
Description: Third edition. | Boca Raton, FL : Taylor & Francis Group, LLC, 2019. | Series: Series in maternal-fetal medicine | Includes bibliographical references and index.
Identifiers: LCCN 2018012336| ISBN 9781498771764 (pack- hardback and ebook : alk. paper) | ISBN 9780429461118 (ebook)
Subjects: | MESH: Heart Diseases--diagnosis | Heart Diseases--therapy | Fetal Heart--physiopathology | Infant, Newborn | Prenatal Diagnosis
Classification: LCC RG618 | NLM WS 290 | DDC 618.3/261--dc23
LC record available at https://lccn.loc.gov/2018012336

**Visit the Taylor & Francis Web site at**
**http://www.taylorandfrancis.com**

**and the CRC Press Web site at**
**http://www.crcpress.com**

For being our inspiration, for their endless patience, we lovingly dedicate this volume to our wives, Noemie Yagel, Gabi Gembruch, and Heather Silverman

Taylor & Francis
Taylor & Francis Group
http://taylorandfrancis.com

# Contents

Taylor & Francis
Taylor & Francis Group
http://taylorandfrancis.com

# Preface

This third edition of *Fetal Cardiology: Embryology, Genetics, Physiology, Echocardiographic Evaluation, Diagnosis, and Perinatal Management of Cardiac Diseases* marks a new beginning in our specialty. Like the first two editions, this edition was created through the generosity of the many professionals who shared their expertise: obstetricians, pediatric cardiologists, sonographers, molecular biologists, and medical physicists. This latest edition adds a complement of twelve new chapters, reflecting the immense strides made in recent years. We are delighted to welcome many new contributors, leaders in their specialties writing on diverse topics, to our team.

The fields of fetal imaging and cardiac therapies and interventions are rapidly changing and developing. Whereas in the preface to the second edition we showcased the three-dimensional/four-dimensional revolution in fetal cardiology, the highlight of the third edition is a pair of chapters focusing on fetal cardiac magnetic resonance imaging. This exciting and innovative discipline promises to enhance fetal diagnosis, inform perinatal management and postnatal treatment, and open new avenues in research.

This new edition comprises expanded and revised chapters on treatment options and pharmacological or surgical interventions available to affected fetuses, as well as all life stages of heart disease, from embryology to the neonate, to the reproductive health of women with congenital heart disease and the counseling of families affected by congenital heart disease. Progress in prenatal genetic investigations and counseling is canvassed in a new chapter on chromosome microarray analysis, exome, and whole genome sequencing of the fetal heart. Two chapters are devoted to the complex issue of the intrauterine and postnatal neurodevelopment of fetuses diagnosed with congenital heart disease and the management strategies available to them. An expanded chapter describes the evaluation of fetal cardiac function with advanced Doppler techniques, while another focuses on fetal bradydysrhythmia and the long Q-T syndrome, prior knowledge of which may save lives, not only of the fetus or newborn, but may lead to diagnosis and effective preventative treatment for affected but asymptomatic family members as well.

*Congenital heart disease* is a broad classification, estimated to affect 8:1,000 live births and to occur at a similar rate in aborti. This underlines the necessity to integrate comprehensive fetal echocardiography in every targeted organ scan. *Fetal Cardiology*, third edition, is a comprehensive guide intended for everyone interested in fetal development: anyone having an interest in the fetal heart, we believe, will find it useful. It is our hope that this volume will bridge the specialties of obstetrics, perinatology, pediatric and general cardiology, and radiology.

**Simcha Yagel**
**Norman H. Silverman**
**Ulrich Gembruch**

Taylor & Francis
Taylor & Francis Group
http://taylorandfrancis.com

# List of contributors

**Alfred Abuhamad**
Department of Obstetrics and Gynecology
Eastern Virginia Medical School
Norfolk, Virginia

**Reuven Achiron**
Chaim Sheba Medical Center
Sackler School of Medicine
Tel Aviv University
Tel Aviv, Israel

**Silvia G.V. Alvarez**
Department of Pediatric Cardiology and Congenital Heart Disease in Adolescents and Adults
"Dante Pazzanese" Institute of Cardiology
São Paulo, Brazil

**Hagai Amsalem**
Department of Obstetrics and Gynecology
Hadassah-Hebrew University Medical Center
Mt. Scopus, Jerusalem, Israel

**Margot M. Bartelings**
Department of Anatomy and Embryology
Leiden University Medical Center
Leiden, The Netherlands

**Ahmet A. Baschat**
The Johns Hopkins Center for Fetal Therapy
Department of Gynecology and Obstetrics
Johns Hopkins University School of Medicine
Baltimore, Maryland

**Christoph Berg**
Department of Obstetrics and Prenatal Medicine
University of Bonn
Bonn, Germany

**Einat Birk**
Pediatric Cardiology
Pediatric Heart Institute
Schneider Children's Medical Center
Petach Tikva, Israel

**Sean C. Blackwell**
Division of Maternal-Fetal Medicine
Department of Obstetrics and Gynecology
University of Texas Health Sciences
Houston, Texas

**Graham J. Burton**
The Centre for Trophoblast Research
Department of Physiology, Development, and Neuroscience
University of Cambridge
Cambridge, United Kingdom

**Javier Caradeux**
BCNatal. Barcelona Center for Maternal-Fetal and Neonatal Medicine (Hospital Clínic and Hospital Sant Joan de Deu)
Institut Clínic de Ginecologia
Obstetricia i Neonatologia Fetal i+D Fetal Medicine Research Center
Barcelona, Spain

and

Fetal Medicine Unit
Clínica Dávila
Santiago, Chile

**Julene S. Carvalho**
Professor of Practice and Consultant in Fetal Cardiology
Head of Brompton Centre for Fetal Cardiology
Royal Brompton Hospital
and
Fetal Medicine Unit
St George's University Hospital
and
Molecular and Clinical Sciences Research Institute
St George's, University of London
London, United Kingdom

**Frank Cetta**
Division of Pediatric Cardiology
Department of Cardiovascular Diseases
Mayo Clinic
Rochester, Minnesota

**Rabih Chaoui**
Center for Prenatal Diagnosis and Human Genetics
Berlin, Germany

**Sarah M. Cohen**
Department of Obstetrics and Gynecology
Hadassah-Hebrew University Medical Center
Jerusalem, Israel

**Bettina F. Cuneo**
Children's Hospital Colorado Heart Institute
Colorado Fetal Care Center
University of Colorado School of Medicine
Aurora, Colorado

**Pe'er Dar**
Department of Obstetrics and Gynecology and Women's Health
Montefiore Medical Center
Albert Einstein College of Medicine
New York City, New York

**Mary T. Donofrio**
Professor of Pediatrics
George Washington University
and
Director of the Fetal Heart Program and Critical Care Delivery Program
Co-Director of the Cardiac Neurodevelopmental Outcome Program
Children's National Medical Center
Washington, DC

**Luke Eckersley**
Fetal and Neonatal Cardiac Program
Pediatric Cardiology
Stollery Children's Hospital
University of Alberta
Edmonton, Canada

**Mark I. Evans**
Fetal Medicine Foundation of America
Comprehensive Genetics PLLC
and
Department of Obstetrics and Gynecology
Mt. Sinai School of Medicine
New York City, New York

**Laurent Fermont**
Shaare Zedek Medical Center
Jerusalem, Israel

**Francesc Figueras**
BCNatal. Barcelona Center for Maternal-Fetal and Neonatal Medicine (Hospital Clínic and Hospital Sant Joan de Deu)
Institut Clínic de Ginecologia
Obstetricia i Neonatologia Fetal i+D Fetal Medicine Research Center
Barcelona, Spain

and

Center for Biomedical Research on Rare Diseases (CIBER-ER)
Madrid, Spain

**Lindsay R. Freud**
Assistant Professor
Division of Pediatric Cardiology
Department of Pediatrics
Morgan Stanley Children's Hospital of New York-Presbyterian
Columbia University Medical Center
New York City, New York

**Helena M. Gardiner**
The Fetal Center
UTHealth McGovern School of Medicine
Houston, Texas

**Annegret Geipel**
Department of Obstetrics and Prenatal Medicine
University of Bonn
Bonn, Germany

**Ulrich Gembruch**
Department of Obstetrics and Prenatal Medicine
University Bonn Medical School
Bonn, Germany

**Adriana C. Gittenberger–de Groot**
Department of Cardiology
Leiden University Medical Center
Leiden, The Netherlands

**Max E. Godfrey**
Pediatric Cardiology
Shaare Zedek Medical Center
Jerusalem, Israel

and

Schneider Children's Medical Center
Petah Tikva, Israel

**Debra S. Goldman-Wohl**
Magda and Richard Hoffman Center for Human Placenta Research
Department of Obstetrics and Gynecology
Hadassah-Hebrew University Medical Center
Jerusalem, Israel

**Luís F. Gonçalves**
Professor and Co-Director, Fetal Imaging
Phoenix Children's Hospital
Professor, Departments of Child Health and Radiology
University of Arizona College of Medicine-Phoenix
Phoenix, Arizona

**Frank L. Hanley**
Professor, Cardiothoracic Surgery
Executive Director, Betty Irene Moore Children's Heart Center
Lucille Packard Children's Hospital
Stanford University
Stanford, California

**Astrid Hellmund**
Department of Obstetrics and Prenatal Medicine
University of Bonn
Bonn, Germany

**Ulrike Herberg**
Department of Pediatric Cardiology
University of Bonn
Bonn, Germany

**Julien I.E. Hoffman**
Department of Pediatrics
Cardiovascular Research Institute
University of California
San Francisco, California

**Wolfgang Holzgreve**
University Clinic
University of Bonn
Bonn, Germany

**Lisa K. Hornberger**
Fetal and Neonatal Cardiac Program, Pediatric Cardiology
Stollery Children's Hospital
Department of Pediatrics and Obstetrics and Gynecology
University of Alberta
Edmonton, Canada

**Lucile Houyel**
Centre Marie Lannelongue
Le Plessis-Robinson, France

**Hedwig H. Hövels-Gürich**
Department of Pediatric Cardiology
Children's Heart Center
RWTH Aachen University
Aachen, Germany

**James C. Huhta**
Perinatal Cardiologist
MEDNAX Services, Inc.
Tampa, Florida

**Jon Hyett**
RPA Women and Babies
Royal Prince Alfred Hospital
New South Wales, Australia

**Edgar T. Jaeggi**
Department of Pediatrics
Fetal Cardiac Program
Labatt Family Heart Center
The Hospital for Sick Children
University of Toronto Faculty of Medicine
Toronto, Canada

**Eric Jauniaux**
EGA Institute for Women's Health
Faculty of Population Health Sciences
University College London
London, United Kingdom

**Monique R.M. Jongbloed**
Departments of Cardiology, Anatomy, and Embryology
Leiden University Medical Center
Leiden, The Netherlands

**Torvid Kiserud**
Department of Clinical Science
University of Bergen
and
Department of Obstetrics and Gynecology
Haukeland University Hospital
Bergen, Norway

**Diego A. Lara**
Pediatric Cardiology
Department of Pediatrics
Ochsner Hospital for Children
New Orleans, Louisiana

**Michael Y. Liu**
Fetal Heart Program
The Cardiac Center
Children's Hospital of Philadelphia
and
Department of Pediatrics
Perelman School of Medicine
University of Pennsylvania
Philadelphia, Pennsylvania

**Alexander Lowenthal**
Pediatric Cardiologist
Heart Institute
Schneider Children's Medical Center of Israel
Petach-Tikvah, Israel

**Davide Marini**
Labatt Family Heart Centre
The SickKids Hospital
Toronto, Canada

**Angela McBrien**
Department of Pediatrics and Obstetrics and Gynecology
Stollery Children's Hospital
University of Alberta
Edmonton, Canada

**Christopher G. McCusker**
School of Applied Psychology
University College Cork
Cork, Ireland

**Waltraut M. Merz**
Department of Obstetrics and Prenatal Medicine
Center of Obstetrics and Gynecology
University of Bonn
Bonn, Germany

**Baruch Messing**
Ma'ayanei HaYeshua Medical Center
Bnei Brak, Israel

and

Chaim Sheba Medical Center
Ramat Gan, Israel

**Ritu Mogra**
RPA Women and Babies
Royal Prince Alfred Hospital
New South Wales, Australia

**Anita J. Moon-Grady**
Division of Cardiology
Department of Pediatrics
University of California San Francisco
and
Fetal Cardiovascular Program
UCSF Benioff Children's Hospital
San Francisco, California

**Shaine A. Morris**
Division of Pediatric Cardiology
Department of Pediatrics
Texas Children's Hospital and Baylor College of Medicine
Houston, Texas

**Karina Seidl Nall**
Certified Genetic Counselor
Steward Healthcare
Fetal Diagnostic Center
Gilbert, Arizona

and

Metis Genetics
Addison, Texas

**Andrew J. Parry**
Department of Paediatric Surgery
Bristol Royal Hospital for Children
Bristol, United Kingdom

**Carlos A.C. Pedra**
Pediatric Interventional Program
Instituto Dante Pazzanese de Cardiologia
and
Pediatric Interventional Laboratory
Hospital do Coração
Sao Paulo, Brazil

**Simone R.F. Fontes Pedra**
Fetal and Pediatric Echocardiography Laboratory
Instituto Dante Pazzanese de Cardiologia
and
Fetal Unit
Hospital do Coração
Sao Paulo, Brazil

**Shabnam Peyvandi**
Division of Cardiology
Department of Pediatrics
University of California San Francisco
and
Fetal Cardiovascular Program
UCSF Benioff Children's Hospital
San Francisco, California

**Sabrina D. Phillips**
Department of Cardiovascular Diseases
Mayo Clinic
Jacksonville, Florida

**Robert E. Poelmann**
Departments of Cardiology
and
Institute of Biology Leiden
Sylvius Laboratory
Leiden University
Leiden, The Netherlands

**Sharon Portnoy**
Department of Physiology and Experimental Medicine
University of Toronto and Hospital for Sick Children
Toronto, Canada

**Michael D. Puchalski**
Division of Pediatric Cardiology
Department of Pediatrics
Primary Children's Hospital
University of Utah School of Medicine
Salt Lake City, Utah

**Sabine Rudnik-Schöneborn**
Sektion für Humangenetik der Medizinischen Universität
Innsbruck
Zentrum Medizinische Genetik Innsbruck
Innsbruck, Austria

**Abraham M. Rudolph**
Department of Pediatrics
University of California
San Francisco, California

**Marco C. de Ruiter**
Department of Anatomy and Embryology
Leiden University Medical Center
Leiden, The Netherlands

**Jack Rychik**
Professor
Fetal Heart Program
The Cardiac Center
Children's Hospital of Philadelphia
and
Department of Pediatrics
Perelman School of Medicine
University of Pennsylvania
Philadelphia, Pennsylvania

**David Sahn**
Professor Emeritus
Oregon Health and Sciences University
Portland, Oregon

**Mike Seed**
Associate Professor
Division of Cardiology
Hospital for Sick Children
Department of Paediatrics
University of Toronto
Toronto, Canada

**Viola Seravalli**
The Johns Hopkins Center for Fetal Therapy
Department of Gynecology and Obstetrics
Johns Hopkins University School of Medicine
Baltimore, Maryland

**Hagit Shani**
Department of Obstetrics and Gynecology and Women's Health
Montefiore Medical Center
Albert Einstein College of Medicine
New York City, New York

and

The Josef Buchman Gynecology and Maternity Center
Sheba Medical Center
Ramat Gan, Israel

**Israel Shapiro**
Department of Obstetrics and Gynecology
Bnai-Zion Medical Center
Technion, Faculty of Medicine
Haifa, Israel

**Ori Shen**
Shaare Zedek Medical Center
Jerusalem, Israel

**Norman H. Silverman**
Professor of Pediatrics (Cardiolgy)
University of California San Francisco
San Francisco, California

and

Professor of Pediatrics (Emeritus)
Division of Pediatric Cardiology
Stanford University
Stanford, California

and

Honorary Professor of Pediatrics
University of Cape Town
Cape Town, South Africa

**Elena S. Sinkovskaya**
Associate Professor
Department of Obstetrics and Gynecology
Eastern Virginia Medical School
Norfolk, Virginia

**Brian S. Snarr**
Fetal Heart Program
The Cardiac Center
Children's Hospital of Philadelphia
and
Department of Pediatrics
Perelman School of Medicine
University of Pennsylvania
Philadelphia, Pennsylvania

**Julia Solomon**
Director Fetal Diagnostic Center
Physicians Group of Arizona
Steward Healthcare
Gilbert, Arizona

**Yoram Sorokin**
Department of Obstetrics and Gynecology
Wayne State University School of Medicine
Detroit, Michigan

**Diane E. Spicer**
Department of Pediatric Cardiology
Congenital Heart Center
University of Florida
Gainesville, Florida

**Varsha Thakur**
Division of Cardiology
Department of Pediatrics
The Hospital for Sick Children
University of Toronto Faculty of Medicine
Toronto, Canada

**Boris Tutschek**
Professor of Obstetrics and Gynecology
Prenatal Zurich
Zürich, Switzerland

and

Medical Faculty
Heinrich Heine University
Düsseldorf, Germany

**Wayne Tworetzky**
Department of Cardiology
Boston Children's Hospital
Harvard Medical School
Boston, Massachusetts

**Dan V. Valsky**
Division of Obstetrics and Gynecology
Hadassah-Hebrew University Medical Center
Jerusalem, Israel

**Christoph Wohlmuth**
The Fetal Center
UTHealth McGovern School of Medicine
Houston, Texas

and

Department of Obstetrics and Gynecology
Paracelsus Medical University
Salzburg, Austria

**Simcha Yagel**
Magda and Richard Hoffman Center for Human Placenta Research
Division of Obstetrics and Gynecology
Hadassah-Hebrew University Medical Center
Jerusalem, Israel

**Shi-Joon Yoo**
Department of Diagnostic Imaging
The Hospital for Sick Children
University of Toronto Faculty of Medicine
Toronto, Canada

**Yaron Zalel**
Sackler School of Medicine
Tel Aviv University
Tel Aviv, Israel

**Klaus Zerres**
Institut für Humangenetik der RWTH Aachen
Aachen, Germany

# 1

# Cardiac morphogenesis

Adriana C. Gittenberger-de Groot, Monique R.M. Jongbloed, Marco C. de Ruiter, Margot M. Bartelings, and Robert E. Poelmann

## Introduction

Cardiovascular development and the regulatory mechanisms underlying this major embryonic event have become essential knowledge for the fetal cardiologist. The increased potential of ultrasound technology to detect morphology of the growing heart requires more insight into the morphogenetic and epigenetic pathways essential for normal and abnormal development. This area is now expanding with the possibilities of acquiring data from patients by human exome screening, transcriptome analysis, single nuleotide polymorphism (SNIP) technology, and chromatin remodeling.[1–3] It is essential to link these genetic, epigenetic, and environmental clues from patient material to advance our understanding of the complicated interactive processes that govern heart development. The crucial processes in human cardiac development take place within the first 6 weeks of embryogenesis and, as such, cannot be pursued using *in vivo* diagnostics. It is, therefore, still imminent that essential knowledge is incorporated from animal models such as (transgenic) mouse, chicken, and, more recently, zebrafish, as basic principles of heart formation can be compared between various animal models and human development, even profiting from an evolutionary-developmental approach.[4,5] One has to take into account, however, important species differences such as, for instance, a double-sided aortic arch in fish and reptiles, a right-sided aortic arch system in birds, as compared to a left-sided system in mammals,[6] a persisting left-sided caval vein in mice, and the lack of cardiac septation in fish and many reptiles with only a two- or three-chambered heart tube as a final result. The influence of hemodynamics on the developing system has long been underestimated or neglected because of insufficient refined technology to study this *in vivo* in the developing embryo. Currently, newly designed techniques including microparticle image velocimetry have opened up this research field.[7,8] For the fetal cardiologist, particle image velocimetry is a very interesting new development, as noninvasive techniques such as echo-Doppler add physiologic insight to morphology.

The various converging fields of research have sometimes resulted in a confusing use of terminology, which is not easily solved,[9] and which will undoubtedly continue with future new discoveries. This chapter describes in brief the major events in cardiac development.[10] There is a focus specifically on the continuous recruitment of myocardium from the second heart field[11,12] and on extracardiac cellular contributions[13] to the heart and their modulatory role.[14] Genetic and epigenetic causal pathways will be briefly discussed. (For all abbreviations of genes and gene products, see Table 1.1; for all embryological and anatomical abbreviations, see Table 1.2.)

## Primary cardiogenesis

The primary heart tube (Figure 1.1a) develops from the precardiac mesoderm, also referred to as the first heart field (FHF) (Figure 1.2), which is located bilaterally in the splanchnic layer of the lateral plate mesoderm of the embryo. These cardiogenic plates fuse rostrally in the midline and form a crescent-shaped structure that will develop into the primary heart tube.[15] The inner lining of this tube is formed by cardiac jelly and endocardial cells that are continuous with the endothelium of the embryonic vascular plexus. The endocardium is most probably a heterogeneous population both in origin and in function depending on the site in the heart. The endoderm of the adjoining developing primary gut plays an important inductive role[16] in the differentiation of the primary heart tube through a cascade of inductive signaling molecules, such as the bone morphogenetic protein (BMP) and fibroblast growth factor (FGF), as well as the inhibitor wingless-related integration site (Wnt) families.[17] The primary heart tube is therefore not just a small homunculus in which all future segments of the heart are already present. This has become generally accepted, and many reviews and book chapters now provide these new insights.[11,14,18,19] Data on the components of the primary heart tube are somewhat confusing, but the most recent data, based on extensive and minute tracing studies, are in favor of an initial small atrial compartment, a myocardial atrioventricular (AV) canal, in which cardiac jelly is remodeled into AV endocardial cushions (putative AV valves),[20] and a primitive ventricle (Figure 1.1b) connecting to the arterial pole.[21] In the human embryo, this primary heart tube already starts to beat with peristaltic contractions at 3 weeks of development. The formed primary heart tube is never completely symmetric (Figure 1.1a), and

**Table 1.1** Mentioned genes and gene products

**14-3-3 epsilon:** Eluted in the 14th fraction on positions 3.3
**Actc:** Cardiac muscle α actin
**Acvr2b:** Activin A receptor type B
**Alk2:** Activing receptor-like kinase
**BMP:** Bone morphogenetic protein
**CHD7:** Chromodomain helicase DNA binding protein 7
**Cited2:** cbp/300-interacting transactivator 2
**DSCAM:** Down syndrome cell adhesion molecule
**eNOS:** Endothelial nitric oxide synthase
**ET1:** Endothelin-1
**FGF:** Fibroblast growth factor
**GATA:** Transcription factors binding to the GATA sequence
**GJA1:** Gap junction α-1 protein
**HAND2:** Heart and neural crest derivatives
**HCN4:** Potassium/sodium hyperpolarization-activated cyclic nucleotide-gated channel 4
**Isl1:** Insulin gene enhancer protein 1
**Irx4:** Iroquois homeobox protein
**KLF2:** Krüppel-like factor-2
**Lrp2:** Low-density lipoprotein-related protein-2
**Mef2c:** Myocyte-specific enhancer factor
**MHC:** Myosin heavy chain
**MYH 6,7:** Myosin heavy chain
**NFATc1:** Nuclear factor of activated T cells
**NKx2.5:** Nk2 homeobox 5
**Nodal:** Member of transforming growth factor superfamily
**Notch1:** Notch homolog-1
**Pax3:** Paired box transcription factor
**Pitx2c:** Paired-like homeodomain transcription factor
**Pdgfrα:** Platelet-derived growth factor receptor-α
**Podoplanin:** Encoded by the PDPN gene
**Raldh2:** Retinaldehyde dehydrogenase-2
**RhoA:** Ras homolog gene family
**SALL4:** Spalt-like transcription factor
**Shox2:** Short stature homeobox
**Tbx:** T-box proteins
**TGFβ:** Transforming growth factor
**Wnt:** Wingless-related integration site
**VEGF:** Vascular endothelial growth factor

genetic determinants of sidedness[22] and cardiac looping[23] are present. Many mouse knockout studies of genes that are essential for primary cardiogenesis lead to early embryonic lethality. Heterozygous mutations of some of these genes in the human population can lead to congenital malformations such as, for example, those described for Nkx2.5 mutation.[3,24]

## Secondary cardiogenesis and organogenesis

Early marker experiments in chicken embryos,[5,16] as well as elegant tracing of cell clones in mouse embryos,[21] have proved that essential parts of the cardiac myocardium at both the outflow and the inflow of the primary heart tube are newly recruited. Transgenic reporter mice with cardiac progenitor-specific marker genes like Isl1, Mef2c, and Nkx2.5 have further supported these findings.[11,18] As the splanchnic mesoderm forming the primary heart tube is referred to as the FHF, the newly recruited cardiac cells derive from mesenchyme referred to as the second heart field (SHF) (Figures 1.1d and 1.2), which is initially positioned medially, but eventually attains a dorsal position between the endoderm of the gut and the primary heart tube. As the dorsal mesocardium is interrupted in its midportion, these SHF-derived cells can only reach the heart tube at the arterial and the venous poles (Figure 1.2). The specific contributions of the SHF to the developing heart are discussed in the next paragraph.

The addition of SHF cardiac cells from a proliferating dorsal pericardial wall source[25] results in a lengthening of the primary heart tube concomitant with ongoing dextral looping that is also governed by genetic factors like asymmetric Pitx2c expression.[23,26]

## Recruitment of second heart field cardiac progenitors

Experimental studies show specific characteristics of the addition of cardiac cells. Here details at the outflow tract (OFT) (arterial pole) and inflow tract (venous pole) are described separately.[27]

### *The arterial pole*

Dependent on the marker experiments and reporter gene constructs, several temporospatial patterns of contribution of SHF myocardium have been distinguished, in its most extensive form comprising the complete right ventricle, including the arterial outflow tract and the right side of the ventricular septum[27] (Figures 1.1c and 1.3a). Ongoing scientific insight resulted in changes in nomenclature that might be somewhat confusing (Figure 1.2). The contribution of the SHF-derived cells to the outflow tract is not symmetric, as we and others[28,29] have recently shown. There is a marked deposition toward the (embryonic left) pulmonary side of the OFT forming the right ventricular outflow tract myocardium and components of the pulmonary arterial wall (Figure 1.3b). This process is actually responsible for lifting of the pulmonary orifice anteriorly and to the right of the aortic orifice and as such explains rotation of the orifices and great arteries at the arterial pole (Figure 1.3 and Video 1.1). We have called this anterior SHF-directed process the "pulmonary push."[28] Our

**Table 1.2** Embryological and anatomical abbreviations

| | | | |
|---|---|---|---|
| A | Atrium | MB | Moderator band |
| Ao | Aorta | MC | Mesenchymal cap |
| AoS | Aortic sac | MO | Mitral orifice |
| AP | Arterial pole | NCC | Neural crest cells |
| AS | Atrial septum | OFT | Outflow tract |
| ASD | Atrium septum defect | OS | Ostium secundum |
| AV | Atrioventricular | OTS | Outflow tract septum |
| AVC | Atrioventricular canal | OVM | Ligament of Marshall |
| AVSD | Atrioventricular septum defect | PAA | Pharyngeal arch arteries |
| CAT | Common arterial trunk | PEO | Proepicardial organ |
| CCS | Cardiac conduction system | PS | Primary interatrial septum |
| CCV | Common cardiac vein | PT | Pulmonary trunk |
| CJ | Cardiac jelly | PV | Pulmonary vein |
| CS | Coronary sinus | RA | Right atrium |
| CV | Cardinal vein | RC | Right cardinal vein |
| DA | Ductus arteriosus | RV | (Primitive) right ventricle |
| DMP | Dorsal mesenchymal protrusion | RVOT | Right ventricular outflow tract |
| EC | Endocardial cushion | SAN | Sinoatrial node |
| EPDC | Epicardium derived cells | SB | Septal band |
| FD | Flow divider | SCV | Superior caval vein |
| FS | Folding septum | SHF | Second heart field |
| GCV | Great cardinal vein | SS | Secondary interatrial septum |
| ICV | Inferior caval vein | SV | Sinus venosus |
| IFT | Inflow tract | TO | Tricuspid orifice |
| IS | Inlet septum | TS | Trabecular septum |
| LA | Left atrium | VCAC | Ventriculo-coronary arterial communication |
| LCV | Left cardinal vein | VP | Venous pole |
| LV | (Primitive) left ventricle | VSD | Ventricular septum defect |
| LVOT | Left ventricular outflow tract | | |

findings are in line with earlier observations that a specific sensitivity of the pulmonary outflow tract myocardium might relate to distinct genetic coding areas in the subpulmonary and subaortic outflow tract region, which are important for the rotation of the outflow tract.[30]

## The venous pole

At the venous pole, the contribution of SHF is important for the growth of the atria. The incorporation of sinus venosus myocardium in the dorsal wall of the atria is an important mechanism (Figure 1.1b). In parallel with the *anterior SHF* at the outflow tract, we have introduced the term *posterior SHF* for this region (Figures 1.1d and 1.2), which is now generally accepted.[11,27,31] We and others have discovered that the sinus venosus myocardium is initially Nkx2.5-negative[32,33] (Figure 1.4a,b).

Tracing of Isl1-positive progenitor cells has shown the extent of the incorporation. In contrast to the outflow tract, this area and the derived sinus venosus myocardium have specific gene expression patterns, including Tbx18,[34] Shox2,[35,36] BMPs,[31,37] and podoplanin.[33] Based on specific gene expression patterns studied in various research centers, there has arisen some controversy concerning whether or not a specific pulmonary venous progenitor myocardium exists.[37–39] A recent publication, using LaacZ tracing of posterior SHF cells, shows the common origin of sinus venosus cells with cells incorporated at the posterior atrial wall, including the pulmonary venous myocardium.[40] Subsequent differentiation with specific gene patterns for each region has most probably led to the controversy.

Not only myocardial wall is added to the venous pole, but also an SHF-derived mesenchymal component, the dorsal mesenchymal protrusion (DMP), is incorporated, being essential for AV septation.[41] The SHF also gives rise to the

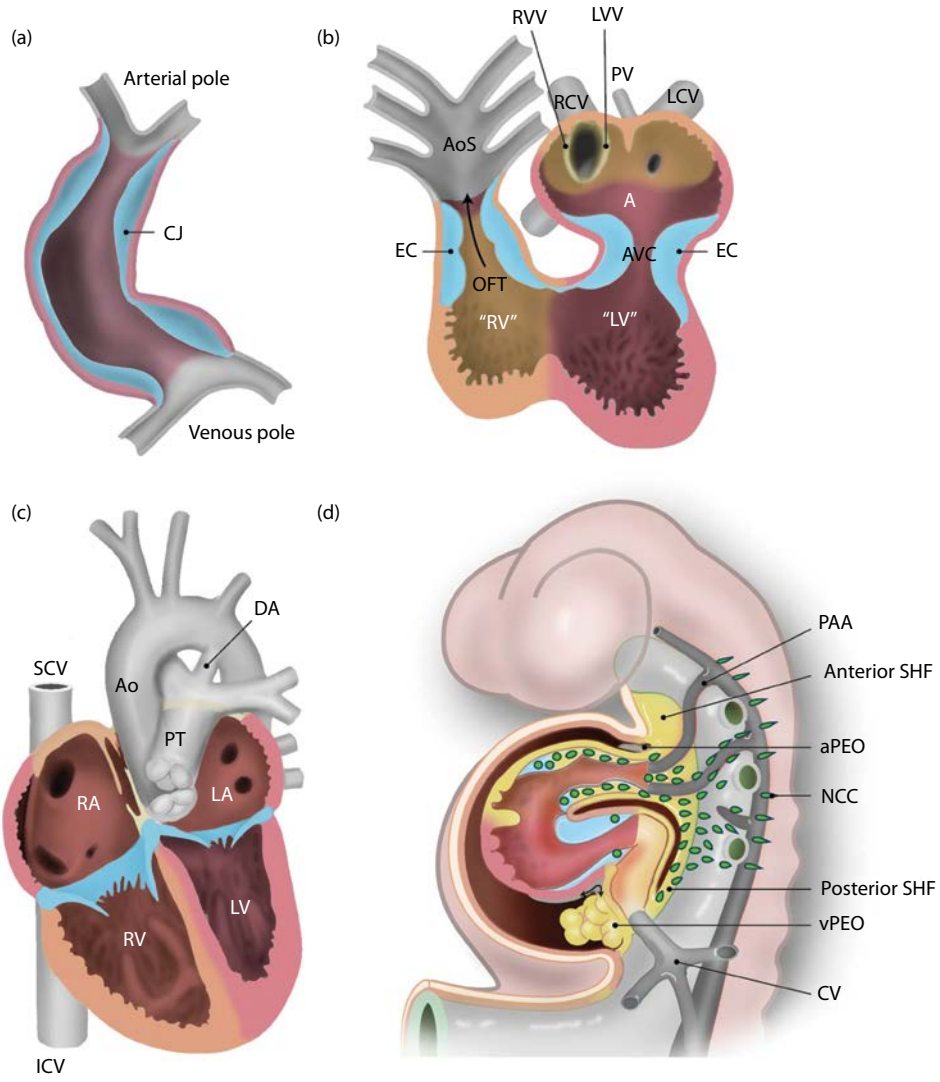


**Figure 1.1**
Stages of cardiac development. (a) The primary heart tube in an early phase of dextral looping lined on the inside by cardiac jelly (CJ). (b) A more advanced stage of development, depicted for clarity in one plane with the unseptated aortic sac (AoS) and common atrium (A) in a side-to-side position. The entrance of the common pulmonary vein (PV) is on the left side of the atrium is and the entrance of the sinus venosus, flanked by the right (RVV) and left (LVV) valves, on the right side. First (pink) and second heart field (SHF, yellow) derived myocardium is indicated. AV canal (AVC) and outflow tract (OFT) carry the respective endocardial cushions (EC) in blue. The AoS connects to a symmetric set of pharyngeal arch arteries. LCV left cardinal vein, "LV" primitive left ventricle, RC right cardinal vein, "RV" primitive right ventricle. (c) Fully formed four-chambered heart. The interventricular septum is derived from both first and second heart field derived cells. Ao aorta, DA ductus arteriosus, ICV inferior caval vein, LA left atrium, LV left ventricle, PT pulmonary trunk, RA right atrium, RV right ventricle, SCV superior caval vein. (d) Sagittal section of a stage comparable to (b). Migrating neural crest cells (NCCs, green) are depicted, mainly reaching the OFT with few cells to the AV cushions. The proepicardial organ at the venous pole (vPEO) and the smaller one at arterial pole (aPEO) are indicated, although the latter emerges slightly later in development. (CV, common cardinal vein; PAA, pharyngeal arch arteries.) (Modified after Gittenberger de Groot AC et al. In: Moller JH, Hoffmann JIE, eds. *Pediatric Cardiovascular Medicine*, 2nd edn. Wiley-Blackwell; Hoboken, New Jersey, 2012:1–22.[19])

proepicardial organ (Figure 1.1d), which is described in more detail in the section "Epicardium."

## The neural crest

A contributing population to the developing heart are the neural crest cells (NCCs) migrating from the crest of the neural tube through the splanchnic mesoderm-derived SHF (Figures 1.1d, 1.2, and 1.5). The relevance of cardiac NCC was first studied in the avian embryo, and its distribution has initially been detected by quail chick-chimera experiments[5,16] and confirmed by retroviral reporter gene transfer[42] showing the deposition of NCC in the arterial outflow tract as well as the differentiation into smooth muscle cells of part of the wall of the great arteries and aortic arch tributaries. At both the

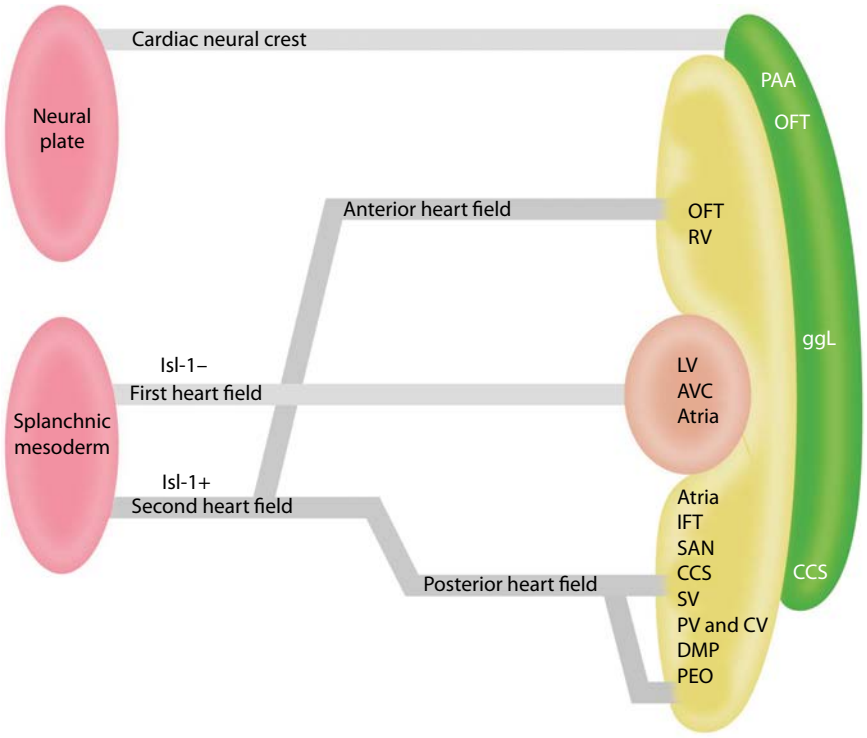


**Figure 1.2**
The various lineages showing contribution from first and second heart fields as well as the neural crest that arise from the crest of the neural plate and migrate into the pharyngeal arches and the heart. Part of the early splanchnic mesoderm gives rise to the first and second heart field. The first heart field differentiates into the primary heart tube (left ventricle, AV canal and part of the atria). The second heart field separates in an anterior (arterial pole) and a posterior (venous pole) part with many derivatives. (AVC, atrioventricular canal; CCS, cardiac conduction system; CV, cardinal veins; DMP, dorsal mesenchymal protrusion; ggL, autonomic ganglia; IFT, inflow tract; LV, left ventricle; OFT, outflow tract; PAA, pharyngeal arch arteries; PEO, proepicardial organ; PV, pulmonary veins; RV, right ventricle; SAN, sinoatrial node; SV, sinus venosus.) (Modified after Gittenberger-de Groot AC, Poelmann RE. In: Yagel S, Silverman NH, Gembruch U, eds. *Fetal Cardiology*. Informa Healthcare; New York, 2009:9–17.[109])

inflow and outflow tract, NCCs (Figure 1.5a) contribute to the sympathetic and parasympathetic innervation,[43] including a marked ring around the pulmonary venous anlage.[44]

Based on NCC ablation experiments,[42,45] topical deficiency of this cell type was held responsible for many cardiac outflow tract malformations such as common arterial trunk (CAT), pulmonary stenosis and atresia, tetralogy of Fallot, double-outlet right ventricle, and aortic arch malformations. This spectrum is ideally exemplified in the human 22q11 deletion syndrome that also shows other neural crest cell-influenced abnormalities in, for example, the face and thymus. The most essential gene in the 22q11 deletion syndrome, however, is Tbx1[46] that is not expressed in the NCCs but in the SHF mesenchyme providing cells to the arterial pole and, as was recently shown, also to the venous pole.[27] This leads to the important conclusion that it is the disturbed interaction of SHF and NCCs at various levels that is essential for the spectrum of cardiac malformations. It explains also that mutations in a great number of genes expressed in either cell population can evoke comparable malformations, broadening immensely our scope of understanding of the pathomorphogenesis of outflow tract anomalies.

# Epicardium

Epicardial cells derive from the posterior SHF and its covering coelomic wall mesothelium (Figure 1.1d). These mesothelial cells not only differentiate into the already described sinus venosus myocardium but also form an epithelial structure at the venous pole next to the sinus venosus referred to as the proepicardial organ (PEO)[47,48] (Figure 1.6a,b). Epicardial cells detach from the PEO and migrate over the initially naked myocardial heart tube.[49] It is evident that retinaldehyde dehydrogenase (RALDH) and retinoic acid play an important role in guiding this process.[50] After covering the heart, the epicardial cells undergo EMT migrating into a mesenchymal subepicardial layer as epicardium-derived cells (EPDCs).[51–53] Subsequently, these EPDCs migrate between the atrial and ventricular cardiomyocytes to form the interstitial fibroblasts and even take up a subendocardial position (Figure 1.6). A second wave of epicardial EMT is seen when the coronary capillary plexus is remodeled into an arterial and venous system in which the EPDCs are the source of smooth muscle cells and periarterial (adventitial) fibroblasts (Figure 1.6c,d). At this stage, the EPDCs are also essential in dissociating the

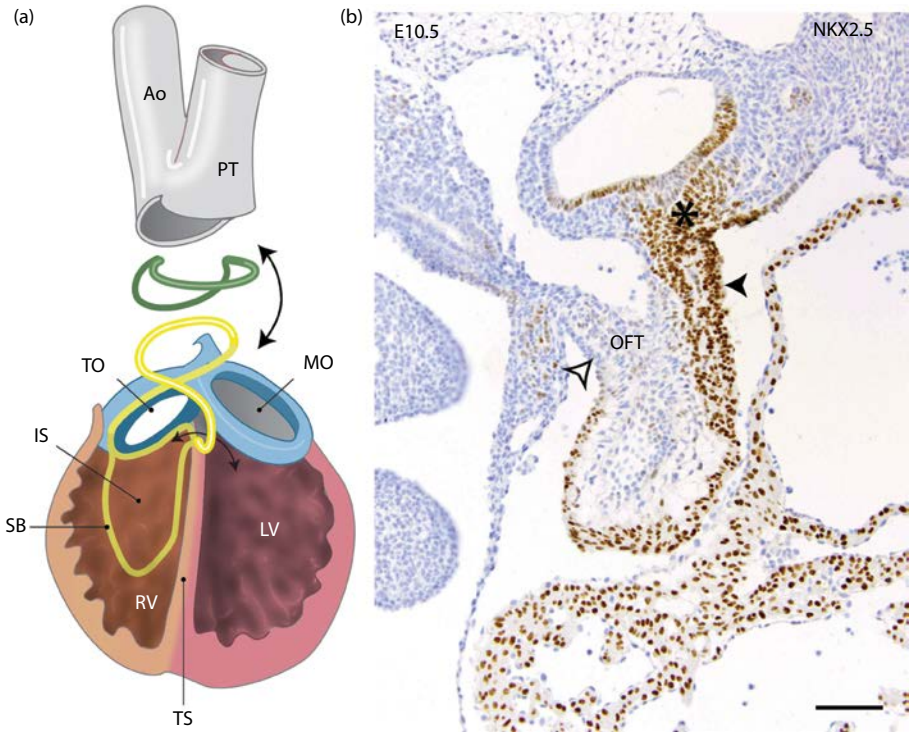


**Figure 1.3**
(a) Exploded view of the outflow tract with a still unseptated aorta (Ao) and pulmonary trunk (PT). The green ring represents the saddle-shaped semilunar valve level; note that the pulmonary part is more cranial than the aortic part. The curved double-headed arrow represents the pulmonary push. The semilunar valve level is located ventral to the atrioventricular canal (blue) with the mitral (MO) and tricuspid (TO) orifices. The yellow band represents the primary ring, mainly the border between first and second heart field myocardial derivatives. In the right ventricle (RV), the primary ring has expanded to allow formation of the inlet septum (IS) of which the septal band (SB) is the visible representative. The interventricular communication is indicated (small double-headed arrow). (LV, left ventricle; TS, trabecular septum.) (b) Section of the cardiac outflow tract (OFT) of a mouse embryo stained for expression of NKx2.5. The nuclear staining is encountered in differentiated myocardial cells as well as in its second heart field precursors (asterisk) showing a clear asymmetry with a marked preference for the pulmonary side (closed arrow head) as opposed to the aortic side (open arrow head). The pulmonary side is relevant for the pulmonary push.

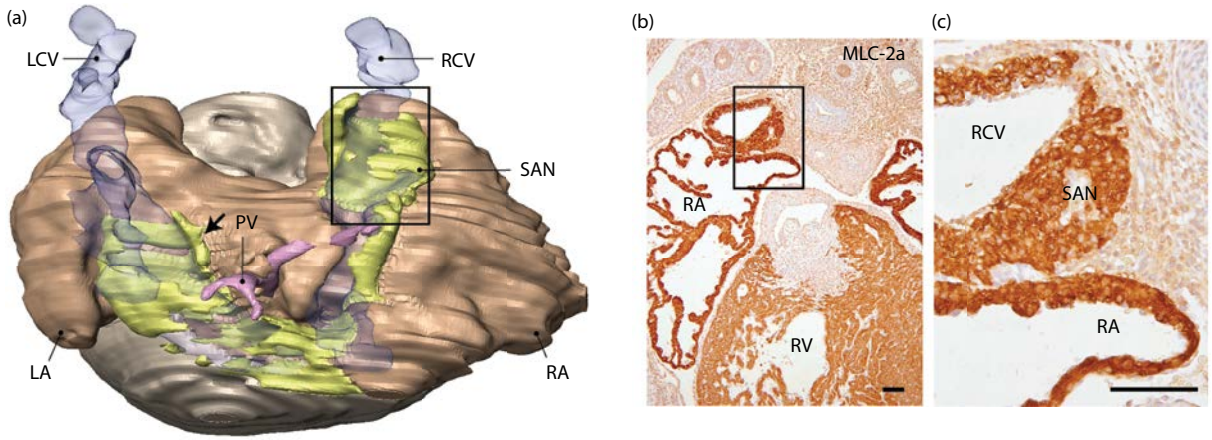


**Figure 1.4**
(a) Three-dimensional reconstruction of a mouse embryo heart viewed from dorsal. The NKx2.5 negative myocardium (green) is seen as a U-shaped part of the mesoderm connecting and covering the left (LCV) and right (RCV) cardinal veins and encircling the pulmonary vein (PV). At this site, a transient left sinoatrial node (arrow) is seen, while at the right side this is a far larger area that will persist as the definitive right-sided sinoatrial node (SAN). Color codes: right (RA) and left (LA) atria are in brown, the LCV and the RCV in blue, and the PV in pink. (b,c) (magnification) A MLC2a stained section incorporating both Nkx2.5 positive and negative myocardium showing the SAN at the entrance of the RCV into the RA. Note that this segment of the cardinal vein also expresses the atrial myocardial light-chain protein (MLC2a staining) marking it as myocardium. (Modified after Gittenberger-de Groot AC et al. *Anat Rec* 2007;290:115–22.[33])

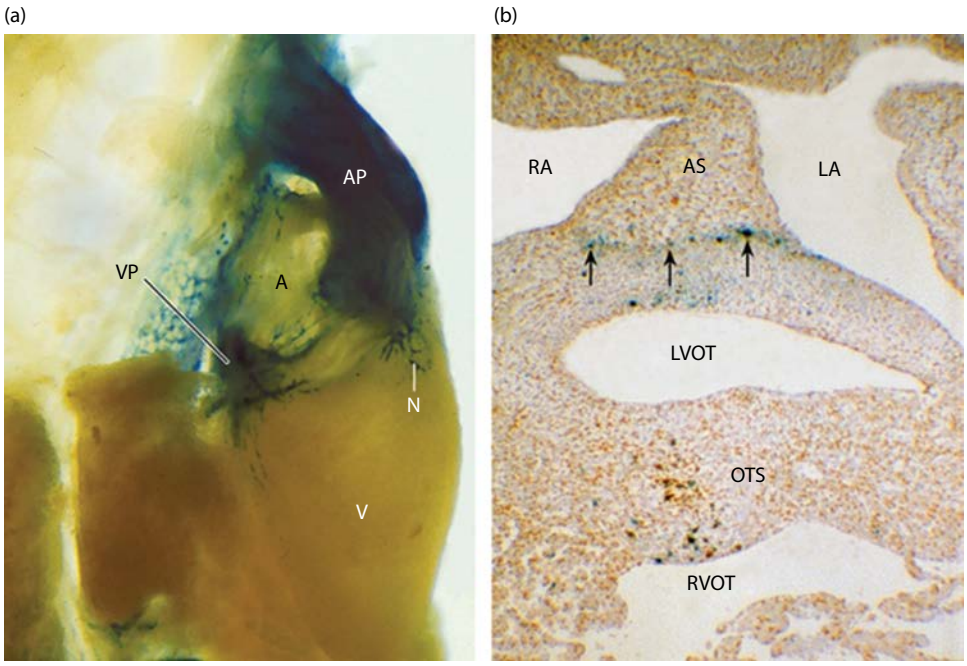


**Figure 1.5**
Early chicken embryo (HH10) received injection of a retrovirus harboring the marker gene LacZ into the neural tube, thereby infecting neural crest cells. The migrated NCCs are turned blue by chemical staining. (a) Whole mount of resulting heart with massive NCC presence in aorta and pulmonary trunk and in the venous pole (VP). Atrium and ventricles are negative but for some subepicardial neuronal cells. (A, atrium; AP, arterial pole; N, neurons; V, ventricle.) (b) Section encompassing the base of the atrial septum (AS) and the outflow tract septum. Blue NCCs are present both at the border of atrial septum with left ventricular outlet (LVOT), as well as in the outflow tract septum (OTS). Incidentally, many of the blue NCCs become apoptotic in this combined staining that includes terminal deoxynucleotidyl transferase-mediated dUTP nick-end-labeling (TUNEL) for DNA fragments (brown cells). (LA, left atrium; RA, right atrium; RVOT, right ventricular outflow tract.) (Modified after Gittenberger de Groot AC et al. In: Moller JH, Hoffmann JIE, eds. *Pediatric Cardiovascular Medicine*, 2nd edn. Wiley-Blackwell; Hoboken, New Jersey, 2012:1–22; Poelmann RE, Gittenberger-de Groot AC. *Dev Biol* 1999;207:271–86.[19,110])

atrial from the ventricular myocardium by migrating into the AV endocardial cushions (Figure 1.6c,d), where they contribute to the formation of the fibrous annulus (part of the fibrous heart skeleton) and the AV valves.[51,54,55] The differentiation capacities of the EPDCs are still under investigation, with a main controversial issue being whether they are also the source of the coronary endothelial cells.[56,57] Furthermore, we have shown by PEO inhibition and rescue studies that EPDCs are essential for compaction of the myocardium,[58] the ingrowth and stabilization of the main coronary arteries,[59,60] and the differentiation of the Purkinje network[61] (Figure 1.6e).

At the root of the aorta and pulmonary trunk, the venous pole–derived cardiac epicardium "meets" the coelomic lining at the arterial pole referred to as cephalic[62] or arterial epicardium that forms bleb-like structures strongly resembling the venous PEO.[12] After ablation of the PEO in chicken embryos resulting in the absence of the PEO-epicardium, the arterial lining will expand, partially covering the OFT myocardium.[58]

## Endocardial cushions

The endocardial cushions are major players in both cardiac septation and formation of the AV and semilunar valves. They develop from cardiac jelly that is populated by cells in the AV and OFT regions. The endocardial cushion cells derive from multiple origins by EMT from the lining endocardium[20] but also receive cells from the epicardium (predominantly in the AV cushions) and from the neural crest (mainly in the outflow tract cushions). With regard to cardiac septation, the superior and inferior AV cushions that line the upper rim of the ventricular inlet septum fuse with the atrial mesenchymal cap covering the lower part of the primary atrium septum to separate the left mitral and right tricuspid orifice (Figure 1.7a,b). The AV cushions are continuous with the two proximal (parietal and septal) endocardial outflow tract cushions. Proper fusion of AV and outflow tract endocardial cushion components results in completing cardiac septation forming a separated four-chambered heart (Figure 1.1b,c).

## Atrium formation, septation, and vein incorporation

The venous pole of the heart consists of the sinus venosus (receiving the blood from the left and right cardinal veins, the omphalomesenteric and umbilical veins) and the common atrium (Figure 1.7). The common atrium (Figure 1.1b)

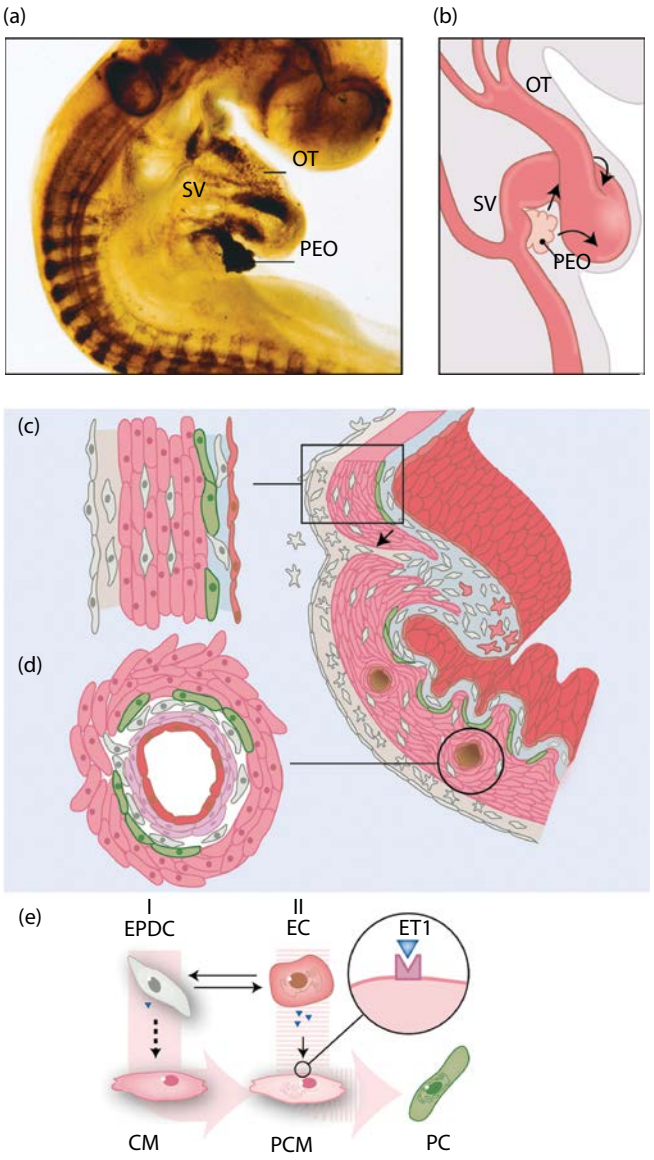


**Figure 1.6**
Development of the epicardium. (a) In an early embryo the proepicardial organ (PEO) is present near the sinus venosus (SV). (b) Cells from the PEO attach to the myocardial wall of atrium and ventricle and migrate to form the epicardial epithelium eventually covering the heart until the myocardial border at the outflow tract (OT). (c,d) The epithelial cells go into epithelium-mesenchymal transition to form epicardium-derived cells (EPDCs) in the subepicardial space, and migrate further into the myocardium to differentiate into interstitial fibroblasts (gray cells in between pink myocardium). Subendocardially located myocardial cells may be induced to form Purkinje cells (green). Note the breach (arrow) between atrial and ventricular myocardium filled with EPDCs (future annulus fibrosis) also using this route to reach the AV cushions, also filled by endocardium-derived cells (red cells). (e) Schematized cross-talk between EPDCs and myocardial cells (CM), and by endothelial (EC) endothelin-1(ET1) signaling leading to the differentiation of primitive cardiomyocytes (PCM) into Purkinje cells (PC). ([c,d] Modified after Winter EM, Gittenberger-de Groot AC. *Cell Mol Life Sci* 2007;64:692–703.[52] [e] Modified after Eralp I et al. *Anat Rec* 2006;288A:1272–80.[61])

expands asymmetrically, concomitant with a rightward shift of its connection to the sinus venosus, including its tributing cardinal veins that will be incorporated into the right atrium as the superior and inferior caval veins. The left cardinal vein in humans becomes the ligament of Marshall, and only the coronary sinus connecting the coronary venous system to the right atrium persists (Figure 1.7c,d). At the same time, the connections with the lung circulation start to develop. The volume of the left atrium is influenced by incorporation of the pulmonary veins. In early stages, the first connections from the pulmonary splanchnic plexus are with the (systemic) cardinal veins, the later and definitive connections are via the pulmonary vasculature. This drainage of the lungs is located in the dorsal mesocardium, while the systemic connections gradually disappear.[39] The single pulmonary vein primordium is, concomitant with formation of the primary atrial septum, incorporated in the posterior atrial wall of the left atrium. Progression of this pulmonary venous incorporation results in four pulmonary vein orifices (two left and two right pulmonary veins) (Figure 1.7b). In this process, the inner vascular lining of endothelium and smooth muscle cells of the pulmonary veins forms the lining of the body of the left atrium (yellow in Figure 1.7b), while the left atrial appendage still has an endocardial lining (red in Figure 1.7b).

Atrial septation is accompanied by the mesenchymal posterior SHF-derived DMP[63] (Figure 1.7a,b), also known as the spina vestibuli, that develops between the entrances of the pulmonary and systemic veins. The DMP extends toward the inferior AV cushion and contributes to the atrioventricular septal complex by closure of the ostium primum (Figure 1.7a,b). The primary atrial septum is initially formed from a double layer of posterior SHF-derived myocardium and is lined at its underrim by a mesenchymal cap (Figure 1.7a) that is continuous with the inferior endocardial AV cushion. In the human embryo, at the right side of the primary atrial septum, an infolding of the atrial roof develops, the *secondary atrial septum*. The free rim is referred to in the adult situation as the limbus fossae ovalis. This secondary septum usually fuses after birth with the (in the meantime fibrotic) primary atrial septum now called the valve of the foramen ovale. The latter is the persistent opening before birth that allows oxygen-rich blood from the placenta to bypass the nonfunctioning lung circulation, reaching directly the left atrium and ventricle and thus the systemic circulation. Complicated gene interactions, including sonic hedgehog signaling,[64] are involved in the formation of the atrial septum.

## *Relevance for understanding atrial septal defects and abnormal pulmonary venous return*

Severe developmental inflow tract malformations are seen in disturbed contribution of posterior SHF-derived myocardium

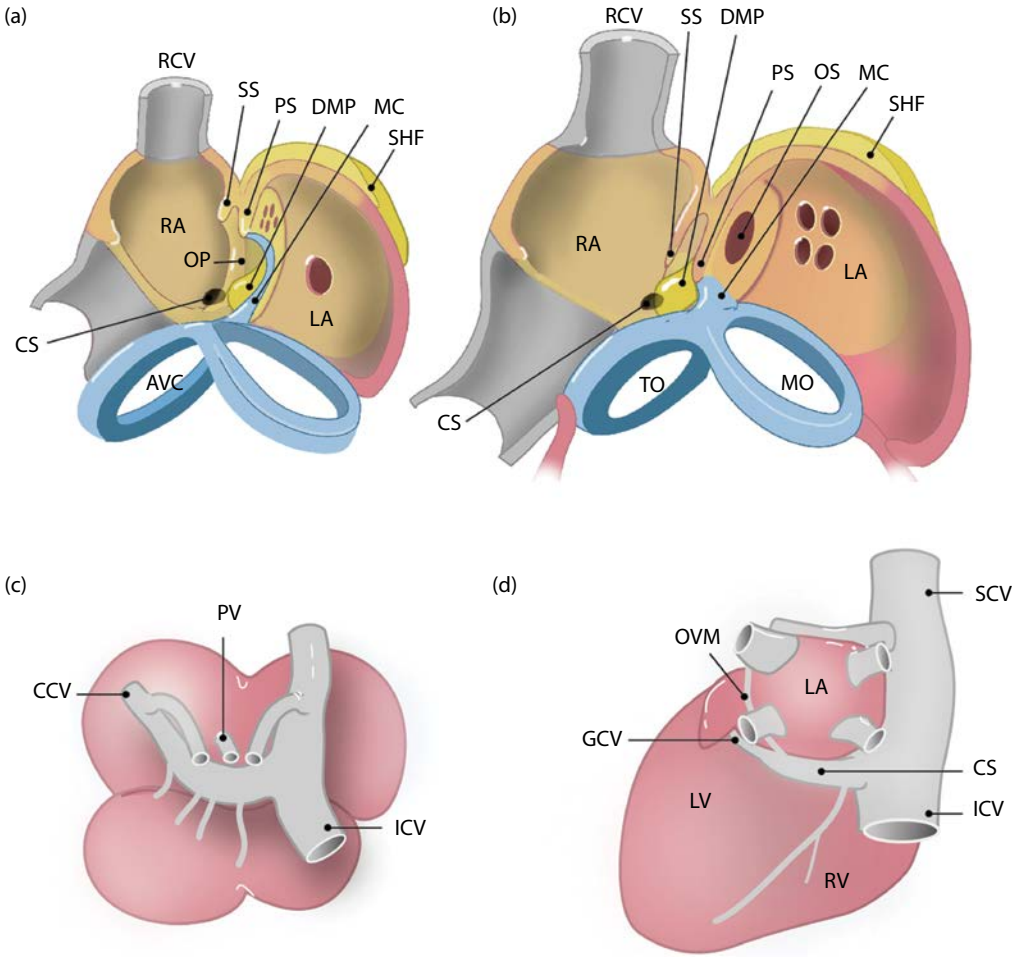


**Figure 1.7**
(a,b) Dorsal aspect of the atria during two stages of formation of the primary (PS) and secondary (SS) interatrial septum. The entrance of the sinus venosus is always in the right atrium (RA) including the coronary sinus (CS). The pulmonary vein (PV) becomes incorporated in the dorsal wall of the left atrium (LA). The second heart field-derived dorsal mesenchymal protrusion (DMP) is central to atrial septation. The mesenchymal cap (MC) of the PS fuses with both AV cushions closing the ostium primum (OP). (AVC, atrioventricular canal; LA, left atrium; MO, mitral orifice; OS, ostium secundum; SHF, second heart field; RCV, right cardinal vein; TO, tricuspid orifice.) (c,d) Dorsal aspects showing the venous contributions to the atria. (CCV, common cardiac vein; GCV, great cardiac vein; ICV, inferior cardinal vein; OVM, ligament of Marshall; SCV, superior cardinal vein.) ([a,b] Modified after Gittenberger de Groot AC et al. In: Moller JH, Hoffmann JIE, eds. *Pediatric Cardiovascular Medicine*, 2nd edn. Wiley-Blackwell; Hoboken, New Jersey, 2012:1–22.[19])

and mesenchyme including atrial septal defects, abnormal pulmonary venous return, and atrial sidedness. For the latter Pitx2 is a very important gene directing left-sidedness in the heart[26] revealing interesting information on atrial isomerism and differentiation of the posterior SHF-derived sinus venosus myocardium, including the sinoatrial node (SAN)[32] and the pulmonary vascular system.[39] Abnormal pulmonary venous return can also be evoked by mutation of SHF-expressed genes like podoplanin[65] and Pdgfrα[66] that result in absent development from the left side of the posterior SHF of the myocardial pulmonary sleeve.

Our observations suggest that all atrial septal components as well as the development of parts of the conduction system might be disturbed when sinus venosus myocardium is not properly differentiated.[33,39]

## Ventricular chamber formation, septation, and myocardial differentiation

Ventricular septation is a relatively restricted event in evolution as it is absent in fish, amphibians, and most reptiles, but appears separately in mammals, crocodiles, and birds. The ventricular septum develops early in organogenesis inside the, as yet, unseptated looping cardiac tube. Its myocardial components (Figure 1.8a) align three-dimensionally with the respective atrial and outflow tract septal elements. Several concepts have been put forward regarding the origin of the septum components.[67] Recent evolutionary-developmental backed research[4] strongly supports separate origins of the

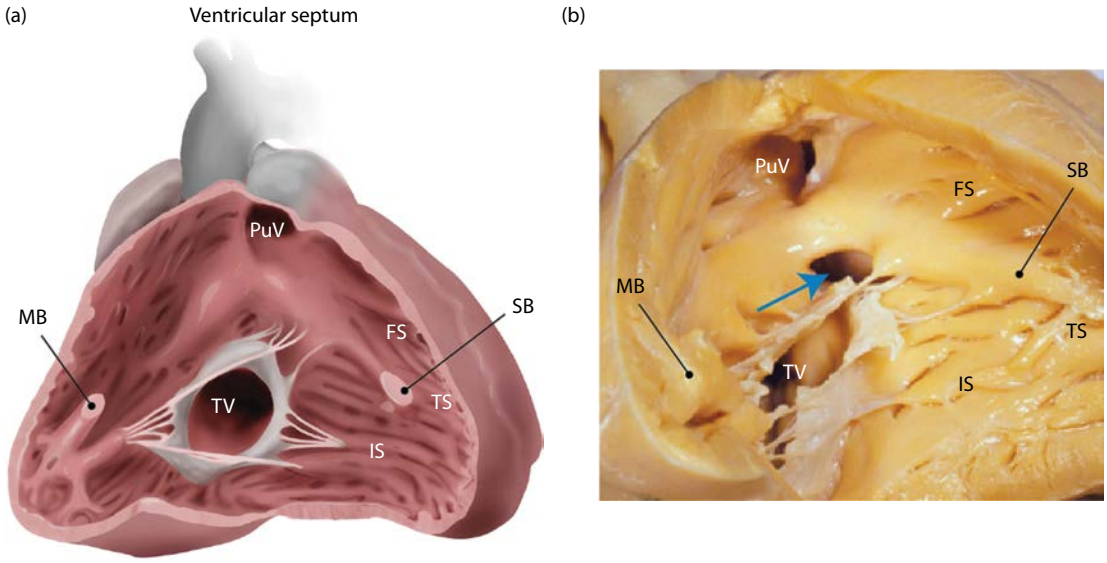


**Figure 1.8**
(a) Opened right ventricle, showing the anterior and lateral walls and the interventricular septum. (FS, folding septum; IS, inlet septum; MB, moderator band; PuV, pulmonary valve; SB, septal band; TS, trabecular septum; TV, tricuspid valve and orifice.) The arrow in (b) points toward a ventricular septal defect. (Modified after Gittenberger-de Groot AC et al. *Ann Med* 2014;46:640–52; Gittenberger de Groot AC et al. In: Moller JH, Hoffmann JIE, eds. *Pediatric Cardiovascular Medicine*, 2nd edn. Wiley-Blackwell; Hoboken, New Jersey, 2012:1–22.[14,19])

posteriorly located inlet septum and the anteriorly located trabecular or folding septum complemented by the outflow tract septum for final division of the right and left sides of the heart. By rightward movement of the initially slit-like right-sided part of the AV canal (future tricuspid orifice), the posterior wall of the right ventricle expands, forming the inlet portion of the right ventricle allowing the right atrium to connect to the right ventricle.[68,69] The anteriorly located trabecular or folding septum forms because of the combination of *ballooning* of the ventricular chambers and the concomitant *infolding* of the left and right ventricular walls with the epicardium sandwiched in between.[4] The formation of the anterior folding septum starts in the inner curvature, which is rich in subepicardial tissue and continues in an apical direction where it becomes more trabecular and spongiose. The inlet septum, including the septal band and the moderator band, merges with the anterior folding septum to form the major part of the interventricular septum. The superior and inferior AV cushions that line the upper rim of the inlet septum fuse with the atrial mesenchymal cap covering the lower part of the primary atrium septum to separate the left mitral and right tricuspid orifice (Figure 1.7a,b).

## *Relevance for ventricular septation defects*

Most ventricular septal defects (VSDs), including AV septal defects (AVSDs), are the result of malalignment, hypoplasia, or even absence of a septal component.[14] Sometimes multiple processes are disturbed at the same time. The problem can be of myocardial origin or based on nonfusion of endocardial cushions. It is remarkable that a relatively restricted number of gene pathways are involved in development of VSDs.[14] Most VSDs are located in the outflow tract region, and deviation of septum components often results in malalignment. Defects resulting from abnormal fusion or development of the inlet septum and the anterior folding septum can be found on their merging borderline that is at the position of the septal band (Figure 1.8a,b). The central muscular VSD is an example. Also the myocardial structure can be deficient as seen in some EPDC-deficient embryos with a spongy septum. This can result in multiple muscular VSDs.

Myocardial differentiation takes place from an initial two-layered structure, not yet covered by epicardium, to a multilayered sheet that consists of an inner trabecular layer and an outer compact layer.[70] Development of the myocardial wall knows many interactive players and inductive signals. The work in zebrafish in which part of the ventricles was removed and regenerated afterward is revealing as to the role of endocardium and epicardium in this process.[71] Recent work[72] shows how dissociation of the inner myocardial layer favors trabecular formation being also effective in endocardial cushion delamination, which is essential for AV valve formation.

## *Relevance for understanding of myocardial disease*

Noncompaction and abnormal thinning of the myocardium can be evoked by abnormal gene patterning and untimely interactions of the various contributing cell types. Mutations of myocardial genes of course play an essential role,[73] leading not only to a dysfunctional myocardial cell but also to abnormal interactions with, for example, the endocardium and the EPDCs. Also an abnormal inductive role of EPDCs in

formation of the compact myocardium might be of relevance for the understanding of some cardiomyopathies, including spongy myocardium or myocardial noncompaction, as well as abnormally thin myocardium (e.g., Uhl anomaly). Defects in either or both might lead to abnormal myocardial differentiation.[12] Also myocardial-to-endocardial interaction disturbances as seen in the 14-3-3 epsilon mutant mouse may lead to an abnormally thin myocardium.[74]

## Remodeling and septation of the outflow tract

Cell–cell and cell–matrix interaction of SHF and NCC based on their specific gene expression patterns[46,75,76] is essential for normal development of the outflow tract and the great arteries. An additional (epigenetic) candidate that is emerging as an important modulating factor is the role of hemodynamics and shear stress on the outflow tract wall and pharyngeal arch arteries.[77] Essential genes such as endothelin-1,[78] Kruppel-like factor-2 (Klf2),[78] transforming growth factor (Tgfβ2),[79] and, as recently shown, possibly also Lrp2[80] might have their effect through mechanosensors, including the possible role of the cytoskeleton through an endocardial/endothelial cilia system.[81] The two proximal (parietal and septal) endocardial OFT cushions after secondary myocardialization fuse resulting in outflow tract separation, with a long subpulmonary infundibulum and a short left ventricular outflow tract, due to the pulmonary push of SHF contribution. The actual outflow tract septum in a normal heart is minimal in size and cannot be recognized as a separate structure.[10]

## *Relevance for understanding outflow tract congenital malformations*

The above findings imply that many genetic as well as environmental pathways can lead to the spectrum of outflow tract malformations. Hampering SHF myocardial recruitment at the outflow tract will lead to outflow tract shortening and abnormal remodeling of the inner curvature myocardium. As a consequence, the pulmonary push (Figure 1.3b, Video 1.1) does not take place properly, and the aortic orifice is not properly wedged in between the atria remaining in a relative dextral position. The resulting abnormalities are dextroposition of the aorta with a double-outlet right ventricle as its most severe form (the most common anomaly in animal models). In these cases, NCCs can still migrate and reach the pharyngeal arch arteries and the endocardial outflow tract cushions as in normal outflow tract septation (Figure 1.9a,b). We have recently described a new model for development of a CAT in a Lrp2 mutant. In this case, there is essentially a rerouting of the NCCs by the absence of leftward expansion of the SHF (Figure 1.9c,d). The NCCs now migrate around the pulmonary trunk and reach the outflow tract cushions, without filling the aorta-pulmonary septum.[80] A similar mechanism, in which both

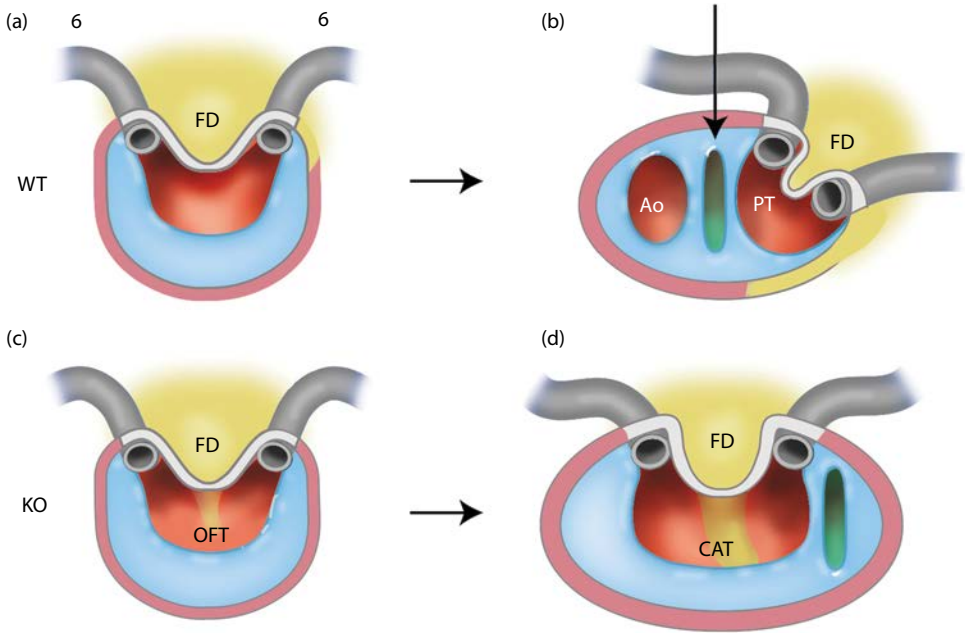


**Figure 1.9**
A model describing outflow tract septation combining neural crest (green) and second heart field-derived (yellow) cells. (a,b) In wild-type (WT) mouse embryos the flow divider (FD) separates the left and right sixth pharyngeal arch arteries, while the neural crest separates (arrow) the aorta (Ao) and pulmonary trunk (PT). (c,d) In the described knockout (KO), the FD has not expanded to the left and the neural crest does not separate the Ao and PT resulting in a common arterial trunk (CAT). 6: Sixth pharyngeal arch artery (the pulmonary artery). (Modified after Baardman ME et al. *Dis Model Mech* 2016;9:413–25.[80])

outflow and inflow tracts show a diminished SHF contribution, is postulated for the mutant Pdgfra knockout mouse (KO)[66] and the Tgfβ2 KO mouse.[82]

Primary NCC defects can lead to a similar spectrum of anomalies including CAT as described for NCC ablation embryos[45] and for mutant NCCs-deficient mouse embryos,[76,83] in which the NCC-filled aorto-pulmonary septum does not complete the septation at orifice level of the great arteries. If the endocardial outflow tract cushions do not fuse properly with the AV cushion mass, outflow tract VSDs develop. Based on their location and surrounding tissues, these are often referred to as perimembranous VSDs.[14] In these cases, the outflow tract septum, in contrast with the normal heart, is distinguishable and often deviated toward either the left ventricle (rare) or the right ventricle (more common) as in tetralogy of Fallot.

Based on the above described interactions of cellular components contributing to the outflow tract, we now have a better understanding of development of the tetralogy of Fallot with subpulmonary stenosis. In a vascular endothelial growth factor (VEGF) 120/120 model,[84] with a tetralogy of Fallot phenotype, an aberrant upregulation of VEGF120 in the subpulmonary outflow tract is present.[84] More recently, we discovered that the expected pulmonary push has not taken place properly.[28]

Epigenetic factors such as hyperglycemia in diabetic pregnancies may likewise lead to similar malformations, most probably affecting SHF as well as NCCs.[85–87]

## Atrioventricular valve formation

The cushion complexes in the AV canal as well as in the OFT are involved in valve formation. In the AV canal, the superior and inferior cushions and the two smaller parietal cushions develop separately and are involved in AV valve formation.[88] The parietal cushions receive preferentially EPDCs[89] as part of the isolation of the atrial and ventricular myocardium during annulus fibrosis formation by the epicardium.[54,90] Thus, the AV valve leaflets have a differential cellular composition. In addition, the underlying right- and left-sided myocardium shows different signaling profiles (TGFβ2 and myosin heavy chain). This relates to the different etiology of delamination of the AV endocardial cushions from the myocardial wall to eventually form the fibrous (bicuspid) mitral and tricuspid leaflets attached (Figure 1.10a–e) by also endocardial cushion–derived chordae tendinae to their papillary muscles.[72]

### *Relevance for congenital malformations*

Atrioventricular endocardial cushion defects can lead to a number of congenital heart malformations. The most common problem is nonfusion of the inferior and superior cushions to each other and the mesenchymal cap of the primary atrial septum, resulting in AVSD. Dependent on the supposed causal factor, this anomaly has initially been referred to as endocardial cushion defect or AV canal defect, a term now considered obsolete. AVSD in the neonate most commonly occurs in the setting of trisomy 21 (Down syndrome) or other syndromes but can also occur as nonsyndromal disease. Many genes have been related to the development of AVSD.[91] Current knowledge from human embryos[92] as well as mouse models shows the effects of a hypoplastic DMP (or spina vestibuli).[41] A deficient contribution of EPDCs to the border of the atrioventricular cushion with the underlying myocardium might inhibit delamination of the tricuspid valve and lead to an equivalent of Ebstein malformation.[93]

## Semilunar valve formation

After fusion of the septal and the parietal endocardial OFT cushions, complemented by two intercalated cushions, three

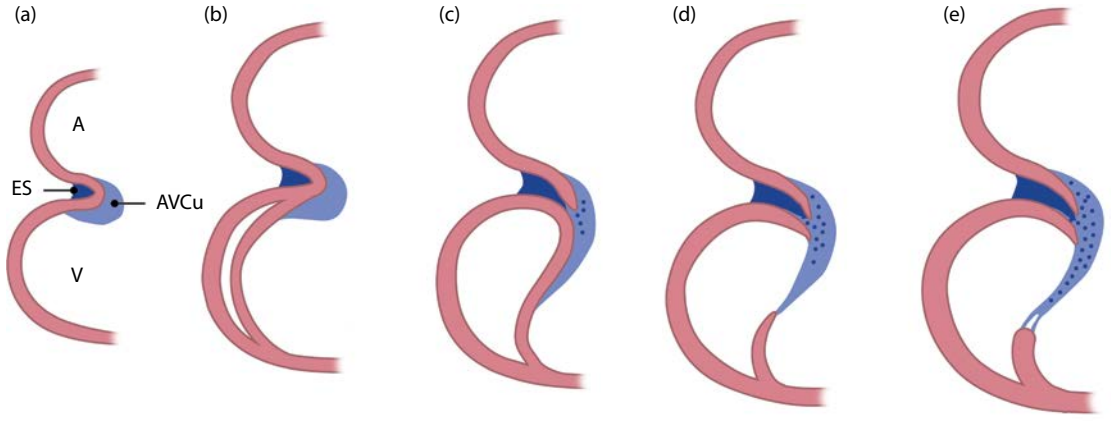


**Figure 1.10**
Formation of atrioventricular valves. (a) AV cushions (AVCu, light blue) lining the atrioventricular canal, while the AV groove is filled with EPDCs (ES, dark blue). (b) Ventricular myocardium delaminates still provide a scaffold for the endocardial cushion. (c) Atrial (A) and ventricular (V) myocardium become separated by subepicardium in the formation of the annulus fibrosis. (d) Part of tendon apparatus develops. Papillary muscle and chordae tendinae are present.

semilunar valve leaflets develop in both the aortic and pulmonary root at the border of the myocardium and the arterial vascular wall. In the formation of semilunar valves, several cell populations participate, in particular the endocardium, and endocardial cushion cells, that are derived after EMT. Furthermore, the NCCs[5,45] that fill the central part of the endocardial outflow tract cushions and the arterial epicardium contribute to the formation of the annulus fibrosis between the arterial wall and the myocardial rim.[12] As a consequence, developmental or signaling disturbances in any of these populations might result in congenital valve malformations as exemplified by the neural crest related Pax3 signaling pathway[94] (Figure 1.11a–d).

## *Relevance for septation and valve formation abnormalities*

The most common congenital heart malformation is the bicuspid aortic valve (BAV) (Figure 1.11e). Many mutant mouse models are related to BAV, including mice with mutations of eNOS, FGF8, Nkx2.5, GATA5, and RhoA. In humans, mutations in Notch1 and NFATc1 were found to be associated with BAV. Most probably we are dealing with a heterogenous cause as many cell populations including the anterior SHF and the NCC are involved as exemplified by NCC-related Pax3 signaling pathway[94] and the eNOS mutation in the endothelium of the developing valves.[95] Dilation (aneurysm) of the ascending aorta is associated with BAV, which is not a surprise as the same cells contribute to both the aortic wall and the valve.[96]

# Cardiac conduction system

In the primary heart tube stage, peristaltic contractions initiated at the sinus venosus propel the blood column toward the outflow tract. Concurrent with the addition of SHF myocardium to the venous pole, differentiation takes place toward working myocardium and specialized (conducting) myocardium.[97] The definitive conduction system consists of the (right-sided) sinus node (SAN), AV-node, penetrating bundle of His, the right and left bundle branches, and the ventricular Purkinje fibers.

Early in development the entire sinus venosus has the capacity to generate action potentials,[98] resulting in a peristaltic heart contraction. Gradually this becomes restricted to the right side of the sinus venosus, marking the entry of the right cardinal vein in the right atrium. The wall of the left cardinal vein (containing a transient left SAN) (Figure 1.4a) develops into the sinus coronarius and will lose its pacemaking capacity, which is also the case of the wall of the pulmonary veins entering the left atrium. The absence of Nkx2.5 characterizes normal SAN development.[33,99] Further transcription factors, including Tbx18 and the repressor Tbx3, mark the development of the right-sided SAN.[99] The ion channel HCN4 is essential for

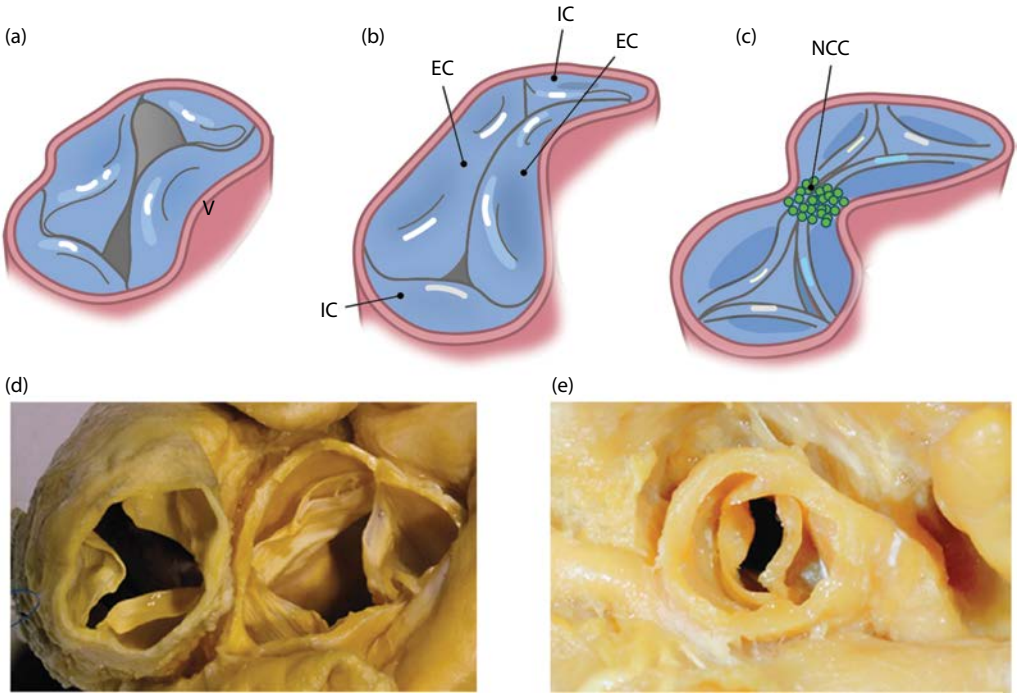


**Figure 1.11**
(a–c) Four OFT cushions develop into six semilunar valve leaflets. Fusion of septal and parietal endocardial cushion (EC) by involvement of neural crest cells (green) forms the facing valve leaflets in aortic and pulmonary orifice. Note the saddle shape of the orifice level with the AP-septum at the highest point. (d) Human heart with the two semilunar valves and six leaflets. AP-septum is central between the four facing leaflets. (e) Neonatal aorta with a bicuspid valve.

pacemaker activity of the sinus node. Of interest, HCN4 is initially expressed in the entire heart tube and only in later stages restricted to the cardiac conduction system, corresponding to an initially broad pacemaking capacity of the heart tube.[100]

EPDCs are essential for formation of the fibrous annulus, resulting in the electrical isolation of atrial and ventricular myocardium, necessary for the mature ventricular apex to base conduction propagation.[54] The AV node remains the sole gateway to the ventricles relaying to the His bundle. Progressive compaction of trabeculations accompanies Purkinje fiber differentiation.[11]

The signaling cascades[97,99] involved in formation of the AV node from the AV myocardium include BMP, TBX20, and, in contrast to the sinus node, Nkx2.5. Furthermore, the ion channel protein HCN4 is expressed, but not the fast conducting connexin CX40. The fast conducting His bundle and bundle branches are characterized by the expression of CX40.

### *Relevance for arrhythmias*

Clinically, a spectrum of rhythm disturbances can be explained by the fact that the embryonic conduction system covers a broad area that will later be restricted to the definitive elements of the adult cardiac conduction system. Areas initially showing a pacemaking phenotype during development remain predilection sites for arrhythmogenic foci in the child and adult heart, indicating a reactivation of embryonic cell capacities, a cause of arrhythmias in selected cases.[97] Relatively late progress of annulus fibrosis formation and electrical isolation of atrial and ventricular myocardium during formation of the right AV orifice might explain transient late fetal rhythm disturbances and Wolff–Parkinson–White syndrome.[54,90]

## Coronary vascular system

The coronary system consists of the left coronary artery (which divides into a left anterior and a left circumflex) and a right coronary artery that connect to the aorta. These main coronary arteries supply the myocardium by branching into smaller arteries connecting to an extensive capillary bed that drains into the coronary venous system.[101]

It has recently been confirmed in mouse models that the coronary endothelial cells use the subepicardial space as a migration matrix[57] but are otherwise derived from the sinus venosus lining and the liver endothelium.[102,103] Also, there is an indication that at later stages of development an endocardial luminal contribution to the coronary endothelium takes place.[103]

### *Implications for coronary vascular anomalies*

The differential cell sources contributing to coronary artery development may relate to the variety of congenital coronary artery anomalies.[101] The inductive and formative role of EPDCs also sheds light on the anlage and differentiation of the coronary vascular system. We have shown that partial inhibition of EPDC differentiation can lead to abnormalities of the main coronary arteries, including pinpoint orifices and complete absence of main coronary stems.[59,60] In the latter case, aberrant connections with the cardiac lumen, fistulae, or ventriculo-coronary arterial communication (VCAC) will develop to sustain myocardial perfusion.[59,60] In a clinical setting, this background knowledge is important for differentiating between cases with pulmonary atresia without ventricular septal defect (VSD) that can present with or without VCAC. Fetal ultrasound diagnostics revealed the early presence of fetal VCAC in combination with pulmonary stenosis that later developed into pulmonary atresia.[104] Histopathology showed already severe coronary malformations with intimal thickening and even complete closure of vessels, and the presence of large VCAC.[105] We hypothesize that these fetuses suffer from a primary coronary vessel (EPDC-derived) anomaly, whereas in cases with primary pulmonary atresia and a normal coronary vasculature the original problem might have been SHF or NCC derived. Absent to deficient formation of the coronary ostia is seen in animal models with disturbed EPDC migration.[59,60] Environmental (epigenetic) influences on several embryonic cell types as in in induced diabetes in mice led to a deficient microvascular coronary bed.[87]

## Molecular genetic and epigenetic considerations

In this chapter, we alluded throughout the text to important genes and morphogenetic and transcription factors that are crucial for normal cardiac development. There is quite an improvement in our understanding of the genetics of CHD in recent years.[1–3] If cardiac-relevant genes are spontaneously mutated in humans or induced in mouse models, deficiency can lead to CHD or even embryonic death. In KO mouse models, it has been shown that many die early in embryonic life.[106] In the human population, it is known that 60%–80% of conceptions do not survive 4–6 weeks of pregnancy. It is to be expected that many of these embryos die of a cardiac cause in which first heart field expressed splanchnic mesoderm genes may be involved. The addition of the SHF mesoderm, followed by neural crest cells, with many essential expressed genes, leads to most of the cardiac malformations that we encounter neonatally and which are currently already detected in the fetal period through prenatal echocardiographic diagnosis. Although several cardiac malformations are lethal in the fetal period, fetuses with CHD can survive as the fetus is still on oxygen supply by the mother. Also early cardiac morphogenetic genes of the TGFβ superfamily like nodal, activin, BMPs, but also Nkx2.5 are in most cases still present in the nonaffected allele so that most human embryos with mutations and CHD are heterozygous for that particular gene. Recently,[3] the myriad of cardiogenic interactions is charted, and the pathways and interactions involved in the

development of congenital cardiac diseases are investigated. They studied both genes and gene pathways in nonsyndromic and syndromic congenital heart disease. As expected, important genes in cardiac morphogenesis were found to be linked to congenital cardiac anomalies, such as BMP, Notch1, NFATc, Nkx2.5, GATA 4,6, VEGF, and the TGFβ-linked EMT.

A further important factor in our knowledge of causes for CHD is the 85% of cases that are considered to be "multifactorial" in origin. This implies a genetic susceptibility in combination with an environmental cause. The genetic susceptibility might be variably present depending on modulating factors like the role of micro-RNAs or methylation and histone modification genes. All are known to regulate expression of otherwise nonmutated genes. Methylation and histon modifications play important roles in normal cell differentiation during development in which, for example, a pluripotent stem cell differentiates toward a plethora of known differentiated cells like endothelial cells, smooth muscle cells, or cardiomyocytes. New knowledge in this field has led to the now extensive stem cell research in which pluripotency is tried to recover or enable repair of tissues. Also in cancer research, where cells "spontaneously" acquire an unwanted pluripotency and mitotic capacity, these regulatory genetic mechanisms are extensively investigated. With regard to the frequency of CHD, we have not been able to significantly diminish the incidence of these anomalies indicating that we are still greatly at loss with regard to causal factors as a whole.

In the following paragraph we briefly refer to the contribution of (epi)genetic (modulatory) pathways. As an example, we take our knowledge on the genetic variability in cardiac septation defects (Figure 1.12).[14] It is remarkable that only a relatively small number of genes and gene pathways are involved. These findings are supported not only by research of human mutations but also by transgenic overexpression and KO mouse embryo studies. There is a great overlap in the early patterning of morphogenetic genes like GATA4/5, Tbx1/5, Nkx2.5, BMP2/4, and NODAL and VEGF pathways. Both a spectrum of ASDs and various types of VSDs are linked to related genes and pathways. The difference between ending up with a simple ASD or more complex VSDs is most probably linked to a tight spatiotemporal pattern of sequential and overlapping events in cardiac development in combination with hemodynamic effects.

A new very enlightening discovery has been through whole genome screening procedures in children with CHD and their parents.[2] It turned out that not a great number of novel mutated genes were discovered but that modulating genes were mutated, bringing in the already mentioned epigenetic influence. It has been shown that in 10% of cases there were mutations in the methylation and histone modification genes, which can down- or upregulate gene expression. The link to CHD becomes evident when it became clear that, for instance, essential cardiac morphogenetic genes like Nkx2.5 and Tbx5 are regulated in this way.

A next very informative step is that methylation and histone modification pathways can also be influenced by environmental factors such as homocysteine[107] and diet-induced

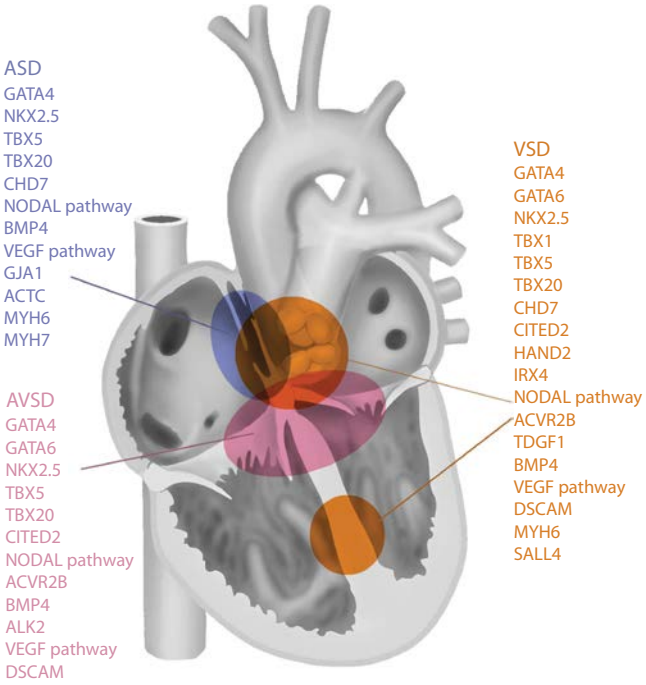


**Figure 1.12**
The atrial (ASD), ventricular (VSD), and atrioventricular septal defects (AVSD) with the genes indicated either in mouse models or the human population that are related to the development of the CHD. It is remarkable that there is a great overlap of genes involved and thereby a relative paucity of genes involved. (From Gittenberger-de Groot AC et al. *Ann Med* 2014;46:640–52, with permission.[14])

hypercholesterolemia.[108] Hyperglycemia, as occurs in diabetes, can act through reactive oxygen species pathways, and experiments both in chicken[85,86] and in mouse[95] have shown that lowering the oxidative stress ratio can lead to a diminishment of CHD by 80%.

A final not to be neglected factor is the specific role of hemodynamics and shear stress in cardiac development and maintenance. After formation of the primary cardiac heart tube and already before advanced looping and septation processes, the heart is beating and propelling blood from the venous to the arterial pole along the endocardial cells. These are adapting by altering gene expression patterns.[78] In the already mentioned transcriptome study,[3] the finding that eventually the right and left ventricle present with a similar gene expression pattern, although they differ in heart field origin, is also considered an indication that heart function might influence gene expression patterns. The relevance of the endothelial/endocardial cilium has been described to some extent in the section "Remodelling and septation of the outflow tract."[81] It turns out that a number of patients with isolated CHD as well as syndromic CHD fall within the category of ciliopathies and thus may have additional hemodynamic factors in their causal background.

In conclusion, to unravel the above indicated factors, it is essential to continue molecular biological approaches in mouse models based on the now more detailed knowledge derived from large human genome studies.[2,3]

The relative paucity of genes involved supports the already mentioned tight temporospatial framework that makes study in an early human embryonic developmental setting as yet unsuitable and unsatisfactory. Particularly for CHD, it is imminent that more attention needs to be directed to the hitherto not so sexy epigenetic and environmental influences on the complex genetic pathways that lead to CHD.

## Acknowledgments

We would like to thank Ron Slagter, medical artist, for most of the drawn illustrations and Bert Wisse for the three-dimensional animations.

## Video

**Video 1.1** (https://youtu.be/7cLT122l1mQ)
In this video illustrating both the pulmonary push and the swing of the AV canal to the right (bringing the tricuspid orifice above the right ventricle), it is shown how, with asymmetric and leftward expansion of the second heart field contribution, the pulmonary orifice and trunk are brought anterior and rightward to the aorta. This is a relatively simple explanation for the rotation process of the outflow tract during development, including a tightening of the inner curvature and a rightward movement of the AV canal. (From Scherptong RW et al. *Dev Dyn* 2012;241:1413–22, with permission.[28])

## References


1. Gelb BD. *Curr Opin Pediatr* 2013;25:561–6.
2. Zaidi S et al. *Nature* 2013;498:220–3.
3. Li X et al. *Physiol Genomics* 2014;46:482–95.
4. Poelmann RE et al. *PLOS ONE* 2014;9(9):e106569.
5. Hutson MR, Kirby ML. *Semin Cell Dev Biol* 2007;18:101–10.
6. Keyte AL et al. *Birth Defects Res C Embryo Today* 2014;102:309–23.
7. Hove JR et al. *Nature* 2003;421:172–7.
8. Vennemann P et al. *J Biomech* 2006;39:1191–200.
9. Pexieder T et al. *Int J Cardiol* 1989;25:255–64.
10. Gittenberger-de Groot AC et al. *Pediatr Res* 2005;57:169–76.
11. Miquerol L et al. *Dev Dyn* 2013;242:665–77.
12. Gittenberger-de Groot AC et al. *Differentiation* 2012;84:41–53.
13. Keyte A, Hutson MR. *Differentiation* 2012;84:25–40.
14. Gittenberger-de Groot AC et al. *Ann Med* 2014;46:640–52.
15. DeRuiter MC et al. *Anat Embryol (Berl)* 1992;185:461–73.
16. Waldo K et al. *J Clin Invest* 1999;103:1499–507.
17. Lough J, Sugi Y. *Dev Dyn* 2000;217:327–42.
18. Zaffran S, Kelly RG. *Differentiation* 2012;84:17–24.
19. Gittenberger de Groot AC et al. Normal and abnormal cardiac development. In: Moller JH, Hoffmann JIE, eds. *Pediatric Cardiovascular Medicine*, 2nd edn. Wiley-Blackwell; Hoboken, New Jersey, 2012:1–22.
20. Eisenberg LM, Markwald RR. *Circ Res* 1995;77:1–6.
21. Meilhac SM et al. *Dev Cell* 2004;6:685–98.
22. Levin M. *Mech Dev* 2005;122:3–25. Erratum in: *Mech Dev* 2005;122:621.
23. Linask KK, Vanauker M. *Scientific World Journal* 2007;7:280–98.
24. Benson DW et al. *J Clin Invest* 1999;104:1567–73.
25. Van den Berg G et al. *Circ Res* 2009;104:179–88.
26. Franco D et al. *Trends Cardiovasc Med* 2014;24:23–31.
27. Rana MS et al. *Circ Res* 2014;115:790–9.
28. Scherptong RW et al. *Dev Dyn* 2012;241:1413–22.
29. Henderson DJ, Chaudhry B. *Birth Defects Res A Clin Mol Teratol* 2011;91:460–7.
30. Bajolle F et al. *Circ Res* 2006;98:421–8.
31. Briggs LE et al. *Circ Res* 2013;112:1420–32.
32. Christoffels VM et al. *Circ Res* 2006;98:1555–63.
33. Gittenberger-de Groot AC et al. *Anat Rec* 2007;290:115–22.
34. Greulich F et al. *Cardiovasc Res* 2011;91:212–22.
35. Blaschke RJ et al. *Circulation* 2007;115:1830–8.
36. Puskaric S et al. *Hum Mol Genet* 2010;19:4625–33.
37. Mommersteeg MT et al. *Cardiovasc Res* 2010;87:92–101.
38. Sizarov A et al. *Circulation* 2010;122:798–807.
39. Douglas YL et al. *Int J Cardiol* 2011;147:13–24.
40. Lescroart F et al. *Circ Res* 2012;111:1313–22.
41. Briggs LE et al. *Differentiation* 2012;84:117–30.
42. Boot MJ et al. *Anat Rec A Discov Mol Cell Evol Biol* 2003;275:1009–18.
43. Verberne ME et al. *Dev Dyn* 2000;217:191–204.
44. Poelmann RE et al. *Anat Embryol* 2004;208:389–93.
45. Hutson MR, Kirby ML. *Birth Defects Res C Embryo Today* 2003;69:2–13.
46. Lindsay EA et al. *Nature* 2001;410:97–101.
47. Viragh S et al. *Anat Embryol (Berl)* 1993;188:381–93.
48. Schlueter J, Brand T. *J Cardiovasc Transl Res* 2012;5:641–53.
49. Vrancken Peeters M-PFM et al. *Anat Embryol (Berl)* 1995;191:503–8.
50. Xavier-Neto J et al. *Dev Biol* 2000;219:129–41.
51. Gittenberger-de Groot AC et al. *Circ Res* 1998;82:1043–52.
52. Winter EM, Gittenberger-de Groot AC. *Cell Mol Life Sci* 2007;64:692–703.
53. Perez-Pomares JM et al. *Int J Dev Biol* 2001;45:S155–6.
54. Kolditz DP et al. *Circulation* 2008;117:1508–17.
55. Zhou B et al. *Dev Biol* 2010;338:251–61.
56. Perez-Pomares JM et al. *Int J Dev Biol* 2002;46:1005–13.
57. Poelmann RE et al. *Circ Res* 1993;73:559–68.
58. Gittenberger-de Groot AC et al. *Circ Res* 2000;87:969–71.
59. Eralp I et al. *Circ Res* 2005;96:526–34.
60. Lie-Venema H et al. *Circ Res* 2003;92:749–56.
61. Eralp I et al. *Anat Rec* 2006;288A:1272–80.
62. Pérez-Pomares JM et al. *Dev Dyn* 2003;227:56–68.
63. Snarr BS et al. *Dev Dyn* 2007;236:1287–94.
64. Hoffmann AD et al. *PLOS Genet* 2014;10(10):e1004604.
65. Mahtab EA et al. *Dev Dyn* 2009;238:183–93.
66. Bax NA et al. *Dev Dyn* 2010;239:2307–17.
67. Van Mierop LH, Kutsche LM. *Heart Vessels* 1985;1:114–19.
68. Lamers WH et al. *Circulation* 1995;91:111–21.
69. Wenink AC et al. *Anat Rec* 1994;239:216–23.
70. Wessels A, Sedmera D. *Physiol Genomics* 2003;15:165–76.
71. Kikuchi K et al. *Dev Cell* 2011;20:397–404.
72. Kruithof BP et al. *Int J Dev Biol* 2013;57:853–63.
73. Ahmad F et al. *PLOS ONE* 2008;3(7):e2642.
74. Kosaka Y et al. *Mol Cell Biol* 2012;32:5089–102.
75. Huynh T et al. *Genesis* 2007;45:470–75.
76. Conway SJ et al. *Cardiovasc Res* 1997;36:163–73.
77. Hogers B et al. *Circ Res* 1997;80:473–81.
78. Groenendijk BCW et al. *Circ Res* 2005;96:1291–8.
79. Gittenberger-de Groot AC et al. *Trends Cardiovasc Med* 2006;16:1–6.
80. Baardman ME et al. *Dis Model Mech* 2016;9:413–25.
81. Van der Heiden K et al. *Dev Dyn* 2006;235:19–28.

82. Bartram U et al. *Circulation* 2001;103:2745–52.
83. Anderson RH et al. *Cardiovasc Res* 2012;95:108–15.
84. Van den Akker NMS et al. *Circ Res* 2007;100:842–9.
85. Molin DG et al. *Birth Defects Res A Clin Mol Teratol* 2004;70:927–38.
86. Roest PAM et al. *Birth Defects Res A Clin Mol Teratol* 2007; 79:231–5.
87. Moazzen H et al. *Cardiovasc Diabetol* 2014;13:46.
88. Oosthoek PW et al. *Anat Embryol (Berlin)* 1998;198:317–29.
89. Lockhart MM et al. *J Dev Biol* 2014;2:1–17.
90. Hahurij ND et al. *Pediatr Res* 2011;70:37–43.
91. Calkoen EE et al. *Int J Cardiol* 2016;202:784–95.
92. Blom NA et al. *Circulation* 1999;99:800–6. Erratum in: *Circulation* 2005;112:e71.
93. Lie-Venema H et al. *Differentiation* 2008;76:809–19.
94. Jain R et al. *J Clin Invest* 2011;121:422–30.
95. Liu Y, Feng Q. *Differentiation* 2012;84:54–61.
96. Grewal N et al. *J Thorac Cardiovasc Surg* 2014;148:1583–90.
97. Jongbloed MR et al. *J Cardiovasc Electrophysiol* 2004;15:349–55.
98. Vicente-Steijn R et al. *J Cardiovasc Electrophysiol* 2010;21: 1284–92.
99. Van Weerd JH, Christoffels VM. *Development* 2016;143: 197–210.
100. Vicente-Steijn R et al. *Heart Rhythm* 2011;8:1254–63.
101. Pérez-Pomares JM et al. *Cardiovasc Res* 2016;109:204–16.
102. Red-Horse K et al. *Nature* 2010;464:549–53.
103. Tian X et al. *Circ Res* 2015;116:515–30.
104. Chaoui R et al. *Ultrasound Obstet Gynecol* 2000;15(2):160–2.
105. Gittenberger-de Groot AC et al. *Prog Ped Cardiol* 2001;13: 157–64.
106. Conway SJ et al. *Genesis* 2003;35:1–21.
107. Boot MJ et al. *Cardiovasc Res* 2004;64:365–73.
108. Alkemade FE et al. *Am J Pathol* 2010;176:542–8.
109. Gittenberger-de Groot AC, Poelmann RE. Cardiac morphogenesis. In: Yagel S, Silverman NH, Gembruch U, eds. *Fetal Cardiology*. Informa Healthcare; New York, 2009:9–17.
110. Poelmann RE, Gittenberger-de Groot AC. *Dev Biol* 1999; 207:271–86.

# 2

# Cardiac anatomy and examination of specimens

Diane E. Spicer

## Introduction

The quality of prenatal echocardiography has greatly improved in the recent past, secondary to increased experience of diagnosticians and improvement in equipment, both identifying cardiac structures with greater detail. Congenital heart disease is now detected earlier in gestation and can play an important part in decisions concerning termination of pregnancy. The link between early echocardiographic and pathologic diagnosis is an important one, with the autopsy being the final arbiter. Dilation and evacuation procedures can provide nearly as much information as a full autopsy if the examination is done with extreme care. Pathologic confirmation of echocardiographic findings serves to educate the echocardiographer, the maternal fetal medicine physician, and most importantly, the family. The nature and scope of counseling for the family can be impacted based on the specificity of the pathologic diagnosis.

The diagnosis of congenital heart disease is not difficult when the principles of the morphologic method are employed. It provides for a logical analysis of the congenitally malformed heart and uses the most constant feature to identify each of the cardiac segments. Along with the morphologic method, sequential segmental analysis provides a simple, straightforward approach to describing any congenital cardiac malformation or constellation of defects. This approach is dependent on the recognition of the three cardiac segments, namely, the atriums, the ventricles, and the arterial trunks, each classified by their intrinsic morphologic characteristics. The progression of cardiac analysis then moves to the description of the junctional variations, which cannot be described without first knowing the morphology of each segment.

Throughout this chapter, the morphologic characteristics of each of the cardiac segments and their junctional variations, both atrioventricular and ventriculo-arterial, will be described. Topology and cardiac position are also important descriptive characteristics for both the echocardiographer and the pathologist or pathologists' assistant.

## Position of the heart

There are differences in the cardiac position and size during early gestation. Anatomic differences in size and shape of other organs in the body also occur, including the liver, ovaries, intestine, kidneys, and adrenals, with the liver having the most impact on the position of the heart early on. In the very young fetus, the apex of the heart is well away from the left chest wall, with the position of the heart impacted by the size of the fetal liver. Early on, the liver has a somewhat symmetric appearance with a large left lobe that tends to tilt the cardiac apex cranially with the base of the heart angled toward the posterior mediastinum. The position of the heart and its apex are directed toward the midline when compared with the axis of the spine, and the apex lies just to the left of the midline (Figure 2.1a). As gestation progresses, the liver remodels, and the left lobe becomes smaller, directly impacting the position of the heart. The heart moves into the left chest with a leftward and caudally directed apex. The aorta and pulmonary trunk also move toward the anterior mediastinum (Figure 2.1b).

The position of the apex and the position of the heart within the chest should be assessed as two separate descriptive variables. If the heart is displaced in the chest, it can still be structurally normal. This is usually related to another malformation or force occurring within the thorax or abdomen, including hydrops, diaphragmatic hernia, cystic malformations of the lung, omphalocele, and so on. Abnormal position can be a helpful hint for predicting other abnormalities. The angle of the long axis of the heart to the midline is an important consideration and can be assessed both echocardiographically and pathologically with the normal angle of the interventricular septum to the midline of the thorax at about 45° (Figure 2.2). If the cardiac axis is displaced leftward, the septum will be almost at a right angle to the midline. If the displacement is rightward, the septum will be almost parallel to the midline. Laterality defects must be considered if the cardiac position and apex are noted to be abnormal. Mirror image arrangement of the organs, ectopia cordis (Figure 2.3), and absence of the pericardium are rare conditions but can also directly affect the position of the heart and its apex.

## Morphologic method and sequential segmental analysis

The key to understanding and analyzing hearts with congenital cardiac malformations is utilization of the "morphologic

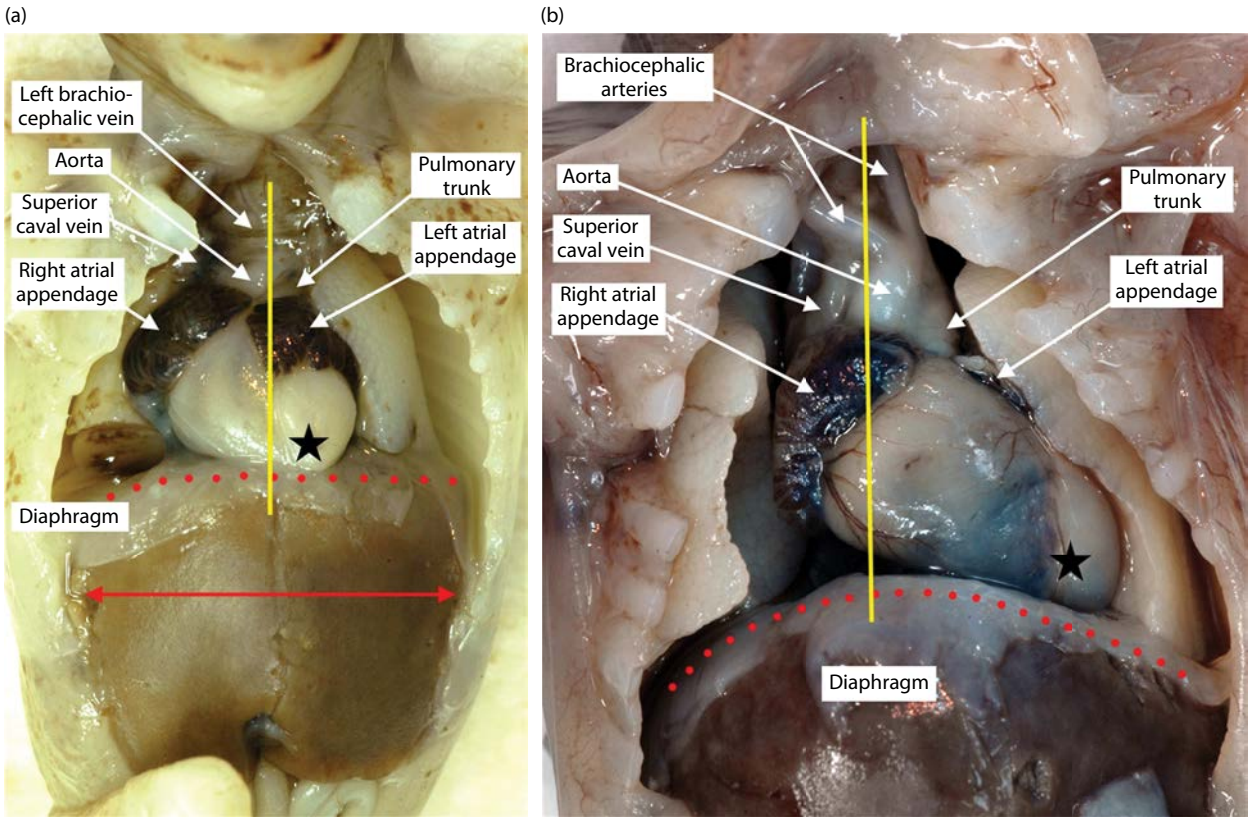


**Figure 2.1**
(a) This *in situ* view of the fetus shows the symmetric nature (double-headed red arrow) and large size of the liver in this 13-week fetus. The superior aspect of the liver is nearly flat (red dots), and the apex of the heart (black star) is just to the left of the midline (yellow line). The aorta and pulmonary trunk are not easily appreciated. (b) A similar view of an 18-week fetus shows the remodeling of the liver with a convex superior aspect (red dots). The apex of the heart (black star) and the ventricular mass are now well into the left chest. The aorta and pulmonary trunk are easily appreciated.

method." The concept was initially put forth by Van Praagh and colleagues and was based on some of the initial work of Lev. This principle states that one anatomic feature that is variable should not be used to define another feature that is itself variable. This system allows for the morphologic distinction of the atriums, the ventricles, and the arterial trunks.

The most constant morphological characteristics of the atriums are the atrial appendages and the extent of the pectinate muscles. Establishing the arrangement of the atrial appendages is the cornerstone of sequential segmental analysis. Ventricular morphology is determined by the apical trabecular component. Once the atrial arrangement is determined, the type of connection at the atrioventricular junction can be assessed and is a separate feature from the morphology of the atrioventricular valve. The normal heart has two atrioventricular junctions, each guarded by its own atrioventricular valve. Determining atrial and ventricular morphology allows for adequate assessment of the atrioventricular junctions, ventricular topology, and the relationships of the chambers within the ventricular mass. The morphology of the arterial trunks is next in the scope of analysis, followed by the description of the ventriculo-arterial junctions and the relationships of the arterial trunks to one another as they exit the ventricular mass.

## *Morphologically right atrium*

On outward appearance, many think that the triangular tip of the right atrium is its appendage, when in reality the entire anterior wall of the right atrium is the appendage. The right atrium is composed of a venous component, a vestibule, a septum, and an appendage (Figure 2.4a,b).

The appendage has a broad attachment to the smooth-walled venous component, this junction marked by the terminal groove. The superior and inferior caval veins serve as the systemic venous return with the venous return from the heart draining via the coronary sinus. The inferior caval vein and the coronary sinus join the right atrium inferiorly and along the diaphragmatic aspect. The superior caval vein joins the roof of the right atrium with the terminal crest crossing this junction anteriorly. The terminal crest is a prominent muscle bundle on the interior surface of the right atrium lying immediately adjacent to the above-mentioned terminal groove that marks the outward junction of the appendage with the venous component. Arising from the terminal crest are the pectinate muscles, which run in parallel fashion and extend laterally into the appendage. The morphologically right atrium is characterized by the pectinate muscles extending around the atrioventricular junction, this being the most

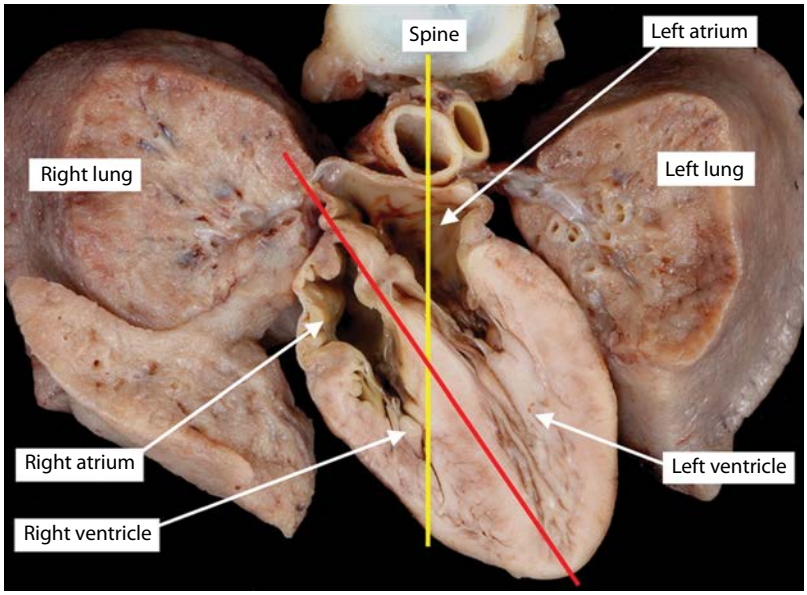


**Figure 2.2**
This cross section of the heart and lungs demonstrates the long axis of the heart (red line) compared to the long axis of the body (yellow line).

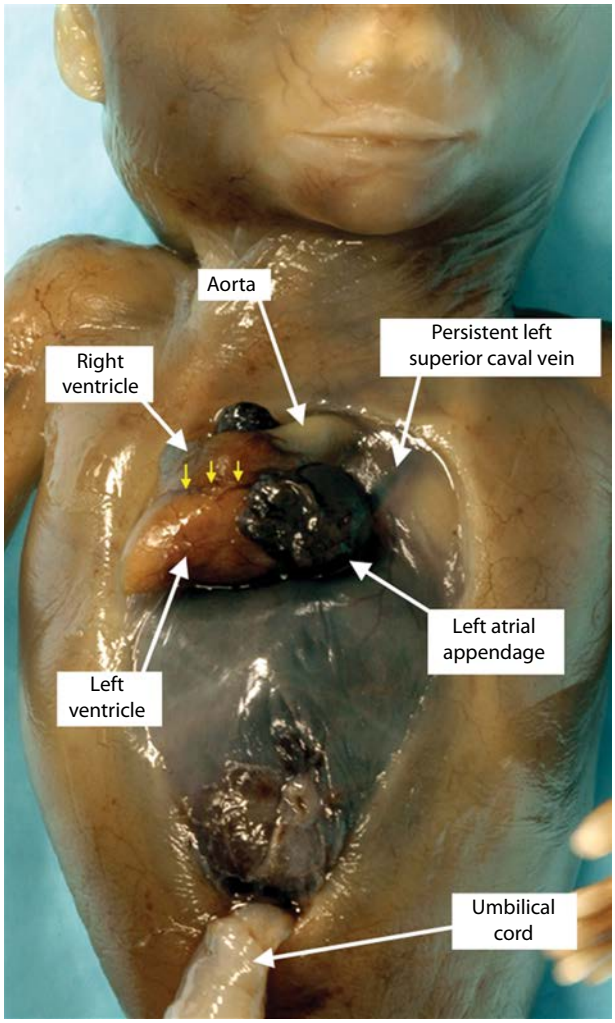


**Figure 2.3**
This 16-week fetus was stillborn with the heart located outside of the chest. The position of the heart and its apex are to the right. The right ventricle is hypoplastic, the yellow arrows marking the anterior interventricular coronary artery.

important and constant morphologic feature. The pectinate muscles extend to the crux and into the diverticulum inferior to the orifice of the coronary sinus or the sub-thebesian sinus. The Eustachian and Thebesian valves take origin from the terminal crest and guard the openings of the inferior caval vein and the coronary sinus. The right atrial vestibule is the narrow, smooth-walled portion of the atrium that inserts into the hinge point of the tricuspid valve.

## *Morphologically left atrium*

The left atrium also has a venous component, a vestibule, a septum, and an appendage, and it is the most posterior of the cardiac chambers. Outwardly, the left appendage has a tubular appearance, sometimes with a hooked tip, and is often scalloped along its outer border with a narrow attachment to the venous component (Figure 2.5a). Unlike the right atrium, this area is not marked by a terminal groove or terminal crest. The most constant morphological feature is the extent of the pectinate muscles, which are typically confined to the appendage. The left atrial vestibule is typically smooth, particularly the portion surrounding the posterior aspect of the atrioventricular groove (Figure 2.5b). The pulmonary veins enter the four corners of the roof of the smooth-walled vestibule, and the septal surface is formed by the flap valve at the floor of the oval fossa. The flap valve overlaps the prominent superior interatrial fold and has a characteristic "horseshoe" appearance in this area. Where the flap valve becomes adherent, there can be trabeculated areas, and this should not be confused with extension of the pectinate muscles. The left atrium has a significant body, which is the area joining the appendage, vestibule, and septum. The body remains prominent even when there is anomalous pulmonary venous drainage.

The coronary sinus runs in the left atrioventricular groove, and although it drains to the right atrium, embryologically,

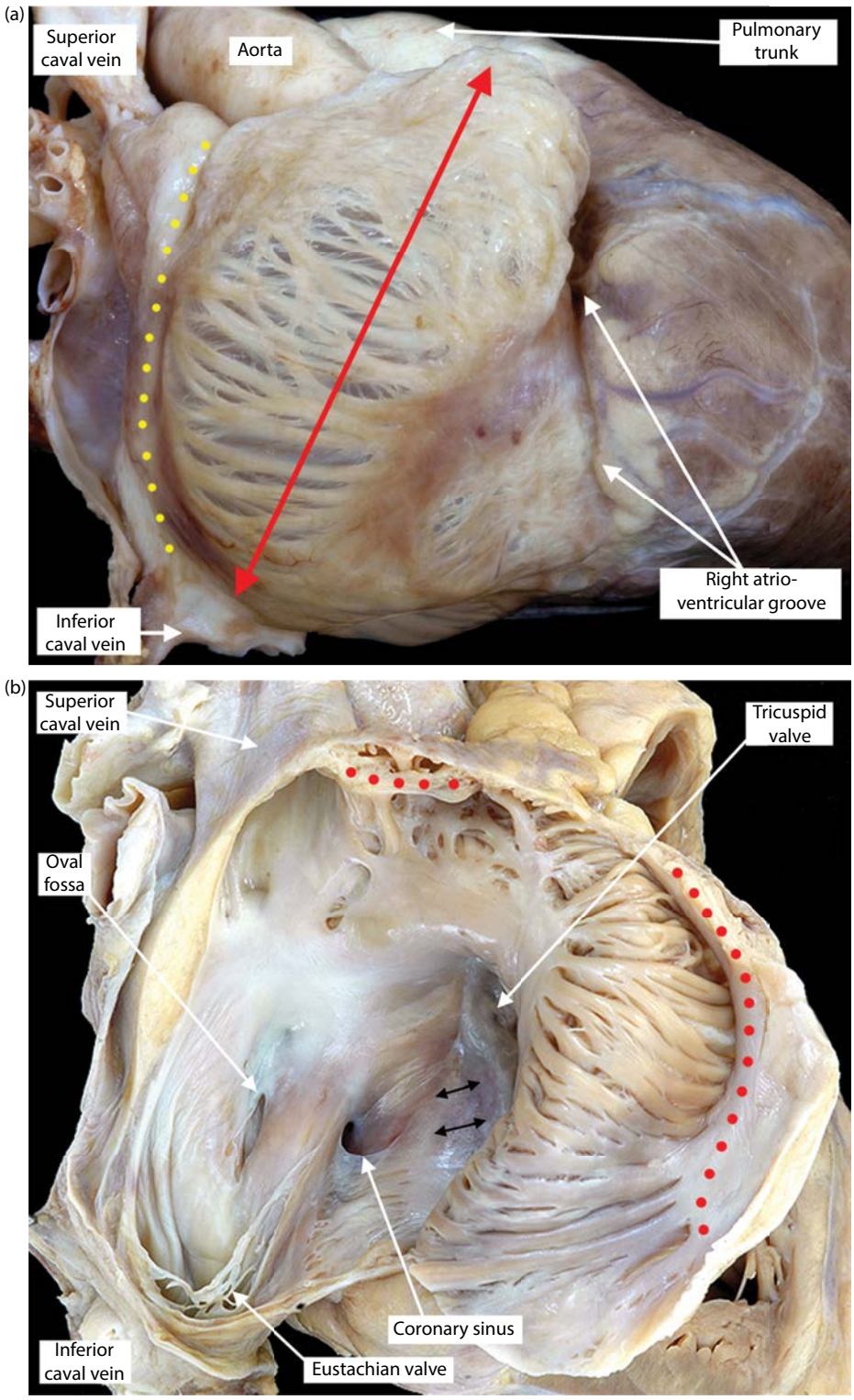


**Figure 2.4**
(a) The anterior view of the morphologically right atrium demonstrates the extent of the appendage (double-headed red arrow) along with its triangular tip and the broad attachment with the venous component (yellow dots). (b) The right atrial appendage has been cut along the venous junction, and the appendage is folded back. The pectinate muscles arise from the terminal crest (red dots) and extend around the atrioventricular junction. There is a narrow, smooth vestibule (black double-headed arrows) that inserts into the hinge point of the tricuspid valve.

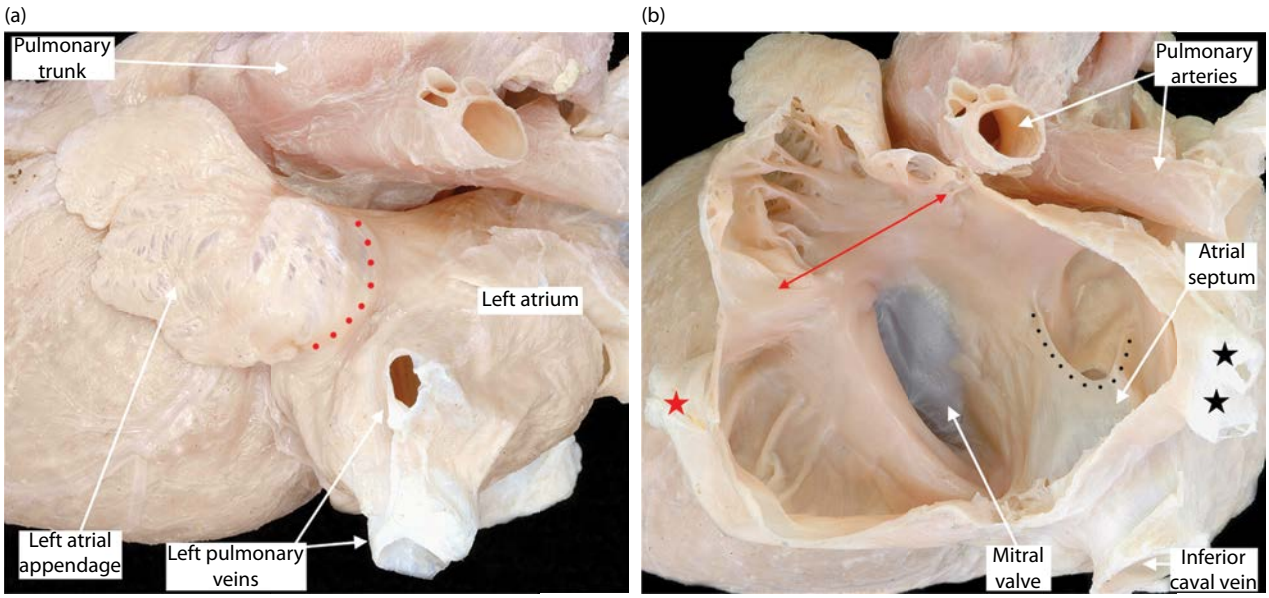


**Figure 2.5**
(a) The outward view of the left atrial appendage shows its tubular nature, the scalloped borders, and the narrow attachment (red dots) to the venous component. (b) The opened left atrium demonstrates the smooth vestibule and the pectinate muscles confined (red double-headed arrow) to the appendage. The flap valve at the floor of the oval fossa is marked with black dots, and the right (black stars) and left (red star) pulmonary veins are easily appreciated.

it is a left-sided structure. On long-axis echocardiographic views, the coronary sinus is a good anatomic marker for the morphologically left atrium (Figure 2.6).

## *The morphologically right ventricle*

The muscular walls of the right ventricle make up the majority of the anterior aspect of the ventricular mass. The ventricles are assessed in a tripartite fashion and are composed of an inlet, an apical trabecular component, and an outlet. The tricuspid valve guards the inlet, which extends from its hinge point to the attachments of the tendinous cords. The tricuspid valve has attachments to the septum and to papillary muscles. The septal leaflet lies adjacent to the ventricular septum. The anterosuperior leaflet is supported by the anterior papillary muscle and the medial papillary muscle (muscle of Lancisi). The inferior leaflet is in part supported by a single smaller or

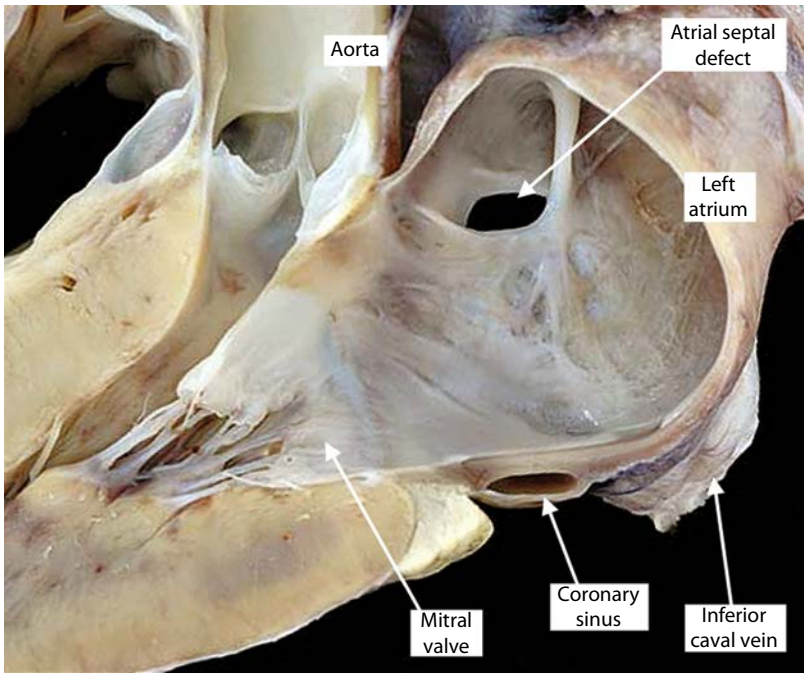


**Figure 2.6**
Long axis view of the left atrioventricular junction shows the coronary sinus within the left atrioventricular groove.

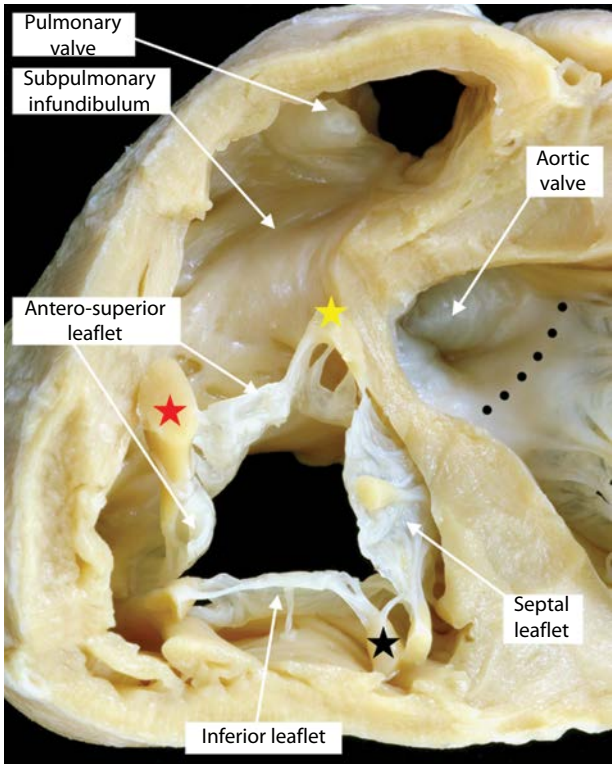


**Figure 2.7**
This apical short axis view of the tricuspid valve shows the three leaflets along with the papillary muscles that support it; medial (yellow star), anterosuperior (red star), and inferior (black star). Note the aortic valve at the center of the heart. (Black dots represent the aorta to mitral fibrous continuity.)

multiple smaller papillary muscles along the diaphragmatic aspect (Figure 2.7).

The apical trabecular component is the most constant morphological feature of the ventricles. Within the right ventricle, the apical trabeculations are coarse, and the septal surface is often trabeculated with a prominent trabeculation known as the septomarginal trabeculation or septal band. Toward the base of the ventricle, it divides into two limbs that join the supraventricular crest, one oriented in a cephalic direction and the other caudally. The medial papillary muscle arises from the caudal limb, while the anterior papillary muscle extends from the body of the septal band. The moderator band is a well-formed muscular bundle extending between the anterior papillary muscle and the parietal wall of the right ventricle. It is an anatomic, echocardiographic marker for the right ventricle. The septal band also gives rise to a series of trabeculations that extend from its anterior surface to the parietal wall of the right ventricle, known as septoparietal trabeculations (Figure 2.8a,b).

Within the outlet component of the right ventricle, the pulmonary valve is supported by a free-standing muscular sleeve or subpulmonary muscular infundibulum (Figure 2.8b). This sleeve of muscle lifts the pulmonary valve away from the ventricular mass. The fibroelastic wall of the pulmonary trunk joins this muscular sleeve around its entire circumference, forming a true ring at the ventriculo-arterial junction. The pulmonary valve consists of three, semilunar leaflets that cross the ventriculo-arterial junction, incorporating a crescent of muscle at the base of each sinus. In the right ventricle, the atrioventricular or tricuspid valve is separated from the arterial or pulmonary valve by the subpulmonary muscular infundibulum. It is not a septal structure and is in part composed of the inner curvature of the right ventricular musculature, typically called the ventriculo-infundibular fold (Figure 2.8b).

## *The morphologically left ventricle*

The left ventricle has three components just as in the right ventricle: an inlet, an outlet, and an apical trabecular component. The mitral valve lies in the inlet, and it consists of two leaflets supported by tendinous cords that extend to two papillary muscles. When the two leaflets are in the closed position, there is a solitary zone of apposition or commissure (Figure 2.9a). The posterior or mural leaflet guards two-thirds of the valvar circumference, and it is a rather shallow leaflet. The anterior or aortic leaflet guards the remaining one-third, and it is broad. This anterior leaflet is in fibrous continuity with the left coronary and nonadjacent leaflets of the aortic valve, and for this reason, it is sometimes referred to as the aortic leaflet. Each of the mitral valve leaflets is supported for the most part by tendinous cords that extend in a relatively equal fashion to each of the papillary muscles. The mitral valve has no attachments to the ventricular septum, with the deep subaortic outflow separating the aortic leaflet from the smooth septal surface of the left ventricle proximal to the aortic root (Figure 2.9b). The papillary muscles attach to the parietal wall of the left ventricle. When assessed in attitudinally appropriate fashion, they are located in superolateral and inferoseptal positions rather than posteromedial and anterolateral positions when viewed with the heart on its apex in the "Valentine" position.

The apical trabecular component is the most constant component of the left ventricle. Beyond the papillary muscles, the trabeculations are fine and criss-crossing with a smooth septal surface toward the outlet (Figure 2.10). The aortic root marks the outlet of the left ventricle and is supported by muscle and fibrous tissue. The leaflets and sinuses of the aortic valve are named according to the origin of the coronary arteries from the aortic sinuses and with reference to their relative position to the pulmonary trunk. These are designated as the right coronary or right-facing sinus, the left coronary or left-facing sinus, and the nonfacing or nonadjacent sinus (Figure 2.11). The term *noncoronary sinus* poses a problem when a coronary artery arises from it. This is rare but does occur. The three semilunar leaflets that make up the aortic valve are inserted in similar fashion to the pulmonary valve with crescents of muscle incorporated into the base of the right coronary aortic sinus in its entirety and a portion of the left coronary aortic sinus. The remainder of the left coronary aortic sinus and the entire nonadjacent aortic sinus have fibrous support in the area of aorta to mitral valve fibrous continuity.

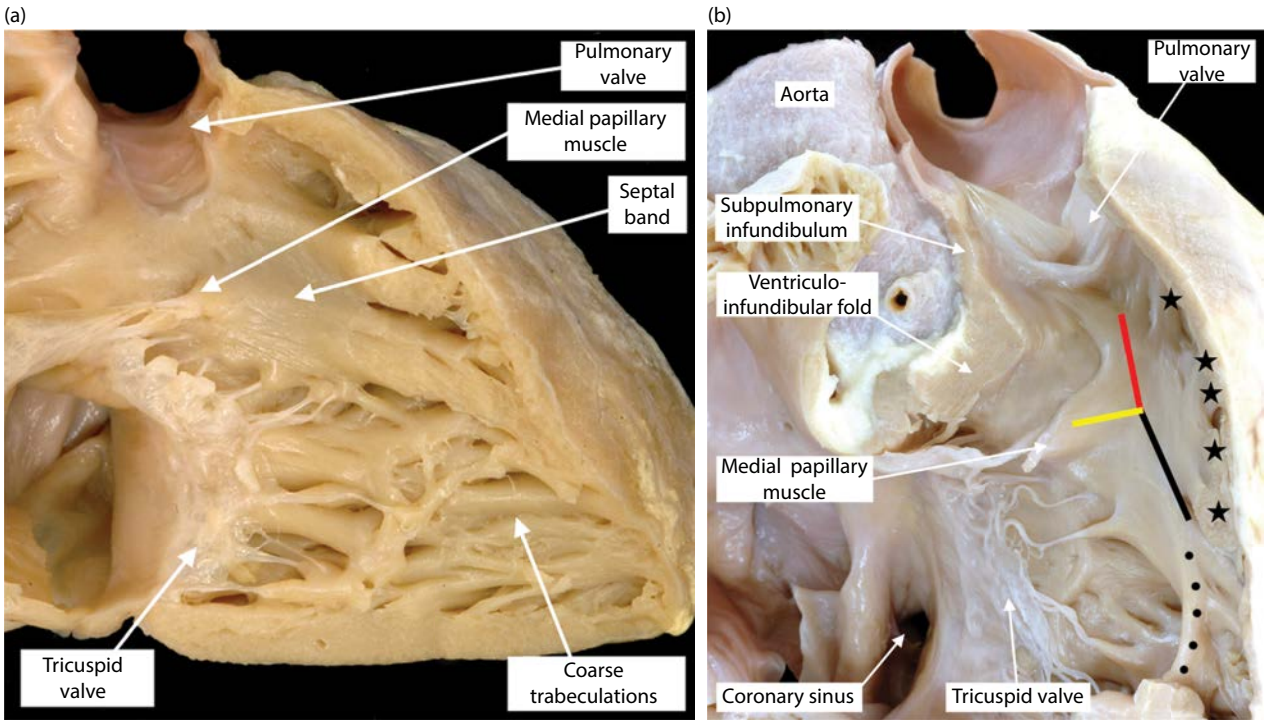


**Figure 2.8**
(a) The anatomic view of the right ventricle shows the coarse apical trabecular component and the trabeculated septal surface. (b) The free wall of the right ventricle has been removed demonstrating the components of the septal band (black line). There are cephalic (red line) and caudal (yellow line) arms along with septoparietal extensions (black stars). The moderator band (black dots) arises from the inferior aspect.

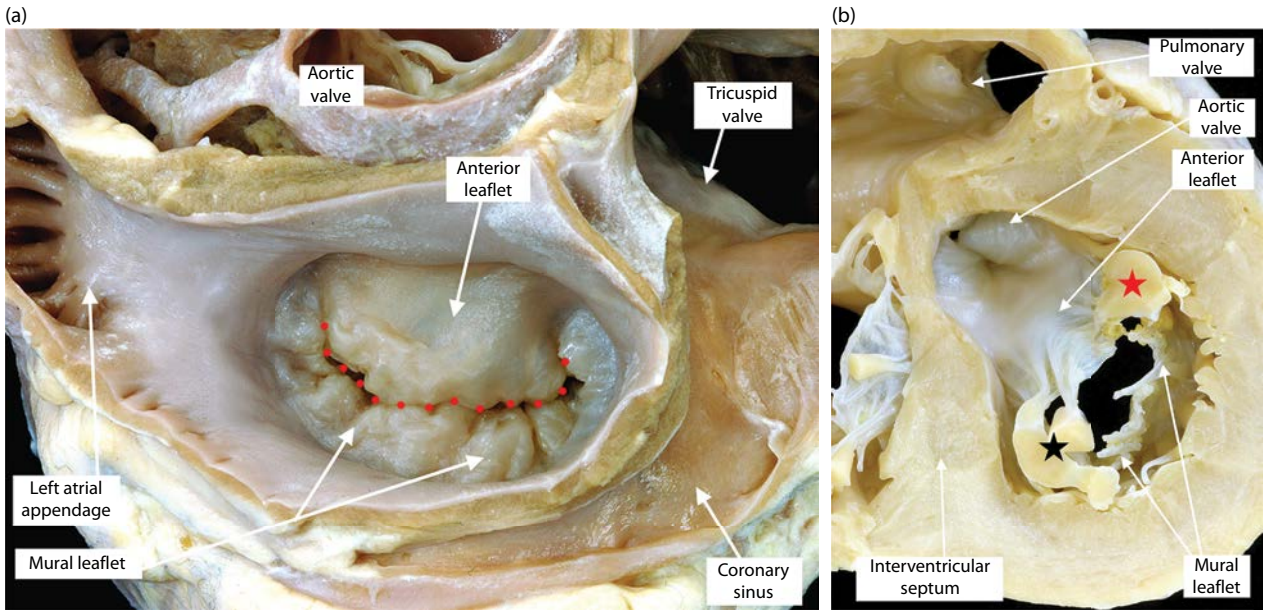


**Figure 2.9**
(a) The mitral valve is viewed from the base of the heart, and the single zone of apposition is marked with red dots. The anterior leaflet is broad, while the mural or posterior leaflet is shallow. (b) The apical short axis view shows the fibrous continuity between the anterior leaflet and the aortic valve. The superolateral (red star) and the inferoseptal (black star) papillary muscles equally support both leaflets.

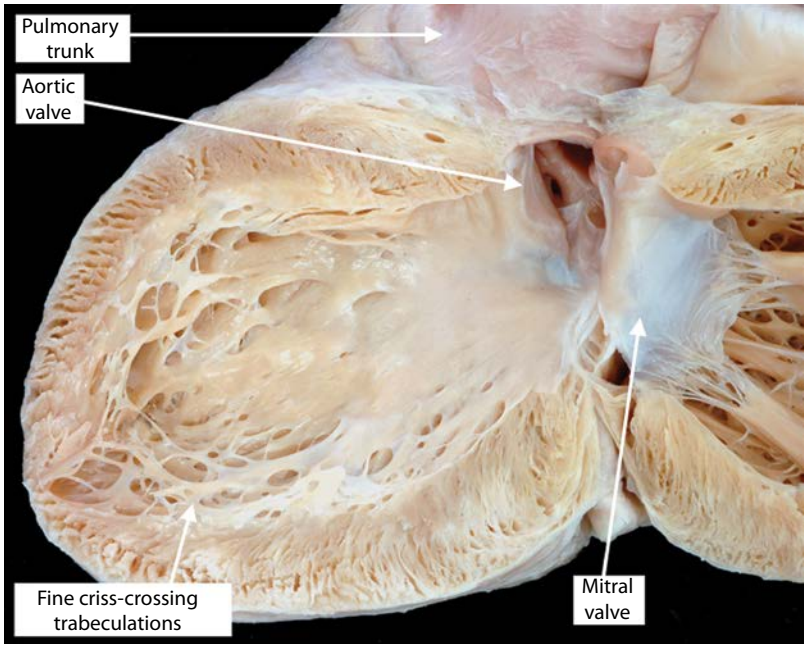


**Figure 2.10**
The left ventricle has been opened in clam-shell fashion demonstrating the fine, criss-crossing apical trabecular component and the smooth septal surface toward the outlet.

## *The arterial trunks*

The arterial trunks, namely, the pulmonary trunk and the aorta, make up the third segment of the heart and are identified morphologically by their branching pattern. The aorta is the center piece of the heart, spiraling from behind the pulmonary trunk, which lies anterior to it as the arterial trunks rise from the ventricular mass. Both arterial trunks extend superiorly into the mediastinum and have an intra- and extrapericardial component (Figure 2.12). The intrapericardial segment of the aorta is typically referred to as the ascending aorta or the tubular portion. This portion of the aorta can be defined as the area between the sinutubular junction and the area just proximal to the bifurcation of the brachiocephalic arteries. The coronary arteries are the first branches from the aorta, the right coronary artery arising

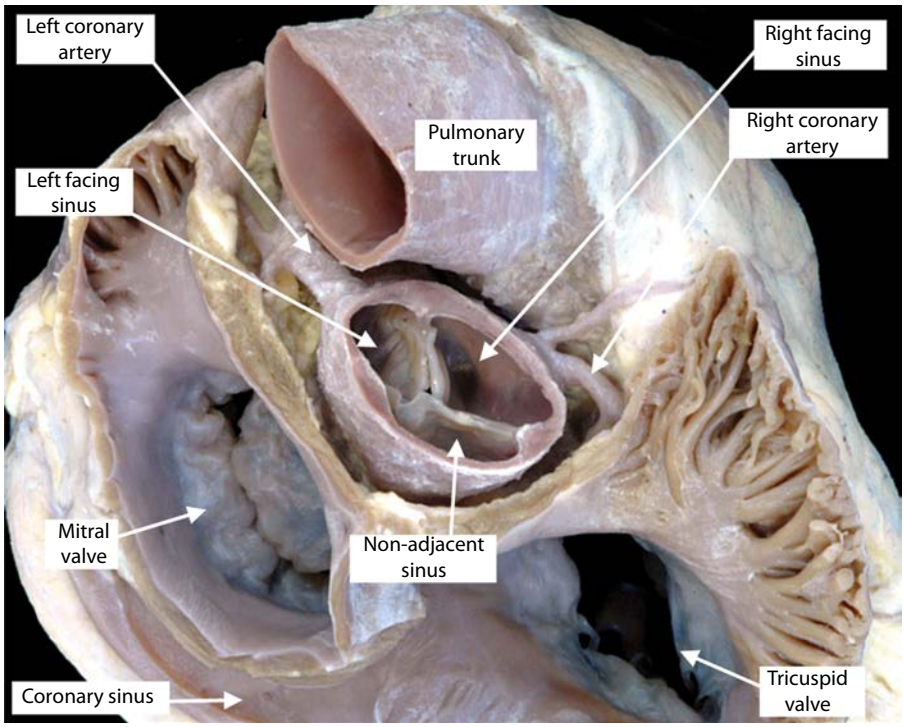


**Figure 2.11**
The short axis view from the base demonstrates the central position of the aorta and the valvar sinuses as they are related to the pulmonary trunk.

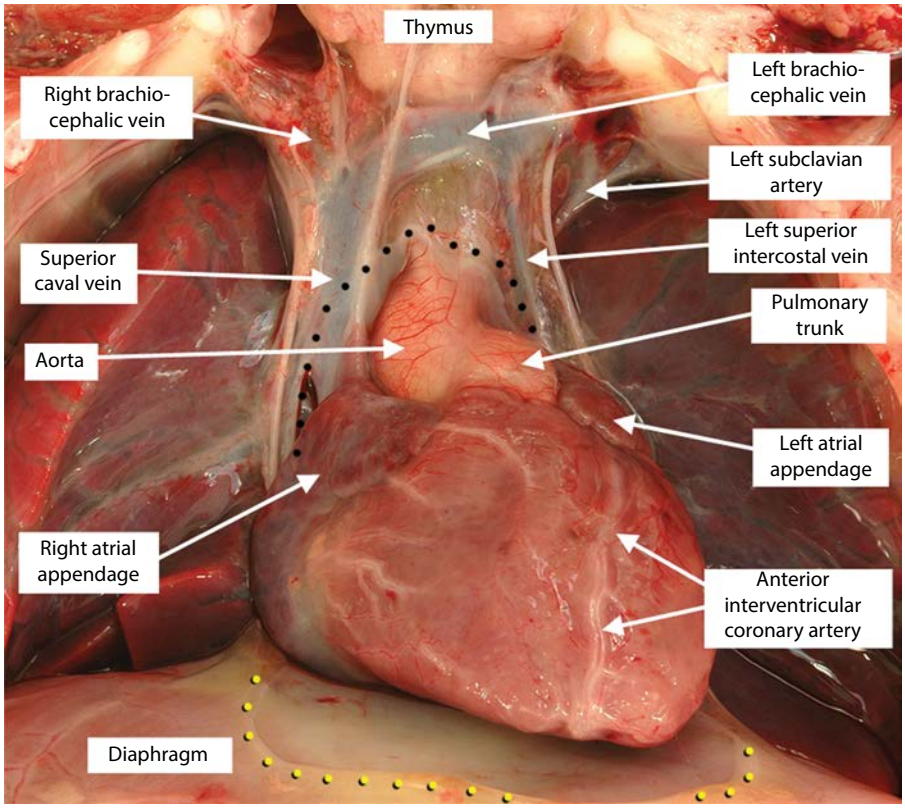


**Figure 2.12**
This *in situ* view of the heart marks the extent of the pericardial refection, separating the intra- and extrapericardial components (black dots) of the aorta and pulmonary trunk. The aorta and pulmonary trunk are normally related. The yellow dots mark the diaphragmatic margin of the pericardium.

from the right-facing or the right coronary sinus, and the left coronary artery from the left-facing or the left coronary sinus (see Figure 2.11). This is the normal relationship, and although there can be variations such as a coronary artery arising from the nonadjacent sinus or even from the pulmonary trunk, both are rare occurrences. The brachiocephalic arteries branch from the aortic arch at or slightly distal to where the pericardial reflection crosses the anterior aspect of the aorta. This portion of the aorta is known as the transverse arch, and it runs in a relatively horizontal plane. The brachiocephalic trunk is the first branch, followed by the left common carotid and left subclavian arteries. The aortic arch extends to the left, over the left main bronchus and along the spine. The area between the origin of the left subclavian artery and the junction of the arterial duct is known as the isthmus. Beyond the insertion of the arterial duct is the descending aorta (Figure 2.13).

The pulmonary trunk takes a short intrapericardial course prior to bifurcating into the right and left pulmonary arteries. The pericardial reflection crosses over the area where the left pulmonary artery bifurcates from the pulmonary trunk to extend to the hilar region of the left lung. The right pulmonary artery bifurcates slightly lower than the left pulmonary artery and extends posterior to the aorta and superior caval vein to the hilar region of the right lung. The arterial duct originates from the upper surface of the pulmonary trunk and very close to the bifurcation of the left pulmonary artery. It extends to insert into the aorta between the isthmus and the descending aorta (Figure 2.13).

## Topology and ventricular mass

Abnormal positions of the heart and its apex are highly suggestive of congenital cardiac malformations. The ventricles should be described in a tripartite fashion with mention of the inlet, outlet, and apical trabecular components. Abnormal ventricles can be described according to how the inlet and outlet components are shared between the apical trabecular components. The extent of the ventricular myocardium is from the atrioventricular junction to the ventriculo-arterial junction.

The shape of the ventricular mass can be described as three sided with inferior diaphragmatic, anterior sternocostal, and posterior pulmonary surfaces. There are sharp and rounded or obtuse borders over the outer surface, the borders between the diaphragmatic and sternocostal margins being quite sharp and known as the acute margin (Figure 2.14). The morphologically right ventricle makes up the majority of the anterior surface of the heart with only a small portion of the left ventricle visualized toward the apex.

Ventricular size is an important feature along with the ventricular topology. Topology describes the relationship

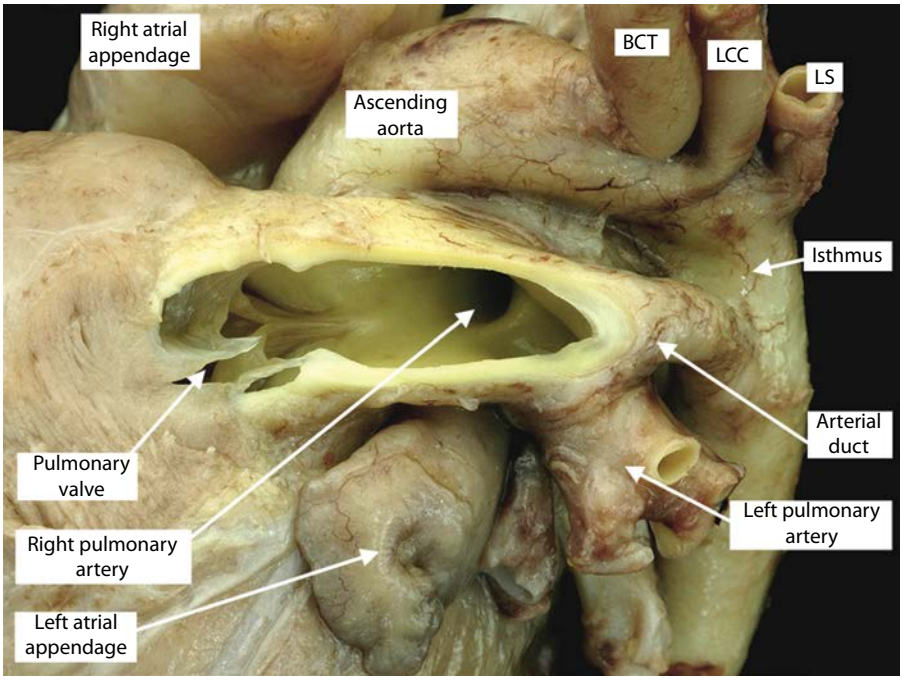


**Figure 2.13**
The pulmonary trunk has been windowed in this left lateral view demonstrating the bifurcation of the right and left pulmonary arteries and the arterial duct. Note the insertion of the arterial duct into the aortic isthmus. The ascending aorta gives way to the left arch, the brachiocephalic arteries branching in normal fashion from the arch.

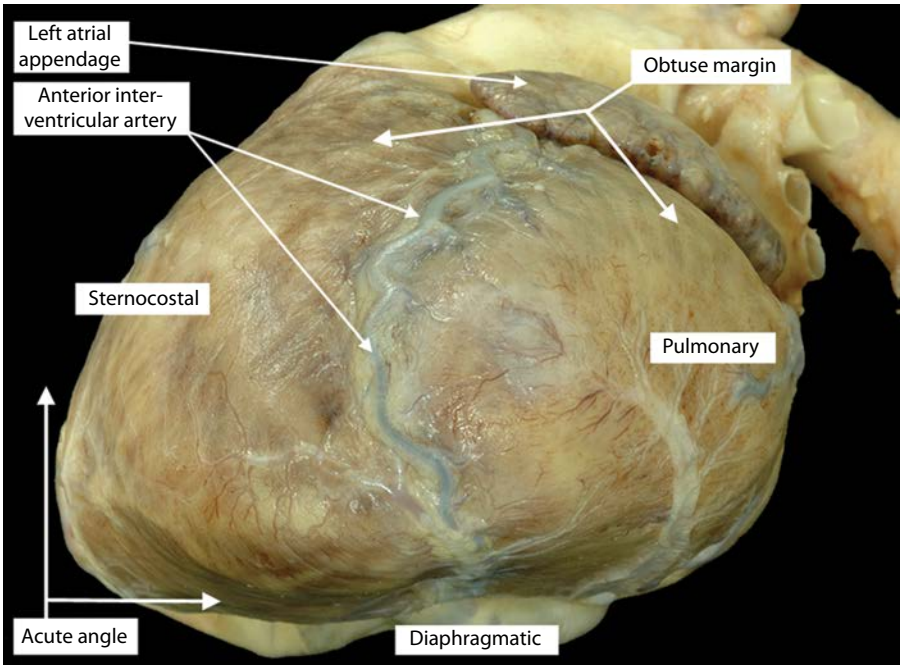


**Figure 2.14**
The anatomic borders of the heart are easily appreciated when the heart is viewed from the apex toward the base.

of the two ventricles within the ventricular mass, and there are two basic patterns that are mirror images of one another. Ventricular topology can best be described as a right-hand or a left-hand pattern and utilizes the septal surface of the morphologically right ventricle as the guide. A morphologically right ventricle in the normal heart will allow for the palmar surface of the right hand to be placed on the septal surface of the right ventricle with the thumb in the inlet and the fingers in the outlet. This is right-hand ventricular topology (Figure 2.15a) and is the

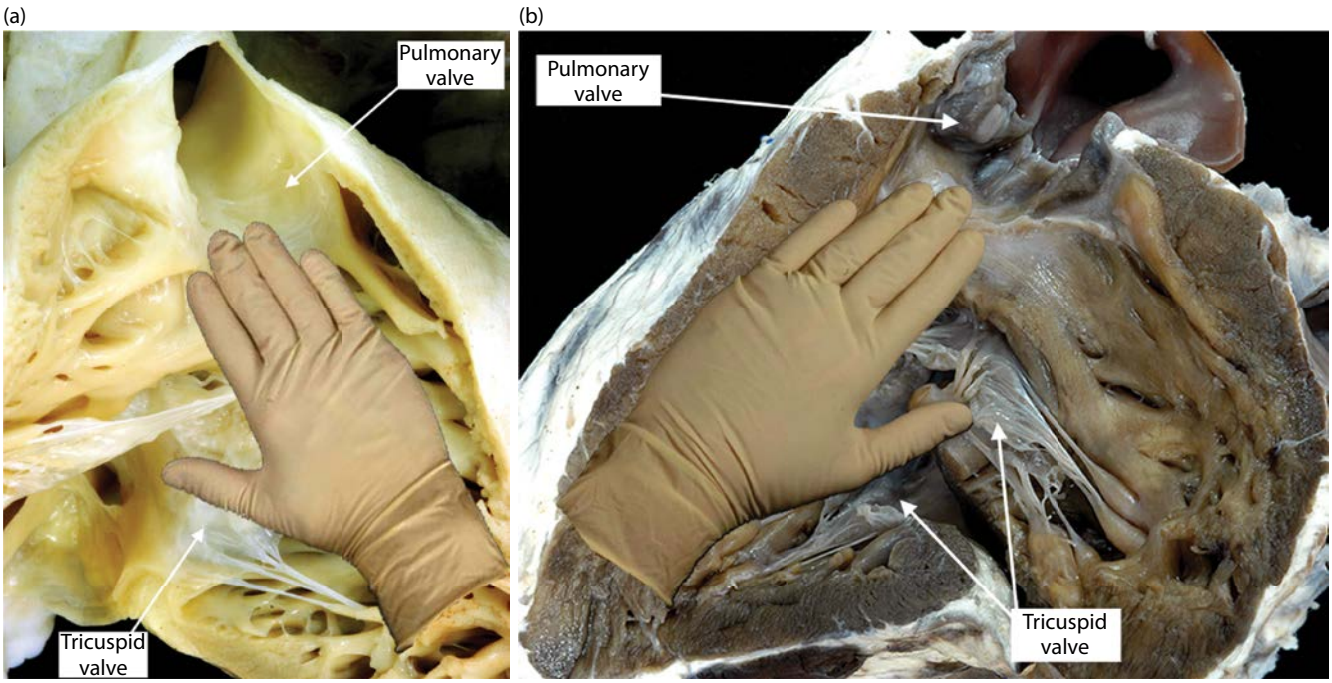


**Figure 2.15**
(a) Right-hand topology. (b) Left-hand topology.

usual pattern in the normal heart. In the mirror image of the normal heart or in those hearts with congenitally corrected transposition with usual atrial arrangement, the palmar surface of the left hand can only be placed on the septal surface of the right ventricle with the thumb in the inlet and the fingers in the outlet, constituting left-hand ventricular topology (Figure 2.15b). Ventricular topology can always be described, irrespective of the position of the ventricles within the ventricular mass.

When there is a univentricular, atrioventricular connection (double-inlet connection or absent connection, described in the section "Atrial arrangement and variation at the atrioventricular junction"), a rudimentary chamber is usually present. This small chamber may be virtually unrecognizable by both clinical and pathological diagnostic techniques. The relationship of the small chamber must be described as to its position relative to the larger ventricular chamber and in terms of right–left, superior–inferior, and anterior–posterior positions. The trabecular and outlet components of the rudimentary chamber should also be described. A heart with one big and one small ventricle should be referred to as a functionally univentricular heart, allowing for the recognition and description of both ventricular chambers. Hearts with a solitary indeterminate ventricle have been described but are rare. The apical trabecular component in this group exhibits neither the right nor left type of apical trabeculation. These ventricles are typically coarsely trabeculated with multiple large muscle bundles traversing the chamber and rendering the morphology as indeterminate.

## *Septal structures*

Within the right atrium, there is a narrow, smooth vestibule that extends to the hinge point of the tricuspid valve. This area gives way to the atrioventricular muscular sandwich, which is formed by the overlapping portions of atrial and ventricular musculature with a small amount of fibrofatty tissue between them (Figure 2.16a). This overlap exists as a result of the more apical insertion of the tricuspid valve relative to the mitral valve. Here, the overlapping segments of the atrial and ventricular musculature are separated by the inferior atrioventricular groove, which contains the fibrofatty tissue that makes up the "meat" of the sandwich. This area is confluent with the walls that separate the inferior caval vein from the coronary sinus, sometimes referred to as the sinus septum (Figure 2.16b). Many include this area along with the area extending to the junction of the superior caval vein and the oval fossa as the atrial septal surface, while only the floor of the oval fossa and its antero-inferior rim make up the true interatrial septum. Superiorly, the atrial walls are largely separated by an extensive area of infolding or the "septum secundum" (Figure 2.16c). This superior fold is often extensive and separates the superior caval vein from the right pulmonary veins, also known as Waterston's or Sondergaard's groove. The flap valve at the floor of the oval fossa overlaps the superior interatrial fold on the left side, eventually becoming adherent in this area after birth. The prominent antero-inferior muscular rim of the oval fossa is formed by the muscularization of the vestibular spine during development of the heart.

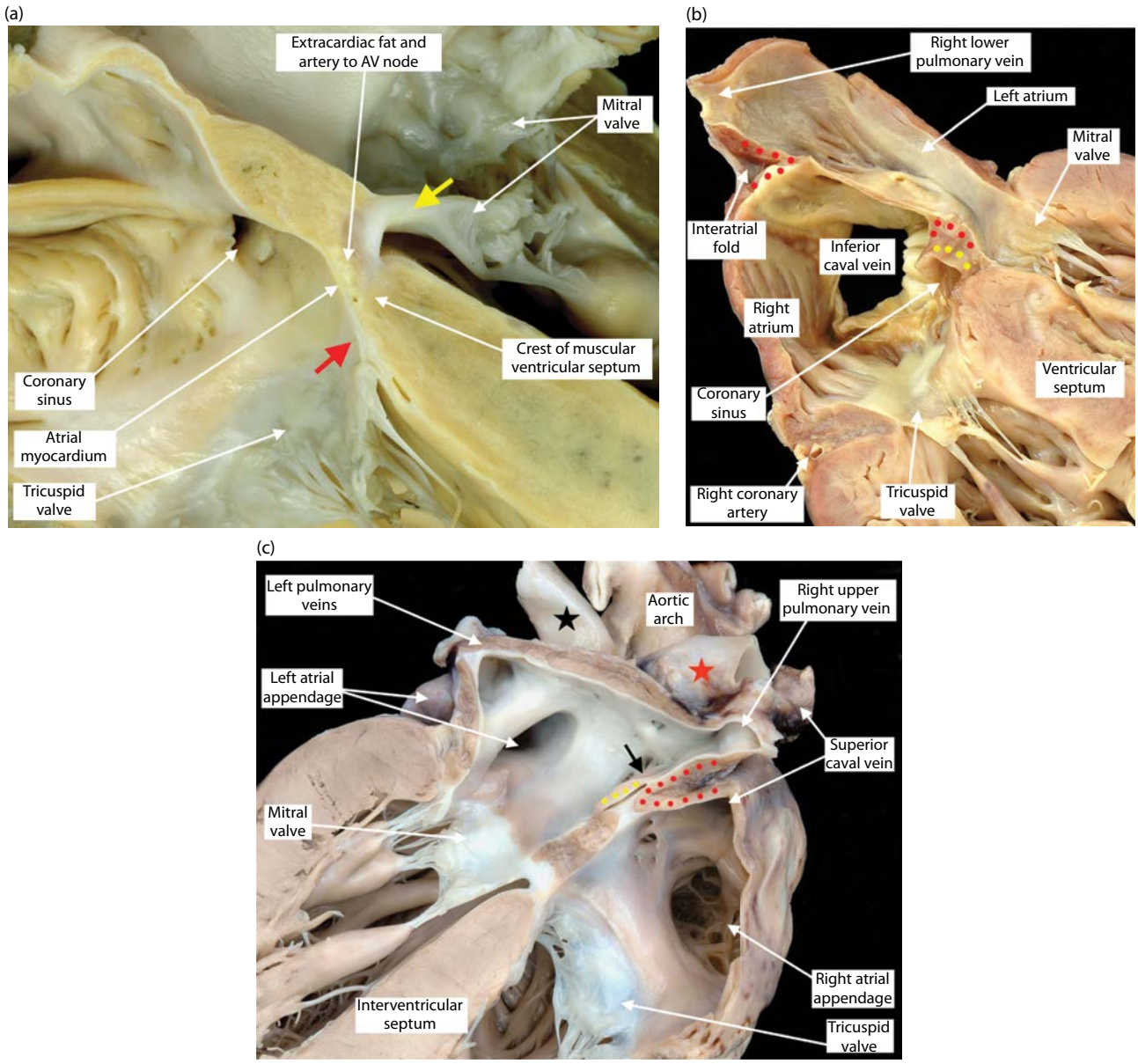


**Figure 2.16**
All images have been cut in a four chamber plane. (a) This close up inferior view demonstrates the "atrioventricular muscular sandwich" with the extracardiac fat forming the "meat" of the sandwich between the atrial myocardium and the crest of the muscular ventricular septum. (Red arrow—apical insertion of the tricuspid valve, yellow arrow—insertion of the mitral valve). (b) The inferior portion of the heart shows the interatrial folds (red dots) related to the inferior caval vein and the coronary sinus (yellow dots). (c) This image is viewed from posterior to anterior and shows the superior interatrial fold (red dots) and the overlap (black arrow) of the flap valve at the floor of the oval fossa (yellow dots). (Red star-right pulmonary artery, black star-left pulmonary artery).

The majority of the interventricular septum is muscular with a much smaller membranous component. The muscular interventricular septum often has a slight sigmoid curvature and separates the right ventricular inlet from the subaortic outflow tract (Figure 2.17a). The muscular septum should be described as a whole, since there are no specific boundaries to divide it into component parts.

The membranous septum is very small when compared to the muscular septum, and it is divided into atrioventricular and interventricular components. These two components can vary from heart to heart and are divided by the hinge line or attachment of the tricuspid valve (Figure 2.17b). The membranous septum is continuous with the fibrous interleaflet triangle that separates the right coronary from the nonadjacent aortic valvar leaflets and extends to the right aspect of the fibrous attachment of the mitral valve or the right fibrous trigone that supports the aortic root within the left ventricular outflow tract. The junction of the right fibrous trigone and the membranous septum is known as the central fibrous body (Figure 2.17c). The cavity of the right ventricle is separated from the subaortic outflow tract by the interventricular component of the membranous septum.

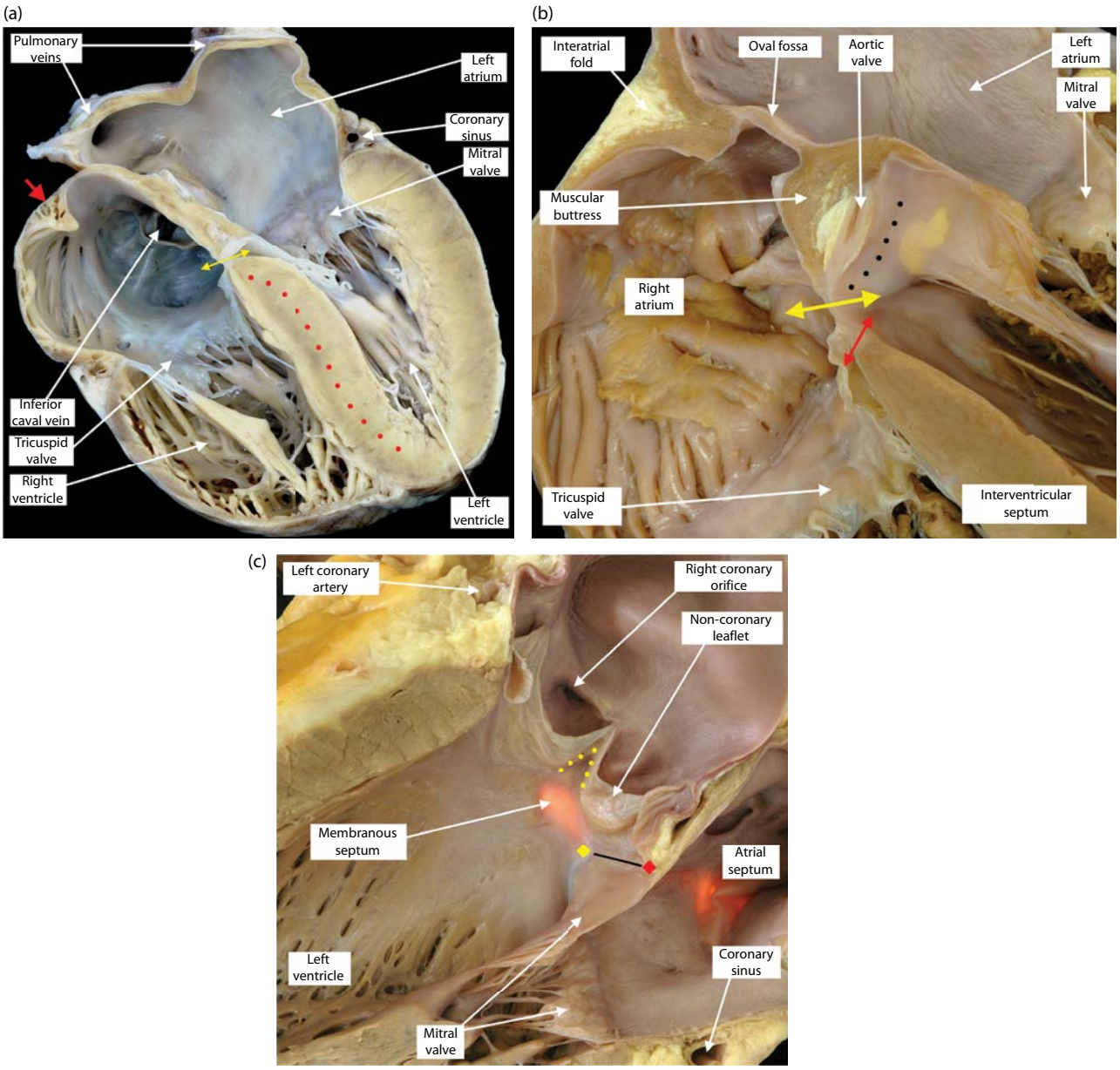


**Figure 2.17**
(a) The heart is sectioned in a four-chamber plane demonstrating the atrioventricular component (yellow double-headed arrow) of the membranous septum and the interventricular muscular septum (red dots). (Red arrow represents the terminal crest.) (b) The heart is sectioned in a four-chamber plane and demonstrates the components of the membranous septum. The atrioventricular portion is marked with a double-headed yellow arrow, and in this area there is potential for right atrial to left ventricular communication. The interventricular component is marked with the double-headed red arrow. (c) This long axis view of the left ventricle shows a backlit membranous septum and its relationship with the interleaflet triangle (yellow dots) between the right coronary and nonadjacent sinuses along with the right fibrous trigone (yellow diamond) in the area of aorta to mitral valve fibrous continuity (black line). (Red diamond represents the left fibrous trigone.)

# Analyzing the heart

Echocardiographically, the heart is always examined in its attitudinally correct position within the fetal chest and should also be examined in this way pathologically. Once morphology of the atrial and ventricular chambers and arterial segments are determined, then the atrioventricular and ventriculo-arterial connections can be assessed.

## *Atrial arrangement and variation at the atrioventricular junction*

The arrangement of and the morphology of the atrial appendages are of particular importance. Once the atrial morphology has been determined, the classifications are as follows: usual arrangement, mirror image arrangement, or presence

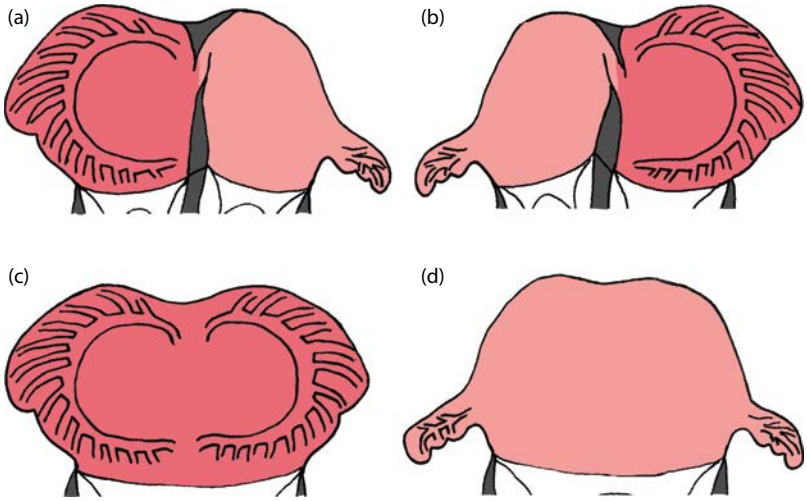


**Figure 2.18**
(a) Usual atrial arrangement. (b) Mirror image atrial arrangement. (c) Isomerism of the right atrial appendages. (d) Isomerism of the left atrial appendages.

of bilateral morphologically right or morphologically left atrial appendages (isomerism) (Figure 2.18).

The bronchial morphology, in most cases, will correlate with the morphology of the atriums, and clinically, this can be used as a morphological marker. The morphologically right main bronchus is approximately half as long as the morphologically left main bronchus. The first branch of the morphologically right bronchus is eparterial or above the pulmonary artery that extends to the lower lobe of the lung (Figure 2.19a). The right lung normally has three lobes. The morphologically left bronchus is hyparterial or below the pulmonary artery extending to the lower lobe of the lung (Figure 2.19b). The left lung normally has two lobes. The positions of the organs within the abdomen and thorax will often correlate with one another but can also be quite variable in their presentation. The bronchial morphology can be isomeric and usually correlates well in those cases that have isomerism of the right or left atrial appendages (Figure 2.19c,d). Echocardiographically, the organs can be assessed and lend predictability to the presence of congenital heart disease. Even though bronchial morphology and the position of the organs within the body can be used as indicators, these features are not always consistent.

There are five basic types of atrioventricular connection (Figure 2.20). In the normal arrangement, the morphologically right atrium is connected to a morphologically right ventricle, and the morphologically left atrium is connected to a morphologically left ventricle. This represents concordant atrioventricular connections and a biventricular connection (Figure 2.20a). Discordant atrioventricular connections are represented by a morphologically right atrium connected to a morphologically left ventricle and a morphologically left atrium connected to a morphologically right ventricle. This connection also represents a biventricular connection (Figure 2.20a). When isomeric atrial chambers are connected to separate ventricular inlets, this renders the terms concordant and discordant as inappropriate. These connections are biventricular and mixed (Figure 2.20b). The remaining two types of atrioventricular connection are those that are univentricular and characterized by both atriums opening to a dominant ventricle (double-inlet connection) or absence of either the right or left atrioventricular connection. A double-inlet connection consists of both atriums and their associated ventricular inlet components connecting to the same ventricular trabecular component. The morphology of the dominant ventricle may be of right, left, or indeterminate morphology (Figure 2.20c). When both inlets are committed to a large ventricle that is of left or right morphology, there will be an incomplete, rudimentary ventricular chamber that will lack an inlet component. When the incomplete, rudimentary ventricle is of right morphology, it is typically located in an anterosuperior position and when of left morphology in a posterior or posteroinferior position within the ventricular mass. A univentricular connection can be described as absence of the right or left atrioventricular connection. In other words, one atrium is connected to a ventricular inlet component. In this case, there is no potential for an atrioventricular connection and there is typically an associated incomplete, rudimentary ventricular component that lacks an inlet.

The morphology of the atrioventricular valves guarding the atrioventricular junctions is an independent feature that is dependent on the above-described variations at the atrioventricular junction. When separate right and left atrioventricular junctions are present, they can be guarded by two patent valves, one patent and one atretic valve, by a common atrioventricular valve, or by valves that can straddle and override. Atresia of the right or left atrioventricular valve can have two presentations. First, an imperforate valve has the potential for an atrioventricular connection with a diaphragm of valve tissue blocking the flow of blood between atrium and ventricle. The second type of atresia exists when there is no valve tissue at the atrioventricular junction, and in this case, the floor of the atrium is typically muscular with no possibility for an atrioventricular connection. A common valve will guard the right and left atrioventricular junctions regardless of morphology and can exist in a balanced or unbalanced arrangement. Straddling valves are defined as having tension apparatus on either side of the ventricular septum and supporting the valve within both ventricles. A valve overrides when the atrioventricular junction is connected to ventricles on both sides of a septal structure. Overriding

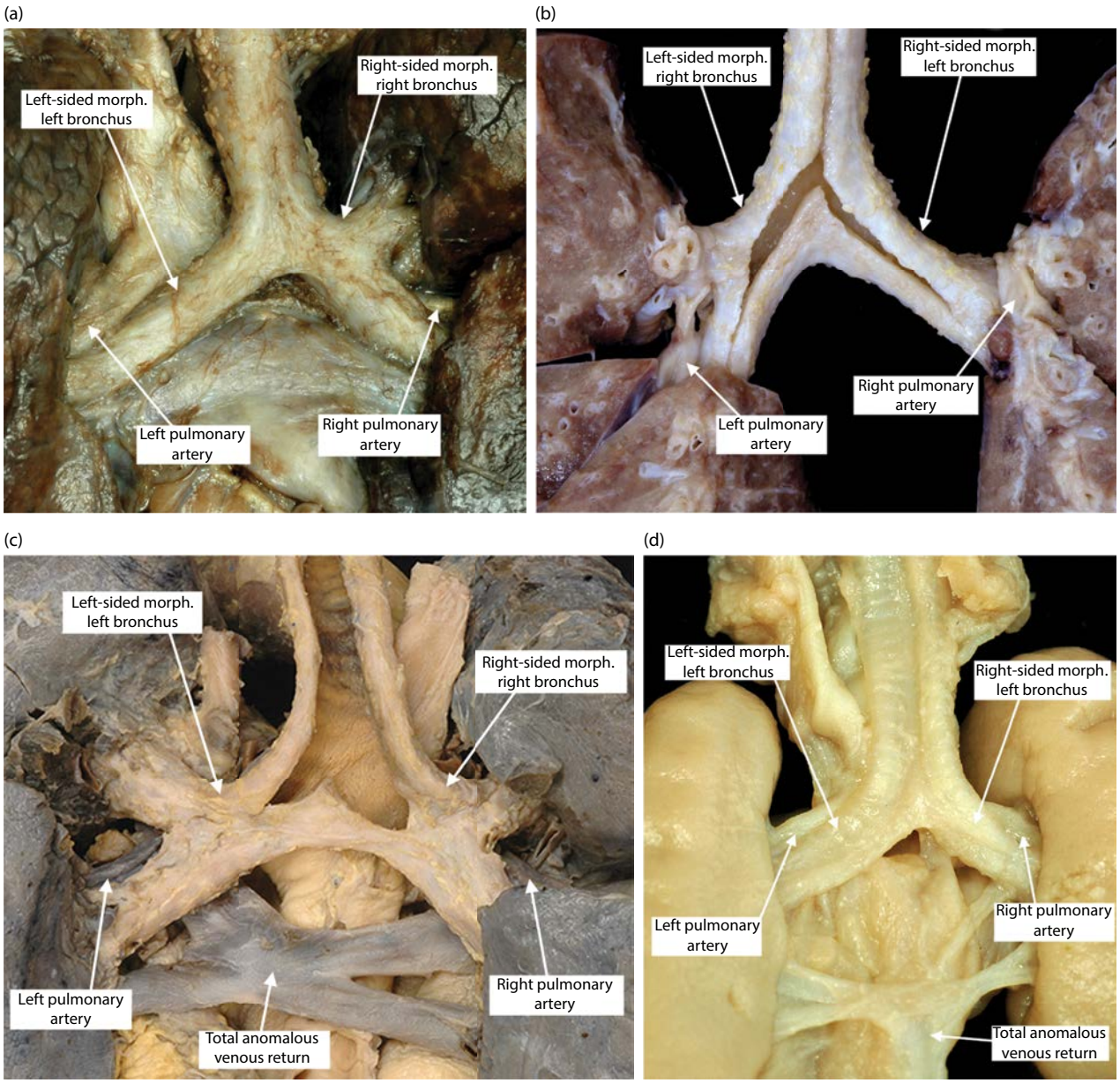


**Figure 2.19**
(a) Usual bronchial arrangement. (b) Mirror image bronchial arrangement. (c) Right bronchial isomerism. (d) Left bronchial isomerism. (morph.—morphologically)

valves must be described as to the degree of commitment of the atrioventricular junction to the ventricles relative to the ventricular septum. This produces a spectrum that defines how the atriums and ventricles are joined together, ranging from biventricular atrioventricular connections with minimal overriding (Figure 2.21a), to a univentricular atrioventricular connection or a double-inlet ventricle (Figure 2.21b) that can be of either right or left morphology. Rare, uniatrial but biventricular connections do exist in which case there is absence of one atrioventricular connection. This connection can be right- or left-sided, and a solitary atrioventricular valve is present. It is straddling and overriding of the solitary valve that produce the uniatrial, but biventricular atrioventricular connection.

## *Arterial relationships*

In the normal heart, there are two arterial trunks with the aorta essentially forming the center piece of the heart and occupying a deeply wedged position between the two atrioventricular valves (see Figures 2.11 and 2.12). The pulmonary trunk lies anterior to the aortic root as the arterial trunks leave the ventricular mass with the aortic valve, posterior and to the right of the pulmonary valve. The pulmonary valve is lifted from the ventricular mass by the subpulmonary muscular infundibulum. The aortic and pulmonary valves should be described in terms of their anterior–posterior and right–left positions relative to one another, taking note that any relationship can exist with any ventriculo-arterial connection. Three components must be assessed when analyzing

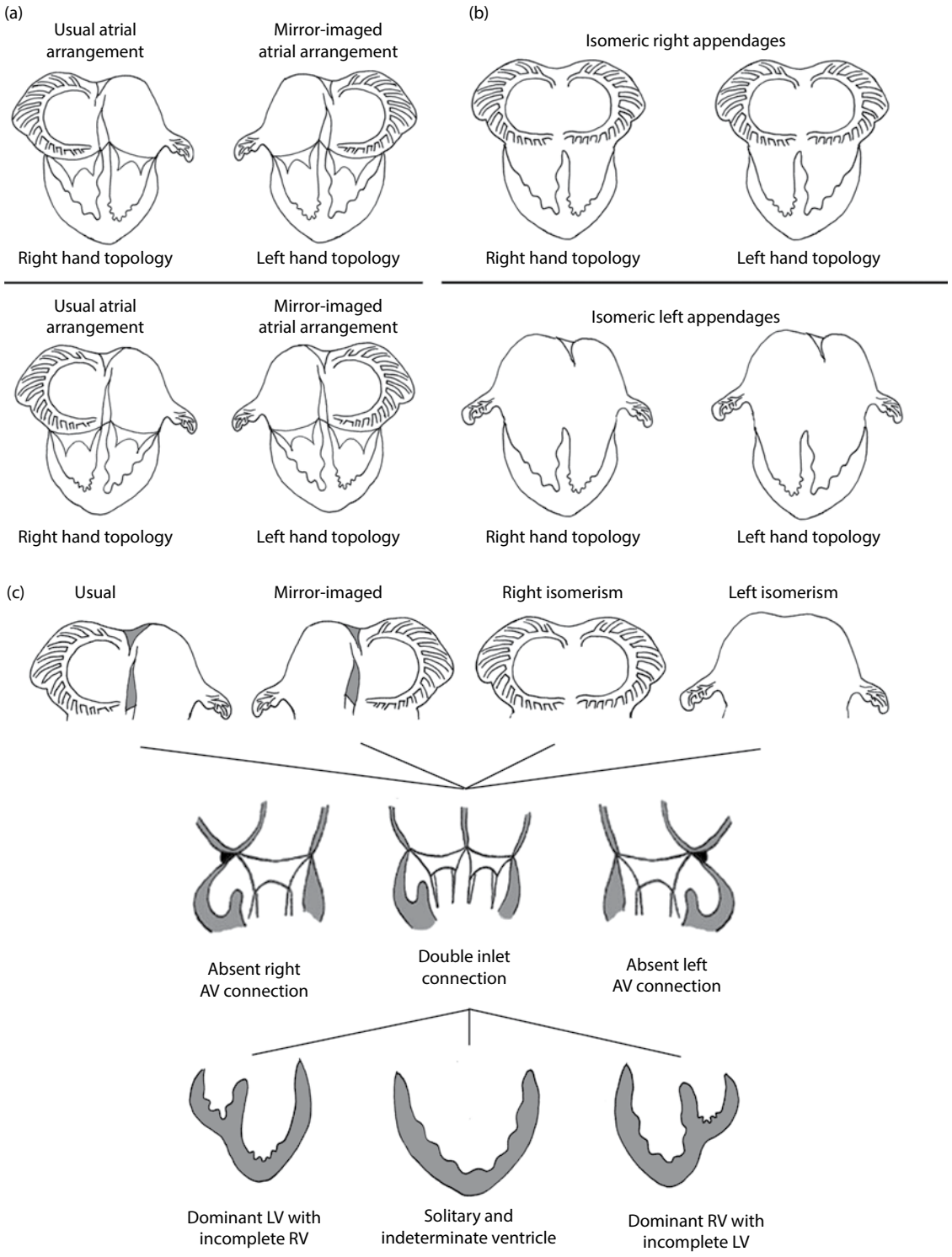


**Figure 2.20**
(a) Concordant (top) and discordant (bottom) atrioventricular connections can exist with usual or mirror-imaged patterns. Typically, with concordant connections, the atriums with usually arranged appendages are connected to a ventricular mass with right-hand topology, and those atriums with mirror-imaged appendages are connected to a ventricular mass with left-hand topology. (b) Isomeric atrial appendages (right top and right bottom) exhibit biventricular and mixed connections, no matter the ventricular topology. In this case, it is necessary to specify both the morphology of the atrial appendages and ventricular topology. (c) This image is representative of the potential univentricular atrioventricular connections. The atrial appendage possibilities are listed in the top row, with the types of atrioventricular connection in the second row (absent right, double inlet, or left atrioventricular [AV] connection) and the ventricular component in the bottom row (dominant left ventricle [LV], solitary and indeterminate ventricle, or dominant right ventricle [RV]). The positions of the incomplete ventricles and the ventriculo-arterial connections in this group exhibit further variability.

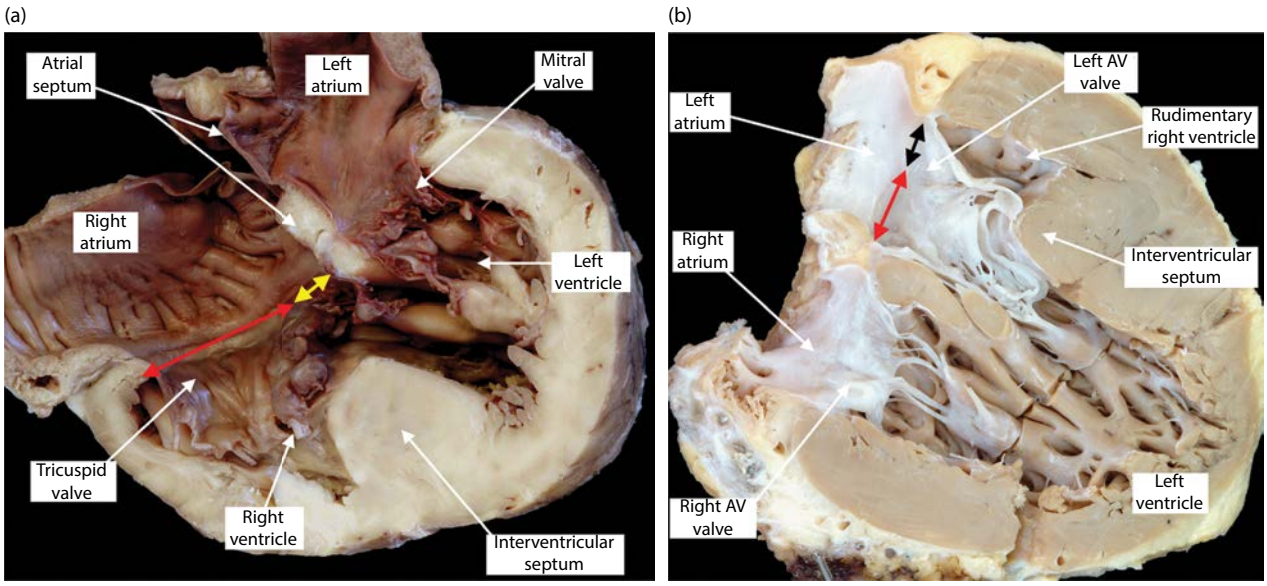


**Figure 2.21**
This pair of images demonstrates the spectrum of overriding atrioventricular junctions with the lesser part of the overriding junction illustrated in (a), rendering this as a biventricular connection. The tricuspid valve is committed mostly to the right ventricle (double-headed red arrow) with a small portion (double-headed yellow arrow) overriding the interventricular septum and supported by a papillary muscle within the left ventricle. In (b) the lesser part of the overriding junction (double-headed black arrow) is committed to the rudimentary right ventricle with the remainder of the left-sided atrioventricular valve (double-headed red arrow) committed to the dominant left ventricle in this specimen with double-inlet left ventricle. Straddling and overriding valves can be found with any combination of atrial chambers and ventricles.

the ventriculo-arterial junctions: first, the nature of the connection between the arterial trunks and the ventricles; next, the relationship of the arteries to one another; and last, the morphology of the outlet component that supports the arterial valves.

## *Ventriculo-arterial connections*

There are four possible types of ventriculo-arterial connections (Figure 2.22). Concordant ventriculo-arterial connections are seen in the normal heart where the pulmonary trunk arises from the morphologically right ventricle and the aorta arises from the morphologically left ventricle (Figure 2.22a). The reverse of the normal relationship is described as a discordant ventriculo-arterial connection with the aorta arising from the morphologically right ventricle and the pulmonary trunk from the morphologically left ventricle (Figure 2.22a). When both arteries arise from the same ventricular chamber, the ventriculo-arterial connection is a double-outlet connection. The ventricle can be of right or left ventricular morphology or a solitary, indeterminate ventricle (Figure 2.22b). Use of the 50% rule is helpful when the entirety of both trunks do not arise from the same ventricular chamber. When an arterial trunk is 50% or less committed to a ventricle, then the connection should be assessed as a concordant or discordant connection with both arterial trunks arising predominantly from their own ventricle. When one arterial trunk is overriding the interventricular septum and is greater than 50% committed to a ventricle, the connection then becomes double outlet. There are several scenarios for the last type of ventriculo-arterial connection, which is a single outlet (Figure 2.22c). This can exist when there are two identifiable, intrapericardial trunks or with a single, intrapericardial arterial trunk. When there are two intrapericardial arterial trunks, one or the other of the pulmonary trunk or the aorta is patent and the other is atretic, leaving a single outlet from the ventricular mass. A common arterial trunk and a solitary arterial trunk are other forms of single-outlet ventriculo-arterial connections and must be differentiated. A common arterial trunk supplies the coronary, pulmonary, and systemic circulations and is typically shared between the ventricles to different degrees. A solitary arterial trunk occurs when two intrapericardial arterial trunks cannot be identified, and the single outlet supplies the coronary and systemic circulations with the pulmonary circulation arising distal to the brachiocephalic arteries along the descending portion of the aorta. A single outlet corresponding to any of the above-mentioned types can arise from a chamber with right or left ventricular morphology, can be shared between the two chambers, or can arise from a solitary ventricular chamber with indeterminate morphology.

## Acknowledgment

All of the images in this chapter are from the Web Portal of the Archiving Working Group of The International Society for Nomenclature of Paediatric and Congenital Heart Disease (ISNPCHD) (http://ipccc-awg.net) and appear courtesy of Diane E. Spicer BS, PA (ASCP) (University of Florida, Department of Pediatric Pathology, Gainesville, Florida).

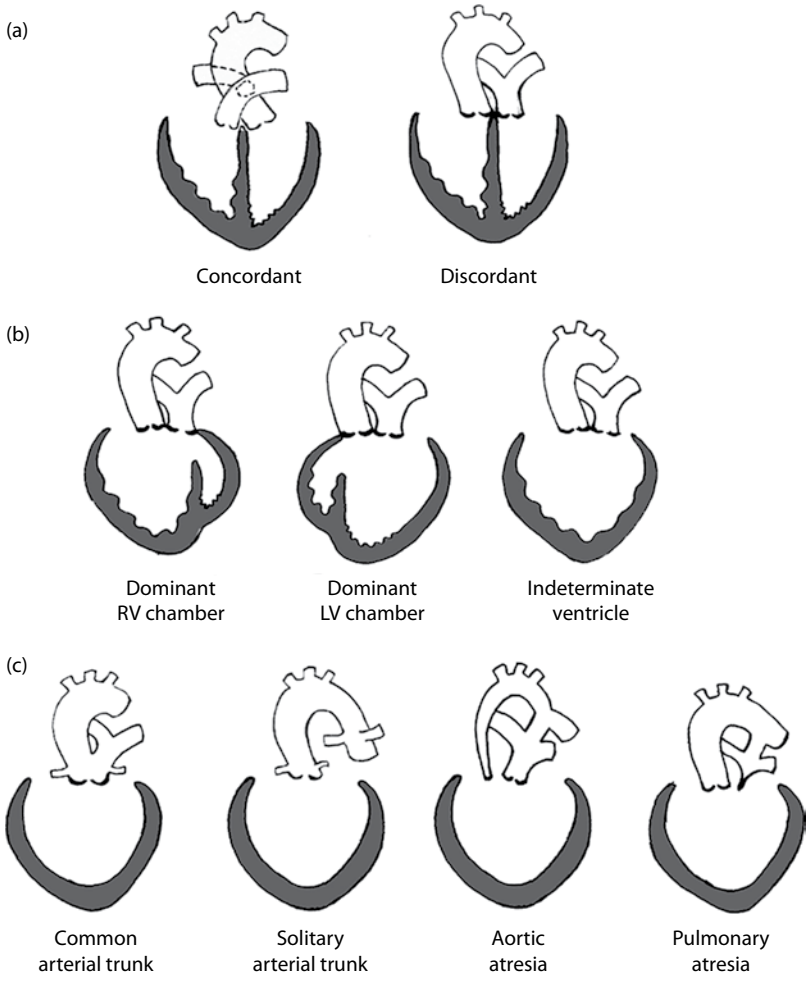


**Figure 2.22**
(a) The left panel represents concordant ventriculo-arterial connections with the pulmonary trunk arising from the morphologically right ventricle and the aorta from the morphologically left ventricle. In the right panel, discordant ventriculo-arterial connections are represented with the aorta arising from the morphologically right ventricle and the pulmonary trunk from the morphologically left ventricle. (b) When the arterial trunks arise from the same ventricle, this is described as a double-outlet ventriculo-arterial connection whether the arterial trunks arise from the morphologically right (RV), morphologically left (LV), or a ventricle with indeterminate morphology. (c) A single outlet from the heart is represented here. On the left the single outlet from the ventricular mass is formed by a common arterial trunk, which will supply the coronary, pulmonary, and systemic circulation. The left middle represents a solitary arterial trunk. In this instance, two intrapericardial arterial trunks cannot be identified, and the single outlet supplies the coronary and systemic circulation with the pulmonary circulation supplied by arteries that arise from the descending aorta, distal to the brachiocephalic arteries. In the right middle, the single outlet is represented by the pulmonary trunk with atresia of the aorta. To the right, the single outlet is represented by the aorta with atresia of the pulmonary trunk. It is important to note that with atresia of either of the arterial trunks, the ventricular origin of the trunks must be described. The origin may be exclusively from a right or left ventricle or override the ventricular septum taking its origin from both ventricles.

# Bibliography


1. Van Praagh R et al. *Circulation* 1980;61:1057–8.
2. Van Praagh R. *Circulation* 1977;56:139–43.
3. Anderson RH et al. *Pediatr Cardiol* 1984;5:281–8.
4. Anderson RH et al. *Pediatric Cardiology*, 3rd ed. Philadelphia, PA: Churchill Livingstone Elsevier, 2002.
5. Anderson RH et al. *Anat Rec* 2000;260:81–91.
6. Cook AC, Anderson RH. Editorial. *Heart* 2002;87:503–6.
7. Anderson RH et al. *J Cardiovasc Trans Res* 2013;6(2):118–23.
8. Spicer DE, Anderson RH. *J Cardiovasc Trans Res* 2013;6(2): 145–54.
9. Aiello VD et al. *Cardiol Young* 2007;17(suppl. 2):97–103.
10. Anderson RH. *Heart Rhythm* 2015;12:515–6.
11. Anderson RH, Loukas M. *Clin Anat* 2009;22:47–51.
12. Gilbert-Barness E et al. *Handbook of Pediatric Autopsy Pathology*, 2nd ed. Ch. 8. Springer-Verlag, 2013.
13. Loomba RS et al. *Cardiovasc Pathology* 2016;25(3):173–80.

# 3

# Placental implantation and development

Simcha Yagel and Debra S. Goldman-Wohl

## Introduction

The placenta, it must always be remembered, is fetal in origin. Any aberration affecting the placenta has serious consequences for the developing fetus. The size and function of the placenta have a profound effect on normal fetal growth and development, as the organ responsible for the supply of oxygen to the fetus. Therefore, placental pathology is most relevant to fetal well-being, and has far-reaching effects on healthy cardiovascular function and development. This makes the understanding of normal and pathological placental implantation and function indispensable in a text dealing with fetal cardiology.

The fetal heart pumps blood not only to the fetal brain and other organs, but also—in similar quantity to that within the fetal venous system—to the placenta. The placenta functions as the fetal lung in gas exchange, as well as the fetal kidney in waste removal, the fetal digestive system in nutrient acquisition, the fetal endocrine system in hormone production, and more.

In this chapter, we in no way attempt to provide an exhaustive review of placental form and function: whole texts have been devoted to this topic; rather, we focus our discussion on selected aspects of placental development having particular influence on the fetal cardiovascular system, among them intrauterine growth restriction (IUGR) and preeclampsia (PE). Other chapters in this text deal with the physiology of placentation and placental function, and their effects on fetal cardiac development and function, while here we focus on the cellular and molecular processes involved in placental development and implantation.

## Villous development

In 12–18 days postconception (pc), trophoblastic trabeculae begin to proliferate and form the primary villi, finger-like protrusions into the maternal blood surrounding them. Two days later, these primary villi are invaded by embryonic connective tissue and thus transformed into secondary villi. From days 18–20, the first fetal capillaries appear. At their appearance, the tertiary villi begin to develop. The first generation of tertiary villi make up the mesenchymal villi, which are the first structures to provide surface area for maternal-fetal exchange of nutrients, gases, and wastes. By term, the surface area of the placenta reaches an astounding 12M$^2$.[1] Between days 20 and 42 pc, the first generations of mesenchymal villi begin vasculogenesis, i.e., new capillaries are formed from mesenchymal precursor cells. The mesenchymal villi form the only pool for subsequent villous sprouting and development of the villous trees.[2–10]

The mesenchymal villi can differentiate into several types of specialized villi. Increased diameter and numerous stromal channels characterize the immature intermediate villi. These eventually become stem villi through stromal fibrosis. Mature intermediate villi begin to differentiate from the mesenchymal villi from about pregnancy week 23. These differ from immature intermediate villi in that they do not mature into stem villi. Rather, they produce many terminal villi along their surfaces. The terminal villi are highly capillarized and efficient vessels for maternal-fetal diffusional exchange. Some mesenchymal villi and immature intermediate villi are retained in the centers of the villous trees, forming a sort of growth reserve (Figure 3.1).[9]

The process of branching morphogenesis begins with selection of a cell subgroup induced toward motility and invasivity. This invasiveness may be a general characteristic of branching morphogenesis or its driving force, as branches enter surrounding tissues.[11] Fibroblast growth factor (FGF) signaling through their receptor tyrosine kinases (RTK) coordinates varied biological processes: angiogenesis, proliferation, differentiation, and branching morphogenesis.

We examined human placental branching morphogenesis through the expression of FGFR 1–4 and FGF10 in placentea and decidua. We found that FGFR 1–4 are expressed in placenta but not in the decidua, while FGF10 is expressed by decidual cells and by the placenta, especially the extravillous trophoblasts (EVTs).[12] We also showed that *Spry* 2 is expressed in the three trimesters of pregnancy by the placental villous macrophages (Hofbauer cells)[12] and that FGF10 induces *Spry2* expression in Hofbauer cell culture, suggesting that mesenchymal-epithelial interaction and cross talk among the different placenta cell types may play a role in regulation of placental development.[12]

Exogenous FGF10 promotes invasion and outgrowth of villi in organ culture, and upregulates metalloprotease activity in trophoblast cell culture, as well as increasing migration of single-cell trophoblasts through Matrigel (a biologically

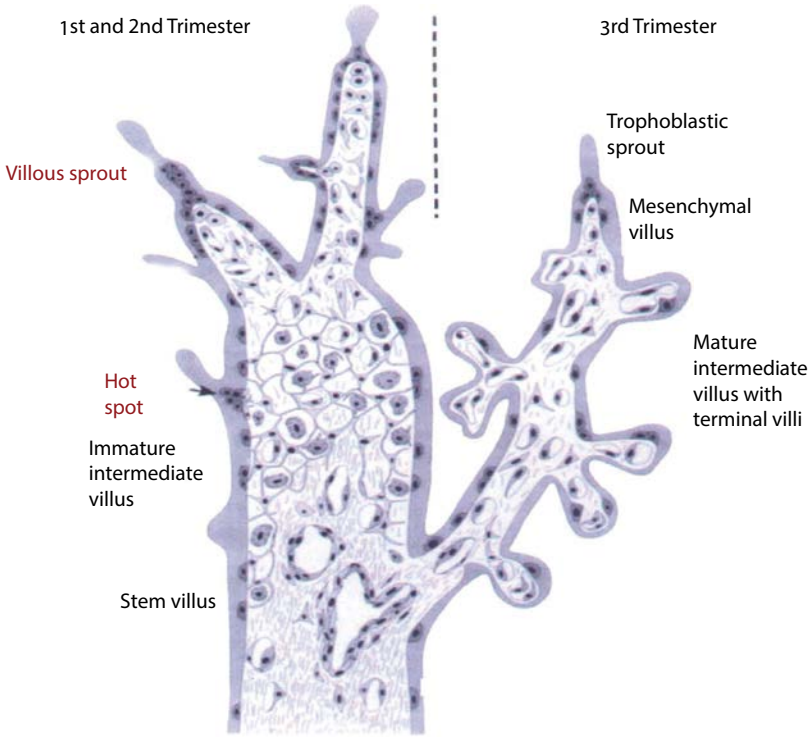


**Figure 3.1**
Formation and differentiation of placental villi during early and late pregnancy. Histological characteristics of the various villous types and their typical topographical relationships. Note the immature intermediate villus (left) showing a "hot spot," which subsequently (top of the left villus) develops via trophoblastic and villous sprouts into a new mesenchymal villus. Hot spots correspondingly mark the sites of future villous branching. (Modified with permission from Castellucci M. et al. *Hum Reprod Update* 2000;6:485–94.[9])

active extracellular matrix). Silencing of *Spry*2 expression by siRNA also enhanced the outgrowth of trophoblasts.[13]

*Spry*2 was shown to be a potential regulator of FGF10 activity; FGF10 is in turn a strong inducer of cell migration and collagenolitic activity. We speculate that trophoblast outgrowth and invasion at the fetal-maternal interface are in part positively regulated by FGF10, and negatively by Sprouty 2.[12,14]

## Invasion and implantation

Trophoblasts are the first cells to differentiate in the embryo. These cells adhere to the uterus and initiate the implantation process (Figure 3.2).[15] In fact, without appropriate and timed trophectoderm development, conception can occur but not implantation or pregnancy. Trophoblasts retain a stem cell population of villous cytotrophoblasts throughout pregnancy, and differentiation of trophoblasts into two major cell lineages, the syncytiotrophoblast and the invasive trophoblast, also continues to the end of pregnancy.

The syncytiotrophoblast of the chorionic villi is responsible for placental nutrient and gas exchange, as well as most placental hormone and growth factor production. It is within the chorionic villi that the fetal placental arteries and veins develop. The syncytiotrophoblast is a terminally differentiated tissue without cell borders separating the nuclei. It expands and is repaired via cell fusion of the underlying cytotrophoblast progenitor cells. The nuclei exit the cell cycle prior to or perhaps upon fusion, and the syncytiotrophoblast is thus composed of nuclei incorporated at varied times of gestation. This is reflected in the diverse appearance of the nuclei from euchromatin to heterochromatin and may reflect functional capability of the particular nuclei[1] reviewed in Huppertz.[16] With an amazing $60 \times 10^9$ nuclei at term, a mechanism must have developed that controls transcription and translation in the syncytiotrophoblast. One possible mechanism used to attenuate transcription in this huge number of nuclei would be to reduce transcription in a subset of the nuclei. Transcriptional activity in the syncytiotrophoblast has been studied using varied methodologies and has not surprisingly yielded mixed results.[16–20]

We demonstrated that snRNA is reduced in many syncytiotrophoblast nuclei. Since mRNA splicing guided by snRNAs is intimately associated with transcriptional activity, reduced snRNA indirectly points to reduced transcriptional activity.[20] However, the overall mechanisms of transcriptional and translational control in the syncytiotrophoblast as well as lateral cross talk among the nuclei remain to be elucidated.

The second lineage derived from the cytotrophoblasts, the invasive extravillous trophoblast may be defined as endovascular or interstitial. Early in pregnancy, the cytotrophoblasts begin to proliferate and form cell columns. It is from these cell columns that extravillous trophoblasts emanate and from which the interstitial and endovascular invasive trophoblasts

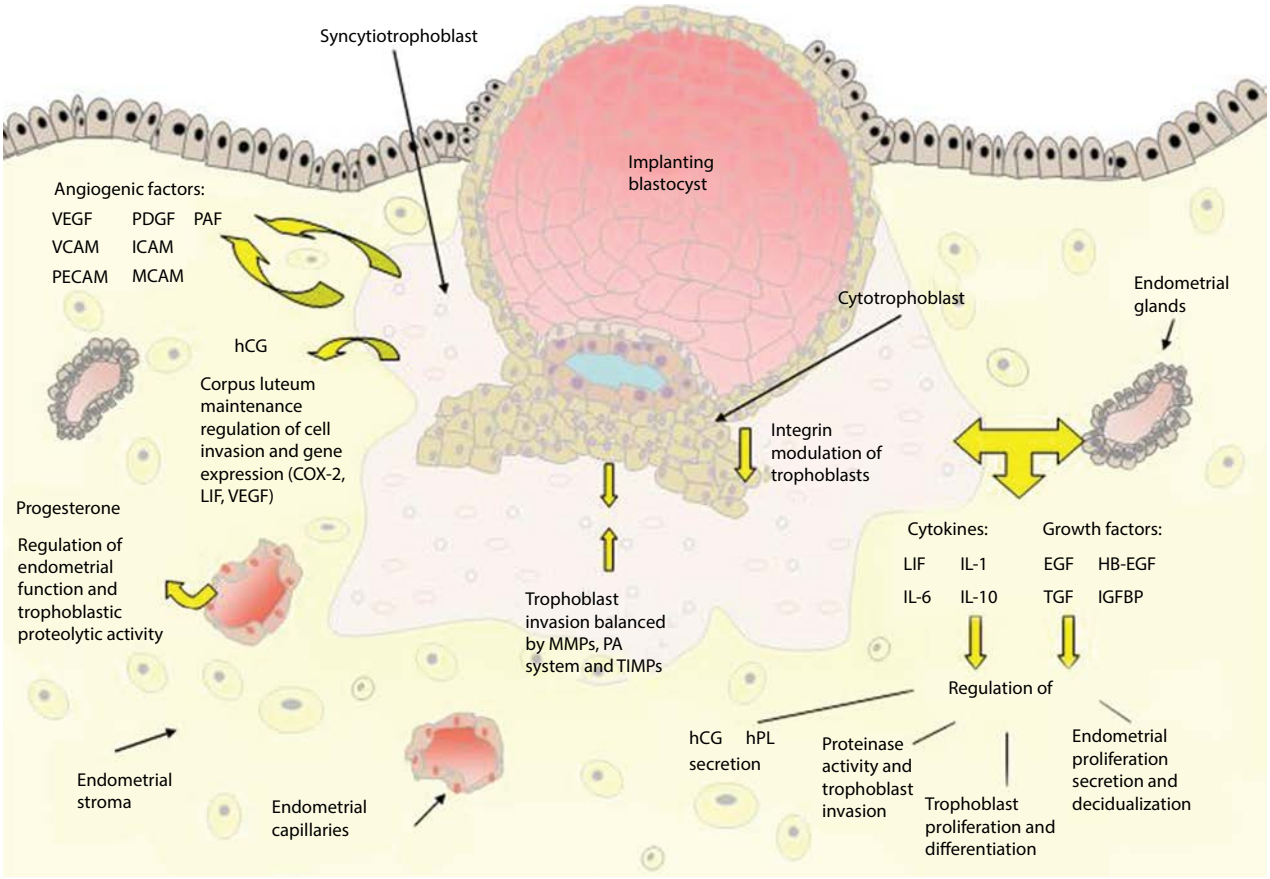


**Figure 3.2**
An implanting blastocyst, highlighting interactions between trophoblastic and endometrial cells, including integrins, growth factors, cytokines, hormones, and proteases. (Reproduced with permission from Staun-Ram E, Shalev E. *Reprod Biol Endocrinol* 2005;3:56.[170])

are derived. The former migrate through and invade the uterine tissue and anchor the placenta to the uterus, while the latter migrate to the maternal uterine spiral arteries. In the spiral arteries, the endovascular invasive trophoblasts begin the work of conversion of the spiral arteries, by displacing and replacing the endothelial cell lining of the vessels. This aids the process of forming a vessel of low resistance and high capacitance, equipped to meet the ever-increasing demand for blood flow required to maintain the growing pregnancy. This trophoblast-mediated conversion of the spiral arteries must occur by the end of the first trimester for a healthy pregnancy to continue.

Failure of the trophoblasts to invade the uterus appropriately, whether through shallow trophoblast invasion, fewer invasive trophoblasts, or failure to convert the spiral arteries, is often observed in placentas of preeclampsia.[21–26] In fact, disorders termed the *great obstetrical syndromes*, are associated with failures in deep placentation.[27] These complications of pregnancy, including preeclampsia, IUGR, preterm labor, preterm premature rupture of membranes, late spontaneous abortion, and abruption placentae, may show different degrees of spiral artery remodeling and may be instrumental in the development of these syndromes.[27]

Conversion of the maternal spiral arteries is mediated by trophoblast invasion. This is coincident with loss of the muscle and elastic tissue surrounding the arteries and replacement of the endothelial cells with trophoblasts, as discussed by Pijnenborg et al.[28] Interstitial endovascular invasion may be superficial in preeclampsia, not penetrating to one-third of the myometrial layer proximal to the endometrium, as is observed in healthy pregnancies. Spiral artery mean diameter remains low: persistence of unmodified narrow spiral arteries results in reduced placental perfusion. Additionally, the narrow spiral arteries of preeclampsia might result in high-pressure blood flow into the intervillous space, thus damaging the chorionic villi, and may be a critical factor in the development of the maternal syndrome (Figure 3.3).[25,29,30]

Some light has been shed on the mechanisms of cytotrophoblast induction of vessel remodeling in a transplantation model of placental villi into severe combined immunodeficiency disease (SCID) mice. Investigators showed that trophoblasts mediated both maternal endothelial cell and vascular smooth muscle cell apoptosis. Conversion of the spiral arteries depends on these modeling steps.[31] Other molecular mechanisms necessary for trophoblast invasion include transcription factor expression and differentiation to the invasive phenotype, mechanisms of migration and invasion, digestion of the extracellular matrix (ECM), expression of angiogenic factors involved in spiral artery remodeling. and ultimately, trophoblast immune cell cross talk and induction of chemokines and

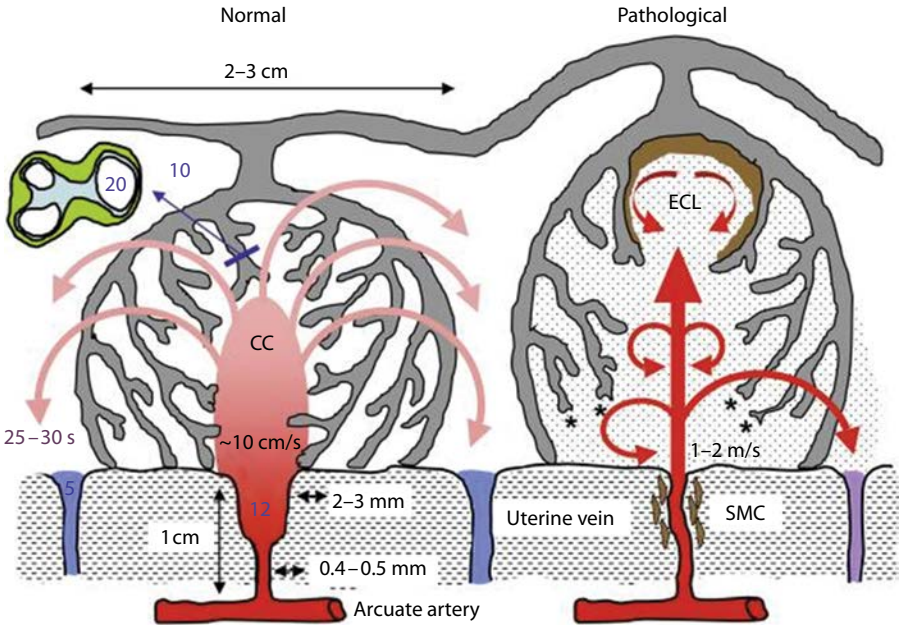


**Figure 3.3**
The effects of spiral artery conversion on the inflow of maternal blood into the intervillous space and on lobule architecture predicted by modeling (not to scale). Dilation of the distal segment in normal pregnancies will reduce the velocity of incoming blood, and the residual momentum will carry the blood into the central cavity (CC) of the lobule, from where it will disperse evenly through the villous tree. Transit time to the uterine vein is estimated to be in the order of 25–30 seconds, allowing adequate time for oxygen exchange. The pressure of the maternal blood, indicated in millimeters of Mercury (mm Hg) by the figures in blue, will drop across the nondilated segment of the spiral artery, the dimensions of which are given alongside. In pathological pregnancies, where no or very limited conversion occurs, the maternal blood will enter the intervillous space at speeds of 1–2 m/s. The high Reynolds number predicts turbulent flow, indicated by the circular arrows. We suggest that the high momentum ruptures anchoring villi (asterisks) and displaces others to form echogenic cystic lesions (ECL) lined by thrombus (brown). The transit time will be reduced, so that oxygen exchange is impaired and blood leaves in the uterine vein with a higher oxygen concentration than normal. Trophoblastic microparticulate debris (dotted) may be dislodged from the villous surface, leading to maternal endothelial cell activation. Finally, the retention of smooth muscle cells (SMCs) around the spiral artery will increase the risk of spontaneous vasoconstriction and ischaemia-reperfusion injury. (Reprinted with permission from Burton GJ. et al. *Placenta* 2009;30(6):473–82.[29])

cytokines that govern trophoblast migration and angiogenesis. More recently, researchers have begun to investigate the role that epithelial to mesenchymal transition (EMT) plays in cell migration of the cytotrophoblast, including similarities and differences in gene expression and highlighting the role that transcription factors play in this process.[32,33] This was recently reviewed by Davies et al.[33] In analogy to other systems with cells "on the move," particularly tumor biology, a role for hypoxia in early placental development akin to oxygen-starved tumors may mediate, respectively, trophoblast migration and tumor metastasis.[34]

## Extracellular matrix degradation

Trophoblast invasion and digestion of the extracellular matrix are governed by intrinsic trophoblast cell programming as well as interaction with the maternal cellular environment. To achieve successful invasion, trophoblasts must induce the repertoire of genes involved in digestion of the extracellular matrix. For example, MMP (92-kD matrix metalloproteinase, gelatinase B) is closely associated with the invasive phenotype of trophoblasts.[35,36] When trophoblast invasion is shallow (e.g., in preeclampsia) gene expression and the activity of several molecules involved in the degradation of extracellular matrix are abnormal,[37] including expression of MMP, which fails to be upregulated in preeclampsia. The enzymatic activities of urokinase plasminogen activator and plasminogen inhibitor are also altered in preeclampsia, suggesting a role for these molecules in invasion and migration of trophoblasts.[38]

In their pioneering work, Genbacev and colleagues[39] showed that the 5%–8% $O_2$ conditions of the late first-trimester fetal-maternal interface favor the invasive trophoblast phenotype. Under 2% $O_2$ conditions, trophoblast proliferation is preferentially observed. It has also been shown that under hypoxic conditions, trophoblasts retain adhesion molecule properties mimicking those of trophoblasts of preeclampsia.[26,40] It has also been demonstrated[41] that hypoxia-inducible factor (HIF1-$\alpha$) and its downregulating response to higher oxygen tension can adjust trophoblast invasion through inhibition of TGF$\beta$3, thus enhancing the invasive phenotype. Furthermore, expression of the tumor suppressor protein von Hippel-Lindau (pVHL), which is

critical for HIF1-α and HIF1-β regulation,[42] was shown to be downregulated as trophoblasts enter the more invasive oxygen-enriched environment.

## Expression of adhesion molecules by trophoblasts

Adhesion molecules and integrins play an important role in cell migration. Extravillous trophoblasts express the stage-specific repertoire of adhesion molecules (aVβ4, α1β1, VE-cadherin, VCAM-1, and PECAM-1). Certain adhesion molecules characterizing the stem cell population of villous cytotrophoblasts inhibit invasion: these molecules are downregulated as trophoblasts enter the invasive pathway of differentiation (α6β4, αVβ6, and E-cadherin).[26,40,43] Invasive trophoblasts undergo an epithelial-to-endothelial cell transformation and express endothelial cell-specific adhesion molecules. If the endovascular invasive trophoblasts do not undertake the function of the endothelial cells, which normally line the spiral artery, inadequate spiral arteries result, leading to deficient placentation and its sequelae. Defects in the molecules responsible for trophoblast invasion and degradation of the extracellular matrix, through which trophoblasts must migrate, and failure to acquire endovascular integrin markers, are indicative of a problem in a fetal pathway of trophoblast migration.[15]

## Placental vasculogenesis and angiogenesis

Angiogenesis is the formation of new vascular beds and is critical to normal tissue growth and development.[44–46] Placentation includes angiogenesis in both fetal and maternal tissues to ensure sufficiently increased uterine and umbilical blood flow[47–52] to afford the most favorable surroundings for meeting the demands of the developing fetus. Later in pregnancy, angiogenesis factors influence physiological exchange.[47,51,53] Decreased vascular development and increased vascular resistance have been shown to be associated with early embryo loss.[54,55]

One of the earliest stages in embryonic development is the establishment of functional circulation.[56–58] Increased transplacental exchange, which makes possible the rapid growth of the fetus in the second half of pregnancy, is supported by the extensive increase in uterine and umbilical blood flow.[51,59]

Major angiogenic factors have been identified, including those involved in placental vascularization processes. Among them are vascular endothelial growth factor (VEGF), fibroblast growth factor (FGF), and the angiopoietin (ANG) protein families, and their respective receptors.[45,60–63] VEGF and FGF are involved in most of the heparin-binding angiogenic activity produced by both ovarian[64] and placental[65–69] tissues. VEGF's specific stimulation of vascular permeability and vascular endothelial cell protease production and migration all influence the angiogenic process.[44–46,61,64] VEGF has also been shown to increase angiogenesis in both *in vivo* and *in vitro* models,[70–72] and has been implicated in the primary regulation of angiogenesis in normal and pathological processes, such as luteal growth, wound healing, coronary ischemia, and tumor growth.[61,73]

Mouse models have been used to study various aspects of placentation, including angiogenesis. During early pregnancy, VEGF mRNA is expressed in fetal placental, more than in maternal (endometrial) placental tissues, while basic FGF (bFGF) mRNA is expressed more in endometrial than in fetal placental tissues. In late pregnancy, VEGF mRNA is increasingly expressed in the placentome and intercotyledonary fetal membranes, while bFGF is greatest in the intercotyledonary fetal membranes.[74] Gene knockout studies show a central role for VEGF in fetal and placental angiogenesis. In mice, homozygous knockouts of the genes for vascular endothelial growth factor receptors (VEGFRs) led to defects in the initial formation of placental vasculature and angiogenesis, which led to fetal demise before midgestation.[75,76] Defects included abnormal vascular formation, organization, patterning, and endothelial morphology. Homozygous knockouts of VEGF were lethal by day 11 and led to dramatic cardiovascular defects: delayed and abnormal development of the heart, aorta, major vessels, and extraembryonic vasculature, including the yolk sac and the placenta.[77,78] Heterozygous knockout embryos with decreased VEGF expression showed similar defects and also died by day 11–12,[77,78] which may point to a threshold level of VEGF expression for normal vascular development to occur.

Just over a decade ago, our knowledge of the association between deficient angiogenensis and preeclampsia took a dramatic leap forward with the publication of several investigations conducted by Karumanchi and colleagues. Employing gene microarray analysis on placental RNA from placenta, Karumanchi observed that the soluble receptor, fms-like tyrosine kinase 1 (sFlt1), an antagonist of both VEGF and placental growth factor (PlGF), is highly upregulated in preeclamptic as compared to normal placentas. They also found that the soluble endoglin receptor that binds TGFβ, was upregulated in preeclampsia[79–82] (Figure 3.4).[83] This observation, combined with functional experimentation in animal models, set the tone for clinical investigations of circulating angiogenic factors in preeclamptic and normal women. Investigators posited a possible role for sFlt1 in the pathogenesis of preeclampsia and as a predictive indicator for preeclampsia, especially when associated with IUGR. Mechanistically, the sFlt1 receptor acts as an anti-angiogenic factor, by binding to circulating proteins, VEGF and PlGF, preventing them from interacting with the cell-bound Flt1 receptor to initiate angiogenesis. At the time of these important studies, the isoform sFlt1 was known as an endothelial cell alternate splice mRNA, Flt1-13, yielding a truncated protein not bound to the cell membrane. Subsequently, we, in collaboration with the Keshet group and colleagues, were able to demonstrate that the preeclamptic form of sFlt1 was a different alternate splice than that found in endothelial

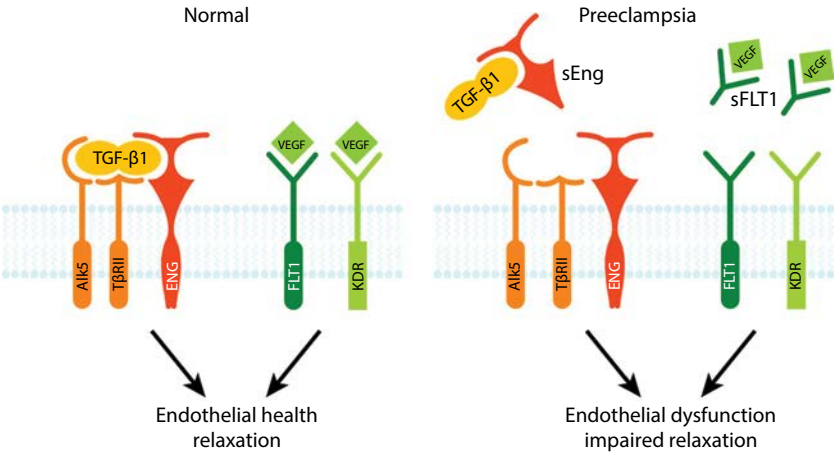


**Figure 3.4**
sFlt1 and soluble endoglin (sEng) cause endothelial dysfunction by antagonizing vascular endothelial growth factor (VEGF) and transforming growth factor-β1 (TGF-β1) signaling. There is mounting evidence that VEGF and TGF-β1 are required to maintain endothelial health in several tissues including the kidney and perhaps the placenta. During normal pregnancy, vascular homeostasis is maintained by physiological levels of VEGF and TGF-β1 signaling in the vasculature. In preeclampsia, excess placental secretion of sFlt1 and sEng (2 endogenous circulating antiangiogenic proteins) inhibits VEGF and TGF-β1 signaling, respectively, in the vasculature. This results in endothelial cell dysfunction, including decreased prostacyclin, nitric oxide production, and release of procoagulant proteins. TβRII indicates transforming growth factor-β type II receptor. (Reprinted with permission from Powe CE. et al. *Circulation* 2011;123:2856–69.[83])

cells.[84] This novel human-specific isoform, termed sFlt1-14, is expressed primarily in nonendothelial cells, e.g., in vascular smooth muscle cells, and is highly expressed in degenerative syncytiotrophoblast-syncytial knots (Figure 3.5).[84] Its normal function may be to protect nonendothelial cells from adverse angiogenic signaling. Pathologically, it acts to block angiogenic signaling necessary to maintain a healthy pregnancy, resulting in or exacerbating the maternal cascade of events in preeclampsia.

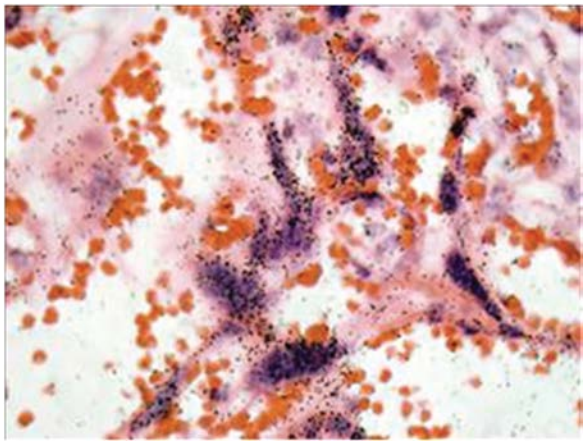

**Figure 3.5**
Syncytial knots, degenerative structures typifying a preeclamptic placenta, are the major source of the novel human-specific soluble VEGF receptor, previously implicated in preeclampsia causation. *In situ* hybridization of a preeclamptic placenta with a riboprobe specific to the novel soluble VEGF receptor, designated sFlt1-14. (Reprinted with permission from Sela et al. *Circ Res* 2008;102(2):1574–66.[84])

The avenue of investigation into antiangiogenic factors and preeclampsia spearheaded by Karumanchi and colleagues triggered active investigations searching for predictive biomarkers of preeclampsia with a special focus on serum levels of the ratio of sFlt1:PlGF,[85,86] as well as a search for treatment options based on these antiantiogenic findings in preeclampsia. These studies have promise in predicting the development as well as severity of preeclampsia. With this in mind, Litwinska and colleagues devised a risk model for development of early or late-onset preeclampsia based on maternal characteristics and medical history with multiples of the median (MoM) values of mean arterial pressure (MAP), uterine artery pulsatility index (UtA-PI), PlGF, and sFlt-1. The investigators showed that this model identified a group of women that constitutes less than 1% of the total population and contains greater than 95% of those who will develop PE before 32 weeks' gestation, as well as a group that constitutes less then 20% of the total and contains greater than 90% of patients who will develop PE at 32–35 weeks.

Zeisler et al. investigated whether a ratio of serum sFlt-1 to PlGF had predictive value for the development of preeclampsia in at-risk women.[163] The researchers found that a sFlt-1:PlGF ratio at or below 38 predicted the absence of preeclampsia within 1 week from testing; a score above 38 was mildly predictive of preeclampsia developing in the ensuing 4 weeks.

These investigations highlighted the importance and the central role for the placenta in the development of preeclampsia. However, one was still left with the chicken or the egg question.[164] Was placental overexpression of sFlt1 and lower circulating levels of VEGF and PlGF an actual cause of preeclampsia or part of the maternal cascade of events responding to endothelial cell dysfunction characteristic of preeclampsia?

FGFs are also potent angiogenesis factors and have been shown to stimulate *in vivo* and *in vitro* uterine arterial and fetal placental arterial endothelial cell proliferation.[44,45,87,88] FGFs are unique among the angiogenic growth factors in that they are pleiotropic and influence angiogenesis and other developmental and differentiated functions.[89]

VEGF and FGF regulate placental blood flow. Upregulation of endometrial expression of VEGF and bFGF mRNA, as well as increased uterine vascularization and blood flow, were demonstrated following estrogen treatment in ovariectomized ewes and mice.[52,90–92] Both VEGF and bFGF stimulate endothelial production of nitric oxide (NO), a local vasodilator, which has been shown to mediate estrogen-induced increase in uterine blood flow.[88,93–97] NO also regulates the expression of VEGF and bFGF.[98,99] ANGs have also been shown to be major angiogenic factors that regulate (both increase and decrease) vascular growth and development.[60,100–102] Like VEGF, ANG1 and ANG2 appear to be vascular-specific growth factors, because the receptor Tie2 is present primarily on endothelial cells.[60,103] ANG2 is a natural Tie2 antagonist, leading to vascular regression and modulation of vascular growth. ANG1 is a Tie2 agonist, critical in embryonic vascular development. Lack of ANG1 leads to significant cardiovascular defects and demise by midgestation.[60,100] Mice with null mutations of Tie1, Tie2, and ANG1 die later than VEGFR knockouts, pointing to a later role for Tie and ANG in vascular development.

VEGFR knockouts lack primary vascular growth and organization, while ANG and Tie knockouts are affected at the stage of vascular remodeling.[104] ANG does not affect endothelial cell proliferation but increases microvascular organization and endothelial cell survival.[102,105–108] In addition, ANG1 is produced by periendothelial cells, and partners VEGF in the angiogenic process.

The endothelial cell-specific receptors Tie1 and Tie2 and the angiopoietin ligands of Tie2 play fundamental roles in angiogenesis and in remodeling of vessel structure, but not in cell proliferation. Specifically, Ang2, an antagonist ligand for Tie2, is involved in the widening of vessels and disruption of vessel integrity.[103] We have described the expression patterns of Tie2 and its antagonist ligand ANG2 at the fetal maternal interface.[104] Ang2 is expressed in the syncytiotrophoblast and Tie2 in both fetal and maternal endothelial cells.[104,109] This receptor ligand interaction and fetal-maternal cross talk have the potential to mediate widening of both fetal and maternal vessels, as reviewed by Pijnenborg et al.[28]

The ephrin subfamily of endothelial cell ligands and receptors plays a role in endothelial cell and nerve cell targeting and migration, but not proliferation.[109] The downregulation of EPHB4 and upregulation of ephrin B1 in cytotrophoblasts is associated with endovascular migration.[110] We investigated whether the ligand, ephrin-Al, is involved in trophoblast targeting as well as angiogenesis in the placenta. Using RNA *in situ* hybridization analysis, we found ephrin-Al expressed in cell columns of extravillous trophoblast in first trimester placenta.[111] In late first trimester and in second and third trimesters, ephrin-Al is found in the extravillous trophoblast cells that have invaded the decidua. We did not observe ephrin-Al in syncytiotrophoblast or in cytotrophoblasts. The cell-specific distribution of ephrin-Al suggests that it may play a role in migration of trophoblasts and in the vascular remodeling induced by the invading extravillous trophoblasts. Ephrin-Al's role in the defective cell invasion observed in preeclampsia remains to be investigated. A role for ephrin-B2 and EPHB4 regulated miRNA expression may play a role in the development of preeclampsia.[112]

## The role of natural killer cells: When killers become builders

Natural killer (NK) cell cytotoxicity is regulated by both inhibitory and activating receptors.[113] Groundbreaking population-based genetic studies[114] showed evidence that certain combinations of fetal and maternal genotypes, specifically HLA-C2 genotypes in the fetus and specific genotypes of maternal NK killer cell immunoglobulin-like receptors (KIRs), KIR-AA, increased the risk for preeclampsia. Conversely, the presence of the maternal KIR-B haplotype was protective for preeclampsia. This overinhibitory model necessitated an intellectual shift among researchers, that genotypes that encode greater inhibition of NK cells are associated with the development of preeclampsia, whereas previous theories of preeclampsia had focused on the need to inhibit the NK cell response as a prerequisite for allowing trophoblast invasion.

These observations[114] can be reconciled through the pioneering work in mouse models.[115] Research into animal models over the past decade laid the foundation for a theory of uterine NK cells' pivotal role in angiogenesis and artery remodeling at the fetal-maternal interface.[115] The role of decidual NK cells' interactions with extravillous trophoblasts, growth factor secretion, cytokines, and angiogenic stimulators that have the potential to enhance spiral artery widening and trophoblast invasion[116] demonstrate these observations at the human fetal-maternal interface. Furthermore, we demonstrated that the genetic interactions described by Hiby et al.[114] cause overinhibition of NK cells, which in turn increase the risk for preeclampsia, lead to decreased secretion of specific cytokines interleukin 8, interferon-$\gamma$ inducible protein-10 (IL-8, IP-10), as well as angiogenic factors VEGF and placental growth factor (PLGF).[116]

This NK cell regulation of spiral artery conversion can extend to their effect on trophoblast attraction and migration throughout the decidua. The molecular signals partly responsible for trophoblast attraction are revealed through chemokine receptor expression on invading trophoblasts and chemokine ligand expression by the NK cells populating the maternal-fetal interface. Specifically, Hanna et al.[116] demonstrated that trophoblasts expressing the chemokine receptors CXCR1 and CXCR3 are attracted to decidual NK cells. These express their respective ligands, IL-8 and IP-10. In addition, activated decidual NK cells express higher levels of IP-10 and IL-8.

It remains to be demonstrated that the maternal-fetal immune genetic interactions that predispose a pregnancy to

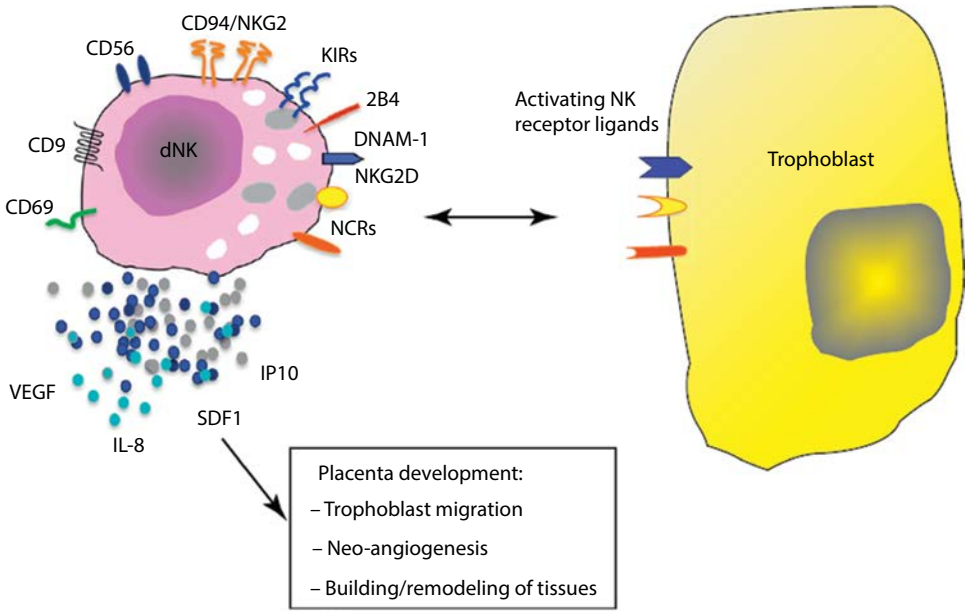


**Figure 3.6**
Molecular interactions between dNK and trophoblast cells. The dNK/trophoblast cross talk is mediated by a number of receptor-ligand interactions. As a consequence, dNK cells release cytokines/chemokines that play a major role in neoangiogenesis, and building/remodeling of tissues. dNK cells appear to contribute also to the placenta development by promoting migration of trophoblast cells. (Reprinted with permission from Vacca P. et al. *Trends Immunol* 2011;32:517–23.[118])

preeclampsia actually result in narrow, unconverted spiral arteries, establishing a placental insufficiency ripe for the development of preeclampsia. This maternal NK cell and fetal trophoblast cross talk would exemplify how immune interactions between the mother and fetus at the maternal-fetal interface could contribute to the development of preeclampsia by both failure of trophoblasts to invade and lack of the angiogenic signals necessary to convert the spiral arteries leading to utero-placental blood flow insufficiency[117] (Figure 3.6).[118]

## Maternal immune tolerance to the fetus

Mother and fetus are distinct genetically, and maternal and fetal tissues are in intimate contact at the placenta and maternal decidua across the maternal-fetal interface. This intimate contact could be expected to generate a maternal immune rejection response, but in most cases it does not. Maternal immune rejection of the developing fetus has been implicated in pathologies of pregnancy such as recurrent miscarriage and preeclampsia.[119–121] Since trophoblasts are the placental cell population most in contact with the maternal immune system, research focuses on maternal immune recognition of these cells. The mechanisms involved in placental trophoblast, and thereby fetal, avoidance of maternal immune surveillance remain inadequately understood.

Trophoblasts invade maternal tissue while eluding maternal immune surveillance. Protection of trophoblasts from attack by NK cells is of critical importance, since in a normal pregnancy trophoblasts closely associate with NK cells at the implantation site, where they represent the major lymphocyte population.[122] Several mechanisms work to maintain the delicate balance between immune tolerance and activation, which could lead to rejection of the embryo by the decidual lymphocytes. Both EVT and decidual lymphocytes are involved in these mechanisms. One of the chief activities of leukocytic and nonleukocytic cells at the maternal-fetal interface is to produce and release cytokines. The cytokine cross talk occurring across this interface has been the subject of extensive research; cytokines help facilitate communication between the host and guest cells. Modulation of the local cytokine profile[123] is thought to control EVT invasion. Therefore, the cytokine release of decidual lymphocytes is closely regulated. EVT also expresses two nonclassical class I MHC proteins, the HLA-E[124] and HLA-G,[125] along with the classical HLA-C protein, but do not express the HLA-A and HLA-B proteins.[126] This unique pattern of expression of class I MHC may prevent rejection of the semi-allogeneic fetus by the mother's immune system, as most of the CTL are directed against HLA-A and HLA-B proteins.

Activated T cells (Th0 cells) produce a variety of cytokines; activated $CD4^+$ T cells (Th1 and Th2 cells) are grouped according to the cytokines they produce. Thl cytokines, interleukin-2 (IL-2) and interferon-$\gamma$, help macrophages and cytotoxic T lymphocyte–mediated responses. Th2 cells help antibody production by B cells. These two types of response may be mutually exclusive.[127–129]

Cytokine secretion by fetal and maternal tissues at the interface seems to be high. Receptors for a number of cytokines have been found on fetal trophoblasts.[130,131] Cytokines

or growth factors produced by the decidua may potentially affect trophoblast growth and invasion. The question of local suppression of Th1-type cytokines in human pregnancy remains open. Interferon-γ is expressed in the placenta and found in amniotic fluid at term.[132,133] IL-2, however, is absent from uteroplacental tissues. Since large granulated lymphocytes' cytotoxicity against trophoblasts is induced *in vitro* only following activation by IL-2, its absence may be a method of large granulated lymphocytes cytolytic behavior regulation.[130–137]

Of the Th2 cytokines, IL-4 and IL-6 have been found in maternal and fetal tissues at the fetal-maternal interface, and cytotrophoblasts and maternal lymphocytes produce IL-10. The role of cytokines at the maternal-fetal interface is not yet fully understood.[138–140]

There is epidemiological evidence to indicate that primipaternity, insemination with donor sperm, and pregnancy without prior cohabitation increase the risk of preeclampsia, which suggests an immune component for the development of the disease.[141–143] HLA-G expression is absent or reduced in preeclampsia as compared to normal placenta.[37,144–146] It has been suggested that HLA-G, perhaps in conjunction with HLA-E, protects invasive trophoblasts from attack by NK cells.[147] When invasive trophoblasts lacking HLA-G encounter decidual NK cells, they are destroyed.

The decidua is heavily infiltrated by NK cells, and attention has focused on maternal NK cell response to HLA-G.[123] It is possible, if the maternal NK cell recognition HLA-G is defective, then the HLA-G positive trophoblasts will be unable to infiltrate the decidua. Reduced HLA-G expression in preeclampsia, and vulnerability to attack by the maternal NK cells, support the idea that disruption of trophoblast invasion would lead to failure of spiral artery conversion, and thereby initiate the cascade of events observed in preeclampsia.[148,149] This preeclampsia model, in turn, exemplifies the balancing act of escaping maternal immune surveillance.[146]

The Fas receptor and its ligand FasL belong to the tumor necrosis factor and nerve growth factor receptor family. They are known to be involved in immune response regulation. Kauma et al. showed that FasL is expressed on trophoblasts at the maternal-fetal interface, and that these cells induce apoptosis in activated lymphocytes. These findings may help elucidate a mechanism for maternal immune tolerance of the developing fetus.[119–121,150–152]

Preeclampsia may be considered as a two-step disease, with its initiating factor narrowing spiral arteries, which result in insufficient placental blood flow, leading to a hypoxic uterine environment and endothelial dysfunction, finally resulting in the maternal syndrome. Many of the mechanisms discussed previously, and in addition such maternal factors as risk for atherosclerosis, would lead to narrow spiral arteries. That is, narrow spiral arteries and poor placental perfusion may be the consequence of a fetal pathway of shallow trophoblast invasion and unconverted spiral arteries or a maternal pathway of normally converted spiral arteries that become blocked; these pathways converge in the maternal disease of preeclampsia.[117]

## Exosomes and microparticles

The study of circulating placental debris, particularly apoptotic particles of villous trophoblast, has gained high-profile attention as cell-free fetal DNA (more accurately, placental DNA) is the basis for the revolutionary technology of noninvasive prenatal testing (NIPT).[153,154] There are many open questions in the field regarding a correlation between placental health and production and release of these placental apoptotic particles. The syncytiotrophoblast releases microparticles composed of exosomes, microvesicles, and larger syncytial aggregates.[155] The exosomes, microvesicles, and larger syncytial aggregates (at times referred to as apoptotic bodies) differ in particle size and origin. Whereas syncytial exosomes are cell-derived vesicles, microvesicles are fragments of the cell plasma membrane. The larger syncytial aggregates may be indicative of cellular debris released postapoptosis. These extracellular vesicles (EVs) released into the maternal circulation throughout pregnancy contain a myriad of molecules including mRNA, miRNA, proteins, and lipids, which contribute to intercellular communication.[156] The field of study is complicated by a lack of standardization or consensus regarding methods of isolation, high number of platelet debris found in circulation, size of the particle, and biological markers used to identify and aid in isolation of syncytiotrophoblast-derived particles from maternal circulation. To circumvent some of these technical problems, villous explant culture can be performed over mesh and the shed products evaluated.[157] The Redman-Sargent group advanced the study of the increased numbers of extracellular vesicles found in maternal circulation in preeclampsia[158] by pioneering the use of nanoparticle tracking analysis, which affords characterization of EVs down to the 50 nm size range, whereas conventional flow cytometry can be used to phenotype to the 300 nm range.[159]

Related to this finding may be the hypoxia-reoxygenation hypothesis, which proposes placental damage and hence perhaps the release of placental debris from the syncytiotrophoblast, as the blood of the narrow spiral artery spurts out into the intervillous space, as opposed to controlled smooth flow from appropriately modified widened spiral arteries[160] (Figure 3.3).[29] One of the prominent roles of exosomes is thought to be immune modification at both the maternal-fetal interface and perhaps through the maternal circulation to distant sites. These exosomes induce pro-inflammatory cytokines, and inhibit NK cell, T-cell, and macrophage responses.[155,156,161] Of particular note is that syncytial extracellular vesicles released from the placentas of preeclampsia increase platelet activation and may provide a link between the increased circulating "placental debris" found in preeclampsia with the clotting disturbances complicating preeclampsia.[162] Extracellular vesicles derived from maternal platelets induce a thromboinflammatory response in the placenta via purinergic signaling.[163] Thus, cross talk between placental-derived EVs and maternal-derived EVs may play an important role in the etiology of preeclampsia. Furthermore, the Sadovsky

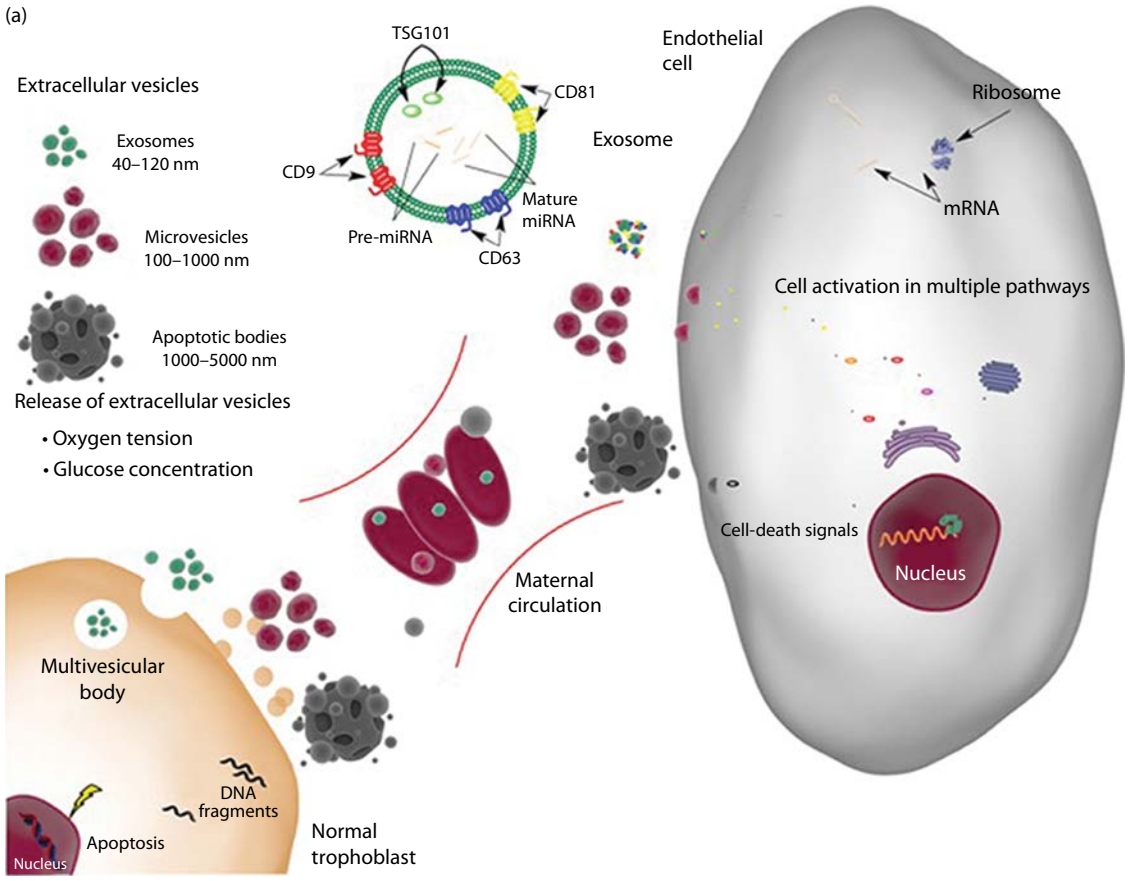


**Figure 3.7**
(a) Extracellular vesicles released from placenta in normal pregnancy. Extracellular vesicles (EVs) include exosomes, microvesicles, and apoptotic bodies all with different sizes and origins. With adequate blood flow from the mother to the placenta resulting in normal oxygen tension and glucose (nutrient) concentration, a limited number of EVs are shed from the placenta into the maternal circulation. Cargo and function of the EVs are not completely understood. However, they may constitute a common language between fetal-placental tissue and mother with interchange of information leading to normal blood flow supply (from the mother to the placenta). Fetal-placental extracellular vesicles may also modulate maternal endothelial cell function. The cargo of exosomes, of endosomal origin, including proteins and nucleic acids, such as microRNAs may be "planned" by the placenta. This cargo controls endothelial cell protein expression leading modifying multiple pathways including among others metabolic and survival-death signals. Appropriate communication allows successful pregnancy and fetal development. (*Continued*)

group has shown that nanosized exosomes isolated from the plasma of pregnant women and from the media of cultured primary human trophoblasts displayed antiviral activity.[165] Their work demonstrated the differing properties and compositions of placental extracellular vesicles, microparticles, placental debris, and exosomes. Interestingly, among the proteins and mRNAs found in circulating syncytial aggregates is the antiangiogenic soluble receptor for VEGF and PlGF, sFlt1.[157] Thus, we have a link between placental microparticles and an avenue for the high amounts of sFlt produced in the placenta entering the maternal circulation (Figure 3.7a,b).[166]

A brave new frontier has opened with the finding that microparticles play a role in blastocyst-trophoblast endometrial communication and may be instrumental in the regulation of implantation.[167,168] Endometrial embryonic cross talk could perhaps be bidirectional, as the endometrium produces exosomes containing miRNAs that are internalized by embryos and that modify expression of embryonic adhesion molecules, while the inner cell mass produces microparticles that stimulate the trophectoderm of the blastocyst, enhancing implantation.[167,169]

## Conclusions

In the last decade, tremendous progress has been made in our knowledge of the cellular and molecular mechanisms precipitating the development of the placenta and placental-based syndromes, especially preeclampsia. Insights into properties of the fetal-maternal interface based on studies of vasculogenesis and angiogenesis of placental and maternal blood vessels, the role that immunology plays in developing the placental bed, exosomes, and placental particles have all recently

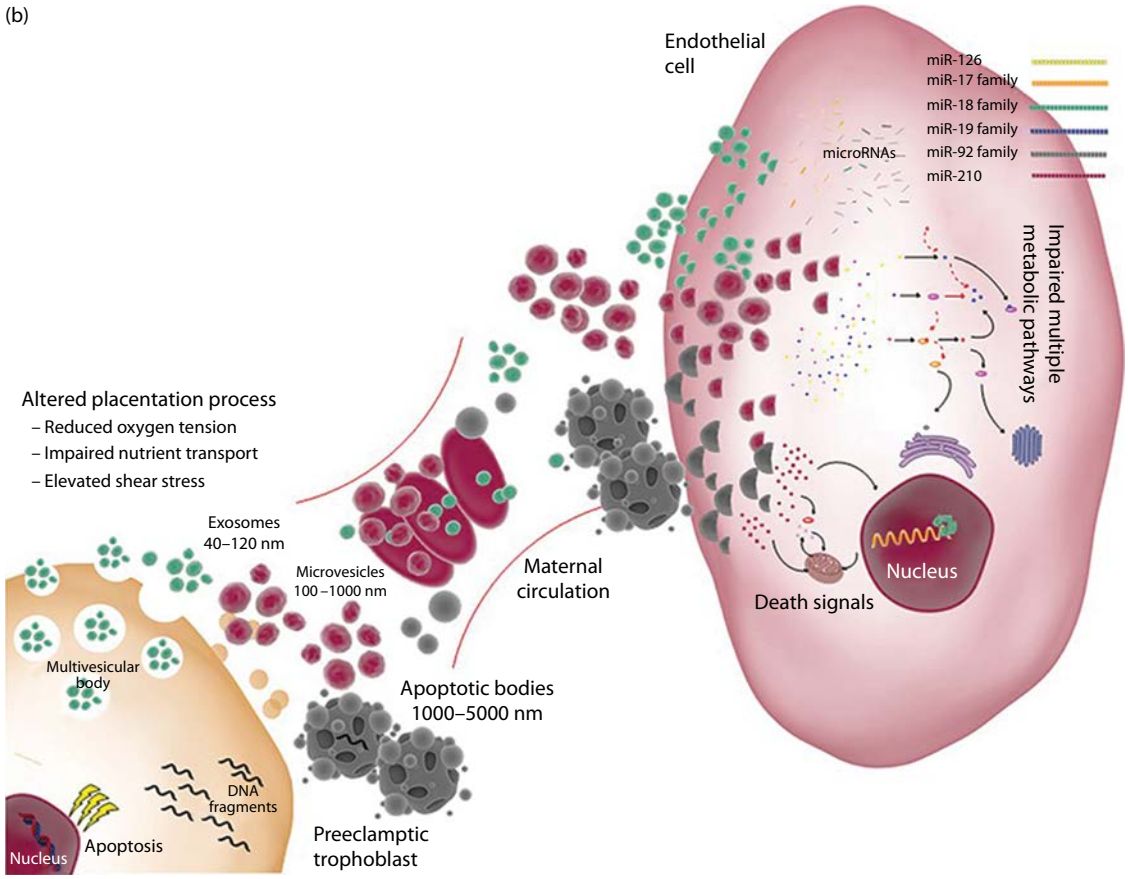


**Figure 3.7 (Continued)**
(b) Exosomes released from the placenta: focus on preeclampsia. As in normal pregnancy, extracellular vesicles (EVs) include exosomes, microvesicles, and apoptotic bodies all with different sizes and origins. However, abnormal placentation secondary to reduced trophoblast invasion and failed remodeling of spiral arteries leads to reduced oxygen tension, impaired nutrient transport, and exposure to increased shear stress for the syncytiotrophoblast. Under these stressful conditions, more EVs are shed from the placenta into the maternal circulation. Messages carried by the EVs are not completely understood; however, it is proposed that they cause endothelial dysfunction with associated elevation of maternal blood pressure. This figure indicates some of miscommunication generated by the placenta via exosomes and its cargo, microRNAs. Potential effects on maternal endothelial cells by the family of miR-126, miR-17, miR-18, miR-19, miR-92, and miR-210 are detailed in the manuscript. In preeclampsia, multiple pathways may be impaired including metabolic and death signaling by microRNAs among others. (Reprinted with permission from Escudero CA. et al. *Front Physiol* 2016;7:98.[166])

contributed to our understanding of establishing and maintaining a healthy pregnancy. However, many key questions are still open for further investigation, to continue to elucidate the complex processes involved in placental implantation and development.

# References


1. Mayhew TM, Simpson RA. *Placenta* 1994;15(8):837–44.
2. Boyd JD, Hamilton WJ. *The Human Placenta*. Cambridge, UK: Heffner; 1970.
3. Castellucci M, Kaufmann P. *Placenta* 1982;3(3):269–85.
4. King BF. *Am J Anat* 1987;178(1):30–44.
5. Enders AC, King BF. *Am J Anat* 1988;181(4):327–40.
6. Demir R et al. *Acta Anat (Basel)* 1989;136(3):190–203.
7. Castellucci M et al. *Anat Embryol (Berlin)* 1990;181(2):117–28.
8. Benirschke K, Kaufmann P, eds. *The Pathology of the Human Placenta*. New York, NY: Springer; 2000.
9. Castellucci M et al. *Hum Reprod Update* 2000;6(5):485–94.
10. Kaufmann P, Kingdom JC. Development of the vascular system in the placenta. In: Risau W, Rubanyi G, eds. *Morphogenesis of Endothelium*. Amsterdam: Harwood; 2000:225–75.
11. Affolter M et al. *Dev Cell* 2003;4(1):11–8.
12. Anteby EY et al. *Eur J Obstet Gynecol Reprod Biol* 2005b; 119(1):27–35.
13. Natanson-Yaron S et al. *Mol Hum Reprod* 2007;13(7):511–9.
14. Anteby EY et al. *Placenta* 2005a;26(6):476–83.
15. Norwitz ER et al. *N Engl J Med* 2001;345(19):1400–8.
16. Huppertz B. *Placenta* 2010;31(suppl):S75–81.
17. Ellery PM et al. *Placenta* 2009;30(4):329–34.
18. Fogarty NM et al. *J Anat* 2011;219(5):601–10.
19. Fogarty NM et al. *Am J Pathol* 2013;183(1):144–52.
20. Goldman-Wohl D et al. *Mol Hum Reprod* 2013;19(11):737–44.
21. Brosens IA et al. *Obstet Gynecol Annu* 1972;1:177–91.
22. Gerretsen G et al. *Br J Obstet Gynaecol* 1981;88(9):876–81.
23. Khong TY et al. *Br J Obstet Gynaecol* 1986;93(10):1049–59.
24. Moodley J, Ramsaroop R. *S Afr Med J* 1989;75(8):376–8.
25. Meekins JW et al. *Br J Obstet Gynaecol* 1994;101(8):669–74.
26. Zhou Y et al. *J Clin Invest* 1997;99(9):2152–64.

27. Brosens I et al. *Am J Obstet Gynecol* 2011;204(3):193–201.
28. Pijnenborg R et al. *Placenta* 2006;27(9–10):939–58.
29. Burton GJ et al. *Placenta* 2009;30(6):473–82.
30. Hung TH et al. *Am J Pathol* 2001;159(3):1031–43.
31. Red-Horse K et al. *J Clin Invest* 2006;116(10):2643–52.
32. DaSilva-Arnold S et al. *Placenta* 2015;36(12):1412–8.
33. Davies JE et al. *Cell Adh Migr* 2016;10(3):310–21.
34. Burton GJ et al. *Placenta* 2017;56:14–8.
35. Librach CL et al. *J Cell Biol* 1991;113(2):437–49.
36. Shimonovitz S et al. *Am J Obstet Gynecol* 1994;171(3):832–8.
37. Lim KH et al. *Am J Pathol* 1997;151(6):1809–18.
38. Graham CH, McCrae KR. *Am J Obstet Gynecol* 1996;175(3 Pt 1):555–62.
39. Genbacev O et al. *Science* 1997;277(5332):1669–1672.
40. Zhou Y et al. *J Clin Invest* 1997;99(9):2139–51.
41. Caniggia I et al. *J Clin Invest* 2000;105(5):577–87.
42. Genbacev O et al. *Dev Biol* 2001;233(2):526–36.
43. Damsky CH et al. *J Clin Invest* 1992;89(1):210–22.
44. Folkman J, Klagsbrun M. *Science* 1987; 235(4787):442–7.
45. Klagsbrun M, D'Amore PA. *Annu Rev Physiol* 1991;53:217–39.
46. Reynolds LP et al. *FASEB J* 1992;6(3):886–92.
47. Assheton R. *Phil Trans R Soc B* 1906;198:143–200.
48. Greiss FC, Jr., Anderson SG. *Am J Obstet Gynecol* 1970;106(1): 30–8.
49. Reynolds LP et al. *J Anim Sci* 1984;58(2):423–9.
50. Reynolds LP. *J Anim Sci* 1986;62(suppl 2):47–61.
51. Reynolds LP, Redmer DA. *J Anim Sci* 1995;73(6):1839–51.
52. Magness RR. Maternal cardiovascular and other physiological responses to the endocrinology of pregnancy. In: Bazer FW, ed. *The Endocrinology of Pregnancy*. Totowa, NJ: Humana Press; 1998:507–39.
53. Bell AW et al. *Am J Physiol* 1986;250(5 Pt 1):E538–44.
54. Meegdes BH et al. *Fertil Steril* 1988;49(2):216–20.
55. Bassil S et al. *Hum Reprod* 1995;10(6):1497–501.
56. Witschi E. *Development of Vertebrates*. Philadelphia, PA: W.B. Saunders; 1956.
57. Patten BM. *Foundations of Embryology*. New York, NY: McGraw-Hill; 1964.
58. Ramsey EM. *The Placenta, Human and Animal*. New York, NY: Praeger; 1982.
59. Meschia G. Circulation to female reproductive organs. In: Abboud FM, Shepherd JT, eds. *Handbook of Physiology*. Bethesda, MD: American Physiologocal Society; 1983;III, part 1:241–69.
60. Breier G et al. *Thromb Haemost* 1997;78(1):678–83.
61. Ferrara N, Davis-Smyth T. *Endocr Rev* 1997;18(1):4–25.
62. Hanahan D. *Science* 1997;277(5322):48–50.
63. Neufeld G et al. *FASEB J* 1999;13(1):9–22.
64. Reynolds LP et al. *Endocrine* 2000;12(1):1–9.
65. Reynolds LP et al. *Reprod Fertil* 1987;81(1):233–40.
66. Reynolds LP, Redmer DA. *J Reprod Fertil* 1988;83(1):497–502.
67. Millaway DS et al. *J Reprod Fertil* 1989;86(2):689–96.
68. Zheng J et al. *J Soc Gynecol Invest* 1995;2(2):289.
69. Zheng J et al. *Biochem Cell Biol* 1998;76(1):89–96.
70. Leung DW et al. *Science* 1989;246(4935):1306–9.
71. Nicosia RF et al. *Am J Pathol* 1994;145(5):1023–9.
72. Phillips GD et al. *In Vivo* 1994;8(6):961–5.
73. Fraser HM et al. *Endocrinology* 2000;141(3):995–1000.
74. Reynolds LP, Redmer DA. *Biol Reprod* 2001;64(4):1033–40.
75. Fong GH et al. *Nature* 1995;376(6535):66–70.
76. Shalaby F et al. *Nature* 1995;376(6535):62–6.
77. Carmeliet P et al. *Nature* 1996;380(6573):435–9.
78. Ferrara N et al. *Nature* 1996;380(6573):439–42.
79. Maynard SE et al. *J Clin Invest* 2003;111(5):649–58.
80. Levine RJ et al. *N Engl J Med* 2004;350(7):672–83.
81. Thadhani R et al. *J Clin Endocrinol Metab* 2004;89(2):770–5.
82. Levine RJ et al. *N Engl J Med* 2006;355(10):992–1005.
83. Powe CE et al. *Circulation* 2011;123(24):2856–69.
84. Sela S et al. *Circ Res* 2008;102(12):1574–66.
85. Zeisler H et al. *N Engl J Med* 2016;374(1):13–22.
86. Litwinska M et al. *Ultrasound Obstet Gynecol* 2017;50(3):367–72.
87. Cale JM et al. *J Soc Gynecol Investig* 1997;4(6):284–92.
88. Zheng J et al. *Endocrinology* 1995;140(3):1399–407.
89. Gospodarowicz D. *Ann N Y Acad Sci* 1991;638:1–8.
90. Cullinan-Bove K, Koos RD. *Endocrinology* 1993;133(2):829–37.
91. Reynolds LP et al. *Biol Reprod* 1998a;59(3):606–12.
92. Reynolds LP et al. *Biol Reprod* 1998b;59(3):613–20.
93. Rosenfeld CR et al. *J Clin Invest* 1996;98(9):2158–66.
94. Babaei S et al. *Circ Res* 1998;82(9):1007–15.
95. Hood JD et al. *Am J Physiol* 1998;274(3 Pt 2):H1054–8.
96. Kroll J, Waltenberger J. *Biochem Biophys Res Commun* 1998; 252(3):743–6.
97. Vagnoni KE et al. *Am J Physiol* 1998;275(5 Pt 2):H1845–56.
98. Sasaki K et al. *J Biochem* 1998;123(3):431–9.
99. Frank S et al. *Biochem J* 1999;338(Pt 2): 367–74.
100. Suri C et al. *Cell* 1996;87(7):1171–80.
101. Lindahl P et al. *Curr Opin Lipidol* 1998;9(5):407–11.
102. Patan S. *Microvasc Res* 1998;56(1):1–21.
103. Maisonpierre PC et al. *Science* 1997;277(5322):55–6.
104. Goldman-Wohl DS et al. *Mol Hum Reprod* 2000b;6(1):81–7.
105. Hayes AJ et al. *Microvasc Res* 1999;58(3):224–37.
106. Kwak HJ et al. *FEBS Lett* 1999;448(2-3):249–53.
107. Papapetropoulos A et al. *Lab Invest* 1999;79(2):213–23.
108. Thurston G et al. *Science* 1999;286(5449):2511–4.
109. Yancopoulos GD et al. *Nature* 2000;407(6801):242–8.
110. Red-Horse K et al. *Development* 2005;132(18):4097–106.
111. Goldman-Wohl D et al. *Placenta* 2004;25(7):623–30.
112. Wang W et al. *J Clin Endocrinol Metab* 2012;97(6):E1051–9.
113. Hanna J, Mandelboim O. *Trends Immunol* 2007;28(5):201–6.
114. Hiby SE et al. *J Exp Med* 2004;200(8):957–65.
115. Croy BA et al. *J Reprod Immunol* 2003;59(2):175–91.
116. Hanna J et al. *Nat Med* 2006;12(9):1065–74.
117. Goldman-Wohl DS, Yagel S. *J Reprod Immunol* 2007;76(1–2): 54–60.
118. Vacca P et al. *Trends Immunol* 2011;32(11):517–23.
119. McIntyre JA et al. *Obstet Gynecol* 1986;67(2):169–75.
120. Gill T, Wegmann T. Immune recognition, genetic regulation and the life of the fetus. In: Gill T, Wegmann T, Nisbet-Brown E, eds. *Immunoregulation and Fetal Survival*. New York, NY: Oxford University Press; 1987:3–11.
121. Cross JC et al. *Science* 1994;266(5190):1508–18.
122. Loke YW, King A. *Mol Med Today* 1997;3(4):153–9.
123. King A et al. *Placenta* 2000c;21(suppl A):S81–5.
124. King A et al. *Eur J Immunol* 2000a;30(6):1623–31.
125. Rouas-Freiss N et al. *Proc Natl Acad Sci U S A* 1997;94(21): 11520–5.
126. King A et al. *Placenta* 2000b;21(4):376–87.
127. Wegmann TG et al. *Immunol Today* 1993;14(7):353–6.
128. Robertson SA et al. *Crit Rev Immunol* 1994;14(3–4):239–92.
129. Vince GS, Johnson PM. *Biochem Soc Trans* 2000;28(2):191–5.
130. Hampson J et al. *Immunology* 79(3):485–90.
131. Yelavarthi KK, Hunt JS. *Am J Pathol* 1993;143(4):1131–41.
132. Bulmer JN et al. *Am J Reprod Immunol* 1990;22(3–4):109–16.
133. Olah KS et al. *J Reprod Immunol* 1996;32(1):89–98.

134. Ferry BL et al. *Cell Immunol* 1991;132(1):140–9.
135. Grabstein KH et al. *Science* 264(5161):965–8.
136. Armitage RJ et al. *J Immunol* 1995;154(2):483–90.
137. King A et al. *Cytokine* 1995;7(4):364–71.
138. Nishino E et al. *J Clin Endocrinol Metab* 1990;71(2):436–41.
139. Roth I et al. *J Exp Med* 1996;184(2):539–48.
140. de Moraes-Pinto MI et al. *Immunology* 1997;90(1):87–94.
141. Need JA. *Br Med J* 1975;1(5957):548–9.
142. Robillard PY et al. *Lancet* 1994;344(8928):973–5.
143. Smith GN et al. *Am J Obstet Gynecol* 1997;177(2):455–8.
144. Colbern GT et al. *Am J Obstet Gynecol* 1994;170(5 Pt 1):1244–50.
145. Hara N et al. *Am J Reprod Immunol* 1996;36(6):349–58.
146. Goldman-Wohl DS et al. *Mol Hum Reprod* 2000a;6(1):88–95.
147. Navarro F et al. *Eur J Immunol* 1999;29(1): 277–83.
148. Dekker GA, Sibai BM. *Am J Obstet Gynecol* 1998;179(5):1359–75.
149. Thellin O et al. *Curr Opin Immunol* 2000;12(6):731–7.
150. Marti JJ, Herrmann U. *Am J Obstet Gynecol* 1977;128(5):489–93.
151. Nagata S. *Adv Immunol* 1994;57:129–44.
152. Kauma SW et al. *J Clin Endocrinol Metab* 1999;84(6):2188–94.
153. Chiu RW et al. *BMJ* 2011;342:c740.1.
154. Taglauer ES et al. *Placenta* 2014;35(suppl):S64–8.
155. Tannetta D et al. *J Reprod Immunol* 2017;119:98–106.
156. Mitchell MD et al. *Am J Obstet Gynecol* 2015;213(4 Suppl): S173–81.
157. Rajakumar A et al. *Hypertension* 2012;59(2):256–64.
158. Redman CW et al. *Placenta* 2012;33(suppl):S48–54.
159. Dragovic RA et al. *Methods* 2015;87:64–74.
160. Hung TH et al. *Circ Res* 2002;90(12):1274–81.
161. Redman CW, Sargent IL. *J Reprod Immunol* 2007;76(1–2): 61–7.
162. Tannetta DS et al. *PLOS ONE* 2015;10(11):e0142538.
163. Kohli S et al. *Blood* 2016;128(17):2153–64.
164. Karumanchi SA, Bdolah Y. *Endocrinology*. 2004;145(11): 4835–7.
165. Ouyang Y et al. *Placenta* 2016;47:86–95.
166. Escudero CA et al. *Front Physiol* 2016;7:98.
167. Desrochers LM et al. *Nat Commun* 2016;7:11958.
168. Greening DW et al. *Biol Reprod* 2016;94(2):38.
169. Vilella F et al. *Development* 2015;142(18):3210–21.
170. Staun-Ram E, Shalev E. *Reprod Biol Endocrinol* 2005;3:56.

# 4

# Placental circulations

Eric Jauniaux and Graham J. Burton

## Introduction

Normal human pregnancy demands that two distinct, but interrelated, changes in cardiovascular function take place in parallel.[1] Ample dilatation of the maternal uteroplacental circulation together with rapid villous angiogenesis are the key factors necessary for adequate placental development and function, and subsequent fetal growth.[2]

Human placentation is almost unique among mammals in that it is highly invasive and the gestational sac embeds itself completely within the uterine endometrium and adjacent myometrium.[1,2] The development of a low resistance to blood flow in the placental circulation is essentially the result of anatomical transformations and/or biochemically induced vasomotor mechanisms. The correlation of Doppler ultrasound findings with anatomical and physiological features suggests that the establishment of high volume–low resistance flow in both placental circulations is primarily the consequence of the considerable increase in the diameter of the corresponding vascular beds. The length of the vascular network and the blood viscosity have much smaller influences.

Placental-related disorders of pregnancy are almost unique to the human species. These disorders, which affect around a third of human pregnancies, primarily include miscarriages, preeclampsia, fetal growth restriction (FGR), spontaneous preterm labor, and preterm premature rupture of the membranes. In other mammalian species, the incidence of these disorders is extremely low.[3] In humans, these disorders may relate to the fact that our invasive form of implantation, and subsequent hemochorial placentation, poses special hemodynamic challenges. These complications are often associated with abnormal maternal adaptations to pregnancy in the second trimester, including failure to gain weight, lack of blood pressure reduction, and persistent, nonpregnant hematocrit levels.[1–3]

In this chapter, we reviewed the basic hemodynamic concepts of the placental circulations and their relationships to maternal cardiac adaptations to pregnancy and embryonic, and subsequently fetal, cardiac development in normal pregnancies and in pregnancies complicated by placental-related disorders.

## Normal development of the uteroplacental circulation

The human uterine vasculature comprises a complex vessel network that anastomoses with branches of the ovarian and vaginal arteries to establish a vascular arcade perfusing the internal genital organs.[4,5] The left and right uterine arteries are the main blood supply to the uterus. They ascend along the lateral aspect within the broad ligament and give off approximately 8–10 arcuate branches, which divide almost immediately into anterior and posterior branches. The arcuate arteries run circumferentially between the outer and middle thirds of the myometrium, and anastomose freely with their counterparts from the opposite side in the midline (Figure 4.1). The arcuate arteries give rise to the radial arteries that are directed toward the lumen of the uterus. In the region of the myometrial-endometrial boundary, each radial artery gives off lateral branches, the basal arteries that supply the myometrium and the deeper basalis parts of the endometrium, and continues as a spiral artery. As it passes through the endometrium, each spiral artery also gives off small branches supplying the capillary plexuses surrounding the uterine glands.

In the nonpregnant state, the walls of the spiral and radial arteries contain large quantities of smooth muscle equipped with a rich autonomic innervation and, therefore, are highly responsive to both exogenous and endogenous adrenergic stimuli.[5,6] The segment of the radial artery just proximal to the myometrial-endometrial junction is particularly important in this respect, and the inner myometrium is described as a specialized region, often referred to as the junctional zone (JZ).[6–9]

### *Physiological transformation of the uterine circulation*

At term, the spiral arteries that, in the nonpregnant state, transport just a few milliliters (mL) of blood per minute need to carry around 600 mL per minute.[5] The basis of the increase in the maternal placental flow rates is the transformation of

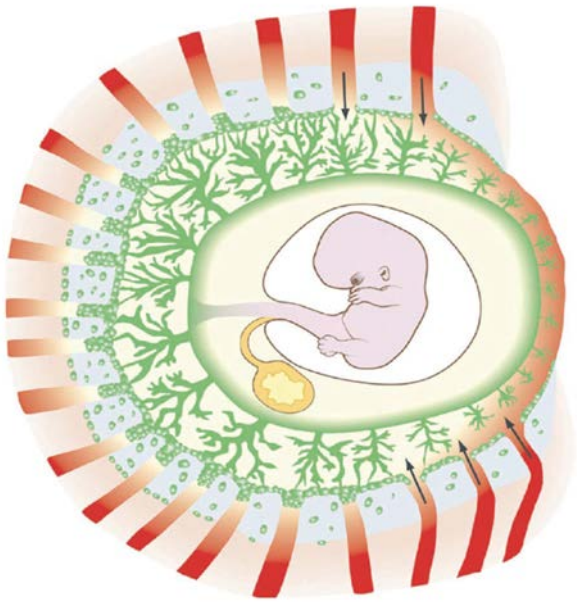

**Figure 4.1**
A complete gestational sac at 8 weeks of gestation showing the presence of the trophoblastic shell and intravascular spiral artery plugs in the center of the placental bed, whereas in the periphery an intervillous circulation is established (arrows).

the uterine vasculature, which is associated with the peripheral widening of the supplying arteries by tissue growth and remodeling of the arterial wall. It is a gradual process that starts at implantation and is then linked to the trophoblastic infiltration of the endometrium and superficial layer of the myometrium. Anatomical and radiographic studies including uterine perfusion experiments have demonstrated that the uterine vascular network elongates and dilates steadily throughout pregnancy.[5]

When the blastocyst attaches to the uterine wall, trophoblastic cells infiltrate the decidua from the proliferating tip of the anchoring villi and from the trophoblastic shell.[6,7] Cells on the outer surface of the shell differentiate into nonproliferative, trophoblast cells that invade the decidual stroma, collectively called extravillous trophoblast (EVT). They differentiate primarily into interstitial and endovascular subpopulations that migrate through the decidual stroma and down the lumens of the spiral arteries, respectively.[7,9] They gradually extend laterally, reaching the periphery of the placenta around midgestation. Depth-wise, the changes normally extend as far as the inner third of the uterine myometrium within the central region of the placental bed, but the extent of the EVT invasion is progressively shallower toward the periphery.[7,10] The EVTs penetrate the myometrium as far as the JZ via the intercellular ground substance, affecting its mechanical and electrophysiological properties.[11]

Human placentation is also characterized by remodeling of the spiral arteries. The architecture of their decidual and myometrial parts is disrupted, with the loss of myocytes from the media and the internal elastic lamina. These essential arterial components are progressively replaced by fibrinoid material.[6–9] Consequently, the vessels lose their responsiveness to circulating vasoactive compounds. In normal pregnancies, the transformation of spiral arteries into uteroplacental arteries is described as being complete around midgestation. However, there is a gradient in the infiltration of the trophoblast along a spiral artery, and even in normal pregnancies, not all spiral arteries are completely transformed.[12] This transformation, termed *physiological changes*, results in the metamorphosis of small-caliber spiral vessels into flaccid distended uteroplacental arteries with a 5- to 10-fold dilation at the vessel mouth. Around 30–60 spiral arteries are recruited into the basal plate of the definitive placenta. The extent of the spiral arteries conversion is greatest in the central region where the EVT is most extensive.[8] Within this context, the uteroplacental circulation differs from other vascular beds in that the diameter of the vessels increases, rather than decreases, as they approach their target organ.

Using conventional radiology, Burchell[13] found that the diameter of the uterine artery doubled by 6.5 weeks of pregnancy, and that by midpregnancy the diameter of the arcuate arteries exceeded that of the uterine arteries. At term some of the arcuate arteries are twice the diameter of the uterine arteries, and equal to that of the internal iliac arteries. The main aim of these major vascular changes is to optimize the distribution of maternal blood into a low-resistance uterine vascular network, and ultimately inside the placental intervillous chamber. However, the physiological conversion may not be so important in terms of volume of intervillous blood flow, but it may play a pivotal role in affecting the quality of that flow in terms of the perfusion pressure, the pulsatility and rate of blood flow, and the consistency of the flow.[1]

In the past, it has been assumed that the principal function of the placenta is to supply the fetus with as much oxygen as possible, and to a large extent that is the case during the second and third trimesters of pregnancy when fetal weight gain and growth are greatest. However, during the first trimester our combined *in vivo–in vitro* investigations have shown that the placenta limits, rather than facilitates, oxygen supply to the fetus.[3,14] It is now established that fetal organ development and growth during the first trimester of pregnancy occur in a physiologically low oxygen microenvironment, stimulated by secretions from the endometrial glands that are rich in nutrients and growth factors.[15,16] A normal fetal-placental development is therefore very closely linked to well-coordinated development of the uteroplacental circulation and well-controlled entry of maternal blood inside the placenta.

## Development of the intervillous circulation

The intervillous circulation in the hemochorial placenta has been referred to as an open system compared to other circulatory beds where the blood is retained within arteries, through capillary beds to veins.[17,18] Because the spiral arteries open into essentially a large lake of blood and the intervillous space does not impose any impedance to flow, the human

placenta has been considered to act as a large arteriovenous shunt. Modern anatomic and *in vivo* studies have shown that human placentation is in fact not truly hemochorial in early pregnancy.[19–22] These studies have demonstrated that before the main invasion of the uterine decidua by the EVT takes place, these cells form a continuous shell at the level of the maternal-fetal interface (Figure 4.1).

In the human, placental development is precocious, and the conceptus is fully embedded in the uterine wall before the primitive streak has formed. Consequently, other strategies need to be employed to restrict exposure of the fetus to oxygen, and as a result the human placenta is exposed to major fluctuations in $O_2$ concentration from conception to delivery.[23–25] In normal pregnancies, this is a very well-controlled phenomenon that has to provide a delicate balance between the metabolic needs of the fetus and its placenta and the potential danger of oxygen-free radicals (OFRs). The plugging of the spiral arteries also creates a uteroplacental $O_2$ gradient, which exerts a regulatory effect on placental tissue development and function. In particular, it influences cytotrophoblast proliferation and differentiation along the invasive pathway, villous vasculogenesis, and formation of the chorion laeve or free placental membranes.[26]

Placental trophoblastic cells are extremely sensitive to oxidative stress because of their extensive cell divisions and the concomitant exposure of their DNA.[25] Excessive production of OFRs results in oxidative stress, and there are two examples when this occurs physiologically during human pregnancy. First, at the end of the first trimester, a physiological increase of oxidative stress occurs in the periphery of the early placenta.[23] The underlying uteroplacental circulation in this area is never plugged by the trophoblastic shell, allowing limited maternal blood flow to enter the placenta from 8 to 9 weeks of gestation (Figure 4.1). This leads to higher local oxygen concentrations at a stage of pregnancy when the trophoblast possesses low concentrations and activities of the main antioxidant enzymes superoxide dismutase, catalase, and glutathione peroxidase. Focal trophoblastic oxidative damage and progressive villous degeneration trigger the formation of the fetal membranes,[27] which is an essential developmental step enabling vaginal delivery. The second example involves an ischemia-reperfusion (I/R) phenomenon. Angiographic studies of the uterine vasculature of the rhesus monkey have demonstrated that during normal pregnancy, flow from spiral arteries into the intervillous space is often intermittent, arising from spontaneous vasoconstriction.[28] Although equivalent studies have not been performed in the human, the general similarity of the uteroplacental vasculature and delivery of blood into the intervillous space to those of the rhesus monkey has led to the assumption that intermittent perfusion of the intervillous space also occurs in our species. Some degree of I/R stimulus may therefore be a feature of normal human pregnancy, especially toward term when the fetus and placenta are extracting large quantities of $O_2$ from the intervillous space.[29] There is good evidence that it also occurs during labor when the contractions prevent uterine arterial blood flow.[30]

During organogenesis, the placental villi display only a few capillaries and fetal erythrocytes are nucleated,[2,14] suggesting that the fetal blood is extremely viscous and that consequently the fetal-placental circulation is limited. Furthermore, during the first trimester the villous membrane is twice the thickness it will be in the second, and the early placenta and fetus are separated by the exocoelomic cavity (Figure 4.2), which occupies most of the space inside the gestational sac.[31] During the period when there is no true maternal blood circulation entering the placenta, the endometrial glands deliver nutrient-rich secretions through the shell directly into the intervillous space until at least 10 weeks.[15,32] These secretions are a heterogenous mix of maternal proteins, carbohydrates, including glycogen, and lipid droplets, and are phagocytosed by the syncytiotrophoblast indicating a histotrophic nutrition through the primitive placenta.

At the end of the first trimester, the trophoblastic plugs are progressively dislocated, allowing maternal blood to flow progressively, freely, and continuously within the intervillous space. During the transitional phase of 10–14 weeks' gestation, two-thirds of the primitive placenta disappears, and the exocoelomic cavity is obliterated by the growth of the amniotic sac.[2,14,31] This brings the maternal blood closer to the fetal tissues, facilitating nutrient and gaseous exchange between the two circulations. These morphological changes are a reflection of millions of years of adaptation to changes in oxygen concentration in the earth's atmospheric environment. The absence of a continuous maternal circulation inside most of the primitive placenta during the first trimester placental barrier is essential to control the oxygen levels inside the gestational sac during organogenesis. It also adds to the natural defense of the fetus against parasites and viruses when it is at its most vulnerable.[33]

## *Maternal hemodynamic changes and regulation of the uteroplacental circulation*

The maternal plasma volume increases gradually from the first month of gestation to a plateau in the third trimester, about 45% above the nonpregnant level.[34,35] Plasma volume expansion is essential to meet the greater circulatory needs of the placenta and the maternal organs (e.g., uterus, breasts, skin, and kidneys). The gradual pattern of plasma volume expansion is out of phase with the rapid increase in maternal cardiac output and drop in arterial pressure. There are vast differences among women, however, from a minimal change to a doubling in plasma volume. Several factors can influence plasma volume expansion, including maternal prepregnancy body mass index, parity, and multiple gestation pregnancy. The mechanisms regulating these changes in human pregnancy are still unknown.

Most of the 30%–60% increase in cardiac output and half of the 10% fall in arterial pressure is accomplished in the first trimester,[36] and cardiac output continues to increase even in

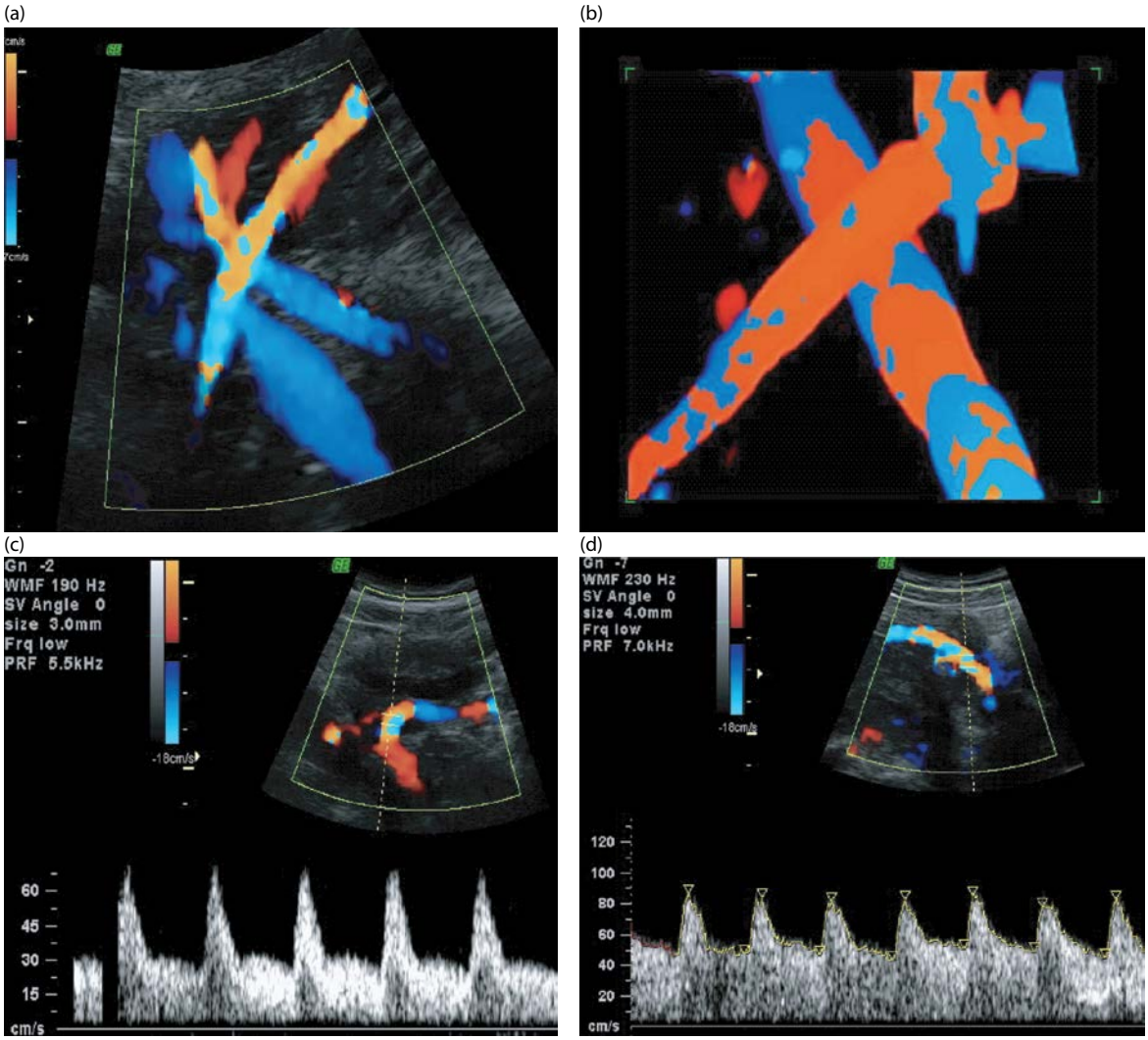


**Figure 4.2**
Two-dimensional (a) and three-dimensional (b) color flow mapping of the main uterine artery crossing the iliac vessels. Spectral analysis of blood velocity waveforms obtained from the main uterine artery at 14 weeks (c) and 20 weeks (d) of gestation. Note the protodiastolic notch at 14 weeks (c).

late pregnancy.[37] It has been suggested that the fall in peripheral systemic vascular tone is the main factor triggering the rise in cardiac output in early pregnancy.[38] The resulting rapid fall in preload and afterload leads to a compensatory increase in heart rate, and activation of the volume-restoring mechanisms. It is only from the end of the first trimester onward that this increased cardiac output is due to an increase in stroke volume. Blood viscosity is directly related to the hematocrit. Maternal total red cell volume increases steadily throughout gestation.[35] The increment varies from 18% to 30% of nonpregnant values, and its extent is considerably influenced by oral iron intake. However, at the same time, plasma volume increases by about 40%, resulting in hemodilution and, therefore, in a decrease of maternal blood hematocrit and blood viscosity. A lower maternal blood viscosity potentiates the fall in peripheral vascular resistance.

A variety of hormones are known to influence the uterine artery resistance. Their role is emphasized by the fact that in the human, the decrease in uterine vascular resistance starts during the luteal phase of the menstrual cycle[39] and is similar in intra- and extrauterine placentation. Furthermore, in some animal species, such as horses, pigs, and cows, maternal tissue is not infiltrated by trophoblastic cells, and the conceptus is adequately perfused by maternal blood. It is well established that estrogen produces important changes in uterine blood flow in both human and various animal species. For example, direct intra-arterial uterine infusion of estradiol in ewes induces a dramatic increase of the uterine blood flow in both the pregnant and nonpregnant uterine vascular bed, while progesterone partially inhibits the vascular effect of estradiol.[40] A similar response is observed in postmenopausal women receiving hormone replacement therapy.[41] At physiological levels, estradiol decreases the resistance to flow in the uterine circulation, and this is partially reversed by progesterone. Maternal serum 17β-estradiol levels may also have

a significant influence on uterine resistance to blood flow during pregnancy.[42] In addition, independent of gestational age, maternal serum levels of relaxin may be a significant contributor to uterine resistance to blood flow as assessed by Doppler indices.[43]

A close temporal relationship has been found between the Doppler detection of a continuous intervillous flow and the human chorionic gonadotropin (hCG) peak.[44] Although there is no obvious role for the hCG molecule in the regulation of uteroplacental hemodynamics, this finding suggests that hCG secretion may be influenced by changes in intraplacental hemodynamics and possibly by changes in placental oxygen tension. Maternal antenatal betamethasone resulted in a significant transient change in the velocity waveform and a decrease in the pulsatility index in the umbilical artery and ductus venosus but did not influence the uteroplacental circulation.[45]

## *Ultrasound/Doppler features of the uteroplacental circulation*

The various branches of the uterine circulation can be differentiated by means of color Doppler imaging, and the overall Doppler mapping features correlate well with the classical and modern anatomic findings.[46] However, the uteroplacental circulation is a dynamic model in which the magnitude of blood flow through a single vessel may vary significantly (Figures 4.2 and 4.3). Thus, the evaluation of blood flow in single uteroplacental vessels is often difficult to interpret and of limited value in understanding the pathophysiology of placental-related pregnancy disorders.

In nonpregnant women and during the first half of normal pregnancy, flow velocity waveforms (FVWs) from the main uterine arteries are characterized by a well-defined protodiastolic "notch" (Figure 4.2). End-diastolic flow (EDF) starts to increase in the main uterine arteries and their branches during the second half of the menstrual cycle, and continues as pregnancy advances. In 85% of pregnancies, the protodiastolic notch disappears before 20 weeks of gestation[47] and may reflect the end of the implantation process and its associated physiological changes. Blood flows in the spiral arteries are characterized in pregnancy by a low-impedance irregular flow pattern (Figure 4.3), which shows no significant changes in shape throughout pregnancy.[46]

Doppler studies have demonstrated a progressive decrease in the downstream resistance to blood flow in the uterine circulation from implantation to term.[48–54] This decrease can be observed in all segments of the uterine circulation. Impedance to blood flow through spiral arteries in the second trimester is lower in the central area of the placental bed than in peripheral areas.[51] These Doppler data are in agreement with histologic data.[2,8] The resistance index (RI) or the pulsatility index (PI) measured from the FVWs recorded at the level of the main uterine arteries reflects the downstream flow impedance in the whole uterine circulation.[2] Both left and right main arteries must be investigated at the same time, as unilateral measurement may provide erroneous results concerning true uterine perfusion. Between 12 and 14 weeks of gestation, there is a rapid increase from 50 to 120 cm/s in the mean peak systolic velocity (PSV) of the main uterine artery. A decrease of the resistance and pulsatility indices from the main uterine artery toward the spiral arteries can also be demonstrated at different stages of pregnancy.[49]

When comparing Doppler features of the placental circulation at different gestational ages, we found that a nonpulsatile signal corresponding to maternal intraplacental blood flow could not be identified inside the intervillous space before 10 weeks of gestation.[2,55,56] In view of the deleterious effect of oxidative stress, it is likely that onset of maternal blood flow to the placenta is normally a progressive phenomenon, with communication between the uteroplacental arteries and the intervillous space being established in a small number of vessels at a time from the end of the second month of pregnancy onward. In normal pregnancies, the intervillous circulation is gradually established between the beginning of the third month and the end of the fourth month of gestation.[27,57] Doppler studies also demonstrate that, in normal pregnancies, onset of maternal blood flow is most often initiated in the peripheral regions of the placenta, and this may be related to regional differences in the extent of plugging of the maternal arteries. The evidence available suggests, therefore, that the normal establishment of a continuous intervillous circulation is an incremental phenomenon, starting in the periphery and expanding progressively to the rest of the placenta thereafter. This concept is supported by the immunohistochemical and morphological evidence of temporospatial differences in the degree of trophoblastic oxidative stress.[27]

# Abnormal development of the uteroplacental circulation

Placental-related disorders of pregnancy, including miscarriage, preeclampsia, and FGR, are almost unique to the human species, for their incidence in other mammalian species is extremely low. In humans these disorders may relate to the fact that our invasive form of implantation, and subsequent hemochorial placentation, poses special hemodynamic challenges. Preeclampsia is often associated with abnormal maternal adaptations to pregnancy in the second trimester, including failure to gain weight, lack of blood pressure reduction, and persistent nonpregnant hematocrit levels.[58] In particular, failure of physiological hemodilution during the second trimester is associated with an increased risk for the development of subsequent placental-related pregnancy complications.[59]

There is mounting evidence that oxidative stress or an imbalance in the oxidant/antioxidant activity in uteroplacental tissues plays a pivotal role in the development of placental-related diseases.[60] In about two-thirds of early pregnancy failures, there is anatomical evidence of defective placentation, which is mainly characterized by a thinner

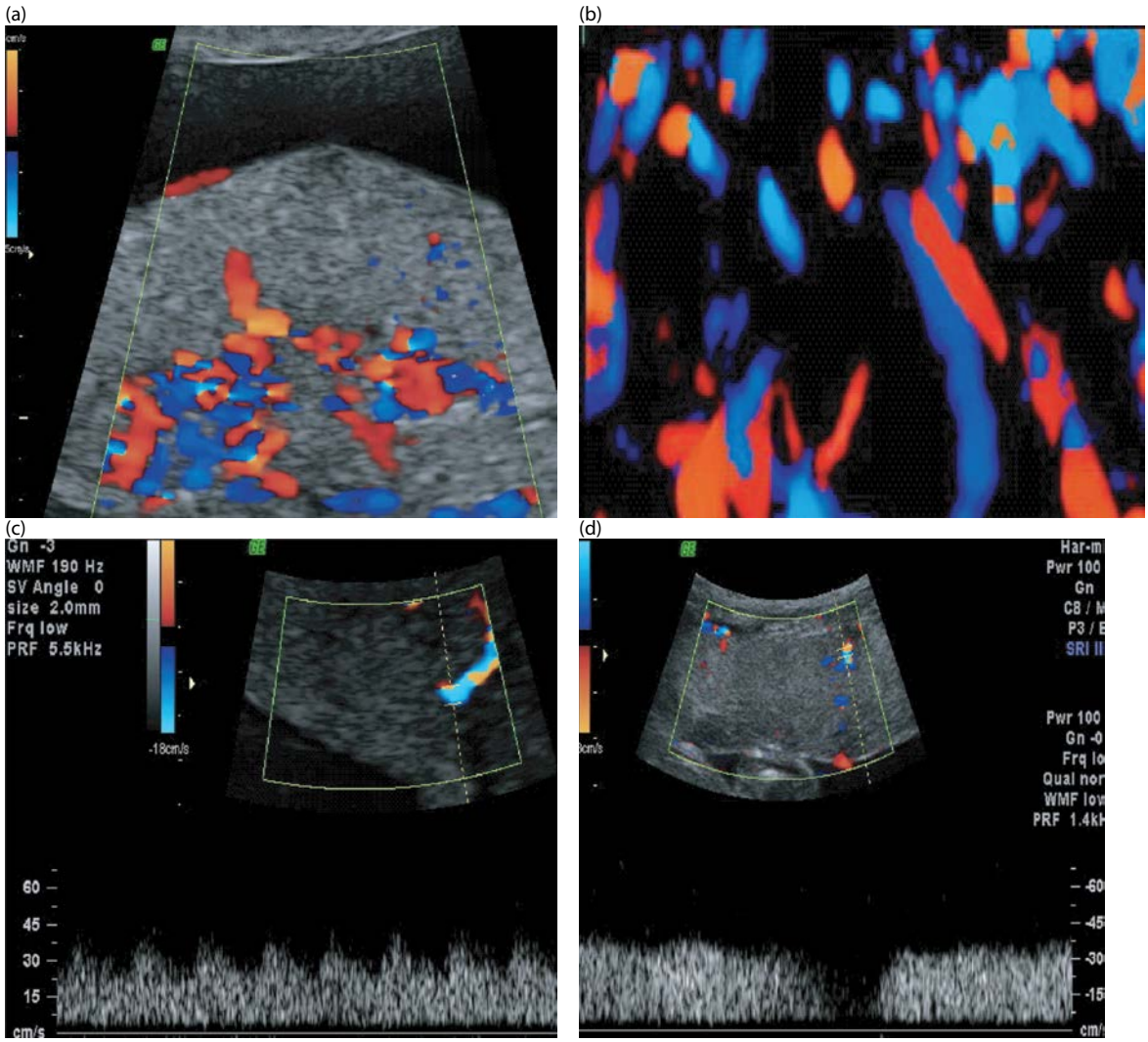


**Figure 4.3**
Two-dimensional (a) and three-dimensional (b) color flow mapping of the placental bed. Spectral analysis of blood velocity waveforms obtained from spiral artery at 10 weeks of gestation (c) and from the intervillous space at 14 weeks of gestation (d). Note the discontinuous blood flow with a venous pattern (i.e., intervillous flow) in (d).

and fragmented trophoblast shell, reduced cytotrophoblast invasion of the endometrium, and incomplete plugging of the lumen at the tips of the spiral arteries.[3,27,61–63] This is associated with the absence of physiological changes in most spiral arteries and leads to a premature onset of the maternal circulation throughout the entire placenta (Figure 4.4). Independent of the etiology of the miscarriage, the excessive entry of maternal blood into the intervillous space has two effects: a direct mechanical effect on the villous tissue, which becomes progressively enmeshed inside large intervillous blood thrombi, and indirect $O_2$-mediated widespread trophoblastic oxidative damage and increased apoptosis.[10,63–65] Overall, the consequences are placental degeneration with complete loss of syncytiotrophoblast function and detachment of the placenta from the uterine wall. This mechanism is common to all miscarriages, the time at which it occurs in the first trimester depending on the etiology.[27] Therefore, miscarriages are the consequences of an extreme disorder of placentation with rapid degeneration of the placental tissue.

Preeclampsia stems from a similar, though lesser, defect in early trophoblast invasion where placentation is sufficient to allow the normal development of the fetus into the second trimester, but it is insufficient to fully convert most the spiral arteries into low-resistance channels.[9,66] There is increasing evidence that preeclampsia is a heterogeneous syndrome, and early and late-onset forms are now recognized with a distinction of onset before (early) or after (late) 34 weeks of gestation.[67,68] In early onset, there is clear evidence that a certain proportion of the spiral and basal arteries are not transformed resulting in the retention of smooth muscle cells within their walls, and so some vasoreactivity. This progressively leads not only to diminished perfusion of the intervillous space, but more importantly to greater risk of intermittent perfusion. Since the placenta and fetus continually extract oxygen, transient hypoxia will result, and consequently, the placenta

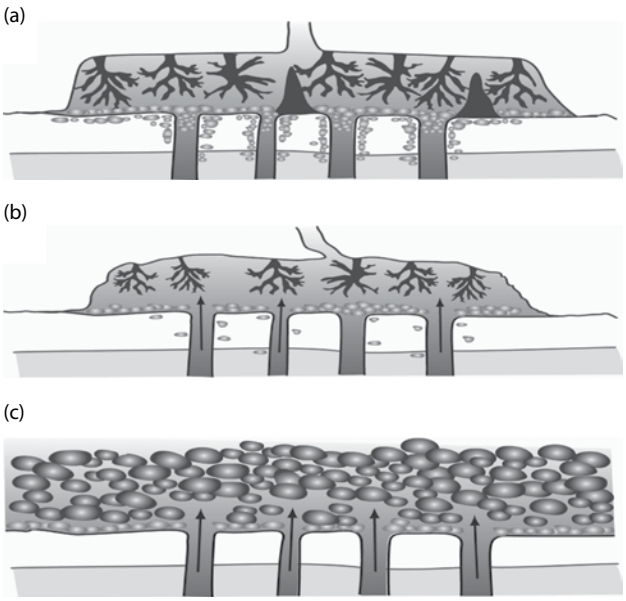


**Figure 4.4**
Placentation in a normal ongoing pregnancy (a), in an early pregnancy failure (b), and in a complete hydatidiform mole (c). Note in (a) the continuous trophoblastic shell, the plugs in the lumens of the spiral arteries, and the interstitial migration of the extravillous trophoblast through the decidua down to the superficial layer of the myometrium; in (b) the discontinuous trophoblastic shell, the absence of plugs, and the reduced migration of extravillous trophoblastic cells; in (c) the absence of trophoblastic plugs and interstitial migration.

suffers a chronic low-grade ischemia reperfusion–type injury.[69] This would impair the placentation process, leading to chronic oxidative stress in the placenta and finally to diffuse maternal endothelial cell dysfunction.[3,60,70] The timing of the appearance of the maternal and fetal symptoms is probably linked to the proportion of spiral arteries that are transformed by 22–24 weeks of gestation. By contrast, late-onset preeclampsia is thought to reflect maternal predisposition to cardiovascular disease.[67]

In cases of isolated FGR of maternal vascular origin, there is evidence that the level of oxidative, and in particular endoplasmic reticulum (ER), stress is intermediate between a normal control and an early onset preeclamptic placenta.[1,60] The molecular pathology of these placentas indicates a selective suppression of protein synthesis, which when recapitulated in placental cell lines results in reduced rates of proliferation. It is likely that these stresses originate at a low level from the time of onset of the maternal circulation onward, and this hypothesis is consistent with the reduced rate of growth of the placenta observed with serial ultrasound scans in these cases.[71]

## *In vivo features of abnormal placentation*

In early pregnancy failure, the premature and massive entry of maternal blood inside the placenta is associated with major changes of the placental structure on ultrasound imaging. In most missed miscarriages, the placenta appears on color flow mapping to be hypervascularized (Figure 4.5) well before the end of the first trimester.[61,62] In these cases, there is extensive dislocation of the trophoblastic shell and a continuous intervillous blood flow on color mapping before 12 weeks of gestation. These findings suggest that in early pregnancy failure, the initial central trophoblastic migration and vascular plugging are insufficient, allowing the entry of larger than normal quantities of maternal blood into the placenta. As a consequence, oxidative damage to the trophoblast is significantly increased, and this will prevent the normal villous trees from developing and hence compromise placentation. The premature entry of maternal blood into the intervillous space at this stage of pregnancy disrupts the placental shell and is probably the mechanical cause of the abortion. This mechanism is common to all miscarriages, the time at which it occurs in the first trimester depending on the etiology.[3,27] The predictive value of Doppler measurements in early pregnancy is limited. All Doppler studies in the first trimester have failed to demonstrate abnormal blood flow indices in the uteroplacental circulation of pregnancies that subsequently ended in early pregnancy failure, even in high-risk patients.[72]

The failure of complete conversion of the spiral and basal arteries network observed in preeclampsia should by itself not significantly influence the volume of maternal blood to the placenta, as this is mainly determined by changes in the radial and arcuate arteries.[1] Rather, maternal blood flow will enter the intervillous space at greater velocity in excess of 1 m/s than normal, a phenomenon that we described as the "hose effect."[1,60,73] On ultrasound the inflow appears as jet-like streams surrounded by turbulence. The force is sufficient to drive apart the villous branches and form intervillous lakes (also called maternal lakes). In contrast to the physiological central cavities of lobules, these lakes are often lined by thrombotic material, consistent with the pattern of turbulent inflow. In the most severe cases, there is evidence of an abnormal intervillous circulation from the beginning of the second trimester, which is characterized by major placental anatomical changes that have been described on ultrasound as "jelly like" or "wobbly."[1,60,74] These features refer to the overall appearance of the placenta, with its chorionic plate being pushed up by jet-like bloodstreams (Figure 4.6), with an overall reduction in the placental mass echogenicity. They are thought to arise from reduced numbers of, or rupture of remaining, anchoring villi. Rupture of the anchoring villi will have a profound effect on placental architecture but will also interrupt the supply of extravillous trophoblast, impairing further arterial modification.

Several Doppler screening studies, both in the second and more recently in the first trimester of pregnancy, have demonstrated an association between increased impedance to flow in the uterine arteries and subsequent development of preeclampsia, FGR, and perinatal death.[75] Most studies have focused on the fact that an increased impedance to flow in the uteroplacental circulation and persistent uterine

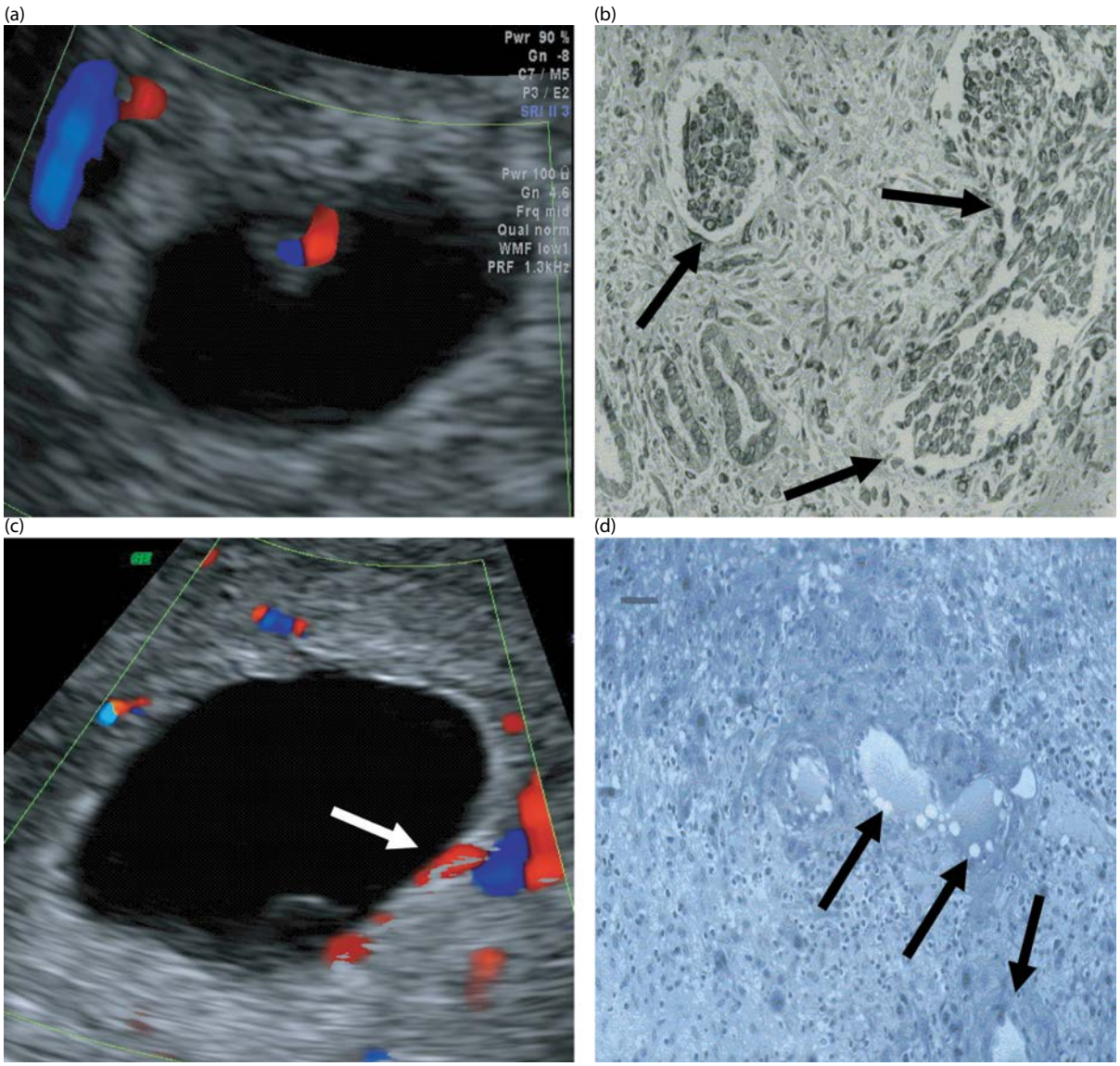


**Figure 4.5**
(a) Color flow mapping of a gestational sac containing a 5 mm embryo with a heart activity and showing the placental bed circulation. (b) Histological view of a decidual biopsy collected from the area under the definitive placenta showing trophoblastic plugs inside the lumen of the tips of the spiral arteries at 9 weeks of gestation (arrows). (c) Color flow mapping of a gestational sac in a missed miscarriage at 9 weeks (last menstrual period) showing diffuse intervillous signals (arrow). (d) Histological view of a decidual biopsy in a similar case of missed miscarriage at 9 weeks showing the poor transformation of the tip of the spiral arteries and the absence of trophoblastic plugs (arrows).

artery notching at midgestation predict the development of placental-related pregnancy disorders. Initial screening by continuous-wave Doppler was carried out at 18–20 weeks of gestation, and the examination was repeated in those with increased impedance to flow at around 24 weeks. The differences in Doppler technique employed in the different studies might partly explain their discrepant results. Other factors, such as the definition of abnormal flow, the populations, the gestational age at which women were examined, and the criteria for the diagnosis of preeclampsia and FGR may also have contributed to the wide variation in detection rates.[75] Recent data suggest that increased impedance at 23–24 weeks identifies about 40% of those cases that subsequently develop preeclampsia, and about 20% of those that develop FGR.[76] Overall, abnormal Doppler is better at predicting early onset disease, and the sensitivity of abnormal Doppler features for preeclampsia requiring delivery prior to 34 weeks of gestation is about 80%, and for FGR it is about 60%. Uterine Doppler screening at 23–24 weeks can be used in detecting pregnancies at risk of adverse outcome and in selecting cases for more intense surveillance. There is an increasing interest in first-trimester risk prediction models for preeclampsia.[76] A recent meta-analysis has shown that first-trimester uterine artery Doppler is a useful tool for predicting early onset preeclampsia, as well as other adverse pregnancy outcomes.[77]

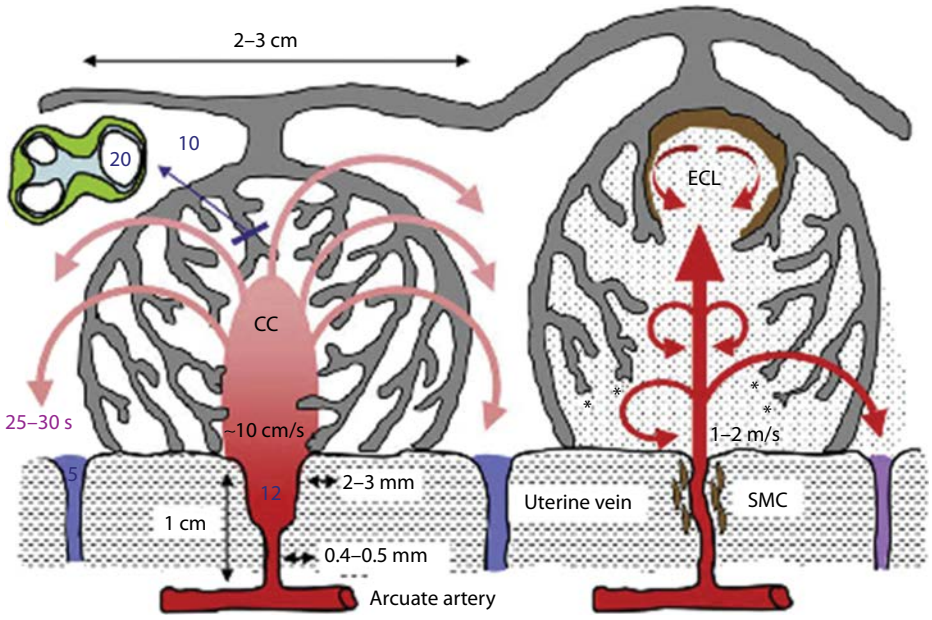


**Figure 4.6**
The effects of spiral artery conversion on the inflow of maternal blood into the intervillous space in normal and in pregnancies complicated by insufficient transformation of the spiral arteries (diagram not to scale). The retention of smooth muscle cells around the spiral artery will increase the risk of spontaneous vasoconstriction and ischemia-reperfusion injury. (CC, central cavity; ECL, echogenic cystic lesions.) (From Burton GJ et al. *Placenta* 2009;30:473–82, with permission.[1])

## Normal development of the umbilicoplacental circulation

The development of the fetal vasculature begins during the third week postconception (fifth week of pregnancy) with the *de novo* formation of hemangioblastic cell cords within the villous stromal core. By the beginning of the fourth week, the cords have developed lumens and the endothelial cells become flattened. Surrounding mesenchymal cells become closely apposed to the tubes and differentiate to form pericytes.[78] During the next few days, connections form between neighboring tubes to create a plexus, and this ultimately unites with the allantoic vessels developing in the connecting stalk to establish the fetal circulation to the placenta. Around 28 days postovulation (six completed menstrual weeks), the villous vasculature is connected with the primitive heart and the vascular plexus of the yolk sac via the vessels of the connecting stalk.

Around the end of the fifth week of gestation, the primitive heart begins to beat, and this pivotal phenomenon has been documented *in utero* on ultrasound as early as 36 days, menstrual age. From 6 to 9 weeks, there is a rapid increase of the mean heart rate to a plateau in the second and third trimesters. The fetal-placental circulation is established from around 8 weeks of gestation.[2] The development of the fetal-placental circulation is characterized by a progressive rise in blood flow and decrease in vascular resistance to flow. Because of the absence of innervation beyond the proximal 1–2 cm of the umbilical cord, the umbilicoplacental circulation is considered to be a passive circulation in which the flow rate is determined by the mean effective perfusion pressure and local vasoactive factors.[79]

### *Development of the villous circulation*

Early in pregnancy, the capillary network is labile and undergoes considerable remodeling. Angiogenesis continues until term through a series of different phases, which most probably reflect different concentrations and combinations of growth factors induced by the changing intrauterine environment.[80] From 25 weeks onward, terminal capillary loops are produced; indeed it is thought that the differential elongation of the capillary network to that of the containing villus causes vascular loops to obtrude from the surface, so creating a new terminal villus. The caliber of the fetal capillaries is not constant within intermediate and terminal villi, and frequently on the apex of a tight bend the capillaries become greatly dilated, forming sinusoids. These regions may help to reduce vascular resistance and so facilitate distribution of fetal blood flow through the villous trees.[2] They also serve to reduce the diffusion distance between the fetal and maternal circulations.

Placental capillary formation is only completed by midgestation. *De novo* formation of capillaries from the transformation of mesenchymal cells is rare in mature placental tissue and only occurs in persisting mesenchymal villi.[81] The villous circulation of the definitive placenta is composed of muscularized stem arteries (750 μm), branching more than 10 times and ending in long capillary loops, 15–20 μm in diameter, and perivascular capillary networks.

## Hemodynamics of the umbilicoplacental circulation

During the second half of pregnancy, the vascular network with the lowest resistance in the entire fetal circulatory system is at the level of the placental vascular bed.[2,46] According to Poiseuille law, a decrease in blood viscosity and/or in the vascular system length and an increase in the mean radius of the vascular system collectively decrease the resistance to flow.[82] The latter effect is particularly strong, the resistance depending on the radius to the fourth power. The number of fetal capillaries per villous profile and the proportion of the villi (volume fraction) occupied by the fetal capillaries remain low (1–2/villi) during the first 2 months of pregnancy.[83] Furthermore, up to the middle of the second month of gestation, all embryonic erythrocytes are nucleated, indicating that the fetal blood viscosity is high in early pregnancy.[2] Subsequently, the number of nucleated erythrocytes decreases rapidly, and by 12 weeks of gestation, these cells account for less than 10% of the total red cell population in the fetal circulation. Thus, as the mean radius of the villous vascular system is low and the viscosity high, the resistance to flow in the early umbilicoplacental circulation must be high.[2] This suggests that for at least the first 2 months of gestation, the extraembryonic circulation is mainly vitelline to the yolk sac (as opposed to placental).

The mechanism by which a reduction in vascular impedance through the fetal-placental circulation occurs during the second trimester is not known. Since umbilical vessels are not innervated, vasodilatation must occur through one of two mechanisms: through a direct vasorelaxant paracrine effect of an agent acting upon vascular smooth muscle, or through angiogenesis. From an anatomical perspective, the villous capillary bed has the greatest potential to influence total umbilicoplacental vascular impedance. However, the formation of villous capillaries is progressive and does not appear to be directly related to the rapid drop in umbilical artery impedance observed between 12 and 14 weeks' gestation.[2] Computational analysis of steady blood flow through the chorionic arteries of a mature placenta has shown that the combination of dichotomous and monopodial bifurcation in a normal chorionic plate ensures a uniform blood perfusion of the placenta.[84] Simulations with narrow daughter and intraplacental vessels did not result in significant changes in the main mother tubes, supporting clinical observations in which umbilical blood flow remains normal, although some peripheral vessels may be occluded.

Several humoral factors are known to modulate the tone of the cord and villous vessels of the term placenta. Vasoconstrictor substances include thromboxane $A_2$ produced by the platelets and the umbilical vessels, angiotensin II produced by the fetal kidney, and endothelin-1 synthesized locally within the placenta.[85] Possible vasodilators produced by the fetus are the atrial natriuretic peptide, nitric oxide (NO), and prostacyclin.[86] Maternal serum hCG and relaxin levels have an independent correlation with the fetal heart rate,[87] but the influence of other maternal or placental factors on the hemodynamics of the developing umbilicoplacental circulation remains uncertain. NO and cyclic guanosine monophosphate (cGMP) concentrations are positively correlated with umbilical artery impedance between 9 and 15 weeks' gestation.[88] These data suggest that NO and cGMP may play an important part in maintaining flow through the early first trimester fetal-placental circulation. As pregnancy advances, the reduction in impedance occurs despite a decrease in NO production, indicating that another vascular-endothelial mechanism, or new villous vessel formation, is responsible for reducing umbilical artery resistance at this critical stage in the development of the fetal-placental circulation. The passage of fetal blood through an anatomically high-resistance circuit could lead to endothelial stimulation of nitric oxide synthase (NOS) activity, thus maintaining vasodilatation within the umbilicoplacental circulation until anatomical changes occur. Shear stresses may be highest in the first trimester umbilicoplacental circulation, prior to the development of new villous blood vessels and the appearance of a low-impedance, positive end-diastolic flow umbilical artery velocity waveform. This changing pattern of blood flow after 12 weeks could lead to reduced endothelial stimulation and, consequently, to a rapid reduction of both NOS and GMP levels from the villous trophoblast.[88]

## In vivo features of the umbilicoplacental circulation

Development of the heart and the placenta are likely to be closely interlinked through several mechanisms.[89] In the first 3 months of gestation, umbilical arteries show a high degree of vascular resistance to blood flow expressed by narrow systolic waveforms, absence of EDF, and high PI values (Figure 4.7). PI values from the umbilical artery remain high, which suggests minor changes in umbilical placental vascular resistance until the end of the first trimester.[2] Between 12 and 14 weeks, the EDF develops rapidly but is incomplete and/or inconsistently present. Diastolic frequencies throughout the entire cardiac cycle are recorded in the umbilical artery of the normally developing fetus from 14 weeks onward (Figure 4.7). After that period, the trend in the RI or PI shows a gradual decrease until the end of the third trimester. End-diastolic velocities are present at the level of intracerebral arteries 2 weeks earlier than in the umbilical artery.[89]

In early pregnancy, there are no relationships among umbilical artery Doppler impedance indices, fetal heart rate,[89] or villous angiogenesis.[2] There are also no correlations between umbilical artery resistance to flow and fetal blood hematocrit or umbilical cord length later in pregnancy,[90] although maternal smoking and iron supplementation increase fetal blood viscosity at term.[91] In early pregnancy, the rapid appearance of the EDF in the umbilical circulation and the drop in umbilical artery PI value coincide with the time of the establishment of the intervillous circulation. Changes in the pressure gradient due to the expansion of the

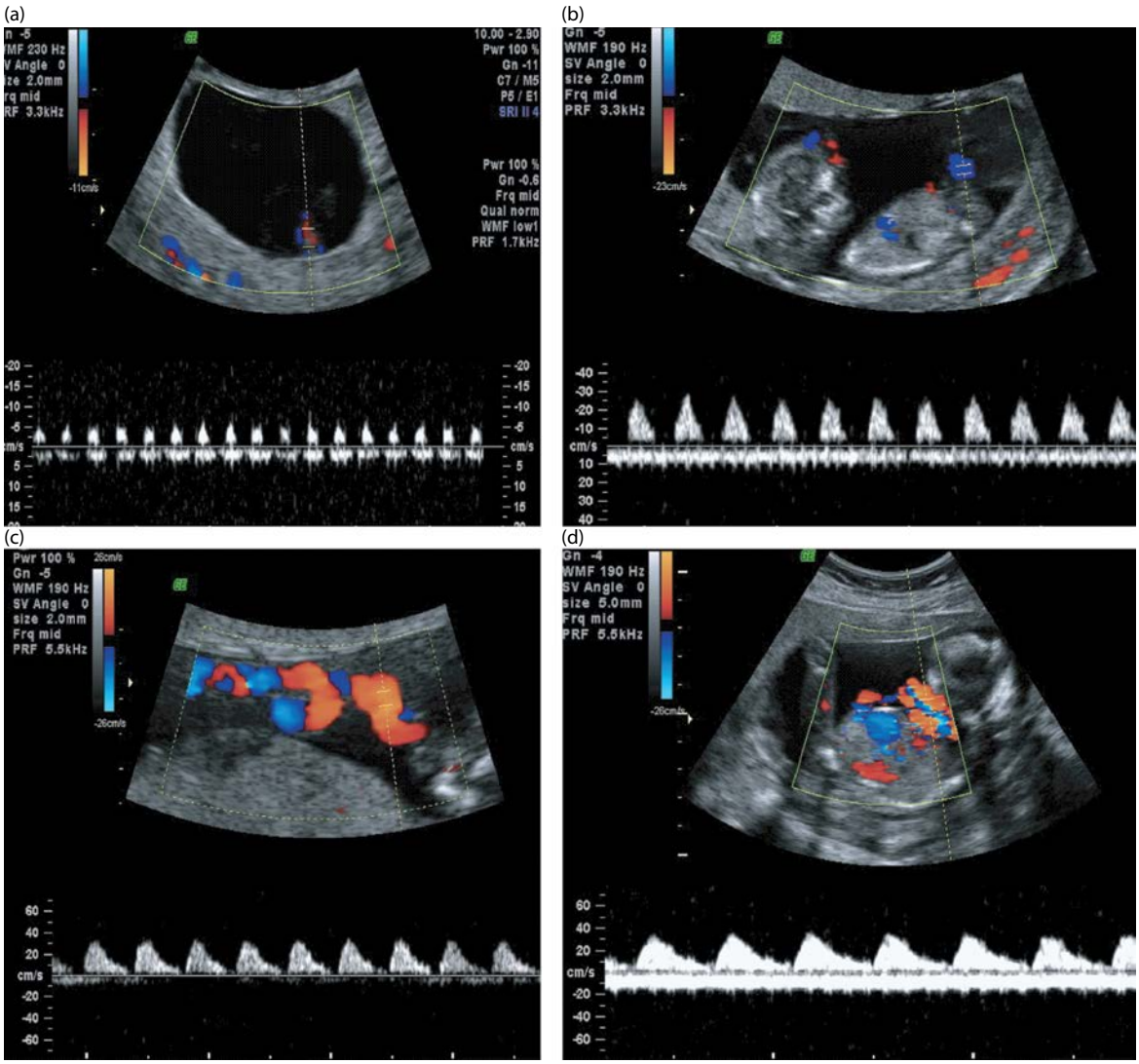


**Figure 4.7**
Color Doppler mapping and spectral analysis of the umbilical cord blood flow at 7 weeks (a), 11 weeks (b), 14 weeks (c), and 16 weeks (d). Note the progressive appearance of the end-diastolic flow.

intervillous space and/or a modification of the local concentration of vasodilators could also influence relaxation of the small placental arteries.

The addition of color flow mapping to Doppler equipment, three-dimensional (3D) power Doppler, multigate spectral velocimetry, and more recently spectral Doppler index mapping have facilitated the visualization of smaller intraplacental vessels,[2,49,92–94] and clearly visualize umbilical cord coiling (Figure 4.8). As for the uteroplacental circulation, Doppler signals can be obtained from the different segments of the umbilicoplacental circulation (Figure 4.8), and spectral analysis also shows a decline in resistance indices with advancing gestation and toward the intraplacental arterioles.[2,49] However, Doppler investigation of the branches of the umbilicoplacental circulation is limited to chorionic and mainstem villous (approximately 750 μm in internal diameter) vessels, and the villous capillary bed cannot be directly explored with these techniques.

## *Abnormal villous vascular development*

Primary anomalies of villus angiogenesis are rare, and include mainly chorioangioma and molar villi. Secondary anomalies are more common, and are found within the context of FGR associated with congenital infection or chromosomal abnormalities and disorders of uteroplacental circulation leading to chronic fetal hypoxia. It has been proposed that the placenta is hyperoxic, rather than hypoxic as is commonly assumed, in cases of severe intrauterine growth restriction.[95] This theory may explain the basis for many of the morphological changes observed but does not account for how the hyperoxia is initiated.

The absence and a reverse of EDF in the umbilical arteries are common findings in pregnancies complicated by severe FGR. From analysis of the umbilical waveform, it is possible to assess

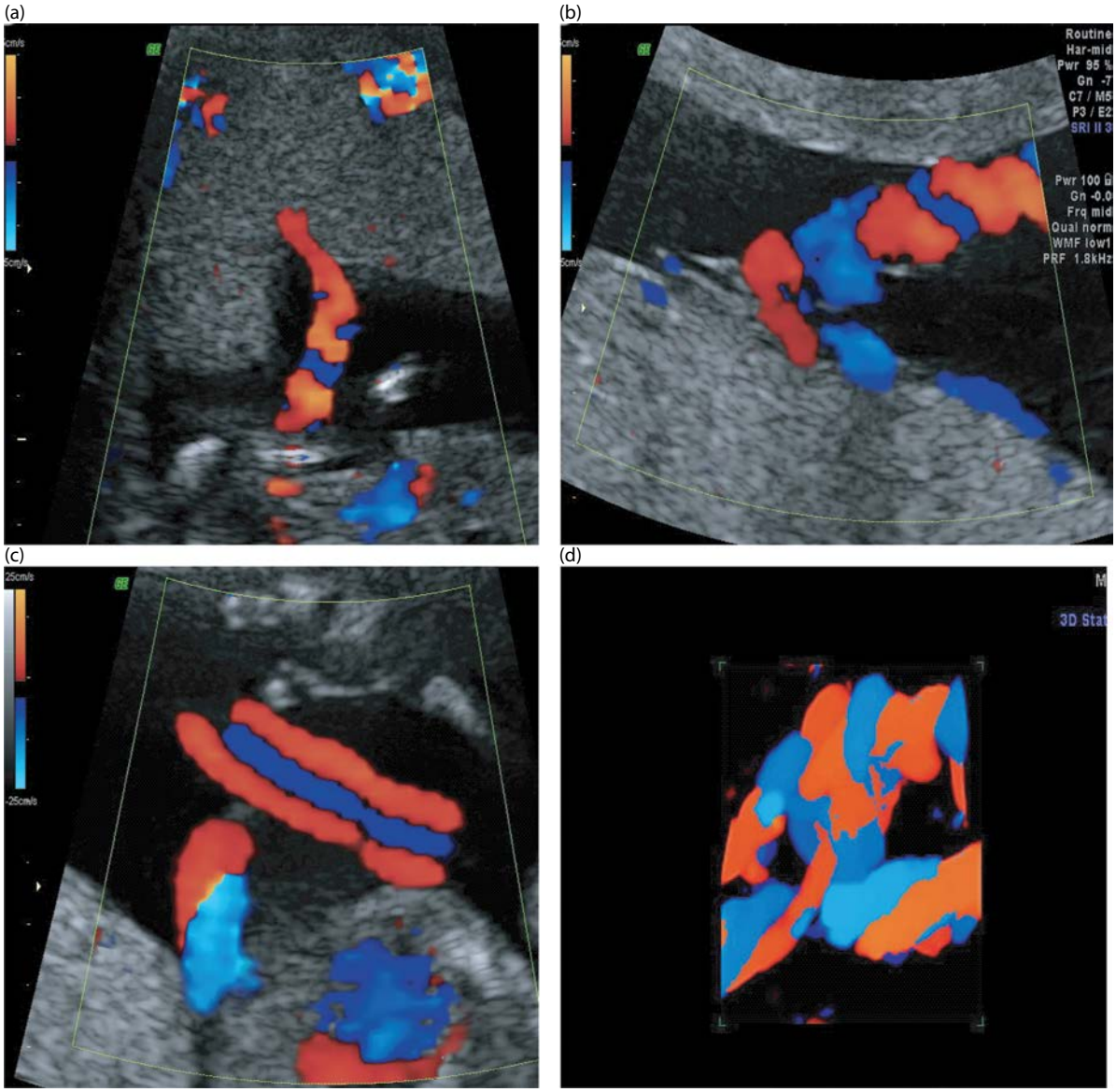


**Figure 4.8**
Color Doppler mapping of the umbilical cord placental insertion at 12 weeks (a) and 20 weeks of gestation (b). Note the entry of one of the umbilical arteries inside the placenta (a) and the branching of the chorionic vessels on the surface of the placenta (b). Two-dimensional and three-dimensional color Doppler mapping of a free loop of umbilical cord at 16 weeks (c) and 32 weeks (d). Note the difference in coiling of the cord between the second- and the third-trimester views.

the impedance to placental blood flow, and to accurately predict fetal hypoxia.[96] Various attempts have been made to correlate the Doppler abnormalities with placental structural changes in order to provide a mechanistic explanation for their origin. The results have been varied, ranging from claims of a reduction in the number of arteries within the supporting stem villi to a reduction in the capillary vascular bed within the terminal villi, the principal site of gaseous exchange. Histomorphometric features are consistent with previous findings that increasing severity of abnormal Doppler waveforms in the uterine and umbilical circulations is associated with fetal distress and hypoxia.[97] Abnormal intraplacental blood flow at 28–34 weeks of gestation is also strongly associated with FGR.[98] Blood flow resistance indices are lower in the superficial and deep placenta compared with the cord insertion area.[2,49] Absent or opposite gradient between the umbilical artery and the placental vessels is associated with adverse pregnancy outcome.[99]

Aberrant hemodynamics in the umbilico-placental circulation may influence cardiac development. As this circulation is only established toward the end of the period of cardiac organogenesis, it is more likely that placental problems influence cardiac differentiation biomechanically later in pregnancy when the placenta receives ~40% of fetal cardiac output.[89] Failure of correct placentation results in fetal growth restriction, and an impaired nutrient supply or adverse fetal endocrine environment may have non-specific effects on the growth and differentiation of many organ systems, including the fetal heart.[89] Changes in the umbilical vascular resistance

through thrombotic vasculopathy or medial hyperplasia in the stem villus arteries could affect differentiation of the cardiomyocytes, resulting in hypo- or hyperplastic syndromes.

The underlying cause of the placental lesions is not known, although the fact that Doppler changes in the umbilical circulation are invariably seen subsequent to similar changes in the uterine arteries strongly suggests that they are a secondary phenomenon. We speculate that deficient trophoblast invasion during early pregnancy leads to incomplete conversion of the spiral arteries. These vessels remain of higher resistance than normal, and the retention of smooth muscle within the spiral arteries exacerbates their normal contractility, resulting in longer periods of vasoconstriction and hence greater fluctuations in oxygen tension. This, in turn, promotes a mild ischemia-reperfusion injury in the placental tissues, leading to oxidative stress in the fetal vasculature. Oxidative stress could downregulate expression of the CSE enzyme but is also a powerful inducer of endothelial cell apoptosis. Repeated insults during midpregnancy may lead to regression of the peripheral capillaries, particularly as a high percentage are not stabilized by a pericyte covering.[97] These two effects would increase vascular impedance in a reverse of the pattern seen during normal pregnancy, and so account for the changes in umbilical waveform observed. The intermediate and terminal villi are the principal sites of gaseous exchange, and decreased vascularization will inevitably impair placental exchange. This will lead to fetal hypoxia and growth retardation, but also reduced oxygen extraction from the intervillous space and so hyperoxia on the venous side of the placenta as a tertiary event.

## References


1. Burton GJ et al. *Placenta* 2009;30:473–82.
2. Jauniaux E et al. *Ultrasound Obstet Gynecol* 1991;1:435–45.
3. Jauniaux E et al. *Hum Reprod Update* 2006;12:747–55.
4. Itskovitz J et al. *Obstet Gynecol* 1980;55:67–70.
5. Ramsey EM, Donner NW. *Placental Vasculature and Circulation*. Stuttgart: Georg Thieme; 1980.
6. Pijnenborg R et al. *Placenta* 1980;1:3–19.
7. Pijnenborg R et al. *Placenta* 1981;2:303–16.
8. Pijnenborg R et al. *Placenta* 1983;4:397–414.
9. Pijnenborg R et al. *Best Pract Res Clin Obstet Gynaecol* 2011;25:273–85.
10. Hempstock J et al. *Hum Pathol* 2003;34:1265–75.
11. Wood C. *J Obstet Gynaecol Br Commonw* 1964;71:615–20.
12. Meekins JW et al. *Br J Obstet Gynaecol* 1994;101:669–74.
13. Burchell C. *Am J Obstet Gynecol* 1969;98:303–11.
14. Jauniaux E et al. *Placenta* 2003;24(suppl A):S86–93.
15. Burton GJ et al. *Int J Dev Biol* 2010;54:303–12.
16. Burton GJ, Jauniaux E. *Am J Obstet Gynecol* 2015;213(4 suppl):S6.e1–4.
17. Moll W et al. *Eur J Obstet Gynecol Reprod Biol* 1975;5:67–74.
18. Moll W. *Eur J Obstet Gynecol Reprod Biol* 2003;110:S19–27.
19. Hustin J et al. *Placenta* 1990;11:477–86.
20. Hustin J, Jauniaux E. Morphology and mechanisms of abortion. In: Barnea E, Hustin J, Jauniaux E, eds. *The First Twelve Weeks of Gestation: A New Frontier for Investigation and Intervention*. Heidelberg: Springer-Verlag; 1992:469–85.
21. Hustin J, Schaaps JP. *Am J Obstet Gynecol* 1987;157:162–8.
22. Burton GJ et al. *Am J Obstet Gynecol* 1999;181:718–24.
23. Jauniaux E et al. *Am J Pathol* 2000;157:2111–22.
24. Jauniaux E et al. *Am J Obstet Gynecol* 2001;184:998–1003.
25. Burton GJ et al. *Reprod Biomed Online* 2003;6:84–96.
26. Burton GJ. *J Anat* 2009;215:27–35.
27. Jauniaux E et al. *Am J Pathol* 2003;162:115–25.
28. Martin CB et al. *Am J Obstet Gynecol* 1964;90:819–23.
29. Hung TH et al. *Am J Pathol* 2001;159:1031–43.
30. Cindrova-Davies T et al. *Am J Pathol* 2007;171:1168–79.
31. Jauniaux E, Gulbis B. *Hum Reprod Update* 2000;6:268–78.
32. Burton GJ et al. *J Clin Endocrinol Metab* 2002;87:2954–9.
33. Carlier Y et al. *Acta Tropica* 2012;121:55–70.
34. Blackburn ST, Loper DL. *Maternal, Fetal, and Neonatal Physiology. A Clinical Perspective*. Philadelphia, PA: W.B. Saunders; 1992:160–2, 171, 202–3, 222–8.
35. Faupel-Badger JM et al. *Cancer Epidemiol Biomarkers Prev* 2007;16:1720–3.
36. Clapp J et al. *Am J Obstet Gynecol* 1988;159:1456–60.
37. Mabie WC et al. *Am J Obstet Gynecol* 1994;170:849–56.
38. Duvekot JJ et al. *Am J Obstet Gynecol* 1993;169:1382–92.
39. Jurkovic D et al. Doppler ultrasound investigations of pelvic circulation during the menstrual cycle and early pregnancy. In: Barnea E, Hustin J, Jauniaux E, eds. *The First Twelve Weeks of Gestation: A New Frontier for Investigation and Intervention*. Heidelberg: Springer-Verlag; 1992:78–96.
40. Resnik R et al. *Am J Obstet Gynecol* 1977;128:251–4.
41. de Ziegler D et al. *Fertil Steril* 1991;55:775–9.
42. Jauniaux E et al. *Hum Reprod* 1992;7:1467–73.
43. Jauniaux E et al. *Obstet Gynecol* 1994;84:338–42.
44. Meuris S et al. *Hum Reprod* 1995;10:947–50.
45. Thuring A et al. *Ultrasound Obstet Gynecol* 2011;37:668–72.
46. Jauniaux E et al. *Am J Obstet Gynecol* 1991;164:486–8.
47. Bower S et al. *Obstet Gynecol* 1993;82:78–83.
48. Jurkovic D et al. *Obstet Gynecol* 1991;77:365–9.
49. Jauniaux E et al. *Am J Obstet Gynecol* 1992;166:585–7.
50. Dickey RP et al. *Hum Reprod* 1995;10:2676–9.
51. Matijevic R et al. *Obstet Gynecol* 1995;86:289–92.
52. Coppens M et al. *Ultrasound Obstet Gynecol* 1996;7:114–21.
53. Valentin L et al. *Am J Obstet Gynecol* 1996;174:768–75.
54. Makikallio K et al. *Gynecol Obstet Invest* 2004;58:49–54.
55. Jaffe R et al. *Am J Obstet Gynecol* 1997;176:695–705.
56. Jauniaux E. *Ultrasound Obstet Gynecol* 1996;8:73–6.
57. Jauniaux E et al. *Fertil Steril* 2003;79:100–6.
58. Thorburn J et al. *Br J Obstet Gynaecol* 1982;89:117–22.
59. Soliman AA et al. *Clin Hemorheol Microcirc* 2015;59:1–15.
60. Burton GJ, Jauniaux E. *Am J Obstet Gynecol* 2018;218: S745–61.
61. Jauniaux E et al. *Hum Reprod* 1994;9:2432–7.
62. Greenwold N et al. *Fertil Steril* 2003;79:1373–9.
63. Jauniaux E, Burton GJ. *Placenta* 2005;26:114–23.
64. Calleja-Agius J et al. *Am J Reprod Immunol* 2012;67:515–25.
65. Pang W et al. *Placenta* 2013;34:436–42.
66. Brosens I et al. *Am J Obstet Gynecol* 2011;204:193–201.
67. Tranquilli AL, Landi B. *Pregnancy Hypertension* 2013;3:44–7.
68. Yung HW et al. *J Pathol* 2014;234:262–76.
69. Hung TH et al. *Am J Pathol* 2001;159:1031–43.
70. Redman CW, Staff AC. *Am J Obstet Gynecol* 2015;213:S9–11.
71. Suri G et al. *Placenta* 2013;34:745–50.
72. Yildiz G et al. *Clin Exp Obstet Gynecol* 2012;39:326–9.
73. Jauniaux E, Nicolaides KH. *Ultrasound Obstet Gynecol* 1996;7: 141–4.
74. Jauniaux E et al. *Am J Obstet Gynecol* 1994;170:130–7.

75. Khalil A, Thilaganathan B. *Best Pract Res Clin Obstet Gynaecol* 2017;38:38–47.
76. Li N et al. *Acta Obstet Gynecol Scand* 2014;93(12):1276–81.
77. Velauthar L et al. *Ultrasound Obstet Gynecol* 2014;43:500–7.
78. Dempsey EW. *Am J Anat* 1972;134:221–38.
79. Berman W et al. *Circ Res* 1976;38:262–6.
80. Kaufmann P et al. *Placenta* 2004;25:114–26.
81. Demir R et al. *Acta Anat* 1989;136:190–203.
82. Maulik D. *Ultrasound Obstet Gynecol* 1993;3:219–27.
83. Jauniaux E et al. *Placenta* 1991;12:269–76.
84. Gordon Z et al. *Ann N Y Acad Sci* 2007;1101:250–65.
85. Kingdom JCP et al. *Ultrasound Obstet Gynecol* 1997;9:271–86.
86. McCarthy AL et al. *Am J Obstet Gynecol* 1994;170:945–51.
87. Johnson MR et al. *Br J Obstet Gynaecol* 1994;101:1003–4.
88. Lees C et al. *Obstet Gynecol* 1998;91:761–5.
89. Burton GJ, Jauniaux E. *Front Physiol* 2018;9:373.
90. Wright JW, Ridgway LE. *Am J Obstet Gynecol* 1990;163:1788–91.
91. Csorba R et al. *J Matern Fetal Neonatal Med* 2015;28:969–76.
92. Kirkinen P et al. *Acta Obstet Gynecol Scand* 1994;73:220–4.
93. Yagel S et al. *Ultrasound Obstet Gynecol* 1999;14:256–61.
94. Abramowicz JS, Sheiner E. *Placenta* 2008;29(11):921–9.
95. Kingdom JCP, Kaufmann P. *Placenta* 1997;18:613–21.
96. Bilardo CM et al. *Am J Obstet Gynecol* 1990;162:115–20.
97. Kuzmina IY et al. *Eur J Obstet Gynecol Reprod Biol* 2005;120:139–45.
98. Yagel S et al. *Ultrasound Obstet Gynecol* 1999;14:262–6.
99. Daniel-Spiegel E et al. *J Matern Fetal Neonatal Med* 2005;17: 133–6.

# 5

# Technical advances in fetal echocardiography

Boris Tutschek and David Sahn

## Introduction

Structural congenital heart disease (CHD) is among the most common anomalies in prenatal ultrasound studies. Prenatal detection can significantly improve perinatal outcome at least in certain types of CHD.[1–4] Various technical advances in ultrasound systems have promised improvements specifically for fetal echocardiography, but prenatal detection rates vary considerably and depend on factors like operator training and experience.[5–8] Screening for fetal heart disease and detailed diagnosis of fetal heart disease require technologies of different complexities.[9] This chapter attempts to review technical advances regarding fetal echocardiography.

## Improved acquisition, processing, and display

### *Electronic focusing and two-dimensional matrix array transducers*

Lateral resolution describes the minimal distance between neighboring objects in the plane of the ultrasound beam that can be resolved. Resolution depends on the distance between adjacent transducer elements and on the lateral width of the ultrasound beam (slice thickness) used to interrogate a certain depth.

Figure 5.1 shows an ultrasound phantom insonated with good and poor lateral discrimination. Focusing of the ultrasound beam can be achieved by electronic "steering": adjacent elements are activated at different time points so that the wave fronts they generate converge at the level of the selected depth (or focus). This electronic focusing has been used in one-dimensional (1D) array transducer over many years. However, it affects the image only in the plane of the ultrasound elements. Perpendicular to the plane of the ultrasound elements, the focus zone cannot be changed in 1D arrays; the "focus" of the beam perpendicular to the long axis of the elements is fixed. Recently two-dimensional (2D) matrix array transducers that can overcome this limitation have become available (Video 5.1). Using matrix array transducers, focusing perpendicular to the long axis of the transducer is possible, avoiding artifacts from structures immediately adjacent to the insonated plane. Figure 5.2 shows a phantom with cystic objects insonated with either a conventional 1D or with a new 2D array transducer capable of electronic focusing in two planes.

### *Tissue harmonic imaging*

Lower-frequency ultrasound signals have better tissue penetration. Decreasing the insonation frequency, however, also lowers image resolution. Tissue penetration of ultrasound waves also depends on tissue properties like tissue density, pressure, temperature, and others; emitted sound waves also exceed pressure and, therefore, change as they travel through tissue, are reflected and received. The further the ultrasound waves travel through the tissue, the more their waveform changes from the emitted pure sinus wave to a compound waveform, consisting of the original and of additional waveforms of smaller amplitude but higher frequency. These lower-amplitude, higher-frequency waves occur at multitudes of the insonation (fundamental) frequency and are called harmonic frequencies.[10] Signals recorded at twice the insonation frequency are called first harmonic frequencies. Harmonic

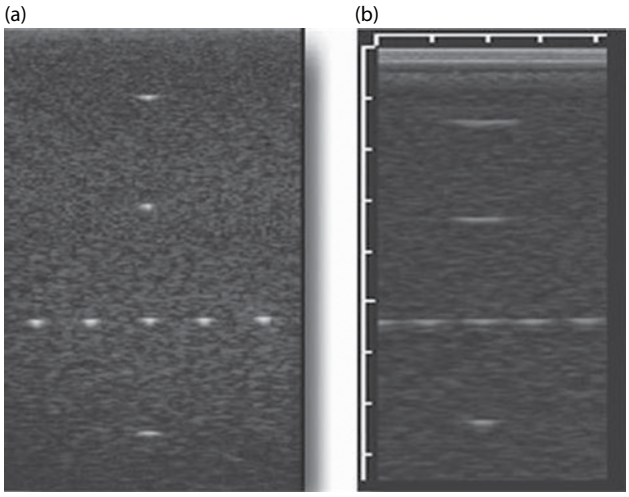


**Figure 5.1**
Lateral resolution of 0.3 mm nylon threads in a phantom insonated with good (a) and poor (b) lateral resolution. (Image kindly provided by H. Dudwiesus, GE Healthcare.)

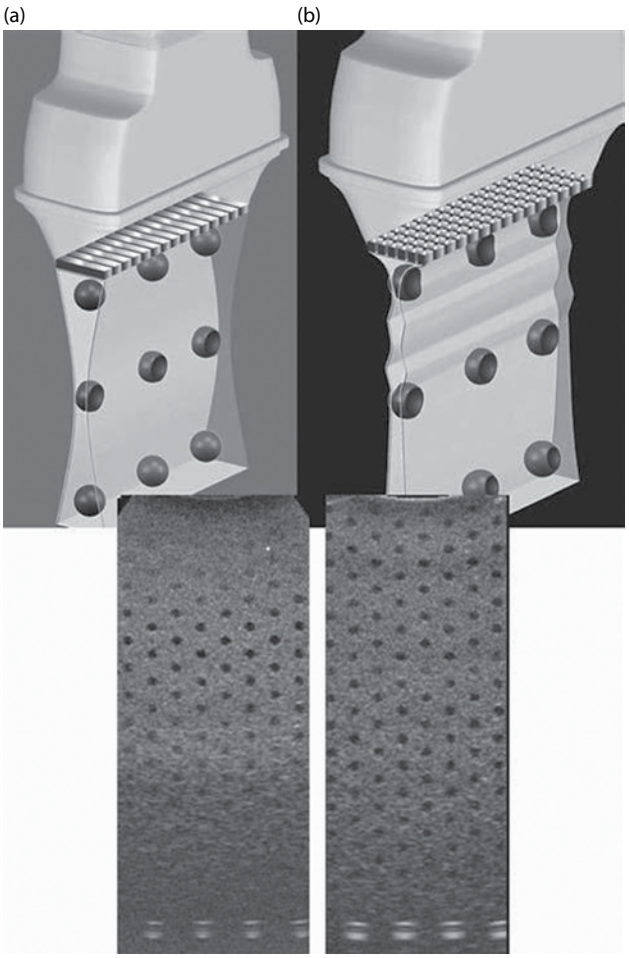


**Figure 5.2**
Improved resolution using a two-dimensional matrix array transducer (b) versus a conventional, one-dimensional array transducer (a). Using a matrix transducer, focusing is possible also perpendicular to the transducer's longitudinal axis. The small cystic structures in the phantom are resolved better and over a greater depth field. (Image kindly provided by H. Dudwiesus, GE Healthcare.)

imaging removes the fundamental frequencies using filters and typically shows a narrower main lobe, yielding better axial and lateral resolution, as well as better side-lobe suppression.[11] Tissue harmonic imaging can improve imaging of fluid-filled structures, providing better border definition and contrast as well as decreasing artifacts. Harmonic imaging can be implemented without increasing power output. Tissue harmonic imaging (THI) shows a significant improvement in grayscale imaging, especially in difficult scanning conditions as for example in obese patients.[12,13] THI improved the resolution in half of the pregnant patients studied by Treadwell et al.,[14] in particular in obese women. Kovalchin et al.[15] compared fundamental and harmonic imaging in a group of fetuses from mothers, 71% of whom had difficult scanning conditions. Image quality and visualization of the ventricles, valves, and the aortic and ductal arches were better using harmonic imaging. The authors concluded that harmonic imaging improved the image quality and that it was a useful adjunct to fundamental imaging in fetal echocardiography. Paladini et al.[16] performed a detailed study on harmonic imaging in fetal echocardiography. They studied 50 women in three groups receiving fetal echocardiography with either fundamental or harmonic imaging. In general, the diagnostic results were equal, but resolution from harmonic imaging was poorer, leading the authors to the conclusion that in pregnant women of normal weight, fundamental imaging still is the technique of choice for fetal echocardiography. In obese women and those with inadequate imaging in fundamental imaging, however, harmonic imaging performed better ("rescue" modality). With the wide availability of harmonic imaging in most newer ultrasound systems, it is often a standard modality in routine imaging.

## *Real-time compound imaging*

In conventional ultrasound imaging, ultrasound beams are emitted at right angles to the elements. If the beams hit the interface between structures of different echogenicity (a reflector) at a 90° angle, most echoes are returned to the transducer. At other angles, reflections are diverted away from the transducer, reducing the received signal intensity. In the worst case, when the beam is parallel to the interface, little or no reflection occurs. Real-time spatial compound imaging uses electronic beam steering of a transducer array to acquire several overlapping scans of an object from different view angles (see Figure 5.3). Individual views of the same plane, but acquired from slightly different angles (up to nine different angles are being used), are compounded into a multiangle image in real time. Reflections or signal losses occurring on cystic structures or irregular-shaped borders are reduced using compound imaging (CI) (for an example of compound imaging of the fetal

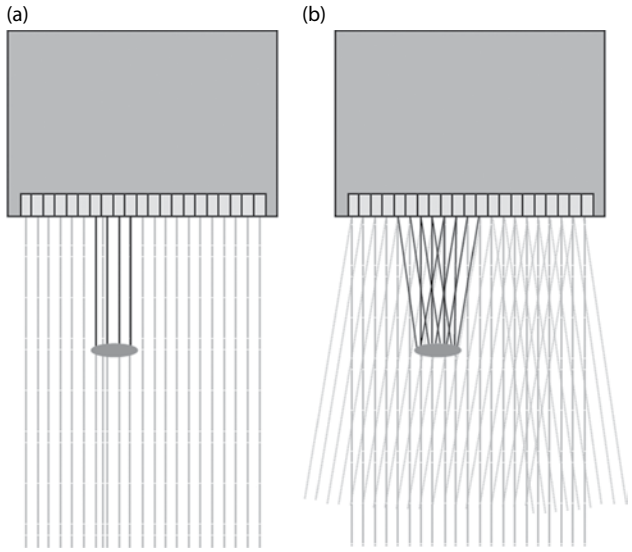


**Figure 5.3**
Conventional "single line of sight" (a) and real-time compound imaging (b). By electronically steering the ultrasound beams to "look" at objects from different angles, true reflectors can be better differentiated from artifacts because their reflections appear consistently in several of the angled views.

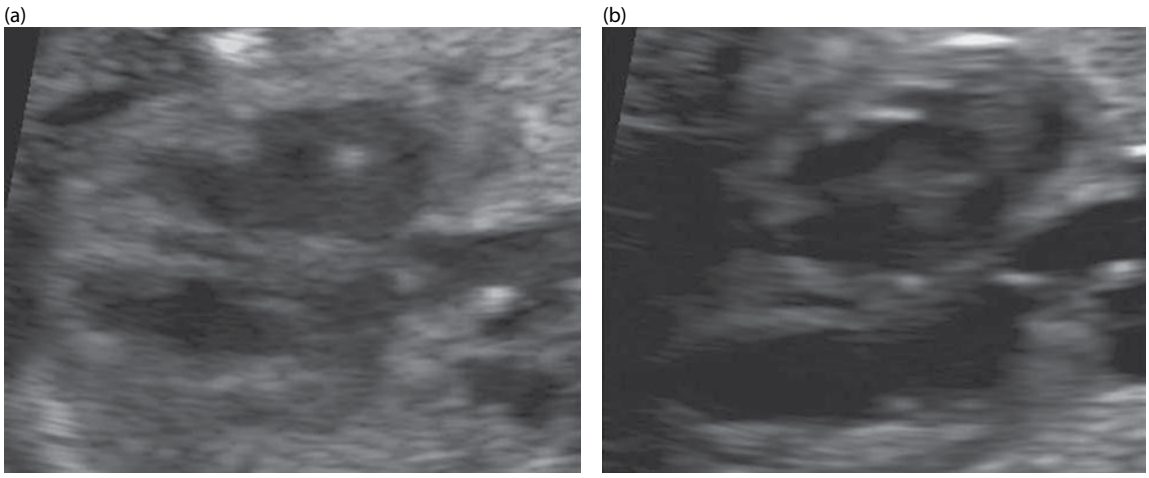


**Figure 5.4**
A normal fetal heart (at 23 weeks' gestation) imaged without (a) and with compound imaging (b) (but otherwise with identical settings).

heart, see Figure 5.4. The actual frame rate, however, drops because views are acquired from different angles, then compounded (computed) before the image can be displayed. CI has been marketed under various names (e.g., Philips: SonoCT, GE Healthcare: Cross Beam Imaging). CI reduces ultrasonic artifacts like speckle, promising improved contrast resolution and tissue differentiation.[17] In a clinical study of breast tissue, for example, CI increased signal-to-noise ratio but also increased the apparent target width.[18] A fetal study on compound and harmonic imaging in fetal diagnostic scanning at 11–14 weeks' gestation reported an improved visualization in various anatomical regions for studies for the combination of compound and harmonic imaging. For the fetal heart, there was a small (but probably not significant) improvement over conventional B-mode versus compound plus harmonic imaging.[19] Compound imaging alters contrast ratios,[20] similar to using a higher-frequency transducer,[21] which must be kept in mind when qualitative assessment, for example of fetal bowel echogenicity or cardiac valve or myocardium appearance, is to be based on subjective contrast impression using harmonics and compound imaging. In addition, averaging multiple frames for CI invariably reduces the frame rate, limiting its practical use.

## Volume contrast enhancement

The availability of volume data acquired using mechanical sweep or electronic 2D array transducers, combined with sufficient processing power, enables another form of real-time compounding: volume contrast enhancement. Volume contrast enhancement works by comparing voxels in neighboring parallel planes acquired in real time or nearly real time. Signals present in more than one plane are considered true signals and amplified; signals present in only one section are considered noise and suppressed. Volume contrast enhancement can be applied to single (static) volumes, but also in real-time scanning. The diagnostic effect depends on the slice thickness used for enhancement. Volume contrast enhancement in and parallel to the acquisition plane can also be used to study the fetal heart. It improves the perception of tissue interfaces and depth and structure around the heart. For an example, see Video 5.2. The aortic arch, head and neck vessels and inferior vena cava, liver veins, and umbilical vein can be recognized in practically the same section.

## Speckle reduction

Speckles are artefactual ultrasound signals caused by the interference of reflected ultrasound energy from scatters that are too small and too close to be resolved with the frequency used. Speckles appear as a pseudostructure in histologically homogenous tissue due to wave interference of reflected signals.[22] Speckle reduces the spatial and contrast resolution in ultrasound images and results in an artificial "sono-texture" that becomes apparent when the highest magnifications

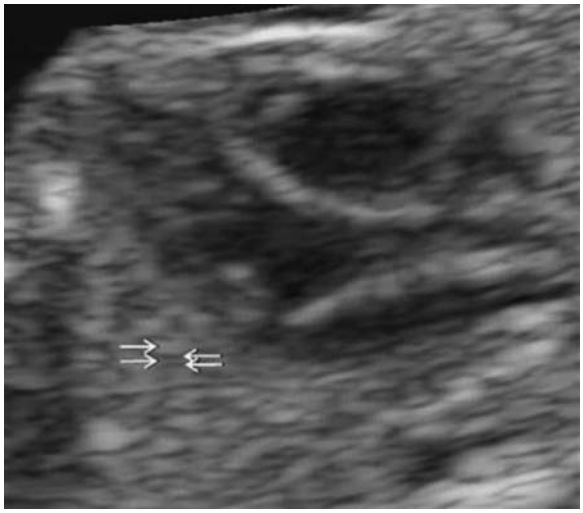

**Figure 5.5**
Ultrasound speckles. Interference of the reflected ultrasound waves at the level of the resolution limit causes an artifactual pattern appearance (see alternating white and dark areas indicated by the arrows) without histological correlate in the tissue.

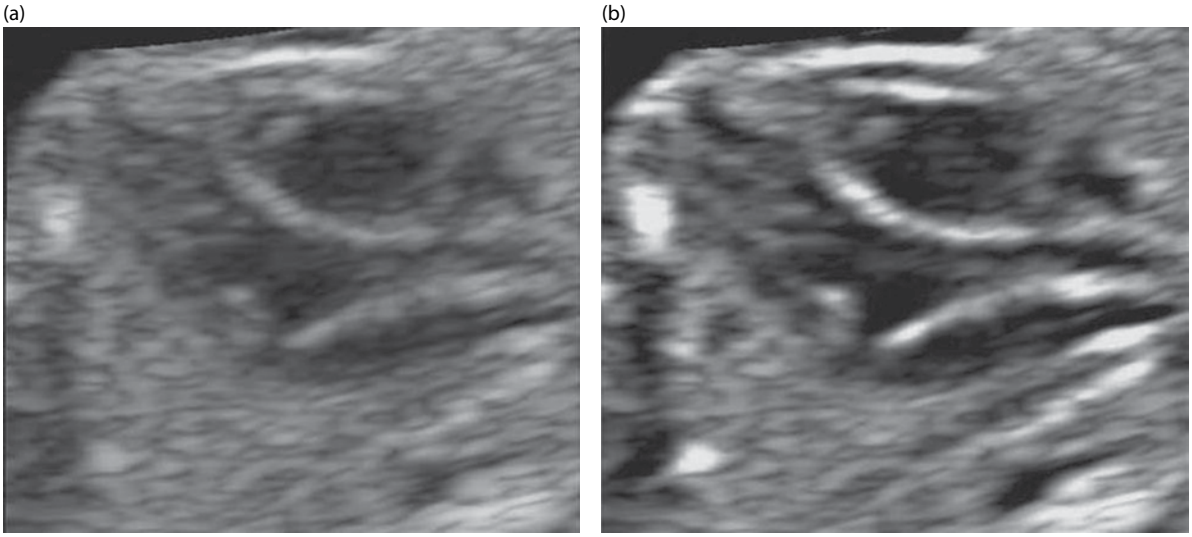


**Figure 5.6**
Speckle reduction. Postprocessing algorithms in modern ultrasound systems reduce speckles by real-time image analysis and interposition of gray tones to ameliorate the speckled appearance. (a) High magnification shows the artifactual pattern of the tissue (speckles); (b) speckle reduction applied to the identical still image.

are used (see Figure 5.5). A prominent speckle structure in a diagnostic image can obscure true objects with little contrast to the neighboring tissue. To reduce speckles, techniques have been employed for (1) improved resolution like higher-frequency transducers, coded excitation, matrix-array transducers, and harmonic imaging; (2) temporal averaging and spatial compounding; and (3) postprocessing approaches involving different types of filters.[22] Speckle reduction algorithms aim to remove the distracting speckle pattern without reducing the detail in the ultrasound image (see Figure 5.6). The techniques of geometric filtering to reduce speckle were first applied to radar images and later also to ultrasound images.[23] Postprocessing algorithms for speckle reduction have been introduced under different names (e.g., Philips: XRES, ContextVision: GOPView,[24] GE Healthcare: speckle reduction imaging SRI[22]). It should be mentioned that using harmonic and also compound imaging, subtle anatomical details may appear different also in size from fundamental imaging, a fact that has also been noted regarding other subtle anatomical details like the nuchal translucency or smallest distance measurements. In an ultrasound phantom designed to measure distance below 1 mm, fundamental imaging combined with speckle reduction, but without compound and harmonic imaging, showed the most accurate distance measurements (see Figure 5.7).[25]

## *The use of colors in B-mode imaging*

The physiology of human visual perception involves two types of receptors in the retina: The rods are specialized for perception of low light intensities, the scotopic vision, providing

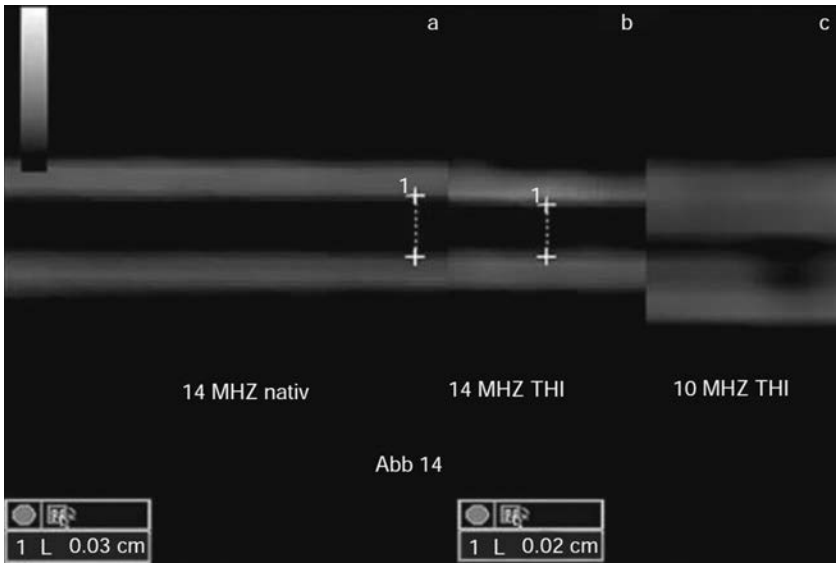


**Figure 5.7**
Measuring accuracy of fundamental and tissue harmonic imaging in an ultrasound phantom with membranes 0.3 mm apart. (a) Fundamental imaging at 14 MHz; (b,c) harmonic imaging at 14 and 10 MHz. (Reproduced with permission from Wunsch R et al. *Fortschr Röntgenstr* 2007; 179:65–71.[25])

sharp vision in low light surroundings. Photopic vision is performed by the cones, which are the dominant receptors in the fovea centralis where they provide the highest-resolution perception. Rods typically resolve between 20 and 60, under ideal circumstances up to 250 gray levels, but cones, utilizing color, saturation, and intensity, enable differentiation of up to seven million colors in photopic vision.[26] "Photopic ultrasound imaging" was available on a commercial ultrasound system also used for fetal studies (Elegra, Siemens Medical Ultrasound, Erlangen, Germany). In this implementation, the wide dynamic range available from raw ultrasound data was transformed in real time from the conventional shades from a grayscale (scotopic) into a photopic image, enabling much finer delineation over a wide dynamic range. Photopic imaging has been studied in internal medicine, but no fetal studies have been published. This ultrasound system providing photopic imaging is now no longer in production, but color to enhance the visual perception, for example, monochromatic coloring of B-mode images, is available in many ultrasound systems. Rendered 3D images are often produced using a colored display. In one commercial system (Aplio, Toshiba Europe Medical Systems), there is a palette using several colors in substitution for the conventional simple grayscale. Another way of exploiting colors to display ultrasound data has been implemented for 3D imaging in various commercial ultrasound systems to enhance depth perception by coloring elements in the foreground differently from those in the background. Video 5.3 shows the application of dynamic colorizations for a fetal 3D studies.

## *Advanced methods for motion detection*

### B-Flow

Conventional Doppler techniques in vascular imaging tend to exaggerate the real size of a vessel ("bleeding" of the color). In addition, the morphological information detected and displayed by grayscale B-mode imaging may be lost by the overlying color or power Doppler signals. B-mode imaging can be extended to detect blood flow independent of Doppler-derived signals by using digitally encoded ultrasound.[91,92] An ultrasound beam is encoded in two separate beams: The reflection of the first is used to reconstruct the cross-sectional imaging, while the reflections of the second, amplified beam are analyzed for the moving blood particles. Both signals are displayed in the same grayscale image. When compared to fetal Doppler ultrasound, B-flow has higher resolution and frame rates, and disadvantages of Doppler-based flow detection like aliasing and signal dropout at orthogonal scanning angles are avoided. B-flow alone or in combination with spatiotemporal image correlation (STIC) allows visualization of fine small vessels with low velocity, such as pulmonary veins, offering potential for the detection of small cardiac vessels, such as total anomalous pulmonary venous return (Pooh et al. 2000).[53] Volpe et al.[57] showed that B-flow in combination with STIC was superior to 2D grayscale and color Doppler alone in the detection of small pulmonary vessels (major pulmonary collateral arteries) that may crucially aid in diagnosing complex cardiac malformations with pulmonary vascular involvement.

### Directional power Doppler

The reflected signal from Doppler insonation contains different information that can be used in various display modalities. The frequency shift of the reflected signals indicates the velocity of the reflectors, for example, the cells in the moving blood, whereas the amplitude of the reflected signal correlates with the reflected energy. Traditionally, color Doppler has been used to encode motion direction, for example, using red and blue denoting flow toward and away from the transducer and velocity encoded in the brightness of the color signal. Power Doppler, however, displays the amplitude component of the reflected signals. The combination of both yields a sensitive motion display with directional information. Sensitive flow modalities based on power Doppler imaging with directional information for fetal studies including fetal echocardiography often provide imaging superior to conventional color Doppler vascular imaging with higher resolution, good lateral discrimination, and higher sensitivity, providing flow information almost in B-mode image quality.

# Navigation and display of ultrasound volume data

## *Reconstructed fetal 3D echocardiography: STIC*

Reconstructed 3D echocardiography currently is the dominant clinical technique for fetal 3D echocardiography. A sequence of sonographic data from a series of cross-sectional images is acquired while an automated probe sweeps the ultrasound plane across the fetal heart. Offline reconstruction then generates a virtual cardiac cycle comprising data from multiple heartbeats, which are rearranged using an algorithm that composes volume data from multiple cross-sectional images[28]; for a review, see Deng and Rodeck.[29,90] Clinical systems commercially available today use STIC for grayscale and color Doppler,[30,31] but the reconstructed nature of the volume leaves room for motion artifacts. Other approaches have also been studied (for reviews, see Deng and Rodeck[32] and Sklansky[33]) but are not yet available for broad clinical use. STIC was first introduced into a commercially available ultrasound system by Kretz Ultrasound (now GE Healthcare) and is today incorporated into ultrasound systems from several other companies. Volume data from STIC displayed as multiplanar imaging; reconstruction of 3D views ("rendering")[27,93]; the combination with color Doppler, tomographic, and invert modes[31,34–39]; and the ability to quantify fetal cardiac volumes[40–42] have provided fascinating insights into and very graphic 3D representation of the fetal heart. STIC is described extensively in other

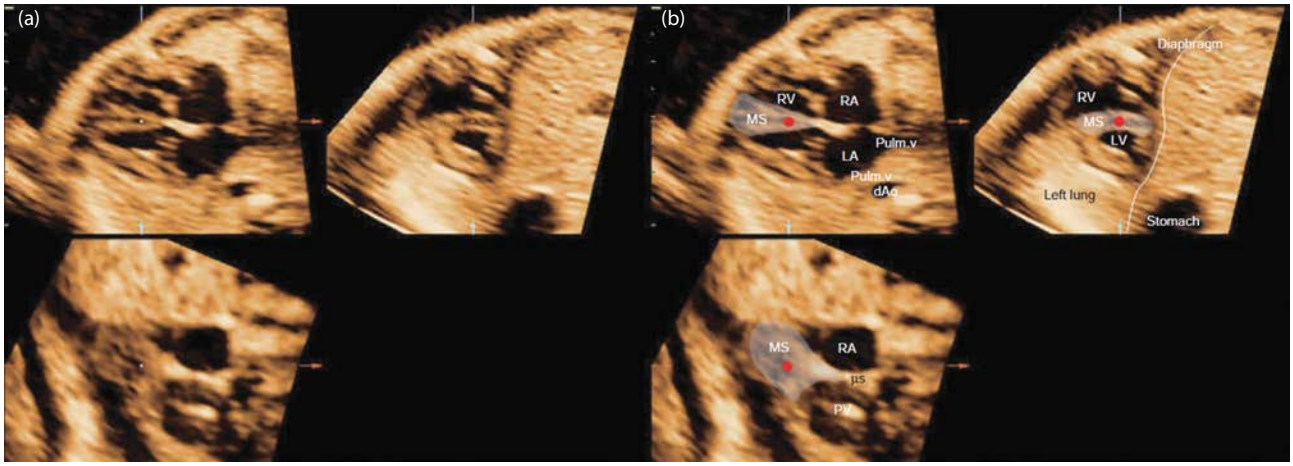


**Figure 5.8**
Multiplanar imaging of a normal fetal heart at 23 weeks' gestation. (a) The display shows three orthogonal cross sections with four-chamber view (top left), short-axis view (top right), and *en face* view of the interventricular septum (IVS). (b) Annotated image with the intersection of all three planes represented by the red dot; gray shaded area: IVS; RV/RA, right ventricle/atrium; LV/LA, left ventricle/atrium; Pulm.v, Pulmonary vein(s); PV, pulmonary valve; IAS, interatrial septum. (See also corresponding Video 5.4.)

chapters of this book. Therefore, we only briefly describe the display modalities available from volume echocardiographic data. Three-dimensional sequences of the fetal heart can be displayed in various forms. One (or several) cross-sectional plane(s) can be placed anywhere within a volume, enabling interactive scrolling through the heart offline, either in the plane of acquisition (highest spatial resolution) or any other (reconstructed) plane. Multiplanar imaging describes a display with three orthogonal planes (see Figure 5.8). If a whole cardiac cycle has been reconstructed, all structures can be viewed at different times in the cardiac cycle. Inspecting adjacent cross-sectional planes in a volume scan is particularly useful for the examination of the great arteries. Using 2D only, the outflow tracts can be visualized by moving the transducer toward the fetal head to obtain cross sections and by rotation and slight angulation to obtain views along the vessels. This may, however, be difficult due to an unfavorable fetal position, movements, or lacking operator experience.[43] In contrast, a stored volume (sequence) can be manipulated digitally, overcoming some of these limitations. Because of the given anatomical position and relation of the normal structures, views of the great arteries can be derived virtually from the standard four-chamber view, provided the volume covers these structures. Failure to be able to do so may even hint at structural heart disease. For example, if a fetal cardiac volume has been acquired in the four-chamber view insonation, cross or longitudinal sections of great arteries can be extracted from the data set following a simple algorithm (e.g., the "spin" technique[43]).

Typical 2D echocardiography aligns its standard planes with one of the ventricular axes, while primarily digital imaging modalities (magnetic resonance imaging [MRI] and computed tomography [CT]) display structures in relation to standard anatomical orientations (sagittal, coronal, and transverse) and in parallel planes or cross sections. Volume echocardiography can combine the conventional 2D imaging and orientation standards. In tomographic imaging several parallel cross-sectional planes through the same volume are displayed similar to a typical CT or MRI study (see Figure 5.9 and Video 5.5). Tomographic displays of ultrasound volume data have been given different commercial names (multislice, tomographic ultrasound imaging [TUI], and iSlice). Tomographic imaging of 3D fetal echocardiographic data can elegantly display normal or structurally abnormal planes from one insonation angle (see Figure 5.10 and Video 5.6). Tomographic imaging has successfully been applied to the heart at different gestations and to CHD.[37,38,44] With a slice distance setting appropriate for the size of the fetal heart, which increases with gestation, tomographic displays can be generated to show the four-chamber view and both ventricular outflow tracts, highlighting, for example, the normal and the abnormal arrangement of the great arteries (see Videos 5.7 and 5.8). A semiautomatic algorithm can help to display the relevant cardiac structures in one or several tomographic or multiplanar panels.[45–47] In the current releases of various ultrasound systems, automated approaches are available commercially.[48,49]

Rendering modes are an alternative to the cross-sectional modes. Rendering displays either external or internal surfaces of organs from volume data. Using specific settings for display thresholds, apparent tissue transparency, and shading techniques, 3D representations can be displayed on a 2D computer monitor or in a printed image. Surface rendering was originally developed to display the outer surfaces of solid objects like the fetal face or the skeleton in 3D.[33,93] For rendered images of the fetal heart, cropping into the heart will display its internal surfaces,[27,50] like cutting the heart in halves at the level of the four-chamber view or looking from an *en face* view of the valve plane, generating a more plastic impression than the thin slice usually displayed in a conventional B-mode image (see Figure 5.11). An example for a rendered view inside a normal fetal heart, alongside three

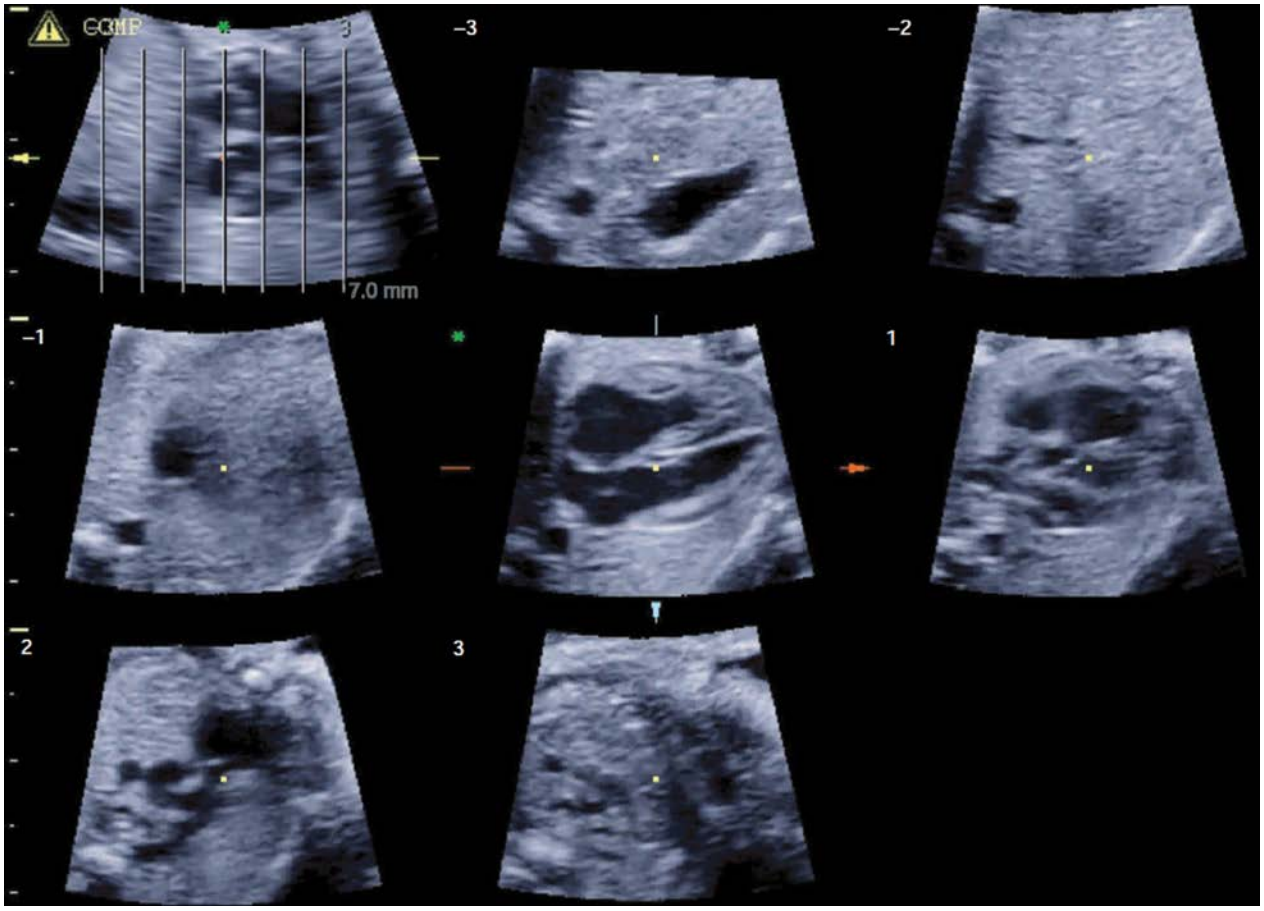


**Figure 5.9**
Tomographic display of a fetal volume containing parallel cross sections of the upper fetal abdomen and thorax. Panel 3 shows the fetal stomach; panel 2: hepatic veins converging toward inferior vena cava (IVC); panel 1: IVC passing through the diaphragm; *: indicates the level of the four-chamber view; 1: origin of the aorta; 2: origin and branching of the main pulmonary artery; 3: cross section of the head and neck vessels in the upper mediastinum. The top left image shows a sagittal section orthogonal to the other views, indicating the spatial relationship of the horizontal sections. (See also Video 5.5.)

orthogonal cross-sectional planes, is shown in Video 5.9 (the bottom right panel of this video shows an *en face* view of the atrioventricular valve plane).

Rendering in inversion mode shows only fluid-filled spaces (see Figure 5.11f), generating "digital casts" of the fetal heart and vasculature both in normal and structurally abnormal cases.[34,36,51,52] STIC can be combined with color and power Doppler, generating structural and functional cardiac information and angiography-like images.[31,35,39,53,54,91] Due to its high sensitivity for low velocities, power Doppler can also demonstrate extracardiac structures like pulmonary vasculature, teratoma, and chorioangioma.[55,56] Examples of this surface rendering of blood flow signals are the 3D display of vessels close to the heart (Videos 5.10 and 5.11) and of blood flow within the heart, for example, in ventricular septal defects (Videos 5.12 and 5.13). B-flow combined with STIC as well as these rendering techniques provide even more detailed visualization of small normal and aberrant vessels.[36,57]

STIC is an excellent tool for teleconsultation among experienced users[35,39] or between radiologists, obstetricians, and cardiologists, as well as for teaching.[58]

Clinically, STIC may have a future role to improve screening of pregnancies for CHD, in particular if combined with telemedicine.[59]

## Semiautomatic quantification

Functional and quantitative analysis of the fetal heart is yet another promising new area of volumetric fetal echocardiography research. Technically different 3D technologies have been applied to measure cardiac ventricular volumes and masses[40–42,60–62] (Messing et al. 2007[63,94]). The first report on 3D measurement of fetal cardiac ventricles by Chang et al.,[60] using a fast, automated sweep, demonstrated a linear increase of the cardiac volume between 20 and 30 weeks and that 3D volumetry had a better reproducibility than 2D measurements. Initial experiments using nongated 3D from free-hand acquisition confirmed the correlation between ventricular chamber volumes and gestational age.[61,62] *In vitro* experiments using STIC demonstrated acceptable accuracy for volume and even mass estimations in the range comparable with mid- and late-gestation fetal hearts.[40,41] 3D inversion mode

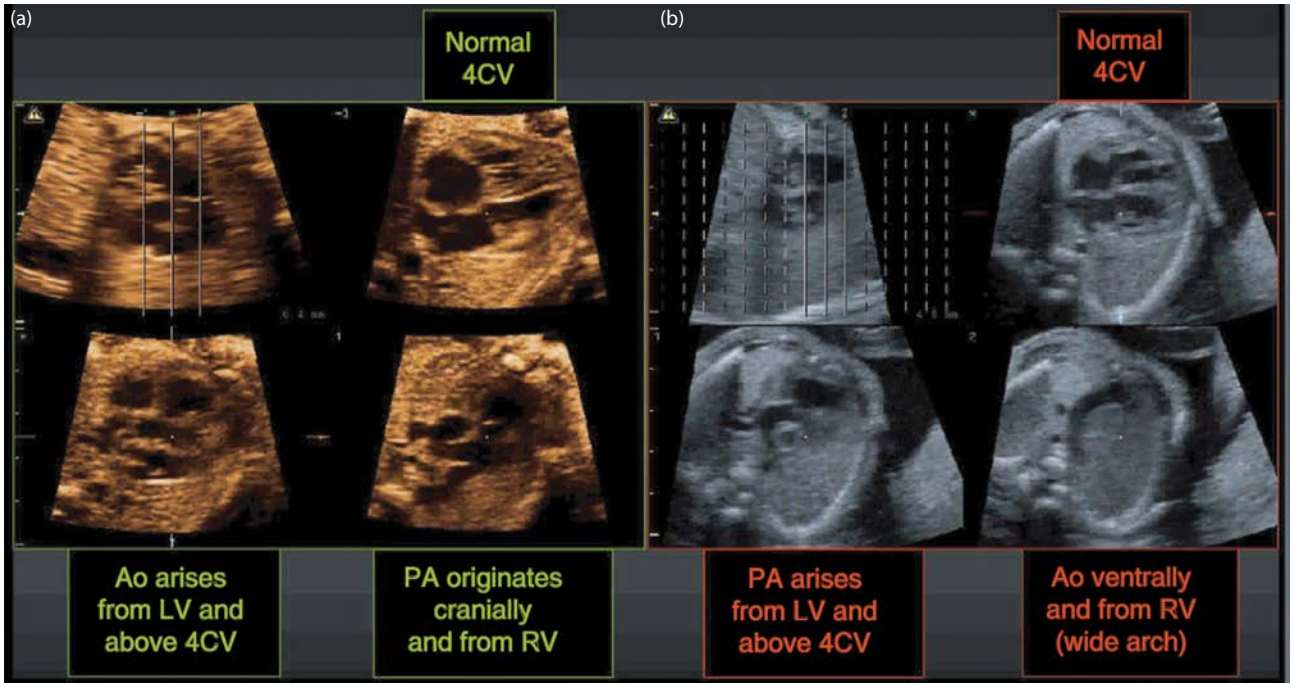


**Figure 5.10**
Tomographic imaging of a normal heart (a) and a dextrotransposition of the great arteries (b). For the same gestational age, identical settings of slice distances at three different levels at and above the four-chamber view (4CV) display the diagnostic sections. (See also Video 5.6.) (Ao, aorta; LV, left ventricle; PA, pulmonary artery; RV, right ventricle.)

sonography combined with STIC represents another and possibly more reproducible method for estimating fetal cardiac ventricle volume (Messing et al. 2007). Live 3D using newer transducer technologies, that is, 2D matrix array transducers, holds the promise of measurements in nonreconstructed data sets. Preliminary data show that nonreconstructed fetal cardiac volumetry and STIC technology exhibit reasonable concordance between these two measurement approaches.[63]

## Live 3D using matrix array transducers

### *Matrix array transducer*

Transducers with more elements and broader frequency bandwidths improve both resolution and tissue penetration. A major goal in transducer technology has been the development of an electronic 2D array, enabling full beam steering in three dimensions.[64]

### *Sparse and full array matrix transducer*

The first 2D-array transducer available used a sparse 2D array (Volumetric Medical Imaging Inc. 1997, Durham, North Carolina),[65–67] but soon a full 2D-array transducer with some 2,800 individual elements, miniaturized multiplexers build into the probe handle and capable of generating more than 20 B-mode volumes per second and even color duplex volumes was introduced (Philips Medical System 2001). Maulik et al.[68] used such a 4 MHz 2D array transducer in 12 fetuses between 16 and 37 weeks. They concluded that the system allowed comprehensive visualization of fetal cardiac anatomy and color Doppler flow unattainable by 2D approaches and suggested that live 3D fetal echocardiography could be a significant tool for prenatal diagnosis and assessment of congenital heart disease. Sklansky et al.[69] studied 30 fetuses with this matrix system, focusing on rendered images of the fetal heart in comparison to conventional cross-sectional imaging. Volume-rendered displays identified all major abnormalities and enabled offline retrieval of views not visualized during the actual scans; volume-rendered displays had only slightly inferior image quality compared with conventional 2D. Acar et al. (2005)[98] reported their experience with biplane (simultaneous display of two different cross sections, e.g., simultaneous display of both outflow tracts) and live-3D (rendered) imaging with the same system in 60 fetuses between 22 and 34 weeks. In pathologic fetal hearts 3D was helpful, for example, for localizing multiple cardiac tumors, estimating size and function of the right and left ventricles, and evaluating the mechanism of valvular regurgitation and pulmonary obstruction. Several other transducers have been introduced for adult or pediatric as well as for fetal volumetric imaging (Philips Medical Systems, GE Healthcare). Real-time 3D echocardiography should provide an accurate means of determining chamber volumes and cardiac mass.[70] These systems show that they can also be used for fetal cardiac volumetry (see Figures 5.12 and 5.13).[63]

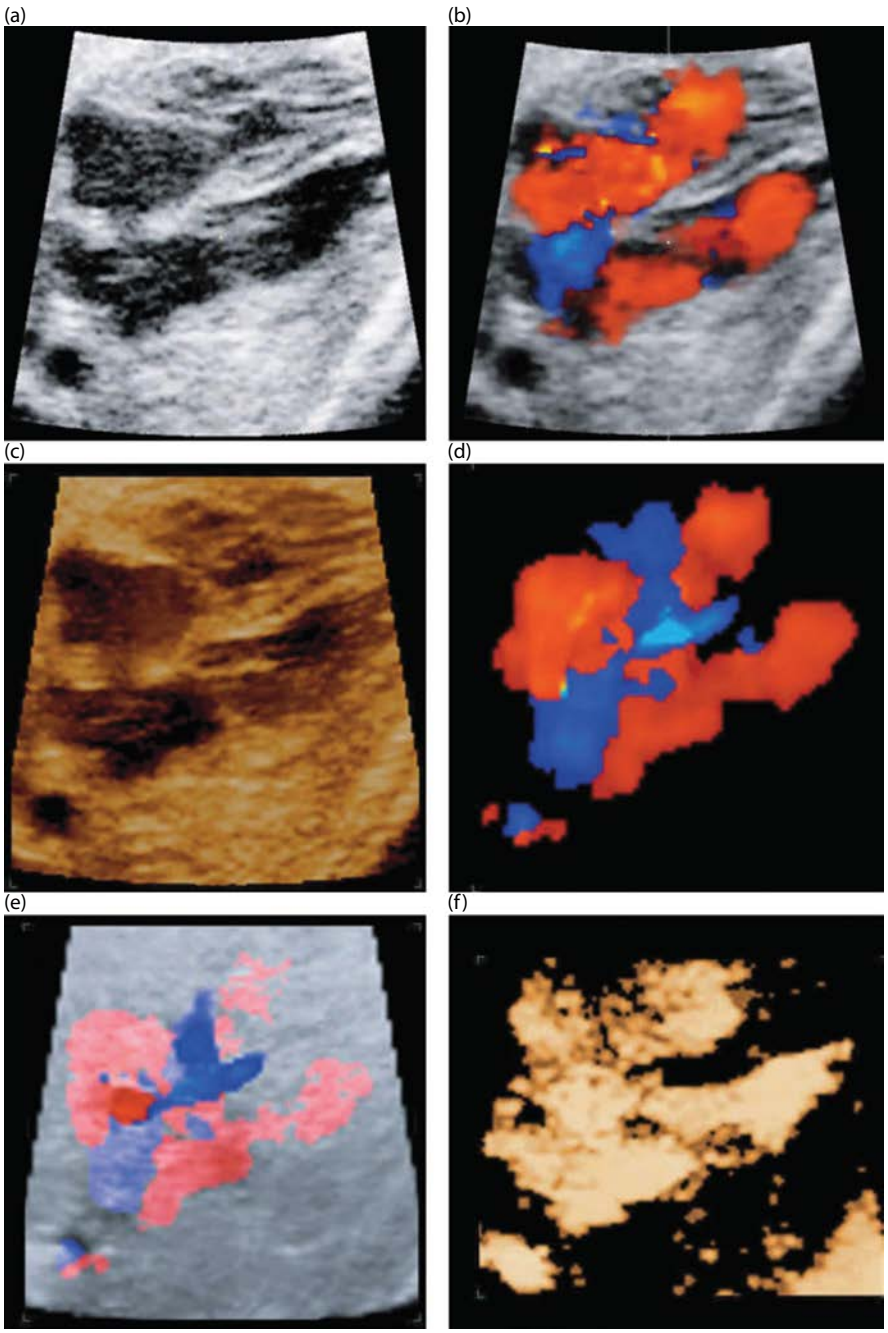


**Figure 5.11**
Cross-sectional and rendered views of a normal fetal heart at 29 weeks' gestation. (All images derived from a spatiotemporal image correlation [STIC] volume acquired in a four-chamber view plane.) Cross sections: (a) B-mode, (b) color duplex with biventricular inflow (in red); rendered images: (c) surface-rendered view, cropped to display only the "cranial half" of the heart, (d) color-only rendering of the whole volume with display of hepatic veins and inferior vena cava (blue) and ventricular inflow, (e) "glass-body": region of interest as in (d) but with transparent tissue rendering over color Doppler, (f) inversion mode (thin volume slice cropped to display only the four-chamber plane). (Reproduced with permission from Tutschek B and Sahn DJ. *Cardiol Clin* 2007;25:341–55.[97])

## Fetal cardiac MRI

MRI has increasingly been used over the last decade for fetal studies, but the use of MRI for studies of the fetal heart has been hampered by obstacles not present in the pediatric or adult patient: small size, fetal movements, and lack of gating in the absence of a fetal electrocardiogram.[71] Initial studies using MRI to investigate the fetal heart date back over a decade[72] but have not led to routine protocols for its clinical use.[73]

A recently published case series highlighted the utility of MRI in studying vasculature near the fetal heart as a potential current application, based on the fact that aortic arch und pulmonary vascular anomalies are among the most challenging tasks for fetal echocardiography.[73]

Compared to ultrasound technology, MRI is more expensive and less readily available, yet it offers attractive potential advantages compared to ultrasound: independence from fetal position, shadowing from maternal structures and fetal parts, as well as other factors.[73]

The use of MRI for fetal cardiac studies may increase if high-resolution, gated fetal cardiac MRI studies can be performed. Such fetal studies are possible in chronically instrumented sheep.[74] Further developments such as metric-optimized gating[75] may in the future create a clinical role for gated fetal cardiac MRI, which, at present, remains a research tool.

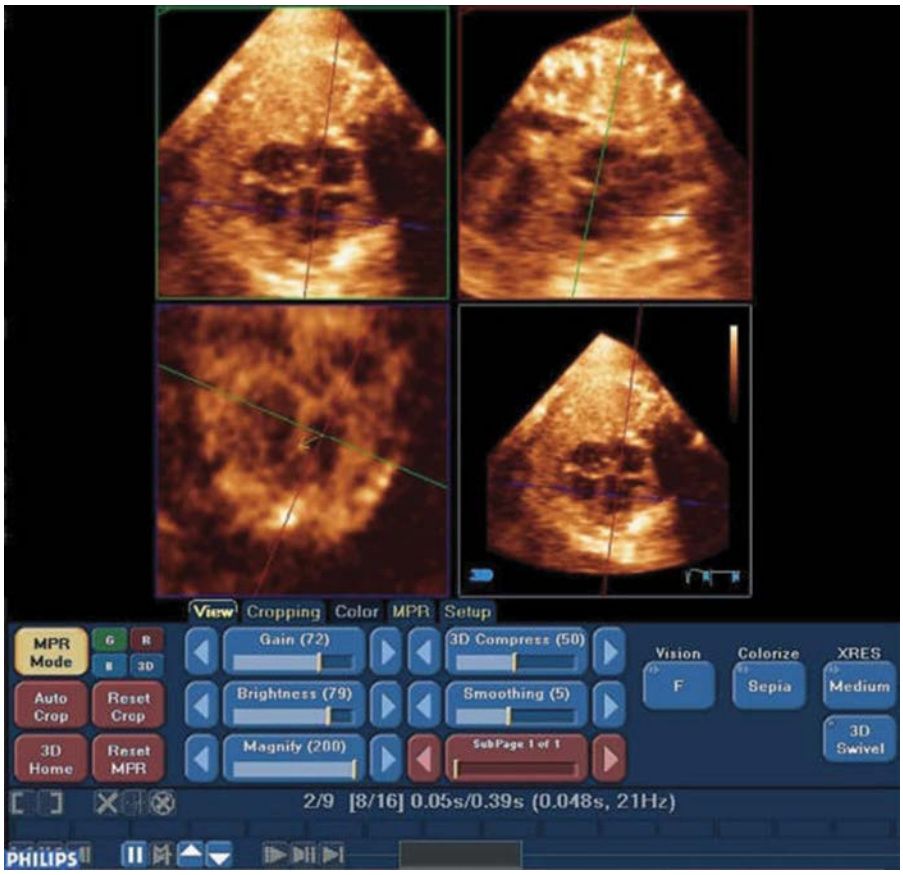


**Figure 5.12**
Real-time fetal 3D echocardiography using a fully electronically steerable two-dimensional matrix array transducer (x3-1/iE33 and software QLab 3DQ Advanced; Philips Medical Systems, Bothell, Washington). The ultrasound images represent three cross sections orthogonal to each other and a 3D niche view of a normal 26-week fetal heart.

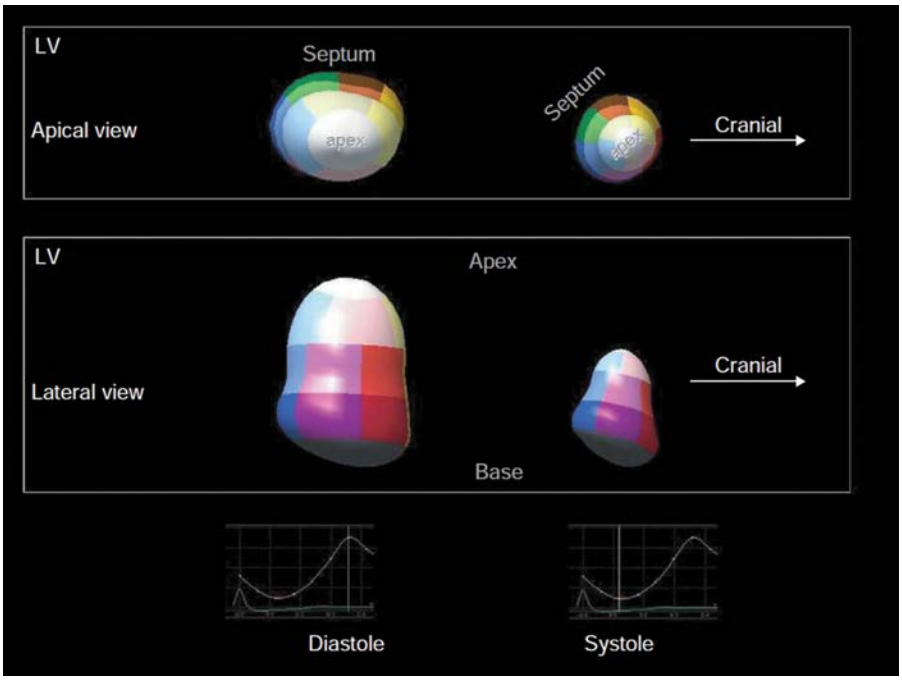


**Figure 5.13**
Virtual endocardial casts of the normal human left cardiac ventricle in a 28-week fetus in diastole and systole and endocardial volume curves, generated using semiautomatic volume calculation software from a volume loop acquired using real-time 3D echocardiography (QLab 3DQ Advanced and x3-1/iE33; Phillips Medical Systems, Bothell, Washington).

# Cardiac mechanics

## *Motion detection, contractility*

Motion of the fetal heart and of its individual regions as well as intracardiac blood flow can be studied to describe the cardiac mechanical function globally or locally.[95] Sonographic measurement of cardiac function can be based on ventricular dimensions (fractional shortening calculated from M-mode or B-mode imaging to estimate the ejection fraction or from 3D measurement, as described previously) or on velocities of intracardiac blood flow or cardiac structures (tissue Doppler echocardiography). Blood flow Doppler studies provide data from velocity waveform analysis across the atrioventricular valves, in the great arteries, or in the veins close to the heart; quantitative data include acceleration times, mechanical cardiac intervals, or computation of cardiac output from flow velocities and vessel diameters.[76,77]

## *Tissue Doppler*

Fetal tissue Doppler echocardiography (TDE) has been used to assess regional diastolic and systolic wall excursions and for functional assessment of the fetal heart[96] (Harada et al. 1999[78–82,99]). Figure 5.14 and the accompanying Video 5.14 show color tissue Doppler imaging of a normal fetal heart. Quantitative information can be obtained by using either color or pulsed wave Doppler TDE, also enabling diagnosis of fetal cardiac rhythm disturbances.[81,83,84] Figure 5.15 shows an example of normal and abnormal fetal cardiac rhythm. The accompanying Video 5.15 shows a normal cardiac pulsed wave TDE study.

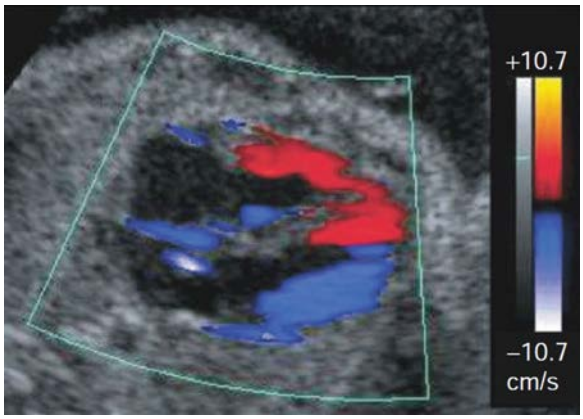


**Figure 5.14**
Color tissue Doppler image of a normal fetal heart. (Reproduced with permission from Tutschek B et al. *Ultrasound Obstet Gynecol* 2003;21(1):26–32.[82]; See also Video 5.14.)

## *Strain and strain rate, speckle tracking*

Di Salvo et al.[85] studied regional myocardial deformation (strain and strain rate) using tissue Doppler in 75 normal human fetuses. They described the characteristics of ventricular filling and found an increase of longitudinal

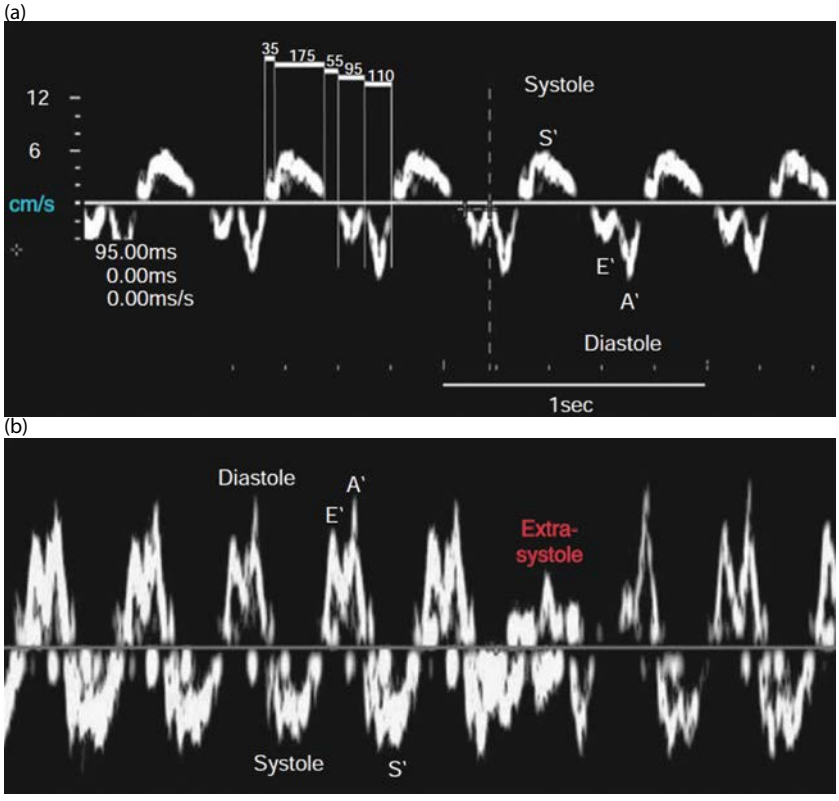


**Figure 5.15**
(a) Normal pulsed wave (PW) tissue Doppler (TDE) tracing of the right ventricular valve annulus and (b) PW TDE showing an extrasystole. The systolic (S′) and diastolic (E′ and A′) peaks can be seen and the segments of the mechanical action of the heart can be measured in milliseconds. ([b] Reproduced with permission from Tutschek B et al. *Ultrasound Obstet Gynecol* 2003;21(1): 26–32.[82])

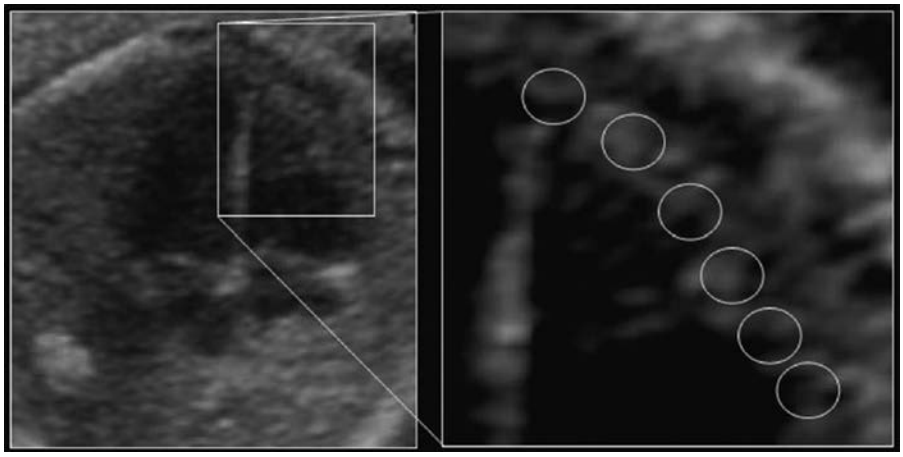

**Figure 5.16**
Speckle tracking uses the artifactual, but region-specific pattern generated by wave interference to track smallest tissue regions (magnified from a cross-sectional image sequence throughout the cardiac cycle).

deformation with gestational age. Larsen et al. (2006)[100] obtained tissue Doppler sequences to calculate fetal strain and strain rate in three normal fetuses and one fetus with aortic valve atresia, showing severely reduced strain rates in the affected ventricle. Doppler-based measurements, however, suffer from the limitation of angle dependency. In addition, quantitative analysis based on Doppler data is hampered by measurement errors and by its angle dependency. Strain rate imaging by speckle tracking imaging (STI) is less affected by these factors and is the only sonographic measurement that allows rotational or twist analysis of the left ventricle of the heart. STI exploits the sonographic texture of the cardiac walls in a 2D images sequence of the beating heart. Individual segments of the beating heart, that is, regions along the myocardial walls in long or short axis views, can be tagged and tracked by a semiautomatic image analysis algorithm due to their "speckled" appearance (speckle tracking; see Figure 5.16). The deformation (or stretching) of tissue, normalized to its original size or shape, is called cardiac strain. The rate at which this tissue deformation occurs is called strain rate (D'hooge et al. 2000[101]). The higher the strain rate, the faster the deformation occurs between individual points in the myocardium, or, in other words, the faster the myocardium contracts or relaxes. Strain rate imaging has been used in various adult cardiac conditions including ischemic heart disease and myocardial dys-synchrony (for an extensive review, see Stoylen[86]). STI can be used to assess longitudinal strain in the human fetus (see Video 5.16). One intriguing aspect of the complex architecture of the left ventricle is the ability to produce torsion of the ventricle, similar to wringing a towel dry. This fundamental component of left ventricular function may be caused by the helical arrangement of myocardial layers.[87] STI can also be used to study left ventricular torsion in the human fetus (see Video 5.17).

Miranda et al. have used speckle tracking to both systolic and diastolic ventricular deformation in fetuses with coarctation of the aorta. The affected fetuses had lower LV systolic longitudinal strain, systolic strain rate, and diastolic strain rate than controls, suggesting functional changes that may lead to structural alterations that may or may not be obvious from structural analysis alone.[88]

The current uses of additional methodologies have recently been addressed in a detailed overview of cardiac diagnosis and treatment commissioned by the American Heart Association.[71] Table 5.1 shows a summary of the technologies and their current and possible future uses.

**Table 5.1** Current and future technological advances in fetal heart studies

| *Technique* | *Current uses in fetal cardiology* | *Potential future uses* |
|---|---|---|
| 3D/4D echocardiography | Detailed assessment and reconstruction of (small) vessels' courses and complex spatial relationships<br>Teleconsulting<br>Education/teaching/self-study | Screening for structural heart disease<br>Qualitative assessment of cardiac structure<br>Quantitative assessment of cardiac function and volumes |
| Tissue Doppler | Evaluation of time intervals and rhythm | Evaluation of ventricular function |
| Strain and strain rate imaging | Investigational | Evaluation of ventricular function |
| Cardiovascular MRI | Investigational<br>In addition to evaluation of visceroatrial situs, venous returns, and associated extracardiac malformations | Studies of extracardiac vasculature in suspected CHD<br>With gating, assessment of cardiac structure and ventricular volume and function |

*Source:* Donofrio MT et al. *Circulation* 2014;129(21):2183–242.[71]

# Future developments

## *Automated 3D/4D studies of ventricular volumes and chamber mechanics*

The ability to acquire, compute, and measure 3D/four-dimensional (4D) images of the fetal heart will continue to improve. Automated and tailored methods for edge detection should substantially improve the ability to integrate cardiac volume measurements into the clinical realm of fetal echocardiography. Likewise, high frame rate 3D/4D acquisitions are now possible, in particular with 2D-matrix array transducers, providing high resolution. Further refinements will allow for speckle cluster mechanics that should yield methods for defining cardiac mechanics, strain, twist, and torsion measurements of the fetal ventricles and for assessing right and ventricular interaction, taking into account the effect of through-plane motion.

A breakpoint will occur that clearly sets different data and analysis formats for fetal cardiac imaging, as distinct from the other 3D methods used in perinatology.

## *The pathway for matrix array implementation*

Matrix array development will proceed in two directions: for transabdominal imaging of the fetal heart larger aperture, more complex or even curved plane matrix arrays will be developed. For denser acquisitions, high-resolution fetal cardiac imaging will correct aberrations that occur along the imaging pathway. The growing interest and understanding of the potential for changing the natural history of heart disease with prenatal cardiac interventions will lead to developments of miniaturized devices for intrauterine applications.

These will provide 4D near-field imaging and potentially offer integrated therapeutic options like radiofrequency, laser, or high-intensity focused ultrasound therapies. They will incorporate the latest nonceramic ultrasound sensors, such as computer micromachined ultrasound transducers (CMUTs) (see Figure 5.17), which have agility for controlling frequency and power output[89] far beyond what exists today.

# Conclusion

Continuing technological ultrasound advances have increased the image quality available for fetal cardiology. The possibilities of volume ultrasound together with offline processing have pushed the field forward tremendously. Currently, STIC is the clinically dominant 3D modality, but continuing advances in array technology have almost made nonreconstructed, truly live 3D imaging a clinical reality.

Pushing the limits at another front, highest-frequency transvaginal probes, together with the general trend toward earlier prenatal diagnosis, are available now, too, and their use in fetal echo will further push the limits of detection in expert hands.

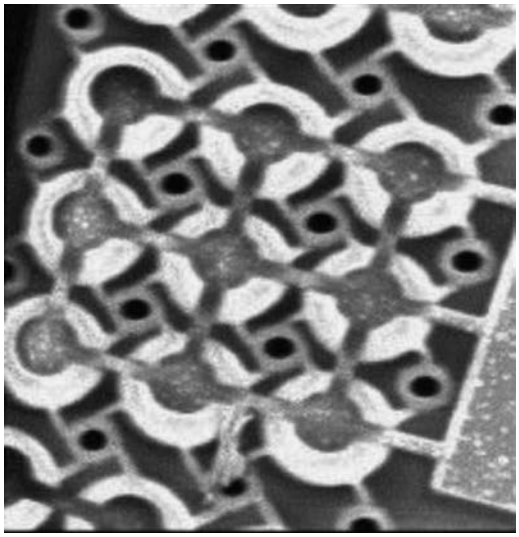

**Figure 5.17**
Capacitive micromachined ultrasound transducers (CMUTs) (scanning electron microscope image).

It can be expected that these developments will be accompanied by further automation, including detection algorithms that enable tracking of tissue borders, automatic assessment of relaxation and contraction, automatic volume and mass quantification, and flow measurements.

Despite all of the technological improvements, the main factor likely to improve the detection rate of fetal cardiac defects remains the operator's ability to obtain the diagnostic views. Especially the offline image or volume analysis methods and the novel ways of analyzing and presenting fetal echocardiography data will improve the general level of scanning technique and personnel expertise.

# Videos

**Video 5.1** (https://youtu.be/d2PVwxRWbCM)
High-resolution real-time three-dimensional (3D) view of a beating normal fetal heart (22 weeks' gestation). Using a two-dimensional matrix array transducer, instantaneous or real-time 3D scanning with sufficiently high spatial and temporal resolution is possible.

**Video 5.2** (https://youtu.be/vvWleBz9FAs)
Volume contrast enhancement during real-time scanning: fetal abdomen, 20 weeks, sagittal section.

**Video 5.3** (https://youtu.be/O7hw9VHmMcE)
Dynamic colorization. Dynamic colorization refers to the differential coloring of fore- and background objects in three-dimensional rendering. In this example of a real-time 3D study of a normal fetus at 16 weeks' gestation, the fetal legs and umbilical cord in the foreground are colored in amber while the structures farther away from the viewer are shaded in blue. (Reproduced with permission from Tutschek B and Sahn DJ. *Cardiol Clin* 2007;25:341–55.[97])

**Video 5.4** (https://youtu.be/dZruW7S-4mc)
Multiplanar reconstruction (MPR) of a virtual cardiac cycle acquired using spatiotemporal image correlation (STIC). In this video, three orthogonal sections through a looping virtual cardiac cycle are shown; the intersection of planes is denoted by little yellow or red dots. The top left panel (A-plane) is the acquisition plane, adjusted to display the four-chamber view, the top right panel B the short axis view of the ventricles, and the bottom left panel C the interventricular septum *en face*. (Reproduced with permission from Tutschek B and Sahn DJ. *Cardiol Clin* 2007;25:341–55.[97])

**Video 5.5** (https://youtu.be/AiDZzaBATcc)
Tomographic imaging of a virtual cardiac cycle (from a STIC acquisition). A stack of sections parallel to the four-chamber view is displayed from a virtual cardiac cycle (captured using STIC). By adjusting the center of the volume in the middle panel and selecting the appropriate distance between the sections, several relevant planes can be displayed dynamically and at once (top left panel: short-axis view displaying the "slice" levels). (Reproduced with permission from Tutschek B and Sahn DJ. *Cardiol Clin* 2007;25:341–55.[97])

**Video 5.6** (https://youtu.be/81NHNobAbhw)
Tomographic imaging of a normal heart (left panel) and a heart with d-transposition of the great arteries (TGA, right panel; reduced playback speed). Both hearts are displayed using the same settings to demonstrate the striking differences in analogous planes. (Reproduced with permission from Tutschek B and Sahn DJ. *Cardiol Clin* 2007;25:341–55.[97])

**Video 5.7** (https://youtu.be/14CrSoMlEpw)
Tomographic imaging of the fetal heart: normal fetal heart (midtrimester).

**Video 5.8** (https://youtu.be/eg7APAVYoWM)
Tomographic imaging of the fetal heart: d-TGA (midtrimester).

**Video 5.9** (https://youtu.be/74nXtb6x0xc)
Multiplanar display of the heart plus rendered view of the cardiac valves.

**Video 5.10** (https://youtu.be/B_9FEAQ5Bl8)
Surface rendering of color Doppler signals from STIC: 3D angiogram normal midtrimester fetus (one cardiac cycle).

**Video 5.11** (https://youtu.be/fUTsWGpknXI)
Surface rendering of color Doppler signals from STIC: 3D angiogram (still) normal midtrimester fetus (rotation).

**Video 5.12** (https://youtu.be/CmbRDQENYWM)
Muscular VSD: glass-body mode, showing color Doppler signals "surface rendered" inside the transparently rendered tissue.

**Video 5.13** (https://youtu.be/VScLdScfGf4)
Muscular VSD: rotating view of the "surface-rendered" color Doppler signals (single volume).

**Video 5.14** (https://youtu.be/c2EmGFWxkcg)
Color tissue Doppler of a normal fetal heart at midtrimester. By reducing the wall filter, pulse repetition frequency, and gain, the tissue motion is shown in color. Note the synchronicity of the atria and ventricles, the foramen ovale flap, and how the septum moves with the free wall of the right ventricle.

**Video 5.15** (https://youtu.be/1yFo70OK4GQ)
Pulsed-wave tissue Doppler study of a normal fetal heart. The fetal heart is imaged in an apical four-chamber view and the PW sample volume placed to cover the excursion of the lateral part of the tricuspid valve annulus. The wall filter and pulse repetition frequencies as well as the gain are lowered and the sweep speed increased. The resulting PW tracing shows the tissue excursion with the typical two-peak diastolic (E′ and A′, movement away from transducer, negative velocities) and the systolic peak (S′, toward the transducer, positive velocity). Arrhythmias show distinctly altered typical patterns, and timing of the mechanical segment of the cardiac cycle can be measured from the PW tracing. (Reproduced with permission from Tutschek B and Schmidt KG. *Ultrasound Obstet Gynecol* 2004;24(3):229.[81])

**Video 5.16** (https://youtu.be/6up2npOwSwY)
Longitudinal strain in the fetus measured using speckle tracking in an apical four-chamber view. The colors in the top left panel indicate longitudinal shortening and lengthening (tissue deformation, strain). The graph on the right shows longitudinal strain over time during one cardiac cycle.

**Video 5.17** (https://youtu.be/Cay5tQx69tw)
Application of speckle tracking to measure circumferential strain of the fetal right ventricle in a short-axis view. The colors in the top left panel indicate circumferential shortening and lengthening (tissue deformation, strain). The graph on the right shows circumferential strain over time during one cardiac cycle.

# References


1. Bonnet D et al. *Circulation* 1999;99:916–8.
2. Crane JP et al. *Am J Obstet Gynecol* 1994;171:392–9.
3. Fuchs IB et al. *Ultrasound Obstet Gynecol* 2007;29:38–43.
4. Tworetzky W et al. *Circulation* 2001;103:1269–73.
5. Carvalho JS et al. *Heart* 2002;88:387–91.
6. Sharland GK, Allan LD. *Br J Obstet Gynaecol* 1992;99:220–5.
7. Simpson LL. *Obstet Gynecol Clin North Am* 2004;31:51–9.
8. Tegnander E, Eik-Nes SH. *Ultrasound Obstet Gynecol* 2006; 28:8–14.
9. Ville Y. *Ultrasound Obstet Gynecol* 2007;29:1–5.
10. Forsberg L. *Ultrasonics* 2004;42:17–27.
11. Fowlkes JB, Averkiou M. Contrast and tissue harmonics imaging. In Goldman LW, Fowlkes JB, eds. *Categorial Course in Diagnostic Radiology Physics: CT and US Cross-Sectional Imaging*. Oak Brook, Illinois: RSNA; 2000:77.
12. Shapiro RS et al. *AJR Am J Roentgenol* 1998;171:1203–6.
13. Tranquart F et al. *Ultrasound Med Biol* 1999;25:889–94.
14. Treadwell MC et al. *Am J Obstet Gynecol* 2000;182:1620–2.
15. Kovalchin JP et al. *J Am Soc Echocardiogr* 2001;14(10):1025–9.
16. Paladini D et al. *Ultrasound Obstet Gynecol* 2004;23(2): 159–64.
17. Entrekin RR et al. *Semin Ultrasound CT MR* 2001;22(1): 50–64.
18. Dahl JJ et al. *Ultrason Imaging* 2004;26(4):203–16.

19. von Kaisenberg CS et al. *Am J Obstet Gynecol* 2005;192(2): 535–42.
20. Lee HJ, Cho JY. *J Clin Ultrasound* 2003;31(6):302–7.
21. Vincoff NS et al. *J Ultrasound Med* 1999;18(12):799–803. quiz 805–6.
22. Milkowski A et al. 2003 GE Medical Systems. Available from http://www.gehealthcare.com/euen/ultraosund/docs/education/whitepapers/whitepaper_SRI.pdf, accessed June 2007.
23. Busse LJ et al. *1995 IEEE Ultrasonics Symposium 95CH35844*; 1995:1353–6.
24. Floreby L. 2005, http://www.contextvision.com, accessed June 2007.
25. Wunsch R et al. *Fortschr Röntgenstr* 2007;179:65–71.
26. Gebel M et al. *Electromedica* 2000;68(1):59–64.
27. Yagel S et al. *Ultrasound Obstet Gynecol* 2006;28:266–74.
28. Nelson TR et al. *J Ultrasound Med* 1996;15:1–9.
29. Deng J, Rodeck CH. *Prenat Diagn* 2004;24:1092–103.
30. DeVore GR et al. *Ultrasound Obstet Gynecol* 2003;22(4):380–7.
31. Chaoui R et al. *Ultrasound Obstet Gynecol* 2004;23:535–45.
32. Deng J, Rodeck CH. *Curr Opin Obstet Gynecol* 2006;18: 177–84.
33. Sklansky M. *Pediatr Cardiol* 2004;25:307–21.
34. Espinoza J et al. *Ultrasound Obstet Gynecol* 2005;25:428–34.
35. Goncalves LF et al. *Ultrasound Obstet Gynecol* 2004a;24(6): 696–8.
36. Goncalves LF et al. *J Ultrasound Med* 2005;24:415–24.
37. Goncalves LF et al. *J Perinat Med* 2006a;34(1):39–55.
38. Goncalves LF et al. *Ultrasound Obstet Gynecol* 2006b;27: 336–48.
39. Goncalves LF et al. *J Ultrasound Med* 2004b;23:473–81.
40. Bhat AH et al. *Circulation* 2004;110:1054–60.
41. Bhat AH et al. *J Ultrasound Med* 2004;23:1151–9.
42. Messing B et al. *Ultrasound Obstet Gynecol* 2006;28(suppl):397.
43. DeVore GR et al. *Ultrasound Obstet Gynecol* 2004;24:72–82.
44. Paladini D et al. *Ultrasound Obstet Gynecol* 2006;27:555–61.
45. Abuhamad A. *J Ultrasound Med* 2004;23:573–6.
46. Abuhamad AZ, Falkensammer P. *Ultrasound Obstet Gynecol* 2006;28:359–411.
47. Espinoza J et al. *J Ultrasound Med* 2006;25:947–56.
48. Stoeckl Ch. SonoVCADheart – Sonography-based Volume Computer Aided Display. An automated approach to visualize standard views of the fetal heart. New findings, new visualization planes – Update 2009. GE Healthcare Zipf, Austria. https://www.volusonclub.net/emea/search/An%20automated%20approach%20to%20visualize%20standard%20views%20of%20the%20fetal%20heart.
49. Yeo L, Romero R. *Ultrasound Obstet Gynecol* 2013;42(3):268–84.
50. Vinals F et al. *Ultrasound Obstet Gynecol* 2006;28:26–31.
51. Ghi T et al. *Ultrasound Obstet Gynecol* 2005;26:679–86.
52. Lee W et al. *J Ultrasound Med* 2005;24:201–7.
53. Yagel S et al. *Ultrasound Obstet Gynecol* 2007;29:81–95.
54. Yagel S et al. *Ultrasound Obstet Gynecol* 2005;25(1):97–8.
55. Ruano R et al. *Ultrasound Obstet Gynecol* 2005;25(2):128–33.
56. Sciaky-Tamir Y et al. *Am J Obstet Gynecol* 2006;194(1):274–81.
57. Volpe P et al. *Ultrasound Obstet Gynecol* 2006;28:40–6.
58. Shen O, Yagel S. *Ultrasound Obstet Gynecol* 2010;35(3):260–2.
59. Michailidis GD et al. *Ultrasound Obstet Gynecol* 2001;18(4): 325–8.
60. Chang FM et al. *Ultrasound Obstet Gynecol* 1997;9:42–8.
61. Esh-Broder E et al. *Ultrasound Obstet Gynecol* 2004;23(6): 546–51.
62. Meyer-Wittkopf M et al. *J Ultrasound Med* 2001;20(4):317–27.
63. Tutschek B et al. *J Am Coll Cardiol* 2007;49(suppl A):254A.
64. Light ED et al. *Ultrason Imag* 1998; 20:235.
65. Ota T et al. *Am Heart J* 1999;137:958–66.
66. Shiota T et al. *Circulation* 1998;97:1897–900.
67. Stetten G et al. *J Cardiovasc Diagn Procedures* 1998;15:73–84.
68. Maulik D et al. *Echocardiography* 2003;20:715.
69. Sklansky MS et al. *J Ultrasound Med* 2004;23:283–9.
70. Rusk RA et al. *J Am Soc Echocardiogr* 2000;13:910–7.
71. Donofrio MT et al. *Circulation* 2014;129(21):2183–242.
72. Fogel MA et al. *Fetal Diagn Ther* 2005;20(5):475–80.
73. Lloyd DF et al. *Prenat Diagn* 2016;36(10):916–25.
74. Yamamura J et al. *Eur Radiol* 2009;19(10):2383–90.
75. Jansz MS et al. *Magn Reson Med* 2010;64(5):1304–14.
76. Tutschek B, Schmidt KG. *Ultraschall Med* 2012;33(7):E16–24.
77. Tutschek B, Schmidt KG. *Ultraschall Med* 2012;33(3):236–44.
78. Twining P. *Ultrasound Obstet Gynecol* 1999;13(4):255–9.
79. Pacileo G et al. *Ultrasound Obstet Gynecol* 2000;16(2):128–32.
80. Paladini D et al. *Ultrasound Obstet Gynecol* 2000;16(6):530–5.
81. Tutschek B, Schmidt KG. *Ultrasound Obstet Gynecol* 2004; 24(3):229.
82. Tutschek B et al. *Ultrasound Obstet Gynecol* 2003;21(1):26–32.
83. Rein AJJT et al. *J A Soc Echocard* 2001;14(2):149–51.
84. Rein AJJT et al. *Circulation* 2002;106:1827–33.
85. Di Salvo G et al. *Ultrasound Med Biol* 2005;31(9):1159–62.
86. Stoylen A. 2006. http://folk.ntnu.no/stoylen/strainrate/, accessed June 2007.
87. Thomas JD, Popovic ZB. *JACC* 2006;48:2012–25.
88. Miranda JO et al. *Ultrasound Obstet Gynecol* 2017;49:623–9.
89. Yeh DT et al. *IEEE Trans Ultrason Ferroelect Freq Contr* 2006;5(6):1202–11.
90. Deng J. *Ultrasound Obstet Gynecol* 2003;22:336–44.
91. Heling KS et al. *Ultraschall Med* 2004;25:280–4.
92. Pooh RK. *Ultrasound Obstet Gynecol* 2000;15:163.
93. Riccabona M et al. *J Clin Ultrasound* 1997;25(4):157–67.
94. Messing B et al. *Ultras Obstet Gynecol* 2007;30:142–51.
95. Sklansky MS et al. *J Ultras Med* 1999;18:745–52.
96. Tutschek B et al. *Ultrasound Obstet Gynecol* 2000;16(s1):53–4.
97. Tutschek B, Sahn DJ. *Cardiol Clin* 2007;25:341–55.
98. Acar P et al. *Prenat Diagn* 2005;25:370–5.
99. Harada K. *Int J Cardiol* 1999;71:227–34.
100. Larsen LU et al. *Ultras Obstet Gynecol* 2006;27:210–3.
101. D'hooge J et al. *Eur J Echocardiogr* 2000;1:154–70.

# 6

# Epidemiology of congenital heart disease: Etiology, pathogenesis, and incidence

Julien I.E. Hoffman

## Introduction

Congenital heart disease (CHD), the most serious birth defect, is cardiovascular disease present at birth. Most CHD is due to gross structural developmental cardiovascular anomalies such as septal defects, stenosis or atresia of valves, hypoplasia or absence of one or other ventricle, or abnormal connections between great vessels and the heart. A few children are born with arrhythmias, and some are born with genetic diseases (Marfan syndrome, cardiomyopathy) that usually present later in life. Some genetic defects affect major arteries. Even though asphyxial heart disease is present at birth, it is not included as CHD.

## Incidence of CHD

The incidence of CHD is determined accurately only if ascertainment of the anomalies is complete. Two barriers exist. Some CHD causes death in the first few days after birth. A specific diagnosis might not have been made by the time of death, and without an autopsy examination, the incidence of these serious malformations might be seriously underestimated.[1] Conversely, children with minimal pulmonic stenosis or small atrial or ventricular septal defects might never be included in any cardiologist's practice so that their frequency is also underestimated.

Other factors that influence our estimates of the true incidence of CHD are as follows:

1. Patent ductus arteriosus of prematurity, a maturational disorder rather than a cardiovascular anomaly, is common. An unknown number of these may be included in any collected series, thereby inflating the incidence of the anomaly.
2. A bicuspid aortic valve occurs in approximately 1% of the population.[2] If some patients with this lesion are classified as aortic stenosis, it will alter the apparent incidence of the latter lesion. Alternatively, if subjects with bicuspid valves and small pressure gradients across them are not classified as aortic stenosis, the incidence of aortic stenosis will appear to be smaller than it should be.
3. Atrioventricular septal (atrioventricular canal) defects are more frequent in children with trisomy 21, and trisomy 21 is more frequent in mothers over 35 years old. Therefore, frequency of this lesion in any series depends on how many older mothers there are and on how many pregnancies of fetuses with trisomy 21 are terminated medically.
4. Fetuses with serious CHD were electively terminated in as many as 50% of pregnancies in some series.[3,4]
5. As many as 5% of neonates have tiny muscular ventricular septal defects, about 95% of which close spontaneously within 6–12 months after birth.[5] Therefore, the incidence of ventricular septal defects and of all CHD (because ventricular septal defects are the most common forms of CHD) depends on how many of these trivial defects are included in the series.[6] If they are included, the incidence of CHD might be 5%–6% of all live births. If they are excluded, the incidence drops to about 1% of live births. Over the last 10 years, the incidence of CHD has been rising slowly, not because of a true increase in all congenital heart lesions but because of an increasing number of patients with small ventricular septal defects who are now being diagnosed.[2,7–9]
6. In one study, the investigators did not include mild pulmonic stenosis with systolic gradients across the pulmonary valve less than 25 mm Hg.[10] Some children with mild pulmonic stenosis may be classified as having innocent murmurs.
7. Small atrial septal defects occur in 24%–80% of neonates. Most of these defects close spontaneously within the first year.[11,12]
8. Certain lesions, particularly ventricular septal defects, detected *in utero* have disappeared at the time of birth.

Therefore, it is difficult to assess accurately the incidence of CHD at conception or birth. If we consider only those defects present at 1 year of age or requiring treatment in infancy, the incidence is approximately 12 per thousand live births. A similar number of children have bicuspid aortic valves that usually do not cause problems until later life.[2] The incidence is much higher in fetuses, especially those with chromosomal defects.[13,14]

The incidence of CHD is given in Table 6.1, both as percentages of all CHD and as numbers per million live births.[6]

**Table 6.1** Incidence of CHD in live-born children

| *Anomaly* | *Percentage of all CHD* | *Per million live births* |
|---|---|---|
| Ventricular septal defect* | 32.4 | 2,829 |
| Patent ductus arteriosus | 6.8 | 567 |
| Atrial septal defect | 7.5 | 564 |
| Atrioventricular septal defect | 3.8 | 340 |
| Pulmonic stenosis | 7.0 | 532 |
| Aortic stenosis | 3.9 | 256 |
| Coarctation of the aorta | 4.8 | 356 |
| Transposition of the great arteries | 4.4 | 303 |
| Tetralogy of Fallot | 5.2 | 356 |
| Persistent truncus arteriosus | 1.4 | 94 |
| Hypoplastic left heart | 2.8 | 226 |
| Hypoplastic right heart | 2.2 | 160 |
| Double-inlet left ventricle | 1.5 | 85 |
| Double-outlet right ventricle | 1.8 | 115 |
| Total anomalous pulmonary venous connection | 1.0 | 91 |
| Miscellaneous | 10.1 | |

*Source:* Data about percentages from Hoffman JIE. In: Anderson RH et al., eds. *Paediatric Cardiology*. 2nd ed. London: Churchill Livingstone; 2002:111–39;[50] Data about incidence per million from Hoffman JIE, Kaplan S. *J Am Coll Cardiol* 2002;39:1890–900[6].

*Note:* Numbers are median values.

*Excluding tiny muscular defects that close soon after birth.

A ventricular septal defect is the most frequent form of CHD and is the most frequently observed CHD in subjects with chromosomal and genetic defects. The ventricular septum is formed from multiple portions of the developing heart,[15] so that many different ways of interfering with cardiac development will cause a ventricular septal defect.

## Cardiac development

Cardiovascular development involves complex processes, each of which must occur at the right time under the orchestration of genes and gene products.[16–20] Many are found in chick and mouse heart development, some have been identified in humans, but many are yet to be discovered. In general, the further upstream (closer to initiation of development) a gene is, the more its malfunction will affect major cardiac architecture. There are multiple genes required for cardiogenesis, including GATA4, TBX5, Nkx2.5, Wnt, nodal, lefty, and notch genes that are present in the earliest heart formation.[18,20] Any given cardiac anomaly could result from ineffective expression of one of several genes (Tables 6.2 and 6.3).

The mammalian heart develops from the primary heart tube formed by myocardial and endothelial cells that have differentiated from splanchnic mesoderm and will form the atria and left ventricle. Medial to these cells are myocardial precursors of the secondary heart field that develop the outflow tract and right ventricle[21,22] (Figure 6.1). The two cell populations fuse early in development but remain clonally distinct. Integration of the secondary and primary fields depends in part on cells in the neural crest.[20,23,24] The proepicardial organ provides cells that form the epicardium and the coronary arteries.[17,20]

This fused heart precursor is a straight tube that contains, in sequence from the caudal end, segments that form the atria, left ventricle, right ventricle, and truncus arteriosus. The tube elongates and twists into a d-loop, so that the right ventricle moves to the right of the left ventricle, and the normal cardiac asymmetry is initiated.[15] The earliest asymmetry occurs in Hensen node with unidirectional swirling of the monocilia that dip from the nodal cells into the extracellular embryonic fluid.[25,26] The proteins that drive the cilia-kinesin and dynein are subject to mutations that can alter normal asymmetry. This asymmetrical rotation affects some early expressed genes (*lefty, nodal, fibroblastic growth factor 8, zic3*); faulty expression of these genes produces dextrocardias, l-loops, situs abnormalities (heterotaxies), and complex heart disease.

The future atria are connected to the left ventricle, which is connected to the right ventricle that leads to the truncus arteriosus, the precursor of the aorta and main pulmonary artery. Then the primary atrial and ventricular septa form, and the atrioventricular and semilunar valve rings move to allow the right and left atria to connect to the right and left ventricles, respectively, and the ventricles to communicate with their respective great arteries. Coordinating these changes are genes involved in cell migration and the formation of the extracellular matrix, so that their malfunction produces developmental arrest at a primitive stage such as double-inlet left ventricle, double-outlet right ventricle, and truncus arteriosus. These abnormalities are in part related to abnormal function of the endocardial cushions, and other abnormalities of these cushions lead to the relatively gross distortions of architecture found in atrioventricular septal (endocardial cushion) defects.[16]

## Genetic factors

Genetic abnormalities may be chromosomal rearrangements, copy number variants (CNVs)—microdeletions and microduplications (both of which affect many genes), or isolated point mutations. Epigenetic factors, probably acting via micro-RNA inhibition or DNA methylation, inhibit gene expression. Finally, nonspecific factors and random errors in cell migration produce various defects or influence the severity of others.

### *Chromosomal defects*

These vary from trisomies or monosomies to deletion syndromes and microdeletions that involve contiguous genes. About 0.30%–2.27% (median 0.67%) of live births are associated with chromosomal defects; these are usually the

**Table 6.2** Chromosomal defects and CHD (partial listing)

| *Chromosomal defect* | *Incidence/1,000 live births* | *Percentage with CHD* | *Predominant types of CHD* |
|---|---|---|---|
| **Trisomies** | | | |
| 21 (Down syndrome) | 1–1.5 | 50–60 | AVSD, VSD |
| 18 (Edward syndrome) | 0.2–0.3 | 95 | VSD, PDA, ASD, polyvalvar disease |
| 13 (Patau syndrome) | 0.1–0.2 | 90 | VSD, ASD, PDA, polyvalvar disease |
| 9 | – | 65–80 | VSD, PDA, PA, DORV |
| **Duplications** | | | |
| 3q26-27 duplication (Cornelia de Lange) | – | – | VSD |
| 4p | – | 10–15 | – |
| 5p (Opitz) | – | 10 | – |
| 8 | – | 20 | – |
| 9p | – | Low | – |
| 10q | – | 50 | – |
| 11p | – | Low | VSD |
| 12p (Pallister-Killian; Fryn) | – | 25 | VSD+, coarctation, PDA, ASD, AS, absent pericardium |
| 22p11 (cat eye) | – | 40 | TAPVC, ToF |
| **Monosomy** | | | |
| X (Turner) | 0.1–0.2 | 25–50 | Coarctation of the aorta; aortic stenosis or bicuspid aortic valve; aortic rupture |
| **Deletion syndromes** | | | |
| 4p– (Wolf-Hirshhorn) | – | 50 | ASD |
| 4q– | – | 60 | VSD, PDA, PPS, AS, tricuspid atresia, ASD, coarctation, ToF |
| 5p–(cri-du-chat) | – | 30 | Variable, mainly VSD |
| 7q11.23 (Williams syndrome) | – | 53–85 | Supravalvar AS and PS, PPS |
| 8p | – | 50–75 | AVSD, PS, VSD, ToF |
| 8p21 (CHARGE) | 1/10,000 | – | Conotruncal, arch anomalies |
| 10p | – | 50 | BAV, ASD, VSD, PDA, PS, Coarc |
| 11q23 (Jacobsen) | – | 60 | HLHS, AS, VSD, Coarc, Shone complex |
| 13q– | – | 50 | VSD |
| 18p– | – | 10 | |
| 18q– | – | Low | VSD |
| JAG1, NOTCH2 on 20p12- (Alagille) | – | High | PPS, PS, TOF |
| **Microdeletion syndromes** | | | |
| 22q11 (DiGeorge: CATCH-22); Shprintzen (velo-cardio-facial) | – | – | Aortic arch anomalies 24%<br>IAA- 50%–89%<br>TA- 34%–41%<br>Tetralogy of Fallot 8%–35%<br>some VSD (3% isolated, 45% with arch anomaly) |
| *CLIP2*, *ELN*, *GTF2I*, *GTF2IRD1*, and *LIMK1 on ch* 7q11.23 (Williams) | – | High | Supravalvar AS, PPS, |
| 16p13.3 (Rubinstein-Taybi) | – | 25 | PDA, VSD, ASD |
| 5.15.2 Cri-du-Chat | – | 10%–55% | VSD, PDA, ASD, ToF |

*Source:* Based on Burn J, Goodship J. In: Emery AE, Rimoin DL, eds. *Principles and Practice of Medical Genetics*. Edinburgh: Churchill Livingstone; 1997:767–828;[51] Richards AA, Garg V. *Curr Cardiol Rev* 2010;6:91–7;[19] Pierpont ME. et al. *Circulation* 2007;115:3015–38;[28] and Greenwood RD. *Clin Pediatr (Phila)* 1984;23:145–51.[40]

*Note:* Other CNV syndromes in Table 6.2 of Fahed AC. et al. *Circ Res* 2013;112:707–20.[34]

*Abbreviations:* AS, aortic stenosis; ASD, atrial septal defect (secundum); AVSD, atrioventricular septal defect (endocardial cushion defect); BAV, bicuspid aortic valve; coarc, coarctation of the aorta; DILV, double-inlet left ventricle; DORV, double-outlet right ventricle; d-TGA, transposition of the great arteries; HLHS, hypoplastic left heart syndrome; HRHS, hypoplastic right heart syndrome; IAA, interrupted aortic arch; PAPVC, partial anomalous pulmonary venous connection; PDA, patent ductus arteriosus; PS, pulmonic stenosis (valvar); PPS, peripheral pulmonic stenosis; TA, truncus arteriosus; TAPVC, total anomalous pulmonary venous connection; ToF, tetralogy of Fallot; VSD, ventricular septal defect.

**Table 6.3** CHD caused by gene mutations (syndromic and nonsyndromic)

| *Syndrome* | *Chromosome (ch) or gene* | *Percent with CHD* | *CHD* |
|---|---|---|---|
| Noonan | PTPN11 on 12q24, 12p12.1 also SOS1, KRAS, etc. | 80 | Pulmonic stenosis; hypertrophic cardiomyopathy |
| Apert | 10q26 | – | VSD, coarctation of aorta, PS |
| Holt-Oram | TBX5 transcription factor 12q24.1 | 75–100 | ASD+, VSD, AVSD, truncus arteriosus, anomalies of radius |
| Ellis-van Creveld | EVC or EVC2 on 4p16 | >50 | Single atrium, AVSD, polydactyly |
| Marfan | FBN1 on 15q21 | High | Dilatation and rupture of aorta; aortic or mitral regurgitation |
| Ehlers-Danlos type IV | COL3A1 on 2q31-32.3 | High | Arterial rupture |
| Loeys-Dietz | SMAD3 on 15q22.33, TGFβ2 on 1q.41, TGFβR1 on 9q22, TGFβR2 on 3p22 | High | Arterial aneurysms and dissection |
| Osteogenesis imperfecta | COL1A on 17q21.33, COL1A2 on 7q22.1, CRTAP on 3p22.3, P3H1 on 1p34.1 | Low | Aortic root dilatation, aortic or mitral incompetence |
| Pseudoxanthoma elasticum | ABCC6 on 16p3.1 | High | Mitral valve prolapse, coronary arterial disease, restrictive cardiomyopathy |
| Mucopolysaccharidoses | **I**-IDUA on 4p16.3; **II**-DS on Xq28; **III**-GNS on 12q14, HGSNAT on 8p11.1, NAGLU on 17q21, SGSH on 17q25.3; **IV**-GLB1 on 3p21.33; **V**-IDUA on 4p16.3; **VI**-ARSB on 5p14.1; **VII**-GUSB on 7q21.11 | >50% | Aortic or mitral incompetence; coronary artery narrowing |
| Hypertrophic cardiomyopathy | MYH7 on 14q12,<br>MYBPC3 on 11p11.2,<br>TNNT2 on 1q32,<br>TNNI3 on 19q13.4<br>and genes on<br>2q24.3, 3p, 3p25, 7q31, 12q23-24, 15q14, 15q22.1, 20q13.3 | High | Asymmetric ventricular hypertrophy due to mutations in sarcomeric proteins: myosin heavy and light chains, actin, tropomyosin, titin, troponin, caveolin, and myosin binding protein C |
| Dilated cardiomyopathy | Xp21.2, Xq28, 1q21, 1q32, 1q42-43, 2q31, 2q35, 5q33, 6q22.1, 10q212.3-q23.2, 10q22-q23, 11p11, 11p15.1, 14q12, 15q14, 15q22 | – | Dilated (congestive) cardiomyopathy due mainly to abnormal cytoskeletal but also sarcomeric proteins: dystrophin, tafazzin, lamin A/C, cardiac troponin T, α-actinin, titin, desmin, δ-sarcoglycan, phospholamban, metavinculin, myosin binding protein C, muscle LIM protein, β-myosin heavy chain, cardiac actin, α-tropomyosin |
| Noncompaction of left ventricle | Xq28, 18q12.1-12.2, 11p15 | High | Cardiomyopathy |
| Osler-Rendu-Weber | 9q34.1; also 5q31.3, 12q11 | High | Pulmonary arteriovenous fistulae |
| Long QT | QT1-11p15.5, QT2-12p11.1, QT3-3p21, QT4-4q25-27, QT5-21q22.1, QT6-21q22.1 | High | Long QT interval, arrhythmias, sudden death |
| CHARGE syndrome | CHD7; SEMA3E on 8p21<br>7q21.11 | – | VSD, ToF |
| Williams syndrome | 7q11.23 | 50%–85% | Supravalvar AS, ps, PPS |

(*Continued*)

**Table 6.3 (Continued)** CHD caused by gene mutations (syndromic and nonsyndromic)

| *Syndrome* | *Chromosome (ch) or gene* | *Percent with CHD* | *CHD* |
|---|---|---|---|
| Heterotaxy | ZIC3, CFC1 | >75% | DILV, DORV, d-TGA, AVSD, VSD, ASD, PS |
| | NKX2.5 | ? high | ASD, AVSD, ToF, AV block, DORV, HLHS, coarc, IAA; tricuspid valve abnormalities, TGA, Ebstein |
| | GATA4 | – | ASD, VSD, AVSD, ToF, HRHS, PAPVC |
| | MYH6 | – | ASD, HCM |
| | CRELD1, ALK2 | – | AVSD |
| | NOTCH1 | – | BAV, early calcification |
| | PROSIT-240 | – | d-TGA |

*Source:* Based on data from Burn J. In: Anderson RH et al., eds. *Paediatric Cardiology*. 1. London: Churchill Livingstone; 2002;141–213;[32] Ackerman MJ. *J Electrocardiol* 2004;37(suppl):1–6;[52] Jefferies JL, Towbin JA. *Lancet* 2010;375:752–62;[35] and Online Mendelian Inheritance in Man (OMIM). A knowledgebase of human genes and genetic disorders. omim.org.[33]

*Abbreviations:* AS, aortic stenosis; ASD, atrial septal defect (secundum); AV, atrio-ventricular; AVSD, atrioventricular septal defect (endocardial cushion defect); BAV, bicuspid aortic valve; coarc, coarctation of the aorta; DILV, double-inlet left ventricle; DORV, double-outlet right ventricle; d-TGA, transposition of the great arteries; HCM, hypertrophic cardiomyopathy; HLHS, hypoplastic left heart syndrome; HRHS, hypoplastic right heart syndrome; IAA, interrupted aortic arch; PAPVC, partial anomalous pulmonary venous connection; PDA, patent ductus arteriosus; PS, pulmonic stenosis (valvar); PPS, peripheral pulmonic stenosis; TA, truncus arteriosus; TAPVC, total anomalous pulmonary venous connection; ToF, tetralogy of Fallot; VSD, ventricular septal defect.

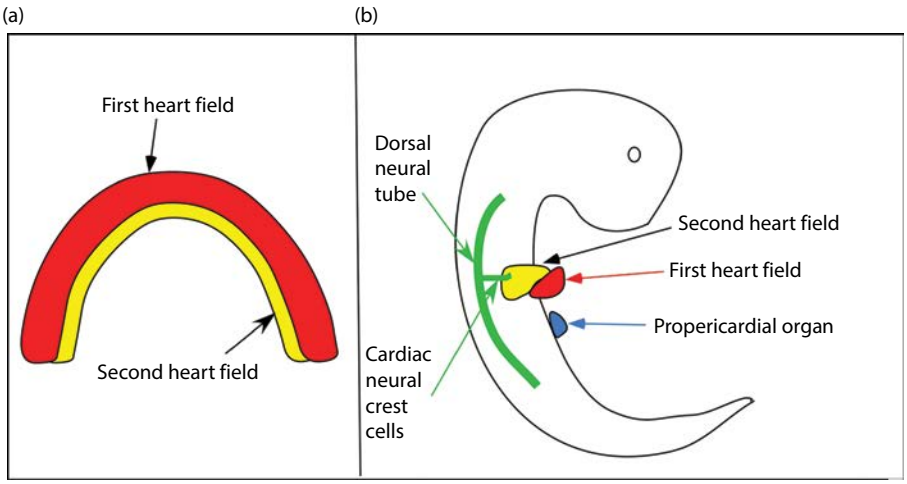


**Figure 6.1**
(a) Primitive first and second heart fields. (b) Later stage showing neural crest contributions to second heart field.

aneuploidies (trisomy 21, 18, and 13) and the sex polysomies (e.g., XXX and XYY) that increase with maternal age, and monosomy X that is inversely related to maternal age[13] (Table 6.2). Infants with these abnormalities are survivors of a much larger cohort of fetuses with chromosomal defects. In first trimester fetuses aborted for nonmedical reasons, 2.6%–6.4% (median 4.5%) have chromosomal defects, so that only about 15% of fetuses with chromosomal defects survive to birth. Among spontaneous abortions, the incidence of chromosomal abnormalities is 15.7%–69.8% (median 46.6%). The chances of survival to birth depend on the defect. It is about 1% for trisomy 21, 18, and 13, and for X monosomy, but as high as 80% for the sex polysomies[13] (Table 6.2). Sex polysomies do not have an increased incidence of CHD except that approximately 50% of subjects with Klinefelter syndrome (49XXXXY type) have a patent ductus arteriosus or atrial septal defect.[27,28] The percentage of aborted fetuses with chromosomal anomalies is greatest in the youngest fetuses, and decreases to 6%–15.9% (median 11.7%) beyond 20 weeks' gestational age. Therefore, the earlier the echocardiographic study, the greater is the chance of finding a chromosomal abnormality in a fetus with CHD.

Because most chromosomal defects have a very high association with CHD (Table 6.2), the incidence of CHD in general depends on how many fetuses are conceived by older mothers and how many affected fetuses reach term alive. As a group, chromosomal defects account for about 6% of all CHD in live-born infants,[29] but this figure could change depending

on increased survival of the affected fetuses or the frequency of therapeutic abortion.

## Genetic abnormalities

Single gene defects are common and account for approximately 3% of all CHD. Some gene mutations cause defects in more than one organ system and produce recognizable syndromes. These genes are probably general or "upstream" and function early in development to affect several systems. The Holt-Oram syndrome, due to mutations in the Tbx5 transcription factor,[30] is associated with septal defects, hypoplastic left heart syndrome, and abnormalities of the radius or thumb. The Noonan syndrome, about half due to mutation of the PDPN11 gene on chromosome 12,[31] shows characteristic body habitus and facies, dysplastic pulmonary valves, and hypertrophic cardiomyopathy. Some of the better-known genetic syndromes with CHD are listed in Table 6.3; more detailed lists are available.[32,33] Other genes, however, are specific or "downstream" and function later in development to affect only one organ or part of one organ. Many gene mutations have been found in CHD, usually not as part of a general syndrome. None of these genetic defects are frequent. In development of any part of the cardiovascular system, there is usually a cascade of genes and gene products involved, and mutation in any of the members of the cascade would cause a specific cardiac defect; multiple genotypic abnormalities may converge on a similar phenotype. In addition, some genes modify mutations in other genes, with subtle differences in timing or level of expression that will influence the phenotype. CNVs that involve many genes account for more congenital heart disease.[34]

About 30%–50% of dilated cardiomyopathies are familial and genetically determined,[35] and most hypertrophic cardiomyopathies are due to isolated gene mutations[36] (Table 6.3). Although most cardiomyopathies do not present in the fetus or the neonate, they do have a genetic origin. This is also true for certain arrhythmias such as the long QT and Brugada syndromes,[37,38] and those associated with arrhythmogenic right ventricular dysplasia.[39] A normal echocardiogram in the face of an abnormal family history of one of these diseases does not exclude the genetic defect.

Patients with one congenital abnormality often have abnormalities of other systems.[40] For example, abnormalities of the genitourinary tract occur in about 30% of patients with congenital heart disease, and patients with tetralogy of Fallot often have omphaloceles.[40–42] Neurodevelopmental abnormalities occur in approximately 40%.

These are not usually regarded as syndromes, and it is not clear if these associations stem from a common genetic origin or from some other disturbance during fetal development.

The concept of multifactorial inheritance in CHD[43] and cardiovascular disease in general[44] is that certain lesions may be due to the interaction of several genes (polygenic inheritance), the outcome being modulated by environmental factors. This could explain why CHD could be genetically caused without manifesting classical Mendelian genetic frequencies. For example, if one parent (especially the mother) has CHD, there is increased risk of 5%–10% for CHD in the children, unlike the 50% risk found for autosomal dominant disease or the 25% risk associated with recessive disease. Criteria needed to indicate a multifactorial model have been described by Burn.[32] Recurrence risk to siblings and offspring is approximately the square root of the population incidence. The risk to siblings is comparable to the risk to offspring.

The only CHD that fits the multifactorial model is the patent ductus arteriosus (Zetterqvist, cited by Burn[32]). If so, then how do we explain the other forms of CHD? One possible answer lies in experiments reported by Kurnit and colleagues.[45] During endocardial cushion development, cell adhesion molecules such as platelet endothelial cell adhesion molecules are downregulated when endocardial cells undergo mesenchymal transformation. The quintessential lesion related to endocardial cushion defects, the atrioventricular septal defect, is particularly common in trisomy 21. In trisomy 21, fibroblasts cultured from the lung have abnormally increased adhesiveness. Kurnit and colleagues developed a computer model of embryological development in which they programmed differing degrees of adhesiveness, random migration, and certain rules for when migration and cell division would cease. With normal cell adhesiveness, the atrioventricular canal region developed normally in their model. With abnormally increased adhesiveness, some but not all of the atrioventricular canals were abnormally formed, just as in an atrioventricular canal defect. Therefore, the abnormality produced in their model was *due* to abnormal adhesiveness, but its expression depended in part on random events in cell migration. Thus, failure to fit classical Mendelian genetics is not an argument against a genetic cause of CHD.

## Environmental factors

CHD has been associated with environmental toxic or infectious factors[46] (Table 6.4). We do not know if these act by affecting gene expression directly or by blocking the action of the gene product. None of them are known to affect the genome itself. Phenylketonuria, a genetic defect itself, affects the fetus through the increased maternal blood levels of phenylalanine and phenylpyruvic acid. In addition, taking folic acid during pregnancy might reduce the incidence of congenital heart disease.[46]

A link between environmental and genetic events occurs with retinoic acid and its metabolites. The development of the aorticopulmonary and truncal septa depends on the migration into the embryonic heart of cells from the cranial neural crest.[21] If these cells are removed experimentally, there is a high incidence of conotruncal defects such as ventricular septal defects, double-outlet right ventricles, and truncus arteriosus. Because these neural crest cells also aid in the formation of the pharyngeal arches and pouches (from which the thymus and parathyroid glands are derived) and the aortic arches, this may explain why

**Table 6.4** Environmental causes of CHD

| *Environmental factor* | *CHD* | *Percentage (%) frequency of CHD* |
|---|---|---|
| Rubella virus | PDA, PPS, PS, ASD, VSD | >35 |
| Mumps | Endocardial fibroelastosis | – |
| Lithium | Mitral and tricuspid incompetence, Ebstein syndrome, ASD | – |
| Diabetes in pregnancy | Outflow tract lesions, especially TGA, coarctation of the aorta; d-TGA | 3–5 |
| Alcohol | VSD, ASD, ToF | 25–70 |
| Retinoic acid | Cono-truncal anomalies | – |
| Phenylketonuria | ToF, VSD, coarctation, PDA, SV, ASD | 25–50 |
| Trimethadione | TGA, ToF, HLH | 15–30 |
| Phenytoin | PS, AS, PDA, coarctation of the aorta | 2–3 |
| Systemic lupus erythematosus | Complete heart block | 20–40 |
| Coumadin | PDA, PPS | – |
| Thalidomide | Truncus arteriosus, ToF, septal defects, coarctation, PS, TGA, TAPVC | 5–10 |

*Source:* Data taken from Jackson BT. *N Engl J Med* 1968;279:80–9 concl.;[53] Michels VV, Riccardi VM. In: Emery AE, Rimoin DL, eds. *Principles and Practice of Medical Genetics*. Edinburgh: Churchill Livingstone; 1990:1207–37;[54] Burn J. In: Anderson RH et al., eds. *Paediatric Cardiology*. 1. London: Churchill Livingstone; 2002:141–213;[32] and Jenkins KJ. et al. *Circulation* 2007;115:2995–3014.[46]

*Abbreviations:* AS, aortic stenosis; ASD, atrial septal defect (secundum); AVSD, atrioventricular septal defect (endocardial cushion or atrioventricular canal defect); DA, patent ductus arteriosus; HLH, hypoplastic left heart syndrome; PDA, patent ductus arteriosus; PPS, peripheral pulmonic stenosis; PS, pulmonic stenosis (valvar); SV, single ventricle; TAPVC, total anomalous pulmonary venous connection; TGA, complete transposition of the great arteries; ToF, tetralogy of Fallot; VSD, ventricular septal defect.

aortic arch anomalies and truncus arteriosus are so frequently associated with the DiGeorge (CATCH 22) syndrome.[47] Certain chemicals are now known to interfere with migration of these neural crest cells. Thus, giving bis-diamine, isotretoin, or all-*trans*-retinoic acid produces lesions resembling those found in Kirby's experiments.[48] It is thus possible that some outflow tract lesions might be due either to genetically or to environmentally determined defects of neural crest cell migration.

## Conclusions

Worldwide, CHD occurs in about 1,500,000 live births annually.[49] Today, most subjects with CHD survive to become adults and to raise their own families. This progress comes at considerable economic cost; furthermore, CHD remains a major cause of morbidity and premature death, and is often a barrier to employment. Because the children of these parents have an increased incidence of CHD, the total incidence of CHD is likely to increase slowly, generation by generation.

## Acknowledgments

I thank Dr. Harold Bernstein and Dr. James Bristow for valuable advice and criticism.

## References

1. Abu-Harb M et al. *Arch Dis Child* 1994;71:3–7.
2. Hoffman JI et al. *Am Heart J* 2004;147:425–39.
3. Allan LD et al. *J Am Coll Cardiol* 1994;23:1452–8.
4. Daubeney PE et al. *Circulation* 1998;98:562–6.
5. Roguin N et al. *J Am Coll Cardiol* 1995;26:1545–8.
6. Hoffman JIE, Kaplan S. *J Am Coll Cardiol* 2002;39:1890–900.
7. Fixler DE et al. *Circulation* 1990;81:137–42.
8. Meberg A et al. *Tidsskr Nor Laegeforen* 1990;110:354–7.
9. Spooner EW et al. *Teratology* 1988;37:21–8.
10. Bound JP, Logan WF. *Br Heart J* 1977;39:445–50.
11. Fukazawa M et al. *Am Heart J* 1988;116:123–7.
12. Senocak F et al. *Int J Cardiol* 1996;53:221–6.
13. Hoffman JI. *Pediatr Cardiol* 1995;16:155–65.
14. Wren C. The epidemiology of cardiovascular malformations. In: Moller JH, Hoffman JIE, Benson DW, van Hare GF, Wren C, eds. *Pediatric Cardiovascular Medicine*. Oxford, England: Wiley-Blackwell; 2012:268–75.
15. Harvey RP, Rosenthal N. *Heart Development*. San Diego, CA: Academic Press; 1999.
16. Bruneau BG. *Nature* 2008;451:943–8.
17. Kodo K, Yamagishi H. *Circ J* 2011;75:2296–304.
18. McCulley DJ, Black BL. *Curr Top Dev Biol* 2012;100:253–77.
19. Richards AA, Garg V. *Curr Cardiol Rev* 2010;6:91–7.
20. Vincent SD, Buckingham ME. *Curr Top Dev Biol* 2010;90:1–41.
21. Kelly RG. *Trends Cardiovasc Med* 2005;15:51–6.
22. Zaffran S et al. *Circ Res* 2004;95:261–8.

23. Kirby ML. Contribution of neural crest to heart and vessel morphology. In: Harvey RP, Rosenthal N, eds. *Heart Development*. San Diego, CA: Academic Press; 1999:1179–93.
24. Waldo KL et al. *Dev Biol* 2005;281:66–77.
25. McGrath J et al. *Cell* 2003;114:61–73.
26. Schneider H, Brueckner M. *Am J Genet (Sem Med Genet)* 2000;97:258–70.
27. Visootsak J et al. *Clin Pediatr (Phila)* 2001;40:639–51.
28. Pierpont ME et al. *Circulation* 2007;115:3015–38.
29. Greenwood RD et al. *Pediatrics* 1975;55:485–92.
30. Bruneau BG et al. *Dev Biol* 1999;211:100–8.
31. Jongmans M et al. *Am J Med Genet A* 2005;134:165–70.
32. Burn J. The aetiology of congenital heart disease. In: Anderson RH, Baker EJ, Macartney FJ, Rigby ML, Shinebourne EA, Tynan M, eds. *Paediatric Cardiology*. 1. London: Churchill Livingstone; 2002:141–213.
33. Online Mendelian Inheritance in Man (OMIM). omim.org.
34. Fahed AC et al. *Circ Res* 2013;112:707–20.
35. Jefferies JL, Towbin JA. *Lancet* 2010;375:752–62.
36. Maron BJ et al. *J Am Coll Cardiol* 2012;60:705–15.
37. Antzelevitch C. *J Electrocardiol* 2001;34(suppl):177–81.
38. Morita H et al. *Lancet* 2008;372:750–63.
39. Iyer VR, Chin AJ. *Am J Med Genet C Sem Med Genet* 2013;163C:185–97.
40. Greenwood RD. *Clin Pediatr (Phila)* 1984;23:145–51.
41. Kramer HH et al. *Am J Dis Child* 1987;141:789–95.
42. Zahka KJ. Associated abnormalities in children with congenital heart disease. In: Emmanouilides GC, Riemenschneider TA, Allen HD, Gutgesell HP, eds. *Heart Disease in Infants, Children and Adolescents, Including the Fetus and Young Adult*. 1. 5th ed. Baltimore, MD: Williams and Wilkins; 1989:614–28.
43. Nora JJ. *Circulation* 1968;38:604–17.
44. van Asselt KM et al. *Circulation* 2006;113:1136–9.
45. Kurnit DM et al. *Am J Hum Genet* 1987;41:979–95.
46. Jenkins KJ et al. *Circulation* 2007;115:2995–3014.
47. Hong R. *Clin Rev Allergy Immunol* 2001;20:43–60.
48. Lammer EJ et al. *N Engl J Med* 1985;313:837–41.
49. Hoffman JIE. *Cardiol Young* 1994;4:208–23.
50. Hoffman JIE. Incidence, mortality, and natural history. In: Anderson RH, Baker EJ, Macartney FJ, Rigby ML, Shinebourne EA, Tynan M, eds. *Paediatric Cardiology*. 2nd ed. London: Churchill Livingstone; 2002:111–39.
51. Burn J, Goodship J. Congenital heart disease. In: Emery AE, Rimoin DL, eds. *Principles and Practice of Medical Genetics*. Edinburgh: Churchill Livingstone; 1997:767–828.
52. Ackerman MJ. *J Electrocardiol* 2004;37(suppl):1–6.
53. Jackson BT. *N Engl J Med* 1968;279:80–9 concl.
54. Michels VV, Riccardi VM. Congenital heart defects. In: Emery AE, Rimoin DL, eds. *Principles and Practice of Medical Genetics*. Edinburgh: Churchill Livingstone; 1990:1207–37.

# 7

# Indications for fetal echocardiography: Screening in low- and high-risk populations

Anita J. Moon-Grady, Mary T. Donofrio, Sarah M. Cohen, and Simcha Yagel

## Introduction

The incidence of congenital heart disease (CHD) has been estimated at 6–12 per 1,000 live births depending on the population studied and the time of ascertainment.[1–4] If bicuspid aortic valve and small septal defects are included, this figure becomes much higher, with estimations between 20 and 50 per 1,000 live births.[5] Though several studies have evaluated the incidence of serious CHD in live-born infants and estimated it to be on the order of 3–4 per 1,000 births,[2,6] data from nonselected populations in fetuses are less forthcoming. A Belgian study[6] reported an incidence of 8.3% in euploid live-born and stillborn infants of 26 or more weeks' gestation, and a study from Norway[3] reported an incidence of 3.3% in a population-based sample. Of note is that an even higher incidence is expected in fetuses evaluated at an earlier gestation given spontaneous and intentional pregnancy termination in the presence of serious defects.

The difficulty in ascertaining the degree to which specific maternal or fetal factors may confer an increased risk becomes evident given that the incidence varies depending on the population studied as highlighted above. Regardless of these issues, there are some valid, established maternal and fetal risk factors that portend CHD, as will be detailed in this chapter. The reality of clinical practice, however, is that the majority of new cases of CHD are diagnosed in low-risk women. For this reason, obstetric scanning of the fetal heart, which is usually performed as part of the midgestation scan of fetal anatomy, should be a detailed screening examination with a goal to detect serious CHD. Strategies to improve detection rates of CHD during screening examination will facilitate identification of abnormal findings and prompt referral for a comprehensive fetal echocardiogram, either in the same center or in a specialized facility. Concern or suspicion for fetal CHD during screening is therefore an important indication for fetal echocardiogram referral, and for this reason, this chapter summarizes the fetal cardiac assessment at the time of obstetric screening with subsequent discussion related to additional aspects of risk and triggers for higher levels of evaluation.

Guidelines for the elements needed for fetal heart screening[7–13] differ depending on the source. The application of color and pulse wave Doppler modalities, functional evaluation to assess the severity of cardiac lesions, and their prognosis are among the parameters available in referral examinations but not required at the screening level. Nevertheless, as there is agreement that the majority of CHD cases will occur in women without recognized risk criteria, the importance of proficient fetal heart scanning at the time of midtrimester anatomy scanning cannot be overemphasized. Obstetric fetal anomaly screening is a window of opportunity to identify nominally low-risk women carrying a fetus with CHD.

## Screening for congenital heart disease: The obstetric screening examination of the fetal heart

Fetal heart screening varies in different health systems based on local recommendations for prenatal screening including timing and requirements, the availability of providers, as well as other factors. In some areas and dependent on individual providers, fetal heart screening may include only limited views, whereas in other practices the fetal heart screening examination is much more comprehensive and includes most or all elements of a complete fetal echocardiogram. In practice, obstetric fetal heart screening and fetal echocardiography probably represent a continuum, rather than being mutually exclusive. According to current practice guidelines, the fetal heart screening examination[8,9] should include the four-chamber view as well as the left and right ventricular outflow tracts views (LVOT, RVOT); the three vessel and trachea (3VT) view should also be visualized.[14] These views can be obtained by sweeping the transducer cephalad visualizing first the four-chamber view, then continuing to the LVOT, RVOT, and 3VT, as shown in the five planes approach (Figure 7.1).[8,15] This approach to fetal heart screening has been adopted by several organizations[7–12] given that the streamlined methodology can be integrated easily into the routine

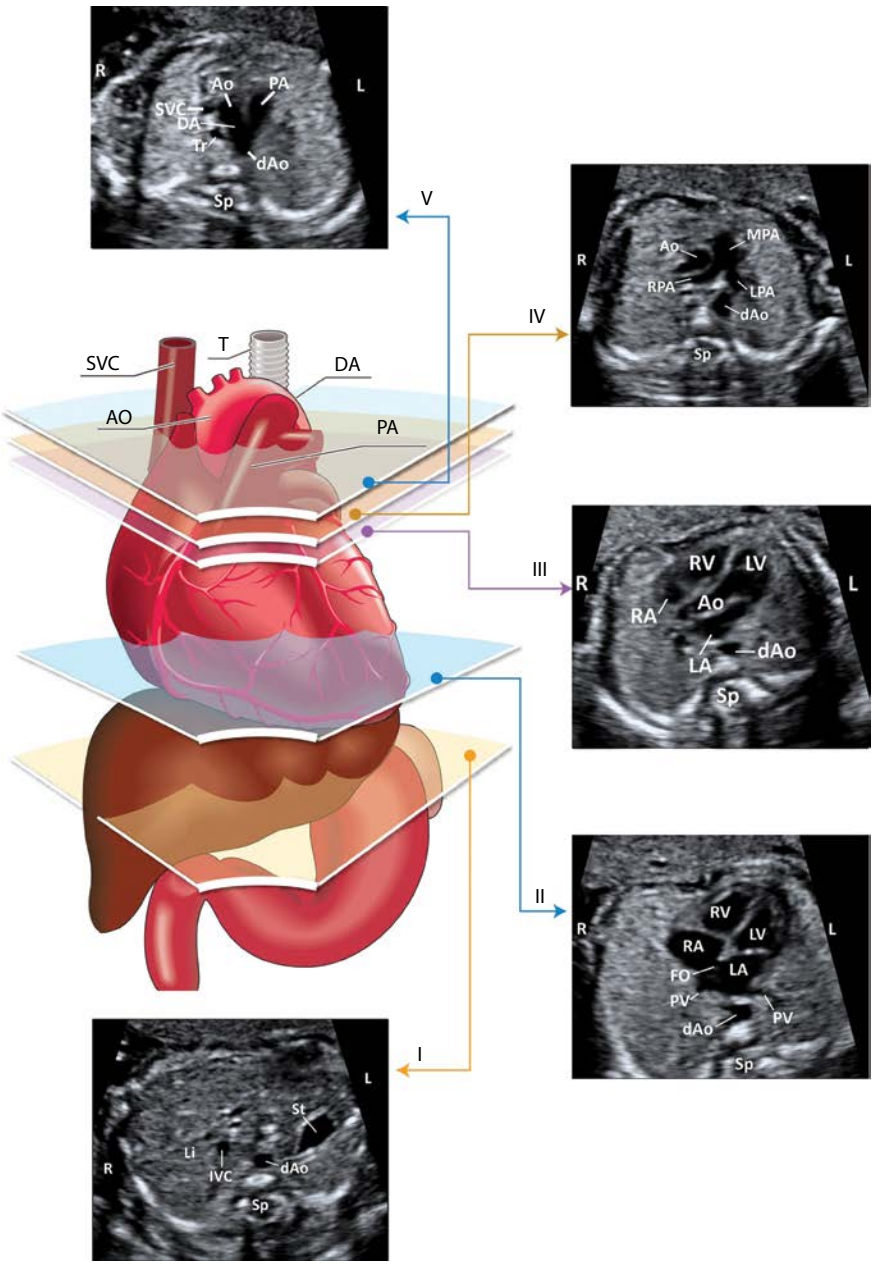


**Figure 7.1**
The five axial views for optimal fetal heart screening. The color image shows the trachea (Tr), heart and great vessels, liver, and stomach, with the five planes of insonation indicated by polygons corresponding to the grayscale images, as indicated. (I) Most caudal plane, showing the fetal stomach (St), cross section of the descending aorta (dAo), spine (Sp), and liver (Li). (II) Four-chamber view of the fetal heart, showing the right and left ventricles (RV, LV) and atria (RA, LA), foramen ovale (FO), and pulmonary veins (PV) to the right and left of the dAo. (III) Left ventricular outflow tract view, showing the aortic root (Ao), LV, RV, LA, and RA and a cross section of the dAo. (IV) Slightly more cephalad view (right ventricular outflow tract view) showing the main pulmonary artery (MPA) and the bifurcation into the right (RPA) and left (LPA) pulmonary arteries and cross sections of the ascending aorta (Ao) and dAo aorta. (V) Three vessels and trachea view showing the superior vena cava (SVC), pulmonary artery (PA), ductus arteriosus (DA), transverse aortic arch (from proximal Ao to dAo), and trachea (Tr). IVC, inferior vena cava; L, left; R, right. (For full details please see Chapter 12, Videos 12.1–12.9.) (Modified with permission from Yagel S et al. *Ultrasound Obstet Gynecol* 2001;17(5):367–9[15], as appeared in International Society of Ultrasound in Obstetrics and Gynecology, Carvalho JS et al. *Ultrasound Obstet Gynecol* 2013;41(3):348–59.[8])

obstetric anatomy scan. Recent reviews of the effectiveness of fetal heart screening have shown that protocols that mirror the five planes approach by including the four-chamber view, outflow tracts views, and 3VT view have the highest sensitivity and specificity to detect CHD.[16,17] This approach was shown to achieve higher sensitivity for detection than those obtained in studies applying the four-chamber view alone or with only the outflow tracts or only the 3VT view.

The establishment of abdominal situs and cardiac position should be the first step in evaluation of the fetal cardiovascular

system, noting in normal fetuses the stomach and heart are oriented on the fetal left. The heart should occupy about one-third of the area of the thorax, and there should be no hypertrophy or pericardial effusion, though a slight hypoechoic appearance around the heart, if an isolated finding, can be a normal variant.[18,19] The cardiac axis is normally oriented approximately 45° (±20°) toward the fetal left. Deviation in cardiac situs, axis, or position requires evaluation for situs abnormalities and structural or chromosomal anomalies (Figure 7.2). In addition, a shift in cardiac position can be indicative of space-occupying lesions or diaphragmatic hernia.

The mainstay of the fetal heart screening examination traditionally has been visualization of the four-chamber view[11,20–22] (Figure 7.1, Plane II). What is important to note is that seeing the four-chamber view does not imply merely counting four cardiac chambers. Examination of this plane through the heart should include a general overview of the heart size and position and evaluation of the chambers and valve anatomy and function, as well as an assessment of heart rate and rhythm.

The cardiac atria should be approximately equal in size, and the foramen ovale flap should be observed opening toward the left atrium. Atrial septum primum should be visualized. In most cases, the pulmonary veins can be seen at their entry into the left atrium. Failure to demonstrate normal atrial configuration, or presence of a structure posterior to the left atrium other than the normal descending aorta, should raise suspicion for anomalous pulmonary venous connection and prompt further evaluation.

The ventricles are also approximately equal in size, with the morphological right ventricle distinguished by the characteristic moderator band at the apex. While some disparity in ventricle size may be normal, particularly in late gestation, marked difference in size should raise suspicion of CHD, for example, such defects as hypoplastic left heart or coarctation of the aorta. The ventricular septum should be visualized intact from the apex to the crux, and no cardiac wall or septal hypertrophy should be present. Both atrioventricular valves should be seen to open and move freely, with the tricuspid valve leaflet insertion into the ventricular septum found somewhat closer to the cardiac apex than that of the mitral valve (Figure 7.3).

The utility of adding the outflow tracts to fetal heart screening is well established in the literature[23–30] and supported by international guidelines[8,9,11] to increase anomaly detection,[23,25,31–33] particularly in those cases that may present with a normal-appearing four-chamber view, such as tetralogy of Fallot, transposition of the great arteries, or double-outlet right ventricle. The outflow tracts are imaged by sweeping the transducer cephalad from the four-chamber view.[15] The aorta should be seen originating from the morphologic left ventricle when imaging the LVOT. The aortic valve leaflets should move freely and not appear thickened. The anterior aortic wall should be observed in continuity to the ventricular septum. This continuity is important to exclude the overriding aorta of tetralogy of Fallot (Figure 7.4) as well as other conotruncal anomalies. The RVOT is the next sequential plane, imaged just cephalad to the LVOT. In this plane, the pulmonary artery (PA) is seen originating from the morphologic right ventricle. The bifurcation to right and left pulmonary arteries is usually observed, lying left of the aorta and superior vena cava and anterior to the descending aorta (DAo), the latter

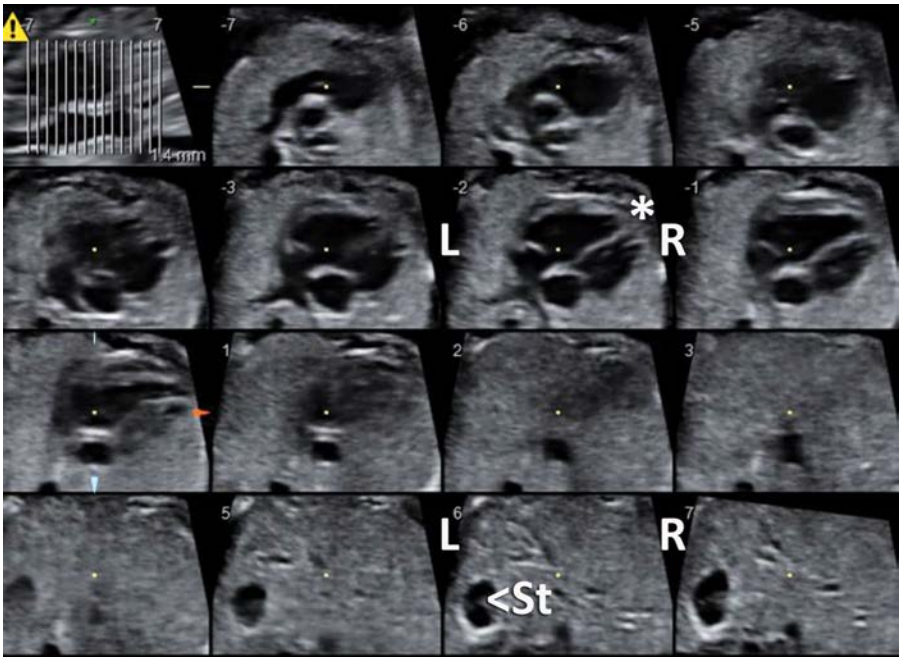


**Figure 7.2**
A case of dextrocardia rendered in tomographic ultrasound imaging (TUI). While this modality is not necessary for screening, the figure demonstrates the importance of the abdominal plane (Plane I in Figure 7.1) to orient directionality in the exam and establish normal situs (bottom row of the TUI matrix) stomach (St) is on the left. Second row from the top shows the heart in four-chamber view, with the cardiac axis (*) oriented toward the fetal right (Video 7.1).

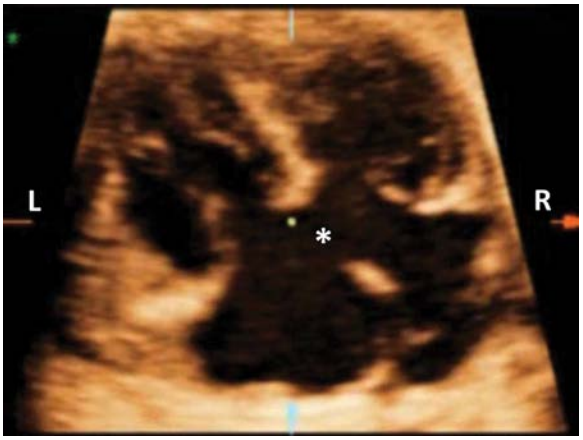


**Figure 7.3**
A case of atrioventricular canal defect (AV-Canal) seen in the four-chamber view. Compare Figure 7.1, Plane II, the four-chamber view plane: the valve leaflets and septa are markedly malformed. *The crux is missing (Video 7.2).

seen in cross section. Angling the transducer just slightly more cephalad reveals the ductus arteriosus coursing toward the DAo. The pulmonary valve should be visualized moving freely, with no apparent thickening. In lesions such as transposition of the great arteries, the configuration of the ventricles and great vessels is abnormal (Figure 7.5).

The 3VT view is visualized just cephalad to the RVOT, revealing the ductal and aortic arches in a V-shaped configuration, anterior and to the left of the trachea and SVC. The trachea appears as a small echogenic ring surrounding a small hypoechoic space. The SVC can be seen in cross section. The 3VT plane demonstrates vessel size, number, arrangement, and alignment relative to each other and to the trachea.[14] This view is useful to confirm or exclude anomalies,[34–36] such as persistent left superior vena cava, coarctation of the aorta, right or double aortic arch, and interrupted aortic arch (Figure 7.6).

The normal fetal heart rate is 120–160 beats/min. Mild transient bradycardia (<110 bpm) is not usually a cause for

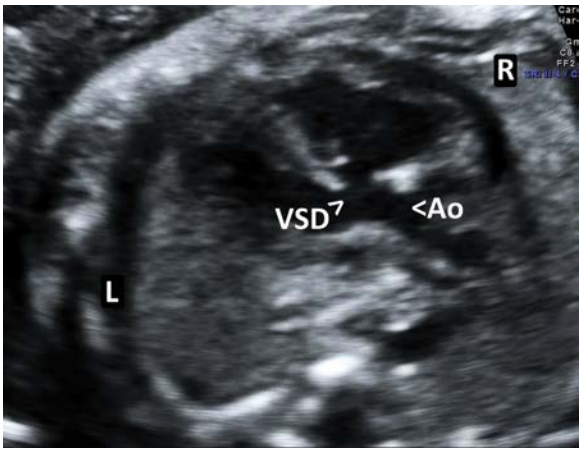


**Figure 7.4**
A case of tetralogy of Fallot with the characteristic VSD with overriding aorta (Ao). Compare with Figure 7.1, Plane III, the left outflow tract plane (Video 7.3).

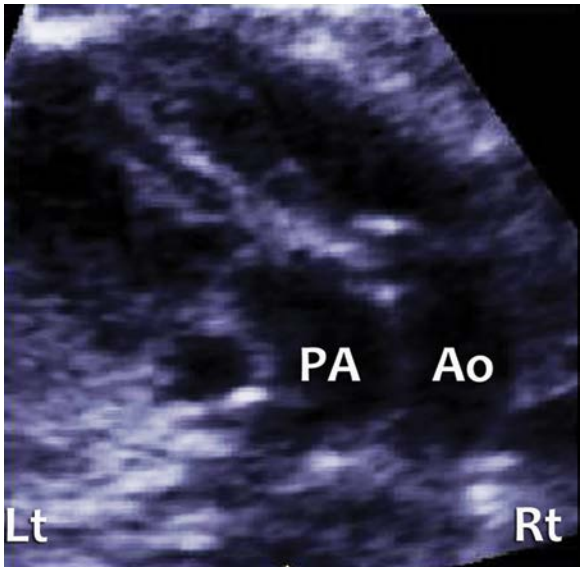


**Figure 7.5**
A case of transposition of the great arteries. Compare with Figure 7.1, Plane IV, the right outflow tract plane. The great vessels, which normally would not be imaged in the same plane, are seen to run parallel at the RVOT plane. Pulmonary artery (PA) on the left and aorta (Ao) on the right, are marked (Video 7. 4).

concern; however, fixed bradycardia or missed beats may require further evaluation. Mild transient tachycardia (>160) is generally associated with fetal movement. Persistent tachycardia or tachycardia at rates greater than 180–200 may be cause for concern and should be evaluated further.

The optimal timing of fetal heart screening is the subject of some debate. Early scanning at the end of the first trimester during NT screening has been advocated, as have late first or early second trimester scanning and midgestation imaging.[37–40] There is general agreement that early screening

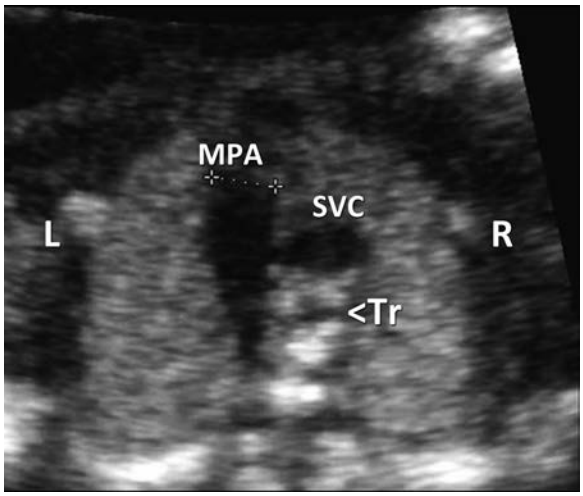


**Figure 7.6**
A case of interrupted aortic arch with its characteristic 3VT configuration: the main pulmonary artery (MPA), SVC, and trachea (Tr) are seen, but the aortic arch is missing in this plane. Compare Figure 7.1, Plane V, the 3VT plane.

necessitates repeated examination at midgestation, owing to the evolution of CHD *in utero*.[41–45]

## Obstetric fetal heart screening, limitations and pitfalls

Fetal echocardiography has been shown to have a much higher sensitivity for the detection of CHD than routine obstetric scanning. In fact, fetal echocardiography in experienced hands may detect up to 90% of serious abnormalities in a low-risk population.[33,42] Because of the very low yield of CHD detection during obstetrical screening (10%–26%)[46–48] in some populations, it has been suggested[49] that routine fetal echocardiography should be performed for all pregnancies. The feasibility of this approach, however, is a matter of serious question, and obstetric heart screening protocols incorporating the aforementioned views of the fetal heart are currently the mainstay of screening for fetal cardiac malformations.

The four-chamber view can be reliably obtained in 95%–98% of pregnancies within 1–2 minutes[22,31] and theoretically will detect over 50% of serious cardiac malformations when performed in midgestation. Addition of outflow tract views or 3VT views increases sensitivity, possibly to as high as 90%.[23,25,35,50,51] The sensitivity and specificity of these views for detection of cardiac malformations, however, have been shown to vary by operator training, level of experience, and the population studied.[3,26,31,44,52–54]

Institution of rigorous population-based screening programs that include training of the individuals performing and interpreting the examinations has proven useful, providing up to 80%–91% detection of serious CHD in unselected populations.[50,51] Most of the published improvements in detection associated with a training intervention have gone beyond the four-chamber view, incorporating outflow tract views and/or 3VT view, which may account for some of the improvement in detection. The American College of Obstetricians and Gynecologists, the American Institute of Ultrasound in Medicine, the International Society of Ultrasound in Obstetrics and Gynecology, and the American College of Radiology each recognize the benefit of including outflow tracts. In recent years, the recommendations for imaging have changed: now most guidelines incorporate the outflow tracts or the five axial plane approach as routine, and it is expected that future reports will demonstrate higher prenatal diagnosis rates than were previously reported for the general population.

# Beyond routine obstetric screening: Indications for a comprehensive evaluation of the fetal heart

Despite the increased detection of CHD afforded by a more rigorous screening approach and adoption of recommendations by most professional organizations to include the outflow tracts and 3VT views, there remains a clear role for more specialized and comprehensive evaluation of the fetal heart. Fetal echocardiography in this case is not a screening test, as it is intended to give precise details of the diagnosis, hemodynamics, and prognosis for the fetus. For some patients, the screening obstetric ultrasound will have suggested the presence of an anomaly, and fetal echocardiography will further refine the diagnosis and help guide therapy. For others, screening may have been equivocal or even normal, but given a significant elevation in risk, a detailed cardiac evaluation by fetal echocardiography is performed.

There are a multitude of factors that have been shown to be associated with an increased risk of CHD in the fetus that are related to familial, maternal, or fetal conditions. Factors such as maternal metabolic disease or family history of CHD may be reasons for referral; however, many of these indications have been estimated to carry a less than 5%–10% risk. Whether any increase over the baseline risk of 0.3%–1.2% necessitates additional expenditure of resources, and at what level, will depend on the health-care system environment, skill of screening operators, and available resources. Thus, recommendations regarding indications for referral for fetal echocardiogram must take into account risk for CHD in individual populations. In general, when risk approximates that of the general population (<1%), fetal echocardiography is probably not indicated. However, whenever the individual risk exceeds population risk, fetal echo should be considered. What follows represents a discussion regarding in which cases fetal echocardiography is or might be indicated (see also Table 7.1), though clinical decisions may always be tailored to the specific patient or situation.

## Fetal factors

### Suspected cardiac abnormality on obstetric ultrasound

The diagnostic yield for fetal echocardiographic detection of cardiac structural disease when the referral indication was an abnormal four-chamber screening view on obstetric ultrasound is over 40%.[31,55–57] Suspicion of an abnormality of the outflows or great vessels on a screening ultrasound increases the detection rate, especially for conotruncal anomalies associated with a normal four-chamber view, such as d-transposition of the great arteries or tetralogy of Fallot. Addition of the 3VT view into screening obstetric examinations[35,58–60] has a very high specificity. Therefore, any abnormality of this view or even an equivocal or unobtainable view should be considered an abnormal screening examination. If repeat screening in cases of unclear views on initial assessment remains unconvincing, fetal echocardiography is a reasonable next step. It is likely and expected that approximately 50% of fetal echocardiograms in this scenario will yield a normal result. Conversely, if the screening ultrasound suggests an abnormality due to abnormal cardiac axis or position, and the fetal

**Table 7.1** Commonly cited indications for referral for fetal echocardiogram with associated *a priori* risk

| *Condition* | *Risk* |
|---|---|
| **Abnormal anatomy scan/obstetric ultrasound** | |
| Suspected cardiac anomaly | 50%–60% |
| Extracardiac anomaly | 20%–45% |
| Hydrops | 15% |
| Tachyarrhythmia, isolated ectopy | 0.3%–1% |
| Bradycardia/heart block | 35%–50% |
| **Abnormal screening in first trimester** | |
| NT > 3.5 mm or >99%ile | 3%–6% (increases with increasing NT value, see Table 7.3) |
| Chromosome abnormality confirmed | As high as 90%, depending on abnormality |
| **Monochorionic twinning** | |
| With TTTS | 7.5%–10% |
| Without known TTTS | 4.5% |
| **Maternal disease or exposure** | |
| Pregestational diabetes | 3%–5% |
| Phenylketonuria | 12%–14% |
| Obesity | 1%–2% |
| Febrile illness | 1.2%–1.4% |
| Teratogen exposure | 1%–2% |
| Antidepressants | 1%–2% |
| Antihypertensives | 3% |
| Autoimmune disease | 1%–5% |
| *In vitro* fertilization | 1.3%–3.3% |
| **Familial disease** | |
| Maternal CHD | 3%–8% |
| Paternal CHD | 2%–3% |
| Sibling with HLHS | 8% |
| Sibling with other CHD | 3% |
| First- or second-degree relative with structural CHD associated with disease of Mendelian inheritance | Up to 50% |

*Source:* Derived from data from Donofrio MT et al. *Circulation* 2014;129(21):2183–242 and Jenkins KJ et al. *Circulation* 2007;115(23):2995–3014.[10,155]

*Abbreviations:* CHD, congenital heart disease; HLHS, hypoplastic left heart syndrome; NT, nuchal translucency; TTTS, twin-twin transfusion syndrome.

echocardiogram is normal, then evaluation for extracardiac pathology (i.e., diaphragmatic defect or lung pathology) can be repeated.

Abnormalities of fetal heart rate or rhythm are occasionally appreciated during routine obstetric visits, either by Doppler or ultrasound imaging, and are usually benign—especially premature atrial contractions or transient bradycardias. Rarely, abnormalities in rhythm are pathologic, in the form of tachy- or bradyarrhythmia requiring treatment. Fetal tachycardias are seldom associated with cardiac structural disease in the absence of significant tricuspid regurgitation (tricuspid valve abnormalities or right ventricular outflow obstruction may be an exception). However, detailed fetal echocardiography should be performed in all cases to ascertain the mechanism of tachycardia (supraventricular tachycardia, atrial flutter, or ventricular tachycardia) and to guide therapy. Fetal bradycardia in the form of sinus bradycardia may be associated with structural heart disease; fetal bradycardia due to channelopathies, specifically long QT syndrome, may present as isolated mild sinus bradycardia or 2:1 AV block.[61–64] Heart block is associated with structural heart disease in approximately 50%–55% of cases[65] and idiopathic in a small number (approximately 5%–10%), with the remainder due to maternal autoantibody disease. Irregularity of fetal rhythm caused by premature atrial contractions is not generally associated with structural heart disease (0.3%, 95% confidence interval [CI] 0%–0.7% in one series[66]), but may precede more malignant arrhythmias in approximately 2% of patients.[66]

## Abnormalities of the umbilical cord or venous system

The presence of a single umbilical artery (SUA) has been associated with an increased prevalence of CHD in the fetus; more than twice as many infants with SUA have congenital cardiac malformations than infants with a normal cord.[67,68] Anomalies of the human fetal venous system occur sporadically and have often been associated with cardiac malformations.[69–71] The true incidence of such venous malformations is undefined, but because of frequently reported cooccurrence of cardiac malformations,[72] including up to 8% for persistent right umbilical vein,[73] some have advocated for fetal cardiac evaluation in the fetus with a venous anomaly. Certainly, abnormalities of umbilical venous connection, particularly infrahepatic or suprahepatic (directly to the right atrium) ectopic insertion of the umbilical vein, have been associated with life-threatening volume overload and should prompt a thorough investigation of cardiac structure and function.[74]

## Extracardiac fetal anomalies

Malformations of the central nervous system, as well as the gastrointestinal and genitourinary systems, are often seen in association with cardiovascular malformations (Table 7.2). The overall incidence of CHD in the presence of one or more extracardiac malformations is estimated at approximately 20%–45% depending on the population studied and the gestational age at which ultrasound screening is performed.[68,75–81]

**Table 7.2** Congenital heart disease risk in fetuses with identified extracardiac anomalies

| *Extracardiac anomaly* | *Number (%)* | *Reference* | *Estimated from multiple studies (1)* |
|---|---|---|---|
| Central nervous system | 49/409 (11.7%) | Copel et al. (2) | 5%–15% |
| Diaphragmatic hernia | 11/48 (23%), 2/11 (18%) | Greenwood et al. (3), Fogel et al. (4) | Up to 30% |
| Gastrointestinal, all | 53/240 (22%), 38/166 (23%) | Thompson and Mulholland (5), Tulloh et al. (6) | 4%–25% |
| Gastrointestinal, nonsyndromic | 29/203 (14%) | Thompson and Mulholland (5) | – |
| Tracheoesophageal fistula | 48/326 (15%), 22/57 (39%) | Greenwood and Rosenthal (7), Tulloh et al. (6) | – |
| Omphalocoele | 31/159 (19%), 4/20 (20%), 13/37 (35%) | Greenwood et al. (8)<br>Tulloh et al. (6)<br>Fogel et al. (4) | 30% |
| Genitourinary | 34/453 (8%) | Greenwood et al. (9) | 8%–71% |
| Single umbilical Artery | High-risk pop (19%), 59/1694 (3.5%) | Martinez-Frias et al. (10), Lilja (11) | 3.9% |
| Left superior vena cava | 262/449 (58%) | Gustapane et al. (12) | – |
| Any | 14/25 (56%) | Clur et al. (13) | 20%–45% |

*Source:*

1. Donofrio MT et al. *Circulation* 2014;129(21):2183–242.
2. Copel JA et al. *Am J Obstet Gynecol* 1986;154(5):1121–32.
3. Greenwood RD et al. *Pediatrics* 1976;57(1):92–7.
4. Fogel M et al. *Am J Perinatol* 1991;8(6):411–6.
5. Thompson AJ, Mulholland HC. *Ulster Med J* 2000;69(1):23–6.
6. Tulloh RM et al. *Arch Dis Child Fetal Neonatal Ed* 1994;70(3):F206–8.
7. Greenwood RD, Rosenthal A. *Pediatrics* 1976;57(1):87–91.
8. Greenwood RD et al. *J Pediatr* 1974;85(6):818–21.
9. Greenwood RD et al. *Clin Pediatr (Phila)* 1976;15(12):1101–4.
10. Martinez-Frias ML et al. *Am J Med Genet A* 2008;146A(1):15–25.
11. Lilja M. *Paediatr Perinat Epidemiol* 1992;6(4):416–22.
12. Gustapane S et al. *Ultrasound Obstet Gynecol* 2016.
13. Clur SA et al. *Prenat Diagn* 2011;31(12):1134–40.

Though the cooccurrence of CHD with extracardiac anomalies is highest in fetuses with aneuploidy, CHD may be present in a large number of euploid fetuses with extracardiac malformations as well[76]; therefore, fetal echocardiography is recommended for most fetuses with ultrasonographic extracardiac abnormalities, regardless of results of genetic testing.

## Known or suspected chromosomal abnormality

If genetic testing has been undertaken and discloses a known genetic mutation, deletion, rearrangement, or aneuploidy in the fetus, fetal echocardiography should probably be performed even if screening obstetric ultrasound is normal, as the implications of minor lesions such as coarctation and small to moderate ventricular septal defects (VSDs) in these fetuses may be different from patients without aneuploidy.[5] Though it is known that approximately 7% of fetuses with apparently isolated CHD have been found to have copy number variants when subjected to chromosomal microarray analysis,[82] the yield for fetal echocardiography in patients found to have a variant of uncertain significance is at present unstudied.

## Abnormal first-trimester screening

The 10–14 week "nuchal translucency" (NT) can be reliably measured by trained, experienced ultrasound operators and when increased has been shown to correlate with increased risk of aneuploidy and other malformations.[83–85] The etiology is speculative; studies of cardiac function at this gestation do not support a causal relation between heart function and increased nuchal fluid.[86,87] Abnormalities of development or function of lymphatic, neural crest tissue, or early endothelial precursors have been suggested as possible etiologies,[88] as has disturbance of early fetal blood flow/hemodynamics.[84,89] The accumulation is generally a transient phenomenon and begins to resolve at 14 weeks. Normal values have been established; the 95th centile varies with gestational age (or crown-rump length) but approximates 2.5 mm, while the 99th centile cutoff will approximate 3.5 mm; it should be noted, however, that these last two are not equivalent in terms of risk.[90]

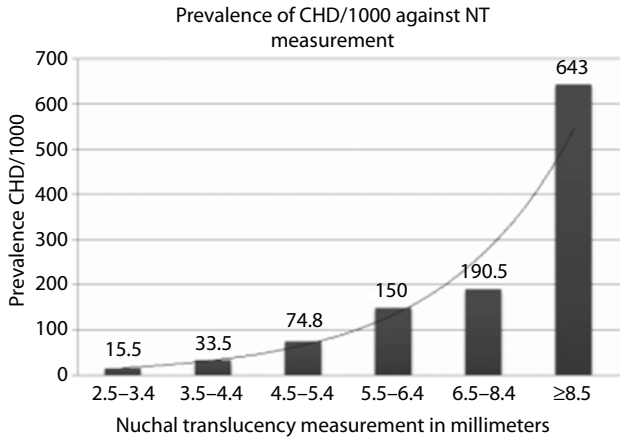


**Figure 7.7**
Prevalence of congenital heart defects in relation to nuchal translucency measurement. (CHD, congenital heart disease; NT, nuchal translucency.) (Data from Clur SA et al. *Prenat Diagn* 2009;29[8]:739–48.[101])

The association of abnormally increased NT and CHD in chromosomally normal fetuses was first recognized by Hyett et al. in 1996,[91] and has been the subject of a number of studies. The degree of increased risk of CHD in chromosomally normal fetuses has however been variably reported. Difficulties in interpreting the literature lie in part in differing study methodologies and in the differing populations studied (high risk versus low risk) and cutoff points for abnormal values (95th versus 99th centile, >2.5 mm versus ≥3.5 mm, or multiples of the median of 1.7, 2, 2.5, or 3). A sensitivity for detection of up to 56% using the 95th centile cutoff[92] in early reports suggested value of NT as a screening tool for CHD; unfortunately, subsequent studies have demonstrated a much lower sensitivity, as low as 6%–15%[90,93–97] in low-risk populations with the 99th centile threshold, making NT likely ineffective in terms of screening the general population. The likelihood of the fetus having CHD once an increased NT is detected rises (above the 0.4%–0.8% for the general population) to approximately 3% for NT > 95th, and to approximately 6% for NT ≥ 99th centile across nearly all of the published studies.[94–96,98,99] The risk for CHD rises exponentially with increasing NT[98,100] (summarized in Clur[101]) (Figure 7.7 and Table 7.3). Currently, many advocate for fetal echocardiography for all euploid fetuses with NT ≥ 3.5 mm or alternately greater than the 99th centile[90] with some even suggesting that the cutoff be as low as greater than the 95th centile (though at this threshold, 5% of the screened population would require fetal echocardiography).

Abnormal ductus venosus (DV) Doppler in the first trimester, defined as absence or reversal of flow with atrial contraction, has been associated with increased risk of CHD, aneuploidy, and poor outcome in the fetus.[102,103] In populations with NT ≥ 95th centile, an 83% sensitivity (95% CI, 51%–95%) with a positive likelihood ratio of 4.35 (1.5–12.1) translated to a 15% incidence of major heart malformation in euploid fetuses with both increased NT and abnormal DV in a meta-analysis.[104] When NT is ≥99th centile (3.5 mm), sensitivity decreases to 68.8% (11/16 fetuses); the LR is similar while CHD incidence increases to approximately 20%.[105] These results suggest that the addition of DV Doppler analysis may be useful for identifying those at greatest risk among the high-risk screening population. DV flow abnormalities in the absence of an increased NT are not a useful screening test (sensitivity <20%).[104] The addition of evaluation for tricuspid regurgitation present by Doppler at the time of the NT examination (Figure 7.8) has also been shown to increase sensitivity for detection of CHD[106] but requires some technical expertise and may not be applicable to large-scale screening in low-risk populations.

## Monochorionic twinning

Monozygous twinning, in which division of the early embryonic cell mass between days 3 and 8 of gestation results in two fetuses with identical genomes, comprises roughly 3–4 per 1,000 live births, with two-thirds being monochorionic (MC) (single shared placenta) and one-third dichorionic.[107] Dizygotic twinning, far more common, results from two separate fertilized ova, and these twin fetuses are essentially always dichorionic. Twin pregnancies have higher rates of congenital malformations (including cardiac malformations) than singleton gestations; however, observations of higher than expected frequencies of congenital malformations in MC twins[107] have led to the speculation that the etiologic basis of cardiac malformations differs in monozygotic twinning versus dizygotic twinning (in which the higher incidence of abnormalities in affected pregnancies may be attributed to the increased fetal number alone).[108]

Reports of large series of MC twins have for the most part originated from referral centers and thus may overestimate

**Table 7.3** Prevalence of congenital heart defects in relation to nuchal translucency measurement

| *NT measurement (mm)* | *2.5–3.4* | *3.5–4.4* | *4.5–5.4* | *5.5–6.4* | *6.5–8.4* | *≥8.5* |
|---|---|---|---|---|---|---|
| Percentage (%) with CHD | 1.55% | 3.35% | 7.48% | 15% | 19.1% | 64.3% |
| Based on absolute number (CHD/total) | 78/5039 | 43/1284 | 30/401 | 9/60 | 8/42 | 9/14 |

*Source:* Data from Clur SA et al. *Prenat Diagn* 2009;29(8):739–48.[101]

*Abbreviations:* CHD, congenital heart disease; NT, nuchal translucency.

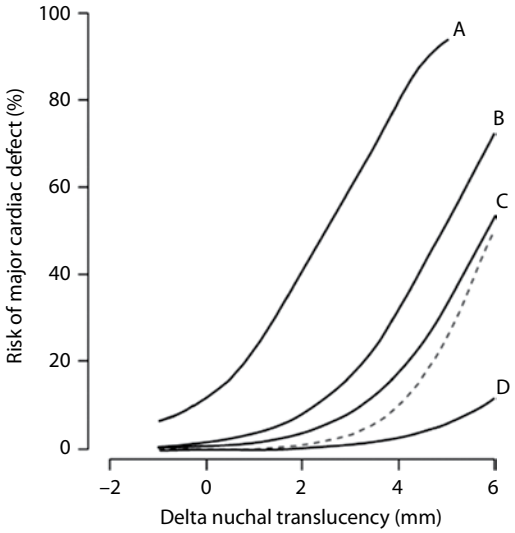


**Figure 7.8**
Patient-specific risk for major cardiac defects according to fetal nuchal translucency (NT) in isolation (dotted line) and NT combined with interpretation of blood flow pattern in the ductus venosus (DV) and presence of tricuspid regurgitation (TR) in a representative fetus with crown-rump length of 65 mm (lines A–D). (A) TR and DV "A" wave reversal; (B) TR and normal DV flow; (C) DV "A" wave reversal alone; (D) no TR, normal DV flow. (From Pereira S et al. *Obstet Gynecol* 2011;117(6):1384–91, with permission.[106])

the true risk of cardiac malformations in these twins. Nevertheless, MC twins do appear to be at increased risk, and when malformation occurs, discordance is the rule rather than the exception.[109] Overall, in a meta-analysis,[110] the prevalence of congenital cardiac malformations among MC twins was increased approximately ninefold regardless of the presence or absence of additional complications (range depending on reference population from relative risk [RR] 9.18; 95% CI, 5.51–15.29 to RR 15.04; 95% CI, 9.78–23.13) versus singletons in the general population. More recently, Pettit et al.[111] reported a cohort of more than 900 MC, mostly diamniotic twin infants with a prevalence of CHD of 7.5%. The most common CHD were ventricular septal defects and atrial septal defects, affecting approximately 4% and 2%, respectively, though in about 1% of the infants, the cardiac defect was more severe, enough to require surgery in the first year of life or to cause neonatal death in the absence of surgery. For the much less common monoamniotic pairs, the risk for anomalies is even higher, with reports of up to 57%.[112]

Twin-twin transfusion syndrome (TTTS), in which MC twins with a shared placental mass (and therefore vascular anastomoses which allow transfer of blood and vasoactive substances), has been associated with acquired RVOT obstruction in approximately 10% of recipient fetuses[112,113] and atrial septal defects postnatally in either twin.[113,114] Recently, acquired mitral valve dysplasia has been reported in recipient fetuses as well.[115] The incidence of pulmonary stenosis is decreased to about 2% if the pregnancy is successfully treated with invasive laser photocoagulation of the intertwin anastomosis in midgestation.[113,114,116]

## Known or suspected anemia

Increased middle cerebral artery peak systolic Doppler velocity can be used to estimate degree of abnormality in fetal hemoglobin levels. Velocity over 1.5 multiples of the median corresponds to moderate to severe anemia.[117] Though measurable increase in cardiac output in the face of moderate to severe anemia is expected,[118] fetal echocardiography has not been used routinely for the purpose of diagnosing or treating fetal anemia. In the presence of high output, ventricular failure and hydrops may ensue (see the following section), but the role for fetal echocardiography in prehydropic fetuses with or at risk for anemia has not been examined.

## Nonimmune hydrops, effusions, and polyhydramnios

Fetal hydrops refers to the pathologic accumulation of fluid in two or more fetal compartments including the pleural or pericardial spaces, abdominal cavity, integument, or placenta. Polyhydramnios may also be considered a criterion. The mechanism of development of hydrops in the fetus is thought to be similar to that of postnatal edema formation, due to a combination of increased hydrostatic pressure, decreased oncotic pressure, and in some relative lymphatic obstruction. Up to 25% of cases of nonimmune fetal hydrops are due to cardiac structural abnormalities or arrhythmias,[119,120] with an additional 10% due to high cardiac output states such as are seen in anemia or other more rare pregnancy complications, including placental arteriovenous malformations, acardiac twinning, sacrococcygeal teratoma, and other vascular malformations.

Due in part to the passive nature of the venous portion of the fetoplacental circulation, the fetus develops hydrops in the presence of relatively small increases in venous pressure resulting from abnormalities of myocardial relaxation or compliance. Increases in venous pressure resulting from volume overload due to atrioventricular or semilunar valve regurgitation, pressure overload from biventricular outflow obstruction, or decreased diastolic filling time in tachycardia are among the cardiac causes for fetal hydrops that can be detected with fetal echocardiography. Evaluation of the hydropic fetus using fetal echocardiography is therefore indicated to assess for both structural disease and myocardial dysfunction (whether primary or secondary to infectious, infiltrative, genetic, rhythm-related, or high-output effects on myocardial function). This recommendation can be extended to the evaluation of the at-risk fetus and to the fetus with effusions in the absence of overt hydrops (isolated pericardial or pleural effusion, ascites). Additionally, up to 11% of fetuses with unexplained severe polyhydramnios (Amniotic Fluid Index >35 cm) may have associated congenital anomalies; up to 25% of these anomalous infants will have cardiac structural malformations, most of which can be detected by fetal echocardiography.[121]

# Maternal factors

## Maternal diabetes

Diabetes mellitus is extremely common in the obstetric population, complicating up to 10% of pregnancies. Of these, 20% of women were diabetic prior to conception. Overall the congenital malformation rate in fetuses of pregestational diabetics is increased to triple that of the general population, and nearly half of affected infants manifest cardiac malformations, resulting in a nearly fivefold (3%–5%) increase in CHD.[122] Gestational diabetes, or insulin resistance acquired only during the third trimester of pregnancy, does not appear to confer this same increased risk of cardiovascular malformation in the fetus. However, whether women with abnormal early pregnancy glucose screening or those with metabolic syndrome and pregestational insulin resistance without a diagnosis of diabetes are at increased risk for CHD in their offspring is not known.

In the pregestational diabetic population, early studies indicated that lack of preconceptional glycemic control, as evidenced by elevation in serum hemoglobin A1C levels greater than 8.5% in the first trimester, was associated with increases in all congenital malformations,[123] while strict glycemic control before conception and during pregnancy could reduce risk to a level comparable to the nondiabetic population.[124,125] A meta-analysis published in 2001 found that preconception care likely reduces the risk of all congenital anomalies.[126] However, subsequent studies have suggested that there is no specific threshold hemoglobin A1C value for fetal cardiac anomalies[127–129] and that all pregestational diabetics remain at increased risk for congenital cardiac malformation in their offspring. Diabetes increases the risk of some specific cardiac malformations, with odds ratios of 6.22 for heterotaxy, 4.72 for truncus arteriosus, 2.85 for transposition of the great arteries, and 18.24 for single ventricle in one series. In the same paper, hemoglobin A1C values only slightly above the normal range (mean 6.4%) were nevertheless associated with risk of cardiac malformation of 2.5%–6.1% in the offspring.[127] Therefore, it appears that although the risk may be highest in those with hemoglobin A1C levels over 8.5%, all pregnancies in pregestational diabetics are at some increased risk.

Fetuses may develop ventricular hypertrophy late in gestation in the presence of poorly controlled maternal diabetes; the degree of hypertrophy has been shown to be an effect of glycemic control.[130] However, in pregnancies with hemoglobin A1C levels less than 6% in the second half of pregnancy, the effects are mild and do not warrant repeated fetal cardiac evaluation.[131]

## Phenylketonuria

Untreated maternal phenylketonuria (PKU) results in adverse pregnancy outcomes including mental retardation, microcephaly, growth restriction, and congenital anomalies.[132–134] Elevated maternal serum levels of phenylalanine (>15 mg/dL) are associated with a 10- to 15-fold increased risk of congenital heart disease in the infant.[10,133,135] While the risk for CHD in the fetus remains as high as 12% if control is not achieved by 10 weeks' gestation,[136] with periconceptional dietary control this risk can be greatly reduced. One large prospective international collaborative study of 576 completed pregnancies in women with PKU and 101 controls without PKU found phenylalanine levels greater than 10 mg/dL to be associated with congenital heart disease in 14% of live-born infants[135]; however, the fetal risk may be higher, as some affected pregnancies were electively terminated due to CHD detected in the midtrimester.[137] No cases of CHD in the fetus were identified if maternal phenylalanine levels were less than 6 mg/dL prior to conception and during early organogenesis,[135] suggesting that for women with well-controlled PKU, with preconception and first trimester phenylalanine levels less than 10 mg/dL, risk may revert to baseline.

## Maternal autoimmune disease and autoantibody positivity

The association of maternal lupus and other connective tissue diseases with congenital atrioventricular block (CAVB) is well established[138,139]; the fetus may be affected even if the mother has no overt clinical symptoms of disease. The reported incidence of fetal CAVB has been reported to be as high as 1%–5% in known seropositive (anti-Ro/SSA, anti-La/SSB) mothers. The number of affected pregnancies rises to 11%–19% for those with a previously affected child with heart block.[140–144] Recent studies have suggested that high anti-Ro values (≥50 U/mL) correlate with increased fetal risk.[144] A minority of antibody-exposed fetuses may also develop cardiomyopathies, including myocardial inflammation or endocardial fibroelastosis, or may exhibit atrioventricular valve apparatus dysfunction.[145–148]

The fetal mechanical PR interval can be measured using either M-mode or spectral Doppler techniques, and gestational age–adjusted normal values have been published.[149] Though direct evidence is not well established, expert consensus holds that serial assessment at 1- to 2-week intervals through 24–28 weeks' gestation should be offered[10,143,150] due to the potential for treatment with dexamethasone, intravenous immune globulin (IVIG), or both, which may mitigate development of worsening manifestations of fetal disease.[148,151] Additionally, a proportion (estimated at 16%) of affected fetuses with cardiac findings will go on to develop isolated effusions, ascites, or hydrops, presumably due to prolonged bradycardia and myocardial involvement,[152] which may justify additional assessment, even into the third trimester.

## Maternal obesity

Maternal obesity, defined as a body mass index (BMI) (kg/m$^2$) greater than 30 as per criteria established by the Centers for Disease Control and Prevention (CDC) and the World Health Organization (WHO), has been associated with increased maternal risk, adverse pregnancy outcomes, and increased incidence of congenital defects including neural tube defects and omphalocele in offspring. It is likely that these risks exist even controlling for maternal comorbidities,

including hypertension and pregestational diabetes, though it has been difficult to separate these from a practical standpoint in smaller studies. Recent studies suggest an association between maternal prepregnancy obesity and CHD in the fetus, with risk ratios on the order of 1.1–1.5 (increasing with increasing maternal BMI), with a particularly strong association with conotruncal defects.[153,154] Clearly, however, the implications of excessive maternal BMI for ultrasound detection of less severe defects needs to be considered, as acoustic windows may be very limited in these women, thereby increasing the rates of inconclusive evaluations.

## Teratogen exposure

The current state of knowledge regarding maternal therapeutic and nontherapeutic drug and alcohol exposure has been reviewed extensively.[155] Several issues surround constructing reasonable risk estimates with respect to maternal medication and drug exposures, including recall bias, the retrospective or registry-reported nature of most series, and the era of ascertainment, which all may dramatically over- or underestimate the true prevalence of fetal heart disease in these pregnancies. Moreover, drug safety (or the converse) in animal testing does not always translate to the human. Nevertheless, it is agreed that intake of certain medications or binge consumption of alcohol may increase the risk of congenital cardiac malformation in the fetus (Table 7.4).

## Maternal infection

Many women experience symptoms of mild to moderate viral illness during pregnancy, and the vast majority will have no effect on the fetus, with a few notable exceptions, which may lead the provider to perform a repeat or more detailed assessment of the fetal heart. Fever in and of itself is generally tolerated, though in one population-based study, maternal febrile illness was positively associated with the occurrence of heart defects in the offspring (odds ratio [OR] = 1.8; 95% CI = 1.4–2.4)[156] and a recent meta-analysis[157] calculated an OR of 1.54 (CI = 1.37–1.74) for any CHD with maternal pyrexia in the first trimester. Certain infections, specifically maternal rubella, have been associated with a higher incidence of specific cardiac malformations,[158] though the majority of reported defects were patent ductus arteriosus and peripheral pulmonic stenosis, which would not be detected prenatally. Parvovirus, coxsackievirus, adenovirus, and cytomegalovirus have been implicated in fetal myocarditis but not structural disease *per se*.

## Assisted reproduction

The use of assisted reproductive technologies has been dramatically increasing over the last two decades. In 2005, an estimated 1% of all live births in the United States were conceived with the use of *in vitro* fertilization (IVF) with or without intracytoplasmic sperm injection (ICSI).[159] There are conflicting reports in the literature regarding association of the use of this technology with malformations in the offspring,[160–162] but three meta-analyses in 2004–2005 suggested that there was an increase in the expected prevalence of all malformations to as high as 9.5% and of congenital cardiac malformation to approximately 1.2%, in infants conceived with IVF with or without ICSI.[161,163,164] Since that time, some reports have suggested that the increase in birth incidence of CHD in these pregnancies may be attributable to an increased risk specifically in multiple gestations, and that singletons conceived with IVF are not at increased risk.[165] There does not seem to be increased risk overall with the use of ICSI versus IVF alone.[163] Unfortunately, the relative effect attributable to the technology is difficult to ascertain. Because of known influence of advanced maternal age on CHD risk[166] and the known increased risk (see the following text) associated with monozygous twinning (increased with IVF), as well as the unknown impact of the underlying etiology of subfertility in couples using IVF/ICSI on risk for cardiac and other malformations in the fetus, a direct causation remains unproven.[164,167–169] Nevertheless, overall risk of cardiac malformations in infants conceived through IVF seems to be slightly higher than that for reference populations, on the order of 1.1%–3.3%,[163,165,167,170] and though a recent report[171] showed an increased risk of tetralogy of Fallot attributable to IVF, the majority of CHD seem to be septal defects, which may not be detectable in fetal life.

# *Family history*

Most literature pertaining to large-scale estimates of familial risk was published prior to the era of genetic testing, some in the era prior to the introduction of routine echocardiography. As advances are made in genetic testing (including microarray technology and whole exome sequencing), the ambiguity surrounding these risk estimates is likely to change.

## Maternal congenital heart disease

The risk of recurrence of nonsyndromic, nonchromosomal cardiac disease is over twice as high as the general population if the mother is the affected parent rather than the father or a prior offspring.[172,173] It is important to determine the exact nature of maternal disease, especially if she has had prior surgical correction that may also affect her care during pregnancy. Unfortunately, many women are not aware of the details of their cardiac diagnosis. For the majority of maternal cardiac diagnoses, the risk of recurrence in the offspring is in the range of 3%–7%,[10] with recurrence for nonsyndromic tetralogy of Fallot and d-transposition of the great arteries 3% or less.[172,174] Risk is higher for euploid women with atrioventricular septal defects, at approximately 10%–14%[172,174,175] and aortic stenosis at as high as 13%–18%.[174,176,177]

## Paternal congenital heart disease

Most studies in which the male parent is affected with nonsyndromic cardiac malformation (excluding bicuspid aortic valve and single-gene disorders) give a 2%–3% risk of cardiac malformation in the infant or fetus,[172,174,176,178] consistent with a multifactorial mode of inheritance. A single study reported a 7.5% recurrence when fetal echocardiogram ascertainment

**Table 7.4** Select teratogens associated with increased incidence of fetal cardiac malformations

| *Drug or drug class* | *Association* | *Estimated risk* | *References* |
|---|---|---|---|
| Anticonvulsants | Any | RR 4.2 | Jenkins et al. (1) |
| Carbamazepine | Not specified | 1.8% | Matalon et al. (2) |
| Lithium | Ebstein anomaly | 8% (likely biased) | Nora et al. (3) |
| | | No risk RR 1.1 (95%CI 0.1–16.6) | Jacobson et al. (4) |
| Retinoic acid | Conotruncal, aortic arch | 8%–20% | Lammer et al. (5) |
| Smoking | Septal defects, RVOT obstruction | RR 1.11 (1.02–1.21) | Lee et al. (6) |
| | | OR 2.35, CI 1.21–4.53 | Malik et al. (7) |
| Alcohol | ASD, TGA, VSD | Conflicting; from no increase to up to 2.1 (1.1–4.2) | Sun et al. (8) |
| Alcohol (binge drinking) + smoking | Not specified | Up to OR 9.45 (CI 2.53–35.31) | Mateja et al. (9) |
| Antidepressants | N/A | No association | Ericson et al. (10), Louik et al. (11), Reis and Kallen (12) |
| SSRI (general) | N/A | No higher than baseline | Alwan et al. (13), Louik et al. (11), Lattimore et al. (14), Bar-Oz et al. (15) |
| Paroxetine | RVOT abnormality | 1%–2% | Bar-Oz et al. (15), Louik et al. (11), Reis and Kallen (12) |
| Angiotensin-converting enzyme inhibitors | ASD, PDA | 2.9%; may be lower or due to underlying disease | Cooper et al. (16); Li et al. (17) |
| Vitamin K agonists (Coumadin, other) | N/A | 0.3% | Schaefer et al. (18) |
| Organic solvents | Conotruncal, valve stenosis, TGA, TOF, CoA, septal defects, Ebstein anomaly | RR 2–6 | Patel and Burns (19) |
| Cyanide, heavy metals | Not specified | RR 1.5–2.2 | Shaw et al. (20) |

*Source:* Data from references as noted.

1. Jenkins KJ et al. *Circulation* 2007;115(23):2995–3014.
2. Matalon S et al. *Reprod Toxicol* 2002;16(1):9–17.
3. Nora JJ et al. *Lancet* 1974;2(7880):594–5.
4. Jacobson SJ et al. *Lancet* 1992;339(8792):530–3.
5. Lammer EJ et al. *N Engl J Med* 1985;313(14):837–41.
6. Lee LJ, Lupo PJ. *Pediatr Cardiol* 2013;34(2):398–407.
7. Malik S et al. *Pediatrics* 2008;121(4):e810–6.
8. Sun J et al. *Congenit Heart Dis* 2015;10(5):E216–24.
9. Mateja WA et al. *J Womens Health (Larchmt)* 2012;21(1):26–34.
10. Ericson A et al. *Eur J Clin Pharmacol* 1999;55(7):503–8.
11. Louik C et al. *N Engl J Med* 2007;356(26):2675–83.
12. Reis M, Kallen B. *Psychol Med* 2010;40(10):1723–33.
13. Alwan S et al. *N Engl J Med* 2007;356(26):2684–92.
14. Lattimore KA et al. *J Perinatol* 2005;25(9):595–604.
15. Bar-Oz B et al. *Clin Ther* 2007;29(5):918–26.
16. Cooper WO et al. *N Engl J Med* 2006;354(23):2443–51.
17. Li DK et al. *BMJ* 2011;343:d5931.
18. Schaefer C et al. *Thromb Haemost* 2006;95(6):949–57.
19. Patel SS, Burns TL. *Pediatr Cardiol* 2013;34(7):1535–55.
20. Shaw GM et al. *Arch Environ Health* 1992;47(2):147–54.

*Abbreviations:* ASD, atrial septal defect; CHD, congenital heart disease; CoA, coarctation of the aorta; OR, odds ratio; PDA, patent ductus arteriosus; RR, relative risk; RVOT, right ventricular outflow tract; SSRI, selective serotonin reuptake inhibitor; TGA, transposition of the great arteries; TOF, tetralogy of Fallot; VSD, ventricular septal defect.

was used in addition to postnatal evaluation for detection of defects[179]; this study included small ventricular septal defects and atrial septal defects, which were not detectable on fetal echocardiography, and the majority of cases were discordant with the paternal diagnosis. Recurrence risk for aortic stenosis may be higher,[176] though in some populations bicuspid aortic valve has been shown to be more highly heritable than some other defects,[180] which may account for this difference. The highest estimate of recurrence risk was reported in a population of adults with moderate to severe cardiac malformations who had been followed since childhood; a 13% incidence of any cardiac diagnosis in offspring was reported,[177] though considerable bias may have been introduced by the study design in this case.

## Prior affected fetus or child

Studies suggest that recurrence risk for a sibling of a prior affected child with unaffected parents is 2%–6%,[2,172,176,181] with birth prevalence nearly fourfold higher in siblings of a prior child with cardiac disease versus those with unaffected older siblings.[182] A sibling recurrence risk of 4.4% for conotruncal defects with high degree of defect concordance has been reported in a single study.[183] An 8% recurrence risk for hypoplastic left heart syndrome has been reported,[184] suggesting higher heritability for this lesion in particular. For most other defects, less than 50% concordance has been observed, though exact concordance may be in the range of 20%–35% for the majority of cardiac malformations.[172,178,179] Risk for recurrence increases if more than one prior sibling is affected.[179,185]

## Second-degree relatives of the fetus

Recent studies have established a high heritability for left-sided obstructive lesions and aortic valve abnormalities,[180,184,186] leading some to advocate echocardiographic screening for all first- and second-degree relatives of affected individuals. However, the overall risk of all malformations in second- and third-degree relatives of a proband are otherwise quite small (RR 1.39, CI 1.25–1.54 and RR 1.18, CI 1.05–1.32).[173] In one small series of 316 probands, there were 11 affected relatives (3.5%), but syndromic cases were not excluded[179]; therefore, the true recurrence risk in this cohort is probably lower. When both a first- and a second-degree relative are affected, recurrence risk may be much higher: reported as 40% in one study,[177] underscoring the importance of obtaining a thorough family history when congenital heart disease is suspected.

## Diseases, disorders, or syndromes with Mendelian inheritance

The current state of knowledge regarding heritable causes of cardiovascular malformations was recently reviewed (for detailed discussion, please refer to that publication).[5] In pregnancies in which a prior child is affected by a recessively inherited disease or a parent is affected by an autosomal dominant genetic disorder with increased risk for cardiac malformation or a deletion syndrome known to be associated with high incidence of cardiac phenotype (22q11 deletion, Alagille syndrome, Williams syndrome), the recurrence risk in the fetus will be high but variable, depending on issues of penetrance and expressivity.

There is little value to fetal echocardiography in evaluation for disease with postnatal onset of cardiovascular manifestations such as hypertrophic cardiomyopathy, Marfan, Ehlers-Danlos, Williams–Beuren, or Noonan syndromes. This should be disclosed to the patient, and fetal echocardiography should not be considered a substitute for genetic testing. However, since occasionally there will be abnormalities present in fetal life, increased vigilance in performing the screening examination is needed if the fetus has had genetic testing confirming a causative mutation.

# Summary

Only 10% of fetuses with CHD present with an identifiable fetal or maternal "risk factor," while the other 90% are not nominally at increased risk but potentially may be referred for echocardiography with only an abnormal obstetric screening examination as a clue to underlying cardiac disease.[33] It is suggested, therefore, that "all fetuses regardless of maternal, familial, or fetal factors be approached as if they have the potential to have a cardiac malformation."[10] Only if this strategy is embraced will the detection rates of cardiac disease be improved beyond current practice. Data and experience suggest that the four-chamber view is inadequate in isolation, and the outflow tracts and 3VT view should be obtained as part of every routine obstetric ultrasound screening examination as outlined in this chapter and supported by professional guidelines. Fetal heart screening studies should be critically evaluated by trained examiners, and if not conclusively normal, additional evaluation should be undertaken. It is distressing that recent studies have shown that nearly 50% of four-chamber abnormalities were missed in a low-risk population based study in Nevada.[49] Nationwide in the United States contemporary detection rates for CHD are even lower.[187] Additional visualization of the outflow tracts or 3VT view should increase sensitivity for detection of CHD in a low-risk screening population to at least 65%[26] to as high as 75%–97%.[31,35] It is important to note that the detection rates for CHD will vary by type of ultrasound practice and the level and type of training of the examiner.[26,188,189] However, it has been documented that increased detection is possible. Educational programs and reinforced training have both been shown to improve detection dramatically.[50,51] Recently, reports have shown that in both low- and high-risk populations evaluated in university settings, a normal obstetrical anatomic survey that includes outflow tracts will minimize the need for detailed fetal echocardiography, as even in high-risk populations the yield of fetal echocardiography after a normal screening examination is reported to be extremely low.[190–192] Ultimately, the goal will be to improve screening to the point where detailed fetal echocardiography supervised

by physicians specifically trained in cardiac diseases of the fetus is reserved for those patients in whom routine obstetric scanning suggests the possibility of an abnormality, making obsolete the multitude of other risk-based "indications" for fetal echocardiography referral.

## Videos

**Video 7.1** (https://youtu.be/OcXbzx4uff0)
A case of dextrocardia rendered in tomographic ultrasound imaging (TUI).

**Video 7.2** (https://youtu.be/resOW0oxcg4)
Four-chamber view of a case of atrioventricular canal defect (AV-Canal).

**Video 7.3** (https://youtu.be/9bGcJP332W0)
A case of tetralogy of Fallot with the characteristic VSD with overriding aorta (Ao), demonstrating the abnormal left ventricular outflow tract plane.

**Video 7.4** (https://youtu.be/6_-aCAxBi_s)
A case of transposition of the great arteries, demonstrating the abnormal right ventricular outflow tract view.

## References


1. Ferencz C et al. *Am J Epidemiol* 1985;121(1):31–6.
2. Hoffman JI. *Pediatr Clin North Am* 1990;37(1):25–43.
3. Tegnander E, Eik-Nes SH. *Ultrasound Obstet Gynecol* 2006;28(1):8–14.
4. Wren C et al. *Heart* 2000;83(4):414–9.
5. Pierpont ME et al. *Circulation* 2007;115(23):3015–38.
6. Moons P et al. *Acta Paediatr* 2009;98(3):472–7.
7. Sharland G et al. Revised April 2012. Accessed June 27, 2016. Available from: http://www.bcs.com/documents/Fetal_Cardiology_Standards_2012_final_version.pdf.
8. International Society of Ultrasound in Obstetrics and Gynecology, Carvalho JS, et al. *Ultrasound Obstet Gynecol* 2013;41(3):348–59.
9. American Institute of Ultrasound in Medicine. *J Ultrasound Med* 2013;32(6):1067–82.
10. Donofrio MT et al. *Circulation* 2014;129(21):2183–242.
11. International Society of Ultrasound in Obstetrics & Gynecology. *Ultrasound Obstet Gynecol* 2006;27(1):107–13.
12. Lee W et al. *Ultrasound Obstet Gynecol* 2008;32(2):239–42.
13. Wax J et al. *J Ultrasound Med* 2014;33(2):189–95.
14. Yagel S et al. *Ultrasound Obstet Gynecol* 2002;20(4):340–5.
15. Yagel S et al. *Ultrasound Obstet Gynecol* 2001;17(5):367–9.
16. Li Y et al. *PLOS ONE* 2013;8(6):e65484.
17. Zhang YF et al. *Medicine (Baltimore)* 2015;94(42):e1759.
18. Yoo SJ et al. *Ultrasound Obstet Gynecol* 2001;18(3):248–52.
19. Di Salvo DN et al. *J Ultrasound Med* 1994;13(4):291–3.
20. Allan LD et al. *Br Med J (Clin Res Ed)* 1986;292(6537):1717–9.
21. Copel JA et al. *Am J Obstet Gynecol* 1987;157(3):648–55.
22. Tegnander E et al. *Ultrasound Obstet Gynecol* 1994;4(1): 24–8.
23. Achiron R et al. *BMJ* 1992;304(6828):671–4.
24. DeVore GR. *J Ultrasound Med* 1992;11(7):345–8.
25. Kirk JS et al. *Obstet Gynecol* 1994;84(3):427–31.
26. Ogge G et al. *Ultrasound Obstet Gynecol* 2006;28(6):779–84.
27. Barboza JM et al. *Radiographics* 2002;22(5):1125–37; discussion 37–8.
28. Achiron R et al. *Ultrasound Obstet Gynecol* 2002;20(6):553–7.
29. Berg C et al. *Ultraschall Med* 2009;30(3):230–51.
30. Berg C et al. *Ultraschall Med* 2009;30(2):128–44; quiz 45–9.
31. Carvalho JS et al. *Heart* 2002;88(4):387–91.
32. Bromley B et al. *Am J Obstet Gynecol* 1992;166(5):1473–81.
33. Stumpflen I et al. *Lancet* 1996;348(9031):854–7.
34. Vinals F et al. *Ultrasound Obstet Gynecol* 2003;22(4):358–67.
35. Del Bianco A et al. *J Perinat Med* 2006;34(4):309–12.
36. Zalel Y et al. *Prenat Diagn* 2004;24(3):174–8.
37. Yagel S et al. *J Ultrasound Med* 2015;34(1):143–9.
38. Persico N et al. *Ultrasound Obstet Gynecol* 2011;37(3):296–301.
39. Smrcek JM et al. *J Ultrasound Med* 2006;25(2):187–96.
40. Smrcek JM et al. *J Ultrasound Med* 2006;25(2):173–82; quiz 83–5.
41. Khalil A, Nicolaides KH. *Semin Fetal Neonatal Med* 2013;18(5):251–60.
42. Yagel S et al. *Circulation* 1997;96(2):550–5.
43. Zidere V et al. *Ultrasound Obstet Gynecol* 2013;42(6):679–86.
44. Clur SA, Bilardo CM. *Prenat Diagn* 2014;34(13):1235–45.
45. Moon-Grady A et al. *J Am Soc Echocardiogr* 2012;25(12):1342–52.
46. Ewigman BG et al. *N Engl J Med* 1993;329(12):821–7.
47. Garne E et al. *Ultrasound Obstet Gynecol* 2001;17(5):386–91.
48. Tegnander E et al. *Ultrasound Obstet Gynecol* 1995;5(6):372–80.
49. Acherman RJ et al. *J Ultrasound Med* 2007;26(12):1715–9; quiz 20–1.
50. Corcoran S et al. *Eur J Obstet Gynecol Reprod Biol* 2016;203:260–3.
51. Marek J et al. *Heart* 2011;97(2):124–30.
52. Friedberg MK, Silverman NH. *Prenat Diagn* 2004;24(10):781–6.
53. Ott WJ. *Am J Obstet Gynecol* 1995;172(6):1741–7; discussed 7–9.
54. Randall P et al. *BJOG* 2005;112(1):24–30.
55. Callan NA et al. *Am J Perinatol* 1991;8(6):390–4.
56. Simpson LL. *J Clin Ultrasound* 2004;32(3):123–8.
57. Thorisdottir S et al. *Laeknabladid* 2010;96(2):93–8.
58. Chaoui R, McEwing R. *Ultrasound Obstet Gynecol* 2003;21(1):81–93.
59. Wu Q et al. *J Ultrasound Med* 2009;28(10):1319–24.
60. Yoo SJ et al. *Ultrasound Obstet Gynecol* 1997;9(3):173–82.
61. Hofbeck M et al. *Heart* 1997;77(3):198–204.
62. Lin MT et al. *Am Heart J* 2004;147(3):540–4.
63. Tomek V et al. *Pediatr Cardiol* 2009;30(2):194–6.
64. Mitchell JL et al. *Circulation* 2012;126(23):2688–95.
65. Schmidt KG et al. *J Am Coll Cardiol* 1991;17(6):1360–6.
66. Copel JA et al. *Am J Obstet Gynecol* 2000;182(4):813–7; discussion 7–9.
67. Lilja M. *Paediatr Perinat Epidemiol* 1992;6(4):416–22.
68. Martinez-Frias ML et al. *Am J Med Genet A* 2008;146A(1):15–25.
69. Fasouliotis SJ et al. *J Ultrasound Med* 2002;21(10):1145–58.
70. Yagel S et al. *Ultrasound Obstet Gynecol* 2010;36(1):93–111.
71. Yagel S et al. *Ultrasound Obstet Gynecol* 2010;35(6):741–50.
72. Weichert J et al. *Ultrasound Obstet Gynecol* 2011;37(5):543–8.
73. Lide B et al. *J Ultrasound Med* 2016;35(1):1–5.
74. Berg C et al. *Ultrasound Obstet Gynecol* 2006;28(3):275–81.
75. Copel JA et al. *Am J Obstet Gynecol* 1986;154(5):1121–32.
76. Fogel M et al. *Am J Perinatol* 1991;8(6):411–6.
77. Greenwood RD et al. *J Pediatr* 1974;85(6):818–21.

78. Greenwood RD et al. *J Pediatr* 1975;86(4):576–9.
79. Greenwood RD et al. *Clin Pediatr (Phila)* 1976;15(12):1101–4.
80. Greenwood RD et al. *Pediatrics* 1976;57(1):92–7.
81. Tennstedt C et al. *Heart* 1999;82(1):34–9.
82. Jansen FA et al. *Ultrasound Obstet Gynecol* 2015;45(1):27–35.
83. Nicolaides KH et al. *BMJ* 1992;304(6831):867–9.
84. Nicolaides KH et al. *Prenat Diagn* 2002;22(4):308–15.
85. Snijders RJ et al. *Lancet* 1998;352(9125):343–6.
86. Huggon IC et al. *Ultrasound Obstet Gynecol* 2004;24(4):390–8.
87. Haak MC et al. *Ultrasound Obstet Gynecol* 2005;25(3):246–52.
88. Burger NB et al. *Prenat Diagn* 2015;35(6):517–28.
89. Allan LD. *Cardiol Young* 2006;16(1):11–7.
90. Jelliffe-Pawlowski LL et al. *Am J Obstet Gynecol* 2015;212(4): 518e1–10.
91. Hyett J et al. *Ultrasound Obstet Gynecol* 1996;7(4):245–50.
92. Hyett J et al. *BMJ* 1999;318(7176):81–5.
93. Bahado-Singh RO et al. *Am J Obstet Gynecol* 2005;192(5): 1357–61.
94. Mavrides E et al. *Ultrasound Obstet Gynecol* 2001;17(2):106–10.
95. Muller MA et al. *Prenat Diagn* 2007;27(2):164–9.
96. Simpson LL et al. *Obstet Gynecol* 2007;109(2 Pt 1):376–83.
97. Westin M et al. *Ultrasound Obstet Gynecol* 2006;27(6):632–9.
98. Ghi T et al. *Ultrasound Obstet Gynecol* 2001;18(6):610–4.
99. Makrydimas G et al. *Am J Obstet Gynecol* 2003;189(5):1330–5.
100. Atzei A et al. *Ultrasound Obstet Gynecol* 2005;26(2):154–7.
101. Clur SA et al. *Prenat Diagn* 2009;29(8):739–48.
102. Bilardo CM et al. *Ultrasound Obstet Gynecol* 2001;17(4):288–94.
103. Matias A et al. *Ultrasound Obstet Gynecol* 1999;14(5):307–10.
104. Papatheodorou SI et al. *BJOG* 2011;118(12):1438–45.
105. Maiz N et al. *Ultrasound Obstet Gynecol* 2008;31(3):256–60.
106. Pereira S et al. *Obstet Gynecol* 2011;117(6):1384–91.
107. Karatza AA et al. *Heart* 2002;88(3):271–7.
108. AlRais F et al. *Prenat Diagn* 2011;31(10):978–84.
109. Nora JJ et al. *N Engl J Med* 1967;277(11):568–71.
110. Bahtiyar MO et al. *J Ultrasound Med* 2007;26(11):1491–8.
111. Pettit KE et al. *J Perinatol* 2013;33(6):457–61.
112. Manning N, Archer N. *Prenat Diagn* 2006;26(11):1062–4.
113. Herberg U et al. *Heart* 2006;92(1):95–100.
114. Pruetz JD et al. *Prenat Diagn* 2011;31(10):973–7.
115. Losada E et al. *Circulation* 2010;122(15):1456–63.
116. Moon-Grady AJ et al. *Ultrasound Obstet Gynecol* 2011;37(1): 27–33.
117. Mari G et al. *N Engl J Med* 2000;342(1):9–14.
118. Copel JA et al. *Am J Obstet Gynecol* 1989;161(2):361–5.
119. Machin GA. *Am J Med Genet* 1981;9(4):341–50.
120. Society for Maternal-Fetal Medicine (SMFM), Norton ME et al. *Am J Obstet Gynecol* 2015;212(2):127–39.
121. Dashe JS et al. *Obstet Gynecol* 2002;100(1):134–9.
122. Rowland TW et al. *J Pediatr* 1973;83(5):815–20.
123. Miller E et al. *N Engl J Med* 1981;304(22):1331–4.
124. Cousins L. *Clin Obstet Gynecol* 1991;34(3):481–93.
125. Ylinen K et al. *Br Med J (Clin Res Ed)* 1984;289(6441):345–6.
126. Ray JG et al. *QJM* 2001;94(8):435–44.
127. Lisowski LA et al. *Herz* 2010;35(1):19–26.
128. Shields LE et al. *Obstet Gynecol* 1993;81(6):954–7.
129. Starikov R et al. *Pediatr Cardiol* 2013;34(7):1716–22.
130. Weber HS et al. *J Pediatr* 1991;118(1):103–7.
131. Jaeggi ET et al. *Ultrasound Obstet Gynecol* 2001;17(4):311–5.
132. Lee PJ et al. *Pediatrics* 2003;112 (6 Pt 2):1553–6.
133. Lenke RR, Levy HL. *N Engl J Med* 1980;303(21):1202–8.
134. Levy HL, Waisbren SE. *N Engl J Med* 1983;309(21):1269–74.
135. Platt LD et al. *Am J Obstet Gynecol* 2000;182(2):326–33.
136. Koch R et al. *Eur J Pediatr* 2000;159(suppl 2):S156–60.
137. Levy HL et al. *Prenat Diagn* 1996;16(7):599–604.
138. Chameides L et al. *N Engl J Med* 1977;297(22):1204–7.
139. McCue CM et al. *Circulation* 1977;56(1):82–90.
140. Brucato A et al. *Arthritis Rheum* 2001;44(8):1832–5.
141. Buyon JP et al. *J Am Coll Cardiol* 1998;31(7):1658–66.
142. Costedoat-Chalumeau N et al. *Arthritis Rheum* 2004;50(10): 3187–94.
143. Friedman DM et al. *Circulation* 2008;117(4):485–93.
144. Jaeggi E et al. *J Am Coll Cardiol* 2010;55(24):2778–84.
145. Cuneo BF et al. *Am J Cardiol* 2011;107(5):761–6.
146. Krishnan AN et al. *J Matern Fetal Neonatal Med* 2008;21(11): 776–82.
147. Nield LE et al. *J Am Coll Cardiol* 2002;40(4):796–802.
148. Trucco SM et al. *J Am Coll Cardiol* 2011;57(6):715–23.
149. Nii M et al. *Heart* 2006;92(12):1831–7.
150. Small M, Copel JA. *Pediatr Cardiol* 2004;25(3):210–22.
151. Krishnan A et al. *Prenat Diagn* 2014;34(12):1207–12.
152. Saleeb S et al. *Arthritis Rheum* 1999;42(11):2335–45.
153. Madsen NL et al. *Congenit Heart Dis* 2013;8(2):131–41.
154. Gilboa SM et al. *Am J Obstet Gynecol* 2010;202(1):5e11–e10.
155. Jenkins KJ et al. *Circulation* 2007;115(23):2995–3014.
156. Botto LD et al. *Epidemiology* 2001;12(5):485–90.
157. Dreier JW et al. *Pediatrics* 2014;133(3):e674–88.
158. Stuckey D. *Br Heart J* 1956;18(4):519–22.
159. Wright VC et al. *MMWR Surveill Summ* 2008;57(5):1–23.
160. Ericson A, Kallen B. *Hum Reprod* 2001;16(3):504–9.
161. Hansen M et al. *N Engl J Med* 2002;346(10):725–30.
162. Koivurova S et al. *Hum Reprod* 2002;17(5):1391–8.
163. Lie RT et al. *Int J Epidemiol* 2005;34(3):696–701.
164. Rimm AA et al. *J Assist Reprod Genet* 2004;21(12):437–43.
165. Bahtiyar MO et al. *J Ultrasound Med* 2010;29(6):917–22.
166. Reefhuis J, Honein MA. *Birth Defects Res A Clin Mol Teratol* 2004;70(9):572–9.
167. Katalinic A et al. *Fertil Steril* 2004;81(6):1604–16.
168. Olson CK et al. *Fertil Steril* 2005;84(5):1308–15.
169. Rimm AA et al. *J Assist Reprod Genet* 2011;28(8):699–705.
170. Reefhuis J et al. *Hum Reprod* 2009;24(2):360–6.
171. Tararbit K et al. *Hum Reprod* 2013;28(2):367–74.
172. Burn J et al. *Lancet* 1998;351(9099):311–6.
173. Oyen N et al. *Circulation* 2009;120(4):295–301.
174. Nora JJ, Nora AH. *Am J Cardiol* 1987;59(5):459–63.
175. Emanuel R et al. *Br Heart J* 1983;49(2):144–7.
176. Rose V et al. *J Am Coll Cardiol* 1985;6(2):376–82.
177. Whittemore R et al. *J Am Coll Cardiol* 1994;23(6):1459–67.
178. Gill HK et al. *J Am Coll Cardiol* 2003;42(5):923–9.
179. Fesslova V et al. *J Pregnancy* 2011;2011:368067.
180. Cripe L et al. *J Am Coll Cardiol* 2004;44(1):138–43.
181. Nora JJ, Nora AH. *Prog Med Genet* 1983;5:91–137.
182. Pradat P. *Genet Epidemiol* 1994;11(2):131–40.
183. Peyvandi S et al. *Am J Med Genet A* 2014;164A(6):1490–5.
184. Hinton RB, Jr. et al. *J Am Coll Cardiol* 2007;50(16): 1590–5.
185. Calcagni G et al. *Eur J Pediatr* 2007;166(2):111–6.
186. McBride KL et al. *Am J Med Genet A* 2005;134A(2):180–6.
187. Quartermain MD et al. *Pediatrics* 2015;136(2):e378–85.
188. Friedberg MK et al. *J Pediatr* 2009;155(1):26–31, e1.
189. Pinto NM et al. *Ultrasound Obstet Gynecol* 2012;40(4):418–25.
190. Friedman AM et al. *Obstet Gynecol* 2011;118(4):921–7.
191. Skeels M et al. *Pediatr Cardiol* 2002;23(6):594–7.
192. Starikov RS et al. *J Ultrasound Med* 2009;28(5):603–8.

# 8

# Circulation in the normal fetus and cardiovascular adaptations to birth

Abraham M. Rudolph

## Fetal circulation

Postnatally, oxygen uptake and carbon dioxide removal from the body occur in the lungs. Energy substrates are absorbed in the gastrointestinal tract and delivered to the liver through the portal venous system before entering the general circulation. In the mammalian fetus, oxygen uptake and carbon dioxide removal are accomplished in the placenta through the umbilical circulation. Energy substrates diffuse or are actively transported from the maternal circulation across the placental membrane and are transferred to the fetal body via the umbilical vein. Although a proportion of the substrates enter the hepatic circulation, a variable amount bypasses the liver to enter the general fetal circulation via the ductus venosus.

### *Course of the circulation*

Postnatally, the pulmonary circulation is completely separated from the systemic circulation. Well-oxygenated arterial blood ejected by the left ventricle flows through the systemic arteries to supply all tissues of the body with oxygen and nutrients. Blood then enters the systemic venous system and returns to the right atrium and ventricle; it is ejected into the pulmonary arterial circulation and returns to the left atrium and ventricle through the pulmonary veins. Blood thus flows serially through the circulation and, apart from passage of a small amount of coronary venous blood into the left ventricular cavity through thebesian veins, no mixing of arterial and venous blood occurs.

In the fetus, oxygenated blood returns to the body through the umbilical venous system. This blood mixes with systemic venous blood before entering the cardiac ventricles to be ejected to perfuse the fetal body. As seen in Figure 8.1, the umbilical vein enters the porta hepatis and gives rise to several branches that are distributed to the left lobe of the liver.[1] Distal to the branches supplying the left lobe, the ductus venosus originates and passes first posteriorly and then superiorly to connect with the inferior vena cava. The umbilical vein then arches to the right lobe, where it is joined by the portal vein. After this junction, branches are distributed to the right lobe of the liver. The left hepatic vein drains into the inferior vena cava in close proximity to the ductus venosus. In the sheep fetus, the left hepatic vein and ductus venosus drain through a common orifice on the left posterior aspect of the vena cava. In the human, the two vessels drain through adjacent orifices separated by a sharp ridge. In the fetal lamb, a thin valve-like membrane covers the distal orifice of the ductus venosus and left hepatic vein.[2,3] Although the function of this membrane has not been defined, I have proposed that it facilitates preferential streaming of blood flow, as mentioned in the following text. The right hepatic vein drains separately into the right and posterior aspect of the inferior vena cava, and the orifice is also partly covered by a distal valve-like membrane. Based on angiographic studies in which contrast medium was injected into the umbilical vein, Lind et al. suggested that umbilical venous blood passing through the ductus venosus flowed largely to the left atrium through the foramen ovale.[4] We have studied the distribution of umbilical and portal venous and inferior vena cava blood in fetal lambs by injecting radionuclide-labeled microspheres into each vessel and determining the distribution of the spheres in the fetal body.[5,6] Umbilical venous blood is distributed to the left lobe of the liver, which receives about 90% of its blood supply from this source; the remaining 10% is derived from the descending aorta through the hepatic artery. Almost all the blood passing through the ductus venosus (92%–95%) is from the umbilical vein; the remaining small amount is contributed by the portal vein. Umbilical venous blood is distributed to the right lobe of the liver through the arcuate connection to the portal vein. Most portal venous blood flows to the right lobe of the liver. Only a small amount passes through the ductus venosus, and none is distributed to the left lobe of the liver. The ductus venosus acts as a bypass for umbilical venous blood. To some extent it reduces the resistance to the flow of umbilical venous blood to the inferior vena cava by diverting it away from the hepatic microcirculation. The proportion of umbilical venous blood that passes through the ductus varies greatly, both in the lamb and in the human fetus, from about 20%–90%, with an average of about 50%.[7,8]

Ductus venosus blood is preferentially distributed through the foramen ovale into the left atrium and left ventricle, whereas abdominal inferior vena cava blood flows preferentially through the tricuspid valve to the right ventricle.

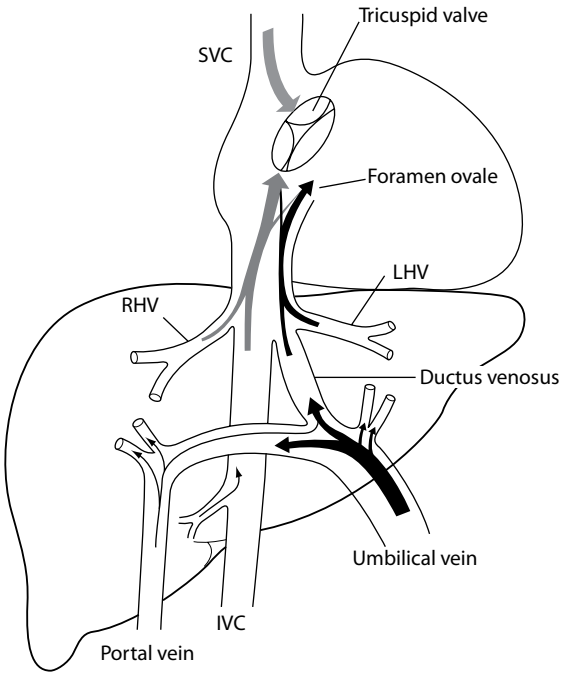


**Figure 8.1**
Course of blood flow in the region of the porta hepatis. Umbilical venous blood is distributed to the left lobe of the liver. The ductus venosus arises from the umbilical vein, which then arches to the right to join the portal vein. Portal venous blood is largely distributed to the right liver lobe and only a small proportion passes through the ductus venosus. (Reproduced with permission from Rudolph AM. *Congenital Diseases of the Heart*. Chichester, UK: Wiley; 2009.[1])

The distribution of blood from the left and right hepatic veins was also examined using radionuclide-labeled microspheres in fetal sheep. Blood from the left hepatic vein, which enters the inferior vena cava through the same orifice as the ductus venosus, also flows preferentially across the foramen ovale. In contrast, right hepatic venous blood streams preferentially across the tricuspid valve, similarly to the flow of abdominal inferior vena caval blood (Figure 8.1). These streaming patterns of abdominal inferior vena cava blood and ductus venosus blood can be identified by direct observation of the thin-walled inferior vena cava in the thorax of the fetal lamb *in utero*. A stream of well-oxygenated blood from the ductus venosus and left hepatic vein can be identified on the left anterior aspect of the vena cava; a poorly oxygenated stream from the abdominal inferior vena cava and right hepatic vein is observed on the posterior right aspect of the vena cava. Similar streaming has been observed in the inferior vena cava and atria in fetal sheep by color flow Doppler studies.[9] The ductus venosus stream is directed largely through the foramen ovale, whereas distal inferior vena cava blood streams across the tricuspid valve. Ultrasound examinations of human fetuses have also shown similar flow patterns of blood in the ductus venosus and abdominal inferior vena cava.[10,11]

The mechanisms responsible for this selective streaming have not been fully defined. In the sheep fetus, the valvelike structures over the entrance of the ductus venosus and left hepatic vein may direct the blood draining from these vessels toward the foramen ovale. Similarly, right hepatic venous blood may be deflected by the valve toward the tricuspid valve. These valves are not well defined in the human fetus, so other mechanisms must account for preferential streaming. The inferior margin of the atrial septum separates the entrance of the inferior vena cava from the left atrium. The crista dividens, the crescentic edge of the superior portion of the atrial septum, overlies the inferior vena cava, so that the posterior left portion of the inferior vena cava connects directly through the foramen ovale to the left atrium. During phases of the cardiac cycle, the eustachian valve and the lower portion of the atrial septum move in unison, either to the left, to facilitate blood through the foramen ovale, or to the right, to direct flow through the tricuspid valve.[9] This will tend to direct blood on the left posterior aspect of the vena cava through the foramen ovale. Another mechanism that has been proposed is that different velocities of the streams tend to allow separation in the inferior vena cava.[9–11] The mean velocity of the abdominal inferior vena cava stream is relatively low (about 15 cm/s). The ductus venosus mean velocity is, however, much higher (about 55–60 cm/s). It is suggested that this high velocity permits the stream to maintain a degree of separation from the abdominal inferior vena cava stream in the thoracic portion of the inferior vena cava and carry the blood through the foramen ovale. This preferential streaming of ductus venosus and left hepatic venous blood through the foramen ovale provides blood of higher oxygen saturation to the left atrium and ventricle and thus into the ascending aorta. Abdominal inferior vena cava blood and the right hepatic venous blood of lower oxygen saturation are preferentially distributed into the right ventricle and pulmonary artery.

Flow across the foramen ovale into the left atrium is influenced by two other factors: magnitude of pulmonary blood flow and left ventricular end-systolic volume. If pulmonary blood flow is high, the large pulmonary venous return would elevate left atrial pressure and thus flow across the foramen ovale would be decreased; a decrease in pulmonary blood flow would result in an increase of right to left flow through the foramen ovale. Left ventricular end-systolic volume may be increased if afterload on the left ventricle is increased, as with left ventricular outflow obstruction. Pressure during early diastole would thus be elevated, and this would limit flow across the foramen ovale and mitral valve into the left ventricle. Effective emptying of the left ventricle during systole, as may occur if afterload is low, will be associated with a reduction in end-systolic volume, and flow across the foramen ovale would be increased.

Almost all superior vena cava blood passes through the tricuspid valve into the right ventricle. Normally, about 5% or less flows through the foramen ovale into the left atrium. Ultrasound studies in fetal lambs demonstrated that the small amount of superior vena cava blood that enters the foramen ovale does so indirectly. It is first diverted in a retrograde direction into the upper portion of the inferior vena cava during atrial systole and then enters the foramen during the rapid inflow phase from the inferior vena cava.[9]

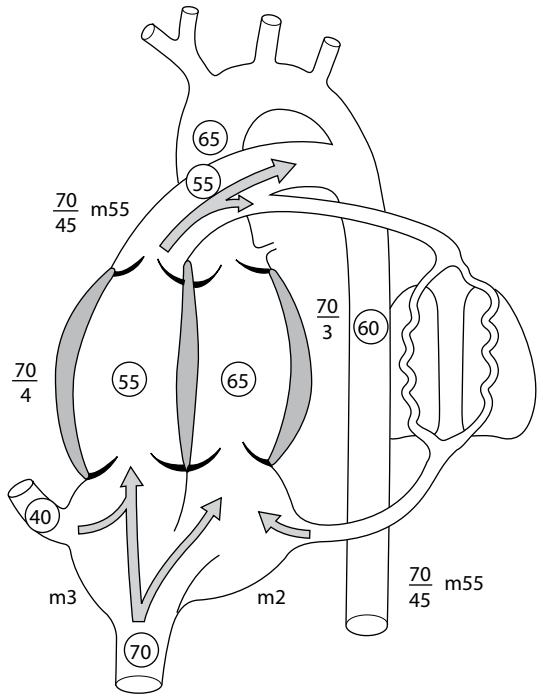


**Figure 8.2**
Course of the circulation in the heart and great vessels in the late-gestation fetal lamb. The figures in circles within the chambers and vessels represent percent oxygen saturation levels. The figures alongside the chambers and vessels are pressures in millimeters of mercury (mm Hg) related to amniotic pressure level as zero. (m, mean pressure.) (Reproduced with permission from Rudolph AM. *Congenital Diseases of the Heart*. Chichester, UK: Wiley; 2009.[1])

Right ventricular blood is ejected into the pulmonary trunk; a small proportion passes into the pulmonary circulation but the majority is directed through the ductus arteriosus to the descending aorta (Figure 8.2). Normally, none of the blood flowing through the ductus arteriosus passes in a retrograde fashion across the aortic isthmus to the ascending aorta and its branches. The left atrium receives blood from the foramen ovale and pulmonary veins, and then empties into the left ventricle, which ejects into the ascending aorta. Most ascending aortic blood is distributed to the coronary circulation, head and cerebral circulation, and upper extremities; only a small proportion passes across the aortic isthmus into the descending aorta. Descending aortic blood is distributed to the abdominal organs and the tissues of the lower trunk and lower extremities, but a large amount enters the umbilical-placental circulation.

## Admixture of oxygenated and systemic venous blood

In the adult circulation, there is essentially no mixing of oxygenated pulmonary venous and systemic venous blood. However, oxygenated umbilical venous and poorly oxygenated systemic venous blood mix at several sites in the fetal circulation before being distributed to the systemic arteries. A proportion of umbilical venous blood mixes with portal venous blood and enters the central circulation through the right hepatic vein. Blood from the ductus venosus, left and right hepatic veins, and abdominal inferior vena cava all enter the thoracic portion of the inferior vena cava. Preferential streaming of blood from the ductus venosus and left hepatic vein to some extent separates well-oxygenated and poorly oxygenated blood. In the left atrium, blood entering the foramen ovale from the inferior vena cava is joined by pulmonary venous blood, which, in the fetus, has a relatively low oxygen saturation. Systemic venous blood is preferentially directed into the right ventricle, pulmonary trunk, and ductus arteriosus to the descending aorta and its branches to supply the arterial branches of the lower body, as well as the placenta. Thus, blood delivered to all fetal tissues and to the placenta is a mixture of oxygenated umbilical venous and systemic venous blood.

Some umbilical venous blood is returned to the placenta without first being delivered to fetal tissues to permit oxygen uptake. This arrangement is inefficient because it imposes an additional workload on the heart to supply oxygen to the tissues. Similarly, blood returning to the heart from the superior and inferior vena cava that is distributed to the fetal tissues without first being delivered to the placenta for oxygenation contributes to the inefficiency of the fetal circulation. In the sheep fetus under normal conditions, about 45% of superior vena cava blood and 53% of inferior vena cava blood are returned to the fetal tissues without having had the opportunity to take up oxygen in the placenta. About 22% of umbilical venous blood is returned to the placenta without first passing through the systemic microcirculation. The inefficiency resulting from systemic venous and umbilical venous recirculation constitutes about 33% of the combined ventricular output of the fetal heart.

## Fetal vascular pressures

The fetus is surrounded by amniotic fluid in the uterus within the abdomen; it is customary to relate all vascular pressures to amniotic cavity pressure. Fetal pressures are thus raised by increases in intra-abdominal pressure as occurs with straining, gaseous distension, feeding, or uterine contraction. In the quietly standing ewe, intra-amniotic pressure is usually about 8–10 mm Hg above atmospheric pressure. Pressures in the cardiac chambers and major vessels in the lamb fetus are shown in Figure 8.2. All pressures are presented with amniotic pressure as baseline.

Umbilical venous pressure is about 8–10 mm Hg near the umbilical ring and 2–3 mm Hg higher near the placenta. Normally, the pressure shows a continuous flat contour, with no phasic change during atrial or ventricular systole. This lack of pulsatile pressure extends into the porta hepatis, where the mean pressure is 5–6 mm Hg. This is in contrast to the inferior and superior vena cavae, which show variations of pressure with the cardiac cycle. Postnatally, the left atrial is higher than the right atrial mean pressure; the right atrial

pressure contour shows a dominant a-wave, whereas the left atrium shows a dominant v-wave. In the fetus, the mean pressure in the superior and inferior vena cava and the right atrium is about 2–3 mm Hg, and a- and v-wave pressures are both about 4–5 mm Hg. Left atrial pressure has a contour similar to that of the right atrium, and the mean pressure is 1–2 mm Hg lower than right atrial pressure.

Right and left systolic and end-diastolic pressures are similar. In the lamb fetus, the right ventricular and pulmonary arterial systolic pressures tend to exceed the left ventricular and aortic pressures by 5–8 mm Hg during late gestation; this is probably the result of mild constriction of the ductus arteriosus. Aortic pressure increases with gestational age in the lamb fetus, from a mean level of 25–30 mm Hg at about 60 days' gestation to 60–70 mm Hg close to term, at about 145 days' gestation.

## Blood gases and oxygen saturation

Maternal arterial blood in the pregnant ewe has a $PO_2$ (partial pressure of oxygen) of 90–100 mm Hg and a $PCO_2$ of about 35 mm Hg. There is a large $PO_2$ gradient across the placenta; the $PO_2$ of umbilical venous blood is 32–35 mm Hg. Umbilical venous blood $PCO_2$ is about 40 mm Hg and the pH is 7.40. The P50 (the $PO_2$ at which hemoglobin is 50% saturated with oxygen) for fetal blood in the sheep is considerably lower (about 27 mm Hg) than that of adult blood (about 38 mm Hg). Therefore, when $PO_2$ of umbilical venous blood is 32–35 mm Hg, oxygen saturation is about 90%. Oxygen saturations of blood in various cardiac chambers and great vessels measured in the fetal lamb are shown in Figures 8.2 and 8.3. Umbilical venous blood has an oxygen saturation of 80%–90%. The left hepatic venous blood oxygen saturation is about 75%, whereas right hepatic venous blood oxygen saturation is lower, at about 65%. This is related to the difference in the blood supplying the left and right lobes of the liver, as discussed previously.

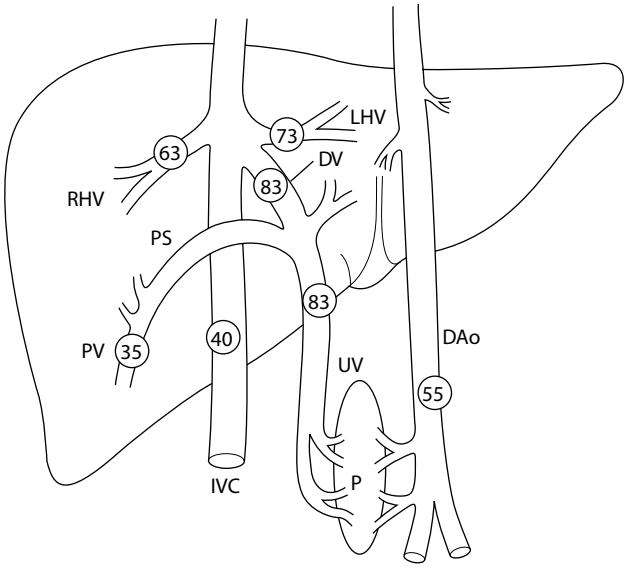


**Figure 8.3**
Oxygen saturations of blood in the vessels in the region of the porta hepatis and in the inferior vena cava and hepatic veins. (Reproduced with permission from Rudolph AM. *Congenital Diseases of the Heart*. Chichester, UK: Wiley; 2009.[1])

Blood in the abdominal inferior vena cava distal to the entrance of the ductus venosus and hepatic veins has a $PO_2$ of about 12–14 mm Hg and an oxygen saturation of 35%–40%. The $PO_2$ and oxygen saturation in superior vena cava blood are similar. The $PO_2$ of right ventricular and pulmonary arterial blood is 18–20 mm Hg, and oxygen saturation is about 50%. Left ventricular and ascending aortic blood has a $PO_2$ of about 25–28 mm Hg and an oxygen saturation of about 65%, whereas descending aortic blood has a $PO_2$ of 20–23 mm Hg and an oxygen saturation of about 55%. Systemic arterial blood has a $PCO_2$ of 43–45 mm Hg and a pH of about 7.38–7.39. Reliable values for blood gases and oxygen saturations for the human fetus *in utero* are not available.

## Effects of administering oxygen to the mother

Administering 100% oxygen to the ewe raises her arterial oxygen saturation to 100% and the $PO_2$ to more than 400 mm Hg. Umbilical venous blood $PO_2$ in the fetal lamb increases to 40–50 mm Hg, and oxygen saturation reaches 95%–100%. Arterial $PO_2$ increases to only 30–35 mm Hg, with an oxygen saturation of about 80%. The large oxygen difference between the maternal arterial and fetal umbilical venous $PO_2$ is the result of diffusion limitation across the placental membrane. The separation between the maternal and fetal circulations in the sheep is fairly broad, because the sheep has a syndesmochorial placenta. It is possible that the maternal-fetal oxygen gradient is lower in the human fetus because the placental membrane has fewer layers.

## Cardiac output and its distribution

Postnatally blood is ejected by the left ventricle into the aorta and distributed to the tissues; it returns through the veins to the right atrium and is ejected by the right ventricle to the pulmonary circulation and returns to the left atrium and ventricle. In this circulation, the volume of blood ejected by each ventricle is similar and is termed the *cardiac output*. In the fetus, as mentioned previously, systemic and umbilical venous blood mix, and the mixed blood is distributed to the various parts of the body and to the placenta; blood to many organs is derived from both ventricles. Unlike in the postnatal circulation, the volumes of blood ejected by left and right ventricles are different in the fetus. The output of the heart is usually expressed as combined ventricular output (CVO), the sum of the volumes ejected by the two ventricles. In chronically instrumented fetal lambs during the later months of gestation (term is about 145 days), the combined ventricular output is about 450 mL/min/kg fetal body weight.[12,13]

Umbilical-placental blood flow is about 200 mL/min/kg body weight, and blood flow to the fetal body is about 250 mL/min/kg. The right ventricle ejects about two-thirds and the left ventricle about one-third of combined ventricular output in the fetal lamb (Figures 8.4 and 8.5).

Umbilical-placental flow of about 200 mL/min/kg represents 40%–45% of CVO. Although the proportions vary, about 55% of umbilical venous blood passes through the ductus venosus and 45% through the hepatic circulation. Thus, about 110 mL/min/kg passes through the ductus venosus. The right and left lobes of the liver receive a total of about 90 mL/min/kg fetal body weight of blood from the umbilical vein, and the right lobe receives ~30 mL/min/kg fetal body weight from the portal vein. Inferior vena cava blood distal to the entrance of the hepatic veins and ductus venosus (abdominal inferior vena cava) is derived from the lower body organs and the lower extremities as well as the lower portion of the trunk. In the fetal lamb, this is approximately 30% of CVO or about 135 mL/min/kg.

The blood entering the heart from the inferior vena cava includes blood from the ductus venosus, left and right hepatic veins, and abdominal inferior vena cava, and constitutes about 70% of CVO, or about 315 mL/min/kg (Figures 8.4 and 8.5). About 115 mL/min/kg or about 25% of CVO passes through the foramen ovale to the left atrium; this blood is derived predominantly from the ductus venosus. Venous return from the superior vena cava is 90–95 mL/min/kg, representing about 21% of CVO, and is largely directed across the tricuspid valve into the right ventricle. About 200 mL/min/kg of inferior vena cava blood as well as coronary venous blood enters the right ventricle. The right ventricle ejects about 66% of CVO, or about 300 mL/min/kg. Only about 10%–15% of the blood ejected by the right ventricle is directed to the pulmonary circulation; this constitutes about 8% of CVO or about 35 mL/min/kg fetal weight. The remaining 58% of CVO, about 265 mL/min/kg, passes through the ductus arteriosus.

The left ventricle receives the 115 mL/min/kg of blood that passes through the foramen ovale as well as about 35 mL/min/kg from pulmonary venous return. It ejects about 150 mL/min/kg, representing about 33% of CVO. Less than a third of the blood ejected by the left ventricle passes across the aortic isthmus to the descending aorta. This represents about 10% of CVO or about 45 mL/min/kg. The coronary circulation receives about 3% of CVO; about 20% of CVO, or about 90 mL/min/kg, is distributed to the head, brain, upper extremities, and upper portion of the trunk. The magnitude of blood flow through the major arteries is reflected by the relative diameters of these vessels. The pulmonary trunk is very large, and the ascending aorta somewhat narrower; the descending aorta is also very wide, whereas the isthmus of the aorta is much narrower than the ascending or descending aorta and the ductus arteriosus.

The combined ventricular output is about 450 mL/min/kg fetal body weight. In the sheep fetus it is fairly constant in

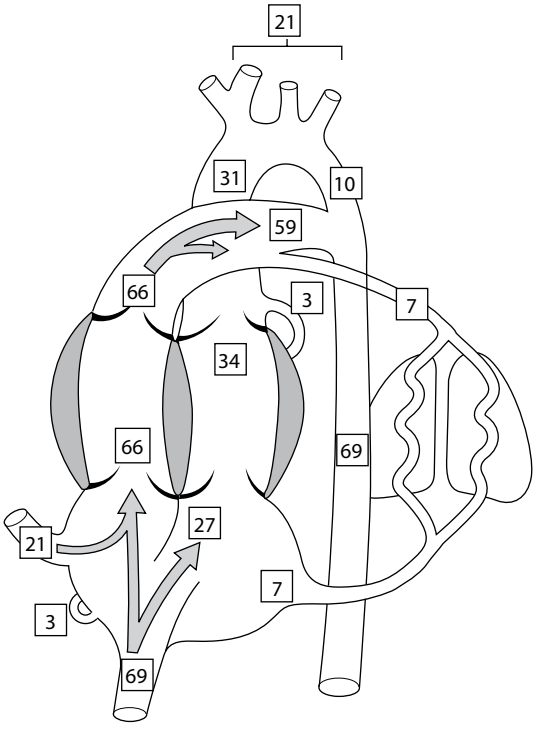


**Figure 8.4**
The percentages of the combined ventricular output that return to the fetal heart that are ejected by each ventricle and that flow through the main vascular channels. Figures represent values for late-gestation lambs. (Reproduced with permission from Rudolph AM. *Congenital Diseases of the Heart*. Chichester, UK: Wiley; 2009.[1])

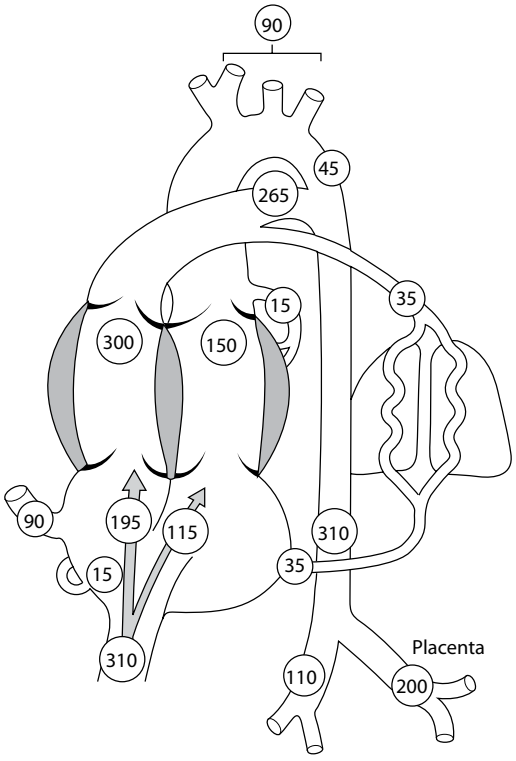


**Figure 8.5**
The volumes of blood flowing through cardiac chambers and great vessels for the late-gestation fetal lamb (mL/min/kg body weight). (Reproduced with permission from Rudolph AM. *Congenital Diseases of the Heart*. Chichester, UK: Wiley; 2009.[1])

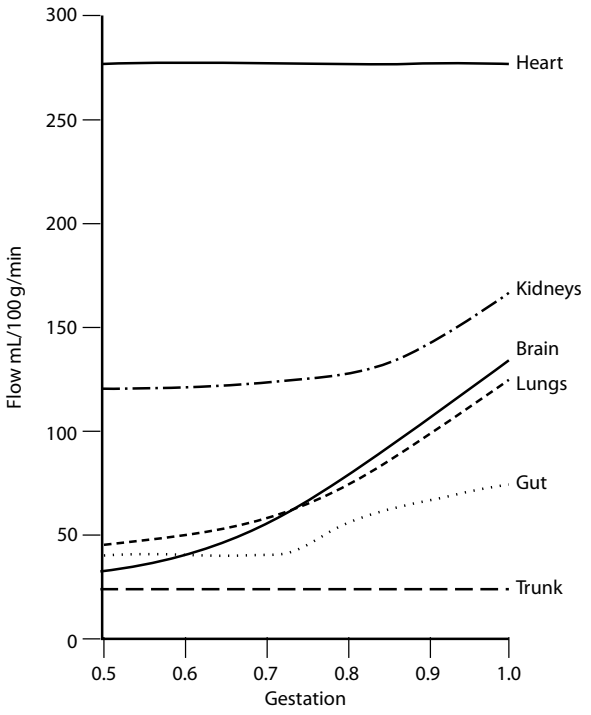


**Figure 8.6**
Changes in blood flow to various organs in relation to tissue weight in the fetal lamb during the latter half of gestation. (Reproduced with permission from Rudolph AM. *Congenital Diseases of the Heart*. Chichester, UK: Wiley; 2009.[1])

relation to fetal body weight from about 90 to 140 days' gestation (term is 140–145 days). In the last few days of pregnancy, there is a modest fall in CVO related to body weight. This could be related to uterine contraction or other unidentified factors. The proportions of CVO distributed to different organs change during gestational development. In the fetal lamb, the placenta receives about 42%–44% of CVO at 75–90 days' gestation; the proportion falls slightly to 36%–38% in the latter weeks of gestation. The percentage distributed to the brain and lungs increases with gestational age. This change during growth is more striking when the changes in blood flow per unit of organ tissue weight are examined. Changes in organ blood flow per 100 g of weight, during development of the fetal lamb, are shown in Figure 8.6. At about 110 days (0.75 gestation), blood flow per 100 g organ weight progressively increases to the brain, gut, and lungs. The cause of the increase in flow to these organs is not known; it could be related to an increase in size of the vascular bed due to the growth of new vessels, or to increased metabolic activity with vasodilatation, or a combination of these factors.

## *Circulation in the human fetus*

Blood flows in the human fetus have been studied using Doppler flow analysis and also using magnetic resonance imaging (MRI).[14–18] The general course of the circulation in the human fetus is similar to that in the lamb. The pattern of flow in the liver region of the human also appears to be similar to that of the lamb fetus. In fetal lambs, Doppler flow studies demonstrated a blood flow velocity of 55–60 cm/s in the ductus venosus, whereas the velocity in the abdominal inferior vena cava was only about 16 cm/s.[20] The ductus venosus stream was directed preferentially through the foramen ovale (see section "Course of the circulation"). In the human fetus, blood flow velocity in the ductus venosus has been reported to be 65–75 cm/s, and the ductus venosus stream also preferentially flows through the foramen ovale.[19,20]

Although reports of left and right ventricular output vary considerably, the combined ventricular output appears to be similar to that in the sheep fetus at about 450–500 mL/min/kg estimated weight. However, the proportions of combined ventricular output distributed to body organs differ, because of differences in body configuration and the relative weights of some organs.

## Cardiac output and its distribution in the human fetus

The ratio of right to left ventricular output, which in the sheep is about 2:1, is about 1.2–1.3:1 in the human.[14–16] Thus, whereas right ventricular output is about 66% and left ventricular output about 33% of combined ventricular output in the lamb fetus, in the human fetus the right ventricle ejects about 55%–60% and the left ventricle 40%–45% of combined ventricular output. There are also major differences in the proportions of cardiac output that are distributed to some organs, particularly the brain, the lungs, and the placenta.

Perhaps the most important factor is brain size; in the human fetus the brain constitutes 12%–13% of body weight, as compared with 2%–3% in the lamb. Near term, both human and sheep fetal body weights are about 3.5 kg, and brain weights are about 75 g in the sheep and 420 g in the human. In the fetal sheep, brain blood flow changes dramatically with advancing gestation. At 0.5 gestation, brain blood flow is about 30 mL/min/100 g brain weight, and this represents about 2.5% of combined ventricular output. Near term, brain blood flow increases to about 120 mL/min/100 g, and this requires about 3.5% of combined ventricular output in the lamb. If it is assumed that brain flow in relation to brain weight changes similarly in the human fetus with gestational age, because of the relatively much greater weight of the brain, blood flow to the brain would require about 10% of combined ventricular output at 20 weeks' gestation, but 35%–40% near term. This would place a considerable extra volume load on the heart.

In the sheep fetus, about 4% of combined ventricular output is distributed to the lungs at 0.5 gestation, and this increases to 7%–8% near term. Pulmonary blood flow is considerably higher in the human fetus; it is about 12%–13% of combined ventricular output at 20 weeks and increases markedly to about 25% after 30 weeks' gestation.[21,22] Blood flow to the left ventricle is derived from the pulmonary venous return and right-to-left flow of blood across the foramen ovale. In the sheep fetus, because pulmonary blood is relatively low, the

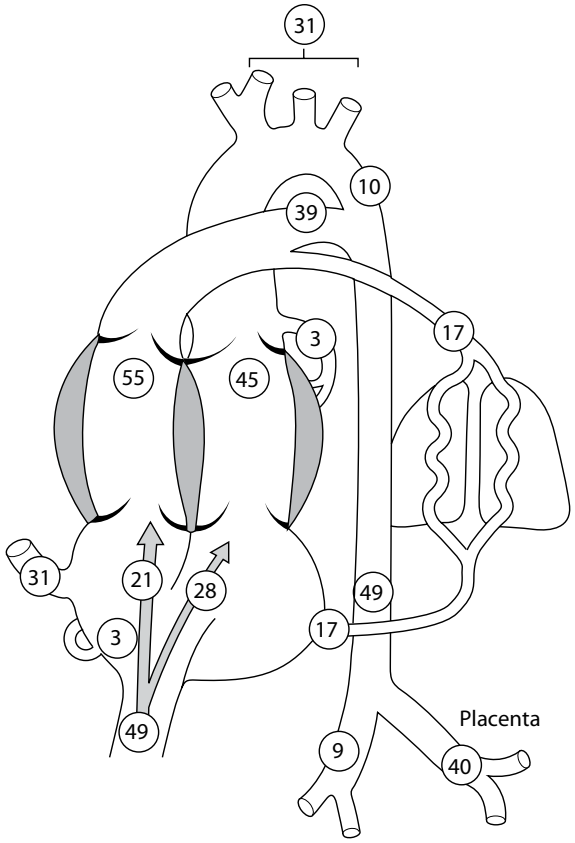


**Figure 8.7**
The percentages of the combined ventricular output that return to the fetal heart that are ejected by each ventricle and that flow through the main vascular channels for the late-gestation human fetus. (Modified from Rudolph AM. *Congenital Diseases of the Heart*. Chichester, UK: Wiley; 2009.[1])

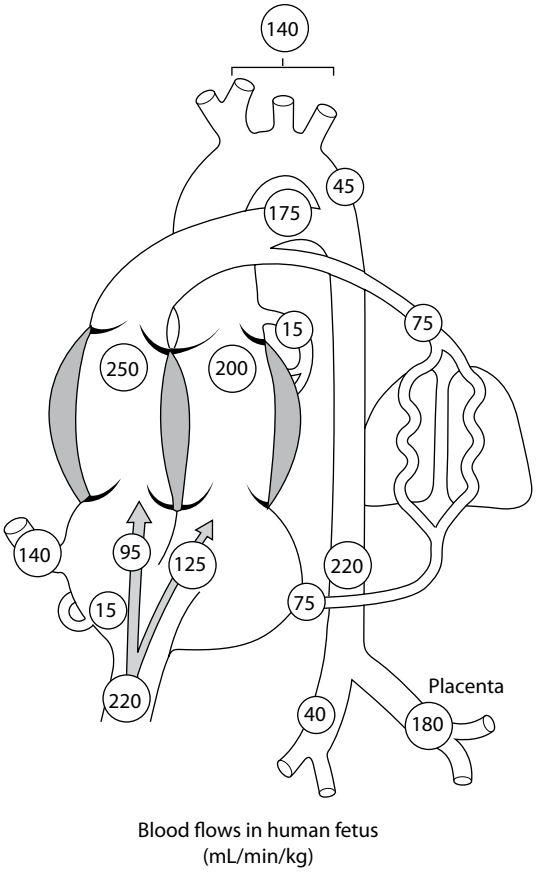


**Figure 8.8**
The volumes of blood (mL/min/kg) flowing through cardiac chambers and great vessels of the late-gestation human fetus. (Modified from Rudolph AM. *Congenital Diseases of the Heart*. Chichester, UK: Wiley; 2009.[1])

major proportion of flow into the left ventricle is derived from flow across the foramen ovale; this does not change much with gestation, because the increase on pulmonary blood flow with advancing gestation is relatively small. However, in the human fetus, at 20 weeks' gestation, pulmonary blood flow constitutes 13% of combined ventricular output and foramen ovale flow 34%. Beyond 30 weeks, pulmonary blood flow increases to 25%, but foramen ovale flow falls to 18% of combined ventricular output.[21]

Umbilical-placental blood flow is about 180 mL/min/kg fetal weight, and about 40% of combined ventricular output in the sheep, and it does not change significantly throughout gestation. Although umbilical blood flow has been reported to be about 180 mL/min/kg estimated fetal weight in the human,[16] more recent studies have reported lower flows of about 120–140 mL/min/kg.[19,20] It is also important that umbilical blood flow falls relative to fetal weight during the latter half of gestation, from about 140–150 mL/min/kg or about 33% of combine ventricular output at 20 weeks, to 120–125 mL/min/kg, or about 25% of combined ventricular output at 40 weeks' gestation. This fall in umbilical blood flow relative to fetal weight would restrict the amount of oxygen delivered to the fetus. To compensate for this, fetal hemoglobin concentration is adjusted. Thus, in the lamb, in which umbilical blood flow falls only slightly with advancing gestation, hemoglobin concentration rises from 8 g/dL at 0.5 gestation to 9 g/dL at term. However, in the human fetus it increases from 10 g/dL at 20 weeks' gestation to 16 g/dL at term.

The percentages of combined ventricular output ejected by the heart and distributed to the major vessels near term are shown in Figure 8.7, and the blood flows through various great vessels and ejected by each ventricle are depicted in Figure 8.8.

## *Flow velocity contours*

### Arterial flow

Patterns of blood flow in various sites of the circulation in the fetus have been studied in fetal lambs by electromagnetic or ultrasonic means, and in human fetuses by means of Doppler ultrasound. Velocity recordings in the ascending aorta and main pulmonary trunk are similar to those in the adult. However, in the fetal lamb, there are distinct differences between aortic and pulmonary blood flow patterns. The velocity in the main pulmonary trunk rises

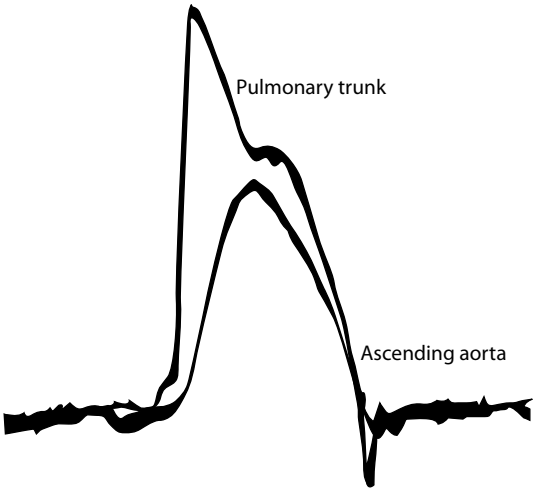


**Figure 8.9**
Blood flow velocities were recorded simultaneously from the ascending aorta and the pulmonary trunk with electromagnetic flow transducers in a late-gestation fetal lamb *in utero*. The calibration for the two flows is identical. Note that stroke volume, the area under the curve, is almost twice as great from the right as from the left ventricle. The differences in flow contours are discussed in the text.

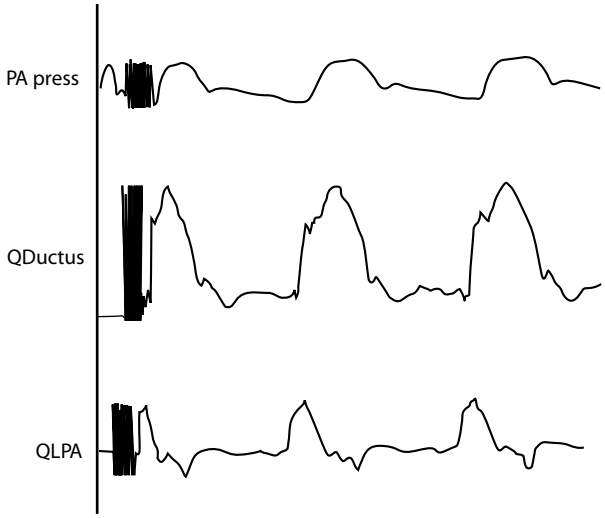


**Figure 8.10**
Simultaneous recordings of blood flow velocities in the ductus arteriosus and left pulmonary artery (LPA), using ultrasonic flowmeters and pulmonary arterial pressure (PA Press) in a fetal lamb *in utero*. See text for discussion. (Reproduced with permission from Rudolph AM. *Congenital Diseases of the Heart*. Chichester, UK: Wiley; 2009.[1])

rapidly after the onset of ejection to reach its peak early in systole. It then falls rapidly initially, but the rapid decrease in velocity is interrupted and a definite incisura in the velocity profile is frequently noted (Figure 8.9). The ascending aortic velocity shows a slower rise at the onset of ejection, and peak velocity is achieved in about midsystole. The peak of aortic velocity is close to the incisura on the downslope of the pulmonary trunk velocity tracing. The mechanisms responsible for these differences in the velocity patterns have not been defined. One possible explanation is that there are marked differences in impedance in the two circulations. The left ventricle ejects into the ascending aorta, which in the fetal lamb carries only about a third of CVO. The aortic isthmus is relatively narrow, and it transmits only about 10% of CVO; it imposes some degree of obstruction to flow from the ascending to the descending aorta. The arterial system into which the left ventricle ejects has a relatively low compliance, and this may explain the slow rise and late peaking of velocity. The right ventricle ejects predominantly through the ductus arteriosus to the descending aorta, from which the relatively low-resistance umbilical-placental circulation arises. The ejection into this highly compliant circulation could explain the rapid rise and early peaking of the velocity. The incisura on the downslope of the pulmonary trunk velocity tracing indicates that the fall in velocity is briefly interrupted. A possible explanation for this phenomenon is that when blood ejected by the left ventricle crosses the aortic isthmus to reach the ductus arteriosus, it interferes with flow from the pulmonary trunk through the ductus and thus slows the fall in velocity momentarily. This hypothesis is supported by the fact that the incisura coincides with the peak of the aortic velocity profile.

The velocity pattern of blood flow in the branch pulmonary arteries is distinctive in the fetal lamb.[23] In the normal lamb, velocity increases rapidly early in systole, but forward flow ceases about halfway through systole, and a variable amount of retrograde flow occurs through the remainder of systole (Figure 8.10). No antegrade flow is evident during diastole, but a small amount of retrograde flow continues through much of diastole. The factors contributing to this pattern of flow have not been fully defined, but it appears to be related to the low compliance of the large pulmonary arteries, the high resistance of the pulmonary circulation, and the presence of the ductus arteriosus. During the early phase of right ventricular systole, blood flows into the main and branch pulmonary arteries, as well as through the ductus arteriosus. Owing to the high vascular resistance, flow into the lung ceases, but flow through the ductus continues. The recoil of the large pulmonary arteries results in reversed flow of blood through the ductus into the low-resistance circulation of the lower body and placenta, resulting in retrograde flow at the site of recording of the velocity profile. The interruption of the rapid decline in forward flow in the ductus is evident in the velocity tracing of the ductus, coincident with the retrograde flow in the left pulmonary artery tracing.

The velocity profile in the branch pulmonary arteries is markedly altered by changes in pulmonary vascular resistance. Administration of a pulmonary vasodilator such as acetylcholine to the fetal lamb results in an increase in pulmonary blood flow. The duration of the forward flow phase in the branch pulmonary arteries is prolonged, the degree depending on the magnitude of the vasodilatation and the decrease in the duration and amount of retrograde flow (Figure 8.11). An increase in pulmonary vascular resistance resulting from

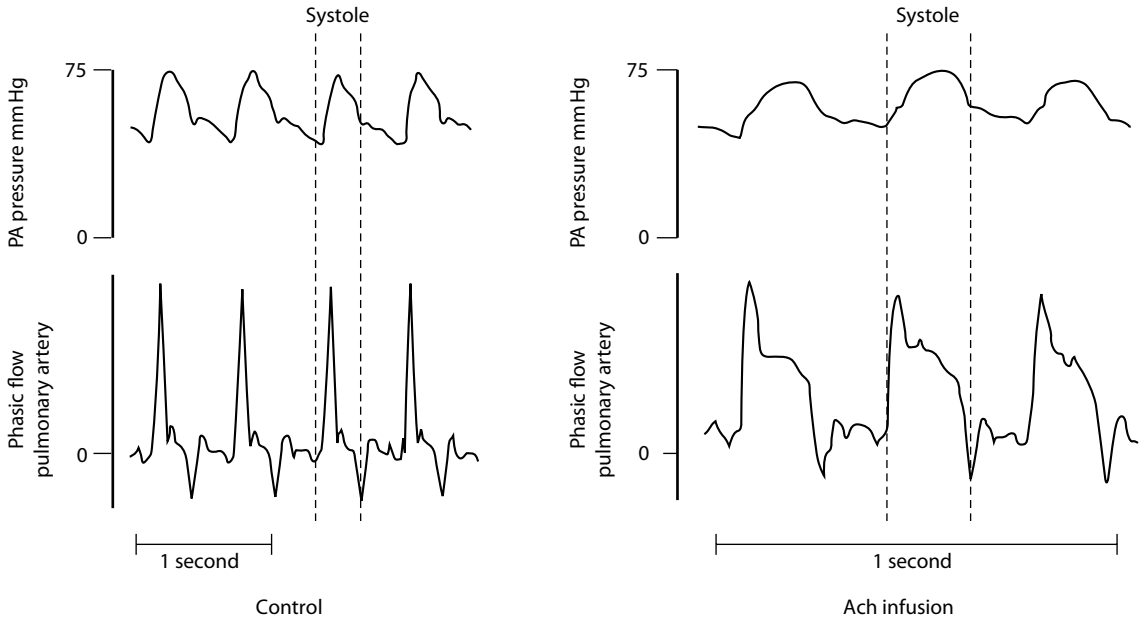


**Figure 8.11**
The pattern of blood flow in the left pulmonary artery is shown before (left panel) and during (right panel) infusion of acetylcholine (Ach) into the pulmonary artery. See text for discussion.

induced hypoxia in the lamb markedly reduces the duration and magnitude of the forward flow phase and increases the duration and degree of retrograde flow.

The velocity profile in the branch pulmonary arteries of the human fetus is different, because in later gestation, pulmonary vascular resistance is lower and pulmonary blood flow is relatively higher in the human than in the lamb (see previous text); thus, the forward flow phase would be longer and the retrograde flow less significant than in the lamb. Defining the velocity profile in human fetuses could provide useful information about the status of pulmonary vascular resistance.

## Venous flow

Patterns of flow in the superior and inferior venae cavae are similar, and in the normal fetus they do not differ significantly from postnatal flow patterns (Figure 8.12). The flow contours are related inversely to the pressure tracing. Coincident with atrial systole, there is a short phase of retrograde flow, followed by forward flow during ventricular systole; this forward flow is enhanced at the end of ventricular systole, coincident with the phase of rapid inflow into the ventricle. As is evident in Figure 8.12, venous flow is markedly altered during fetal respiratory movements; flow is greatly enhanced during inspiratory movements and reduced during expiration. The velocity profile is markedly affected by alterations in heart rate and vascular resistance. Bradycardia results in an exaggeration of retrograde flow during atrial systole, as does an increase in peripheral vascular resistance.

Flow in the umbilical vein is continuous, and the phasic changes associated with the cardiac cycle are normally not evident, so that the velocity profile is flat. However, induction

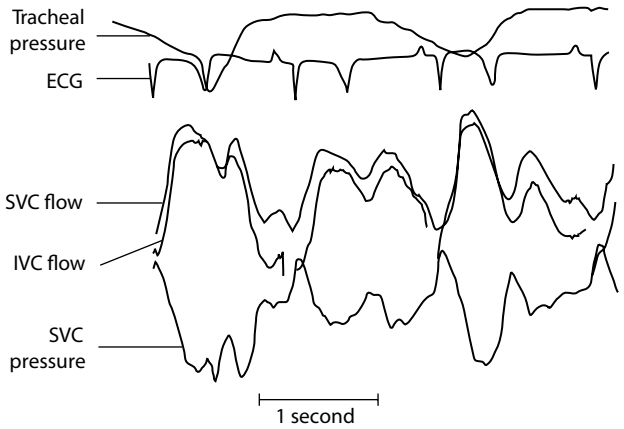


**Figure 8.12**
Simultaneous recordings of blood flow velocities in the superior (SVC) and inferior vena cava (IVC) by electromagnetic flow transducers placed around the vessels in the thorax, and vena cava and intratracheal pressures in a fetal lamb *in utero*. Note the increase in forward flow in both vessels associated with inspiratory effort (decrease in intratracheal pressure). For detailed description see text.

of hypoxia in the lamb fetus results in some degree of phasic change in umbilical flow velocity. This is probably related to the fact that a greater proportion of umbilical venous blood traverses the ductus venosus and dilates the vessel, allowing transmission of central venous pressure.

## *Determinants of cardiac output*

Cardiac ventricular output is the product of heart rate and stroke volume. Stroke volume is determined by preload,

afterload, and myocardial contractility. Preload determines the degree to which the ventricular muscle is stretched immediately prior to contraction. In the intact heart, ventricular volume at end diastole determines the length of the cardiac myocytes and thus sarcomere length. The greater the length of the sarcomere, up to an optimal level, immediately before contraction occurs, the greater is the force generated during contraction. An increase in end-diastolic ventricular volume increases the force of contraction of the muscle and, in the intact heart, increases the stroke volume if other factors are unchanged. Afterload, or load on the heart muscle during development of active force, determines the degree of shortening of the sarcomeres and thus the volume ejected during systole. With the same force of ventricular contraction, the chamber will empty more if the afterload is low, and the ejection volume will be lower if the afterload is increased. In the intact circulation, afterload is influenced by several factors, such as arterial pressure, compliance of the arterial system, and peripheral vascular resistance. Contractility is the intrinsic force of contraction of the muscle; with isolated muscle, increased contractility increases the force developed and, in the intact heart, increases the stroke volume, or developed pressure. In the intact circulation, heart rate, preload, afterload, and contractility are interrelated, and a change in one factor may modify other parameters. It is therefore important to consider possible changes in these other parameters when assessing the effects of alteration of one regulatory factor.

## Effects of heart rate

In the adult, cardiac output is relatively constant over a wide range of heart rates. Increasing the heart rate to 150 beats/min or decreasing it to 50 beats/min from a resting rate of about 70 beats/min does not significantly alter output. Greater increases in heart rate may decrease cardiac output because the reduction in diastolic filling time does not permit adequate filling to maintain stroke volume. With very slow heart rates, stroke volume is increased to maintain cardiac output, but when maximum diastolic filling has been achieved, further slowing results in a decrease of ventricular output.

In studies in fetal sheep, spontaneous increases in heart rate above the resting level of about 160 beats/min are associated with increases of ventricular output of up to 15%–20%, and spontaneous decreases in heart rate result in a fall in output.[24] In these studies, it was not apparent whether the tachycardia was directly responsible for the increase in cardiac output. It is possible that the factors inducing the increase in heart rate also affected loading conditions or contractility. The effects of electrical pacing of the right or left atrium to increase rates to 240–300 beats/min were studied in fetal lambs. Pacing the right atrium resulted in an increase of left ventricular output of up to 15%, with only a small increase or no change in right ventricular output. At rates above 300–320 beats/min, ventricular output fell progressively with increasing rate, presumably because diastolic filling time was greatly reduced. Pacing the left atrium increased right ventricular output modestly, but decreased left ventricular output. Normally in the fetus, the right atrial pressure is slightly higher than that in the left atrium throughout the cardiac cycle. During pacing, the left atrial pressure pulse is altered so that the left atrial pressure exceeds that in the right atrium during some phases of the cycle and interferes with flow through the foramen ovale into the left atrium, reducing the left ventricular filling and output.

Vagal stimulation decreased the output of both ventricles by about 15%–20%, associated with bradycardia. However, the decrease in output could not be ascribed entirely to the decrease in heart rate, because vagal stimulation increases systemic arterial pressure and elevates afterload; this could contribute to the fall in ventricular output.

## Effects of preload and afterload

Preload and afterload are discussed together, because there is usually an interaction between them in the intact circulation. If afterload is increased, the volume ejected by the ventricle during systole is reduced and residual ventricular volume increases. If ventricular filling is maintained, preload is greater with the next beat. *In utero* studies of fetal lambs have been performed to assess the role of preload on cardiac output. In most of these studies, ventricular end-diastolic or atrial pressures have been used as an index of preload. Pressure measurements may not, however, be a reliable indicator of volume, because ventricular compliance determines the volume at any particular pressure. Studies in isolated myocardium and intact hearts have shown that fetal myocardium is less compliant than that of the adult.[25]

Rapid intravenous infusions of 0.9% NaCl solution raised cardiac output associated with an increase in atrial pressure in newborn lambs.[26] Cardiac output increased progressively with elevation of atrial pressure to levels of about 15 mm Hg. Several investigators have studied the effects of decreasing or increasing preload in fetal lambs *in utero*.[27–30] Preload was decreased by reducing fetal blood volume by removal of blood, and increased by rapid intravenous infusion of electrolyte solution. A fall in right atrial and right ventricular end-diastolic pressure resulted in a marked decrease in cardiac output. Output rose when atrial pressure increased by 2–4 mm Hg above resting levels, but further increases in pressure did not result in greater output by the ventricle (Figure 8.13). This response is distinctly different from that in the postnatal lamb, in which increases of atrial pressure to levels of 15–20 mm Hg are associated with a progressive increase in ventricular output. Based on these studies, it was proposed by Gilbert[27,28] that the fetal heart is normally operating near the top of its ventricular function curve. It was suggested that the elevation of cardiac output associated with an increase in preload is limited because myocardial performance, or contractility, is relatively poor in the fetus. However, a decrease in atrial pressure reduces preload, resulting in a fall in cardiac output.

In these studies, the effects of rapid infusion of electrolytes on arterial pressure were not considered. Associated with the

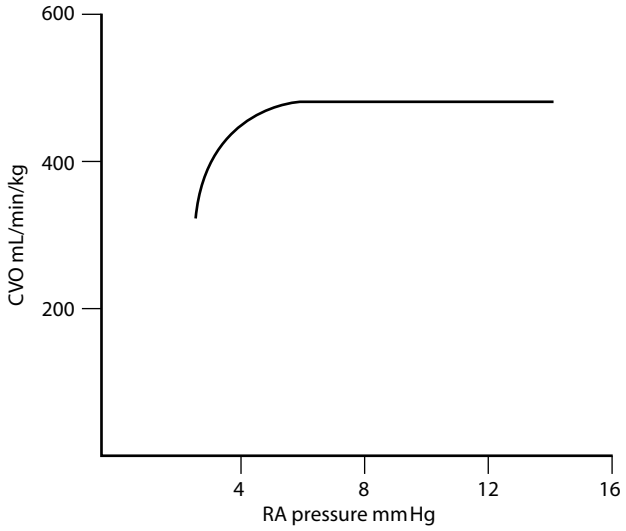


**Figure 8.13**
Changes in combined ventricular output (CVO) associated with acute reduction of atrial pressure by blood removal and increase of atrial pressure by infusion of electrolyte solution in fetal lambs. (Reproduced with permission from Rudolph AM. *Congenital Diseases of the Heart*. Chichester, UK: Wiley; 2009.[1])

infusion, fetal arterial pressure also increases and thus changes afterload. We examined the effects of changing preload at various constant levels of arterial pressure.[31] Arterial pressure elevation dramatically reduced left ventricular stroke volume at all levels of mean atrial pressure (Figure 8.14). At constant arterial pressure levels, progressive elevation of left atrial pressure increased left ventricular stroke volume even with atrial pressures of 10–12 mm Hg. This study demonstrated that the fetal heart responds to increases in preload by increasing its output. It did not, however, resolve whether performances of the fetal and adult myocardium are comparable.

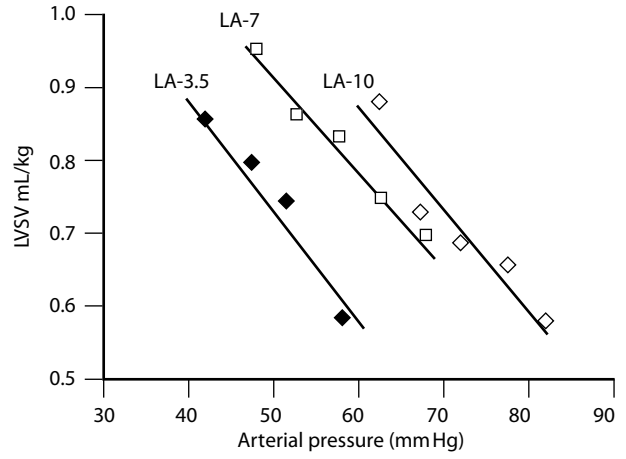


**Figure 8.14**
When systemic arterial pressure is regulated, an increase in pressure results in a fall of left ventricular stroke volume (LVSV) at fixed left atrial (LA) pressure. At any level of arterial pressure, an increase in left atrial pressure increases left ventricular stroke volume. (Reproduced with permission from Rudolph AM. *Congenital Diseases of the Heart*. Chichester, UK: Wiley; 2009.[1])

# Myocardial performance

Studies of isolated myocardium from fetal and adult sheep have demonstrated that fetal myocardium develops less active tension than adult myocardium at similar muscle lengths.[32] Also, the maximum force that can be generated is considerably lower for fetal than for adult myocardium. Several differences in morphological and biochemical parameters of myocardium have been described that could account for the lesser contractility of fetal myocardium. It was suggested that fetal myocardium contains fewer sarcomeres, or contractile units, in each myocyte.

Another factor that may be important is development of the sarcoplasmic reticulum, which regulates the movement of calcium ions, essential for myocardial contraction. The fetal myocardial sarcoplasmic reticulum is well developed, but the T-tubular system, representing the extension of the sarcoplasmic reticulum to provide closer relations with the contractile elements, is either poorly developed or absent in the immature myocardium. Not only are there structural differences in the sarcoplasmic reticulum, but, in studies with isolated sarcoplasmic reticulum vesicles, calcium uptake was found to be impaired in fetal myocardium.[33]

Local release of norepinephrine (noradrenaline) at sympathetic nerve endings is an important mechanism for increasing myocardial contractility. Sympathetic nerve endings are sparse or even absent in fetal myocardium. The abundance of sympathetic nerve endings varies greatly during development in different species. In the guinea pig, myocardial sympathetic innervation is almost fully developed at birth,[34] whereas in the rabbit and the rat there is almost no innervation at birth, but it develops within 14–21 days after birth.[35] The sheep fetus has no detectable sympathetic innervation at 75 days (midgestation), but innervation begins to appear at 90–100 days, and is abundant but not yet fully developed just before birth.[36]

In addition to the difference in sympathetic innervation, β-adrenergic receptor concentration is lower in fetal than in adult myocardium.[37] Although these differences in sympathetic innervation and β-adrenoreceptor concentration may not be important in the resting fetal heart, they could influence the ability to respond to stress.

# *Regulation of the circulation in the fetus*

In the adult, the systemic and pulmonary circulations are separate. Each ventricle is subjected to a potentially different preload and afterload, and the stroke volume of each ventricle might vary greatly. The Frank-Starling mechanism is useful for adjusting the outputs of the two ventricles so that over a short period, the ventricles eject similar volumes. A reduction in venous return to the right atrium reduces the filling pressure and end-diastolic volume of the right ventricle, resulting in a decrease of stroke volume. Pulmonary blood flow and venous return to the left atrium and ventricle is reduced, and

stroke volume falls. An increase in systemic arterial pressure will restrict left ventricular stroke volume; end-diastolic volume will increase so that, with the next beat, greater force is generated to increase stroke volume.

In the fetus, the presence of the foramen ovale tends to make right and left atrial pressures equal throughout the cardiac cycle. The ductus arteriosus provides a large communication between the aorta and the pulmonary artery, resulting in almost identical pressures in the two vessels. In view of the similar atrial pressures and similar aortic and pulmonary arterial pressures, differences in stroke volumes of the left and right ventricles in the fetal lamb are probably due to differences in afterload on the ventricles. The aortic isthmus, which in the fetus is narrower than the ascending and descending aorta, to some extent functionally separates the upper and lower body circulations. The left ventricle ejects into the ascending aorta and the vessels of the head and neck, a circulation that in the lamb fetus is poorly compliant and has a relatively high vascular resistance. The right ventricle ejects into the pulmonary trunk and directly through the large ductus arteriosus into the descending aorta and its branches. This circulation has a higher compliance and a lower resistance because it includes the umbilical-placental vasculature. This functional separation of the aorta at the isthmus has been demonstrated in fetal lambs. A rapid reduction in peripheral vascular resistance in the lower body circulation, induced by a vasodilator, causes a decrease in descending aortic pressure and an increase in right ventricular stroke volume for several beats, whereas the ascending aortic pressure and left ventricular output do not change. Similarly, injection of a vasodilator into the ascending aorta causes an evanescent decrease of ascending aortic pressure and increase in left ventricular stroke volume.

# Reflex regulation

## *Chemoreflexes*

Previous studies on the role of chemoreflexes in control of the fetal circulation were conflicting. Some investigators suggested that aortic and carotid chemoreceptors are relatively inactive in the fetus, but these studies were performed in anesthetized exteriorized fetal lambs.[38] Other studies indicated that aortic receptors were important in causing a bradycardic response to hypoxia.[39] More recent studies in fetal lambs have shown that they are active, at least in the last third of gestation.[40] Responses to carotid chemoreceptor stimulation are much greater than to aortic receptor stimulation.[41] The chemoreceptors are stimulated by hypoxemia, and experimentally can be activated by intravascular injection of small doses of sodium cyanide. The cardiovascular response dominates, with bradycardia and immediate hypotension, but respiratory gasps are noted. The bradycardia can be abolished if the lambs are pretreated with atropine, indicating that the bradycardia is induced by vagus nerve stimulation. Confirmation of the fact that the cyanide response is the result of chemoreceptor stimulation was obtained by demonstrating the loss of the cardiovascular and respiratory responses to cyanide in fetal lambs in which sinoaortic denervation had been accomplished.[40,41]

In the adult, chemoreceptor stimulation results in reflex peripheral vasoconstriction. It is likely that the peripheral vasoconstriction induced by fetal hypoxemia is largely mediated by chemoreceptor stimulation. From the studies in fetal lambs, it is apparent that their chemoreflex responses are different from those in the adult. The respiratory response in the adult animal dominates, whereas chemoreceptor stimulation in the fetus causes only a minor respiratory response. There is as yet no explanation for this difference in response.

## *Baroreflexes*

In the adult, arterial pressure is maintained over a fairly narrow range through the control of baroreceptors. Stimulation of aortic and carotid baroreceptors by a rise in arterial pressure induces bradycardia, depression of myocardial contractility, and peripheral vasodilatation, all of which tend to decrease arterial pressure.[42] Ablation of aortic and carotid baroreceptors, by bilateral section of the aortic and carotid afferent nerves, results in an initial increase in resting heart rate and arterial pressure, but within 1–2 days these parameters return to average levels that were present during the predenervation period. Wide swings of arterial pressure and heart rate occur around the average pressure and rate, in association with stimuli that produce only small changes in the normal animal.[43]

Arterial baroreceptors are functional in the fetus relatively early in gestation, but their importance in regulating fetal arterial pressure has been questioned. In fetal lambs, baroreflex sensitivity increases with gestational age from about 80 days' gestation; near term gestation, the bradycardia induced by increased arterial pressure is equal to that noted postnatally. In fetal lambs, sinoaortic denervation results in the same wide variation in heart rate and blood pressure as observed in adult animals.[39] It is thus apparent that baroreflexes are important in stabilizing arterial blood pressure in the fetus as well.

# Birth-associated changes in the circulation

Delivery of the fetus from the uterus disrupts the umbilical-placental circulation. The functions of oxygen uptake and carbon dioxide removal are transferred to the lungs. Pulmonary ventilation has to be established to provide gas exchange. During fetal life, pulmonary blood flow is relatively low and has to increase to allow oxygen uptake adequate for postnatal survival. The well-oxygenated blood from the umbilical veins and poorly oxygenated blood from the vena cava mix partially, and venous blood is diverted away from the lungs through the foramen ovale and the ductus arteriosus.

In the adult, blood circulates in series. All venous blood is returned to the right atrium and ventricle, ejected into the lungs where it is oxygenated, and then passes to the left atrium and ventricle to be ejected into the systemic arterial circulation. Apart from the return of minor amounts of venous blood into the left ventricle via thebesian veins, there is no mixing of arterial and venous blood.

The foramen ovale and ductus arteriosus have to be closed functionally or anatomically to establish the adult circulation.

As the fetus is delivered, several events occur in a short time period. Fluid in the fetal airways is removed either by expulsion through the mouth as a result of chest compression, or by absorption into the pulmonary circulation with the onset of breathing. Regular ventilation is established, and the umbilical-placental circulation is terminated by disruption or clamping of the umbilical cord. Ventilation by room air is associated with an increase in the alveolar oxygen concentration and also with the rhythmic physical expansion of the lung and removal of alveolar fluid. It has been difficult to assess the role of each of these factors in contributing to the circulatory changes associated with birth, because they occur almost simultaneously. We developed a fetal lamb preparation to examine the role of individual birth events in these changes.[44] Catheters were implanted in various fetal vessels, a tube was inserted into the trachea, and an inflatable balloon occluder was placed around the umbilical cord. All of the catheters were exteriorized to the maternal flank, and the ewe and fetus were allowed to recover from surgery. Fetal vascular pressures and blood gases were monitored, and blood flows were measured repeatedly by the radionuclide-labeled microsphere technique. The effect of rhythmic expansion of the lung was assessed by ventilating the fetus with a gas mixture of 5% carbon dioxide, 3% oxygen, and 92% nitrogen. This did not significantly change fetal blood gas levels of $PO_2$ 21 mm Hg and $PCO_2$ 40 mm Hg in descending aortic blood. The fetus was then ventilated with 100% oxygen; this raised fetal descending aortic $PO_2$ to about 50 mm Hg and oxygen saturation to above 90%. With the fetus well oxygenated, the effect of occluding the umbilical cord was then assessed.

The proportions of CVO ejected by each ventricle and distributed to the major vessels are shown in Figure 8.7. Rhythmic ventilation without altering fetal blood gases produced a considerable increase in pulmonary blood flow (Figure 8.15) and a decrease in pulmonary vascular resistance (Figure 8.16).[45] The proportion of CVO passing to the lungs increased from 9% to 31%. Interestingly, pulmonary arterial pressure did not fall, suggesting that the ductus arteriosus was still widely patent and that aortic pressure was transmitted to the pulmonary artery. Associated with the increased pulmonary blood flow, pulmonary venous return to the left atrium increased, and the proportion of CVO passing through the foramen ovale decreased (Figure 8.17). Although CVO did not change, right ventricular output constituted about 52% of CVO, as compared with 65% in the unventilated fetus. Also, only 24% of CVO passed through the ductus arteriosus to the descending aorta, compared with 57% in the control state. Left ventricular output increased from 34% to 48% of CVO, so that the outputs of the two ventricles were now similar.

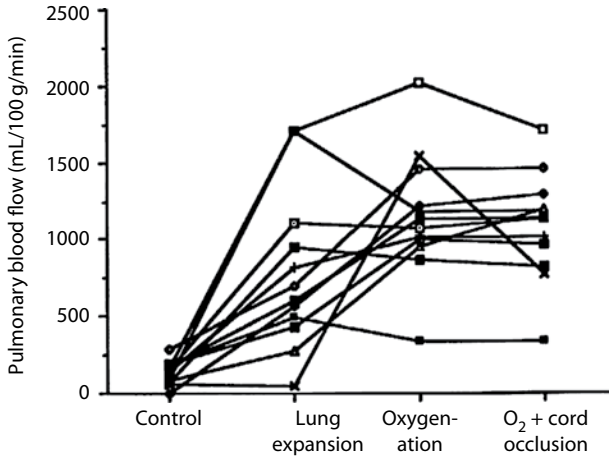


**Figure 8.15**
Changes in pulmonary blood flow resulting from physical expansion of the lung, ventilation with oxygen, and umbilical cord occlusion in fetal lambs. (Reproduced with permission from Rudolph AM. *Congenital Diseases of the Heart*. Chichester, UK: Wiley; 2009.[1])

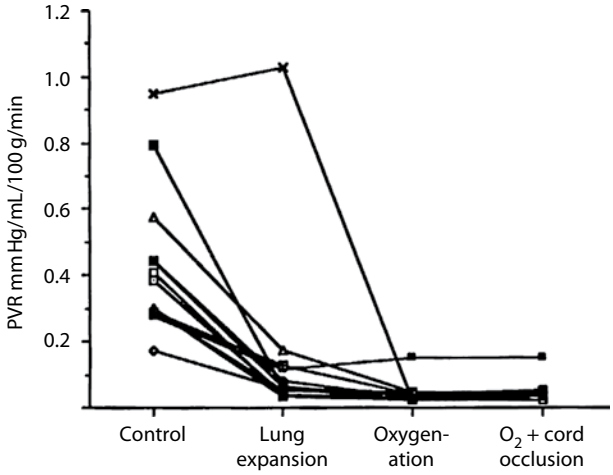


**Figure 8.16**
Changes in pulmonary vascular resistance (PVR) resulting from physical expansion of the lung, ventilation with oxygen, and umbilical cord occlusion in fetal lambs. (Reproduced with permission from Rudolph AM. *Congenital Diseases of the Heart*. Chichester, UK: Wiley; 2009.[1])

Ventilation with oxygen resulted in a further decline in pulmonary vascular resistance and a rise in pulmonary blood flow (Figure 8.18). Only a minor proportion of blood ejected by the right ventricle passed through the ductus arteriosus to the descending aorta, almost all being distributed to the pulmonary circulation. The large venous return to the left atrium elevated left atrial pressure above that in the systemic veins and right atrium; this resulted in closure of the foramen ovale, with only insignificant flow from the right to the left atrium. Total CVO did not change significantly, but left ventricular output exceeded right ventricular output, with 55% of CVO contributed by the left and 45% by the right ventricle. This higher output by the left ventricle was the result of the development of a shunt from the aorta to the pulmonary

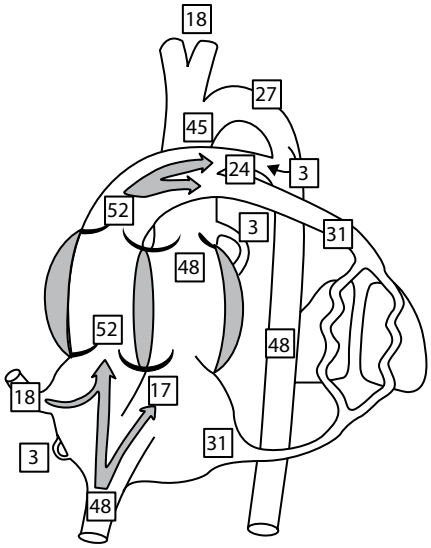


**Figure 8.17**
Proportions of combined ventricular output ejected by the right and left ventricles and flowing through great vessels in fetal lambs during ventilation without changing fetal blood gases. (Reproduced with permission from Itskovitz J, Rudolph AM. *Am J Physiol*. 1987;252:H916–22.[40])

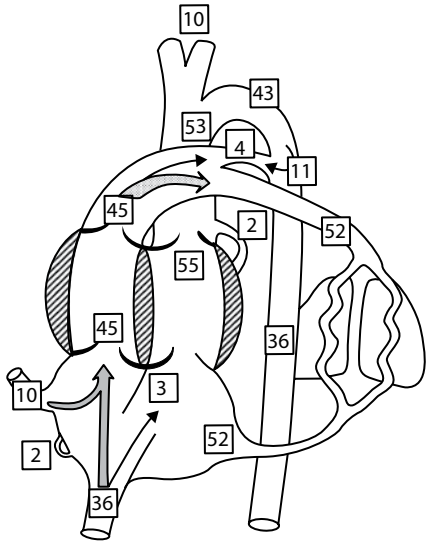


**Figure 8.18**
Proportions of combined ventricular output ejected by the right and left ventricles and flowing through great vessels in fetal lambs during ventilation with oxygen. (Reproduced with permission from Itskovitz J, Rudolph AM. *Am J Physiol*. 1987;252:H916–22.[40])

artery through the still open ductus arteriosus, constituting about 10% of CVO. Pulmonary arterial pressure gradually and progressively decreased below aortic levels. This reflected the separation of systemic and pulmonary arteries by constriction of the ductus arteriosus.

Occlusion of the umbilical cord completely eliminated umbilical blood flow. It resulted in a modest increase in systemic arterial pressure and a small increase in the shunt through the ductus arteriosus from the aorta to the

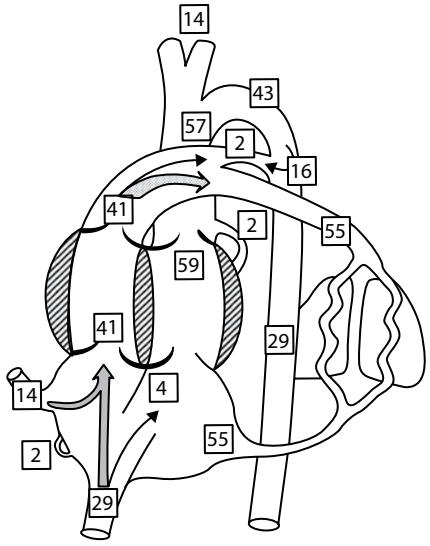


**Figure 8.19**
Proportions of combined ventricular output ejected by the right and left ventricles and flowing through great vessels in fetal lambs after occlusion of the umbilical cord during ventilation with oxygen. (Reproduced with permission from Itskovitz J, Rudolph AM. *Am J Physiol*. 1987;252:H916–22.[40])

pulmonary artery. However, no other additional changes occurred, and CVO was still similar to that in the control fetal state (Figure 8.19).

From these studies, it is apparent that the dramatic decrease in pulmonary vascular resistance resulting from ventilation of the lungs is the dominant factor contributing to the circulatory changes during the perinatal period. The elevation in left atrial pressure resulting from increased pulmonary venous return to the left atrium closes the foramen ovale. The cessation of umbilical venous return may also contribute to closure of the foramen. Constriction of the ductus arteriosus (*vide infra*) completes the separation between the left and right sides of the heart and the major arteries, resulting in the series circulation characteristic of the adult.

## Perinatal changes in the pulmonary circulation

Rhythmic physical expansion of the lungs and an increase in oxygen levels in the ventilating gas mixture have independent but complementary roles in pulmonary vasodilatation. The mechanisms by which these processes reduce pulmonary vascular resistance have been investigated but are not yet fully resolved. There is considerable evidence suggesting that rhythmic expansion of the lungs results in the production of the prostaglandin, prostacyclin ($PGI_2$), probably from endothelial cells.[46] $PGI_2$ is a pulmonary vasodilator and could be responsible for the effect of ventilation. Although inhibition of prostaglandin production in the sheep fetus limits the degree of pulmonary vasodilatation with ventilation, it does not completely prevent it, suggesting that other factors may be involved. The possibility should be entertained that the removal of fluid present in fetal airways and the replacement

with gas could contribute to a decrease in pulmonary vascular resistance based on physical phenomena alone. During fetal life, the alveoli contain fluid, and the positive pressure from the amniotic cavity is transmitted through the thorax to the lungs. This would tend to compress the pulmonary vessels alongside the alveoli and small bronchi. During delivery of the fetus, airway fluid is removed; spontaneous breathing results in the development of a negative intrapleural pressure, with a gradient from the airways outward to the pleura, and this tends to dilate pulmonary vessels.

However, as shown experimentally in fetal lambs, positive-pressure ventilation with no change in blood gas concentrations also reduces pulmonary vascular resistance. Physical factors that could possibly contribute to this are changes in surface forces on the alveoli. During fetal life, there is a fluid-fluid interface on the alveolar surface with no significant surface tension forces. When the alveoli are filled with gas, a strong surface tension at the gas-fluid interface tends to collapse the alveoli. This would result in a force tending to dilate pulmonary vessels associated with the alveoli, and thus decrease pulmonary vascular resistance.

During fetal life, the pulmonary vessels are exposed to the $PO_2$ of blood in the pulmonary arteries, which, in fetal lambs, is about 18 mm Hg. Fetal pulmonary vessels are markedly constricted when $PO_2$ is reduced below and dilated by an increase of $PO_2$ above control levels. Ventilation with air increases the $PO_2$ in precapillary pulmonary vessels, because oxygen diffuses into these vessels from surrounding alveoli, resulting in vasodilatation. It has been suggested that the response to changes in $PO_2$ may be due to a direct effect on smooth muscle cells, and could be related to transmembrane movement of potassium via oxygen-sensitive potassium channels. A reduction in $PO_2$ blocks potassium channels and results in constriction, whereas a rise in $PO_2$ opens the channels, causing vasodilatation. The role of potassium channels in the response is supported by studies in fetal lambs showing that potassium channel blockers cause pulmonary vasoconstriction.[47]

The vasodilator effect of oxygen on pulmonary arterioles has also been shown to be associated with nitric oxide (NO) mechanisms. NO production by endothelial cells, which is associated with an increase in $PO_2$, induces relaxation of vascular smooth muscle cells, resulting in a fall in pulmonary vascular resistance. *N*-nitro-L-arginine inhibits NO production; in studies in fetal lambs, it markedly limited the reduction in pulmonary vascular resistance associated with oxygenation.[48]

In the lamb, the rapid increase in pulmonary blood flow with ventilation is associated with a drop in pulmonary vascular resistance from the fetal level of 1.6–0.3 mm Hg/mL/min/kg. Functional responses of the pulmonary circulation are considerably greater in the fetus than in the adult, due to differences in morphology of the small pulmonary arteries. The pre-acinar arteries in the fetal lung have a thick wall with a prominent smooth muscle layer. The intra-acinar arteries, associated with bronchioli, are partly muscular or nonmuscular, and more distal vessels do not have smooth muscle cells. The muscular medial layer does not change significantly during the latter half of gestation, but the number of intra-acinar and alveolar duct arteries increases with lung growth during fetal development. After birth, the pulmonary arterioles have a thinner muscular media as a result of an increase in lumen size. Subsequently, the smooth muscle layer gradually regresses, so that pre-acinar arteries develop the morphological features of adult vessels with the thin wall and large lumen/wall ratio. These changes occur over several weeks.

The normal development of the pulmonary circulation before and after birth may be influenced by alteration of the $PO_2$ and the intraluminal pressure to which the arteries are exposed. Interference with normal oxygenation after birth may delay the normal regression of smooth muscle. Individuals born and continuing to live at high altitude are exposed to a lower partial pressure of oxygen in inspired air; they retain a greater amount of smooth muscle in pulmonary vessels and have higher pulmonary arterial pressures than individuals at sea level.[49]

An increase of pulmonary arterial pressure in the fetus, as may occur with constriction of the ductus arteriosus, results in increased development of the pulmonary arteriolar smooth muscle layer.[50] The greater amount of smooth muscle may interfere with postnatal adaptation, and the fall in pulmonary arterial pressure may be slower than normal as a result of the higher pulmonary vascular resistance. After birth, pulmonary arterial pressure may not fall normally if there is a congenital cardiovascular malformation with a large communication between the left and right ventricles or the aorta and pulmonary artery. The large communication results in a tendency for pressures on the left and right sides of the heart to equalize, and thus pulmonary arterial pressure does not fall as in the normal infant. Persistence of the high pulmonary arterial pressure delays normal maturation of the pulmonary vessels, and the smooth muscle component persists. The role of the pulmonary circulation in the hemodynamic and clinical manifestations of congenital cardiovascular malformations is discussed in Chapter 53.

## Persistent pulmonary hypertension of the newborn

If pulmonary vascular resistance does not fall normally after birth, pulmonary arterial pressure will not drop to normal postnatal levels, and pulmonary blood flow adequate for oxygen needs may not be established. This phenomenon has been named persistent pulmonary hypertension of the newborn and may result from several conditions.

An inability to establish normal respiration after birth will interfere with the expansion of alveoli with air, and thus the $PO_2$ will not be increased normally, and pulmonary vasoconstriction will persist. This may occur in babies who are depressed as a result of sedative drugs given to the mother. It may also result from an obstruction to airways, as with meconium aspiration. In these infants, development of the lung and pulmonary vasculature may be normal, but pulmonary

vasoconstriction persists because alveolar oxygen concentration does not increase. Relief of airway obstruction or stimulation of breathing results in a rapid fall of pulmonary vascular resistance.

Failure of the normal postnatal decrease in pulmonary vascular resistance may be the result of abnormal prenatal development of the pulmonary resistance arteries. As mentioned previously, an increase of pulmonary arterial pressure in the fetus, as may result from constriction of the ductus arteriosus, induces increased development of the pulmonary vascular smooth muscle.[47] This may interfere with the achievement of normal postnatal pulmonary vascular resistance. These vessels are exquisitely sensitive to changes in $PO_2$, and even mild degrees of hypoxemia may result in marked pulmonary vasoconstriction. The muscle does regress slowly postnatally, but normal pulmonary arterial pressure and flow after birth may not be achieved for several weeks. Persistent pulmonary hypertension of the newborn may occur in infants when the fetus has been exposed to indomethacin *in utero*, because prostaglandin inhibition causes ductus arteriosus constriction.[51] Experimental studies have suggested that prolonged fetal hypoxia may also induce an increase in pulmonary vascular smooth muscle.

Persistent pulmonary hypertension of the newborn may be associated with inadequate cross-sectional area of the pulmonary vascular bed. This is most commonly the result of an interference with lung development resulting from encroachment of a space-occupying lesion in the thorax, such as a large lung cyst, or by intestine herniating through a diaphragmatic hernia. It may also be the result of agenesis of a lung. Since pulmonary vascular development parallels the growth of alveolar units, lack of lung development will be associated with a reduced size of the pulmonary vascular bed. Adequate development of the pulmonary circulation after birth will occur only slowly, as new alveolar units are added with growth of the lung.

## Ductus arteriosus closure after birth

The ductus arteriosus connects the pulmonary trunk, before origin of the left and right pulmonary arteries, to the descending aorta, just beyond the origin of the left subclavian artery, in the human fetus. The wall of the ductus is morphologically quite different from that of the aorta and pulmonary artery. Whereas the walls of these arteries are largely composed of elastic tissue, the predominant tissue in media of the ductus is smooth muscle. During fetal life, the ductus arteriosus diverts a major proportion of right ventricular output away from the lungs to the descending aorta. In the sheep fetus, right ventricular output is about 66% of combined ventricular output and almost 90% of right ventricular blood passes through the ductus arteriosus. Estimates of flow through the ductus arteriosus, measured by ultrasound in human fetuses, show considerable variation. The proportion of right ventricular output distributed to the lungs is greater in the human, and it is estimated that about 60% of the blood ejected by the right ventricle passes though the ductus. The ductus remains widely patent throughout gestation, and no pressure gradient between the pulmonary trunk and the descending aorta can be detected. However, during the latter weeks of gestation, mild constriction may occur, as evidenced by a 5–8 mm Hg drop in systolic pressure across the ductus. After birth, the ductus constricts rapidly; the rate of constriction appears to vary in different species. In the rat, rabbit, and guinea pig, it is essentially closed within minutes. In the sheep the process is somewhat slower, closure usually being achieved within an hour. In full-term human infants, functional closure usually occurs within 12–15 hours. During the first few hours, a bidirectional shunt may be detected by ultrasound, but after about 6 hours, only a small left-to-right shunt may occur for up to about 15 hours. Prior to complete closure, the ductus responds to a decrease of $PO_2$ by dilatation and, with the increase of pulmonary arterial pressure resulting from pulmonary vasoconstriction, some degree of shunting from the pulmonary artery to the aorta may again occur.

The $PO_2$ to which the ductus arteriosus is subjected is an important determinant of the degree of constriction. In the fetus, right ventricular blood with a $PO_2$ of about 18 mm Hg in the lamb passes through the ductus to the descending aorta. The ductus arteriosus is constricted by an increase in oxygen levels. This has been observed in ductus rings in a tissue bath[52] or in isolated perfused ductus preparations,[53] as well as in fetuses *in utero*. In a tissue bath, ductus preparations are relaxed at $PO_2$ of 25–30 mm Hg; they show a progressive increase in the degree of constriction from $PO_2$ of about 40–100 mm Hg. With air breathing, the $PO_2$ of arterial blood increases to 90–100 mm Hg. The mechanism by which oxygen constricts the ductus has not yet been resolved. The magnitude of response to oxygen is dependent on gestational age. The more immature is the fetus, the less is the constrictor response, and the level of $PO_2$ required to initiate constriction is greater.

The ductus arteriosus has also been shown to be very sensitive to prostaglandins. The ductus is relaxed by prostaglandin $E_2$ and prostaglandin $I_2$ (prostacyclin); both are produced by the ductus wall, but they are also produced elsewhere in the fetus, and circulating levels of $PGE_2$ are elevated as compared with postnatally. Although large amounts of $PGI_2$ are produced by the ductus, $PGE_2$ is probably more important in regulating its tone, because the ductus muscle is much more sensitive to $PGE_2$. Prostaglandins are synthesized from arachidonic acid by the cyclooxygenase enzymes. Inhibition of prostaglandin synthesis by agents such as aspirin or indomethacin in the lamb fetus results in constriction of the ductus,[51] confirming the fact that prostaglandins are important in maintaining its patency prenatally.

Blood $PGE_2$ concentrations fall rapidly after birth, and the relative contributions of the removal of $PGE_2$ and the increase in blood oxygen levels to ductus constriction after birth have yet to be resolved. Studies by Clyman et al. indicate that the rise in $PO_2$ is more important than the fall in $PGE_2$ levels in late gestation, whereas in the second and early part of the third trimester, the ductus is more sensitive to the removal of

prostaglandin than to the increase in $PO_2$.[54] Studies in fetal lambs indicate that the sensitivity of the ductus to oxygen and $PGE_2$ can be matured by administering corticosteroids to the immature fetus.

Recently, the role of NO in influencing the ductus has been demonstrated. NO relaxes the ductus muscle. In prematurely delivered baboons, a cyclooxygenase inhibitor did not induce complete closure of the ductus, but combination with an inhibitor of NO production caused complete closure.[55] The role of NO in normal regulation of the ductus is yet to be determined.

The mechanisms by which permanent closure of the ductus arteriosus is achieved have not yet been fully resolved. Constriction results in thickening of the intima and the development of intimal mounds that encroach on the lumen. Disruption of the internal elastic lamina results in migration of endothelial and smooth muscle cells. Clyman et al. have suggested that the middle layers of the ductus receive oxygen supply from blood in the lumen. Constriction results in thickening of the wall and severe hypoxia of the middle portion of the wall.[56] This results in cell damage, with replacement by fibrous tissue. Permanent closure of the ductus is usually complete within a week but may not occur for up to 3 weeks in some infants. While the ductus is still patent, a small shunt from the aorta to the pulmonary artery (left to right shunt) may be detected by ultrasound.

## The ductus arteriosus in the preterm infant

Postnatal closure of the ductus arteriosus is frequently delayed in infants born prematurely. The younger the gestational age at birth, the more likely it is that the ductus will not close soon after birth. In preterm infants with birth weights under 750 g, more than 80% have persistent patency of the ductus beyond the third day after birth. In infants with birth weights of 1000–1500 g, the incidence of persistent patency of the ductus is 40%–50%, whereas in infants weighing 1500–1750 g at birth, the incidence is about 20%. Most of the more immature infants also have severe respiratory distress syndrome. Several possible explanations for delayed closure of the ductus in preterm infants have been proposed. It was first suggested that the preterm infant did not achieve an adequate elevation of arterial $PO_2$ due to poor ventilation, but this possibility has been excluded because, with assisted ventilation, $PO_2$ may be raised to levels normal for mature infants and ductus patency persists. As mentioned previously, the ductus arteriosus of the immature animal is more sensitive to the effect of removal of prostaglandins than to an increase of $PO_2$, and even the high $PO_2$ achieved may not induce complete closure. The possibility that $PGE_2$ levels do not fall postnatally as rapidly as in the mature infant has also been examined. Results of these studies indicate that there is a delay in the fall of blood $PGE_2$ concentrations after birth in preterm infants, and levels may be elevated for as long as 2–4 weeks postnatally. However, although $PGE_2$ concentrations have been elevated in many infants with respiratory distress syndrome, only some had ductus arteriosus patency.

## Postnatal changes in cardiac output

The combined ventricular output (CVO) of the left and right ventricles is about 400–450 mL/min/kg body weight in term fetal lambs *in utero*. Measurements in newborn lambs showed cardiac output levels of 400–450 mL/min/kg. Since left and right ventricular outputs are the same postnatally, the output of each ventricle is about 400–450 mL/min/kg, and combined output is 800–900 mL/min/kg, about twice that in the fetus. In the fetus, right ventricular output is about 66% of CVO, or about 300 mL/min/kg; it increases by about 50% after birth. The left ventricle, which in the fetus ejects about 150 mL/min/kg, increases its output almost threefold to 400–450 mL/min/kg after birth. The factors contributing to this rise of cardiac output postnatally have not been fully assessed. The studies mentioned previously in fetal lambs *in utero*, in which we sequentially induced physical expansion of the lungs, oxygenation, and umbilical cord occlusion, indicated that none of these events resulted in a rise of CVO. The proportion of CVO ejected by the left ventricle increased, and that by the right ventricle decreased. The possibility was considered that delivery from the *in utero* environment with a temperature of about 39°C into a room air environment with a temperature of about 25°C could contribute to the increase in CVO. In studies in which we measured CVO in nonbreathing fetal lambs delivered into a water bath but with no alteration of umbilical-placental flow, changing the bath temperature from 37°C to 25°C did not result in a significant change of CVO.[57]

In these experimental studies, the fetuses did not breathe spontaneously and were not exposed to the stress of delivery. It has been proposed that fetal cardiac output is regulated by a high pericardial pressure transmitted from the intrauterine cavity across the thorax and fluid-filled lungs; this high pericardial pressure restricts filling of the ventricles and limits stroke volume.[58] Spontaneous ventilation after birth results in the development of a negative intrapleural (relative to atmospheric) pressure, also creating a negative intrapericardial pressure, which facilitates filling of the ventricles. This greater diastolic filling of the ventricles would, if myocardial function is adequate, result in a higher stroke volume and greater ventricular output.

Several hormones are recognized as having important roles in the perinatal circulatory adjustments. Plasma catecholamine concentrations increase during delivery and could, by their effect of increasing myocardial contractility, facilitate the increase in cardiac output occurring after natural vaginal delivery. In the experimental studies, the fetuses were not exposed to the stress of delivery and, thus, may not have experienced catecholamine stimulation of the myocardium.

In sheep, plasma cortisol concentrations increase slowly from about 120 days' gestation, and 2–3 days prior to delivery (at about 150 days) they rise sharply, severalfold. Cortisol plays an important role in maturing the myocardium in the

perinatal period; it has been shown to reduce nuclear proliferation and to increase protein concentration in fetal myocytes; this could be a factor in providing an increase in cardiac output after birth.[59]

Thyroid hormone has long been known to affect the myocardium in adults. Deficiency of the thyroid results in a depression of myocardial performance. The number of β-adrenoreceptors in the myocardium is greatly reduced in adult animals with thyroid deficiency. Although decreased response to catecholamine stimulation resulting from reduced β-adrenoreceptors could well contribute to the decreased function, thyroid hormone may have additional effects by modifying heavy-chain myosin expression. The role of thyroid hormone on cardiac performance in the perinatal period has been demonstrated in sheep.

In fetal lambs, plasma tri-iodothyronine ($T_3$) concentration is about 1 ng/mL. After vaginal delivery, it rises to about 4 ng/mL within 30–60 minutes. This is unlikely to be a factor in the rapid increase in cardiac output, because, in adults, the effect of thyroid hormone is noted within days rather than minutes. In studies of fetal lambs, we observed that complete thyroidectomy performed just prior to delivery resulted in no increase in $T_3$ concentrations, but the lambs showed the expected increase in cardiac output.[60] However, if thyroidectomy was done about 10 days before delivery, fetal $T_3$ levels were undetectable, and after delivery, the lambs showed a limitation of cardiac output as well as a blunted response to catecholamine infusion. This suggested that $T_3$ was important prenatally for normal myocardial development, and we showed that β-adrenoreceptor numbers in ventricular muscle were significantly reduced.[61]

## Morphological changes in the myocardium after birth

Histological studies of adult and fetal myocardium show dramatic differences. The adult myocyte in the sheep heart has a diameter of about 15–20 μm, whereas in the fetal lamb heart myocytes are much smaller, with a diameter of 5–7 μm. The nucleus in adult myocytes is relatively small, and polyploidy is very common. In the fetal myocyte, the nucleus is relatively larger, and most cells have a single nucleus. Observations in fetal lambs over the latter half of gestation show no significant change in myocyte diameter.[62] Since the weight of the heart increases greatly, the increase in muscle mass is almost exclusively by an increase in cell numbers, or by hyperplasia. Postnatally, myocyte size increases dramatically, and almost all growth is the result of hypertrophy; minimal mitosis occurs postnatally. Measurements of the DNA and protein content of the myocardium during fetal and postnatal life confirm this difference in growth patterns. DNA concentration reflects the number of nuclei in tissues; protein concentration reflects the total tissue mass. A high DNA/protein ratio suggests a relatively large number of nuclei, indicating that cells are small. The reverse suggests that the cells are large relative to nuclear numbers. During fetal life, the lamb heart shows a relatively high DNA/protein ratio, but after birth the DNA/protein ratio falls, reflecting the cessation of mitosis and the increase in myocyte size. Although all the factors responsible for the dramatic change in the pattern of myocardial growth after birth are not determined, cortisol at least appears to be important. In studies in fetal lambs, in which we infused cortisol into the left coronary artery for up to 96 hours *in utero*, the DNA/protein ratio of the myocardium fell, in a similar manner to that noted normally after birth.[59]

## Postnatal changes in hepatic and ductus venosus blood flow after birth

Prenatally, umbilical venous blood enters the porta hepatis; about 50% is distributed to the left and right lobes of the liver, and 50% passes through the ductus venosus. Portal venous flow in the fetal lamb is quite low, and almost all is distributed to the right lobe of the liver, with less than 10% passing through the ductus venosus.

The liver receives a very large blood supply of almost 450 mL/min per 100 g liver weight. After birth, umbilical blood flow ceases, and apart from a small amount of flow from the hepatic artery, all hepatic flow is derived from the portal vein. After birth the hepatic blood flow is about 100 mL/min per 100 g liver weight; the flow increases to 140 mL/min per 100 g and then increases rapidly after feeding to about 300 mL/min/kg liver weight.[63]

The ductus venosus had been thought to react passively to the intraluminal pressure, but it was shown that prostaglandin is partly responsible for maintaining patency of the ductus venosus. Postnatally, removal of prostaglandins and cessation of flow from the umbilical vein contribute to closure of the ductus venosus. Soon after birth, considerable proportions of portal venous blood may pass through the ductus venosus, but by 3–4 days this becomes negligible, and by about 6–10 days after birth the ductus closes.

## References


1. Rudolph AM. *Congenital Diseases of the Heart*. Chichester, UK: Wiley; 2009.
2. Bristow J et al. *J Dev Physiol* 1981;3:255–66.
3. Rudolph AM. *Hepatology* 1983;3:254–8.
4. Lind J et al. *Human Foetal and Neonatal Circulation*. Springfield, IL: C.C. Thomas; 1964.
5. Reuss ML et al. *Am J Obstet Gynecol* 1981;141:427–32.
6. Edelstone DI, Rudolph AM. *Am J Physiol* 1979;237:H724–9.
7. Edelstone DI et al. *Circ Res* 1978;42:426–33.
8. Rudolph AM et al. *Pediatr Res* 1971;5:452–65.
9. Schmidt KG et al. *Circulation* 1996;93:826–33.
10. Kiserud T. *Eur J Obstet Gynecol Reprod Biol* 1999;84:139–47.
11. Kiserud T. *J Perinat Med* 2000;28:90–6.
12. Rudolph AM, Heymann MA. *Circ Res* 1967;21:163–8.
13. Rudolph AM, Heymann MA. *Circ Res* 1970;26:289–99.
14. Sutton MG et al. *Cardiovasc Res* 1991;25:603–8.
15. Meijboom EJ et al. *Circulation* 1985;71:551–6.
16. Mielke G, Benda N. *Circulation* 2001;103:1662–8.
17. Seed M et al. *J Cardiovasc Magn Reson* 2012;14:79.

18. Prsa M et al. *Circ Cardiovasc Imaging* 2014;7:663–70.
19. Kiserud T et al. *Am J Obstet Gynecol* 2000;182:147–53.
20. Kohl T, Silverman NH. *J Ultrasound Med* 1996;15:465–73.
21. Rasanen J et al. *Circulation* 1996;94:1068–73.
22. Rasanen J et al. *Circulation* 1998;97:257–62.
23. Lewis AB et al. *Circ Res* 1976;39:536–41.
24. Rudolph AM, Heymann MA. *Am J Obstet Gynecol* 1976;124: 183–92.
25. Romero T et al. *Am J Physiol* 1972;222:1285–90.
26. Klopfenstein HS, Rudolph AM. *Circ Res* 1978;42:839–45.
27. Gilbert RD. *Am J Physiol* 1980;238:H80–6.
28. Gilbert RD. *J Dev Physiol* 1982;4:299–309.
29. Thornburg KL, Morton MJ. *Am J Physiol* 1983;244:H656–63.
30. Thornburg KL, Morton MJ. *Am J Physiol* 1986;251:H961–8.
31. Hawkins J et al. *Circ Res* 1989;65:127–34.
32. Friedman WF. *Prog Cardiovasc Dis* 1972;15:87–111.
33. Mahony L, Jones LR. *J Biol Chem* 1986;261:15257–65.
34. Lipp JA, Rudolph AM. *Biol Neonate* 1972;21:76–82.
35. Friedman WF et al. *Circ Res* 1968;23:25–32.
36. Lebowitz EA et al. *Pediatr Res* 1972;6:887–93.
37. Birk E et al. *Pediatr Res* 1992;31:468–73.
38. Jansen AH, Chernick V. *J Appl Physiol* 1974;36:1–5.
39. Dawes GS. *Foetal and Neonatal Physiology*. Chicago, IL: YearBook; 1968.
40. Itskovitz J, Rudolph AM. *Am J Physiol* 1987;252:H916–22.
41. Bartelds B et al. *Pediatr Res* 1993;34:51–5.
42. Cowley AW, Jr. et al. *Circ Res* 1973;32:564–76.
43. Itskovitz J et al. *Circ Res* 1983;52:589–96.
44. Teitel DF et al. *Pediatr Res* 1987;22:557–66.
45. Teitel DF et al. *Pediatr Res* 1990;27:372–8.
46. Leffler CW et al. *Pediatr Res* 1984;18:938–42.
47. Mital S, Konduri GG. *Biol Neonate* 2000;77:58–68.
48. Moore P et al. *J Appl Physiol* 1992;73:2151–7.
49. Sime F et al. *Am J Cardiol* 1963;11:143–9.
50. Levin DL et al. *J Pediatr* 1978;92:265–9.
51. Heymann MA, Rudolph AM. *Circ Res* 1976;38:418–22.
52. Oberhansli-Weiss I et al. *Pediatr Res* 1972;6:693–700.
53. McMurphy DM et al. *Pediatr Res* 1972;6:231–8.
54. Clyman RI et al. *Prostaglandins* 1978;15:993–8.
55. Keller RL et al. *Pediatr Res* 2005;58:1216–21.
56. Kajino H et al. *Pediatr Res* 2002;51:228–35.
57. van Bel F et al. *Pediatr Res* 1993;34:47–50.
58. Grant DA et al. *Circulation* 1992;86:1615–21.
59. Rudolph AM et al. *Pediatr Res* 1999;46:141–6.
60. Breall JA et al. *J Clin Invest* 1984;73:1418–24.
61. Birk E et al. *Pediatr Res* 1992;31:468–73.
62. Smolich JJ et al. *Am J Physiol* 1989;257:H1–9.
63. Townsend SF et al. *Pediatr Res* 1989;25:300–4.

# 9

# Development of fetal cardiac and extracardiac Doppler flows in early gestation

Viola Seravalli, Ulrich Gembruch, and Ahmet A. Baschat

## Introduction

The onset of rhythmic contractions of the primitive embryonic heart between 21 and 24 days after conception initiates an important sequence in the functional development of the embryonic cardiovascular system. The normal development of the embryonic cardiovascular system and the fetoplacental unit are necessary to ensure adequate blood flow, oxygen delivery, and gas and nutrient exchange at organ and cellular levels. As the placenta is the major respiratory organ *in utero*, the normal maturation of these two circulatory systems is important for adequate fetal growth and development. The first trimester is a period of rapid development in many organ systems coupled with exponential embryonic growth. Thereafter, fetal growth and development continue toward term in a more steady fashion. The cardiovascular system has to match these needs of the growing and developing embryo. It is therefore not surprising that there are important changes in fetal cardiac function that take place in the first and second trimesters.

Since its introduction by FitzGerald and Drumm,[1] Doppler sonography has evolved as an important tool for the noninvasive examination of the fetal cardiovascular system in uncomplicated pregnancies and fetal disease. The wide application of Doppler sonography has greatly enhanced our knowledge of the maturation of the embryonic cardiovascular system. The study of these cardiovascular developmental changes has been of importance for several reasons.

Studies investigating the normal and abnormal development of the human fetal cardiovascular system indicate that there are important differences from other mammalian species. Therefore, data that have been gathered in sheep and primate experiments may have to be applied with caution to the human fetus. Greater understanding of normal early vascular development allows Doppler flow studies to be integrated into prenatal diagnosis. In this context, the integration of ductus venosus (DV) Doppler studies into first-trimester anomaly and aneuploidy screening, and application in pregnancies at high risk for chromosomal defects, have been investigated.[2–4] Previous observations have indicated that certain cardiac defects may produce a unique hemodynamic or structural impact in early gestation, which ultimately contributes to their poor prognosis.[5,6] Examination of DV blood flow is often abnormal under such circumstances. This explains why abnormal DV blood flow in chromosomally normal fetuses with increased nuchal translucency may be beneficial in identifying fetuses with underlying major cardiac defects.[3,4] Preliminary results suggest that the application of this information in pregnancies at high risk for chromosomal defects based on nuchal translucency thickness, and incorporation of DV Doppler screening into the nuchal translucency scan may result in a major reduction in the need for invasive testing.[2] When the nuchal translucency is normal, ductus venosus blood flow assessment shows low sensitivity as a single screening parameter.[7–9]

This example illustrates that the understanding of embryonic and fetal cardiovascular dynamics is likely to gain increasing importance in the future. This chapter outlines functional cardiovascular changes in the fetus with particular emphasis on the first and second trimesters.

## Cardiovascular control mechanisms

The heart undergoes a repetitive orderly sequence of cardiac contraction and valvular action, which is responsible for the antegrade delivery of blood. These events are summarized in the cardiac cycle, and the level of cardiac function determines the efficiency with which adequate blood flow can be provided to the body under physiological and pathological conditions. A detailed knowledge of the physiology underlying the cardiac cycle is helpful in the application and interpretation of Doppler waveforms obtained from the fetal circulation. The principal events that constitute the cardiac cycle are ventricular diastole, when the atrioventricular (AV) valves are open and the ventricles receive blood, and ventricular systole, when the aortic and pulmonary valves are open and blood is ejected into the circulation. In addition, discrete phases of the cardiac cycle have been identified, which further subdivide the two principal events. Evaluation of fetal cardiac function requires knowledge about the characteristics of these phases and their relationship to flow and pressure events. Since Doppler waveforms display only time and

velocity information, any deductions about cardiovascular pressures are made from our understanding of the phases underlying the cardiac cycle. Nonetheless, important differences between fetal and adult cardiac function have been identified using the Doppler technique.

## Cardiac cycle: Diastole

Ventricular diastolic filling in the adult is subdivided into a passive phase and an active phase. Initial passive filling is rapid and reaches a plateau (diastasis), which is followed by atrial contraction triggered by the electrical discharge at the sinoatrial node, initiating active filling. The initial rapid inflow of blood into the ventricles causes a proportionate fall in atrial pressure, which is reflected in a fall in the venous pulse (Y-descent). Subsequent contraction of the atria results in a rapid rise in the atrial pressure, which is reflected in a rise in the venous pulse (a-wave). The two phases of ventricular inflow produce a biphasic flow velocity waveform across the AV valve consisting of an early peak (E-wave) and a second shorter peak during atrial contraction (A-wave). In the adult heart, the majority of ventricular filling (90%) occurs during the E-wave, while the A-wave contributes to the remainder when a person is at rest. However, if the heart rate is very high (e.g., during exercise), the atrial contraction may account for up to 40% of ventricular filling. In such situations, the "atrial kick" contributes to a larger proportion of ventricular filling; therefore, the relationship of the E- and A-waves may reverse.[10] Atrial contribution to ventricular filling therefore varies inversely with duration of ventricular diastole and directly with atrial contractility. After atrial contraction is complete, the atrial pressure begins to fall, causing a pressure gradient reversal across the AV valves. This causes the valves to float upward (pre-position) before complete closure during the beginning of systole. At this time, the ventricular volumes are maximal, and this ventricular end-diastolic volume constitutes the ventricular preload (Figure 9.1).

## Cardiac cycle: Systole

When the electrical impulses traverse the annulus fibrosus and reach the ventricular conduction system, ventricular myocardial contraction is initiated. Elevation of intraventricular pressures above the atrial pressures results in closure of the tricuspid and mitral valves. Following closure of the atrioventricular valves initially there is a period of rapid rise in intraventricular pressures (isovolumetric contraction). During this phase of isovolumetric contraction, there

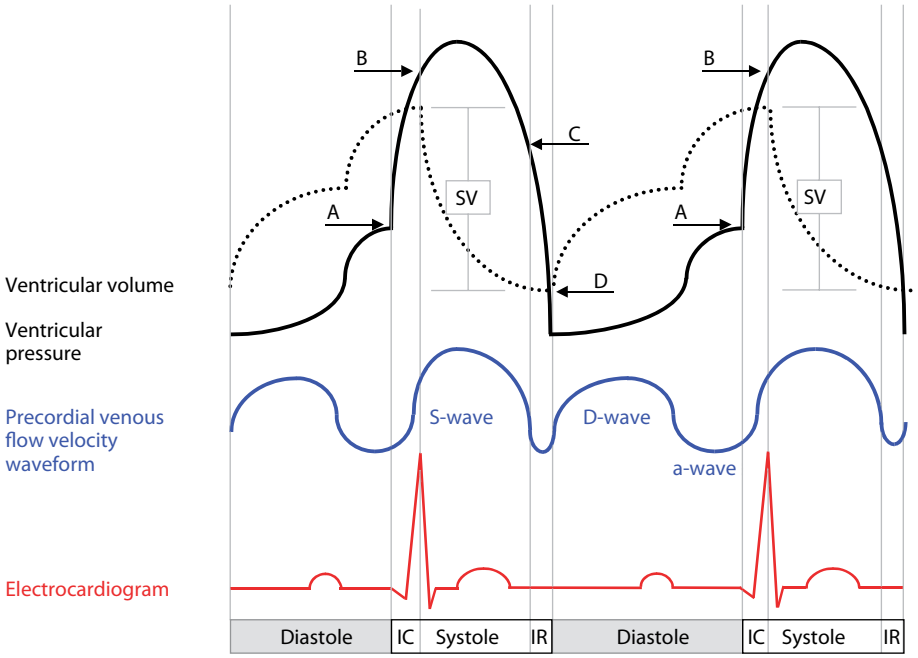


**Figure 9.1**
The cardiac cycle. The relationship between intraventricular pressure and volume and precordial venous flow velocity waveforms during the cardiac cycle. Electrical activity precedes atrial and ventricular contractions. In the fetus a larger proportion of ventricular filling occurs by atrial contraction in late diastole. The rapid rise in atrial pressure is transmitted into the venous system, decreasing antegrade flow (a-wave). With onset of ventricular contraction, atrioventricular valves close (A) and intraventricular pressure rapidly rises without ventricular shortening (IC, isovolumetric contraction) until it exceeds pressure in the great vessels, and semilunar valves open (B). Ventricular shortening during ejection of the stroke volume (SV) causes rapid descent of the atrioventricular valve ring, allowing increased precordial venous forward flow (S-wave). When ventricular pressure falls below diastolic pressures in the major vessels, the semilunar valves close (C). When intraventricular pressure falls below atrial pressure, the atrioventricular valves open (D) at the end of isovolumetric relaxation (IR). The rapid inflow into the ventricle is reflected by increased precordial venous flow (D-wave).

may be bulging of the AV valves, resulting in a temporary increase in atrial pressures transmitted to the venous pressure waveform. Once the intraventricular pressures exceed those of the great arteries, the pulmonary and aortic valves open; left ventricular blood is ejected into the ascending aorta, and right ventricular blood is ejected into the main pulmonary artery during this rapid ejection phase of ventricular systole. The rapid ventricular shortening results in a descent of the AV-ring which causes atrial pressures to fall below venous pressures (X-wave); atrial filling begins at this time. This period corresponds to the S-wave in the venous flow velocity waveform (see section "Doppler investigation of the cardiovascular system"). Following rapid ejection, the rate of outflow from the ventricle decreases, and the ventricular and aortic pressures start to decrease. At this point muscle fibers have shortened, are repolarizing, and can no longer contract forcefully. This causes ventricular active tension to decrease and the rate of ejection and ventricular emptying to fall. When the ventricular ejection falls to zero, the intraventricular pressures fall below the diastolic pressures in the major vessels, resulting in closure of the aortic and pulmonary valves. Ongoing ventricular relaxation ensures decreasing intraventricular pressures until these fall below atrial pressure and the atrioventricular valves open at the end of isovolumetric relaxation. The volume of blood that remains in the ventricle prior to the opening of the AV valves is called the end-systolic volume. The difference between the end-diastolic volume and the end-systolic volume is the stroke volume (Figure 9.1).

## *Indices of cardiac function*

Individual ventricular blood volumes ejected in 1 minute define the ventricular outputs representing the product of individual ventricular stroke volumes and heartbeats per minute. The combined cardiac output is simply the sum of right ventricular and left ventricular outputs. The parallel arrangement of the fetal circulation results in the unique feature that the relative contribution of the individual chambers to the combined cardiac output can change under physiological and pathological conditions. The blood pressure generated by the combined effects of ventricular contraction force, vessel wall resistance, and downstream vascular resistance determines fetoplacental perfusion. For any organ, the perfusion is passively regulated by the pressure drop across the arterial and venous ends of its vascular supply. In addition, many organs have the potential to optimize perfusion by local changes in resistance vessel diameter by a process called *autoregulation*.[11] The downstream resistance experienced by each ventricle is determined by the sum of blood flow resistance in individual downstream vascular beds. The product of the cardiac output and peripheral resistance determines the blood pressure generated.

Although the mechanisms involved in the cardiac cycle appear relatively straightforward at first, it is important to realize the presence of many interacting factors. Changes in cardiac output may be due to variations in heart rate and/or stroke volume. Changes in the filling state of the heart (preload), changes of downstream resistance (afterload), and variations in myocardial contractility can achieve alterations of the stroke volume. Preload can be defined as the initial stretching of the cardiac myocytes prior to contraction, and is related to the sarcomere length. Sarcomere length cannot be determined in the intact heart, so other indexes such as ventricular end-diastolic volume or pressure are substituted. Neither of these measures is ideal, because they do not accurately reflect sarcomere length. Nevertheless, end-diastolic pressure and, particularly, end-diastolic volume are used as clinical indices of preload.

Other factors influencing cardiac function are valvular competence, blood viscosity and inertia of the blood, and myocardial muscle mass. The heart rate is predetermined by the sinoatrial node, which is the cardiac pacemaker with the highest rate of intrinsic automaticity. There is superimposed modulation of heart rate and intracardiac conduction through the AV node by the autonomic nervous system. The overall control of vascular tone and blood pressure is integrated at the level of the vasomotor center.[12] Under physiological circumstances, preload is primarily determined by venous return and blood volume. Heart rate, by affecting filling time, can have a pronounced inverse effect on preload. If preload is viewed as end-diastolic volume, then preload is determined ultimately by the end-diastolic pressure and the compliance of the ventricle. Therefore, a decrease in compliance, as occurs with ventricular hypertrophy, will lead to a reduction in preload unless there is a corresponding increase in end-diastolic pressure.

In the adult heart, an increase in preload or a decrease in afterload within a physiological range will result in an increase of stroke volume. The Frank-Starling mechanism describes the ability of the myocardium to increase stroke volume in response to increases in preload. The efficiency of the Frank-Starling mechanism is strongly influenced by diastolic and systolic myocardial properties. Degree and velocity of myocardial relaxation are the major determinants of ventricular compliance and therefore resistance of the ventricles to diastolic filling. A low ventricular compliance is associated with an exaggerated increase in intraventricular pressure when preload is increased. Under such circumstances, ventricular filling becomes increasingly dependent on atrial contraction, displacing the effective period of filling to late diastole. The decreased ventricular filling capacity is prohibitive for an increase in the stroke volume. In addition, myocardial contractility has to be of sufficient force to oppose the effects of afterload. Contractility and contraction velocity are the main determinants of stroke volume in circumstances of increased afterload. The functionality of the myocardium is one of the factors responsible for the efficiency with which cardiovascular control mechanisms can modulate cardiac output. Slower systolic contraction velocity and strength and low diastolic compliance have a significant impact on cardiac function and the efficiency of cardiovascular reflex mechanisms.

## The fetal circulation

The unique arrangement of the fetal circulation impacts significantly on cardiac function and distribution of cardiac output. According to data from sheep studies, approximately 50% of oxygenated blood of placental origin reaches the fetal heart via the umbilical vein through the DV after bypassing the hepatic circulation.[12,13] The DV develops at approximately 7 weeks of gestation and, in contrast to the other veins, which grow with the embryo, shows little increase in size.[14] The narrow diameter of the ductus is responsible for a marked acceleration of the entering blood.[14,15] Blood with lower oxygen content enters the right atrium via the inferior and superior caval veins and the coronary sinus. Differential directionality of right atrial venous inflow and the crista dividens of the foramen ovale results in an interatrial right-to-left passage of well-oxygenated blood that was also confirmed for the human fetus.[16,17] One of these bloodstreams originates in the umbilical sinus, reaching the left atrium via the left upper portion of the inferior vena cava after considerable flow acceleration in the DV; middle and left hepatic venous blood joins this stream. A second stream originating in the abdominal portion of the inferior vena cava is joined by right hepatic venous blood entering the right atrium via the right upper portion of the inferior vena cava. This stream meets with blood from the superior vena cava and coronary sinus and enters the right ventricle through the tricuspid valve. Pulmonary venous return reaches the left ventricle via the left atrium. The relative separation of right atrial inflow and little admixture from the pulmonary veins ensures that in the fetal lamb the left ventricle receives approximately 65% of the well-oxygenated blood, which has a 15%–20% higher oxygen content than right ventricular blood.

Because of the parallel arrangement of the fetal circulation, the afterload acts separately on each ventricle. Right ventricular afterload is predominantly determined by vascular resistance in the main pulmonary artery, the ductus arteriosus, and the descending aorta with its organ branches, and the combined resistance of the fetoplacental circulations. Vascular resistance in the ascending aorta and the brachiocephalic circulation predominantly determines left ventricular afterload. The relative separation of the venous ventricular inflows also has the effect that right ventricular preload comprises mainly the superior and inferior venae cavae, while left ventricular preload comprises the pulmonary veins and the left hepatic vein and DV. The characteristics of the fetal circulation have been extensively studied in the fetal lamb. Because of the parallel arrangement, there is a differential distribution of right and left ventricular outputs with a predominant contribution of the right ventricle. In the fetal sheep, the ratio of right-to-left ventricular output is 1.8:1. Owing to the high pulmonary vascular resistance and the orientation of the ductus arteriosus, only 13% of the right ventricular output is distributed to the lungs and the remaining 87% reaches the descending aorta.[13,18,19] Approximately two-thirds of this blood reaches the placental vascular bed for oxygenation via the umbilical arteries. Left ventricular output is predominantly distributed to the coronary and brachiocephalic circulations. Of the 29% of left ventricular output reaching the descending aorta, two-thirds reaches the placenta. The right ventricle therefore has the role to deliver oxygen-poor blood to the placenta for oxygenation, while the left ventricle delivers well-oxygenated blood to the brain and heart. In the fetal lamb, the majority (41%) of the combined cardiac output is delivered to the placenta, while 22% supplies the upper part of the body, 8% the lungs, and 3% the myocardium.[13,18,19] A change in distribution of the cardiac output with advancing gestation has been documented for the fetal lamb. The proportion of cardiac output reaching the brachiocephalic circulation increases from approximately 20% at midgestation to term. At this time, the brachiocephalic circulation receives approximately 35% of the common cardiac output, while the placenta and the remaining body receive 30% each. The high resistance in the fetal peripheral circulation and the constantly falling blood flow resistance in the placental bed ensure that a considerable proportion of aortic blood flow is diverted to the placenta via the umbilical arteries for oxygenation. The differential downstream distribution of blood volume passing through the descending aorta changes with gestation. At midgestation, 59% of the blood flow reaches the placenta while 41% reaches the lower half of the body. This proportion changes toward term, when only 33% of blood flow reaches the placenta, and 67% is distributed to the lower body[13,18–20] (Figure 9.2).

More recently, other animal models have also been proposed for the study of fetal circulation. In particular, pregnant murine and rabbit models have placental characteristics similar to those of humans, with shorter gestational periods, requiring smaller experimental areas.[21] In pregnant murine models, the use of high-frequency ultrasound facilitates a detailed characterization of the embryonic cardiovascular system.[22–24] The study of fetal Doppler parameters in pregnant mice has yielded similar results to those obtained during human fetal surveillance. An increase in Doppler velocities and decrease in resistance index have been observed in all fetal vascular territories toward the end of pregnancy, indicating a continuous development of fetal organ vascular networks.[23] Future research on hemodynamic changes in experimentally induced pathologic conditions (e.g., preeclampsia, intrauterine growth restriction, diabetes) in mouse models using high-frequency ultrasound will provide a better understanding of the process of adaptation or deterioration related to obstetrical complications.

The noninvasive Doppler examination of the human fetal circulation seems to confirm the developmental changes observed in other mammalian species. However, there are some important differences that have been identified in the human fetus. The dominance of the right ventricle contributing approximately 53% of the combined cardiac output has also been demonstrated for the human fetus.[25–27] The ratio of right-to-left ventricular output is lower in the human fetus than in fetal sheep (1.1–1.2 versus 1.8, respectively).[26,28] The difference from the sheep fetus is due to the fact that the human fetus has a relatively larger brain mass.[26] Another important difference from the fetal lamb is that in the human fetus, a higher proportion of umbilical blood is directed to

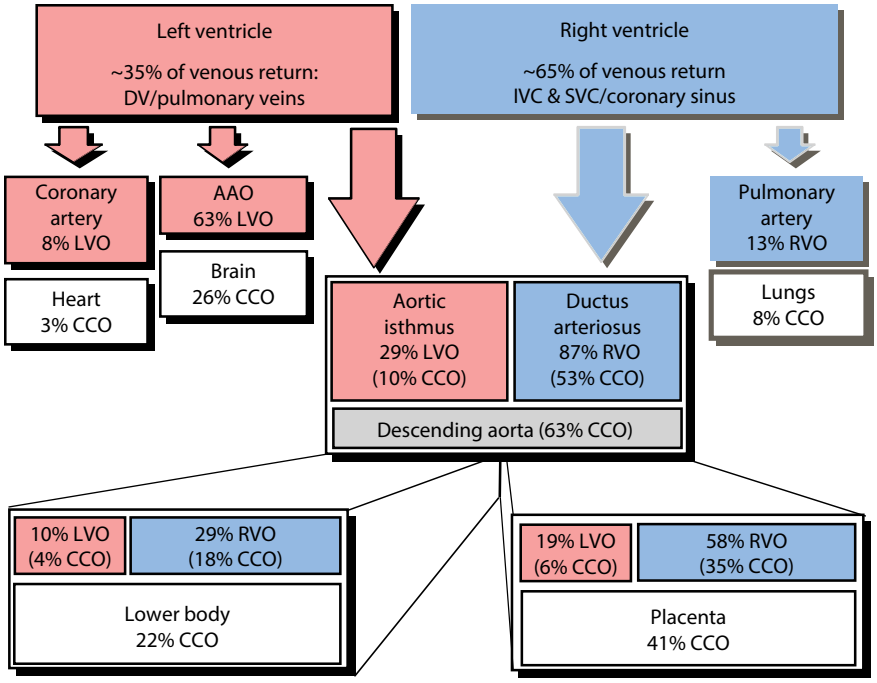


**Figure 9.2**
The fetal circulation. The distribution of right and left ventricular output (RVO, LVO) and the combined cardiac output (CCO) in the circulation of the fetal lamb. The largest proportion of the CCO is distributed to the placenta for oxygenation. Through preferential streaming, well-oxygenated left ventricular blood supplies the brain and heart, while right ventricular blood with lower oxygen content is predominantly distributed to the placenta. (AAO, ascending aorta; DV, ductus venosus; IVC, inferior vena cava; SVC, superior vena cava.)

the liver and less is shunted through the DV. Compared to the 50% shunting of umbilical blood through the DV found in animal experiments, the degree of shunting in the human fetus under physiological conditions is considerably less, about 25% of the umbilical venous blood, suggesting a higher priority of the fetal liver than was previously realized.[29,30] These findings indicate that there are important differences in regional blood flows in different mammalian species that may have important consequences in pathological states. Further studies are necessary to delineate these differences in greater detail to elucidate fetal adaptation to intrauterine life.

The stroke volume and cardiac output have been measured in the human fetus from the first trimester to term using either two-dimensional (2D) or three-dimensional (3D) ultrasound, with the latter being considered more accurate.[31] Heart volumes are smaller when measured by 3D ultrasound as compared to 2D ultrasound, and this has been explained by the fact that in the estimation of volume by 2D ultrasound it is assumed that the heart has an elliptical or spherical shape.[26,28,32,33] The modern four-dimensional spatiotemporal imaging correlation (STIC) ultrasound technique and the Virtual Organ Computer-aided AnaLysis (VOCAL) technique have been recently used to establish reference ranges for stroke volume and cardiac output in normal fetuses. These parameters increase exponentially with gestation. At 12 weeks, the mean stroke volume and cardiac output are 0.02 mL and 2.39 mL/min for the left ventricle, and 0.01 mL and 1.80 mL/min for the right ventricle. At 34 weeks, the respective mean values are 2.08 mL and 284.71 mL/min for the left ventricle and 2.67 mL and 365.99 mL/min for the right ventricle. The ratio of right to left stroke volume and cardiac output increases significantly with gestation from about 0.97 at 12 weeks to 1.13 at 34 weeks.[28] However, it remains relatively constant between 20 and 30 weeks of gestation.

The ventricular ejection force has been measured as early as 12 weeks in the human fetus. It increases with advancing gestation, and it is similar between the two ventricles.[34–36] This increase is believed to be mostly due to the increase in myocardial contractility as the heart develops, since the ventricular ejection force is relatively independent of the peripheral vascular resistance.[35]

## Structural and functional maturation of the fetal myocardium

The immature fetal myocardium has decreased contractility and compliance, as well as slower contraction and relaxation rates than the adult or neonatal myocardium. The Frank-Starling mechanism is necessary for optimal cardiac output at various filling stages of the heart. It was long presumed that the human fetus was unable to increase cardiac output by the Frank-Starling mechanism. However, the demonstration of postextrasystolic potentiation in cases of fetal arrhythmia suggests that the Frank-Starling mechanism is operational in the human fetus from 20 weeks onward, but working at the upper limit.[37,38]

The fetal myocardial response to increases in afterload is another limitation when compared to neonatal and adult myocardium. Investigations in the fetal lamb have demonstrated that resting fetal cardiac function is normally near maximum, very sensitive to changes in afterload, and largely unaffected by baroreceptors.[39,40] There is a sharp drop of cardiac output with minimal increases in afterload. In addition, cardiac output experiences only a slight increase if afterload falls. For these reasons, fetal cardiac function is described

as being relatively afterload-sensitive.[19,39,40] Cardiac output can be increased with volume loading and β-adrenoceptor stimulation, provided arterial pressure does not increase.[40,41] This indicates that alteration of preload is an important determinant of cardiac output *in utero*. The majority of the fetal blood volume is contained in the placental circulation situated between the arterial and venous limbs of the circulation. Since this large proportion of the vascular volume is extracorporeal, the ability to increase preload by alteration of venous return is limited.[42] Finally, the presence of central shunting through the foramen ovale also results in equalization of pressures between the two ventricles (interdependence). Owing to this effect, preload of both ventricles is equally affected, impairing the ability for selective regulation of ventricular output by this mechanism.

The sarcomere and its protein components actin, myosin, troponin, and tropomyosin constitute the contractile unit of the cardiac muscle. After β-adrenergic stimulation, electrical impulses travel across the sarcoplasmic reticulum resulting in calcium ion release from the T-tubule system. These calcium ions bind to troponin at the actin-to-myosin binding site. Conversion of adenosine triphosphate (ATP) to adenosine diphosphate (ADP) by a myosin-bound enzyme (ATPase) releases energy that is necessary for the relative motion between actin and myosin. Activation of troponin by the binding of calcium ions is permissive for this electromechanical coupling, which results in shortening of the sarcomere and ultimately contraction of the muscle fiber. The density of β-adrenoceptors, number of sarcomeres, development of the sarcoplasmic reticulum and the T-tubule system, structure of contractile proteins, and the number of calcium binding sites on the troponin influence the strength of contractility of the muscle fiber. In contrast, the contraction velocity is determined by the reaction rate of the myosin ATPase.[43,44]

Contraction velocity and maximal contractile force of isolated fetal cardiac muscle fibers are significantly lower than in the neonate or adult.[19] Many mammalian experimental studies have documented structural and functional maturation of the myocardium in fetal and neonatal life. These changes presumably also occur in the human fetus. Fetal myocardium has approximately 30% less contractile elements per gram of muscle fiber[43,44] as well as a lower concentration of contractile proteins.[45,46] The myosin ATPase bound to the heavy-chain myosin isoforms has a slower reaction rate than that bound to adult isoforms.[47–49] Fetal troponin isoforms display a lower affinity and sensitivity for calcium ion binding than their adult counterparts.[45–50] The fetal sarcoplasmic reticulum and the transverse tubular system are less well developed and have a lower capacity for calcium ions than in the adult or neonate.[50,51] A number of ultrastructural changes have a significant impact on fetal myocardial function with advancing gestational age. An increase in myocardial adrenergic receptor density and maturation of the sarcoplasmic reticulum ultimately allow more effective stimulation of the sarcomere. Increased capacity and distribution of calcium ions within the sarcoplasmic reticulum enhance delivery of this important contractile substrate to troponin binding sites.[45–52] There is a switch in the expression of isoforms of the contractile proteins to more mature adult forms, which contributes to an increase in contractility and maximal generated contractile force.[53] The combination of enhanced calcium delivery in response to stimulation and changes in contractile elements results in a markedly increased efficiency of electromechanical coupling.[19] An important modulator of this maturational process is the concentration of thyroxine.[54,55] The marked rise in thyroxine concentrations prior to term may contribute to improved cardiac function by an upregulation of myocardial β-adrenergic receptors.[54,55] However, the sequence and timing of these changes have not been fully delineated. There is an up to 40-fold increase of thyroid hormones in the embryonic tissues from the 9th to the 12th week of gestation, and a steady further increase toward term.[56–58] This increase may promote the development of cardiac adrenoceptors as well as switching to adult forms of myosin heavy chains, therefore having a more profound effect on cardiac functional development. Experiments on sheep fetuses showed that the Tri-iodo-L-thyronine ($T_3$) promotes maturation and hypertrophy of fetal cardiomyocytes, and that the normal development of the near-term fetal heart requires $T_3$ concentrations to be maintained within a defined range. In these animal models, $T_3$ infusion promotes cell maturation by producing cell enlargement, increasing cell binucleation, and suppressing proliferation. Conversely, thyroidectomized fetuses have reduced cell cycle activity and binucleation.[59]

The cardiac weight increases 200-fold between 8 and 20 weeks of gestation. Both ventricles are structurally identical at this time.[19] Between 13 and 17 weeks of gestation, there is a significant linear increase of all cardiac dimensions, which correlates with fetal growth and gestational age. The ratios between right and left ventricles and pulmonary trunk and aorta remain relatively constant at 1:1 and 1:1.1, respectively.[60] In addition to the changes in cardiac dimensions, a significant change in embryonic heart rates with advancing gestation has been documented in response to peripheral and central maturation of autonomic cardiac control.

Tissue Doppler imaging represents a recent evolution of the Doppler technique that allows measurements of contraction and relaxation velocities directly from the myocardium.[61,62] The use of this technique in the study of fetal heart showed that the myocardial velocity gradient demonstrated in adults also exists in the fetus.[62,63] Ventricular myocardial velocities change in relation to advancing gestational age, with peak velocities ranging from 0.1 to 4.8 cm/s. Myocardial velocities appear to be higher in the left than in the right ventricle during systole, whereas the reverse occurs during early diastole.[62]

## Development of the fetal cardiac conduction system and autonomic innervation

Fetal cardiac activity is initiated by contracting ventricular myocytes on the caudal region of the straight heart tube

between days 21 and 23 after conception. Development of the cardiac conduction system is ongoing during the folding and looping process of the embryonic heart, and its maturation continues until after delivery. The sinoatrial and AV nodes persist as remnants of the primary myocardium of the sinus venosus and AV junction. As the atria and ventricles become electrically isolated by growth of the endocardial cushions, the AV node provides the only conductive pathway between these chambers. The ventricular conduction system develops concomitantly with ventricular septation and first becomes detectable in the myocardium surrounding the interventricular foramen. Cardiac contractions are initiated at the time of development when truncoventricular fusion commences, involving the atria and the sinus venosus. Therefore, the primitive heart pumps blood before rotation and septation.

In normal pregnancies, the mean heart rate is in the region of 110 beats/minute at 5 weeks of gestation. This is followed by a rise to approximately 170 beats/minute at 9–10 weeks, with a subsequent fall to 150 beats/minute at 14–15 weeks, and a continuing gradual further drop to term.[60,64–66] The initial changes in heart rate are primarily attributed to the changes in cardiac morphology.

The increasing heart rate in the early first trimester is predominantly due to the fusion of the sinus venous with the atria and ventricles and the development of the conductive tissue. This allows the establishment of the sinoatrial node as the primary cardiac pacemaker with the highest intrinsic spontaneous rate of rhythmicity.[67,68] The subsequent decrease in heart rate is thought to reflect increasing parasympathetic modulation,[69] improved ventricular contractility, increasing ventricular muscle mass,[70] and improved atrioventricular valvular function.[19] The successive decline of baseline rate and increasing heart rate variability toward term reflect a relative increase in parasympathetic cardiac innervation and central maturation of autonomic control.

In the human fetus, the parasympathetic inhibition of the sinoatrial node appears to be established between 12 and 17 weeks, followed by sympathetic nerves between 22 and 24 weeks.[5] Marked episodes of sinus bradycardia with excellent prognosis may be observed until this period in gestation. With formation of the AV node and the junctional connection to the ventricles, development of the conduction system is generally completed at 12 weeks. The complete formation of the annulus fibrosus may be disturbed or delayed, resulting in persistence of abnormal conduction pathways. These allow establishment of aberrant reentry conduction in some cases. Completion of the annulus fibrosus eventually leads to cessation of aberrant conduction.[18,71]

The sequential changes of embryonic heart rate are relatively constant. It has been realized that bradycardia is associated with a higher risk for chromosomal anomalies, such as trisomy 18, and/or spontaneous miscarriage.[72,73] An increase in the embryonic heart rate is associated with a higher risk for trisomy 13.[72,74] It, therefore, appears that the human embryonic heart goes through an ultrastructural maturation sequence, which is coupled with the growth of the cardiac structures and the development of receptor and neural connections. The association between abnormal structural cardiac development and the presence of transient thickening of the nuchal fold suggests that intravascular volume handling in the human embryo and early fetus may be particularly vulnerable to cardiac dysfunction.

Evidence of maturation of the autonomic innervation of the fetal heart has been gathered using Doppler ultrasound. Between 10 and 20 weeks of gestation, increasing variability of fetal heart rate and time-averaged velocity have been documented in the abdominal aorta.[75] In addition, umbilical artery peak systolic velocity variability and fetal heart rate variability also increase in this period.[76] The heart rate variability is considered as evidence of maturation of the parasympathetic nervous system, whereas peak systolic velocity variability reflects the activation of a hemodynamic feedback mechanism.[77,78] The documented inverse relationship between umbilical artery flow velocity and fetal heart rate during this time has been considered as evidence that the Frank-Starling mechanism regulates cardiovascular control as early as the late first and early second trimesters of pregnancy.[75–78]

## Doppler investigation of the cardiovascular system

The Doppler equation can be used to describe the relationship between the Doppler shift frequency and the absolute blood flow velocity. After resolution of the equation, the velocity can be calculated from the Doppler shift frequency if the velocity and angle of insonation are known. The processing of incoming signals via fast Fourier transformation allows the graphic display of the calculated velocities in a 2D image. In such an image, the flow velocity waveform is displayed, with the velocities on the ordinate and the time on the abscissa (Figure 9.3). The integral under the waveform corresponds to the maximal velocity in the time interval examined.[79] The flow velocity waveform can be analyzed by quantitative or qualitative waveform analysis. Quantitative analysis utilizes formulas to calculate absolute velocities and volume flow, as shown in Figure 9.4.

Quantitative analysis is predominantly utilized for intracardiac flow velocity waveforms. The primary parameters utilized include the absolute diastolic and systolic velocities, time-averaged velocity (TAV), time-averaged maximum velocity (TAMX), and time to peak velocity. The TAV can be used to calculate volume flow if the vessel diameter is known. Since inaccuracies in vessel diameter are raised to the square, measurement of absolute volume flow by Doppler requires stringent adherence to correct anatomic planes using an insonation angle close to 0°.[79–81] The intracardiac flows that have been predominantly investigated include the diastolic filling across the atrioventricular valves, the systolic output across the aortic and pulmonary valves, and the flow across the foramen ovale. The study of fetal intracardiac flows also includes the assessment of the time intervals spent during the various phases of the fetal cardiac cycle, in order to calculate the myocardial performance index (MPI). Such index,

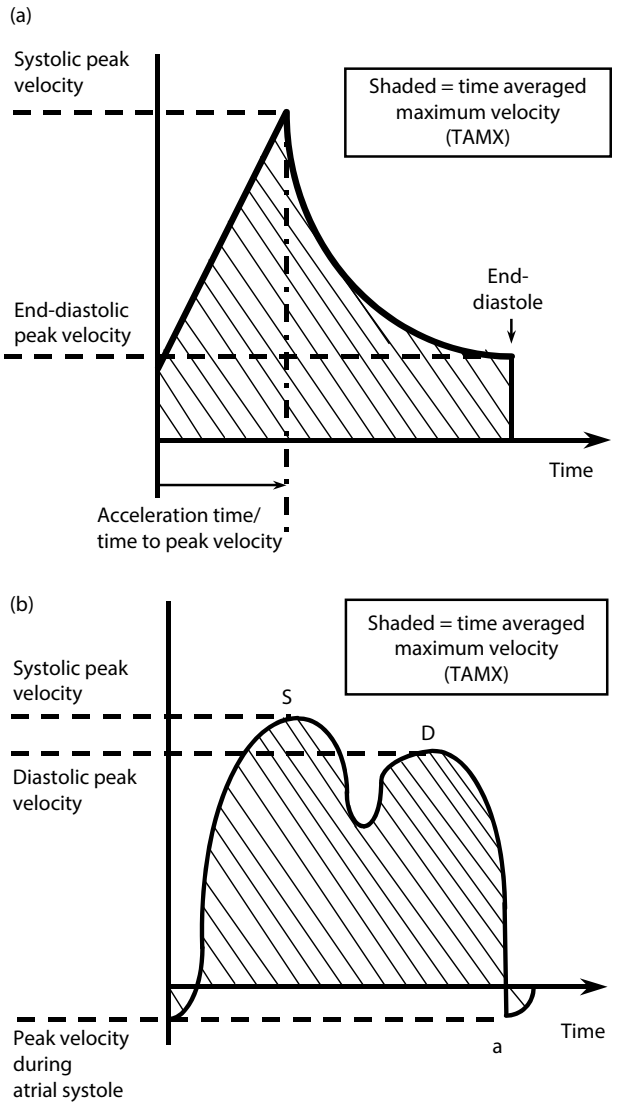


**Figure 9.3**
Arterial flow velocity waveform. (a) An arterial flow velocity waveform. The marked velocities are utilized for the calculation of indexes, while the acceleration time is used as an absolute measurement. (b) A venous flow velocity waveform. The triphasic waveform (S, systole; D, diastole; a, atrial contraction) reflects volume flow changes during the cardiac cycle (see text).

originally proposed by Tei et al.[82] for adult cardiac evaluation, has been applied to fetal echocardiography.[83–85] It is defined as the sum of isovolumetric contraction and relaxation times, divided by the left ventricle ejection time.

Extracardiac Doppler ultrasound predominantly uses qualitative waveform analysis based on angle-independent indexes. The main features of the waveform are the same for all arterial vessels except the coronary circulation where predominant flow is in diastole. The indexes used in fetal medicine utilize the systolic, end-diastolic, and TAMX velocities. Using these indices avoids the sources of error inherent in the use of quantitative waveform analysis and the calculation of absolute volume flow. The systolic/diastolic ratio, resistance index, and pulsatility index predominantly reflect downstream flow resistance and filling pressure of the arterial bed.[86,87] Many authors prefer the use of the pulsatility index, since this allows ongoing waveform analysis in cases of absent or reversed end-diastolic blood flow velocities.[78] An increase of downstream vascular resistance results in a relative decrease of end-diastolic velocities and a subsequent increase of these three indices (Figure 9.4). The middle cerebral artery is one of the main branches of the circle of Willis and, because of its anatomic location, it can be imaged easily with a 0° insonation angle. The Doppler interrogation of this vessel is used to study not only cerebral blood flow resistance indices, but also absolute velocities, particularly the peak systolic velocity (PSV). The absolute flow velocities depend on cardiac and blood dynamics and tend to increase with fetal anemia and decrease with polycythemia.[88] Under physiologic conditions, fetal pCO2 is the primary regulator of the middle cerebral artery PSV. Accordingly, increases in the fetal pCO2, sometimes observed in advanced placental insufficiency, may ultimately result in an increase in this parameter.[89]

Since the beginning of the 1990s, examination of the venous system has been increasingly incorporated into the assessment of the human fetus. These studies have allowed greater insight into the effects of many conditions on cardiac preload. The vessels most commonly utilized in this context are the inferior vena cava, DV, hepatic veins, and the free umbilical vein. The flow velocity waveform of the inferior vena cava is influenced more by right ventricular function, while those of the left hepatic vein and the DV more closely represent left ventricular function.[90–92] The venous flow velocity waveform consists of two peaks and troughs. The systolic and diastolic peaks (the S-wave and D-wave, respectively) are each followed by a trough. The S-wave is produced by descent of the AV-ring during ventricular systole, while the D-wave results from passive ventricular filling during early diastole. The trough that follows the S-wave (v-wave) is produced by ascent of the AV-ring as the ventricle relaxes. The sudden increase in right atrial pressure with atrial contraction in late diastole causes a variable amount of reverse flow, producing a second trough after the D-wave (the a-wave) (Figure 9.3b). The degree of reverse flow during atrial contraction varies considerably in individual veins. There may be reverse flow during atrial contraction in the inferior vena cava and hepatic veins. In contrast, normal blood flow in the DV is antegrade also during atrial systole. The most widely applied indices for the assessment of venous Doppler-derived flow are the percentage of reverse flow,[93] peak velocity index for veins, pulsatility index for veins,[94] and the preload index.[95] Venous indices are believed primarily to reflect cardiac function and to a lesser extent cardiac afterload[90–98] (Figure 9.4). Except for the preload index, all indices mentioned increase when there is a decrease in antegrade flow, such as that associated with increased reverse flow during atrial systole. Such situations occur with increased atrial and ultimately increased central venous pressure. However, it has been observed that the DV a-wave related indices, such as the pulsatility index for veins, do not correlate with the myocardial performance parameters.[99,100] Accordingly, when these indices are used, waveform analysis is not able to differentiate

**Cardiac indexes**

E/A ratio = $\frac{E}{A}$

Volume flow (Q) = TAV x $\pi r^2$

Acceleration time

**Arterial indexes**

Pulsatility index = $\frac{S - D}{TAV}$

Resistance index = $\frac{S - D}{S}$

Systolic diastolic ratio = $\frac{S}{D}$

**Venous indexes**

% Reverse flow = $\frac{TVI\ (S+D)}{TVI\ a}$

S/A ratio = $\frac{S}{a}$

Preload index = $\frac{S - a}{S}$

Peak velocity index = $\frac{S - a}{D}$

Pulsatility index = $\frac{S - a}{TAMX}$

**Figure 9.4**
Formulas used for quantitative and qualitative waveform analysis.

the underlying pathology. Since these indices provide an overall but nonspecific reflection of cardiac forward function, any detection of changes in the DV flow profile should prompt a detailed ultrasound examination of the fetal heart. Recently, the use of Doppler velocity ratios of individual phases of the DV waveform (such as the the S/v and v/D ratios) has been suggested, and reference ranges have been described in normal pregnancies.[101] These ratios seem to more accurately reflect the different events of the cardiac cycle. However, their clinical application has not yet been defined.[100]

The umbilical venous flow velocity waveform has a constant pattern in the second and third trimesters. Pulsations in the umbilical vein are considered evidence of retrograde transmission of elevated central venous pressures. The pulsations correspond to the maximal reverse flow component of atrial contraction.[102]

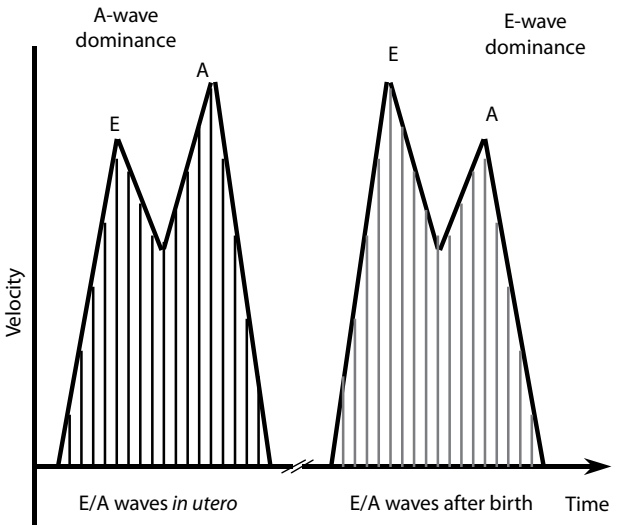


**Figure 9.5**
E/A diagram in the adult and fetus. The flow velocity waveform across atrioventricular valves. In the fetus, a greater proportion of diastolic filling occurs during atrial systole, resulting in a higher peak velocity during this part of the cardiac cycle (A). After birth the relationship between velocities during early diastole (E) and A-wave reverses (see text).

## Development of intracardiac flow velocity waveforms

Diastolic ventricular filling is examined by positioning the Doppler gate immediately distal to the respective AV valves. The characteristic waveform has two peaks representing early diastolic ventricular filling (E-wave) and ventricular filling during atrial systole (A-wave) (Figure 9.5). The ratio between the E- and A-wave peak velocities is a generally accepted angle-independent index for quantification of the waveform across the AV valves. The index is thought to reflect changes in ventricular diastolic function, relaxation velocity and compliance, and pre- and afterload of the respective ventricle. In the adult, diastolic filling occurs predominantly in the early passive phase of diastole resulting in an E/A ratio of greater than 1. In contrast, during fetal life, diastolic filling relies mainly on atrial contraction. Subsequently, the A-wave is generally predominant *in utero*, resulting in an E/A ratio of less than 1. This A-wave dominance *in utero* is presumed to be due to the lower compliance and relaxation time of the fetal myocardium when compared to the adult. Low ventricular compliance is associated with impaired filling during the passive early phase of diastole, requiring atrial contraction to contribute to the major part of ventricular filling. Therefore, a lower E/A ratio is thought to reflect these properties of the ventricle.

Doppler measurements of the transatrioventricular flow velocity waveforms showed that monophasic AV flow velocity waveforms become biphasic as early as 8 weeks.[103,104] A significant gestational age-dependent increase was observed for all AV waveform parameters, which showed a linear relationship with the crown-rump length.[103–105] An increase in cardiac size and atrioventricular valve area contributes to an increase in atrioventricular blood flow volume and thus ventricular

preload. In both the first and the second trimesters, the transtricuspid blood flow volume exceeds that across the mitral valve.[105,106] This is in keeping with the fact that the right ventricle contributes to a greater proportion of the combined cardiac output *in utero*. If the atrioventricular flow profiles are used for calculation of the ventricular output, reproducible results have been obtained, showing right ventricular dominance.[26] When the ventricular volumes measured by 3D and 4D ultrasound are used for the calculation of the cardiac output, smaller values are obtained, but still the right ventricle predominance is confirmed from 17 weeks' gestation on.[28]

With advancing gestation, there is an increase of both transtricuspid and transmitral peak E, but little change in peak A, resulting in a substantial increase in the E/A ratio from approximately 0.5 at 13 weeks of gestation to 0.8–0.9 at 36–38 weeks' gestation.[99,106–110] This is thought to reflect the combined effects of decreasing afterload and improved diastolic ventricular function and both myocardial relaxation and compliance, which are likely to result in a decrease of ventricular diastolic pressures, favoring passive filling during early diastole.[106–110] During the second and third trimesters of pregnancy, a lack of correlation between the Doppler echocardiographically assessed ventricular filling pressures, which were determined by measuring the ratio between flow velocity (E) and annular velocity ($E_A$) with PW-Doppler tissue imaging in early diastole, and gestational age was shown.[111] This suggests the absence of a significant change in ventricular filling pressure and a constant compliance, respectively. Therefore, progressive enhancement of active relaxation and changes in loading conditions are more likely to explain variations in fetal AV blood flow than changes in ventricular compliance.[111]

When the Doppler gate is adjusted to include the inflow across the AV valve and the outflow tract of the respective ventricles, the isovolumetric period and the duration of the ejection period can be measured to calculate the MPI.[83] This parameter has been studied mostly for the left ventricle, where it can be evaluated during the same Doppler waveform. Poor agreement in estimated normal values of MPI exists in different fetal studies. The use of the modified technique suggested by Hernandez et al. seems to allow a better interobserver reproducibility.[112] Throughout gestation, the left-ventricle MPI is relatively constant, showing only a slight increase as pregnancy advances (from $0.35 \pm 0.027$ at 19 weeks to $0.37 \pm 0.029$ at 39 weeks). Of the three components, the isovolumetric contraction time (ICT) remains constant, while the isovolumetric relaxation time (IRT) increases, and the ejection time (ET) slightly decreases.[112] This reflects the progressive improvement of diastolic ventricular function (increase in myocardial relaxation and compliance) and reduction of ejection time that characterizes fetal cardiac maturation. Fetal heart rate has no effect on the MPI, but the duration of IRT, ICT, and ET decreased by 13%–15% when the fetal heart rate increased from 130 to 160 beats per minute.[112] A decrease in myocardial performance in pathological conditions is associated with a prolongation of the isovolumetric period and a reduction in ejection time, thus resulting in an increase in the MPI.

## Flow velocity waveforms in the outflow tracts

Peak velocities in the ascending aorta and the main pulmonary artery are predominantly determined by cardiac contractility and afterload and, therefore, are accepted parameters of ventricular systolic performance. Measurement of outflow tract peak blood flow velocities has been performed as early as 10 weeks of gestation. In these examinations, peak blood flow velocities in the ascending aorta were found to exceed those in the main pulmonary artery.[106,109,110] The improvement in systolic cardiac function between 13 and 20 weeks results in an increase in output from both ventricles, which is also associated with increasing peak blood flow velocities in both outflow tracts. At 13 weeks, outflow tract velocities average 30 cm/s. By 20 weeks, the peak blood flow velocity in the ascending aorta averages 60 cm/s and in the main pulmonary artery 54 cm/s. With continuing gradual increase toward term, these velocities increase to 60–120 cm/s in the ascending aorta and 50–110 cm/s in the main pulmonary artery.[91,113] Calculation of the valvular area allows the estimation of the cardiac output when the TAV and heart rate are known or if the velocity integral and the heart rate are known, because a flat velocity profile can be suggested for the blood flow in the ascending aorta and the pulmonary valve directly behind the semilunar valves. In the human fetus, it has been confirmed that the pulmonary arterial diameter consistently exceeds the aortic diameter, with both vessels showing a linear increase with gestational age.[60] Since the pulmonary artery has a slightly larger diameter than the aorta (approximately 1.3:1), it is expected that the right ventricle contributes to a larger proportion of the cardiac output. This assumption, which was previously documented in an animal experiment, has also been confirmed in the human fetus. These findings confirm animal experimental data suggesting the intrauterine dominance of the right ventricle. A positive relationship between stroke volume and gestational age has been shown and is consistent among studies. However, different absolute values of ventricular cardiac output are obtained when different methods for cardiac output assessment are used (measurement of valve area and flow velocity waveform by 2D and Doppler ultrasound or volume measurement by 3D and 4D ultrasound techniques).[28,113]

The time to peak velocity (TPV) or acceleration time of the arterial flow velocity waveform is primarily determined by mean arterial pressure and to a lesser degree by ventricular contractility. There is an inverse relationship between the TPV and the mean arterial pressure. Several studies have come to different conclusions regarding the TPV, and there is still controversy about the utility and significance of TPV investigation in the human fetus.[114] Machado et al. found that between 16 and 30 weeks the TPV was significantly shorter in the pulmonary artery than in the aorta (32.1 ms compared to 43.7 ms), suggesting that in the midtrimester fetus, the mean pulmonary arterial pressure is higher than in the aorta.[115] Van Splunder et al.[104] have confirmed these findings

for the first-trimester fetus. In contrast, Rizzo et al.[116] found no major differences between these two vessels, while Sutton et al. documented a consistently higher TPV in the aorta.[36] Chaoui et al.[117] were able to document that the TPV and the ratio between TPV and the ejection time increased significantly between 18 weeks and term. These changes throughout gestation are in accordance with animal experiments and suggest that the mean arterial pressure in the main pulmonary artery is higher than in the ascending aorta. In addition, the changes in ejection times and vascular resistances indicate an increase in perfusion as well as a decrease in the vascular resistance and pressure in the pulmonary circulation.[117] The majority of authors agree that the difference in TPV between the aorta and the pulmonary artery becomes less marked and may be negligible close to term.

## Flow velocity waveform in the aortic isthmus

Located between the origin of the left subclavian artery and the aortic end of the ductus arteriosus, the aortic isthmus establishes communication between the two arterial outlets that perfuse in parallel the upper and lower body of the fetus.[118] Its blood flow reflects the relative contribution of the left and right ventricular output (during systole), as well as the balance between the vascular impedances of the upper and lower body (during systole and diastole), especially of the brain and the placenta. Under normal physiological circumstances, antegrade flow throughout the entire cardiac cycle is observed, due to the lower placental vascular impedance in comparison with the impedance of the brachiocephalic circulation. A progressive reduction in the forward flow is observed as gestation advances, with a possible brief reversal flow occurring at the end of systole from 25 weeks on.[119] The mean peak systolic blood flow velocity significantly increases with advancing gestation, from 29 cm/s at 11 weeks' gestation to 102 cm/s near term. The mean end-diastolic flow velocity increases in the first half of pregnancy, while it remains constant at 8.3–8.8 cm/s from 20 weeks to term.[120,121] The PI increases with gestation, most likely secondary to the fall in the impedance of cerebral circulation, while the RI remains relatively stable.[120,121] A significant increase in the blood flow volume of the aortic isthmus is observed from 11 to 20 weeks.[121] This could be explained by relative changes in the ventricles' output, as well as by the low placental impedance relative to cerebral impedance, as an effect of the rapid growth in the cross section of the placental vascular bed during this gestational period.

Conditions of increased placental vascular resistance, reduced cerebral vascular impedance, and fetal hypo-oxygenation can all cause a reversal of the aortic isthmus blood flow.[122,123] The amount and direction of blood through the aortic isthmus are best assessed by using the isthmic flow index (IFI). This is obtained by dividing the sum of the systolic (S) and diastole (D) Doppler flow velocity integrals by the systolic flow integrals. The IFI slightly decreases from $1.33 \pm 0.03$ at 18 weeks to $1.23 \pm 0.16$ at 39 weeks.[124] Five flow patterns (type I–V IFI) have been described that correlate with fetal outcome. Clinical conditions in which such classification can be applied include ventricular functional impairment and stenotic lesions, to predict postnatal ductal dependency, or conditions affecting peripheral vascular resistance, such as placental insufficiency.

## Flow velocity waveforms in the ductus arteriosus

The ductus arteriosus provides a conduit between the main pulmonary artery and the descending aorta. It originates near the origin of the left pulmonary artery and ends in the descending aorta immediately distal to the left subclavian artery. From approximately 26 weeks of gestation, the ductus arteriosus exhibits increasing sensitivity toward prostaglandin.[125] Most authors agree that right ventricular pressures are predominantly determined by the blood flow resistance in the ductus arteriosus. Systolic peak blood flow velocities in this vessel increase from 50 cm/s at 15 weeks' gestation to 130–160 cm/s near term.[126] End-diastolic flow can first be detected between 13 and 14 weeks' gestation and is generally established by 17 weeks' gestation.[127] The pulsatility index in the ductus arteriosus is relatively high ($2.46 \pm 0.52$) and remains relatively constant throughout pregnancy.[128] In constriction of the ductus arteriosus, there is an increase of arterial peak blood velocities, which is more marked in diastole. This results in a fall of the pulsatility index below 1.9 in mild cases and as low as 1 with associated tricuspid insufficiency in severe constriction.[125–128]

Measurement of the timing of cardiac contractions has allowed a comparison to be made between the duration of individual cardiac cycle phases for individual ventricles. A longer diastolic filling time has been found on the left side of the heart (197 ms) compared with the right (174 ms). In contrast, the ejection time is shorter for the left ventricle (174 ms) than on the right side of the heart (189 ms).[129,130] The significant decrease in heart rate between 10 and 20 weeks' gestation results in a lengthening of the cardiac cycle from 373 to 406 ms. Concurrently, there is a significant increase of the diastolic filling time associated with a linear decrease in isovolumetric relaxation and ejection time. This development documents several maturation processes in fetal cardiac function including elevation of myocardial relaxation velocity, increasing compliance, improved ventricular contractility, and decreasing cardiac afterload.[104,105]

## Extracardiac arterial Doppler indexes

The blood flow resistance in the ascending aorta and therefore left ventricular afterload are predominantly determined by the brachiocephalic circulation (predominantly the common

carotid arteries and to a lesser extent the left subclavian artery).[131] Accordingly, changes in vascular resistance in the common carotid arteries reflect predominantly cerebral vascular blood flow resistance (external carotid, internal carotid, and cerebral arteries). The blood flow resistance in these vessels develops similarly, and therefore, many authors prefer the middle cerebral artery, since it is readily accessible at close to 0° insonation. Right ventricular afterload is determined by the blood flow velocities in the pulmonary circulation, the ductus arteriosus, and the vascular beds distal to the ductus (descending aorta with its organ branches, fetoplacental circulation).

## The cerebral circulation

Intracerebral flow velocity waveforms have been visualized as early as 10 weeks of gestation. This early in pregnancy, it is often not possible to distinguish between the individual cerebral arteries.[132] It is of note that in intracerebral vessels, end-diastolic velocities are present between 11 and 13 weeks. The pulsatility index of the intracerebral vessels and the internal carotid artery is relatively constant until 20 weeks of gestation.[131,132] Thereafter, a decrease in the pulsatility index is observed in all cerebral vessels toward term. The pulsatility index in the middle cerebral artery is higher than in all other cerebral vessels. Most authors report a modest rise in the pulsatility index until approximately 26 weeks, with a subsequent fall toward term.[133,134] A similar pattern has been described for the anterior cerebral artery, where there is an increase in the PI until 28–32 weeks of gestation, followed by a reduction until the end of pregnancy.[135] Since the pulsatility index is also influenced by filling pressure, an increase in cerebral blood flow volume may be an explanation for this observation. The decrease of the pulsatility index with advancing gestation suggests a decrease in cerebral blood flow resistance.

## The pulmonary circulation

The vascular connections between intrapulmonary arterioles and the main pulmonary vessels are established between 35 and 50 days after conception. After 16 weeks, there is increasing arborization of the pulmonary vascular tree, which continues toward term.[136,137] The intrapulmonary arteries possess a relatively thick muscular coat and therefore have a small lumen. *In utero* the pulmonary circulation is a low-flow, high-resistance vascular bed. In the fetal lamb, only 3.7% of the common cardiac output reaches the pulmonary circulation in midgestation. This proportion increases to 7% at term.[138] In the human fetus, the pulmonary blood flow and the percentage of cardiac output delivered to the lung (11%) seem to be higher than the values in the fetal lamb.[32]

The high blood flow resistance in the pulmonary circulation is predominantly determined by the overall small cross-sectional area of the pulmonary vascular bed.[138,139] Therefore, fetoplacental blood flow resistance is a more important determinant of the flow velocity in the main pulmonary artery.[19] Several studies have been undertaken to investigate vascular development in the branch pulmonary arteries and have yielded inconsistent results. The pulmonary blood flow pattern at the proximal and middle branch level is characterized by a rapid early systolic flow acceleration, a sharp midsystolic deceleration, a deep notch or reverse flow in early diastole, and a low diastolic forward flow.[140,141] The high pulmonary vascular resistance compared to the fetal systemic circulation and the preferential blood flow through the patent ductus arteriosus into the descending aorta may explain this blood flow pattern. The distal branches, however, show a monophasic forward flow pattern with lower pulsatility and acceleration and deceleration velocities.[140,141] The peak velocity and pulsatility of blood flow significantly decrease if the Doppler interrogation moves from the proximal to the distal arterial branches.[140,141] A high pulsatility index has been documented by several investigators, but findings regarding the development of the pulsatility index from 15 weeks to term differ among investigators.[140–143] Laudy et al. found no significant change in the pulsatility index in the proximal pulmonary branch artery, but a significant gestational age-related drop in the systolic/diastolic (S/D) ratio.[142] Their findings suggest that analysis of the unique waveform of the branch pulmonary arteries using the pulsatility index may not accurately reflect downstream vascular resistance. It is likely that there is a fall in the pulmonary vascular impedance with gestational age. Rasanen et al. found a decreasing pulsatility index with gestational age in the proximal and distal branch pulmonary arteries. This decrease was linear until approximately 31 weeks and then remained relatively unchanged.[143] Laudy et al. demonstrated a similar decrease in the pulsatility index between 20 and 30 weeks followed by a significant increase from 31 weeks until term.[140] They concluded that fetal branch pulmonary arterial vascular impedance decreases significantly between 20 and 30 weeks and suggested an increase of pulmonary vascular resistance during the last 8–10 weeks of pregnancy.[140–143] Recently, Sivan et al. found a slight constant increase of pulsatility index in the proximal, middle, and distal segments of the branch pulmonary artery, but without statistical significance.[141] The lack of change in branch pulmonary artery pulsatility index in later gestation could suggest that during this time lung growth and increase in vascular cross-sectional area result in an overall increase in blood flow in this area.[140–144] Sutton et al. found that blood flow through the lungs increased exponentially with gestational age by almost fourfold between 18 and 37 weeks and was a mean of 22% of combined ventricular output.[16] Foramen ovale blood flow increased exponentially threefold, representing between 17% and 31% of combined ventricular output. The proportions of these flows remained unchanged through the second and third trimesters of pregnancy.[16] Similarly, Rasanen et al. established that from 20 to 30 weeks of gestation, the proportion of pulmonary blood flow increased from 13% to 25% and maintained a constant pattern thereafter, accompanied with a significant decrease in pulmonary vascular resistance, as a result of the increased pulmonary vascular bed.[145] However, they documented that the proportion of foramen ovale blood flow

decreased from 34% to 18% with little change in the proportions after 30 weeks. At 38 weeks, the right ventricular output was 60% of the combined cardiac output, indicating that the development of the human fetal pulmonary circulation has an important role in the distribution of cardiac output.[145] Despite this increase in total pulmonary flow during the second half of gestation, the TAMX and peak systolic velocity at the proximal, middle, and distal pulmonary branch levels did not reveal significant gestational age-related change, suggesting that the increase of vessel diameter, rather than a rise of flow velocities, determines the observed increase of pulmonary blood flow.[140,141] Further research into these relationships is necessary. It appears safe to assume that there is a progressive increase in pulmonary blood flow with advancing gestation in the human fetus. In the second trimester, this may be due to a decrease in pulmonary vascular impedance to blood flow, while in the third trimester an increase in lung volume and overall vascular cross-sectional area may be the major contributor to this development.[117,140–145]

Maternal hyperoxygenation has no effect on the reactivity of the pulmonary circulation in the human fetus at 20–30 weeks. With advancing gestation, pulmonary vessels also acquire increased vasoreactivity, and the pulmonary circulation at 30–38 weeks responds to maternal hyperoxygenation with increased blood flow and decreased vascular resistance.[145,146]

## *Descending aorta and fetal visceral blood flow*

In the descending aorta, end-diastolic blood flow velocities become detectable between 13 and 15 weeks of gestation, therefore later than in the cerebral circulation. Between 16 and 20 weeks, there is a rapid fall of the pulsatility index. After this time, the pulsatility index in the descending aorta remains relatively constant toward term, despite a linear increase in blood flow volume.[147] This is analogous to the development in the ductus arteriosus, indicating that there is relatively little change in blood flow resistance in these vessels after 20 weeks of gestation. This has been attributed to divergent development of blood flow resistance in distal vascular beds. Doppler sonography has been performed in many vascular territories originating from the descending aorta. These include splenic, hepatic, mesenteric, adrenal, renal, and iliac arteries, and, further distally, the femoral arteries[148–154] (Figure 9.6).

In the renal and adrenal arteries, a linear decrease in the pulsatility index has been observed from 20 to 38 weeks.[151,152,154] The splenic artery shows a temporary rise in the pulsatility index in midgestation with a subsequent decline toward term,[148] while the mesenteric and hepatic arteries represent high-impedance vascular beds.[149,152,153] Distal to the bifurcation into the iliac arteries, the vascular beds behave differently with respect to the development of resistance indexes. The examination of the external iliac arteries and femoral arteries reflects development of vascular resistance in the lower body. In the femoral artery, there is a linear increase in the pulsatility index with advancing gestation.[150,152] Throughout gestation, there is a diastolic flow reversal in this vessel and the external iliac artery, indicating the high blood flow resistance in these vessels.[150] The blood flow pattern in the internal iliac artery is predominantly determined by placental and umbilical cord blood flow resistance and therefore shows a different development during gestation. End-diastolic blood flow is established at a similar time in gestation to that in the umbilical artery. Thereafter, there is a continuous decrease in pulsatility index paralleling the development in the placental circulation. Since the pulsatility index in the descending aorta remains relatively constant, it is presumed that the sum of all of these divergent changes in flow resistance overall cause little change in aortic blood flow resistance.[147,152] Importantly, the different blood flow resistance is likely to have an impact on the regional distribution of blood flow in the vascular beds distal to the descending aorta. Because the descending aorta

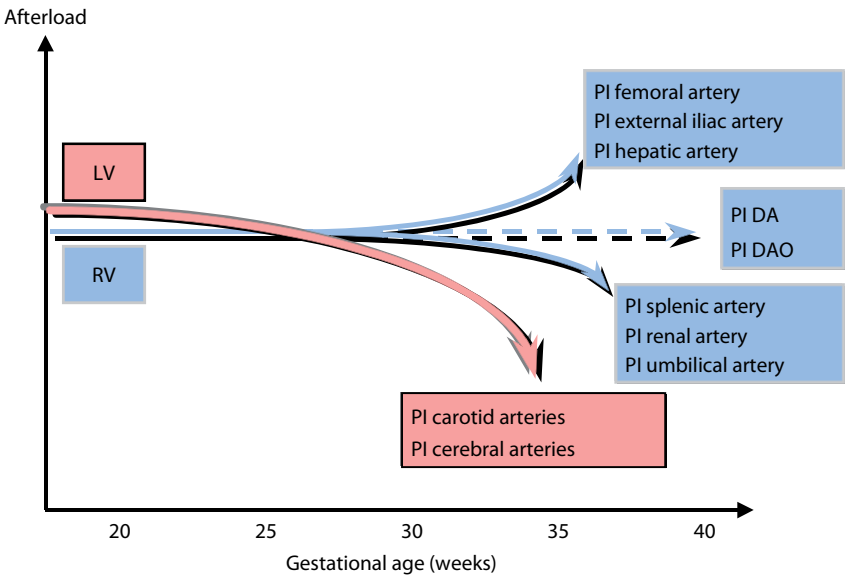


**Figure 9.6**
Development of ventricular afterload in gestation. With advancing gestation, there is a steady decrease in the pulsatility index (PI) in the cerebral circulation and therefore left ventricular (LV) afterload. In contrast, there is little change in the pulsatility index in the ductus arteriosus (DA) and descending aorta (DAO). This may be due to the divergent development of blood flow resistance in downstream vascular beds. (RV, right ventricle.)

Doppler provides similar information to the umbilical vessels and it is technically more difficult to obtain, umbilical artery Doppler is usually preferred in the study of placental function.[155]

## *Uteroplacental blood flow*

The development of the flow velocity waveform in the maternal and fetal compartments of the placenta is suggestive of a progressive fall in vascular resistance with advancing gestational age. Normal uterine artery waveforms in the first trimester show a high pulsatility index and an early diastolic notch as an indicator of significant vascular recoil. The trophoblastic transformation of placental vascular tree is characterized by a decrease in the amount of muscle in the walls of these vessels with advancing gestation.[156] The diastolic notch in the spiral artery flow velocity waveform disappears by 13 weeks' gestation, followed by the arcuate arteries within a further 2 weeks; intervillous flow fully develops by 14 weeks' gestation.[157,158] To evaluate the placental blood flow resistance in the fetal compartment, the umbilical arteries were examined. Increasing differentiation of the villous vascular tree into tertiary villi results in an overall decrease in placental blood flow resistance. End-diastolic flow is first appreciable at 13–15 weeks' gestation, and there is a continuous rise in end-diastolic velocities contributing to the linear fall in umbilical artery pulsatility index toward term.[158–160] Examination of the umbilical flow velocity waveform using Laplace transform techniques suggests that vessel wall tone also decreases at the beginning of the second trimester.[161] These changes in flow velocity waveforms show the increased development of the villous vascular tree and the development of tertiary villi.

# Extracardiac venous Doppler indexes

The blood flow volume in the umbilical vein approximates 140–180 mL/kg/min in the second trimester and decreases slightly to 110–170 mL/kg/min toward term.[159,162,163] It is of note that, although umbilical venous volume flow increases linearly with fetal weight, the volume flow per unit body weight changes little with gestational age. In the first trimester, the umbilical vein has a pulsatile flow pattern, and a constant Doppler flow pattern is generally established at approximately 13 weeks' gestation, because the isthmus of the ductus venosus attenuates the retrograde transmission of the atrial pressure-volume changes.[164,165] Still thereafter, monophasic pulsation corresponding to atrial systole in a floating cord segment are observed in up to 20% of normal fetuses.[166] In contrast, biphasic or triphasic pulsations are always abnormal. There are differences in flow velocity waveforms in precordial venous vessels. The inferior vena cava and hepatic veins have a flow velocity waveform with reverse flow during atrial contraction. In contrast, ductus venosus blood flow is antegrade throughout the cardiac cycle. This is partly due to the fact that there is marked antegrade acceleration of blood flow as umbilical venous blood enters the ductus venosus. Therefore, the highest venous blood flow velocities are found in the ductus venosus. Here, the peak systolic velocity increases from 48 cm/s to 66–71 cm/s from 14 to 41 weeks' gestation, and the end-diastolic velocity shows a continuous increase from 36 cm/s to 43–51 cm/s at term.[167,168] With increasing gestational age, there is a continuous decrease in venous Doppler indices, which is apparent for the precordial veins.[167,169–171] The ductus venosus pulsatility index for veins decreases from 0.57 at 21 weeks to 0.44 at 40 weeks.[168] This is predominantly due to an increased antegrade flow component during atrial systole. This decrease in indices is most marked between 13 and 20 weeks' gestation and is likely to represent the combined effects of improved cardiac diastolic function and decreasing afterload, resulting in an overall decrease in intraventricular end-diastolic pressures. Concurrent with the decrease in venous Doppler indices the proportion of fetuses with pulsatile flow in the free umbilical vein decreases, especially between 11 and 13 weeks of gestation.[97,102,164,169–172]

The flow velocity waveform in the pulmonary veins has a biphasic profile with a systolic peak and a second peak during the early part of ventricular diastole, and is inversely related to the left atrial pressure pulsations.[173–175] In contrast to the adult,[174] there is continuous antegrade flow toward the left atrium in the human fetus.[173–176] This continuous forward flow even during atrial systole suggests that the fetal extraparenchymal pulmonary venous system is not spacious and compliant. Therefore, extraparenchymal pulmonary venous pressure may be higher than the left atrial pressure even at atrial systole.[176] From approximately 20 weeks onward, there is a marked increase in antegrade peak blood flow velocities, contributing to a significant decrease in the S/D ratio.[173] This development is likely to be the result of several factors. There may be a significant increase in pulmonary blood flow volume during this time. In addition, there may be a decrease in the pressure gradient toward the left ventricle,[173] presumably due to improved diastolic ventricular filling facilitating atrial emptying during diastole. Therefore, the decreasing S/D ratio in the pulmonary venous vessels documents improved left ventricular diastolic function and increased preload.[174,175]

# Sequential changes of flow velocity waveforms

The immature fetal heart has limited diastolic and systolic function in the first trimester, limiting its ability to accommodate changes in cardiac preload and afterload. Cardiac development during the following weeks results in improved cardiac function throughout the cardiac cycle. Enhanced diastolic function is manifested by changes in intracardiac and extracardiac flow velocity waveforms—there is change from a monophasic to a biphasic flow velocity profile during

ventricular inflow by 8–10 weeks, which is followed by elevation of the E/A ratio. The latter changes occur in association with a decrease of pulsatility in precordial venous Doppler flow velocity waveform and disappearance of venous pulsation in the free umbilical portion of the umbilical vein. These changes indicate an enhanced antegrade venous flow toward the atrial chambers, which ultimately results in an increase in preload. Between 10 and 20 weeks of gestation, there is a significant increase in cardiac cycle length due to a decrease in fetal heart rate. Despite this lengthening of the cardiac cycle, ejection time and isovolumic relaxation time show a significant decrease.[105] The concomitant improvement of diastolic function is necessary for an efficient accommodation of this increased preload. A significant decrease in the atrial contribution to ventricular filling has been demonstrated between 10 and 14 weeks of gestation, indicating improved diastolic function and the increase in cardiac output necessary to maintain adequate growth.[105,177]

Changes in ventricular afterload are of special significance in regulating organ flow in the fetus, since the "after-load sensitivity" of the fetal ventricular myocardium limits the ability to regulate cardiac output by other mechanisms. At 6 weeks of gestation, approximately 20% of the cardiac cycle is occupied by the isovolumic contraction, while isovolumic relaxation occupies approximately 16%.[103] The isovolumic contraction time shortens progressively and is not measurable after 12 weeks, suggesting effective heart compliance by this time.[103] The persistent decrease in right and left ventricular afterload in the first and early second trimesters associated with the increase in preload and growth of the fetal heart result in an exponential increase in combined cardiac output. During the second and third trimesters, relative distribution of the right and left ventricular outputs is influenced by the changes in afterload of the individual ventricles.[178] End-diastolic velocities are discernible in the cerebral circulation before the fetoplacental circulation. With ongoing development, there is a progressive drop in the pulsatility indexes and presumably also blood flow resistance in the brachiocephalic circulation. At the same time, from 20 weeks onward, pulsatility indexes in the ductus arteriosus and the descending aorta remain relatively constant. This divergent development of ventricular afterload results in physiological redistribution of the cardiac output in favor of the left ventricle and, therefore, the upper body. In the vascular beds distal to the descending aorta, development of Doppler indexes is also divergent in pregnancy. While vascular resistance in the limbs and therefore the external iliac arteries increases, there is a steady decrease in the umbilical artery and therefore the internal iliac pulsatility index. Owing to this development, the major proportion of descending aorta blood flow is distributed to the placental vascular bed for oxygenation. The combined cardiac output increases steadily toward term. The increased contractility and preload and decrease in afterload are associated with increased peak blood flow velocities and an exponential increase of cardiac output during gestation. After 18 weeks' gestation, the relationship between cardiac output and fetal body weight remains relatively constant at 450 mL/kg/min. Although placental blood flow increases from 115 mL/min from 20 weeks to 415 mL/min at term, it decreases in relation to fetal body weight, resulting in relative placental insufficiency at term.[163]

Improved resolution of modern ultrasound machines allows the study of small-caliber vessels. Studies of human fetuses with growth restriction suggest that the cerebral, adrenal, and coronary circulations are capable of autoregulation in the second trimester.[131,151,179–181] In addition, the liver and spleen appear to be preferentially perfused organ systems.[148,149] With delivery of the fetus, the fetal circulation gathers its postnatal functionality by closure of the central shunts[182] (Figure 9.7).

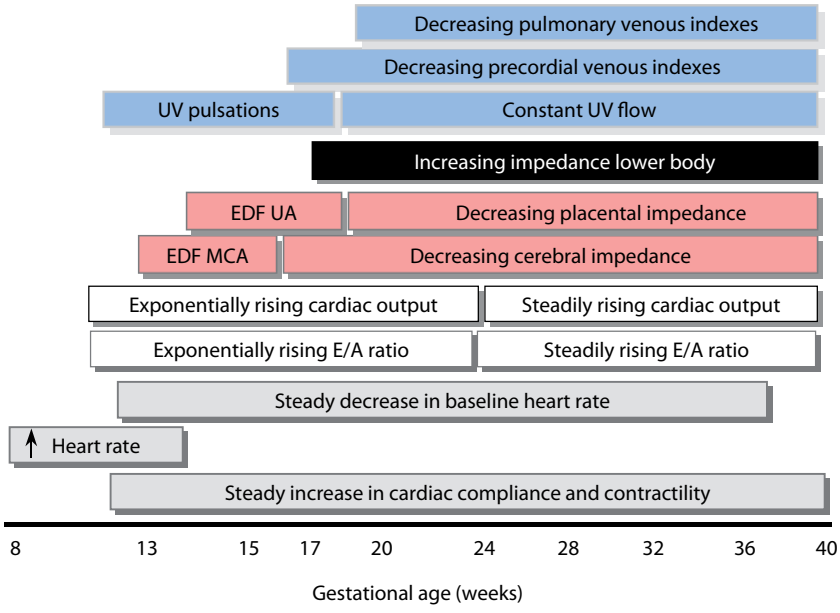


**Figure 9.7**
Development of cardiac and extracardiac functionality with gestation. The approximate temporal relationship of arterial and venous flow velocity changes and cardiac function with advancing gestational age. (EDF, end-diastolic flow; MCA, middle cerebral artery; UA, umbilical artery; UV, umbilical vein.)

# References


1. FitzGerald DE, Drumm JE. *Br Med J* 1977;2(6100):1450–1.
2. Matias A et al. *Ultrasound Obstet Gynecol* 1998;12(6):380–4.
3. Matias A et al. *Ultrasound Obstet Gynecol* 1999;14(5):307–10.
4. Maiz N et al. *Ultrasound Obstet Gynecol* 2008;31(3):256–60.
5. Allan LD et al. *Int J Cardiol* 1989;25(3):341–3.
6. Baschat AA et al. *Ultrasound Obstet Gynecol* 1999;14(5):311–4.
7. Papatheodorou SI et al. *BJOG* 2011;118(12):1438–45.
8. Geipel A, Gembruch U. *Z Geburtshilfe Neonatol* 2012;216(4): 157–61.
9. Prats P et al. *Fetal Diagn Ther* 2012;32(1–2):138–43.
10. Nagueh SF et al. *Circulation* 1998;98(16):1644–50.
11. Guyton AC et al. *Circ Res* 1964;15(suppl I):60–9.
12. Edelstone DI et al. *Circ Res* 1978;42(3):426–33.
13. Rudolph AM. *Circ Res* 1985;57(6):811–21.
14. Chacko AW, Reynolds SR. *Anat Rec* 1953;115(2):151–73.
15. Kiserud T et al. *Lancet* 1991;338(8780): 1412–4.
16. Sutton MS et al. *Br Heart J* 1994;71(3):232–7.
17. Wilson AD et al. *J Am Soc Echocardiogr* 1990;3(6):491–4.
18. Long WA, Henry GW. Autonomic and central neuroregulation of fetal cardiovascular function. In: Polin RA, Fox WW, eds. *Fetal and Neonatal Physiology*. Philadelphia, PA: WB Saunders; 1992:629–45.
19. Sutton MS et al. Functional anatomic development in the fetal heart. In: Polin RA, Fox WW, eds. *Fetal and Neonatal Physiology*. Philadelphia, PA: WB Saunders; 1992:598–609.
20. Teitel DF. Physiologic development of the cardiovascular system of the fetus. In: Polin RA, Fox WW, eds. *Fetal and Neonatal Physiology*. Philadelphia, PA: WB Saunders; 1992:609–19.
21. Malassine A et al. *Hum Reprod Update* 2003;9(6):531–9.
22. Greco A et al. *Reprod Sci* 2015;22(12):1649–55.
23. Hernandez-Andrade E et al. *Ultrasound Med Biol* 2014;40(2): 351–60.
24. Khankin EV et al. *Pregnancy Hypertens* 2012;2(2):84–92.
25. Allan LD et al. *Br Heart J* 1987;57(6):528–33.
26. De Smedt MC et al. *Am J Cardiol* 1987;60(4):338–42.
27. Kenny J et al. *Circulation* 1987;76(1):52–8.
28. Molina FS et al. *Ultrasound Obstet Gynecol* 2008;32(2):181–7.
29. Kiserud T. *J Perinat Med* 2000;28(2):90–6.
30. Kiserud T et al. *Am J Obstet Gynecol* 2000;182:147–53.
31. Gutierrez-Chico JL et al. *Am J Cardiol* 2005;95(6):809–13.
32. Mielke G, Benda N. *Circulation* 2001;103(12):1662–8.
33. Chang FM et al. *Ultrasound Obstet Gynecol* 1997;9(1):42–8.
34. Parasuraman R et al. *J Obstet Gynaecol Res* 2012;38(1):160–4.
35. Rizzo G et al. *Ultrasound Obstet Gynecol* 1995;5(4):247–55.
36. Sutton MS et al. *Br Heart J* 1991;66(4):285–9.
37. Reed KL et al. *Obstet Gynecol* 1987;70(1):1–6.
38. Tonge HM et al. *J Clin Ultrasound* 1986;14(8):607–12.
39. Gilbert RD. *J Dev Physiol* 1982;4(5):299–309.
40. Hawkins J et al. *Circ Res* 1989;65(1):127–34.
41. Moise KJ, Jr., Mari G, Fisher DJ et al. *Am J Obstet Gynecol* 1990; 163(3):776–84.
42. Indik JH, Reed KL. *Am J Obstet Gynecol* 1990;163:1792–6.
43. Barany M. *J Gen Physiol* 1967;50(6 suppl):197–218.
44. Schwartz K et al. *J Mol Cell Cardiol* 1981;13(12):1071–5.
45. Nassar R et al. *Circ Res* 1987;61(3):465–83.
46. Sweeney LJ et al. *Circ Res* 1987;61(2):287–95.
47. Cummins P et al. *J Muscle Res Cell Motil* 1980;1(3):357–66.
48. Ingwall JS et al. *Pediatr Res* 1981;15(8):1128–33.
49. Nakanishi T et al. *Pediatr Res* 1987;22(2):201–7.
50. Maylie JG. *Am J Physiol* 1982;242(5):H834–43.
51. Mahony L, Jones LR. *J Biol Chem* 1986;261(32):15257–65.
52. Mahdavi V et al. *Circ Res* 1987;60(6):804–14.
53. Nadal-Ginard B, Mahdavi V. *J Clin Invest* 1989;84(6):1693–700.
54. Whitsett JA et al. ß *Pediatr Res* 1982;16(6):463–9.
55. Williams LT et al. *J Biol Chem* 1977;252(8):2787–9.
56. Costa A et al. *J Endocrinol Invest* 1991;14(7):559–68.
57. Edwards JG et al. *Biochem Biophys Res Commun* 1994;199(3): 1482–8.
58. Nathanielsz PW et al. *J Endocrinol* 1973;58(3):683–4.
59. Chattergoon NN et al. *FASEB J* 2012;26(1):397–408.
60. Gembruch U et al. *Fetal Diagn Ther* 2000;15(1):20–31.
61. Tutschek B et al. *Ultrasound Obstet Gynecol* 2003;21(1):26–32.
62. Paladini D et al. *Ultrasound Obstet Gynecol* 2000;16(6):530–5.
63. Yang Y et al. *Echocardiography* 2012;29(2):182–6.
64. Schats R et al. *Br J Obstet Gynaecol* 1990;97(11):989–94.
65. Shenker L et al. *J Reprod Med* 1986;31(5):333–5.
66. Wisser J, Dirschedl P. *Early Hum Dev* 1994;37(2):107–15.
67. James TN. *Am J Cardiol* 1970;25(2):213–26.
68. Yamauchi A. *Z Anat Entwicklungsgesch* 1965;124(6):562–87.
69. Friedman WF et al. *Circ Res* 1968;23(1):25–32.
70. Clark EB et al. *Am J Physiol* 1986;250(3 Pt 2):H407–13.
71. Kirby ML. Development of the fetal heart. In: Polin RA, Fox WW, eds. *Fetal and Neonatal Physiology*. Philadelphia, PA: WB Saunders; 1992:589–97.
72. Papaioannou GK et al. *Early Hum Dev* 2011;87(7):453–6.
73. Papaioannou GI et al. *Hum Reprod* 2011;26(7): 1685–92.
74. Hyett JA et al. *Ultrasound Obstet Gynecol* 1996;7(4):239–44.
75. Ursem NT et al. *Ultrasound Obstet Gynecol* 1999;14(6):397–401.
76. Ursem NT et al. *Clin Sci (Lond)* 1998;95(5):539–45.
77. Montenegro N et al. *Ultrasound Obstet Gynecol* 1998;11(4): 274–6.
78. Ursem NT et al. *Cardiovasc Res* 1998;37(3):601–5.
79. Kremkau FW. *Doppler Ultrasound—Principles and Instruments*. Philadelphia, PA: WB Saunders; 1995.
80. Beeby AR et al. *Br J Obstet Gynaecol* 1991;98(8):807–14.
81. Maulik D, Yarlaggada P. In vitro validation of Doppler waveforms indices. In: Maulik D, McNellis D, eds. *Doppler Ultrasound Measurement of Normal Fetal Hemodynamics*. New York, NY: Perinatology Press; 1987:257–82.
82. Tei C et al. *J Am Soc Echocardiogr* 1997;10(2):169–78.
83. Hernandez-Andrade E et al. *Ultrasound Obstet Gynecol* 2005;26(3):227–32.
84. Friedman D et al. *Ultrasound Obstet Gynecol* 2003;21(1):33–6.
85. Raboisson MJ et al. *Am J Cardiol* 2003;91(7):919–21.
86. Gosling RG et al. *Ultrasound Obstet Gynecol* 1991;1(3):175–9.
87. Maulik D et al. *J Ultrasound Med* 1995;14(12):939–47.
88. Mari G et al. *N Engl J Med* 2000;342(1):9–14.
89. Picklesimer AH et al. *Am J Obstet Gynecol* 2007;197(5):526 e1–4.
90. Hecher K et al. *Circulation* 1995;91(1):129–38.
91. Rizzo G et al. *Ultrasound Obstet Gynecol* 1992;2(6):434–45.
92. Rizzo G et al. *Br J Obstet Gynaecol* 1988;95(1):65–9.
93. Rizzo G et al. *Br J Obstet Gynaecol* 1995;102(12):963–9.
94. Hecher K et al. *Ultrasound Obstet Gynecol* 1994;4(5):381–90.
95. Kanzaki T, Chiba Y. *Fetal Diagn Ther* 1990;5(3–4):168–74.
96. Reed KL, Anderson CF. *Am J Obstet Gynecol* 2000;182(4):835–38; discussion 738–40.
97. Reed KL et al. *Obstet Gynecol* 1996;87(4):617–20.
98. Severi FM et al. *Fetal Diagn Ther* 2000;15(1):8–19.
99. Rozmus-Warcholinska W et al. *Ultrasound Obstet Gynecol* 2010;35(5):540–7.
100. Sanapo L et al. *Ultrasound Obstet Gynecol* 2014;43(5):515–9.

101. Turan OM et al. *J Ultrasound Med* 2014;33(2):329–36.
102. Reed KL et al. *Obstet Gynecol* 1997;89(6):953–6.
103. Leiva MC et al. *Ultrasound Obstet Gynecol* 1999;14(3):169–74.
104. van Splunder P et al. *Circulation* 1996;94(6):1372–8.
105. van Splunder IP, Wladimiroff JW. *Ultrasound Obstet Gynecol* 1996;7(6):411–5.
106. Reed KL et al. *Circulation* 1986;73(1):41–6.
107. Labovitz AJ, Pearson AC. *Am Heart J* 1987;114(4 Pt 1):836–51.
108. Stoddard MF et al. *Circulation* 1989;79(6):1226–36.
109. van der Mooren K et al. *Am J Obstet Gynecol* 1991;165(3):668–74.
110. Wladimiroff JW et al. *Am J Obstet Gynecol* 1992;167(3):736–9.
111. Pacileo G et al. *Ultrasound Obstet Gynecol* 2000;16(2):128–32.
112. Hernandez-Andrade E et al. *Ultrasound Obstet Gynecol* 2007; 29(3):321–5.
113. Kenny JF et al. *Circulation* 1986;74(6):1208–16.
114. Silverman NH. *Br Heart J* 1988;59(5):639–40.
115. Machado MV et al. *Br Heart J* 1987;58(1):15–8.
116. Rizzo G et al. *Br J Obstet Gynaecol* 1990;97(7):603–7.
117. Chaoui R et al. *Ultrasound Obstet Gynecol* 1998;11(3):173–9.
118. Fouron JC. *Ultrasound Obstet Gynecol* 2003;22(5):441–7.
119. Fouron JC et al. *Am J Cardiol* 1994;74(5):483–6.
120. Del Rio M et al. *Ultrasound Obstet Gynecol* 2006;28(1):71–6.
121. Vimpeli T et al. *Ultrasound Obstet Gynecol* 2009;33(3):265–71.
122. Fouron JC et al. *Am J Obstet Gynecol* 1999;181(5 Pt 1):1102–7.
123. Makikallio K et al. *Am J Obstet Gynecol* 2006;194(2):542–50.
124. Ruskamp J et al. *Ultrasound Obstet Gynecol* 2003;21(5):441–4.
125. Huhta JC. The fetal ductus arteriosus. In: Copel JA, Reed KL, eds. *Doppler Ultrasound in Obstetrics and Gynecology*. New York, NY: Raven Press; 1994:325–32.
126. Huhta JC et al. *J Am Soc Echocardiogr* 1990;3(1):30–4.
127. Brezinka C et al. *Ultrasound Obstet Gynecol* 1992;2(6):397–401.
128. Tulzer G et al. *J Am Coll Cardiol* 1991;18(2):532–6.
129. Anderson CF et al. *AIUM Annual Meeting*, New Orleans, 1987.
130. Reed KL et al. *J Am Coll Cardiol* 1986;8(2):391–5.
131. Wladimiroff JW et al. *Br J Obstet Gynaecol* 1986;93(5):471–5.
132. van den Wijngaard JA et al. *Br J Obstet Gynaecol* 1989;96(7): 845–9.
133. Arduini D et al. *Obstet Gynecol* 1992;79(4):605–10.
134. Vyas S et al. *Br J Obstet Gynaecol* 1990;97(9):797–803.
135. Benavides-Serralde JA et al. *Gynecol Obstet Invest* 2010;69(1): 33–9.
136. Hislop A, Reid, L. *J Anat* 1972;113:35–48.
137. Levin DL et al. *Circulation* 1976;53(1):144–51.
138. Rudolph AM, Heymann MA. *Circ Res* 1970;26(3):289–99.
139. Long W. Developmental pulmonary circulatory physiology. In: Long W, ed. *Fetal and Neonatal Cardiology*. Philadelphia, PA: WB Saunders; 1990.
140. Laudy JA et al. *Ultrasound Obstet Gynecol* 2000;15(6):479–86.
141. Sivan E et al. *Ultrasound Obstet Gynecol* 2000;16(5):453–6.
142. Laudy JA et al. *Pediatr Res* 1997;41(6):897–901.
143. Rasanen J et al. *Am J Obstet Gynecol* 1996;174(5):1441–9.
144. Rizzo G et al. *Ultrasound Obstet Gynecol* 1996;8(2):87–92.
145. Rasanen J et al. *Circulation* 1996;94(5):1068–73.
146. Rasanen J et al. *Circulation* 1998;97(3):257–62.
147. Tonge HM et al. *Clin Cardiol* 1984;7(6):323–9.
148. Abuhamad AZ et al. *Am J Obstet Gynecol* 1995;172(3):820–5.
149. Kilavuz O, Vetter K. *J Perinat Med* 1999;27(2):103–6.
150. Mari G. *Am J Obstet Gynecol* 1991;165(1):143–51.
151. Mari G et al. *Ultrasound Obstet Gynecol* 1996;8(2):82–6.
152. Mari G, Copel A. Peripheral fetal circulation. In: Copel JA, Reed K, eds. *Doppler Ultrasound in Obstetrics and Gynecology*. New York, NY: Raven Press; 1994:125–32.
153. Rhee E et al. *J Matern Fetal Med* 1998;7(3):120–3.
154. Vyas S et al. *Am J Obstet Gynecol* 1989;161(1):168–72.
155. Baschat AA. *Semin Fetal Neonatal Med* 2011;16(1):2–12.
156. Pijnenborg R et al. *Placenta* 1983;4(4):397–413.
157. Coppens M et al. *Ultrasound Obstet Gynecol* 1996;7(2):114–21.
158. den Ouden M et al. *Br J Obstet Gynaecol* 1990;97(8):716–9.
159. Gill RW, Warren PS. Doppler measurements of umbilical blood flow. In: Sanders JC, James AE, eds. *The Principles and Practice of Ultrasonography in Obstetrics and Gynecology*. Norwalk, CT: Appleton-Century-Crofts; 1985:87–97.
160. Wladimiroff JW et al. *Obstet Gynecol* 1991;78:812–4.
161. Brackley KJ et al. *Br J Obstet Gynaecol* 1998;105(1):78–82.
162. Lees C et al. *Ultrasound Obstet Gynecol* 1999;14(4):250–5.
163. Sutton MS et al. *Pediatr Res* 1990;28(4):383–7.
164. Rizzo G et al. *Am J Obstet Gynecol* 1992;167(3):675–7.
165. Rizzo G et al. *Biol Neonate* 1995;68(3):163–8.
166. van Splunder IP et al. *Ultrasound Obstet Gynecol* 1994;4(1): 49–53.
167. Bahlmann F et al. *Prenat Diagn* 2000;20(8):623–34.
168. Kessler J et al. *Ultrasound Obstet Gynecol* 2006;28(7):890–8.
169. Rizzo G et al. *Am J Obstet Gynecol* 1992;166(4):1271–80.
170. Wladimiroff JW et al. *Am J Obstet Gynecol* 1992;166(3):921–4.
171. Huisman TW et al. *Ultrasound Med Biol* 1993;19(6):441–5.
172. Wladimiroff JW et al. *J Am Coll Cardiol* 1991;17(6):1357–9.
173. Laudy JA et al. *Ultrasound Obstet Gynecol* 1995;6(4):277–81.
174. Rajagopalan B et al. *Cardiovasc Res* 1979;13(12):667–76.
175. Rudolph AM. *Annu Rev Physiol* 1979;41:383–95.
176. Hong Y, Choi J. *Fetal Diagn Ther* 1999;14(2):86–91.
177. Thornburg KL, Morton MJ. *Am J Physiol* 1983;244(5):H656–63.
178. St John Sutton MG et al. *Circulation* 1984;70(6):935–41.
179. Baschat AA et al. *Ultrasound Obstet Gynecol* 2000;16(5):425–31.
180. Baschat AA et al. *Ultrasound Obstet Gynecol* 1997;9(3):162–72.
181. Dubiel M et al. *Ultrasound Obstet Gynecol* 2000;16(5):414–8.
182. Teitel DF et al. *Pediatr Res* 1987;22(5):557–66.

# 10

# Examination of the normal fetal heart using two-dimensional echocardiography

Rabih Chaoui

## Introduction

Despite the introduction of numerous tools in the antenatal assessment of the fetal heart in the last three decades, the two-dimensional (2D) grayscale examination is still considered as the basis of a fetal cardiac examination. In recent years, a huge improvement has been observed in image resolution, not only at centers with high-level ultrasound machines but also at primary and secondary institutions with equipment available for performing antenatal screening. In this chapter, the basics of a cardiac examination performed in 2D grayscale ultrasound are presented. We first present the actual International Society of Ultrasound in Obstetrics and Gynecology (ISUOG) guidelines followed by discussion of the different cardiac planes.

## Guidelines from the international society of ultrasound in obstetrics and gynecology: The sonographic cardiac screening

Cardiac screening programs are in general integrated into routine screening in pregnancy and are thus made available to all pregnant women. Pregnancies at high-risk for congenital heart disease (CHD) or suspected heart anomalies will, however, require a more comprehensive fetal echocardiography, which includes also the use of color Doppler. The ISUOG published in 2013 the updated practice guidelines for the sonographic screening of the fetal heart.[1] Fetal cardiac screening is most optimally performed between 18 and 22 weeks' gestation. Ultrasound examinations performed in early gestation are discussed in Chapter 14. The fetal cardiac screening examination, as defined by the ISUOG practice guidelines, includes the visualization of the upper abdomen, the four-chamber view, and the outflow tracts[1] (Figure 10.1). The left and right outflow tracts are in ISUOG guidelines as part of the fetal cardiac screening examination. Normal anatomy of the great vessels can be ascertained by obtaining transverse views from the four-chamber view and into the upper mediastinum. In this sweep, the five-chamber view can first be seen, followed by the pulmonary view, the three-vessel view, and then the three-vessel trachea view (Figures 10.1 and 10.2). The ISUOG cardiac screening guidelines state that visualization of the three-vessel trachea view is desirable and should be attempted as part of the routine cardiac screening examination. The three-vessel trachea view is discussed later in this chapter and in Chapter 11.

## Technical aspects

### *Transducer choice*

The choice of the appropriate transducer is a prerequisite for a good or best image on ultrasound. The optimized image quality is an important component to confirm normality or to clearly describe the diagnosis in abnormal hearts. Many examiners consistently use one or two preferred transducers, which provide good images in the majority of patients. Most obstetric transducers are curved array with a frequency range of 3–9 MHz. In general, the examiner decides between two types of transducers: the transducer with low-frequency range (range 2–5 MHz) (Figure 10.2), which allows good penetration, or the transducer with high-frequency range (range 5–8 MHz) (Figure 10.2),[2] which is used for higher resolution but less penetration. Recently, linear transducers that are commonly used for soft tissue imaging in radiology have been adapted to obstetric imaging.[3] These linear transducers are desirable because of their high resolution and thus are primarily used when detailed anatomic information is needed (Figure 10.2).

### *Image optimization*

A prerequisite of a good image is in addition to the choice of the proper transducer, the adjustments of the different presets, characteristic for cardiac presets.[2] It is beyond the scope of this chapter to discuss the adjustments of optimal cardiac presets, which are summarized in Table 10.1.

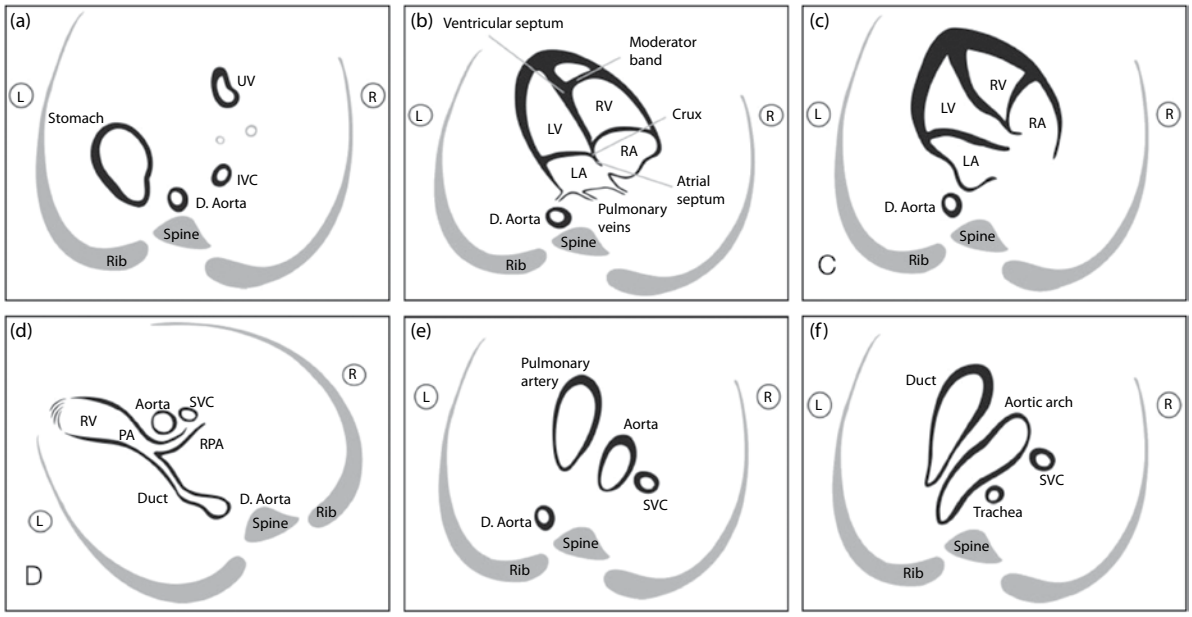


**Figure 10.1**
Views of fetal cardiac screening as recommended by the International Society of Ultrasound in Obstetrics and Gynecology. (a) abdominal situs, (b) four-chamber view, (c) left ventricular outflow tract view, (d) right ventricular outflow tract view, (e) three-vessel view, and (f) three-vessel-trachea view. (D. Aorta, descending aorta; Duct, ductus arteriosus; IVC, inferior vena cava; L, left; LA, left atrium; LV, left ventricle; PA, pulmonary artery; RA, right atrium; RPA, right pulmonary artery; RV, right ventricle; R, right; SVC, superior vena cava; UV, umbilical vein.) (Modified with permission from Carvalho JS et al. *Ultrasound Obstet Gynecol* 2013;41:348–59.[1])

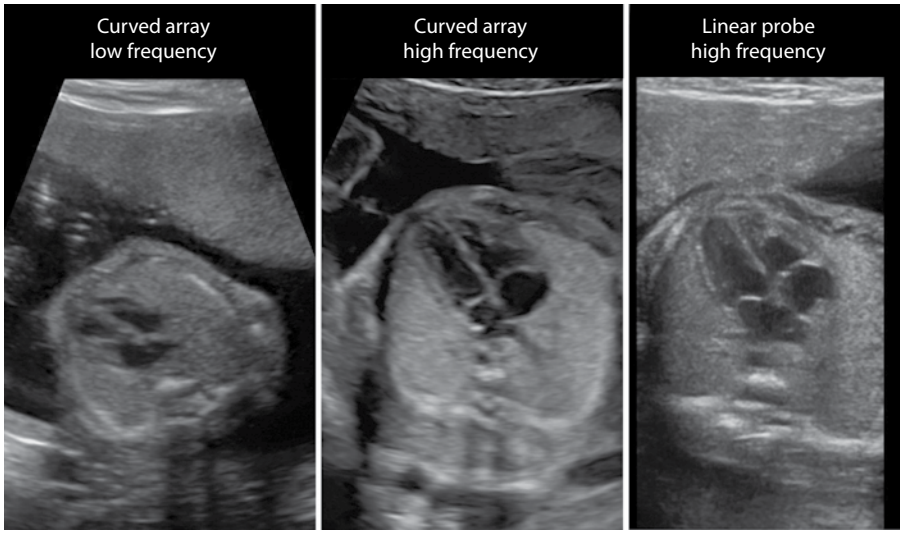


**Figure 10.2**
The four-chamber view shown with three different transducers (Left): Low-frequency curved array probe (e.g., 2–5 MHz), which is used here due to the needed penetration in a fetus deep lying with anterior placenta. (Middle): High-frequency curved array probe. (Right): High-frequency linear probe with a high resolution image.

**Table 10.1** Checklist of image optimization in 2D fetal cardiac scan

- Choose the transducer according to scanning conditions
- Narrow the image sector
- Reduce the image depth
- Use one focal zone positioned at the level of the heart
- Combine harmonic imaging, compound imaging, and speckle reduction
- Magnify or zoom the image to visualize heart and thorax
- Select high-contrast image
- Adapt image resolution for higher frame rate
- Use cine loop to analyze cardiac and valves motion

## Cardiac planes

Examination of the fetal heart in 2D ultrasound should be achieved by acquiring different axial, oblique, and longitudinal planes. The aim is to achieve a comprehensive segmental assessment of the cardiac connections. Different approaches were proposed in the past, either slightly modifying the pediatric cardiologic planes or creating "new" fetal planes with more flexibility.[4,5] The advantage of the latter is that they are easier to learn in obstetric ultrasound. This chapter concentrates on planes we proposed in the past[5] (Figures 10.3 and 10.4) and planes recommended in national and international guidelines (Figure 10.1).

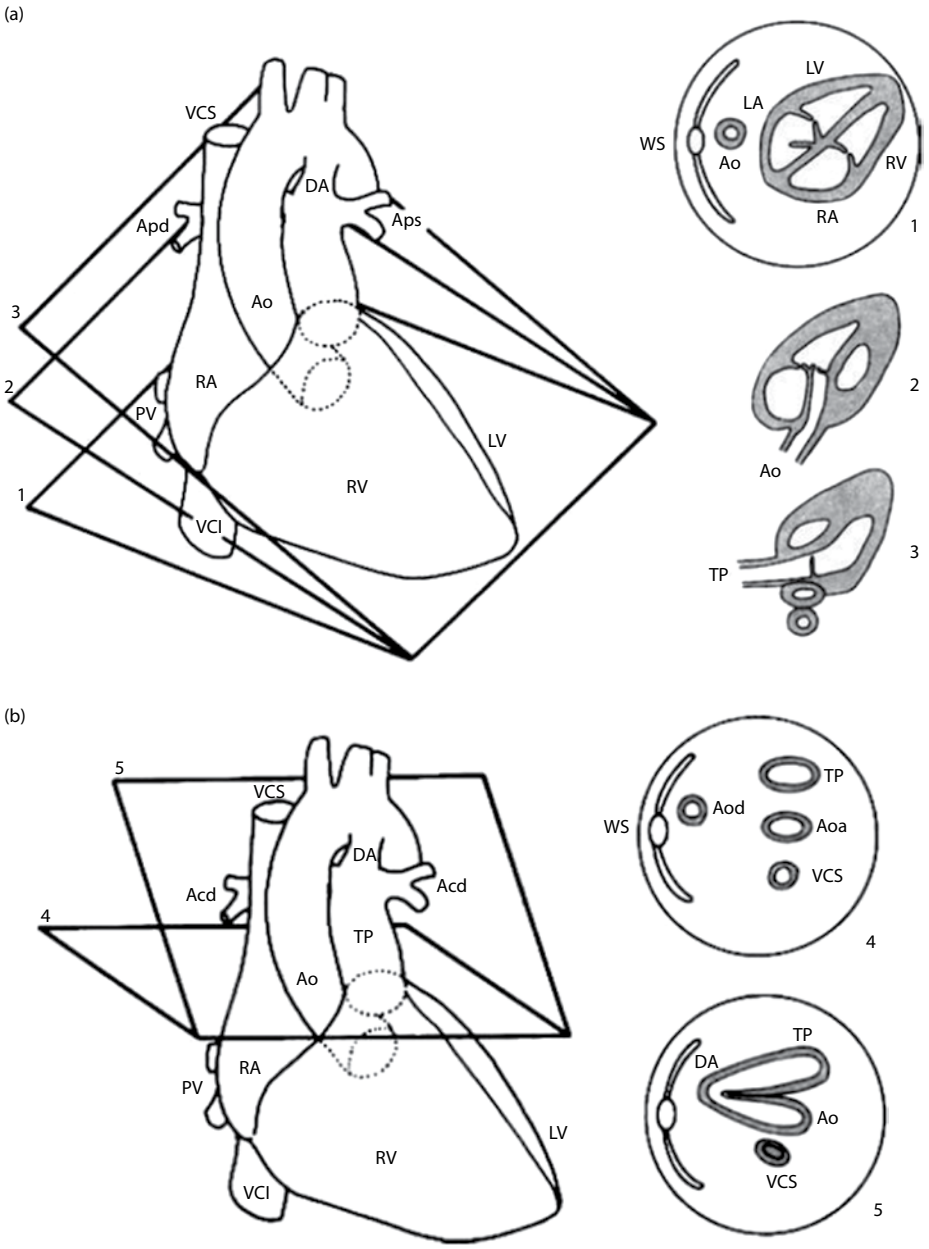


**Figure 10.3**
(a) The different cross sections from the four-chamber view to the five-chamber and pulmonary views. (b) A cross section of the upper thorax to obtain the three-vessel view. (Ao, aorta; Aoa, ascending aorta; Aod, descending aorta; Apd, right pulmonary artery; Aps, left pulmonary artery; DA, ductus arteriosus; LV, left ventricle; PV, pulmonary vein; RA, right atrium; RV, right ventricle; TP, pulmonary trunk; VCI, inferior vena cava; VCS, superior vena cava; WS, spine.) (From Chaoui R et al. *Ultraschall Klin Prax* 1991;6:1–15.[5])

## The upper abdomen

Assessment of the upper abdomen is an integral part of the fetal echocardiographic examination (Table 10.2). Heart malformations associated with abnormalities of the situs are known to be more severe and complex. Furthermore, a careful analysis of the upper abdomen provides a better orientation when examining the fetal heart. The examiner begins with the assessment of the fetal position *in utero*, in order to distinguish the right and left sides of the fetus. The upper abdomen is ideally visualized in a cross-sectional plane (Figure 10.5). An imaginary anterior-posterior line is drawn, dividing a left and a right side. On the left side, the stomach and the descending aorta are seen. On the right side, the liver and the inferior vena cava are found, the inferior vena cava lying anterior to the aorta. By tilting the transducer slightly cranial, the confluence of the three liver veins toward the inferior vena cava is seen. In a lower plane, the umbilical vein enters the liver and continues to the right side into the portal sinus. To the right of the umbilical vein, the gallbladder can be seen. From the upper abdomen, the transducer is then moved slightly cranially to visualize the next plane, i.e., the four-chamber view (Figure 10.4). During this movement, the connection of the inferior vena cava with the right atrium is checked (venoatrial connection).

## The four-chamber view

Since its introduction in the 1980s, the four-chamber-view (4CV) plane is still considered as the most important plane in the examination of the fetal heart. The main cardiac

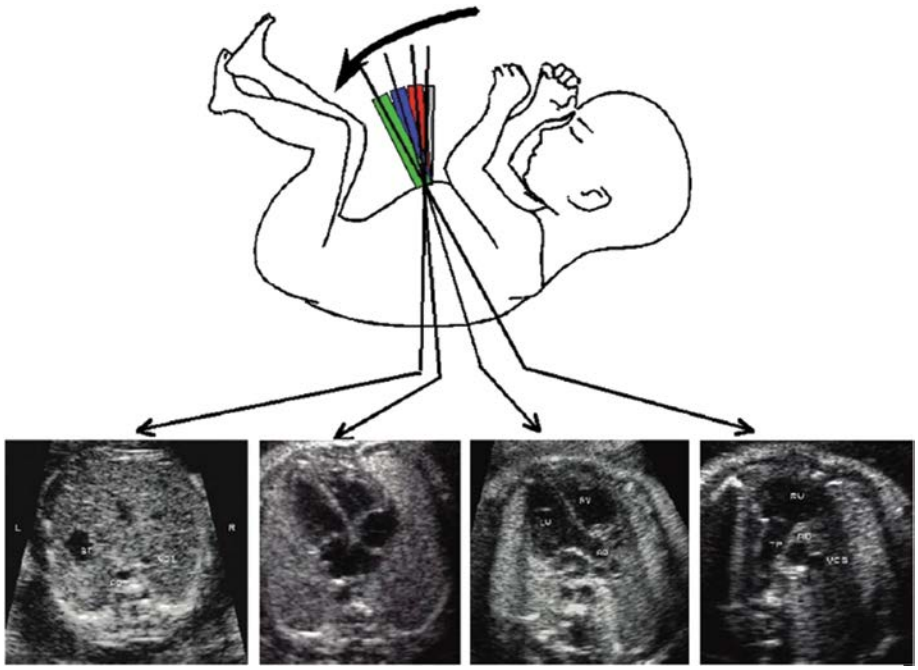

**Figure 10.4**
The approach to obtain the different planes from the abdominal plane to the four- and five-chamber views toward the pulmonary view. See also corresponding Video 10.5.

**Table 10.2** Checklist of the plane of the upper abdomen

- Filled stomach is on the left side
- Aorta is on the left side of the spine
- Liver is on the right side
- Inferior vena cava is on the right side of the spine, ventral and lateral to the aorta
- Inferior vena cava receives the hepatic veins and is connected to the right atrium

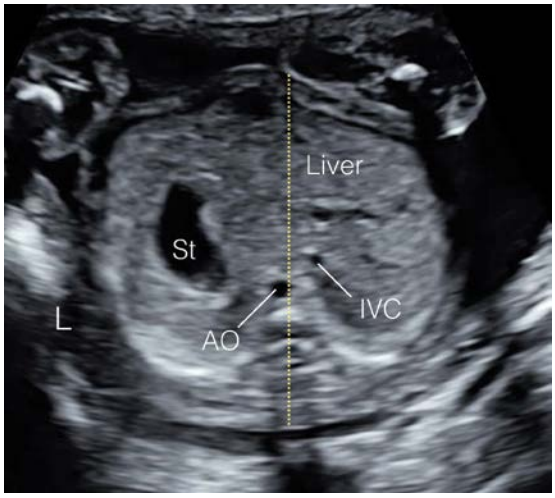


**Figure 10.5**
Cross section of the upper abdomen. The line divides the left and right sides. Visualized are the stomach (ST) and the descending aorta (AO) on the left (L) and the inferior vena cava (IVC) on the right.

structures—the position, the size, the rhythm, and the contractility of the fetal heart—can all be analyzed (Table 10.3). In the 4CV, the simultaneous visualization of atria, ventricles, atrioventricular valves, and interventricular and interatrial septa is achieved (Figure 10.6) (Video 10.1). This plane is important because it is accurate in detecting a wide range of fetal heart defects, and it can be easily learned. Owing to the fluid-filled lungs in prenatal life, as well as to the late calcification of the ribs, different insonation views of the four-chamber plane can be obtained, reducing the disadvantage of the different fetal positions on fetal examination (Figure 10.7). The correct plane should include both patent atrioventricular valves connecting the atria with the corresponding ventricles (Figure 10.6).

**Table 10.3** Checklist of the four-chamber view plane

- Position of the heart in the thorax
- Cardiac axis
- Size of the heart
- Rhythm
- Contractility
- Size of the left and right atria
- Size of the left and right ventricles
- Size relationship of the left and right sides
- Position and function of the tricuspid and mitral valves
- Continuity of the interventricular septum
- Position and form of the interatrial septum and the valve of the foramen ovale
- Connections of the pulmonary veins to the left atrium

- *Cardiac position and axis:* Once the four-chamber plane is visualized, an imaginary anteroposterior line is drawn, dividing the thorax into two equal left and right sides (Figure 10.6). In normal levocardia, one-third of the heart is on the right side and two-thirds are on the left, with the heart axis pointing to the left. In recent years, the assessment of the cardiac axis was added as a new parameter in the analysis of heart position.[6] Compared to the sagittal axis, the cardiac axis is at 45° ± 15° and is abnormal in many heart defects, especially those involving the great vessels. The pericardium of the heart is recognized as a slight double layer around the outer cardiac wall. At the level of the atrioventricular valves, a tiny amount of pericardial fluid can be seen and should not be diagnosed as an abnormal effusion.
- *Cardiac size:* Analysis of the heart size is important in order to distinguish between cardiomegaly, generally due to atrioventricular valve insufficiency associated with right atrium dilatation, and the normal heart in a small thorax in growth-restricted fetuses. In doubtful cases, the examiner can perform cardiac measurements derived in the four-chamber view, measuring the heart length, width, area, and cardiothoracic ratio.
- *Cardiac contractility and rhythm:* The analysis of heart contractility enables the detection of hypokinesia of the myocardium. An abnormal heart rhythm is easily detected with real-time sonography, but its classification is more reliably performed by using M-mode.
- *Left and right atria:* After general evaluation of the heart, the examiner continues with the assessment of the cardiac structures. After localization of the heart's left and right sides, as well as the atria and ventricles, the cavities are then compared with one another. Important landmarks to remember are that the lumen of the right is slightly smaller than the left ventricle, and the foramen ovale flap bulges into the left atrium. Anterolaterally to the spine, the descending aorta is recognized as a circular, pulsating structure and the esophagus in front of it. The first cardiac structure ventrally adjacent to the aorta and esophagus is the left atrium. The left atrium is situated most posteriorly in the chest and is recognized by the connections of the pulmonary veins and

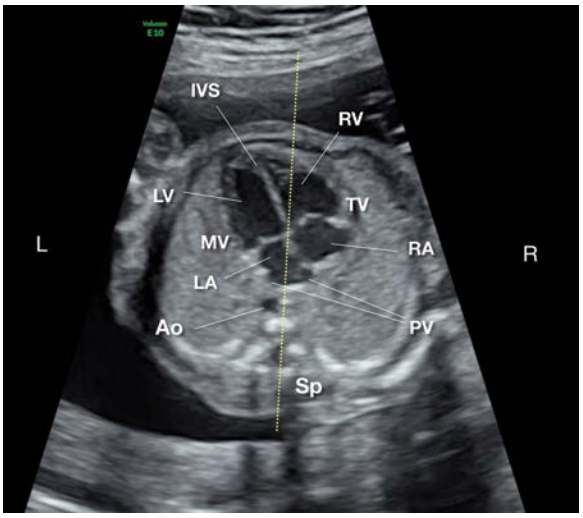


**Figure 10.6**
Apical four-chamber view of the fetal heart with the right atrium (RA), left atrium (LA), right ventricle (RV), left ventricle (LV), and interventricular (IVS) septum. The tricuspid valve (TV) inserts more apically in comparison to the mitral valve (MV). The right and left (inferior) pulmonary veins (PV) can be seen to enter the left atrium posteriorly on either side of the descending aorta (AO). (L, left; R, right; Sp, spine.)

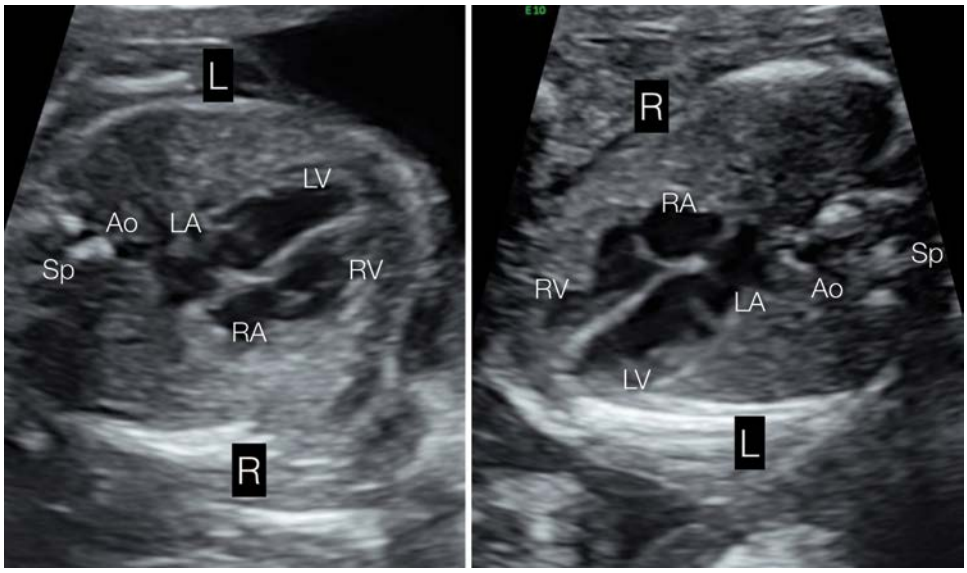


**Figure 10.7**
Four-chamber view seen from the left side (left) and from the right (right). The advantage of the fetal examination is that the four-chamber view can be visualized in different fetal positions. In the lateral approaches, the septum can be better estimated. (L, left; R, right; RA, LA, right and left atrium; RV, LV, right and left ventricle.)

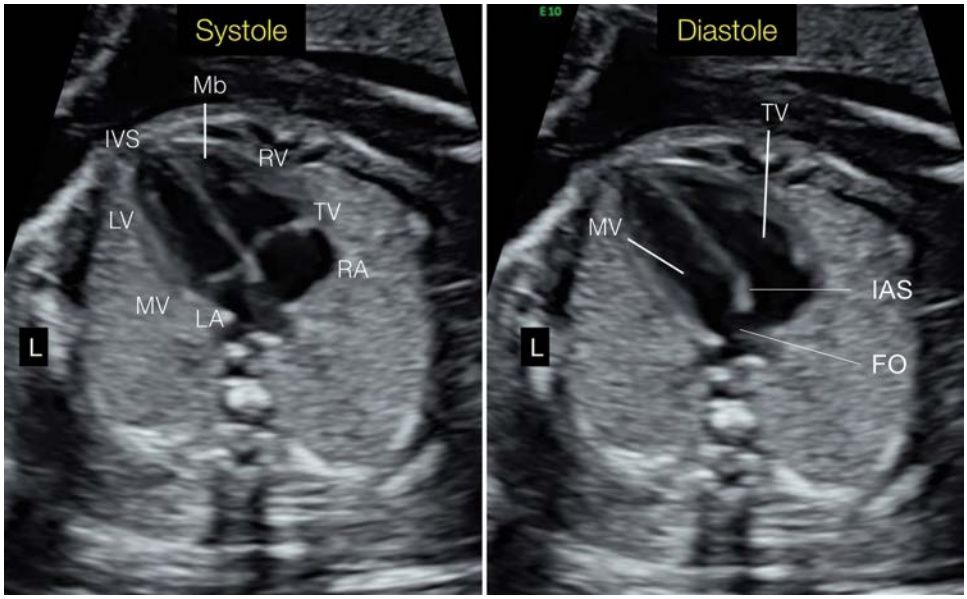


**Figure 10.8**
Apical four-chamber view in systole (left) and diastole (right). Using a cine-loop, the visualization of different phases of the heart cycle is easier. During diastole, the opened valves are well recognized, as well as the bulging of the flap of the foramen ovale (FO) (septum primum). See also corresponding Video 10.1.

the leaflet of the foramen ovale. The foramen ovale "flap" is the free part of the septum primum, which closes during embryological development of the septum primum. Owing to the right-to-left shunt at the atrial level, the flap bulges into the left atrium, showing a wide variation in its size and shape. This structure is semilunar and is best seen using a left-sided approach to the heart. The right atrium is on the right side of the left atrium and communicates with the latter via the foramen ovale (i.e., the ostium secundum). By slightly angulating the transducer cranially and/or caudally, or by tilting the transducer into a longitudinal plane, the connections of the inferior and superior venae cavae can be identified. Both atria are nearly equal in size and are best recognized by the vein connections. Another feature is visualization of the appendages: the left atrial appendage is finger-like and has a narrow base, whereas the right atrial appendage is pyramidal in shape with a broad base. The appendages can be visualized in a plane slightly cranial to the four-chamber view but are not identified reliably under many conditions.

- *Left and right ventricle:* Directly behind the sternum, the right ventricle appears as the most anterior cardiac structure. The left ventricle is adjacent and posterior to the right ventricle and is the most left-sided cardiac structure (Figure 10.8). Many features can be used to differentiate the right from the left ventricle. The right ventricle is trabeculated and the cavity is irregular, whereas the inner shape of the left ventricle is smooth. The lumen of the left ventricle is longer than that of the right ventricle, and reaches the apex of the heart. The right ventricle shows a short lumen, mainly owing to the moderator band (septomarginal trabeculum) coursing from the interventricular septum to the lower free wall of the right ventricle (Figure 10.9). The ventricles can also be recognized owing to the related atrioventricular valve: the left ventricle receives the mitral valve and the right ventricle the tricuspid valve. The tricuspid valve inserts slightly more apically than the mitral valve on the interventricular septum (Figure 10.8).
- *Interventricular septum:* Both ventricles are separated by the interventricular septum. The septum begins as a

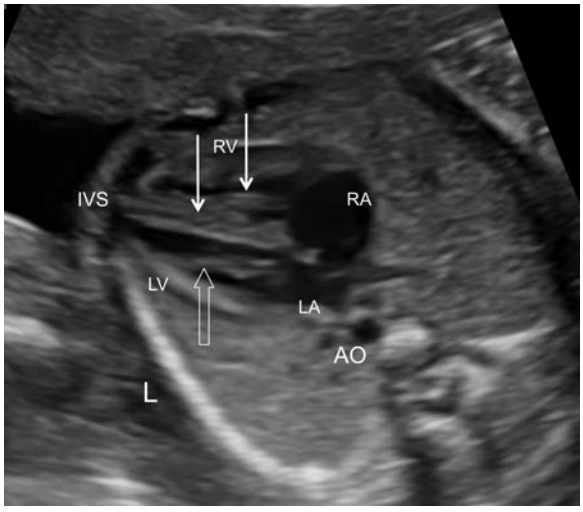


**Figure 10.9**
Lateral view of the fetal heart at the level of the four-chamber view. Note in the right ventricle (RV) the apical insertion of the chordae tendineae of the tricuspid valve to the right ventricular wall and apex of the heart (two solid arrows). Open arrow in the left ventricle (LV) points to the free wall attachment of the papillary muscle of the mitral valve. (AO, aorta; IVS, interventricular septum; L, left; LA, left atrium; RA, right atrium.)

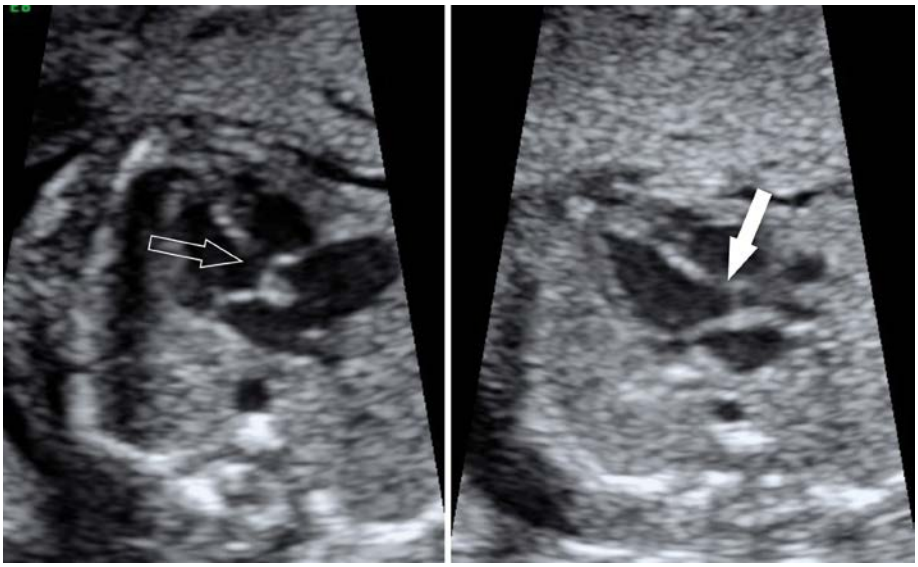

**Figure 10.10**
Apical four chamber more apical (left) and more lateral (right). This "dropout" effect (empty arrow) may mimic a septal defect but is due to the insonation angle almost parallel to the membranous septum. By angulating the transducer more laterally (right), the intact septum is better recognized (solid arrow).

wide, thickened structure at the apex of the heart, and it becomes thinner as it reaches the level of the atrioventricular valves. This is due to the development and anatomic structure of the septum, with a muscular part in the lower two-thirds, and a membranous part at the junction with the atrioventricular and semilunar valves. Around 20 weeks of gestation, this thin membranous part is not correctly visualized by an apical approach. This dropout effect sometimes leads to a false-positive suspicion of septal defects (Figure 10.10). In these conditions, the heart should be examined using a lateral view, allowing better visualization of the septum. Thickness of the septum, ranging between 2 and 4 mm during gestation, should also be measured by the lateral approach.

## The area behind the heart

For years examiners have focused on the assessment of the cardiac chambers in the standard 4CV plane. In 2007 Berg and colleagues[7] emphasized that focus should be placed on the region behind the heart while examining the 4CV (Figure 10.11). Anterior and left lateral to the spine, the descending aorta is recognized. Just anterior to the aorta, the esophagus is seen as an echogenic circular structure. To the right side of the aorta and directly anterior to the spine, the azygos vein can be seen and has about a third of the size of the aorta. Table 10.4 summarizes some abnormal findings in this region behind the heart.

## The left and right ventricular outflow tracts

In the next planes, the five-chamber view and the pulmonary view, the arising of the aorta from the left ventricle and the pulmonary trunk from the right ventricle are visualized. Assessment of the ventriculoarterial concordance is mandatory in analyzing heart anatomy.

Once the four-chamber plane is visualized, the examiner tilts the transducer slightly cranially (Figure 10.3) and focuses attention on the center of the heart in the left ventricle, where

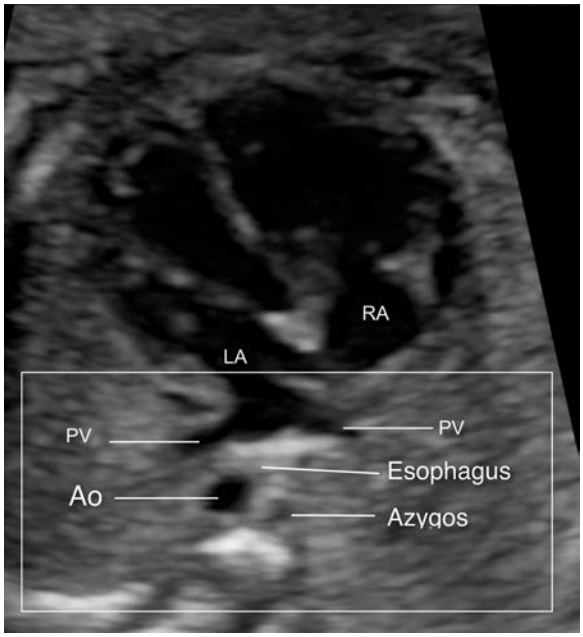


**Figure 10.11**
The area behind the heart with the presence of the aorta (AO) to the left of the spine and the azygos vein, as a small vessel, to the right of the spine. Between the AO and left atrium (LA), the esophagus is found as an echogenic structure. The two inferior pulmonary veins (PV) are seen to enter the left atrium in this plane. (RA, right atrium.)

**Table 10.4** The area behind the heart normal findings and suspicious findings

| | *Normal finding* | *Suspicious finding* |
|---|---|---|
| Descending aorta | Lies left anterior to the spine | Aorta in the middle or to the right of the spine in fetuses with right aortic arch, double aortic arch, or some cardiac malpositions |
| Azygos vein | Lies to the right of the aorta directly anterior to the spine; tiny vessel, diameter less than one-third of aorta | Azygos vein dilated and similar in size to aorta in interrupted vena cava inferior, e.g., in left isomerism |
| Esophagus | Is an echogenic dot, anterior to aorta and posterior to left atrium | May be dilated during fetal swallowing and should not be confused with azygos vein dilation |
| Left atrium and pulmonary veins | Posterior aspect of left atrium irregular and two inferior pulmonary veins enter the left atrium | Posterior aspect of left atrium smooth, and a venous confluence is found between aorta and left atrium where the pulmonary veins connect in fetuses with abnormal pulmonary venous connections |

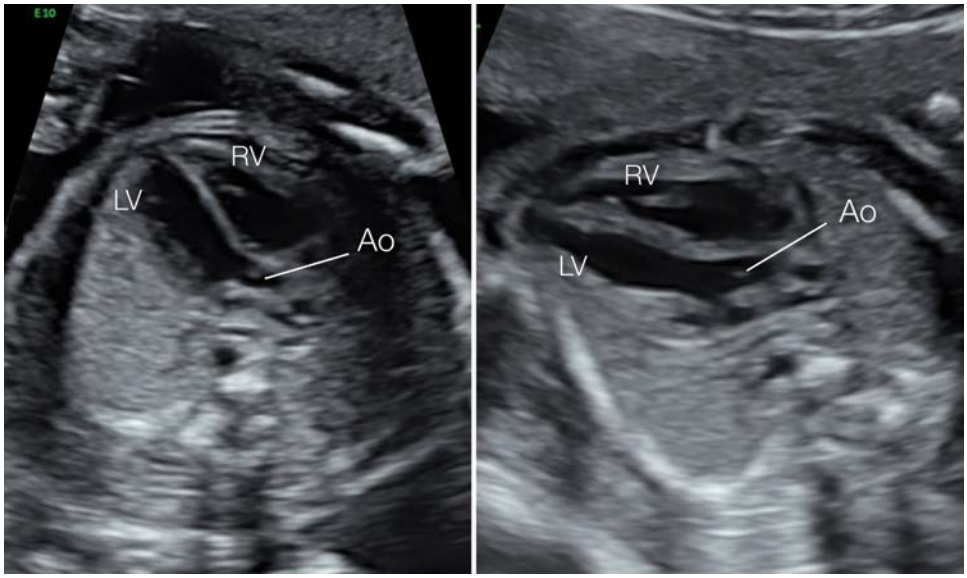


**Figure 10.12**
The "five-chamber view" (left) with the aorta (Ao) arising from the left ventricle (LV) from an apical and a lateral view (right). (RV, right ventricle.)

**Table 10.5** Checklist of outflow tract assessment

- Normal connection of the aorta to the left ventricle and pulmonary trunk to the right ventricle
- Both vessels cross over each other
- Compare caliber of pulmonary trunk (PT) and aorta (PT > aorta)
- Assess opening excursion of aortic and pulmonary valves
- Continuity of ventricular septum to the aortic root
- Normal course and caliber of great vessels and superior vena cava in the upper thorax
- Assess aortic isthmus and ductus arteriosus
- Rule out atypical vessels (e.g., left persisting superior vena cava)

the mitral valve connects with the ventricular septum. The aorta arises as a vessel continuing the ventricular septum but pointing slightly to the right side (Figure 10.12) (Video 10.2). The other border of the aortic wall shows a close connection to the mitral valve. Within the aortic root, the aortic valve can be recognized as an echogenic dot. In this plane, the examiner checks (Table 10.5) the continuity of the septum and aorta, the angulation of the aorta and septum, the size of the aortic root, and the ascending aorta, as well as the opening movements of the aortic valve (most ventricular septal defects can be detected in this plane).

The pulmonary trunk can be visualized by further tilting the transducer cranially (Figure 10.4), but some authors recommend the short-axis view (Figure 10.13) (Video 10.3). This plane is easy to obtain by noncardiologists and can be obtained by successive tilting from the four- and five-chamber planes. Once the five-chamber view is obtained, the examiner focuses attention during further tilting of the transducer on the connection of the right ventricle with the descending aorta (vessel toward the spine). The vessel then arising is the pulmonary trunk, continuing as the ductus arteriosus. The pulmonary trunk crosses perpendicularly over the ascending aorta and then becomes the

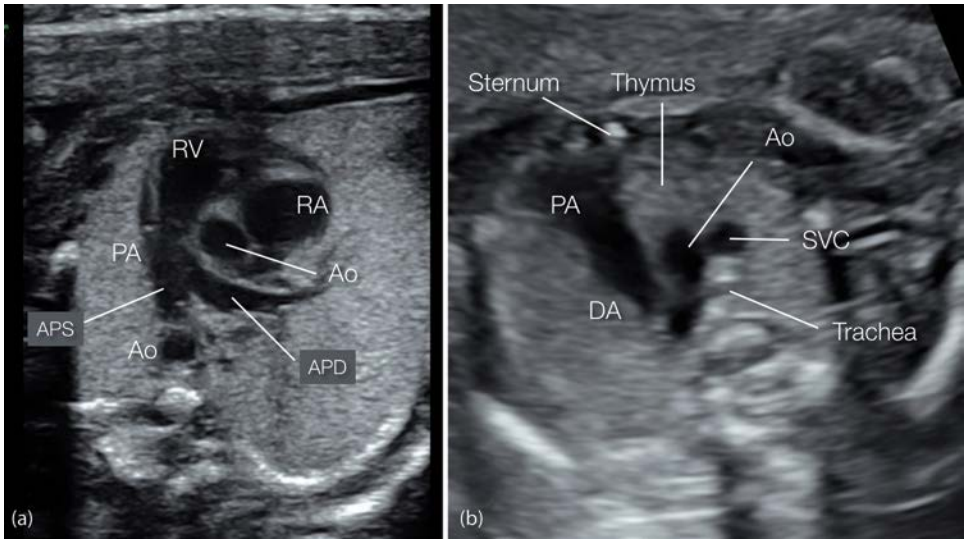


**Figure 10.13**
(a) Short-axis view of the aorta (Ao) in the center and around it the right atrium (RA), the right ventricle (RV), the pulmonary artery (PA) with its bifurcation into the right (APD) and left (APS) pulmonary arteries. (b) Three-vessel-trachea view in the upper thorax visualizing the aorta (Ao) with isthmus, the pulmonary artery (PA) with ductus arteriosus (DA), and the superior vena cava. The trachea is recognized as an echogenic circle on the right side of the two great vessels and behind the superior vena cava (SVC). The thymus gland is between the sternum and the great vessels.

vessel on the left. On its right side, two vessels in cross section can be recognized: the ascending aorta and the superior vena cava. During the tilting movement from the five-chamber view, the examiner checks for the correct connection of the right ventricle and pulmonary trunk, as well as the crossing of the pulmonary trunk. The size of the pulmonary trunk has a slightly larger caliber compared to that of the aorta, and the valve is seen as a white dot showing opening and closing movements.

In heart defects affecting the great arteries, it is often important to correctly differentiate the vessels involved. Aorta and pulmonary trunk can be differentiated by the origin of the stem vessels for the aorta, and the bifurcation of the right and left pulmonary arteries for the pulmonary trunk. Whereas the three arterial branches are seen during the visualization of the aortic arch, the pulmonary arteries are best visualized by obtaining a short-axis view of the heart. This is achieved by visualizing the five-chamber view, and then rotating the transducer in order to obtain a plane from the right hip to the left shoulder, demonstrating the "circle and sausage" sign, with the aorta in the center, and the right atrium, right ventricle, pulmonary trunk, and bifurcation around it (Figure 10.13).

## The three-vessel-trachea view

From the four-chamber plane, the transducer is moved parallel in the direction of the upper thorax. In this sagittal cross section of the upper thorax, the three vessels of the pulmonary trunk—the ductus arteriosus, aortic arch with aortic isthmus, and superior vena cava—can be seen (Figure 10.13 right) (Videos 10.4 and 10.5). The aortic and the ductus arches are seen in a tangential cross section and build a V-form pointing to the posterior thorax on the left side of the spine (Figure 10.13) with the trachea to the right of both vessels.[8,9] The trachea prior to its bifurcation is recognized as a circular structure with an echogenic wall adjacent to and on the right side of the aortic isthmus and anterior to the spine. In front of the trachea and on the right side of the aortic arch, the superior vena cava is recognized. On the left and right sides of these vessels, lung tissue can be recognized (Figure 10.13).[9] In front of these three vessels the thymus is recognized as a structure with a less echogenic appearance (Figure 10.13) (Video 10.6).[9,10] The assessment of the three-vessel-trachea view has been emphasized in the past few years since it allows the detection of many outflow tract anomalies.[9] Thymus measurements have been proposed, which was reported to be small not only in microdeletion 22q11[10] but also in trisomy 21 and 18.[11] Furthermore, the position of the trachea in comparison to these vessels can be used as a landmark to distinguish the correct left-sided aortic arch from an abnormal right-sided aortic arch. The advantage of this plane is that it allows the visualization of both arches in most positions of the fetus, allowing easier detection of possible abnormalities. The slightly larger size of the pulmonary trunk compared to the size of the aorta can be checked, as can the continuity of the aortic arch, or the presence of a fourth vessel on the left of the pulmonary trunk, as a left persisting superior vena cava.

## Longitudinal views of the veins and outflow tracts

Longitudinal views during the fetal cardiac examination are displayed mainly to demonstrate the course of the vessels.

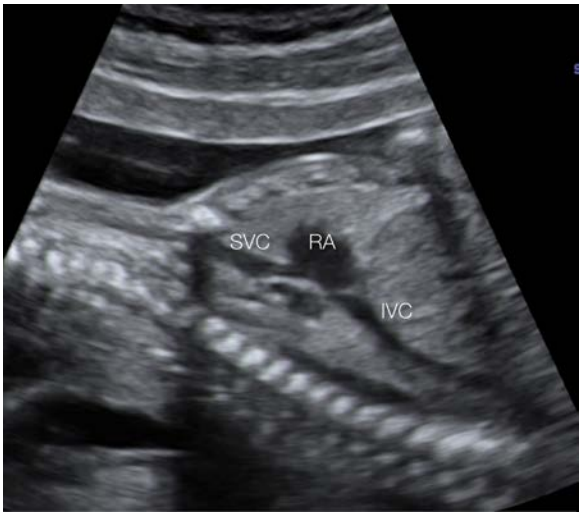


**Figure 10.14**
Parasagittal right-sided longitudinal view demonstrating the connection of the superior (SVC) and inferior vena cava (IVC) to the right atrium (RA) in the bicaval view.

A parasagittal view on the right of the heart demonstrates the connection of the superior and inferior caval veins into the right atrium in the plane called bicaval view (Figure 10.14). The longitudinal planes of the outflow tracts are visualized to assess the aortic and the ductus arteriosus arches. In these planes, the continuity and form of the arches are seen, as well as the brachiocephalic vessels arising from the aorta to the head and upper extremity (Video 10.7). The examiner obtains a parasagittal plane slightly to the left, including the aortic valve and the descending aorta, and can thus visualize the aortic arch (Figure 10.15). In this plane, the aortic arch appears to

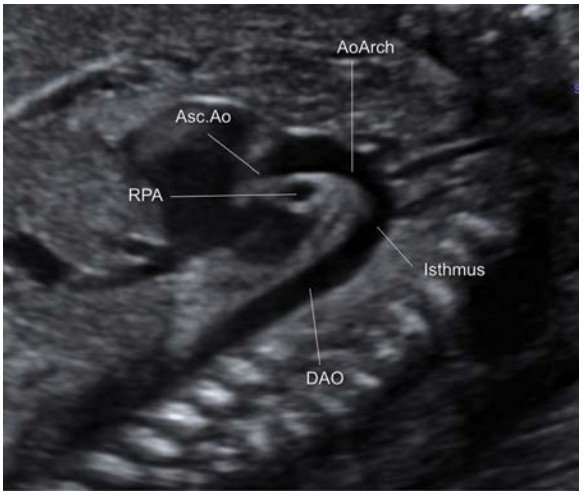


**Figure 10.15**
Longitudinal view of the aortic arch with the ascending aorta (Asc. Ao), the transverse aortic arch (AoArch) continuing into the isthmus and descending aorta (DAO). The aortic arch resembles a "candy cane." One can easily recognize the three vessels to the head and upper limbs. Under the aortic arch, the right pulmonary artery (RPA) is seen in cross section.

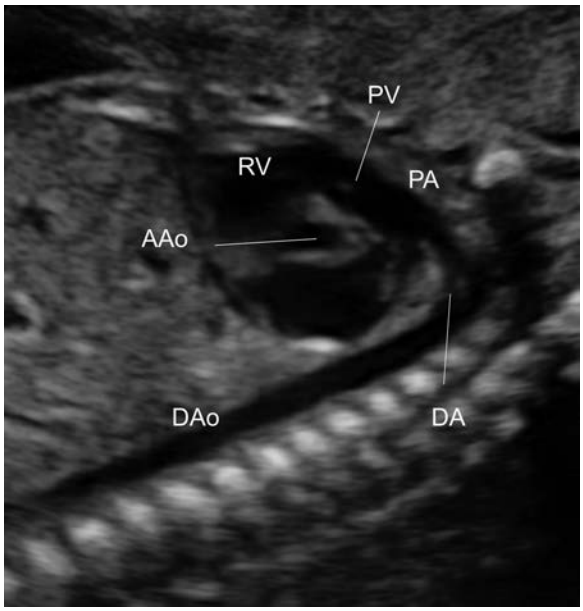


**Figure 10.16**
Longitudinal view of the ductus arteriosus arch. The pulmonary artery (PA) arises from the anteriorly positioned right ventricle (RV) and courses toward the descending aorta (DAo). The ascending aorta (AAo) is under the pulmonary artery (PA). This arch has a nearly perpendicular shape and resembles a "hockey stick."

emerge from the center of the heart and shows a circular shape ("candy cane"). Under the ascending aorta, a cross section of the right pulmonary artery can be recognized. In the next adjacent plane to the left, the longitudinal view of the pulmonary trunk with the ductus arteriosus can be recognized (Figure 10.16) (Video 10.8). The right ventricle and the pulmonary valve are seen anteriorly, and the ductus arteriosus arch courses perpendicularly to connect with the descending aorta, recognized as having a more angular shape ("hockey stick").

## Videos

**Video 10.1** (https://youtu.be/f8-eOjZRjW4)
The four-chamber view with atria, atrioventricular valves, and ventricles.

**Video 10.2** (https://youtu.be/SSzwCaUeRHc)
Left ventricular outflow tract with the aorta arising from the left ventricle.

**Video 10.3** (https://youtu.be/4fmY5-PJp1c)
Transition from the four-chamber view to the short-axis view.

**Video 10.4** (https://youtu.be/j6jXwTLh0a8)
Transition from the five-chamber view to the three-vessel-trachea view.

**Video 10.5** (https://youtu.be/dwNq-RoS3tI)
Complete sweep from the upper abdomen to the three-vessel-trachea view in the axial plane.

**Video 10.6** (https://youtu.be/Qn17puu9qNk)
Sagittal view of the aortic arch.

**Video 10.7** (https://youtu.be/R4xop82cQpU)
Sagittal view of the ductal arch.

**Video 10.8** (https://youtu.be/6dR4AKmmE60)
Axial view at the 3VT level showing the thymus clearly at 30 weeks.

# References


1. Carvalho JS et al. *Ultrasound Obstet Gynecol* 2013;41:348–59.
2. Abuhamad A, Chaoui R. *A Practical Guide to Fetal Echocardiography: Normal and Abnormal Hearts*. 3rd ed. Philadelphia, PA: Lippincott-Williams Wilkins; 2015.
3. Persico N et al. *Ultrasound Obstet Gynecol* 2011;37:296–301.
4. DeVore GR. *J Clin Ultrasound* 1985;13:229–45.
5. Chaoui R et al. *Ultraschall Klin Prax* 1991;6:1–15.
6. Smith R et al. *Obstet Gynecol* 1995;85:187–91.
7. Berg C et al. *Ultrasound Obstet Gynecol* 2007;30:721–7.
8. Yagel S et al. *Ultrasound Obstet Gynecol* 2002;20:340–5.
9. Gardiner H, Chaoui R. *Semin Fetal Neonatal Med* 2013;18: 261–8.
10. Chaoui R et al. *Ultrasound Obstet Gynecol* 2011;37:397–403.
11. Karl K et al. *Ultrasound Obstet Gynecol* 2012;40:412–7.

# 11

# The three vessel and tracheal view

Julia Solomon

Four-chamber view screening of the fetal heart began in the 1980s as a way to detect congenital heart disease prenatally. However, the four-chamber view alone demonstrated only modest success at detecting major congenital heart disease and failed to reliably detect many conotruncal abnormalities, such as tetralogy of Fallot and d-transposition of the great arteries.[1] The concept of an "extended" fetal echocardiogram was proposed in 1992 by Achiron et al.,[2] specifically as a mechanism to increase the detection of complex outflow tract and ductal-dependent lesions. Early echocardiographic teaching recommended obtaining sagittal views of the ductal and aortic arches. While continuity of both arches may be assessed in this plane, both arches cannot be imaged simultaneously, so discordance or subtle lack of continuity may be missed.[3] The ability to obtain these views is also more dependent on fetal lie and operator skill.

The three-vessel view (3VV) of the fetal mediastinum was first described formally in 1997 by Yoo et al.[4] It refers to an axial view of the fetal chest, above the level of the four-chamber view, where an oblique section of the main pulmonary artery/ductus arteriosus, ascending aorta, and superior vena cava can be obtained in a single image. Since the plane of image acquisition is identical (though more cephalad) to that used to obtain a four-chamber view (4CV), advanced scanning expertise is not required (Video 11.1—3VT view superimposed on rendered 4CV for perspective). The term "three vessel tracheal" (3VT) view is often used interchangeably with three-vessel view but was described as a distinct entity several years later.[5] The tracheal view is minimally more cephalad again, with the scanning plane inclined slightly toward the right fetal shoulder, as the transverse aortic arch is rightward and cephalad to the ductal arch. The 3VT view offers the added ability to identify the transverse aortic arch, assess arch laterality, and assess ductal and aortic arch calibers simultaneously.[3] A satisfactory 3VT view is defined as one that demonstrates the main pulmonary trunk in direct communication with the ductus arteriosus, with the transverse aortic arch lying to the right of the main pulmonary artery (MPA).[5] The addition of color flow imaging permits directional assessment and confirmation of anterograde flow in both arches. Currently, most sonologists prefer the 3VT view for these added advantages, understanding that both views are imaged almost simultaneously. Because of the incorporation of both outflow tracts as well as their size and orientation in the scanning plane, this view permits increased detection of many conotruncal and ductal-dependent lesions, which contribute significantly to neonatal morbidity and mortality when undiagnosed.[6]

## Ultrasound anatomy of the normal three-vessel/tracheal view

An axial view of the upper mediastinum allows demonstration of the arrangement, course, size, and alignment of the ductal and aortic arches, their position relative to the trachea, and assessment of size and location of the superior vena cava. The thymus gland, when normal, is often visualized in the anterior mediastinum at the same level as a structure slightly hypoechoic relative to surrounding lung tissue. A normal 3VV is demonstrated schematically in Figure 11.1a; the corresponding 3VT view is shown in Figure 11.1b.

A normal 3VT view will have several notable characteristics (Figure 11.2). In keeping with the nomenclature, there should be three vessels identified. From left to right in the transverse fetal chest are the main pulmonary artery/ductus arteriosus, aorta, and superior vena cava. The main pulmonary artery is closest to the anterior chest wall and should be of the largest caliber. The vessels progressively become more posteriorly located and smaller in size as one moves from left to right, with these relationships preserved throughout gestation. In the midtrimester, the mean pulmonary artery to aorta diameter ratio is 1.16.[7] When the vessels are normally configured, a straight line can be drawn along the anterior borders of the vessels. The trachea is identified as a small sonolucency anterior to the fetal spine, often accompanied by a brightly echogenic border. A normal left-sided aortic arch will lie to the left of the trachea, and intersect the ductal arch in a "V"-shaped configuration at the isthmic region. Superimposed color flow or power Doppler with directional information allows confirmation of anterograde flow in both transverse arches, with minimal aliasing often visualized in the distal ductal arch (Figure 11.3, Video 11.2—normal 3VT with color flow).

At the level of the 3VT or slightly more cephalad, other normal vascular structures may be easily documented. The left brachiocephalic vein, which drains blood from the left upper extremity, head, and neck, can be visualized as a vessel running transversely across the fetal chest, anterior to the ductal and aortic arches, and draining into the superior vena cava (Figure 11.4).

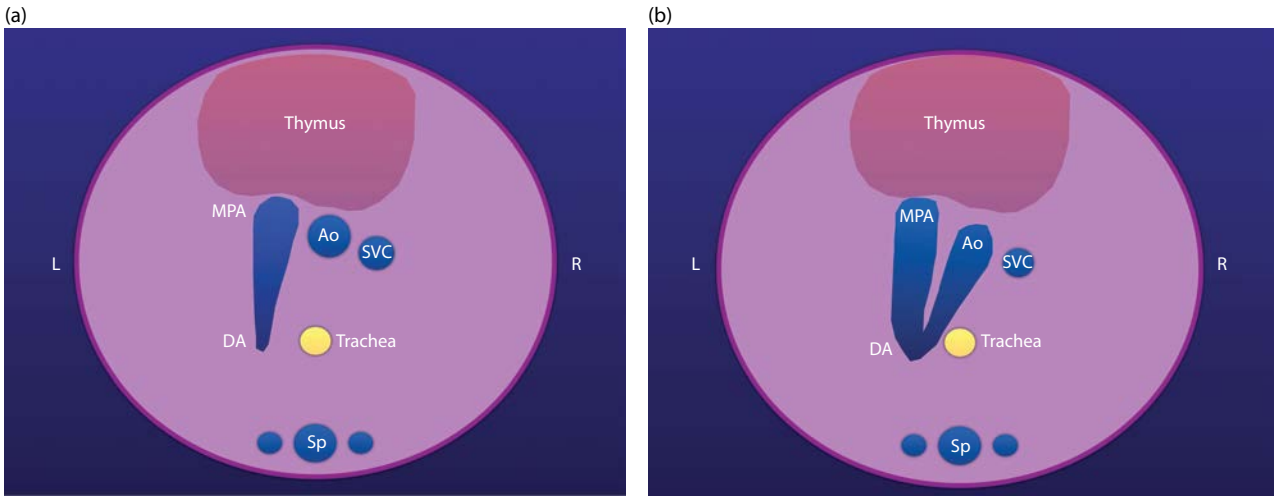


**Figure 11.1**
(a) A normal three-vessel view. (Ao, ascending aorta; DA, ductus arteriosus; MPA, main pulmonary artery; Sp, spine; SVC, superior vena cava.) (b) A normal three-vessel tracheal view. (Ao, aorta including transverse arch; DA, ductus arteriosus; MPA, main pulmonary artery; Sp, spine; SVC, superior vena cava.)

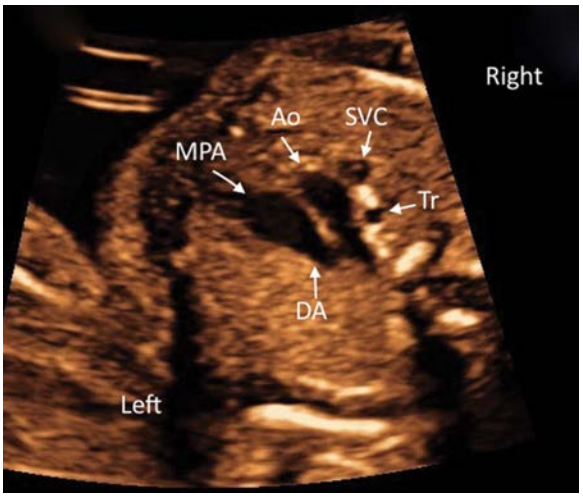


**Figure 11.2**
Grayscale image of a normal three-vessel tracheal view. (Ao, aorta including transverse arch; DA, ductus arteriosus; MPA, main pulmonary artery; SVC, superior vena cava; Tr, trachea.)

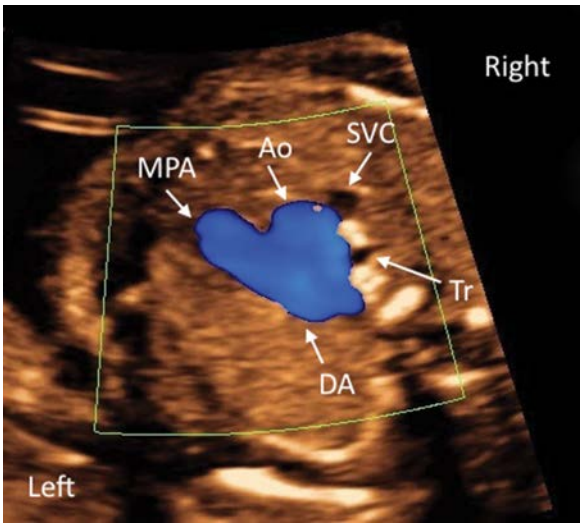


**Figure 11.3**
Color flow imaging of a normal three-vessel tracheal view. (Ao, aorta including transverse arch; DA, ductus arteriosus; MPA, main pulmonary artery; SVC, superior vena cava; Tr, trachea. Anterograde flow (blue) is noted in both ductal and aortic arches.)

The azygous vein may also be identified in a right paraspinal location, draining into the superior vena cava (Figure 11.5).

Several authors have created nomograms and reference values for measurements of the individual vessels noted in the 3VT as a function of gestational age.[8,9] Z-scores have also been reported for the transverse arch and duct in the 3VT for the evaluation of possible arch hypoplasia or coarctation.[10]

## Assessment and interpretation of the three-vessel trachea view

A systematic approach to interpretation of the 3VT has been advocated by several authors, with slight variations on the categories (see Table 11.1).[3–5,11,12] Evaluation of this view should include assessment for the following parameters, understanding that any given lesion may have features of more than one category:

1. Abnormal vessel number
2. Abnormal vessel course or alignment
3. Abnormal vessel size
4. Abnormal color flow/directional signal

## Abnormal vessel number

Abnormalities associated with abnormal vessel number include both benign variants as well as significant congenital

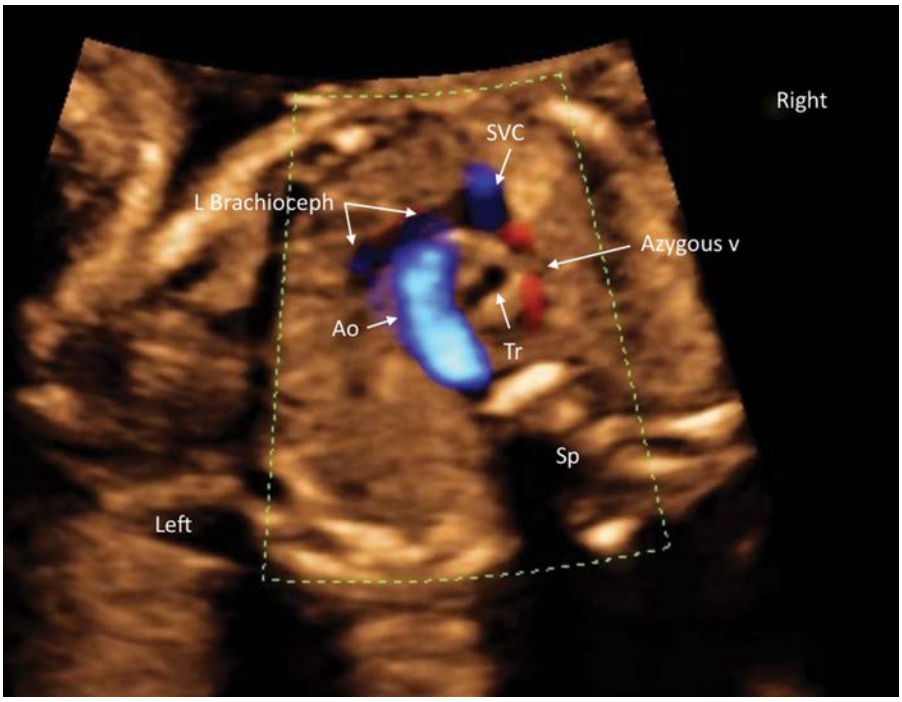


**Figure 11.4**
Left brachiocephalic and azygous vein drainage. (Ao, aorta; azygous v, azygous vein draining to SVC; L brachioceph, left brachiocephalic vein draining to SVC; Sp, spine; SVC, superior vena cava; Tr, trachea.)

heart disease, typically involving either two or four vessel configurations. The presence of bilateral superior venae cavae will cause a fourth vessel to be visualized, located leftward of the ductal arch, in addition to the normally located right superior vena cava (Figure 11.6).

A common abnormality identified by this view is d-transposition of the great arteries, where only one vessel is seen in addition to the superior vena cava. In the case of d-TGA, this is due to the spatial orientation of outflow tracts, where the anteriorly transposed aorta lies at the usual level of the 3VT, with the pulmonary artery generally lying below—or caudal to—the plane of imaging (Figure 11.7, Video 11.3—3VT for d-TGA abnormality). This has been termed the "I-sign" by several authors,[13,14] representing an elongated, anteriorly transposed aortic arch running in an anteroposterior direction across the fetal chest. It could be visualized in 92% of cases in one study[14] and resulted in a sensitivity of 96.8%–100% for detection of this abnormality.[13,14] When anteriorly transposed, the aortic arch arises much closer to the anterior chest wall than when outflow tracts are normally related. In addition to the anterior origin, the transposed aorta also typically displays a rightward convexity.[15]

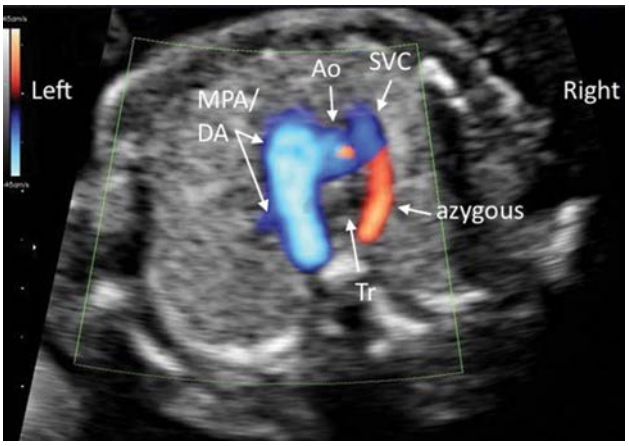


**Figure 11.5**
Azygous arch and 3VV. (Ao, aorta; azygous, azygous vein; MPA/DA, main pulmonary artery and ductus arteriosus; SVC, superior vena cava; Tr, trachea.)

In abnormalities involving a solitary outflow tract, such as common arterial trunk, only two vessels will be visualized (Figure 11.8a). Depending on the configuration of the pulmonary arteries and their origin off the common trunk, they may also be visualized in the 3VT view (Figure 11.8b). Abnormalities with severe hypoplasia or atresia of one of the outflow tracts may appear to demonstrate only two vessels on the 3VT, such as tetralogy of Fallot with pulmonary atresia or hypoplastic left heart syndrome (HLHS)/aortic atresia. Occasionally, superimposed color flow will identify an abnormally small vessel not seen in grayscale. In cases of hypoplastic left heart syndrome, the solitary ductal arch may produce a similar appearance to the "I-sign" of d-TGA, though subtle differences in vessel location and orientation are noted. In HLHS, there is a space between the visible (ductal) arch and superior vena cava, usually occupied by the transverse aortic arch. The vessel also lacks the rightward convexity noted with aortic transposition, in favor of an almost straight trajectory. In d-TGA, the aortic arch is immediately leftward

**Table 11.1** Categorization of congenital heart abnormalities according to the principal three vessels and trachea (3VT) findings

*Abnormal vessel size*:
- Small pulmonary artery (PA)
- Small aortic arch (TAoA)
- Enlarged arterial vessel
- Enlarged superior vena cava

*Abnormal vessel alignment*:
- PA-Ao-SVC not in a straight line, but their overall left-to-right order is preserved

*Abnormal vessel arrangement*:
- Left-to-right order of the three vessels is distorted

*Abnormal vessel number*:
- Two vessels
- Four vessels

*Abnormal location of the transverse aortic arch in relation to the trachea*:
- Trachea located between PA and TAoA
- [a]Trachea located to the left of both PA and TAoA

*Reversed flow (color Doppler)*:
- Reversed flow in TAoA
- Reversed flow in PA

*Turbulent flow (color Doppler)*:
- Pulmonary stenosis
- Aortic stenosis

*Source:* Vinals F et al. *Ultrasound Obstet Gynecol* 2003;22:358–67, with permission.[11]

*Abbreviations:* PA, pulmonary artery; SVC, superior vena cava; TAoA, transverse aortic arch.

[a] Not contained in initial reference; added for additional diagnostic accuracy.

and adjacent to the superior vena cava. Finally, certain variants of a double-outlet right ventricle may produce a similar sonographic appearance, depending on the specific spatial configuration of the outflow tracts.

In cases of supracardiac anomalous pulmonary venous return, it may be possible to visualize the vertical vein as a fourth vessel at the level of 3VT. This vertical vein originates from a common venous confluence and proceeds cephalad to enter the systemic venous circulation.[16] A dilated azygous vein may also be visualized in this plane, seen in conjunction with interruption of the inferior vena cava.[11]

## Abnormal vessel course or alignment

Abnormal orientation of the outflow tracts may be inferred when the typical left-sided "V" confluence of the arches is

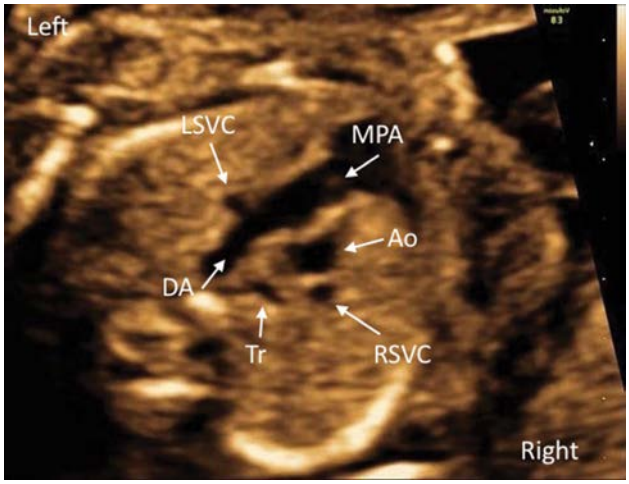


**Figure 11.6**
Three-vessel view of bilateral superior venae cavae. (Ao, ascending aorta; DA, ductus arteriosus; LSVC, left superior vena cava; MPA, main pulmonary artery; RSVC, right superior vena cava; Tr, trachea.)

absent and the superior vena cava is not right sided. The presence of a persistent left-sided superior vena cava can easily be detected in this view as a vessel leftward of the ductal arch, with absence of a normally located right-sided vessel (Figure 11.9). Typical drainage of a persistent left superior vena cava (LSVC) (whether alone or in the setting of bilateral SVCs) is to a dilated coronary sinus, which can be visualized in the left atrium at the level of the four-chamber view. It then drains transversely posterior to the atria and into the right atrium (Video 11.4—LSVC with drainage to coronary sinus at the level of 4CV).

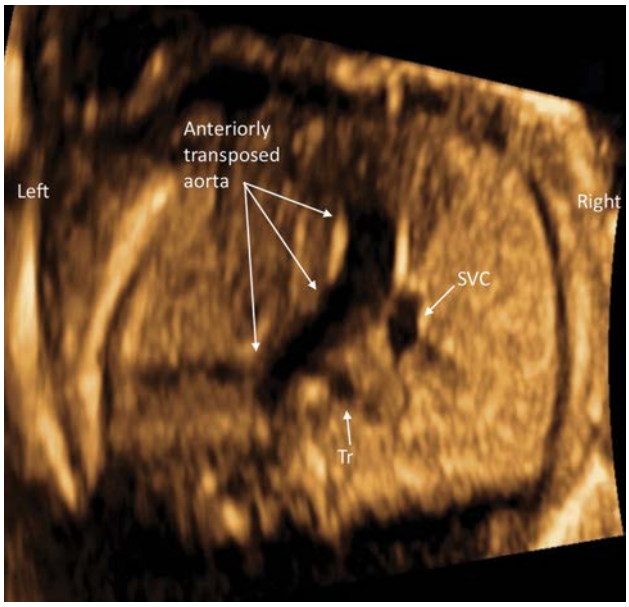


**Figure 11.7**
Three-vessel tracheal view of d-transposition of the great arteries. (Anteriorly transposed aorta, as labeled; SVC, superior vena cava; Tr, trachea.)

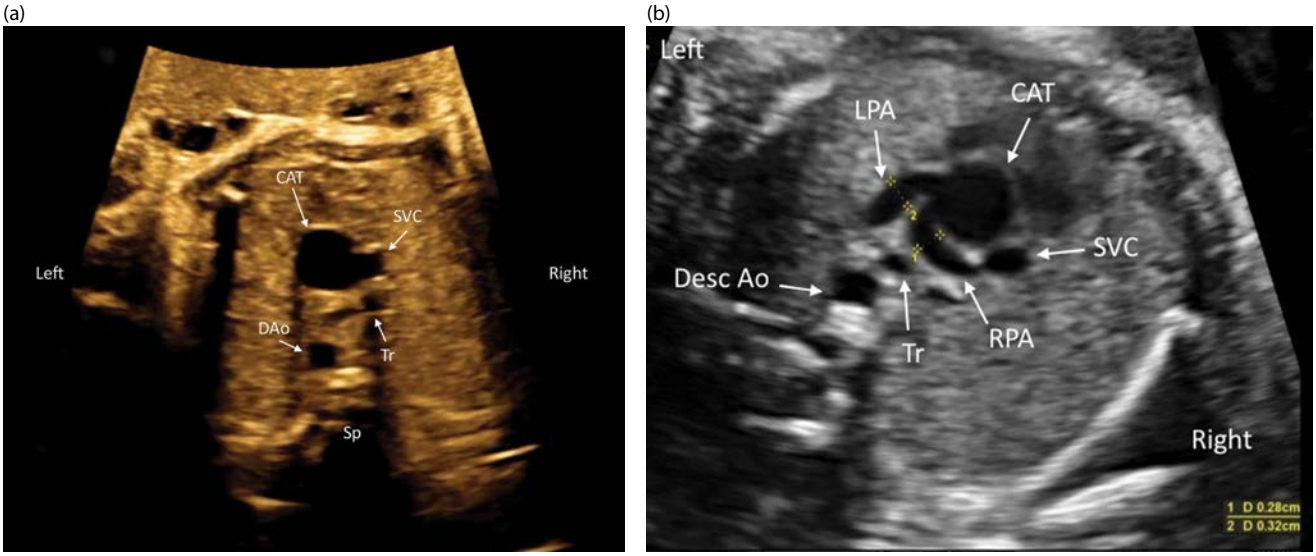


**Figure 11.8**
(a) Three-vessel view of a common arterial trunk. (CAT, common arterial trunk; Dao, descending aorta; Sp, spine; SVC, superior vena cava; Tr, trachea.) (b) Three-vessel view of common arterial trunk with discrete pulmonary arteries arising from the posterior trunk. (CAT, common arterial trunk; Dao, descending aorta; LPA, left pulmonary artery; RPA, right pulmonary artery; Sp, spine; SVC, superior vena cava; Tr, trachea.)

Abnormalities of the aortic arches, including vascular rings, are particularly sensitive to detection using the 3VT and have been reported by numerous authors.[17–21] Evaluation of arch laterality is limited in the postnatal period due to shadowing from air bronchograms, and must be inferred by the branching pattern of the brachiocephalic vessels. In fetal life, the presence of fluid-filled lungs and trachea as well as access to the axial plane affords a unique window for diagnosis of arch abnormalities and sidedness. In the case of a right aortic arch with a left ductus arteriosus, the presence of a leftward "V" confluence of the arches is replaced by a "U"-shaped vascular signal, with the trachea sitting between the two arches (Figure 11.10, Videos 11.5 and 11.6—grayscale and four-dimensional glass-body spatiotemporal image correlation [STIC] of right aortic arch-left ductus vascular configuration). The ductal arch remains leftward of the trachea, whereas the aortic arch is right sided, and the base of the "U" represents the confluence of both arches. A large retrospective review of the 3VT images obtained in over 18,000 midtrimester scans by Achiron et al. identified 19 cases of a right aortic arch with left ductus, including one case of a double aortic arch, all confirmed postnatally.[17]

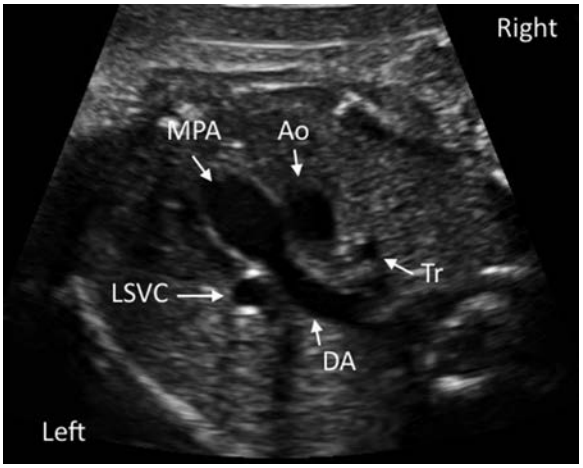


**Figure 11.9**
Three-vessel view of a left superior vena cava. (Ao, ascending aorta; DA, ductus arteriosus; LSVC, left superior vena cava; MPA, main pulmonary artery; Tr, trachea.)

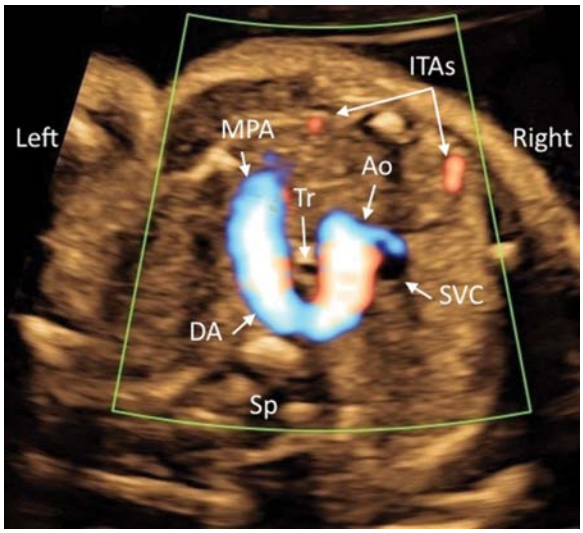


**Figure 11.10**
Three-vessel tracheal view of a right aortic arch with left ductus arteriosus vascular ring. The "U"-shaped vessel indicates confluence of the arches posterior to the trachea. (Ao, aorta and aortic arch; DA, ductus arteriosus; MPA, main pulmonary artery; Sp, spine; SVC, superior vena cava; Tr, trachea.)

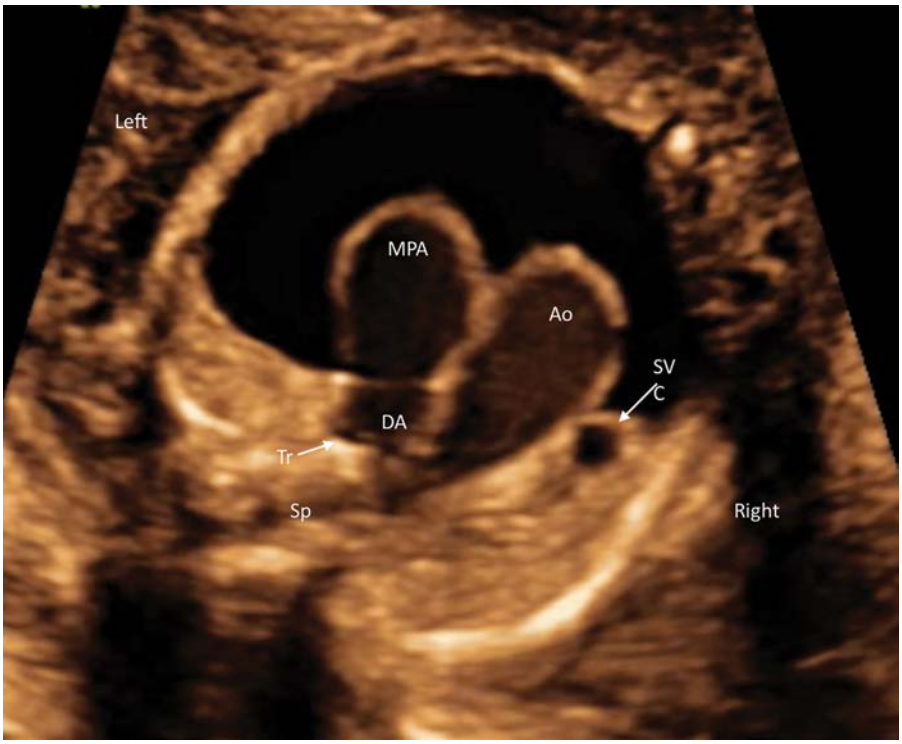


**Figure 11.11**
Three-vessel tracheal view of a right aortic arch with mirror image branching, associated with a right ductus arteriosus; the confluence of the arches meets as a "V" to the right of the trachea. In this case, there are also large pleural effusions and enlargement of both outflow tracts due to valvar regurgitation. (Ao, aorta and aortic arch; DA, ductus arteriosus; MPA, main pulmonary artery; Sp, spine; SVC, superior vena cava; Tr, trachea.)

A right aortic arch with mirror image branching—where both the ductus and aortic arch are right sided—can also be detected on a 3VT. This abnormality is somewhat subtler as the arches meet in a typical "V" confluence, but the "V" is rightward, located on the same side as the superior vena cava (Figure 11.11). This variant is strongly associated with additional cardiac abnormalities, particularly tetralogy of Fallot, common arterial trunk, or other malalignment abnormalities of the outflow tracts.[18]

A double aortic arch may be identified in the same plane by encirclement of the trachea by a vascular ring.[22] This abnormality may be seen as a complete type, where there is an "O"-shaped vascular encirclement of the trachea, or an incomplete "C" type, where one branch is narrowed or atretic, frequently the left side. In a large series of congenital arch anomalies, over half were isolated and lacked other sonographic abnormalities, furthering the importance of the 3VT for detection of these defects.[20]

Interruption of the aortic arch may also be detected in this manner. In addition to a size discrepancy between a much larger main pulmonary artery and smaller ascending aorta (Figure 11.12), the transverse segment of the aortic arch will not be identified with cephalad progression from the standard 3VV to the 3VT.[23] Almost all variants of interrupted aortic arch are accompanied by a ventricular septal defect of the posterior malalignment type (Video 11.7—3VV of interrupted aortic arch, with pan down to 4CV where posteriorly malaligned VSD is noted).

Abnormalities of subclavian arteries are frequently seen in conjunction with aortic arch variants and may be identified on a 3VT. A normal right subclavian artery arises from the first (brachiocephalic) branch of the aortic arch, in conjunction with the right common carotid artery. An aberrant

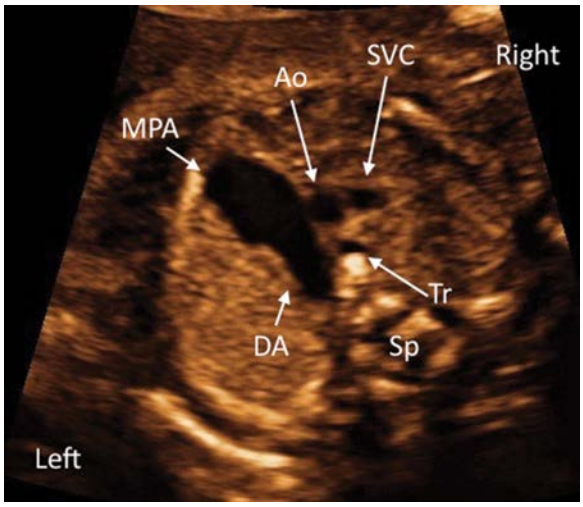


**Figure 11.12**
Three-vessel view of an interrupted aortic arch, with a small ascending aorta noted. (Ao, ascending aorta; DA, ductus arteriosus; MPA, main pulmonary artery; Sp, spine; SVC, superior vena cava; Tr, trachea.)

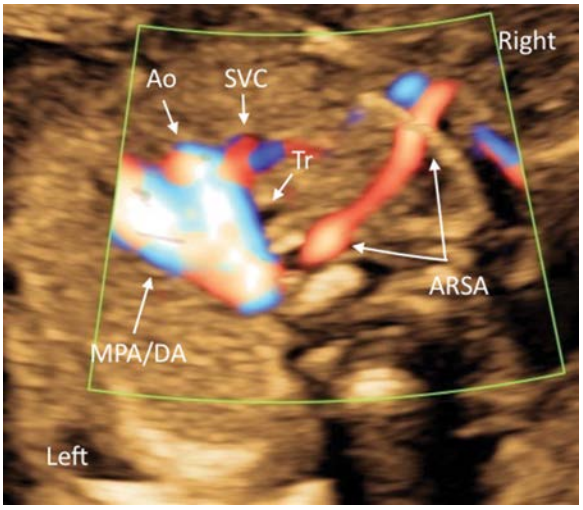


**Figure 11.13**
Three-vessel view demonstrating an aberrant right subclavian artery originating from the distal transverse arch and coursing toward the right shoulder. (Ao, aorta; ARSA, aberrant right subclavian artery; MPA/DA, main pulmonary artery ductus arteriosus; SVC, superior vena cava; Tr, trachea.)

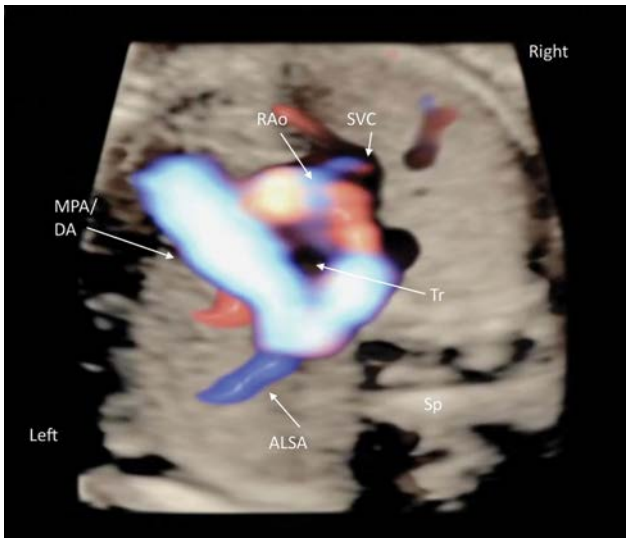


**Figure 11.14**
Three-vessel view of a right aortic arch with left ductus arteriosus and an aberrant right subclavian artery vascular ring abnormality, which originates from the distal right-sided arch and courses toward the left fetal shoulder. (ALSA, aberrant left subclavian artery; MPA/DA, main pulmonary artery/ductus arteriosus; RAo, right-sided aortic arch; Sp, spine; SVC, superior vena cava; Tr, trachea.)

right subclavian artery, conversely, arises as a discrete fourth branch distally on the arch, and the vessel courses behind the trachea and esophagus in an oblique manner across the fetal chest toward the right shoulder (Figure 11.13). In a recent large meta-analysis, the course of the right subclavian artery could be visualized in the axial 3VT plane in over 98% of fetuses, with all cases of an aberrant vessel course successfully identified in this plane. The approximate incidence of the finding was 1%. This finding has an increased incidence in fetuses with Down syndrome, with varying likelihood ratios depending on the study and whether the finding is isolated or not.[24]

As part of a right aortic arch–left ductus arteriosus variant, an aberrant left subclavian artery can also be identified in the 3VT.[25] When the aortic arch is right sided, the branching pattern is reversed such that the first (brachiocephalic) branch divides into the left common carotid and left subclavian arteries. An aberrant course of the left subclavian artery demonstrates an origin from the distal right-sided aortic arch, with an oblique course that runs posterior to the trachea and esophagus and toward the left fetal shoulder (Figure 11.14, Video 11.8—3VT of right arch with aberrant left subclavian artery vascular ring).

## Abnormal vessel size

Alterations from the expected vessel caliber seen on the 3VT represent significant clues to underlying conotruncal disease. The relative sizes of the vessels in a normal configuration are such that they become smaller as one moves from left to right across the axial view of the chest; the pulmonary artery/ductus arteriosus is slightly larger than the aorta, which is larger than the cross section of the superior vena cava.[5] Variations in this arrangement, where any one vessel may be dilated, hypoplastic, or absent, are strongly suggestive of an abnormality of the outflow tracts.

Tetralogy of Fallot can be identified in this view as a result of the abnormal vessel sizes that are typical of this disorder. The classic form of tetralogy of Fallot is characterized by pulmonary stenosis—with a small main and branch pulmonary arteries—as well as dilation of the ascending aorta. This produces an image on the 3VT of a small caliber pulmonary artery and a significantly larger aorta (Figure 11.15,

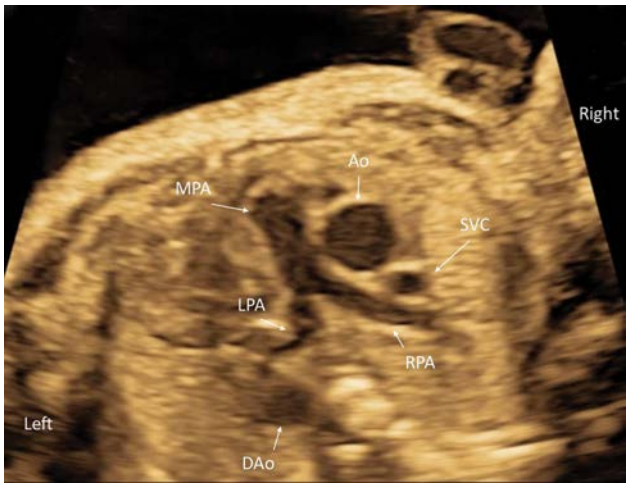


**Figure 11.15**
Three-vessel view of a classic tetralogy of Fallot, with a small main and branch pulmonary arteries, large ascending aorta, and hypoplastic thymus. (DAo, descending aorta; LPA, left pulmonary artery; MPA, main pulmonary artery; RPA, right pulmonary artery; SVC, superior vena cava.)

Video 11.9—3VV of classic tetralogy of Fallot; small main and branch pulmonary arteries, large aorta, with close proximity of vessels to anterior chest wall due to thymic hypoplasia). A narrow pulmonary artery may be found in several additional disorders, including some forms of double-outlet right ventricle with a subaortic ventricular septal defect, Ebstein anomaly, tricuspid atresia, or any complex abnormality associated with progressive hypoplasia of the right outflow tract.[3] In cases associated with a 22q11 microdeletion, where the thymus gland may be either hypoplastic or absent, the vessels are also noted in closer proximity to the anterior chest wall.

The aorta will appear smaller than expected in the context of several forms of left ventricular outflow obstruction. In the case of an interrupted aortic arch, the ascending aorta is smaller than expected and demonstrates a visible discrepancy in size from the main pulmonary artery on the 3VV; the transverse arch will remain nonvisualized on the 3VT.[23] Coarctation of the aorta may also produce a visible difference in sizes of the transverse arches, with a narrowed or hypoplastic aortic arch noted in the 3VT.[26]

Abnormalities of the semilunar valves may also result in altered vessel size. Valvar stenosis with associated flow acceleration commonly results in postvalvar dilation of the vessel, altering its appearance on the 3VT. An additional clue to this finding is an echogenic semilunar valve that is visualized throughout the cardiac cycle (Video 11.10—3VT with pulmonary stenosis including thickened echogenic pulmonary valve and poststenotic dilation of the MPA). In tetralogy of Fallot with absent pulmonary valve syndrome, both the main and branch pulmonary arteries are massively dilated in the 3VT.[27]

## Abnormal color flow pattern/ directional signal

In a structurally normal heart, both transverse arches should demonstrate anterograde flow represented by the same color signal. Abnormal color or directional power Doppler signals obtained in the 3VT can be noted in several instances.

In the case of atresia of one of the great arteries, there is a discrepancy noted in the color signal with anterograde flow noted in the patent artery and retrograde flow (via ductal perfusion) noted in the atretic one. For example, in cases of HLHS with aortic atresia, retrograde flow may be identified in a smaller hypoplastic aortic arch on the 3VT (Figure 11.16). Conversely, with pulmonary atresia, the most leftward vessel will demonstrate retrograde flow, consistent with ductal perfusion via a patent aortic arch (Figure 11.17). In a study by Vinals et al., prenatal detection of reversed flow in one of the transverse arches was consistently associated with complex congenital heart disease, diminution of flow to the corresponding great vessel, and accurately predicted ductal dependence.[28]

When anterograde flow is preserved but there is stenosis of or obstruction across a semilunar valve, turbulent flow may produce an appearance of aliasing on the color signal (Figure 11.18). This is frequently accompanied by the postvalvar dilation described previously.

## Additional vascular assessment

Abnormalities involving the brachiocephalic and azygous veins may also be evaluated in the 3VT view. Unusual

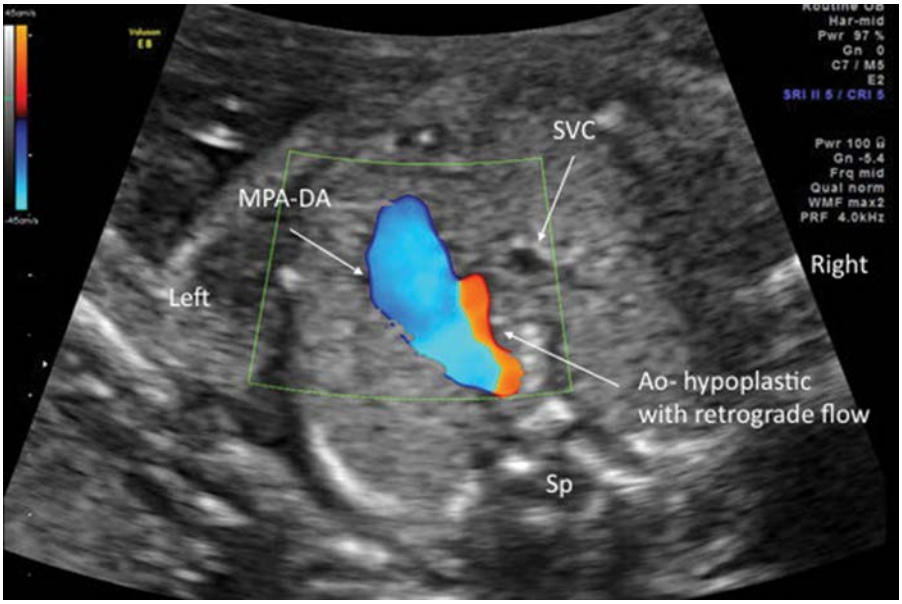


**Figure 11.16**
3VT of hypoplastic left heart syndrome due to mitral/aortic atresia. There is a large main pulmonary artery with anterograde flow, and a small aorta with retrograde flow via the ductus arteriosus.

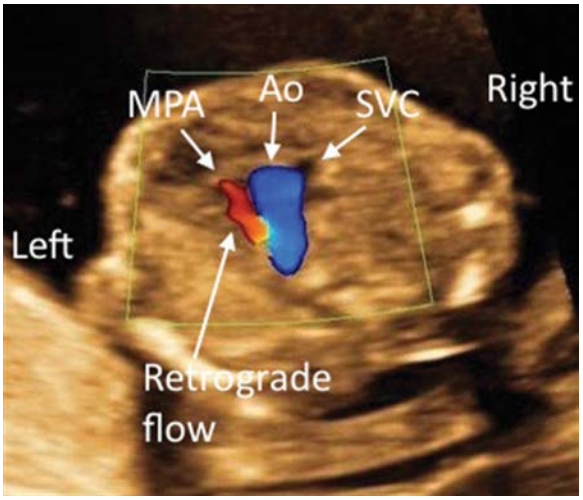


**Figure 11.17**
3VT of pulmonary atresia, demonstrating retrograde flow in the pulmonary artery, which is also hypoplastic. (Ao, aorta; MPA, main pulmonary artery; SVC, superior vena cava.)

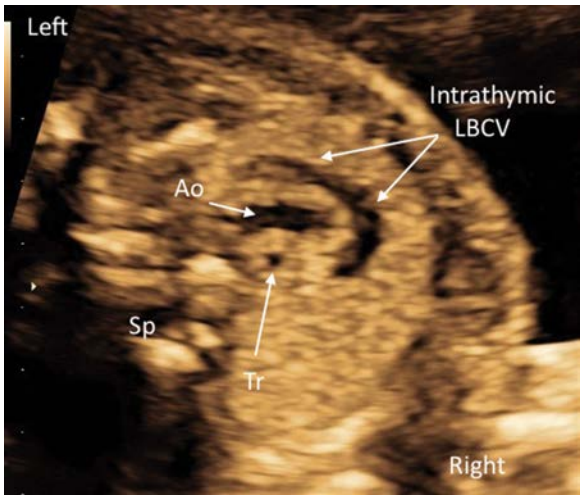


**Figure 11.19**
Intrathymic course of a left brachiocephalic vein, just above the level of the 3VT. (Ao, aorta; LBCV, left brachiocephalic vein; Tr, trachea.)

prominence or dilation of the left brachiocephalic vein entering the superior vena cava may indicate an increased volume load, such as supracardiac drainage of anomalous venous return or a cerebral venous malformation. If the superior vena cava is left sided, the brachiocephalic vein enters from the right side and is typically absent in the case of bilateral SVCs. Alternate courses of the left brachiocephalic vein, such as an intrathymic trajectory, may be identified on this view (Figure 11.19).[29] A normally small azygous arch, seen at the level of the 3VT, may also appear larger than expected in cases of interrupted inferior vena cava with azygous continuation, or with infracardiac anomalous venous return via the azygous vein.[11]

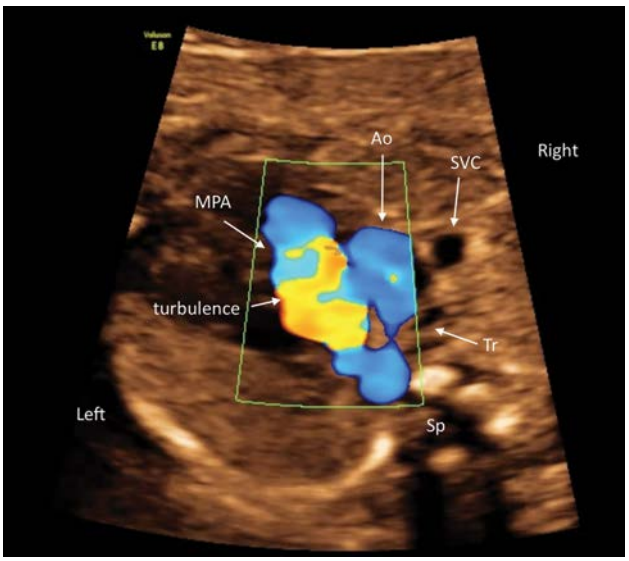


**Figure 11.18**
3VT of pulmonary stenosis, where aliasing and turbulent flow is noted in the postvalvar region. (Ao, aorta; MPA, main pulmonary artery; Sp, spine; SVC, superior vena cava; Tr, trachea.)

## Thymic assessment

Due to the anatomic level of the 3VT on axial imaging of the fetal chest, the thymus gland can also be evaluated. There is a strong association of conotruncal disease with a 22q11 microdeletion, the spectrum of which may include agenesis or hypoplasia of the thymus gland. Thymic size can be assessed subjectively, related to the proximity of the anterior borders of the vessels to the fetal chest/sternum as a result of the reduced thymic volume.[30] Gestational age–appropriate nomograms have also been created for thymic width.[31] However, a simple approach to evaluation of the thymus was published by Chaoui et al. A "thymic-thoracic ratio" was devised as a means to quantify thymic volume in the anterior chest. The measurement is taken as a ratio of two midline diameters: (1) from the posterior sternal border to the anterior border of the ascending aorta (as a surrogate measurement of thymic volume) and (2) from the posterior sternal border to the anterior aspect of the thoracic vertebral body, and described as a ratio (Figure 11.20a). This ratio was found to be stable across gestational ages, simplifying interpretation. It also reliably segregated the population with conotruncal disease and 22q11.2 microdeletion from both normal fetuses and those with conotruncal disease and no microdeletion. The mean ratio was 0.44 in normal fetuses and abnormal fetuses without the microdeletion, whereas the mean ratio was 0.25 (and always less than 0.3) in those with conotruncal disease and the 22q11.2 microdeletion, indicating closer proximity of the great arteries to the anterior chest wall as a function of reduced thymic volume[32] (Figure 11.20b). Finally, depending on color settings, the internal thoracic arteries may be visualized, delimiting the thymic capsule on each side (Figure 11.10).

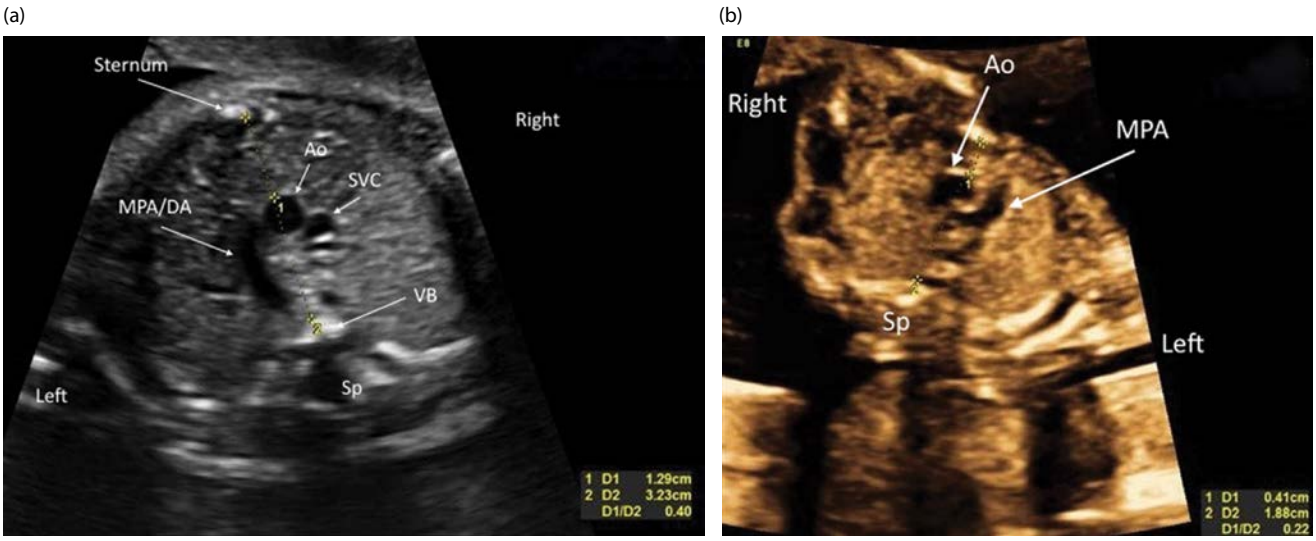


**Figure 11.20**
(a) Normal thymic-thoracic ratio (0.40), also showing the slightly hypoechoic thymus gland in the anterior mediastinum. (Ao, aorta; MPA/DA, main pulmonary artery-ductus arteriosus; Sp, spine; SVC, superior vena cava; VB, anterior border of vertebral body.) (b) Abnormal thymic thoracic ratio (0.22) as a result of a hypoplastic thymus gland. (Ao, aorta; MPA, main pulmonary artery; Sp, spine.)

## Screening recommendations and the 3VT

As of 2013, incorporation of the 3VT into fetal cardiac was required by both the International Society of Ultrasound in Obstetrics and Gynecology[33] and the American Institute of Ultrasound in Medicine.[34] Both governing bodies mandate this view in their published guidelines, recognizing the importance of this view for the detection of congenital heart disease.

## Detection of congenital heart disease using the 3VT

The 3VT provides specific information regarding outflow tract/conotruncal anatomy and would be expected to increase the detection rate of complex defects above that noted with four-chamber screening alone, since many conotruncal abnormalities exist in the setting of a normal four-chamber view. Multiple authors have investigated the added benefit of the 3VT for congenital heart disease. In a large prospective study of routine prenatal screening for congenital heart disease, Wu et al. noted a sensitivity of only 65.6% for the four-chamber view alone, increasing to 81.3% with incorporation of the 3VV.[12] The 3VV/3VT were integrated as a single approach—termed the "complete" three-vessel view—by Tongsong et al. Excluding septal defects, the complete 3VV demonstrated an 89% detection rate for conotruncal disease.[35] Utility of an isolated three-vessel view image has also been studied. Brandt et al. reported a 91% sensitivity for detection of isolated outflow tract abnormalities was achieved, with an 88% sensitivity for combined anomalies. All cases of tetralogy of Fallot and d-transposition of the great arteries were identified with an isolated 3VV.[36] This benefit has also been documented in the first trimester, where the addition of the 3VT to four-chamber view color flow screening resulted in a virtual doubling of the detection rate of congenital heart defects, from 45.7% to 88.6%.[37]

## Conclusion

The 3VT is an easy axial plane to acquire across all gestational ages. It provides information that allows the detection of most conotruncal abnormalities and ductal-dependent lesions, as the majority of these disorders are associated with an abnormal 3VT. Sensitivity is increased with the addition of color Doppler, which will help detect atresia of the great vessels and evolving flow-related abnormalities such as acquired stenoses. Additional vascular features, such as brachiocephalic and azygous vein malformations, may also be identified using the 3VT and a slightly more cephalic plane. Finally, the thymus gland may be evaluated, which may be absent or hypoplastic in the setting of conotruncal disease and the 22q11.2 deletion.

## Videos

**Video 11.1** (https://youtu.be/IslA6RbvzWs)
Four-dimensional STIC glass-body rendering, depicting outflow tracts (blue) as seen in the three-vessel tracheal view, with the perspective of the four-chamber view and ventricular inflow caudally located.

**Video 11.2** (https://youtu.be/IHR_40krgVE)
Color flow imaging of a normal 3VT; slight aliasing is commonly seen in the ductus arteriosus. Anterograde flow is noted in both ductal and aortic arches.

**Video 11.3** (https://youtu.be/xNNTynVT53g)
3VT of a d-TGA abnormality in grayscale. Note the anteriorly transposed aorta appears as a solitary outflow leftward of the superior vena cava, with a slight convexity toward the left side. The aorta also originates much closer to the anterior chest wall due to the transposed position.

**Video 11.4** (https://youtu.be/TUjc9UUpRRk)
Sweep from 3VT to four-chamber view demonstrating a left-sided superior vena cava, with drainage via a dilated coronary sinus noted at the level of the left atrium in the four-chamber view.

**Video 11.5** (https://youtu.be/xvVPvIKsZyU)
Right aortic arch with left-sided ductus; the "U"-shaped vascular signal represents both arches with the transverse aortic arch to the right side of the trachea, which appears as a sonolucency in the middle of the "U." Confluence of the arches is represented by the base of the "U."

**Video 11.6** (https://youtu.be/M0cCeUfv9R0)
Four-dimensional glass-body STIC representation of a right aortic arch–left ductus arteriosus. The left pulmonary artery can be seen originating from the main pulmonary trunk below the ductus. The trachea is visible as a sonolucency in the center of the "U."

**Video 11.7** (https://youtu.be/YXHcWXqvr8E)
3VV of an interrupted aortic arch, type B. The video starts at the 3vv, demonstrating a small ascending aorta (smaller than adjacent SVC) and a large main pulmonary artery. As the video sweeps to the 4cv, we see the small, hypoplastic aortic root and aortic valve, in association with a posteriorly malaligned ventricular septal defect, which is typical of this abnormality.

**Video 11.8** (https://youtu.be/qrzVLjv3waM)
R3VT of a left ductus arteriosus and a right aortic arch; there is an aberrant left subclavian artery originating at the distal right arch and coursing toward the left fetal shoulder. The trachea is a central sonolucency in the middle of the "U."

**Video 11.9** (https://youtu.be/lxydK_4ro8w)
3VV of classic tetralogy of Fallot. The main and branch pulmonary arteries are hypoplastic (stenosis), and there is a large, dilated ascending aorta. Also note the proximity of the vessels to the anterior chest wall due to thymic hypoplasia, though there is some hypoechoic thymus tissue noted.

**Video 11.10** (https://youtu.be/wnVbiArjWCs)
3VT of pulmonary stenosis, demonstrating a thickened echogenic pulmonary valve, which is visible throughout the cardiac cycle. There is also evidence of postvalvar dilation of the main pulmonary artery due to turbulence and flow acceleration.

# References


1. Kirk JS et al. *Obstet Gynecol* 1997;89:227–32.
2. Achiron R et al. *BMJ* 1992;304:671–4.
3. Gardiner H, Chaoui R. *Semin Fetal Neonatal Med* 2013;18(5): 261–8.
4. Yoo SJ et al. *Ultrasound Obstet Gynecol* 1997;9:173–82.
5. Yagel S et al. *Ultrasound Obstet Gynecol* 2002;20:340–5.
6. Mielke G et al. *Ultrasound Obstet Gynecol* 1997;9:25–9.
7. Wong SF et al. *Ultrasound Obstet Gynecol* 2007;30:275–80.
8. Zalel Y et al. *Prenat Diagn* 2004;24:174–8.
9. Moon MH et al. *Prenat Diagn* 2007;27:158–63.
10. Pasquini L et al. *Ultrasound Obstet Gynecol* 2007;29:628–33.
11. Vinals, F et al. *Ultrasound Obstet Gynecol* 2003;22:358–67.
12. Wu Q et al. *J Ultrasound Med* 2009;28:1319–24.
13. Ishii Y et al. *Ultrasound Obstet Gynecol* 2013;41:667–71.
14. Palatnik A et al. *J Ultrasound Med* 2015;34:1329–35.
15. Menahem S et al. *Ultrasound Obstet Gynecol* 2013;41: 168–71.
16. Abuhamad A, Chaoui R. *A Practical Guide to Fetal Echocardiography: Normal and Abnormal Hearts*, Chapter 31, 3rd ed. 2016, Wolters Kluwer, Philadelphia, Pennsylvania.
17. Achiron R et al. *Ultrasound Obstet Gynecol* 2002;20:553–7.
18. Yoo SJ et al. *Ultrasound Obstet Gynecol* 2003;22:535–46.
19. Jain S et al. *J Ultrasound Med* 2010;29:287–94.
20. Li, S et al. *Prenat Diagn* 2011;31:334–46.
21. Bravo C et al. *J Ultrasound Med* 2016;35:e17–31.
22. Trobo D et al. *J Ultrasound Med* 2015;34:1921–7.
23. Slodki M et al. *Ultrasound Med Biol* 2011;37(11):1808–13.
24. De Leon-Luis J et al. *Ultrasound Obstet Gynecol* 2014;44: 147–53.
25. Hsu KC et al. *Taiwan J Obstet Gynecol* 2011;50(3):353–8.
26. Pasquini L et al. *Ultrasound Obstet Gynecol* 2007;29:628–33. (erratum in *Ultrasound Obstet Gynecol* 2007;29:366).
27. Abuhamad A, Chaoui R. *A Practical Guide to Fetal Echocardiography: Normal and Abnormal Hearts*, Chapter 8, 3rd ed. 2016, Wolters Kluwer, Philadelphia, Pennsylvania.
28. Vinals F et al. *Ultrasound Obstet Gynecol* 2002;19:246–9.
29. Sinkovskaya E et al. *Ultrasound Obstet Gynecol* 2012;40: 542–8.
30. Chaoui R et al. *Ultrasound Obstet Gynecol* 2002;20:546–52.
31. Barrea C et al. *Prenat Diagn* 2003;23(1):9–15.
32. Chaoui R et al. *Ultrasound Obstet Gynecol* 2011;37:397–403.
33. *Ultrasound Obstet Gynecol* 2013;41:348–59.
34. *J Ultrasound Med* 2013;32:1067–82.
35. Tongsong T et al. *Prenat Diagn* 2010;30:23–9.
36. Brandt JS et al. *J Ultrasound Med* 2015;34:1415–21.
37. Wiechec M et al. *J Ultrasound Med* 2015;34:585–94.

# 12

# First and early second trimester fetal heart screening

Simcha Yagel, Sarah M. Cohen, Reuven Achiron, Yaron Zalel, and Alfred Abuhamad

## Introduction

Congenital heart disease (CHD) is the most common major congenital malformation, affecting approximately 6:1,000 live births.[1] The epidemiology of CHD is discussed in Chapter 6. The majority of cases of CHD do not cluster in families or populations, but rather occur in low-risk patients. In addition, a fetus diagnosed with CHD is at increased risk of chromosomal abnormalities.[2–6] Cardiac malformations are common in spontaneously aborted fetuses.[7] Major chromosomal abnormalities are found in spontaneously aborted fetuses (57%),[6] midtrimester fetuses (18%), and live births affected by significant CHD (12%).[2,3] When extracardiac malformations are present, this rate can be as high as 66%.[5] The overall risk of aneuploidy in a fetus with CHD is estimated to be 30%.[2–4,6] Therefore, the prenatal diagnosis of CHD is an indication for fetal genetic investigation. While CHD is one of the most clinically significant malformations amenable to prenatal ultrasonographic diagnosis, it is also the most commonly missed during fetal scans.

Targeted organ scanning for fetal heart anomalies was traditionally scheduled at 20–22 weeks' gestation and performed by the transabdominal approach in specialized referral centers. However, the first systematic investigation of fetal cardiac anatomy has now shifted in many areas to the first and early second trimesters of pregnancy. Cases of heart anomalies detected before 15–16 weeks' gestation by transabdominal sonography (TAS) have been reported since the 1980s.[8] The increasing acceptance of transvaginal sonography (TVS) and the use of high-frequency (4–8 MHz RAB6), high-resolution TAS probes, along with substantial improvements in magnification imaging and signal processing, have dramatically increased our ability to visualize and examine the developing fetal heart. Characteristic changes in structural anatomy, once the province of the embryologist and pathologist, can now be imaged in great detail. The terms *sonoembryology*[9] and *embryography*[10] have been coined and used in this context. The point has been reached where embryonic development, rather than technical obstacles, is the limiting factor in early imaging and detection of structural anomalies.

## Benefits of early fetal echocardiography

Certain advantages are offered by the earlier diagnosis of CHD: (1) early confirmation of normal cardiac anatomy may help to relieve the anxiety of high-risk patients, or facilitate earlier and safer termination of pregnancy in cases where severe anomalies are detected; (2) there is sufficient time for fetal karyotyping and genetic counseling for parents with affected fetuses; and (3) in selected cases there is a possibility of pharmacological therapy with subsequent improvement in fetal condition. Early detection of CHD allows advance planning for the optimal timing and venue of delivery, at a center with appropriate neonatal care facilities. Intrauterine, rather than postnatal, transfer improves neonatal condition for surgery and may reduce early morbidity and mortality.[11–13] Early screening must be repeated at midgestation, and a third-trimester scan should be performed, if possible, to rule out developmental CHD.[14–18]

### *Normal early anatomy and its visualization*

Organogenesis occurs over a relatively short period: by the end of the first trimester, organogenesis is complete and all the major organ systems can be imaged by ultrasound. By 56 days postfertilization, the fetal heart is formed and a four-chamber structure established.[19] Description, knowledge, and understanding of the anatomic landmarks of fetal cardiovascular development, with recognition of our ability to adequately visualize normal cardiac anatomy and appreciation of our limitations, are essential before assessment of anomalous development can be attempted early in the course of pregnancy. Without this knowledge, abnormalities may be either missed or misdiagnosed, or suspected where they do not exist.

Several investigators have described normal fetal heart anatomy in early gestation.[20–30] The cardiovascular system begins to mature during the third developmental week, and

the first beats of the embryonic heart, the sine qua non of embryonic viability, can be clearly discerned from the first days of the sixth gestational week, when the crown-rump length (CRL) is about 3 mm. The heart gradually attains a tubular structure that resembles a triocular cavity at the end of the 10th gestational week.[19] Formations of the septae and arterial and venous connections are completed only after 8 weeks of gestation. The aorta can be seen at the end of the ninth week, and by the end of the 12th week the brachiocephalic and carotid arteries are readily seen in every fetus.[19] The defined cardiac structures visible the earliest by sonography in the first trimester are probably the mitral and tricuspid valves. It has been shown that each atrioventricular valve can be individually visualized by the 10th week of gestation, along with the normal offset position of the tricuspid valve,[24] the 3VT, the ventricular outflow tracts, the aortic arch, and the ductus arteriosus.[29] The superior and inferior venae cavae can be reliably visualized from 11 to 15 weeks' gestation and the pulmonary veins by 12–14 weeks' gestation.[29]

While complete echocardiography including all scanning parameters cannot be reliably performed at 10 gestational weeks, it is possible transvaginally in 90% of cases by 12–14 weeks and in 100% by 15 weeks.[29] In our experience[31] and others' reports,[32–36] the use of the transvaginal approach along with cardiac imaging at 12–14 weeks of gestation improves visualization rates of fetal anatomy and detection rates of cardiac anomalies. Shapiro et al.[28] performed transvaginal measurements of the fetal heart from 14 to 17 weeks' gestation, and transabdominally thereafter, to term. Linear correlation was found between gestational age and measurements of the right and left ventricles. The ratio between the fetal heart and the transverse diameter of the chest was almost constant at that period. The size of the embryonic heart has also been correlated with that of the CRL and abdominal diameter.[28]

Since the 1990s, many groups have examined the feasibility of early fetal heart scanning, whether by the transvaginal or transabdominal approach, or both, or comparing the two.[29,37–43] More recently, investigators have applied three-dimensional (3D)/four-dimensional (4D) ultrasound modalities to early scanning, in order to improve detection rates of CHD.[44–46]

Two factors critically influence the accuracy of early fetal cardiac imaging: the ultrasound equipment and the operator.[36,47] In our ultrasound unit, we use 4–8 MHz transducers, which provide a higher resolution than the 5 MHz transducers that are commonly used. The advantage of these high-frequency transducers is the ability to provide a clearer image because of greater axial and lateral resolution,[23,27] making small structures more distinguishable. With regard to the operator, the technique of TVS requires a substantial amount of experience. Certain views may be limited by the fixed linear axis of the ultrasound probe during the transvaginal examination, and fetal position often dictates the views that can be imaged. Consequently, certain maneuvers and manipulations are frequently needed in order to obtain the best planes and views in a reasonable examination time. Systematic evaluation of the fetal heart and other organs in early gestation is primarily performed by the OB/GYN sonologists and sonographers who are well acquainted with the TVS technique. In our experience, the average duration of fetal ultrasound examination is approximately 30 minutes, and in many cases the echocardiographic examination requires less than 5 minutes of the scanner's time with a favorable fetal lie.[48,49]

## The extended fetal echocardiographic examination

As early as the early 1980s,[50] echocardiography proved to be a reliable tool in the diagnosis of CHD, and incorporation of the four-chamber view (FCV) of the fetal heart into screening made possible the detection of 60% of severe cardiac anomalies.[51] The importance of a normal FCV was emphasized by Copel et al.,[52] who showed that if TAS revealed normal views, more than 90% of CHD could be ruled out, and that the FCV was abnormal in 96% of fetuses with structural heart defects. When patients were referred with a suspected diagnosis of FCV abnormalities, CHD was confirmed in over 80% of cases.[51] Therefore, the American Institute of Ultrasound in Medicine (AIUM) and the American College of Radiology (ACR) in their obstetrical ultrasound guidelines recommended inclusion of the FCV in routine prenatal anatomy scanning programs.[53] However, prompted by the limitations discovered in the FCV approach, the ventricular outflow tracts views have been incorporated into screening programs since the early 1990s.[54,55]

According to current practice guidelines, the fetal heart screening examination,[56,57] including the four-chamber view as well as the left and right ventricular outflow tracts (LVOT, RVOT) views, and when possible, the three vessel with trachea (3VT) view should also be visualized.[58] These views can be obtained by sweeping the transducer cephalad visualizing first the four-chamber view, then continuing to the LVOT, RVOT, and 3VT views, as shown in the five planes approach (Figure 12.1).[56,59] This approach to fetal heart screening has been adopted by several organizations[56,57,60–63] given that the streamlined methodology can be integrated easily into the routine obstetric anatomy scan. Recent reviews of the effectiveness of fetal heart screening have shown that protocols that mirror the five planes approach by including the four-chamber view, outflow tracts views, and 3VT view have the highest sensitivity and specificity to detect CHD.[64,65] This approach was shown to achieve higher sensitivity for detection than those obtained in studies applying the four-chamber view alone or with only the outflow tracts or only the 3VT view.

The establishment of abdominal situs and cardiac position should be the first step in the evaluation of the fetal cardiovascular system. This is performed by identifying the stomach and heart in the fetal left side. The heart should occupy about one-third of the area of the thorax, and there should be no hypertrophy or pericardial effusion, though a slight hypoechoic appearance around the heart, if an isolated finding, can be a normal variant.[66,67] The cardiac axis is normally oriented approximately 45° (±20°) toward the fetal

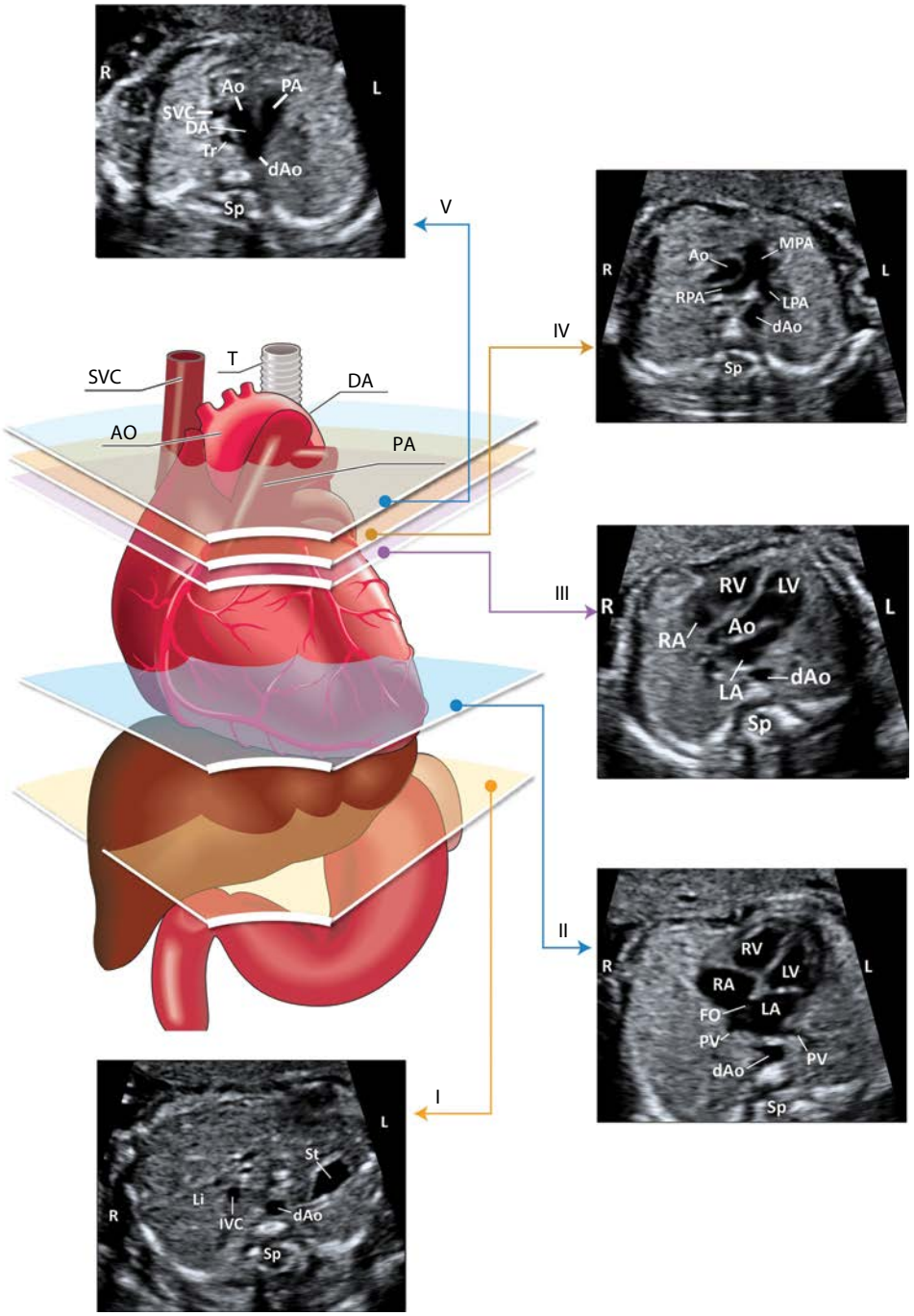


**Figure 12.1**
The five short-axis views for optimal fetal heart screening. The color image shows the trachea, heart and great vessels, liver, and stomach with the five planes of insonation superimposed. Polygons show the angle of the transducer and are assigned to the relevant grayscale images (LT, left; RT right). (I) The most caudal plane, showing the fetal stomach (ST), cross section of the abdominal aorta (AO), spine (SP), and liver (LI). (II) The four-chamber view of the fetal heart, showing the right and left ventricles (RV, LV) and atria (RA, LA), foramen ovale (FO), and pulmonary veins (PV) to the right and left of the aorta (AO). (III) The five-chamber view, showing the aortic root (AO), left and right ventricles (LV, RV), atria (LA, RA), and a cross section of the descending aorta (AO with arrow). (IV) The slightly more cephalad view showing the main pulmonary artery (MPA) and the bifurcation of left and right pulmonary arteries (LPA, RPA) and cross sections of the ascending and descending aortae (AO and AO with arrow, respectively). (V) The 3VT plane of insonation, showing the pulmonary trunk (P), proximal aorta ([P]Ao), ductus arteriosus (DA), distal aorta ([D]Ao), superior vena cava (SVC), and the trachea (T). See accompanying videos of the five planes (Videos 12.1–12.9). (Reprinted with permission from International Society of Ultrasound in Obstetrics and Gynecology, Carvalho JS et al. *Ultrasound Obstet Gynecol* 2013;41:348–59.[56])

left. Abnormalities in cardiac situs, axis, or position require detailed evaluation for situs abnormalities, and structural or chromosomal anomalies. In addition, a shift in cardiac position can be indicative of space-occupying lesions or diaphragmatic hernia.

The mainstay of the fetal heart screening examination remains visualization of the four-chamber view[51,52,61,68] (Figure 12.1, Plane II). What is important to note is that seeing the four-chamber view does not imply merely counting four cardiac chambers. Examination of this plane through the heart should include a general overview of the heart size and position and evaluation of the chambers and valve anatomy and function, as well as an assessment of heart rate and rhythm.

The cardiac atria should be approximately equal in size, and the foramen ovale flap should be observed opening toward the left atrium. Atrial septum primum should be visualized. In most cases, the pulmonary veins can be seen at their entry into the left atrium. Failure to demonstrate normal atrial configuration, or the presence of a structure posterior to the left atrium other than the normal descending aorta, should raise suspicion for anomalous pulmonary venous connection and prompt further evaluation.

The ventricles are also approximately equal in size, with the morphological right ventricle distinguished by the characteristic moderator band at the apex. While some disparity in ventricle size may be normal particularly in late gestation, marked difference in size should raise suspicion of such defects as hypoplastic left heart or coarctation of the aorta. The ventricular septum should be visualized intact from the apex to the crux, and no cardiac wall or septal hypertrophy should be present. Both atrioventricular valves should be seen to open and move freely, with the tricuspid valve leaflet insertion into the ventricular septum found somewhat closer to the cardiac apex than that of the mitral valve (Figures 12.2 through 12.5).

The utility of adding the outflow tracts to fetal heart screening is well established in the literature,[54,69–75] supported by international guidelines,[56,57,61] and has been shown to increase anomaly detection,[54,55,70,76,77] particularly in

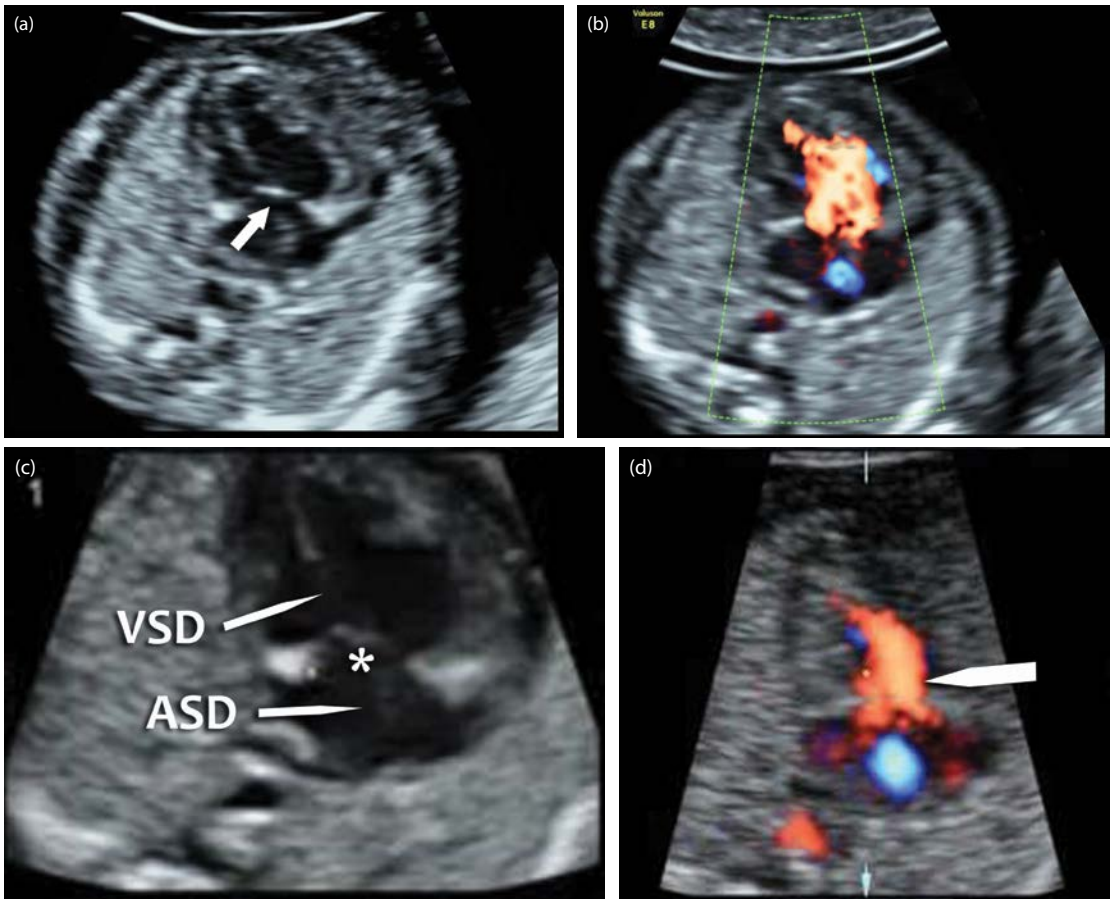


**Figure 12.2**
(a) 2DUS grayscale image of a case of atrioventricular canal defect diagnosed at $12^{+4}$ weeks' gestational age. Arrow indicates the common AV-valve. (See accompanying Video 12.10.) (b) 2DUS with Doppler mapping of the same case shows the single atrioventricular inflow jet. (See accompanying Video 12.11.) (c) Case of AV canal diagnosed at $12^{+4}$ weeks. 4DUS grayscale STIC volume rendered with TUI. Frame was extracted from the TUI matrix. Please see accompanying Video 12.12, which shows the full TUI screen. Arrows indicate the ventricular septal defect (VSD) and atrial septal defect (ASD); asterisk shows the common AV-valve. (d) 4DUS STIC volume with color Doppler rendered with TUI showing the single atrioventricular inflow jet. Frame was extracted from the TUI matrix. Please see accompanying Video 12.13, which shows the full TUI screen.

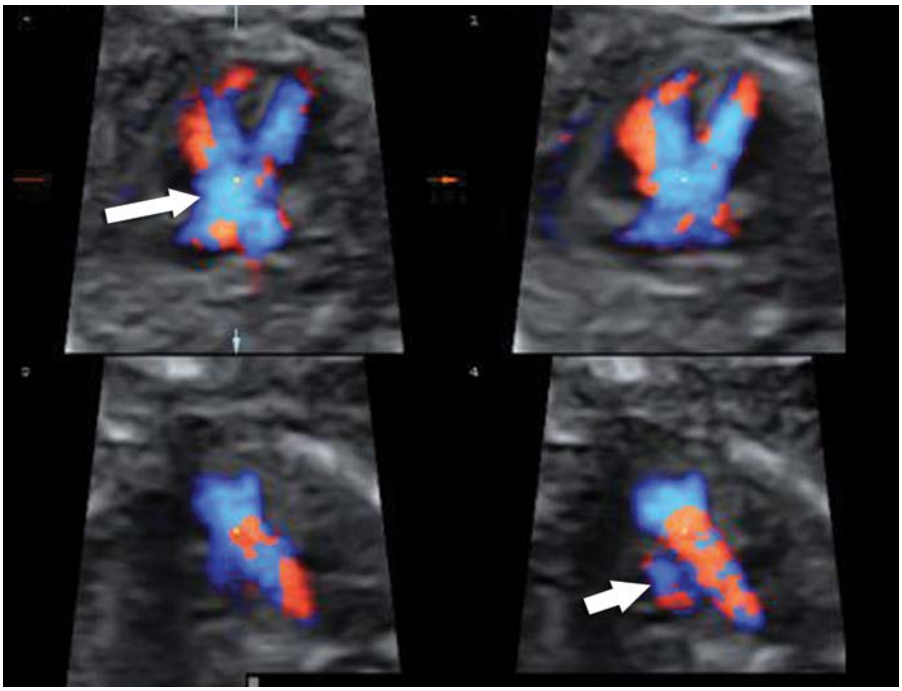

**Figure 12.3**
4DUS STIC acquisition of AV canal in a case of heterotaxy diagnosed at 14 weeks, rendered in TUI. Long arrow indicates the flow across the common AV valve; short arrow indicates the aortic stenosis. Four center frames are shown from the TUI; see accompanying Video 12.14 for the full TUI matrix.

those cases that may present with a normal-appearing four-chamber view, such as tetralogy of Fallot, transposition of the great arteries, or double-outlet right ventricle. The outflow tracts are imaged by sweeping the transducer cephalad from the four-chamber view.[59] The aorta should be seen originating from the morphologic left ventricle when imaging the LVOT. The aortic valve leaflets should move freely and not appear thickened. The anterior aortic wall should be observed in continuity to the ventricular septum. This continuity is important in order to exclude an overriding aorta in tetralogy of Fallot (Figure 12.6a) as well as other conotruncal anomalies (Figures 12.6 and 12.7). The RVOT is the next sequential plane, imaged just cephalad to the LVOT. In this plane, the pulmonary artery is seen originating from the morphologic right ventricle. The bifurcation to right and left pulmonary arteries is usually observed, lying left of the aorta and superior vena cava and anterior to the descending aorta (DAo), the latter seen in cross section. Angling the transducer just slightly more cephalad reveals the ductus arteriosus coursing toward the DAo. The pulmonary valve should be visualized moving freely, with no apparent thickening. In lesions such as transposition of the great arteries, the configuration of the ventricles and great vessels is abnormal (Figure 12.6b,c).

The 3VT view is visualized just cephalad to the RVOT, revealing the ductal and aortic arches in a V-shaped configuration, anterior and to the left of the trachea and SVC. The trachea appears as a small echogenic ring surrounding a small hypoechoic space. The SVC can be seen in cross section. The 3VT plane demonstrates vessel size, number, arrangement, and alignment relative to each other and to the trachea.[58] This view is useful to confirm or exclude anomalies,[78–80] such as persistent left superior vena cava, coarctation of the aorta, right or double aortic arch, interrupted aortic arch, and aberrant right subclavian artery (ARSA) (Figure 12.7a–d).

The normal fetal heart rate is 120–160 beats/minute. Mild transient bradycardia (<110 bpm) is not usually a cause for concern; however, persistent bradycardia or frequent missed beats may require further evaluation. Mild transient tachycardia (>160) is generally associated with fetal movement. Persistent tachycardia or tachycardia at rates greater than 180–200 may be cause for concern and should be evaluated further (Figure 12.8).

The optimal timing of fetal heart screening is the subject of some debate. Early scanning at the end of the first trimester during nuchal translucency (NT) screening has been advocated, as have late first or early second trimester scanning and midgestation imaging.[29,31,43,81,82] Zalel et al.[83] advocate fetal cardiac scanning following a result of increased NT, before the performance of fetal karyotyping. When NT $\geq$ 99th percentile, the likelihood of significant anatomic abnormality markedly increases; anatomic abnormality in this context is a strong predictor of aneuploidy.[83] There is general agreement that early screening necessitates repeated examination at midgestation owing to the evolution of CHD *in utero*.[14,34,84–86]

Whenever a cardiac abnormality is suspected or detected, further evaluation is performed in collaboration with the

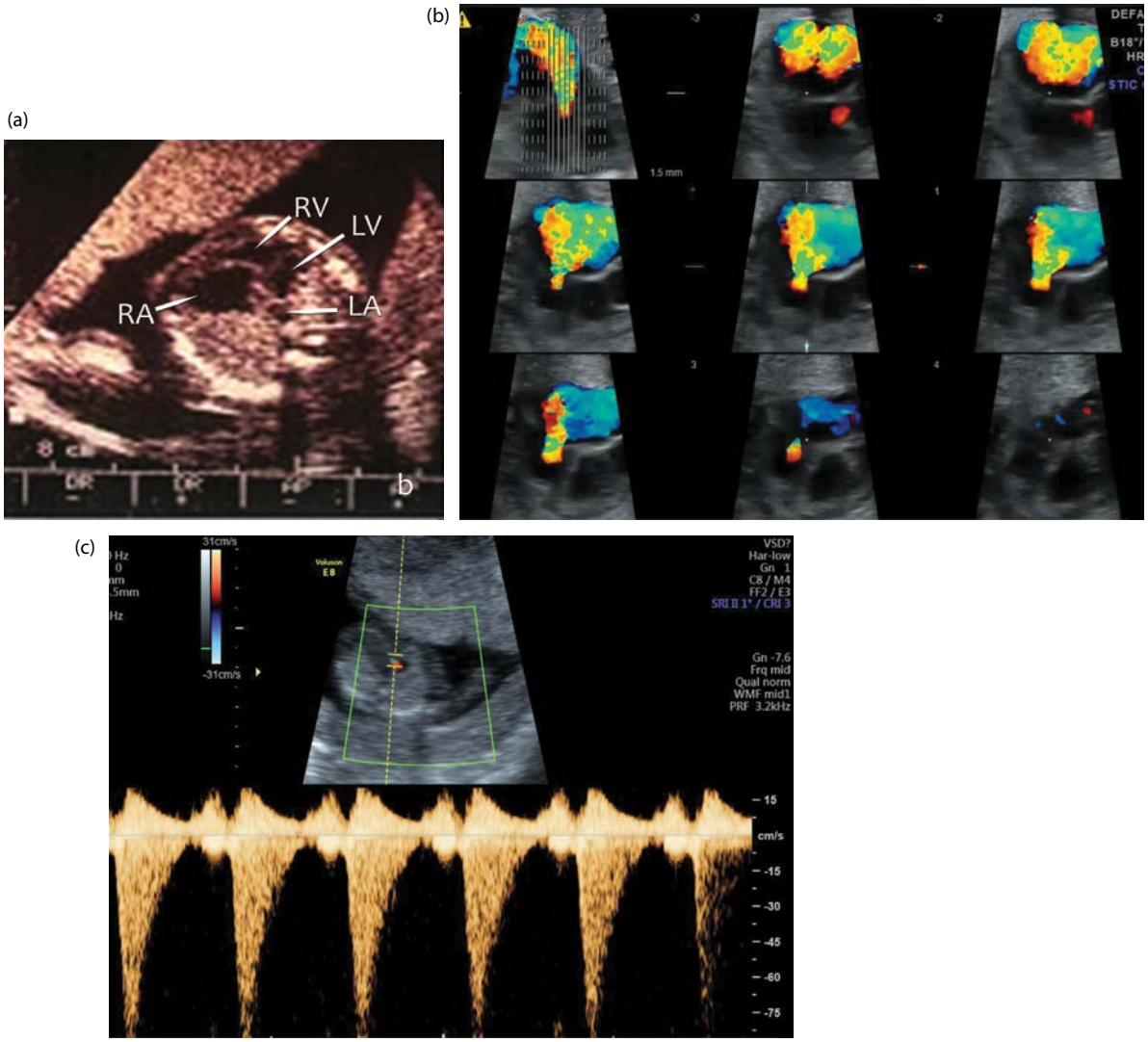


**Figure 12.4**
(a) Ebstein anomaly diagnosed at 13 weeks' gestation. Note the differential sizes of the four heart chambers. (LA, left atrium; LV, left ventricle; RA, right atrium; RV, right ventricle.) (b) 3D/4DUS STIC volume rendered with TUI shows severe tricuspid regurgitation in a case of Ebstein anomaly diagnosed at $13^{+4}$ weeks. See also accompanying Video 12.15. (c) Duplex image shows holosystolic moderate tricuspid regurgitation.

pediatric cardiologist and management team. We routinely schedule a second echocardiographic examination, using the transabdominal approach, at 20–23 weeks' gestation for all our patients, and recommend a third examination in the third trimester, at 30–32 weeks, whenever possible.

## The fetal venous system

Examination of the fetal venous system is important for comprehensive understanding of the fetal cardiovascular system. The venous system develops from three paired veins. At the end of the first trimester, several abnormal connections of the fetal venous system are recognized and are classified as follows: pathologies of the cardinal vein, umbilical veins, vitelline veins, and anomalous pulmonary venous connections. (For detailed description see Chapter 35.)

## Diagnostic early echocardiography

Diagnosis of cardiac anomalies follows the segmental approach to fetal echocardiography.[87–89] The first reports of diagnostic transvaginal fetal echocardiography date back to 1990. Gembruch et al.[90] used a 5 MHz transvaginal probe to diagnose complete atrioventricular canal defect and complete heart block at 11 weeks' gestation, and subsequently performed an elective abortion on the basis of this information. Bronshtein et al.[91] used a high-frequency 6.5 MHz probe to diagnose a VSD associated with an overriding aorta, and an isolated VSD with pericardial effusion, both at 14 weeks' gestation. The same group later reported a series of 10 fetuses with CHD diagnosed by the same technique at 12–16 weeks' gestation.[92] A further series of eight fetuses with cardiac abnormalities detected between 10 and 12 weeks' gestation was reported by our group.[93]

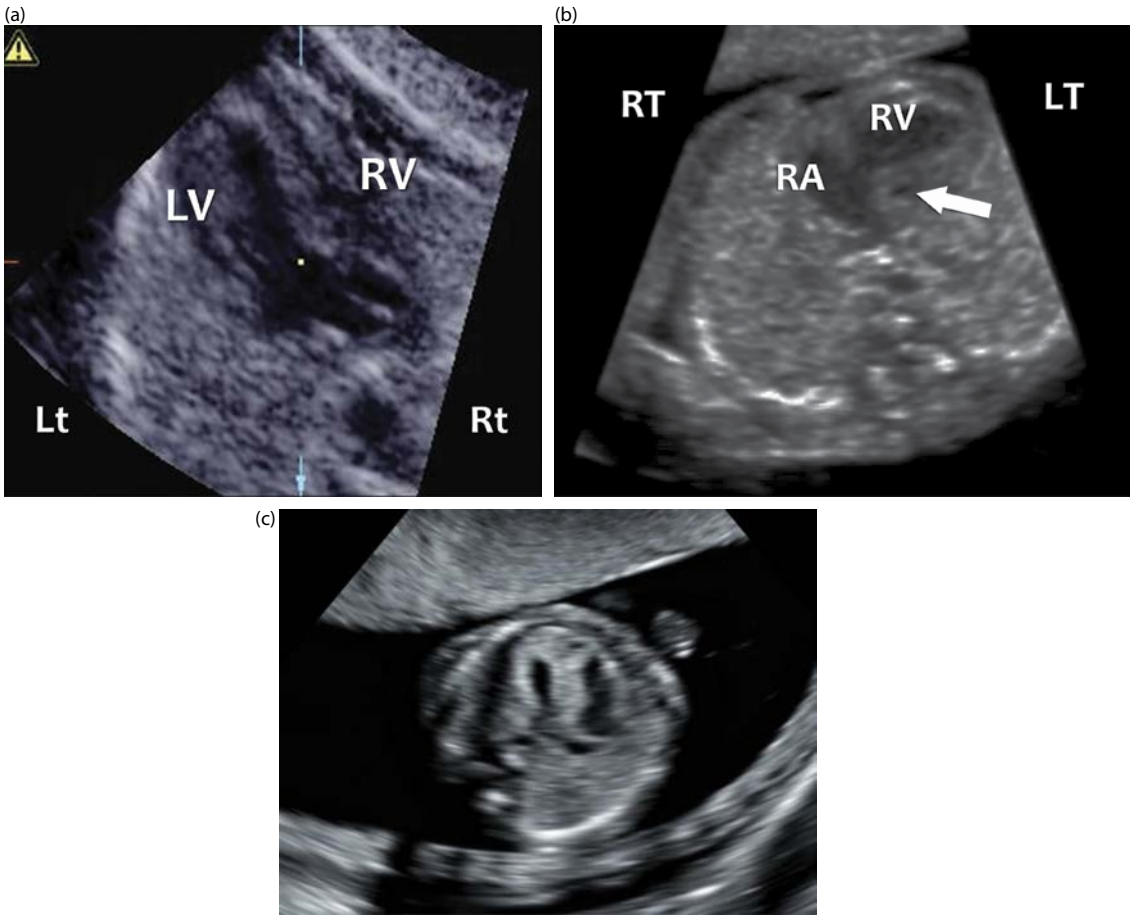


**Figure 12.5**
Anomalous 4CV: (a) A case of hypoplastic right heart diagnosed at 13 weeks. Note the right ventricle (RV) is much smaller than the left (LV). (b) Case of hypoplastic left heart diagnosed at 14 weeks. Note the diminutive left ventricle (arrow) (RA, right atrium; RV, right ventricle). (c) Anomalous four-chamber view: 2DUS grayscale image showing thickened ventricular septum in a case of ventricle mass diagnosed at 14 weeks. See accompanying Video 12.16.

Examples of heart defects detected during the first and early second trimesters are shown in Figures 12.2 through 12.9. From the series and case reports that followed over the next several years,[48,90–92,94,95] we learned that transvaginal echocardiography provides accurate diagnosis of practically all classes and types of CHD. One of the largest series, including 12,793 patients over a 5-year period, originated in Israel and was reported by Bronshtein et al.[91]

Gembruch et al.[90] and our group[93] reported experiences with transvaginal echocardiography in both low- and high-risk patients, reaching high sensitivities and specificities. Over the ensuing years since these seminal studies, early fetal echocardiography has been rigorously evaluated in large studies (Table 12.1).[14,29,37–46,48,49,70,91,96–98]

## *The 3D revolution in fetal echocardiography*

Three- and four-dimensional ultrasound (3D/4DUS) have revolutionized fetal echocardiography.[46,99] The various techniques of volume acquisition and analysis are described in detail in Chapter 13. The application of 3D/4DUS to the diagnosis and evaluation of the fetus with congenital heart disease as it applies to specific groups of lesions appears in Chapter 14 and other relevant chapters.

The 3D/4DUS modalities are also applicable to screening fetal echocardiography examinations.[44,46] Of particular note is the spatiotemporal image correlation (STIC) modality (see Chapter 13).[100–102] Briefly, a wedge-shaped scanning volume is acquired from the fetal upper abdomen moving cephalad through the fetal thorax by tilting the transducer through approximately 15°–25°. The five planes of fetal echocardiography are contained within this volume and are acquired in a single sweep. Acquisition speed varies from 7.5 to 15 seconds and should preferably be performed with the fetus in a quiet state. Slower scanning speed will provide higher resolution, but the fetus will have more opportunity to move or breathe. This will introduce artifacts that compromise scan quality. Therefore, younger fetal age shortens examination time, thus making STIC an excellent tool for early fetal echocardiography. (See Chapter 13 and 14 for details.)

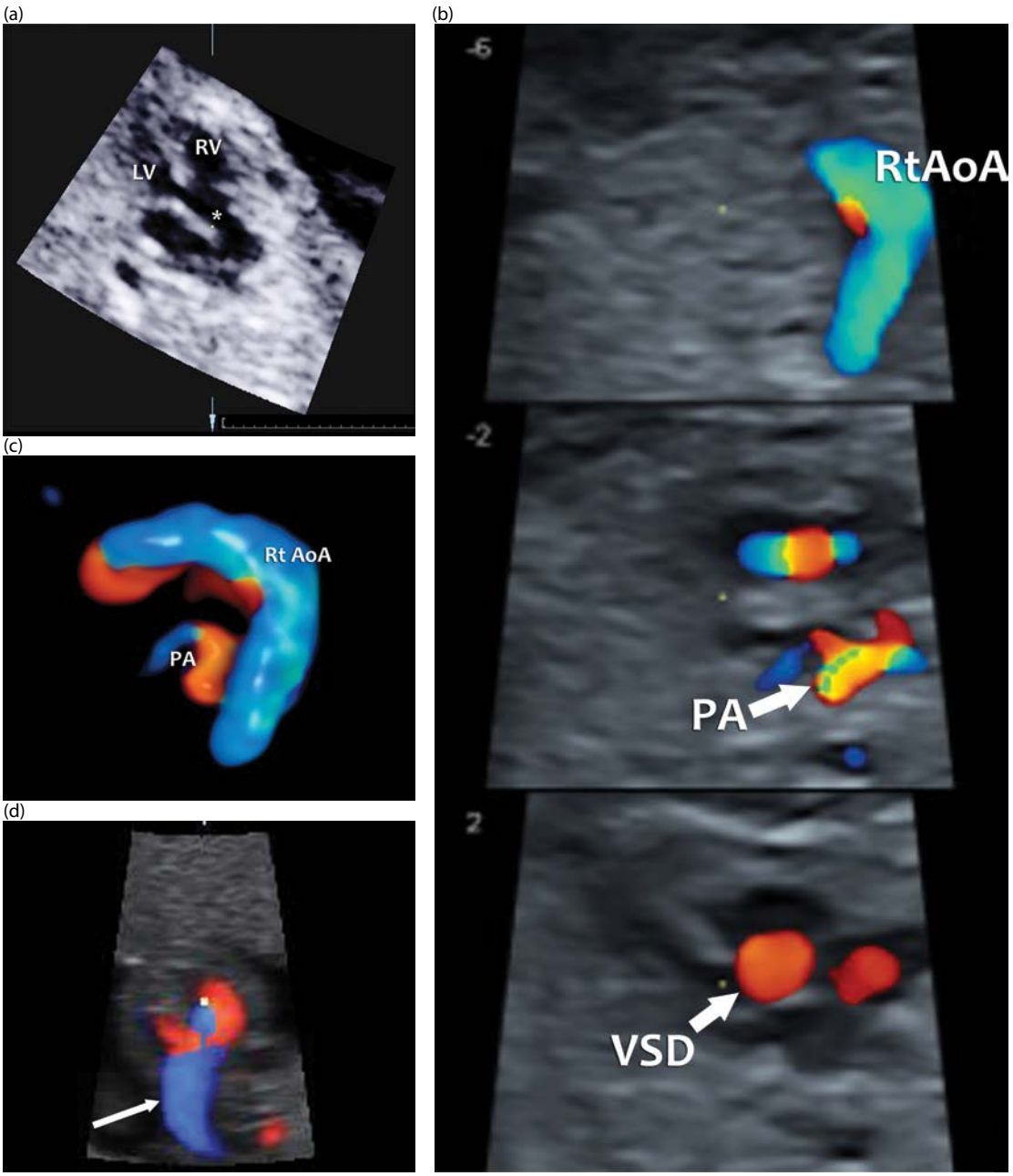


**Figure 12.6**
(a) 2DUS grayscale image of tetralogy of Fallot diagnosed at 14 weeks. Note the overriding aorta (asterisk) in this five-chamber view image (LV, left ventricle; RV, right ventricle). (b,c) 4DUS STIC acquisition of a case dTGA diagnosed at 14 weeks, rendered in TUI. (b) Right column images are three frames of the TUI matrix. Top frame shows the right aortic arch (RtAoA), middle frame shows the pulmonary artery (PA) on the left, and bottom frame shows the ventricular septal defect (VSD). Accompanying Video 12.17 shows the full TUI matrix. (c) HD color Doppler is applied to show the aorta on the right and pulmonary artery on the left. See accompanying Video 12.18. (d) Persistent truncus arteriosus diagnosed at 12 weeks. 4DUS STIC acquisition with color Doppler, rendered in TUI, showing the persistent truncus arteriosus (arrow). Frame extracted from a TUI matrix; see accompanying Video 12.19 for full TUI.

Once acquired, the volume contains the complete cardiac cycle (with or without color Doppler) and is available for postprocessing analysis. Within a well-executed volume, all the planes necessary for complete fetal cardiac scanning are available for evaluation.[58,59] Planes not accessible to direct scanning with conventional 2DUS can now be obtained and evaluated, such as the *en face* view of the interventricular septum and the coronal atrioventricular valves plane, showing the "surgical plane" through the level of the heart valves.[103,104] (See supplemental videos accompanying Figure 12.1.)

Other examples of 3D/4DUS modalities applicable to fetal echocardiography screening examinations include

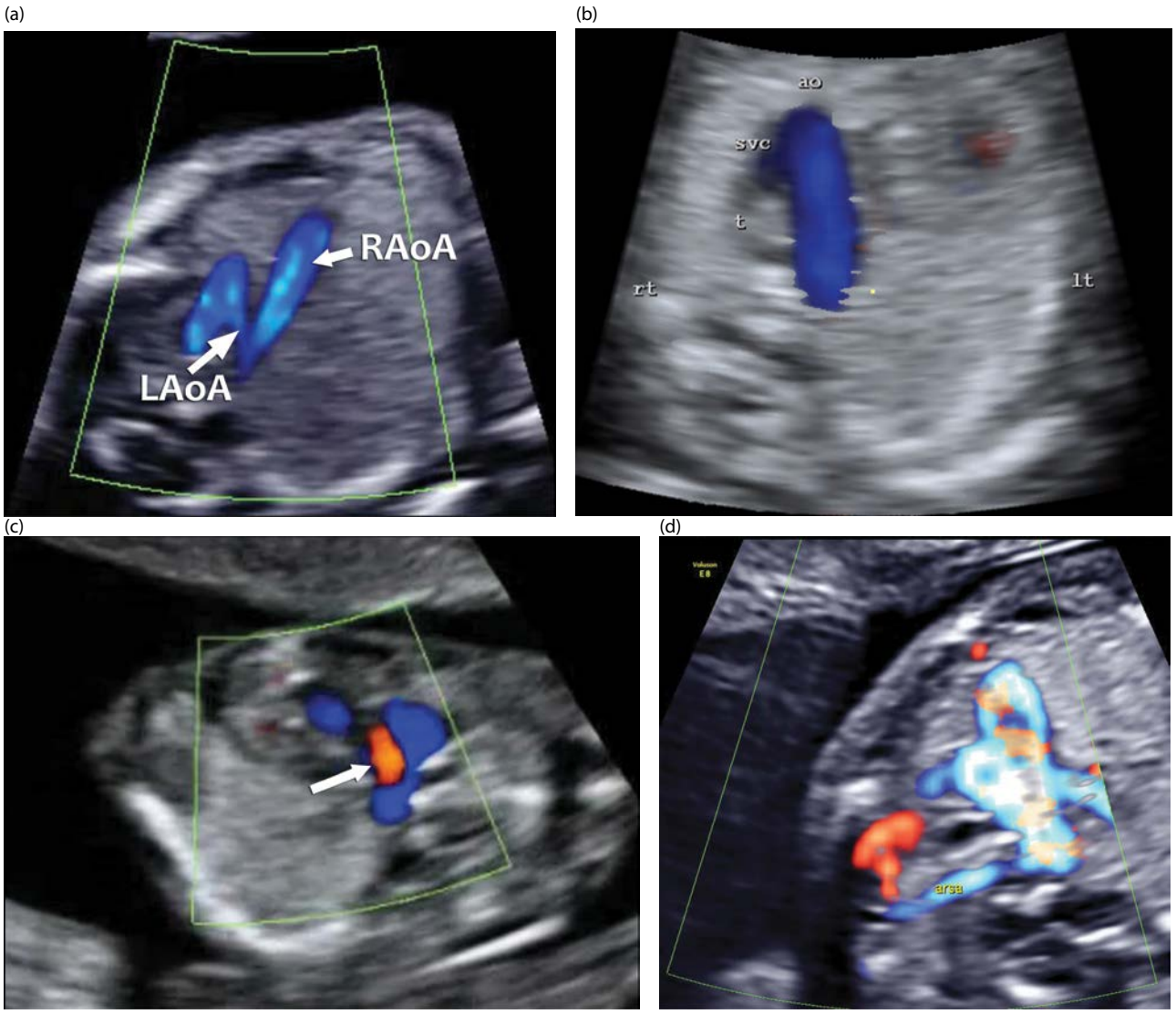


**Figure 12.7**
(a) Double aortic arch diagnosed at 14 weeks, showing the characteristic anomalous 3VT view (LAoA, left aortic arch; RAoA, right aortic arch). See accompanying Video 12.20. (b) Pulmonary atresia diagnosed at 14 weeks shows the characteristic single vessel in the 3VT view. Note the trachea is seen (t) with the superior vena cava (svc) and aorta (ao). (c) Another case of pulmonary atresia diagnosed at 14 weeks, showing reversed flow in the ductus arteriosus (arrow) in the 3VT plane. (d) Aberrant right subclavian artery (ARSA) imaged in the 3VT view. See accompanying Video 12.21.

acquisition tools such as B-flow, 3D power Doppler (3DPD), and high-definition power Doppler, along with postprocessing tools such as tomographic ultrasound imaging (TUI) and inversion mode (IM). Various postprocessing modalities and their application to fetal echocardiography have also been investigated[103–109] and are all more fully described in Chapter 14.

Another advantage of 3D/4D modalities is the digital archiving and sharing capabilities designed into these systems. Once the volume is acquired, it is stored to the system database and can be transferred by Internet link to any connected computer for analysis. This opens unlimited possibilities for onsite and offsite multidisciplinary consultations, quality review of screening programs, and teaching. Perhaps most importantly for screening echocardiography, this allows outlying or poorly served areas to be reached more effectively, since volumes acquired "in the field" by local practitioners can be analyzed offsite by fetal cardiology specialists.[110,111]

## Embryonic and fetal heart rate

Quantitative evaluation of embryonic and fetal heart rate (HR) in cases of suspected CHD is both feasible and important. Extreme deviations of the HR from the norm (120–160 bpm) convey a poor prognosis. Abnormal rates may aid not only in raising suspicion of CHD, but also in predicting fetuses possibly destined to undergo spontaneous abortion.[112] Nomograms for embryonic HR are helpful in the diagnosis of bradycardia or tachycardia in the first trimester, which signal the need for a detailed anatomic evaluation.[112–115] Significant fetal tachycardia (above the upper

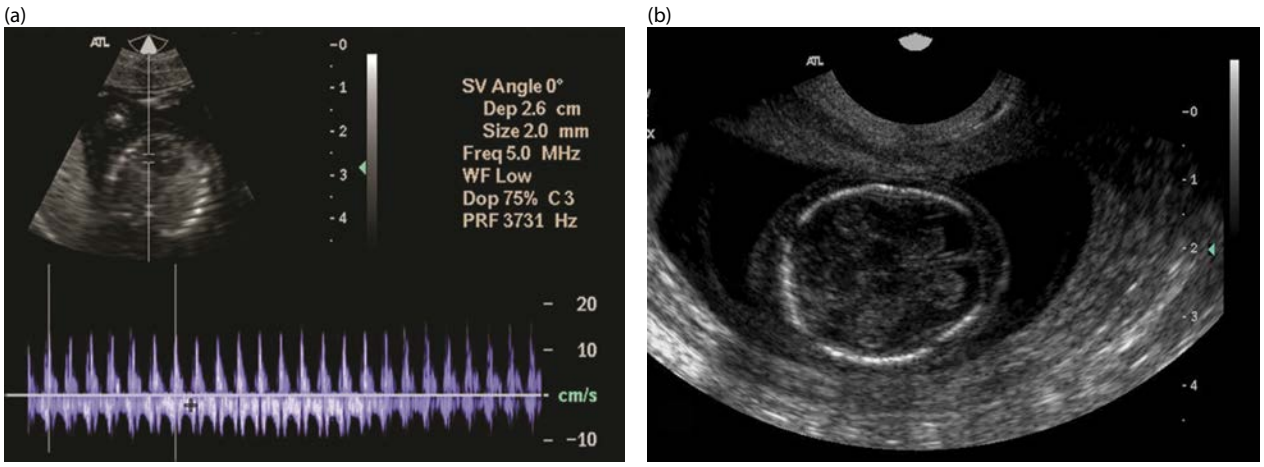


**Figure 12.8**
(a) Supraventricular tachycardia (SVT) to 292 beats/min, diagnosed at 13 weeks' gestation and associated with severe fetal hydrops. The fetus responded well to transplacental treatment of the SVT, with resolution of hydrops. (b) At presentation, signs of cardiac failure included increased scalp skin thickness. (Reproduced with permission from Porat S et al. *Ultrasound Obstet Gynecol* 2003;21:302–5.[114])

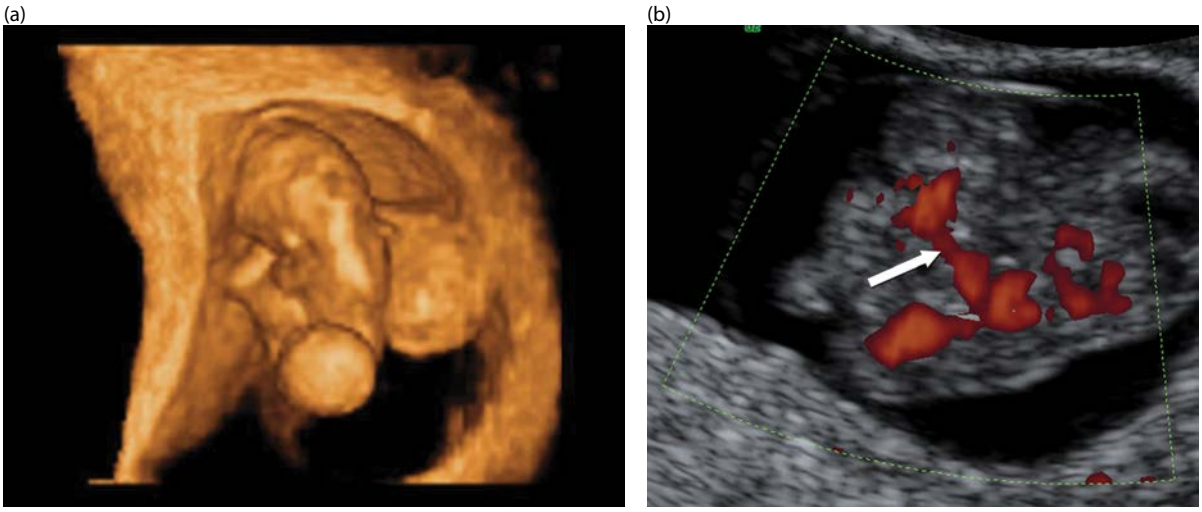


**Figure 12.9**
Conjoined twins diagnosed with 3DUS at $9^{+5}$ (a); 2DUS with color Doppler shows the shared blood flow between the fetal hearts (b) (Video 12.22).

95% confidence interval) often induces cardiac decompensation, manifested by hydrothorax and ascites (Figure 12.8). In addition, the diagnosis of fetal tachycardia or arrhythmia early in pregnancy provides the opportunity for medical treatment for patients who desire to continue the pregnancy.[112–115]

## The integration of noninvasive prenatal testing into first trimester screening programs

The introduction of noninvasive prenatal testing (NIPT)[116–126] and its enthusiastic uptake by patients and providers have necessitated rethinking of first trimester screening programs. There is some debate as to the optimal way to integrate NIPT into existing programs.[125,127–130] NIPT can be performed from about 10 weeks' gestation, prior to the timing of NT and other first trimester screening. In most cases, the test informs patients whether their fetus is euploid or is affected by one of the most common aneuploidies (trisomies 21, 18, 13) or sex chromosome syndromes. Positive results must be confirmed by invasive testing (chorionic villus sampling or amniocentesis). To many patients, NT and other first trimester screening may appear unnecessary. However, first trimester screening targets have been shown to be effective tools not only in the identification of fetuses at high risk for chromosomal anomalies, but also those at high risk for CHD, with or without associated anomaly,[96,131–137] as well as other obstetric complications. It has been proposed that NIPT be delayed until after first trimester NT and anatomic screening are performed[138] to

**Table 12.1** Studies of early screening echocardiographic examination

| *Author/year* | *Echocardiographic views employed* | *Gestational age at examination* | *Sensitivity* | *Population prevalence of CHD* | *Number of patients* |
|---|---|---|---|---|---|
| Bronshtein/1993 (mixed risk)[91] | FCV+RLVOT | 12–16 weeks | 77% | 0.36% | 12,793 |
| Achiron/1994 (low risk)[48] | FCV+RLVOT | 13–15 weeks | 50% | 0.9% | 660 |
| Kirk/1994[70] | FCV+AoR | 14+ | 78% | 0.85% | 5,967 |
| Yagel/1997[14] | FCV+RLVOT+PA+Ao | 13–22 | 64%–85% | 0.76% | 22,050 |
| Comas Gabriel/2002 (high risk)[42] | Segmental approach+D+Col | 12–17 weeks (14.2) | 79.2% | 14.4% | 330 |
| McAuliff/2005 (high risk)[38] | FCV+RLVOT+AVV | 11–16 weeks (13.5) | 70% | 12.5 | 160 |
| Smrcek/2006 (mixed risk)[43] | 5 planes+D+col | $11–13^{+6}$, 22 | 63%, 87% | 7.6% | 2,165 |
| Becker/2006 (medium risk)[37] | FCV+RLVOT+RLVIT+COL+VW+AVd+GVd | $11–13^{+6}$, 22 | 84.2%, 92% | 1.2% | 3,094 |
| Yagel/2011[46] | ISUOG Consensus Statement (REF 2008)+AoA+DV | 14–16, 22–24 | 93.8% | 1.47% | 13,101 (3,447 early scans) |
| Volpe/2011 (low risk)[97] | FCV+LVOT+RVOT+anterior V-sign+3VT 2DUS and color Doppler | At NT screening, repeated second, third trimesters | 61.9%, 92.8% | 0.9% | 4,445 |
| Iliescu/2013 (low risk)[45] | 5 planes + color Doppler TVS and 3DUS as necessary | 12–13+6 | 90% | 0.55% | 5472 |
| Turan/2014 (very high risk)[44] | STIC acquisition, TUI, and color Doppler to obtain 12 anatomical landmarks | 11–13+6 | 91% | 13% | 164 |
| Wiechec/2015 (high risk)[98] | FCV+3VTV+color Doppler | 11+0–13+6 weeks (CRL 45–84 mm) | 88.6% | 3.2% | 1,084 |

*Abbreviations:* Ao, aorta; AoA, aortic arch; AoR, aortic root; AVd, atrioventricular valves' diameters; COL, color flow mapping; D, Doppler; FCV, four-chamber view; GVd, great vessels' diameters; PA, pulmonary arteries; RLVIT, right/left ventricular inflow tracts; RLVOT, right/left ventricular outflow tracts; VW, ventricular width.

prevent cases of parents being falsely reassured of the "normality" of the fetus, when in fact grave anatomic findings are present.[138] Some investigators advocate the performance of fetal echocardiography as part of comprehensive anatomic screening at the time of NT screening, when other ultrasound and maternal biochemical screening tests are performed, but studies of the visualization rates of cardiac and other anatomy, and the detection rates of anomalies, have shown mixed results.[31–35,45,84,96,139–141] Regardless of the screening algorithm that is adopted in a given region or health system, it is essential to stress with patients three salient facts: (1) NIPT does not test for all genetic anomalies; (2) NIPT does not exclude anatomic malformations in the fetus; and (3) most cases of fetal anatomic malformations occur in chromosomally normal fetuses. Since congenital heart defects are the most common of fetal anomalies, it follows that fetal heart scanning should be an integral part of all prenatal screening programs.

## Natural course and *in utero* development of CHD

In terms of the aforementioned, delayed or even missed diagnoses in some cardiac malformations occur despite detailed echocardiographic examination by experienced operators. Evidence has accrued that progression of cardiac disease may occur and may be observed *in utero* with advancing gestational age.[14–18,43,84,142–146] Thus, some CHD may develop *in utero*, leading to a varying appearance over time. Therefore, a normal echocardiographic appearance of the heart at any gestational age does not always mean that subsequent development can be assumed to be normal, and cannot completely rule out subsequent diagnosis of structural heart disease in late gestation, or even in the postnatal period.

Our group undertook a study that attempted to further characterize the development of cardiac defects *in utero*, and

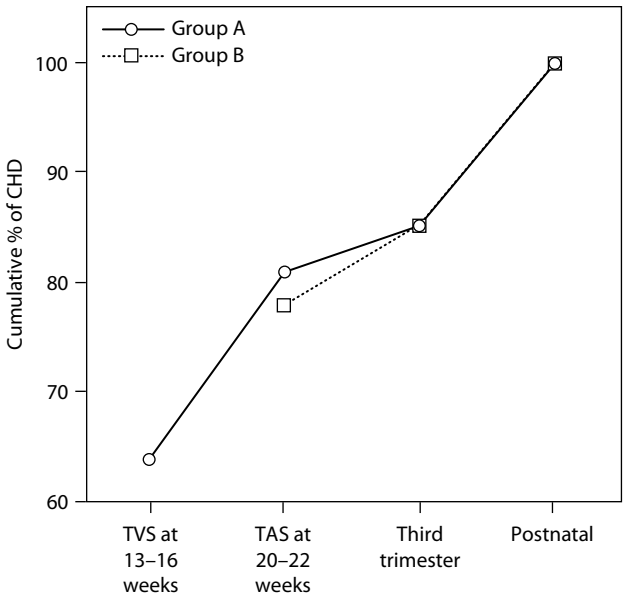


**Figure 12.10**
Cumulative percentage of heart defects identified at transvaginal, transabdominal, and third trimester scans and postnatally. (Reprinted with permission from Yagel S et al. *Circulation* 1997;96:550–5.[14])

to evaluate the effects of this newly recognized entity on the accuracy of prenatal diagnosis of CHD.[14] In a retrospective study, we reviewed the medical records of 22,050 pregnant women and their newborns, of a mixed high- and low-risk population for CHD. Patients were divided into two groups: 6,294 who had initial TVS at 13–16 weeks' gestation, followed by TAS at 20–22 weeks, and 15,126 who had initial TAS at 20–22 weeks. Both groups were subsequently examined in the third trimester, and all newborns were examined by certified pediatricians. CHD was diagnosed in 168 babies: 66 in group A and 102 in group B, for an overall rate of 7.6:1,000. In group A (Figure 12.10), 42 malformations (64%) were detected at the first TVS examination, and 11 (17%) were diagnosed during the subsequent TAS. Three additional anomalies (4%) were found during the third trimester, and 10 malformations (15%) were detected postnatally. In group B, 80 malformations (78%) were detected at the initial TAS scan at midtrimester, and an additional 7 (7%) were found in the third trimester, whereas 15 (15%) were diagnosed postnatally. Overall, 85% of the affected children were diagnosed prenatally. The 10 anomalies that were diagnosed only during the third trimester included aortic stenosis ($n = 2$), cardiac rhabdomyoma ($n = 2$), subaortic stenosis ($n = 1$), tetralogy of Fallot ($n = 1$), aortic coarctation ($n = 1$), sealed foramen ovale ($n = 1$), ventricular septal defect ($n = 1$), and hypertrophic cardiomyopathy ($n = 1$).[14]

Possible causes for delayed diagnosis may be classified into three major categories: limited resolution, which may be related to both instrumentation and fetal size and position (category A); progression of lesions *in utero*, leading to late onset of CHD (category B); and errors in diagnosis (category C). Isolated VSDs are probably the most commonly missed CHD during prenatal sonographic scanning, and this is probably the result of a combination of limited ultrasound resolution, as well as erroneous diagnosis. Lesions that may evolve and progress *in utero* are of major interest. Examples of such lesions include major vessel stenosis and ventricular outflow tract obstruction. Abnormal pressure gradients may result in focal hypoplasia and structural remodeling, which can predominate anatomically. For example, narrowing of the outflow tract will first prompt ventricular asymmetry. Later, chamber hypoplasia, fibroelastosis, or both, may ensue. These forms of outflow tract lesions may not appear to be obvious during the first half of pregnancy, mainly because the process of arrested valve growth is not significant enough to be delineated so early by ultrasound. Therefore, although the heart will have completed its structural development by the end of the first trimester, an apparently normal appearance of the heart at that time does not exclude major CHD. Furthermore, physicians and patients should be aware that rarely, serious defects may develop even after midtrimester. Consequently, follow-up examinations are of major importance and should be performed throughout pregnancy, especially in high-risk patients.

## Precautions and recommendations

Transabdominal ultrasound can effectively visualize the fetal heart sufficiently to perform complete fetal echocardiography assessment from 14 weeks' gestation.[31] Visualization rates and anomaly detection rates are lower during the NT window of 11–13 weeks.[31] Larger fetal size and the application of transvaginal scanning improve visualization and detection rates.[32,34–36,84]

However, some caveats concerning early cardiac diagnosis should be emphasized. First is the fact that pathologic confirmation of an echocardiographic diagnosis of fetal CHD is essential if the pregnancy is terminated. The small size of the specimens after pregnancy interruption during the first or midtrimester can render this task difficult, irrespective of the technique used for termination. Postmortem confirmation of the diagnosis is almost impossible after vacuum evacuation of the uterus. By using dilatation and evacuation, we found that confirmation was possible in only 62% of our cases.[93] This requires certain expertise and careful inspection of the products of conception, and even filtering to avoid loss of the fetal heart, which measures about 7–8 mm at this gestational age. While termination of pregnancy by prostaglandins permits a more gentle extraction of the embryo or fetus so that pathologic confirmation may be achieved in nearly all cases,[147] it has the disadvantage of being an inpatient procedure that carries considerable physical and psychological morbidity.

Second, cardiac abnormalities diagnosed early in pregnancy tend to be more complex than those detected in the second half of pregnancy, and cause more severe hemodynamic disturbances in the small, developing fetus. For example, a common feature in seven of eight fetuses in one

of our previously reported series[93] was the demonstration of fluid accumulation, that is, ascites, pleural-pericardial effusion, and a huge generalized hygroma enveloping the entire fetal body surface, as was also described by Gembruch et al.[147] In comparison, only 2 of 23 fetuses with CHD detected during the second trimester had such fluid accumulation.[54] Furthermore, because of the complexity and lethality of many of the anomalies amenable to diagnosis early in pregnancy, spontaneous miscarriage occurs frequently. Similarly, the incidence of CHD in second-trimester abortions is high,[5–7] as are abnormal karyotypes.[3,4] This should be borne in mind while considering the management of fetuses with complex CHD, and while counseling their parents.

Third, considerable experience in the techniques of TVS and fetal echocardiography is obligatory before attempting early diagnosis of CHD, since only an operator who is well acquainted with both of these techniques can perform transvaginal echocardiography.

Given that the FCV and great arteries are almost uniformly imaged by TVS by 12 weeks' gestation, cardiac screening can thus be performed at this early gestation. If performed transabdominally, we prefer to perform early fetal echocardiography at 14–16 weeks' gestation.[31] This is the time when the combination of the sufficient anatomical size of the heart and the higher resolution of the new TAS transducers gives the best results. The benefits of early cardiac diagnosis may still be preserved at that period. Large studies have confirmed the feasibility and high sensitivity of early fetal echocardiography. However, it must be stressed that repeated examination at midtrimester to rule out developmental CHD is essential.

## Videos

**Video 12.1** (https://youtu.be/URJvM9Z4jAo)
The most caudal plane in the five planes approach, showing the fetal stomach, cross-section of the abdominal aorta, spine, and liver.

**Video 12.2** (https://youtu.be/vzxmUKdEctU)
The four-chamber view of the fetal heart, showing the right and left ventricles and atria, the foramen ovale, and the pulmonary veins to the right and left of the aorta.

**Video 12.3** (https://youtu.be/wGVmEbmil30)
The four-chamber view of the fetal heart with color Doppler mapping, showing the right and left ventricles and atria, the foramen ovale, and the pulmonary veins to the right and left of the aorta.

**Video 12.4** (https://youtu.be/gNrW1fIU6F0)
The 'five-chamber' view, showing the aortic root, left and right ventricles and atria, and a cross-section of the descending aorta.

**Video 12.5** (https://youtu.be/ESd7cQOY97I)
The 'five-chamber' view with color Doppler mapping, showing the aortic root, left and right ventricles and atria, and a cross-section of the descending aorta.

**Video 12.6** (https://youtu.be/SfJPaNmmhWU)
The fourth, slightly more cephalad view showing the main pulmonary artery and the bifurcation of left and right pulmonary arteries and cross-sections of the ascending and descending aortae.

**Video 12.7** (https://youtu.be/vo-UJW9M_mk)
The fourth, slightly more cephalad view with color Doppler mapping, showing the main pulmonary artery and the bifurcation of left and right pulmonary arteries, and cross-sections of the ascending and descending aortae.

**Video 12.8** (https://youtu.be/VaeT2xPQvhk)
The 3VT plane of insonation, showing the pulmonary trunk, proximal aorta, ductus arteriosus, distal aorta, superior vena cava, and the trachea.

**Video 12.9** (https://youtu.be/gCzc85_IzP8)
The 3VT plane of insonation with color Doppler mapping, showing the pulmonary trunk, proximal aorta, ductus arteriosus, distal aorta, superior vena cava, and the trachea.

**Video 12.10** (https://youtu.be/vOqJeoxDfD8)
2DUS grayscale image of a case of atrioventricular canal defect diagnosed at $12^{+4}$ weeks gestational age. Note the common AV-valve.

**Video 12.11** (https://youtu.be/czhuEFpJNwc)
2DUS with Doppler mapping of the same case as Figure 12.2a and Video 12.10 shows the single atrioventricular inflow jet.

**Video 12.12** (https://youtu.be/vHBoTDXdobM)
The full TUI screen from Figure 12.2c, showing a case of AV canal diagnosed at $12^{+4}$ weeks imaged with 4DUS grayscale STIC volume rendered with TUI. Note the ventricular septal defect the atrial septal defect and the common AV-valve.

**Video 12.13** (https://youtu.be/gtiFKA8D2jg)
The full TUI screen from Figure 12.2d. 4DUS STIC volume with color Doppler rendered with TUI showing the single atrioventricular inflow jet.

**Video 12.14** (https://youtu.be/hQuZUyLu-oM)
4DUS STIC acquisition of AV canal in a case of heterotaxy diagnosed at 14 weeks, rendered in TUI. Note the flow across the common AV-valve and the aortic stenosis.

**Video 12.15** (https://youtu.be/gwpgFJdbwgY)
3D/4DUS STIC volume rendered with TUI shows severe tricuspid regurgitation in a case of Ebstein anomaly diagnosed at $13^{+4}$ weeks.

**Video 12.16** (https://youtu.be/HHVfvESa2ek)
Anomalous four chamber view: 2DUS grayscale image showing the thickened ventricular septum in a case of ventricle mass diagnosed at 14 weeks.

**Video 12.17** (https://youtu.be/BDiXAE2CxRQ)
4DUS STIC acquisition of a case dTGA diagnosed at 14 weeks, rendered in TUI. Note the right aortic arch, pulmonary artery on the left, and the ventricular septal defect.

**Video 12.18** (https://youtu.be/KvXaIMK-XEw)
HD color Doppler is applied to show the aorta on the right and pulmonary artery on the left.

**Video 12.19** (https://youtu.be/5bKMu_SDhAw)
Full TUI matrix shown in Figure 12.6d. Persistent truncus arteriosus diagnosed at 12 weeks. 4DUS STIC acquisition with color Doppler, rendered in TUI, showing the persistent truncus arteriosus.

**Video 12.20** (https://youtu.be/KblAKsQLpaM)
Double aortic arch diagnosed at 14 weeks, showing the characteristic anomalous 3VT view.

**Video 12.21** (https://youtu.be/siWx5eES2Js)
Aberrant right subclavian artery (ARSA) imaged in the 3VT view.

**Video 12.22** (https://youtu.be/1350LHTuIm0)
Rendered image of conjoined twins diagnosed with 3DUS at $9^{+5}$.

# References


1. Hoffman JI, Kaplan S. *J Am Coll Cardiol* 2002;39:1890–900.
2. Allan LD et al. *Ultrasound Obstet Gynecol* 1991;1:8–11.
3. Copel JA et al. *A J Obstet Gynecol* 1988;158:409–13.
4. Ferencz C et al. *J Pediatr* 1989;114:79–86.
5. Nicolaides KH et al. *Lancet* 1992;340:704–7.
6. Ursell PC et al. *Circulation* 1985;72:1232–6.
7. Gerlis LM. *Int J Cardiol* 1985;7:29–46.
8. DeVore GR et al. *Obstet Gynecol* 1987;69:494–7.
9. Timor-Tritsch IE et al. *JCU* 1990;18:286–98.
10. Neiman HL. *Semin Ultrasound CT MR* 1990;11:22–33.
11. Bonnet D et al. *Circulation* 1999;99:916–8.
12. Jaeggi ET et al. *Ultrasound Obstet Gynecol* 2001;17:380–5.
13. Verheijen PM et al. *J Thorac Cardiovasc Surg* 2001;121:798–803.
14. Yagel S et al. *Circulation* 1997;96:550–5.
15. Todros T et al. *Int J Cardiol* 1988;19:355–62.
16. Allan LD. *Circulation* 1997;96:391–2.
17. Hornberger LK et al. *J Am Coll Cardiol* 1995;25:739–45.
18. Yagel S et al. *Am J Obstet Gynecol* 1995;172:971–5.
19. Moore KL, Persaud, TVN. eds. The cardiovascular system. In: *The Developing Human: Clinically Oriented Embryology*. 6th ed. Philadelphia, PA: WB Saunders; 1998:349–404.
20. Achiron R et al. *Ultrasound Obstet Gynecol* 1998;11:180–4.
21. Achiron R et al. *Ultrasound Obstet Gynecol* 2000;15:226–30.
22. Blaas HG et al. *Ultrasound Obstet Gynecol* 1995;6:240–9.
23. D'Amelio R et al. *Prenat Diagn* 1991;11:69–75.
24. Dolkart LA, Reimers FT. *A J Obstet Gynecol* 1991;165:688–91.
25. Firpo C et al. *Am J Cardiol* 2001;87:594–600.
26. Gembruch U et al. *Fetal Diagn Ther* 2000;15:20–31.
27. Rottem S, Chervenak FA. *Obstet Gynecol Clin North Am* 1990; 17:17–40.
28. Shapiro I et al. *Ultrasound Obstet Gynecol* 1998;12:404–18.
29. Smrcek JM et al. *J Ultrasound Med* 2006;25:173–82; quiz 83–5.
30. Timor-Tritsch IE et al. *Am J Obstet Gynecol* 1988;159:676–81.
31. Yagel S et al. *J Ultrasound Med* 2015;34:143–9.
32. Rossi AC, Prefumo F. *Obstet Gynecol* 2013;122:1160–7.
33. Syngelaki A et al. *Prenat Diagn* 2011;31:90–102.
34. Khalil A, Nicolaides KH. *Semin Fetal Neonatal Med* 2013;18: 251–60.
35. Ebrashy A et al. *Ultrasound Obstet Gynecol* 2010;35:292–6.
36. Timor-Tritsch IE et al. *Am J Obstet Gynecol* 2004;191:1247–52.
37. Becker R, Wegner RD. *Ultrasound Obstet Gynecol* 2006;27:613–8.
38. McAuliffe FM et al. *Am J Obstet Gynecol* 2005;193:1253–9.
39. Carvalho MH et al. *Prenat Diagn* 2002;22:1–4.
40. Haak MC et al. *Ultrasound Obstet Gynecol* 2002;20:9–13.
41. Simpsom JM et al. *BJOG* 2000;107:1492–7.
42. Comas Gabriel C et al. *Prenat Diagn* 2002;22:586–93.
43. Smrcek JM et al. *J Ultrasound Med* 2006;25:187–96.
44. Turan S et al. *Ultrasound Obstet Gynecol* 2014;44:562–7.
45. Iliescu D et al. *Ultrasound Obstet Gynecol* 2013;42:300–9.
46. Yagel S et al. *Ultrasound Obstet Gynecol* 2011;37:432–7.
47. Abu-Rustum RS et al. *J Ultrasound Med* 2011;30:695–700.
48. Achiron R et al. *J Ultrasound Med* 1994;13:783–9.
49. Weissman A, Achiron R. Ultrasound diagnosis of congenital anomalies in early pregnancy. In: Jauniaux Ja, Jurkovic, D, eds. *Progress in Obstetric and Gynecological Sonography Series*. CRC Press; 1995:95–120.
50. Kleinman CS et al. *Pediatrics* 1980;65:1059–67.
51. Allan LD et al. *BMJ* 1986;292:1717–9.
52. Copel JA et al. *Am J Obstet Gynecol* 1987;157:648–55.
53. Leopold GR. *J Ultrasound Med* 1986;5:241–2.
54. Achiron R et al. *BMJ* 1992;304:671–4.
55. Bromley B et al. *Am J Obstet Gynecol* 1992;166:1473–81.
56. International Society of Ultrasound in Obstetrics and Gynecology, Carvalho JS et al. *Ultrasound Obstet Gynecol* 2013;41:348–59.
57. American Institute of Ultrasound in M. *J Ultrasound Med* 2013;32:1067–82.
58. Yagel S et al. *Ultrasound Obstet Gynecol* 2002;20:340–5.
59. Yagel S et al. *Ultrasound Obstet Gynecol* 2001;17:367–9.
60. Donofrio MT et al. *Circulation* 2014;129:2183–242.
61. International Society of Ultrasound in Obstetrics and Gynecology. *Ultrasound Obstet Gynecol* 2006;27:107–13.
62. Lee W et al. *Ultrasound Obstet Gynecol* 2008;32:239–42.
63. Sharland G et al. *BCCA Fetal Cardiology Standards*. Revised. 2 ed. London, UK: British Congenital Cardiology Association; 2012.
64. Li Y et al. *PLOS ONE* 2013;8:e65484.
65. Zhang YF et al. *Medicine* 2015;94:e1759.
66. Yoo SJ et al. *Ultrasound Obstet Gynecol* 2001;18:248–52.
67. Di Salvo DN et al. *J Ultrasound Med* 1994;13:291–3.
68. Tegnander E et al. *Ultrasound Obstet Gynecol* 1994;4:24–8.
69. DeVore GR. *J Ultrasound Med* 1992;11:345–8.
70. Kirk JS et al. *Obstet Gynecol* 1994;84:427–31.
71. Ogge G et al. *Ultrasound Obstet Gynecol* 2006;28:779–84.
72. Barboza JM et al. *Radiographics* 2002;22:1125–37; discussion 37–8.
73. Achiron R et al. *Ultrasound Obstet Gynecol* 2002;20:553–7.
74. Berg C et al. *Ultraschall in der Medizin* 2009;30:230–51.
75. Berg C et al. *Ultraschall in der Medizin* 2009;30:128–44; quiz 45–9.
76. Carvalho JS et al. *Heart* 2002;88:387–91.
77. Stumpflen I et al. *Lancet* 1996;348:854–7.
78. Vinals F et al. *Ultrasound Obstet Gynecol* 2003;22:358–67.
79. Del Bianco A et al. *J Perinat Med* 2006;34:309–12.
80. Zalel Y et al. *Prenat Diagn* 2004;24:174–8.
81. Persico N et al. *Ultrasound Obstet Gynecol* 2011;37:296–301.
82. Sairam S, Carvalho JS. *Early Hum Dev* 2012;88:269–72.
83. Zalel Y et al. *Prenat Diagn* 2017;37:235–43.
84. Zidere V et al. *Ultrasound Obstet Gynecol* 2013;42:679–86.
85. Clur SA, Bilardo CM. *Prenat Diagn* 2014;34:1235–45.
86. Moon-Grady A et al. *J Am Soc Echocardiog* 2012;25:1342–52.
87. Shinebourne EA et al. *Br Heart J* 1976;38:327–40.

88. Carvalho JS et al. *Ultrasound Obstet Gynecol* 2005;26:105–11.
89. Van Praagh R. *Circulation* 1977;56:139–43.
90. Gembruch U et al. *Obstet Gynecol* 1990;75:496–8.
91. Bronshtein M et al. *Obstet Gynecol* 1993;82:225–9.
92. Bronshtein M et al. *Prenat Diagn* 1990;10:697–702.
93. Achiron R et al. *Obstet Gynecol* 1994;84:69–72.
94. Bronshtein M et al. *Obstet Gynecol* 1991;78:374–8.
95. Rustico MA et al. *Ultrasound Obstet Gynecol* 1995;5:202–5.
96. Huggon IC et al. *Ultrasound Obstet Gynecol* 2002;20:22–9.
97. Volpe P et al. *Prenat Diagn* 2011;31:1054–61.
98. Wiechec M et al. *J Ultrasound Med* 2015;34:585–94.
99. Yagel S et al. *Ultrasound Obstet Gynecol* 2007;29:81–95.
100. DeVore GR et al. *Ultrasound Obstet Gynecol* 2003;22: 380–7.
101. Goncalves LF et al. *Am J Obstet Gynecol* 2003;189:1792–802.
102. Goncalves LF et al. *Ultrasound Obstet Gynecol* 2006;27:336–48.
103. Paladini D et al. *Prenat Diagn* 2003;23:1052–5.
104. Yagel S et al. *Ultrasound Obstet Gynecol* 2006;28: 266–74.
105. Abuhamad A. *J Ultrasound Med* 2004;23:573–6.
106. DeVore GR et al. *Ultrasound Obstet Gynecol* 2004;24:72–82.
107. Espinoza J et al. *J Ultrasound Med* 2006; 25:947–56.
108. Goncalves LF et al. *J Ultrasound Med* 2005;24:415–24.
109. Sciaky-Tamir Y et al. *Am J Obstet Gynecol* 2006;194:274–81.
110. Michailidis GD et al. *Ultrasound Obstet Gynecol* 2001;18:325–8.
111. Vinals F et al. *Ultrasound Obstet Gynecol* 2005;25:25–31.
112. Achiron R et al. *Obstet Gynecol* 1991;78:330–4.
113. Baschat AA et al. *Ultrasound Obstet Gynecol* 1999;14:311–4.
114. Porat S et al. *Ultrasound Obstet Gynecol* 2003;21:302–5.
115. Sciarrone A et al. *Prenat Diagn* 2005;25:1129–32.
116. Lo YM et al. *Lancet* 1997;350:485–7.
117. Chiu RW et al. *BMJ* 2011;342:c7401.
118. Ehrich M et al. *Am J Obstet Gynecol* 2011;204:205 e1–11.
119. Palomaki GE et al. *Genet Med* 2011;13:913–20.
120. Dan S et al. *Prenat Diagn* 2012;32:1225–32.
121. Nicolaides KH et al. *Am J Obstet Gynecol* 2012;207:374 e1–6.
122. Norton ME et al. *Am J Obstet Gynecol* 2012;207:137 e1–8.
123. Sparks AB et al. *Am J Obstet Gynecol* 2012;206:319 e1–9.
124. Zimmermann B et al. *Prenat Diagn* 2012;32:1233–41.
125. Benn P et al. *Ultrasound Obstet Gynecol* 2013;42:15–33.
126. Bianchi DW et al. *N Engl J Med* 2014;370:799–808.
127. Yagel S et al. *J Ultrasound Med* 2015;34:363–9.
128. Cuckle H et al. *Prenat Diagn* 2013;33:636–42.
129. Gil MM et al. *Ultrasound Obstet Gynecol* 2013;42:34–40.
130. Nicolaides KH et al. *Fetal Diagn Ther* 2014;35:185–92.
131. Hyett JA et al. *Ultrasound Obstet Gynecol* 1997;10:242–6.
132. Hyett J et al. *BMJ* 1999;318:81–5.
133. Snijders RJ et al. *Lancet* 1998;352:343–6.
134. Haak MC et al. *Ultrasound Obstet Gynecol* 2002;20:14–21.
135. Makrydimas G et al. *Am J Obstet Gynecol* 2005;192:89–95.
136. Lopes LM et al. *Ultrasound Obstet Gynecol* 2003;22:470–8.
137. Borrell A et al. *Ultrasound Obstet Gynecol* 2013;42:51–7.
138. Zalel Y. *Ultrasound Obstet Gynecol* 2015;45:115–6.
139. Grande M et al. *Ultrasound Obstet Gynecol* 2012;39:157–63.
140. Souka AP et al. *Am J Obstet Gynecol* 2006;194:393–6.
141. Weisz B et al. *Reprod Biomed Online* 2005;10:541–53.
142. Allan LD et al. *Br Heart J* 1984;52:471–3.
143. Allan LD et al. *Int J Cardiol* 1989;25:341–3.
144. Marasini M et al. *JCU* 1993;21:65–8.
145. Rice MJ et al. *Am J Perinatol* 1993;10:424–7.
146. Achiron R et al. *Prenat Diagn* 1988;8:73–7.
147. Gembruch U et al. *Ultrasound Obstet Gynecol* 1993;3:310–7.

# 13

# Four-dimensional ultrasound examination of the fetal heart using spatiotemporal image correlation (STIC)

Luís F. Gonçalves

## Introduction

Prenatal evaluation of the fetal heart is one of the most challenging components of the obstetrical ultrasound examination. Sonographers must conduct a comprehensive examination, which includes a detailed assessment of the four-chamber view (Table 13.1),[1,2] the connections of the great vessels to the ventricular chambers, the venous return to the heart, and cardiac rhythm. Besides the limited amount of time that is usually available for a comprehensive ultrasound examination in clinical practice, other challenges that are of particular relevance to the examination of the fetal heart include the following, which may negatively impact image quality: (1) maternal obesity, abdominal scars, anterior placentas, and oligohydramnios; (2) frequent movement or breathing during the examination; (3) less than ideal fetal position that cannot be controlled by the operator; and (4) faster heart rates than adult and pediatric patients.[3–6] Thus, extensive training is required to develop the skills necessary to effectively examine the fetal heart. Operator skill is considered one of the most important factors affecting prenatal diagnosis of congenital heart disease.[7–12] Failure to diagnose a life-threatening cardiac disorder *in utero* may negatively impact survival, since there is evidence that prompt intervention after delivery is associated with improved outcomes for disorders such as transposition of the great arteries, hypoplastic left heart syndrome, and coarctation of the aorta.[13–17]

Four-dimensional ultrasonography (4DUS) with spatiotemporal image correlation (STIC) allows examiners to acquire volume datasets of the fetal heart using grayscale imaging only or with the addition of blood flow information from color Doppler, power Doppler, or B-flow imaging.[5,18–25] Once acquired, volume datasets can be examined using the standard planes of section of two-dimensional ultrasonography (2DUS), as well as novel planes that are only possible by volumetric imaging. These volume datasets can be thought of as "digital specimens" of the fetal heart, akin to actual heart specimens that are examined by pathologists during a necropsy. The "digital heart" can be oriented on the screen to be displayed in a standardized position, after which standard planes of section are obtained with the use of "digital scalpel" tools that allow visualization of one or more slices of the "digital heart." Moreover, sophisticated three-dimensional (3D) rendering techniques can be applied to display "digital casts" of cardiac chambers and great vessels that look similar to postmortem casts obtained by injecting silicone rubber into cardiovascular structures.[22,26–28] Advantages of the "digital specimen" when compared to the "actual specimen" include the following: (1) functional information is preserved since heartbeats are included in the volume dataset; (2) the direction of blood flow can be analyzed in volume datasets acquired with color or power Doppler; and (3) if the examiner accidentally makes a mistake during the review of the volume dataset, the "digital specimen" is not damaged forever, and all that it takes to begin the examination all over again is to reset it to its original state with the click of a button.

In this chapter, we review techniques that can be used to examine the fetal heart by 4DUS with STIC in normal fetuses as well as in those with congenital heart disease.

## Technology

The term 4DUS is used to describe volume datasets that incorporate information about the three spatial dimensions plus the temporal dimension.[29] 4DUS of the heart presents unique technical challenges, since the phases of the cardiac cycle must be not only included in the final volume dataset, but also synchronized with the acquired spatial information. This synchronization is termed *cardiac gating*. In adults and children, a cardiac gating signal is obtained by simultaneous recording of an electrocardiogram. Since electrocardiographic signals are difficult to obtain in the fetus, other gating methods have been proposed.[30–38] TIC is a gating algorithm based on the analysis of cardiac motion.[32,37] The fundamental fetal heart rate is directly extracted from the volume dataset (Figure 13.1).[5,18,19] Although retrospective, gating is quickly performed immediately after the volume scan, while the patient is still on the scanning table.[4] The end result is a volume dataset containing 3D plus temporal information that

**Table 13.1** Basic cardiac screening examination

**General**
- Normal cardiac situs, axis, and position
- Heart occupies a third of thoracic area
- Majority of heart in left chest
- Four cardiac chambers present
- No pericardial effusion or hypertrophy

**Atria**
- Atria approximately equal in size
- Foramen ovale flap in left atrium
- Atrial septum primum present

**Ventricles**
- Ventricles about equal in size
- No cardiac wall hypertrophy
- Moderator band at right ventricular apex
- Ventricular septum intact (apex to crux)

**Atrioventricular valves**
- Both atrioventricular valves open and move freely
- Tricuspid valve leaflet inserts on ventricular septum closer to the cardiac apex than to the mitral valve

*Source:* From Lee W. *J Ultrasound Med* 1998;17:601–7, with permission.[70] Erratum in *J Ultrasound Med* 1998;17:796.

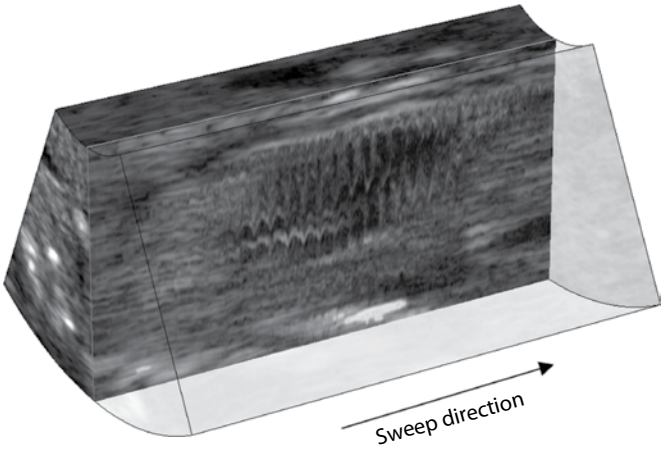


**Figure 13.1**
Raw data image used to calculate the fetal heart rate. This image is generated after the STIC acquisition is performed as a single, slow sweep. Information from this raw data is used to rearrange the 2D frames. This particular image is orthogonal to the original 2D frame. Because of the long acquisition time (7.5 to 15 seconds from the left to the right end of this image), the beating heart draws a motion pattern. This pattern is analyzed in terms of periodical changes of grayscale information, and the fetal heart rate is calculated. Beat-to-beat changes of the heart rate would appear as shortening or elongation of the above motion pattern. This image is not visible on the system during STIC acquisition but helps to understand the technique. (Figure 9 from Gonçalves LF et al. *Am J Obstet Gynecol* 2003;189(6):1792–802, with permission.[18])

allows the interactive display of cardiac structures in any plane of section as well as 3D reconstruction by rendering techniques.

## Volume acquisition

Volume acquisition is a crucial aspect of 4DUS with STIC. It may be performed using mechanical volumetric probes or matrix array electronic probes. Mechanical probes are more widely available and perform very well with STIC technology (Figure 13.2). Matrix array probes are fully electronic transducers that are capable of imaging the fetal heart using both STIC and real-time volumetric imaging (Figure 13.3).[39,40] Volumes are obtained faster with matrix array probes, and this minimizes motion artifacts; however, given the more sophisticated technology incorporated into these probes, they tend to be more expensive than their mechanical counterparts, at least at the time of this writing. Regardless of the type of probe used, the final quality of the volume dataset is heavily dependent on the adjustment of 2D grayscale and

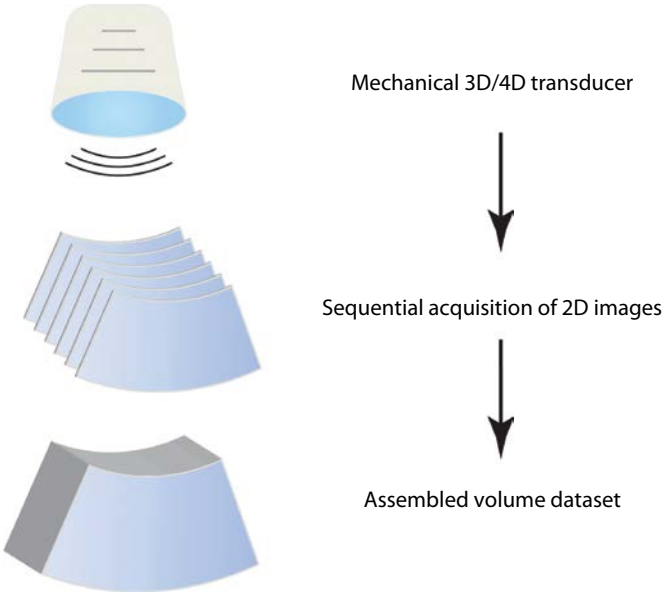


**Figure 13.2**
Scanners equipped with mechanical 3D transducers such as the ones used in the current study generate 3D volume datasets by automatically acquiring a sequence of 2D images through a region of interest selected by the examiner. The images are reassembled into a final volume dataset that can be explored using postprocessing tools. The examiner can re-slice the volume in virtually any plane, either to obtain rendered 3D images, or to perform volumetric measurements. Most mechanical 3D transducers are also capable of four-dimensional ultrasound (4DUS) imaging, whereby multiple volume datasets are continuously acquired and quickly updated on the screen. With this technology, motion (temporal dimension) is added to the three spatial dimensions, allowing real-time visualization of 3D images. The primary limitation of 4DUS is that spatial resolution is often sacrificed at the expense of temporal resolution. (Reproduced with permission from Goncalves LF et al. *Pediatr Radiol* 2011;41:1047–56.[71])

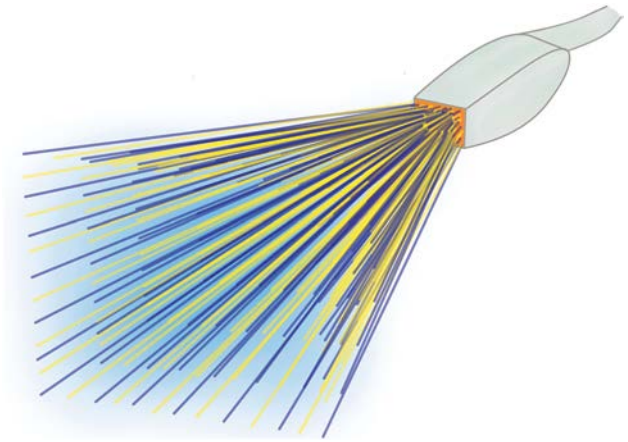

**Figure 13.3**
Matrix array probes are electronic 3D probes with thousands of transducer elements arranged as a 2D matrix on the probe surface. The probe is able to insonate a full volume of tissue at once to produce real-time 4D images. In addition, it is possible to fire each row of the matrix array in sequence as a very fast sweep to produce 3D or 4D volumes in a manner similar to that of a mechanical probe, only much faster.

color Doppler parameters.[41] Fetal echocardiography presets characterized by low persistence, high contrast, and high frame rate are favored. Magnification should be performed prior to acquisition. Harmonic imaging may improve image quality in selected cases (e.g., obese patients).[42,43]

Once the 2D image is optimized, a region of interest is selected on the screen, and volume acquisition is performed with a single automated sweep of the transducer. Depending on the manufacturer and probe used, volume acquisition may take from 5 to 15 seconds. The STIC technology detects the fundamental heart rate based on the rhythmic pattern of changes in cardiac diameter and uses this information for gating. Frames acquired during the same phase of the cardiac cycle, although from a different position in space, are merged into the same volume dataset. This process is repeated for all phases of the cardiac cycle. After image rearrangement, an ordered sequence of volume datasets is displayed on the screen as a continuous cine loop containing all phases of the cardiac cycle, and the data are ready for examination.[5,18] This can be performed either at the time of patient examination or offline, and the volumes can be saved on a hard drive for later review or transmission to a remote diagnosis center.[19,37,44]

# *Tips to optimize volume acquisition*

## Original plane of acquisition

Volume acquisition using transverse sweeps across the fetal thorax are preferred when the examiner is interested in the evaluation of the four-chamber view, five-chamber view, outflow tracts, three-vessel view, and three-vessel with trachea view.[41] Conversely, if the examiner is mainly interested in obtaining images of the aortic and ductal arches, high-quality volume datasets are acquired with sagittal sweeps through the fetal thorax.

## Fetal position

The ideal fetal position to examine the fetal heart is with the fetus lying on its back (i.e., with the spine oriented at approximately the 6 o'clock position on the screen). Since this is not always possible, volume datasets of sufficient quality may also be obtained when the spine is up, provided that it is not positioned between 11 and 1 o'clock. Under these circumstances, acoustic shadowing from the spine and ribs frequently compromises fetal heart imaging.

## Selecting a region of interest

The region of interest (ROI) determines the width and height of the volume dataset ($x$- and $y$-planes). When an examiner begins to use 4DUS with STIC, the tendency is to select a large ROI, including not only the heart, but also the surrounding anatomical structures such as the lungs, ribs, and amniotic fluid. The reader is reminded that the selection of wide ROIs is associated with lower than expected frame rates during acquisition, and this may negatively impact the temporal resolution of the final volume dataset. This is particularly important during color or power Doppler acquisitions, since both technologies negatively affect the frame rate. Thus, ROIs should be set as narrow as possible and include only the information that the examiner is interested in. This practice maximizes the frame rate during acquisition and, therefore, the final temporal resolution of the volume dataset.

## Setting the acquisition angle

The acquisition angle determines the amount of information acquired in the "$z$" or azimuth plane. For acquisitions performed in the transverse plane (e.g., the four-chamber view plane), images from the upper mediastinum all the way down to the upper abdomen should be ideally included in the volume dataset.[19] This practice ensures that all standard planes of section, including the three-vessel and trachea view, superiorly, and the transverse section of the fetal abdomen containing the stomach, aorta, and inferior vena cava (IVC), inferiorly, will be available for the examination. For second trimester fetuses, acquisition angles between 25° and 30° should suffice. Adjustments may be necessary when examining smaller or larger fetuses.

## Setting the acquisition time

Acquisition time determines the speed that is used by the transducer to sweep through the ROI. Depending on equipment manufacturer, acquisition time ranges from 5 to 15 seconds. Ideally, volume datasets should be acquired using the longest acquisition time possible to improve spatial resolution. Unfortunately, in the presence of intense fetal movements or breathing, examiners may be forced to select a shorter acquisition time to minimize motion artifacts. This results in a volume dataset with lower spatial resolution. In practice, we preset the equipment to sweep for 10 or 12.5 seconds and adjust the acquisition time according to the presence or absence of active fetal movement or breathing. Mothers may also move during acquisition, and abdominal breathing by the mother may cause motion artifacts. Therefore, we have found it useful to ask mothers to

momentarily withhold moving or breathing during acquisition. This applies mainly to mechanical transducers, since, as noted before, volume acquisition using modern matrix array transducers can be performed much faster or even in real time.

# Examination of the fetal heart with STIC

## *Image optimization*

Once the volume dataset has been acquired and is displayed on the screen, the image may be further optimized by adjusting brightness and contrast, as well as color filters (e.g., sepia) that may improve tissue contrast resolution.

## *Scrolling through the volume dataset*

The most basic approach to examine a volume dataset of the fetal heart acquired with STIC is to scroll through the volume dataset from top to bottom along the original plane of acquisition. For volumes acquired using transverse sweeps through the fetal chest, this approach allows examiners to visualize the transverse planes of section proposed by Yoo et al.[45] and Yagel et al.[46] (1) transverse view of the upper abdomen; (2) four-chamber view; (3) five-chamber view; (4) three-vessel view; and (5) three-vessel view and trachea view (Figure 13.4).

Viñals et al.[19] evaluated this approach in 100 volume datasets acquired by sonologists with little experience in the examination of the fetal heart. A specialist in fetal echocardiography, who was not involved in volume acquisition, examined the volume

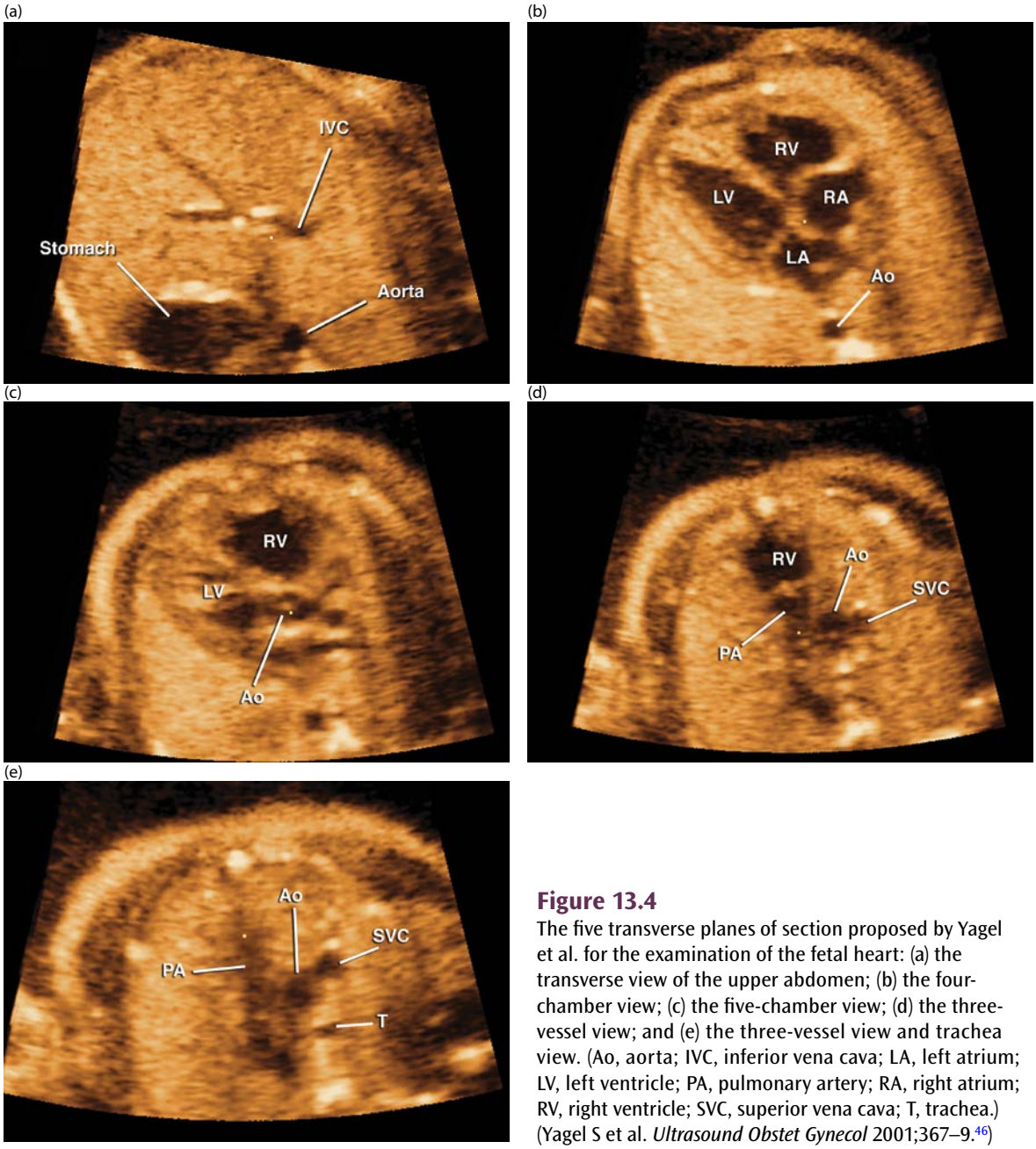


**Figure 13.4**
The five transverse planes of section proposed by Yagel et al. for the examination of the fetal heart: (a) the transverse view of the upper abdomen; (b) the four-chamber view; (c) the five-chamber view; (d) the three-vessel view; and (e) the three-vessel view and trachea view. (Ao, aorta; IVC, inferior vena cava; LA, left atrium; LV, left ventricle; PA, pulmonary artery; RA, right atrium; RV, right ventricle; SVC, superior vena cava; T, trachea.) (Yagel S et al. *Ultrasound Obstet Gynecol* 2001;367–9.[46])

datasets. Visualization rates for the four-chamber view, the left and right ventricular outflow tracts, the three-vessel view, and the three-vessel and trachea view ranged from 81% to 100%. The lowest visualization rates were observed for structures located either at the upper abdomen or upper mediastinum. This occurred because acquisition angles were not properly set, that is, the sweep angle was not wide enough to include information from the upper mediastinum through the upper abdomen in some cases. This methodology has also been used for remote diagnosis of congenital heart disease (TELESTIC).[44,47]

## Automated multiplanar slicing

Several ultrasound manufacturers now provide software to automatically slice 3D and 4D volume datasets (Multislice View, Accuvix, Medison, Seoul, Korea; Tomographic Ultrasound Imaging, GE Healthcare, Milwaukee, Wisconsin; iSlice, Philips Medical Systems, Bothell, Washington; Multi-Slice View, Siemens Medical Solutions, Malvern, Pennsylvania). This technology allows an examiner to automatically obtain a series of tomographic parallel images on a single screen, akin to display methods commonly used in computerized tomography and magnetic resonance imaging.[47] With STIC, since motion information is preserved, multiple slices of the beating heart can be visualized and examined at the same time.[48,49] The user can adjust the number and position of slices with specific software controls until the desired planes of section can be visualized in the same image.[48,50] Hue, brightness, and contrast can also be adjusted to optimize image quality. This approach represents an alternative to manually scrolling through the volume datasets to obtain standard cardiac views and may decrease the time spent in the evaluation of cardiac anatomy during screening and consultative examinations by allowing examiners to simultaneously view the spatial relationships of the transverse views described by Yoo et al.[45] and Yagel et al.[46] (Figures 13.5 and 13.6).[48]

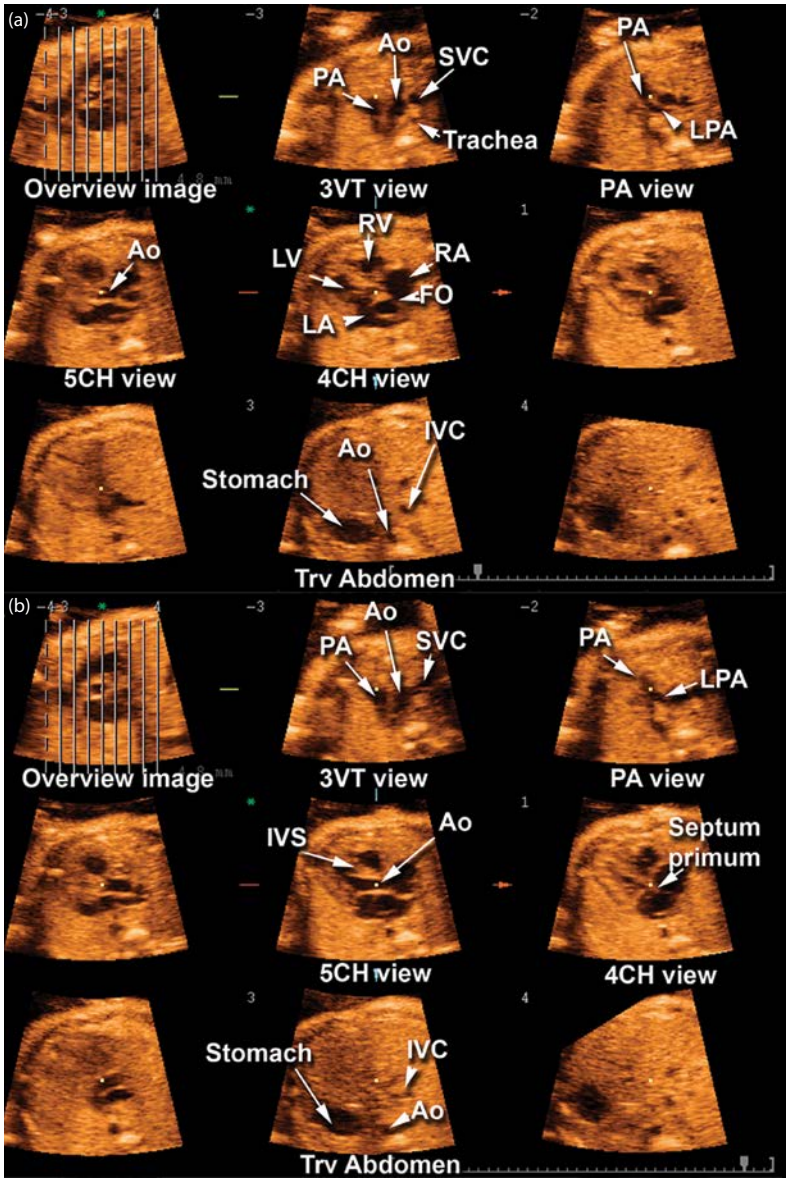


**Figure 13.5**
Tomographic ultrasound imaging (TUI) of a normal fetal heart in systole (a) and diastole (b). The overview image on the left upper panel of each figure shows the orthogonal sagittal plane to the sections that are being displayed. Each line represents a slice. The center slice is marked with an asterisk (*), and each subsequent plane to the right or left is marked with numbers ranging from −4 to +4. The plane marked by the dotted line is not displayed. In this volume dataset, the five transverse planes of section proposed by Yagel et al.[46] for the examination of the fetal heart are visualized. Please note that the five-chamber view was better visualized during systole. (Ao, aorta; FO, foramen ovale; IVC, inferior vena cava; IVS, interventricular septum; LA, left atrium; LPA, left pulmonary artery; LV, left ventricle; PA, pulmonary artery; RA, right atrium; RV, right ventricle; SVC, superior vena cava; 4CH, four-chamber; 5CH, five-chamber.) (From Gonçalves LF et al. *J Perinat Med* 2006;34(1):39–55, with permission.[49])

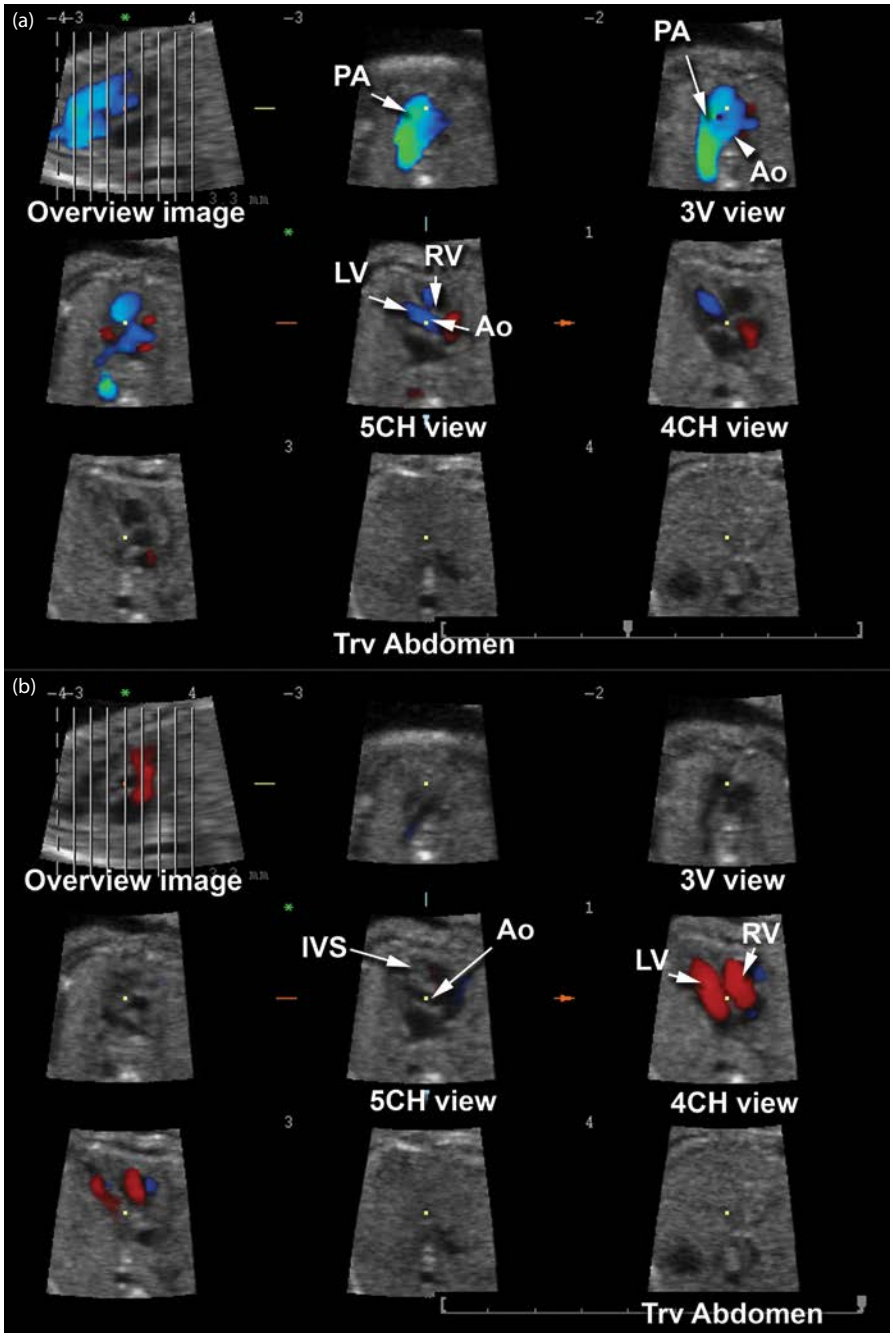


**Figure 13.6**
Tomographic ultrasound imaging (TUI) of a normal fetal heart in systole (a) and diastole (b). The volume datasets were acquired using B-mode and color Doppler imaging. The overview image on the left upper panel of each figure shows the orthogonal sagittal plane to the sections that are being displayed. Each line represents a slice. The center slice is marked with an asterisk (*) and each subsequent plane to the right or left are marked with numbers ranging from −4 to +4. The plane marked by the dotted line is not displayed. In this volume dataset, the three planes of section proposed by Chaoui et al.[72] for the examination of the fetal heart are visualized. (Ao, aorta; IVS, interventricular septum; LV, left ventricle; PA, pulmonary artery; RV, right ventricle; 4CH, four-chamber; 5CH, five-chamber.) (From Gonçalves LF et al. *J Perinat Med* 2006;34(1):39–55, with permission.[49])

Previous studies have demonstrated that the five basic axial planes of section for the examination of the fetal heart can be automatically obtained in the majority of patients.[48–50] Manual adjustment of the interslice distance when all views are not obtained by automatically slicing the volume dataset with the equipment presets improves the visualization rates of the transverse planes of section proposed by Yoo et al.[45] and Yagel et al.[46] The optimal interslice distance to automatically slice the volume dataset and simultaneously visualize these planes of section changes with gestational age (Table 13.2). In addition, the visualization rate for the five-chamber view improves by approximately 14% over what is possible by gray-scale imaging alone for volumes acquired with color Doppler imaging.[49]

## *Systematic approach for visualization of the great vessels*

There are now several approaches to systematically demonstrate the great vessels in volume datasets acquired with STIC.[18,23,51–53] In 2003, we proposed and subsequently validated a technique designed to simultaneously display the long-axis view of the left ventricular outflow tract and the short-axis view of the right ventricular outflow tract on panels A and B of the multiplanar display.[18,23] The technique was developed for volume datasets acquired by sweeping the fetal thorax on the transverse plane of section using the four-chamber view as the starting point and is illustrated in detail in Figure 13.7.

**Table 13.2** Interslice distance according to gestational age

| *Gestational age (weeks)* | *n* | *Minimum (mm)* | *Maximum (mm)* | *Mean (mm)* | *SD (mm)* |
|---|---|---|---|---|---|
| 12–15 | 11 | 0.7 | 1.4 | 1.14 | 0.26 |
| 16–19 | 10 | 1.4 | 2.6 | 1.78 | 0.34 |
| 20–24 | 44 | 2.2 | 3.4 | 2.82 | 0.27 |
| 25–29 | 15 | 2.2 | 4.6 | 3.63 | 0.65 |
| 30–34 | 17 | 3.4 | 5.3 | 4.37 | 0.56 |
| 35–40 | 6 | 4.3 | 5.3 | 4.75 | 0.37 |

*Source:* From Paladini D et al. *Ultrasound Obstet Gynecol* 2006;27(5):555–61, with permission.[50]

*Abbreviation:* SD, standard deviation.

More recently, Espinoza et al.[53] developed an enhanced algorithm combining tomographic ultrasound imaging and standardized manipulations of the volume dataset to simultaneously display the three-vessel and trachea view, the four-chamber view, and both outflow tracts on the same screen. The algorithm was developed to overcome a limitation of automatic slicing using tomographic ultrasound imaging alone, which is that the simple use of parallel planes to the four-chamber view of the heart does not allow for visualization of the long-axis view of the left outflow tract and the short-axis view of the aorta, which are considered part of an integral examination of the fetal heart. Details of the algorithm are described in Figure 13.8a–f. In a study that included 227 volume datasets of fetuses with ($n = 14$) and without ($n = 138$) congenital heart disease, simultaneous visualization of the short axis of the aorta, three-vessel and trachea view, left outflow tract, and four-chamber view was achieved in 78% (152/195) of the volume datasets from fetuses without and 40% (8/20) of those with congenital heart disease. The lower visualization rates of standard planes of section in cases of congenital heart disease may reflect abnormal spatial relationships between cardiovascular structures and may prove helpful in the identification of specific patterns of congenital heart disease in the future.

## Visualization of the aortic and ductal arches

Ideal visualization of the aortic and ductal arches requires that the volume dataset be acquired with sagittal sweeps through the fetal chest. The original technique describing how to systematically visualize the aortic and ductal arches was originally published by Bega et al.[54] in 2001 and is illustrated in Figure 13.9.

## Spin technique

DeVore et al.[20] proposed in 2004 a technique to display the ascending aorta and transverse aortic arch, the main pulmonary artery and bifurcation of the right and left pulmonary arteries, the ductus arteriosus and superior vena cava. The technique is simple and can be applied to any structure of interest during the examination of volume datasets of the fetal heart, simply by positioning the reference dot in the center of the structure and "spinning" the volume dataset around the *y*-axis until the structure is "opened up" and visualized in its entirety. Figure 13.10 illustrates the application of the spin technique to identify an abnormal vessel visualized in the three-vessel and trachea view as a persistent left superior vena cava draining into a dilated coronary sinus.

## FAST technique

The FAST technique (four-chamber view and swing technique) uses a technology called OmniView (4DView, GE Healthcare, Waukesha, Wisconsin) to visualize the following planes of the fetal heart in a single image: longitudinal view of the ductal ach, three-vessels and trachea view, five-chamber view, and four-chamber view (Figure 13.11). The long-axis view of the aorta is obtained by one additional rotation of the volume around the *y*-axis (Figure 13.12). In an initial study of 50 normal fetuses, all planes could be seen simultaneously 98% of the time.[55]

## STAR technique

The STAR technique (simple targeted arterial rendering) also uses OmniView technology (4DView, GE Healthcare, Waukesha, Wisconsin) to simultaneously visualize the fetal cardiac outflow tracts and ventricular septum from an original volume containing the four-chamber view. The method is illustrated in Figure 13.13.

## Automatic extraction of fetal echocardiographic planes from volume datasets

The latest approach to obtaining standard planes of section by manipulation of the volume dataset has been referred to as "automated sonography."[1,2] According to this concept, the standard planes of section for examination of the fetal heart can be automatically displayed by the equipment once the

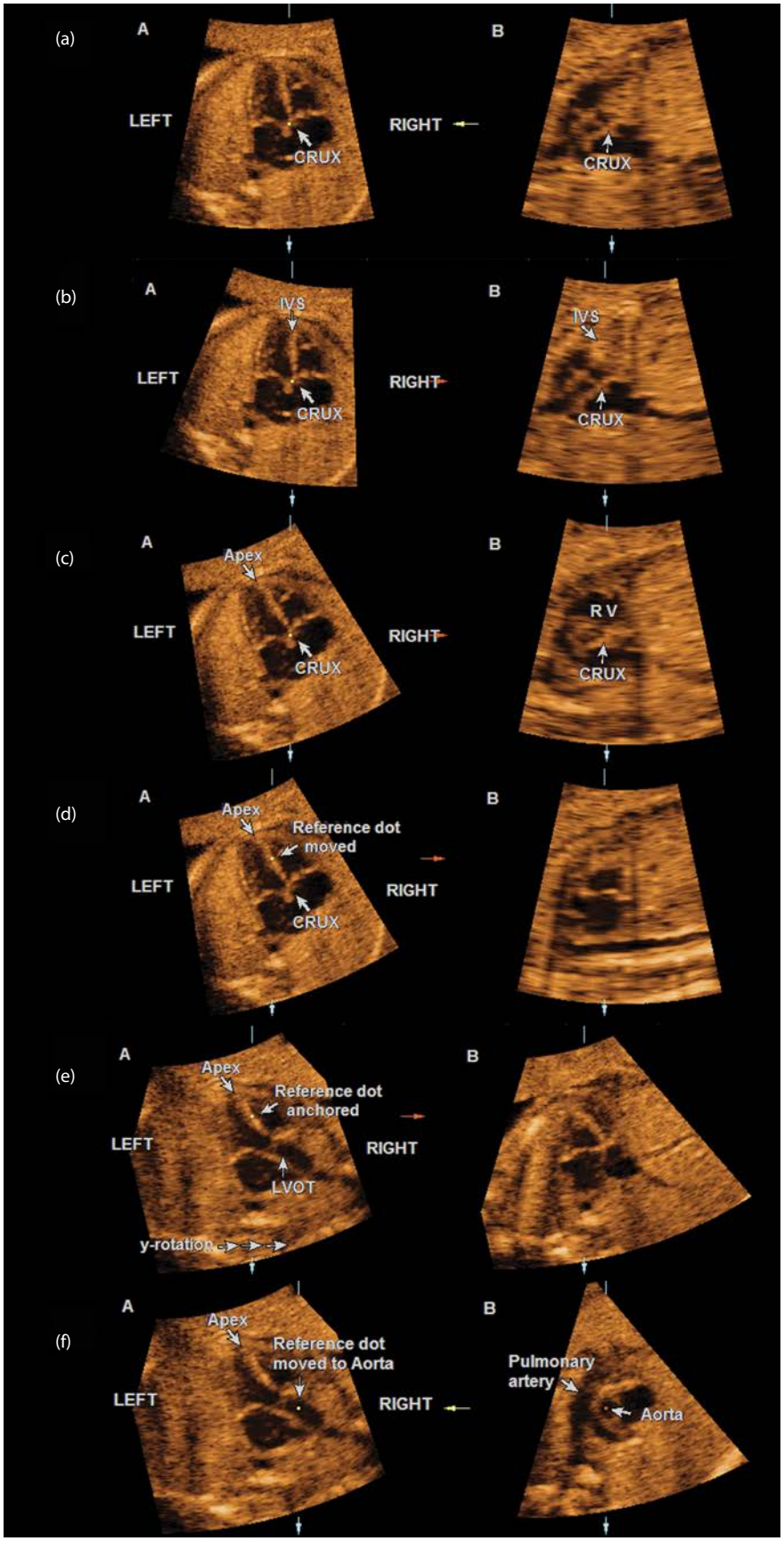


**Figure 13.7**
Technique to systematically visualize the left and right outflow tracts in volume datasets acquired with spatiotemporal image correlation (STIC). Only panels A (original plane of acquisition, transverse) and B (sagittal plane) are displayed. (a) The first step in this technique consists of making sure that the left side of the heart is located on the left side of the image, and the right side of the heart is on the right side of the image; if necessary, rotate the volume around the *y*-axis until this is achieved. The reference dot is then positioned in the crux of the heart, on both the transverse and the sagittal planes. (b) The volume dataset is rotated around the *z*-axis until a perfect apical four-chamber view is obtained. (c) The volume is then rotated around the *z*-axis counterclockwise until the angle between the apex and the transducer is approximately 30°–40°. (d) The crucial step is to position the reference dot in the interventricular septum, midway between the crux of the heart and the apex; this will anchor the three orthogonal planes for the next rotation movement, which will display the left ventricular outflow tract. (e) The volume dataset is now rotated around the *y*-axis; this will open up the continuity between the interventricular septum and the anterior wall of the aorta; the anterior leaflet of the mitral valve is seen in continuity with the posterior wall of the aorta. (f) Once the reference dot is moved above the aortic valve, the short-axis view of the right ventricular outflow tract is displayed on the sagittal plane. (IVS, interventricular septum; LVOT, left ventricular outflow tract; RV, right ventricle.) (From Gonçalves LF et al. *Ultrasound Obstet Gynecol* 2006;27(3):336–48, with permission.[41])

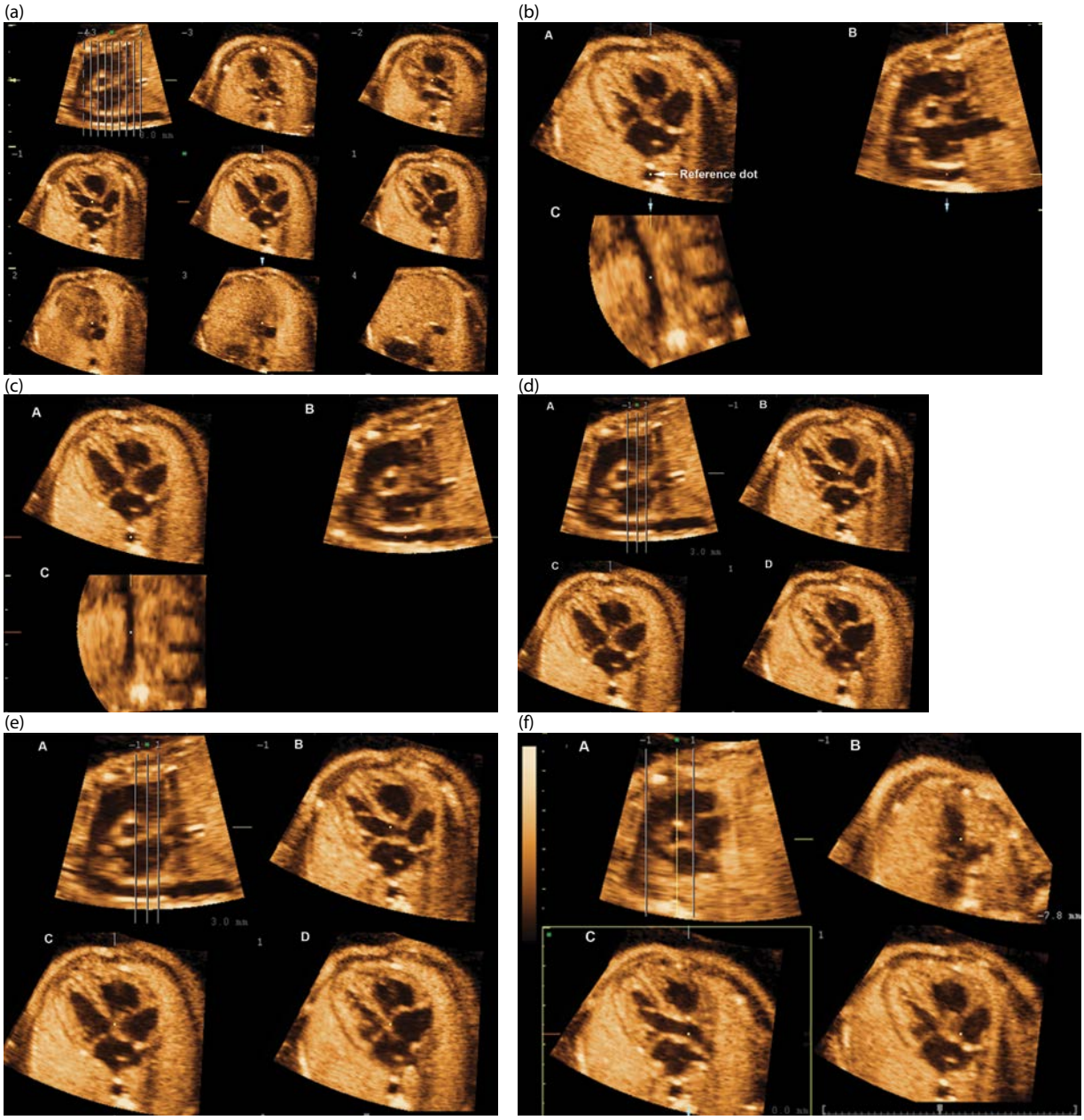


**Figure 13.8**
(a) An "overview image" is shown on the upper left corner. The parallel lines determine the position of the eight orthogonal planes to the plane containing the "overview image." (b) The orthogonal planes were reduced to three. Volume datasets were adjusted to display the four-chamber view in panel A, where the fetal aorta was aligned with the crux of the heart in the vertical plane. The reference dot was positioned in the aorta allowing the visualization of the coronal view of the descending aorta in panel C. (c) In panel C the image was rotated to display the aorta in a vertical position, when necessary. This allowed for the visualization of the longitudinal view of the ductal arch in panel B. (d) Only three planes were selected, using the "Slices" option, including the plane that crosses the reference dot (which is labeled with an asterisk in the software), one plane to the left ("−1"), and one to the right ("+1") to the plane crossing the reference dot. These images were magnified using the four panel "Display format." (e) In panel A, the image was moved until the reference dot was positioned in the center of the aorta. The "Adjust" option was selected to align the "−1" plane with the ductal arch and the "+1" plane with the external edge of the aorta. This allowed for the simultaneous visualization of the ductal arch in panel A, the three-vessel and trachea view in panel B, the five-chamber view in panel C, and the four-chamber view in panel D. (f) The "Rotation Y" was selected by clicking on the bar, and the five-chamber view was rotated by scrolling on the *y*-axis until the left outflow tract was visualized in panel B. This allowed for the simultaneous visualization of the short axis of the aorta in panel A, the three vessel and trachea view in panel B, the long axis of the left outflow tract on panel C, and the four-chamber view on panel D. (From Espinoza J et al. *J Ultrasound Med* 2006;25(8):947–56, with permission.[53])

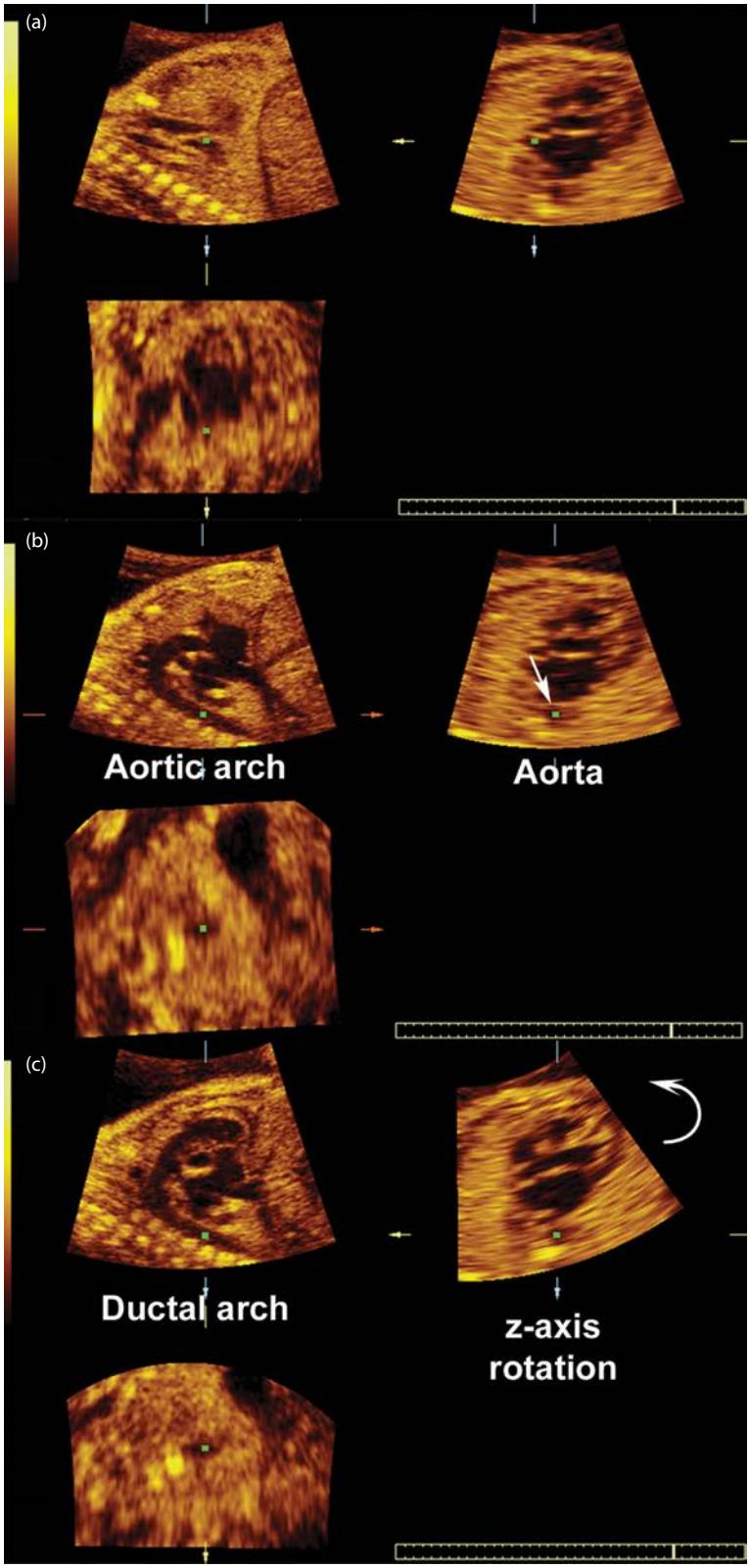


**Figure 13.9**
3D multiplanar slicing of the aortic and ductal arches. (a) 3D multiplanar image of the fetal thorax in the original acquisition plane (sagittal). (b) The reference dot was manipulated in the right upper panel and moved to the center of the aorta (white arrow). The resulting image in the left upper panel was a sagittal view of the aorta. Minor adjustment of this image around the *y*-axis was required to demonstrate the aortic arch. (c) To demonstrate the ductal arch, the right upper panel image was simply rotated counterclockwise around the *z*-axis (curved arrow). (Figure 3 from Gonçalves LF et al. *Am J Obstet Gynecol* 2003;189(6):1792–802, with permission.[18])

four-chamber view is selected as the reference plane. The spatial relationships of the standard planes of section to the four-chamber view[1,2] as well as the geometric changes that the fetal heart undergoes as gestational age progresses[28] have been studied as a preliminary step for the development of such algorithms. In the first study validating the concept, Abuhamad et al.[56] obtained 3D static volumes of the fetal chest in 72 fetuses between 18 and 23 weeks of gestation. The left ventricular outflow tract, right ventricular outflow tract, and abdominal circumference plane were automatically extracted by software in 94.4%, 91.7%, and 97.2% of volumes, respectively.

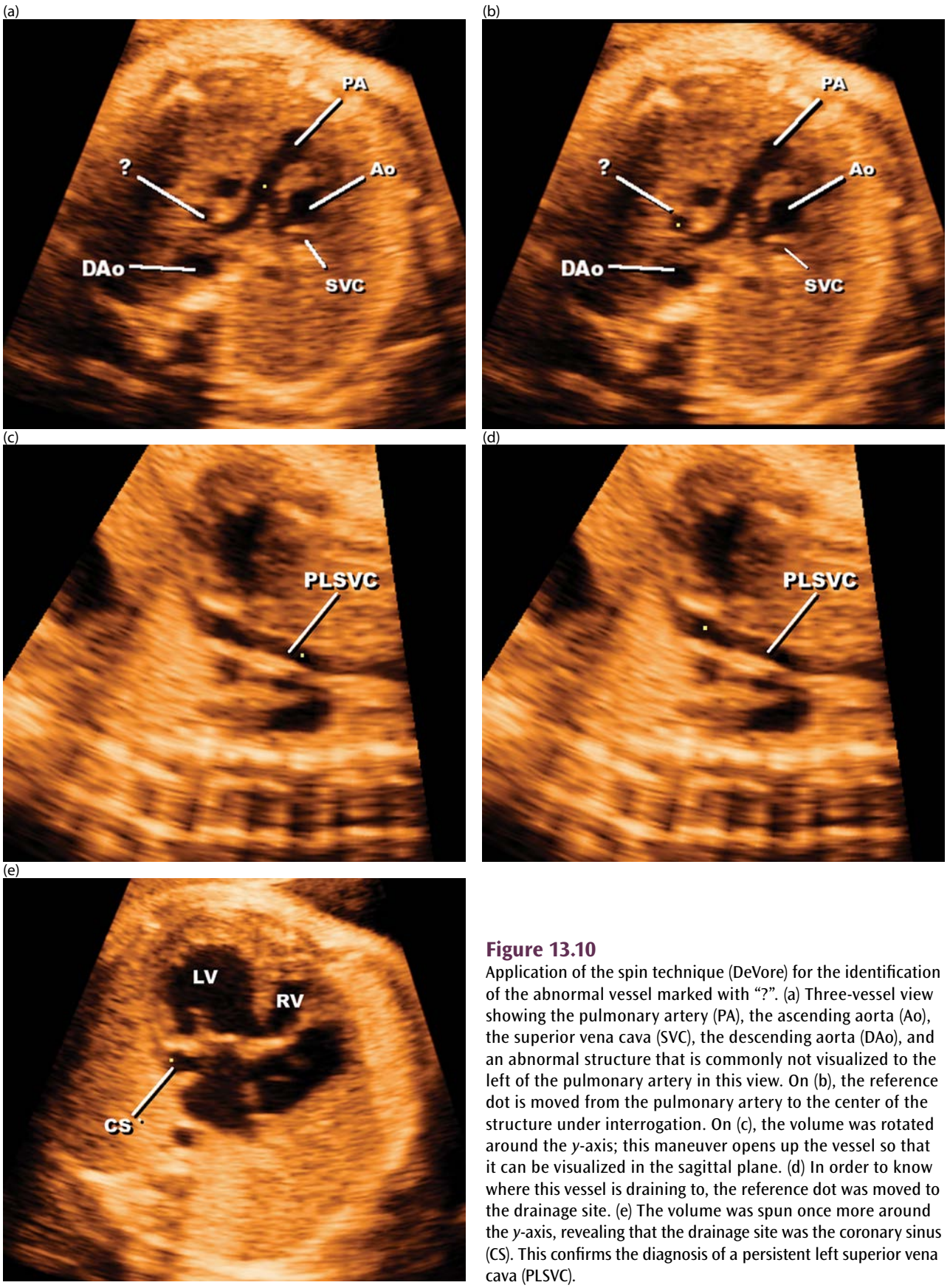


**Figure 13.10**
Application of the spin technique (DeVore) for the identification of the abnormal vessel marked with "?". (a) Three-vessel view showing the pulmonary artery (PA), the ascending aorta (Ao), the superior vena cava (SVC), the descending aorta (DAo), and an abnormal structure that is commonly not visualized to the left of the pulmonary artery in this view. On (b), the reference dot is moved from the pulmonary artery to the center of the structure under interrogation. On (c), the volume was rotated around the *y*-axis; this maneuver opens up the vessel so that it can be visualized in the sagittal plane. (d) In order to know where this vessel is draining to, the reference dot was moved to the drainage site. (e) The volume was spun once more around the *y*-axis, revealing that the drainage site was the coronary sinus (CS). This confirms the diagnosis of a persistent left superior vena cava (PLSVC).

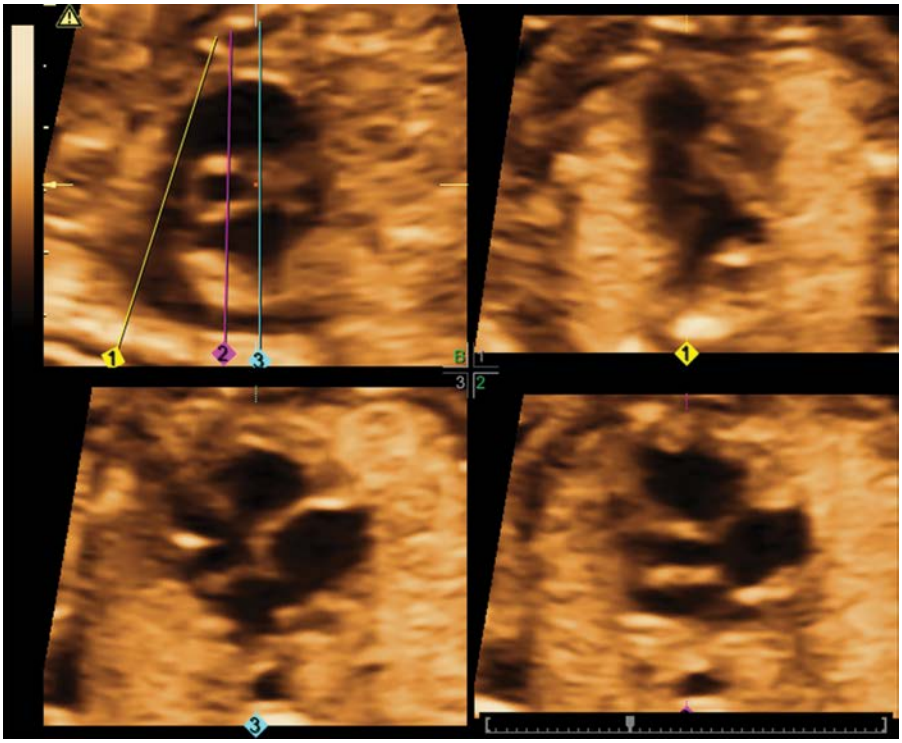

**Figure 13.11**
Image obtained using OmniView technology on 4DView software (GE Healthcare, Waukesha, Wisconsin), simultaneously showing the ductal arch (B), three-vessels and trachea view (1), five-chamber view (2), and four-chamber view (3). The planes are obtained by manually drawing the lines through the ductal arch (yellow), aortic root (magenta), and base of the heart (blue) on the sagittal view of the ductal arch seen on panel B.

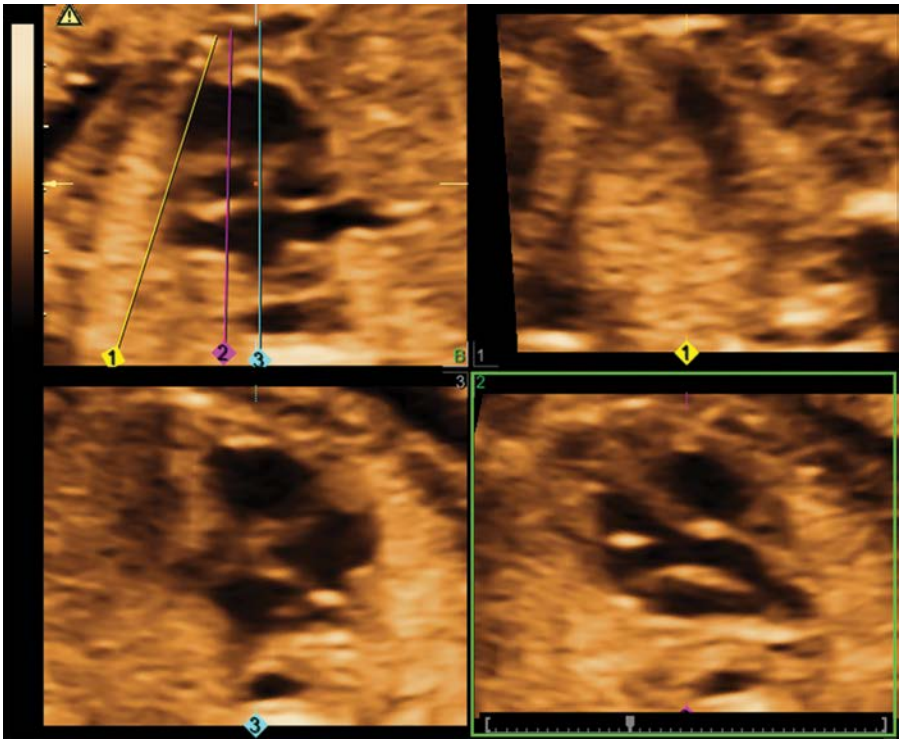

**Figure 13.12**
The left outflow tract (panel 2, highlighted in green) is seen after rotating the volume around the *y*-axis from the original position seen in Figure 13.9.

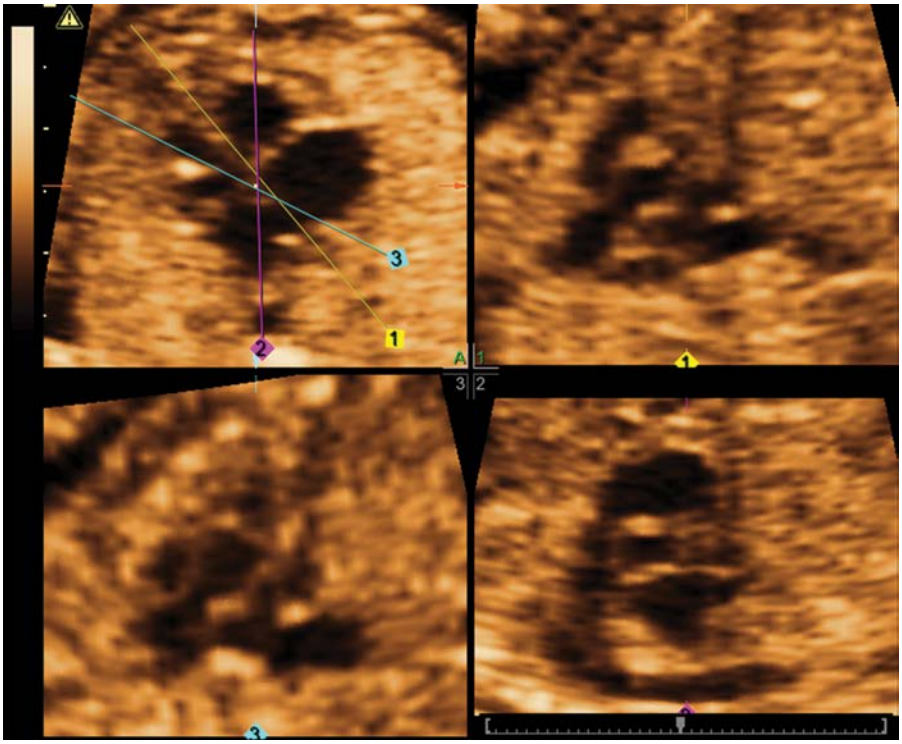


**Figure 13.13**
STAR (simple targeted arterial rendering) technique to extract a sagittal view of the ventricular septum (yellow line, panel 1), ductal arch view (magenta line, panel 2), and left ventricular outflow tract (blue line, panel 3) from a four-chamber view (panel A).

More recently, a method called FINE (fetal intelligent navigation echocardiography) has been developed to demonstrate nine diagnostic echocardiographic planes (four-chamber view, five-chamber view, left ventricular outflow tract, short-axis view of the great vessels/right ventricular outflow tract, three vessels and trachea view, abdomen/stomach, ductal arch, aortic arch, and superior and inferior vena cava).[57] The method is based on the identification of seven anatomical structures seen on axial views of the fetal chest: (1) a cross section of the aorta at the level of the stomach, (2) a cross section of the aorta at the level of the four-chamber view, (3) the crux of the heart, (4) the right atrial wall, (5) the pulmonary valve, (6) a cross section of the superior vena cava, and (7) the transverse aortic arch. In the initial study including 50 volume datasets, the success rate to obtain the nine diagnostic echocardiographic planes as described ranged from 78% for the ductal arch view to 100% for the abdomen/stomach view. Using an additional tool named Virtual Intelligent Sonographer Assistance (VIS-Assistance), which automatically performs additional sonographic navigation on each of the nine planes using specific pivot points and sequential movements optimized for each plane, the visualization rates improved to 98% for the three vessels and trachea view and 100% for the remaining planes. This technology has been subsequently validated in two larger prospective studies. The first was a study of STIC volumes obtained from 207 women undergoing an ultrasound examination. Diagnostic quality STIC volumes could be obtained from 72.5% (150/270) of the patients, and nine diagnostic planes were visualized by a combination of FINE and/or VIS-Assistance in 98%–100% of the cases.[58] In the second study, which included 246 patients, nine diagnostic planes were obtained through a combination of FINE and/or VIS-Assistance in 96%–100% of the cases.[59]

## *Rendering techniques for visualization of intracardiac structures and valves*

Rendering techniques can be applied to the visualization of intracardiac structures to obtain a depth perspective of the area under examination. Rendering techniques can also be used to optimize contrast of myocardial borders, septa, and valves, or to obtain realistic 4D images of particular structures of interest.

In Figure 13.14, "thick-slice" rendering was applied to the atrioventricular valves to visualize the leaflets *en face*, as if the examiner was observing them from the ventricular chambers.[9,36] This view can also be obtained by selecting the direction of rendering from the atrial chambers. Yagel et al.[60] were able to consistently obtain this rendered view in 93% of 136 normal fetuses examined between 21 and 26 weeks of gestational age. In 5 of 35 abnormal cases examined in their study, this rendered view provided additional diagnostic

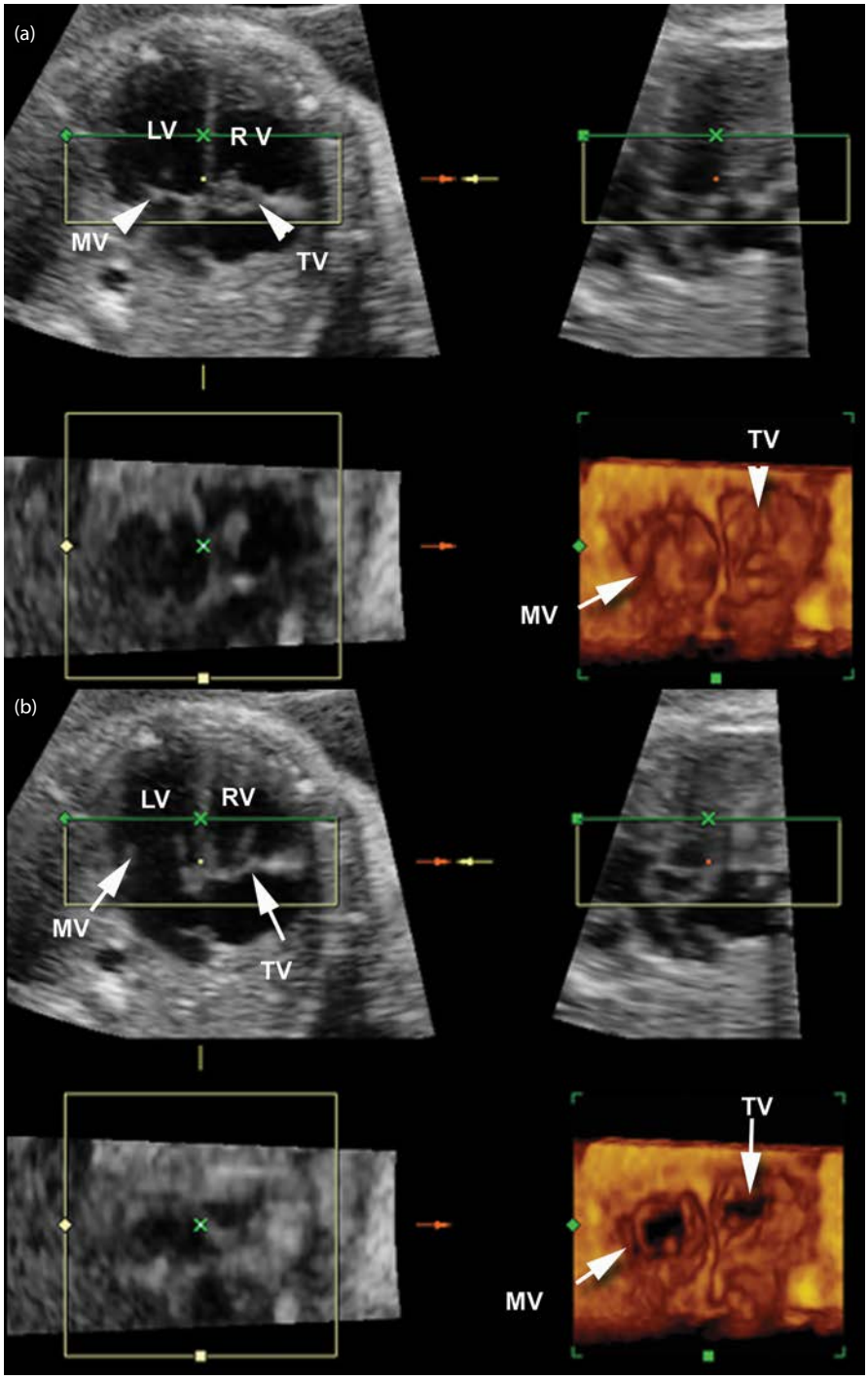


**Figure 13.14**
"Thick-slice" rendering of the atrioventricular valves of a normal fetus in systole (panel a) and diastole (panel b). The key to obtaining the rendered image (right lower corner) is the position and size of the region of interest (ROI), encompassing only the atrioventricular valves. The green line indicates the direction of view, which is the direction that the computer software will use to convert the voxels along the projection path to pixel information to be displayed on the two-dimensional screen. In this case, the position of the green line indicates that the atrioventricular valves are being visualized from the ventricular chambers. This volume dataset was rendered using a combination (mix) of 60% gradient light and 40% surface mode. (LV, left ventricle; MV, mitral valve; RV, right ventricle; TV, tricuspid valve.) (From Gonçalves LF et al. *Ultrasound Obstet Gynecol* 2006;27(3):336–48, with permission.[41])

information regarding the relative position of the great vessels to the atrioventricular valves as well as the appearance of the semilunar valves. Figure 13.15 presents a comparison of atrioventricular valves visualized *en face* in a normal case, in a case of complete atrioventricular canal, and in a case of a hypoplastic tricuspid valve associated with pulmonary atresia.

In Figure 13.16, we demonstrate the use of thick-slice rendering with inversion mode to emphasize the abnormal insertion of the tricuspid valve in a case of Ebstein anomaly.[22] This technique has been reported as helpful in characterizing the hypokinetic motion of the ventricular wall in a case of congenital left ventricular aneurysm.[61] Figure 13.17 shows another example of thick-slice rendering to visualize an overriding aorta in a case of tetralogy of Fallot associated with absent pulmonary valve syndrome. Figure 13.18 shows the pulmonary artery, which is constricted at the level of the pulmonary valves, the poststenotic dilatation, and, as a result of the depth perspective provided by rendering, a cross section of the dilated left pulmonary artery is also visualized. This is a

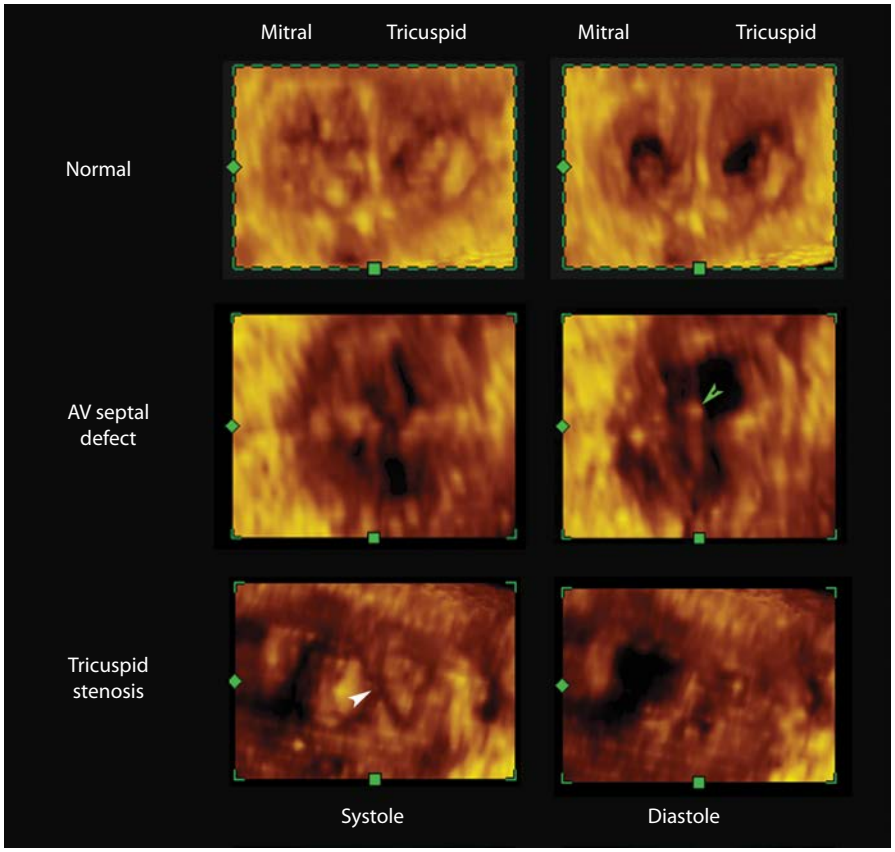


**Figure 13.15**
Comparison of 3D surface rendering of the atrioventricular valves: normal fetus (top), atrioventricular septal defect (middle), and tricuspid stenosis (bottom). The bright echogenic spot in the center of the image of the atrioventricular septal defect case (green arrowhead, diastole), corresponds to the atrial septum secundum viewed from above. In the tricuspid stenosis with ventricular septal defect case, the tricuspid valve is very small with limited excursion during diastole. Loss of continuity of the interventricular septum is observed during systole (white arrowhead). (Figure 7 from Gonçalves LF et al. *Am J Obstet Gynecol* 2003;189(6):1792–802, with permission.[18])

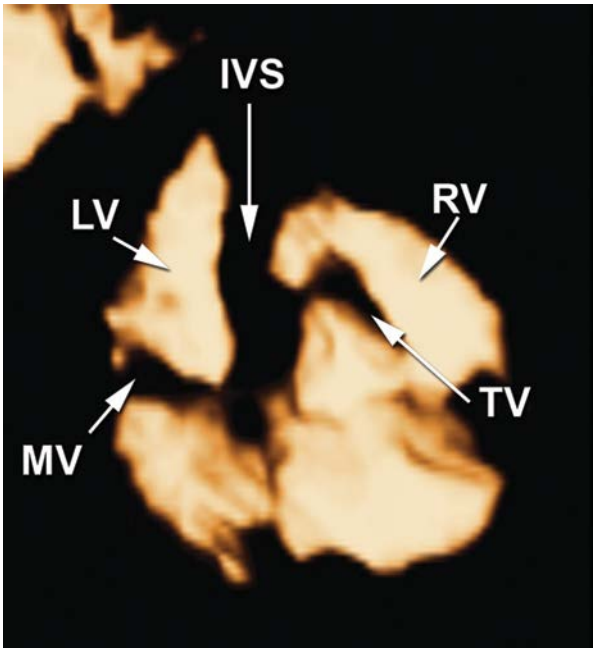


**Figure 13.16**
"Thick-slice" rendering of the atrioventricular valves using inversion mode in a fetus with Ebstein anomaly. This mode provides great contrast for the visualization of the myocardium and atrioventricular valves. Note the abnormal apical insertion of the tricuspid valve and the small right ventricle. (IVS, interventricular septum; LV, left ventricle; MV, mitral valve; RV, right ventricle; TV, tricuspid valve.) (From Gonçalves LF et al. *Ultrasound Obstet Gynecol* 2006;27(3):336–48, with permission.[41])

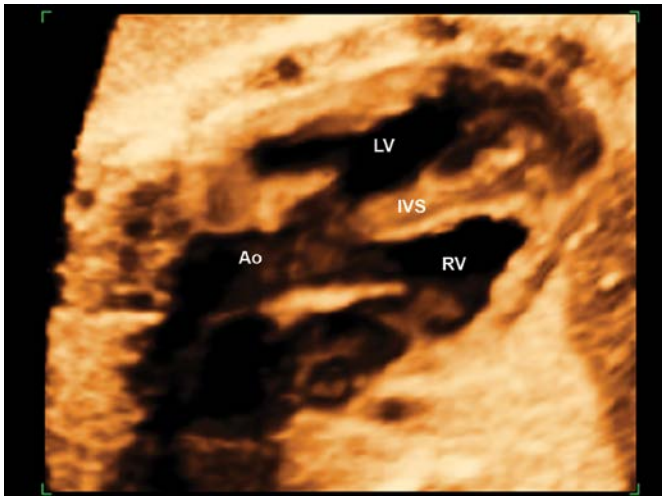


**Figure 13.17**
"Thick-slice" rendered image of the aorta (Ao) overriding the interventricular septum (IVS) in a case of absent pulmonary valve syndrome associated with tetralogy of Fallot. (LV, left ventricle; RV, right ventricle.) The algorithm used for rendering was the "gradient light" mode. (From Gonçalves LF et al. *Ultrasound Obstet Gynecol* 2006;27(3):336–48, with permission.[41])

common finding in absent pulmonary valve syndrome associated with tetralogy of Fallot. Figure 13.19 shows rendered views of the atrial and ventricular septum in the sagittal plane using a technique described by Yagel et al.[60] This view may contribute to further elucidation of atrial and ventricular septal defects.

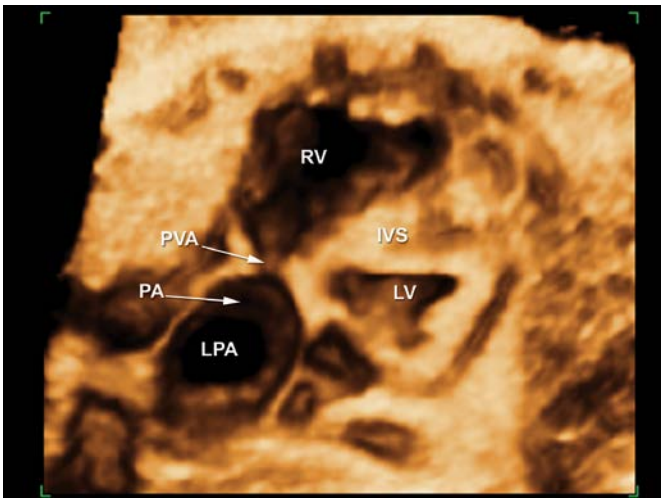


**Figure 13.18**
Thick-slice rendered image of the right ventricle (RV) and pulmonary artery (PA) in a case of absent pulmonary valve syndrome associated with tetralogy of Fallot. The stenotic pulmonary valve annulus (PVA), the poststenotic dilatation of the pulmonary artery, and a cross section of the dilated annulus of the left pulmonary artery (LPA) are demonstrated in a single image. The algorithm used for rendering was the "gradient light" mode. (From Gonçalves LF et al. *Ultrasound Obstet Gynecol* 2006;27(3):336–48, with permission.[41])

## *Rendering techniques for visualization of the great vessels*

Several rendering algorithms have been described for visualization of the 3D structure and spatial relationships of great vessels and venous return to the heart. These images can be obtained by acquiring volume datasets with color Doppler,[21,24,33,35] power Doppler,[21,24,62] or B-flow imaging,[22,63,64] as well as by rendering grayscale volume datasets with inversion mode.[22,27,37,65] Crisscrossing of the pulmonary artery over the ascending aorta as these vessels leave the ventricular chambers is best visualized in volume datasets acquired using transverse sweeps through the fetal thorax. Sagittal acquisitions are preferred when the objective is to visualize the aortic and ductal arches.

Figure 13.20 shows the technique that we frequently use in our unit to visualize the crisscrossing of the outflow tracts as they leave the ventricular chambers. As described in the previous paragraph, volume datasets are acquired using the four-chamber view as the starting point. For the sake of reproducibility, we reorient the heart on the screen whenever necessary by rotating the volume dataset around the *y*- and *z*-axes until the four-chamber view is in the apical position, and the left side of the heart is displayed on the left side of the screen. Next, the rendering box is selected and adjusted in panel B to include the whole heart within the region of interest (in this case, from the heart base touching the diaphragm to the great vessels close to the neck). In order to visualize the great vessels leaving the heart, the user must set the direction of view to project the heart from the great vessels toward its base. In our example, the direction of view was set from left to right, using panel B as a reference. The resulting rendered image is shown in panel D. Figure 13.21 shows examples of the normal pulmonary artery crisscrossing over the aorta in volume datasets acquired with color Doppler (Figure 13.21a), power Doppler (Figure 13.21b), inversion mode (Figure 13.21c), and B-flow imaging (Figure 13.21d). In Figure 13.22, the application of this technique for the diagnosis of transposition of the great arteries is demonstrated.[66]

## *Inversion Mode and B-flow*

Inversion of grayscale voxels to visualize blood pools from cardiac structures was originally described by Nelson et al.[37] in 1996. This principle has been more recently incorporated into commercially available ultrasound equipment and is known as inversion mode. With inversion mode, anechoic structures such as the heart chambers, vessel lumen, stomach, gallbladder, renal pelvis, and bladder appear echogenic in the rendered images, whereas structures that are normally echogenic before grayscale inversion (e.g., bones) appear anechoic. Postprocessing adjustments are performed as necessary, including gamma-curve correction to optimize contrast resolution, and grayscale threshold and transparency to improve image quality. The technique allows examiners to obtain 4D rendered images of cardiovascular structures from volume datasets acquired with grayscale only, without the need for color Doppler, power Doppler, or B-flow imaging (Figure 13.23). An example of the applicability of this technique is provided in Figure 13.24, which illustrates the 3D rendering of a case of interrupted IVC with azygous continuation.[27]

B-flow technology digitally enhances weak blood reflector signals from vessels and, at the same time, suppresses strong signals from the surrounding tissues.[63,67] Since this technology does not use Doppler methods to display blood flow, it is angle independent and does not interfere with frame rate as much as color or power Doppler.[67] Due to its high sensitivity and angle independence to blood flow, B-flow is potentially advantageous over color or power Doppler imaging for visualization of the great vessels and venous return to the heart,[22] as well as for visualization of small vessels such as the coronary arteries[68] and aortopulmonary collateral branches in cases of pulmonary atresia with a ventricular septal defect. In Figure 13.25, the aortic and ductal arches of a normal fetus have been rendered using a volume dataset acquired with B-flow imaging and the gradient light algorithm.

# Limitations

Factors that affect image quality of conventional 2D ultrasonography are likely to impact the quality of STIC volume

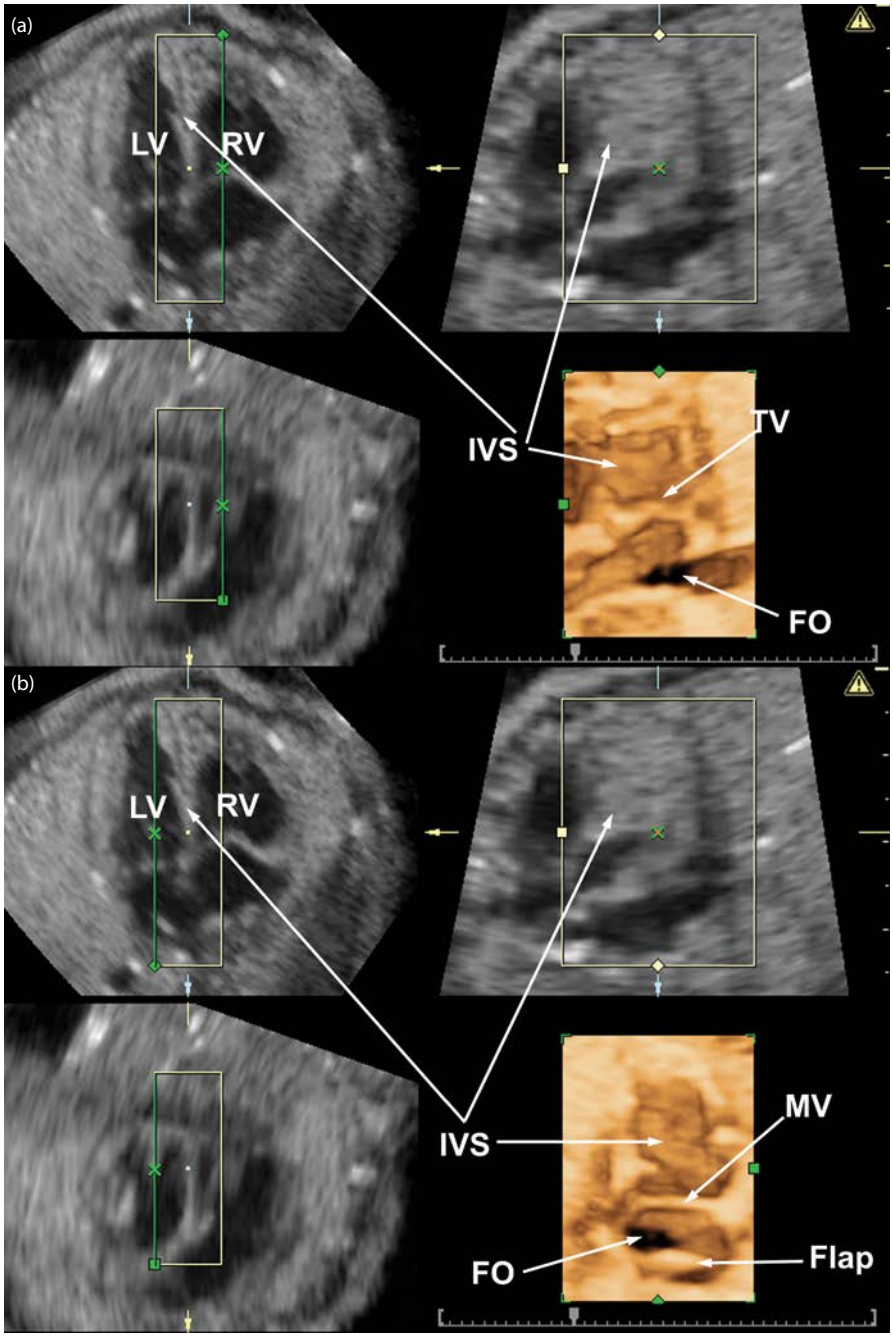


**Figure 13.19**
Rendered images of the interventricular septum (IVS). On (a) the interventricular septum is rendered with the direction of view (green line) set from the right ventricle (RV). On (b), the direction of view was set so that the volume was reconstructed with the IVS visualized from the left ventricle (LV). (Flap, flap of the foramen ovale; FO, foramen ovale; MV, mitral valves; TV, tricuspid valve.)

datasets. These factors include early gestational age, unfavorable fetal position, and maternal obesity. Fetal movement and sudden changes in fetal heart rate (e.g., fetal arrhythmias) during acquisition are additional factors that may affect the technique and cause misregistration of the information required for precise reconstruction of moving cardiac structures.[18] We have observed such an artifact in a case of a fetus with transposition of the great arteries, which was misinterpreted during analysis of the 4D volume dataset as double-outlet right ventricle. In this case, significant fetal movement during acquisition artificially shifted the connections of the outflow tracts to appear as exiting from the right ventricle.[69] Therefore, we caution that in case of a suspected malalignment defect (e.g., overriding ventricular septal defect, tetralogy of Fallot, double-outlet right ventricle, truncus arteriosus, pulmonary atresia with a ventricular septal defect) that is observed first by volumetric imaging, the finding should be confirmed by conventional 2D ultrasonography prior to establishing the final diagnosis.

## Conclusion

In this chapter, we describe a practical approach for the examination of the fetal heart by 3D/4D ultrasonography

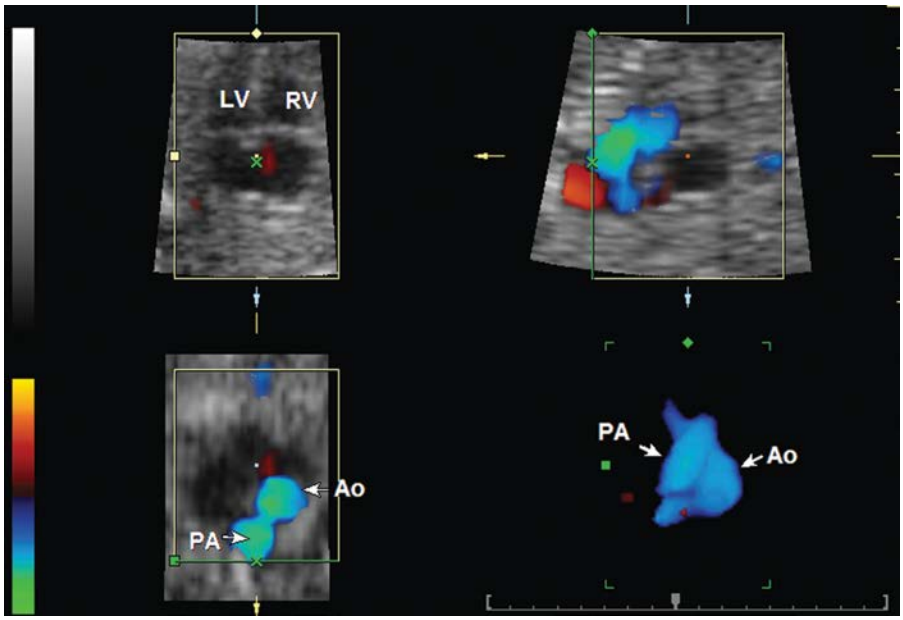


**Figure 13.20**
Technique to obtain rendered images of the outflow tracts using color Doppler. The rendering box is adjusted to encompass the heart and great vessels. The direction of view (green line) is set to project the rendered image from anterior (pulmonary artery) to posterior (aorta and ventricular chambers). The same technique can be applied to volume datasets acquired with power Doppler and B-flow imaging, as well as for volume datasets acquired with B-mode imaging but rendered using inversion mode. (Ao, aorta; LV, left ventricle; PA, pulmonary artery; RV, right ventricle.) (From Gonçalves LF et al. *Ultrasound Obstet Gynecol* 2006;27(3):336–48, with permission.[41])

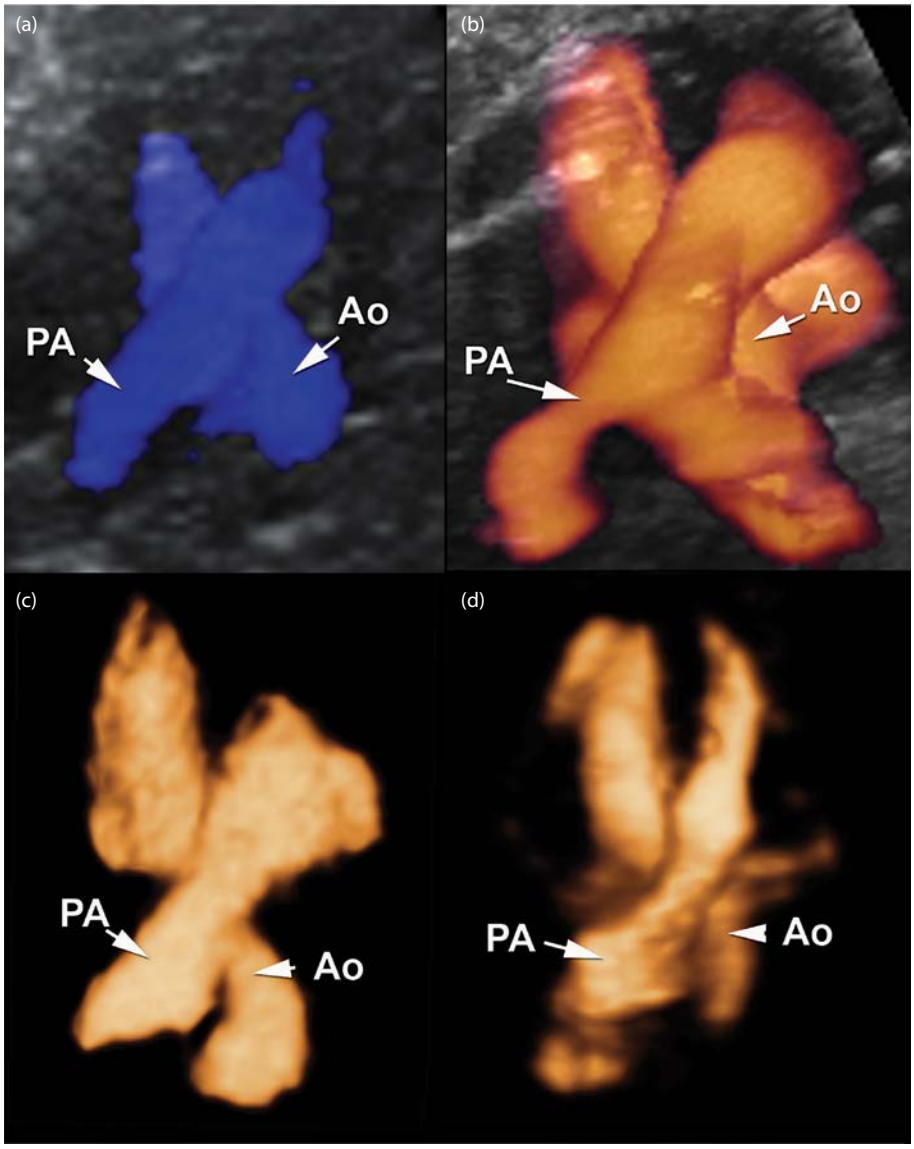


**Figure 13.21**
Crisscrossing of the outflow tracts as they exit the ventricular chambers. The pulmonary artery always crosses in front of the aorta. The rendered images were obtained with the technique described in Figure 13.15. The volume datasets were acquired with color Doppler (a), power Doppler (b), grayscale (then rendered with inversion mode) (c), and B-flow (d). (From Gonçalves LF et al. *Ultrasound Obstet Gynecol* 2006;27(3):336–48, with permission.[41])

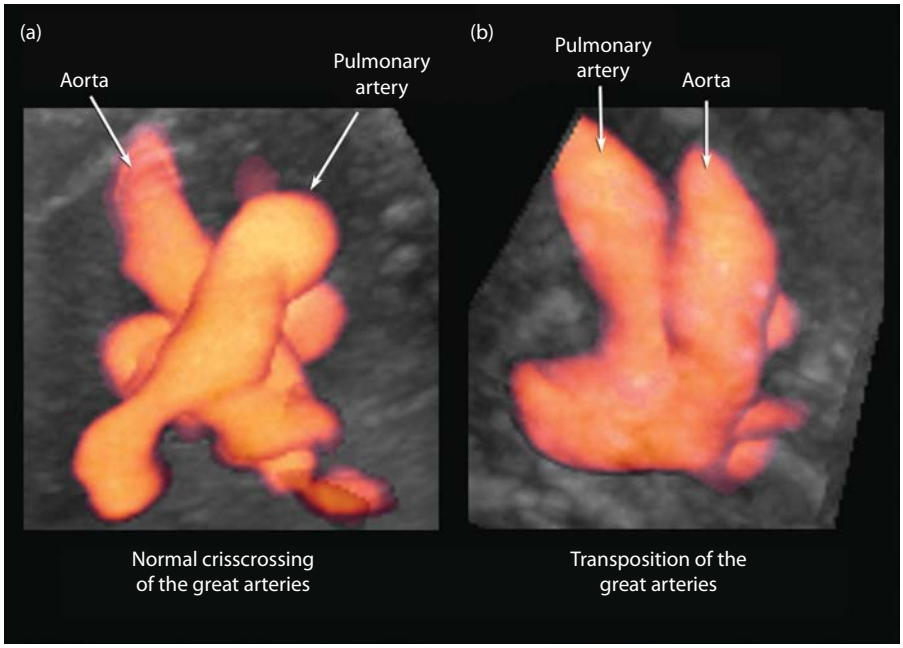


**Figure 13.22**
Rendered images from volume datasets of the fetal heart in a normal case (a) and transposition of the great arteries (b). The volumes were acquired through a transverse sweep of the fetal chest, using power Doppler four-dimensional ultrasonography with STIC. In the normal fetus, normal crisscrossing of the great arteries is observed, whereas in transposition of the great arteries, the vessels leave the ventricles in parallel. The technique utilized to render the volume datasets is explained in Figure 13.15. (From Gonçalves LF et al. *J Ultrasound Med* 2004;23(9):1225–31, with permission.[66])

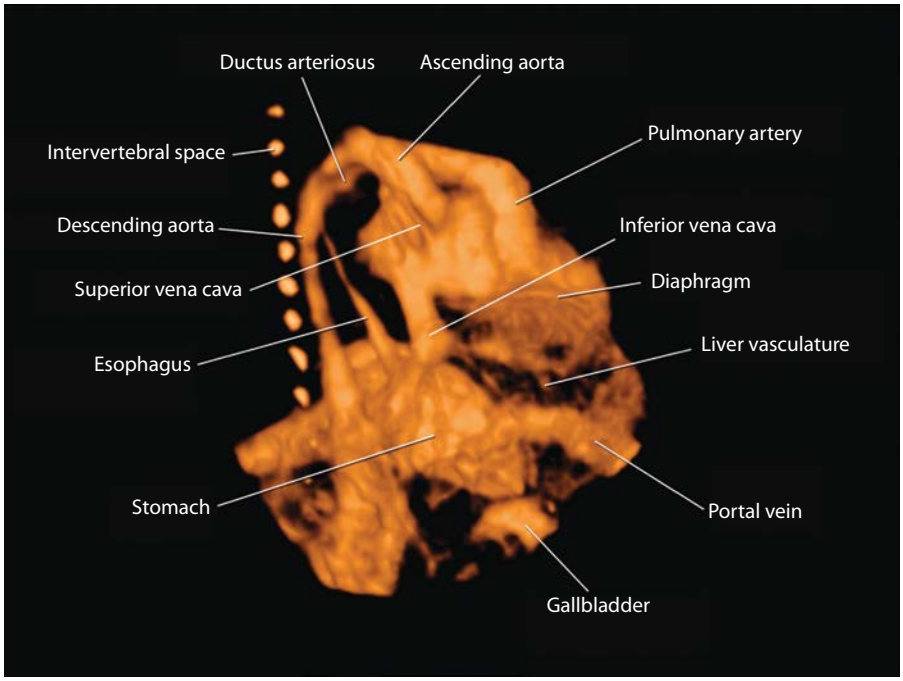


**Figure 13.23**
"Digital casts" of the aortic and ductal arches obtained with inversion mode. (From Gonçalves LF et al. *Ultrasound Obstet Gynecol* 2004;24(6):696–8, with permission.[65])

with STIC. This technology allows (1) navigation through the volume dataset and examination of the fetal heart in the absence of the patient; (2) the use of techniques to systematically visualize the outflow tracts in volume datasets acquired using the four-chamber view image as the starting point; (3) examination of the fetal heart using a tomographic approach similar to what is used to read computerized tomography and magnetic resonance imaging examinations; and (4) 3D and 4D rendering of cardiovascular structures to visualize the relationships, size, and course of the outflow tracts in normal fetuses and those with congenital heart disease. The 3D and 4D rendering of the great vessels, in particular, has been previously possible only during postmortem examination by injection of silicon rubber to produce pathological casts of the cardiovascular system. For the expert in fetal echocardiography, these techniques may represent additional tools to complement the 2D examination of the fetal heart.

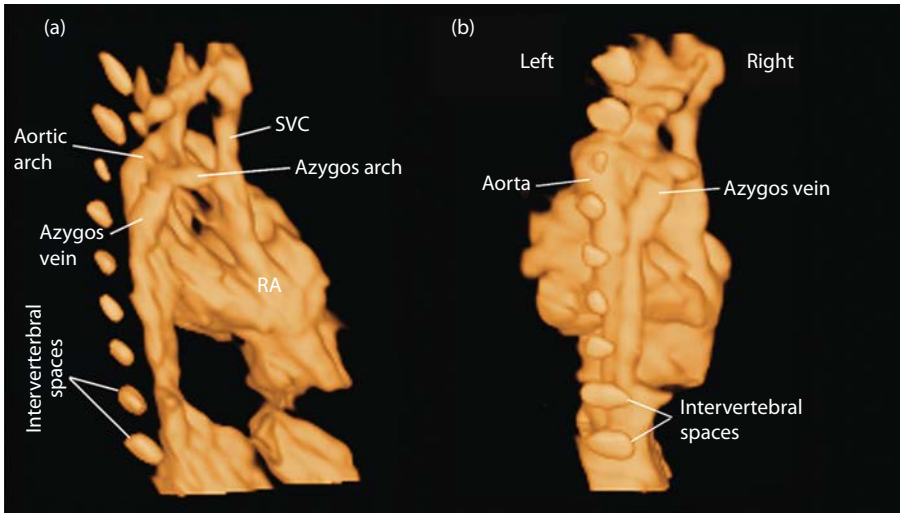


**Figure 13.24**
Three-dimensional images of a fetal heart rendered with the inversion mode in a case of interrupted inferior vena cava with azygos vein continuation associated with omphalocele. (a) From the right side of the heart showing that the arch of the azygos vein joins the superior vena cava (SVC) before entering the right atrium. (b) Posterior view of the fetal heart showing a dilated azygos vein located to the right of the descending aorta. The arch of this vein forms a Y image with the aortic arch before joining the SVC. (RA, right atrium.) (From Gonçalves LF et al. *Ultrasound in Obstet Gynecol* 2004;24(6):696–8, with permission.[65])

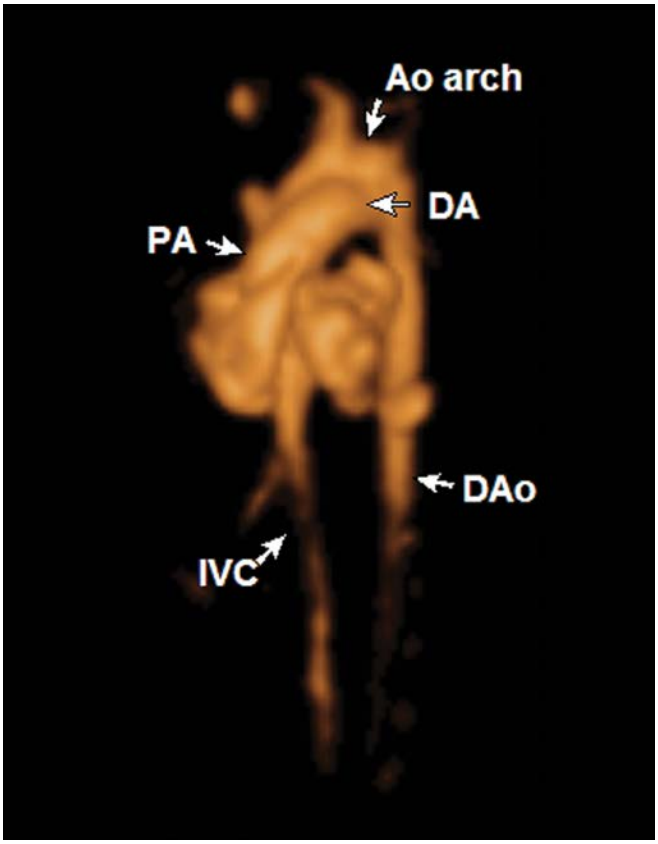


**Figure 13.25**
Rendered image of the aortic and ductal arches obtained from a volume dataset acquired with B-flow imaging, using a similar acquisition and rendering technique as illustrated in Figure 15. (Ao arch, aortic arch; DA, ductus arteriosus; DAo, descending aorta; IVC, inferior vena cava; PA, pulmonary artery.) (From Gonçalves LF et al. *Ultrasound Obstet Gynecol* 2006;27[3]:336–48, with permission.[41])

# References


1. American Institute of Ultrasound in Medicine. *J Ultrasound Med* 2013;32(6):1067–82.
2. International Society of Ultrasound in Obstetrics and Gynecology, Carvalho JS et al. *Ultrasound Obstet Gynecol* 2013;41(3):348–59.
3. Chaoui R, Heling KS. *Semin Fetal Neonatal Med* 2005;10(6): 567–77.
4. Deng J, Rodeck CH. *Curr Opin Obstet Gynecol* 2006;18(2): 177–84.
5. DeVore GR et al. *Ultrasound Obstet Gynecol* 2003;22(4):380–7.
6. DeVore GR et al. *J Ultrasound Med* 1993;12(11):659–63.
7. Allan L et al. *Ultrasound Obstet Gynecol* 2001;17(5):370–9.
8. Carvalho JS. *Heart* 2002;88(4):387–91.
9. Hunter S et al. *Heart* 2000;84(3):294–8.
10. Rustico MA et al. *Ultrasound Obstet Gynecol* 2000;16(7):614–9.
11. Tegnander E, Eik-Nes SH. *Ultrasound Obstet Gynecol* 2006; 28(1):8–14.
12. Wong SF et al. *Ultrasound Obstet Gynecol* 2003;21(1):19–25.
13. Bonnet D et al. *Circulation* 1999;99(7):916–8.
14. Calderon J et al. *J Pediatr* 2012;161(1):94–9.
15. Tworetzky W et al. *Circulation* 2001;103(9):1269–73.
16. Mahle WT et al. *Pediatrics* 2001;107(6):1277–82.
17. Tzifa A et al. *Arch Dis Child Fetal Neonatal Ed* 2007;92(3): F199–203.
18. Gonçalves LF et al. *Am J Obstet Gynecol* 2003;189(6):1792–802.
19. Viñals F et al. *Ultrasound Obstet Gynecol* 2003;22(4):388–94.
20. DeVore GR et al. *Ultrasound Obstet Gynecol* 2004;24(1):72–82.
21. Chaoui R et al. *Ultrasound Obstet Gynecol* 2004;23(6):535–45.
22. Gonçalves LF et al. *J Ultrasound Med* 2005;24(4):415–24.
23. Gonçalves LF et al. *J Matern Fetal Neonatal Med* 2005;17(5): 323–31.
24. Gonçalves LF et al. *J Ultrasound Med* 2004;23(4):473–81.
25. Yagel S et al. *Ultrasound Obstet Gynecol* 2005;25(1):97–8.
26. Cook AC et al. *Br Heart J* 1992;68(5):481–4.
27. Espinoza J et al. *Ultrasound Obstet Gynecol* 2005;25(5):428–34.
28. Lee W et al. *Ultrasound Obstet Gynecol* 2010;35(1):124–5.
29. Deng J. *Ultrasound Obstet Gynecol* 2003;22(4):336–44.
30. Brekke S et al. *Ultrasound Obstet Gynecol* 2004;24(2):192–8.
31. Deng J et al. *Ultrasound Med Biol* 2001;27(1):51–9.
32. Deng J et al. *Ultrasound Med Biol* 1996;22(8):979–86.

33. Deng J, Richards R. *Ultrasound Obstet Gynecol* 2002;20(2):209.
34. Deng J et al. *Ultrasound Med Biol* 2000;26(6):1021–32.
35. Deng J et al. *Ultrasound Med Biol* 2001;27(1):43–50.
36. Herberg U et al. *Ultrasound Obstet Gynecol* 2003;22(5):493–502.
37. Nelson TR et al. *J Ultrasound Med* 1996;15(1):1–9.
38. Sklansky MS et al. *Am J Cardiol* 1997;80(5):665–8.
39. Maulik D et al. *Echocardiography* 2003;20(8):715–21.
40. Zheng M et al. *PLOS ONE* 2013;8(3):e58494.
41. Gonçalves LF et al. *Ultrasound Obstet Gynecol* 2006;27(3): 336–48.
42. Kovalchin JP et al. *J Am Soc Echocardiogr* 2001;14(10):1025–9.
43. Paladini D et al. *Ultrasound Obstet Gynecol* 2004;23(2):159–64.
44. Viñals F et al. *Ultrasound Obstet Gynecol* 2005;25(1):25–31.
45. Yoo SJ et al. *Ultrasound Obstet Gynecol* 1997;9(3):173–82.
46. Yagel S et al. *Ultrasound Obstet Gynecol* 2001;17:367–9.
47. Viñals F et al. *Ultrasound Obstet Gynecol* 2006;28(1):22–5.
48. Devore GR, Polanko B. *J Ultrasound Med* 2005;24(12):1685–96.
49. Gonçalves LF et al. *J Perinat Med* 2006;34(1):39–55.
50. Paladini D et al. *Ultrasound Obstet Gynecol* 2006;27(5):555–61.
51. Abuhamad A. *J Ultrasound Med* 2004;23(5):573–6.
52. Abuhamad A et al. *J Ultrasound Med* 2007;26(4):501–7.
53. Espinoza J et al. *J Ultrasound Med* 2006;25(8):947–56.
54. Bega G et al. *J Ultrasound Med* 2001;20(4):307–13.
55. Yeo L et al. *Ultrasound Obstet Gynecol* 2011;37(4):423–31.
56. Abuhamad A et al. *Ultrasound Obstet Gynecol* 2008;31(1):30–6.
57. Yeo L, Romero R. *Ultrasound Obstet Gynecol* 2013;42(3):268–84.
58. Garcia M et al. *Ultrasound Obstet Gynecol* 2016;47(4):450–9.
59. Veronese P et al. *Fetal Diagn Ther* 2017;41(2):89–99.
60. Yagel S et al. *Ultrasound Obstet Gynecol* 2006;28(3):266–74.
61. Chiang Y-C et al. *Ultrasound Obstet Gynecol* 2006;28(3):345–7.
62. Chaoui R, Kalache KD. *Ultrasound Obstet Gynecol* 2001;17(5): 455–6.
63. Pooh RK, Korai A. *Croat Med J* 2005;46(5):808–11.
64. Volpe P et al. *Ultrasound Obstet Gynecol* 2006;28(1):40–6.
65. Gonçalves LF et al. *Ultrasound Obstet Gynecol* 2004;24(6): 696–8.
66. Gonçalves LF et al. *J Ultrasound Med* 2004;23(9):1225–31.
67. Deane C. *Ultrasound Obstet Gynecol* 2000;15(2):96–7.
68. Gonçalves LF et al. *Ultrasound Obstet Gynecol* 2005;26(4):366–7.
69. Gonçalves LF et al. *J Ultrasound Med* 2006;25(6):691–9.
70. Lee W. *J Ultrasound Med* 1998;17:601–7. (Erratum in *J Ultrasound Med* 1998;17:796.)
71. Gonçalves LF et al. *Pediatr Radiol* 2011;41:1047–56.
72. Chaoui et al. *Ultrasound Obstet Gynecol* 2003;21:81–93.

# 14

# Three- and four-dimensional ultrasound in fetal echocardiography: A new look at the fetal heart

Simcha Yagel, Sarah M. Cohen, Israel Shapiro, Baruch Messing, and Dan V. Valsky

## Background

Three- and four-dimensional (3D/4D) applications in fetal ultrasound scanning have made impressive strides in the past three decades, with particularly dramatic improvement in fetal echocardiography. Recent technological developments in motion-gated scanning allow almost real-time 3D/4D cardiac examination. It appears that 3D/4D ultrasound applications will make a significant contribution to our understanding of the developing fetal heart in both normal and anomalous cases, to interdisciplinary management team consultation, to parental counseling, and to professional training. 3D/4D echocardiography may facilitate screening methods, and with its offline networking capabilities may improve health-care delivery systems by extending the benefits of prenatal cardiac screening to poorly served areas. The introduction of "virtual planes" to fetal cardiac scanning has helped sonographers obtain views of the fetal heart not generally accessible with a standard two-dimensional (2D) approach. There is no doubt that 3D/4D gives us another look at the fetal heart.

3D/4D cardiac scanning has been extensively applied in clinical practice and investigated as to whether it improves the accuracy of fetal echocardiography. In this chapter, we summarize the 3D/4D acquisition and postprocessing modalities in 3D/4D fetal echocardiography, demonstrating their use through normal and anomalous case examples.

## Three- and four-dimensional techniques and their application to fetal cardiac scanning

### *Acquisition modalities*

#### Spatiotemporal image correlation

Spatiotemporal image correlation (STIC) acquisition is an indirect motion-gated offline scanning mode.[1–5] The methodology of STIC is comprehensively described in Chapter 13. Briefly, automated volume acquisition is made possible by the array in the transducer performing a slow single sweep, recording a single 3D dataset consisting of many 2D frames, one behind the other. The volume of interest (VOI) is acquired over a period of 7.5 to about 30 seconds at a sweep angle of approximately 20°–40° (depending on the size of the fetus) and frame rate of about 150 frames per second. A 10-second, 25° acquisition would contain 1,500 B-mode images.[3] When using the newer electronic 4D eSTIC acquisitions, the acquisition principle is split into subvolumes, and frame rates are in the range of 800 frames per second.

Following acquisition, mathematical algorithms are applied to the volume data to detect systolic peaks that are used to calculate the fetal heart rate. The B-mode images are arranged in order according to their spatial and temporal domain, correlated to the internal trigger, the systolic peaks that define the heart cycle[3] (Figure 14.1). The result is a reconstructed complete heart cycle that displays in an endless loop. This cine-like file of a beating fetal heart can be manipulated to display any acquired scanning plane at any stage in the cardiac cycle (Figure 14.2). This reconstruction takes place directly following the scan in a matter of seconds, allowing the STIC acquisition to be reviewed with the patient still present and repeated if necessary, and saved to the scanning machine, personal computer (PC), or network.

STIC acquisition can be combined with other applications by selecting the appropriate setting before acquisition (B-flow, color and power Doppler, tissue Doppler, high-definition flow Doppler) or with postprocessing visualization modalities (3D volume rendering, VOCAL [virtual organ computer-aided analysis], inversion mode, tomographic ultrasound imaging [TUI]).

#### B-flow

B-flow is an old-new technology that images blood flow without relying on Doppler shift; rather, B-flow is an outgrowth of B-mode imaging. With the advent of faster

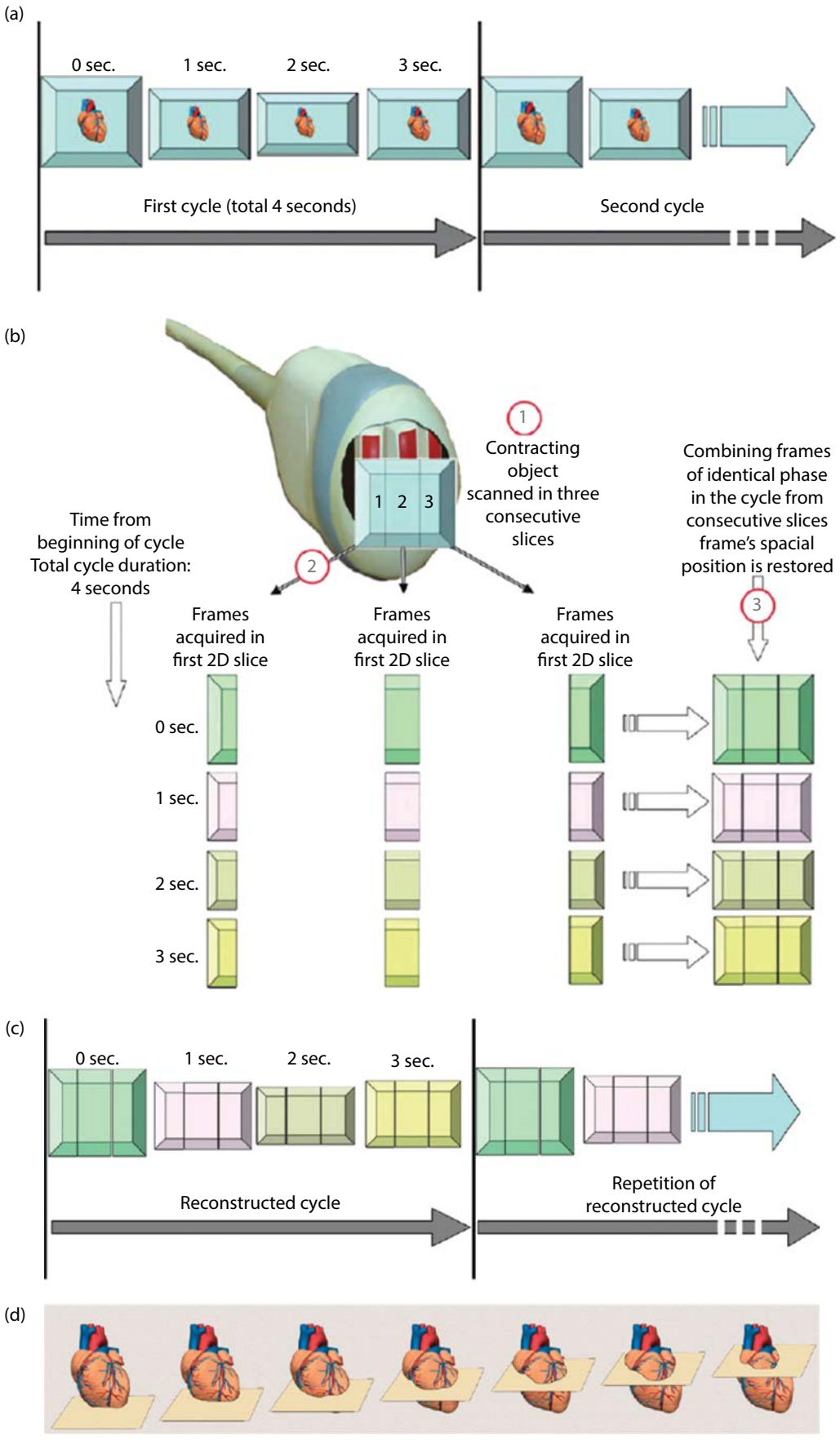
(a)
0 sec.
1 sec.
2 sec.
3 sec.
First cycle (total 4 seconds)
Second cycle
(b)
1
Contracting object scanned in three consecutive slices
1 2 3
2
Combining frames of identical phase in the cycle from consecutive slices frame's spacial position is restored
3
Time from beginning of cycle
Total cycle duration: 4 seconds
Frames acquired in first 2D slice
Frames acquired in first 2D slice
Frames acquired in first 2D slice
0 sec.
1 sec.
2 sec.
3 sec.
(c)
0 sec.
1 sec.
2 sec.
3 sec.
Reconstructed cycle
Repetition of reconstructed cycle
(d)

frame rates and computer processing, B-flow directly depicts blood cell reflectors. It avoids some of the pitfalls of Doppler, such as aliasing and signal dropout at orthogonal scanning angles. The resulting image is a live grayscale depiction of blood flow and part of the surrounding lumen, creating sensitive "digital casts" of blood vessels and cardiac chambers (Figure 14.3 and Video 14.1; Figure 14.4 and Video 14.2). B-flow is also a sensitive acquisition tool for volume measurement. B-flow modality is a direct-volume nongated scanning method able to show blood flow in the heart and great vessels in real time, without color Doppler flow information.[6] B-flow combined with STIC can provide real-time dynamic angiographic features of extracardiac vessels.[7] These capabilities make it an invaluable tool in fetal echocardiography.

## 3D/4D with color Doppler, 3D power Doppler (3DPD), and 3D high-definition power flow Doppler

Color and power Doppler have been extensively applied to fetal echocardiography; scanning is incomplete today without color Doppler. Color or power Doppler, and the most recent development, high-definition flow Doppler, can be combined with static 3D direct volume nongated scanning to obtain 3D volume files with two-color Doppler information or one-color 3DPD.

Color Doppler can be used more effectively in 3D/4D when combined with STIC acquisition[8] in fetal echocardiography, resulting in a volume file that reconstructs the cardiac cycle, as above, with color flow information. (Extreme care must be taken when working with Doppler applications in postprocessing, however, to avoid misinterpretation of flow direction as the volume is rotated.) This joins the Doppler flow to cardiac events[1] and provides all the advantages of analysis (multiplanar reconstruction [MPR] rendering, TUI) with color. This combination of modalities is very sensitive for detecting intracardiac Doppler flow signals throughout the cardiac cycle, for example, mild tricuspid regurgitation occurring very early in systole or very briefly.[9]

3DPD is directionless, one-color Doppler that is most effectively joined with static 3D scanning.[1] 3DPD uses Doppler shift technology to reconstruct the blood vessels in the VOI, isolated from the rest of the volume. Using the "glass body" mode in postprocessing, surrounding tissue is not shown, while the vascular portion of the scan is isolated for evaluation. The operator can scroll spatially to any plane in the volume (but not temporally: in this case, color Doppler with STIC is more effective, see above). In 3DPD, the vascular tree of the fetal abdomen and thorax is reconstructed,[10,11] obviating the necessity of reconstructing a mental picture of the idiosyncratic course of an anomalous vessel from a series of 2D planes. This has been shown to aid our understanding of the normal and anomalous anatomy and pathophysiology of vascular lesions[12] (Figure 14.5).

High-definition power flow Doppler, the newest development in color Doppler applications, uses high resolution and a small sample volume to produce images with two-color directional information, with less "blooming" of color for more realistic representation of vessel size. It depicts flow at a lower velocity than color or power Doppler, while retaining the advantage of flow directional information, thereby combining high-resolution bidirectional flow Doppler with the anatomic acuity associated with power Doppler. It can be used with static 3D or 4D gated acquisition (STIC) and the glass-body mode, to produce high-resolution images of the vascular tree with bidirectional color coding (Figure 14.6 and Video 14.3). It is particularly sensitive for imaging small vessels. Systolic and diastolic flow are observed at the same time owing to the sensitivity of the modality. For example, when used with STIC acquisition, the ductus venosus is shown to remain filled in both systole and diastole. Doppler applications in 3D/4DUS reconstructions have improved steadily over the years, now providing sharper, more defined appearance of blood flowing in its

**Figure 14.1 (opposite page)**
Demonstration of spatiotemporal image correlation (STIC) technology. Cycle duration, number of slices, and number of frames per slice were chosen to simplify illustration. The scale applicable to fetal cardiac examination is discussed in the text. (a) An object is contracting in a cyclical manner (4 seconds per cycle). The shape of the object is presented at four points during the cycle. Assume that the contraction rate is too high to scan the whole object in conventional real-time 3D. (b) The object is scanned in three consecutive slices adjacent to each other (1). At least one complete cycle is recorded in real-time 2D ultrasound, thus acquiring many frames per slice. In this example, four frames are recorded in each slice (2). By simultaneous analysis of the tissue movements, the software identifies the beginning of each cycle and sets the time that each frame was acquired in respect of the beginning of the cycle. Knowing the time and position of each frame, the software reconstructs the 3D shape of the complete object in each phase of the cycle (3). The shape is constructed from frames arranged side by side according to their position in the object (hence *spatio*temporal). Though each frame composing the object was acquired in a different cycle, their phase in respect of the beginning of the cycle is identical (hence spatio*temporal*). (c) The system completes its task by creating an endless loop animation composed of the consecutive reconstructed volumes of the cycle, resulting in a moving volume resembling real-time 3D. The procedure takes only a few seconds; the stored reconstructed volumes are now available for analysis with postprocessing techniques as described in the text. (d) Demonstration of the multiple slices through the heart acquired during a single STIC scan. The dedicated transducer automatically changes its scanning angle, either by means of a small motor in some systems, or electronically by using a phased matrix of elements. (Reproduced with permission from Yagel S et al. *Ultrasound Obstet Gynecol* 2007;29:81–95.[82] © International Society of Ultrasound in Obstetrics and Gynecology. Permission is granted by John Wiley and Sons Ltd on behalf of ISUOG.)

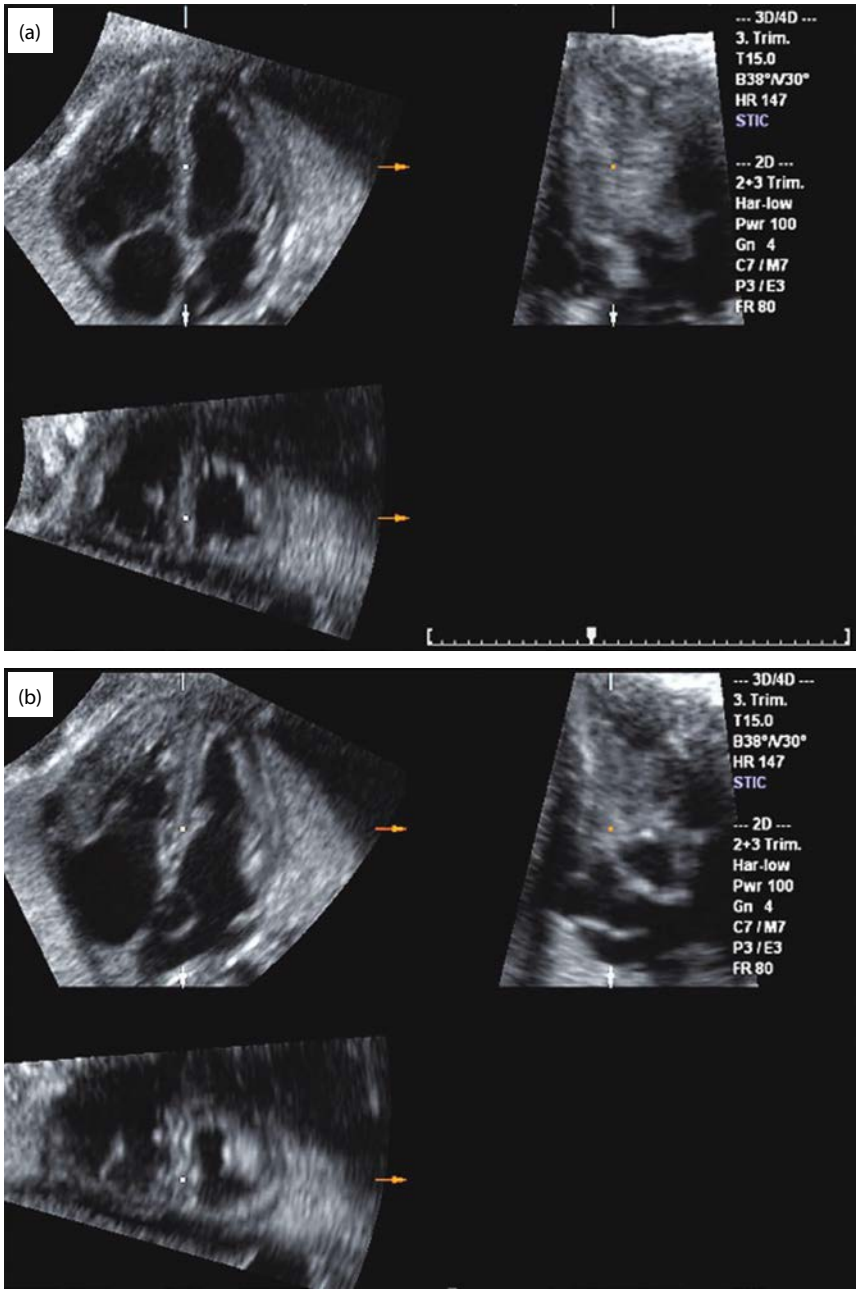


**Figure 14.2**
The four-chamber view from a STIC acquisition in a third-trimester fetus in systole (a) and diastole (b). By applying multiplanar reconstruction (MPR), the operator optimizes the four-chamber view (FCV) plane, adjusting the image both spatially along the *x*-, *y*-, and *z*-axes, and to the desired stage of the cardiac cycle. The navigation point is placed on the interventricular septum in the A-plane; the B-plane shows the septum *en face*, and the C-plane shows a coronal plane through the ventricles. (Reproduced with permission from Yagel S et al. *Ultrasound Obstet Gynecol* 2007;29:81–95.[82] © International Society of Ultrasound in Obstetrics and Gynecology. Permission is granted by John Wiley and Sons Ltd on behalf of ISUOG.)

vessels with two-color information.[13] Figure 14.7a–c (and Videos 14.4 and 14.5) show a normal heart and vessels imaged with this modality.

## Real-time 3DUS

Real-time 3DUS with a matrix-array probe and the live xPlane modality provide a moving 3D display of two orthogonal images simultaneously: the primary image scanned by the operator, and the secondary image, which is extracted from the volume along the line placed by the operator on the primary image. This approach has been shown to be a feasible method to image the five planes of fetal echocardiography as well as the ductal arch view, giving it added value in diagnosing conotruncal anomalies, and the interventricular septum.[14–16] However, this approach may require manual adjustment to accommodate fetal position or an abnormal left ventricular outflow tract (LVOT).[17]

Herberg and colleagues[18] found that real-time 3DUS with a matrix transducer is a valid and reliable method for ventricle volume measurement, and showed a strong inter- and intraobserver variability with a mean intraclass correlation coefficient (ICC) of 0.997. In a further study, they compared the visualization rates of specific structures with real-time 3DUS (RT3D), reconstructed 3DUS (3DR), and 2DUS. The investigators found that RT3D had a better visualization rate than 2DUS, and that 2DUS and RT3D had higher sensitivity for identification of anomalies than 3DR.[19]

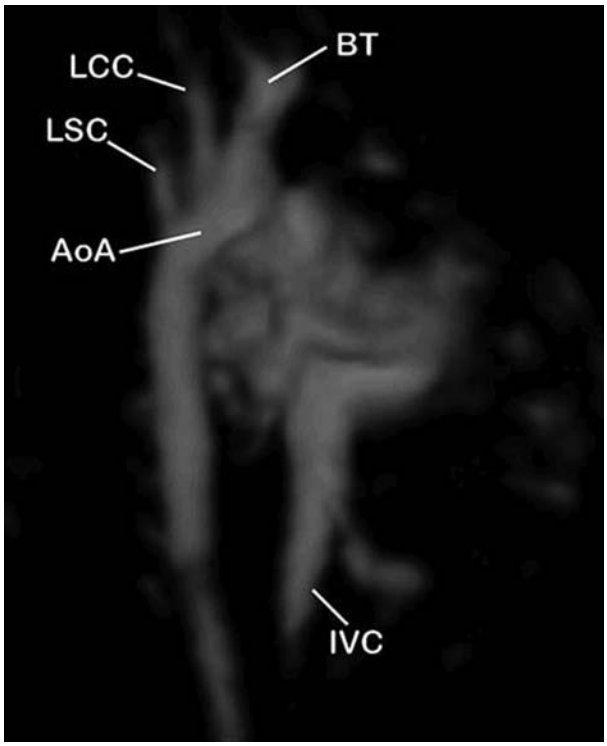


**Figure 14.3**
B-flow image of normal heart and aortic arch. Brachiocephalic trunk (BT), left common carotid (LCC), and left subclavian artery (LSA) are seen projecting from the aortic arch (AoA). Inferior vena cava (IVC) is indicated. See also corresponding Video 14.1. (Reproduced with permission from Yagel Set al. *Ultrasound Obstet Gynecol* 2007;29:81–95.[82] © International Society of Ultrasound in Obstetrics and Gynecology. Permission is granted by John Wiley and Sons Ltd on behalf of ISUOG.)

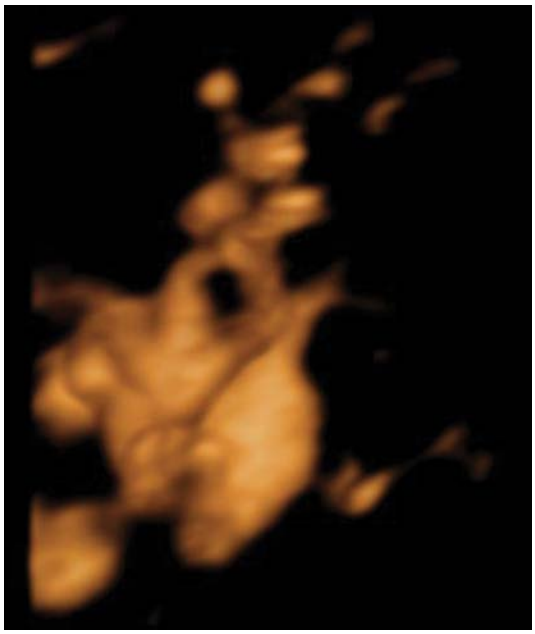

**Figure 14.4**
B-flow: A case of aortic ring imaged in B-flow. (See accompanying Video 14.2.)

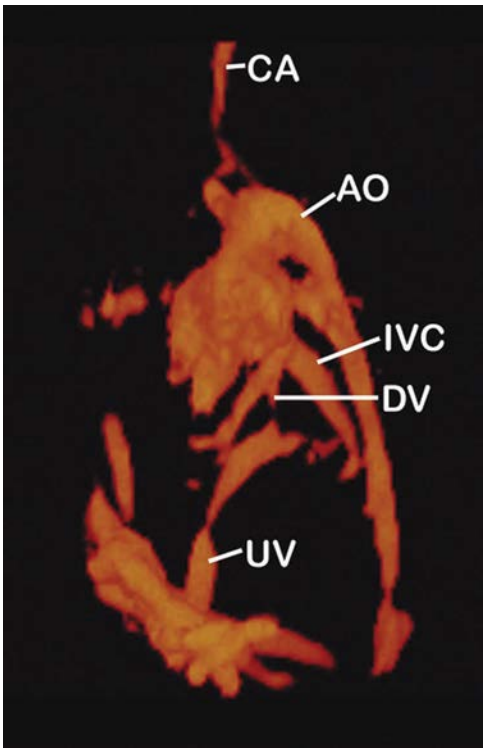


**Figure 14.5**
3D power Doppler of the heart and major vessels. Noted are the carotid artery (CA); aorta (AO); inferior vena cava (IVC); ductus venosus (DV); and umbilical vein (UV). (Reproduced with permission from Yagel S et al. *Ultrasound Obstet Gynecol* 2007;29:81–95.[82] © International Society of Ultrasound in Obstetrics and Gynecology. Permission is granted by John Wiley and Sons Ltd on behalf of ISUOG.)

Zhu et al.[20] applied real-time 3D echocardiography *in vivo* and *in vitro* in an animal study to determine the feasibility of this modality to measure fetal stroke volume, left ventricular mass, and myocardial strain, finding excellent correlation with reference values based on a balloon pump model.

## *Postprocessing modalities*

In postprocessing, various methodologies have been proposed to optimize the acquired volumes to demonstrate the classic planes of fetal echocardiography[21,22] (Figure 14.8), as well as "virtual planes" that are generally inaccessible in 2D cardiac scanning.[23–27] These views, once obtained, are stored to the patient file, in addition to the original volume, either as static images or 4D motion files. Any of the stored information can be shared for expert review, interdisciplinary consultation, parental counseling, or teaching.

### MPR, 3D rendering, and TUI

3D/4D volume sets contain a "block" of information; this is generally a wedge-shaped chunk of the targeted area. In order to analyze this effectively, the operator displays 2D planes in either MPR mode (Figure 14.2) or 3D volume rendering.

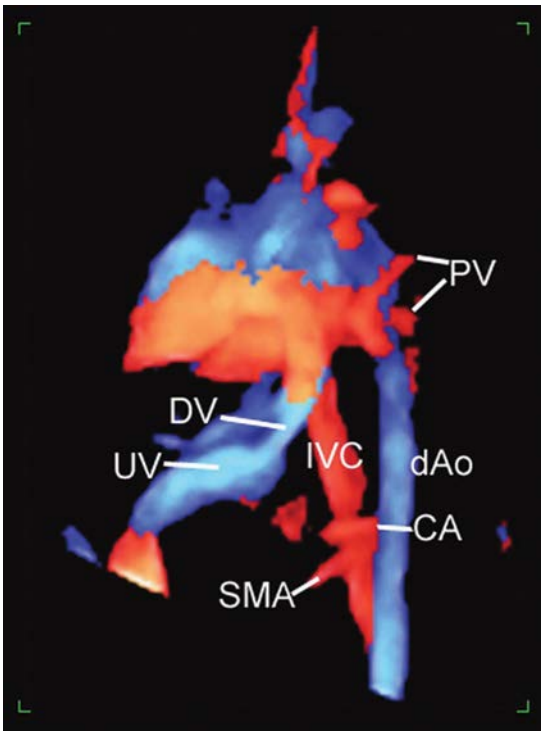


**Figure 14.6**
Normal heart and great vessels: STIC acquisition with high definition power flow Doppler. (CA, celiac artery; dAo, descending aorta; DV, ductus venosus; IVC inferior vena cava; PV, pulmonary veins; SMA, superior mesenteric artery; UV, umbilical vein. (See accompanying Video 14.3.) (Reproduced with permission from Yagel S et al. *Ultrasound Obstet Gynecol* 2007;29:81–95.[82] © International Society of Ultrasound in Obstetrics and Gynecology. Permission is granted by John Wiley and Sons Ltd on behalf of ISUOG.)

In MPR, the screen is divided into four frames, referred to as A (upper left), B, C, and the fourth frame (lower right) showing either the volume model for reference, or the rendered image. Each of the three frames shows one of the three orthogonal planes of the volume. The reference dot guides the operator in navigating within the volume, as it is anchored at the point of intersection of all three planes. By moving the point, the operator manipulates the volume to display any plane within the volume; if temporal information was acquired, the same plane can be displayed at any stage of the scanned cycle.

From a good STIC acquisition,[5] the operator can scroll through the acquired volume to obtain sequentially each of the classic five planes[21] of fetal echocardiography, and any plane may be viewed at any time-point throughout the reconstructed cardiac cycle loop. The cycle can be run or stopped "frame by frame" to allow examination of all phases of the cardiac cycle, for example, opening and closing of the atrioventricular valves.

By comparing the A- and B-frames of the MPR display, the operator can view complex cardiac anatomy in corresponding transverse and longitudinal planes simultaneously. So, for example, an anomalous vessel that might be disregarded in cross section is confirmed in the longitudinal plane.

3D rendering is another analysis capability of an acquired volume. It is familiar from static 3D applications, such as imaging the fetal face in surface rendering mode. In fetal echocardiography, it is readily applied to 4D scanning. The operator places a bounding box around the region of interest within the volume (after arriving at the desired plane and time) to show a slice of the volume whose depth reflects the thickness of the slice. For example, with the A-frame showing a good four-chamber view, the operator places the bounding box tightly around the interventricular septum. The rendered image in the D-frame will show an *en face* view of the septum. The operator can determine whether the plane will be displayed from the left or right (i.e., the septum from within the left or the right ventricle); the thickness of the slice will determine the depth of the final image, for example, to show the texture of the trabeculations within the right ventricle (Figure 14.9).

Figures 14.10, 14.11, and Videos 14.6 through 14.8 present rendered images of aberrant right subclavian artery and of aortic atresia that were acquired in STIC with high-definition power Doppler and rendered to display the relevant anatomy.

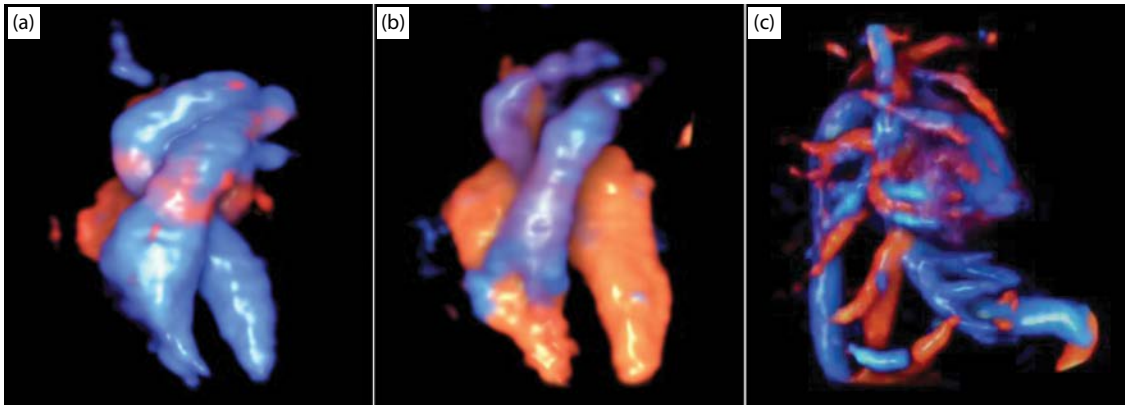


**Figure 14.7**
STIC combined with high-definition power Doppler: Normal heart and great vessels from a STIC acquisition with high-definition power Doppler of the heart in systole (a) and diastole (b). (c) The normal heart and vessels in longitudinal view. (See accompanying Videos 14.4 and 14.5.)

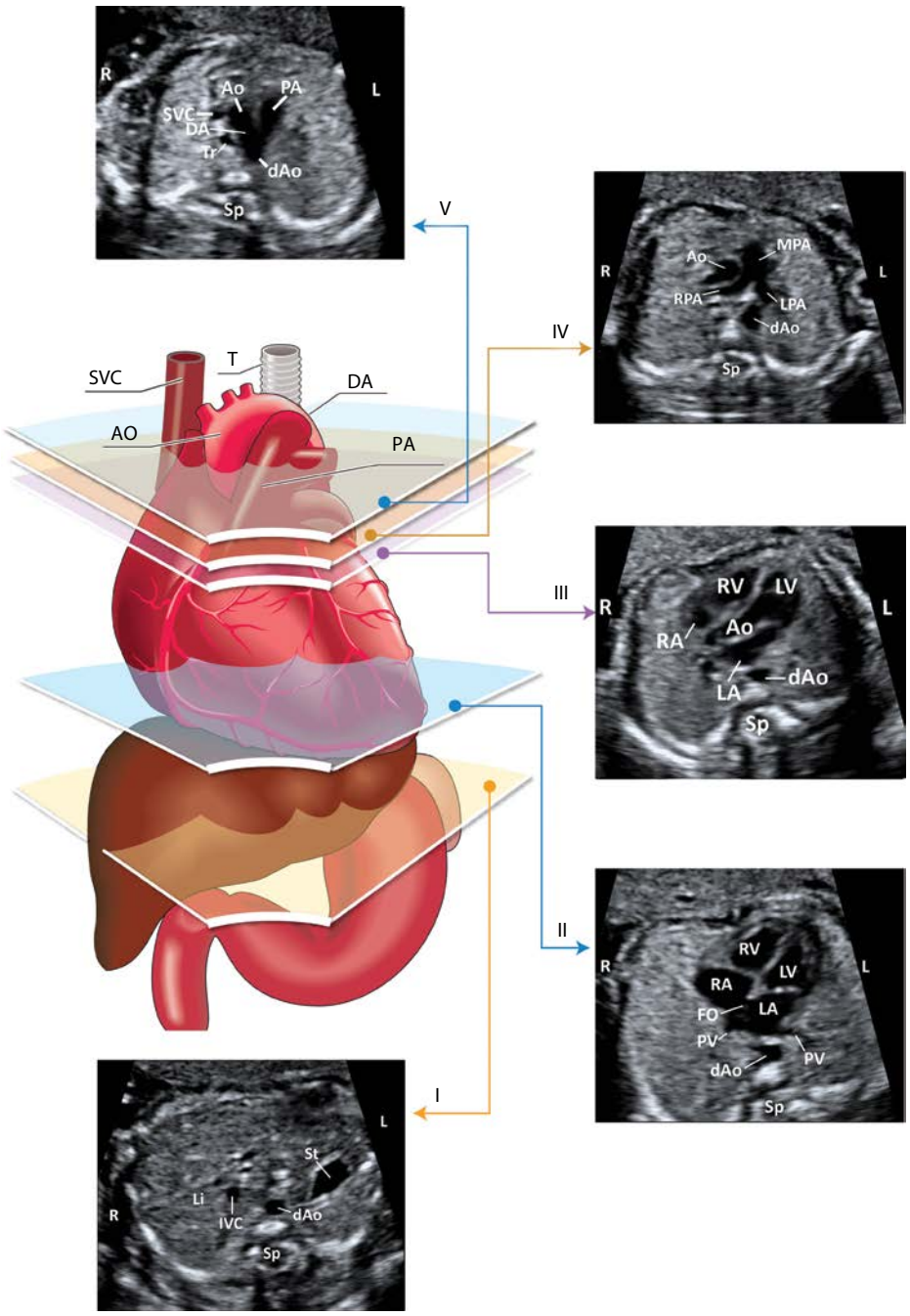


**Figure 14.8**
The five planes of fetal echocardiography. See Chapter 12, Figure 12.1 for full explanation. (Reprinted with permission from International Society of Ultrasound in Obstetrics and Gynecology, Carvalho JS et al. *Ultrasound Obstet Gynecol* 2013; 41:348–59.[37])

TUI application extends the capabilities of MPR and rendering modes. This multislice analysis mode resembles a magnetic resonance imaging or computer-assisted tomography display. A matrix displays parallel slices simultaneously, centered around the plane of interest (the "zero" plane). The matrix comprises an adjustable number of sequential views (from –5 through +5, for example), dependent on the thickness of the slices, i.e., the distance of one plane to the next, which is regulated by the operator. The upper left frame of the display shows the position of each plane within the region of interest, relative to the reference plane. This display of sequential parallel planes gives a more complete picture of the fetal heart (Figure 14.12 through 14.15 and Videos 14.9 through 14.12).

VOCAL (Virtual Organ Computer-aided AnaLysis) mode is a semiautomated 3D measurement mode that performs rotational measurement of volume. The saved volume file is rotated 180° about a fixed central axis through a preset number of rotation steps based on the operator-chosen angle of rotation, 6%, 9%, 15%, or 30%. Setting the rotation angle at 15°, for example, results in 12 planes available for measurement. The computer mouse is used to manually define the contours of the measured object (for example, a heart ventricle) at each plane serially. Alternatively, the operator can opt for the system to draw the contours automatically, according to varying degrees of sensitivity. Once an outline is drawn around each plane of the target, the system reconstructs a contour model of the target. This postprocessing

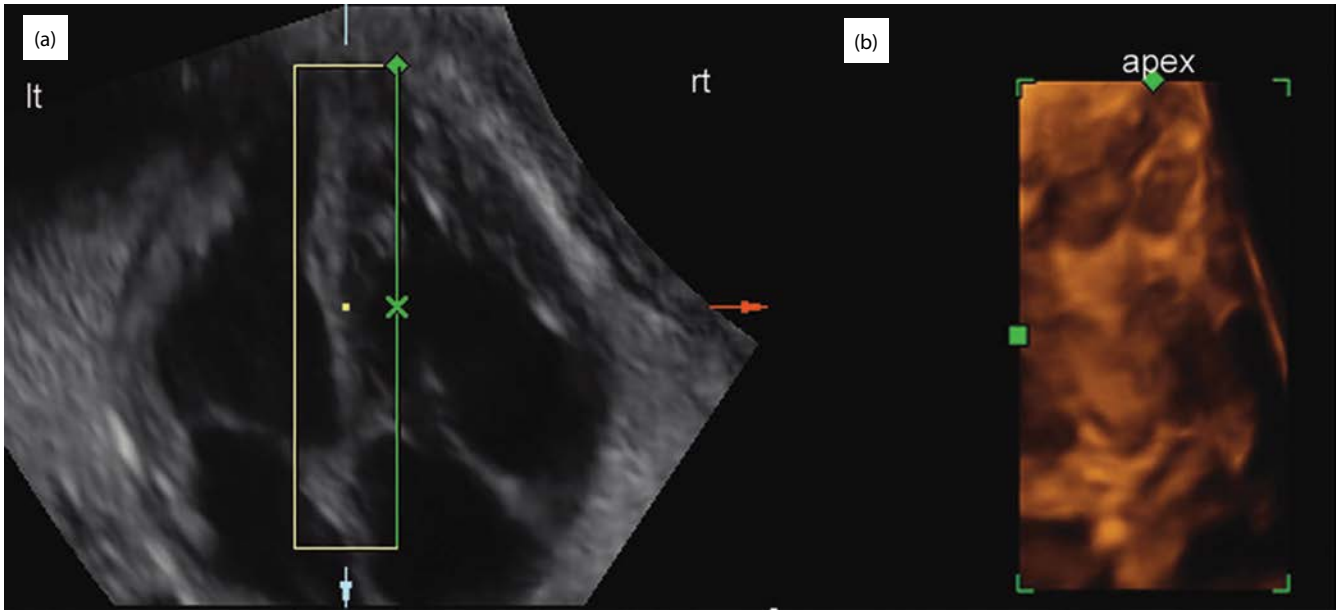


**Figure 14.9**
Normal interventricular septum in 3D rendering mode. In frame A (a), the bounding box is placed tightly around the septum with the active side (green line) on the right. The D-frame (b) shows the septum *en face*: note the rough appearance of the septum from within the trabeculated right ventricle. (Reproduced with permission from Yagel S et al. *Ultrasound Obstet Gynecol* 2007;29:81–95.[82] © International Society of Ultrasound in Obstetrics and Gynecology. Permission is granted by John Wiley and Sons Ltd on behalf of ISUOG.)

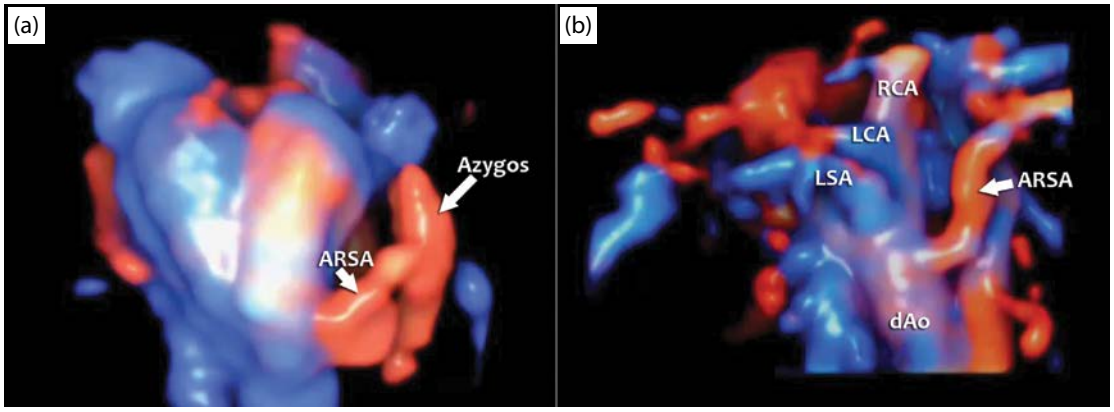


**Figure 14.10**
Rendered image of case of aberrant right subclavian artery (ARSA). Left image (a) shows the 3VT plane with ARSA. The azygos vein (azygos) is marked. Right image (b) shows the ARSA and the relative positions of the aortic branches, the left subclavian artery (LSA), left carotid artery (LCA), right carotid artery (RCA), and the descending aorta (dAo). Rendered image derived from a STIC acquisition with high-definition power Doppler of a case of aortic atresia. Arrow indicates reverse flow in the narrow aorta. (See corresponding Videos 14.6 and 14.7.)

modality has been applied to volume calculation of numerous fetal organs, including heart, lungs, and others.[28–30]

## Inversion mode

Inversion mode (IM) is another postprocessing visualization modality that can be combined with static 3D or STIC acquisition.[28,31,32] IM analyzes the echogenicity of tissue (white) and fluid-filled (black) pixels in a volume and inverts their presentation, i.e., fluid-filled spaces such as the cardiac chambers now appear white, while the myocardium has disappeared. In fetal echocardiography, it can be applied to create "digital casts"[33] of the cardiac chambers, outflow tracts, and great vessels in normal and anomalous cases.[34] It can also produce a reconstruction of the extracardiac vascular tree, similar to 3DPD. IM has the additional advantage of showing the stomach and gallbladder as white structures, which can aid the operator in navigating within a complex anomaly scan. IM can be joined with STIC and VOCAL to quantify fetal cardiac ventricular volumes or mass, and can also be applied to the evaluation of fetal heart function.[28,35,36]

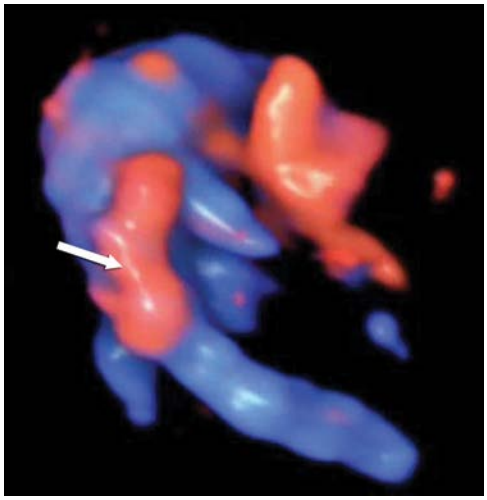

**Figure 14.11**
Rendered image derived from a STIC acquisition with high-definition power Doppler of a case of aortic atresia. Arrow indicates reverse flow in the narrow aorta. (See corresponding Video 14.8.)

# Screening examination of the fetal heart with three- and four-dimensional ultrasound

## *Guidelines*

Guidelines for the performance of fetal heart examination have been published by the International Society of Ultrasound in Obstetrics and Gynecology (ISUOG).[37] These guidelines for fetal cardiac scanning can incorporate 3D/4D applications and 3D/4D ultrasound can enhance fetal cardiac scans, as well as the evaluation of congenital anomalies. Many research teams have applied 3D ultrasound and STIC acquisition to fetal echocardiography, and various techniques have been put forward to optimize the use of this modality.

A well-executed STIC acquisition (see Chapter 13) contains all the necessary planes for evaluation of the five classic transverse planes of fetal echocardiography.[21,22] The operator can examine the fetal upper abdomen and

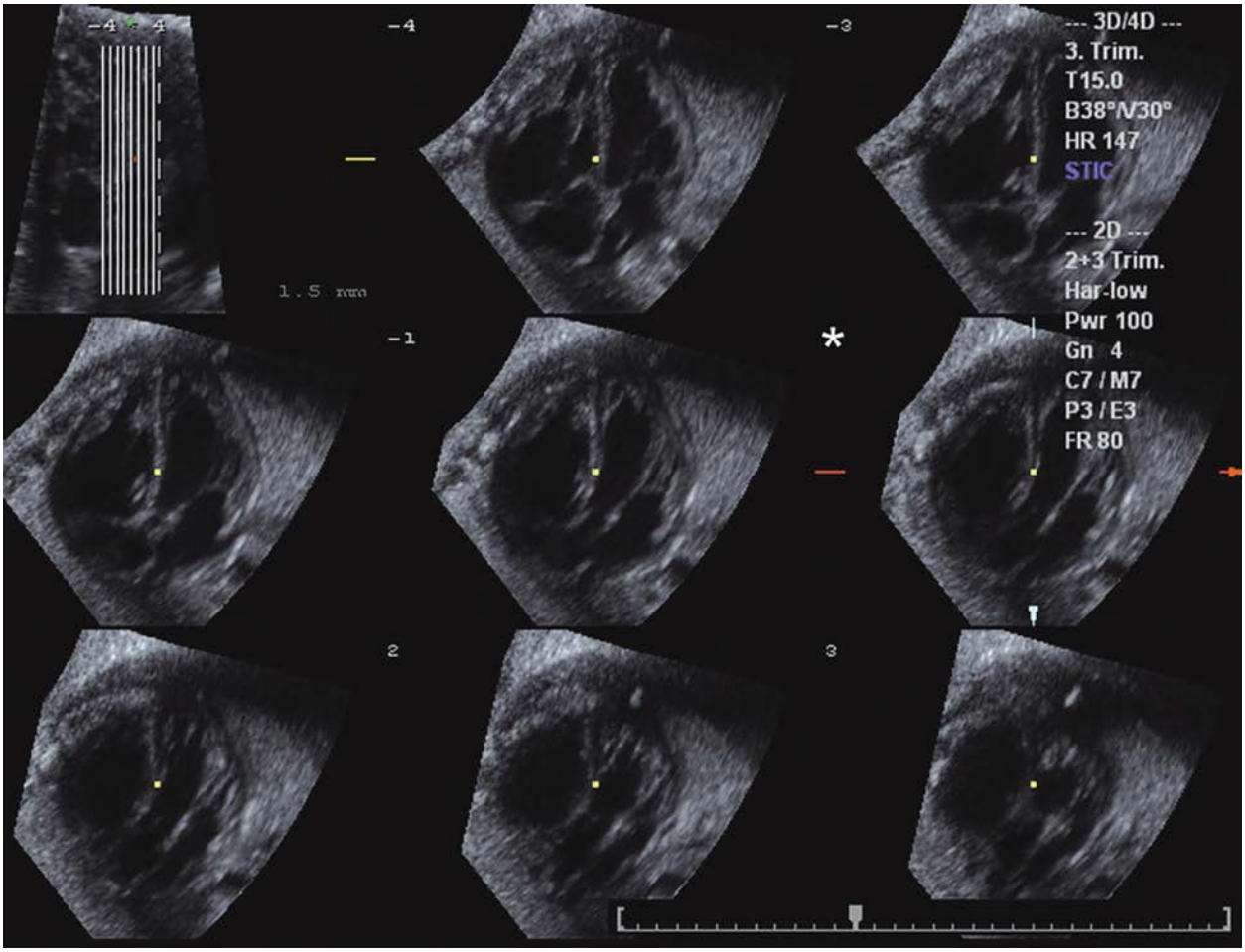


**Figure 14.12**
Tomographic ultrasound imaging (TUI): the –4 plane (top row, center) shows the FCV, while the zero plane (asterisk, middle row, right) shows the outflow tract view, and the +3 plane shows the great vessels (bottom, right). (Reproduced with permission from Yagel S et al. *Ultrasound Obstet Gynecol* 2007;29:81–95.[82] © International Society of Ultrasound in Obstetrics and Gynecology. Permission is granted by John Wiley and Sons Ltd on behalf of ISUOG.)

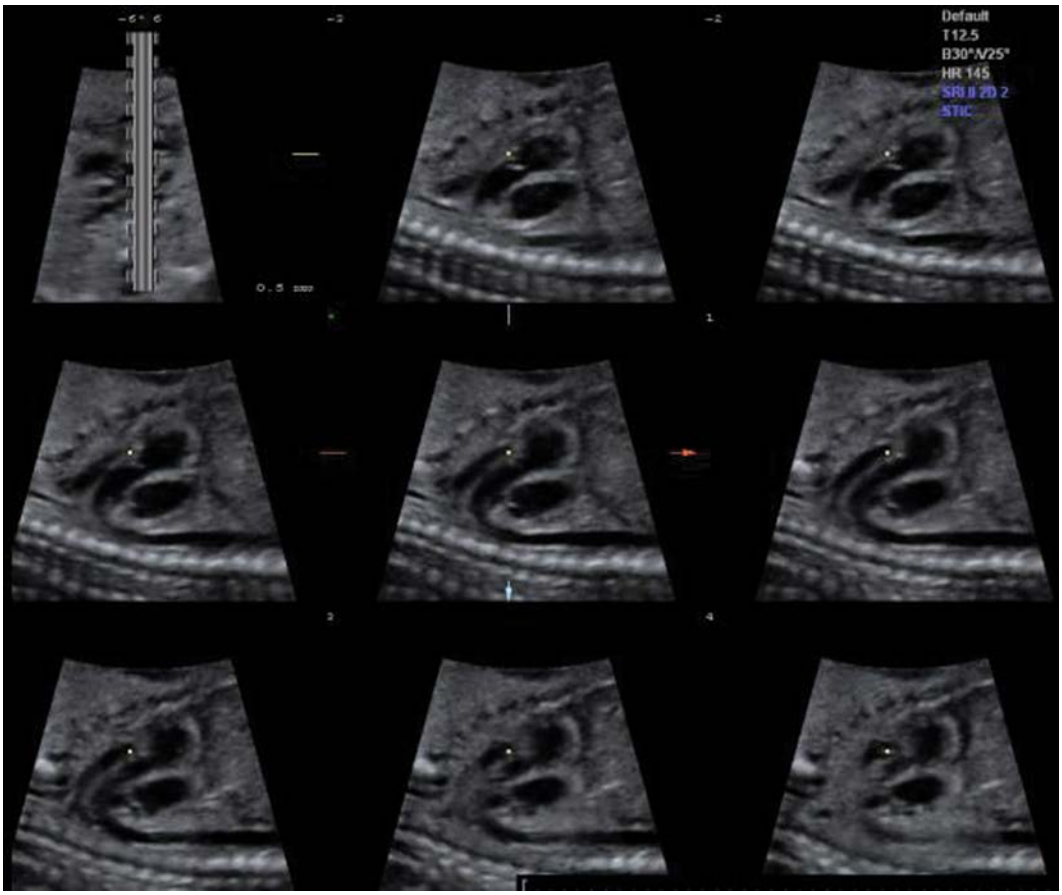


**Figure 14.13**
Tomographic ultrasound imaging (TUI): A TUI image from a grayscale STIC acquisition showing a case of transposition of the great arteries with parallel vessels. The serial images clearly display the aorta anterior to the pulmonary artery. (See corresponding Video 14.9.)

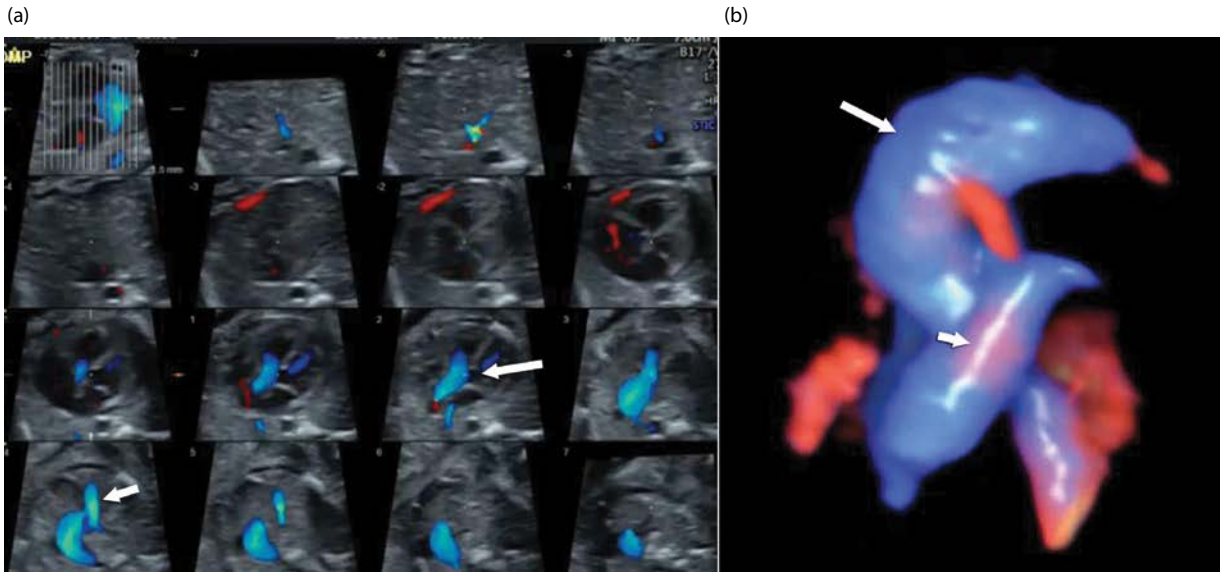


**Figure 14.14**
Tetralogy of Fallot shown in TUI (a) and in a rendered image from STIC acquired with high-definition power Doppler (b). TUI image shows the pulmonary stenosis (small arrow) and dilated overriding aorta (long arrow). Rendered image shows the narrow pulmonary artery (small arrow) and dilated aortic arch (long arrow). (See corresponding Videos 14.10 and 14.11.)

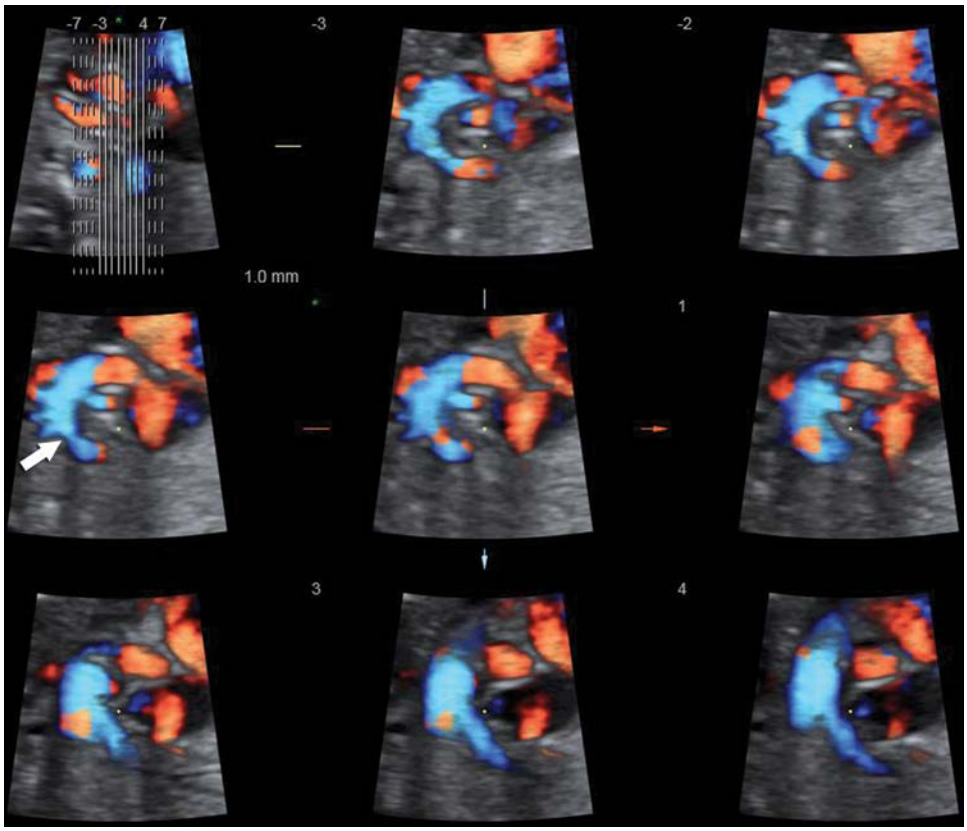


**Figure 14.15**
TUI with color Doppler shows postductal coarctation of the aorta. Arrow indicates the lesion. (See corresponding Video 14.12.)

stomach, then scroll cephalad to obtain the familiar four-chamber view, the five-chamber view, the bifurcation of the pulmonary arteries, and finally the three-vessel and trachea view. Slight adjustment along the *x*- or *y*-axes may be necessary to optimize the images. Performed properly, this methodology will provide the examiner with all the necessary planes to conform to the guidelines, above. However, it must be remembered that STIC acquisition that was degraded by maternal or fetal movements, including fetal breathing movements, will contain artifacts within the scan volume.

## Applications

Among the most attractive facets of 3D/4D scanning are the potential for digital archiving and sharing of examination data over a network.[38–43] These capabilities were applied by Viñals and colleagues[39–41] to increase delivery of prenatal cardiac scanning to poorly served areas. Local practitioners in distant areas acquired and stored 3D volume sets at their centers; they were subsequently sent over an Internet link and analyzed by expert examiners in central locations.[39,40] Rizzo et al. showed that cardiac volumes acquired by 4D sonography in peripheral centers showed high enough quality to allow satisfactory diagnostic cardiac views.[42] This can have important implications in increasing the penetration of prenatal ultrasound services in poorly served or outlying areas of many countries.

STIC also has a role in education and training of examiners.[40,42,44,45] We devised a study to apply STIC specifically to train nonexpert examiners to perform fetal echocardiography.[44] Two sonographers without formal training in fetal echocardiography received theoretical instruction on the five classic planes of fetal echocardiography, as well as STIC technology. They acquired and stored STIC volumes, which were evaluated offline according to a standardized protocol that required the trainee to mark 30 specified structures on the five required axial planes. Volumes were then reviewed by an expert examiner for quality of acquisition and correct identification of specified structures. Trainees succeeded in identifying 97%–98% of structures, with a highly significant degree of agreement with the expert's analysis ($p < 0.001$).[44]

DeVore and colleagues presented the "spin" technique,[25] combining MPR and STIC acquisition to analyze acquired volumes and simplify demonstration of the ventricular outflow tracts. Using this technique, the operator acquires a VOI from a transverse sweep of the fetal mediastinum that includes the sequential planes of fetal echocardiography. In postprocessing, the outflow tract view is imaged in the A-plane, and outflow tract and adjacent vessels are then examined by placing the reference point over each vessel and rotating the image along the *x*- and *y*-axes until the full length of each vessel is identified.[25]

Abuhamad proposed an automated approach to extract the required planes from an acquired volume, coining the term *automated multiplanar imaging* (AMI).[24] Based on the idea

that the scanned 3D volume contains all possible planes of the scanned organ, it should be possible to define the geometric planes within that volume that would be required to display each of the diagnostic planes of a given organ, for example, the sequential scanning planes of fetal echocardiography. Beginning from the four-chamber view, all the other planes are in constant anatomic relationship to this plane, and a computer-automated program could present those planes once the appropriate volume block is acquired.[24]

Espinoza and colleagues introduced a novel algorithm combining STIC and TUI[26] to image the diagnostic planes of the fetal heart simultaneously, and facilitate visualization of the long-axis view of the aortic arch. Turan et al. proposed a similar approach to employ STIC and TUI to standardize fetal echocardiography; the investigators achieved successful imaging of target views in one panel in 91% of cases.[46]

Yeo and colleagues[47] investigated the application of fetal intelligent navigation echocardiography (FINE) to acquired STIC volumes, to visualize nine diagnostic planes and virtual intelligent sonographer assistance (VIS-Assistance) to navigate the anatomy surrounding each plane. The system automatically generates the abdomen/stomach plane, four-chamber, five-chamber (aortic root), left ventricular outflow tract, right ventricular outflow tract, and three vessels and trachea views as well as the ductal and aortic arches and the superior vena cava (SVC) and inferior vena cava (IVC) views. Veronese and colleagues subsequently applied these modalities to STIC volumes of fetuses in the second and third trimesters and found that both modalities, singly or in combination, were effective in identifying the nine diagnostic planes required for fetal echocardiography.[47]

However, in any postprocessing technique, if the original volume was suboptimal, subsequent analysis will be prone to lower image quality and the introduction of artifacts.

Nuchal translucency screening programs will refer approximately 3%–5% of patients for fetal echocardiography as high risk,[48,49] increasing demand for fetal cardiac screening programs. The integration of noninvasive prenatal diagnosis to first-trimester screening programs may move targeted anatomy scanning to earlier gestational ages.[50] STIC acquisition is amenable to younger gestational ages, as the smaller fetal heart can be scanned in a shorter acquisition time, thus reducing the chance of acquisition degradation from fetal movements. It has been shown to be suitable for use in a screening setting.[51]

## *Functional evaluation of the fetal heart: Ventricular volume, mass, and functional measurements*

Evaluation of fetal heart functional parameters has long challenged fetal echocardiographers.[52] While duplex and color Doppler flow nomograms have been quantified and are long-established in 2D fetal echo, many of the pediatric and adult measures are based on end-systolic and end-diastolic ventricular volumes: stroke volume, ejection fraction, and cardiac output. Without electrical trace or clinically applicable segmentation methods to determine the ventricular volume, these parameters have eluded practical prenatal quantification. 3D ultrasound opens new avenues for exploration into ventricular volumetry[28,36,53–55] and mass[35,56,57] measurement.

Bhat and colleagues used nongated static 3D acquisition and STIC to obtain mid-diastolic scans of fetal hearts, and applied VOCAL analysis to determine cavity volume. The result was multiplied by myocardial density (1.050 g/cm$^3$) to obtain the mass.[56,57] A recent animal study showed the validity of 4DUS acquired volume analysis to determine ventricular mass in a model of ventricular hypertrophy.[58]

We published[28] a methodology combining STIC acquisition to determine the end-systolic and end-diastolic stages in the cardiac cycle, then inversion mode to isolate the fluid-filled ventricular volume, which was measured using VOCAL analysis (Figure 14.16 and Video 14.13). The resulting volumes allowed quantification of stroke volume and ejection fraction.[28] It was found that both the inversion mode and VOCAL analysis were highly dependent on operator-determined threshold parameters, which affect the intensity of the signal to be colored and included in the volumetry.

Subsequent studies refined the technique and validated the repeatability and reproducibility of the STIC with VOCAL approach for ventricular volume measurement.[55,59,60] Reference ranges for the ventricular walls and interventricular septum were calculated with this approach,[61,62] which was also shown to be applicable in cases of congenital heart disease.[61] 3D/4DUS methodologies have also been applied to obtain fetal cardiac functional parameters based on ventricular volumes, including stroke volume (SV), cardiac output (CO), and ejection fraction (EF).[18,20,36,54,63–65] The measurements have been validated in mechanical[57,60] and animal models.[20]

STIC combined with IM and VOCAL approach can be extended to mass measurement. We measured fetal ventricular mass[35] based on STIC volumes analyzed with inversion mode and VOCAL. The VOCAL trace included the entire ventricle and walls; IM colors the fluid-filled chamber, which was subtracted from the total volume. The remainder was multiplied by the estimated fetal myocardial density (1.050 g/cm$^3$). We created scatterplots for fetal right and left ventricular mass in the second half of gestation. Several anomalous cases that were diagnosed during the study period showed deviation from normal values of ventricle mass.[35]

We applied STIC to acquire and analyze fetal tricuspid annular plane systolic excursion (f-TAPSE).[66] f-TAPSE is a modified method to measure the vertical movement of the tricuspid valve annulus. This is traditionally done by M-mode ultrasound; it is a recognized measure to assess the fetal right heart. We evaluated the usefulness of STIC M-mode in obtaining it, and compared conventional M-mode and STIC M-mode–based measures of f-TAPSE. First, conventional M-mode was applied to the tricuspid

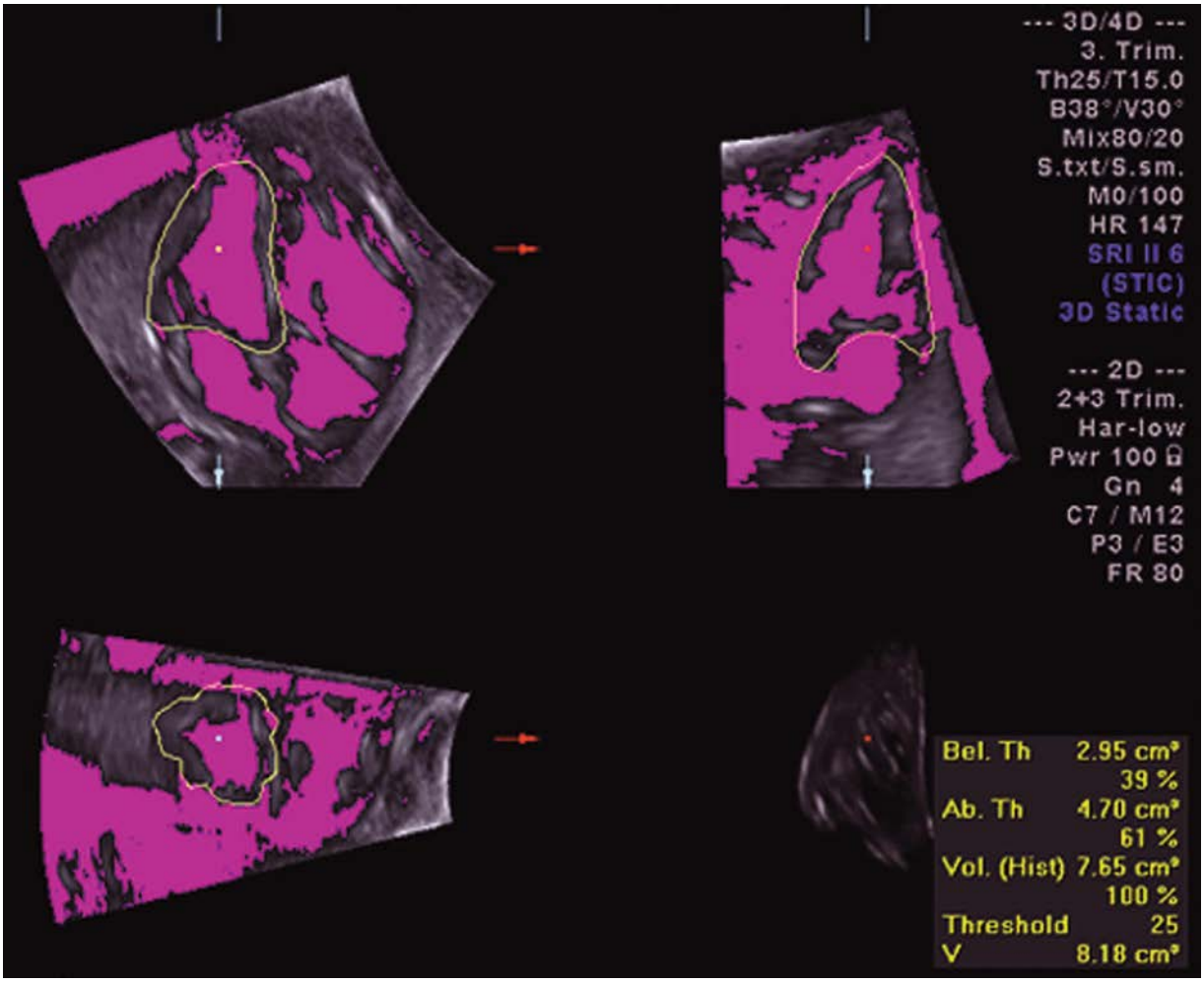


**Figure 14.16**
STIC acquisition combined with inversion mode (IM) and virtual organ computer-aided analysis (VOCAL) for fetal cardiac ventricle volumetry. The resulting measurements appear in the box, bottom right. See also corresponding Video 14.13. (Reproduced with permission from Yagel S et al. *Ultrasound Obstet Gynecol* 2007;29:81–95.[82] © International Society of Ultrasound in Obstetrics and Gynecology. Permission is granted by John Wiley and Sons Ltd on behalf of ISUOG.)

annulus, parallel to the ventricular septum, and the amplitude of the resulting wave was measured. A STIC volume was then acquired and saved; the volume was rotated in postprocessing to show an apical four-chamber view, and f-TAPSE was measured. Scatterplots of f-TAPSE measures obtained with conventional M-mode and with STIC M-mode were created for gestational age and estimated fetal weight. f-TAPSE increased linearly with GA and with EFW, and good correlation was found between the two methods (Pearson $R^2 = 0.904$). Inter- and intraobserver variation (ICC) in conventional M-mode and STIC M-mode f-TAPSE measures were 0.94 and 0.97, respectively.[66]

STIC M-mode has also been applied[67] to produce reference ranges of fetal cardiac biometric parameters, including thicknesses of the right and left ventricular walls and intraventricular septum. A subgroup of fetuses with congenital heart disease (CHD) were studied; these cardiac biometric measurements were found to deviate from the reference ranges (>95th centile or <5th centile) in these fetuses.[68]

## Three- and four-dimensional ultrasound in the diagnosis of congenital heart disease

One of the great advantages of a 3D/4D system is its digital archiving capabilities. Examination volumes are stored for later analysis, away from the patient and the time constraints of a busy clinic. In cases of CHD, other professionals can be invited to view the examination. They can do this anywhere that an Internet link is available.[39] The first examiner can consult with the attending physician, cardiologist, surgical[69] or other management teams, genetic counselors, and parents. Complex malformations can be elucidated through interdisciplinary discussion and made clear to laymen. In addition, stored data from cases of CHD are invaluable teaching materials for professional education.[44]

Many teams have applied 3D/4D ultrasound capabilities to the diagnosis of congenital cardiovascular malformations.

Each of the modalities and applications described above lends itself to different facets of this complex endeavor.

## Virtual planes

As described above, a properly executed STIC acquisition results in a "volume block," which is a reconstructed complete cardiac cycle. This block of spatial and temporal image data contains and makes available many scanning planes that are not readily accessible in 2D ultrasound. The term *virtual planes* was coined to refer to these rendered scanning planes. The interventricular and interatrial septa (IVS, IAS) planes, and the coronal atrioventricular (CAV) plane of the cardiac valves' annuli, have been investigated and applied to the evaluation of CHD.[27] They were shown to have added value in the diagnosis of ventricular septal defect, restrictive foramen ovale, alignment of the ventricles and great vessels, and evaluation of the atrioventricular (AV) valves.[67]

## Segmental approach

The segmental approach to CHD has helped to standardize the description of cardiac lesions. In addition, it has contributed to understanding the pathophysiology of the malformed developing fetal heart, and subsequently to our conceptualization and diagnostic imaging. The sequential segmental approach essentially divides the heart into three basic segments: the atria, the ventricles, and the great arteries. These are divided and joined at the level of the atrioventricular valves, and at the ventriculoarterial junctions. The segmental approach to diagnosis of CHD is comprehensively and concisely described elsewhere[70]; we follow this sequence in describing the application and added value of 3D/4D in the diagnosis of CHD, through index cases of anomalies diagnosed in our center.

## Veins and atria: Total anomalous pulmonary venous connection and interrupted inferior vena cava with azygos continuation

Total anomalous pulmonary venous connection (TAPVC) is a many-faceted group of malformations affecting the pulmonary veins[71]; the variations and classification are described in detail in Chapter 19. Essentially, in these anomalies the pulmonary veins do not drain into the left atrium, but rather to various other locations: the right atrium, great veins, or abdominal veins. The present case was an intradiaphragmatic variation with drainage of the pulmonary veins to the portal vein.

3D/4D ultrasound can have a significant contribution to the understanding of the fetal venous system. Figure 14.17a and Video 14.14 show the use of MPR with the reference point to navigate this complex lesion. Placement of the reference point in the suspected anomalous blood vessel in cross section (A-frame) showed the vessel in longitudinal plane in the B-frame. This confirmed that the finding was not an artifact, but rather the characteristic vertical vein. 3D power flow Doppler displayed the idiosyncratic vascular tree and absence of the pulmonary veins (Figure 14.17b and Video 14.15); rotation of the image in postprocessing allowed overall examination of the lesion in 360°.

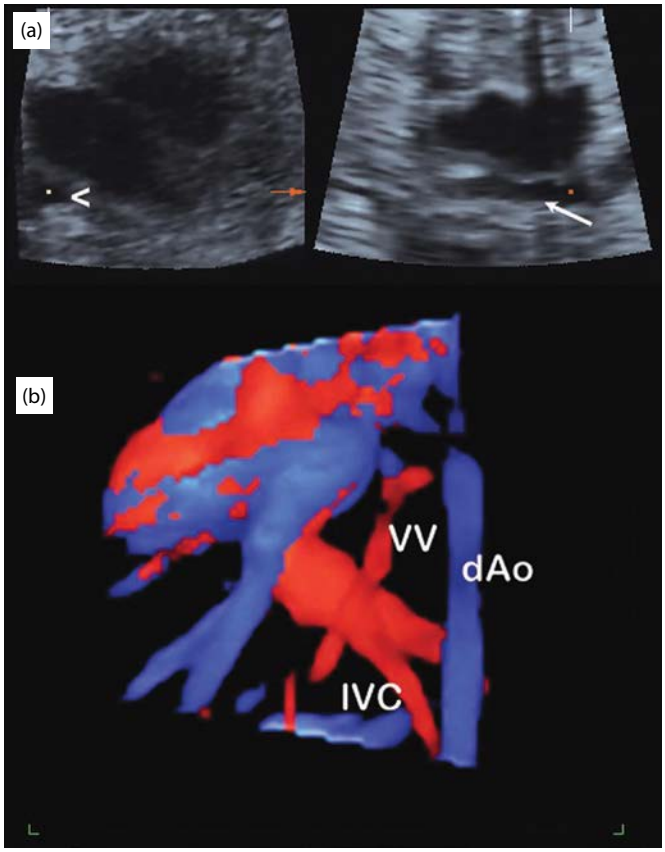


**Figure 14.17**
(a) STIC acquisition in a case of total anomalous pulmonary venous connection (TAPVC). The A-plane shown raised suspicion of an anomalous vessel (caret), which is confirmed in the B-plane (arrow). (b) The heart and great vessels of this fetus: STIC acquisition and high-definition power flow Doppler confirmed the characteristic vertical vein (VV). Note also the absence of pulmonary veins (compare Figure 14.6). See also corresponding Videos 14.14 and 14.15. (Reproduced with permission from Yagel S et al. *Ultrasound Obstet Gynecol* 2007;29:81–95.[82] © International Society of Ultrasound in Obstetrics and Gynecology. Permission is granted by John Wiley and Sons Ltd on behalf of ISUOG.)

Interrupted inferior vena cava (IVC) with azygos continuation is shown in Figure 14.18 and Video 14.16. This cardinal vein anomaly results from primary failure of the right subcardinal vein to connect to the hepatic segment of the IVC.[72] Blood is shunted directly into the right supracardinal vein (which will become the SVC) and blood from the lower body flows through the azygos vein to the SVC. In this instance, B-flow acquisition provided real-time representation of the anomalous course of the IVC and connection to the fetal heart. It showed the azygos vein draining into the SVC, as well as the aorta in one 3D image that would be impossible to obtain with 2D color Doppler scanning. B-flow scanning provided superior imaging of the slower blood flow in the azygos vein than was demonstrated with 3DPD.

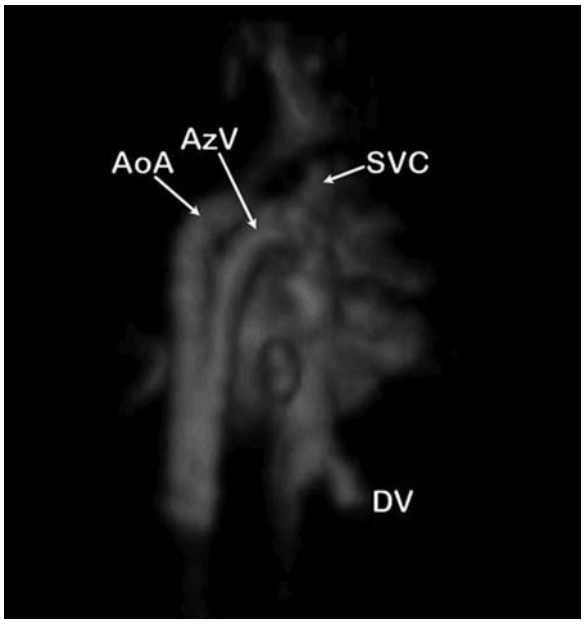


**Figure 14.18**
B-flow image of the heart and great vessels in a fetus with interrupted inferior vena cava with azygos continuation. See also corresponding Video 14.16. (AoA, ascending aorta; AzV, azygos vein; DV, ductus venosus; SVC, superior vena cava.) (Reproduced with permission from Yagel S et al. *Ultrasound Obstet Gynecol* 2007;29:81–95.[82] © International Society of Ultrasound in Obstetrics and Gynecology. Permission is granted by John Wiley and Sons Ltd on behalf of ISUOG.)

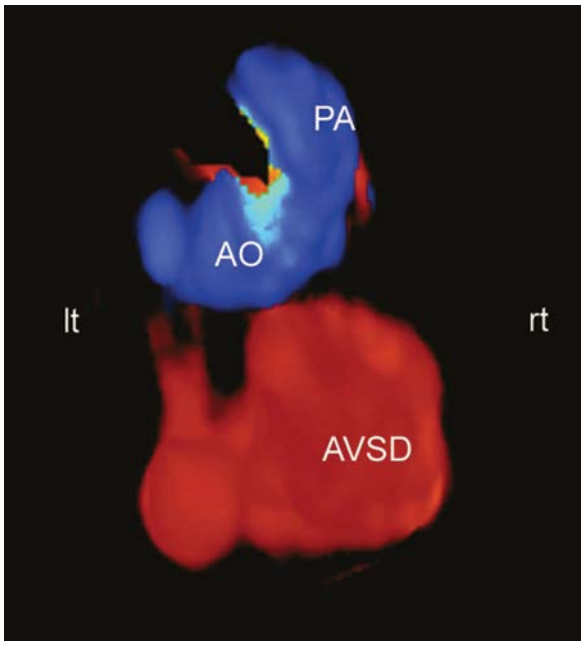


**Figure 14.19**
The coronal atrioventricular plane from STIC acquisition with color Doppler mapping in a case of atrioventricular septal defect. (AO, aorta; AVSD, atrioventricular septal defect; PA, pulmonary artery.) (Reproduced with permission from Yagel S et al. *Ultrasound Obstet Gynecol* 2007;29:81–95.[82] © International Society of Ultrasound in Obstetrics and Gynecology. Permission is granted by John Wiley and Sons Ltd on behalf of ISUOG.)

## *Atrioventricular junction: Atrioventricular septal defect and tricuspid valve stenosis*

Atrioventricular septal defect (AVSD) is characterized by incomplete atrial and ventricular septation, forming a common atrioventricular junction. AVSD has many forms; all involve an abnormality of the AV valves. Figure 14.19 shows the use of 3D rendering of a STIC volume acquired with color Doppler to demonstrate the anomalous intracardiac flow resulting from the AVSD.

Another group of AV valve lesions is mitral or tricuspid valve atresia, dysplasia, or stenosis. Figure 14.20 shows the CAV plane in a case of tricuspid stenosis. This "virtual plane 2" is obtained from a STIC volume with color Doppler, by placing the bounding box tightly around the level of the AV connection in the four-chamber view, with the superior side active (frame A); the plane is slightly adjusted along the *x*- and *y*-axes; the rendered image (frame D) shows the AV valves with anomalous anatomy (compare normal CAV plane, inset). This virtual plane provides a 3D look at the AV and semilunar valves' annuli, resembling the surgical plane seen when the heart is opened in surgery.

## *Ventricles: Ventricular septal defects*

Ventricular septal defects are perhaps the most common—and most commonly missed—congenital heart defect. The natural history and *in utero* development of these lesions are described in Chapter 21 (Intracardiac shunt malformations). Several groups have proposed methods for evaluation of the interventricular septum.[16,27,73,74] By using MPR, with the reference point placed on the septum with the four-chamber view in the A-frame, the B-frame will show the septum and defect *en face* (Figure 14.21 and Video 14.17). We recommend, however, the use of the bounding box in 3D rendering from STIC acquisition with color Doppler. The operator places the "active" side of the box to the right or left (i.e., from within the left or right ventricle) and obtains an image (in the D-frame) having more depth, for a more detailed examination of the size and nature (and number) of the VSD(s). The addition of color Doppler demonstrates blood flow across the lesion and shows at what stage in the cardiac cycle and to what degree shunting occurs.

## *Ventriculoarterial junctions (conotruncal anomalies): Transposition of the great arteries, tetralogy of Fallot*

Transposition (or malposition or malalignment) of the great arteries (TGA) is the general name for a complex group of anomalies with widely varying anatomic and clinical presentations. When the sequential segmental approach is applied to

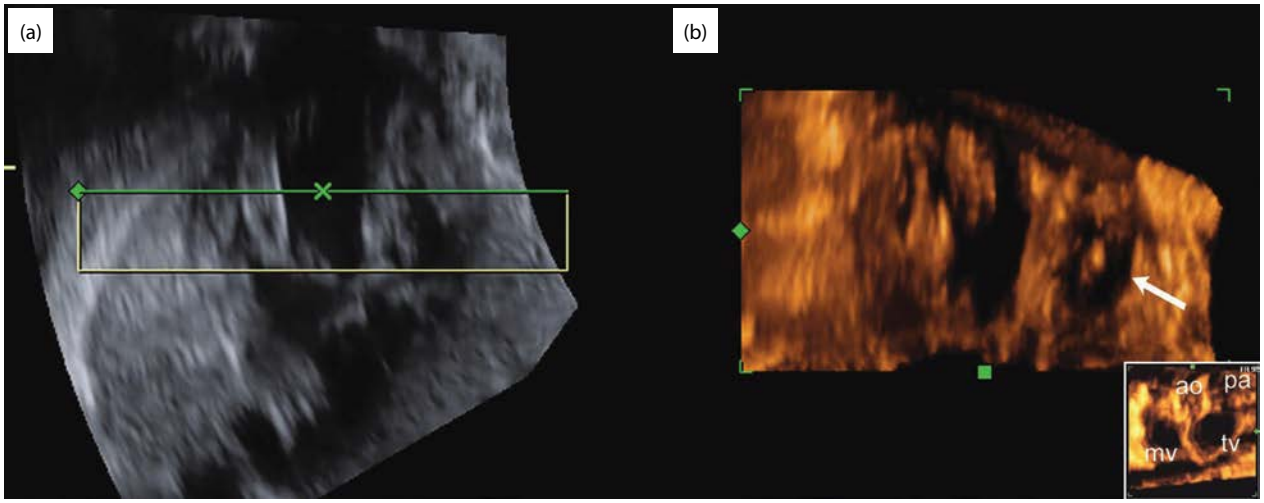


**Figure 14.20**
Tricuspid stenosis evaluated with 3D rendering and the CAV plane. The bounding box is placed tightly around the level of the AV valves in the A-frame (a); the D-frame (b) clearly shows the stenotic valve (arrow). Compare normal CAV plane in diastole, inset: ao, aortic valve; mv, mitral valve annulus; pa, pulmonary valve; tv, tricuspid valve annulus. (Reproduced with permission from Yagel S et al. *Ultrasound Obstet Gynecol* 2007; 29: 81–95.[82] © International Society of Ultrasound in Obstetrics and Gynecology. Permission is granted by John Wiley and Sons Ltd on behalf of ISUOG.)

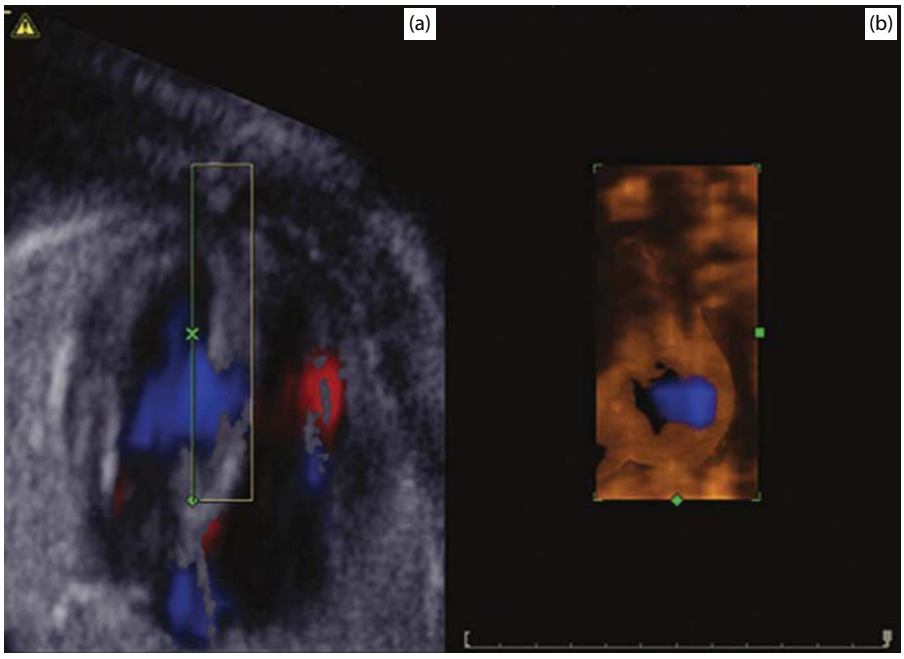


**Figure 14.21**
The interventricular septum (IVS) "virtual plane" with color Doppler in evaluation of ventricular septal defect (VSD). The navigation point is placed on the septum in the A-plane (a); the D-frame (b) shows the rendered IVS with flow across the defect from right to left. See also corresponding Video 14.17. (Reproduced with permission from Yagel S et al. *Ultrasound Obstet Gynecol* 2007;29:81–95.[82] © International Society of Ultrasound in Obstetrics and Gynecology. Permission is granted by John Wiley and Sons Ltd on behalf of ISUOG.)

systematic diagnosis of CHD,[70] the morphology of each successive anatomic segment is assessed in turn. The morphologic right and left atria and ventricles are established; now the examiner addresses the ventriculoarterial junction and the accordance or discordance of the great arteries and ventricles.

3D rendering with color Doppler was applied to the evaluation of suspected malalignment of the great vessels, by examining the CAV ("surgical plane") at the level of the AV and semilunar valves' annuli.

We applied B-flow scanning to the evaluation of TGA and found that it was more effective than 3DPD or inversion mode in visualizing the great vessels' structure and relationships. Figure 14.22 and Video 14.18 show a case of complete dextrotransposition of the great arteries. The B-flow scan clearly showed blood flow into the ventricles and out through the malaligned vessels. This demonstration of the anatomic variant of the anomaly aided our consultations with the parents and their attending physician.

Tetralogy of Fallot is a conotruncal defect characterized by ventricular septal defect (VSD), aortic valve overriding the ventricular septum, narrowing of the right ventricular outflow tract (RVOT), and right ventricular hypertrophy. Figure 14.23 and Video 14.19 show a case of tetralogy of Fallot imaged in TUI, clearly showing the dilated overriding aorta.

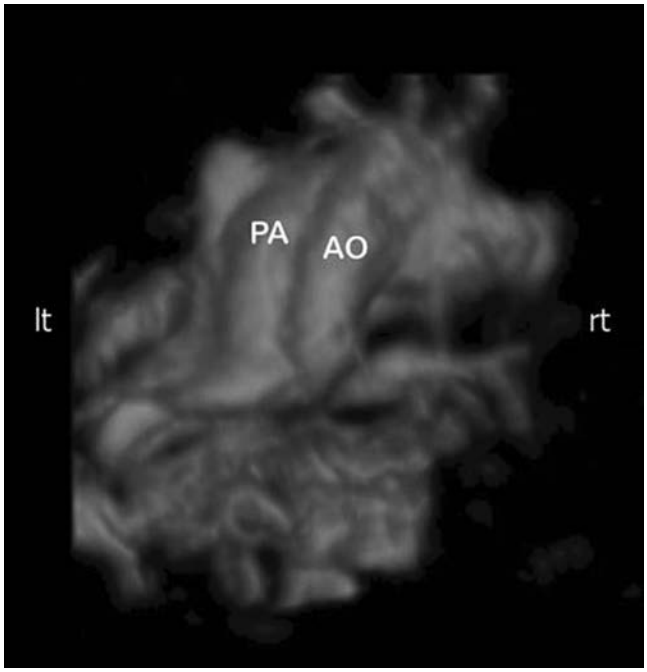


**Figure 14.22**
B-flow modality showed the parallel great vessels in a case of transposition. Application of this modality clearly shows the blood flow in the malaligned vessels. See also corresponding Video 14.18. (AO, aorta; PA, pulmonary artery.) (Reproduced with permission from Yagel S et al. *Ultrasound obstet Gynecol* 2007;29:81–95.[82] © International Society of Ultrasound in obstetrics and Gynecology. Permission is granted by John Wiley and Sons Ltd on behalf of ISUOG.)

## *Arterial trunks: Pulmonary stenosis and right aortic arch*

The use of 3D rendering of a STIC acquisition with or without color Doppler to obtain virtual planes was discussed previously. The CAV plane is an excellent tool for evaluation of the semilunar valves. Once the CAV plane is obtained, the 4D-cine option is initiated and blood flow across the valves evaluated through the cardiac cycle. Figure 14.24 shows a case of critical pulmonary stenosis with retrograde flow in the main pulmonary artery (MPA). Figure 14.25 shows another case, of severe pulmonary stenosis with post-stenotic dilatation of the pulmonary artery rendered with TUI. See also corresponding Videos 14.20 and 14.21.

Right aortic arch defect results from persistence of the right dorsal aorta and involution of the distal part of the left dorsal aorta. There are two main types, with or without a retroesophageal component.[72] Figure 14.26 shows a case of right aortic arch diagnosed with B-flow; this modality showed the characteristic course of the aortic arch to the right of the trachea.

## *Functional evaluation: Ventricular volumes*

Messing et al.[28] published a novel methodology combining STIC acquisition with postprocessing application of inversion mode and VOCAL to quantify end-systolic and end-diastolic ventricular volumes. Nomograms were created from

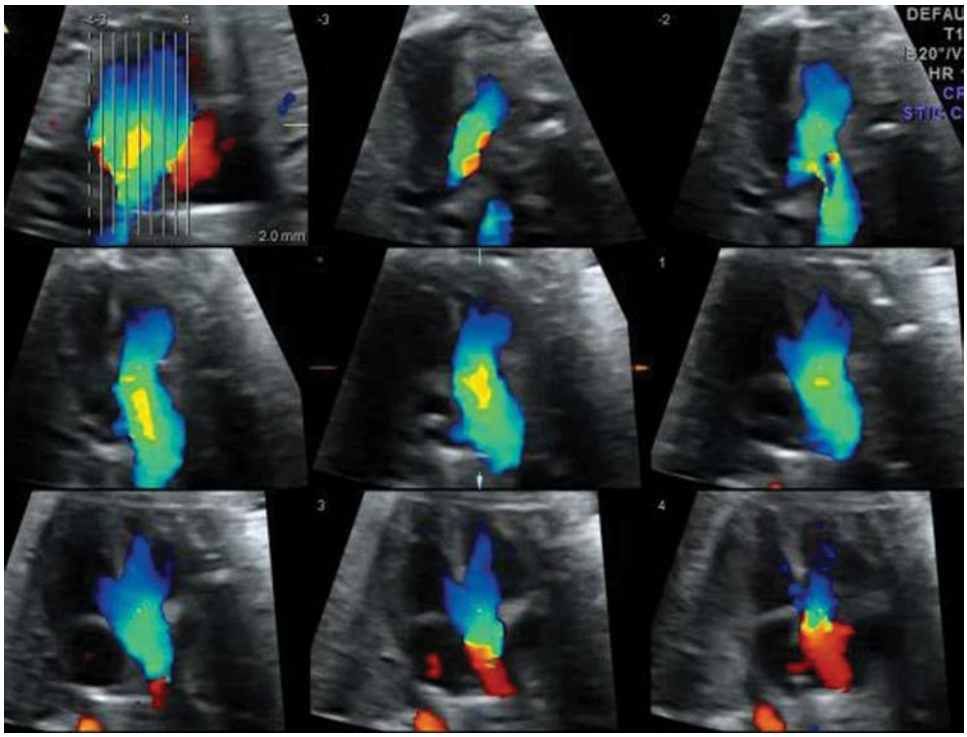


**Figure 14.23**
TUI image of the left ventricular outflow tract (LVOT) in a case of tetralogy of Fallot, showing the dilated overriding aorta. (See corresponding Video 14.19.)

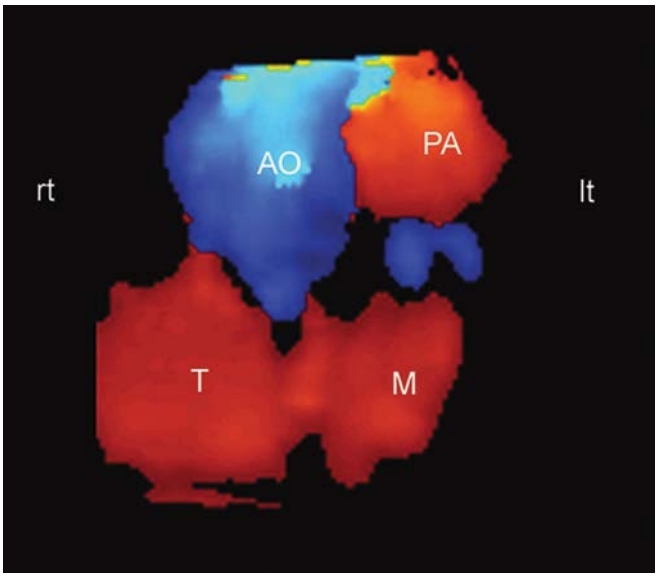


**Figure 14.24**
The CAV plane from STIC acquisition with color Doppler mapping in a case of transposition of the great arteries and pulmonary stenosis with retrograde flow in the main pulmonary artery. (AO, aorta; M, mitral annulus; PA, pulmonary artery; T, tricuspid annulus.) (Reproduced with permission from Yagel S et al. *Ultrasound Obstet Gynecol* 2007;29:81–95.[82] © International Society of Ultrasound in Obstetrics and Gynecology. Permission is granted by John Wiley and Sons Ltd on behalf of ISUOG.)

right and left ventricle end-systolic and end-diastolic volumes from 100 fetuses examined between 20 and 40 gestational weeks. The resulting measurements correlated strongly with gestational age and estimated fetal weight. The measured volumes were used to create nomograms for fetal stroke volume and cardiac ejection fraction.

The methodology was applied to saved STIC volumes of cases with cardiac anomaly or dysfunction that involved changes in ventricular volume, stroke volume, or ejection fraction. These included critical pulmonary stenosis, twin-to-twin transfusion syndrome with secondary pulmonary stenosis, aortic valve stenosis with hypoplastic aortic arch, Ebstein anomaly, supraventricular tachycardia, and vein of Galen aneurysm.[28]

Our normal cases showed the effectiveness of fetal heart ventricle volumetry in cardiac evaluation and quantification; such volumetry is not readily available in 2D echocardiography. The pathological cases showed the potential added value of this methodology. In the case of critical pulmonary stenosis, for example, the diagnosis was more serious than suspected by 2D echocardiography. Ventricle volumetry also provided insight into the pathophysiology of lesions such as supraventricular tachycardia (SVT) and vein of Galen aneurysm, among others.[28]

Subsequently, other teams[36,55] paired STIC with VOCAL to investigate fetal ventricular volume. Hamill and colleagues found that STIC and VOCAL allowed repeatable and reproducible calculation of ventricular volumes[55] and can be used to quantify normal fetal right and left stroke volume, cardiac

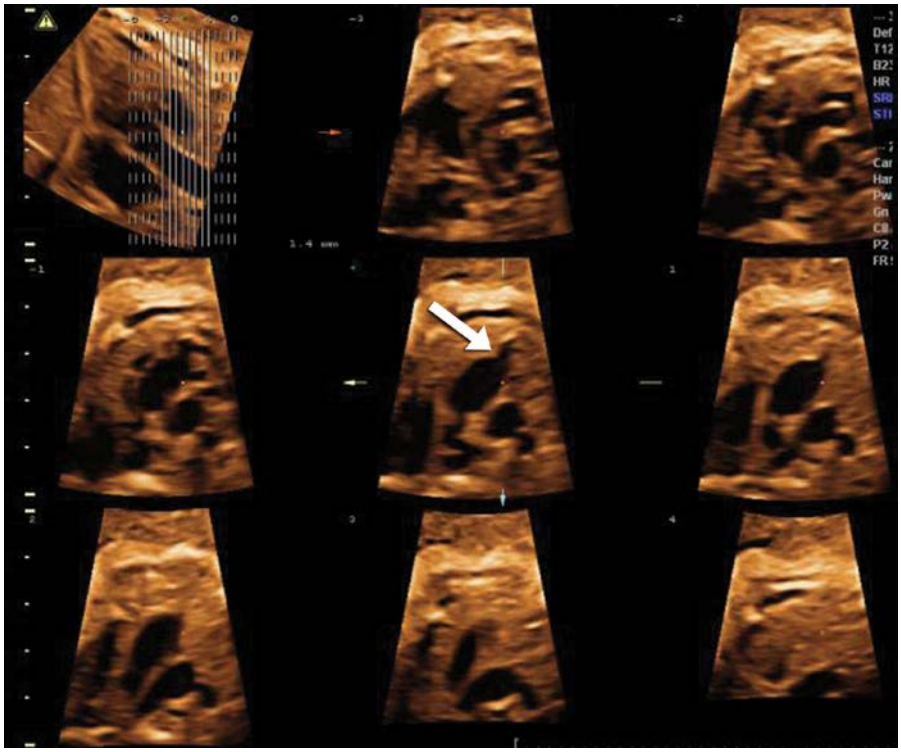

**Figure 14.25**
Severe pulmonary stenosis rendered with TUI. Arrow indicates the marked narrowing at the valve and post-stenotic dilatation of the pulmonary artery. (See corresponding Videos 14.20 and 14.21.)

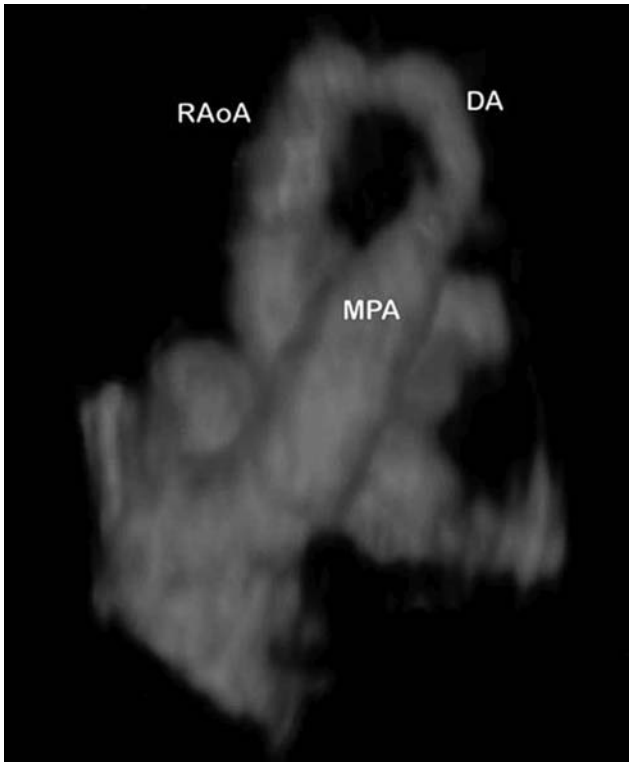


**Figure 14.26**
B-flow modality in a case of right aortic arch (RAoA). (DA, ductus arteriosus; MPA, main pulmonary artery.) (Reproduced with permission from Yagel S et al. *Ultrasound Obstet Gynecol* 2007;29: 81–95.[82] © International Society of Ultrasound in Obstetrics and Gynecology. Permission is granted by John Wiley and Sons Ltd on behalf of ISUOG.)

output (CO), adjusted CO, and right and left ejection fraction. They found that the larger right volume and greater left ejection fraction resulted in similar right and left SV and CO.[36] Hamill and colleagues[65] applied STIC combined with VOCAL in a cross-sectional study of 34 fetuses with umbilical artery pulsatility index >95th percentile. Ventricular volume at end-systole and end-diastole, SV, CO, adjusted CO, and EF were compared to those of 184 normal fetuses. The investigators found that mean ventricular volumes were lower in fetuses with PI > 95th centile, as were mean left and right SV, CO, and adjusted CO. Right ventricular volume, SV, CO, and adjusted CO exceeded the left in these fetuses, while mean EF was greater than that observed in controls. The authors concluded that increased placental vascular impedance to flow is associated with changes in fetal cardiac function.[65]

# Potential pitfalls of three- and four-dimensional echocardiography

3D/4D fetal echocardiography scanning is prone to artifacts similar to those encountered in 2D ultrasound, and some that are specific to 3D/4D acquisition and postprocessing.

## *STIC acquisition quality*

The quality of a STIC acquisition may be adversely affected by fetal body or "breathing" movements. To improve scan quality, the fetus should be in a quiet state and the shortest scan time possible employed. When reviewing a STIC acquisition, the B-frame reveals artifacts introduced by fetal breathing movements Figure 14.27. If the B-frame appears sound, the volume is usually acceptable and can be used for further investigation. The quality of the original acquisition impacts on all further stages of postprocessing and evaluation.

## *Original angle of insonation*

The original angle at which a scan was performed will impact on the quality of all the planes acquired. It is important to achieve an optimal beginning 2D plane, before starting 3D or 4D acquisition.

## *Acoustic shadows*

Shadowing artifacts pose a particular problem to 3D/4D ultrasound. When commencing scanning from the 2D plane, acoustic shadows may not be apparent. However, they may be present within the acquired volume block. It is imperative to review suspected defects with repeated 2D and 3D scanning to confirm their presence in additional scanning planes.

## *Three-dimensional rendering*

3D rendering creates virtual images. Application of some algorithms designed to smooth the image can lead to loss of data from the original scan. 3D rendering should always be used in conjunction with the A-frame 2D image for comparison.

## *Flow direction*

An acquired volume containing Doppler flow information is available for manipulation and may be sliced and rotated around the *x*-, *y*-, and *z*-axes for analysis. However, rotation of the volume with Doppler directional flow information can mislead the operator: if the directions are reversed, flow data can be misinterpreted. The operator must confirm any suspected pathological flow patterns by confirming the original direction of scanning, whether flow was toward or away from the transducer during the acquisition scan.

## Accuracy

Multiple studies have compared imaging yield between 2D and 3D/4D fetal echocardiography, and others have examined the feasibility of 3D/4D and STIC in screening programs, and still others have described the application of various 3D/4D modalities to diagnosis or evaluation of fetal cardiovascular anomalies. We investigated[23] the contribution of 3D/4D to diagnostic accuracy and precision in our fetal echocardiography screening program. Patients ($n = 13{,}101$) underwent complete fetal

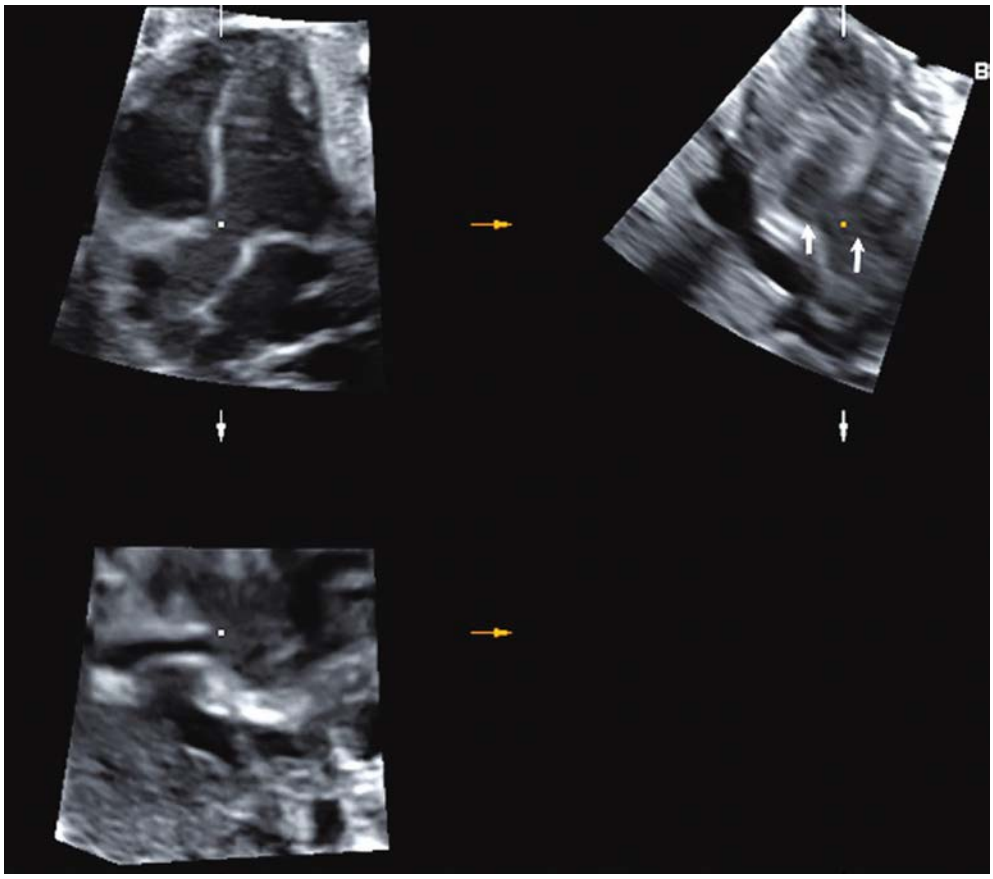

**Figure 14.27**
Artifacts and pitfalls. STIC acquisition in a 26-week fetus: the A-frame shows left ventricular outflow tract plane. Note that the B-frame, however, is degraded by fetal breathing artifacts (arrows). (Reproduced with permission from Yagel S et al. *Ultrasound Obstet Gynecol* 2007;29:81–95.[82] © International Society of Ultrasound in Obstetrics and Gynecology. Permission is granted by John Wiley and Sons Ltd on behalf of ISUOG.)

echocardiography according to our five-planes protocol, as well as examination of the ductus venosus and longitudinal aortic arch planes, performed with 2D ultrasound combined with 2D color Doppler, STIC, STIC with color Doppler, and STIC with B-flow. Stored 2DUS cine-loops and 4DUS volumes were reviewed separately according to a standardized table of 23 specified structures on five required planes of visualization. During the study, there were 181 diagnosed cases of CHD, and 12 false-negative and 0 false-positive results. In 12 cases, 3D/4DUS added to the accuracy of our diagnosis: one right aortic arch with anomalous branching; one transposition of the great arteries with pulmonary atresia diagnosed with TUI; one segmental interrupted aortic arch diagnosed with TUI; one right ventricle aneurysm diagnosed with B-flow; two agenesis of ductus venosus to the coronary sinus diagnosed by multiplanar reconstruction (MPR) and B-flow; two total anomalous pulmonary venous connection diagnosed with MPR; and four ventricular septal defects (VSDs) diagnosed with the aid of virtual planes. We found that overall, 3D/4D ultrasound modalities had impact on diagnostic precision and accuracy in about 6% of cases of fetal anatomical cardiovascular anomalies.[23]

In order to test the reliability and interobserver agreement of 3D/4DUS, Espinoza and colleagues[75] designed a study including seven centers with expertise in 4D fetal echocardiography; each center submitted volume datasets of normal and anomalous cases, which were uploaded onto a centralized server, and blinded analysis by all centers was performed. Intercenter agreement was determined. Ninety volume datasets were randomly selected for analysis. Overall, the median (range) sensitivity, specificity, positive and negative predictive values, and false-positive and false-negative rates for the identification of fetuses with CHDs were 93% (77%–100%), 96% (84%–100%), 96% (83%–100%), 93% (79%–100%), 4.8% (2.7%–25%), and 6.8% (5%–22%), respectively. The most frequent CHDs were conotruncal anomalies (36%). There was excellent intercenter agreement ($\kappa = 0.97$). The authors concluded that 4DUS volume datasets can be remotely acquired and accurately interpreted by different centers, and that in experienced hands, 4DUS is an accurate and reliable method for fetal echocardiography.[75]

Benasar et al.[76] investigated the accuracy of STIC in the diagnosis of CHD in a referral population. STIC volumes were obtained during the (2DUS) referral examinations and stored. The volumes were analyzed at least 1 year later by an examiner blinded to the original results and fetal outcomes. The new diagnoses were compared to 2DUS and postnatal or postmortem examinations of the fetuses. The accuracy, sensitivity, specificity, and positive and negative predictive values of STIC to diagnose the presence or absence of CHD were 91.6%,

94.9%, 88.1%, 89.7%, and 94.0%, respectively. STIC-based diagnoses concurred with the specific postnatal diagnosis of CHD in 74.3% of cases, as compared with 81.7% for 2DUS.[76]

Levental and coworkers compared 2D and nongated 3D ultrasound to obtain standard cardiac views.[77] Meyer-Wittkopf and colleagues[78] evaluated 2D and Doppler-gated 3D in obtaining standard echocardiography scanning planes in normal hearts. They found that 3D provided additional structural depth and allowed a dynamic 3D perspective of valvar morphology and ventricular wall motion.[78]

In evaluating CHD, Meyer-Wittkopf and coworkers[79] evaluated gated 3D volume sets of 2D-diagnosed cardiac lesions, and compared key views of the heart in both modalities. They determined that 3D had added value in a small proportion of lesions.[79] Wang and colleagues[80] compared 3D and 2D scanning of fetuses in the spine-anterior position. This group found that only in the pulmonary outflow tract was 3D ultrasound superior to 2D.

Espinoza and colleagues[31] examined the added value of IM in the evaluation of anomalous venous connections. The investigators found that IM improved visualization of cases of dilated azygos or hemiazygos veins and their spatial relationships with the surrounding vascular structures.

Benacerraf and colleagues[81] compared acquisition and analysis times for 2D and 3D fetal anatomy scanning at 17–21 gestational weeks. 3D ultrasound compared favorably with 2D in mean scanning time and accuracy of fetal biometry.

The data archiving and networking capabilities of 3D/4D fetal echocardiography with STIC acquisition open new avenues for disseminating fetal echocardiography programs to outlying or poorly served areas. This can have important public health implications in these populations. Michailidis and coworkers[43] and Viñals and colleagues[39,40] have shown the feasibility and success of programs based on 3D/4D examination volumes acquired in one center, and reviewed by experts in a center connected by telemedicine Internet link.[38]

## Acknowledgment

An earlier version of this chapter originally appeared as Yagel S, Cohen SM, Shapiro I, Valsky DV. 3D and 4D ultrasound in fetal cardiac scanning: A new look at the fetal heart. *Ultrasound Obstet Gynecol* 2007;29:81–95. It is reproduced with permission.

## Videos

**Video 14.1** (https://youtu.be/u6pUEoMHyjM)
B-flow of normal heart and aortic arch. Brachocephalic trunk (BT), left common carotid (LCC), and left subclavian artery (LSA) are seen projecting from the aortic arch (AoA). Inferior vena cava (IVC) is indicated.

**Video 14.2** (https://youtu.be/n-hz4-Y0HtU)
B-flow: A case of aortic ring imaged in B-flow.

**Video 14.3** (https://youtu.be/ChPaDYkldXo)
Normal heart and great vessels: STIC acquisition with high-definition power flow Doppler. (CA, celiac artery; dAo, descending aorta; DV, ductus venosus; IVC, inferior vena cava; PV, pulmonary veins; SMA, superior mesenteric artery; UV, umbilical vein.)

**Video 14.4** (https://youtu.be/zuEvv_-9RRA)
STIC combined with high-definition power Doppler: Normal heart and great vessels from a STIC acquisition with high-definition power Doppler.

**Video 14.5** (https://youtu.be/y1uzchqi1Ys)
STIC combined with high-definition power Doppler: The normal heart and vessels in longitudinal view.

**Video 14.6** (https://youtu.be/sJERZ-vY9hs)
Rendered image of case of aberrant right subclavian artery (ARSA). The 3VT plane with ARSA. The azygos vein (azygos) is marked.

**Video 14.7** (https://youtu.be/ou4gGReuEGM)
Rendered image of case of aberrant right subclavian artery (ARSA). The ARSA and the relative positions of the aortic branches, the left subclavian artery (LSA), left carotid artery (LCA), right carotid artery (RCA), and the descending aorta (dAo).

**Video 14.8** (https://youtu.be/Xz4PeczEiB8)
Rendered image derived from a STIC acquisition with high-definition power Doppler of a case of aortic atresia. Arrow indicates reverse flow in the narrow aorta.

**Video 14.9** (https://youtu.be/edpgo6Vu1xo)
Tomographic ultrasound imaging (TUI): A TUI image from a grayscale STIC acquisition showing a case of transposition of the great arteries with parallel vessels. The serial images clearly display the aorta anterior to the pulmonary artery.

**Video 14.10** (https://youtu.be/TAtCO9p5juU)
Tetralogy of Fallot shown in TUI. TUI image shows the pulmonary stenosis (small arrow) and dilated overriding aorta (long arrow).

**Video 14.11** (https://youtu.be/uLoRyEZvmMc)
Tetralogy of Fallot in a rendered image from STIC acquired with high-definition power Doppler. Rendered image shows the narrow pulmonary artery (small arrow) and dilated aortic arch (long arrow).

**Video 14.12** (https://youtu.be/65oaeHb-5r4)
TUI with color Doppler shows postductal coarctation of the aorta. Arrow indicates the lesion.

**Video 14.13** (https://youtu.be/V2_FiFxUqXI)
STIC acquisition combined with IM and VOCAL analysis for fetal cardiac ventricle volumetry. The computer mouse was used to manually define the contours of the ventricle at sequential planes. The resulting measurements appear in the box, bottom right.

**Video 14.14** (https://youtu.be/FOXymTHuWwc)
STIC acquisition in a case of TAPVC. The A-plane showed raised suspicion of an anomalous vessel (caret), which is confirmed in the B-plane (arrow).

**Video 14.15** (https://youtu.be/coRLXfehYBE)
The heart and great vessels of this fetus: STIC acquisition and high-definition power flow Doppler confirmed the characteristic vertical vein. (dAo, descending aorta; IVC, inferior vena cava; VV, vertical vein.) Note also the absence of pulmonary veins (compare Figure 14.6).

**Video 14.16** (https://youtu.be/nRP52FleAJo)
B-flow of the heart and great vessels in a fetus with interrupted inferior vena cava with azygos continuation. (AoA, aortic arch; AzV, azygos vein; DV, ductus venosus; SVC, superior vena cava.)

**Video 14.17** (https://youtu.be/RoZVzWQfCvo)
The IVS "virtual plane" with color Doppler in evaluation of VSD shows the rendered IVS plane, demonstrating flow across the defect from right to left.

**Video 14.18** (https://youtu.be/JgafyNqOlLo)
B-flow modality showing the parallel great vessels in a case of transposition. Application of this modality clearly shows the blood flow in the malaligned vessels. (AO, aorta; PA, pulmonary artery.)

**Video 14.19** (https://youtu.be/y7erGZekE6g)
TUI image of the left ventricular outflow tract (LVOT) in a case of tetralogy of Fallot, showing the dilated overriding aorta.

**Video 14.20** (https://youtu.be/K-lTX8QYKDo)
TUI of severe pulmonary stenosis. Note the stenotic pulmonary valve and post-stenotic dilatation of the pulmonary artery.

**Video 14.21** (https://youtu.be/NsVUFowf-Pc)
TUI with color Doppler mapping. Note the pulmonary stenosis with retrograde flow, leading to post-stenotic dilatation in the pulmonary artery.

# References


1. Deng J. *Ultrasound Obstet Gynecol* 2003;22:336–44.
2. DeVore GR et al. *Ultrasound Obstet Gynecol* 2003;22:380–7.
3. Falkensammer P. *Spatio-Temporal Image Correlation for Volume Ultrasound. Studies of the Fetal Heart*. GE Healthcare; Zipf, Austria, 2005.
4. Goncalves LF et al. *Am J Obstet Gynecol* 2003;189:1792–802.
5. Goncalves LF et al. *Ultrasound Obstet Gynecol* 2006;27:336–48.
6. Volpe P et al. *Ultrasound Obstet Gynecol* 2006;28:40–6.
7. Hongmei W et al. *Echocardiography* 2012;29:614–9.
8. Goncalves LF et al. *J Ultrasound Med* 2004;23:473–81.
9. Messing B et al. *Ultrasound Obstet Gynecol* 2005;26:606–9; discussion 610.
10. Chaoui R et al. *Ultrasound Obstet Gynecol* 2004;23:535–45.
11. Chaoui R et al. *Ultrasound Obstet Gynecol* 2001;17:22–9.
12. Sciaky-Tamir Y et al. *Am J Obstet Gynecol* 2006;194:274–81.
13. Yagel S et al. *Ultrasound Obstet Gynecol* 2017;50:283–3.
14. Xiong Y et al. *Ultrasound Obstet Gynecol* 2012;39:316–21.
15. Xiong Y et al. *Prenat Diagn* 2013;33:462–6.
16. Xiong Y et al. *Ultrasound Obstet Gynecol* 2010;35:754–5.
17. Yuan Y et al. *Ultrasound Obstet Gynecol* 2011;37:302–9.
18. Herberg U et al. *Ultraschall Med* 2011;32:46–53.
19. Herberg U et al. *Ultraschall Med* 2011;32:293–301.
20. Zhu M et al. Real time three-dimensional echocardiographic evaluations of fetal left ventricular stroke volume, mass, and myocardial strain: In vitro and in vivo experimental study. *Echocardiography* 2015;32:1697–706.
21. Yagel S et al. *Ultrasound Obstet Gynecol* 2001;17:367–9.
22. Yagel S et al. *Ultrasound Obstet Gynecol* 2002;20:340–5.
23. Yagel S et al. *Ultrasound Obstet Gynecol* 2011;37:432–7.
24. Abuhamad A. *J Ultrasound Med* 2004;23:573–6.
25. DeVore GR et al. *Ultrasound Obstet Gynecol* 2004;24:72–82.
26. Espinoza J et al. *J Ultrasound Med* 2006;25:947–56.
27. Yagel S et al. *Ultrasound Obstet Gynecol* 2006;28:266–74.
28. Messing B et al. *Ultrasound Obstet Gynecol* 2007;30:142–51.
29. Peralta CF et al. *Ultrasound Obstet Gynecol* 2006;27:128–33.
30. Ruano R et al. *J Ultrasound Med* 2006;25:701–9.
31. Espinoza J et al. *Ultrasound Obstet Gynecol* 2005;25:428–34.
32. Goncalves LF et al. *Ultrasound Obstet Gynecol* 2004;24:696–8.
33. Goncalves LF et al. *J Ultrasound Med* 2005;24:415–24.
34. Hata T et al. *J Obstet Gynaecol Res* 2010;36:513–8.
35. Messing B et al. *Ultrasound Obstet Gynecol* 2011;38:191–7.
36. Hamill N et al. et al. *Am J Obstet Gynecol* 2011;205:76 e71–10.
37. Carvalho JS et al. *Ultrasound Obstet Gynecol* 2013;41:348–59.
38. Adriaanse BM et al. *Ultrasound Obstet Gynecol* 2012;39:203–9.
39. Vinals F et al. *Ultrasound Obstet Gynecol* 2008;31:633–8.
40. Vinals F et al. *Ultrasound Obstet Gynecol* 2005;25:25–31.
41. Vinals F et al. *Ultrasound Obstet Gynecol* 2003;22:388–94.
42. Rizzo G et al. *J Ultrasound Med* 2011;30:93–9.
43. Michailidis GD et al. *Ultrasound Obstet Gynecol* 2001;18:325–8.
44. Avnet H et al. *J Ultrasound Med* 2016;35:111–9.
45. Tutschek B, Sahn DJ. *Ultrasound Obstet Gynecol* 2008;32:176–80.
46. Turan S et al. *Ultrasound Obstet Gynecol* 2009;33:652–6.
47. Yeo L, Romero R. *Ultrasound Obstet Gynecol* 2013;42:268–84.
48. Hyett J et al. *BMJ* 1999;318:81–5.
49. Hyett JA et al. *Ultrasound Obstet Gynecol* 1997;10:242–6.
50. Yagel S et al. *J Ultrasound Med* 2015;34:363–9.
51. Uittenbogaard LB et al. *Ultrasound Obstet Gynecol* 2008;31:625–32.
52. Godfrey ME et al. *Ultrasound Obstet Gynecol* 2012;39:131–44.
53. Meyer-Wittkopf M et al. *J Ultrasound Med* 2001;20:317–27.
54. Esh-Broder E et al. *Ultrasound Obstet Gynecol* 2004;23:546–51.
55. Hamill N et al. et al. *J Ultrasound Med* 2009;28:1301–11.
56. Bhat AH et al. et al. *Circulation* 2004;110:1054–60.
57. Bhat AH et al. *J Ultrasound Med* 2004;23:1151–9.
58. Liu X et al. Image-derived assessment of left ventricular mass in fetal myocardial hypertrophy by 4-dimensional echocardiography: An in vitro study. *J Ultrasound Med* 2016;35:943–9.
59. Rizzo G et al. *J Ultrasound Med* 2010;29:261–70.
60. Uittenbogaard LB et al. *Ultrasound Obstet Gynecol* 2010;35:324–31.
61. Barros FS et al. *Prenat Diagn* 2015;35:65–73.
62. Rolo LC et al. *J Matern Fetal Neonatal Med* 2015;28:1388–93.
63. DeKoninck P et al. *Fetal Diagn Ther* 2012;32:72–8.
64. Uittenbogaard LB et al. *Ultrasound Obstet Gynecol* 2010;36:308–14.
65. Hamill N et al. et al. *Am J Obstet Gynecol* 2013;208:153.e1–13.
66. Messing B et al. *Ultrasound Obstet Gynecol* 2013;42:182–8.
67. Rolo LC et al. *Prenat Diagn* 2013;33:50–5.
68. Tedesco GD et al. *Pediatr Cardiol* 2017;38:271–9.
69. Zidere V et al. *Ultrasound Obstet Gynecol* 2013;42:421–5.
70. Carvalho JS et al. *Ultrasound Obstet Gynecol* 2005;26:105–11.
71. Yagel S et al. *Ultrasound Obstet Gynecol* 2010;36:93–111.
72. Moore KL, Persaud, TVN. The cardiovascular system. In: *The Developing Human: Clinically Oriented Embryology*. Philadelphia, PA: WB Saunders; 349–404.
73. Paladini D et al. *Prenat Diagn* 2003;23:1052–55.
74. Yagel S et al. *Ultrasound Obstet Gynecol* 2005;25:97–8.
75. Espinoza J et al. *J Ultrasound Med* 2010;29:1573–80.
76. Bennasar M et al. *Ultrasound Obstet Gynecol* 2010;36:458–64.
77. Levental M et al. *J Ultrasound Med* 1998;17:341–8.
78. Meyer-Wittkopf M et al. *Ultrasound Obstet Gynecol* 2000;15:397–402.
79. Meyer-Wittkopf M et al. *Ultrasound Obstet Gynecol* 2001;17:485–92.
80. Wang PH et al. *Int J Cardiovasc Imaging* 2002;18:17–23.
81. Benacerraf BR et al. *Radiology* 2006;238:988–96.
82. Yagel S et al. *Ultrasound Obstet Gynecol* 2007;29:81–95.

# 15

# Magnetic resonance imaging: Techniques and normal fetal cardiovascular physiology

Davide Marini, Sharon Portnoy, and Mike Seed

## Introduction

Fetal magnetic resonance imaging (MRI) was initially reported in 1983, and its clinical utility as an adjunct to ultrasound, particularly for the assessment of central nervous system malformations and for the evaluation of invasive disorders of the placenta, is now well established. The increasing variety of quantitative MRI techniques being developed has prompted a number of groups to investigate the potential of this imaging modality for assessing fetal cardiovascular and placental pathophysiology. Unlike ultrasound, MRI can provide direct information about fetal oxygenation and perfusion, while diffusion-weighted imaging and magnetic resonance spectroscopy offer the possibility of assessing tissue microstructure and metabolism. Pre- and postnatal brain imaging incorporating these quantitative techniques has been used to gauge the impact of fetal congenital heart disease (CHD) and intrauterine growth restriction (IUGR) on *in utero* brain development. However, these applications remain largely within the realms of research, and there is currently limited use of MRI in clinical fetal cardiology practice. In this chapter, presented are some potential MRI approaches to examining the fetal cardiovascular and central nervous systems and reviewed are observations made about normal fetal circulatory physiology using MRI. Chapter 16 covers some of the findings reported in pregnancies affected by fetal cardiovascular disorders.

## Methods

### *Safety*

Animal experiments and human studies have raised concerns about the safety of MRI in pregnancy. Possible adverse effects are thought to relate to the static magnetic field, while consideration has also been given to the potential for harm arising from the radiofrequency energy needed to produce MR images and its associated heating effect, and the noise associated with gradient changes during imaging.[1] A series of animal experiments demonstrated general deleterious embryonic effects.[2–4] The major period of risk appears to be during the embryonic period, which is completed in humans during the first trimester of pregnancy, and this has led to recommendations by the American College of Radiology that fetal MRI be performed only after 17–18 weeks in humans.[5] In addition, recent studies have raised concerns about DNA damage in circulating lymphocytes in adult subjects undergoing cardiovascular MRI.[6] However, the results of a number of subsequent studies that have looked into the effect of MRI on DNA have mainly been reassuring. A number of follow-up studies have been performed following fetal MRI in humans and in pregnant MRI workers, none of which have detected any adverse impact on overall outcome or neurodevelopment.[7–9] However, an increased incidence of rheumatologic disease has recently been reported in children following fetal MRI that involved the administration of gadolinium contrast agents.[10] Given the known association between nephrogenic sclerosing fibrosis and gadolinium in adult subjects with renal impairment, gadolinium-containing contrast agents are therefore relatively contraindicated during pregnancy.

In summary, the ACR guidelines have suggested fetal MRI can be performed on a routine basis provided gadolinium is avoiding and the attending radiologist considers the relative benefits outweigh the risks of conducting the examination.[5] The guidelines emphasize how the use of MRI should be limited to those situations when it offers additional information over ultrasound. A recent review of fetal MRI safety concluded that when the equipment is used correctly and the specific absorption rate (SAR) kept to a minimum, fetal MRI at 1.5 Tesla would appear to be safe for the mother and fetus.[11] While there is less experience with higher field strengths, one recent article suggested clinical imaging can be performed with equivalent SAR and with no evidence of additional heating of the fetus, and an increasing number of clinical fetal MRI examinations are now being conducted at 3T.[12]

### *Central nervous system*

Conventional T1- and T2-weighted imaging of the fetal brain offers superior tissue contrast and visualization of cerebral cortical structure over ultrasound and has become the modality of choice when a suspicion is raised during the prenatal period about a central nervous system malformation.[13]

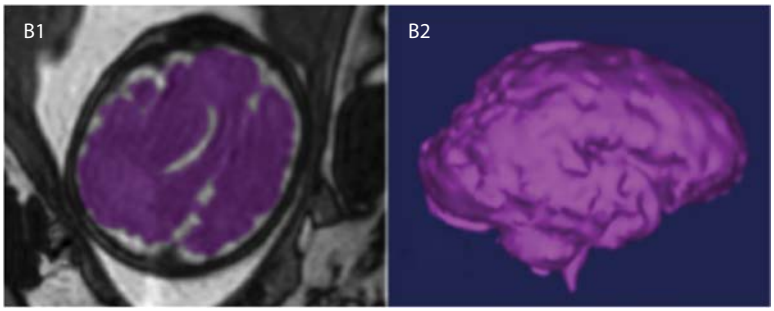


**Figure 15.1**
Segmented three-dimensional steady-state free precession image of the late gestation fetal brain with volume rendered reconstruction allowing quantification of fetal brain volume. (From Zhu MY et al. *Am J Obstet Gynecol* 2016;214:367, with permission.[65])

Accelerated acquisitions have resulted in improvements in artifacts resulting from fetal motion, with single-shot T2-weighted fast spin echo with half Fourier reconstruction the most frequently used sequence. T1WI is usually performed using gradient echo (sometimes with inversion recovery), while steady-state free precession (SSFP), which gives contrast with T2/T1 weighting, is another option for acquiring rapid fetal imaging. By acquiring the SSFP as a three-dimensional acquisition, it is possible to take advantage of the contrast between the bright cerebrospinal fluid and lower signal in the brain to segment the brain and measure brain volume using automated software (Figure 15.1).

More sophisticated reconstructions of T2-weighted two-dimensional acquisitions acquired in three planes have also been used to obtain high-resolution whole brain and regional brain volumetric measurements. Quantitative information about perinatal brain development has also been obtained using diffusion-weighted imaging (DWI) and diffusion tensor imaging (DTI).[14,15] These modalities measure the extent of water diffusion in brain tissue, and when DWI is applied in many directions, information about the direction of the diffusion is also acquired (DTI). As white and deep gray matter tracts mature, the diffusion of water in directions tangential to the axonal pathways becomes increasingly limited, while diffusion along the axons is facilitated, resulting in higher fractional anisotropy and reduced mean diffusivity. Conversely, as cortical connections become more complex with normal maturation, fractional anisotropy falls. An example of a fractional anisotropy map is shown in Figure 15.2.

Another tool for assessing brain maturation is proton magnetic resonance spectroscopy (MRS). In normal human brain development, the concentration of certain amino acids and brain metabolites changes with maturation.[16] For example, the ratio of the neuronal metabolite *N*-acetyl aspartate to choline, a component of cell membranes, increases through gestation. An example of a proton spectrum from a term neonate is shown in Figure 15.3.

Finally, blood oxygen level dependent (BOLD) imaging is a technique that takes advantage of the different magnetic properties of oxygenated and deoxygenated blood. In older children this forms the basis of functional MRI, where neuronal activation-mediated cerebral vasodilation results in increased cerebral blood flow in more metabolically active regions of the brain. This local increase in flow is associated with a drop in the oxygen extraction fraction and increase in the venous oxygen saturation and therefore the BOLD signal. Similar approaches have been reported in the fetus, and BOLD imaging has also been used to assess changes in tissue oxygenation during maternal hyperoxygenation in humans.[17] Similar experiments incorporating episodes of hypoxia have been reported in fetal sheep and mice.[18,19]

While in the human fetus many of these quantitative measures are subject to artifacts arising from fetal motion, ongoing technical developments are addressing these issues through faster acquisitions and postprocessing methods to correct for fetal motion. Movement artifacts can also be

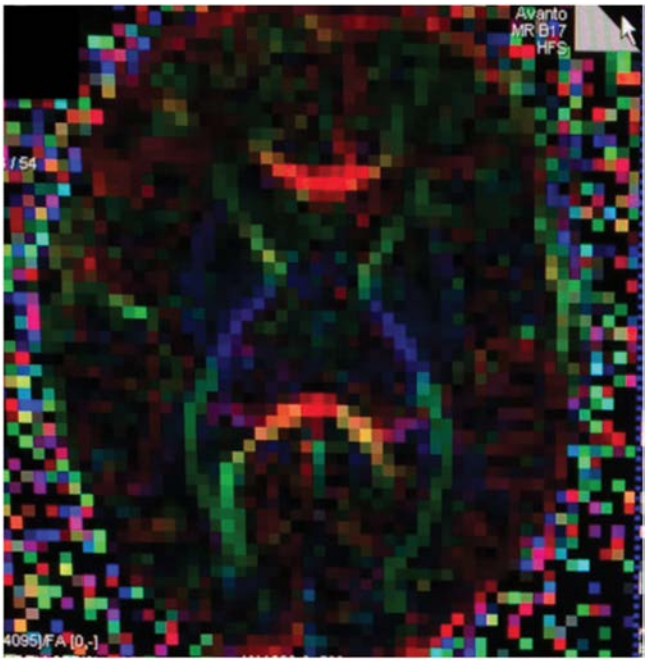


**Figure 15.2**
Example of a fractional anisotropy map of the neonatal brain acquired at 1.5 Tesla. The color coding represents the orientation of the diffusion. Prominent white matter tracts in the anterior and posterior limbs of the internal capsule, the corpus callosum, and optic radiations are clearly seen.

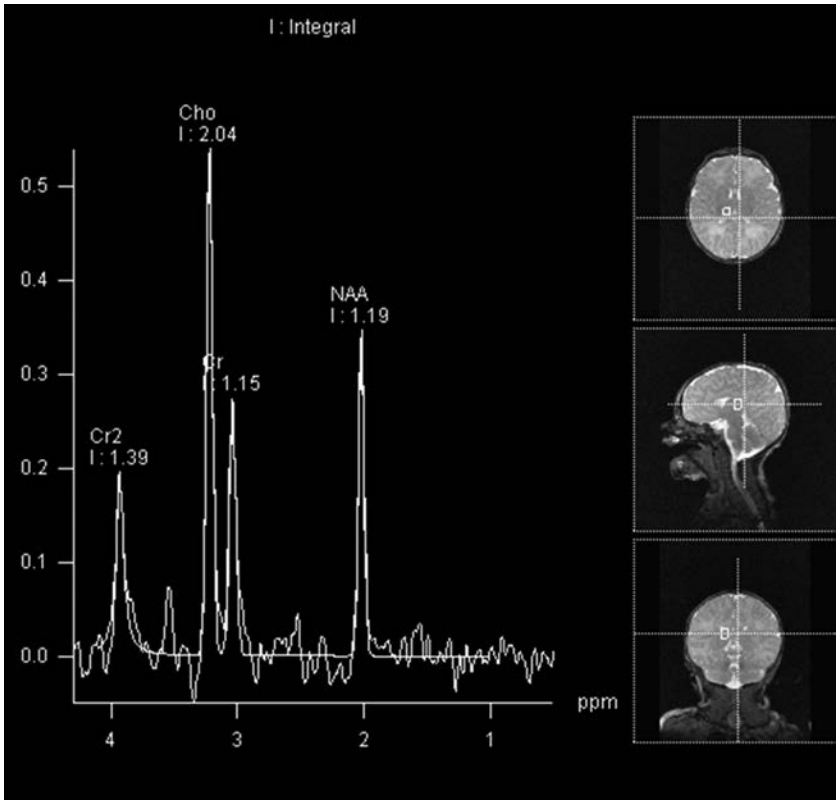


**Figure 15.3**
Example of a normal proton spectrum from the right thalamus in a term neonate showing the relative sizes of the *N*-acetyl aspartate (NAA), choline (Cho), and creatine peaks.

overcome by waiting until birth, when it is often possible to achieve high-quality neonatal brain imaging without sedation during natural sleep.[20]

## Placental MRI

Conventional T1- and T2-weighted imaging have been used to describe placental size, position, and morphology, as well as the degree of placental invasion beyond the endometrium.[21,22] The most established MRI methods for measuring perfusion involve the administration of a gadolinium-containing contrast agent, which is relatively contraindicated in human pregnancies. However, contrast-enhanced dynamic perfusion MRI has been investigated in animal models, while noncontrast techniques such as intravoxel incoherent motion imaging and arterial spin labeling have been used to measure placental perfusion in human pregnancies.[23,24] Placental function has also been interrogated with diffusion-weighted imaging and MRS using both proton and phosphorous MRS.[25–27] The assessment of placental function by MRI is an area of active research, and the potential clinical role of the various techniques available is considered in a recent review article on the subject.[28]

## Maternal cardiovascular system

MRI methods for studying the maternal cardiovascular system during pregnancy include standard techniques for performing ventricular volumetry and flow quantification (Figure 15.4). Several groups have reported measurements of right and left ventricular mass, end-systolic, end-diastolic, and stroke volumes and ejection fractions using short-axis cine steady-state free precession imaging.[29] We have found that by combining standard anatomical surveys through the thorax with noncontrast angiography of the maternal pelvis, it is possible to prescribe through-plane cine phase contrast imaging in the maternal ascending aorta, superior vena cava, descending aorta, main and branch pulmonary arteries, and right and left uterine arteries.[30] In late pregnancy, the venous return from the placenta appears to be largely via the ovarian veins, which can also be interrogated with cine phase contrast MRI, while an estimation of any additional uterine venous return can be approximated by subtracting the venous return from the legs (measured in the external iliac veins) from inferior vena caval flow just above the common iliac venous confluence. By combining this approach to measuring perfusion with the oximetry measurements described in the following text in maternal, fetal, and umbilical vessels, we have made preliminary measurements of placental oxygen exchange and fetal and placental oxygen consumption.

## Fetal cardiovascular system

A range of cardiovascular MRI techniques have been used to assess the fetal heart and vessels. Examples of these and some

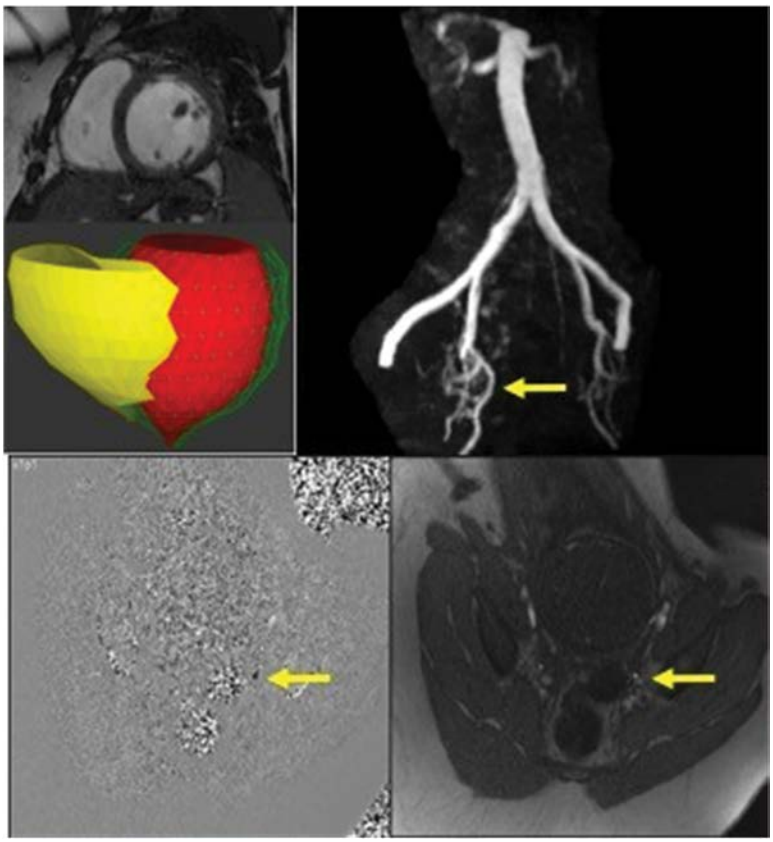

**Figure 15.4**
Cardiovascular MRI techniques for assessing the maternal circulation. Top left: segmented short-axis cine SSFP slice for ventricular volumetry. Top right: noncontrast time-of-flight angiography for localizing the pelvic vessels (arrow indicates uterine artery). Bottom: cine phase contrast MRI of the uterine arteries.

proposed imaging parameters are listed in Table 15.1. Virtually all examinations will include some attempt to visualize basic cardiac and vascular anatomy and SSFP has been used by a number of investigators to make static images of the fetal heart.[32,33] The excellent contrast between the high signal returned by flowing blood and lower signal generated by the myocardium are ideal for delineating cardiac structures and blood vessels. Furthermore, the short acquisition times afforded by the very short echo times and repetition times possible with SSFP allow for reasonable anatomical imaging without any attempt to address fetal or cardiac motion. However, even with this ultrafast sequence, a single image acquired with the requisite in-plane spatial resolution of 1–2 mm still requires a scan time of several cardiac cycles, and this results in blurring of cardiac structures caused by cardiac motion. As in postnatal MRI, cardiac imaging is therefore enhanced by some form of triggering, whereby cardiac motion can be "frozen." Each image then consists of data obtained during a limited part of the cardiac cycle. Such an approach can also be employed to produce a series of images, one at each cardiac phase, which can be displayed as a movie. Imaging of the beating heart provides superior visualization of cardiac structures and also yields information about cardiac function. Unfortunately, the usual electrocardiographic triggering signal for cardiovascular MRI is not easily obtained from the fetus, particularly in an MRI environment.

## *Gating for fetal cardiovascular MRI*

Several approaches to achieving cardiac triggering, or "gating," using other approaches have been described for use in the fetus. In a fetal sheep model, a Doppler ultrasound trigger has been obtained during MRI using a cardiotocogram (CTG) modified for use in the magnet.[34] This method has been used for anatomical cine imaging of the heart, and for velocity encoded cine phase contrast MRI. Techniques incorporating MRI data about the cardiac cycle acquired during imaging, which can be used to organize the timing of the acquisition known as "self-gating," have also been employed successfully in animal models.[35] "Metric optimized gating" is a retrospective technique whereby the imaging data are acquired using an artificial trigger and then subjected to iterative reconstruction through a range of candidate heart rates until an image metric identifies the correct average fetal heart rate present during the acquisition through the lack of artifact in the resulting images, as shown in Figure 15.5.[36] The acquisition can be divided up with metric optimized gating applied to shorter periods of the acquisition, although this requires additional postprocessing time. We have found that a two-parameter model is suitable for cine phase contrast flow measurements, with scan times of 20–30 seconds for each vessel. A combination of phase contrast flow measurements made

**Table 15.1** Fetal cardiovascular MR sequence parameters

| *Sequence* | *Type* | *Gating* | *Resp. comp.* | *Parallel Imaging factor* | *NSA* | *TE (ms)* | *TR (ms)* | *Slice thick (mm)* | *Matrix size* | *FOV (mm)* | *Temp. resol. (ms)* | *Scan time(s)* |
|---|---|---|---|---|---|---|---|---|---|---|---|---|
| 3D-SSFP | 3D | – | Breath-hold | 2 | 1 | 1.74 | 3.99 | 2 | 256 × 205 × 80 | 400 | – | 13 |
| Static SSFP | 2D | – | – | – | 1 | 1.3 | 6.33 | 4 | 320 × 211 | 350 | 1336 | 24 (15 slices) |
| Cine SSFP | 2D | MOG | – | 2 | 1 | 1.26 | 3.04 | 5 | 340 × 310 | 340 | 46 | 55 (10 slices) |
| Phase contrast[a] | 2D | MOG | – | – | 1 | 3.15 | 6.78 | 3 | 240 × 240 | 240 | 54 | 36 |
| T2 mapping[b] | 2D | PG | – | 2 | 1 | 1.15[c] | 3.97[c] | 6 | 224 × 181 | 350 | 4000 | 16 |

*Source:* Seed M. Fetal cardiovascular MRI. In: Kline-fath B, Bahado-Singh R, Bulas D, eds. *Diagnostic Imaging of Fetal Anomalies: Ultrasound and MRI*. Philadelphia, PA: Lippincott Williams and Wilkins; 2015:228–34, with permission.[31]

*Abbreviations*: FOV, field of view; MOG, metric optimized gating (R-R interval 545 ms); NSA, number of signal averages; PG, pseudo-gating (based on estimated R-R interval); TE, echo time; TR, repetition time.

[a] Velocity encoding sensitivity tailored according to vessel: 150 cm/s for arteries, 100 cm/s for veins, and 50 cm/s for umbilical vein. Number of segments per cardiac cycle = 4.

[b] T2 mapping used five T2 preparation times, tailored to span the expected T2 of a given vessel (0 ms, 0.33∗T2, 0.66∗T2, 1.00∗T2, and 1.33∗T2), with 4000 ms of magnetization recovery between successive T2 preparations.

[c] Rapid imaging of the T2-prepared magnetization was performed using a single-shot SSFP sequence with the indicated TE/TR values.

in each of the major fetal vessels can be used to determine the distribution of the fetal circulation.[37] It is important to prescribe these vessels perpendicular to the long axis of the vessel for accurate quantification of through-plane flow. The correct positioning of the imaging plane can be determined using two orthogonal long-axis views of the vessel. We use static SSFP surveys in coronal, axial, and sagittal orientation to the fetal thorax, as shown in Figure 15.6. These surveys can be repeated between the flow measurements when the fetus is active to ensure up-to-date planning of slice prescription. For more detailed anatomic imaging, and to obtain information about ventricular function, metric-optimized gating can also be used for anatomical cine imaging using SSFP.[38,64] The code for MOG is available as a free Internet download for use on MATLAB® software (http://metricoptimizedgating.github.io/MOG-Public/).

## Quantitative methods for assessing fetal and placental oxygenation

The differing magnetic properties of oxygenated and deoxygenated hemoglobin have been exploited to gauge tissue oxygenation and the oxygen saturation of blood in postnatal subjects, and these approaches can be applied to the fetus. BOLD imaging is the basis of postnatal functional neuroimaging, where neuronal activation results in regional increases in cerebral perfusion resulting in a reduction in the fraction of oxygen extracted from blood reaching the cerebral veins, i.e., an increase in venous oxygen saturation with a corresponding increase in T2∗. Similarly, the BOLD signal has been measured in the human and animal fetus to compare tissue oxygenation in various fetal organs at baseline and during episodes of hypoxia and hyperoxia.[17,18] One advantage of BOLD is that when it is used to interrogate tissue oxygenation in fetal organs, the requirements for spatial resolution are reasonable. However, in addition to the oxygen saturation of the blood in the arteries and veins supplying and draining an organ, a number of other factors including vessel density, underlying tissue characteristics, and local magnetic field inhomogeneity influence T2∗. This can lead to difficulties in the interpretation of differences in baseline BOLD between fetal organs and variation in the signal returned by individual organs under different conditions. An alternative approach attempts to quantify the oxygen saturation of blood within the larger fetal vessels and is most appropriately termed *magnetic resonance oximetry*. MR oximetry was initially described in 1991 and has subsequently gained some popularity for the quantification of cerebral oxygen consumption, which is measured by combining a measurement of cerebral blood flow with arterial and venous oxygen saturation.[39] Cerebral venous oxygen saturation has usually been quantified by interrogating the superior sagittal sinus.[40] The following section describes one possible approach to fetal MR oximetry.

## Measurement of fetal vessel oxygen saturation, hematocrit, and oxygen content

T1 and T2 are fundamental properties of any tissue including blood. They describe the exponential recovery of longitudinal magnetization (T1) and the decay of transverse magnetization (T2) that occurs following a radiofrequency pulse in a magnetic field. Due to their differing physical properties, different tissues vary in their rates of recovery and decay, and these differences can be exploited to characterize them. This basic principle of MRI provides a method for measuring the oxygen content of

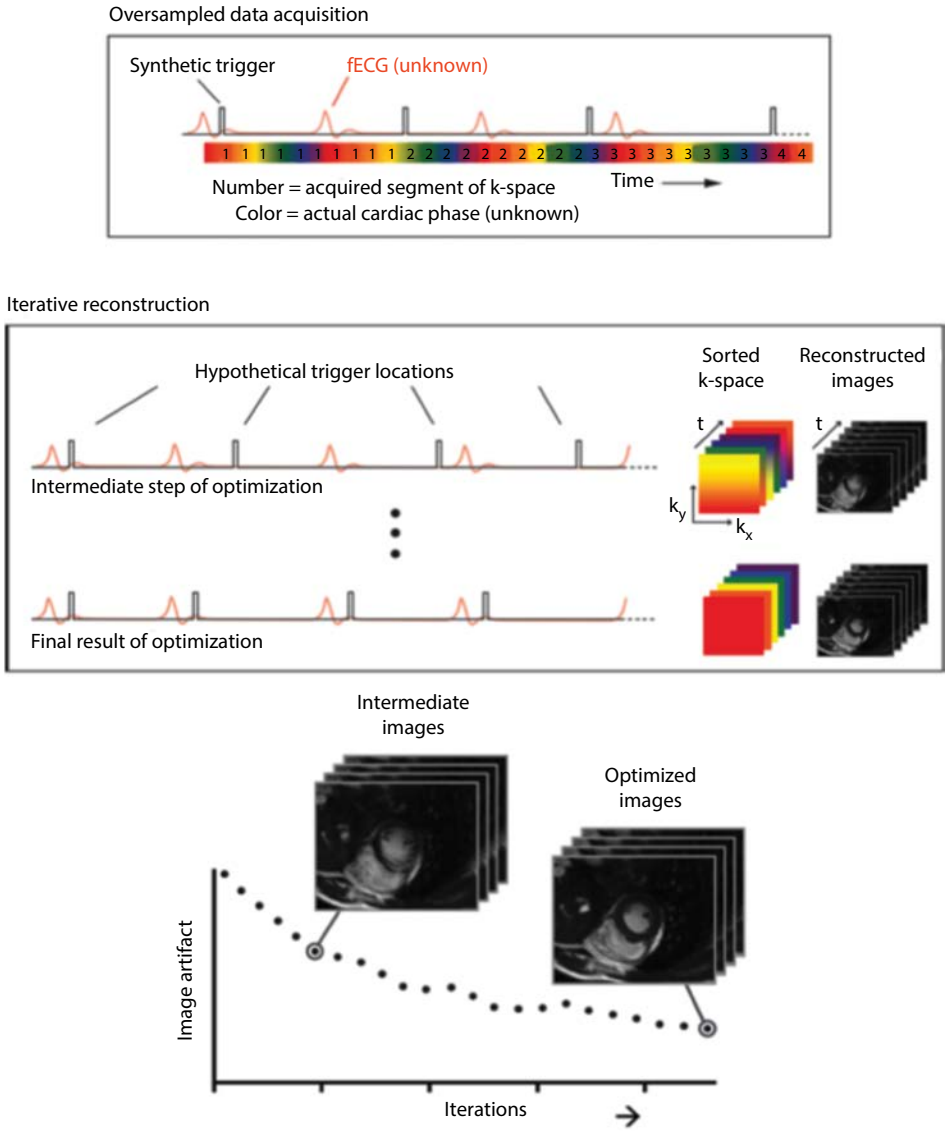


**Figure 15.5**
Metric-optimized gating. A synthetic trigger with longer R-R interval is used to acquire the k-space data. Hypothetic trigger locations are then retrospectively applied to the data, which is iteratively reconstructed with the correct average R-R interval identified as the reconstruction with the least image artifact. (From Seed M. Fetal cardiovascular MRI. In: Kline-fath B, Bahado-Singh R, Bulas D, eds. *Diagnostic Imaging of Fetal Anomalies: Ultrasound and MRI*. Philadelphia, PA: Lippincott Williams and Wilkins; 2015:228–34, with permission.[31])

blood in a fetal blood vessel. Blood oxygen content is the product of oxygen saturation and hemoglobin concentration:

$$\text{Oxygen content} = \text{Oxygen saturation} \times \text{Hemoglobin concentration} \times 1.36$$

where 1.36 is the number of milliliters of oxygen bound to 1 g of hemoglobin at one atmosphere.[41] This calculation ignores the amount of oxygen dissolved in plasma, which is negligible in the fetus.[42] As paramagnetic deoxyhemoglobin shortens T2 relaxation, there is a predictable relationship between oxygen saturation and T2, which is also dependent on the magnetic field strength.[39] The relationship between T2 and oxygen saturation for adult and fetal hemoglobin at 1.5 Tesla is shown in Figure 15.7.[43]

The T2 of flowing blood can be measured using a three-dimensional T2 preparation pulse using a technique called T2 mapping.[44,45] A series of images are generated with varying T2 preparation intervals, and the signal intensity returned from the vessel reflects the exponential decay of transverse magnetization. T2 is the time constant for this curve, indicating the time taken for a 63% reduction of the initial signal, as shown in Figure 15.8. The effect of turbulent flow on the T2 of blood can be minimized by using a short refocusing pulse for the T2 preparation.[46]

While the T2 of blood is primarily determined by its oxygen saturation, it is also influenced by hemoglobin concentration.[39] This is analogous to clinical cyanosis, which is more obvious in the presence of polycythemia. Variation in hemoglobin concentration (and therefore hematocrit) is expected in the setting of fetal circulatory disease. For example, fetuses

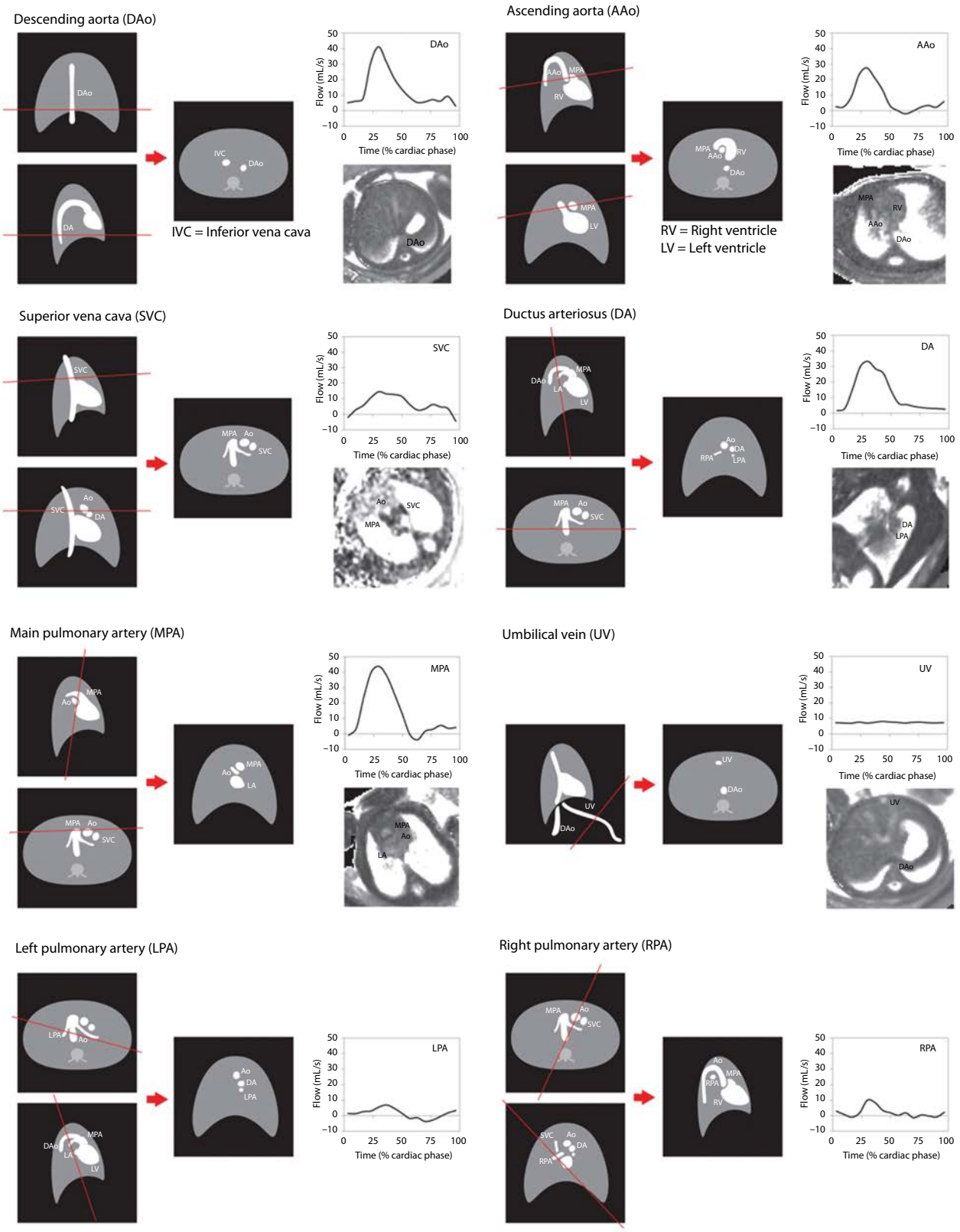


**Figure 15.6**
Orientation of phase contrast (PC) and T2 acquisitions from coronal, sagittal, and axial localizers showing expected appearances of modulus PC images, representative flow curves, and examples of T2 maps for each of the target vessels. (From Seed M. Fetal cardiovascular MRI. In: Kline-fath B, Bahado-Singh R, Bulas D, eds. *Diagnostic Imaging of Fetal Anomalies: Ultrasound and MRI*. Philadelphia, PA: Lippincott Williams and Wilkins; 2015:228–34. with permission.[31])

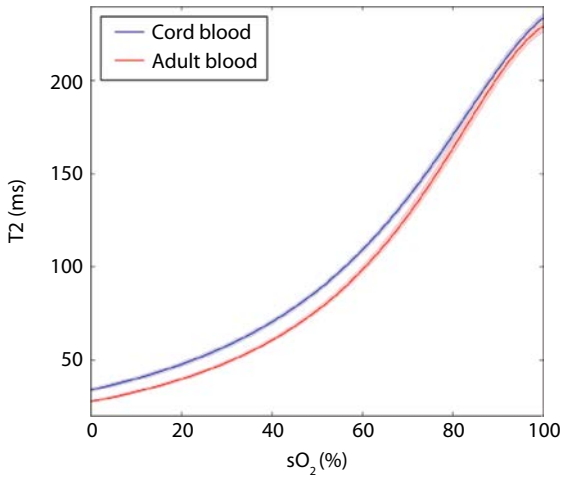


**Figure 15.7**
Relationship of T2 to $SaO_2$ of blood (adult and fetal). (From Portnoy S et al. *Magn Reson Med* 2017;77:1678–90, with permission.[43])

subjected to chronic hypoxia become polycythemic as part of an adaptative response to hypoxia that results in improved tissue oxygenation.[47] Fetal anemia due to alloimmunization, parvovirus, and congenital hemoglobinopathies are also common clinical conditions. Significant inaccuracies in fetal MR oximetry in fetuses with circulatory and hematologic abnormalities can then be expected unless T2 mapping can be corrected for variation in hematocrit. However, the T1 of blood is strongly related to hematocrit, with higher hematocrits associated with a shortening of T1.[43] Within expected physiologic ranges, we have shown through experimental manipulation of umbilical cord blood samples scanned *in vitro* that a unique solution exists for both hematocrit and oxygen saturation for any pair of T1 and T2 that might coexist in a fetal blood vessel.[48] Figure 15.9 illustrates variation in T2 according to oxygen saturation and hematocrit. Figure 15.10 shows the variation in T1 according to hematocrit and oxygen saturation. Figure 15.11 shows how the combination of

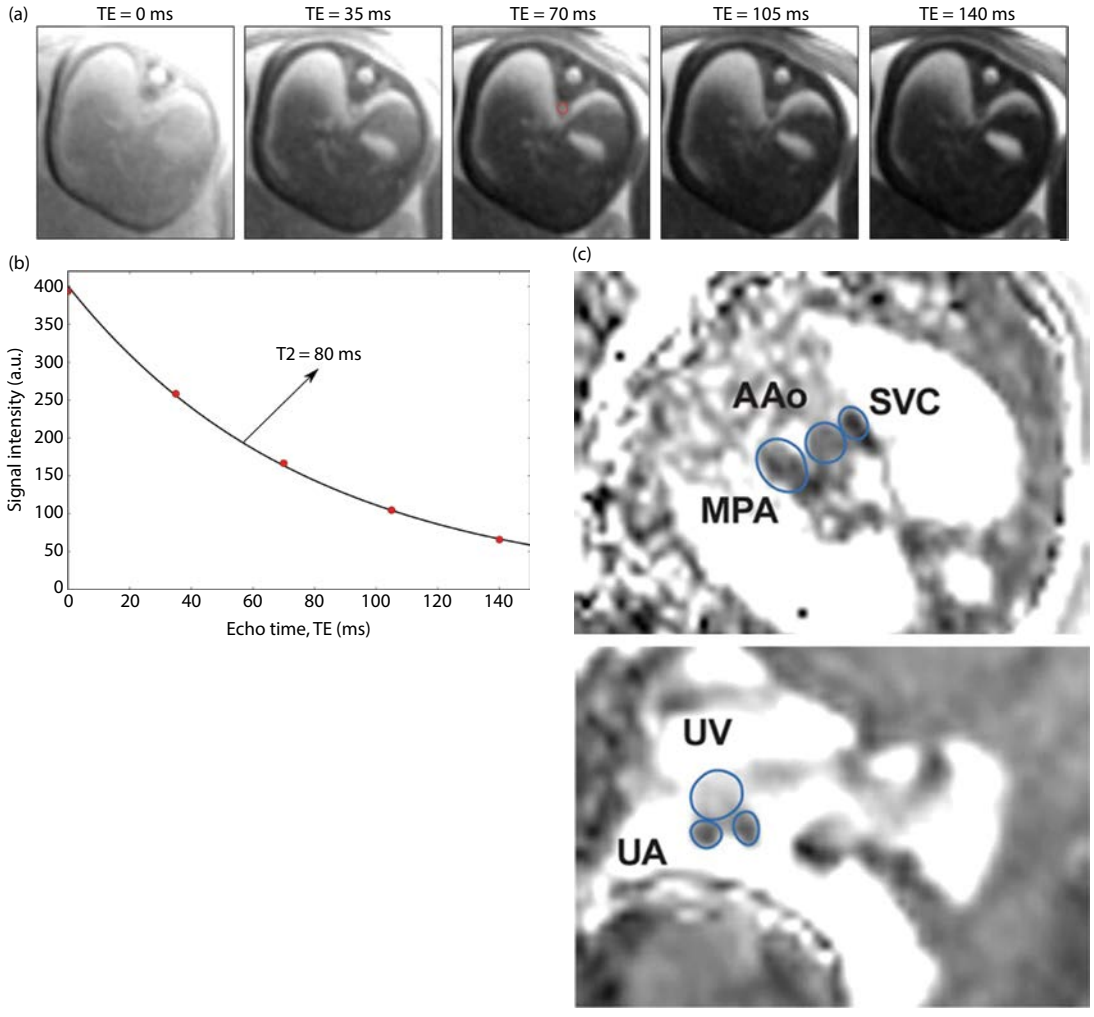


**Figure 15.8**
Fetal T2 mapping. (a) Individual T2 preparation images showing variable echo times. (b) Corresponding T2 curve for the descending aorta. (c) Examples of T2 maps in the umbilical cord and the mediastinum showing higher signal intensity in those vessels with higher oxygen saturation. (AAo, ascending aorta; MPA, main pulmonary artery; SVC, superior vena cava; UA, umbilical artery; UV, umbilical vein.) (Adapted from Sun L et al. *Circulation* 2015;131:1313–23, with permission.[66])

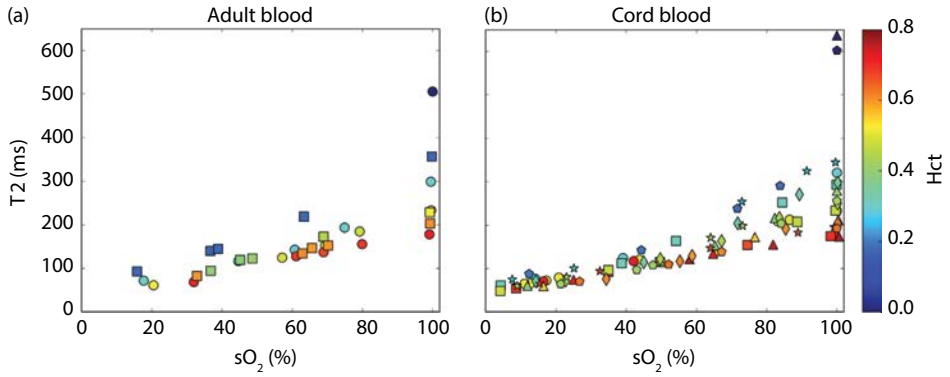


**Figure 15.9**
Variation in T2 with respect to oxygen saturation and hematocrit for adult blood (a) and fetal blood (b). T2 lengthens with increasing oxygen saturation but is shortened by increasing hematocrit. (From Portnoy S et al. *Magn Reson Med* 2017;77:1678–90, with permission.[43])

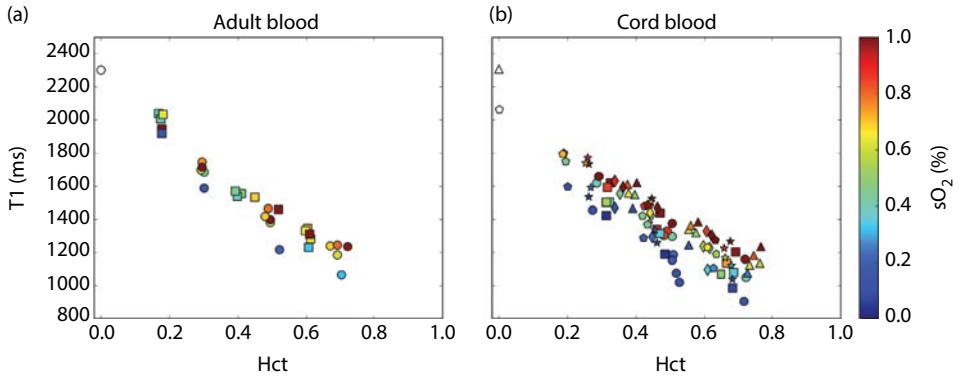


**Figure 15.10**
Variation in T1 with respect to hematocrit and oxygen saturation for adult blood (a) and fetal blood (b). T1 shortens with increasing hematocrit but is lengthened by increasing oxygen saturation. (From Portnoy S et al. *Magn Reson Med* 2017;77:1678–90, with permission.[43])

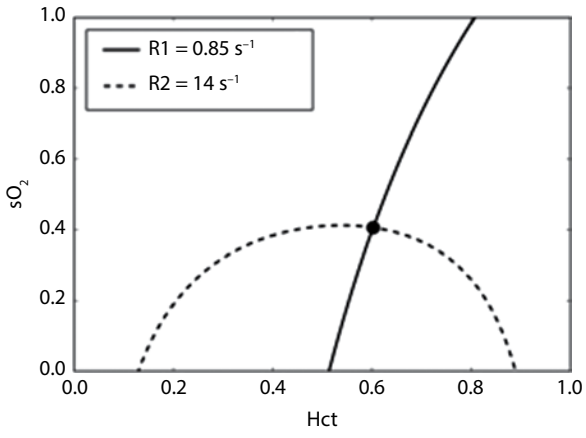


**Figure 15.11**
Intersection of the lines expressing the relationships between T1 relaxation rate (R1) and T2, oxygen saturation (*y*-axis) and hematocrit (*x*-axis), and T2 relaxation rate (R2), oxygen saturation and hematocrit represents the unique solution for all four variables. (From Portnoy S et al. *Magn Reson Med* 2017;77:1678–90, with permission.[43])

T1 and T2 measured in a vessel can be used to solve for both oxygen saturation and hematocrit.

This combined T1 and T2 mapping approach therefore provides the basis of the only currently available noninvasive method to measure the oxygen content in human fetal vessels. However, criteria for the accurate measurement of the T2 of flowing blood have been defined and include adequate spatial resolution to avoid partial volume artifacts.[49] With current clinical MRI systems in unsedated fetuses, fetal MR oximetry with T2 is therefore limited to the larger vessels in late gestation fetuses.[31]

## *Measurement of fetal oxygen delivery, consumption, and extraction fraction*

A combination of the measurements described can be used to quantify additional fetal hemodynamic parameters.[42] This is similar to the conventional Fick method for measuring cardiac output and pulmonary vascular resistance in postnatal subjects where measurements of oxygen consumption obtained using mass spectroscopy of expired air are combined with arterial and venous blood gases obtained

at cardiac catheterization in order to calculate blood flow.[41] In fetal cardiovascular MRI, a combination of vessel flow measurements made with phase contrast and oxygen content measurements made with T1 and T2 mapping can be used to calculate oxygen delivery ($DO_2$), consumption ($VO_2$), and the oxygen extraction fraction (OEF) as follows:

$$\text{Fetal } DO_2 = \text{Umbilical vein oxygen content} \times \text{Umbilical vein flow}$$
$$\text{Fetal } VO_2 = (\text{Umbilical vein} - \text{Umbilical artery oxygen content}) \times \text{Umbilical vein flow}$$
$$\text{Fetal OEF} = \text{Fetal } DO_2 \div \text{Fetal } VO_2$$

These measurements provide an additional way to assess placental function, fetal metabolism, and fetal circulatory physiology. A similar approach to assessing these parameters in individual fetal organs is potentially also possible. In practice this is limited by the requirements for resolution and adequate signal-to-noise ratio that are difficult to achieve in the fetus because of the need for short acquisitions that is imposed by fetal motion. However, by taking superior vena caval (SVC) flow as a surrogate for cerebral blood flow, we have attempted to quantify fetal cerebral hemodynamics by combining SVC flow with oximetry in the ascending aorta (AAo) and SVC:

$$\text{Fetal cerebral } DO_2 = \text{AAo oxygen content} \times \text{SVC flow}$$
$$\text{Fetal cerebral } VO_2 = (\text{SVC} - \text{AAo oxygen content}) \times \text{SVC flow}$$
$$\text{Fetal cerebral OEF} = \text{Fetal cerebral } DO_2 \div \text{Fetal cerebral } VO_2$$

# Results

## Normal brain development

The MR imaging appearances of the normal brain including the development of transient structures and changes in signal intensity throughout the second and third trimester have been described.[14,50] During this period, remarkable changes take place in brain structure with the ongoing migration of neurons from the germinal matrix to the cerebral cortex, which becomes increasingly complex in terms of its folding into the various sulci and gyri. Myelination begins in the third trimester and continues after birth, but it is interesting to note that in contrast with other organ systems, around 75% of brain growth is complete by 2 years of age, with the period of maximal brain growth velocity starting in late pregnancy.[51] As the brain matures and neuronal pathways become more established and myelinated, fractional anisotropy increases in the white matter and deep gray structures, and mean diffusivity drops.[15] The opposite is true in the cerebral cortex, where neurons lose their predominantly radial orientation with the advancing complexity of dendritic arborization. Progressive reductions in white matter mean diffusivity and N-acetyl aspartate to choline ratios have also been described in the normal fetus using diffusion tensor imaging and MRS.[16,52]

## Maternal circulation

The demands placed on the maternal circulation by pregnancy result in significant cardiac remodeling. Using short-axis cine SSFP imaging, Ducas et al. described increases in left ventricular end-diastolic volume from 99 ± 6 mL to 128 ± 5 mL and right ventricular end diastolic volume from 93 ± 4 mL to 115 ± 4 mL between baseline (postpartum) and the third trimester.[29] Right and left ventricular ejection fractions were unchanged, while left ventricular stroke volume increased from 68 ± 7 mL to 79 ± 4 mL and heart rate increased from 62 ± 8 mL to 97 ± 6 mL, resulting in an 85% increase in cardiac output. This was associated with a 48% increase in left ventricular mass. Using a similar approach, two other studies reported reductions in cardiac output and stroke volume during the third trimester in normal weight women when supine compared with a lateral decubitus position.[53,54] The effect of maternal position is less important in early pregnancy and in overweight subjects throughout pregnancy. Pates et al. attempted to use cine phase contrast MRI to measure uterine blood flow during pregnancy but concluded this was not feasible due to problems encountered in interrogating the ovarian arteries.[55] However, using a similar approach, we measured uterine artery blood flow in 12 normal late gestation pregnancies at 1137 ± 311 mL/min.[30] A noncontrast magnetic resonance angiogram using a quiescent-interval single-shot steady-state free precession acquisition was used to identify the uterine arteries, and a cine phase contrast MRI imaging plan was oriented perpendicular to the long axis of the vessel to measure through-plane flow. Based on the small size and lack of signal in the ovarian vessels in our study, we concluded that these vessels do not contribute significantly to uteroplacental flow in human pregnancies. In our preliminary study, we also attempted to measure venous return and uteroplacental oxygen extraction in late gestation. While we were unable to interrogate the uterine veins directly using this approach, we estimated uterine venous return as the difference between inferior vena caval and combined external iliac vein oxygen flow. For the total uteroplacental venous return, we combined this with oxygen flow in the ovarian veins (which would appear to carry the majority of the uteroplacental venous return in late pregnancy). Using this approach in conjunction with fetal oxygen consumption measured in the umbilical and fetal vessels as described previously, we have approximated placental oxygen exchange and consumption. The preliminary findings indicate a luxurious supply of oxygen to the pregnant uterus with only about one-sixth taken up by the uteroplacental unit. Of the total uptake of the uterus, approximately one-third is used by the placenta and two-thirds by the fetus, which is in keeping with previous measurements in pregnant sheep made using invasive techniques.[56]

## Fetal and placental BOLD

A series of experiments in fetal lambs have demonstrated changes in the BOLD signal of various fetal organs and the

**Table 15.2** Mean and SD flows and oximetry in 30 late gestation human fetuses

| | *CVO* | *UV* | *AAO* | *MPA* | *SVC* | *DAO* | *DA* | *PBF* | *FO* |
|---|---|---|---|---|---|---|---|---|---|
| Mean flow (mL/min/kg) | 467 ± 57 | 129 ± 28 | 196 ± 37 | 251 ± 30 | 137 ± 33 | 233 ± 40 | 175 ± 37 | 77 ± 29 | 105 ± 15 |
| Mean flow (% CVO) | | 28 ± 7 | 42 ± 6 | 55 ± 6 | 30 ± 8 | 50 ± 8 | 38 ± 8 | 16 ± 5 | 23 ± 3 |
| Mean $SaO_2$ % | | 84 ± 10 | 69 ± 13 | 55 ± 12 | 38 ± 11 | 56 ± 12 | | | |

*Source:* Seed M. Fetal cardiovascular MRI. In: Kline-fath, B, Bahado-Singh, R, Bulas, D, eds. *Diagnostic Imaging of Fetal Anomalies: Ultrasound and MRI*. Philadelphia, PA: Lippincott Williams and Wilkins; 2015:228–34, with permission.[31]

*Abbreviations:* AAo, ascending aorta; CVO, combined ventricular output; DA, ductus arteriosus; Dao, descending aorta; FO, foramen ovale; MPA, main pulmonary artery; PBF, pulmonary blood flow; $SaO_2$, oxygen saturation; SVC, superior vena cava; UV, umbilical vein.

placenta during challenges with maternal hyperoxygenation and ventilation with hypoxic gases.[18,57,58] These reveal modest changes or no change in brain BOLD compared with more dramatic changes in placenta, renal, liver, and spleen BOLD. The reason for this is not clear but may relate to the relatively low density of blood vessels in the brain compared with those other organs. "Brain-sparing physiology" refers to the redistribution of the fetal circulation that occurs in response to acute fetal hypoxia. This mechanism is facilitated by the connections between different compartments of the fetal circulation and is driven by the combination of cerebral and coronary vasodilation and peripheral and pulmonary vasoconstriction and serves to preserve oxygen delivery to the most metabolically active organs: the heart and brain. Brain-sparing may also partly account for the relatively stable BOLD signal in the setting of fetal hypoxia in fetal sheep. The opposite effect, which has been referred to as "reverse brain-sparing" has been proposed as a possible explanation for the lack of increase in BOLD during maternal hyperoxygenation in human fetuses.[17] It is interesting to consider whether delivery of blood with a relatively narrow range of blood oxygen content to the cerebral circulation may be important for normal fetal brain development, as the results of recent murine experiments have suggested.[59]

## *Distribution of blood flow and oxygen saturations in the normal human fetal circulation*

Using a combination of blood flow measurements made with cine phase contrast MRI with metric optimized gating and oxygen saturation measurements made using T2 mapping, we have provided preliminary reference ranges for the distribution of blood flow and oxygen transport in the late gestation human fetus, as shown in Table 15.2.

The results shown here are largely in keeping with previous estimates regarding the human fetal circulation made by Rudolph, based on his invasive measurements made in fetal sheep.[42] As Rudolph suggested, compared with the sheep fetus, the human fetus has higher cerebral and pulmonary blood flow and lower umbilical flow. The increase in SVC flow likely reflects the larger size of the fetal brain in the human, while the reduction in umbilical flow may reflect the higher hemoglobin concentration, which allows similar fetal oxygen delivery despite lower flow due to the increased oxygen-carrying capacity of human fetal blood. This is supported by the MRI-based calculations of fetal oxygen delivery and consumption, which are similar to those for fetal sheep, as shown in Table 15.3.

Human fetal $DO_2$ and $VO_2$ measurements reported by Acharya and Sitras were made using ultrasound measurements of flow and conventional umbilical artery and vein blood gases collected at the time of delivery.[60] The lower oxygen delivery in these fetuses resulted from the lower umbilical flow observed in these perinatal subjects. These umbilical flow measurements are lower than prior late gestation human ultrasound measurements, and it is possible that this reflects physiologic reductions in placental perfusion during the early stages of labor. This might account for the higher oxygen extraction fraction found in the human study compared with prior fetal sheep studies and our MRI results.

The human MRI oximetry data support the presence of the same streaming of oxygenated blood from the umbilical

**Table 15.3** Comparison of mean human fetal oxygen delivery ($DO_2$) and oxygen consumption ($VO_2$) obtained by MRI with reference lamb data and human data using conventional blood gases

| | *Fetal lamb* | *Human at term delivery* | *Late gestation human by MRI* |
|---|---|---|---|
| $DO_2$ | ~20 | 13.4 | 24.2 |
| $VO_2$ | 7–8 | 6.58 | 7.7 |

*Source:* Rudolph, A. The fetal circulation. In: *Congenital Diseases of the Heart—Clinical-Physiological Considerations*. 3rd ed. Chichester: Wiley-Blackwell; 2009:1–24;[42] Acharya G, Sitras V 2009. *Acta Obstetricia et Gynecologica* 88:104–9;[61] Seed M. Fetal cardiovascular MRI. In: Kline-fath B, Bahado-Singh R, Bulas D, eds. *Diagnostic Imaging of Fetal Anomalies: Ultrasound and MRI*. Philadelphia, PA: Lippincott Williams and Wilkins; 2015:228–34, with permission.[31]

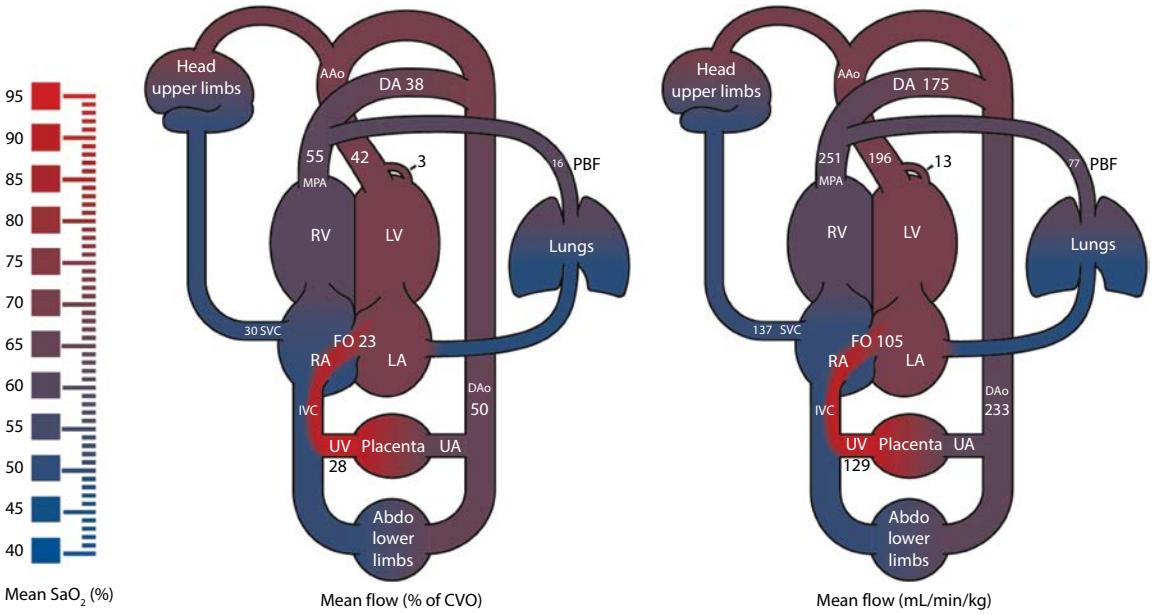


**Figure 15.12**
Distribution of blood flow and oxygen saturations in the major vessels of the human fetal circulation by phase contrast MRI and T2 mapping. Mean flows are shown in mL/min/kg (right) and as % of CVO (left). Mean oxygen saturations ($SaO_2$) are represented by the color coding and confirm higher saturations on the left side of the heart and ascending aorta than the right, likely due to streaming of the umbilical venous return across the foramen ovale. (AAo, ascending aorta; DA, ductus arteriosus; Dao, descending aorta; FO, foramen ovale; LA, left atrium; LV, left ventricle; MPA, main pulmonary artery; PBF, pulmonary blood flow; RA, right atrium; RV, right ventricle; SVC, superior vena cava; UA, umbilical artery; UV, umbilical vein.) (From Seed, M. Fetal cardiovascular MRI. In: Kline-fath B, Bahado-Singh R, Bulas D, eds. *Diagnostic Imaging of Fetal Anomalies: Ultrasound and MRI*. Philadelphia, PA: Lippincott Williams and Wilkins; 2015:228–34, with permission.[31])

vein to the left heart via the ductus venosus and foramen ovale that has previously been demonstrated in the fetal sheep, as shown in Figure 15.12.[42] This results in a remarkable mechanism, whereby two columns of blood moving at different speeds and with different oxygen saturations coexist in the suprahepatic inferior vena cava. More oxygenated blood is then directed toward the foramen ovale by the ductus arteriosus, presumably to ensure an adequate supply of glucose and oxygen to the brain and heart, the most metabolically active fetal organs. Streaming also results in transport of more deoxygenated blood back to the placenta via the ductus arteriosus, descending aorta, and umbilical arteries. This blood is also presented to the pulmonary circulation, where its relatively low oxygen content maintains the high pulmonary vascular resistance typical of the fetal circulation.

In late gestation, there is considerable variability in pulmonary blood flow, which may partly reflect variation in the oxygen content of the blood presented to the fetal lungs.[61] Certainly an episode of acute maternal hyperoxygenation results in an increase in the oxygen content of blood in the umbilical vein and pulmonary vasodilation with increased pulmonary blood flow in human fetuses.[62] However, in fetal lambs exposed to longer episodes of maternal hyperoxygenation, the pulmonary vasodilatory effect of oxygen appears to wear off after a matter of hours.[63] An important fetal circulatory mechanism known as "brain-sparing physiology" involves redistribution of the combined ventricular output to favor cerebral and cardiac oxygen delivery at the expense of the abdominal viscera, carcass, and lungs.[42] This response results from opposing changes in the vascular resistance of the different circulatory compartments in the setting of hypoxia and is facilitated by the presence of connections between the systemic and pulmonary circulations at the arterial duct and foramen ovale. The relationship between arterial and venous oxygen saturations and cerebral, pulmonary, and umbilical flow in human fetuses investigated with MRI is illustrated by the plots shown in Figure 15.13. These graphs combine measurements from 55 late gestation human fetuses, nine of which had evidence of fetal growth restriction. In keeping with prior invasive fetal sheep experiments in which acute fetal hypoxia was induced through uterine or umbilical cord occlusion, we found evidence of cerebral vasodilation and pulmonary vasoconstriction in response to reduced arterial oxygen content. There was a less consistent relationship between umbilical vein oxygen content and umbilical flow. However, the findings were in keeping with impaired oxygen exchange and increased placental resistance in the setting of fetal growth restriction.

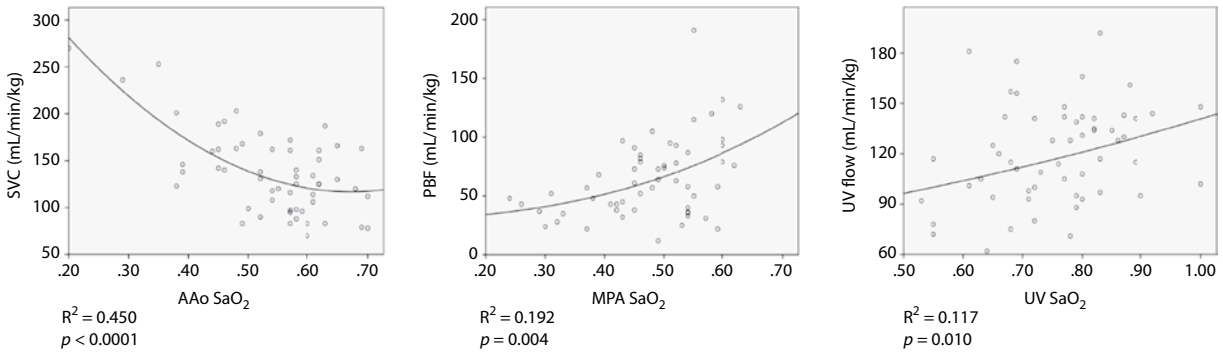


**Figure 15.13**
Relationship between superior vena caval (SVC), umbilical vein (UV), pulmonary blood flow (PBF), and oxygen saturation in the ascending aorta (AAo), umbilical vein (UV), and main pulmonary artery (MPA), respectively.

# Conclusion

Innovations in MR technology have enabled the application of this versatile imaging modality to the examination of the fetal cardiovascular system. In situations in which ultrasound imaging is hampered, for example, in the late gestation fetus with oligohydramnios, MRI can provide superior cardiac anatomical visualization, which may aid in the prenatal diagnosis of congenital heart disease. However, our experience has been that it is MRI's potential for providing new insights into the relationships between fetal, placental, and maternal cardiovascular physiology and fetal growth and development that has been of most interest to researchers and health-care providers in reproductive medicine. In this chapter, we have reviewed MRI observations made by our group and others that confirm human fetal cardiovascular physiology has much in common with what we have learned from invasive measurements in animal models, particularly sheep. Some preliminary observations regarding human fetal circulatory changes made using these techniques in the setting of fetal cardiac and placental disease are reported in Chapter 16. However, with the relatively recent development of these techniques and somewhat limited availability of MRI, there remains much to be learned about the possible utility of this exciting technology for improving patient care.

# References


1. De Wilde J et al. *Prog Biophys Mol Biol* 2005;87:335–53.
2. Narra V et al. *Inves Radiol* 1996;31:586–90.
3. Espinar A et al. *Bioelectromagnetics* 1997;18:36–46.
4. Tyndall D, Sulik K. *Teratology* 1991;4:263–75.
5. Expert Panel on MR Safety. *J Magn Reson Imag* 2013;37:501–30.
6. Simi S et al. *Mol Mech Mutagenesis* 2008;645:39–43.
7. Kanal E. *Magn Reson Imag Clin N Am* 1994;2:309–17.
8. Baker P et al. *Am J Obstet Gynecol* 1994;170:32–3.
9. Bouyssi-Kobar M et al. *Pediatr Radiol* 2015;45:1823–30.
10. Ray J et al. *JAMA* 2016;316:952–61.
11. Gowland P. Safety of fetal MRI scanning. In: Prayer D, ed. *Fetal MRI*. Berlin: Springer Berlin Heidelberg; 2011:49–54.
12. Victoria T et al. *Pediatr Radiol* 2014;44:376–86.
13. Pugash D et al. *Eur J Radiol* 2008;68:214–26.
14. Prayer D et al. *Eur J Radiol* 2006;57:199–216.
15. Brain Development Cooperative Group. *NeuroImage* 2006;30:184–202.
16. Girard N et al. *Magn Reson Med* 2006;56:768–75.
17. Sorensen A et al. *Prenat Diagn* 2013;33:141–5.
18. Wedergartner U et al. *Radiology* 2006;238:872–80.
19. Cahill L et al. *J Cereb Blood Flow Metab* 2014;34:1082–8.
20. Windram J et al. *Pediatr Radiol* 2012;42:183–7.
21. Blaicher W et al. *Eur J Radiol* 2006;57:256–60.
22. Derman A et al. *Am J Roentgen* 2011;197:1514–21.
23. Moore R et al. *Placenta* 2000;21(7):726–32.
24. Francis S et al. *Lancet* 1998;351:1397–9.
25. Bonel H et al. *Radiology* 2010;257:810–9.
26. Denison F et al. *PLOS ONE* 2012;7:e42926.
27. Sohlberg S et al. *Placenta* 2014;35:318–23.
28. Siauve N et al. *Am J Obstet Gynecol* 2015; 213(4Suppl):S103–14.
29. Ducas R et al. *J Cardiovasc Magn Reson* 2014;16:1.
30. Saini B et al. *Ultrasound Obstet Gynecol* 2016;48(SI):148–8.
31. Seed M. Fetal cardiovascular MRI. In: Kline-fath, B, Bahado-Singh, R, Bulas, D, eds. *Diagnostic Imaging of Fetal Anomalies: Ultrasound and MRI*. Philadelphia, PA: Lippincott Williams and Wilkins; 2015:228–34.
32. Saleem S. *Am J Roentgenol* 2008;191:1208–15.
33. Dong S et al. *J Cardiovasc Magn Reson* 2013;15:40.
34. Yamamura J et al. 2012;35:1071–6.
35. Yamamura J et al. *Eur Radiol* 2011;21:142–9.
36. Jansz M et al. *Magn Reson Med* 2010;64(5):1304–14.
37. Seed M et al. *J Cardiovasc Magn Reson* 2012;14:79.
38. Roy C et al. *Magn Reson Med* 2013;70(6):1598–607.
39. Wright G et al. *JMRI* 1991;1:275–83.
40. Ge Y et al. *J Cerebr Blood Flow Metab* 2012;32:403–12.
41. Wilkinson J. *Heart* 2001;85:113–20.
42. Rudolph, A. The fetal circulation. In: *Congenital Diseases of the Heart—Clinical-Physiological Considerations*. 3rd ed. Chichester: Wiley-Blackwell; 2009:1–24.
43. Portnoy S et al. *Magn Reson Med* 2017;77:1678–90.
44. Nield L et al. *Pediatr Radiol* 2005;35:179–85.
45. Wedergartner U et al. *Magn Reson Med* 2010;64:32–41.
46. Varghese J et al. *J Cardiovasc Magn Reson* 2015;17(S1):W31.
47. Richardson B, Bocking A. *Comp Biochem Physiol* 1998;119A(3):717–23.

48. Portnoy S et al. *Magn Reson Med* 2017;78:2352–9.
49. Stainsby J, Wright G. *Magn Reson Med* 1998;40(3):494–9.
50. Garel C et al. *Child's Nervous System* 2003;19:422–5.
51. Dobbing J, Sands J. *Arch Dis Child* 1973;48:757–67.
52. Huang H et al. *J Neurosci* 2009;29:4263–73.
53. Rossi A et al. *J Cardiovasc Magn Reson* 2011;13:31.
54. Nelson D et al. *Am J Perinatol* 2015;32:1318–23.
55. Pates J et al. *Magn Reson Imag* 2010;28:507–10.
56. Carter A *Placenta* 2000;21(SA):S31–7.
57. Sorensen A et al. *Ultrasound Obstet Gynecol* 2009;34:687–92.
58. Sorensen A et al. *Ultrasound Obstet Gynecol* 2011;38:665–72.
59. Yuen T et al. *Cell* 2014;158:383–96.
60. Acharya G, Sitras V. *Acta Obstetricia et Gynecologica* 2009;88: 104–9.
61. Prsa M et al. *Circulation Cardiovasc Imaging* 2014;7:663–70.
62. Porayette P et al. *Prenat Diag* 2016;36:274–81.
63. Accurso F et al. *Resp Physiol* 1986;63:43–52.
64. Roy C et al. *Magn Reson Med* 2017;77:2125–35.
65. Zhu MY et al. *Am J Obstet Gynecol* 2016;214:367.
66. Sun L et al. *Circulation* 2015;131:1313–23.

# 16

# Magnetic resonance imaging: Abnormalities of the fetal circulation

Davide Marini, Sharon Portnoy, and Mike Seed

## Introduction

In the previous chapter, some of the magnetic resonance imaging (MRI) techniques available for examining maternal, placental, and fetal cardiovascular physiology and perinatal brain development were described. Outlined were some initial observations about normal human fetal circulatory physiology made using MRI. In this chapter, we report the preliminary findings of researchers studying abnormalities of the fetal cardiovascular system using MRI, in particular, the distribution of blood flow and oxygen saturations across the circulation in fetuses with congenital heart disease (CHD) and intrauterine growth restriction (IUGR). As noted in Chapter 15, this approach is currently limited to a small number of centers performing research in this field. The techniques we describe currently require several hours of postprocessing time to generate the data for a single case. Furthermore, due to limitations imposed by the inherent trade-off between achieving adequate signal-to-noise ratio and spatial resolution when acquiring the images quickly enough to overcome fetal motion artifacts, our approach is currently only feasible in late gestation. However, using this approach, we have been able to examine some of the concepts that have been considered by previous investigators regarding the impact of cardiac malformations and placental dysfunction on fetal circulatory physiology. In particular, we have focused on the relationship between these cardiovascular changes and delays in fetal brain development.

## Fetal hemodynamic patterns of congenital heart malformations

The mean vessel flows and oxygen saturations found in a preliminary group of fetuses with a range of more severe forms of CHD obtained using the MRI techniques described in Chapter 15 are provided in Table 16.1.[1] Although the number of patients in each group is relatively small, particularly for the oximetry, some expected hemodynamic patterns can still be appreciated. Many of these are very much expected and straightforward. For example, when one side of the heart is obstructed, there is a compensatory increase in blood flow through the unobstructed side. For example, in hypoplastic left heart syndrome, ascending aortic flow is significantly reduced, while flow across the main pulmonary artery and ductus arteriosus are markedly increased. Similarly, in lesions characterized by right heart obstruction, like tetralogy of Fallot and tricuspid atresia, we have observed significant increases in ascending aortic flow with diminished flow in the main pulmonary artery and arterial duct. In transposition of the great arteries, we have noted a reversal of the normal relationship between main pulmonary artery and ascending aortic flows. In the normal fetal circulation, main pulmonary artery flow exceeds ascending aortic flow. This is possible in the fetal circulation because of the presence of shunts at the foramen ovale and ductus arterious and presumably reflects the greater venous return to the right ventricle. In transposition, ascending aortic flow is higher than main pulmonary artery flow, likely due to the discordant ventriculo-arterial connections that result in the aorta being connected to the dominant right ventricle. Despite these variations in the outputs of the right and left heart, fetal organ perfusion appears to be reasonably well maintained. For example, pulmonary blood flow is rather stable across all of these forms of CHD, and similar to pulmonary blood flow in normal controls. If superior vena caval flow is taken as a surrogate for cerebral blood flow, then cerebral blood flow is also well maintained in most forms of CHD. The exception to this may be in those fetuses with more severe forms of Ebstein anomaly. Fetal Ebstein anomaly is associated with the lowest combined ventricular outputs we have observed in fetuses with CHD, and appears to be prone to lower cerebral blood flow. Other types of CHD with single ventricle physiology are also associated with a reduction of combined ventricular output in the range of 10%–20%. While cerebral and pulmonary perfusion are relatively well maintained, this reduction in cardiac output is associated with a drop in umbilical blood flow.

In addition to the reductions in umbilical flow seen in fetuses with single ventricle hearts, CHD appears to be associated with modest reductions in the oxygen content of umbilical venous blood. This may reflect structural differences that have been described on pathologic examination of the placenta in pregnancies affected by fetal CHD.[2–4] In our preliminary experience of performing fetal MR oximetry, the other striking

**Table 16.1** Mean flows and oxygen saturations in the major vessels of the fetal circulation in normal fetuses and fetuses with congenital heart disease by MRI

| | *Mean blood flow (mL/min/kg)* | | | | | | | | | *Mean $SaO_2$ (%)* | | | | | |
|---|---|---|---|---|---|---|---|---|---|---|---|---|---|---|---|
| | *n* | *CVO* | *AAo* | *MPA* | *SVC* | *DAo* | *UV* | *DA* | *PBF* | *n* | *UV* | *AAo* | *MPA* | *DAo* | *SVC* |
| Normal | 33 | 469 | 208 | 246 | 137 | 237 | 130 | 180 | 71 | 33 | 80 | 59 | 52 | 53 | 45 |
| HLHS | 14 | 429 | 56 | 368 | 141 | 220 | 120 | 298 | 78 | 5 | 80 | 48 | 48 | 50 | 36 |
| TOF | 12 | 482 | 387 | 84 | 129 | 261 | 140 | 78 | 79 | 10 | 68 | 53 | 50 | 50 | 38 |
| TGA | 13 | 498 | 272 | 211 | 170 | 250 | 133 | 133 | 83 | 7 | 71 | 46 | 53 | 49 | 39 |
| Ebstein | 5 | 285 | 207 | 150 | 101 | 162 | 112 | 110 | 71 | 4 | 78 | 46 | 44 | 45 | 33 |
| Tricuspid atresia | 7 | 414 | 229 | 173 | 138 | 195 | 80 | 125 | 73 | 5 | 73 | 47 | 50 | 47 | 36 |

*Abbreviations:* HLHS, hypoplastic left heart syndrome; TGA, transposition of the great arteries; TOF, tetralogy of Fallot.

and almost universal finding in fetuses with CHD was the reduction in ascending aortic oxygen saturation. Individual examples of oximetry data collected from fetuses with different types of CHD are shown in Figure 16.1 and illustrate some of the different hemodynamic mechanisms leading to this aortic desaturation. For example, in transposition, the usual streaming of well-oxygenated blood toward the left heart via the ductus venosus and foramen ovale results in this blood being directed toward the pulmonary circulation. Meanwhile, more desaturated blood from the inferior vena cava combines with superior vena caval blood returning from the cerebral circulation and is redirected to the ascending aorta. Similarly, in tetralogy of Fallot, although the usual streaming may result in normal oxygen saturations in left atrium and ventricle, right-to-left shunting at the ventricular septal defect resulting from right ventricular outflow tract obstruction dilutes the left ventricular output with more deoxygenated blood from the right heart. In hypoplastic left heart syndrome, there can be no effective streaming because flow through the left side of the heart is completely obstructed, and there is effectively only one cardiac outlet. In this arrangement there is mixing of the entire venous return in the right atrium and ventricle, and all compartments of the fetal circulation are supplied with blood of a similar oxygen content. In addition to the interruption of the usual preferential streaming of oxygenated blood toward the ascending aorta, the reduction in combined ventricular output and associated drop in umbilical flow results in a reduction in overall fetal oxygen delivery. This combination of hemodynamic effects is associated with some of the lowest ascending aortic saturations we have observed. Fetal brain BOLD (blood oxygen level dependent) measurements obtained in normal controls and fetuses with CHD (Mette Lauridson, personal communication) also suggest that oxygen saturations are lower in the brains of fetuses with CHD, and the implications of this finding in terms of brain development are discussed in more detail below.

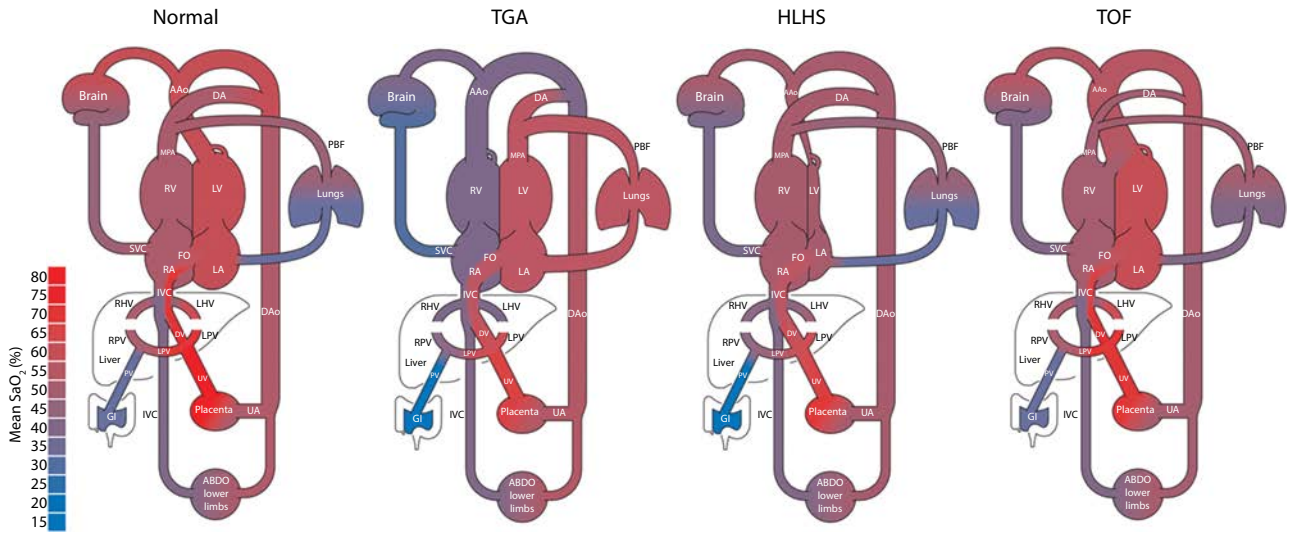


**Figure 16.1**
Oxygen saturations across the normal fetal circulation with examples of oximetry data from congenital heart disease cases by magnetic resonance oximetry. (HLHS, hypoplastic left heart syndrome; TGA, transposition of the great arteries; TOF, tetralogy of Fallot.) (From Sun L et al. *Circulation* 2015;131:1313–23, with permission.[8])

## Congenital heart disease: Hemodynamic consequences

The effects of CHD on fetal oxygen delivery ($DO_2$), oxygen consumption ($VO_2$), fetal cerebral oxygen delivery ($CDO_2$), and consumption ($CVO_2$) are shown in Tables 16.2 and 16.3.[5] Here, a range of different CHD types have been combined into a single group and compared with a large group of control fetuses. To obtain blood oxygen content, we estimated hemoglobin concentration based on gestational age–appropriate reference data and converted T2 to $SaO_2$ using prior experiments in which the relationship between the $SaO_2$ of adult blood and T2 was determined.[6,7] Using this approach, we found a reduction of 25% in fetal $DO_2$ resulting from diminished umbilical vein flow and oxygen content.[8] This reduction in fetal $DO_2$ was associated with a corresponding drop in fetal $VO_2$. As previously described, the reduction in fetal $DO_2$ combined with interruption of the usual streaming of oxygenated blood from the placenta to fetal brain was associated with an average reduction in oxygen saturation of 10% in the ascending aorta. In keeping with the concept of brain-sparing physiology described in Chapter 15, this reduction in ascending aortic saturation was associated with an increase in superior vena cava flow, although this was only apparent when superior vena cava flow was indexed to brain volume. In our studies of late-gestation CHD fetuses, their brains have been 10%–15% smaller than those of normal controls, while fetal weight has not been significantly different. When superior vena cava flow and $CDO_2$ are indexed to fetal weight, cerebral oxygen delivery and consumption are reduced in fetuses with CHD, while $CDO_2$ and $CVO_2$ indexed to fetal brain weight are not significantly different between fetuses with CHD and normal controls.

## Fetal hemodynamics and brain growth and development

In keeping with the findings of prior investigations, the brains of newborns with CHD in our studies have been smaller and had abnormal white matter and deep gray matter microstructure by diffusion tensor imaging compared with normal controls.[9,10] These findings have been interpreted as evidence of delayed brain development, a concept that is supported by the immature electrophysiology of term newborns with CHD and infant

**Table 16.2** Fetal hemodynamics in control fetuses and fetuses with congenital heart disease by MRI

| | *CHD (n = 40)* | *Normal (n = 46)* | *P-value* |
|---|---|---|---|
| Fetal GA (weeks) | 36.5 ± 1.0 | 36.5 ± 1.3 | 0.9 |
| Estimated fetal weight (kg) | 3.0 ± 0.4 | 2.9 ± 0.4 | 0.2 |
| $DO_2$ (indexed to fetal weight) (mL/min/kg) | 15.8 [13.9, 20.9] | 21.0 [16.4, 23.7] | **0.003** |
| QUV (indexed to fetal weight) (mL/min/kg) | 115.4 ± 32.3 | 130.2 ± 28.6 | **0.03** |
| UV $SaO_2$ (%) | 73.5 [68.3, 79.0] | 79.0 [73.8, 83.0] | **0.01** |
| AAo $SaO_2$ (%) | 48 [40, 54] | 58 [52, 64] | **0.0001** |
| SVC flow (indexed to fetal weight) (mL/min/kg) | 128.5 [106.0, 169.0] | 126.5 [103.0, 151.3] | 0.4 |
| SVC flow (indexed to fetal brain weight) (mL/min/g) | 1.41 ± 0.08 | 1.20 ± 0.06 | **0.03** |

*Note:* Bold values are those with statistical significance <0.05.

*Abbreviations:* AAo $SaO_2$, ascending aortic oxygen saturation; $DO_2$, oxygen delivery; GA, gestational age; SVC, superior vena cava; QUV, umblical vein flow; UV $SaO_2$, umbilical vein oxygen saturation.

**Table 16.3** Fetal cerebral hemodynamics and measures of neonatal brain growth and development in control fetuses and fetuses with congenital heart disease by MRI

| | *CHD (n = 40)* | *Normal (n = 46)* | *P-value* |
|---|---|---|---|
| $CDO_2$ (indexed to fetal weight) (mL $O_2$/min/kg) | 12.8 [10.3, 14.8] | 14.7 [11.4, 17.6] | **0.04** |
| $CDO_2$ (indexed to fetal brain weight) (mL $O_2$/min/g) | 0.14 ± 0.01 | 0.14 ± 0.01 | 0.75 |
| $CVO_2$ (indexed to fetal weight) (mL $O_2$/min/kg) | 2.8 [1.5, 4.1] | 3.6 [2.7, 5.0] | **0.01** |
| $CVO_2$ (indexed to fetal brain weight) (mL $O_2$/min/g) | 0.03 [0.02, 0.05] | 0.03 [0.02, 0.05] | 0.17 |
| Neonatal GA (weeks) | 39.7 ± 1.8 | 40.2 ± 1.4 | 0.2 |
| Neonatal brain volume (mL) | 344.1 ± 42.4 | 379.2 ± 52.0 | **0.0008** |
| WM ADC ($mm^2$/s) | 1705 [1634, 1780] | 1572 [1493, 1701] | **0.0004** |

*Note:* Bold values are those with statistical significance <0.05.

*Abbreviations:* $CDO_2$, cerebral oxygen delivery; $CVO_2$, cerebral oxygen consumption; GA, gestational age; WM ADC, mean white matter apparent diffusion coefficient.

behavior that is more characteristic of newborns with normal hearts born in the late preterm period.[11,12] Limperopoulos et al. used MRI to measure brain growth and metabolism in fetuses with CHD and found a slowing of brain growth and metabolism, particularly during the third trimester.[13] We and others have speculated that this could have resulted from *in utero* cerebral hypoxia. The principle of "oxygen conformance" has been established at a cellular level *in vitro*, whereby even small reductions in cellular oxygen delivery result in a series of metabolic adaptions that serve to downregulate cellular requirements for oxygen, thus protecting the cell against energetic collapse.[14] The cellular mechanisms involved in oxygen conformance include hypoxic inducible factor-mediated changes in gene expression, the switch from aerobic to anaerobic respiration, the reduction of cellular respiration, and slowing of the electron transfer chain, as well as downregulation of the cell's requirement for ATP. Modification of these pathways results in downstream effects on protein synthesis and cell cycling. Similarly, in fetal animal models, chronic hypoxia has been associated with a slowing of neuronal metabolism and reductions in synaptogenesis and myelination.[15,16] These would be in keeping with the apparent matching of substrate delivery and brain growth and metabolism indicated by the results shown in Tables 16.2 and 16.3. However, a causal relationship between diminished cerebral oxygen delivery and brain growth and maturation has yet to be established in human fetuses with CHD. Recent whole genome sequencing evidence obtained from children with CHD revealed a high rate of *de novo* mutations, particularly in those children with neurodevelopmental delay.[17] Interestingly, some of these mutations have also been associated with neurodevelopmental delay in children with normal hearts, and it has been suggested that intrinsic genetic factors may be more important than cerebral hemodynamics for brain development in children with CHD. Thus, the reduced cerebral oxygen delivery we observed in fetuses with CHD could reflect innate differences in the rate of brain growth arising from genes or epigenetic factors that influence brain development. One approach to investigating the relationship between $CDO_2$ and brain development is to attempt to augment $CDO_2$. A clinical trial that aims to test the hypothesis that chronic maternal hyperoxygenation enhances fetal brain development in the setting of single-ventricle CHD is currently underway. However, the benefit of accelerating fetal brain maturation in CHD patients through fetal intervention is also uncertain. The etiology of the neurodevelopmental deficits reported in children with CHD is likely to be multifactorial. Our serial postnatal MRI studies of children undergoing neonatal cardiac surgery suggest that postnatal derangements in cardiovascular physiology and perioperative injury are potentially more important than the subtle delays of brain growth and development typical of the fetal period.[18]

## Maternal hyperoxygenation and the pulmonary circulation

The impact of supplementary inhaled maternal oxygen on the fetal circulation has been studied intensively in humans and animals. It has been known since the 1960s that human umbilical cord oxygen saturations could be increased during labor by administering inhaled oxygen to the mother. More extensive studies in monkeys, lambs, and guinea pigs have characterized the relationship between increases in maternal $PaO_2$ and fetal oxygen saturation, whereby the most dramatic increases in fetal $SaO_2$ result from initial increases in maternal $FiO_2$ from room air (21%) up to 40%, with more modest increments in fetal $SaO_2$ achieved with further increases in maternal $FiO_2$ up to 100%.[19] The increase in placental oxygen exchange resulting from an increased diffusion gradient between maternal and fetal blood may be partly offset by a uterine vasoconstrictor effect of maternal hyperoxygenation that has been shown in sheep.[20] However, a number of animal and human studies have demonstrated consistent fetal circulatory changes in response to acute maternal hyperoxygenation.[21,22] Perhaps the best known of these is the pulmonary vasodilatory impact of an acute increase in fetal $SaO_2$. This was first described by Rudolph et al. who controlled ovine maternal $FiO_2$ using oxygen chambers while measuring fetal pulmonary blood flow using flow probes.[21] These studies confirmed an inverse relationship between fetal $SaO_2$ and pulmonary vascular resistance, which is more pronounced with advancing gestation. Subsequent work defined the biochemical basis of hyperoxic pulmonary vasodilation, which involves the nitric oxide and endothelin pathways.[23] The absence of a pulmonary vasodilatory response to maternal hyperoxygenation has been proposed as a way to identify atrial septal restriction in fetuses with hypoplastic left heart,[24] and this is in keeping with the abnormal pulmonary venous velocity profiles, low pulmonary blood flow, and abnormal pulmonary vascular development seen on histology in patients with this anatomy.[25]

The therapeutic potential of inducing pulmonary vasodilation, thereby improving left ventricular filling and promoting growth, has been explored by a number of investigators. Thomas Kohl used intermittent third trimester maternal hyperoxygenation in fetuses with underdeveloped ventricles and reported improvements in the size of the hypoplastic structures in some individuals.[26] More modest improvements in left heart growth were reported by a group of investigators from Texas Children's Hospital, while a group from the Second Xiangya Hospital, Changsha, reported a dramatic reduction in the need for coarctation surgery in fetuses with prenatally suspected coarctation treated with intermittent third trimester maternal hyperoxygenation.[27,28] The pulmonary vasodilatory effect of acute maternal hyperoxygenation has been shown using T2 mapping and phase contrast MRI in the normal human fetus and in fetuses with CHD, although in one case of borderline left ventricular hypoplasia, we found no associated increase in ascending aortic flow.[29,30] BOLD MRI studies have reported changes in fetal and placental oxygenation during ventilation with hypoxic and hyperoxic gas mixtures in sheep and mice.[31,32] The impact of maternal hyperoxygenation has also been studied in normal human pregnancies and pregnancies affected by CHD and intrauterine growth restriction (IUGR), where a diminished BOLD response was associated with an adverse perinatal outcome.[33–35]

## The hemodynamics of intrauterine growth restriction

In Chapter 15, we introduced the concept of "brain-sparing physiology," whereby redistribution of the fetal circulation occurs in response to hypoxia, with increased flow delivered to the brain and heart, and reduced flow delivered to the pulmonary circulation, musculoskeletal system, and abdominal viscera. This response has been extensively characterized in fetal sheep using microspheres and flow probes, and is used to identify human fetal distress through demonstration of reduced pulsatility in the middle cerebral artery on Doppler ultrasound.[21,36] Brain-sparing occurs through several mechanisms, including the local action of adenosine released by brain parenchymal cells on the cerebral vasculature.[15] Norepinephrine and nitric oxide released via the carotid chemoreceptor-mediated response to hypoxemia also act on cerebral vessel smooth muscle to induce vasodilation. Dramatic increases in cerebral blood flow and maintenance of cerebral oxygen delivery are achieved with minimal changes in combined ventricular output through redistribution of the fetal circulation induced by a combination of cerebral vasodilation and hypoxic pulmonary vasoconstriction and catecholamine-induced peripheral vasoconstriction. We measured the distributions of fetal circulation in 13 fetuses with late-onset IUGR and compared them with 26 normal controls.[37] T2 mapping was used to estimate vessel oxygen saturations using a conversion to oxygen saturation based on previous *in vitro* experiments performed using adult blood.[7] We estimated hemoglobin concentration based on reference data from conventional hematologic measurements of cord blood samples to quantify fetal $DO_2$ and $VO_2$ and fetal $CDO_2$ and $CVO_2$.[6]

The results of the flow and T2 measurements are shown in Figures 16.2 and 16.3. Total fetal $DO_2$ and $VO_2$ and fetal $DO_2$ and $VO_2$ indexed to fetal weight are shown in Figure 16.4. Figure 16.5 shows absolute fetal $CDO_2$ and $CDO_2$ indexed to fetal weight. Figure 16.6 reveals the difference in neonatal brain weight Z-score for the IUGR and control subjects, while Figure 16.7 compares total white matter and basal ganglia fractional anisotropy for the two groups. Figure 16.8 illustrates the relationship between fetal $CDO_2$ and neonatal brain weight Z-score. The results are in keeping with prior research conducted in fetal sheep[21] and demonstrate redistribution of the fetal circulation in the setting of hypoxemia with preferential flow to the brain and a reduction in pulmonary blood flow. The increase in cerebral blood flow results in relative sparing of $CDO_2$, although our findings in IUGR are similar to those described previously in CHD, with modest reductions in $CDO_2$ that appear to match decrements in brain growth. The associated reductions in white matter fractional anisotropy would appear to be in keeping with the diminished myelination seen in fetal sheep following chronic hypoxemia.[16] Importantly, $CDO_2$ correlates with neonatal brain size, in keeping with the concept that restriction of oxygen (and other metabolic fuels) may be limiting brain growth and metabolism in subjects with placental dysfunction. However, it is worth noting that a number of studies have demonstrated postnatal catch-up growth following IUGR, including catch-up of head circumference.[38] We also wish to emphasize that our findings should not necessarily be interpreted as evidence that earlier delivery in the setting of IUGR would lead to improvements in brain development. Premature exposure to the high oxygen tensions associated with extrauterine life has been shown to impair cerebral angiogenesis in mice, which could contribute to the white matter dysmaturation and injury typical of premature infants.[39]

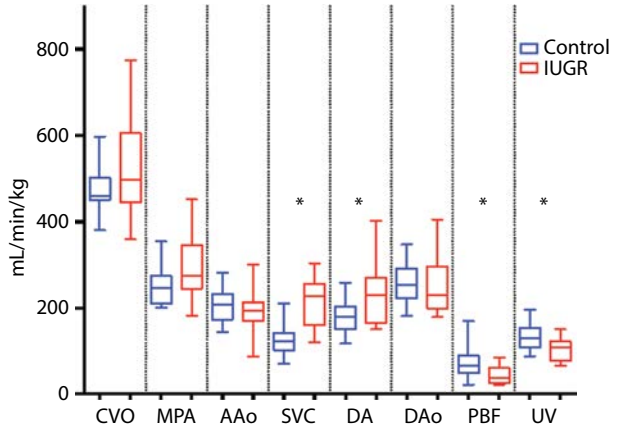


**Figure 16.2**
Distribution of blood flow in human fetuses with late-onset IUGR compared with normal controls by phase contrast MRI. (AAo, ascending aorta; CVO, combined ventricular output; DA, ductus arteriosus; DAo, descending aorta; MPA, main pulmonary artery; PBF, pulmonary blood flow; SVC, superior vena cava; UV, umbilical vein.) (From Zhu MY et al. *Am J Obstet Gynecol* 2016;214:367, with permission.[37])

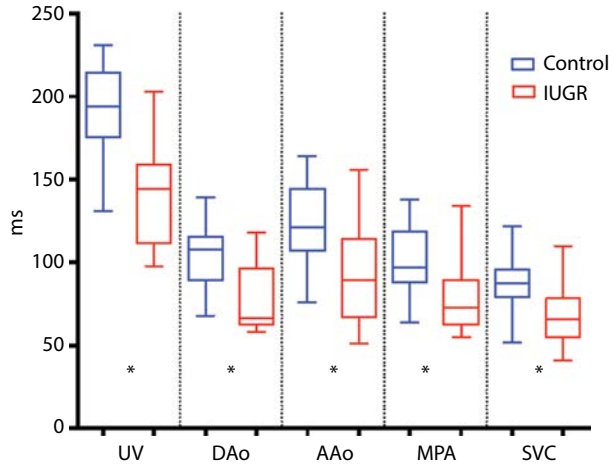


**Figure 16.3**
Vessel T2s (a measure of oxygen saturation) in human fetuses with late-onset IUGR compared with normal controls by MRI. (AAo, ascending aorta; DAo, descending aorta; MPA, main pulmonary artery; SVC, superior vena cava; UV, umbilical vein.) (From Zhu MY et al. *Am J Obstet Gynecol* 2016;214:367, with permission.[37])

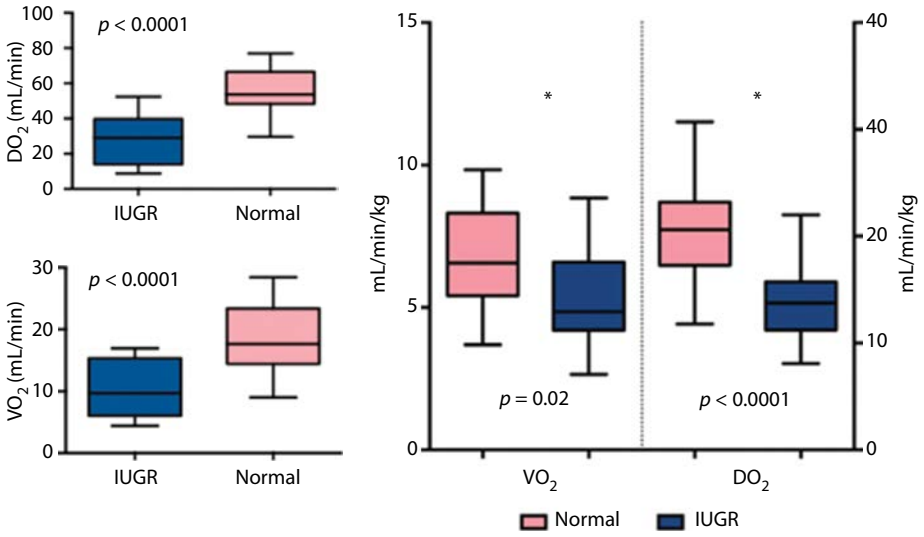


**Figure 16.4**
Absolute fetal oxygen delivery and consumption (left) and fetal oxygen delivery and consumption indexed to fetal weight (right) in human fetuses with late-onset IUGR by MRI. ($DO_2$, oxygen delivery; IUGR, intrauterine growth restriction; $VO_2$, oxygen consumption.) (From Zhu MY et al. *Am J Obstet Gynecol* 2016;214:367, with permission.[37])

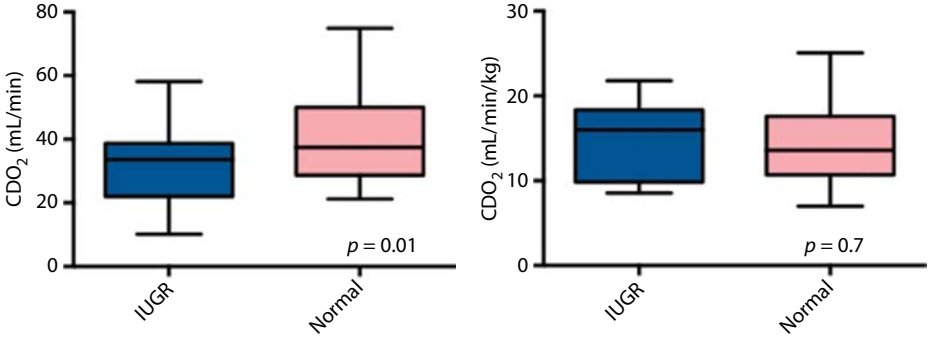


**Figure 16.5**
Cerebral oxygen delivery ($CDO_2$) in human fetuses with late-onset IUGR compared with controls by MRI.

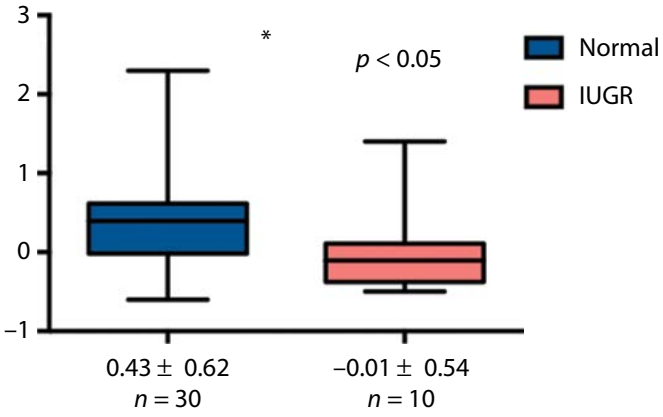


**Figure 16.6**
Brain weight Z-score in newborns following late-onset IUGR compared with normal controls by MRI.

One notable observation of our study of late-onset IUGR was the demonstration of placental dysfunction without circulatory redistribution in approximately one-third of our subjects.[37] An example of a set of serial hemodynamic measurements and the growth chart of one of these fetuses is shown in Figure 16.9. The data reveal a progressive reduction in oxygen delivery resulting from worsening desaturation of umbilical vein blood. However, this fetus appears to adapt to the reduction in $DO_2$ without classical brain-sparing physiology. Presumably, in the setting of stable placental dysfunction, gradual fetal metabolic adaption with downregulation of $VO_2$ can occur without the dramatic changes in cerebral and pulmonary blood flow seen in other fetuses subjected to more acute placental dysfunction. These findings may have implications with regard to the identification of late-onset IUGR and are in keeping with prior

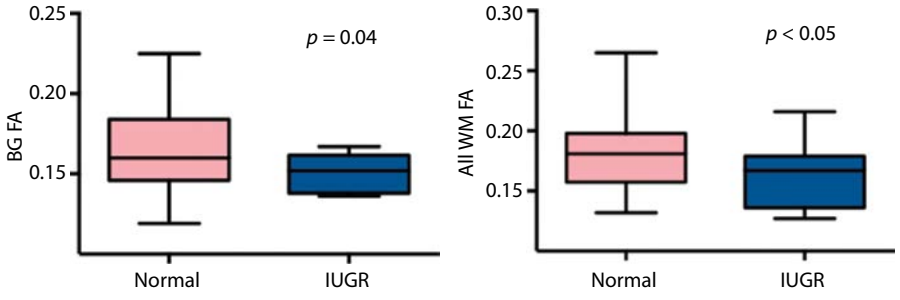


**Figure 16.7**
Fractional anisotropy (FA) in the basal ganglia (BG) and white matter (WM) of newborns following late-onset IUGR compared with controls by diffusion tensor imaging.

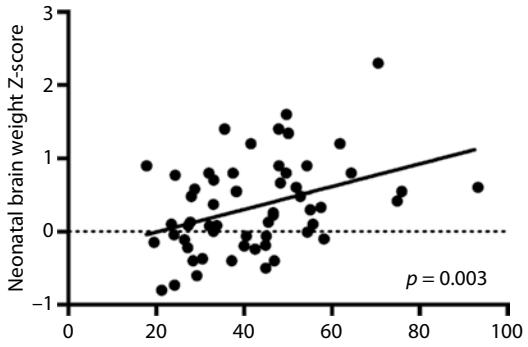


**Figure 16.8**
Relationship between prenatal cerebral oxygen delivery ($CDO_2$) and neonatal brain size by MRI.

studies showing that the typical Doppler changes seen in association with redistribution of the fetal circulation may only be present in a minority of affected fetuses.[40] It would appear that this subtler form of fetal growth restriction might only be confirmed with serial growth measurements or by approaches that provide direct measures of fetal oxygenation such as MRI.

## Associated fetal MRI findings

Associated fetal MRI findings in the setting of IUGR include asymmetric growth restriction with reduced liver volume, reduced subcutaneous fat, oligohydramnios, and morphologic abnormalities of the placenta. In CHD, MRI has been proposed as a useful adjunct to ultrasound, as it may provide evidence of anomalies of other organ systems.[41] One potentially clinically useful finding is the demonstration of secondary pulmonary lymphangiectasia in the setting of chronic pulmonary venous obstruction, for example, in hypoplastic left heart syndrome with intact or highly restrictive atrial septum, as shown in Figure 16.10.[42,43] At our institution, this has been used to aid decision-making regarding the use of fetal atrial septostomy to improve lung development and stabilize neonatal oxygenation in this most challenging form of HLHS.

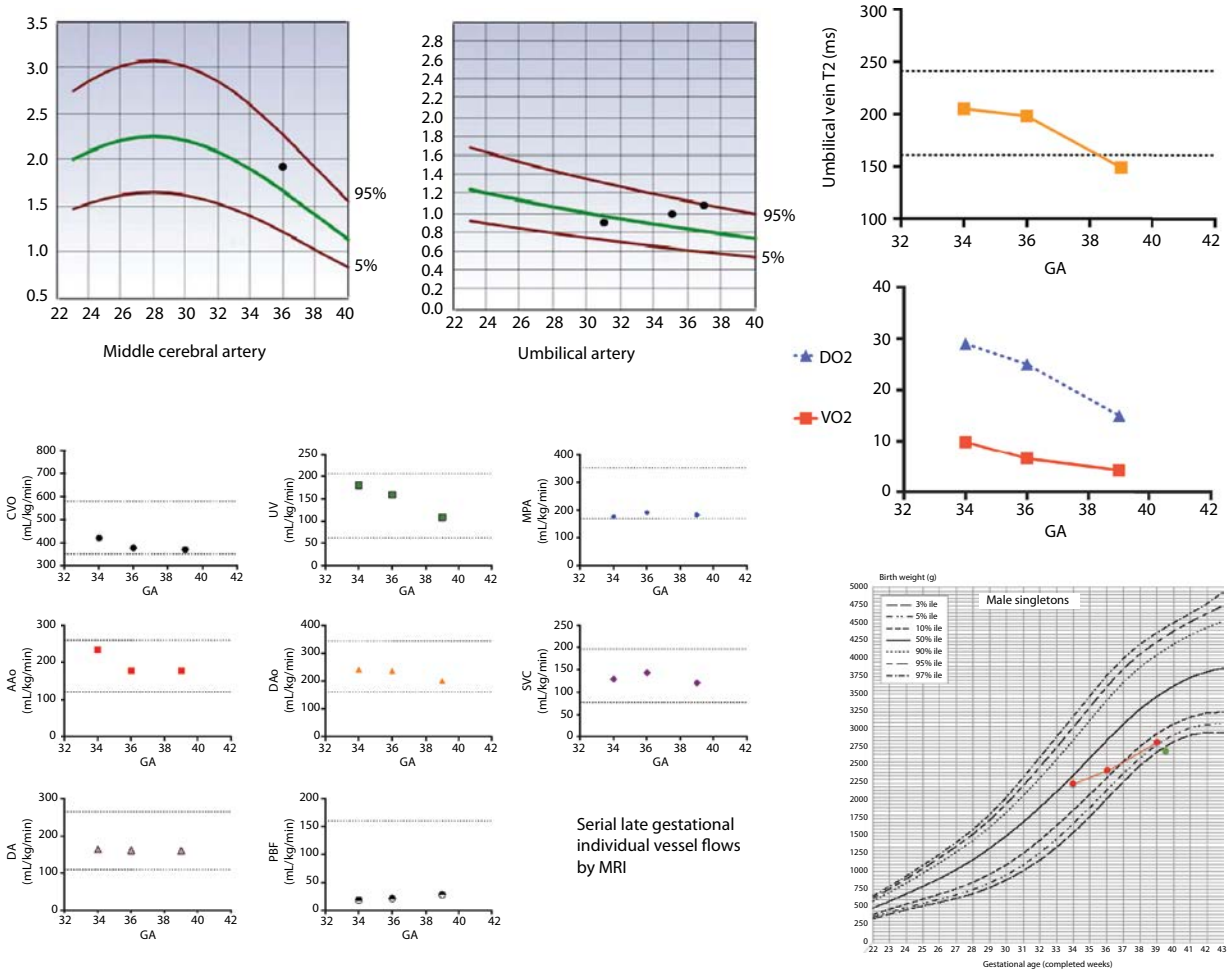


**Figure 16.9**
Doppler measurements of pulsatility index (top left), serial flow (bottom right), umbilical vein T2 and fetal oxygen delivery ($DO_2$) and consumption ($VO_2$) (top right) and fetal growth chart (Hadlock formula) in a fetus with late-onset IUGR without evidence of brain-sparing physiology. (From Zhu MY et al. *J Cardiovasc Magn Reson* 2015;17[S1]:P27, with permission.[45])

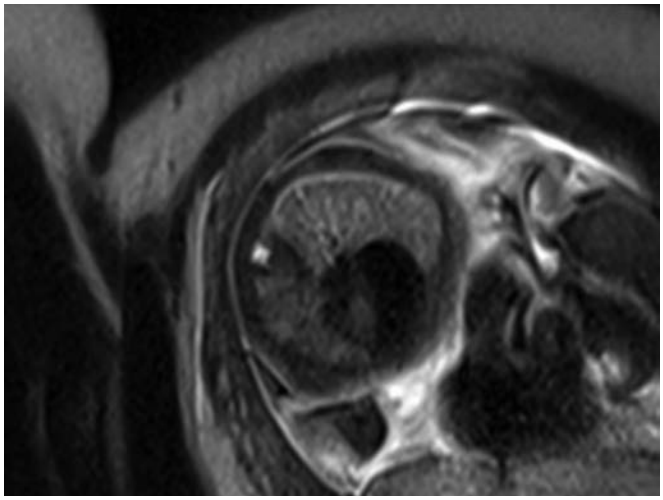

**Figure 16.10**
Pulmonary lymphangiectasia secondary to congenital heart disease with obstructed pulmonary venous drainage characterized by hyperintense branching structure extending through peribronchovascular and interlobular septal spaces demonstrated by T2-weighted fast spin echo MRI.

## Conclusion

Examples have been provided of how our understanding of fetal cardiovascular physiology has been enhanced through the application of a combination of vessel blood flow and oximetry measurements. Evidence is provided for a link between reductions in cerebral oxygen delivery resulting from placental and cardiac diseases and impaired brain development. The clinical significance of these findings remains uncertain, and there are currently no established clinical indications for fetal cardiac MRI. The relatively limited familiarity of obstetric clinicians with MRI technology, lack of access, and higher cost of MRI compared with ultrasound may hinder the widespread adoption of these new techniques. However, as researchers seek to evaluate new forms of fetal treatment such as maternal hyperoxygenation, there would appear to be potential utility for a modality that allows for the direct quantification of fetal oxygenation. Similarly, such an approach may offer increased accuracy in the diagnosis of late-onset IUGR. Finally, the detailed information we have acquired regarding normal fetal cardiovascular physiology may be helpful as we seek to translate the promise of *ex utero* physiologic support of the premature lamb using umbilical extracorporeal membrane oxygenation and fluid incubation to the management of human prematurity and other fetal conditions.[44]

## References


1. Porayette P et al. Abstract: ISMRM 2015.
2. Jones HN et al. *Placenta* 2015;36:1078–86.
3. Goff DA et al. *Circulation* 2011;124:A11260.
4. Albalawi A et al. *J Ultrasound Med* 2017;36:965–72.
5. Lim J et al. *Ultrasound Obstet Gynecol* 2016;48(suppl. 1): 44–5.
6. Nicolaides K et al. *The Lancet* 1988;331: 1073–5.
7. Wright G et al. *J Magn Reson Imaging* 1991;1:275–83.
8. Sun L et al. *Circulation* 2015;131:1313–23.
9. Miller SP et al. *N Engl J Med* 2007;357:1928–38.
10. Licht DJ et al. *J Thorac Cardiovasc Surg* 2009;137:529–37.
11. Limperopoulos C et al. *Pediatrics* 1999;103:402–8.
12. Birca A et al. *Ann Clin Transl Neurol* 2016;3(9):708–22.
13. Limperopoulos C et al. *Circulation* 2010;121(1):26–33.
14. Wheaton WW, Chandel NS. *Am J Physiol Cell Physiol* 2011;300: C385–93.
15. Pearce W. *J Appl Physiol* 2006;100:731–8.
16. Rees S et al. *Int J Dev Neurosci* 2011;29:551–63.
17. Homsy J et al. *Science* 2015;350:1262–6.
18. Porayette P et al. *J Cardiovasc Magn Reson* 2016;18:P156.
19. Longo LD. Respiratory gas exchange in the placenta. *Compr Physiol* Supplement 13: Handbook of Physiology, The Respiratory System, Gas Exchange 2011: pp 351–401. 10.1002/cphy.cp020418.
20. Tervilä L et al. *Acta Obstet Gynecol Scand* 1973;52:177–81.
21. Rudolph A. The fetal circulation. In: *Congenital Diseases of the Heart—Clinical-Physiological Considerations*. 3rd ed. Chichester: Wiley-Blackwell; 2009:1–24.
22. Rasanen J et al. *Circulation* 1998;97:257–62.
23. Heymann MA. *Eur J Obstet Gynecol Reprod Biol* 1999;84:127–32.
24. Szwast A et al. *Circulation Cardiovasc Imaging* 2010;3:172–8.
25. Rychik J et al. *J Am Coll Cardiol* 1999;34:554–60.
26. Kohl T. *Pediatr Cardiol* 2010;31:250–63.
27. Lara DA et al. *J Am Soc Echocardiogr* 2015;28:B8.
28. Zeng S et al. *Sci Rep* 2016;6:39304.
29. Porayette P et al. *Prenat Diagn* 2016;36:274–81.
30. Borik S et al. *Cardiol Young* 2015;25:1214–7.
31. Sørensen A et al. *Ultrasound Obstet Gynecol* 2009;34:687–92.
32. Cahill LS et al. *J Cereb Blood Flow Metab* 2014;34:1082–8.
33. Sørensen A et al. *Prenat Diagn* 2013;33:141–5.
34. You W et al. *Circulation* 2015;132:A19532.
35. Sinding M et al. *Ultrasound Obstet Gynecol* 2016;47:748–54.
36. Wladimiroff JW et al. *BJOG* 1986;93(5):471–5.
37. Zhu MY et al. *Am J Obstet Gynecol* 2016;214:367.
38. de Wit CC et al. *J Pediatr* 2013;162:415–20.
39. Yuen TJ et al. *Cell* 2014;158:383–96.
40. Oros D et al. *Ultrasound Obstet Gynecol* 2011;37:191–5.
41. Manganaro L et al. *Eur J Radiol* 2009;72:172–80.
42. Seed M et al. *Pediatr Radiol* 2009;39:747–9.
43. Al Nafisi B et al. *J Cardiovasc Magn Reson* 2013;15:65.
44. Partridge EA et al. *Nat Commun* 2017;8:15112.
45. Zhu MY et al. *J Cardiovasc Magn Reson* 2015;17[S1]:P27.

# 17

# Abnormal visceral and atrial situs and congenital heart disease

Varsha Thakur, Edgar T. Jaeggi, and Shi-Joon Yoo

## Introduction

Congenital heart disease (CHD) should be analyzed in a sequential segmental manner, especially when an abnormality of situs exists.[1,2] The term "situs" is used to define the right-left orientation or arrangement of the body organs at three anatomical levels: abdominal, bronchopulmonary, and atrial.[3–8] The term *situs*, however, does not define cardiac position. Usually there is an asymmetry of the abdominal and thoracic organs (Figure 17.1, Table 17.1). Abdominal asymmetry is characterized by a specific rightward-leftward orientation of the nonpaired solitary organs including the liver, stomach, and spleen, whereas thoracic asymmetry is due to asymmetry of the forms of the paired organs including the lungs, bronchi, pulmonary arteries, and atria. The organ arrangement at one level is usually consistent with other levels, but exceedingly rarely, abdominal, bronchopulmonary, and atrial arrangements may also be discordant.[3,6,9–13] Three types of situs are possible: situs solitus, situs inversus, and heterotaxy (Figure 17.2, Table 17.2). *Situs solitus* indicates the normal arrangement of organs at the abdominal, atrial, and bronchopulmonary levels. *Situs inversus* refers to an inverted or mirror image arrangement of these organs. *Heterotaxy* (Greek, *heteros* [other or different] + *taxis* [arrangement]) indicates that the arrangement of the organs is different from the usual arrangement of situs solitus or situs inversus.[4,12]

## *How to determine visceral and atrial situs*

Laterality disorders (situs inversus and heterotaxy) affect about 1.1–1.2 per 10,000 live births.[14] As these abnormalities of situs are harbingers of CHD and other anomalies, it is very important to routinely define the situs prior to the detailed fetal cardiac evaluation. The assessment should first begin with the determination of right and left sides of the fetus.[15] Once the sonographer has clarified the "sidedness" of the fetus, the evaluation of situs at all three levels can be commenced. The abdominal situs is determined by observing the location of the liver, stomach, spleen, abdominal aorta, and inferior vena cava in the transverse view of the upper abdomen (Figure 17.3).[1] In situs solitus, the larger lobe of the liver is seen on the right, and the stomach and spleen are seen on the left (Figure 17.3a). The abdominal aorta is located posteriorly at the left anterior aspect of the spine, and the inferior vena cava is located more anteriorly on the right, almost always entering the right atrium. In situs inversus, this right-left relationship is mirror imaged (Figure 17.3b). In heterotaxy with right isomerism or asplenia, the liver is characteristically symmetrical and the stomach tends to be located near the midline either on the right or on the left (Figures 17.3c,d). Occasionally, a part of the stomach is seen in the lower thorax.[16] In most but not all cases with right isomerism, there is asplenia: by evaluating the posterior and lateral aspects of the stomach, the spleen can be identified if it is present. In most cases of heterotaxy and asplenia, a posteriorly located abdominal aorta and an anteriorly positioned inferior vena cava are seen on the same side of the spine as "juxtaposed" vascular structures.[1,17]

In heterotaxy with left isomerism or polysplenia, symmetry of the liver may appear less evident with its major portion often lying to one side of the abdomen (Figures 17.3d and 17.4).[3,4] The arrangement of the liver and stomach often mimics that of either situs solitus or situs inversus. As the spleen develops in the dorsal mesogastrium, multiple spleens (polysplenia) aggregate in a single location along the greater curvature of the stomach[18] (Figure 17.3d). Occasionally, multiple spleens may fuse together to form a single but multilobulated mass. This is in contrast to accessory spleens, in which a dominant spleen is present together with multiple small splenules that can be found anywhere in the peritoneal cavity. Polysplenia is commonly associated with interruption of the suprarenal infrahepatic segment of the inferior vena cava (interrupted IVC) and continuation of the lower-body venous drainage via the azygos or hemiazygos venous system (Figure 17.5). Although it can also occur with other types of body situs, interruption of the IVC is highly suggestive of heterotaxy with polysplenia. It can be diagnosed when the coronal or sagittal sonograms do not show the usual IVC connection to the atrial segment (Figure 17.5a).[17,19–21] It can also be suspected when two equally sized vessels are seen in the posterior mediastinum in either the coronal or the transverse view, the posterior one being the dilated azygos or hemiazygos vein

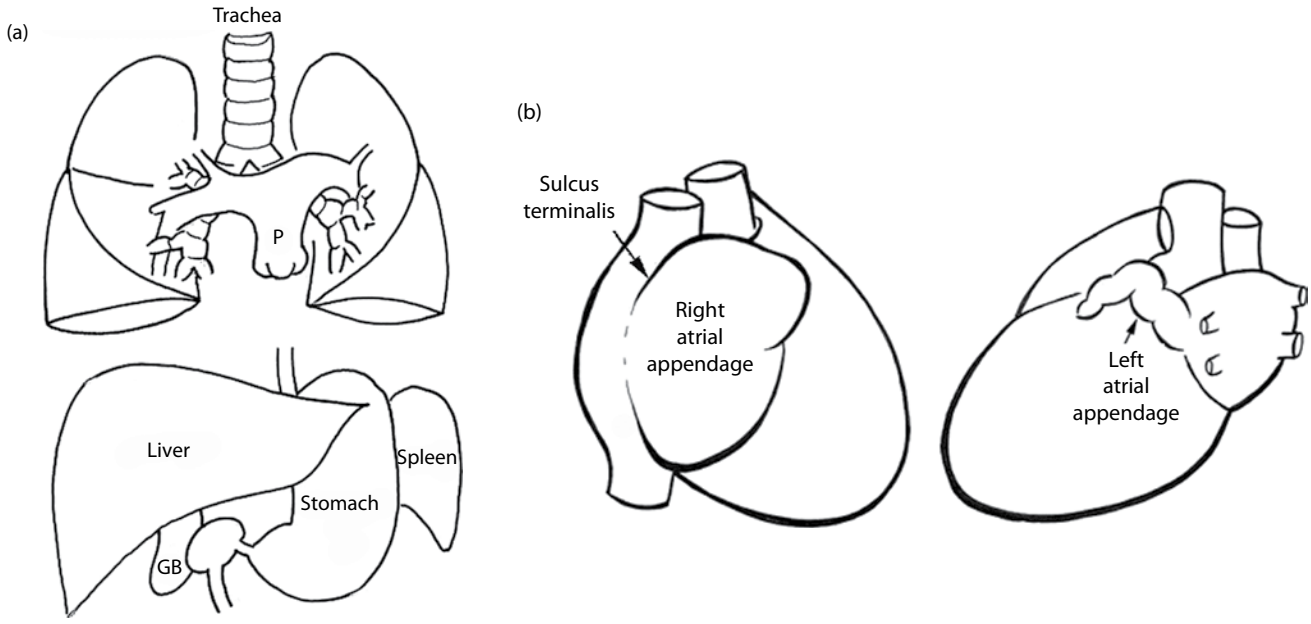


**Figure 17.1**
Normal asymmetry of the thoracic and abdominal organs (a) and the heart (b). Note the asymmetric forms of the paired organs of the thorax and the asymmetric arrangement of the nonpaired abdominal organs. Asymmetric shape of the atrial appendages, presence or absence of sulcus and crista terminalis, and asymmetric extent of the atrial pectinate muscles relative to the atrioventricular junction characterizes the cardiac asymmetry. (GB, gall bladder; P, pulmonary artery.)

**Table 17.1** Features characterizing normal asymmetry of body organs

| | *Right* | *Left* |
|---|---|---|
| Abdominal organs | • Larger lobe of the liver | • Spleen and stomach |
| Lung lobation | • Three lobes | • Two lobes |
| Main bronchus | • Short, eparterial | • Long, hyparterial |
| Pulmonary artery | • Transverse course in front of the right main bronchus<br>• Origin of the first branch proximally in the mediastinum | • Oblique course crossing over the left main bronchus (epobronchial)<br>• Origin of the first branch distally at the hilum |
| Atrium | • Triangular appendage with wide junction demarcated by crista terminalis<br>• Appendage with pectinate muscle reaching the atrioventricular junction<br>• Fossa ovalis with limbus | • Finger-like appendage with narrow junction not demarcated by crista terminalis<br>• Appendage and its pectinate muscles at distance from the atrioventricular junction<br>• No fossa ovalis |

and the other anterior structure being the descending aorta (Figures 17.5b–d).[1,17,19–21] On color Doppler examination, the blood flow through these two parallel vessels is in opposite directions with the azygous vein seen draining into the superior vena cava (Figure 17.5d).

On examination of anatomical specimens, determination of the atrial situs is based on the morphology of the atrial appendages (Figure 17.1b).[10,11,22] In this regard, it should be known that the atrial appendage is characterized internally by the presence of pectinate muscles in contrast to the smooth inner surface of the rest of the atrium. The right atrial appendage is triangular and has a wide orifice that is demarcated by a prominent crest termed the *crista terminalis*. The right atrial appendage with its pectinate muscles reaches the atrioventricular junction. The left atrial appendage is finger-like and has a narrow orifice that is not demarcated by a crest. The left atrial appendage as well as its pectinate muscles do not reach the atrioventricular junction.[22] The atrial appendages can be visualized by echocardiography (Figure 17.6),[1,23,24] but it is difficult to reliably differentiate a morphological right from a left atrial appendage by prenatal and postnatal two-dimensional ultrasound imaging.[20] Furthermore, although the pectinate muscles may be visualized, it is very difficult to evaluate the extent of these muscles. Therefore, we consider it impractical to define atrial situs based on the atrial morphological appearance. The atrial situs can reliably be inferred from the abdominal situs as the atrial and visceral situs are concordant apart from rare exceptions to this "viscero-atrial concordance rule."[3,6,9–11,25,26]

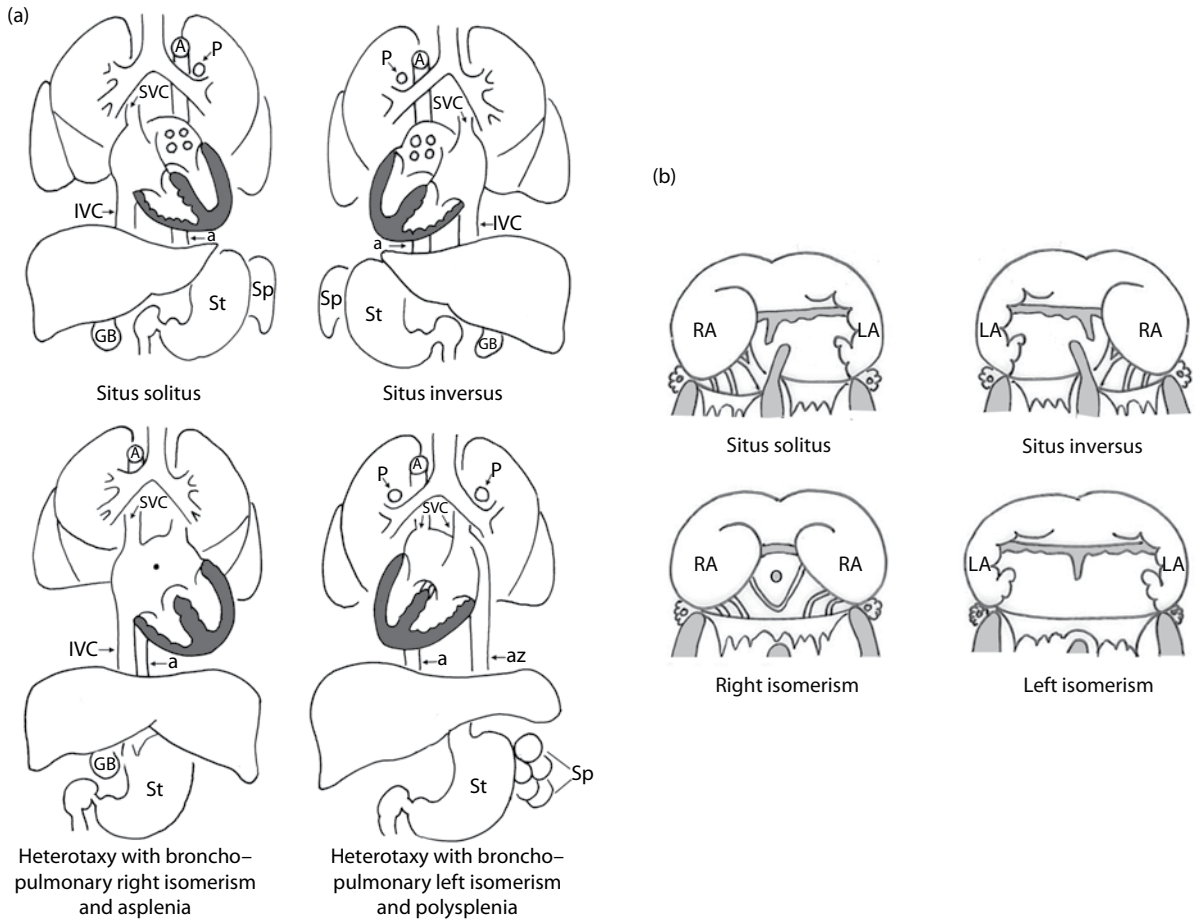


**Figure 17.2**
Classical types of visceral (a) and atrial (b) situs. (A, aortic arch; a, descending aorta; az, azygos vein; GB, gall bladder; IVC, inferior vena cava; P, pulmonary artery; Sp, spleen; St, stomach; SVC, superior vena cava.)

**Table 17.2** Types of visceral and atrial situs

| *Abdominal situs* | *Bronchopulmonary situs* | *Atrial situs* |
|---|---|---|
| Situs solitus | Situs solitus | Situs solitus |
| Situs inversus | Situs inversus | Situs inversus |
| Heterotaxy | Heterotaxy | Heterotaxy |
| With asplenia | With right isomerism | With right isomerism |
| With polysplenia | With left isomerism | With left isomerism |
| With normal spleen | | With ambiguous atrial morphology |

# Situs inversus

## *Incidence, genetics, and associated abnormalities*

The reported incidence of situs inversus ranges from 1 in 2,500 to 1 in 25,000 live births. In a mass radiographic survey of adults, it was found 1 per 7,000–8,000.[27,28]

Dextrocardia is the usual and appropriate position of the heart of patients with situs inversus (Figure 17.7, Video 17.1), although levocardia and mesocardia are not infrequent findings. The prevalence of CHD that occurs in association with situs inversus varies with the cardiac position. CHD is less prevalent with dextrocardia, although exact numbers are unknown because of problems with ascertainment of asymptomatic cases with less severe anomalies. Main lesions include tetralogy of Fallot, ventricular and atrial septal defects, transposition of the great arteries, and double-outlet right ventricle, while single ventricle lesions are infrequent.[29–31]

Levocardia and mesocardia in patients with situs inversus are rare but almost always associated with CHD. The

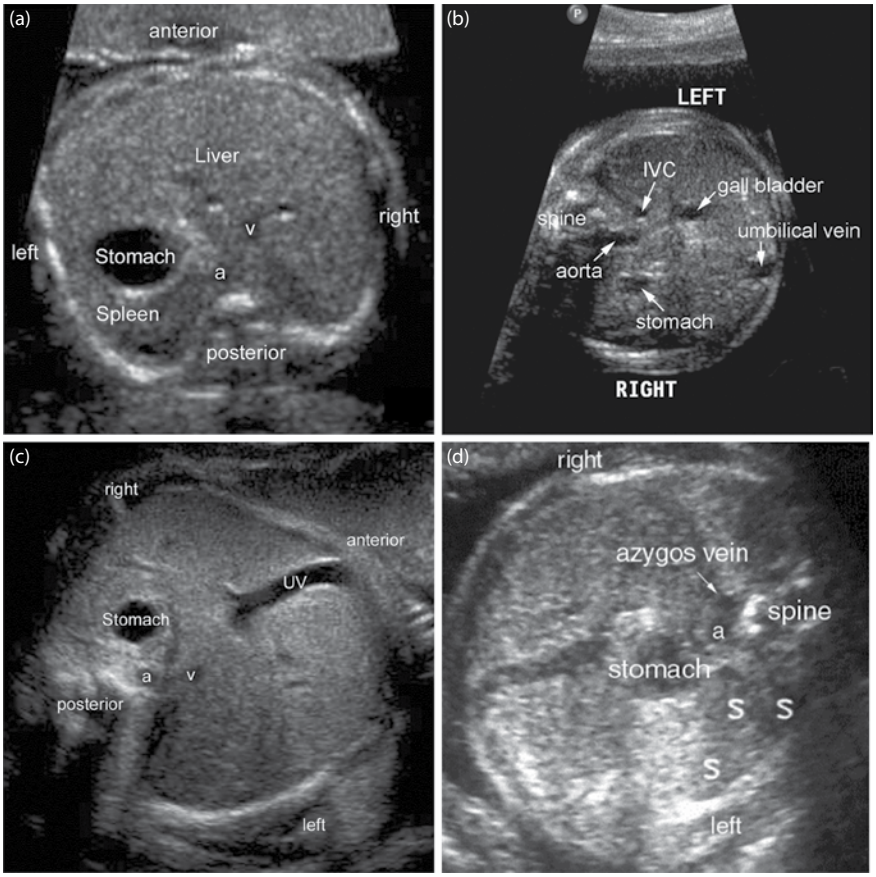


**Figure 17.3**
Transverse sonograms of the upper abdomen showing the arrangement of the abdominal organs in situs solitus (a), situs inversus (b), heterotaxy with asplenia (c), and heterotaxy with polysplenia (d). The abdominal situs is determined by observing the location of the liver, stomach, spleen, abdominal aorta (a), and inferior vena cava (v). In situs inversus, there is mirror image arrangement of the abdominal organs (b). In heterotaxy, the orderly pattern of the organ arrangement is disrupted. In asplenia the aorta and inferior vena cava are seen back-to-back on the same side (c). In polysplenia the aorta and dilated azygos vein are seen side-by-side or back-to-back in front of the spine (d). Multiple spleens (S) are seen behind the stomach. (UV, umbilical vein.)

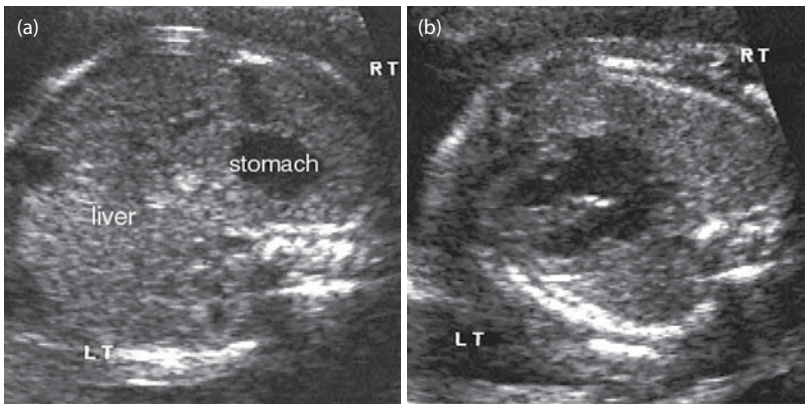


**Figure 17.4**
Left isomerism with probable polysplenia. (a) Transverse sonogram of the upper abdomen shows the right-sided stomach and left-sided larger lobe of the liver. (b) Four-chamber view of the heart shows levocardia and normal cardiac anatomy. (Lt, left; Rt, right.)

typical pathology of patients with a discordant heart axis is congenitally corrected transposition of the great arteries[32,33] in association with additional significant cardiac defects.

The majority of patients with situs inversus will have ciliary dysfunction.[28,34] Conversely, situs inversus occurs in 50% of patients with primary ciliary dyskinesia or immotile cilia syndrome, a combination known as Kartagener syndrome.[35]

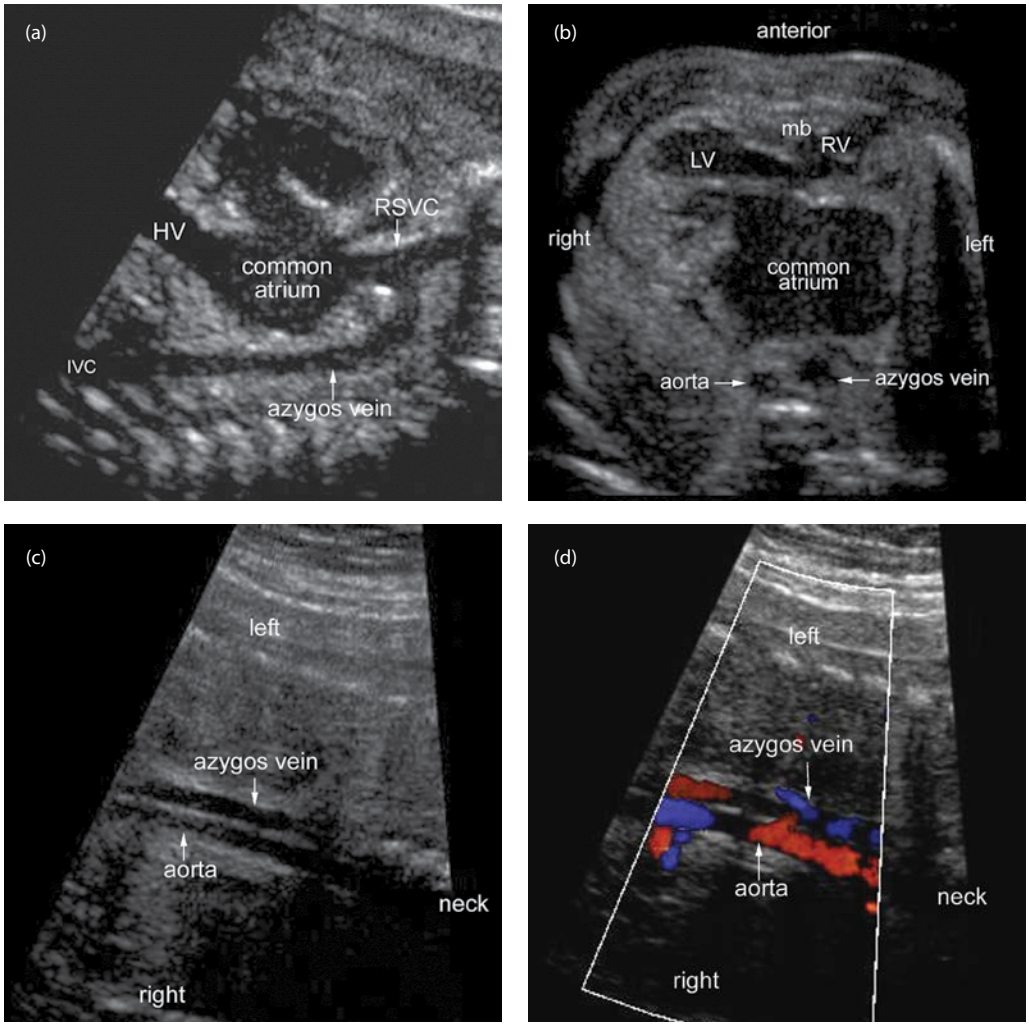


**Figure 17.5**
Interruption of the inferior vena cava with azygos continuation. (a) Sagittal view showing the inferior vena cava that does not connect to the atrium but to the dilated azygos vein. (b) Four-chamber view shows complete atrioventricular septal defect with a common atrium. There are two vessels in the posterior mediastinum. They are the descending aorta and the dilated azygos vein draining the interrupted inferior vena cava (c and d). Oblique coronal views of the thorax shows two parallel vessels, the aorta and azygos vein that show opposite blood flow direction. (HV, hepatic vein; LV, left ventricle; mb, moderator band; RSVC, right superior vena cava; RV, right ventricle.)

Primary ciliary dyskinesia disorder has an autosomal recessive inheritance pattern with extensive genetic heterogeneity, although autosomal dominant gene mutations have been reported.[36]

Intra-abdominal pathologies such as duodenal atresia, biliary atresia, and gastroschisis with malrotation affected 58% of referrals with situs inversus to a large tertiary care center.[37] Other known associations include Dandy-Walker malformation, limb deficiencies, and ear anomalies (anotia, microtia).[14,38]

## *Fetal and neonatal outcomes*

Outcomes largely depend on the severity of cardiac and noncardiac anomalies. Most cardiac lesions are usually repairable with good results. A significant number of patients with dextrocardia may have no symptoms, and the diagnosis is made incidentally by an abnormal ultrasound exam or x-ray.[39]

The main consequences of primary ciliary dyskinesia are susceptibility to chronic recurrent respiratory infections, including sinusitis, bronchitis, pneumonia, and otitis media due to reduced or absent mucus clearance from the lungs that can evolve to progressive bronchiectasis beginning in early childhood. Immotile sperm can lead to infertility, although conception remains possible through the use of *in vitro* fertilization.

# Heterotaxy

## *Diagnostic features*

Fetal diagnosis of heterotaxy with asplenia or polysplenia can be highly accurate due to telltale abnormalities found in arrangement of the abdominal organs in association with CHD.[17] Heterotaxy has often been called *situs ambiguous*

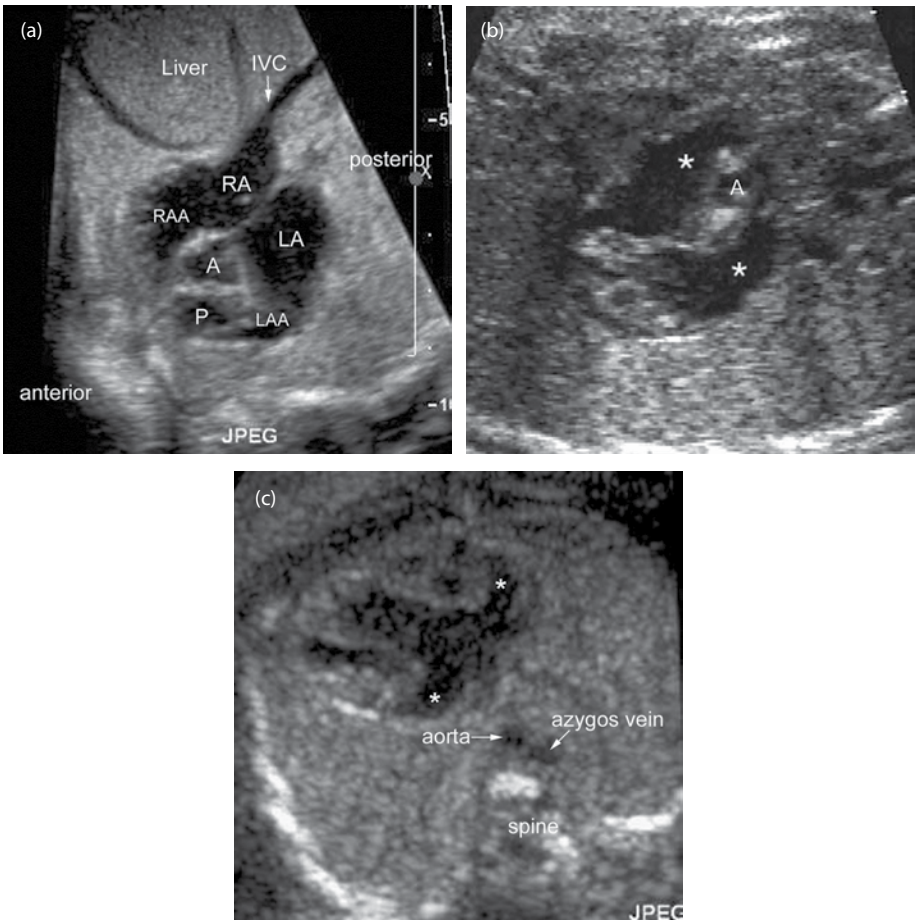


**Figure 17.6**
Atrial appendages. (a) Short-axis echocardiogram of a normal fetal heart showing the appendages of the right (RA) and left (LA) atriums. The appendages embrace the aortic root (A) and pulmonary trunk (P) from behind. The pectinate muscles are seen as small nodular structures along the lateral wall of the right atrial appendage (RAA). The right atrial appendage is large and has a wide opening; the left atrial appendage (LAA) is small and tubular and has a narrow opening (b and c). Symmetrical appendages (asterisks) in right (b) and left (c) isomerism. (IVC, inferior vena cava.)

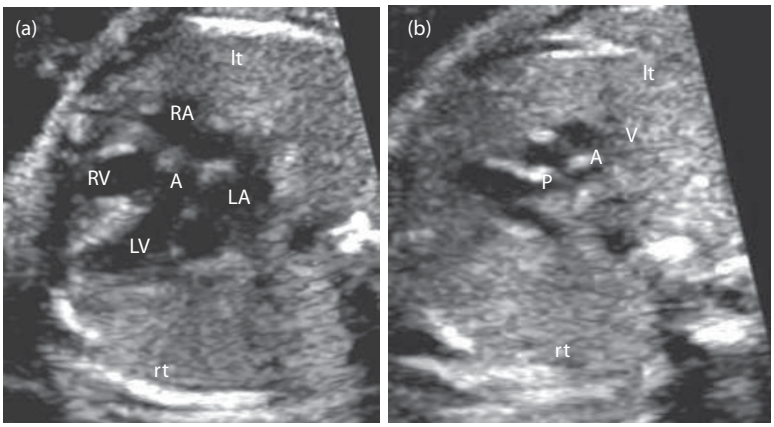


**Figure 17.7**
Situs inversus totalis. (a) Four chamber view showing dextrocardia with mirror image atrial arrangement and concordant atrioventricular connections. Correct diagnosis of situs inversus totalis relies on the appropriate determination of the right and left side of the fetus (Video 17.1). (b) Mirror image three-vessel view found in situs inversus totalis. The pulmonary artery is rightward and anterior to the aorta. (A, aorta; LA, left atrium; lt, left; LV, left ventricle; P, pulmonary; RA, right atrium; rt, right; RV, right ventricle; V, superior vena cava.)

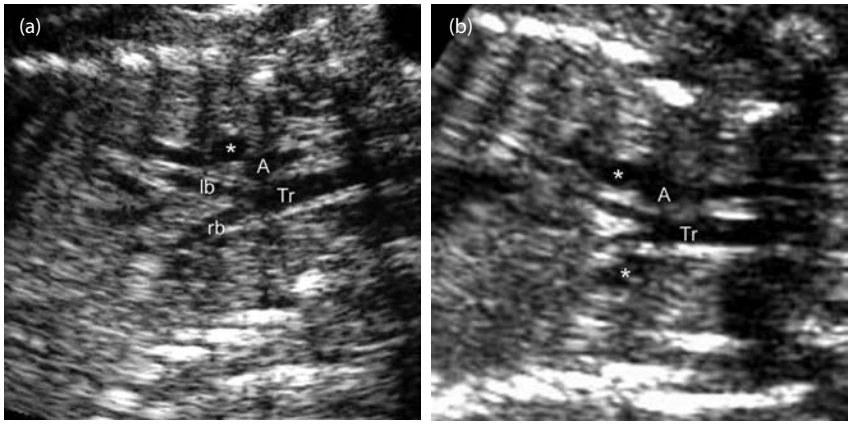


**Figure 17.8**
Bronchopulmonary anatomy seen in coronal sonograms. (a) Normal bronchopulmonary anatomy. The trachea (Tr) bifurcates into the right (rb) and left (lb) main bronchi. The left aortic arch (A) and left pulmonary artery (asterisk) course above the left main bronchus. The right pulmonary artery does not course above the right main bronchus. (b) Left isomeric bronchopulmonary anatomy. Both pulmonary arteries (asterisks) are seen to course above the ipsilateral bronchi. Although it is possible to demonstrate the anatomy, the practical usefulness of this is questionable.

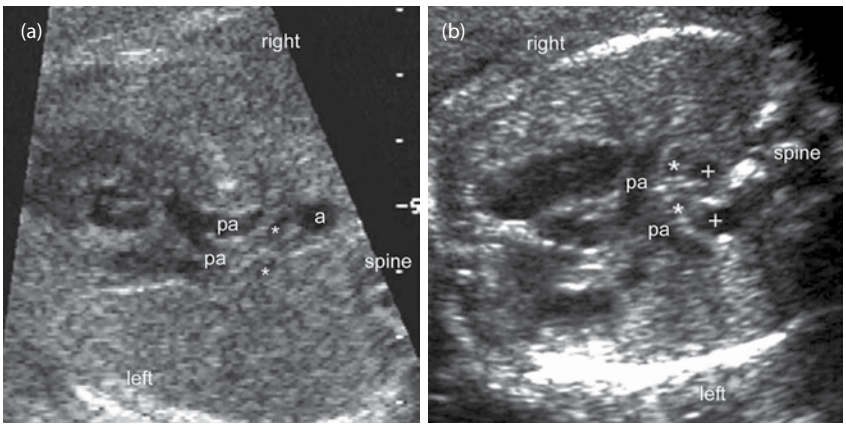


**Figure 17.9**
Bronchopulmonary anatomy seen in transverse sonograms of right (a) and left (b) isomerism. The pulmonary arterial branching is symmetrical in both cases. Asterisks depict the main bronchi. The difference between the two is not evident. Note the two vessels (crosses) in front of the spine in (b). One is the aorta and the other is the dilated azygos vein in this case of left isomerism. (a, descending aorta; pa, pulmonary artery.)

(uncertain situs).[5,6,9] However, *situs ambiguous* is not an appropriate term, as the organ arrangement in heterotaxy is not uncertain but rather complex or difficult to define.[1] Abdominal heterotaxy is characterized by jumbled-up arrangement of the nonpaired solitary organs.[1,3–6,9–13,18,40–44] The liver and stomach may be disposed in a random fashion as far as their location on the right or left side is concerned. The intestine is commonly malrotated. In most cases, the spleen is either absent (asplenia), or multiple spleens are present on the right or on the left (polysplenia). Rarely, a normal spleen is found. Bronchopulmonary heterotaxy is characterized by the symmetric arrangement of the lungs, bronchi, and pulmonary arteries (Figures 17.8 and 17.9).[18,41–44] The symmetry is the result of duplication of either the right- or the left-sided structures, thereby dividing thoracic heterotaxy into left and right isomeric subtypes. Atrial heterotaxy is characterized by symmetry of atrial appendage morphology and, therefore, the relation of the pectinate muscles to the atrioventricular junction (Figure 17.6).[6,10,11] Atrial heterotaxy can also be divided into right and left atrial isomerisms. Generally, asplenia occurs with right bronchopulmonary and atrial isomerism, while polysplenia occurs with left bronchopulmonary and atrial isomerism. However, polysplenia can occur with right isomerism, and asplenia with left isomerism. Isomerisms may even occur with a normal spleen. While splenic morphology is somewhat variable, there is tighter concordance between bronchopulmonary situs and atrial situs so that the bronchopulmonary arrangement usually reflects the atrial arrangement.[10,11]

## *Incidence and genetics*

The incidence of heterotaxy is approximately 1–1.44 per 10,000 births[13,27,28,45,46] but is likely underestimated as not all

children with left isomerism will become clinically symptomatic after birth. In the New England Regional Infant Cardiac Program, heterotaxy was found in 4.2% of infants with CHD.[47] In fetal series, although the relative incidences of right and left isomerism vary, left isomerism is consistently more common than right isomerism.[43,44,46,48] In postnatal series, most reports describe a higher incidence of right isomerism,[42] while a postnatal series from our institution showed a similar predominance of left isomerism after birth.[46] It has been postulated that the combination of heart block and atrioventricular valve insufficiency in left isomerism leads to fetal demise and a lower postnatal incidence. Another explanation is that left atrial isomerism without CHD may go unnoticed after birth, while right isomerism is always associated with major forms of CHD and thus is unlikely to be missed. There is evidence to suggest that heterotaxy may have a genetic etiology,[13,27,45,49–53] although genetic anomalies were unusual diagnoses in our institutional experience[46] with heterotaxy patients.

Similarly, other studies have not found that there is a significantly increased risk for chromosomal abnormalities in heterotaxy.[52,54] It has also been suggested that abnormal visceral situs is strongly predictive of a normal karyotype.[55]

Recurrence rates of visceral heterotaxy of 5%–10% were reported if a sibling was affected.[13,45,51] Moreover, there are reports of rare cases of familial heterotaxy caused by single gene mutations inherited in an autosomal dominant or recessive or x-linked pattern.[27,50,56–61] All possible situs variants, solitus, inversus, and heterotaxy may appear in the same family.[55] Given the genetic complexity of these disorders, genetic counseling is indicated and the option of genetic testing presented to affected families.

## Associated abnormalities

CHD is exceedingly common when there is heterotaxy. As such, we are unaware of any documented case of right isomerism that was not affected by CHD. It is also accepted that most cases of left isomerism do also have CHD, but types of lesions are more variable and usually less severe than that found in association with right isomerism. Moreover, left isomerism may be found incidentally without any clinical evidence of a cardiac defect.[18,62] In some of these asymptomatic individuals with left isomerism, an interrupted inferior vena cava and multiple spleens may be the only detectable anomalies by fetal echocardiography. Nonetheless, there is considerable overlap in the cardiac malformations within the two types of isomerism (Table 17.3).[18,27,28,35,41–44,48,63–67] Bilateral superior venae cavae (Figure 17.10) and complete atrioventricular septal defect (Figures 17.11 and 17.12) are common in both right and left isomerisms. In right isomerism more than left isomerism, the atrioventricular septal defect is usually characterized by an unbalanced commitment of the atrioventricular

**Table 17.3** Common congenital cardiac defects in right and left isomerism (Videos 17.2 and 17.3)

| | *Right isomerism* | *Left isomerism* |
|---|---|---|
| Bilateral superior venae cavae | 45% | 45% |
| Bilateral systemic venous drainage | 70% | 60% |
| Absence of coronary sinus | ~100% | ~60% |
| Interruption of the inferior vena cava | <2.5% | 80% |
| Juxtaposition of the aorta and inferior vena cava | ~90% | Uncommon |
| Extra cardiac type of total anomalous pulmonary venous connection with/without obstruction | 50%, with obstruction in 50% | Rare |
| Pulmonary venous connection to ipsilateral atriums | 4% | 45% |
| Atrioventricular septal defect | 90% | 50% |
| Atrial septum | Functionally common atrium in 50% | Usually better formed, intact in ~20% |
| Atrioventricular connection | Univentricular in 70% | Biventricular in ~75% |
| Ventriculoarterial connection | Concordant only in 4% | Concordant in ~70% |
| Pulmonary atresia or stenosis | 80% | 30% |
| Left-sided obstructive lesion | <5% | ~30% |
| Heart block/bradycardia | Rare | 25–70% |

*Source:* Composite data from Uemura H et al. *Am J Cardiol* 1995;76(11):846–9;[10] Uemura H et al. *Ann Thorac Surg* 1995;60(3):561–9;[11] Berg C et al. *Ultrasound Obstet Gynecol* 2003;22(5):451–9;[17] Peoples WM et al. *Pediatr Cardiol* 1983;4(2):129–37;[18] Phoon CK, Neill CA. *Am J Cardiol* 1994;73(8):581–7;[42] Lim JS et al. *Circulation* 2005;112(16):2454–61;[46] Taketazu M et al. *Am J Cardiol* 2006;97(5):720–4;[48] Gilljam T et al. *J Am Coll Cardiol* 2000;36(3):908–16;[63] Rubino M et al. *J Thorac Cardiovasc Surg* 1995;110(3):641–50;[64] Hashmi A et al. *J Am Coll Cardiol* 1998;31(5):1120–6;[65] Patel CR et al. *Ultrasound Obstet Gynecol* 2001;17(3):268–71;[66] Huggon IC et al. *J Am Coll Cardiol* 2000;36(2):593–601;[67] Wren C et al. *Am J Cardiol* 1987;59(12):1156–8;[69] Shenker L et al. *Am J Obstet Gynecol* 1987;157(2):248–53;[70] Baschat AA et al. *Ultrasound Obstet Gynecol* 1999;14(5):311–4;[71] Berg C et al. *Ultrasound Obstet Gynecol* 2005;26(1):4–15;[72] Jaeggi ET et al. *Ultrasound Obstet Gynecol* 2005;26(1):16–21.[74]

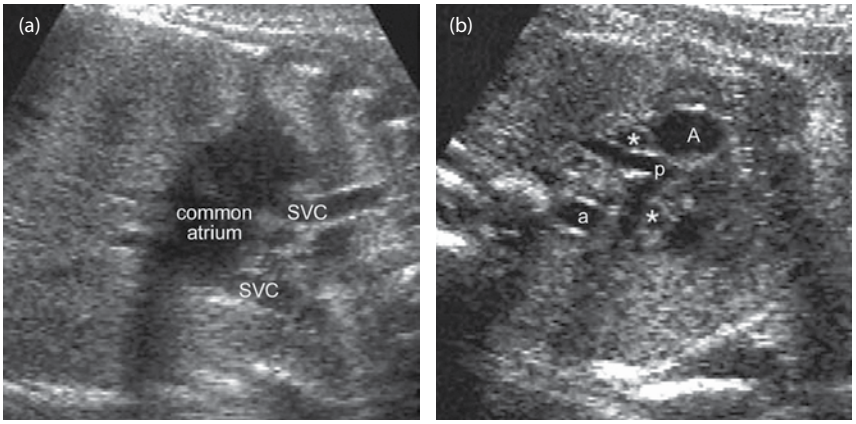


**Figure 17.10**
Bilateral superior venae cavae. (a) Coronal view from a fetus with right isomerism showing bilateral superior venae cavae (SVC) connected to the roof of the common atrium. (b) Three-vessel view from another fetus with right isomerism showing bilateral superior venae cavae (asterisks). Note the symmetric pulmonary arterial branching (p). The pulmonary artery is much smaller than the aorta (A) because of severe pulmonary stenosis. (a, descending aorta.)

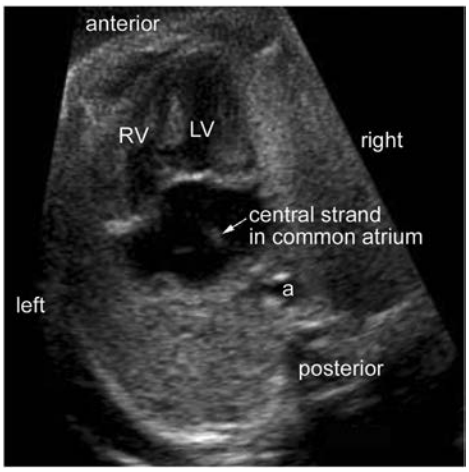


**Figure 17.11**
Complete atrioventricular septal defect in right isomerism. Four-chamber view shows atrioventricular septal defect. The right ventricle (RV) is slightly smaller than the left ventricle (LV). The atrium is a common chamber with a small strand of remnant atrial septum seen as a dot (central dot sign). (a, descending aorta.)

valve to the underlying ventricular mass with resultant discrepancy in the size of the left and right ventricles.[46,67] Other cardiac lesions show noticeable predilection to one type of isomerism. In right isomerism, cardiac lesions are typically complex and usually affect the heart at multiple levels. Supra- (Figure 17.12) or infracardiac total anomalous pulmonary venous connection, often with pulmonary venous obstruction (Figure 17.13), is particularly common in right isomerism[68] but uncommon in left isomerism. When the pulmonary veins are connected to the atrium or atria in the presence of right isomerism, the connection is usually through a narrow confluent channel (Figure 17.14). In left isomerism, the pulmonary veins from each lung tend to separately enter the posterior wall of the ipsilateral atrium. As previously mentioned, IVC interruption with azygos continuation is a key feature of left isomerism, while the aorta and the patent IVC are juxtaposed on the same side in right isomerism. In both conditions, the hepatic veins may have separate openings in the floor of the atrium or atria, rather than forming a confluence. The atrial septation is also different in right and left isomerism. In 50% of cases of right isomerism, there is a common atrium, and in most cases only a strand of remnant atrial septum is seen traversing the atrial cavity (Figure 17.11). In a four-chamber view, this strand is seen as a dot in the center of the common atrium (the "central dot sign"), which is pathognomonic for right isomerism. In left isomerism, the atrial septum is usually better formed or well developed in two-thirds of cases. The atrioventricular connection is more often univentricular in right isomerism (to a dominant chamber of right ventricular morphology) and biventricular in left isomerism. The morphology of the ventricular chambers in univentricular atrioventricular connection may be difficult to define by trabeculations. It is, however, useful to determine ventricular morphology indirectly by assessing the spatial relationship between the dominant and rudimentary ventricle, respectively. When the rudimentary chamber is related to the crux cordis and therefore is located along the posterior and inferior surfaces of the ventricular mass, it is the morphologically left ventricle; thus, the dominant chamber is the morphologically right ventricle. When the rudimentary chamber is not in contact with the crux cordis but is located anteriorly and superiorly, either on the right or on the left, it is the morphologically right ventricle; thus, the dominant chamber is the morphologically left ventricle. When only one ventricle is identified, the ventricular morphology is hard to define and called indeterminate. In most cases of right isomerism, the ventriculo-arterial connection is abnormal and discordant, and can be that of transposition of the great arteries, double-outlet right ventricle (with malposed great arteries), or a single outlet (usually the aorta) (Figures 17.15 through 17.17). Pulmonary stenosis or atresia is present in approximately 80% of the right isomerism cases. The

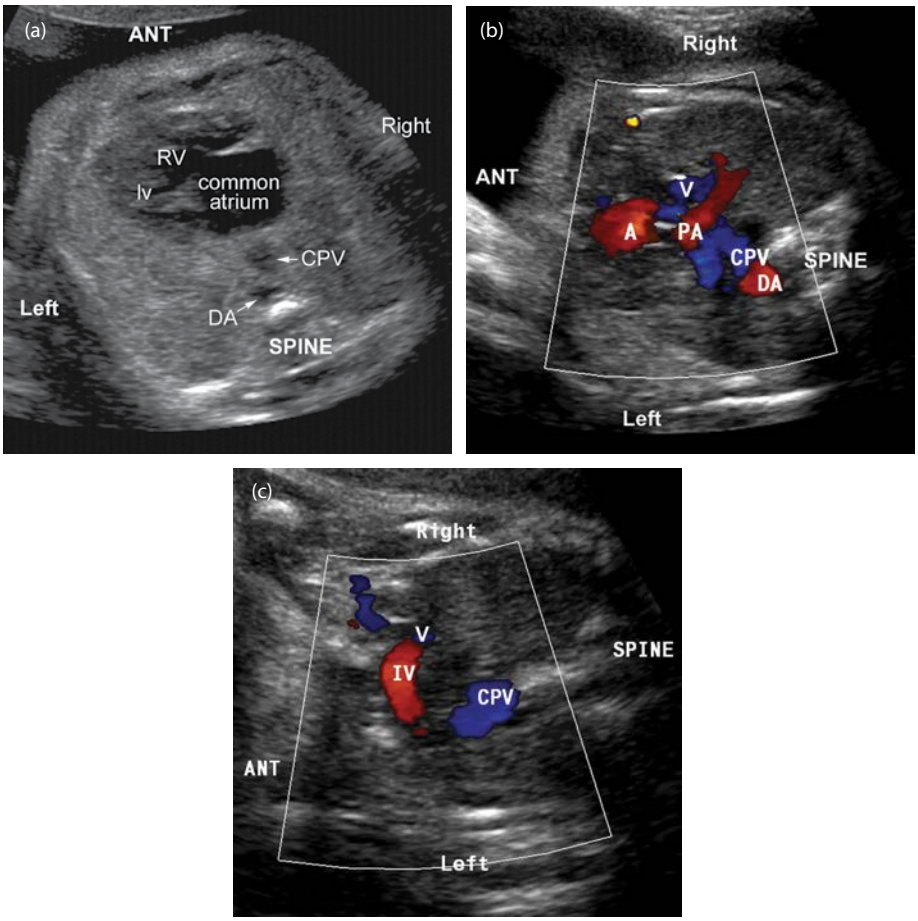


**Figure 17.12**
Unbalanced atrioventricular septal defect and total anomalous pulmonary venous connection to the brachiocephalic vein in right isomerism. (a) Four-chamber view demonstrates the pulmonary venous confluence (CPV) behind the atrium. There is unbalanced complete atrioventricular septal defect with a dominant right ventricle (RV) and a small left ventricle (lv). (b) Three-vessel view shows the antero-posterior relationship of the ascending aorta (A) and pulmonary artery (PA). The confluent common pulmonary vein courses backward and leftward in front of the descending aorta (DA). The superior vena cava (V) is on the right. Note the symmetric branching pattern of the pulmonary artery. (c) Oblique axial view shows the common pulmonary vein connecting to the innominate vein (IV).

pulmonary artery can be nonconfluent with the right and left pulmonary arteries being supplied by bilateral ductus arteriosus. Concordant ventriculo-arterial connection is rare in right isomerism. In contrast, in up to 70% of cases of left isomerism, the ventriculo-arterial connection is concordant and pulmonary stenosis or atresia far less common (approximately 30% of cases), while left-sided obstructive lesions are found in about 20%–30%.

Bradycardia secondary to high degree or complete heart block is a feared prenatal association with left isomerism when there is an atrioventricular septal defect (Figure 17.18, Video 17.4).[13,43,46,48,63,69–72] Left isomerism is the leading cause of fetal heart block if there is CHD. The condition is explained by the anatomical discontinuity between the atrioventricular (AV) node and the conduction axis.[73] Most cases will present with CHB in the first trimester, but progressive heart block is possible later in pregnancy. The risk of heart block in left isomerism is much higher in fetal series than in postnatal series.[43,46,63,71,72,74] The hearts with right isomerism typically have two atrioventricular nodes and bundles and thus are not affected by heart block. This arrangement carries a small risk of fetal reentrant supraventricular tachycardia due to antegrade electrical conduction via one AV node and retrograde conduction via the second node.[61,75] Fetal diagnosis of arrhythmia is reported elsewhere in more detail (Figure 17.18).

Heterotaxy is associated with abnormal arrangement of internal organs.[68,76] Bowel malrotation is associated with heterotaxy, which carries a risk of volvulus or obstruction[37,77–80] that may need surgical intervention.[80] In up to 20%, left isomerism was found associated with biliary atresia, absence or hypoplasia of the gall bladder, and short pancreas,[63,81] while conversely, approximately 6% of biliary atresia cases are associated with left isomerism. When biliary atresia is present, pulmonary arteriovenous malformations may develop later in life. Polysplenia may also be associated with extra hepatic portosystemic shunt[82] and agenesis or hypoplasia of the portal vein.

In right isomerism, part of the stomach may be seen in the thorax,[16] usually due to a hiatal hernia. Adrenal, genitourinary, and anal anomalies, such as horseshoe kidneys and

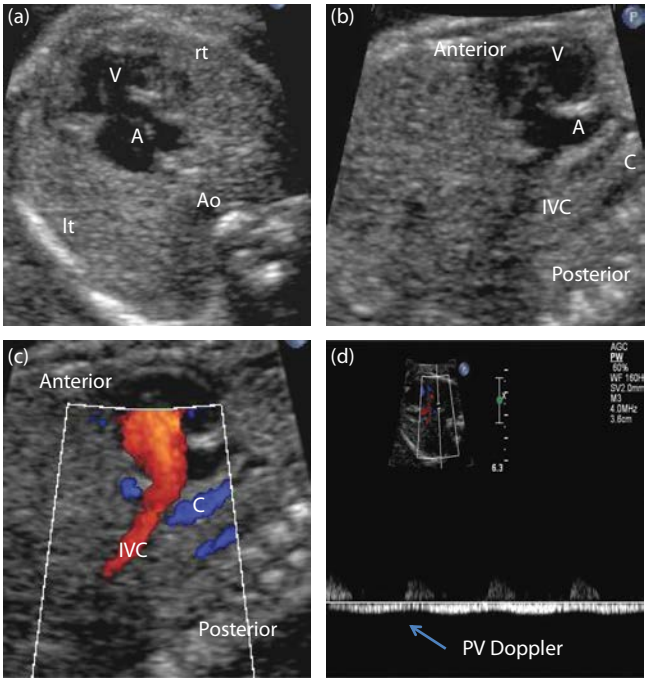


**Figure 17.13**
Right atrial isomerism with obstructed infradiaphragmatic total anomalous pulmonary venous return. (a) Four-chamber view showing dextrocardia and an unbalanced AVSD. Although the pulmonary venous confluence is not seen well behind the common atrium, there is a large gap between the common atrium and the descending aorta that should raise suspicion for a confluence and anomalous pulmonary veins. (b) Two-dimensional long-axis view in the same fetus, which shows a confluence behind the common atrium that has a vertical vein draining into the liver. (c) Color Doppler of the same long-axis view that shows the confluence drains into the ductus venosus. (d) Pulse Doppler of a pulmonary vein in this fetus showing continuous low-velocity flow; there is loss of the biphasic flow pattern, typically seen in the pulmonary vein, that is suggestive of obstruction.

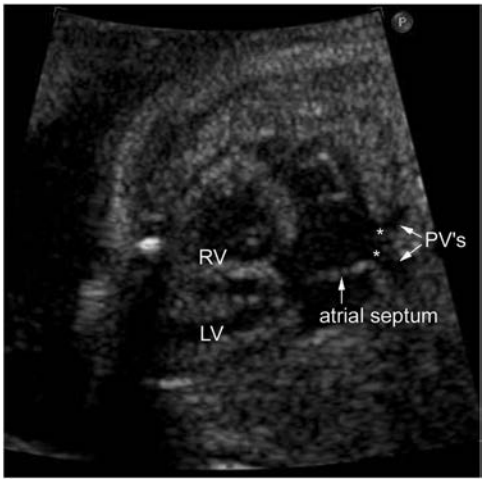


**Figure 17.14**
Right isomerism with the pulmonary veins connected to the common atrium. Four-chamber view shows the close proximity of the orifices of the pulmonary veins (asterisks). (LV, left ventricle; RV, right ventricle.)

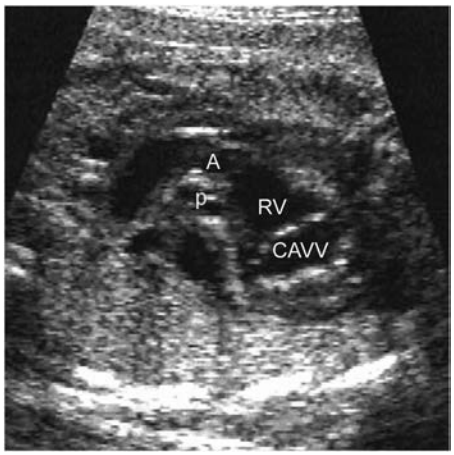


**Figure 17.15**
Transposition in right isomerism. Ventricular outflow tract view shows the aorta (A) arising from the right ventricle (RV) and the pulmonary artery (P) from the left ventricle (LV). A large ventricular septal defect (d) is seen. (l-a, left-sided atrium.)

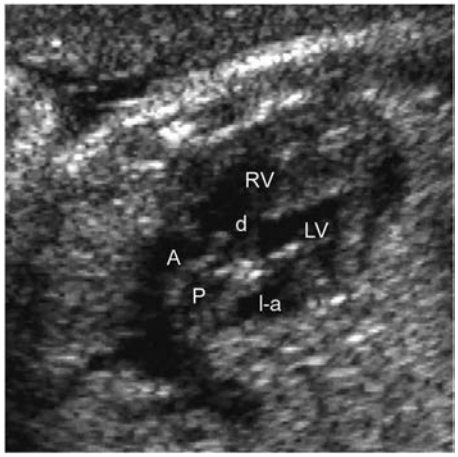


**Figure 17.16**
Double-outlet right ventricle in right isomerism. Ventricular outflow tract view shows that both the aorta (A) and the pulmonary artery (p) arise from the right ventricle (RV). A common atrioventricular valve (CAVV) is seen in the right ventricle. The pulmonary artery is smaller because of stenosis.

adrenals and anal stenosis and atresia, are not uncommon in right isomerism.[83] There is a rare association of primarily ciliary dyskinesia with heterotaxy, and children with bronchiectasis or recurrent sinusitis should be evaluated for this respiratory disorder.[34,84] Patients born with asplenia or polysplenia with functional asplenia carry a significant risk of infections and will require lifelong preventive antibiotic prophylaxis for potentially life-threatening infection-related complications.[85]

## *Fetal and neonatal outcomes*

Spontaneous fetal death is uncommon in heterotaxy unless there is left isomerism with bradycardia due to high-degree heart block,[43,44,46] which is typically a lethal association

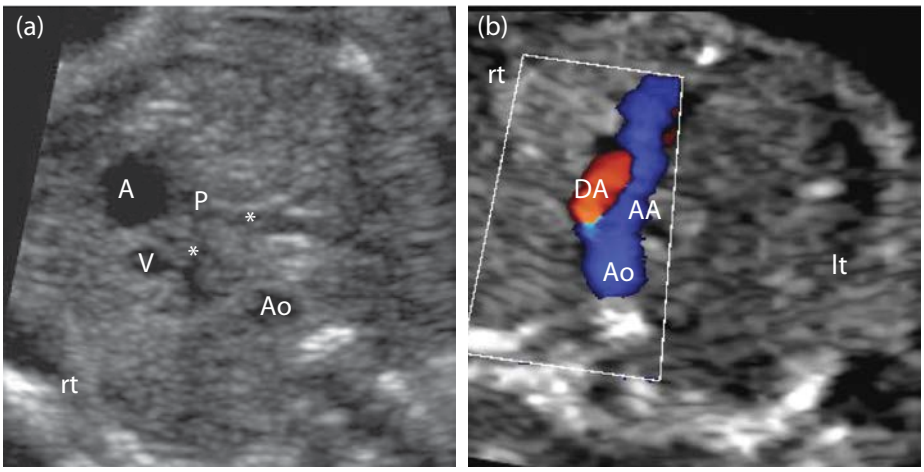


**Figure 17.17**
Right atrial isomerism with single outlet (pulmonary atresia). (a) The two-dimensional three-vessel view shows a large anterior and rightward aorta. The pulmonary artery is quite hypoplastic in keeping with pulmonary atresia. The branch pulmonary arteries are symmetric in keeping with right atrial isomerism. (b) Color Doppler in the tracheal three vessel view shows antegrade flow in the aortic arch. Retrograde flow is seen in the ductal arch in keeping with pulmonary atresia. (A, aorta; AA, aortic arch; A0, descending aorta; DA, ductal arch; lt, left; P, pulmonary artery; rt, right; V, superior vena cava; *, branch pulmonary arteries.)

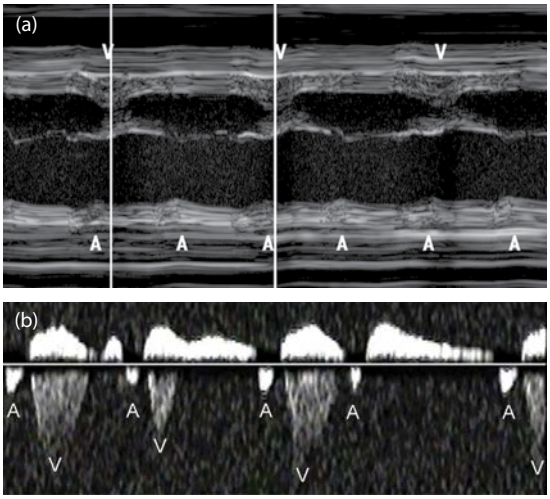


**Figure 17.18**
Atrioventricular dissociation in left isomerism. (a) M-mode echocardiogram through the atrial and ventricular walls shows that the ventricular beats (V) are independent of the atrial beats (A). (b) Simultaneous Doppler tracing of the pulmonary artery and vein shows a similar pattern of atrioventricular dissociation. The letter "V" indicates forward flow through the pulmonary artery peaking during ventricular systole. The letter "A" indicate reversed flow through the pulmonary vein during atrial systole.

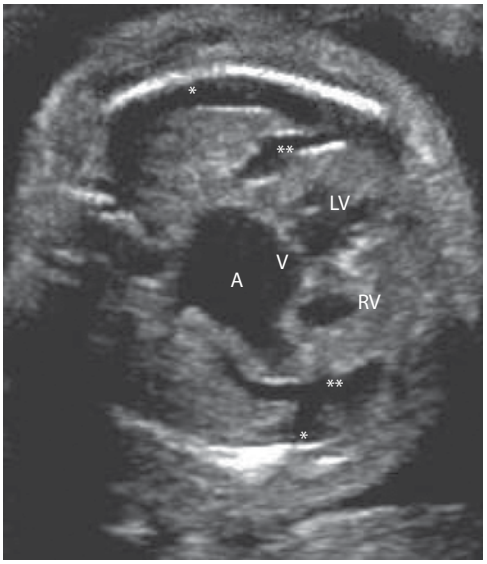


**Figure 17.19**
Hydrops in fetus with left isomerism. The fetus has a balanced AVSD. Hydrops has developed secondary to severe bradycardia due to complete heart block. Bilateral pleural effusions and a pericardial effusion are seen. (A, common atrium; LV, left ventricle; RV, right ventricle; V, common AV valve; *, pleural effusion; **, pericardial effusion.)

(Figure 17.19, Video 17.4)[43,46,72,74] or bilateral outflow obstruction. Left atrial isomerism with complete heart block is often seen in association ventricular noncompaction.[86]

The postnatal prognosis is largely dependent on the severity of cardiac and extracardiac anomalies. Data from our institution showed that antenatal diagnosis did not improve overall survival in both left and right isomerism.[46] Right isomerism carries a significantly worse prognosis than left isomerism.[41,42,46] The high postnatal mortality in right isomerism is related to the high incidence of total anomalous pulmonary venous connection, severe pulmonary outflow tract obstruction, and functionally single ventricle that usually relates to an unbalanced atrioventricular septal defect. When pulmonary outflow tract obstruction is significant, administration of prostaglandin is necessary immediately after delivery to maintain patency of the ductus arteriosus. Right isomerism with obstructive total anomalous pulmonary venous connection is associated with a particularly poor prognosis due to

the additional lung pathology.[87] In our experience, the majority of patients with right isomerism were not candidates for a biventricular repair and if attempted did not survive to hospital discharge.[46] Of cases with primary single ventricle palliation, only one-third of cases eventually underwent the Fontan operation. Risk factors for mortality other than right isomerism included total anomalous pulmonary venous connection with obstruction, underdeveloped pulmonary arterial bed, functionally single ventricle, and the need for early surgical intervention. In addition, complex anatomy of the systemic as well as pulmonary venous connections, presence of bilateral superior venae cavae, unusual spatial relationship of the ventricles, and complex outflow tract pathology are also important in determining the complexity of postnatal surgical repair and long-term need for reintervention. Postnatal outcomes were also related to the extracardiac anomalies and their resultant complications, including biliary atresia and intestinal obstruction.

## Videos

**Video 17.1a** (https://youtu.be/bhrUZV5eri0)
Video demonstrating Cordes method showing the heart is on the right side of the chest.

**Video 17.1b** (https://youtu.be/pQmfjaZGLhk)
A transverse sweep from abdomen to neck shows situs inversus showing the liver on the left and stomach on the right with dextrocardia, mirror image atrial arrangement, and concordant AV and VA connections with a right aortic arch and right ductal arch.

**Video 17.2a** (https://youtu.be/WI7bHSr_90E)
Two-dimensional imaging showing heterotaxy with asplenia and right atrial isomerism. Sweep using method by Cordes et al. showing that the stomach and heart are on the right side. The aorta and IVC are juxtaposed on the left side.

**Video 17.2b** (https://youtu.be/DgNAZKYT-A4)
A transverse two-dimensional view showing the right-sided stomach with left-sided IVC and aorta. The liver appears to be midline.

**Video 17.2c** (https://youtu.be/yP4udtDwoyE)
Sweep from the four-chamber view showing dextrocardia with an unbalanced AVSD with a dominant left-sided right ventricle and hypoplastic right-sided left ventricle. There is double-outlet right ventricle with malposed great vessels with an anterior aorta. Pulmonary outflow is hypoplastic. There are confluent, symmetric branch pulmonary arteries. Total anomalous pulmonary veins are seen with drainage to the left SVC via a vertical vein. In addition, there is a left SVC. There is good ventricular function.

**Video 17.3a** (https://youtu.be/B8tzVOD1FEk)
Two-dimensional imaging in a fetus with heterotaxy and left atrial isomerism. Clip using method by Cordes et al. showing stomach on the right with levocardia. There is an azygous vein seen posterior to the aorta. There is a common atrium with an unbalanced AVSD with a mildly smaller but apex-forming left ventricle.

**Video 17.3b** (https://youtu.be/gS80XXYIZd8)
Video showing the four-chamber view with a common atrium and mildly unbalanced AVSD with a mildly smaller but apex-forming left ventricle. There is good biventricular function. The VSD component is small.

**Video 17.3c** (https://youtu.be/yMo69ZacxvI)
Transverse view at the level of the abdomen showing the azygous vein posterior to the aorta. The stomach is right sided, and the liver is midline.

**Video 17.3d** (https://youtu.be/hIOSzivhKIM)
Three-vessel view showing a prominent azygos vein draining into the right SVC. There is an additional LSVC. Pulmonary artery is leftward and anterior to the aorta.

**Video 17.4** (https://youtu.be/Pajy31QqwOo)
Two-dimensional video of fetus with left atrial isomerism. There is a balanced AVSD. There is significant bradycardia secondary to complete heart block. A moderately sized pericardial effusion has developed.

## References


1. Yoo SJ et al. *Cardiol Young* 1999;9(4):430–44.
2. Carvalho JS et al. *Ultrasound Obstet Gynecol* 2005;26(2):105–11.
3. Bartram U et al. *Biol Neonate* 2005;88(4):278–90.
4. Stanger P et al. *Circulation* 1977;56(2):159–72.
5. Van Praagh R. *Circulation* 1977;56(2):139–43.
6. Tynan MJ et al. *Br Heart J* 1979;41(5):544–53.
7. Ivemark BI. *Acta Paediatr Suppl* 1955;44(Suppl 104):7–110.
8. Polhemus DW, Schafer WB. *Pediatrics* 1952;9(6):696–708.
9. Macartney FJ et al. *Br Heart J* 1980;44(6):657–67.
10. Uemura H et al. *Am J Cardiol* 1995;76(11):846–9.
11. Uemura H et al. *Ann Thorac Surg* 1995;60(3):561–9.
12. Nagel BH et al. *Cardiol Young* 2005;15(5):469–73.
13. Freedom RM et al. *Cardiol Young* 2005;15(6):554–67.
14. Lin AE et al. *Am J Med Genet A* 2014;164A(10):2581–91.
15. Cordes TM et al. *J Am Soc Echocardiogr*1994;7(1):47–53.
16. Wang JK et al. *Eur J Pediatr* 1993;152(5):418–20.
17. Berg C et al. *Ultrasound Obstet Gynecol* 2003;22(5):451–9.
18. Peoples WM et al. *Pediatr Cardiol* 1983;4(2):129–37.
19. Celentano C et al. *Ultrasound Obstet Gynecol* 1999;14(3):215–8.
20. Atkinson DE, Drant S. *Am J Cardiol* 1998;82(9):1147–9, A10.
21. Espinoza J et al. *Ultrasound Obstet Gynecol* 2005;25(5):428–34.
22. Anderson RH. Terminology. In: Anderson RH, Baker EJ, Macartney FJ, Rigby ML, Shinebourne EA, Tynan M, eds. *Paediatric Cardiology*. Edinburgh: Churchill Livingstone; 2002, 19–36.
23. Colloridi V et al. *Prenat Diagn* 1994;14(4):299–302.
24. Berg C et al. *Ultrasound Obstet Gynecol* 2005;26(5):538–45.
25. Mauser I et al. *Br Heart J* 1991;65(5):293–5.
26. Stewart PA et al. *J Am Coll Cardiol* 1984;4(5):1015–20.
27. Bowers PN et al. *Semin Perinatol* 1996;20(6): 577–88.
28. Zhu L et al. *Eur J Hum Genet* 2006;14(1):17–25.
29. Evans WN et al. *Pediatr Cardiol* 2010;31(1):1–6.
30. Bohun CM et al. *Am J Cardiol* 2007;100(2):305–9.
31. Dilorenzo M et al. *Tex Heart Inst J* 2013;40(4):481–3.
32. Oliver JM et al. *Am J Cardiol* 2012;110(11):1687–91.
33. de Lezo JS et al. *Tex Heart Inst J* 1983;10(3):293–9.
34. Shapiro AJ et al. *Cardiol Young* 2015;25(4):752–9.
35. Bush A et al. *Eur Respir J* 1998;12(4):982–8.
36. Bataille S et al. *Am J Kidney Dis*2011;58(3):456–60.
37. Lee SE et al. *J Pediatr Surg* 2006;41(7):1237–42.

38. Hu J et al. *J Plast Reconstr Aesthet Surg* 2015;68(2):e35–6.
39. Douard R et al. *Surg Radiol Anat* 2000;22(5–6):293–7.
40. Van Mierop LH, Gessner IH. *Prog Cardiovasc Dis* 1972;15(1): 67–85.
41. Moller JH et al. *Circulation* 1967;36(5):789–99.
42. Phoon CK, Neill CA. *Am J Cardiol* 1994;73(8):581–7.
43. Phoon CK et al. *Am J Cardiol* 1996;77(12):1083–8.
44. Ho SY et al. *Pediatr Pathol* 1991;11(4): 589–608.
45. Lin AE et al. *Genet Med* 2000;2(3):157–72.
46. Lim JS et al. *Circulation* 2005;112(16):2454–61.
47. Fyler DC. *Pediatrics* 1980;65(2):375–461.
48. Taketazu M et al. *Am J Cardiol* 2006;97(5):720–4.
49. Kathiriya IS, Srivastava D. *Am J Med Genet* 2000;97(4):271–9.
50. Morelli SH et al. *Am J Med Genet* 2001;101(4):388–92.
51. Allan LD et al. *Am J Cardiol* 1986;58(3):334–7.
52. Allan LD et al. *Ultrasound Obstet Gynecol* 1991;1(1):8–11.
53. Eronen M et al. *Pediatr Cardiol* 2004;25(2):141–4.
54. Brown DL et al. *J Ultrasound Med* 1993;12(3):153–61.
55. Casey B. *Hum Mol Genet* 1998;7(10):1565–71.
56. Boskovski MT et al. *Nature* 2013;504(7480):456–9.
57. Cowan J et al. *Hum Mutat* 2014;35(1):66–75.
58. Izumi K et al. *Eur J Med Genet* 2014;57(10):558–61.
59. Tsai EA et al. *Hum Mutat* 2015;36(6):631–7.
60. Sutherland MJ et al. *Hum Mol Genet* 2013;22(10):1913–23.
61. D'Alessandro LC et al. *Congenit Heart Dis* 2013;8(2):E36–40.
62. Slavotinek A et al. *Clin Dysmorphol* 1996;5(3):241–7.
63. Gilljam T et al. *J Am Coll Cardiol* 2000;36(3):908–16.
64. Rubino M et al. *J Thorac Cardiovasc Surg* 1995;110(3):641–50.
65. Hashmi A et al. *J Am Coll Cardiol* 1998;31(5):1120–6.
66. Patel CR et al. *Ultrasound Obstet Gynecol* 2001;17(3):268–71.
67. Huggon IC et al. *J Am Coll Cardiol* 2000;36(2):593–601.
68. Burton EC et al. *Pediatr Dev Pathol* 2014;17(4):250–64.
69. Wren C et al. *Am J Cardiol* 1987;59(12):1156–8.
70. Shenker L et al. *Am J Obstet Gynecol* 1987;157(2):248–53.
71. Baschat AA et al. *Ultrasound Obstet Gynecol* 1999;14(5):311–4.
72. Berg C et al. *Ultrasound Obstet Gynecol* 2005;26(1):4–15.
73. Ho SY et al. *J Am Coll Cardiol* 1992;20(4):904–10.
74. Jaeggi ET et al. *Ultrasound Obstet Gynecol* 2005;26(1):16–21.
75. Wu MH et al. *J Am Coll Cardiol* 1998;32:773–9.
76. Salomon LJ et al. *Prenat Diagn* 2006;26(3):282–5.
77. Elder CT et al. *J Pediatr Surg* 2014;49(12):1746–8.
78. Pockett CR et al. *J Pediatr Surg* 2013;48(10):2078–83.
79. Chang J et al. *J Pediatr Surg* 1993;28(10):1281–4;discussion 5.
80. Choi M et al. *Arch Dis Child* 2005;90(8):813–5.
81. Carmi R et al. *Am J Med Genet* 1993;45(6):683–93.
82. Murray CP et al. *Pediatr Radiol* 2003;33(9):614–20.
83. Ticho BS et al. *Am J Cardiol* 2000;85(6): 729–34.
84. Shapiro AJ et al. *Chest* 2014;146(5):1176–86.
85. Prendiville TW et al. *Pediatr Cardiol* 2010;31(7):1052–8.
86. Friedberg MK et al. *Am J Cardiol* 2005;96(7):985–90.
87. Escobar-Diaz MC et al. *Am J Cardiol* 2014;114(4):612–7.

# 18

# Cardiac malpositions and syndromes with right or left atrial isomerism

Rabih Chaoui

Isomerism and related cardiac malpositions belong to the most difficult fields in pediatric cardiology. According to the Baltimore-Washington Infant Study,[1] which analyzed 4,390 congenital heart defects (CHDs) detected in the first year of life over a period of 10 years (1981–1989), isomerism was found in 99 cases, accounting for 2.2% of CHDs. The mortality in this small group was 51% within the first year of life. In the fetus, the true prevalence is, however, not known, since some forms, especially when associated with heart block and fetal hydrops, would end as fetal death, and some other more mild forms of cardiac malposition or isolated situs inversus may be overlooked even in a child. The early prenatal detection of an abnormality of this group has a large impact on counseling the pregnant woman, especially because small details can radically change the prognosis. There are difficulties in achieving a final fetal diagnosis, as the examiner can rely only on ultrasound, where there are limited possibilities for the precise differentiation of structures. Furthermore, some basic knowledge is needed in order to understand some definitions as well as the classification of defects. In this chapter, not all aspects of these abnormalities can be covered in detail. It is tried, rather, to supply the reader with basic information for a practical approach when abnormal conditions are suspected.

## Developmental aspects and normal body configuration

In contrast to other embryological organs, the thoracic and abdominal structures develop asymmetrically. There are well-defined right-sided and left-sided organs and structures. After completion of lateralization, the "normal" and most common condition found is then called *situs solitus* for the visceral arrangement, and *levocardia* (heart on the left side) for the thoracic arrangement (Figure 18.1). In Chapter 10, on fetal cardiac anatomy, the focus was on the segmental analysis of the upper abdomen and the heart, showing that under normal conditions, in situs solitus the stomach and descending aorta are on the left and the liver and the inferior vena cava on the right. The umbilical vein bends to the right, continuing with the portal sinus. In levocardia the heart apex points to the left anterior thoracic cavity with normal atrial and ventricular arrangement (Figure 18.1) and, under normal conditions, the inferior vena cava is connected to the right atrium and the pulmonary veins to the left atrium.

## Situs inversus, malrotations, and malpositions of the heart

Compared to the most common condition of situs solitus and levocardia, there is rarely a situation where all organs are rotated exactly to the opposite side, leading to a mirror-image arrangement. This situation is called situs inversus. When this mirror-image rotation of abdominal and intrathoracic organs is complete, the liver and inferior vena cava are on the left, whereas the stomach and the descending aorta are on the right (Figures 18.2 and 18.3). Since the inferior vena cava and the right atrium are concordant, the right atrium and right ventricle are on the left anteriorly, and the left atrium and left ventricle are on the right posteriorly, and the heart axis points to the right anterior thorax, a situation called dextrocardia (Figure 18.3) (mirror-image dextrocardia or situs inversus with dextrocardia, or situs inversus completus). In these conditions, associated heart defects are rare. The true incidence of this situation is low, but also not exactly known, since persons with this abnormality are asymptomatic and are not identified until an x-ray, ultrasound, or medical intervention is performed. Because this condition is extremely rare, it can be recommended that before making this diagnosis, the examiner checks the fetal position and the transducer orientation. According to our experience, we have found that a high risk for situs inversus was in a family with a previous child with this condition, in consanguineous couples, and in the offspring of diabetic mothers. However, there are other conditions where the mirror-image arrangement is partial: either only affecting the heart, as in dextrocardia (with situs solitus); or affecting the visceral organs, as in situs inversus with levocardia.[2] In these conditions, heart defects are more common.

The heart position and axis are important features to check while analyzing the heart. Compared to its normal position in the left chest with a normal base-apex axis of 45° to the left side, cardiac malpositions are divided into dextrocardia, levocardia, mesocardia, and ectopia cordis.

As already stated, dextrocardia is present when the heart is in the right hemithorax with the axis pointing to the right.

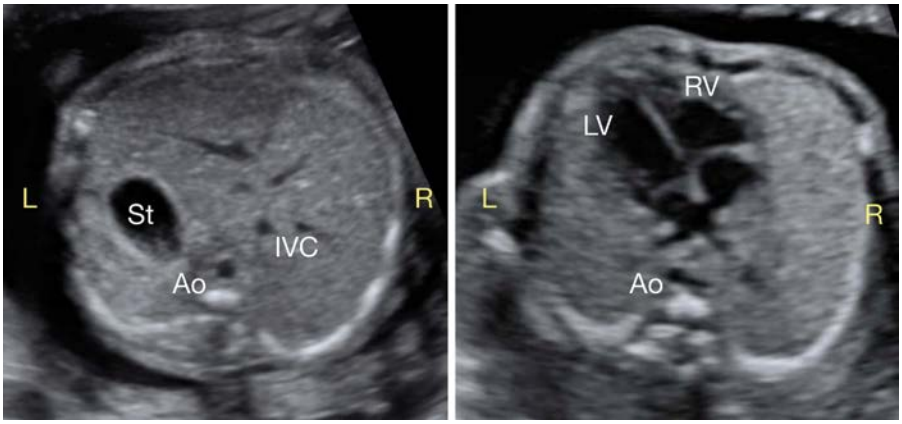


**Figure 18.1**
The two important planes in assessing isomerism and other cardiac malpositions. The normal sonoanatomy of the upper abdomen with situs solitus (left) and the heart in levocardia (right). (Ao, aorta; IVC, inferior vena cava; L, left; LV, left ventricle; R, right; RV, right ventricle; St, stomach.)

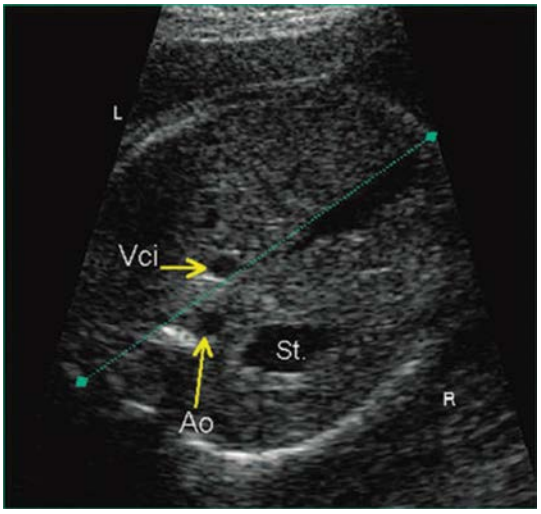


**Figure 18.2**
Situs inversus. The fetus is in vertex position and in the upper abdomen a mirror-image rotation is found with the stomach (St.) and the aorta (Ao) on the right side and the inferior vena cava (Vci) and liver on the left side.

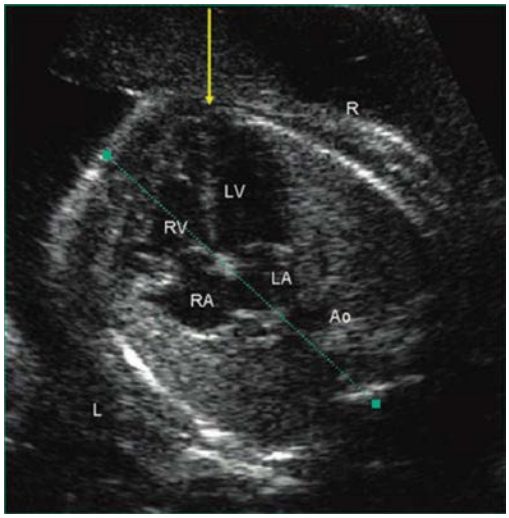


**Figure 18.3**
The heart in a fetus with complete situs inversus and mirror-image dextrocardia. The fetus is in vertex position. The heart points to the right anterior thorax (arrow). The right ventricle (RV) (with trabeculation) is on the left side and in the anterior thorax. The descending aorta (Ao) is on the right side. (LA, left atrium; RA, right atrium.)

In these conditions, not only the isomerism conditions discussed below should be considered but also cardiac anomalies as congenital corrected transposition of the great arteries (Figure 18.4). Mesocardia is found when the heart points to the midline of the thorax. Many children having mesocardia are incorrectly grouped in the dextrocardia group, since on x-ray, the heart seems more on the right side. Levocardia (heart on the left, i.e., the normal position) is mainly considered when there is a situs inversus or ambiguus, to stress that the heart still points to the left side.

Cardiac dextroposition (displacement to the right) is found when the heart is shifted into the right chest with the axis still pointing to the left, as observed in left-sided congenital diaphragmatic hernia (Figure 18.5), left-sided intrathoracic masses, or fluid accumulation, in agenesis of the right lung, or in scimitar syndrome.

Similarly, levoposition (displacement to the left) is seen when the heart is shifted into the left thoracic cavity with the axis still pointing to the left, as typically found in right-sided diaphragmatic hernia or some other right-sided thoracic lesions.

## Right and left atrial isomerisms in the fetus

Conversely to the above-cited very rare abnormalities with a mirror-image arrangement of the visceral and intrathoracic organs, there are more common conditions with an incomplete lateralization (heterotaxy) of the abdominal organs during embryological rotation, showing an indeterminate

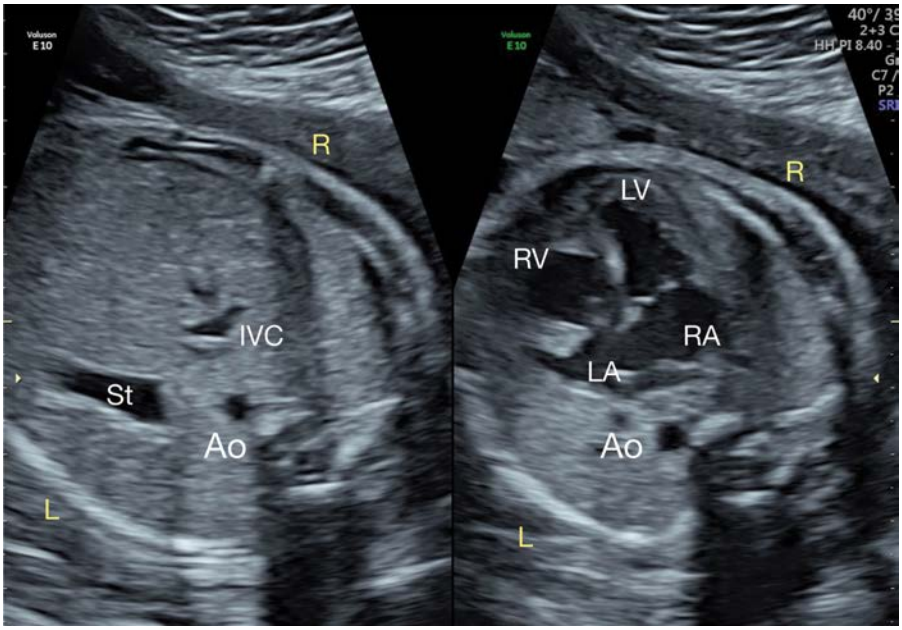


**Figure 18.4**
Fetus with a normal abdominal situs (solitus) and with a dextrocardia. The descending aorta is on the left, the heart on the right, right and left atria are seen, but the anatomy of the ventricles shows an atrioventricular discordance characteristic for the congenital corrected transposition, which often is associated with a dextrocardia.

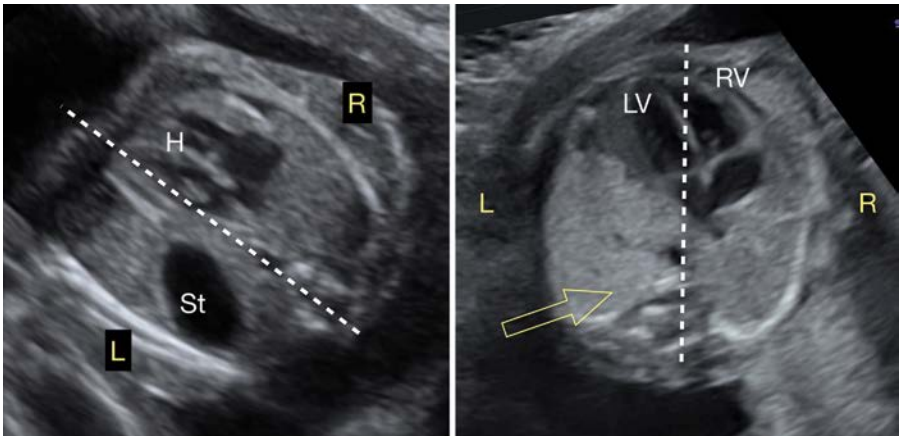


**Figure 18.5**
Two examples of dextropositions: on the left, a fetus with left-sided congenital diaphragmatic hernia (ST, stomach) with a shifting of the heart (H) into the right hemithorax; on the right, a fetus with a hyperechogenic enlarged left lung in a fetus with bronchopulmonary sequestration. The heart is shifted to the right side. Compare with Figure 18.16.

visceral situs. In these conditions, the arrangement is called situs ambiguus (indeterminate or uncertain situs) and is the most complex form of visceral and atrial arrangement. This group of defects has many synonyms, such as heterotaxy syndromes, cardiosplenic syndromes, or asplenia-polysplenia syndromes or isomerisms, and the conditions are regularly associated with complex cardiac defects.

In these abnormal lateralizations of the visceral and intrathoracic structures, there is a tendency to symmetric development of the normally asymmetric organs, associated with either a bilateral right-sidedness (right isomerism) or bilateral left-sidedness (left isomerism). Ivemark[3] noted the association of spleen anomalies with some cardiac defects. Because the spleen develops as a left-sided organ, it was in the past a sign for classification, asplenia being the previous name of right isomerism and polysplenia of left isomerism. This group of developmental defects was therefore called cardiosplenic syndromes. However, it was found that spleen presence, position, and number do not have definitive diagnostic value, and this terminology was abandoned[4] (although it is often still used in clinical pediatric cardiology).

Knowing that the heart develops according to well-defined cardiac segments, Van Praagh[5] proposed a classification according to the anatomy and connections of these segments, known as the segmental approach. The constant starting point for classifying these conditions is the anatomy of the

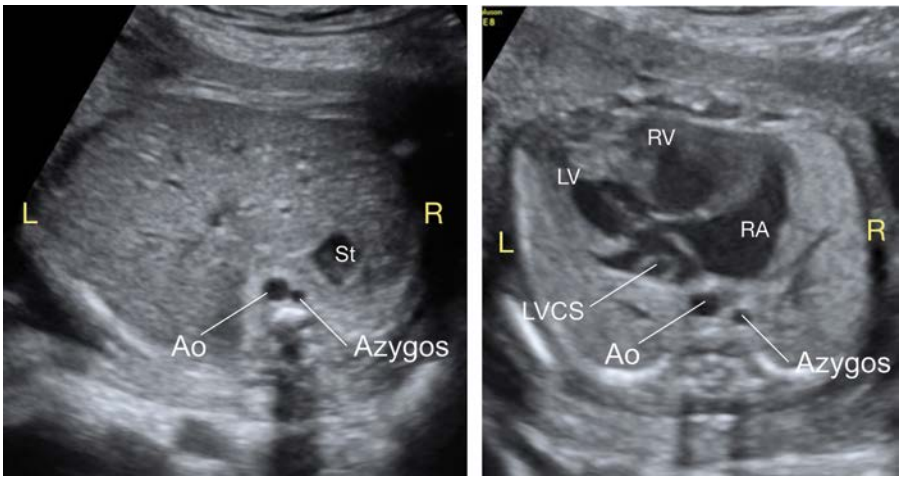


**Figure 18.6**
Fetus with left isomerism showing, in the upper abdomen, situs ambiguus with the stomach (ST) on the right side (R) and an interruption of the inferior vena cava with azygos (AZ) vein continuation. The double-vessel sign is typical of left isomerism. In the four-chamber view, the heart shows an atrioventricular septal defect and behind the heart again the double-vessel aorta (Ao) and azygos, left vena cava superior (LVCS).

atria. Therefore, diseases with isomerism are now divided into right atrial and left atrial isomerism.

The identification of these anomalies and their differentiation may be easier for the pathologist during necropsy. In the fetus the diagnostic possibilities are reduced, and the reliable diagnosis or differentiation between right or left isomerism can be very difficult to be achieved prenatally.[6] Even for the experienced examiner, this group of anomalies is considered a challenge. The diagnostic approach using ultrasound is based on the approach proposed by Huhta et al.[7] for neonatal echocardiography, focusing on the upper abdomen and the relationship between the venous system and the atria. The central point of diagnosis is the anatomy of the atria defined by their shape and their appendages. The left atrial appendage is finger-like and has a narrow base, whereas the right atrial appendage is pyramidal in shape and its base is rather broad. The appendages can be visualized in a plane slightly cranial to the four-chamber view but are not identified reliably under many conditions. In a recent retrospective study[8] on 30 fetuses with isomerism, it was, however, shown that

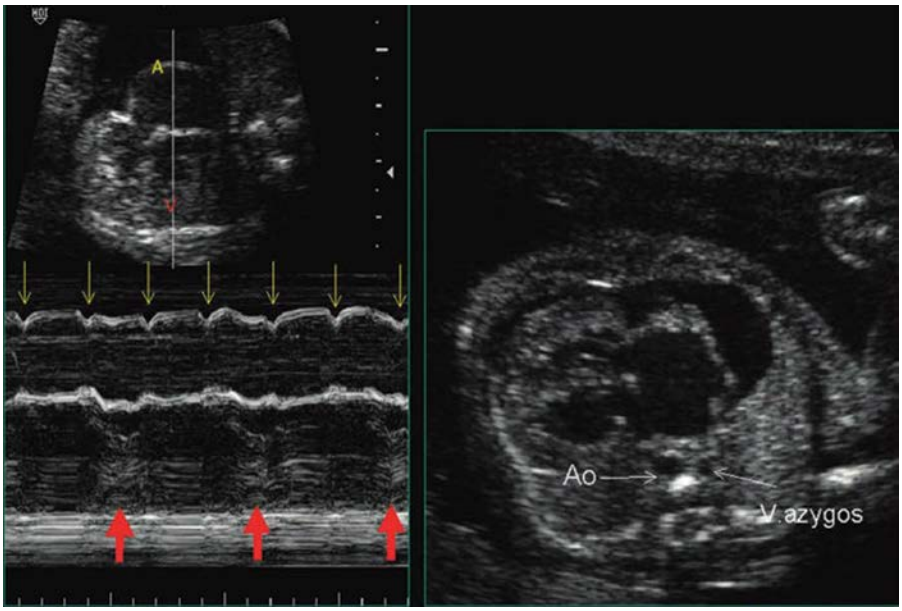


**Figure 18.7**
This fetus was referred with bradycardia. M-mode shows the presence of a complete heart block: the atria (A) have a normal sinus rhythm (yellow arrows), whereas the ventricles show bradycardia (50 beats per minute) (red arrows). Examination of the four-chamber view reveals the diagnosis: a dilated heart with pericardial effusion, and behind the heart side-by-side with the descending aorta there is a second vessel, which is the dilated azygos vein; this is a typical finding in left isomerism.

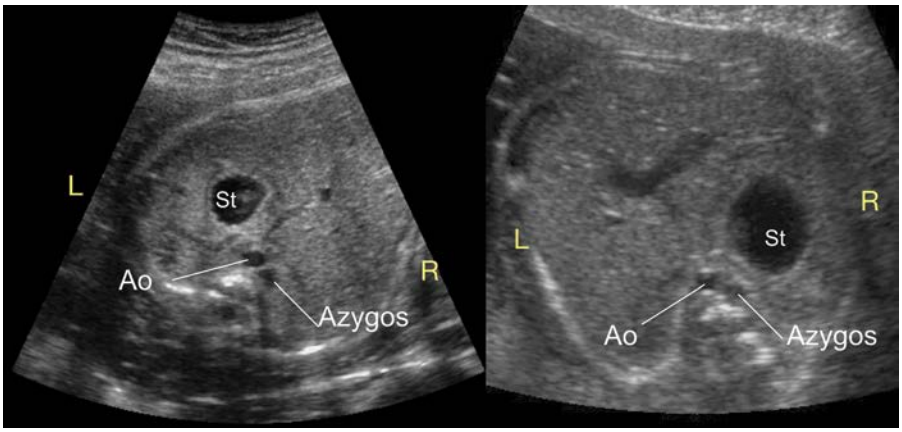


**Figure 18.8**
Two examples of left isomerism with the "double-vessel sign" (dilated azygos and aorta side by side) with the stomach on the left (left case) and on the right (right case).

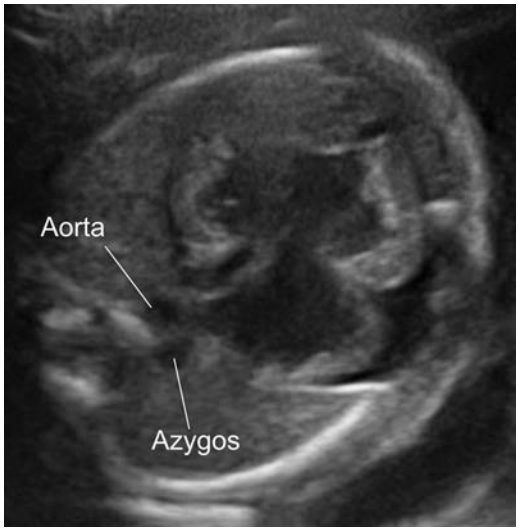


**Figure 18.9**
Left isomerism with AV septal defect with azygos continuation side by side with the aorta.

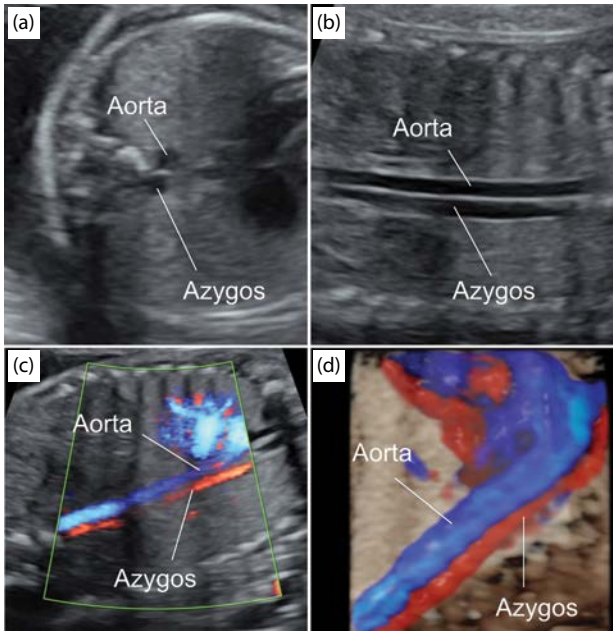


**Figure 18.10**
Thoracic cross section (a) and longitudinal view of descending aorta and dilated azygos vein (b). (c) The double-vessel sign seen in color Doppler. (d) Color Doppler in combination with three-dimensional glass-body mode.

prenatally the morphology of the atrial appendages could have been suspicious in 19 cases, with the typical bilateral sickle-shape appearance in left and the blunt-shape appearance in right isomerism.

Since the connecting veins are part of the atrial anatomy, the venoatrial connection is the leading diagnostic sign for diagnosis. However, there are no heart defects that are pathognomonic for the one or the other diagnostic group.

In the following sections, some features associated with each anomaly are enumerated, which might help in making diagnoses.

## *Left atrial isomerism*

In this condition of double left-sidedness, right-sided structures such as the inferior vena cava and the right atrium with sinus node are absent or may have developed abnormally. Therefore, two leading signs in left isomerism can be expected: first, the interruption of the inferior vena cava in its intrahepatic part and its continuation as the azygos (or hemiazygos) vein (Figures 18.6 through 18.11, Videos 18.1 and 18.2); second, arrhythmia with heart block (malformed sinus node) (Figures 18.6 and 18.11). The azygos continuation of the interrupted inferior vena cava has been shown to be present in most cases with left isomerism (>80%). It can be recognized by the observation of the aorta and the (dilated) azygos vein on its right or left side (hemiazygos) either in the upper abdomen (Figures 18.6 and 18.8) or at the level of the four-chamber view (Figures 18.9 and 18.11).[9] Sheley et al.[10] described it as the "double-vessel sign," and found it in all

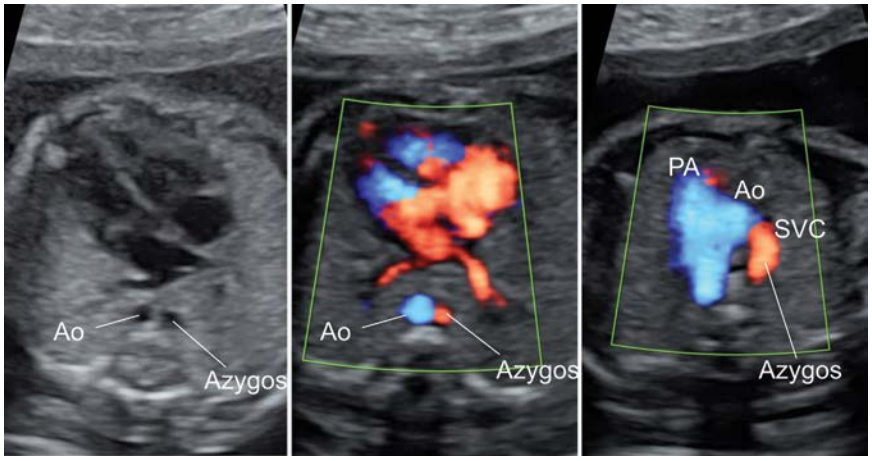


**Figure 18.11**
Fetus with left isomerism and azygos continuation: (Left) Four-chamber view with the aorta (Ao) and the dilated azygos vein side by side; (Middle) Color Doppler showing the different direction of flow in aorta and azygos vein; (Right) Three-vessel-trachea view with the dilated azygos vein draining into the superior vena cava (SVC). (PA, pulmonary artery.)

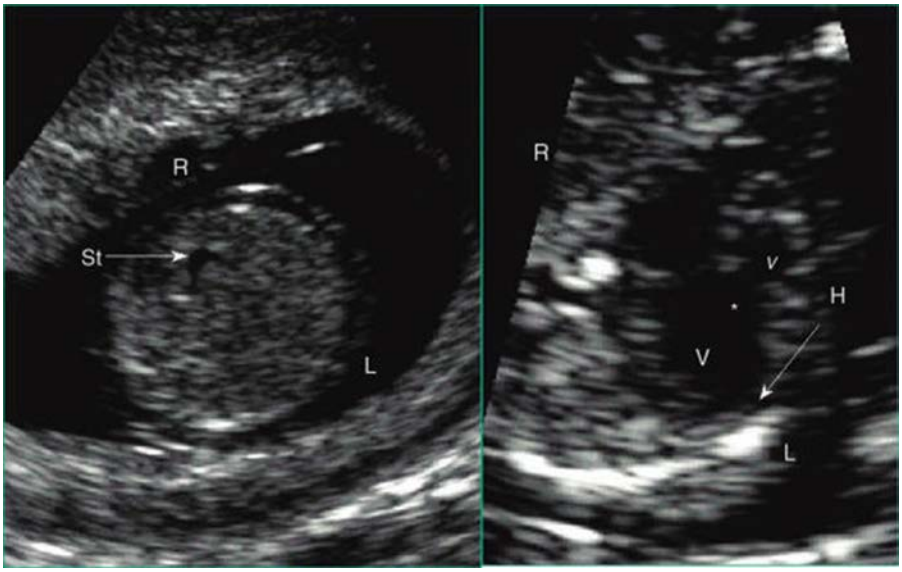


**Figure 18.12**
This fetus was referred at 14 weeks because of nuchal edema (and beginning hydrops) associated with bradycardia. We found a heart block, a stomach (St) on the right side (left), and levocardia (H) with a heart defect. The heart showed a univentricular atrioventricular connection with a small (v) and a dilated ventricle (V) connected by a ventricular septal defect (*). The liver lay centrally. After termination of pregnancy because of suspected left isomerism, the diagnosis was confirmed at autopsy (see Figure 18.13).

eight fetuses with left isomerism that they examined, but also in one false-positive case with right isomerism. In a study in 22 fetuses with left isomerism,[11] 21 showed this azygos continuation sign. If the examiner is aware of this sign, he can easily detect it prenatally on real-time imaging and confirm it using color Doppler (Figures 18.10 and 18.11, Video 18.3). The azygos vein is then visualized draining into the superior vena cava or into a persisting left superior vena cava (Figure 18.11).

The types of cardiac malformation associated with left and right isomerism are complex, showing a considerable overlap. Except for the azygos continuation of the inferior vena cava, considered as a typical sign of left isomerism, there are no cardiac defects permitting a strict classification into one or other group of isomerism. The conditions of a heart with left atrial isomerism seem to be less severe than those with right isomerism, demonstrating a normal ventriculoarterial junction in almost 70% of cases.[12] These hearts tend to be biventricular, and on many occasions, a ventricular septal defect or an atrioventricular septal defect is present.[4,13] The association of an atrioventricular septal defect with complete heart block is considered to be pathognomonic for left atrial isomerism[6] and should prompt careful examination of the venous connections. Heart block detected in the late first trimester is also very likely to be due to left isomerism and not to maternal autoantibodies[14] (Figures 18.12 and 18.13). In the study reported previously, in 22 fetuses with left isomerism,

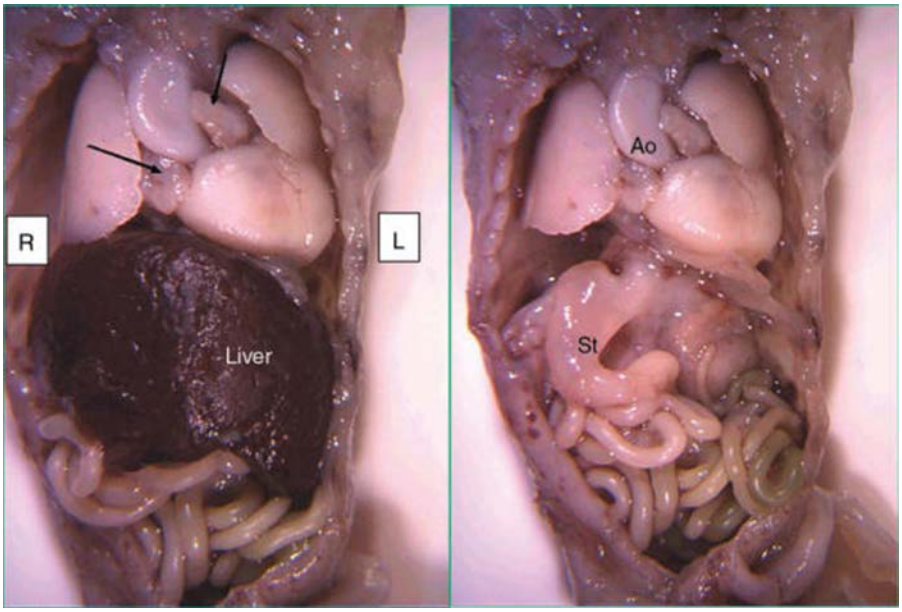


**Figure 18.13**
Necropsy of the 14-week fetus shown in Figure 18.12, demonstrating the central liver (left), the heart with two left atrial appendages (arrows), and, after removing the liver, the stomach (St) on the right side.

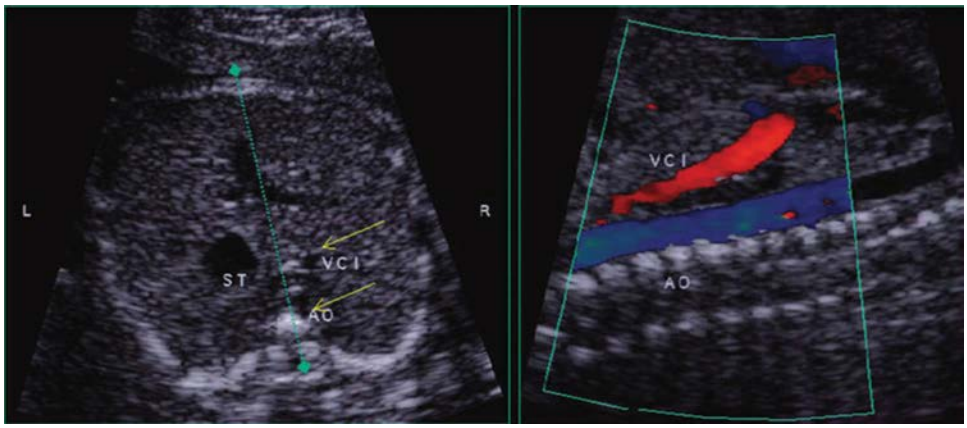


**Figure 18.14**
Right atrial isomerism. In the upper abdomen, the aorta (AO) and inferior vena cava (VCI) are on the same side (here the right side [R]) and the inferior vena cava is anterior to the aorta (arrows). The stomach (ST) is nearer the midline than on the left. In a longitudinal plane (right), both the aorta (blue) and the inferior vena cava (red) are seen in one plane and are both directly anterior to the spine.

a persisting bradycardia was found in 12/22 cases.[11] The position of the heart can be on the left, on the right, or in the midline. The most severe complex extracardiac malformation observed in left isomerism is extrahepatic biliary atresia with absence of the gallbladder.

## *Right atrial isomerism*

In this condition of double right-sidedness, left-sided structures such as the left atrium, the pulmonary veins, and the upper gastrointestinal tract are likely to be found malformed. In this group of complex malformations, there are no characteristic features, such as interruption of the inferior vena cava or the heart block described for left isomerism.

The inferior vena cava is present and is generally on the same side as the descending aorta (Figures 18.14 and 18.15, Video 18.4). The visceral heterotaxy is more common and severe in right isomerism, and anomalies of the upper abdomen are more likely to be found in right than in left isomerism; these include not only the common absence of the spleen, but also the symmetrical liver, and nonfixation of the gastrointestinal tract leading to various degrees of malrotation (Figures 18.15 through 18.17). Atresia of the esophagus or duodenum can be found as well as the herniation of a midline-positioned stomach. Heart defects in right isomerism are likely to be more severe than those with left isomerism. Among the cardiac defects, total anomalous pulmonary venous drainage is found in 70% of cases (rarely in

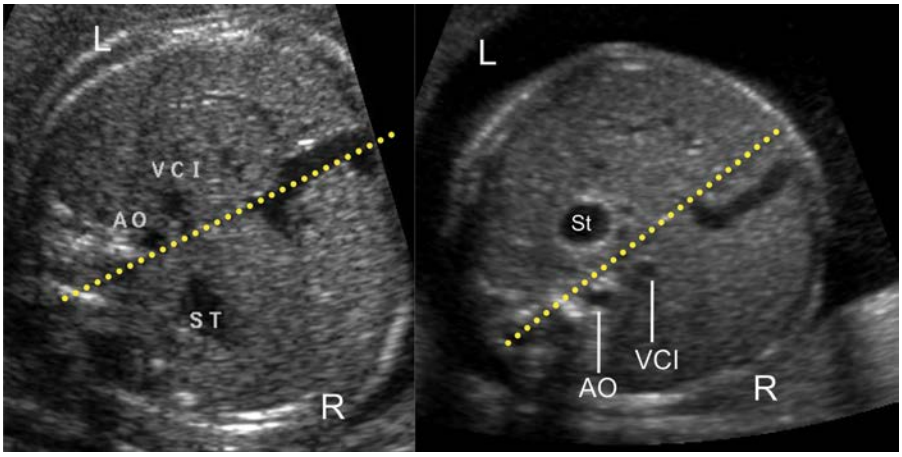


**Figure 18.15**
Right isomerism with the typical sign of the juxtaposition of IVC and aorta—that is, it is on the same side of the descending aorta, either on the left (left case) or on the right side of the spine (right case). The position of the stomach can be on the right or on the left side (the stomach is more central).

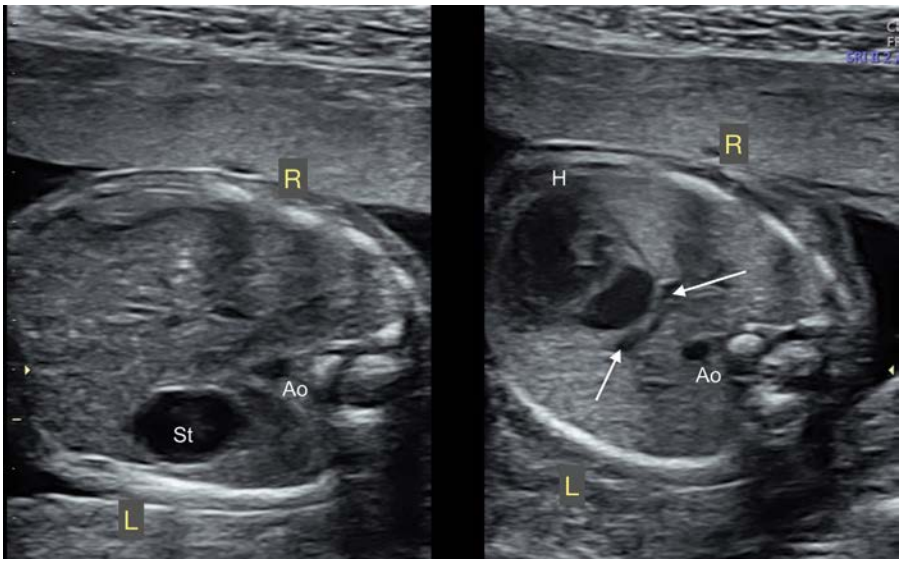


**Figure 18.16**
Fetus with right isomerism with left-sided stomach (St) and dextrocardia. The heart (H) is on the right and shows a univentricular connection with a confluence vein behind the heart (arrows) as a sign of the associated anomalous pulmonary venous drainage. (Ao, aorta; L, left; R, right.)

left isomerism) (Figure 18.16, Videos 18.4 and 18.5). Hearts with right atrial isomerism can also show an atrioventricular septal defect but are more likely to be associated with a univentricular atrioventricular connection (Figures 18.16 and 18.17) and exhibit a much higher incidence of abnormal ventriculoarterial connections (double-outlet ventricle, malposition of the great arteries) (Figure 18.17). These hearts show a much higher frequency of pulmonary stenosis or atresia. An absence of the coronary sinus is found in 85% of cases. A left persisting superior vena cava is found frequently. In a study of 21 fetuses with right isomerism,[15] 20 had complex cardiac anomalies, predominantly atrioventricular septal defects and right ventricular obstruction in 62% and 48%, respectively. Only 12 fetuses in this study showed a juxtaposition of aorta and inferior vena cava, and out of six cases with anomalous pulmonary venous return, four were not diagnosed prenatally. Therefore, when right isomerism is suspected in a fetus, the connections of the pulmonary veins should be examined carefully to rule out anomalous pulmonary venous return.[16]

## *Prognosis in isomerism*

It is known that left and right isomerisms are associated with a poor prognosis.[4,13] Individual differences, depending on the specific finding, should be considered when counseling

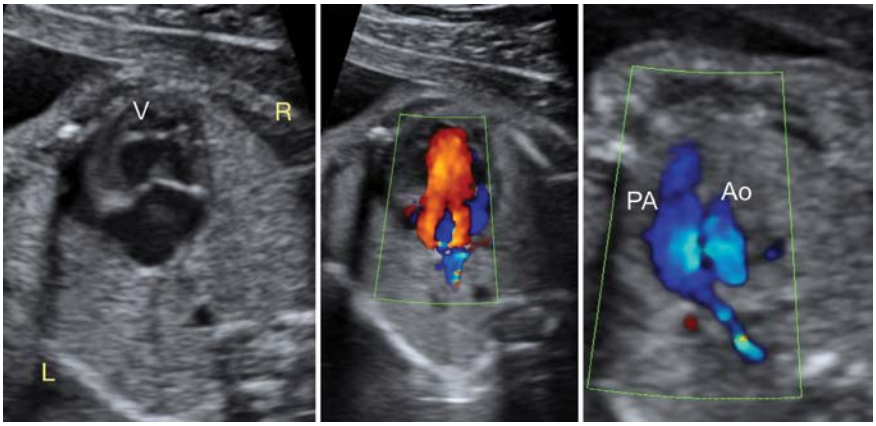


**Figure 18.17**
Fetus with right isomerism and dextrocardia. (Left) There is a univentricular atrioventricular connection to one ventricle (V). (Middle) Color Doppler shows the univentricular flow into the single ventricle. (Right) The outflow tract evaluation reveals antegrade flow into aorta (Ao) and pulmonary artery (PA). (L, left; R, right.)

parents after a prenatal diagnosis, but it is often difficult to assess the prognosis from the prenatal scan in these conditions. Fetuses with left isomerism show a poor prognosis *in utero* when associated with complete heart block and hydrops. Cardiac failure and hydrops may occur very early, leading to spontaneous *in utero* demise. Postnatally, the prognosis may be further complicated by the underlying heart defect, although this is generally less severe than in right isomerism. Among extracardiac anomalies, biliary atresia can be considered as the most severe finding, which cannot be definitively ruled out *in utero*. Under some conditions, children with left isomerism show a better survival rate than those with right isomerism.

The diagnosis of right atrial isomerism is very difficult *in utero* and should be considered in every fetus with a complex cardiac malformation, especially when cardiac or situs

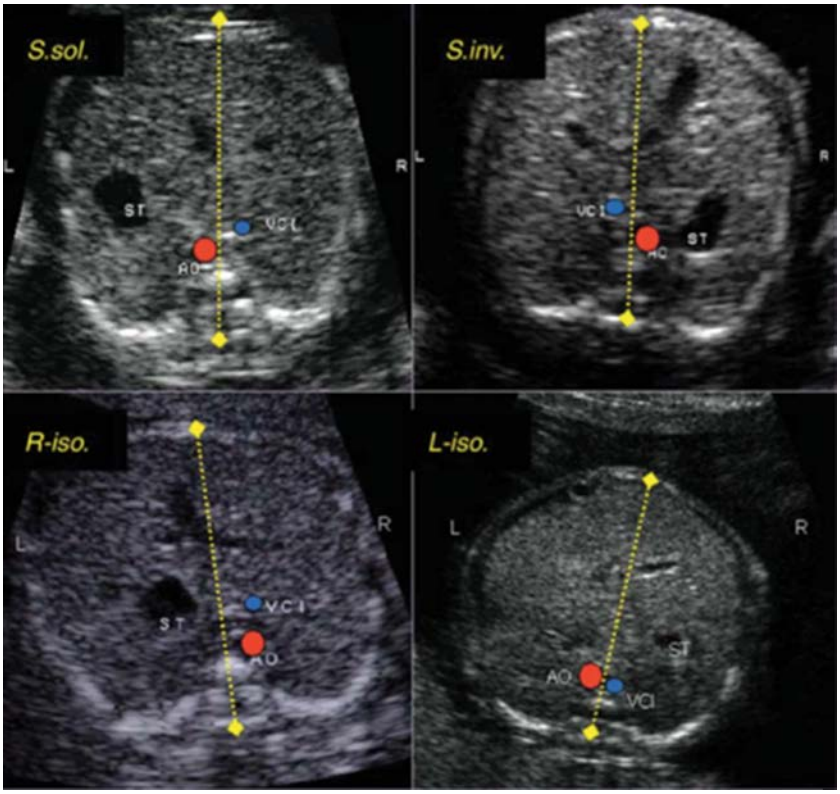


**Figure 18.18**
Summary of the four typical findings in the upper abdomen in situs solitus (top left), situs inversus (top right), right isomerism (bottom left), and left isomerism (bottom right). The inferior vena cava (blue) and its position relative to the aorta (red) are main landmarks.

malposition is suspected. The severity of the disease usually appears postnatally and is due to the abnormal pulmonary venous connection, to the ductus-dependent pulmonary perfusion in right outflow tract obstruction, or to the complex chamber anatomy. Within the first year of life, 79%–94% of all children with right isomerism were reported to die, with or without operation.[13] A long-term risk in patients with right isomerism is also infection due to asplenia, which is often associated.

The association with chromosomal aberrations such as trisomy 21, 13, 18, or others is extremely rare, since the diagnosis of isomerism rather rules out such chromosomal aberrations. Yates et al.[17] reported, however, a fetus with isomerism associated with a 22q11 deletion.

## Conclusion

Every fetal heart defect should be analyzed in a segmental approach in order to detect (or rule out) an isomerism (Figure 18.18). This approach can be difficult to achieve in some cases and even omitted in others. Therefore, the examiner should always rule out isomerism when the following ultrasound signs are found: cardiac or stomach malpositions, a complex cardiac defect, fetal heart block, abnormal venous connections, and dilatation of the azygos vein.

## Videos

**Video 18.1** (https://youtu.be/CN2xdtDw5rQ)
Fetus with left isomerism. Sweep from the abdominal plane to the cardiac plane reveals the aorta and azygos vein side by side with the absence of the inferior vena cava, the left position of the stomach with the right-sided heart, and the complex cardiac anomaly.

**Video 18.2** (https://youtu.be/WS3Tt7hZtOc)
Fetus with left isomerism with a single ventricle showing the symmetry of the atria due to the two left atrial appendages.

**Video 18.3** (https://youtu.be/XugddVH5OpY)
Fetus with left isomerism. The double-vessel sign of aorta and azygos continuity is best demonstrated by color Doppler showing both vessels side by side with opposite color (aorta red, azygos blue).

**Video 18.4** (https://youtu.be/LX_RVVaJyO0)
Fetus with right isomerism: sweep from the abdominal plane to the cardiac plane reveals the aorta and inferior vena cava on the right side (juxtaposition), the left position of the stomach with the right-sided heart and the complex cardiac anomaly. Behind the heart, one could recognize a vein confluence suggesting an anomalous pulmonary venous connection.

**Video 18.5** (https://youtu.be/Sh9HTxR5KVA)
Fetus with right isomerism: the cardiac plane reveals the dextrocardia with the complex cardiac anomaly and between heart and descending aorta one can recognize the vein confluence as the collecting site of the pulmonary veins in an anomalous pulmonary venous connection.

## References


1. Ferencz C et al. The epidemiology of congenital heart disease, the Baltimore-Washington Infant Study 1981–1989. In: *Perspectives in Pediatric Cardiology*, Ferencz C et al. (Eds) 4. Mount Kisco, NY: Futura; 1993 pp. 32–66.
2. Blaas H-G et al. *Fetus* 1991;1:75–93.
3. Ivemark BI. *Acta Paediatr* 1955;44(suppl 104):7–110.
4. Freedom RM, Smallhorn JF. Syndromes of right or left atrial isomerism. In: Freedom R, Benson L, Smallhorn J, eds. *Neonatal Heart Disease*. New York, NY: Springer; 1995:543–60.
5. Van Praagh R. *Birth Defects* 1972;8:4–23.
6. Hobbins JC, Drose JA. Cardiosplenic syndromes. In: Drose J, ed. *Fetal echocardiography*. Philadelphia, PA: WB Saunders; 1998:253–62.
7. Huhta J et al. *Br Heart J* 1982;48:97–108.
8. Berg C et al. *Ultrasound Obstet Gynecol* 2005;26:538–45.
9. Phoon CK et al. *Am J Cardiol* 1996;77:1083–8.
10. Sheley RC et al. *J Ultrasound Med* 1995;14:381–7.
11. Berg C et al. *J Ultrasound Med* 2005;24:921–31.
12. Peoples WM et al. *Pediatr Cardiol* 1983;4:129–37.
13. Hagler DJ, O'Leary P. Cardiac malpositions and abnormalities of atrial and visceral situs. In: Emmanouilides G, Allen H, Riemenschneider T, Gutgesell H, eds. *Moss and Adams' Heart Disease in Infants, Children and Adolescents*. Baltimore, MD: Williams and Wilkins; 1995:1307–36.
14. Baschat A et al. *Ultrasound Obstet Gynecol* 1999;14:311–14.
15. Berg C et al. *Ultraschall Med* 2006;27:225–33.
16. Batukan C et al. *Ultraschall Med* 2005;26:234–8.
17. Yates RW et al. *Heart* 1996;76:548–9.

# 19

# Pulmonary vein anomalies

Anita J. Moon-Grady

## Introduction

Prenatal diagnosis of abnormal pulmonary venous connections is considered very challenging for an obstetric sonographer or sonologist and may also elude the fetal echocardiographer. Anomalies of the pulmonary veins are rarely detected in the fetus on second-trimester obstetric screening due to their low incidence and difficulty in obtaining detailed imaging.[1] Over the last two decades, refinement in ultrasound technology and cumulative operator experience has helped improve recognition of these conditions. Case series of over a dozen cases from single center experiences began appearing in the early 2000s (including Valsangiacomo et al.[2] and Patel et al.[3]). More recently, several centers have reported the potential for improvement in prenatal detection rates of pulmonary venous anomalies even with standard obstetric screening views.[4–7] Most infants with partial anomalous pulmonary venous connection (PAPVC) will be asymptomatic early in life, but the condition does require surgical repair in order to preserve functional status later in life. Though a majority of infants with total anomalous pulmonary venous connection (TAPVC) will present with nonspecific respiratory symptoms or feeding issues and mild desaturation, the condition can be life threatening within minutes to hours of birth if the pulmonary venous drainage is obstructed, and in cases with associated cardiac abnormalities, anomalies of the pulmonary veins may greatly alter surgical approach and prognosis. Therefore, an understanding of these anomalies is of paramount importance, and timely, accurate prenatal diagnosis dictates that evaluation of the pulmonary veins should be part of any complete fetal cardiac evaluation.

## Total anomalous pulmonary venous connection

Although TAPVC accounts for only 0.5%–2% of all cardiovascular malformations and occurs in approximately 8.7 of 100,000 live births,[8,9] it is the fifth most common cause of critical heart disease in infants.[8] In a large population-based report, 6/422 affected live-born babies had a sibling with TAPVC, supporting a genetic etiology in at least some patients.[10] The fundamental sign of the malformation is failure of the pulmonary veins to connect normally to the left atrium; instead they either drain directly or through the systemic veins to the right atrium. Abnormal pulmonary venous drainage can be isolated or may be a component of a more complex cardiac malformation such as may be seen with right and left atrial isomerism. Recent experimental evidence has disclosed that the origin of the pulmonary veins is distinct from the systemic veins.

## Embryology

The formation of the systemic and pulmonary veins and venous pole of the heart in the human is complex and incompletely understood. The developing systemic veins and right atrium are under the control of different transcription factors than the left atrium and pulmonary veins; systemic venous return derives from Nkx2-5–negative precursors, the pulmonary myocardium derives from Nkx2-5–expressing precursors, indicating distinct origins of the two.[11] Systemic venous development also requires transcription factor TBX18, whereas normal development of the pulmonary venous system and left atrium do not.[12,13] In mice, Pitx2c expressing pulmonary myocardial cells have been shown to be important in formation of the common pulmonary vein,[11] which runs through the mesenchyme of the dorsal mesocardium and drains initially at the pulmonary pit (a structure arising from the atrium). Early work in mice shows that the pulmonary veins form from a plexus draining the primitive foregut and lung buds (which arise from the foregut), and the speculation arose that persistence of early capillary connections from this plexus to the developing cardinal and splanchnic veins along with absence of development of the normal connection of the common pulmonary vein were responsible for the anomalous venous drainage of the lungs.[14] These anomalous connections, however, have never been clearly demonstrated in normal development. Newer information has emerged that the secreted guidance molecule semaphorin 3d (Sema3d) is necessary for normal development of pulmonary veins. Normally, Sema3d provides a repulsive cue to endothelial cells in the region of the developing foregut and posterior to the developing atrium, establishing a boundary; in the absence of Sema3d, endothelial tubes form in a region that is normally avascular, resulting in aberrant connections (Figure 19.1). This mutation has been observed in individuals with TAPVR and thus forms the basis of an alternate developmental model in these patients,[15] in which it is not a failure

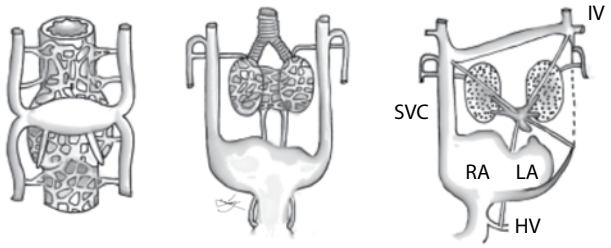


**Figure 19.1**
Conceptual framework for classification of anomalous pulmonary venous connections. Diagrammed is persistence of normal embryologic connections of the venous plexus draining the primitive foregut-derived lung bud to the embryo's cardinal and umbilicovitelline venous system. New research is suggesting that actual formation of such connections is only seen when signaling pathways are disrupted in very early development, suggesting that in normal embryos, these connections never exist, but the framework is useful in explaining the course of anomalous connections that are seen in the fetus and postnatal patient. Connection to the innominate vein (IV) or coronary sinus (CS) (left anterior cardinal vein or left common cardinal), superior vena cava (SVC) (right anterior cardinal vein), portal or hepatic veins (HV) (umbilicovitelline veins) is thus illustrated. (LA, left atrium; RA, right atrium.)

of regression of primitive connections to the systemic venous system but rather a failure to suppress development of them.[16]

## Anatomy

In TAPVC, there is no direct connection between the pulmonary veins and the left atrium. Rather, the pulmonary veins drain directly or via the systemic veins to the right atrium. Thus, postnatally systemic cardiac output is reliant on right-to-left shunting at the atrial level, or in more complex anomalies on admixture at the atrial or ventricular levels or both. An estimated one-third of patients present with an associated anomaly, while two-thirds present with isolated TAPVC.

An anatomic classification system has been described by Darling[17] (Figures 19.2 through 19.4):

1. Connection at the supracardiac level or type I (45%): In this variant, most commonly the pulmonary veins drain to a posterior confluence, which in turn is drained to the systemic venous system via a "vertical" vein with connection to the left innominate vein. The vertical vein can also drain to the azygous vein or to the right superior vena cava. The innominate vein and superior vena cava (SVC) may be normal or dilated in the fetus and are usually dilated postnatally. The site of obstruction may be at the left pulmonary artery and bronchus, at the connection to the innominate vein or SVC, or at the trachea as the vein passes posteriorly.
2. Connection at the cardiac level or type II (25%): When isolated, the most common anatomy is a connection of the pulmonary veins to the coronary sinus. Direct connection to the right atrium may also occur, more commonly with heterotaxy syndromes and other more complex malformations.

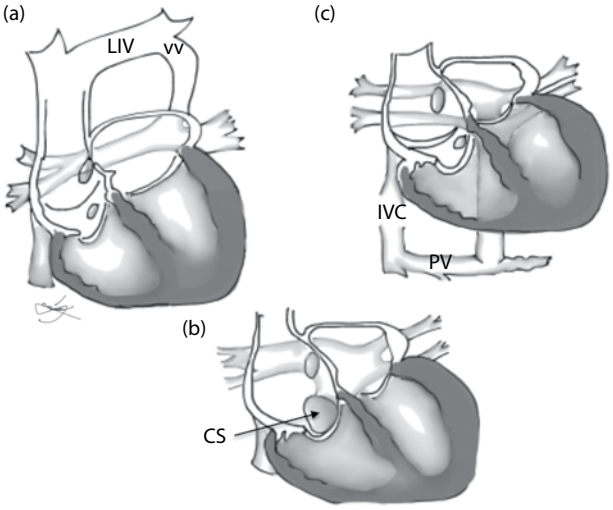


**Figure 19.2**
Common forms of total anomalous pulmonary venous connection. (a) Supracardiac or type I, to the left innominate vein (LIV) by way of a vertical vein (VV). (b) Cardiac (type II) to the coronary sinus. The pulmonary veins join to form a confluence that is continuous with the coronary sinus. (c) Infracardiac/infradiaphragmatic or type III, to the portal or hepatic vein (PV). The pulmonary veins form a confluence, from which an anomalous channel arises. This connects to the portal vein, which communicates with the inferior vena cava (IVC) by way of the ductus venosus or the hepatic sinusoids. (Redrawn with modification after Wilson A. In: Alejos J, Windle M, Moore J, Herzberg G, Berger S, eds. *Medscape Reference: Drugs, Diseases and Procedures*; 2012. Retrieved from http://emedicine.medscape.com/article/899491-overview.[52])


**Figure 19.3**
Supracardiac (type I) total anomalous pulmonary venous connection in an autopsy specimen. The pulmonary veins are seen posterior to the heart (which is reflected cranially here). They emerge from the hilum normally, accompanying the pulmonary artery (PA) but join at a confluence (c) rather than to the left atrium. The vertical vein is seen coursing over the left pulmonary artery (*), where obstruction in fetal life led to a severe degree of pulmonary fibrosis evident on the gross specimen. (Courtesy of Phil Ursell MD.)

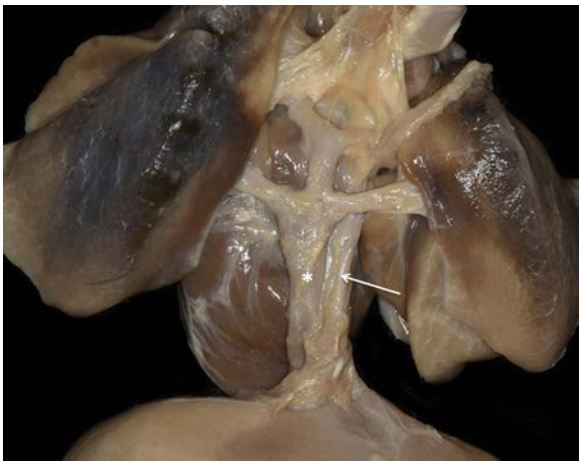

**Figure 19.4**
Infracardiac (type III) total anomalous pulmonary venous connection. Viewed from posterior. The pulmonary veins are seen draining separately each lobe of both lungs in an inverted pine tree formation. The vertical vein (*) is seen coursing inferiorly next to the esophagus (arrow) and through the diaphragm. (Courtesy of Phil Ursell MD.)

3. Connection at the infracardiac level type III (25%): In this type, there is often a less well-defined confluence and the pulmonary veins drain to a tubular structure behind the atrium, which then continues inferiorly passing through the diaphragm at the esophageal hiatus level (where there may be some physiologic obstruction) before connecting to the portal, hepatic, or less commonly other systemic veins. This type of TAPVC is nearly always physiologically obstructed due to the long course of the vertical vein, the abnormal connections within the intra-abdominal venous system, location of connection distal to the ductus venosus, and need to decompress through the hepatic circulation, or frank obstruction at the site of connection.
4. "Mixed" connections (type IV) occur at two or more of the above levels (10%).

The presence of obstruction in the pulmonary venous channel or at the atrial septum influences the hemodynamic state and clinical presentation of TAPVC. Obstruction may be intrinsic or extrinsic to the venous connections and may present as anatomic, physiologic, or combined lesions of varying degrees. Obstruction is nearly universal in the infradiaphragmatic type, while supracardiac drainage is obstructed in approximately 40% of patients, and cardiac-type TAPVC is only occasionally obstructed. One-third of patients will present with an associated major anomaly: atrioventricular septal defect, single ventricle, truncus arteriosus, transposition of the great arteries, pulmonary atresia, coarctation, hypoplastic left ventricle, and anomalies of the systemic veins.

## Pathophysiology

The nature of the fetal circulation and, in particular, fetal shunts allows TAPVC to be well tolerated *in utero*. Because pulmonary blood flow is a small portion of the combined ventricular output, even obstructed TAPVC rarely presents with any circulatory symptoms in the fetus. However, once postnatal transition occurs, there is complete mixing of the pulmonary and systemic circulations in the right heart, and the infant will be cyanotic and may have difficulty feeding in the first weeks and months of life even in the absence of other abnormalities. In some newborns, respiratory distress and decompensation occur very early in the neonatal period if there is significant obstruction to pulmonary venous return; obstruction results in elevated pulmonary venous and arterial pressures, decreased pulmonary blood flow, pulmonary edema, and decreased systemic oxygen delivery. The condition can quickly become life threatening unless the diagnosis is promptly recognized and surgical intervention arranged.

In early descriptions of prenatal appearance of TAPVC, right heart greater than left heart size discrepancy was reported as an important feature,[8] although it was present in only some fetuses. In abnormally connected pulmonary veins, the volume of blood returning from the lungs passes through the right heart instead of the left initially, and it has been suggested that this abnormal connection may produce right greater than left chamber discrepancy on the four-chamber view. However, in the middle of the second trimester, only 15% of the combined ventricular output passes through the lungs,[18,19] increasing to about 25%–35% of the cardiac output in the third trimester. The small amount of blood flow return from the lungs early in gestation, with flow increase only in later gestation may be a reason for inconsistent evidence of chamber discrepancy before 28 weeks.[8,10]

Because of the abnormal connections of the veins, flow dynamics in TAPVC are different from the normal as evidenced by spectral Doppler flow patterns. A normal pulmonary venous Doppler signal consists of pulsatile flow toward the left atrium throughout the cardiac cycle with biphasic peaks in systole and diastole. There is an initial peak followed by continuous flow during ventricular systole, which corresponds to the atrial filling phase and is represented as a recognizable "s." This is followed by another peak in early diastole due to atrial emptying into the ventricle and seen as "d." Following this, there is a period of reduced antegrade (or sometimes retrograde) flow during atrial contraction recognizable as the "a" wave.[20–22] Pulsed Doppler waveforms, then, in normal pulmonary venous connections are fairly predictable and uniform in their appearance. In abnormally connected veins, unique Doppler waveform patterns will reflect pathophysiological alterations due to the relative lack of left atrial influences, and may possibly be further affected by resistance to flow within the abnormal pulmonary veins and confluence/vertical vein to connect to the systemic veins, which may be of varying length. This produces distinctly abnormal waveforms (Figures 19.5 and 19.6) that should be considered diagnostic of anomalous connection of the pulmonary vein in the fetus.[4,23,24]

## Diagnosis

Pulmonary venous abnormalities are notoriously difficult to diagnose, especially in an obstetric screening setting,

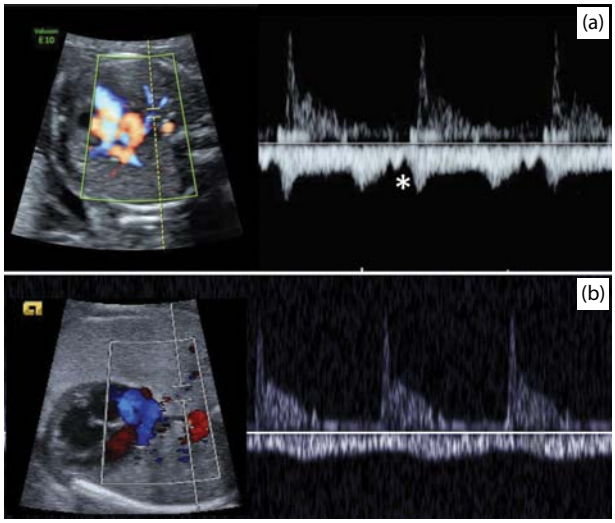


**Figure 19.5**
Pulsed-wave spectral Doppler for detection of abnormal connection of the pulmonary veins in the fetus. (a) Normal and (b) abnormal Doppler traces obtained with a sample gate encompassing both the pulmonary artery and pulmonary vein as they enter the hilum of the lung. The pulmonary artery Doppler gives a timing reference for systole; note the normal "a" wave corresponding with decreased forward flow in the pulmonary vein due to atrial contraction when the vein is connected normally to the left atrium (*). This normal "a" wave flow decrease or reversal is absent in fetuses with connection of the pulmonary veins to systemic venous structures or a confluence (supracardiac and infracardiac TAPVC) and in some patients with PAPVC.

and the diagnosis is difficult even in a specialized setting, particularly when the anomaly is isolated. In a large multicenter series of 424 cases, very low rates of diagnosis—less than 2%—were reported as diagnosed on routine screening.[10] Higher success rates have been reported (up to 60%) in smaller series, illustrating that it is possible to improve on detection rates in an obstetric screening setting. Higher detection rates, ranging from 57% to 96%, have been consistently reported in recent eras in the fetal echocardiography literature.

TAPVC should be suspected in the fetus when pulmonary veins cannot be visualized entering the left atrium on the axial scan. In addition, a common pulmonary venous confluence may be identified posterior to the left atrium. In supracardiac forms of TAPVC, the confluence will usually drain to an ascending "vertical vein," which in turn may be followed to a dilated systemic venous structure, most commonly the left innominate vein or right superior vena cava or less commonly the azygous vein near its junction with the superior vena cava. Doppler studies reveal flow in this vertical vessel to be cephalad, as opposed to the normal flow of blood in the systemic veins toward the heart. In infradiaphragmatic forms of TAPVC, the "vertical vein" can be seen draining the confluence and may be followed to the site of its connection to the hepatic or portal venous system. A diagnosis of cardiac-type TAPVC with drainage to the coronary sinus should be considered in cases with grossly dilated coronary sinus in the absence of left superior vena cava.[25] A simplified algorithm for enhancing recognition of TAPVC at the time of the routine anatomic scan has been proposed and is shown in Figure 19.7.

Echocardiographic evaluation of suspected TAPVC (Figures 19.8 through 19.12 and Videos 19.1 through 19.8) must locate the site of connection of the common pulmonary vein, evaluate any obstruction of the pulmonary veins or vertical vein, and confirm or exclude associated cardiac lesions. Doppler evaluation is invaluable in the diagnosis of all forms of TAPVC. Key features of the diagnosis include the following:

*Four-chamber view.* Lack of visualization of normal right and left pulmonary veins connecting to the

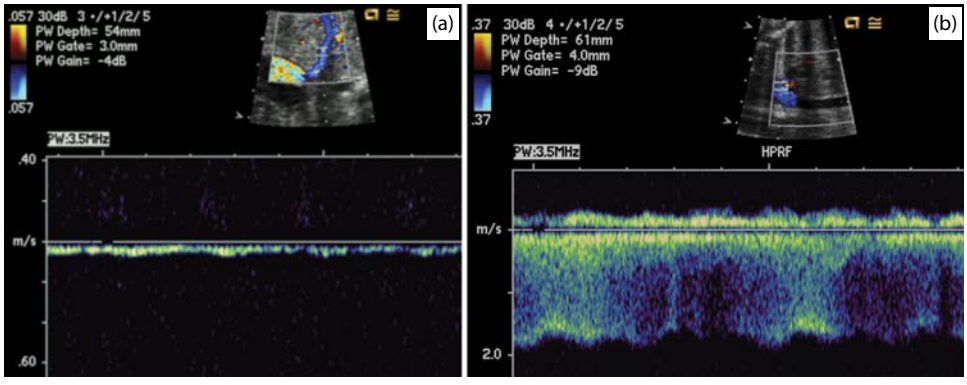


**Figure 19.6**
Severe pulmonary venous obstruction in a fetus suggested by spectral Doppler flow pattern in the individual pulmonary veins. Continuous extremely low velocity flow (a) in the pulmonary veins as they emerge from the lung, near the hilum, is a clue to severe obstruction distally and may portend the presence of abnormal lung vascular and lymphatic development by term. Fetuses with this degree of obstruction may exhibit profound cyanosis at birth with lung fibrosis and lymphangiectasis that may not be reversible. Because the percent of combined ventricular output dedicated to pulmonary blood flow in the fetus is normally low, and because of the inherent obstruction in the long venous channels leading from the confluence to the systemic venous connection, velocity of flow at the obstruction site (b) is unreliable in predicting the postnatal physiology.

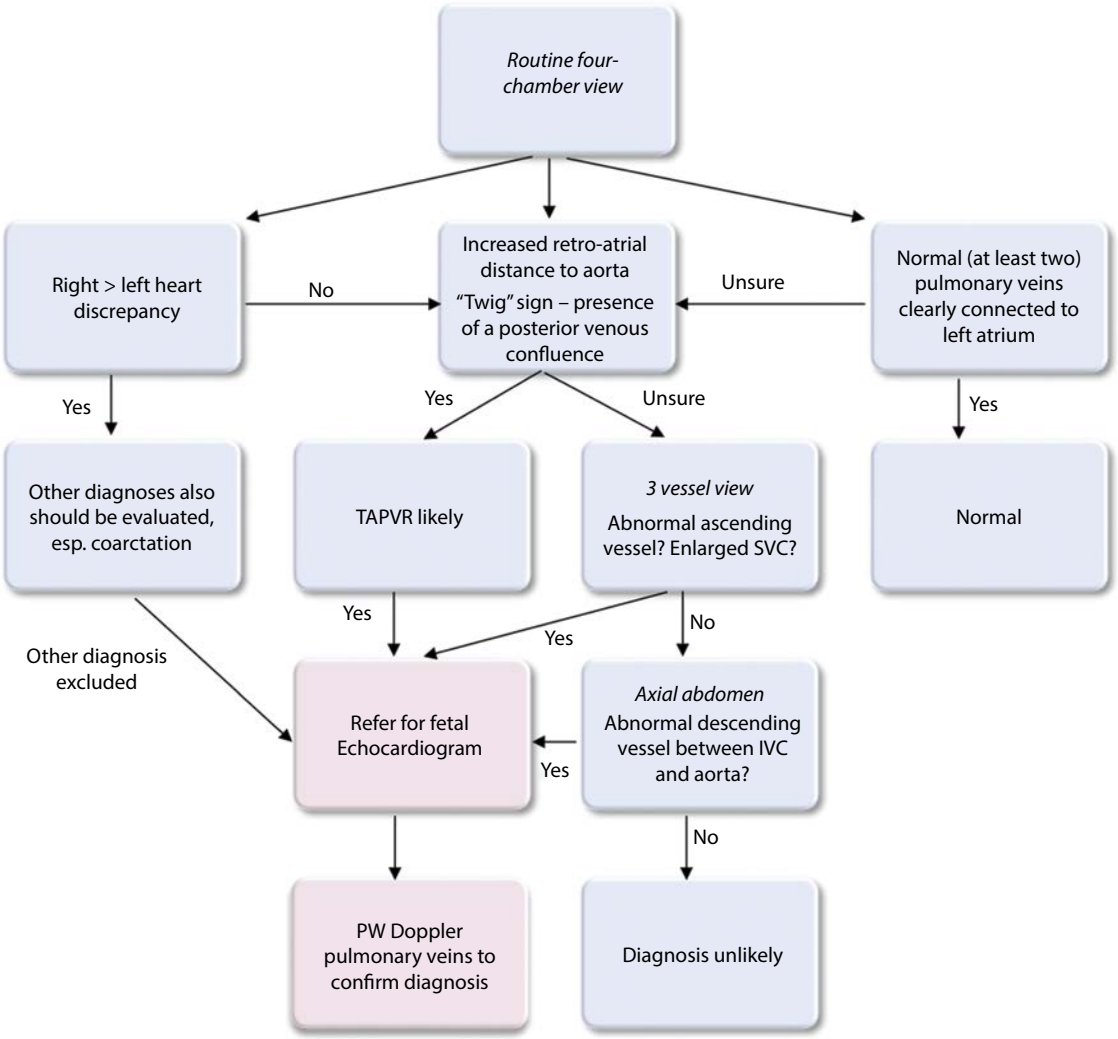


**Figure 19.7**
Flowchart for assessment of pulmonary venous return within a routine obstetric anatomy scan. (Reproduced with permission from Ganesan S et al. *J Ultrasound Med* 2014;33(7):1193–207.[4])

left atrium, with a smooth posterior left atrial surface and an abnormally wide space between the left atrium and the descending aorta (Figures 19.8, 19.9, and 19.11). Quantification of an increased post-left atrial space has been suggested as a screening tool by several groups,[6,26,27] with a cutoff of greater than 1.27 considered abnormal. The axial four-chamber view also may have a tubular vascular confluence situated posterior to the atria described as a "twig" sign due to its similar appearance in most cases (Figure 19.8). Color mapping aids in the diagnosis but may also falsely "connect" the veins to the left atrium and so must be interpreted with caution; the flow velocity may be very low in the veins, due to distal obstruction, and therefore requiring a particularly low pulse repetition frequency (PRF) in order to fill the veins should alert the examiner to the possibility of the diagnosis (Figure 19.10). Relative right ventricle greater than left ventricle chamber asymmetry may be present, especially later in gestation,[8] but is not found in all cases.

*Three-vessel view.* The presence of an additional vascular channel apart from the normal superior vena cava, aorta, and pulmonary artery, once a left superior vena cava or azygous is excluded, should alert the examiner to the possibility of type I supracardiac TAPVC. Relative prominence of the superior vena cava has also been described.

*Abdominal views.* The descending vertical vein in infradiaphragmatic TAPVC can be seen passing through the esophageal hiatus between the aorta and the inferior vena cava. Longitudinal or sagittal views will identify these "vertical" venous connections. Color Doppler imaging to identify flow direction and location of obstruction should be added to confirm the nature of these venous structures (Figures 19.11 and 19.12, and Videos 19.6 through 19.8).

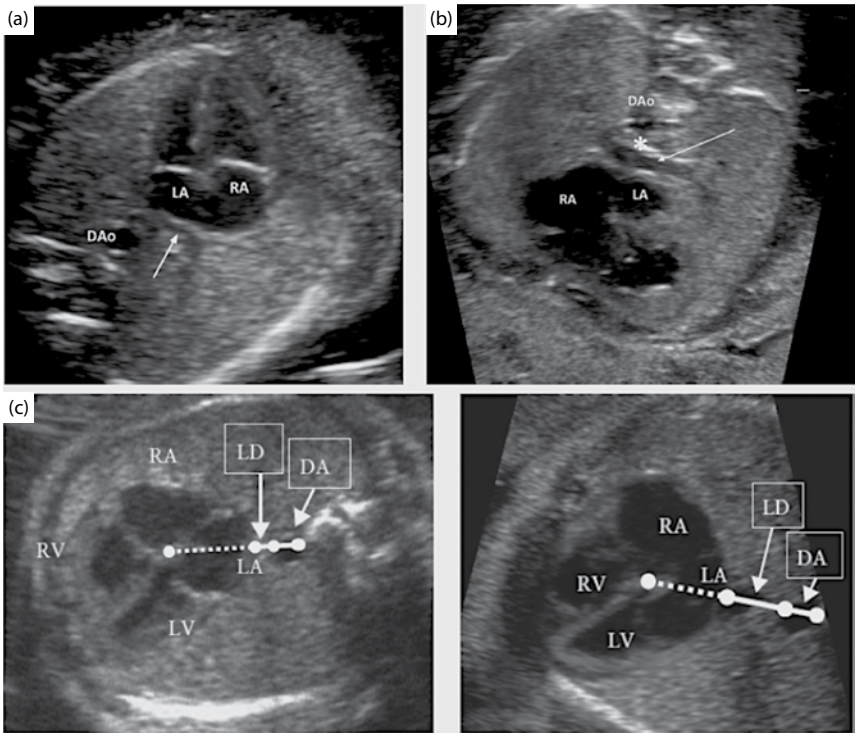


**Figure 19.8**
Posterior venous confluence, increased posterior left atrial space, and post-LA space index measurement. (a) Axial four-chamber recognition of the abnormality will lead to the diagnosis as the confluence is seen and the pulmonary veins do not join the atrium "twig sign" (arrow). The venous structure represents the confluence of the pulmonary veins; the draining vein may ascend (type I), descend (type III), or connect to the coronary sinus (type II) and would not be visible in this view. DAo indicates descending aorta; LA, left atrium; and RA, right atrium. (b) Exaggerated space behind the left atrium (*) in a fetus with complex heart disease. The "twig sign" is also visible (arrow). (c) The post-left atrial space index measurement (the ratio of the distance between the left atrium and descending aorta [LD] to the diameter of the descending aorta [DA]) in normal (left panel) and abnormal (right panel) fetuses. (Reprinted with permission from Kawazu Y et al. *Ultrasound Obstet Gynecol* 2014;44(6):682–7.[27])

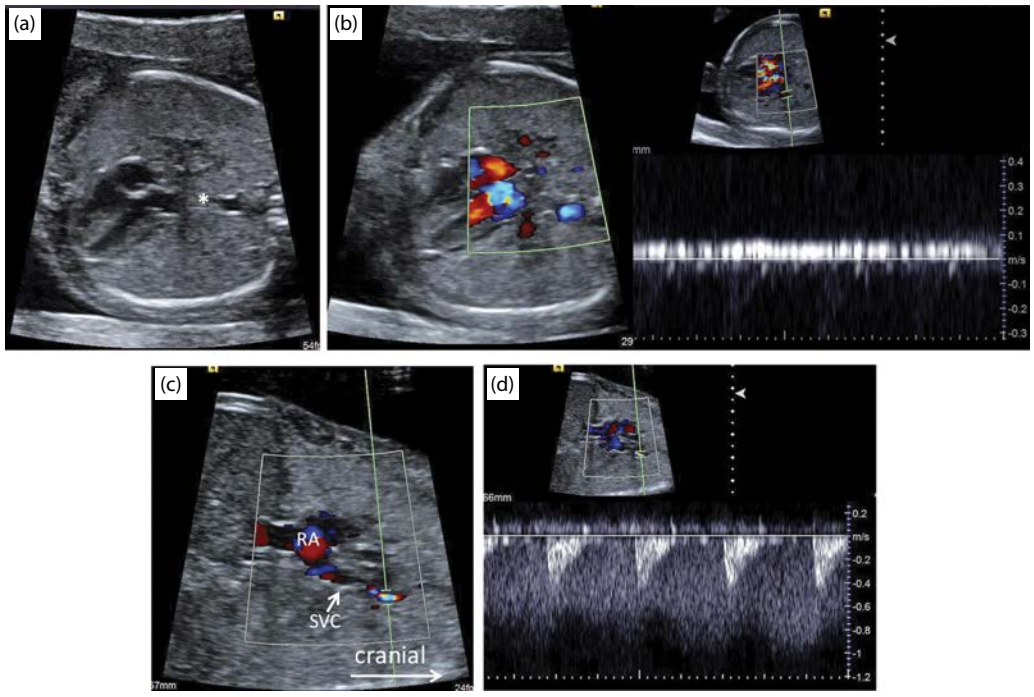


**Figure 19.9**
Isolated total anomalous pulmonary venous connection (TAPVC) with supracardiac drainage to the left innominate vein. (a) Axial grayscale image at the four-chamber view with characteristic increased post-left atrial space (*) and smooth-walled posterior left atrium. (b) Color Doppler and corresponding spectral Doppler trace in the left lower pulmonary vein as it enters the hilum. Note the very low PRF needed to detect antegrade flow. Flow is nonphasic by spectral Doppler, lacking the characteristic "a" wave of normal pulmonary venous flow and characteristic of severe distal obstruction. (c) Sagittal image of the vertical vein demonstrating its obstructed connection to the superior vena cava (SVC). Spectral Doppler (d) reveals severe obstruction at this point. See also corresponding Videos 19.1 and 19.2.

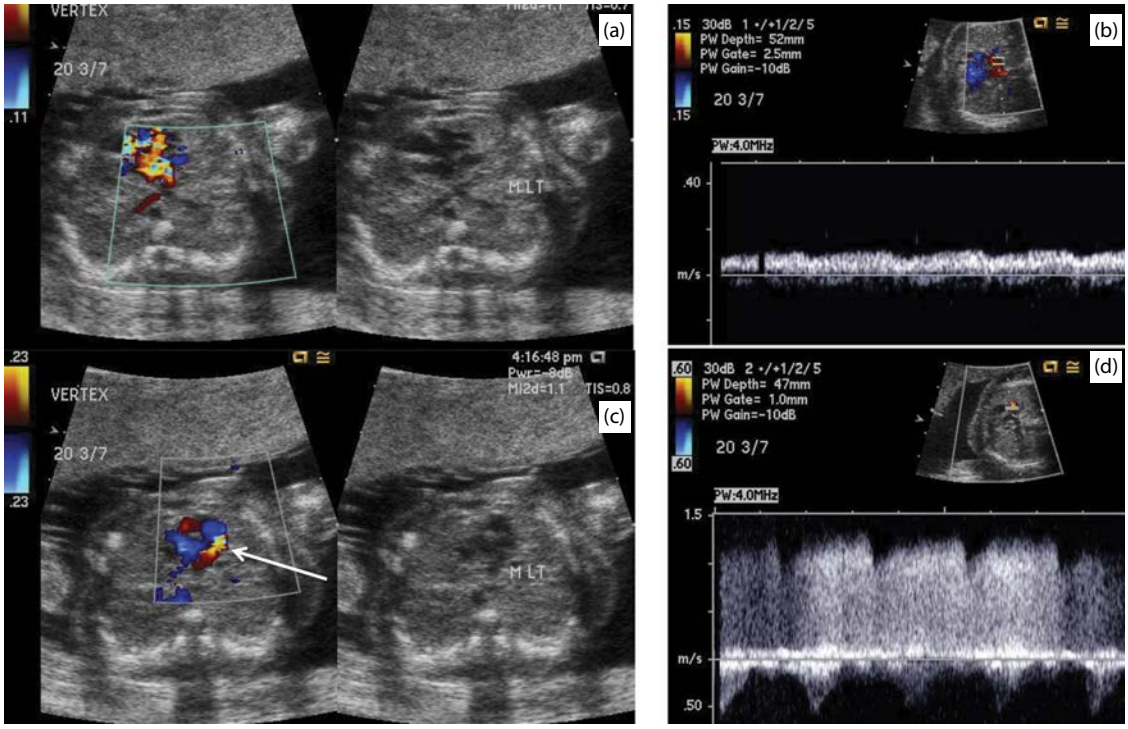


**Figure 19.10**
Total anomalous pulmonary venous connection (TAPVC) with supracardiac drainage in a fetus with heterotaxy. (a) Note the very low PRF needed to detect antegrade flow in the pulmonary veins toward the confluence posterior to the left atrium. At this low PRF, color may artifactually appear to "connect" the pulmonary veins to the atrium, but the corresponding grayscale image suggests the diagnosis with a smooth-walled posterior left atrium and the "twig sign" of the pulmonary veins. (b) Further, the flow is nonphasic by spectral Doppler, lacking the characteristic "a" wave of normal pulmonary venous flow and characteristic of veins lacking a direct connection to the atrium. (c) Scan cranially to follow the vertical vein as it demonstrates its course over the top of the right pulmonary artery before connecting to the right superior vena cava (arrow). Spectral Doppler (d) reveals moderate obstruction at this point. See also corresponding Videos 19.3 and 19.4.

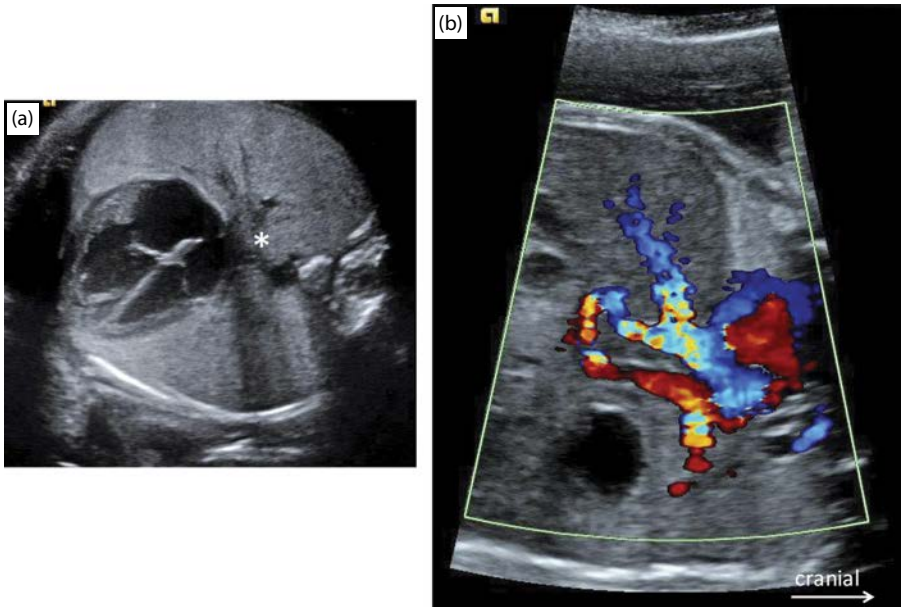


**Figure 19.11**
Isolated total anomalous pulmonary venous connection (TAPVC) with infracardiac drainage. (a) Axial grayscale image at the four-chamber view with characteristic increased post-left atrial space (*) and smooth-walled posterior left atrium. (b) Sagittal image with low-PRF color Doppler shows pulmonary veins draining to the venous channel behind the left atrium, which courses posteriorly through the diaphragm near the esophageal hiatus and connects to the infradiaphragmatic venous system. Here the umbilical or portal vein is near the ductus venosus, which is the primary source of obstruction in this patient. See also corresponding Videos 19.5 and 19.6.

*Spectral (pulsed-wave) Doppler Interrogation of the Pulmonary Veins.*

Normal fetal pulmonary venous flow can be either tri- or biphasic and pulsatile, and dynamically influenced by the left atrial pressure changes as noted above[28–31] (Figure 19.5). With atrial systole, there is a decrease in forward flow to a minimum during the cardiac cycle (biphasic); atrial reversal of flow ("a" wave, triphasic) is noted in about 10% in the fetal

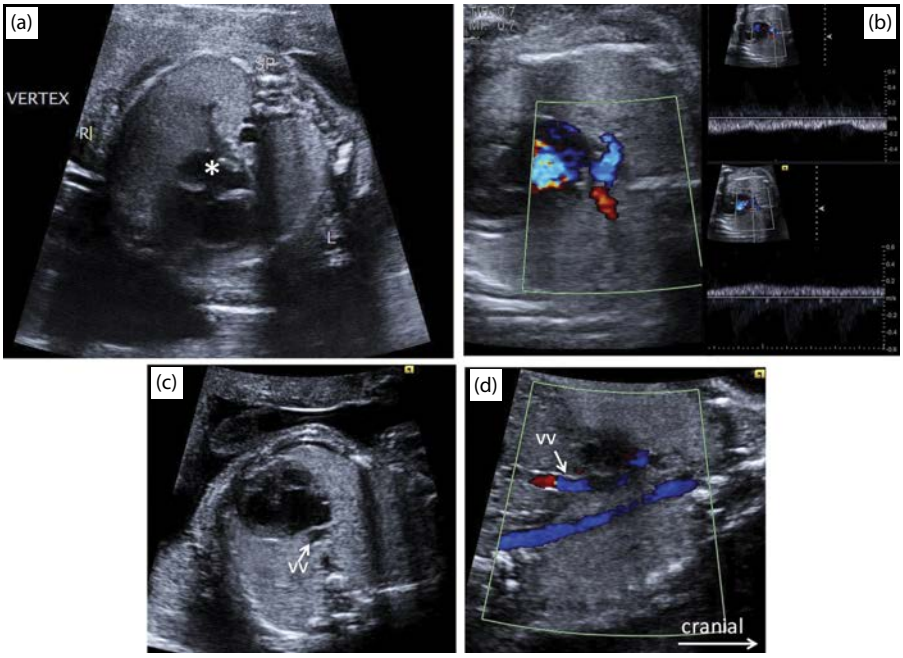


**Figure 19.12**
Total anomalous pulmonary venous connection (TAPVC) with infracardiac drainage in a fetus with heterotaxy. (a) Axial imaging showing right-sided stomach, leftward apex, and "twig sign" posterior to the common atrium (*). (b) Color Doppler of pulmonary veins. Note the very low PRF needed to detect antegrade flow in the pulmonary veins toward the confluence posterior to the left atrium. At this low PRF, color may artifactually appear to "connect" the pulmonary veins to the atrium, but the corresponding spectral Doppler lacks the characteristic "a" wave of normal pulmonary venous flow and characteristic of veins lacking a direct connection to the atrium. (See also corresponding Videos 19.7 and 19.8.) (c) Axial and (d) sagittal images of the vertical vein (vv) as it descends through the diaphragm with color Doppler in the same direction as aortic flow (away from the heart), making it impossible for the structure to be mistaken for a normal venous structure such as inferior vena cava or azygous vein (in which flow would be the opposite direction).

period.[29] Four distinct abnormal patterns in the pulmonary venous waveforms, all recognizably different from normal, have been observed in fetuses with TAPVC:

- Pseudonormal, bi- or triphasic and pulsatile but with abnormal appearance: Seen in supracardiac connections directly to the low superior vena cava or right atrium
- Biphasic with decreased pulsatility: Seen typically in supracardiac connection but also occasionally infradiaphragmatic TAPVC
- Monophasic but pulsatile: Seen in most cases of infradiaphragmatic connection and some with supracardiac connection
- Monophasic and nonpulsatile: Seen in both infradiaphragmatic and supracardiac in the presence of severe obstruction of the vertical vein[2,4]

In addition, spectral Doppler interrogation of the ascending or descending vertical vein at the suspected site of obstruction may show a turbulent or continuous high-velocity flow signal (Figures 19.6 and 19.9, Video 19.2).

## Clinical presentation

If obstruction is severe, profound cyanosis, pulmonary edema, metabolic acidosis, circulatory collapse, and death may ensue within hours of birth. Temporary improvement may be seen with institution of measures to decrease oxygen consumption and increase pulmonary vascular resistance, but medical management is merely temporizing for these neonates.

## Treatment

Surgery for TAPVC is generally curative. Reported survival at 20 years is over 83%. The rate of re-intervention due to postoperative pulmonary vein obstruction has decreased to around 10% for simple TAPVR in recent literature.[32] Primary sutureless repair[33,34] at the time of initial surgical intervention may mitigate the risk of postrepair and recurrent pulmonary vein stenosis. Morbidity and mortality are higher in patients with mixed-type (type IV) TAPVC.[35,36]

## Prognosis

Mortality after TAPVC repair in biventricular patients in the current era is quite low; risk factors for perioperative death include small size, younger age, and preoperative obstruction. Isolated TAPVC appears to be at the highest risk for perioperative mortality or late postoperative obstruction when clinical obstruction is present preoperatively; patients who present for elective repair without significant symptoms almost universally do well in the short term, and pulmonary vein stenosis as a late complication is

unusual in these patients.[37] Risk-adjusted estimated 1-year survival for a patient repaired at birth with unfavorable morphology approaches 20%–50% compared with 96% for those with favorable morphology repaired at 1 year of age in one large series. Freedom from reoperation in the same series was 82% a decade after repair, with increased risk for reoperation associated with mixed connection type and postoperative pulmonary venous obstruction.[35] Reoperation for postoperative pulmonary vein obstruction carries significant risk for death; these patients represent a subset with particularly poor (<60%) long-term survival.[38] Long-term survivors may exhibit decreased exercise tolerance thought to be due to relative diastolic dysfunction[39] but in general can expect to be reasonably asymptomatic well into adulthood.

## Partial anomalous pulmonary venous connection

Isolated partial anomalous pulmonary venous connection (PAPVC) is rarely identified in the fetus. The lesion involves one or more, but not all, of the pulmonary veins connecting to the right atrium or a tributary (Figure 19.13).

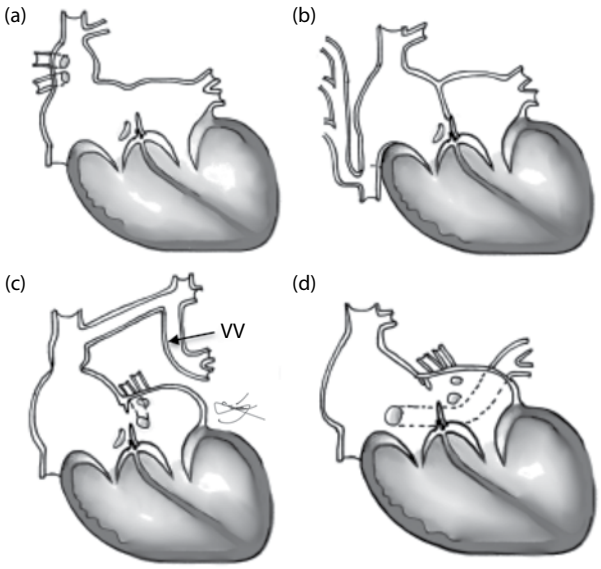


**Figure 19.13**
Common forms of partial anomalous pulmonary venous connection. (a) Anomalous connection of the right pulmonary veins to superior vena cava. A high or sinus venous defect is usual in this anomaly. (b) Anomalous connections of the right pulmonary veins to the inferior vena cava, also called *scimitar syndrome*. The right lung commonly drains by one pulmonary vein without its usual anatomic divisions. Parenchymal abnormalities of the right lung are common, and the atrial septum is usually intact. (c) Anomalous connection of the left pulmonary veins to the left innominate vein by way of a vertical vein (vv). An additional left-to-right shunt may occur through the atrial septal defect. (d) Anomalous connection of the left pulmonary veins to the coronary sinus. (Redrawn after Krabill KA, Lucas RV. In: Emmanouilides GC, Riemenschneider TA, Allen HD, Gutgesell HP, eds. *Moss and Adams' Heart Disease in Infants, Children, and Adolescents*, 5th ed. Baltimore, MD: Williams and Wilkins; 1995:841–9.[40])

The entire lung may be involved in up to 20% of cases, but usually only part of the lung is involved—most commonly the right. In isolated PAPVC, an atrial septal defect (ASD) is often present postnatally but may be difficult to diagnose in the fetus. There are several variant presentations of this anomaly:[2,3,8,40]

1. The right pulmonary veins enter the superior vena cava (SVC) (Figure 19.13a). In this variant, most commonly the right upper and middle lung lobes drain into the SVC, while in some cases the upper lobe may drain into the SVC below the azygous vein, the middle lobe into the SVC at its junction with the right atrium, or the right lower lobe may drain into the left or right atrium. The proximal SVC between the azygous vein and the right atrium may be normal or dilated. A sinus venosus ASD may be visualized and is often present. Other types of ASD are found less often. The right pulmonary veins may alternately connect directly to the right atrium.
2. The right pulmonary veins enter the inferior vena cava (IVC) (Figure 19.13b). In this variation, all or only the middle and lower lobes of the right lung are drained into the IVC, just above or below the diaphragm. This variant of PAPVC, called *scimitar syndrome* because of the characteristic chest radiographic appearance of the right pulmonary vein contour as it descends toward the inferior vena cava (Figure 19.14), is frequently associated with hypoplasia of the right lung, anomalies of the bronchial system, dextroposition of the heart, hypoplasia of the right pulmonary artery, anomalous arterial connection to the right lung from the aorta, and other cardiac anomalies, and can be suspected when mild dextroposition of the fetal heart is noted on axial scanning without associated chest pathology.
3. The left pulmonary veins enter the left innominate vein (Figure 19.13c). In this anomaly, veins from either the left upper lobe or all lobes of the left lung enter the left innominate vein by way of an anomalous vertical vein. It is often associated with cardiac defects and syndromes including polysplenia-asplenia syndrome, and Turner and Noonan syndromes, and generally, there is an atrial septal defect present postnatally, though patients may also experience normal postnatal closure of the foramen ovale and have no ASD.
4. Less commonly, the left pulmonary veins connect anomalously to the coronary sinus (Figure 19.13d) or to the IVC, right SVC, right atrium, or left subclavian vein. Very rarely, the right pulmonary veins may connect to the azygous vein or coronary sinus.

PAPVC is often present in association with complex anomalies; therefore, careful attention to the pulmonary venous connections should be sought for any initial evaluation for complex CHD. Echocardiographic diagnosis of PAPVC is made by visualizing pulmonary veins connecting to the systemic venous structure involved. A postnatal finding of right ventricular volume overload with an intact atrial septum and otherwise normal intracardiac anatomy may indicate

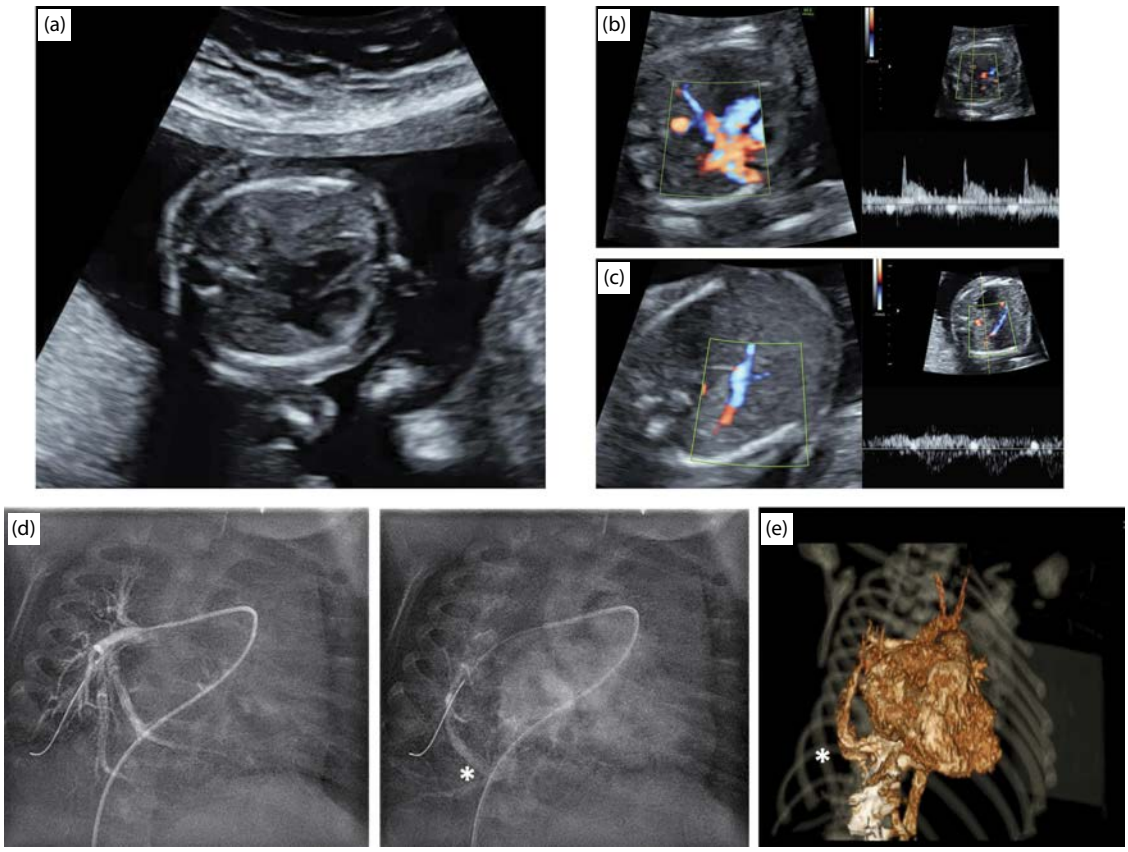


**Figure 19.14**
Partial anomalous pulmonary venous connection (PAPVC) in a fetus with scimitar confirmed postnatally. (a) Axial grayscale image at the four-chamber view shows mild dextroposition of the heart with abnormal cardiac axis but no clear left lung pathology, which should suggest the diagnosis of right lung hypoplasia and/or PAPVC. (b) Directional power Doppler and spectral Doppler demonstrate normal left pulmonary venous connection, while (c) venous drainage from the right lung appears to be to the inferior vena cava by color Doppler; spectral Doppler interrogation clearly reveals the pulmonary venous nature of the identified venous structure. Postnatal right pulmonary artery angiography in this patient (d) shows levophase return of contrast to the inferior vena cava with the curved appearance (*) of a "scimitar blade" from which this anomaly derives its name. (e) Three-dimensional reconstruction from computerized tomography images obtained in a similar neonate. Note again the "scimitar" vein draining the right lung to the inferior vena cava (*). (See also corresponding Videos 19.9 and 19.10.) (Figure (e) courtesy of Wayne Tworetzky MD.)

that PAPVC is present. The diagnosis may be suspected in the ill neonate with pulmonary hypertension or abnormal chest radiographic findings, or may be incidentally detected on echocardiography performed for other indications. The diagnosis of PAPVC versus TAPVC may be suspected in the neonate if abnormal connections of pulmonary veins are detected but color flow at the atrial septum (through the foramen ovale or an ASD) is left-to-right rather than the characteristic right-to-left postnatal flow expected for TAPVC. Doppler flow studies and color mapping of individual systemic and pulmonary venous connections are indispensable in identification and classification of this group of anomalies,[6] and adjunctive modalities may also prove helpful.[41–45]

Prognosis is good for isolated PAPVC or PAPVC with associated atrial septal defect.[46] For anomalous left pulmonary venous connection, anastomosis of the veins to the left atrial appendage has been reported with excellent long-term survival and very low rates of re-stenosis.[47]

## Other pulmonary venous anomalies

The common pulmonary vein is an embryologic structure that is usually not normally present beyond the embryonic period. The developing common pulmonary vein uses the dorsal mesocardium to reach the primary atrial segment. Initially, the pulmonary pit, which will become the portal of entry for the pulmonary vein, is located along the embryologic midline surrounded by ridges, and subsequent tissue remodeling results in the incorporation of the portal of entry of the pulmonary vein in left atrial myocardium.[48] The mesenchyme containing the common pulmonary vein is surrounded by cells belonging to the second heart field. This mesenchyme differentiates into cardiomyocytes forming the myocardial pulmonary venous sleeves, and ultimately, the pulmonary venous connection to the left atrium becomes several separate orifices. Persistence of a single stenotic or even atretic orifice, with no decompressing vein, is usually lethal and may present *in utero* with

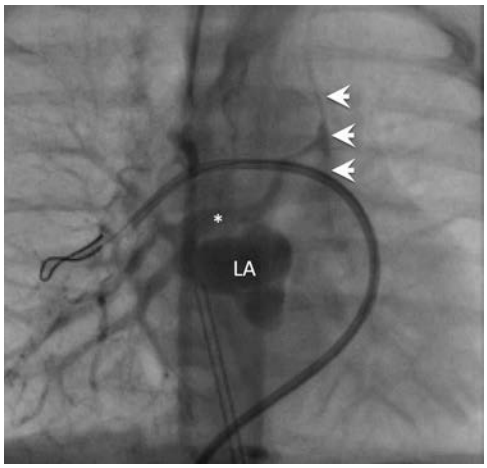


**Figure 19.15**
Levoatriocardinal vein. Neonate with a prenatal diagnosis of mitral atresia, intact atrial septum, and decompressing levoatriocardinal vein. Shown is the levophase after a right pulmonary artery injection, demonstrating the right pulmonary veins connecting normally to the left atrium (LA), with a decompressing vein (*) coursing from the right upper pulmonary vein to a persistent left superior vena cava (arrowheads).

bilateral hydrothorax or postnatally with severe pulmonary hypertension.[49]

Levoatriocardinal vein is a term used to describe a venous structure arising directly from the left atrium or one of the pulmonary veins (usually the left upper) decompressing the left atrium to the systemic venous circulation.[50] This leads to a situation of "normally connected but anomalously draining" pulmonary veins, and presents similarly to TAPVR. The condition is most commonly associated with severe left heart obstructive disease with intact or severely restrictive interatrial septum.[51] Prenatal recognition of the levoatriocardinal vein relies on similar tools to those discussed for TAPVR, including abnormal pulmonary vein appearance, spectral Doppler patterns consistent with left atrial hypertension (with increased retrograde "a" wave velocity and duration), and color Doppler demonstration of the venous vessel ascending posterior to the left atrium; however, identification can be very challenging (Figure 19.15). Prognosis is generally poor, similar to that for hypoplastic left heart syndrome with severe atrial septal restriction (see Chapter 30).

## Videos

**Video 19.1** (https://youtu.be/hq-CqNtc_Fo)
Isolated total anomalous pulmonary venous connection (TAPVC) with supracardiac drainage to the left innominate vein, axial grayscale 4-chamber view.

**Video 19.2** (https://youtu.be/KHWQt0GJ3hA)
Isolated total anomalous pulmonary venous connection (TAPVC) with supracardiac drainage to the left innominate vein, sagittal color Doppler bicaval view.

**Video 19.3** (https://youtu.be/Xk3DZhhgOTg)
Total anomalous pulmonary venous connection (TAPVC) with supracardiac drainage in a fetus with heterotaxy, color Doppler and corresponding grayscale demonstrating pulmonary veins and confluence.

**Video 19.4** (https://youtu.be/0EeWGOPiHSI)
Total anomalous pulmonary venous connection (TAPVC) with supracardiac drainage in a fetus with heterotaxy, color Doppler and corresponding grayscale demonstrating course of the vertical vein in the three-vessel view.

**Video 19.5** (https://youtu.be/FWkQmvt7HT4)
Isolated total anomalous pulmonary venous connection (TAPVC) with infracardiac drainage, axial grayscale image at the 4-chamber view.

**Video 19.6** (https://youtu.be/Rm4rcIrrTJ4)
Isolated total anomalous pulmonary venous connection (TAPVC) with infracardiac drainage, sagittal image with low-PRF color Doppler show pulmonary veins draining to the venous channel behind the left atrium.

**Video 19.7** (https://youtu.be/KH3g-bYGnr0)
Total anomalous pulmonary venous connection (TAPVC) with infracardiac drainage in a fetus with heterotaxy, axial grayscale sweep from stomach on right to heart with leftward apex.

**Video 19.8** (https://youtu.be/gqpxNBUgFb4)
Total anomalous pulmonary venous connection (TAPVC) with infracardiac drainage in a fetus with heterotaxy, axial image with color Doppler and corresponding grayscale demonstrating pulmonary veins coursing toward posterior confluence.

**Video 19.9** (https://youtu.be/YFmTzZfmA1A)
Partial Anomalous Pulmonary Venous Connection (PAPVC) in a fetus with scimitar confirmed postnatally, axial sweep from chest to abdomen follows the anomalous pulmonary vein course.

**Video 19.10** (https://youtu.be/CoP3WTE-NFk)
Partial Anomalous Pulmonary Venous Connection (PAPVC) in a fetus with scimitar confirmed postnatally: postnatal right pulmonary artery angiography with levophase contrast return.

## References

1. Bromley B et al. *Am J Obstet Gynecol* 1992;166(5):1473–81.
2. Valsangiacomo ER et al. *Ultrasound Obstet Gynecol* 2003;22(3):257–63.
3. Patel CR et al. *J Ultrasound Med* 2005;24(9):1191–8.
4. Ganesan S et al. *J Ultrasound Med* 2014;33(7):1193–207.
5. Laux D et al. *Ultrasound Obstet Gynecol* 2013;41(3):291–7.
6. Olsen R et al. *J Ultrasound Med* 2016;35(6):1193–206.
7. Tongsong T et al. *J Ultrasound Med* 2016;35(7):1601–7.
8. Allan LD, Sharland GK. *Heart* 2001;85(4):433–7.
9. Hoffman JI. *Postnatal Incidence Pediatr Cardiol* 1995;16(3):103–13.
10. Seale AN et al. *Ultrasound Obstet Gynecol* 2012;40(3):310–8.

11. Mommersteeg MT et al. *Circ Res* 2007;101(9):902–9.
12. Christoffels VM et al. *Circ Res* 2006;98(12):1555–63.
13. Sizarov A et al. *Circulation* 2010;122(8):798–807.
14. DeRuiter MC et al. *Circulation* 1993;87(4):1306–19.
15. Degenhardt K et al. *Nat Med* 2013;19(6):760–5.
16. Sizarov A et al. Development of the heart: Morphogenesis, growth, and molecular regulation of differentiation. In: Allen HD, Shaddy RE, Penny DJ, Cetta F, Feltes TF, eds. *Moss and Adams' Heart Disease in Infants, Children, and Adolescents*. 1. 9th ed. Philadelphia, PA: Wolters Kluwer Health/Lippincott Williams and Wilkins; 2016:1–54.
17. Craig JM et al. *Lab Invest* 1957;6(1):44–64.
18. Rasanen J et al. *Circulation* 1996;94(5):1068–73.
19. Rudolph AM. *Circ Res* 1985;57(6):811–21.
20. Anteby EY et al. *Ultrasound Obstet Gynecol* 1994;4(3):208–10.
21. Better DJ et al. *J Am Soc Echocardiogr* 1996;9(3):281–5.
22. Laudy JA et al. *Ultrasound Obstet Gynecol* 1995;6(4):277–81.
23. Feller Printz B, Allan LD. *Ultrasound Obstet Gynecol* 1997; 9(5):347–9.
24. Lenz F, Chaoui R. *Ultrasound Obstet Gynecol* 2006;28(1):63–70.
25. Karl K et al. *Ultrasound Obstet Gynecol* 2011;38(6):729–31.
26. Akkurt MO et al. *J Perinat Med* 2016;44(6):613–7.
27. Kawazu Y et al. *Ultrasound Obstet Gynecol* 2014;44(6):682–7.
28. Hecher K et al. *Am J Obstet Gynecol* 1995;173(1):10–5.
29. Hong Y, Choi J. *Fetal Diagn Ther* 1999;14(2):86–91.
30. Hong YM, Choi JY. *Early Hum Dev* 2000;57(2):95–103.
31. Paladini D et al. *Ultrasound Obstet Gynecol* 1997;10(1):27–31.
32. Yong MS et al. *Ann Thorac Surg* 2011;91(6):1921–7.
33. Alsoufi B. *World J Pediatr Congenit Heart Surg* 2014;5(2):302–5.
34. Yanagawa B et al. *J Thorac Cardiovasc Surg* 2011;141(6):1346–54.
35. Karamlou T et al. *Circulation* 2007;115(12):1591–8.
36. Kogon B et al. *Cardiol Young* 2017;27(5):870–6.
37. Frommelt PC et al. *Pediatr Cardiol* 2010;31(8):1191–7.
38. Seale AN et al. *Circulation* 2010;122(25):2718–26.
39. Marcondes LD et al. *J Thorac Cardiovasc Surg* 2014;148(1): 238–44.
40. Krabill KA, Lucas RV. Abnormal pulmonary venous connections. In: Emmanouilides GC, Riemenschneider TA, Allen HD, Gutgesell HP, eds. *Moss and Adams' Heart Disease in Infants, Children, and Adolescents*, 5th ed. Baltimore, MD: Williams and Wilkins; 1995:841–9.
41. Lee W et al. *Ultrasound Obstet Gynecol* 2010;35(1):124–5.
42. Peng R et al. *J Ultrasound Med* 2012;31(10):1651–8.
43. Valsangiacomo ER et al. *Pediatr Radiol* 2003;33(2):92–8.
44. Volpe P et al. *Ultrasound Obstet Gynecol* 2007;30(6):830–7.
45. Espinoza J et al. *Ultrasound Obstet Gynecol* 2005;25(5):428–34.
46. Alsoufi B et al. *Ann Thorac Surg* 2007;84(6):2020–6; discussion 6.
47. Naimo PS et al. *Interact Cardiovasc Thorac Surg* 2015;21(2):254–6.
48. Wessels A et al. *Anat Rec* 2000;259(3):288–300.
49. Samuel N et al. *J Ultrasound Med* 1988;7(1):25–8.
50. Bernstein HS et al. *J Am Coll Cardiol* 1995;26(4):995–1001.
51. Hayashi T et al. *Pediatr Int* 2016;58(7):656–9.
52. Wilson A. Total anomalous venous connection. In: Alejos J, Windle M, Moore J, Herzberg G, Berger S, eds. *Medscape Reference: Drugs, Diseases and Procedures*. 2012. Retrieved from http://emedicine.medscape.com/article/899491-overview

# 20

# Ebstein malformation and tricuspid valve pathology

Lindsay R. Freud, Wayne Tworetzky, and Norman H. Silverman

## Introduction

Congenital tricuspid valve malformations, which include apical displacement of the tricuspid valve (Ebstein malformation) or dysplasia, are rare forms of structural heart disease that predominantly lead to tricuspid regurgitation. The postnatal incidence has been estimated at approximately 50–100 per 1 million live births, which comprises up to 1% of congenital heart disease.[1–3] However, the prenatal incidence has been noted to be substantially higher, comprising up to 8% of congenital heart disease.[4] Ebstein malformation or tricuspid valve dysplasia that leads to severe tricuspid regurgitation is poorly tolerated in the fetus, with the development of cardiomegaly, ventricular dysfunction, and hydrops. Perinatal mortality, including fetal demise or neonatal death, was reported to be as high as 45% in a recent, large contemporary series across North America.[5] Advances in fetal echocardiography have led to the prenatal diagnosis of more mild forms of disease, with mild or less tricuspid regurgitation. Such patients are uncommonly affected early in life and may remain asymptomatic until adolescence or adulthood.

## Genetics and the environment

While the etiology of Ebstein malformation and other congenital tricuspid valve pathology is not well understood, there is emerging data to suggest genetic heterogeneity. Up to 28% of cases are syndromic and/or associated with extracardiac anomalies, including trisomy 18 and 21, del1p36, and 8p23 deletion (likely involving the GATA4 gene).[1,5,6] In nonsyndromic cases, mutations in the NKX2.5 transcription factor known to affect cardiac embryogenesis have been reported.[7] Among cases of Ebstein malformation associated with left ventricular noncompaction, analysis of unrelated probands revealed mutations in the sarcomere gene MYH7, which encodes ß-myosin heavy chain. Family members of mutation-positive probands were also found to have congenital heart disease and/or left ventricular noncompaction.[8,9]

The Baltimore-Washington study, a regional case-control investigation of congenital heart disease, identified the following risk factors among patients with Ebstein malformation as compared to controls: twin gestation, family history of congenital heart disease, white race, prior miscarriages, maternal use of benzodiazepines, and exposure to varnishing agents.[1] Although several retrospective series in the 1970s demonstrated a strong association between lithium exposure and Ebstein malformation, with relative risks as high as 400, this association has since been reevaluated. Cohen et al. examined two recent, controlled cohort studies and estimated the relative risk to be 1.2–7.7.[10]

## Embryology

The tricuspid valve is composed of three leaflets: anterior, mural (also termed inferior or posterior), and septal. Embryologically, the valve leaflets develop from endocardial cushion tissue and become mobile after delamination from the ventricular myocardium. The anterior leaflet delaminates from the supraventricular crest, while the mural and septal leaflets delaminate from the ventricular septum.[11] Tricuspid valve malformations predominantly involve the septal and/or mural leaflets; therefore, failure of delamination from the ventricular septum, in particular, is felt to be a critical step in pathogenesis.

## Pathology

Congenital tricuspid valve malformations that lead to severe tricuspid regurgitation are often divided into two categories. The first is Ebstein malformation, which was first described by Wilhelm Ebstein in 1866[12] and primarily involves apical displacement of the tricuspid valve from the atrioventricular junction. The second, tricuspid valve dysplasia, is characterized by malformation of the tricuspid valve leaflets without displacement.

Among fetuses and neonates with Ebstein malformation (Figure 20.1), the following pathologic characteristics have been described: apical displacement of the septal and/or mural leaflet without displacement of the anterior leaflet from the atrioventricular junction, dysplastic features of the valve leaflets (beyond their displacement), and atrialization of the inlet portion of the right ventricle (with or without thinning of the atrialized myocardium).[13] The redundant and "sail-like" nature of the anterior leaflet may lead to a one-leaflet valve mechanism with anterosuperior displacement of the valve orifice toward the right ventricular outflow tract.[14] Abnormalities of the subvalvar apparatus, including

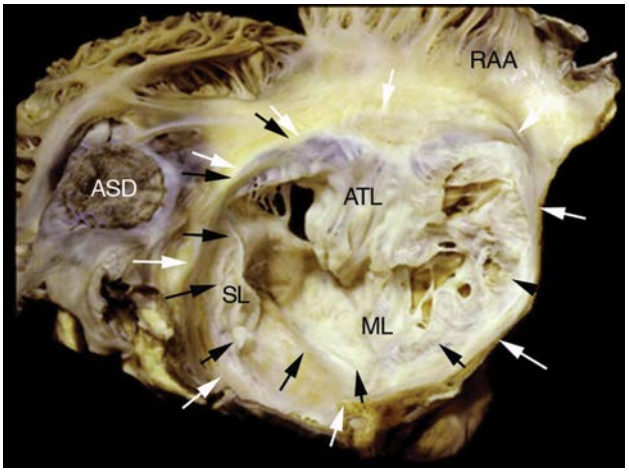


**Figure 20.1**
Autopsied heart of a young boy with Ebstein malformation who had his atrial septal defect (ASD) closed due to cyanosis. The specimen is viewed from the right atrial aspect; the ASD has been closed by a patch, and the right atrial appendage (RAA) is present. The white arrows represent the tricuspid atrioventricular junction, whereas the black arrows represent the displaced attachments of the septal (SL) and mural (ML) leaflets to the underlying myocardium. The anterior leaflet (ATL) is not displaced. The area between the two groups of arrows represents the atrialized right ventricle.

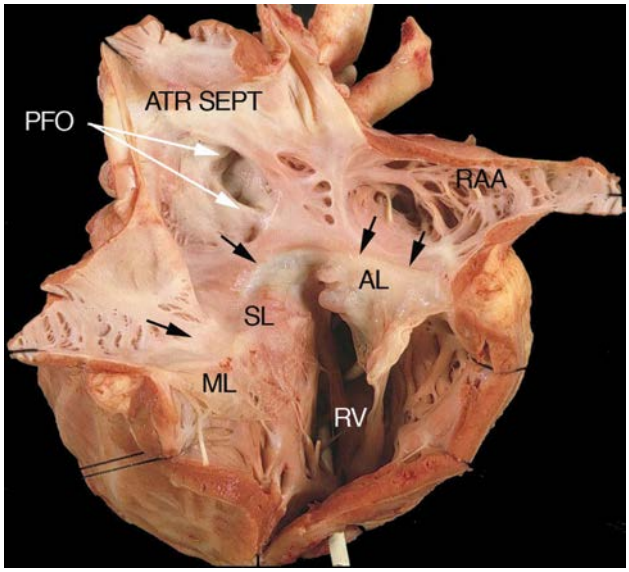


**Figure 20.2**
Specimen viewed from the posterior aspect of the right atrium and right ventricle (RV). A patent foramen ovale (PFO), depicted by the white arrows, is noted in the atrial septum (ATR SEPT). The nondisplaced attachment of the tricuspid valve leaflets to the atrioventricular junction is noted by the black arrows. All three leaflets are abnormal: the septal leaflet (SL) is hypoplastic, and the mural (ML) and anterior (AL) leaflets have nodular thickening with rolling of the edges and abnormal chordae tendinae. (RAA, right atrial appendage.)

anomalous or tethered chordal attachments and/or papillary muscles, further contribute to the morphologic spectrum of Ebstein malformation.

Fetuses and neonates with tricuspid valve dysplasia (Figure 20.2) have nodular thickening and rolling of the leaflet edges without displacement of the valve leaflets from the atrioventricular junction. The septal and mural leaflets are most commonly affected; however, all three leaflets may be involved.[4,13] In severe cases of tricuspid valve dysplasia, all three leaflets may be hypoplastic, tethered, and nonfunctional, leading to a variant of unguarded tricuspid valve.[15–17] In the original pathologic report of an unguarded tricuspid valve orifice by Kanjuh et al., however, the tricuspid valve annulus was noted to be "devoid of any valvular tissue."[18]

Other rare types of congenital tricuspid valve malformations that may lead to regurgitation include a cleft tricuspid valve and deformities associated with Uhl anomaly (absence of the right ventricular myocardium).[19] Tricuspid stenosis is rarely seen in the fetus.

## Associated cardiac defects

Associated cardiac defects are common, and many occur as a consequence of the altered physiology of Ebstein malformation or tricuspid valve dysplasia during fetal development. The most common associated cardiac defect among patients postnatally is a patent foramen ovale or atrial septal defect,[20] which may lead to right-to-left shunting and cyanosis. There is also likely greater than normal physiologic right-to-left shunting *in utero* due to the severity of the tricuspid regurgitation and associated right ventricular dysfunction. Right ventricular outflow tract obstruction may occur in up 40% of patients with Ebstein malformation and 66% with tricuspid valve dysplasia.[13] Etiologies include obstructive chords in the subpulmonary region owing to an abnormal valvar apparatus; hypoplastic infundibulum, which may be due to poor antegrade flow; pulmonary stenosis with abnormal leaflet morphology or dysplasia; and muscular or membranous pulmonary atresia (Figure 20.3). It is important to distinguish between true or anatomic pulmonary atresia and "functional" pulmonary atresia, wherein there is no antegrade flow across the pulmonary valve due to severe tricuspid regurgitation (and elevated pulmonary vascular resistance postnatally) despite normal pulmonary valve leaflets. Hypoplastic pulmonary arteries may be observed, particularly in the context of anatomic pulmonary atresia. A ventricular septal defect, typically of the perimembranous type, may also be present, with or without right ventricular outflow tract obstruction.[4,13,15]

Left-sided lesions may also occur; namely, coarctation, bicuspid aortic valve, and mitral valve prolapse or dysplasia.[20–22] Noncompaction of the left ventricle may be present in up to 18% of adult patients with Ebstein malformation, with effects on both left ventricular systolic and diastolic dysfunction.[22] Ebstein malformation and other tricuspid valve pathology may also occur in the context of congenitally corrected transposition of the great arteries (cc-TGA). Although tricuspid valve pathology may occur in up to 50% of patients

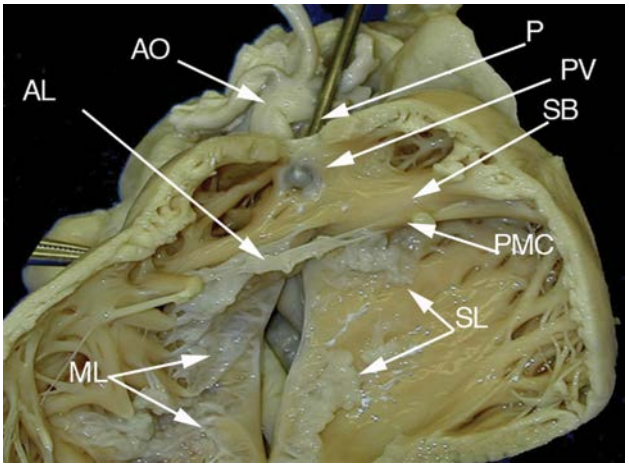


**Figure 20.3**
A 38-week fetopsy specimen with Ebstein malformation and anatomic right ventricular outflow tract obstruction with membranous pulmonary atresia. The specimen is open from the right ventricular aspect. The septal leaflet (SL) of the tricuspid valve is vestigial and displaced from the atrioventricular junction. The mural leaflet (ML) is also displaced. The nondisplaced anterior leaflet (AL) stretches from the anterior papillary muscle to the papillary muscle of the conus (PMC). The supraventricular crest with the septal band (SB) is interposed between the tricuspid valve and the atretic pulmonary valve (PV), which has no evidence of leaflets. A probe has been placed in the pulmonary artery (P) to highlight the anatomic atresia. Of note, the right ventricle is also dilated and thin walled. (AO, aorta.)

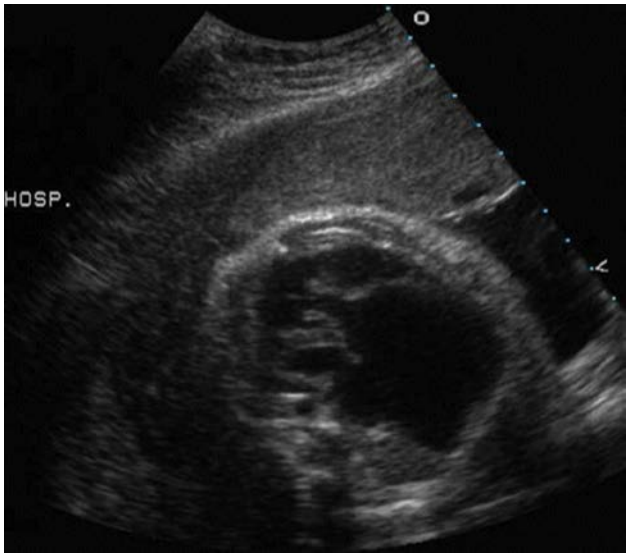


**Figure 20.4**
Significant cardiomegaly that may be observed in fetuses with Ebstein malformation or tricuspid valve dysplasia.

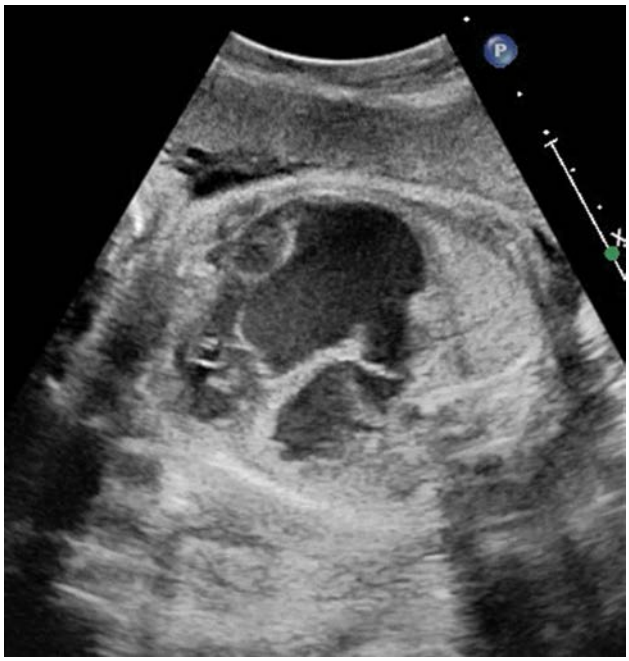


**Figure 20.5**
Ebstein malformation with displacement of the septal leaflet of the tricuspid valve.

with cc-TGA, the morphologic aspects of the valve differ, and significant annular and right ventricular dilation occurs less frequently.[23,24]

Finally, conduction abnormalities may occur in the context of Ebstein malformation. Accessory pathways leading to supraventricular tachycardia and other atrial arrhythmias may be present in up to 17% of children.[25] The likelihood of rhythm disturbances increases with age, regardless of surgical intervention.[26] The incidence of fetal arrhythmias has not been well defined.

# Fetal echocardiography

## *Pathophysiology*

Fetuses with tricuspid valve pathology are often detected due to cardiomegaly, with dilation of the right heart in particular on the four-chamber view (Figure 20.4). The ability to discern Ebstein malformation or tricuspid valve dysplasia by fetal echocardiography is possible[27] (Figures 20.5 and 20.6, Videos 20.1 through 20.4). However, the lesions exist along a spectrum. Regardless of the underlying pathology, tricuspid regurgitation is the common pathophysiologic insult, producing a volume load on both the right atrium and ventricle that may lead to ventricular dysfunction and progression of disease throughout gestation. As such, fetuses diagnosed with tricuspid valve pathology should be followed closely throughout gestation with serial echocardiograms.

In cases of severe right ventricular outflow tract obstruction, that is, pulmonary stenosis or anatomic pulmonary atresia, the flow in the ductus arteriosus is retrograde (left-to-right) to supply blood flow to the pulmonary arteries from early in gestation. Functional pulmonary atresia, on the other hand, may develop throughout the course of gestation as blood is unable to be ejected antegrade. The right atrium is a more compliant chamber than the right ventricle. Severe tricuspid regurgitation

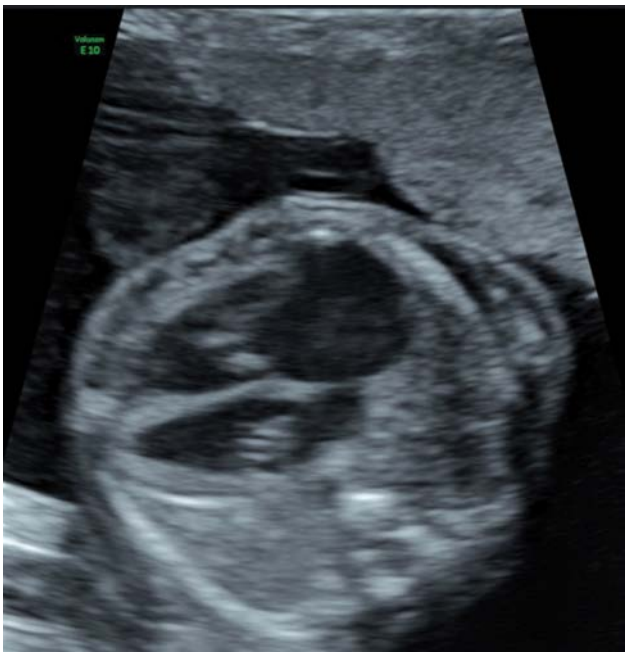

**Figure 20.6**
Tricuspid valve dysplasia with abnormal but nondisplaced leaflets from the atrioventricular junction.

also produces a chronic volume overload on the right ventricle, which may exacerbate underlying myocardial abnormalities. Systolic dysfunction may ensue, and the right ventricle may fail to generate adequate pressure to eject antegrade. Therefore, as disease progresses, flow in the ductus arteriosus may reverse from antegrade (right-to-left) to retrograde (left-to-right) to supply the pulmonary arteries (Figure 20.7).

In the most severe cases, the development of functional pulmonary atresia with retrograde flow in the ductus arteriosus leads to pulmonary regurgitation (Figure 20.8, Video 20.5). This may occur as a result of the increased afterload (systemic fetal blood pressure from the ductus arteriosus) onto an already struggling right ventricle that cannot generate pressure. Pulmonary regurgitation is a particularly ominous sign, since it completes the vicious cycle of ineffective blood flow known as "circular shunting" (Figure 20.9). With circular shunting, blood that enters the right ventricle as a result of pulmonary regurgitation subsequently passes into the right atrium due to the tricuspid valve pathology. As in the normal intrauterine circulation, blood flows right to left across the foramen ovale and passes through the left side of the heart into the aorta. In the aorta, however, blood proceeds retrograde through the ductus arteriosus and regurgitates back through the pulmonary valve into the right ventricle for the vicious cycle to begin anew. This ineffective shunting exacerbates the volume overload on the right heart, leading to further cardiomegaly and lung compression, and, most importantly, steals from the fetus's systemic circulation. If this physiology continues postnatally, then blood flow also bypasses the pulmonary capillary bed for gas exchange, producing a lethal combination of cyanosis and low cardiac output.

There are two other important mechanisms by which severe tricuspid regurgitation may produce low cardiac output in the fetus. First, the right atrium may become massively dilated and bow into the left atrium. With the atrial septum abutting the lateral wall of the left atrium, flow across the foramen ovale may become diminished. Indeed, the size of the foramen ovale has been noted to correlate with left ventricular output in fetuses with Ebstein malformation.[28] Furthermore, right ventricular dilation, with septal displacement and paradoxical septal wall motion, leads to abnormal left ventricular geometry, diminished left ventricular filling, and impaired left ventricular systolic function.[29,30] In a series of 31 fetuses with severe tricuspid valve disease, Inamura et al. found worse left ventricular myocardial performance in patients with pulmonary atresia or regurgitation, as compared to fetuses with antegrade pulmonary blood flow. Poor left ventricular myocardial performance was associated with fetal demise or neonatal death.[31]

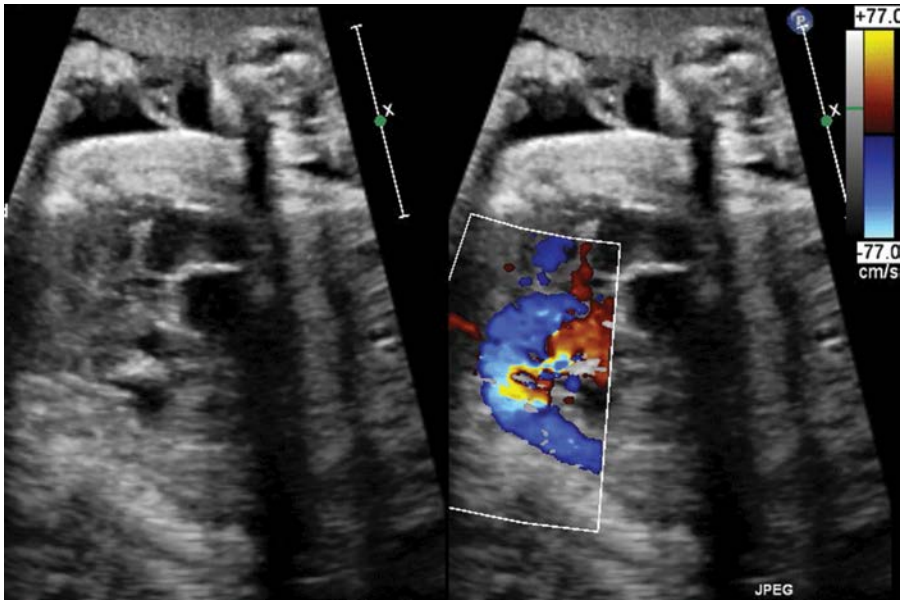


**Figure 20.7**
Retrograde (left-to-right) flow through the ductus arteriosus in a fetus with severe Ebstein malformation and functional pulmonary atresia.

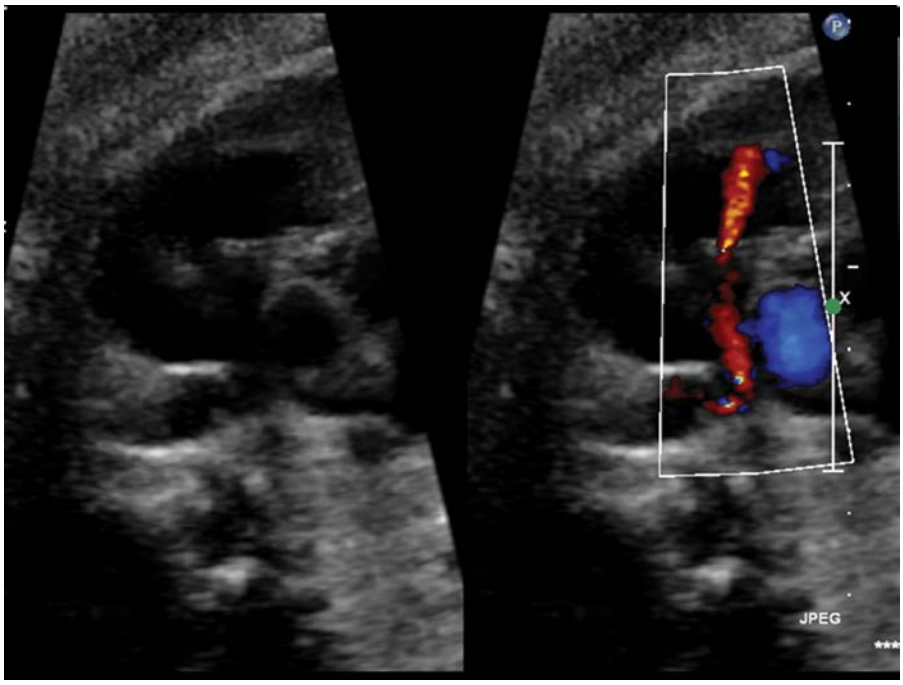


**Figure 20.8**
In addition to retrograde flow through the ductus arteriosus, this fetus has developed pulmonary regurgitation, which completes the cycle of circular shunting.

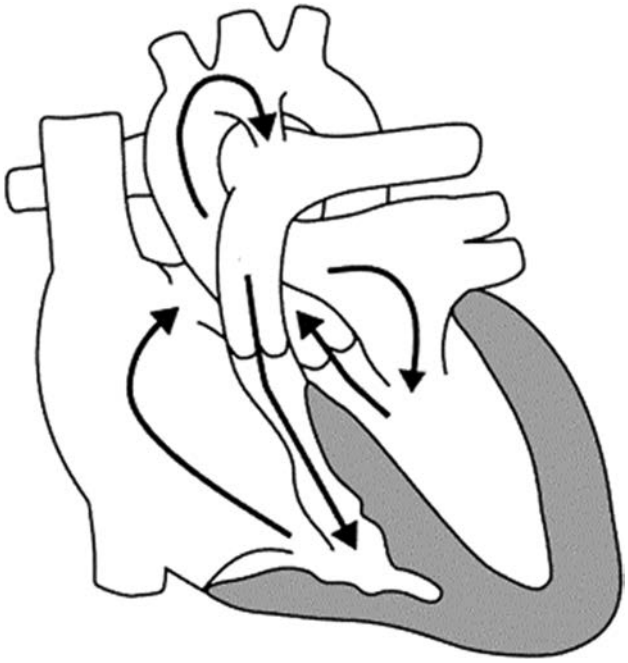

**Figure 20.9**
This cartoon depicts circular shunting physiology in the context of severe tricuspid regurgitation in the fetus or neonate. (Adapted with permission from Wald RM et al. *Am J Cardiol* 2005;96(6):851–6.[50])

Finally, Ebstein malformation or tricuspid valve dysplasia may produce hydrops in the fetus (Figure 20.10, Video 20.6), presumably as a result of elevated right atrial and systemic venous pressures from severe tricuspid regurgitation. The combination of hydrops and low cardiac output likely accelerates diminished end-organ perfusion and acidosis and leads to the high rate of fetal demise.[4,5,15] In a case-control investigation of fetuses with various types of cardiac pathology, those with Ebstein malformation or tricuspid valve dysplasia had among the highest prevalence of fetal demise at 27%.[32]

## *Predictors of perinatal mortality*

Given the high rate of fetal demise and neonatal death, multiple investigators have attempted to define risk factors for perinatal mortality based on fetal echocardiographic findings. The right atrial area index is a measure that was first reported in fetuses and neonates with tricuspid valve disease in 1989. This index is the ratio of the area of the right atrium and atrialized right ventricle to the area of the functional right ventricle and left heart from a four-chamber view. Roberson et al. initially demonstrated that higher ratios were associated with perinatal mortality.[33] Celermajer et al. applied this index to a larger group of neonates and demonstrated that incrementally higher ratios correlated with greater mortality.[34] However, the right atrial area index has had inconsistent associations with mortality in more recent fetal series,[35,36] which may be due to the difficult nature of reliably measuring fetal cardiac areas.

Nearly all studies have found that lack of antegrade pulmonary blood flow and/or retrograde flow in the ductus arteriosus is associated with perinatal mortality.[36–39] In fact, Barre et al. demonstrated that the presence or absence of antegrade pulmonary blood flow alone was just as reliable a prognostic factor as more complex scoring systems developed to predict mortality.[35] Additional factors that have been reported to predict perinatal mortality include earlier era of medical and surgical management, increased cardiothoracic area ratio, depressed right or left ventricular systolic function, reduced right ventricular pressure, and the presence of fetal distress.[36–40]

Until recently, the literature on this topic consisted of small, single-center case series, often spanning multiple decades to

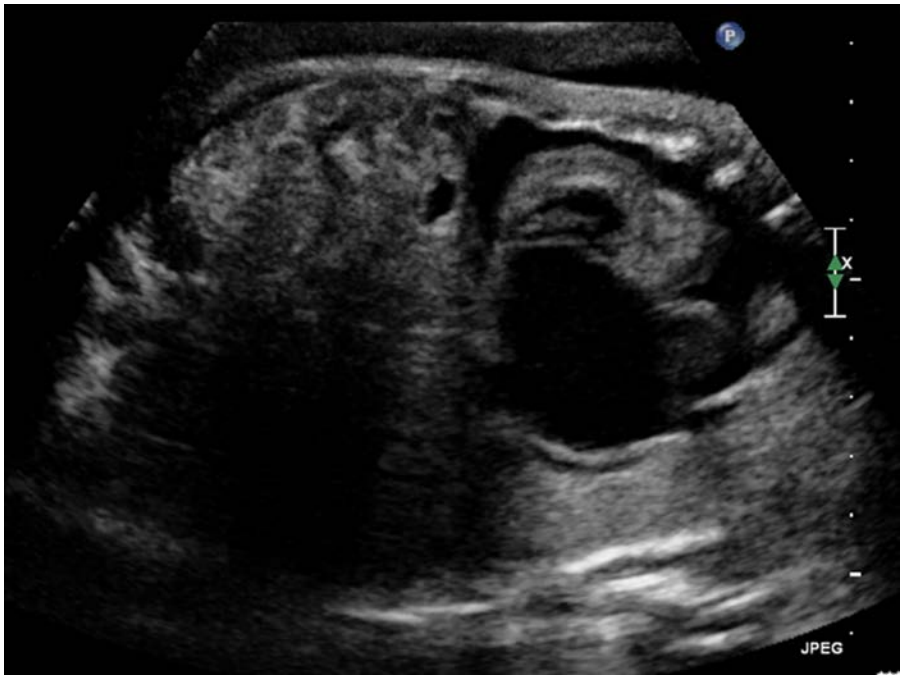


**Figure 20.10**
Sagittal image illustrating a fetus with cardiomegaly and hydrops (pericardial effusion, ascites, and subcutaneous edema) due to tricuspid valve dysplasia.

capture sufficient patients for analysis. In addition, owing to limited sample sizes, these studies were not able to analyze hemodynamic factors at different times in gestation. In 2015, Freud et al. published a contemporary series of 243 fetuses with Ebstein malformation or tricuspid valve dysplasia from 23 centers across North America. The following clinical and echocardiographic factors were found to be predictive of perinatal mortality at the time of diagnosis: gestational age less than 32 weeks, larger tricuspid valve annulus *z*-score, the presence of pulmonary regurgitation, and a pericardial effusion. The larger tricuspid valve annulus *z*-score represented greater right-sided dilation, while the presence of a pericardial effusion was often a harbinger for the development of hydrops. Pulmonary regurgitation emerged as a potent hemodynamic predictor of risk, indicating circular shunt physiology. In fact, fetuses that developed pulmonary regurgitation at any point during gestation were nearly twice as likely to experience fetal demise or neonatal death.[5]

Since disease often progresses throughout the course of gestation, an analysis of late gestation (>30 weeks) echocardiographic findings in 160 fetuses was also performed. A larger cardiothoracic area ratio, indicating greater cardiomegaly; a lower tricuspid regurgitation jet velocity, reflective of a failing right ventricle; lack of antegrade pulmonary blood flow; and depressed left ventricular systolic function were associated with perinatal mortality.[5]

# Management

## *Prenatal management and counseling*

When Ebstein malformation or tricuspid valve dysplasia is diagnosed prenatally, evaluation for extracardiac anomalies and chromosomal abnormalities should be performed. As mentioned previously, up to 28% of cases may be syndromic, and outcomes of congenital heart disease, in general, are known to be affected by such diagnoses.[41–43] Magnetic resonance imaging to assess fetal lung volumes (Figure 20.11) may be considered to assist with both prognosis and perinatal management.[44] However, the lung hypoplasia that results from severe tricuspid valve disease is histologically distinct from that which develops as a result of other conditions that affect fetal lung growth and maturity; namely, congenital diaphragmatic hernia.[45] Therefore, further investigations are necessary to understand the implications of low fetal lung volumes in this setting.

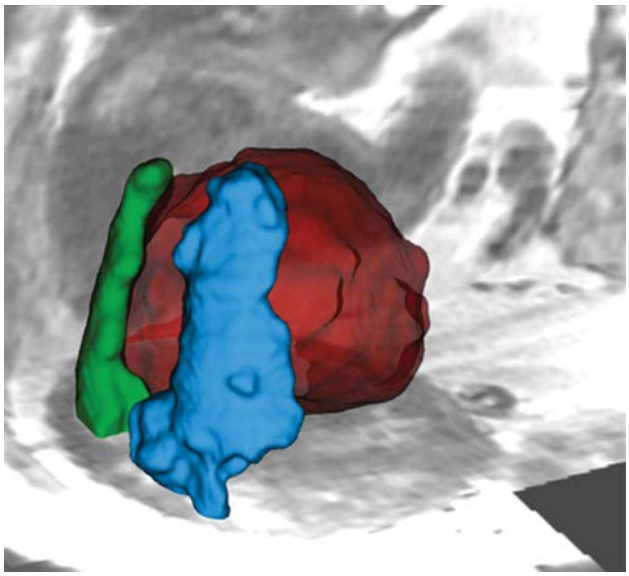

**Figure 20.11**
Reconstructed magnetic resonance image of hypoplastic lungs (depicted in green and blue) as a result of severe cardiomegaly (red) in a fetus with Ebstein malformation.

Since disease progresses throughout gestation, serial fetal echocardiograms are essential. Mild disease in the second trimester may rapidly advance to severe disease in the third trimester. Reliable predictors of disease progression are currently unknown, which is important to discuss at the time of counseling. In the third trimester, there should be a low threshold for performing nonstress testing or a biophysical profile.[46] Whether an abnormal test would indicate delivery, however, is an important question that would need to be discussed carefully with the obstetrical team, particularly in light of the gestational age of the fetus. Premature delivery of infants with congenital heart disease, in general, and severe tricuspid valve disease, in particular, is associated with worse neonatal outcomes, even when delivery occurs at 36 or 37 weeks' gestational age.[5,47,48] To date, no transplacental or interventional therapies for the prevention or treatment of fetal arrhythmias, ventricular dysfunction, or hydrops associated with severe tricuspid valve disease have been systematically evaluated.

## *Postnatal management*

Fetuses with severe tricuspid valve disease often have difficulty transitioning to a neonatal circulation. Inadequate pulmonary blood flow and lung hypoplasia contribute to cyanosis, while ventricular dysfunction and poor left ventricular filling may produce low cardiac output. In the most severe cases, circular shunting physiology leads to both profound cyanosis and low cardiac output, and death in the delivery room may occur. Therefore, delivery of fetuses with high-risk physiology in the third trimester, as defined by Freud et al.,[5] should be a coordinated effort among obstetrical, cardiac, and neonatal teams.[49]

The most important initial strategy for neonates with severe tricuspid valve disease and functional pulmonary atresia or pulmonary regurgitation is to lower the pulmonary vascular resistance with oxygen, nitric oxide, and/or phosphodiesterase inhibitors and avoid prostaglandin therapy. Once the pulmonary artery pressure is lower than the right ventricular pressure, the pulmonary valve will open, and antegrade pulmonary blood flow will ensue, with improved left ventricular filling. Cyanosis should be tolerated, as long as end-organ perfusion is adequate. As in the fetus, the ductus arteriosus plays a pathologic role by limiting antegrade pulmonary blood flow and promoting circular shunting. If prostaglandin therapy is necessary for profound cyanosis, then the neonate should be trialed off as soon as feasible, with close hemodynamic monitoring in the intensive care unit.[50] In the most severe cases of high pulmonary vascular resistance despite aggressive pulmonary vasodilation and evolving cardiogenic shock, extracorporeal membrane oxygenation may be necessary.

With intensive medical management and sufficient time for the pulmonary vascular resistance to fall, some neonates, even with severe tricuspid regurgitation and circular shunting at birth, will be able to avoid surgery in the neonatal period. For other neonates, there are a range of catheter-based or surgical interventions depending on the patient's anatomy and physiology. For cases of functional pulmonary atresia where medical management is the first-line therapy, as described previously, there are instances in which the right ventricle has recovered and is ejecting antegrade, but hemodynamic instability persists due to patency of the ductus arteriosus. Therefore, ductal ligation may be necessary.[50] In cases of right ventricular outflow tract obstruction, that is, pulmonary stenosis or anatomic pulmonary atresia, patients will require prostaglandin therapy until either a catheter-based or surgical intervention is performed to relieve the obstruction.

Occasionally, the neonate is unable to be weaned from support, but the right ventricle is felt to be adequate. In such instances, repair of the tricuspid valve may be attempted. Knott-Craig et al. have reported up to 74% survival with this approach. However, survival was significantly diminished when anatomic pulmonary atresia was present.[51–53] If the right ventricle is either hypoplastic or persistently failing and/or anatomic pulmonary atresia is present, then a neonatal biventricular repair may not be feasible. An aortopulmonary shunt may be placed to augment pulmonary blood flow, with a biventricular, one-and-a-half ventricular, or univentricular approach pursued later. Alternatively, a right ventricular exclusion procedure, also known as the Starnes procedure, may be performed. This operation involves fenestrated tricuspid valve closure with right atrioplasty and ventriculoplasty and placement of an aortopulmonary shunt with main pulmonary artery ligation. Neonatal hospital survival of 69% was reported by Starnes and colleagues, with survivors proceeding to the Glenn and Fontan operations to complete univentricular palliation. Intermediate-term follow-up demonstrated regression of right ventricular size, creating less septal impingement and normalization of left ventricular systolic function.[54–56]

# Outcomes beyond the neonatal period

Despite high perinatal mortality, survival improves substantially beyond the neonatal period. In a series of fetuses and neonates, Yu et al. reported 1- and 5-year survival of 78% and 76%, respectively.[36] Similarly, Kapusta et al. found that, despite early mortality, survival stabilized by 3 years of age at 80%, with little attrition throughout older childhood and adolescence.[57] Various series have reported that approximately one-third of patients will require surgery at some point.[57,58] Although arrhythmias are less common early in life,[25] increased arrhythmia burden with age contributes to morbidity and impaired quality of life.[26,58,59] Women with Ebstein malformation may become pregnant, but they are at increased risk of adverse cardiac events, with higher rates of cesarean section and preterm delivery, and warrant close monitoring throughout pregnancy.[26,60,61]

# Videos

**Video 20.1** (https://youtu.be/Y1eZs-Wqn5Y)
Ebstein's malformation with displacement of the septal leaflet of the tricuspid valve. Severe right atrial and ventricular dilation is present.

**Video 20.2** (https://youtu.be/afAe59_YcRE)
Color Doppler images of Ebstein's malformation, demonstrating severe tricuspid regurgitation.

**Video 20.3** (https://youtu.be/_6NQ0C1HXII)
Tricuspid valve dysplasia with thickened and restricted, but non-displaced, leaflets. Severe right atrial and ventricular dilation is also present.

**Video 20.4** (https://youtu.be/huDU9RQ5tjA)
Color Doppler images of tricuspid valve dysplasia, demonstrating severe tricuspid regurgitation.

**Video 20.5** (https://youtu.be/89oQohdQQVs)
In addition to retrograde flow through the ductus arteriosus, this fetus has developed pulmonary regurgitation, which completes the cycle of circular shunting. A pericardial effusion is also present. This patient was delivered at 37 weeks and died in the delivery room.

**Video 20.6** (https://youtu.be/RKwNhoVo1-M)
Third-trimester fetus with hydrops and biventricular systolic dysfunction.

# References


1. Correa-Villasenor A et al. *Teratology* 1994;50(2):137–47.
2. Hoffman JI, Kaplan S. *J Am Coll Cardiol* 2002;39(12):1890–900.
3. Talner CN. *Pediatrics*, 1980;65(Suppl):375–461. *Pediatrics*. 1998;102(1 Pt 2):258–9.
4. Sharland GK et al. *J Am Coll Cardiol* 1991;17(4):944–9.
5. Freud LR et al. *Circulation* 2015;132(6):481–9.
6. Digilio MC et al. *Am J Med Genet A* 2011;155A(9):2196–202.
7. Gioli-Pereira L et al. *Int J Cardiol* 2010;138(3):261–5.
8. Postma AV et al. *Circ Cardiovasc Genet* 2011;4(1):43–50.
9. van Engelen K et al. *Neth Heart J* 2013;21(3):113–7.
10. Cohen LS et al. *JAMA* 1994;271(2):146–50.
11. Lamers WH et al. *Circulation* 1995;91(1):111–21.
12. van Son JA et al. *Eur J Cardiothorac Surg* 2001;20(5):1082–5.
13. Lang D et al. *J Am Coll Cardiol* 1991;17(5):1161–7.
14. Schreiber C et al. *J Thorac Cardiovasc Surg* 1999;117(1):148–55.
15. Hornberger LK et al. *J Am Coll Cardiol* 1991;17(1):167–73.
16. Wong KK et al. *Cardiol Young* 2004;14(5):557–9.
17. Mohan JC et al. *Int J Cardiol* 2000;74(2–3):153–7.
18. Kanjuh VI et al. *Circulation* 1964;30:911–7.
19. Vaujois L et al. *Cardiol Young* 2015;25(3): 580–3.
20. Barbara DW et al. *Cardiovasc Pathol* 2008;17(3):166–71.
21. Gerlis LM et al. *Am J Cardiovasc Pathol* 1993;4(4):294–301.
22. Attenhofer Jost CH et al. *Mayo Clin Proc* 2005;80(3):361–8.
23. Anderson KR et al. *Circulation* 1978;58(3 Pt 2):I87–91.
24. Silverman NH et al. *Am J Cardiol* 1995;76(17):1277–83.
25. Delhaas T et al. *Pediatr Cardiol* 2010;31(2):229–33.
26. Brown ML et al. *J Am Coll Cardiol* 2008;52(6):460–6.
27. Oberhoffer R et al. *Br Heart J* 1992;68(6):580–5.
28. Pavlova M et al. *Am Heart J* 1998;135(6 Pt 1):1081–5.
29. Ishii T et al. *Ultrasound Obstet Gynecology* 2012;40(1):55–61.
30. Lasa JJ et al. *Prenat Diagn* 2012;32(3):245–51.
31. Inamura N et al. *Am J Perinatol* 2005;22(2):91–7.
32. MacColl CE et al. *Pediatr Cardiol* 2014;35(8):1403–14.
33. Roberson DA, Silverman NH. *J Am Coll Cardiol* 1989;14(5): 1300–7.
34. Celermajer DS et al. *J Am Coll Cardiol* 1992;19(5):1041–6.
35. Barre E et al. *Pediatr Cardiol* 2012;33(8):1391–6.
36. Yu JJ et al. *Pediatr Cardiol* 2013;34(7):1590–6.
37. Yetman AT et al. *Am J Cardiol* 1998;81(6):749–54.
38. McElhinney DB et al. *Am J Cardiol* 2005;96(4):582–6.
39. Andrews RE et al. *Am J Cardiol* 2008;101(7):1046–50.
40. Freire G et al. *Cardiol Young* 2014;24(6):1049–56.
41. Anaclerio S et al. *Ital Heart J* 2004;5(8):624–8.
42. Michielon G et al. *J Thorac Cardiovasc Surg* 2009;138(3): 565–70 e2.
43. Patel A et al. *Ann Thorac Surg* 2010;89(6):1805–13; discussion 13–4.
44. Nathan AT et al. *Fetal Diagn Ther* 2010;27(2):101–5.
45. Tanaka T et al. *Pediatr Cardiol* 1998;19(2):133–8.
46. Donofrio MT et al. *Circulation* 2014;129(21):2183–242.
47. Costello JM et al. *Pediatrics* 2010;126(2):277–84.
48. Costello JM et al. *Circulation* 2014;129(24):2511–7.
49. Donofrio MT et al. *J Am Soc Echocardiogr* 2015;28(11): 1339–49.
50. Wald RM et al. *Am J Cardiol* 2005;96(6):851–6.
51. Knott-Craig CJ et al. *Ann Thorac Surg* 2000;69(5):1505–10.
52. Knott-Craig CJ et al. *Ann Thorac Surg* 2002;73(6):1786–92; discussion 92–3.
53. Knott-Craig CJ et al. *Ann Thorac Surg* 2007;84(2):587–92; discussion 92–3.
54. Starnes VA et al. *J Thorac Cardiovasc Surg* 1991;101(6): 1082–7.
55. Reemtsen BL et al. *J Thorac Cardiovasc Surg* 2006;132(6): 1285–90.
56. Reemtsen BL et al. *J Thorac Cardiovasc Surg* 2007;134(6):1406–10; discussion 10–2.
57. Kapusta L et al. *Eur Heart J* 2007;28(21): 2661–6.
58. Celermajer DS et al. *J Am Coll Cardiol* 1994;23(1):170–6.
59. Attie F et al. *Medicine (Baltimore)* 2000;79(1):27–36.
60. Katsuragi S et al. *Am J Obstet Gynecol* 2013;209(5):452 e1–6.
61. Lima FV et al. *Arch Cardiovasc Dis* 2016;109(6–7):390–8.

# 21

# Intracardiac shunt malformations

Einat Birk and Norman H. Silverman

Intracardiac malformations leading to a cardiac left-to-right shunt postnatally include atrial septal defects (ASDs), atrioventricular septal defects (AVSDs), and ventricular septal defects (VSDs). These lesions constitute the largest group of cardiac defects detected during fetal life, the most common being VSD and AVSD.[1,2]

## Defects of the atrial septum

### *Anatomy*

An ASD is a common congenital defect seen in children, occurring in 1 in 1500 live births.[3] It can present as an isolated defect or in association with complex congenital heart defects. Several mechanisms cause the formation of an atrial communication, leading to several defect types (Figure 21.1):

- Secundum ASD
- Primum ASD (also named AVSD—partial or transitional type)
- Sinus venosus ASD (superior and inferior types)
- Coronary sinus ASD

Secundum ASD is the most common atrial communication in children. It occurs when the septum primum fails to cover the oval fossa, which is patent and allows right-to-left flow of oxygenated blood to the heart and brain during fetal life. This failure of the septum primum can result in a single defect or fenestrated defect, as well as a wide range of defect sizes.

A primum ASD involves the lower part of the atrial septum and is part of the AVSD spectrum, which is discussed separately.

A sinus venosus ASD is located in the posterosuperior or posteroinferior portion of the atrial septum. The superior defect is the more common, lying at the junction of the superior vena cava, right upper pulmonary vein, and atrial septum. The superior vena cava appears to override the defect, which tends to be large. The inferior defect occurs at the junction of the inferior vena cava and the atrial septum. It is a less common defect and also tends to be of significant size. These defects result from a developmental malformation in the sinus venosus or from a primary failure in the partitioning of the true embryonic septum secundum.[4]

A coronary sinus ASD is a rare defect believed to occur when the atrio-sinus venosus fold fails to form. Therefore, instead of the normal draining of the coronary sinus into the right atrium via its usual orifice, there is a persistence of the wide communication between the sinus venosus and both atria, allowing a left-to-right shunt after birth.[4] Persistent left superior vena cava terminating in the left atrium is almost always present. Unlike a large coronary sinus receiving a persistent left superior vena cava that eventually drains into the right atrium, this defect allows a communication between the two atria, and the left superior vena cava drains directly into the left atrium.

During fetal life, the normal atrial communication at the oval fossa allows right-to-left atrial flow, allowing oxygen-rich blood to flow to the left heart and, consequently, to the brain and the heart. Some time after birth, following the normal decrease in pulmonary pressure and resistance, and immediate increase of systemic vascular resistance caused by the loss of the placenta, the foramen should close and prevent intra-atrial shunting. The foraminal mechanism has been found to be substantially less efficient than was previously believed, since the advent of modern postnatal cardiac ultrasound has shown that a substantial number of infants under 6 months of age have intra-atrial left-to-right shunts. This is due to incomplete closure of the fossa ovalis by the septum primum.

When the septum primum is deficient, the right atrial and ventricular pressure decreases gradually as the compliance increases, leading to a predominant left-to-right shunting across the atrial communication. The amount of left-to-right shunting is determined by the size of the atrial defect and by the relative atrial and ventricular diastolic pressure differences.

## Ostium secundum atrial septal defect

During fetal life, there is normally a communication between the right and left atria, which is located at the secundum septum, namely, the foramen ovale. Relatively oxygenated blood streams from the ductus venosus via the inferior vena cava and into the left atrium by diverting the septum primum flap, which lies on the left side of the septum. This flap of atrial tissue is pushed open during most

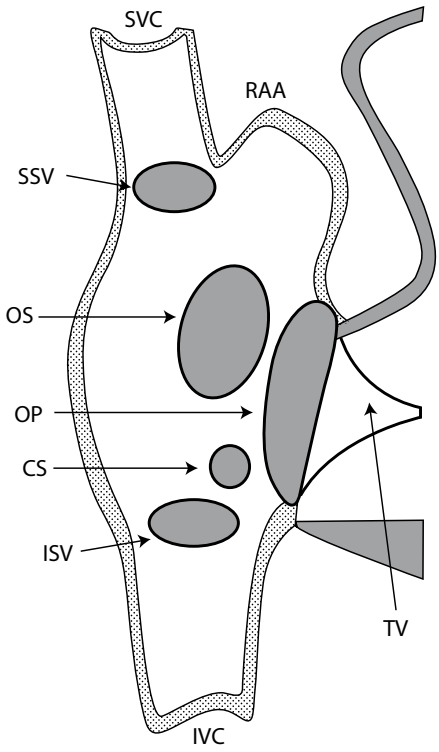


**Figure 21.1**
The different types of interatrial septal communications as seen from the right aspect of the atrial septum. (CS, coronary sinus; ISV, inferior sinus venosus; IVC, inferior vena cava; OP, ostium primum; OS, ostium secundum; RAA, right atrial appendage; SSV, superior sinus venosus; SVC, superior vena cava; TV, tricuspid valve.)

of the cardiac cycle. The foramen ovale lies in the middle third of the atrial septum and grows with gestation. The normal foramen size is similar to the aortic diameter[5] and grows from approximately 3 mm at 20 weeks of gestation to 8 mm at term.[6]

After birth, placental flow is eliminated, and two processes occur: pulmonary venous flow increases and left atrial pressure rises above right atrial pressure. The flap of the septum primum is then pushed against the foramen ovale, leading to a functional closure of the atrial communication. Only when this flap valve mechanism fails to close the foramen ovale is the communication termed a *secundum defect*. Since the size of the fetal foramen ovale and the primum flap varies widely in the normal fetus, it is impossible to predict the failure of the closure process during fetal life. Therefore, in contrast with postnatal life, when a secundum ASD is the most common atrial defect, the fetal diagnosis of such an ASD possesses inherent difficulty and is rarely possible.[1]

Ostium secundum ASD can be a part of many forms of complex congenital heart defect, from anomalies of pulmonary venous return through to coarctation of the aorta. It is an essential part of defects such as tricuspid atresia. As in an isolated defect, it is rarely associated with extracardiac anomalies or genetic disorders.

## Ostium primum atrial septal defect (partial atrioventricular septal defect)

One of the most commonly diagnosed atrial communications *in utero* is the primum ASD.[1] This lesion is a form of common atrioventricular canal defect without a ventricular component. In this defect, the lower portion of the atrial septal fusion to the underlying atrioventricular valve junction is absent; both atrioventricular valves are attached to the crest of the ventricular septum and lose their normal differential appearance. The left atrioventricular valve is referred to as being "cleft," showing a commissure between the primitive anterosuperior and posteroinferior bridging leaflets. Mild degrees of valvar insufficiency from this site can be detected in some fetuses. The four-chamber view is a useful plane in detecting this lesion. With this plane, a series of scans should be looked at in a sequential fashion in order to define appropriate morphological information (Figure 21.2). The posterior cross-sectional cut reveals the coronary sinus emptying into the right atrium just above the tricuspid valve. This view may lead to the impression that both atrioventricular valves insert into the ventricular septum at the same level. However, a more anterior coronal cut will show that both atrioventricular valves open and close with their normal differential insertion. This cut is also ideal for color Doppler interrogation of both valves. A more anterior angulation will reveal the left ventricular outflow tract including the aortic valve and ascending aorta. The coronal cut where both atrioventricular valves open is probably the most useful in the diagnosis of a primum ASD (Figure 21.3a). In this view, the lower atrial septum is missing, and both atrioventricular valves insert into the ventricular septum at the same level. A mild degree of left atrioventricular valve insufficiency may be detected as well as occasional right atrioventricular valve insufficiency. The more posterior cut, where the coronary sinus is displayed together with the tricuspid valve, can lead to the false impression that both atrioventricular valves are at the same level, leading to the erroneous diagnosis of a primum ASD. This error is even more likely to occur when the coronary sinus is enlarged (Figure 21.3b). This is the case when a persistent left superior vena cava drains into the coronary sinus; however, this vessel can usually be detected from other views. The cleft in the left atrioventricular valve is best seen in a cross section from the parasternal or subcostal short-axis views.

When a primum ASD is detected, a complete sequential analysis of the heart is mandatory. Primum ASD is associated with situs anomalies such as right or left atrial isomerism, when the atrial septum tends to be small, leading to the appearance of a common atrium. Left heart hypoplasia, subaortic narrowing, and coarctation of the aorta are known associated anomalies. A secundum ASD is a common associated finding. Primum ASD is associated with extracardiac anomalies, the most common being trisomy 21. It has also been rarely associated with DiGeorge syndrome and Ellis-van

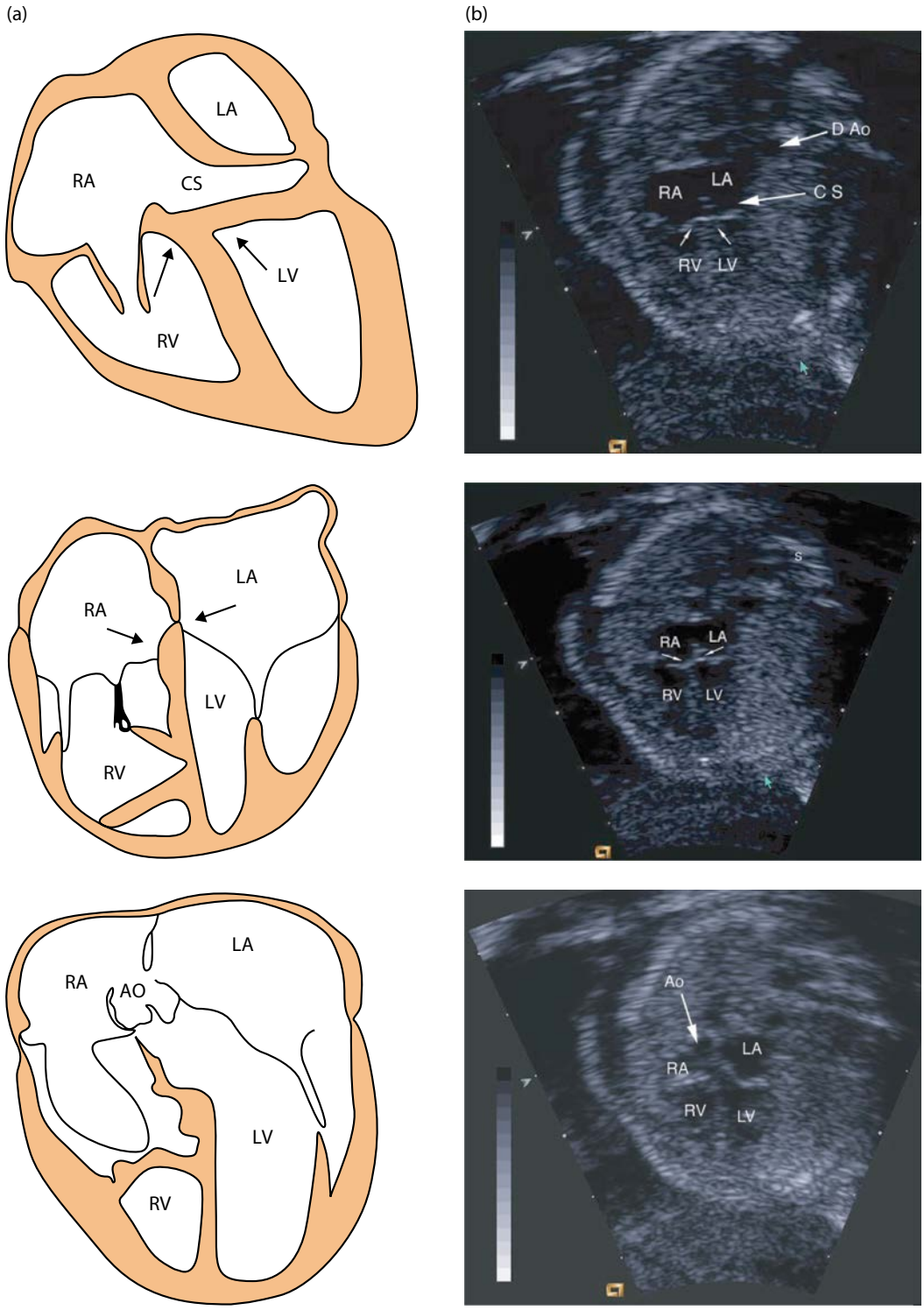


**Figure 21.2**
(a) A series of four-chamber cuts as scanned from the back to the front of the heart. (Top) Posterior cross-sectional cut reveals the coronary sinus (CS) emptying into the right atrium (RA) just above the tricuspid valve. This view may lead to a false impression that both atrioventricular valves insert into the ventricular septum at the same level (arrows). (Middle) A more anterior conventional four-chamber cut will show that both atrioventricular valves open and close with their normal differential insertion (arrows). This cut is also ideal for color Doppler interrogation of both valves. (Bottom) A more anterior cut will reveal the left ventricular (LV) outflow tract including the aortic valve (AO) and ascending aorta. The coronal cut where both atrioventricular valves open is probably the most useful in the diagnosis of a primum atrial septal defect. (b) (Top-bottom) This series of ultrasonic cuts in the four-chamber plane corresponds to the series shown in Figure 21.2a. (LA, left atrium; RV, right ventricle; D Ao, descending aorta.)

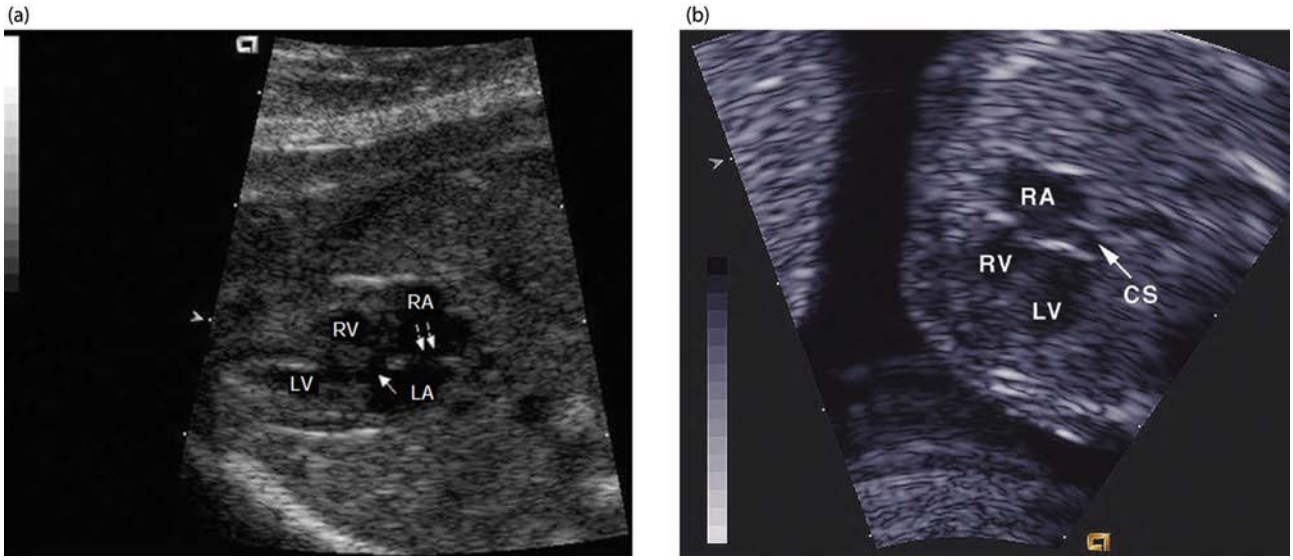


**Figure 21.3**
(a) The heart is imaged in the four-chamber view showing both atrioventricular valves inserting into the ventricular septum at the same level. The single arrow points to the missing lower atrial septum, indicating the presence of a primum atrial septal defect. The double arrow points to the foramen ovale, the site of a normal fetal atrial communication. (b) This frame is a four-chamber cut showing the enlarged coronary sinus (CS, arrow) entering the right atrium (RA), which reflects the increased flow from a persistent left superior vena cava entering the upper portion of the coronary sinus. The coronary sinus enlargement may give the false impression of an ostium primum type of interatrial communication.

Creveld syndrome. Karyotyping should be performed when the diagnosis of primum ASD is made.

## Sinus venosus and coronary sinus atrial septal defect

To the best of our knowledge, both sinus venosus and coronary sinus ASDs have not yet been reported in the fetus. These lesions are rarely associated with cardiac, extracardiac, or chromosomal anomalies.

### *Natural history and outcome*

Small secundum ASDs usually close spontaneously during the first 2 years of life. Defects persisting beyond 2 years of age tend to stay open and lead to a left-to-right atrial shunting of variable amount.

Primum ASDs (or partial AVSDs) do not close spontaneously and usually lead to a significant left-to-right shunting as well as the risk of pulmonary hypertension and pulmonary vascular disease. Some will develop substantial insufficiency of the left atrioventricular valve.

Sinus venosus ASDs never close spontaneously and almost always have a large concomitant left-to-right atrial shunt.

Even patients with a large left-to-right atrial shunt may be asymptomatic for many years. Some will develop right ventricular dysfunction and atrial arrhythmias during late adult life. A serious but rare complication is the development of secondary pulmonary hypertension and pulmonary artery thrombosis. Closing the defect can prevent all complications. For most secundum defects, transcatheter closure has become available in many centers. Larger defects as well as all primum and sinus venosus atrial septal defects have to be closed surgically. The closure of a primum ASD involves repair of the left atrioventricular valve. Some of these patients will eventually need additional surgery for left atrioventricular valve repair or replacement. A smaller group will require further surgery to alleviate progressive obstruction of the left ventricular outflow tract. While life quality and expectancy after secundum ASD repair during childhood are similar to those of the general population,[7] patients following primum ASD repair have somewhat poorer results. Approximately 10% will need repeated surgery, and life expectancy is shorter than that of the normal population.[8] When a primum defect is associated with left heart anomalies such as hypoplasia of the left atrioventricular valve, hypoplasia of the left ventricle, subaortic obstruction, or coarctation of the aorta, the overall prognosis is guarded. In rare cases the left heart hypoplasia will not allow a biventricular repair, leading to palliative solutions such as the Fontan-type repair.

### *Restrictive foramen ovale*

As discussed previously, the normal fetal foramen ovale has a wide range of what is considered to be normal size. The normal flow across it is of low velocity, ranging between 20 and 40 cm/s on pulsed Doppler.[6] Restrictive flow across it corresponds to an increase in flow velocity, usually above 100 cm/s. Most case reports of restrictive flow across the foramen ovale are associated with various forms of hypoplasia of the left heart.[9] In these cases, the expected increase in left

atrial pressure results in the opposition of the primum septum to the atrial septum and therefore a decrease in the flap valve diameter. Some authors believe that a restrictive foramen may lead to the development of hypoplastic left heart, since foraminal flow provides most flow into the left ventricle. Restrictive flow across the fetal foramen ovale with structurally normal heart is rare and usually carries good prognosis.[10]

# Complete atrioventricular septal defect

## Anatomy

A complete AVSD is one of the more common cardiac defects detected prenatally.[1,11,12] This lesion is also known by the terms *endocardial cushion defect* or *atrioventricular canal defect*. In this lesion the atrial and ventricular septation is not complete and the separation between mitral and tricuspid orifices does not occur. Instead, there is a common atrioventricular junction. This lesion can be found as a spectrum of anomalies, ranging from a complete form (when both atrial and ventricular septation is incomplete, leading to a communication at both atrial and ventricular level) to a partial, or incomplete, form (when only the atrial or ventricular communication persists). All forms involve an intrinsic abnormality of the atrioventricular valves.

In most cases of AVSD, the atrioventricular junction is connected to the right and left ventricles so that the blood flows relatively evenly into each ventricle. This relationship is also described as a balanced AVSD. When the atrioventricular junction is predominantly connected to one of the ventricles, there is usually hypoplasia of the ventricle receiving the smaller portion of the atrioventricular orifice. This relationship is also described as an unbalanced AVSD, and right or left dominance can be identified[13] (Video 21.1).

## Fetal diagnosis

The goals of the fetal cardiac ultrasound examination are as follows:

1. Identify the presence and extent of the AVSD.
2. Assess the relationship of the atrioventricular junction to the underlying ventricles.
3. Assess the size of both ventricles.
4. Assess the degree of atrioventricular valve regurgitation.
5. Identify associated anomalies.

The apical four-chamber view is the most commonly used cut to identify an AVSD (Figure 21.4). In the normal heart, the tricuspid septal leaflet is attached to the ventricular septum, while the mitral valve has no septal attachment and inserts into the crux of the heart at a slightly more cranial position. In an AVSD, the left atrioventricular valve is attached to the ventricular septum at the same level, as is the right atrioventricular valve. Therefore, both atrioventricular valves are at the same level, losing the normal differential insertion. The

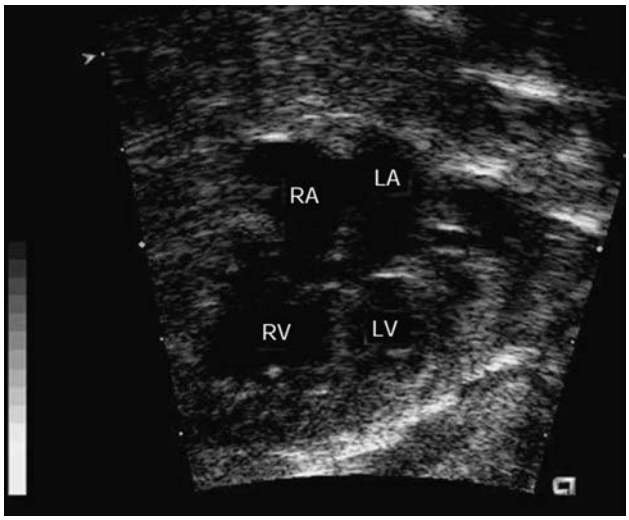


**Figure 21.4**
The heart is imaged in the apical equivalent four-chamber view, showing a typical picture of an atrioventricular septal defect. Both atrioventricular valves insert into the ventricular septum at the same level. Atrial and ventricular septal defects are seen above and below this insertion.

primum septum that can be easily identified in the normal four-chamber view is absent. A ventricular communication can usually be identified in this view; in most cases this defect is large, although smaller defects can exist and are usually more difficult to identify. The apical four-chamber view is ideal for assessing the relationship of the atrioventricular junction to the underlying ventricles as well as the size of both ventricles. In this plane, the ventricles should be of similar size. The atrial septum can be malaligned with the ventricular septum: when the atrial septum is deviated to the left, the right atrium drains to both ventricles (also described as double-outlet right atrium). When the atrial septum is shifted to the right, the left atrium drains to both ventricles. Such an anomaly can be corrected by surgery. A less favorable variation is when one ventricle is significantly smaller than the other. This is also known as an unbalanced AVSD, and in extreme situations will lead to a single ventricle solution. The apical four-chamber view is also ideal for flow interrogation of the atrioventricular valves. Insufficiency of both atrioventricular valves, which is common in the newborn with an AVSD, is less commonly seen during fetal life (Figure 21.5). The short-axis views obtained from the parasternal or subcostal equivalent angles provide a detailed picture of the atrioventricular valve anatomy. In rare cases, the insertion of the right or left atrioventricular valve is on the other side of the ventricular septum. These are more difficult to repair and may lead to a worse prognosis. A more common variation is when the anterior bridging leaflet has no attachment to the interventricular septum. This anatomical form of AVSD is often associated with tetralogy of Fallot and can be diagnosed in the fetus (Video 21.2). To the best of our knowledge, this has not yet been reported in the fetus. As in the case of primum ASD, the presence of a large coronary sinus may be

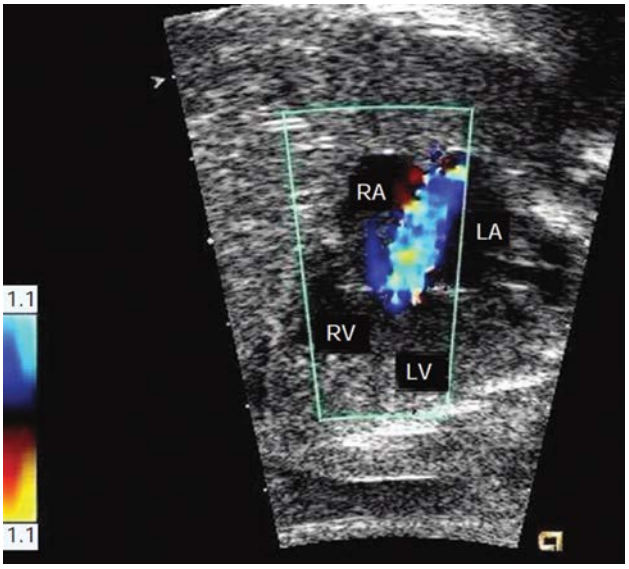


**Figure 21.5**
Color Doppler interrogation of the atrioventricular valves demonstrates a systolic jet of valve insufficiency, as shown in this four-chamber cut.

misdiagnosed as an AVSD.[14] The coronary sinus lies behind the left atrium and is usually enlarged by additional flow from a persistent left superior vena cava draining into the coronary sinus. A posterior coronal four-chamber view can create the illusion of both tricuspid and mitral valves inserting into the ventricular septum at the same level. However, a more anterior cut (Figure 21.2) will reveal the real relationship between the valve insertions, where they can be demonstrated in both open and closed position. The normal offset can then be demonstrated, avoiding the false diagnosis of an AVSD. One should keep in mind that persistent left superior vena cava and dilated coronary sinus can coexist with an AVSD.

## Associated lesions

When an AVSD is detected, a complete sequential analysis of the heart is mandatory. An AVSD is associated with situs anomalies such as right and left isomerism. Tetralogy of Fallot and double-outlet right ventricle are well-known associated lesions, more common in fetuses with trisomy 21. Left heart hypoplasia, subaortic narrowing, and coarctation of the aorta are all known associated cardiac anomalies, usually in fetuses with normal chromosomes. Another common association is a secundum ASD. The most common extracardiac anomaly associated with an AVSD is trisomy 21. An AVSD is also associated with other chromosomal anomalies such as trisomies 18 and 13. The fetal karyotype, therefore, should be examined whenever this diagnosis is made. It can also be a part of other syndromes such as Ellis–van Creveld, VACTERL (vertebral anomalies, anal atresia, congenital heart disease, tracheoesophageal fistula, renal dysplasia, and limb abnormalities), CHARGE (coloboma of the eye, heart defects, atresia of the choanae, retardation of growth and/or development, genital and/or urinary abnormalities, and ear abnormalities or deafness), Cornelia de Lange, and Goldenhar syndromes.[15] In a recent study,[16] out of 301 fetuses with an AVSD, only 51% had isolated AVSD. Right isomerism occurred in 12% and left isomerism in 20%. Extracardiac abnormalities and nonkaryotypic syndromes were evident in 13%; 39% had trisomy 21 and 10% had other chromosomal abnormalities. Similar findings were found by other groups.[11,17]

## Natural history and outcome

During fetal life AVSD is usually well tolerated, and most fetuses reach term and are delivered according to routine obstetric practice. A few will develop congestive heart failure and nonimmune hydrops because of severe insufficiency of the atrioventricular valve or heart block, especially in left atrial isomerism.[16,19,20] In these cases, the odds for fetal or neonatal demise are high. According to a recent study, 15% of fetuses diagnosed with this lesion whose parents opted to continue with the pregnancy died *in utero*.[16]

The infant with an isolated AVSD will remain asymptomatic for a few weeks. Most will develop signs of congestive heart failure during the first 4–8 weeks of life as pulmonary vascular resistance falls. All will require surgical repair, which is usually carried out during the first 6 months of life. Survival after AVSD repair is high, exceeding 90%, although some patients (especially the group with normal chromosomes) will require additional surgery because of the development of left atrioventricular valve insufficiency or narrowing of the left ventricular outflow tract. The odds for a successful repair decline when additional cardiac anomalies are present. Again, the chance of survival to 3 years is significantly lower in the group followed since intrauterine life when compared to the surgical literature and is quoted as low as 38%.[16]

# Ventricular septal defect

## Anatomy

VSD is the most common congenital heart defect diagnosed during the first year of life.[21,22] VSD is also a common cardiac defect detected prenatally, at a rate lower than that of prenatal detection of an AVSD.[1,2]

The ventricular septum is arbitrarily divided into four sections: the inlet, membranous, trabecular, and outlet components, which have different embryological origins.

When viewed from the right ventricle, the inlet septum has a lightly trabecular surface and is bounded by the tricuspid annulus and the attachments of the papillary muscles to the ventricular septum.

The membranous septum is a relatively small segment lying beneath the septal leaflet of the tricuspid valve and adjacent to the aortic and mitral valves. Viewed from the left ventricle, the membranous septum lies adjacent to the right fibrous trigone just beneath the aortic valve. The membranous septum is a thin translucent structure and therefore cannot be well

imaged in all planes, and it is often difficult to image even after birth. This may result in the false impression of a VSD in some views, especially in the fetus.

The trabecular septum, which derives its name from its heavily trabeculated appearance, extends from the inlet septum to the region of the outlet septum just proximal to the pulmonary valve, and does not lie in a single plane. It contains the moderator band (or septomarginal trabeculation, which is also called the septal band of the crista supraventricularis), which extends in a Y-shaped fashion below the pulmonary valve. Its anterior portion abuts the outlet septum, while its posterior portion is the papillary muscle of the conus (muscle of Lancisi). Inferiorly, the septomarginal trabeculation extends as a broad muscle bundle. This portion of the muscle, the septomarginal trabeculation, is also referred to as the septal limb of the crista supraventricularis. The ventricular infundibular fold, also called the parietal band of the crista supraventricularis, is the right ventricular muscle lying between the tricuspid and the pulmonary valves. The outlet septum (also named conus septum) is a small segment extending from the septomarginal trabecula to the pulmonary valve.

VSDs can occur in any of the septal locations and also at the sites of fusion between them; for example, defects found around the membranous septum are termed *perimembranous*. They can also be named for their area of extension, such as perimembranous-inlet, perimembranous-trabecular, and perimembranous-outlet defects. Perimembranous defects comprise about 75% of all VSDs.[23] When the defects are surrounded entirely by muscle, they are termed *muscular-inlet*, *muscular-trabecular*, and *muscular-outlet defects*. Muscular defects comprise 10%–15% of all ventricular septal defects. Defects of the outlet septum most commonly are adjacent to the pulmonary and aortic valves and are termed *subarterial doubly committed* or *supracristal defects*. Such defects constitute about 5% of the VSDs but are more common in Asian populations.[23]

When the different portions of the septum adjacent to the VSD are malaligned, they are termed a malalignment VSD. The VSD can be malaligned between the outlet and trabecular septum or with respect to the atrioventricular valves, associated with straddling of an atrioventricular valve.

The size of ventricular septal defects varies from very small to large, involving a third or more of the ventricular septum. Since the septum does not lie in a single plane, it can be difficult to assess the VSD size. Defects may be isolated or multiple and are commonly a part of, or associated with, other cardiac lesions.

## Fetal diagnosis

The goals of the ultrasound examination are as follows:

1. Identify the presence of a VSD.
2. Define which segment of the septum is involved.
3. Identify additional anomalies.

The fetal ventricular septum is easily seen in the four-chamber view, which can be visualized from an apical equivalent or from a lateral orientation. In the apical equivalent four-chamber view the ultrasound beam is parallel to the ventricular septum using lateral resolution (Figure 21.6). Since the membranous part of the septum is thin, the ventricular septum "disappears" toward the internal crux of the heart. This may result in the appearance of a dropout in the septum, leading to a false diagnosis of a VSD.[24] In order to achieve a different angle, the transducer can be moved to a different location on the maternal abdomen so that the ultrasound beam will be perpendicular to the ventricular septum, using axial resolution. The parasternal short-axis equivalent cut is also useful, when the ultrasound beam is perpendicular to the ventricular septum; the different parts of the septum can be visualized in great detail. This view is especially useful in identifying a subarterial doubly committed VSD, also known as a supracristal VSD (Video 21.3).

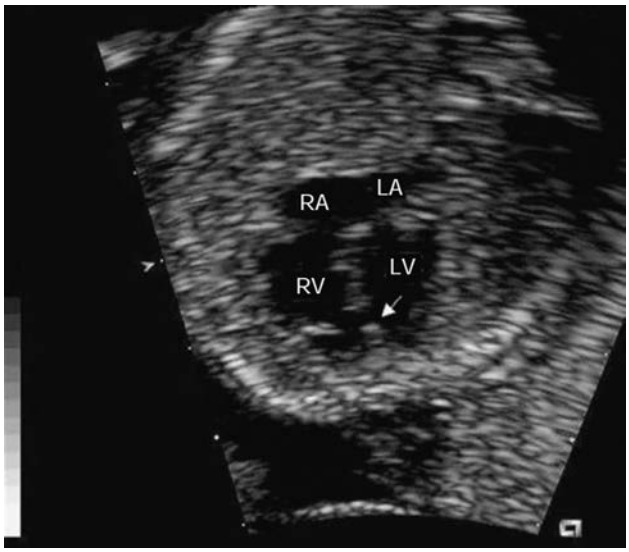


**Figure 21.6**
The ventricular septum of a 20-week fetus is visualized in a four-chamber view. A muscular septal defect is identified at the lower portion of the septum (arrow). Note the "T" artifact at the defect edges.

A useful physical sign of a septal defect is the "T" artifact: high impedance exists at the blood-tissue interface producing ballooning of echoes at the rim of a defect, creating bright spots at the defect edges.[24] The "T" artifact is not created when the septum is thin, leading to a simple dropout. The use of color flow Doppler imaging may augment the ability to identify a VSD in the fetus (Figures 21.7 and 21.8). Once again, when this is performed from the apical equivalent four-chamber view, the ultrasound beam is parallel to the ventricular septum so that the color tends to "cover" the thin part of the septum, leading to the impression of flow across a VSD. However, when the ultrasound beam is perpendicular to the ventricular septum, color Doppler flow can be detected more accurately when flow is crossing the septum, usually in a bidirectional fashion.[25,26] Since the pressure is similar in the fetal right and left ventricles, the potential pressure gradient across a VSD is small. Color flow velocity should therefore be reduced to a low Nyquist limit in order to detect low-velocity jets.

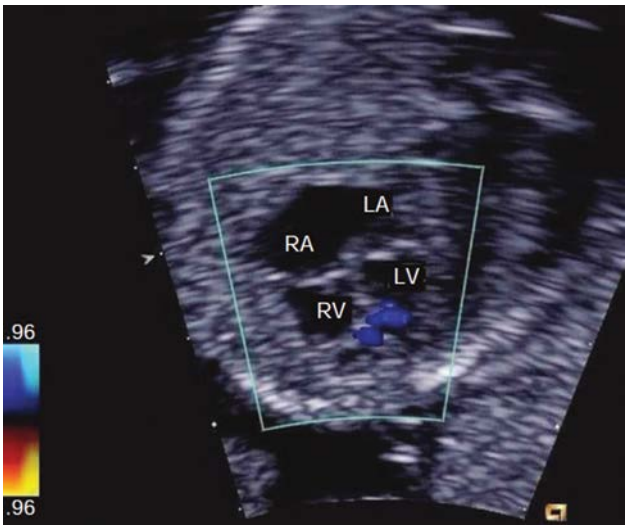


**Figure 21.7**
Flow across this muscular ventricular septal defect can be detected using color flow mapping.

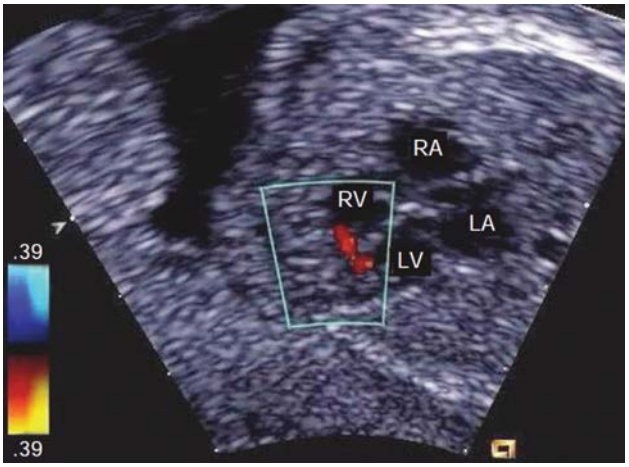


**Figure 21.8**
The same ventricular septal defect as in Figure 21.7 can be shown by color flow Doppler when the ventricular septum is imaged with the ultrasound beam perpendicular to the defect.

Using new echocardiographic technology allowing three-dimensional reconstruction adds to the anatomical understanding of ventricular septal defects in the fetal heart[26,27] (Figure 21.9 and Video 21.5).

## *Associated lesions*

When a VSD is detected, a complete sequential analysis of the heart is mandatory. An isolated VSD is rarely associated with situs anomalies. However, it is commonly found as part of complex cardiac lesions, some of which are not obvious when the study is performed during early pregnancy. When a VSD is identified, both right and left ventricular outflow tracts should be examined in detail. Since a VSD can be a part of tetralogy of Fallot, the size of the right ventricular outflow

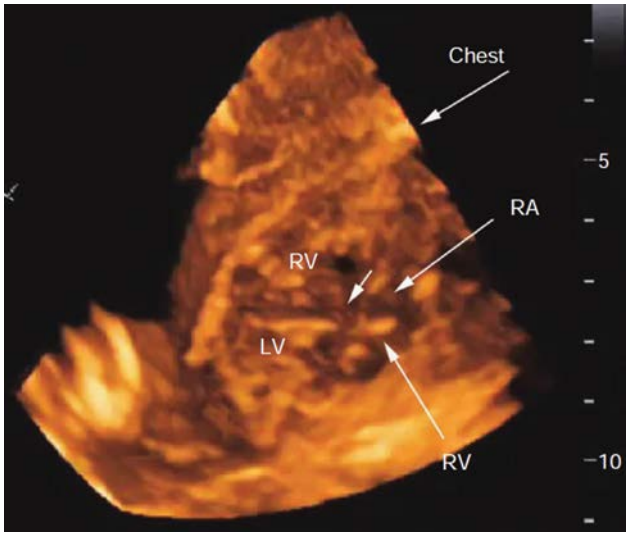


**Figure 21.9**
This three-dimensional image is taken from a fetus of 26 weeks' gestation, with a perimembranous ventricular septal defect, shown by an unlabeled short arrow at the top of the septum. The chest, the right atrium (RA), right ventricle (RV), left atrium (LA), and left ventricle (LV) are labeled. Additionally, the atrial and ventricular septa can be clearly identified between their respective chambers. See also corresponding Video 21.4.

tract and main and branch pulmonary arteries, as well as the flow across these structures, should be examined. The usual anterior malalignment of the outflow septum in tetralogy of Fallot is not as easy to identify during fetal life as it is in postnatal life. This diagnosis should be suspected whenever the pulmonary artery is smaller than expected or a pressure gradient is detected across the right ventricular outflow tract. The associations of other lesions with ventricular septal defects are numerous and include left heart obstructions such as subaortic narrowing, aortic valve stenosis, coarctation of the aorta, and interrupted aortic arch. Close inspection of the VSD from a parasternal echocardiographic cut allows a better assessment of the outflow septum and facilitated the identification of anterior or posterior malalignment. When posterior malalignment is identified (Video 21.4), mitral and aortic valves anomalies as well as aortic coarctation should be suspected and carefully evaluated. Since both right and left outflow obstructions can evolve during pregnancy and postnatal life, reassessment during late gestation is advised. A VSD can also be a part of complex lesions such as transposition of the great arteries and double-outlet right ventricle.

Extracardiac anomalies associated with a VSD include chromosomal anomaly in over 40% according to some series.[1,2] Such anomalies included trisomies 21, 13, and 18. This rate is significantly higher than expected from postnatal series and may relate to the selection of patients referred for fetal echocardiography as well as to spontaneous fetal loss in chromosomally abnormal fetuses that would not be included in postnatal series. Other extracardiac anomalies associated with a VSD include a deletion in 22q11 and nonchromosomal multiply malformed fetuses.[2]

## Natural history and outcome

During fetal life, a VSD is well tolerated, and most fetuses reach term and are delivered according to routine obstetric practice. The odds for fetal demise are higher when extracardiac anomalies are present. Isolated perimembranous and muscular ventricular septal defects detected and followed through pregnancy show a high rate of spontaneous closure.[28–30] No correlation was found between the size of the defect prenatally and its chance for spontaneous closure.[28] We have data to show that smaller VSDs have a greater chance of closure than larger defects (postnatally). Infants with an isolated VSD may remain asymptomatic for a few weeks; those with relatively large defects will develop signs of congestive heart failure after a few weeks of life as pulmonary vascular resistance falls. Over 50% of VSDs located in the perimembranous or muscular septum will close spontaneously, usually during the first year of life; only a minority of such defects will require surgical repair. Defects in the inlet or outlet septum do not close spontaneously and require surgical repair. Surgery is usually carried out during the first year of life and, when isolated, carries a low mortality and complication rate.[18] Multiple defects or a single large apical muscular defect carries a higher risk of surgical repair due to limited access. Such infants may need the placement of pulmonary arterial banding to decrease pulmonary flow and pressure during the first months of life, followed by surgical or transcatheter closure of the defects coupled with pulmonary debanding later in life. When associated cardiac anomalies are present, the odds for a successful repair depend on the severity and nature of the additional cardiac defects.

## Videos

**Video 21.1** (https://youtu.be/0UbotCVcerI)
Four-chamber view of an atrioventricular septal defect (AVSD) with a smaller left atrioventricular connection when compared to the right, seen both on two-dimensional image (a) and with color flow across the inlets (b).

**Video 21.2** (https://youtu.be/1eBwPsWOWt0)
The superior (sup) leaflet of the AVSD does not have any attachment to the interventricular septum (type C according to the Rastelli classification). In many cases, this type of AVSD is associated with tetralogy of Fallot.

**Video 21.3** (https://youtu.be/cKOFcLlq9Pg)
(a) In this fetus with transposition of the great arteries, a septal defect is clearly seen in the outlet portion of the interventricular septum. Such a VSD is termed subarterial doubly committed or supracristal defect. (b) Same video using color Doppler to demonstrate flow across the defect (in this case the flow is directed from the left ventricle via the VSD into the anterior aorta). (c) A sweep across the outlets of the right and left ventricles shows the VSD adjacent to both semilunar valves. In this fetus, the aorta is the anterior vessel and the pulmonary artery is the posterior vessel.

**Video 21.4** (https://youtu.be/D5SPZmKQ9Pw)
Parasternal echocardiographic cut allows a better assessment of the outflow septum and its relation to the VSD. The left ventricular (LV) outflow tract, VSD, posterior malalignment of the outflow septum (arrow), and the ascending aorta (AO) are seen well on this view.

**Video 21.5** (https://youtu.be/EES2Z4gRcaI)
Three-dimensional reconstruction of a perimembranous VSD in a fetus of 26 weeks' gestation, with a perimembranous ventricular septal defect. The chest, the right atrium (RA), right ventricle (RV), left atrium (LA), and left ventricle (LV) are labeled. Additionally, the atrial and ventricular septa can be clearly identified between their respective chambers.

## References


1. Allan LD et al. *J Am Coll Cardiol* 1994;23:1452–8.
2. Stoll C et al. *Prenat Diagn* 2001;21:243–52.
3. Fyler DC. *Pediatrics* 1980;65:375–461.
4. Goor DA, Lillehei CW. *Congenital Malformations of the Heart*. New York, NY: Grune and Stratton; 1975.
5. Wilson AD et al. *J Am Soc Echocardiogr* 1990;3:491–4.
6. Phillipos EZ et al. *J Am Soc Echocardiogr* 1994;7:257–63.
7. Nieminen HP et al. *Circulation* 2001;104:570–5.
8. El-Najdawi EK et al. *J Thorac Cardiovasc Surg* 2000;119:880–90.
9. Cohbot V et al. *J Am Soc Echocardiogr* 1990;3:15–19.
10. Uzun O et al. *Pediatr Cardiol* 2014;35:943–952.
11. Allan LD. *Am J Obstet Gynecol* 1999;181:1250–3.
12. Silverman NH. *Pediatric Echocardiography*. Baltimore, MD: Williams and Wilkins; 1993.
13. Pitkanen OM et al. *Am Heart J* 2006;152:163.e1–7.
14. Park JR et al. *Ultrasound Obstet Gynecol* 1997;10:126–9.
15. Feldt RH et al. Atrioventricular septal defects. In: Emmanouilides GC, Riemenschneider TA, Allan HD, Gutgesell HP, eds. *Moss and Adams' Heart Disease in Infants, Children and Adolescents*, 5th ed. Baltimore, MD: Williams and Wilkins; 1995:704–24.
16. Huggon IC et al. *J Am Coll Cardiol* 2000;36:593–601.
17. Delisle MF et al. *Obstet Gynecol* 1999;94:763–7.
18. Masuda M et al. *Jpn J Thorac Cardiovasc Surg* 2001;49:497–503.
19. Silverman NH et al. *Circulation* 1985;72:825–32.
20. Schmidt KG et al. *J Am Coll Cardiol* 1991;17:1360–6.
21. Anderson RH et al. Ventricular septal defects. In: Anderson RH, ed. *Paediatric Cardiology*. London, England: McGraw-Hill; 1987:565–90.
22. Ferencz C et al., eds. The epidemiology of congenital heart disease, the Baltimore–Washington Infant Study 1981–1989. *Perspectives in Pediatric Cardiology*, Vol. 4. Mount Kisco, NY: Futura Publishing; 1993:31–3.
23. Rudolph AM. *Congenital Disease of the Heart: Clinical–Physiological Considerations*. Mount Kisco, NY: Futura Publishing; 2001:198–9.
24. Canale JM et al. *Circulation* 1981;63:689–97.
25. Lethor JP et al. *Circulation* 2000;101:e93.
26. Chao RC et al. *Am Heart J* 1994;127:955–8.
27. Yagel S et al. *Ultrasound Obstet Gynecol* 2006;28:266–74.
28. Paladini D et al. *Ultrasound Obstet Gynecol* 2000;16:118–22.
29. Axt-Fliender R et al. *Ultrasound Obstet Gynecol* 2006;27:266–73.
30. Bahtiyar MO et al. *J Ultrasound Med* 2008;27:715–720.

# 22

# Atrioventricular septal defect ("atrioventricular canal")

Laurent Fermont and Lucile Houyel

## Anatomy

The definition of atrioventricular (AV) canal is both embryologic and anatomic: the AV canal is the zone of junction between the atria and the ventricles, including the vestibular septum (lowest part of the atrial septum), the AV valves, and the inlet septum (inferior part of the ventricular septum). Morphologically, the congenital heart defect named the "atrioventricular canal" or "atrioventricular septal defect" (AVSD) is defined as the persistence of a common AV junction guarded by a common AV valve and is associated with anomalies of varying degrees in these three components.[1]

This common origin explains the anatomic characteristics common to all anatomic types of AVSD:

- The common AV junction with a common five-leaflet AV valve: two leaflets in the morphological right ventricle, one in the morphological left ventricle, and two bridging leaflets, anterosuperior and posteroinferior, which have insertions in both ventricles.
- The disproportion between outlet and inlet portions of the left ventricle: contrary to the normal heart, the length of the outlet part of the left ventricle (from the anterior insertion of the aortic valve to the apex) and the length of its inlet part (from the inferior part of the left AV valve to the apex) are not identical, the outlet being longer than the inlet in AVSD[2] (Figure 22.1). This discrepancy results from the defect of formation of the inlet part of the ventricular septum, with the characteristic scooped-out aspect of the ventricular septum viewed from the left ventricle. The anatomic consequences of this inlet defect are a higher location of the aortic valve, which does not achieve its normal position between the mitral and the tricuspid valve, resulting in both "unwedging" of the aortic valve, and elongation and narrowing of the outflow tract (Figure 22.2).
- The defect of the inlet part of the ventricular septum, with or without a shunt at the ventricular level, is thus present whatever the anatomic type of AVSD.

The different anatomic types of AVSD result from the extent of the attachments of the bridging leaflets on the crest of the ventricular and atrial septum[3] (Figure 22.3). Rastelli[3] clarified the surgical approach, describing the AV septal defects in three groups: (1) group A: evenly divided anterior hemivalve with attachments to the ventricular crest (multiple chordae on the crest); (2) group B with unevenly divided anterior hemivalve with attachments to the papillary muscles; and (3) group C with undivided anterior hemivalve free and floating attached on papillary muscles of the two ventricles.

The existence and the localization of the intracardiac shunts depend on these attachments in the complete form (complete AV canal); the two bridging leaflets are not fused together or to the crest of the ventricular and atrial septum, resulting in interventricular and interatrial communications (inlet VSD and ostium primum ASD) and a common AV orifice. In the partial form (partial AV canal) (Figure 22.4), the two bridging leaflets are fused together and to the crest of the ventricular septum, leaving only an interatrial communication (ostium primum ASD) and separating the common AV valve into two valvar orifices with a three-leaflet left AV valve. The "cleft" of the left component of the common AV valve is indeed the zone of apposition between the left parts of the two bridging leaflets. Less frequently, the two bridging leaflets fuse together and to the atrial septal crest, leaving an inlet VSD associated with a common AV junction and a three-leaflet AV valve. The "intermediate" form results from an incomplete fusion of the bridging leaflets with the ventricular septal crest, leaving one or several small, restrictive, interventricular communications. Finally, AVSD can exist without any shunt: common AV junction with a three-leaflet AV valve, and common AV junction without a cleft of the left AV valve. This last anatomic form is responsible for the echocardiographic sign called "linear insertion of the AV valves" in the fetal heart and considered for some authors an anatomic landmark for trisomy 21.[4]

## Embryology

During embryonic cardiac development, the AV canal is the zone of junction between the atria and the ventricles, bordered by the mesenchyme of the AV endocardial cushions. Immediately after cardiac looping, the AV canal opens in the developing left ventricle exclusively. While the right ventricle grows by addition of myocardial cells of the anterior second

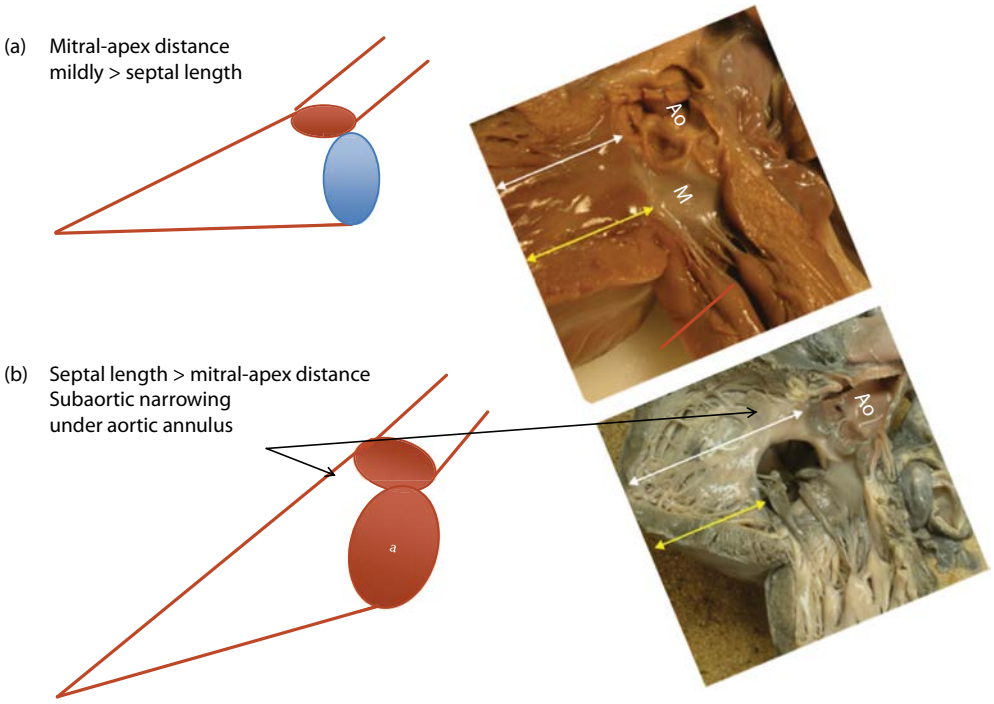


**Figure 22.1**
Differential septal length in normal (a) and AVSD (b).

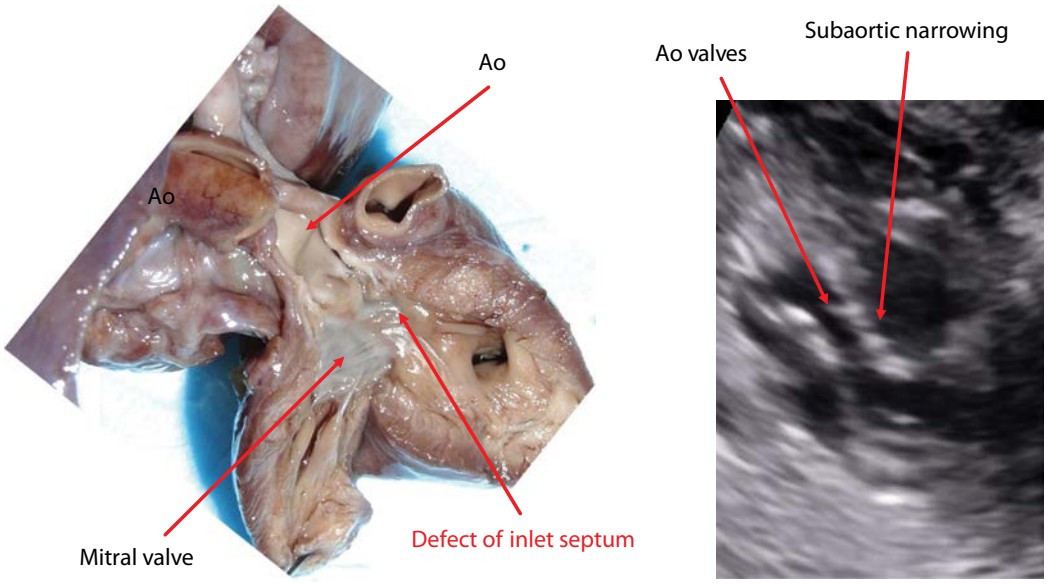


**Figure 22.2**
Partial AVSD, with a "goose-neck aspect" elongation of the subaortic outflow tract.

heart field, the right AV junction develops from the dorsal part of the primary fold, between the inner curvature and the right part of the AV canal.

AV canal, or AV septal defect, was considered for a long time to be due to an anomaly of structure and development of the AV endocardial cushions and, hence, the term "endocardial cushion defect." The anatomic analysis presented previously proves that AVSD is primarily due to an anomaly of septation of the AV junction, with a common AV valve and a defect of formation of the vestibular atrial septum and of the inlet part of the ventricular septum. Two experimental studies on human embryos with Down syndrome[5] and mouse embryos with trisomy 16, the murine equivalent of human trisomy 21,[6] demonstrate that the major determinant of the persistence of a common AV junction in these cases is defective growth of the vestibular spine or dorsal mesenchymal protrusion, itself derived from the posterior second heart field via the dorsal mesocardium.[7–9] This lack of growth prevents appropriate fusion of the AV mesenchymal components that normally close the primitive interatrial foramen or ostium primum (Figure 22.4): the mesenchymal cap on the leading edge of the primitive atrial septum, the endocardial cushions of the AV canal, and the vestibular spine itself. These three components are known as the AV mesenchymal complex.[10] This leads to the persistence of the common AV junction, with persistence of the ostium primum and failure of normal development of the inlet part of the ventricular septum. The embryonic origin of the inlet septum is still controversial. Experimental studies

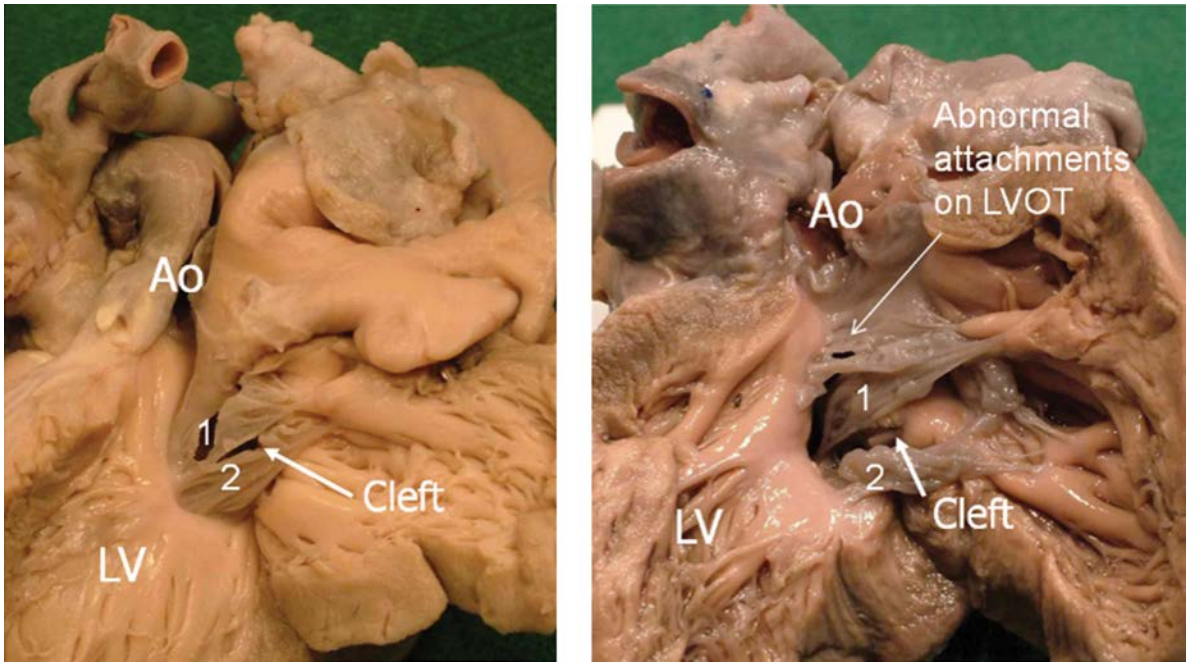


**Figure 22.3**
Subvalvar anatomy: septal attachments of chordae.

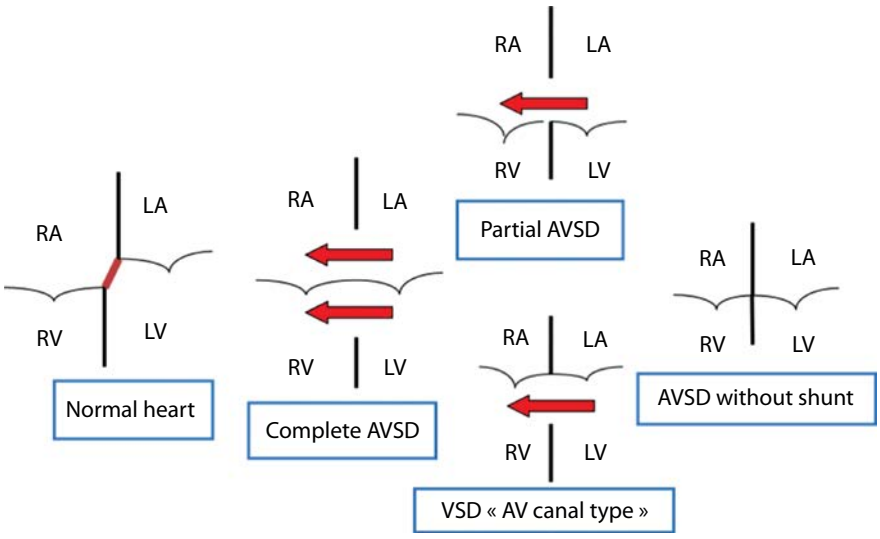


**Figure 22.4**
Spectrum of AVSD.

in the mouse embryo demonstrate that the larger part of the central mesenchymal mass created by the fusion of the mesenchymal tissues of the vestibular spine, the mesenchymal cap of the primitive atrial septum, and the AV cushions, becomes muscularized to form the inferior margin of the oval fossa.[11] The occurrence of muscularization in the inferior part of the mass (the part that is lacking in hearts with a common AV junction, forming the inlet VSD) has been demonstrated in the chick embryo[12] but not in mammals, in which the inferior part of the ventricular septum would derive from the growth of the caudal part of the developing trabeculated muscular septum, after the rightward expansion of the embryologic AV canal.[13,14] The endocardial cushions have a normal structure in AV septal defects, and the major determinant of AVSD is impaired proliferation and cell migration in the posterior second heart field.[15–17]

## *Prenatal diagnosis of AVSD*

AV septal defects do not usually alter the prenatal hemodynamic conditions except in those with major leakage of the AV valves or high-degree complete AV block with low heart rates (<50/bpm) and cardiomyopathies (hypertrophic or noncompacted).[17] Prenatal detection may be obtained from examinations performed in two conditions: (1) Multiple factors increase the risks of cardiac malformations and define a "high-risk" group. These factors include maternal age over

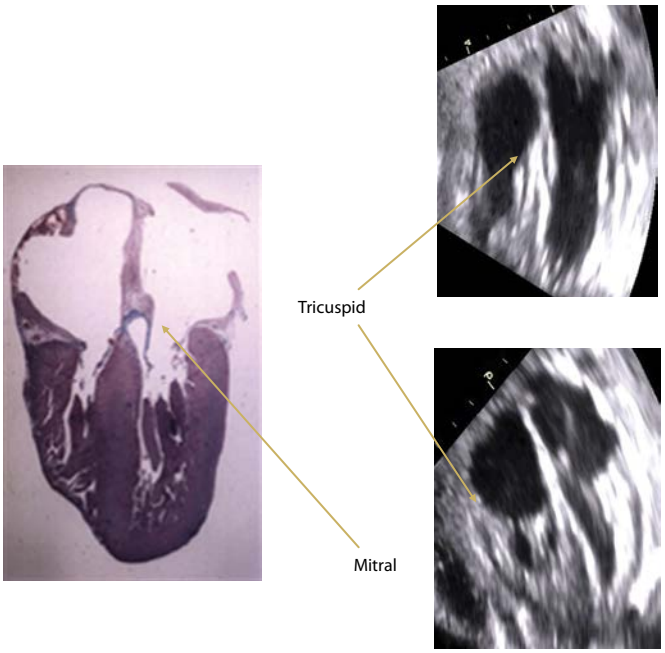


**Figure 22.5**
Echo-anatomic correlation: normal four-chambers view.

36 years or familial antecedents of cardiopathy, aneuploidy, or monogenic syndrome, or at least one ultrasonic marker, such as nuchal translucency, minor specific sonographic signs such as length of the nasal bones, growth retardation, excess of amniotic fluid or oligohydramnios, or detection of any extracardiac malformation. (2) Most prenatally detected cases occur in the "low-risk" population and are identified by general sonographers,[19–20] who must be trained to always include specific views of the fetal heart in their examinations performed after 18 weeks of gestation—that is, at least the four-chambers view (Figure 22.5). Every anatomical change compared to usual aspects may be of paramount importance in term of diagnosis and prognosis as well.[18] Every sonographer practitioner must especially focus on the disposition of the mitral and tricuspid valves, paying strong attention to a slightly more apical position of the tricuspid ring with respect to the more posterior mitral one, a disposition similar to the aspects described postnatally.[21,22] Studies of the arterial and venous anatomies and atriovisceral situs and concordances are equally important. These views[23,24] are adapted to increase prenatal diagnosis of most structural cardiac malformations, AV defects included.[25,26]

Linear and horizontal arrangements of the mitro-tricuspid annulus and insertions of chordae on the septal crest as described by pathologists and neonatal cardiologists (Figures 22.6 through 22.8) raise the possibility of an AV septal defect. This appears mainly on the four-chambers views and differs strikingly from normal structure.

Transverse views at the level of the AV apparatus and valves may be useful as well. They also show a horizontal disposition of the common AV ring and that the anterior mitral valve is proximal to the interventricular septum (7a: mitro-tricuspid valves open and close as "butterfly wings" above the septum) reproducing the anatomical data: A dominant anterosuperior leaflet crossing the interventricular septum, a posterior leaflet also crossing the septum, and a lateral mural leaflet. In cases of intact interventricular septum, the right and left segments of the AV valves appear to be horizontally inserted on the septal crest leading to an amazing appearance of "spectacles" (Figure 22.9). The characteristic "scooped out" mitral valve creates an elongation of the left ventricular outflow tract, sometimes stenotic, as illustrated by the traditional "goose-necked" aspect in longitudinal views (Figure 22.2). Below the valvar configuration (Figure 22.10a), the papillary muscles and chordae may be analyzed: number, size, position, and function are assessed. Normally, the two papillary muscles (one anterior and one posterior) are oriented toward the low-positioned aortic ring continuous to the mitral ring. In cases of AV septal defects, a counterclockwise rotation of the papillary muscles is seen (Figure 22.10b,c). They may be abnormal in number (one papillary muscle, called a "parachute") (Figure 22.11), in attachments on the septum, or in position (higher or lateral); rarely there are two mitral orifices (Figure 22.12).

*Atrial septal defects* are present in almost all cases: the atrial defect of AV septal defects can be visualized as a lack at the lower part of the atrial septum in the vestibular septum, thus

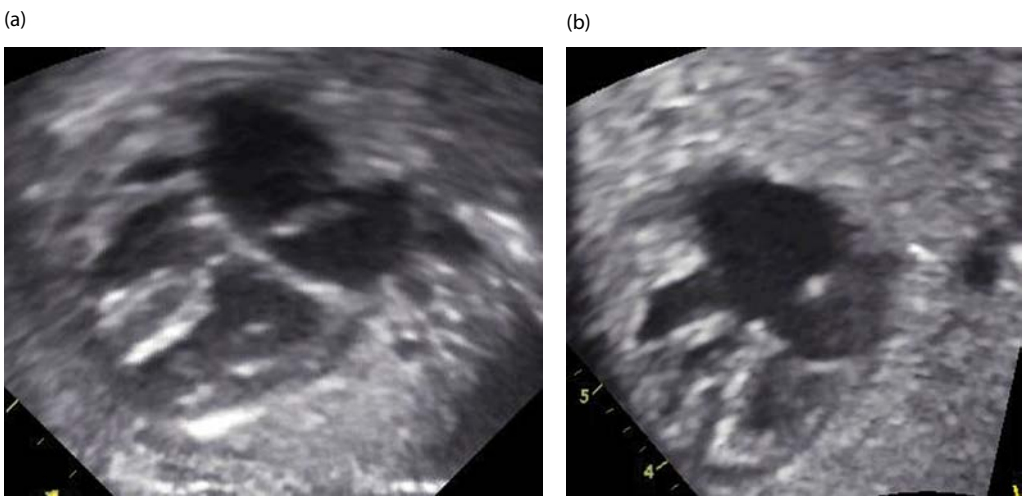


**Figure 22.6**
"Four-chambers view": (a) complete and (b) partial AV canal.

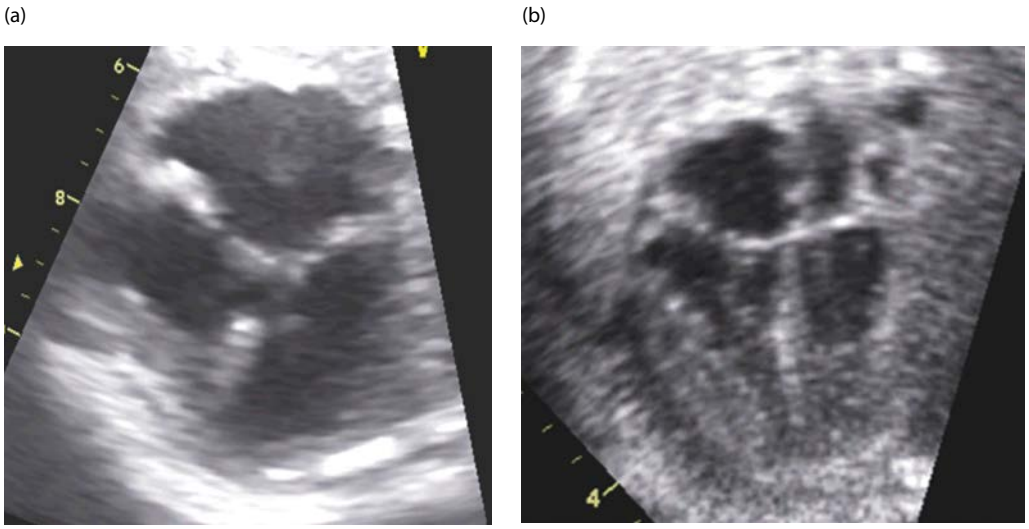


**Figure 22.7**
Spectrum of anatomic forms: (a) major; (b) minor: horizontal disposition of the AV valve.

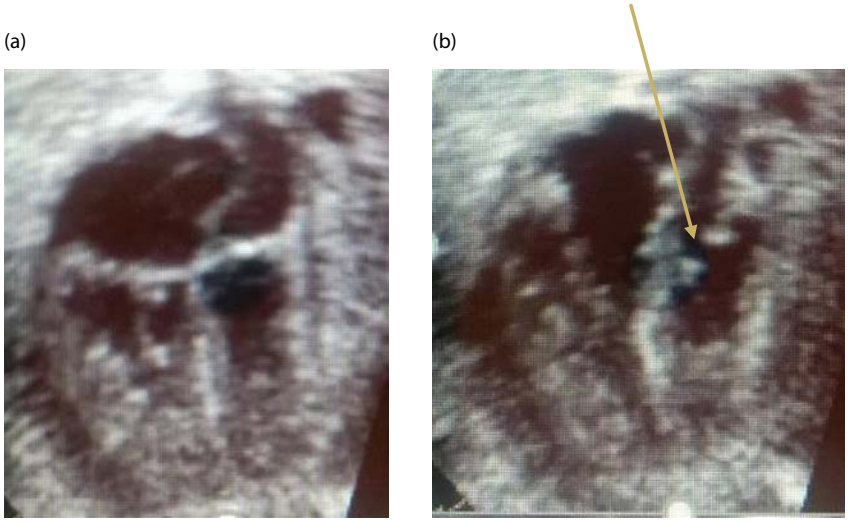


**Figure 22.8**
Minor AVSD: (a) systole; (b) diastole, cleft mitral arrow valve.

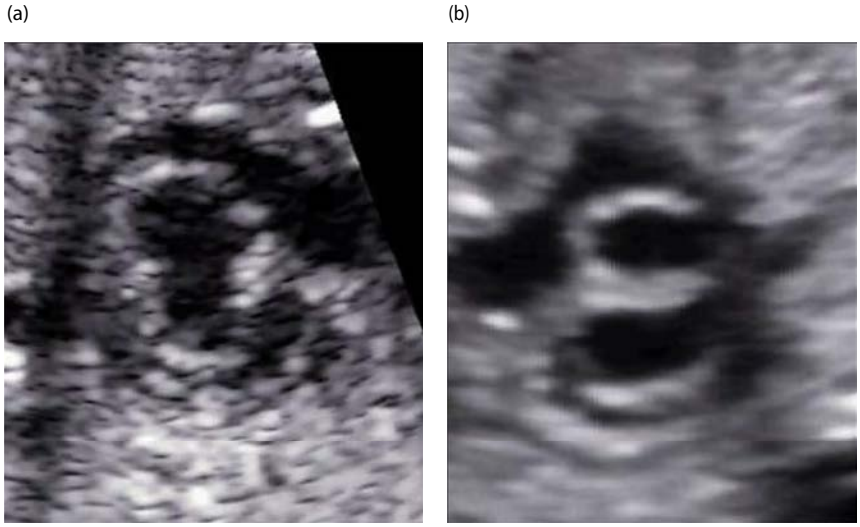


**Figure 22.9**
Transverse view at the valvar level: (a) complete; (b) partial AV canal.

found adjacent to the valvar plane. Their diameters are quite variable from one case to the other, generally of medium size ranging from 10% to 50% of the interatrial septal length (measured between the auriculoventricular plane and the posterior wall of the atrium).[27] In some instances, the atrial septum may be completely missing, showing itself as a "single atrium," usually part of a left heterotaxy (Figure 22.7a). Elsewhere, the defect may be tiny, diminutive, or even absent. These cases are at high risk of missed diagnosis, whether the examination is performed by general obstetric sonographers or specialists in

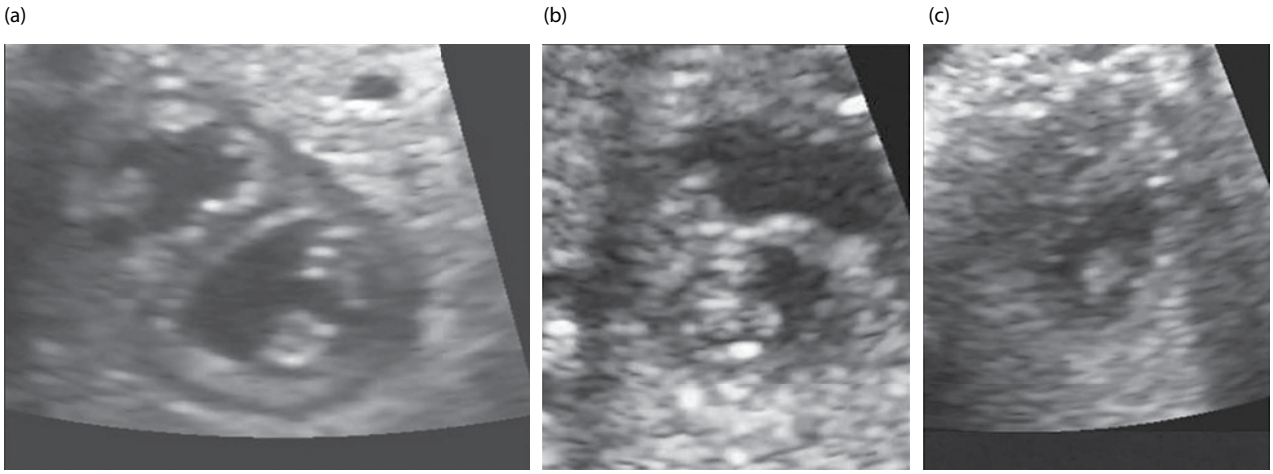


**Figure 22.10**
Transverse view of papillary muscles: (a) normal; (b) closed and counterclockwise rotated; (c) unique.

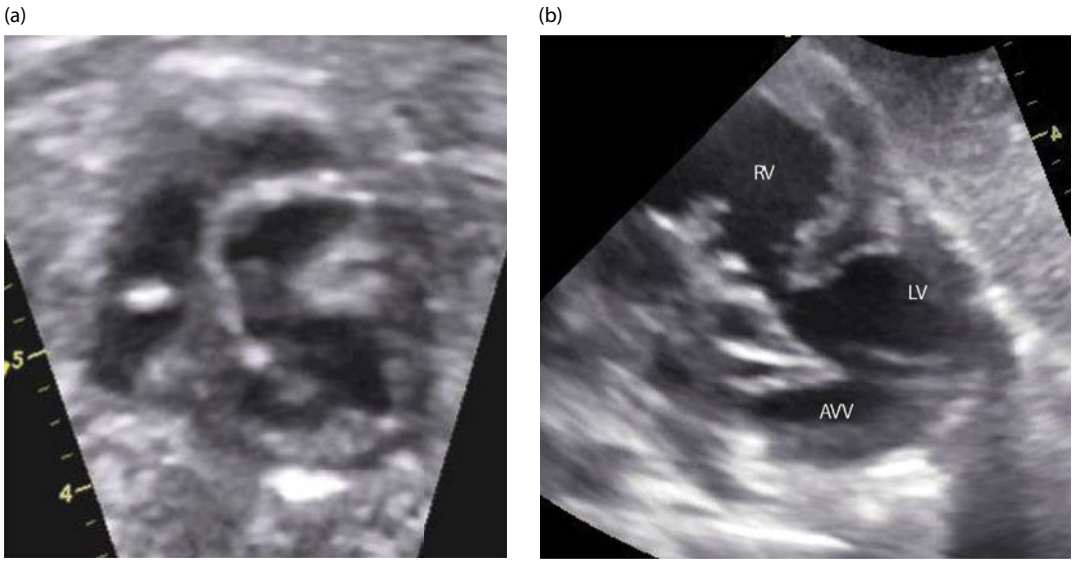


**Figure 22.11**
Abnormal insertion on single papillary muscles, transverse view: (a) complete AVSD; (b) insertion of chordae.

fetal echocardiography (Figure 22.7b). AV septal defects might only be suspected upon observation of the horizontal aspect of the AV valve.[28] Similarly, the tissue of the mural mitral valve must be carefully reviewed to appreciate the quality of the valvar components, which are sometimes hypoplastic, and to detect a cleft mitral valve (Figure 22.8).

*Interventricular septal defects* (VSDs) are present in 75% of patients. In this malformation, they involve the posterior part of the interventricular septum within the "inlet septum," located in the plane of the AV valves. Chordae inserted on the septal crest may limit the size of the defect inferiorly. This may confuse the examiner, resulting in false appearance of an intact interventricular septation, which in turn could lead to overlooking the defect.

Ventricular defects may range from total absence of any septal structure (univentricular hearts or the "cor biloculare," which is usually part of a heterotaxy) to small and restrictive communications, sometimes barely noticeable. In some cases, only perimembranous or trabeculated defects, which are unrelated to the development of AV septal defects, are present. Total absence of any septal defect is extremely rare. The horizontal disposition of the AV annulus can be the sole clue to the presence of an AV septal defect, even without a cleft mitral valve[4,29,30]; nevertheless, these fetuses bear an increased risk of associated Down syndrome.[31] On the contrary, AV septal defects may be diagnosed in excess, for example, a dilated coronary sinus secondary to increased flow from an abnormal intracardiac pulmonary venous drainage, or a persistent left superior vena cava, may be mistaken for AVSD.

AVSDs can be categorized to two main groups based on their septal anatomy (Figure 22.4)[32,33]:

- *Partial AV canal defects*, ostium primum–type atrial septal defects are here present without the typical "inlet" ventricular septal defect. The focus on the leaflets in four chambers and transverse views visualizes the "cleft" in the mitral valve (Figure 22.8). Interventricular perimembranous or trabeculated defects with intact inlet septum may

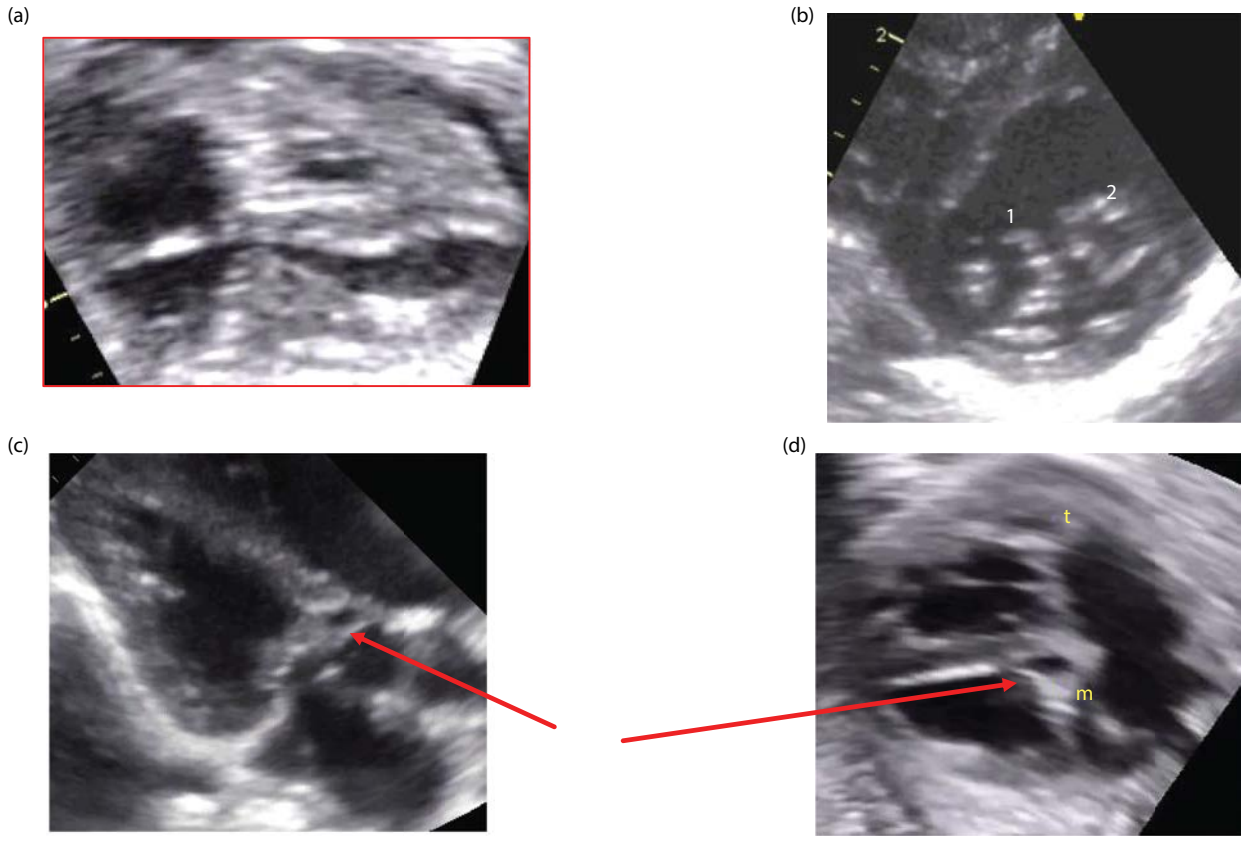


**Figure 22.12**
(a) Double mitral orifice prenatally; (b) double mitral orifice postnatally (same patient as in [a]); (c) septal subaortic insertions of chordae (arrowed), LV-AO view; (d) septal subaortic insertions of chordae (arrowed), four-chambers view.

be described. Those cases can be classified as partial (elsewhere "intermediate"). As with all AV defects, there is a higher prevalence of Down syndrome (around 10%).[34]

- *Complete AV canal defects* include the specific AV disposition and the mitral anomaly ("cleft") associated with an "ostium primum–type" atrial septal defect and a posterior interventricular septal defect found in the "inlet" septum. Inlet ventricular septal defects may also be isolated without ostium primum or even any valvar anomaly. There is a higher prevalence of Down syndrome (around 40%), especially in balanced forms or with associations (*cardiac*: persistent left superior vena cava or tetralogy of Fallot; or *extracardiac*: digestive system anomalies or all associated anomalies that could raise the possibility of any monogenic syndrome).

The effectiveness of screening examinations is related to the severity of the anatomic abnormalities. In severe cases, it is enough to include systematically the visualization of the four-chambers view on any ultrasound examination according to the rules described to fulfill the current obligation of prenatal detection of significant congenital cardiopathies. Univentricular hearts or large septal defects are—or should be—systematically detected in the "low-risk" population on examinations done during the second trimester, even if such detection was possible earlier (Figure 22.13). Diagnosis may be extremely difficult in cases of "near to normal" four-chambered hearts with minor septal defects or an intact septum. In addition, technical difficulties may preclude visualization of an adequate four-chambers view. Figures 22.14 and 22.15 demonstrate how easy it is to overlook this diagnosis. As mentioned previously, these limitations might be overcome if general sonographers are keen to pay special attention to the AV disposition in the four-chambers and transverse views and to review or to refer doubtful cases to pediatric cardiologists or other specialists in fetal echocardiography.

## Factors in prognosis

Neonatal symptoms are not necessarily related to severity of the anatomic defect. Large septal defects may be clinically tolerated in cases without significant atrioventricular valve anatomical malformation or significant insufficiency. Indeed, persistent high pulmonary resistances may transiently "protect" neonates against clinical effects of pulmonary overflows. But, this "clinical protective effect" is actually dangerous and must lead to irreversible and fixed pulmonary high resistances, especially and quickly in babies with Down's syndroms. Therefore, surgical indications, even palliative, are often mandatory before the age of 3 months to avoid further development of irreversible pulmonary arterial hypertension and Eisenmenger syndrome. These possible sequelae underline the importance of prenatal diagnosis.

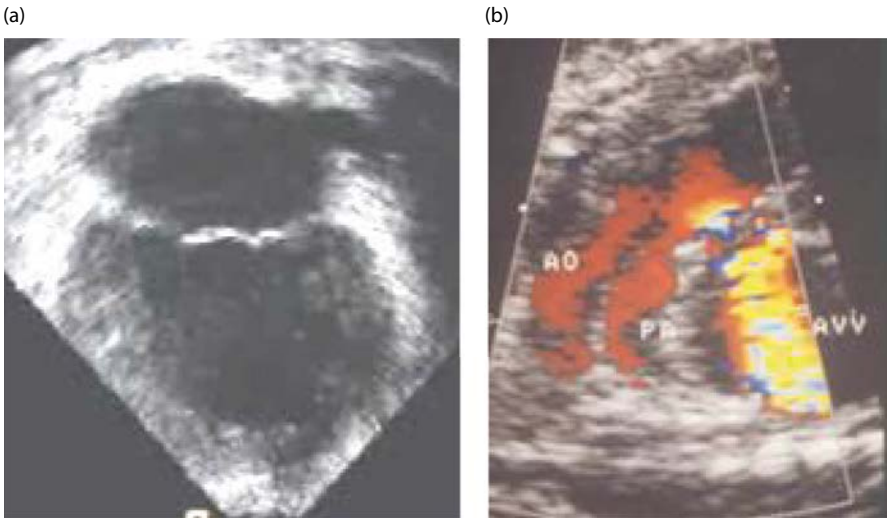


**Figure 22.13**
Cor biloculare: (a) common AV valve insufficiency; (b) severe regurgitation of AV valve in color Doppler.

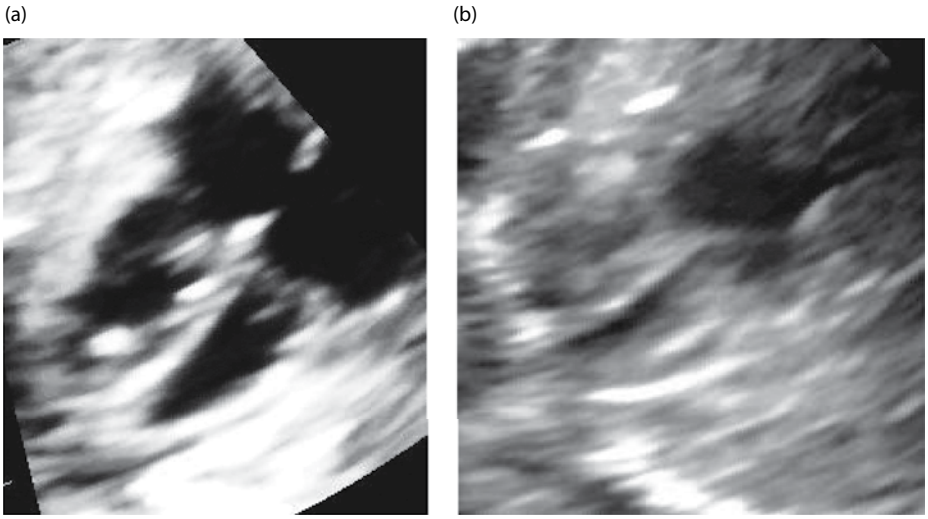


**Figure 22.14**
Risk of false positive: (a) Risk of false negative. An ostium secundum ASD is observed while a tiny ostium primum is overlooked; (b) Same patient: usual aspect of the AV valve.

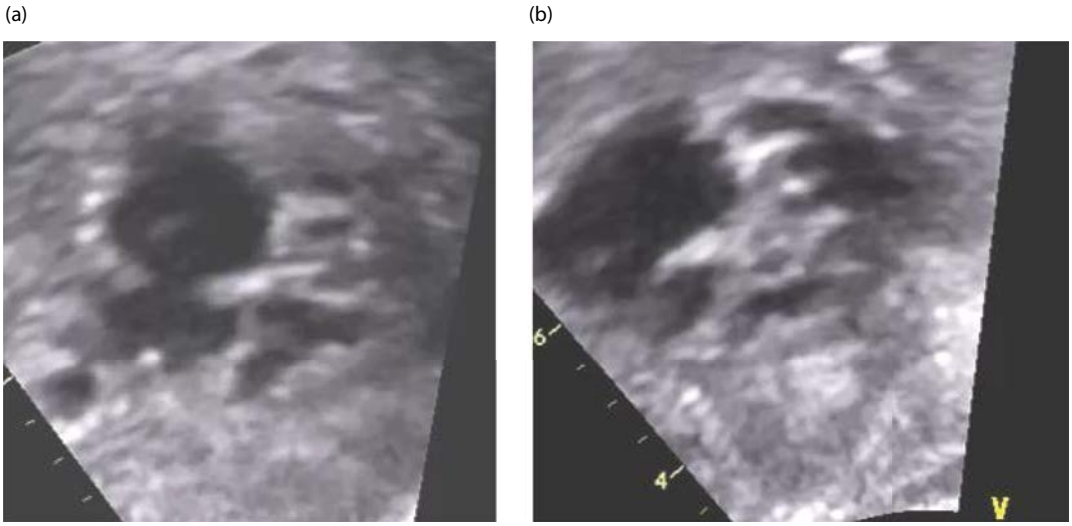


**Figure 22.15**
Risk of false positive: (a) near to normal; (b) same patient, mitral aspect of AVSD.

To maintain or restore hearts with four chambers and two concordant arteries is the core of every surgical cardiac repair of congenital heart defects. It must be reiterated that there is a wide range of severity, from simple anatomical forms to cor biloculare (Figure 22.13) or single atria. These severe malformations, while not necessarily lethal, are beyond the scope of satisfactory anatomical repairs and are amenable to early prenatal diagnosis, thus raising major ethical issues regarding continuation of the pregnancy. There is a correlation between the degree of anatomic alteration of the structures of

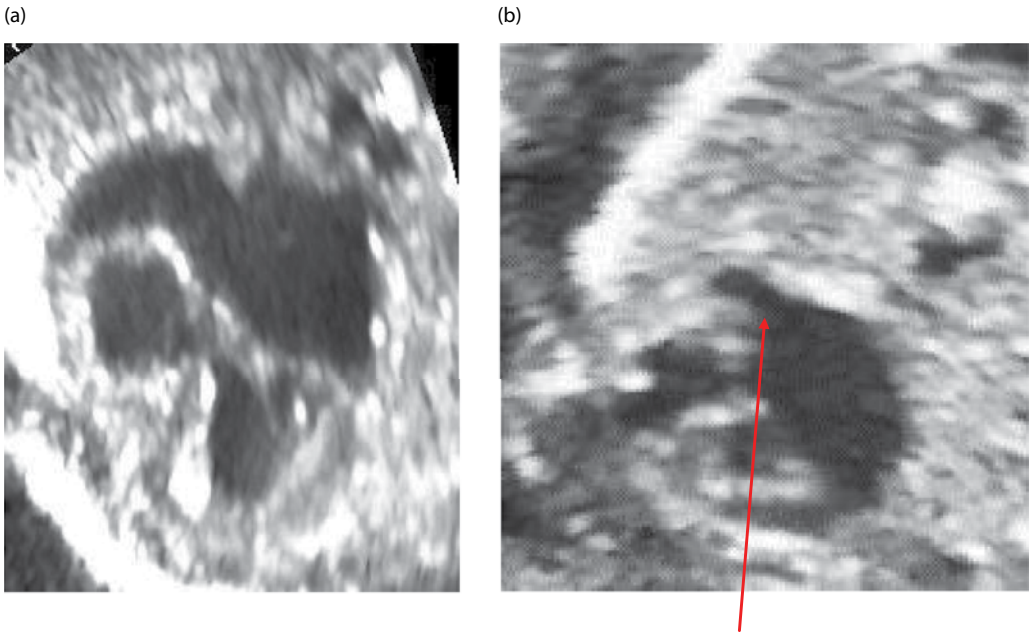


**Figure 22.16**
(a) Single atria; (b) first trimester, note right-sided left appendage (finger aspect, arrowed).

the AV septal defects and the surgical potential to repair each component of the malformation. Single atria, generally components of a left heterotaxy, do not prevent septation. The severity of this malformation generally stems from anomalies of the mitral apparatus or of the venous drainage, as well as complete AV blocks. Right-sided position of a left appendage may be seen (Figure 22.16) even in first-trimester examinations.

Absent or very short interventricular septa are by themselves compatible with life, and most of these newborns, even those seriously affected, may survive spontaneously if there are no lethal or ductus-dependent malformations associated. However, biventricular (anatomic) repairs will be surely impossible, thus leading to univentricular palliative repairs (Fontan circulation).

The tissue of one valvar component may be underdeveloped[35] and lead to perinatal leakage, raising major difficulties in achieving proper surgical repair. Similarly, chordae may be inserted on the septal left narrowed ventricular outflow tract, which may sometimes be difficult to fix. These abnormal mitral chordal insertions may raise the possibility of an AV septal defect, even in minor anatomical forms (Figure 22.15).

Development and size of the ventricles must be carefully assessed. Anatomic biventricular repairs necessarily need proper balance of the ventricles and the AV annulus.[36,37] It is widely accepted that balanced AV septal defects are often seen in cases of Down syndrome, sometimes associated with other malformations, such as tetralogy of Fallot and persistent left superior vena cava. In fact, all types of chromosomal or monogenic syndromes may be diagnosed in this context.[38,39] The left ventricle may be dominant (hypoplasia of the right ventricle of variable degree, sometimes major) (Figure 22.17a). Conversely, the right ventricle may be dominant (hypoplasia of the left ventricle of variable degree, sometimes major), leading to the description of an associated hypoplastic left ventricle and mitral atresia or major hypoplasia (Figure 22.17b). An unbalanced structure may raise suspicion of related downstream anomalies, some of them reparable, such as coarctation of the aorta. In those functional cases, postoperative rehabilitation of the left ventricle is possible[40] (Figure 22.18). Recognition of such functional aspects of diminutive ventricles, as opposed to developmental hypoplastic

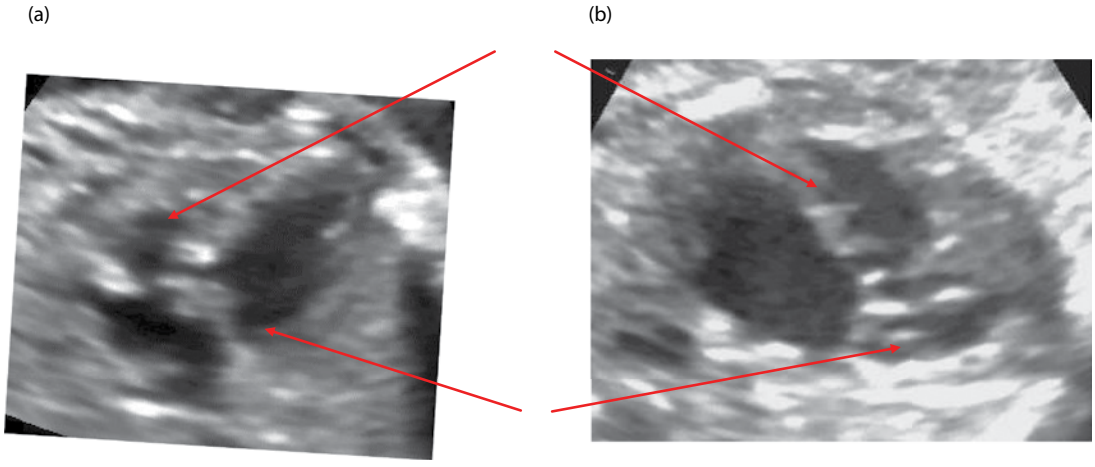


**Figure 22.17**
Unbalanced ventricles in AVSD: (a) left dominant; (b) right dominance (top arrow, RV; lower arrow, LV).

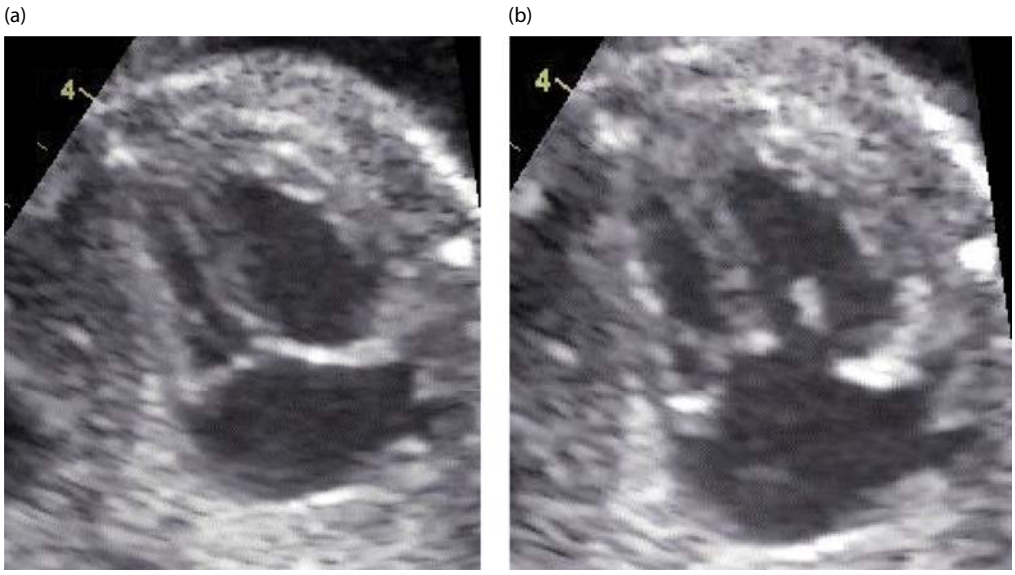


**Figure 22.18**
(a,b) Partial AVSD with coarctation: right dominance, proper left ventricle geometry.

ventricles, is therefore of crucial importance to avoid excess diagnoses of hypoplastic left heart syndrome associated with AV septal defect. These events occur principally in cases of "partial" AVSDs. The neonatal course depends on the anatomy and the function of the mitral apparatus and on possible left ventricular tract obstructions ("tunnel-like"). Multiple interventions may sometimes be required. Because of these associations, in cases of AV septal defect, "partial" does not mean "benign," and balanced complete forms may be easier to repair surgically.

## Associated malformations

Besides cardiac malformations associated with AVSDs, all types of malformations can be associated with this anomaly. Detection of any malformation must lead to thorough examination of the fetal heart. Few are prenatally lethal, such as major valvar insufficiency, which occurs especially in heterotaxy, or cardiomyopathies (hypertrophic or noncompacted) with anomalies of AV conduction (Figure 22.19). Associations may worsen prognosis and increase the difficulty of surgery.

First, tetralogy of Fallot is not a rare association. Its detection should prompt referral to genetic counseling (associated trisomies 21 or 18 might be more probable than microdeletion 22q1.1). More complex conotruncal malformations, such as tetralogy of Fallot with pulmonary atresia and transposition of the great arteries, as well as all types of double-outlet right ventricle, which are not lethal in cases of preserved pulmonary anterograde flow but are often refractory to repair (Figure 22.20). These malformations are frequently part of heterotaxy syndromes (most often right but also left) and are particularly severe if associated with total anomalous pulmonary venous return, especially the infradiaphragmatic variant (Figure 22.21). Left or right heterotaxies may be diagnosed if the AV defect is associated with an anomaly of the AV situs or a double-outlet right ventricle. Nevertheless, a left heterotaxy is much more probable in case of single atria, azygos continuation, or AV block.

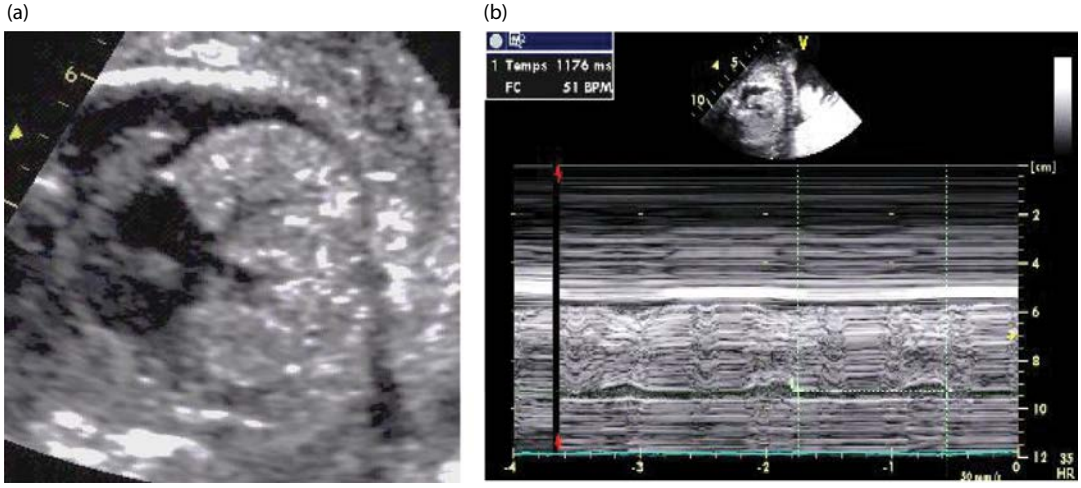


**Figure 22.19**
AVSD, lethal prenatally: (a) with cardiomyopathy; (b) with AV block.

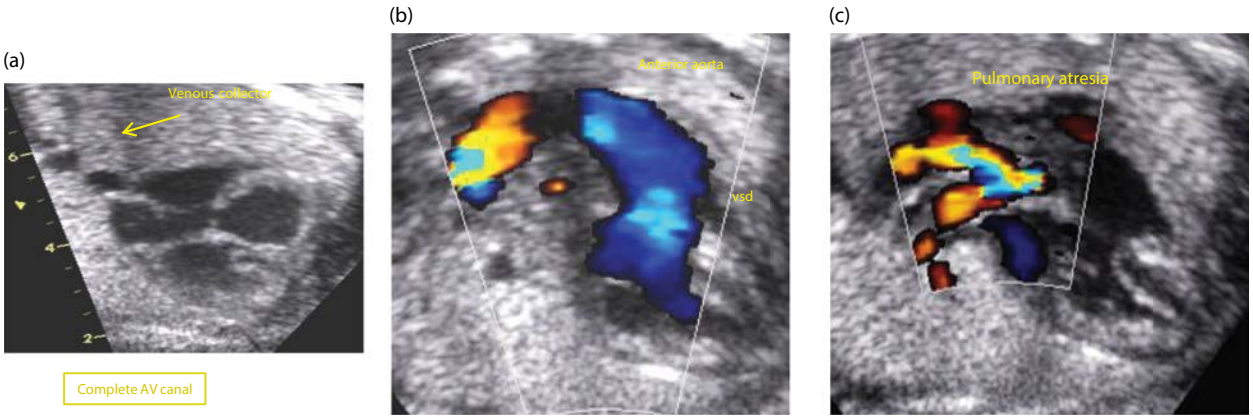


**Figure 22.20**
AVSD at 25 weeks: (a) with double-outlet right ventricle; (b) with pulmonary atresia; (c) TAPVD.

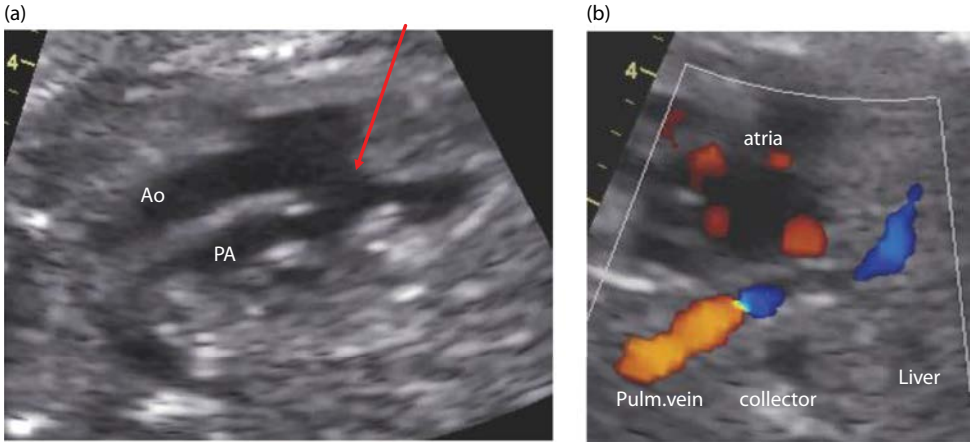


**Figure 22.21**
Complete AVSD: (a) with transposition of great arteries and TAPVR (arrow, complete AV canal); (b) nonreparable form of AVSD (infradiaphragmatic TAPVD).

## *Extracardiac malformations associated with AVSD*

From a genetic point of view, all variants of AV septal defects represent a major marker of chromosomal anomalies, mainly trisomy 21. It is most commonly seen in balanced complete forms but may also occur in partial AVSD, or cases with an inlet ventricular septal defect, or even isolated mitral cleft and abnormal insertions to the septum. Approximately half of patients with an AV septal defect also suffer from Down syndrome, but only 25% of patients with trisomy 21 have an AV septal defect.[15] This suggests a multifactorial origin for the malformation, with the participation of genetic modifiers,[9] like CRELD1 and VEGFA, which have been demonstrated to be risk factors for AVSD.[15] Many other chromosomal anomalies may be associated, such as trisomy 18 or microdeletions (8p, 3p). In fact, all types of disorders may be encountered and must be investigated by new genetic technologies. AV septal defects are also part of the phenotype of a great number of syndromes, including Holt-Oram, Ellis-van Creveld, Smith-Lemli-Opitz, and CHARGE syndromes. AV septal defects are also extremely frequent (more than 80%) in heterotaxy syndromes. This indicates an important role of the laterality genes in the normal development of the AV junction.[16] Finally, AVSD, which is primarily an anomaly of the posterior second heart field, can coexist with anomalies of the anterior second heart field like tetralogy of Fallot, especially in patients with trisomy 21.[17]

AVSD is amenable to diagnosis by general sonographers, though cases of minor or mild anatomic variants may be more challenging. The importance of prenatal diagnosis in low-risk populations is increased because of the frequent association with other cardiopathies, extracardiac malformations, or genetic disorders. To achieve this goal, general sonographers should be trained to identify suspicious anatomy and should be overseen by level III obstetrician sonographers and pediatric cardiologists, who can confirm the diagnosis, assess prognosis, and determine perinatal management. Prenatal detection improves care to fetuses and neonates, which is always demanding in these evolving[41] and complex malformations.

# References

1. Anderson RH et al. *Word J Pediatr Congenit Heart Surg* 2010; 1:59–67.

2. Penskoke PA et al. *J Thorac Cardiovasc Surg* 1985;90:611–22.
3. Rastelli, GC et al. *J Thoracovasc Surg* 1968;55:299–308.
4. Fredouille C et al. *Fetal Diagn Ther* 2002;17:188–92.
5. Blom NA et al. *Am J Cardiol* 2003;91:180–4.
6. Webb S et al. *Circ Res* 1999;84:897–905.
7. Snarr BS et al. *Circ Res* 2007;101:971–4.
8. Goddeeris MM et al. *Development* 2008;135:1887–95.
9. Briggs LE et al. *Differentiation* 2012;84:117–30.
10. Snarr BS et al. *Dev Dyn* 2007;236:1287–94.
11. Webb S et al. *Circ Res* 1998;82:645–56.
12. De la Cruz MV et al. *Anat Rec* 1997;247:512–20.
13. Kim JS et al. *Circ Res* 2001;88:395–402.
14. Anderson RH et al. *Heart* 2003;89:949–58.
15. Redig JK et al. *AIMS Genet* 2014;1:1–19.
16. Calkoen EE et al. *Int J Cardiol* 2016;202:784–95.
17. Nguyen HH, Jay PY. *J Pediatr* 2014;165:194–6.
18. Bader RS et al. *Congenit Heart Dis* 2014;9:286–93.
19. Gembruch U et al. *Am Heart J* 1991;121: 1489–97.
20. Allan LD. *Am J Obstet Gynecol* 1999;181:1250–1.
21. Smallhorn JF. *Echocardiography* 2001;18:415–32.
22. Ando M, Takahashi Y. *Ann Thorac Surg* 2010;90:614–21.
23. Khoshnood B et al. *Heart* 2012 Nov;98:1667–73.
24. Marek J et al. *Heart* 2011;97:124–30.
25. Huggon IC et al. *J Am Coll Cardiol* 2000;36:593–601.
26. Craig B. *Heart* 2006;92:1879–85.
27. Machlitt A et al. *Ultrasound Obstet Gynecol* 2004;24:618–22.
28. Silverman NH, Moon-Grady AJ. *J Am Coll Cardiol* 2016;68: 931–3.
29. Silverman NH et al. *Int J Cardiol* 1984;5:567–73.
30. Kaski JP et al. *Heart* 2006;92:832–5.
31. Calkoen E et al. *Fetal Diagn Ther* 2016;39(1):13–20.
32. Fesslova V et al. *Cardiol Young* 2002;12:18–26.
33. Friedberg MK et al. *Congenit Heart Dis* 2007;2:110–14.
34. Paladini D et al. *Ultrasound Obstet Gynecol* 2009;34:268–73.
35. Davey BT, Rychik J. *Pediatr Cardiol* 2016;37:50–4.
36. Mone F et al. *Prenat Diagn* 2015;35(6):577–82.
37. Rasiah SV et al. *Prenat Diagn* 2008;28:95–101.
38. Langford K et al. *Prenat Diagn* 2005;25:137–9.
39. Pierpont ME et al. *Am J Med Genet* 2000;97:289–96.
40. Jouannic JM et al. *Am J Obstet Gynecol* 2003;22:527–30.
41. Davey B et al. *Pediatr Cardiol* 2013;34:1797–802.

# 23

# Double-inlet ventricle

Astrid Hellmund and Ulrich Gembruch

## Introduction

Double-inlet left or right ventricle (DILV or DIRV) or double-inlet ventricle (DIV), when the origin of the single chamber cannot be established, is a rare form of congenital heart disease with a prevalence of 0.1–0.08 per 1,000 live births. It accounts for 1.25%–1.8% of all congenital heart disease.[1–3] It belongs to a variety of heart diseases comprising a functionally single ventricle. A double-inlet single ventricle is present when two normally developed atria connect via separate right and left atrioventricular (AV) valves to a common ventricle in which the ventricular inlet is unseptated.[4,5]

However, in many of these cases, one of the AV valves is atretic, and the distinction between DIV and other forms of functional univentricular hearts like tricuspid atresia is difficult. Moreover, there is a controversial discussion of the nomenclature of single-ventricle hearts.

## Etiology

Little is known about the etiology or epidemiologic associations. Familial aggregation of single-ventricle malformations or other congenital heart defects in siblings are described, but rare (2.8%). In one study of 223 patients with univentricular heart defects, only one sibling (0.5%) of 102 patients with DILV had a congenital heart defect, whereas patients with more complex univentricular defects more often had siblings with heart defects (5%).[3] One study showed an association to paternal smoking and alcohol consumption.[2] Chromosomal abnormalities in patients with single ventricle are possible, but rare (2/223, 0.9%).[3] However, univentricular heart defects, especially in cases of a common inlet, are often associated with left or right isomerism.[2,4]

## Nomenclature

Many terms have been used to describe hearts with a functional single ventricle: common ventricle, single ventricle, primitive ventricle, univentricular heart, and double-inlet ventricle. However, most authors agree to the categorization of single-ventricle hearts in three morphological types:

- Left-ventricle type with or without rudimentary right ventricle
- Right-ventricle type with or without rudimentary left ventricle
- Indeterminate or undifferentiated type

Further subcategorization can be achieved by regarding the atrial situs (solitus, inversus, and indeterminate), the type of AV connection (double inlet, absent right, or absent left)[6] and right- or left-hand pattern of ventricular organization and ventriculoatrial connection (concordant, discordant, double-outlet aorta, single-outlet aorta, single-outlet pulmonary trunk, and common arterial trunk).[4]

## Ventricular morphology

The distinction between double-inlet left, right, or undifferentiated type of ventricle is made by characterization of the ventricular morphology such as trabecular structure, papillary muscles, and septal surface.[7] Whereas the left ventricular myocardium appears smooth and has fine trabeculations, the right ventricular myocardium is irregular and coarse. Postnatally angiographic investigations can confirm the morphology of the ventricle in most cases.[8] In an angiographic study, the ventricular morphology was determined in 476 patients undergoing Fontan procedure. A dominant left ventricle was identified in 72%, a dominant right ventricle in 16%, and a ventricle of indeterminate morphology was detected in 1%.[9] In contrast, a Chinese study of 60 patients with double-inlet ventricle (age range from 1 day to 15 years) examined by echocardiography found a dominant right ventricle in 60% (36/60), a dominant left ventricle in 28% (28/60), and an indeterminate ventricle in 12% (7/60); right atrial isomerism was present in the majority of patients with DIRV (30/36), in 5/17 in cases of DILV, and 6/7 in ventricles of indeterminate morphology.[10]

In about 60%–80%, DIV is a double inlet into a morphologic left ventricle (double-inlet left ventricle). In this situation, a small underdeveloped right ventricle is often present and communicates with the single ventricle via a ventricular septal defect, the bulboventricular foramen, or outlet foramen. Both terms describe the same morphologic structure, the interventricular communication between a dominant ventricle and a rudimentary outlet chamber.[11] This rudimentary outlet chamber may be located right sided and anterior or left sided and anterior.

Other forms of DIV include a double-inlet right ventricle (5%–25%), a ventricle of mixed morphology, and a ventricle of undetermined morphology (<5%).[4] The single right ventricle is often associated to viscero-atrial heterotaxy, particularly to right isomerism. The rudimentary left chamber is situated at the inferior, posterior, or diaphragmatic side of the ventricle. In the type of a single ventricle with indeterminate morphology, any form of abnormality of the outflow tracts, AV valves, and pulmonary veins is common and may complicate the situation.

## Morphologic differentiation between DILV with one imperforate valve and tricuspid atresia

When the right AV connection is absent and the left atrium is connected to a dominant left ventricle, the situation is classically named *tricuspid atresia*. In contrast, in case of continuity of the AV connection—visible in pathologic studies because of the continuity of the parietal wall of atrium and ventricle—combined with an atretic valve, the type of functionally univentricular heart is called double-inlet left ventricle. Moreover, in case of a tricuspid atresia, the rudimentary right ventricle is situated at the anterosuperior shoulder of the ventricular mass with the trabecular component to the right, whereas in DIV the trabeculation of the anterosuperior rudimentary outlet chamber can be either left sided, right sided, or anterior.[5] In the majority of DIV, the ventriculo-arterial connection is discordant,[5] whereas in classic tricuspid atresia both discordant and concordant ventriculo-arterial connection can be found nearly equally, in a larger study of 54 cases of tricuspid atresia in 46.3% versus 51.9%.[12]

## Outflow tract anomalies

The outflow tracts usually are in malposition and can arise from the single ventricle or the small outlet chamber. The more uncommon case of a right-sided rudimentary right ventricle and a normal ventriculo-arterial connection is called Holmes heart. The incidence of a concordant ventriculo-arterial connection is 15% of all cases of DILV.[13] First described by Dr. Andrew Holmes in 1823 was a double-inlet left ventricle with a large aorta originating from the left ventricle, a rather restrictive bulboventricular foramen, and a small outlet chamber with subpulmonary stenosis in the presence of a normal situs.[14] Cifarelli et al. found four possible types of Holmes heart in which the rudimentary right chamber is located right or left sided, and the left AV connection is present or absent.[15]

The bulboventricular foramen is almost always surrounded by muscle in case of a dominant left ventricle, and the size and degree of restriction are important for development of the vessel originating from the rudimentary outlet chamber behind the foramen. However, in case of DIRV, the foramen is usually perimembraneous and both vessels can originate from the dominant right ventricle, so that the size of the foramen ovale is of less importance.[5]

In case of a restrictive bulboventricular foramen, the vessel arising from the small outlet chamber is usually small. Therefore, aortic coarctation or pulmonary stenosis are common findings. In a study of 43 live-born, prenatally diagnosed fetuses with DILV, 49% had systemic obstruction, 28% pulmonary obstruction, and only 21% no obstruction of the outflow tract.[16]

Systemic outflow tract obstruction such as subaortic stenosis or atresia may be present at birth or may be acquired postnatally. Most frequently, congenital subaortic stenosis is found in the situation of a DILV with a rudimentary right chamber and malposition of the great arteries, where the blood supply for systemic circulation passes a small bulboventricular foramen. In those cases, pulmonary stenosis is uncommon. In contrast, the bulboventricular foramen tends to be large in case of pulmonary outflow obstruction; therefore, subaortic stenosis is less frequent. However, aortic stenosis may rarely be present or develop postnatally even in cases with pulmonary outflow obstruction. In fetuses with DIV of right ventricular type, aortic outflow obstruction may also be present or develop. In this situation, the aortic outflow tract is narrowed and wedged between the ventriculo-infundibular fold and the infundibular septum.[4]

Furthermore, anomalies of the continuity of the great vessels such as discontinuous pulmonary arteries or interrupted aortic arch can be present and have to be evaluated. Anomalies of the venous connections are infrequent, although any kind of cardiac abnormality must be anticipated in these hearts.

## Differential diagnosis

Differential diagnosis of DIV and DILV includes tricuspid atresia, hypoplastic left heart, and unbalanced AV septal defect in cases of heterotaxy (Table 23.1).

## Ultrasound findings

In case of DIV, ultrasound examination reveals an abnormal four-chamber view of the heart, showing only a single ventricle without ventricular septum (Figures 23.1 and 23.2). This finding can already be detected by early fetal echocardiography in case of sufficient ultrasound conditions.[17] Additionally, an increased nuchal translucency may be present as a nonspecific hint to a congenital cardiac defect.[18]

**Table 23.1** Differential diagnosis of cardiac anomalies with single ventricle

- Tricuspid atresia with ventricular septal defect
- Hypoplastic left heart syndrome
- Unbalanced atrioventricular septal defect
- Double inlet ventricle
- Pulmonary atresia with intact septum (hypoplastic right ventricle)
- Heterotaxy syndrome

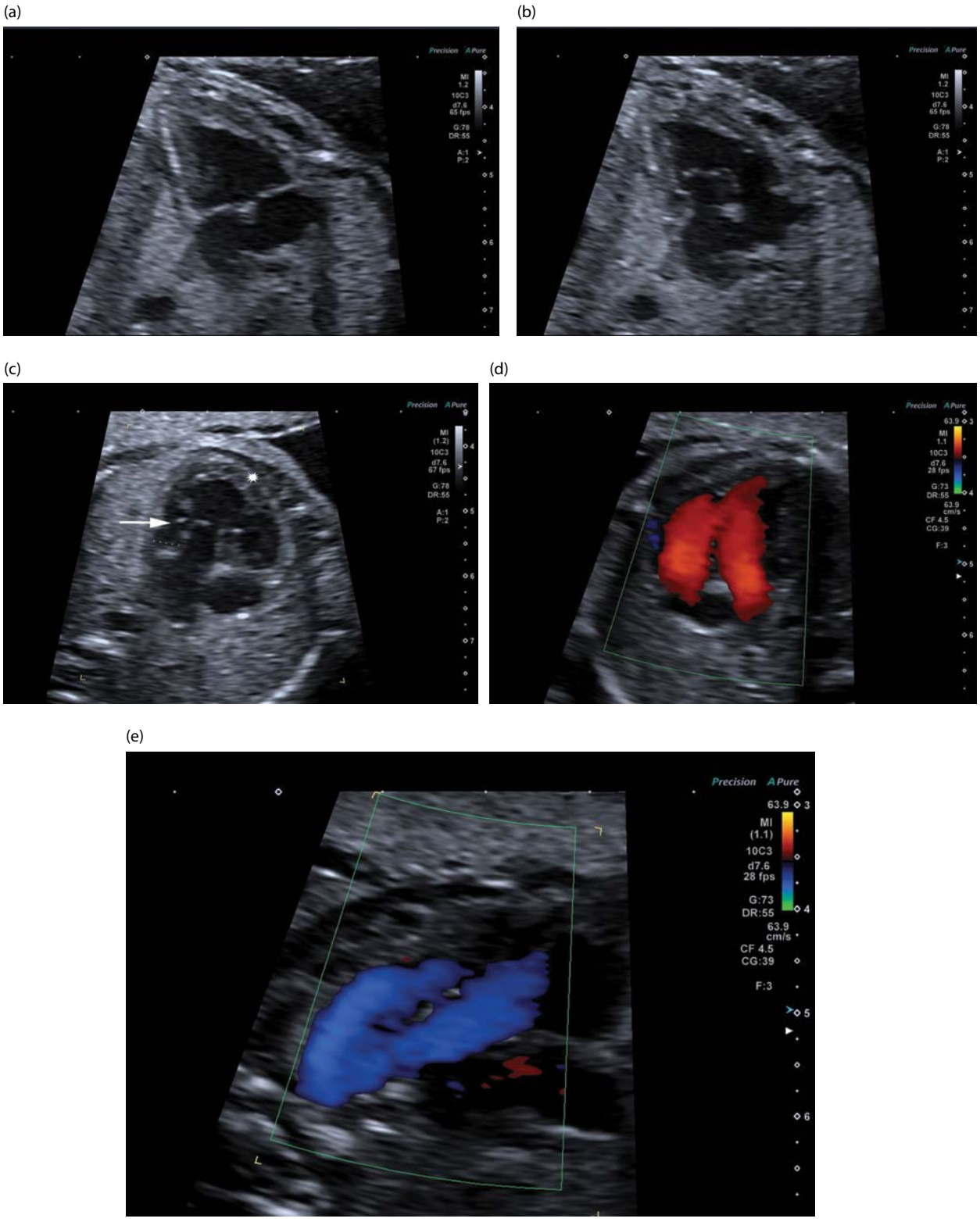


**Figure 23.1**
(a) Double-inlet right ventricle is shown in a fetus at 22 + 5 weeks' gestation. Two regular atria and two patent atrioventricular valves opening into a single ventricle are present. The rudimentary outlet chamber cannot be visualized in the four-chamber view. (b) The two regular atria and two patent atrioventricular valves opening into one unseptated ventricle. (c) A small outlet chamber is situated at the left side of the dominant ventricle (white arrow). The trabeculation of the dominant ventricle is coarse and irregular, indicating a morphologic right ventricle (white star). (d) By color Doppler imaging, the blood flow across two patent atrioventricular valves into a single unseptated ventricle is demonstrated. (e) The outflow tracts arise parallel in a dextro-malposition: the aorta is originating from the dominant right ventricle; the pulmonary trunk from the small left-sided outlet chamber without obstruction.

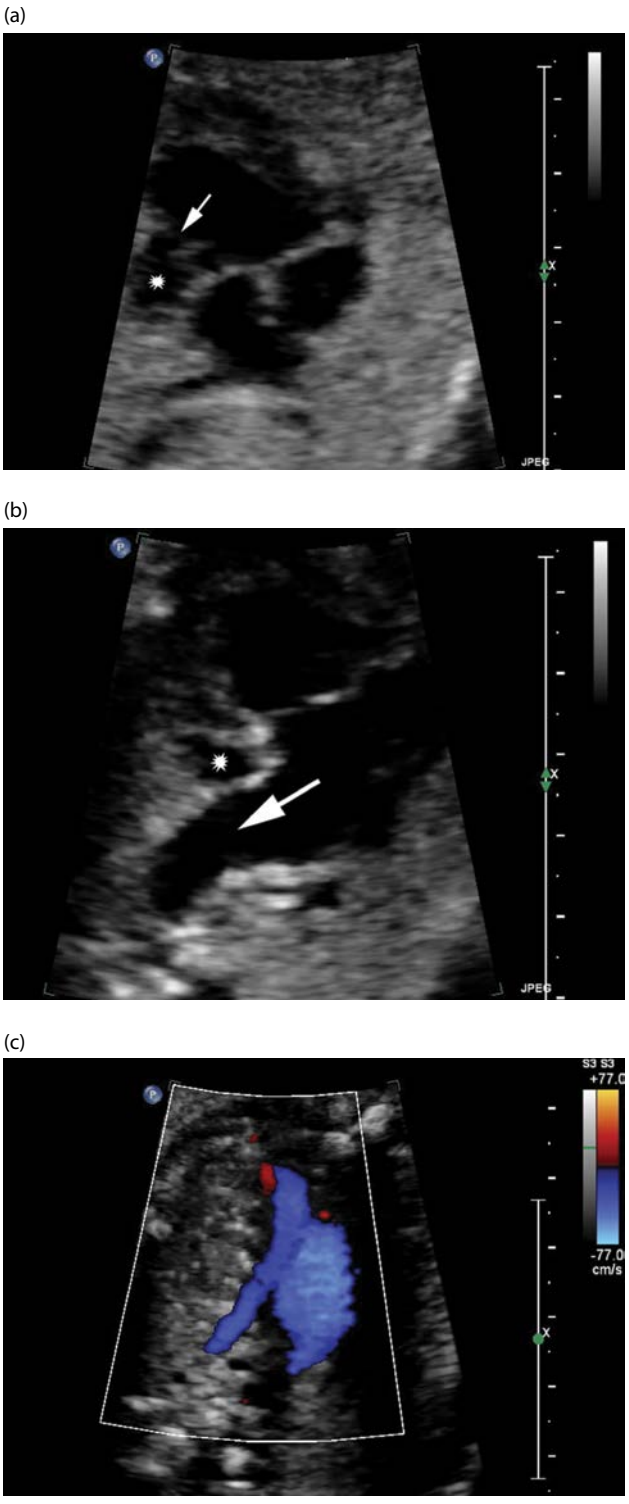


**Figure 23.2**
(a) Double-inlet left ventricle is shown in a fetus at 20 + 1 weeks' gestation. Two atria, two separate and patent atrioventricular valves opening into a single ventricle, and a small right-sided outlet chamber (white star) with bulboventricular foramen (white arrow) are visualized. (b) Levo-malposition of the great arteries with a narrow aorta (aortic coarctation) (white star), and a large pulmonary outflow (white arrow). (c) By color Doppler imaging, the blood flow into the narrow aorta (additional aortic coarctation) and the large pulmonary trunk is demonstrated.

As mentioned previously, a connection between two atria and a single ventricle is mandatory for the diagnosis of DIV. In case of two functionally intact AV valves draining into one ventricle, the diagnosis is obvious. However, in case of atresia of one of the AV valves, differential diagnosis is not easy. Tricuspid atresia and DILV with atresia of the right AV valve present quite similar in fetal echocardiography. The identification of the morphology of the dominant ventricle by means of the anatomic characteristics such as trabecular structure is possible in many cases, as described above.

In contrast to findings in hypoplastic left or hypoplastic right heart, the rudimentary chamber of the right ventricle in DILV is not located at the plane of the four-chamber view but can be visualized in a more cranial plane on the left or right side of the ventricle. In some cases, visualization of the rudimentary outlet chamber and the bulboventricular foramen is difficult. More often, the small outlet chamber is located at the left side of the ventricle, and the great arteries arise in levo-malposition. In cases of right-sided small outlet chamber, the great arteries arise in dextro-malposition or ventriculo-arterial concordance with origin of the pulmonary artery from the small-outlet chamber. Color Doppler adds information about the patency of the AV valves and restriction of flow across the bulboventricular foramen. Present outflow tract obstructions are visualized due to size discrepancy.

## Associated extracardiac findings

Anomalies of the situs such as right/left isomerism are associated to univentricular hearts and point to the differential diagnosis of heterotaxy.

In DILV, extracardiac anomalies and chromosomal abnormalities are possible but rare.[19,20] However, in a series of 65 fetuses diagnosed with DILV, there were three fetuses with additional nonchromosomal anomalies (cystic hygroma $n = 1$, congenital diaphragmatic hernia $n = 2$), one with Klinefelter syndrome, and one with trisomy 18. Among 106 postnatally diagnosed patients, 10% had extracardiac congenital anomalies or chromosomal anomalies (Goldenhar syndrome $n = 1$, DiGeorge syndrome $n = 1$).[16]

## Course of pregnancy

Because of the usual absence of chromosomal anomalies, additional associated extracardiac anomalies, and patent cardiac function, the course of pregnancy is commonly uneventful for most affected fetuses. However, serial follow-up scans are mandatory for detection of worsening of outflow tract obstructions or insufficiency of AV valves.[13]

## Outcome

Without operation, the survival rate for patients with univentricular heart defect is approximately 38% within the first year of life with further deterioration in youth. All patients

with DIV or DILV require surgery with univentricular repair. In cases of unobstructed pulmonary flow, timely pulmonary banding is necessary to restrict unlimited pulmonary blood flow and to avoid subsequent development of pulmonary hypertension.[13] In 1999, a survival study comprising 815,569 children with congenital heart disease and surgical therapy found 67 cases with DIV. This report showed a 77.6% survival rate after the first week of life and that declined to 41.8% after 6 months. At 1 year of life, the survival rate was 38.8%, which continued to the age of 10 years.[1]

A more recent report from 2008 revealed 65 prenatally diagnosed cases of DILV, of which 43 were live-born, and 106 patients diagnosed in the first 3 months of life (median 3 days). Transplantation-free survival rates were 88%, 82%, 79%, and 76% for 1 month, 1 year, 5 years, and 10 years, respectively. The necessity of neonatal surgery was associated with worse outcome; prenatal diagnosis was not associated with better postnatal survival.[16]

Another study of 312 patients with functionally single ventricle cardiac defects, including 29 patients with DIV, 44 cases of tricuspid atresia, and 72 cases of hypoplastic left heart found a lower transplantation-free survival after 7 years for fetuses with a dominant RV compared with fetuses with a dominant LV.[21]

The presence of outflow obstruction is known to be a major factor for postnatal survival. Patients presenting with DILV, malposition, and pulmonary outflow obstruction had predicted survival rates of 90% at 1 year and 79% at 10 years, whereas patients with unobstructed pulmonary flow and systemic outflow tract obstruction survived in 36% and 11% their first and tenth years of life, respectively.[22–24]

A recent review of 105 patients with DILV showed 23% overall mortality with a medium follow-up of 7.7 years (range 0.01–28 years). The survival rates were 89%, 80%, and 63% at 5, 15, and 25 years. Whereas the presence of arrhythmia and pacemaker requirement was an independent risk factor of mortality in that study, pulmonary atresia or stenosis and pulmonary artery banding were associated with decreased mortality. Gender, aortic arch anomaly, and systemic outflow obstruction were no risk factors. The authors state that systemic outflow obstruction was not an independent risk factor for mortality due to the early recognition and timely treatment of these obstructions.[25]

Postnatal development of subaortic stenosis is possible and was detected in 72% of 43 patients with DILV, rudimentary right chamber and malposition of great arteries after banding of the pulmonary artery. The median interval to the detection of subaortic stenosis was 2.5 years.[26] Different explanations for this development include increasing myocardial hypertrophy after pulmonary artery banding, diminishing the size of the bulboventricular foramen, and changing of ventricular volumes and pressure gradients across the bulboventricular foramen after the Fontan operation. Worsening of pulmonary outflow obstruction over time is also common.[4]

Postnatal complications besides outflow tract obstructions include development of pulmonary vascular obstruction or hypertension, progressive left heart hypertension in cases of restrictive interatrial connection, heart block, and progressive AV valve regurgitation as much as elevated venous pressure, thromboembolism, and protein-losing enteropathy.

In summary, DIV and DILV can be associated with variable neonatal outcome depending on the associated cardiac anomalies.

## References


1. Samanek M, Voriskova M. *Pediatr Cardiol* 1999;20:411–7.
2. Steinberger EK et al. *Teratology* 2002;65:106–15.
3. Weigel TJ et al. *Am J Cardiol* 1989;64:768–71.
4. Freedom RM, Yoo SJ. The double-inlet ventricle. In: Freedom RM, Yoo SJ, Mikailian H, Williams WG, eds. *The Natural and Modified History of Congenital Heart Disease*. Elmsford, NY: Wiley-Blackwell; 2003:408–22.
5. Anderson RH. Terminology. In: Anderson RH, Macartney FJ, Shinebourne EA, Tynan M, eds. *Paediatric Cardiology*. Edinburgh, NY: Churchill Livingstone; 1987:65–82.
6. Anderson RH et al. *Am J Cardiol* 1984;54:822–8.
7. VanPraagh R et al. *Am J Cardiol* 1965;15:345–66.
8. Julsrud PR et al. *Pediatr Cardiol* 1997;18:208–12.
9. Julsrud PR et al. *Am J Cardiol* 2000;86:319–23.
10. Wang JK et al. *Am J Cardiol* 1993;72:85–9.
11. Anderson RH. *J Am Coll Cardiol* 1988;11:674–5.
12. Berg C et al. *Ultrasound Obstet Gynecol* 2010;35:183–90.
13. Weichert J et al. *Congenit Heart Dis* 2013;8:579–84.
14. Dobell AR, Van Praagh R. *Am Heart J* 1996;132:437–45.
15. Cifarelli A et al. *Int J Cardiol* 1989;25:21–6.
16. Tham EB et al. *Am J Cardiol* 2008;101:1652–6.
17. Smrcek JM et al. *J Ultrasound Med* 2006;25:187–96.
18. Wald NJ et al. *Prenat Diagn* 2008;28:1094–104.
19. Abuhamad A, Chaoui R. *A Practical Guide to Fetal Echocardiography: Normal and Abnormal Hearts*, 2nd edn. Philadelphia, PA: Lippincott Williams and Wilkins; 2010: 229–34.
20. Gidvani M et al. *AJP Rep* 2011;1:123–8.
21. Beroukhim RS et al. *Ultrasound Obstet Gynecol* 2015;45:657–63.
22. Franklin RC et al. *J Thorac Cardiovasc Surg* 1991;101:767–76.
23. Franklin RC et al. *J Thorac Cardiovasc Surg* 1991;101:917–23.
24. Franklin RC et al. *J Thorac Cardiovasc Surg* 1991;101:924–34.
25. Lan YT et al. *J Am Coll Cardiol* 2004;43:113–9.
26. Freedom RM et al. *Circulation* 1986;73:758–64.

# 24

# Lesions of the right heart

Julene S. Carvalho

## Lesions of the right heart

This chapter covers two conditions affecting the right-sided cardiac structures, namely, pulmonary atresia with intact ventricular septum and tricuspid atresia. From the morphological point of view, these are two distinct entities. However, depending on the exact sequential segmental analysis[1] some overlap exists with regard to the pathophysiology; consequently, surgical strategies may overlap.

## *Pulmonary atresia with intact ventricular septum*

### Introduction

Pulmonary atresia with intact ventricular septum (PAIVS) is a rare abnormality but one that has fascinated pediatric cardiologists over the years, both for the heterogeneity of the anatomical findings and for the challenges posed regarding optimal management to improve actuarial survival and to reduce morbidity. First descriptions of the anomaly date back to the late 1700s and mid-1800s.[2,3] It is, however, relatively recent publications that have contributed to our understanding of the anatomical variability and the pathophysiological implications.

Not infrequently, PAIVS is described as "hypoplastic right heart," but this terminology is best avoided, as the right ventricle (RV) is not always hypoplastic, and right ventricular hypoplasia is not pathognomonic of PAIVS. Essentially, in PAIVS there is complete obstruction to the pulmonary outflow tract (at valvar or subvalvar level) in the presence of an intact ventricular septum. This is usually associated with underdevelopment of the right ventricular cavity, which is hypertrophied, muscle bound, and hypertensive. Coronary abnormalities are common. However, variations do occur. In a minority of cases, there is important tricuspid regurgitation, the RV is dilated and may be thin walled with low pressure.

PAIVS with a very small RV is commonly diagnosed in midgestation due to an abnormal four-chamber view (Figure 24.1a–c). This diagnosis can also be made in the first and early second trimester as either atresia (Figure 24.2a,b) or critical stenosis. It is not uncommon for the RV to be of a relatively good size at 18–22 weeks (Figure 24.3a), and such examples may be overlooked in screening programs. This is of importance, as right ventricular growth may be subsequently impaired leading to a much smaller ventricular size at birth. Thus, fetal intervention to relieve the outflow tract obstruction may be considered in cases of either valve atresia or critical pulmonary stenosis in the hope that this may preserve right ventricular size and function.

Whatever the morphological variations and prenatal history, the neonate with PAIVS will present with a duct-dependent circulation, and thus will require immediate medical/surgical attention to maintain hemodynamic stability. Management strategies will depend on the nature of outflow tract obstruction and adequacy (or not) of the right ventricular structures to maintain (or not) a biventricular circulation in the medium to long term.

### Incidence

PAIVS accounts for approximately 1%–3% of babies with congenital heart disease,[4,5] whereas the incidence at birth obtained from a 20-year population-based study in Sweden (1980–1999) is 4.2 cases per 100,000 live births, with similar sex distribution.[6] An equivalent overall incidence of 4.5 per 100,000 live births (186 cases) was seen in the UK-Eire collaborative multicenter study (1991–1995), which is also population based.[7] Higher incidences of 7.1 and 8.1 per 100,000 live births were previously reported by the New England Infant Cardiac Program[4] and the Baltimore-Washington Infant study,[8] respectively. In the UK-Eire series, significant regional variations did occur, being lower in England and Wales and higher in Eire and Northern Ireland. As this latter study also included fetal cases of PAIVS, the influence of prenatal diagnosis on postnatal incidence can be appreciated. Pregnancy was terminated in 61% of the 86 cases diagnosed prenatally, and a further 4% of fetuses died spontaneously. Live birth incidence would have been higher at 5.6 per 100,000 in England and Wales, but unchanged in Eire and Northern Ireland, where no pregnancies were terminated. This clearly shows the impact of fetal diagnosis on postnatal incidence. More recently, data from a nationwide large inpatient database in the United States, which included all birth hospitalizations in the year 2008, showed an incidence of PAIVS at birth to be 3 per 100,000 live births, with a male-to-female ratio of 0.5.[9]

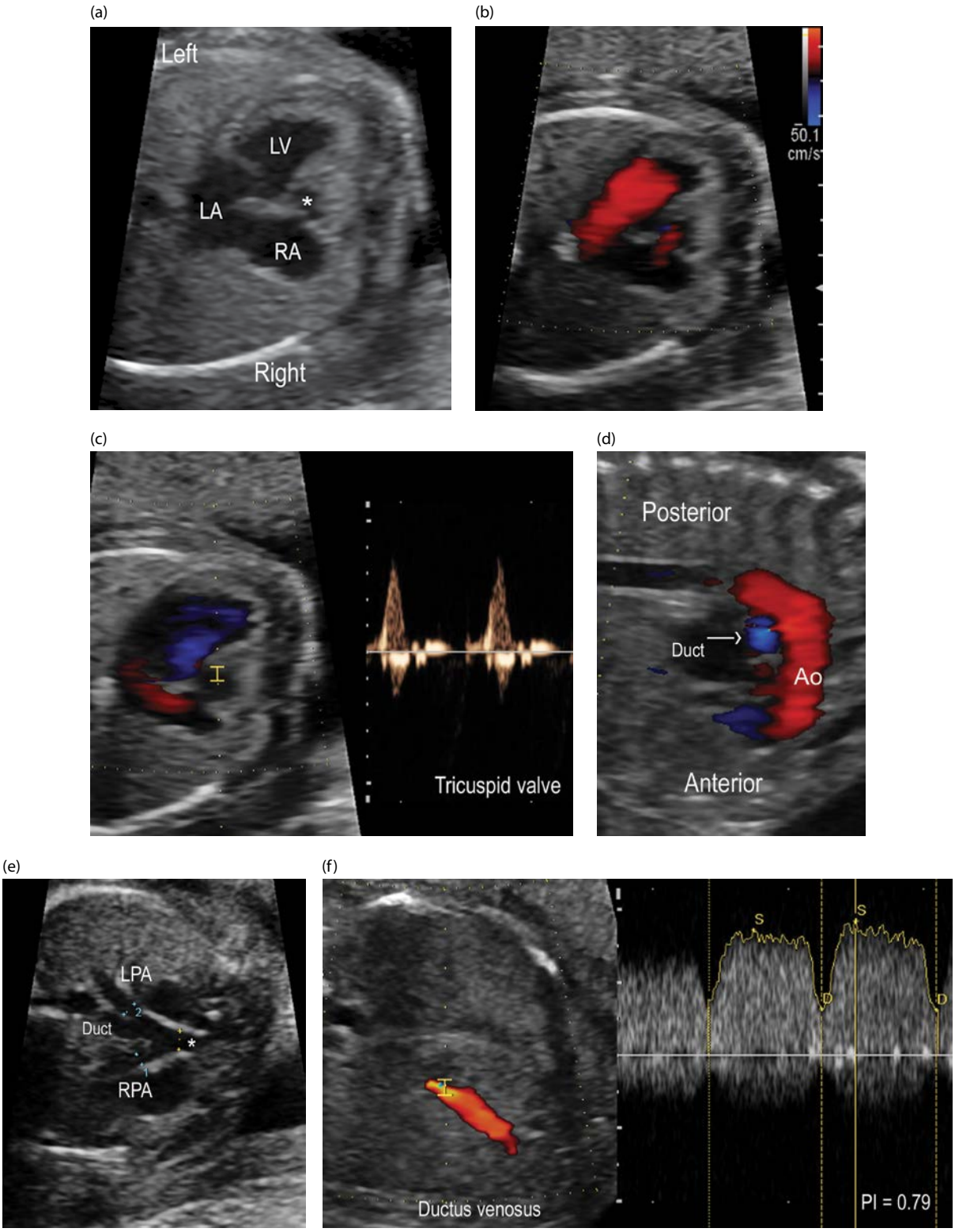


**Figure 24.1**
Images obtained from a 22-week fetus with muscular pulmonary atresia with intact ventricular septum and a small right ventricle (RV). (a–c) Four-chamber views show small RV cavity (indicated by the asterisk). Note a minute tricuspid valve with forward flow seen on color (b) and a monophasic, abnormal flow profile on pulsed wave Doppler (c, right panel). (d) Sagittal view of the aorta (Ao). Note the abnormal position of the arterial duct and reversed flow on color. (e) Axial view at the level of the RV outflow tract. The asterisk shows a small, blind ending main pulmonary artery (PA). Note that right and left PA branches (RPA and LPA) are confluent and of adequate size: RPA = 1.6 mm (Z-score = −1.8) and LPA = 2 mm (Z-score = +0.13). (f) Pulsed-wave Doppler across the ductus venosus shows normal pattern and normal pulsatility index (PI). (LA, left atrium; LV, left ventricle; RA, right atrium.)

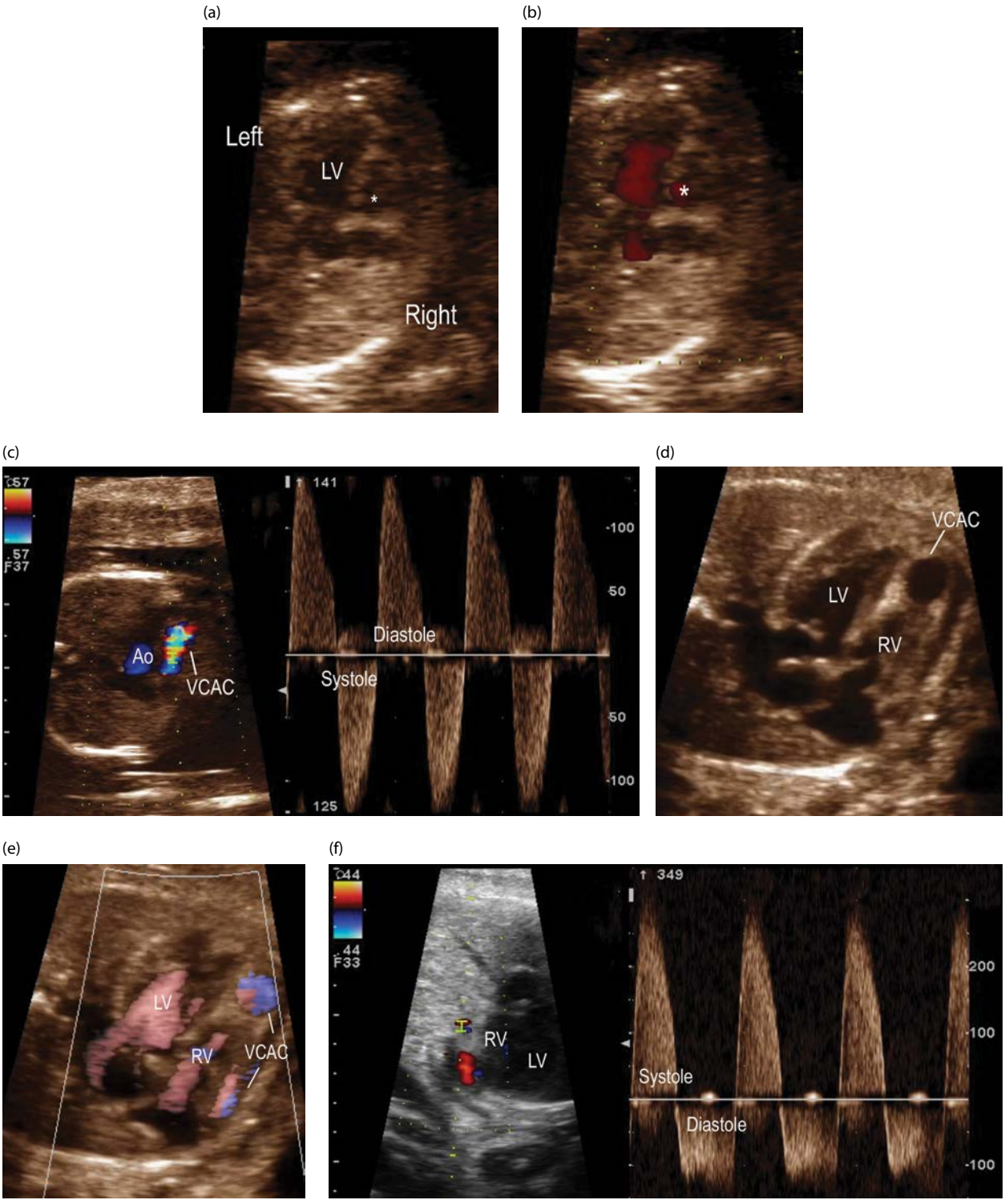


**Figure 24.2**
Images obtained at 16 weeks (a–c) and 22 weeks (d–f) of gestation from a fetus with muscular pulmonary atresia with intact ventricular septum. At 16 weeks: (a,b) note the small cavity of the right ventricle (RV) indicated by the asterisk. (c) Large ventriculo-coronary arterial connection (VCAC): left panel shows the VCAC on color flow mapping, and right panel shows pulsed-wave Doppler signal with diastolic flow toward the RV and systolic flow toward the aorta. At 22 weeks: (d,e) note the small inlet portion of the RV but also the presence of an abnormal cavity at the RV apex, which was part of a large VCAC. (f) Pulsed-wave Doppler shows high systolic velocity within the VCAC of ~350 cm/s, suggestive of stenosis. (Ao, aorta; LV, left ventricle.) This case was considered inoperable.

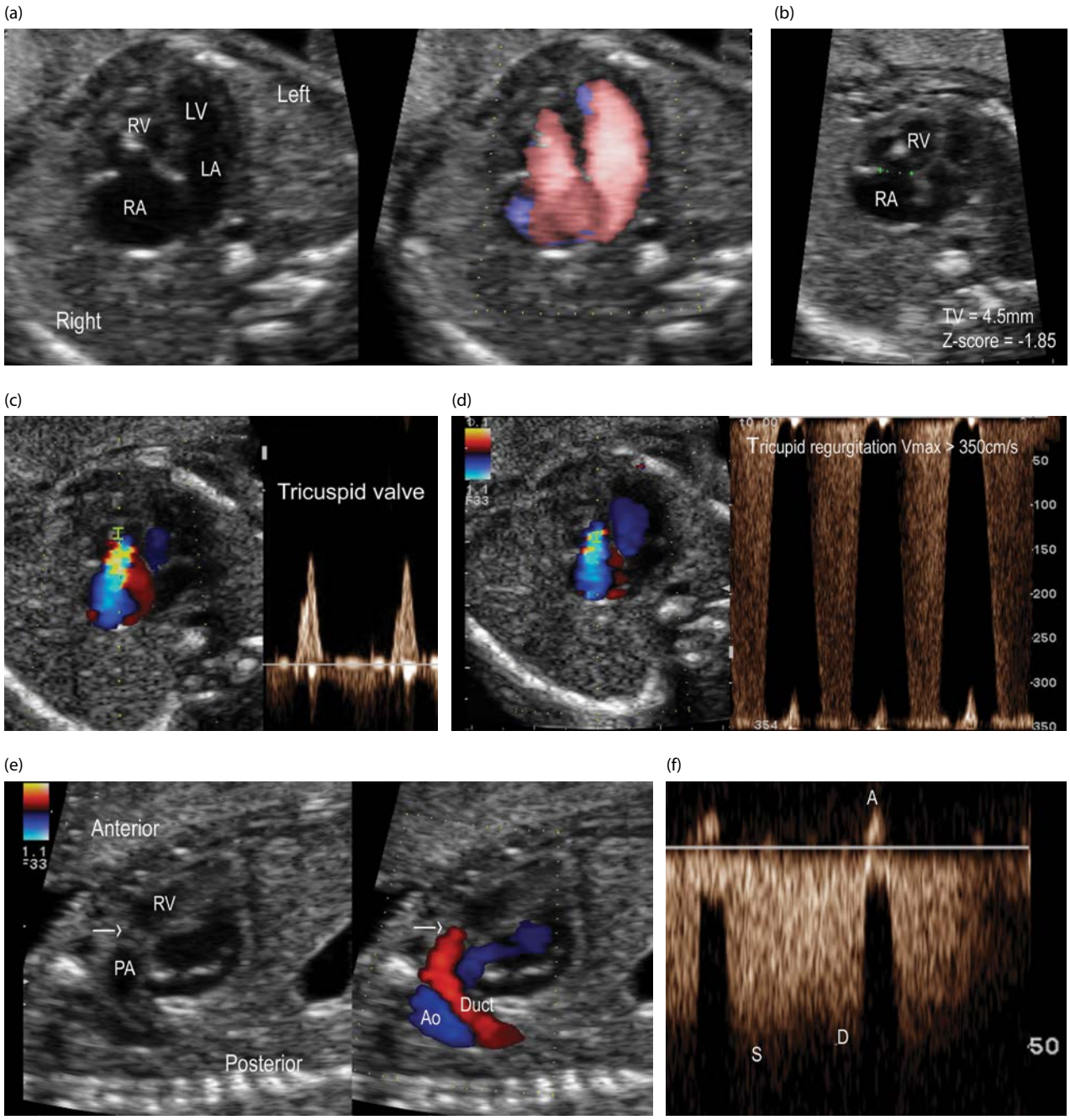


**Figure 24.3**
Images obtained from a 20-week fetus with membranous pulmonary atresia with intact ventricular septum and adequate size right ventricle (RV). (a) Four-chamber view: note a hypertrophied RV with apical muscular overgrowth (left panel) and adequate cavity as seen by color flow (right panel), with RV length similar to that of the left ventricle (LV). (b) Tricuspid valve size indicates potential for a postnatal biventricular circulation (Z-score = −1.85). (c) A biphasic pulsed-wave Doppler pattern can just be seen of the flow velocity profile across the TV. (d) Peak velocity of tricuspid regurgitation indicates high RV pressure (~55 mm Hg). (e) Sagittal views of RV outflow tract. Note the area of valvar atresia (indicated by the arrow, left and right panels) and retrograde flow through the arterial duct, up to the level of the atretic valve. (f) Ductus venosus signal with high pulsatility index. This case achieved a biventricular circulation. (A, atrial contraction; Ao, aorta; D, diastole; PA, pulmonary artery; S, systole.)

## Anatomical findings and ultrasound correlates

In sequential segmental analysis,[1] PAIVS usually occurs in the setting of normal atrial situs with concordant cardiac connections and a left-sided aortic arch. PAIVS can also be seen in association with discordant atrioventricular (AV) and ventriculo-arterial (VA) connections.[10] Although this is a rare occurrence, we have observed one case in our prenatal series.

The morphological spectrum of PAIVS varies from the most common form with a small right ventricular cavity (Figures 24.1 and 24.2) to that of a dilated RV (Figure 24.4). Consequently, the cardiothoracic ratio is normal in the majority of fetuses, but there may be variable degrees of cardiomegaly. The worst cases of increased cardiothoracic ratio lead to the "wall-to-wall" hearts, which are often associated with a poor prognosis.[11] Branch pulmonary arteries are usually confluent and supplied by a left-sided arterial duct,[12] although nonconfluent arteries supplied by bilateral ducts are

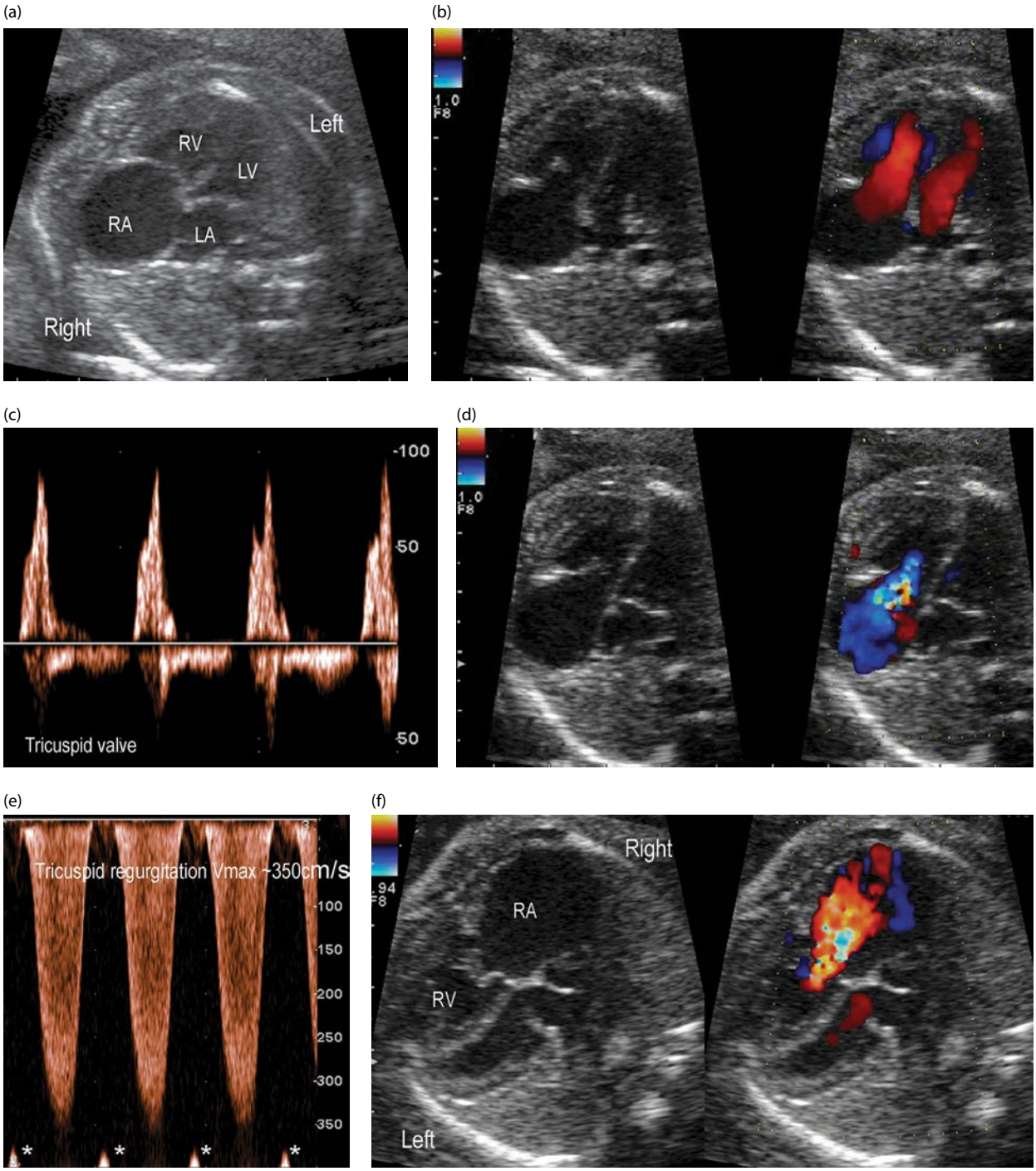


**Figure 24.4**
Images obtained at 22 weeks (a–e) and 25 weeks of gestation (f) from a fetus with pulmonary atresia with intact ventricular septum and cardiomegaly. (a,b,d) At 22 weeks, four-chamber views show a significantly dilated right atrium (RA) and a large RV. (b) Diastolic frame: note a wider color flow signal into the RV compared to the left ventricle (LV) and in (c), a biphasic flow pattern across the tricuspid valve (TV). (d) Systolic frame: note failure of coaption of the TV leaflets (left panel) with significant regurgitation on color flow mapping (right panel). (e) Peak velocity of tricuspid regurgitation indicates high RV pressure (~55 mm Hg). (f) At 25 weeks: four-chamber view shows a "wall-to-wall" heart with dilated RA and RV. (LA, left atrium.)

also reported. The occurrence of systemic-to-pulmonary collateral arteries as source of pulmonary blood flow is rare.[13]

### The right ventricle, tricuspid valve, and right ventricular infundibulum in PAIVS

Although the three components of the RV (inlet, trabecular, and outlet) are present in hearts with PAIVS,[14] there is a variable degree of ventricular hypertrophy and intracavity muscular overgrowth, which can lead to obliteration of one or two of these components. A related nomenclature labels ventricles as being "unipartite," "bipartite," or "tripartite."[15] Unipartite ventricles are those in which only one portion (inlet) is not obliterated; bipartite ventricles have two of the ventricular components; and a tripartite chamber shows all three portions. At birth, tripartite ventricles are more common (59%) than bipartite (~34%), whereas unipartite ventricles account for less than 8% of cases.[16]

The tricuspid valve (TV) morphology is also variable. Its diameter is commonly expressed as "Z-scores" or the number of standard deviations by which a measurement (in this case, TV diameter) deviates from the population mean for a given patient size (in this case, fetal size). In children, Z-scores are often normalized for body surface area, while in the fetus, they can be calculated in relation to femur length, biparietal diameter, or gestational age.[17–19] The TV can be severely stenotic and, as might be expected, unipartite and bipartite ventricles typically have a small valve. As a group, TV mean Z-score at birth is –5, but again there is considerable variability.[16] A severely regurgitant valve is associated with a dilated annulus and is often dysplastic, with or without apical displacement of its leaflets, the latter being a feature of Ebstein malformation, which occurs in approximately 10% of cases.[16,20] In the most severe forms with massive tricuspid regurgitation, the right ventricular cavity may be significantly dilated with a thin myocardium and a "wall-to-wall" heart. In some of these cases, the atresia may be functional rather than anatomical.

The morphological substrate for the outflow tract obstruction is most commonly at valve level, when there is fusion of the valve leaflets and a patent infundibulum, also called membranous atresia. Valvar atresia accounted for 75% of cases in the UK-Eire study, the remainder showing muscular atresia with infundibular obliteration.[16] In this particular series, there were no examples of isolated infundibular obliteration.

The anatomical variability of inlet, trabecular, and outlet components of the RV is reflected by the wide spectrum of ultrasound images observed during fetal echocardiography. On the four-chamber view, the right ventricular cavity may be diminutive due to apical obliteration (Figure 24.1a,b). This is accompanied by a small and stenotic TV with abnormal Doppler signal, which shows a monophasic waveform of short duration (Figure 24.1c). Tricuspid regurgitation, if present, is trivial. These cases have additional muscular overgrowth of the outflow area, often leading to infundibular atresia (Figure 24.1e), thus characterizing a unipartite ventricle. Occasionally, there may be hyperechogenicity of the endocardial wall, which is likely to reflect endocardial fibroelastosis.

At the other end of the spectrum, the RV and right atrium are dilated (Figure 24.4). This is usually associated with an abnormality of the TV, which may show dysplastic leaflets and rolled edges with or without apical displacement (Ebstein malformation). The valve diameter may be larger than normal. Color flow mapping shows severe tricuspid regurgitation. Most cases of PAIVS have an elevated right ventricular pressure, and the pulsed or continuous wave Doppler signal is expected to show a high-velocity tricuspid regurgitation jet (Figure 24.4e). The presence of low-velocity regurgitation may imply that pulmonary atresia is functional rather than anatomical—that is, when there is no effective forward flow through the pulmonary valve due to the massive tricuspid regurgitation.

In between these two extremes of ventricular morphology, the RV may show near-normal dimensions on the four-chamber view with reasonably well-developed inlet and apical portions (Figure 24.3). Careful examination, however, will show increased ventricular wall thickness (Figure 24.3a) and decreased myocardial contractility. High-velocity tricuspid regurgitation is often present and can be promptly identified on color flow mapping (Figure 24.3c,d). These ventricles are usually tripartite structures, with atresia at valve level (i.e., membranous atresia) and, almost invariably, a well-developed infundibulum (Figure 24.3e). The pulmonary valve shows thickened and immobile leaflets.

### Ventriculo-coronary connections and the RV-dependent circulation

Abnormal connections between the right ventricular cavity and the coronary arterial system were first described in 1926 in a pathological specimen of PAIVS,[21] and at angiography in 1964.[22] It was 10 years later that Freedom and Harrington[23] suggested that these communications serve as passive conduits to egress of flow from the blind-end RV and may contribute to myocardial ischemia due to the impairment of diastolic coronary flow. Since then, their importance to the outcome of children with PAIVS has been increasingly recognized.[24]

These connections have been described as "coronary sinusoids," but this terminology is best avoided as it is considered to be incorrect.[24] Ventriculo-coronary arterial connections (VCACs) or fistulas are better descriptions for such communications, which consist of thick-walled, distended intertrabecular myocardial spaces between a more-or-less distended capillary bed and the subepicardial coronary arteries.[25] Typically, VCACs are seen in cases of PAIVS with an underdeveloped right ventricular cavity, stenotic TV, and hypertrophied ventricular walls that often obliterate the apical and outlet portions of the ventricles, leading to suprasystemic ventricular pressures. In pathological fetal series, coronary artery abnormalities were more common in cases with smaller ventricles.[26] Dilated, thin-walled, and nonhypertensive ventricles with abnormal TV leaflets and massive regurgitation are not associated with VCACs.

As a consequence of such communications, there may be an RV-dependent coronary circulation (RVDCC), meaning that adequate flow to the coronary arteries depends on the hypertensive RV to drive the blood from its cavity through

the VCAC and into the coronary territory. Such a circuit may be compromised when there is right ventricular decompression, for example, with surgical or catheter relief of the outflow tract obstruction. An RVDCC is diagnosed when there is a connection between the RV and a coronary artery but no communication between the coronary artery itself and the aorta, or when there is significant stenosis of a major epicardial coronary artery. A review of the literature suggests that VCACs occur in about two-fifths of cases of PAIVS, and that approximately one-fifth of these have an RVDCC.[24] This is similar to the 8% encountered in a population-based study[16] but lower than the 39% reported in a series of 72 patients investigated by angiography in a tertiary center.[27] In the latter, nearly all cases with muscular atresia (96%, 23 of 24), had an RVDCC compared to 10% of those with membranous atresia (5 of 46). Additionally, coronary ostium atresia was only seen in cases of muscular atresia (14 of 23).

In the fetus, the presence of VCACs can be evaluated systematically when scanning the aortic root and right ventricular myocardium during color flow mapping (Figure 24.2) with the velocity scale set at a relatively low level (~30 cm/s). This is often obtained in a transverse view of the fetal chest just superior to the five-chamber view (Figure 24.2c). Pulsed wave Doppler interrogation shows bidirectional flow (Figure 24.2c,f), which is forward and of lower velocity in diastole and retrograde and of higher velocity in systole.[28] Such connections have been recognized as early as the first trimester of pregnancy.[29] We have also observed a case with large VCAC at 16 weeks' gestation. Postnatally, there was myocardial dysfunction, and the neonate was considered inoperable (Figure 24.2). Generally, however, prenatal identification of VCAC, *per se*, does not allow distinction between those who may have an RVDCC and those who may not.

### The pulmonary arteries

Although the presence of confluent pulmonary arteries is the rule in cases of PAIVS, it is important that they are imaged during fetal echocardiography in order to document their size and subsequent growth as pregnancy advances. The branch pulmonary arteries can usually be demonstrated on transverse views of the fetal chest. They are more readily seen in cases of valvar atresia with a thickened pulmonary valve and anatomical continuity between the right ventricular infundibulum and the main pulmonary artery. In such cases of membranous atresia, the main pulmonary artery is often of relatively good size, and the arterial duct is in its usual position (Figure 24.3e). Thus, the three-vessel view may seem normal on two-dimensional imaging. Color flow mapping, however, will show retrograde flow in the arterial duct. On sagittal views, the normal angle (obtuse) between the duct and the descending aorta can be appreciated (Figure 24.3e). This angle is thought to reflect cases where there had been forward flow from the RV to the pulmonary artery at earlier stages of development. That is, there was severe pulmonary stenosis that progressed to atresia.[30]

Alternatively, the arterial duct may arise from the undersurface of the aortic arch, forming an acute angle with the aorta (Figure 24.1d). This represents the direction of flow from the aorta to the pulmonary artery in early stages of gestation.[30] In such cases, the duct is usually a tortuous vessel with a sigmoid shape. This abnormal ductal take-off from the aorta is often seen in cases of muscular pulmonary atresia, and it is often more difficult to visualize the main pulmonary artery (Figure 24.1e). The combination of a small or absent main pulmonary artery and the anomalous position and shape of the arterial duct mean that the three-vessel view is abnormal, and the arterial duct cannot be imaged in the usual way in this standard plane. Its visualization often requires the use of color flow mapping while performing a careful transverse sweep from the level of the proximal ascending aorta (five-chamber view) toward the aortic arch. The duct can then be seen to arise from underneath the aortic arch, at the midpoint between the proximal transverse arch and the descending aorta.

## Pathophysiology and ultrasound findings

In PAIVS, the fetal circulation is dependent on the patency of the foramen ovale and arterial duct. Flow from the right atrium is diverted to the left atrium, left ventricle (LV), and aorta. On fetal echocardiography, left ventricular end-diastolic dimension and stroke volume are increased. Accordingly, Doppler velocities across the mitral and aortic valves may also be increased. On real-time two-dimensional imaging, left-sided volume load is more easily observed in cases with minute TV and diminished flow circulating through the right heart than in cases with a reasonable right ventricular size and tricuspid regurgitation. Difficulty with forward flow through the right heart can also be reflected in the ductus venosus Doppler signal (Figures 24.1f and 24.3f), which may show normal or increased pulsatility index or reversal of flow during atrial contraction. However, this finding does not appear to correlate with outcome.[31]

Color flow mapping will confirm a right-to-left shunt across the atrial septum and left-to-right (reversed) flow across the arterial duct (Figures 24.1d and 24.3e). The foramen ovale is often of adequate size, but restriction to flow at this level may lead to unusually high velocities across it. A restrictive foramen ovale may also contribute to the abnormally low forward velocities or reversed flow in the ductus venosus during atrial systole.

## Prenatal history and associated abnormalities

Progression of pulmonary stenosis *in utero* is well documented.[7,32] In one series, six cases diagnosed as critical stenosis at a mean gestational age of 22 weeks evolved to atresia by 31 weeks.[7] Pulmonary stenosis of varying severity, including critical obstruction and PAIVS, is not infrequently diagnosed in twins, especially in the recipient twin of monochorionic diamniotic pregnancies with twin-to-twin transfusion syndrome (TTTS).[33–36] The pathophysiological mechanisms of such an association are not fully understood, but hemodynamic changes are likely to play a role.[37,38] Pulmonary

stenosis or atresia was found in approximately 11% of recipient twins, prior to laser therapy for TTTS, of which about one-third (36%) died, one-third (32%) regressed, and one-third (32%) had obstruction that persisted and required postnatal intervention.[39] Regression following laser therapy had also been documented by others.[40] In a recent review of 385 live-born recipients in twin pregnancies receiving laser therapy for TTTS, 11 newborns had right ventricular outflow tract obstruction (3%). Based on this and using the unaffected twin recipients as controls, a predictive model showed that early gestational age, abnormal ductus venosus Doppler flow pattern, and pericardial effusion at diagnosis of TTTS were the strongest indicators of development of right ventricular outflow tract obstruction.[36]

Spontaneous fetal death occurs in a small number of cases, accounting for 5% of ongoing pregnancies in one series.[7] A grossly dilated RV with important regurgitation also appears negatively to influence perinatal outcome, it being present in a significant number of cases that died.[32,41]

Chromosomal and extracardiac abnormalities are uncommon, but examples of trisomy 18, trisomy 21, and 4p deletion as well as Dandy-Walker malformation have been reported.[7,28,42,43] From a large series of fetuses with major congenital heart disease, including 30 with PAIVS, 70% were isolated cases; among those with extracardiac but no chromosomal abnormalities, urogenital malformations were the most common (11%).[43] In our prenatal series, we have also encountered one case of trisomy 18 in a fetus presenting with increased nuchal translucency and in whom PAIVS was diagnosed at 16 weeks' gestation.

## Fetal intervention

Following initial reports of prenatal intervention in fetuses with severe valvar pulmonary stenosis/PAIVS,[44–46] fetal pulmonary valvuloplasty continues to be performed, to preserve ventricular growth in the hope that this will maximize the chances of achieving a biventricular repair. In 2006, the UK National Institute for Health and Care Excellence (NICE) issued clinical guidelines on percutaneous fetal balloon valvuloplasty. NICE stated that "Not only numbers are small, but there are no long term follow up data and no clear-cut selection criteria as to which cases may benefit from prenatal intervention." To date, there have been no updates made to the 2006 NICE guidelines.[47] Worldwide experience is still limited and consists of case reports and relatively small series.[48–52]

The goal is to alter natural history, and ideally, only fetuses deemed to have postnatal univentricular surgical palliation should have fetal intervention. It would therefore be important to predict the type of postnatal repair from prenatal ultrasound. Currently, there are no accepted criteria, but attempts have been made to predict postnatal outcome based on natural history cases. Table 24.1 summarizes studies reporting potential predictors of outcome that can guide prenatal counseling and may facilitate decision-making as to which fetuses may benefit from prenatal intervention. Tricuspid valve dimension stands out as an important indicator of eventual biventricular outcome. Perhaps not surprisingly, this is also important on postnatal decision-making. However, the validity of using such measures in the midgestation fetus is limited and can only be proven with large prospective randomized trials. In the absence of such trials, it remains unknown if successful fetal valvuloplasty cases would have achieved a biventricular circulation had prenatal intervention not been performed. In 2009, the Boston group reported successful pulmonary valvuloplasty in 6 out of 10 cases. The procedure was carried out either percutaneously or through a limited laparotomy.[53] By 2011, another six cases were performed by the Austrian group, of which four were successful and three had a biventricular outcome.[54] More recently, another relatively small number of cases were reported through an international registry.[55] Of 30 pregnancies evaluated, 16 underwent fetal intervention at a median gestational age of 26 weeks (range 23–29 weeks). There were no maternal complications, but two fetal deaths were related to the procedure. Other complications requiring treatment included bradycardia ($n = 7$) and hemopericardium ($n = 9$). There were five term and four preterm live births. Six babies achieved a biventricular repair. Although *in utero* pulmonary valvuloplasty is technically feasible, postnatal survival and quality of life need to be considered. Data on long-term outcome are still lacking, and although the rationale for intervention seems logical, there is still no decisive evidence that benefits outweigh the risks.[52] It is also worth noting that in expert hands, interventional cardiac catheterization can be performed in neonates weighting around 1.8–2 kg, thus offering the possibility of early delivery followed by neonatal intervention, as an alternative approach to fetal intervention.[56]

## Postnatal diagnosis and management

The neonate presents with cyanosis and, without prenatal diagnosis, may collapse upon constriction of the arterial duct. However, if the diagnosis is made antenatally, postnatal hemodynamic stability is maintained with the elective use of intravenous prostaglandin E, which maintains ductal patency. On auscultation, there is a single second heart sound. The chest radiograph shows oligemic lung fields, often with a normal heart size, although important cardiomegaly is seen in a minority of cases. The 12-lead electrocardiogram is abnormal and shows dominance of left ventricular forces (S-wave in V1 and R-wave in V6) as opposed to the normal neonatal pattern of right ventricular dominance (R-wave in V1 and S-wave in V6).

Postnatal cross-sectional echocardiography quickly establishes the diagnosis if this had not already been made prenatally. The timing and role of diagnostic cardiac catheterization are contentious, but it is performed in selected cases, often to delineate coronary arterial abnormalities (Figure 24.5a,b), whereas interventional catheterization is frequently carried out with the intent to perforate and dilate the pulmonary valve in cases of membranous atresia (Figure 24.5e–g). If necessary, balloon atrial septostomy can be performed at the same time or under ultrasound guidance.

**Table 24.1** Fetal indicators of postnatal outcome and type of repair in PAIVS

| *Authors* | *Indicators of UV outcome* | *Indicators of BV outcome* | *Comments* |
|---|---|---|---|
| Peterson et al.[96] | TV Z-score ≤−4 after 23 weeks<br>TV annulus ≤5 mm after 30 weeks<br>RV/LV length or width <0.5 and/or no tricuspid regurgitation | | |
| Salvin et al.[97] | | TV Z-score >−3 | More likely to achieve a BV repair |
| Roman et al.[98] | RV/LV length <0.6<br>TV/MV maximum diameter <0.7<br>TV inflow duration <31.5% cardiac cycle length<br>Presence of coronary fistulas | | Before 31 weeks, if three of four criteria were met: 100% sensitivity and 75% specificity for a non-BV repair |
| Gardiner et al.[99] | | PV Z-score >−1 or TV Z-score >−3.4 before 23 weeks<br>Median TV Z-score >−3.95 before 26 weeks<br>Median PV Z-score >−2.8 and medium TV/MV ratio >0.7 at 26–31 weeks<br>Median TV Z-score >−3.9 and medium TV/MV ratio >0.59 after 31 weeks | TV Z-score was a good predictor at all gestational ages |
| Iacobelli et al.[100] | Absence of tricuspid regurgitation<br>TV/MV ratio <0.56 | | Strong predictor of VCAC and risk of UV outcome |
| Gomez-Montes et al.[101] | TV/MV ratio ≤0.83<br>PV/AV ratio ≤0.75<br>TV inflow duration ≤36.5% of cardiac cycle length<br>RV/LV length ratio ≤0.64 | | Before 28 weeks, if three of four markers are present: 100% sensitivity and 92% specificity for a non-BV outcome. If all four criteria are fulfilled, 100% sensitivity and specificity |
| Lowental et al.[102] | | TV/MV ratio >0.63<br>Antegrade flow across PV<br>At least moderate tricuspid regurgitation | Predicts favorable TV Z-score at birth leading to BV repair |

*Abbreviations:* BV, biventricular; LV, left ventricle; MV, mitral valve; PAIVS, pulmonary atresia with intact ventricular septum; PV, pulmonary valve; RV, right ventricle; TV, tricuspid valve; UV, univentricular; VCAC, ventriculo-coronary arterial connections.

This means enlargement of the interatrial communication to ensure an unrestricted right-to-left shunt to avoid development of right atrial hypertension. Once the neonate is stable on a prostaglandin infusion, the next step is to determine whether the baby will be suitable for a biventricular or univentricular repair.

When the RV is unipartite and there is muscular infundibular obstruction, or an RVDCC, a biventricular repair is not possible, and the long-term strategy is geared toward a univentricular circulation. This is when systemic and pulmonary circulations are separated, there is only one functioning ventricle (in this case, the LV), and systemic venous return bypasses the heart. The initial palliation involves securing pulmonary blood flow, which is often achieved surgically with creation of an anastomosis (by interposing a graft) between the subclavian artery and the pulmonary artery (i.e., a modified Blalock-Taussig [BT] shunt). This may be preceded or followed by balloon atrial septostomy or sometimes surgical septectomy (i.e., surgical enlargement of the atrial communication). Subsequent management consists of a bidirectional Glenn procedure (i.e., superior vena cava to right pulmonary artery end-to-side anastomosis) with later placement of an extracardiac conduit between the inferior vena cava and pulmonary artery, thus completing a total cavopulmonary connection (TCPC, which is a univentricular palliation).

In the presence of a tripartite ventricle, with tricuspid Z-score greater than or equal to 2.4 and valvar atresia, the management strategy is for a biventricular repair.[57] Not infrequently, relief of the outflow obstruction can be achieved during cardiac catheterization (Figure 24.5e–g), using laser or radiofrequency perforation of the atretic valve followed by standard balloon dilatation.[58,59] This is performed percutaneously, usually through the femoral vein. If necessary, a surgical valvotomy can be performed. The creation of anatomical

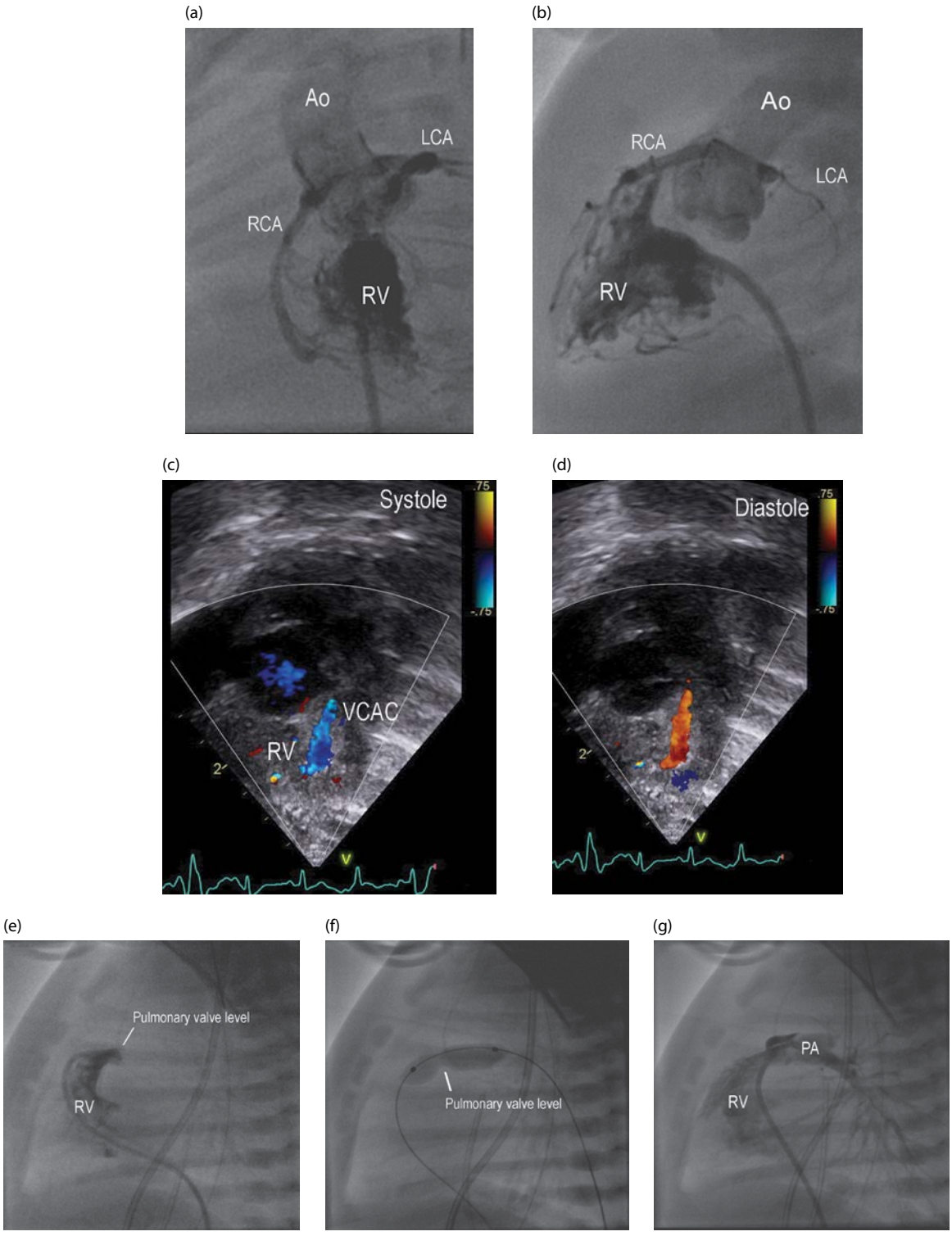


**Figure 24.5**
Postnatal images obtained from two neonates with pulmonary atresia with intact ventricular septum: (a–d) one with muscular atresia and (e–g) one with membranous atresia. (a,b) Injection into the right ventricle (RV) in (a) anteroposterior and (b) lateral projection shows a small RV cavity, opacification of both right and left coronary arteries (RCA and LCA), and retrograde filling of the aorta (Ao), demonstrating significant ventriculo-coronary artery connections (VCAC). (c,d) Echocardiographic images from the same neonate. Note the presence of VCAC on the surface of the RV with (c) systolic and (d) diastolic flow. (e–g) Lateral projection (e) before, (f) during, and (g) after interventional cardiac catheterization. (e) RV injection shows a blind infundibulum with contrast seen up to the level of the atretic pulmonary valve. (b) Balloon dilatation of the pulmonary valve, which followed the initial radiofrequency perforation of the valve. Note a "waist" on the opacified balloon, which corresponds to the level of the valve. (g) Angiogram demonstrating continuity between the RV and pulmonary artery (PA) after successful intervention.

continuity between the RV and the pulmonary artery may suffice to allow adequate antegrade flow. If not, creation of a BT shunt or stenting the arterial duct may be necessary to provide additional source of pulmonary blood flow and to ensure adequate systemic saturation. The shunt or the stent can be closed at a later stage, when the RV is able to maintain pulmonary blood flow, thus achieving a biventricular circulation.

Stenting the arterial duct in the catheter laboratory was first described in 1992[60] and has gained popularity over a surgical BT anastomosis, being also an option as the initial palliation for a univentricular circulation. Overall success rate in duct-dependent pulmonary lesions from a multicenter experience over 18 years is reported as 80%. For cases of PAIVS treated since 2001, success rate was 94%. Failure to stent the duct was related to univentricular physiology and its tortuosity.[61]

However, it is not always certain whether the RV is suitable for a biventricular repair. Various criteria have been used for decision-making with regard to surgical strategies.[62–64] but if the RV is thought to be inadequate, there is the option of a "one-and-a-half" repair[65] in which pulmonary blood flow is via a combination of forward flow from the RV to the pulmonary artery and a Glenn anastomosis.

In the less common form of PAIVS with significant tricuspid regurgitation and a thin-walled RV, the TV can be converted to an atretic valve, this being combined with a modified BT shunt and later univentricular palliation (TCPC).[66]

## Outcome and follow-up

The outcome of babies with PAIVS had been considered relatively poor, but better understanding of the anatomy and pathophysiology of this condition including the significance of VCAC and RVDCC has led to improved surgical strategies and outcomes. In the UK-Eire population-based study published in 2005,[67] actuarial survival at 1 and 5 years, excluding those who did not undergo surgery, was 71% and 64%, respectively. The risk of death was higher in the first 6 months and decreased over the next 12 months, with no deaths occurring after 4 years up to 9 years' follow-up. Others have since reported overall actuarial survival of 82%[64] and 86%[68] at 10 years. A breakdown of surgical results according to type of repair is given by Pawade et al.,[62] who reported a 10-year actuarial survival of 93% for those with a well-developed infundibulum and 75% at 3 years for those without. More recently, 10-year survival for 81 patients operated between 1990 and 2006 was 80% (38% had biventricular repair, 17% univentricular palliation, and 12% had one and a half circulation).[69] For births in the years 2000–2009, the Denmark population-based study reported a 5-year actuarial survival of 78%.

Earlier results following interventional cardiac catheterization showed 85% survival at medium follow-up of 5.5 years, but only 35% were free from surgery.[70] A biventricular repair was more likely with TV Z-score greater than or equal to 2. Chubb et al. reported long-term results (up to 21 years) of a more aggressive approach to perforation of the pulmonary valve ($n = 39$), where overall mortality was 21%.[71] In their series, there was important right ventricular hypoplasia as seen by mean TV Z-scores of −5.1 (SD, 3.4). Simultaneous stenting of the arterial duct was also done in a significant proportion of cases ($n = 14$). Of note, those achieving a biventricular repair had less ventricular hypoplasia compared to those having a non-biventricular pathway (TV Z-score, mean [SD] = −3.92 [2.1] versus −7.01 [1.8], respectively). Schwartz et al. attempted radio-frequency perforation of the pulmonary valve in cases with good size TV (median Z-score of –0.2, range −2.22 to +2.3). They found that residual pulmonary gradient and TV size were predictors of need for outflow tract surgery and additional source of pulmonary blood flow, respectively.[72] Conversely, Rathgeber et al. report their results for pulmonary valve perforation among hearts with a much wider range of TV diameter, with no mortality.[73] Tricuspid to mitral valve median ratios for patients who underwent a biventricular and a non-biventricular repair were 0.82 (IQR, 0.71–0.90) and 0.59 (IQR, 0.39–0.76), respectively, while median Z-scores for TV were −3.2 (range −4.9 to −2.6) and −6.8 (range −9.7 to −4.8), in keeping with the importance of TV size as a surrogate for right ventricular size and type of eventual repair.

Guleserian et al.[74] reviewed the medium-term outcome of patients with an RVDCC whose management was directed to a univentricular circulation. Of 32 patients (all had a modified BT shunt), overall mortality was 19%, all deaths occurred within 3 months of the shunt, and all three patients with aortic coronary atresia died. Actuarial survival for all patients was 81% at 5, 10, and 15 years.

It is generally assumed that a biventricular repair is preferable to that of a univentricular circulation in terms of exercise tolerance. The evidence for this in PAIVS, however, is limited, as even after a biventricular repair, right ventricular diastolic function may remain markedly abnormal,[75] and this may affect exercise performance.[76] Similarly, Numata et al.[65] found no effective difference in exercise capacity at 5 and 10 years after a one-and-a-half repair compared with a univentricular repair. A recent report on outcomes of one-and-a-half repair performed for a variety of diagnoses showed good functional results with most patients in New York functional categories I and II, but this series only included a few patients with PAIVS.[77]

## Summary

PAIVS remains a challenging lesion. Fetal diagnosis facilitates optimal management at birth, has provided the option to perform fetal intervention, but has also resulted in a reduced live birth incidence due to elective termination of pregnancy. Management strategies for PAIVS must include assessment of right ventricular and infundibular morphology as well as the coronary circulation. At one end of the spectrum, interventional cardiac catheterization may suffice as the only treatment pathway leading to a biventricular circulation, while cases with severe right ventricular hypoplasia, VCAC, and RVDCC are associated with higher mortality and may be deemed inoperable.

# *Tricuspid atresia*

## Introduction

Tricuspid atresia is a rare form of cyanotic congenital heart disease in which the only egress of blood from the atrium receiving the systemic venous return is across the atrial septum and into the contralateral atrium, which receives the pulmonary venous return.[78] By far, the most common morphological substrate for this clinical entity is absence of a potential communication between the right atrium and the RV (i.e., absent connection), with the left atrium connecting with a dominant chamber, which is often of left ventricular morphology. The RV, which lacks its inlet portion, is usually small. In most cases, the VA connection is concordant—with the aorta arising from the LV and the pulmonary artery from the smaller RV. In a smaller proportion of cases, there is discordant VA connection, that is, the vessels are transposed. A ventricular septal defect (VSD) is often present but varies in size. Through this defect, blood reaches the RV and the corresponding artery connected to it. Right ventricular dimensions are related to size of the VSD, which in turn is the main determinant of the degree of outflow tract obstruction. If the VSD is restrictive, there will be pulmonary obstruction in hearts with concordant VA connection, but aortic obstruction in cases of transposed vessels. Clinical presentation will depend mainly on the presence and degree of either pulmonary or aortic obstruction.

The first description of obstruction to the TV orifice is attributed to Friedrich Ludwig Kreysig in 1817, as cited by Rashkind,[79] but the term *tricuspid atresia* was first used by Schuberg in 1861,[80] who described the most common variant and what is considered "classical tricuspid atresia."[81] However, anatomical variations do occur and have led to controversy with the use of terminology such as "univentricular hearts" or even in some cases, the appropriateness of the name "tricuspid atresia" in cases where the main chamber is of right ventricular morphology. Other variations also include the rarer form of tricuspid atresia when there is a biventricular connection, but the TV is imperforate. Additionally, hearts with this anomaly are sometimes described as "hypoplastic right heart syndrome," but similarly to PAIVS, it is preferable to avoid this term, as the pulmonary artery is not always small. Instead, the use of sequential segmental analysis allows appropriate description of the fetal heart.[1] All morphological variations may be encountered in prenatal life, so it is important that those performing fetal echocardiography and counseling families are aware of the whole morphological spectrum. Accuracy of diagnosis is even more relevant in the current era, when complex forms of congenital heart disease are diagnosed in the late first and early second trimester of pregnancy. Therefore, this section addresses the spectrum of anatomical malformations in which the atrium receiving the systemic venous return has no direct communication with the ventricular mass, thus leading to the clinical picture of tricuspid atresia.

## Incidence

Tricuspid atresia is a rare anomaly. It accounted for approximately 4% of cases in one prenatal series,[82] a figure likely to be higher than in postnatal life due to cases of interruption of pregnancy. In 2002, Hoffmann provided an incidence of 7.9 per 100,000 live births based on review of published series,[83] which is higher than a previously reported figure of 3.9 per 100,000 live births, for the years 1981–1982. From a more recent study based on hospital births across the United States in the year 2008, incidence was shown to be 5 cases per 100,000 live births, with no difference between sexes.[9] Tricuspid atresia also accounted for 44% of cases with a dominant LV in the Boston fetal series of physiologically single ventricles.[84]

## Anatomical findings and ultrasound correlates

Emphasis has to be given to the most common form of tricuspid atresia, when there is absence of the right AV connection, a dominant LV, a small RV, and normally related great arteries (i.e., concordant VA connection, Figure 24.6). To avoid errors, however, it is preferable to describe the anatomy and, as seen by fetal echocardiography, in a systematic manner.[1]

### Atrial situs and cardiac position

Typically, tricuspid atresia occurs with atrial situs solitus or usual arrangement of the atrial chambers (Figures 24.6 through 24.8). In the child, atrial situs is usually inferred by the arrangement of the abdominal vessels at the level of T10.[85] Prenatally, this can be determined through the abdominal circumference section, which is part of the morphological assessment of the fetus (Figures 24.6a and 24.8a). But it is essential that fetal laterality be determined first; that is, distinguishing the right and left sides of the fetus.[1,86] After ascertaining atrial situs, the heart and cardiac apex position are easily identified at the level of the four-chamber view. In a postnatal series, usual atrial arrangement was seen in 57/60 cases, whereas situs inversus was present in the remaining three cases.[78] In a pathological review of 31 cases of tricuspid atresia with absent AV connection, atrial situs was normal in all but one case with left isomerism.[87] In our own fetal series of about 35 cases, we observed two examples of situs inversus (Figure 24.9), one of left isomerism (Figure 24.10), and the remaining were situs solitus. In the latter group, the heart was left sided in all but one, in which the heart was located in the right chest with apex pointing to the right (Figure 24.8b). In the two cases of situs inversus, the heart was right sided in one but left sided in the other (Figure 24.9), while it was left sided in the only example of left isomerism (Figure 24.10). The cardiothoracic ratio is usually normal, but the four-chamber view will be abnormal.

### Atrioventricular connection

Having established atrial situs, the next step is to determine the type of AV connection, which is best shown on the four-chamber section. In most cases, there is absence of one AV

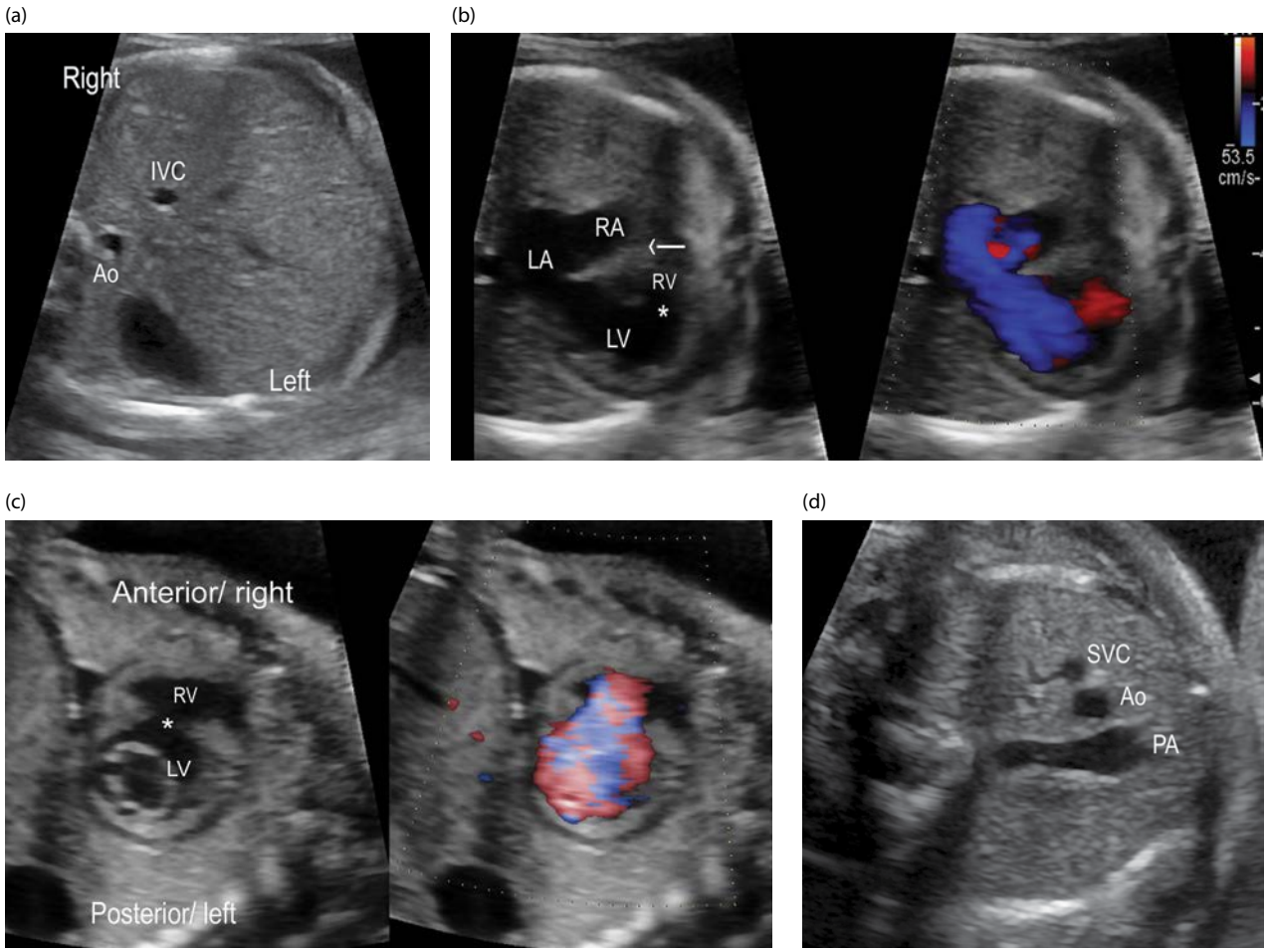


**Figure 24.6**
Images obtained from a 24-week fetus with tricuspid atresia and concordant ventriculo-arterial connection. (a) Abdominal short-axis view shows normal situs, compatible with usual atrial arrangement. Note aorta (Ao) to the left and inferior vena cava (IVC) to the right of the spine and a left-sided stomach. (b) Four-chamber view. The heart is on the left. Note the absence of the right atrioventricular connection (arrow), typical of tricuspid atresia. In the right panel, color flow mapping shows flow from right atrium (RA) to left atrium (LA) and left ventricle (LV). Through a large ventricular septal defect (VSD, indicated by the asterisk), flow reaches the smaller right ventricle (RV) situated anteriorly and to the right. (c) Short-axis views through the ventricles. Note the large VSD (asterisk), which allows unrestrictive flow to the RV. (d) Axial view at the level of the three-vessel view shows normal size, arrangement, and alignment of the pulmonary artery (PA), aorta (Ao), and superior vena cava (SVC) in keeping with normally related great arteries and no significant obstruction.

connection. This is absent right connection in situs solitus (Figures 24.6b; 24.7a,b; and 24.8b) but absent left connection in the setting of situs inversus (Figure 24.9a,b,f). On ultrasound, the absent connection is seen as a hyperechoic tissue in the anticipated site of the AV valve. Anatomically, this corresponds to a prominent fibro-fatty tissue in the AV groove, which occupies the space between adjacent layers of atrial and ventricular myocardium.[81] Thus, when examining a heart specimen, it is possible to place one's hands into this space, without reaching either the right atrium or the ventricular mass. More rarely, but well described in anatomical specimens and postnatal literature, there is TV tissue but the valve is imperforate and blocks the egress of flow from the atrium.[78,81,87] In our fetal series, we have observed one case of imperforate valve, but interestingly, valve tissue could not be easily demonstrated on postnatal echocardiography.

### The ventricular mass and ventricular septal defect

Although most examples of tricuspid atresia constitute a type of univentricular AV connection, these hearts often possess two ventricles, and almost invariably, the RV is small, incomplete, and rudimentary, while the LV is large and dominant. Less often, the RV is the dominant ventricle and the LV is the rudimentary chamber. Very occasionally there may be a solitary and indeterminate ventricle.[88] Rigby et al. found only two examples of a dominant right and two of an indeterminate ventricle among 60 postnatal cases.[78] Similarly, most fetuses in our series showed a dominant LV (Figures 24.6b; 24.7a,b; 24.10b,c), with one example each of a dominant RV (Figure 24.9b–d) and of a dominant chamber of indeterminate morphology (Figure 24.8b). The right ventricular chamber, which lacks its inlet portion, sits anterosuperiorly in relation to the main LV, with its trabecular component almost always to the

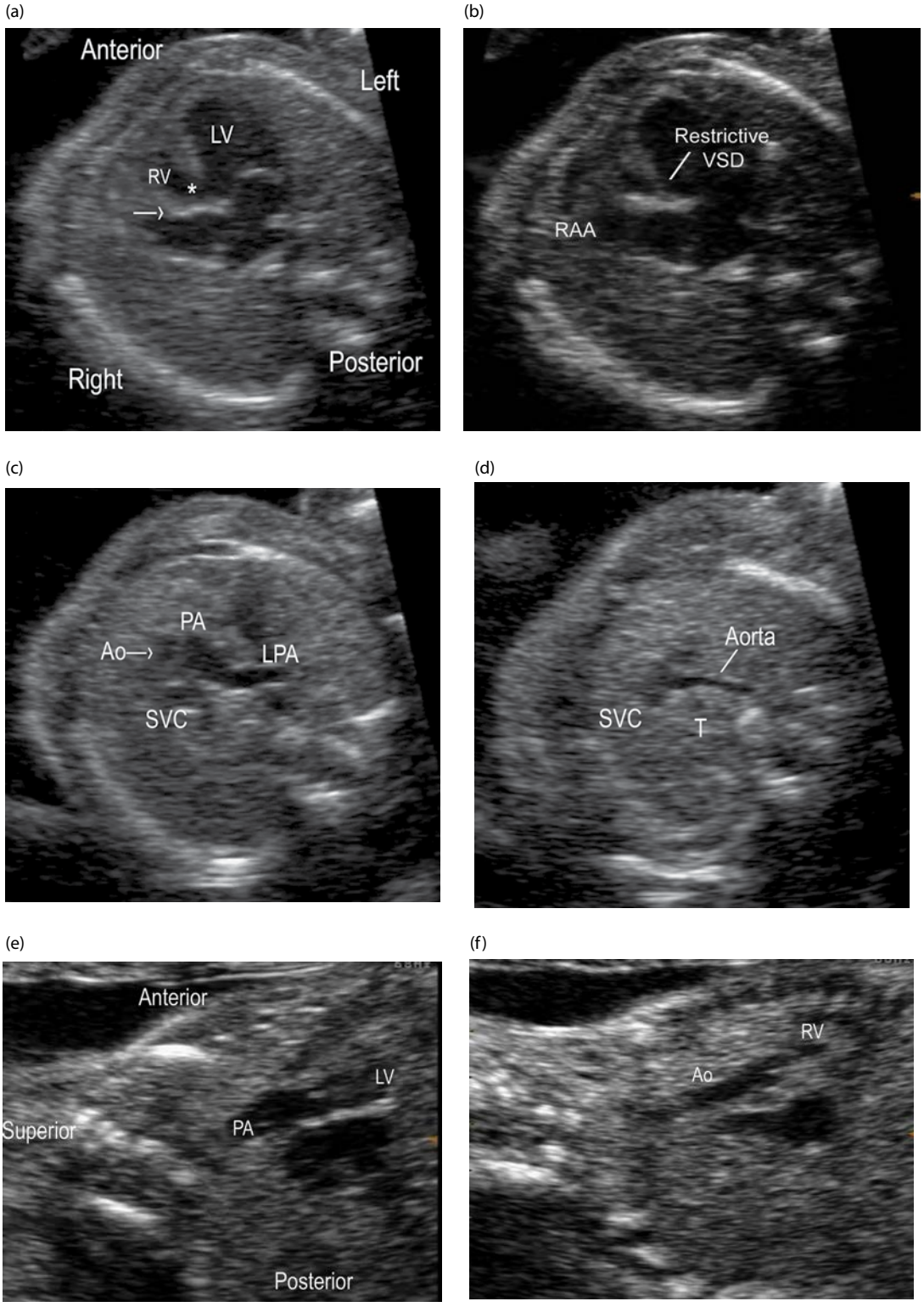


**Figure 24.7**
Images obtained from a 21-week fetus with tricuspid atresia and transposed great arteries. The situs view is normal (not shown). (a,b) Four-chamber views show absent right atrioventricular connection (arrow). The left ventricle (LV) is the main chamber. The right ventricle (RV) is a rudimentary chamber located anterior and to the right. The ventricular septal defect (VSD, indicated by the asterisk) is small. (c,d) Axial views of the outflow tracts. (c) The pulmonary artery (PA), which arises unobstructed from the LV is posterior and larger than the aorta (Ao). (d) The transverse aortic arch is hypoplastic, reflecting aortic obstruction at the VSD level and RV. (e,f), Sagittal views of the great arteries. (e) Larger PA arising from posterior LV. (f) The small Ao arises from the anterior rudimentary RV and is interrupted. (LPA, left PA; RAA, right atrial appendage; SVC, superior vena cava; T, trachea.)

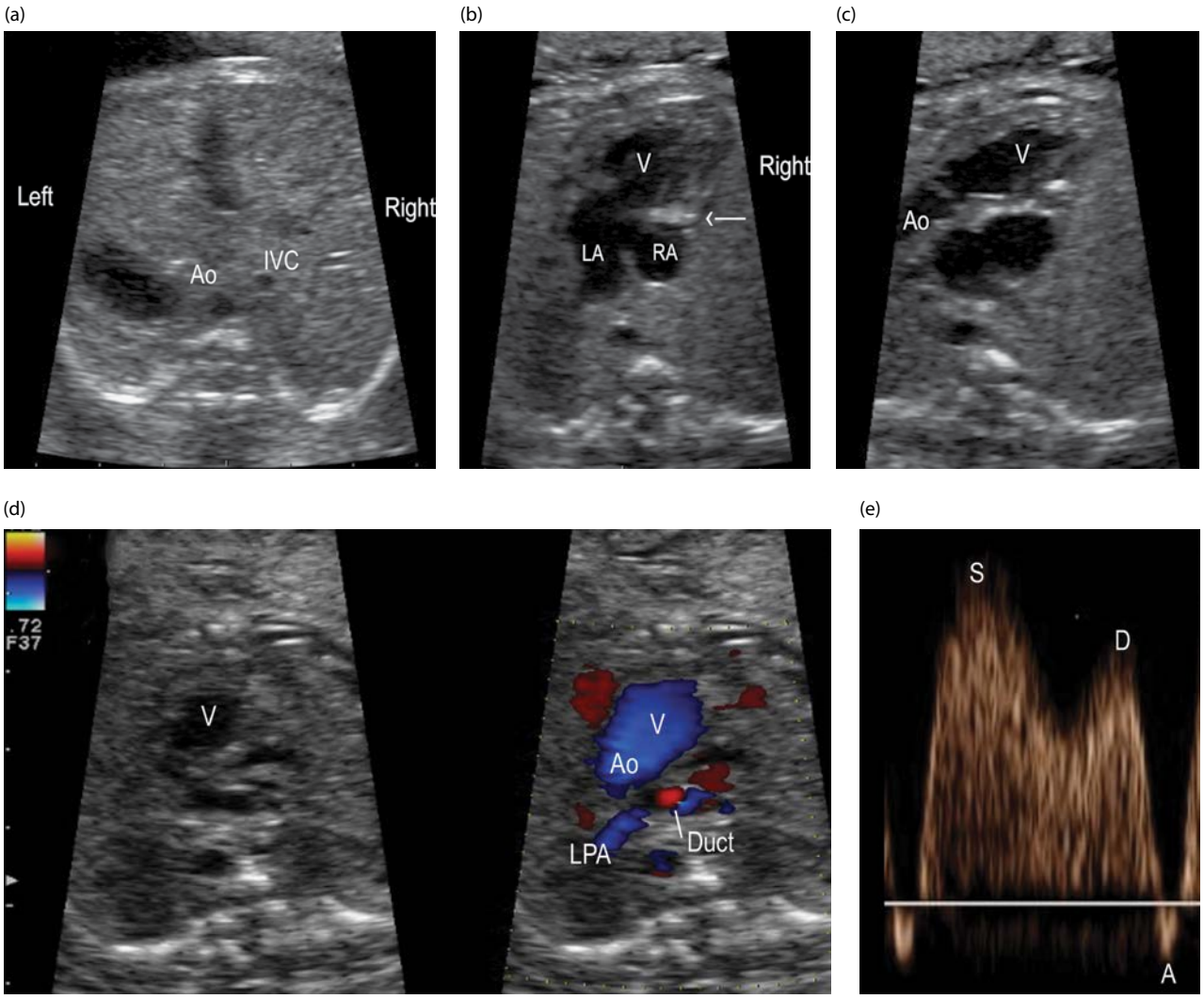


**Figure 24.8**
Images obtained from a 25-week fetus with normal situs and a right-sided heart. (a) Abdominal short-axis view of situs, compatible with usual atrial arrangement. The stomach is to the left. (b) Four-chamber view shows a right-sided heart with a right-sided apex. The arrow points to the absent right atrioventricular connection. Only one ventricular chamber can be imaged, corresponding to a ventricle (V) of indeterminate morphology. (c) This ventricle connects to the aorta (Ao). (d) Axial views at the level of outflow tracts. Note the anterior Ao and posterior branch pulmonary arteries, which fill retrogradely via the arterial duct (right panel). (e) Abnormal flow profile at the ductus venosus with reversed signal during atrial contraction (a). (D, diastole; IVC, inferior vena cava; LA, left atrium; LPA, left pulmonary artery; RA, right atrium; S, systole.)

right. More rarely, the RV is either directly anterior or to the left.[81] Right ventricular size varies and depends on the dimensions of the VSD. The smaller the VSD, the smaller the RV.

On echocardiography, ventricular morphology in hearts with a univentricular AV connection, such as in tricuspid atresia, is best determined by the relative position of the two ventricles The RV is recognized by its anterosuperior position (Figures 24.6b,c; 24.7a,b; 24.10b,c), while the LV is situated posteroinferiorly (Figure 24.9b,c). In tricuspid atresia with normal situs and absent right AV connection, the RV is often to the right side of the main ventricular chamber.

### Ventriculo-arterial connection

The main type of VA connection is concordant, where the aorta arises from the LV and the pulmonary artery from the rudimentary RV (Figure 24.6). This arrangement accounts for approximately 60%–80% of cases. In about 10%–20%, there is VA discordance (Figure 24.7), in which case the RV is connected to the aorta and the pulmonary artery to the LV. Almost invariably, the vessel arising from the main chamber is unobstructed and of normal size or large, while size of the vessel arising from the rudimentary RV will be greatly influenced by size of the VSD. However, other anatomical variables such as morphology of the semilunar valve and subvalvar area will also influence the degree of any systemic or pulmonary obstruction.

From a pediatric cohort ($n = 60$) seen at the Royal Brompton Hospital, most cases showed either concordant (60%) or discordant (22%) VA connection with the remaining being either double outlet (12%) or single outlet (6%).[78]

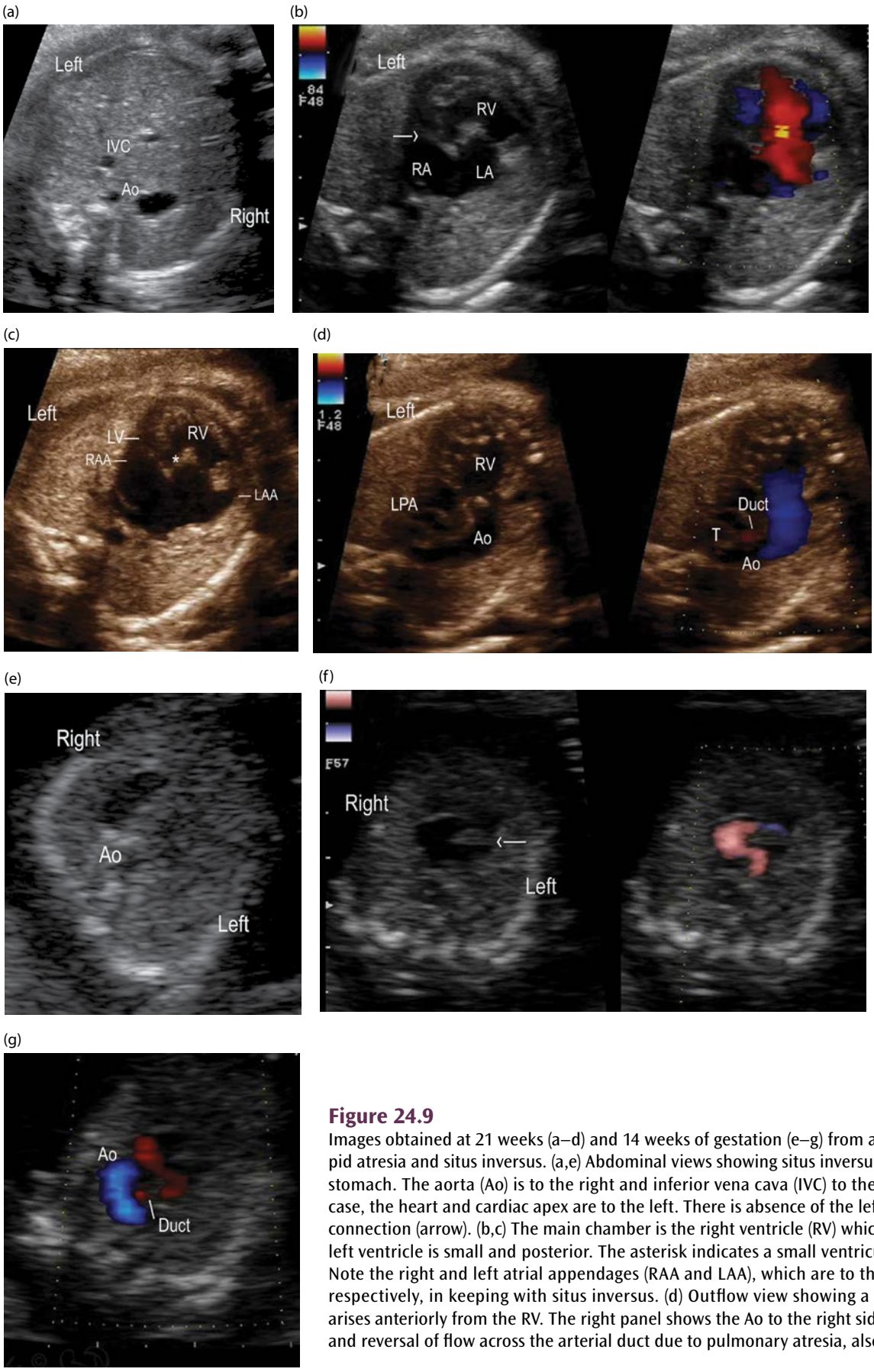


**Figure 24.9**
Images obtained at 21 weeks (a–d) and 14 weeks of gestation (e–g) from a fetus with tricuspid atresia and situs inversus. (a,e) Abdominal views showing situs inversus. Note a right-sided stomach. The aorta (Ao) is to the right and inferior vena cava (IVC) to the left. (b,f) In this case, the heart and cardiac apex are to the left. There is absence of the left atrioventricular connection (arrow). (b,c) The main chamber is the right ventricle (RV) which is anterior. (c) The left ventricle is small and posterior. The asterisk indicates a small ventricular septal defect. Note the right and left atrial appendages (RAA and LAA), which are to the left and right, respectively, in keeping with situs inversus. (d) Outflow view showing a large aorta, which arises anteriorly from the RV. The right panel shows the Ao to the right side of the trachea (T) and reversal of flow across the arterial duct due to pulmonary atresia, also shown in (g).

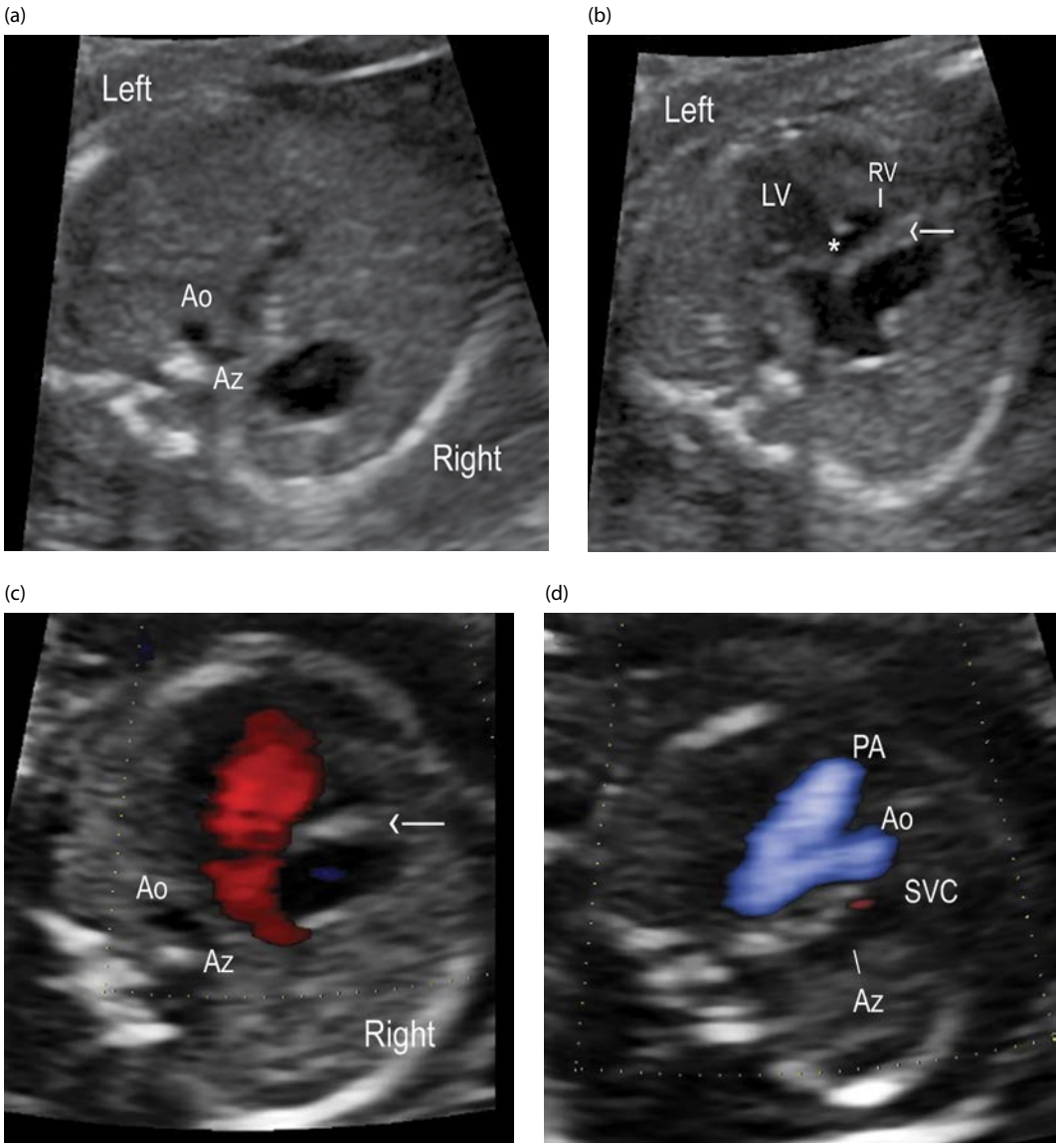


**Figure 24.10**
Images obtained from a 21-week fetus with tricuspid atresia and left isomerism. (a) Situs view shows a right-sided stomach, central aorta (Ao), and posterior, right-sided azygos vein (Az). (b,c) Four-chamber views shows a left-sided heart with a left apex. The arrow points to the absent right atrioventricular connection. Note the Az to the right. The main chamber is the left ventricle (LV). The right ventricle (RV) is smaller and anterior. The asterisk indicates the ventricular septal defect. (d) Three-vessel and trachea view shows normal relationship of the Ao and pulmonary artery (PA) and normal transverse aortic and ductal arches. Note also the Az, which joins the superior vena cava (SVC).

In a recent and large fetal series ($n = 54$), there was only a slight predominance of concordant VA connection (52%) compared with cases of transposed great arteries (46%). In the remaining case, there was a single outlet heart with a common arterial trunk. Pulmonary obstruction was identified in half of those with normally related arteries and aortic obstruction in just over half of those with transposed great arteries. In the latter group, although the pulmonary artery was connected to the main chamber, obstruction to pulmonary flow still occurred in nearly one-quarter of the cases. In contrast, in the Italian anatomical collection, single-outlet hearts were overrepresented and accounted for 23% of the 31 cases of tricuspid atresia, where 52% had concordant and 19% discordant VA connection. Double-outlet RV was present in the minority (6%).[87]

Ultrasound images of the great arteries will reflect the underlying VA connection and degree of arterial obstruction, if any. Thus, in cases of normally related great arteries, vessel arrangement and alignment in the three-vessel view are normal (Figure 24.6d), but relative sizes of aorta and pulmonary artery will depend on the presence and degree of obstruction. As indicated, many of these cases will have pulmonary stenosis; thus, the pulmonary artery will be smaller than the aorta. If there is no obstruction, the three-vessel

and three-vessel-trachea view will be normal (Figure 24.6d). Similarly, cases with transposed vessels will almost invariably show abnormal upper mediastinal views of the great arteries (Figure 24.7c,d). The aorta, which arises from the rudimentary RV, will have an anterior course, its size being related to presence and degree of aortic obstruction. Not infrequently, there will be associated aortic arch obstruction, either coarctation of the aorta or less often, interruption of the aortic arch (Figure 24.7f). Aortic arch abnormalities may be suspected on axial views, but the morphology is best shown on sagittal views. Figures 24.8 and 24.9 show examples of tricuspid atresia with single-outlet heart with the aorta arising from the main chamber and the pulmonary arteries being supplied by the arterial duct (Figures 24.8d and 24.9d,g).

## Pathophysiology and ultrasound findings

In tricuspid atresia, the fetal circulation is dependent on patency of the foramen ovale. In its common form, blood from the right atrium passes through the foramen ovale into the left atrium and LV (Figure 24.6). With concordant VA connection, the LV ejects into the aorta, and through the VSD, blood reaches the smaller RV and pulmonary artery. In cases with transposed great arteries, the LV ejects into the pulmonary artery, and via the VSD, it reaches the aorta. This mixing situation means all fetal venous return is primarily ejected by one ventricle into both great arteries. The balance between how much reaches the aorta and how much reaches the main pulmonary artery and ductal arch depends on presence and degree of systolic or pulmonary obstruction, which can occur at multiple sites. The VSD size plays a significant role in restricting blood to either pulmonary artery or aorta, but obstruction is also seen at valve and subvalvar area as well as further downstream, at aortic arch level.

On color flow mapping, there is obligatory right-to-left flow through the foramen ovale, across the mitral valve, and into the LV. Left ventricular end-diastolic dimension will be increased, reflecting increased preload. Accordingly, Doppler velocity across the mitral valve will also be increased. Going forward from the LV, color flow mapping delineates flow across the VSD and flow through the great arteries, depending on the VA connection and associated arterial obstruction. If there is significant pulmonary obstruction, flow in the arterial duct may be retrograde, indicating a duct-dependent circulation (Figures 24.8d and 24.9d,g). Conversely, in cases of aortic obstruction, the arterial duct is large and the main source of blood supply to the lower body.

Flow signal across the ductus venosus may show increased pulsatility or even reversal of the "A" wave at end diastole (Figure 24.8e). This abnormal pattern does not necessarily indicate cardiac failure and does not seem to have prognostic implication regarding survival to the neonatal period.[31]

## Prenatal history and associated extracardiac abnormalities

The fetus with tricuspid atresia is usually stable throughout pregnancy. Spontaneous fetal demise is relatively uncommon. It accounted for 4.5% of all cases but 6.5% of ongoing pregnancies in a large multicenter series.[89] A similar figure (3.7%) is reported by others.[90] Reported cases of termination of pregnancy in recent series varied between 11% and 31.5%[89–91] but 51% of cases if diagnosed before 24 weeks.[89] From midgestation onward, fetal hydrops is uncommon, but reported.[84]

Abnormal extracardiac findings are reported as relatively uncommon,[92] but they are well described. In Wald's multicenter series of fetal diagnosis,[89] only two of 58 live-born children had chromosomal abnormalities (one trisomy 18, one with chromosome 8 deletion), and another two had a syndrome. One pregnancy affected with trisomy 21 was also terminated. However, the authors pointed out these numbers might have been underestimated as most cases were not fully investigated and only 18% had invasive tests. Accordingly, in another series, which addressed the prevalence of extracardiac abnormalities in fetuses with major forms of CHD, there was a surprisingly large number of associated problems in fetuses with tricuspid atresia.[43] Of 30 cases, 60% were isolated, 30% had extracardiac but no chromosomal defects, and 10% had both. In Berg's series, about 78% were isolated cases, while 22% had extracardiac anomalies including trisomy 13, 18, and Vertebral anomalies, Anal atresia, Cardiac anomalies, Tracheo-oesophageal fistula with Oesophageal atresia, Radial and Renal dysplasia and Limb anomalies (VACTERL) association, among others.[90] In a prenatal series of single-ventricle defects, three of 46 cases of tricuspid atresia had an associated omphalocele.[84] These studies highlight the need for a detailed assessment of the fetus in a multidisciplinary approach. With the advent of more sophisticated genetic tests, it is possible that more cases will be linked to chromosomal defects.

## Postnatal diagnosis and management

In the early neonatal period, clinical presentation of tricuspid atresia varies according to the exact sequential segmental analysis and associated abnormalities. In the absence of pulmonary or systemic obstruction, the newborn baby will be hemodynamically stable, with minimal cyanosis. As pulmonary vascular resistance falls, there will be increasing signs of heart failure with breathlessness, feeding difficulties, and slow weight gain. In these cases, the initial surgical procedure involves placement of a pulmonary artery band to control pulmonary blood flow. On the other end of the spectrum, there may be a duct-dependent circulation, for which the neonate will require early intervention. Cyanosis is the predominant clinical finding in cases of duct-dependent pulmonary circulation (e.g., pulmonary atresia of significant stenosis), while acidosis and cardiovascular collapse are seen in those babies with duct-dependent systemic circulation (e.g., severe aortic obstruction, coarctation, or interrupted aortic arch). Initial palliative procedures include creation of a systemic to pulmonary shunt (e.g., BT shunt) or relief of aortic obstruction (e.g., coarctation repair). In some instances, for example, in cases with transposed vessels with a restrictive VSD a Damus-Kaye-Stansel procedure may be needed. This involves anastomosing the proximal pulmonary artery to the ascending aorta. In extreme cases of aortic hypoplasia, a modified Norwood procedure may be needed. In

between these two extremes, the most common scenario is that of an infant who is cyanosed but with a balanced circulation. An elective BT shunt may be needed if cyanosis progresses, but the first operation may involve a Glenn anastomosis at around 4–6 months of age. This is the first step of univentricular palliation, prior to completion of TCPC, which is performed at a later stage around 2–4 years of age.

## Postnatal outcome and follow-up

The endpoint of surgical treatment for patients with tricuspid atresia will be, by necessity, a univentricular circulation. Results of this palliative surgical pathway from the current era have been recently reported by Alsoufi et al.[93] Out of 105 neonates, about a quarter (26%) were stable enough in early life so that initial surgery was the first stage of TCPC (i.e., a Glenn procedure). The majority (74%) however, required surgery in the neonatal period with type of initial procedure reflecting the anatomical variability of the condition. Those with pulmonary obstruction had a modified BT shunt (44%), those with important aortic outflow obstruction had a Norwood procedure (17%), while pulmonary artery band was needed in the remaining (13%). Survival at 1 month and 1 year for the entire group was 98% and 90%, respectively. Eight-year survival following band of the pulmonary artery was 93% compared with 87% after primary Glenn, 83% after BT shunt, and 78% after Norwood. Genetic and extracardiac anomalies were important risk factors for death, a hazard that persisted for nearly 1 year after surgery. Previously, Wald et al. also highlighted the significance of extracardiac abnormalities on survival with Kaplan-Meyer estimates of 91% at 1 month and 83% at 1 year. In their series, the presence of a chromosomal anomaly or syndrome, although present only in a small proportion of live births, was an independent predictor of mortality, with a hazard ratio of 13.3 (95% confidence interval 2.21–19.6).[89]

In the early 1990s, Franklin et al. identified the presence of associated aortic arch obstruction as a significant risk factor for death or subsequent development of subaortic stenosis.[94] In a recently reported series, which spanned three decades, the importance of systemic outflow tract obstruction at birth remained a significant factor influencing survival, with no apparent effect of surgical era on outcome of children with tricuspid atresia,[95] while in other series, systemic obstruction did not seem to affect survival at the time of first palliation.[93]

## Summary

Clinical presentation of tricuspid atresia varies and is due primarily to variability of VA connection and size of the VSD. Accordingly, treatment options will also depend on these same variables, which will largely influence the balance between pulmonary and systemic circulation. Ultimately, however, all treatment pathways will lead toward univentricular palliation. Survival following surgery has improved over the years and is negatively affected by associated extracardiac abnormalities/genetic syndromes. The rate of termination of pregnancy is high if the diagnosis is made before 24 weeks of gestation.

# References


1. Carvalho JS et al. *Ultrasound Obstet Gynecol* 2005;26(2):105–11.
2. Hunter J. *Med Obs Inquiries* 1784;6(291):294.
3. Hare CJ. *Cyanosis Trans Pathol Soc London* 1853;4(81):85.
4. Fyler DC. *Pediatrics* 1980;65(suppl):376–461.
5. Ferencz C et al. *Am J Epidemiol* 1985;121(1):31–6.
6. Ekman Joelsson BM et al. *Scand Cardiovasc J* 2001;35(3):192–8.
7. Daubeney PE et al. *Circulation* 1998;98(6):562–6.
8. Fyler DC et al. Infants with congenital heart disease: The cases. In: Ferencz C, Rubin JD, Loffredo CA, Magee CA, eds. *Epidemiology of Congenital Heart Disease: The Baltimore-Washington Infant Study 1981–1989*. Mount Kysco, NY: Futura; 1993:38.
9. Egbe A et al. *Pediatr Cardiol* 2014;35(6):975–82.
10. Patel CR et al. *Cardiol Young* 2000;10(3):268–70.
11. Freedom RM et al. *Cardiol Young* 2006;16(1):18–29.
12. Zuberbuhler JR, Anderson RH. *Br Heart J* 1979;41(3):281–8.
13. Albanese SB et al. *Ann Thorac Surg* 2002;73(4):1322–4.
14. Anderson RH, Ho SY. *Ann Thorac Surg* 1998;66(2):673–7.
15. Bull C et al. *Circulation* 1982;66(2):266–72.
16. Daubeney PE et al. *J Am Coll Cardiol* 2002;39(10):1670–9.
17. Schneider C et al. *Ultrasound Obstet Gynecol* 2005;26(6):599–605.
18. DeVore GR. *Ultrasound Obstet Gynecol* 2005;26(6):596–8.
19. Krishnan A et al. *J Am Soc Echocardiogr* 2016;29(12):1197–206.
20. Stellin G et al. *J Thorac Cardiovasc Surg* 1993;106(2):255–61.
21. Grant RT. *Heart* 1926;13:273–83.
22. Lauer RM et al. *N Engl J Med* 1964;271:68–72.
23. Freedom RM, Harrington DP. *Br Heart J* 1974;36(11):1061–5.
24. Freedom RM et al. *Cardiol Young* 2005;15(5):447–68.
25. Gittenberger-De Groot AC et al. *Prog Pediatr Cardiol* 1991;13:157–64.
26. Sandor GG et al. *Cardiol Young* 2002;12(5):436–44.
27. Kipps AK et al. *Congenit Heart Dis* 2011;6(5):444–50.
28. Maeno YV et al. *Heart* 1999;81(6):661–8.
29. Chaoui R et al. *Ultrasound Obstet Gynecol* 2000;15(2):160–2.
30. Santos MA et al. *Circulation* 1980;62(4):818–22.
31. Berg C et al. *Ultrasound Obstet Gynecol* 2006;28(2):137–42.
32. Todros T et al. *Ultrasound Obstet Gynecol* 2003;21(3):228–33.
33. Zosmer N et al. *Br Heart J* 1994;72(1):74–9.
34. Lougheed J et al. *J Am Coll Cardiol* 2001;38(5):1533–8.
35. Herberg U et al. *Heart* 2006;92(1):95–100.
36. Eschbach SJ et al. *Ultrasound Obstet Gynecol* 2017;49(6):737–43.
37. Mahieu-Caputo D et al. *Prenatal Diagnosis* 2003;23(8):640–5.
38. Wohlmuth C et al. *Acta Obstet Gynecol Scand* 2016;95(6):664–71.
39. Ortiz JU et al. *Fetal Diagn Ther* 2017;41(3):191–6.
40. Stagnati V et al. *Prenat Diagn* 2015;35(11):1085–92.
41. Allan LD et al. *J Am Coll Cardiol* 1986;8(5):1131–6.
42. Sharland G. Pulmonary valve abnormalities. In: Allan L, Hornberger L, Sharland G, eds. *Textbook of Fetal Cardiology*. London: Greenwich Medical Media; 2000:233–47.
43. Song MS et al. *Ultrasound Obstet Gynecol* 2009;33(5):552–9.
44. Arzt W et al. *Ultrasound Obstet Gynecol* 2003;21(2):186–8.
45. Tulzer G et al. *Lancet* 2002;360(9345):1567–8.
46. Galindo A et al. *Fetal Diagn Ther* 2006;21(1):100–4.
47. NICE guidelines N. Available from: https://www.nice.org.uk/guidance/IPG176/chapter/4-Changes-since-publication.
48. Gomez Montes E et al. *Cardiol Res Pract* 2012;2012:592403.
49. Polat T, Danisman N. *Images Paediatr Cardiol* 2012;14(3):6–11.

50. Pedra SR et al. *Pediatr Cardiol* 2014;35(3):399–405.
51. Freud LR, Tworetzky W. *Curr Opin Pediatr* 2016;28(2):156–62.
52. Tulzer G, Arzt W. *Semin Fetal Neonatal Med* 2013;18(5):298–301.
53. Tworetzky W et al. *Pediatrics* 2009;124(3):e510–8.
54. Arzt W, Tulzer G. *Prenat Diagn* 2011;31(7):695–8.
55. Moon-Grady AJ et al. *J Am Coll Cardiol* 2015;66(4):388–99.
56. Rigby ML. *Early Hum Dev* 2012;88(5):291–4.
57. Bull C et al. *J Thorac Cardiovasc Surg* 1994;107(2):359–66.
58. Rosenthal E et al. *Br Heart J* 1993;69(4):347–51.
59. Parsons JM et al. *Br Heart J* 1991;66(1):36–8.
60. Gibbs JL et al. *Br Heart J* 1992;67(3):240–5.
61. Udink Ten Cate FE et al. *Catheter Cardiovasc Interv* 2013;82(3): E233–43.
62. Pawade A et al. *J Card Surg* 1993;8(3):371–83.
63. de Leval M et al. *Circulation* 1982;66(2):272–80.
64. Yoshimura N et al. *J Thorac Cardiovasc Surg* 2003;126(5):1417–26.
65. Numata S et al. *Eur J Cardiothorac Surg* 2003;24(4):516–20.
66. Starnes VA et al. *J Thorac Cardiovasc Surg* 1991;101(6):1082–7.
67. Daubeney PE et al. *J Thorac Cardiovasc Surg* 2005;130(4):1071.
68. Odim J et al. *Ann Thorac Surg* 2006;81(2):678–84.
69. Liava'a M et al. *Eur J Cardiothorac Surg* 2011;40(6):1406–11.
70. Agnoletti G et al. *J Am Coll Cardiol* 2003;41(8):1399–403.
71. Chubb H et al. *J Am Coll Cardiol* 2012;59(16):1468–76.
72. Schwartz MC et al. *Pediatr Cardiol* 2014;35(1):22–9.
73. Rathgeber S et al. *Pediatr Cardiol* 2017;38(1):170–5.
74. Guleserian KJ et al. *Ann Thorac Surg* 2006;81(6):2250–7.
75. Redington AN et al. *Cardiol Young* 1992;2:382–6.
76. Sanghavi DM et al. *Am J Cardiol* 2006;97(11):1638–43.
77. Lee YO et al. *Eur J Cardiothorac Surg* 2011;39(5):711–5.
78. Rigby ML et al. *Int J Cardiol* 1990;27(1):1–17.
79. Rashkind WJ. *Pediatr Cardiol* 1982;2(1):85–8.
80. Schuberg W. *Virchows Arch Path Anat* 1861;20:294–7.
81. Rigby ML, Anderson RH. Tricuspid atresia and the Fontan operation. In: Anderson RH, Baker EJ, Macartney FJ, Rigby ML, Shinebourne EA, Tynan M, eds. *Paediatric Cardiology. 2*. London: Churchill Livingstone; 2002:1047–73.
82. Sharland G. Abnormalities of the atrioventricular junction. In: Allan L, Hornberger L, Sharland G, eds. *Textbook of Fetal Cardiology*. London: Greenwich Medical Media; 2000: 133–47.
83. Hoffman JI, Kaplan S. *J Am Coll Cardiol* 2002;39(12):1890–900.
84. Beroukhim RS et al. *Ultrasound Obstet Gynecol* 2015;45(6): 657–63.
85. Huhta JC et al. *Br Heart J* 1982;48(2):97–108.
86. Carvalho JS et al. Identification of fetal laterality and visceral situs should be part of routine fetal anomaly scans. In: Momma K, Imai Y, eds. *World Congress of Pediatric Cardiology and Cardiac Surgery*; May 11–15, 1997; Honolulu, Hawaii. Armonk, NY: Futura Publishing; 1997:117.
87. Frescura C, Thiene G. *Front Pediatr* 2014;2:62.
88. Anderson RH et al. *Am J Cardiol* 1984;54(7):822–8.
89. Wald RM et al. *Am Heart J* 2007;153(5):772–8.
90. Berg C et al. *Ultrasound Obstet Gynecol* 2010;35(2):183–90.
91. Idorn L et al. *Int J Cardiol* 2013;167(4):1311–6.
92. Sharland G. Tricuspid valve abnormalities. In: Allan L, Hornberger L, Sharland G, eds. *Textbook of Fetal Cardiology*. London: Greenwich Medical Media; 2000:133–47.
93. Alsoufi B et al. *Ann Thorac Surg* 2015;100(4):1403–9; discussion 1409–10.
94. Franklin RC et al. *J Am Coll Cardiol* 1990;16(6):1455–64.
95. Franken LC et al. *Eur J Cardiothorac Surg* 2017;51(6):1051–7.
96. Peterson RE et al. *J Am Soc Echocardiogr* 2006;19(11):1393–400.
97. Salvin JW et al. *Pediatrics* 2006;118(2):415–20.
98. Roman KS et al. *Am J Cardiol* 2007;99(5):699–703.
99. Gardiner HM et al. *J Am Coll Cardiol* 2008;51(13):1299–308.
100. Iacobelli R et al. *Ultrasound Obstet Gynecol* 2008;32(1):31–5.
101. Gomez-Montes E et al. *Prenat Diagn* 2011;31(4):372–9.
102. Lowenthal A et al. *Fetal Diagn Ther* 2014;35(2):101–7.

# 25

# Ventricular outflow tract anomalies ("conotruncal anomalies")

Varsha Thakur, Edgar T. Jaeggi, and Shi-Joon Yoo

This chapter discusses the normal anatomy of the ventricular outflow tracts, the fetal echocardiographic techniques for their evaluation, and the echocardiographic findings and postnatal outcomes of conotruncal anomalies (CTAs). Prenatal detection of CTA is of critical importance, as many of these lesions will require immediate treatment after birth.

Ventricular outflow tract anomalies can be classified into two categories: (1) as isolated lesions in an otherwise structurally normal heart, and (2) as more complex anomalies that occur in association with abnormal ventriculo-arterial connections and/or abnormal great arterial relationship. The latter group, known as conotruncal or truncoconal anomalies, includes simple and corrected transposition of the great arteries, double-outlet ventricle, and common arterial trunk. Interruption of the aortic arch and tetralogy of Fallot are also considered conotruncal anomalies and are discussed elsewhere in this book. CTA is considered to result from an errant development of the conotruncal region of the embryonic heart[1] and accounts for 25%–30% of children born with CHD.[2–4] The reported prevalence is lower in fetal series,[5] which is explained by the lower detection rate of ventricular outflow and arch anomalies before birth, in particular, if the cardiac four-chamber view is used alone for prenatal ultrasound screening.[6,7] Nonetheless, with the inclusion of the outflow tract views in more recent prenatal screening recommendations, the prenatal detection of these anomalies continues to steadily improve.[8–11]

## Normal anatomy of the ventricular outflow tracts

The right and left ventricular outflow tracts exhibit significant morphological differences (Figure 25.1). The major difference is the existence of the crista supraventricularis in the right ventricle, which is a muscular crest that separates the pulmonary and tricuspid valves in the normal right ventricle.[12] The major part of the crista is a parietal structure, which is called the ventriculoinfundibular fold. Only a small part of the crista, the *outlet* or *infundibular septum*, is truly a septal structure. The outlet septum is cradled between the two limbs of the trabecula septomarginalis. The crista supraventricularis completes the muscular funnel of the right ventricular outflow tract. In the left ventricle, the aortic valve is deeply wedged between the tricuspid and mitral valves (Figure 25.1c,d). This unique position allows a fibrous continuity between the aortic and mitral valves, and there is no muscular crest between the two valves. The two ventricular outflow tracts cross each other (Figure 25.2). The right ventricular outflow tract is anterior and then angles leftward of the left ventricular outflow tract.

## Echocardiographic techniques for fetal ventricular outflow tract evaluation

In the evaluation of the ventricular outflow tracts, the ventricles and great arteries should be identified according to the morphological criteria and the ventriculoarterial connections and great arterial relationship should be evaluated as follows (Figures 25.3 and 25.4):[13–18]

1. Left ventricular outflow tract view
2. Right ventricular outflow tract view
3. Basal ventricular short-axis view
4. Three-vessel view (3VV)

The left and right ventricular outflow tract views are necessary for determining the ventriculo-arterial (VA) connections. Once the four-chamber view is obtained, the transducer is moved radially around the maternal abdomen, keeping the four-chamber plane in view, until the ventricular septum is aligned perpendicular to the sonographic beam axis. From this particular transducer position, the left ventricular outflow tract view can be obtained simply by rotating the transducer through 40°–50° clockwise or counterclockwise toward the cardiac apex. The transducer is then moved slightly upward until the right ventricular outflow tract view is visualized. It should be noted that the normal right and left ventricular outflow tracts cross each other and cannot be visualized in a single two-dimensional imaging plane (Figures 25.2 through 25.5).

The basal ventricular short-axis view is the optimal plane for evaluating the morphology of the infundibular or outlet septum and the right ventricular outflow tract. The short-axis plane can be found by placing the transducer to connect

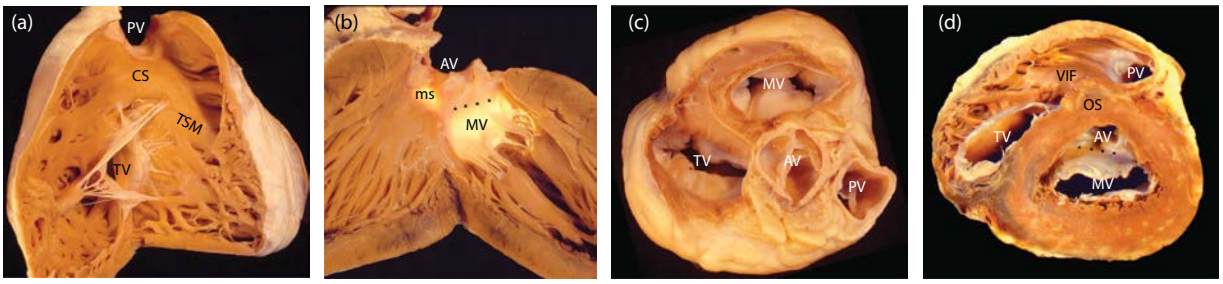


**Figure 25.1**
A normal cardiac specimen. Opened right (a) and left (b) ventricles, and the base of the ventricles seen from above (c) and below (d). As the crista supraventricularis (CS) intervenes between the tricuspid (TV) and pulmonary (PV) valves, the right ventricular outflow tract is a completely muscular funnel. The crista supraventricularis consists of parietal and septal parts; the ventriculoinfundibular fold (VIF) and outlet septum (OS), respectively. The left ventricular outflow tract is partly devoid of muscular wall because of the fibrous continuity (dots in [b] and [d]) between the mitral (MV) and aortic (AV) valves. Notice the deeply wedged position of the aortic valve between the tricuspid and mitral valves in (c). (ms, membranous septum; TSM, trabecula septomarginalis.)

the right lobe of the liver and the left shoulder of the fetus (Figure 25.3). The transducer is moved upward or downward along the fetal thorax with some cranial or caudal tilt until the aortic valve is located in the center of the cardiovascular section that visualizes the right atrium, right ventricle, main pulmonary artery, and right pulmonary artery. An alternative view is the vertical long-axis view of the right ventricle (Figure 25.6). This view can be obtained from the coronal view by displacing the transducer to the left anterior or right posterior part of the chest wall.

The 3VV is an orthogonal transverse view of the upper mediastinum, where normally the oblique section of the main pulmonary artery and cross sections of the ascending aorta and superior vena cava are arranged in a straight line from left anterior to right posterior with a decreasing order of their size (Figure 25.4).[14–17] The 3VV is useful in the evaluation of the spatial relationship and size of the great arteries, and can be obtained simply by sliding the transducer upward from the four-chamber plane toward the fetal upper mediastinum.[19] The 3VV is abnormal in almost all cases with a ventricular outflow tract anomaly.[20] Sliding the transducer

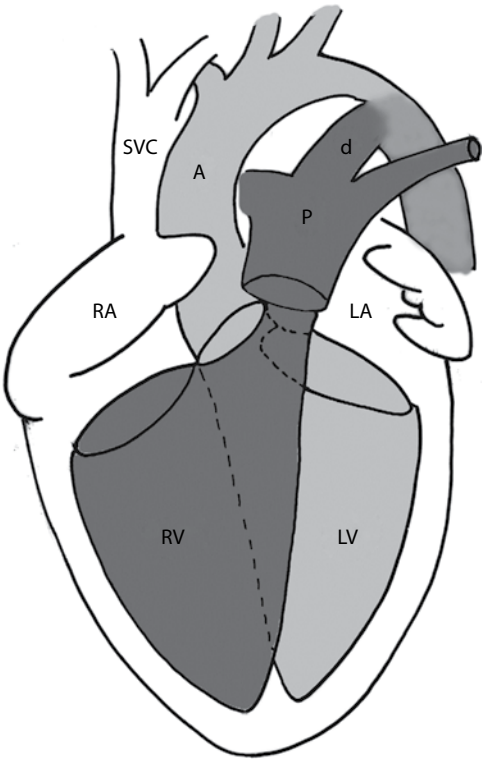


**Figure 25.2**
The long-axis view of the normal right (RV) and left (LV) ventricles. The two outflow tracts cross each other. (A, aorta; d, ductus arteriosus; LA, left atrium; P, pulmonary artery; RA, right atrium; SVC, superior vena cava.)

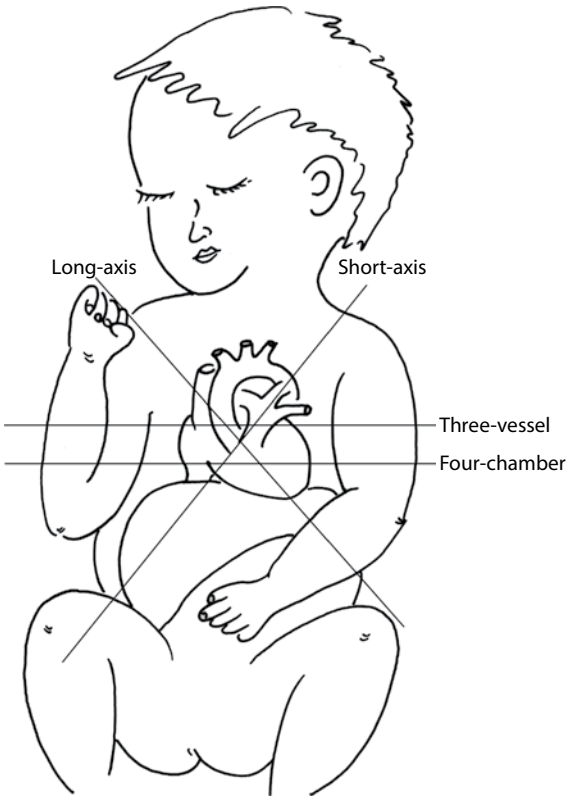


**Figure 25.3**
The imaging planes for echocardiographic views.

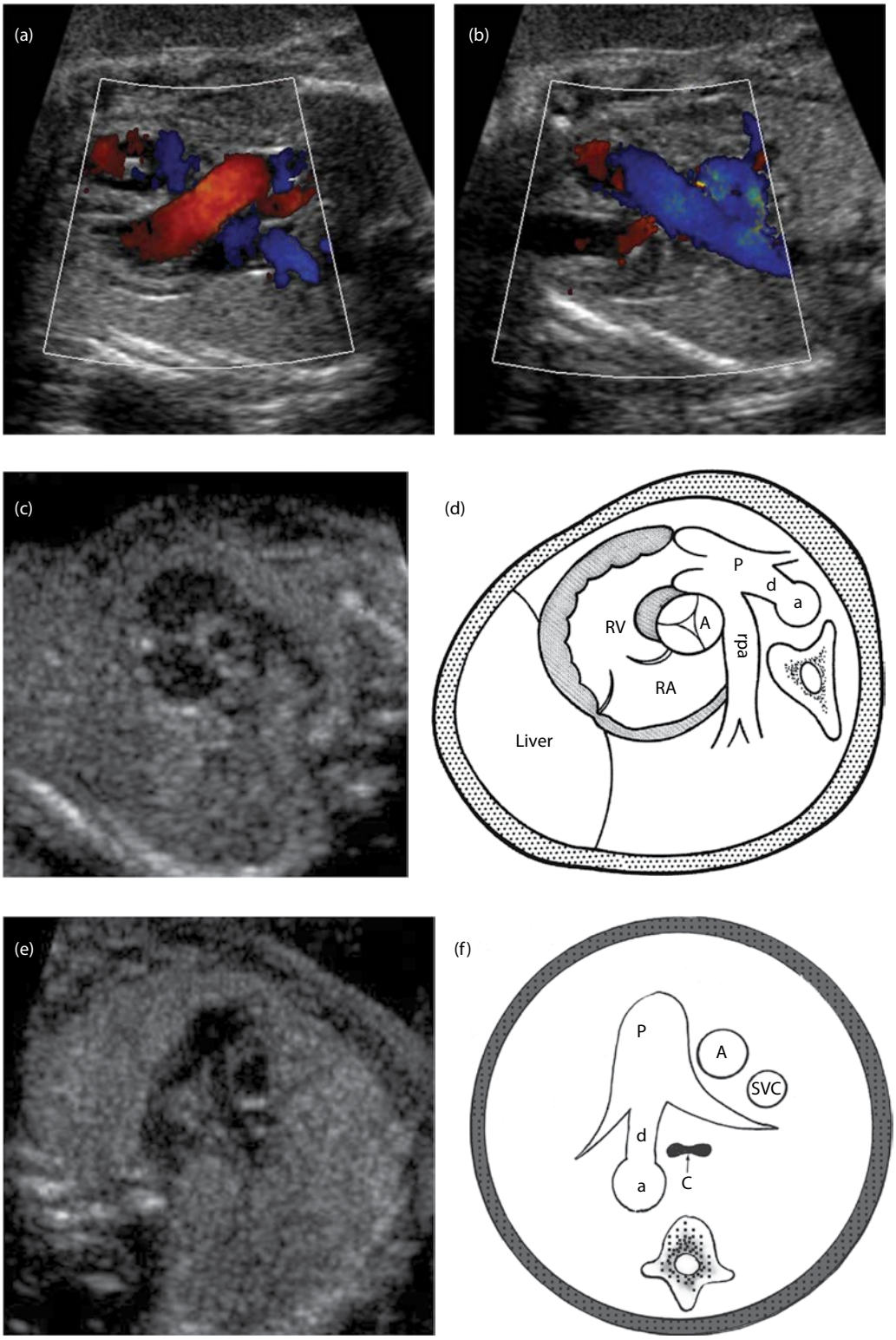


**Figure 25.4**
Echocardiograms and corresponding diagrams for ventricular outflow tract examination. (a) Left ventricular outflow tract view. (b) Right ventricular outflow tract view. (c,d) Short-axis view of the base of the ventricles. (e,f) 3VV. (A, ascending aorta; a, descending aorta; C, carina; d, ductus arteriosus; P, main pulmonary artery; RA, right atrium; rpa, right pulmonary artery; RV, right ventricle; SVC, superior vena cava.)

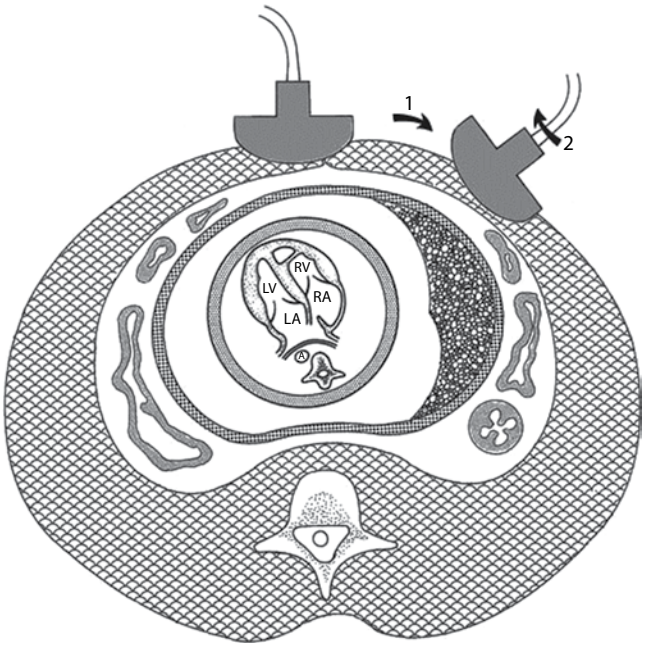


**Figure 25.5**
The maneuver for scanning the ventricular outflow tracts in a fetus in cephalic presentation and supine position. The examination starts from the position providing the four-chamber view. The transducer is moved radially around the maternal abdomen (arrow 1) until the ventricular septum is aligned perpendicular to the sonographic beam axis. Then the left ventricular outflow tract is obtained by rotating the transducer toward the cardiac apex (arrow 2). By sliding the transducer upward along the fetal thorax, the right ventricular outflow tract view is obtained. (A, descending aorta; LA, left atrium; LV, left ventricle; RA, right atrium; RV, right ventricle.) (Reprinted with permission from Yoo SJ et al. *Ultrasound Obstet Gynecol* 1997;9(3):173–82.[14])

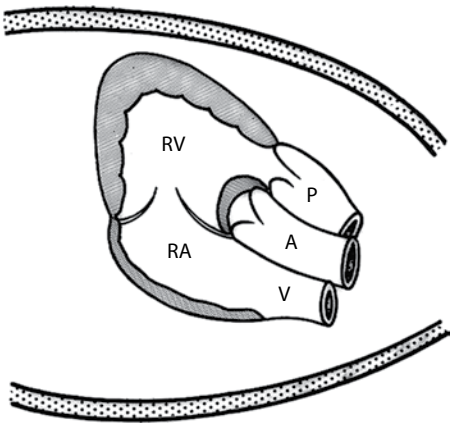


**Figure 25.6**
Vertical long-axis view of the right ventricle and corresponding diagram. This semicoronal view is equivalent to the angiographic right anterior oblique view. The long-axis cuts of the three vessels are aligned from the left anterior to the right posterior aspect of the fetal thorax. (A, aorta; P, pulmonary artery; RA, right atrium; RV, right ventricle; V, superior vena cava.)

further superiorly leads to the three-vessel tracheal view, which forms a "V" in the fetus with a normal left aortic arch and left ductal arch. In fetuses with outflow tract anomalies, the three-vessel tracheal view is also abnormal and quite useful in the diagnosis of CTA.

Three-dimensional (3D) and four-dimensional (4D) ultrasound enhances two-dimensional (2D) diagnostic approaches to fetal outflow tract abnormalities.[21–24] Using the spin technique, a 3D transducer acquires a volume dataset from the four-chamber plane, through the three-vessel plane to the plane for the aortic and ductal arches by using static 3D or spatiotemporal image correlation (STIC) technique. From the volume dataset, the images described can be reconstructed for ventricular outflow tract assessment. Doppler interrogation is an important adjunct to 2D imaging and demonstrates the direction and velocity of the blood flow through the outflow tracts. It also demonstrates the flow direction and velocity through the ductus arteriosus, which is important for recognition of a possible "duct-dependent" pulmonary or systemic circulation after birth. Power and color Doppler mapping facilitates identification of the vessels.

# Individual lesions

## *Transposition of the great arteries*

Transposition of the great arteries (TGA) refers to a condition in which the aorta arises from the right ventricle and the pulmonary artery from the left ventricle and is synonymous with the term "discordant VA connection," "d-TGA," "simple" TGA, or "complete" TGA. When transposition occurs with concordant atrioventricular connection—that is, the right atrium connects to the right ventricle and the left atrium to the left ventricle—it is called complete transposition (Figure 25.7; Video 25.1). When it occurs with discordant atrioventricular connection—that is, the right atrium connects to the left ventricle and the left atrium to the right ventricle—it is called congenitally corrected transposition.

The incidence of TGA is 5%–7% of all live births with CHD. Most cases occur with situs solitus, levocardia, and normally positioned ventricles. The four-chamber view is normal unless there are associated lesions.[25] The spatial great arterial relationship is almost always abnormal and easily recognized in the 3VV (Figure 25.8a).[14–17] The aorta is supported by a muscular infundibulum, while the pulmonary artery is not. The pulmonary valve is in fibrous continuity with the mitral valve. In this classic setting, the aorta is anterior to and to the right of the pulmonary artery. Rarely, the aorta may be located posterior to or to the left of the pulmonary artery.[26] The ventricular outflow tracts are usually parallel, allowing visualization of both outflow tracts in a single imaging plane (Figure 25.8b,c). Finally, the aortic arch is shaped like a "hockey stick" and thus can be mistaken for a ductal arch (Figure 25.8d).

In approximately one-third of cases, TGA occurs in association with isolated or multiple ventricular septal defects (VSDs) (Figure 25.9; Video 25.2). VSDs may occur in any part

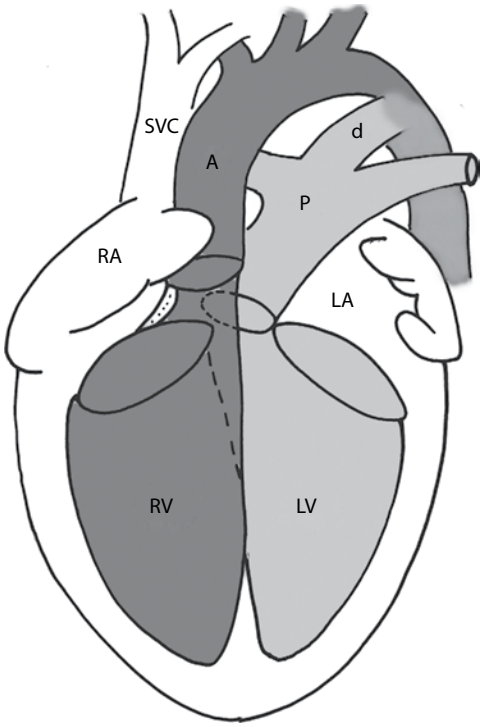


**Figure 25.7**
Pathology of complete transposition of the great arteries. (A, aorta; d, ductus arteriosus; LA, left atrium; LV, left ventricle; P, pulmonary artery; RA, right atrium; RV, right ventricle; SVC, superior vena cava.)

of the septum, but outlet septal defects with or without posterior or anterior septal malalignment tend to be most common. When there is posterior malalignment of the ventricular outlet septum, the subpulmonary outflow tract usually becomes narrowed (Figure 25.9; Video 25.3), while the aortic outflow may override the ventricular septum. When there is anterior malalignment, the subaortic outflow tract appears narrowed, and the pulmonary valve may override the ventricular septum. With a greater degree of overriding of the aortic or pulmonary valve, transposition merges into double-outlet left or right ventricle with malposed great arteries.

Left ventricular outflow tract obstruction (pulmonary stenosis) is common in TGA[27] and may be due to posterior malalignment of the outlet septum. Obstruction due to fibrous ridge, fibromuscular tunnel, or accessory mitral valve tissue can exist with an intact ventricular septum as well as in association with a ventricular septal defect. With a significant left ventricular outflow tract obstruction, the main pulmonary artery is smaller than the ascending aorta. The pulmonary valve may be stenotic (Figure 25.9). In contrast, right ventricular outflow tract obstruction is less common. It may be due to anterior malalignment of the outlet septum as described and is often dynamic. When there is subaortic stenosis, an obstructive lesion of the aortic arch may be present. Hypoplasia of the morphologically right ventricle is also seen in this setting (Figure 25.10; Video 25.4).

TGA without or with only a small VSD can be a life-threatening malformation in neonates. Due to the discordant great arterial connection, oxygenated blood returning from the pulmonary veins to the left heart is ejected again into the

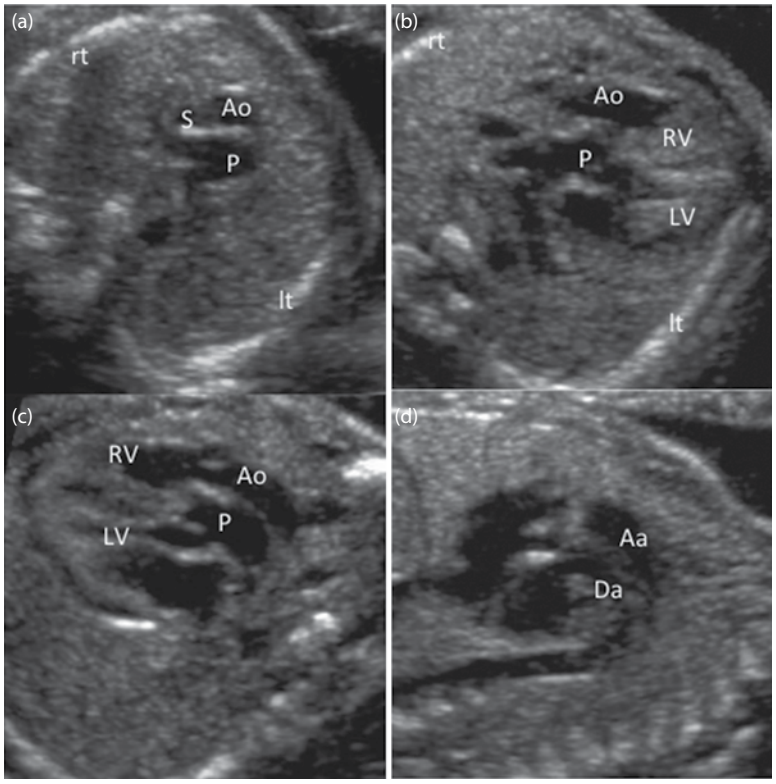


**Figure 25.8**
Complete transposition of the great arteries. (a) Three-vessel view shows the classic great arterial relationship of complete transposition. The three vessels are arranged in a triangular fashion with the right superior vena cava (S), right anterior aorta (A), and left posterior pulmonary artery (P). (b) Ventricular outflow tract view shows discordant ventriculoarterial connection. As the right and left ventricular outflow tracts are parallel to each other, they are imaged in a single plane. (c) Ventricular outflow tract view, again showing the discordant ventriculoarterial connection. (d) Sagittal view of the aortic arch (Aa) and the ductal arch (Da). The aortic arch forms a wide arc with a configuration of a hockey stick. It gives rise to the head and neck branches. (A, aorta; Aa, aortic arch; Da, ductal arch; S, superior vena cava; P, pulmonary artery; lt, left; LV, left ventricle; rt, right; RV, right ventricle.)

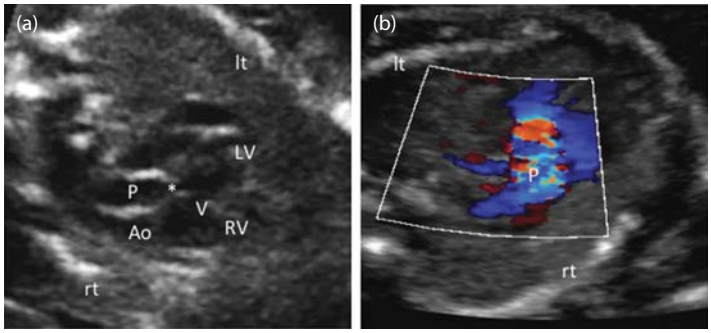


**Figure 25.9**
(a) Complete transposition of the great arteries with ventricular septal defect and left ventricular outflow tract obstruction. Ventricular outflow tract view shows discordant ventriculoarterial connection. The left ventricular outflow tract is narrow because of posteriorly deviated outlet septum, and there is subpulmonary obstruction (asterisk). (b) Color Doppler shows flow acceleration across the narrowed left ventricular outflow tract secondary to the subpulmonary obstruction. (Ao, aorta; V, ventricular septal defect; lt, left; LV, left ventricle; P, pulmonary artery; rt, right; RV, right ventricle; *, subpulmonary obstruction.)

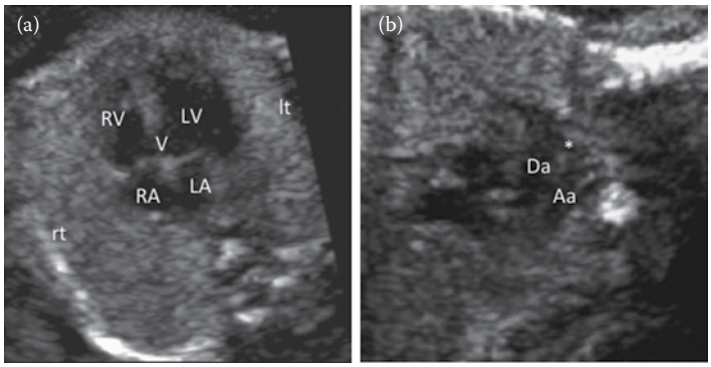


**Figure 25.10**
(a) Complete transposition of the great arteries with ventricular septal defect and coarctation of the aorta. There is discrepancy of the sizes of the right and left ventricles, with a smaller but apex-forming right ventricle in the four-chamber view. (b) The sagittal view shows a diminutive aortic arch with a coarctation (asterisk). (Ao, aorta; Aa, aortic arch; Da, ductal arch; *, coarctation; V, ventricular septal defect; LA, left atrium; lt, left; LV, left ventricle; RA, right atrium; rt, right; RV, right ventricle.)

pulmonary arteries, while desaturated blood from the systemic veins enters the right heart and is ejected to the aorta. Systemic arterial oxygenation and thus the degree of cyanosis depends on the amount of oxygenated blood that is able to pass across an intracardiac (atrial septal defect, ventricular septal defect) and/or extracardiac (ductus arteriosus) communication to the right heart and aorta. Newborns with isolated d-TGA may present with severe cyanosis and develop metabolic acidosis and eventually multiorgan failure unless there is adequate shunting between the systemic and pulmonary circulations via an arterial duct that is maintained patent by the neonatal administration of intravenous prostaglandin and intracardiac communications, such as a sufficiently large atrial septal defect, which is often only achieved by neonatal atrial balloon septostomy in the first hours of life. Delay in diagnosis and treatment may result in significant morbidity and mortality. In a study by Bonnet et al., 12% of neonates without prenatal diagnosis died prior to hospital discharge versus no mortality if TGA was diagnosed prenatally.[25]

Predicting by fetal echocardiography that a fetus has TGA and, in particular, which fetus will immediately present with profound cyanosis and need immediate neonatal attention is extremely important but often also challenging.[28,29] Evaluation of the size and shunt across the foramen ovale and the ductus arteriosus may help in detecting possible restriction of blood flow across these structures after birth.[31] A ductus arteriosus with high-velocity continuous antegrade flow suggests prenatal ductal obstruction. Bidirectional ductal flow has been associated with an increased risk of persistent postnatal pulmonary arterial hypertension.[30]

Complete TGA is only rarely associated with extracardiac and/or genetic anomalies.[7,32] Despite the low yield, prenatal screening for associated lesions is advised.

Current management strategies for complete TGA include (a) delivery at a tertiary care center with expertise in managing newborns with critical CHD, (b) initiation of prostaglandin immediately after birth to maintain ductal patency, and (c) a balloon atrial septostomy to improve mixing of oxygenated and deoxygenated blood if the atrial communication is small. Surgical options include arterial switch operation (ASO)[33] in the first days of life. In the absence of significant other cardiac lesions, long-term outcomes of TGA are good with 97% survival to 20 years, low morbidity, and low rates of surgical and catheter-based reinterventions during childhood.[34] Mortality is increased in neonates with rare coronary abnormalities, particularly intramural coronaries,[35,36] which is not detectable by fetal echocardiography. The presence of a ventricular septal defect in combination with a left ventricular outflow tract obstruction or arch obstruction requires change in surgical management, so these lesions are appropriately addressed. In the presence of left ventricular outflow obstruction, either ASO with resection of the obstructing tissue versus Rastelli operation, REV (Réparation à l'Etage Ventriculaire), or Nikaidoh are possible surgical options to consider,[37,38] although long-term outcomes are inferior to that of simple TGA,[39–41] and there is usually a need for reintervention, that is, to replace pulmonary artery conduits.[40–44]

## *Congenitally corrected transposition of the great arteries*

Congenitally corrected transposition of the great arteries (cc-TGA) is a relatively rare form of CHD with an incidence of less than 1%.[45] In this anomaly, the ventricles are inverted, and the atrioventricular and ventricular arterial connections

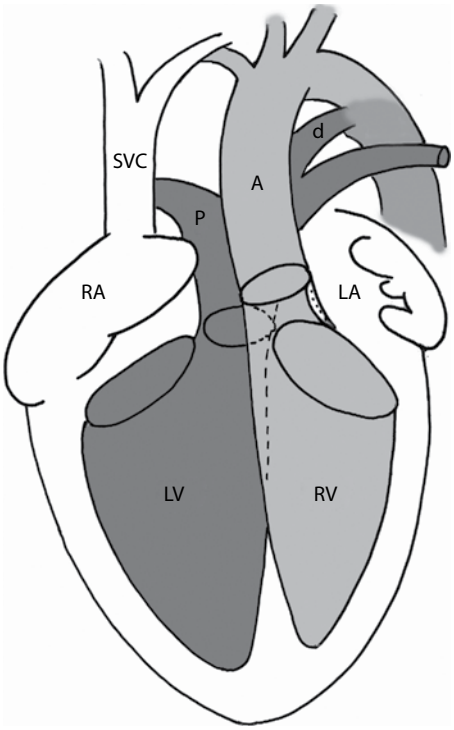


**Figure 25.11**
Pathology of corrected transposition of the great arteries. (A, aorta; d, ductus arteriosus; LA, left atrium; LV, left ventricle; P, pulmonary artery; RA, right atrium; RV, right ventricle; SVC, superior vena cava.)

are therefore discordant (Figure 25.11). This means that after birth, the right ventricle will function as the systemic ventricle and pump oxygenated blood from the left atrium into the aorta, while the left ventricle will pump deoxygenated blood from the systemic veins into the pulmonary vasculature. The lesion is therefore hemodynamically "corrected" to the extent that the newborn will not present with cyanosis at birth unless there are other associated anomalies The usual situs is solitus and levocardia, but mesocardia and dextrocardia are not uncommon.[46–49] An unusual more midline or rightward cardiac position is an important diagnostic feature of cc-TGA among other lesions. Discordant atrioventricular connection can be readily recognized at the four-chamber view (Figure 25.12a; Video 25.5). In situs solitus, the left-sided ventricle is the morphologically right ventricle that can be identified by the presence of a moderator band and more apical attachment of its atrioventricular valve to the ventricular septum. Occasionally, the ventricles may be related in a superior-inferior fashion. The aorta is usually supported by a completely muscular infundibulum, while the pulmonary artery is not. The pulmonary valve is in fibrous continuity with the mitral valve in classic cases. In the majority of cases with cc-TGA, the aorta is located anterior and to the left of the pulmonary artery, which can be easily recognized at the 3VV (Figure 25.12b).[14–17] The ventricular outflow tracts are usually parallel, which allows visualization of both outflow tracts in a single imaging plane (Figure 25.12c).

Most cases of corrected transposition will have additional cardiac lesions, with only 10% occurring as an isolated anomaly.[46–48,50] Most (70% of the cases) have a ventricular septal

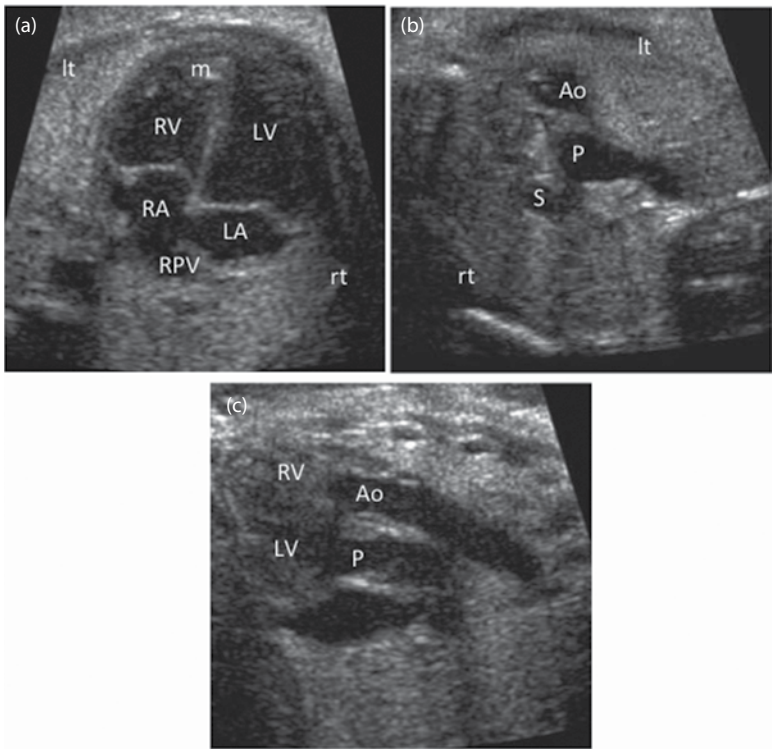


**Figure 25.12**
Corrected transposition of the great arteries. (a) Four-chamber view shows that there are discordant atrioventricular connections. The apical part of the left-sided ventricle is obliterated by the moderator band (m), suggesting it is the morphologically right ventricle (RV). In addition, the left-sided AV valve is more apically displaced in keeping with a tricuspid valve, also suggesting a morphologic right ventricle. (b) 3VV shows that the aorta is located leftward and slightly anterior to the pulmonary artery. (c) Ventricular outflow tract view shows that the right and left ventricular outflow tracts are parallel and connected to the aorta (Ao) and pulmonary artery (P), respectively. (LA, left atrium; LV, left ventricle; lt, left; RA, right atrium; RPV, right pulmonary vein; rt, right; RV, right ventricle; S, superior vena cava.)

defect that is usually in the perimembranous septum and may extend into the ventricular inlet. Left ventricular outflow tract obstruction is another common association, occurring in 40%–50% of cases. The nature of the obstruction may be a fibrous ridge, fibromuscular tunnel, aneurysm of the membranous septum, accessory mitral valve tissue, or stenosis of the pulmonary valve. The cc-TGA may infrequently be complicated by pulmonary atresia. Right ventricular outflow tract obstruction is less common. The left-sided tricuspid valve is abnormal in approximately 30%–45% of cases. The most common pathology is valve dysplasia with a variable degree of regurgitation. Associations with cc-TGA include Ebstein anomaly of the tricuspid valve, which may be accompanied by an obstructive lesion of the aortic arch.[51] Straddling of either atrioventricular valve with hypoplasia of one ventricle is not uncommon. Bradycardia with complete atrioventricular block has been reported to occur in approximately up to 20% of fetuses with congenitally corrected transposition before birth.[46–48] Of cases with normal AV conduction, there is a 1% risk of developing congential heart block (CHB) per patient-year. There is, however, a low risk of genetic or extracardiac anomalies associated with cc-TGA.[7,18]

Management of cc-TGA is quite variable, depending on associated findings or if it occurs in isolation. Without any associated lesions, surgical repair may not be necessary, and patients with this type of pathology may only be diagnosed incidentally.[52] Patients with isolated cc-TGA can be monitored for development of heart block or valve regurgitation that may require intervention. In the presence of a VSD or outflow tract obstruction, an anatomic repair, in which the left ventricle functions as the systemic pump, versus a physiologic repair in which the right ventricle acts as the systemic pump, is considered. Anatomic repair seems to have a better short-term mortality compared to physiologic repair.[53] Biventricular anatomic repair requires Mustard or Senning atrial switch operation and arterial switch or Rastelli-type operation. Biventricular anatomic repair with arterial switch (double switch) procedure is associated with 91% survival short term, while repair with Rastelli-type of repair is associated with 60% survival due to high incidence of residual left ventricle outflow obstruction.[54] On the contrary, patients receiving a Rastelli-type repair tend to have a slightly better 10-year survival rate of about 84% compared to 77% in patients receiving a double switch.[55] Long-term follow-up is required to monitor for ventricular dysfunction, development of heart block or tachyarrhythmias, and need for reintervention.[45] Single-ventricle palliation is usually required for cc-TGA if there is a straddling AV valve, severe Ebstein anomaly of the tricuspid valve, significant ventricular hypoplasia, and in some cases of right ventricular dysfunction. Careful evaluation of fetuses with cc-TGA is required to determine appropriate postnatal management and accurately provide counseling about long-term outcomes to families.

## Double-outlet ventricle

Double-outlet right or left ventricle is defined as both great arteries arising predominantly from either the morphologically right or left ventricle (Figure 25.13)[56,57] A great artery is connected to a ventricle when more than half of its valve is committed to that ventricle. The incidence of double-outlet right ventricle (DORV) is 1.5% of CHD,[4] while double-outlet left ventricle is exceedingly rare.

DORV can occur with any atrial situs and any type of atrioventricular connection. It most commonly occurs with situs solitus and concordant atrioventricular connections. Another common association is with right or left atrial isomerism. In situs solitus, the aorta is usually located to the right of the pulmonary artery, and the great vessels tend to have a side-by-side relationship; however, any great arterial relationship can be found. Subpulmonary or subaortic obstruction can be suspected when one great artery is significantly smaller than the other at the 3VV. A large ventricular septal defect is almost always present.

The postnatal hemodynamic physiology of DORV is determined by the spatial relationship of the VSD to the great arterial valves and the presence or absence of outflow tract obstruction. The VSD may be subaortic (Video 25.6), subpulmonary, doubly committed, or noncommitted in location (Figure 25.13). When there is a subaortic defect and normally related great arteries, the physiology may be that of an isolated ventricular septal defect (Figure 25.14) or, in the presence of anterior deviation of the outlet septum, that of tetralogy of Fallot (Figure 25.15; Video 25.7). When there is a subpulmonary defect, the physiology is that of TGA with a VSD (Figure 25.16; Video 25.8). This subtype of DORV is also known as Taussig-Bing malformation. In the presence of a subpulmonary VSD, aortic outflow obstruction may be present and carries a risk of aortic arch hypoplasia and coarctation. A doubly committed VSD opens beneath both arterial valves. As the outlet septum is deficient with this defect, a common right ventricular outflow tract leads to the great arteries. A noncommitted VSD is remote from both arterial outlets and involves either the inlet or trabecular part of the ventricular septum. An atrioventricular septal defect is another possible form of a noncommitted intracardiac communication. When the defect is doubly committed or non committed, the physiology depends on the intracardiac streaming of blood flow. Finally, the VSD in DORV may be rarely restrictive, and extremely rarely, the ventricular septum is intact.[58]

Double-outlet left ventricle is extremely rare.[59] As with DORV, the VSD in DOLV is most commonly subaortic,[60] less frequently subpulmonary, and least commonly doubly committed or noncommitted. It was once considered that a bilaterally deficient infundibulum is the hallmark of double-outlet left ventricle. A subsequent study, however, verified that any infundibular morphology is found in double-outlet left ventricle and that a subpulmonary or subaortic infundibulum is more common than bilaterally deficient infundibulum.

DORV can be associated with extracardiac and chromosomal anomalies, particularly with trisomy 21, 13, or 18 and 22q11 microdeletion.[7,32,39,56] Rarely, DORV can be associated with ectopia cordis[61] or pentalogy of Cantrell.[62]

Postnatal management of DORV is variable, depending on the type of VSD and its location in relation to the great arteries

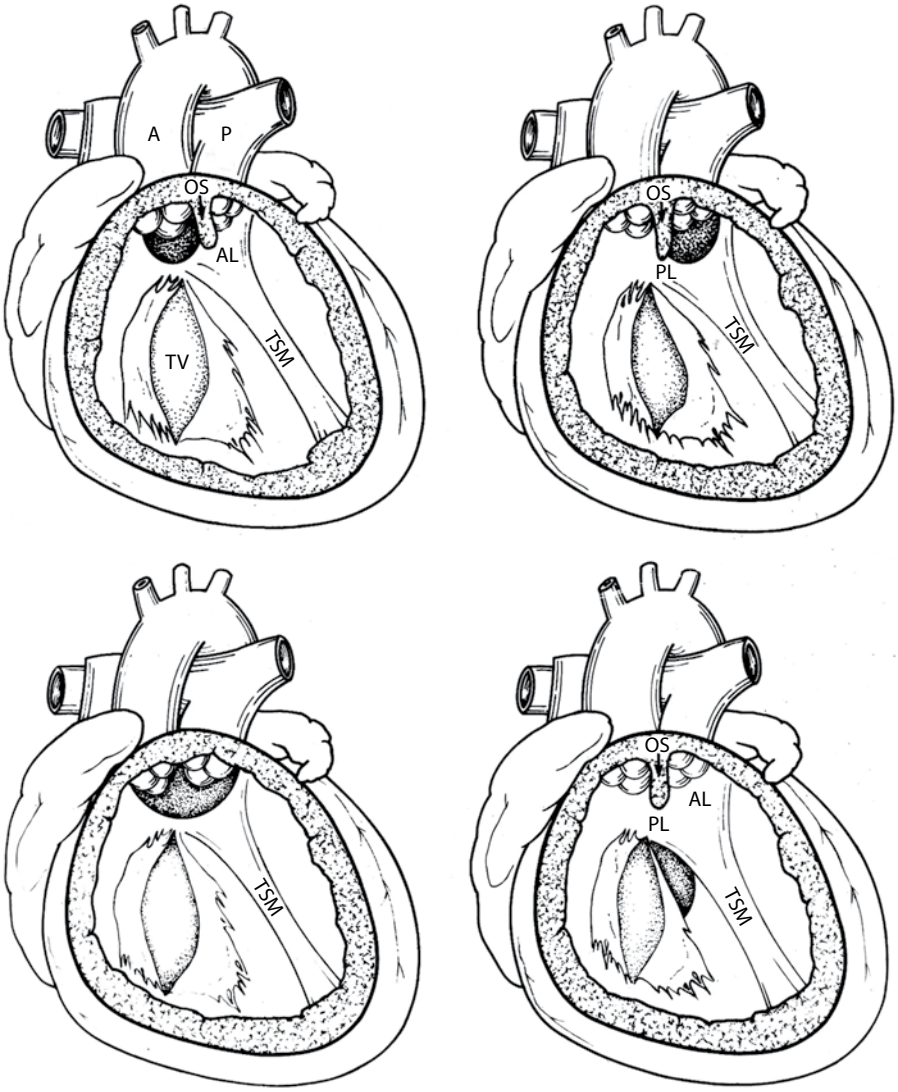


**Figure 25.13**
Pathology of double-outlet right ventricle. The ventricular septal defect is classified according to its location relative to the semilunar valves. (A, aorta; AL, anterior limb of trabecula septomarginalis; OS, outlet septum; P, pulmonary artery; PL, posterior limb of trabecula septomarginalis; TSM, trabecula septomarginalis; TV, tricuspid valve.)

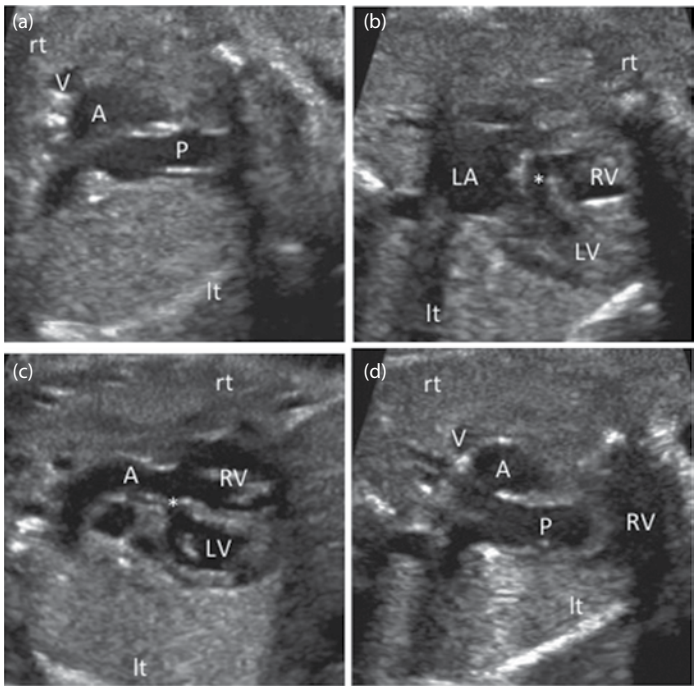


**Figure 25.14**
Double-outlet right ventricle with subaortic ventricular septal defect. (a) 3VV showing normally related great vessels. (b) Four-chamber view showing a VSD that has extension in the inlet. (c) Left ventricular outflow tract view (LVOT) view showing the perimembranous VSD that is more committed to the aorta. There is greater than 50% override of the aorta, which is mostly committed to the right ventricle. (d) Sweeping a little more anteriorly and superiorly, the pulmonary artery is seen arising leftward to the aorta, entirely committed to the right ventricle. (A, aorta; LA, left atrium; lt, left; LV, left ventricle; P, pulmonary; rt, right; RV, right ventricle; V, superior vena cava; *, ventricular septal defect.)

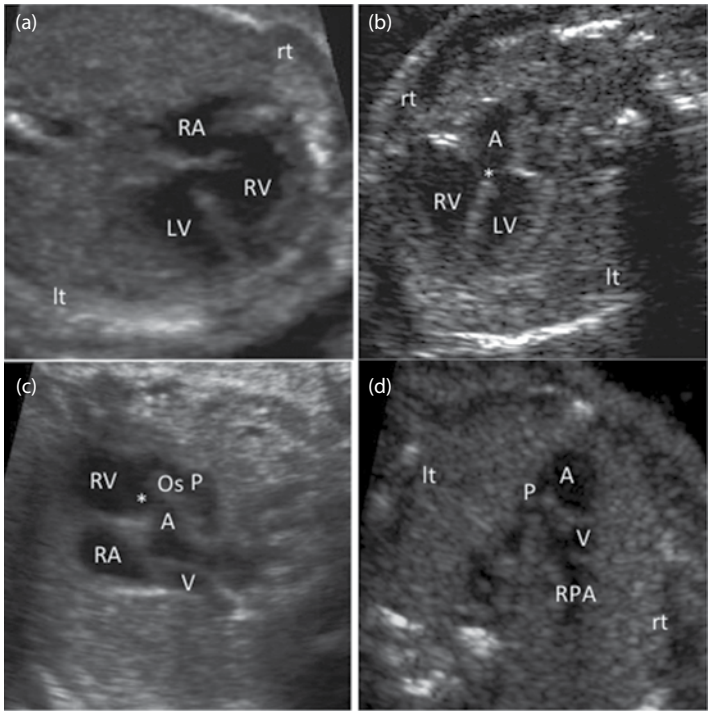


**Figure 25.15**
DORV with subaortic VSD and anterior deviation of the outlet septum (tetralogy of Fallot type DORV). (a) Four-chamber view showing a ventricular septal defect that extends toward the inlet. (b) Subaortic perimembranous VSD which is more committed to the aorta. There is greater than 50% override of the aorta, which is more committed to the right ventricle. (c) RAO view showing the anteriorly deviated outlet septum causing subpulmonary obstruction as typically seen in tetralogy of Fallot. (d) 3VV showing normally arranged great vessels with a large aorta and diminutive pulmonary artery as seen with tetralogy of Fallot. (A, aorta; lt, left; LV, left ventricle; Os, outlet septum; P, pulmonary artery; RA, right atrium; RPA, right pulmonary artery; rt, right; RV, right ventricle; V, superior vena cava; *, ventricular septal defect.)

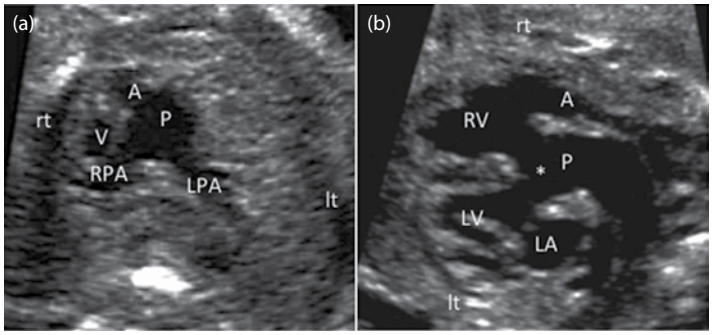


**Figure 25.16**
Double-outlet right ventricle with subpulmonary ventricular septal defect. (a) 3VV shows the triangular arrangement of the aorta, pulmonary artery, and superior vena cava that is seen with double-outlet right ventricle with a subpulmonary VSD and malposed great vessels. The aorta is anterior and rightward to the pulmonary artery. The aorta is also diminutive suggesting coarctation of the aorta, which can commonly be seen with this type of double-outlet right ventricle. (b) Outflow view showing a large perimembranous VSD that is committed to the pulmonary outflow. The pulmonary outflow is greater than 50% committed to the right ventricle. In addition, parallel outflows are seen, with the aorta arising rightward to the pulmonary artery, entirely committed to the right ventricle. (A, aorta; LA, left atrium; LPA, left pulmonary artery; lt, left; LV, left ventricle; P, pulmonary artery; RPA, right pulmonary artery; rt, right; RV, right ventricle; V, superior vena cava; *, ventricular septal defect.)

and concomitant outflow obstruction.[63,64] Surgical repair of DORV with subaortic VSD may entail an intraventricular VSD. Patch enlargement of the pulmonary outflow or conduit placement from the right ventricle to the pulmonary artery is required to repair tetralogy-like pulmonary stenosis. In the case of DORV with subpulmonary VSD, options of surgical management may include an arterial switch operation with VSD closure among others. Postoperative mortality is increased in DORV with a subpulmonary VSD as compared to DORV with a subaortic VSD.[65] With a subpulmonary VSD, most mortality occurs in the first year of life with an 86% survival beyond this age; however, there is frequent need for reintervention, specifically in cases associated with aortic arch obstruction.[66] In cases of ventricular hypoplasia, as commonly seen with DORV associated with heterotaxy, single-ventricle palliation is required.[67]

## Common arterial trunk

Common arterial trunk (CAT) or truncus arteriosus is a condition in which one great artery arises from the base of the ventricles to give rise directly to the systemic, coronary, and pulmonary arteries (Figure 25.17).[68] The incidence of CAT is 1.5% of newborns with CHD.[4]

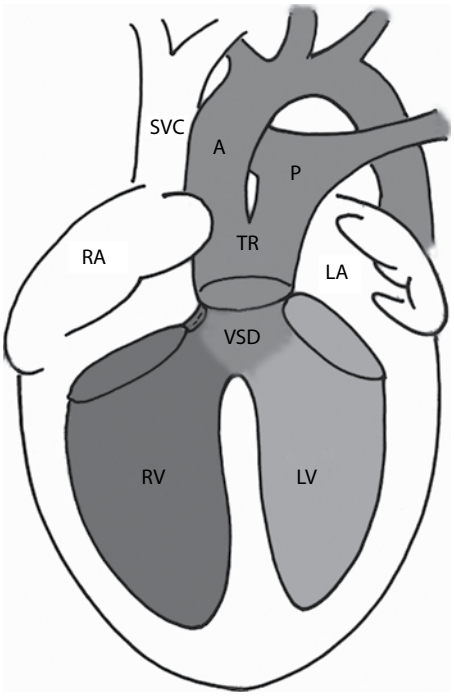


**Figure 25.17**
Pathology of truncus arteriosus. (A, aorta; LA, left atrium; LV, left ventricle; P, pulmonary artery; RA, right atrium; RV, right ventricle; SVC, superior vena cava; TR, truncus; VSD, ventricular septal defect.)

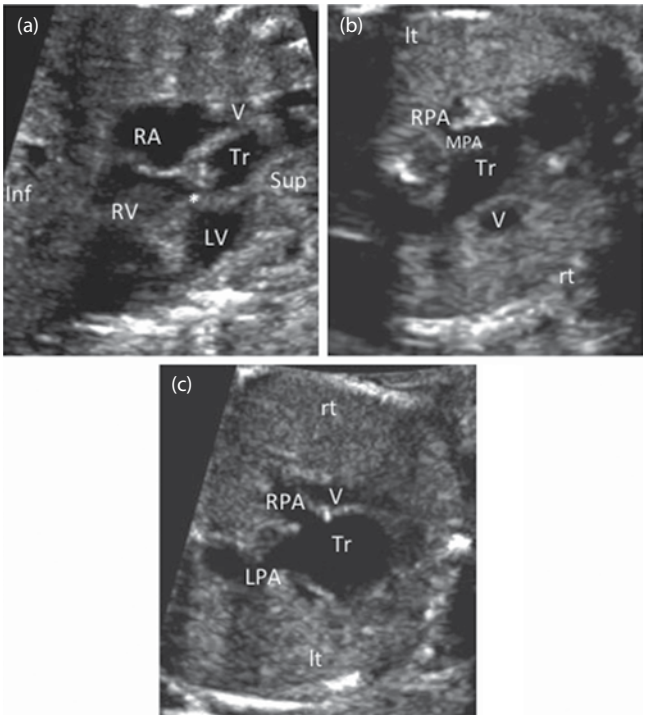


**Figure 25.18**
Common arterial trunk. (a) Coronal view of the common arterial trunk overriding a large outlet ventricular septal defect. The truncal valve is dysplastic. (b) 3VV showing two vessels, the common trunk and superior vena cava. A short main pulmonary artery arises out of the trunk and gives rise to the RPA (the LPA also arises off the main pulmonary artery but not shown in image) in keeping with a type I common arterial trunk. (c) Another 3VV showing two vessels, the common trunk and the superior vena cava. The branch pulmonary arteries arise separately from the common arterial trunk. (LPA, left pulmonary artery; lt, left; LV, left ventricle; MPA, main pulmonary artery; RA, right atrium; RPA, right pulmonary artery; rt, right; RV, right ventricle; Tr, common arterial trunk; V, superior vena cava; *, ventricular septal defect.)

In almost all cases, there is a large ventricular septal defect immediately underneath the common arterial valve, which usually overrides the ventricular septum.[69,70] Occasionally, the common arterial trunk arises exclusively from the right or left ventricle. A ventricular septal defect involving the outlet part of the septum underneath the truncal valve is an essential part of the pathology, although a few exceptional cases with an intact ventricular septum have been reported. The truncal valve is almost always in fibrous continuity with the mitral valve, while a muscular rim separates the truncal valve from the tricuspid valve. In approximately 20% of the cases, the truncal valve is in direct contact with the tricuspid valve, characterizing the VSD as a perimembranous defect. The VSD can be best demonstrated in the left ventricular outflow tract view as in tetralogy (Figure 25.18a; Video 25.9). The truncal valve consists of two to five cusps[71] and is often regurgitant and less commonly stenotic.[30] Evaluating the degree of truncal valve regurgitation is important as there is an increased risk of hydrops and *in utero* demise and worse postnatal outcomes in the presence of a severely regurgitant truncal valve. As there is a single arterial trunk, only two vessels are seen at the 3VV (Figure 25.18b,c; Video 25.10).[14–17] Only two vessels in the 3VV also apply to pulmonary atresia with a VSD and an absent or hypoplastic main pulmonary arterial trunk, which is the main differential diagnosis to CAT. In CAT, however, the pulmonary arteries will arise from the common arterial trunk either with or without a short segment of a main pulmonary artery (Figure 25.18b,c) and is classified according to the Collett and Edwards classification system.[68] Recently, there has been discussion on describing the common arterial trunk as having an aortic or pulmonary dominance, as this is more useful in guiding surgical decision-making.[72] Leftward deviation of the cardiac axis is common in truncus.[73,74] Otherwise, the four-chamber view usually does not show any defect in orientation.

The ductus arteriosus is absent in most cases of CAT unless the aortic arch is interrupted.[52,53] Other more frequent associations include a right aortic arch occurring in approximately one-third of cases, interruption of the aortic arch,[75] and/or unilateral absence of one pulmonary artery.

There is a significant incidence of genetic and extracardiac anomalies associated with CAT.[7,32] Deletion in chromosomal region 22q11 is a common chromosomal abnormality[76–78] associated with CAT and DORV. A large fetal series showed 20% incidence of chromosome 22q11 deletion in fetuses with ventricular outflow tract abnormalities or interruption of the aortic arch. The incidence is higher when truncus arteriosus

is associated with obstructive aortic arch anomalies, including interrupted aortic arch.[26,78,79] This specific chromosomal abnormality usually occurs in a syndromic pattern, such as DiGeorge syndrome, velo-cardio-facial (or Shprintzen) syndrome, conotruncal face syndrome, and Cayler cardiofacial syndrome. As the patients share clinical and laboratory features, an acronym CATCH-22 (*c*ardiac defect, *a*bnormal facies, *t*hymic hypoplasia, *c*left palate, *h*ypocalcemia, and deletion in chromosome *22*) has been used.[77] Thymic hypoplasia can be appreciated at fetal ultrasound.[78,80,81] The transverse diameter of the normal thymus in millimeters is slightly smaller than the gestational age in weeks in the second trimester and becomes slightly larger as the pregnancy approaches term.[82] The combination of associated aortic arch anomalies, thymic hypoplasia or aplasia, and intrauterine growth restriction is highly suggestive of chromosome 22q11 deletion.[82] Prenatal genetic testing and screening for extracardiac anomalies should be strongly considered in fetuses with common arterial trunk. Chromosomal analysis with FISH (fluorescent *in situ* hybridization) for deletion 22q11 is recommended in fetuses with a conotruncal anomaly in addition to karyotyping. Although it occurs *de novo* in 90% of cases, parental screening is indicated in familial cases, as there is a 50% recurrence risk.

The surgical management of CAT consists of separating the pulmonary arteries from the common trunk and allowing the truncal valve to work as a neoaortic valve. The pulmonary arteries are connected to the right ventricle with a conduit.

The neonatal survival rate ranges from 42% to 68%.[83] There is an increased risk of mortality in common arterial trunk with associated arch obstruction.[84] In childhood, there is a significant risk of surgical- or catheter-based reintervention, mainly to readdress conduit stenosis or the pulmonary arteries.[85–87] Exercise capacity and health-related quality of life may also be significantly diminished.[85]

## *Summary*

Accurate diagnosis of conotruncal anomalies is essential to provide appropriate postnatal management, including location of delivery and transfer of the neonate to a neonatal or cardiac care unit for appropriate ongoing management. Many conotruncal lesions require the use of intravenous prostaglandin for their short-term management and may require intervention in the neonatal period. Careful assessment of the outflows, 3VV, and three-vessel tracheal view in addition to the four-chamber view are essential in the diagnosis of CTA. Surgical management and long-term prognosis are quite variable depending on the presence and severity of associated lesions.

## Videos

**Video 25.1** (https://youtu.be/dZiWGNR52EA)
Transposition of the great arteries with intact ventricular septum. Video showing a sweep from the four-chamber view to the 3VV. The ventricular septum is intact. As the probe moves anteriorly and superiorly, the pulmonary artery is seen arising from the left ventricle and the aorta arises in parallel from the right ventricle. The 3VV shows the abnormal triangular arrangement of the great vessels, with the aorta anterior and rightward to the pulmonary artery.

**Video 25.2** (https://youtu.be/FI-WKw3W2Cs)
Transposition of the great arteries with a ventricular septal defect. Video showing a sweep from the four-chamber view to the three-vessel view. The four-chamber view shows a perimembranous VSD that is subpulmonary that extends toward the inlet. As the probe moves anteriorly and superiorly, the pulmonary artery is seen arising from the left ventricle and the aorta arises in parallel from the right ventricle. The 3VV shows the abnormal triangular arrangement of the great vessels, with the aorta anterior and rightward to the pulmonary artery.

**Video 25.3a** (https://youtu.be/DfC5FVJc-xQ)
Transposition of the great arteries with a ventricular septal defect and pulmonary stenosis. (a) Video showing the pulmonary artery arising from the left ventricle. There is subpulmonary narrowing and the pulmonary valve is mildly thickened.

**Video 25.3b** (https://youtu.be/Q6evmtXE1KA)
(b) Color Doppler showing flow acceleration across the LVOT secondary to the subpulmonary narrowing and thickened pulmonary valve.

**Video 25.4** (https://youtu.be/nwm8ugqACxo)
Transposition of the great arteries with a ventricular septal defect and coarctation. Video showing a sweep from the four-chamber view to the 3VV. There is size discrepancy between the two ventricles with a smaller but apex forming right ventricle. The great vessels are seen arising in parallel from the ventricles. There is a size discrepancy in the great vessels with a smaller aorta in comparison to the pulmonary artery in keeping with a coarctation of the aorta.

**Video 25.5** (https://youtu.be/jNYGWJZsXvk)
Congenitally corrected transposition of the great arteries. The video shows a sweep from the four-chamber view to the 3VV. The morphologic left atrium connects into the left-sided right ventricle. The morphologic right atrium is connected to the right-sided morphologic left ventricle. As the sweep moves anteriorly and superiorly, the pulmonary artery is seen arising from the left ventricle and the aorta is seen arising from the right ventricle. In the 3VV, the aorta is seen anterior and leftward to the pulmonary artery.

**Video 25.6** (https://youtu.be/XQszwWw6UcI)
Double-outlet right ventricle with subaortic VSD. Video showing a sweep from the four-chamber view to the 3VV. Both great arteries are mainly committed to the right ventricle. The great vessels are normally related.

**Video 25.7** (https://youtu.be/NX4ynEMgSBQ)
Double-outlet right ventricle with subaortic VSD, tetralogy of Fallot type. Video showing a sweep from the four-chamber view to the 3VV. Both great arteries are mainly committed to the right ventricle. The great vessels are normally related, with a hypoplastic pulmonary artery. The pulmonary valve is mildly thickened.

**Video 25.8** (https://youtu.be/mBFe3FYGKqg)
Double-outlet right ventricle with subpulmonary VSD. Video showing a sweep from the four-chamber view to the 3VV. Both great vessels are mainly committed to the right ventricle. The great vessels are malposed with the pulmonary artery posterior and leftward of the aorta. The 3VV is triangular as seen in transposition of the great arteries.

**Video 25.9** (https://youtu.be/YdFPIWQfhpQ)
Common arterial trunk. Video showing a sweep from the four-chamber view to the 3VV. A single outlet is seen arising from both ventricles which overrides an outlet VSD. The single outflow gives rise to the aorta and a small main pulmonary artery, which is seen arising from the left side of the common trunk. The truncal valve is thick and quite dysplastic.

**Video 25.10** (https://youtu.be/Hxbp5M2-9t4)
Common arterial trunk. Video showing the 3VV. A small main pulmonary artery is seen arising from the common trunk, which then bifurcates into the right and left pulmonary arteries.

# References


1. Restivo A et al. *Anat Rec A, Discov Mol Cell Evol Biol* 2006; 288(9):936–43.
2. Scott DJ et al. *Br Heart J* 1984;52(3):248–57.
3. Moller JH et al. *Pediatr Cardiol* 1995;16(5):216–22.
4. Ferencz C et al. *Am J Epidemiol* 1985;121(1):31–6.
5. Allan LD et al. *J Am Coll Cardiol* 1994;23(6):1452–8.
6. Tegnander E et al. *Ultrasound Obstet Gynecol* 2006;27(3): 252–65.
7. Paladini D et al. *Ultrasound Obstet Gynecol* 1996;8(4):241–6.
8. Tometzki AJ et al. *J Am Coll Cardiol* 1999;33(6):1696–701.
9. Sivanandam S et al. *Am J Perinatol* 2006;23(4):241–5.
10. Wigton TR et al. *Obstet Gynecol* 1993;82(2):219–24.
11. Khoshnood B et al. *Pediatrics* 2005;115(1):95–101.
12. Anderson RH et al. *Br Heart J* 1977;39(8):856–9.
13. Achiron R et al. *Bmj* 1992;304(6828):671–4.
14. Yoo SJ et al. *Ultrasound Obstet Gynecol* 1997;9(3):173–82.
15. Yoo SJ et al. *AJR Am J Roentgenol* 1999;172(3):825–30.
16. Yoo SJ et al. *Cardiol Young* 1999;9(4):430–44.
17. Vinals F et al. *Ultrasound Obstet Gynecol* 2003;22(4):358–67.
18. International Society of Ultrasound in O, Gynecology. *Ultrasound Obstet Gynecol* 2006;27(1):107–13.
19. Brandt JS et al. *J Ultrasound Med* 2015;34(8):1415–21.
20. Palatnik A et al. *J Ultrasound Med* 2015;34(7):1329–35.
21. DeVore GR et al. *Ultrasound Obstet Gynecol* 2004;24(1):72–82.
22. Zhang Y et al. *Prenat Diagn* 2011;31(6):529–35.
23. Yeo L et al. *Ultrasound Obstet Gynecol* 2011;37(5):549–56.
24. Zidere V et al. *Ultrasound Obstet Gynecol* 2013;42(4):421–5.
25. Bonnet D et al. *Circulation* 1999;99(7):916–8.
26. Van Praagh R et al. *Am J Cardiol* 1971;28(6):621–31.
27. Jex RK et al. *J Thorac Cardiovasc Surg* 1990;100(5):682–6.
28. Maeno YV et al. *Circulation* 1999;99(9):1209–14.
29. Punn R, Silverman NH. *J Am Soc Echocardiogr* 2011;24(4): 425–30.
30. Freire G et al. *Cardiol Young* 2012;22(6):671–6.
31. Donofrio MT. *Circulation* 2002;105(11):e65–6.
32. Allan LD et al. *Ultrasound Obstet Gynecol* 1991;1(1):8–11.
33. Jatene AD et al. *Arq Bras Cardiol* 1975;28(4):461–64.
34. Tobler D et al. *J Am Coll Cardiol* 2010;56(1):58–64.
35. Metton O et al. *Eur J Cardiothorac Surg* 2010;37(6):1246–53.
36. Lalezari S et al. *Ann Thorac Surg* 2011;92(3):973–9.
37. Al-Jughiman MK et al. *Pediatr Cardiol* 2015;36(5):896–905.
38. Honjo O et al. *Eur J Cardiothorac Surg* 2013;44(6):1085–94; discussion 94.
39. Hartge DR et al. *J Mater Fetal Neonatal Med* 2012;25(1):58–63.
40. Hazekamp MG et al. *Eur J Cardiothorac Surg* 2010;38(6): 699–706.
41. Kreutzer C et al. *J Thorac Cardiovasc Surg* 2000;120(2):211–23.
42. Brown JW et al. *Ann Thorac Surg* 2011;91(1):188–93; discussion 93–4.
43. Emani SM et al. *Circulation* 2009;120(11 suppl):S53–8.
44. Raju V et al. *J Thorac Cardiovasc Surg* 2015;149(5):1349–55.
45. Connelly MS et al. *J Am Coll Cardiol* 1996;27(5):1238–43.
46. Chiappa E et al. *Cardiol Young* 2004;14(3):265–76.
47. Sharland G et al. *Heart* 2005;91(11):1453–8.
48. Paladini D et al. *Ultrasound Obstet Gynecol* 2006;27(3):281–5.
49. Bernasconi A et al. *Heart* 2005;91(12):1590–4.
50. Rudolph AM. *Pediatr Res* 2007;61(3):375–80.
51. Bader R et al. *Fetal Pediatr Pathol* 2004;23(4):257–63.
52. Kwon SH, Oh JH. *J Thorac Imaging* 2011;26(4):W137–9.
53. Alghamdi AA et al. *Ann Thorac Surg* 2006;81(4):1529–35.
54. Gaies MG et al. *Ann Thorac Surg* 2009;88(6):1952–60.
55. Murtuza B et al. *J Thorac Cardiovasc Surg* 2011;142(6):1348–57 e1.
56. Smith RS et al. *Ultrasound Obstet Gynecol* 1999;14(5):315–9.
57. Kim N et al. *Prenat Diagn* 2006;26(8):740–5.
58. Singla M et al. *Pediatr Cardiol* 2013;34(8):1941–4.
59. Imai-Compton C et al. *Congenit Heart Dis* 2010;5(6):532–6.
60. Menon SC, Hagler DJ. *Curr Treat Options Cardiovasc Med* 2008;10(5):448–52.
61. Malik R et al. *Echocardiography* 2015;32(3):589–91.
62. Ootaki Y et al. *Cardiol Young* 2011;21(2):235–7.
63. Villemain O et al. *J Thorac Cardiovasc Surg* 2016;152(3): 698–706. e3.
64. Bradley TJ et al. *J Thorac Cardiovasc Surg* 2007;134(4):967–73 e6.
65. Lagopoulos ME et al. *Am Heart J* 2010;160(4):692–700.
66. Vergnat M et al. *J Thorac Cardiovasc Surg* 2015;149(4):1124–30; discussion 30–2.
67. Takeuchi K et al. *Ann Thorac Surg* 2006;82(1):146–52.
68. Collett RW, Edwards JE. *Surg Clin North Am* 1949;29(4):1245–70.
69. Duke C et al. *Am J Cardiol* 2001;88(12):1379–84.
70. Volpe P et al. *Heart* 2003;89(12):1437–41.
71. Fuglestad SJ et al. *Am J Cardiovasc Pathol* 1988;2(1):39–47.
72. Russell HM et al. *J Thorac Cardiovasc Surg* 2011;141(3):645–53.
73. Shipp TD et al. *Obstet Gynecol* 1995;85(1):97–102.
74. Smith RS et al. *Obstet Gynecol* 1995;85(2):187–91.
75. Mair DD et al. *Circulation* 1974;49(1):144–51.
76. Goldmuntz E et al. *J Am Coll Cardiol* 1998;32(2):492–8.
77. Wilson DI et al. *J Med Genet* 1993;30(10):852–6.
78. Volpe P et al. *Prenat Diagn* 2003;23(9):752–7.
79. Vesel S et al. *Heart* 2006;92(10):1501–5.
80. Barrea C et al. *Prenat Diagn* 2003;23(1):9–15.
81. Chaoui R et al. *Ultrasound Obstet Gynecol* 2002;20(6):546–52.
82. Cho JY et al. *Ultrasound Obstet Gynecol* 2007;29(6):634–8.
83. Swanson TM et al. *Pediatr Cardiol* 2009;30(3):256–61.
84. Konstantinov IE et al. *Ann Thorac Surg* 2006;81(1):214–22.
85. O'Byrne ML et al. *Am Heart J* 2013;166(3):512–8.
86. Lund AM et al. *Am J Cardiol* 2011;108(1):106–13.
87. Bohuta L et al. *Ann Thorac Surg* 2011;91(5):1473–7.

# 26

# Tetralogy of Fallot

Michael D. Puchalski

## Introduction

Tetralogy of Fallot (TOF) was described by Etienne-Louis Arthur Fallot[1] in 1888,[2] but earlier descriptions appear almost three hundred years ago.[3,4] TOF is the most common cyanotic heart defect and serves as the classic example of a "blue baby" secondary to right to left shunting through a ventricular septal defect. The lesion that Fallot described consisted of four anatomical features: a ventricular septal defect, subpulmonary stenosis, overriding aorta, and right ventricular hypertrophy (Figure 26.1).[5,2] This malformation is a consequence of anterior, superior, and leftward deviation of the outlet septum from the rest of the ventricular septum and is considered the central pathology of TOF (Figure 26.2). In fact, the most important determinant of the degree of cyanosis is the severity of this right ventricular outflow tract obstruction, not the degree of aortic override or size of the ventricular septal defect.

Patients with TOF have symptoms and signs that range from cardiac failure with no cyanosis to severe cyanosis with hypoxemia and acidemia. No treatment was known for this abnormality until a landmark publication by Blalock and Taussig in 1945,[6] in which an aortic-to-pulmonary shunt was successfully introduced in three patients with marked relief

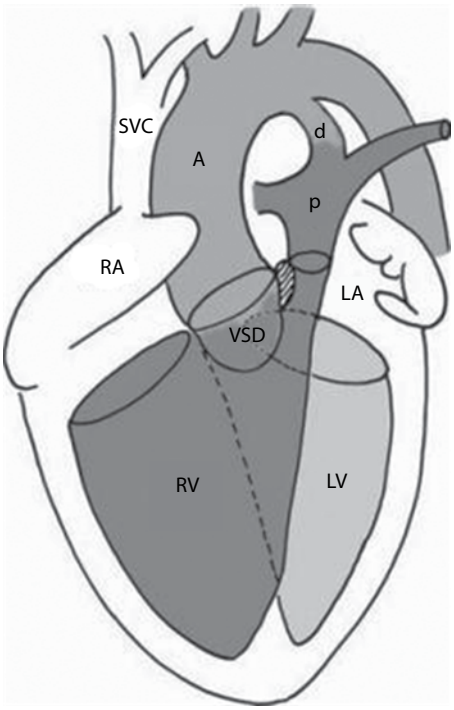


**Figure 26.1**
Pathology of tetralogy of Fallot in a long axial oblique view. (VSD, ventricular septal defect.)

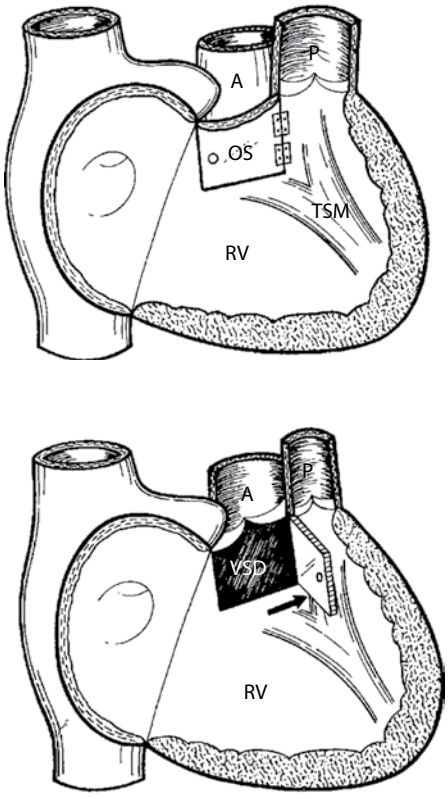


**Figure 26.2**
Central pathology of tetralogy of Fallot. The outlet septum (OS) is supported by the hinges along its left anterior margin. It is pulled anteriorly into the right ventricular outflow tract in tetralogy, leaving a ventricular septal defect (VSD) of anterior malalignment type. The aortic valve overrides the ventricular septum because it is displaced anteriorly with the outlet septum. The deviated outlet septum encroaches on the subpulmonary outflow tract dimension.

of cyanosis. This remarkable achievement opened the door for successful palliation of many patients with cyanotic heart disease and is still used today in select patients. From a fetal standpoint, predicting the presence of significant cyanosis after birth can help with delivery planning and consultation regarding the need for early surgical intervention.

## Incidence

TOF occurs in approximately 0.34 per 1,000 live births.[7] The prevalence of TOF has increased over the last few decades due to successful surgical repair. TOF has a nearly equal sex distribution with a slight increase in boys and is associated with chromosomal abnormalities in approximately 10% of patients,[8] most of whom have 22q11 microdeletion. The recurrence risk for TOF in families with one affected child is approximately 2%–3%. For parents with TOF, the transmission risk for CHD in offspring is approximately 5%.[9]

## Anatomy

In most cases with TOF, the situs is solitis, and there is levocardia. The four-chamber view, if obtained at the level of the AV valves, will look perfectly normal with an intact ventricular septum (Figure 26.3) and therefore can easily be missed during first-line sonographic screening. One needs to tip anteriorly toward the outflow tracts, a five-chamber view, to see the large ventricular septal defect with a dilated aorta overriding the septum (Figure 26.4a). Most commonly, this has a perimembranous extension in which the tricuspid valve is in fibrous continuity with the aortic valve through the posterior inferior border of the defect.[1,5] The perimembranous defect is seen immediately below the overriding aortic valve in the left ventricular outflow tract view with color (Figure 26.4b). It is also seen in the short axis view or vertical long axis view of the right ventricle as a defect extending from the tricuspid annulus toward the ventricular outlet (Figure 26.5). The ventricular septal defect is less frequently a muscular outlet type, in which a muscular fold runs

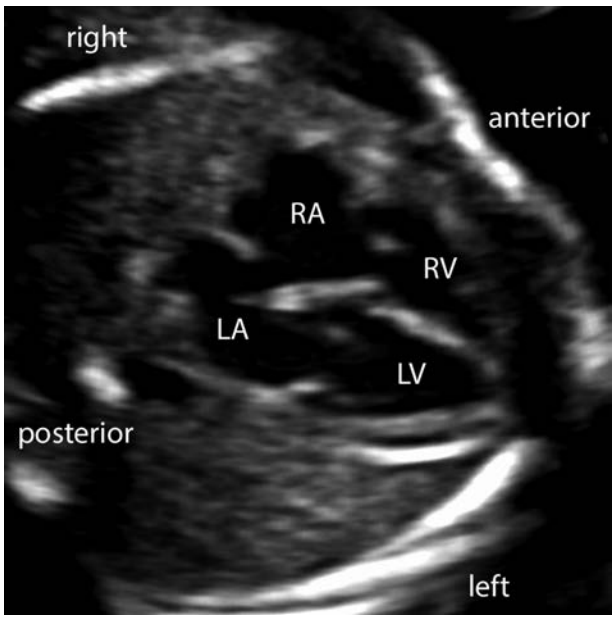


**Figure 26.3**
Tetralogy of Fallot. Four-chamber view shows no defect. The cardiac axis is deviated slightly to the left. The descending aorta is seen on the left anterior aspect of the spine. This fetus had a left aortic arch.

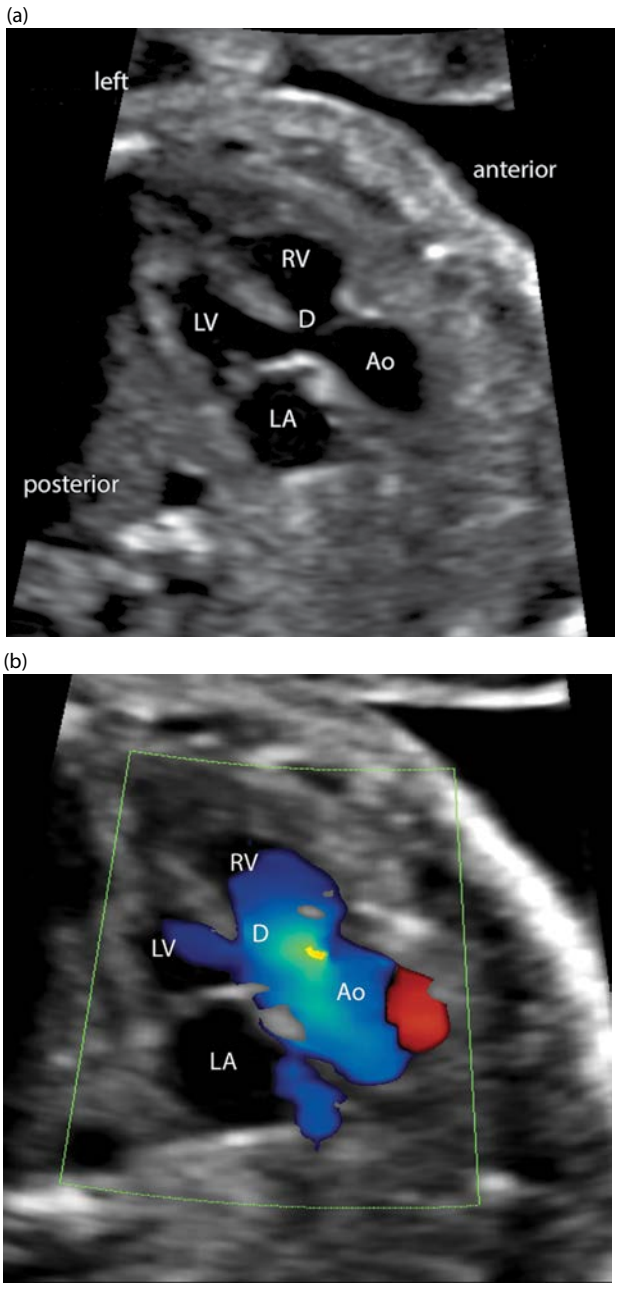


**Figure 26.4**
Tetralogy of Fallot with a perimembranous ventricular septal defect. (a) Left ventricular outflow tract view shows the ventricular septal defect (D) with an overriding aorta (Ao). (b) Color Doppler of the same imaging plane shows blood flow from the left ventricle (LV) and the right ventricle (RV) merging together at the ventricular septal defect (D) prior to exiting the heart through the aorta (Ao).

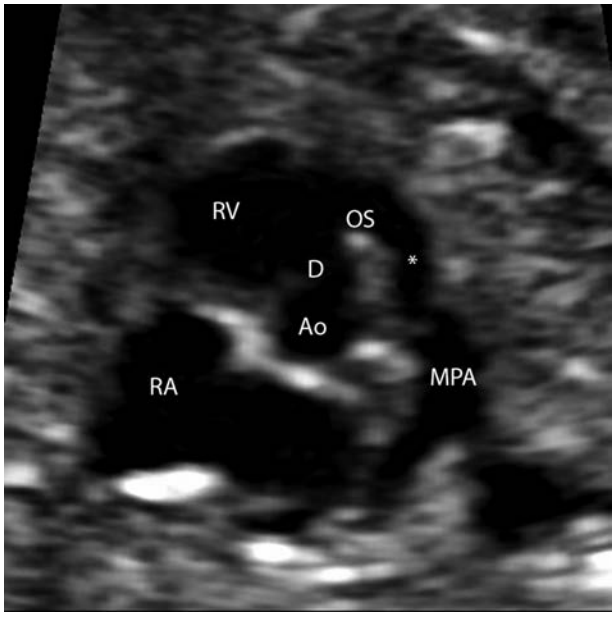


**Figure 26.5**
Tetralogy of Fallot with a perimembranous ventricular septal defect (D) in the short-axis view. The outlet septum (OS) is deviated anterior and superior into the right ventricular outflow tract (*).

inferoposteriorly separating the tricuspid valve from the aortic valve. The least common type of defect is a doubly committed juxta-arterial type, which is characterized by the absence or extreme hypoplasia of the outlet septum. In this type, the aortic and pulmonary valves are in direct contact through the anterior superior border of the defect (Figure 26.6). Both muscular outlet and doubly committed defects are barely visible in the left ventricular outflow tract view but can be visualized in the short-axis view of the ventricular outflow tracts. Uncommonly, TOF may coexist with an atrioventricular septal defect, or additional muscular ventricular septal defects may be present.[10]

A ventricular septal defect with an overriding aorta alone does not make the diagnosis of TOF; careful evaluation of the right ventricular outflow tract should be undertaken. Deviation of the outlet septum from the rest of the septum can be best shown in a basal short-axis or vertical long-axis view of the right ventricle (Figures 26.5 and 26.7).

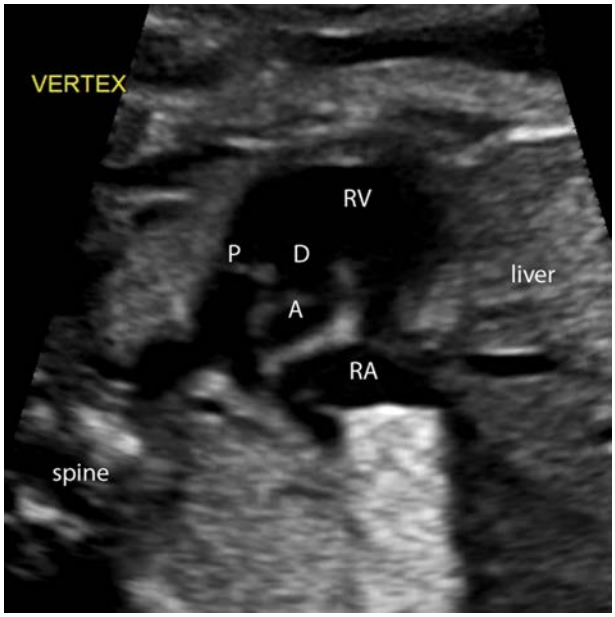


**Figure 26.6**
Tetralogy of Fallot with a doubly committed, juxta-arterial–type ventricular septal defect (D). The aortic (A) and pulmonary valves (P) are in direct continuity through the anterosuperior border of the defect.

(a)

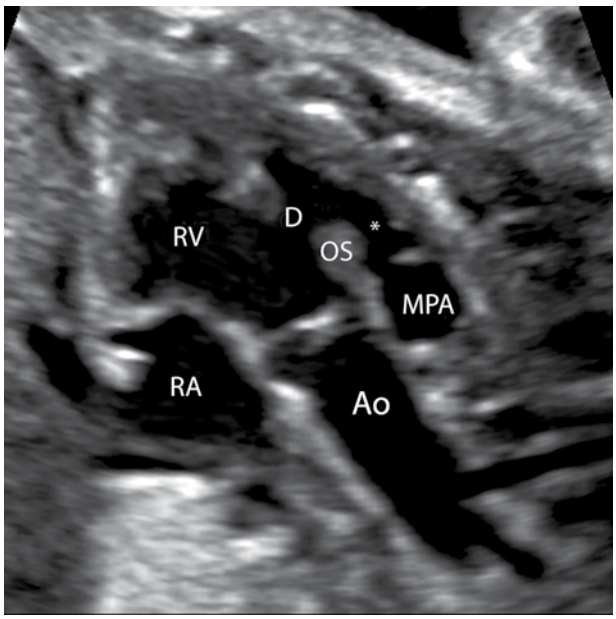


(b)

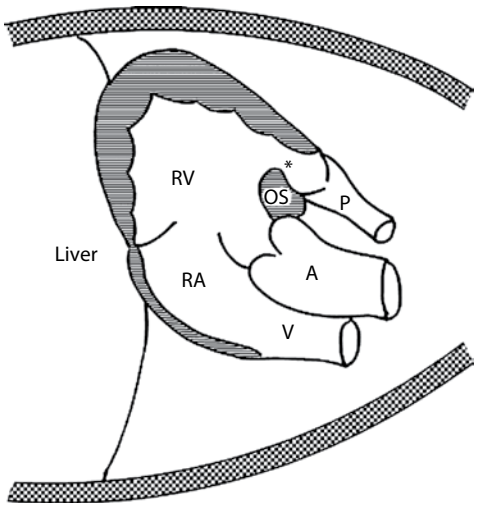


**Figure 26.7**
Tetralogy of Fallot in the vertical long-axis view of the right ventricle (a) with the corresponding diagram (b) showing the right ventricular outflow tract (*) being encroached on by the anteriorly deviated outlet septum (OS). The perimembranous ventricular septal defect (D) is seen behind the outlet septum and below the aorta (Ao).

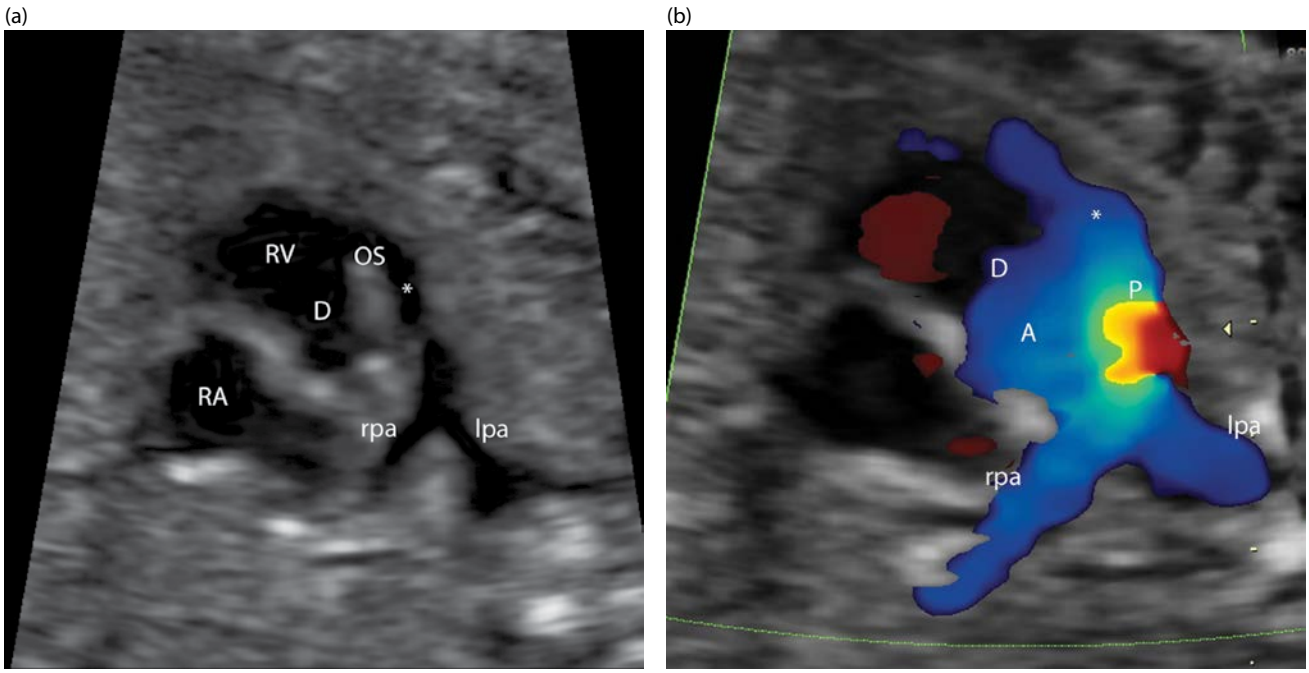


**Figure 26.8**
Tetralogy of Fallot. Side by side 2D (a) and color (b) images in a short-axis plane show that even with a small outflow tract (*) due to deviation of the outlet septum, and a dysplastic and small pulmonary valve (P), there is only trivial flow turbulence due to decompression of the right ventricle toward the aortic valve (A).

The deviated outlet septum encroaches on the outflow tract typically leading to a small pulmonary valve. The amount of deviation or lack thereof dictates the size of the pulmonary annulus and pulmonary arteries. If the outlet septum is completely missing, the pulmonary valve annulus may be more normal in size, whereas if the outlet septum is nearly obstructing the right ventricular outflow tract, the pulmonary valve will be small and the main and branch pulmonary arteries will be hypoplastic yielding clues as to the severity of the disease.[11,12] In addition, the pulmonary valve may be dysplastic and stenotic, but Doppler velocities are typically normal or only mildly increased due to diminished flow across this area due to the presence of the ventricular septal defect, which allows decompression of the right ventricle toward the aorta (Figure 26.8a,b). This is in contrast to postnatal findings where obstruction can easily be seen and infants are cyanotic.

Disproportion between the diameters of the main pulmonary and the ascending aorta, showing a larger aorta and a smaller main pulmonary artery, may help with the diagnosis. The size discrepancy of the arterial trunks may be subtle and may not be apparent in the early stage of gestation but becomes more evident with advancing gestation. In fact, the three-vessel view is ideally suited for this comparison (Figure 26.9).[13,14] Direct visual comparison can be done, but measurements with Z-scores and ratios between the great vessels in a serial fashion on subsequent echoes are most helpful. Increasing discrepancy between the great vessels favoring the aorta should raise suspicion of right-sided subvalvar or valvar obstruction as progression of the outflow tract obstruction is well documented.[11]

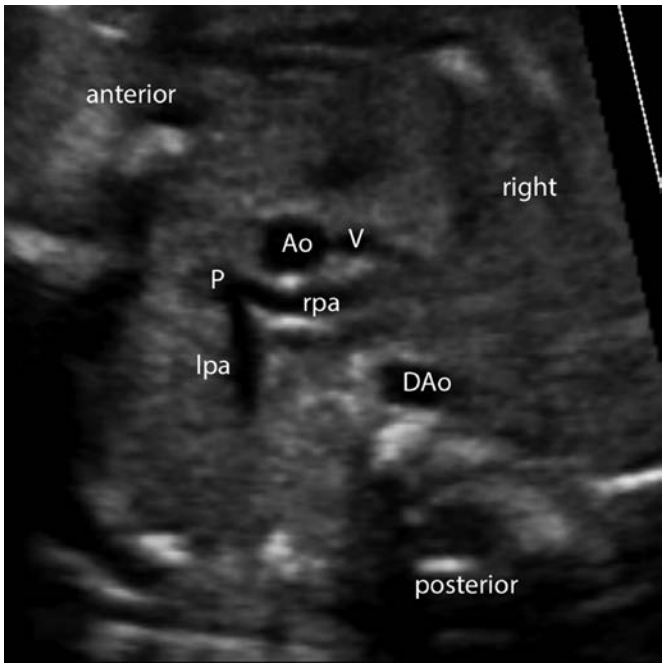


**Figure 26.9**
Three-vessel view shows the abnormal alignment and size of the three vessels. The ascending aorta (Ao) is dilated and displaced anteriorly. The main pulmonary artery (P) is small and displaced posteriorly. The superior vena cava (V) is normal in size as are the right and left pulmonary arteries (rpa and lpa). The descending aorta (DAo) is located on the right side of the spine in this patient with a right aortic arch.

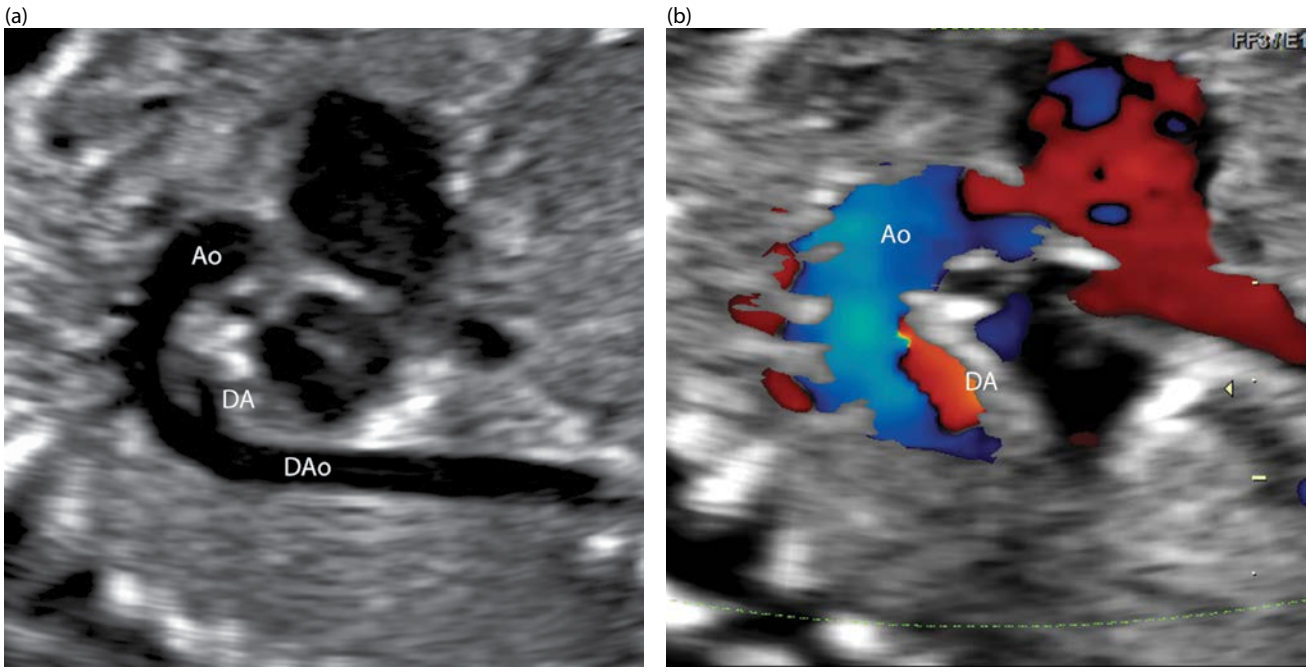


**Figure 26.10**
Tetralogy of Fallot with a left aortic arch. Side-by-side 2D (a) and color (b) images showing a ductus arteriosus (DA) coming off the undersurface of the aortic arch with blood flow being directed retrograde toward the main pulmonary artery suggesting severe outflow tract obstruction.

The ductus arteriosus is characteristically small and sometimes even absent in many patients with conotruncal defects, including TOF. It is often difficult to identify the ductus in TOF, as it usually arises from the undersurface of the aortic arch (Figure 26.10), but nonetheless, it is an additional criterion for severity assessment. A mirror-image right aortic arch is common in TOF, and in this case, the patent ductus is the left ductus that arises from the left innominate or subclavian artery. In the more common left aortic arch, the ductus inserts on the undersurface of the aortic arch after taking a circuitous course. The blood flow through the ductus varies considerably according to the severity of subpulmonary stenosis.[1,12,15] The ductal flow may be right to left, bidirectional, or left or right. A left-to-right shunt through the ductus from the aorta to the pulmonary artery is predictive of severe disease as it suggests right ventricular output is not sufficient to maintain normal flow through the lungs. These infants may require prostaglandin therapy immediately after birth and surgical correction in early life.[16] If the ductus is shunting all right to left like normal, it suggests there is adequate antegrade flow from the right ventricle and the infant will be a "pink" TOF, allowing time for growth before elective surgical repair (Figure 26.11). In rare circumstances such as TOF with an absent pulmonary valve, the ductus arteriosus is typically absent.[17–21]

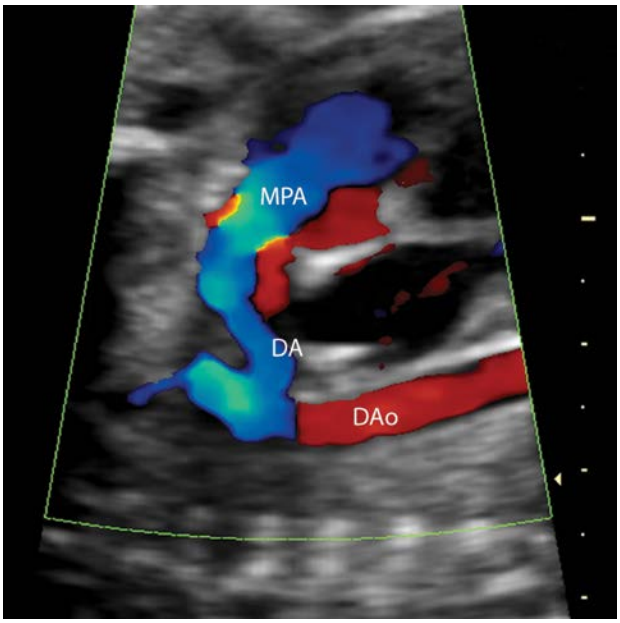


**Figure 26.11**
Tetralogy of Fallot with minimal pulmonary stenosis as evidenced by normal right-to-left shunting from the main pulmonary artery (MPA) to the descending aorta (DAo) through the ductus arteriosus (DA).

## Clinical outcome

The clinical condition of fetuses with TOF is usually excellent. Combined cardiac output remains within normal limits with a higher proportion of combined output coming from the aorta compared to the pulmonary artery. Consequently, the aortic arch and isthmus are well

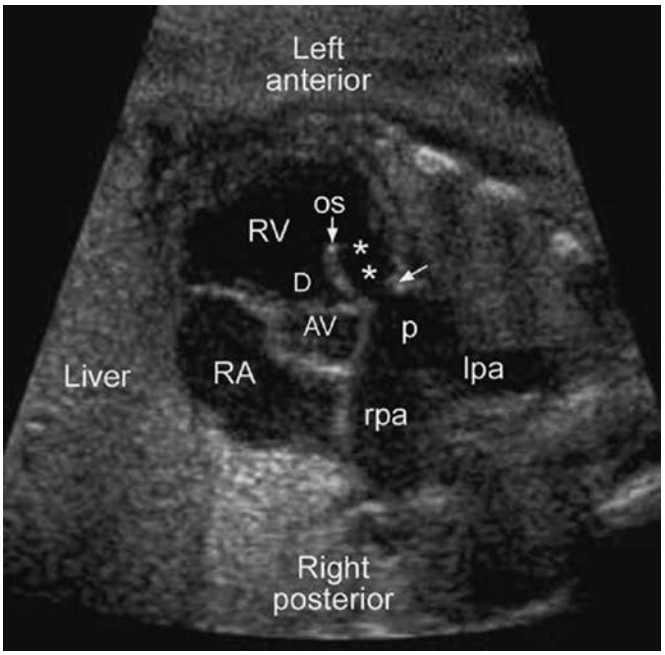


**Figure 26.12**
Absent pulmonary valve syndrome in tetralogy of Fallot. Basal short-axis view of the ventricles shows narrowing of the subpulmonary outflow tract (asterisks) due to anterior cephalad deviation of the outlet septum (os). The main pulmonary artery (p) and branch pulmonary arteries (rpa and lpa) are markedly dilated, while the pulmonary valve annulus is small (arrow). The pulmonary valve leaflets are not identifiable.

developed, and coarctation of the aorta is, for all practical purposes, never described in association with tetralogy of Fallot. Unfortunately, there is a relatively high incidence of chromosomal and extracardiac anomalies with microdeletion of chromosome 22 being detected in up to 20% of infants with TOF.[22] Note that this proportion is greater in patients with a right-sided aortic arch. Delivery should be vaginal in most cases as there is no indication, in isolated TOF, for extraction by cesarean section. The immediate postnatal condition and management will be influenced by the severity of the stenosis and associated extracardiac anomalies. As described, cases with severe right ventricular outflow tract obstruction and retrograde flow through the ductus arteriosus to provide pulmonary blood flow will require specialized care immediately after birth to maintain ductal patency. Ideally, all fetuses with TOF should be delivered in a tertiary center so there can be close monitoring of the clinical condition after normal closure of the ductus arteriosus. Most centers perform elective surgical repair of TOF by 6 months of age with close clinical follow-up prior to that time. For those few patients who are symptomatic prior to that time, management is variable, ranging from catheter interventions in the right ventricular outflow tract and pulmonary valve to placement of a surgical Blalock-Taussig shunt or complete repair depending on institutional philosophy. Outcomes are excellent with greater than 96% chance of hospital survival and greater than 90% survival 30 years after complete repair.[23–26]

## *Tetralogy of Fallot with absent or dysplastic pulmonary valve*

Tetralogy of Fallot with absent pulmonary valve occurs in a small, distinct subgroup of patients whose presentation is very different than classical TOF. This condition is characterized by severe dilatation of the pulmonary arteries,[27,28] free insufficiency of the pulmonary valve which appears dysplastic or rudimentary, right ventricular dilatation, and absence of a ductus arteriosus. The only similarity to classical TOF is a large ventricular septal defect with an overriding aorta. TOF with absent pulmonary valve accounts for 3%–6% of all cases with TOF, and there is an equal distribution among males and females.[29,30]

Ultrasonographic diagnosis of this form of TOF is easier than in the classical form, especially during fetal life.[31] During routine ultrasonographic screening, suspicion is raised by dilatation of the right ventricular cavity on four-chamber view but is confirmed when tipping anteriorly into the right ventricular outflow tract, which shows the dilated pulmonary artery with an abnormal or absent pulmonary valve. Doppler investigation of the dilated pulmonary artery will disclose systolic antegrade and diastolic retrograde flow caused by severe pulmonary insufficiency (Figure 26.13c). In an axial view through the chest, the dilated peripheral pulmonary arteries can be clearly seen with two-dimensional (2D) or color Doppler interrogation (Figure 26.12). This is a constant feature after 22 weeks' gestation and is considered to be due to the combined effect of poststenotic dilatation, severe pulmonary regurgitation, and absence of ductal runoff of blood through the main pulmonary artery into the systemic circulation. The dilated pulmonary arteries do taper down in the lungs, but when they are massively dilated they can be mistaken for a cystic mass in the mediastinum. Careful investigation with both real-time and color Doppler echocardiography will confirm absence of the ductus arteriosus in the majority of cases. In those cases where the ductus arteriosus is patent, the pulmonary artery dilatation is not severe.

The intrauterine prognosis of TOF with absent pulmonary valve is poor.[17] The dilated pulmonary arteries can compress the tracheobronchial tree and esophagus resulting in polyhydramnios and or hydrops.[32] In addition, the *in utero* pulmonary insufficiency may result in elevated right ventricular end-diastolic pressure, impaired diastolic filling, and increased systemic venous pressure resulting in hydrops.[28] For those that survive to birth, life-threatening airway compromise is often an immediate problem.[33] The best surgical approach for this condition is still being debated, and many children continue to have long-term respiratory problems even after complete repair.[34–36]

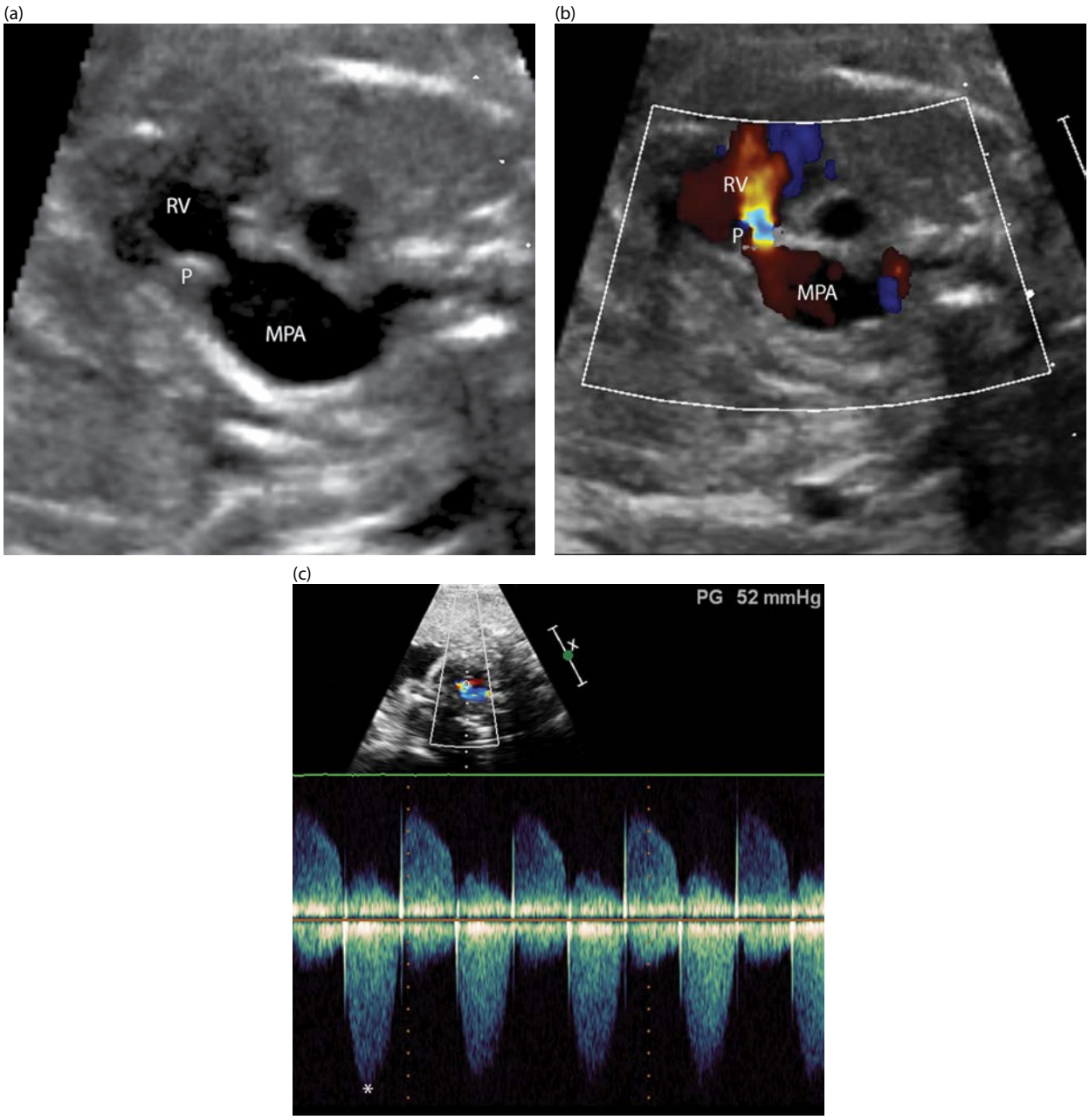


**Figure 26.13**
Tetralogy of Fallot with absent pulmonary valve in the short axis view is shown in 2D (a) and color (b). A rudimentary pulmonary valve (P) with no discernable leaflets is seen as well as the dilated main pulmonary artery (MPA) with a jet of diastolic retrograde pulmonary blood flow from severe insufficiency crossing into the right ventricle (RV). Pulsed Doppler interrogation across the pulmonary valve (c) shows pulmonary stenosis with a peak gradient of 52 mm Hg and severe holodiastolic pulmonary insufficiency.

# References


1. Yoo SJ et al. *Ultrasound Obstet Gynecol* 1999;14:29–37.
2. Fallot E. *Marseille-Med* 1888;25:33–45.
3. Peacock T. *On Malformations of the Heart*. 2nd ed. London: Churchill; 1866.
4. Van Praagh R. *Semin Thorac Cardiovasc Surg Pediatr Card Surg Annu* 2009;12(1):19–38.
5. Shinebourne EA et al. *Heart* 2006;92:1353–9.
6. Blalock A, Taussig HB. *JAMA* 1984;251:2123–38.
7. van der Linde D et al. *J Am Coll Cardiol* 2011;58:2241–7.
8. Lammer EJ et al. *Birth Defects Res A Clin Mol Teratol* 2009;85: 30–5.
9. Chin-Yee NJ et al. *Circ Cardiovasc Genet* 2014;7:102–9.
10. Poon LC et al. *Ultrasound Obstet Gynecol* 2007;29:625–7.
11. Hornberger LK et al. *J Am Coll Cardiol* 1995;25:739–45.
12. Pepas LP et al. *Cardiol Young* 2003;13:240–7.
13. Brandt JS et al. *J Ultrasound Med* 2015;34:1415–21.
14. Palatnik A et al. *J Ultrasound Med* 2016;35(8):1799–809.
15. Mielke G et al. *Ultrasound Obstet Gynecol* 1997;9:25–9.
16. Arya B et al. *Pediatr Cardiol* 2014;35:810–6.
17. Moon-Grady AJ et al. *Am J Cardiol* 2002;89:1280–5.

18. Razavi RS et al. *Am J Cardiol* 2003;91:429–32.
19. Volpe P et al. *Ultrasound Obstet Gynecol* 2004;24:623–8.
20. Galindo A et al. *Ultrasound Obstet Gynecol* 2006;28:32–9.
21. Qureshi MY et al. *Tex Heart Inst J* 2014;41:664–7.
22. Webber SA et al. *J Pediatr* 1996;129:26–32.
23. Gibbs JL et al. *BMJ* 2004;328:611.
24. van Dongen EI et al. *J Thorac Cardiovasc Surg* 2003;126:703–10.
25. Murphy JG et al. *N Engl J Med* 1993;329:593–9.
26. Parry AJ et al. *J Am Coll Cardiol* 2000;36:2279–83.
27. Emmanoulides GC et al. *Am J Cardiol* 1976;37:403–9.
28. Lakier JB et al. *Circulation* 1974;50:167–75.
29. Calder AL et al. *Am J Cardiol* 1980;46:106–16.
30. Lev M, Eckner FA. *Dis Chest* 1964;45:251–61.
31. Fouron JC et al. *Am J Cardiol* 1989;64:547–9.
32. Sameshima H et al. *Fetal Diagn Ther* 1993;8:305–8.
33. Donofrio MT et al. *J Am Soc Echocardiogr* 1997;10:556–61.
34. McDonnell BE et al. *Ann Thorac Surg* 1999;67:1391–5; discussion 1395–6.
35. Rabinovitch M et al. *Am J Cardiol* 1982;50:804–13.
36. Sakamoto T et al. *J Thorac Cardiovasc Surg* 2005;130:1717–8.

# 27

# Double-outlet right ventricle

Luke Eckersley and Lisa K. Hornberger

## Introduction

It has been said that a student with a complete understanding of double-outlet right ventricle (DORV) will understand a significant proportion of congenital heart disease. Knowledge of the embryological origins of DORV provides insight into other outflow tract disorders, and DORV physiology can bear resemblance to most other forms of congenital heart disease. This chapter approaches the specific challenges of fetal DORV, with a focus on correct diagnosis of the cardiac and noncardiac features in order to provide effective and accurate counseling regarding the possible surgical pathways, outcome, and appropriate perinatal management strategy.

## Morphological definition and embryology

DORV has been used to describe a spectrum of conditions in which both great arteries arise from the morphological right ventricle. It is best defined as a type of ventriculo-arterial connection rather than a single cardiac entity. This alleviates the need for a precise distinction between DORV and tetralogy of Fallot (in the case of a subaortic ventricular septal defect [VSD] and normally related great vessels) or transposition of the great arteries with VSD (in the case of d-malposed/transposed great vessels). The most commonly accepted definition has considered a diagnosis of DORV, where the aortic valve overrides the ventricular septum toward the right ventricle by greater than 50%.[1,2] Fibrous continuity of one arterial valve with the left atrioventricular valve has been shown not to prelude a diagnosis of DORV.[3]

In normal cardiac embryogenesis, the conoventricular junction and subsequently the truncal valve rotate and shift leftward, placing the left outflow tract posterior and leftward. The right inner heart curvature remains muscular, forming the ventriculoinfundibular fold (VIF) between the tricuspid and aortic valves, whereas the leftward component regresses resulting in aortic-mitral fibrous continuity.[4,5] The spiraling truncal septum is continuous caudally with the conal septal, which fuses with the interventricular septum and assigns the outflow tracts to their respective ventricles (Figure 27.1). DORV likely results from early failure of these three processes at variable times in early development, explaining the anatomical variation in aortic position, extent of persistent subaortic VIF, and crowding of the right ventricular outflow tract by a leftward and anteriorly deviated infundibular septum. The ventricular communication most commonly found in DORV is secondary to failure of leftward translocation and fusion of the infundibular septum with the muscular interventricular septum,[6] and is frequently perimembranous.

The relationship of the great arteries at semilunar valve level, and the relationship of the interventricular communication have been useful in the classification of DORV, as this description will likely determine the clinical presentation and type of surgical repair. In two-thirds of cases, the aorta is to the right with side-by-side semilunar valve arrangement (Figure 27.2). In one-quarter, the aorta is rightward and anterior to the pulmonary artery. Less than one-tenth of the cases have an aorta that is leftward of the pulmonary artery.

Classically, the ventricular septal defect (VSD) in DORV is described as subaortic, subpulmonary, doubly committed, or noncommitted. It has been argued that the term VSD should be reserved to describe the plane that would be closed by the surgeon, for example, in reconnecting the aorta to the left ventricle in a subaortic defect. The term *interventricular communication* is then used to describe the outlet from the left ventricle. In the first three cases, the interventricular communication is in fact constant and positioned between the anterior and posterior limbs of the septomarginal trabeculation (TSM), or septal band, above the crest of the muscular interventricular septum, and roofed by the inner heart curvature. The association of the VSD with a great artery and therefore flow streaming arises from variable infundibular fusion: in two-thirds of cases with a subaortic VSD, the infundibular septum is fused with the anterior limb of the TSM, separating the pulmonary outflow from the defect. In one-quarter of cases with a subpulmonary VSD, the infundibular septum is fused with the posterior limb of the TSM, separating the aortic outflow from the defect. The extent of the left VIF determines the proximity of the defect to the great arteries. In the less than 5% with doubly committed defects, the infundibular septum is absent, allowing both outflow tracts to override the crest of the interventricular septum. The remaining cases have a VSD that is not committed to either outflow tract—predominantly these are perimembranous defects with inlet extension, or occur as part of an atrioventricular septal defect[7,8] or less commonly may be muscular defects.

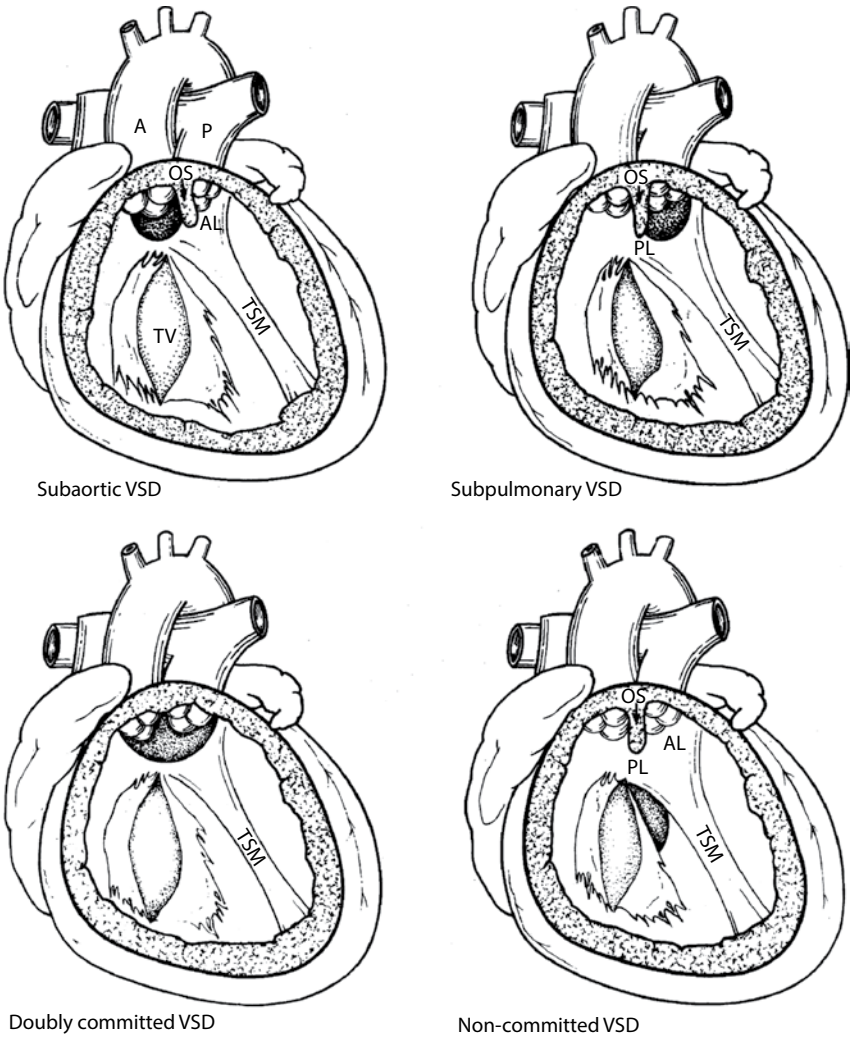


**Figure 27.1**
Examples of double-outlet right ventricle. The ventricular septal defect (VSD) is classified according to its location relative to the semilunar valves. (A, aorta; AL, anterior limb of the trabecula septomarginalos; OS, outlet or infundibular septum; P, pulmonary artery; PL, posterior limb of trabecula septomarginalis; TSM, trabecular septomarginalis; TV, tricuspid valve.)

## Associated cardiac malformations

Some features associated with DORV are predictable from the conoventricular embryological failure underlying the condition. A subaortic VSD, for instance, is usually characterized by a variable degree of subpulmonary or pulmonary valve obstruction secondary to infundibular septal malalignment with features much like that of tetralogy of Fallot. A subpulmonary VSD is associated with an anterior aorta and a subaortic infundibular septum, which may cause obstruction. Subaortic obstruction is associated with aortic arch hypoplasia, coarctation, or interruption, and is also defined as the Taussig-Bing anomaly. Straddle and override of a cleft mitral valve is also an important association with this lesion. In some cases, despite an anterior aorta, there is subpulmonary obstruction due to a posteriorly deviated infundibulum. Noncommitted defects with inlet extension of a perimembranous defect can be associated with straddling of the tricuspid valve. Left ventricular hypoplasia can be observed, particularly in association with abnormalities of the mitral valve. DORV has been reported rarely in association with an intact ventricular septum.

DORV is a frequent finding in isomerism of the right atrial appendage in association with an atrioventricular septal defect and can, in this context, also be associated with pulmonary and systemic venous abnormalities. Anomalous pulmonary venous connections are often associated with an anterior aorta and pulmonary obstruction.[9] There is usually left ventricular hypoplasia in the setting of a functionally univentricular heart.

DORV can also occur in association with tricuspid atresia, in double-inlet left ventricle, or in the context of dextrocardia and discordant atrioventricular connections.

## Epidemiology and genetics

The incidence of DORV is approximately 0.1–0.2 cases per 1,000 live births; 1%–1.5% of congenital heart disease.[10,11]

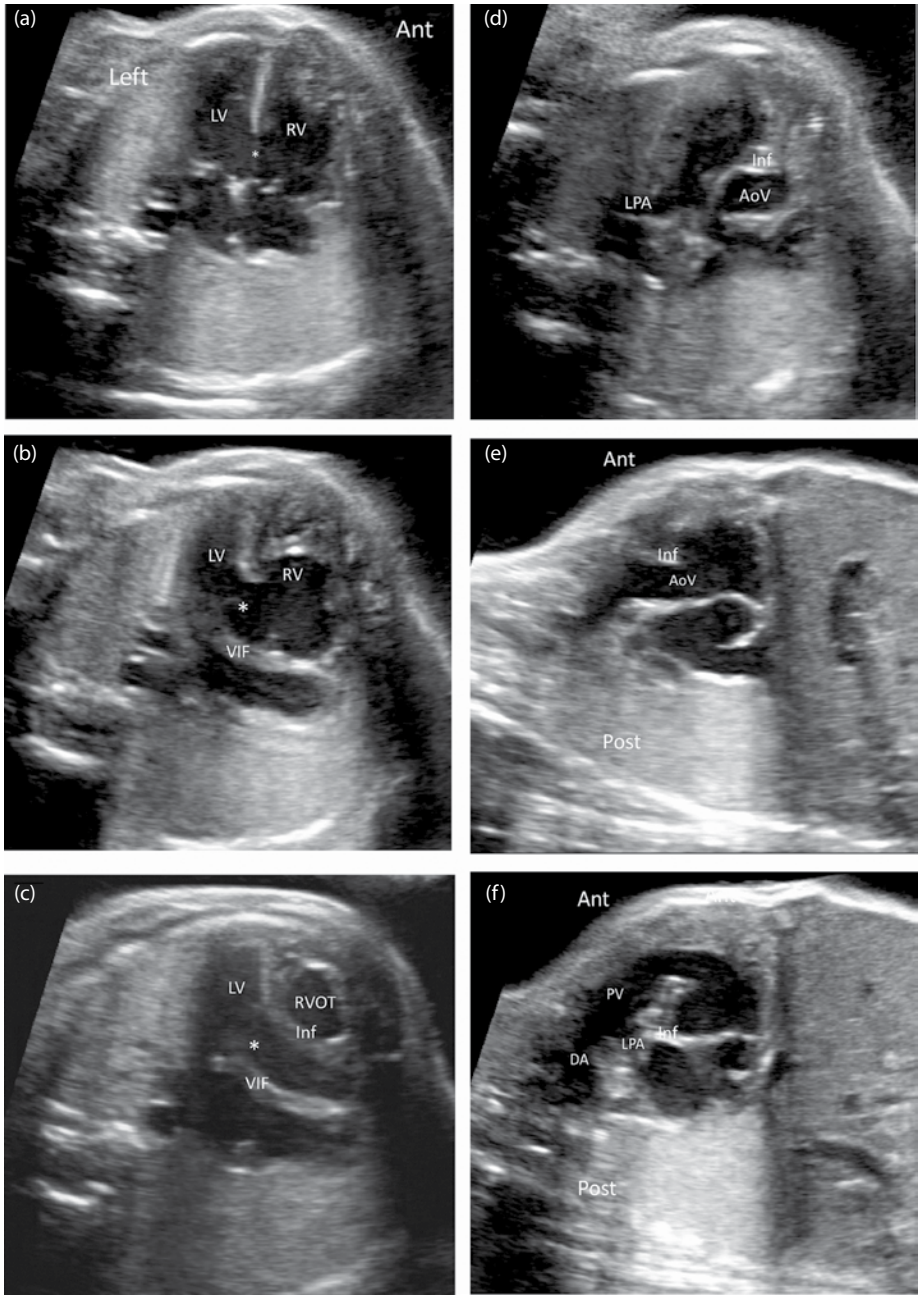


**Figure 27.2**
Double-outlet right ventricle with subaortic ventricular septal defect, in a 33-week gestational age fetus. (a–d) Consecutive two-dimensional cross-sectional views from the four-chamber view at the level of the ventricular communication (*) and extending superiorly. The pathway from the ventricular communication to the aortic valve (AoV) is bounded anteriorly by the infundibular (inf) septum, and posteriorly by the ventriculoinfundibular fold (VIF). The aortic valve is rightward and almost side by side with the pulmonary valve (PV). (e–f) Sagittal views further demonstrate the relationship of the pulmonary and aortic outflows to the infundibular septum. (Ant, anterior; DA, ductus arteriosus; LV, left ventricle; LPA, left pulmonary artery; Post, posterior; PV, pulmonary valve; RV, right ventricle.)

There is no known racial or gender susceptibility. The prevalence of chromosomal abnormalities in fetal series is from 18% to 29%.[12,13] DORV has been seen in association with trisomy 18, 13, and 21 and Klinefelter syndrome (XXY). Microdeletion of 22q11.2 has been reported in up to 11% of prenatally diagnosed DORV cases.[14] Interestingly, where cases with fibrous continuity of mitral and aortic valve are excluded, 22q11.2 occurs in less than 1% of postnatal cases.[14]

A variety of mutations in genes encoding transcription factors have been associated with increased prevalence of DORV, including NkX2.6.[15] A TBX20 mutation in association with DORV showing autosomal dominant transmission and complete penetrance was identified in three generations of one family.[16] Targeted deletion of the helix-loop-helix transcription factor Hand2 in neural crest cells results in DORV in mice.[17]

## Associated extracardiac malformations

Fetal series often report a very high prevalence of extracardiac malformations in association with DORV and other conotruncal anomalies (30%–45%); however, this certainly is affected by ascertainment bias, as the reason for referral is often the extracardiac anomaly.[18] Most extracardiac malformations are in the context of visceral heterotaxy (such as asplenia, midgut malrotation), major chromosomal anomalies, or syndromic conditions. Isolated extracardiac malformations have been reported in 10% of patients, mainly involving the central nervous system and renal tracts.[12] VACTERL association and omphalocele have also been reported in DORV series.

## Physiology and postnatal course

The symptoms and signs exhibited by infants with DORV relate most frequently to the relationship of the VSD to the great arteries and the presence of obstruction to outflow.

The most common form of DORV—that associated with a subaortic defect and subpulmonary stenosis—presents similarly to tetralogy of Fallot, with a variable degree of cyanosis and a harsh systolic murmur at the left upper sternal border, radiating into the lung fields. Patients without severe obstruction are likely to be asymptomatic in the perinatal period and can be discharged for outpatient follow-up.

Infants with a subpulmonary VSD are more likely to present with cyanosis due to streaming of systemic venous blood into the aorta, and oxygenated blood into the pulmonary artery, "transposition streaming." If there is no pulmonary outflow tract obstruction, there may also be pulmonary congestion with increased work of breathing, hepatomegaly, and failure to thrive. If pulmonary outflow tract obstruction is significant, cyanosis may be severe. In this group, an early operative procedure may be necessary to alleviate cyanosis and/or pulmonary congestion. Others may require a balloon atrial septostomy to increase intracardiac mixing, which results in more deoxygenated blood being ejected into the pulmonary artery.

Infants with a subpulmonary VSD and systemic outflow tract obstruction, often at both subaortic and juxtaductal levels, present with a "reversed differential" in oxygen saturations—systemic venous blood perfuses the upper limbs via the aorta, whereas oxygenated blood perfuses the lower limbs via the pulmonary artery and ductus arteriosus. If the ductus becomes restrictive or closes, femoral pulses will be reduced or absent, and the infant is at risk of developing shock. Conversely, an unobstructed pulmonary outflow could lead to the simultaneous development of congestive cardiac failure in the setting of cyanosis and poor femoral pulses.

The presentation of DORV with a VSD remote from the outflow tracts is dependent on the streaming of venous and arterial blood flow to the outflow tracts and the presence of outflow tract obstruction. Most have mixing at atrial and ventricular levels resulting in cyanosis.

## Surgical options

The optimal surgical procedure in DORV is dependent on first, the ability of the left ventricle to support the systemic circulation, and second, the potential to create a pathway from the left ventricle to either one of the outflow tracts. In the biventricular repair of DORV, it is thus not the actual VSD that is closed; rather, the VSD becomes the origin of the outflow tract for the systemic circulation, and closure of the "interventricular communication" is within the right ventricle. Where possible, the left ventricle is connected to the aortic valve via a baffle, and outflow tract obstruction is relieved.

In the setting of a subaortic VSD without or with minimal outflow obstruction, the baby can present with symptoms consistent with a large VSD in isolation with gradual evidence of heart failure. Surgical repair of the VSD with or without resection of subaortic muscle and often performed by 6 months results in a full repair. Where there is subpulmonary obstruction from anteriorly deviate outlet or conal septum, the repair is virtually identical to that associated with tetralogy of Fallot with VSD closure, leaving the left ventricle (LV) ejecting through the aortic valve. The right ventricular communication with the main pulmonary is restored using the required combination of subpulmonary resection, pulmonary valvuloplasty/patch annuloplasty, or right ventricular to pulmonary artery conduit. In cases where the aortic valve is more anterior and rightward, the position of the pulmonary valve may require that it is oversewn and an RV to PA conduit placed in order for the LV-to-aortic baffle placement to be possible (a Rastelli procedure). The long-term risks associated with this repair are nearly identical to those of tetralogy of Fallot; however, there is an increased incidence of subaortic obstruction, particularly if the VSD decreases in size.

In the case of a subpulmonary VSD, in which the great arteries are in a more transposed relationship, it may be possible to perform an arterial switch operation and then baffle the VSD to the neo-aortic root. If the pulmonary outflow is minimally obstructed, an arterial switch may still be performed; however, more significant obstruction must be dealt with differently. First, if the pulmonary outflow is not critically obstructed, balloon atrial septostomy to improve mixing of oxygenated and deoxygenated blood at atrial level may leave the patient sufficiently saturated to be followed as an outpatient for weeks and sometimes months. This allows the surgical intervention to be delayed. Surgical repair in this lesion may be in the form of a Rastelli procedure in which the VSD is baffled to a more remote rightward aorta, and an RV-PA conduit may be placed. This approach increases the risk of LV outflow obstruction and need to long-term. More recently, the Nikaidoh procedure, in which the aortic root is translocated to the pulmonary position leaving no LV outflow obstruction, has become popular. In the latter, VSD closure and placement of an RV-PA conduit is necessary, resulting in a lifelong need for reoperations to replace the conduit. Where there is subaortic obstruction and aortic arch obstruction, the VSD is typically baffled to the pulmonary valve, an arterial switch is formed, enlargement of the right ventricular outflow

is performed if necessary, and the aortic arch is reconstructed. Long-term risks include the need for reintervention for the aortic arch, and the pulmonary outflow tract due to progressive obstruction at subvalvar, valvar, and supravalvar levels.

The major impediments to a biventricular repair are a hypoplastic ventricle incapable of supporting the circulation, or a VSD that is remote from the outflow tracts—usually in the inflow or trabecular region, with the distance and tricuspid valve chordal involvement making baffling impossible. Major straddling of an atrioventricular (AV) valve may also preclude the placement of an LV to outflow tract baffle.

Cases with associated ventricular hypoplasia usually follow a single ventricle pathway, with early palliation in the form of a systemic to pulmonary artery shunt in the setting of severe pulmonary outflow tract obstruction, or pulmonary artery band in those with unobstructed pulmonary blood flow. Close follow-up is required for cases with less severe pulmonary outflow tract obstruction. Others with severe obstruction to aortic outflow are candidates for a Norwood. In all cases, a subsequent bidirectional cavopulmonary shunt and a Fontan are performed. In cases where bilateral SVCs are present, a delay in timing of stage 2 may allow a technically simpler procedure due to growth of the smaller vein.

## Prenatal diagnosis of DORV

The rate of fetal diagnosis of DORV is likely to be extremely variable between health systems and dependant on whether outflow tract views are included in routine obstetric screening ultrasound protocols. In population-based studies from countries with well-developed fetal screening programs, the rate is about 60%, and up to 78% has been reported where national fetal cardiac screening is implemented.[19]

Traditionally, DORV has represented a particularly challenging group in which to obtain an accurate fetal diagnosis. The reported rate of correct diagnosis of DORV subtypes in fetal cardiology programs is approximately 76%–90%, with inaccuracies including in severity of pulmonary outflow or arch obstruction, and in differentiation from tetralogy of Fallot and from posterior malalignment VSDs with arch obstruction. Improvements in diagnostic accuracy occur with multiple prenatal examinations,[13] and the type of surgery required can be predicted in 90% of cases.[20] The precise definition is less important than identification of features that may preclude or make a biventricular repair difficult, such as ventricular hypoplasia, straddling of an atrioventricular valve, or ventricular septal defect distant from the outflow tracts.

## Diagnostic features in the fetus

Fetal echocardiography in suspected DORV is complex and requires a thorough and detailed segmental approach using two-dimensional (2D) imaging, measurement of relevant structures, color-flow imaging, and Doppler interrogation. Sweeps through the heart are particularly useful to correctly identify relationships of structures. Examples of fetal images

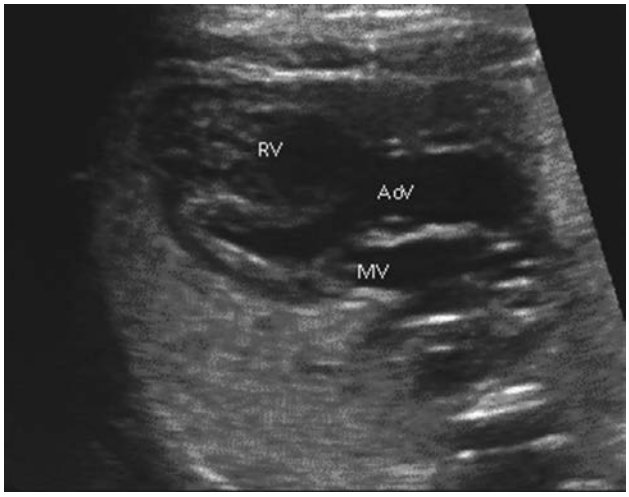


**Figure 27.3**
Double-outlet right ventricle with subaortic ventricular septal defect at 28 weeks ("Tetralogy-like DORV"). This cross-sectional view at the level of the aortic outflow tract demonstrates mitral-aortic fibrous continuity can exist in the context of DORV. (AoV, aortic valve; MV, mitral valve; RV, right ventricle.)

obtained from the most common types of DORV are presented in Figures 27.3 through 27.5 and Videos 27.1 through 27.4.

### *Situs*

The position of the fetus in the uterus should first be established, and left and right sidedness determined. A cross-sectional sweep using 2D and color-flow imaging from the abdomen at the level of the inferior vena cava (IVC) and abdominal aorta up through the fetal heart to the level of the head and neck vessels is used to determine vessel, valve, and chamber relationships and connections. In cases of right or left isomerism, visceroatrial situs is ambiguous. The stomach may be right-sided, and the liver in the midline. In cases of right isomerism, a more posterior stomach position may be a clue to the presence of associated asplenia. The aorta and IVC may both be on the right. In left isomerism, the IVC is usually interrupted, with a dilated azygous vein seen adjacent to the spine in the axial plane, and posterior to the aorta in the sagittal plane. Rarely, situs inversus totalis may be present in DORV in the absence of heterotaxy syndrome.

### *Four-chamber view*

Ventricles: Ventricles should be identified according to morphological criteria. Symmetry of the ventricles must be determined, and if there is suspicion of imbalance, causes identified, such as override of an AV valve into the dominant ventricle or hypoplasia and/or stenosis and hypoplasia of the ipsilateral AV valve. A right ventricle to left ventricle diameter ratio Z-score of greater than 2 is considered borderline for the LV, with an apex forming borderline LV a positive indicator for biventricular repair.[21] Rarely, DORV may occur in the

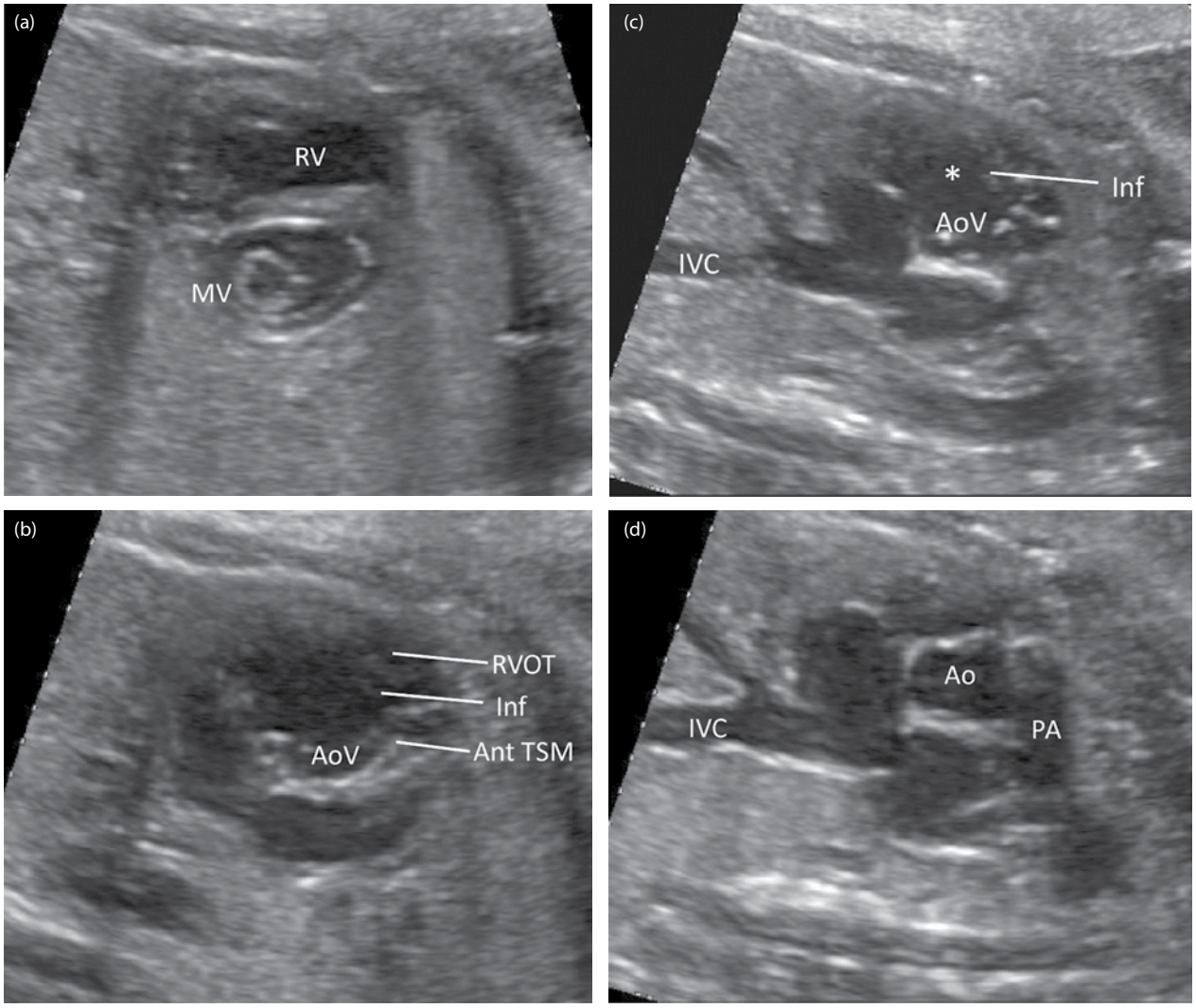


**Figure 27.4**
Double-outlet right ventricle with subaortic ventricular septal defect ("Tetralogy-like DORV") at 28 weeks. (a–d) Serial short-axis views from the level of the mitral valve. In this case, the mitral valve is hypoplastic (a). The aortic valve is seen centrally; the asterisk (*) demonstrates the position for placement of a patch to commit the aortic valve to the LV. The infundibular septum (inf) is fused with the anterior limb of the trabecular septomarginalis (ant TSM), which separates the pulmonary outflow tract from the interventricular communication, which actually lies out of plane posterior to the aortic valve. (AoV, aortic valve; Ao, ascending aorta; IVC, inferior vena cava; MV, mitral valve; PA, pulmonary artery; RV, right ventricle; RVOT, right ventricular outflow tract.)

presence of L-ventricular looping in situs solitus, and usually this is associated with a left and anterior aorta as is typical of L-transposition or physiologically corrected transposition of the great arteries (see Chapter 29). The right ventricle, in this context, is on the left side of the heart, and a ventricular septal defect is present. The great arteries are often configured more akin to L-transposition with an anterior and leftward aorta.

## Atrioventricular connections

A common AV valve should be excluded by confirmation of two separate AV valves with offset in septal attachment and an intact atrial septum above the valves from the four-chamber view. The size and relationship of the AV valves to the ventricular septal defect must be determined as there could be attachments that preclude surgical baffling for two-ventricle repair. This is particularly true in the setting of straddling of one of the AV valves. The tricuspid valve more typically straddles an inlet defect, whereas the mitral valve typically straddles an outlet ventricular septal defect usually through the presence of a cleft. A clue to the presence of a straddling tricuspid valve is the association of a foreshortened right ventricle, whereas with mitral valve straddling the left ventricle may be hypoplastic and the anterior mitral valve leaflet fails to pull away from the ventricular septum due to the presence of a cleft.

## Ventricular septum

The ventricular septal defect is most commonly singular and large; however, other significant muscular ventricular septal defects should be identified. Defects are most easily

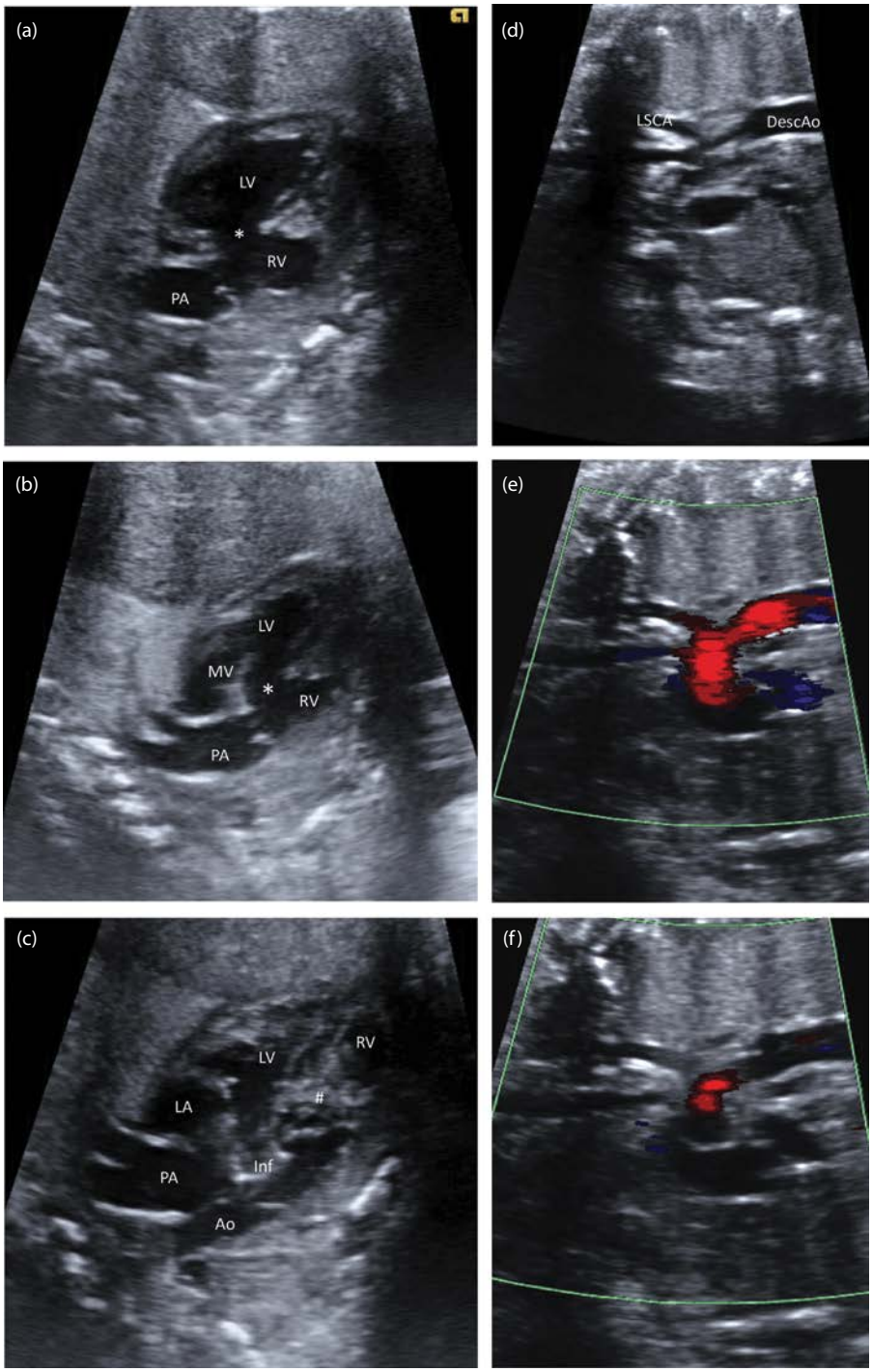


**Figure 27.5**
Double-outlet right ventricle with a subpulmonary ventricular septal defect, subaortic obstruction, and arch hypoplasia (Taussig-Bing anomaly). (a–c) Oblique views of the outflow tracts from inferior to superior. The ventricular communication (*) is seen in the same plane as the pulmonary valve (a,b). There is subaortic outflow septum (Inf) and tricuspid accessory tissue (#) obstructing the aortic outflow tract (c) (Ao). (d–f) Sagittal views of the aorta in the same case show a diminutive aortic arch with abnormal continuous flow in diastole. (DescAO, descending aorta; LA, left atrium; LSCA, left subclavian artery; LV, left ventricle; MV, mitral valve; PA, pulmonary artery; RV, right ventricle.)

identified if the septum lies perpendicular to the plane of insonation. The size and location of the defect and its relationship to the outflow tracts are critical factors in determining the likely surgical approach, and are therefore important in providing accurate counseling. Oblique orientation of the imaging plane can demonstrate the pathway from the left ventricle through the VSD to the outlets, with the outlet most related to the VSD the one most likely used for a two-ventricle repair through intracardiac baffling to eject to the body.

## Pulmonary veins

Pulmonary venous drainage is usually normal in isolated DORV, but there is often total anomalous pulmonary venous drainage in association with right isomerism, with pulmonary veins forming a confluence posterior to the back wall of the atrial mass and either directly entering the atrium, or draining anomalously through a vertical vein to a systemic vein below (infradiaphragmatic) or above (supradiaphragmatic) the diaphragm. A nonpulsatile, low-velocity pulmonary vein Doppler profile is a feature of

obstructed anomalous pulmonary veins. In left isomerism, there are frequently bilateral pulmonary venous connections.

## Outflow tracts

Superior to the four-chamber view, the outflow tracts can be identified. A degree of clockwise or anticlockwise rotation is often necessary to obtain a long axis of each.

The position, relationship, relative size, and subvalvar regions of both outflow tracts must be carefully examined. Where the ventricular septal defect is subaortic, subvalvar pulmonary stenosis is present in around 75% of cases.[13] In subpulmonary VSDs, subaortic crowding is also possible. A gradient through an obstructed outflow tract is not typical, as blood can be ejected through the unobstructed outlet. Visualization of deviation of the outlet or infundibular septum into the pulmonary or aortic outflow and hypoplasia of the semilunar valve through the obstructed outflow may be demonstrated. Great artery size discrepancy is a sign of outlet obstruction, where the outlet that is obstructed is typically smaller than the other. In addition to measuring the size of the ascending aorta and main pulmonary artery, assessment of the branch pulmonary arteries including their diameters should be considered. Recording the Z-score, or number of standard deviations from the average value for gestation, femur length, or biparietal diameter, allows for tracking of growth on serial studies.

## Three-vessel view (3VV) and three-vessel and trachea view (3VT)

By scanning superiorly from the outflow tracts in cross section, the great arteries can be further examined. The aortic and ductal arch sidedness, relative size, and flow direction should be carefully examined. Subaortic narrowing is often associated with aortic arch obstruction, either coarctation or interruption. A right aortic arch confers an elevated risk for microdeletion of 22q11.2.[14] Rarely, there is flow reversal in the aortic arch, and only with critical aortic outflow obstruction. Retrograde flow in the ductus arteriosus is indicative of critical pulmonary outflow tract obstruction. In both cases, abnormal direction of flow in the arches is an indication for commencement of a prostaglandin infusion shortly following birth. Bilateral superior vena cava may be identified if present anterior to the adjacent pulmonary arteries.

## Sagittal view and short axis

Sagittal and short-axis sweeps are important in the prenatal evaluation of DORV. In isolated DORV, there is an increased incidence of left SVC draining to the coronary sinus, which can be demonstrated in this view. Coronal images can demonstrate bilateral superior vena cava. Assessment of atrial septal anatomy and flow is important from these views. The atrial septum in the absence of significant left AV valve obstruction usually bows into the left atrium, and the flow across the atrial septum is most commonly right to left. Left to right flow indicates obstruction to flow through the left heart; the mitral valve and ventricular septal defect size and flow patterns should be carefully examined. A common atrium is frequently seen in isomerism. The anatomy of the mitral and tricuspid valves should be assessed from the short-axis view, and any straddling chordal attachments identified. Short-axis sweeps through the heart assist with deciphering the position of the VSD and its relationship to the outflow tracts. From these views, the diameter of the outflow tracts and valves may be more accurately measured with the plane of imaging axial to the plane of measurement (perpendicular to the vessel or valve). Obstruction below the level of the aortic and pulmonary valves due to a deviated infundibular septum is most easily identified in this view. Discrepancy in the great arteries, again, suggests the presence of outflow obstruction, usually toward the vessel with the smallest diameter.

The long axis views of the ductal and aortic arches can be imaged from sagittal views when the spine is either almost directly anterior or posterior. There may be hypoplasia of the transverse and distal aorta, and bidirectional or retrograde flow may suggest a severe or critical obstruction to aortic outflow, particularly in the context of the Taussig-Bing anomaly.

# Fetal progression and monitoring

Fetal instability or demise secondary to the cardiac lesion in isolated DORV is rare; evidence of evolving hydrops fetalis, growth failure, or abnormal umbilical Doppler profiles should alert the physician to a possible underlying chromosomal/syndromic disorder or placental insufficiency. Severe AV valve insufficiency is usually seen in those with an associated atrioventricular septal defect, in particular, in the setting of isomerism. The majority of cases with DORV have sinus rhythm, but those in association with left isomerism have a higher incidence of heart block or atrial bradycardia, and in this context, noncompaction cardiomyopathy may be present. The frequency of repeat fetal echocardiography will depend on the initial findings. Repeat examination should be focused on further definition of features that may alter the type of surgical repair, or may increase necessary support for the neonate in the perinatal period. Where ventricular discrepancy exists, the growth of the hypoplastic ventricle and mitral valve should be monitored as a guide to potential for biventricular repair. The interventricular communication, representing the sole outlet to the left ventricle, should be confirmed as unrestrictive on each echocardiogram using 2D, color-flow, and Doppler imaging. An abnormal inflow Doppler profile through the mitral valve may be a clue to restriction. The severity of subvalvar outflow tract obstruction should be monitored by 2D and color-flow imaging. Progressive outflow obstruction is common in DORV. Monitoring ascending aorta and main pulmonary artery growth as well as flow direction in either arch is important for anticipating the need for intervention early after birth. In the case of the Taussig-Bing anomaly, the severity of aortic arch obstruction including growth of the transverse and distal arch should be monitored.

## Recent developments in imaging

In postnatal DORV, three-dimensional echocardiographic imaging has the potential distinct advantage over 2D imaging of the capability (a) to assess the size of the interventricular communication accurately using multiplanar reconstruction to create nonstandard 2D views; (b) to accurately assess the degree of AV valve override and the course of any straddling chordae; and (c) to demonstrate the relationship of the VSD to the outflow tracts. The use of spatiotemporal imaging correlation techniques may prove of similar benefit in the fetus, and this requires further examination.[22]

## Outcome

Counseling regarding the risk of a poor outcome in DORV is highly individualized to the presenting case. The presence and severity of noncardiac congenital anomalies and karyotypic disorders are likely to modify the risk significantly. DORV with obstructed pulmonary venous drainage (often in right isomerism) or heart block in the context of left isomerism can be considered to have an extremely poor prognosis. In contrast, a simple DORV with a subaortic VSD and no or mild pulmonary outflow obstruction may have a more positive long-term prognosis in the absence of major extracardiac pathology with many not requiring reintervention long term.

In a published series of fetal DORV, 14/33 (42%) underwent biventricular repair—four had an arterial switch, five had ventricular septal defect closure with relief of pulmonary outflow obstruction, and five had placement of a right ventricle to pulmonary artery conduit. In the 19/33 (58%) who underwent single ventricle palliation, five had primary cavopulmonary anastomosis, nine aortopulmonary shunt, and five a Norwood procedure.[20]

The overall survival at 1 year of pre- and postnatally diagnosed DORV is 80%–90% when not associated with heterotaxy, AVSD, ventricular hypoplasia or syndromes/chromosomal disorders,[12] falling to around 50%–60% where these comorbidities are present.[13,20] There is increased risk associated with even mild prematurity or small for gestational age birth.

## Videos

**Video 27.1a** (https://youtu.be/4xBnp1D5PAY)
Double-outlet right ventricle with a large subaortic ventricular septal defect and no significant outflow tract obstruction. (a) In a four-chamber sweep, the aortic outflow is seen to be most related to the left ventricle and ventricular septal defect, but the aortic valve is positioned very rightward due to a muscular disconnect from the anterior mitral valve leaflet also known as a ventricular-infundibular fold. The aortic valve is in fact arising from the right ventricle.

**Video 27.1b** (https://youtu.be/C5UVaOUsRMs)
(b) Color Doppler demonstrates flow from the left ventricle through the ventricular septal defect to the aortic valve.

**Video 27.2** (https://youtu.be/sssm3EjQSJk)
Double-outlet right ventricle associated with unobstructed outflow tracts in a 13-week gestational age fetus. The location of the ventricular septal defect is less clear in this image, but discrepancy in ventricular size with a smaller left ventricle can be seen in the four chambers. This suggests the presence of a mitral valve abnormality, which cannot be fully delineated in this early gestational age. The pregnancy was refereed for increased nuchal translucency (5.5 mm), and chorionic villous sampling revealed trisomy 18.

**Video 27.3a** (https://youtu.be/34feU9_m6Wg)
Four-chamber image in a fetus with tetralogy of Fallot type of double-outlet right ventricle. In this sweep, the aorta is seen overriding the ventricular septum more than 50%, resulting in a greater commitment to the right ventricle. The great arteries are obviously discrepant with a smaller pulmonary valve and artery due to anterior malalignment of outlet septum.

**Video 27.3b** (https://youtu.be/ei39YRUQ8jA)
The sagittal view again demonstrates a large subaortic ventricular septal defect and discrepancy in the great arteries.

**Video 27.4a** (https://youtu.be/FA9VEFWrNHs)
An image obtained in a fetus with Taussig-Bing form of double-outlet right ventricle that demonstrates the outlet anatomy and position of the ventricular septal defect (VSD). The pulmonary artery is large and overrides a large VSD. There is anterior malalignment of infundibular or outlet septum, which impinges on the subaortic area. The aorta is rightward and significantly smaller than the pulmonary artery.

**Video 27.4b** (https://youtu.be/uP1WOSTb78c)
The aortic arch is hypoplastic in this condition, and there may be a posterior shelf, which suggests coarctation of the aorta.

## References


1. Lev M et al. *J Thorac Cardiovasc Surg* 1972;64(2):271–81.
2. Wilcox BR et al. *J Thorac Cardiovasc Surg* 1981;82(3):405–17.
3. Wilcox BR, Anderson RH. *Surgical Anatomy of the Heart*. 2nd ed. London: Gower Medical Publishing; 1992.
4. Praagh RV. *World J Pediatr Congenit Heart Surg* 2010;1(3): 364–85.
5. Bharucha T et al. *Cardiol Young* 2017;27(1):1–15.
6. Goor DA, Edwards JE. *Circulation* 1973;48(2):406–15.
7. Stellin G et al. *J Thorac Cardiovasc Surg* 1991;102(6):849–55.
8. Beekman RP et al. *J Thorac Cardiovasc Surg* 2002;124(5):984–90.
9. Freedom RM et al. *Cardiol Young* 2005;15(6):554–67.
10. Mitchell SC et al. *Circulation* 1971;43(3):323–32.
11. Zhao QM et al. *Acta Paediatrica* 2013;102(4):397–402.
12. Lagopoulos ME et al. *Am Heart J* 2010;160(4):692–700.
13. Galindo A et al. *Eur J Obstet Gynecol Reprod Biol* 2009;146(1): 55–60.
14. Peyvandi S et al. *Pediatr Cardiol* 2013;34(7):1687–94.
15. Zhao L et al. *Eur J Med Genet* 2014;57(10):579–86.
16. Pan Y et al. *Int J Mol Med* 2015;35(4):1058–66.
17. Holler KL et al. *Dev Biol* 2010;341(1):291–304.
18. Paladini D, Tartaglione A. *Ultrasound Obstet Gynecol* 2000;15: 104–8.
19. Marek J et al. *Heart* 2011;97(2): 124–30.
20. Gelehrter S et al. *Congenit Heart Dis* 2007;2(1):32–7.
21. Pitkanen OM et al. *Am Heart J* 2006;152(1):163.e1–7.
22. Hongmei W et al. *Echocardiography* 2012;29(5):614–9.

# 28

# Truncus arteriosus

Shaine A. Morris and Diego A. Lara

## Definition

Truncus arteriosus (TA), also called common arterial trunk in Andersonian nomenclature, is a conotruncal cardiac lesion in which a single artery arises from the heart, which gives origin to the coronary arteries, the pulmonary arteries, and the ascending aorta (Figure 28.1).[1]

## Epidemiology

The fetal prevalence of TA is unknown, as birth prevalence likely significantly underestimates fetal prevalence given a relatively high rate of miscarriage, elective termination, and *in utero* fetal demise.[2] Fetal death in prenatally diagnosed patients with TA has been estimated to range from 5% to 9%.[3,4] It has been postulated that the discrepancy between fetal prevalence and birth prevalence has increased over the last few decades due to improved rates of prenatal diagnosis and subsequent increased rates of elective termination.[5] In a meta-analysis of studies ranging from 1955 to 2002, Hoffman and coworkers estimated a median incidence of TA among live-born infants of 9.4 per 100,000 (interquartile range of 6.1–13.6).[6] However, a later population-based study from Reller and colleagues reported a prevalence of 6 per 100,000 live births in metropolitan Atlanta from 1998 to 2005.[7] Egbe and colleagues specifically evaluated the changing birth prevalence of TA in the United States from 1999–2000 to 2007–2008 using different methodology and noted a significant decline in birth prevalence from 23 per 100,000 live births to 18 per 100,000, again consistent with decreasing birth prevalence. TA appears to affect males and females with similar frequency.[8,9]

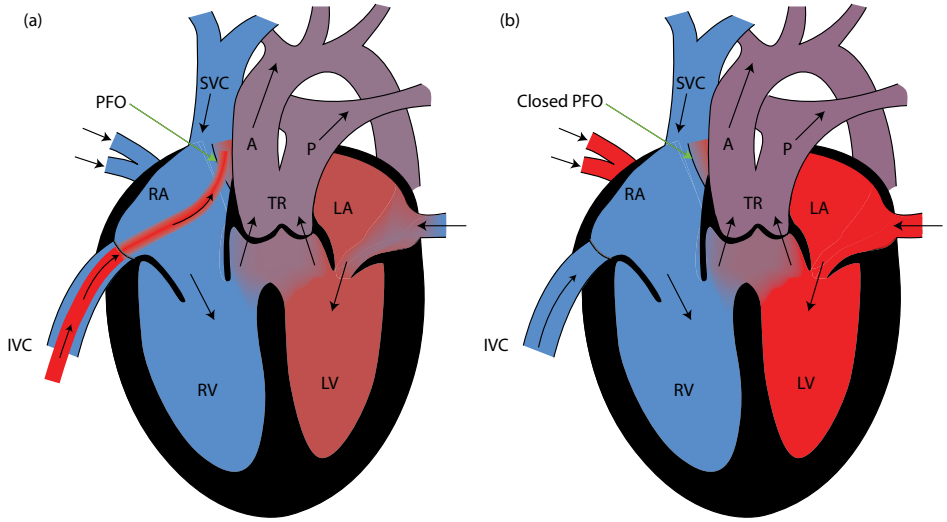


**Figure 28.1**
Truncus arteriosus anomaly: the aorta, pulmonary arteries, and coronary arteries all arise from the same vessel, and a large ventricular septal defect is typically present. (a) Prenatal truncus arteriosus: arrows indicate blood flow. In prenatal life, flow from the umbilical vein courses through the ductus venosus into the inferior vena cava (IVC), and the Eustachian valve directs that oxygenated blood from the right atrium (RA) through the foramen ovale (FO) into the left atrium (LA). The pulmonary veins deliver a small amount of deoxygenated blood to the LA, which mixes with the oxygenated blood. This blood then courses to the LV. At the same time, deoxygenated blood that is returning from the fetus' head and body returns though the fetal superior vena cava (SVC) and IVC, and courses from the RA to the right ventricle (RV). Both the primarily deoxygenated RV blood and the oxygenated LV blood mix across the ventricular septal defect (VSD) and in the truncal root (TR) before being redistributed to the fetus' brain and body. (b) After birth, foraminal flow switches to left-to-right, and the FO often closes. All oxygen to the fetus is provided through the fetal lungs. Oxygenated blood is delivered to the left atrium through the pulmonary veins. Mixing of oxygenated and deoxygenated blood occurs across the VSD and in the truncus again.

## Etiology

The etiology of TA is likely multifactorial, as studies have suggested both genetic and environmental influences. It is suggested in mouse models that normal development of the outflow tracts depends on at least two processes that utilize cells derived from the second heart field: the first is elongation of the common outflow tract and repositioning from over the right ventricle to over the ventricular septum.[10–12] The second process is septation of the outflow tract that occurs as a result of formation of cushions that grow toward each other. It is thought that failure of the first process results in double-outlet right ventricle, while failure of the second process results in TA.[13] Failure of both processes results in TA arising from only the right ventricle. It has been shown that mutations in genes critical for proper development of the second heart field can result in conotruncal abnormalities including truncus arteriosus.[14–17]

Multiple maternal conditions and exposures have also been associated with increased risk of truncus arteriosus, including maternal diabetes, maternal phenylketonuria, smoking in the first trimester, maternal isotretinoin use, maternal fever, and high exposure to air pollutants.[18–23] Although a clear role of folic acid has not been proven, multiple studies suggest that increased folic acid supplementation during pregnancy results in a lower likelihood of conotruncal defects.[23–26]

## Anatomy

TA is a conotruncal cardiac lesion in which there is a single outlet from the ventricular mass. From the TA arises the coronary arteries, the pulmonary arteries, and the ascending aorta. There are at least three commonly used classifications of TA: that described by Collett and Edwards, by Van Praagh, and by Anderson (Figure 28.2).[27,28] Collett and Edwards type IV has been widely accepted as a different diagnosis, pulmonary atresia with aortopulmonary collateral arteries, and is only discussed further in this chapter when helping differentiate it from TA. The Andersonian nomenclature describes each variant sequentially rather than using alphanumeric classification.[97] Anderson also groups lesion types into those with aortic dominance (patent arch), those with pulmonary dominance (with arch hypoplasia/coarctation/interruption), and those with balanced aortic and pulmonary pathways.

Collett and Edwards type I is the same as Van Praagh type A-1, and is present when the branch pulmonary arteries arise from a common pulmonary trunk. Collett and Edwards types 2 and 3 are included in the Van Praagh classification type A-2, and occur when the branch pulmonary arteries arise separately from the truncal artery. Of note, types I and II may be difficult to distinguish from each other.[8] The Van Praagh type A-3 is not included in the Collett and Edwards classification and includes an origin of one of the pulmonary arteries from the aorta via a collateral vessel or the ductus arteriosus. It is often referred to TA "with absent pulmonary artery," although this is a misnomer, as the pulmonary artery has an anomalous origin. If the anomalous origin is via the ductus arteriosus and the ductus closes postnatally, there will be no blood flow to that branch pulmonary artery, and it will appear to be absent. The Van Praagh type A-4 is TA in association with coarctation, hypoplasia, atresia, or interruption of the aortic arch. While the vast majority of patients with TA have an absent ductus arteriosus, type A-4 always has a ductus arteriosus, as this is the only adequate blood supply to the descending aorta.[8,28,29] Interrupted arches are most often type B (84%), with the interruption between the left carotid artery and the left subclavian artery, and are much less frequently type A (~16%), with the interruption distal to the left subclavian artery.[30] Van Praagh also described a "type B" subset of truncus arteriosus lesions without ventricular septal defects (Figure 28.2). These are exquisitely rare.

Type I/A-1 TA is the most common, present in 46% to 58% of patients, followed by type II/A-2 (22%–34%), and type III/A-2 (6%–32%).[30,31] Between 8% and 16% of patients have an "absent" pulmonary artery, which is generally on the same side as the aortic arch.[8,32] The Van Praagh type A-4 is found in 11%–19% of patients.[28,29]

The truncal valve has a biventricular origin in 68% to 83% of patients; alternatively, in 11%–29% of patients, the truncal valve lies over the right ventricle, and in 3%–6% it originates from the left ventricle.[27,31] A right aortic arch is present in 34%–36% of patients.[8,29] An aberrant subclavian artery (right or left) may also be present (14%).[30,31] A double arch has also been described.[33–35] Rarely, TA is seen in conjunction with other complex congenital heart disease, including tricuspid atresia, mitral atresia, total anomalous pulmonary venous return, and atrioventricular canal defect.[4,36–39]

The morphology of the truncal valve varies, although it is most commonly tricuspid (69% of patients); it is quadricuspid in ~22%, bicuspid in ~9%, pentacuspid in ~0.3%, and unicuspid in ~0.3%.[40] Truncal valve leaflet thickening is also very common; it was present in 66% of patients in one study, with 67% of those valve leaflets considered at least moderately thickened. Frank truncal stenosis was present in 11% of patients.[8] Truncal valve regurgitation has been found in 20%–37% of patients.[8,40] Secundum atrial septal defect is present in 9%–20% of patients.[31,41] A left superior vena cava is found in 4%.[31]

Given the many variations of truncus arteriosus, a systematic approach can be used to detail the anatomy (Figure 28.3). Accurate diagnosis of the subtype of TA is critical, as some variations are ductal dependent (denoted in Figure 28.3).

## Fetal imaging

The four-chamber view is typically normal in a patient with TA (Figure 28.4a–c; Video 28.1), as the ventricles, atria, and atrioventricular valves are typically normal. The only clue to an abnormality may be an abnormal axis (Figure 28.4b,c) or the descending aorta to the right of the spine in the presence of a right aortic arch (Figure 28.4c). However, a cephalad

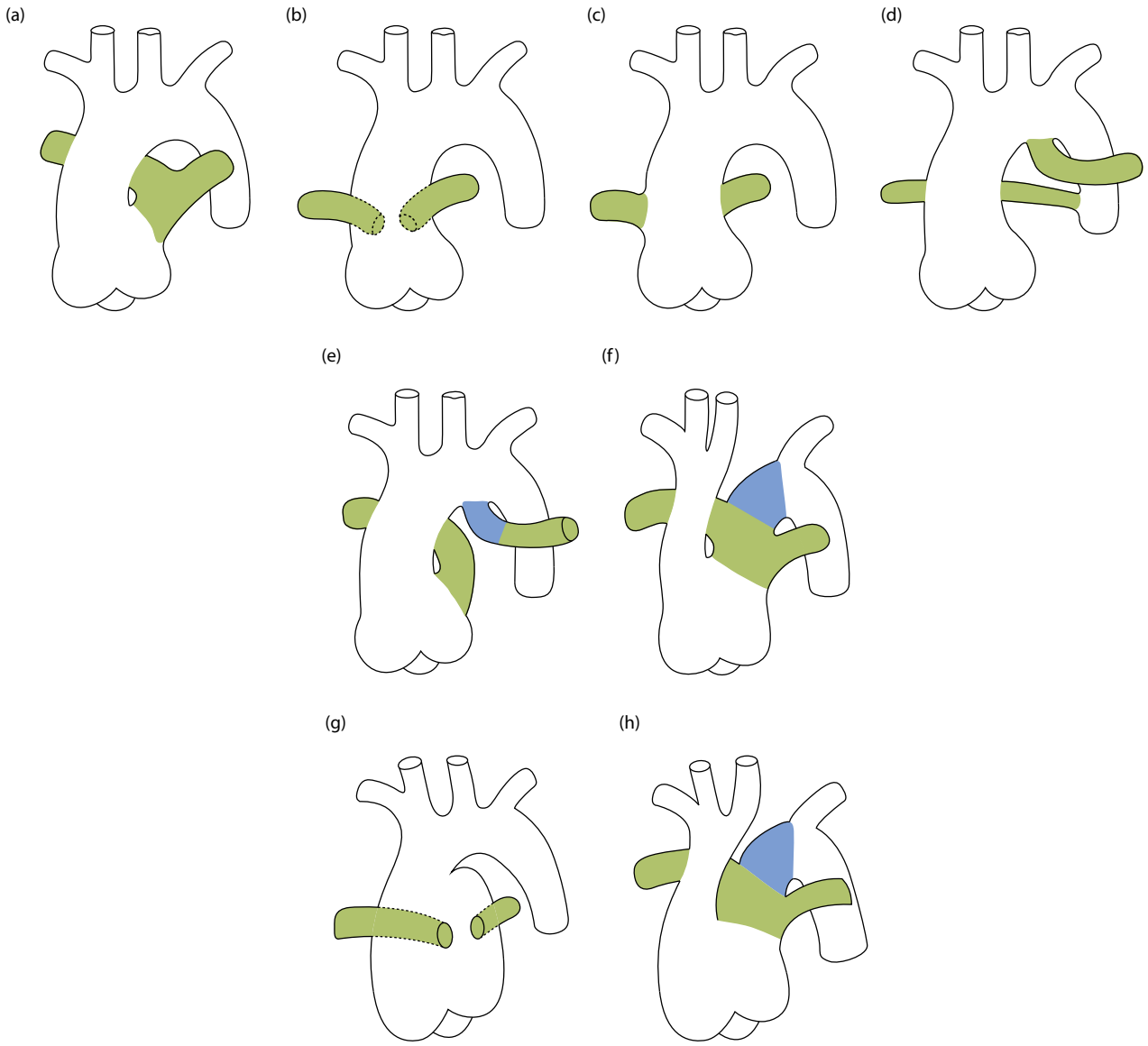


**Figure 28.2**
Classification systems for anatomical variations of truncus arteriosus: PDA, patent ductus arteriosus; VSD, ventricular septal defect; blue indicates ductal tissue; green indicates the pulmonary blood flow.

(a) Collett and Edwards: Type I
Van Praagh: Type A1
Anderson: Common arterial trunk with aortic dominance, with pulmonary arteries arising from a confluent pulmonary segment
VSD, yes; PDA, no

(b) Collett and Edwards: Type II
Van Praagh: Type A2
Anderson: Common arterial trunk with aortic dominance, with pulmonary arteries arising separately from the posterior aspect of the intrapericardial common arterial trunk
VSD, yes; PDA, no

(c) Collett and Edwards: Type III
Van Praagh: Type A2
Anderson: Common arterial trunk with aortic dominance, with pulmonary arteries arising separately from opposite sides of the trunk
VSD, yes; PDA, no

(d) Collett and Edwards: Type IV
Van Praagh: Pulmonary atresia with major aortopulmonary collateral arteries
Anderson: Solitary arterial trunk with pulmonary arteries arising separately from the descending aorta (versus with multiple systemic-to-pulmonary collateral arteries)
VSD, yes; PDA, not usually

(*Continued*)

## Figure 28.2 (Continued)

(e) Collett and Edwards: not described
Van Praagh: Type A3
Anderson: Common arterial trunk with aortic dominance, with right pulmonary artery arising from the arterial trunk and left lung supply arising from a ductus or collateral vessel
VSD, yes; PDA, possibly (versus collateral)

(f) Collett and Edwards: not described
Van Praagh: Type A4
Anderson: Common arterial trunk with aortic dominance, with pulmonary arteries arising from a confluent pulmonary segment with an interrupted aortic arch or coarctation of the aorta
VSD, yes; PDA, yes

(g) Collett and Edwards: not described
Van Praagh: Type B2
Anderson: Common arterial trunk with intact ventricular septum and aortic dominance, with pulmonary arteries arising separately from the posterior aspect of the intrapericardial common arterial trunk
VSD, no; PDA, possibly

(h) Collett and Edwards: not described
Van Praagh: Type B4
Anderson: Common arterial trunk with intact ventricular septum and pulmonary dominance, with pulmonary arteries arising separately from the posterior aspect of the intrapericardial common arterial trunk
VSD, no; PDA, yes

(Adapted from Allen HD et al., eds. *Moss and Adams' Heart Disease in Infants, Children, and Adolescents*. 8th ed. Lippincott Williams and Wilkins; 2013:990–1002.[96])

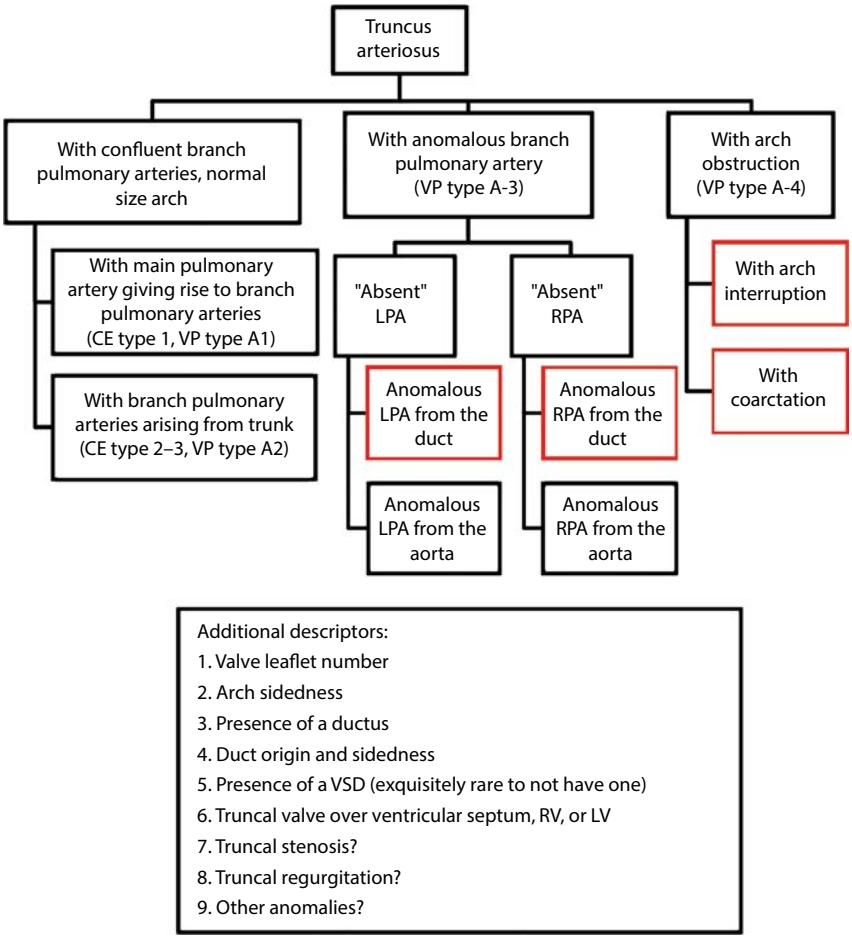


## Figure 28.3

Flow diagram delineating how to characterize truncus arteriosus lesions. Those outlined in red are ductal dependent for either branch pulmonary artery flow or flow to the lower systemic circulation. (CE, Collett and Edwards; LPA, left pulmonary artery; RPA, right pulmonary artery; VP, Van Praagh.)

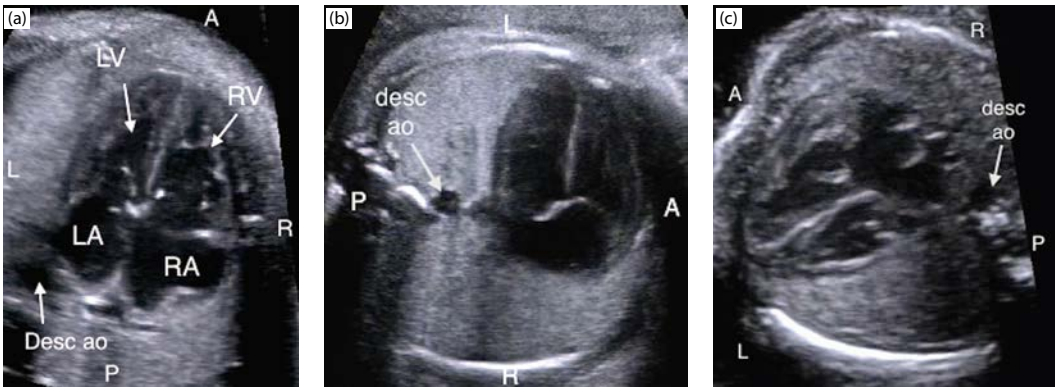


**Figure 28.4**
Two-dimensional imaging in the four-chamber views of fetuses with truncus arteriosus (a–c). In this view, the cardiac anatomy appears normal. Clues to an abnormality may be an abnormal cardiac axis (b,c), or the descending aorta to the right of spine (c). (A, anterior; Desc ao, descending aorta; L, left; LA, left atrium; LV, left ventricle; P, posterior; R, right; RA, right atrium; RV, right ventricle.)

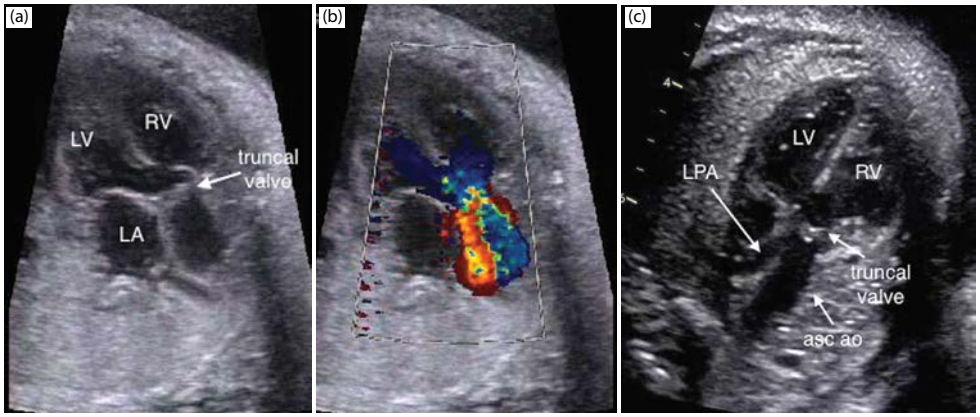


**Figure 28.5**
Fetuses with truncus arteriosus in the left ventricular outflow tract view. The truncal valve and artery override the ventricular septum and ventricular septal defect (a–c). The truncal valve appears thick and echobright (b,c). Color Doppler across the valve (a) shows aliasing of flow across the valve, and swirling of blood in the dilated truncal root. (asc ao, ascending aorta; LA, left atrium; LV, left ventricle; LPA, left pulmonary artery; RV, right ventricle.)

sweep to the outflow tracts (five-chamber view) will demonstrate only one semilunar valve sitting over a ventricular septal defect and leading to the TA (Figure 28.5a,b; Video 28.2). The VSD is generally juxta-arterial, lying immediately underneath the truncal valve. When the truncal valve lies mainly over the right ventricle, the VSD can be very small in diameter. Flow across the VSD will typically be bidirectional.

As the sweep proceeds more cephalad, one can distinguish one of the most critical parts of the fetal echocardiographic examination of TA—the origin of the pulmonary arteries. Remember, for all classification schemes, this feature defines the type of TA in question. Often for a fetus with Collett and Edwards types I or II, pulmonary artery origin is fairly straightforward (Figure 28.6a,b; Videos 28.3 and 28.4). However, for branch pulmonary arteries that arise separately (with one typically arising from either the ductus arteriosus or aorta), it can be difficult (Figure 28.7a–d; Video 28.5). One strategy that can be employed in this situation is to look for the distal branch PAs within the lung by color Doppler and then trace them back to their origin.

Sweeping more cephalad, one can see that the three-vessel view is distinctly abnormal with only two vessels present, the truncus and the superior vena cava. Finishing the sweep, the three-vessel and trachea view will typically be abnormal, as only one arch will be seen (Figures 28.6b; 28.7c,d; 28.8a–d). This vessel will typically be the aortic arch, as most patients with TA do not have a ductus arteriosus. The exceptions to this are when there is severe arch hypoplasia or arch interruption, as seen in type A-4 (Figure 28.8a–d; Video 28.6 through 28.8). With severe arch hypoplasia, there will be a hypoplastic arch and a ductus. With arch interruption, the only arch will be the ductus arteriosus. One can follow the ascending aorta as it arises from the TA and determine the arch sidedness by delineating on which side of the trachea the aorta crosses. This is an important point to note, as a conotruncal anomaly in the setting of a right aortic arch increases the risk of chromosome 22q11.2 deletion (DiGeorge) syndrome.

The truncal valve leaflets are commonly thickened and may show poor excursion (Figure 28.9a).[42] The degree of

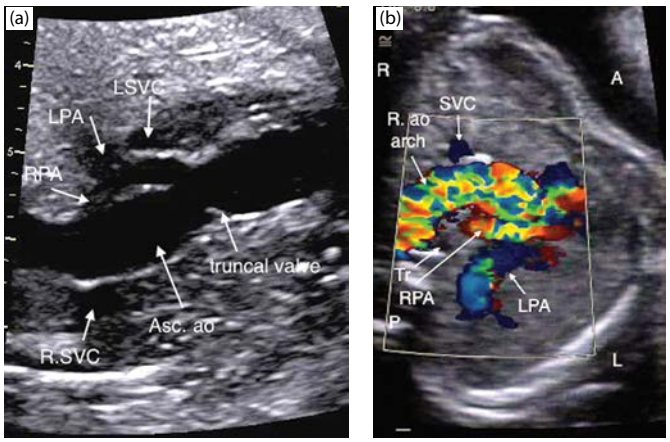


**Figure 28.6**
Collett and Edwards type I, Van Praagh type A-1 truncus arteriosus. In an oblique outflow tract view (a) and in the three-vessel and trachea view (b). The branch pulmonary arteries are seen bifurcating from the main pulmonary artery that arises from the truncal artery. In these examples, the aortic arch is right sided. Aliasing of color Doppler flow is noted in the aortic arch given more proximal truncal valve stenosis. (A, anterior; Asc ao, ascending aorta; L, left; LPA, left pulmonary artery; LSVC, left superior vena cava; P, posterior; R, right; R ao arch, right aortic arch; RPA, right pulmonary artery; RSVC, right superior vena cava; SVC, superior vena cava; Tr, trachea.)

stenosis and/or regurgitation present can be delineated by color and spectral Doppler examination (Figure 28.9b). The degree of truncal regurgitation is an important prognostic sign, so this should be very clearly defined. The morphology of the truncal valve can be difficult to distinguish in fetal life, although this is best evaluated from the *en face* view of the truncal valve (Figure 28.10; Video 28.9).

From the short-axis and arch views, the VSD can be seen in the ventricular short-axis view as one sweeps to the outflow tracts, helping to determine the size of the defect (Figure 28.11). The arch view can help determine if a fetal ductus arteriosus is present. If a ductus is present in TA (Figure 28.8c,d), it is essentially pathognomonic for an arch interruption, which would be a ductal-dependent lesion after birth and require prostaglandin infusion, unlike the majority of patients with TA.

Although not traditionally part of the fetal echocardiogram, the thymus can be easily visualized just cephalad of the three-vessel and trachea view. Absence or hypoplasia of the thymus on fetal ultrasound should strongly increase the suspicion for 22q11.2 deletion syndrome, with a reported sensitivity of 90% and specificity of 98.5%.[43]

## Differential diagnosis

TA can be easily confused with several other congenital heart lesions, including pulmonary atresia with ventricular septal defect (PA-VSD), tetralogy of Fallot (TOF), double-outlet right ventricle, and aortic atresia with ventricular septal defect.[3,44]

The hallmark anatomical features of TA are a single semilunar valve with a ventricular septal defect. These features are also present in patients with PA-VSD and aortic atresia with VSD. However, each of these lesions has specific echocardiographic characteristics that help distinguish among them, as Swanson and colleagues delineated.[3] In TA, the pulmonary arteries arise proximally to the first brachiocephalic vessel, and the flow in the pulmonary arteries is pulsatile.

In pulmonary atresia/VSD, the lungs are supplied by confluent pulmonary arteries supplied by a ductus arteriosus or aortopulmonary collateral artery, which generally arise distal to the first brachiocephalic vessel. Further, the flow in these vessels is generally continuous given that the collateral vessel or ductus arteriosus in these conditions is generally tortuous (Figure 28.12).

In aortic atresia/VSD, the aortic arch is supplied retrograde from the ductus arteriosus. In our experience, the best way to distinguish aortic atresia with VSD from truncus arteriosus is to sweep between the three-vessel view and three-vessel and trachea view with a medium Nyquist limit. In aortic atresia with VSD, one large vessel with prograde flow will be seen, which will be the ductal arch, and there will be a second very narrow vessel with retrograde flow, which will be the hypoplastic aortic arch. For fetuses with TA, there will be only a single arch seen, which will be normal size with prograde flow. For most cases, this will be the aortic arch since the ductus is typically absent. For TA with interrupted arch, only the ductus will be present.

Traisrisilp and coworkers found that the following abnormalities in the truncal root were significantly associated with a fetal diagnosis of TA: (1) a thickened, echogenic semilunar valve; (2) semilunar valve stenosis or regurgitation; and (3) an overall abnormal appearance of the semilunar valve.[45] Tetralogy of Fallot, double-outlet right ventricle, and aortopulmonary window are also included in the differential diagnosis of fetal TA but can both be correctly identified by the presence of a second semilunar valve.

## Genetics

When a fetal practitioner diagnoses truncus arteriosus, diagnosis and counseling about genetic disorders are crucial.

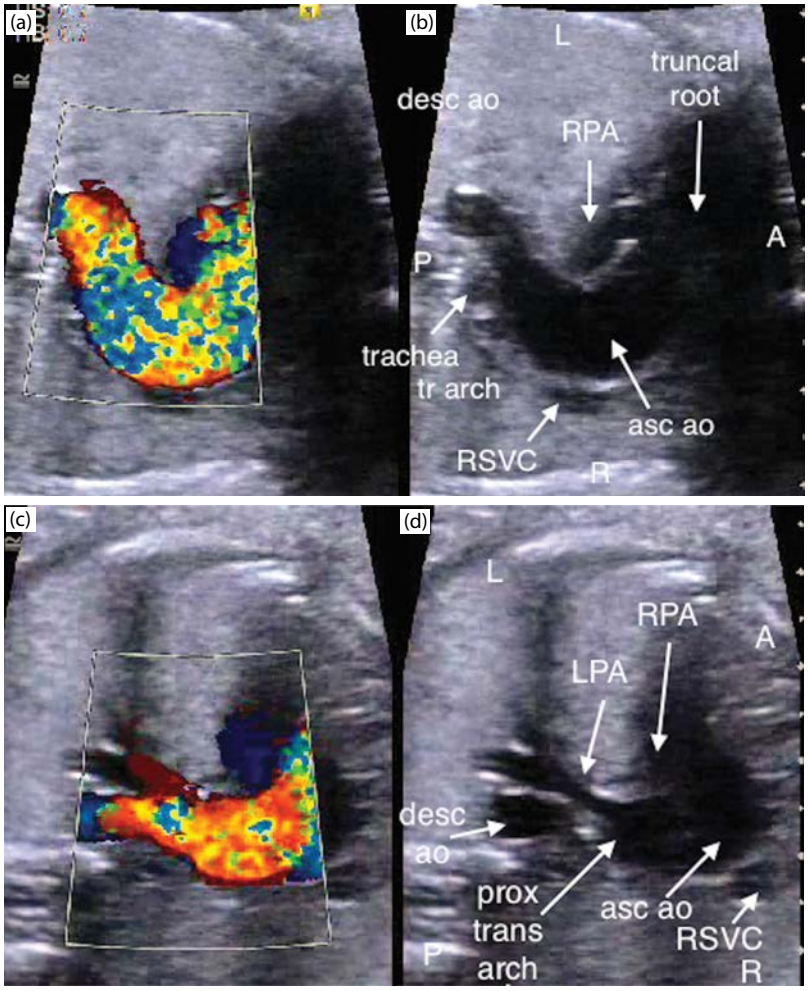


**Figure 28.7**
Van Praagh type A-3 truncus arteriosus with the right pulmonary artery (RPA) arising from the proximal truncal root, and the left pulmonary artery (LPA) arising from the transverse aortic arch in a patient with a left aortic arch. (a,b) Two-dimensional and color Doppler imaging just as the truncus arises from the cardiac mass, and the RPA is seen branching off before diving posteriorly to the ascending aorta. The arch is seen crossing left of the trachea. (c,d) A more cephalad and slightly oblique view. A small portion of the RPA is still seen near the truncal root, but now the LPA is more easily seen branching from the transverse arch and into the left lung field. (A, anterior; asc ao, ascending aorta; desc ao, descending aorta; L, left; LPA, left pulmonary artery; P, posterior; prox trans arch, proximal transverse arch; R, right; RPA, right pulmonary artery; RSVC, right superior vena cava; tr arch, transverse arch.)

Approximately 50% of patients with truncus arteriosus will have an identifiable genetic disorder, the most common of which is 22q11.2 deletion syndrome (DiGeorge syndrome).[46,47] Frequencies of 22q11.2 deletion syndrome by variation of TA are listed in Table 28.1. Other genetic conditions that have been associated with truncus arteriosus include trisomy 18, trisomies 13, 21, and 22; Turner syndrome; 14q deletion; VACTERL syndrome; CHARGE sequence; Alagille syndrome; GATA6 mutations; and chromosome 3q22.3 deletions.[4,48–54]

Given the very high risk of genetic abnormalities, all fetuses with TA should be offered genetic testing, including, at a minimum, evaluation for aneuploidy and 22q11.2 deletion. In prior years, a fluorescent *in situ* hybridization (FISH) study for 22q11.2 deletion was most commonly performed in conjunction with testing for aneuploidy. Recently, chromosomal microarray has been advocated for as a single more cost-effective test in lieu of FISH and/or karyotype given its ability to detect both aneuploidy and 22q11.2 deletions.[55] Other microdeletion or microduplication syndromes may also be discovered with a microarray. While cell-free DNA testing for autosomal aneuploidy is reasonably reliable, current evidence regarding performance for 22q11.2 deletion is based on scant data.[56] Therefore, cell-free DNA testing for 22q11.2 deletion is currently unsupported by sufficient clinical evidence. If the family declines prenatal genetic testing, this should be performed after birth to help identify risk for associated anomalies and developmental delays. If a 22q11.2 deletion is found in the fetus or neonate, given its autosomal dominant inheritance pattern, parents should also be evaluated for 22q11.2 deletion syndrome.

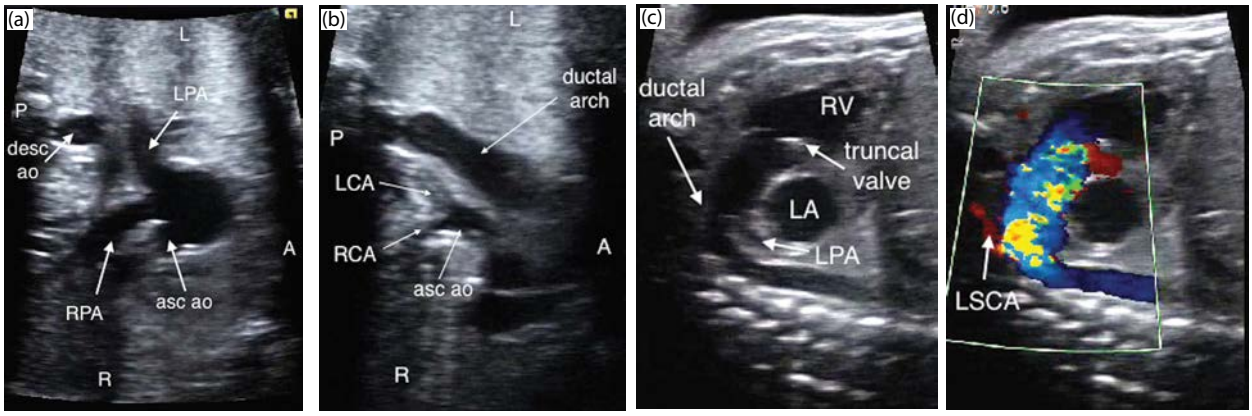


**Figure 28.8**
Van Praagh type A-4 truncus arteriosus with interrupted aortic arch and aberrant right subclavian artery from the descending aorta. (a) Two-dimensional view similar to a high right ventricular outflow tract view. The confluent branch pulmonary arteries are seen bifurcating from the truncal root, as is the hypoplastic ascending aorta. (b) A more cephalad view, similar to a three-vessel and trachea view, although slightly oblique coronally to optimize visualization of the bifurcation of the ascending aorta. The ductal arch is seen and appears normal. The hypoplastic ascending aorta is seen only bifurcating into the left and right carotid arteries, and no aortic arch is present. The aberrant right subclavian artery is not seen in these images. (c,d) A ductal arch view. The ductal arch appears similar to that of a normal fetal heart. However, the left subclavian artery (LSCA) is seen arising from the descending aorta with retrograde flow. (A, anterior; asc ao, ascending aorta; desc ao, descending aorta; L, left; LA, left atrium; LCA, left carotid artery; LPA, left pulmonary artery; LSCA, left subclavian artery; P, posterior; R, right; RCA, right carotid artery; RPA, right pulmonary artery; RV, right ventricle.)

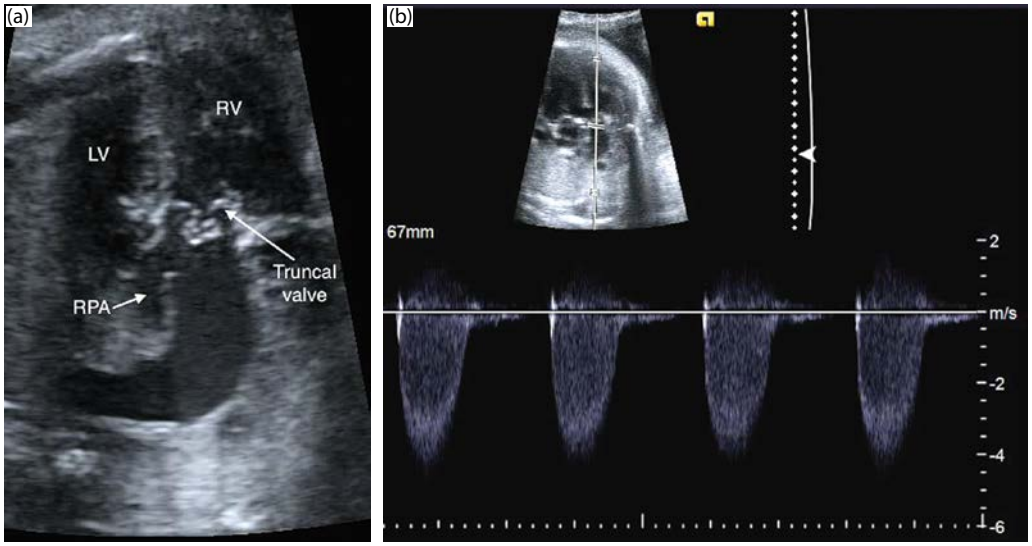


**Figure 28.9**
Truncal valve stenosis. (a) Two-dimensional image that demonstrates the thickened and rolled truncal valve leaflets. (b) A spectral Doppler image showing severe stenosis, with a peak velocity of nearly 4 m/s. (LV, left ventricle; RPA, right pulmonary artery; RV, right ventricle.)

## Prenatal diagnosis rates, impact, and outcomes

TA diagnosis in the fetus has been described since the mid-1980s.[67–69] However, since TA is primarily detected in the outflow tract views, which were not previously part of a standard obstetric screening examination, cases of prenatal diagnosis were previously described only primarily in small series.[4,70] The detection rate has increased over time, likely secondary to improved imaging techniques, and incorporation of outflow tracts view into prenatal screening.[3,71] Current estimates of the rate of prenatal diagnosis are approximately 30%–40%.[3,72] Some studies suggest that the presence of extracardiac anomalies increases the likelihood of prenatal detection of TA.[3] Prenatal diagnosis of TA has now been described even in the first trimester using transvaginal ultrasound.[73–75] The primary factor that seems to be associated with fetal death is severe truncal valve regurgitation.[3,4]

Studying the effect of prenatal diagnosis in TA on postnatal outcomes would be challenging. Most of the studies demonstrating a beneficial effect on early morbidity or mortality have been in lesions that are ductal dependent for

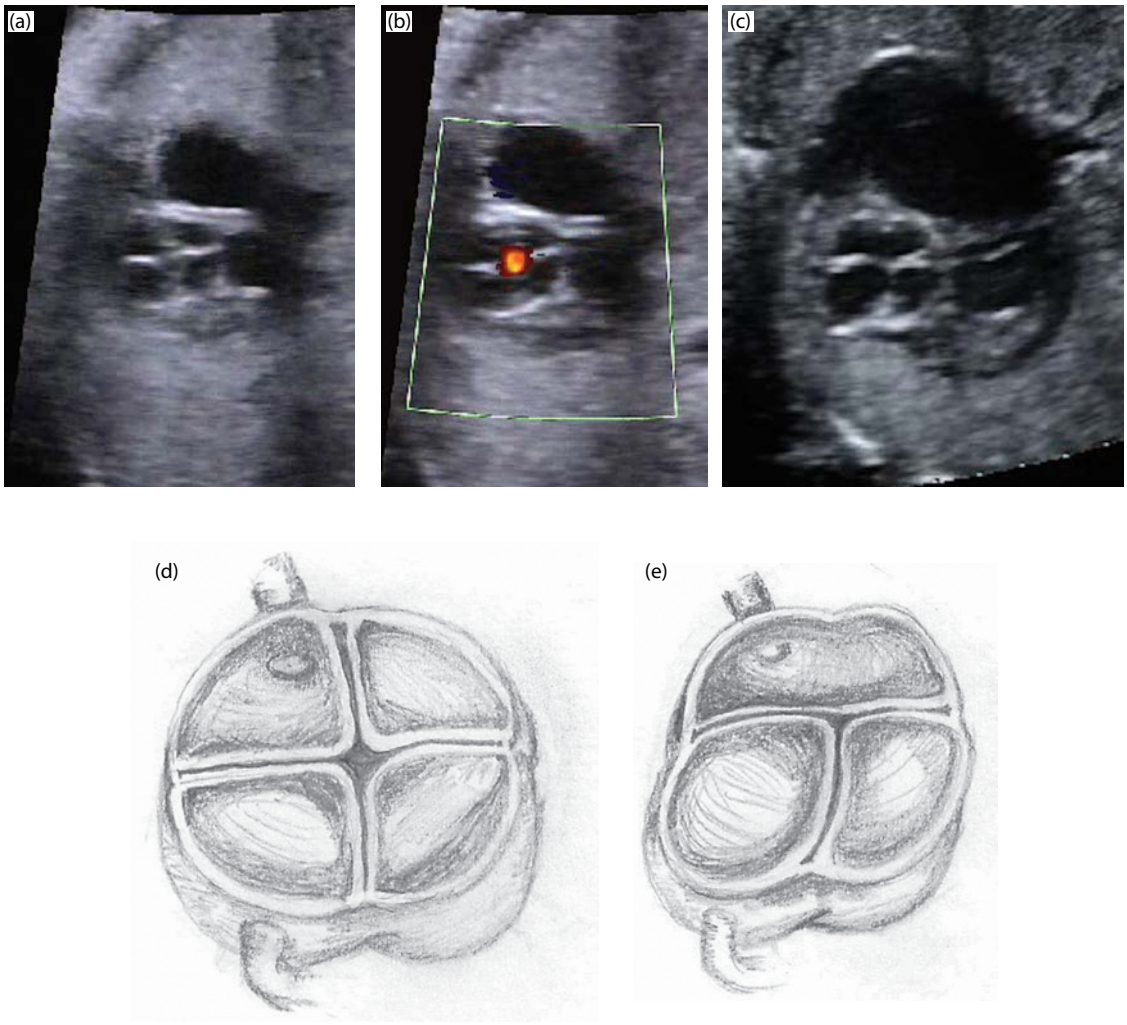


**Figure 28.10**
Varying truncal valve morphology. (a) Two-dimensional image of a quadricuspid truncal valve *en face*. (b) Image with color, showing a central area of valve regurgitation. (c) Two-dimensional image of another fetus with a tricuspid truncal valve. The leaflets are asymmetric. (d) Quadricuspid aortic valve as viewed from the ventricles. (e) The valve as viewed from the ventricles.

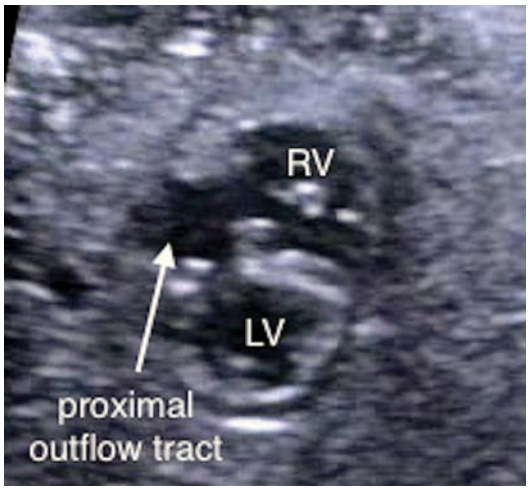


**Figure 28.11**
Short-axis view of the ventricles slightly tilted toward the truncal valve. The outflow tract overrides the ventricular septal defect.

systemic circulation or transposition of the great arteries.[76–78] The natural history of TA without intervention is congestive heart failure with cyanosis, which would usually be detected clinically before cardiac death.[79] However, prenatal diagnosis gives families the opportunity to learn about the condition, perform genetic testing, possibly undergo termination of pregnancy, and plan delivery at an experienced center.[80] Early diagnosis may also allow for earlier surgery and prevention of complications of untreated TA, including necrotizing enterocolitis.[3]

## Delivery, postnatal treatment, and outcomes

Given the potential for compromised circulation after birth, delivery of infants with prenatally diagnosed TA should occur at a center with a neonatologist and access to pediatric cardiology consultation.[80] If the delivery center is not a neonatal cardiac

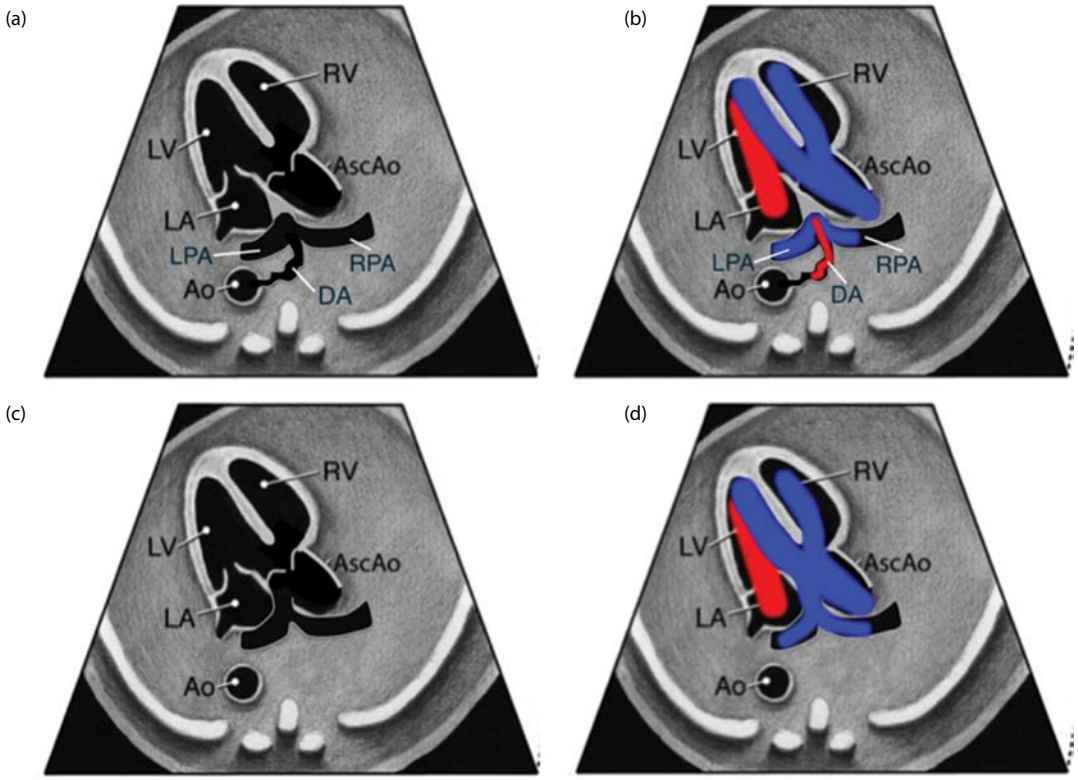


**Figure 28.12**
Truncus arteriosus (TA) from pulmonary atresia with ventricular septal defect (PA-VSD). (a,b) PA-VSD—how outflows look with subtle superior sweeping with and without color Doppler. A tortuous ductus arteriosus (DA) will typically originate from the descending aorta (may originate from the right subclavian artery or innominate artery with a right arch) and will feed the branch pulmonary arteries retrograde, via the main pulmonary artery stump. (c,d) TA—no ductus arteriosus is present, and the branch pulmonary arteries are fed prograde via the truncal root. (With permission from Morris SA et al. In: *Callen's Ultrasonography in Obstetrics and Gynecology*. 6th edn. Norton M, Scoutt L, Feldstein V, eds. Philadelphia, PA: Elsevier; 2016;[98] figures adapted with permission from American Institute of Ultrasound in Medicine: AIUM practice guideline for the performance of fetal echocardiography. *J Ultrasound Med* 2013;32:1067–82.[99])

surgical center, transfer should be arranged when surgery is anticipated, as surgery is typically performed prior to neonatal discharge.[81] If there is any suspicion for aortic arch obstruction or the origin of a pulmonary artery from the ductus arteriosus, prostaglandin infusion should be initiated shortly after birth.

After birth, an infant with TA will be cyanotic due to the compete mixing of systemic and pulmonary circulations. If there is significant arch obstruction (type A-4), the infant will develop cardiogenic shock if the ductus arteriosus closes. For all infants with TA, as the patient's pulmonary vascular resistance falls, saturations will rise, but the infant will quickly develop signs of heart failure due to pulmonary overcirculation. This heart failure can present as respiratory distress or difficulty feeding and gaining weight. If the infant has 22q11.2 deletion, severe hypocalcemia can present with seizure, arrhythmia, and tetany.

Initial medical therapy should be used to stabilize the patient until an early definitive surgical repair. Medical treatment can include diuretics and angiotensin-converting enzyme inhibition for heart failure symptoms, and ventilator support for lung disease associated with pulmonary overcirculation. Careful and close monitoring of feeding is recommended due to the high incidence of necrotizing enterocolitis in TA.[82] In the most ill infants, mechanical ventilator and inotropic support may be necessary prior to surgery. Calcium supplementation may be necessary in those patients with significant hypocalcemia.

In the contemporary era, surgical correction is generally done during the first month of life.[81] Survival at 1 year is very good at greater than 90% compared to approximately 15% for uncorrected patients.[83] Surgical correction is done via median sternotomy while under deep hypothermia and on cardiopulmonary bypass. The specific surgical procedure depends on the individual surgeon, but in general it involves the following steps: (1) excision of the ascending aorta and pulmonary arteries from the truncal root, (2) VSD patch closure through an infundibular incision, (3) anastomosis of the right ventricle to pulmonary artery conduit (RV to PA conduit) to the branch pulmonary arteries, (4) truncal valve repair, (5) anastomosis of the ascending aorta to the truncal root, (6) and anastomosis of the RV to PA conduit to the infundibular incision.[84]

A 2016 review of the Society of Thoracic Surgeons Congenital Heart Surgery Database showed an overall in-hospital mortality rate of 9.6%.[85] However, more complex cases of TA have higher mortality rates. A prior paper using the STS database showed concomitant repair of TA and

**Table 28.1** Rates of 22q11.2 deletion in TA by anatomic variation

| *Lesion* | *Percentage (%) with 22q11.2 deletion* |
|---|---|
| Truncus arteriosus | 30–41 |
| Type A-1 | 25–42 |
| Type A-2 | 17–33 |
| Type A-3 | 63–100 |
| Type A-4 | 25–50 |
| With right aortic arch | 57 |
| With tricuspid truncal valve | 38 |
| With other than tricuspid truncal valve | 35 |

*Source:* Goldmuntz E et al. Genetic aspects of congenital heart defects. In: Allen HD et al. eds. *Moss and Adams' Heart Disease in Infants, Children, and Adolescents*. 8th ed. Philadelphia, PA: Lippincott Williams and Wilkins; 2013:617–43;[57] Boudjemline Y et al., *J Pediatr* 2001;138(4):520–4;[58] Iserin L et al. *Eur J Pediatr* 1998;157(11):881–4;[59] Song MS et al. *Ultrasound Obstetr Gynecol* 2009;33(5):552–9;[60] Momma K et al. *Pediatr Cardiol* 1999;20(2):97–102;[61] Momma K. *Am J Cardiol* 2010;105(11):1617–24;[62] Frohn-Mulder IM et al. *Genet Couns* 1999;10(1):35–41;[63] Peyvandi S et al. *Pediatr Cardiol* 2013;34(7):1687–94;[64] O'Byrne ML et al. *J Thorac Cardiovasc Surg* 2014;148(4):1597–605;[65] McElhinney DB et al. *Pediatr Cardiol* 2003;24(6):569–73.[66]

interrupted aortic arch (IAA) had a mortality of 24%; concomitant truncal valve repair had a mortality of 23%; and TA repair with both IAA and truncal valve repair had a dismal mortality of 60%.[86] The presence of 22q11.2 deletion has not been associated with significantly higher surgical or hospital mortality in infants with TA but is associated with complex hospital courses.[65,87]

Long-term survival tends to be quite good, with one study from the University of California, San Francisco, reporting 90% survival at 5 years, 85% at 10 years, and 83% at 15 years.[88] However, fairly frequent reintervention is almost the rule, as the RV-to-PA conduit becomes stenotic as the patient outgrows it and it becomes calcified. Studies have estimated the mean time to reoperation to be 5.5–5.8 years.[88,89] In a 2016 paper from Texas Children's Hospital, Mery and colleagues in a large single-center study found freedom from first surgical or transcatheter reintervention at 5, 10, and 15 years was 73%, 45%, and 23%, respectively.[90] Reoperation on the truncal valve is also a long-term concern, but the data are mixed. One American study cited freedom from reoperation of 70% at 5 years and 50% at 7 years, while a French study found 82% freedom from reoperation at 10 years and 63% at 18 years.[91,92] Aortic root dilation is common in patients with TA, but studies have not found an increased risk of dissection.[93,94] Children with TA are at risk for neurodevelopmental delay and should be referred to a specialist for assessment and follow-up.[95]

## Acknowledgments

Thank you to Maggie Nguyen, RDCS, and Lacey Schoppe, RDCS, for their consistently exceptional work in fetal imaging resulting in the large majority of images included in this chapter, and thank you to Maggie Nguyen for assistance with creating the videos.

## Videos

**Video 28.1** (https://youtu.be/LMRCbdnQxLc)
Two-dimensional video in the four-chamber view of a fetus with truncus arteriosus. In this view, the cardiac anatomy appears normal.

**Video 28.2** (https://youtu.be/haBigH3dv-w)
Two-dimensional video of a sweep from the inferior/posterior four-chamber view cephalad to the outflow tracts, in a fetus with truncus arteriosus. The truncal artery overrides the ventricular septum and the large ventricular septal defect, although at the end of the sweep the truncus appears to arise more from the right ventricle. The truncal valve leaflets are thickened, and the left pulmonary artery and ascending aorta are visible arising from the truncal artery. The right pulmonary artery is not easily seen in this video. Of note, the fetus also has a large atrial septal defect and a left superior vena cave to a dilated left coronary sinus.

**Video 28.3** (https://youtu.be/-6EwaTpk3V0)
Collett and Edwards type I, Van Praagh type A-1 truncus arteriosus with right aortic arch and bilateral superior vena cava, two-dimensional sweep.

**Video 28.4** (https://youtu.be/Obd0NZ2aqUQ)
Collett and Edwards type I, Van Praagh type A-1 truncus arteriosus with right aortic arch and bilateral superior vena cava, color Doppler sweep.

**Video 28.5** (https://youtu.be/uCRrRM6Ises)
Van Praagh type A-3 truncus arteriosus with the right pulmonary artery (RPA) arising from the proximal truncal root, and the left pulmonary artery (LPA) arising from the transverse aortic arch in patient with a left aortic arch, sweeps in color Doppler and two-dimensional view. The truncus arises from the cardiac mass, and the RPA is seen branching off before diving posteriorly to the ascending aorta. The arch is seen crossing left of the trachea. A more cephalad

sweep shows the LPA branching from the transverse arch and into the left lung field.

**Video 28.6–28.8** (https://youtu.be/dRtl-D5vi3Q; https://youtu.be/lIZLAmvRtdM; https://youtu.be/BGCIQAsIwIg)
Van Praagh type A-4 truncus arteriosus with interrupted aortic arch and aberrant right subclavian artery from the descending aorta. Confluent branch pulmonary arteries are seen bifurcating from the truncal root, as is the hypoplastic ascending aorta. The ascending aorta bifurcated into the right and left carotid arteries, and the transverse aortic arch is interrupted (absent). The ductal arch is seen and appears normal. The aberrant right subclavian artery is seen originating from the descending aorta inferior to the ductal insertion, coursing rightward. The color sweep shows aliasing across the truncal valve in systole and mild to moderate truncal regurgitation.

**Video 28.9** (https://youtu.be/tV3__mm0WKI)
*En face* view of a quadricuspid truncal valve.

# References


1. Anderson RH, Thiene G. *Eur J Cardiothorac Surg* 1989;3(6):481–7.
2. Hoffman JI. *Pediatr Cardiol* 1995;16(4):155–65.
3. Swanson TM et al. *Pediatr Cardiol* 2009;30(3):256–61.
4. Volpe P et al. *Heart* 2003;89(12):1437–41.
5. Egbe A et al. *Pediatr Cardiol* 2014;35(7):1232–8.
6. Hoffman JIE, Kaplan S. *JACC* 2002;39(12):1890–900.
7. Reller MD et al. *J Pediatr* 2008;153(6):807–13.
8. Calder L et al. *Am Heart J* 1976;92(1):23–38.
9. Pradat P et al. *Pediatr Cardiol* 2003;24(3):195–221.
10. Kelly RG et al. *Dev Cell* 2001;1(3):435–40.
11. Waldo KL et al. 2001;128(16):3179–88.
12. Mjaatvedt CH et al. *Dev Biol* 2001;238(1):97–109.
13. Srivastava D, Baldwin HS. Molecular determinants of cardiac development and disease. In: Allen HD, Driscoll DJ, Shaddy RE, Feltes TF, eds. *Moss and Adams' Heart Disease in Infants, Children, and Adolescents*. 8th ed. Philadelphia, PA: Lippincott Williams and Wilkins; 2013:560–76.
14. Jia Q et al. *Dev Biol* 2007;311(1):172–84.
15. Ta-Shma A et al. *J Med Genet* 2014;51(4):268–70.
16. Baardman ME et al. *Dis Model Mech* 2016;9(4):413–25.
17. Ma MC et al. *Dev Biol* 2016;409(1):272–6.
18. Lisowski LA et al. *Herz [Internet]* 2010;35(1):19–26. Available from: http://link.springer.com.ezproxyhost.library.tmc.edu/article/10.1007/s00059-010-3244-3.
19. Seagraves NJ, McBride KL. *Mol Genet Metab* 2012;107(4):650–8.
20. Alverson CJ et al. *Pediatrics* 2011;127(3):e647–53.
21. Lammer EJ et al. *N Engl J Med* 1985;313(14):837–41.
22. Tanner JP et al. *Environ Res* 2015;142:345–53.
23. Csaky-Szunyogh M et al. *Am J Med Genet* 2013;161A(10):2444–52.
24. Scanlon KS et al. *Epidemiology* 1998;9(1):95–8.
25. Shaw GM et al. *Am J Med Genet* 1995;59(4):536–45.
26. Werler MM et al. *Am J Epidemiol* 1999;150(7):675–82.
27. Collett RW, Edwards JE. *Surg Clin North Am* 1949;29(4):1245–70.
28. Van Praagh R, Van Praagh S. *Am J Cardiol* 1965;16(3):406–25.
29. Butto F et al. *Pediatr Cardiol* 1986;7(2):95–101.
30. Konstantinov IE et al. *Ann Thorac Surg* 2006;81(1):214–22.
31. Bharati S et al. *J Thorac Cardiovasc Surg* 1974;67(4):501–10.
32. Mair DD et al. *Circulation* 1974;49(1):144–51.
33. Imai K et al. *Pediatr Cardiol* 2013;34(8):2024–6.
34. Huang S-C et al. *Cardiology* 2008;111(1):16–20.
35. Bhan A et al. *Pediatr Cardiol* 2006;27(3):378–80.
36. Tonni G et al. *Arch Gynecol Obstet* 2010;281(2):255–9.
37. Marino B et al. *Am J Med Genet* 1997;72(1):40–2.
38. Chintala K et al. *Prenat Diagn* 2007;27(6):560–2.
39. Peterson RE, Haynes SE. *Echocardiography* 2016;33(6):939–42.
40. Fuglestad SJ et al. *Am J Cardiovasc Pathol* 1988;2(1):39–47.
41. Marcelletti C et al. *Circulation* 1977;55(4):636–41.
42. Freire G et al. *Cardiol Young* 2012;22(6):671–6.
43. Chaoui R et al. *Ultrasound Obstet Gynecol* 2002;20(6):546–52.
44. Gómez O et al. *Fetal Diagn Ther* 2016;39(2):90–9.
45. Traisrisilp K et al. *Ultrasound Obstet Gynecol* 2015;46(5):564–70.
46. Long J et al. *Birth Defects Res A Clin Mol Teratol* 2010;88(11):971–9.
47. Goldmuntz E et al. *J Am Coll Cardiol* 1998;32(2):492–8.
48. Moore JW et al. *Pediatr Cardiol* 1994;15(3):154–6.
49. Francalanci P et al. *Am J Cardiol* 1997;79(2):245–7.
50. Oehl-Jaschkowitz B et al. *Am J Med Genet* 2013;164(3):620–6.
51. Gong M et al. *Horm Res Paediatr* 2013;79(4):250–6.
52. Rea G et al. *Eur J Med Genet* 2010;53(3):162–7.
53. Patel A et al. *Ann Thorac Surg* 2016;102:1607–14.
54. Galindo A et al. *Eur J Obstet Gynecol Reprod Biol* 2009;146(1):55–60.
55. Geddes GC et al. *Pediatr Cardiol* 2015;36(3):531–6.
56. Yaron Y et al. *Obstet Gynecol* 2015;126(5):1095–9.
57. Goldmuntz E et al. Genetic aspects of congenital heart defects. In: Allen HD, Driscoll DJ, Shaddy RE, Feltes TF, eds. *Moss and Adams' Heart Disease in Infants, Children, and Adolescents*. 8th ed. Philadelphia, PA: Lippincott Williams and Wilkins; 2013:617–43.
58. Boudjemline Y et al. *J Pediatr* 2001;138(4):520–4.
59. Iserin L et al. *Eur J Pediatr* 1998;157(11):881–4.
60. Song MS et al. *Ultrasound Obstetr Gynecol* 2009;33(5):552–9.
61. Momma K et al. *Pediatr Cardiol* 1999;20(2):97–102.
62. Momma K. *Am J Cardiol* 2010;105(11):1617–24.
63. Frohn-Mulder IM et al. *Genet Couns* 1999;10(1):35–41.
64. Peyvandi S et al. *Pediatr Cardiol* 2013;34(7):1687–94.
65. O'Byrne ML et al. *J Thorac Cardiovasc Surg* 2014;148(4):1597–605.
66. McElhinney DB et al. *Pediatr Cardiol* 2003;24(6):569–73.
67. Allan LD et al. *Am J Cardiol* 1986;58(3):334–7.
68. de Araujo LM et al. *Pediatr Cardiol* 1987;8(4):261–3.
69. Marasini M et al. *Eur Heart J* 1987;8(8):921–4.
70. Duke C et al. *Am J Cardiol* 2001;88(12):1379–84.
71. Carvalho JS et al. *Heart* 2002;88(4):387–91.
72. Quartermain MD et al. *Pediatrics* 2015;136(2):e378–85.
73. AboEllail MAM et al. *Ultrasound Obstet Gynecol* 2015;45(6):759–60.
74. Turan S et al. *Ultrasound Obstet Gynecol* 2014;44(5):562–7.
75. Achiron R et al. *Obstet Gynecol* 1994;84(1):69–72.
76. Tworetzky W et al. *Circulation* 2001;103(9):1269–73.
77. Morris SA et al. *Circulation* 2014;129(3):285–92.
78. Bonnet D et al. *Circulation* 1999;99(7):916–8.
79. Marcelletti C et al. *Circulation* 1976;54(1):108–11.
80. Donofrio MT et al. *Circulation* 2014;129(21):2183–242.
81. Williams JM et al. *JACC* 1999;34(2):545–53.
82. McElhinney DB et al. *Pediatrics* 2000;106(5):1080–7.
83. Thompson LD et al. *ATS* 2001;72(2):391–5.

84. Jonas RA. Truncus arteriosus. In: *Comprehensive Surgical Management of Congenital Heart Disease*. 2nd ed. London, England: Boca Raton, FL: CRC Press; 2014:571–84.
85. Jacobs JP et al. *Ann Thorac Surg* 2016;101(3):850–62.
86. Russell HM et al. *ATS* 2012;93(1):164–9, discussion 169.
87. McDonald R et al. *Pediatr Cardiol* 2013;34(2):341–7.
88. Rajasinghe HA et al. *J Thorac Cardiovasc Surg* 1997;113(5):869–78, discussion 878–9.
89. Tlaskal T et al. *Eur J Cardiothorac Surg* 2010;37(6):1278–84.
90. Mery CM et al. *J Thorac Cardiovasc Surg* 2016;151(2):432–441.e2.
91. Kaza AK et al. *Ann Thorac Surg* 2010;90(4):1307–12, discussion 1312.
92. Henaine R et al. *Ann Thorac Surg* 2008;85(1):172–8.
93. Carlo WF et al. *Congenit Heart Dis* 2011;6(3):228–33.
94. Frischhertz BP et al. *Int J Cardiol* 2015;184:521–7.
95. Marino BS et al. *Circulation* 2012;126(9):1143–72.
96. Allen HD et al. eds. *Moss and Adams' Heart Disease in Infants, Children, and Adolescents*. 8th ed. Lippincott Williams and Wilkins; 2013:990–1002.
97. Ezon D et al. *Atlas of Congenital Heart Disease Nomenclature*. Lexington, Ky: Ezon Educational Services, 2015.
98. Morris SA et al. In: *Callen's Ultrasonography in Obstetrics and Gynecology*. 6th edn. Norton M, Scoutt L, Feldstein V, eds. Philadelphia, PA: Elsevier; 2016.
99. AIUM practice guideline for the performance of fetal echocardiography. *J Ultrasound Med* 2013;32:1067–82.

# 29

# Transposition of the great arteries

Silvia G.V. Alvarez and Lisa K. Hornberger

## Introduction

Transposition of the great arteries (TGA) describes cardiac pathology in which the aorta arises from the morphological right ventricle and the main pulmonary artery (MPA) from the morphological left ventricle, also known as ventriculo-arterial (VA) discordance. This pathology was first described in 1797 by Matthew Baillie; however, the term *TGA* was coined by John Farre in 1814.[1,2] TGA is most frequently associated with normal atrioventricular (AV) connections (or D-ventricular looping with a morphological right ventricle rightward and anterior and morphological left ventricle leftward and posterior) or AV concordance, a lesion also referred to as D-TGA or complete TGA (Figure 29.1). Far less commonly, there may be concomitant AV and VA discordance, in which the ventricles are inverted (or L-looped) and the great arteries again arise from the incorrect ventricle: aorta from the left-sided morphological right ventricle and MPA from the right-sided morphological left ventricle (Figure 29.1). The latter, first described by Karl von Ritansky in 1875,[3] is also referred to as L-TGA or physiologically and congenitally corrected TGA: as the pulmonary venous flow is ejected through the aorta to the body and the systemic venous flow through the pulmonary artery to the lungs. Defining the AV connection and the VA connection is crucial to determine the pathophysiology and clinical manifestations of the patient postnatally. These two entities have entirely different pathophysiology; therefore, they are approached separately in this chapter.

## Dextro-transposition of the great arteries

Dextro-transposition of the great arteries (D-TGA) is the most common cyanotic congenital heart disease (CHD) with presentation in the first week of life, often within the first few hours after birth. Associated cardiac lesions may influence the prognosis; however, overall mortality of patients left untreated is 28.7% in 1 week, 51.6% by 1 month, and 89.3% by 1 year of age.[4]

### *Morphological definition and embryology*

The great artery arrangement in D-TGA is usually that of an anterior and rightward aorta with a well-developed subaortic conus, and a posterior and leftward pulmonary artery with fibrous continuity between the pulmonary and mitral valve. A series with 119 patients reported this as the most common arrangement occurring in 88.2% of their patients.[5] However, in 6.2%, they found the presence of bilateral subarterial conus, in 3.4% a subpulmonary conus with an absent or very deficient subaortic conus, and in 1.7% the subarterial conus was bilaterally absent. These differences in the conus anatomy may influence the relationship between the great arteries; however, it is still the VA discordance that defines this pathological and pathophysiological entity.

The embryogenesis of D-TGA is still not fully understood. In normal hearts, the VA connections are formed by the fusion of the muscularized proximal outflow cushions to the primary muscular ventricular septum with the elliptical outflow tract in a position superior to the AV canal. As the fetal heart develops, the angle between the left ventricle and the outflow tract progressively increases as the outflow cushions spiral in a counterclockwise direction downstream, and the pulmonary trunk spirals around the aorta as it exits from the right ventricle.[6,7] It has been theorized that in order to form the proper VA connections, this remodeling requires adequate timing and degree of rotation as well as appropriate shortening of the left outflow tract.[7,8]

Animal studies have explored the pathogenesis of TGA. Costell et al.[9] found the disruption of outflow tract mesenchyme cells results in formation of a straight outlet septum rather than a spiraling septum. The absence of a spiraling septum would then prevent the connection between left ventricle and aorta and the right ventricle and pulmonary trunk. Yasui et al.[10] demonstrated that murine fetuses treated with retinoic acid developed hypoplasia of conal swellings. They suggested the lack of well-developed proximal endocardial ridges in the outflow tract was the primary event leading to TGA by preventing the proximal rotation of the aortic and pulmonary orifices.

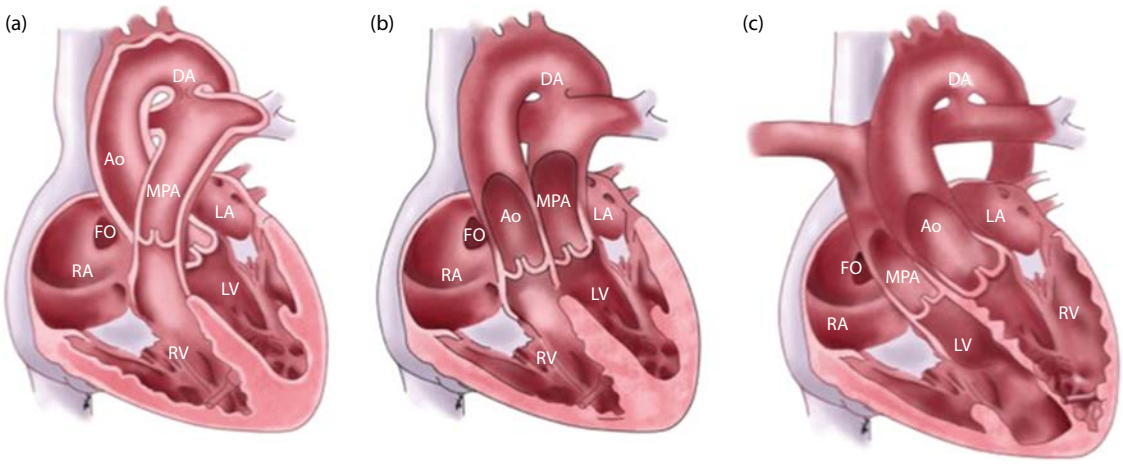


**Figure 29.1**
(a) A normal heart, demonstrating normal atrial situs, normal ventricular (D) looping and normally related great arteries, in other words, atrioventricular concordance and ventriculo-arterial concordance. (b) A D-TGA, demonstrating atrioventricular concordance (normal atrial situs and D-ventricular looping) and ventriculo-arterial discordance. (c) L-TGA, demonstrating atrioventricular (situs solitus, L-ventricular looping) and ventriculo-arterial discordance. (Ao, aorta; DA, ductus arteriosus; FO, foramen ovale; LA, left atrium; LV, left ventricle; MPA, main pulmonary artery; RA, right atrium; RV, right ventricle.)

## Epidemiology and genetics

The prevalence of TGA has been reported to be 4 in 10,000 live births, accounting for about 5% of all CHD,[11,12] with an increased incidence in boys (male/female ratio of 2.1:1[12]).

Its etiology is still unknown, and it is not associated with the most common chromosomal abnormalities.[13,14] Maternal factors such as pregestational diabetes[15] and maternal alcohol consumption[16] have been investigated and suggested to be causal in some. Although most cases of TGA with D- or L-looped ventricles are sporadic and less likely to have genetic origin, a large prospective study suggests some forms of TGA may have a multigenetic origin, likely with contribution of multiple pathogenic mechanisms.[17] A subsequent study demonstrated an association of mutation in laterality genes and some cases of familial TGA.[18]

## Associated cardiac malformations

D-TGAs can be classified as simple or complex based on the associated cardiac malformations. Morphological variants may have an impact on the transitional circulation, the neonatal physiology, and outcome, and consequently, requiring unique clinical and surgical management. Simple D-TGA defined as D-TGA in which the ventricular septum is intact or in which there are hemodynamically insignificant VSDs, accounts for 50%–70% of the patients.[4,19] Complex D-TGA includes those forms with one or more additional cardiac abnormalities: moderate or large ventricular septal defects, left or right outflow tract obstruction, aortic arch obstruction, and AV valve pathology such as overriding, straddling, stenosis, or atresia with hypoplasia of one of the ventricles.

A hemodynamically significant muscular or perimembranous ventricular septal defect (VSD) is reported in up to 20%–30% of the patients.[4,19] LV outflow tract obstruction is observed in 25%–30% of patients with VSD,[4] accounting for almost 10% of all D-TGAs. LV outflow tract obstruction may include valvar stenosis or subvalvar pathology from posteriorly malaligned conal, infundibular, or outlet septum; AV valve tissue, including clefts in the mitral valve; or mobile aneurysm of membranous septum that may be associated with a perimembranous VSD. Where there is subpulmonary stenosis due to posteriorly deviated outlet septum, the ventricular septal defect frequently relates more so to the aorta. RV or aortic outflow tract obstruction is uncommon in simple D-TGA. It is most often caused by anterior malalignment of outlet septum and often associated with aortic arch hypoplasia and coarctation of the aorta, occurring in less than 5% of D-TGA cases.[1,16] The VSD often found in association with aortic coarctation in D-TGA and anteriorly maligned outlet septum is typically subpulmonary. In more complex D-TGA, there may be straddling of the AV valves. The mitral valve most often straddles outlet VSDs, whereas the tricuspid valve straddles inlet VSDs. Mitral and tricuspid stenosis or atresia with a large VSD and hypoplastic left and right ventricle, respectively, are rare forms, each occurring in approximately 5% of the patients with D-TGA. Single-ventricle anatomy has been reported in 3.9% and AV septal defect in less than 2% of D-TGA.[4]

## Associated extracardiac malformations

D-TGA is not commonly associated with extracardiac anomalies. Extracardiac pathology has been reported in 16%–26% of cases in two large fetal series and a necropsy series.[13,20,21] Interestingly, the Baltimore-Washington Infant Study[22] reported a lower incidence of 7.8%, which could relate to biases

associated with referral indications and presentation between fetal, necropsy, and postnatal series.

## Pathophysiology and postnatal course

In D-TGA, systemic venous blood courses from the right atrium into the right ventricle to the aorta, therefore, being ejected back into the systemic circulation. The pulmonary venous blood courses from the left atrium into the left ventricle to the pulmonary artery, therefore, being ejected back into the pulmonary circulation in a parallel manner. While the pathophysiology of D-TGA is well tolerated prenatally due to the shunts at atrial and ductal levels,[23] with this parallel arrangement between the systemic and pulmonary circulation, after birth it can be lethal if there is an inadequate site of mixing of systemic and pulmonary venous blood, most importantly, an atrial shunt. The aforementioned associated cardiac abnormalities, VSDs, left and/or right outflow obstruction, and AV valve pathology,[24] contribute to the clinical presentation and have an impact on the management and outcomes of affected neonates.

### Simple D-TGA

In patients with D-TGA and intact ventricular septum, after delivery, while the pulmonary vascular resistance is still high, there is bidirectional flow across the ductus arteriosus. In systole, the shunt is from the MPA to aorta, and in diastole from the aorta to MPA. As the pulmonary resistance decreases, the shunting across the ductus arteriosus becomes predominantly from the AO to the MPA. The increased blood flow to the lungs increases pulmonary venous return resulting in increased left atrial pressure, which forces oxygenated blood through the atrial level communication into the right atrium, delivering oxygenated blood to the right ventricle and ultimately to the body. For a balanced neonatal circulation prior to surgery, the presence of an unrestrictive atrial shunt and decrease in pulmonary vascular resistance with or without a ductus arteriosus are necessary. The presence of a restrictive atrial-level communication and/or significant pulmonary hypertension will lead to severe hypoxemia, particularly preductal, causing a metabolic acidosis and poor outcome.[25,26]

Increased $PaO_2$ of the blood ejected into the lungs from the left ventricle is believed to be the primary cause of atrial septal defect restriction before birth in D-TGA as originally proposed by Rudolph et al.[27] and later reconsidered in a series of prenatally diagnosed D-TGA by Maeno et al.[25] Minimal increases in $PaO_2$ as might be expected from normal ductus venosus streaming into the left ventricle can cause a reduction in pulmonary vascular resistance in the fetus. Increased pulmonary blood flow leading to increased pulmonary venous return, again, potentially increases the left atrial pressure resulting in a reduction in normal right-to-left shunting through the foramen ovale and closer approximation of septum primum to septum secundum on the left atrial side. In keeping with changes in pulmonary vascular resistances and blood flow due to the unique pathophysiology of D-TGA, the ductus arteriosus diameter has been shown to be relatively small in fetuses with D-TGA compared to normal fetuses.[25] Rarely, there may be frank ductus arteriosus constriction, which has been proposed to be secondary to the altered pulmonary vascular bed with less flow traversing the ductus arteriosus, and may even be a direct consequence of increased $PaO_2$.[25] Ductus arteriosus constriction *in utero* is associated with persistent high pulmonary pressures after birth,[28] and this may impede the effective intercirculatory shunting at ductal and atrial levels necessary for hemodynamic stability of these patients.[23,26,29] Balloon atrial septostomy performed within minutes to hours after delivery to enlarge the atrial-level communication is life-saving for many affected infants.[29–32] Thus, delivery in a tertiary care center that has the capability of such an intervention is critical, as it provides an opportunity for planned perinatal management where personnel are able to perform an atrial septostomy on site. The presence of ductal constriction has also been suggested as an indication for an exit procedure given the severe compromise of affected neonates.[25]

Prenatal detection has been known to improve morbidity and mortality[33]; however, until recently, D-TGA has remained one of the less frequently detected forms of congenital heart disease before birth.[34–37] This is likely due to the fact that it is typically associated with a normal four-chamber view, it is usually an isolated abnormality, and it is typically observed in healthy women.[38] Only with the integration of outflow tract and great artery assessments at routine obstetrical ultrasound[39] have detection rates for D-TGA substantially improved from less than 30% in most reports to the majority in more recent years.[38,40]

### Complex D-TGA

The presence of associated cardiac pathology in D-TGA impacts the presentation and ultimate course of an affected baby. A significant ventricular-level shunt may offer a site of mixing of systemic and pulmonary venous blood resulting in less need for urgent balloon atrial septostomy.[41] Left ventricular or pulmonary outflow obstruction will impact the degree of cyanosis of an affected baby and dictate the timing and type of surgical intervention.[42] Critical left ventricular outflow obstruction requires use of prostaglandins in the neonatal period until surgical intervention.[43] D-TGA with right ventricular outflow obstruction and aortic arch hypoplasia and coarctation of the aorta may present with cyanosis and heart failure, as the outflow tract and arch obstruction drives flow through the ventricular septal defect increasing blood flow to the lungs.[44]

## Postnatal management and surgical options

All patients diagnosed prenatally should have prostaglandins commenced soon after delivery until their stability is assured. Once a transthoracic echocardiogram is performed and the associated lesions are confirmed, including the coronary

artery anatomy, surgical plans can be made. Patients with simple D-TGA, in most centers around the world, have an arterial switch operation with the Lecompte maneuver in the first week of life. In the presence of a moderate or large atrial septal defect or moderate-large VSD, the prostaglandins can often be discontinued assuming the $PaO_2$ is acceptable and the neonate not acidotic. With a larger VSD that is not likely to become restricted, particularly when there is more complex cardiac pathology, repair may be postponed for a few weeks assuming there is adequate intracardiac mixing.[41,42]

Patients with a VSD and subvalvar pulmonary stenosis require prostaglandin therapy only if the obstruction is critical, and then, either definitive repair or a systemic to pulmonary shunt may be performed. If the obstruction is mild, an arterial switch may still be possible; however, if the LV outflow tract obstruction is more significant, assuming there is adequate atrial mixing and a ventricular septal defect, surgical intervention may be postponed for weeks or months. The eventual corrective surgery may include a Rastelli procedure with baffling of the left ventricle to the aorta or a Nikaidoh operation with translocation of the aortic root into the posterior and leftward pulmonary position, both requiring placement of a right ventricle to pulmonary artery conduit.[43,45] The surgical technique varies depending on the degree of obstruction, size of the VSD, and abnormalities of the AV valves.[42] Long-term outcomes include need for reintervention to replace the pulmonary conduit, and, in some, particularly those following a Rastelli procedure, need to alleviate subaortic obstruction. Straddling or significant stenosis of one of the AV valves in D-TGA may preclude a biventricular repair.[43,45]

## *Prenatal diagnosis of D-TGA*

D-TGA is typically associated with situs solitus of the viscera and atria, levocardia, and a normal four-chamber view. These characteristics make D-TGA a challenge to detect on routine fetal ultrasound. Detection rates vary widely between centers.[34–37,40] The key to the diagnosis lies in the evaluation of the outflow tracts and the upper mediastinal views (three-vessel view and three-vessel and trachea view). Sagittal views may also aid in confirming the diagnosis and in the exclusion of coarctation of the aorta, abnormalities of the AV valves and abnormal systemic venous return. Most of the associated cardiac abnormalities with the exception of coronary anomalies can be identified prenatally.

### Systemic and pulmonary venous connections

D-TGA is usually associated with both normal systemic and pulmonary venous connections, which can be identified from both four-chamber and sagittal sweeps.

### Four-chamber view

The majority of fetuses with D-TGA have a normal cardiac size, axis, and four-chamber view (Figure 29.2), with symmetry of the four chambers, normal A-V connections, and

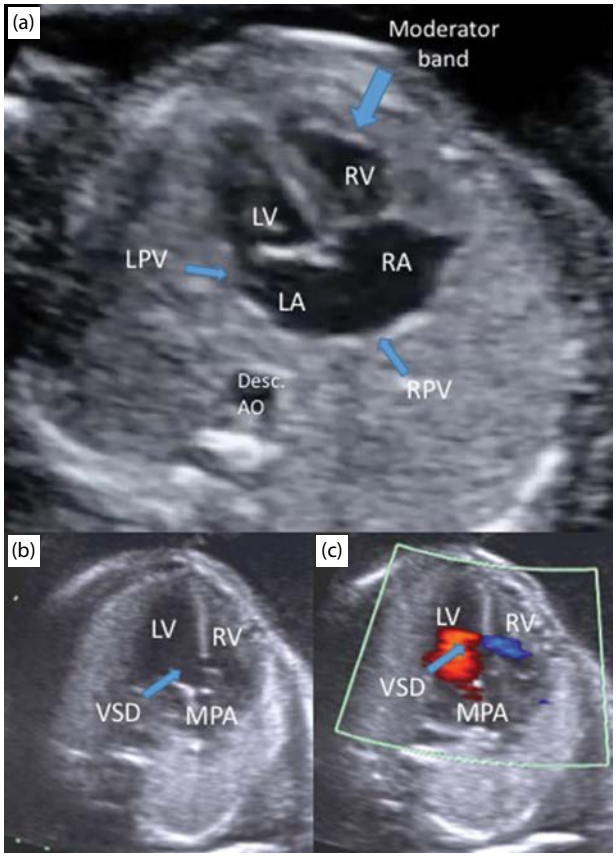


**Figure 29.2**
Fetal four-chamber view of a D-TGA demonstrating atrioventricular concordance. Two pulmonary veins can be seen draining into the left atrium that is most posterior and connects with the left ventricle that is also more posterior. The right atrium is more anterior and is to the right ventricle that is also more anterior and additionally has a moderator band and a more apically positioned atrioventricular valve. There is an intact interventricular septum.

normal (D) ventricular looping (morphological right ventricle on the right side of the heart) (Video 29.1). Most will have normal mitral and tricuspid valves; however, from the four-chamber view, normal morphology, size, and motion of the mitral and tricuspid valves and symmetric flow into both ventricles need to be demonstrated. AV valve asymmetry could suggest pathology that could impact surgical options and outcome. AV valve straddling and/or stenosis may be associated with hypoplasia of the ipsilateral ventricle. As ventricular septal defects are common in D-TGA, detailed assessment of the ventricular septum from four-chamber, long-axis, and short-axis sweeps is important. Demonstrating the location and size of a VSD and its relationship to the great arteries is also crucial, particularly if outflow obstruction is suspected. The ventricular septum is best evaluated perpendicular to the ultrasound beam allowing for maximal axial resolution and color and pulsed-wave Doppler interrogation of flow traversing the VSD.

Detailed evaluation of atrial septal anatomy in both sagittal and four-chamber views, with the plane of imaging perpendicular to the plane of the septum, is critical in evaluating fetal

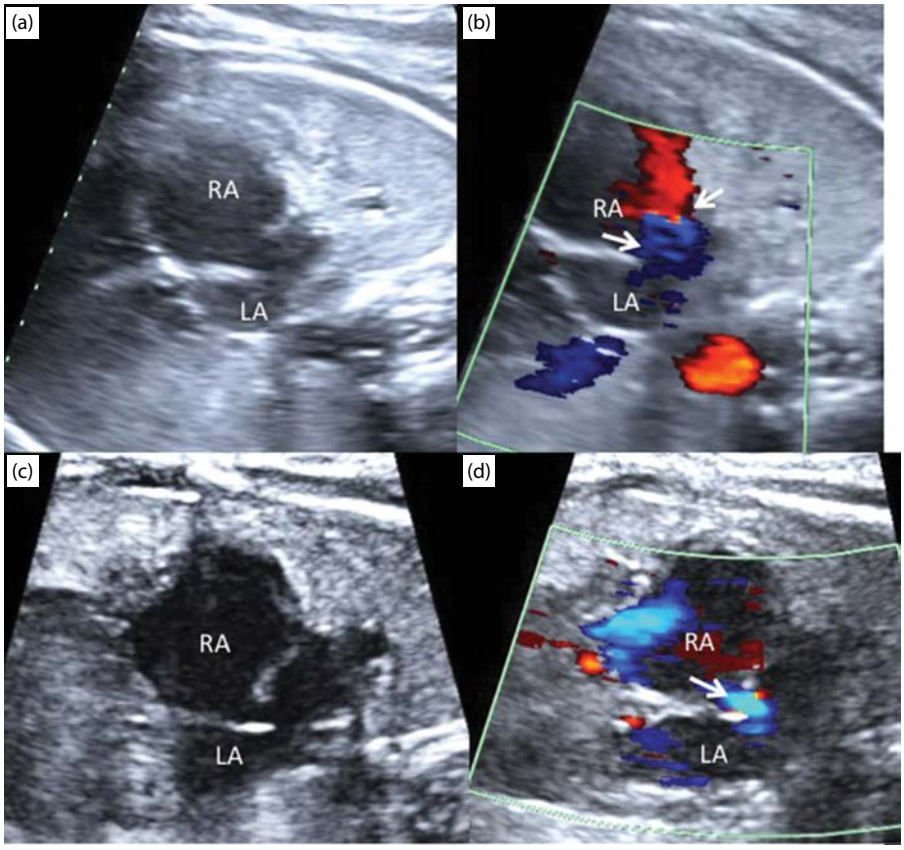


**Figure 29.3**
Evaluation of the atrial septum from a fetal four-chamber view. (a) Two-dimensional grayscale with a fossa ovales that has a reasonable diameter. (b) Color Doppler assessment in the same view, demonstrating laminar flow from the right to the left atrium (arrows demonstrate the flow orifice). (c) Two-dimensional grayscale with a restrictive atrial flow: small size of the fossa ovale and narrow angle between the septum primum and the rest of the atrial septum can be appreciated. (d) Color Doppler assessment in the same view demonstrating a small amount of flow across the septum with accelerated flow (arrow). The increased atrial septal thickness can also be appreciated. (LA, left atrium; RA, right atrium.)

D-TGA. Septum primum can be seen flapping freely, usually in the left atrium, and the fossa ovales flow orifice should be of good size with laminar flow (Figure 29.3a,b; Video 29.2a–d). Signs suggestive of atrial restriction include increased septal thickness (Figure 29.3c), fixed bowing of the septum into the left or right atrium,[46] a narrow angle between septum primum and the rest of the atrial septum (<30°)[24] and a hypermobile state.[24,25,31,46] Color Doppler often confirms the presence of a small flow orifice with accelerated flow (Figure 29.3d) or no clear flow traversing the septum. Pulsed Doppler can confirm the presence of high-velocity continuous flow.

Sweeping from the four-chamber image toward the outlets (Video 29.1a) demonstrates the abnormal relationship of the great arteries. While in the normal heart the great arteries cross and cannot be both demonstrated in long or short axes, in D-TGA, the great arteries run parallel and their long or short axes can be demonstrated in one image (Figure 29.4). A sweep from the four-chamber view toward the fetal head in D-TGA demonstrates that the MPA arises posteriorly and leftward from the LV and is seen bifurcating early (Figure 29.5a). Sweeping more cephalad in the four-chamber view, the aorta arises from the RV outflow tract anterior and rightward, just under the anterior chest wall (Figure 29.5b). The parallel great artery relationship may be demonstrated with these sweeps. Patency of both outflows should be assessed by careful examination on two-dimensional grayscale, as well as with color

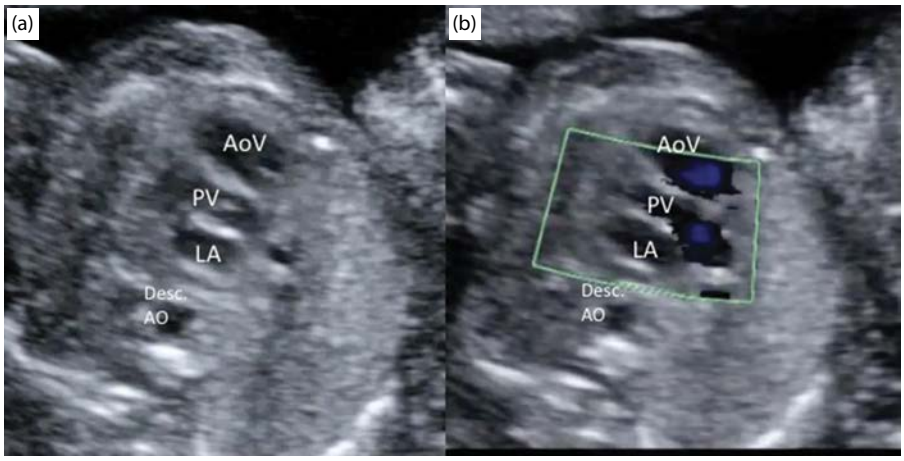


**Figure 29.4**
Oblique cross-sectional view (between the four-chamber and outflow tracts) of a D-TGA. (a) The great arteries can be seen in their parallel orientation, with the aorta sitting anterior to the PA. (AoV, aortic valve; Desc Ao, descending aorta; LA, left atrium; PV, pulmonary valve.) (b) Color Doppler assessment of the same view. (AoV, aortic valve; Desc Ao, descending aorta; LA, left atrium; PV, pulmonary valve.)

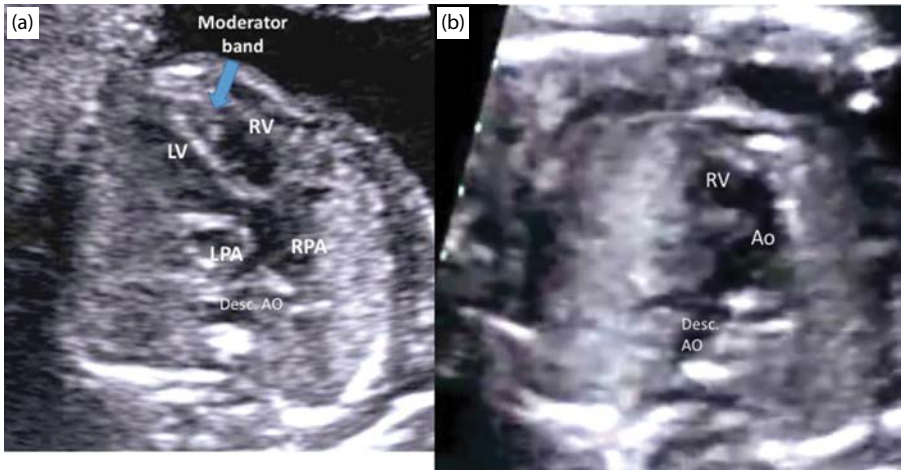


**Figure 29.5**
(a) Sweeping from the four-chamber image, the left ventricular outflow tract is encountered first in D-TGA. The most posterior ventricle is a morphological left ventricle, and it gives rise to the MPA, which bifurcates into RPA and LPA. (b) Sweeping more cephalad and anterior from the four-chamber view, the right ventricular outflow is demonstrated. The more anterior right ventricle gives rise to the aorta. (Desc Ao, descending aorta; LPA, left pulmonary artery; LV, left ventricle; RPA, right pulmonary artery; RV, right ventricle.)

and pulsed-Doppler interrogation to exclude subvalvar and/or valvar obstruction. The semilunar valves should be symmetric and moving freely.

## Three-vessel view and three-vessel and trachea view

The three-vessel and three-vessel tracheal views should be assessed for alignment, arrangement, and size of the great vessels and SVC (Video 29.1b). In most forms of D-TGA, the arrangement of the vessels in these views is abnormal with the aorta anterior and to the right along with the pulmonary artery posterior and to the left. With the SVC posterior and rightward of the aorta, the three-vessel and trachea view as a triangle shape (Figure 29.6). If there is no outflow obstruction, the size of the great vessels should be similar, with the SVC smaller sitting posteriorly and to the right.[47] In D-TGA, only one arch is seen at a time, as they often have a superior/inferior

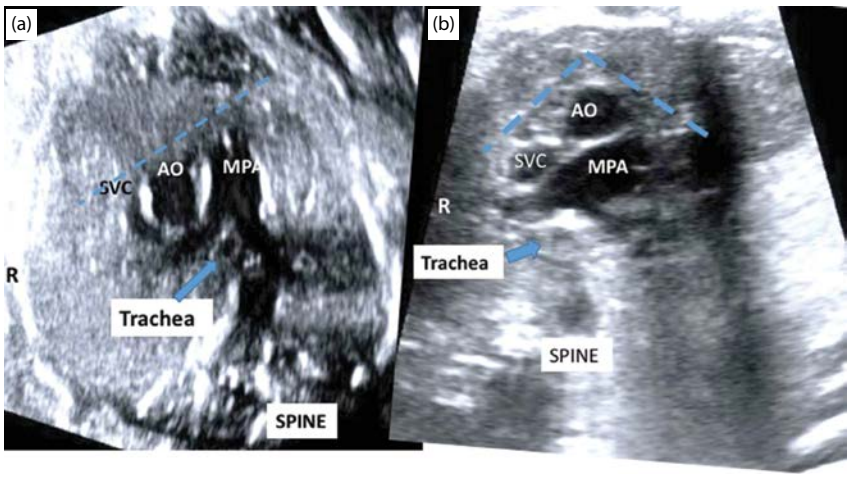


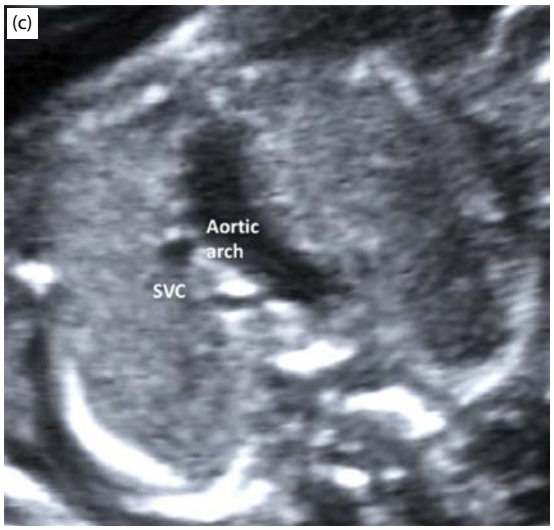


**Figure 29.6**
The three-vessel and trachea view (3VT). (a) 3VT view of a normal heart. The three vessels are aligned diagonally with the MPA being the most anterior and the superior vena cava (SVC) the most posterior and arranged from left to right: MPA, Aorta, and SVC. (b) The 3VT view in D-TGA demonstrates a triangle with the aorta being the most anterior, with the SVC positioned posterior and to the right and the MPA posterior and to the left. (Ao, aorta; MPA, main pulmonary artery; R, right side of the fetal chest; SVC, superior vena cava.) (c) Sweeping more cephalad, the arches in D-TGA are essentially superimposed, the "I' sign. In normal heart both arches can be seen simultaneously from this view joining the descending aorta, forming a "V." In D-TGA, because the ductal and aortic arches have a superior/inferior relationship, only one arch can be seen at a time from a cross-sectional view. The SVC can be seen to the right of the aortic arch.

relationship, which is known as the "i" sign and has been reported to aid in the diagnosis of D-TGA[48] (Figure 29.6c). The aortic and ductal arches almost always course to the left of the trachea.

## Sagittal view

From a sagittal view of the fetus, the aortic and ductal arches can often be seen in the same plane in D-TGA[49] (Figure 29.7; Video 29.3a,b), as opposed to normal hearts, where the arches have a spiraling relationship. This is an optimal view to assess the DA for size and flow. Normal ductal arch flow is considered anterograde throughout the cardiac cycle, biphasic, with peak systolic gradient under 16 mm Hg, end-diastolic velocities (0.12–0.3 m/s), and pulsatility index higher than 1.9. In D-TGA, while MPA to aortic flow is normal, there may be bidirectional flow likely related to low pulmonary resistance with retrograde flow in diastole (Figure 29.7), or where there is constriction, high velocity or continuous flow (restrictive DA) (Figure 29.7e).

By angling the transducer to the fetal right, the bicaval view and atrial septal anatomy can also be demonstrated (Figure 29.8). The superior aspect of the atrial septum where the superior vena cava joins the right atrium is in a fixed position, whereas septum primum, again, is often mobile, flapping into the left atrium in the normal fetus but often flapping back and forth between the two atria in D-TGA. A reduced angle between septum primum and the superior aspect of septum primum, a thickened atrial septum, small fossa ovales, and small flow orifice can be demonstrated from this view in fetuses with restricted atrial septum. Similar to the four-chamber view, color-Doppler interrogation enables evaluation of flow through the fossa ovales into the left atrium.

## Short axis

D-TGA will demonstrate a normal relationship of the ventricles, with the morphological left ventricle, with the "septophobic" mitral valve to the left, on the same side as the stomach. Sweeping toward the left, the parallel relationship of the great arteries can again be demonstrated (Figure 29.9a,b). Sweeping through the short axis, VSDs can be excluded, and the outflow tracts can be evaluated for obstruction.

# *Fetal progression and monitoring*

Fetal monitoring should be performed every 6–8 weeks until delivery to assess the status of the ductus arteriosus and

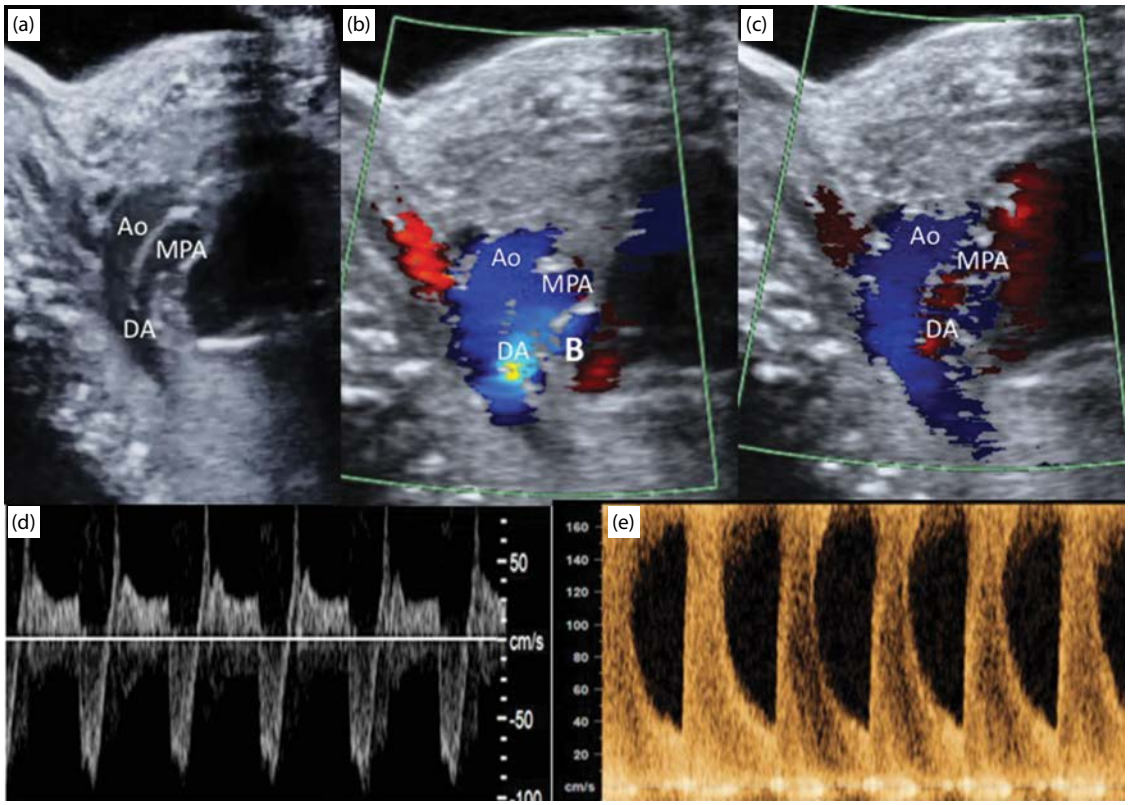


**Figure 29.7**
Sagittal image of the aortic and ductal arches, which can both be demonstrated simultaneously in D-TGA. (a) Two-dimensional grayscale image, with the aorta superior to the ductal arch. The ductus arteriosus can be seen as the arches connect with the descending artery. (b) Color Doppler assessment showing bidirectional flow in the ductus arteriosus (DA), anterograde in systole. (c) Retrograde flow in diastole. (d) Pulsed-wave Doppler assessment of the DA demonstrating the bidirectional flow of the DA. (e) High-velocity more continuous and unidirectional flow in systole and diastole in the DA suggest constriction has occurred before birth. Affected fetuses are at high risk of profound cyanosis at delivery with this feature.

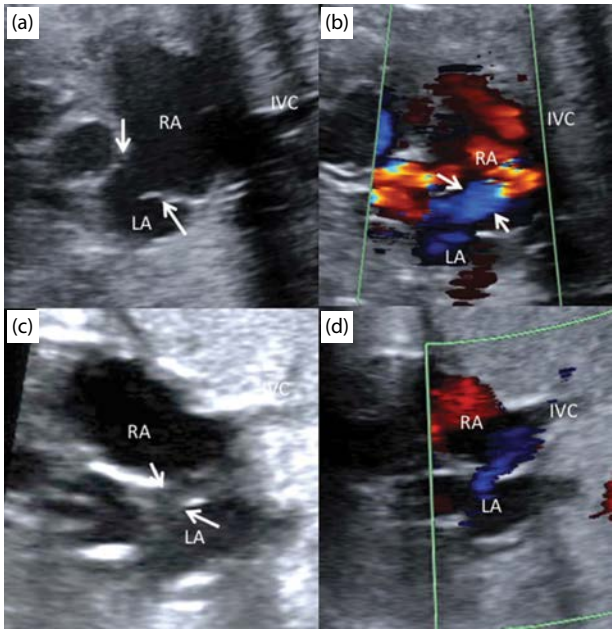


**Figure 29.8**
Evaluation of the atrial septum from the bicaval view. (a) Two-dimensional grayscale with a fossa ovales with good size. (b) Color Doppler assessment in the same view, demonstrating a large flow orifice (arrows) and laminar flow from the right to the left atrium. (c) Two-dimensional grayscale with a restrictive atrial flow: small size of the fossa ovales (arrows) and narrow angle between the septum primum and the rest of the atrial septum can be appreciated. (d) Color Doppler assessment in the same view demonstrating small flow orifice. Increased atrial septal thickness can also be appreciated. (LA, left atrium; RA, right atrium.)

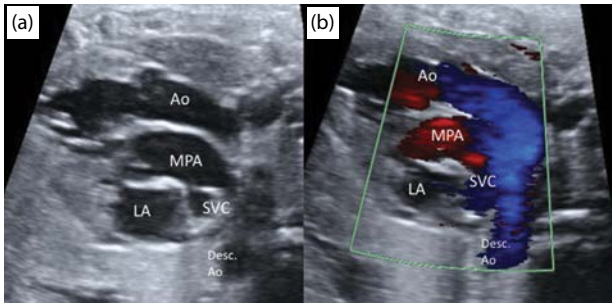


**Figure 29.9**
Sagittal short-axis view of a D-TGA. (a) Two-dimensional view of the great arteries can be seen in their parallel orientation, with the aorta sitting anterior to the PA. The sizes of the great arteries are similar in keeping with no significant outflow obstruction. (b) Color Doppler assessment of the same view. (Ao, aorta; Desc Ao, descending aorta; LA, left atrium; MPA, main pulmonary artery; SVC, superior vena cava.)

foramen ovale as well as to exclude outflow tract obstruction[50] and progressive AV valve pathology.[51] Late in gestation, it may be helpful to evaluate the atrial septum and ductus arteriosus more than once given that restriction of either likely occurs only within the last several weeks.[46]

## Imaging complex D-TGA

More complex D-TGA can be assessed in a similar approach to simple D-TGA. Confirmation of symmetry of the four chambers is important, as any asymmetry could suggest the presence of more complex anatomy. VSD location, size, and relationship to one or both great arteries should be defined. Evaluation for outflow tract obstruction with posterior malalignment of outlet septum crowding the subpulmonary area (Figure 29.10a,b; Videos 29.4a,b) and anterior malalignment of conal septum crowding the subaortic area should be performed (Figure 29.11a,b; Video 29.5). In the latter, the aortic arch is often hypoplastic, and there may be aortic coarctation (Figure 29.11c). Discrepancy in great artery size with a smaller vessel arising from the outlet with obstruction is a typical feature and is useful in anticipating more subtle obstruction. Evaluation of the size relationship and morphology of the aortic arch is important for exclusion of coarctation.

## *Delivery planning in D-TGA*

The mode and timing of delivery should be decided based on obstetrical indications and whether or not there is need for emergent intervention, and this decision should be made as close to term as possible.[52–54] If there are concerns that the atrial septum has restricted flow, with or without abnormal shunting across the DA, plans for an emergent balloon septostomy should be in place, as well as equipment necessary to deal with possible associated pulmonary hypertension.[50] This may require, for some centers, that the baby is delivered by cesarean section.

## *Outcome in D-TGA*

The outcome of neonates with simple d-TGA depends more so on the status of the ductus arteriosus and foramen ovale, which again dictates the severity of cyanosis and compromise at birth. A balloon atrial septostomy may be necessary in 25%–50% depending on the center and carries a low risk of rupture, embolic phenomenon, and bleeding.[55,56] If infants can be stabilized with or without atrial septostomy and undergo arterial switch operation, the outcome can be excellent with an approximate 98% survival for most larger surgical programs.[41,57]

In the setting of VSD and pulmonary stenosis, the outcome is still reasonable, but the surgery usually involves the use of a conduit for pulmonary blood flow, which has its own risks with a need for reoperation long-term for conduit replacement and other nonsurgical interventional procedures.[58] VSD with coarctation as well can result in successful repair with low operative risks, but long term, there is a risk for recurrent coarctation and right ventricular outflow obstruction. If there is hypoplasia of one of the ventricles, or major straddling of AV valves precluding a biventricular repair, these patients are likely to have mid- and long-term outcomes similar to those with a single ventricle.[59,60]

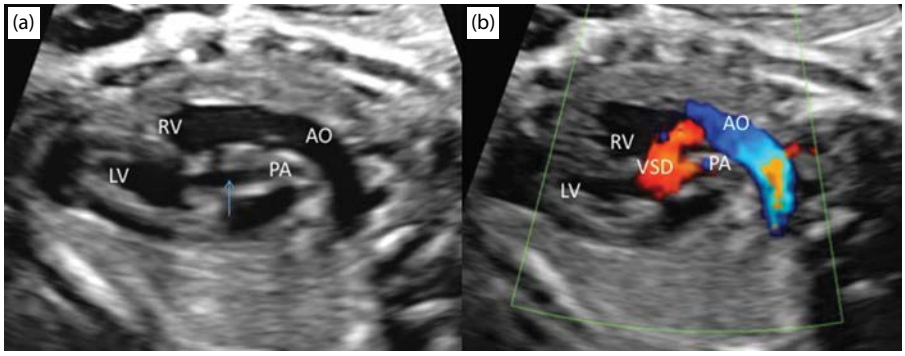


**Figure 29.10**
Two-dimensional grayscale of a fetal D-TGA with deviation of the infundibular septum with a malaligned ventricular septal defect (VSD). (a) Posterior deviation of the infundibular septum crowding the subvalvar area (arrow) and a small pulmonary valve. (b) Color Doppler assessment of the same view with left-to-right shunt across the VSD and unobstructed flow across the aortic valve. The ascending aorta (AO) is clearly larger than the posterior main pulmonary artery (PA) in both images. (AO, ascending aorta; LV, left ventricle; PA, pulmonary artery; RV, right ventricle; VSD, ventricular septal defect.)

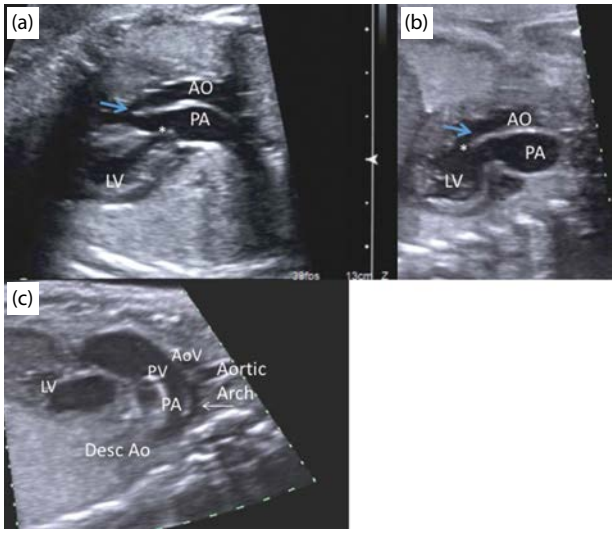


**Figure 29.11**
A 22-week fetus with D-TGA, VSD, and subAS. From a four-chamber image sweeping toward the fetal head (a) and a sagittal image (b) the aortiorly deviate infundibular septum (arrow) can be seen crowing the subaortic area. The pulmonary valve overrides the ventricular septal defect (*), and there is clear size discrepancy with a larger pulmonary artery (PA) relative to the aorta (AO). (c) The aortic and ductal arches; the aortic arch is hypoplastic, and there is a suggestion of a posterior shelf in keeping with coarctation. (DescAo, descending aorta; LV, left ventricle.)

Coronary abnormalities can only be truly assessed postnatally, and although the most common anomalies will not impact severely the prognosis in early life, an abnormal origin and particularly intramural course may complicate the surgical repair, adding to the surgical risk of the arterial switch procedure, which involves the translocation of the coronary arteries to the neoaorta.[57] Although the most common variants such as retropulmonary looping of the entire left coronary artery or just the circumflex artery (when it arises from the right coronary artery), have shown improved outcome over the years, more complex coronary patterns such as single coronary artery and those with an intramural course have been reported to be associated with worse outcomes.[61–63]

The most frequent long-term complications of the arterial switch are neoaortic root dilation present in almost all patients, with some degree of neoaortic valve regurgitation. Supravalvar stenosis may also be present and has been reported in the MPA in 10% of the patients and in the ascending aorta in 5%. Branch pulmonary artery stenosis is another common complication of the arterial switch operation and is less amenable to balloon angioplasty at catheterization. Finally, arrhythmias, including sinus node disease, can be present in up to 10% of the patients in the long term.[64]

## Levo-transposition of the great arteries

Levo-transposition of the great arteries (L-TGA) is an uncommon form of CHD which, when in isolation, may not be detected until later in life due to the normal physiological shunting of systemic venous blood into the pulmonary artery and pulmonary venous blood to the aorta.[24] Ninety percent of affected patients, however, have associated cardiac anomalies, which importantly contribute to both clinical presentation and outcomes. Overall survival to the age of 5 has been reported between 70% and 92%, and to the age of 10 years, 64%–91%.[49,65]

### *Morphological definition and embryology*

Also known as congenitally corrected transposition, in L-TGA the aorta arises leftward and anterior to the pulmonary artery from the morphological left-sided right ventricle, while the pulmonary artery arises posterior and rightward, from the morphological right-sided left ventricle (Figure 29.1c). The pulmonary valve is usually wedged between the atrial septum

and the mitral valve, and there is fibrous continuity between the two mentioned valves.[66] This abnormal arrangement causes a malalignment between atrial and ventricular septum and, consequently, an abnormal pathway of the cardiac conduction system.[66–68]

The causative embryological mechanism of L-TGA is the abnormal looping of primitive heart tube and abnormal remodeling of the outflow tract.[66] Instead of looping to the right, the cardiac tube loops to the left causing the morphological right ventricle to be leftward to the morphological left ventricle. As is true for D-TGA, the primitive outflows rotate abnormally leading to the parallel relationship of the great arteries with an anterior and leftward aorta in the majority of cases.

The abnormal twist and relationship of the ventricles vary in degree and may be extreme to the point of causing a superior-inferior relationship of the ventricles (criss-cross heart).[69]

The AV valves, most commonly the right-sided tricuspid valve, will often also present with abnormalities such as dysplasia,[66] straddling,[68] and more rarely can be stenotic or even atretic demonstrating single-ventricle physiology.[70] The usual pattern of the coronary arteries is also inverted compared to that of D-TGA. Similarly to the normal heart, the anterior descending and circumflex arteries supply the anatomically left ventricle, and the right coronary artery, the morphologic right ventricle.[66,71]

## Epidemiology and genetics

L-TGA is far less common than D-TGA with a prevalence of 0.15 in 10.000 live births[72] and accounts for only 0.05% of all CHD,[72] with no gender difference. Like D-TGA, its etiology is unknown, and it is likely multifactorial[18] with possible association to environmental factors.[73] Associated chromosomal abnormalities are also exceedingly uncommon.[74]

## Associated cardiac malformations

Population-based, anatomic, and fetal series have reported up to 90% of associated cardiac abnormalities.[66,72,74,75] Nonetheless, unless there is severe outflow obstruction or significant abnormality of an AV valve, affected patients usually do not present with any clinical symptoms at birth. An autopsy study of 32 hearts with L-TGA[71] reported VSDs in 80% of the cases, usually in the perimembranous region, tricuspid valve abnormalities in up to 90% of the cases, and pulmonary outflow obstruction in 40%. In 10% of the cases, the mitral valve will also be abnormal.[70] Lesions such as mitral or tricuspid atresia, double-outlet right ventricle, and crossed AV connections may also be found in the setting of L-TGA but are less frequent and will impact clinical presentation.[71] Anatomic studies have reported an incidence of up to 45% of coronary artery abnormalities that may complicate surgical repair.[76] In fetal series, the detection of tricuspid valve dysplasia has been lower, between 30% and 45%,[74,77] most likely due to the difficulty of demonstration of subtle abnormalities of AV valve abnormalities *in utero*. Cardiac malposition, dextro or mesocardia, can occur in 17%–50% of the cases.[74,77,78]

Rhythm disturbances are common in L-TGA due to the abnormal pathway of the conduction system. The most common arrhythmia is that of AV block, which has been demonstrated in up to 20% of prenatally diagnosed cases and typically evolves in the third trimester.[74,79] Presentation bias with fetal bradycardia being a feature that would prompt fetal echocardiography may contribute to such a high incidence.

## Associated extracardiac malformations

Prenatally diagnosed L-TGA is not commonly associated with extracardiac anomalies.[13,20] One population-based study reported that 30% of patients encountered before and after birth had extracardiac abnormalities.[73]

## Pathophysiology and postnatal course

Due to the fact that this is a rare form of CHD, there is a paucity of data regarding the natural history of these patients compared to D-TGA. These patients display an in-series circulation with unsaturated blood returning to the right atrium through the systemic veins flowing into the left ventricle and being ejected to the lungs, and saturated blood returning via the pulmonary veins to the left atrium, flowing to the right ventricle, and then being ejected into the aorta to the body. Therefore, affected patients have quite different physiology than D-TGA patients and require completely different postnatal management. However, in spite of a physiologically corrected circulation, even in patients who have no other associated abnormalities, the natural history and postnatal hemodynamics are quite different from a person with normal anatomy in the short and long term.

Fetuses diagnosed with L-TGA have an increased chance of developing rhythm disturbances and progression of tricuspid valve regurgitation throughout the pregnancy.[74,77,79] Again, this could relate to the bias of fetal referrals.

Features of the pathology such as a morphological RV facing the systemic afterload, various degrees of tricuspid valve dysplasia, and an abnormal AV conduction pathway contribute to the less favorable outcome over the course of a normal life span.[80] The systemic RV, in time, often evolves with dysfunction in response to chronic high afterload, which can lead to congestive heart failure. Depending on the associated cardiac lesions and need for surgical intervention, the evolution of heart failure may be accelerated. A multi-institution study with 182 patients[81] showed that by the age of 45%, 67% of the patients with associated lesions and 25% without associated lesions, had systemic ventricular dysfunction and congestive heart failure. There is a strong association of tricuspid regurgitation and RV failure; however, it is still

unclear if this is causative or represents a secondary complication. Tricuspid valve dysplasia is present in the vast majority of cases and likely contributes to the increased likelihood of valve dysfunction long term.[81] The commonly associated cardiac abnormalities,[72,75] such as tricuspid valve dysplasia and regurgitation, ventricular septal defects, and pulmonary outflow obstruction, influence RV pre- and afterload and may, in so doing, impact the interventricular relationship, ultimately negatively affecting outcomes. Additionally, the abnormal conduction anatomy results in increasing incidence of congenital heart block with age (roughly 1%–2% per year), adding further to the morbidity and mortality risks of the patient.[82] Tachyarrhythmias may also occur in the presence of dual AV nodal pathways or accessory muscular AV connection.[77]

## Postnatal management and surgical options

Most neonates with L-TGA are clinically stable at birth, many without signs or symptoms of congenital heart disease. In the majority of cases, there is no critical outflow obstruction; therefore, prostaglandins are not necessary. In the absence of other intracardiac pathology, affected patients can be clinically well for many years and may even go unrecognized until later in life. AV block remains a lifelong risk for these patients, as does evolution of right ventricular dysfunction, tricuspid insufficiency, and heart failure. With such risks, over the past two decades, some have advocated for surgical intervention in the form of an atrial and arterial switch operation, which leaves the LV to function as the systemic and the RV the pulmonary ventricle. This procedure must be done early in infancy while the LV is still prepared to manage the systemic afterload. The difficulty is that the operation is usually performed on a clinically very well infant who could go decades without requiring intervention for the potential benefit of having a systemic LV. Furthermore, this procedure is not without risks, including risks associated with atrial baffling[83] and risks related to the arterial switch. Additionally, the risk of spontaneous AV block remains.[84,85]

Other more complex L-TGA pathology may be repaired or palliated such that the RV is left as the systemic ventricle ("physiological repair") or the LV is made the systemic ventricle (also referred to as "anatomical repair"). For simpler defects, such as a large VSD, VSD closure is often chosen as the risks are not dissimilar to long-term risks of isolated L-TGA. Whereas, in more complex outflow obstruction, most often pulmonary, baffling of a favorable VSD that is not too remote from the aorta, creating a connection between the RV and the pulmonary artery and atrial switch may be considered as it leaves the LV to function as the systemic ventricle. A large retrospective, multicenter study reported the outcome of 167 patients diagnosed with L-TGA who underwent biventricular repair. Of these, 123 were addressed through a "physiological repair" (14 patients had ASD and/or VSD closure, 21 had TV surgery, 54 required a LV to PA conduit interposition, 26 needed relief of PV outflow tract obstruction, and 8 had *réparation à l'étage ventriculaire)*. The remaining 44 patients underwent an "anatomical repair" (10 had "double-switch" procedure, and 34 had atrial switch plus intraventricular rerouting). Patients were followed for a mean of $9.3 \pm 6.6$ years. In patients who underwent physiological repair, early mortality was 9.7%, reoperation was required in 50.9% of cases, AV block occurred in 21.9%, and in the last follow-up echocardiographic assessment the TR and RV function had significantly deteriorated in all. Additionally, late mortality was 5.9%. In the "anatomically" repaired group, early mortality was 15.9%, 29.7% needed further surgical procedure, and 6.8% developed complete AV block. Interestingly, in the last follow-up echocardiogram, there was no significant change in TR severity, and the RV function had not deteriorated; additionally, late mortality was 0%. This study suggested that late functional outcomes of anatomic repair were superior to physiologic repair,[85] but the findings from this study are limited by its retrospective design.

## Prenatal diagnosis of L-TGA

L-TGA can be detected prenatally through close inspection of the four-chamber view. For many fetuses, the cardiac axis or position is not normal with mesocardia or dextrocardia.[77,78] In the presence of a normal cardiac axis, the absence of other abnormalities in the four-chamber view may make this diagnosis a challenge.[86] Associated cardiac pathology such as dysplastic TV, outflow tract pathology suspicion of VSD, and fetal bradycardia may be the initial reasons for referral.[74]

### Situs

As with D-TGA, L-TGA is typically associated with situs solitus, but *situs inversus* and *situs ambiguous* have also been rarely reported in L-TGA.[67,71] A rightward intact inferior vena cava connecting with the right atrium irrespective of the cardiac position is usually demonstrated and critical in defining the full segmental anatomy.

### Four-chamber view

The most reliable feature that clinches the diagnosis of L-TGA is the demonstration of A-V discordance in which the atrium with the systemic venous connections (inferior and superior vena cava) connects with the morphological LV and the atrium with the pulmonary venous connections connects with the morphological right ventricle (Figure 29.12; Video 29.6a). The inverted relationship of the AV valves results in the left AV valve (the tricuspid valve) being more apically displaced than the right AV valve (the mitral valve). The presence of the moderator band helps to define the RV, which in most cases of L-TGA is visible on the left side of the heart. The AV valves are often dysplastic. This is particularly true of the tricuspid valve, which may be thickened, redundant, and have morphological features of Ebstein anomaly. Such tricuspid valves are often regurgitant, and when severe, this may contribute to the

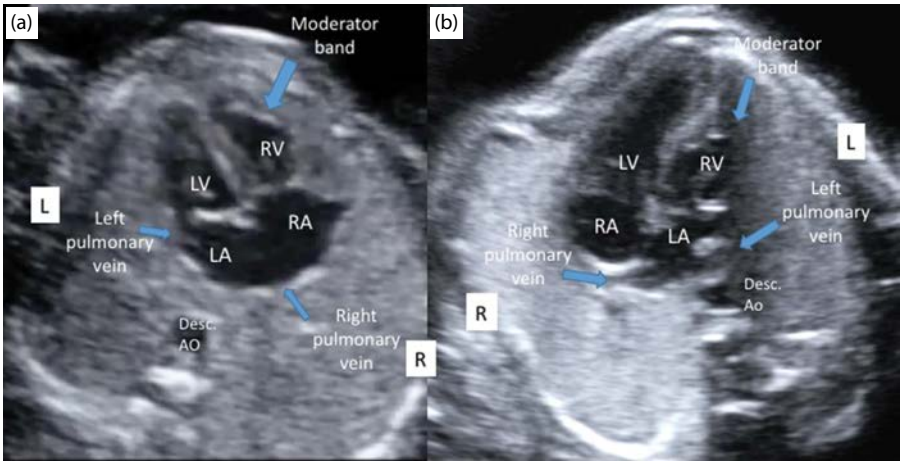


**Figure 29.12**
Fetal four-chamber view. (a) Normal four-chamber view with normal atrioventricular concordance. (b) Four-chamber view in L-TGA with levocardia: Two pulmonary veins can be seen connecting with the left atrium that is most posterior and connects to the ventricle that is also more posterior; however, this more posterior ventricle has a moderator band and a more apical displacement of the atrioventricular valve along the septum, findings in keeping with a right ventricle. The right atrium is more anterior and connects with the more anterior and rightward left ventricle which is less trabeculated, is more bullet shaped, and has a higher attachment of the AV valve (mitral) along the septum.

evolution of felt heart failure and hydrops.[74,77] AV valve size, morphology, patency and function, ventricular symmetry and function, and sweeps for VSDs, defining their size and position (particular relationship with the great arteries) are important to assess in the four-chamber view. Finally, an initial evaluation of rhythm including acquisition of pulsed-wave Doppler tracings to measure the A-V interval for evidence of AV block can be performed in the four-chamber view.

From the four-chamber view, sweeping cephalad to the ventricular outlets confirms the presence of V-A discordance (Video 29.6b,c). Although the spatial relationship of the vessels cannot be fully appreciated in this view, the LV to pulmonary connection will be encountered first as the pulmonary valve typically has continuity with the rightward mitral valve and is posterior and rightward of the aortic outflow tract (Figure 29.13a). Sweeping further cephalad, the aorta in most forms of L-TGA arises from the RV outlet or infundibulum anterior and leftward of the pulmonary artery (Figure 29.13b). Examining the morphology of the outflow tracts including the subvalvar area, the semilunar valve morphology and function, and great artery position and size relationship are important in excluding associated cardiac pathology in L-TGA that may complicate the postnatal course of affected babies. The presence of a subarterial VSD, for instance,

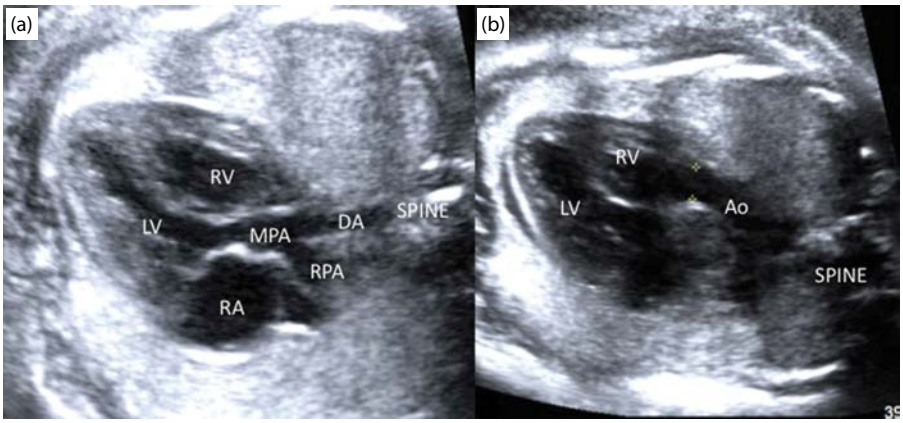


**Figure 29.13**
Sweeping from the four-chamber image the left ventricular outflow tract is encountered first in L-TGA. The most anterior/rightward ventricle is a morphological left ventricle (without the moderator band), and it gives rise to the MPA, which bifurcates into RPA and LPA. (a) Long-axis view of the LVOT of a L-TGA. The most anterior ventricle (LV) is giving rise to the main pulmonary artery, and the bifurcation of this vessel can be seen. (b) Long-axis view of the RVOT of a L-TGA. The most posterior/leftward ventricle (RV) is giving rise to the aorta. (Ao, aorta; DA, ductus arteriosus; LV, left ventricle; MPA, main pulmonary artery; RA, right atrium; RPA, right pulmonary artery; RV, right ventricle.)

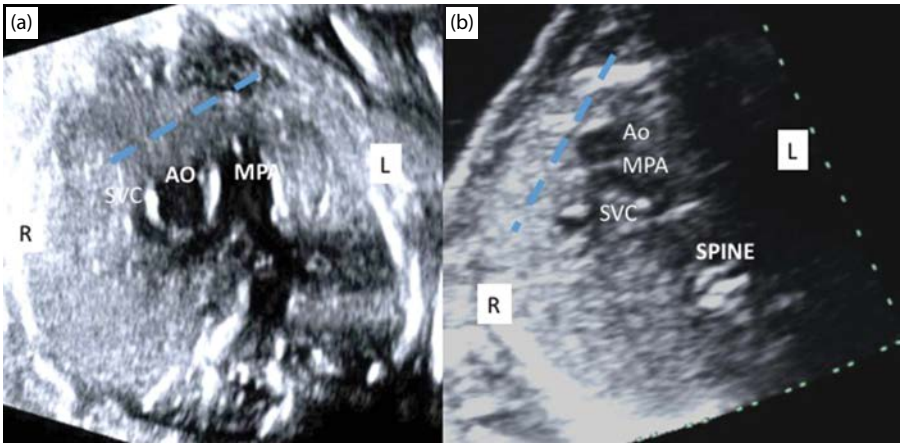


**Figure 29.14**
Cross-sectional view of the upper mediastinum demonstrating the three-vessel and trachea view (3VT). (a) 3VT view of a normal heart. The three vessels are aligned diagonally with the MPA being the most anterior and the SVC the most posterior and arranged from left to right: MPA, aorta, and SVC. (b) The 3VT view in L-TGA. The three vessels are still arranged in a linear fashion, but the aorta is the most anterior and leftward vessel, the MPA is positioned posterior and leftward to the aorta, and the SVC is the most posterior and rightward vessel. (Ao, aorta; MPA, main pulmonary artery; SVC, superior vena cava.)

should lead one to examine whether there is outlet septum malalignment that if posteriorly malaligned could impinge on the subpulmonary area and if anteriorly malaligned could obstruct the subaortic area. AV valve attachments may also contribute to outflow tract obstruction. Long-axis sweeps in a plane that is perpendicular to the ventricular septum from the four-chamber view may demonstrate the parallel relationship of the great arteries.

## Three-vessel view and three-vessel and trachea view

The three-vessel view (3VV) in L-TGA is always abnormal with the pulmonary trunk positioned between the SVC and the aorta. The aorta is typically the most anterior and leftward vessel. The pulmonary artery sits posterior and rightward of the aorta, and the superior vena cava is most often right-sided and posterior to the MPA. Given their parallel relationship, the great arteries are usually both demonstrated in their short axis in the 3VV (Figure 29.14). Discrepancy in the size of the great arteries potentially suggests the presence of outflow obstruction with the smaller vessel ipsilateral to the obstructed outflow tract. The three-vessel tracheal sweep typically demonstrates that the aortic and ductal arches remain to the left of the trachea. The aortic arch course to the descending thoracic aorta is not normal in L-TGA, as it remains to the left of the midline from anterior to posterior, never crossing the midline as is true of the normal great artery relationship. In fact, the aortic and ductal arches are almost superimposed in these sweeps. Aortic arch obstruction may be suggested if its diameter is smaller than that of the ductal arch.

## Sagittal view

Sagittal sweeps in the fetus confirm the presence of AV discordance, the abnormal relationship between the ventricles and AV valves, as well as VA discordance. When there is levocardia in L-TGA, the most anterior ventricle is typically the LV often defined by the bileaflet mitral valve and papillary muscles (Figure 29.15; Video 29.6d); whereas the RV is more posterior as defined by the trileaflet tricuspid valve and the presence of outlet portions separating the tricuspid valve from the aortic valve. Slow sweeps through the ventricular septum from the AV valves to the apex are important for excluding VSDs. From sagittal sweeps, the aortic arch can be examined for hypoplasia and a posterior shelf that suggests the presence of coarctation. The ductal arch should be assessed for its size and direction of flow. Retrograde ductal flow, as is true for other complex pathologies, is in keeping with critical pulmonary outflow obstruction.

# *Fetal progression and monitoring*

If the diagnosis is performed before the third trimester, follow-up should be performed every 6–8 weeks to reassess possible progressive outflow tract obstruction, competency and patency of the AV valves, and cardiac rhythm, particularly A-V conduction.

# *Outcome following prenatal diagnosis*

Little data exist regarding the outcomes following a prenatal diagnosis of L-TGA. One fetal series reported an 80% live birth rate among fetal L-TGA cases, 96% among continued pregnancies,[74] and an adjusted survival of 87.5% (21/24) at 56 months. Termination of pregnancy in this series for three cases was for more severe intracardiac pathology, which could have contributed to fetal demise. Outcomes after birth largely depend on associated cardiac pathology and range from no need for intervention and no clinical symptoms to need for

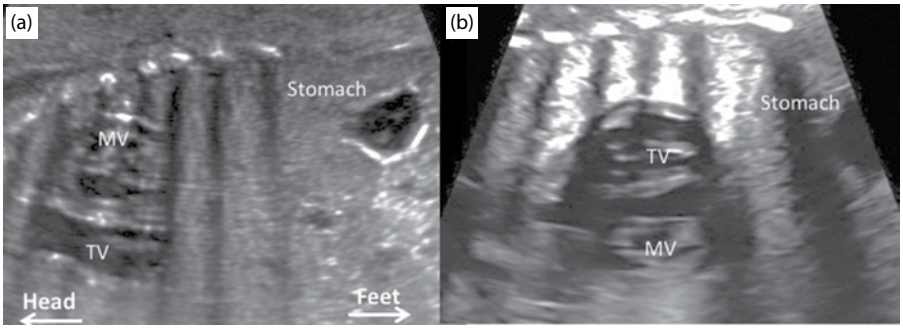


**Figure 29.15**
Sagittal view of the fetus with short-axis view of the ventricles and a cross-sectional view of the stomach. (a) The mitral valve is sitting ipsilateral to the stomach, demonstrating the morphological left ventricle is on the left and posterior. (b) In contrast, in L-TGA, the tricuspid valve is on the same side as the stomach, demonstrating the morphological right ventricle is on the right and often posterior and the left ventricle is rightward and often anterior.

surgical intervention in infancy and repeated interventions. Signs of severe tricuspid dysplasia with regurgitation, pulmonary stenosis, and rhythm disturbances have been associated with guarded prognosis as they impact RV function.[87]

## *Recent developments in imaging*

Although the prenatal detection rates for D-TGA and L-TGA have been improving,[36,40] they are still considered low in many parts of the world. Some groups have been exploring four-dimensional echocardiography and spatiotemporal image correlation (STIC) for their incremental benefit over conventional two-dimensional imaging for D-TGA and L-TGA with encouraging results regarding improved understanding of the anomaly.[88–90]

## Videos

**Video 29.1a** (https://youtu.be/AMHQL555idI)
Sweep from a fetal four-chamber view of a D-TGA into the outflows. This sweep demonstrates atrioventricular concordance and atrioventricular discordance. Two pulmonary veins can be seen draining into the left atrium that is most posterior, connected to the ventricle that is also more posterior. The right atrium is more anterior and connected to the ventricle that is also more anterior and additionally has a moderator band and a more apical placed atrioventricular valve. Intact interventricular septum. Sweeping cephalad from the four-chamber image, the left ventricular outflow tract is encountered first in D-TGA. The most posterior ventricle is a morphological left ventricle (without the moderator band), and it gives rise to the MPA, which bifurcates into RPA and LPA. Sweeping more cephalad and anterior from the four-chamber view, the right ventricular outflow is demonstrated. The more anterior right ventricle gives rise to the aorta. (Desc Ao, descending aorta; LV, left ventricle; LPA, left pulmonary artery; RPA, right pulmonary artery; RV, right ventricle.)

**Video 29.1b** (https://youtu.be/pFsmm59MwQQ)
The three-vessel and trachea view (3VT) in a D-TGA. This video in D-TGA demonstrates a triangle with the aorta being the most anterior, with the SVC positioned posterior and to the right, and the MPA posterior and to the left. This is different from a normal heart where the three vessels are aligned diagonally, with the MPA being the most anterior and the SVC the most posterior, as well as arranged from left to right: MPA, aorta, and SVC. (Ao, aorta; MPA, main pulmonary artery; SVC, superior vena cava.)

**Video 29.2a** (https://youtu.be/_zCPdkjotcE)
Two-dimensional grayscale of the fetal four-chamber view focusing on the atrial septum. The fossa ovales (FO) with good size and the FO flap can be seen moving freely in the left atrium; however, there are no signs of hypermobility of the flap. These are in keeping with an unrestrictive atrial septum at delivery.

**Video 29.2b** (https://youtu.be/7xIkG6dKWjs)
Color Doppler assessment of the four-chamber view focusing on the atrial septum. In this video, laminar flow from the right to the left atrium is demonstrated, again reassuring unrestrictive atrial shunt at delivery.

**Video 29.2c** (https://youtu.be/yvaaUHGy7eU)
Two-dimensional grayscale of the fetal four-chamber view focusing on the atrial septum with restrictive signs. The atrial septum is more fixed, causing a narrow angle between the septum primum and the rest of the atrial septum, and as a result, a small size of the fossa ovale can be appreciated.

**Video 29.2d** (https://youtu.be/1qUr2WVAeRQ)
Color Doppler assessment of the four-chamber view focusing on the atrial septum demonstrating a small amount of flow across the septum with accelerated flow, the increased atrial septal thickness and the more fixed atrial septum can also be appreciated.

**Video 29.3a** (https://youtu.be/aAlGIfiMkgs)
Sagittal image of the aortic and ductal arches, which can both be demonstrated simultaneously in D-TGA. (a) Two-dimensional grayscale image, with the aorta superior to the ductal arch. The ductus arteriosus can be seen as the arches connect with the descending artery.

**Video 29.3b** (https://youtu.be/LJekhMC9UsY)
(b) Color Doppler assessment of the aortic and ductal arches showing bidirectional flow in the ductus arteriosus (DA), anterograde in systole, and retrograde flow in diastole.

**Video 29.4a** (https://youtu.be/ONFPLFlDL3g)
Two-dimensional grayscale of a fetal D-TGA with a view of the LVOT (similar view to a parasternal long axis in a transthoracic echo). The deviation of the infundibular septum causing subvalvar PS with a malaligned VSD is demonstrated.

**Video 29.4b** (https://youtu.be/_4ZYeQsB0Ww)
Color Doppler assessment of a fetal D-TGA with a view of the LVOT with left-to-right shunt across the VSD and unobstructed flow across the aortic valve.

**Video 29.5** (https://youtu.be/Y4CeOMB96-M)
Two-dimensional grayscale of a fetal D-TGA with anterior deviation of the infundibular septum, crowding the subaortic area.

**Video 29.6a** (https://youtu.be/vp_JR0eZHPY)
Two-dimensional grayscale of a sweep from a fetal four-chamber view of a L-TGA. Two pulmonary veins can be seen connecting with the left atrium that is most posterior and connects to the ventricle that is also more posterior; however, this more posterior ventricle has a moderator band and a more apical displacement of the atrioventricular valve along the septum, findings in keeping with a right ventricle. The right atrium is more anterior and connects with the more anterior and rightward left ventricle, which is less trabeculated, is more bullet shaped, and has a higher attachment of the AV valve (mitral) along the septum. There is a large ventricular septal defect (VSD) suggested by the presence of T artifact.

**Video 29.6b** (https://youtu.be/nswHzSj9Wns)
Two-dimensional grayscale of a fetal L-TGA. In the sweep cephalad from the four-chamber image, the left ventricular outflow tract is encountered first in L-TGA. The most anterior/rightward ventricle is a morphological left ventricle, and it gives rise to the MPA, which bifurcates into right and left pulmonary artery. Continuing to sweep cephalad, the most posterior/leftward ventricle is giving rise to the aorta.

**Video 29.6c** (https://youtu.be/VqpvUnL4hvQ)
Color Doppler assessment of a fetal L-TGA. In the sweep cephalad from the four-chamber image, the left ventricular outflow tract is encountered first in L-TGA. The most anterior/rightward ventricle is a morphological left ventricle, and it gives rise to the MPA, which bifurcates into RPA and LPA. Continuing to sweep cephalad, the most posterior/leftward ventricle (RV) is giving rise to the aorta.

**Video 29.6d** (https://youtu.be/fFGDOFU0Dtg)
Two-dimensional grayscale of a fetal L-TGA from a short-axis of the ventricles up to the three-vessel and trachea view. A large VSD can be appreciated in the beginning of the sweep. As the sweep reaches the upper mediastinum, the 3VT view of a L-TGA can be seen: the three vessels are arranged in a more linear fashion, the aorta is the most anterior and leftward, the main pulmonary artery (MPA) is the most posterior vessel and sits between the aorta and superior vena cava (SVC), which is to the right.

# References


1. Baillie M. Diseased appearance of the heart. In: *The Morbid Anatomy of Some of the Most Important Parts of the Human Body*. 2nd ed. London: Johnson J and Nicol G. 1797:38.
2. Farre JR. Imperfect double heart: Transposition of the aorta and the pulmonary artery. In: *On Malformations of the Human Heart*. London: Longman, Hurst, Rees, Orme, Brown; 1814:28.
3. Von Rokitansky K. Deutung der Entwicklungsgeschichtlichen Daten: Construction der normalen Septa—Anwendung auf die Transpositionen—anomale septa (Interpretation of development history: Construction of normal septa—application to transpositions—abnormal septa.) In: *Die Defecte der Scheidewände des Herzens (Defects in the Septa of the Heart)*. Vienna: Wilhelm Braumüller, 1875:83–6.
4. Liebman J et al. *Circulation* 1969;40(2):237–62.
5. Pasquini L et al. *J Am Coll Cardiol* 1993;21(7):1712–21.
6. Moorman A et al. *Heart* 2003;89(1):1110–8.
7. Lomonico MP et al. *Anat Rec* 1986;216(4):544–9.
8. Watanabe M et al. *Development* 1998;125(19):3809–20.
9. Costell M et al. *Circ Res* 2002;91(2):158–64.
10. Yasui H et al. *Circulation* 1995;91(9):2478–86.
11. Mitchell S et al. *Circulation* 1971;43:323–32.
12. Samanek M. *Cardiol Young* 2000;10(3): 179–85.
13. Song MS et al. *Ultrasound Obstet Gynecol* 2009;33(5):552–9.
14. Unolt M et al. *Front Pediatr* 2013;1(June):11.
15. Wren C et al. *Heart* 2003;89(10):1217–20.
16. Grewal J et al. *Birth Defects Res Part A Clin Mol Teratol* 2008;82(7):519–26.
17. Digilio MC et al. *Circulation* 2001;104(23):2809–14.
18. De Luca A et al. *Heart* 2010;96(9):673–7.
19. Losay J et al. *J Am Coll Cardiol* 2006;47(10):2057–62.
20. Fesslova V et al. *Heart* 1999;82(5):594–9.
21. Tennstedt C et al. *Heart* 1999;82(1):34–9.
22. Ferencz C et al. *Am J Epidemiol* 1985;121(1):31–6.
23. Rudolph AM. *Pediatr Res* 2007;61(3):375–80.
24. Anderson R, Weinberg P. *Cardiol Young* 2005;15:76–87.
25. Maeno Y V et al. *Circulation* 1999;99(9):1209–14.
26. Soongswang J et al. *J Am Coll Cardiol* 1998;32(3):753–7.
27. Rudolf AM. *Congenital Diseases of the Heart*. Chicago, IL: Year Book; 1974:446–68.
28. Gewillig M et al. *Eur Heart J* 2009;30(12):1530–6.
29. Jouannic JM et al. *Circulation* 2004;110(13):1743–6.
30. Petit CJ et al. *Circulation* 2009;119(5):709–16.
31. Punn R, Silverman NH. *J Am Soc Echocardiogr* 2011;24(4): 425–30.
32. Baylen BG et al. *J Am Coll Cardiol* 1992;19(5):1025–31.
33. Bonnet D et al. *Circulation* 1999;99(7):916–8.
34. Chaoui R. *Ultrasound Obstet Gynecol* 2003;22(1):3–10.
35. Gardiner HM et al. *Heart* 2013;100(5):375–82.
36. Escobar-Diaz MC et al. *Ultrasound Obstet Gynecol* 2015;45(6): 678–82.
37. Debost-Legrand A et al. *Birth Defects Res (Part A)* 2015;106: 178–84.
38. Ravi P et al. *J Am Coll Cardiol* 2016;67(13):956.
39. The International Society of Ultrasound in Obstetrics. *Ultrasound Obstet Gynecol* 2013;41(3):348–59.
40. Ravi P et al. *Ultrasound Obstet Gynecol* 2018;51(5):659–64.
41. Wetter J et al. *Eur J Cardiothorac Surg* 2001;20(4):816–23.
42. Kalfa DM et al. *Ann Thorac Surg* 2013;95(6):2097–103.
43. Honjo O et al. *Eur J Cardiothorac Surg* 2013;44(6):1085–94.
44. Milanesi O et al. *Br Hear J* 1982;48:566–71.
45. Hazekamp M et al. *Eur J Cardiothorac Surg* 2007;31(5): 879–87.
46. Vigneswaran TV et al. *Am J Cardiol* 2017;119(9):1463–7.
47. Yooo S-J et al. *Am J Roentgenol* 1999;172: 825–30.
48. Palatnik A et al. *J Ultrasound Med* 2015;34(7):1329–35.
49. Huhta JC. *Cardiol Young* 2005;15(1 suppl):88–92.

50. Donofrio MT et al. *Am J Cardiol* 2013;111(5):737–47.
51. Donofrio MT et al. *Circulation* 2014;129(21):2183–242.
52. Costello JM et al. *Pediatrics* 2010;126(2):277–84.
53. Sanapo L et al. *Clin Perinatol* 2016;43(1):55–71.
54. Cheng YW et al. *Am J Obstet Gynecol* 2008;199(4):370.e1–7.
55. Beca J et al. *J Am Coll Cardiol* 2009;53(19): 1807–11.
56. Polito A et al. *Cardiol Young* 2012;22(1):1–7.
57. Wernovsky G et al. *J Thorac Cardiovasc Surg* 1995;109(1983): 289–301,302.
58. Selamet Tierney ES et al. *J Thorac Cardiovasc Surg* 2005;130(2): 282–6.
59. Rogers LS et al. *J Am Coll Cardiol* 2012;60(11):1018–25.
60. Zou M et al. *J Thorac Dis* 2016;8(1):43–51.
61. Pasquali SK et al. *Circulation* 2002;106(20):2575–80.
62. Massoudy P et al. *Circulation* 2002;106(15):1980–4.
63. Stoica S et al. *Ann Thorac Surg* 2012;93(6):1977–83.
64. Villafañe J et al. *J Am Coll Cardiol* 2014;64(5):498–511.
65. Rutledge JM et al. *Pediatr Cardiol* 2002;23(2):137–45.
66. Wallis G et al. *Orphanet J Rare Dis* 2011;6(1):1–12.
67. Hosseinpour AR et al. *Ann Thorac Surg* 2004;77(6):2163–6.
68. Becker AE et al. *Circulation* 1980;61(6):1133–41.
69. Freedom RM et al. *Am J Cardiol* 1978;42(4):620–8.
70. Penny DJ et al. *Br Heart J* 1992;68(5):498–500.
71. Allwork SP et al. *Am J Cardiol* 1976;38(December):910–23.
72. Fyler DC et al. *Pediatrics* 1980;65:375–461.
73. Kuehl KS, Loffredo CA. *Birth Defects Res Part A Clin Mol Teratol* 2003;67(3):162–7.
74. Paladini D et al. *Ultrasound Obstet Gynecol* 2006;27(3): 281–5.
75. Presbitero P et al. *Br Hear J* 1995;74(1):57–9.
76. Ismat FA et al. *Int J Cardiol* 2002;86(2–3):207–16.
77. Chiappa E et al. *Cardiol Young* 2004;14:265–76.
78. Sharland G et al. *Heart* 2005;91(11):1453–8.
79. Paladini D et al. *Prenat Diagn* 2002;22(7):545–52.
80. Prieto LR et al. *Circulation* 1998;98(10):997–1005.
81. Graham TP et al. *J Am Coll Cardiol* 2000;36(1):255–61.
82. Huhta JC et al. *Circulation* 1983;67(6):1374–7.
83. Barron DJ et al. *Semin Thorac Cardiovasc Surg Pediatr Card Surg Annu* 2011;14(1):109–15.
84. Hiramatsu T et al. *Eur J Cardio-Thoracic Surg* 2012;42(6): 1004–8.
85. Lim H-G et al. *Ann Thorac Surg* 2010;89(1):159–67.
86. McEwing RL, Chaoui R. *Ultrasound Obstet Gynecol* 2004; 23(1):68–72.
87. Acar P et al. *Heart* 1998;80(5):479–83.
88. Shih J-C et al. *J Med Ultrasound* 2012;20(2):65–71.
89. Shih JC et al. *Ultrasound Obstet Gynecol* 2008;32(6):762–8.
90. Zhang Y et al. *Prenat Diagn* 2011;31(10):529–35.

# 30

# Left heart malformations

Brian S. Snarr, Michael Y. Liu, and Jack Rychik

## Introduction

Left heart malformations account for nearly 9% of all congenital heart defects.[1] Proper development of the inflow and outflow structures of the left heart are crucial to ensuring a fully oxygenated cardiac output is delivered to the rest of the body. In the early stages of embryogenesis, a sequence of carefully orchestrated molecular events establishes the left atrium as the receiving chamber of pulmonary venous return, left ventricular (LV) inflow through a mitral apparatus, and connection of the LV outflow to the aorta. Perturbation of these events results in various forms of left-sided congenital heart disease. In this chapter, we review the development, pathology, and pathophysiology of left-sided heart malformations, as well as their implications in fetal and postnatal care.

## Development of the left heart

One of the earliest recognizable structures of the primordial heart is the linear heart tube, which is suspended from the embryo along its length by the dorsal mesocardium.[2,3] The combination of left-right patterning molecular signaling cascades and the regression of the middle portions of the dorsal mesocardium will facilitate the heart tube to undergo its characteristic "D-loop," positioning the primitive left ventricle in a relatively leftward and posterior position.[2] The looped heart has an inner and outer curvature and remains in a series configuration with the atrioventricular junction located entirely over the LV. A series of morphogenetic movements that take place at the inner curvature will position the subaortic outflow tract over the LV.[4] The mitral valve leaflets and the associated chordae tendinae derive from the endocardial cushions. These are localized tissue swellings in the atrioventricular junction that are populated mostly by cells that have undergone an epithelial-to-mesenchymal transformation of the endocardial lining.[3,5] The supporting papillary muscles, however, originate from ridges of myocardium in the left ventricle.[6] The aortic valve leaflets arise from outflow tract cushions that are largely composed of endocardial-derived cells, in a manner analogous to the atrioventricular valve development from the endocardial cushions.[3,5] While the specific morphologic mechanisms regulating the development of the left heart structures are poorly understood, interruption of these carefully timed events has a profound impact on the anatomical end result and ultimately a potent impact on the clinical manifestation of left heart disease.

## Left heart physiology in fetal circulation

The fetal circulation is configured in a parallel arrangement between right and left sides with only about one-third of the combined cardiac output provided by the LV.[7] The left atrium receives inflow contributions from the pulmonary veins as well as oxygenated blood from the ductus venosus (DV) and left hepatic vein, flow streams that are directed to the left atrium across the foramen ovale.[8] As the blood traverses the mitral and aortic valves, it continues on to the ascending and transverse aorta and to the aortic isthmus (region of aorta just prior to insertion of the ductus arteriosus), thus preferentially supplying the coronaries, brain, and upper body with more highly oxygenated blood.[8] Any level of interruption of this left-sided circulation in the prenatal period may result in a wide spectrum of congenital malformations and potentially have severe postnatal consequences. Perturbations of left-sided circulation with reduction in volume of flow are often indicated as the cause for arrested development of downstream structures, following a "no flow, no grow" concept. However, it is also plausible to speculate that a primary structural left-sided heart defect may influence upstream flow characteristics, with reduction in flow as a consequence. This debate continues, with examples to support either argument present in nature in a variety of left heart anomalies.

Most left-sided malformations are well-tolerated *in utero* from a cardiovascular, hemodynamic perspective due to the ability of the right ventricle to compensate for the left-sided impairments and provide blood flow to critical structures retrograde through the ductus arteriosus. The fetus may continue to grow and otherwise demonstrate ostensible measures of clinical well-being under the permissive conditions of the fetal circulation. Not surprisingly, there has been great interest in restoring optimal left-sided blood flow *in utero* through fetal interventions in hopes of improving postnatal outcomes.[9] However, at a deeper level, left-sided heart malformations often lead to alterations in flow streams with differences in potential oxygen delivery from normal. Hence,

the impact of left-heart malformation on brain development, somatic growth, and overall heart function is a topic of current interest and investigation.

# *Individual lesions*

## Hypoplastic left heart syndrome

Hypoplastic left heart syndrome (HLHS) is a constellation of congenital anomalies in which the left side of the heart is unable from a structural perspective to undertake its assigned task of perfusion of the systemic circulation. Most commonly, the mitral and aortic valves are poorly developed or absent (atresia) (Figure 30.1) with a diminutive LV cavity (Figure 30.2). Noncardiac anomalies are seen in approximately a third of HLHS infants.[10] Prenatal diagnosis of this lesion has been associated with improvement in presurgical status and decrease in adverse neurologic events.[11] There are still conflicting reports as to whether prenatal diagnosis actually improves outcomes.[12,13] The postnatal management strategy has changed and evolved substantially over the last four decades. While a lethal anomaly if not treated, the current era offers a three-stage palliative surgical strategy that culminates in survival of most born with this condition. The resulting physiology includes a systemic perfusion via a right ventricle delivering blood through a reconstructed aorta and pulmonary blood flow through the connection of systemic venous return directly to the lungs via the Fontan procedure.[14]

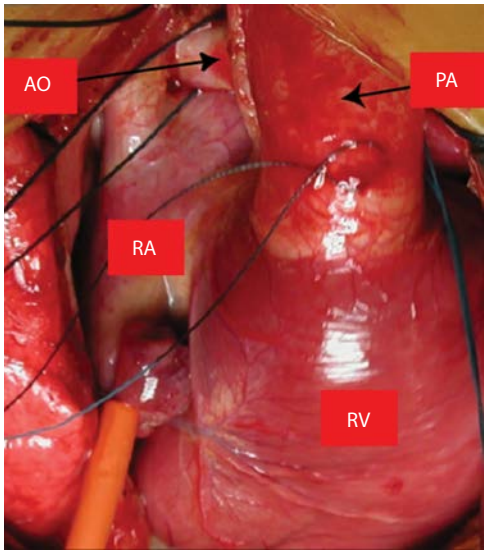


**Figure 30.1**
Operating room image of a live newborn heart with HLHS. Note the miniscule hypoplastic ascending aorta, which measures 1 mm in diameter, in comparison to the dilated pulmonary artery. (AO, severely hypoplastic ascending aorta; PA, pulmonary artery; RA, right atrium; RV, right ventricle.)

HLHS represents between 4% and 8% of all congenital heart defects and is present in 2.6 per 10,000 births.[15] There are multiple levels of evidence that point to a genetic predisposition to developing HLHS, including a higher recurrence risk of congenital heart disease and HLHS in other family members of patients diagnosed with HLHS.[16]

Despite our advances in molecular biology and genetics, the etiologic role of genetics in HLHS pathogenesis is still poorly understood with no monogenic cause identified. There are two general working hypotheses used to explain HLHS development. The first focuses on interruption of the left heart fetal flow patterns, such as abnormal mitral and or aortic valve development, which results in arrested development of left-sided structures secondary to the altered flow conditions. The second hypothesis proposes abnormal ventricular chamber signaling pathways responsible for normal growth and development of the left ventricle.[16] As our molecular understanding of HLHS increases, the relative contribution of each of these hypotheses to HLHS pathogenesis will become more evident.

### Prenatal physiology and management

There are significant differences from normal in the pathway of blood flow in fetuses with HLHS. The systemic venous return is typical to the right atrium. The eustachian valve, which usually directs blood from the inferior vena cava (IVC) toward the atrial septum, is often hypoplastic.[17] Because there is either very little or no antegrade blood flow through the LV

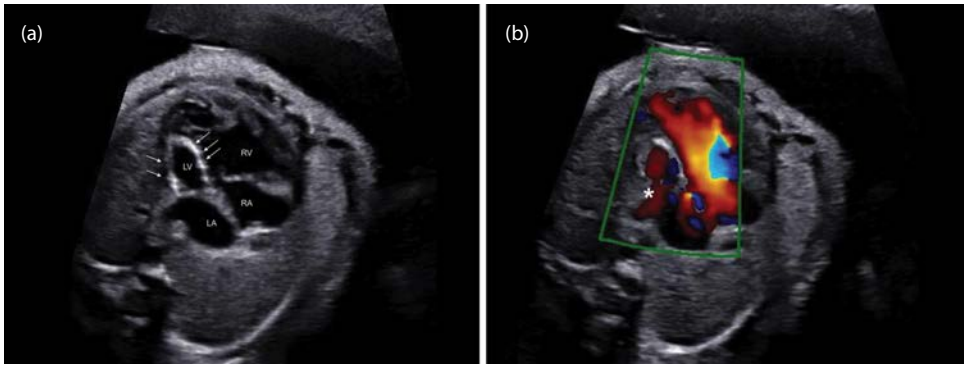


**Figure 30.2**
(a) Fetal echocardiographic image of HLHS at 28 weeks' gestation. The LV is severely hypoplastic and has an echobright appearance (arrows) from endocardial fibroelastosis. (b) Color Doppler during diastole demonstrates mitral valve hypoplasia (asterisk). (LA, left atrium; LV, left ventricle; RA, right atrium; RV, right ventricle.)

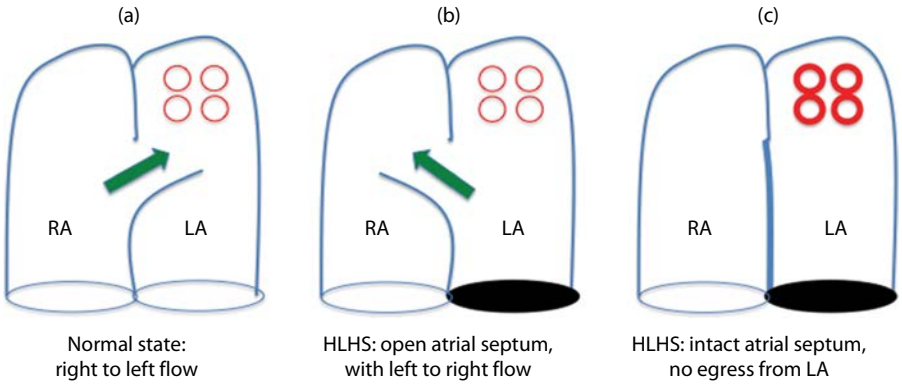


**Figure 30.3**
Demonstrating direction of flow across the atrial septum. (a) Normal state of right to left flow. (b) Hypoplastic left heart syndrome with open atrial septum. As blood cannot traverse the left side, pulmonary venous return flows left to right across the atrial septum. (c) Hypoplastic left heart syndrome with intact atrial septum. Pulmonary venous return cannot find ready egress from the left atrium, resulting in pulmonary vein congestion and developmental abnormalities of the pulmonary vasculature.

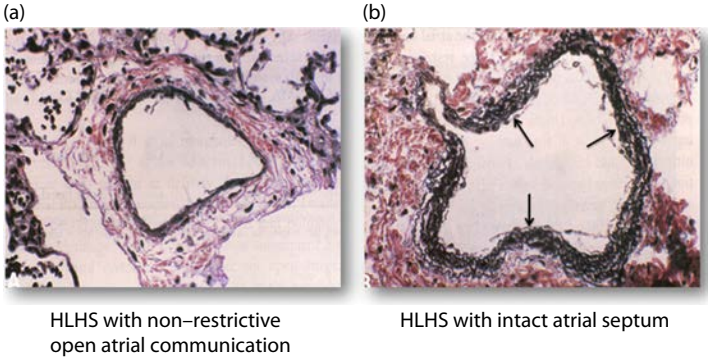


**Figure 30.4**
Hematoxylin and eosin-stained slides of pulmonary veins. (a) Case of a newborn with hypoplastic left heart syndrome and open atrial communication displaying normal vessel wall internal membrane. (b) Case of a newborn with hypoplastic left heart syndrome and intact atrial septum. Note the multiple elastic laminae of the internal vessel wall (arrows) indicating "arterialization" of the pulmonary vein.

and aorta, with both structural and functional impediment to forward flow through the left side, blood flow from the pulmonary veins entering the left atrium shunts from the left to the right atria across the atrial septum to decompress the left atrium (Figure 30.3). During transitional physiology at birth with separation from the placenta, blood flow increases to the lungs and thus leads to increased return to the pulmonary veins and left atrium. This pulmonary venous blood must readily exit the left atrium and mix with systemic venous return in the right atrium as it drains into the right ventricle, thus allowing for oxygenated blood in a mixed manner to be delivered to the body.

Determining the patency of the atrial septum and degree of decompression of the left atrium is important for risk stratifying the fetus with HLHS. Patients with highly restrictive or intact atrial septum are at high risk for postnatal mortality.[18,19] The fetus itself is usually asymptomatic as the placenta provides oxygenated blood to the body. Nevertheless, impediment to left atrial drainage *in utero* can lead to abnormalities of pulmonary vascular development with "arterialization" of pulmonary veins (Figure 30.4). No clinical manifestations may be present while on placental circulation; however, at birth once the infants' lungs are open, oxygenated blood returning to the left atrium (LA) cannot mix with systemic venous return in the right atrium (RA), leading to the potential for profound hypoxemia and early death.

To determine the degree of atrial septal restriction, one can directly visualize the septum with two-dimensional and color imaging, but also measure Doppler wave patterns in the pulmonary veins.[20] The normal pulmonary vein Doppler flow pattern is one of predominantly antegrade flow with a small amount of retrograde flow with atrial contraction. If there is atrial septal restriction, the interval and velocity of the retrograde atrial wave will be increased (Figure 30.5). Michelfelder et al. demonstrated that a velocity-time integral ratio of antegrade to retrograde flow of less than five suggests atrial level restriction and potential need for urgent postnatal intervention.[21] Maternal hyperoxygenation as a provocative test of fetal pulmonary vasoreactivity has also been used to assist in diagnosis of a restrictive atrial septum and its impact on pulmonary vascular development in HLHS. Fetuses with HLHS with an intact or highly restrictive atrial septum had very little pulmonary vasoreactivity and little change in pulmonary artery pulsatility index (PI) after mothers were offered 100% $FiO_2$ through a non-re-breather face mask for 15 minutes.[22,23] Recently, fetal magnetic resonance imaging techniques have been applied to help characterize lung make-up in HLHS. T2-weighted imaging sequences specific to identifying water content have been used to help identify lymphatic congestion or "lymphangiecstasia" in the setting of atrial-level restriction with the presence of a "nutmeg lung" appearance[24] (Figure 30.6). The longitudinal physiological

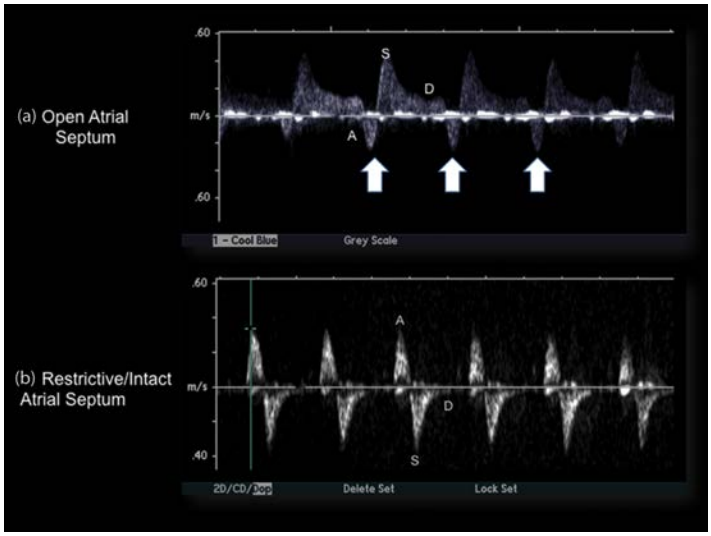


**Figure 30.5**
Doppler interrogation of pulmonary veins. (a) Open atrial septum with predominantly antegrade flow as noted above the baseline. White arrows point to small normal amount of retrograde flow in pulmonary veins with atrial contraction. (b) Highly restrictive atrial septum indicating an equal amount of to-and-from antegrade and retrograde flow. This pattern suggests a high degree of impediment to left atrial egress and high left atrial pressure. (A, atrial contraction wave; D, diastolic wave; S, systolic wave.)

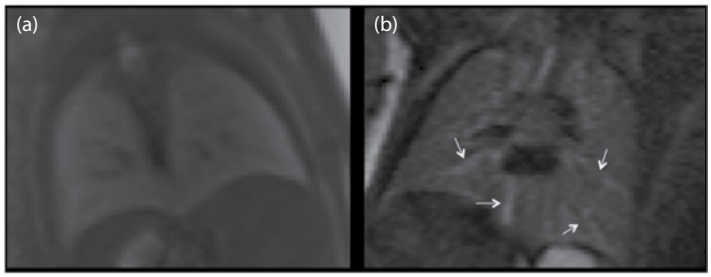


**Figure 30.6**
Fetal lung magnetic resonance imaging with T2-weighted sequences performed at approximately 30 weeks' gestation. (a) Normal lung. (b) Fetus with HLHS and atrial level restriction demonstrating "nutmeg" lung. Arrows point to regions or "septae" of high-intensity signal, suggesting increased water content, indicating presence of lymphatic congestion.

connection between lymphatic abnormalities now being recognized with increasing frequency in the child and adult after staged reconstruction in single ventricle[25] and the prenatal findings of fetal lung lymphangiectasia, and perhaps even first trimester increased nuchal translucency, suggest a derangement of the lymphatic system as a possible common physiological theme in HLHS and other single-ventricle conditions.

In HLHS, the cerebral vasculature is predominantly supplied retrograde from the ductus arteriosus. Fetuses with HLHS have lower cerebrovascular resistance compared to normal and other lesions as measured by lower middle cerebral artery PI.[26] One explanation may be that the brain is autoregulating blood flow to optimize cerebral perfusion. In the face of anatomical impediment due to a small aorta, limited aortic flow may lead to cerebral vasodilation in a compensatory manner. Whether this cerebrovascular vasodilation is sufficiently compensatory or not is unclear. Although neurocognitive deficits in children with HLHS are now well documented, the direct linkage to cerebral blood flow *in utero* remains unclear.[27,28]

In HLHS, the right ventricle is the systemic ventricle. Although it has features of the morphology of a right ventricle, it is rarely of normal appearance and geometry as it adapts during prenatal life to its task of systemic perfusion. In the absence of significant tricuspid regurgitation, or primary ventricular dysfunction, the right ventricle is usually capable of supporting systemic perfusion in fetuses with HLHS. This is why fetal hydrops is rare in HLHS as the right side usually manages well. However, the mechanics of RV contraction, even *in utero*, are different from normal. The presence of a small noncontributory left ventricle such as in the condition of mitral hypoplasia with a left ventricle that displays endocardial fibroelastosis may influence the mechanics of RV contraction (Figure 30.7). Such small ventricles may also have coronary-cameral connections (Figure 30.8) that may impact coronary distribution to healthy RV myocardium and thus influence RV myocardial blood flow.[29] In a Doppler blood flow and myocardial tissue velocity study, comparing normal RV free wall mechanics to the RV free wall of fetuses with HLHS and no visible LV cavity compared to HLHS with a visible small LV with endocardial fibroelastosis (EFE), significant differences in systolic velocity are identified. Furthermore, diastolic function and compliance of the RV as reflected by the ratio of RV early blood flow diastolic velocity (RV E wave velocity) to RV early myocardial movement diastolic velocity (RV Ea wave velocity) is higher in the HLHS fetus with a small LV and EFE than in the HLHS with no LV. The RV E-to-RV Ea ratio, reflecting a "stiffer" right ventricle with higher filling pressure, is noted in the HLHS fetus throughout gestation in comparison to the normal LV (Figure 30.9).

The RV and tricuspid valve often dilate to accommodate the increased blood volume, as the entire or majority of the cardiac output must now traverse the RV. However, it has been shown that fetuses with HLHS have, on average, a 20% decrease in cardiac output relative to normal fetuses.[30] In a gestational age-matched study, Doppler-derived functional characteristics of the fetal RV in HLHS were compared to the normal

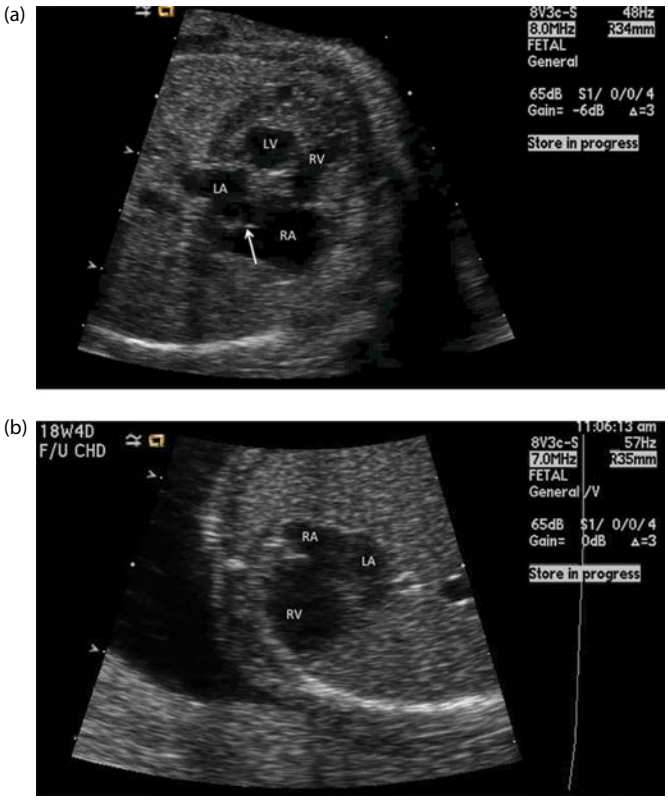


**Figure 30.7**
Variability in RV geometry in HLHS. (a) Case of HLHS with mitral hypoplasia and a small LV. Arrow points to atrial septum bowing left to right indicating inadequacy of the small LV. The RV appearance is oblong and ellipsoid. (b) Case of HLHS with mitral atresia and no visible LV. The RV is much more rounded in its geometry. (LA, left atrium; LV, left ventricle; RA, right atrium; RV, right ventricle.)

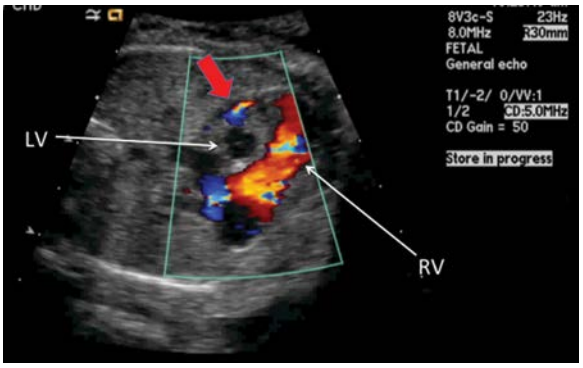


**Figure 30.8**
Case of HLHS with mitral stenosis, a hypoplastic left ventricular cavity that is filling through the mitral valve but with aortic atresia. The arrow points to a coronary-cameral fistula.

fetal RV. Parameters such as the combined cardiac output and the myocardial performance index (MPI), a reflection of global myocardial efficiency (ratio of combined isovolumic contraction and relaxation times to the ejection time) were compared. Lower myocardial performance indices reflect more efficient

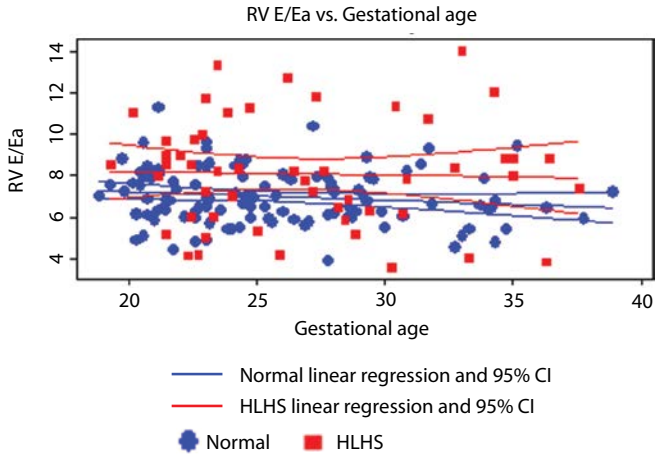


**Figure 30.9**
Graph of Doppler blood flow and tissue imaging derived RV E/Ea ratio—a measure of RV diastolic function—versus gestational age for normal fetuses ($n$ = 115) marked as blue boxes, and HLHS fetuses ($n$ = 85) marked as red boxes. Regression and 95% confidence intervals are displayed. As a whole, the HLHS group has a higher RV E/Ea than normal. Many of the highest values of RV E/Ea above 10 are in those fetuses with HLHS and a sizable LV with endocardial fibroelastosis. (Data from Natarajan S et al. *J Am Soc Echocardiogr* 2013;26(5):515–20.[29])

**Table 30.1** Comparison of measures of ventricular function between hypoplastic left heart syndrome and normal gestational-age matched control fetuses

| *Variable* | *HLHS (n = 44)* | *Normal (n = 76)* | *P value* |
|---|---|---|---|
| GA (weeks) | 26.7 ± 5.1 | 25.9 ± 5.2 | 0.38 |
| Fetal weight (kg) | 0.89 (0.28–3.17) | 0.82 (0.20–3.84) | 0.61 |
| RV MPI | 0.47 ± 0.09 | 0.43 ± 0.05 | 0.005 |
| LV MPI | – | 0.40 ± 0.05 | – |
| RV ejection force (mN) | 9.39 (1.56–84.9) | 6.62 (0.97–28.5) | <0.001 |
| LV ejection force (mN) | – | 5.82 (0.73–24.2) | – |
| Combined cardiac output (mL/min/kg) | 385 | 477 | <0.001 |

*Abbreviations:* GA, gestational age; kg, kilogram; mN, milliNewton; LV, left ventricle; RV, right ventricle; wks, weeks.

and better global ventricular function. In addition, a unique parameter, the "ventricular ejection force," was measured, which is a reflection of systolic ventricular performance derived from Newton's laws, with a higher value corresponding to greater force exerted in ejection. In HLHS the RV myocardial performance index (MPI) is higher, and ejection force is higher than normal, while combined cardiac output is lower than normal (Table 30.1). Hence, in fetal life the RV in HLHS (1) has greater burden of work than normal by virtue of an increased

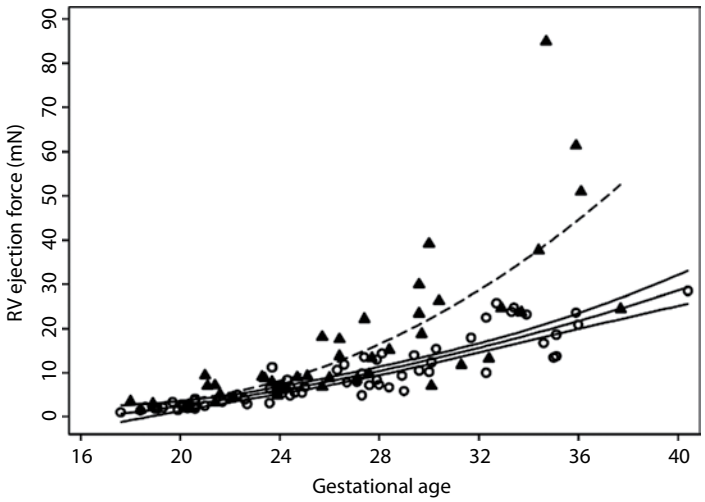


**Figure 30.10**
Graph of Doppler-derived RV ejection force for fetuses with HLHS (closed triangles) versus normal controls (open circles) over gestation. Note the increase in ejection force, which begins to appear at approximately 26–28 weeks' gestation. (mN, milliNewtons, a measure of force.) (Data from Szwast A et al. *Ann Thorac Surg* 2009;87:1214–9.[30])

ejection force, (2) is less efficient than normal with higher MPI, and (3) provides an overall lower cardiac output than normal. Variability in these parameters during fetal life may help predict which right ventricles may be best able to tolerate sustained long-term functionality as a systemic ventricle after surgical staged reconstruction. Of note, RV ejection force begins to differ from the normal RV at approximately 26 weeks' gestation but is more similar to normal prior to that, perhaps suggesting an accommodation to loading conditions at approximately the beginning of the third trimester of pregnancy (Figure 30.10).

### Postnatal management

Infants with HLHS are typically cyanotic at birth, but in those with a large interatrial communication, a plethora of pulmonary blood flow, and a wide open ductus arteriosus, there can be a picture of a well-oxygenated, relatively pink infant. Systemic output is dependent on flow through the patent ductus arteriosus. Hypotension, hypoperfusion, and metabolic acidosis ensue with natural constriction of the ductus, and a state of pulmonary overcirculation develops as more blood is forced into the pathway of least resistance into the lungs. With no intervention, patients will die shortly after ductal closure, which typically occurs within hours to days after birth. Administration of prostaglandin E1 is used to maintain ductal patency until surgical intervention can occur. A three-stage palliative surgical reconstruction is the most common management strategy today.[31] The first stage is performed in the newborn period and establishes reliable systemic output through construction of a neo-aorta, and controlled pulmonary blood flow through the placement of a Blalock-Taussig (BT) shunt or right ventricle to pulmonary artery conduit. There is also an alternative "hybrid" approach that combines the use of catheter-based and surgical interventions to accomplish the same physiologic objectives as the first-stage procedure.[13]

Outcomes after stage 1 Norwood palliation continue to improve. Stratification based on risk factors has been proposed. High-risk factors for mortality after initial surgery include the following: (1) presence of extracardiac anomalies; (2) genetic, chromosomal, or syndromic anomalies; (3) prematurity prior to 34 weeks' gestation; (4) intact or highly restrictive atrial septum; or (5) severe tricuspid regurgitation. Absence of these risk factors defines the standard risk patient. Overall survival through the initial surgery at experienced centers can be greater than 90%, with high-risk survival only slightly higher than 50% (Figure 30.11). This information is important for counseling of families and highlights the importance of rigorous and comprehensive evaluation of these fetuses. The subsequent palliative stages are performed later, including a superior cavopulmonary connection (bidirectional Glenn operation) at approximately 4–6 months of age and culminating in a total cavopulmonary anastomosis (Fontan procedure) usually at 2–4 years of age. Survival up to 20 years is now approaching 70%–80%[32,33]; however, the end-organ consequences of the Fontan circulation are many with a substantial burden of morbidity present for many patients.[34]

## Mitral valve anomalies

In the normal fetal heart, the coordinated movements of the mitral valve and its associated chordae facilitate LV filling from pulmonary venous blood and oxygenated blood streaming across the foramen ovale. The subsequent closure of the mitral valve during systole prevents backflow into the left atrium, and maximizes the efficiency of LV ejection during systolic contraction. Mitral valve abnormalities generally include stenosis, atresia, and insufficiency. Severe mitral stenosis and mitral atresia are discussed in context with hypoplastic left heart syndrome. Mitral valve dysplasia syndrome, although pathophysiologically similar to HLHS, is discussed separately in this section.

### *Mitral stenosis*

Mitral valve stenosis may occur as a result of abnormal development of the mitral valve leaflets proper. This is often associated with shortened chordae tendinae with little or no interchordal spaces (commonly called a "mitral arcade"). There also may be abnormal spacing of the papillary muscles,

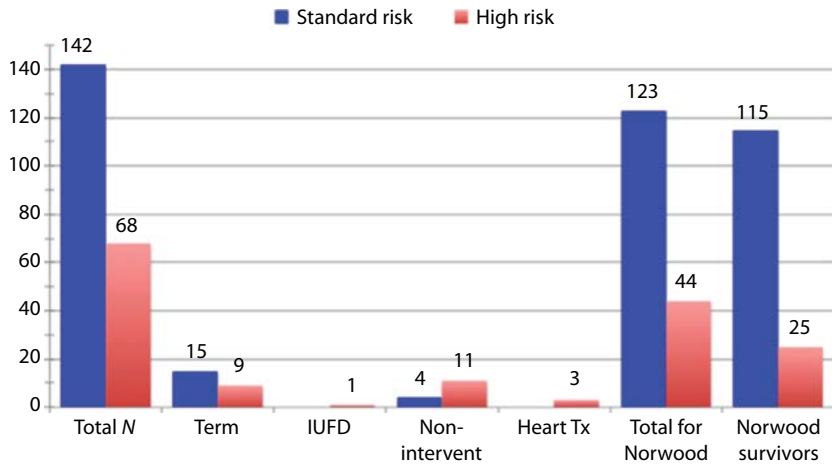


**Figure 30.11**
Outcomes for 210 fetuses with HLHS from point of initial prenatal presentation through stage 1 Norwood operation. In blue are the standard-risk and red the high-risk fetuses, high risk defined as having one or more of the following: (1) extracardiac anomaly, (2) genetic or chromosomal anomaly, (3) prematurity less than 34 weeks' gestation, (4) intact or highly restrictive atrial septum, or (5) severe tricuspid regurgitation. Of those presenting at birth with intention to treat, 115 of 123 standard risk (93%) survived through stage 1 Norwood, while only 25 of 44 high risk (57%) survived stage 1 Norwood surgery. (Heart Tx, heart transplantation pathway; IUFD, intrauterine fetal demise; Non-Intervent, no intervention at birth with palliative care chosen; Term, termination of pregnancy at prior to 24 weeks' gestation.) (Data from Rychik J et al. *Ultrasound Obstet Gynecol* 2010;36:465–70.[19])

or the chordae may attach solely to a single papillary muscle in the "parachute" mitral valve.[6,35] Mitral stenosis can also exist with a supravalvar mitral ring, which may occur in isolation or in combination with other abnormalities such as a parachute mitral valve, left ventricular outflow tract obstruction, and coarctation of the aorta in the "Shone complex."[36] Mitral stenosis results in an increase of left atrial pressure and may cause left to right flow across the foramen ovale. In the case of an unrestrictive foramen ovale, the Doppler gradient across the mitral valve will underrepresent the true degree of stenosis, as blood is shunted away from the obstruction into the right side of the heart. Severe stenosis decreases the amount of blood flow to the left heart and may result in underdeveloped left-sided structures as in HLHS. Fetal mitral stenosis should also prompt thorough evaluation of the left ventricular outflow tract and aorta to look for serial downstream obstructive lesions such as seen in the Shone complex. Postnatal management of mitral stenosis is dependent on its severity and the constellation of other malformations with which it is associated. Severe mitral stenosis associated with HLHS will require the first stage of single-ventricle palliation in the newborn period (discussed in the HLHS section).

## Mitral regurgitation

Fetal mitral regurgitation may occur as a result of abnormal formation of the mitral valve leaflets, supporting chordae, or papillary muscles. An isolated "cleft" or other abnormality of the valve may impair complete closure during systole leading to regurgitation. It may also be associated with coarctation or occur as a consequence of LV dysfunction, such as in cardiomyopathy.[37] Regurgitant flow across the mitral valve is readily assessed with color flow and Doppler interrogation. Depending on the severity of the regurgitation, there may be left ventricular dilation. Left atrial dilation is also possible but more likely if there is a restrictive atrial septum.

## Mitral valve dysplasia syndrome

Mitral valve dysplasia syndrome (MVDS) is a rare condition that is often discussed in the context of its similar physiology with HLHS, but it also has some distinctive characteristics that are worthy of description separately. MVDS is defined by a thick and dysplastic arcade mitral valve that results in both mitral stenosis and severe mitral regurgitation. Severe left ventricular outflow obstruction is also present in the form of aortic stenosis or atresia. The combination of these features produces a significantly dilated left atrium and dilated left ventricle with diminished left ventricular function (Figure 30.12). Ironically, some consider this part of the HLHS spectrum, despite the fact that the LV is not hypoplastic but rather dilated, yet it fulfills the definition of a structural abnormality leading to inadequacy of the LV to support the systemic circulation. Restriction of flow across the atrial septum is another key feature that is likely the result of an increased left atrial pressure causing partial or even complete closure of the foramen ovale.[38] Pulmonary venous Doppler interrogation is useful in assessing the degree of mitral regurgitation and atrial restriction and may demonstrate a unique flow reversal pattern during atrial systole. Severe cases may also demonstrate flow reversal during ventricular systole producing a rather unique "double-reversal" flow pattern. EFE is a common finding in the dilated and poorly functioning

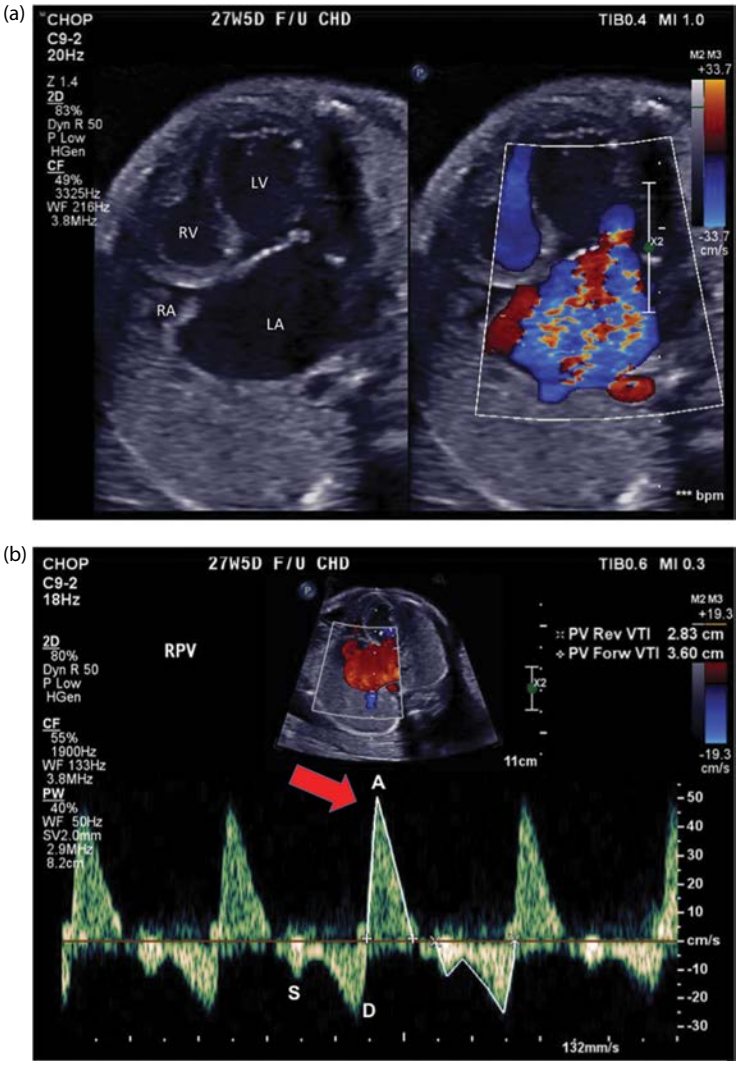


**Figure 30.12**
Fetal echocardiogram of a patient with MVDS at 27 weeks' gestation. (a) Severely dilated LA and LV. Color Doppler shows severe mitral regurgitation. (b) Pulmonary vein pulse wave Doppler interrogation demonstrates significant flow reversal (arrow) during atrial contraction (A) suggestive of elevated LA pressures. (A, atrial contraction; D, diastole; LA, left atrium; LV, left ventricle; RA, right atrium; RPV, right pulmonary vein; RV, right ventricle; S, systole.)

left ventricle. Significant left ventricular dilation may impair right ventricular function. Unlike other forms of HLHS in which hydrops rarely occurs, fetal hydrops is common in MVDS.

Prenatal management includes serial echocardiograms evaluating left heart dilation and the degree of atrial septal restriction as predictors of mortality and the need for urgent postnatal intervention.[38] Fetal hydrops is also assessed, which may be present if right ventricular outflow is compromised. Fetal interventions upon the aortic valve and the atrial septum have been attempted and technically successful in a limited number of patients; however, disappointingly, these efforts have failed to reliably result in recruitment of the left ventricle to enable a well-functioning two-ventricle repair.[38,39] The most significant risk related to the postnatal transition for these patients lies within the severity of restriction at the atrial septum. Thus, delivery in a facility with access to immediate postnatal intervention is imperative. Those without significant atrial septal restriction undergo postnatal management similar to that of patients with HLHS.

## Aortic valve and aortic anomalies

The normal trileaflet aortic valve forms the gateway from the left ventricular outflow tract to the aorta. In the fetal circulation, only about 30%–40% of the combined cardiac output will traverse the aortic valve, providing the more highly oxygenated blood supply to the heart and brain.[7] Fetal anomalies of the aortic valve that interrupt this circulation generally include aortic stenosis and atresia. Aortico-left ventricular tunnel is a rare condition that physiologically resembles aortic insufficiency. True aortic insufficiency in the fetus is uncommon.

### *Aortic stenosis*

Aortic stenosis (AS) broadly refers to an impediment to LV egress and may be a result of valvar, subvalvar, or supravalvar pathology. Of these, valvar aortic stenosis is the most common presentation, with bicuspid aortic valve representing the most common morphology.[15,40] Valvar stenosis may involve decreased annulus size, dysplastic valve leaflets, or abnormal development

of the separate commissures (as in bicuspid aortic valve). Supravalvar aortic stenosis is most commonly associated with Williams syndrome and with mutations in the elastin gene.[41] Subvalvar aortic stenosis may be present in numerous settings, including a posterior malalignment of the conal/infundibular septum in the presence of a malalignment-type ventricular septal defect. Subaortic stenosis can be seen as part of a constellation of left-sided serial obstructions in Shone complex, part of dynamic outflow tract obstruction in hypertrophic cardiomyopathy, or due to atrioventricular (AV) valve attachments in a common AV canal defect. Acquired subvalvar aortic stenosis in the form of a subaortic membrane may develop in the presence of a ventricular septal defect and is common after birth, but this is rare in the fetus.[42] The genetics of aortic stenosis are poorly understood, which is likely due to the large spectrum of malformations that may cause AS, and the multifactorial nature of the disease. AS may occur in isolation or in association with other forms of congenital heart disease. The isolated form has a 3:1 male predominance.[43] AS may be a manifestation as part of a larger syndrome such as Turner or Williams syndromes,[41,44] a pattern of familial left-sided congenital heart malformations,[45] or a result of a single gene mutation.[46] Any left-sided heart disease in a female fetus should prompt investigation for Turner syndrome (45, X0 chromosomes).

## Prenatal physiology and management

AS is generally well tolerated by the fetus, regardless of severity, due to the ductus arteriosus enabling retrograde perfusion of the coronaries and aortic arch vessels in the presence of left ventricular outflow tract obstruction. Severe AS places an increase in afterload upon the left ventricle and results in decreased left ventricular stroke volume, as well as an increase in end systolic ventricular volume. These changes may manifest as left ventricular hypertrophy, dilation, decreased ventricular compliance, and even EFE. If critical AS is present, retrograde flow from the ductus arteriosus will be readily appreciated upon color Doppler evaluation. With increased left ventricular filling pressures, left atrial pressure will rise, and the net right-to-left flow across the foramen ovale may decrease. Importantly, the presence of (1) right to left flow on Doppler interrogation and/or (2) bowing of the atrial septum right to left indicating right atrium to left atrium pressure gradient, are strong indicators of proper adequacy of the left side of the heart. Conversely, predominant left to right atrial shunting should raise concern for an LV and the possible development of HLHS through structural evolution during gestation. Flow across the aortic valve should be evaluated and will usually demonstrate turbulent flow with a normal to mildly elevated systolic velocity by Doppler (Figure 30.13). The severity of narrowing is not necessarily reflected by the presence of a relatively low gradient across the aortic valve. Severe stenosis may be present even if there is a low gradient. This phenomenon is due to decreased flow traversing the left ventricle and is also influenced by ventricular function.

A significant concern for prenatal AS is the potential for impaired growth of left-sided structures and the development of HLHS.[47] Although in our overall experience making up only a small proportion of all forms of HLHS (<5%), the phenomenon of evolving aortic stenosis into HLHS is quite dramatic (Figure 30.14). This has led to the development of fetal aortic valvuloplasty as a potential strategy to relieve aortic valve obstruction and avoid progression to HLHS.[9] The strategy is still controversial, as the criteria for candidacy continues to be debated.[48] Some fetuses have clearly benefitted and have gone on to a successful two-ventricle repair. However, in other cases, important left-sided residual lesions have persisted, leading to repeated operations on the left heart with potential need for prosthetic mitral valve implantation and pulmonary hypertension. Such outcomes raise the question of whether it is of benefit to have a challenged two-ventricle repair with suboptimal outcome versus a single-ventricle Fontan-type palliation. A report on the first 100 patients undergoing this procedure demonstrated promising results on the technical feasibility of fetal aortic valvuloplasty; however, less than half of successfully performed procedures resulted in a postnatal two-ventricular circulation.[49] The concept of potentially altering prenatal course and evolution of a congenital malformation either through catheter-based means of relief of obstruction or perhaps through pharmacological manipulation of fetal blood flow is extremely attractive and remains an active area of interest and investigation.

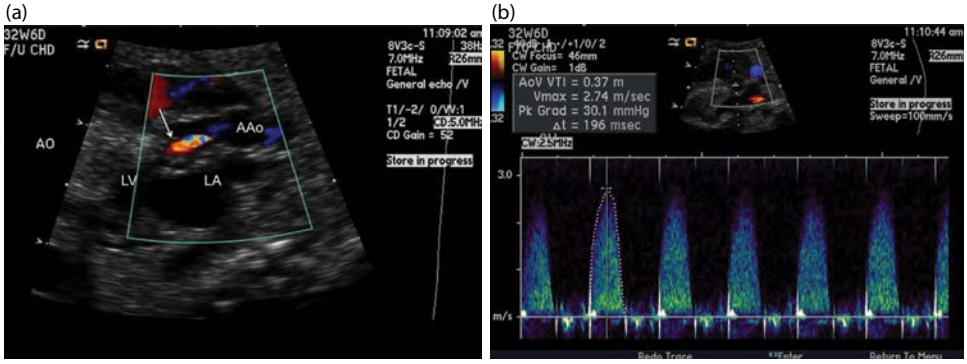


**Figure 30.13**
Fetal echocardiogram of a patient with aortic stenosis at 32 weeks' gestation. (a) Color Doppler shows flow acceleration across the stenotic aortic valve (arrow). (b) Continuous-wave Doppler demonstrates the corresponding elevated flow velocity across the aortic valve. (AAo, ascending aorta; LA, left atrium; LV, left ventricle.)

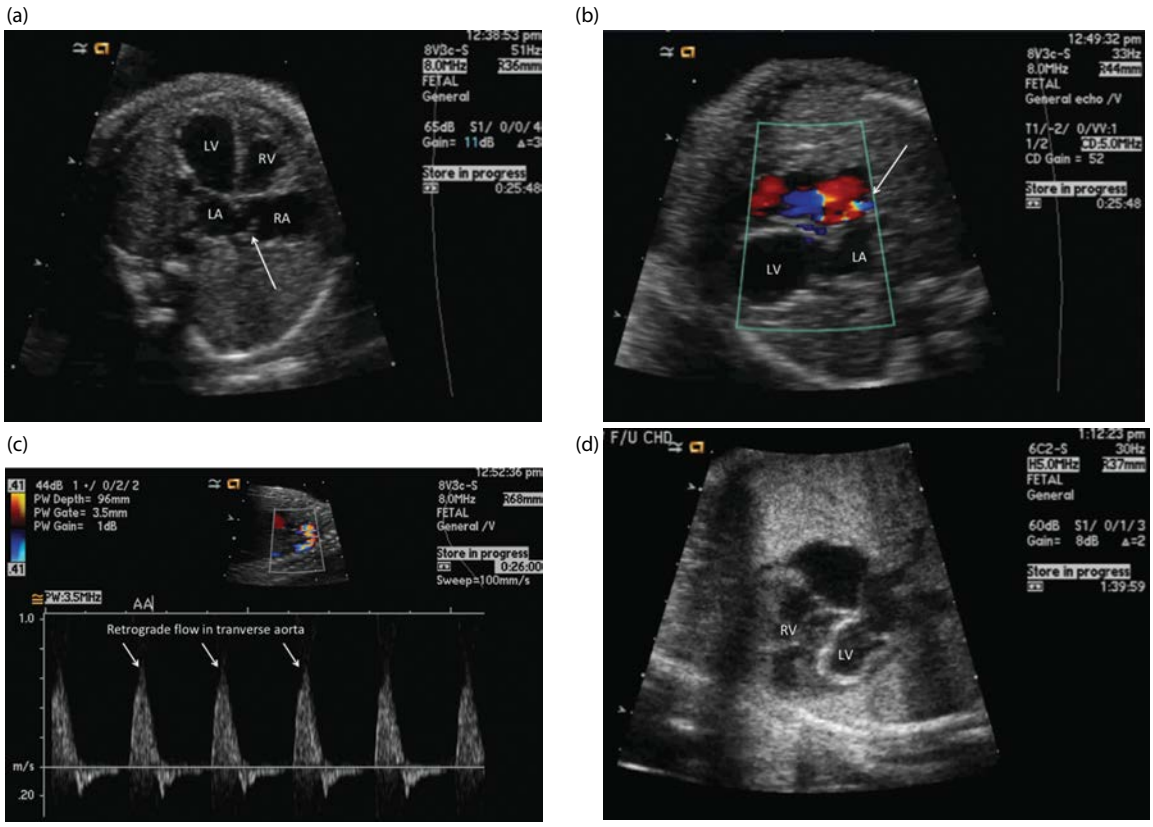


**Figure 30.14**
A case of fetal aortic stenosis that has evolved into HLHS. (a) Four-chamber view at 21 weeks' gestation shows a dilated left ventricle. There is some echo brightness to the LV endocardium suggesting endocardial fibroelastosis. The arrow points to the atrial septum bowing left to right. (b) The left ventricle is dilated, with echo brightness of the ventricular septum. The arrow points to left to right shunting across the atrial septum. (c) Doppler interrogation of the transverse aortic arch demonstrates retrograde flow, indicating perfusion of the aorta via the ductus arteriosus. (d) Same patient now at 33 weeks' gestation. Note the dramatic change in relative size of the left ventricle in comparison to the right ventricle. There is more prominent echo brightness indicating endocardial fibroelastosis. The picture is now one of clear HLHS that has developed from aortic stenosis and a dilated left ventricle. (LA, left atrium; LV, left ventricle; RA, right atrium; RV, right ventricle.)

## Postnatal physiology and management

Postnatal closure of the ductus arteriosus requires the LV to pump a full cardiac output across its outflow tract. With mild to moderate AS, this may be well tolerated by the newborn, and interventions may be postponed into childhood or the condition followed expectantly, depending on severity. If there is concern for severe or critical (ductal dependent) AS, planning for immediate neonatal intervention should take place. Patients with critical AS are safely maintained on prostaglandin infusion while awaiting catheter-based or surgical intervention with the objective of maintaining a two ventricular circulation. If the left ventricle is deemed inadequate to support a full cardiac output in the postnatal state, the patient will require single-ventricle palliation.

## *Aortic atresia*

Complete atresia of the aortic valve is associated with HLHS and follows the prenatal physiology described in more detail in the HLHS section. The absence of antegrade flow across the aortic valve and the presence of retrograde ductal flow into the hypoplastic ascending aorta are key echocardiographic findings supporting the diagnosis. When combined with mitral atresia, the left ventricle is tiny and often not discernible. With mitral valve patency, however, a small echo bright ventricle may be identified. Of note, aortic atresia with extremely tiny ascending aorta can be seen in association with a completely normal mitral valve and totally normal left ventricle when there is a large malalignment ventricular septal defect. This interesting condition is believed to develop due to a severe degree of posterior conal deviation obliterating the formation of the LV outflow tract and aortic valve complex early in development. In such cases, a complex operation can be performed after birth in which the aorta and pulmonary artery are anastomosed, the aortic arch reconstructed (along similar lines to the stage 1 Norwood operation), and the ventricular septal defect then baffled to the native pulmonary artery ("neo-aorta") and a conduit interposed between the right ventricle and the branch pulmonary arteries, thus resulting in a satisfactory two-ventricle repair.[50]

## Aortico-left ventricular tunnel

Aortico-left ventricular tunnel is an extremely rare malformation that consists of an abnormal communication from the ascending aorta to the left ventricle.[51] This connection creates a physiology similar to that of aortic regurgitation: volume loads the left ventricle and results in dilation of the left ventricle and ascending aorta.[52] These features are particularly helpful for echocardiographic diagnosis of aortic-left ventricular tunnel in the prenatal period.[52] Unrepaired aortic-left ventricular tunnel has a poor prognosis, but there have been reports of late presentation as an adult.[51,53] Nonetheless, when this lesion is identified *in utero*, postnatal surgical planning to eliminate the tunnel should commence as hemodynamic instability may present at birth. Surgical repair has had overall positive results, although patients may still eventually develop progressive aortic regurgitation.[54] Transcatheter device closure of aortic-left ventricular tunnel as a primary procedure, and after incomplete surgical closure, is also possible.[53,55]

## Coarctation of the aorta

Coarctation of the aorta is defined as narrowing of the aorta in the region beyond the take-off of the head and neck vessels in the descending aortic portion. Coarctation can be divided into the broad categories of discrete and long-segment narrowing. Discrete stenosis can occur anywhere along the descending aorta but most often occurs at the aortic isthmus, defined as the region just distal to the origin of the left subclavian artery and the insertion of the ductus arteriosus. In long segment or tubular hypoplasia, the isthmus and the region proximally or the entire transverse arch can be hypoplastic. Fetal coarctation can sometimes be a combination of these two types of coarctation, where the arch may be small with a concomitant discrete narrowing of the aorta where the ductal arch inserts.

There are several anatomical associations that are common with coarctation of the aorta, including (1) LV to RV size discrepancy, (2) bicuspid aortic valve, or (3) ventricular septal defect (especially posterior malalignment type). Coarctation of the aorta can also be associated with HLHS, complete atrioventricular canal (in particular, unbalanced atrioventricular canal), and transposition of the great arteries. Isolated coarctation occurs more frequently in males than females and is seen in 35% of patients affected by Turner syndrome (45, XO).[44]

### Prenatal physiology and management

The aortic isthmus is also a very informative site for assessment and evaluation of the balance of flows between the forces driving blood in this region, including (1) forward in systole through ventricular ejection with competing streams from RV and LV, (2) forward through downstream low placental impedance drawing blood forward, and (3) retrograde in relation to upper body and cerebral vascular resistances, as advocated by Fouron.[56] In the normal fetal circulation, the LV fills predominantly by right to left shunting across the foramen ovale of blood that is preferentially streamed across by the angulation and geometry of the ductus venosus. The LV then ejects blood into the ascending aorta and coronary arteries, with the aortic arch delivering blood to the head and neck vessels. By the time the column of LV ejected blood reaches the aortic isthmus, it comprises only approximately 10%–15% of the fetal combined cardiac output. It is no wonder that the aortic isthmus normally appears relatively small compared to the ascending or descending aorta, especially at the point of ductal insertion (Figure 30.15). This may also explain why any diminution in LV blood volume ejected, even if relatively minimal, can have a strong impact on the volume of blood traversing the aortic isthmus and thus lead to development of coarctation. It is also the reason why natural diversions of blood away from the LV, such as in the presence of a left superior vena cava potentially altering left atrial compliance,[57] or the presence of an interrupted inferior vena cava with azygous continuation, can make the aortic isthmus appear smaller than normal. Alterations in foramen streaming can mildly underfill the LV and make the downstream

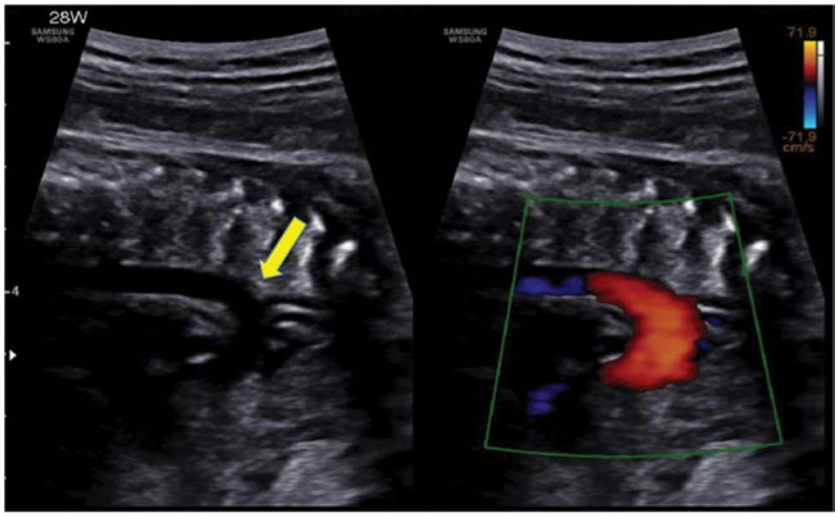


**Figure 30.15**
Normal aortic arch at 28 weeks' gestation. Normal two-dimensional and color flow image. There is a slight diminution in vessel caliber (arrow) at the aortic isthmus which is normal.

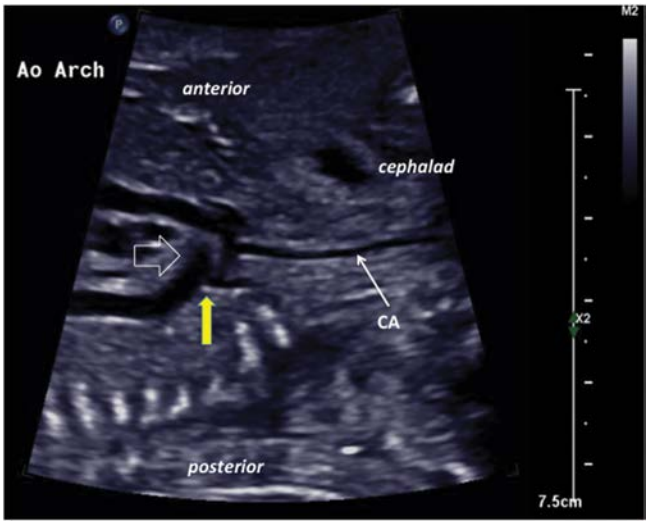


**Figure 30.16**
Fetus at 21 weeks' gestation with coarctation of the aorta. The aortic isthmus (arrow) is small as is the transverse aorta just proximally. Note the abnormal shape of the arch as it inserts into the descending aorta. Open arrow indicates the insertion site of the ductus arteriosus (DA). (CA, carotid artery.)

aortic isthmus appear small, even in the absence of a true "anatomical" coarctation of the aorta.

Detecting a true anatomical coarctation of the aorta in fetal life can be a challenge (Figure 30.16). Blood flow alterations and diversions for a variety of reasons can lead to LV-RV size discrepancy with a relatively small LV, and is now a commonly noted finding considering the ubiquity of obstetrical imaging and fetal echocardiography. Further compounding the problem is the fact that in subtle cases of aortic isthmus narrowing, significant obstruction may only become manifest once the ductus arteriosus closes, unmasking an underlying narrowing. Ductal tissue surrounding the aortic isthmus can itself be the cause of aortic narrowing, as it normally constricts after birth in the region of the insertion site into the descending aorta.

In fetal life, distinguishing a small but normal aortic isthmus from a true anatomical coarctation that will require postnatal surgery is difficult and has led to the practice of often observing at-risk newborns with fetal suspicion of coarctation in a care unit until ductal closure is confirmed and no aortic narrowing is observed. Some fetal echo criteria to aid in detecting a postnatal coarctation have been suggested[58,59] and are listed in Table 30.2.

**Table 30.2** Proposed prenatal echocardiographic features that help in predicting the presence of a postnatal coarctation of the aorta

| *Echocardiographic Feature* |
|---|
| • Right ventricle-to-left ventricle size disproportion |
| • Abnormal contour of aortic isthmus and aortic arch ("3-sign") |
| • Aorta-to-pulmonary artery size disproportion $<0.5$ |
| • Aortic isthmus measurement $<3$ mm at $\geq 32$ weeks' gestation |
| • Long segment distance take-off between left subclavian and left carotid artery |
| • High-velocity color Doppler jet in descending aorta |
| • Continuous sawtooth Doppler flow pattern (typical in postnatal life after ductal closure, rare in the fetus) |

## Postnatal physiology and management

Immediately after birth, the ductus arteriosus can remain patent for hours to days. If the ductus arteriosus is unrestrictive, there is no blood pressure gradient across the upper to lower extremities even in the presence of a coarctation. The ductus arteriosus naturally begins to constrict on the pulmonary end first. It can take weeks for the aortic end to fully constrict, which explains the diagnosis of coarctation later on in the neonatal period or even in infancy. If a coarctation is severe enough that systemic output is ductal dependent (critical coarctation), then intravenous access should be immediately obtained after birth and prostaglandins should be initiated. Sometimes in the absence of any other significant cardiac disease and depending on the severity of the coarctation, a trial off of prostaglandins may be appropriate in order to "test" the area of presumptive narrowing for adequacy. The patient should be monitored in an intensive care setting for possible extremis associated with ductal closure. However, the identification of right to left shunting across the ductus arteriosus after birth reflects ductal dependency of systemic outflow and should preclude turning off the prostaglandin infusion.

LV hypoplasia can be associated with coarctation, although the LV may still be viable as the systemic ventricle. In the presence of coarctation of the aorta with arch hypoplasia, one may have a very small but structurally normal mitral valve and a narrow but long shaped LV. Mitral valve size as small as z-score of less than –3 has been described in association with arch hypoplasia/coarctation of the aorta, in which the LV is still viable at birth.[60] A strategy recently undertaken has been to await a drop in pulmonary vascular resistance and allow for better filling of the left ventricle for a period of time at birth with increased pulmonary venous return, before making a final decision as to the viability of the LV, or lack thereof. Waiting a few days for transitional physiology to be completed and imaging at that point can often demonstrate a much more viable LV. Whether such "testing" and evaluation of a small borderline size LV in association with coarctation of the aorta can be undertaken with provocative maternal hyperoxygenation in fetuses at near-term is an intriguing notion and is being explored.[61]

If the coarctation is discrete and at the isthmus, surgical repair can be performed via a left lateral thoracotomy (incision under the left arm axilla).[62] The area of coarctation is resected with subsequent end-to-end anastomosis performed; this is typically done without cardiopulmonary bypass. When there is arch hypoplasia or long segment narrowing, a median sternotomy is utilized followed by arch augmentation with homograft patch reconstruction. Outcomes after surgical repair are favorable, with mortality rates of approximately 1%–2% at large centers.[63,64] Residual coarctation occurs in approximately 10% of patients and can be successfully ameliorated by balloon angioplasty in the catheterization laboratory.[65]

# References


1. van der Linde D et al. *J Am Coll Cardiol* 2011;58:2241–7.
2. Moorman AF, Christoffels VM. *Physiol Rev* 2003;83:1223–67.
3. Snarr BS et al. *Dev Dyn: An Off Pub the Am Assoc Anatomists* 2008;237:2804–19.
4. Moorman A et al. *Heart* 2003;89:806–14.
5. de Lange FJ et al. *Circ Res* 2004;95:645–54.
6. Oosthoek PW et al. *J Thorac Cardiovasc Surg* 1998;116:36–46.
7. Rudolph AM. *Circ Res* 1985;57:811–21.
8. Kiserud T. *Semin Fetal Neonatal Med* 2005;10:493–503.
9. Freud LR, Tworetzky W. *Curr Opin Pediatr* 2016;28:156–62.
10. Natowicz M et al. *Pediatrics* 1988;82:698–706.
11. Mahle WT et al. *Pediatrics* 2001;107:1277–82.
12. Tworetzky W et al. *Circulation* 2001;103:1269–73.
13. Feinstein JA et al. *J Am Coll Cardiol* 2012;59:S1–42.
14. Rogers LS et al. *J Am Coll Cardiol* 2012;60:1018–25.
15. Hoffman JI, Kaplan S. *J Am Coll Cardiol* 2002;39:1890–900.
16. Benson DW et al. *J Pediatr* 2016;173:25–31.
17. Remmell-Dow DR et al. *Am Heart J* 1995;130:148–52.
18. Rychik J et al. *J Am Coll Cardiol* 1999;34:554–60.
19. Rychik J et al. *Ultrasound Obstet Gynecol* 2010;36:465–70.
20. Chintala K et al. *Heart* 2008;94:1446–9.
21. Michelfelder E et al. *Circulation* 2005;112:2974–9.
22. Szwast A, Rychik J. *Clin Perinatol* 2005;32:857–75, viii.
23. Szwast A et al. *Circ Cardiovasc Imaging* 2010;3:172–8.
24. Saul D et al. *Pediatr Radiol* 2016;46:483–9.
25. Dori Y et al. *Circulation* 2016;133:1160–70.
26. Kaltman JR et al. *Ultrasound Obstet Gynecol* 2005;25:32–6.
27. Williams IA et al. *Am Heart J* 2013;165:544–50.e1.
28. Hahn E et al. *Ultrasound Obstet Gynecol* 2016;47:460–5.
29. Natarajan S et al. *J Am Soc Echocardiogr* 2013;26:515–20.
30. Szwast A et al. *Ann Thorac Surg* 2009;87:1214–9.
31. Ohye RG et al. *Circulation* 2016;134:1265–79.
32. Downing TE et al. *J Thorac Cardiovasc Surg* 2017;154:243–53.e2.
33. d'Udekem Y et al. *Circulation* 2014;130:S32–8.
34. Rychik J. *Semin Thorac Cardiovasc Surg Pediatr Card Surg Annu* 2016;19:37–43.
35. Marino BS et al. *J Thorac Cardiovasc Surg* 2009;137:385–93.e4.
36. Toscano A et al. *J Thorac Cardiovasc Surg* 2009;137:538–42.
37. Pedra SR et al. *Circulation* 2002;106:585–91.
38. Rogers LS et al. *J Thorac Cardiovasc Surg* 2011;142:1381–7.
39. Vogel M et al. *J Am Coll Cardiol* 2011;57:348–55.
40. Ward C. *Heart* 2000;83:81–5.
41. Ewart AK et al. *J Clin Invest* 1994;93:1071–7.
42. Marasini M et al. *Ann Thorac Surg* 2003;75:1763–8.
43. Campbell M. *Br Heart J* 1968;30:514–26.
44. Gøtzsche CO et al. *Arch Dis Child* 1994;71:433–6.
45. Wessels MW et al. *Am J Med Genet Part A* 2005;134A:171–9.
46. Garg V et al. *Nature* 2005;437:270–4.
47. Hornberger LK et al. *A longitudinal study. Circulation* 1995;92:1531–8.
48. Gardiner HM et al. *Ultrasound Obstet Gynecol* 2016;48:373–81.
49. Freud LR et al. *Circulation* 2014;130:638–45.
50. Nakano T et al. *Eur J Cardiothorac Surg* 2014;45:e166–72.
51. Sousa-Uva M et al. *Ann Thorac Surg* 1996;61:1805–10.
52. Cook AC et al. *Br Heart J* 1995;74:443–8.
53. Kathare P et al. *Ann Pediatr Cardiol* 2015;8:103–7.
54. Kim RW, Spray TL. *Semin Thorac Cardiovasc Surg Pediatr Card Surg Annu* 2006:177–9.
55. Chessa M et al. *Am J Cardiol* 2000;86:253–4.
56. Fouron JC. *Ultrasound Obstet* 2003;22:441–7.
57. Liu X et al. *Pediatr Cardiol* 2016;37:1085–90.
58. Quartermain MD et al. *J Am Soc Echocardiogr* 2009;22:1296–301.
59. Jowett V et al. *Ultrasound Obstet Gynecol* 2012;40:47–54.
60. Tani LY et al. *J Thorac Cardiovasc Surg* 1999;118:81–6.
61. Channing A et al. *Ultrasound Obstet Gynecol* 2015;45:664–9.
62. Ungerleider RM et al. *J Thorac Cardiovasc Surg* 2013;145:150–7; discussion 157–8.
63. Wright GE et al. *Ann Thorac Surg* 2005;80:1453–9.
64. Corno AF et al. *Eur J Cardiothorac Surg: Off J Eur Assoc Cardiothorac Surg* 2001;20:1202–6.
65. Dodge-Khatami A et al. *J Card Surg* 2000;15:369–77.

# 31

# Aortic arch anomalies

Varsha Thakur, Edgar T. Jaeggi, and Shi-Joon Yoo

The aortic arch is the part of the aorta that transitions from the ascending to the descending aorta (Figure 31.1). As the ascending aorta transitions into the transverse arch, it gives rise to the right brachiocephalic (innominate), left common carotid, and left subclavian arteries in sequence. The aortic arch lies obliquely on the left side of the trachea and esophagus and above the proximal part of the left main bronchus and is divided into two parts; the proximal and distal arches by the origin of the left common carotid artery. The aortic isthmus is the short segment of the aorta between the origin of the left subclavian artery and the insertion of the ductus arteriosus.[1]

Aortic arch anomalies refer to congenital abnormalities of the position or branching pattern of the aortic arch alone or in combination. While certain aortic arch anomalies are asymptomatic, others may encircle the trachea and/or esophagus completely (vascular ring) or partially (vascular sling) and cause variable compression of these structures. Aortic arch anomalies are often associated with other congenital cardiac defects and/or chromosomal abnormalities, such as chromosome 22q11 deletion.[2,3]

## Hypothetical double-arch model

Understanding embryogenesis and fetal circulation is essential in understanding the pathology and pathophysiology of aortic arch anomalies.[4] Normal and abnormal aortic arch development can be easily understood by reference to the hypothetical double aortic arch model introduced by the frontier pathologist, Dr. Jesse E. Edward in 1948.[5,6] The model (Figure 31.2) illustrates a fairly late stage of development in that the aortic sac has been divided into the ascending aorta and pulmonary arterial trunk, and the descending aorta occupies a neutral position.[7] Two aortic arches connect the ascending and descending aorta, forming a complete vascular ring around the trachea and esophagus. Each aortic arch gives rise to an ipsilateral common carotid artery, a subclavian artery, and an arterial duct that connects the distal part of the aortic arch to the adjacent branch pulmonary artery. Normally, the left aortic arch and left arterial duct persist, while the right aortic arch distal to the origin of the right subclavian artery and the right ductus regress (Figure 31.3a). As a result, the proximal part of the embryological right aortic arch becomes the right brachiocephalic (innominate) artery that bifurcates into the right common carotid and subclavian arteries. Most of the malformations showing abnormal position and branching of the aortic arch are assumed to result from abnormal persistence of a part or parts that should have regressed and/or from abnormal regression of a part or parts that should have persisted.[5,6]

## Evaluation of aortic arch anomalies

The evaluation of the aortic arch anomalies should include the following three basic components:

1. The left- or right-sidedness of the aortic arch relative to the trachea and main bronchus
2. The branching pattern of the head and neck arteries of the aortic arch; determining the absence or presence of an aberrant artery arising from the descending aorta and having a retroesophageal course
3. The left- or right-sidedness of the patent or ligamentous ductus arteriosus

### *Left aortic arch*

A left aortic arch refers to an aortic arch that is located on the left side of the trachea and arches over the proximal part of the left main bronchus. It is formed by interruption of a segment of the embryological right aortic arch. Interruption of the right arch distal to the origin of the right subclavian artery results in a normal left aortic arch (Figure 31.3). Interruption of the right arch between the origins of the right common carotid and right subclavian artery leaves the right subclavian artery attached to the distal part of the right aortic arch. As a consequence, the distal part of the embryological right aortic arch and right subclavian artery together constitute the aberrant right subclavian artery of the developed aortic arch (Figure 31.4).[7–11] With interruption of the right aortic arch proximal to the origin of the right common carotid artery, the distal part of the right aortic arch will persist as the aberrant right innominate artery that gives rise to the right subclavian and right common carotid arteries. Each of these three forms of left aortic arch may have either left or right ductus arteriosus. Bilateral arterial ducts are exceedingly rare. When the left aortic arch has a normal branching pattern of the head and neck branches, no vascular ring or sling is formed around the trachea and esophagus

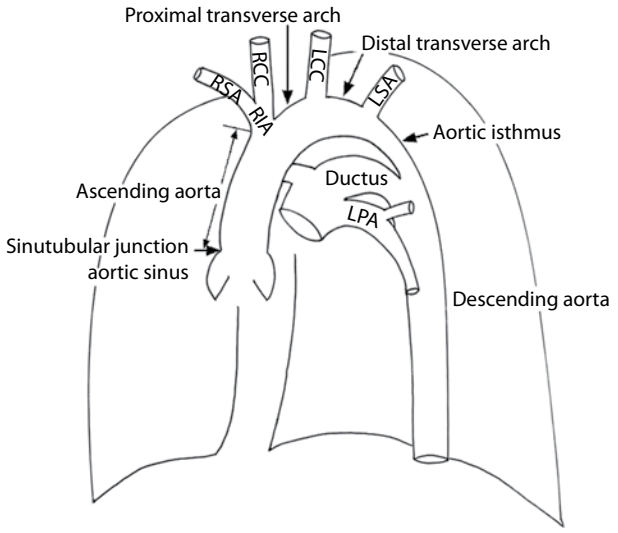


**Figure 31.1**
Nomenclature of the segments of the normal left aortic arch. The aortic arch consists of the proximal and distal transverse arch and isthmus. The aortic isthmus can be absent when the ductus arteriosus has attachment to the aortic arch proximal to the last branch or when the ductus arises from a subclavian artery.

regardless of the presence of a left or right ductus arteriosus. When there is an aberrant origin of the right subclavian or innominate artery, the aberrant artery has an oblique retroesophageal course. When the right ductus is present between the aberrant artery and the right pulmonary artery, a complete vascular ring is formed around the trachea and esophagus. The ring consists of the ascending aorta, the left aortic arch, the descending aorta, the aberrant right subclavian or innominate artery, the right ductus arteriosus, the right pulmonary artery, and the pulmonary arterial trunk with the underlying heart completing the circle. When the left ductus arteriosus persists instead, the circle is not completed, and a vascular sling is formed around the left side of the trachea and esophagus.

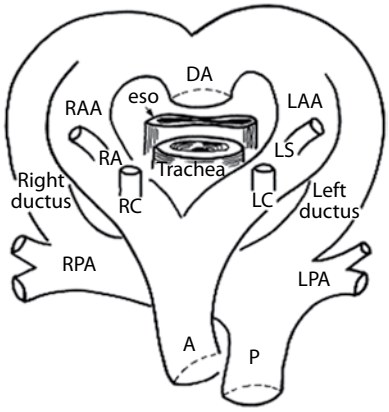


**Figure 31.2**
Hypothetical double aortic arch model of Jesse E. Edward.

## Right aortic arch

A right aortic arch (Figure 31.5; Video 31.1) refers to an aortic arch that is located on the right side of the trachea and arches over the proximal part of the right main bronchus. It is formed by interruption of a segment of the embryological left aortic arch. Interruption distal to the origin of the left subclavian artery results in a right aortic arch with a mirror image of normal branching pattern (Figure 31.5). Interruption of the left arch between the origins of the left common carotid and left subclavian arteries or proximal to the left common carotid artery results in a right aortic arch with aberrant left subclavian (Figure 31.6)[7–12] or left innominate artery. Each of these forms of right aortic arch may have either left or right ductus arteriosus, while bilateral ducts are exceedingly rare. The right aortic arch with a mirror image of normal branching pattern does not cause a vascular ring or sling regardless of the presence of a left or right arterial duct except for a very few reported cases in which there is a left duct between the right descending aorta and the left pulmonary artery.[13–16] When there is an aberrant origin of the left subclavian or left innominate artery, the aberrant artery has an oblique retroesophageal course. When the left duct is present between the aberrant artery and the left pulmonary artery, a complete vascular ring is formed around the trachea and esophagus (Figure 31.7). The ring consists of the ascending aorta, the right aortic arch, the descending aorta, the aberrant left subclavian or innominate artery, the left ductus arteriosus, the left pulmonary artery, and the pulmonary arterial trunk with the underlying heart completing the circle (Video 31.2). When the right arterial duct persists instead, the encirclement is incomplete, and a vascular sling is formed around the right side of the trachea and esophagus. The right aortic arch may be found in isolation, but the finding should alert the examiner to evaluate the fetus for the possibility of a vascular ring and/or intracardiac anomalies.[17,18]

## Double aortic arch

The term *double aortic arch* (Video 31.3) refers to the presence of two aortic arches, one on each side of the trachea.[7–10] It is in contrast to double barrel or double-lumen aortic arch, in which two aortic arches are present on the same side of the trachea. In double aortic arch, the hypothetical double aortic arch model persists without interruption of any segment of the right and left arches (Figure 31.8). One arterial duct, usually the left one, persists, although bilateral ducts have been reported.[19] As a consequence, a ring is formed around the trachea and esophagus. The ring consists of the two aortic arches joined together at the descending aorta. Each aortic arch gives rise to the ipsilateral common carotid and subclavian arteries. In the majority of the cases with double aortic arch, both arches are patent. Rarely, an atretic segment may exist in either arch.[20]

When the aortic arch is on the left, the descending aorta usually stays on the left side in its entire course to enter the

abdomen through the aortic hiatus in the diaphragm. When there is a right aortic arch, the descending aorta starts on the right side and makes a gentle curve to the left to enter the abdomen through the normal aortic hiatus in the diaphragm on the left side. As this midline shift of the descending aorta is gradual, the trachea is not crossed by the descending aorta, while the lower part of the esophagus may be mildly compressed.

## *Circumflex retroesophageal aortic arch*

In this rare malformation, the proximal part of the descending aorta is on the contralateral side of the aortic arch (Figure 31.9).[21,22] This set requires the aortic arch to make an additional arc to the other side behind the trachea and esophagus to reach the descending aorta. The morphogenetic mechanism for development of this rare malformation has been explained by many but will not be introduced in this chapter because it is hardly a help in understanding this rather complex and variable morphology. It occurs much more frequently with a right aortic arch than with a left arch. When it occurs with a right aortic arch, the arch gives rise to the left common carotid artery, followed by the right common carotid and right subclavian arteries from its segment on the right side of the trachea (Figure 31.9). Then the aortic arch makes a sharp turn to the left side to have an oblique leftward and usually downward course to the contralateral descending aorta. The left subclavian artery arises from the transitional point of the arch to the descending aorta.[22] It can be considered an aberrant artery in the sense that it is the last instead of the first branch of the right aortic arch. However, it does not have a retroesophageal component that the other forms of aberrant arteries have. In most cases, the left subclavian artery arises from the aorta through a diverticulum. The apex of the diverticulum connects to the left pulmonary artery through the ductus arteriosus, and a complete vascular ring is formed around the trachea and esophagus. The circumflex retroesophageal

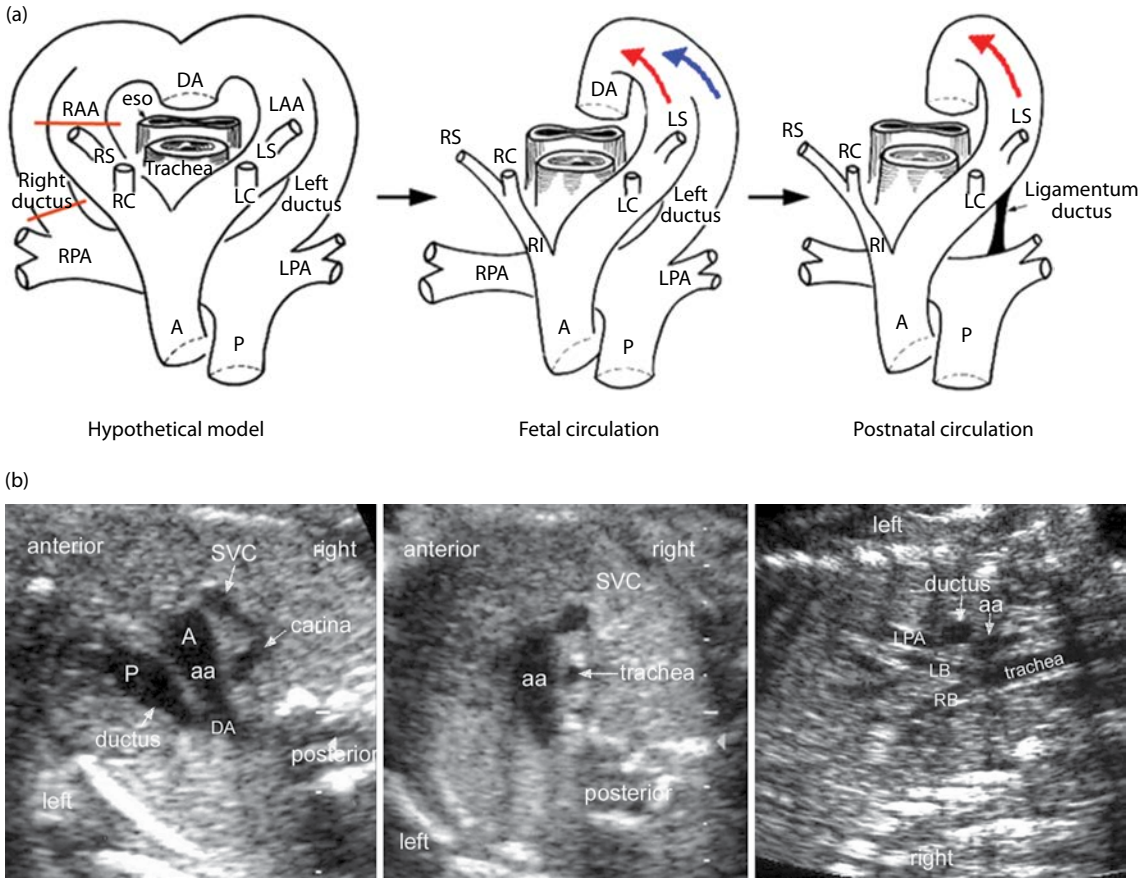


**Figure 31.3**
Normal left aortic arch with left ductus arteriosus. (a) Hypothetical models. In the left-hand diagram, the red bars in left-hand diagram indicate the segments that regress. In the fetal circulation, the aortic arch (red arrow) and the left ductus arteriosus (blue arrow) make a "V"-shaped confluence at the descending aorta. In the postnatal circulation, the left ductus arteriosus closes and persists only as the ligamentum ductus arteriosum. (b) Fetal echocardiograms. In the axial view (left panel), the aortic and ductal arches make a "V" shape as they connect into the descending aorta on the left side of the carina. In a slightly higher axial view (middle panel), the sausage-shaped aortic arch is seen on the left side of the trachea. In the coronal view (right-hand panel), the cross section of the aortic arch is seen on the left side of the distal trachea. The ductal arch is seen inferior and lateral to the aortic arch. (*Continued*)

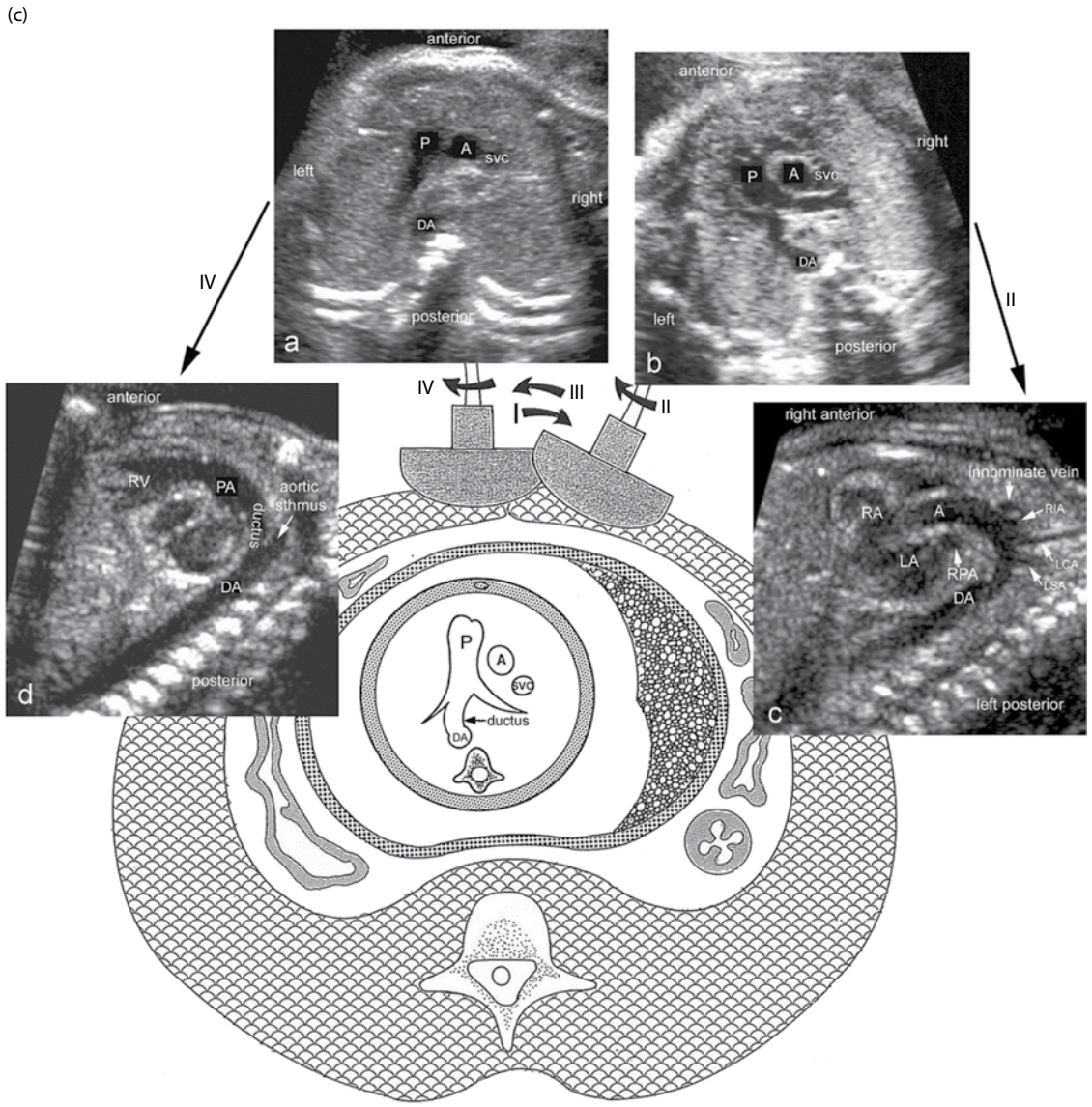


**Figure 31.3 (Continued)**
(c) Composite diagram showing how the aortic and ductal arch views are obtained in a fetus in supine cephalic presentation. The scan starts from any transducer position for a three-vessel view (panel a). Step I. The transducer is moved around the fetal chest until the ascending aorta and descending aorta are aligned vertically in the three-vessel view (panel b). Step II. The transducer is rotated 90° either clockwise or counterclockwise until the aortic arch is seen as a candy cane-like structure (panel c). Step III. The transducer is moved back to a three-vessel view and moved around the fetal chest until the main pulmonary artery and the descending aorta are vertically aligned (panel a). Step IV. The transducer is rotated 90° either clockwise or counterclockwise until the ductal arch is seen as a hockey stick–like structure (panel d). ([a] Reprinted with permission from Yoo SJ et al. *Ultrasound Obstet Gynecol* 2003;22(5):535–46.[7] [c] Modified with permission from Yoo et al. *Ultrasound Obstet Gynecol* 1999;14(1):29–37.[36])

aortic arch is different from a similar situation in which the proximal descending aorta makes a bend to the other side, causing esophageal compression with variable tracheal compression.

## *Cervical aortic arch*

The aortic arch may have a very high position in the upper mediastinum, for which the term *cervical aortic arch* (Video 31.4) has been entertained. It is defined as the aortic arch reaching above the level of the clavicle. It may occur with a right aortic and/or an abnormal branching pattern of the head and neck vessels. Its association with a retroesophageal aortic arch has been recognized. In addition, unusual tortuosity, obstruction, and aneurysm of the aortic arch are found in a significant number of cases with a cervical aortic arch.

The aortic arch anomalies thus discussed can be categorized into three groups according to the presence or absence of a vascular ring or sling: (1) those with a vascular ring or rings, (2) those with a vascular sling, and (3) those without a ring or sling (Table 31.1).

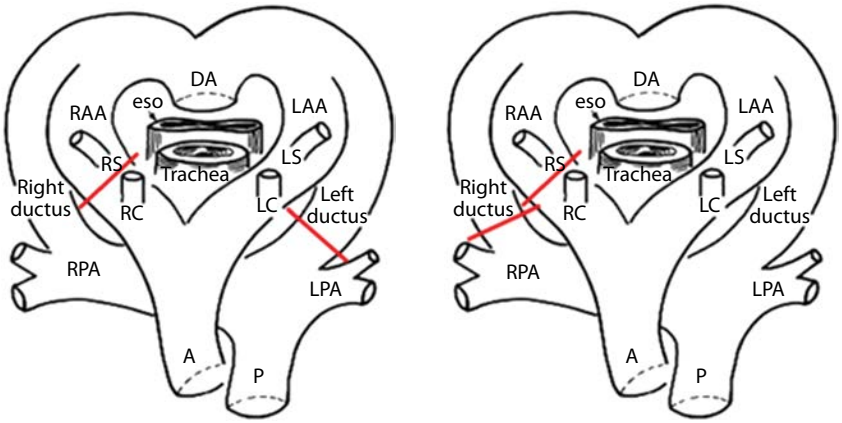


**Figure 31.4**
Developmental models of left aortic arch with aberrant right subclavian artery. The red bars indicate the segments that regress. In this setting, the left ductus persists in most cases, and a vascular sling is formed. Uncommonly, the right ductus persists, and a vascular ring is formed along the left side of the trachea and esophagus.

(a)

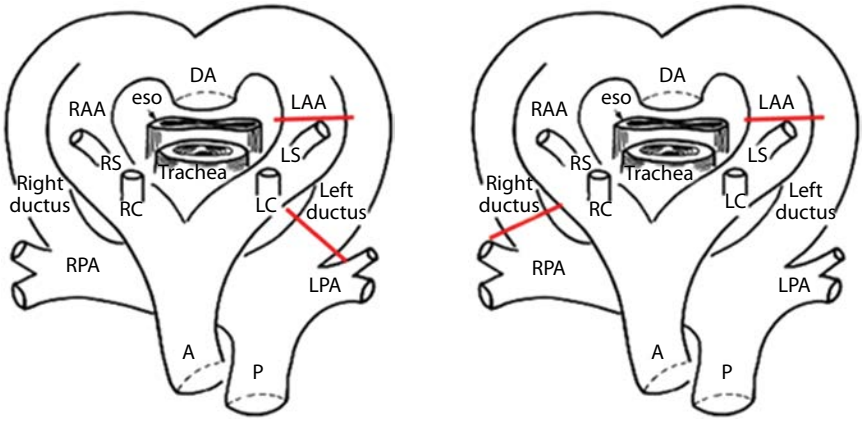


(b)

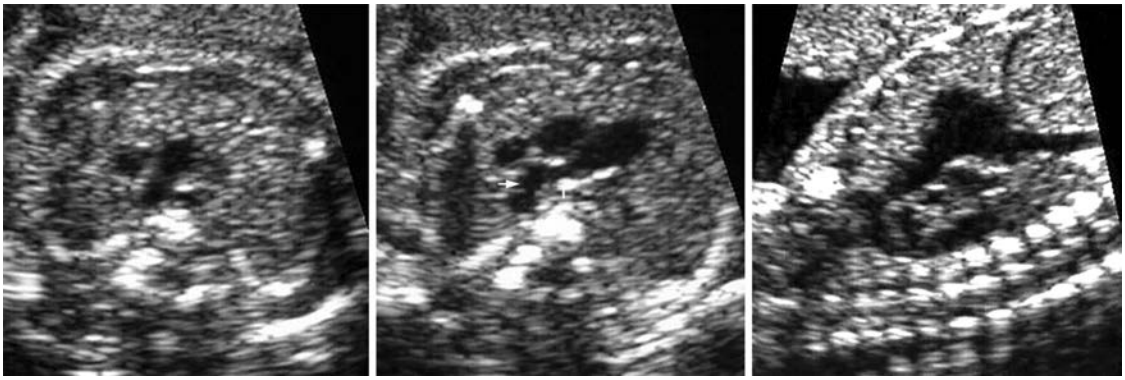

**Figure 31.5**
Right aortic arch with mirror-image branching of the heart and arm arteries. (a) Developmental models. The red bars indicate the segments that regress. In this setting, the persisting ductus arteriosus is usually the left ductus as shown in the right-hand diagram. In either form, no vascular ring or sling is formed around the trachea and esophagus. (b) Fetal echocardiogram in axial plane (left-hand panel) shows that the aortic arch is on the right side of the trachea. Fetal echocardiograms in axial plane underneath the aortic arch plane and in sagittal plane show that the patent ductus arteriosus connects the undersurface of the right aortic arch and the right pulmonary artery. This fetus had tetralogy of Fallot.

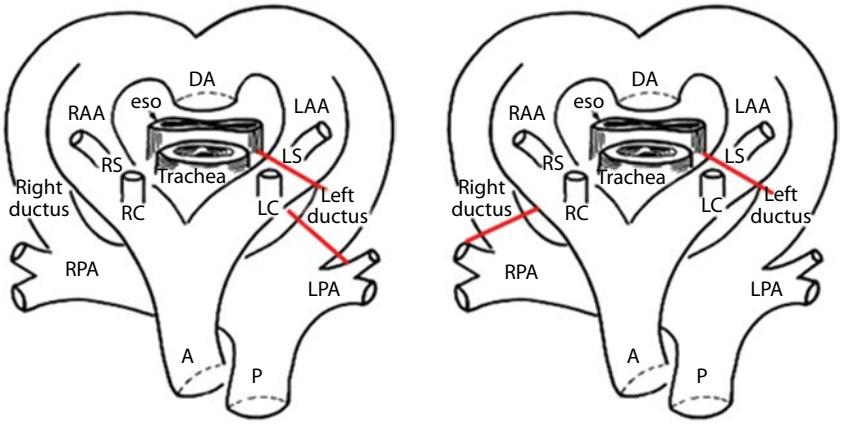


**Figure 31.6**
Developmental models of right aortic arch with aberrant left subclavian artery. The red bars indicate the segments that regress. In this setting, the persisting ductus arteriosus is usually the left ductus, and a vascular ring is formed around the trachea and esophagus. Less commonly, the right ductus persists, and a vascular encirclement of the trachea and esophagus is incomplete.

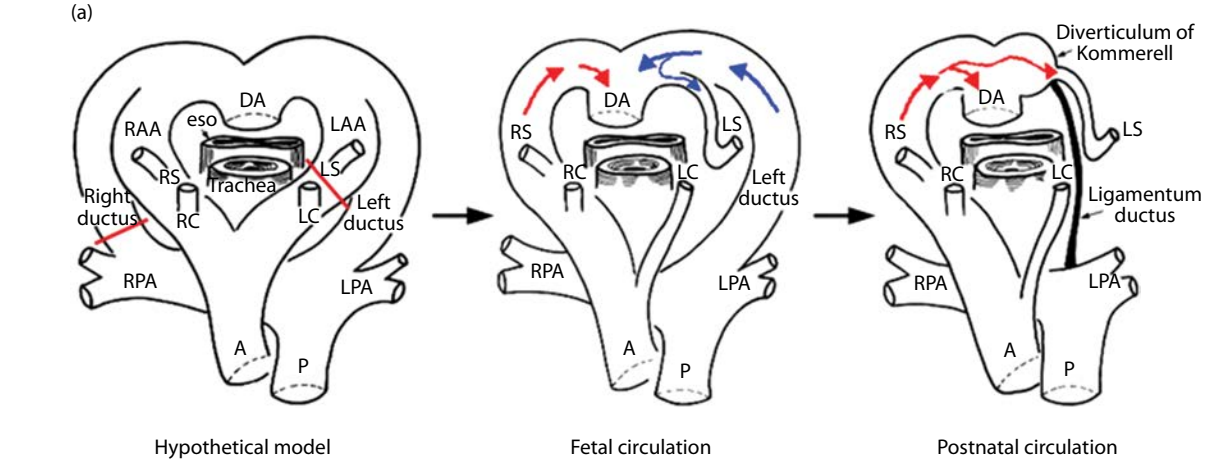


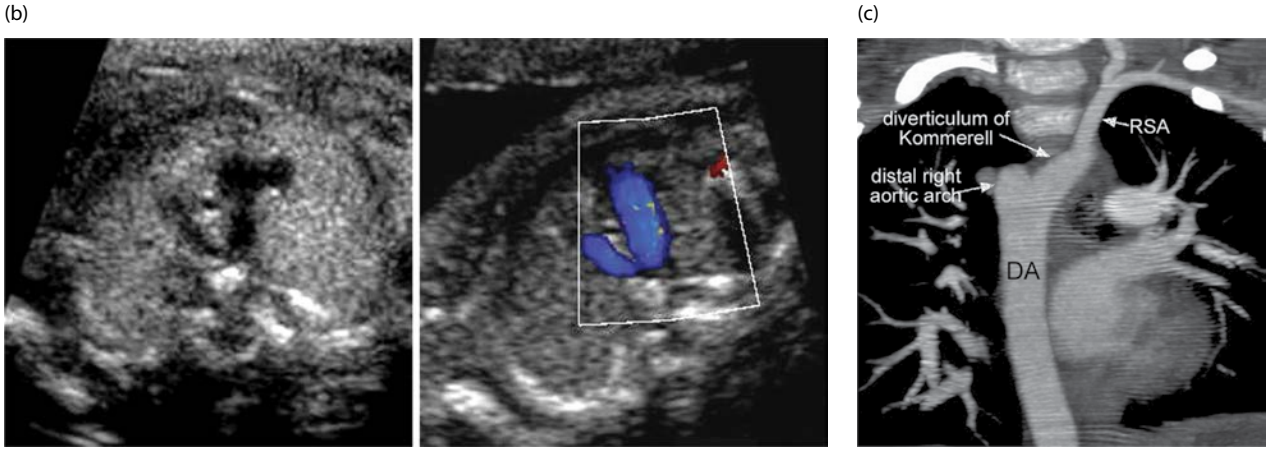


**Figure 31.7**
Right aortic arch with aberrant left subclavian artery and left ductus arteriosus. (a) Developmental model. The red bars indicate the segments that regress. In fetal life, the right aortic arch, the distal left aortic arch, the left ductus arteriosus, and the main pulmonary arterial trunk constitute a "U"-shaped vascular loop around the trachea and esophagus. As the two limbs of the "U"-loop are attached to the heart, a complete vascular ring is formed. Postnatally, when the ductus arteriosus closes, the proximal part of the aberrant left subclavian artery, which is embryologically the distal part of the left aortic arch, persists as the diverticulum of Kommerell. Note that the blood flow in this particular segment of the left subclavian artery is in an opposite direction in fetal life. (b) Fetal echocardiograms show a "U"-shaped vascular loop around the side and posterior aspect of the trachea. Note a rather wide gap between the ascending aorta and main pulmonary arterial trunk. (c) Postnatal computed tomography angiogram from a different patient shows a right aortic arch with aberrant left subclavian artery that arises from the diverticulum of Kommerell.

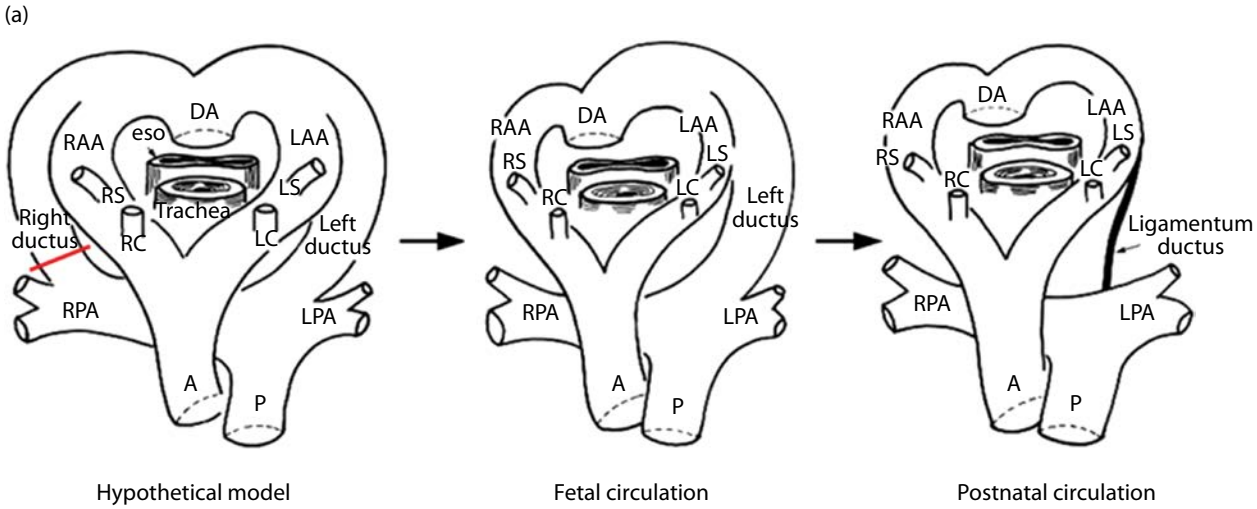


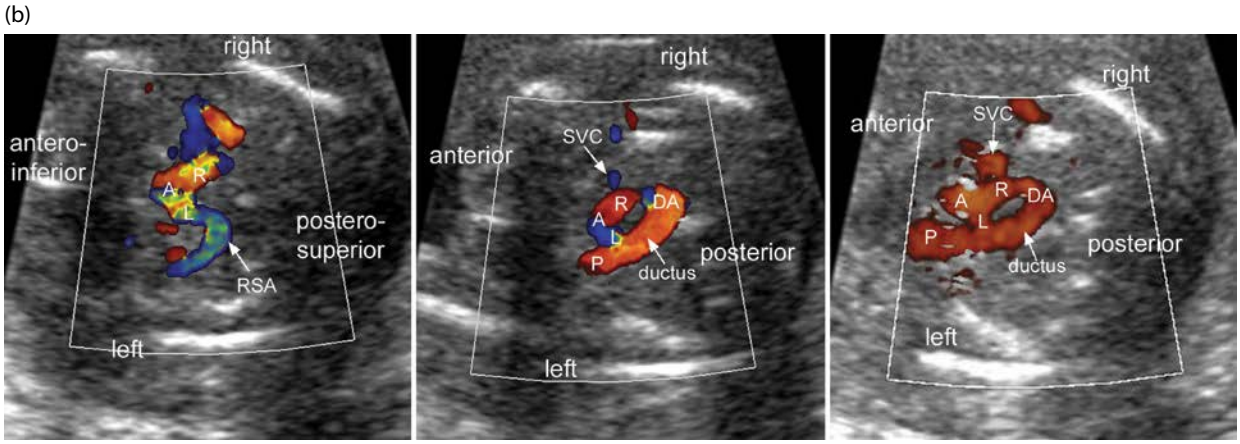


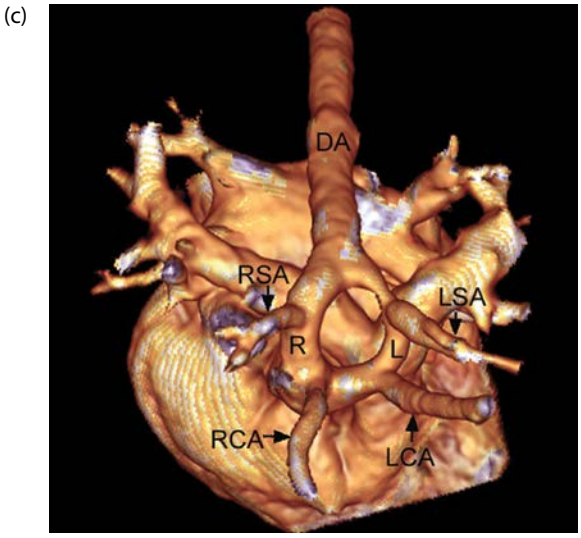


**Figure 31.8**
Double aortic arch. (a) Developmental model. The two patent arches encircle the trachea and esophagus. The left ductus is usually patent. (b) Fetal echocardiograms show a figure of "9" configuration of the vascular complex encircling the trachea (T). (c) Postnatal computed tomography angiogram from a different patient shows double aortic arch. The right arch (R) is bigger than the left (L). Each arch gives rise to the ipsilateral common carotid and subclavian arteries. ([b] Reprinted with permission from Yoo SJ et al. *Ultrasound Obstet Gynecol* 2003;22(5):535–46.[7])

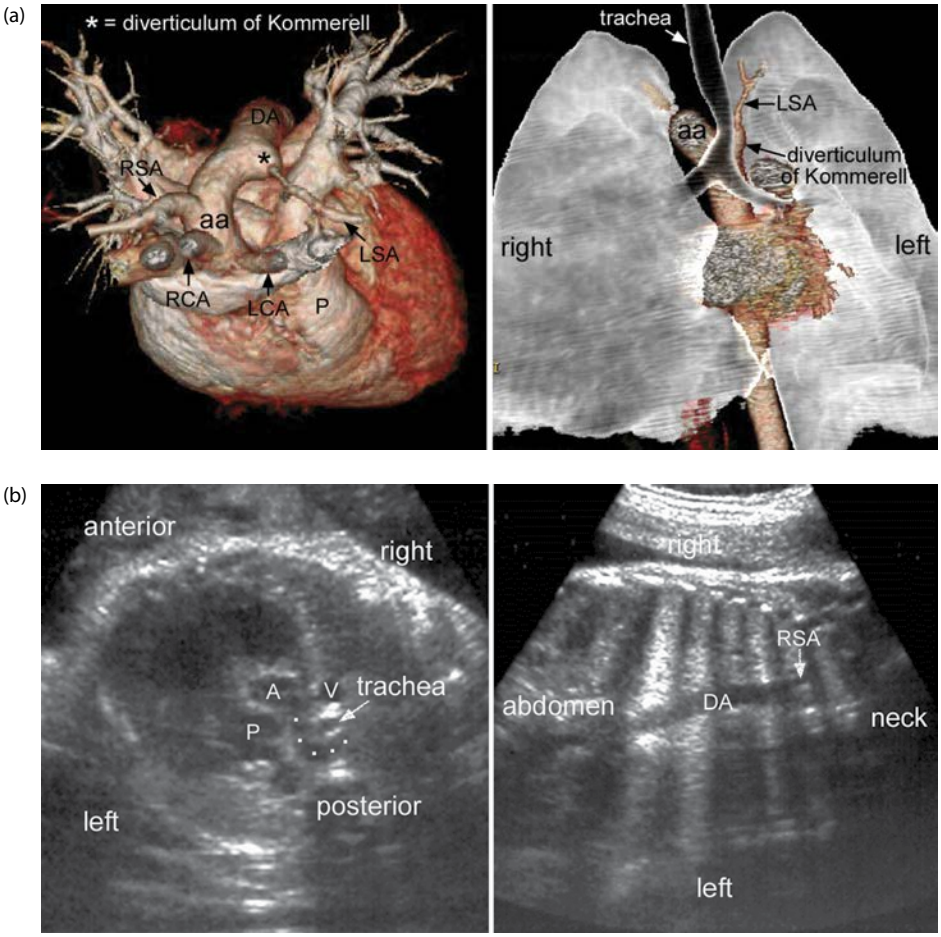


**Figure 31.9**
Circumflex retroesophageal aortic arch. (a) Volume-rendered three-dimensional computed tomography angiograms in a postnatal patient show a right aortic arch that makes an additional arc behind the trachea (and esophagus) to reach the descending aorta on the left side. The left subclavian artery arises from the top of the descending aorta through a diverticulum of Kommerell. (b) Fetal echocardiograms from a different fetus. In the transverse view (left-hand panel), the aorta forms an arch on the left side of the trachea and turns to the right to course behind the trachea. The course of the aorta and aortic arch is marked by white dots. In the coronal view (right-hand panel), the descending aorta is on the right. (Part [b] reprinted with permission from Yoo SJ et al. *Ultrasound Obstet Gynecol* 2003;22(5):535–46.[7])

# Fetal sonographic approach to aortic arch anomalies

## *Normal aortic arch*

The aortic arch and ductus arteriosus can be evaluated by using orthogonal transverse views and oblique sagittal views along the aortic and ductal arches.[7,23–29] Two- and three-dimensional color and power Doppler interrogation facilitates examination of the mediastinal vascular structures.[26,30–32] The assessment of the aortic arch can be started from a three-vessel view. In this plane, the ascending aorta is situated slightly to the right of the midline and the descending aorta at the left anterior aspect of the spine. In a slightly cephalad plane, the ascending and descending aorta join together through a sausage-shaped aortic arch on the left side of the trachea that is filled with fluid. In the same or slightly caudal imaging plane, the ductus arteriosus connects the main pulmonary artery to the descending aorta further laterally on the left side. The aortic arch and ductus arteriosus together make a "V"-shaped confluence at the descending aorta. The confluence may be seen as a "Y"-shaped structure

**Table 31.1** Aortic arch anomalies with or without a vascular ring or sling

*With a vascular ring:*

1. Double aortic arch
2. Right aortic arch with aberrant left subclavian or innominate artery and left ductus arteriosus
3. Right aortic arch with mirror-image branching and left ductus arteriosus between the left pulmonary artery and a right-sided descending aorta
4. Left aortic arch with aberrant right subclavian or innominate artery and right ductus arteriosus
5. Circumflex retroesophageal aortic arch

*With a vascular sling:*

1. Left aortic arch with aberrant right subclavian or innominate artery and left ductus arteriosus
2. Right aortic arch with aberrant left subclavian or innominate artery and right ductus arteriosus
3. Circumflex retroesophageal aortic arch

*Without a ring or sling:*

Right aortic arch with mirror-image branching and either right or left ductus arteriosus

in a slightly tilted position. In these views, the ductus arteriosus has a uniform diameter, while the aortic arch becomes narrower distally as it gives off the head and arm branches. The aortic isthmus is the narrowest part of the aortic arch and has a similar diameter as the arterial duct.[33] It is worth emphasizing that no major vascular structure crosses the midline behind the trachea. Any vessel seen behind the trachea may safely be considered as an aberrant branch of the aortic arch or the aortic arch itself that has an abnormal retroesophageal course or an aberrant left pulmonary artery in a pulmonary artery sling that has an abnormal course between the trachea and esophagus. Evaluating the three-vessel view and examining the relationship of the aortic and ductal arches in relation to the trachea with cephalad sweeps are essential in fetal diagnosis of vascular rings.[34,35] The relationship between the aortic arch and the trachea can also be appreciated in a slanted coronal plane along the trachea.[7,26] In this plane, the cross section of the aortic arch is seen above the proximal part of the left main bronchus, and the cross section of the ductus arteriosus or an oblique cut of the left pulmonary artery is seen above the distal part of the left main bronchus (Figure 31.3b, right-hand panel). The aortic and ductal arches seen in oblique sagittal views are compared to a "candy-cane" and a "hockey stick," respectively. Proper imaging planes for these views can be chosen from a three-vessel view (Figure 31.3c).[36] For a candy-cane view of the aortic arch, the transducer should be aligned with the ascending and descending aorta in a three-vessel view, from which position the transducer is rotated 90° either clockwise or counterclockwise. The aortic arch typically arises from the space between the cranial parts of the right and left atria deep in the center of the mediastinum. It gives rise to the head and arm arteries. For a hockey stick view of the ductal arch, the transducer should be aligned with the main pulmonary artery and descending aorta in a three-vessel view, from which the transducer is rotated 90°. As the ductus arteriosus is an extension of the main pulmonary artery, the ductal arch appears to arise from the anterior mediastinum immediately behind the anterior chest wall. It should be emphasized that the aortic arch has a hockey stick appearance and the ductal arch a candy-cane appearance when there is transposition of the great arteries, because the ascending aorta is located more anterior to the main pulmonary artery in most cases. Therefore, identification of the aortic and ductal arches should not solely rely on the shape of the arches; the aortic arch should be identified as the vessel that gives rise to the head and neck vessels.

## Vascular rings

The best approach to vascular rings is to make a slow sweep through the fetal upper mediastinum in multiple echocardiographic transverse planes.[7,23–29] Some forms of vascular ring can be detected easily by two-dimensional imaging, while others require mental or physical three-dimensional reconstruction. Among the five forms of vascular rings listed in Table 31.1, the double aortic arch is the only form of vascular ring that consists solely of vascular structures. In other forms, the vascular ring is completed by the heart. Therefore, a classic form of double aortic arch can readily be identified as a true vascular ring by echocardiography (Figure 31.8), while other forms are visualized as a loop appearing open anteriorly (Figure 31.7).

One should also be aware that there are many variations in morphology and size in each form of vascular ring. In double aortic arch, one arch is larger and higher than the other in approximately 90% of cases. In the majority of the cases having situs solitus, the right aortic arch is the larger vessel, and there is a left ductus arteriosus and a left-sided descending aorta. The vascular ring and ductus can be imaged in a single plane, giving the appearance of a figure of "6" or "9."[7,27] When the ascending aorta is out of plane in an oblique view, the two aortic arches and arterial ducts merge to the descending aorta giving rise to an appearance of a trident.[37] Uncommonly, one of the two arches is atretic. This condition is almost impossible to differentiate from a unilateral arch with an abnormal branching pattern, because the atretic segment of the vessel cannot be identified.

The rare circumflex retroesophageal aortic arch[7,21,22] occurs in most cases with a right aortic arch and a left ductus arteriosus, and a complete vascular ring is formed. After taking an oblique backward course on the right side of the trachea, the arch makes a rather sharp leftward and downward turn to connect to the descending aorta on the left. It is indistinguishable from a double aortic arch with an atretic segment. Commonly, the aortic arch extends to the level of the thoracic inlet forming a cervical arch.

The right aortic arch with an aberrant left subclavian or innominate artery and a left ductus arteriosus is not uncommon. In this combination, a "U"-shaped vascular loop is seen on three-vessel and adjacent views.[7,25–29] The open end of the "U"-loop faces forward, and the apex of the loop is located behind the fluid-filled trachea (Figure 31.7b). The limbs of the "U"-loop are the aortic and ductal arches that connect to the heart through the ascending aorta and main pulmonary arterial trunk, respectively. When there is no ventricular outflow tract obstruction, the limbs are of a similar size. Additional telltale signs of a right aortic arch include a gap between the pulmonary arterial trunk and ascending aorta at three-vessel view and a right-sided or midline descending aorta on the three-vessel and four-chamber views. A left aortic arch with an aberrant right subclavian or innominate artery and a right arterial duct forming a vascular ring is rare.[38] In this setting, the proximal limbs of the vascular loop, i.e., the ascending aorta and the pulmonary arterial trunk, cross one another as they arise from the heart, forming a "γ" or "ribbon"-shaped loop (Figure 31.4). Another rare form of vascular ring is associated with a right aortic arch with mirror-image branching of the head and arm arteries in which a left duct connects the left pulmonary artery to a right-sided descending aorta coursing behind and on the left side of the trachea and esophagus.[14–16]

## Vascular sling

Vascular sling represents an incomplete encirclement of the airway and/or esophagus by a single or composite vascular structure. A vascular sling is seen in left or right aortic arch with an aberrant subclavian or innominate artery and with the ductus arteriosus on the same side of the aortic arch (Figures 31.4 and 31.6). The ascending aorta, aortic arch, and aberrant artery together form a vascular sling around the trachea and esophagus, which is open-ended on the opposite side of the aortic arch. The aberrant subclavian or innominate artery is seen as a rather small vascular structure coursing to the other side of the aortic arch behind the trachea. This combination is much more commonly seen with a left than with a right aortic arch. This is in contrast to the case forming a vascular ring, which is much more common with a right aortic arch.

Another rare but well-known form of vascular sling is the pulmonary arterial sling in which the left pulmonary artery has a very distal origin from the pulmonary arterial trunk at the right anterior aspect of the trachea and makes a turn to course to the left lung through the space between the airway and esophagus (Figure 31.10).[39] The pulmonary arterial sling is commonly associated with an abnormal branching and stenosis of the airway.

## Aortic arch anomalies without a vascular ring or sling

As is the normal left aortic arch, the right aortic arch with a mirror-image branching pattern is not associated with a vascular ring or sling (Figure 31.5b), except for the exceedingly rare cases as discussed.[14–16] Additionally, the ductus arteriosus is not usually mirror imaged, and the left instead of the right ductus arteriosus persists between the innominate artery and the left pulmonary artery in most cases.

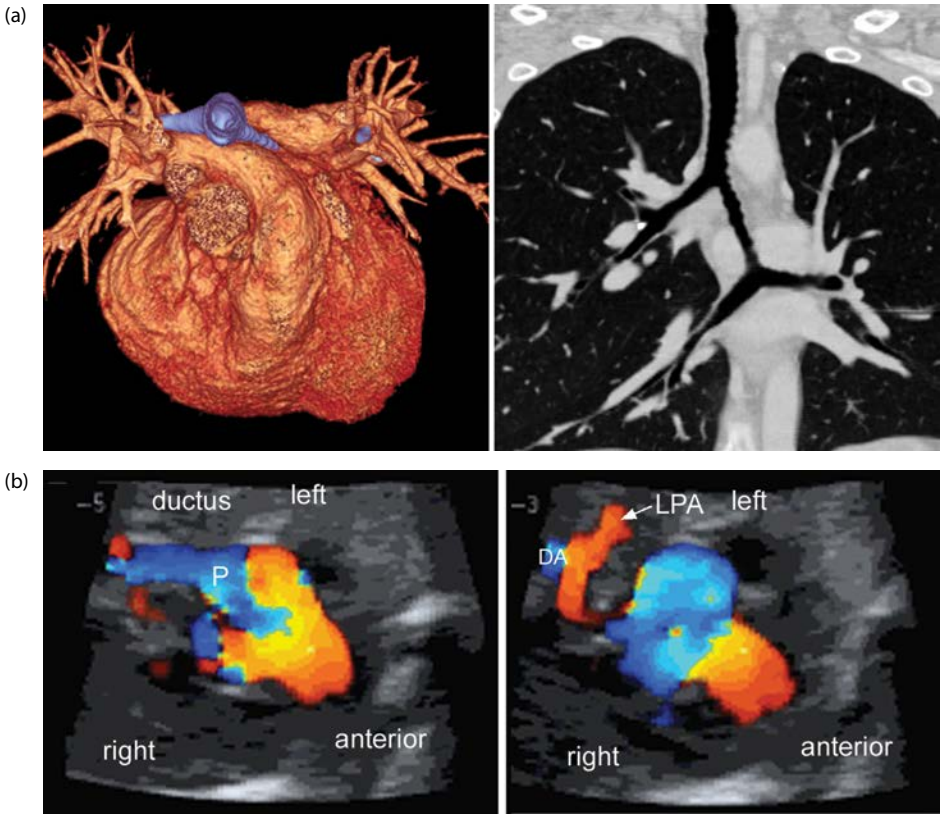


**Figure 31.10**
Pulmonary artery sling. (a) Volume-rendered three-dimensional computed tomography angiogram from a patient shows that the left pulmonary artery arises very distal from the main pulmonary artery and courses to the left behind the trachea and in front of the esophagus. Minimal-intensity thick section shows abnormal branching pattern of the tracheobronchial tree. There is a long segment narrowing of the distal trachea between the abnormal bronchus to the right upper and middle lobes and the tracheal bifurcation. The upper tracheal bifurcation is too high for normal carina, while the lower bifurcation is too low. Some consider the upper bifurcation as the carina, the vertical narrowed part as the left main bronchus, and the bronchus to the right lower lobe as a "bridging bronchus." (b) Fetal echocardiograms from a different fetus show that the left pulmonary artery has an unusual rightward sweep in front of the descending aorta (right-hand panel). It courses to the left through the space below the ductus arteriosus. (Courtesy of Dr. Hirokazu Yorioka, Kansai Medical University, Hirakata Hospital, Japan.)

## Incidence and associated abnormalities

The reported incidence of individual aortic arch anomalies varies according to the study population. The left aortic arch with aberrant right subclavian artery was reported as the most common aortic arch anomaly in a large autopsy series, occurring in 0.5% of cases.[6] In low-risk fetal cohorts, however, a right aortic arch with an aberrant left subclavian artery was the most common association with an incidence of 0.1%.[24,28] The discrepancy between postmortem and prenatal series may be due to the difficulty in detecting a left aortic arch with an aberrant right subclavian artery by fetal sonography. Isolated right aortic arch is uncommon and has no significant associated morbidity or mortality.[18,40,41] Finally, a right aortic arch with mirror-image branching is associated with congenital heart disease in more than 90% of cases.[5,12,14] This association is particularly common in patients with tetralogy of Fallot or truncus arteriosus, with incidences ranging from 15% to 35% of affected patients.[42] Right aortic arch with aberrant left subclavian artery is significantly less associated (<20%) with congenital heart disease,[42] and most commonly with ventricular septal defects. The left aortic arch with an aberrant right subclavian artery is an infrequent association with congenital heart disease. Double aortic arch is usually found in isolation but rarely may occur in association with other cardiac defects such as transposition of the great arteries,[43] interrupted aortic arch,[44] or crossed branch pulmonary arteries.[45] Circumflex retroesophageal aortic arch is usually found in isolation but rarely can be associated with ventricular septal defects and bicuspid aortic valve.[46]

Chromosome 22q11 deletion is a common association with aortic arch anomalies.[2,18,28,40,44,47,48] A fetal series showed an 8% incidence of 22q11 deletion in fetuses with a right aortic arch as an isolated abnormality and 46% if this was associated with CHD.[28] In postnatal series, however, 20%–25% of cases with a right aortic arch as the sole anomaly had 22q11 deletion.[2,18,47] Moreover, more than 50% of patients with an intracardiac anomaly and 22q11 deletion also had an aortic arch anomaly.[49] In patients with conotruncal malformation, anomalies of the subclavian arteries are important anatomical markers for chromosome 22q11 deletion, independent of the laterality of the aortic arch.[50] The subclavian arterial anomalies encompass aberrant origin from the descending aorta, isolated origin, distal ductal origin from the pulmonary artery, and cervical origin of the subclavian artery. Chromosome 22q11 deletion was associated in over 75% of patients with conotruncal malformation and subclavian arterial anomaly, while it was present in less than 30% when there was no subclavian artery anomaly. It has also been shown that there is increased risk for Down syndrome where there is an aberrant right subclavian artery.[51,52] When an aortic arch anomaly is found, fetal karyotyping is therefore recommended, especially when it is associated with congenital heart disease, extracardiac malformations, or an increased nuchal translucency.[28]

## Postnatal clinical manifestations and management

The aortic arch anomalies constituting a vascular ring may cause symptoms and signs of airway and/or esophageal compression that include stridor, cough, asthma, respiratory distress, apnea, recurrent episodes of pneumonia, dysphagia, and episodes of choking.[53,54] Typically, the more severe the airway and/or esophageal compression is, the earlier the age at presentation will be.[9–11,40,48,54–58] A vascular ring in double aortic arch is usually tight, and the affected child usually presents early in life. Nonetheless, a double aortic arch may also be found incidentally in an asymptomatic child.[59] A vascular ring in the right aortic arch with an aberrant left subclavian artery and left ductus tends to be less obstructive, and clinical manifestations of airway/esophagus obstruction are often not present.[60] Most children affected by a vascular sling will have no significant symptom of airway or esophageal compression with the exception of pulmonary artery slings that commonly result in long segment intrinsic narrowing of the distal trachea.

Management includes surgical division of the structures contributing to the vascular ring.[8–10,55] Video-assisted thoracoscopic division of vascular rings in pediatric patients can be performed safely and is a growing trend.[61–63] The aberrant subclavian artery causing significant airway or esophageal compression can be divided and connected to the ipsilateral common carotid artery. A large Kommerell diverticulum can be remodeled, because it may develop aneurysmal dilatation and continue to compress the trachea and esophagus even after the ring has been released.[12,64–66] Patients with associated tracheomalacia may continue to have symptoms that can last for months but may resolve with time.[67]

## Videos

**Video 31.1a** (https://youtu.be/D5FB9NdUveg)
Two-dimensional clip showing a right aortic arch and right ductus arteriosus. The fetus did not have intracardiac anomalies and only had a right aortic arch and right ductus arteriosus in isolation.

**Video 31.1b** (https://youtu.be/P4SWHl38vvM)
Color Doppler showing the right aortic arch and ductus arteriosus.

**Video 31.1c** (https://youtu.be/0OAGOblZi40)
Power Doppler showing the right aortic arch and ductus arteriosus.

**Video 31.2a** (https://youtu.be/FU-YoP1YxmE)
Two-dimensional image of the three-vessel view demonstrating a vascular ring. There is a right-sided aortic arch with left-sided ductus arteriosus and an aberrant left subclavian that form the vascular ring. The ductus arteriosus and aortic arch form a "U" shape.

**Video 31.2b** (https://youtu.be/FV5CQf2flG0)
Same view with color Doppler.

**Video 31.2c** (https://youtu.be/6H5B3L7UZno)
Same view with power Doppler.

**Video 31.3a** (https://youtu.be/8y_7c7gybfA)
Two-dimensional imaging in the three-vessel view showing a double aortic arch. Sweeping cephalad, we see the right and left aortic arches that encircle the trachea.

**Video 31.3b** (https://youtu.be/MHssoSsAhuA)
Double arch seen by color Doppler.

**Video 31.4a** (https://youtu.be/VKWsqAepQWM)
Two-dimensional image of the three-vessel view demonstrating a cervical aortic arch.

**Video 31.4b** (https://youtu.be/YTA9gOHCRa8)
Same view with color Doppler.

**Video 31.4c** (https://youtu.be/j7tkubQTmaU)
Same view with power Doppler.

# Abbreviations used in figures

| | |
|---|---|
| A | ascending (ventral) aorta |
| aa | aortic arch |
| DA | descending (dorsal) aorta |
| eso | esophagus |
| IVC | inferior vena cava |
| LA | left atrium |
| LAA | left aortic arch |
| LB | left main bronchus |
| LC | left common carotid artery |
| LPA | left pulmonary artery |
| LS | left subclavian artery |
| P | main pulmonary artery |
| RA | right atrium |
| RAA | right aortic arch |
| RB | right main bronchus |
| RC | right common carotid artery |
| RI | right innominate artery |
| RPA | right pulmonary artery |
| RS | right subclavian artery |
| RV | right ventricle |
| SVC | Superior vena cava |

# References


1. Moulaert AJ et al. *Circulation* 1976;53(6):1011–15.
2. McElhinney DB et al. *J Am Coll Cardiol* 2001;37(8):2114–9.
3. Digilio M et al. *Images Paediatr Cardiol* 2005;7(2):23–34.
4. Becker AEAR. *Cardiac Embryology: A Help or a Hindrance in Understanding Congenital Heart Disease*. New York, NY: Futura; 1984.
5. Edwards JE. *Med Clin North Am* 1948;32:925–49.
6. Edwards JE. *Lab Investig; A J Tech Methods Pathol* 1953;2(1): 56–75.
7. Yoo SJ et al. *Ultrasound Obstet Gynecol* 2003;22(5):535–46.
8. Chun K et al. *Ann Thorac Surg* 1992;53(4):597–602; discussion 3.
9. Van Son JA et al. *Mayo Clinic Proc* 1993;68(8):743–7.
10. Kocis KC et al. *Pediatr Cardiol* 1997;18(2):127–32.
11. Donnelly LF et al. *AJR Am J Roentgenol* 2002;178(5):1269–74.
12. Cina CS et al. *J Vasc Surg* 2004;39(1):131–9.
13. Schlesinger AE et al. *Pediatr Radiol* 1995;25(6):455–7.
14. McElhinney DB et al. *Pediatr Cardiol* 2001;22(4):285–91.
15. Han JJ et al. *Ann Thorac Surg* 2001;71(2):729–31.
16. Zachary CH et al. *Pediatr Cardiol* 2001;22(1):71–3.
17. Razon Y et al. *J Am Soc Echocardiogr* 2014;27(12):1352–8.
18. Miranda JO et al. *Heart* 2014;100(1):54–9.
19. Peirone A et al. *Cardiol Young* 2002;12(3):272–7.
20. Holmes KW et al. *Pediatr Cardiol* 2006;27(3):316–20.
21. Schneeweiss A et al. *Pediatr Cardiol* 1984;5(3):191–5.
22. Philip S et al. *Int J Cardiol* 2001;79(2–3):133–41.
23. Yagel S et al. *Ultrasound Obstet Gynecol* 2002;20(4):340–5.
24. Vinals F et al. *Ultrasound Obstet Gynecol* 2002;19(3):246–9.
25. Achiron R et al. *Ultrasound Obstet Gynecol* 2002;20(6):553–7.
26. Chaoui R et al. *Ultrasound Obstet Gynecol* 2003;22(6):661–3.
27. Patel CR et al. *J Ultrasound Med* 2006;25(2):251–7.
28. Zidere V et al. *Ultrasound Obstet Gynecol* 2006;28(7):876–81.
29. Berg C et al. *Ultrasound Obstet Gynecol* 2006;28(7):882–9.
30. Chaoui R, McEwing R. *Ultrasound Obstet Gynecol* 2003; 21(1):81–93.
31. Chaoui R et al. *Ultrasound Obstet Gynecol* 2004;23(6):535–45.
32. Yagel S et al. *Ultrasound Obstet Gynecol* 2007;29(1):81–95.
33. Matsui H et al. *Circulation* 2008;118(18):1793–801.
34. Jain S et al. *J Ultrasound Med* 2010;29(2):287–94.
35. Li S et al. *Prenat Diagn* 2011;31(4):334–46.
36. Yoo SJ et al. *Ultrasound Obstet Gynecol* 1999;14(1):29–37.
37. Trobo Marina D et al. *J Obstet Gynaecol* 2016;36(4):526–8.
38. Nguyen HH et al. *Circulation* 2015;131(15):e404–5.
39. Yorioka H et al. *Ultrasound Obstet Gynecol* 2011;37(2):245–6.
40. D'Antonio F et al. *Ultrasound Obstet Gynecol* 2016;47(4): 423–32.
41. Nakata M et al. *J Obstet Gynecol Res* 2013;39(5):1077–80.
42. Glew D, Hartnell GG. *Clinical Radio* 1991;43(5):305–7.
43. Cui W et al. *Echocardiography* 2008;25(1):91–5.
44. Fuchigami T et al. *Ann Thorac Surg* 2016;101(2):e41–3.
45. Zaqout M et al. *Cardiol Young* 2014;24(4):723–4.
46. Tissot C et al. *Heart Surg Forum* 2015;18(3):E114–5.
47. Momma K et al. *Pediatr Cardiol* 1999;20(2):97–102.
48. Trobo D et al. *J Ultrasound Med* 2015;34(11):1921–7.
49. Park IS et al. *Int J Cardiol* 2007;114(2):230–5.
50. Rauch R et al. *Eur J Pediatr* 2004;163(11):642–5.
51. Goldstein WB. *Am J Roentgenol Radium Ther Nucl Med* 1965; 95:131–4.
52. Chaoui R et al. *Am J Obstet Gynecol* 2005;192(1):257–63.
53. Licari A et al. *Pediatr Pulmonol* 2015;50(5):511–24.
54. Robson EA et al. *BMJ Case Rep* 2014;June 3.
55. Alsenaidi K et al. *Pediatrics* 2006;118(5):e1336–41.
56. Humphrey C et al. *Pediatrics* 2006;117(5):e903–8.
57. Olivieri LJ et al. *Pediatr Cardiol* 2012;33(2):351–3.
58. Oppido G et al. *Pediatr Cardiol* 2008;29(2):469–70.
59. Tomos I et al. *Ann Thorac Surg* 2015;100(6):2371.
60. Raimondi F et al. *Ann Pediatr Cardiol* 2016;9(2):170–2.
61. Koontz CS et al. *Am Surg* 2005;71(4):289–91.
62. Slater BJ, Rothenberg SS. *J Laparoendosc Adv Surg Tech A* 2016; 26(1):66–9.
63. Lee JH et al. *Korean J Thorac Cardiovasc Surg* 2015;48(1):78–81.
64. Ota T et al. *J Thorac Cardiovasc Surg* 2006;131(3):574–8.
65. Kouchoukos NT, Masetti P. *J Thorac Cardiovasc Surg* 2007; 133(4):888–92.
66. Luciano D et al. *Ann Thorac Surg* 2015;100(6):2293–7.
67. Iwaki R et al. *World J Pediatr Congenital Heart Surg* 2015;6(3): 458–61.

# 32

# Coarctation of the aorta and interrupted aortic arch

Max E. Godfrey and Wayne Tworetzky

## Background

Coarctation (from the Latin for "constriction") refers to a narrowing of the aorta, usually at the isthmus, and usually with a discrete "posterior shelf" of tissue causing the narrowing of the isthmic lumen. This is one of the more common forms of congenital heart disease, constituting 5% of cases, with an incidence of 3–5 cases per 10,000 live births.[1–4] Despite coarctation being relatively common, it is considered one of the more difficult lesions to diagnose in the fetus,[5] with approximately a third of cases diagnosed prenatally.[6,7] As discussed in this chapter, this low rate of detection is probably due to the unique nature of fetal circulation, the physiologic and anatomic changes that occur in the perinatal period, and, in particular, the relationship between the ductus arteriosus and the aortic isthmus.

## Theories of coarctation

There are a number of theories regarding the embryology of aortic coarctation, which are relevant to the ways in which this condition can be diagnosed in the fetus. In the mid-nineteenth century, there was debate as to whether coarctation was caused by an "inflammation" at some point in postnatal life, or if it was a congenital malformation.[8,9] An early theory was that constriction of ductal tissue within the aorta causes a discrete narrowing,[9] in which case the development of coarctation would be a postnatal event. However, subsequent research showed that, while there is indeed a sling of ductal tissue encircling the isthmus, which is not present in the normal fetus, it seems that a combination of the presence of a coarctation shelf, formed by an abnormal entry of the aortic arch into the ductal arch-descending aorta, together with the postnatal constriction of the ductal tissue, causes the hemodynamic lesion[10–12] (Figures 32.1 and 32.2).

The acknowledged difficulty in diagnosing coarctation in the fetus is due in part to the frequently normal four-chamber view,[5] as well as the lack of clinically significant obstruction at the site of the posterior shelf. In the fetus, there is no constriction of ductal tissue, and the aortic end of the fetal ductus arteriosus widens the channel through which blood can flow across the otherwise narrowed isthmus. Moreover, there is normally low flow across the isthmus in fetal life.[13] In fact, there is no obligate flow across the isthmus prenatally, as the upper body is supplied exclusively by the left ventricle and aortic arch, and the lower body and placenta by the right ventricle, via the ductus arteriosus. Therefore, the presence of any obstacle to flow will simply cause a redistribution of flow. Thus, it should not be surprising that only a half to two-thirds of fetuses who required neonatal surgery for coarctation had a visible posterior shelf or documented flow acceleration at the aortic isthmus.[14,15]

## Fetal diagnosis

The majority of attempts to diagnose coarctation in the fetus have focused on surrogate markers, rather than on demonstrating the presence of isthmic narrowing and a coarctation shelf. Ironically, one of the earliest reports of fetal diagnosis in the literature demonstrated a discrete shelf.[16] However, the first systematic study of coarctation in the fetus looked at 24 fetuses in whom the diagnosis was suspected on the basis of ventricular disproportion, namely, that the right ventricle and pulmonary artery were larger than the left ventricle and aorta. While they also examined the arch subjectively, they did not find a discrete shelf in any of the fetuses, although hypoplasia of the arch was seen in eight patients. They correctly diagnosed an arch abnormality in 18 of these 24 fetuses, although they acknowledged the difficulty in differentiating between coarctation and interrupted aortic arch (see the following text).[17] This was the first of several studies to highlight ventricular disproportion in the fetus as a possible indicator of postnatal coarctation,[15,18–21] although with varying degrees of sensitivity and specificity.[22] A number of groups subsequently looked at measurements of the aortic arch, isthmus, and ductus arteriosus, or abnormalities of the "three-vessel" or "three-vessel and trachea" views[14,15,21,23–28] (Figure 32.3). Similar to the ventricular disproportion studies, many of these studies showed that relative size discrepancies between the left-sided structure (i.e., the aorta) and the right-sided structure (the main pulmonary artery or ductus arteriosus) are indicative of coarctation, with the actual demonstration of a coarctation shelf rarely of importance. Of note, however, measurements of the aortic isthmus and transverse arch were shown to be important in this diagnosis.[15,21,26]

The role of the presence of a left superior vena cava (LSVC) draining to the coronary sinus in the diagnosis of coarctation

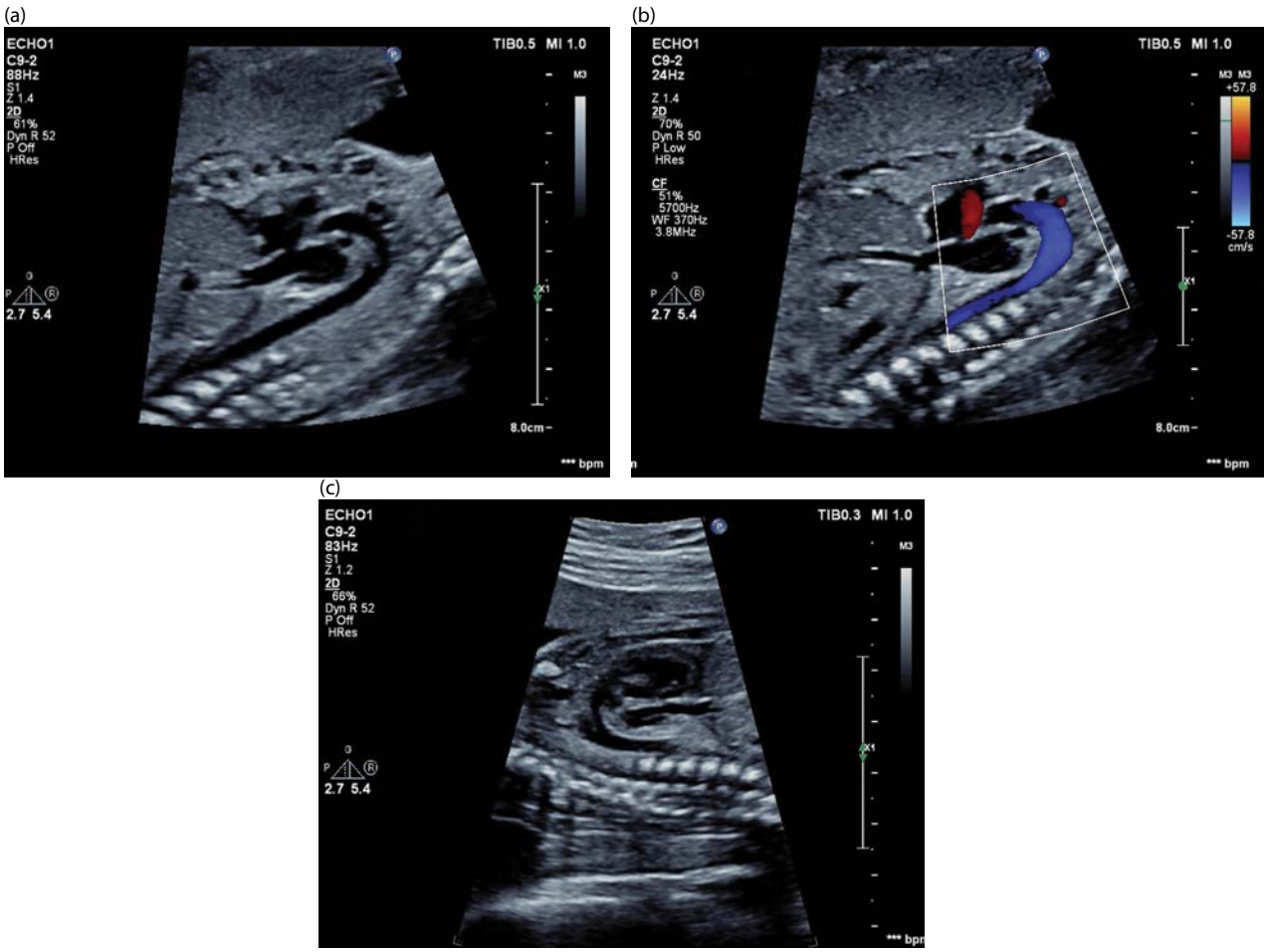


**Figure 32.1**
The normal fetal aortic arch. (a,b) The normal aortic arch, with a smooth posterior wall and no disturbance to flow at the isthmus. (c) The area of the isthmus at the convergence of the ductal and aortic arches.

is somewhat controversial. The finding of an LSVC was found to be strongly associated with the presence of coarctation in one study, in which half of the fetuses with coarctation had this anomaly, compared to a background incidence of 0.3%.[29] However, another paper published soon after found that while fetuses with cardiac disproportion did have an increased incidence of LSVC, the incidence of LSVC was similar for those fetuses with disproportion, regardless of the presence of coarctation,[30] and another study showed the presence of an LSVC to decrease the likelihood of requiring surgery for coarctation.[15] Thus, LSVC would seem to be a marker of ventricular disproportion rather than of coarctation.

The cause of the relatively small left-sided structures in the fetus with coarctation has not been precisely explained. It has been suggested to be caused by raised left ventricular end diastolic pressure (due to the coarctation), reducing right to left shunting at the foramen ovale, with an increased volume load on the right ventricle, and concomitant underfilling of the left ventricle.[15,31] In keeping with this theory, it has been reported that there is an increased incidence of left to right atrial shunting in fetuses with postnatally proven coarctation.[27,32] However, there is a subset of fetuses in which restriction or closure of the foramen ovale is the primary event, resulting in reduced right to left shunting and flow through the left-sided structures, in turn causing reduced growth with resultant coarctation.

One of the problems with using ventricular size discrepancy as a marker of the presence of coarctation is that relative right-left ventricular disproportion can be a normal phenomenon, particularly in the third trimester[33] (Figure 32.4). This has led to a number of studies finding that the diagnostic accuracy for coarctation is reduced as gestation advances,[15,21,32,34] and although there may be certain findings that are more discriminatory at later gestation than at earlier, the sensitivity and specificity are reduced.[28]

There are a number of other considerations regarding the fetal diagnosis of coarctation, unrelated to size discrepancy between left- and right-sided structures. The presence of lesions that are commonly associated with coarctation should raise the index of suspicion and may increase diagnostic accuracy[35] (Table 32.1). Bicuspid aortic valve is present in about 60% of patients with coarctation[36] and can occasionally be diagnosed by fetal echocardiography.[37] Similarly, many cases of coarctation are associated with intracardiac pathology, in

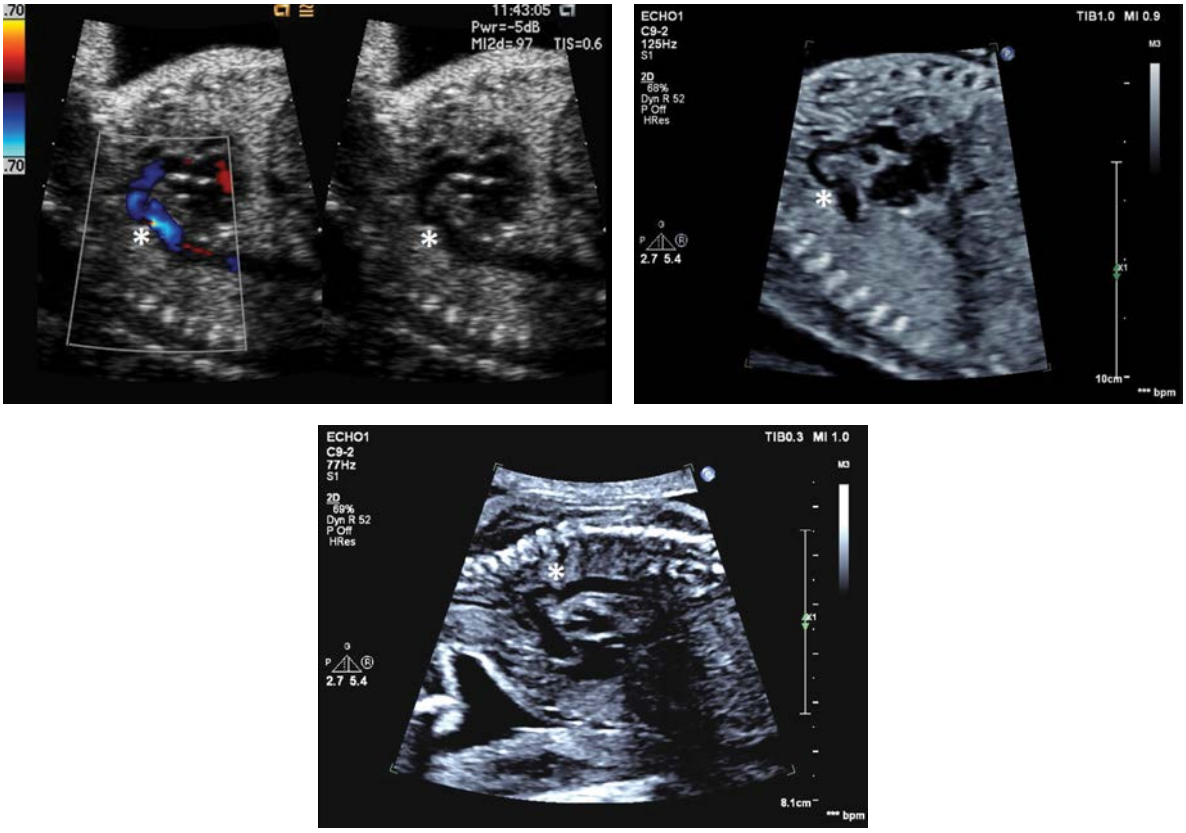


**Figure 32.2**
The aortic arch in the fetus with coarctation. Note the "figure-of-3" appearance of the insertion of the aortic arch into the ductal arch. The asterisk denotes the posterior shelf, with flow disturbance visible at that site in the color image.

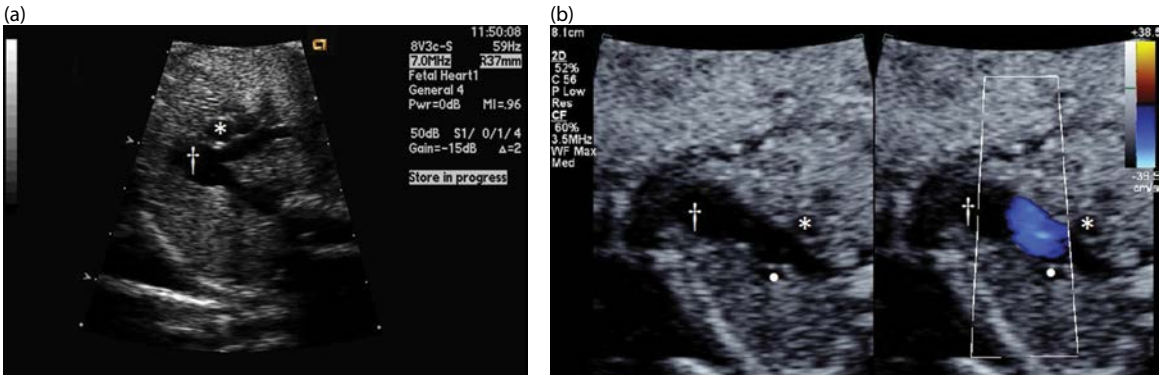


**Figure 32.3**
Abnormal three-vessel view. (a,b) Note the small aorta (*) as compared to the main pulmonary artery (†). (b) A left SVC (•).

particular, ventricular septal defects, mitral anomalies, and left ventricular outflow tract obstruction,[38,39] as well as more complex congenital heart disease, including unbalanced AV canal defect, double-inlet left ventricle, "transposition complex" with systemic obstruction, double-outlet right ventricle, and, more specifically, the Taussig-Bing anomaly.[26,40–47] Although not an associated lesion as such, the left subclavian artery has long been known to be distally displaced in coarctation of the aorta,[48,49] and this finding has been shown to be useful in the prenatal diagnosis of coarctation in the presence of ventricular discrepancy.[50]

Certain genetic syndromes are commonly associated with coarctation, and their presence prompts a higher index of suspicion than normal. These include Turner syndrome,[51] PHACE association,[52] VACTERL association,[53] and Kabuki syndrome.[54]

Conversely, the presence of a single right aortic arch seems to make the diagnosis of coarctation less likely. This

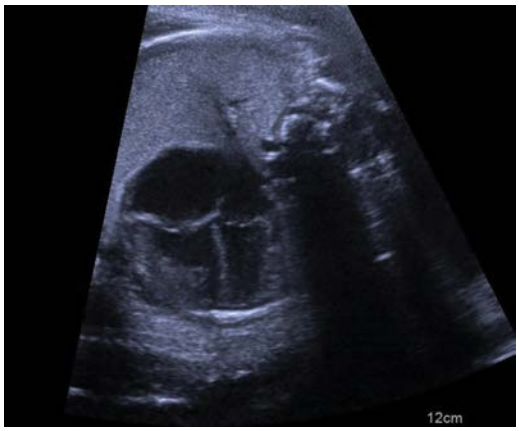


**Figure 32.4**
Right-left disproportion, with much larger right-sided chambers, in a 32-week fetus referred for suspected coarctation, with a normal postnatal examination.

is thought to be due to the different geometry of the aortic and ductal arches in the setting of a right aortic arch, causing relatively more flow across the aortic arch and isthmus, and less across the ductus.[10,55] Likewise, lesions with reduced pulmonary blood flow are very unlikely to be associated with coarctation of the aorta.[56]

Increasing diagnostic accuracy for this condition is important, as coarctation is overrepresented in missed and delayed diagnoses of congenital heart defects,[6,57] and while missing the diagnosis can be catastrophic, prenatal diagnosis is associated with improved outcome.[19] However, in light of the multiple studies cited here, we have not yet achieved diagnostic certainty in this condition, and in particular, we lack a high negative predictive value.

Our institutional clinical practice is to counsel the mother that we suspect coarctation, and explain our limited ability to be certain of the diagnosis. We mention the possibility of associated lesions and genetic syndromes. This counseling is a discussion with the mother of the risks and benefits of different delivery plans. Our advice is, of necessity, to err on the side of caution if there is any suspicion of coarctation. We call this the "good news–good news" model. We recommend delivery in a hospital with on-site pediatric cardiology support. If on postnatal examination, after ductus arteriosus closure, the baby is found not to have a coarctation—that is good news! If the baby indeed has coarctation, then the good news is that the baby is in the right place to receive appropriate treatment.

**Table 32.1** Common clinical and genetic associations in coarctation and interrupted aortic arch

| *Finding* | *Coarctation* | *Interrupted aortic arch* |
|---|---|---|
| Fetal cardiac right:left discrepancy | Common | Common |
| Bicuspid aortic valve | Common | Common |
| VSD | Common | Very common |
| Right aortic arch | Rare | Rare |
| 22q11 microdeletion | Rare | Very common |
| Turner syndrome | Common | Rare |
| PHACE syndrome | Common | Rare |

## Interrupted aortic arch

Interrupted aortic arch (IAA) refers to a loss of luminal continuity between the ascending and descending aorta.[58] Celoria and Patton classified interrupted aortic arch into three subgroups[59] (Figure 32.5): type A (interruption distal to the origin of the left subclavian artery, which can be thought of as an extreme form of coarctation), type B (interruption between the origins of the left common carotid and left subclavian arteries), and type C (interruption between the innominate and left common carotid arteries). Type B is the most common, accounting for 52%–84% of cases, with 13%–47% type A, and only 1%–3% type C.[60–65] Interrupted aortic arch is a rare anomaly, with a prevalence of 2 per 100,000 live births,[4] with even tertiary referral fetal echo centers probably seeing approximately one fetal case a year.[66,67] Interrupted aortic arch can be a difficult diagnosis to make in the fetus, and in particular, it can be difficult to differentiate between coarctation and interruption, especially in light of the physiological similarity between coarctation and IAA type A.[17,30,66] Interrupted aortic arch is associated with a ventricular septal defect (VSD) in 92%–100% of cases, particularly a posterior malalignment VSD[65,68,69] (Figure 32.6), as opposed to approximately 25%–50% of cases of coarctation.[38,70,71] In all fetuses

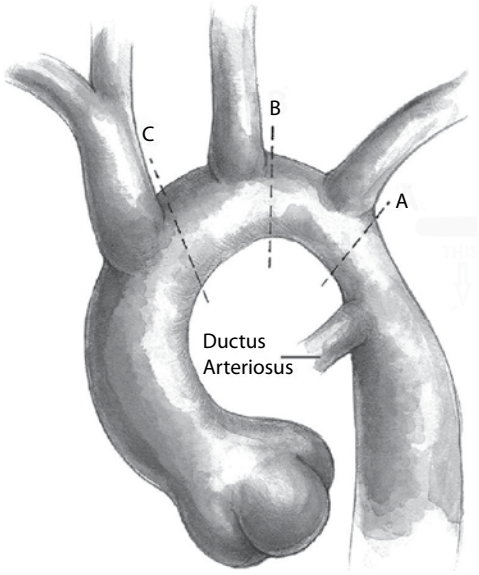


**Figure 32.5**
Celoria and Patton classification of interrupted aortic arch. (Modified from Jonas RA. *Comprehensive Surgical Management of Congenital Heart Disease*. 2nd ed. Boca Raton, FL: CRC Press; 2002.[97])

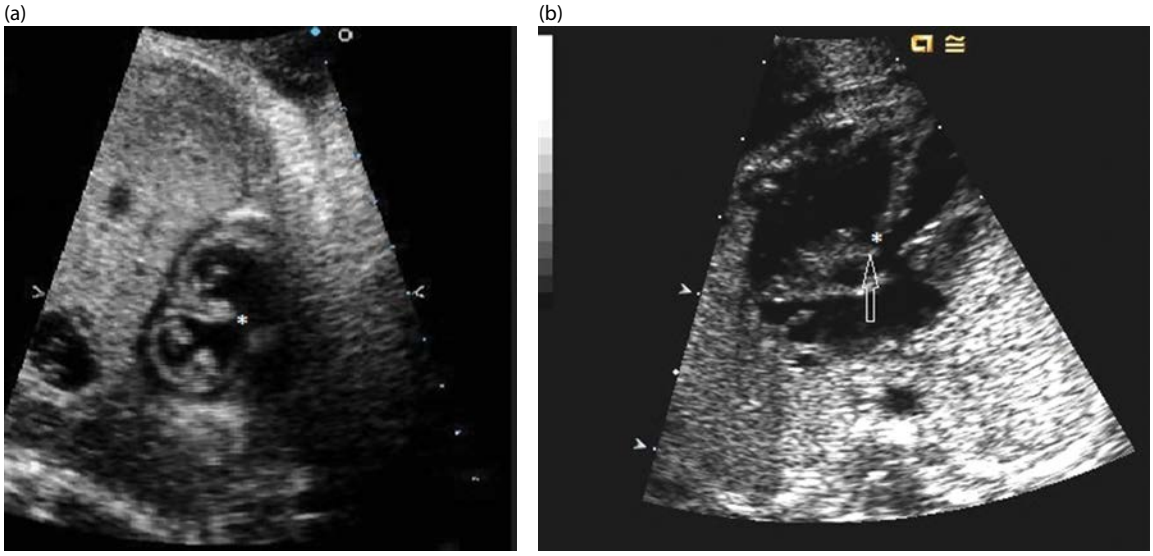


**Figure 32.6**
VSD in IAA. The asterisks indicate the site of the defect. (a) A large conoventricular septal defect. (b) The posterior deviation of the conal septum (arrow), encroaching on the left ventricular outflow tract.

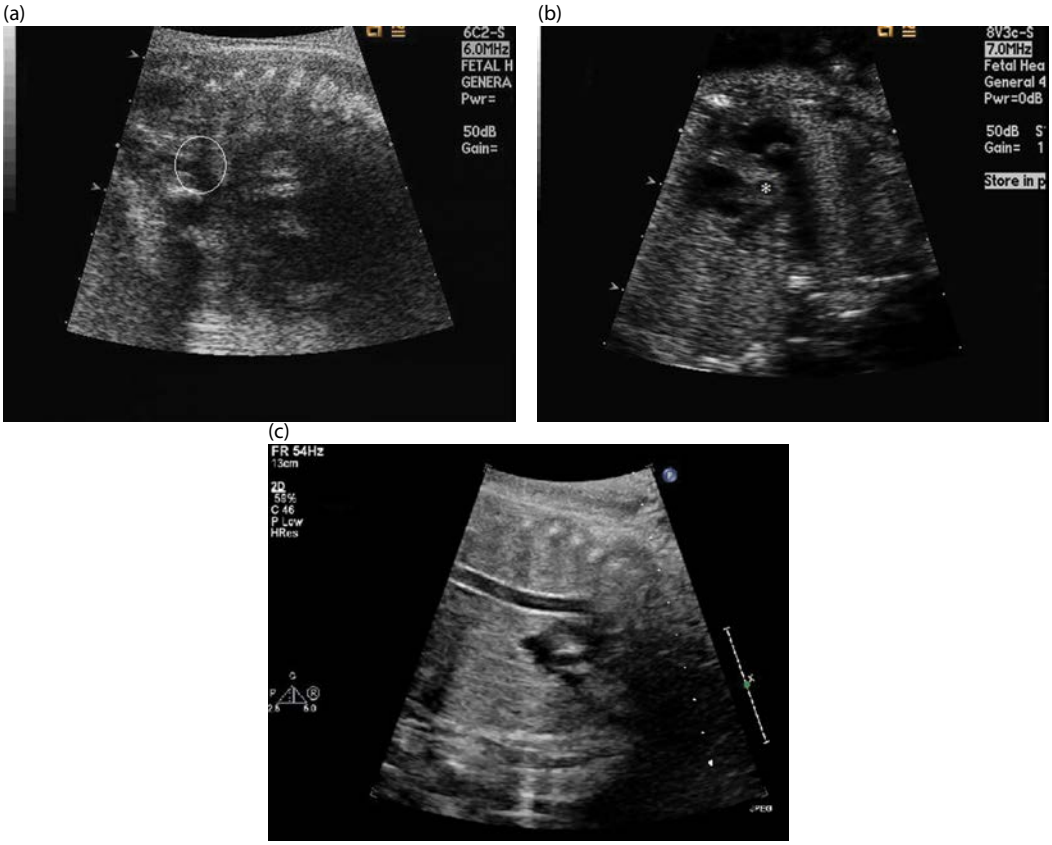


**Figure 32.7**
The aorta in IAA. (a) The "Y-sign" (circled) formed by the ascending aorta branching into the right and left common carotid arteries in a type B IAA (this fetus had an aberrant right subclavian artery). Note the gap between the ascending aorta in the circle and the ductal arch to the right. (b) A very small ascending aorta in cross section (*). (c) An example of how the ductal arch can be mistaken for a normal aortic arch in a fetus with IAA.

referred for suspected VSD, it is prudent to consider the diagnosis of coarctation or IAA as well, as it may be the referral for VSD that prompts the diagnosis of arch obstruction. The frequency of prenatal diagnosis of IAA in the current era is uncertain, but it has been increasing, and it is probably slightly higher than that of coarctation, at 43%–62%.[66,72,73]

The physiology of IAA in the fetus is subtly different from coarctation, as there is no luminal continuity between the aortic arch and the ductal arch. Therefore, the entire blood supply to the lower body (and, depending on the site of interruption, to portions of the upper body) must go through the main pulmonary artery-ductus arteriosus. Accordingly, fetuses with IAA have discrepancy between left- and right-sided structures, in particular, a small aortic valve and a low aortic to pulmonary valve dimension ratio, and a low ascending aorta to main pulmonary artery dimension ratio.[66,74] It is unclear whether these findings are more pronounced in IAA than in coarctation, although one could speculate that, hemodynamically, this should be the case.

On fetal echocardiography, IAA may be apparent by the lack of a connection between the ductal and aortic arches, as well as the "Y appearance" as the ascending aorta runs directly cranially, branching into the innominate (or right common carotid in the case of aberrant right subclavian artery) and left common carotid arteries (Figure 32.7). However, the common association with the 22q11.2 microdeletion (see the following text) and its attendant agenesis of the thymus can make arch imaging more challenging, as the thymus provides sonographic contrast for the arch.[66] Absence of the thymus may be one of the clues prompting the diagnosis of IAA.[75] Use of three- and four-dimensional echocardiographic techniques may provide some added diagnostic sensitivity, in particular, in the detection of arch branching anomalies.[67,76]

Interrupted aortic arch may, like coarctation, be associated with transposition and its variations, as well as double-outlet right ventricle, and in particular, the Taussig-Bing anomaly.[42–44,46,61,64] However, IAA is also associated with specific cardiac structural anomalies, namely, truncus arteriosus and aortopulmonary window. Interruption of the aortic arch is present in 11%–23% of cases of truncus arteriosus,[77–80] and conversely, truncus arteriosus represents 11% of cases of interrupted aortic arch.[81] Similarly, IAA is the most common associated lesion in cases of aortopulmonary window, present in 12%–38% of cases,[82–85] with aortopulmonary window present in 7.3% of patients with interrupted aortic arch.[86] Thus, the diagnosis of any of these lesions in a fetus should prompt a high index of suspicion for the presence of arch obstruction or interruption.

Interrupted aortic arch may be associated with several genetic syndromes, including Turner syndrome and

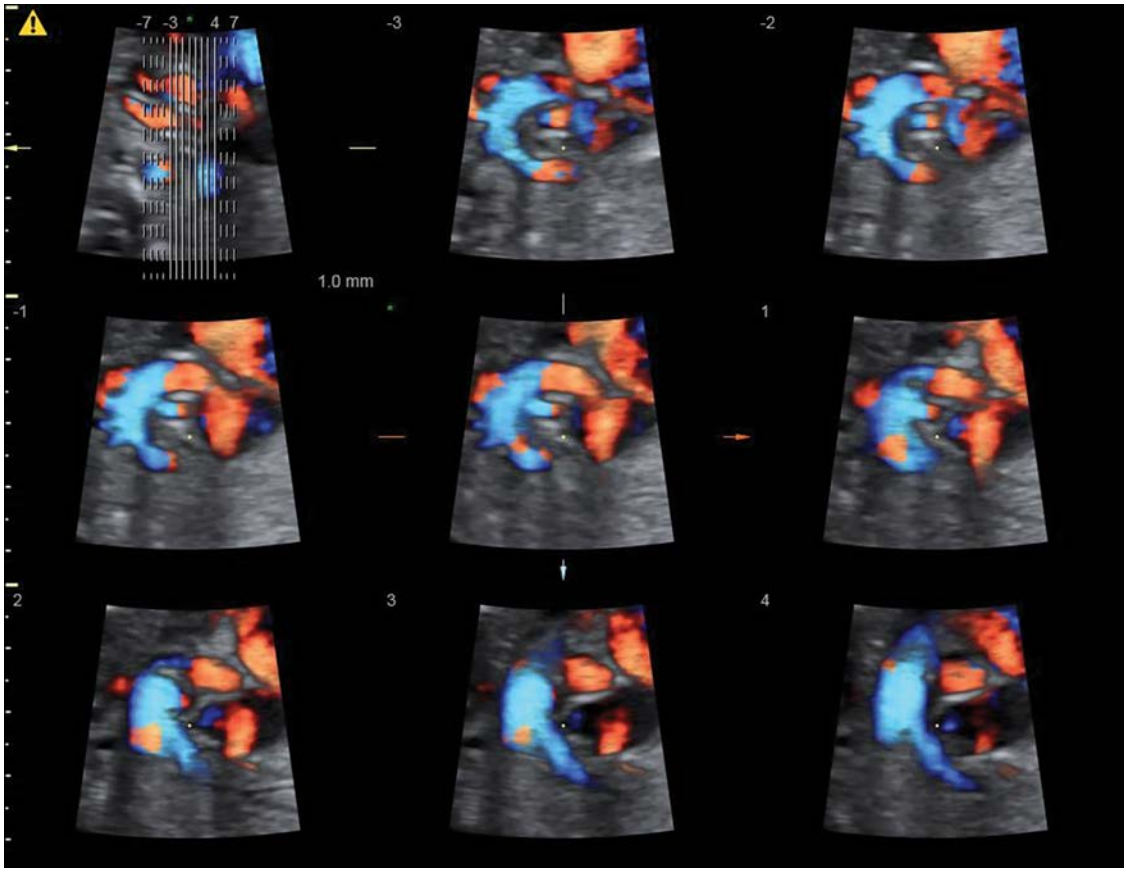


**Figure 32.8**
Fetal coarctation by tomographic ultrasound imaging (TUI) from a spatiotemporal image correlation (STIC) volume data set. (Courtesy of S. Yagel and S. Cohen.)

VACTERL association.[66] However, it is most commonly seen in association with 22q11.2 microdeletion, and it is one of the most common forms of conotruncal malformation seen with this genotype. The 22q11.2 microdeletion is present in 45%–57% of fetuses with IAA[66,67,87–89] and seems to be even more prevalent if arch branching anomalies are present.[89] The association between 22q11.2 microdeletion and IAA is particularly strong in IAA type B, while it is much rarer in type A.[67,89,90]

## Conclusion

The prenatal diagnoses of both coarctation and IAA are challenging, although it is to be hoped that with improving technology, as well as increased awareness among clinicians performing primary screening, the detection rate for both will increase. Imaging of the whole aortic arch is recommended by some,[91,92] but not all,[93] professional societies. It is our institutional practice to examine the aortic arch in both sagittal (the "candy-cane" view) and axial planes, with both two-dimensional and color Doppler imaging, in all fetuses whenever possible. We find it is almost always possible to achieve this, with the candy-cane view often the most easily attainable view when the fetus is spine up. Many centers are using three- and four-dimensional techniques to image the fetal aortic arch (Figure 32.8; Video 32.1), although the added diagnostic value is currently modest.[94–96] Meanwhile, a high index of suspicion, where clinically indicated, coupled with a low threshold for postnatal evaluation, seem to be appropriate.

## Video

**Video 32.1** (https://youtu.be/8sG_9LHvQaM)
A case of coarctation imaged with tomographic ultrasound imaging (TUI) from a spatiotemporal image correlation (STIC) volume data set.

## References


1. Hoffman JI. 1995. *Pediatr Cardiol* 1995;16:103–13.
2. Samanek M et al. *Pediatr Cardiol* 1989;10:205–11.
3. Hoffman JI, Kaplan S. *J Am Coll Cardiol* 2002;39:1890–900.
4. Samanek M, Voriskova M. *Pediatr Cardiol* 1999;20:411–7.
5. Simpson JM. *Ann Pediatr Cardiol* 2009;2:41–50.
6. Liberman RF et al. *Pediatrics* 2014;134:e373–81.
7. McCandless RT et al. *Pediatr Cardiol* 2012;33:1160–4.
8. Anonymous. *Edinb Med Surg J* 1846;65:413–48.
9. Craigie D. *Edinb Med Surg J* 1841;56:427–62.
10. Rudolph AM et al. *Am J Cardiol* 1972;30:514–25.
11. Rosenberg HS. *Perspect Pediatr Pathol* 1973;1:339–68.
12. Ho SY, Anderson RH. *Br Heart J* 1979;41:268–74.
13. Rudolph AM. *Circ Res* 1985;57:811–21.
14. Jowett V et al. *Ultrasound Obstet Gynecol* 2012;40:47–54.
15. Matsui H et al. *Circulation* 2008;118:1793–801.
16. Allan LD et al. *Br Heart J* 52:471–3.
17. Allan LD et al. *Br Heart J* 1988;59:356–60.
18. Benacerraf BR et al. *J Ultrasound Med* 1989;8:65–9.
19. Franklin O et al. *Heart* 2002;87:67–9.
20. Quartermain MD et al. *J Am Soc Echocardiogr* 2009;22:1296–301.
21. Gómez-Montes E et al. *Ultrasound Obstet Gynecol* 2013;41:298–305.
22. Brown DL et al. *J Ultrasound Med* 1997;16:95–9.
23. Vinals F et al. *Ultrasound Obstet Gynecol* 2003;22:358–67.
24. Slodki M et al. *J Ultrasound Med* 2009;28:1313–7.
25. Hornberger LK et al. *Circulation* 1992;86:741–7.
26. Hornberger LK et al. *J Am Coll Cardiol* 1994;23:417–23.
27. Bronshtein M, Zimmer EZ. *Ultrasound Obstet Gynecol* 1998;11:254–7.
28. Gómez-Montes E et al. *Prenatal Diagnosis*. 2014;34(12):1198–206.
29. Pasquini L et al. *Heart* 2005;91:539–40.
30. Head CEG et al. *Heart* 2005;91:1070–4.
31. Kenny D, Hijazi ZM. *Cardiol J* 2011;18:487–95.
32. Sharland GK et al. *Heart* 1994;71:70–5.
33. Sharland GK, Allan LD. *Ultrasound Obstet Gynecol* 1992;2:175–81.
34. Jung E et al. *Prenat Diagn* 2007;27:695–8.
35. Durand I et al. *Pediatr Cardiol* 2015;36:1248–54.
36. Roos-Hesselink JW et al. *Heart* 2003;89:1074–7.
37. Paladini D et al. *Ultrasound Obstet Gynecol* 2002;20:30–4.
38. Becker AE et al. *Circulation* 1970;41:1067–75.
39. Anderson RH et al. *Br Heart J* 1983;50:176–81.
40. Parr GV et al. *J Thorac Cardiovasc Surg* 1983;86:280–7.
41. Bevilacqua M et al. *J Am Coll Cardiol* 1991;18:559–68.
42. Huber C et al. *Eur J Cardiothorac Surg* 2011;39:213–20.
43. Tchervenkov CI, Korkola SJ. *Semin Thorac Cardiovasc Surg Pediatr Card Surg Annu* 2001;4:71–82.
44. Lacour-Gayet F et al. *Circulation* 1997;96:II-328–34.
45. Wetter J et al. *Eur J Cardiothorac Surg* 20:816–23.
46. Choi KH et al. *Pediatr Cardiol* 2016;37:160–6.
47. Alsoufi B et al. *Eur J Cardiothorac Surg* 2008;33:244–50.
48. Kantoch M et al. *Pediatr Cardiol* 1992;13:164–9.
49. Dodge-Khatami A et al. *Ann Thorac Surg* 2005;80:1652–7.
50. Sivanandam S et al. *Pediatr Cardiol* 36:1376–81.
51. Sybert VP. *Pediatrics* 1998;101:E11.
52. Metry D et al. *Pediatrics* 2009;124:1447–56.
53. Khoury MJ et al. *Pediatrics* 1983;71:815–20.
54. Digilio MC et al. *Am J Med Genet* 2001;100:269–74.
55. McElhinney DB et al. *Ann Thorac Surg* 1999;67:1194–1202.
56. Hutchins GM. *Am J Pathol* 1971;63:203–14.
57. Chang RK et al. *Arch Pediatr Adolesc Med* 2008;162:969–74.
58. Backer CL, Mavroudis C. *Ann Thorac Surg* 69:S298–307.
59. Celoria GC, Patton RB. *Am Heart J* 1959;58:407–13.
60. Schreiber C et al. *Eur J Cardiothorac Surg* 1997;12:466–9; discussion 469–70.
61. Serraf A et al. *J Thorac Cardiovasc Surg* 1996;112:1150–60.
62. Menahem S et al. *Pediatr Cardiol* 1992;13:214–21.
63. McCrindle BW et al. *J Thorac Cardiovasc Surg* 2005;129:343–50.
64. Brown JW et al. *Eur J Cardiothorac Surg* 2006;29:666–73; discussion 673–4.
65. Freedom RM et al. *Am J Cardiol* 1977;39:572–82.
66. Vogel M et al. *Am J Cardiol* 2010;105:727–34.
67. Volpe P et al. *Ultrasound Obstet Gynecol* 2010;35:302–9.
68. Van Praagh R et al. *Am J Cardiol* 1971;27:200–11.
69. Oosterhof T et al. *Ann Thorac Surg* 2004;78:1696–702.
70. Moene RJ et al. *Am J Cardiol* 1987;59:952–5.
71. Shinebourne EA et al. *Br Heart J* 1976;38:375–80.
72. Axt-Fliedner R et al. *Fetal Diagn Ther* 2011;30:299–305.
73. Hill GD et al. *Prenat Diagn* 2015;35:859–63.

74. Slodki M et al. *Ultrasound Med Biol* 2011;37:1808–13.
75. Volpe P et al. *Prenat Diagn* 2003;23:752–7.
76. Zhang D et al. *Echocardiography* 2016;33:90–8.
77. Van Praagh R, Van Praagh S. *Am J Cardiol* 1965;16:406–25.
78. Calder L et al. *Am Heart J* 1976;92:23–38.
79. Butto F et al. *Pediatr Cardiol* 1986;7:95–101.
80. Miyamoto T et al. *Ann Thorac Surg* 2005;79:2077–82.
81. Konstantinov IE et al. *Ann Thorac Surg* 2006;81:214–22.
82. McElhinney DB et al. *Am J Cardiol* 1998;81:195–201.
83. Jansen C et al. *Pediatr Cardiol* 2006;27:552–6.
84. Blieden LC, Moller JH. *Br Heart J* 36:630–5.
85. Naimo PS et al. *Ann Thorac Surg* 2014;98:1674–9.
86. Murin P et al. *Thorac Cardiovasc Surg* 2012;60:215–20.
87. Goldmuntz E et al. *J Am Coll Cardiol* 1998;32:492–8.
88. Boudjemline Y et al. *J Pediatr* 2001;138:520–4.
89. Peyvandi S et al. *Pediatr Cardiol* 2013;34:1687–94.
90. Volpe P et al. *Prenat Diagn* 2002;22:371–4.
91. American Institute of Ultrasound in M. *J Ultrasound Med* 2013;32:1067–82.
92. Donofrio MT et al. *Circulation* 2014;129:2183–242.
93. International Society of Ultrasound in O, Gynecology, Carvalho JS et al. *Ultrasound Obstet Gynecol* 2013;41:348–59.
94. Xiong Y et al. *Ultrasound Obstet Gynecol* 2012;39:316–21.
95. Turan S et al. *J Clin Ultrasound* 37:253–7.
96. Yagel S et al. *Ultrasound Obstet Gynecol* 2011;37:432–7.
97. Jonas RA. *Comprehensive Surgical Management of Congenital Heart Disease*. 2nd ed. Boca Raton, FL: CRC Press; 2002.

# 33

# Diseases of the myocardium, endocardium, and pericardium during fetal life and cardiomyopathy in the fetus

Simone R.F. Fontes Pedra and Carlos A.C. Pedra

## Introduction

Diseases of the endocardium, myocardium, and pericardium may present with very variable forms, etiology, and natural history.[1] Since the advent of fetal echocardiography, these abnormalities have been described in fetal life.[2–8] Fetal echocardiography allows for an early recognition of myocardial and endocardial diseases, based on the pattern of dilated and hypocontractile ventricles and/or the degree and localization of ventricular hypertrophy. They may result from systemic abnormalities, maternal diseases, or some other specific conditions such as twin-to-twin transfusion syndrome or anemia.[2,6–8] In the era of fetal echocardiography, referral to check possible familial myocardial disease is quite frequent.[9] This chapter aims to give an overview of these uncommon diseases that may have a poor outcome prenatally or soon after birth.

## Diseases of endocardium

### *Endocardial fibroelastosis*

Endocardial fibroelastosis (EFE) is characterized by deposition of elastin and collagen in the endomyocardium, ventricular hypertrophy, and endocardial thickening.[10] The fibrotic scars compromise systolic and diastolic function due to increased content of noncontractile elements in the fetal myocardium.[11] Endocardial thickening is probably caused by persistent and increased wall tension in the ventricles, possibly secondary to an ischemic and damaged myocardium, mitral regurgitation, or a combination of factors. In addition, the degree of EFE seems to progress with aging. There are multiple conditions associated with its etiology: maternal viral infections, hypoxia, vascular and metabolic diseases, and chromosomal abnormalities. It may also be considered idiopathic.[10,12–14] Although the pathogenesis of EFE is unknown, inflammatory processes have been proposed to play a role.[15] The disease is usually sporadic, but familial cases have been reported in about 10%.[10] Observations that favor a viral etiology include a clinical presentation similar to that of chronic myocarditis, findings of myocarditis or myocardial fibrosis in the affected patients.

There are two pathologic forms of primary EFE: dilated, which is the most common form, and contracted.[16] Dilated EFE is characterized by a markedly enlarged globular heart, mainly involving the left ventricle (LV) and left atrium (LA). The LV endocardium is opaque, glistening, milky white, and diffusely thickened reaching about 1–2 mm. The thickening is most marked in the outflow tract. Endocardial thickening extends to the LA, right ventricle (RV), and right atrium (RA). In approximately 50% of patients, the mitral and aortic valves are involved, often resulting in marked anatomic deformity and either valvar regurgitation or stenosis. The less common contracted type of primary EFE is associated with a relatively hypoplastic or normal LV size. The right and left atria and the RV may be markedly enlarged and hypertrophied. An early event in fetal life is believed to result in dilated EFE, which later changes to a contracted type[16] (Figure 33.1). The same process may affect the RV myocardium. Figure 33.2 illustrates a case of a contracted form of RV EFE (Video 33.1). In this case, the fetus presented with noncontractile and slightly hypoplastic RV with functional pulmonary atresia. Runs of supraventricular tachycardia and hydrops were controlled with oral digoxin. The baby was born with moderate to severe RV hypoplasia and no antegrade pulmonary blood flow. RV systolic function was very poor. The first procedure performed was ductal stenting. The baby was placed on extracorporeal membrane oxygenation (ECMO) and listed for transplant but died waiting for an organ donor. His pathological specimen is depicted in Figure 33.2d. Of note, his previous sibling had presented with similar findings and died of uncontrolled arrhythmia after a Blalock-Taussig shunt.

Secondary EFE, associated with cardiac malformations, is attributed to cardiac hypertrophy and consequent imbalance in the myocardial oxygen supply-demand relationship. Resultant fibroelastotic thickening may be focal or diffuse, with its severity related to the degree and time of exposure to the underlying disease. Congenital cardiac malformations that result from left- or right-sided obstructive lesions such as critical aortic stenosis (CAS), hypoplastic left heart

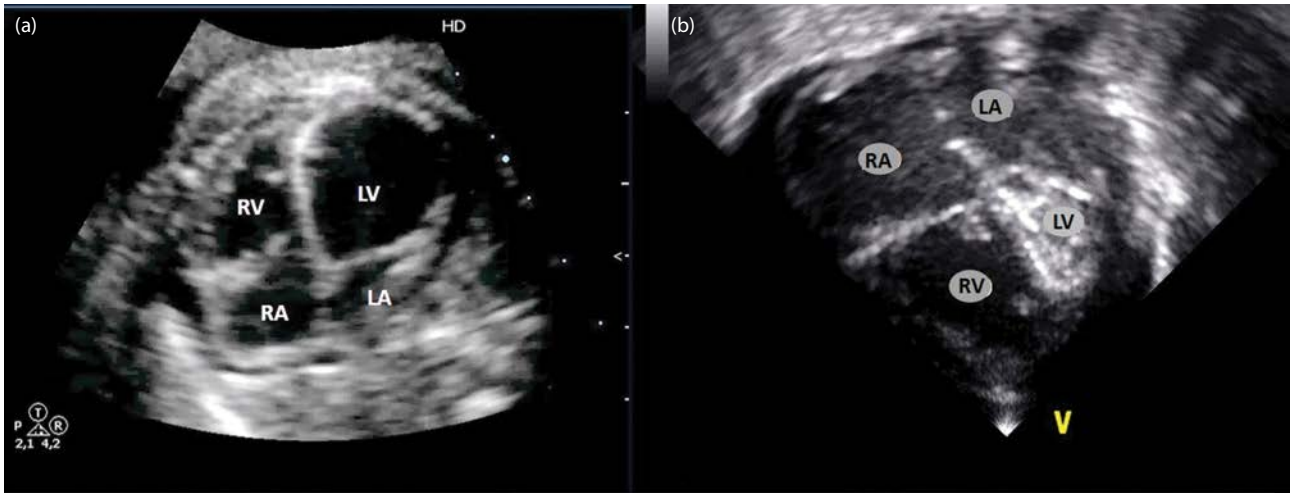


**Figure 33.1**
A case of a dilated form of left ventricular endocardial fibroelastosis at 29 weeks' gestation (a) that presented with severe LV hypoplasia (contracted form) at birth (b). (LA, left atrium; LV, left ventricle; RA, right atrium; RV, right ventricle.)

syndrome, and critical right ventricular outflow obstruction may cause secondary left and right ventricular EFE.

Familial recurrence is well-documented in some case series,[17,18] suggesting a genetic basis for the pathology. Autosomal dominant transmission has been reported, but there are also reports of X-linked inheritance and gene mutations.[19,20]

The prognosis of fetal endocardial fibroelastosis is poor. This disorder, in its primary or secondary form, may be the cause of congestive heart failure, fetal hydrops, and demise.[12,13] Moreover, 80% of children born with EFE present congestive heart failure during the first year of life.[13]

Successful fetal aortic valvuloplasty performed between the 22nd and 30th weeks of gestation may stop the progression

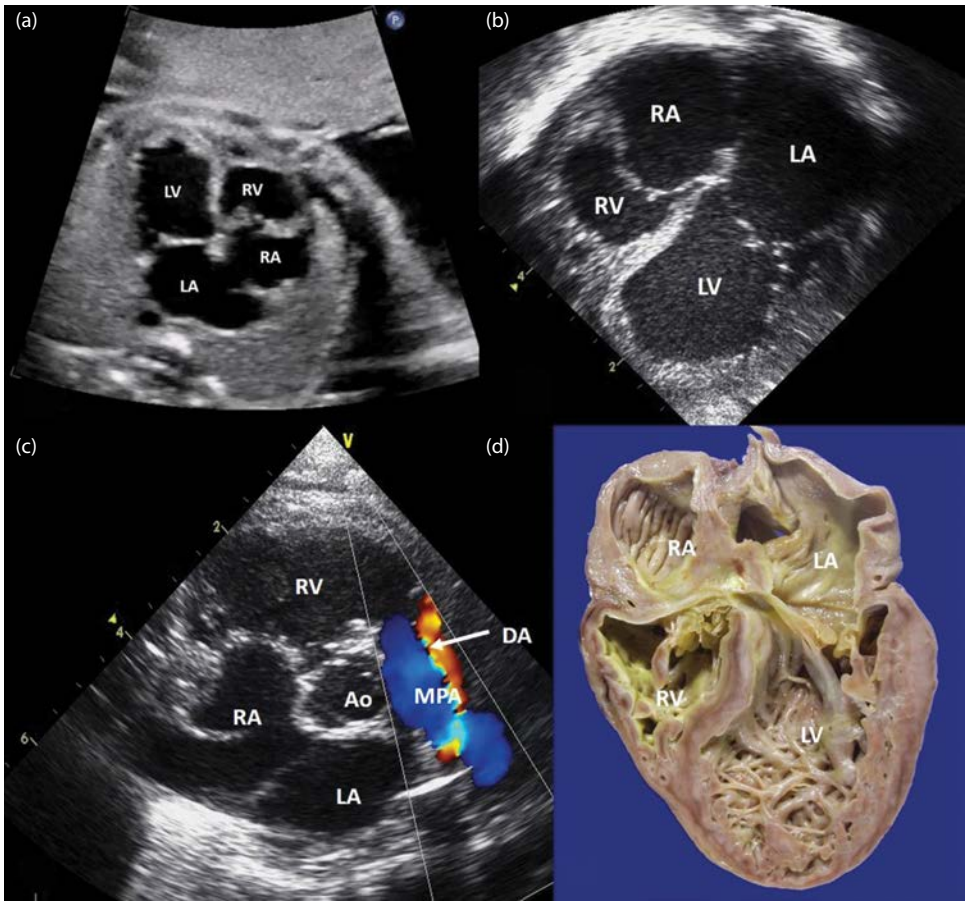


**Figure 33.2**
Fetal and neonatal echocardiograms and pathological specimen of a case of right ventricular EFE contracted form. Note that the RV was already hypoplastic intra-utero at 28 weeks' gestation (a). Same RV hypoplasia observed in the four chamber view during the neontal echocardiogram (b). There was no pulmonary antegrade flow (functional pulmonary atresia) because of severe systolic dysfunction. The baby was kept on IV prostaglandin soon after birth (c). On pathology, diffuse EFE was identified on the RV and, the LV was hypertrabeculated (d). (Ao, aorta; DA, ductus arteriosus; MPA, main pulmonary artery; LA, left atrium; LV, left ventricle; RA, right atrium; RV, right ventricle.)

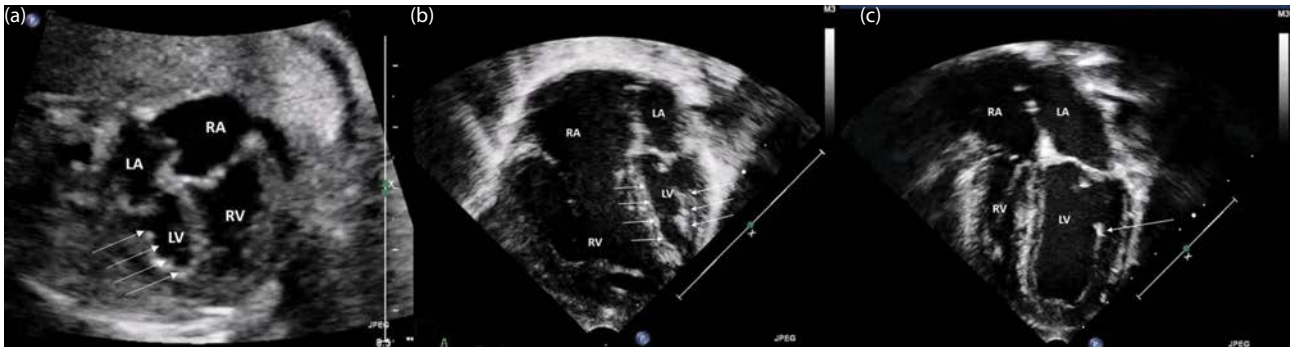


**Figure 33.3**
LV evolution from fetal life to 24 months of age of a baby with secondary EFE due to critical aortic stenosis diagnosed at 26 weeks' gestation (a). After a successful aortic valvuloplasty, the baby was born with borderline LV (b) and was managed with a hybrid procedure (bilateral PA bands and ductal stent). At 13 months, he underwent biventricular repair with PA bands and stent removal associated with EFE overhaul and aortic valve plasty. (c) This four-chamber view at 24 months of age demonstrates significant LV growth reaching normal size. (LA, left atrium; LV, left ventricle; RA, right atrium; RV, right ventricle.)

of left ventricular EFE secondary to critical aortic stenosis in selected cases.[21,22] After adequate relief of the obstruction, if the myocardium is not severely affected, the left ventricular systolic function may recover.[21–23] However, diastolic dysfunction may persist.[24] Many therapeutic strategies have been proposed to rehabilitate the compromised LV, depending on the size of the cavity and on the experience of the pediatric cardiology program. In our center, when the LV is still borderline in size and functional after birth, the first step in the neonatal period is early palliation employing a hybrid procedure and repeated balloon aortic valvuloplasty if there is still significant stenosis.[23] The child is followed with serial echocardiographic scans. When the LV function recovers and if the LV volume is acceptable in the setting of adequate mitral and aortic valves annulus diameters, the child undergoes a LV overhaul, which includes taking down the hybrid procedure, correcting arch hypoplasia if necessary, and performing aortic valve plasty with commissurotomy and leaflet thinning and LV EFE removal. With this staged strategy, we have achieved a 55% rate of biventricular repair in patients with CAS and impending hypoplastic left heart syndrome. The Boston group also employs a staged strategy, but they typically start off with a Norwood procedure with or without an aortic valve plasty, and if possible, an initial EFE resection.[25] Figure 33.3 illustrates a patient with CAS and hypoplastic LV who underwent the strategy described and achieved biventricular circulation at 13 months of age.

## Diseases of the myocardium

Cardiomyopathies correspond to a spectrum of heart muscle disorders that affect cardiac filling, contraction, or both, in the absence of structural heart disease.[1] They are classified as dilated, hypertrophic, and restrictive according to the clinical and anatomical presentation, and may be diagnosed in fetal life. Fetal cardiomyopathies correspond to a heterogeneous group of diseases with many different etiologies involved. They account for approximately 2%–4% of all cardiac disease diagnosed during fetal life and are associated with significant perinatal mortality.[26]

## Dilated cardiomyopathies

In fetal life, dilated cardiomyopathies may affect the RV, the LV, or both. They are defined as dilated and hypocontractile ventricles with ventricular enlargement greater than 2 z-scores for the specific gestational age.[6] Because of ventricular dilation, atrioventricular valve regurgitation is common. Diastolic dysfunction is frequently associated, and according to the degree of dysfunction, hydrops may occur. The cardiothoracic ratio is often markedly increased. Systolic function can be assessed by M-mode, two-dimensional echo and Doppler indexes.[2,6] Ventricular shortening fractions (right, left, or both) are less than 28%. Diastolic Doppler tracings across the atrioventricular valves and in the inferior vena cava, ductus venosus, and umbilical vein are prognostic and may precede fetal hydrops and demise[2] (Video 33.2). The cardiovascular profile score fits perfectly in this group of diseases, being very useful for family counseling.[27,28]

Dilated cardiomyopathy (DCM) may be the end result of a number of different disease processes, including metabolic, genetic, infective, hematological, renal, and immune mediated.[2,6–8] Although mandatory extensive investigation to determine their etiology is now available, close to 50% of the cases remain with no identifiable cause and are considered idiopathic. Table 33.1 lists the most frequent causes of fetal DCM according to the largest series published since the year 2000.

Investigation for the underlying possible causes should commence immediately after the diagnosis of fetal DCM is made. It may result from a viral myocarditis due to infective agents crossing the placenta. Common agents linked to fetal myocarditis include parvovirus, Coxsackievirus, toxoplasma, HIV, and cytomegalovirus.[11] Therefore, maternal blood samples should be drawn to check for possible maternal infection. If Doppler examination of the mean cerebral artery is suspicious for anemia, rapid maternal testing for recent parvovirus

**Table 33.1** Underlying causes of dilated fetal cardiomyopathy according to the four most recent series published

| *Etiology* | *Pedra*[2] | *Sivasankaran*[3] | *Fesslova*[7] | *Weber*[6] | *Total* |
|---|---|---|---|---|---|
| Genetic/ metabolic | 2 | 11 | 1 | 13 | 27 |
| Infective | 6 | 11 | 12 | 3 | 32 |
| Inflammatory | 5 | | | 6 | 11 |
| Anemia | | 5 | | | 5 |
| Renal | | 5 | 2 | | 7 |
| Idiopathic | 9 | 13 | 12 | 18 | 52 |
| Other | | 5 | 4 | | 9 |
| Total | 22 | 50 | 31 | 40 | 143 |

infection should be performed. A fetal blood sample can be obtained by cordocentesis and checked for anemia and acute infection. In most cases, the mother is asymptomatic or has nonspecific symptoms. Fetal echocardiography can demonstrate cardiac dysfunction and pericardial effusions in the setting of inflammation of the myocardium. Fetal tachyarrhythmia may be the first cardiac finding. Although cardiac dysfunction may resolve, functional abnormalities may persist if significant myocardial damage occurs. It is important to exclude intermittent tachycardia that may be the cause or consequence of the disease. Figure 33.4 refers to a case of acute myocarditis due to Coxsackie confirmed by positive mother's serology. The fetus presented in the 32nd week of gestation with ventricular tachycardia and severe biventricular dysfunction. The heart was globally dilated. There was mitral and tricuspid insufficiency. Despite the use of transplacental antiarrhythmic medication and intracordal steroids and immunoglobulin, hydrops progressed. The baby was born by cesarean section in the 33rd week of gestation but died 6 hours after birth with intractable ventricular arrhythmia and low cardiac output (Video 33.3).

Detailed morphological and Doppler fetal ultrasound scanning to exclude the association of extracardiac abnormalities such as renal diseases and dysmorphism should be performed.

Maternal autoimmune diseases, such as lupus and Sjögren syndrome, can result in DCM due to myocardial inflammation with or without associated conduction disease related to SS-A and SS-B antibodies.[29,30] Unique echo-bright regions of the myocardium within the atrium, AV groove, or crux of the heart have been seen in fetuses exposed to these autoimmune processes.[31]

Many metabolic and genetic causes are linked to DCM in the fetus. Mutations on the X chromosome, such as the mutation of the tafazzin gene (TAZ), can cause the disease. Barth syndrome is a disorder caused by a TAZ gene mutation and can result in DCM with cyclic neutropenia and growth impairment.[32]

An echocardiogram of the first-degree relatives (parents and siblings) should be performed to rule out occult forms of familial cardiomyopathies.[9]

Infantile arterial calcinosis is another rare entity that can cause DCM. It is characterized by calcification of the arterial walls of the great vessels and other medium and large vessels.[33] Diminished myocardial function in patients with infantile arterial calcinosis is thought to be secondary to coronary artery calcification with myocardial ischemia. Hypertension resulting from renal artery calcification can also occur.

Sialic acid storage disease and mitochondrial disorders are also causes of DCM.[6–8]

In case of fetal or neonatal death or transplant, anatomical and histological examination of the affected specimen may define the underlying etiology.

In addition to the finding of dilated and hypocontractile chambers, increased filling pressures are also observed, characterized by single waves across the atrioventricular valve inflow, flow reversal in the ductus venosus with atrial contraction, and umbilical venous pulsations (Figure 33.5). These are signs of poor prognosis and are part of the Cardiovascular Profile Score that should be performed during echocardiographic scan. Serial monitoring is certainly indicated in these high-risk patients.[2,26]

Prognosis for fetuses diagnosed with DCM is generally poor. One series demonstrated a survival rate of 50% for non-hydropic fetuses and only an 18% survival rate for hydropic fetuses.[8] Postnatally, cardiac transplant can be considered if function fails to improve in the setting of heart failure.

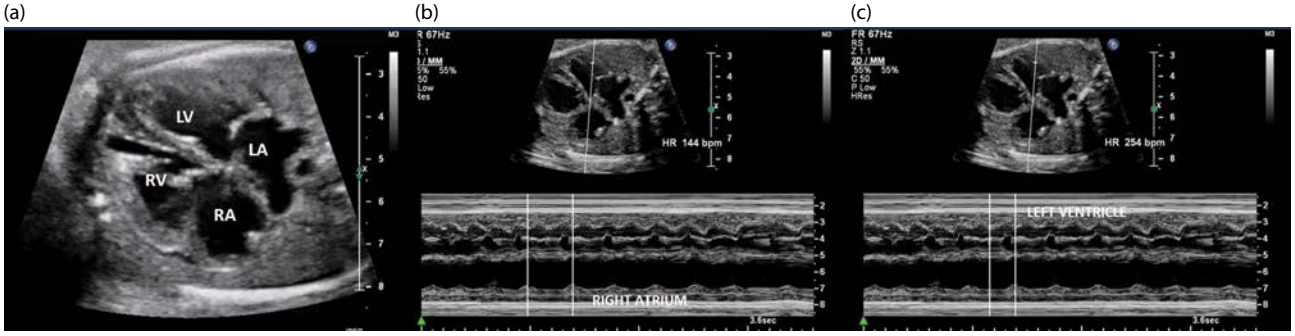


**Figure 33.4**
Four-chamber view of a case with acute myocarditis that presented at 28 weeks' gestation with increased cardiothoracic ratio (a) and uncontrolled ventricular tachycardia, with atrial rate (b) slower than the ventricular rate (c). (LA, left atrium; LV, left ventricle; RA, right atrium; RV, right ventricle.)

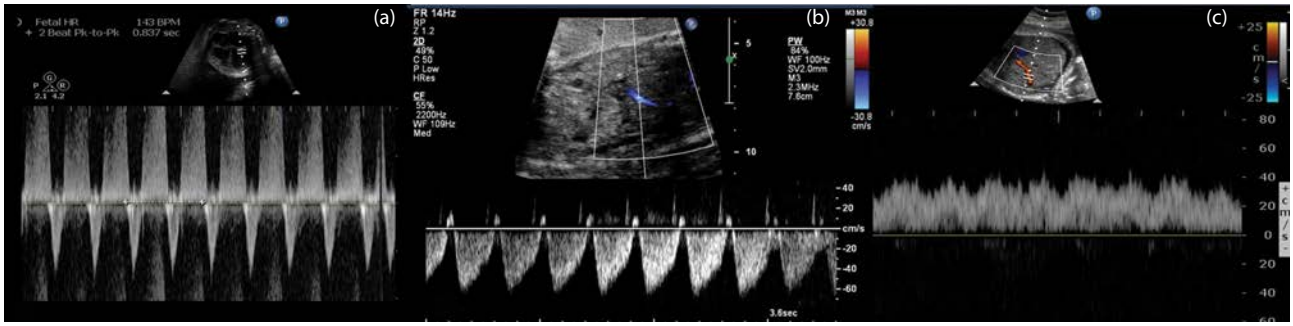


**Figure 33.5**
Abnormal Doppler tracings of a fetus with dilated cardiomyopathy and increased filling pressures. (a) Single inflow wave across the mitral valve; (b) reverse "a" in the ductus venosus; (c) umbilical venous pulsations.

## Fetal therapy for dilated cardiomyopathy

Few situations may be treatable and improve the outcome of dilated cardiomyopathies. Transfusion may rapidly improve when anemia is resulting in ventricular dysfunction and hydrops. Presumed or confirmed acute viral myocarditis can be addressed with steroids and immunoglobulins (IVIG) infused directly in the umbilical cord. However, there is no evidence in the literature that supports its efficacy. Digoxin can also be utilized as it crosses the placenta easily and improves heart function and hydrops.[26] Antiarrhythmic drug therapy should be started whenever tachyarrhythmias are detected. Treatment of maternal autoantibody-mediated fetal cardiomyopathy/endocardial fibroelastosis with IVIG and corticosteroids potentially improves the outcome of affected fetuses. However, the optimal dose and timing of IVIG administration are not well known.[34,35]

## Ventricular noncompaction

Ventricular noncompaction is considered by the World Health Organization as a distinctive form of unclassified cardiomyopathy, not included in the classical dilated, hypertrophic, and restrictive forms.[36] It is more frequently associated with significant systolic dysfunction. It has become increasingly identified prenatally, occurring in isolation or in association with structural heart disease, fetal hydrops, and demise.[7,37–40] It is caused by arrest of the compaction process between the fifth and eighth weeks of embryonic life.[41]

This condition is characterized by deep crypts within the myocardium, usually toward the apex of the left and/or right ventricles. The layer of noncompacted myocardium is thicker than the layer of compacted myocardium, whereas in normal cases, the width of the ventricular wall formed by trabeculations never exceeds the thickness of the compacted layer. Ventricular trabeculations are usually confined to the apical and midventricular myocardial segments of the LV. The standard criteria include crypts in the myocardium that are more than twice the depth of the compact layer of the myocardium. Different from sinusoids, the recesses in noncompacted cardiomyopathy do not connect with the coronary arteries.[42] This condition may be familial, and hence, investigation of parents is warranted. Mutation of the tafazzin gene (TAZ) also can cause the noncompaction. Barth syndrome is a disorder caused by a TAZ gene mutation and can result in ventricular noncompaction as well as dilated cardiomyopathy. Because the symptomatology is extremely variable, the affected parents may be entirely asymptomatic.[43]

Familial, both X-linked and dominant, forms of left ventricular noncompaction have been described, representing 20%–50% of cases. However, sporadic cases have also been reported.[44] Noncompaction of the ventricular myocardium has been described in infancy in association with severe left and right ventricular obstructive lesions,[45,46] as well as in cases of anomalous origin of the coronary arteries from the pulmonary artery,[47] or even in association with more complex congenital heart defects.[47]

Figure 33.6 demonstrates a case of noncompation myocardium (NCM) diagnosed at 29 weeks' gestation associated with pulmonary atresia and intact ventricular septum with good size RV.

## Hypertrophic cardiomyopathies

Hypertrophic cardiomyopathy (HCM) is defined by ventricular hypertrophy that is not explained by any structural cardiac abnormality with significant obstruction of the left or right ventricular outflows. It can affect all ventricular walls, just one ventricle, or may predominate in the interventricular septum. HCM is diagnosed on the basis of an increased parietal thickness above 97.5% of normal standards for gestational age.[48,49] In some fetuses, severe hypertrophy of the interventricular septum may lead to a dynamic obstruction of the outflow tract by the hypertrophied muscle (Video 33.4). Measurement of the ventricular wall may be performed by two-dimensional echocardiography or M-mode and be compared to the normal ranges according to gestational age. Severe HCM may be associated with intrauterine fetal death or adverse postnatal outcome. There are many causes involved in the genesis of HCM in fetal life. Maternal uncontrolled diabetes mellitus is the most frequent etiology.[50] Table 33.2 shows the different causes described in the most recent series reported in the literature.

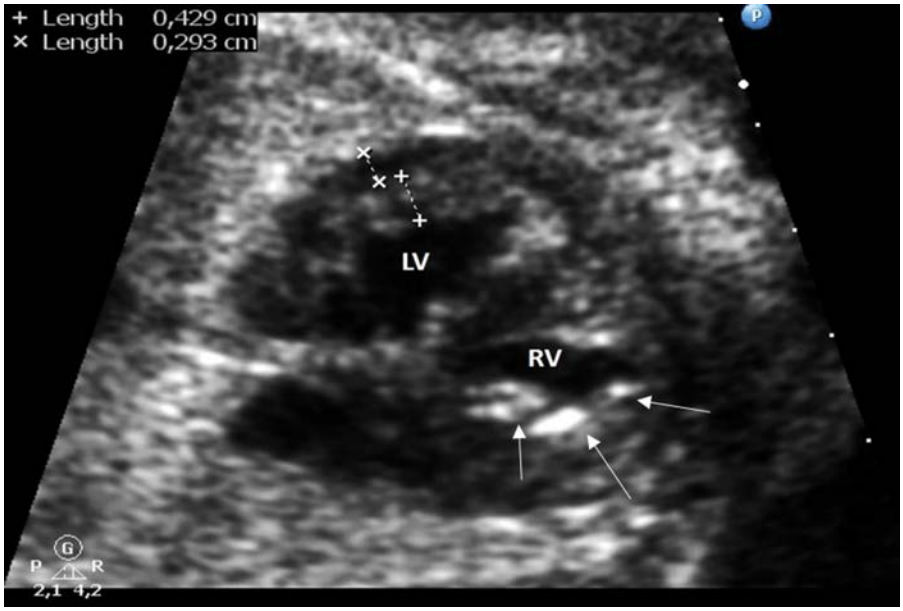


**Figure 33.6**
Fetal echocardiography of a fetus with pulmonary atresia and intact ventricular septum with bright echoes in the RV (arrow) and left ventricular non-compaction myocardium. (LV, left ventricle; RV, right ventricle.)

**Table 33.2** Underlying causes of hypertrophic fetal cardiomyopathy according to the three most recent series published

| *Etiology* | *Pedra*[2] | *Fesslova*[7] | *Weber*[6] | *Total* |
|---|---|---|---|---|
| Genetic/Metabolic | 12 | 26 | 12 | 50 |
| Maternal diabetes | 7 | 17 | | |
| Familial | 1 | 5 | 1 | |
| Noonan's | 2 | 1 | 2 | |
| Alfa thalassemia | 2 | | 5 | |
| Other | | 3 | 4 | |
| TTTS | 18 | | | 18 |
| Renal | | 16 | | 16 |
| Idiopathic | 3 | 16 | 9 | 28 |
| Other | | 2 | | 2 |
| Total | 33 | 60 | 21 | 114 |

*Abbreviation:* TTTS, twin-to-twin transfusion syndrome.

Few cases of myocardial hypertrophy during fetal life due to mitochondrial cytopathies are reported in the literature. Therefore, detailed metabolic investigations are indicated for unexplained ventricular hypertrophy.[7] Congenital disorder of glycosylation and ATPase deficiency were identified among 21 cases of HCM recently reported by Weber et al.[6]

Fetal hypertension due to severe renal disorders may be involved in the genesis of hypertrophic cardiomyopathy occasionally observed in cases with malformation of the genitourinary tract (Figure 33.7).

Diabetes mellitus affects the fetal heart during early and late gestation. During embryology, it impairs the proper expression of genes needed for the correct development of the fetal heart, causing structural cardiac defects.[51] During late gestation, especially in the third trimester, fetal hyperinsulinemia secondary to inappropriate maternal glycemic control stimulates the fetal insulin cardiac receptors, causing hyperplasia and hypertrophy of the fetal myocardium, leading to HCM.[52] Ventricular walls become hypertrophied, but the most commonly affected area is the interventricular septum, which has abundant insulin receptors.[53,54] HCM corresponds to 40% of all cardiac disease presented in infants of diabetic mothers. Fortunately, cardiac hypertrophy is transient with spontaneous resolution within the first 6 months of life, requiring no therapy in the majority of cases. Transient tachypnea, respiratory distress, and cyanosis may present early after birth, and about 5% of neonates may suffer from congestive heart failure due to left ventricular outflow obstruction or diastolic dysfunction. In order to detect diabetic cardiomyopathy prenatally, fetal echocardiography should be serially performed in late pregnancy of diabetic mothers.

Higher thickness values for interventricular septum (IVS), RMW, and LMW (right and left ventricular myocardial wall) are related to uncontrolled diabetic cases (HbA1c >6.5%). A prenatal IVS thickness of ≥4.5 mm or an IVS/LMWT (left myocardial wall thickness) ratio of ≥1.18 was associated with almost twofold higher risk of intrauterine fetal death and almost threefold higher risk of possibly relevant perinatal mortality according to an interesting study performed by Elmekkawi et al.[55] Figure 33.8 depicts a case of a fetus of a diabetic mother at 34 weeks' gestation with uncontrolled glycemic levels with severe biventricular hypertrophy and diastolic dysfunction.

Familial hypertrophic cardiomyopathy has been detected prenatally. However, the time at which the development of LVH most often occurs is during adolescence.[56] For this reason, a normal fetal echocardiogram does not exclude this diagnosis.

Other genetic disorders associated with HCM are Noonan syndrome, alpha thalassemia, trisomy 13, Tomas and Hurler syndromes, among others. Noonan syndrome is the most frequently diagnosed prenatally. It is frequently associated with

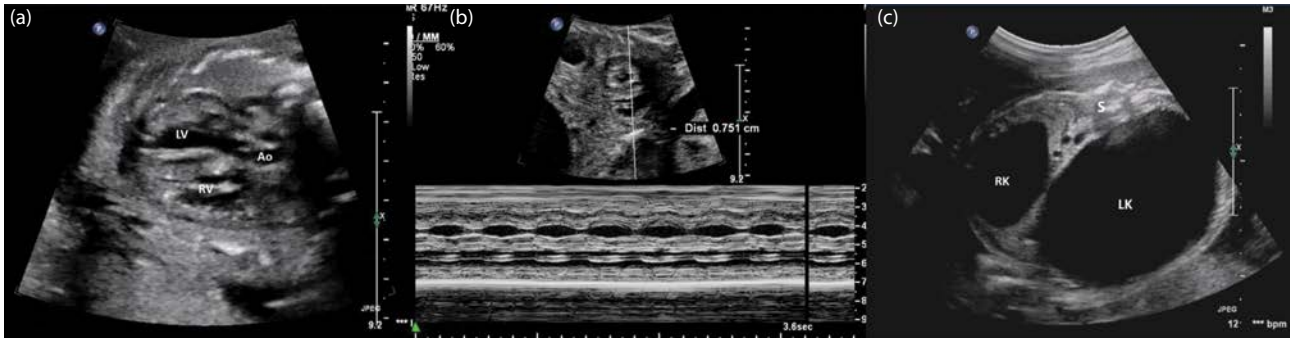


**Figure 33.7**
Hypertrophic cardiomyopathy secondary to bilateral severe hydronephrosis: (a) Two-dimensional image of the left ventricular outflow tract demonstrating severe hypertrophy of the LV walls; (b) M mode tracing of the ventricular chambers showing increased ventricular wall thickness; (c) bilateral hydronephrosis. (Ao, aorta; LK, left kidney; LV, left ventricle; RK, right kidney; RV, right ventricle.)

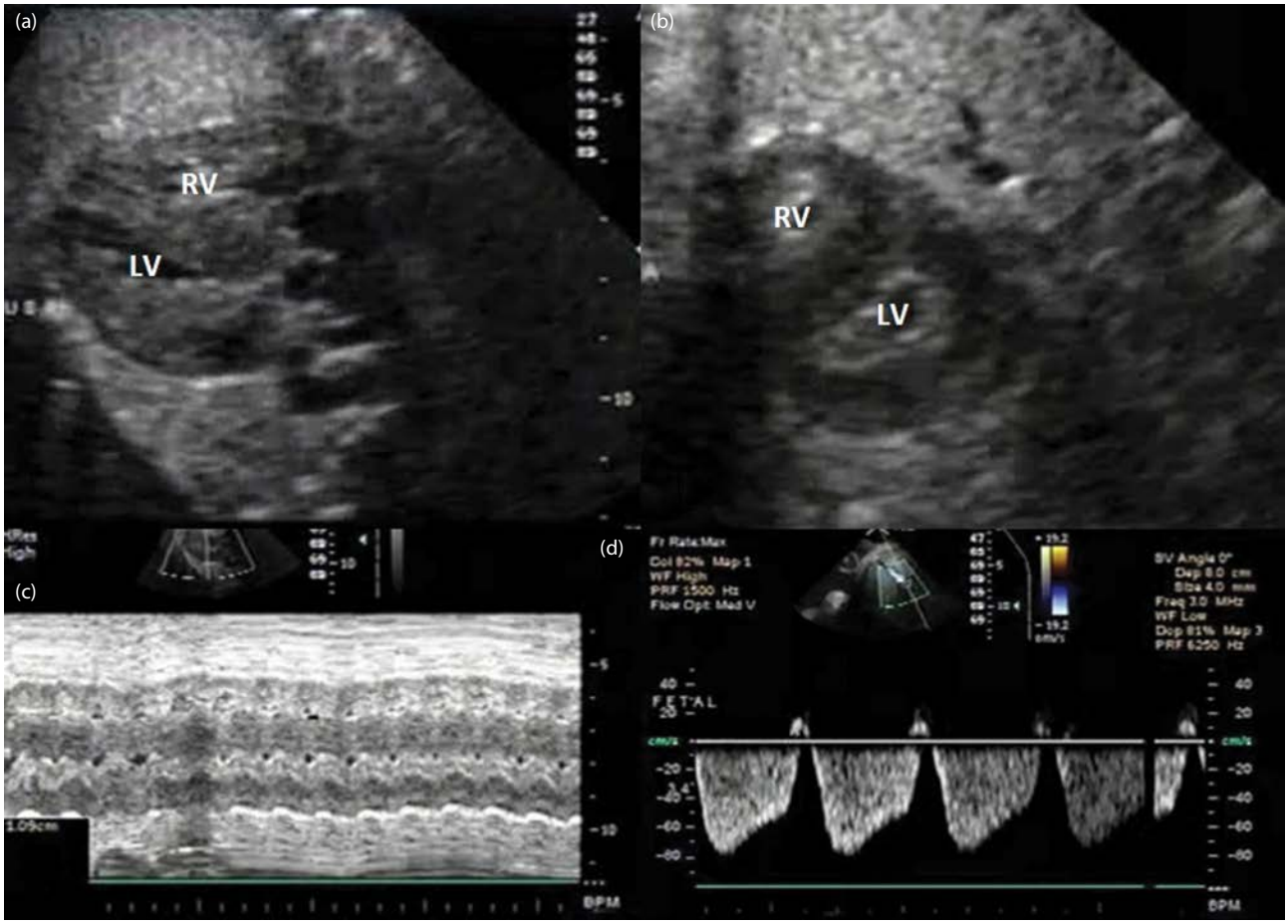


**Figure 33.8**
Fetal echocardiogram of a fetus of a diabetic mother performed at 34 weeks' gestation. (a) Severe biventricular hypertrophy with diminished ventricular cavities seen in four-chamber view. (b) Same aspect on short-axis view of the ventricles. (c) M-mode tracing of the ventricular walls and (d) reverse "a" wave in the ductus venosus Doppler tracing. (LV, left ventricle; RV, right ventricle.)

increased nuchal translucency and normal karyotype in the first trimester. Polyhydramnios, hydrops fetalis, renal anomalies, distended jugular lymphatic sacks (JLS), hydrothorax, cystic hygroma, and ascites are strong markers of Noonan syndrome when associated with HCM. This should prompt genetic testing using PTPN11, RAF1, and KRAS,[57] when available.

LEOPARD syndrome is an autosomal dominant disorder that is associated with mutations on the PTPN11 gene that may cause HCM in the fetus. This disorder is associated with additional skin, skeletal, and sensorineural abnormalities.

Fetal HCM can be found in families with HCM, and genetic testing for the specific mutation may be available.[58]

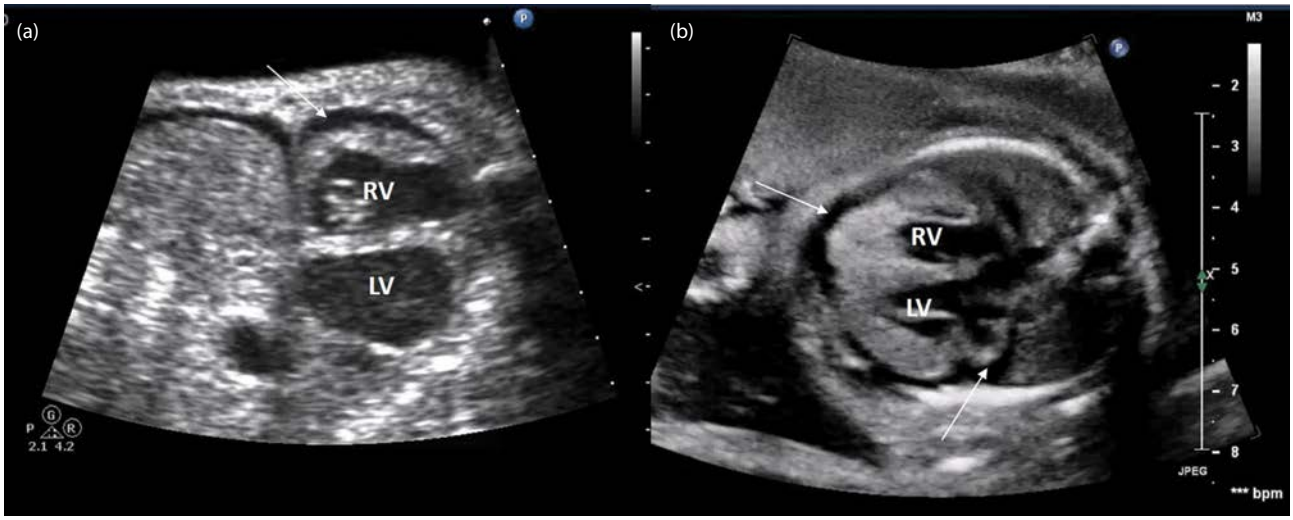


**Figure 33.9**
Two examples of abnormal pericardial effusion: (a) dilated cardiomyopathy with increased ventricular sizes and signs of fetal hydrops due to pericardial effusion and ascites; (b) hypertrophic cardiomyopathy with no confirmed etiology associated with significant pericardial effusion. (LV, left ventricle; RV, right ventricle.)

HCM may occur in the recipient fetus of the twin-to-twin transfusion syndrome. Cardiovascular disorders in recipients may result from increased preload caused by chronic hypervolemia. However, it is the increased afterload resulting from increased arterial resistance and pressure that has been identified by many as a key factor in the pathogenesis of cardiomyopathy.[59–64] As such, in about half the cases, the heart is enlarged as a result of hypertrophy rather than ventricular dilatation. The thickened, dysfunctional myocardium causes alterations in ventricular filling.[65] As such, diastolic functional impairment is frequently present before the development of systolic dysfunction. Resultant prolonged relaxation time is more important than systolic dysfunction in compromising fetal circulation and producing hydrops[66] (Video 33.5). The development of right ventricular outflow obstruction, observed in approximately 10% of all recipient twins, is likely multifactorial, occurring as a consequence of increased preload, afterload, and circulating factors such as renin, angiotensin, endothelin, and atrial and brain natriuretic peptides.[67]

## Diseases of the pericardium

Fetal pericardial effusions occur when there is an accumulation of pericardial fluid *in utero*. It is generally accepted as abnormal when the pericardial fluid thickness is greater than 2 mm.[68] Small amounts of pericardial fluid during routine prenatal ultrasound are common and can be seen in 40%–50% of normal fetuses, especially during the second half of gestation.[69] Greater amounts may be secondary to conditions associated with nonimmune fetal hydrops, most commonly related to structural cardiac malformations and arrhythmias. Other conditions associated with fetal hydrops include chromosomal and genetic anomalies, metabolic diseases, tumors (pericardial teratoma), hematologic abnormalities, and congenital infections[26] (Figure 33.9). A ventricular aneurysm or diverticulum is commonly described in association with pericardial effusion. Tamponade may ensue in case of rupture.[70] However, there are cases in which the amount of fluid around the heart exceeds 2 mm in thickness, and there are no anatomical or functional abnormalities detected.[71] In these cases, the pericardial effusion may disappear spontaneously, and the fetal prognosis is similar to that of the normal population.[72]

Because of commonly associated disorders, a complete diagnostic workup is mandatory. It should comprise fetal ultrasonography with Doppler fetal echocardiography, amniocentesis, and, when necessary, cord sampling and pericardiocentesis. The purpose is to provide optimal genetic counseling in a prenatal tertiary center and appropriate clinical management pre- and postnatally.

## Videos

**Video 33.1** (https://youtu.be/yKs4bKhoOkY)
Movie 1 is an example of right ventricular endocardial fibroelastoses, contracted form that presented with supraventricular tachycardia, which improved after transplacental digoxin. There is a global dilation of the heart, with biventricular systolic function compromise. The right ventricle is slightly hypoplastic. There is functional pulmonary valve atresia with retrograde ductal flow. Doppler tracings of the mitral and tricuspid valves show single inflow waves and there is retrograde atrial contraction flow at the ductus venosus.

**Video 33.2** (https://youtu.be/rslWE6iT3W0)
Movie 2 is a case of dilated cardiomyopathy. The heart is diffusely dilated, particularly the left ventricle, which demonstrates severe systolic dysfunction. Color flow mapping shows severe mitral and mild tricuspid regurgitations. There is ascites and pericardial effusion and decreased left ventricular shortening fraction. The

aortic valve is thin and does not open. There is retrograde aortic flow in the ascending aorta, uniphasic left ventricular inflow, and holosystolic mitral regurgitation. Doppler tracings of ductus venosus and umbilical vein demonstrate high filling pressures.

**Video 33.3** (https://youtu.be/KOPDgjb2dxI)
This fetus presented on the 28th week of gestation with runs of ventricular tachycardia. Besides the abnormal rhythm, there was severe biventricular systolic dysfunction and global heart dilation. There is some pericardial effusion. Mother serology was positive for acute Coxsackie B infection.

**Video 33.4** (https://youtu.be/oPjAJUwQm4A)
This is an example of hypertrophic cardiomyopathy of unknown etiology. There is severe concentric left ventricular hypertrophy. There is significant left ventricular outflow obstruction and evident systolic anterior motion of the mitral valve, with a peak systolic left ventricular to aorta gradient of 44 mmHg. Ductus venosus tracing demonstrates reversal "a" wave.

**Video 33.5** (https://youtu.be/BttxdicsxSk)
This is a late stage of twin-to-twin transfusion syndrome. The recipient twin is on the left-hand side and has moderate ascites. The donor twin is stuck and can be seen on the lower right side. The heart examination is focused on the recipient twin whose heart is grossly dilated. There is biventricular hypertrophy and systolic dysfunction. There is mitral and tricuspid insufficiency and no right ventricular outflow obstruction.

# References


1. Maron BJ et al. *Circulation* 2006;113(14):1807–16.
2. Pedra SR et al. *Circulation* 2002;106(5): 585–91.
3. Schmidt KG et al. *Am J Cardiol* 1989;63(9):599–605.
4. Sivasankaran S et al. *Cardiol Young* 2005;15(4):409–16.
5. Yinon Y et al. *Prenat Diagn* 2007;27(1):23–8.
6. Weber R et al. *JACC Heart Fail* 2014;2(4):403–11.
7. Fesslova V et al. *Int J Pediatr* 2010;2010:628451.
8. Sivasankaran S et al. *Cardiol Young* 2005;15(4):409–16.
9. Pedra SR et al. *Pediatr Cardiol* 2005;26(5):543–52.
10. Fishbein MC et al. *Arch Pathol Lab Med* 1977;101(1):49–54.
11. Rychik J. *Pediatr Cardiol* 2004;25(3):201–9.
12. Greenwood RD et al. *Am Heart J* 1976;92(5):549–60.
13. Ino T et al. *Am J Cardiol* 1988;62(7):431–4.
14. Bennett MJ et al. *Clin Cardiol* 1996;19(3):243–6.
15. van der Geld H et al. *Lancet* 1966;2(7475):1210–3.
16. Carceller AM et al. *Br Heart J* 1990;63(5):311–3.
17. Tannouri F et al. *J Ultrasound Med* 1998;17(1):63–6.
18. Lazda EJ. *Pediatr Dev Pathol* 1998;1(6):522–7.
19. Steward CG et al. *Prenat Diagn* 2010;30(10):970–6.
20. Hodgson S et al. *J Med Genet* 1987;24(4):210–4.
21. Mäkikallio K et al. *Circulation* 2006;113(11):1401–5.
22. Tworetzky W et al. *Circulation* 2004;110(15):2125–31.
23. Pedra SR et al. *Pediatr Cardiol* 2014;35(3):399–405.
24. Friedman KG et al. *Am J Cardiol* 2011;108(4):556–60.
25. Emani SM et al. *J Am Coll Cardiol* 2012;60(19):1966–74.
26. Davey B et al. *Minerva Pediatr* 2012;64(5):471–92.
27. Huhta JC. *Semin Fetal Neonatal Med* 2005;10(6):542–52.
28. Hofstaetter C et al. *J Matern Fetal Neonatal Med* 2006;19(7): 407–13.
29. Nield LE et al. *Circulation* 2002;105(7):843–8.
30. Nield LE et al. *J Am Coll Cardiol* 2002;40(4):796–802.
31. Kaur A, Lai WW. *Ultrasound Obstet Gynecol* 2007;30(3):351–3.
32. Steward CG et al. *Prenat Diagn* 2010;30(10):970–6.
33. Chong CR, Hutchins GM. *Pediatr Dev Pathol* 2008;11(5):405–15.
34. Jaeggi ET et al. *Circulation* 2004;110(12):1542–8.
35. Trucco SM et al. *J Am Coll Cardiol* 2011;57(6):715–23.
36. Richardson P et al. *Circulation* 1996;93(5):841–2.
37. Arunamata A et al. *J Am Soc Echocardiogr* 2012;25(1):112–20.
38. Friedberg MK et al. *Am J Cardiol* 2005;96(7):985–90.
39. Karatza AA et al. *Ultrasound Obstet Gynecol* 2003;21(1):75–80.
40. Moura C et al. *Cardiol Young* 2002;12(3):278–83.
41. Sedmera D, Thomas PS. *Bioessays* 1996;18(7):607.
42. Freedom RM et al. *Cardiol Young* 2005;15(4):345–64.
43. Captur G, Nihoyannopoulos P. *Int J Cardiol* 2010;140(2): 145–53.
44. Raghib G et al. *Am Heart J* 1965;70(4):476–80.
45. Davignon AL et al. *Am Heart J* 1961;62:690–7.
46. Dusek J et al. *Arch Pathol* 1975;99(6):312–7.
47. Feldt RH et al. *Am J Cardiol* 1969;23(5):732–4.
48. Tan J et al. *Am J Cardiol* 1992;70(18):1459–67.
49. DeVore GR et al. *Am J Obstet Gynecol* 1984;150(8):981–8.
50. Veille JC et al. *Obstet Gynecol* 1992;79(1):51–4.
51. Molin DG et al. *Birth Defects Res A Clin Mol Teratol* 2004;70(12):927–38.
52. Menezes HS et al. *Cardiol Young* 2001;11(6):609–13.
53. Mehta A, Hussain K. *Arch Dis Child* 2003;88(9):822–4.
54. Thorsson AV, Hintz RL. *N Engl J Med* 1977;297(17):908–12.
55. Elmekkawi SF et al. *Clin Med Insights Womens Health* 2015;8: 39–43.
56. Maron BJ, Maron MS. *Lancet* 2013;381(9862):242–55.
57. Croonen EA et al. *Eur J Hum Genet* 2013;21(9):936–42.
58. Maron BJ et al. *J Am Coll Cardiol* 2014;64(1):83–99.
59. Lopriore E et al. *Congenit Heart Dis* 2007;2(1):38–43.
60. Halvorsen CP et al. *Acta Paediatr* 2009;98(9): 1468–74.
61. Mahieu-Caputo D et al. *Fetal Diagn Ther* 2001;16(4):241–4.
62. Mahieu-Caputo D et al. *Prenat Diagn* 2003;23(8):640–5.
63. Manning N. *Early Hum Dev* 2008;84(3):173–9.
64. Van Mieghem T et al. *Int J Pediatr* 2010;2010. pii: 379792.
65. Bajoria R et al. *Hum Reprod* 1999;14(6):1614–8.
66. Van Mieghem T et al. *Int J Pediatr* 2010;2010. pii: 379792.
67. Lougheed J et al. *J Am Coll Cardiol* 2001;38(5):1533–8.
68. Brown DL et al. *AJR Am J Roentgenol* 1993;160(6):1251–5.
69. Jeanty P et al. *Am J Obstet Gynecol* 1984;149(5):529–32.
70. McAuliffe FM et al. *Ultrasound Obstet Gynecol* 2005;25(4): 401–4.
71. Slesnick TC et al. *Am J Cardiol* 2005;96(4):599–601.
72. Di Salvo DN et al. *J Ultrasound Med* 1994;13(4):291–3.

# 34

# Ultrasound examination of the fetal coronary circulation

Ahmet A. Baschat, Ulrich Gembruch, and Viola Seravalli

## Introduction

The coronary circulation provides blood supply to the myocardium. For one of the most critical fetal organs, matching myocardial blood flow and demand is necessary to ensure cardiac function over a wide variety of physiologic and pathologic conditions. For this reason, the examination of coronary vascular dynamics is becoming increasingly relevant in various fetal conditions. Ultrasound examination of the fetal coronary circulation has become possible through advances in ultrasound technology and a better understanding of human fetal cardiovascular physiology. Although not yet standard clinical practice, continuing trends in ultrasound technology and spreading familiarity with the examination and interpretation are likely to expand clinical applications in the future.[1]

Ultrasound examination of the fetal coronary system utilizes grayscale, zoom, and cine-loop techniques, and requires optimal spatial and temporal settings of the Doppler modalities. Proper setup of the ultrasound system is therefore a necessary prerequisite. Traditional ultrasound planes used in cardiac scanning are modified to provide best visualization of the coronary vessels. A comprehensive survey of extracardiac vascular dynamics is often necessary to provide the clinical context for interpretation of intracardiac and coronary flow dynamics. This chapter reviews embryology, functional anatomy, animal experiments, ultrasound technique, and clinical utility of ultrasound evaluation of the fetal coronary circulation.

## Embryology and functional anatomy of the coronary circulation

Oxygenated blood supply to the myocardium is delivered through the right (RCAs) and left coronary arteries (LCAs), arising from the ipsilateral anterior and posterior aortic sinuses, respectively, and the left anterior descending (LAD) branch of the LCA.[2,3] Left ventricular venous return drains mainly into a superficial system through the coronary sinus and anterior cardiac veins, constituting approximately two-thirds of myocardial venous return. The deep system consisting of arterioluminal vessels, arteriosinusoidal vessels, and thebesian veins drains the remaining venous return directly into the cardiac chambers.[2–4]

In embryonic life, endothelial cells originating from the septum transversarium in the hepatic region form epicardial blood islands that eventually coalesce into vascular networks throughout the epicardium and myocardium.[5,6] Concurrently, the RCA and LCA originate as microvessels and penetrate the aortic root, acquiring a muscular coat in this process. Connection of the mainstem coronary arteries and myocardial vascular channels marks the initiation of a functional coronary circulation. Venous drainage develops independently of the arterial system and becomes fully functional when the coronary sinus, as a remnant of the left horn of the sinus venosus, becomes incorporated into the inferior wall of the right atrium and thebesian veins gain access to the ventricular cavities. The coronary circulation is completely functional by the sixth week of embryonic life and ensures myocardial blood supply by the time the embryonic circulation is established.

Coronary vascular development can be modulated by stimuli such as local oxygen tension, mechanical wall stress, and myocardial and vascular shear forces.[6–9] As a result, the coronary circulation is subject to great anatomic and functional variation. Under physiologic conditions, modulation of vascular growth enables the matching of coronary vascular development to myocardial growth, ensuring a balanced relationship between ventricular mass and vascular density.[10] Persistent, or progressive, tissue hypoxemia may exaggerate this physiologic process, resulting in a marked increase in vascular cross-sectional area in the coronary circulation.[11–14] Under these circumstances, vascular reactivity to physiologic stimuli is also enhanced.[15] Similarly, abnormal intracardiac pressure relationships such as those found in outflow tract obstructive lesions may force the development of accessory vascular channels between the coronary vessels and the ventricular cavity (ventriculo-coronary fistulae).[16] The plasticity of the coronary circulation is responsible for the variation in myocardial vascular territories and blood flow found in various fetal conditions, illustrating the importance of myocardial oxygenation for proper cardiac function.

# Regulation of myocardial perfusion

Myocardial metabolism is almost exclusively aerobic and, in the presence of adequate oxygen, various substrates including carbohydrates, glucose, lactate, and lipids can be metabolized.[17–20] In fetal life, myocardial glycogen stores and lactate oxidation constitute the major sources of energy, while fatty acid oxidation rapidly becomes the primary energy source after birth. To maintain metabolism, myocardial oxygen extraction is as high as 70%–80% in the resting state. Consequently, the coronary atrioventricular oxygen difference of 14 mL/dL exceeds that of most other vascular beds and allows little further extraction of oxygen unless the blood flow is significantly augmented. Therefore, coronary blood flow is closely regulated to match myocardial oxygen demands.

The regulation of myocardial perfusion operates at several levels and time frames. The unique parallel arrangement of the fetal circulation allows delivery of well-oxygenated blood through the ductus venosus to the left ventricle and thus the ascending aorta. In the fetal lamb, the coronary circulation receives approximately 8% of the left ventricular output at rest.[21]

This proportion may be higher in the human fetus, and may be further altered by modulating the degree of shunting through the ductus venosus.[22] Once blood enters the coronary vessels from the ascending aorta, the pressure difference to the right atrium becomes the primary driving force for coronary blood flow. This perfusion pressure is further subjected to changes in vascular tone and extravascular pressure. Autonomic innervation of coronary resistance vessels regulates overall vascular tone,[23,24] but ventricular contractions are the main contributor to extravascular resistance, with significant impacts on the flow velocity waveform.[25–27] Myocardial perfusion predominantly occurs during diastole when the ventricles relax and pose little extravascular resistance. This diastolic timing of predominant perfusion is unique to the coronary circulation and distinguishes it from other vascular beds in the human body. In the adult, increases above a resting heart rate of 70 beats per minute result in a disproportionate shortening of diastole. At fetal heart rates of 120–160 beats per minute, this places special demands on dynamic vascular mechanisms to regulate the myocardial blood flow volume.

The efficiency of myocardial oxygen delivery is further enhanced by active autoregulatory control mechanisms, ensuring optimal myocardial blood flow despite fluctuations in arterial perfusion pressure.[28,29] This is achieved through caliber adjustment of precapillary resistance vessels, allowing channeling of blood flow to areas of greatest oxygen demand.[30,31] With maximal dilatation of these sphincters, myocardial blood flow may be elevated four times above basal flow. This increase in blood flow volume that can be achieved under these circumstances is the myocardial blood flow reserve. If myocardial oxygenation cannot be upheld long term, adaptation with the formation of new blood vessels may be invoked, thus increasing the myocardial blood flow reserve.[32–34] Such elevated myocardial blood flow reserve allows marked augmentation of blood flow during periods of acutely worsening hypoxemia or increased cardiac work, and increases as high as 12 times the basal flow have been reported.[15,35,36]

## *Coronary blood flow under various conditions in the animal model*

The arrangement of the fetal circulation and the role of the placenta as the primary source of oxygen, water, and nutrients have important implications for fetal vascular homeostasis. Partitioning of oxygen-rich umbilical venous blood occurs at several levels that can affect coronary perfusion. Increased diversion of umbilical venous blood through the ductus venosus increases the proportion of this oxygenated blood that reaches the left ventricle, while differential changes in right and left ventricular afterload can shift the proportion of cardiac output toward the ventricle with the lowest downstream blood flow resistance. This unique arrangement of the fetal circulation is responsible for a number of cardiovascular responses observed in fetuses with uteroplacental insufficiency.

Studies of the coronary circulation in the fetal lamb indicate functional autoregulation under conditions of acute hypoxemia,[19,21,25,37] increased afterload,[35] and acute-on-chronic hypoxemia.[25,27] The fetal heart is remarkably tolerant of a hypoxic environment and is capable of sustaining normal cardiac function in the presence of a 50% reduction in oxygen level. Subjected to acute hypoxemia, a four- to fivefold increase in myocardial blood flow, corresponding to changes in the adult human heart, is observed. Selective elevation of right ventricular afterload is associated with a global increase in myocardial blood flow.[35] This may be due to increased oxygen demands of cardiac pressure work, suggesting functional extracardiac control by humoral and/or neurogenic factors.[27,35,38–40] However, the most striking changes in myocardial blood flow can be observed in fetuses subjected to acute hypoxemia after a period of chronic hypoxemia. In this setting of acute-on-chronic hypoxemia, maximal myocardial flow reserve is increased to 12-fold the basal flow, and is among the highest flows observed under any condition. This increase in flow reserve most likely reflects the effects of chronic hypoxemia on coronary vascular remodeling and reactivity. The alterations in the vascular tree allow recruitment of much larger blood volume during acute hypoxemia, resulting in markedly enhanced blood flow.[25,27,33,34] In chronically hypoxemic, intrauterine growth–restricted sheep fetuses, no change in blood flow to the heart is observed, confirming that increased cardiac perfusion is only observed in acute hypoxemia.[41]

# Ultrasound examination technique

## *Ultrasound setup*

The setup of the ultrasound system determines the spatial and temporal resolution of the ultrasound image and is therefore

of major importance for successful examination of the fetal coronary arteries. Grayscale ultrasound and color and pulsed wave Doppler need to be optimized for complementary use. Although visualization of coronary vessels can be achieved using 4 MHz transducers, higher frequencies improve resolution and therefore detection. The dynamic range of the grayscale image should be set to an intermediate level that is generally used in cardiac setups. Zoom magnification of the area of interest limits the computing power that needs to be allocated to the generation of the grayscale image. These two maneuvers will improve the frame repetition rate and should therefore be applied before adding color Doppler imaging. When adding color Doppler imaging, the filter should be set to a high degree of motion discrimination, and the color box and gate are kept as small as possible to optimize spatial and temporal resolution of this Doppler modality. The lateral dimension of the color box has the greatest impact on computing power and therefore frame rate. The color amplification gain is set to eliminate background noise on the screen. The persistence is set to a low level to minimize frame averaging. The color velocity scale is adjusted to a range that allows visualization of intra- and extracardiac flows without aliasing and suppression of wall-motion artifacts. A useful velocity range for coronary arteries is between 0.3 and 0.7 m/s for coronary arteries and between 0.1 and 0.3 m/s for the coronary sinus. Since initial detection of the coronary arteries relies on color Doppler, these aspects of the setup are essential preliminary steps. Once the coronary vessel is identified using these techniques, the transducer position should be adjusted to provide an insonation angle close to 0° prior to obtaining pulsed wave measurements. The pulsed wave Doppler gate should be adjusted to exclude other cardiac and extracardiac flows and should be the only active display when measurements are taken. Concurrent activation of multiple image modalities (duplex or triplex mode) drastically increases computing requirements and affects the spatial and temporal resolution of the spectral Doppler waveform.

Recently, the B-flow sonographic technique has been developed to provide direct visualization of blood flow with grayscale sonography. This non-Doppler technology uses digitally encoding techniques to improve sensitivity for direct visualization of blood flow, resulting in higher spatial, temporal, and contrast resolution imaging. Application of B-flow to cardiac imaging has been described, and its combination with four-dimensional spatiotemporal image correlation (STIC) has been suggested as a promising new tool for fetal intracardiac and extracardiac hemodynamics.[42,43] The application of this novel technique to the study of the coronary circulation could improve the visualization of this specific vascular territory.

## Examination of coronary arteries

Using grayscale ultrasound, the coronary ostia are discernable in late gestation. Before this time, the size of the mainstem arteries is below 1 mm in diameter and thus frequently below the resolution threshold of current sonographic equipment in the majority of cases.[44] For this reason, color and pulsed wave Doppler ultrasound are necessary to detect and verify coronary artery blood flow. Doppler examination of the fetal coronary vessels has been adopted from techniques developed for infants and neonates. The mainstem right and left coronary arteries are best examined in a long-axis view of the left ventricular outflow tract and ascending aorta or a precordial short-axis view of the aorta. The left anterior descending branch of the LCA is best identified in an apical short-axis view. In the standard precordial short-axis view, the left coronary artery runs forward, while the right runs more parallel. This view, therefore, facilitates examination of the LCA. In the lateral or long-axis view of the left ventricular outflow tract, the RCA is more readily imaged from the right side of the fetus. In this view, it may also be possible to visualize both coronary arteries (Figure 34.1).[45,46] The LAD may be identified from the apical four-chamber view by tilting the transducer cephalad until the level of the superior cardiac surface and interventricular groove is reached.[47] The course of the LAD is visualized along the interventricular septum. Cardiac wall motion, high blood flow velocities in the ventricles and ventricular outflow tracts, and movement of pericardial fluid can all interfere with the relatively low coronary blood flow velocities on color Doppler imaging. Back and forward motion of pericardial fluid outlining the ventricular walls in particular may be mistaken for a coronary artery.[48] For these reasons, identification of coronary artery blood flow by color Doppler imaging should always be followed by verification of the typical waveform pattern by pulsed wave Doppler to provide assurance that the coronary arteries have indeed been identified. The coronary artery blood flow can also be visualized using B-flow imaging (Figure 34.2).

Spectral Doppler measurement of coronary blood flow velocities is easiest proximally, since vessel diameter is greatest, and motion during the cardiac cycle is less than distally. After coronary vessels are identified by color Doppler, the pulsed wave Doppler gate is positioned at their origin. The gate may require adjustment to achieve continuous sampling of the waveform, allowing for movement of the aortic root in the cardiac cycle. The coronary artery flow velocity waveform has a biphasic pattern, with systolic and diastolic peaks and antegrade flow throughout the cardiac cycle (Figure 34.3).[49] The coronary waveform is unique. Due to the predominant diastolic perfusion, velocities are higher during diastole than systole. In normal fetuses, coronary blood flow has been visualized from 29 weeks onward (median gestational age of 33 + 6 weeks). The median systolic and diastolic peak blood flow velocities are 0.21 and 0.43 m/s, respectively, and show little change during the latter part of gestation (Figures 34.4 and 34.5).[50]

## Examination of the coronary sinus

The larger size and location of the coronary sinus facilitates its ultrasound examination.[51,52] The coronary sinus runs in the atrioventricular groove and enters the right atrium below

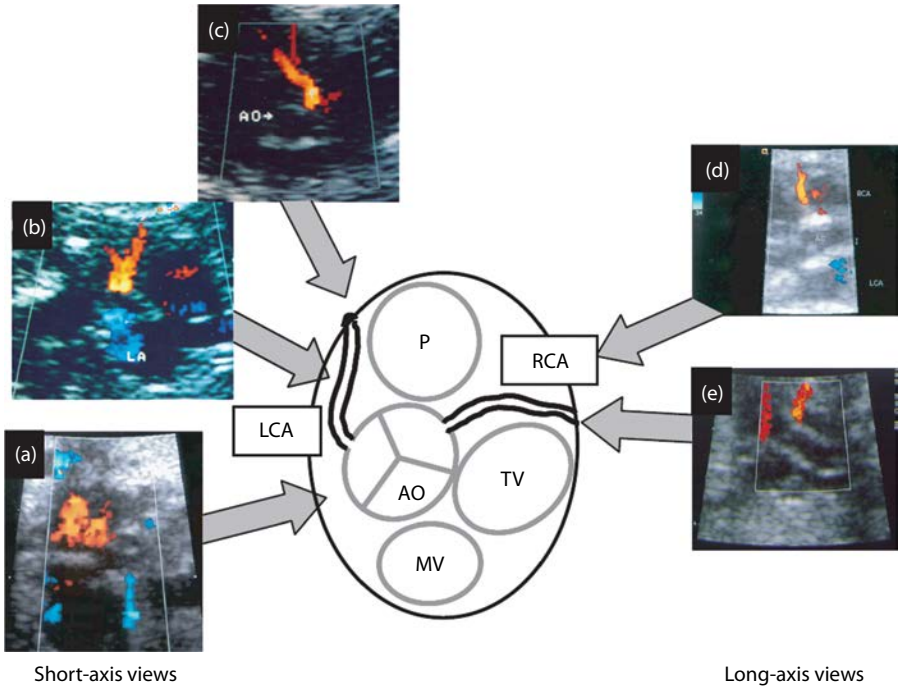


**Figure 34.1**
The origin of the great vessels and the atrioventricular valves shows the course of the left and right coronary arteries (RCA and LCA, respectively) in relationship to the aorta (AO), pulmonary artery (P), mitral (MV), and tricuspid valves (TV). The angle of insonation and type of cardiac axis determines the orientation of the coronary arteries on the ultrasound image. Short-axis views facilitate examination of the left coronary artery (b) and may enable visualization of both coronary arteries (c), occasionally also allowing demonstration of the origin of the left anterior descending branch (b,c). Although the right coronary artery can be examined in the short-axis view (a), it is easier to identify this vessel in a right lateral long-axis view of the left ventricular outflow tract (e). This view also allows simultaneous visualization of both coronary arteries (d).

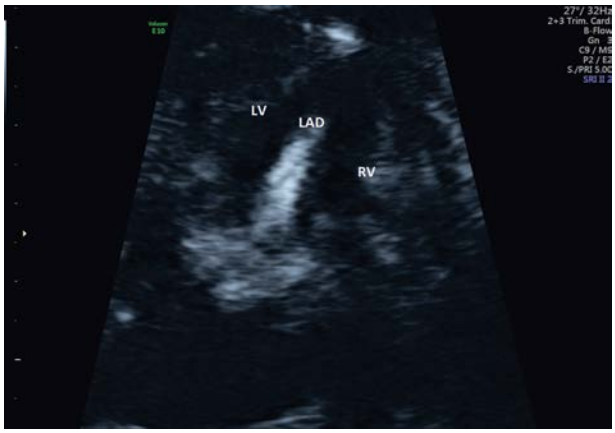


**Figure 34.2**
B-Flow imaging demonstrating the left anterior descending (LAD) branch of the left coronary artery in a 32-week-old fetus. (LV, left ventricle; RV, right ventricle.)

the level of the foramen ovale just above the valve of the inferior vena cava. Because of its position, apical or basal four-chamber views provide the best opportunity for grayscale biometry, while lateral four-chamber views provide a more favorable insonation angle for color and spectral Doppler imaging (Figures 34.6 and 34.7).

Grayscale and M-mode echocardiography have both been used to obtain normative data on the length and diameter of the coronary sinus. The caliber of the coronary sinus undergoes cyclic changes, with the cardiac cycle being smallest at the beginning of diastole and largest in mid-systole with maximal descent of the atrioventricular (AV) ring. M-mode echocardiography allows precise documentation of caliber and dynamic changes (Figure 34.8). The coronary sinus has a maximum diameter ranging from 1 to 3 mm with advancing gestation. The method utilized to obtain these measurements influences the reference limits.[51,53] Figures 34.9 and 34.10 show gestational reference ranges for the maximal diastolic and systolic dimensions measured with M-mode. Appreciating the phenomenon of variations in coronary sinus diameter may call for verification using this M-mode technique when dilatation of the coronary sinus is suspected.

Color Doppler identification of coronary sinus blood flow is successful in approximately 50% of normal fetuses. During diastole, the direction of blood flow from the coronary sinus is toward the right atrium, whereas blood flow across the foramen ovale is directed toward the left atrium (Figure 34.11).[54] B-flow imaging can also be used for the identification of coronary sinus blood flow (Figure 34.12). Despite its straight course, allowing exact placement of the sample volume, spectral Doppler measurements are only possible in

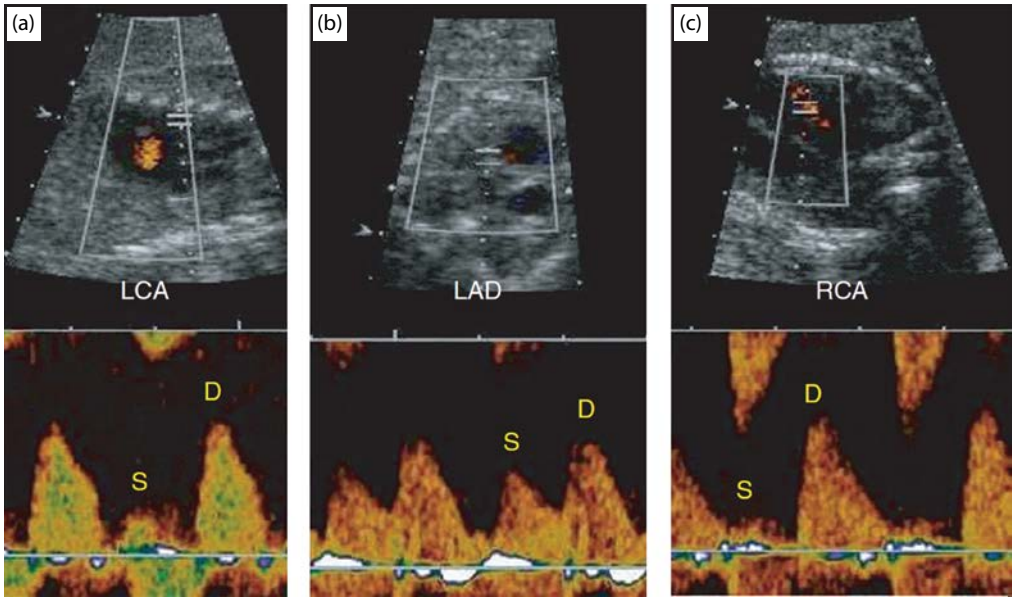


**Figure 34.3**
Pulsed wave Doppler images of the left coronary (LCA, a), left anterior descending (LAD, b), and right coronary arteries (RCA, c) are obtained in a 29-week fetus. Of note is the predominance of blood flow during diastole (D) that is observed in all three vessels. (Reproduced with permission from Baschat AA, Gembruch U. *Ultrasound Obstet Gynecol* 2002;20(4):405–12.[49])

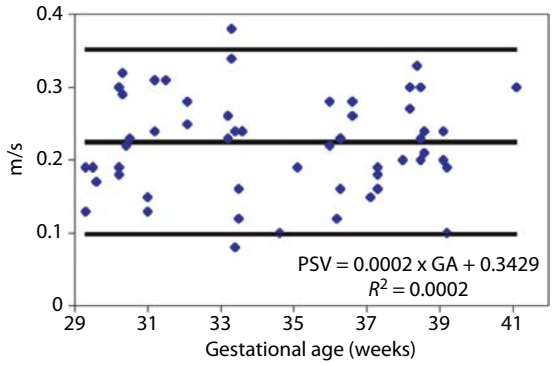


**Figure 34.4**
The median and 95% confidence interval for the peak systolic velocity (PSV) in the coronary artery of appropriately grown fetuses in relation to gestational age (GA). (Reproduced with permission from Baschat AA et al. *Ultrasound Obstet Gynecol* 2003; 21(5):426–9.[50])

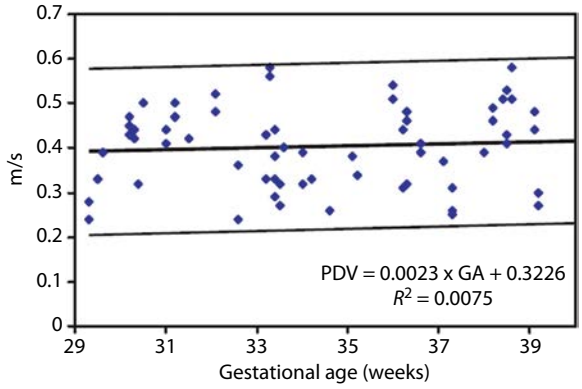


**Figure 34.5**
The median and 95% confidence interval for the peak diastolic velocity (PDV) in the coronary artery of appropriately grown fetuses in relation to gestational age (GA). (Reproduced with permission from Baschat AA et al. *Ultrasound Obstet Gynecol* 2003;21(5):426–9.[50])

approximately 10% of fetuses. This low success rate is partly due to lower coronary sinus blood flow velocities and interference caused by intra-atrial blood flows and/or cardiac and atrioventricular valve movement. The coronary sinus flow velocity waveform has a triphasic pattern, with systolic and diastolic antegrade flow and occasional reversal during atrial contraction (Figure 34.13). Similar to the coronary arteries, diastolic forward velocities (median 0.38 m/s) exceed systolic velocities (median 0.18 m/s). These velocities are related to the periods of predominant myocardial blood flow.

Methods to relate coronary sinus velocities to myocardial flow reserve have been described in neonates and adults,[55,56] but these are currently not practicable for validation in the human fetus.

## Clinical applications in fetuses with normal cardiac anatomy

There are several conditions in fetuses with normal cardiac anatomy that have prominent cardiovascular manifestations. In some of these conditions, coronary blood flow dynamics may be altered to accommodate changes in myocardial oxygen requirements. Since spectral Doppler of the coronary

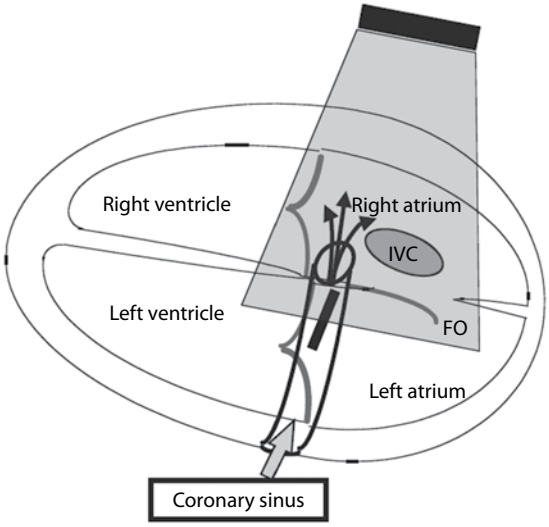


**Figure 34.6**
The fetal heart shows the course of the coronary sinus in the right lateral four-chamber view. The coronary sinus runs in the atrioventricular groove and opens into the right atrium near the atrioventricular valve, in close proximity to the inferior vena cava (IVC) and foramen ovale (FO). In this imaging plane, the direction of blood flow is toward the transducer beam. (Reproduced with permission from Baschat AA, Gembruch U. *Ultrasound Obstet Gynecol* 1998;11(4):410–4.[54])

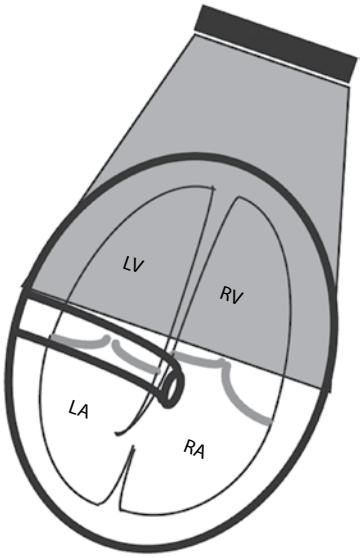


**Figure 34.7**
The fetal heart imaged in the apical four-chamber view showing the left and right ventricles (LV and RV) and the corresponding atria (LA and RA). The coronary sinus runs in the atrioventricular groove parallel to the mitral valve leaflets. The coronary sinus is visualized by tilting the transducer toward the inferior cardiac surface until the valve leaflets disappear. (Reproduced with permission from Abello KC et al. *Ultrasound Obstet Gynecol* 2002;20(2):137–41.[51])

sinus is rarely achieved, clinical observations revolve primarily around color and pulsed wave Doppler characteristics in coronary arterial vessels.

## *The "heart-sparing effect" in fetal growth restriction*

Severe intrauterine growth restriction (IUGR) can progress to decompensation of cardiovascular status documented through progressive deterioration of arterial and venous Doppler studies.[57] This progression often accompanies the deterioration of acid-base status from chronic hypoxemia to acidemia.[58–61] Under these circumstances, the combination of elevated central venous pressure, elevated afterload, and worsening oxygenation places unique demands on myocardial oxygen balance. Elevated afterload increases myocardial oxygen demand because of an increase in cardiac work. Elevated central venous pressure and aortic pressure decrease the pressure difference across the coronary vascular bed and therefore

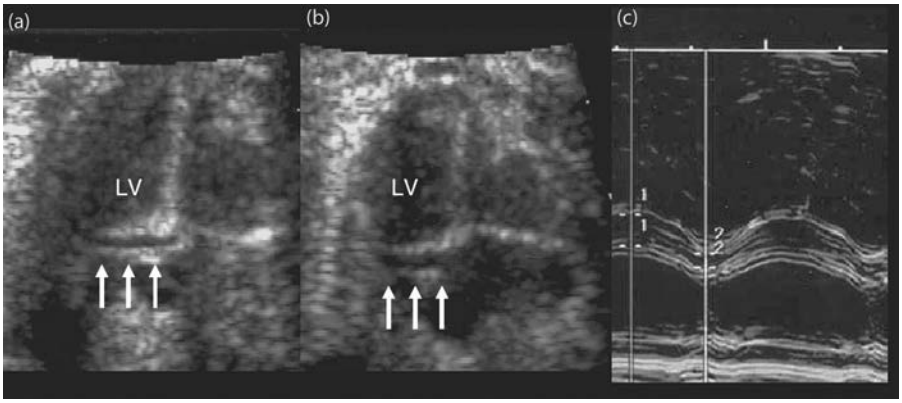


**Figure 34.8**
The fetal heart imaged in an apical four-chamber view at 28 + 4 weeks' gestation. The coronary sinus (arrows) can be seen running in the atrioventricular groove between the left ventricle (LV) and atrium. Using the cine-loop technique a difference in diameter between end-systolic (a) and mid-systolic (b) diameters can be appreciated. An M-mode tracing obtained from a normal coronary sinus at 29 weeks' gestation demonstrates fluctuations during systole and diastole (c). The cursors are placed on the anterior and posterior walls of the coronary sinus. (Reproduced with permission from Abello KC et al. *Ultrasound Obstet Gynecol* 2002;20(2):137–41.[51])

diminish the driving force for coronary perfusion. The summation of these factors has detrimental effects on coronary perfusion at a time when myocardial oxygen balance and fetal metabolic state are drastically increased. Consequently, adaptive mechanisms need to be evoked in order to maintain myocardial oxygen balance. The necessary augmentation of coronary blood flow can be achieved in two principal ways. One is to increase the proportion of oxygenated left ventricular output available for myocardial delivery. The second is through autoregulation-mediated coronary vasodilatation.

Several mechanisms operate in IUGR fetuses that increase the potential delivery of oxygenated blood to the myocardium (Figure 34.14). Under conditions of elevated placental resistance, the relative proportion of left ventricular output increases[60,62–65] (first phase). Decreases in oxygen tension may further increase the proportion of oxygenated umbilical venous blood that is delivered through the ductus venosus to the left side of the heart.[66,67] Prolonged chronic myocardial hypoxemia allows angiogenesis and increases in vascular cross-sectional area and, therefore, myocardial flow reserve (second phase). These responses constitute chronic heart sparing in IUGR. When acute worsening of cardiovascular status and/or oxygenation is superimposed, the only mechanism to significantly augment myocardial blood flow is marked coronary vasodilatation, with massive recruitment of coronary vascular reserve (third phase). This vascular response is more acute, often occurring over the course of 24 hours, and is most consistently associated with severe elevation of precordial venous Doppler indices.[68,69]

The chronic initial phase of heart sparing can be implied by demonstrating certain Doppler abnormalities in the arterial and venous circulations. These include absent or reversed umbilical artery end-diastolic velocity and/or end-diastolic blood flow reversal in the aortic isthmus.[70] In the second trimester, the magnitude of coronary blood flow may still be below the visualization threshold of ultrasound equipment. Therefore, augmentation of coronary blood flow cannot be documented by spectral Doppler measurement of coronary arteries. With acute worsening of fetal cardiovascular and respiratory status, color and pulsed wave Doppler measurement of coronary artery blood flow is readily achieved as a reflection of maximal augmentation of coronary blood flow, now exceeding the visualization threshold[45] (Figure 34.15 and 34.16). In IUGR, both diastolic and systolic coronary artery peak blood flow velocities are significantly higher than in appropriately grown fetuses, providing additional evidence of blood flow augmentation. There are no associated changes in the coronary sinus diameter as evidence of increased coronary venous return.[53] Heart sparing in IUGR fetuses has been described in the presence of a normal myocardial performance index and cardiovascular profile score, suggesting that neither systolic nor diastolic cardiac dysfunction is the primary drive for increased coronary perfusion.[71] Since coronary artery blood flow may be visualized in normal and IUGR fetuses at overlapping gestational ages, concurrent examination of arterial and venous circulations and biophysical variables is mandatory to assess fetal status, and clinical management cannot be based on the evaluation of coronary vascular dynamics. In IUGR fetuses with abnormal arterial and venous Doppler and heart sparing, the prognosis is poor, with a high perinatal mortality and a high risk for acidemia and neonatal circulatory insufficiency requiring the highest level of neonatal care. The visualization of coronary blood flow has been correlated with fetal and neonatal outcome. In a series of 21 fetuses showing the heart-sparing effect before 32 weeks' gestation, the outcome was poor, with a 50% perinatal mortality.[72] Fetuses with visible coronary artery blood flow require earlier delivery, have lower birth weight, lower cord pH and cord $pO_2$, compared to IUGR fetuses in which coronary blood flow

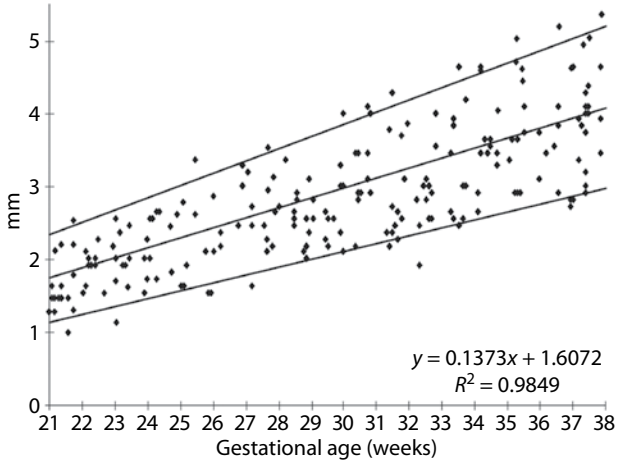


**Figure 34.9**
Scattergram showing individual measurements, the mean, and 95% confidence interval of the maximum systolic diameter of the coronary sinus with respect to gestational age. (Reproduced from Abello KC et al. *Ultrasound Obstet Gynecol* 2002;20(2):137–41.[51])

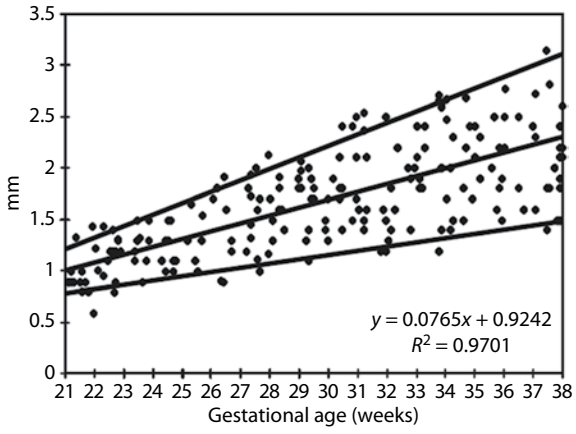


**Figure 34.10**
Scattergram showing individual measurements, the mean, and 95% confidence interval of the maximum diastolic diameter of the coronary sinus with respect to gestational age. (Reproduced with permission from Abello KC et al. *Ultrasound Obstet Gynecol* 2002;20(2):137–41.[51])

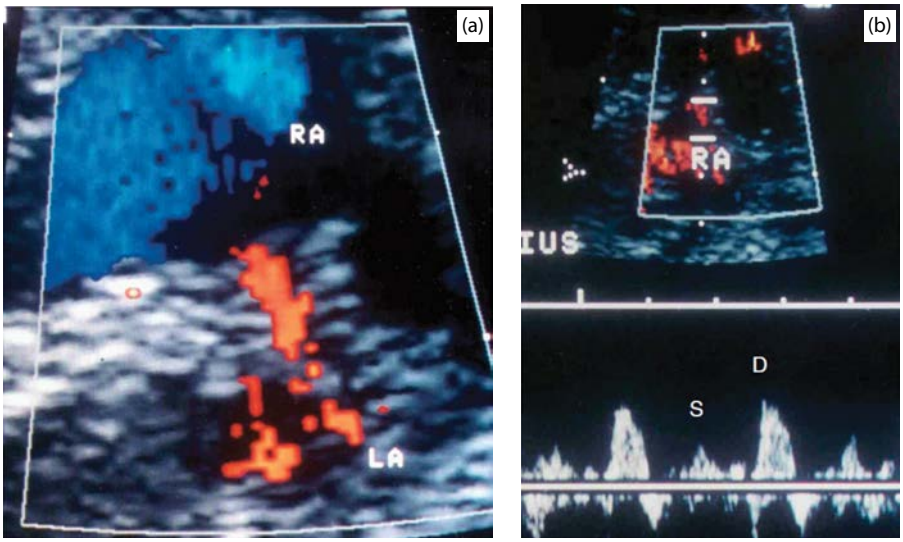


**Figure 34.11**
The fetal heart is imaged in a lateral four-chamber view and coronary sinus blood flow toward the right atrium (RA) is identified with color Doppler imaging (a). Pulsed wave Doppler shows a triphasic flow profile with a small systolic (S) and a larger diastolic peak (D) followed by brief reversal during atrial contraction (b). (Reproduced with permission from Baschat AA, Gembruch U. *Ultrasound Obstet Gynecol* 2002;20(4):405–12.[49])

is not visualized.[69,73] In IUGR fetuses with reverse velocity waveforms in the DV, visualization of coronary circulation is associated with higher incidence of intrauterine fetal demise and a shorter time interval between the Doppler diagnosis and delivery or fetal death.[73]

## *Fetal anemia*

Severe fetal anemia eventually leads to a reduction of the oxygen-carrying capacity in blood, and subsequently impaired myocardial oxygenation. Fetal hydrops with tricuspid insufficiency and abnormal precordial venous flow is associated with elevated right heart pressures and a decline in coronary perfusion pressure. Under these circumstances, short-term augmentation of myocardial blood flow of four to five times basal flow can be achieved through autoregulation. Coronary artery blood flow has been measured in circumstances of acute fetomaternal hemorrhage, nonimmune hydrops, and hemolytic disease.[50,74] Under these circumstances, peak diastolic velocities as high as 1 m/s and peak systolic velocities of 0.5 m/s may be observed, significantly exceeding those observed in any other fetal condition. Blood velocities were responsive to maternal oxygen therapy and fetal blood transfusion, and fell below the visualization threshold after normalization of the fetal hematocrit. With

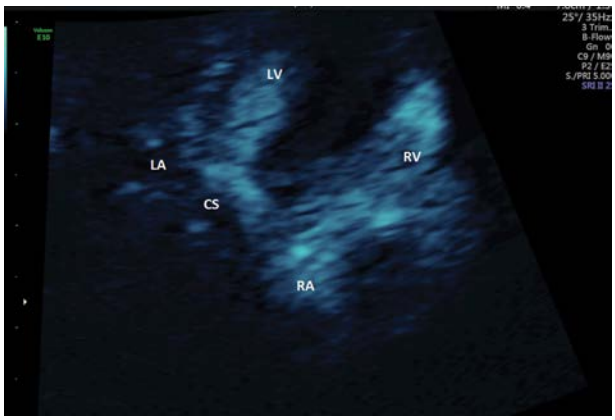


**Figure 34.12**
B-Flow imaging demonstrating the coronary sinus (CS) blood flow toward the right atrium (RA) in a 32-week fetus. (LA, left atrium; LV, left ventricle; RV, right ventricle.)

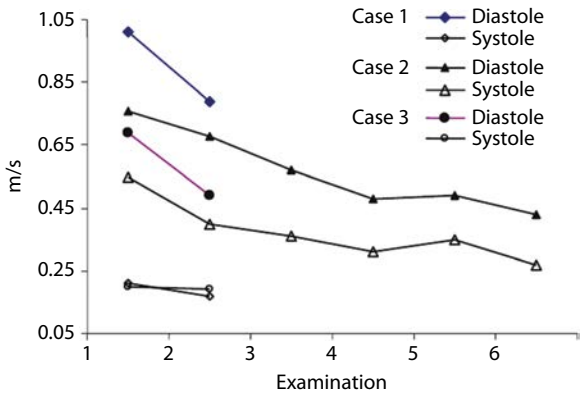


**Figure 34.13**
Systolic and diastolic peak blood flow measurements in three cases of severe fetal anemia. In cases 1 and 3, velocities were obtained in hydropic fetuses prior to transfusion. In case 1 a hematocrit of 9% was corrected to 39.8%, and in case 3 from 14% to 42.8%. In the second case of maternal trauma, repeat transfusions were necessary on days 1 and 5 for hematocrit levels of 21% and 24%, respectively. (Reproduced with permission from Baschat AA et al. *Ultrasound Obstet Gynecol* 2003;21(5):426–9.[50])

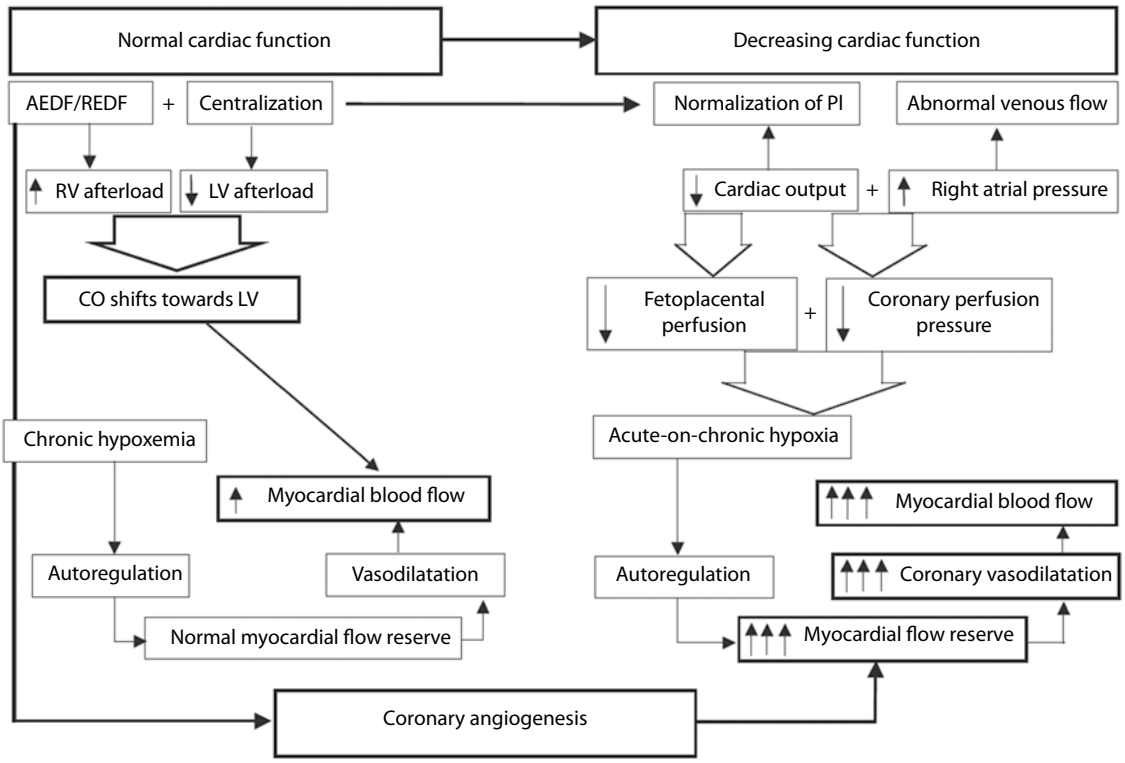


**Figure 34.14**
The stages of fetal heart sparing. In the first stage, the increased afterload of the right ventricle and decreased afterload of the left ventricle result in redistribution of cardiac output (CO) toward the left ventricle, thus providing increased perfusion to the myocardium. In addition, chronic intrauterine hypoxemia stimulates coronary vasodilatation and coronary angiogenesis. The magnitude of myocardial blood flow enhancement is below the visualization threshold of current ultrasound equipment. In the second stage, coronary angiogenesis results in increasing myocardial flow reserve. In the late stage, there is cardiovascular decompensation associated with acute-on-chronic hypoxemia. An altered myocardial vascular bed allows recruitment of a larger myocardial flow reserve, and the magnitude of coronary blood flow is now above the visualization threshold. (AEDF, absent end-diastolic flow; PI, pulsatility index; REDF, reversed end-diastolic flow.) (Reproduced with permission from Baschat AA et al. *J Perinat Med* 1998;26(3):143–56.[63])

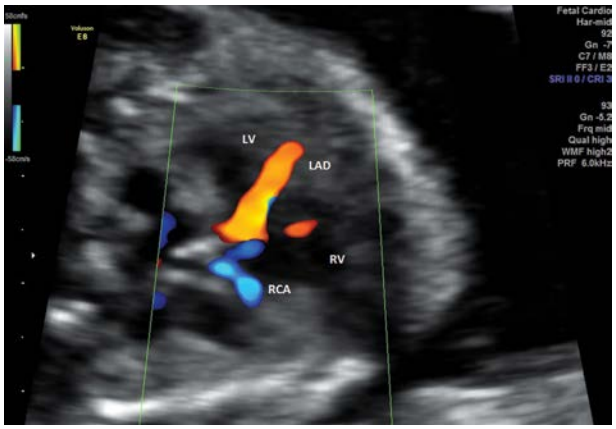


**Figure 34.15**
Coronary arterial blood flow in a severely growth-restricted fetus. By color Doppler flow mapping, the right coronary artery (RCA) and the left anterior descending (LAD) branch in an apical four-chamber view are visualized at 26 weeks' gestation.

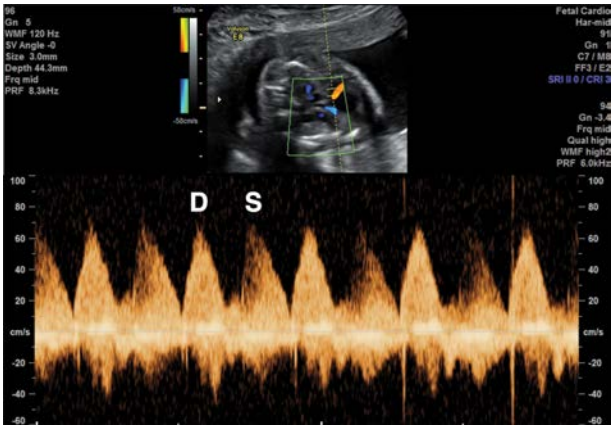


**Figure 34.16**
Pulsed wave Doppler waveform of the proximal right coronary artery obtained at 26 weeks' gestation in a severely growth-restricted fetus, showing a higher peak velocity (70 cm/s) during diastole than during systole (50 cm/s). No reverse flow was observed.

the development of fetal hydrops, decreases in coronary sinus dynamics can be observed. This finding is analogous to observations in adults with heart failure, where coronary sinus caliber changes are attenuated, presumably due to elevations in coronary venous pressures.[51]

## Ductus arteriosus constriction

Maternal indomethacin therapy for preterm labor carries the risk of constriction of the ductus arteriosus in the fetus. As a conduit for the right ventricle to the systemic circulation, constriction of this vessel raises afterload and, therefore, cardiac work and oxygen requirement. In severe constriction, tricuspid insufficiency and abnormal venous indices may develop. There is evidence for coronary blood flow augmentation, and color and pulsed wave Doppler measurement of coronary artery blood flow becomes possible. While the peak velocities are not significantly elevated, the gestational age at visualization is determined by the onset of the clinical condition. With resolution of ductus arteriosus constriction following discontinuation of indomethacin, coronary blood flow could no longer be visualized.

## Other fetal conditions

Acute changes in fetal oxygenation and cardiac pre- and afterload also cause arterial and venous redistribution in favor of the organs essential for fetal life. These heart-, brain-, and adrenal gland-sparing phenomena have been described in different animal models. The few observations made by Doppler ultrasound in the human fetus support the presence of the same protective mechanisms. Transient brain- and heart-sparing phenomena were observed in a 30-week fetus following acute bradycardia after umbilical fetal blood sampling. Sudden visualization of coronary blood flow, brain-sparing, and highly pulsatile precordial venous flow persisted for a long period after the 12-minute bradycardia[75] (Figure 34.17). Heart sparing has also been observed in a group of normally grown, nonanemic fetuses with cardiac dysfunction, as expressed by elevated myocardial performance index and reduced cardiovascular profile score, in the absence of Doppler changes consistent with uteroplacental insufficiency and/or brain sparing.[71] This suggests that fetal blood flow redistribution also occurs in response to isolated myocardial dysfunction and not only as a generalized response to acute hypoxia.[71] Coronary artery blood flow enhancement has been described in a fetus with supraventricular tachycardia, and it disappeared when fetal heart rate was converted to normal sinus rhythm.[76] Also, changes in coronary sinus dynamics have been documented in a fetus with supraventricular tachycardia.[51] It is likely that more observations of alterations in coronary arterial and venous dynamics will be reported, as familiarity with the examination technique and advances in ultrasound technology facilitate examination.

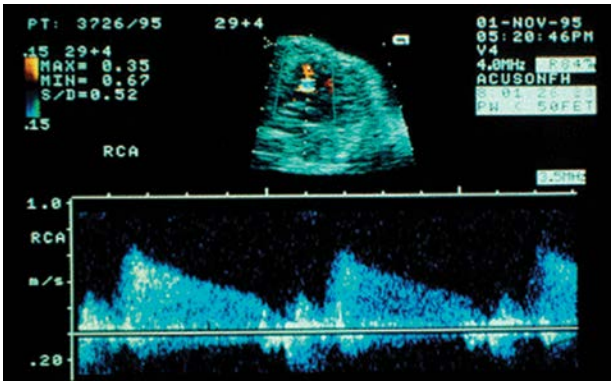


**Figure 34.17**
In a fetus with multiple malformations, fetal bradycardia of 56 beats per minute was provoked by percutaneous ultrasound-directed puncture of the umbilical vein for blood sampling at 29 + 4 weeks' gestation. The blood flow velocity waveform of the right coronary artery after 240 seconds of bradycardia showed a short systolic peak (peak blood flow velocity = 35 cm/s) and a prolonged diastolic flow (peak blood flow velocity = 69 cm/s). (Reproduced with permission from Gembruch U, Baschat AA. *Ultrasound Obstet Gynecol* 2000;15(5):424–7.[75])

# Clinical applications in fetal cardiac abnormalities

Due to the vascular properties of the coronary arterial circulation, abnormalities frequently develop in cardiac lesions that are associated with disturbed intracardiac pressure/volume relationships during embryonic organogenesis. Due to the embryology of the coronary sinus, abnormalities involving this vessel frequently involve anomalous central venous drainage (both systemic and/or pulmonary). Ultrasound biometry and assessment of coronary sinus dynamics have clinical relevance and may be the only apparent clue pointing in the direction of such anomalies.

## Ventriculo-coronary connections in the human fetus

Ventriculo-coronary connections are frequently noted in fetuses and newborns with pulmonary atresia, hypoplastic right ventricle, intact ventricular septum, or restrictive ventricular septal defect.[77] In cases of hypoplastic left heart with aortic atresia, intact ventricular septum and patent mitral valve ventriculo-coronary connections may also be present but are less common. The genesis of these vascular abnormalities was previously discussed. The abnormal coronary channels may provide a conduit to release intraventricular pressures and may partially avert hypoplasia and fibroelastosis. However, coronary blood flow dynamics may be significantly compromised, impacting on prognosis and approach to postpartum surgical management.[78–80] While coronary perfusion may be well maintained *in utero*, the situation may change after birth. Right ventricular–dependent coronary circulation may occur

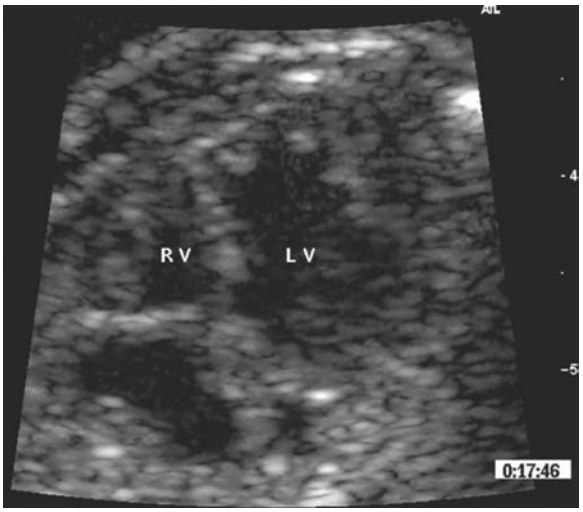


**Figure 34.18**
A fetus with severe pulmonary stenosis and intact interventricular septum at 21 + weeks' gestation. The four-chamber view demonstrated hypoplasia of the right ventricle.

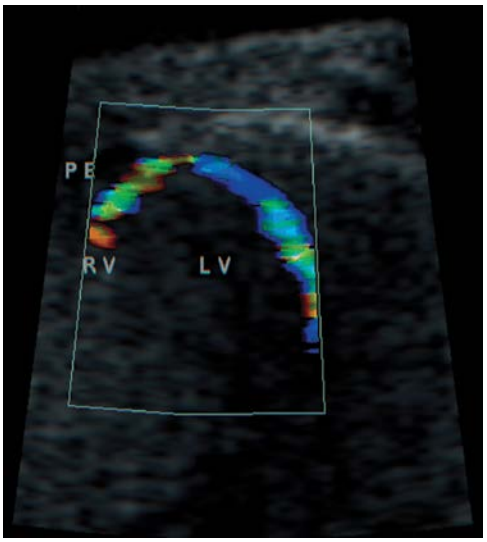


**Figure 34.19**
Color Doppler imaging demonstrating a ventriculo-coronary connection between the right ventricle and the aortic sinus.

and result in acute or chronic global myocardial ischemia or infarction due to coronary steal and segmental vascular obstruction. Because of these potential impacts, prenatally detected outflow tract obstructive lesions with relatively preserved ventricular architecture should prompt the search for ventriculo-coronary fistula.

Prenatal diagnosis of ventriculo-coronary fistula is achieved by the demonstration of high-velocity bidirectional flow in the coronary artery by color Doppler flow mapping, and verified by pulsed wave Doppler examination. A severely dilated coronary artery may also be imaged by two-dimensional echocardiography. In cases of right ventricular outflow tract obstruction, diastolic flow from the aortic sinus is directed toward the hypoplastic right ventricle. Pressures are reversed during ventricular systole, and blood flows from the right ventricle to the aorta (Figure 34.18 through 34.20).[77,81,82]

## *Coronary arteriovenous fistula in the human fetus*

Congenital coronary fistulae may occur rarely if cardiac anatomy is otherwise normal. The majority of these involve a single coronary artery, and less often multiple branches. Connections may involve the coronary arterial tree, right atrium, coronary sinus, caval veins, right ventricle, and pulmonary trunk. Drainage into a low-pressure system can result in a large left-to-right shunt, already causing symptoms in childhood such as congestive heart failure, myocardial ischemia from coronary artery steal, right chamber enlargement, arrhythmia, thrombosis with consecutive embolization, and bacterial endocarditis.[83] In the majority of cases, symptoms appear in the second and third decades of life. In a 20-week fetus, prenatal detection of an isolated coronary fistula connecting to the right ventricle has been reported with demonstration of a progressive increase in size as well as tortuosity of the fistula during gestation.[84] A similar case with a fistula between the LCA and the right atrium has also recently been described.[85] The shunting blood caused high-velocity flow in the dilated coronary sinus. In addition to the prenatal findings, a persistent left superior vena cava and a small ventricular septal defect were also identified postnatally. Following coil embolization of the coronary fistula, the further clinical course was reported as uneventful.

## *Idiopathic arterial calcification in the human fetus*

The idiopathic arterial calcification has an unknown etiology and is characterized by generalized arterial calcification

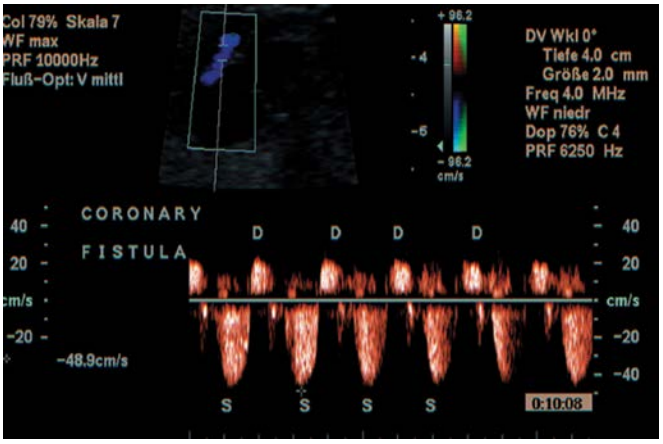


**Figure 34.20**
In the same fetus as in Figure 34.17, pulsed wave Doppler examination showed a disturbed to-and-fro blood flow with a systolic flow from the right ventricle to the aortic sinus (S) and a diastolic reversal (D).

and stenoses, especially of the walls in the arterial trunk of the pulmonary artery and aorta.[86,87] Most commonly, the coronary arteries are also affected, but peripheral arteries of the gastrointestinal tract, liver, kidneys, brain, extremities, and placenta may also be involved. Severe myocardial dysfunction may cause severe fetal hydrops, tissue ischemia, and fetal death in the late second or third trimester.[88] In less severe cases, especially in the absence of hydrops, palliative treatment postpartum may be started with steroids and bisphosphonates in order to stop or delay the progression of the disease.[89] However, most infants with idiopathic arterial calcification die within the first year of life, complicated by cardiac and pulmonary failure, severe hypertension, renal infarction, peripheral gangrene, and bowel infarction.[87]

## Critical aortic stenosis

Critical aortic stenosis in fetal life can be associated with a marked decrease in left ventricular output and reversal of shunting across the foramen ovale. Under these circumstances, coronary perfusion pressure is affected by a decrease in arterial and an elevation of right atrial pressure, thereby decreasing the driving force across the coronary vascular bed. Concurrently, left ventricular work and therefore myocardial oxygen demand are increased. The development of acute heart sparing has been documented in a fetus presenting with severe left ventricular outflow tract obstruction and nonimmune hydrops due to critical aortic stenosis. While these findings were ameliorated initially by transplacental digoxin therapy, visualization of coronary blood flow became visible at 39 weeks, coinciding with shunt reversal across the foramen ovale.[90]

## Persistent left superior vena cava

While Doppler examination of the coronary sinus has limited utility in the human fetus, substantial dilatation may result from volume overload from a persistent left superior vena cava draining into the coronary sinus.[91–93] The frequency of a persistence of the left vena cava is 1–2 per 1,000 but may be as high as 9% in the presence of congenital heart defects.[94] The degree of dilatation is often marked and lies appreciably above normal reference limits. This dilatation appears to be predominantly related to vascular volume changes and is independent of associated cardiac defects.[69] Other causes of coronary sinus dilatation in the human fetus may be a coronary arteriovenous fistula and anomalous pulmonary vein drainage into the coronary sinus. Ectopic connection of the ductus venosus in an enlarged coronary sinus has also been described in a small number of cases, and it should be considered in cases of isolated coronary sinus dilatation after exclusion of left superior vena cava and totally anomalous pulmonary vein connection.[95,96]

It is important to note that because of its close proximity to the insertion of the atrioventricular valve, a dilated coronary sinus has been mistaken for an atrial septal defect of ostium primum type and/or an atrioventricular septal defect, respectively.[97–99] Coronary sinus dynamics may be attenuated in fetal conditions associated with elevated right heart pressures, severe fetal cardiac dysfunction, and hydrops. These alterations in dynamics may indicate elevated coronary sinus pressures, or changes in coronary blood flow.[51]

# References


1. Abuhamad A. *Ultrasound Obstet Gynecol* 2003;21(5):423–5.
2. McAlpine W. *Heart and Coronary Arteries*. New York, NY: Springer-Verlag; 1975.
3. Williams PL, Warwick, R. *Gray's Anatomy*. New York, NY: Churchill Livingstone; 1983.
4. Ganong W. *Review of Medical Physiology*. Norwalk, CT: Appleton and Lange; 1989.
5. Larsen W. *Human Embryology*. New York, NY: Churchill Livingstone; 1993.
6. Tomanek RJ. *Cardiovasc Res* 1996;31:E46–51.
7. Hudlicka O, Brown MD. *J Vasc Res* 1996;33(4):266–87.
8. Poole TJ, Coffin JD. *J Exp Zool* 1989;251(2):224–31.
9. Skalak TC, Price RJ. *Microcirculation* 1996;3(2):143–65.
10. Engelmann GL et al. *Circ Res* 1993;72(1):7–19.
11. Banai S et al. *Cardiovasc Res* 1994;28(8):1176–9.
12. Levy AP et al. *Circ Res* 1995;76(5):758–66.
13. Ratajska A et al. *Dev Dyn* 1995;203(4):399–407.
14. Scheel KW et al. *Am J Physiol* 1984;246(6 Pt 2):H768–75.
15. Reller MD et al. *Am J Physiol* 1992;263(4 Pt 2):H1327–9.
16. Baschat AA et al. *Ultrasound Obstet Gynecol* 2001;18(1):39–43.
17. Ascuitto RJ, Ross-Ascuitto NT. *Semin Perinatol* 1996;20(6): 542–63.
18. Bartelds B et al. *Circulation* 1999;99(14):1892–7.
19. Fisher DJ et al. *Am J Physiol* 1982;242(4):H657–61.
20. Spahr R et al. *Basic Res Cardiol* 1985;80(suppl 1):53–6.
21. Rudolph AM. *Circ Res* 1985;57(6):811–21.
22. Kiserud T et al. *Am J Obstet Gynecol* 2000;182(1 Pt 1):147–53.
23. Krajcar M, Heusch G. *Basic Res Cardiol* 1993;88(suppl 1): 25–42.
24. Bassenge E. *Pflugers Arch* 1978;373:R6.
25. Cannon PJ et al. *Am J Cardiol* 1975;36(6):783–92.
26. Mantero S et al. *J Biomed Eng* 1992;14(2):109–16.
27. Thornburg KL, Reller MD. *Am J Physiol* 1999;277(5 Pt 2): R1249–60.
28. Guyton AC et al. *Circ Res* 1964;15(suppl):60–9.
29. Mosher P et al. *Circ Res* 1964;14:250–9.
30. Barnea O, Santamore WP. *Basic Res Cardiol* 1992;87(3):290–301.
31. Hoffman JI. *Circulation* 1984;70(2):153–9.
32. Campbell SE et al. *Can J Cardiol* 1991;7(5):234–44.
33. Holmes G, Epstein ML. *Pediatr Res* 1993;33(5):527–32.
34. Muller JM et al. *Cardiovasc Res* 1996;32(4):668–78.
35. Reller MD et al. *Circulation* 1992;86(2):581–8.
36. Thompson LP et al. *Am J Physiol Regul Integr Comp Physiol* 2000;279(5):R1813–20.
37. Reller MD et al. *Am J Physiol* 1995;269(6 Pt 2):H2074–81.
38. Behrman RE et al. *Am J Obstet Gynecol* 1970;108(6):956–69.
39. Block BS et al. *Am J Obstet Gynecol* 1984;148(7):878–85.
40. Reuss ML, Rudolph AM. *J Dev Physiol* 1980;2(1–2):71–84.
41. Poudel R et al. *Am J Physiol Regul Integr Comp Physiol* 2015; 308(3):R151–62.
42. Hata T et al. *J Clin Ultrasound* 2008;36(4):204–7.

43. Pooh RK, Korai A. *Croat Med J* 2005;46(5):808–11.
44. Oberhoffer R et al. *Eur J Pediatr* 1989;148(5):389–92.
45. Baschat AA et al. *Ultrasound Obstet Gynecol* 1997;9(3):162–72.
46. Gembruch U, Baschat AA. *Ultrasound Obstet Gynecol* 1996; 7(1):10–6.
47. Mielke G, Wallwiener D. *Ultrasound Obstet Gynecol* 2001; 18(4):407.
48. Yoo SJ et al. *Ultrasound Obstet Gynecol* 2001;18(3):248–52.
49. Baschat AA, Gembruch U. *Ultrasound Obstet Gynecol* 2002; 20(4):405–12.
50. Baschat AA et al. *Ultrasound Obstet Gynecol* 2003;21(5):426–9.
51. Abello KC et al. *Ultrasound Obstet Gynecol* 2002;20(2):137–41.
52. Rein AJ et al. *Ultrasound Obstet Gynecol* 2000;15(6):468–72.
53. Chaoui R et al. *Prenat Diagn* 2003;23(7):552–7.
54. Baschat AA, Gembruch U. *Ultrasound Obstet Gynecol* 1998; 11(6):410–4.
55. Mundigler G et al. *Clin Cardiol* 1997;20(3):225–31.
56. Zehetgruber M et al. *J Am Coll Cardiol* 1995;25(5):1039–45.
57. Hecher K et al. *Circulation* 1995;91(1):129–38.
58. Hecher K et al. *Am J Obstet Gynecol* 1995;173(1):10–5.
59. Nicolaides KH et al. *BMJ* 1988;297(6655):1026–7.
60. Rizzo G et al. *Ultrasound Obstet Gynecol* 1996;7(6):401–10.
61. Weiner CP. *Am J Obstet Gynecol* 1990;162(5):1198–202.
62. al-Ghazali W et al. *Br J Obstet Gynaecol* 1989;96(6):697–704.
63. Baschat AA et al. *J Perinat Med* 1998;26(3):143–56.
64. Reed KL et al. *Am J Obstet Gynecol* 1987;157(3):774–9.
65. Rizzo G, Arduini D. *Am J Obstet Gynecol* 1991;165(4 Pt 1): 876–82.
66. Tchirikov M et al. *Ultrasound Obstet Gynecol* 1998;11(6):426–31.
67. Tchirikov M et al. *Am J Obstet Gynecol* 1998;178(5):943–9.
68. Baschat AA, Gembruch U. *Ultrasound Obstet Gynecol* 1996; 8(3):201–5.
69. Baschat AA et al. *Ultrasound Obstet Gynecol* 2000;16(5):425–31.
70. Makikallio K et al. *Ultrasound Obstet Gynecol* 2002;19(2): 147–52.
71. Bui YK et al. *J Matern Fetal Neonatal Med* 2016;29(10):1536–40.
72. Chaoui R. *Acta Paediatr Suppl* 2004;93(446):6–12.
73. Rizzo G et al. *J Matern Fetal Neonatal Med* 2009;22(7):547–51.
74. Baschat AA et al. *Ultrasound Obstet Gynecol* 1998;12(2):128–31.
75. Gembruch U, Baschat AA. *Ultrasound Obstet Gynecol* 2000; 15(5):424–7.
76. Uerpairojkit B et al. *Prenat Diagn* 2009;29(3):274–6.
77. Maeno YV et al. *Heart* 1999;81(6):661–8.
78. Coles JG et al. *Ann Thorac Surg* 1989;47(2):213–7.
79. Giglia TM et al. *Circulation* 1992;86(5):1516–28.
80. Hanley FL et al. *J Thorac Cardiovasc Surg* 1993;105(3):406–23, 24–7; discussion 23–4.
81. Arabin B et al. *Ultrasound Obstet Gynecol* 1996;7(6):461–2.
82. Chaoui R et al. *Ultrasound Obstet Gynecol* 1997;9(3):194–7.
83. Liberthson RR et al. *Circulation* 1979;59(5):849–54.
84. Sharland GK et al. *Heart* 1996;76(1):79–81.
85. Mielke G et al. *Ultrasound Obstet Gynecol* 2002;19(6):612–5.
86. Hajdu J et al. *Prenat Diagn* 1998;18(11):1186–90.
87. Moran JJ. *Pathol Annu* 1975;10:393–417.
88. Juul S et al. *Am J Dis Child* 1990;144(2):229–33.
89. Bellah RD et al. *J Pediatr* 1992;121(6):930–3.
90. Schmider A et al. *Ultrasound Obstet Gynecol* 2000;16(3):275–8.
91. Papa M et al. *Br Heart J* 1995;73(4):355–8.
92. Rostagno C et al. *Cardiologia* 1999;44(2):203–6.
93. Snider AR et al. *Circulation* 1979;60(4):721–7.
94. Nsah EN et al. *Pediatr Pathol* 1991;11(2):261–9.
95. Ben Brahim F et al. *J Ultrasound Med* 2014;33(3):535–42.
96. Qian Y et al. *Echocardiography* 2016;33(1):154–6.
97. Allan LD, Sharland GK. *Heart* 2001;85(4):433–7.
98. Gembruch U et al. *Ultrasound Obstet Gynecol* 1993;3(5):310–7.
99. Park JK et al. *Ultrasound Obstet Gynecol* 1997;10(2):126–9.

# 35

# The fetal venous system: Normal embryology, anatomy, and physiology and the development and appearance of anomalies

Simcha Yagel, Ori Shen, Sarah M. Cohen, and Dan V. Valsky

## Part I: Normal embryology, anatomy, hemodynamics, ultrasound evaluation, and Doppler investigation

### *Introduction*

Sonographic investigation of the fetal venous system has developed rapidly since its introduction in the mid-1980s. Elucidation of normal venous anatomy, its role in normal fetal development and in the evaluation and management of intrauterine growth restriction (IUGR) and other cardiovascular disorders, as well as its association as a part of complex structural anomalies, are the subjects of intensive research.

In addition to recognition of the normal and anomalous sonographic appearance of the fetal venous system, knowledge of its embryology and physiology is vital to better inform our management decisions and provide appropriate parental counseling when an anomaly is encountered.

This chapter is composed of two parts. Part I discusses the embryology of the fetal venous system, continuing with normal fetal anatomy and hemodynamics, Doppler investigation of various vessels, and finally the application of three- and four-dimensional ultrasound (3D/4DUS) technology to this system. Part II describes pathophysiology, the embryological basis and ultrasound appearance of anomalies, and Doppler flow studies in circulatory compromise.

### *Embryology of the human venous system*

The cardiovascular system is the first organ system to develop in the human embryo, and the heart begins to beat by day 23 of embryonic development.

Three symmetric paired veins form the basis of the early venous system in the 4-week embryo (6 weeks menstrual age [MA]), draining into the heart: the umbilical veins (UVs), vitelline veins (VVs), and cardinal veins (CVs). The UVs drain the chorion, the VVs the yolk sac, and the CVs the body of the embryo. All three pairs open to the right and left horn of the sinus venosus. Also at this stage, the liver buds begin to develop from the ventral endodermal wall of the foregut. These cells invade mesenchymal tissue, called the septum transversum, which will form the connective tissue of the future liver[1–3] (Figure 35.1a).

Between 4 and 6 weeks (6–8 weeks MA), a complex pattern of vessel growth, anastomosis, and asymmetric degeneration occurs. The VV and UV systems, which represent the afferent venous vessels of the liver, are modified by their proximity to the developing liver in the septum transversum. The liver cords growing into the septum transversum interrupt the cranial portion of both veins between the liver and the heart with an extensive vascular network: the hepatic sinusoids. The growing hepatic sinusoids first become linked to both VVs, and by day 32 have tapped into the UV (Figure 35.1b).

By the fifth week of development (seventh week MA), the left cranial part of the VV atrophies and disappears. The remaining right proximal VV, which will give rise to the hepatocardiac segment of the inferior vena cava (IVC), is connected to the intrahepatic efferent veins: the left, medial, and right hepatic veins. Meanwhile, distal sections of the left and right VVs and the anastomoses between them become the portal vein (PV), while other segments of the right and left VVs collapse and disappear (Figure 35.1c).

These changes in the VVs are accompanied by changes in the UVs. The entire right UV and the left cranial segment of the left UV will atrophy and disappear; the left UV becomes the dominant conduit of blood from the placenta. During the eighth week of development (10th week MA), the intrahepatic portion of the VV, and more specifically the left portal branch, forms an anastomosis between the intrahepatic segment of left UV and the ductus venosus (DV), which is formed by the coalescence of the hepatic sinusoids and drains into the hepatocardiac segment of the IVC (Figure 35.1d).

The CVs drain the embryo body, with the anterior and posterior CVs draining the cranial and caudal parts of the body,

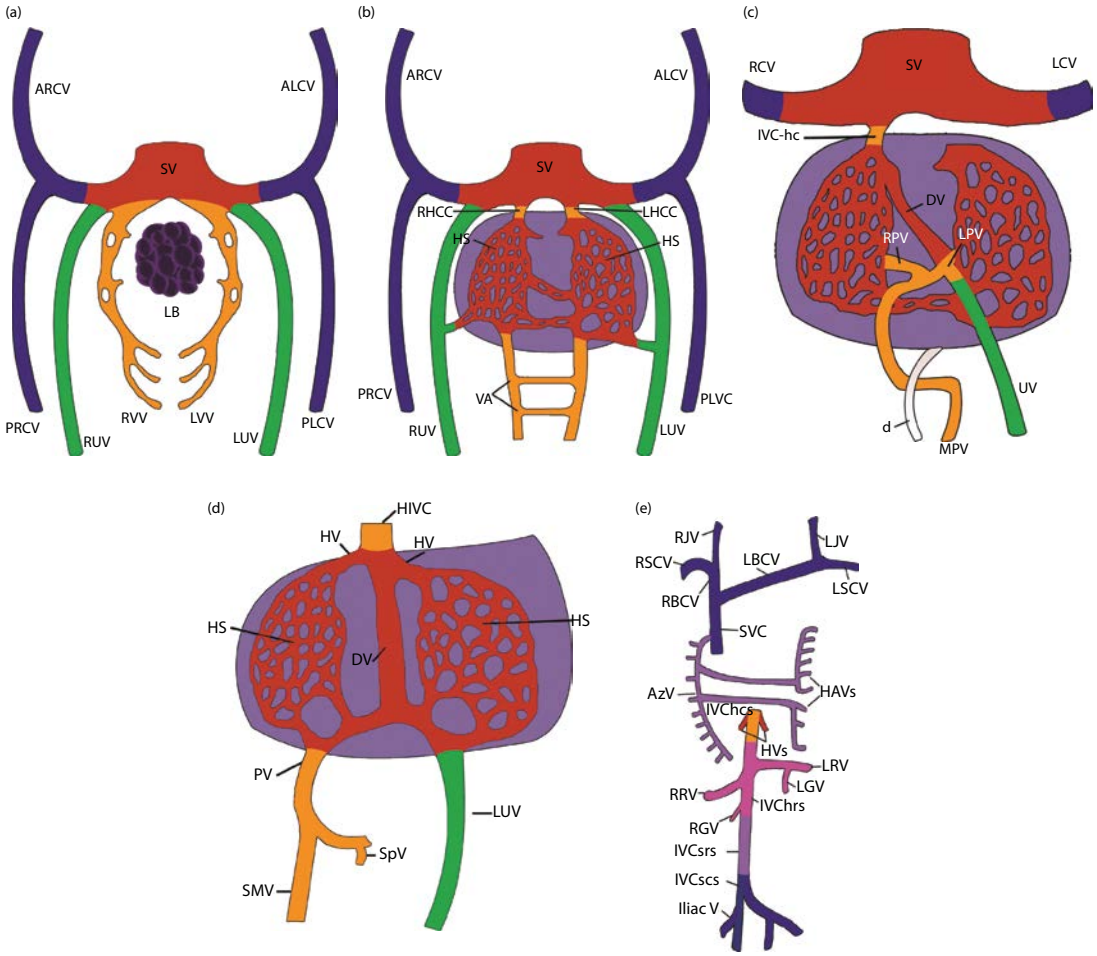


**Figure 35.1**
Embryological development of the human venous system at sequential stages. See text for details. (a) In the 4-week embryo (6 weeks menstrual age), three symmetric paired veins are observed: umbilical veins (green), vitelline veins (orange), and cardinal veins (blue). (Red indicates all the rest.) (ALCV, anterior left cardinal vein; ARCV, anterior right cardinal vein; LB, liver buds; LUV, left umbilical vein; LVV, left vitelline vein; PLCV, posterior left cardinal vein; PRCV, posterior right cardinal vein; RUV, right umbilical vein; RVV, right vitelline vein; SV, sinus venosus.) (b) Embryo from fifth to eighth weeks of development (7–10 weeks menstrual age): liver cords growing into the septum transversum interrupt the cranial portion of the umbilical and vitelline systems, the early liver, and surround the hepatic sinuses. (HS, hepatic sinus; LHCC, left hepatic common cardinal vein; RHCC, right hepatic common cardinal vein; VA, vitelline anastomoses. Green, umbilical veins; orange, vitelline veins; blue, cardinal veins; red all the rest.) (c) Fifth–eighth weeks of development (7–10 weeks menstrual age), the asymmetric stage. The intrahepatic umbilico-portal-ductus venosus anastomosis. (d, duodenum; DV, ductus venosus; IVChc, inferior vena cava hepatocardiac segment; LCV, left cardinal vein; LPV, left portal vein; MPV, main portal vein; RCV, right cardinal vein; RPV, right portal vein; SV, sinus venosus; UV, umbilical vein. Green, umbilical veins; orange, vitelline veins; blue, cardinal veins; red, all the rest.) (d) Changes in the vitelline veins are accompanied by changes in the umbilical veins. (DV, ductus venosus; HIVC, hepatic portion of the IVC; HS, hepatic sinus; HV, hepatic veins; LUV, left umbilical vein; PV, portal vein; SMV, sup-mesenteric vein; SpV, splenic vein.) (e) Fifth–eighth weeks of development (7–10 weeks menstrual age), the cardinal veins, asymmetric stage. Vessels having their origin in the cardinal system (blue): IVCscs, inferior vena cava sacro-cardinal segment; iliac veins; LBCV, left brachiocephalic vein; LJV, left jugular vein; LScV, left subclavian vein; RBCV, right brachiocephalic vein; RJV, right jugular vein; RScV, right subclavian vein. Vessels having their origin in the subcardinal system (pink): IVChrs, inferior vena cava hepatorenal segment; LGV, left gonadal vein; LRV, left renal vein; RGV, right gonadal vein; RRV, right renal vein. Vessels originating from the supracardinal system (purple): AZV, azygos vein; HAZV, hemiazygos vein; IVCsrs, inferior vena cava sacrorenal segment. Vessels of the vitelline system (orange): HVs, hepatic veins; IVChcs, inferior vena cava hepatocardiac segment. (Red, all the rest.) (Modified from Sadler T. *Langman's Medical Embryology*; 1985;[1] and Larsen WJ. *Essentials of Human Embryology*. London, UK: Churchill Livingstone; 1998;[3] Reprinted with permission from Yagel S et al. *Ultrasound Obstet Gynecol* 2010;35:741–50.[7])

respectively. Both veins empty into the common CVs: the third venous system entering the sinus venosus of the embryonic heart (Figure 35.1a). From the fifth week of development (seventh week MA), the posterior branches are obliterated and only the most caudal part persists, giving rise to the common iliac vein and the most caudal segment of the IVC, the sacral. They are replaced by two pairs of veins: the subcardinal and the supracardinal veins. The subcardinal vein drains the kidney and gonads. By the 9th–10th week MA, the proximal left subcardinal vein obliterates and connects with

the right branch, which then forms the renal-hepatic (suprarenal) segment of the IVC.

The supracardinal veins drain the thoracic wall and the iliac veins. The inferior portion of the left supracardinal vein obliterates and connects to the right subcardinal vein, forming the sacro-renal (prerenal) segment of the IVC. The superior segment of the supracardinal vein is divided into the left branch, called the hemiazygos vein, which forms a cross-anastomosis to the right branch, called the azygos vein, which drains into the superior vena cava (SVC) (Figure 35.1e).

The IVC, therefore, is formed from four different embryonic sources in a caudo-cranial order (the first three have their origin from the posterior CV):

1. The most caudal, sacrocardinal segment is formed from the posterior CV
2. The prerenal, sacrorenal segment from the right supracardinal vein
3. The suprarenal, hepatic renal segment from the right subcardinal vein
4. The most cranial, heptocardiac segment originates from the right VV

During the same period, the proximal left anterior CV regresses and disconnects from the sinus venosus. A shunt to the right anterior CV is then created, forming the left brachiocephalic vein. The right anterior CV is transformed to the right brachiocephalic vein. The segment between the junction of the left and right brachiocephalic veins and the right atria develops meanwhile into the SVC.

Within the developing fetal liver, afferent and efferent venous networks develop. The afferent system includes the UV, PV, and DV, while the efferent is composed of the hepatic veins. They form two apposing systems in the caudal and cranial portions of the liver, respectively.[1,3–5]

## The pulmonary veins

During the fourth week of embryonic development (sixth week MA, 4 mm embryo), blood coming from the developing lungs drains into the splanchnic plexus and then to the common CVs and the umbilical and VVs. These connections are maintained until the beginning of the fifth week, when the first pulmonary vein appears as a single dorsal invagination of the left atrium and meets the pulmonary venous plexus. This process continues, and as the atrial cavity develops through the fifth embryonic week, two right and two left branches of the pulmonary stem enter the atrial cavity via four orifices. These veins anastomose with the veins developing from the pulmonary mesoderm to form the definitive pulmonary veins.[1,3] The pulmonary venous plexus gradually loses its connection to the vitelline and CVs.

# *Anatomy of the fetal precordial venous system*

## Imaging the venous system in three planes

Examination of the fetal venous system is feasible with the application of three or six abdominal planes.[6–8] We recently described[6] a systematic approach to imaging the fetal precordial venous system, composed of two-dimensional ultrasound (2DUS) color Doppler scanning of the fetal abdomen in three discrete planes: two transverse and one longitudinal (Figure 35.2a–c). The more caudal plane is obtained in a ventral or lateral transverse abdominal plane to image the UV, left portal vein (LPV), portal sinus (PS), anterior right portal vein (ARPV), posterior right portal

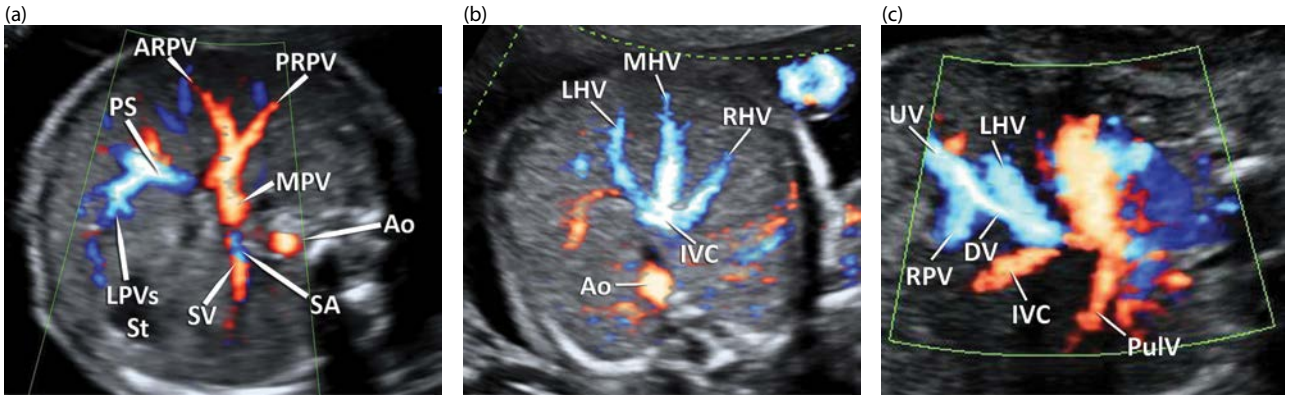


**Figure 35.2**
The fetal precordial venous system in three planes.[6] Frame a: Lateral transverse plane through the fetal abdomen from right to left. The splenic artery is shown (SA, blue jet) as it is always observed with the splenic vein. (Ao, aorta; ARPV, anterior right portal vein; LPVs, left portal veins; MPV, main portal vein; PRPV, posterior right portal vein; PS, portal sinus; SA, splenic artery; St, stomach; SV, splenic vein.) Frame b: Anterior-posterior transverse plane through the upper fetal abdomen showing the normal "trident sign" of the hepatic veins. (Ao, aorta; LHV, left hepatic vein; MHV, middle hepatic vein; RHV, right hepatic vein.) Frame c: Typical longitudinal plane showing the umbilical vein (UV); left hepatic vein (LHV); right portal vein (RPV); ductus venosus (DV); inferior vena cava (IVC); and pulmonary vein (PulV). The DV is best seen in this plane, as it arises from the umbilical vein. (Reprinted with permission from Yagel S et al. *Ultrasound Obstet Gynecol* 2015;45:578–83.[6])

vein (PRPV), main portal vein (MPV), and splenic vein and artery. Moving cephalad, a ventral or lateral transverse plane is obtained to image the right, middle, and left hepatic veins and inferior vena cava (IVC). Finally, a longitudinal anterior-posterior plane shows the UV, DV, IVC, and left hepatic vein.

Plane A is a ventral or slightly lateral transverse plane through the fetal abdomen at the level of the left PS (Figure 35.2a). In this plane, the UV, LPV, PS, ARPV, PRPV, MPV, and splenic vein and artery are imaged. The splenic artery was included because it is always seen with the splenic vein. The transducer is then moved cephalad to view Plane B, a ventral or slightly lateral transverse plane, wherein the right hepatic vein, middle hepatic vein, and left hepatic vein were visualized where they drain into the IVC (Figure 35.2b). To obtain Plane C, the transducer is rotated toward a longitudinal plane and the UV, DV, left hepatic vein, and IVC were visualized where they converge proximal to the right atrium (Figure 35.2c). This plane corresponds to the classic sagittal ductus venous plane proposed by Kiserud.[9] When necessary, the pulse Doppler waveform of a given target vessel is examined, as described in the following text.

In the fetus, oxygen- and nutrient-rich blood from the placenta is delivered through the UV and DV to the fetal heart. The intra-abdominal segment of the UV courses via the falciform ligament to merge with the LPV. This segment is also known as the umbilical segment of the LPV. It is similar in diameter to the LPV and is usually wider than the right portal vein (RPV). The intrahepatic point of separation between the UV and the PV is represented by the inferior branch of the left portal vein (LPVi).

The LPV gives rise to the DV, which is aligned with the UV, just before turning almost 90° to the right to join the RPV. This portion of the LPV is known also as the pars transversa or PS, and it extends from the LPVi to the point of bifurcation of the MPV to the RPV. The DV connects to the IVC distally, together with the left and middle hepatic veins, just proximal to the entrance into the right atrium (Figure 35.2).

The DV is a branchless, hourglass-shaped vessel narrowing to 1–2 mm, approximately one-third of the width of the UV, which forms a direct shunt between the junction of the left portal and intra-abdominal UVs and the separate connection to the IVC. Some investigators report a "sphincter" regulating blood flow through the DV; an oxygen concentration–dependent mechanism may control the activity of this sphincter.[10,11] However, Mavrides et al.,[12] in their histological study, demonstrated that this narrowing zone consists of a multilayered elastine, shelf-like stricture, with no sphincter formation. The rest of the DV is covered by a single layer of muscular, elastine, and endothelial cells.

The RPV receives poorly oxygenated blood, primarily through the MPV. The greater volume and higher oxygen content of blood flowing through the left lobe of the liver as compared to the right results in a noticeably larger left than right lobe during fetal life. When the UV and DV atrophy after birth, this situation is reversed.

### The fetal portal system

Within the developing fetal liver, two apposed venous systems develop: afferent and efferent. The afferent venous system of the fetal liver (the UV, PV, PS, and DV) and the efferent venous system (the hepatic veins) form two systems positioned in the caudal and cranial portions of the liver, respectively.[7]

The MPV enters the liver in the porta hepatis or main fissure, posterior to the hepatic artery and the common hepatic duct. This fissure divides the liver into its right and left lobes. The site of connection of the MPV to the PS represents the anatomic point of division between its right and left branches and is situated to the right and inferiorly to the origin of the DV.

The LPV is divided into three main branches: the inferior, superior, and medial (LPVi, LPVs, and LPVm, respectively) and lies approximately at the level of origin of the LPVi. The right branch of the MPV becomes the right portal vein (RPV) and bifurcates into two major branches, the ARPV and PRPV, at varying distances from the MPV-PS junction (Figure 35.2).

The junction of the MPV and the PS displays a continuum of morphologic variation in the angle of communication, ranging from 90° to a completely parallel course and a disjunction of two paired vessels: the MPV/PRPV and LPV/ARPV, connected only by a thin bridging vessel. Among the variations, three main subtypes can be identified[13,14]:

1. T-shape, end-to-side anastomosis (the most common, identified in 68% of cases)
2. X-shape, side-to-side anastomosis (12% of cases)
3. H-shape, parallel anastomosis (15% of the cases) (Figure 35.3a–c)[14]

## The hepatic veins

The efferent venous drainage of the liver is situated topographically superior and apposed to the afferent system. It is trident shaped and consists of three main hepatic veins: right, left, and middle. The hepatic veins course anteriorly to the DV and open to the subdiaphragmatic vestibulum, a funnel-shaped dilatation of the hepatocardiac IVC segment. The vestibulum continues through the diaphragm to the right atrium.[10] Sonographically, all three branches can be depicted in the same plane, using a coronal, oblique, downward projection as shown in Figure 35.2b.

# *Hemodynamics of the fetal venous system*

The main goal of the fetal venous system is to deliver blood rich with oxygen and nutrients from the placenta to the fetal heart. The DV plays a critical role in this important function. The venous system represents one component of the four that comprise the feto-maternal vascular system, the others being the heart, the placenta, and the arterial system. Their functions individually and as part of an integrated system depend on the healthy performance of each component.

In order to facilitate smooth blood flow toward the heart, low placental resistance combined with improved cardiac contraction must work in synergy. A pressure gradient is created between the atria and ventricles, which reduces the

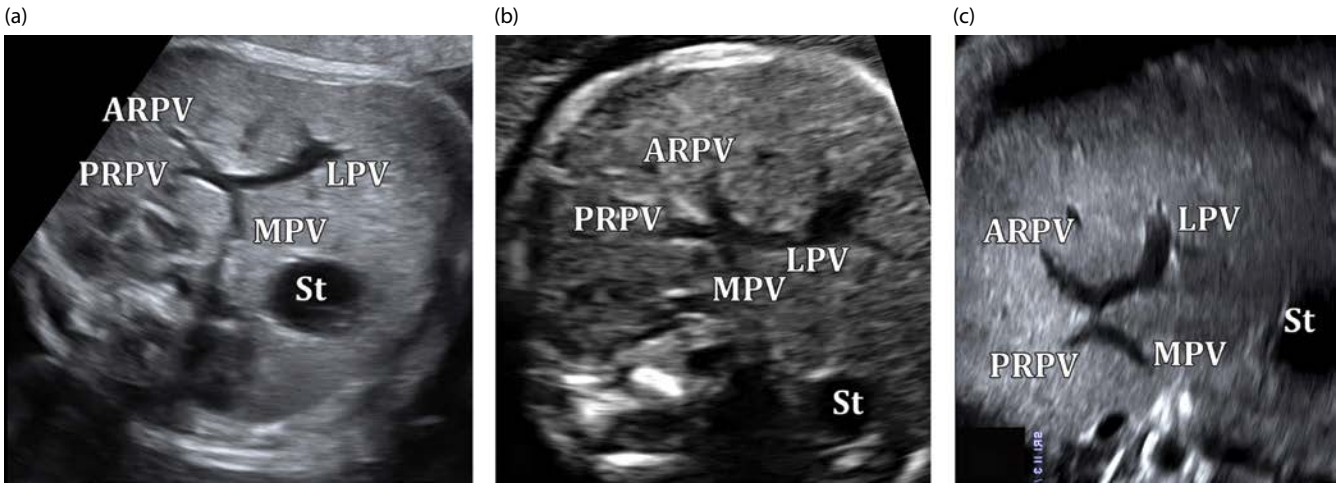


**Figure 35.3**
Normal anatomic variants in the intrahepatic portal veins connection. Three main types of the MPV/PS junction are identified. Type 1, a T-shape, end-to-side anastomosis (a). Type 2, an X shape, side-to-side anastomosis (b). Type 3, an H shape, parallel anastomosis (c). (ARPV, anterior right portal vein; LPV, left portal vein; MPV, main portal vein; PRPV, posterior right portal vein; St, stomach.) (Reprinted with permission from Yagel S et al. *Ultrasound Obstet Gynecol* 2010;35:741–50.[7])

preload in the venous circulatory system and allows blood to flow toward the heart. This pressure gradient is further accentuated by the physiologic stenosis of the DV. At this point, blood velocity increases from 16.3 cm/s in the intrahepatic segment of the UV[9] to 65–75 cm/s in the DV, causing an increase in the umbilico-caval pressure gradient.

The fetal venous system and the other elements of the fetal circulation demonstrate their physiologic interdependence during fetal breathing movements.[15,16] It has been shown[15–18] that change in the pressure gradient between the intra-abdominal and intrathoracic cavities created by fetal breathing movements alters blood flow in the venous system. During inspiration, the pressure gradient between the abdominal cavity (as it contracts inward) and thoracic cavity (as it expands outward) rises from some 0–3 mm Hg to about 22 mm Hg. This raises the pressure gradient between the UV and the thoracic segment of the IVC (umbilico-caval pressure gradient), and in turn, flow velocity in the UV rises. The opposite effect is observed during expiration.[17]

Intrathoracic pressure variations caused by fetal breathing movements have been demonstrated to affect both venous return to the heart and the arterial system.[18] When blood flow to the heart decreases, changes are observed in placental blood flow on the fetal side of the interface. Increased venous preload prevents the placenta from emptying, increasing resistance and causing a drop in arterial diastolic flow. Additionally, ineffective filling of the cardiac ventricles from decreased venous return causes a drop in arterial systolic blood flow. The diastolic phase of the cardiac cycle shows the most marked effects. An increase in venous flow to the heart is accompanied at the next heartbeat by a rise in systolic and diastolic arterial blood flow. The placenta, therefore, is a system capable of transmitting pressure changes occurring within the heart and thorax. The changes in intracavity pressure and flow velocities at inspiration and expiration are summarized in Figure 35.4.

Fetal blood volume has been estimated at approximately 10%–12% of body weight, as compared to 7%–8% in the adult.[19,20] The variation between the fetus and adult comes from the large reservoir of blood in the placenta. The proportional volume of blood in the placenta decreases as gestation progresses. Doppler-based estimates of fetal cardiac output indicate that about one-third of combined cardiac output is sent to the placenta at 20–32 weeks; this proportion declines to about one-fifth after 32 weeks.[21,22]

*In utero* human studies have shown that fetal umbilical venous flow increases per unit of time with advancing pregnancy from 33 to 54 mL/min at 20–23 weeks of gestation, to 221–320 mL/min at 36–38 weeks of gestation. However, when volume blood flow is calculated per unit of weight, umbilical venous flow decreases from 117–125 mL/min/kg at 20–23 weeks to 63–104 mL/min/kg at 36–38 weeks of gestation.[23,24]

Animal[25] and human[26] studies have shown that under normal conditions, 70%–75% of the blood flow in the UV is distributed to the liver, while only 25%–30% flows to the DV. Of the blood volume flowing to the liver, approximately 75% supplies the left lobe and 25% the right. This constitutes 50% of the blood supply to the right liver lobe, while the remainder is supplied by the PV. The fetal liver is thus divided into two physiologically different lobes: the left, supplied by blood rich in oxygen and nutrients, and the right, which receives a mixed supply of blood. The LPV represents a watershed between the umbilical and portal circulations, as coined by Kiserud and colleagues.[27]

The thoracic IVC blood flow is uniquely characterized by a double streaming of flow. It is composed of high-velocity DV flow, running along the left dorsal portion of the IVC, and directed by the crista dividens toward the foramen ovale, and low-velocity IVC flow, which runs on the right-ventral portion of the IVC and is directed toward the tricuspid valve. The final result is a preferential supply of high-quality

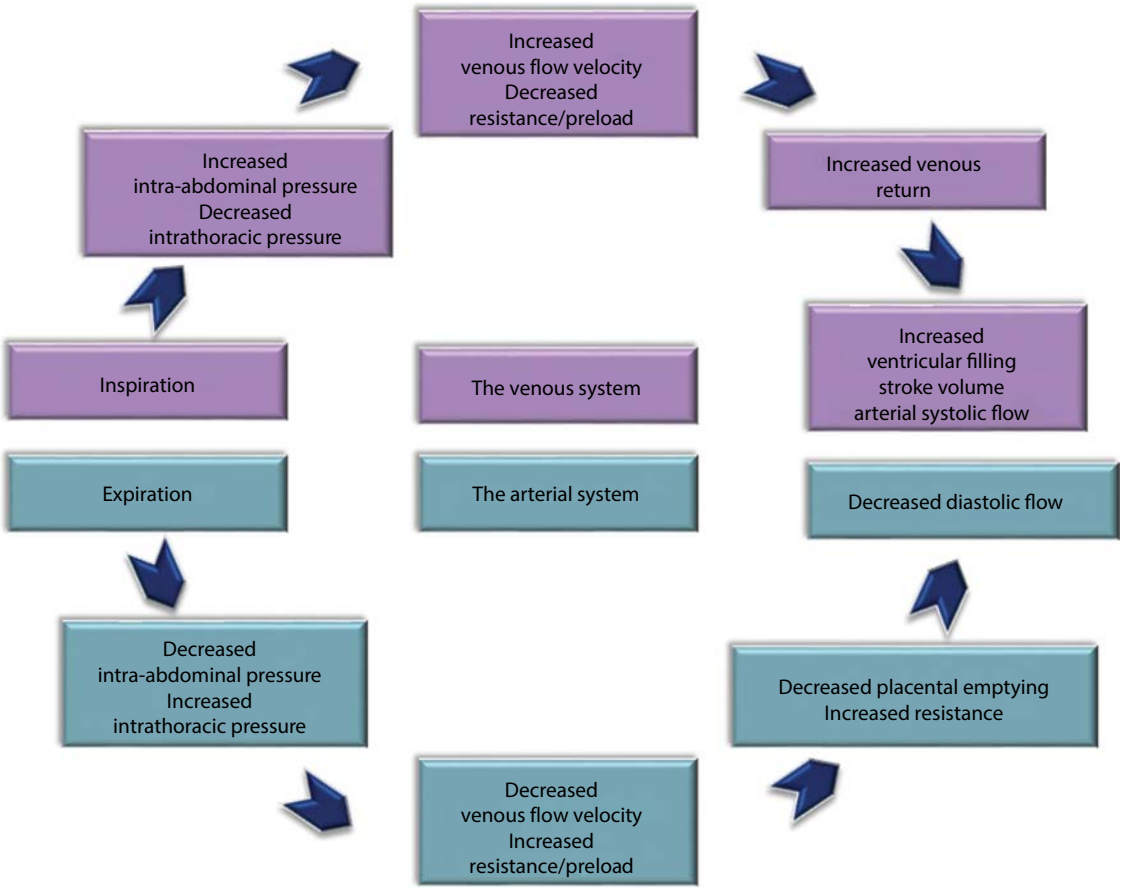


**Figure 35.4**
Venous-placental-arterial interaction during fetal breathing movements.

placental blood to the most essential organs, the heart and the brain.[9,28–30]

## *Doppler waveforms of the normal fetal venous system*

Doppler waveforms of the fetal precordial veins mirror the heart cycle. Their typical three-peak form represents the ventricular systolic phase (s), passive diastolic phase (d), and active diastolic phase (a). As opposed to the IVC and hepatic veins, DV blood flows forward throughout the entire heart cycle, assuring constant high-quality blood supply to the heart. Various methods have been proposed to evaluate venous system preload index,[31–34] similar to the arterial system. A gradual decrease in preload index with progression of pregnancy was consistently shown.[32,35] Doppler investigation of the most commonly investigated vessels is shown in Figure 35.5.

### Umbilical vein

UV Doppler patterns are evaluated in the intra-abdominal portion of the vein (Figure 35.5). Although linear forward flow reflects the normal functioning of a positive umbilicocaval pressure gradient, pulsatile flow may be considered a normal feature until 15 weeks of gestation, before the low resistance placental vascular bed is established by the second trophoblast invasion.[36] As mentioned above, UV pulsations are also associated with fetal breathing movements in the second half of pregnancy. Van Splunder and colleagues showed that, proceeding from the free-loop UV to the intrahepatic, porto-umbilical connection, the retrograde atrial contraction waveform propagation is more pronounced, and the incidence of pulsations increased from 19.6% to 78.4%, respectively.[37]

### Ductus venosus

The DV is sampled at its inlet with a large sample volume in a near-sagittal scan at a low angle of insonation.[9] Alternatively, DV flow can be sampled in an oblique transverse section of the fetal abdomen. Normally, about 30% of blood is shunted through the DV at 20 weeks' gestation, while about 20% of blood is so shunted at 30 weeks.[23,26,38] Changes in DV flow are seen in hypoxia and hypovolemia in experimental animal models and in human fetuses.[39–43] These changes are discussed in detail in Part II.

### Inferior vena cava

The IVC is usually sampled in the fetal abdomen, caudal to the hepatic confluence and DV outlet, to avoid interference from neighboring vessels (Figure 35.5). Reference ranges for normal IVC flow parameters have been established. It is normal to observe a negative a-wave in the IVC because of the

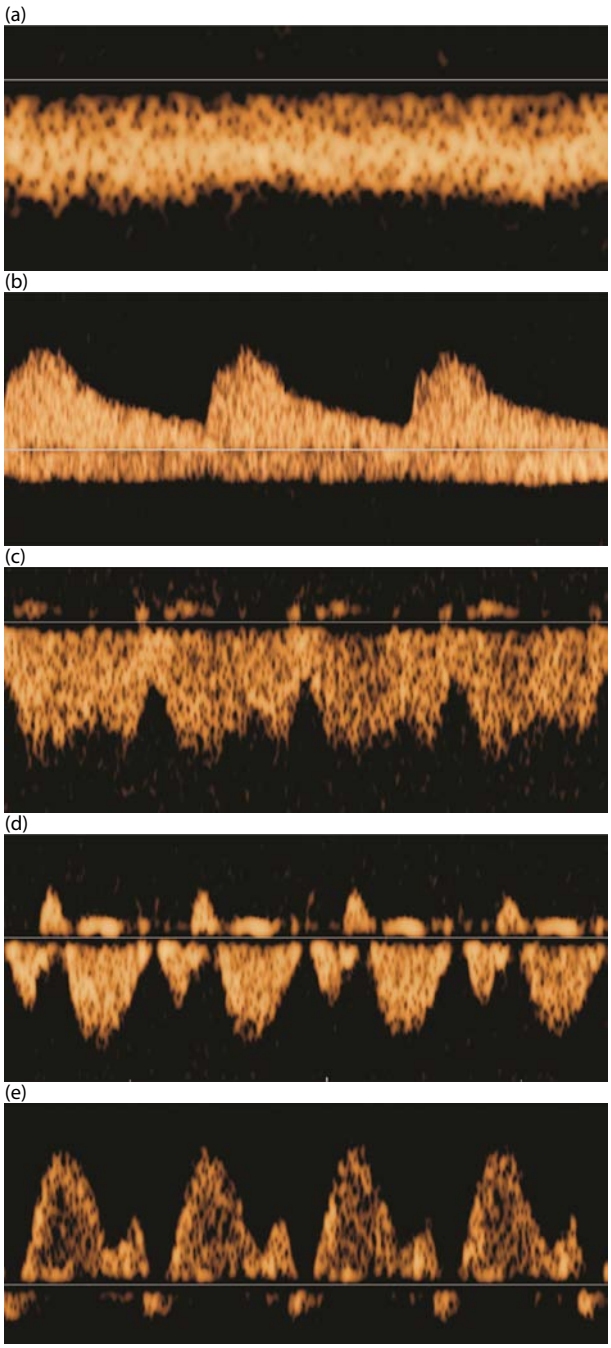


**Figure 35.5**
Characteristic Doppler waveforms of the studied vessels: (a) umbilical vein; (b) splenic artery and vein (note that the arterial and venous waves appear together: as mentioned, the splenic artery and vein are always imaged together); (c) ductus venosus; (d) left hepatic vein; (e) inferior vena cava. (Reprinted with permission from Yagel S et al. *Ultrasound Obstet Gynecol* 2015;45:578–83.[6])

vessel's normally lower velocities.[44–47] The rate of flow reversal is estimated as the percentage of the total forward flow (S + D waves), and decreases as pregnancy advances from 16% at 16 weeks of gestation to 7% at term.[45]

The IVC is the preferred vessel for postnatal evaluation of SGA neonates and is familiar to pediatricians, so it is often sampled in the fetus.[38]

## Hepatic and portal veins

The hepatic veins, while easy to sample, have not been widely studied.[48–53] As compared with the DV and IVC, the hepatic veins show lower increase in peak velocity and decrease in resistance indices with advancing gestational age. This renders them less suitable as targets for monitoring fetal well-being. The waveform is similar to that of the IVC, presenting a characteristic reverse a-wave. The signs of cardiac compromise observed in the hepatic vein are similar to those apparent in the DV and IVC.[38,50] Hepatic venous Doppler has been shown to differentiate between types of extrasystoles.[51]

## The portal system

The MPV exclusively supplies the right liver lobe, delivering 50% of the right lobe venous blood supply. This constitutes only 20% of all the venous supply to the liver, the remainder coming from the UV and the main trunk of the LPV. As mentioned previously, the LPV is the watershed of the fetal venous circulation, as the meeting point between the umbilical and portal systems, bridging to the DV.[27,54] Under normal conditions its flow is directed toward the right liver lobe. The higher velocity of the UV, and higher umbilico-caval pressure gradient[55,56] prevent blood from the MPV from flowing toward the DV.

MPV blood flow is directed toward the right branch, with a monophasic (sometimes pulsatile) waveform. Blood volume and velocity increase gradually from 20 weeks of gestation to term. Velocity almost doubles from 8.4 to 14.9 cm/s. The flow volume increases from 5 to 41 mL/min, and when calculated per unit of weight, from 10 to 13 mL/min/kg. This is in contrast to UV blood flow, indicating a preferential flow to the liver as pregnancy progresses.[57]

The pulsatility of the waveform diminishes as the vessel is sampled distally from the insertion of the MPV toward the right and left branches. The nature of these pulsations is not clear. They may originate from adjacent pulsation of the hepatic artery, or represent the reverse propagation of the atrial contraction (a-wave) to the portal system. The latter origin is supported by the fact that in hemodynamically compromised fetuses, Kiserud et al.[27] showed that accentuation of LPV peak velocity mirrored the DV a-wave.

# *3D/4D Ultrasound in the evaluation of the fetal venous system*

3D/4DUS modalities were recently reviewed.[58] Spatiotemporal image correlation, B-flow, 3D power Doppler, 3D high-definition power flow Doppler, multiplanar reconstruction, 3D rendering, inversion mode, Virtual Organ Computer-aided AnaLysis (VOCAL) and tomographic ultrasound imaging have been applied to evaluation of the normal and anomalous fetal venous system[59–68] and have been extensively described over the last decade. They have been shown to have utility in improving anatomic evaluation of this system, and most recently have been applied to functional evaluation. Specific applications are shown in the illustrating figures; for a full description of these various modalities and their applications, please see Chapters 9, 13, 14, and 34.

## Comment

Understanding the normal embryology of the venous system is essential to appreciating the complex malformations in this system. Ultrasound has been shown to be an effective tool for imaging the normal developing venous system and may have more to offer than traditional embryology. Over the years, many ultrasound images of the venous system have appeared in the literature. The embryological and anatomic knowledge accumulated from these images potentially surpasses that of traditional embryological illustrations, as it is based on hundreds of ultrasound images from dozens of imaging planes in many subjects. Ultrasound has also shown us rare variants of anatomy and shown others to be not as rare as previously believed. 2DUS, 3D/4DUS, and color and power Doppler, are all effective tools in the ultrasound evaluation of the venous system, adding to our understanding of complex anatomy and assisting in providing cogent advice to patients.

# Part II: Congenital anomalies of the fetal venous system: Etiology and sonographic appearance

Abnormal development of the fetal venous system can stem from any of its four embryonic systems: umbilical, vitelline, cardinal, and pulmonary. We speculate that the normal developmental course of the fetal venous system may be disturbed in two ways: (1) primary failure of a system or part of a system to form or to create critical anastomosis, and (2) secondary occlusion of an already transformed system. We proposed[69,70] a classification that expands on the four major embryologic groups mentioned previously.

**Classification System of Fetal Venous System Anomalies**

1. Cardinal veins
   a. Complex malformations: heterotaxy syndromes
   b. Isolated malformations: persistent left SVC or double SVC, interrupted IVC, persistent left IVC, double IVC, etc.
2. Umbilical veins
   a. Primary failure to create the critical anastomosis: abnormal connection of the UV with agenesis of DV (with intra- or extrahepatic systemic shunt of the UV)
   b. Persistent right UV with or without left UV and/or DV
3. Vitelline veins
   a. Primary failure to create critical anastomosis
      i. Complete agenesis of the portal system (portosystemic shunt)
      ii. Partial agenesis of the right, left, or both portal branches (porto-hepato-systemic shunt)
4. Anomalous pulmonary venous connection (described in detail in Chapter 19)
   a. Total anomalous pulmonary venous connection
   b. Partial anomalous pulmonary venous connection

Achiron et al. have suggested other possible classification systems.[71]

## Cardinal vein

### Heterotaxy syndromes

Heterotaxy syndromes, or incomplete errors of lateralization, are an abnormal placement of organs owing to failure to establish normal left-right patterning. It is important to differentiate these anomalies from complete situs inversus in which all organs (visceral and thoracic) are rotated to the opposite side, and which is usually asymptomatic. Therefore, the first step in evaluating venous system malformations is to determine the fetal visceral and thoracic situs.

The incidence of heterotaxy syndromes in newborns is approximately 1:1,000,[72,73] constituting 2%–4% of all congenital heart diseases.[74] These syndromes may present in two main forms: asplenia and polysplenia. In asplenia, the fetus will have predominant right-sidedness and right atrial isomerism, resulting in a fetus whose left side is a mirror image of its right side. Congenital heart malformations are frequent (50%–100%) and severe and represent the most important prognostic factors. The most frequent venous system malformations associated with asplenia include persistent left SVC, anomalous pulmonary venous return, and left-side IVC, resulting in a characteristic juxtaposition of the abdominal aorta and IVC.

Polysplenia is characterized by predominant left-sidedness and left atrial isomerism, resulting in a fetus whose right side is a mirror image of its left side, with polysplenia. Cardiac malformations are rare and less severe than in asplenia; the most common being an A-V septal defect with complete heart block. The characteristic venous malformation is an interrupted IVC with azygos continuation to the SVC. This anomaly arises from a failure to form the right subcardinal-hepatic anastomosis, resulting in absence of the hepatic segment of the IVC. The sonographic landmark is a dilated azygos vein alongside the aorta on the abdominal circumference plane and four-chamber view plane, and atrioventricular block bradycardia. In the sagittal abdominal plane, the descending aorta and azygos vein run side by side with opposite flow directions (Figure 35.6a–e; Videos 35.1 through 35.3).

Interrupted IVC has also been reported as an isolated entity.[75–79] In such cases, it is usually clinically silent.

### Persistent left SVC

Persistent left SVC (PLSVC) is a known variant of venous return observed in 0.3% of adults without cardiac malformation[80] and in approximately 4% of patients with congenital heart disease. Galindo et al.[81] found a respective incidence of 0.2%, and 9% of fetuses sent for echocardiographic examination, in a tertiary center, calculating an odds ratio for congenital heart disease of 49.9 for a fetus with PLSVC.

PLSVC results when the left anterior CV fails to atrophy following formation of the oblique anastomosis with the right CV (the innominate vein). The PLSVC is a remnant of the proximal left anterior CV (Figure 35.7a–d; Video 35.4). The vessel most often drains into the coronary sinus.[82,83] It is

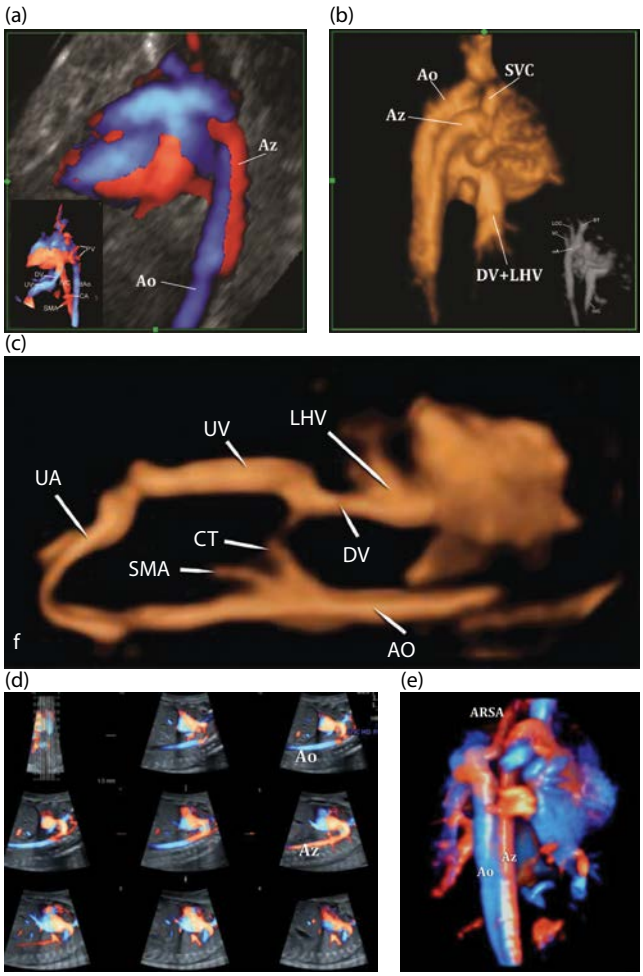


**Figure 35.6**
Interrupted IVC anomaly with azygos continuation imaged in (a) high-definition power flow Doppler (HDPD) and (b) in B-flow. Note the dilated azygos vein draining into the SVC, with flow in the opposite direction to the flow in the aorta. Compare with insets showing HDPD and B-flow images of the normal heart and great vessels. (c) Another case, imaged in 4DUS with B-flow imaging in the longitudinal plane, showing the umbilical vein draining into the ductus venosus, which flows into the left hepatic vein. The inferior vena cava was interrupted, with azygos continuation, and could not be visualized in the plane as normal (See also Video 35.1.) (d) Tomographic ultrasound imaging (TUI) of a case of interrupted IVC. The aorta is seen in blue in frame 3 (top) and the azygos in red in frame 6 (second row). (See Video 35.2.) (e) Newer high-definition power Doppler shows the same case with an associated aberrant right subclavian artery (ARSA) apparent in this frame. (See Video 35.3.) The child is alive and well. (Ao, aorta; Az, azygos vein; DV, ductus venosus; LHV, left hepatic vein; SVC, superior vena cava.) ([b] Insets reprinted with permission from Yagel S et al. *Ultrasound Obstet Gynecol* 2007;29:81–95.[58] [c] Reprinted with permission from Yagel S et al. *Ultrasound Obstet Gynecol* 2015;45:578–83.[6])

diagnosed by fetal echocardiography on observation of a dilated coronary sinus (though this may not always be present) and an extraneous vessel identified to the left of the ductal arch in the three-vessel and trachea (3VT) view of the fetal heart. In rare instances, PLSVC may be seen with absent right SVC.[84] In this case, the 3VT view will show three vessels: the LSVC, ductal arch, and aortic arch.[85] Multiplanar reconstruction mode in 4DUS has been shown to be useful in diagnosis of the PLSVC anomaly.[86]

When isolated, the anomaly usually has no clinical significance; however, this was reported to occur in only 9% of cases. PLSVC is more often seen in association with other anomalies: cardiac (23%)—atrioventricular septal defect, double-outlet right ventricle, left outflow tract obstructive anomalies, conotruncal anomalies, VSD, or other extracardiac malformations, including heterotaxy syndrome (41%–45%), esophageal atresia, diaphragmatic hernia, IVC malformations, complex malformation syndromes, and chromosomal anomalies. Significant morbidity and mortality may be seen with PLSVC; these arise from the associated anomalies rather than the lesion itself.[81,87]

Other rare anomalies of the vena cava have been reported in the pediatric literature and were extensively reviewed.[88]

## *Umbilical veins*

Anomalies of the UVs and PVs are the largest group of congenital venous anomalies detected *in utero*. They comprise three main entities:

1. Agenesis of DV with extrahepatic umbilico-systemic shunt or with intrahepatic umbilico-hepatic shunt
2. Persistent right UV with or without intact DV
3. UV varix

### Agenesis of the ductus venosus

Agenesis of the ductus venosus (ADV) results from failure to form the "critical anastomosis": no connection is established between the UV and DV, and this in turn leads to the shunting of umbilical blood through an aberrant vessel that may flow into one of the extrahepatic veins such as the iliac vein, IVC, SVC, right atrium,[89–98] or coronary sinus[99]; or via an intrahepatic venous network (umbilico-hepatic shunt), or through the PS to hepatic sinusoid (umbilico-portal-hepatic shunt), or even directly into the right atrium (Figure 35.8a–j; Videos 35.5 through 35.12). The prevalence of the anomaly has been estimated at 1:2,500 fetal examinations.[100] The anomaly is often associated with cardiac, extracardiac, and chromosomal anomalies, and syndromes such as Noonan syndrome, in 24%–65% of cases. It may be associated with agenesis of the PV in as many as 50% of cases, or with partial or total agenesis of the portal system in others. Hydrops and generalized edema are encountered in 33%–52% of cases,[101,102] which may require postnatal device occlusion.[98] In only 35%–59%, DV agenesis presented as an isolated finding. In such cases, however, the majority had a normal outcome.[101–104] While only sporadic cases were reported in neonates before the advent of ultrasound, prenatal diagnosis of DV agenesis is feasible, and many case series have appeared in the literature.[69,98,104,105]

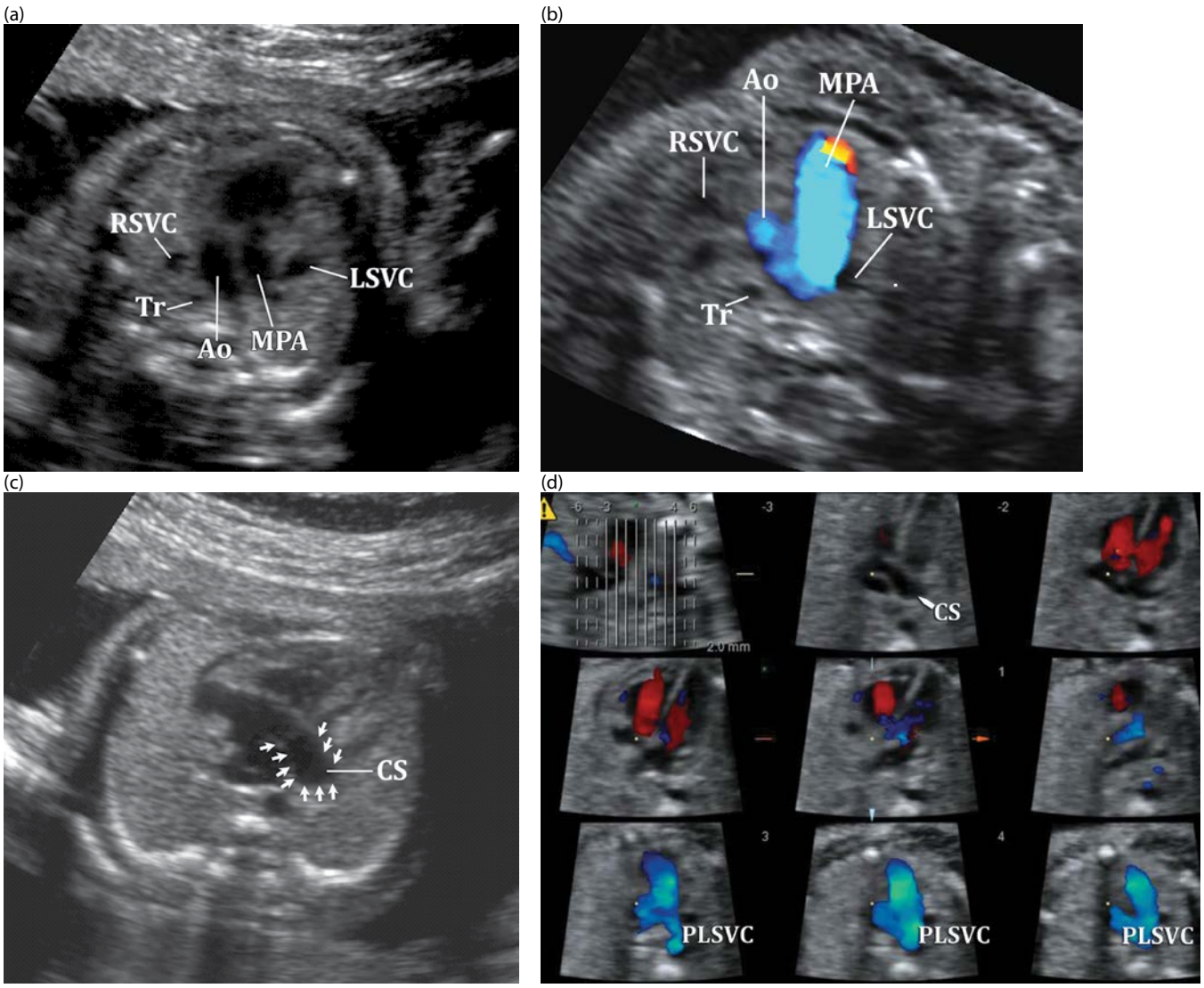


**Figure 35.7**
Persistent left SVC anomaly imaged in (a) grayscale and (b) with color Doppler. (Ao, aorta; LSVC, left superior vena cava; MPA, main pulmonary artery; RSVC, right superior vena cava; Tr, trachea.) (c) Dilated coronary sinus (CS, highlighted with arrows), where the persistent LSVC drains into it. (d) PLSVC in a case with absent right SVC; CS indicates the dilated coronary sinus. (See Video 35.4.) (Reprinted with permission from Yagel S et al. *Ultrasound Obstet Gynecol* 2010;36:93–111.[70])

Among fetuses with no or minor associated anomalies, location of the umbilical drainage site seems to impact on prognosis, with a better outcome expected in cases without liver bypass.[91,102,106] Jaeggi et al.,[91] when reviewing the literature, reported a mortality rate of 17% from congestive heart failure. Associated malformations were reported in 87% of the cases with extrahepatic shunt; single umbilical artery was the most common. In the intrahepatic type, the rate of associated malformation was much lower. Gorincour et al.[107] reported an incidence of 45% of severe hemodynamic disturbance leading to perinatal death or termination of pregnancy, and 18% mild changes, manifested by cardiomegaly with or without hepatomegaly. IUGR was found in 60% of the cases, and increased abdominal circumference in 40%, reflecting liver congestion. Reviewing 42 cases reported in the literature, the authors noted that hemodynamic distress and fetal or neonatal demise after 25 weeks' gestation were frequent in cases with shunt to the IVC (63%) or to the iliac veins (92%). No cases of hemodynamic disturbance or fetal demise were encountered in cases where intrahepatic shunts or shunts to the right atrium were observed.[107]

From our observations, we suggest that the parameter that most influences outcome in cases of agenesis of the DV is the development of the portal system. We recently presented data that support the notion that if the shunt is a narrower, ductus-like connection, some or all of the portal system will have

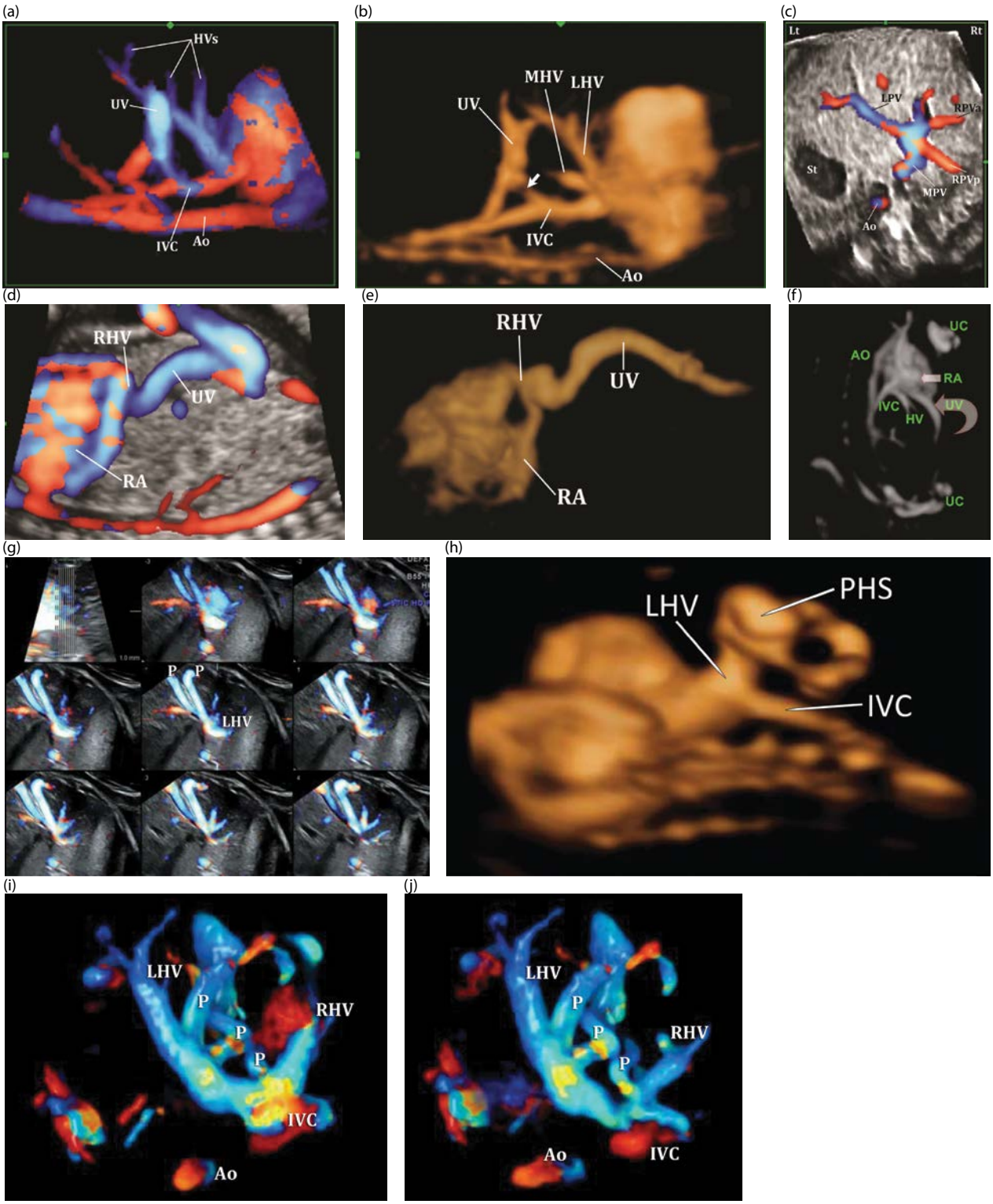


**Figure 35.8**

Variations of the agenesis of ductus venosus anomaly. (a–c) Case of agenesis of the DV with narrow extrahepatic shunt from the umbilical vein (UV) to the inferior vena cava (IVC), imaged with high-definition power flow Doppler (HDPD) (a,c) and B-flow (b). (See Videos 35.5 and 35.6.) In (c), the appropriately developed portal system is shown. (Az, azygos vein; LHV, left hepatic vein; LPV, left portal vein; MHV, main hepatic vein; RPVa and p, anterior and posterior branches of right portal vein; St, stomach.) (d,e) Another case of agenesis of the DV with intrahepatic shunt of the UV to the right hepatic vein (RHV), imaged in HDPD and B-flow. (See Video 35.7.) (f) 4D ultrasound B-flow image of absent DV, with UV drainage to the right atrium (RA). (Ao, aorta; HV, hepatic veins; UC, umbilical cord.) (See Video 35.8.) (g) Tomographic ultrasound imaging showing the portal veins (PV) and left hepatic vein (LHV). (See Video 35.9.) (h) 4D-US B-flow image in the longitudinal plane, showing left portohepatic shunt (See also Video 35.10). (i,j) The portal veins shunt to the IVC; imaged with high-definition power Doppler. (See Videos 35.11 and 35.12.)

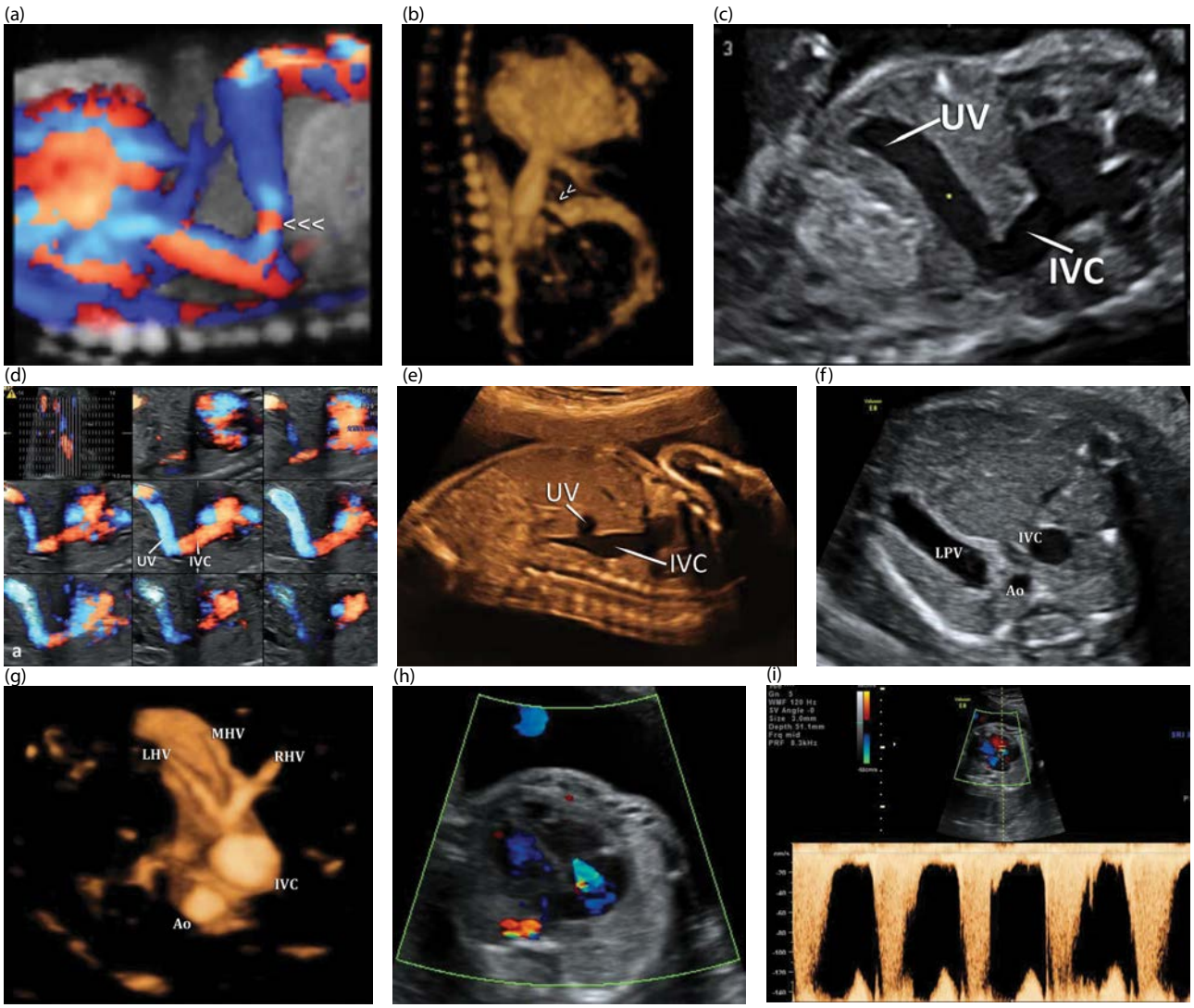


**Figure 35.9**
Hemodynamic effects of agenesis of ductus venosus with a wide versus narrow shunt: (a) and (b) show cases of a narrow shunt in power Doppler and b-flow. Carets indicate the shunts. (See Videos 35.13 and 35.14.) (c–i): The impact of the wide shunt: (c) the umbilical vein (UV) draining into the IVC, agenesis of the ductus venosus with wide shunt to the inferior vena cava (IVC) in grayscale tomographic ultrasound imaging (TUI), and (d) 4DUS with high definition power flow Doppler TUI of the longitudinal plane. (See Video 35.15.) (e) Sepia image of the umbilical vein and enlarged IVC. (See Video 35.16.) (f) a grayscale image shows the enlarged IVC and left portal vein (LPV). The right portal vein was absent. (See Video 35.17.) (g) 4DUS B-flow image shows the enlarged IVC and the hepatic veins. (See Video 35.18.) (h,i) Increased preload led to tricuspid regurgitation. (See Videos 35.19 and 35.20.) ([d] Reprinted with permission from Yagel S et al. *Ultrasound Obstet Gynecol* 2015;45:578–83.[6])

developed (Figure 35.9a,b; Videos 35.13 through 35.20). This, in turn, impacts on prognosis.[97] A wide shunt will tend to have greater impact on cardiovascular hemodynamics. Figure 35.9c–i shows a case of ADV with wide shunt. The shunt led to dilatation of the IVC and increased preload, demonstrated by marked tricuspid regurgitation.

## Persistent right umbilical vein

In the course of normal embryological development, the right UV degenerates, and the left UV is left to carry blood from the placenta to the fetus. Failure of right UV involution results in the persistent right umbilical vein (PRUV) anomaly[90,108–110] (Figure 35.10; Video 35.21). PRUV is the most frequently detected fetal venous system anomaly. Its prevalence has been estimated to range from 1:250 to 1:1,000 in various studies.[72,108,110–112] The PRUV might replace the left UV or might be found as an intrahepatic supernumerary vein, connecting to the RPV. The right UV might also bypass the liver, causing an aberrant drainage of blood into the IVC or right atrium.[111,113,114] It has been suggested that primary or secondary occlusion by thromboembolic events arising from the placenta may lead to early streaming of blood through the right UV to cause this anomaly.[115] Teratogenic agents such as retinoic acid or deficient folate induced the PRUV anomaly in rats.[116] Secondary formation of UV anomalies may result

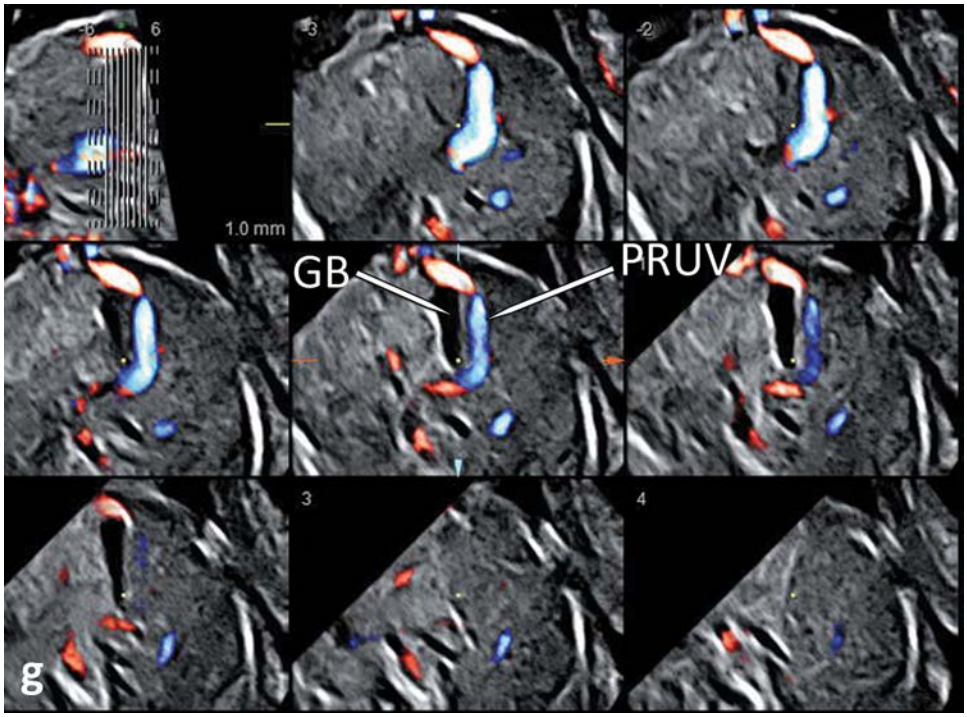


**Figure 35.10**

Typical appearance of the persistent right umbilical vein anomaly: TUI with high-definition power flow Doppler in caudal transverse plane, in a typical case of persistent right umbilical vein. The umbilical vein is seen passing laterally right of the gall bladder. (GB, gall bladder; PRUV, persistent right umbilical vein.) (See Video 35.21.) (From Yagel S et al. *Ultrasound Obstet Gynecol* 2015;45:578–83, with permission.[6])

from thromboembolytic events occluding the DV or other veins. Echogenic foci situated within the fetal liver suggest this etiology.

Of the 240 cases reviewed by Lide et al., 76% were isolated, while the remainder had other abnormalities, including 19 (7.9%) cardiac, 9 (3.8%) central nervous system, 15 (6.3%) genitourinary, 3 (1.3%) genetic, and 17 (7%) placental/cord.[117] Two of the 74 cases reviewed by De Catte et al. had Noonan syndrome, and one had trisomy 18, all with multiple associated anomalies.[118] While early reports seemed to indicate that PRUV was a worrisome finding in prenatal ultrasound,[113,115] accumulated experience has shown that isolated, intrahepatic PRUV with normal DV connection is usually a normal anatomic variant with no clinical significance.[72,108,110,111,117,119,120] However, it should prompt meticulous examination of other organ systems.[71,117,120] If associated anomalies are identified, genetic investigation is appropriate.[71,117] Ultrasound identification of PRUV is made by visualizing the aberrant vein passing laterally to the right of the gall bladder at the plane of measurement of the abdominal circumference (Figure 35.10).

## Fetal intra-abdominal umbilical vein varix

UV varix is a focal dilatation of vein diameter. It is an uncommon finding with estimated intrauterine incidence of about 1:1,000.[121] Most reported UV varices were of the intra-abdominal UV, but extra-abdominal UV varices have been reported.[122] Fetal intra-abdominal UV (FIUV) varix is diagnosed when a sonographically anechoic cystic mass is seen between the abdominal wall and lower liver edge. Color Doppler ultrasonography helps to distinguish this vascular anomaly from other cystic lesions in this area (Figure 35.11a,b).

The diameter of most varices ranges from 8[117] to 14 mm.[123] FIUV varix has been variously defined as an intra-abdominal UV diameter at least 1.5 times the diameter of the intrahepatic UV,[124] or as an intraabdominal UV diameter exceeding 9 mm.[125]

In a review of 91 cases, Fung et al.[126] reported that 68% of cases presented as an isolated finding, and of these, 74% had a normal outcome. However, 8.1% (5/62) resulted in intrauterine death in which no specific cause could be identified, and one case (1.6%) had trisomy 21. In the group with associated sonographic findings, only 27.6% had normal outcomes. Congenital abnormalities and syndromes were confirmed after birth in 20.7% (6/29); 27.6% had chromosomal abnormalities. The overall incidence of aneuploidy was 9.9%, the majority were trisomies 21 and 18. The incidence of sudden intrauterine demise was 5.5%, occurring between 29 and 38 weeks of gestation.

The diameter of the UV at first diagnosis and the maximum diameter of the UV over the course of pregnancy were not found to be related to the occurrence of obstetric complications. Diagnosis of FIUV varix warrants a detailed anatomic search for additional anomalies, karyotyping, echocardiography, and close monitoring of the fetus for sonographic signs of hemodynamic disturbance. Fetal heart monitoring

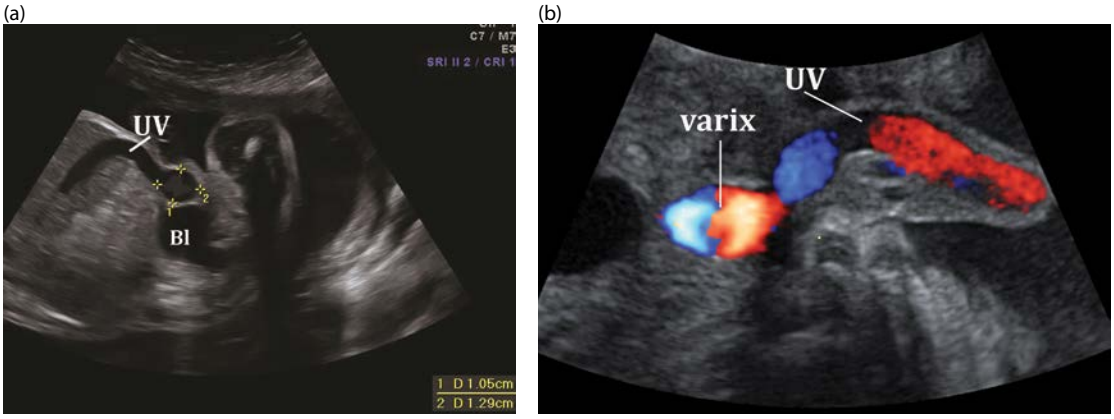


**Figure 35.11**
Fetal intra-abdominal umbilical vein varix: An anechoic cystic mass is seen between the abdominal wall and lower liver edge in a longitudinal section (a) and imaged with HDPD (b). The varix is shown to be 1.5 times the diameter of the UV.

is advised from 28 weeks of gestation. The optimal timing for delivery remains the subject of debate.[104] In light of the apparent high risk of unfavorable outcome, including sudden intrauterine demise even in isolated FIUV varix, the option of induction of labor when lung maturity is ascertained may be considered.[127]

## *Vitelline veins*

### Complete or incomplete agenesis of the portal system

Anomalies of the VVs are extremely rare, and few cases have been reported during fetal life.[128–133] Morgan and Superina[134] proposed classifying portal agenesis into two types: type I, in which there is a complete diversion of the portal blood into the vena cava (portosystemic shunt); and type II, in which the PVs are preserved but a portion of portal blood is diverted into the systemic venous circulation through the liver (portohepatic shunt). Both types were further classified into two subtypes: subtype a, in which the splenic vein (SpV) and superior mesenteric vein (SMV) do not join to form a confluence, and thus there is no anatomical PV; and subtype b, in which the SpV and SMV do join to a confluence that may shunt to the IVC, renal vein, iliac vein, azygos vein, or right atrium.[134]

Complete absence of the portal venous system (CAPVS) is an extreme example of total failure of the VVs to transform into the portal system; that is, there is primary failure to form the critical anastomosis with the hepatic sinusoids or UVs (Figure 35.12). As a result, the enterohepatic circulation is disturbed, and the portal venous blood is shunted systemically. Liver development is supplied by the hepatic arteries. Mesenteric and splenic venous blood may drain directly into the IVC, the renal veins, hepatic veins, or via caput medusa to the heart.[135] Associated anomalies are frequent. Northrup et al.[136] reported an incidence of heterotaxy-polysplenia in

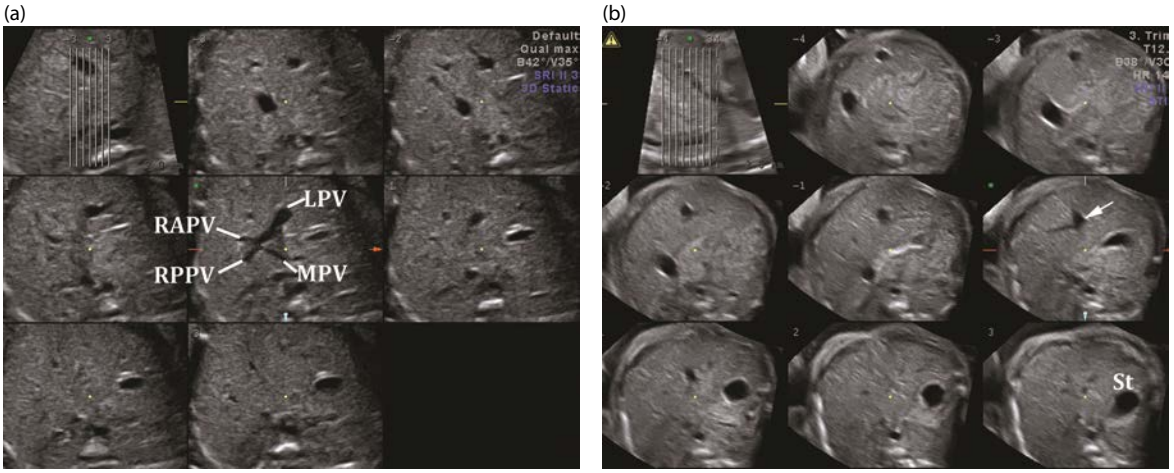


**Figure 35.12**
Complete agenesis of the portal venous system (CAPVS). (a) Tomographic ultrasound imaging (TUI) of the normal portal system. (LPV, left portal vein; MPV, main portal vein; RAPV, right anterior portal vein; RPPV, right posterior portal vein.) (b) TUI in a case of complete agenesis of the portal venous system. The arrow indicates the only remnant of the portal system. (St, stomach.) (Reprinted with permission from Yagel S et al. *Ultrasound Obstet Gynecol* 2010;36:93–111.[70])

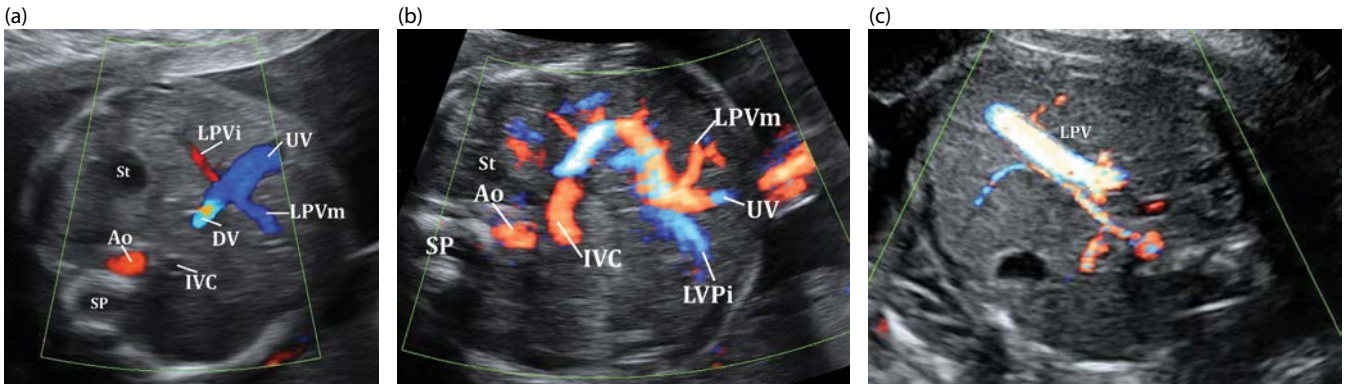


**Figure 35.13**
Incomplete absence of the portal venous system (IAPVS). (a) Incomplete absence of the portal venous system (IAPVS): Absent right portal vein and portal sinus. An X-shape configuration formed by the UV, LPV branches, and the DV, at the standard transverse plane for abdominal circumference measurement. (b) Another form of the intrahepatic portal vein abnormal circulation in IAPVS: dilated aberrant "horseshoe-shaped" arrangement of vessels encircling the right hepatic lobe. (Ao, aorta; IVC, inferior vena cava, LPV, left portal vein; LPVi, left portal vein inferior branch; LPVm, left portal vein medial branch; UV, umbilical vein; St, stomach; SP, spine.) (c) Another case of incomplete absence of the portal venous system imaged with color Doppler mapping, showing the preserved left portal vein. (See Video 35.22.)

25% of their cases, congenital heart disease in 30%, most frequently atrial septal defect and/or ventricular septal defect, and Goldenhar syndrome in 10%. Achiron et al. reported associated malformations, including trisomy 21, in four of their five cases.[132]

Incomplete absence of the portal venous system (IAPVS) or partial failure to form critical anastomosis may represent a more benign form of VV abnormalities and may result in agenesis of the right portal system, with a persistent left VV connected directly to the HV (portohepatic shunt) and an absent or preserved DV (Figure 35.13a–b; Video 35.22).

Neonatal spontaneous resolution may occur. Prenatal diagnosis of partial absence of the PV, with agenesis of RPVs and LPVs, associated with a porto-hepatic-systemic shunt, was reported by Gonçalves et al.[128] Achiron et al. reported four cases, none with associated malformations; in three, the shunts resolved spontaneously postnatally.[132]

Prognosis of IAPVS depends on the presence of associated malformations and the development of hemodynamic imbalance with signs of heart failure, cardiomegaly, and hydrops. As opposed to CAPVS, IAPVS is rarely associated with malformations, and hemodynamic compromise depends on the intrahepatic shunt ratio, leading to IUGR.[137]

Hepatic bypass of the portal circulation is known to cause the hepatic artery buffer effect,[138] which compensates for the decreased portal supply by increasing blood flow in the hepatic artery. This results in a prominent Doppler signal,[132] increased blood flow velocity, and decreased pulsatility index in the hepatic artery.[138]

Portosystemic shunting is known to have long-term metabolic sequelae, as reported in the postnatal literature, and include hypergalactosemia[139]; hyperbilirubinemia; hyperammonemia[140]; liver masses including focal nodular hyperplasia, adenoma, hepatoblastoma, and hepatocellular carcinoma; and rarely, encephalopathy.[141,142]

## Abernethy malformation

Abernethy malformation is a postnatal diagnosis of congenital extrahepatic portosystemic shunt, made when the portomesenteric blood drains into a systemic vein, bypassing the liver through a complete or partial shunt.[143,144] These rare malformations are among the variations of congenital portosystemic venous shunts, which may be intrahepatic or extrahepatic; the intrahepatic types are characterized by venous connections between branches of the PV, after its division, with the hepatic veins and other systemic veins. Other classification systems have been devised,[144] based on the type and nature of these communications within the liver.

Abernethy malformation, or congenital extrahepatic portosystemic shunt, is characterized by absent intrahepatic portal branches and complete diversion of the portal venous flow shunted to the systemic circulation.[143] Abernethy malformation is usually divided to types 1a and 1b, and type 2.[143] In type 1a, the splenic vein and superior mesenteric vein drain separately into a systemic vein, while in type 1b the SV and SMV form a common vessel to drain into the systemic vein. In Abernethy type 2, the intrahepatic PV is intact, but part of the portal flow is diverted to the IVC through a side-to-side shunt. Figure 35.14 shows a schematic of Abernethy malformation subtypes and a case of prenatally diagnosed congenital extrahepatic portosystemic shunt. In this case, the fetal PV was visualized draining into the IVC. During prenatal life, the intrahepatic drainage was apparently dependent on the UV. In the newborn, this system collapsed after closure of the UV. Venous blood from the digestive system flowed into the MPV, which drained into the IVC. The neonate underwent surgical correction at age 3 months and is alive and well. See also Video 35.23.

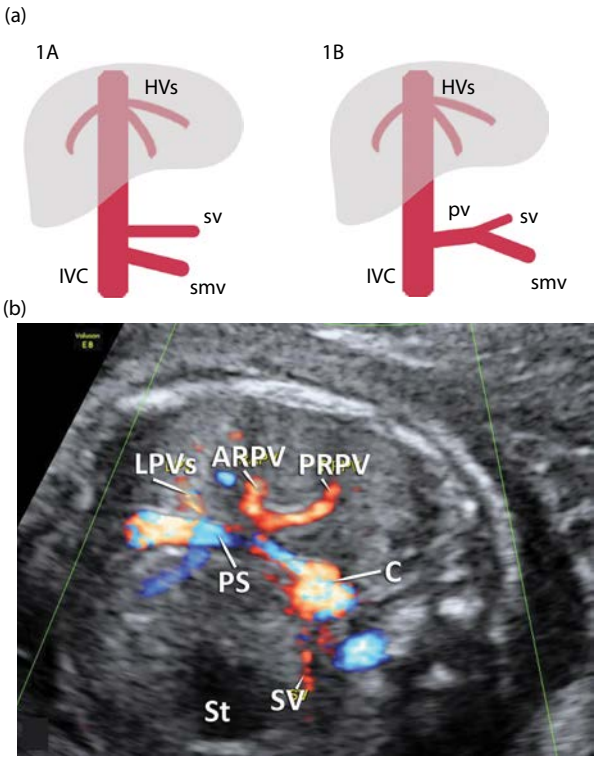


**Figure 35.14**
Abernethy malformation. (a) Abernethy types 1A and 1B. (b) Lateral caudal transverse plane on 2DUS, showing side-to-side portocaval shunt, with confluence of the main portal vein with the inferior vena cava. (See also Video 35.23.) Abernethy was confirmed postnatally; the shunt was corrected at age 3 months. The child is alive and well, aged 5 years. ([a] Modified from Alonso-Gamarra E et al. *Radiographics* 2011;31:707–22.[143])

## Vitelline vein aneurysm

There are scattered case reports of prenatal diagnosis of PS or VV aneurysms.[133,145,146] Figure 35.15 shows a case of an aneurysmal VV. Normal right and left PVs were preserved. Careful examination of the portal system is critical to differentiate this rare anomaly from FIUV varix. Prenatal diagnosis can alert caregivers to the necessity of postpartum surveillance and timely surgical intervention. See Videos 35.24–35.27.

# *The fetal venous system in pathological conditions*

In the physiology section of Part I of this chapter, we emphasized the unique role of the venous system in maintaining a positive umbilico-caval pressure gradient. This assures a low preload index, which is essential for optimal cardiac drainage. Cardiac output progressively increases, and resistance of the placental vascular bed decreases, while the umbilicocaval pressure gradient is maintained steady during the third trimester of pregnancy.[147] Any situation hampering this hemodynamic balance initiates compensatory mechanisms in the arterial and venous systems. These compensatory mechanisms are gradual and sequential, in correlation with the severity of the hypoxic insult, hence creating an efficient monitoring tool of evolving fetal distress.

The most frequent pathologic condition affecting the feto-placental hemodynamic balance is placental dysfunction. Other etiologies are cardiac (malformations, arrhythmias, or increased preload blood volume), and conditions resulting in elevation of ventricular end-diastolic pressure, atrial pressure, and consequently, precordial venous pressure. We focus here on uteroplacental insufficiency and the gradual hemodynamic changes that accompany its compromised vascular function.

Reduced placental supply to the fetus initiates multiple compensatory-vasodilatory mechanisms involving various arterial and venous systems. In the arterial system, the organ most widely studied and clinically evaluated is the brain (brain-sparing effect).[148,149] Evaluation of various parts of the arterial circulation in the fetus with circulatory compromise has been widely studied and reviewed[150–153] and is not discussed here.

Hemodynamic changes in the placenta, heart, and brain characterize the cascade of evolving circulatory compromise. The fetal circulation may be viewed in two compartments, with the division at the aortic isthmus: the right ventricle/placenta, of high resistance, and the second, the left ventricle/brain, of low resistance, the reverse of the norm. The ratios between the resistance indices of the two compartments have been used clinically as monitoring tools of fetal compensatory mechanisms and the magnitude of hypoxic insult.[154–156] The implications of these changes for the venous system are fourfold: reduced blood supply from the placenta to the liver, an increased portion (also per unit of weight) of cardiac output diverted to the fetal body and consequently to the IVC, increased blood flow through the SVC resulting from the brain-sparing effect, all faced with an increased afterload on the right ventricle. These hemodynamic changes lead to increased preload indices that hamper the supply of high-quality blood flow from the placenta.

Venous compensatory mechanisms aim to improve placental supply to the heart by increasing the proportion of DV shunting from the PS. Human Doppler studies have reported variable results. Belloti et al. found that the percentage of UV blood flow shunted through the DV increased from 26.5% in normally grown fetuses to 90.3% in growth-retarded fetuses, with a consequent increased normalized blood flow volume from 30.8 mL/min/kg to 41.3 mL/min/kg.[26] Others showed more moderate changes. Tchirikov et al. reported an increase from 43% to 62%,[157] and Kiserud et al. from 25% to a mean of 39% in normally grown and IUGR fetuses, respectively.[158] The authors found that the degree of shunting in IUGR fetuses is positively correlated with the severity of placental insufficiency as reflected by the umbilical artery diastolic flow. Significant increase in shunting to the DV was found only in IUGR fetuses with

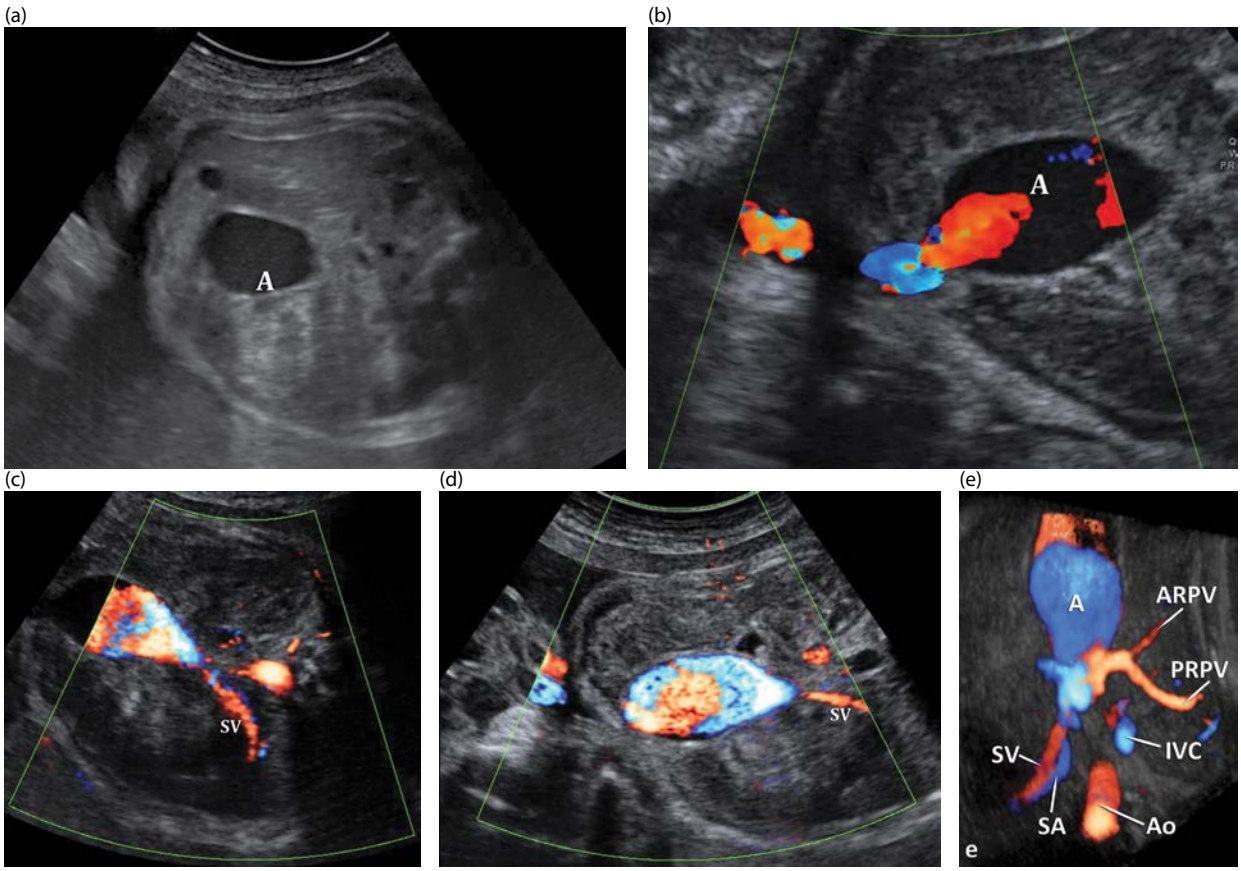


**Figure 35.15**
Vitelline vein aneurysm: (a) Grayscale image and (b–d) color Doppler mapping of the aneurysmal vitelline vein. (e) Modified caudal transverse plane with high-definition three-dimensional power flow Doppler, showing the aneurysmal vitelline vein. (See Videos 35.24–35.27.) Chromosomal microarray (CMA) was normal, the aneurysm gradually resolved postnatally, and the child is alive and well. (A, aneurysm; ARPV, anterior right portal vein; IVC: inferior vena cava; PRPV: posterior right portal vein; SV: splenic vein; SA: splenic artery; Ao: aorta.) (Reprinted with permission from Yagel S et al. *Ultrasound Obstet Gynecol* 2015;45:578–83.[6])

umbilical artery (UA) pulsatility index (PI) above the 97.5 percentile, and in those with absent/reversed diastolic flow, 35% and 57%, respectively.[158]

Preferential flow through the DV results from reciprocal hemodynamic changes inside the liver. The presence of a sphincter in the isthmic portion of the DV was never confirmed.[12] Tchirikov et al. showed *in vitro* that there was a differential adrenergic response in rings of portal venous branches and those from the DV, the PVs showing a considerably stronger constriction. During hypoxia this may come into play, in addition to the fact that there is an active nitric oxide–mediated DV distension, as shown experimentally.[159] This intrahepatic shift of blood from the portal system to the DV was supported by an *in vivo* Doppler study. Kessler et al. demonstrated that in IUGR fetuses with UA PI above the 97.5 percentile, total liver perfusion is decreased equally to the left and right lobes. However, as placenta insufficiency increased (as measured by the oxygen partial pressure in the umbilical artery), the proportion of left PV contribution to the right lobe decreased and was replaced by increased flow from the main PV.[160]

In summary, placental vasculopathy leads to reduced umbilical flow to the heart. This initiates an intrahepatic compensatory mechanism, which consists of shifting blood from the liver to the DV. The liver plays a central role in regulating fetal growth. Reduced liver perfusion may provide the first clinical evidence of placental insufficiency, restricted fetal growth, and decreased weight.

## *Doppler studies of the fetal venous system*

Doppler investigation is the only noninvasive *in utero* method for assessing feto-placental hemodynamic status. Each component of the feto-maternal circulation has a different role in placental function and fetal well-being. Doppler evaluation of the venous system aims to assess fetal cardiac function, which in severe cases may deteriorate to an acute event of congestive heart failure (CHF).

The Cardiovascular Profile Score (CVP)[161–163] combines sonographic markers of fetal cardiovascular status based on

parameters found to be correlated with perinatal mortality. The parameters most strongly predictive of adverse outcome were cardiomegaly, monophasic atrioventricular filling or holosystolic tricuspid regurgitation, and pulsations in the UV among growth-restricted fetuses,[163] and UV or DV Doppler in hydropic fetuses.[161] This concurs with previous studies showing that in the temporal sequence of events prior to the appearance of abnormal fetal heart rate pattern, atonia, or fetal demise, the arterial Doppler changes precede those of the venous system[164] but were too early a sign to be used to time delivery decision. This was particularly evident in cases of early onset IUGR, before 32 weeks of gestation.[153,165]

Adverse perinatal outcome is related to gestational age and the degree of placental insufficiency. Decision-making concerning the time of delivery aims to strike a balance between fetal injury related to prematurity, and that related to placental insufficiency.[166]

Results of the GRIT study[167] indicated some short-term gain in terms of stillbirth rate when delivery was immediate. However, this was refuted by the findings at 2 years of follow-up: the rate of cerebral palsy in the immediate delivery group was as expected (10%), while in the delayed delivery group it was 0%, suggesting that deferred delivery could be a protective management.

In a prospective multicenter study, Baschat et al.[152] found that gestational age is the best predictor for intact survival until 29 weeks or 800 g, with sensitivity of 68% and 72%, respectively. Above these thresholds, DV velocity, forward or absent/reversed, was the only statistically significant predictor of intact survival, and as such is the only parameter to use as a trigger for delivery.

Turan et al.[151] found a well-ordered sequence of Doppler abnormalities, beginning from early onset Doppler abnormalities including increased UA resistance and brain-sparing effect, to late-onset Doppler abnormalities, such as absent/reversed UA diastolic velocity, absent/reversed DV a-wave, and UV pulsation. The rate of progression correlated significantly with gestational age. When appearing as early as 26–27 weeks of gestation, it usually presented as a severe form, progressing from one Doppler abnormality to the next in approximately 7–10 days. When Doppler abnormalities emerged near 30 weeks' gestation, progression intervals were longer, up to 14 days, and cases presented clinically as more mild. Changes were limited to the arterial system, with median age of delivery of 33 weeks.

These findings are in contrast of those of Arduini and colleagues.[154] That group showed time intervals between arterial Doppler changes and delivery for late fetal heart rate decelerations were statistically significantly longer when Doppler abnormalities appeared before 29 weeks of gestation (mean 13.5 days, range 3–26 days), as compared to late-onset cases, where the mean interval between changes was 3 days (range 1–9 days). Other studies[153,168] have shown that venous Doppler abnormalities preceded the appearance of late decelerations or reduced short-term variability (<2.2 msec), by 6–7 days.

In conclusion, a well-documented sequence of biophysical and Doppler abnormalities corresponds with placental insufficiency and fetal growth restriction (Figure 35.16). Abnormalities in venous system Doppler waveforms are sensitive tools for the assessment of fetal well-being before 32 weeks' gestation and may help fine-tune our decision-making concerning time of delivery of affected fetuses.

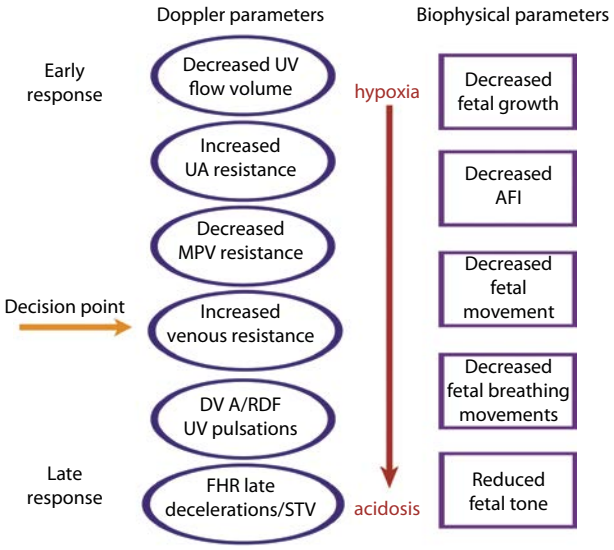


**Figure 35.16**
A proposed graphic representation of the cascade of deterioration in fetal circulatory compromise. Changes in Doppler and physiological parameters follow a temporal sequence. See text for full explanation. (UV, umbilical vein; UA, umbilical artery; MPV, main portal vein; DV, ductus venosus; AFI, amniotic fluid index; A/RDF, absent or reversed diastolic flow; FHR, fetal heart rate; STV, short term variability.) (Reproduced with permission from reference Yagel S et al. *Ultrasound Obstet Gynecol* 2010;36:93–111.[70])

Venous Doppler patterns in normal and IUGR fetuses have been established in large longitudinal and cross-sectional studies; normal Doppler patterns are discussed in Part I of this chapter. Doppler abnormalities seen in the most commonly investigated vessels are described in the following text (Figure 35.17a–c).

## Umbilical vein

UV Doppler patterns are usually evaluated in the intra-abdominal portion of the vein. Sample volume should include the whole cross section of the vessel with angle of insonation at or as close as possible to zero. Since the IUGR state includes increased impedance in the feto-placental circulation, reduced UV flow and lower velocity result. However, considerable overlap with normal ranges precludes the usefulness of UV flow velocity as a measure of IUGR.[38]

The appearance of pulsatile flow in the UV is a simple and reliable marker of circulatory compromise, long recognized as a marker of asphyxia in small for gestational age fetuses and in cases of nonimmune hydrops.[169,170] Pulsatility in the UV can result from two main sources of pressure waves. Atrial contraction can cause a sharp deflection (notch) in UV flow, or a wave from neighboring arterial flow, which will

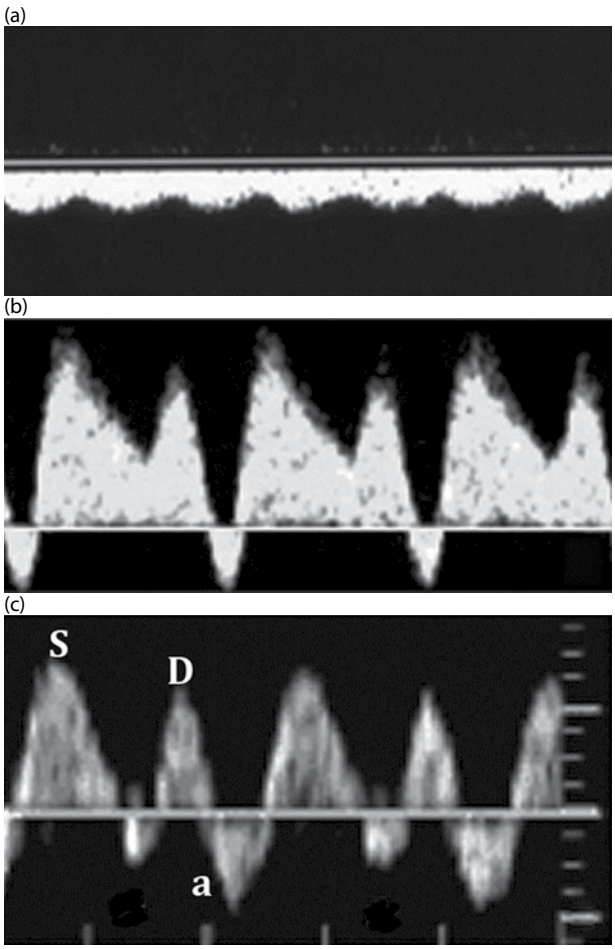


**Figure 35.17**
Abnormal Doppler waveforms in the umbilical vein, IVC, and ductus venosus. (a) Abnormal UV waveform in hemodynamically compromised fetuses is characterized by the appearance of pulsations. (b) Abnormal DV waveform: DV normally has forward blood flow throughout the cardiac cycle. In compromised fetuses, a drop in atrial systolic forward velocities will be observed. As central venous pressure increases, blood flow may be reversed during atrial systole. (c) Abnormal IVC waveforms in IUGR will show a decrease in forward flow during the S- and D-waves and accentuation of reversed flow in the a-wave. As the condition deteriorates, the D-wave may be reversed. (a, a-wave; D, D-wave; S, S-wave.) (Reprinted with permission from Yagel S et al. *Ultrasound Obstet Gynecol* 2010;36:93–111.[70])

be traveling in the same direction as UV flow, can cause an increment in UV flow. The resulting pulsatile UV Doppler pattern may be only an a-wave notch, or in some severe cases, a triphasic waveform that mirrors the whole cardiac cycle may appear[38] (Figure 35.17a).

## Ductus venosus

Changes in DV flow are seen in hypoxia and hypovolemia in experimental animal models and in human fetuses.[39–43,171] The DV is sampled at its inlet with a large sample volume in a near-sagittal scan at a low angle of insonation.[9,23] Alternatively, DV flow can be sampled in an oblique transverse section of the fetal abdomen. Normally, about 30% of blood is shunted through the DV at 20 weeks' gestation, while about 20% of blood is so shunted at 30 weeks.[23,26,38,172] In SGA fetuses, a much higher proportion of blood is shunted through the DV, and earlier placental compromise will show a more pronounced shunt and distension of the DV.[38]

Cardiac events are apparent in the DV waveform. Reversed or zero flow in the a-wave is a simple sign of disordered cardiac function. There is reduced velocity in the a-wave in IUGR, as well as alterations in time intervals in the systolic (S) and diastolic (D) components,[171] where the S(DV) time interval decreases while the D(DV) interval increases.[171] As the situation worsens, flow is further deflected owing to increased afterload and preload, as well as increased end-diastolic pressure, the direct effects of hypoxia, and increased adrenergic drive. Taken together, these effects produce an augmented atrial contraction and strong deflection during the a-wave in the DV waveform[164,173,174] (Figure 35.17b).

These factors, coupled with distension of the DV, which lessens wave reflection at the junction with the UV by lessening the difference in the vessels' diameters, produces a greater effect on UV flow. Further deterioration leads to decreased velocity between the systolic and diastolic peaks; these effects are most apparent in the second trimester. Early appearing disorders are usually the result of chromosomal aberration as opposed to cardiac decompensation.[173,175–178] These effects are rarely observed in the third trimester, when improved endocrine control operates to attenuate them.[179–181]

## Inferior vena cava

The IVC is usually sampled in the fetal abdomen, caudal to the hepatic confluence and DV outlet to avoid interference from neighboring vessels. Reference ranges for normal IVC flow parameters have been established. The IVC is the preferred vessel for postnatal evaluation of SGA neonates and is familiar to pediatricians, so it is often sampled in the fetus. It is normal to observe a negative a-wave in the IVC because of the vessel's normally lower velocities.[35,44–47] In compromised fetuses, abnormal IVC flow velocity waveform will show a decrease in forward flow during the S- and D-waves, and an accentuated reversed flow in the a-wave (Figure 35.17c). In severe cases, the D-wave may be reversed.

## Hepatic and portal veins

The hepatic vein, while easy to sample, is only infrequently employed as a parameter in IUGR studies. The signs of cardiac compromise observed in the hepatic vein are similar to those apparent in the DV and IVC.[48–51]

## The left portal vein as the watershed of the fetal venous circulation

The LPV has been suggested as a simple marker of circulatory compromise.[27,88,182] The vessel is sampled in the left portal branch between the DV inlet and the junction with the main portal stem. Disturbed blood flow in the umbilical arteries is indicative of increased resistance to blood flow in the right

heart and right liver lobe. Under these pressures, flow in the LPV is reduced and may become pulsatile, bidirectional, or reversed. If reversed, oxygen-poor blood from the spleen and gut will mix with oxygenated blood from the UV as it courses to the DV, supplying oxygen-poor blood to the fetal organs. Ultimately, during reversal, more blood could be flowing through the DV than the UV that supplies it, possibly creating suction on the LPV.[183] Kilavuz and colleagues showed that in IUGR fetuses having absent or reversed end-diastolic (ARED) flow in the umbilical arteries, while UV flow remained normal, LPV flow was normal in mildly affected fetuses, pulsatile in fetuses with increased resistive index (RI) or zero-flow in the UA, and reversed in fetuses with reversed flow in the UA. The investigators showed a significant correlation between reverse flow in the LPV and increased RI in the UA.[183]

The normal distribution of blood flow between the left and right liver lobes is approximately 60% and 40%, respectively. Most UV blood (70%–80%) perfuses the fetal liver, while 20%–30% is shunted to the DV, as previously described. Blood flow in the UV is directed to the left liver lobe and the DV, with only a minority diverted to the left PV and right liver lobe.[57] Low or reversed flow in the left portal branch is an expression of prioritized umbilical perfusion of the left liver lobe at the expense of the right.[172]

## *Comment*

Congenital malformations of the venous system are a complex and varied group of lesions. There is much that we do not know about this system and its anomalies, but knowledge of the embryological development of affected vessels is key to understanding the *in utero* progress and prognosis of these cases. Whenever anomalies of the cardinal, vitelline, or umbilical system are diagnosed, they should prompt thorough investigation of the other segments of the cardiovascular system. It would appear that anomalies of the venous system are not as rare as formerly believed, and that more will be diagnosed if practitioners are cognizant of their sonographic appearance and associated anomalies.

## Videos

**Video 35.1** (https://youtu.be/B5bOw2AMB3s)
Interrupted IVC imaged in 4DUS with B-flow imaging in the longitudinal plane, showing the umbilical vein draining into the ductus venosus, which flows into the left hepatic vein.

**Video 35.2** (https://youtu.be/PMsBWvrsGPg)
Tomographic ultrasound imaging (TUI) of a case of interrupted IVC. The aorta is seen in blue in frame 3 (top) and the azygos in red in frame 6 (second row).

**Video 35.3** (https://youtu.be/K7yr6Vjj344)
Newer high definition power Doppler shows the same case of interrupted IVC with an associated aberrant right subclavian artery (ARSA) apparent in this frame.

**Video 35.4** (https://youtu.be/h3Cde9ST7WM)
PLSVC with absent right SVC rendered in TUI with color Doppler mapping.

**Video 35.5** (https://youtu.be/cYNKqmiTRec)
Agenesis of the DV with narrow extrahepatic shunt from the umbilical vein to the inferior vena cava, imaged with high definition power flow Doppler (HDPD).

**Video 35.6** (https://youtu.be/uW0F8Vbtdw0)
Agenesis of the DV with narrow extrahepatic shunt from the umbilical vein to the inferior vena cava imaged with B-flow.

**Video 35.7** (https://youtu.be/878RmMsHxfU)
Agenesis of the DV with intrahepatic shunt of the UV to the right hepatic vein (RHV), imaged in B-flow.

**Video 35.8** (https://youtu.be/PS027XuULnk)
Agenesis of the DV with UV drainage to the right atrium, imaged in B-flow.

**Video 35.9** (https://youtu.be/gXaDYMJPf8A)
TUI rendering of agenesis of DV showing the portal veins and left hepatic vein.

**Video 35.10** (https://youtu.be/e7-xi-8_Bcw)
Left porto-hepatic shunt in the longitudinal plane, imaged in 4DUS and B-flow.

**Video 35.11** (https://youtu.be/CiJdBDEXmHQ)
Portal vein shunts draining into the IVC imaged in high definition power Doppler.

**Video 35.12** (https://youtu.be/JH1ZkawE9lE)
Portal vein shunts draining into the IVC imaged in high definition power Doppler.

**Video 35.13** (https://youtu.be/YuAuYJzz_vg)
Agenesis of DV with a narrow shunt imaged in power Doppler Carets indicate the shunts.

**Video 35.14** (https://youtu.be/9ZEU_-xibbk)
Agenesis of DV with a narrow shunt imaged in B-flow. Carets indicate the shunts.

**Video 35.15** (https://youtu.be/dP1FtSxncMM)
Agenesis of DV with a wide shunt imaged at the longitudinal plane with 4DUS and high definition power flow Doppler, rendered TUI.

**Video 35.16** (https://youtu.be/ehRG_5aprYw)
Sepia image of the umbilical vein and enlarged IVC.

**Video 35.17** (https://youtu.be/IPErzoJ7AE8)
Grayscale image shows the enlarged IVC and left portal vein (LPV). The right portal vein was absent.

**Video 35.18** (https://youtu.be/67F1T2hUxhg)
4DUS B-flow image shows the enlarged IVC and the hepatic veins.

**Video 35.19** (https://youtu.be/WESegQ7YlJg)
Increased preload led to tricuspid regurgitation.

**Video 35.20** (https://youtu.be/KLqeWQHipxQ)
Increased preload led to tricuspid regurgitation.

**Video 35.21** (https://youtu.be/JOFWrJ0hNYY)
PRUV anomaly imaged with color Doppler.

**Video 35.22** (https://youtu.be/zZK1K7_SZOo)
Incomplete absence of the portal venous system imaged with color Doppler mapping, showing the preserved left portal vein.

**Video 35.23** (https://youtu.be/ZIOAQ9QQ4G4)
Lateral caudal transverse plane on 2DUS with color Doppler mapping, showing side-to-side portocaval shunt, with confluence of the main portal vein with the inferior vena cava.

**Video 35.24** (https://youtu.be/4aZ7LzTdPOM)
Grayscale 2DUS cineloop of the aneurysmal vitelline vein.

**Video 35.25** (https://youtu.be/nQN1034y5ZU)
Color Doppler mapping of the aneurysmal vitelline vein.

**Video 35.26** (https://youtu.be/JFEiirwa2uQ)
Color Doppler mapping of the aneurysmal vitelline vein.

**Video 35.27** (https://youtu.be/kiQMbinyqaA)
Color Doppler mapping of the aneurysmal vitelline vein.

# References


1. Sadler TW, Langman J. *Langman's Medical Embryology*. 5th ed. Philadelphia: Williams & Wilkins. 1985.
2. Moore KL, Persaud TVN. *The Developing Human, Clinically Oriented Embryology*. 6th ed. Philadelphia: Saunders, 1998.
3. Larsen WJ. *Essentials of Human Embryology*. London, UK: Churchill Livingstone, 1998.
4. Yagel S et al. *Ultrasound Obstet Gynecol* 2009;34:123.
5. Collardeau-Frachon S, Scoazec JY. *Anat Rec (Hoboken)* 2008;291:614–27.
6. Yagel S et al. *Ultrasound Obstet Gynecol* 2015;45:578–83.
7. Yagel S et al. *Ultrasound Obstet Gynecol* 2010;35:741–50.
8. Sinkovskaya E et al. *Semin Fetal Neonatal Med* 2013;18:269–78.
9. Kiserud T et al. *Lancet* 1991;338:1412–4.
10. Huisman TW et al. *Pediatr Res* 1992;32:338–41.
11. Pearson AA, Sauter RW. *Am J Obstet Gynecol* 1971;110:560–5.
12. Mavrides E et al. *Ultrasound Obstet Gynecol* 2002;19:39–46.
13. Czubalski A, Aleksandrowicz R. *Folia Morphol (Warsz)* 2000;59:97–8.
14. Kivilevitch Z et al. *Ultrasound Obstet Gynecol* 2009;34:634–42.
15. Huisman TW et al. *Ultrasound Obstet Gynecol* 1993;3:26–30.
16. Nyberg MK et al. *Ultrasound Obstet Gynecol* 2010;36:718–23.
17. Chiba Y et al. *Ultrasound Med Biol* 1985;11:43–9.
18. Indik JH, Reed KL. *Am J Obstet Gynecol* 1990;163:1792–6.
19. Brace RA. Regulation of blood volume in utero. In: Hanson MA, Specer JAD, Rodeck CH, eds. *Fetal and Neonate. Physiology and Clinical Application*. Cambridge, UK: Cambridge University Press; 1993:75–99.
20. Kiserud T, Acharya G. *Prenat Diagn* 2004;24:1049–59.
21. Kiserud T et al. *Ultrasound Obstet Gynecol* 2006;28:126–36.
22. Sutton MG et al. *Cardiovasc Res* 1991;25:603–8.
23. Kiserud T et al. *Am J Obstet Gynecol* 2000;182:147–53.
24. Boito S et al. *Ultrasound Obstet Gynecol* 2002;19:344–9.
25. Edelstone DI et al. *Circ Res* 1978;42:426–33.
26. Bellotti M et al. *Am J Physiol Heart Circ Physiol* 2000;279:H1256–63.
27. Kiserud T et al. *Ultrasound Obstet Gynecol* 2003;21:359–64.
28. Edelstone DI, Rudolph AM. *Am J Physiol* 1979;237:H724–9.
29. Schmidt KG et al. *Circulation* 1996;93:826–33.
30. Kiserud T et al. *Ultrasound Obstet Gynecol* 1992;2:389–96.
31. Rizzo G et al. *Ultrasound Obstet Gynecol* 1996;7:401–10.
32. Baschat AA. *Ultrasound Obstet Gynecol* 2003;22:561–6.
33. Baschat AA et al. *Am J Obstet Gynecol* 2004;191:277–84.
34. Ott WJ. *Am J Perinatol* 1999;16:429–34.
35. Hecher K et al. *Ultrasound Obstet Gynecol* 1994;4:381–90.
36. Rizzo G et al. *Am J Obstet Gynecol* 1992;167:675–7.
37. van Splunder IP et al. *Ultrasound Obstet Gynecol* 1994;4:49–53.
38. Kiserud T. Venous flow in intrauterine growth restriction and cardiac decompensation. In: Yagel S, Silverman NH, Gembruch U, eds. *Fetal Cardiology*. New York, NY: Informa Healthcare; 2009:547–60.
39. Behrman RE et al. *Am J Obstet Gynecol* 1970;108:956–69.
40. Edelstone DI et al. *Am J Physiol* 1980;238:H656–63.
41. Itskovitz J et al. *Am J Physiol* 1987;252:H100–9.
42. Meyers RL et al. *J Dev Physiol* 1991;15:189–97.
43. Paulick RP et al. *Am J Obstet Gynecol* 1990;163:1357–63.
44. Reed KL et al. *Circulation* 1990;81:498–505.
45. Rizzo G et al. *Am J Obstet Gynecol* 1992;166:1271–80.
46. Huisman TW et al. *Ultrasound Med Biol* 1993;19:441–5.
47. Huisman TW et al. *Ultrasound Med Biol* 1991;17:679–82.
48. Bellotti M et al. *Am J Obstet Gynecol* 2004;190:1347–58.
49. Axt-Fliedner R et al. *Arch Gynecol Obstet* 2004;270:46–55.
50. Hofstaetter C et al. *Eur J Ultrasound* 1996;4:153–60.
51. Saemundsson Y et al. *Ultrasound Obstet Gynecol* 2011;37:179–83.
52. Kaji T et al. *Ultrasound Obstet Gynecol* 2012;39:357–9.
53. Gindes L et al. *J Ultrasound Med* 2009;28:977–88.
54. Haugen G et al. *Ultrasound Obstet Gynecol* 2004;24:599–605.
55. Acharya G et al. *Prenat Diagn* 2005;25:99–111.
56. Kiserud T. *Semin Fetal Neonatal Med* 2005;10:493–503.
57. Kessler J et al. *Ultrasound Obstet Gynecol* 2007;30:52–60.
58. Yagel S et al. *Ultrasound Obstet Gynecol* 2007;29:81–95.
59. Kim SH et al. *J Ultrasound Med* 2008;27:1491–501.
60. Abuhamad A. *J Ultrasound Med* 2004;23:573–6.
61. Abuhamad A et al. *Ultrasound Obstet Gynecol* 2008;31:30–6.
62. Chaoui R et al. *Ultrasound Obstet Gynecol* 2004;23:535–45.
63. Chaoui R, Kalache KD. *Ultrasound Obstet Gynecol* 2001;17:455–6.
64. Chaoui R et al. *Ultrasound Obstet Gynecol* 2001;17:22–9.
65. Espinoza J et al. *Ultrasound Obstet Gynecol* 2005;25:428–34.
66. Goncalves LF et al. *J Ultrasound Med* 2005;24:415–24.
67. Goncalves LF et al. *J Ultrasound Med* 2004;23:473–81.
68. Sciaky-Tamir Y et al. *Am J Obstet Gynecol* 2006;194:274–81.
69. Fasouliotis SJ et al. *J Ultrasound Med* 2002;21:1145–58.
70. Yagel S et al. *Ultrasound Obstet Gynecol* 2010;36:93–111.
71. Achiron R, Kivilevitch Z. *Ultrasound Obstet Gynecol* 2016;47:739–47.
72. Lin AE et al. *Genet Med* 2000;2:157–72.
73. Berg C et al. *Ultrasound Obstet Gynecol* 2005;26:538–45.
74. Bowers PN et al. *Semin Perinatol* 1996;20:577–88.
75. Vijayaraghavan SB et al. *J Ultrasound Med* 2003;22:747–52.
76. Mihmanli I et al. *Eur J Ultrasound* 2001;14:179–82.
77. Koc Z, Oguzkurt L. *Eur J Radiol* 2007;62:257–66.
78. Bartram U et al. *Pediatr Dev Pathol* 2008;11:266–73.

79. Sheley RC et al. *J Ultrasound Med* 1995;14:381–7.
80. Biffi M et al. *Chest* 2001;120:139–44.
81. Galindo A et al. *Ultrasound Obstet Gynecol* 2007;30:152–61.
82. Guarnieri GF et al. *Pediatr Cardiol* 2006;27:646–8.
83. Sarodia BD, Stoller JK. *Respir Care* 2000;45:411–6.
84. Freund M et al. *Ultrasound Obstet Gynecol* 2008;32:593–4.
85. Pasquini L et al. *Prenat Diagn* 2006;26:700–2.
86. Rizzo G et al. *J Ultrasound Med* 2008;27:497–8.
87. Berg C et al. *Ultrasound Obstet Gynecol* 2006;27:274–80.
88. Minniti S et al. *Eur Radiol* 2002;12:2040–55.
89. Currarino G et al. *Pediatr Radiol* 1991;21:265–6.
90. Kinare AS et al. *J Clin Ultrasound* 1996;24:333–8.
91. Jaeggi ET et al. *Am J Obstet Gynecol* 2002;187:1031–7.
92. Langman G et al. *Pediatr Dev Pathol* 2001;4:298–303.
93. Leonidas JC, Fellows RA. *AJR Am J Roentgenol* 1976;126:892–5.
94. Siven M et al. *Pediatr Pathol Lab Med* 1995;15:39–50.
95. Sothinathan U et al. *Acta Paediatr* 2006;95:620–1.
96. Volpe P et al. *Prenat Diagn* 2002;22:995–1000.
97. Shen O et al. *Ultrasound Obstet Gynecol* 2011;37:184–90.
98. Acherman RJ et al. *J Ultrasound Med* 2007;26:1077–82.
99. Perles Z et al. *Fetal Diagn Ther* 2003;18:247–51.
100. Staboulidou I et al. *Fetal Diagn Ther* 2011;30:35–40.
101. Contratti G et al. *Ultrasound Obstet Gynecol* 2001;18:605–9.
102. Berg C et al. *Ultrasound Obstet Gynecol* 2006;28:275–81.
103. Hoppen T et al. *J Perinat Med* 2000;28:69–73.
104. Thomas JT et al. *Prenat Diagn* 2012;32:686–91.
105. Moaddab A et al. *J Matern Fetal Neonatal Med* 2016;29:3606–14.
106. Sau A et al. *Prenat Diagn* 2004;24:418–23.
107. Gorincour G et al. *Am J Roentgenol* 2005;184:163–8.
108. Shen O et al. *Ultrasound Obstet Gynecol* 1996;8:31–3.
109. Bell AD et al. *Int J Cardiol* 1986;10:167–76.
110. Hill LM et al. *Obstet Gynecol* 1994;84:923–5.
111. Blazer S et al. *Obstet Gynecol* 2000;95:433–6.
112. Kirsch CF et al. *J Ultrasound Med* 1996;15:371–4.
113. Greiss HB, McGahan JP. *J Ultrasound Med* 1992;11:111–3.
114. Jouk PS, Champetier J. *Surg Radiol Anat* 1991;13:59–62.
115. Jeanty P. *Radiology* 1990;177:735–8.
116. Monie IW et al. *Circ Res* 1957;5:187–90.
117. Lide B et al. *J Ultrasound Med* 2016;35:1–5.
118. De Catte L et al. *J Ultrasound Med* 1998;17:775–9.
119. Weichert J et al. *Ultrasound Obstet Gynecol* 2011;37:543–8.
120. Wolman I et al. *Ultrasound Obstet Gynecol* 2002;19:562–4.
121. Byers BD et al. *Ultrasound Obstet Gynecol* 2009;33:282–6.
122. White SP, Kofinas A. *J Ultrasound Med* 1994;13:992–4.
123. Mahony BS et al. *J Ultrasound Med* 1992;11:73–6.
124. Sepulveda W et al. *J Ultrasound Med* 1998;17:171–5.
125. Allen SL et al. *J Ultrasound Med* 1998;17:189–92.
126. Fung TY et al. *Ultrasound Obstet Gynecol* 2005;25:149–54.
127. Valsky DV et al. *Prenat Diagn* 2004;24:451–4.
128. Goncalves LF et al. *J Ultrasound Med* 1995;14:849–52.
129. Laverdiere JT et al. *Pediatr Radiol* 1995;25:52–3.
130. Manning N et al. *Prenat Diagn* 2004;24:537–40.
131. Venkat-Raman N et al. *Ultrasound Obstet Gynecol* 2001;17:71–5.
132. Achiron R et al. *Ultrasound Obstet Gynecol* 2009;34:643–52.
133. Kivilevitch Z, Achiron R. *J Ultrasound Med* 2010;29:1651–6.
134. Morgan G, Superina R. *J Pediatr Surg* 1994;29:1239–41.
135. Niwa T et al. *J Comput Assist Tomogr* 2002;26:681–6.
136. Northrup M et al. *J Ultrasound Med* 2002;21:569–72.
137. Delle Chiaie L et al. *Ultrasound Obstet Gynecol* 2008;32:233–5.
138. Ebbing C et al. *Reprod Sci* 2008;15:166–78.
139. Kim SZ et al. *Eur J Pediatr* 1998;157:608–9.
140. Usuki N, Miyamoto T. *J Comput Assist Tomogr* 1998;22: 728–9.
141. Matsuoka Y et al. *Gastrointest Radiol* 1992;17:31–3.
142. Grazioli L et al. *Eur Radiol* 2000;10:820–5.
143. Alonso-Gamarra E et al. *Radiographics* 2011;31:707–22.
144. Guerin F et al. *Semin Pediatr Surg* 2012;21:233–44.
145. Benoist G et al. *Ultrasound Obstet Gynecol* 2007;29:708–11.
146. Hery G et al. *J Pediatr Surg* 2013;48:e1–4.
147. Kessler J et al. *Ultrasound Obstet Gynecol* 2006;28:890–8.
148. Wladimiroff JW et al. *Br J Obstet Gynaecol* 1986;93:471–5.
149. Mari G, Deter RL. *Am J Obstet Gynecol* 1992;166:1262–70.
150. Miller J et al. *Semin Perinatol* 2008;32:274–80.
151. Turan OM et al. *Ultrasound Obstet Gynecol* 2008;32:160–7.
152. Baschat AA et al. *Obstet Gynecol* 2007;109:253–61.
153. Ferrazzi E et al. *Ultrasound Obstet Gynecol* 2002;19:140–6.
154. Arduini D, Rizzo G. *J Perinat Med* 1992;20:29–38.
155. Hecher K et al. *Ultrasound Obstet Gynecol* 1992;2:266–71.
156. Harrington K et al. *Ultrasound Obstet Gynecol* 1995;6:19–28.
157. Tchirikov M et al. *Am J Obstet Gynecol* 1998;178:943–9.
158. Kiserud T et al. *Ultrasound Obstet Gynecol* 2006;28:143–9.
159. Tchirikov M et al. *Ultrasound Obstet Gynecol* 2006;27:452–61.
160. Kessler J et al. *Pediatr Res* 2009;66:113–7.
161. Hofstaetter C et al. *J Matern Fetal Neonatal Med* 2006;19:407–13.
162. Huhta JC. *Semin Fetal Neonatal Med* 2005;10:542–52.
163. Makikallio K et al. *Ultrasound Obstet Gynecol* 2008;31:48–54.
164. Hecher K et al. *Circulation* 1995;91: 129–38.
165. Bilardo CM et al. *Ultrasound Obstet Gynecol* 2004;23:119–25.
166. Baschat AA et al. *Ultrasound Obstet Gynecol* 2000;16:407–13.
167. Thornton JG et al. *Lancet* 2004;364:513–20.
168. Hecher K et al. *Ultrasound Obstet Gynecol* 2001;18:564–70.
169. Gudmundsson S et al. *Am J Obstet Gynecol* 1991;164:33–7.
170. Lingman G et al. *Biol Neonate* 1986;49:66–73.
171. Wada N et al. *Ultrasound Obstet Gynecol* 2015;46:221–6.
172. Kessler J et al. *Pediatr Res* 2008;63:315–20.
173. Kiserud T et al. *Ultrasound Obstet Gynecol* 1994;4:109–14.
174. Matias A et al. *Ultrasound Obstet Gynecol* 1999;14:307–10.
175. Borrell A et al. *Am J Obstet Gynecol* 1998;179:1612–7.
176. Kiserud T. *Eur J Obstet Gynecol Reprod Biol* 1999;84:139–47.
177. Matias A et al. *Ultrasound Obstet Gynecol* 1998;12:380–4.
178. Murta CG et al. *Fetal Diagn Ther* 2002;17:308–14.
179. Hanson MA. *Eur J Obstet Gynecol Reprod Biol* 1997;75:55–61.
180. Iwamoto HS et al. *Am J Physiol* 1989;256:H613–20.
181. Kiserud T et al. *BJOG* 2001;108:359–64.
182. Kessler J et al. *Ultrasound Obstet Gynecol* 2007;30:757–64.
183. Kilavuz O et al. *J Perinat Med* 2003;31:184–7.

# 36

# Fetal cardiac tumors

Lisa K. Hornberger and Angela McBrien

Fetal cardiac tumors are relatively rare pathologies, representing 0.02% to 0.13% of cases in fetal cardiac series.[1–3] Over the past two decades, with advances in ultrasound technology and experience, there has been a substantial improvement in their prenatal detection. The majority of fetal cardiac tumors are identified in the second and third trimesters of pregnancy.[1,3,4–8] Although the diagnosis of a particular tumor is best confirmed by pathological examination, most can be suspected on the basis of specific anatomical features typically defined by echocardiography that include its location, its echogenicity relative to the surrounding myocardium, whether it is well circumscribed or amorphous, homogeneous or heterogeneous, sessile or pedunculated, single or multiple, or whether there are associated arrhythmias or pericardial effusion. While many tumors are benign, some can result in significant obstruction of ventricular inflows and outflows or general cardiac compression causing the evolution of fetal heart failure/hydrops and even fetal demise, or the need for surgical intervention in the neonatal period. Others may be associated with fetal arrhythmias or conduction abnormalities that can also contribute to cardiovascular compromise. Table 36.1 summarizes more commonly detected fetal cardiac tumors, the characteristics of the tumor, and associated cardiac and extracardiac pathologies.

The following sections review the characteristic features, associated abnormalities, and known outcomes of the most common types of fetal cardiac tumors, including rhabdomyomas, pericardial teratomas, fibromas, hemangiomas, and myxomas.

## Cardiac rhabdomyoma

Cardiac rhabdomyomas are by far the most common fetal cardiac tumors accounting for 70%–80% of cases in reported fetal series.[1–9] Cardiac rhabdomyomas are nonmalignant tumors of striated muscle cells. Echocardiography reveals a homogeneous, typically well-circumscribed mass that is significantly more echogenic relative to the myocardium (Figure 36.1a–d). Cardiac rhabdomyoma may be intracavitary or intramural, found within the ventricular free wall, the ventricular septum, papillary muscles, or less commonly, within the atria. They are usually sessile but can occasionally be mobile. In most affected fetuses there are multiple tumors, and this assists with the diagnosis (Video 36.1).[10] Often when there are multiple tumors, however, some tumors may be less obvious and require careful sweeping through the myocardium from different approaches to identify. Cardiac rhabdomyoma may grow in size prior to 32 weeks, regressing thereafter.[1,3,6,9,11–15] They may cause ventricular inflow or outflow obstruction; however, surgical intervention is rarely necessary and has been reported in no more than 6% of fetal diagnoses. In up to 5% of cases, cardiac rhabdomyomas may be so large that they cause cardiac compression leading to fetal hydrops and demise (Video 36.2). Fetal rhabdomyoma are also associated with atrioventricular valve regurgitation as well as arrhythmias and conduction abnormalities in 10%–20% of cases, including atrial and ventricular ectopy, supraventricular tachycardia (especially those associated with preexcitation), ventricular tachycardias, repolarization abnormalities, and rarely, atrioventricular block.[1,3,6,13,15,16] Given the risk of progression, serial assessment of an affected pregnancy is important particularly prior to 32 weeks. Furthermore, assessment of pregnancies at risk for fetal tuberous sclerosis should include serial evaluation after 22–23 weeks through 32 weeks, as the tumors may only become evident later in the second or early third trimesters.

## *Tuberous Sclerosis*

Although the tumor itself is usually benign, fetal cardiac rhabdomyoma may be associated with tuberous sclerosis complex (TSC) in up to 78%–80% of cases.[1,3,6,10,12,14,15] Tuberous sclerosis occurs in the majority of affected patients as a consequence of mutations in the tumor suppressor genes TSC1, which encodes the protein hemartin, or TSC2, which encodes protein tuberin.[17] TSC is an autosomal dominantly inherited condition with variable expression; however, up to two-thirds of affected cases represent spontaneous mutations. TSC is associated with hamartomas and low-grade neoplasms of multiple organ systems.[17] In addition to cardiac rhabdomyoma, TSC is associated with specific skin lesions such as hypomelanotic macules, shagreen patches and angiofibromas, renal angiolipomas, retinal hamartomas, and central nervous system findings such as cortical tubers, subependymal nodules, and giant cell astrocytomas.[17] Extracardiac pathologies associated with TSC can be defined even prenatally by ultrasound and fetal magnetic resonance imaging[18] (Figure 36.2). With respect to fetal cardiac rhabdomyomas, the presence of multiple tumors is associated with TSC in 95%; whereas, the finding of an isolated rhabdomyoma has a risk of only 23%.[10] Thus, defining whether there are multiple tumors is a critical aspect of the evaluation and counseling of affected pregnancies. The neurocognitive

**Table 36.1** Most common fetal cardiac tumors

| *Tumor type* | *Location* | *Echo characteristics* | *Single/multiple* | *Associated pathology* |
|---|---|---|---|---|
| Rhabdomyoma | IVS, LV, and RV free walls, papillary muscles, atria intramural, endocardial, epicardial | Very echogenic, homogeneous, well circumscribed | Single or multiple | Atrial and ventricular ectopy, SVT, VT, AV block, LV or RV inflow or outflow obstruction, compression, TSC |
| Myocardial fibroma | IVS, LV, and RV | Heterogeneous, cystic degeneration | Single | Ventricular ectopy and tachycardia, LV or RV outflow obstruction |
| Pericardial teratoma | SVC-Ao pericardial reflection | Heterogeneous, echogenic, solid and cystic elements | Single | Compression especially of right atrium |
| Myxoma | LV, RV, or atria | Sessile or pedunculated | Sngle | Obstruction of ventricular inflows and outflows, AV valve regurgitation, emboli, arrhythmias |
| Hemangioma | Right atrium | Lobulated and sessile, mixed echogenicity, may see vascularity with Doppler | Single | Compression, arrhythmias, high-output failure, pericardial effusion |
| Hamartoma | LV but may be associated with valves | Sessile, homogenous, similar echogenicity to myocardium (represents overgrowth of myocardial cells with less order) | Single or multiple | Ventricular ectopy, obstruction and compression |
| Lipoma | Any cardiac chamber | Homogeneous, nodular echogenicity | Single or multiple | Ventricular outflow or inflow obstruction |

*Abbreviations:* AV, atrioventricular; IVS, interventricular septum; LV, left ventricle; RV, right ventricle; SVC-Ao, superior vena cava-aortic; SVT, supraventricular tachycardia; TSC, tuberous sclerosis complex; VT, ventricular tachycardia.

complications associated with TSC have the greatest impact on the long-term outcome of affected patients. These include seizures in more than 80% of affected patients, which represent infantile spasms in up to a third, and neurodevelopmental delay in up to 68%, including spectrum of autism disorder.[17,19]

Interestingly and importantly, the spectrum of associated neurocognitive abnormalities may be different among prenatally versus postnatally diagnosed patients. This is likely in part due to presentation bias.[14] A fetal diagnosis is typically suspected as a consequence of identification of a cardiac tumor on routine obstetrical ultrasound. In contrast, those diagnosed postnatally most often come to medical attention as a consequence of neurocognitive manifestations. In a small series comparing prenatally versus postnatally diagnosed patients with a definitive diagnosis of TSC, Bader and colleagues demonstrated that only 40% of prenatally diagnosed patients manifested clinical symptoms (seizures and/or developmental delay), and this was despite the finding of central nervous system pathology by imaging in 71% of cases.[14] In contrast, 88% of those with a postnatal diagnosis demonstrated significant clinical neurocognitive abnormalities. Although some centers offer genetic testing and routinely perform fetal magnetic resonance imaging to examine for noncardiac features of TSC, the finding of fetal abnormalities does not necessarily predict the clinical outcome. This has been further emphasized in a case report reported by Chadha et al. in which the clinically asymptomatic father of a set of affected dizygotic twins had a TSC2 mutation and multiple cortical tubers.[20] Further work is necessary to better define the full clinical spectrum and risks associated with a fetal diagnosis of rhabdomyoma, including prenatally predictive features, which will lead to more appropriate prenatal evaluations and, importantly, more accurate prenatal counseling.

## Fetal pericardial teratomas

Pericardial teratomas account for 10%–15% of cardiac tumors identified in fetal life. They consist of endodermal, mesodermal, and ectodermal germinal cell layers and are typically found within the pericardial reflection at the junction of the superior vena cava, right atrium, and ascending aorta.[9] Pericardial teratomas are encapsulated, single, heterogeneous masses with calcified and cystic elements (Figure 36.3; Video 36.3).[1,3,4,9,21–25] Teratomas can also be identified in other locations within the body, including the mediastinum and very rarely within the heart (Figure 36.4). Pericardial teratomas are consistently associated with a pericardial effusion, which is often large and the first feature identified at routine ultrasound (Figure 36.3; Video 36.3). As many as 70%–80% of pericardial teratomas are associated with the evolution of fetal hydrops, typically occurring in the second and third trimesters, and this is most often observed in the presence of larger masses.[25,26] Some pericardial teratomas can rapidly grow, and,

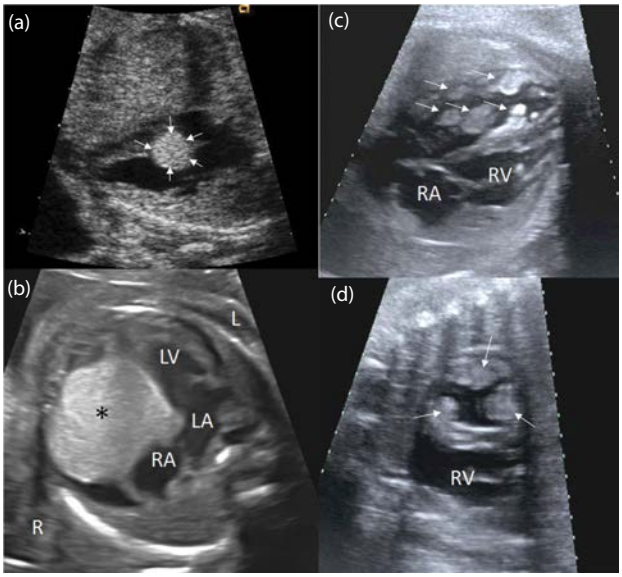


**Figure 36.1**
Examples of fetal cardiac rhabdomyomas. (a) Isolated ventricular septal rhabdomyoma at 26 weeks of gestation. Note the echogenic, well-circumscribed, homogenous, and globular appearance of this isolated tumor (arrows) that is confined to the interventricular septum. (b) This massive fetal rhabdomyoma (*) in a 25-week fetus is again well-circumscribed, echogenic relative to the myocardium and homogeneous. It is largely a part of the inferior or diaphragmatic surface of both the right and left ventricles, extending outside of the heart. This tumor eventually led to the evolution of hydrops and fetal demise at 28 weeks. (c) Multiple cardiac rhabdomyomas are present in this 34-week fetus largely present in the LV, but there was at least one tumor in the RV, none of which caused ventricular inflow or outflow obstruction. (d) The sagittal image for the same 34-week fetus demonstrating rhabdomyomas along the left ventricular free wall and the ventricular septum as well as attached to the left ventricular papillary muscles. (LA, left atrium; LV, left ventricle; PA, pulmonary artery; RA, right atria; RV, right ventricle.)

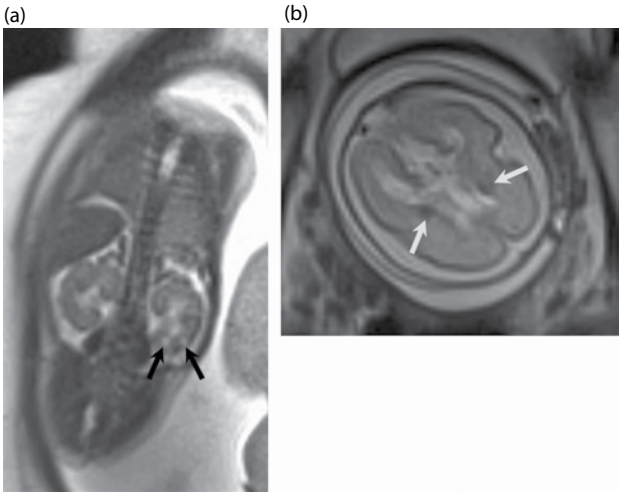


**Figure 36.2**
Fetal magnetic resonance images demonstrating extracardiac findings in tuberous sclerosis complex including (a) renal angiolipomas (black arrows) and (b) hamartomas represented as low-intensity signals in the periventricular area of the fetal brain (arrows).

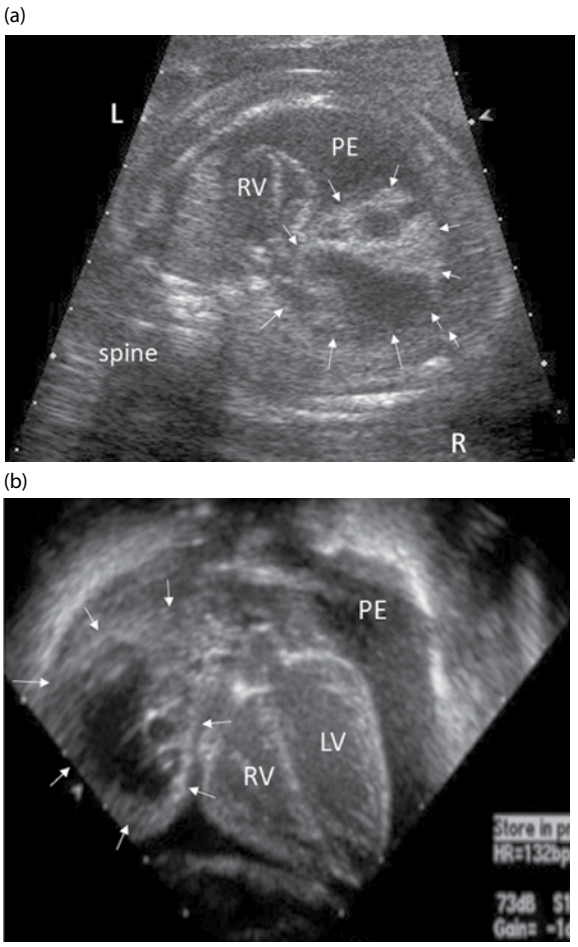


**Figure 36.3**
Pericardial teratoma in a 28-week fetus and neonate. (a) Fetus with a large mass attached to the base of the heart with cystic and solid elements (white arrows) as well as the large pericardial effusion (PE) that is a key feature of this type of tumor. (b) Images from a neonate with similar features. The arrows outline the mass. The cystic component of the mass is very large. (L, left; R, right; RV, right ventricle.)

with compression of right heart structures, this likely contributes to more acute cardiovascular compromise.[26] Venous Doppler changes have been demonstrated in the presence of larger pericardial teratomas associated with the evolution of hydrops.[25,26] Serial assessment of tumor growth, combined cardiac output, and venous Doppler may be helpful in anticipating potential for cardiovascular compromise.

Although in the past, pericardial teratomas have been associated with a high perinatal loss, especially with evolving hydrops, the advent and success of fetal intervention, particularly resection of the tumor, may result in optimized outcomes.[26–28] All without prenatal intervention require surgical resection after birth.

## Fetal myocardial fibroma

Fetal myocardial fibromas account for 5%–10% of fetal cardiac tumors. They are connective tissue tumors derived

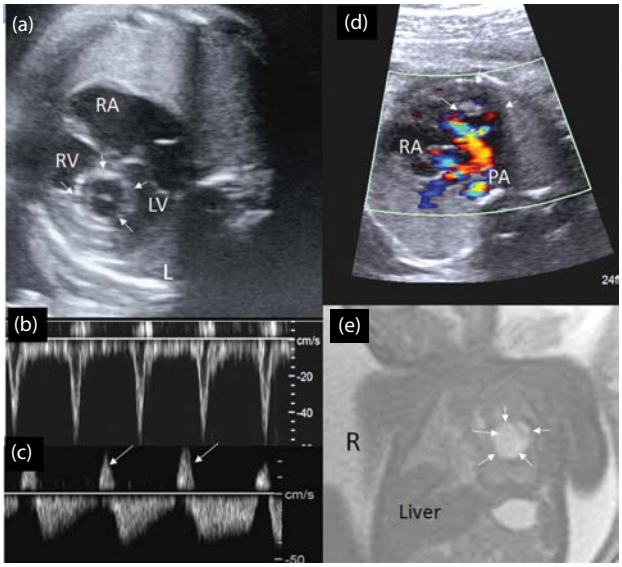


**Figure 36.4**
A very rarely found intracardiac teratoma in a 32-week fetus. (a) A large cystic and solid mass was visible in the right ventricular cavity extending into the outflow tract (arrow). The left ventricle (LV) was compressed. (b) The presence of the large mass impacted right ventricular (RV) function with both tricuspid insufficiency and altered diastolic filling (Doppler tracing shown). (c) There was also increased a-wave velocities in the inferior vena cava (arrow) in keeping with increased central venous pressures. (d) Color Doppler demonstrated streaming of blood around the tumor in the right ventricular outflow tract, and there was retrograde flow in the ductus arteriosus in keeping with severe right ventricular outflow obstruction. (e) Fetal magnetic resonance imaging was performed, which demonstrated a rounded flask-shaped T2 hyperintense mass lesion within the right ventricle (arrows) with a neck that extended into the outflow tract. The lesion was hypointense to fluid on T1-weighted sequences. The findings further suggested a teratoma involving the ventricular septum, which was confirmed with surgical resection. (L, left; PA, pulmonary artery; R, right; RA, right atrium.)

from fibroblasts and myofibroblasts and are also called fibromatosis, myofibromatosis, fibrous hemartoma, and congenital mesoblastic tumor.[9] Myocardial fibromas are typically single intramural tumors that are most often found within the ventricular septum, but they may also be found within the left or right ventricular free walls[1,3,4,9,29–31] (Figure 36.5; Video 36.4). By echocardiography, they are typically echogenic relative to the surrounding myocardium, but often less so compared to rhabdomyomas. They may be cystic with central degeneration, which results in the less homogeneous appearance.

Myocardial fibromas can be associated with arrhythmias, which may include ventricular ectopy, ventricular tachycardia, and atrioventricular block.[9] Fibromas may cause ventricular inflow or outflow obstruction, in some resulting in significant cyanosis in the neonatal period; can cause heart failure; rarely can cause distortion of atrioventricular valves leading to insufficiency; and rarely may be associated with embolic events. Unlike cardiac rhabdomyomas, fibromas do not regress, and they require surgical intervention postnatally to partially or completely remove the tumor. Due to their infiltrative nature, occasionally resection of cardiac fibromas is not possible, and cardiac transplantation or, in the case of severe obstruction or cavity obliteration, single-ventricle palliation may be considered.[31] Rarely, extracardiac pathology has been identified with cardiac fibromas, including cleft lip and palate, hydrocephalus, cystic renal dysplasia, Beckwith–Wiedemann syndrome, and nevoid basal cell carcinoma syndrome (Gorlin syndrome).[9] Roughly 50% of affected fetuses survive the neonatal period.[9] With newer strategies and more aggressive perinatal and postnatal intervention, including single ventricle palliation and transplantation, this may improve.[31] In the absence of significant hydrops, survival associated with neonatal teratomas has been reported based on a review of the literature to be as high as 85%.[9]

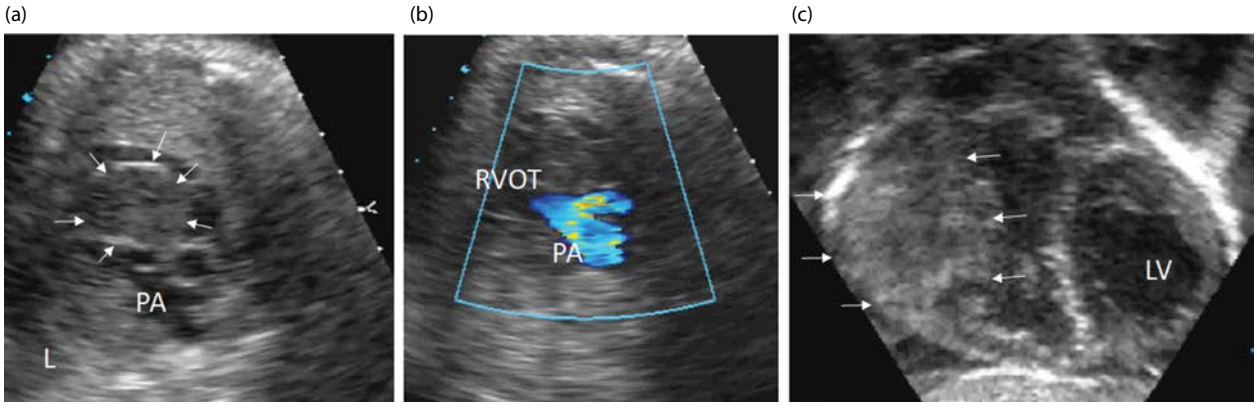


**Figure 36.5**
Fetal cardiac fibroma infiltrating the right ventricular free wall and right ventricular cavity. (a) The mass, which has infiltrated the right ventricular free wall extending into the right ventricular outflow tract (arrows), is not as easily distinguished from the myocardium. It is less homogenous and echogenic than the rhabdomyoma. (b) By color Doppler, there is patency of the pulmonary outflow with forward (blue) flow through the main pulmonary artery and ductus arteriosus. (c) Postnatally, the tumor was more easily demonstrated as shown in this subcostal view (arrows). The diagnosis of a fibroma was confirmed after the tumor was surgically resected in early infancy to relieve right ventricular outflow obstruction. (LV, left ventricle; PA, pulmonary artery; RVOT, right ventricular outflow tract.)

## Fetal cardiac hemangiomas

Hemangiomas are vascular tumors that can be classified into three main types based on the caliber of the vessel lumen: cavernous hemangioma consisting of many dilated thin-walled vessels; capillary hemangioma composed of lobules of smaller vessels; and mixed, composed of both types.[9] Cardiac hemangiomas are rarely identified in the fetus and neonate, observed in 6%–7% of 89 cases in one review of the literature from 2004.[9] They are usually single tumors, which by echocardiography may be homogeneous or may have mixed cystic and solid components (Figure 36.6; Video 36.5). The most common site of origin of cardiac hemangiomas is the base of the heart adjacent to the right atrium,[9,32–35] where they may even be fed by the right coronary artery[32]; however, they can be seen in any cardiac chamber, may involve the endocardium or myocardium, and may even be primarily associated with the pericardium. Although for most the vascular nature may not be demonstrable as the vessels are often microscopic, occasionally the feeding vessel may be visible by color Doppler, and when highly vascular and large, power Doppler interrogation has assisted with the diagnosis.[35] Cardiac hemangiomas, when large, may be associated with high-output failure or compression, arrhythmias, and consumption of blood products. They are secretory in nature and may be associated with a pericardial effusion. Cardiac hemangiomas have been rarely reported to spontaneously regress.[35] Most ultimately require surgical resection after birth, when there are relevant symptoms that are associated with good early and long-term outcomes with at least 85% survival and a small risk of recurrence.[9,32]

## Fetal cardiac myxomas

Cardiac myxomas, myxoid tumors composed of primitive connective tissue, are the most common cardiac tumors in adolescents and adults but are rarely identified before birth.[9,36–38] They are usually single and, although most often associated with the atrial septum and atrial free walls after birth, in fetal life they may also be observed within the ventricles.[36,37] Cardiac myxomas may be echogenic relative to the myocardium, and may be either well-circumscribed or amorphous. Myxomas may be intracavitary or intramural, and they can occasionally be epicardial. Unlike most other cardiac tumors, they are often, but not always, pedunculated and mobile. When pedunculated, movement in and out of the atrioventricular valves or outflow tracts can result in obstruction or negatively affect valve function. Myxomas can rarely be associated with pericardial effusions and among postnatal cases have been associated with embolic phenomenon. Finally, cardiac myxomas are observed in Carney complex, an autosomal dominant syndrome that manifests after birth and consists of spotty skin pigmentation, benign and malignant tumors of the endocrine glands, and endocrinopathies. Surgical intervention is the treatment for cardiac myxomas after birth, which is typically curative with good early and long-term outcomes and low risk of recurrence.[9]

## Other fetal cardiac tumors

Other types of cardiac tumors have been reported in isolated cases, most in the neonatal period suggesting the potential for prenatal diagnosis. These would include nonneoplastic tumors such as hamartomas and lipomas, and malignancies including fibrosarcomas and rhabdomyosarcomas.[9,39–43]

## Fetal echocardiography general considerations

### *Performing the Fetal Echocardiogram*

When a fetal cardiac tumor is suspected, fetal echocardiography should include detailed 2D evaluation of the fetal atria,

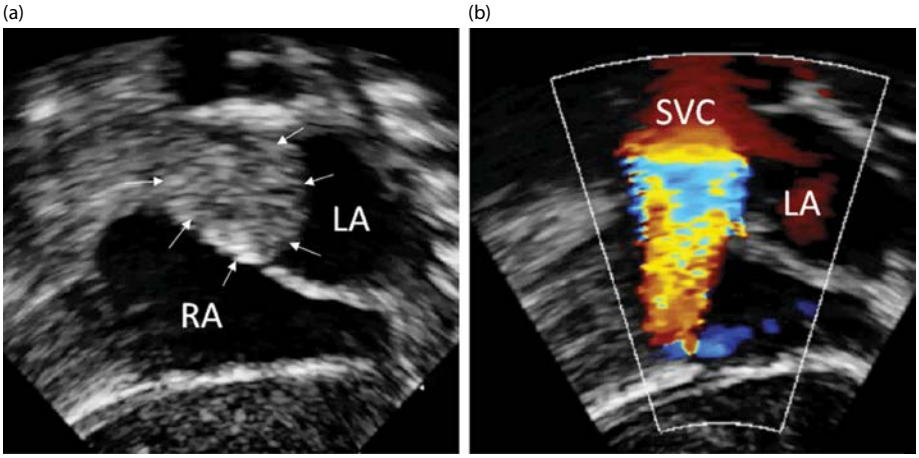


**Figure 36.6**
Hemangioma diagnosed in a neonate. (a) The tumor was found attached to the atrial septum near the right atrial-superior vena cava junction (arrows). It was well circumscribed but less echogenic, and not homogeneous. Color Doppler did not demonstrate flow within the mass due to the microscopic nature of the vascular contents. (b) Turbulent flow in the superior vena cava (SVC) suggested the presence of obstruction, which led to surgical resection. (LA, left atrium; RA, right atrium.)

ventricles, and ventricular septum. Descriptions of the location, characteristics, and size of the tumor or tumors are important in defining the nature of the tumor, determining its potential for obstruction of ventricular inflows or outflows, and determining risks of compression and cardiovascular compromise, whether it is progressing or regressing. Color and spectral Doppler interrogations of ventricular inflows, outflows, and arches are necessary to further define risks or the presence of severe ventricular inflow or outflow obstruction and to exclude the presence of significant atrioventricular valve insufficiency. Assessment of systemic venous, ductus venosus, and umbilical venous flow patterns may be useful to exclude evidence of increased cardiac filling pressures or cardiac compression. Cardiac output assessment may be useful where potential for or presence of cardiac compression is suspected. A detailed assessment for fetal arrhythmias and conduction abnormalities as well as for effusions is also important for many types of cardiac tumors. Serial assessment is recommended for fetal cardiac tumors, particularly those associated with progression in tumor size, risk of cardiovascular compromise, and evolution of arrhythmias. For certain cardiac tumors, fetal magnetic resonance imaging may be helpful to further delineate the type and extent of the tumor.[44,45]

## *Prenatal Counseling for Fetal Cardiac Tumors*

Counseling for fetal tumors requires knowledge of the most likely type or types of cardiac tumors, associated cardiac and extracardiac pathology, likelihood of progression or regression, and risks of arrhythmias and cardiovascular compromise. It also requires understanding the likely need of surgical intervention after or even before birth. For rhabdomyomas in particular, given the risk of TSC, consultation with a prenatal geneticist is warranted.

## *Perinatal Management for Fetal Cardiac Tumors*

Management planning particularly for larger tumors requires input from a multidisciplinary team that includes, in addition to the maternal fetal medicine specialist, fetal cardiologist and neonatologist, and a fetal or pediatric cardiovascular or general surgeon. If there is evolving hydrops, early delivery at a viable age may be necessary with plans for neonatal intervention. For some tumors, fetal surgery has been reported with increasing success. Planning of perinatal management requires anticipating potential for compromise. While many particularly with rhabdomyoma, for instance, may be clinically well at birth, critical obstruction of a ventricular inflow or outflow tract may necessitate initiation of a prostaglandin infusion to stabilize the neonate. The presence of a very large tumor and evolving hydrops due to cardiac compression may result in the need for an *ex utero* intrapartum treatment (EXIT) to a full circulatory support approach until the tumor can be resected.

# Videos

**Video 36.1a** (https://youtu.be/DBDzeu0waoA)
Example of fetal cardiac rhabdomyoma. (a) Four-chamber view demonstrates many masses within the left ventricle and a single mass in the right ventricle.

**Video 36.1b** (https://youtu.be/KWCsEYPjbaY)
(b) Color Doppler excluded clear evidence of ventricular inflow and outflow tract obstruction.

**Video 36.2** (https://youtu.be/bjJQAq-nAtQ)
A massive cardiac rhabdomyoma on the inferior surface of the ventricles associated with evolving hydrops including ascites and a pericardial effusion. Atrial ectopy was also present.

**Video 36.3** (https://youtu.be/ulX-zSzR8N0)
Example of a pericardial teratoma resulting in the evolution of a large pericardial effusion and eventual hydrops.

**Video 36.4a** (https://youtu.be/ah1NRGpD5VQ)
A 32-week fetus with a right ventricular fibroma. (a) Two-dimensional imaging demonstrated a fairly subtle mass adherent to the right ventricular free wall but not causing significant obstruction by color Doppler.

**Video 36.4b** (https://youtu.be/Q7L63a0qXVY)
(b) Postnatal echo confirmed a classic appearance of a fibroma, a solitary tumor invading the right ventricular free wall with less echogenicity relative to the myocardium and not homogenous.

**Video 36.4c** (https://youtu.be/IxXmRf0os8M)
(c) Postnatal appearance of the fibroma that nearly obliterated the right ventricular cavity.

**Video 36.5a** (https://youtu.be/ctFU53InHu4)
Hemangioma in a neonate arising from the atrial septum near the right atrial-superior vena cava junction. (a) The mass is not very hyperechoic relative to the myocardium and is not homogeneous. Its location provided some clue to its nature.

**Video 36.5b** (https://youtu.be/9lv7lp1q-bY)
(b) Color Doppler demonstrated obstruction to inflow from the superior vena cava. Growth of the tumor with progressive superior vena caval obstruction led to the need for intervention.

# References


1. Holley D et al. *J Am Coll Cardiol* 1995;26:516–20.
2. Allan L. Fetal cardiac tumors. In: Allan L, Hornberger L, Sharland G, eds. *Textbook of Fetal Cardiology*. London: Greenwich Medical Media Limited; 2000:358–65.
3. Yinon Y et al. *Prenatal Diagnosis* 2010;30:941–9.
4. Groves AM et al. *Arch Dis Child* 1992;67:1189–92.
5. Niewiadomska-Jarosik K et al. *Prenat Diagn* 2010;30:882–7.
6. Paladini D et al. *Ultrasound Obstet Gynecol* 1996;7:84–5.
7. Geipel A et al. *Ultrasound Obstetr Gyn* 2001;17(1):17–21.

8. Zhou QC et al. *Ultrasound Obstet Gynecol* 2004;23:165–71.
9. Isaacs H. *Pediatr Cardiol* 2004;25:252–73.
10. Tworetzky W et al. *Am J Cardiol* 2003;92(4):487–9.
11. Farooki ZQ et al. *Am J Cardiol* 1991;67(9):897–9.
12. D'Addario V et al. *J Perinat Med* 2002;30(2):170–5.
13. Fesslova V et al. *Prenat Diagn* 2004;24(4):241–8.
14. Bader RS et al. *J Pediatr* 2003;143(5):620–4.
15. Chao AS et al. *Ultrasound Obstet Gynecol* 2008;31(3):289–95.
16. Wacker-Gussmann A et al. *Heart Rhythm* 2014;11:677–83.
17. Northrup H, Krueger DA. *Pediatr Neurol* 2013;49:243–54.
18. Sgro M et al. *Ultrasound Obstet Gynecol* 1999;14(5):356–9.
19. Degueldre SC et al. *Cardiol Young* 2010;20(1):18–24.
20. Chada R et al. *J Obstet Gynaecol Can* 2011;33(8):854–7.
21. Catanzarite V et al. *Ultrasound Obstet Gynecol* 1994;4:505–7.
22. Cyr DR et al. *J Ultrasound Med* 1988;7:87–90.
23. Sklansky M et al. *Obstet Gynecol* 1997;89:807–9.
24. Tollens T et al. *Ann Thorac Surg* 1998;66:559–60.
25. Bader R et al. *Am J Perinatol* 2006;23(1):53–8.
26. Rychik J et al. *Am J Obstet Gynecol* 2016;215:780.e1–7.
27. Merchant AM et al. *J Pediatr Surg* 2005;40(1):228–31.
28. Sydorak RM et al. *Fetal Diagn Ther* 2002;17(5):281–5.
29. Malisch TW, Jeanty P. *Fetus* 1991;1:1.
30. Munoz H et al. *J Ultrasound Med* 1995;14:479–81.
31. Lee C et al. *Ann Thorac Surg* 2010;90(3):1011–4.
32. Sharma J et al. *Cardiol Young* 2009;19:403–6.
33. Hou CF et al. *Eur J Obstet Gynecol Reprod Biol* 2007;130(2): 271–2.
34. Tseng JJ et al. In utero diagnosis of cardiac hemangioma. *Ultrasound Obstet Gynecol* 1999;13(5):363–5.
35. Tongsong T et al. *Ultrasound Obstet Gynecol* 2004;24:207–9.
36. Yuan SM. *Z Geburtshilfe Neonatol* 2017;221(4):175–9.
37. Paladini D et al. *Obstet Gynecol* 2003;102(5 Pt 2):1174–6.
38. Ríos JC et al. *World J Pediatr Congenit Heart Surg* 2013;4(2): 210–2.
39. Schmaltz AA, Apitz J. *Pediatr Cardiol* 1982;2:73–5.
40. Lazarus KH et al. *Am J Pediatr Hematol Oncol* 1989;11:343–7.
41. Isaacs Jr H. *Tumors of the Fetus and Newborn*. Vol 35. Philadelphia, PA: Saunders; 1999:330–43.
42. Gedikbasi A et al. *Fetal Pediatr Pathol* 2010;29(5):330–7.
43. Satgé D et al. *Fetal Diagn Ther* 2005;20(1):44–7. Review.
44. Fieno DS et al. *J Cardiovasc Magn Reson* 2006;8(6):839–53.
45. Kiaffas MG et al. *Am J Cardiol* 2002;89(10):1229–33.

# 37

# The fetal thymus

Elena S. Sinkovskaya and Alfred Abuhamad

## Introduction

The thymus gland is a lymphoepithelial organ that plays an important role in immune response before and after birth. It is located in the central compartment of the thoracic cavity, above the heart and behind the sternum, and can be consistently identified on routine obstetrical ultrasound using high-resolution transducers.[1–4] The thymus gland was first described by Galen of Pergamum in 216 AD.[5] It remained, however, an "organ of mystery" for more than 2,000 years until its function was finally fully understood in the 1960s. In recent years, there has been a growing interest in assessing the fetal thymus due to increasing evidence in the literature supporting strong association between thymus abnormalities and a wide range of fetal and maternal complications during pregnancy, such as chromosomal aberrations, intrauterine growth restriction, preterm labor, or chorioamnionitis.[6–12] Furthermore, it is well known that small or absent thymus gland is identified in fetuses diagnosed with congenital heart defects, in particular, conotruncal anomalies, with increased fetal risk for DiGeorge syndrome.[13,14] We believe it is important for ultrasound specialists performing fetal echocardiography to be familiar with the current approach to sonographic evaluation of the fetal thymus. This chapter presents the embryologic development, normal anatomy, and typical sonographic appearance of the fetal thymus. Measurement techniques commonly used for assessment of the thymus size on obstetrical ultrasound are also presented.

## Embryogenesis and development of the thymus

The thymus gland originates from the ventral part of the third pharyngeal pouch and cleft complex on each side of the embryo.[15] By the sixth week postconception, it can be recognized as two elongated diverticula, which start to grow caudally into the surrounding neural crest mesenchyme. During the eighth week of development, each diverticulum continues its rapid descent toward the final destination within the thoracic cavity, where both diverticula merge together at the midline forming a bilobed structure containing by then elements derived from the three germinal layers.[15–18] Around the same time, the thymus completely loses its connection with pharyngeal pouches. Recent studies have suggested that neural crest cells play a critical role in organogenesis and morphogenesis of the thymus.[16] The thymus proliferation, descent, and positioning, as well as its separation from the pharynx are thought to depend on a series of signals from the surrounding neural crest mesenchyme. In addition, neural crest mesenchyme contributes to formation of the connective tissue, which forms the capsule and septa, contributing to the lobulated architecture of the thymic gland. Until the eighth week, the thymus primarily consists of epithelial elements. At this time, colonization of the thymus by hematopoietic stem cells (initially from the yolk sac and fetal liver and later from the bone marrow) begins, and by the end of the 10th week, over 95% of thymic cells belong to the T-cell lineage.[19,20] At 14–16 weeks, further differentiation of the thymic structure into cortex and medulla occurs.[21,22] The morphogenesis of the thymus is completed by 16–20 gestational weeks; however, its maturation and growth continue throughout fetal and neonatal life.[16,18]

The thymus undergoes significant changes over its lifetime. It reaches its greatest weight relative to body weight at birth with a mass approximately 15 grams.[23] It measures about 4–6 cm long, 2.5–5 cm wide, and 1 cm thick.[23] It continues to grow during the first year of life until it weighs about 20 grams and subsequently remains at this mass. As puberty is reached, the involution of the thymus begins to be characterized by a progressive decrease of the total amount of active lymphoid tissue and increased adipose infiltration.[18,23]

## Anatomy and function of the thymus

The thymus gland is a bilobed soft tissue organ that extends from the level of the fourth costal cartilage in the chest inferiorly up to the basis of the neck superiorly, sometimes as high as the lower border of the thyroid gland or even higher[23]—Figures 37.1 through 37.4. Lateral borders of the thymus are in direct contact with the pleura. The upper part of the trachea, anterior surface of the heart, and vessels of the superior mediastinum (left brachiocephalic vein, aortic arch, and pulmonary artery) are located along the posterior border of

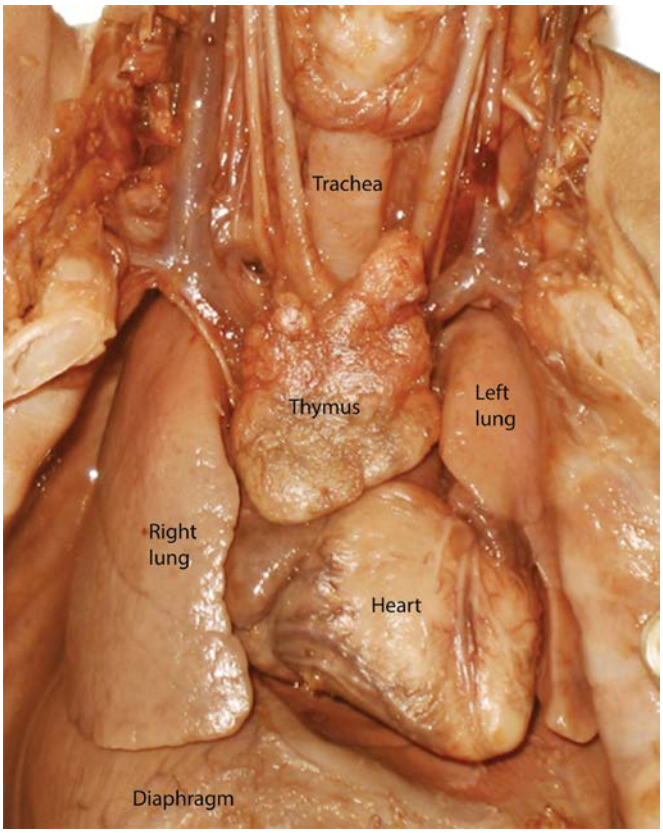


**Figure 37.1**
Anatomic specimen of the fetal thorax viewed from the front. Note the location of the thymus in the mediastinum and its relationship to the heart, lungs, and trachea.

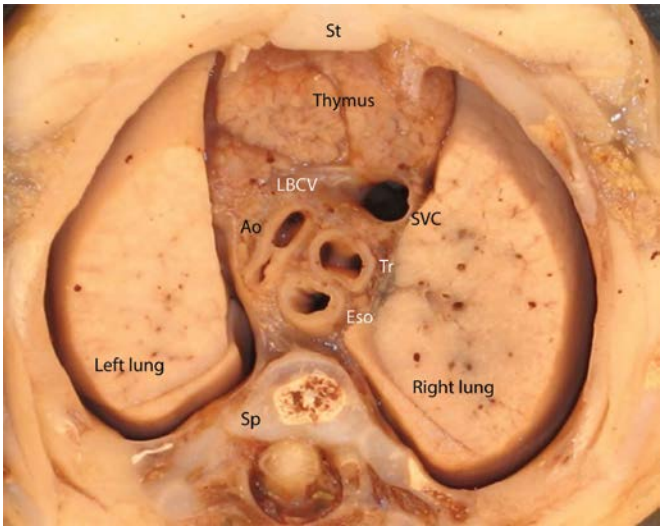


**Figure 37.2**
Anatomic specimen of the cross section of the upper fetal chest. Note two thymic lobes in typical location between manubrium sterni anteriorly and left brachiocephalic vein draining into superior vena cava posteriorly. (Ao, transverse aortic arch; Eso, esophagus; L, left; LBCV, left brachiocephalic vein; R, right; Sp, spine; St, sternum; SVC, superior vena cava; Tr, trachea.)

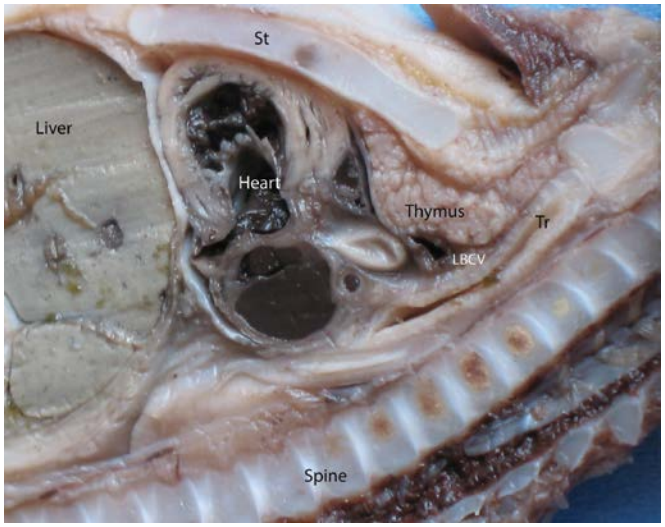


**Figure 37.3**
Anatomic specimen of the sagittal section of the fetal thorax. Note extension of the thymus from anterior surface of the heart in the chest inferiorly to the basis of the neck superiorly. Left brachiocephalic vein and trachea can be identified along posterior border of the thymus. (LBCV, left brachiocephalic vein; St, sternum; Tr, trachea.)

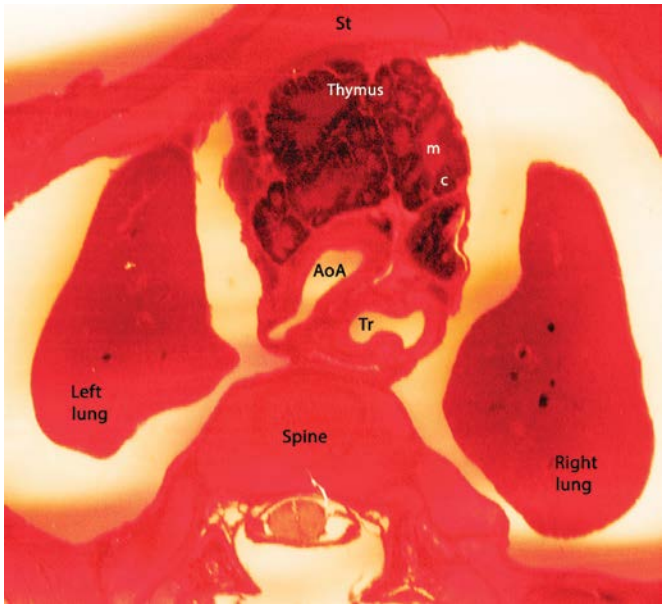


**Figure 37.4**
Histologic specimen of the fetal chest at 16 weeks gestation. Note multiple lobules of different size and orientation compose the structure of the thymus. The central medulla (m), containing mostly epithelial cells, and the outer cortex (c), containing thymic lymphocytes, can be recognized within each lobule. (AoA, transverse aortic arch; St, sternum; Tr, trachea.)

the thymus. The anterior surface of the thymus is covered by manubrium sterni and origins of the sternohyoid and sternothyroid muscles (Figure 37.3). The upper pole of the left lobe usually extends higher to the neck region than the upper pole of the right lobe (Figure 37.1). Conversely, the lower end of the

right lobe is located deeper in the chest and commonly lies between the right side of the ascending aorta and the right lung. Prenatally and at birth, the anterior-posterior diameter of the thymic lobes is thickest inferiorly and thins out toward its superior aspect.

Thymic lobes come into close contact at the midline in the superior mediastinum (Figure 37.2). Histologically, within each lobe capsule, cortex, medulla, and vascular corticomedullary junction can be distinguished.[24] A thin connective tissue capsule surrounds each lobe and gives rise to multiple septa, which partially subdivide the thymus into interconnecting lobules of variable size and orientation.[25] The cortex is densely populated by thymic lymphocytes, also called thymocytes, whereas the medulla is composed primarily of epithelial cells.[22]

The thymus receives blood supply mainly from the branches of the internal thoracic and inferior thyroid arteries. Venous return from the thymus occurs via corresponding small veins into internal thoracic, inferior thyroid, and left brachiocephalic veins or, in rare instances, directly into the superior vena cava.

The role of the thymus as an immune organ was uncovered by Australian immunologist Jacques Miller in 1961.[26] Since that revolutionary discovery, the function of the thymus and the role that it plays in the immune response were extensively investigated and reported. Generating functional T-lymphocytes is considered to be the primary role of the thymus in cellular immunity. Thymic epithelial cells provide a unique environment for T-lymphocyte development, maturation, and differentiation.[16] The process of positive and negative selection also occurs in the thymus to ensure the specificity of produced T cells.

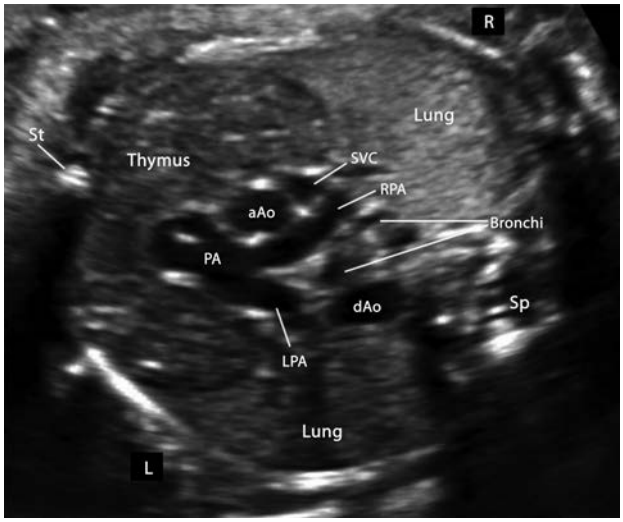


**Figure 37.5**
Cross section of the chest at the level of the three vessel view in a normal fetus at 27 weeks gestation. Typical location of the thymus behind the anterior thoracic wall and in front of the great vessels is shown. Note oval shape of the thymus gland with slight hypoechogenicity in comparison to the surrounding lungs parenchyma. (aAo, ascending aorta; dAo, descending aorta; LPA, left pulmonary artery; PA, pulmonary artery; RPA, right pulmonary artery; Sp, spine; St, sternum; SVC, superior vena cava; Tr, trachea; L, left; R, right.)

## Visualization techniques

On routine grayscale ultrasound, the thymus gland can be demonstrated in several transverse and sagittal views of the fetal chest (Figures 37.5 through 37.11). It is visualized as soft tissue, which occupies space in the anterior mediastinum between the sternum and great vessels of the heart. Echo-structure of the thymus is mostly homogeneous, but some echogenic linear elements can be present within its texture. Usually the thymic tissue appears slightly less echogenic than surrounding lung parenchyma and shows no significant change in its sonolucency between 14 and 38 weeks' gestation.[2]

The three-vessel trachea view is most commonly used for evaluation of the fetal thymus. In this plane, the thymus can be identified between the lungs and directly behind the anterior thoracic wall, with an oval or rectangular shape (Figure 37.6). The thymus gland can also be identified in the sagittal plane of the chest, where it is triangular in appearance (Figures 37.9 through 37.11). The visualization of the posterior border of the thymus can be best achieved in a slightly more cranial plane to the three-vessel trachea view, demonstrating a course of left brachiocephalic (innominate) vein (Figure 37.8). In this view, the left brachiocephalic vein is shown in longitudinal orientation as it crosses the mediastinum along the posterior border of the thymus and drains into the superior vena cava. Therefore, the differentiation of the thymic area from surrounding lungs tissue can be improved by implementing the "thy-box" technique proposed by Paladini. This method utilizes color Doppler mapping of the course of the internal thoracic arteries as a landmark to enhance the visualization of lateral thymic borders (Figure 37.12) and has been shown to be helpful in recognizing the fetal thymus in normal and abnormal conditions.[27] The high-frequency convex or linear transabdominal transducers and low-scale Doppler presets are required for imaging optimization.[27]

Several studies have demonstrated the utility of three-dimensional and spatiotemporal image correlation (STIC) ultrasound in imaging of the fetal thymus in normal and abnormal conditions.[4,28] The main advantage of these modalities lies in the ability to reconstruct the fetal thymus in its entirety and display its shape as well as its spatial relationship with other anatomical structures of the mediastinum. Therefore, three-dimensional (3D) ultrasound can ease the visualization of the perithymic course of the mammary arteries when the "thy-box" technique is used by providing thicker slices for analysis (Figure 37.13).[27] Thus, 3D or four-dimensional (4D) ultrasound can be particularly useful for the differential diagnosis of thymus anomalies and may improve the accuracy of prenatal diagnosis of fetal conditions associated with abnormal thymus.

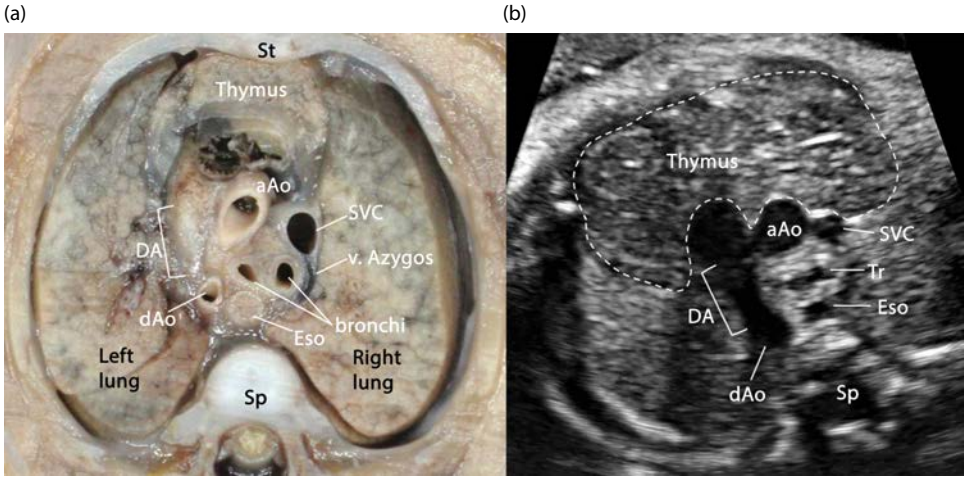


**Figure 37.6**
Transverse section of the upper fetal chest at the level of transverse view of arterial duct in anatomic specimen (a) and gray scale ultrasound (b) in a normal fetus at 30 weeks gestation. (aAo, ascending aorta; DA, ductus arteriosus; dAo, descending aorta; Eso, esophagus; PA, pulmonary artery; Sp, spine; St, sternum; SVC, superior vena cava; Tr, trachea; L, left; R, right.)

Successful ultrasound evaluation of fetal thymus also has been reported in early gestation using high-resolution transabdominal or transvaginal transducers.[29,30] Borgelt et al. performed a retrospective evaluation of the fetal thymus on a large cohort of 971 singleton pregnancies between 11 + 0 and 13 + 6 weeks of gestation using stored images of the fetal midsagittal plane.[29] In this view, the fetal thymus was identified as tissue between the internal border of the sternum and the external border of the ascending aorta (Figure 37.14). Visualization of the thymus between 13 and 16 weeks is also possible in the transverse plane of the upper mediastinum, at the level of the three-vessel trachea view, using both the grayscale mode and color Doppler "thy-box" techniques (Figure 37.15).[30]

Multiple prospective and retrospective studies have demonstrated that ultrasound assessment of the thymic structure, shape, and size is feasible and can be consistently achieved throughout gestation. In 1989, Felker et al., for the first time, showed that the thymus can be imaged by ultrasound in most fetuses in the second and third trimesters with a successful visualization rate of 74%.[1] Substantial advancements in technical aspects of ultrasound imaging in the last three decades allowed significant improvement in our ability to perform detailed evaluation of the fetal anatomical structures including the thymus. Recent studies have reported that assessment of the fetal thymus using 2D and 3D is possible in 95%–99% of cases between 17 and 39 weeks.[2,4] Moreover, visualization of the thymus

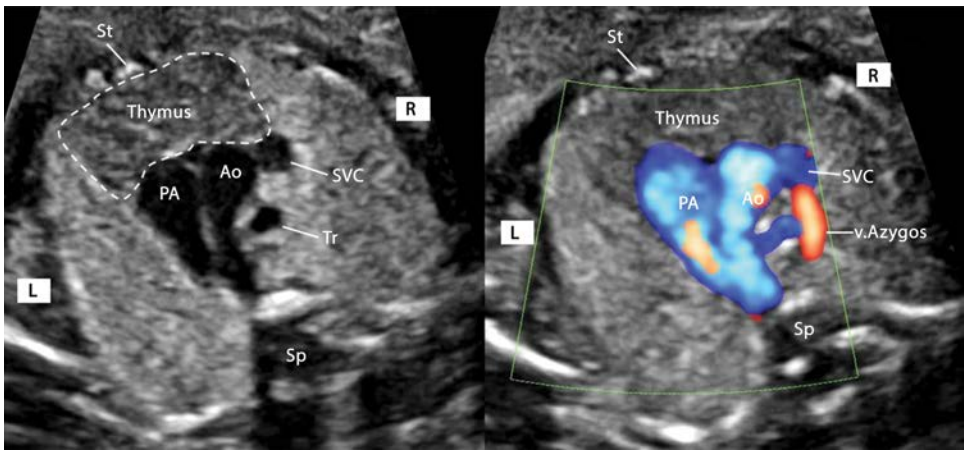


**Figure 37.7**
Transverse oblique section of the upper fetal chest at the level of three vessel trachea view in gray scale (a) and color Doppler imaging (b) in a normal fetus at 24 weeks gestation. Note that the thymus has rectangular shape (traced using dashed line) and can be identified directly behind the anterior thoracic wall. (Ao, ascending aorta; PA, pulmonary artery; Sp, spine; St, sternum; SVC, superior vena cava; Tr, trachea; L, left; R, right.)

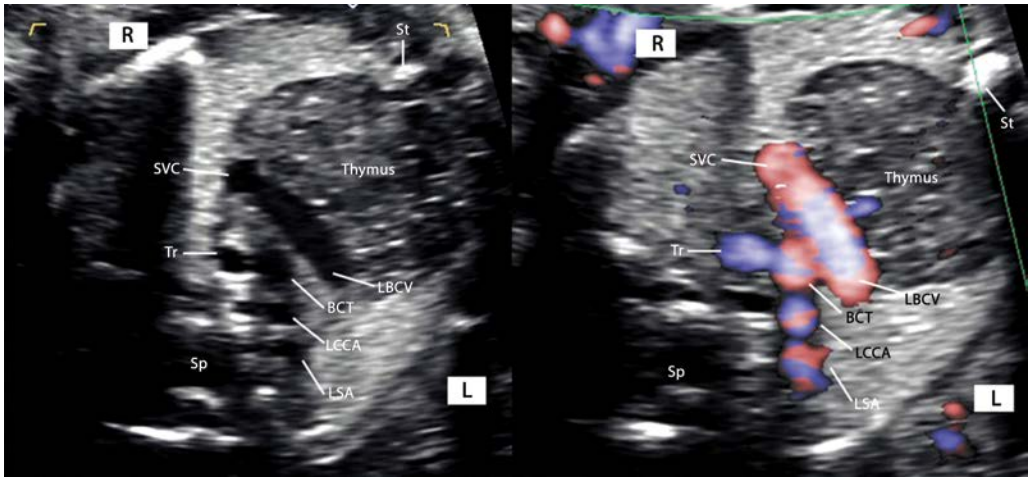


**Figure 37.8**
Transverse oblique section of the upper fetal chest at the level of drainage of left brachiocephalic vein into superior vena cava in gray scale (a) and color Doppler imaging (b) in a normal fetus at 32 weeks gestation. Thymus has oval shape with multiple linear bright echos within its structure. Note that at this level, left brachiocephalic vein runs along the posterior border of the thymus and can be used as a landmark facilitating thymus visualization. (BCT, brachiocephalic trunk; LBCV, left brachiocephalic vein; LCCA, left common carotid artery; LSA, left subclavian artery; Sp, spine; St, sternum; SVC, superior vena cava; Tr, trachea; L, left; R, right.)

can be equally successful in singleton and twin pregnancies at this gestational age.[4,31] Color Doppler sonography can further enhance the imaging, thus providing a reliable tool for thymic evaluation from 13 weeks' gestation onward.[30] By applying the "thy-box" technique in a group of 287 low-risk singleton pregnancies in early gestation, Weissmann-Brenner et al. demonstrated that visualization of the thymus can be achieved in 75% of cases at 13 weeks, in 96% of cases between 14 and 15 weeks, and in 94% of fetuses at 16 weeks' gestation.[30] Assessment of the fetal thymus using 3D/4D or STIC modalities was reported to be successful in 78%–95% of uncomplicated pregnancies.[4,28]

However, despite recent advances in ultrasound technologies, there are still some limitations to thymus visualization. The delineation of the thymus margins can be suboptimal due to unfavorable fetal position or maternal body habitus; those factors also make it especially challenging in early gestation. In addition, visualization of the fetal thymus can be limited by the presence of fetal thoracic or cardiac abnormalities, such as severe cardiomegaly, diaphragmatic hernia,

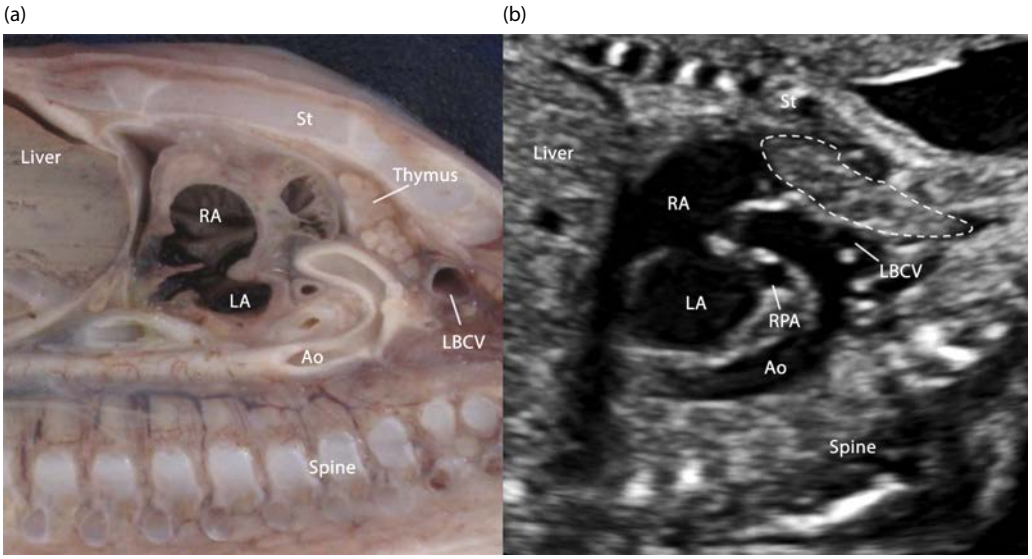


**Figure 37.9**
Sagittal view of the fetal chest at the level of aortic arch in pathology specimen (a) and gray scale imaging (b) in a normal fetus at 23 weeks gestation. Note shape of the thymus, which looks more triangular (traced with dashed line). (Ao, aorta; LA, left atrium; LBCV, left brachiocephalic vein; RA, right atrium; RPA, right pulmonary artery; St, sternum.)

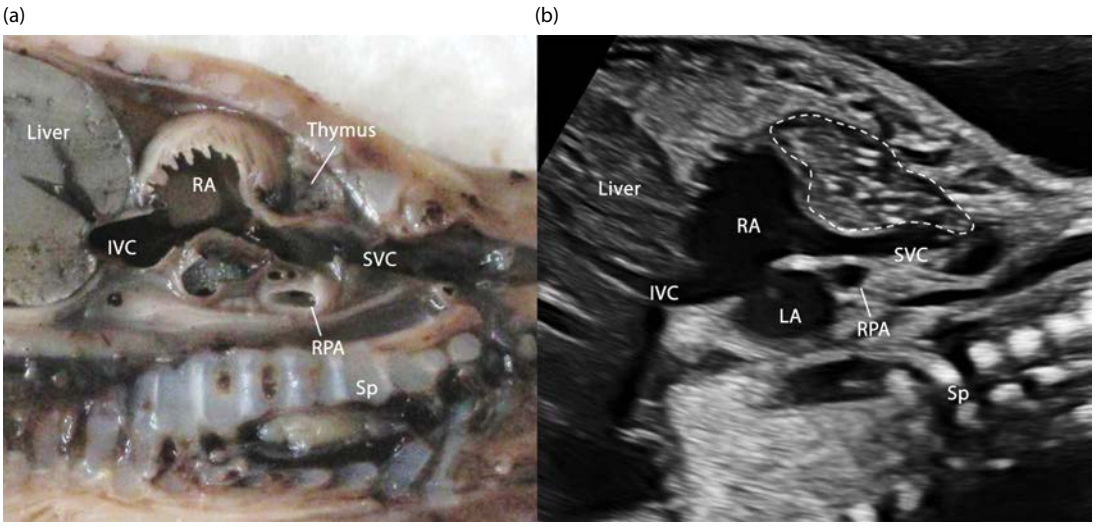


**Figure 37.10**
Right parasagittal view of the fetal chest at the level of caval veins drainage into the right atrium in pathology specimen (a) and gray scale imaging (b) in a normal fetus at 25 weeks gestation. Note shape of the thymus (traced with dashed line). (IVC, inferior vena cava; LA, left atrium; RA, right atrium; RPA, right pulmonary artery; SVC, superior vena cava.)

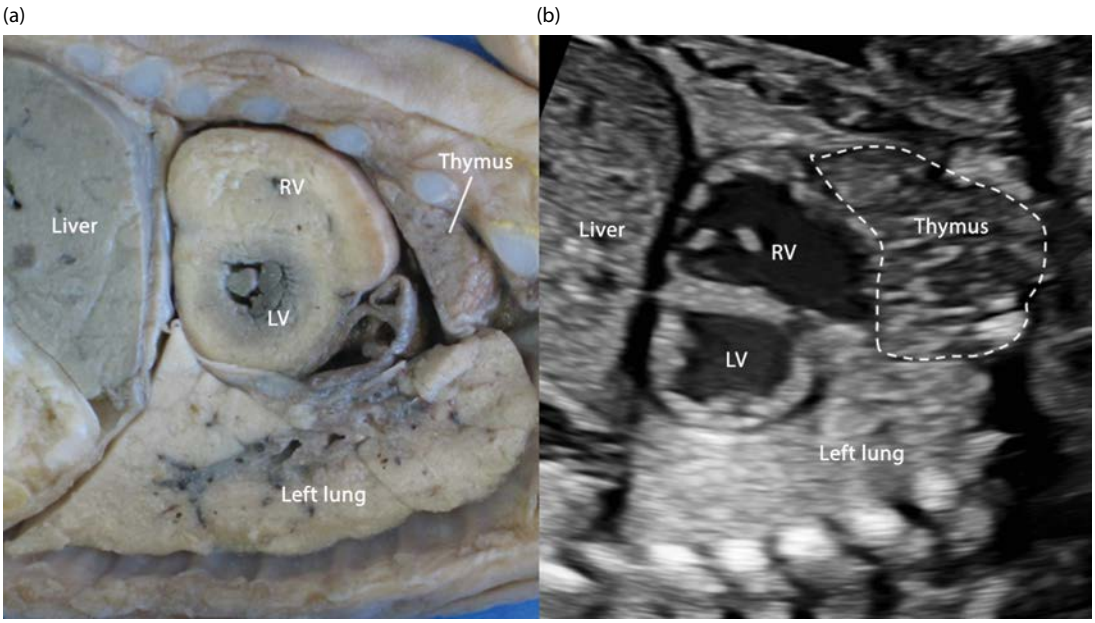


**Figure 37.11**
Left parasagittal view of the fetal chest at the level of ventricular short axis in pathology specimen (a) and gray scale imaging (b) in a normal fetus at 25 weeks gestation. Note shape of the thymus (traced with dashed line). (LV, left atrium; RV, right atrium.)

cystic lung lesions, hydrothorax, and pericardial effusion or tumor resulting in thymus compression and displacement from its typical position (Figure 37.16). Acoustic shadows from ribs, extremities, or sternum, as well as fetal movements can prevent full depiction of the thymus during 3D/4D or STIC acquisition. Leon-Luis et al. demonstrated that ultrafast magnetic resonance imaging (MRI) can be successfully used to image the fetal thymus and potentially may help to overcome some limitations inherent to ultrasound technology[32] (Figure 37.17).

## Thymus size assessment

Assessment of thymus dimensions is not required to be performed routinely in fetal ultrasound examinations but can be strongly indicated in certain clinical situations. Thus, it is important to be familiar with different ultrasound techniques used for thymus biometry. Several sonographic parameters were proposed for quantitative evaluation of the thymus size, including anterior-posterior diameter, transverse diameter, superior-inferior diameter, transverse

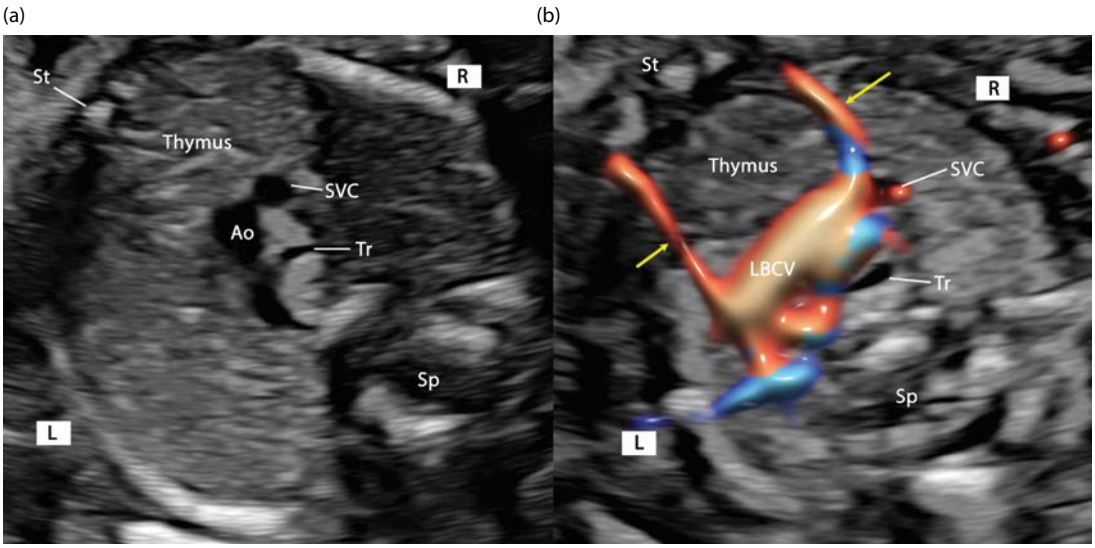


**Figure 37.12**
Transverse section of the upper fetal chest at the level of transverse view of aortic arch in gray scale (a) and color Doppler imaging—"Thy-Box" technique (b) in a normal fetus at 23 weeks gestation. Note course of internal thoracic arteries (yellow arrows), allowing better delineation of the lateral margins of the thymus in comparison to just 2D imaging. (Ao, aorta; LBCV, left brachiocephalic vein; Sp, spine; St, sternum; SVC, superior vena cava; Tr, trachea; L, left; R, right.)

perimeter/area, thymic-thoracic ratio (TT-ratio), and thymus volume measurements (Figures 37.18 through 37.24). The majority of these measurements can be performed in the transverse planes of the upper mediastinum at the level of the three-vessel trachea view, which is routinely obtained during midtrimester screening evaluation (Figure 37.18d). Fetal thymus size is similar in fetuses from singleton and twin pregnancies and is not influenced by fetal gender.[4,31,33,34]

On initial report in the late 1980s anterior-posterior diameter or thickness was found to be the most consistently obtainable measurement of the thymus prenatally.[1] The anterior-posterior diameter of the thymus is measured along the midline of the fetal thorax with calipers placed at the internal border of the chest wall anteriorly and at the leading age of the transverse aortic arch posteriorly. Mean thymic thickness increases with advancing gestation from 2 mm at 14 weeks to about 21 mm at term, showing large

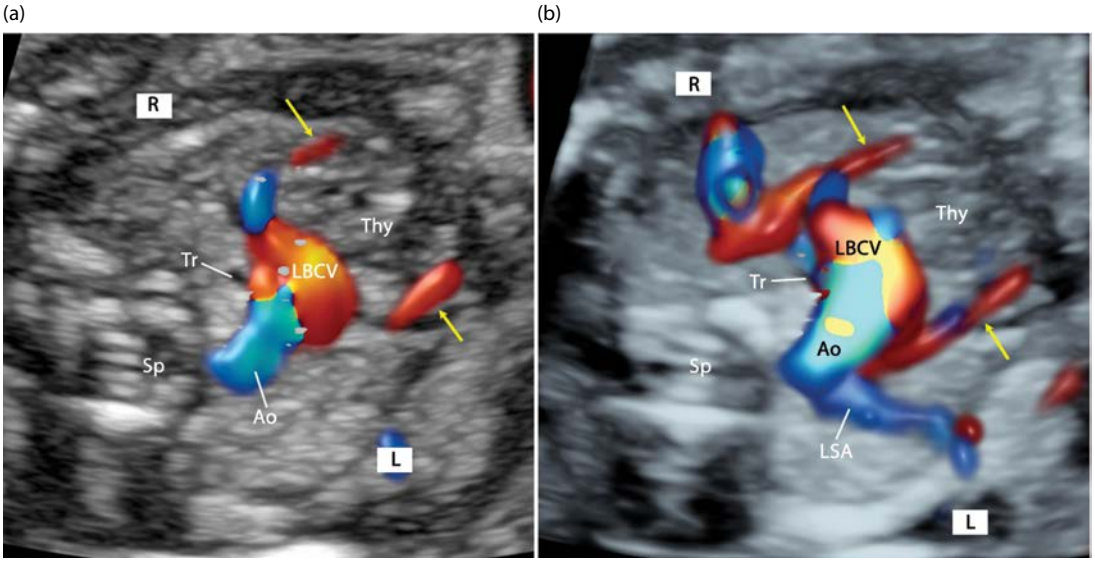


**Figure 37.13**
"Thy-box" technique for evaluation of the fetal thymus using 2D (a) and 3D (b) ultrasound imaging on the same normal fetus at 22 weeks gestation. Note that thicker slice obtained by 3D ultrasound allows better visualization of the internal thoracic arteries (yellow arrows) highlighting the lateral borders of the thymus. (Ao, aorta; LBCV, left brachiocephalic vein; LSA, left subclavian artery; Sp, spine; Thy, thymus; Tr, trachea; L, left; R, right.)

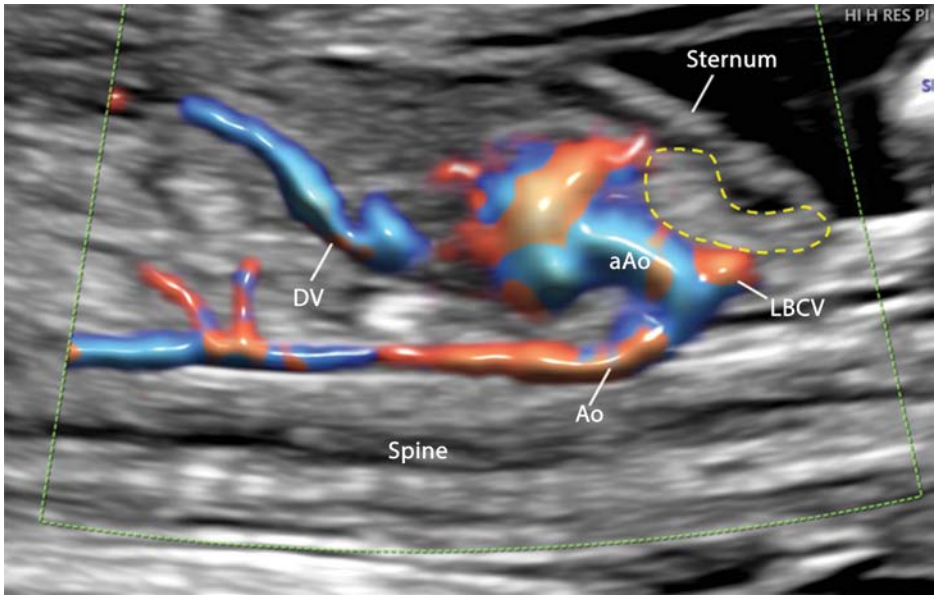


**Figure 37.14**
Mid-sagittal view of the fetus at $12^{+6}$ weeks gestation using transabdominal 2D ultrasound imaging. Note shape (traced with dashed line) and typical location of the thymus between ascending aorta and anterior chest wall. (aAo, ascending aorta; Ao, descending aorta; DV, ductus venosus; LBCV, left brachiocephalic vein.)

measurement variation after 30 weeks.[1] When performing first-trimester screening, measurement of the anterior-posterior thymic diameter can be reliably obtained in the midsagittal plane of the fetal chest.[29] Calipers should be placed between the internal border of the thoracic wall and the anterior wall of the ascending aorta and had to be perpendicular to a tangent to the skin (Figure 37.20). This measurement shows positive linear correlation with crown-rump length.

Thymic maximum perimeter and area measurements can be obtained by manual tracing with electronic calipers along the margins of the thymus gland on the three-vessel trachea plane (Figure 37.18c). Both parameters show linear growth during pregnancy.[2,4] Mean thymus perimeter measures about 22 mm at 14 gestational weeks and extends to 128 at 38 weeks.[2] In the same ultrasound image, maximum transverse diameter of the thymus can be assessed (Figure 37.18b). To perform this measurement, calipers are placed at the lateral thymic borders and

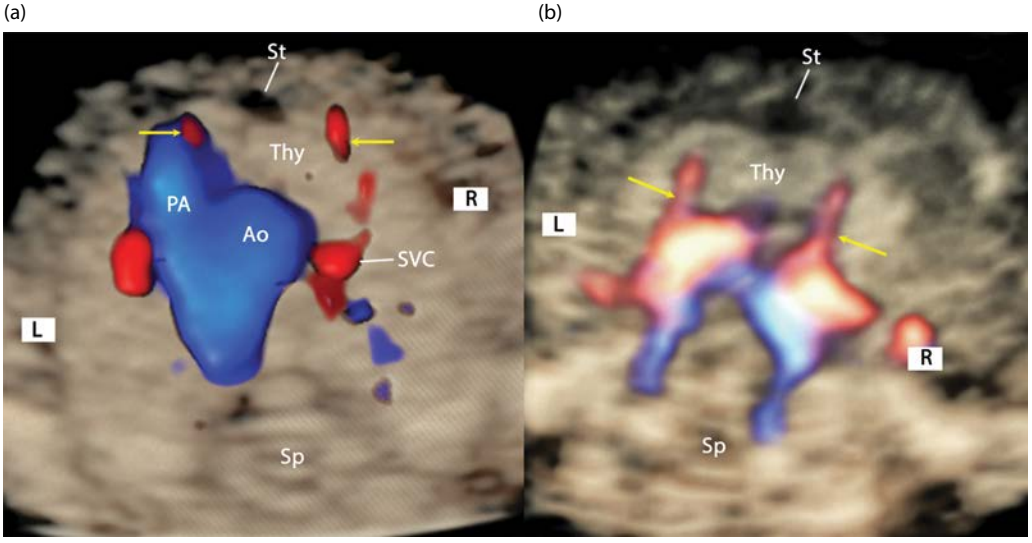


**Figure 37.15**
"Thy-box" technique for evaluation of the thymus using transvaginal 3D ultrasound imaging on a normal fetus at $13^{+3}$ weeks gestation. Note course of internal thoracic arteries (yellow arrows) allowing better delineation of the lateral margins of the thymus on the three vessel trachea view (a) and slightly higher plane (b). (Ao, aorta; PA, pulmonary artery; Sp, spine; St, sternum; SVC, superior vena cava; Thy, thymus; L, left; R, right.)

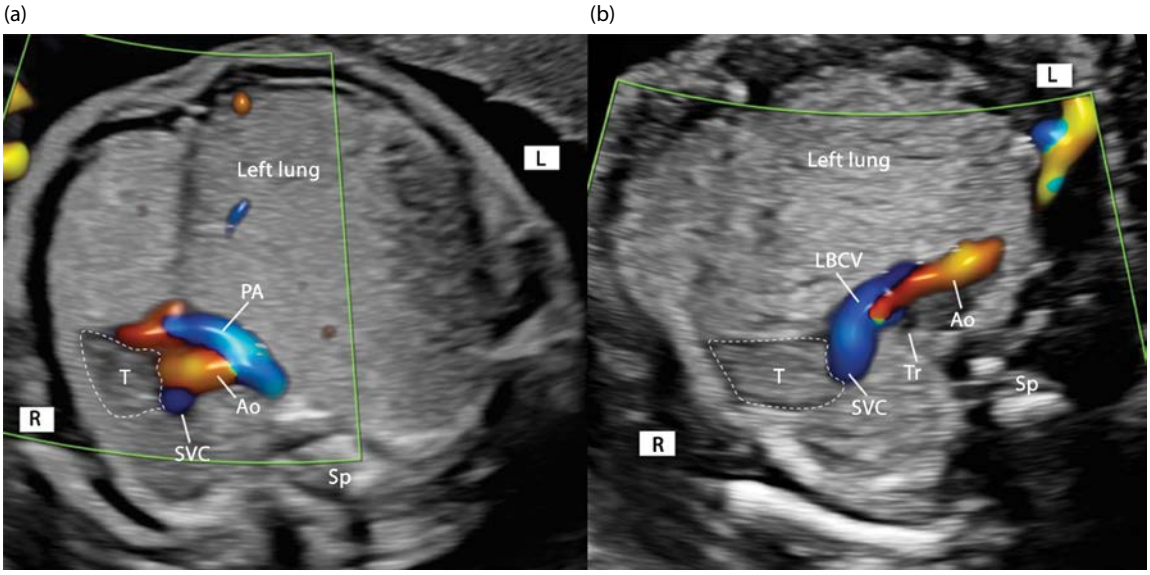


**Figure 37.16**
Transverse oblique section of the upper fetal chest at the level of three vessel trachea view (a) and slightly higher plane (b) in a fetus at 24 weeks gestation with large left-sided congenital cystic adenomatoid malformation. Note that the thymus (traced using dashed line) and great vessels are displaced from their typical position into the right chest. (Ao, aorta; LBCV, left brachiocephalic vein; PA, pulmonary artery; Sp, spine; SVC, superior vena cava; Tr, trachea; L, left; R, right.)

perpendicular to the anterior-posterior line, which divides the chest into two equal halves by connecting the sternum to the spine. The transverse diameter of the fetal thymus correlates with gestational age and parameters of fetal biometry (biparietal diameter [BPD], femur length [FL], and abdominal circumference [AC]) in a linear manner.[3] Accuracy of the transverse thymic diameter measurement can be improved by utilizing thy-box technique, which allows better delineation of the lateral thymic borders.[34]

Despite excellent feasibility, linear measurements of the thymic size can demonstrate significant inter- and intraob-server variability, especially when image quality is suboptimal, which can limit their clinical applicability. In addition, the normal thymus demonstrates a great deal of variation in shape, size, and volume, which can make a single measurement insufficient for objective representation of the organ's size.

The alternative method to estimate size of the fetal thymus was recently proposed by Chaoui et al. and called the "thymic-thoracic ratio" or TT-ratio.[35] The TT-ratio is calculated by dividing the anterior-posterior thymic diameter over the intrathoracic mediastinal diameter (Figure 37.18d). Measurement of the anterior-posterior thymic diameter is

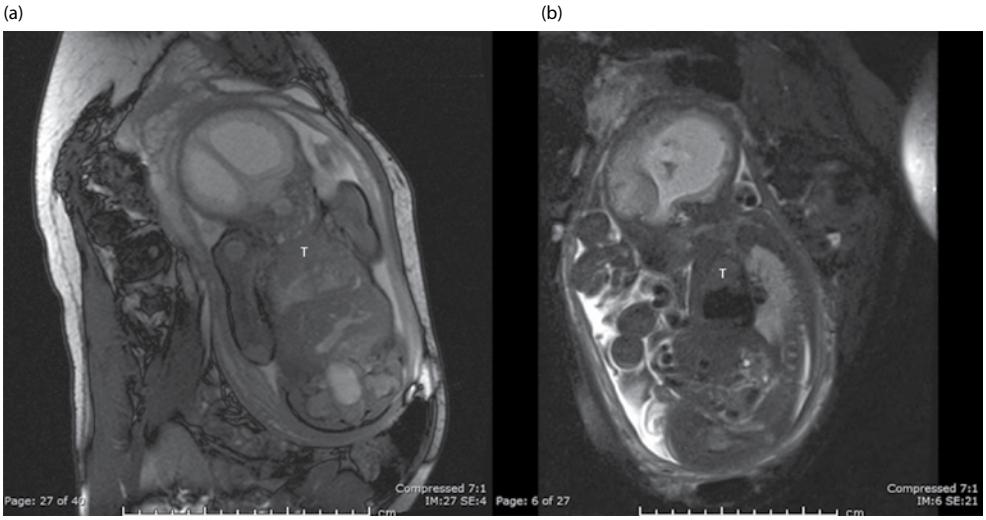


**Figure 37.17**
Fetal MRI "HASTE" T2-weighted sequence at 30 weeks gestation. Fetal thymus (T) is shown in coronal (a) and sagittal (b) plane. (Courtesy of Wendy T. Brown MD, MPH.)

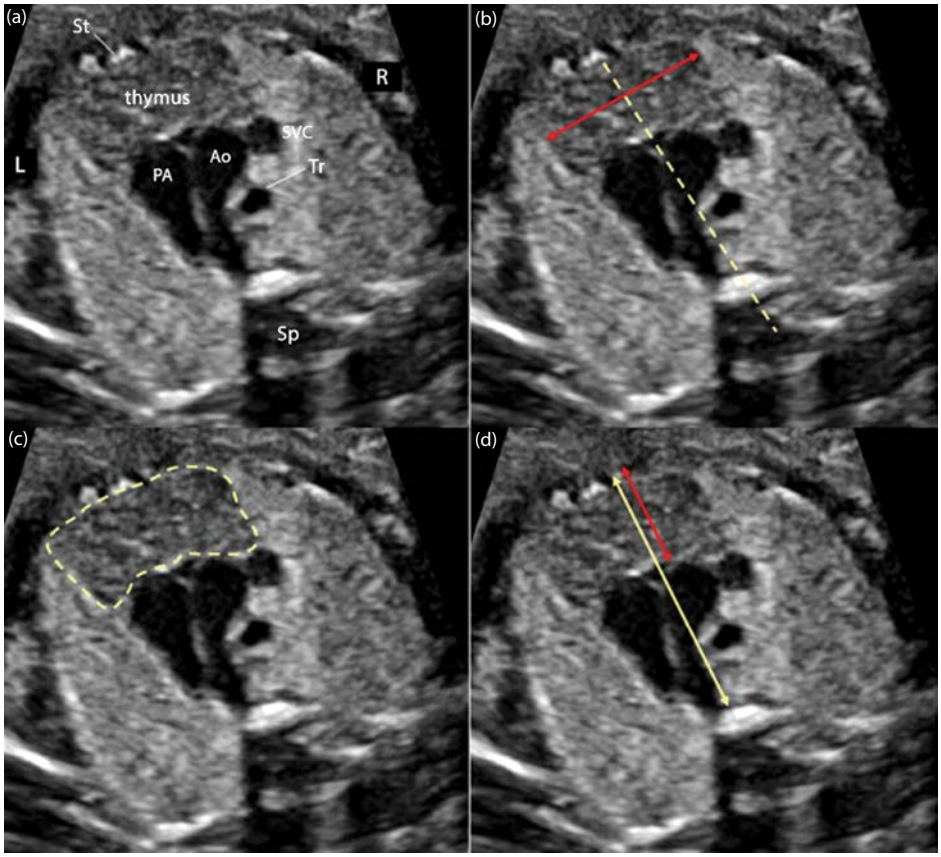


**Figure 37.18**
Assessment of the thymus size using transverse oblique section of the upper fetal chest at the level of three vessel trachea view. (a) Anatomical landmarks of the three vessel Atrachea view; (b) measurement of maximum transverse thymus diameter by placing calipers at the lateral thymic borders and perpendicular to the mid-line of the chest; (c) thymic maximum perimeter and area measurements obtained by manual tracing with electronic calipers along the margins of the thymus gland; (d) measurements required for TT-ratio calculation. The anterior–posterior diameter of the thymus (red line) is measured along the mid-line of the fetal thorax with calipers placed at the internal border of the chest wall anteriorly and at the leading edge of the transverse aortic arch posteriorly. The intrathoracic mediastinal diameter (yellow line) is measured along the mid-line of the fetal thorax with calipers placed at the internal border of the chest wall and anterior edge of the thoracic vertebral body. (Ao, aorta; PA, pulmonary artery; Sp, spine; St, sternum; SVC, superior vena cava; Tr, trachea; L, left; R, right.)

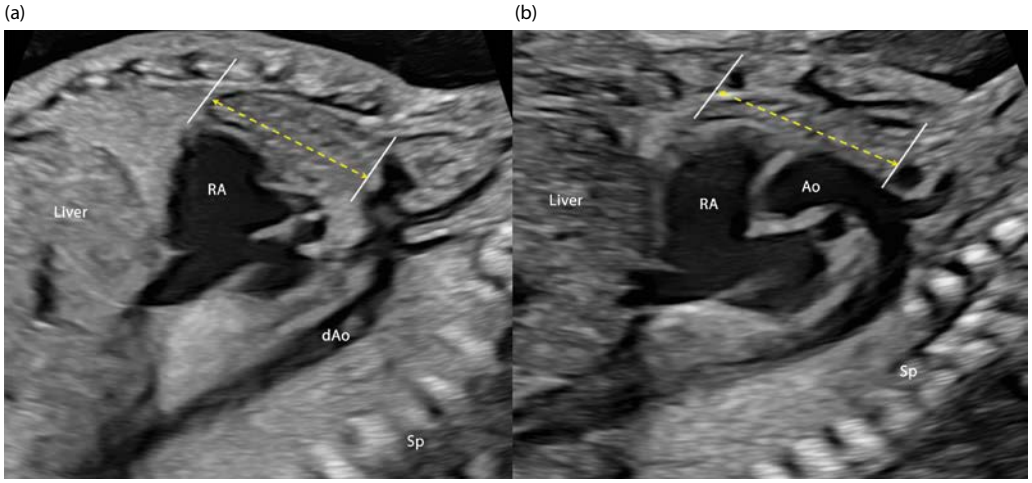


**Figure 37.19**
Assessment of the thymus size using sagittal view of the fetal chest at the level of aortic arch view. Measurement of superior–inferior diameter in two fetuses with right-sided (a) and left-sided (b) aortic arch is demonstrated. (Ao, ascending aorta; dAo, descending aorta; RA, right atrium; Sp, spine.)

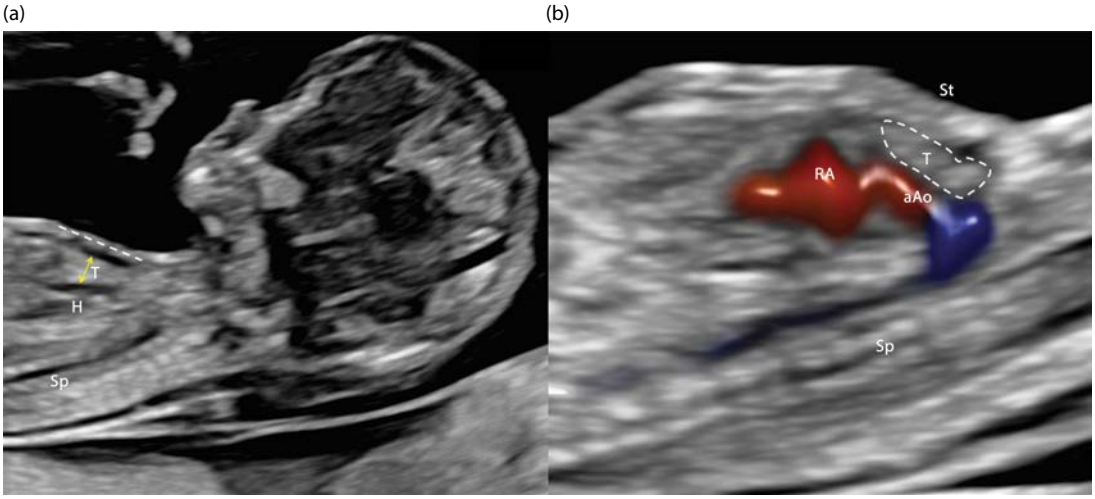


**Figure 37.20**
Assessment of the thymus size in the first trimester using mid-sagittal view. The anterior–posterior thymic diameter measurement obtained by placing calipers between the internal border of the thoracic wall and the anterior wall of the ascending aorta and had to be perpendicular to a tangent to the skin (a). Using magnified image with better contrast resolution, thymus perimeter also can be traced (b). (aAo, ascending aorta, H, heart; RA, right atrium; Sp, spine; St, sternum; T, thymus.)

performed using the technique described previously. The intrathoracic mediastinal diameter is measured along the midline of the fetal thorax with calipers placed at the internal border of the chest wall and anterior edge of the thoracic vertebral body. The TT-ratio has important advantages over other parameters, as it shows no change during pregnancy with a mean value of $0.44 \pm 0.04$, which makes interpretation of the results easier.[35]

Thymic volume can be estimated using Virtual Organ Computer-aided AnaLysis (VOCAL) software applied to offline analysis of the 3D or STIC volume datasets acquired at the axial plane of the fetal upper chest (Figures 37.21 through

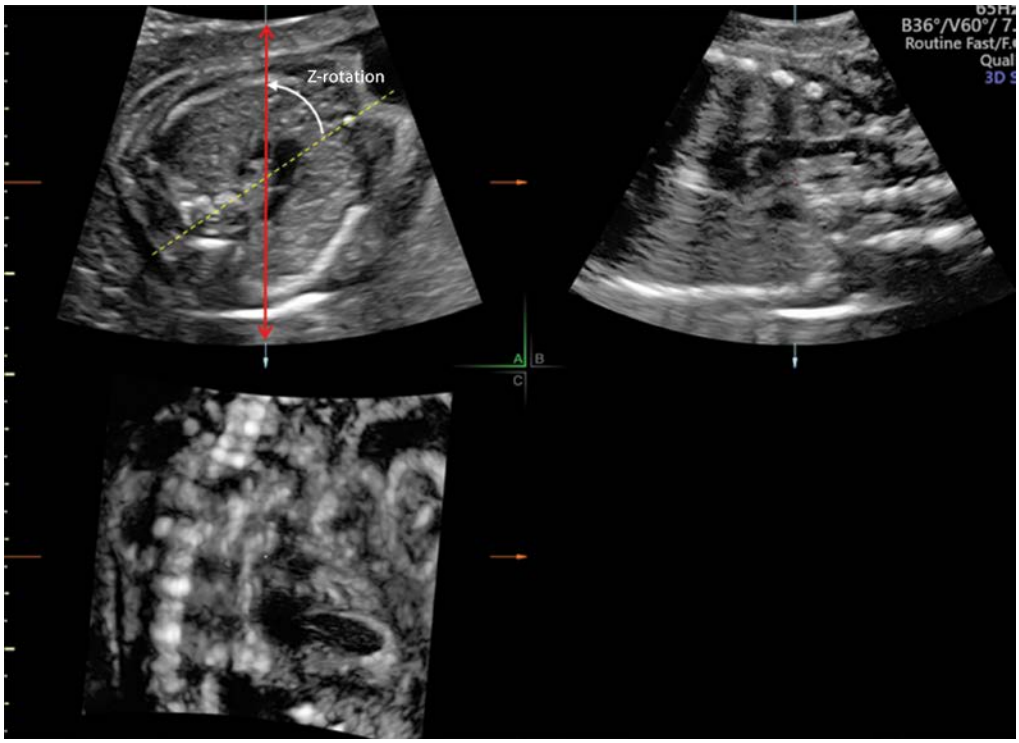


**Figure 37.21**
Assessment of the thymic volume using virtual organ computer-aided analysis (VOCAL). Initial multiplanar view of a 3-D sonographic volume of the fetal chest.

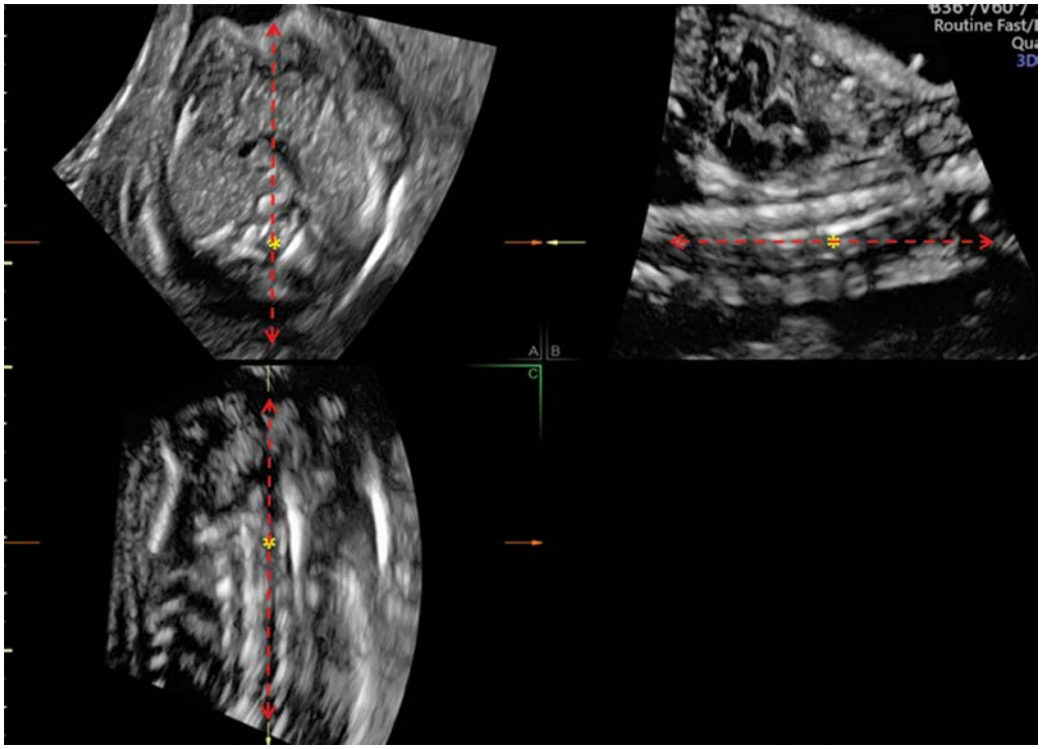


**Figure 37.22**
Assessment of the thymic volume using virtual organ computer-aided analysis (VOCAL). Standardization of volume display. Plane A is rotated along the z-axis until the spine was at the 6-o'clock position. Reference/rotational point is placed in the fetal spine in plane A. Standardization in planes B and C is achieved when the spine is aligned horizontally and vertically in planes B and C, respectively.

37.24). Initially, 3D volume datasets need to be displayed in the multiplanar format and standardized. The multiplanar display of 3D volumes will show the reference plane (plane of acquisition—the axial plane of the fetal upper chest) in the left upper plane (plane A) and the two orthogonal planes to the reference plane in the right upper plane (plane B) and left lower plane (plane C), respectively. Standardization of the volume dataset display can be achieved by ensuring a uniform orientation of the spine in planes A, B, and C, respectively. This is accomplished by rotating plane A along the *z*-axis (*z*-rotation) to place the spine at the 6 o'clock position (Figure 37.21). When the reference point is placed on the fetal spine in plane A, a longitudinal view of the spine is displayed in planes B and C. Standardization in planes B and C is achieved when the spine is aligned horizontally and vertically in planes B and C, respectively (*z*-rotation in each plane) (Figure 37.22). As standardization is complete, the VOCAL tool can be enabled. This software allows rotation of the plane A 180° around a fixed central axis with a rotation step of 6°, 9°, 15°, or 30°, resulting in automatic extraction of the multiple 2D planes from the volume. The contour of the thymus is required to be traced manually on each plane (Figure 37.23), and after that, software automatically generates a 3D reconstructive image of the thymus together with thymic volume measurement (Figure 37.24). Lie et al. first reported on using 3D ultrasound to evaluate the volume of the developing fetal thymus.[4] Results of this study suggest that thymic volume is more significantly correlated with gestational age than are linear measurements such as diameter or perimeter, as it better accounts for thymus shape. Therefore, normal values for thymus volume during uncomplicated pregnancy were established (Table 37.1).

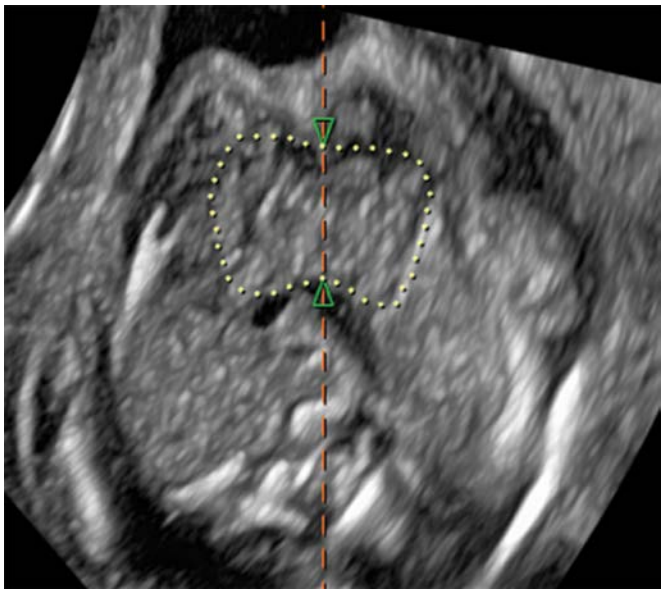

**Figure 37.23**
Assessment of the thymic volume using virtual organ computer-aided analysis (VOCAL). Manual tracing of the thymus contour.

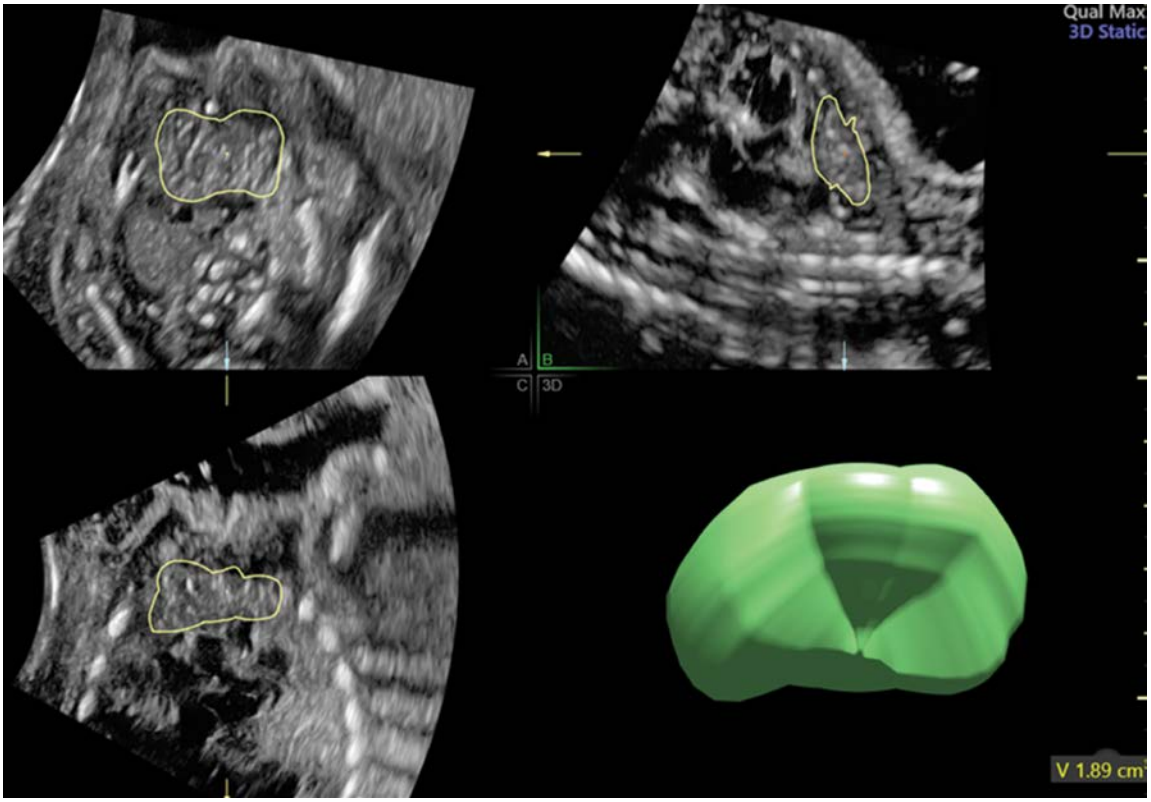


**Figure 37.24**
Assessment of the thymic volume using virtual organ computer-aided analysis (VOCAL). Software automatically generates 3D reconstructive image of the thymus together with thymic volume measurement.

Finally, in selected cases, fetal MRI can be of help to measure the fetal thymus. Excellent correlation was found between measurements of the transverse diameter and perimeter of the thymus obtained by ultrafast MRI and ultrasound.[32] Moreover, it was suggested that reference nomograms for thymic size evaluation established based on ultrasound data also can be used for interpretation of the MRI-retrieved dimensions, as the mean difference between MRI and ultrasound measurements was less than 5% (Figure 37.25).[32] Nomograms of the fetal transverse thymic diameter and perimeter are presented in Figures 37.26 and 37.27. For additional information, please refer to the literature.[1–4,29,35,36]

## Abnormalities of the fetal thymus

Absence or diminutive size is the most common abnormality of the fetal thymus that can be detected on prenatal ultrasound (Figures 37.19 through 37.24). Despite this, nomograms for thymus growth during uncomplicated pregnancy have been established using 2D and 3D ultrasound, but well-defined criteria for diagnosis of the thymus hypoplasia do not yet exist. It is generally accepted that fetal thymus can be defined as small or hypoplastic when its diameter, perimeter, or volume measures below the fifth percentile for given gestational age. If the TT-ratio is used for thymus size evaluation, the value of 0.35 was suggested to be a cut-off.[35] In addition, visualization of the great vessels right behind the anterior thoracic wall should immediately raise suspicion for absent or hypoplastic thymus (Figures 37.28 through 37.33). This observation was supported by data reported by Paladini, revealing that visualization of the internal thoracic arteries is difficult or not possible due to significant anterior displacement of the great arteries in case of thymus aplasia[27] (Figure 37.30). Therefore, use of the thy-box technique in the presence of hypoplastic thymus usually demonstrates a converse rather than parallel course of the mammary vessels.

Strong association between thymus hypoplasia/aplasia and fetal risk for chromosomal aberrations, especially 22q11.2 microdeletion, is well established and extensively published in the literature.[13,37–40] Deletion in the specific region q11.2 in chromosome 22 can be phenotypically presented as a wide range of syndromes, including DiGeorge syndrome (hypoglycemia secondary to parathyroid hypoplasia, T-cell deficiency due to thymus hypoplasia/aplasia, and cardiac anomaly), velocardiofacial or Shprintzen syndrome (facial abnormality, cleft palate, and cardiac anomaly), and Takao syndrome (cardiac anomaly and facial anomaly). As these syndromes share genetic and embryologic origins and demonstrate significant overlap in clinical presentation, the acronym CARCH22 is frequently used to refer to these conditions.

In clinical practice, ultrasound diagnosis of the fetal cardiac malformation in particular conotruncal anomaly can be

**Table 37.1** Fetal thymus volume according to gestational age for normal singleton gestation

| | *Fetal thymus volume (mL)* | | |
|---|---|---|---|
| *Gestational age (weeks)* | *Mean (SD)* | *Fifth centile* | *95th centile* |
| 17 + 0 to 17 + 6 | 0.9 (0.382) | 0.27 | 1.53 |
| 18 + 0 to 18 + 6 | 1.15 (0.383) | 0.52 | 1.78 |
| 19 + 0 to 19 + 6 | 1.53 (0.383) | 0.90 | 2.16 |
| 20 + 0 to 20 + 6 | 1.61 (0.383) | 0.98 | 2.24 |
| 21 + 0 to 21 + 6 | 1.95 (0.384) | 1.32 | 2.58 |
| 22 + 0 to 22 + 6 | 2.36 (0.384) | 1.73 | 2.99 |
| 23 + 0 to 23 + 6 | 2.90 (0.384) | 2.27 | 3.53 |
| 24 + 0 to 24 + 6 | 3.67 (0.385) | 3.04 | 4.30 |
| 25 + 0 to 25 + 6 | 4.09 (0.385) | 3.46 | 4.72 |
| 26 + 0 to 26 + 6 | 4.59 (0.386) | 3.96 | 5.22 |
| 27 + 0 to 27 + 6 | 5.37 (0.386) | 4.73 | 6.01 |
| 28 + 0 to 28 + 6 | 5.47 (0.387) | 4.83 | 6.11 |
| 29 + 0 to 29 + 6 | 6.21 (0.388) | 5.57 | 6.85 |
| 30 + 0 to 30 + 6 | 6.47 (0.388) | 5.83 | 7.11 |
| 31 + 0 to 31 + 6 | 6.52 (0.388) | 5.88 | 7.16 |
| 32 + 0 to 32 + 6 | 6.76 (0.388) | 6.12 | 7.40 |
| 33 + 0 to 33 + 6 | 6.97 (0.389) | 6.33 | 7.61 |
| 34 + 0 to 34 + 6 | 7.81 (0.389) | 7.17 | 8.45 |
| 35 + 0 to 35 + 6 | 8.72 (0.389) | 8.08 | 9.36 |
| 36 + 0 to 36 + 6 | 9.13 (0.390) | 8.49 | 9.77 |
| 37 + 0 to 37 + 6 | 9.67 (0.390) | 9.03 | 10.31 |
| 38 + 0 to 38 + 6 | 10.31 (0.391) | 9.67 | 10.95 |

*Source:* Li L et al.: Assessment of the fetal thymus by two- and three-dimensional ultrasound during normal human gestation and in fetuses with congenital heart defects. *Ultrasound Obstet Gynecol* 2011;37:404–9. Copyright Wiley-VCH Verlag GmbH & Co. KGaA. Reproduced with permission.[4]

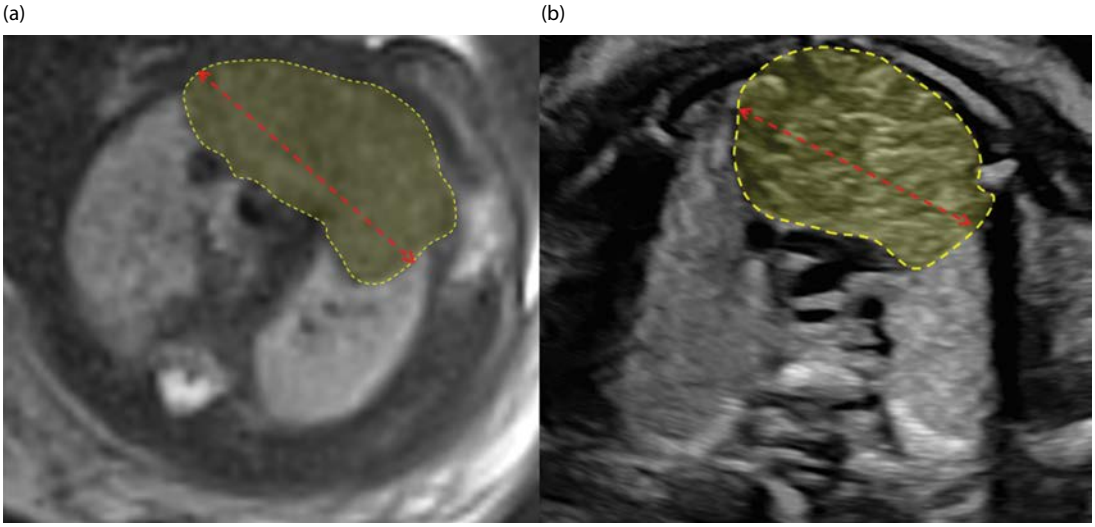


**Figure 37.25**
Assessment of the thymus size using transverse view of the fetal chest. Measurements of maximum transverse thymus diameter and perimeter by 2D ultrasound (a) and fetal MRI (b) are demonstrated. (Sp, spine.) (MRI image is courtesy of Wendy T. Brown, MD, MPH.)

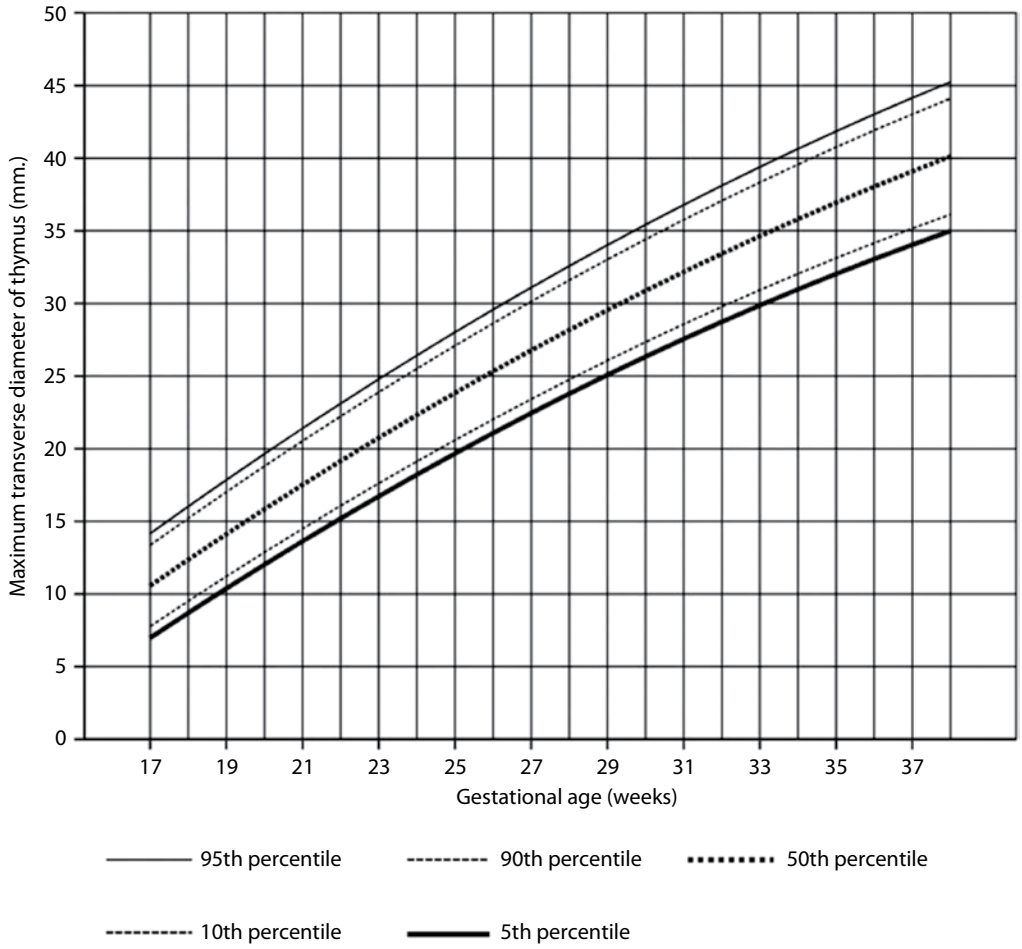


**Figure 37.26**
Normal gestational age ranges of the thymus maximum transverse diameter assessed by 2D ultrasound with the 5th, 10th, 50th, 90th and 95th percentiles. (Reproduced with permission from Tangshewinsirikul C and Panburana P. *J Clin Ultrasound* 2017;45(3):150–9.[36])

the first clue to prenatal detection of del22q11.2 (Figures 37.34 through 37.37). Chaoui et al. reported that the prevalence of 22q11.2 microdeletion within an unselected group of fetal cardiac anomalies is about 7% but increases to 13% in a subgroup of conotruncal anomalies.[39] Similar incidence of 22q11.2 microdeletion was reported in fetuses and neonates with different conotruncal anomalies. This chromosomal aberration is commonly associated with Fallot complex and is present in 10%–15% of fetuses with classic tetralogy of Fallot (with pulmonary stenosis), 18%–25% of fetuses with pulmonary atresia and ventricular septal defect, and up to 50% in fetuses with absent pulmonary valve.[41] The highest incidence of 22q11.2 microdeletion is found in the common arterial trunk (30%–40%) and interrupted aortic arch type B (50%).[41] Isolated minor vascular anomalies such as aberrant right subclavian artery and right aortic arch can also be associated with del22q11.2 in a clinically significant proportion of cases.[42] Identification of small or absent thymus in fetuses with conotruncal anomalies allows for the detection of 22q11.2 microdeletion with sensitivity of 90%, specificity of 98.5%, positive predictive value of 81.8%, and negative predictive value of 99.2%.[14] In fetuses affected by 22q11.2 deletion, TT-ratio is significantly decreased. Perolo et al. reported that the 100% detection rate of the 22q11.2 deletion can be achieved in fetuses with isolated right aortic arch if TT-ratio is used for thymus hypoplasia evaluation.[42] Thus, assessment of the thymus size is strongly recommended in fetuses with congenital heart disease (CHD) and can help to identify patients at risk for del22q11.2 who may benefit from genetic testing for this condition.

Fetuses with isolated cardiac abnormalities are also expected to have smaller than normal thymus as the embryogenesis of the thymus and conotruncal region of the heart are intimately linked through neural crest cells, which are equally contributing to development of both structures.[16] Results of a prospective study performed by Li et al. supported this theory, demonstrating that thymic volume estimated by 3D ultrasound was significantly lower in fetuses with CHD than in normal controls.[4]

Development of the immune system can also be compromised in fetuses with aneuploidies.[43–45] A study conducted by Karl et al. demonstrated that reduced thymus size can be observed in about one-third of fetuses with trisomy 21, 18, and 13.[6] However, the mechanism of the thymus underdevelopment may be different in fetuses with trisomies and those with microdeletion 22q11.2. The authors

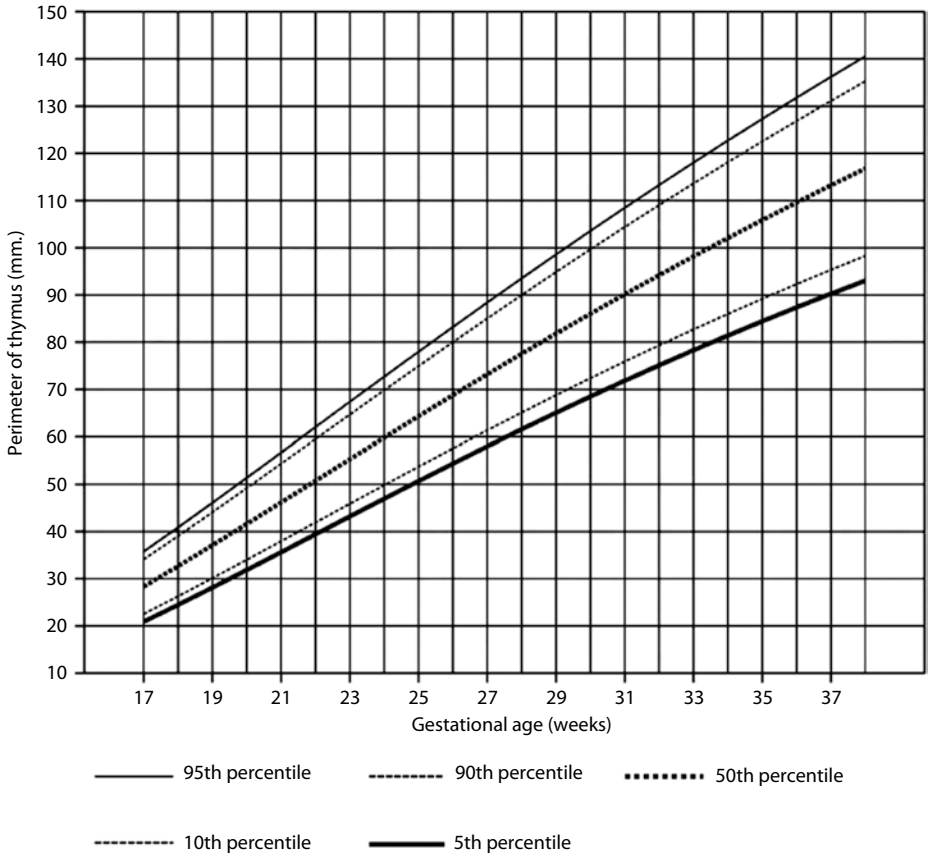


**Figure 37.27**
Normal gestational age ranges of the thymus perimeter assessed by 2D ultrasound with the 5th, 10th, 50th, 90th and 95th percentiles. (Reproduced with permission from Tangshewinsirikul C and Panburana P. *J Clin Ultrasound* 2017;45(3):150–9.[36])

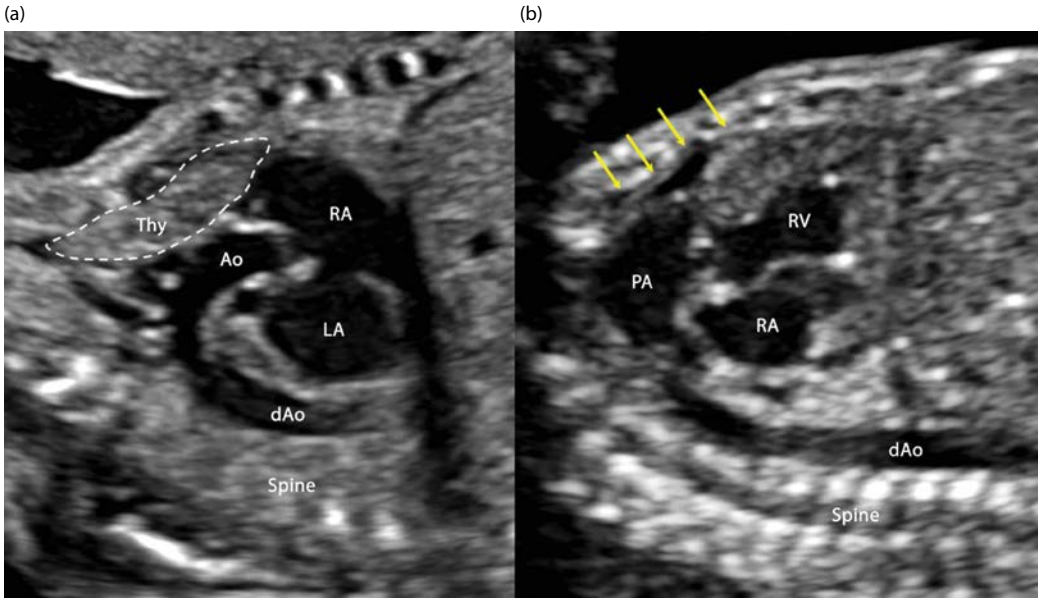


**Figure 37.28**
Mid-sagittal view of the fetal chest in two fetuses in the second trimester. (a) Typical appearance and location of thymus between ascending aorta and anterior chest wall in normal fetus; (b) absent thymus in a fetus with interrupted aortic arch and deletion 22q11. Note that heart and great vessels are visualized right behind the anterior thoracic wall (yellow arrows). (Ao, ascending aorta; dAo, descending aorta; LA, left atrium; PA, pulmonary artery; RA, right atrium; RV, right ventricle; Sp, spine; Thy, thymus.)

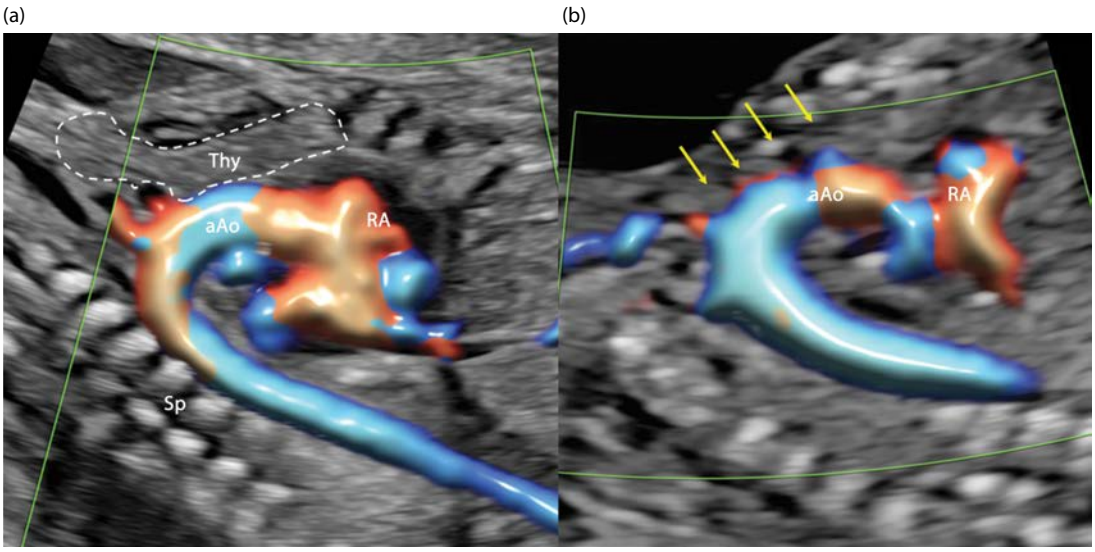


**Figure 37.29**
Sagittal view of the fetal chest demonstrating aortic arch in two fetuses with normal cardiac anatomy at 23 weeks gestation. (a) Normal thymus size and location (traced using dashed line); (b) absent thymus. Note anterior displacement of the ascending aorta due to absent thymus (yellow arrows). (aAo, ascending aorta; RA, right atrium; Thy, thymus.)

suggested that smaller than normal thymus size in fetuses with trisomy 21 is primarily caused by an *in utero* involution enhanced by growth restriction rather than abnormal embryogenesis.

The size of the thymus can also be affected by *in utero* infection and inflammation related to pregnancy complication such as preterm labor and chorioamnionitis.[7–9] The role of the thymus in the development of the fetal inflammatory response syndrome was well investigated in human and animal studies.[46,47] Systematic review and meta-analysis performed by Caissutti et al. demonstrated that in patients with high obstetrical risk due to preterm premature rupture of membranes or presenting with symptoms of preterm labor, identification of small fetal thymus increases the risk of preterm birth, chorioamnionitis, neonatal sepsis, and neonatal morbidity.[48] However, in a low-risk population, this association was not confirmed. There was no sufficient evidence noted to correlate small thymus with increased risk for intrauterine growth restriction and preeclampsia.

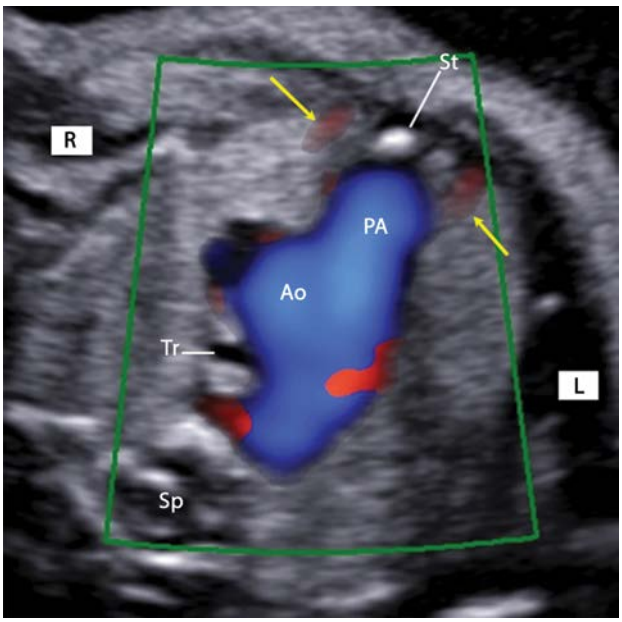


**Figure 37.30**
Transverse section of the upper chest at the level of three vessel trachea view in a fetus with absent thymus at 25 weeks gestation. Note anterior displacement of the great arteries due to thymus aplasia. Arrows indicate course of internal thoracic arteries. (Ao, aorta; PA, pulmonary artery; Sp, spine; St, sternum; Tr, trachea; L, left; R, right.)

There is some new evidence that size of the fetal thymus can be affected in pregnancies complicated by maternal diabetes. Dörnemann et al. observed reduced fetal TT-ratio in patients with gestational and pregestational diabetes regardless of type of control.[49] A recent study by Warby et al. showed no difference in the fetal TT-ratio in pregnancies affected by rheumatic disease compared to controls between 19 and 37 weeks of gestation.[50] However, an increasing trend in the subgroup of pregnancies affected by antiphospholipid syndrome was observed.

Other congenital abnormalities of the thymus include undescended thymus and ectopic accessory thymic lobes, which are usually diagnosed after birth. In rare occasions, small simple cysts can be identified within the thymus (Figure 37.38). There are few case reports in the literature on prenatal diagnosis of congenital thymic cysts.[51–53] These lesions account for about 3% of all anterior mediastinal masses, but their incidence in the fetus remains unknown. Thymic cysts found to have no association with other fetal

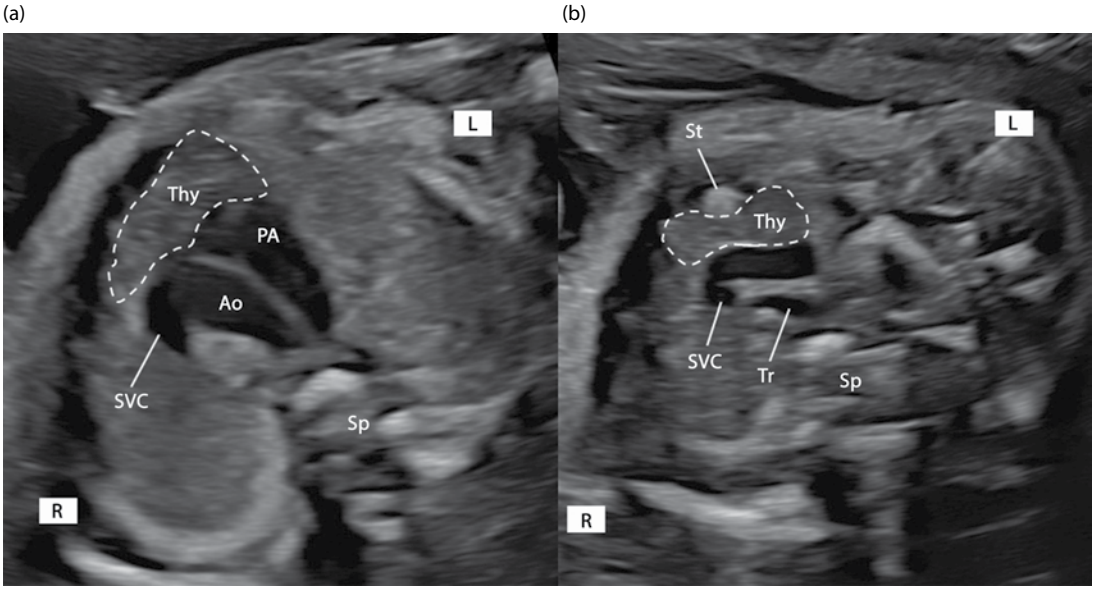


**Figure 37.31**
Transverse oblique section of the upper fetal chest at the level of three vessel trachea view (a) and slightly higher plane (b) in a fetus at 26 weeks gestation with severe IUGR and abnormal karyotype (trisomy 18). Note hypoplastic thymus (traced using dashed line). (Ao, aorta; PA, pulmonary artery; Sp, spine; St, sternum; SVC, superior vena cava; Thy, thymus; Tr, trachea; L, left; R, right.)

anomalies tend to be asymptomatic and reported to undergo spontaneous resolution soon after birth.

Finally, unusual appearance of the thymus can be observed in fetuses with anomalies of the left brachiocephalic vein (Figures 37.39 through 37.41). The left brachiocephalic vein (BCV) can be partially or completely embedded into thymic tissue, making the thymus look smaller than usual. This condition was described as the intrathymic course of left brachiocephalic vein and can be seen in approximately 1/60 fetuses examined in the midtrimester.[54] The clue to the presence of intrathymic course of the left BCV is the arch-like rather than the straight shape of this vessel observed in the transverse view of the upper chest (Figures 37.39a and 37.40). A sagittal view reveals left BCV located in the middle of the gland surrounded by thymic tissue (Figure 37.39b). The intrathymic course of left BCV as an isolated finding on routine ultrasound examination should be considered a normal variant and has no impact on the fetal well-being and does not require referral for fetal echocardiogram or further follow-up. The intrathymic course of the left BCV can be an incidental finding in fetuses with

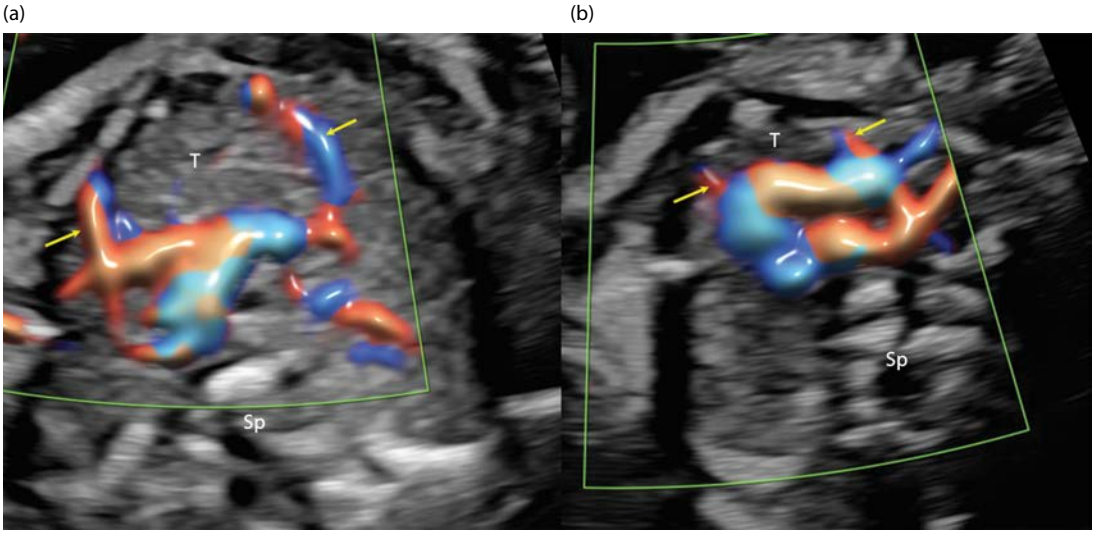


**Figure 37.32**
The thymus size evaluated using "Thy-box" technique in a normal fetus at 24 weeks gestation (a) and fetus with severe thymus hypoplasia at similar gestational age (b). Arrows indicate course of internal thoracic arteries. (Sp, spine; T, thymus.)

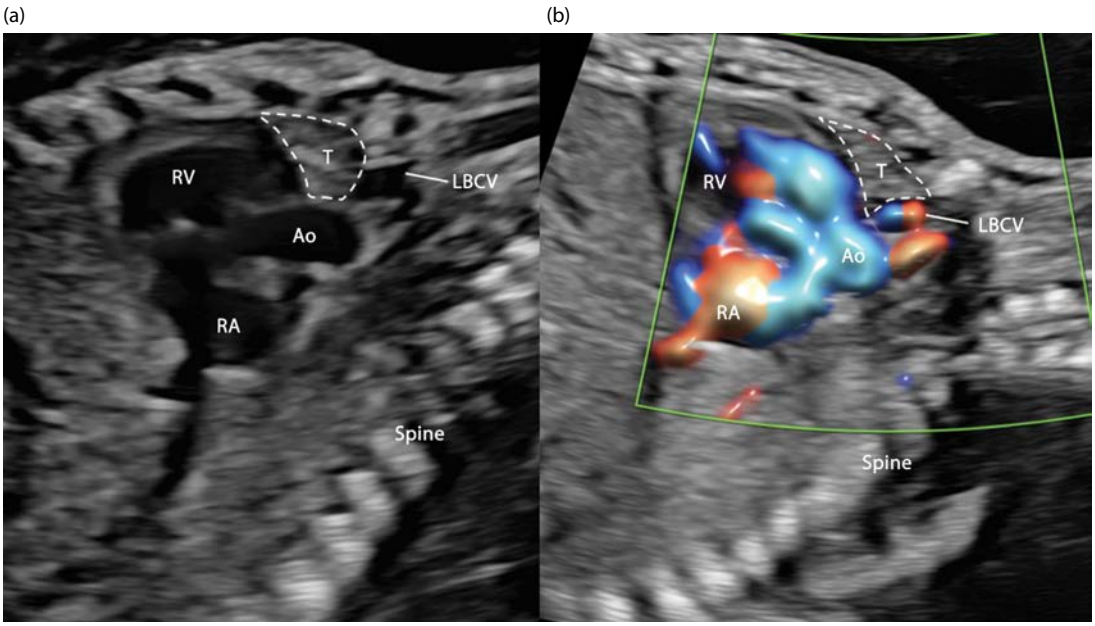


**Figure 37.33**
Sagittal view of the fetal chest in a fetus with severe IUGR and CMV infection at 24 weeks gestation. Note hypoplastic thymus (traced using dashed line). (Ao, ascending aorta; LBCV, left brachiocephalic vein; RA, right atrium; RV, right ventricle; T, thymus.)

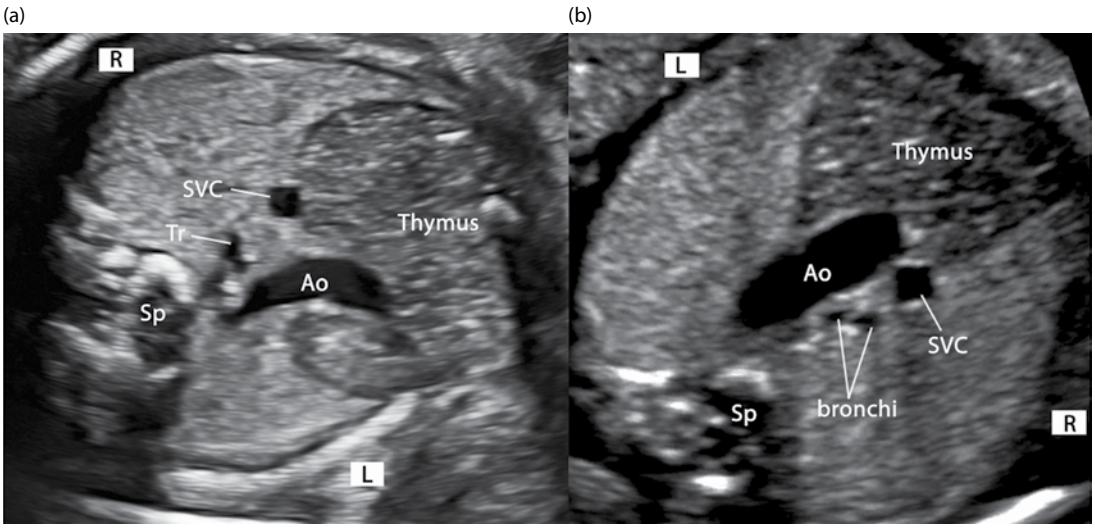


**Figure 37.34**
Transverse section of the upper chest at the level of transverse aortic arch in two second trimester fetuses with normal growth and normal karyotype (a) with transposition of the grate arteries (D-TGA) and (b) with tetralogy of Fallot. Note different shape, but normal size of the thymus. (Ao, aortic arch; SVC, superior vena cava; Sp, spine; Tr, trachea; L, left; R, right.)

cardiac or extracardiac anomalies without a specific association being reported as yet. Therefore, it is important to notify surgeons about this condition if thoracic intervention involving thymus removal is planned after birth to avoid unnecessary complications. The fetal thymus may appear smaller than usual due to compression by a dilated left BCV (Figure 37.41). Significant dilation of the left BCV occurs secondary to cerebral arteriovenous malformations such as vein of Galen aneurysm, supracardiac type of total anomalous pulmonary venous return, and at advanced stage of intrauterine growth restriction.[55]

In conclusion, the fetal thymus is a lymphoepithelial organ that plays an important role in the development of the immune system and is responsible for proper T-lymphocyte differentiation and selection. With recent improvements in ultrasound technology, the fetal thymus can be easily visualized and measured from 13 weeks' gestation onward by using 2D, 3D, and color Doppler modalities. There is currently sufficient

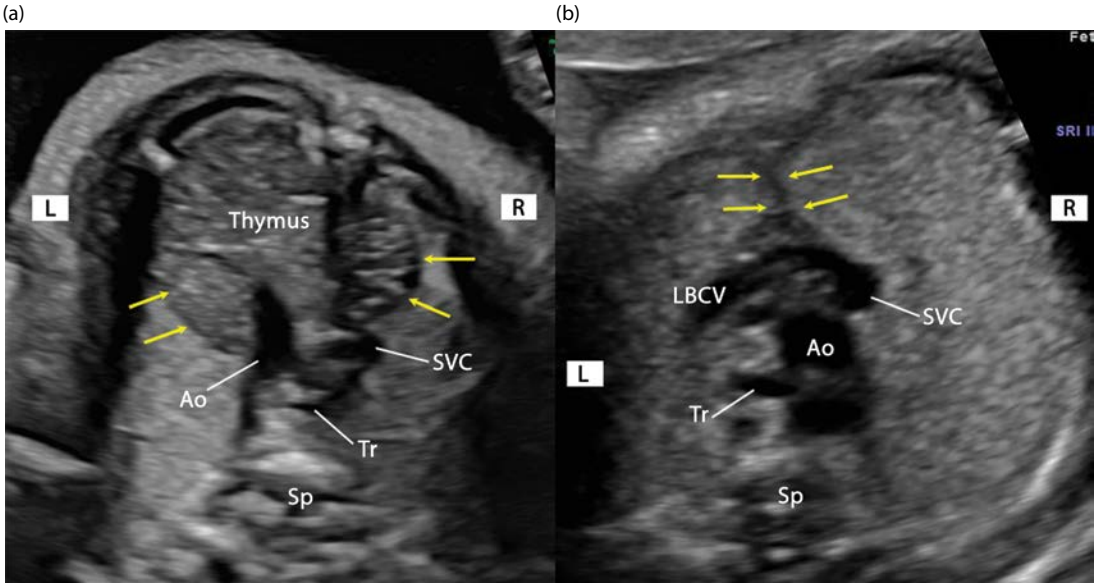


**Figure 37.35**
Transverse section of the upper chest at the level of transverse aortic arch in two fetuses with common arterial trunk type IV (solitary trunk) in the second trimester. (a) Normal thymus is visualized in typical location between lungs (thymus-lung border is pointed by yellow arrows); left-sided aortic arch is present; normal growth and normal karyotype were also reported for this fetus. (b) Absent thymus; right-sided aortic arch is demonstrated in a growth restricted fetus positive for deletion 22q11. Note direct contact between the left and right lung at the mid-line (pointed by yellow arrows). (Ao, aortic arch; SVC, superior vena cava; LBCV, left brachiocephalic vein; Sp, spine; Tr, trachea; L, left; R, right.)

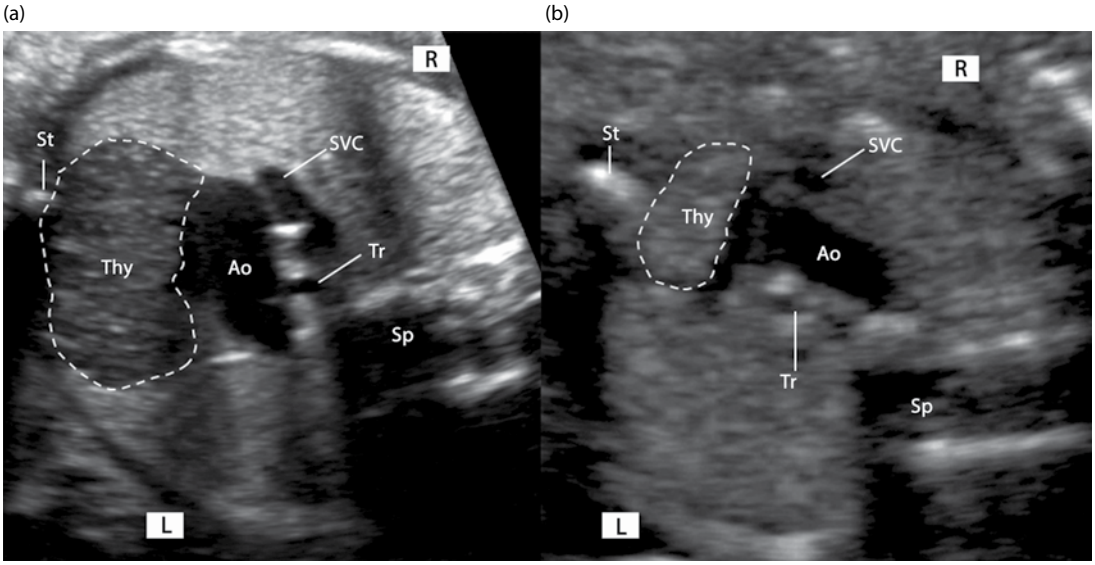


**Figure 37.36**
Transverse section of the upper chest at the level of transverse aortic arch in two fetuses with pulmonary atresia and ventricular septal defect in the third trimester. (a) Normal thymus size; left-sided aortic arch is present; normal growth and normal karyotype were also reported for this fetus. (b) Hypoplastic thymus; right-sided aortic arch is demonstrated in a normally grown fetus positive for deletion 22q11. (Ao, aorta; SVC, superior vena cava; Sp, spine; St, sternum; Thy, thymus; Tr, trachea; L, left; R, right.)

evidence in the literature to suggest that ultrasound assessment of the fetal thymus is indicated when a congenital defect, in particular, conotruncal anomaly, is identified in order to improve detection rates of microdeletion 22q11.2. However, further studies are needed to prove whether small thymus size can be used in clinical practice as an indirect marker for congenital thymic insufficiency as well as a predictor of adverse pregnancy outcomes in patients with high and low obstetrical risk. Until then, ultrasound assessment of fetal thymus should not be performed routinely.

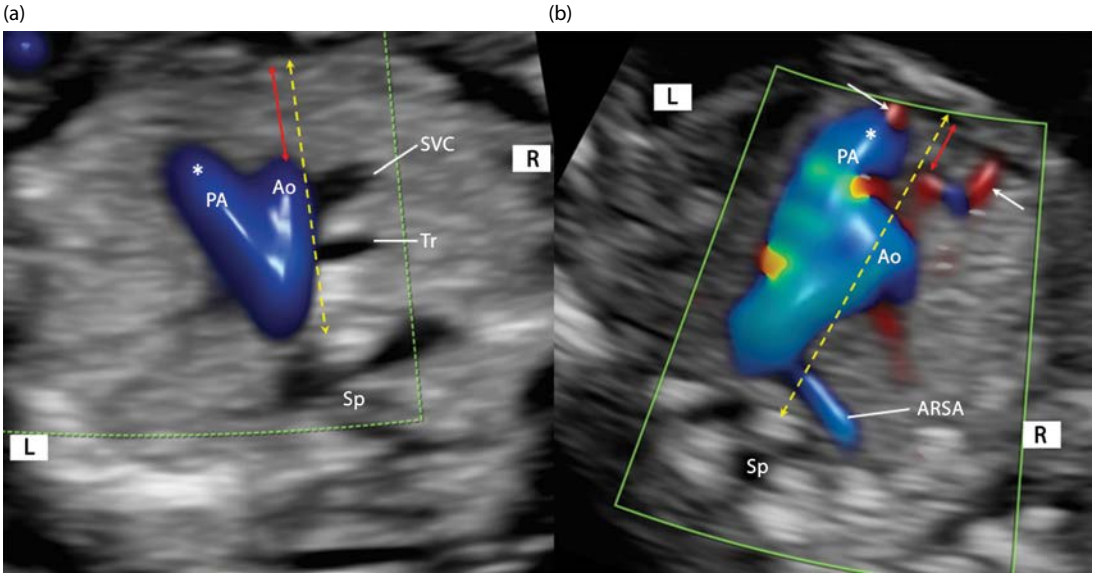


**Figure 37.37**
Transverse section of the upper chest at the level of three vessel trachea view in two fetuses in the first trimester. (a) Normal appearance of the thymus; normal karyotype and cardiac anatomy were reported for this fetus. (b) Hypoplastic thymus; aberrant right subclavian artery (ARSA) is present without major CHD. The fetus and mother were diagnosed with deletion 22q11. Note reduced TT-ratio and more anterior position of the pulmonary artery (labeled as *) in this fetus compared to normal fetus shown in image A. Arrows indicate course of internal thoracic arteries. (Ao, aorta; PA, pulmonary artery; SVC, superior vena cava; Sp, spine; Tr, trachea; L, left; R, right.)

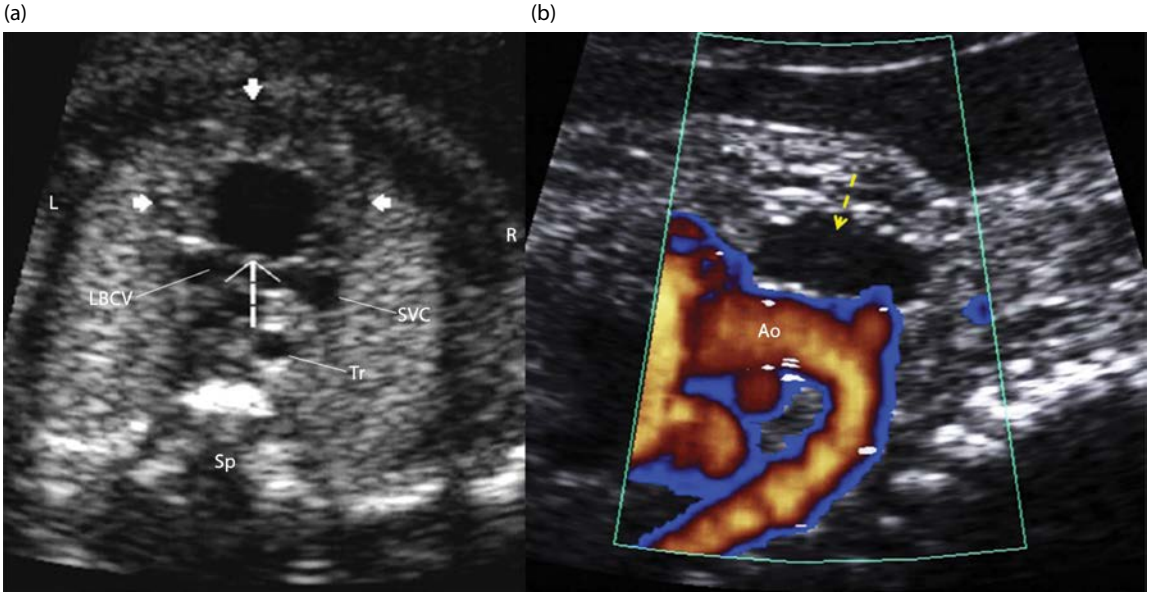


**Figure 37.38**
Transverse oblique view of the upper fetal chest at the level of drainage of the left brachiocephalic vein (LBCV) into superior vena cava (a) and sagittal view at the level of the aortic arch (b) showing a thymic cyst – pointed by dashed arrow. Note the compression of the thymic tissue by the cyst. (Courtesy of Professor R. Chaoui.)

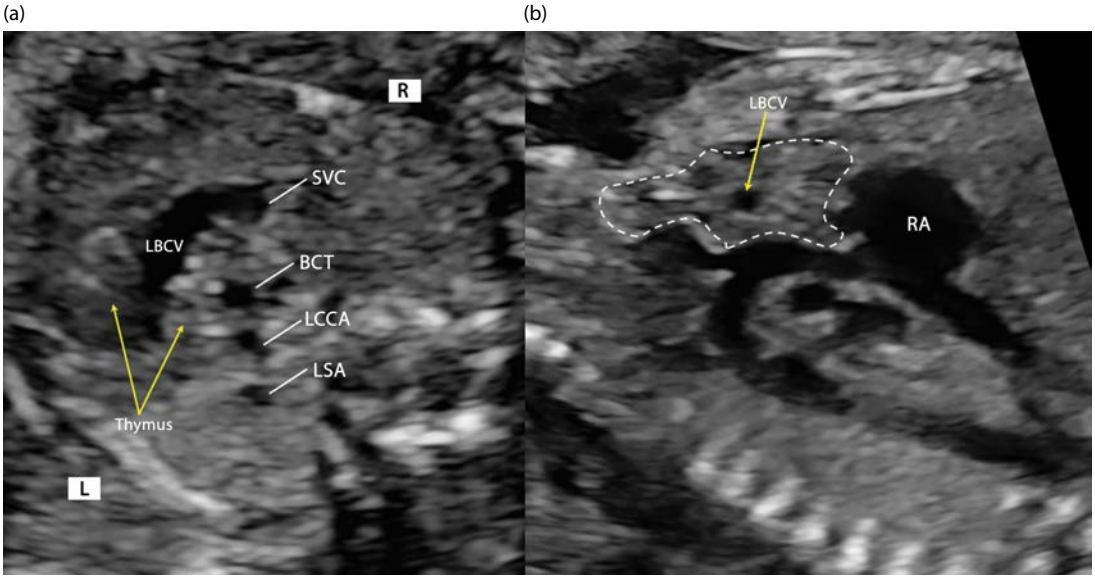


**Figure 37.39**
Transverse oblique view of the upper fetal chest at the level of drainage of the left brachiocephalic vein (LBCV) into superior vena cava (a) and sagittal view at the level of the aortic arch (b) showing an intrathymic course of the LBCV. Note that LBCV is located in the middle of the gland surrounded by thymic tissue. (BCT, braciocephalic trunk; LBCV, left brachiocephalic vein; LCCA, left common carotid artery; LSA, left subclavian artery; RA, right atrium; SVC, superior vena cava; L, left; R, right.)

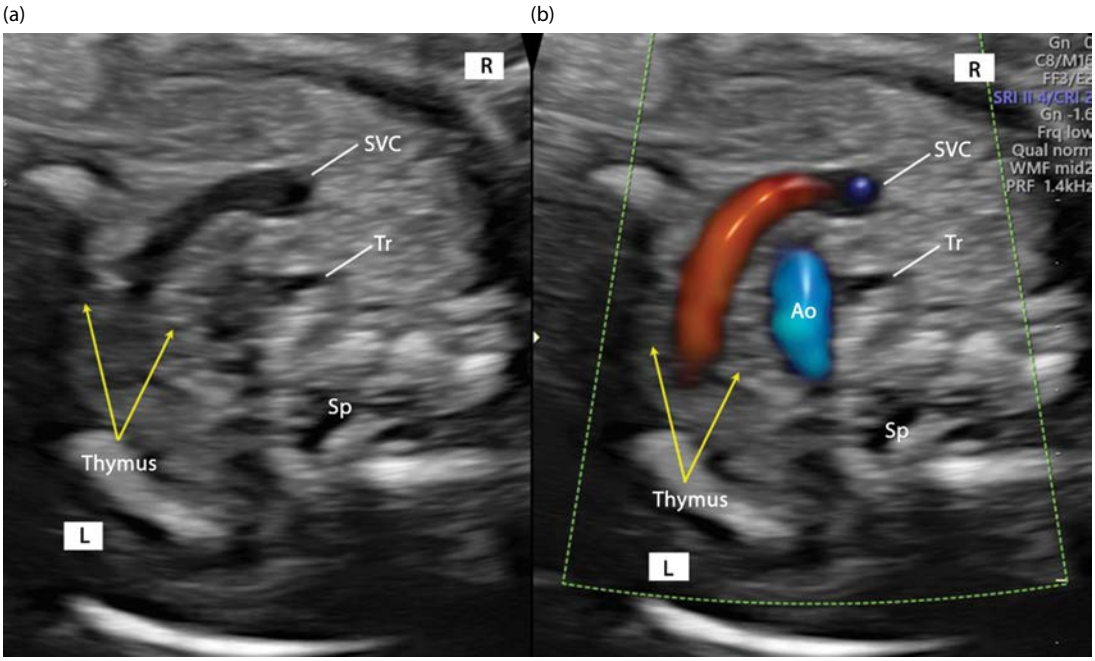


**Figure 37.40**
Transverse oblique view of the upper fetal chest at the level of drainage of the left brachiocephalic vein (LBCV) into superior vena cava (SVC) showing an abnormal course of the LBCV through the thymus in gray scale (a) and color Doppler imaging (b). Note the "arch-like" rather than strait course of the vessel. (Ao, aorta; Sp, spine; SVC, superior vena cava; L, left; R, right.)

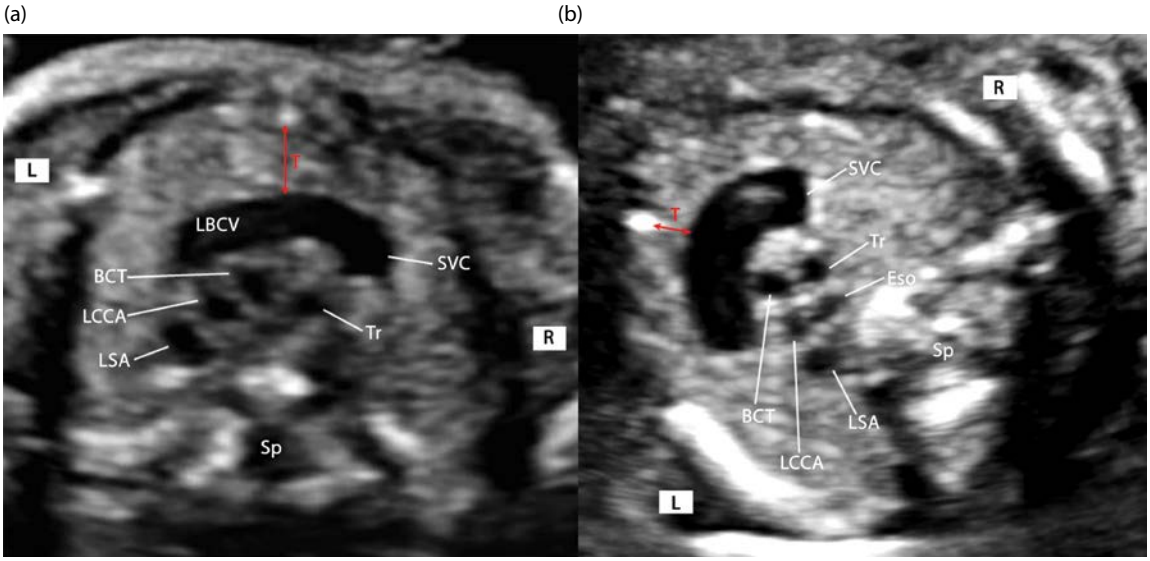


**Figure 37.41**
Transverse oblique view of the upper fetal chest at the level of drainage of the left brachiocephalic vein (LBCV) into superior vena cava (SVC) showing dilated LBCV in fetus with v. Galen aneurysm (a) and in fetus with supracardiac form of total anomalous pulmonary venous return (b). Note compression of the thymus (T) resulted in reduced anterior–posterior diameter. (BCT, braciocephalic trunk; Eso, esophagus; LBCV, left brachiocephalic vein; LCCA, left common carotid artery; LSA, left subclavian artery; Sp, spine; SVC, superior vena cava; T, thymus; Tr, trachea; L, left; R, right.)

## Acknowledgment

Thanks are extended to the Department of Human Anatomy, Orenburg State Medical Academy of Federal Agency for Healthcare and Social Development, Orenburg, Russia, for providing the pathology specimens illustrations.

## References

1. Felker RE et al. *J Ultrasound Med* 1989;8:669–73.
2. Zalel Y et al. *Prenat Diagn* 2002;22:114–7.
3. Cho JY et al. *Ultrasound Obstet Gynecol* 2007;29:634–8.
4. Li L et al. *Ultrasound Obstet Gynecol* 2011;37:404–9.
5. May MT. *Galen on the Usefulness of the Parts of the Body*. Ithaca, NY: Cornell University Press; 1968:30.
6. Karl K et al. *Ultrasound Obstet Gynecol* 2012;40:412–7.
7. Sciaky-Tamir Y et al. *Prenat Diagn* 2015;35:413–9.
8. El-Haieg DO et al. *BJOG* 2008;115:836.
9. Yinon Y et al. *Ultrasound Obstet Gynecol* 2007;29:639.
10. Toti P et al. *Hum Pathol* 2000;31:1121–8.
11. Mohamed N et al. *Ultrasound Obstet Gynecol* 2011;37:410–5.
12. Cromi A et al. *Ultrasound Obstet Gynecol* 2009;33:421.
13. Dodson W et al. *Lancet* 1969;1:574–5.
14. Chaoui R et al. *Ultrasound Obstet Gynecol* 2011;37:397.
15. Langman J. *Medical Embryology*. 4th ed. Baltimore, MD: Williams and Wilkins; 1981.
16. Gordon J, Manley NR. *Development* 2011;138(18):3865–78.
17. Lele SM et al. *Chest Surg Clin N Am* 2001;11:233–53.
18. Moore KL et al. *The Developing Human: Clinically Oriented Embryology*. 10th ed. Philadelphia, PA: Elsevier; 2016.
19. Ygberg S, Nilsson A. *Acta Paediatr* 2012;101(2):120–7.
20. Farley AM et al. *Development* 2011;138:3865–78.
21. Parham P. *The Immune System*. New York, NY: Garland Science; 2009.
22. von Gaudecker B. *Curr Top Pathol* 1986;75:1–42.
23. Gray's Anatomy. *The Anatomical Basis of Clinical Practice*. 40th ed. Spain: Elsevier; 2008.
24. Pearse G. *Toxicol Pathol* 2006;34:504–14.
25. Liu D, Ellis H. *Clinical Anatomy* 2016;29:679–84.
26. Miller JF. *Lancet* 1961;2:748–9.
27. Paladini D. *Ultrasound Obstet Gynecol* 2011;37:488–92.
28. Re C et al. *J Ultrasound Med* 2015;34:847–52.
29. Borgelt JMA et al. *Acta Obstet Gynecol Scand* 2016;95:210–6.
30. Weissmann-Brenner A et al. *J Ultrasound Med* 2015;34:2263–8.
31. Gamez F et al. *Ultrasound Obstet Gynecol* 2010;36:302–7.
32. De Leon-Luis J et al. *J Magn Reson Imaging* 2011;33(5):1100–5.
33. De León-Luis J et al. *J Ultrasound Med* 2009;28:43–8.
34. Muñoz-Chápuli M et al. *J Ultrasound Med* 2015;34:853–8.
35. Chaoui R et al. *Ultrasound Obstet Gynecol* 2011;37:397–403.
36. Tangshewinsirikul C, Panburana P. *J Clin Ultrasound* 2017; 45(3):150–9.
37. Barrea C et al. *Prenat Diagn* 2003;23:9–15.
38. Volpe P et al. *Prenat Diagn* 2003;23:752–7.
39. Chaoui R et al. *Ultrasound Obstet Gynecol* 2002;20:546–52.
40. Oskarsdottir S et al. *Eur J Pediatr* 2005;164:146–53.
41. Abuhamad A, Chaoui R. *A Practical Guide to Fetal Echocardiography: Normal and Abnormal Hearts*. Philadelphia, PA: Lippincott Williams and Wilkins; 2016.
42. Perolo A et al. *Ultrasound Obstet Gynecol* 2016;48:200–3.
43. Makrydimas G et al. *Prenat Diagn* 1994;14:239–41.
44. Zizka Z et al. *Fetal Diagn Ther* 2006;21:510–4.
45. Kusters MAA et al. *Clin Exp Immunol* 2009;156:189–93.
46. Melville JM et al. *Reprod Sci* 2012;19(7):740–7.

47. De Felice C et al. *J Matern-Fetal Neonat Med* 2008;21(4):251–4.
48. Caissutti C et al. *Acta Obstet Gynecol Scand* 2017 Oct 23. doi: 10.1111/aogs.13249. [Epub ahead of print]
49. Dörnemann R et al. *J Perinat Med* 2017;45(5):595–601.
50. Warby AC et al. *J Perinat Med* 2014;42:635–9.
51. McEwing R, Chaoui R. *J Ultrasound Med* 2005;24(1):127–30.
52. de Miguel Campos E et al. *J Ultrasound Med* 1997;16(5): 365–7.
53. Lee D et al. *J Ultrasound Med* 2014;33(5):919–21.
54. Karl K et al. *Ultrasound Obstet Gynecol* 2016;48(4):464–9.
55. Sinkovskaya E et al. *Ultrasound Obstet Gynecol* 2012;40(5): 542–8.

# 38

# Extracardiac Doppler investigation in fetuses with congenital heart disease

Annegret Geipel, Ulrich Gembruch, and Christoph Berg

## Introduction

Since the introduction of Doppler ultrasound in prenatal monitoring, numerous studies have investigated the fetal and uteroplacental circulation in low-risk and high-risk collectives. Arterial and venous Doppler sonography is currently most frequently used in the diagnosis and monitoring of fetuses with intrauterine growth restriction (IUGR). Fetal blood flow is influenced by multiple factors, including the structure and function of the heart as well as impedance of the distal vascular beds. Specific anatomical cardiac defects may therefore lead to alterations of the fetal and uteroplacental blood flow. The significance of Doppler investigations of peripheral fetal blood vessels in congenital heart disease (CHD) has been the subject of an increasing number of studies, with in part contradictory results. Extracardiac Doppler has been evaluated for the purpose of screening, monitoring of the fetus with known CHD, and predicting the postnatal outcome. This chapter focuses on second- and third-trimester Doppler investigations of the umbilical artery (UA), the middle cerebral artery (MCA), the cerebroplacental ratio (CPR), and the ductus venosus (DV) in fetuses with congenital heart disease.

## Umbilical artery

In fetuses with IUGR caused by uteroplacental dysfunction, umbilical artery blood flow velocity waveform may show an increase of pulsatility predominantly reflecting downstream flow resistance caused by a disturbed development of the tertiary villi and consecutive increased resistance at the level of the small arteries and arterioles. The increase of the downstream indices (pulsatility index [PI], resistance index [RI], systolic/diastolic ratio [S/D]) results from a relative decrease of end-diastolic velocities. However, the downstream indices are also influenced by a decrease of filling pressure in the arterial bed as a principal determinant of placental blood flow, and that blood pressure is dependent on cardiac output. Therefore, alterations in umbilical artery blood flow velocity waveform may be secondary to reduced volume flow, reduced cardiac contractility, and increased afterload; in addition, abnormal shunting may also reduce the umbilical arterial filling pressure. A number of earlier studies described increased UA pulsatility in fetuses with CHD.[1] The high incidence of pathological Doppler results of these studies must be considered in the context of associated extracardiac malformations, chromosomal anomalies, or fetal growth restriction observed in the majority of cases, as fetuses with isolated heart disease were not investigated separately.[1,2]

Meise et al. were the first to analyze umbilical and cerebral blood flow patterns in 55 second- and third-trimester fetuses with isolated heart disease, that is, after the exclusion of cases with aneuploidies, extracardiac malformations, and growth restriction.[3] The investigated cases represented a wide spectrum of prenatally diagnosed cardiac malformations, including left heart obstructions, right heart obstructions, outflow-tract disorders, and septal defects. This study demonstrated the insufficiency of Doppler investigation of the UA as a sole screening parameter for CHD (Table 38.1). There were insignificant differences between cases of isolated heart disease and controls with regard to pathological results (PI $>$ 95th centile, 7% versus 4%). As observed by previous studies, a significantly higher percentage of pathological Doppler indexes (48%) was found in the group of nonisolated heart defects ($n = 60$). The isolated heart defects with a UA PI $>$ 95th centile included two cases with reverse perfusion of the pulmonary artery via the ductus arteriosus (tricuspid and pulmonary atresia, pulmonary atresia, and tricuspid dysplasia), one case with reverse perfusion of the aorta (aortic atresia with consecutive hypoplastic left heart), and one case with Ebstein anomaly and a distinct pulmonary valve insufficiency. The increased UA pulsatility of the first three cases was discussed with respect to the right- or left-sided outflow tract obstruction with retrograde perfusion via the ductus arteriosus, with a possible reduction of diastolic blood flow in the descending aorta and in the UA to the extent that an increased umbilical PI resulted. In the fetus with Ebstein anomaly and major pulmonary insufficiency, the reduced diastolic blood flow toward the placenta may have been caused by a disturbance of the low-pressure chamber function ("Windkessel function") of the pulmonary trunk.[3]

Likewise, most of the studies investigating mixed collectives of CDH observed no differences in UA resistance

**Table 38.1** Doppler studies of the umbilical artery in fetuses with isolated congenital heart disease (CHD)

| *Study* | *Type of CHD* | *Number of fetuses* | *Studied parameters* | *Results CHD versus controls* |
|---|---|---|---|---|
| Meise et al.[3] | Mixed | 55 | PI (95th centile) | NS |
| Jouannic et al.[8] | TGA | 23 | PI (median) | NS |
| Donofrio et al.[4] | Mixed | 36 | RI (mean) | NS |
| Kaltman et al.[10] | HLH | 28 | ΔPI | NS |
| | LHO | 13 | ΔPI | NS |
| | RHO | 17 | ΔPI | Increased |
| Modena et al.[5] | Mixed | 71 | PI (mean) | NS |
| Guorong et al.[14] | Mixed | 45 | ΔPI | Increased |
| Itsukaichi et al.[6] | Mixed | 44 | RI (95th centile) | NS |
| Szwast et al.[11] | POTO | 59 | ΔPI | NS |
| | HLH | 72 | ΔPI | NS |
| Yamamoto et al.[9] | HLH | 42 | ΔPI | Increased |
| | CoA | 21 | ΔPI | Increased |
| | TGA | 11 | ΔPI | NS |
| | POTO | 15 | ΔPI | NS |
| Masoller et al.[7] | Mixed | 95 | ΔPI | NS |

*Abbreviations:* CoA, coarctation of the aorta; HLH, hypoplastic left heart; LHO, left heart obstruction; NS, not significant; PI, pulsatility index; POTO, pulmonary outflow tract obstruction; RHO, right heart obstruction; RI, resistance index; TGA, transposition of the great arteries.

compared to controls[4–7] (Table 38.1). Others found no difference in UA Doppler parameters for specific types of CHD, such as transposition of the great arteries (TGA),[8,9] hypoplastic left heart (HLH),[10,11] or pulmonary outflow tract obstruction (POTO).[9,11] In contrast, Yamamoto et al. found higher UA-PI in fetal HLH and isolated coarctation with reversed arch flow[9] (Table 38.1).

In some fetuses with specific cardiac lesions, the filling pressure of the descending aorta and placental arterial bed is drastically reduced, resulting in a significant decrease of end-diastolic blood flow velocities and increased pulsatility in the UA, respectively. In fetuses with tetralogy of Fallot and absent pulmonary valve, even reversed end-diastolic blood flow may be present in the UA and other fetal arteries, if a patent ductus arteriosus allows diastolic shunting from the aorta into the right and left ventricles.[12] Furthermore, some fetuses with Ebstein anomaly and tricuspid dysplasia show tricuspid insufficiency in combination with reduced or missing antegrade flow across the pulmonary valve and pulmonary regurgitation severe enough to cause increased UA pulsatility up to reversed end-diastolic flow.[13] Similar hemodynamic changes with increased pulsatility in the UA can be observed in some recipient fetuses of advanced-state twin-twin transfusion syndrome.

Umbilical artery Doppler in congenital heart disease is not predictive of fetal survival,[3,14] although in the studies of Copel et al. and Meise et al., all fetuses with increased UA pulsatility died either pre- or postnatally, this also applied to five of nine and 19 of 51 fetuses with a normal umbilical Doppler, respectively.[2,3] In some subtypes of CHD, however, a distinct increase of pulsatility in the umbilical artery is caused by reduced filling pressure in the placenta and descending aorta, resulting from low cardiac output state and/or pronounced diastolic shunting away from the descending aorta; those fetuses have an increased perinatal mortality and morbidity.[11,12]

## Middle cerebral artery and cerebroplacental ratio

Congenital heart disease may have an impact on cerebrovascular blood flow dynamics in the fetus. Several structural congenital heart defects are accompanied by an intracardiac mixing of oxygenated and deoxygenated blood. These lesions along with obstructive lesions of the outflow tracts may interfere with normal cerebral oxygen supply and therefore modify cerebrovascular resistance. Alteration of *in utero* cerebral blood flow could be a critical point of later neurodevelopmental outcomes; however, the linkage between these items is not yet fully established.

Meise et al. were the first to investigate the cerebral perfusion of fetuses with isolated CHD.[3] They found no difference in pulsatility of the MCA between the study group and controls, with regard to either ΔPI or 95% reference interval (Table 38.2). In a single case analysis, a reduced PI (<5th centile) was found in four decompensated fetuses with severe obstructive lesions (aortic atresia with HLH, critical aortic stenosis with endocardial fibroelastosis, two cases of severe pulmonary and aortic stenosis), with the latter three fetuses presenting generalized hydrops. Of the four fetuses, three died *in utero* and one postnatally.[3] This finding was confirmed in a more previous study, observing decreased MCA PI in fetuses with CHD complicated with congestive heart failure.[14]

Meanwhile, a number of studies have looked at cerebrovascular resistance as measured by MCA PI and CPR (Tables 38.2

**Table 38.2** Doppler studies of the middle cerebral artery in fetuses with isolated CHD

| *Study* | *Type of CHD* | *Number of fetuses* | *Studied parameters* | *Results CHD versus controls* |
|---|---|---|---|---|
| Meise et al.[3] | Mixed | 55 | PI (<5th centile) | NS |
| | | | ΔPI | NS |
| Jouannic et al.[8] | TGA | 23 | PI (median) | Decreased |
| Donofrio et al.[4] | Mixed | 36 | RI (mean) | Decreased |
| | HLH | 12 | RI (mean) | Decreased |
| | LHO | 4 | RI (mean) | NS |
| | TGA | 4 | RI (mean) | Decreased |
| | TOF | 11 | RI (mean) | Decreased |
| | HRH | 5 | RI (mean) | NS |
| Kaltman et al.[10] | HLH | 28 | ΔPI | Decreased |
| | LHO | 13 | ΔPI | NS |
| | RHO | 17 | ΔPI | NS |
| Modena et al.[5] | Mixed | 71 | PI (mean) | NS |
| | | | PI (<5th centile) | $p = 0.023$ |
| Berg et al.[15] | Mixed | 113 | ΔPI | NS |
| | TGA | 18 | ΔPI | NS |
| | HLH | 46 | ΔPI | Decreased |
| Guorong et al.[14] | Mixed | 45 | ΔPI | NS |
| | LHO | 11 | ΔPI | NS |
| | RHO | 16 | ΔPI | NS |
| Itsukaichi et al.[6] | Mixed | 44 | RI (<5th centile) | $p = 0.002$ |
| Szwast et al.[11] | POTO | 59 | ΔPI | NS |
| | HLH | 72 | ΔPI | Decreased |
| Yamamoto et al.[9] | HLH | 42 | ΔPI | Decreased |
| | CoA | 21 | ΔPI | Decreased |
| | TGA | 11 | ΔPI | NS |
| | POTO | 15 | ΔPI | NS |
| Masoller et al.[7] | Mixed | 95 | ΔPI | Decreased |

*Abbreviations:* CoA, coarctation of the aorta; HLH, hypoplastic left heart; HRH, hypoplastic right heart; LHO, left heart obstruction; NS, not significant; PI, pulsatility index; POTO, pulmonary outflow tract obstruction; RHO, right heart obstruction; TGA, transposition of the great arteries; TOF, tetralogy of Fallot; RI, resistance index.

**Table 38.3** Cerebroplacental ratio (CPR) in fetuses with isolated CHD

| *Study* | *Type of CHD* | *Number of fetuses* | *Studied parameters* | *Results CHD vs controls* |
|---|---|---|---|---|
| Berg et al.[15] | Mixed | 113 | ΔPI | Decreased |
| | TGA | 18 | ΔPI | NS |
| | HLH | 46 | ΔPI | Decreased |
| Itsukaichi et al.[6] | Mixed | 44 | RI < 1 | $p = 0.0007$ |
| Szwast et al.[11] | POTO | 59 | ΔPI | NS |
| | HLH | 72 | ΔPI | Decreased |
| Yamamoto et al.[9] | HLH | 42 | ΔPI | Decreased |
| | CoA | 21 | ΔPI | Decreased |
| | TGA | 11 | ΔPI | NS |
| | POTO | 15 | ΔPI | NS |
| Masoller et al.[7] | Mixed | 95 | ΔPI | Decreased |

*Abbreviations:* CoA, coarctation of the aorta; HLH, hypoplastic left heart; HRH, hypoplastic right heart; LHO, left heart obstruction; PI, pulsatility index; POTO, pulmonary outflow tract obstruction; RHO, right heart obstruction; RI, resistance index; NS, not significant; TGA, transposition of the great arteries.

and 38.3). They demonstrated different alterations of blood flow patterns dependent on the type of structural heart disease present. The number of ventricles (one or two), systemic ventricular morphology (left or right), and nature of flow into the aorta (obstructed or unobstructed) may influence the pathways of blood flow delivery to the aorta, hence potentially altering cerebrovascular blood flow dynamics.

In most of the studies exploring collectives with nonspecific cardiac lesions, no major differences in the mean MCA PI were found between fetuses with CHD and controls.[3,5,14,15]

Jouannic et al.[8] and Donofrio et al.[4] were the first to specifically investigate fetuses with TGA and found a significantly reduced pulsatility of the MCA compared to controls, suggesting that cerebral vasodilatation occurred. However, in two more recent studies, the Doppler findings were not confirmed[9,15] (Table 38.2).

There is growing evidence that cases with HLH show the strongest cerebrovascular alterations detectable by evaluation of MCA Doppler indices and CPR.[4,9–11,15] Compared to other types of CHD, MCA-PI and CPR were significantly decreased in the majority of studies (Tables 38.2 and 38.3). In the study of Berg et al., altered Doppler findings were also found when different periods during gestation were analyzed separately (19–25 weeks', 26–32 weeks', and 33–41 weeks' gestational age).[15] In contrast, Szwast et al. described similar cerebrovascular resistance in normal fetuses and those with HLH at 20 weeks, but observed a drop below the expected normal values in fetuses with HLH at approximately 27 weeks' gestation.[11] Yamamoto et al. found lower MCA-PI and lower PCR in fetal HLH and isolated coarctation with reversed arch flow. In this study, no difference was found between HLH with anatomical coarctation and those without; however, MCA-PI correlated positively with neonatal head circumference in HLH with reversed distal arch flow.[9] The findings of the studies suggest that aortic obstruction is the key anatomic feature influencing cerebrovascular resistance.[9,11,15] In contrast, Jansen et al. did not establish a significant correlation

between aortic flow or oxygen saturation and head circumference growth, even if they demonstrated significant restriction of head circumference growth with increasing gestational age independent on the subtype of CHD.[16] In addition, Hahn et al. showed in fetuses with univentricular hearts that there was less growth in HC from 30 weeks onward compared with the period from 20 to 29 weeks.[17] Decreased fetal somatic growth but not head circumference or MCA-PI may predict developmental abnormalities. In their study, lower cerebrovascular resistance seemed to be protective for neurodevelopment.[17] The observed blood flow alterations may reflect the specific hemodynamic situation in different heart defects. In normal fetal heart anatomy, the ventricles function in parallel with two distinct shunt pathways that equalize pressure differences. While the left ventricle ejects the blood into a high-resistance system, the head, upper body, and across the aortic isthmus, the right ventricle ejects blood into the lower body and the low-resistance placenta. In normal fetal circulation, oxygen saturation of the blood delivered to the heart and the brain is higher (approximately 65%) than that delivered to the rest of the body[18] (Figure 38.1a).

In fetuses with transposition of the great arteries, the oxygenated blood from the left ventricle is ejected into the truncus pulmonalis. Deoxygenated blood with an oxygen saturation of only 55% is ejected from the right ventricle into the aorta ascendens, the coronary arteries, and the brain/arm vessels (Figure 38.1b).[18] In fetuses with hypoplastic left heart, there is intracardiac mixing of oxygenated blood with deoxygenated blood, as well as retrograde perfusion of the aorta, which results in the delivery of blood with a saturation of approximately 60% to the cerebral and coronary arteries[18] (Figure 38.1c). Additional hypoplasia of the aortic arch may lead to a further reduction of blood flow toward the brain. Fetuses with aortic stenosis have blood flow restrictions of various degrees, with only a little intracardiac mixing of blood. In cases with severe restriction, retrograde perfusion of the aortic arch via the ductus arteriosus (DA) with less oxygenated blood occurs. Relatively deoxygenated blood ($O_2$ saturation of about 63%) enters the cerebral circulation due to intracardiac mixing in fetuses with tetralogy of Fallot, and especially in fetuses with HRH (pulmonary atresia, severe pulmonary stenosis, or tricuspid atresia).[18]

In addition to the disruption of streaming of oxygenated blood toward the brain, fetuses with single-ventricle anatomy have a significant reduction of combined cardiac output of approximately 20%.[19] As a consequence, the placental blood flow is reduced as demonstrated by a significantly reduced blood flow and oxygen saturation in the umbilical vein, resulting in a drop of cerebral oxygen delivery in those fetuses.[20]

Finally, there is a high incidence of placental abnormalities found in the setting of CHD.[21,22] This may cause an additional reduction of oxygen saturation in the umbilical venous blood and lower fetal oxygen delivery also in fetuses with normal cardiac output and umbilical venous flow. In the late third trimester and near term, this effect is augmented by the occurrence of a relative placental insufficiency in an increasing percentage of fetuses[22] and may be associated with a decrease of MCA-PI.[23] High incidences of placental abnormalities have been observed on pathology and histopathology, and in the late first trimester, abnormal placentation is more frequent in pregnancies with fetal CHD.[22] Altogether, these studies suggest that CHD may have an intrinsic altered placentation that is more pronounced at the end of pregnancy, with ensuing placental hypoxia.[22]

Considering the location of the most effective fetal chemoreceptors for hypoxemia or hypercapnia in the carotid arteries, the observed cerebral vasodilatation could be a fetal autoregulatory response to moderate hypoxia, as described for the above-mentioned types of heart defects. Compared to fetuses with a classical blood flow redistribution ("brain-sparing effect") in response to generalized hypoxia due to uteroplacental dysfunction, most fetuses with isolated heart disease did not show an increased UA pulsatility, which argues in favor of a rather local response to the receipt of less-oxygenated blood

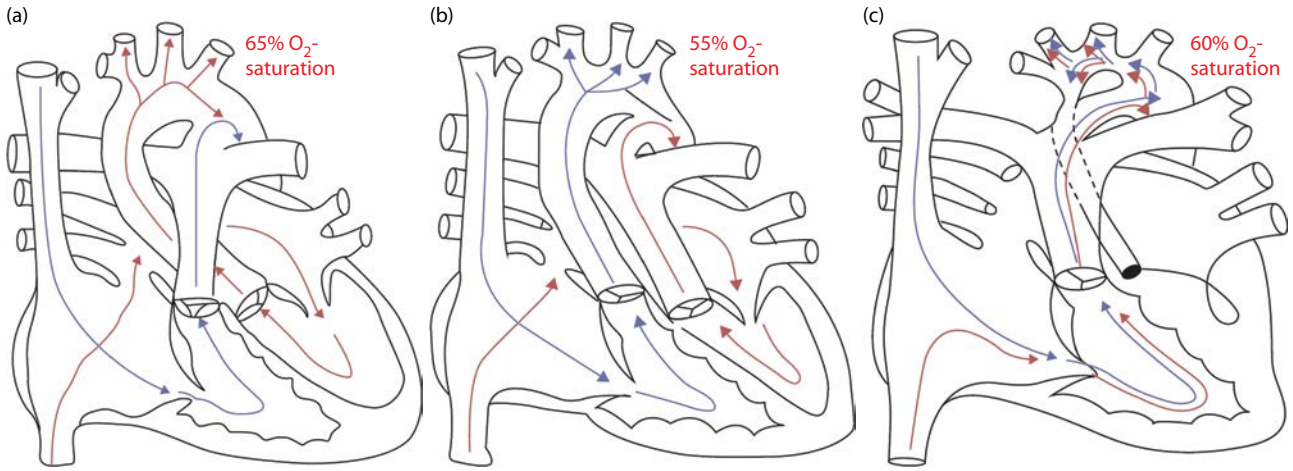


**Figure 38.1**
$O_2$ saturation in normal heart anatomy and congenital heart disease. Red arrows indicate oxygenated blood; blue arrows indicate deoxygenated blood. (a) Normal fetal blood flow. (b) Transposition of the great arteries. (c) Hypoplastic left heart.

from the pre-isthmus aorta.[4,5,8,10] Fetuses with hypoplastic left heart had the most pronounced alteration of flow, suggesting that they had the greatest need for autoregulation. Fetal animal models suggest that after prolonged periods of hypoxia, cerebral vascular tone tends to normalize, with downregulation of neuronal and glial metabolism that results in reduced cerebral oxygen consumption and associated changes in brain growth and development.[24] Investigating fetal hemodynamics, oxygen saturation, and brain volume in fetuses with different CHD by magnetic resonance imaging technology, Sun et al. showed that the mean blood flow in the superior caval vein was unchanged despite the lower oxygen content of the blood supplied to the brain. These findings are even more suggestive that the reduced cerebral oxygen consumption resulting from chronic hypoxia compared to the "brain-sparing physiology" seen in acute fetal hypoxemia leads to reduced brain size and impaired neurodevelopment.[20]

Progressive decline in the mortality rate of cases with CHD has focused attention toward the associated developmental morbidity (Chapter 59). Given the findings of the various studies that assessed the pattern of redistribution of cerebral blood flow, smaller head circumference, and intracranial volume in proportion to weight and brain injury in newborns[25–30] with cardiac defects is most probably multifactorial and cumulative during life, but is also a consequence of disordered fetal circulation at least in some subtypes of CHD.[9,31–33] Placental and (epi)genetic factors may contribute to the restricted cerebral growth and reduced neurodevelopment in fetuses with CHD.

## Ductus venosus

The fetal DV connects the intra-abdominal umbilical vein to the inferior vena cava at its inlet to the heart. The normal triphasic flow pattern reflects the pressure gradient between the DV and the right atrium during different phases of the cardiac cycle. In conditions with increased cardiac afterload, preload, and/or myocardial dysfunction, elevation of the right atrial as well as the central venous pressure occurs, thus resulting in an increased pulsatility of the venous blood flow velocity waveforms. In fetuses with congenital heart disease, the question arises whether abnormal DV flow profiles indicate fetal compromise or rather reflect the specific hemodynamics of the heart defect itself.

Kiserud et al. analyzed the peak systolic and end-diastolic velocities of the DV in 30 fetuses with heart defects, including cases with supraventricular tachycardia. Pathological results had a sensitivity of 64% for the diagnosis of CHD, and 81% sensitivity for malformations involving only atrioventricular valves and great arteries. However, the results were biased by the inclusion of fetuses with arrhythmias, aneuploidies, or other extracardiac defects.[34] DeVore and Horenstein observed an absent forward flow during the a-wave in one fetus with pulmonary atresia and in a second with severe cardiovascular dysfunction, while one fetus with HLH showed a normal DV blood flow pattern.[35]

Gembruch et al. were the first to investigate venous Doppler flow profiles (DV, vena cava inferior) in a large group of heterogeneous heart defects.[36] In this study, isolated heart defects with hydrops ($n = 7$) and without hydrops ($n = 89$) were differentiated from nonisolated heart defects ($n = 50$). Differences in DV pulsatility (peak velocity index for veins [PVIV]) were found between the total group of CHD including nonisolated cases and controls, but not when isolated heart defects were analyzed separately from the other cases. Although 83% of the group of fetuses with cardiogenic hydrops showed an increased DV pulsatility (>95th centile), the results were insignificant due to the small number of cases. However, in the analysis of further subgroups, a significant increase in DV pulsatility was found in fetuses with right heart malformations ($n = 23$) compared to the remaining isolated cases ($n = 71$, Table 38.4).

Venous Doppler sonography was not a reliable predictor of fetal outcome in isolated cases of CHD in this study. Although there was a higher survival (78%) for fetuses with normal DV blood flow, 58% of the fetuses survived despite abnormal Doppler examinations, while 22% of fetuses with a normal DV flow pattern died.[37] The same group observed no association

**Table 38.4** Doppler studies of the ductus venosus in fetuses with isolated CHD

| *Study* | *Type of CHD* | *Number of fetuses* | *Studied parameters* | *Results CHD versus controls* | |
|---|---|---|---|---|---|
| Gembruch et al.[36] | Mixed | 94 | PVIV (95th centile) | NS | |
| | | | ΔPVIV | NS | |
| | RHM | 23 | PVIV (95th centile)<br>ΔPVIV | Increased<br>Increased | (versus remaining isolated CHD) |
| Berg et al.[37] | RHM + VSD | 36 | PVIV (95th centile) | NS | |
| | (DORV, TOF, PA) | | ΔPVIV | NS | |
| | Obstructive RHM | 47 | PVIV (95th centile) | Increased | |
| | (TA + VSD, Ebstein anomaly, PS, PA) | 47 | ΔPVIV | Increased | |

*Abbreviations:* DORV, double-outlet right ventricle; PA, pulmonary atresia; PS, pulmonary stenosis; PVIV, peak velocity index for veins; RHM, right heart malformation; TA, tricuspid atresia; VSD, ventricular septal defect.

between the Doppler indexes of the DV and the survival rate of fetuses with right heart defects.[37] Others, however, found a significantly higher DV-PIV in nonsurvivors than in survivors.[38,39] In the study of Baez et al., 10 out of 13 nonsurvivors (77%) demonstrated an abnormal DV PVIV as compared to 12 out of 36 survivors (33%).[38] The same association was present in a subanalysis of cases with atrioventricular (AV) septal defects and abnormalities predominantly involving the right ventricle.[38] Bianco et al. reported a significantly higher perinatal survival in fetuses with CHD and normal DV resistance (83%) compared to those with abnormal DV (33%). The predictive value in this study was independent of karyotype and gestational age at delivery.[39] The prognosis of cardiogenic hydrops was uniformly bad in all studies, with all of them resulting in either intrauterine or postnatal demise.[36–38]

Building on the results of the first study conducted by Gembruch et al., Berg et al. further analyzed 83 fetuses with isolated right heart lesions divided into two groups: group A with a pressure-equalizing ventricular septal defect (VSD) (double-outlet right ventricle, TOF, pulmonary atresia with VSD) and group B with inflow obstruction (tricuspid atresia with VSD), or outflow obstruction with intact septum (Ebstein anomaly, pulmonary atresia, or pulmonary stenosis). Whereas in group A no significant alterations were found compared to controls, in group B a significantly higher PVIV was observed as well as frequent reverse flow during the a-wave (Figure 38.2). The abnormal DV flow characteristics were not significantly related to signs of heart failure (cardiomegaly, AV-valve insufficiency, or hydrops), therefore more likely reflecting elevated cardiac preload rather than decompensation in those heart defects.[37]

The common pathophysiology of these types of heart defects consists of a relevant increase of right atrial and central venous pressure. In this case, the forward flow during atrial contraction decreases to zero or to retrograde flow, leading to an increased pulsatility of the blood flow profile (Figure 38.3). However, the development of hydrops fetalis is extremely rare in fetuses with right ventricular outflow obstructions, even with an intact ventricular septum, as in most cases, the left ventricle compensates the abnormal hemodynamics of the right ventricle. In order to tolerate the increased transatrial right-to-left shunt, a nonrestrictive foramen ovale is mandatory. So far, none of the studies have investigated longitudinally the prognostic value of DV pulsatility with regard to the development of hydrops. Sequential examination was performed in 15 fetuses of group B by Berg et al.[37] In 10 of the cases, DV pulsatility remained unaltered, in four cases the pulsatility increased, and in one the pulsatility decreased. In none of the cases with a longitudinal increase of DV pulsatility (one with tricuspid atresia, three with pulmonary atresia) was the development of hydrops observed.[37]

However, in some rare cardiac malformations, such as Ebstein anomaly, aortic atresia with restricted foramen ovale, absent pulmonary valve syndrome (APVS), or truncus arteriosus communis (TAC) with severe insufficiency of the common arterial valve, increasing pulsatilities in the flow velocity waveforms of the precordial veins are indicative of increasing

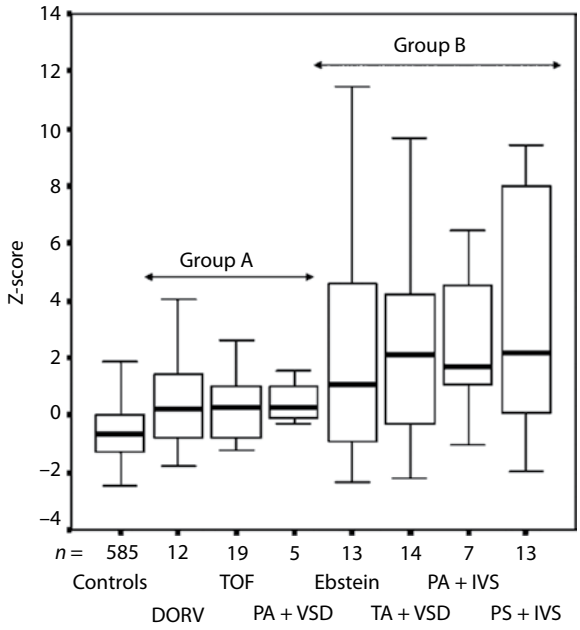


**Figure 38.2**
Z-scores of ductus venosus peak velocity index for veins of 83 fetuses with right-sided cardiac lesions (group A with a large ventricular septal defect equalizing interventricular pressures, group B with obstruction of the inflow or obstruction of the outflow with intact ventricular septum) and 585 fetuses in the control group. (DORV, double-outlet right ventricle; Ebstein, Ebstein anomaly; IVS, intact ventricular septum; PA, pulmonary atresia; PS, pulmonary stenosis; TA, tricuspid atresia; TOF, tetralogy of Fallot; VSD, ventricular septal defect.) (Reproduced from reference Berg C et al. *Ultrasound Obstet Gynecol* 2006;28:137–42, with permission granted by Wiley & Sons Ltd.[37])

venous pressure, announcing cardiac decompensation and impending hydrops fetalis.

The pathophysiology of fetuses with severe Ebstein anomaly with tricuspid insufficiency is more complex and different from that of other right-sided cardiac lesions. The intrauterine hemodynamics depends not only on the size of the fossa ovalis and the function of the left ventricle, but also on the function of the right ventricle, the extent of tricuspid insufficiency, and the right atrial compliance. A relatively small foramen ovale and/or extreme cardiomegaly, both frequently observed in these fetuses, can lead to substantial left ventricular compression with obstruction of volume flow, possibly resulting in cardiac decompensation with development of hydrops fetalis. In this specific situation, an increased DV pulsatility may be a sign of impending hydrops and alert the examiner. Accordingly, Berg et al. reported on significantly higher DV pulsatilities in two hydropic compared to 11 nonhydropic fetuses with Ebstein anomaly.[37]

More recently, Arya et al. compared DV measurements in fetuses with various right-sided congenital heart disease.[40] Fetuses were separated into those with obstructive (group 1) and nonobstructive lesions (group 2). Group 1 included CHD with tricuspid and/or pulmonary stenosis and/or atresia. Group 2 was defined as CHD with dysplasia of the tricuspid

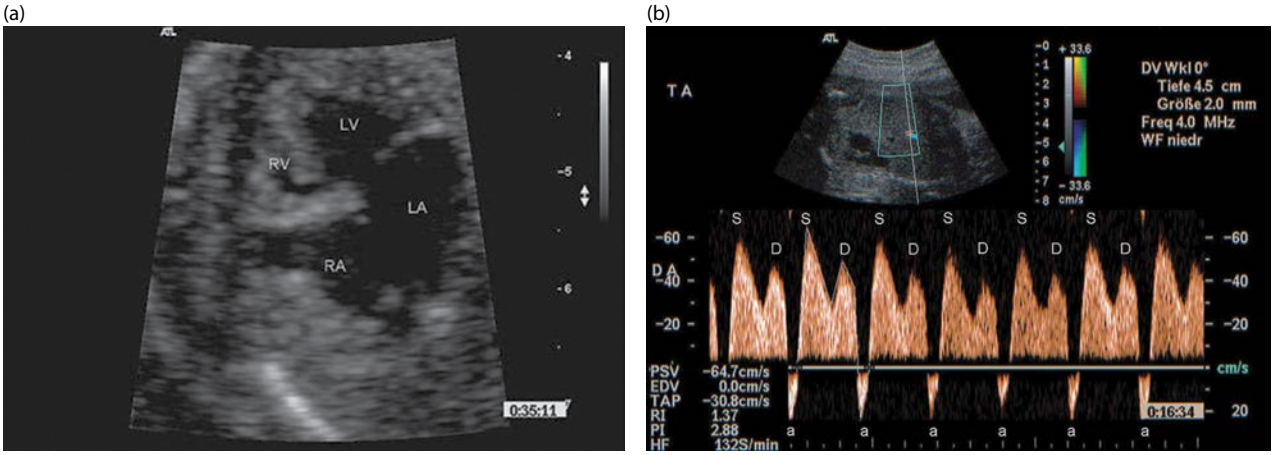


**Figure 38.3**
(a) Sonogram of a fetal heart with tricuspid atresia at 20 + 4 weeks of gestation. (LA, left atrium; LV, left ventricle; RA, right atrium; RV,right ventricle.) (b) The blood flow velocity waveforms of the ductus venosus demonstrate high pulsatilities with reversal of flow during atrial contraction. (a, atrial contraction; D, diastole; S, systole.)

or the pulmonary valve resulting in insufficiency but not severe stenosis, this group included Ebstein anomaly. A-wave reversal in the DV was significantly higher in group 1 than in group 2 (49% versus 13%). Also, fetuses in group 1 had a higher PVIV than fetuses in group 2. For the total group of right-sided CHD, no relationship was observed for DV pulsatility or a-wave reversal and fetal compromise. For both groups, the presence of flow reversal in the DV was not significantly different for those fetuses who died versus those who survived. However, in group 1 the PVIV in the subgroup that died was significantly higher than in those who survived.[40] The findings of this study were not adjusted for extracardiac and/or chromosomal abnormalities.

Fetuses with severe tricuspid regurgitation of various genesis (tachycardia-induced cardiomyopathy after conversion to sinus rhythm, Ebstein anomaly, pulmonary atresia, or rhabdomyomas) are occasionally observed to have atypical flow patterns in the DV, with decrease of the systolic forward flow (Figure 38.4) or systolic notching (Figure 38.5), both consequences of an impairment of the venous flow during systole due to severe tricuspid insufficiency.[36,41] In calculating the venous pulsatility indexes, this shifts the results toward more normal values and should be considered when monitoring these fetuses.

## Summary

Fetuses with isolated structural heart defects predominantly show normal arterial and venous blood flow patterns. Therefore, Doppler sonography of the umbilical artery, MCA, and DV is an insufficient parameter for the purpose of screening. Abnormal blood flow patterns are frequently found in cases additionally complicated by fetal growth restriction, aneuploidies, or extracardiac malformations. Individual groups of heart defects show significant blood flow alterations compared to controls due to their own pathophysiology. This refers especially to cases with severe obstruction of the inflow and outflow. An increased pulsatility of the umbilical artery

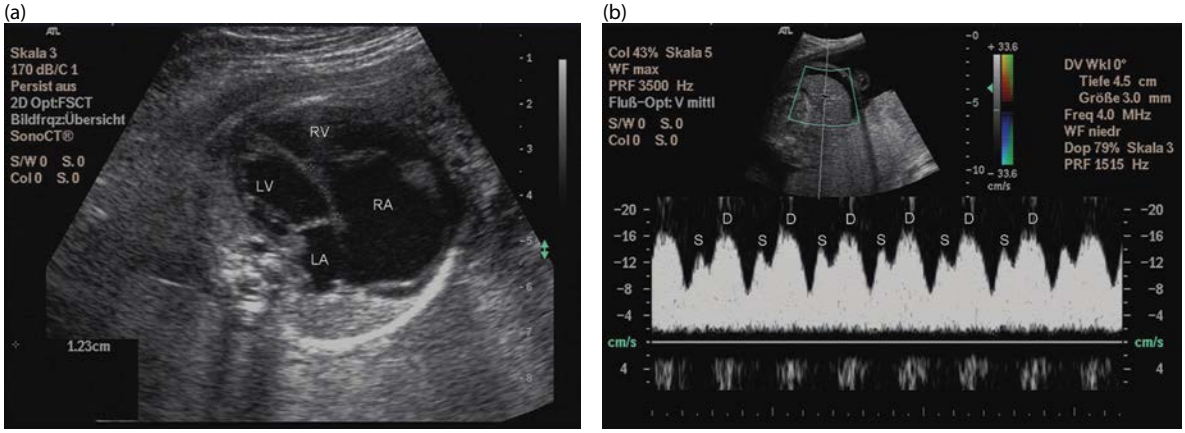


**Figure 38.4**
(a) Sonogram of a fetal heart with Ebstein anomaly at 25 weeks + 3 days of gestation. (b) The blood flow velocity waveforms demonstrate higher velocities during diastole (D) than during systole (S). (LA, left atrium; LV, left ventricle; RA, right atrium; RV,right ventricle.)

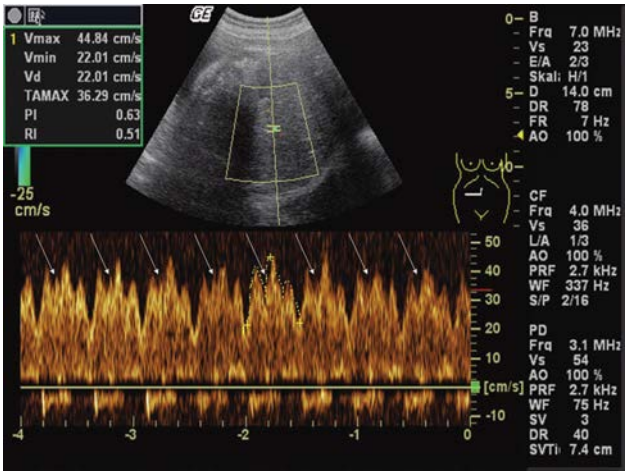


**Figure 38.5**
Ductus venosus blood flow with presence of systolic notching (arrows) at 21 + 1 weeks of gestation in a fetus with Ebstein anomaly and severe tricuspid regurgitation.

has been observed specifically in fetuses with severe outflow obstruction and reverse perfusion via the ductus arteriosus. In contrast to fetuses with IUGR and brain sparing following general circulatory redistribution, those with hypoplastic left heart and severe aortic arch obstruction may have isolated cerebral vasodilatation of the MCA as a local adaptive response to moderate hypoxia. DV pulsatility may be increased, especially in right heart malformations with elevated right atrial pressure, usually without being associated with cardiac compromise.

Neither arterial nor venous Doppler permits reliable prediction of fetal survival; the most determining factors are the type and severity of the underlying heart defect and its influence on postnatal hemodynamics.

# References


1. Al-Gazali W et al. *Br J Obstet Gynaecol* 1987;94:742–5.
2. Copel JA et al. *J Ultrasound Med* 1991;10:323–6.
3. Meise C et al. *Ultrasound Obstet Gynecol* 2001;17:398–402.
4. Donofrio MT et al. *Pediatr Cardiol* 2003;24:436–43.
5. Modena A et al. *Am J Obstet Gynecol* 2006;195:706–10.
6. Itsukaichi M et al. *Fetal Diagn Ther* 2011;30:219–24.
7. Masoller N et al. *Ultrasound Obstet Gynecol* 2014;44:182–7.
8. Jouannic JM et al. *Ultrasound Obstet Gynecol* 2002;20:122–4.
9. Yamamoto Y et al. *Ultrasound Obstet Gynecol* 2013;42:294–9.
10. Kaltman JR et al. *Ultrasound Obstet Gynecol* 2005;25:32–6.
11. Szwast A et al. *Ultrasound Obstet Gynecol* 2012;40:62–7.
12. Gottschalk I et al. *Ultrasound Obstet Gynecol* 2017;49(5):637–42.
13. Wertaschnigg D et al. *Can J Cardiol* 2016;32(12):1500–6.
14. Guorong L et al. *Fetal Diagn Ther* 2009;25:167–72.
15. Berg C et al. *Ultrasound Obstet Gynecol* 2009;34:666–72.
16. Jansen FA et al. *Ultrasound Obstet Gynecol* 2016;48(3):357–64.
17. Hahn E et al. *Ultrasound Obstet Gynecol* 2016;47:460–5.
18. Rudolph AM. *Congenital Diseases of the Heart*. 3rd ed. Chichester, UK: Wiley; 2009.
19. Szwast A et al. *Ann Thorac Surg* 2009;87:1214–9.
20. Sun L et al. *Circulation* 2015;131:1313–23.
21. Wallenstein MB et al. *J Matern Fetal Neonatal Med* 2012;25:662–5.
22. Ruiz A et al. *Ultrasound Obstet Gynecol* 2017;49(3):379–86.
23. Barbu D et al. *Am J Obstet Gynecol* 2009;201:43.e1–7.
24. Pearce W. *J Appl Physiol* 2006;100:731–8.
25. Limperopoulos C et al. *Pediatrics* 1999;103:402–8.
26. Mahle WT et al. *Circulation* 2002;106(suppl 1):109–14.
27. Van Houten JP et al. *Am J Perinatol* 2002;13:47–53.
28. Rosenthal GL. *Am J Epidemiol* 1995;143:505–13.
29. Limperopoulos C et al. *Circulation* 2010;121:26–33.
30. Clouchoux C et al. *Cereb Cortex* 2013;23:2932–43.
31. Masoller N et al. *Ultrasound Obstet Gynecol* 2016;47:65–73.
32. Khalil A et al. *Ultrasound Obstet Gynecol* 2014;43:14–24.
33. Matthiesen NB et al. *Circulation* 2016;133:566–75.
34. Kiserud T et al. *J Matern Fetal Invest* 1993;3:15–20.
35. DeVore GR, Horenstein J. *Ultrasound Obstet Gynecol* 1993;3:338–42.
36. Gembruch U et al. *Ultrasound Obstet Gynecol* 2003;22:345–50.
37. Berg C et al. *Ultrasound Obstet Gynecol* 2006;28:137–42.
38. Baez E et al. *Fetal Diagn Ther* 2005;20:383–9.
39. Bianco K et al. *J Ultrasound Med* 2006;25:979–82.
40. Arya B et al. *J Ultrasound Med* 2014;33:1563–71.
41. Smrcek JM et al. *Ultrasound Obstet Gynecol* 2005;26:180–2.

# 39

# Electrophysiology for the perinatologist

Edgar T. Jaeggi

## Introduction

Disturbances of the heart rhythm and rate are an important aspect of fetal medicine. The primary objective of any newly detected arrhythmia is to determine its underlying mechanism, the hemodynamic consequences and whether treatment is needed and available. The purpose of this chapter is to review the normal physiology of electrical impulse generation and conduction and to then address the mechanisms and diagnostic features of the more common fetal arrhythmias.

## Normal electrophysiology

### *Normal impulse formation and propagation*

The main role of the heart is to pump blood throughout the body to allow adequate supply of oxygen and nutrients to the tissues while removing toxic wastes. Cardiac output (CO), the volume of ejected blood per minute, is equal to the combined ventricular stroke volumes in a single heartbeat times the heart rate. A normal combined fetal CO is ~450 mL/kg/minute during mid- and late gestation. Cardiac actions naturally underlie the control of highly specialized muscle tissue, the cardiac electrical conduction system, that comprises the sinoatrial (SA) node, the atrioventricular (AV) node, and the His–Purkinje system, including the penetrating bundle of His, bundle branches, and the Purkinje fibers (Figure 39.1). The role of the conduction system is to generate the electrical impulse in spontaneously depolarizing SA nodal cells that are located at the upper right atrial wall and to then propagate the action potential across the fibrous ring of the AV junction and throughout the ventricles, allowing the synchronized electrical and mechanical activation of the atrial and ventricular cardiomyocytes with each heartbeat. As the SA node generates electrical impulses the fastest, it overdrives the pacemaker potential of other cardiac tissue that may also exhibit automatic properties such as AV nodal cells. Electrical conduction velocities vary between cardiac tissues and are significantly slower across the AV node (0.05 m/s) when compared to atrial and ventricular myocardium (0.5–1 m/s) and the His-Purkinje system (2–4 m/s). The considerable slowing in impulse propagation across the AV node allows for sufficient time for complete atrial myocardial depolarization and contraction prior to ventricular depolarization with each heartbeat. The cardiac mechanical actions, contraction of myocytes in systole and relaxation in diastole, are orchestrated by rapid cyclic changes in transmembrane $Na^+$, $Ca^{2+}$ and $K^+$ currents with each heartbeat. Following depolarization, the conducted impulse is prevented from immediately reactivating the conduction system and myocardium by refractoriness of the tissue that just has been activated. The heart must then await a new electrical impulse to initiate the next heartbeat. The period of time that a new action potential cannot be initiated by electrical stimulation during a cardiac cycle is termed the effective refractory period (ERP) of the tissue. ERP acts as a protective mechanism against arrhythmias.

### *Assessment of the fetal cardiac rhythm*

After birth, electrocardiography (ECG) is the modality of choice to record the electrical activity of the heart. The normal ECG entails a sinus P wave with a P wave axis between 0 and +90 degrees that precedes each QRS complex within a timely normal PR interval for age. The assessment of the fetal cardiac rhythm before birth is more challenging. While it is also possible to non-invasively record fetal electrical events by maternal transabdominal ECG or, indirectly, by magnetocardiography (MCG),[1–5] suitable recording systems are currently either unavailable (ECG) or too expensive (MCG) to be more widely used in fetal medicine. Fetal echocardiography has therefore been used as a surrogate modality to study the beat-to-beat chronology of atrial and ventricular electrical events by their respective mechanical consequences.[6–11] By way of M-mode (Figure 39.2) or tissue Doppler imaging, it is possible to simultaneously record the sequence and time-relationship of atrial and ventricular systolic wall movements. Similarly, simultaneous pulse wave Doppler evaluation of the mitral inflow and aortic outflow (MV/aorta) or, preferably, the superior vena cava and the ascending aorta (SVC/aorta Doppler) is used to examine the sequence and time-relationship of blood flow events that are secondary to atrial and ventricular contractions (Figure 39.3). The beginning of the retrograde flow in the SVC (a-wave) reflects the onset of atrial systole, whereas the onset of aortic forward flow marks the beginning

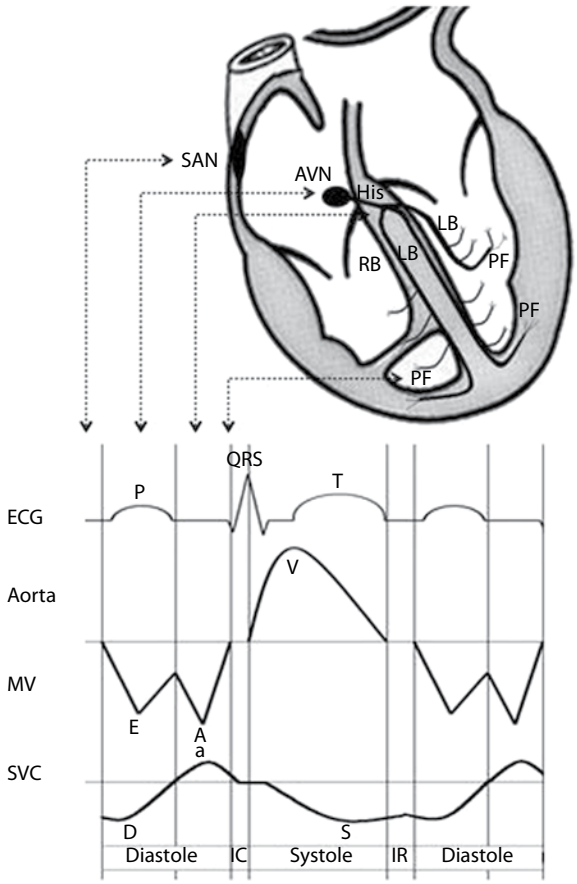


**Figure 39.1**
Electrical conduction system and the relationship between electrical depolarization (ECG) and the mechanical consequences (echocardiography). *Top Section:* The electrical impulse propagates from the sino-atrial node (SAN) along atrial muscle fibers towards the AV junction, stimulating the atrial myocardium to contract. Within the AV node (AVN), providing the only electrical connection between the atria and ventricles across the fibrous ring of the AV junction, the electrical impulse is physiologically delayed thus functioning as a filter against the propagation of abnormally fast atrial rates or very premature atrial beats to the ventricles. After crossing the AV node, the electrical current rapidly passes through the bundle of His, the right (RB) and left (LB) bundle branches and the interweaving network of the Purkinje fibers (PF) to the endocardial surfaces of both ventricles. The electrical depolarization then spreads quickly from one ventricular myocyte to the next, so that both ventricles function as synchronous contractile units. *Bottom Section:* There is a physiological delay between the atrial (P-wave) and ventricular (QRS complex) depolarization and the onset of myocardial contraction and intracardiac blood flow respectively. Mitral valve (MV) A-wave and superior vena cava (SVC) a-wave are late-diastolic events that result from atrial contraction, while forward flow in the ascending aorta (V) is caused by ejection of blood during ventricular contraction. The onsets of the atrial and ventricular systolic flow events are used to assess the mechanical AV relationship by Doppler echocardiography. The degree of correlation between electrophysiological PR and ultrasound-derived mechanical AV intervals is determined by electromechanical cardiac activation and loading conditions and differs among the different ultrasound modalities. Early diastolic flow: E-wave (MV); D-wave (SVC); Late diastolic flow: A-wave (MV); a-wave (SVC); Systolic flow: V-wave (aorta); S-wave (SVC).

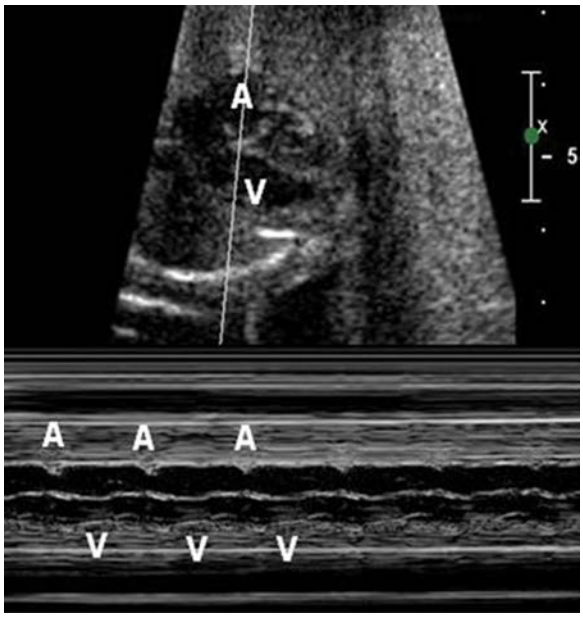


**Figure 39.2**
Simultaneous assessment of atrial and ventricular systolic wall motion by M-mode echocardiography. Guided by real-time two-dimensional echocardiography, the M-mode ultrasound beam is aligned simultaneously through the atrial (A) and ventricular (V) walls to record the sequence of systolic wall motions. A normal M-mode tracing is characterized by regular atrial and ventricular contractions at normal rates that occur within a normal AV time intervals.

of ventricular systole. Applying the same concept, the pulmonary artery and vein flow or the left ventricular inflow and outflow may be simultaneously recorded by pulsed Doppler imaging.

While echocardiography provides useful information on the chronology of systolic atrial and ventricular events including AV conduction, it does not inform on the morphology, duration and amplitude of other electrical events such as QRS waves and QT intervals. Hence, it is, for example, not possible to diagnose long QT syndrome and other repolarization abnormalities solely by fetal echocardiography although this may be suspected from other telltale findings.

With the above limitations in mind, a *normal fetal cardiac rhythm* is assumed by the documentation of:

1. A relatively regular rhythm with atrial and ventricular rates between the 3rd and 97th percentile for gestational age (GA)[12] and
2. A timely normal 1:1 AV relationship (Figure 39.4)

Gestational-age matched reference values of mechanical AV time intervals by different echocardiographic methods have been published.[1,13] AV time measurement is routinely used to monitor the AV nodal conduction of fetuses exposed to maternal anti-Ro/SSA auto-antibodies and thus with a risk of developing complete heart block (CHB). There is some evidence that CHB may be preventable if the disease can be recognized and treated at an early disease manifestation

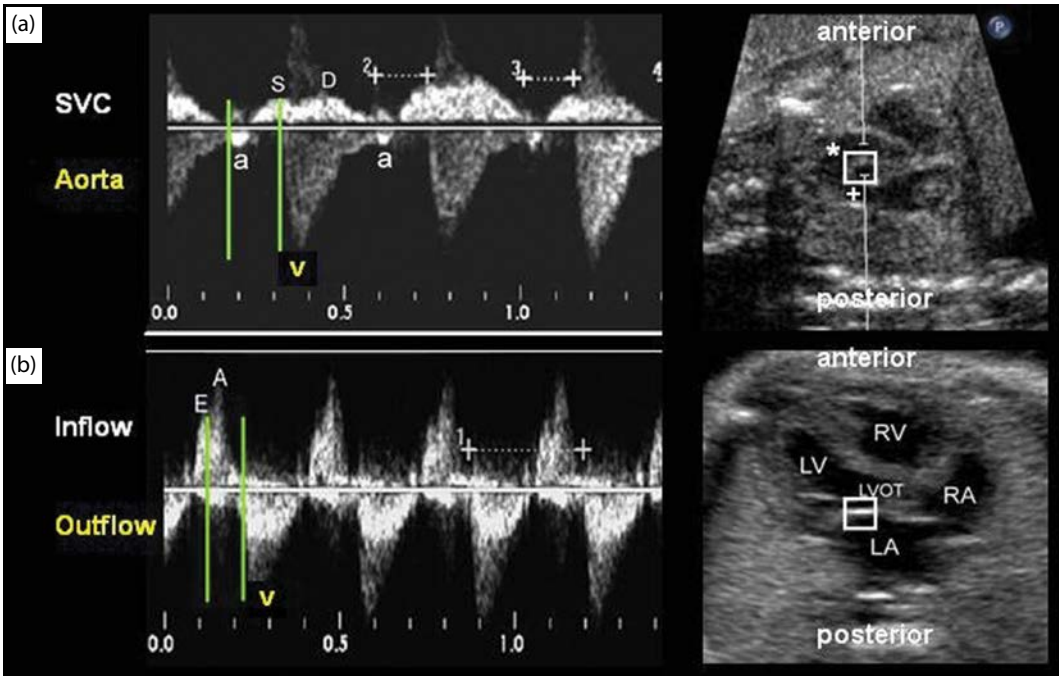


**Figure 39.3**
Simultaneous assessment of atrial and ventricular systolic flow by pulsed Doppler echocardiography. (a) *Superior vena cava/ascending aorta (SVC/Aorta) Doppler.* In the sagittal view of the fetal thorax, the connection of the superior vena cava (+) to the right atrium and part of the adjacent ascending aorta (*) can be seen. Positioning of the enlarged Doppler sample volume □ within both vessels allows simultaneous recording of the SVC and aortic flow (V). SVC Systolic (S-wave) and early diastolic (D-wave) flow is directed towards the fetal heart while it is in the opposite direction during atrial contraction (a-wave). Measurement of the atrio-ventricular interval (AV: from the onset of the a-wave to the onset of V) is illustrated by vertical bars. (b) *Mitral valve/ascending aorta (left ventricular Inflow/Outflow) Doppler.* Simultaneous inflow-outflow Doppler is easily obtained in a cranially angulated four chamber view of the fetal heart with the aorta seen as the fifth chamber. The Doppler sample volume □ is then positioned across the mitral valve and the left ventricular outlet (LVOT). This approach is mainly useful to determine the AV relationship during the normal rhythm. The beginning of the mitral A-wave marks the onset of atrial systole, while the beginning of aortic flow (V) marks the onset of ventricular systole. The technique of measuring the AV interval is illustrated by vertical bars.

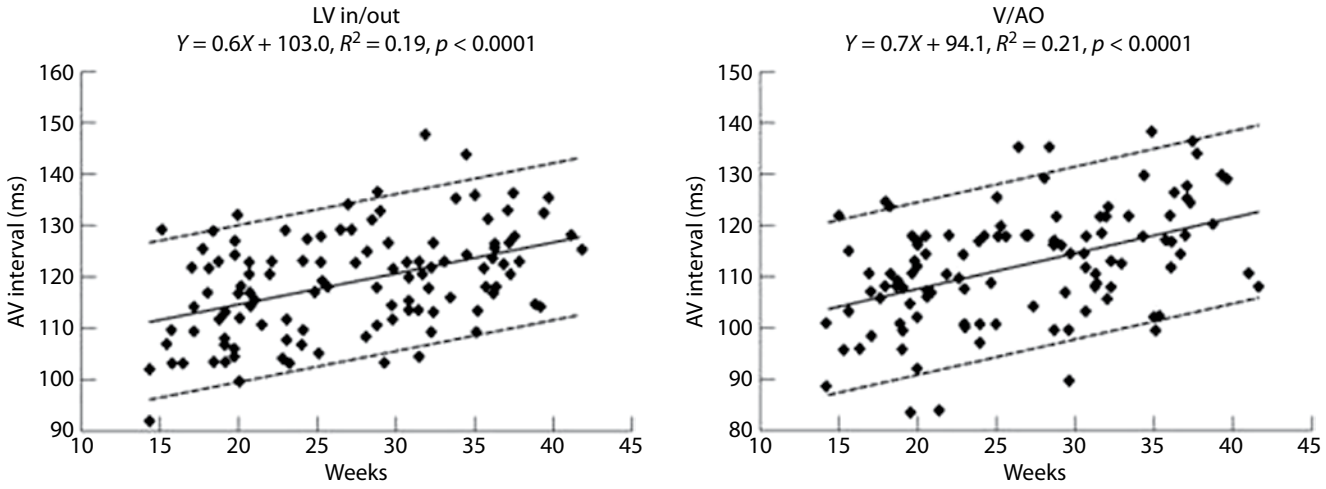


**Figure 39.4**
Gestational-age matched normal AV intervals by pulse-wave Doppler. Lines denote regressions and 95% confidence limits for individual observations. (AV, atrio-ventricular; LV in/out, left ventricular inflow/outflow; $R^2$, coefficient of determination; V/AO, superior vena cava/aorta.) (Reproduced with permission from Nii M et al. *Heart* 2006;92:1831–7.[1])

of incomplete 1st or 2nd degree AV block.[14–17] First degree heart block as the most subtle electrical conduction anomaly is characterized by 1:1 AV conduction with normal regular atrial and ventricular rates, but the AV time intervals are significantly prolonged for the gestational age.[17]

# Fetal arrhythmias

## *Arrhythmia mechanisms*

Arrhythmias other than 1st degree heart block are deviations from the normal cadence of electro-mechanical activity that will either manifest as an irregularity of the rhythm, as a slow or fast heart rate, or as a combination of abnormal rhythm and rate. The contributing causes can be broadly divided into abnormalities in the generation and propagation of electrical impulses and may occur in every region of the heart.[18–20]

### Abnormal impulse generation

Cardiac cells in the atria, AV node and His-Purkinje system may manifest automaticity outside the SA node. Their ability to act as pacemaker cells is typically suppressed by the physiologically faster sinus rate. An ectopic cardiac rhythm occurs when the dominant pacemaker shifts from the SA node to a subsidiary pacemaker because the sinus rate decreases below the intrinsic rate of the secondary pacemaker (e.g., atrial or junctional escape rhythm) or because the intrinsic rate of a secondary pacemaker surpasses the normal sinus rate due to enhanced automaticity (e.g., atrial ectopic tachycardia [AET]; premature atrial contractions [PAC]). Another rhythm disorder whose origin is abnormal impulse generation includes a sinus node that fires at an unusually fast rate (sinus tachycardia) or slow rate (sinus bradycardia).

### Abnormal impulse propagation

"Reentry" is the propagation of an electrical impulse through myocardial tissue already activated by the same impulse in a circular movement. It is the mechanism of most supraventricular tachyarrhythmias (SVA), including atrial flutter (AF) and AV reentrant tachycardia (AVRT). AF is sustained by a reentrant circuit that is confined to atrial tissue. In AVRT, the predominant mechanism of a persistently fast fetal heart rate, the reentrant circuit usually includes the AV node to conduct from the atria to the ventricles and an accessory pathway to propagate the ventricular impulse back to the atria. Delay or blockage of electrical propagation occurs when conduction tissue such as the AV node is diseased (e.g., heart block) or refractory (e.g., blocked PAC).

## *Echocardiographic assessment of fetal arrhythmias*

Most arrhythmias and their clinical relevance can be reliably discerned by a stepwise analysis and interpretation of M-Mode and/or Doppler arrhythmia tracings and other key parameters (Table 39.1). This includes determining:

1. The rate, regularity and chronology of atrial and ventricular events;
2. The hemodynamic consequences; and
3. Contributing or aggravating factors of the arrhythmia.

## *Arrhythmias presenting with an irregular rhythm*

Probably the most frequent presentation of an irregular rhythm disorder is coincidental, during a routine assessment

**Table 39.1** Stepwise approach to the assessment of fetal arrhythmias

- *Atrial (A) rate and rhythm (A-A):*
  A: Absent—slow—normal—fast
  A-A: Regular—irregular—regular-irregular (e.g., atrial bigeminy)
- *Ventricular (V) rate and rhythm (V-V):*
  A: Slow—normal—fast
  A-A: Regular—irregular—regular-irregular (e.g., ventricular bigeminy)
- *Ratio of atrial and ventricular events (A-V ratio):*
  Normal 1:1 (equal A and V)
  >1:1 (more A than V)
  <1:1 (more V and A)
- *Relationship and timing of atrial and ventricular events:*
  Normal AV time—prolonged AV time—A-V dissociation
- *Arrhythmia pattern:*
  Duration: brief (<10%)—intermittent (10%–50%)—sustained (>50%)—incessant (100%)
  Onset/termination: sudden or gradual; triggered by other event (i.e., PAC)
- *Fetal health state:*
  Effusions, heart size and function, AV valve regurgitation; fetal movements; amniotic fluid
- *Structural heart disease and other associations:*
  Heart block: anti-Ro antibodies; left isomerism; congenital corrected transposition
  Sinus tachycardia: Grave's disease; anemia; fetal distress
  Sinus bradycardia: long QT syndrome; anti-Ro/SSA antibodies

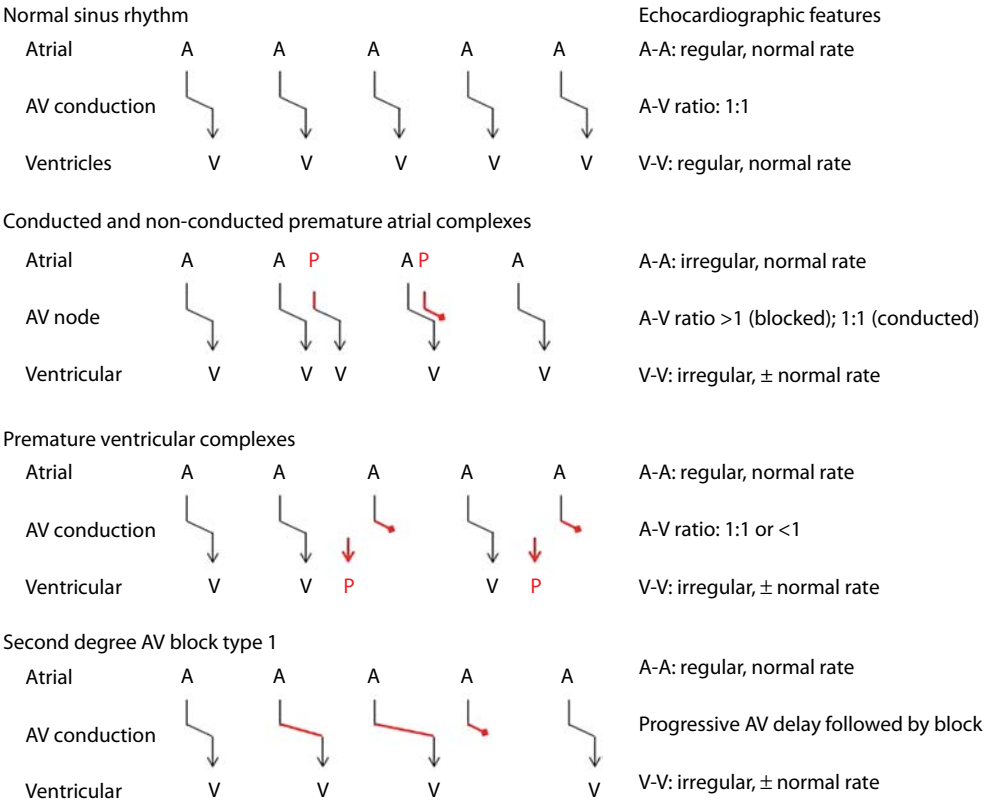


**Figure 39.5**
Mechanisms and echocardiographic features of irregular arrhythmias compared with normal sinus rhythm. (A, normal atrial event; P, premature atrial or ventricular contraction; V, normal ventricular event; —◆, non-conducted atrial beat.)

of an otherwise asymptomatic mother and her fetus. The main differential diagnosis of an irregular heart rhythm includes (Figure 39.5):

- Premature atrial contractions (PAC)
- Premature ventricular contractions (PVC) and
- Second degree AV block type I and type II

*Premature atrial contractions* (Figure 39.5 top section) are by far the most common cause of an irregular fetal heartbeat. By echocardiography, a PAC is detected by a shorter than normal atrial (A-A) time interval.[21,22] If the PAC is premature enough to fail conduction across the refractory AV node, no ventricular event will be observed, which manifests as a skipped heartbeat. If the AV node is not refractory, the premature atrial event will be followed by a timely related premature ventricular contraction.

Conducted PACs are to be distinguished from *premature ventricular contractions* (Figure 39.6 bottom section), which are rare observations in the fetus. By echocardiography, the PVC is not preceded by an atrial beat and atrial intervals are usually normal and regular. A regular-irregular arrhythmia pattern is observed if every second (bigeminy) or third (trigeminy) atrial or ventricular beat occurs prematurely.

Irrespective of the pattern of appearance, isolated PACs and PVCs are hemodynamically insignificant and typically resolve spontaneously without medication. Nonetheless, isolated PACs are associated with a <1% risk of fetal SVA and a risk that is higher if they occur as atrial bigeminy or in couplets.[23,24] Fetal heart rate should therefore be intermittently monitored by an obstetrician or midwife for signs of tachyarrhythmia until the PACs have resolved. In addition, recently published AHA guidelines recommend fetal echocardiography to assess the cardiac structure and function and to establish the mechanism of the arrhythmia if the fetus presents with frequent irregular beats, if there is any question about the arrhythmia mechanism or if the ectopic beats persist beyond 1–2 weeks.[23]

An irregular rhythm can also be rarely due to *2nd degree AV block*, which is characterized by failure of AV conduction of some but not all atrial activity to the ventricles. The atrial rate is normal and the ventricular rate depends on the number of conducted atrial impulses. In 2nd degree AV block Mobitz type I (Wenckebach), the non-conducted atrial event is preceded by progressive AV lengthening while in Mobitz type II the AV conduction is either normal or blocked. Second-degree AV block may be secondary to antibody-mediated AV nodal inflammation and may then benefit from anti-inflammatory treatment to prevent progression to complete heart block.[25,26]

## *Arrhythmias presenting with low heart rates*

The conventional definition of fetal bradycardia is a heart rate <110 bpm, although a more accurate definition would be a

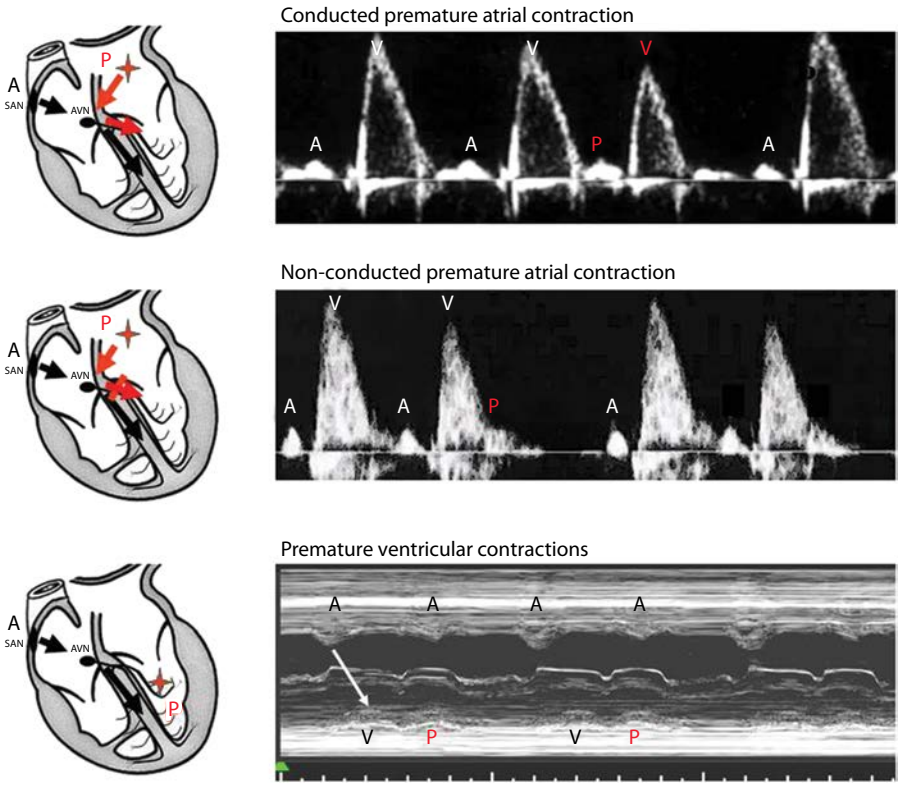


**Figure 39.6**
Premature atrial (PAC) and ventricular (PVC) contractions. *Top and middle: Conducted and non-conducted PACs (SVC/Aorta Doppler)* When compared to the normal atrial-atrial (A-A) intervals, the A–P (PAC) interval is visibly shorter. Conduction of the PAC to the ventricles depends on the refractoriness of the AV node at the time of atrial extrasystole. *Bottom: PVCs (M-Mode)* The atrial rhythm (A-A) is regular, while the ventricular rhythm is irregular, in this case due to prematurity (P) of every alternating ventricular beat (ventricular bigeminy). The average ventricular rate remains normal, despite the fact that only every second atrial beat is conducted (indicated with arrow).

heart rate <3rd percentile for gestational age. Bradycardia mechanisms include (Figure 39.7):

- Sinus bradycardia
- Non-conducted atrial bigeminy
- 2:1 AV block
- Complete heart block (CHB)

*Sinus bradycardia* is defined as a rhythm that originates from the SA node but where the rate is slow for age. A secondary pacemaker may take over if the spontaneous discharge rate of the SA node decreases below that of the subsidiary atrial or junctional pacemaker. By echocardiography, sinus or atrial bradycardia resembles that of a normal rhythm with the only difference that the atrial and ventricular rates are slow for gestational age, usually in the range between 80 and 110 bpm. Sinus bradycardia *per se* is well tolerated. Brief episodes of bradycardia of less than 1–2 minutes are considered benign, particularly if observed early in gestation. More sustained or persistent episodes should trigger an assessment for possible causes, such as fetal distress, sinus node dysfunction (anti-Ro antibody related, left atrial isomerism) and long QT syndrome (KCNQ1 mutation).[12,27–32] The perinatal management of sinus bradycardia depends on the underlying etiology and may include no treatment, anti-inflammatory medication for myocarditis (anti-Ro antibodies), premature delivery (fetal distress), and postnatal therapy with beta-blocker ± pacing (LQTS).

*Functional AV block* may occur when the AV node is still refractory, that is, following recent depolarization or because cardiac repolarization is prolonged. In *non-conducted atrial bigeminy* (Figure 39.8 top section), every second atrial impulse occurs prematurely enough to fail conduction across the refractory AV node. By echocardiography, the inter-atrial intervals are irregular but in a regular pattern alternating between a shorter (A-PAC) and a longer (PAC-A) atrial interval. If each PAC is non-conducted and each normal sinus beat (A) is forwarded to the ventricles, the ventricular rate will be half of that of the averaged atrial rate, which is usually between 60–90 bpm. Non-conducted atrial bigeminy is a not infrequent cause of fetal bradycardia and may sometimes persist for days to weeks. Still, like the other presentations of PACs, atrial bigeminy is well-tolerated and will eventually resolve spontaneously. Because of the increased risk of fetal SVA with atrial bigeminy, weekly heart rate assessment is recommended until the resolution of the arrhythmia.[23]

Atrial bigeminy should not be confused with *2:1 AV block* (Figure 39.8 middle section) which may be related to a congenital QT prolongation.[30,33] Unlike with atrial bigeminy, the atrial rhythm in 2:1 AV-block is regular. In addition, 1:1 AV conduction may recur at slower atrial rates. Similar to other

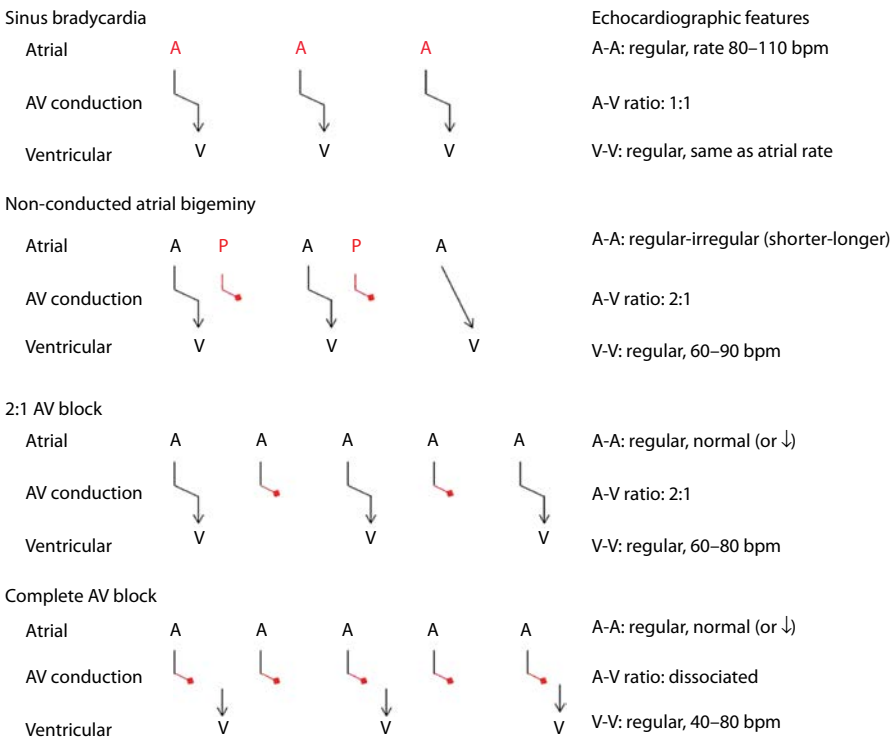


**Figure 39.7**
Mechanisms and echocardiographic features of disorders of a slow heart rate. (A, atrial event; P, premature atrial complex; V, ventricular event; —◆, non-conducted atrial beat.)

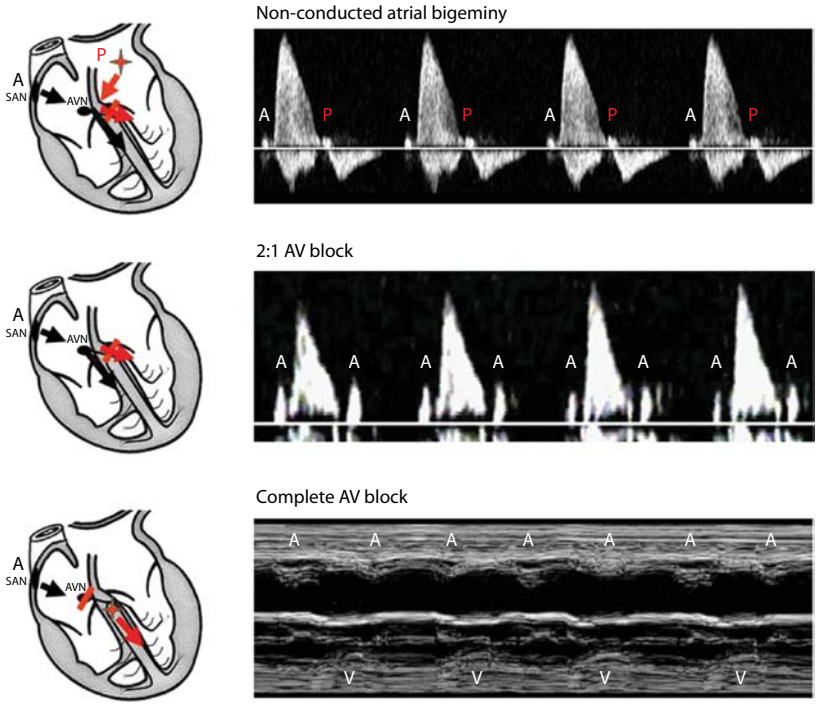


**Figure 39.8**
Atrial bigeminy, 2:1 AV block and complete AV block. *Top: Atrial bigeminy (SVC/Aorta Doppler)* Normal atrial (A) and premature atrial contractions (P) alternate. In this example, the PAC occurs prematurely enough to regularly fail conduction to the ventricles. Sustained atrial bigeminy with blocked premature beats may lower the average heart rate of the fetus to 60–100 beats per minute. *Middle: 2:1 AV block (SVC/Aorta Doppler)* Although the atrial rate is regular and normal, only every second beat is conducted to the ventricles. *Bottom: Complete AV block (M-Mode)* Atria (A) and ventricles (V) beat independently and regularly at their intrinsic rates due to complete failure of electrical AV nodal conduction.

possible manifestations of LQTS such as unexplained sinus bradycardia and ventricular tachycardia, patients with 2:1 AV block and their families should undergo a work-up for the possibility of genetic ion channel disorders. Due to the predisposition of LQTS patients for ventricular tachycardia-related cardiac arrests and sudden death, postnatal treatment with a long-acting β-blocker ± pacemaker or implantable cardioverter defibrillator is usually required.

*Complete heart block (CHB)* (Figure 39.8 bottom section), defined as a failure of propagation of any atrial electrical impulses through the AV node, affects about 1 in every 5,000–10,000 pregnancies. The echocardiographic differentiation between non-conduction across a functionally refractory AV node (as in atrial bigeminy and 2:1 AV block) and CHB is clinically important as the latter is irreversible and represents advanced AV nodal damage. The typical fetal echocardiogram of CHB is that of a regular normal atrial rhythm, while the ventricle beats independently at a much slower rate of between 40–80 bpm. In about half of fetal cases with CHB, this is associated with major structural heart disease, most importantly left atrial isomerism which carries a very high risk of *in-utero* demise.[32,34,35] In the absence of structural heart disease, congenital CHB is strongly linked to the transplacental passage of maternal anti-Ro/SSA antibodies, which are detected in about 2% of pregnant women.[36] In 1%–5% of mothers with high-titer anti-Ro antibodies, immune-mediated fetal cardiac complications including CHB, sinus bradycardia, myocarditis, endocardial fibroelastosis, and/or dilated cardiomyopathy will develop after the first trimester.[36] While isolated fetal CHB is often tolerated, at the severe end of the disease spectrum it may contribute to low cardiac output, fetal hydrops, and perinatal death. Risk factors significantly associated with fetal and neonatal death include fetal hydrops, endocardial fibroelastosis, myocarditis, and bradycardia <50–55 bpm.[37,38]

There is no consensus about the optimal management of patients with CHB including indications of prenatal therapy for isolated immune-mediated CHB. There is no treatment available to reverse CHB.[39] Dexamethasone, intravenous immune globulin (IVIG), β-adrenergic medication and postnatal pacing have been used to prevent or treat more severe immune-mediated myocardial inflammation, to augment cardiac output and to improve the chances of survival.[40,41] In our institution, maternal dexamethasone (8 mg/day for 2 weeks; 4 mg/day to 28 weeks; 2 mg/day to birth) is routinely used to treat immune-mediated cardiac disease from the time of diagnosis to birth to prevent more severe myocardial damage.[42] Maternal IVIG (1 g/kg every 2–3 weeks) is added if we detect signs of endocardial fibroelastosis and ventricular dysfunction. In contrast, isolated CHB that is not associated to maternal anti-Ro antibodies can be managed without anti-inflammatory medication. If the average fetal heart rate is <50 bpm, transplacental salbutamol (10 mg TID or QID oral) and postnatal isoprenaline infusion is used to temporarily increase the ventricular rate and maintain an adequate ventricular output until the neonatal implantation of a permanent pacemaker system. Using this approach, 10-year survival rates in Toronto are >90% following a fetal diagnosis of antibody-mediated bradyarrhythmia.

## Arrhythmias presenting with a fast heart rate

The detection of a fast heart rate >180 bpm in the fetus or newborn constitutes a medical emergency as it carries a risk of hemodynamic compromise and mortality.

Possible mechanisms of a fast rhythm include in the order of frequency (Figure 39.9):

- Supraventricular tachycardia (SVT) including AV re-entrant tachycardia (AVRT), atrial ectopic tachycardia (AET) and permanent junctional reciprocating tachycardia (PJRT)
- Atrial flutter (AF)
- Sinus tachycardia
- Ventricular tachycardia

*AVRT and AF* account for 90% of the fetal tachyarrhythmias.[43] Both arrhythmias are readily distinguished by echocardiography.[6,7,10,44]

*AV re-entrant tachycardia* (Figure 39.10 top section) most commonly manifests as an intermittent or persistent tachycardia between 190 and 300 bpm. It can occur any time after the first trimester. The usual reentrant circuit involves the AV node for anterograde conduction (AV) and a fast retrograde (VA) conducting accessory pathway. AVRT starts suddenly with a PAC and terminates with AV block. Most hearts are structurally normal, but Ebstein anomaly of the tricuspid valve is a known association with right-sided accessory pathways. By fetal echocardiography, the tachycardia has a short VA pattern as the atrial contraction occurs closely after the ventricular contraction. Due to the almost simultaneous atrial and ventricular contraction, the AV valves are functionally closed during atrial systole which leads to pronounced a-wave flow reversal in the precordial veins and the ductus venosus.

*Atrial flutter* (Figure 39.10 middle section) is sustained by a circular macro-reentrant pathway within the atrial wall, while the AV node is not part of the reentry pathway. Atrial rates range between 300 and 500 bpm, which is commonly associated with 2:1 AV conduction and ventricular rates between 150–250 bpm.[44] Normal or near normal ventricular rates are observed in AF with slower (3:1 or 4:1) AV conduction.

*Other fetal tachyarrhythmia mechanisms* are far less common. Fetal sinus tachycardia, persistent junctional reciprocating tachycardia (PJRT) and atrial ectopic tachycardia (AET) present very similar as long VA tachycardia with heart rates <220 bpm and may be difficult to differentiate from each other. *Sinus tachycardia* is usually 20–30 bpm slower than AET and PJRT and characterized by atrial rates of <200 beats per minute, normal 1:1 AV conduction and some variability of the fetal heart rate. *PJR*T is an AV re-entry tachycardia with a relatively slow retrograde conducting accessory pathway which explains the long VA pattern. *AET* (Figure 39.10 bottom section) arises from an ectopic focus within the atria

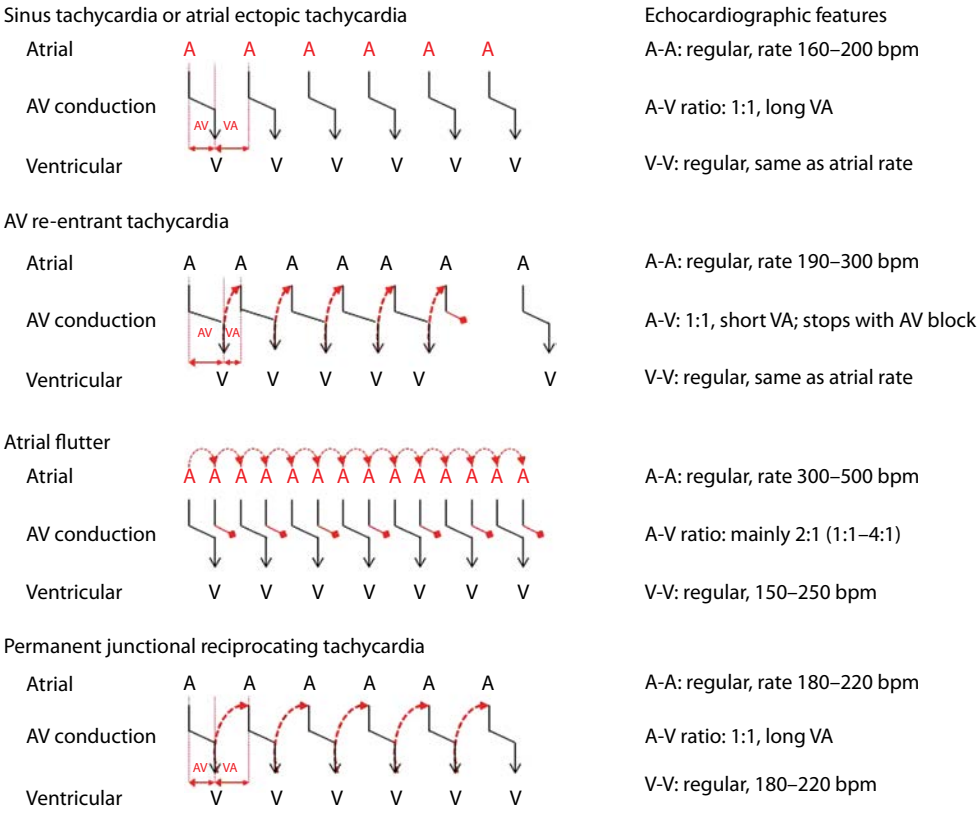


**Figure 39.9**
Mechanisms and echocardiographic features of disorders of a fast heart rate. (A, atrial event; V, ventricular event; —◆, non-conducted atrial event; ----➔, reentrant pathway.) Long VA indicates that the tachycardia VA interval is longer than the AV interval, which is the case in sinus tachycardia, permanent junctional reciprocating tachycardia and atrial ectopic tachycardia. The VA is shorter than the AV interval in AV reentrant tachycardia (short VA).

and is most commonly sustained. During AET, intermittent changes in tachycardia rate with "warming-up and cooling down" may be observed. Although AET is usually 1:1, conduction delay with variable conduction or functional 2:1 AV block may be seen.

*Ventricular tachycardia and junctional ectopic tachycardia* are exceptional causes of fetal tachyarrhythmias.[22,36] The fetal echocardiogram will show a tachycardia <200 bpm that is often incessant on presentation. The ventricular rate is higher than the atrial rate and there is no clear relation between ventricular and atrial events (AV dissociation).

## Management

Close observation without drug therapy may be a safe approach for the fetus with infrequent, brief SVA episodes, as heart failure will only rarely develop unless the arrhythmia is very fast and/or becomes more persistent. Conversely, fetuses with incessant tachyarrhythmia tend to develop heart failure with hydrops if left in tachycardia. Indeed, fetal hydrops, low cardiac output and death are strongly associated with incessant AVRT but even intermittent SVA may have serious consequences.[43,45] Medication that may be used to treat fetal supraventricular tachyarrhythmia include maternal digoxin, flecainide, or sotalol either alone or in combination, while amiodarone and direct fetal therapy are usually reserved for treatment-resistant, poorly tolerated tachycardia.[43–45] After birth, antiarrhythmic treatment, that is, with a beta-blocker is often used to prevent SVT recurrence during the first 6–12 months of life or longer. Neonatal recurrence of AF is unusual and long-term treatment is rarely required.

A variety of fetal, maternal and pregnancy-related conditions may be responsible for sustained sinus tachycardia including distress, anemia, infections and maternal antithyroid autoantibodies. The importance of sinus tachycardia is recognizing and treating the underlying cause. When evaluating a fetus for VT, possible etiologies include viral and anti-Ro antibody-mediated myocarditis, cardiac tumors, structural heart disease, hereditary cardiomyopathy including LQTS, and electrolyte imbalance. Treatment and prognosis depend on the VT mechanism and pattern, the hemodynamic impact, and associated conditions. Before birth, short-term maternal intravenous magnesium has been recommended as first line medication for VT >200 bpm.[23] Other treatments to acutely control VT may include IV lidocaine, oral beta-blocker and mexiletine. In the absence of LQTS, amiodarone, flecainide or sotalol may also be useful.

*In summary*, non-invasive documentation of the underlying arrhythmia mechanism and the fetal well-being is possible by echocardiography. A stepwise diagnostic approach should be used to examine the regularity, rates,

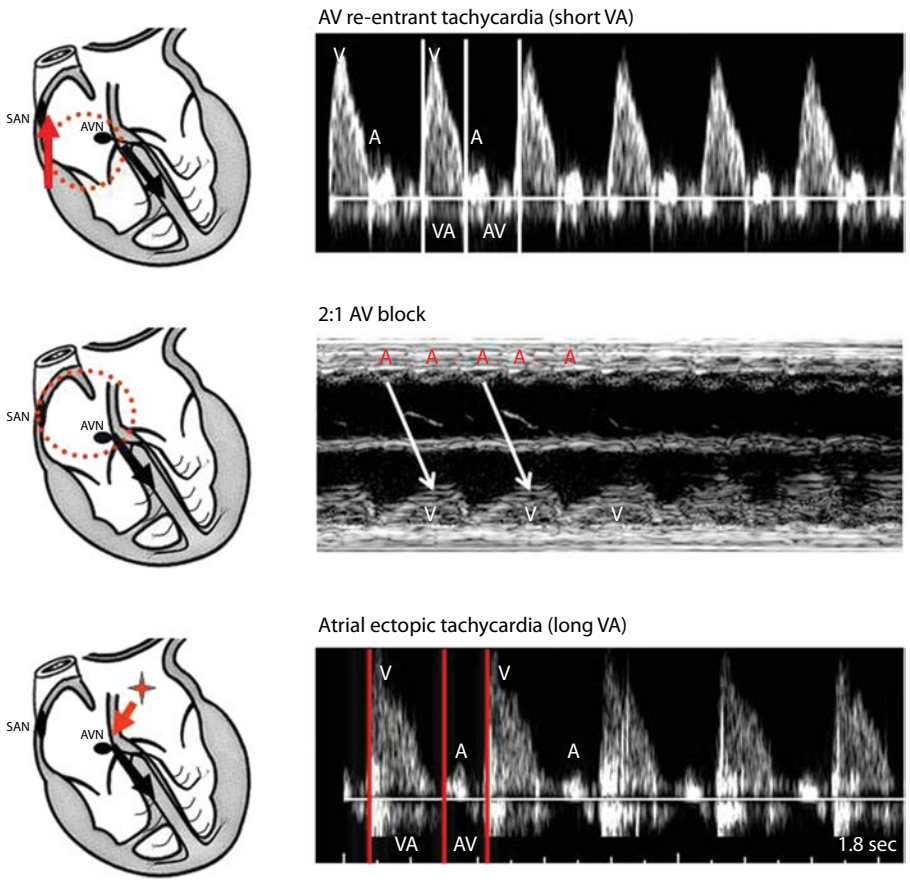


**Figure 39.10**
AV-reentry, atrial flutter and atrial ectopic tachycardia. *Top: AV re-entrant tachycardia (SVC/Aorta Doppler)* The SVC a-wave (A) is seen close to the end of aortic flow wave (V), suggesting that atrial systolic contraction occurs shortly after ventricular systole. Measurement of the AV and VA intervals (marked by vertical bars) indicate a shorter VA than AV interval, which is a characteristic for a reentrant tachycardia that uses the normal (slow) path of the AV node for the antegrade AV conduction, while the atria are excited through a fast, retrogradely (VA) conducting accessory pathway (red arrow). As the VA conduction is faster than the AV conduction, the VA interval is shorter on echocardiography. *Middle: Atrial flutter (AF; M-Mode)* The M-mode tracing shows an atrial (A-A) rate that exceeds 300 bpm and is twice as fast as the ventricular (V-V) rate. This is explained by atrial re-entrant circuit (circle) with conduction of every second atrial event to the ventricles. AF is often already suspected by 2-D echocardiography, because of very fast moving atrial walls. The diagnosis is then best confirmed by M-mode imaging. *Bottom: Atrial ectopic tachycardia (AET; SVC/Aorta Doppler)* The tracing demonstrates a fetal tachycardia with 1:1 AV conduction. The VA interval is significantly longer when compared to the AV interval. This "long VA pattern" may be explained by various arrhythmia mechanisms, including abnormal impulse generation in the SA node (sinus tachycardia) or atria (atrial ectopic tachycardia as in this case), and AV reentry through a slowly retrograde-conducting accessory pathway (permanent junctional reciprocating tachycardia).

chronology and conduction ratio of atrial and ventricular events, and to decide on the most likely rhythm diagnosis and the hemodynamic consequences. This approach will reduce the risk of irrational drug treatment or premature delivery of fetuses with relatively benign findings while it may facilitate the management and improve the outcome of those with major rhythm disturbances such as SVT and CHB. Management and prognosis of the various types of fetal arrhythmias will be discussed in more detail elsewhere in this textbook.

# References


1. Nii M et al. *Heart* 2006;92:1831–7.
2. Taylor MJ et al. *BJOG* 2003;110:668–78.
3. Kiefer-Schmidt I et al. *J Perinat Med* 2012;40:277–86.
4. Strasburger JF et al. *Heart Rhythm* 2008;5:1073–6.
5. Wakai RT et al. *Circulation* 2003;107:307–12.
6. Kleinman CS et al. *Am J Cardiol* 1983;51:237–43.
7. Jaeggi E et al. *Heart* 1998;79:582–7.
8. Rein AJ et al. *Circulation* 2002;106:1827–33.
9. Fouron JC et al. *Obstet Gynecol* 2000;96:732–6.
10. Fouron JC et al. *Heart* 2003;89:1211–6.
11. Carvalho JS et al. *Heart* 2007;93:1448–53.
12. Mitchell JL et al. *Circulation* 2012;126:2688–95.
13. Andelfinger G et al. *Am J Cardiol* 2001;88:1433–6.
14. Sonesson SE et al. *Arthritis Rheum* 2004;50:1253–61.
15. Rein AJ et al. *Circulation* 2009;119:1867–72.
16. Friedman DM et al. *Circulation* 2008;117:485–93.
17. Jaeggi ET et al. *J Am Coll Cardiol* 2011;57:1487–92.
18. Waldo AL, Wit AL. *Lancet* 1993;341:1189–93.
19. Boyden PA. *Am J Cardiol* 1996;78:4–11.

20. Cabo C, Wit AL. *Cardiol Clin* 1997;15:517–38.
21. Fouron JC. *Prenat Diagn* 2004;24:1068–80.
22. Kleinman CS, Nehgme RA. *Pediatr Cardiol* 2004;25:234–51.
23. Donofrio MT et al. *Circulation* 2014;129:2183–242.
24. Sonesson SE et al. *Ultrasound Obstet Gynecol.* 2014;44:171–5.
25. Raboisson MJ et al. *J Am Soc Echocardiogr* 2005;18:375–80.
26. Cuneo BF et al. *Am J Obstet Gynecol* 2016;215:527–8.
27. Maeno Y et al. *Ultrasound Obstet Gynecol* 2003;21:234–8.
28. Beinder E et al. *Am J Obstet Gynecol* 2001;185:743–7.
29. Hofbeck M et al. *Heart* 1997;77:198–204.
30. Cuneo BF et al. *Circ Arrhythm Electrophysiol* 2013;6:946–51.
31. Chockalingam P et al. *J Rheumatol* 2011;38:2682–5.
32. Lim JS et al. *Circulation* 2005;112:2454–61.
33. Horigome H et al. *Circ Arrhythm Electrophysiol* 2010;3:10–7.
34. Berg C et al. *Ultrasound Obstet Gynecol* 2005;26:4–15.
35. Jaeggi ET et al. *Ultrasound Obstet Gynecol* 2005;26:16–21.
36. Jaeggi E et al. *J Am Coll Cardiol* 2010;55:2778–84.
37. Izmirly PM et al. *Circulation* 2011;124:1927–35.
38. Eliasson H et al. *Circulation* 2011;124:1919–26.
39. Saleeb S et al. *Arthritis Rheum* 1999;42:2335–45.
40. Jaeggi ET et al. *Circulation* 2004;110:1542–8.
41. Trucco SM et al. *J Am Coll Cardiol* 2011;57:715–23.
42. Hutter D et al. *Scand J Immunol* 2010;72:235–41.
43. Jaeggi ET et al. *Circulation* 2011;124:1747–54.
44. Jaeggi E et al. *J Pediatr* 1998;132:335–9.
45. Simpson JM, Sharland GK. *Heart* 1998;79:576–81.

# 40

# Fetal bradycardia

Bettina F. Cuneo

## Introduction

Fetal arrhythmias constitute approximately 10% of referrals to perinatal cardiology centers. The vast majority of arrhythmias are atrial and ventricular ectopy, which are benign and require no treatment. Sustained bradycardia is unusual, and in large series, comprises only about 5% of all arrhythmia referrals.[1,2] Bradycardia can be due to primary abnormalities in the cardiac conduction system or secondary to fetal or maternal conditions[3] (Table 40.1). The most likely diagnosis of the bradycardic fetus depends on fetal heart rate and on gestational age at presentation. For example, a 32-week fetus with the new onset of a fetal heart rate of 70–80 bpm is more likely to have blocked atrial bigeminy (BAB) or the functional 2° atrioventricular (AV) block of long QT syndrome than anti-Ro/SSA antibody mediated AV block. The same fetal heart rate in a 15-week fetus is most likely to be AV block due to an abnormal conduction system and complex structural defects. Sinus bradycardia between 20 and 32 weeks can be secondary to any of the causes listed.

## Diagnosis of the bradycardic fetus

The three principal methods to diagnose fetal arrhythmias are echocardiography, electrocardiography (fECG), and magnetocardiography (fMCG). Each method has its benefits and shortcomings (Table 40.2). Spectral Doppler and M-mode echocardiography evaluate the mechanical consequences of electrophysiological events, including the atrial and ventricular beat rates, the AV relationship, and the mechanical surrogate of the AV interval (Figure 40.1). Cardiac anatomy and presence and degree of heart failure can be assessed by fetal echocardiography, but echo cannot evaluate the QT interval and repolarization characteristics, and brief or infrequent salvos of arrhythmias.

In principle, fetal cardiac waveform morphology, cardiac intervals, and repolarization characteristics can be assessed by fECG[4,5] but the electric signals from the fetal heart are attenuated by amniotic fluid and fetal vernix; thus, diagnostic quality signals are usually obtained only with direct fetal contact.[6] Fetal MCG is a noninvasive measurement of the magnetic fields of the fetal heart that has consistently and reliably provided diagnostic quality fetal ECG-like signal from 18 weeks to term using a SQUID magnetometer[7] or, more recently, an optically pumped magnetometer.[8] The fMCG rhythm tracings and signal-averaged waveforms (Figure 40.2) have provided accurate and complete diagnosis of fetal bradycardias and presented unique insights into their electrophysiological features and natural histories.[9–11]

## Definitions of fetal bradycardia

Fetal bradycardia can be diagnosed by the relationship and the atrial and ventricular beat rates. Sinus bradycardia is characterized by a 1:1 AV relationship and a gestational age-independent rate that is 110 bpm or less.[12] Although this definition is well accepted by the obstetrical community, others have suggested that since FHR decreases with advancing gestational age,[13] the definition of "sinus bradycardia" should also decrease with gestational age.[14] If the bradycardic fetus has variable AV conduction, the rhythm will be either BAB or AV block. Bradycardia can occur with a structurally normal heart or with structural cardiac defects.

## Bradycardia with a 1:1 AV relationship

Bradycardia with 1:1 conduction occurs in three settings. First, the fetal sinoatrial node (SAN) can be normal, but there is bradycardia due to either a sympathetic imbalance, such as in long QT syndrome (LQTS)[15] or because of immune-mediated inflammation or fibrosis of the SAN secondary to maternal anti-Ro/SSA (Sjogren's) antibodies. The spectrum of immune-mediated damage to the SAN varies from sinus bradycardia to "atrial standstill" with AV block and junctional bradycardia[16–18] (Figure 40.3). Second, the SAN may be absent or displaced, and the atrial beat rate is set by an ectopic atrial pacemaker. This commonly occurs in right and left atrial isomerism.[19–22] Third, there are heritable causes of SAN dysfunction resulting in bradycardia.[5,23–25] Sporadic, recessive, or autosomal dominant mutations in HCN4 (the gene regulating the I[f] current in the SAN), the homeobox gene Shox2, or the α-subunit of the cardiac sodium channel gene SCN5A have been reported.[5,23–26] Review of the family and maternal histories, fetal heart rate variability, and cardiac anatomy can be helpful in the diagnosis of bradycardia with a 1:1 AV relationship. For example, if there is a family history of syncope, fetal

**Table 40.1** Fetal bradycardia

| | *Causes* |
|---|---|
| *Bradycardia with 1:1 AV conduction: Primary causes* | |
| Ectopic atrial pacemaker | • Absence or abnormal location of SAN in heterotaxy syndromes |
| SAN dysfunction | • Immune-mediated or viral damage to a normal SAN<br>• Genetic causes |
| Channelopathies | • Familial and *de novo* long QT mutations |
| *Bradycardia with 1:1 AV conduction: Secondary causes* | • Fetal distress<br>• CNS or chromosome abnormalities; maternal medications<br>• Maternal thyroid disease |
| *Junctional bradycardia* | • Immune-mediated damage to the SAN and the AVN |
| *Bradycardia with variable AV conduction* | |
| Blocked atrial bigeminy | • Every other atrial beat occurs too early (PAC) to be conducted to the ventricle |
| AV block | • Developmental abnormality of the AV node associated with structural cardiac anomalies<br>• Immune-mediated damage to a normal AV node<br>• Long QT mutations, especially SCN5A or KCNH2 |

**Table 40.2** Techniques to diagnose fetal bradycardia

| *ECHO* | *fMCG* | *fECG* |
|---|---|---|
| 12–40 weeks: Atrial and ventricular rates, AV relationship; approximates only the PR interval | 18–40 weeks: Atrial and ventricular rates, AV conduction; accurately measures all cardiac intervals | 18–40 weeks: Ventricular rates; diagnostic quality tracings limited to scalp electrodes during labor |
| Evaluates cardiac morphology and function | Cannot evaluate cardiac morphology or function | Cannot evaluate cardiac morphology or function |
| Cannot analyze beat-to-beat heart rate/rhythm; brief and transient arrhythmias undetected | Analyzes beat-to-beat heart rate/rhythm for several hours; detects brief and transient arrhythmias | Averages beat-to-beat ventricular contractions similar to continuous external fetal monitoring; brief and transient arrhythmias undetected |
| Detects rhythm changes in response to transplacental therapy | Detailed/accurate analysis of response to therapy by including changes in cardiac intervals | May in some instances detect changes in cardiac intervals |
| Ubiquitous and cost effective | Limited to research; <10 centers worldwide | Limited because of inconsistent/unreliable quality |

heart rate variability is decreased, and the heart is structurally normal, bradycardia is suspicious for a channelopathy.[27]

## Sinus bradycardia and long QT syndrome

The first confirmed case of prenatal LQTS was a fetus with "moderate" bradycardia (fetal heart rates 110–120 bpm) in the late third trimester.[28] The newborn, his mother, and his maternal grandmother had prolonged QTc intervals on 12-lead ECG. The author concluded that "moderate fetal bradycardia (110–120 bpm) does not indicate fetal distress, but indicates that fetuses should be studied for fetal cardiac conduction defects in the newborn period."[28]

Since that publication in 1995, the association between fetal bradycardia and LQTS has been confirmed by other investigators[29–32] and further characterized as repeated fetal heart rate measures less than the third percentile for gestational age[31] or 133 bpm or less in the third trimester.[32] Using the cut-point of $\leq$ 133 bpm in the third trimester confers 50% sensitivity but greater than 97% specificity for LQTS.[32] The degree of bradycardia can suggest the subject's genotype: In a study of 184 fetuses from two KCNQ1 founder populations, the heart rate varied from 134 $\pm$ 8 bpm for fetuses with a single mutation to 111 $\pm$ 6 for those with a double mutation.[32] In a second study, LQTS fetuses with CALM 2, KCNH2 pore mutations, or SCN5A R1623Q mutations had lower heart rates during sinus rhythm than fetuses with KCNQ1 mutations (120.7 $\pm$ 3.6 versus 130.8 $\pm$ 2.4, $p < 0.01$).[33]

Although sinus bradycardia is accepted as a marker of LQTS, its significance as a predictor of LQTS is often overlooked. One reason is that there is considerable overlap between the heart rates of normal and LQTS fetuses resulting in a low sensitivity

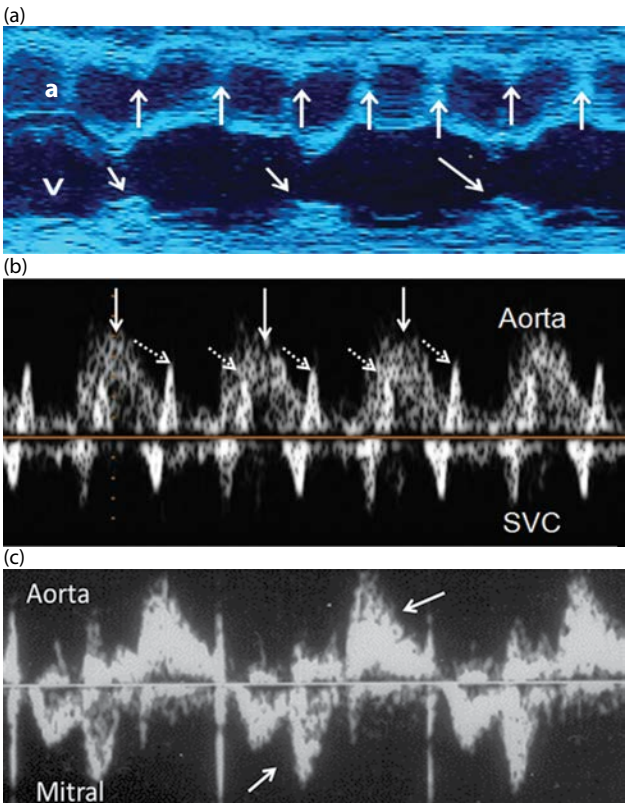


**Figure 40.1**
Methods of arrhythmia diagnosis by fetal echocardiography. (a) Simultaneous m-mode interrogation of the atrium (a, top line) and ventricle (V, bottom line) of a fetus in complete AV block with a normal atrial rate, ventricular bradycardia, and no relationship between atrial and ventricular contractions (AV dissociation). (b) Simultaneous spectral Doppler interrogation of the aorta and superior vena cava (SVC) of a fetus in atrial flutter. The aortic outflow tracings and the retrograde flow during atrial systole in the SVC are above baseline. There are two atrial contractions (dotted arrows, above baseline) for every ventricular contraction (solid arrow). (c) Simultaneous spectral Doppler interrogation of the aortic outflow and mitral inflow of a fetus in sinus rhythm. There is 1:1 AV conduction as seen by the 1:1 relationship between the mitral "a" wave (representing atrial contraction) (arrow, below baseline) and the aortic outflow representing ventricular contraction (arrow, above baseline).

using fetal heart rate to discriminate between affected and nonaffected fetuses.[32,33] A second reason is that the definition of LQTS bradycardia (repeated fetal heart rates less than the third percentile for gestational age or a cut-point less than or equal to 133 bpm in the third trimester) differs from the obstetrical definition of bradycardia (fetal heart rates less than or equal to 110 bpm at any time during gestation).[34] The result is that most fetuses with LQTS bradycardia will be overlooked and not receive postnatal ECGs and/or genetic testing to confirm their diagnosis. The ascertainment of LQTS in a large low-risk fetal population has been reported as only 1/8,658, while in the postnatal population, LQTS occurs in 1/2,000 individuals.[35]

Prospective identification of LQTS before birth is important for several reasons. The disease burden is high: Long QT syndrome accounts for approximately 10% each of sudden infant deaths and unexplained intrauterine fetal demises and approximately 3,000 arrhythmic deaths/year of adolescents and young adults.[36,37] Treatment is extremely effective in preventing the ventricular arrhythmias causing sudden death.[38] If the fetus is recognized to have LQTS, cascade testing can identify asymptomatic family members at risk for sudden death. A fetal diagnosis of LQTS also has implications for the pregnancy: withholding or limiting QT prolonging medications and optimizing maternal magnesium, vitamin D, and calcium levels could reduce the risk of fetal ventricular tachycardia. If it is known that the fetus has LQTS, fetal bradycardia due to functional 2° AV block or a nonreactive fetal heart rate tracing will be attributed to the LQTS phenotype and not mistaken for fetal distress. Last, anticipatory postnatal care from a prenatal diagnosis has been shown to improve outcomes.[39]

Fetal MCG has successfully identified LQTS with 89% sensitivity and specificity.[40] During sinus rhythm, signal-averaged fMCG demonstrates a gestational age–independent QTc interval greater than the 95th percentile (or ≥490 ms).[40] The echo diagnosis of tachycardia with AV dissociation and functional AV block can be confirmed by fMCG to be torsades de pointes and 2:1 AV conduction secondary to prolonged ventricular repolarization. There is excellent correlation between pre- and postnatal QTc and heart rates.[40] Risk factors for LQTS are a family history of LQTS (each fetus is at 50% risk of having the same family mutation), repeated fetal heart rate measures less than the third percentile for gestational age or 133 bpm or less during the third trimester, and the signature LQTS rhythms of functional 2° AV block and ventricular tachycardia detected by fetal echocardiography.

## Bradycardia with greater than 1:1 AV relationship

The differential diagnosis of fetal bradycardia with greater than 1:1 AV relationship (atrial beats > ventricular beats) is AV block or BAB. Both present with a regular rhythm and bradycardia, but the etiologies and prognosis of the two rhythms are vastly different. Differentiating the two rhythms relies on the timing of the second atrial contraction, a′ (Figure 40.4a).

### *Blocked atrial bigeminy*

BAB refers to a specific pattern of premature atrial contractions (PACs). BAB occurs when every other normal atrial contraction (a) is followed by a PAC (a′), which is not conducted to the ventricle. This results in ventricular bradycardia because only the (a) is conducted (Figure 40.4b–d). BAB can occur at any time during gestation and can last several weeks to months. It can be alarming to parents and caregivers but is self-limited with an excellent prognosis. BAB requires no treatment. Since BAB is a form of atrial ectopy, there is a risk that supraventricular tachycardia can develop, so weekly or twice weekly fetal heart rate auscultation is suggested. BAB occurs with structurally normal and abnormal fetal hearts.

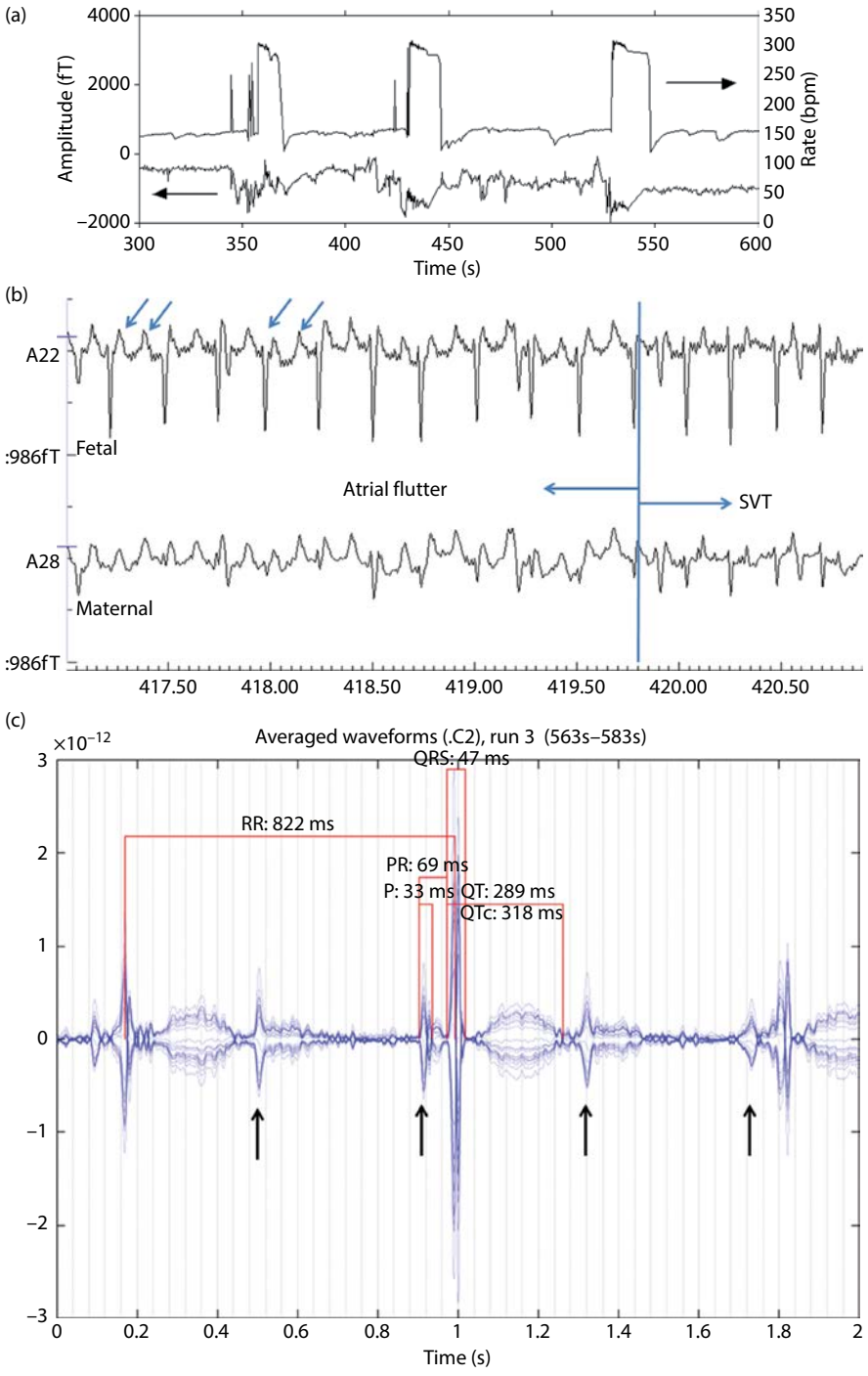


**Figure 40.2**
The spectrum of fMCG. (a) Actocardiogram of fetus with intermittent SVT. The amplitude of fetal movement (bottom tracing) is on the left *y*-axis and the fetal heart rate (top tracing) is on the right *y*-axis. Fetal movement initiates the episodes of SVT. (b) Rhythm tracing of a fetus with both atrial flutter (to the left of blue line) and supraventricular tachycardia. Arrows indicate initial four p-waves. The top tracing is only the fetal rhythm; the bottom tracing includes both the fetal and the maternal waveforms. (c) Signal-averaged tracing of a fetus with anti-Ro/SSA antibody negative 2° AV block. Arrows indicate p-waves. The QT and QTc intervals are normal.

In contrast to the self-limited and benign nature of BAB, fetal AV block heralds the risk of fetal demise from hydrops, cardiomyopathy, or channelopathy, and the likelihood of postnatal cardiac pacing. There are several ways to distinguish AV block from BAB. First, during BAB the coupling interval of (a-a′) is shorter than the coupling interval of (a-a′) during 2° AV block (Figure 40.4). Second, if the rhythm is BAB, the ventricular beat rates are faster ($82 \pm 5.7$ versus $69 \pm 4.2$)[10] and the isovolumic contraction time is shorter ($13.6 \pm 5.8$ versus $60.9 \pm 22.6$, $p = < 0.005$)[41] when compared with AV block (Figure 40.5). Other differences between the two rhythms can be found in the paper by Wiggens et al.[10]

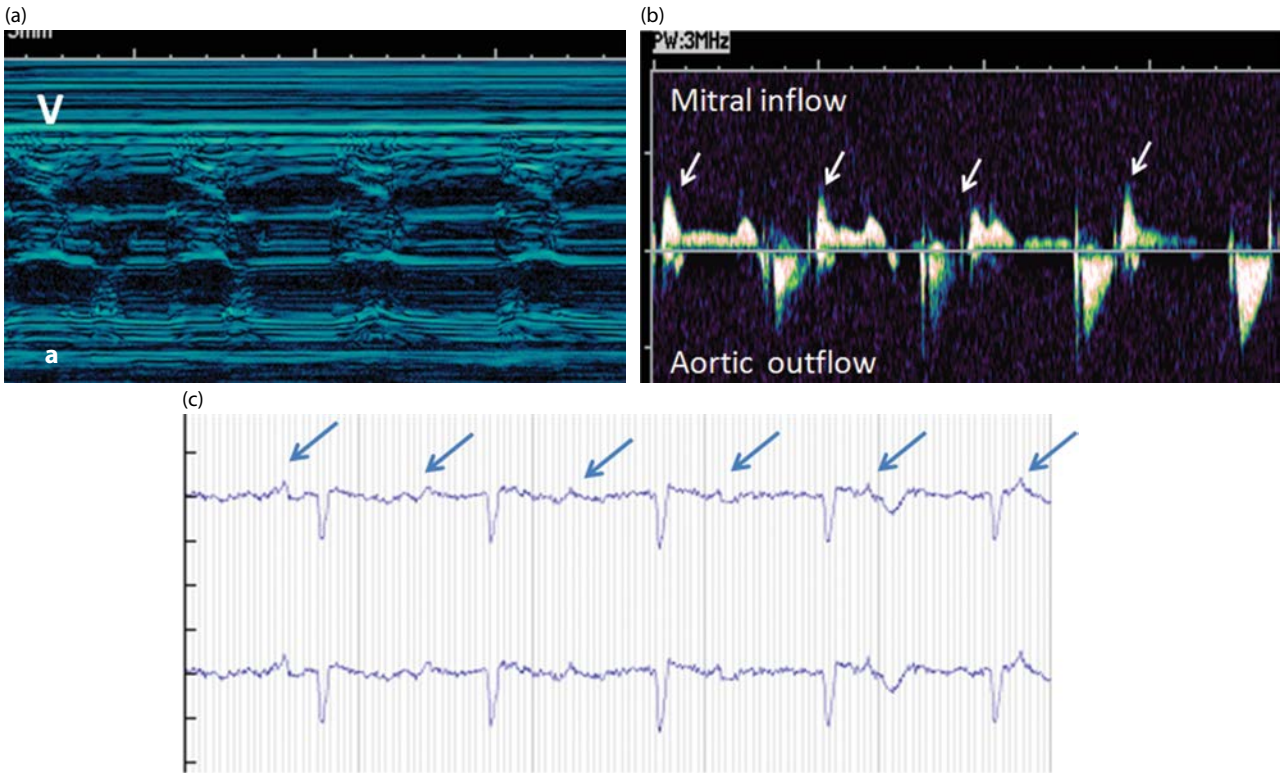


**Figure 40.3**
Fetal echocardiogram and fMCG of a 24-week fetus with immune-mediated sinus node dysfunction and AV block. (a) The M-mode shows ventricular (V) and atrial (a) rates that are equal, but the rates are 70 bpm. (b) Spectral Doppler of mitral inflow (above baseline) and aortic outflow (below baseline) shows a similar beat rates, but the mitral a-wave varies in distance from the aortic outflow suggesting there is no relationship between the two (AV dissociation and AV block). (c) The fMCG clearly demonstrates AV dissociation between the p-wave (arrows) and the QRS complexes.

## *Atrioventricular (AV) block*

Fetal AV block occurs in four situations (Table 40.1). Most commonly, AV block is due to inflammation and fibrosis of a normal AV node secondary to maternal anti-Ro/SSA antibodies. Anti-Ro/SSA antibody mediated AV block typically presents between 18 and 25 weeks of gestation.[42] Fetal AV block can also occur because of an abnormally formed conduction system associated with complex cardiac abnormalities such as congenitally corrected transposition of the great vessels (CC-TGV) or left atrial isomerism (LAI)[43–50] (Table 40.1). The majority of clinical data, including fMCG studies, describe the natural history and electrophysiology of LAI AV block; CC-TGV AV block is much less common. Unlike anti-Ro/SSA antibody mediated AV block, which presents at 18–25 weeks of gestation, AV block and structural cardiac defects can present as early as 12–13 weeks of gestation.

Anti-Ro/SSA antibodies are responsible for 90%–96% of fetal AV block. Antibody-negative fetal AV block with a structurally normal fetal heart[22,51] can occur with viral myocarditis or (if it is 2° AV block) because of prolonged repolarization in LQTS.[52,53] Recently, heritable causes of antibody-negative AV block known as *progressive cardiac conduction disorders* (PCDDs) have been described. PCDD are a genetically heterogeneous group of conduction system abnormalities diagnosed after birth and linked to mutations in the ion channel genes SCN5A, SCN1B, SCN10A, TRPM4, and KCNK17.[54] Conduction system disease has also been reported with variants of the genes coding for cardiac transcription factors, such as NKX2.5 and TBX5. These latter genes are also implicated in the morphogenesis of the heart; thus, conduction system disease can be isolated or occur with atrial or ventricular septal defects.[54–56] Progressive 1° AV block can be part of the Holt-Oram syndrome, which also includes skeletal anomalies of the upper limb.[56] These findings underscore the importance of taking a complete family history and obtaining ECGs on first-degree relatives when evaluating the fetus with antibody-negative AV block.

The different degrees of AV block (1°, 2°, or 3°) can be diagnosed with echocardiography by measuring the AV interval and the relationship and timing of atrial and ventricular systole (Figure 40.6 and Table 40.3).

## *First-degree AV block*

First-degree AV block is defined as a prolonged AV interval measured during spectral Doppler interrogation of mitral

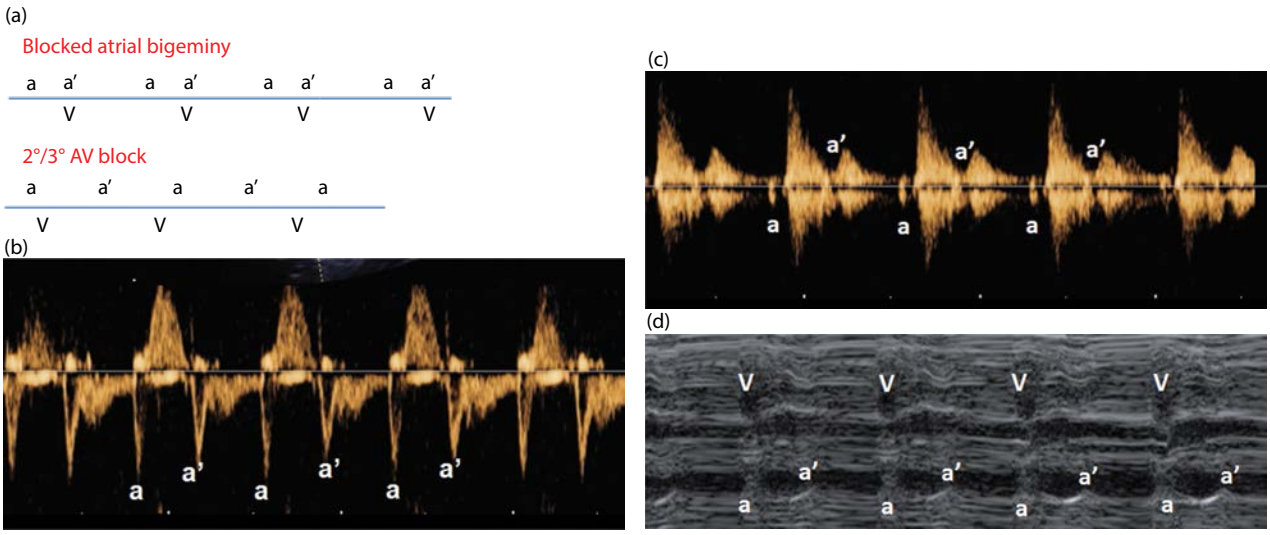


**Figure 40.4**
Blocked atrial bigeminy. (a) A cartoon showing the difference between BAB and AV block. (a) the conducted atrial contraction; (a′) the premature atrial contraction that is not conducted; (V) the ventricular beat. (b) Spectral Doppler of mitral inflow (below baseline) and aortic outflow (above baseline) during BAB. The coupling interval between the conducted atrial contraction (a) and the atrial contraction that is not conducted (a′) is slightly different. (c) Spectral Doppler of superior vena cava inflow and aortic outflow Doppler tracing during BAB. The relationship between (a) and (a′) and between (a) and (V) is clearly shown. (d) M-mode tracing demonstrating the different (a-a′) intervals and their relation to ventricular contraction (V).

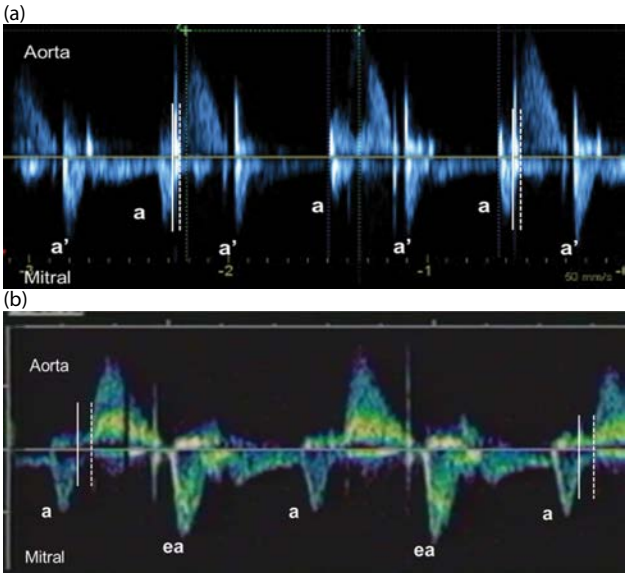


**Figure 40.5**
Isovolumic times in BAB and AV block. (a) Mitral inflow (below baseline) and aortic outflow (above baseline) spectral Doppler tracing of isovolumic contraction time (ICT) in a fetus with BAB. The ICT is the time from mitral valve closure to aortic valve opening. Note the ICT (between the solid and dashed white line) is only approximately 20 ms; the time from mitral valve closure to aortic valve opening is almost simultaneous. Atrial contractions are either conducted (a) or blocked (a′). (b) Mitral inflow (below baseline) and aortic outflow (above baseline) spectral Doppler tracing of isovolumic contraction time (ICT) in a fetus with type 2, 2° AV block. The time from mitral valve closure to aortic valve opening is shown between the solid and dashed white lines. Note the ICT is longer (~75 ms) than in BAB. Atrial contractions are either conducted (a) or fused and blocked (ea).

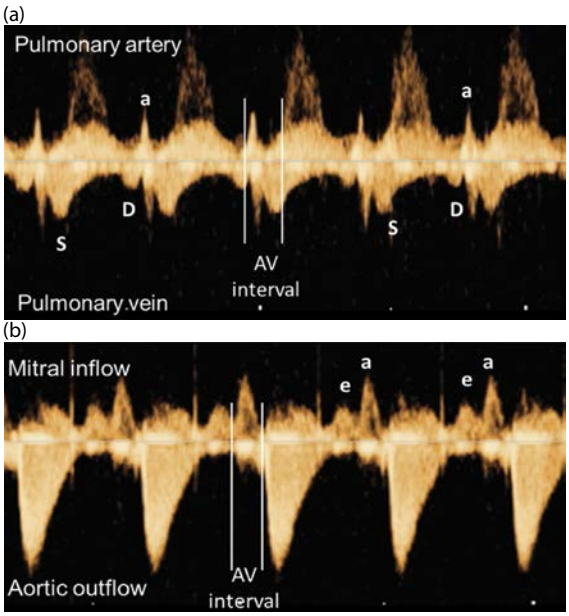


**Figure 40.6**
Two methods of measuring the AV interval. The tracings are in sinus rhythm. (a) Simultaneous pulmonary artery (PA, above baseline) and pulmonary vein (PV, below baseline). The three components of pulmonary venous flow are systole (S), diastole (D), and reversal in the pulmonary vein during atrial systole (a). The AV interval is measured from the onset of pulmonary venous atrial systole (above baseline) to the onset of pulmonary artery systole (above baseline). (b) Simultaneous mitral inflow (above baseline) and aortic outflow (Ao, below baseline). The two components of mitral inflow are passive filling (e) and atrial contraction (a). The AV interval is measured from the onset of the atrial contraction (above baseline) to the onset of aortic flow (below baseline).

**Table 40.3** Characteristics of atrioventricular (AV) conduction

| *AV Conduction* | *Findings* | *Example* |
|---|---|---|
| Normal 1:1 | Atrial rate = ventricular rate, rates are normal<br>Rhythm is regular<br>AV interval <170 ms | 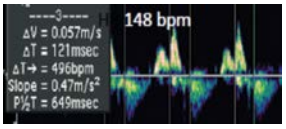 |
| 1° AV block | Atrial rate = ventricular rate, rates are normal<br>Rhythm is regular<br>AV interval ≥170 ms | 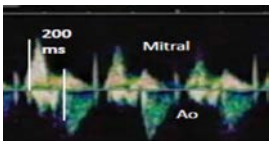 |
| Type 1 or Wenckebach 2° AV block | Atrial rate > ventricular rate, atrial rate is normal, ventricular rate is variable, rhythm is irregular, AV interval prolongs and then a ventricular beat is dropped | 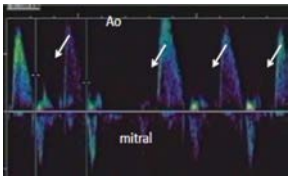 |
| Type 2, 2° AV block | Atrial rate is usually 2× ventricular rate and normal; ventricular rate is slow and rhythm is regular; every other atrial beat is conducted; the AV interval is consistent and not prolonged | 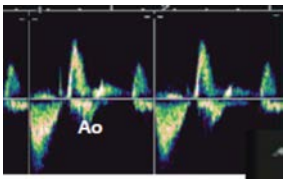 |
| Complete (3°) AV block | Atrial rate is normal; ventricular rate is slow; there is AV dissociation; and the AV interval is variable |  |

inflow and aortic outflow or systemic/pulmonary venous inflow and arterial outflow (Figure 40.6). Normal values have been established for each approach[57]; however, the diagnosis of 1° AV block is not always straightforward. The AV interval reflects conduction time through the atrium and the AV node; thus, a "prolonged" AV interval may be secondary to intra-atrial conduction delay or prolonged atrial repolarization rather than 1° AV block. The echo Doppler AV interval is the mechanical surrogate of the electrocardiographic PR interval and includes the isovolumic contraction time (the time from the onset of myocardial contraction to ventricular ejection). A fetus with a "prolonged" AV interval may have normal conduction through the atrium and the AV node, but a prolonged isovolumic contraction time[58] (Figure 40.7). In studies directly comparing echo and fMCG, the PR interval is 15–16 ms shorter than echo Doppler AV interval.[59] Finally, of 15 untreated fetuses with "1° AV block" (a AV interval of 150–180 ms) only 1 (with a AV interval >170 ms) had a prolonged PR interval after birth.[60]

Other echocardiographic features of fetal 1° AV block are fluctuating AV intervals and intermittent or consistent monophasic filling of the left ventricle, seen as partial or complete fusion of the mitral "e" and "a" waves (Figure 40.8 and Table 40.3). This probably occurs because as the AV interval is prolonged, the mitral "a" wave becomes more and more delayed until atrial contractions occur simultaneously with passive ventricular filling. These findings suggest that the definition of 1° AV block is probably a AV interval greater than or equal to 170 ms and some disturbance of the left ventricular filling pattern.

## Second-degree AV block

There are two types of 2° AV block. Type 1, or Wenckebach AV block, occurs when there is progressive lengthening of the AV interval until the atrial beat does not conduct to the ventricle (Figure 40.9a). After the nonconducted atrial beat, the next atrial beat is conducted to the ventricle with a short or normal AV interval, and the process is repeated. A fetus with type 1, 2° AV block has an irregular rhythm. In contrast, a fetus with type 2, 2° AV block has a regular rhythm and bradycardia, because every other atrial beat is conducted normally to the ventricle, effectively halving the normal ventricular rate (Figure 40.9b,c). As previously mentioned, the isovolumic contraction time is longer and the ventricular beat rate lower in 2° AV block when compared to BAB[10,41] (Figure 40.4, 40.5). The 2° AV block of LQTS can occur with 2:1 or 3:1 AV conduction (Figure 40.10).

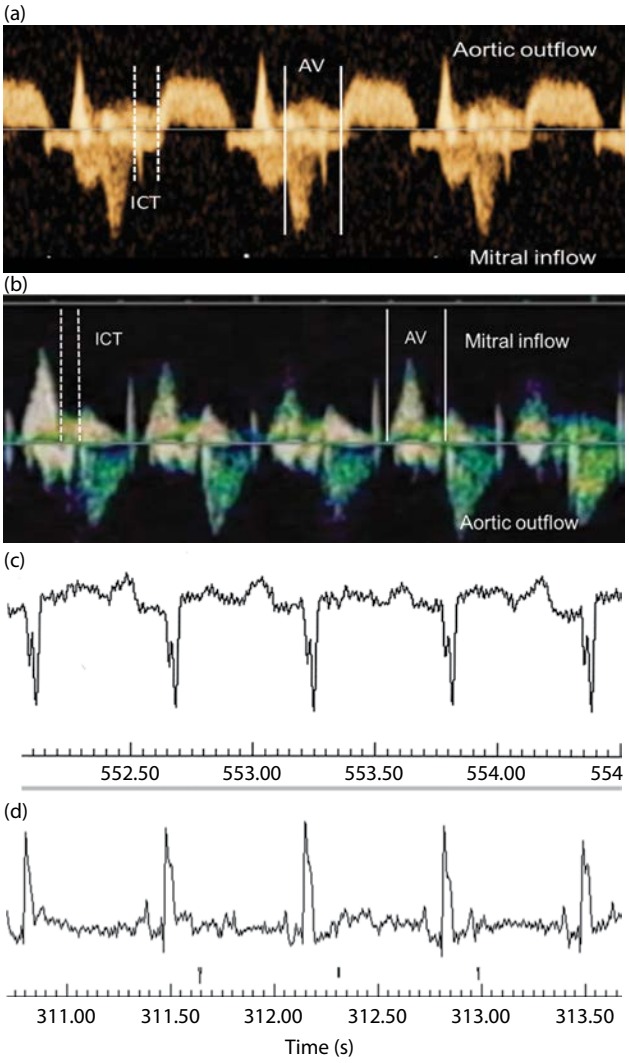


**Figure 40.7**
Echo Doppler and fMCG examples of prolonged AV intervals. (a) Fetus with cardiac dysfunction and negative maternal anti-Ro/SSA antibodies. Each tic (seen at bottom of figure) is 500 ms. The AV interval is 170 ms; the ICT is 85 ms or about half the AV interval. This is prolonged isovolumic contraction time, not 1° AV block. (b) Fetus with maternal anti-Ro/SSA antibodies. Each tic (seen on top of figure) is 200 ms. The AV interval is approximately 200 ms; the isovolumic contraction time (ICT) is approximately 40 ms or about one-quarter of the AV interval. This is 1° AV block. (c) Fetus with AV interval (not shown) and fMCG PR interval of 200 ms. The fMCG shows a broad p-wave suggesting intra-atrial conduction delay rather than AV block. The maternal anti-Ro/SSA antibody screen was negative. (d) Fetus with cardiac dysfunction and a AV interval of 180 ms (not shown) and fMCG PR interval of 140 ms. The maternal anti-Ro/SSA antibody screen was negative.

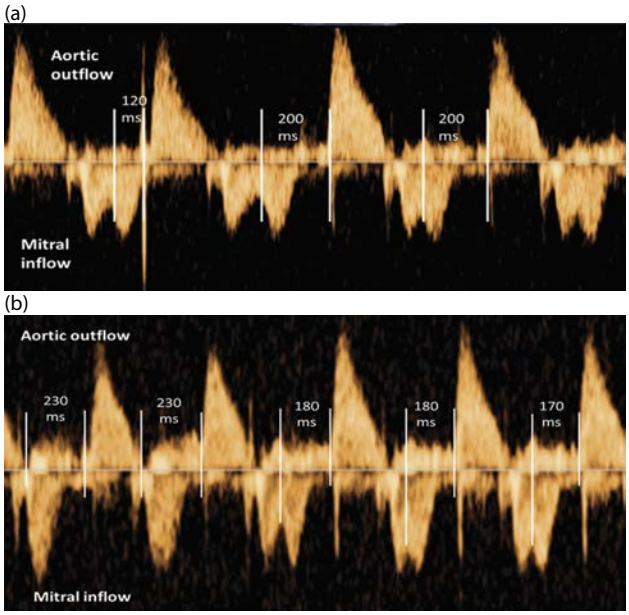


**Figure 40.8**
Evolving 1° AV block in a fetus at 20 weeks of gestation with maternal anti-Ro/SSA antibodies. (a) A normal AV interval (120 ms) is followed by two prolonged AV intervals of 200 ms. The mitral valve (below baseline) filling patterns are not monophasic but differ from beat to beat. (b) Varying AV intervals and mitral valve filling patterns in the same subject.

## *Third-degree AV block*

Third-degree AV block occurs when the atrium and ventricles beat independently of one another (Table 40.3). However, 3° AV block is not a simple bradycardia but is "electophysiologically intricate and dynamic."[61] For example, fetal heart rate patterns during 3° AV block can be reactive or nonreactive based on the ventricular rates and the etiology of the AV block (immune mediated or associated with structural cardiac defects). A reactive fetal heart rate tracing can become nonreactive, but not *vice versa* (Figure 40.11). If the fetus has immune-mediated 3° AV block and the ventricular rate is greater than 56, the fetal heart rate is reactive; below 56 bpm, the fetal heart rate is nonreactive. Regardless of the ventricular rate, fetuses with LAI 3° AV block have nonreactive fetal heart rate patterns regardless of ventricular rate.[61] Even when the ß-agonist terbutaline is given to augment fetal heart rate to greater than 56 bpm, the fetal heart rate pattern remains unreactive.[62] Fetal heart rate reactivity is likely related to the correlation between atrial and ventricular accelerations (Figure 40.12). The atrial rate in 3° AV block can fluctuate between 3 and 10 bpm due to ventriculophasic sinus arrhythmia. Ventriculophasic sinus arrhythmia is increased at lower atrial rates and more prominent at later gestational ages.[60] Fetuses with 3° but not 2° AV block manifest other rhythms, including ventricular ectopy and slow junctional ectopic tachycardia (JET), which can occur soon after diagnosis of AV block only to vanish in weeks to months or, in some cases, continue after delivery.[61] The rate of JET can be within the range of normal fetal heart rates and is often mistakenly diagnosed to be intermittent recovery of normal conduction. Another great pretender of improved conduction is 3° AV block with accrochage, which is the tendency of dissociated atrial and ventricular rhythms to synchronize.[63] This can be mistaken for 2° AV block.

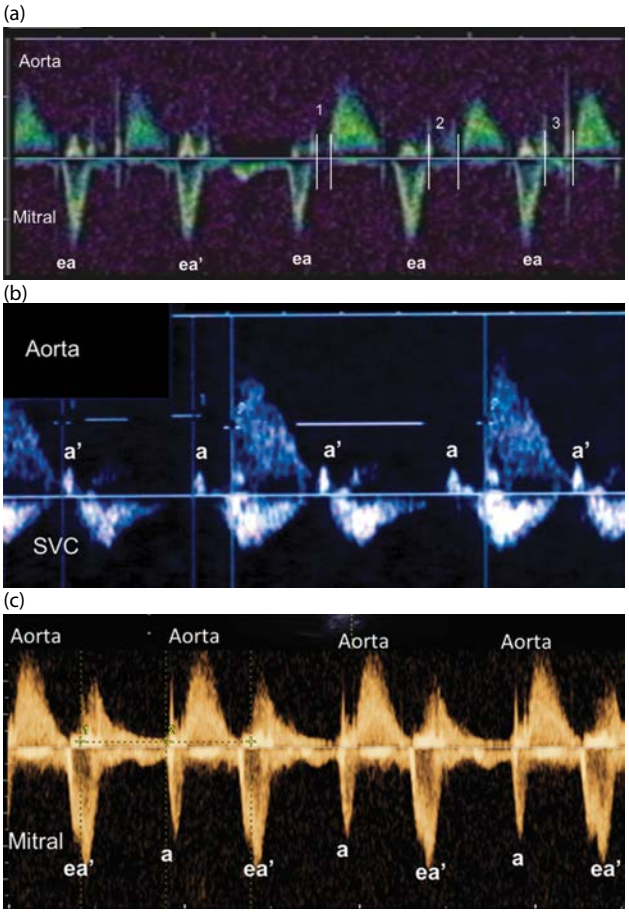


**Figure 40.9**
Spectral Doppler examples of fetal 2° AV block. (a) Wenckebach (type 1) 2° AV block assessed by simultaneous mitral inflow and aortic outflow. The mitral (e) and (a) waves (below baseline) are fused. The second atrial contraction (ea′) is not conducted. The first AV interval (1) after the conducted beat is shorter than the second and third AV intervals (3 and 4). (b) Simultaneous SVC (below baseline) and Ao (above baseline) of type 2, 2° AV block. Reverse flow in the SVC during atrial contraction (a) is seen above baseline. Every other atrial contraction (a) is conducted to the ventricle resulting in aortic outflow; the atrial contraction that is not conducted because of the AV block is marked as (a′). (c) Simultaneous mitral valve inflow (below baseline) and aortic valve outflow (above baseline) of type 2, 2° AV block. The (e) and (a) waves of mitral inflow are fused (ea). Every other atrial contraction is blocked (ea′) and does not conduct to the ventricle.

In addition to fetal heart rate patterns, fMCG has demonstrated other important differences between immune-mediated and LAI AV block. One of these differences is seen in the response to terbutaline. Although the atrial and ventricular rates were no different in the baseline state, the atrial beat rate increased more than the ventricular beat rate in fetuses with immune-mediated 3°AV block, while the ventricular beat rate increased more than the atrial beat rate in fetuses with LAI 3° AV block.[62] This suggests that in those subjects evaluated, immune-mediated fibrosis was more specific to the AV node and distal conduction system and spared the atria. The sinus node is absent in left atrial isomerism, and the subsidiary atrial pacemakers may not be capable of an increased beat rate. The patterns of acceleration in response to terbutaline also differ between LAI and immune-mediated 3° AV block suggesting differences in the subsidiary pacemakers (Figure 40.13).

## *Anti-Ro/SSA antibody mediated AV block*

Maternal anti-Ro/SSA antibodies are found in 1%–2% of the female population.[64] Fetal 3° AV block develops in 2%–4% of pregnant anti-Ro/SSA positive women and 17%–21% if a previous pregnancy has been affected.[42] Approximately 1,000 fetuses/year in the United States are diagnosed with anti-Ro/SSA antibody mediated AV block, but despite its low penetrance, the disease burden is considerable. In large series, the mortality is 17.5%, with the greatest number succumbing before birth (~32%) and during the first 6 months after birth (~46%).[65] Risk factors for a poor outcome include diagnosis of 3° AV block before 20 weeks, a ventricular rate less than 50 bpm, decreased function, and hydrops.[65,66] The majority of fetal and neonatal survivors require permanent cardiac pacing. Although the conduction system, especially the AV node, is the most common target of immune-mediated inflammation and fibrosis, the myocardium and AV valves can also be affected, resulting in endocardial fibroelastosis and/or cardiomyopathy and rupture of the AV valve chordae.[67,68] If conduction system and myocardial disease coexist, the case fatality rate is greater than 30%.[65]

Although fetal AV block occurs in 2% of anti-SSA positive pregnancies, there are several factors that increase the risk. A previously affected offspring increases the risk from 2% to 17%.[42] If maternal anti-Ro/SSA anti-body levels are greater than 100 U/mL, the risk is also increased: from about 15% if titers are 50 U/mL to 85%.[69] Other features conferring a higher risk include concomitant thyroid disease,[70] nonwhite ethnicity[65] and a springtime birth.[71]

Efforts to prevent or mitigate the anti-Ro/SSA antibody mediated effects on the fetal myocardium have been largely unsuccessful. Prophylactic treatment of anti-SSA positive pregnant women with IVIG, plasmapheresis, or dexamethasone has not decreased the rate of fetal AV block.[72–76] A retrospective study of hydroxychloroquine in previously affected anti-Ro/SSA positive pregnancies has provided some hope: the recurrence rate of fetal AV block was 64% lower in mothers treated with hydroxychloroquine at or before 11 weeks of gestation, and the case fatality ratio was 0% compared to a case fatality ratio of 22% in those who were not treated.[77] A prospective trial of hydroxychloroquine is currently underway.

While 3° AV block is irreversible, treatment of 2° or "emergent" 3° AV block has successfully restored sinus rhythm or prevented progression to established 3° AV block (Tables 40.4 and 40.5; Figure 40.14).[78–83] Surveillance to detect and treat emergent 3° AV block to interrupt the progression to

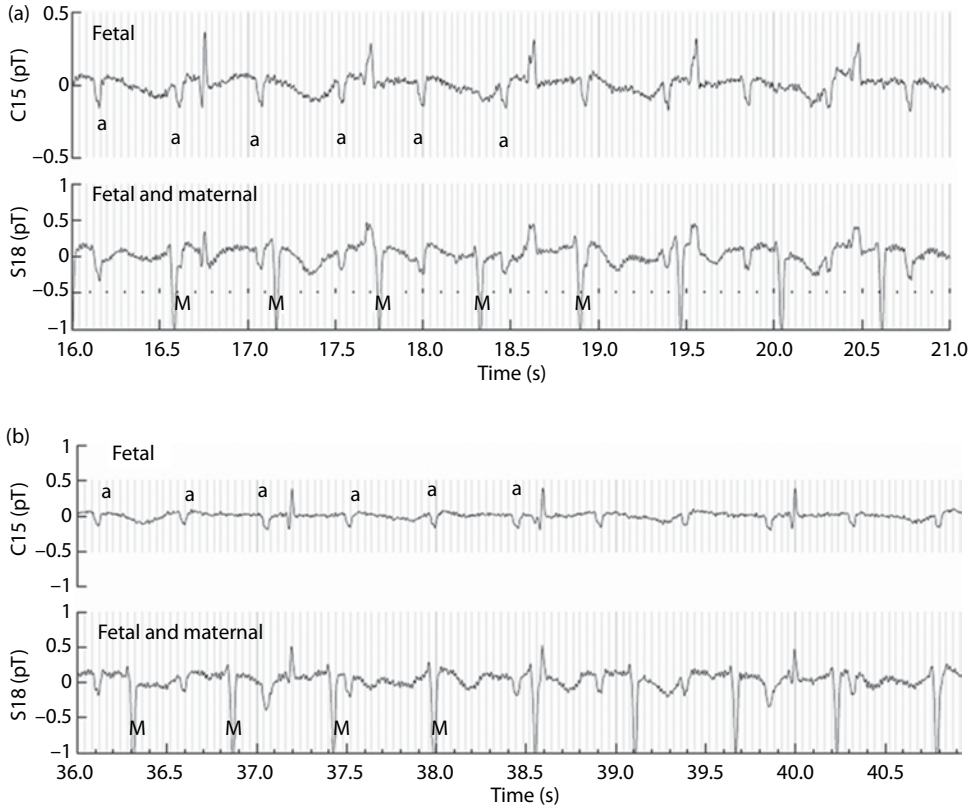


**Figure 40.10**
The fMCG of 2° AV block in a 33-week fetus with long QT syndrome. (a) The top 2 tracings show 2:1 AV conduction (a, atrial contractions) that occur because of prolonged ventricular repolarization. The bottom tracing shows the maternal heart rate. Both maternal heart rate and QTc were normal. (b) The top 2 tracings show 3:1 AV conduction (a, atrial contractions) and the bottom tracing is the maternal heart rate. The QTc (not shown) was over 700 msec. The fetus was stillborn 1 week after the fMCG.

established 3° AV block is logical and intuitive. Unfortunately, even weekly fetal echo surveillance has failed to detect the time period when the normal fetal heart rhythm transitions to emergent 3° AV block at a time when treatment was effective.[84,85] Instead, within 7–10 days of having normal conduction, 3/95 subjects presented with 3° AV block and did not respond to treatment.[84] One reason weekly surveillance was unsuccessful is the recent finding that emergent 3° AV block develops in less than 24 hours.[83] A more frequent method of surveillance such as daily ambulatory fetal heart rate and rhythm monitoring may be more successful in detecting emergent 3° AV block in a time frame when treatment can be successful.[86]

Treatment of anti-Ro/SSA antibody mediated immune-mediated 3° AV block is controversial. It is clear that 3° AV block is irreversible,[12] but whether or not transplacental anti-inflammatory treatment has improved symptoms of disease beyond the AV node is debatable.[87,88] Some studies suggest that dexamethasone monotherapy may not be as beneficial as combination therapy with intravenous immune globulin (IVIG) and/or ß-mimetics such as terbutaline.[89,90] While the risks and side effects of fluorinated steroids have been well delineated, long-term data on the risk/benefit ratio in this population are limited.[91,92] However, preliminary reports are cautiously optimistic regarding the effect of fluorinated steroids on neurocognitive development and suggest differences in development may be due not to steroid use, *per se*, but to other factors, such as fetal ventricular rate.[93] The potential benefits of IVIG more clearly exceed its risks: there is a long history of IVIG treatment for pregnant women with idiopathic thrombocytopenia and infants and children with Kawasaki disease.[94,95] The side effects of IVIG are limited to blood product exposure and occasional allergic reactions.

There are institution-specific protocols for management of the fetus with immune-mediated 3° AV block, but common to most is care by a team of obstetricians and fetal cardiologists. After the initial diagnosis, evaluation, and a counseling session with the parents, the fetus is evaluated weekly for worsening of symptoms such as AV valve insufficiency, ventricular dysfunction, progressive endocardial fibroelastosis, ventricular rates less than 50 or 55 bpm, or the development of effusions. Some protocols suggest chronotropic support if the ventricular rate is less than 50 or 55 bpm and the timing of delivery.[92,96] ß-Mimetics such as terbutaline and salbutamol increase fetal heart rate and decrease vascular resistance, with maternal side effects such as palpitations and "jitteriness" when therapy is initiated.[97,98] Because of the abnormal heart rate and rhythm, nonstress testing is not feasible, but instead, fetal well-being can be assessed

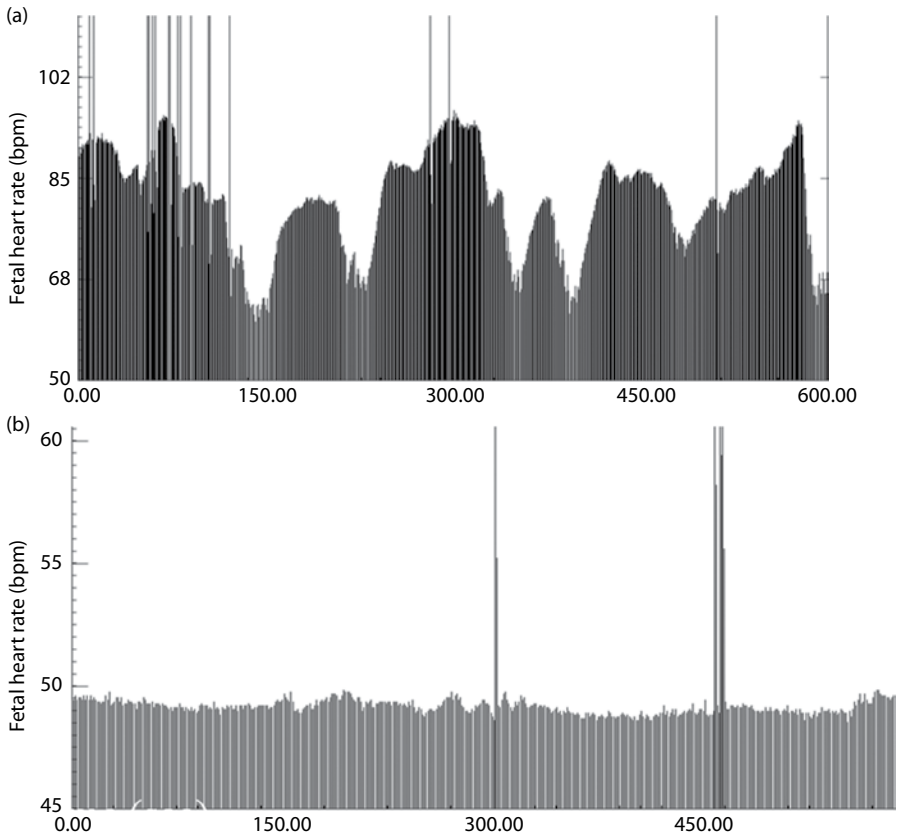


**Figure 40.11**
Fetal heart rate reactivity in a single fetus with anti-Ro mediated CAVB. (a) Early in gestation (~22 weeks), the fetal heart rate is reactive and the ventricular rate in the low 70s. (b) Later in gestation (~34 weeks) the ventricular rate has fallen and the fetal heart rate is no longer reactive. (From Das B et al. *Fetal Diagn Ther* 2008;24(3):282–5, with permission.[114])

during twice weekly biophysical profile assessment. If the fetus is stable, an elective cesarean section delivery can be planned for 39 weeks, but with progression of symptoms or nonreassuring fetal testing, an earlier delivery can be considered. The postnatal care team should be prepared to give isoproterenol, especially if the fetus has required a ß-mimetic for low ventricular rates *in utero*. If pacing is needed in the neonatal period,[99] results suggest that placing the epicardial lead on the left ventricular apex or free wall rather than the right ventricle results in less left ventricular dysfunction and dyschyrony.[100,101] Dual-chamber pacing is feasible in the neonate, but more data are needed

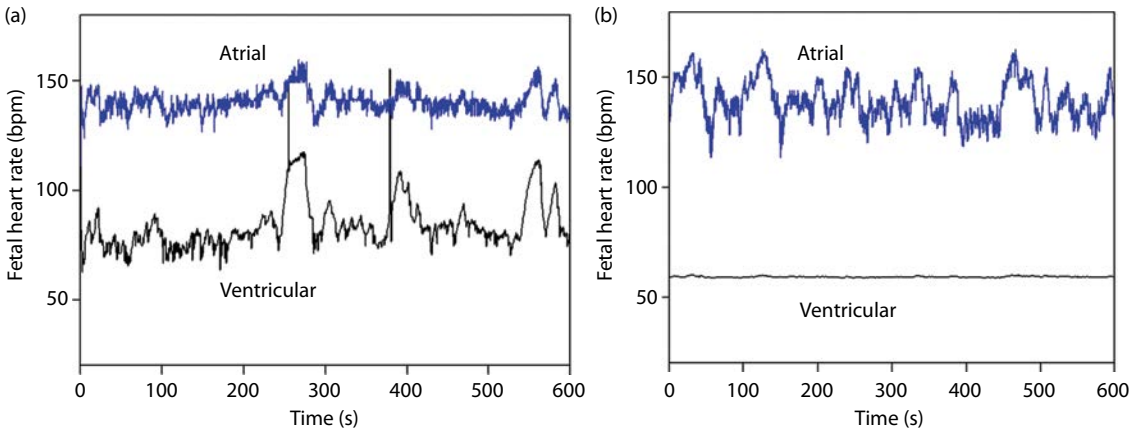


**Figure 40.12**
Relationship between atrial and ventricular reactivity in 3° AV block. (a) At ventricular beat rates greater than 56 bpm, ventricular and atrial reactivity are concordant. (b) At ventricular beat rates less than 56 bpm, reactivity is flat. (From Cuneo BF et al. *Am J Cardiol* 2007;100(4):661–5, with permission.[62])

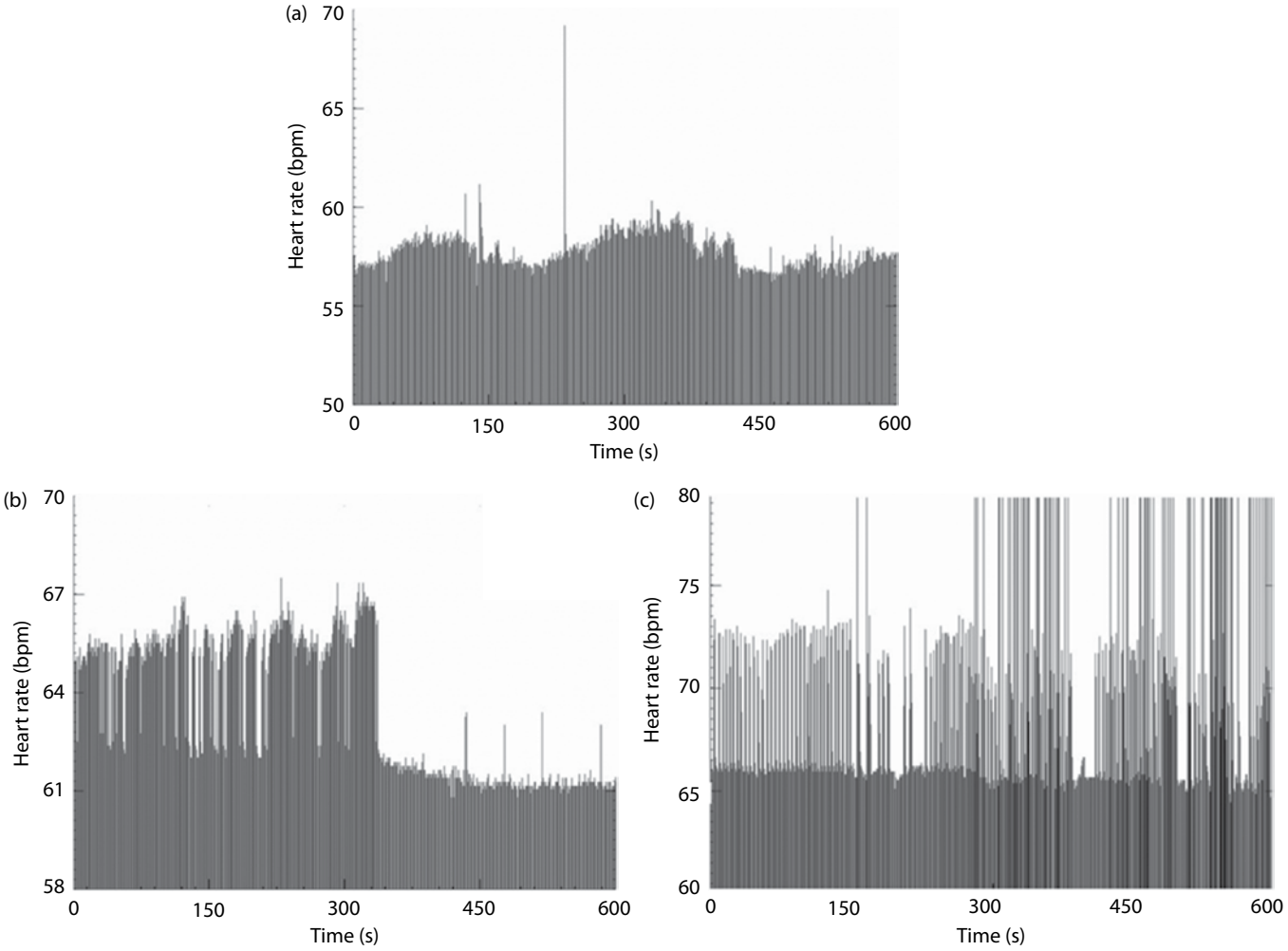


**Figure 40.13**
Fetal heart rate acceleration patterns in terbutaline treated fetuses with 3° AV block. Each black line is an individual heart rate. (a) Slow ramp up and cool down in anti-Ro/SSA antibody mediated AV block. (b,c) Two different patterns of acceleration in LAI AV block. The fetal heart rate vacillates in a very different pattern than (a). (From Cuneo BF et al. *Am J Cardiol* 2007;100(4):661–5, with permission.[62])

**Table 40.4** Published outcomes of emergent 3° AVB treated *in utero*

| *Reference* | *Number with emergent 3° AVB* | *RX* | *In utero rhythm after Rx* | *Postnatal rhythm* | *Percentage (%) restored 1:1 conduction in utero/ postnatal* |
|---|---|---|---|---|---|
| Raboisson[78] | 3 | Dex | (3) SR | (3) SR | 100/100 |
| Saleeb[79] | 4 | Dex | (4) 1° AVB | (4) 1° AVB | 100/100 |
| Izmirly[65] | 13 | Dex | – | (4) 1° AVB or SR<br>(6) No change<br>(3) 3° AVB | –/31 |
| Askanese[80] | 4 | Dex | (2) 1° AVB<br>2 SR | (2) 1° AVB<br>(2) SR | 100/100 |
| David[81] | 1 | IVIG | 1° AVB<br>inter SR | 2° AVB | 100/0 |
| Tunks[82] | 1 | IVIG+Dex | 1° AVB | 1° AVB | 100/100 |
| Cuneo[83] | 2 | IVIG+Dex | (2) 1° AVB | (2) 1° AVB | 100/100 |

**Table 40.5** Published outcomes of fetal 2° AVB not treated *in utero*

| *Reference* | *Number with 2° AVB* | *Rx* | *In utero rhythm after Rx* | *Rhythm after birth* | *Percentage (%) restored 1:1 conduction in utero/postnatal* |
|---|---|---|---|---|---|
| Saleeb[79] | 2 | No Rx | (2) 3° AVB | (2) 3° AVB | 0/0 |
| Izmirly[65] | 8 | No Rx | – | (1) 1° AVB<br>(3) No change<br>(4) 3° AVB | –/12.5 |

*Abbreviations:* AVB, atrioventricular block; Dex, dexamethasone; inter, intermittent; IVIG, intravenous immune globulin; ND, no data; Rx, treatment; SR, sinus rhythm.

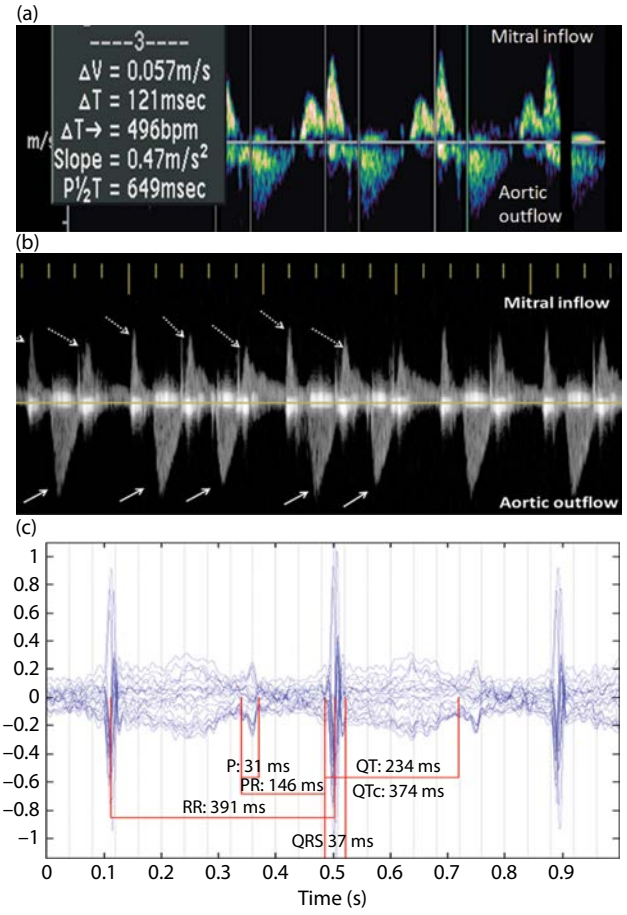


**Figure 40.14**
Emergent 3° AV block in an anti-SSA positive 19 week fetus. (a) Normal spectral Doppler of mitral inflow (above baseline) and aortic outflow (below baseline) at 18 weeks and 5 days of gestation. The AV interval is 121 ms and the heart rate is 148 bpm. (b) Two days later, approximately 4 hours after the mother heard an irregular heart rhythm with a Doppler fetal heart rate monitor at home. The fetus is now in type 1, 2° AV block: the AV interval prolongs and then an atrial beat is not conducted. Mitral (a) waves are shown by dashed arrows above baseline, and aortic outflow is below baseline (solid arrows). The ventricular rate is irregular. (c) Signal averaged fMCG 3 days after IVIG and dexamethasone treatment. The fetus now has 1:1 conduction with 1° AV block. (From Cuneo BF et al. *Am J Cardiol* 2007;100(4):661–5, with permission.[62])

to determine if dual-chamber pacing has an advantage over single-lead ventricular pacing.[102,103]

## AV block and structural heart disease

As previously mentioned, the two most common structural cardiac defects associated with fetal AV block are CC-TGV and LAI. Fetal AV block in the setting of left atrial isomerism can develop as early as 12 weeks of gestation.[104] Fetal AV block occurred in 15%–50% of LAI case series and in all studies was a risk factor for poor outcome.[50,105–111] Additional findings of complex structural defects, hydrops, and noncardiac anomalies lead to dismal postnatal survival rates for LAI AV block of 0%–20%. At some centers, cardiac transplantation is offered as first-line therapy to newborns with LAI-AV block.[50] Treatment with positive chronotropic agents can increase the atrial and ventricular rates and perhaps prolong gestation but do not improve postnatal survival.[62,112]

Although it is much less common, the prognosis for CC-TGV AV block is significantly better than for LAI-AV block. The presentation and outcome of CC-TGV AV block are shown in Table 40.6.

# Conclusion

The evaluation of fetal bradycardia is summarized in Figure 40.15. Many conditions will be benign, and parental counseling can be reassuring. In those conditions with a guarded prognosis, frequent follow-up and a multidisciplinary approach can optimize the outcome. The next steps to improve outcome and mitigate disease depend on the diagnosis. For the fetus at risk for anti-Ro/SSA antibody mediated AV block, this includes developing a surveillance technique to detect the earliest manifestations of disease and defining the best treatments for AV block. For the premature fetus with AV block and incipient heart failure, *in utero* pacing has the potential to delay delivery until maturity.[113] A greater awareness of the possible implications and a detailed evaluation of the fetus at risk for channelopathy either because of a family history or because of a sustained "mild" sinus bradycardia could lead to primary prevention of ventricular arrhythmias and identify asymptomatic family members at risk for sudden death.

**Table 40.6** Presentation and outcome of atrioventricular (AV) block and congenitally corrected transposition of the great vessels

| *Reference* | *N CC-TGV* | *N CC-TGV + AVB* | *GA Dx AVB (weeks)* | *Postnatal survivors (%)* |
|---|---|---|---|---|
| Gembruch et al. (1981–1987)[115,a] | 4 | 4 | 31 (25–36) | 75 |
| Schmidt et al. (1979–1989)[116,a] | 7 | 7 | 31 (22–38) | 57 |
| Jaeggi et al. (1990–2003)[117,a] | 3 | 3 | 32 (28–37) | 100 |
| Sharland et al. (1993–2003)[118,b] | 34 | 2 (~6%) | ND | ND |
| Paladini et al. (1994–2003)[119,b] | 30 | 2 (~7%) | 32 (31–34) | 100 |
| Chiappa et al. (1999–2003)[120,b] | 11 | 2 (18%) | 34 | 100 |
| Wan et al. (1999–2006)[121,b] | 14 | 1 (~7%) | ND | ND |

*Abbreviations:* AVB, atrioventricular block; Dx, diagnosis; FD, fetal demise; GA, gestational age; ND, neonatal demise; TOP, termination of pregnancy.

[a] Series of fetuses with AV block.

[b] Series of fetuses with CC-TGV.

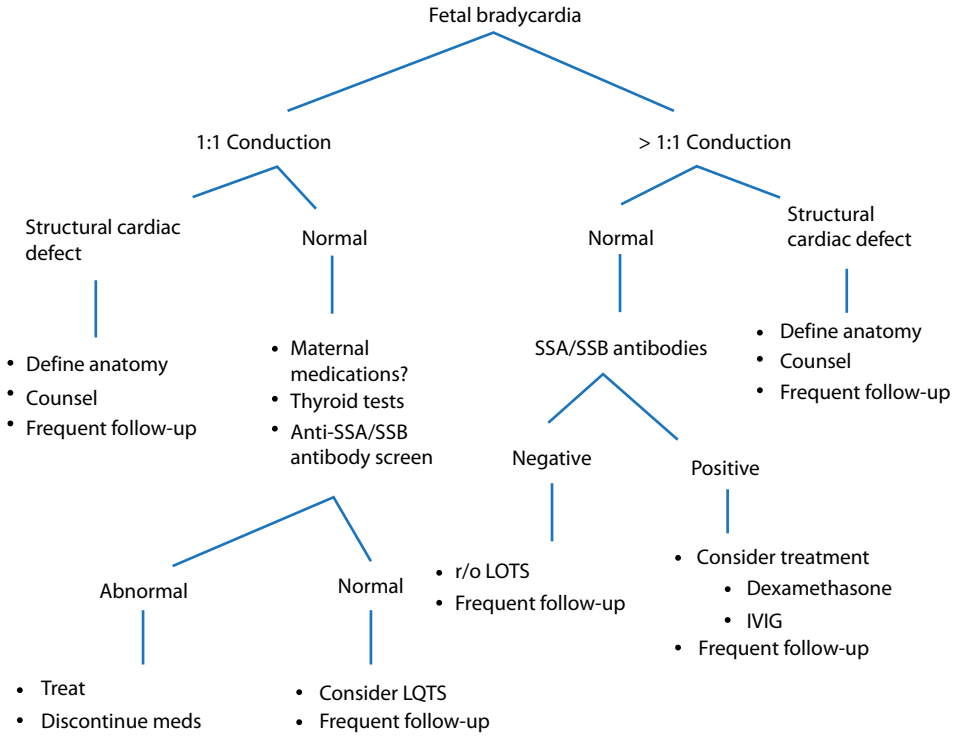


**Figure 40.15**
Decision tree for the evaluation of fetal bradycardia.

## Acknowledgment

I would like to thank Ron Wakai, Ph.D., Janette Strasburger, M.D., and the Biomagnetism Laboratory of the University of Wisconsin-Madison for the fMCG tracings.

## References

1. Eliasson H et al. *Ultrasound Obstet Gynecol* 2011;37(2):172–8.
2. Jaeggi ET, Friedberg MK. *Pacing Clin Electrophysiol* 2008;31 (suppl 1): S50–3.
3. Liao AW et al. *Ultrasound Obstet Gynecol* 2000;16(7):610–3.
4. Taylor MJ et al. *BJOG* 2003;110(7):668–78.
5. Gardiner HM et al. *Heart* 2007;93(11):1454–60.
6. Ojala K et al. *BJOG* 2006;113(4):419–23.
7. Leuthold A et al. *Early Hum Dev* 1999;54(3):235–43.
8. Shah VK, Wakai RT. *Phys Med Biol* 2013;58(22):8153–61.
9. Zhao H et al. *J Am Coll Cardiol* 2008;51(1):77–84.
10. Wiggins DL et al. *Heart Rhythm* 2013;10(8):1192–8.
11. Campbell JQ et al. *Obstet Gynecol* 2006;108(3 Pt 2):767–71.
12. ACOG Committee on Practice Bulletins. *Obstet Gynecol* 2009; 114:192–202.
13. Serra V et al. *Ultrasound Obstet Gynecol* 2009;34:74–9.

14. Mitchell JL et al. *Circulation* 2012;126(23):2688–95.
15. Porta A et al. *J Am Coll Cardiol* 2015;65(4):367–74.
16. Chockalingam P et al. *J Rheumatol* 2011;38(12):2682–5.
17. Cuneo BF et al. *J Matern Fetal Neonatal Med* 2009;22(3):233–8.
18. Jaeggi ET et al. *Heart Rhythm* 2009;6(9):1370–2.
19. Abadir S et al. *J Am Heart Assoc* 2015;4(12):e002676.
20. Dickinson DF et al. *Circulation* 1979;59:879–85.
21. Bharati S, Lev M. *Circulation* 1978;57:163–71.
22. Moorman AF et al. *Heart Rhythm* 2005;8:875–86.
23. Benson DW et al. *J Clin Invest* 2003;112(7):1019–28.
24. Milanesi R et al. *N Engl J Med* 2006;354(2):151–4.
25. Nawathe PA et al. *J Cardiovasc Electrophysiol* 2013;24(9):1021–7.
26. Liu H et al. *Pediatr Cardiol* 2012;33(6):882–9.
27. Heradien MJ et al. *J Am Coll Cardiol* 2006;48(7):1410–5.
28. Vigliani M. *J Reprod Med* 1995;40:725–8.
29. Hofbeck U et al. *Heart* 1997;77:198–204.
30. Lin MT et al. *Am Heart J* 2004;147:540–4.
31. Mitchell M et al. *Circulation* 2012;126(23):2688–95.
32. Winbo A et al. *Circ Arrhythm Electrophysiol* 2015;8(4):806–14.
33. Cuneo BF et al. *Circulation* 2013;128(20):2183–91.
34. ACOG Committee on Practice Bulletins. *Obstet Gynecol* 2009; 114:192–202.
35. Flock A et al. *J Maternal-Fetal Neonatal Medicine* 2015;28:1731–5.
36. Crotti L et al. *JAMA* 2013;309(14):1473–82.
37. Arnestad M et al. *Circulation* 2007;115(3):361–7.
38. Goldenberg I et al. *J Cardiovasc Electrophysiol* 2010;21(8): 893–901.
39. Greene AE et al. *Cardiol Young* 2012;23(1):141–5.
40. Cuneo BF et al. *Circulation* 2013 12;128(20):2183–91.
41. Sonesson SE et al. *Ultrasound Obstet Gynecol* 2014;44(2):171–5.
42. Buyon JP et al. *J Am Coll Cardiol* 1998;31:1658–66.
43. Ho SY et al. *J Am Coll Cardiol* 1992;20:904–10.
44. Sharland G et al. *Heart* 2005;91:1453–8.
45. Jaeggi ET et al. *Ultrasound Obstet Gynecol* 2005;26:16–21.
46. Paladini D et al. *Ultrasound Obstet Gynecol* 2006;27:281–5.
47. Chiappa E et al. *Cardiol Young* 2004;14:265–76.
48. Wan AW et al. *Am J Cardiol* 2009;104:1276–79.
49. Escobar-Diaz MC et al. *Pediatr Cardiol* 2014;35(6):906–13.
50. Cohen MS et al. *Ann Thorac Surg* 2006;82(5):1629–36.
51. Brucato A et al. *J Rheumatol* 2009;36(8):1744–8.
52. Fishman SG et al. *Pediatr Cardiol* 2011;32(1):84–6.
53. Cuneo BF et al. *Circ Arrhythm Electrophysiol* 2013;6(5):946–51.
54. Baruteau AE et al. *Eur J Pediatr* 2016;175(9):1235–48.
55. Schott JJ et al. *Science* 1998;281:108–11.
56. Li, QY et al. *Nat Genet* 1997;15:21–9.
57. Nii M et al. *Heart* 2006;92(12):1831–7.
58. Bergman G et al. *Ultrasound Obstet Gynecol* 2009;34(5):543–9.
59. Kato Y et al. *Fetal Diagn Ther* 2012;32(1-2):109–15.
60. Jaeggi ET et al. *J Am Coll Cardiol* 2011 29;57(13):1487–92.
61. Zhao H et al. *J Am Coll Cardiol* 2008;51(1):77–84.
62. Cuneo BF et al. *Am J Cardiol* 2007 15;100(4):661–5.
63. Marriott HJ. *Circulation* 1956;14(1):38–43.
64. Hornberger LK Rajaa N. *Scand J Immunol* 2010;72(3):189–97.
65. Izmirly PM et al. *Circulation* 2011;124(18):1927–35.
66. Eliasson H et al. *Circulation* 2011;124(18):1919–26.
67. Nield LE et al. *Circulation* 2002;105:843–8.
68. Cuneo BF et al. *Am J Cardiol* 2011;107(5):761–6.
69. Jaeggi E et al. *J Am Coll Cardiol* 2010 15;55(24):2778–84.
70. Spence D et al. *J Rheumatol* 2006;33(1):167–70.
71. Ambrosi A et al. *Ann Rheum Dis* 2012;71(3):334–40.
72. Miyakata S et al. *Ryumachi* 2001;41(4):726–35.
73. Makino S et al. *Acta Obstet Gynecol Scand* 2007;86(9):1145–6.
74. Pisoni CN et al. *Arthritis Rheum* 2010;62(4):1147–52.
75. Friedman DM et al. *Arthritis Rheum* 2010;62(4):1138–46.
76. Costedoat-Chalumeau N et al. *Ann Rheum Dis* 2003;62(10): 1010–2.
77. Izmirly PM et al. *Circulation* 2012;126(1):76–82.
78. Raboisson MJ et al. *J Am Soc Echocardiogr* 2005;18(4):375–80.
79. Saleeb S et al. *Arthritis Rheum* 1999;42(11):2335–45.
80. Askanase AD et al. *Lupus* 2002;11:142–51.
81. David AL et al. *Obstet Gynecol* 2010;116(suppl 2):543–7.
82. Tunks RD et al. *Am J Obstet Gynecol* 2013;208(1):64.e1–7.
83. Cuneo BF et al. *Am J Obstet Gynecol* 2016 Jul 12, 527–8. doi: 10.1016/j.ajog.2016.07.006
84. Friedman DM et al. *Am J Cardiol* 2009;103(8):1102–6.
85. Krishnan A et al. *Prenat Diagn* 2014;34(12):1207–12.
86. Hanif F et al. *J Obstet Gynecol* 2013;208(suppl):S162.
87. Izmirly PM et al. *Ann Rheum Dis* 2016;75(6):1161–5.
88. Trucco SM et al. *J Am Coll Cardiol* 2011;57(6):715–23.
89. Jaeggi ET et al. *Circulation* 2004;110(12):1542–8.
90. Hutter D et al. *Scand J Immunol* 2010;72(3):235–4.
91. Wapner RJ et al. *Semin Perinatol* 2016;40(5):291–7.
92. Cuneo BF et al. *Matern Fetal Neonatal Med* 2010;23(12): 1400–5.
93. Kelly EN et al. *Arthritis Rheumatol* 2014;66(8):2290–6.
94. Howman RA et al. *Fetal Diagn Ther* 2009;25(1):93–7.
95. Newburger JW et al. *Circulation* 2004;110:2747–71.
96. Weber R et al. *Heart Rhythm* 2008;5(9):1347–9.
97. Räsänen J. *Acta Obstet Gynecol Scand* 1990;69:487–92.
98. Benedetti TJ. *Am J Obstet Gynecol* 1983;145:1–6.
99. Gregoratos G et al. *Circulation* 1998;97:1325–35.
100. Silvetti MS et al. *Europace* 2015;17(4):603–10.
101. Silvetti MS et al. *Europace* 2010;12:1316–21.
102. Kelle AM et al. *J Thorac Cardiovasc Surg* 2007;134(5):1188–92.
103. Hauser J et al. *Am J Cardiol* 2011;107(1):92–5.
104. Pipes S et al. *Heart* 2009;95:1974–7.
105. Kuleva M et al. *Prenat Diagn* 2015;35(4):354–61.
106. Taketazu M et al. *Am J Cardiol* 2006 1;97(5):720–4.
107. Phoon CK et al. *Am J Cardiol* 1996;77:1083–88.
108. Atkinson DE, Drant S. *Am J Cardiol* 1998;82:1147–9.
109. Huggon IC et al. *J Am Coll Cardiol* 2000;36:593–601.
110. Lim JS et al. *Circulation* 2005;112:2454–61.
111. Berg C et al. *J Ultrasound Med* 2005;24:921–31.
112. Arunamata A et al. *J Am Soc Echocardiogr* 2012;25(1):112–20.
113. Bar-Cohen Y et al. *Heart Rhythm* 2015;12(7):1683–90.
114. Das B et al. *Fetal Diagn Ther* 2008;24(3):282–5, with permission.
115. Gembruch U et al. *Eur J Obstet Gynecol Reprod Biol* 1989; 31(1):9–22.
116. Schmidt KG et al. *J Am Coll Cardiol* 1991;91:1360–6.
117. Jaeggi ET et al. *Ultrasound Obstet Gynecol* 2005;26(1):16–21.
118. Sharland G et al. *Heart* 2005;91(11):1453–8.
119. Paladini D et al. *Ultrasound Obstet Gynecol* 2006;27(3):281–5.
120. Chiappa E et al. *Cardiol Young* 2004;14(3):265–76.
121. Wan AW et al. *Am J Cardiol* 2009;104(9):1276–9.

# 41

# Fetal tachyarrhythmia

Ulrich Gembruch

Fetal tachyarrhythmias, defined as fetal heart rates about 180–200 beats/minute, are generally subdivided into sinus tachycardia, supraventricular tachyarrhythmia, including supraventricular tachycardia (SVT) and atrial flutter, and ventricular tachyarrhythmia. The most common form of fetal and neonatal SVT, the atrioventricular reentry tachycardia via an accessory pathway, involves the atrium, atrioventricular (AV) node, much of the ventricles, and an accessory pathway as reentry circuit, and therefore is a "whole heart" tachycardia.[1] According to the three electrophysiological levels of the heart, it seems to be more accurate to divide the tachyarrhythmias into atrial tachycardia (atrial flutter or atrial ectopic tachycardia), conduction system tachycardia (atrioventricular reentry tachycardia via an apparent or "concealed" accessory pathway, permanent junctional reciprocating tachycardia, and atrioventricular nodal reentry tachycardia), junctional ectopic tachycardia, and ventricular tachycardia, as well as the rare accelerated idioventricular tachycardia.[1] In fetuses, SVT is more frequent than atrial flutter (70%–75% versus 25%–30%), whereas ventricular tachycardia is very rare.[2] Sustained fetal tachyarrhythmia (SVT with 1:1 atrioventricular conduction, atrial flutter, and ventricular tachycardia) may cause congestive heart failure, leading to elevated right atrial and systemic venous pressure, and may be followed by nonimmune hydrops, placental edema, and polyhydramnios. In addition, associated maternal complications may be complaints due to severe polyhydramnios, preterm contractions and labor, premature rupture of the membranes, and the mirror syndrome or Ballantyne syndrome. These result in a maternal hyperdynamic and hypertensive state with symptoms of preeclampsia, which is sometimes observed associated with fetuses with placental edema and hydrops of various etiologies.[3–5] If remission of hydrops can be achieved, preeclamptic symptoms of the mother may disappear in the ongoing pregnancy.[6–8]

## *In utero* diagnosis of fetal tachyarrhythmia

The majority of fetal tachyarrhythmias are detected during routine obstetric examination in the second and third trimesters of pregnancy. Monitoring of the fetal heart rate by ultrasound, continuous wave Doppler (Doptone), or cardiotocography reveals fetal arrhythmia requiring a detailed echocardiographic examination. Polyhydramnios and fetal hydrops may also lead to the detection of an underlying tachyarrhythmia. If intensive noninvasive and invasive searches for an underlying disease are unsuccessful, paroxysmal supraventricular tachyarrhythmia should always be taken into consideration, particularly if signs of congestive heart failure such as cardiomegaly, atrioventricular valvular regurgitation, and/or increased pulsatility of venous flow velocity waveforms are present. In this situation, repeated sonographic heart rate monitoring, or long-term cardiotocography carried out several times per day, can diagnose or exclude paroxysmal supraventricular tachyarrhythmia as the cause of the hydrops.

Differential diagnosis of fetal arrhythmia and also tachyarrhythmias is performed using echocardiographic techniques with a high time resolution. Tracings of the wall and valve movements and blood flow velocity waveforms of the heart, the arteries, and the veins obtained by M-mode, pulsed wave Doppler, and/or color Doppler M-mode allow indirect conclusions to be drawn from these recordings of the mechanical and flow activities against time to the electrical events (Figures 41.1 and 41.2). Thus, correct diagnosis of the type of fetal arrhythmia is possible in the vast majority of cases (Table 41.1). For cases of fetal arrhythmia, the diagnostic approach is elaborated further in Chapter 39.

New noninvasive methods for diagnosis of fetal arrhythmias are tissue velocity imaging (by pulsed wave Doppler, color-coded M-mode, or color Doppler imaging), and magnetocardiography. Tissue Doppler techniques allow simultaneous sampling of atrial and ventricular wall velocities to yield precise temporal analysis of atrial and ventricular events, similar to the M-mode and Doppler techniques.[9] Significant advantages of tissue Doppler compared to the classical M-mode and Doppler techniques for the diagnosis of fetal arrhythmias have not been obvious so far, particularly as there are some limitations inherent to tissue Doppler imaging techniques.[10] Fetal magnetocardiography records the magnetic fields generated by the electrical activity of the fetal heart, exhibiting significantly better signal quality compared with fetal electrocardiography, because it is largely unaffected by the high electrical resistance of the fetal skin, which attenuates fetal electrocardiography. At present, sensors cooled by liquid helium are positioned several centimeters above the maternal abdomen in a magnetically shielded room. Fetal magnetocardiography offers a more precise

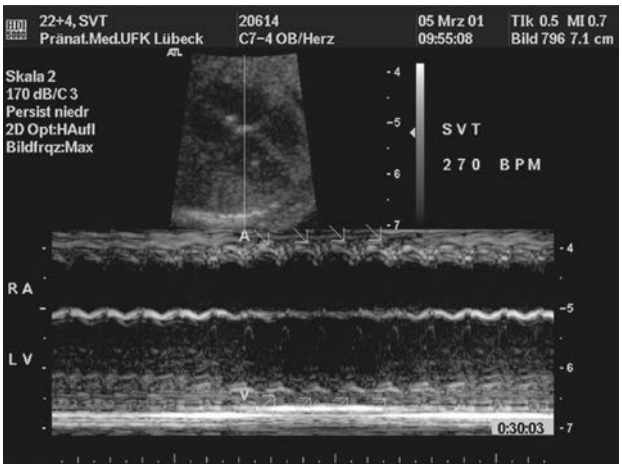


**Figure 41.1**
M-mode echocardiogram of the heart in a fetus at 22 + 4 weeks' gestation. The cursor is positioned across the right atrium (RA) and the left ventricle (LV), producing the M-mode tracing as shown. It reveals a supraventricular reentry tachycardia at 270 beats/minute. Each contraction (marked by arrows) of the atrial wall (A) is followed by one of the ventricular wall (V) indicating a 1:1 atrioventricular conduction.

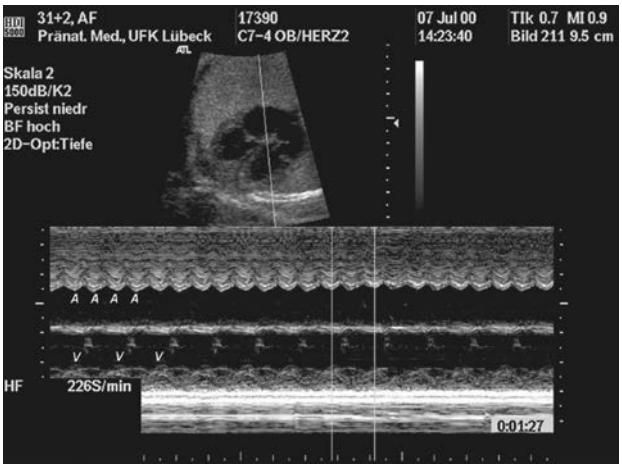


**Figure 41.2**
M-mode echocardiogram of the heart in a fetus at 31 + 2 weeks' gestation. The cursor is positioned across the right atrium (RA) and the left ventricle (LV), producing the M-mode tracing as shown. It reveals an atrial flutter with a 2:1 atrioventricular conduction resulting in an atrial rate of around 450 beats/minute and a ventricular rate of around 225 beats/minute. Each second contraction of the atrial wall (A) is followed by one of the ventricular wall (V).

delineation of fetal electrophysiology, or more precisely, magnetophysiology, allowing measurements of different intervals such as PR, QRS, and QT.[11–16] Diagnosis of the different arrhythmias (Figure 41.3) and long QT syndrome by fetal magnetocardiography has been reported,[12–14,16–19] as well as electrophysiological patterns of initiation and termination of atrioventricular reentrant tachycardia in fetuses.[15] Because of its high technical prerequisites, fetal magnetocardiography is

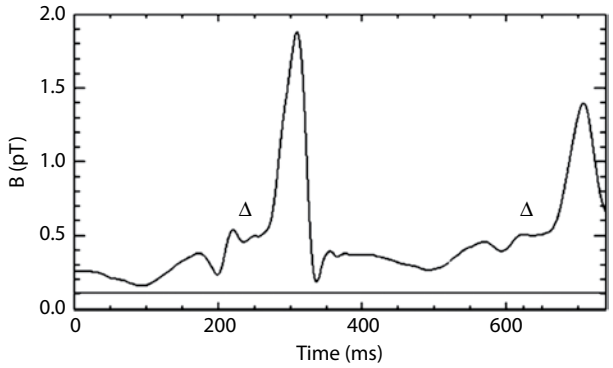


**Figure 41.3**
Fetal magnetocardiogram (averaged QRS complexes) in a fetus with supraventricular tachycardia (SVT) of 240 beats/minute at 34 weeks' gestation. In a normofrequent phase, a delta-wave (Δ) as a part of the R wave could be demonstrated, suggesting the presence of Wolff–Parkinson–White (WPW) syndrome. This was confirmed by neonatal electrocardiogram. B, amplitude. (Courtesy of Uwe Scheider, University of Jena, Germany.)

very expensive and is available in only a few centers around the world. However, improvements of the technique may overcome these problems in the near future.[14]

## Electrophysiological mechanisms of fetal tachyarrhythmia

In general, the natural history and pathophysiology for many of the fetal tachyarrhythmias are documented incompletely. Using M-mode and/or Doppler echocardiography, most prenatal series separate the SVT with a 1:1 AV contraction relation from atrial flutter. A 1:1 AV conduction most probably suggests an atrioventricular reentry tachycardia via an accessory pathway. Moreover, that an atrial ectopic tachycardia and junctional reciprocating tachycardia are also associated with a 1:1 AV contraction relation cannot be excluded, although they are less common. Therefore, the type and prevalence of fetal tachyarrhythmia are inferred from more exact electrophysiological analysis in neonates. It appears that the spectrum of fetal tachyarrhythmia closely resembles that found during the neonatal period. However, the exact definition of the type of fetal tachycardia may still be difficult. Variable outcomes reported in different studies may reflect the presence of different rhythm disturbances rather than a variation in response to the arrhythmia. Therefore, the initial assessment of the type of arrhythmia may have to be revised if there is a failure of response to the common antiarrhythmic treatment. Therefore, knowledge of the mechanism of tachycardia is potentially important, as it will define both the response to treatment and the prognosis.[20–24]

In this context, the timing of the ventriculo-atrial (VA) relation using fetal M-mode or pulsed wave spectral Doppler echocardiography may be helpful in distinguishing short and long VA time interval tachycardias (Table 41.1).[22–24] Simultaneous Doppler recordings of flow velocity waveforms

**Table 41.1** Echocardiographic features of the fetal tachyarrhythmias

| *Type of tachycardia* | *Atrial rate (beats/minute)* | *Ventricular rate (beats/minute)* | *AV relation* | *VA interval* |
|---|---|---|---|---|
| SVT (AV reentry) | 190–280 | 190–280 | 1:1 | Short VA |
| Atrial flutter (AF) | 300–480 | 150–240 | 2:1, rarely 3:1 or 4:1 | |
| Atrial ectopic tachycardia (AET), permanent junctional reciprocating tachycardia (PJRT) | 180–230 | 180–230 | 1:1 | Long VA |
| Ventricular tachycardia (VT) | 120–160 (normal) | 170–230 | Dissociated (<1:1) | Dissociated |
| Accelerated idioventricular rhythm (AIVR) | 120–610 (normal) | 160–180 | Dissociated (<1:1), isorhythmic, bundle branch block | Dissociated |
| Junctional ectopic tachycardia (JET) | 160–210 [or 120–160 (normal)] | 160–210 | 1:1 (or dissociated as VT) | Very short VA (or dissociated) |
| Sinus tachycardia | 160–220 | 160–220 | 1:1 | Long VA |

*Abbreviations:* AV, atrioventricular; SVT, supraventricular tachycardia; VA, ventriculoatrial.

in the superior vena cava and the ascending aorta reflect the VA and atrioventricular (AV) time intervals more accurately than M-mode. Measurements of these intervals by simultaneous recording of left ventricular inflow and outflow are impracticable at heart rates above 160 beats/minute because of mitral E- and A-wave overlap.[23,24] A short VA time interval is characteristic of atrioventricular reentry via an accessory pathway. A long time interval, which is defined as a ratio of the VA to the atrioventricular time interval above 1 (long VA tachycardia), is typical of permanent junctional reciprocating tachycardia or atrial ectopic tachycardia, which are more refractory to antiarrhythmic treatment.[7] Atrial ectopic tachycardia may occur in fetuses and originate from a single abnormal focus or a wandering pacemaker. The more rarely occurring permanent junctional reciprocating tachycardia belongs to the conduction system tachycardias mediated by a concealed, backward conducting accessory pathway with slow AV node-like conduction properties. In both long VA tachycardias, the P-wave is far from the QRS complex, and the venous Doppler a-wave is of normal amplitude (atrial contraction during diastole against open AV valves) with a long VA interval (VA > AV). The atrial ectopic and the permanent junctional reciprocating tachycardia of the fetus are characterized by frequencies between 180 and 220 beats/minute, whereas for atrioventricular reentry, tachycardia frequencies between 220 and 280 beats/minute are typical. A very short VA interval (very short VA tachycardia) with concomitant onset of tall venous atrial and aortic Doppler waves characterizes atrioventricular nodal reentrant tachycardia and junctional ectopic tachycardia.[24] Furthermore, atrial ectopic tachycardia sometimes shows a higher variability of the heart rate, termed a *heating phenomenon*,[8] which is very atypical for the classical atrioventricular reentry tachycardia.

During early human life, the frequency of the various SVTs and their underlying electrophysiological mechanisms varies depending on the age at presentation.[25] Studies in newborns and infants with tachyarrhythmias[25,26] suggest that around 80%–90% of fetal SVTs are atrioventricular reentrant tachycardias. These are based on an accessory atrioventricular conduction pathway besides the atrioventricular node, whereas atrial ectopic tachycardia, chaotic or multifocal atrial tachycardia, atrioventricular nodal reentrant tachycardia, permanent junctional reciprocating tachycardia, and His bundle tachycardia (junctional ectopic tachycardia) are seldom the electrophysiological mechanism of perinatal SVT.[1,20–25,27,28] Accordingly, a Wolff–Parkinson–White syndrome can be confirmed electrocardiographically in approximately 10% of fetuses with SVT. Much less common are other preexcitation syndromes such as the Lown–Ganong–Levine syndrome and the Mahaim syndrome.[28] In the vast majority of atrioventricular reentry tachycardias, there is an "orthodromic" impulse conduction, meaning that the electrical impulse is conducted from the atrium to the ventricle via the atrioventricular node and subsequently back to the atrium via the accessory pathway with fast conduction properties. Therefore, this "orthodromic" atrioventricular reentry tachycardia is a short VA tachycardia characterized by a narrow QRS complex and a retrograde P-wave shortly after the narrow QRS complex in the electrocardiogram; in simultaneous Doppler recording of the superior vena cava and ascending aorta, the venous a-wave in the superior vena cava is superimposed on the aortic wave and is tall because of atrial contraction against closed atrioventricular valves.[23,24] This depolarizing current circuit works independently from the physiological sinoatrial pacemaker. An "antidromic" reciprocating tachycardia may also occur in cases of Wolff–Parkinson–White syndrome and concealed atrioventricular reentry tachycardias with antegrade impulse conduction through a slow accessory pathway. The prerequisite for the appearance of a reentry tachycardia is different electrophysiological properties of both pathways, having a different conduction velocity and/or refractoriness. Under these circumstances, the reentry tachycardia is usually triggered by an incidental supraventricular extrasystole if there is a critical relationship between conduction velocity

and refractory period. The reentrant premature atrial contraction causes delayed antegrade conduction through the AV node with subsequent retrograde conduction through the accessory pathway, thus initiating "orthodromic" atrioventricular reentry tachycardia via an accessory pathway. Atrial ectopy is common in fetuses, with an incidence of 1%–3%. Approximately 0.5%–1% of these fetuses will develop SVT during fetal and neonatal life, resulting in the general recommendation to check the fetal heart rate weekly for detection of an occurrence of SVT. Early occurrence of fetal ectopy, frequent ectopy, and the presence of multiple accessory pathways are risks for the occurrence of reentrant SVT during fetal life. Furthermore, variations in autonomic activity may influence conduction in the AV node and accessory pathway compatible with the association between fetal body movements and patterns of SVT initiation involving premature atrial contractions and sinus acceleration.[15] In atrioventricular reentrant tachycardia, the conduction velocity and the length of the reentrant circuit determine the relatively fixed frequency of the reentrant tachycardia with failed heart rate variability.[20,27] In fetal atrioventricular reentry tachycardia via an accessory pathway, this is between 220 and 280 beats/minute. Drug-induced alteration of conduction velocity and/or refractoriness of the reentrant circuit may stop or prevent the reentry tachycardia. Sometimes a premature ectopic beat may also interrupt a reentry tachycardia as well as parasympathetic excitation. Fetal tachycardias between 180 and 230 beats/minute suggest other electrophysiologic mechanisms and types of tachycardia, most often permanent junctional reciprocating, atrial ectopic tachycardias, and junctional ectopic tachycardia with 1:1 VA conduction, respectively.

The high incidence of atrioventricular reentry tachycardia during fetal and neonatal life and its decrease due to the spontaneous disappearance of SVT suggest the immaturity of the myocardium, and in particular, a delayed development of the annulus fibrosus and/or prolonged persistence of accessory atrioventricular pathways as the most underlying etiology of fetal SVT.[25,29] Much less common are cases due to autosomal dominant inheritance of Wolff–Parkinson–White syndrome, or SVT in fetuses with Ebstein anomaly, rhabdomyoma, or viral myocarditis.

Fetal atrial flutter, which accounts for 25%–30% of all cases of fetal tachyarrhythmias,[2] and atrial fibrillation, which is extremely rare in the fetus, are most commonly generated within the atria themselves by an intra-atrial reentrant circuit. Experiments, and the observation that atrial flutter is observed only during the third trimester, support the favored hypothesis of an atrial macroreentry as the underlying mechanism of fetal atrial flutter. The atrium probably reaches a critical size for establishing a macroreentry circuit at about 27–30 weeks' gestation, associated with a high vulnerability against triggering atrial extrasystoles.[30] The frequency of this atrial reentrant tachycardia is between 350 and 500 beats/minute. The atrioventricular node, which is not part of the reentrant circuit, usually protects the ventricles by variably blocking atrioventricular conduction, with the result of a substantially slower fixed or varying ventricular rate, depending on the degree of AV block, which may be a fixed or varying 2:1, 3:1, or 4:1 block. In some fetuses with atrial flutter, the presence of an accessory atrioventricular pathway has been shown by postnatal transesophageal electrophysiological studies in neonates with previously documented fetal atrial flutter.[28] The association between atrial flutter and intermittent atrioventricular reentrant tachycardia by accessory pathways seems to be rare during fetal life but was recently reported in 5 of 13 fetuses with atrial flutter using prolonged, continuous monitoring by fetal magnetocardiography.[31] In this study, complex atrial ectopy due to reentrant premature supraventricular extrasystoles often accompanied the atrial flutter.[31] Chaotic atrial tachycardia and atrial fibrillation are extremely rare during fetal life.

Distinct atrial dilatation resulting from severe AV valvular regurgitation in cases of Ebstein anomaly and rarely atrioventricular septal defects may sometimes cause atrial flutter during fetal life, similar to the well-known pathomechanism of atrial flutter as a consequence of left atrial dilatation due to mitral valve dysfunction in later life.

Sinus tachycardia is usually characterized by a baseline fetal heart rate between 180 and 220 beats/minute and is commonly a secondary manifestation of an underlying disease. These include maternal fever, chorioamnionitis, fetal distress, fetal thyrotoxicosis, and maternal medication such as β-sympathomimetics. During the late third trimester, longer accelerations, which can be found in a healthy "jogging" fetus in the 4F activity state, must be distinguished from sinus tachycardia. Its association with increased fetal breathing and body movements, its commonly high variability of the fetal heart rate pattern, and particularly its transient occurrence allow distinction. Differentiation from a permanent junctional reciprocating tachycardia (PJRT) showing also a long VA interval may be difficult.

The junctional ectopic tachycardia (previously known as His bundle tachycardia) is the least common form of tachycardia but is often underdetected by current diagnostic means. It is driven by a focus with abnormal automaticity within or immediately adjacent to the atrioventricular (AV) junction of the cardiac conduction system (i.e., AV node–His bundle complex). Junctional ectopic tachycardia is nonsustained, shows heart rates between 160 and 210 beats/minute, slightly slower than ventricular tachycardia, and is mainly associated with anti-SSA antibodies and may be associated with AV block.[32] Junctional ectopic tachycardia is occasionally associated with a 1:1 VA conduction resulting in a 1:1 atrioventricular relation and a very short VA interval or appears similar to ventricular tachycardia with an AV dissociation. The onset (warm-up) and termination of a junctional ectopic tachycardia are gradual.[33] There are only a few reports of fetal ventricular tachycardia. Prenatal diagnosis is usually performed if the ventricular tachycardia shows AV dissociation, with ventricular rates varying from 180 to 300 beats/minute in excess of the atrial rate, as documented by M-mode (Figure 41.4) and/or Doppler echocardiography.[20,27,34,35] This pattern of tachyarrhythmia is highly suggestive of either a ventricular or a junctional

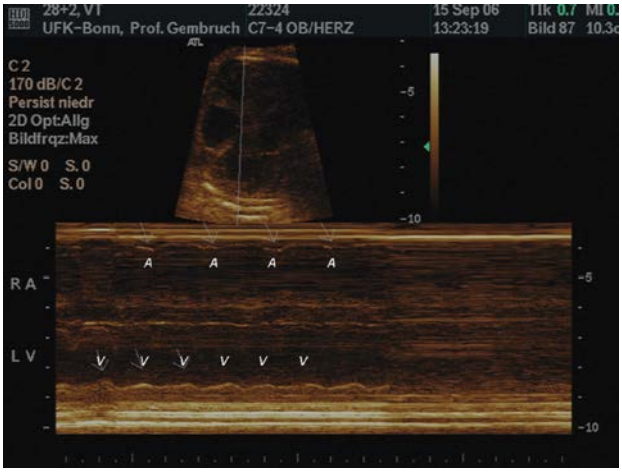


**Figure 41.4**
In a hydropic fetus with severe dilated cardiomegaly, a ventricular tachycardia suddenly occurred at 28 + 4 weeks' gestation. The M-mode echocardiogram—the cursor is positioned across the right atrium (RA) and the left ventricle (LV)—reveals a ventricular tachycardia with an AV dissociation (ventricular rate of 245 beats/minute and atrial rate of 145 beats/minute). Postnatally long QT syndrome was diagnosed.

origin of the tachycardia, whose differentiation seems to be impossible during fetal life. In some cases of ventricular tachycardia, however, retrograde AV conduction may lead to a 1:1 contraction sequence of atria and ventricles, making prenatal differentiation from SVT difficult or impossible. Ventricular tachycardia should be suspected if the fetal heart rate lies outside the normal range of 220–280 beats/minute for SVT, especially if transient AV dissociation is observed in addition. Similar to the more common ventricular tachycardia in coronary heart disease in later adulthood, causing focal alteration of the ventricular myocardium, a locally restricted reentrant circuit may also be the underlying electrophysiological basis of ventricular tachycardia during fetal life. In fetal life, segmental alterations of myocardial oxygen supply may occur in severe myocardial hypertrophy secondary to semilunar valve stenosis and cardiomyopathy, or from cardiac tumors resulting in ventricular tachycardia.[27] Other underlying myocardial diseases are cardiac ventricular aneurysms, cardiac tumors, and myocarditis. Furthermore, fetuses with the long QT syndrome predominantly show sinus bradycardia, sometimes with intermittent AV block and/or torsades de pointes, but seldom also show transient ventricular tachycardia.[17,18,36–43] The episodes of torsades de pointes last between 1 second to almost 8 minutes, its number ranged from 15 to 45 within a 48 minute period with typical manifestation after 30 weeks' gestation.[18] However, torsades de pointes and/or 2:1 AV conduction indicating fetal long QT syndrome occurs in more than 25% of involved fetuses.[18] Sinus bradycardia with repeated fetal heart rates less than the third percentile for gestational age is the main form of fetal presentation.[18,42] The presence of ventricular tachycardia in cases with long QT syndrome appears to be associated with a particularly poor prognosis,[43] and also with a "spongy myocardium."[37,41] In some cases of stillbirth with unknown etiology, hidden arrhythmias and long QT syndrome, respectively, may be the underlying cause.[44] Therefore, sinus bradycardia and particularly the combination of episodes of AV block and periods of ventricular tachycardia are strongly suspicious for fetal long QT syndrome. Because of its dominant inheritance of the underlying channelopathies, the family history should be checked and the corrected QT interval ($QTc > 0.44$; $QTc = QT/\sqrt{RR}$) of both parents should be measured on the electrocardiogram, even if a positive family history may be lacking in infants with prolonged corrected QT interval.[24] Inherited anomalies of myocardial structure and function may induce these arrhythmias. Long QT syndrome (Romano-Ward syndrome) belongs to the ion channel diseases, which are clinically characterized by episodes of disturbed excitability of muscle or nerve cells. For the long QT syndrome, various mutations in cardiac potassium and sodium channel encoding genes inducing changes in channel gating have been reported, showing a different mode of inheritance.[43,45] The type of fetal arrhythmia in long QT syndrome depends on the mutation type.[43] Measurement of the QT interval and prenatal diagnosis of long QT syndrome are possible by fetal electrocardiography, and in particular, by fetal magnetocardiography.[13,14,16,17,43]

During fetal life, accelerated idioventricular rhythm (AIVR) seems to be frequently associated with hydrops.[46] Because of the only slightly increased ventricular rates of around 170 bpm and its transient character, AIVR may often remain undetected. Postnatally, diagnosis is performed by electrocardiography revealing wide monomorphic QRS complexes dissociated from atrial depolarizations, interrupted by variable periods of either sinus rhythm or concomitant atrial and ventricular contractions (isorhythmic AV dissociations) related to atrial or ventricular captures, left or, less frequently, right bundle branch block, and ventricular rates within 15%–20% of the preceding sinus rhythm.[46] Recently, Fouron et al. recommended the following Doppler sonographic approach in identifying AIVR: simultaneous registration of superior vena cava and ascending aorta flow velocity waveforms demonstrates atrioventricular dissociation (ventricular rates within 20% of atrial rates) with related cannon a-waves, but sometimes episodes of isorhythmic AV dissociations; M-mode shows atrioventricular dissociation and normal left ventricular shortening fraction; simultaneous registration of aortic isthmus and ductus arteriosus flow velocity waveforms reveals the presence of right or left bundle branch block; Doppler waveforms of the ductus venosus indicate increased venous pressure with retrograde a-waves in the presence of simultaneous atrial and ventricular contractions.[46] Therefore, in fetuses with unexplained hydrops and increased pulsatility of ductus venosus flow pattern, the presence of AIVR should be ruled out.[46]

## Pathophysiology

Pathophysiologically, there is a substantial shortening of the diastolic period of the cardiac cycle preventing adequate early

diastolic filling of the ventricles, subsequently increasing the systemic venous volume load and the central venous pressure, which is already high in the normal fetal circulation. Furthermore, results from animal studies of left atrial pacing and M-mode echocardiographic studies in human fetuses suggest that initial left atrial depolarization can be tolerated to a lesser degree by the fetus.[27,28] By pre-excitation of the left atrium, partial closure of the foramen ovale may significantly disturb the interatrial right-to-left shunt. This results in a trapping of the venous return in a, by now, volume-overloaded right atrium and right ventricle, with further elevation of central venous pressure. Premature closure of the foramen ovale has also been reported in two fetuses with atrial flutter.[47] The left ventricular output is subsequently diminished. In addition, the most common fetal SVT, "orthodromic" atrioventricular reentry tachycardia, is characterized by a short VA interval with atrial contraction against closed atrioventricular valves causing a higher increase of venous pressure than long VA tachycardias.[23] Furthermore, a very high ventricular rate and a manifestation of tachycardia in earlier gestation may predispose these fetuses to the development of hydrops, because both diastolic and systolic function of the isolated myocardium and the whole heart distinctly improve with advancing gestational age. Finally, ventricular filling is predominantly dependent on the atrial systole due to the relative stiffness of the fetal myocardium. Therefore, a regular 1:1 atrioventricular conduction sequence is important, and intermittent atrial contraction against a closed atrioventricular valve may predispose some fetuses with atrial flutter to the development of hydrops. This explains the observation that some fetuses with atrial flutter develop hydrops in spite of a normal or slightly increased ventricular rate, and why, in some fetuses with atrial flutter, hydrops may persist even if the ventricular rate is normalized by drug-induced higher-degree AV block, and only disappears after the establishment of normal atrial and ventricular rate with 1:1 AV conduction.

Although there are important differences between atrial pacing in animal models and supraventricular reentry tachycardia, atrial flutter, and rapid sinus tachycardia in human fetus atrial pacing, studies in fetal lamb models still give important insights into the pathogenic mechanisms of the development of fetal hydrops.[48–52] In atrial pacing at rates up to 300 beats/minute, there is an increase of ventricular output and a decrease of ventricular end-diastolic pressure. Prolonged left atrial pacing at rates of 300–320 beats/minute results in a decrease of cardiac output and in the development of hydrops within 4–48 hours; this confirms the suggestion that, above a critical heart rate, diastolic filling is impeded especially for the ipsilateral ventricle. In these situations, cardiomegaly and hepatomegaly develop, arterial oxygen tension remains unchanged, and protein, including albumin, concentrations stay stable or slightly decrease later on in the disease process.[48–51] Because no, or only slight, nonsignificant hypoproteinemia may be observed, there is no evidence for an increase of capillary permeability for albumin. In advanced stages of congestive heart failure, however, there may be more distinct hypoproteinemia due to disturbed hepatic synthesis. The aortic pressure remains unchanged, while the mean venous pressure in the inferior vena cava increases by 75%.[52] This elevation may reflect a compensatory increase of venomotor tone for maintenance of adequate cardiac output by an elevation of the preload. However, the abrupt elevation of venous pressure is associated with an immediate appearance of pulsatile reversal of blood flow occurring during diastole (Figures 41.5 through 41.7).[52] This is observed above a "critical" heart rate of 310 beats/minute. Below this heart rate, the venous flow is biphasic, with a systolic and diastolic forward surge that also occurs immediately after the pacing is stopped.[52] Besides the direct impeding of diastolic filling when the diastolic interval is critically shortened, the abrupt occurrence of changes—reduction of ventricular output, immediate elevation of venous pressure, and appearance of pulsatile venous blood flow above a "critical" pacing rate—suggests ventricular dysfunction consistent with alteration of the pressure-volume relationship in association with impaired ventricular relaxation at high pacing rates. The most likely explanation is that oxygen supply to the myocardium by coronary blood flow is inadequate for the increased requirement of the myocardium during tachycardia.[53,54]

Myocardial blood flow is maintained primarily by the pressure gradient across the vascular bed, extravascular pressure, and local autoregulation. Since the extravascular pressure is considerably lower in diastole than in systole, the major portion of coronary blood flow occurs in diastole. In tachycardia, however, the diastolic period is significantly shortened. Moreover, with increased atrial pressure, the myocardial pressure gradients decrease. Severe ventricular dysfunction and even injury of the myocardium may occur in prolonged tachycardia, and may cause reversible

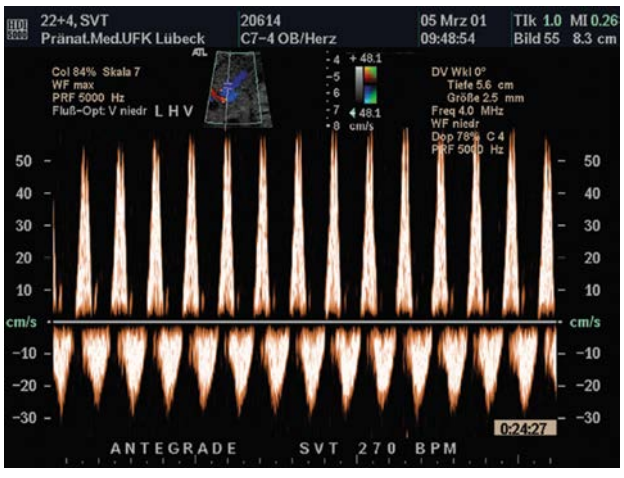


**Figure 41.5**
In a nonhydropic fetus at 22 + 4 weeks' gestation with a supraventricular tachycardia at 270 beats/minute, Doppler measurement in the left hepatic vein revealed a pulsatile reversal of blood flow occurring during diastole. The antegrade blood flow during systole is in the lower channel (away from the transducer), and the reverse blood flow during diastole in the upper channel (toward the transducer).

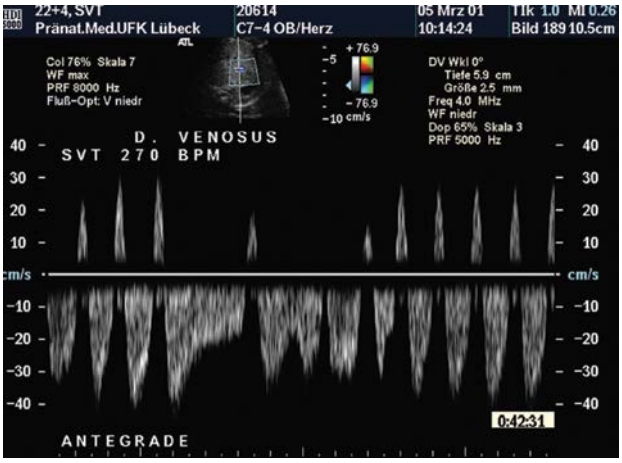


**Figure 41.6**
In a nonhydropic fetus at 22 + 4 weeks' gestation with a supraventricular tachycardia at 270 beats/minute, Doppler measurement in the ductus venosus showed a triphasic venous blood flow pattern with a systolic and diastolic peak during a short period of sinus rhythm. An atrial premature beat is triggering the supraventricular reentry tachycardia associated with an abrupt onset of the pulsatile reversal of blood flow occurring during diastole. The antegrade blood flow during systole is in the lower channel (away from the transducer), and the reverse blood flow during diastole in the upper channel (toward the transducer).

tachycardia-induced "cardiomyopathy" in humans and animals.[53–55] In conjunction with the enormous cardiac dilatation in fetuses with sustained SVT, functional incompetence as indicated by annular enlargement of both atrioventricular valves may be observed, suggesting structural remodeling of the ventricles in the presence of tachycardia-induced "cardiomyopathy" (Figures 41.8 and 41.9).[56] In pigs,

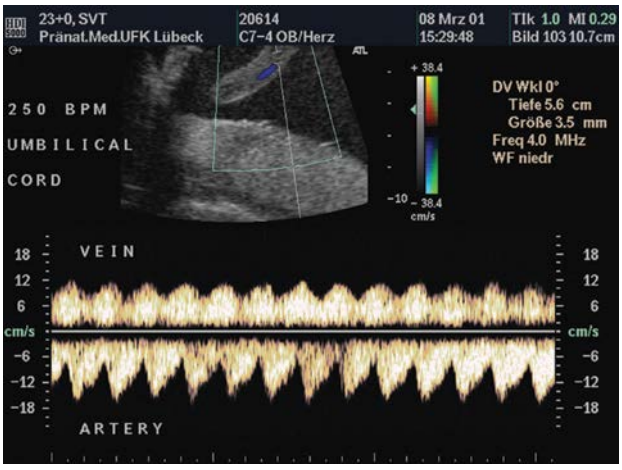


**Figure 41.7**
In a nonhydropic fetus at 22 + 4 weeks' gestation with a supraventricular reentry tachycardia at 270 beats/minute, Doppler measurement in the umbilical cord showed arterial blood flow in the lower channel (away from the transducer) and the umbilical venous blood flow pattern with monophasic pulsations as typically associated with pulsatile reversal of blood flow in the ductus venosus and other precordial veins.

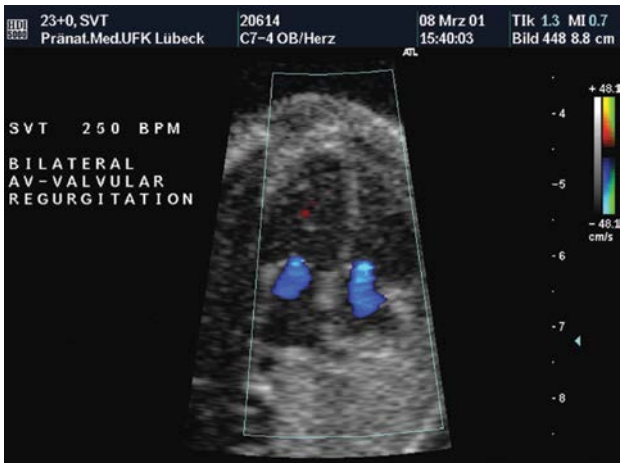


**Figure 41.8**
In a nonhydropic fetus at 22 + 4 weeks' gestation with a supraventricular reentry tachycardia at 250 beats/minute and a consequent cardiomegaly, mild bilateral atrioventricular valvular regurgitations occurred during a short period of sinus rhythm.

recovery from tachycardia-induced "cardiomyopathy" was accompanied by persisting chamber dilatation, significant myocardial hypertrophy, and persisting diastolic dysfunction.[57] During early recovery, left ventricular function and myocardial blood flow normalize at no exertion, but stress results in marked systolic and diastolic left ventricular dysfunction and reduced myocardial blood flow.[53,54] In human fetuses after termination of SVT, cardiac dilatation, myocardial hypertrophy, atrioventricular valve incompetence, and hydrops disappear with immense interindividual differences, which could be explained by different stages of progression of tachycardia-induced "cardiomyopathy" at

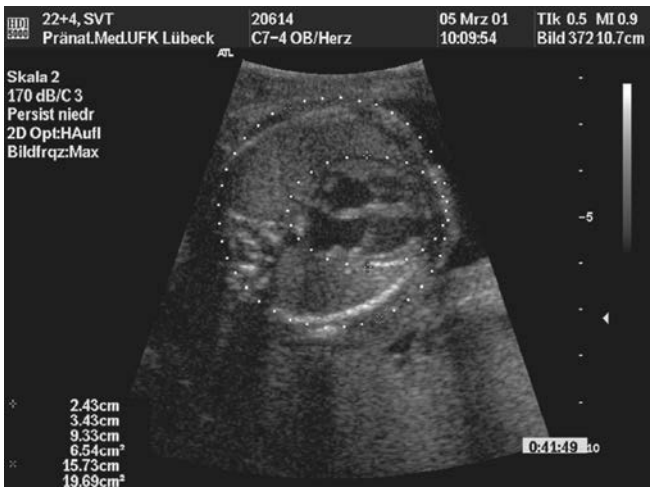


**Figure 41.9**
In a nonhydropic fetus at 22 + 4 weeks' gestation with a supraventricular tachycardia at 270 beats/minute, the size of the heart is moderately increased as indicated by measuring the cardiothoracic ratios (CTRs). The CTR of the circumferences is 0.59 (93/157 mm), and the CTR of the areas is 0.33 (654/1969 $mm^2$).

the time of drug-induced cardioversion.[56] Venous blood flow studies in the human fetus with SVT demonstrate the occurrence of monophasic forward and pulsatile reversed blood flow during diastole in the inferior vena cava, hepatic veins, and ductus venosus as well as of pulsations in the umbilical venous blood flow pattern above a critical heart rate of approximately 210–220 beats/minute.[58] This is in accordance with fetal lamb studies, where this change of venous blood flow pattern was associated with a considerable elevation of venous pressure.[52] Furthermore, in the human fetus, in addition to the persistence of cardiomegaly and atrioventricular valve regurgitation, abnormal indices of venous blood flow during sinus rhythm indicate the existence of altered myocardial function, suggesting the presence of a reversible tachycardia-induced "cardiomyopathy."[59,60] Times for remission of hydrops, disappearance of atrioventricular valve regurgitation, and normalization of the venous blood flow indices show a good correlation with the immense interindividual differences. The hydrops disappears first, then the atrioventricular valve incompetence recovers, and finally the venous Doppler indices become normal.[56,59,60] The time interval from the drug-induced conversion into a constant sinus rhythm may differ from 1 day to 6 weeks.[56,59–61] The time needed for complete normalization of cardiac function may also vary extremely, in accordance with different stages of progression of tachycardia-induced "cardiomyopathy" at the time of conversion into a sinus rhythm.[56,59,60]

In conclusion, the most important pathomechanism in SVT of the human fetus is an impeded ventricular filling due to an inadequately short diastolic period, which may alter the ventricular filling directly and/or by changes of diastolic ventricular function due to inadequate oxygen supply by reduced myocardial blood flow. Both mechanisms result in an elevation of venous pressure, with a subsequently increased rate of transcapillary fluid filtration into the interstitial space, and significant reduction of lymphatic flow, inadequate for drainage of the increasingly produced interstitial fluid back into the vascular space.[51] Data from studies in animals and humans suggest that, in less advanced stages of disease, the elevation of the venous pressure results in a substantially increased transcapillary fluid filtration rate. Furthermore, the impaired lymphatic drainage is the most important pathomechanism in sustained tachyarrhythmia, while hypoxia-induced increase of capillary permeability to water as well as proteins, and alterations of hepatic protein synthesis, are not relevant for the development of hydrops.[51] Therefore, it seems to be advisable to treat fetuses with tachyarrhythmia *in utero*, because the congestive heart failure and the elevation of venous pressure are reversible after drug-induced cardioversion, while tissue hypoxia damaging capillary membranes and/or liver cells seems not to be present in these fetuses. Also, the tachycardia-induced "cardiomyopathy" with diastolic and systolic dysfunction will improve and disappear before birth, if constant sinus rhythm can be established. Thus, adequate prolongation of pregnancy can be achieved.

## Fetal surveillance and assessment of cardiac function in fetal tachyarrhythmia

The assessment of fetal cardiac function and also fetal surveillance appears to be very difficult in fetuses with tachyarrhythmia. The value of fetal heart rate monitoring is limited during tachyarrhythmia, whereas sonography, echocardiography, and Doppler sonography, as noninvasive and repeatable methods, are the most important tools for the diagnosis and surveillance of these fetuses:

1. Detailed sonographic and echocardiographic examination should exclude cardiac and noncardiac malformation, in particular, Ebstein anomaly and cardiac tumors.
2. The amount of amniotic fluid, placental structure and thickness, and, in hydropic fetuses, distribution and extent of fluid accumulation should be assessed.
3. Echocardiography and Doppler sonography of the venous system may indicate or exclude cardiac failure, which may be the primary or the secondary cause in the advanced stage of diseases other than anemia. Cardiac dilatation as well as measurement of the cardiothoracic ratio and search for AV valve incompetence may help to assess the degree of tachycardia-induced cardiomyopathy. Evaluation for the detection of cardiomegaly as a noninvasive assessment of cardiac function in nonimmune hydrops is validated by the measurement of umbilical venous pressure.[62]
4. The value of fetal venous Doppler velocimetry is limited by the fact that, above a critical frequency of fetal tachycardia, which is approximately 210–220 beats/minute for the human fetus, pulsatile venous blood flow with diastolic reversal appears to be independent of the cardiac function and the degree of tachycardia-induced "cardiomyopathy."[58] In other words, reversal of the venous a-wave in the ductus venosus and the occurrence of a pulsatile flow pattern in the umbilical vein correspond to a distinct venous pressure increase, which might be sufficient to cause interstitial water accumulation and hydrops, even if the myocardial function is preserved. Therefore, in fetuses with fetal tachyarrhythmia, increased pulsation in the venous blood flow pattern is not a prognostic marker, and in particular, not an ominous sign. Recurrence of the normal biphasic forward blood flow pattern in the precordial veins seems to indicate a significant drop in the fetal venous pressure. After cardioversion to sinus rhythm, however, measurement of the venous Doppler indices is the best method to evaluate cardiac function.[59,60]
5. Fetal heart rate monitoring should repeatedly be performed for longer periods, for detection of paroxysmal tachyarrhythmia and/or for monitoring the effects of the antiarrhythmic treatment.
6. In addition, sonographic demonstration of fetal breathing and body and extremities movements indicates fetal well-being, whereas fetal heart rate monitoring and Doppler velocimetry in umbilical and fetal arteries are not useful

for fetal surveillance during tachyarrhythmia. However, Doppler velocimetry in the uterine arteries may exclude an associated uteroplacental dysfunction.

# Treatment of fetal tachyarrhythmia

## *Rationale for fetal antiarrhythmic treatment*

*In utero* treatment of fetal tachyarrhythmia has to consider both the fetal and the maternal condition. Therefore, the decision for *in utero* antiarrhythmic treatment should only be made after a detailed risk-benefit analysis and should depend on the presence or absence of hydrops, duration of tachycardic periods, gestational age of the fetus, and type of tachyarrhythmia, and also on the maternal condition and willingness. Detailed counseling of the parents should always be performed. On the one hand, the high mortality and morbidity of preterm newborns with hydrops due to tachyarrhythmia have to be considered; on the other hand, there are favorable results for *in utero* antiarrhythmic treatment. Hence, the rationale for treatment of fetal tachyarrhythmia in hydropic fetuses is to establish a constant sinus rhythm, allowing the fetus to resolve the hydrops and the cardiac dysfunction, and to prolong the pregnancy to birth near term.

A special risk of antiarrhythmic medications administered for the suppression of cardiac rhythm disturbances is the provocation of new, or the exacerbation of existing, arrhythmias. This proarrhythmic effect may affect the mother and the fetus, and may occur as an early proarrhythmic complication after initiation of therapy, varying from nonserious through potentially fatal arrhythmias or manifesting late as enhanced arrhythmic death.[20,27,34,63] Late proarrhythmia may occur during the administration of all antiarrhythmic drugs except for β-blocking agents.[27] Severe sinus and atrioventricular node dysfunction may be initiated by digitalis glycosides and Vaughan Williams class I–IV antiarrhythmic drugs (Table 41.2), atrial tachycardia with variable atrioventricular block and with junctional tachycardia may result from digoxin toxicity, torsades de pointes polymorphic ventricular tachycardia from type Ia and III antiarrhythmic agents prolonging the QT interval, and ventricular tachycardia from Ic agents. Congestive heart failure, hypokalemia, hypocalcemia, and hypomagnesemia may predispose to proarrhythmias.[27] Furthermore, inherited and acquired anomalies and gestational age-specific features of myocardial structure and function, anomalies of ion channels, and anomalies of enzymes of the cytochrome P450 pathway may be the underlying anomalies of proarrhythmic complications, especially in interaction with other antiarrhythmic and non-antiarrhythmic drugs.[27,67] Whereas maternal health and risks can be sufficiently checked by detailed examinations, fetal disposition to proarrhythmia may be only insufficiently assessed. In particular, fetuses with advanced tachycardia-induced cardiomyopathy may be at risk for the negative-inotropic and other unforeseen effects related to antiarrhythmic therapy. Sudden fetal death shortly after the initiation of an antiarrhythmic therapy was reported for flecainide as well as sotalol,[40,68,69] but almost all of these fetuses were hydropic; therefore, it is still unclear whether the fetal death was the consequence of a proarrhythmic drug effect, of a negative-inotropic drug effect, or of end-stage cardiac disease in the reported cases.

Fetal therapy can be best monitored by ultrasound and echocardiographic techniques, demonstrating the extent and distribution of fluid accumulations, the cardiac rhythm, the cardiac size and contractility, and the occurrence of AV valve regurgitation. Sonographic examination of fetal breathing and body and extremity movements provides an assessment of fetal condition. Fetal electrocardiography and magnetocardiography are not useful, because reliable technology to provide high-fidelity recordings of fetal electrocardiograms is lagging behind, and the availability is limited, respectively.

In nonhydropic fetuses with sustained or intermittent tachycardia, observation without antiarrhythmic treatment may be a safe management option close to term, because hydrops will rarely develop, presumably owing to the better intrinsic properties of the fetal heart late in gestation. A trial of transplacental treatment with digoxin, if successful, will facilitate vaginal delivery by allowing the interpretation of fetal heart tracing. If unsuccessful, however, delivery and direct neonatal therapy of SVT appears preferable to intrauterine therapy. Elective cesarean section is the most often recommended mode of delivery in fetuses with SVT. The trial of vaginal delivery, however, appears to be justified in selected cases, because the risk of intrapartum hypoxemia does not seem to be increased in nonhydropic fetuses with SVT in particular, and with arrhythmia in general. After the antenatal assessment of normal uteroplacental function by sonography, biophysical profile, and Doppler sonography, vaginal delivery may be performed. Sometimes increased vagal tone during labor may interrupt the SVT; in other cases, alternative techniques of intrapartum surveillance may be utilized, such as repetitive fetal scalp blood sampling for monitoring the acid-base status alone or in combination with continuous $PO_2$ monitoring.[70,71]

In fetuses with paroxysmal intermittent SVT with short periods of tachycardia, which can be confirmed by heart rate monitoring for 12–24 hours, treatment can be deferred, as was recently shown in fetuses with intermittent SVT.[72] However, close observation is necessary for the early detection of conversion to sustained tachycardia and the occurrence of congestive heart failure and hydrops.[72] If there are long tachycardic episodes, then it would be reasonable to start antiarrhythmic treatment in nonhydropic fetuses, in particular, during the second and early third trimesters. The conversion to sustained tachycardia may take place and/or hydrops may develop in intermittent tachycardia,[66,68,73] decreasing therapeutic options by impairing transplacental passage of drugs in the presence of hydrops.

Elective delivery before 34 weeks of gestation of hydropic fetuses with sustained and intermittent tachyarrhythmia generally results in a mixture of many complications and problems

in the management of premature hydropic fetuses. These are postpartum increase of cardiac work, need for own regulation of body temperature by the neonate, mechanical ventilation, repetitive pleural drainage, congestive heart failure, simultaneous occurrence of pulmonary edema and hyaline membrane disease, reducing the effectiveness of surfactant therapy, severe degree of tachycardia-induced "cardiomyopathy" with impaired diastolic and systolic cardiac function, refractory neonatal tachyarrhythmia, and side-effects of antiarrhythmic and other cardiovascular drugs on the preterm newborn. In consequence, the outcome of this approach is poor, even if the problems and side-effects of transplacental treatment are avoided. Thus, *in utero* antiarrhythmic treatment for adequate control of the arrhythmia and remission of hydrops is prudent in sustained fetal tachyarrhythmia with hydrops, because data from animal and human studies indicate that hydrops results from elevated venous pressure and consecutive obstruction of lymphatic drainage, but not from hypoxic damage to capillaries or other tissues. Therefore, in hydropic fetuses with tachyarrhythmia, intrauterine treatment with digoxin alone or in combination with different antiarrhythmic drugs (flecainide, sotalol, or amiodarone) is the best approach for almost all fetuses. Transplacental treatment is successful in the majority of cases,[2,20, 66,68,74–79] whereas additional direct antiarrhythmic treatment is limited to rare, severely hydropic fetuses with tachyarrhythmia refractory to transplacental treatment. In third-trimester fetuses with atrial flutter refractory to transplacental treatment, delivery may be a good alternative because direct current cardioversion is postnatally highly successful to convert atrial flutter into permanent sinus rhythm.

## Maternal surveillance during fetal antiarrhythmic treatment

Because of its potentially hazardous and life-threatening complications, each antiarrhythmic treatment should be started in an inpatient setting. Before initiation of any antiarrhythmic therapy, an accurate medical examination of the pregnant woman and a 12-lead electrocardiogram must be performed to exclude hidden maternal diseases such as Wolff–Parkinson–White syndrome, prolonged QT interval, myocarditis, or other contraindications for antiarrhythmic treatment in general or for some drugs only. Maternal serum sodium, potassium, chloride, calcium, and magnesium levels should be evaluated as well as those of blood urea nitrogen, creatinine, and albumin. Thyroid function should also be checked, especially if treatment with amiodarone is considered.

Daily maternal electrocardiographic monitoring with special attention to PR, QT, and QRS prolongation and careful recording of signs and symptoms of possible maternal side-effects are the most important parameters of the therapy, whereas the measurement of drug serum concentrations is mainly helpful to document an underdosage. Dangerous complications to the mother and the fetus may further be reduced by lowering the drug dosage at the start of therapy, by incrementally increasing the dosage, and by avoiding hazardous drug combinations, especially during the phase of the change to second- or third-line therapy. High dosages and maternal serum levels of the antiarrhythmic agent as well as allowance of sufficient time to reach adequate drug levels even in the fetal compartments are necessary for successful cardioversion of fetal tachyarrhythmia to a constant sinus rhythm, and, in consequence, may indirectly reduce the risks by avoidance of the application of more dangerous second- or third-line agents.

## Fetal antiarrhythmic treatment protocols

The pharmacology, pharmacokinetics, and bioavailability of antiarrhythmic drugs may be substantially affected by physiological changes during pregnancy, such as increased extra- and intravascular fluid volume, increased glomerular filtration, delayed gastric emptying and intestinal transit, progesterone-induced enhancement of hepatic enzymatic activity, and relative decrease in plasma proteins. Furthermore, many aspects of transplacental transfer and fetal pharmacology of antiarrhythmic drug treatment related to gestational age are still unknown. Additionally, placental transfer of the drugs may vary, influenced by gestational age-dependent changes in the placenta, disorders in development of the villous placenta, mainly disorders of the fetal circulation associated with elevated venous pressure, and placental edema following tachyarrhythmia. Therefore, concentrations of the antiarrhythmic drug measured in the maternal blood may strongly differ from those in the fetal blood. The physiological and pathophysiological changes at muscular and cellular levels in the fetal heart during pregnancy are also significant. Owing to all these reasons, animal models and models of an artificial placenta can illuminate only some of the important aspects of transplacental therapy of fetal tachyarrhythmias. The same applies to data gained from single cases in human fetuses of the transplacental transfer of antiarrhythmic drugs.

*In vitro* examinations of the human placenta showed a dose-related relaxation of arteries and veins with nearly all antiarrhythmic drugs.[80] Only adenosine led to a constriction of these vessels.[80] With a model of a placental lobule perfused from the fetal as well as from the maternal side, it was shown that digoxin reached the fetal compartment very well, flecainide transferred well, and amiodarone transferred only insufficiently.[81,82] At a low perfusion rate, the transplacental transfer of digoxin decreased.[81] An increase of venous pressure with subsequent development of placental edema, a smaller villous surface capillary density, and a widened maternal-fetal diffusion in the early weeks of pregnancy probably decreases the transfer of these drugs *in vivo* to fetuses with tachyarrhythmias during the second and third trimesters.

Choice of appropriate drug and route of administration to achieve a rapid therapeutic level in the fetal compartment, and early detection of maternal and fetal complications, determine successful intrauterine antiarrhythmic treatment of the fetus.

Digoxin was generally used as an agent of first choice for the intrauterine therapy of fetal tachyarrhythmias, especially

**Table 41.2** Antiarrhythmic therapy in fetuses with tachyarrhythmia—Data for the common antiarrhythmic agents

| *Drug* | *Class* | *Indication* | *Metabolism* | *Feto-maternal ratio* | *Dosage* | *Side effects and precautions* | |
|---|---|---|---|---|---|---|---|
| | | | | | | *Maternal* | *Fetal* |
| Digoxin | Cardiac glycoside | SVT, AF | Renal excretion; t1/2: 34–36 hours; therapeutic serum levels: 2.0–2.5 ng/mL | 0.8–1.0; substantially reduced in hydropic fetuses | Loading dose over 2–3 days: IV: 0.3–0.5 mg q8h Maintenance dose: PO: 0.15–0.2 mg q8h; dose adjustment in renal failure | Narrow therapeutic range: nausea, vomiting, anorexia, diarrhea, fatigue, colored vision, confusion, insomnia, sinus bradycardia, ES, AV block, VT; increased toxicity in hypokalemia, hypomagnesemia, hypercalcemia; contraindication: WPW syndrome, VT, AV block II°–III° | Low fetal serum levels in hydropic fetuses; contradicted in WPW syndrome which is not detectable in the fetus; until now there is no report of glycoside-induced VT in the fetus |
| Flecainide | Ic (sodium-channel blockade delaying conduction with normal repolarization) | SVT, AF, VT | Hepatic excretion: 60%; renal excretion: 40%; t1/2: 12–18 hours (therapeutic plasma level: 0.4–1.0 μg/mL) | 0.7–0.8 | PO: 100 mg q(6–)8h | Proarrhythmia, vertigo, nausea, disturbed vision, headache, paresthesia | Negative inotropic effect, proarrhythmia |
| Sotalol | III (+II) (increase of repolarization by potassium-channel blockade and β-adrenoreceptor blockade) | AF, SVT, VT | Renal excretion; t1/2: 15–17 hours; (serum level: 1.5–2.5 μg/mL) | 0.7–0.9 | PO: 80–160 mg q12h; increase to 160 mg q8h; dose adjustment in renal failure | Proarrhythmia: VT; bradycardia; AV block, nausea | Negative inotropic effect, proarrhythmia |

| | | | | | | | |
|---|---|---|---|---|---|---|---|
| Amiodarone | III (increase of repolarization by potassium-channel blockade) | SVT, AF, VT | Hepatic metabolism to active desethylamiodarone; renal excretion of metabolites; t1/2: 14–100 days; (therapeutic plasma level: 1–2 μg/mL amiodarone; desethylamiodarone 1.5–2-fold higher) | 0.1–0.3; substantially reduced in hydropic fetuses | Loading dose over 5–7 days: IV: 1200 mg over 24 hour permanent infusion; or PO: 200 mg q 4–5 hours; maintenance dose: PO: 200 mg q6–8h; direct: 2.5–5 mg/kg estimated fetal body weight (deduction of hydrops) infusion into the umbilical vein over 10 min q6–8h | Proarrhythmia: VT; malfunction of thyroid, corneal microdeposits, photosensitivity, hepatic malfunction; (under sustained treatment: lung fibrosis, neuropathy, myopathy); (anticonception at least until 12 months after treatment) | Malfunction of thyroid: transient hypothyroidism (control of fetal thyroid hormones); corneal microdeposits; mild negative inotropic effect (proarrhythmia) |
| Propranolol | II (β-adrenoreceptor blockade) | SVT, VT | Fast hepatic inactivation ("first pass effect"); t1/2: 3–5 hours (therapeutic plasma level: 50–1000 ng/mL) | 0.1–0.3 | PO: 40–80 mg q8–12h | Bronchospasm (contraindication: asthmatic women with increased bronchic reaction); bradycardia; AV blockade; increased hypoglycemia in diabetic women; cold hands and extremities (contraindication: Raynaud phenomenon) | Negative inotropic effect; bradycardia; AV blockade; newborn: hypoglycemia, bradycardia, and respiratory depression; low birth weight |

*Source:* This table is modified from corresponding tables and data, respectively, in the following publications: Kleinman CS and Copel JA. *Ultrasound Obstet Gynecol* 1991;1:286–97[20]; Kleinman CS et al. In: Creasy RK, Resnik R, eds. *Maternal-Fetal Medicine*, 4th ed. Philadelphia, PA: Saunders; 1999:301–18[34]; Kleinman CS et al. In: Harrison MR et al. eds. *The Unborn Patient: The Art and Science of Fetal Therapy*, 3rd ed. Philadelphia, PA: Saunders; 2001:417–41[27]; Gembruch U and Somville T. *Gynäkologe* 1995;28:329–45[64]; Ito S et al. *Clin Perinatol* 1994;21:543–72[65]; Simpson J. In: Allan L et al. eds. *Textbook of Fetal Cardiology*. London: Greenwich Medical Media; 2000:423–51[66]; Fouron JC. *Prenat Diagn* 2004;24:1068–80[24].

*Note:* Only maternal plasma levels of digoxin are relevant for dose adjustment during fetal treatment. Overdosage can be recognized by serial maternal electrocardiogram controls, PR (digoxin), QRS (flecainide), and QT (class III agents) interval, and typical clinical signs of intoxication.

*Abbreviations:* AF, atrial flutter; AV, atrioventricular; ES, extrasystole; IV, intravenous; PO, oral; SVT, supraventricular tachycardia; VT, ventricular tachyarrhythmia, WPW, Wolff–Parkinson–White.

if a short VA tachycardia suggesting atrioventricular reentry tachycardia is diagnosed. Meanwhile, flecainide is successfully used as first-line drug for transplacental treatment in fetuses with atrioventricular reentry tachycardia. Serum levels in the fetus range from 70% to 100% of the maternal serum level, with normal transplacental passage in the absence of hydrops. In hydropic fetuses, however, the placental passage of digoxin is distinctly impaired, and adequate concentrations of digoxin in the fetal compartments cannot be obtained by transplacental treatment via the mother.[74,83–88] Owing to the increase of glomerular filtration rate toward term, the elimination half-life of digoxin substantially decreases in the second and third trimesters of gestation, resulting in a higher dosage of digoxin for adequate loading and maintenance therapy.[89] For the treatment of fetal tachyarrhythmia, high maternal digoxin levels between 2 and 2.5 ng/mL should be achieved. The measurement of digoxin levels should be performed at least 6–8 hours after the last dose of digoxin, using assays that do not include endogenous digoxin-like immunoreactive substances found in maternal, fetal, and neonatal blood and that are altered by digoxin therapy.[90,91] The addition of amiodarone, flecainide, verapamil, and quinidine results in increased digoxin levels and should be accompanied by a decrease in the maintenance dosage of digoxin. Rapid intravenous loading within 48–72 hours for initiation of therapy followed by oral maintenance is generally preferred, especially in hydropic fetuses.[74] In nonhydropic fetuses, however, the more convenient loading of the mother by oral administration, which is only completed after 6–7 days, can be used, especially if the admission of the pregnant woman to hospital should be avoided.[66] In a case of maternal renal failure, dosage reduction is mandatory, according to the maternal creatinine clearance.

For second- and third-line therapy and for first-line therapy in already hydropic fetuses, other medications, including flecainide, sotalol, and amiodarone, provide an alternative transplacental therapy alone or in combination with digoxin (Table 41.3). Other antiarrhythmic agents, however, such as procainamide, quinidine, disopyramide, propafenone, propranolol, and verapamil, are generally no longer used for *in utero* antiarrhythmic therapy, because of insufficient therapeutic effects and/or substantial side-effects in the fetus and/or the mother.[20,27,28,66]

Flecainide, a class Ic antiarrhythmic agent, strongly blocks the fast sodium channel, which slows the conduction velocity in most cardiac pathways and has no influence on repolarization. Its therapeutic range lies between 200 and 1000 ng/mL of serum levels. Flecainide has an excellent bioavailability of 95% with oral therapy and a good placental passage; 80% of the maternal plasma levels are achieved also in hydropic fetuses.[93] Before final cardioversion, there occurs a gradual slowing of the frequency of the supraventricular reentry in many cases. The time interval from initiation of the flecainide therapy to fetal cardioversion into sinus rhythm may range from 1 to 14 days, mostly occurring on days 2–4.[91,94–97] It is shorter in nonhydropic than in hydropic fetuses and shorter using a high-dose regimen (>300 g/d).[94–96] No fetal mortality even with high doses and high maternal flecainide concentrations was observed. Maternal flecainide concentrations, once therapeutic, do not predict cardioversion in fetuses with SVT.[95] In atrial flutter, however, flecainide may have a negative effect by increasing the ventricular response to atrial flutter and should be used cautiously and in combination with digoxin, because flecainide may increase the ventricular response to atrial flutter. Paradoxical proarrhythmic effects may occur in virtually all of the antiarrhythmic drugs, including provocation or exacerbation of arrhythmia after initiation of therapy;[40,68,69] late arrhythmia-related death could be more common in this class than in other types of antiarrhythmic drug. This was observed in adults treated with flecainide and encainide following myocardial infarction[98] and also in children treated with flecainide or encainide because of supraventricular and ventricular tachycardia, where the incidence of significantly proarrhythmic effects was 7.5%.[99]

Sotalol is a class III antiarrhythmic drug with an additional β-adrenergic receptor blocking effect. It substantially prolongs repolarization and the action potential and has only a mild negative inotropism. Its bioavailability and placental passage are so good that adequate fetal sotalol levels between 70% and 100% of the maternal levels may be achieved within 48–72 hours after the initiation of oral administration.[100] Because of its exclusively renal elimination—the half-life is around 16 hours—dosage reduction is mandatory if maternal renal function is decreased. The class III antiarrhythmic drugs sotalol and amiodarone are also associated with a proarrhythmic risk, especially for the development of torsade de pointes/ventricular fibrillation in the mother. To minimize this risk for the mother, long QT syndrome must be excluded before the initiation of therapy by maternal and family history of arrhythmic events and by electrocardiogram (ECG) and sometimes Holter monitoring; during treatment, the maternal ECG should regularly be evaluated for changes in QTc interval. Meanwhile, there is profound evidence that some drug-induced arrhythmias might also represent cases of "forme fruste" congenital long QT syndrome with a corresponding molecular basis. In these cases, not only cardiac drugs but also noncardiac drugs such as erythromycin, terfenadine, haloperidol, or cisapride, may cause excessive prolongation of the QTc interval and life-threatening arrhythmias.[27] In the future, individuals at risk for proarrhythmic effects may be identified by screening for mutations of candidate genes.[67] Proarrhythmic effects were also observed in children treated with sotalol.[101] Sotalol has proved to be safe and efficacious in the treatment of fetal supraventricular tachycardia refractory to digoxin alone.[102–104] A series of 21 fetuses treated with sotalol, however, showed a relatively high intrauterine mortality of 4 of the total of 21 fetuses and 4 of 10 hydropic fetuses. Three fetuses had supraventricular tachycardia, and one fetus had atrial flutter—with occurrence of fetal death within 1 week after the initiation of sotalol treatment.[40] It appears that the proarrhythmic impact of sotalol is more pronounced in the immature fetal and also the neonatal heart than it is in adult hearts.[40] On the other side, successful first- and second-line therapy of SVT and atrial flutter without any negative side-effect was meanwhile reported in

**Table 41.3** Therapeutic protocol for the antiarrhythmic therapy of fetal tachyarrhythmia currently used in our hospital based on data from the literature[a] and own experience[b]

| *Tachyarrhythmia* | *First choice* | *Second choice* | *Third choice* |
|---|---|---|---|
| PSVT (short term and without hydrops) | Control twice a week | | |
| PSVT (long term and/or with hydrops, especially below 30th week of gestation) | Flecainide | Digoxin + flecainide | Digoxin + amiodarone |
| SVT without hydrops | Flecainide | Digoxin + flecainide | Digoxin + amiodarone |
| SVT with hydrops, without AV valve regurgitation | Flecainide (+ digoxin) | Amiodarone | In addition: amiodarone directly in the umbilical vein |
| SVT with hydrops and severe AV valve regurgitation | Amiodarone (if necessary, directly in addition) | In addition: amiodarone directly in the umbilical vein | |
| Long VT tachycardia without hydrops | Amiodarone or sotalol | Control twice a week | |
| Long VT tachycardia with hydrops | Amiodarone or sotalol | Sotalol or amiodarone, respectively | |
| AF without hydrops | Digoxin | Control twice a week; digoxin + sotalol | |
| AF with hydrops | Digoxin | Digoxin + sotalol; alternatively: digoxin + flecainide | Digoxin + amiodarone (directly and transplacentally) |
| VT without hydrops | Control twice a week | | |
| VT with hydrops | Magnesium IV | Flecainide or propranolol, respectively | Amiodarone (+ digoxin) |

*Notes:*

1. If the frequency of tachycardia can be reduced under flecainide and other antiarrhythmic therapy below 210 beats/minute, and pulsatile monophasic blood flow in the precordial veins is replaced by normal biphasic antegrade blood flow pattern, we can expect a significant reduction of fetal venous pressure, and medication should be continued even if complete cardioversion is not obtained.
2. After the 34th week of gestation, fetuses with supraventricular tachycardia may be delivered, in particular, if hydrops progresses despite antiarrhythmic therapy.
3. After the 34th week of gestation, fetuses with atrial flutter may be delivered, because postnatally electrical cardioversion is available and results in a permanent sinus rhythm in the most neonates.

*Abbreviations:* IV, intravenously; PSVT, paroxysmal supraventricular tachycardia.

[a] From references 2, 19, 20, 27, 40, 65, 67, 68, 93, 94, 96, 101–103, 114, 115.

[b] From references 2, 63, 91, 95.

several studies,[94,102–104] querying stronger negative effects of sotalol compared to other antiarrhythmic drugs. However, sotalol treatment should be restricted to third-line therapy in hydropic fetuses with supraventricular tachycardia refractory to digoxin alone and digoxin and flecainide in combination.[40] In supraventricular tachycardia with long VA time interval (long VA tachycardia) suggestive for permanent junctional reciprocating tachycardia, or atrial ectopic tachycardia, and in atrial flutter with hydrops, the class III agents sotalol and amiodarone are indicated for fetal transplacental therapy.[22–24] Low initiation dosages of sotalol and stepwise dosage increases may decrease the risk of proarrhythmia.[40,100]

Amiodarone, as a class III antiarrhythmic drug, substantially prolongs repolarization and the action potential. In contrast to the other antiarrhythmic drugs, it is characterized by a very long elimination half-life of 1–3 months and has an active hepatic metabolite, desethylamio-darone. With only maternal treatment, it has a low fetal bioavailability but offers the advantage of only minimal negative inotropism. An oral or intravenous loading of the mother with 1200 mg/day for 4–6 days is followed by a maintenance dosage of oral 600–900 mg/day. Although the transplacental transfer is poor, with fetomaternal ratios for amiodarone between 10% and 40%, and seems further impaired in hydropic fetuses, there is a constant increase of fetal serum levels of amiodarone and desethylamiodarone, presumably due to the very long elimination half-life in the fetal compartments. Regarding the duration of treatment, application of amiodarone for fetal tachyarrhythmia during pregnancy is a short-term therapy, since in the majority of infants the tachyarrhythmia can be treated effectively with other drugs after birth. Because of the finite period of administration, the most serious side-effects of long-term amiodarone therapy such as interstitial pneumonia, pulmonary fibrosis,

neuropathy, and myopathy, are unlikely to occur in this context. In contrast, some cases of fetal and neonatal iodine-induced transient hypothyroidism have been reported after maternal and/or fetal direct therapy,[74,86,87,105–109] because 200 mg amiodarone contains 75 mg iodine, even if neonatal hypothyroidism appears to be lacking in the majority of cases with maternal amiodarone therapy during pregnancy. The frequency of transient neonatal hypothyroidism in cases of long-term maternal administration of amiodarone during pregnancy is around 20%, with favorable evolution after a few months.[108,109] Therefore, before and during therapy, monitoring should be carried out of the maternal thyroid gland and thyroid hormones, as well as the neonate directly after birth and during the first weeks of life.[74,86,105] Exclusion of fetal hypothyroidism by cordocentesis and subsequent fetal thyroxin therapy may be an additional option.[74,86] Negative effects of fetal hypothyroidism during the second half of gestation on the later neurophysiological development are in discussion, even when hormone substitution is started immediately after birth.[110,111] Postnatal long-term follow-up examination of the psychomotor development of only a few children exposed transplacentally to amiodarone during their fetal life showed favorable global intelligence quotient (IQ) scores and well-developed social competence, but mild deficits in some nonverbal skills such as reading comprehension, written language, and arithmetic.[112] Nevertheless, this important question has to be validated by larger follow-up studies. Only because of the possible negative effect of amiodarone-induced transient hypothyroidism on fetal and neonatal neurodevelopment did treatment with this highly effective antiarrhythmic drug turn into second- and third-line therapy for selected severely hydropic and otherwise drug-refractory fetuses.[74,85,86,113–116] Particularly if the situation forces direct fetal treatment, amiodarone seems to be the ideal drug, owing to its extremely long elimination half-life and the minimal inotropism as outlined in the following text; the use of amiodarone is justified in advanced stages of this life-threatening disease.[55,74,85,86,113,114]

Adenosine, an endogenous purine nucleoside, has an almost immediate but short-lasting effect mediated by A1-purine receptors. Intravenous application of 100–200 μg adenosine/kg estimated fetal weight (without hydrops) into the umbilical vein resulted in cardioversion within 15–30 seconds.[117] This was mediated by a slowing of conduction time through the atrioventricular node, and may have been accompanied by a direct action on sinus pacemaker cells. The induced atrioventricular block immediately breaks the atrioventricular and atrioventricular nodal reentry tachycardias, but rarely atrial ectopic tachycardia and flutter.[20] Because the anatomical prerequisites for reentry tachycardia, the accessory atrioventricular conduction pathway and the triggering supraventricular extrasystoles, are not influenced, adenosine has no prophylactic effect, and recurrence of reentry tachycardia is generally observed in the fetus unless effective concentrations of another antiarrhythmic drug can prevent this. Therefore, the extremely short duration of action and the absent prophylactic effect limit the use of adenosine as a therapeutic agent in fetal tachycardia, yet it may have a role to aid differential diagnosis.[20] Persistent tachycardia after an adenosine bolus injection strongly suggests an atrial rather than atrioventricular reentry tachycardia, thus allowing some modification of the therapeutic approach.

In severely hydropic fetuses with supraventricular tachycardia refractory to transplacental therapy, the direct application of antiarrhythmic drugs to the fetus as an ultimate method may be successful.[74,85–87,113,114] Especially in the group of hydropic fetuses with substantial grade of AV valvular insufficiency during tachycardia, a most advanced stage of "cardiomyopathy" may be suggested, and rapid cardioversion should be achieved. This may be possible only by direct fetal drug administration in addition to maternal administration.

Injections of digoxin,[74,87,118,119] amiodarone,[56,74,85,86,113,114,120,121] verapamil,[68,74,87] propafenone,[74,85] and adenosine[117] have been reported to be performed into the umbilical vein,[56,66,68,74,85–87,113,114,117,121] the fetal muscle,[88,118,119] the fetal peritoneum,[74,85,86,113,120,121] the amnion,[56,121] and the fetal heart,[68] or by a combination of different routes.[56,66,68,74,85,86,113,121] Meanwhile, intravascular application into the umbilical vein seems to be the best way, allowing direct injection into the intravascular compartment of the fetus for the most rapid loading, and in addition, the monitoring of fetal therapy, measuring concentrations of the antiarrhythmic agents in the fetal blood.[74,85,86,113] Alternatively, in the presence of fetal ascites, intraperitoneal administration of amiodarone is easier than the injection into the umbilical vein; the intraperitoneal route seems to assure delivery of the drug to the severely hydropic fetus, too, and enables increase of the bolus dose compared to the intravenous administration to be delivered for sustained absorption.[87,120,121] Amiodarone appears to be the ideal drug for direct therapy of the hydropic fetus because of its extremely long-lasting elimination half-life of 1–3 months,[74,85,86,113,114,120,121] which differs from all other antiarrhythmic drugs with half-lives between 2 and 18 hours. In these rare cases with severe hydrops, high concentrations of amiodarone in the fetal compartments may rapidly be achieved by repeated injections of amiodarone into the umbilical vein, even if placental passage of the drugs is markedly impaired or absent. In order to avoid the dangerous bolus injection of amiodarone, which may cause severe bradycardia and cardiac arrest, repetitive doses of 2.5–5 mg amiodarone/kg estimated fetal weight (without hydrops) over 10 minutes should be administered several times a day.[56,74,86] Concurrently, the mother should receive oral digoxin and amiodarone according to the dosage outlined previously, to prevent the drug crossing the placenta from the fetus to the mother and to allow transplacental transfer of drug from the mother to the fetus when fetal circulatory recompensation and remission of hydrops are accompanied by a substantial improvement in the placental passage of amiodarone and digoxin.[74,85,86]

Permanent junctional reciprocating tachycardia is often resistant to antiarrhythmic therapy. But because of its relatively low tachycardic frequency between 180 and 220 beats/minute, hydrops rarely occurs in these fetuses. Class III antiarrhythmic drugs such as sotalol and amiodarone,[24] but also flecainide, may be the first choice for *in utero* treatment.[1]

In fetuses with persistent ventricular tachycardia, amiodarone was successfully administered transplacentally.[35] However, first-line transplacental treatment with maternal intravenous magnesium therapy may be indicated because of the proarrhythmic side effects of other antiarrhythmic drugs in cases of long QT syndrome.[122] Alternatively, propranolol or flecainide may be administered in fetal ventricular tachycardia, because underlying long QT syndrome cannot be excluded prenatally, and the sodium channel blocker flecainide effectively decreases the QTc interval in some sodium channel mutations, causing long QT syndrome.[123] In contrast, class III antiarrhythmic agents such as sotalol and amiodarone may induce serious proarrhythmic side effects and death in fetuses with long QT syndrome. Moreover, the proarrhythmic impact of sotalol appears to be more pronounced in the immature fetal and neonatal heart than it is in the adult heart.[66]

## *Effectiveness of fetal antiarrhythmic therapy*

The success of fetal antiarrhythmic treatment has been reviewed in detail by Simpson.[66] In addition, Krapp and colleagues performed a meta-analysis comparing SVT with atrial flutter.[2] At present, no consensus on first-line treatment of SVT exists (Table 41.3); a large randomized multicenter study has been started to find the answer (ClinicalTrials.gov identifier NCT02624765). Between 50% and 75% of nonhydropic fetuses with supraventricular tachycardia will convert to sinus rhythm with transplacental digoxin monotherapy, confirmed by a published series.[69] Flecainide as a second-line agent may be successful in almost all remaining cases.[2,68,72,92,94–97] Alternatively, sotalol and amiodarone are also mostly successful as second-line drugs.[94,115,116] In hydropic fetuses, however, transplacental digoxin monotherapy is rarely effective—in only about 10%–15%.[2,68,69,92,94] Therefore, antiarrhythmic therapy in hydropic fetuses should start directly with flecainide, using sotalol or amiodarone as second-line therapy. These drugs can be combined with digoxin using the positive-inotropic effect of this drug. In rare cases of severely advanced cardiomyopathy, direct fetal therapy with amiodarone may be indicated. With this regime, successful cardioversion to constant sinus rhythm may be obtained in up to 80% of hydropic fetuses.[2] Thus, the arrhythmia-related mortality rate in nonhydropic fetuses with supraventricular tachycardia is nearly zero, whereas approximately 10%–20% of hydropic fetuses have a fatal outcome.[2,66,68,69] In their meta-analysis, Krapp and coworkers found no difference in the success rates of digoxin in SVT and in atrial flutter.[2]

Meanwhile, more centers use flecainide alone or in combination with digoxin as a first-line therapy in fetuses with SVT without hydrops, too, and achieve high cardioversion rates greater than 90%. In both nonhydropic and hydropic fetuses with SVT, time to cardioversion into sinus rhythm is shorter (median time around 3 days, range 1–16 days),[94–97] and the reduction of SVT rate before cardioversion, which acutely improves fetal hemodynamics, is higher with flecainide than with digoxin or sotalol.[92,94–97] A high-dose regimen with daily doses of 400 mg flecainide may achieve sinus rhythm more rapidly.[95,96] Measurement of the ratio between VA and atrioventricular time interval appears to differentiate SVT with short VA time interval, typical of atrioventricular reentrant tachycardia through accessory atrioventricular connection, from SVT with long VA time interval, typical of permanent junctional reciprocating and atrial ectopic tachycardia. The latter are usually incessant and unresponsive to most antiarrhythmic drugs, and may recur postpartum. In these rare types of tachycardia, class III agents are potential drugs of first choice.[22,24,97]

The therapeutic protocol in fetuses with atrial flutter is similar to the treatment of supraventricular tachycardia. In nonhydropic fetuses with paroxysmal atrial flutter, careful monitoring may be justified. In sustained atrial flutter and in paroxysmal atrial flutter with hydrops, however, intravenous loading with digoxin within 48–72 hours is followed by an oral maintenance dosage. Fetal atrial flutter may be suppressed successfully by digoxin alone in only 30%–50%,[2,94] but this therapy may be useful because of its positive inotropic and negative chronotropic properties.[13] Meanwhile, retrospective observational studies in fetuses with atrial flutter without and with hydrops showed that sotalol monotherapy achieves sinus rhythm in up to 80% and superior cardioversion rates after treatment with digoxin or flecainide in combination with digoxin.[94,102,103] However, in the absence of rhythm control and 1:1 atrioventricular conduction, hydrops does not often occur in fetuses with atrial flutter,[2,30] presumably because the lower ventricular rate in fetuses with atrial flutter with 2:1 and/or higher-degree AV block may prevent hydrops;[2] furthermore, atrial flutter seems to start mostly after 30 weeks of gestation, that is, 2.1 weeks later than SVT[2] when the intrinsic properties of the fetal myocardium are more mature. One might speculate that the fetal atrium reaches a critical size at about 27–30 weeks' gestation, allowing atrial macro-reentry, favored as the most likely mechanism of atrial flutter.[30] Therefore, a second-line therapy is uncommonly indicated in fetuses with atrial flutter and should be restricted to those fetuses that develop hydrops. In these cases, the preferred drug is sotalol; amiodarone may be used as second-line therapy,[30,124] because in adults and newborns, class III agents appear to be more effective than class Ic agents in cases of atrial flutter.[40,124]

# Postnatal follow-up in fetuses with tachyarrhythmias

In fetuses with SVT that were treated *in utero*, the postnatal outcome may be complicated by a recurrence of tachyarrhythmia in approximately 50% of the neonates.[74,78] Therefore, prophylactic continuation of antiarrhythmic treatment during the first 6–12 months of life is recommended to prevent recurrent attacks for all newborns or at least for all the newborns with postnatal recurrence of tachyarrhythmia.[66] By maturation of the infant's conduction tissue, annulus fibrosus, and

myocardium, the probability of late recurrence decreases. Only in 10%–20% of infants may the tachycardia persist beyond the first year of life.[28,74] Whereas in atrioventricular reentry tachycardia via an accessory pathway spontaneous resolution of tachycardia occurs in the vast majority of cases, the recurrence rate appears to be higher in other types of tachycardia.[25] Atrial flutter can be relatively easily controlled after birth by direct current cardioversion, by transvenous atrial overdrive pacing, and/or by digoxin alone or in combination with other antiarrhythmic drugs such as sotalol, amiodarone, or flecainide.[30,124] Also, spontaneous termination of atrial flutter may occur directly after birth. When a sinus rhythm has been established, a relapse of atrial flutter is so rare[13] that a prophylactic arrhythmic treatment beyond the neonatal period is not justified.[30,124]

Fetal with atrial ectopic tachycardia and junctional reciprocal tachycardia often persist after birth, and long-term antiarrhythmic treatment may be necessary. The class III antiarrhythmic agents sotalol and amiodarone, but also flecainide, are preferred under these conditions.

In neonates with persistent ventricular tachycardia, even in association with long QT syndrome, the class Ic anti-arrhythmic agents flecainide and propafenone may be administered. Also, propranolol may be given. Amiodarone and sotalol may be useful in therapy-refractory ventricular tachycardias. Some neonates with long QT syndrome, however, require a temporary pacemaker in the neonatal period or a permanent pacemaker, shortening the QT interval and thereby reducing the risk of potentially lethal ventricular tachycardias.[18,37,41] The administration of β-blockers, in addition, may reduce the sympathetic drive to the heart of infants with long QT syndrome.[37,41]

The postnatal long-term outcomes of tachyarrhythmic fetuses have not been prospectively examined. For the vast majority, normal long-term development can be expected after *in utero* and/or postnatal cessation of tachyarrhythmia. Only a few cases with abnormal neurological outcome have been reported in the literature. Schade et al. reviewed six cases from the literature and reported three additional observations.[125] All nine fetuses developed hydrops and were born in a hydropic condition in spite of successful drug-induced cardioversion to sinus rhythm. In some cases, the postnatal course was complicated by severe prematurity, perinatal asphyxia, and/or postnatal recurrence of tachyarrhythmia. Periventricular leukomalacia and hemorrhage diagnosed in some of these cases *in utero* or within a few hours after birth indicated that the occurrence was due to an intrauterine hypoxic-ischemic event. In a retrospective follow-up study of 49 children with fetal tachyarrhythmias, the overall outcome was generally good. At the age of 5 years, only increased motor activity and language development delay were described in a few children.[126] In another study assessing neurologic, mental, and psychomotor development of 27 children with fetal tachyarrhythmias, a normal long-term neurodevelopment was observed.[127] Oudijk et al. retrospectively studied the neurological function of 11 infants, aged 6 months to 12 years, who were prenatally treated for fetal tachyarrhythmia complicated by hydrops.[128] They found that the majority of fetuses tolerate fetal tachyarrhythmia even if hydrops results.[128] Also in this collective, abnormal neurological outcome was associated with prematurity and birth of a hydropic newborn. However, it may be speculated that in fetuses with paroxysmal tachyarrhythmia, abolition of cerebral autoregulation may lead to severe impairment of the maintenance of constant cerebral perfusion.[125,128] Therefore, sudden changes in fetal heart rate may cause significant fluctuations of fetal arterial blood pressure and, consequently, of cerebral perfusion leading to hypoxic-ischemic brain damage,[125] especially in fetuses before 32 weeks' gestation, where the autoregulatory range of systemic blood flow pressures is narrow, and the periventricular vessels are highly vulnerable. Therefore, rapid and persistent control of fetal tachyarrhythmia may prevent fetal neurological damage. This is an additional rationale for intrauterine antiarrhythmic treatment of fetal tachyarrhythmia even if it occurs only intermittently, especially in immature and/or already hydropic fetuses.

## References


1. Kothari DS, Skinner JR. *Arch Dis Child Fetal Neonatal Ed* 2006;91:136–44.
2. Krapp M et al. *Heart* 2003;89:913–17.
3. van Selm M et al. *Obstet Gynecol Surv* 1991;46:285–8.
4. Carbillon L et al. *Obstet Gynecol Surv* 1992;552:310–4.
5. Gherman RB et al. *J Matern Fetal Invest* 1998;7:227–9.
6. Duthie SJ, Walkingshaw SA. *Br J Obstet Gynaecol* 1995;102:1011–3.
7. Midgley DY, Harding K. *Eur J Obstet Gynecol Reprod Biol* 2000;88:201–2.
8. Goeden A, Worthington D. *Obstet Gynecol* 2005;106:1183–6.
9. Rein AJJT et al. *Circulation* 2002;106:1822–33.
10. Thomas G. *Cardiovasc Ultrasound* 2004;2:12.
11. Stinstra J et al. *BJOG* 2002;109:1235–43.
12. Kähler C et al. *Prenat Diagn* 2001;21:176–82.
13. Hosono T et al. *Prenat Diagn* 2002;22:198–200.
14. Schneider U et al. *Prenat Diagn* 2005;25:704–8.
15. Wakai RT et al. *Circulation* 2003;107:307–12.
16. Zhao H et al. *Am J Cardiol* 2006;98:491–6.
17. Cuneo BF et al. *Circulation* 2013;128:2183–91.
18. Cuneo BF et al. *J Electrocardiol* 2016;49:807–13.
19. Wacker-Gussmann A et al. *Am J Perinatol* 2014;31:617–28.
20. Kleinman CS, Copel JA. *Ultrasound Obstet Gynecol* 1991;1:286–97.
21. Wren C. *Heart* 1998;79:536–7.
22. Jaeggi E et al. *Heart* 1998;79:582–7.
23. Fouron JC et al. *Heart* 2003;89:1211–6.
24. Fouron JC. *Prenat Diagn* 2004;24:1068–80.
25. Ko JK et al. *Am J Cardiol* 1992;69:1028–32.
26. Weindling SN et al. *Am Heart J* 1996;131:66–72.
27. Kleinman CS et al. The fetus with cardiac arrhythmia. In: Harrison MR, Evans MI, Adzick NS, Holzgreve W, eds. *The Unborn Patient: The Art and Science of Fetal Therapy*, 3rd ed. Philadelphia, PA: Saunders; 2001:417–41.
28. Naheed ZJ et al. *J Am Coll Cardiol* 1996;27:1736–40.
29. James TN. *Am J Cardiol* 1970;25:213–26.

30. Jaeggi E et al. *J Pediatr* 1998;132:335–9.
31. Wacker-Gussmann A et al. *J Am Heart Assoc* 2016;5(6). doi: 10.1161/JAHA.116.003673.
32. Dubin AM et al. *Heart Rhythm* 2005;2:313–5.
33. Bae EJ et al. *PACE* 2005;28:254–7.
34. Kleinman CS et al. Fetal cardiac arrythmias: Diagnosis and therapy. In: Creasy RK, Resnik R, eds. *Maternal-Fetal Medicine*, 4th ed. Philadelphia, PA: Saunders; 1999:301–18.
35. Schleich JM et al. *Prenat Diagn* 2000;20:449–52.
36. Gembruch U et al. *Eur J Obstet Gynecol Reprod Biol* 1989;31: 9–22.
37. Hofbeck M et al. *Heart* 1997;77:198–204.
38. Lin MT et al. *Am J Perinatol* 1998;15:145–7.
39. Yamada M et al. *Cardiol Young* 1998;8:119–22.
40. Oudijk MA et al. *Circulation* 2000;101: 2721–6.
41. Manning N et al. *Br J Obstet Gynaecol* 2000;107:1049–51.
42. Mitchell JL et al. *Circulation* 2012;126:2688–95.
43. Cuneo BF et al. *Circ Arrhythm Electrophysiol* 2013;6:946–51.
44. Crotti L et al. *JAMA* 2013;309:1473–82.
45. Lehnart SE et al. *Circulation* 2007;116:2325–45.
46. Fouron JC et al. *Ultrasound Obstet Gynecol* 2017;50(5):624–31.
47. Buis-Liem TN et al. *Prenat Diagn* 1987;7:425–31.
48. Stevens DC et al. *Am J Obstet Gynecol* 1982;142:316–22.
49. Nimrod C et al. *Am J Obstet Gynecol* 1987;157:655–9.
50. Gest AL et al. *Am J Physiol* 1990;258:H1159–63.
51. Gest AL et al. *Biol Neonate* 1993;64:325–30.
52. Gest AL et al. *Pediatr Res* 1990;28:223–6.
53. Spinale FG et al. *Circulation* 1992;85:717–29.
54. Spinale FG et al. *Am J Physiol* 1995;268:H836–7.
55. Packer DL et al. *Am J Cardiol* 1986;57:563–70.
56. Gembruch U et al. *Am Heart J* 1993;125:1290–301.
57. Tomita M et al. *Circulation* 1991;83:635–44.
58. Gembruch U et al. *Ultrasound Obstet Gynecol* 1995;5:394–9.
59. Krapp M et al. *Ultrasound Obstet Gynecol* 1992;10:32–40.
60. Gembruch U et al. *Eur J Obstet Gynecol Reprod Biol* 1999;84: 182–92.
61. Petrikovsky B et al. *Fetal Diagn Ther* 1996;11:292–5.
62. Johnson P et al. *Am J Obstet Gynecol* 1992;162:1309–13.
63. Morganroth J. *Cardiol Clin* 1992;10:392–401.
64. Gembruch U, Somville T. *Gynäkologe* 1995;28:329–45.
65. Ito S et al. *Clin Perinatol* 1994;21:543–72.
66. Simpson J. Fetal arrhythmia. In: Allan L, Hornberger L, Sharland G, eds. *Textbook of Fetal Cardiology*. London: Greenwich Medical Media; 2000:423–51.
67. Napolitano C et al. *J Cardiovasc Electrophysiol* 2000;11:691–6.
68. Simpson JM, Sharland GK. *Heart* 1998;29:526–81.
69. Jouannic JM et al. *J Gynecol Obstet Biol Reprod (Paris)* 2003; 32:338–44.
70. Van den Berg P et al. *J Perinat Med* 1989;17:371–4.
71. Afriat R et al. *Acta Obstet Gynecol Scand* 1999;78:827–8.
72. Simpson LL et al. *J Ultrasound Med* 1997;16:459–64.
73. Simpson JM et al. *Pediatr Cardiol* 1992;18:28–83.
74. Hansmann M et al. *Ultrasound Obstet Gynecol* 1991;1:162–70.
75. Kleinman CS et al. *J Clin Ultrasound* 1985;13:265–73.
76. Stewart PA, Wladimiroff JW. *Fetal Ther* 1987;2:7–16.
77. Maxwell DJ et al. *Br Med J* 1988;297:107–10.
78. Van Engelen AD et al. *J Am Coll Cardiol* 1994;24:1371–5.
79. Frohn-Mulder IM et al. *Prenat Diagn* 1995;15:1297–302.
80. Omar HA et al. *J Cardiovasc Electrophysiol* 1996;7:1197–203.
81. Schmolling J et al. *Ther Drug Monit* 1997;19:11–16.
82. Schmolling J et al. *Perinat Med* 1998;10:6–11.
83. Mimura S et al. *Clin Cardiol* 1987;10:63–5.
84. Younis JS, Granat M. *Am J Obstet Gynecol* 1987;157:1268–9.
85. Gembruch U et al. *Am Heart J* 1989;118:1335–8.
86. Gembruch U et al. *Fetal Ther* 1988;3:210–15.
87. Gembruch U et al. *J Perinat Med* 1988;16:39–44.
88. Hallak M et al. *Obstet Gynecol* 1991;28:523–5.
89. Azancot-Benisty A et al. *J Pediatr* 1992;121:608–13.
90. Weiner CP et al. *Am J Obstet Gynecol* 1987;157:368–71.
91. Schlebusch H et al. *Eur J Clin Chem Clin Biochem* 1991;29:57–66.
92. Krapp M et al. *Ultrasound Obstet Gynecol* 2002;19:158–64.
93. Allan LD et al. *Br Heart J* 1991;65:46–8.
94. Jaeggi ET et al. *Circulation* 2011;124:1747–54.
95. Vigneswaran TV et al. *Heart Rhythm* 2014;11:2047–53.
96. Strizek B et al. *Heart Rhythm* 2016;13:1283–8.
97. Sridharan S et al. *Heart Rhythm* 2016;13:1913–9.
98. Echt DS et al. *N Engl J Med* 1991;324:781–8.
99. Fish FA et al. *J Am Coll Cardiol* 1991;18:356–65.
100. Oudijk MA et al. *J Am Coll Cardiol* 2003;42:765–70.
101. Pfammatter JP, Paul T. *Pediatr Cardiol* 1997;18:28–34.
102. Shah A et al. *Am J Cardiol* 2012;109:1614–8.
103. van der Heijden LB et al. *Ultrasound Obstet Gynecol* 2013;42: 285–93.
104. Ekman-Joelsson BM et al. *Acta Paediatr* 2015;104:1090–7.
105. Plomp TA et al. *Eur J Obstet Gynecol Reprod Biol* 1992;43:201–7.
106. Foster CJ, Love HG. *Int J Cardiol* 1988;20:307–16.
107. Grosso S et al. *J Endocrinol Invest* 1998;21:699–702.
108. Laurent M et al. *Am J Cardiol* 1987;60:942.
109. Matsumara LK et al. *Thyroid* 1992;2:279–81.
110. Rovet JF et al. *J Pediatr Psychol* 1992;117:187–213.
111. Haddow JE et al. *N Engl J Med* 1999;341:549–55.
112. Magee LA et al. *Neurotoxicol Teratol* 1999;21:261–5.
113. Flack NJ et al. *Obstet Gynecol* 1993;82:714–16.
114. Mangione R et al. *Eur J Obstet Gynecol Reprod Biol* 1999;86: 105–7.
115. Jouannic JM et al. *Prenat Diagn* 2003;23:152–6.
116. Strasburger JF et al. *Circulation* 2004;109:375–9.
117. Kohl T et al. *Obstet Gynecol* 1995;85:873–4.
118. Weiner CP, Thompson MB. *Am J Obstet Gynecol* 1988;150: 670–3.
119. Parilla BV et al. *Am J Perinatol* 1996;13:483–6.
120. Kang SL et al. *Cardiol Young* 2015;25:447–53.
121. Lin PH et al. *Taiwan J Obstet Gynecol* 2016;55:434–6.
122. Simpson JM et al. *Ultrasound Obstet Gynecol* 2009;34:475–80.
123. Abriel H et al. *Circulation* 2000;102:921–5.
124. Lisowski LA et al. *J Am Coll Cardiol* 2000;35:771–7.
125. Schade RP et al. *Ultrasound Obstet Gynecol* 1999;13:43–7.
126. Krapp M et al. *Ultraschall Med* 2011;32:E175–81.
127. Lopriore E et al. *Am J Obstet Gynecol* 2009;201:46e1–5.
128. Oudijk MA et al. *Ultrasound Obstet Gynecol* 2004;24:154–4.

# 42

# Cardiac diseases in association with hydrops fetalis

Ulrich Gembruch and Wolfgang Holzgreve

## Definition

The Greek-Latin term *hydrops fetalis* is issued for pathologically increased fluid accumulations in fetal soft tissues and serous cavities.[1] *Immune hydrops fetalis* refers to those cases of hydrops that are caused by alloimmune hemolytic anemia in the presence of circulating maternal antibodies against fetal erythrocytes.[2] If there is no evidence of blood group incompatibility (isoimmunization), the hydrops is characterized as being *nonimmune hydrops fetalis*. The prenatal diagnosis of hydrops fetalis is achieved by ultrasound, which demonstrates the skin edema and/or fluid accumulations in serous cavities of the fetus (abdominal ascites, pleural and/or pericardial effusion). Fetal hydrops is defined by the demonstration of fluid accumulations in at least two of these four fluid compartments.[3] But the placenta and the amniotic sac have sometimes been included as additional "fetal compartments." Placentomegaly indicating hydrops placentae can be diagnosed if the placental thickness, from chorionic plate to base, increases by 4 cm or more in the second trimester and by 6 cm or more in the third trimester. Although polyhydramnios defined by an amniotic fluid index above 24 cm is associated in 30%–75% of cases with nonimmune hydrops,[4,5] the amniotic sac should not be considered as one of the compartments for the diagnosis of hydrops, because the pathophysiological mechanisms of the occurrence of polyhydramnios can differ from those leading to an increased rate of interstitial fluid accumulation causing hydrops fetalis and placentae. Furthermore, hydrops may even be associated with oligohydramnios, for example, in some preterminal fetuses with Turner syndrome or in cases with intrauterine cytomegaloviral infection. Some series of nonimmune hydrops also include cases of isolated pleural effusion, abdominal ascites, or generalized skin edema, because fluid accumulation in one site may represent an early stage of a disease that may lead to fluid accumulation in several sites at a more advanced stage, especially in diseases known to result in generalized hydrops fetalis.

Nonimmune hydrops can occur in association with an extremely wide variety of conditions. The list of disorders comprises far more than 150 fetal conditions, but for many of these the association is based on only one or a few case reports,[1,3–12] and the causal relationship to the occurrence of hydrops is sometimes only speculative. The causes and associations of nonimmune hydrops can be differentiated into those that are either more generalized, such as in hematological, infectious, or metabolic disorders, and chromosomal and nonchromosomal syndromes, or more focal, such as in cranial, cardiac, vascular, pulmonary, gastrointestinal, and renal disorders, or tumors.[1,3–14]

The incidence of nonimmune hydrops varies between 1:1,500 and 1:3,000 deliveries.[15–17] Because of the high intrauterine loss rate among hydropic fetuses, the true occurrence rate is most likely to be higher; in some instances, however, fetal hydrops can also regress during gestation. Especially in chromosomally abnormal fetuses, there is a high spontaneous abortion rate between the first and second or third trimesters of pregnancy,[18] following an early appearance of hydrops in the late first and early second trimesters, whereas in chromosomally normal fetuses the hydrops often develops much later.[5,19–21] The large variability in incidence and distribution of causative and associated diseases in the reported series of nonimmune hydrops is strongly influenced by factors such as the presence of a general ultrasound screening program, the gestational age windows of the screening examinations, and the specific referral patterns in any region. The ethnic background of the population also has an effect; for example, homozygous $\alpha$-thalassemia is the most common cause of nonimmune hydrops in Southeast Asians, as opposed to cardiac diseases in Caucasians. The same influences are relevant for the reported survival rates, which vary between 10% and 60% in the literature.[1,3–10,19,22,23]

Although hydrops fetalis in its various manifestations is easily detected by ultrasound (screening), the enormous spectrum of etiologies and associations requires highly specialized knowledge in order to apply the noninvasive and invasive diagnostic and sometimes therapeutic steps in a systematic and effective way. Owing to the time pressure that is often present with progressing severity of hydrops, nonimmune hydrops is a situation in prenatal medicine where good cooperation between screening investigators and specialized centers not only allows a realistic assessment of the prognosis and subsequent proper counseling about recurrence risks, but also can often mean the difference between life and death for an affected child *in utero*. In this context, one of the most important diagnostic steps is a detailed and extensive anatomical and functional assessment of the cardiovascular system, because some of the underlying conditions are primary cardiac diseases, and others may secondarily result in compromised fetal cardiac function, congestive heart failure, and hydrops (Table 42.1).

**Table 42.1** Cardiac and extracardiac diseases causing congestive heart failure and hydrops

*Cardiac abnormalities*

- Structural defects
  - Atrioventricular septal defect in combination with heterotaxia syndrome (situs ambiguus, atrial isomerism) and bradyarrhythmia
  - Tricuspid dysplasia and Ebstein anomaly
  - Severe obstruction of the right ventricular outflow tract by pulmonary stenosis, pulmonary atresia, and premature obstruction of the ductus arteriosus (by indomethacin or spontaneously)
  - Absent pulmonary valve syndrome (mostly combined with tetralogy of Fallot and/or agenesis of the ductus arteriosus)
  - Truncus arteriosus communis with insufficiency of the truncal valve
  - Severe obstruction of the left ventricular outflow tract by aortic stenosis and atresia leading to interatrial left-to-right shunt, high-restriction or premature closure of the foramen ovale
  - Premature closure of the foramen ovale
  - Aortico–left ventricular tunnel
  - Atrioventricular septal defect, isolated or in association with Down syndrome
- Cardiac tumors
  - Rhabdomyoma, often as part of tuberous sclerosis
  - Hemangioma
  - Hamartoma
  - Pericardial teratoma
- Cardiomyopathy
  - Isolated noncompaction of the ventricular myocardium
  - Hypertrophic
  - Dilated (cardiac glycogenoses)
  - Barth syndrome (3-methylglutaconic aciduria type II)
  - Restrictive
- Myocarditis
  - Parvovirus B19
  - Adenovirus
  - Coxsackievirus
  - Chagas disease
- Myocardial infarction
- Coronary fistula
- Arrhythmias
  - Tachyarrhythmias
    - Supraventricular tachycardia
    - Atrial flutter
    - Ventricular tachycardia
    - Ventricular tachycardia as manifestation of prolonged QT syndrome
    - Accelerated idioventricular rhythm
  - Bradyarrhythmias
    - Sinus bradycardia
    - Complete heart block combined with atrial isomerism and structural defect (as listed previously) in the presence of maternal autoimmune antibodies (anti-SSA, anti-SSB)
- Idiopathic arterial calcification

(*Continued*)

**Table 42.1 (Continued)** Cardiac and extracardiac diseases causing congestive heart failure and hydrops

*Extracardiac diseases possibly causing congestive heart failure and hydrops*

- Tumors and vascular disorders
  - Teratoma (sacrococcygeal, mediastinal, intracerebral, pericardial)
  - Mediastinal fibrosarcoma
  - Neuroblastoma
  - Arteriovenous malformation of different localization
    - Vein of Galen aneurysm
    - Hamartoma and hemangioma (liver, neck, chest)
    - Diffuse neonatal hemangiomatosis
    - Pulmonary arteriovenous malformation
    - Coronary fistula
    - Angio-osteohypertrophy syndrome (Klippel-Trenaunay-Weber syndrome)
    - Chorioangioma
    - Chorioangioma as part of Wiedemann-Beckwith syndrome
    - Diffuse placental chorioangiomatosis
- Hematological disorders causing fetal anemia
- Excessive erythrocyte loss
  - Intrinsic hemolysis or abnormal hemoglobins
    - $\alpha$-Thalassemia
    - Erythrocyte enzyme disorders: glucose-6-phosphate dehydrogenase deficiency, pyruvate kinase deficiency, glucose phosphate isomerase deficiency, congenital erythropoietic porphyria
    - Erythrocyte membrane disorders: abnormalities of spectrin
  - Extrinsic hemolysis
    - Kasabach-Merritt sequence (arteriovenous malformations and tumors)
  - Hemorrhage
    - Fetomaternal hemorrhage
    - Fetal closed-space hemorrhage (bowel, intracranial, tumor)
- Erythrocyte underproduction
  - Liver and bone marrow replacement syndromes
    - Transient myeloproliferative disorder (e.g., in fetuses with trisomy 21)
    - Congenital leukemia
  - Red cell aplasia and dyserythropoiesis
    - Parvovirus B19 infection
    - Blackfan-Diamond syndrome
    - Dyserythropoietic anemia
- Metabolic disorders
  - Lysosomal storage diseases
    - Mucopolysaccharidoses
    - Oligosaccharidoses
    - Lysosomal transport defects
    - Sphingolipidoses
    - Mucolipidoses
  - Cardiac glycogen storage disease

(*Continued*)

**Table 42.1 (Continued)** Cardiac and extracardiac diseases causing congestive heart failure and hydrops

- Carnitine deficiency
- Congenital disorders of glycosylation (CDG)
- Hereditary hemochromatosis
- Congenital myotonic dystrophy
- Pleural effusion
- Chest masses
  - Congenital pulmonary airway malformation (CCAML, macrocystic or microcystic)
  - Bronchopulmonary sequestration
  - Mediastinal teratoma
  - Congenital high airway obstruction sequence (CHAOS)
- Gestational alloimmune liver disease (GALD) causing neonatal hemochromatosis
- Fetal renal insufficiency (renal agenesis, polycystic kidney disease)
- Cardiovascular disorders in twin pregnancies
  - Twin-to-twin transfusion syndrome
  - Twin reversed arterial perfusion (TRAP) sequence with a parasitic acardiac twin
  - Conjoined twins

*Source:* Modified from Holzgreve W. In: Harrison MR et al. eds. *The Unborn Patient. Prenatal Diagnosis and Treatment*, 2nd ed. Philadelphia, PA: WB Saunders; 1990:228–45;[1] Society for Maternal-Fetal Medicine (SMFM); Norton ME et al. *Am J Obstet Gynecol* 2015;212:127–39;[3] Holzgreve W et al. *Am J Obstet Gynecol* 1984;148:805–12;[6] Holzgreve W et al. *Semin Perinatol* 1985;9:52–67;[7] Machin GA. *Am J Med Genet* 1989;34:366–90;[10] Jones DC. *Semin Perinatol* 1995;19:447–61;[11] Tercanli S et al. In: Callen PW, ed. *Ultrasonography in Obstetrics and Gynecology*, 4th ed. Philadelphia, PA: WB Saunders; 2000:551–75;[12] Knilans TK. *Semin Perinatol* 1995;19:483–92;[24] Arcasoy MO, Gallagher PG. *Semin Perinatol* 1995;19:502–15;[25] Gembruch U, Holzgreve W. In: Harrison MR et al. eds. *The Unborn Patient: The Art and Science of Fetal Therapy*, 3rd ed. Philadelphia, PA: WB Saunders; 2001:525–82.[26]

# Pathophysiology of hydrops fetalis

There is a constant exchange of extracellular fluids between the intravascular and interstitial compartments. The interstitial space can be subdivided into transcellular and lymphatic fluid components. Under normal conditions, the differences of the hydrostatic and colloid oncotic pressure in the intracapillary and interstitial fluid cause a fluid shift into the interstitial compartment on the arteriolar side of the capillary bed and a flux back into the intravascular compartment on the venule end. The regulation of fluid movement across the capillary membrane is expressed by the Starling equation[27,28]:

$$J_v = \mathrm{CFC}[(P_c - P_i) - \sigma(\pi_c - \pi_i)]$$

The total flow of fluid ($J_v$) across the capillary membrane is influenced by the intracapillary hydrostatic pressure ($P_c$) and the colloid oncotic pressure of the interstitial fluid ($\pi_i$), which are the two driving forces for capillary ultrafiltration into the interstitial fluid. The interstitial hydrostatic pressure (tissue turgor tension) ($P_i$) and the plasma colloid osmotic pressure ($\pi_c$) are the opposite Starling forces. The fluid filtration coefficient (CFC) represents the net amount of fluid crossing the capillary membrane for a given imbalance of the Starling forces, and it is affected by both the conductance of the capillary wall and the ease of fluid movement in the interstitial space. Changes of the permeability of a particular capillary bed change the reflection coefficient for oncotically active solute ($\sigma$), and, therefore, the influence of a given colloid osmotic pressure differs between both compartments. Thus, an increased capillary permeability allows water and protein to leak more easily into the interstitial space of the fetus and/or placenta. Abundant fluid in the interstitial compartment is returned to the vascular space via the lymphatic system. The capacity of lymphatic drainage of the interstitial space is determined by the outflow pressure for the lymphatic flow, which is the central venous pressure.[27–29]

Fetal interstitial fluid accumulation and hydrops generally originate from an imbalance between the higher rate of interstitial fluid formation by capillary ultrafiltration and the lower rate of interstitial fluid return through the venule side of the capillary bed and the lymphatic system back to the circulation. The six classically postulated mechanisms are as follows: (1) primary myocardial failure with decreased cardiac output; (2) high cardiac output failure; (3) decreased colloid oncotic plasma pressure; (4) increased capillary permeability especially secondary to tissue hypoxia or sepsis; (5) obstruction of venous flow; and (6) obstruction of lymphatic flow.[10,27,30]

Data on fluid distribution and regulation of the intercompartmental flow are almost exclusively based on studies in the sheep, and they allow only a cautious extrapolation to the human fetus. Gestational age-dependent maturation of the vascular bed and the mechanisms of its neuronal and humoral government regulating the body fluid distribution by changes of the Starling forces and the lymphatic drainage are relatively unclear in the human fetus. Considering that roughly 30% of the fetal plasma

volume is outside the fetal body, the interstitial space of the fetus seems to be substantially larger in comparison to the postpartum situation, with an elevated ratio of about 4.4:1 compared to 3:1 for the adult sheep. According to fetal lamb studies, several factors facilitate transcapillary fluid filtration into the interstitial space during fetal compared to adult life.[27,28] First, the permeability of the capillary membrane for plasma proteins is 15 times higher than in adult sheep.[31] This decreases the reflection coefficient for the colloids, impairing the effect of the colloid oncotic pressure difference between fetal vascular and interstitial space and, therefore, the driving force of fluid flux back into the vascular space. This lower effect of the colloid oncotic pressure difference on the transcapillary fluid flux in the fetus seems to provide a relative protection for the fetus against the negative effect of hypoproteinemia.[32] Second, the fluid filtration coefficient (CFC) of the capillary bed is roughly fivefold higher in fetal than in adult sheep, facilitating and increasing the fluid flow for any given imbalance in the Starling forces.[33] Third, the compliance of the interstitial space of the fetus is higher than in the adult sheep. Therefore, a greater accumulation of interstitial fluid is necessary in the fetus to increase the interstitial hydrostatic pressure. Expressed in another way, smaller changes in the hydrostatic pressure difference between capillary and interstitial space ($\Delta P = P_c - P_i$) lead to a larger fluid flow across the capillary membrane.[33] The increase of both the fluid filtration coefficient and the compliance of the interstitial space facilitates the transcapillary fluid flow and allows the fetus a more rapid restoration of blood volume after acute blood volume loss and expansion caused by acute hemorrhage and infusion, respectively.[27,29] Changes of the transplacental fluid transfer seem to be without relevance in this context.

The lymphatic system allows the return of fluid and the oncotic active proteins to the vascular space. Studies in sheep have elucidated the importance of this system for the fluid balance between the intravascular and interstitial compartments.[29] Basal lymph flow rates in the fetus are substantially higher than postpartum, reflecting the enhanced transcapillary flow into the interstitial space.[29,34] Very important for the pathogenesis of hydrops is the observation that the lymphatic drainage of the interstitial space is not impeded at a normal outflow pressure for the lymphatic system, which represents the central venous pressure.[29,34,35] The lymphatic flow rate in the thoracic duct of fetal sheep is four- to fivefold higher than in adult sheep.[29,34] If the venous pressure increases over the physiological value of 3–4 mm Hg, the lymphatic flow rate in the fetus is substantially reduced, and ceases at only 16 mm Hg.[29,34,35] In adult sheep, the flow is relatively constant up to 8 mm Hg and only stops at 26 mm Hg. This delicate relationship between venous pressure and lymphatic flow represents one important pathophysiological mechanism for the occurrence of fetal hydrops.[29,34,35]

Elevation of the systemic venous pressure due to circulatory dysfunction seems to be the most important pathogenic mechanism for the development of hydrops, even if increased capillary permeability, decreased plasma oncotic pressure, and obstruction of lymphatic fluid return may also contribute to the fluid accumulation in fetal soft tissue and serous cavities.[27] An increase of venous pressure may be considered as a consequence of homeostatic mechanisms serving to preserve adequate systemic delivery of metabolic substrate when cardiocirculatory function is impaired. Decreased intravascular volume may occur due to blood loss as a result of fetofetal or fetomaternal blood transfusion or of fetal hemorrhage. It may also be due to a relative deficiency of intravascular volume as a result of an increased fluid loss into the interstitial space by increased capillary permeability or decreased plasma oncotic pressure. Tissue hypoxia may cause capillary damage. Hepatocellular injury can lead to hypoproteinemia. Furthermore, local hypoxia may lead to tissue accumulation of lactate, a powerful osmotic agent. Diminished venous return may be caused by local obstruction of venous flow, but more often by a decreased ventricular compliance and by significant shortening of the diastolic period in tachyarrhythmia. Inadequate oxygen supply during the advanced stage of various alterations may decrease the ventricular compliance, possibly also in tachyarrhythmia. This may lead to inadequate myocardial blood flow, because of the substantially shortened duration of diastole. In consequence, diastolic cardiac dysfunction and decreased venous return may result in low cardiac output due to inadequate ventricular filling. Primary myocardial dysfunction may also impair stroke volume and cardiac output, for example in cases of myocarditis, myocardial infarction, or myocardial hypoxia. Furthermore, systolic cardiac dysfunction can occur when right and left ventricular afterload are increased; this is very poorly tolerated by the fetus. In this group, obstructive lesions of the semilunar valves, constriction of the ductus arteriosus, and arterial hypertension in the recipient fetus of a fetofetal transfusion syndrome and in cases with hypoxemia-induced arterial blood flow redistribution with peripheral vasoconstriction can be included. Because of the low heart rate, the cardiac output may be diminished in fetuses with complete heart block, even if the stroke volume is compensatorily increased. Furthermore, diminished supply of organs with oxygen and nutrients may be compensated for by an increase of cardiac output. The product of stroke volume and heart rate leads to high-output cardiac failure, for example, in cases of decreased hemoglobin saturation and/or hemoglobin concentration, in cases of maldistribution of flow, such as in association with tumors and arteriovenous malformations, or in cases of metabolic disorders such as thyrotoxicosis.[26,30]

In all of these pathological conditions, local and systemic compensatory mechanisms become effective and may help the fetus to survive. But at the same time, some of these mechanisms increase the imbalance of Starling forces, resulting in enhanced interstitial fluid accumulation. In advanced disease, an increase of hydrops and fetal deterioration may occur, when the compensatory mechanisms become exhausted, resulting in further elevation of venous pressure by secondary volume overload or myocardial dysfunction with occurrence of atrioventricular valve regurgitation.[26,30] Compensatory mechanisms are as follows[26,30]:

1. The opening of additional capillaries, which may increase the exchange area between the vascular and interstitial space, improving the extraction of oxygen and nutrients.

2. The redistribution of arterial and venous blood flow by selective vasoconstriction, maintaining the supply of heart, brain, and adrenal glands with oxygen and nutrients at the expense of other organs. This is triggered by chemoreceptors followed by neuronal and endocrine-mediated stimulation of vasoconstriction and by local autoregulation.
3. The increase of blood flow and better supply of oxygen and nutrients to organs, which may result from elevation of the cardiac output. This can be achieved by an increase of the heart rate and/or systolic ventricular function as well as by an increase of intravascular blood volume and/or venous pressure. An increase of intravascular volume may be achieved by fluid retention through the kidneys and/or by transcapillary resorption, especially in cases of lowered intravascular volume and venous pressure. Elevation of venous pressure by volume increase or increase of venous tone leads to an improved ventricular filling. However, because of the diminished preload reserve and Frank-Starling mechanism of the fetal heart, which seems to operate near the top of its ventricular function curve, it seems to be difficult for the fetus to convert any increase of myocardial filling into an appropriate augmentation of cardiac output, which limits this compensatory mechanism. Above this limit, atrial distension may lead to a release of atrial natriuretic factor, which provokes relaxation of vascular smooth muscles by inhibiting endothelin secretion and reducing sympathic tone followed by decrease of the pressure and increase of capillary permeability. In human fetuses, increased concentrations of atrial natriuretic factor were demonstrated by cordocentesis in conditions associated with atrial distension, for example, in anemic and acidemic fetuses, in fetuses with congestive heart failure, in the recipient fetus in twin-twin transfusion syndrome, and in fetuses after volume expansion by intrauterine blood transfusion.[36,37]

Regulation of fluid distribution in the fetus may also be modified by the placental circulation, receiving about 40% of the fetal combined cardiac output. Increased hydrostatic pressure or decreased plasma colloid oncotic pressure in the fetus enhance the transcapillary fluid filtration into the interstitial compartment of the fetus and the placenta; in the placenta, this would also drive fluid into the maternal vascular space, at least partially counteracting the fluid retention by the fetus. Studies in fetal sheep show that the fetal placental postcapillary resistance is quite large,[38] while the somatic postcapillary resistance is very low.[39] Therefore, placental capillary pressure may be protected from an elevation of the venous pressure by a small decrease in placental flow, whereas somatic capillary pressure tightly reflects the systemic venous pressure.[40] An elevation of venous pressure cannot result in an increased compensatory fetal fluid flux into the mother.

## Diagnostic approach in the hydropic fetus

Hydrops is an "emergency" condition in fetal life that requires fast diagnosis and therapy. Diagnostic methods and approaches are listed in Table 42.2. Noninvasive examination by maternal blood sampling includes the antibody screening test for exclusion of alloimmune hemolytic anemia, the Kleihauer-Betke stain for hemoglobin F (HbF) cells for diagnosis of fetomaternal hemorrhage, and a search for infectious diseases, such as parvovirus B19, cytomegalovirus, syphilis, toxoplasmosis, and adenovirus, coxsackievirus, and herpes simplex virus infections. If family history or actual findings indicate a special etiology, more sophisticated investigations may be necessary: hemoglobin electrophoresis, determination of enzyme activity, or exclusion of autoimmune antibodies (anti-SSA, anti-SSB).

Sonography, echocardiography, and Doppler sonography as noninvasive and repeatable methods are the most important tools for the diagnosis and surveillance of cases with nonimmune fetal hydrops. The distribution and extent of fluid accumulation, amount of amniotic fluid, and placental structure should be assessed. Sonographic detection of malformations and hygroma colli is suggestive of specific chromosomal and nonchromosomal disorders. Specific causes of hydrops may be detected in other pathological conditions, such as lung masses, tumors, heart defects, arteriovenous malformation, gastrointestinal and renal diseases, fetofetal transfusion, parasitic twins, and sustained arrhythmia. After exclusion of fetal arrhythmia and structural abnormalities, the most important diagnostic step is the measurement of the peak systolic velocity in the middle cerebral artery to assess for the presence of fetal anemia.[2,3] Echocardiography and Doppler sonography of arterial and venous vessels may demonstrate high cardiac output in cases of anemia and arteriovenous malformations. Echocardiography and Doppler sonography of the venous system may indicate or exclude cardiac failure, which may be the primary or the secondary cause in the advanced stage of diseases other than anemia. Cardiac dilatation, atrioventricular (AV) valve incompetence, and increased pulsatility of venous blood flow velocity waveforms are indicative of fetal congestive heart failure. Fetal heart rate monitoring should repeatedly be performed for longer periods during 24 hours to exclude paroxysmal tachyarrhythmia.

For adequate clinical management, rapid karyotyping is mandatory in most situations of hydrops fetalis independent of the underlying disease. Chromosomal microarray analysis is meanwhile mandatory in this setting. Additional techniques for DNA sequencing may also be indicated depending on the findings. The method of sampling depends on the gestational age and the necessity for other invasive procedures. The alternative methods are chorionic villus sampling or placentesis and fetal blood sampling. The last has the advantage of an additional exclusion of many other potential disorders, especially anemia and infection.

Therefore, fetal blood sampling is usually the preferred method for rapid karyotyping. Moreover, its additional advantages are exclusion and differentiation of anemia (reticulocyte count, detection of hemoglobinopathies, and signs of hemolytic anemia), thrombocytopenia, and leukemia, and detection of liver dysfunction and infectious diseases. In special cases, some biochemical tests and DNA analysis are also possible from fetal blood for various diseases such as infections, metabolic disorders, and congenital myotonic

**Table 42.2** Diagnostic approach in cases of nonimmune hydrops fetalis

*Maternal history*

- Ethnic background
- Diseases: anemia, infection, diabetes mellitus, connective tissue disease
- Consanguinity

*Family history*

- Obstetric history
- Previous affected sibling
- Spontaneous abortions/stillbirths

*Pregnancy history*

- Gravida/para
- Gestational age
- Multiple gestations
- Infectious diseases
- Medication

*Maternal studies*

- Blood group typing
- Indirect Coombs' testing
- Complete blood count with indexes such as mean corpuscular volume
- Peripheral blood smear for erythrocyte morphology
- Kleihauer-Betke stain
- Syphilis, parvovirus B19, cytomegalovirus, toxoplasmosis, and other infections
- Additional examinations (as indicated)
  - Hemoglobin electrophoresis
  - Maternal blood chemistry
  - G6PD, pyruvate kinase deficiency screening

*Fetal studies*

- Ultrasound
  - Two- and three-dimensional ultrasound
- Fetal echocardiography
  - Two-dimensional ultrasound (dimension, cardiac structures, rhythm)
  - Pulsed and color flow Doppler (intracardiac and postcardiac for detection of flow abnormalities such as valve regurgitation, stenosis, ductus arteriosus constriction, shunts, high cardiac output)
  - M-mode (dimension, rhythm, contractility)
  - Venous Doppler studies (cardiac function, rhythm)
  - Arterial Doppler (high cardiac output, arteriovenous malformations)
- Cardiotocography
  - Fetal condition
  - Paroxysmal tachyarrhythmia
  - Fetal anemia
- Amniocentesis[a]
  - Fetal karyotype and molecular cytogenetic analysis (array-CGH)
  - α-Fetoprotein
  - Antigen tests by PCR and amniotic fluid culture for syphilis, cytomegalovirus, toxoplasmosis, and other infections
  - Metabolic testing of amniotic fluid
  - Amniotic cell morphology and culture for metabolic disorders

(*Continued*)

**Table 42.2 (Continued)** Diagnostic approach in cases of nonimmune hydrops fetalis

- Fetal blood sampling[a]
  - Fetal karyotype and molecular cytogenetic analysis (array-CGH)
  - Fetal complete blood count with indexes
  - Peripheral blood smear
  - Reticulocyte count
  - White blood cell differentiation
  - Blood group typing
  - Direct Coombs' test
  - Fetal albumin
  - Fetal liver function tests
  - Fetal antigen-specific IgM, IgA, and PCR for infectious causes
- Additional examinations (as indicated)
  - Hemoglobin electrophoresis
  - Osmotic fragility
  - Heinz body preparation
  - Erythrocyte enzyme determination
  - Special testing of erythrocyte membrane skeleton proteins
  - Metabolic testing
- Chorionic villus sampling[a]
  - Fetal karyotype and molecular cytogenetic analysis (array-CGH)
- Additional examinations (as indicated)
  - Morphological examination for storage diseases
  - Metabolic testing

*Source:* Modified from Holzgreve W. In: Harrison MR et al. eds. *The Unborn Patient. Prenatal Diagnosis and Treatment*, 2nd ed. Philadelphia, PA: WB Saunders; 1990:228–45;[1] Society for Maternal-Fetal Medicine (SMFM); Norton ME et al. *Am J Obstet Gynecol* 2015;212:127–39;[3] Holzgreve W et al. *Semin Perinatol* 1985;9:52–67;[7] Machin GA. *Am J Med Genet* 1989;34:366–90;[10] Jones DC. *Semin Perinatol* 1995;19:447–61;[11] Tercanli S et al. In: Callen PW, ed. *Ultrasonography in Obstetrics and Gynecology*, 4th ed. Philadelphia, PA: WB Saunders; 2000:551–75;[12] Arcasoy MO, Gallagher PG. *Semin Perinatol* 1995;19:502–15;[25] Gembruch U, Holzgreve W. In: Harrison MR et al. eds. *The Unborn Patient: The Art and Science of Fetal Therapy*, 3rd ed. Philadelphia, PA: WB Saunders; 2001:525–82.[26]

[a] If there is an index case or specific symptoms, molecular genetic DNA-based analysis can be performed from chorionic villus sampling, fetal blood, and amniotic cells, e.g., for diagnosing storage diseases, some inborn hematological disorders, skeletal dysplasia, or congenital myotonic dystrophy, or whole exome or whole genome sequencing.

dystrophy. Measurement of umbilical venous pressure during fetal blood sampling may assess cardiac function and differentiate between cardiac and noncardiac causes of hydrops.[41,42] Nevertheless, noninvasive measurement of cardiac size and/or venous blood flow pattern shows a good correlation with cardiac function and systemic central venous pressure.[41,43–45]

The first diagnosis of hydrops fetalis is established sonographically. Many causes of hydrops, such as sustained arrhythmias, tumors of the fetus, lung masses, skeletal dysplasia, or twin-twin transfusion syndrome, can often be detected during this first scan.[3,11] Other findings such as cystic nuchal hygroma, indicating chromosomal disorders or rare syndromes, may lead to further diagnostic procedures such as rapid karyotyping. Furthermore, primary ultrasound has to define the exact distribution of the fluid accumulation, such as skin edema, ascites, uni- or bilateral pleural effusion, pericardial effusion, hydrops placentae, and amount of amniotic fluid. A semiquantification of these fluid accumulations is the basis for further monitoring and sometimes for prognostic assessment. Classification into mild, moderate, and severe is helpful and can additionally be specified by measurements such as the prehepatic ascites (diameter of fluid between abdominal wall and liver), the diameter between lung and lateral thoracic wall, the systolic and diastolic diameters of pericardial effusion, the parietal or frontal and abdominal skin thickness, the placental thickness, and the amniotic fluid index or maximal vertical amniotic fluid pocket. The presence and extent of mediastinal shifting and biventricular heart diameter should always be documented. The distribution of fluid accumulations may be helpful for diagnosis of the underlying cause. In hydropic fetuses with anemia, tachyarrhythmia, and complete heart block, signs such as ascites, skin edema, hydrops placentae, and polyhydramnios are usually present, but pleural effusion can be noted only in more advanced stages of the disease.[19,46–49] In other underlying diseases such as alteration of lymphatic

drainage and chromosomal anomalies, pleural effusion is predominant, and other fluid accumulations are less often seen.[19]

If the first sonographic examination does not reveal the etiology of hydrops, a high-level ultrasound examination should immediately be arranged, including fetal echocardiography and Doppler examination of the arterial and venous vessels. This leads to the detection of anomalies causing hydrops that are difficult to diagnose with the usual scan. Anomalies such as associated cardiac defects can be detected, which can again lead to the diagnosis of a chromosomal aberration or a rare syndrome. The peripheral arterial and venous Doppler examination may reveal a high cardiac output by demonstration of increased blood flow velocities and/or a cardiac dysfunction with increased pulsatility of the venous Doppler.

Hydrops without evidence for anemia or other causes can be due to a spontaneous remission of anemia subsequent to an infection with parvovirus B19 and more rarely to fetomaternal transfusion or to fetal bleeding. In these cases, mild cardiomegaly, polyhydramnios, thickened placenta, and an increased number of reticulocytes and normoblasts in fetal blood may be demonstrated. An examination should also be performed in amniotic fluid and fetal blood, including polymerase chain reaction (PCR), as well as assessment of specific immunoglobulin M (IgM). Paroxysmal supraventricular tachycardia should always be taken into consideration. Diagnosis of paroxysmal tachyarrhythmia is best established by repeated sonographic heart rate monitoring, or more easily by long-term cardiotocography several times per day. The diagnosis is confirmed by fetal echocardiography, which also allows identification of the specific type of arrhythmia. In these cases, cardiomegaly, polyhydramnios, and hydrops placentae may be present. In some cases, increased pulsatility of venous Doppler flow velocity waveforms during the periods of sinus rhythm can be seen, indicating tachycardia-induced "cardiomyopathy" due to repeated tachycardia.

The prognosis in cases of nonimmune hydrops mainly depends on the underlying disease. In some disorders, antenatal treatment may be emergently indicated and may be very successful such as in fetuses with tachyarrhythmia and anemia (Table 42.3). Further prognostic indicators are: distribution as well as extent of fluid accumulation and edema, degree of cardiac decompensation, and gestational age at the time of manifestation. Therefore, correct assignment of the precise diagnosis in each case of nonimmune hydrops is mandatory for adequate management of the pregnancy and counseling of the parents. It seems to be very difficult, however, to exclude all potential causes in the large group of heterogeneous disorders when investigating individual cases. Therefore, the following factors should be considered before the diagnostic technique is chosen:

1. Invasive versus noninvasive approach (noninvasive tests such as sonography and maternal blood sampling harbor no risks for the fetus and, therefore, should usually be applied first)
2. Incidence of the potential disorders at the specific gestational age
3. Necessity for prompt exclusion of fetal anemia causing nonimmune hydrops, which is life threatening and can usually be successfully treated if diagnosis is achieved in time

**Table 42.3** Antenatal treatment options for selected etiologies of nonimmune hydrops

| *Etiology* | *Therapeutic option* |
|---|---|
| Fetal anemia (e.g., parvovirus B19, fetomaternal hemorrhage) | Intrauterine transfusion |
| Tachyarrhythmia | Antiarrhythmic therapy (transplacentally, seldom directly) |
| Primary hydrothorax | Thoracoamniotic shunting |
| Bronchopulmonary sequestration with pleural effusion | Thoracoamniotic shunting or intrafetal vascular laser ablation |
| CPAM, macrocystic type | Thoracoamniotic shunting or needle drainage of cyst(s) |
| CPAM, microcystic | Maternal administration of placenta crossing fluorinated corticosteroids or open fetal surgery |
| Aortic stenosis with high restrictive or intact atrial septum | Aortic valvuloplasty or stenting of atrial septum |
| Twin-twin transfusion syndrome | Laser ablation or placental anastomoses |
| Twin-reversed arterial perfusion sequence | Vascular ablation by infrafetal laser of radiofrequency |

Detailed examination of the cardiovascular system is a central part of the diagnostic approach in fetuses with hydrops fetalis. Structural cardiac defects should be excluded, because they can be the primary cause of the hydrops or may be coincident in some underlying disorders such as chromosomal aberrations. Furthermore, in other underlying diseases, hydrops may result from another pathomechanism, but additional congestive heart failure appears in the advanced stage of the disease. Therefore, ultrasonographic examination should be addressed to the detection of signs for fetal congestive heart failure, which means inadequate tissue perfusion. In particular, if a cardiac disease is the primary cause of hydrops, the signs of congestive heart failure may occur before the clinical state of hydrops. Besides fetal hydrops cardiomegaly, abnormal cardiac function and abnormal venous Doppler may be highly indicative of fetal congestive heart failure, resulting in the construction of a cardiovascular profile score for diagnosis of fetal cardiac failure.[50–52] However, the demonstration of arterial blood flow redistribution by Doppler sonography may result from fetal congestive heart failure, but more probably suggests hypoxemia and acidosis in the advanced stage of various diseases such as intrauterine growth restriction and anemia. The demonstration of more than one of these signs makes the diagnosis of fetal congestive heart failure most likely. By the cardiovascular profile score, the severity of heart failure can be assessed, and the prognosis is primarily dependent on the underlying disease.

Calculations of the cardiac output (CO) by two-dimensional echocardiography (e.g., by Simpson rule, and by Doppler echocardiographic measurement following the equation $CO = A \times VTI \times HR$, where A is the area of the artery, VTI the velocity time integral, and HR the heart rate, are difficult and time consuming and have too high a variability in clinical practice at present. Further development of ultrasound equipment may eliminate these limitations. The pathophysiology of this hypoxemia-induced redistribution of cardiac output is covered in detail in Chapter 46. Low cardiac output failure may typically be caused with myocardial diseases (cardiomyopathy or myocarditis), arrhythmia (tachyarrhythmia or complete heart block), some cardiac defects (critical aortic stenosis), and by cardiac compression (pleural and pericardial effusions or chest mass). High cardiac output may result from anemia, arteriovenous malformation, and fistula in tumors, Ebstein anomaly, absent pulmonary valve sequence, twin-twin transfusion, and twin arterial perfusion with parasitic twin (Table 42.1). The more special sonographic parameters for fetal congestive heart failure are discussed later in this chapter.

Measurement of the cardiac time intervals (isovolumetric relaxation time [IRT], isovolumetric contraction time [ICT], and ejection time [ET]) and the derived myocardial performance index (MPI, Tei index; ICT + IRT/ET) of tissue velocity, strain, and strain rate, as well as three- and four-dimensional volumetry provide more detailed information about cardiac, ventricular, and myocardial function in diastole and systole.[53–55] In addition to the blood flow Doppler technique, tissue Doppler (pulsed wave and color Doppler) and speckle tracking are available.[54,55] But the large intra- and interobserver variability, technical problems (registration without electrocardiographic trigger, fetal heart rate variability, relatively low frame rate compared to the fetal heart rate), different algorithms, and, particularly, lack of validation *in utero* result in a high variance and divergency of reported reference ranges for fetuses and avoid, therefore, the broad clinical application of these new techniques. Relatively easy and reproducible are the M-mode and speckle tracking measurements of TAPSE and MAPSE (tricuspidal and mitral annular plane systolic excursion).[54,55] However, just as the conventional techniques, all these new techniques are not only dependent on the myocardial function (relaxation and contractility) but also on the working conditions (loading), tissue properties, and interaction of different segments. In particular, in fetuses with hydrops, the changes of loading condition may be extreme.

NT-proBNP reflects myocardial dysfunction during fetal life and serves postnatally as an integrated biomarker for cardiac structure, function, and loading and to allow prognostic evaluation.[56] BNP acts predominantly in a paracrine manner and is considered as a key player in the regulation of cardiac remodeling. Cardiac remodeling induced by increased ventricular wall stress includes myocardial cell proliferation in size and number, coronary tree remodeling, and an augmented contractile response to hypoxic stress. Independent of the primary cause, fetal NT-proBNP concentration seems to reflect the ventricular wall stress and allow a better understanding of the pathophysiology of intrauterine ventricular and myocardial dysfunction and cardiac remodeling. Distinctly increased NT-proBNP levels are reported in fetuses with anemia correlating with the severity and effectiveness of treatment; with cardiac defects, especially in such defects with pure pressure load as aortic and pulmonary obstruction with intact ventricular septum; with intrauterine growth restriction secondary to uteroplacental dysfunction; and also in fetuses with renal diseases with reduced or absent renal function, which is mostly associated with biventricular hypertrophy.[56] Unfortunately, NT-proBNP measurement requires an invasive procedure to obtain fetal blood. However, in cases in which invasive procedures are part of the treatment, NT-proBNP may prove a valuable tool in assessment of severity of cardiac involvement, case selection, timing of intervention, and control of treatment success.[56]

## Cardiomegaly

Cardiomegaly means the pathological increase of cardiac size by either a more symmetric enlargement of all cardiac chambers or an asymmetric widening of isolated cardiac cavities. Because of the parallel circuit of the fetal circulation, the right atrium is the most common cardiac cavity to express enlargement. This may result from increased right ventricular preload by volume overload, from a relatively restrictive foramen ovale and/or increased left atrial pressure, from a compromised right ventricular contractility and performance, and/or from an increased right ventricular afterload.[27,50,51] Although right atrial distension may be an early sign of fetal congestive heart failure, right atrial enlargement may also be obvious in states of intracardiac compensatory redistribution of blood flow, maintaining adequate combined cardiac output; this occurs in many congenital heart defects during fetal life.[50,51] Therefore, diagnosis of congestive heart failure should always be supported by the demonstration of other criteria. Besides the increase of the absolute cardiac parameters compared to the reported gestational age-dependent normative values,[57–63] advancing enlargement of the cardiac cavities can be more easily documented by measuring the cardiothoracic ratios (Figure 42.1). These different ratios of the cardiac to the thoracic circumference or area remain relatively independent of gestational age during the second and third trimesters when the heart occupies one-third of the thorax and the cardiothoracic circumference ratio is around 0.5.[61–63] Between 10 and 17 weeks of gestation, however, a more significant increase of all the cardiothoracic ratios has been reported, and the thoracic area occupied by the heart increases from one-fifth to one-quarter.[60] In contrast to the absolute biometric measurements of the single cardiac cavities, the cardiothoracic ratios become abnormal only after marked chamber enlargement is manifested. Therefore, these parameters are highly specific but not sensitive in the diagnosis of fetal congestive heart failure.[50,51] By the measurement of umbilical venous pressure, evaluation of the cardiothoracic ratio showing cardiomegaly

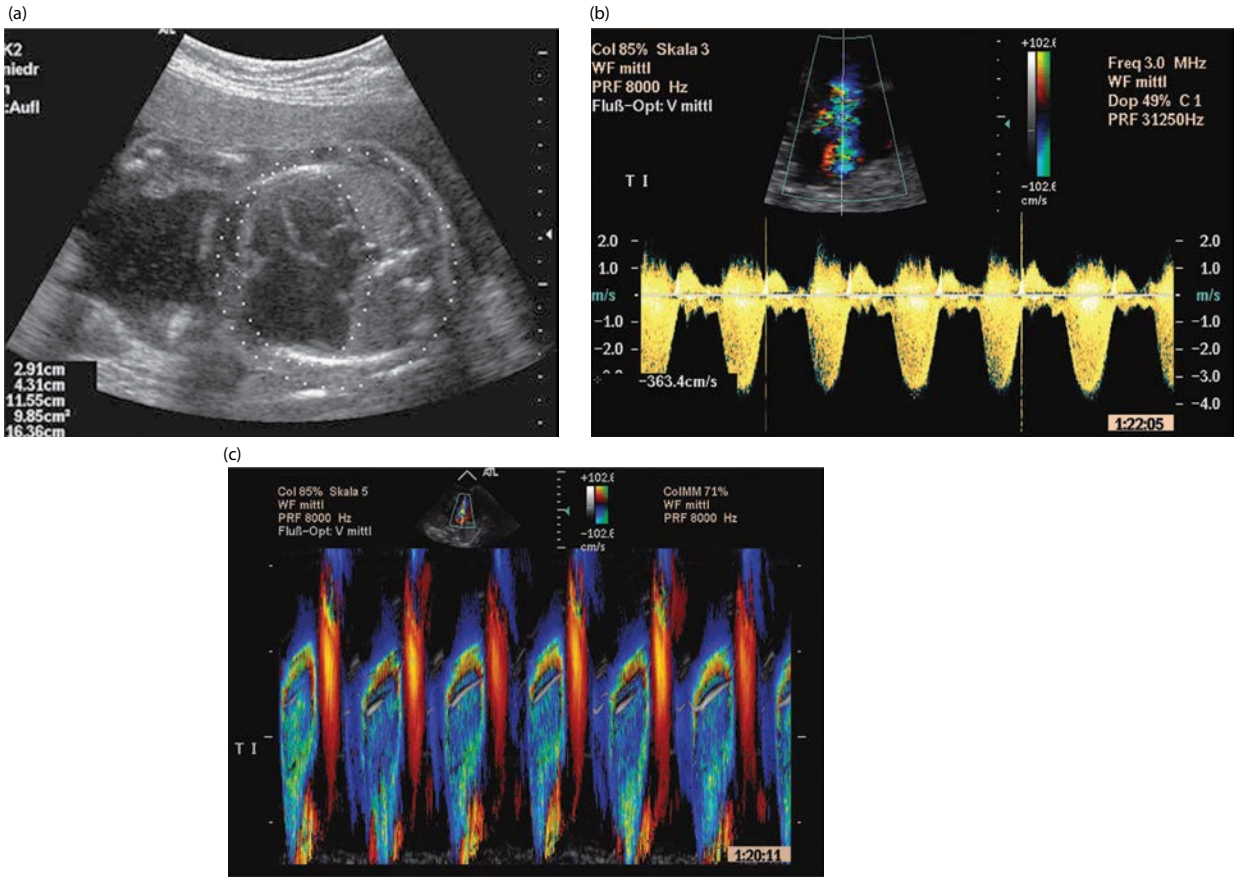


**Figure 42.1**
(a) Cardiomegaly is shown in a fetus with Ebstein anomaly at 24 + 4 weeks' gestation. The cardiothoracic circumference (0.71) and the cardiothoracic area ratio (0.46) are markedly increased. (b) Severe holosystolic tricuspid insufficiency is demonstrated in a fetus with Ebstein anomaly at 24 + 4 weeks' gestation. By continuous wave Doppler, a jet velocity of 3.63 m/s was measured. Using the Bernoulli equation, a pressure gradient of 52.7 mm Hg was calculated. (c) Color Doppler M-mode echocardiography shows the holosystolic character of the tricuspid regurgitation (blue). The systolic right ventricular inflow is colored red–yellow.

has been validated for the assessment of cardiac function in cases of nonimmune hydrops in the human fetus.[41] Therefore, it is not surprising that cardiomegaly is a good prognostic factor in fetuses with nonimmune hydrops, as it is relatively independent of the etiology, indicating a distinct compromise of cardiac function and an unfavorable prognosis.[64]

## *Systolic and diastolic ventricular function*

The systolic myocardial function can best be estimated by determining the ventricular fractional shortening using M-mode echocardiography. The normal ranges for left and right ventricular fractional shortening (FS) are between 28% and 40%, calculated by the following equation:

$$FS = (EDD - ESD)/EDD$$

where EDD is the end-diastolic diameter and ESD the end-systolic diameter.[50,51] Myocardial compromise may result in reduced ventricular shortening and increased ventricular work in more pronounced fractional shortening; however, fractional shortening and the derived calculation of left ventricular ejection fraction by the Teicholz or Simpson formula mainly reflect radial ventricular function and are usually altered only in late stages of myocardial deterioration. Besides myocardial dysfunction, increased afterload and increased ventricular dilatation may also decrease the ventricular fractional shortening. In addition, an unfavorable position of the fetal heart makes it impossible to obtain the standard position for exact measurement with the M-mode line perpendicular to the interventricular septum. Therefore, in prenatal diagnosis, determination of ventricular fractional shortening is not commonly used for the estimation of myocardial dysfunction and diagnosis of congestive heart failure.

The evaluation of the ventricular ejection force is also rarely used to assess fetal systolic myocardial function,[65,66] although this Doppler index appears to be less influenced by changes in ventricular preload and afterload. The velocity ejection force (VEF) is calculated using the following equation:

$$VEF = (1.055 \times \text{Valve area} \times VTIAT) \times (PV/AT)$$

where VTIAT is the velocity time integral during acceleration, PV is the peak velocity, and AT is the acceleration time.

In growth-restricted fetuses, the VEF of both ventricles was found to be significantly decreased, showing the low influence of ventricular afterload on this parameter of myocardial function. A further drop of VEF was related to the appearance of other signs of severe fetal compromise.[66] In hydropic fetuses, this parameter may also be useful but has not yet been studied. Measurement of TAPSE and MAPSE by M-mode and/or tissue Doppler techniques allows a good assessment of systolic ventricular function. Measurement of the systolic annular peak velocity by tissue Doppler imaging seems to be a sensitive and early marker of myocardial dysfunction. Just as in tissue Doppler imaging, the technique of speckle tracking allows measurements of myocardial motion (peak velocities) and deformation parameters (strain and strain rate) in different myocardial segments of ventricular and atrial walls.

Diastolic ventricular function may be assessed by evaluation of the filling pattern of the ventricles. In fetal life, the peak velocities of tricuspid and mitral blood flow during the early diastole (E-wave) are lower than the second peak during atrial contraction (A-wave). The E/A ratio increases during gestation, reflecting maturation processes of the myocardium and the diastolic properties, respectively, during gestation. A decrease of the E/A ratio and, in particular, monophasic filling reflects severe diastolic dysfunction of the ventricle or cardiac tamponade. Furthermore, the IRT and the ventricular inflow duration are sensitive parameters to evaluate the ventricular function. Prolongation of IRT (normally <43 ms) and shortening of ventricular filling duration (normally >38% of the total duration of cardiac cycle) indicate abnormal ventricular diastolic function and filling up to monophasic filling during atrial contraction.[67]

The global cardiac ventricular function may be assessed by the Tei index (MPI), which allows the evaluation of combined systolic and diastolic ventricular myocardial performance and is considered to reflect the global ventricular function.[68] The Tei index is defined as the sum of the isovolumetric contraction time and isovolumetric relaxation time divided by the ejection time (Tei index = [ICT + IRT]/ET). In fetal echocardiography, the modified MPI using the clicks of aortic and mitral valves improves the accuracy and is generally used. Left ventricular MPI is simultaneously available by Doppler registration of mitral inflow and left ventricular outflow, whereas assessment of blood flow Doppler derived right ventricular MPI requires the acquisition of two separate waveforms (tricuspid and pulmonary flow) with inherently less reproducibility; therefore, for the right ventricle tissue, Doppler (pulsed wave or color Doppler) seems to be a better technique for evaluation of right ventricular MPI.[54,55,67] This index is suggested to be independent of ventricular geometry and heart rate and not affected by mitral or tricuspid regurgitation. A gradual decrease in the Tei index represents maturation and increasing myocardial function during gestation. Abnormal Tei indexes were demonstrated in fetuses with intrauterine growth restriction and maternal diabetes.[68] In chronic twin-twin transfusion syndrome, increased myocardial performance indexes of both ventricles were demonstrated in the recipient twin, partly before an increase of venous pulsatility, cardiomegaly, or hydrops occurred. These increases of the myocardial performance indexes in the recipient fetus were mainly caused by prolongation of the isovolemic relaxation time, suggesting myocardial diastolic dysfunction, whereas the indexes of the donor fetus stayed in the normal range.[69,70] In hydropic fetuses, the Tei index may demonstrate global right and/or left ventricular dysfunction.[70,71] Myocardial hypertrophy can also be measured and quantified by M-mode echocardiography. Owing to the high afterload sensitivity of the fetal heart, the obstruction of ventricular outflow usually causes myocardial hypertrophy of the ipsilateral ventricle. Biventricular myocardial hypertrophy is found in the recipient fetuses of twin-twin transfusion syndrome, in fetuses with complete heart block and other forms of sustained bradyarrhythmia, and furthermore, in fetuses with long-standing tachyarrhythmia, chronic anemia, storage diseases, and distinctly reduced or absent renal function (e.g., bilateral renal agenesis, antenatal manifesting polycystic kidney diseases, or bilateral renal dysplasia following severe urethral obstruction by urethral agenesis or posterior urethral valves).[56] Severe myocardial hypertrophy may significantly reduce systolic and diastolic ventricular function, with reduced myocardial blood flow during stress.[72–75] It may also be associated with severe cardiovascular decompensation of the neonate in reaction to the increased cardiac work after birth.[50,51]

## *Incompetence of structurally normal cardiac valves*

Incompetence of structurally normal cardiac valves most commonly concerns the tricuspid valve. Severe insufficiency of the tricuspid valve and also the mitral valve may indicate congestive heart failure based on myocardial dysfunction, increased ventricular preload, and/or afterload.[50,51,67] A trivial tricuspid regurgitation is usually transient, mostly restricted to the early and midsystolic period, and in rare cases, also holosystolic.[76–78] Dependent on the sensitivity of the utilized Doppler equipment, this phenomenon may be demonstrable in around 7% of healthy fetuses without any cardiac or extracardiac pathology.[77] A holosystolic tricuspid regurgitation, however, mostly indicates a pathological significance such as cardiac defects, constriction of the arterial duct or extracardiac disorders increasing right ventricular volume or pressure, and/or compromised myocardial function. The severity of the regurgitation itself does not seem directly related to the occurrence of hydrops. Only additional alterations of intracardiac blood flow such as relative restriction of the fossa ovalis and inadequate left ventricular function may limit the compensatory possibilities if fetal hydrops appears. Pulmonary or aortic valve regurgitation is extremely rare in healthy fetuses.[79] Significant insufficiency of the pulmonary and/or aortic valve usually occurs only in the stage of severe myocardial failure,[51,67] when the support for the semilunar valves is decreased, for example, in fetuses with complete heart block, and with tricuspid valve dysplasia and Ebstein

anomaly (Figure 42.1), and especially in the recipient fetus of twin-twin transfusion syndrome.

For assessment of the severity of AV valve regurgitation, color Doppler–derived parameters of jet morphology are used, particularly the length of the jet related to the distance from the tricuspid valve to the opposite right atrial wall, and the jet area related to the area of the right atrium. Because the color Doppler–visualized jet morphology is more dependent on the velocity than on the volume, and there is a strong influence of color Doppler equipment and operating setting on the jet morphology, most examiners use the temporal duration of the jet related to the systolic period and grade this into non-holosystolic (early and midsystolic) regurgitation and holo- or pansystolic regurgitation.[46,77,78,80] These intervals can be measured by spectral and color Doppler M-mode echocardiography.[46,77,78,80] Especially for intra-individual follow-up studies, AV valve regurgitation sensitively reacts when cardiac function decreases or improves.[46] Except for extremely rare cases, holosystolic regurgitation suggests a substantial alteration of the fetal circulation.

The myocardial contractility can be evaluated using the spectral Doppler-derived shape of the tricuspid or mitral valve regurgitation, measuring the rate of ventricular pressure rise over time (dP/dt) measured between 1 and 3 m/s using the Bernoulli equation ($dP = 4[v^2]$) (in other words, right ventricle [RV] and right atrium [RA] gradient of 4–36 mm Hg, or a 32 mm Hg difference). In the second and third trimesters, fetal atrial pressure is between 3 and 4 mm Hg, and ventricular pressure is between 40 and 60 mm Hg. The pressure gradient over time (dP/dt) reacts very sensitively to changes in ventricular contractility and is relatively independent of afterload during the pre-ejection period.[50,51,67,81] Values lower than 800 mm Hg/s are abnormal, and values above 800–1000 mm Hg/s are normal in fetuses.[50] In a study of 20 fetuses with holosystolic tricuspid regurgitation associated either with ductal constriction or with nonimmune hydrops, the Doppler-derived right ventricular dP/dt appeared to be useful for right ventricular functional assessment in fetuses with tricuspid regurgitation and for prediction of poor outcome if dP/dt was lower than 400 mm Hg/s.[67,81]

## Venous Doppler velocimetry

An increased pulsatility of the blood flow in the pericardial veins indicates compromised cardiac function in fetuses with intrauterine growth restriction and is commonly associated with hypoxemia and also acidemia. A substantial increase of the end-diastolic pressure of the ventricles elevates the right atrial as well as the central venous pressure, and results in decreased venous forward flow during all of diastole, including atrial systole, generating an abnormal venous flow pattern. Therefore, each increase of cardiac afterload, preload, and/or myocardial dysfunction may cause an elevation of the central venous pressure. When sufficient, this results in an increased pulsatility of the venous blood flow velocity waveforms.[45,82] For fetal surveillance, recordings of the blood flow pattern of the inferior vena cava, ductus venosus, and umbilical vein are commonly used in clinical practice. An excess of normal reverse blood flow during atrial systole in the inferior vena cava indicates an increase of central venous pressure as well as reduced antegrade, absent, or reverse blood flow during atrial systole in the ductus venosus, and monophasic as well as biphasic pulsations in the umbilical vein. There are some differences between these three veins:

1. The blood flow of the inferior vena cava is directed into the right ventricle and that of the ductus venosus through the foramen ovale into the left atrium.
2. Hypoxemia increases the proportion of umbilical venous blood, which is preferentially directed to the ductus venosus, bypassing the liver.
3. An active vasodilatation of the ductus venosus may reduce umbilical venous pressure and facilitate a more distal propagation of the pulse wave during atrial contraction.
4. In contrast to the vasodilatation and increased or maintained blood flow of the ductus venosus blood, flow volume in the inferior vena cava is diminished, when hypoxemia-induced arterial blood flow redistribution takes place.
5. In the inferior vena cava, there may be a higher compliance than in the ductus venosus; furthermore, any stress-induced increase in sympathetic tone causes venoconstriction.

However, alterations of blood flow velocity waveforms of the inferior vena cava and ductus venosus seem to be equally good in clinical practice for predicting the extent of fetal hypoxemia and acidemia in growth-restricted fetuses,[83] whereas transmission of the pulsations into the portal and umbilical veins correlates with an increasing degree of compromise.[84]

In fetuses with elevation of the central venous pressure caused by other factors, increased pulsatility in the inferior vena cava and ductus venosus also results and correlates with the pressure increase. Increased pulsatility of venous flow velocity waveforms may be observed in some fetuses with cardiac defects. It is caused by the particular hemodynamics of some cardiac defects causing increased right atrial pressure, such as tricuspid atresia and severe right ventricular outflow obstruction (pulmonary atresia and pulmonary severe stenosis) with intact interventricular septum, and Ebstein anomaly/tricuspid dysplasia with severe tricuspid regurgitation, presumably caused by a relative restriction of the increased transatrial flow through the fossa ovale without other indicators of compromised cardiac function.[85] Therefore, venous Doppler velocimetry in the proximal veins, such as the inferior vena cava, seems to be sensitive to changes of fetal hemodynamics by some cardiac defects and alterations of cardiac function, and may become abnormal if cardiomegaly is still not identifiable. In advanced stages of fetal congestive heart failure, however, where hydrops is often associated, a large increase of atrial and venous pressure results in a strongly pulsatile venous blood flow and in more distal propagation of this pulsatility, especially into the umbilical venous circulation. Thus, fetuses with pulsations in the umbilical venous blood flow have the most serious

compromise of cardiac function. As in fetuses with intrauterine growth restriction,[84] the occurrence of umbilical venous pulsations seems to be the best predictor of intrauterine or perinatal death in fetuses with nonimmune hydrops.[44,86] This is the case even if compared to right and left ventricular fractional shortenings, pulmonary and aortic peak velocities, the aortic and pulmonary valve products of time velocity integral and heart rate, inferior vena caval diameter, and pulsatility of inferior venous blood flow.[86] An important exception is fetal tachyarrhythmia, where pulsation in the umbilical venous blood flow is usually present during supraventricular tachycardia above a critical frequency of 210–220 beats/minute, even in fetuses without hydrops and excellent prognosis.[87–89] Furthermore, good fetal outcome may also occur in some cases of marked fetal bradycardia and complete heart block, showing pulsations in the umbilical vein.

Although changes of ventricular preload and afterload may influence the venous flow velocity waveform, in most clinical situations, a substantial increase of pulsatility in venous blood flow indicates myocardial dysfunction and congestive heart failure. In contrast to the Doppler-derived parameters of tricuspid regurgitation and the ventricular fractional shortening, which have a lower reproducibility and demand an experienced sonographer and excellent equipment, Doppler flow velocity waveforms of the ductus venosus and inferior vena cava can easily and reproducibly be recorded.[88,89] Compared to measurement of the cardiothoracic ratio, venous Doppler velocimetry appears to be more sensitive to congestive heart failure. Therefore, the noninvasive evaluation of the venous Doppler flow velocity waveform to date seems to be the most valuable tool for monitoring cardiac function.

## Cardiovascular anomalies

With documented incidences between 20% and 40%, cardiac anomalies are the most common associations with nonimmune hydrops.[3,6,8,9,17,24] Sustained arrhythmia and/or structural cardiac defects can cause congestive heart failure and resultant nonimmune hydrops,[24] and are in up to 20% the underlying disease of the hydrops fetalis.[17] Because of specific features of the fetal circulation, with the parallel arrangement of the two ventricles and the presence of communications between the atria and the great arteries, anomalies of the right and left ventricular flow may elevate the right atrial and systemic venous pressure. Soft tissue edema and effusion into the serous cavities, but not pulmonary edema, are the consequences. Any dysfunction affecting one side of the heart can be overcome by functional adaptation of the other side, maintaining a combined cardiac ventricular output within the normal limits, even if detailed echocardiographic studies[90] have shown the presence of hemodynamic abnormalities. These include, especially, a reduction of combined cardiac output and stroke volume already in some fetuses with congenital heart disease, but absent hydrops fetalis. This may limit an adequate response to hemodynamic stressors such as birth, transition from fetal to neonatal circulation, and heart surgery.[90] In general, however, the parallel flow circuitry protects the fetus against cardiac decompensation, congestive heart failure, and hydrops. Isolated structural cardiac defects very seldom lead to interstitial fluid accumulation and hydrops. Therefore, it is incorrect from a pathophysiological point of view that in many published reports and review articles a causative relationship between the cardiac lesion and the hydrops is postulated, for example, in cases with ventricular or atrial septal defects, tetralogy of Fallot, or transposition of the great arteries. Therefore, in many cases with hydrops, the presence of a cardiac defect is coincidental, and there is no causal relationship between the cardiac abnormality and the nonimmune hydrops.[24,91] In these cases, different extracardiac factors may have led to hydrops, especially in fetuses with Turner syndrome and autosomal trisomies.

Because of parallel arrangement of the fetal circulation, almost all diseases resulting in a secondary cardiac overload and deterioration involve both ventricles by hypertrophy and/or dilatation. Typically, the earliest signs of cardial dysfunction are observed in the right ventricle. In pathological conditions associated with increased preload or afterload, dilatation, hypertrophy, and diastolic and systolic dysfunction manifest at first in the right ventricle and afterward in the left ventricle due to right heart dominance in the distribution of cardiac output and different geometry and myocardial fiber architecture (trapezoid-shaped right ventricle with predominantly parallel myofibers in the longitudinal direction, and ellipsoid-shaped left ventricle with longitudinal, circumferential, and oblique arrangement of its myocardial fibers resulting in a more homogenous transmural workload and stiffness).[67] Consequently, the right ventricle is more compliant, generates less force, and is significantly less resistant to increased ventricular load,[67] as exemplified by the severe right ventricular dysfunction in some recipient fetuses of advanced twin-twin transfusion sequence.

## Structural cardiac defects

### *Tricuspid valve dysplasia and Ebstein anomaly*

In the group of congenital heart defects with the possibility of developing congestive heart failure followed by hydrops during fetal life, tricuspid valve dysplasia and Ebstein anomaly are two of the most common cardiac malformations. Thickened, nodular, and often redundant tricuspid leaflets with normal attachment at the atrioventricular junction are the diagnostic criteria of tricuspid atresia, whereas Ebstein anomaly is characterized by a displacement of the septal and posterior leaflets from the atrioventricular junction downward into the inlet component of the right ventricle, causing a downward displacement of the functional annulus (septal > posterior > anterior leaflet) and a functional atrialization of a variable portion of the anatomically right

ventricle with variable degrees of hypertrophy and thinning of the wall.[92]

Because of the significant variances between fetal and neonatal circulation, different factors determine intrauterine and postnatal survival.[93] The survival of neonates with Ebstein anomaly and tricuspid dysplasia is essentially dependent on their ability to establish an adequate pulmonary flow. Greater impairment of pulmonary flow results from severe pulmonary obstruction, often associated with severe tricuspid insufficiency and poor right ventricular function. Severe cardiomegaly is also an unfavorable parameter, presumably as cardiac enlargement is most extensive if severe tricuspid incompetence is present (Figure 42.1). In cases with an open pulmonary valve, the occurrence of reverse perfusion of the ductus arteriosus and the pulmonary trunk with severe pulmonary insufficiency suggests severe right ventricular dysfunction and/or severe tricuspid insufficiency. Therefore, a right atrial (RA) area ratio (ratio between the area of the functional right atrium and the added areas of the other cardiac chambers measured in the four-chamber view) greater than one (or >0.75) and no antegrade flow in the pulmonary trunk seem to be the best prenatal parameters predicting an unfavorable postnatal course.[94–98] Functional pulmonary atresia appears if the pulmonary afterload exceeds the pressure generated by the right ventricle. Functional pulmonary atresia is increasingly observed during late gestation, probably as a result of the physiological increase in fetal arterial pressure, the failure of the RV to generate sufficient contractile force, and/or an increase of tricuspid insufficiency.[96–98] In a study by Wertaschnigg and colleagues, fetuses with severe tricuspid regurgitation and without pulmonary forward flow at the last fetal echocardiogram showed a mortality rate of 65% in infancy.[97] In addition to a functional pulmonary atresia, pulmonary insufficiency may appear. Pulmonary regurgitation and severe tricuspid insufficiency cause a circular left-to-right shunt via the arterial duct resulting in further right ventricular overload and critical decrease of the systemic arterial flow due to severe steal effect. Because the blood ineffectively recirculates between both ventricles, low cardiac output is followed by an increase of pulsatility in aortic and umbilical flow velocity waveforms up to absent or reversed end-diastolic flow. In these fetuses, amelioration of the hemodynamic compromise by interruption of a circular shunt may be achieved by premature closure of ductus arteriosus by maternal administration of high doses of indomethacin; this therapeutic concept is currently being evaluated. In addition, LV function and anatomy are abnormal in fetuses with severe Ebstein anomaly and tricuspid valve dysplasia, and may be important contributors to outcome.[99] Compared to a single parameter, the use of a scoring system may improve the prediction of postnatal outcome because diverse mechanisms cause right ventricular and circular deterioration during fetal life. Scoring systems (SAS score[95] or SickKids score[97]) consist of cardiac size, right atrial area index, direction of pulmonary flow, flow pattern in the arterial duct, severity and pressure gradient of tricuspid regurgitation, and pulsatility of flow velocity waveform in the umbilical artery. The presence of hydrops is also associated with poorer outcome but is not a component of both scoring systems. In recently published series, the mortality rates of fetuses with hydrops were approximately 30%–40%.[96–98] The prognostic parameters and the scoring may distinctly deteriorate during fetal life with increasing gestational age, for which reason a prediction of outcome by those echocardiographic parameters is not appropriate in the second trimester and is substantially poorer in the third trimester, as demonstrated in a longitudinal multicenter study of 51 fetuses with Ebstein anomaly or tricuspid valve dysplasia diagnosed before 24 weeks' gestation. Of 18 fetuses (35%) without initial markers for poor hemodynamic status at less than 24 weeks of gestation, 11 (61%) developed at least one marker of poor outcome in the third trimester; functional pulmonary atresia arised in 9 (33%) of 27 fetuses with initially antegrade pulmonary blood flow.[100]

In some fetuses, significant inhibition of lung growth by long-standing compression leading to severe pulmonary hypoplasia may complicate neonatal resuscitation,[101,102] even if significant changes of the pulmonary artery as observed in lung hypoplasia of other etiologies do not occur.[103] But, if adequate pulmonary flow can be established, a decrease of pulmonary vascular resistance and right ventricular afterload may markedly improve tricuspid incompetence after birth. Therefore, fetal hydrops, increased RA area ratio, significant cardiomegaly, pulmonary insufficiency, no antegrade flow in the pulmonary trunk (functional pulmonary atresia), together with a severe tricuspid insufficiency, significantly increased pulsatility of flow velocity waveform in the umbilical artery, diagnosis before 30 weeks' gestation, severe pulmonary valve obstruction, severe tricuspid lesion with tethered distal attachment of the septal leaflet, severe right ventricular dysplasia, and the presence of associated anomalies are the most important prognostic parameters for an unfavorable neonatal outcome.[94–98,104]

In contrast to neonatal survival, fetal survival is not dependent on adequate pulmonary flow but is strongly linked to the ability of the fetal heart to compensatorily increase the left ventricular volume flow. Therefore, the size of the fossa ovalis allowing the required increase of transatrial right-to-left shunt and a sufficient left ventricular diastolic and systolic function are mandatory in fetuses with tricuspid atresia and Ebstein anomaly, to avoid the occurrence of congestive heart failure followed by hydrops and *in utero* fetal death.[93,94]

Pathoanatomical studies in infants and children with tricuspid and pulmonary atresia showed substantially increased rates of foramen ovale over atrial septal area, suggesting that an adequate increase of transatrial flow and a wider than normal size of the fossa ovale are mandatory for *in utero* survival.[105] In a reported series of eight fetuses with Ebstein anomaly, two fetuses became hydropic.[93] These fetuses had the lowest ratio of fossa ovalis diameter over atrial septal length, and accordingly, the lowest left ventricular output, both in the normal range. The six nonhydropic fetuses had an increased size of the fossa ovalis and elevated left ventricular output.[93] There were no significant differences between the

hydropic and nonhydropic fetuses concerning septal leaflet displacement, severity of tricuspid insufficiency, pulmonary valve obstruction, or cardiothoracic ratio.[93] Severe incompetence of the tricuspid valve without or with pulmonary obstruction usually leads to severe tricuspid insufficiency during fetal life, and therefore demands a wider fossa ovalis allowing an adequate increase of left heart volume flow. This makes the occurrence of a relative restriction of the fossa ovalis more probable in these cases. Substantial compression of the left ventricle may act as an additional factor for fetal cardiac decompensation.[104] Venous Doppler velocimetry in the inferior vena cava and ductus venosus can provide early detection of those fetuses with a maladapted circulation developing congestive heart failure and fetal hydrops.[85] Furthermore, the onset of supraventricular tachyarrhythmia—typical is atrioventricular reentry tachycardia via an accessory pathway[92]—may be an additional cause for developing hydrops in Ebstein anomaly, favored by the marked right atrial distension and the higher incidence of preexcitation syndrome associated with Ebstein anomaly. Because fetuses with severe cardiomegaly and hydrops are more easily detectable during obstetric ultrasound examination, the severe end of the spectrum is preferentially referred to the specialized center. This explains the high proportion of these fetuses in prenatal series,[106] the high incidence of associated severe pulmonary valve obstruction,[101,102] and the very poor outcome of prenatally diagnosed fetuses with tricuspid dysplasia and Ebstein anomaly, reaching an overall perinatal mortality of up to 80% as reported[94,101,102,106,107] and in recently published series between 40% and 60%.[96–98]

Because of the poor outcome of hydropic fetuses with Ebstein anomaly and tricuspid dysplasia in the neonatal period (around 30% of all neonates diagnosed with tricuspid valve dysplasia and Ebstein anomaly will not survive 1 month, and fewer than 60% will survive to 5 years of age; in symptomatic neonates, the prognosis is always very poor, particularly if fetal hydrops occurs, and around 70%–90% of these will die during the perinatal period),[92,94–98] termination of pregnancy or expectant acceptance of *in utero* fetal death is the preferred management for these fetuses. In individual cases, however, preterm delivery and aggressive reanimation, including mechanical ventilation, administration of prostaglandins to maintain adequate pulmonary flow, and administration of nitric oxide to reduce pulmonary resistance, may be successful[94] if adequate pulmonary blood flow can be established. In rare cases, different operative interventions may be made. In special situations, transplacental treatment with digoxin may at least temporarily improve cardiac function, with remission of the hydrops, and may be indicated for avoidance of severe prematurity or, in a monochorionic twin pregnancy, for prevention of the risks of *in utero* death in one twin for the healthy co-twin.[108] In fetuses with sustained tachyarrhythmia, transplacental treatment with antiarrhythmic drugs may be successful and should be performed in nonhydropic fetuses with Ebstein anomaly if long-standing reentry tachycardia is associated, in order to prevent the development of hydrops.

## Atrioventricular septal defect

Isolated atrioventricular septal defects very rarely cause congestive heart failure and hydrops during fetal life. Semiquantification of AV valve regurgitation by color Doppler–derived spatial and temporal parameters has shown that AV valve regurgitation can be demonstrated in almost all fetuses with atrioventricular septal defects,[80] but severe AV valve insufficiency is not common in fetuses.[80] In only a small minority of fetuses with atrioventricular septal defect, holosystolic regurgitation correlated with the most severe degree of AV valve regurgitation was nonimmune hydrops associated.[80] In these cases, cardiomegaly and a pathological venous blood flow pattern are usually present and additionally indicate congestive heart failure as the cause of hydrops. Rarely, severe dilatation of the atrium may trigger supraventricular tachyarrhythmia, resulting in hydrops fetalis.[109] In the special situation of heterotaxy syndrome, however, where left atrial isomerism and atrioventricular septal defect are frequently associated with severe bradyarrhythmia, mostly as complete heart block, congestive heart failure followed by hydrops often occurs and leads to *in utero* fetal death.[110–113] The combination of severe bradycardia and compensatory markedly increased stroke volume and ventricular systolic pressure with a malformed and incompetent atrioventricular valve, and ischemia-induced dysfunction of the hypertrophic and structurally remodeled myocardium, may be factors for the occurrence of hydrops in these fetuses. Owing to the extremely poor prognosis of these hydropic fetuses, intrauterine treatment seems not to be justified if an atrioventricular septal defect is associated with complete heart block.

## Incompetence of the semilunar valves

Structural abnormalities with severe insufficiency of the semilunar valves are very rare. A few cases of truncus arteriosus communis with severe incompetence of the truncal valve and the absent pulmonary valve syndrome may cause severe atrioventricular regurgitation with consequent elevation of the right atrial and venous pressure.[114–116] The absent pulmonary valve is mostly associated with tetralogy of Fallot, seldom with intact ventricular septum or discontinuous left pulmonary artery or absent left pulmonary artery. In tetralogy of Fallot with absent pulmonary valve, the regurgitant flow results in a volume overload of both ventricles, especially in fetuses with patent ductus arteriosus if blood flow from the aorta fills both ventricles during diastole. Therefore, patent ductus arteriosus in fetuses with tetralogy of Fallot and absent pulmonary valve causes a severe chronic volume overload of the fetal heart incompatible with fetal life, and results in cardiac failure, hydrops, and fetal death early in gestation.[117,118] Besides hydrops, these fetuses show a characteristic to-and-fro blood flow in the main pulmonary artery, arterial duct, descending aorta, umbilical artery, middle cerebral

artery, and further arteries because of the diastolic "steal effect" and the absence of "Windkessel" function in the pulmonary trunk. Only if the ductus arteriosus is absent—agenesis of the ductus arteriosus is present in 10%–20% of fetuses with tetralogy of Fallot—may the fetus reach the second trimester of gestation, because the regurgitant part of the stroke volume is limited. In these fetuses, enormous dilatation and pulsation of the pulmonary trunk and the right and left pulmonary arteries are the sonographic characteristics, combined with a stenotic and regurgitant to-and-fro blood flow across the rudimentary pulmonary valve (Figure 42.2).[118] The volume overload of both ventricles may result in hydrops, intrauterine death, or a severely ill neonate complicated by severe respiratory distress and bronchotracheomalacia resulting from long-standing compression of the trachea and primary bronchi.[118–122] Fetuses with absent pulmonary valve and intact interventricular septum or discontinuous left pulmonary artery, however, have a much lower volume overload and may survive. In 30%–40% of fetuses with tetralogy of Fallot, absent pulmonary valve, and agenesis of the ductus arteriosus, a microdeletion 22q11.2 is present.[118–122]

## *Aortico-left ventricular tunnel and aortico-right ventricular tunnel*

Aortico-left ventricular tunnel is a rare malformation that comprises a communication between the aortic sinus and the left ventricle, bypassing the aortic valve. The most severe degree of this defect with a large channel can be diagnosed *in utero* by the finding of left ventricular dilatation and dysfunction on obstetric ultrasound examination.[123,124] Exact diagnosis is obtained by demonstration of para-aortic regurgitation into the left ventricle that causes chronic left ventricular volume overload. Sometimes, significant aortic stenosis is associated.[108] Direct visualization of the tunnel as an anechogenic para-aortic structure may be possible by two-dimensional echocardiography.[124] A dilated and thick-walled left ventricle, dilated aortic sinus, bulging of the ascending aorta into the left ventricular outflow tract, and sometimes a thickened aortic valve may be additional findings.[123,124] Uncommonly, when, in fetuses with severe aortic regurgitation, the developing left ventricular dysfunction can no longer be balanced by the right ventricle, *in utero* congestive heart failure and hydrops may occur, suggesting a very poor prognosis.[124]

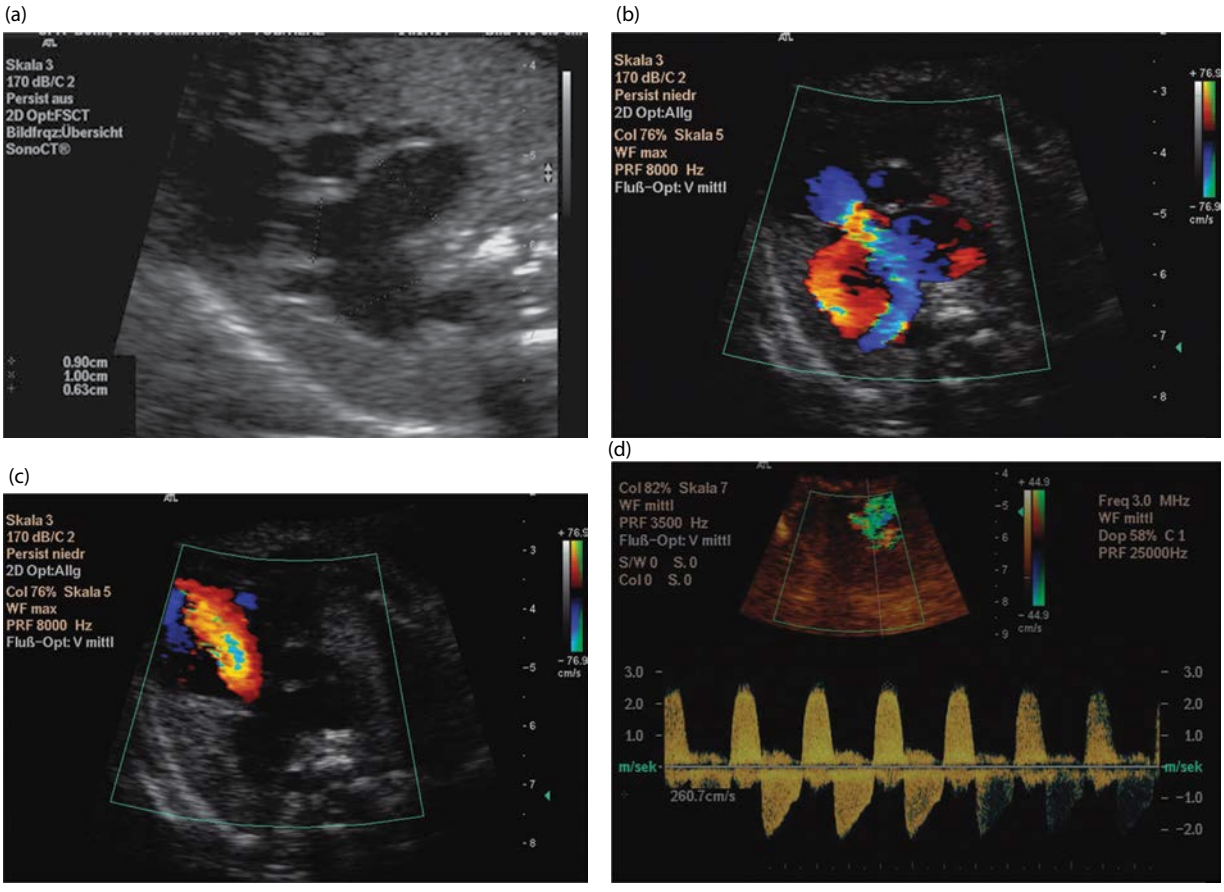


**Figure 42.2**
(a) Absent pulmonary valve syndrome in a fetus with tetralogy of Fallot and agenesis of the ductus arteriosus at 26 + 3 weeks' gestation. The pulmonary trunk and both pulmonary arteries are significantly dilated. (b) During systole, the turbulent blood flow via the rudimentary pulmonary valve and (c) during diastole the severe pulmonary insufficiency are shown. (d) By continuous wave Doppler the systolic jet velocity of 2.61 m/s and the holodiastolic pulmonary insufficiency with a jet velocity of 2.32 m/s are demonstrated.

Aortico-right ventricular tunnel is diagnosed by demonstration of an abnormal connection between the ascending aorta and the right ventricle with bidirectional flow and dilatation of the right and left ventricles, pulmonary trunk, and ascending aorta.[125] Volume overload heart failure and postnatal myocardial hypoperfusion may result in a rapid deterioration of the neonate. The same pathomechanism may explain hydrops and death in fetuses with isolated absence of the aortic valve.

## Constriction and closure of the ductus arteriosus

Significant constriction of the ductus arteriosus leads to an acute increase of right ventricular afterload, resulting in an elevation of right ventricular pressure, right ventricular systolic dysfunction, and severe tricuspid regurgitation, probably caused by papillary muscle dysfunction and/or dilatation of the tricuspid annular ring.[126] Increased transatrial right-to-left shunt and/or pulmonary blood flow may also result in volume load and dilatation of the left ventricle.[127] Sometimes, the occurrence of hydrops fetalis has been reported.[128–131] In the vast majority of cases, ductal constriction or closure is caused by transplacental transfer of indomethacin or other prostaglandin synthesis inhibitors applied to the mother for the treatment of premature contractions and/or polyhydramnios.[126,132,133] After discontinuation of indomethacin therapy, ductal constriction, right ventricular systolic dysfunction, and tricuspid regurgitation usually resolve.[126,127] The risk of drug-induced constriction of the arterial duct is dependent on the dosage of indomethacin and on gestational age, starting after 24 weeks and increasing in advancing pregnancy. Therefore, inhibitors of cyclo-oxygenase enzymes should not be used after 32–34 weeks' gestation, because ductal constriction may lead to *in utero* hydrops and death, or may cause postnatal pulmonary hypertension. Diagnosis of ductal constriction is based on increased systolic and particularly diastolic peak velocities in the ductus arteriosus, resulting in a pulsatility index of less than 1.9, mostly accompanied by severe tricuspid regurgitation with increased peak velocities of 4–5 m/s due to the marked elevation of the right ventricular systolic pressure due to the increased afterload.[134] Spontaneous constriction or complete closure of the ductus arteriosus have been reported, followed by hydrops.[128–130]

## Obstruction of the right and left ventricular outflow tracts

In the same way, afterload mismatch by structural right ventricular outflow tract obstruction (pulmonary atresia with intact interventricular septum and severe pulmonary stenosis) and, rather rarely, left ventricular outflow tract (aortic atresia and severe aortic stenosis) obstruction may cause severe insufficiency of tricuspid or mitral valves, respectively. Although central venous pressure may be increased in fetuses with right heart obstructions (tricuspid atresia, pulmonary stenosis, and atresia with intact interventricular septum), as was demonstrated by increased pulsatility in the ductus venosus,[85] the development of hydrops is very rare in fetuses with right ventricular outflow tract obstruction, because the left ventricle is mostly able to compensate for the alteration of right heart blood flow. Normal function of the left ventricle and a nonrestrictive foramen ovale are mandatory in this situation. Therefore, significant bivalvular obstruction of both pulmonary and aortic valves appears to be a severe complication, resulting in early fetal death and, if surviving early gestation, leading to hydrops in the second trimester.[135]

Most fetuses with a hypoplastic left heart do not become hydropic, and the right ventricle pumps out the whole cardiac output, even if a slightly reduced cardiac output.[136] In some fetuses with severe aortic obstruction and hypoplastic left heart, severe mitral regurgitation may significantly elevate the left atrial pressure, leading to a substantial alteration of flow via the foramen ovale, with the appearance of an accelerated and disturbed left-to-right shunt or complete closure of the foramen ovale.[137–145] In the last group, an extreme enlargement of the left atrium with secondarily increased cardiothoracic ratio may be the consequence (Figure 42.3). In these rare variants of hypoplastic left heart syndrome with highly restrictive (diameter of foramen ovale <2 mm in color Doppler and transatrial peak velocity >60 cm/s) or closed foramen ovale, hydrops may occur despite normal systemic venous Doppler flow profiles, but the pulmonary venous waveforms demonstrate a highly increased pulmonary venous pressure characterized by a short to-and-fro pattern and a decrease in the combined forward-to-reverse flow velocity-time intergral of 3.[142,144] Normally, the parallel arrangement of fetal circulation, pulmonary arteriolar vasoconstriction, limited pulmonary blood flow, and reverse shunting via the foramen ovale prevent a significant increase of pulmonary venous pressure and pulmonary edema. In fetuses with aortic obstruction with highly restrictive or closed atrial septum and severe mitral insufficiency, which is associated with a relatively high left heart volume, a markedly increased pulmonary venous pressure leads to lymphatic pulmonary edema—pulmonary lymphangiectasia is a common finding in such cases—and decreased oncotic pressure owing to the loss of albumin-rich pulmonary fluid into the amniotic sac.[141] Significant anatomical alterations of pulmonary veins and lymphatic vessels occur, and the alveolo-capillary membrane formation is severely disordered.[146] Right ventricular overload combined with an alteration of the right ventricular function by the dilated left ventricle and myocardial dysfunction of the ventricular septum (interventricular dependence) may also result in right atrial and central venous pressure increase.[137–140,142–145] In this situation, treatment with digoxin, delivery by cesarean section, and balloon dilatation of the stenotic aortic valve in the newborn resulted in a successful outcome.[140] In earlier gestation, intrauterine opening and/or stenting of the foramen ovale may stabilize the fetal condition, decrease pulmonary venous pressure, and, in addition, may allow regeneration of the altered pulmonary venous and lymphatic vessels[17–150,144,145] and perhaps

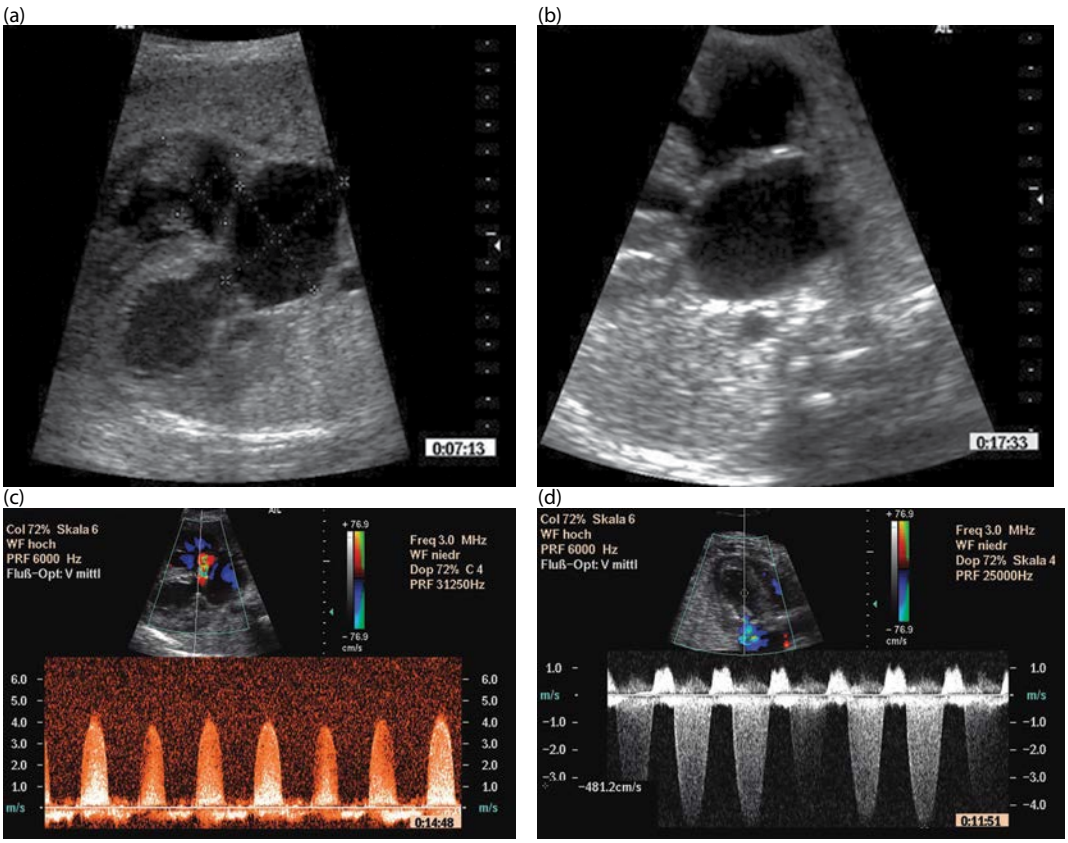


**Figure 42.3**
(a) Critical stenosis of the aortic valve is demonstrated in a fetus at 34 + 2 weeks' gestation. The myocardium of the left ventricle shows marked hypertrophy. The size of the left atrium is significantly increased. (b) The valve of the foramen ovale shows no movement in the two-dimensional echocardiogram. By color Doppler examination, a shunt across the foramen ovale cannot be demonstrated. (c) By continuous wave Doppler a maximal velocity of 4.62 m/s is measured across the stenotic aortic valve. Using the Bernoulli equation a pressure gradient of 85.47 mm Hg is calculated. (d) Severe holosystolic mitral insufficiency is demonstrated by color Doppler imaging. By continuous wave Doppler a jet velocity of 4.81 m/s is measured. Using the Bernoulli equation, a pressure gradient of 92.5 mm Hg is calculated.

improve the poor prognosis of fetuses with hypoplastic left heart syndrome with an intact or highly restrictive atrial septum, although significant improvements in survival have not yet been reported.[144,145,149–151]

## *Primary restriction or complete closure of the foramen ovale*

The concept of primary premature closure of the foramen ovale as an occasional cause of secondary hypoplastic left heart syndrome has now been abandoned. Restriction and smallness of the foramen ovale in hypoplastic left heart syndrome is a common secondary phenomenon in fetuses with severe left ventricular outflow tract obstruction, where a primary patent foramen ovale develops into restriction or complete obstruction in later gestation. A few case reports, however, have described an isolated restriction or premature closure of the foramen ovale in association with nonimmune hydrops.[152–155] In these cases, the left ventricle was normal in size or underdeveloped, whereas the right-sided chambers were substantially enlarged. Diagnosis is based on the demonstration of disturbed blood flow with increased velocities through the foramen ovale or of absent transatrial blood flow in cases of complete closure. In addition, an abnormal blood flow pattern in the pulmonary veins with substantial reversal of blood flow during atrial systole, indicative of elevated left atrial pressure,[156] can be expected in this situation. Owing to the abrupt decrease in pulmonary flow, delivery with consequent disappearance of hydrops and right-sided congestive heart failure is the recommended treatment.[152,153] Restriction of the foramen ovale may also occur in association with tachyarrhythmia.[157] In these cases, initial left atrial depolarization may result in a premature pressure increase in the left atrium, which lowers the interatrial shunt during the short diastole or may lead to premature closure of the foramen ovale. In this group, prenatal normalization of cardiac rhythm may lead to a "reopening" of the foramen ovale and remission of hydrops.

Premature closure of the foramen ovale has also been reported in nonhydropic fetuses.[158] In an autopsy series, this was not significantly increased among hydropic infants

compared to nonhydropic controls, indicating that factors other than premature closure of the foramen ovale are operative in the pathogenesis of nonimmune hydrops.[91]

## Cardiac tumors

Cardiac tumors are a rare cause of nonimmune hydrops. Dependent on their localization, size, and number, cardiac tumors may cause hydrops by impeding diastolic filling, by altering the function of atrioventricular valves, or by obstructing the outflow tract,[159] sometimes indirectly by induction of sustained supraventricular and less often ventricular tachyarrhythmia.[159–161] The vast majority of fetal intracardiac tumors are rhabdomyomata, showing a homogeneous echogenicity, which is increased compared with the normal myocardium. A rhabdomyoma may prominently protrude into the ventricular or atrial cavity or may be confined as a small tumor to the cardiac wall. Spontaneous regression of the rhabdomyomata after birth commonly occurs. In around 50% of fetuses with rhabdomyomata, however, tuberous sclerosis is present, especially in fetuses with multiple cardiac tumors.[160–163] In the case of a rhabdomyoma, a definitive exclusion of tuberous sclerosis may be impossible by prenatal ultrasound, because the pathognomonic giant cell astrocytomata are often undetectable by sonography of the fetal brain, even if high-resolution transvaginal scanning is used in the fetal vertex position.[164] More successful *in utero* diagnosis of associated intracerebral lesions indicating tuberous sclerosis has been reported by magnetic resonance imaging.[165] The sonographic visualization of multiple intracardiac tumors seems to be indicative of tuberous sclerosis. Successful drug-induced cardioversion of a supraventricular tachycardia into sinus rhythm leading to complete remission of hydrops *in utero* has been shown in a fetus with multiple rhabdomyomata.[161] If congestive heart failure and hydrops resulting from tumor obstruction do occur, *in utero* transplacental treatment with digoxin or delivery, depending on gestational age, may be considered. However, such an aggressive treatment may not be indicated, because of the poor prognosis in such hydropic fetuses and the frequent association with tuberous sclerosis. It should be performed only in cases with a special request of the parents after detailed counseling.

Furthermore, the development of fetal hydrops has been seen in a fetus with a right atrial hemangioma[166] showing mixed echogenicity with echogenic and hypoechogenic parts, and in another with a hamartoma of the conduction system in association with tachyarrhythmia and a structural heart defect.[167]

Pericardial teratomata are very rare tumors of variable echogenicity, often containing cysts of varying size. They can grow to a considerable size and are commonly associated with a large pericardial effusion (Figure 42.4). In these situations, the development of hydrops is a more common complication, resulting from a substantial obstruction of intracardiac blood flow due to cardiac compression.[168–179] In such fetuses with cardiac tamponade caused by a massive pericardial effusion, stabilization of cardiac function may be achieved by single or repeated pericardiocenteses or by placement of an indwelling catheter as pericardioamniotic shunt to provide drainage of the pericardial effusion into the amniotic sac, resulting in rapid remission of fetal fluid accumulations and normalization of the pulsatility of venous flow velocity waveforms.[166,173–178] *In utero* open fetal surgery for tumor resection may be an even more invasive alternative in very immature fetuses with hydrops caused by an intrapericardial teratoma,[179] particularly if cardiac tamponade is predominately caused by the tumor.

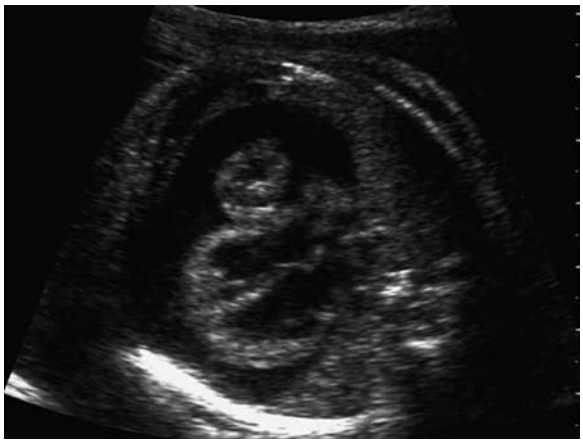

**Figure 42.4**
Four-chamber view demonstrating a pericardial teratoma with a massive pericardial effusion in a fetus at 25 + 0 weeks' gestation. In the following gestation four pericardiocenteses were performed leading to immediate remission of ascites and skin edema and normalization of pulsatility in the ductus venosus. (Reproduced with permission from Kamil et al. *Ultrasound Obstet Gynecol* 2006;28: 972–3.[168])

## Idiopathic arterial calcification

Idiopathic arterial calcification is a rare disease, caused by homozygous or compound heterozygous nonsense mutation for the *ectonucleotide pyrophosphatase/phosphodiesterase 1* (*ENPP1*) gene on chromosome 6q, and characterized by generalized calcification of large and medium-sized arteries, especially in the aorta and pulmonary trunk.[180] In addition, degeneration of elastin fibers and fibrous proliferation in elastic and muscular arteries has been found. Most commonly, the coronary arteries are affected, but peripheral arteries of the gastrointestinal tract, kidneys, extremities, brain, and placenta may also be involved. In these fetuses, ischemia-induced myocardial dysfunction may cause severe hydrops, tissue ischemia, and fetal death in the late second or third trimester.[180–184] In less severe cases, especially if no hydrops is present, palliative treatment postpartum with steroids and diphosphonates may stop the progression of the disease.[180,184] However, almost 90% of affected infants with idiopathic arterial calcification die within the first year of life, complicated by cardiac and pulmonary failure, renal infarction, peripheral gangrene, and bowel infarction.[180,184]

## Tachyarrhythmia

The most common cardiac disease causing fetal hydrops is fetal tachyarrhythmia. Because a separate chapter about fetal tachyarrhythmias is written in this book (Chapter 41), the pathophysiology and the clinical management are only briefly discussed in the context of fetal hydrops. Sustained fetal tachyarrhythmia may cause congestive heart failure, leading to elevated right atrial and systemic venous pressure. It may be followed by nonimmune hydrops, placental edema, and polyhydramnios. In fetuses, supraventricular tachycardia is more frequent than atrial flutter, independent of the presence or absence of hydrops, whereas ventricular tachycardia is very rare.[185,186] Between 80% and 90% of cases with supraventricular tachycardia are atrioventricular reentrant tachycardias based on an accessory atrioventricular conduction pathway beside the atrioventricular node, whereas atrial ectopic, atrioventricular nodal reentrant, and junctional tachycardias are not often the electrophysiological mechanism of perinatal supraventricular tachycardia.[187–190] An accessory atrioventricular connection seems to be present in some fetuses with atrial flutter.[190]

Pathophysiologically, there is a substantial shortening of the diastolic period of the cardiac cycle, which prevents adequate early diastolic filling of the ventricles. Furthermore, it is suggested that initial left atrial depolarization can be tolerated to a lesser degree by the fetus, because the left ventricular output is diminished and the interatrial right-to-left shunt is disturbed.[191] Atrial pacing studies in the fetal lamb have shown an increase of ventricular output and a decrease of ventricular end-diastolic pressure at rates up to 300 beats/minute. Prolonged left atrial pacing at rates of 300–320 beats/minute results in a decrease of cardiac output and in the development of hydrops within 4–48 hours. Cardiomegaly and hepatomegaly develop, whereas arterial oxygen tension and mean aortic pressure remain unchanged.[192–196] Because no or only slight hypoproteinemia may be observed, there is no evidence for an increase of capillary permeability for albumin. Above this "critical" heart rate, the mean venous pressure in the inferior vena cava abruptly increases by 75%.[196] This abrupt elevation of venous pressure is associated with an immediate appearance of pulsatile reversal of blood flow occurring during diastole.[196] Below this heart rate, the venous flow is biphasic with a systolic and diastolic forward surge, which also occurs immediately after the pacing is stopped.[196] Besides the direct impedance of diastolic filling when the diastolic interval is critically shortened, the abrupt occurrence of changes—reduction of ventricular output, the immediate elevation of venous pressure, and appearance of pulsatile venous blood flow above a "critical" pacing rate—suggests ventricular dysfunction consistent with an alteration of the pressure-volume relationship in association with impaired ventricular relaxation and compliance at high pacing rates. The most likely explanation is that oxygen supply to the myocardium by coronary blood flow is inadequate for the increased requirement of the myocardium during tachycardia, in particular due to the significant shortening of the diastolic period when the major portion of coronary blood flow takes place.[72] This hypothesis is supported by the observation that severe ventricular dysfunction and even injury of the myocardium may occur in prolonged tachycardia, and may cause reversible tachycardia-induced "cardiomyopathy" in humans and animals.[72–75] In conjunction with the enormous cardiac enlargement in fetuses with sustained supraventricular tachycardia, functional incompetence of both AV valves may be observed, suggesting structural remodeling of the ventricles in the presence of tachycardia-induced "cardiomyopathy." Recovery from tachycardia-induced "cardiomyopathy" was accompanied by persisting chamber dilatation, significant myocardial hypertrophy, and persisting diastolic and systolic dysfunction.[75] Venous blood flow studies in the human fetus with supraventricular tachycardia have demonstrated the occurrence of monophasic forward and pulsatile reversed blood flow during diastole in the inferior vena cava and ductus venosus above a critical heart rate of approximately 210–220 beats/minute.[87,88] This is in accordance with fetal lamb studies, where this change of venous blood flow pattern was associated with a considerable elevation of venous pressure.[196] After the termination of supraventricular tachycardia, cardiac dilatation, myocardial hypertrophy, atrioventricular valve incompetence, hydrops, and increased pulsatility of venous blood flow disappear with immense interindividual differences. These could be explained by different stages of progression of tachycardia-induced "cardiomyopathy" at the time of drug-induced cardioversion and, accordingly, varying time intervals for normalization of cardiac function.[46,88,89]

In conclusion, these results from animal and human studies indicate that fetal hydrops due to tachyarrhythmia is caused by congestive heart failure leading to elevated venous pressure and consecutive obstruction of lymphatic drainage, but not from hypoxic damage to capillaries or other tissues.[195] Owing to the various problems postpartum in managing premature hydropic fetuses (postpartum increase of cardiac work, regulation of body temperature, mechanical ventilation, repetitive pleural drainage, simultaneous occurrence of lung edema and hyaline membrane disease that reduce the effectiveness of surfactant therapy, severe degree of tachycardia-induced "cardiomyopathy," and refractory neonatal tachyarrhythmia), iatrogenic preterm delivery of hydropic fetuses for better control of arrhythmia often results in a poor outcome. Treatment *in utero* for adequate control of the arrhythmia and remission of hydrops is prudent in sustained tachyarrhythmia of fetuses with and also without hydrops. In hydropic fetuses with tachyarrhythmia, intrauterine treatment with digoxin alone and in combination with different antiarrhythmic drugs (flecainide, sotalol, and amiodarone) is the best approach for almost all fetuses, as elaborated in Chapter 41. Transplacental treatment is successful in the majority of cases.[187,188,197–206] In hydropic fetuses with supraventricular tachycardia refractory to transplacental therapy, the direct intravascular application of antiarrhythmic drugs to the fetus as an ultimate method may be successful.[197,207,208]

## Complete heart block

Complete heart block may also cause fetal hydrops. Because complete heart block is discussed in a separate chapter of this book (Chapter 40), only its association with hydrops is emphasized in the following section. Especially the combination of fetal complete heart block and atrioventricular septal defect in fetuses with left atrial isomerism (Figure 42.5) seems to have a very poor prognosis, with the appearance of hydrops and intrauterine death in the majority of fetuses.[110–113] The combination of a malformed and most severely incompetent AV valve with ventricular bradycardia causing high stroke volume and an increase of ventricular pressure is the pathophysiological mechanism explaining the most common appearance of hydrops in these fetuses. In contrast, the occurrence of hydrops in fetuses with AV block and "corrected" transposition of the great arteries is very rare, because the AV valve apparatus is generally intact in these fetuses.[110,113] This is also the reason why, in fetuses with complete heart block without congenital heart disease, the appearance of hydrops is much less frequently observed, occurring in only approximately 10%–20% of fetuses.[209] In these fetuses, complete heart block is not caused by a malformation of the conduction system, but follows an inflammatory destruction of conduction pathways, especially in the AV nodal region, induced by transplacental transfer of maternal autoimmune antibodies (anti-SSA/Ro and anti-SSB/La antibodies). Hydrops may occur when the ventricular escape rhythm is very low;

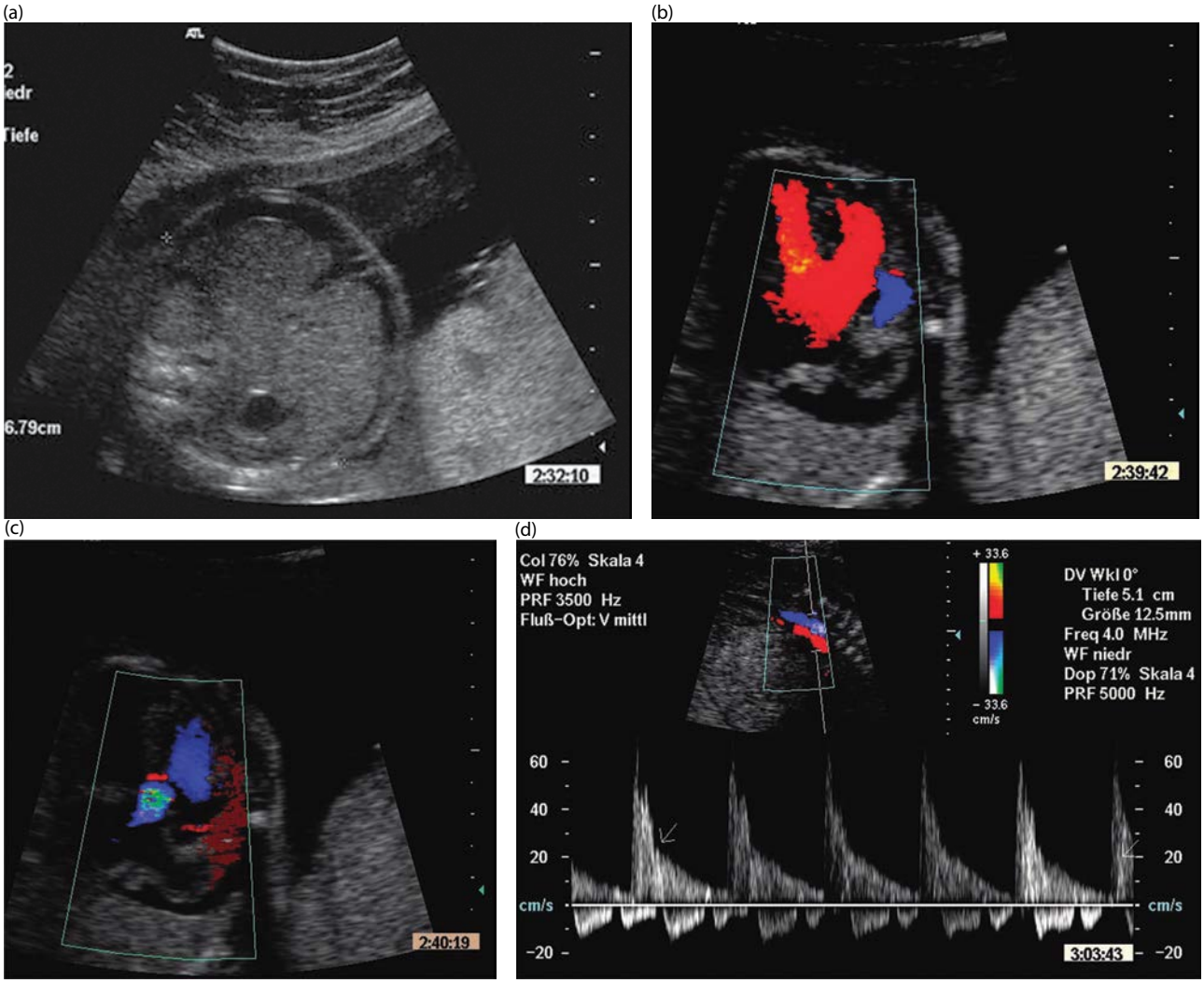


**Figure 42.5**
(a) Abdominal situs of a hydropic fetus with left atrial isomerism (heterotaxia syndrome), atrioventricular septal defect, and complete heart block is shown in a fetus at 23 + 6 weeks' gestation. The stomach is on the right side of the abdomen (situs ambiguus) and moderate ascites is seen. (b) The heart is on the left side. The diastolic inflow across the common atrioventricular valve into both ventricles is colored red. (c) During diastole a regurgitant jet is shown (blue) in the middle of the common atrioventricular valve. (d) In parallel with the aorta (blue) the venous blood flow pattern in the azygos vein (red) is demonstrated in the thorax. By pulsed wave Doppler, the aortic blood flow is recorded in the upper channel showing a ventricular rate of 57 beats/minute. In the lower channel, the venous blood flow pattern demonstrated an atrial rate of 125 beats/minute independent of the ventricular systoles. The reverse flow during two of the atrial systoles is marked by arrows.

furthermore, widespread myocarditis and/or generalized extracardiac inflammation may contribute to the occurrence of hydrops in some of these fetuses. Sometimes hydrops develops only after 30 weeks of gestation, because at this time the required increase of the combined cardiac output cannot be produced by these fetuses. Another cause may be progression of a more generalized myocarditis and/or inflammation of other fetal tissues due to autoantibodies.[210,211]

In complete heart block without a structural cardiac malformation, intrauterine treatment of hydropic fetuses may be successful by transplacental infusion with salbutamol and isoprenaline (positive chronotropic and positive inotropic effects),[212] by treatment with digoxin (positive inotropic effect),[110,213,214] and by dexamethasone[210,211,215] and/or plasmapheresis, impairing the severity of inflammation. This may be not only in the conductive tissue but also in the myocardium and other fetal organs, as elaborated in Chapter 33. Remission of complete heart block, however, cannot be achieved by intrauterine treatment with dexamethasone or plasmapheresis.[216–219] In a few reported cases, direct intrauterine pacing was technically successful, but only for some hours.[220,221] Whether the anti-inflammatory effect of transplacental treatment with dexamethasone in fetuses with already manifested complete heart block may attenuate secondary cardiomyopathy, lower the necessity of pacemaker, and improve the long-term outcome,[215,218] is very controversial[222,223] and must be further evaluated because of the serious side effects of the therapy to the mother and the fetus.

Weekly echocardiographic monitoring of fetal PR interval starting at 16 weeks in pregnant women with anti-SSa/Ro antibodies, and transplacental treatment by dexamethasone if prolongation of the PR interval[224] is demonstrated, seem not to be effective in preventing complete heart block, because fetal complete heart block occurs abruptly without previous prolongation of the PR interval.[225,226] As shown by a retrospective register analysis, in a high-risk collective consisting of pregnant women with a previous child born with complete heart block, the administration of hydroxychloroquine starting before 10 weeks of gestation seems to be effective in prevention of complete heart block.[227]

## Primary and secondary diseases of the myocardium

The cardiomyopathies can be divided into dilated or congestive, hypertrophic, which may be obstructive in addition, and restrictive types. Although myocardial diseases of unknown etiology were originally termed *cardiomyopathy*, this term is more generally used to categorize a wide range of heart muscle diseases not associated with structural cardiac anomalies or pericardial diseases.

The primary form of cardiomyopathy consists in the majority of idiopathic cases,[228] and genetic-metabolic, familial, and inflammatory disorders were also described. Noncompaction of the ventricular myocardium or spongiform cardiomyopathy results from an arrest of compaction of the loose myocardial network during fetal ontogenesis, resulting in a "spongy myocardium" with "persisting sinusoids" that fail to regress, and communicate to the epicardial coronary arteries. This disease may partially or totally involve the left or the right ventricle, and may be associated with other cardiac diseases such as aortic obstruction, or Ebstein anomaly. Isolated noncompaction of the ventricular myocardium may result in impaired ventricular function, heart failure, fetal hydrops, and arrythmias.[229–231] The outcomes of primary fetal cardiomyopathies are very poor, including a high rate of fetal death, especially in those fetuses with hydrops and/or bilateral AV valve insufficiency.[232,233]

The secondary form of cardiomyopathy consists of cases with systemic diseases resulting in significant functional alteration and structural remodeling of the myocardium. In a small number of fetuses, metabolic storage diseases have been reported to significantly reduce *in utero* cardiac function, followed by congestive heart failure and hydrops.[234–237] Cardiac glycogenosis without acid maltase deficiency and carnitine deficiency may very rarely present as nonimmune hydrops fetalis.[234–237] In one hydropic neonate, postnatal oral DL-carnitine supplements resulted in a dramatic improvement of cardiac function, normoglycemia, and restoration of serum carnitine levels to normal.[235] Barth syndrome, an X-linked disorder, may be associated with typically dilated cardiomyopathy with or without endocardial fibroelastosis (EFE) or left ventricular noncompaction, but rarely also with hypertrophic cardiomyopathy (HCM); rarely it manifests antenatally with severe cardiomyopathy, low cardiac output, and hydrops fetalis.[238] Fetuses with Noonan syndrome may develop hydrops fetalis due to lymphatic dysplasia, seldom in association with a hypertrophic cardiomyopathy. Severe cardiomyopathy may also be pathophysiologically relevant in some hydropic fetuses with congenital myotonic dystrophy, an autosomal dominant disease characterized by fetal hypo- and akinesia.[239,240] Myocardial infarction resulting in severe cardiac dysfunction is very rare during fetal life and appears to be mostly induced by coronary thromboembolism.[241]

A chronic high-output cardiac state due to arteriovenous malformation, tumor, and parasitic twin is a more common cause of dilated cardiomyopathy in fetal life, sometimes leading to fetal hydrops. In chronic hemolysis, repetitive fetal maternal hemorrhage, and parvovirus B19 infection, significant fetal anemia causes a high-output cardiac state. In this group of diseases, congestive heart failure appears not to be the primary cause of hydrops but occurs in an advanced stage of fetal compromise, indicated by the appearance of cardiac enlargement, AV valve regurgitation, and increase of pulsatility of venous blood flow velocity waveforms. In earlier stages of the disease, other pathomechanisms may be operating, especially hypoxia-induced capillary damage, reduced colloid oncotic pressure, and portal hypertension due to significant extramedullary erythropoiesis. Accordingly, Doppler studies in fetuses that were anemic because of alloimmunization demonstrated a hyperdynamic circulatory state with increased venous, intracardiac, and arterial blood flow velocities.[242] The studies suggested portal hypertension[243] but

failed to show an increased pulsatility of venous blood flow representing central venous pressure and cardiac function.[242]

In Southeast Asia, the leading cause of hydrops and perinatal death is homozygous α-thalassemia resulting in severe tissue hypoxia.[25,244] Symptoms are anemia ranging from 3 to 10 g/dL, cardiomegaly, hepatosplenomegaly, hydrops fetalis and placentae, and poly- and later oligohydramnios. As in other diseases, placentomegaly is likely to be an important factor for the maternal hyperdynamic and hypertensive state, the "mirror syndrome."[245–250] A thickened placenta seems to be the first sonographic marker, detectable from 10 to 18 weeks of gestation, followed by cardiomegaly, hepatosplenomegaly, and fetal hydrops, which may present as early as the 12th week of gestation and most commonly beyond the 20th week of gestation.[251–254] Demonstration of placentomegaly, cardiomegaly resulting in an increased cardiothoracic ratio, and hydrops is used in Southeast Asia not only if DNA-based prenatal diagnosis is not readily available, but also as an alternative diagnostic means, avoiding the risks related to invasive procedures.[244,252–254] Measurement of cardiothoracic ratios by transvaginal sonography can distinctly identify affected fetuses at 12–13 weeks of gestation.[255] After sonographic detection, diagnosis is confirmed by fetal blood sampling showing hemolytic anemia, abnormal hemoglobin, and hypoxemia.[254,255] Although some anemic fetuses show increased peak velocities at the pulmonary valve and a larger pulmonary valve diameter at 12 and 13 weeks of gestation, there is an extensive overlap between anemic and nonanemic fetuses.[256] Also, nuchal translucency thickness, nuchal edema, and hydrops seem not to be useful for the prediction of anemic fetuses in early gestation.[257]

Cardiomegaly, AV valve regurgitation, and increased pulsatility of the venous blood flow pattern, suggesting congestive heart failure, have been reported in fetuses with transient myeloproliferative disorder and Down syndrome.[258–265] Additional pathogenic mechanisms predisposing to the development of hydrops in these fetuses may be mild to moderate anemia with hemoglobin concentrations between 6 and 10 g/dL causing high cardiac output, capillary damage by hypoxia resulting from anemia and hyperviscosity, increased vascular resistance, extramedullary megakaryoblastic proliferation, and liver fibrosis.

In fetuses with sacrococcygeal teratoma, large tumors with a high proportion of solid tissue demand high amounts of blood for supply of the tumor with nutrients and oxygen. Therefore, a high percentage of combined cardiac output is sacrificed exclusively for the perfusion of the teratoma, causing high cardiac output; furthermore, increased cardiac output may occur due to intratumoral arteriovenous shunting. Development of high-output cardiac failure as demonstrable by Doppler techniques may occur in about one-third of cases with sacrococcygeal teratoma (Figure 42.6). Not so common is the subsequent development of generalized hydrops fetalis and placentae being correlated with a very high spontaneous death rate.[224] Hydrops has also been reported in fetuses with teratoma of other locations.[168–179,266–272] Furthermore, in some fetuses, mostly mild or moderate anemia may be detected, which is caused by spontaneous hemorrhages into the tumor or by the Kasabach-Merritt sequence with signs of microangiopathic hemolytic anemia and consumption coagulopathy. *In utero* treatment of a fetus with a teratoma developing hydrops depends on several factors. In particular, cases with a large intracorporeal portion compressing and displacing other organs have a poorer prognosis than cases with predominantly extracorporeal components. In fetuses with a sacrococcygeal teratoma of the extracorporeal type, the presence of a completely solid tumor with its risk for malignancy and hypervascularization seems to be an important negative prognostic factor.[273] Intrauterine transfusion of packed erythrocytes for correction of anemia and transplacental digitalization may be considered. Ligation, embolization, perivascular sclerosis, and coagulation of the supplying arteries interrupting the blood supply (monopolar cautery, laser ablation, and RFA) or resection of the tumor by open fetal surgery or fetoscopy seem to constitute a causative treatment approach for correcting high-output cardiac failure in immature fetuses. Prenatal debulking of the tumor and devascularization in premature fetuses with sacrococcygeal teratoma and subsequent hydrops may significantly reduce the cardiac output and may thus be the best treatment option prior to viability. However, open fetal surgery is associated with major fetal and maternal risks (preterm prelabor rupture of the membranes, preterm delivery, uterine scarring, and hemorrhage) and shows a high fetal mortality in already hydropic fetuses. However, if pregnancies complicated by high-risk sacrococcygeal teratoma will manifest signs of fetal or maternal decompensation, or both, between 27 and 32 weeks of gestation, preemptive early delivery results in surprisingly good outcomes in the absence of fulminant hydrops.[274] A poor prognostic sign is the development of hydrops in an elsewhere localized teratoma, such as a mediastinal[267,273] or intrapericardial teratoma,[168–179,272] where local compression of the heart, cardiac tamponade, lymphatic drainage, and venous return may occur in addition, similarly to other thoracic masses, such as fibrosarcoma, with origin from the lungs or mediastinum.[275]

Arteriovenous malformations and vascular tumors may also cause hydrops. Examples are liver hemangiomas, cavernous hemangiomas of the chest, nuchal hemangiomas, diffuse neonatal hemangiomatosis,[276,277] intracerebral hemangioma,[278] pulmonary arteriovenous malformation,[279] coronary arteriovenous fistula,[280] umbilical cord hemangioma,[281,282] placental chorioangioma (Figure 42.7),[283–286] and diffuse placental chorioangiomatosis.[287] The most important pathomechanism is high-output cardiac failure due to arteriovenous shunts inside the tumor. In addition, anemia due to a Kasabach-Merritt sequence and/or hemorrhage may occur in these tumors and increase the high cardiac output state. Especially fetuses with a giant hemangioma of the liver[277,288–292] or neck,[293] with diffuse hemangiomatosis,[276,277] or with Klippel-Trenaunay syndrome[294,295] may develop hydrops and Kasabach-Merritt sequence with microangiopathic hemolytic anemia, thrombocytopenia, and consumptive coagulopathy (Figure 42.8). In these situations, treatment options for immature fetuses

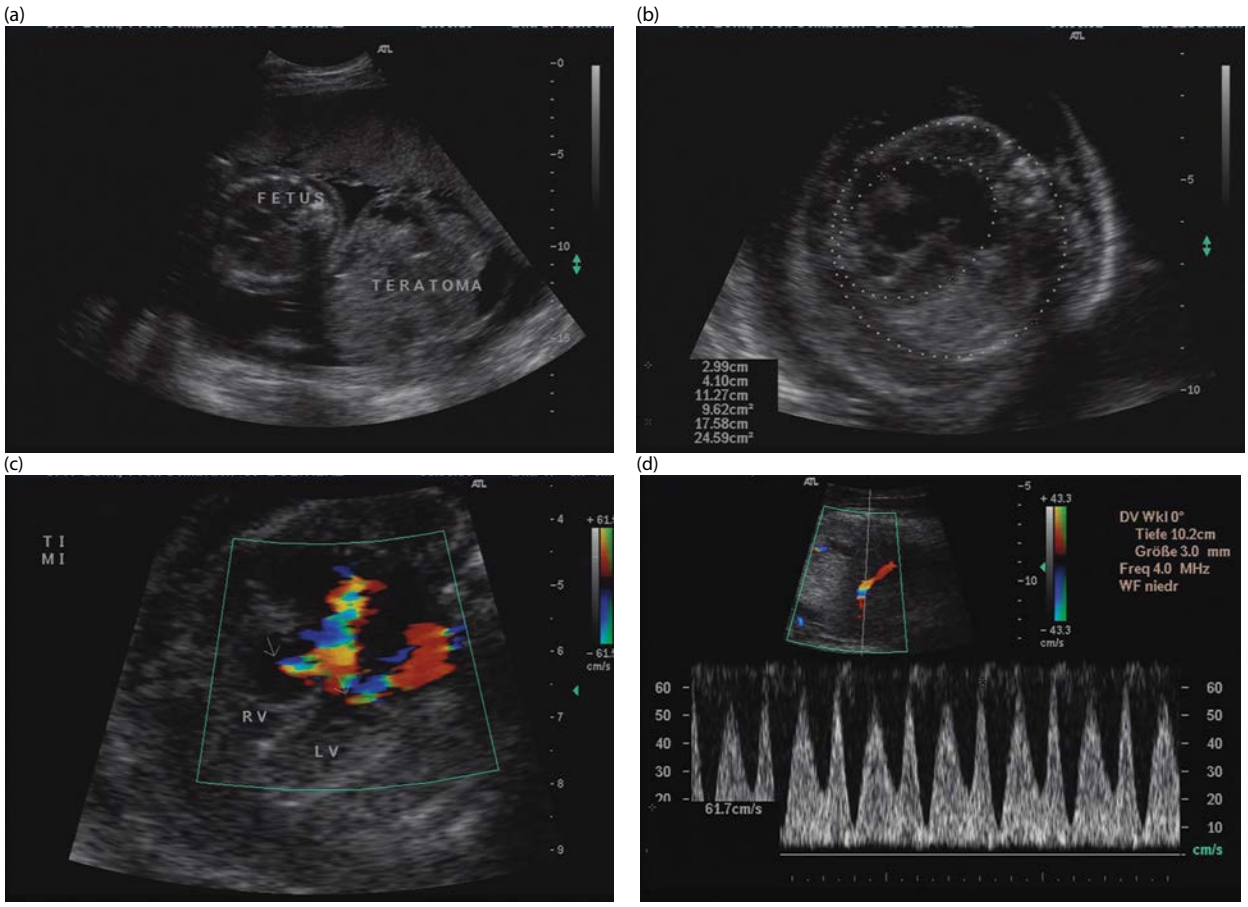


**Figure 42.6**
(a) Large solid sacral teratoma (dimensions 100 × 100 × 110 mm) with severe high-output cardiac failure in a fetus at 23 + 3 weeks' gestation. (b) The fetal heart is markedly dilated and the cardiothoracic circumference (0.64) and the cardiothoracic area (0.39) ratios are increased. A thick generalized skin edema is present. (c) Severe holosystolic insufficiency of both atrioventricular valves is demonstrated by color Doppler imaging. (d) The blood flow velocity pattern of the ductus venosus already shows increased pulsatility.

developing hydrops may be the intrauterine transfusion of packed erythrocytes, if anemia is present, and of thrombocytes, if severe thrombocytopenia is present, and digitalization and high doses of placenta-crossing corticosteroids.[296,297]

Intracerebral arteriovenous malformations may involve and dilate the vein of Galen ("aneurysm" of the vein of Galen), resulting in a significant shunting of blood volume and high-output cardiac failure characterized by cardiomegaly, AV valve insufficiency, and development of hydrops fetalis and placentae as well as polyhydramnios (Figure 42.9).[245,298–301] In addition, brain damage may occur if there is a relevant arteriovenous blood shunting that bypasses the brain parenchyma ("steal" phenomenon). Sinus venosus atrial septal defect with partially anomalous pulmonary venous return and discrete aortic coarctation are probably associated with the increased blood flow through the low resistance circuit of the vein of Galen early in gestation.[299] Palliative treatment with digoxin seems to be the only sensible approach in immature nonviable fetuses with high-output cardiac failure.

Other examples of secondary dilated cardiomyopathies with more direct myocardial damage may be observed in fetuses with infections, for example, coxsackievirus,[302] adenovirus,[303,304] and parvovirus B19,[305–313] or by maternal autoantibody-induced myocarditis, mostly associated with atrioventricular block.[209–211,215–219] *Trypanosoma cruzi,* the agent of Chagas disease in Latin America, may *in utero* transmit to the fetus, resulting in placentitis, fetal anemia, infection of fetal organs including myocarditis, and hydrops.[314,315] Significant hypertrophic cardiomyopathy has rarely been reported *in utero*, particularly in association with maternal diabetes, Noonan syndrome, and lysosomal and glycogen storage diseases.

A secondary cardiomyopathy of dilated but also hypertrophic type can more frequently be found in the recipient twin of twin-twin transfusion syndrome and in fetuses with long-standing tachy- and bradyarrhythmia. In the recipient twin of chronic fetofetal transfusion syndrome, increased pulsatility of the systemic veins suggests elevated central venous blood pressure. Elevated afterload and preload by arterial hypertension and hypervolemia, respectively, cause significant ventricular pressure and volume load. Biventricular myocardial hypertrophy, cardiomegaly, and AV valve incompetence as further signs for congestive heart failure usually appear before the development of hydrops.[316–320] In contrast,

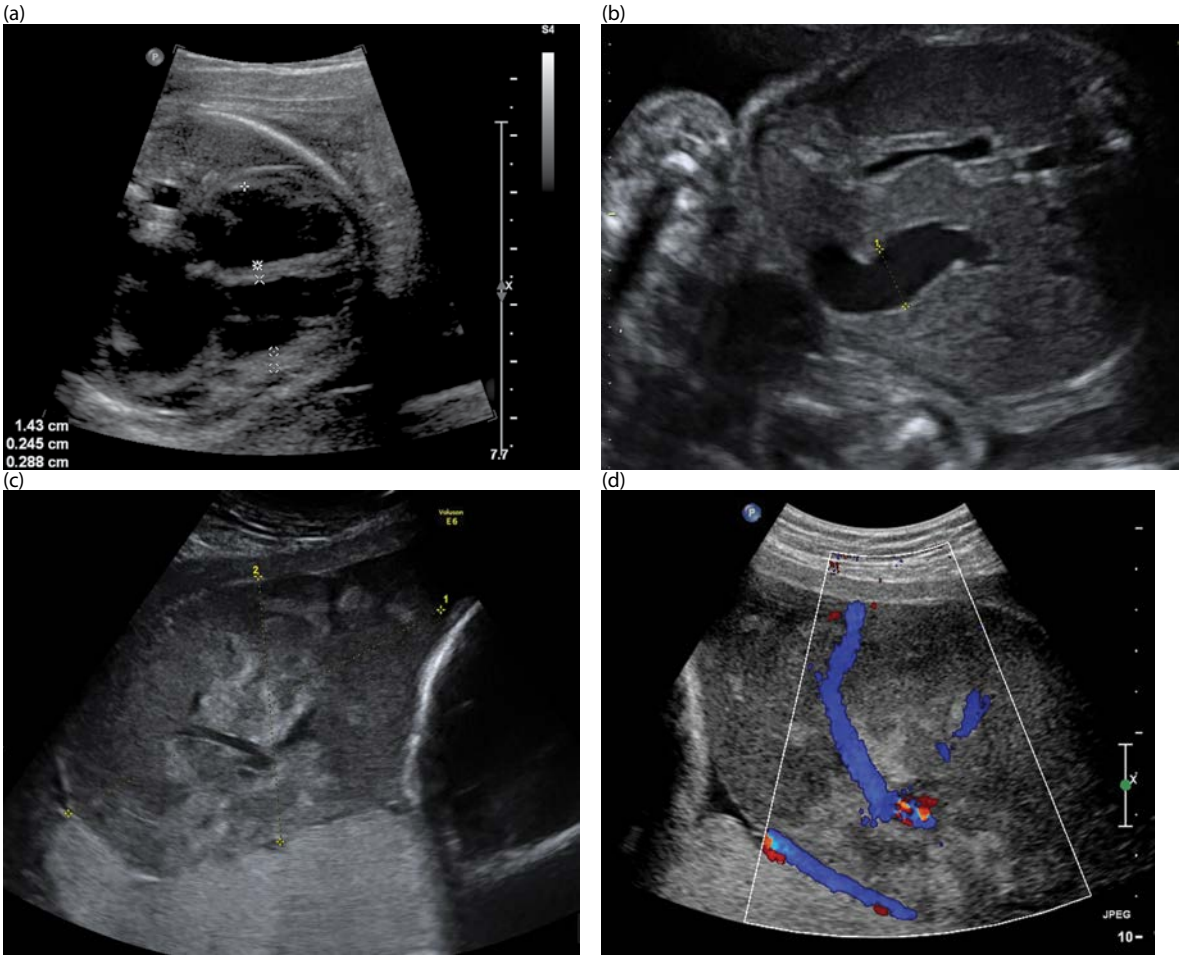


**Figure 42.7**
(a) Biventricular dilatation of the ventricles due to high-output cardiac failure in a fetus at 26 + 1 weeks' gestation. (b) The precordial veins are dilated, on this image the intraabdominal part of the umbilical vein. (c) The underlying disease was a large placental chorangioma (dimensions 123 × 77 × 136 mm). (d) A hypervascularization of the chorangioma was shown by color Doppler imaging.

generalized hydrops, AV valve incompetence, and increased pulsatility of venous blood flow are extremely rare in the donor fetus,[320] which may show only occasionally isolated mild to moderate pericardial effusion and rarely hydrops if severe anemia is present. Furthermore, transient hydrops and significant increase of venous pulsatility may occur in some donor fetuses after laser coagulation for severe twin-twin transfusion syndrome and indicate a hemodynamic adaptation response following interruption of the transfusion process.[321]

Cardiac compression may impair cardiac function. Massive bilateral and unilateral pleural effusion caused by a localized and generalized lymphatic disorder, increased venous pressure, and cardiac compression resulting in generalized hydrops. Under these disorders, primary hydrothoraces most frequently result from a local pleuromediastinal lymph vessel disturbance. More rarely presented are diseases with generalized lymphatic disorders, as Noonan and multiple pterygium colli syndrome, congenital lymphedema syndrome, or congenital pulmonary lymphangiectasia. Large chest masses may also cause cardiac compression with low cardiac output state, and impairment of lymphatic and venous return. Such chest masses are congenital pulmonary airways malformation (CPAM)—also named congenital cystic adenomatoid malformation of the lung (CCAML) with a macrocystic, microcystic, and mixed type—bronchopulmonary sequestration with accompanying pleural effusion, and rarely mediastinal and pericardial teratoma. Cardiac compression, disturbance of venous return, and lymphatic tissue drainage with consecutive hydrops fetalis may also be caused by congenital high airways obstruction sequence, sometimes as part of Fraser syndrome.[322] During fetal life, several end-stage renal diseases, such as polycystic kidney diseases and renal agenesis, are associated with severe biventricular myocardial hypertrophy and dysfunction resulting in low cardiac output and sometimes hydrops fetalis.[323]

Depending on the underlying disease, significant cardiac enlargement and/or myocardial hypertrophy may be present in fetuses with cardiomyopathy. If fetal hydrops is associated, additional signs of congestive heart failure are usually identifiable. These include reduced ventricular fractional shortening, tricuspid and/or mitral valve regurgitation, and increased

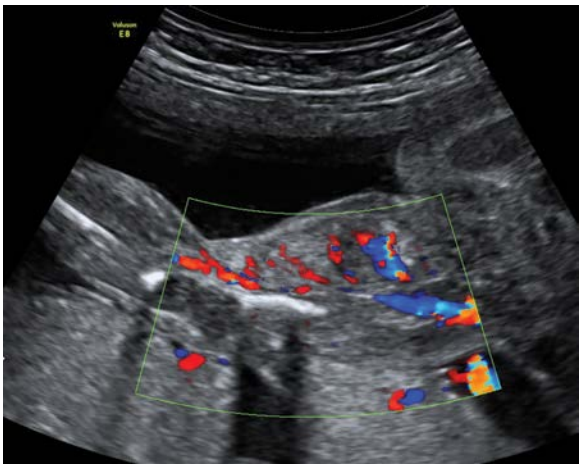

**Figure 42.8**
A Klippel-Trenaunay-Weber syndrome was diagnosed in a hydropic fetus with ascites and cranial skin edema at 23 + 5 weeks' gestation. On his right side, the upper and the lower right leg were edematous and massively swollen by bony and soft tissue hypertrophy, as well. Color Doppler imaging visualized hypervascularization and hyperperfusion of the right upper leg.

pulsatility of the venous Doppler blood flow pattern. Locally circumscribed or more general hyperechogenicity of the ventricular myocardium may suggest myocardial infection. In all cases of fetal cardiomyopathy, a detailed search for the underlying disease should be performed, because the exact diagnosis is the key to the prognosis, perinatal management, and adequate counseling of the parents. In some secondary cardiomyopathies, *in utero* treatment may be successful. This includes intrauterine blood transfusion in fetuses with anemia, transplacental treatment with corticosteroids in fetuses with myocarditis, or laser coagulation of placental anastomosis in fetuses with twin-twin transfusion syndrome. In addition, transplacental treatment with digoxin may result in a nonspecific increase of myocardial inotropy causing remission of hydrops or stabilization of the fetal condition in cases with unclear etiology. Digoxin is known to decrease the catecholamine response to congestive heart failure and may improve filling and low filling pressure, if there is diastolic dysfunction in the fetus.[51] If there is an elevated afterload, however, increase in oxygen consumption could result from increased inotropy without improved myocardial perfusion.[51] It should be kept in mind that the prognosis is usually poor in fetuses with metabolic storage diseases or primary cardiomyopathy, if hydrops develops *in utero*. Therefore, aggressive *in utero* and perinatal management must be carefully considered and may only be performed with informed consent by the extensively counseled parents.

## Hydrops fetalis in early gestation

In the first and early second trimester, many more hydropic fetuses have chromosomal abnormalities compared to hydropic fetuses of the late second and third trimesters.[20,324] Almost all of these fetuses have increased nuchal translucency thickness or cystic hygromata colli; the latter represent distended fluid-filled lymphatic vessels in the nuchal region, frequently associated with generalized malformation of the lymphatic vessels resulting in hydrothorax, ascites, and generalized skin edema.[325] The vast majority of hydropic fetuses die spontaneously. Some fetuses with complex cardiac malformations developing hydrops die spontaneously early in pregnancy. These include fetuses with severe bivalvular stenoses of the pulmonary and aortic valve[326] and fetuses with an absent pulmonary valve and patent arterial duct. Furthermore, in early pregnancy, fetuses with trisomy 21 very often have transient nuchal edema,[327] but in some cases, a generalized skin edema and hydrops fetalis may occur. Both groups contain fetuses without cardiac defects, although the incidence of atrioventricular septal defects and ventricular septal defects is much higher in fetuses with increased nuchal translucency and generalized hydrops.[328] Also, in the group of euploid fetuses, nuchal translucency

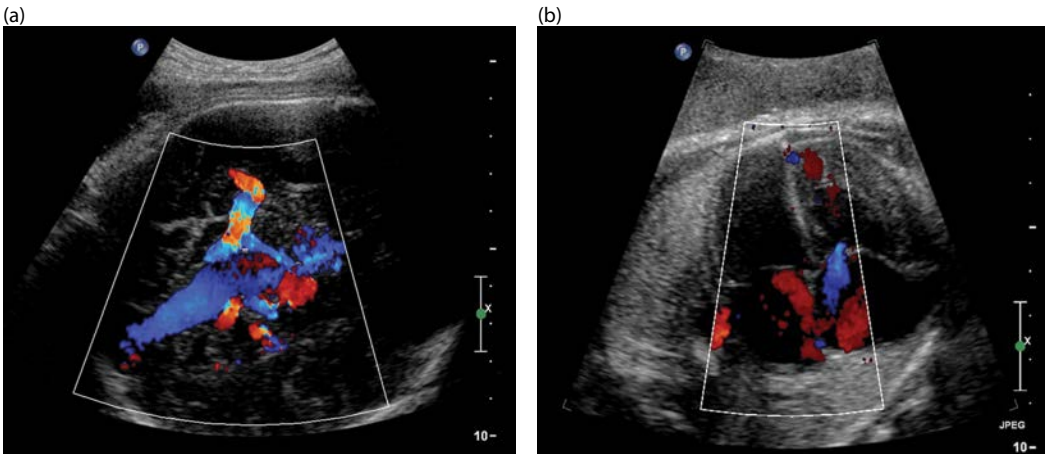


**Figure 42.9**
(a) Intracerebral arteriovenous malformation with a distinctly dilated vein of Galen was demonstrated by color Doppler imaging in a fetus at 35 + 2 weeks' gestation. Intracerebral arteries fistulized with a much dilated median prosencephalic vein of Markowski, which drained into an enlarged straight sinus. (b) The fetal heart showed biventricular dilatation with moderate tricuspid and mitral regurgitation, as well.

thickness correlates with the prevalence of congenital heart disease.[329] Therefore, increased nuchal translucency has been proposed as a screening method for fetal congenital heart diseases in chromosomally normal fetuses.[329] In the majority of both chromosomally abnormal and normal fetuses with isolated increased nuchal translucency, the nuchal fluid accumulation disappears after 14 weeks, most probably because of more efficient drainage of the interstitial fluid by the lymphatic system, increasing myocardial performance, and/or the drop in peripheral arterial resistance.[327,330] In some hydropic fetuses, but also in fetuses with isolated nuchal edema, the presence of AV valve regurgitation and abnormal venous Doppler flow velocity waveforms suggests cardiac congestive heart failure as a pathomechanism for the development of nuchal edema and hydrops.[331,332] But in some hydropic fetuses with trisomy 21, only cardiac defects seem to be associated. In these fetuses and in hydropic trisomy 21 fetuses without cardiac anomalies, other pathomechanisms have to be discussed. These include a transient myeloproliferative disorder and maldevelopment of lymphatic vessels, especially in cases of isolated hydro-/chylothorax that may be found in fetuses with trisomy 21, hypoxia-induced capillary damage, a transient myeloproliferative disorder, and/or altered collagen formation due to a dose effect from responsible genes on chromosome 21.

Nuchal edema and hydrops may be associated with other autosomal trisomies, such as trisomies 18 and 13, and triploidy.[326] Although the isolated nuchal edema may be transient, hydrops already occurring in the first and early second trimester is associated with spontaneous abortion in the vast majority of these fetuses. Septated cystic hygromata colli are associated with monosomy X (Turner syndrome) in two-thirds of fetuses and with a normal karyotype in the majority of the residual cases.[324] Because of a more generalized maldevelopment of the lymphatic vessels, hydrothorax and also hydrops often occur, and the fetuses die during the next few gestational weeks. In these fetuses, a tubular coarctation of the aorta may frequently be present, probably resulting from early compression of the aortic arch by the distended lymphatic vessels.[327]

## Conclusion

During fetal life, fetal hydrops indicates a severe disease, which can easily be detected by obstetric ultrasound. The enormous spectrum of underlying diseases requires a high level of diagnostic knowledge. The prognosis of hydropic fetuses is crucially dependent on the etiology of hydrops, which has to be identified for adequate perinatal management, assessment of prognosis, and counseling of the parents. The examination of the fetal cardiovascular system is one of the most important steps in this context. Cardiovascular diseases may frequently be the etiological disorder in fetal hydrops. Additionally, signs of congestive heart failure may be associated with many extracardiac causes of fetal hydrops. Fetal echocardiography allows repetitive assessment to be made of fetal cardiac function, providing important information about prognosis, fetal surveillance, and monitoring of therapeutic measures. Therefore, fetal hydrops demonstrates the need for a profound knowledge of perinatal cardiology to achieve adequate management. The effective, speedy, and stepwise diagnostic approach from less to more invasive techniques is a valid indicator of the competence of any prenatal care center.

## References


1. Holzgreve W. The fetus with nonimmune hydrops. In: Harrison MR, Golbus MS, Filly RA, eds. *The Unborn Patient. Prenatal Diagnosis and Treatment*, 2nd ed. Philadelphia, PA: WB Saunders; 1990:228–45.
2. Society of Maternal-Fetal Medicine (SFMF); Mari G, Norton ME, Stone J, Berghella V, Sciscione AC, Tate D, Schenone MH. *Am J Obstet Gynecol* 2015;212:697–710.
3. Society for Maternal-Fetal Medicine (SMFM); Norton ME et al. *Am J Obstet Gynecol* 2015;212:127–39.
4. Hutchinson AA et al. *Obstet Gynecol* 1982;59:347–52.
5. McCoy MC et al. *Obstet Gynecol* 1995;85:578–82.
6. Holzgreve W et al. *Am J Obstet Gynecol* 1984;148:805–12.
7. Holzgreve W et al. *Semin Perinatol* 1985;9:52–67.
8. Hansmann M et al. *Fetal Ther* 1989;4:29–36.
9. Hansmann M et al. Management of the fetus with nonimmune hydrops. In: Harrison MR, Golbus MS, Filly RA, eds. *The Unborn Patient. Prenatal Diagnosis and Treatment*, 2nd ed. Philadelphia, PA: WB Saunders; 1990:246–8.
10. Machin GA. *Am J Med Genet* 1989;34:366–90.
11. Jones DC. *Semin Perinatol* 1995;19:447–61.
12. Tercanli S et al. Nonimmune hydrops fetalis: Diagnosis and management. In: Callen PW, ed. *Ultrasonography in Obstetrics and Gynecology*, 4th ed. Philadelphia, PA: WB Saunders; 2000:551–75.
13. Forouzan I. *Obstet Gynecol Surv* 1997;52:130–8.
14. Norton ME. *Semin Perinatol* 1994;18:321–32.
15. Macafee CA et al. *J Obstet Gynaecol Br Commonw* 1970;77:226–37.
16. Maidman JE et al. *Obstet Gynecol* 1980;56:571–6.
17. Bellini C et al. *Am J Med Genet A* 2015;167A:1082–8.
18. Snijders RJM et al. *Prenat Diagn* 1994;14:543–52.
19. Anandakumar C et al. *Ultrasound Obstet Gynecol* 1996;8:196–200.
20. Iskaros J et al. *Obstet Gynecol* 1997;90:321–5.
21. Jauniaux E. *Prenat Diagn* 1997;17:1261–8.
22. Im SS et al. *Am J Obstet Gynecol* 1984;148:566–9.
23. Wafelman LS et al. *Biol Neonate* 1999;75:73–81.
24. Knilans TK. *Semin Perinatol* 1995;19:483–92.
25. Arcasoy MO, Gallagher PG. *Semin Perinatol* 1995;19:502–15.
26. Gembruch U, Holzgreve W. The fetus with nonimmune hydrops. In: Harrison MR, Evans MI, Adzick NS, Holzgreve W, eds. *The Unborn Patient: The Art and Science of Fetal Therapy*, 3rd ed. Philadelphia, PA: WB Saunders; 2001:525–82.
27. Apkon M. *Semin Perinatol* 1995;19:437–46.
28. Wu PYK. Colloid osmotic pressure and osmoregulation in the pregnant woman, fetus, and neonate. In: Polin RA, Fox WW, eds. *Fetal and Neonatal Physiology*, 2nd ed. Philadelphia, PA: WB Saunders; 1998:1721–6.
29. Brace RA. Fluid distribution in the fetus and newborn. In: Polin RA, Fox WW, eds. *Fetal and Neonatal Physiology*, 2nd ed. Philadelphia, PA: WB Saunders; 1998:1703–13.

30. Anderson PAW et al. Cardiovascular function during normal fetal and neonatal development and with hypoxic stress. In: Polin RA, Fox WW, eds. *Fetal and Neonatal Physiology*, 2nd ed. Philadelphia, PA: WB Saunders; 1998:837–90.
31. Gold PS, Brace RA. *Microvasc Res* 1988;36:262–74.
32. Pasman SA et al. *Am J Obstet Gynecol* 2006;194:972–5.
33. Brace RA, Gold PS. *Am J Physiol* 1984;247:R800–5.
34. Brace RA. *Am J Obstet Gynecol* 1989;160:494–7.
35. Gest AL. *Pediatr Res* 1992;32:585–8.
36. Nageotte MP et al. *Obstet Gynecol* 1989;73:867–70.
37. Ville Y et al. *Am J Obstet Gynecol* 1994;171:777–83.
38. Brace RA, Christian JL. *Am J Physiol* 1981;240:H843–7.
39. Adamson SL et al. *Circ Res* 1992;70:761–72.
40. Faber JJ, Anderson DF. *Placenta* 1997;18:313–26.
41. Johnson P et al. *Am J Obstet Gynecol* 1992;167:1309–13.
42. Weiner CP. *Am J Obstet Gynecol* 1993;168:817–23.
43. Hecher K, Campbell S. *Ultrasound Obstet Gynecol* 1996;7: 68–83.
44. Gudmundsson S et al. *Am J Obstet Gynecol* 1991;164:33–7.
45. Reed KL et al. *Obstet Gynecol* 1996;87:617–20.
46. Gembruch U et al. *Am Heart J* 1993;125:1290–301.
47. Saltzman DH et al. *Obstet Gynecol* 1989;74:106–11.
48. Skoll MA et al. *Ultrasound Obstet Gynecol* 1991;1:309–12.
49. Smoleniec J, James D. *Fetal Diagn Ther* 1995;10:95–100.
50. Huhta JC et al. Fetal congestive heart failure. In: Allan L, Hornberger LK, Sharland G, eds. *Textbook of Fetal Cardiology*. London: Greenwich Medical Media; 2000:565–75.
51. Huhta JC. *Semin Fetal Neonatal Med* 2005;10:542–52.
52. Hofstaetter C et al. *J Matern Fetal Neonatal Med* 2006;19:407–13.
53. Bijnens B et al. *Fetal Diagn Ther* 2012;32:5–16.
54. Crispi F, Gratacós E. *Fetal Diagn Ther* 2012;32:47–64.
55. Herberg U et al. *Minerva Pediatr* 2014;66:453–71.
56. Merz WM, Gembruch U. *Ultrasound Obstet Gynecol* 2014;44: 377–85.
57. Sharland GK, Allan LD. *Ultrasound Obstet Gynecol* 1992;2: 175–81.
58. Tan J et al. *Am J Cardiol* 1992;70:1459–67.
59. Shapiro I et al. *Ultrasound Obstet Gynecol* 1998;12:404–18.
60. Gembruch U et al. *Fetal Diagn Ther* 2000;15:20–31.
61. Paladini D et al. *Obstet Gynecol* 1993;81:679–82.
62. Respondek M et al. *Eur J Obstet Gynecol Reprod Biol* 1992;44: 185–8.
63. Chaoui R et al. *Fetal Diagn Ther* 1994;9:92–104.
64. Carlson DE et al. *Am J Obstet Gynecol* 1990;163:1785–7.
65. Sutton MS et al. *Br Heart J* 1991;61:285–9.
66. Rizzo G et al. *Ultrasound Obstet Gynecol* 1995;5:247–52.
67. Thakur V et al. *Can J Cardiol* 2013;29:759–67.
68. Tsutsumi T et al. *Pediatr Int* 1999;41:722–7.
69. Raboisson MJ et al. *Circulation* 2004;110:3043–8.
70. Szwast A et al. *Ultrasound Obstet Gynecol* 2007;30:40–6.
71. Aoki M et al. *J Am Soc Echocardiogr* 2004;17:28–35.
72. Spinale FG et al. *Am J Physiol* 1995;268:H836–47.
73. Packer DL et al. *Am J Cardiol* 1986;57:563–70.
74. Spinale FG et al. *Circulation* 1992;85:717–29.
75. Tomita M et al. *Circulation* 1991;83:635–44.
76. Respondek K et al. *Am J Obstet Gynecol* 1994;171:1265–70.
77. Gembruch U, Smrcek JM. *Ultrasound Obstet Gynecol* 1997;9: 374–82.
78. Smrcek JM, Gembruch U. *Prenat Diagn* 1999;19:197–204.
79. Smrcek JM et al. *Ultrasound Obstet Gynecol* 1998;12:254–9.
80. Gembruch U et al. *Am Heart J* 1991;121:1489–97.
81. Tulzer G et al. *J Matern Fetal Invest* 1991;1:15–18.
82. Reed KL et al. *Obstet Gynecol* 1997;89:953–6.
83. Gudmundsson S et al. *Ultrasound Obstet Gynecol* 1996;7:262–7.
84. Baschat AA et al. *Am J Obstet Gynecol* 2004;191:277–84.
85. Berg C et al. *Ultrasound Obstet Gynecol* 2006;28:137–42.
86. Tulzer G et al. *Ultrasound Obstet Gynecol* 1994;4:279–83.
87. Gembruch U et al. *Ultrasound Obstet Gynecol* 1995;5:394–9.
88. Krapp M et al. *Ultrasound Obstet Gynecol* 1997;10:32–40.
89. Gembruch U et al. *Eur J Obstet Gynecol Reprod Biol* 1999;84: 187–92.
90. Lutin WA et al. *Pediatr Cardiol* 1999;20:390–5.
91. McFadden DE, Taylor GP. *Pediatr Pathol* 1989;9:11–17.
92. Attenhofer Jost CH et al. *Swiss Med Wkly* 2005;135:269–81.
93. Pavlova M et al. *Am Heart J* 1998;135:1081–5.
94. McElhinney DB et al. *Am J Cardiol* 2005;96:582–6.
95. Andrews RE et al. *Am J Cardiol* 2008;101:1046–50.
96. Freud LR et al. *Circulation* 2015;132:481–9.
97. Wertaschnigg D et al. *Can J Cardiol* 2016;32:1500–6.
98. Gottschalk I et al. *Ultraschall Med* 2017;38(4):427–36.
99. Ishii T et al. *Ultrasound Obstet Gynecol* 2012;40:55–61.
100. Selamet Tierney ES et al. *Am J Cardiol* 2017;119:106–11.
101. Sharland GK et al. *J Am Coll Cardiol* 1991;17:944–9.
102. Lang D et al. *J Am Coll Cardiol* 1991;17:1161–7.
103. Tanaka T et al. *Pediatr Cardiol* 1998;19:133–8.
104. Robertson DA, Silverman NH. *J Am Coll Cardiol* 1989;14: 1300–7.
105. Atkins DL et al. *Circulation* 1982;66:281–3.
106. Allan LD et al. *J Am Coll Cardiol* 1994;23:1452–8.
107. Hornberger LK et al. *J Am Coll Cardiol* 1991;17:167–73.
108. Koike T et al. *J Perinat Med* 1997;25:295–7.
109. Gembruch U et al. *Geburtshilfe Frauenheilkd* 1988;48:445–7.
110. Gembruch U et al. *Eur J Obstet Gynecol Reprod Biol* 1989;31: 9–22.
111. Machado MVL et al. *Br Heart J* 1988;60:512–15.
112. Baschat AA et al. *Ultrasound Obstet Gynecol* 1999;14:311–14.
113. Schmidt KG et al. *J Am Coll Cardiol* 1991;17:1360–6.
114. Ettedgui JA et al. *Am J Cardiol* 1990;66:233–4.
115. Persutte WH et al. *J Ultrasound Med* 1990;9:541–5.
116. Liang CC et al. *Gynecol Obstet Invest* 1997;44:61–3.
117. Berg C et al. *Ultrasound Obstet Gynecol* 2007;30:254–8.
118. Gottschalk I et al. *Ultrasound Obstet Gynecol* 2016 May 31. doi:10.1002/uog.15977. [Epub ahead of print].
119. Razavi RS et al. *Am J Cardiol* 2003;91:429–32.
120. Volpe P et al. *Ultrasound Obstet Gynecol* 2004;24:623–8.
121. Galindo A et al. *Ultrasound Obstet Gynecol* 2006;28:32–9.
122. Wertaschnigg D et al. *Ultrasound Obstet Gynecol* 2013;41:162–7.
123. Cook AC et al. *Br Heart J* 1995;74:443–8.
124. Sousa-Uva M et al. *Ann Thorac Surg* 1996;61:1805–10.
125. Freund MW et al. *Fetal Diagn Ther* 2007;2:335–8.
126. Huhta JC. The fetal ductus arteriosus. In: Copel JA, Reed KL, eds. *Doppler Ultrasound in Obstetrics and Gynecology*. New York, NY: Raven Press; 1994:325–31.
127. Harada K et al. *Ultrasound Obstet Gynecol* 1997;10:247–53.
128. Hofstadler G et al. *Am J Obstet Gynecol* 1996;174:879–83.
129. Leal SD et al. *Am J Perinatol* 1997;14:205–10.
130. Harlass FE et al. *Obstet Gynecol Surv* 1989;44:541–3.
131. Chaoui R et al. *Geburtshilfe Frauenheilkd* 1989;49:1096–8.
132. Tulzer G et al. *J Matern Fetal Invest* 1992;1:267–9.
133. Moise KJ. *Am J Obstet Gynecol* 1993;168:1350–3.
134. Tulzer G et al. *J Am Coll Cardiol* 1991;18:532–6.
135. Kohl T et al. *Am J Cardiol* 2000;85:1230–3.
136. Szwast A et al. *Ann Thorac Surg* 2009;87:1214–9.
137. Olson RW et al. *Birth Defect* 1987;23:433–42.

138. Gembruch U et al. *Prenat Diagn* 1990;10:211–17.
139. Bharati S et al. *Am Heart J* 1991;122:597–600.
140. Bitar F et al. *Am J Perinatol* 1997;14:389–91.
141. Williams IA, Kleinman CS. *Ultrasound Obstet Gynecol* 2008; 31:96–9.
142. Yamamoto Y, Hornberger LK. *Early Hum Dev* 2012;88:279–85.
143. Rogers LS et al. *J Thorac Cardiovasc Surg* 2011;142:1381–7.
144. Vogel M et al. *J Am Coll Cardiol* 2011;57:348–55.
145. Herberg U et al. *Cardiol Young* 2014;24(suppl 2):47–54.
146. Goltz D et al. *Prenat Diagn* 2015;35:463–70.
147. Marshall AC et al. *Circulation* 2004;110:253–8.
148. Kohl T et al. *Ultrasound Obstet Gynecol* 2005;26:780–5.
149. Chaturvedi RR et al. *Int J Cardiol* 2013;168:2029–36.
150. Moon-Grady AJ et al. *J Am Coll Cardiol* 2015;66:388–99.
151. Vlahos AP et al. *Circulation* 2004;109:2326–30.
152. Redel DA, Hansmann M. Fetal obstruction of the foramen ovale detected by two-dimensional Doppler echocardiography. In: Rijsterbourgh H, ed. *Echocardiography*. The Hague: Martinus Nijhuis Publishers; 1981:425–9.
153. Pesonen E et al. *Arch Dis Child* 1983;58:1015–6.
154. Jouk PS et al. *Arch Mal Coeur* 1987;80:538–42.
155. Chobot V et al. *J Am Soc Echocardiogr* 1990;3:15–9.
156. Better DJ et al. *Heart* 1999;81:646–50.
157. Buis-Liem TN et al. *Prenat Diagn* 1987;7:425–31.
158. Phillipos EZ et al. *J Am Coll Echocardiogr* 1990;3:342–4.
159. Calhoun BC et al. *J Reprod Med* 1991;36:317–9.
160. Groves AM et al. *Arch Dis Child* 1992;67:1189–92.
161. Geipel A et al. *Ultrasound Obstet Gynecol* 2001;17:17–21.
162. Holley DG et al. *J Am Coll Cardiol* 1995;26:516–20.
163. Beghetti M et al. *Am Heart J* 1997;134:1107–14.
164. Sgro M et al. *Ultrasound Obstet Gynecol* 1999;14:356–9.
165. Sonigo P et al. *Pediatr Radiol* 1996;26:1–4.
166. Platt LD et al. *Am J Obstet Gynecol* 1981;141:107–9.
167. Wedemeyer AL, Breitfeld V. *Am J Dis Child* 1975;129:738–41.
168. Kamil D et al. *Ultrasound Obstet Gynecol* 2006;28:972–3.
169. Rheuban KS et al. *Pediatr Cardiol* 1991;12:54–6.
170. Perez-Aytes A et al. *Prenat Diagn* 1995;15:859–63.
171. Bruch SW et al. *J Pediatr Surg* 1997;32:1113–5.
172. Riskin-Mashiah S et al. *Prenat Diagn* 1998;18:1328–30.
173. Sklansky M et al. *Obstet Gynecol* 1997;89:807–9.
174. Benatar A et al. *Obstet Gynecol* 1992;79:856–9.
175. Czernik C et al. *Ultrasound Obstet Gynecol* 2006;28:973–6.
176. Bader R et al. *Am J Perinatol* 2006;23:53–8.
177. Devlieger R et al. *Fetal Diagn Ther* 2009;25:407–12.
178. Tomek V et al. *Pediatr Cardiol* 2010;31:1236–8.
179. Rychik J et al. *Am J Obstet Gynecol* 2016;215:780.e1–7.
180. Crum AK et al. *Fetus* 1992;2:74781–6.
181. Juul S et al. *Am J Dis Child* 1990;144:229–33.
182. Nagar AM et al. *J Ultrasound Med* 2003;22:553–659.
183. Chong C, Hutchins G. *Pediatr Dev Pathol* 2008;11:405–15.
184. Mastrolia SA et al. *Arch Gynecol Obstet* 2015;291:977–86.
185. Lopes LM et al. *Pediatr Cardiol* 1996;17:192–3.
186. Schleich JM et al. *Prenat Diagn* 2000;20:449–52.
187. Kleinman CS et al. *J Clin Ultrasound* 1985;13:265–73.
188. Kleinman CS, Copel JA. *Ultrasound Obstet Gynecol* 1991;1: 286–97.
189. Ko JK et al. *Am J Cardiol* 1992;69:1028–32.
190. Naheed ZJ et al. *J Am Coll Cardiol* 1996;27:1736–40.
191. Kleinman CS et al. Abstract presented at *2nd World Congress of Pediatric Cardiology and Cardiac Surgery*, Hawaii; 1997: 281ES.
192. Gest AL et al. *Am J Physiol* 1990;258:H1159–63.
193. Stevens DC et al. *Am J Obstet Gynecol* 1982;142:316–22.
194. Nimrod C et al. *Am J Obstet Gynecol* 1987;157:655–9.
195. Gest AL et al. *Biol Neonate* 1993;64:325–30.
196. Gest AL et al. *Pediatr Res* 1990;28:223–6.
197. Hansmann M et al. *Ultrasound Obstet Gynecol* 1991;1:162–70.
198. Van Engelen AD et al. *J Am Coll Cardiol* 1994;24:1371–5.
199. Simpson JM, Sharland GK. *Heart* 1998;79:576–81.
200. Jaeggi E et al. *J Pediatr* 1998;132:336–9.
201. Lisowski LA et al. *J Am Coll Cardiol* 2000;35:771–7.
202. Jaeggi ET et al. *Circulation* 2011;124:1747–54.
203. Vigneswaran TV et al. *Heart Rhythm* 2014;11:2047–53.
204. Strizek B et al. *Heart Rhythm* 2016;13:1283–8.
205. Sridharan S et al. *Heart Rhythm* 2016;13:1913–9.
206. Ekman-Joelsson BM et al. *Acta Paediatr* 2015;104:1090–7.
207. Gembruch U et al. *J Perinat Med* 1988;16:39–44.
208. Gembruch U et al. *Am Heart J* 1989;118:1335–8.
209. Groves AMM et al. *Heart* 1996;75:190–4.
210. Richards DS et al. *Obstet Gynecol* 1990;76:957–9.
211. Copel JA et al. *Am J Obstet Gynecol* 1995;173:1384–90.
212. Groves AM et al. *Circulation* 1995;15:3394–6.
213. Harris JP et al. *Am J Perinatol* 1993;10:217–19.
214. Anandakumar C et al. *Obstet Gynecol* 1996;87:835–7.
215. Trucco SM et al. *J Am Coll Cardiol* 2011;57:715–23.
216. Breur JM et al. *Ultrasound Obstet Gynecol* 2004;24:467–72.
217. Berg C et al. *Ultrasound Obstet Gynecol* 2005;26:4–15.
218. Jaeggi ET et al. *Circulation* 2004;110:1542–8.
219. Maeno Y et al. *Heart* 2005;91:1075–9.
220. Carpenter RJ et al. *J Am Coll Cardiol* 1986;8:1434–6.
221. Walkinshaw SA et al. *Fetal Diagn Ther* 1994;9:183–5.
222. Ho A et al. *Am J Cardiol* 2015;116:142–7.
223. Izmirly PM et al. *Ann Rheum Dis* 2016;75:1161–5.
224. Nii M et al. *Heart* 2006;92:1831–7.
225. Friedman DM et al.; for the PRIDE investigators. *Circulation* 2008;117:485–93.
226. Jaeggi ET et al. *J Am Coll Cardiol* 2011;57:1487–92.
227. Izmirly PM et al. *Circulation* 2012;126:76–82.
228. Schmidt KG et al. *Am J Cardiol* 1989;63:599–605.
229. Grebe S et al. *Fetal Diagn Ther* 2007;22:29–32.
230. Hidaka N et al. *J Ultrasound Med* 2007;26:519–24.
231. Stöllberger C et al. *Pediatr Cardiol* 2016;37:919–24.
232. Weber R et al. *JACC Heart Fail* 2014;2:403–11.
233. Ezon DS et al. *J Ultrasound Med* 2016;35:1949–55.
234. Atkin J et al. *Eur J Pediatr* 1984;142:150.
235. Steenhout P et al. *J Inherit Metab Dis* 1990;13:69–75.
236. Kooper AJA et al. *Clin Chim Acta* 2006;371:176–82.
237. Rodríguez MM et al. *Pediatr Dev Pathol* 2002;5:365–74.
238. Steward CG et al. *Prenat Diagn* 2010;30:970–6.
239. Igarashi H et al. *Pediatr Neurol* 1998;18:366–9.
240. Joseph JT et al. *Neurology* 1997;49:1457–60.
241. Patel CR et al. *J Am Soc Echocardiogr* 1996;9:721–3.
242. Hecher K et al. *Obstet Gynecol* 1995;85:122–8.
243. D'Ancona RL et al. *Ultrasound Obstet Gynecol* 1997;10:333–7.
244. Chui D, Waye S. *Blood* 1998;91:2213–22.
245. Ordorica SA et al. *Am J Obstet Gynecol* 1990;162:1166–7.
246. Van Selm M et al. *Obstet Gynecol Surv* 1991;46:785–8.
247. Carbillon L et al. *Obstet Gynecol Surv* 1997;552:310–14.
248. Gherman RB et al. *J Matern Fetal Med* 1998;7:227–9.
249. Duthie SJ, Walkingshaw SA. *Br J Obstet Gynaecol* 1995;102: 1011–13.
250. Braun T et al. *Fetal Diagn Ther.* 2010;27:191–203.
251. Ko TM et al. *Prenat Diagn* 1995;15:7–10.
252. Tongsong T et al. *J Clin Ultrasound* 1996;24:73–7.
253. Lam YH et al. *Prenat Diagn* 1997;17:267–9.

254. Lam YH, Tang M. *Prenat Diagn* 1997;17:501–4.
255. Lam YH et al. *Am J Obstet Gynecol* 1999;180:148–50.
256. Lam YH et al. *Ultrasound Obstet Gynecol* 1999;13:48–51.
257. Lam YH et al. *Ultrasound Obstet Gynecol* 1999;13:238–40.
258. Baschat AA et al. *Prenat Diagn* 1998;18:731–6.
259. Zerres K et al. *Lancet* 1990;335(8681):117.
260. Hendricks SK et al. *Obstet Gynecol* 1993;82:703–5.
261. Donnenfeld AE et al. *Prenat Diagn* 1994;14:721–4.
262. Macones GA et al. *Fetal Diagn Ther* 1995;10:131–3.
263. Smrcek JM et al. *Ultrasound Obstet Gynecol* 2001;17:403–9.
264. Hojo S et al. *Prenat Diagn* 2007;27:507–11.
265. Tamblyn JA et al. *Arch Dis Child Fetal Neonatal Ed* 2016;101: F67–71.
266. Statile CJ et al. *Ultrasound Obstet Gynecol* 2013;41:54–8.
267. Van Mieghem T et al. *Ultrasound Obstet Gynecol* 2014;43:611–9.
268. Weinraub Z et al. *Prenat Diagn* 1989;9:368–72.
269. Sherer DM et al. *Am J Obstet Gynecol* 1993;168:97–9.
270. Sherer DM, Onyeije CI. *Am J Perinatol* 1998;15:319–28.
271. Kuller JA et al. *J Perinatol* 1991;11:294–6.
272. Cyr DR et al. *J Ultrasound Med* 1988;7:87–90.
273. Holterman A-X et al. *J Pediatr Surg* 1998;33:899–903.
274. Roybal JL et al. *J Pediatr Surg* 2011;46:1325–32.
275. Navajas A et al. *Eur J Pediatr* 1997;156:62–4.
276. Wu TJ, Teng RJ. *Eur J Pediatr* 1994;153:759–61.
277. Gembruch U et al. *Ultrasound Obstet Gynecol* 2002;19:454–60.
278. Drut R et al. *Pediatr Pathol* 1993;13:9–13.
279. Hellmund A et al. *Fetal Diagn Ther* 2014;35:133–6.
280. Çetiner N et al. *Case Rep Obstet Gynecol* 2014;2014:487281.
281. Seifer DB et al. *Obstet Gynecol* 1985;66:283–6.
282. Carles D et al. *Ann Pathol* 1994;14:244–7.
283. Jones CE et al. *Pediatrics* 1972;50:901–7.
284. D'Ercole C et al. *Fetal Diagn Ther* 1996;11:357–60.
285. Horigome H et al. *Fetal Diagn Ther* 1997;12:241–3.
286. Lim FY et al. *Fetal Diagn Ther* 2015;37:18–23.
287. Russell RT et al. *Fetal Diagn Ther* 2007;22:183–5.
288. Anai T et al. *Acta Paediatr Jpn* 1992;34:324–7.
289. Gonen R et al. *Obstet Gynecol* 1989;73:485–7.
290. Skopec LL, Lakatua DJ. *Pediatr Pathol* 1989;9:87–93.
291. Albano G et al. *Acta Paediatr* 1998;87:1307–9.
292. Sharara FI, Khoury AN. *J Reprod Med* 1994;39:547–9.
293. Nakamura Y et al. *Pediatr Pathol* 1989;7:19–30.
294. Mor Z et al. *Am J Obstet Gynecol* 1988;159:1185–6.
295. Peng HH et al. *Prenat Diagn* 2006;26:825–30.
296. Sheu BC et al. *J Ultrasound Med* 1994;13:495–9.
297. Mejides AA et al. *Obstet Gynecol* 1995;85:850–3.
298. Sepulveda W et al. *Ultrasound Obstet Gynecol* 1995;6:282–6.
299. McElhinney DB et al. *Arch Dis Child* 1998;78:548–51.
300. Deloison B et al. *Ultrasound Obstet Gynecol* 2012;40:652–8.
301. Godfrey ME et al. *Fetal Diagn Ther* 2017;41(2):108–14.
302. Benirschke K et al. *Am J Cardiovasc Pathol* 1987;1:131–3.
303. Towbin JA et al. *Pediatr Infect Dis J* 1994;13:144–50.
304. Ranucci-Weiss D et al. *Prenat Diagn* 1998;18:182–5.
305. Porter HJ et al. *Lancet* 1988;5:535–6.
306. Naides SJ, Weiner CP. *Prenat Diagn* 1989;9:105–14.
307. Van Elsacker-Niele AM et al. *Br J Obstet Gynaecol* 1989;96: 768–75.
308. Katz VL et al. *J Perinatol* 1990;10:366–9.
309. Morey AL et al. *Br J Obstet Gynaecol* 1992;99:566–74.
310. Brandenburg H et al. *Prenat Diagn* 1996;16:75–7.
311. von Kaisenberg CS et al. *Fetal Diagn Ther* 2001;16:427–32.
312. von Kaisenberg CS, Jonat W. *Ultrasound Obstet Gynecol* 2001; 18:280–8.
313. Ramirez MM, Mastrobattista JM. *Clin Perinatol* 2005;32: 697–704.
314. Okumura M et al. *Prenat Diagn* 2004;24:179–81.
315. Coura JR. *Mem Inst Oswaldo Cruz* 2007;102(suppl 1):113–22.
316. Gembruch U et al. *J Matern Fetal Investig* 1993;3:201 (abstr).
317. Zosmer N et al. *Br Heart J* 1994;72:74–9.
318. Hecher K et al. *Ultrasound Obstet Gynecol* 1995;5:318–24.
319. Fesslova' V et al. *Am J Obstet Gynecol* 1998;179:1056–62.
320. Zikulnig L et al. *Ultrasound Obstet Gynecol* 1999;14:380–7.
321. Gratacós E et al. *Ultrasound Obstet Gynecol* 2002;19:449–53.
322. Ryan G et al. *Semin Fetal Neonatal Med* 2016;21:230–9.
323. Merz WM et al. *PLOS ONE* 2013;8:e63664.
324. Has R. *Clin Exp Obstet Gynecol* 2001;28:187–90.
325. Malone FD et al. *Obstet Gynecol* 2005;106:288–94.
326. Gembruch U et al. *Ultrasound Obstet Gynecol* 2000;16(suppl 1): 92 (abstr).
327. Snijders RJM et al. *Lancet* 1998;352:343–6.
328. Hyett JA et al. *Am J Med Genet* 1997;69:207–16.
329. Hyett J et al. *Br Med J* 1999;318:81–5.
330. Gembruch U et al. *Ultrasound Obstet Gynecol* 1993;3:310–17.
331. Matias A et al. *Ultrasound Obstet Gynecol* 1998;12:380–4.
332. Matias A et al. *Ultrasound Obstet Gynecol* 1999;14:307–10.

# 43

# Congestive heart failure in the fetus

James C. Huhta

## Introduction

Fetal echocardiography has progressed to be able to diagnose many forms of congenital heart disease and to assess the prognosis of cardiac lesions based on their anatomy and presentation *in utero*. However, the presence of signs of fetal heart failure such as hydrops or valvular regurgitation makes the assessment of prognosis more difficult.

Congestive heart failure, defined as inadequate tissue perfusion for normal organ development and function, is a final common pathway for all fetal disease states that lead to demise *in utero*. A tool for this assessment is the Cardiovascular Profile Score, which combines ultrasonic markers of fetal cardiovascular function based on univariate parameters that have been correlated with perinatal mortality documented in the literature (see the Appendix of this chapter).[1] This profile could then become the "heart failure score" and could potentially be used in the same way as, and in combination with, the Biophysical Profile Score (a noninvasive tool for assessment of brain function). This chapter reviews the pathophysiology of congestive heart failure prenatally and presents a straightforward method for the rapid evaluation of the fetus that may have fetal congestive heart failure. The progression from normal to the prehydropic state, to hydrops, is illustrated. The use of the score in the hydropic fetus to ascertain whether or not there are signs of congestive heart failure as the cause is discussed. Mechanisms of congestive heart failure such as increased afterload (such as seen in the twin-twin transfusion recipient), valvular or myocardial failure (such as seen in Ebstein malformation of the tricuspid valve), or high output failure (such as seen with anemia or sacro-coccygeal teratoma) are illustrated.

## The fetal circulation

After birth, the circulation consists of desaturated venous blood entering the right heart, and passing to the lungs with little or no admixture with oxygenated blood. The pulmonary venous blood is highly oxygenated and passes through the left atrium (LA) and left ventricle (LV) to the aorta. Therefore, the postnatal circulation is a series circuit. The fetal circulation is unique and significantly different from that in the newborn, infant, or child. Knowledge of these morphologic and physiologic differences is crucial for the understanding and assessment of fetal cardiovascular function. Most of this knowledge is derived from experimental animal data and, more recently, ultrasonography, which has allowed direct observation of the circulation in normal and abnormal human fetuses.

In the fetus, the ventricles pump blood in parallel rather than in series, with the LV pumping to the aorta and upper body, and the right ventricle (RV) pumping to the ductus arteriosus and the lower body and placenta.[2] The lungs have a high resistance *in utero*, and the placenta fulfills the role of oxygenating the blood and ridding the body of wastes, requiring a significant proportion of the combined cardiac output. The highly oxygenated blood from the placenta passes to the ductus venosus where a portion bypasses the liver and passes predominantly to the LA. The relatively deoxygenated blood from the upper body passes to the tricuspid valve and then to the ductus arteriosus and lungs. The deoxygenated blood from the inferior vena cava and the right hepatic veins is directed to the right atrium (RA) and predominantly to the tricuspid valve. This distribution of lower body flow is accomplished by the posterior portion of the inferior vena cava connecting directly to the foramen ovale and the superior portion of the atrial septum, the crista dividens, which overlies the inferior vena cava, effectively dividing it into two streams. Therefore, the presence of three shunts (ductus venosus, foramen ovale, and ductus arteriosus) allows the fetal heart to work with two parallel rather than one series circulation. Right and left atrial pressures are almost equal because of the presence of the foramen ovale, and right and left ventricular pressures are equal due to the ductus arteriosus. The LV ejects into the upper body and cerebral circulation, and the RV ejects into the pulmonary arteries and through the ductus arteriosus into the lower body and the placental circulation. The vascular beds of the upper and lower body are connected via the aortic isthmus. As a further consequence of the parallel arrangement of these circulations, ventricular outputs can be different and, in the case of obstruction on one side of the heart, the other side is able to increase its work or even completely supply the whole circulation alone.

## Factors affecting perinatal cardiac output

The cardiac ventricular output is the product of the heart rate and the stroke volume of both the right and LVs. The stroke volume is determined by the preload, afterload, and myocardial contractility of each ventricle. An increase in the stretch of the ventricular chamber will result in an increased contractility and stroke volume according to the Frank-Starling mechanism. This mechanism is now known to be present as early as 8 weeks' gestation in the human. This allows the cardiac output to be unchanged during periods of heart rate change between 50 and 200 beats per minute.

Distribution of cardiac output prenatally is different from that after birth and changes throughout gestation.[3] The fetal RV always ejects more blood than the LV (in the fetal lamb almost twice as much); the lungs are perfused only by a small (8%–25%) proportion of the combined ventricular output (CVO), the aortic isthmus 10%, and the placenta receives up to 40%–45% of the CVO. Umbilical vein flow is divided at the entrance to the liver, where approximately 50% of its highly oxygenated blood is shunted through the ductus venosus directly to the inferior vena cava (IVC), RA, and through the foramen ovale to the LA. The other 50% passes through the liver before reaching the IVC. Streaming within the IVC is such that the higher oxygenated blood, coming from the ductus venosus, is directed to the LA, whereas lower oxygenated blood from the hepatic circulation and superior vena cava (SVC) preferentially enters the RV. As a consequence, the coronary arteries and brain are perfused with higher oxygenated blood. In the case of circulatory compromise, the fetus will take advantage of these shunts to shift more oxygenated blood to the left side of the heart, thus ensuring adequate perfusion of vital organs. Throughout gestation, the distribution of the CVO changes such that, with increasing gestational age, the lower body, lungs, gut, and brain receive a higher percentage, and placenta and kidneys a lower percentage.[4]

Because the pulmonary and systemic circulations are separate in the fetus, each ventricle has a stroke volume determined by the individual preload, afterload, and contractility of that chamber. Both ventricles are linked by a common heart rate and humoral environment. They are also linked by the atrial pressures, which are similar due to the presence of the foramen ovale. They are also linked by the ventricular septum, which is shared by each ventricle, and by the common arterial pressure, which is the result of the widely patent ductus arteriosus. The unique feature of the parallel nature of the ventricular ejection is that if there is increased afterload of one ventricle, the output of that ventricle will fall, and the output of the contralateral ventricle will increase in a compensatory manner. This leads to the commonly observed feature associated with congenital heart disease of disproportionate growth of the normal side of the heart. A functional separation of the ventricles at the level of the aortic isthmus has been observed such that any blood pressure drop in the lower body causes increased right ventricular output without a change of ascending aortic pressure.

The metabolic source of energy for the fetal myocardium is glucose almost exclusively. In adults, fatty acids are the major source of energy for the myocardium. Growth or increased workload in the fetus results in hyperplasia of the myocardium with an increased number of cells, whereas growth of the myocardium after birth is increased only by cell size or hypertrophy (increased protein content of each cell).

Besides the difference in contractility, the fetal heart reacts differently in response to pre- and afterload changes. Several studies in isolated myocardium and intact hearts have demonstrated a reduced compliance of the fetal myocardium.[5] Studies of the effect of preload changes on cardiac output in the fetus have shown that, while a reduction of preload results in a decrease of cardiac output, cardiac output rises only when filling pressures increase 2–4 mm Hg above resting pressures, but a further increase of atrial pressure does not result in greater ventricular output.[4] This is in contrast to postnatal hearts, where a progressive increase in ventricular output is observed with an atrial pressure rise to 15–20 mm Hg. However, there is usually an interaction with afterload. Increased afterload in the fetus is followed by a reduction in myocardial shortening and in stroke volume. So, if arterial pressures are kept constant, ventricular stroke volume increases even with atrial pressures as high as 10–15 mm Hg.[6] Thus, the Frank-Starling mechanism is present in the fetus, although it operates at the upper limit. In the fetus, one has to consider that right ventricular afterload is mainly determined by the vascular bed of the placenta, while left ventricular output is determined by the cerebral circulation.

The effect of heart rate on fetal CVO is much more pronounced than it is postnatally. The fetus has a range of heart rates between 50 and 200 beats per minute, at which the stroke volume of the ventricular chambers can adapt to maintain adequate CVO and tissue perfusion. Outside of this range, heart failure will result.

In summary, the major determinant of cardiac output is the afterload of the fetal ventricle. Any influence that raises the impedance of ejection will inversely lower the ventricular stroke volume by the effect on both the systolic and diastolic functions of the heart. For example, in growth restriction in the fetus due to placental dysfunction, the combined cardiac output drops due to increased placental resistance.

## The transitional circulation

After birth, the function of gas exchange is transferred from the placenta to the lungs. The major changes in the circulation after birth are the decrease in pulmonary vascular resistance and the closure of the ductus arteriosus and foramen ovale. The ductus closes within 2–3 days in the term neonate, and the patency of the ductus during this time results in a significant left-to-right shunt. This raises the left atrial pressure and effectively restricts the right-to-left shunting at the atrial level. Shunting through the ductus venosus ceases normally within 2–3 days after birth.

# The etiology of hydrops fetalis

## *Cardiac failure in the fetus*

End-stage fetal heart failure results in hydrops fetalis. The reduced ability of the fetal heart to contract and to generate force, the lower myocardial compliance and the diminished Frank-Starling mechanism, the higher dependence of cardiac output on heart rate, and the lack of adrenoceptors all contribute to decreased cardiac reserve in response to stress and to a higher susceptibility of the fetus for the development of cardiac failure.

## *Factors contributing to hydrops*

Several features are responsible for fluid accumulation in fetal tissue. The final common pathway of many different conditions compromising the cardiovascular system is elevation of ventricular end-diastolic pressure, atrial pressure, and central venous pressure. In the fetus, even small increases in venous pressure have been shown to have great effects.[7] The younger the fetus, the higher is its extracellular water content and the lower is its tissue pressure. Fluid movement between intravascular and extravascular space is dependent on intra- and extravascular hydrostatic and oncotic pressure, and the fluid filtration coefficient, which is determined by the capillary membrane (in the fetus more permeable for fluid and protein). Albumin concentration, largely responsible for oncotic pressure, is lower in the fetus and increases with gestational age. All of these factors favor fluid movement out of the capillary into tissue. Thus, lymphatic drainage of tissue seems to be much more important in the fetus. An elevated venous pressure may reduce lymphatic flow, further favoring the development of hydrops. A decrease in arterial blood pressure and an elevation of filling pressures additionally trigger hormonal responses, including production of plasma arginine vasopressin (decreases urinary production), angiotensin II (increases fluid accumulation), and atrial natriuretic peptide (increases capillary permeability).

Pulmonary edema as part of congestive heart failure does not usually occur in the fetus. The reason for this is that in the presence of a patent foramen ovale, left atrial hypertension does not develop, the pulmonary arterioles are constricted, and there is a fluid-filled lung, where the positive intra-amniotic pressure is transmitted. However, in the case of total anomalous pulmonary venous drainage with stenosis of the draining vessel, or premature constriction or occlusion of the foramen ovale associated with left-sided obstructions, pulmonary venous hypertension can occur with secondary damage to the fetal lungs, such as pulmonary vascular disease and pulmonary lymphangiectasia.

Faced with the fetus with hydrops fetalis, one must first determine whether the hydrops is cardiac, inflammatory, or metabolic. Many cases of hydrops are now being attributed to fetal systemic infection. New markers are identifying etiologic agents such as parvovirus or adenovirus. The associated hepatitis with these infections can compromise the protein-producing capability of the fetus, thereby decreasing the fetal oncotic pressure in the vascular space and resulting in fluid loss out of the circulation. Immune hydrops must always be considered in the differential diagnosis, but other causes of anemia can cause hydrops, such as hemoglobinopathies. Infections can cause hemolytic anemia, which can be treated by fetal transfusion. High central venous pressure may exceed the oncotic pressure of the interstitial space, causing fluid to pass into spaces such as the abdominal cavity (ascites), pleural or pericardial spaces (effusions), or any of the vital organs. Multiple mechanisms of hydrops may coexist, and the primary cause may not be immediately obvious. Of more importance is determination of the prognosis of hydrops. This task would be aided by a semiquantitative measure of fetal heart failure. In other words, is this hydrops from heart failure? This chapter presents such an assessment tool.

The challenge of hydrops assessment and the diagnosis of heart failure can be summarized as the difficulty in knowing how well the fetal myocardium is performing under changing loading conditions. By combining information from the obstetrical and cardiological evaluations, the perinatal cardiologist can assess whether it is likely that the function abnormality is transient or permanent. The etiology cannot always be known, but the differential is often between infectious, inherited, congenital, or toxin-related.

After birth, the prognosis will depend on the diagnosis and the evolution of the functional abnormality over time. The long-term outcome will be dependent on whether or not the insult is reversible, and whether there were periods of ischemia and/or brain injury. There are several possibilities for the cause of heart failure in the fetus after ruling out fetal infection (Table 43.1).

**Table 43.1** Causes of fetal congestive heart failure

- Fetal arrhythmias (Figure 43.1)
- Anemia
- Congenital heart disease with valvular regurgitation (Figure 43.2)
- Noncardiac malformations such as diaphragmatic hernia or cystic hygroma
- Twin-twin transfusion recipient volume and pressure overload
- Arteriovenous fistula with high cardiac output (Figure 43.3)

# Prognosis of fetal heart failure: Markers of fetal mortality

The cardiovascular system provides a large volume of information about the well-being of the fetus. It is accessible because of rapid developments in the technology of noninvasive techniques, particularly ultrasound. The fetus has become the new patient of the decade, due to the rapid changes in ultrasonic technologies and other fetal assessment techniques. For example, fetal heart rate monitoring

**Table 43.2** Factors that should be considered in the assessment of fetal heart function

- Ventricular shortening less than 0.28
- Valvular regurgitation
- Tricuspid regurgitation (nonholosystolic but greater than 70 ms duration)
  - Significant tricuspid regurgitation (holosystolic)
  - Mitral regurgitation
  - Pulmonary or aortic valve regurgitation
  - Abnormal atrioventricular valve regurgitation dP/dt
    - Normal >1000 mm Hg/s
    - Mortality <400 mm Hg/s
- Ventricular hypertrophy
- Pattern of ventricular filling by pulsed Doppler

by nonfocused ultrasound can detect abnormal rate changes, and a lack of normal variability may be related to ischemia. New techniques examine the signal averaged electrocardiogram (ECG) to detect ST–T wave changes.[8] The fetal biophysical profile is useful to detect changes in fetal well-being, because it assesses brain function indirectly.[9] The decision to deliver a fetus prematurely due to cardiac changes must be made in the context of the risks both pre- and postnatally. Most associations of how cardiovascular changes correlate with other organ function in the fetus have yet to be defined. Therefore, any assessment demands a coordinated team approach between perinatologists, cardiologists, and neonatologists.[10] Table 43.2 lists factors to be considered in assessing fetal cardiac function.

The definition of fetal congestive heart failure is similar to after birth—inadequate tissue perfusion. Inadequate cardiac output results in a series of complex reflexes and adaptations to improve forward flow or direct it to vital organs. This state can be described as a deficiency of flow of blood to the tissues such that certain reflexes are triggered for the survival of the fetus. One is the secretion of an excess of circulating catecholamines, which are produced in response to peripheral vascular detection of abnormal perfusion. Powerful hormonal reflexes are triggered, including those that control salt and water retention, in an attempt to increase myocardial preload, and adrenocorticoid excess, which mobilizes additional calories for the increased metabolic demand that is present. It is now known that the fetus is capable of producing cytokine activation, as well as secreting endothelin, troponin T,[11] tumor necrosis factor, and brain natriuretic peptide (BNP).[12]

The maturational changes of the systemic vascular bed with gestational age are not known, but at some point in the pregnancy, it is thought that vasoconstriction of the fetal systemic resistance vessels occurs in response to stress. How this affects compensation in the fetal circulation is currently being investigated.

The most useful predictor of perinatal death in fetal hydrops is the presence of umbilical venous pulsations.[13] This is true because the most common pathway of perinatal demise is compromised fetal cardiac output—fetal congestive heart failure. What follows is a method to detect this entity, and to attempt to decide which fetus should be referred to a fetal center. Initially, data are collected during fetal echocardiography:

- Cardiac size/thoracic size (C/T): cardiac divided by thoracic area ratio (normal 0.25–0.35) or C/T circumference ratio (normal <0.5) (Figure 43.1)
- Venous Doppler: inferior caval (or hepatic venous) (increased atrial reversal) and umbilical cord vein (pulsations) (Figure 43.2)
- Four-valve Doppler: any leak of the valve should be evaluated further.

If there are abnormalities in any of these measurements, then a cardiac cause or associated physiological problem may be present, and detailed study is indicated to rule out serious cardiovascular involvement.

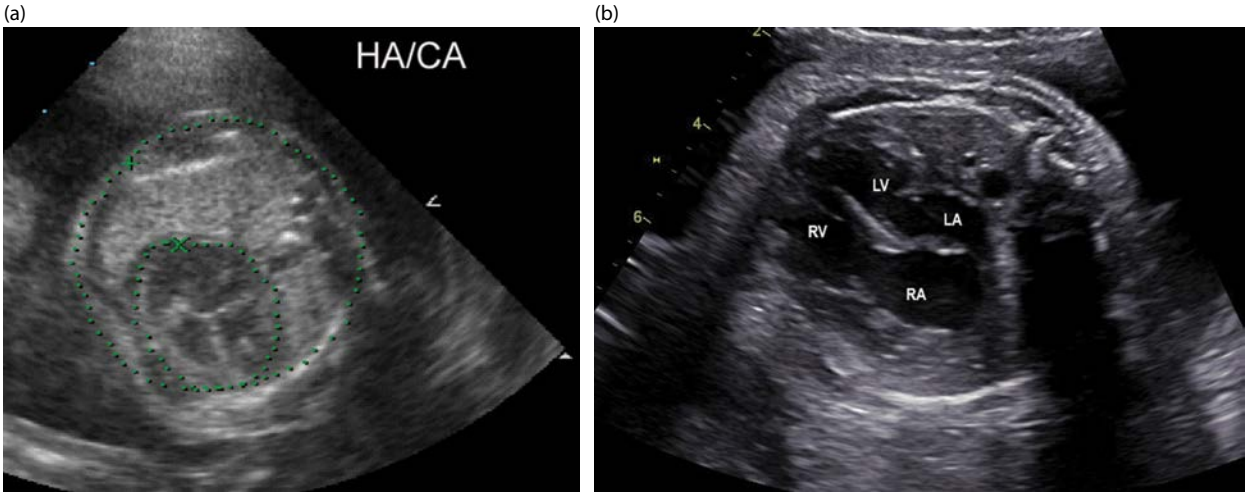


**Figure 43.1**
Heart area to chest area (HA/CA) ratio in a normal fetus showing the area ratio to be less than 0.3 (a). Marked heart enlargement with the HA/CA ratio greater than 0.5 (b) in a fetus with anemia.

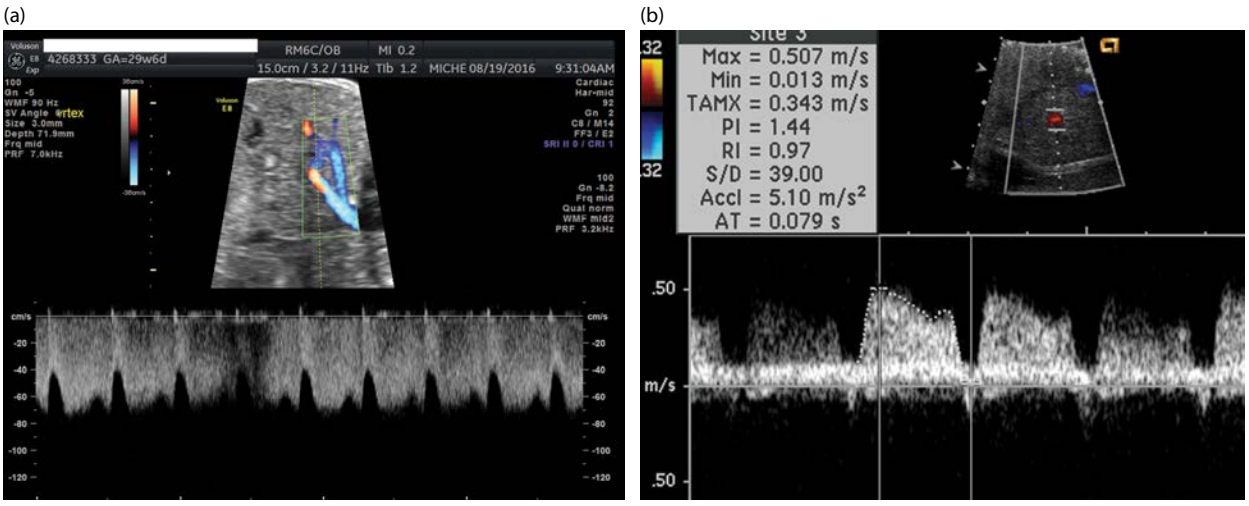


**Figure 43.2**
Ductus venosus Doppler (a) normal, and (b) with increased atrial contractions (increased pulsatility index) and small atrial reversal. Scale is in centimeters per second.

## Ventricular function in the fetus

Most attention has been paid to the right ventricular function in the human fetus, because this ventricle is most likely to show an abnormality during clinical situations associated with increased workload. The RV in the fetus is now understood to be a large contributor to the work output of the fetal myocardium because of the large volume and pressure work required of it. It is observed that the earliest signs of altered function in the fetal heart are a reflection of right heart hemodynamics. For example, isolated right atrial enlargement is a sign of many abnormalities, especially early in gestation. This may be because the RA is at the center of the fetal circulation. Flow from the superior vena cava is passing to the tricuspid valve, directed by the right venous valve inside the RA. Flow from left hepatic veins and the ductus venosus is crossing inferiorly across the RA to reach the foramen ovale and the LA. The normal flow from the RA to the LA reflects the normal right atrial to left atrial pressure gradient. Any increase in flow to the heart, such as with anemia or arteriovenous fistula, will translate into enlargement of the RA. The RV is pumping primarily to the lower body and placenta, and right atrial pressure elevation will result from any increase in the resistance that is seen by this ventricle. For example, placental dysfunction later in gestation will cause right ventricular dysfunction and secondary right atrial enlargement, while the LV will show no signs of dysfunction.

## Normal right ventricle growth and function

The geometry of the RV *in utero* is different from that of the LV. The RV is tripartite with inflow, apical, and outflow portions. Calculating the volume of this chamber is difficult because of the complex shape of the chamber. *In utero*, it is more spherical and more like the LV but still must be measured with nongeometric techniques. After birth, the RV atrophies, and the shape becomes more flattened and thinned. RV volume ejected is greater than LV by echocardiography measurements throughout gestation.[14] The RV supplies the pulmonary arteries, and the descending aorta and placenta via the ductus arteriosus. The high resistance of the pulmonary arteries is in parallel with the lower resistance of the lower body. The workload of the RV is determined by the volume of blood pumped and the afterload. In general, the work of the RV can be described as the product of the afterload (blood pressure) and the stroke volume of ejection. The afterload of the RV is unique because there are pressure reflections from the downstream resistance. These reflections from the proximal arterioles and, more important, from the proximal ductus arteriosus result in increased power expenditure for a given cardiac output. This is illustrated by the shortened acceleration time in the pulmonary valve compared to the aortic valve. In other words, the RV must perform the work of overcoming inertia, moving the mass of blood forward, and the oscillatory work resulting from the downstream pressure reflections that return to the pulmonary valve shortly after the onset of ejection. When the volume of blood pumped by a ventricle is reduced, the overall size of the ventricle becomes smaller than the contralateral side due to redistribution of flow at the atrial level. This finding of disproportion at the ventricular level is an excellent screening marker of ventricular dysfunction or congenital defect. Rarely does pressure overload alone result in ventricular dilatation.

Another indication that the RV is performing more work than the LV is given by data collected in fetal lambs measuring the coronary blood flow of both ventricles. The RV coronary flow was consistently one-third greater than that of the LV.[15] RV size limits the volume of blood that can be pumped with each systolic ejection. In situations with reduced RV size with an intrinsically normal RV, the RV volume can be

reduced by variables such as pericardial fluid, or diastolic stiffness. A hypoplastic RV chamber may limit ejection volume if a step increase in stroke volume is demanded of that chamber. The heart rate also limits the volume of blood that can be ejected by the RV or LV by limiting the filling time of the ventricle. With fetal tachycardia, the cardiac output will drop with increasing heart rate. It is known from clinical experience that the fetus with a heart rate greater than 240 beats per minute can become hydropic in 3–5 days during incessant tachycardia.

## *Changes with increasing gestational age*

The inflow pattern of blood velocity can be useful to determine the diastolic characteristics of the RV. The normal pattern is biphasic, with an early filling wave (E-wave) immediately after opening of the tricuspid valve followed by a later atrial contraction wave (A-wave). The atrial contraction augments RV filling, and the filling waves can sometimes be used to assess the filling properties of the RV. Tulzer and others analyzed longitudinally the filling patterns of the RV[16,17] and showed that the fetal circulation is RV dominant. With increasing gestational age, the early filling wave increases in area, and the peak velocities show increasing E-waves and decreasing A-waves. The right ventricular chamber increases in size, similar to the left during gestation. A normal shortening fraction (diastolic dimension minus systolic dimension divided by diastolic) is greater than 28%. Calculations of the distribution of cardiac output have shown that the RV pumps more than the LV. This distribution is maintained in spite of significant changes in the pulmonary vascular resistance and flow between 20 and 37 weeks' gestation.[18] Foramen ovale flow changes inversely with pulmonary blood flow, thereby maintaining the net RV output greater than the left.[17]

Because the RV is complex in shape, techniques such as calculation of the RV function by nongeometric techniques using inflow and outflow time intervals are employed. The myocardial performance index, or Tei index, of the RV is not dependent on geometrical assumptions of the RV, and can be used as a parameter to follow changes in RV function over time. The Tei index is the sum of the isovolumic time divided by the ejection time. The isovolemic time is the sum of two intervals: the isovolemic relaxation time and the isovolemic contraction time. This term can be measured by subtracting the ejection time from the time of inflow of the RV (the time from tricuspid valve opening to closure). Changes in loading of the RV will result in hypertrophy of the chamber walls, and severe thickening can result in diastolic dysfunction (poor relaxation).

Description of the RV function requires that the loading conditions of the ventricle be known, and this is one of the most important goals in RV assessment in the human fetus. The pulmonary vascular resistance, for example, has been estimated in the fetus, and appears to decrease between 20 and 30 weeks' gestation and then increase again until term.

# Tricuspid valve

The tricuspid valve is intimately associated with the RV function. This valve is normally never regurgitant and is maintained competent by a complex interaction with the RV endocardium from which it arises early in fetal development. Newer techniques of color Doppler may detect a short color jet that appears to be regurgitation; however, the closure of the valve leaflets causes this finding, and it is not regurgitation. A jet of regurgitation that lasts longer than 70 milliseconds is termed *nonholosystolic tricuspid regurgitation*, and it is uncommon but without prognostic significance. Holosystolic tricuspid valve regurgitation, even though trace in severity, is abnormal, and a cause should be investigated. Higher grades of regurgitation (1+, 2+, 3+, or 4+) are all holosystolic and have a peak velocity greater than 2 m/s. The grade of regurgitation can be determined by the width of the jet at the valve and the extent of the jet in the RA.

Any acute increase in RV afterload, such as with acute constriction of the ductus arteriosus, will result in a small amount of tricuspid valve regurgitation within two heartbeats.[19] Sudden relief of this pressure work causes immediate cessation of the regurgitation. This implies that the shape and micromorphology of the RV chamber are intimately associated with tricuspid valve function and that there are constant instantaneous adjustments going on in the fetal RV to maintain the workload. After examining over 1,000 normal fetuses, Respondek et al.[20] concluded that there is rarely any normal tricuspid valve regurgitation (TR) in the human fetus at any time. Monitoring tricuspid valve function in the first trimester, even before the development of the mature tricuspid valvular apparatus, shows the same result—not even a trace of leak. Therefore, this marker of TR is a useful one clinically in detecting the RV that may have dysfunction. The time frame of the TR is also useful in deciding whether the TR could be a sign of disordered myocardial function or is simply a result of normal adjustments to workload. For example, a sudden onset of increased workload does not allow time for the ventricle to adapt, and TR results.

The rapidity of the upstroke of the TR jet along with its peak velocity gives information about the RV function. A calculation of the parameter dP/dt (where P is pressure and t is time) can be performed with a good-quality TR jet.[21] A value of less than 400 mm Hg/second was associated with death in hydropic fetuses. The peak velocity can be used to assess the peak pressure in the RV. Using continuous wave Doppler, the peak velocity is measured, and four times this velocity squared equals the pressure gradient from RV to RA in millimeters of mercury (torr). Therefore, with progressive RV dysfunction, the RV pressure will decrease, while the RA pressure during ventricular systole will increase. The difference between the RV and RA then decreases and is useful in monitoring the interaction of fetal blood pressure and central venous pressure.

Systolic function can also be assessed by analyzing the ejection force of the fetal ventricles. This is done at the outflow valves. The right and left ventricular force development

is estimated by Newton's equation in which force is defined as the product of mass and acceleration, and the ejection force can be assessed using the shape of the ejection curve.[22,23] Such calculations show that the ejection forces of both ventricles are similar. Altered loading conditions can significantly alter the force of ejection.

The most severe forms of RV diastolic dysfunction are manifested by the finding of monophasic inflow velocity, a severe form of diastolic dysfunction. This sign has been associated with compromised prognosis. The ability of the RV to relax is dramatically demonstrated in the rare fetus delivered at term with ductal occlusion. The RV usually stays thick, small, and contracted prior to birth, but immediately after the first breath, the afterload reduces, and the ventricle relaxes and fills. Within days, the RV may be able to change from a small thick ventricle to one that is supporting the majority of the circulation.

# Normal pulmonary valve

The blood velocity pattern of RV ejection through the pulmonary valve can be used to learn whether or not the RV afterload is increased. With decreasing RV output, the time-velocity integral decreases, while the acceleration time shortens. The pulmonary valve function is also affected in relation to the underlying RV function. Normally, the pulmonary valve in the fetus is perfectly competent. With severe and end-stage RV dysfunction, the valve may exhibit regurgitation, and this finding can have significant prognostic implications, such as in the case of associated Ebstein abnormality of the tricuspid valve.

# Normal ductus arteriosus

The ductus arteriosus is a site where much can be learned about the left and right heart circulations.[24] Flow is normally from the pulmonary artery to the descending aorta in systole and diastole. The peak velocity is between 0.8 and 2 m/s and increases with increasing gestational age.

# Abnormal right ventricular function

## *Effects of increased afterload*

### Growth restriction

RV dysfunction has been recognized more commonly in the most severe cases of intrauterine growth restriction.[25] Both systemic and pulmonary vascular resistances are increased, and the placental resistance can be dramatically elevated. The marked decreases in oxygenation in this disease may also play a role in the compromise of RV shortening due to the limitation of RV coronary arterial oxygen extraction. Dilatation of the RV and later decreased RV shortening demand prompt attention, because they can signal acidosis in the fetus or impending difficulty. These signs of heart failure are best assessed using venous Doppler and other cardiac signs. Tricuspid valve regurgitation in this disease also signals compromised RV function and the need for more detailed study.

### Twin-twin circulation

The recipient, larger twin in twin-twin transfusion syndrome can experience marked elevations in cardiac output and blood pressure. Typically, the larger twin maintains a high cardiac output due to the volume transfusion plus a state of vasoconstriction due to vasoactive substances produced by the smaller twin. With slow increases in the workload of the RV, there is compensatory hypertrophy and systolic function and minimal signs of hemodynamic compensation. With more rapid onset of volume and pressure overload, the RV stretches, and the tricuspid valve begins to leak. The coronary perfusion and subendocardial blood flow are progressively compromised by the hypertrophy and increased early systolic workload. These signs are probably associated with increases in the end-diastolic pressure of the RV. This is reflected in the end-diastolic pressure of the RA, which is elevated. These A-contractions against an elevated pressure resistance produce retrograde flow during atrial systole in the hepatic and inferior caval veins. The ductus venosus is the earliest site to see altered flow patterns. With the onset of atrial reversal in this site or umbilical venous pulsations, the onset of metabolic acidosis is imminent. Although many factors influence this outcome, one of the most important is the RV myocardial reserve. The recipient twin manifests biventricular hypertrophy and valvular regurgitation (see Video 43.1).

### Ductal constriction/occlusion

Ductal constriction is defined by the shape of the curve and the estimated mean velocity. Spontaneous or medication-induced constriction of the ductus arteriosus can be detected by the velocity in it, and the severity of ductal constriction can be estimated.[24] One of the most common clinical situations in which to observe RV function changes is during fetal ductal changes. Either drug-induced or naturally occurring constriction or occlusion of the ductus arteriosus will affect RV shortening. In this situation, the overall RV cross-sectional area change with systole and diastole decreases dramatically, so that although the RV moves with contraction, there is little wall movement, and the ejection volume is greatly decreased. The extent of this decrease was shown by Tulzer and others, and the total combined cardiac output may not be normal. One of the most important observations from these data is that decreased shortening *may not* indicate abnormal contractility of the ventricle. This was shown by calculating dP/dt, the first derivative of the pressure change in the RV using the TR jet, and in most cases of acute ductal constriction, this parameter is maintained normal. Therefore, there is no reported case in the literature at this point of hydrops resulting from ductal occlusion or constriction without concomitant restriction of the foramen

ovale. This is a reflection of the redistribution of cardiac output to the LV. Monitoring of venous Doppler is most useful for assessing the impact of altered RV function in this setting. In most cases, the pregnancy progresses without alteration in growth of the fetus, and the RV becomes smaller and thicker.

### *Increased preload: Arteriovenous fistula*

A shunt from the arterial to the venous circulation in the human fetus will result in a large volume of blood returning to the RA. This results in dilated right heart structures and a high cardiac output. The fetal heart is well adapted to handle increasing volume loads if they are imposed gradually. If rapidly increasing severity shunts occur, as is sometimes seen in sacrococcygeal teratoma, then cardiac decompensation and the development of hydrops fetalis can occur quickly. An important sign of RV decompensation in this scenario is valvular regurgitation. Early signs of tricuspid regurgitation, if only very mild, should signal an increase in fetal surveillance. The subsequent development of mitral regurgitation is ominous and is a clear sign of a pre-hydropic state.

## Congenital heart disease

### *Pulmonary valve abnormalities*

The most common right-sided heart abnormality is a bicuspid pulmonary valve. This usually results in trivial narrowing of the right ventricular outflow tract and no significant hemodynamic alteration. Less common is severe pulmonary stenosis with significant pressure increase in the RV. In this lesion, the RV pressure will only increase to suprasystemic levels when it is most severe. At this point, a gradient will be detected by an increased velocity across the pulmonary valve. One can estimate the degree to which the RV pressure is greater than systemic by converting the peak velocity to a gradient using the four times velocity squared equation. This is associated with hypertrophy of the RV and a decrease in the shortening fraction. More severe degrees of RV outflow obstruction occur with pulmonary atresia. In this lesion, the pulmonary valve annulus is smaller than normal, and there are usually signs of endocardial change in the RV such as echogenicity. In congenital heart defects with pulmonary stenosis or atresia and a ventricular septal defect such as tetralogy of Fallot, there are no RV changes, and the RV size is maintained normal and equal to the LV because the pressures are equal. There is an uncommon form of pulmonary atresia with intact ventricular septum where infarction of the RV occurs, and there is tricuspid valve regurgitation which is severe. Then, the RV is larger than normal, and the RA may be massively enlarged.

In the rare tetralogy of Fallot with absent pulmonary valve syndrome, there is no ductus arteriosus and the pulmonary arteries are enlarged. Pulmonary valve regurgitation is moderate or severe because there is no pulmonary valve and it is replaced by a fibrous ring. Both the RV and LV experience the effects of the pulmonary regurgitant volume and are usually seen to be normal. Rarely, there is dysfunction of the RV, which is indicated by disproportion of the ventricular sizes with RV enlargement and segmental RV wall motion abnormalities. In the presence of an open ductus with this heart defect, there is diastolic steal, and heart failure ensues (see Video 43.2).

### *Tricuspid valve abnormalities*

Tricuspid valve congenital abnormalities that result in significant amounts of tricuspid valve regurgitation are often fatal. The most common defect noted in fetal studies in the last decade is known as tricuspid valve dysplasia. In this lesion, the RV and RA are massively dilated, and color Doppler shows that regurgitation is the cause (see Video 43.3). The key issue in this lesion is the nature of the RV outflow tract. If there is no pulmonary stenosis, then the lesion may have occurred later in gestation, and the prognosis is better. The degree of RV cardiomyopathy can be assessed by measurement of the peak velocity of the TR jet. The lower the velocity, the worse are the RV dysfunction and the prognosis.

Ebstein malformation of the tricuspid valve with various severities of pulmonary stenosis or atresia in the fetus is the "cancer" of congenital heart disease. The heart becomes enlarged to occupy more than 60%–70% of the chest, and this is due to RA and atrialized RV enlargement. The pulmonary development can be altered irreparably by compression from the heart if it is severe, is associated with pleural effusions, and occurs in the critical time frame of 20–30 weeks when the lungs are developing. Peak TR velocities of less than 2 m/s are associated with a poor prognosis due to the development of RV myopathy and a peak aortic velocity less than 100 cm/s is a sign of poor prognosis due to decreased left ventricular function (see Video 43.4).

Primary cardiomyopathies of the RV such as Uhl anomaly or arrhythmogenic RV have not been reported in the fetus. However, any intractable ventricular arrhythmia in the fetus should prompt consideration of one of these diagnoses.

## Cardiovascular profile score development

The diagnosis of fetal congestive heart failure, therefore, must be addressed in a clinical fashion similar to that after birth. The classical clinical tetrad of cardiomegaly, tachycardia, tachypnea, and hepatomegaly has been used in neonates and children. This clinical state in the fetus can be characterized by findings in at least five categories, which are obtained during the ultrasonographic examination. The following five categories are each worth 2 points in a 10-point scoring system to assess the cardiovascular system. Abnormalities in the

Cardiovascular Profile Score may occur prior to the clinical state of hydrops fetalis. The five categories are as follows:

- Hydrops
- Umbilical venous Doppler
- Heart size
- Abnormal myocardial function
- Arterial Doppler

Within specific disease entities, more emphasis is placed on certain areas by the attending physician to predict the prognosis. As always, this information can only constitute a portion of the total picture and must be integrated by the attending physician into the diagnostic and treatment plan for the patient.

The Cardiovascular Profile Score gives a semiquantitative score of the fetal cardiac well-being and uses known markers from ultrasound that have been correlated with poor fetal outcome. This profile is normal if the score is 10, and signs of cardiac abnormalities result in a decrease of the score from normal. For example, if there is hydrops with ascites and no other abnormalities, there would be a deduction of 1 point for hydrops (ascites but no skin edema) and no deductions for the other categories, for a score of 9 out of 10.

## *Hydrops*

Hydrops fetalis may present with ascites, pleural effusion, pericardial effusion, or a combination of these findings. In advanced hydrops, there is generalized skin edema seen easily over the scalp and abdominal wall. In scoring hydrops for the Cardiovascular Profile Score, 1 point is deducted for early hydrops and 2 points for skin edema.

## *Umbilical and ductus venosus Doppler*

Fetal venous blood velocities have been examined, and investigations have been clinically promising.[26] Several studies have confirmed that normal flow in the inferior vena cava of the fetus has a pulsatile, triphasic pattern. The first forward wave begins to increase with atrial relaxation, reaches its peak during ventricular systole, and then falls to reach its nadir at the end of ventricular systole. The second forward wave occurs during early diastole, and a reverse flow is usually present in late diastole with atrial contraction. In normal pregnancy, the peak velocities obtained during the first wave of systole are greater than the early diastolic values. The systolic-to-diastolic ratios do not appear to change with advancing gestational age, but a significant decrease in flow reversal with atrial contraction is evident.

Studies in the fetal lamb have shown that this decrease in percentage of reversed flow seen in normal pregnancy is related to the pressure gradient between the RA and the RV during end-diastole. It appears to be related to both ventricular compliance and ventricular end-diastolic pressure and, therefore, is a reflection of central venous pressure. Recording venous blood velocity might thus give important information on fetal cardiac pump function. Previous studies in humans have shown that alterations in central venous blood velocity patterns accurately reflect abnormalities in cardiac hemodynamics. The abnormal pulsatility pattern consists of increased velocity of blood flow reversal away from the heart during atrial contraction, and has been reported in the fetus with congestive heart failure and may be a sign of increased end-diastolic pressure in the ventricles of the failing heart. Abnormal IVC flow velocity patterns have been described in several fetal pathologic conditions including anemia, nonimmune hydrops, and arrhythmias, and in severely growth-restricted fetuses characterized by the absence of end-diastolic flow in the umbilical artery. The compromised fetus with acidosis is known to manifest abnormalities of venous Doppler, including increased atrial reversal in excess of normal in the inferior vena cava at the junction with the RA[27] and increased pulsatility in the ductus venosus. The prognostic importance of these abnormalities has been confirmed in the fetus with intrauterine growth restriction and in the fetus with hydrops. An increased A/S ratio in the ductus venosus (peak atrial reversal divided by the peak filling wave during ventricular systole) appears to be the most useful sign in quantifying the increase of atria contraction in fetuses with growth restriction. Normally, the ratio of the area of the atrial reversal to the entire forward flow area should be less than 7%. Transmission of the venous pulsations into the portal and umbilical circulation correlates with increasing degrees of cardiac compromise. Tulzer et al. studied the cardiac factors related to prognosis in hydrops and noted that umbilical venous pulsations could stand in for a number of cardiac variables in predicting prognosis, including ventricular shortening fraction, ejection velocities, and percentage IVC atrial reversal.[28] In some disease states, abnormal venous Doppler progresses retrograde from the heart in the following order: (1) increased atrial reversal in the IVC, (2) ductus venosus atrial reversal, (3) portal venous atrial pulsations, and (4) umbilical venous atrial pulsations.

The end-stage finding of abnormal venous Doppler is atrial pulsations in the umbilical cord vein. This finding of "diastolic block" predicts perinatal mortality. Double umbilical venous pulsations, or the pattern of the normal IVC in the umbilical vein, are ominous clinical findings.[28] Venous pulsations are not normal in the portal vein, and such a finding may precede the progression to umbilical venous pulsations.

## Venous Doppler in congenital heart disease

Pagatto et al., working with us, studied a group of 41 fetuses diagnosed with congenital cardiac defects *in utero* and confirmed postnatally. The gestational age ranged from 18 to 38 weeks with a mean gestational age of 27.5 weeks. The fetuses were grouped into those with ventricular septal defects ($n = 11$), tricuspid atresia or hypoplasia ($n = 4$), hypoplastic left heart syndrome ($n = 19$), and others ($n = 7$), and

we analyzed the venous Doppler patterns. Abnormal inferior vena caval waveforms were present only in fetuses with tricuspid atresia or other right heart lesions where the returning flow to the heart all passed through the foramen ovale to reach the heart. Umbilical waveforms were nonpulsatile in all patients. We concluded that venous Doppler in fetuses with congenital heart disease without heart failure is normal, with the exception of tricuspid atresia and pulmonary atresia with intact septum, such that the combined cardiac output must pass through the foramen ovale. When abnormal central venous flow patterns occurred in association with cardiac defects *in utero*, they were usually secondary to another process occurring simultaneously, which affected ventricular compliance (such as endocardial fibroelastosis) or rhythm-related hemodynamics (such as complete heart block).

To assess the venous system consistently, pulsed Doppler sampling is obtained in the inferior vena cava, the ductus venosus, the umbilical vein in the abdomen, and the umbilical cord vein as part of each serial examination. Transmission of the atrial reversal into the ductus venosus and later into the portal and cord vein sites over time suggests progression of heart failure. The Cardiovascular Profile Score has deductions for abnormal venous Doppler as follows:

- Ductus venosus atrial reversal, −1 point
- Umbilical venous atrial pulsations, −2 points

Maximum deduction in any category is 2 points.

## Cardiomegaly

Enlargement of the cardiac chambers is a universal sign of heart failure. This is true in the fetus as well, but few of the mechanisms are understood. It is likely that neural humoral reflexes are triggered, resulting in retention of extracellular volume leading to increased end-diastolic volume of the ventricles. At some point, this increased ventricular size indicates increased end-diastolic pressure. However, unlike the postnatal human, it is uncommon to encounter persistent tachycardia with signs of catecholamine excess. It is possible that the levels of humoral agents are modified by the fetal-maternal exchange mechanisms, which exist when the placenta is functioning normally.

The most common cardiac chamber to express enlargement as a sign of impending cardiac failure is the RA. The reasons for this relate to the many causes for heart failure, but the RA is a final pathway for blood flow returning to the heart and will manifest enlargement in situations of relative foramen obstruction, volume overload, tricuspid valve regurgitation, and increased afterload. Increased RA size may be due to increased RV end diastolic pressure, which may be due to increased afterload or coronary insufficiency. The RV may be more susceptible to increased work because of the nature of the afterload and the resultant increased demands for oxygen in the face of increased chamber wall stress. It is generally believed that increased atrial wall stress without increased ventricular work does not lead to clinical difficulties in the fetus. Such a situation could be an early marker of cardiac decompensation and may predispose to supraventricular arrhythmias. Secretion of atrial natriuretic peptide (ANP) could be a marker of this finding.

Slower than normal heart rate or persistent rapid heart rate leads to cardiomegaly. The time frame of the onset of arrhythmia may therefore be estimated by the effect on the cardiac size. For example, an intermittent arrhythmia that has appeared recently would not be expected to cause cardiac enlargement.

Small heart size with external compression has been correlated with hydrops and poor outcome in fetuses with cystic adenomatoid malformation.[29] When heart size was less than 20% of the chest area, fetal outcome was affected. Cardiomegaly is a heart-to-chest-area ratio greater than 0.35 at any time in gestation.

Cardiac size calculations are as follows:

- C/T area ratio = cardiac area/chest area (normal 0.2–0.35)
- C/T circumference ratio = cardiac circumference/chest circumference (normal <0.5)

therefore,

- Normal heart/chest: area ratio ≤0.35 and >0.20
- Mild cardiomegaly: area ratio >0.35 and ≤0.5, −1 point
- Severe cardiomegaly: area ratio >0.50, −2 points
- Small heart: ratio >0.2, −2 points

The maximum deduction is 2 points.

## Abnormal myocardial function

The cardiac function is assessed indirectly by the global shortening (and thickening) of the walls of the ventricles, and by the function of the atrioventricular and semilunar valves.

Both of the RVs and LVs should shorten their diameters more than 28% in systole compared to diastole. Measurements of cardiac dimensions with time are performed using M-mode echocardiography. The shortening fraction of a ventricle is calculated by taking the difference between the diastolic (DD) and systolic dimensions (SD) and dividing by the diastolic dimension:

$$\text{Fractional shortening} = (DD - SD)/DD, \text{ normal} > 0.28$$

An abnormal shortening fraction could reflect myocardial compromise *or* an increase in the fetal ventricular workload. Regardless, an increase in diastolic dimension is often related to a decrease in shortening fraction and should be regarded as an indication for more intensive monitoring.

The atrioventricular and semilunar valves are competent in the normal fetus, and if regurgitation is detected, it is usually a sign of altered cardiovascular physiology. Respondek et al. showed that 7% of fetuses having a fetal echocardiogram display trivial or significant tricuspid valve regurgitation.[20] Most had some reason for this, such as constriction of the ductus arteriosus from indomethacin treatment of preterm labor, but 93% had no trace of regurgitation with state-of-the-art equipment and careful examination. Since tricuspid valve

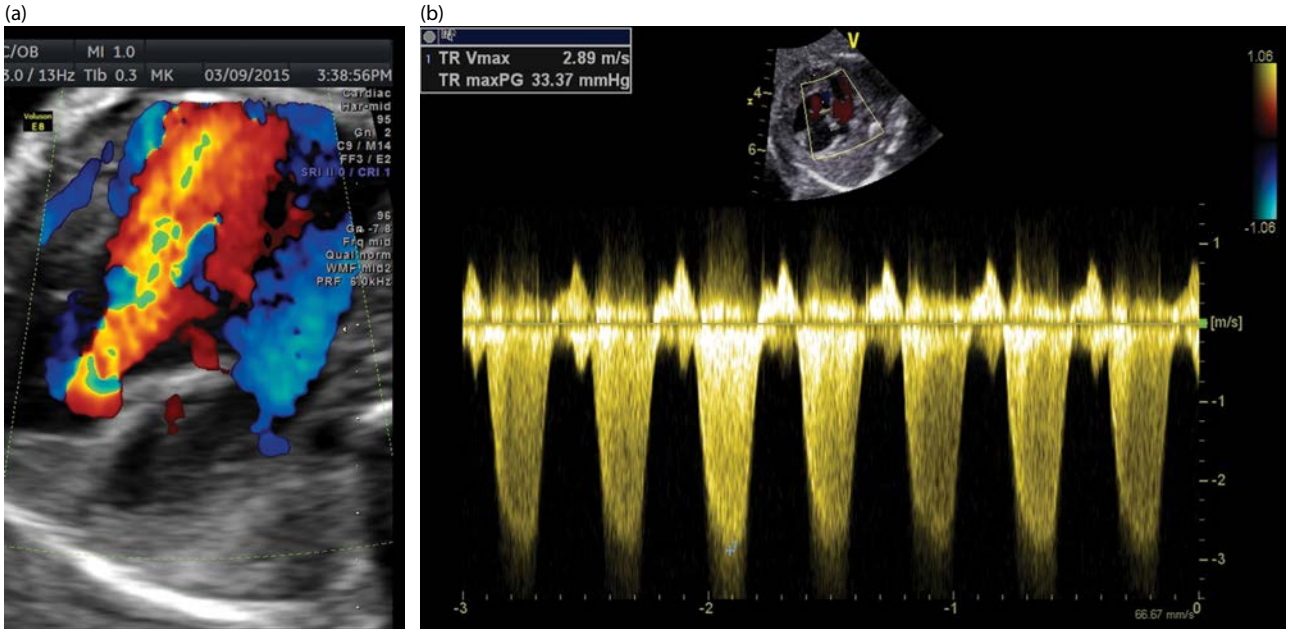


**Figure 43.3**
Severe tricuspid valve (TV) regurgitation, (a) on color Doppler with fetal TV dysplasia and (b) by continuous wave Doppler.

regurgitation is common after birth, we may speculate that the fetal RV is well adapted to systemic pressure work. Therefore, valvular competence is normal, and only in disturbances of cardiovascular physiology where there is increased ventricular wall stress is tricuspid valve regurgitation present. Trace tricuspid regurgitation defined as nonholosystolic regurgitation lasting at least 70 ms is not normal. This may be the first sign of a problem, but it has little prognostic importance. Holosystolic tricuspid regurgitation is abnormal and always indicates the need for further investigation.[19] When regurgitation is detected by color Doppler, it must be confirmed and graded by pulsed Doppler. With congenital diseases of the tricuspid valve, hydrops and fetal death can occur (Figure 43.3).

Regurgitation of other valves is usually a sign of more advanced congestive heart failure and may occur in the moribund fetus with acidosis and severe heart failure as a sign of myocardial compromise. Tricuspid valve regurgitation can be a reversible sign of heart failure, as one observes in fetuses with successful *in utero* therapy for anemia or tachycardia. Progression to mitral valve regurgitation is always a sign of fetal congestive heart failure and usually means that a significant increase in left ventricular wall stress is present. With severe myocardial failure, the support for the semilunar valves is compromised, and pulmonary or aortic valve regurgitation can occur. Similarly, the absence of the pulmonary valve in tetralogy of Fallot with absent pulmonary valve causes severe pulmonary regurgitation (Figure 43.4).

The nature of the velocity waveform of valvular regurgitation has prognostic value in the calculation of fetal ventricular dP/dt. With holosystolic tricuspid valve regurgitation, the time interval from one RV–RA pressure difference to another can be used to calculate the change in pressure over time, or the dP/dt. A value of less than 800 mm Hg/s is abnormal, and a value less than 400 predicts a poor fetal outcome.[20] This measurement requires continuous wave Doppler, and the peak velocity may be from 2.5 to 4.5 m/s. We have found that the most useful range for dP/dt measurement in fetal TR is 0.5–2.5 m/s. In other words, an RV–RA gradient of 1–25 mm Hg or a 24 mm Hg difference.

The fetal ventricles are at equal and systemic pressure throughout gestation; therefore, the blood pressure of the fetus is being estimated by this technique.

The filling pattern of the ventricles in diastole is an indicator of the diastolic function of the heart. Normal values show that the proportion of atrial filling during the atrial contraction is constant from 14 to 40 weeks' gestation.[15] Monophasic filling of the ventricles is a sign of compromised diastolic function and is a sign of fetal heart failure.[29]

Several disease states are now being identified where thickening of the ventricular chambers (myocardial hypertrophy) occurs in the absence of congenital ventricular outflow obstruction. This is assessed by measuring the end-diastolic wall thickness of the LV and comparing it with the normal values for age. Any left ventricle posterior wall (LVPW) thickness greater than or equal to 4 mm is abnormal. The most severe cases of fetal hypertension that have been detected are in the larger of twins in the syndrome known as twin-twin transfusion, where a mortality of over 70% for the fetuses is common. It appears that early identification of cardiomegaly and severe hypertrophy in the larger twin can be useful in patient management (Figure 43.5). Treatment strategies to prevent hydrops in the larger fetus result in improved survival. Postnatally, neonatal hypertension can be severe and life-threatening. *In utero* interventions are currently being explored and appear to be indicated in selected fetuses for this cause of congestive heart failure, including serial amniocentesis and laser

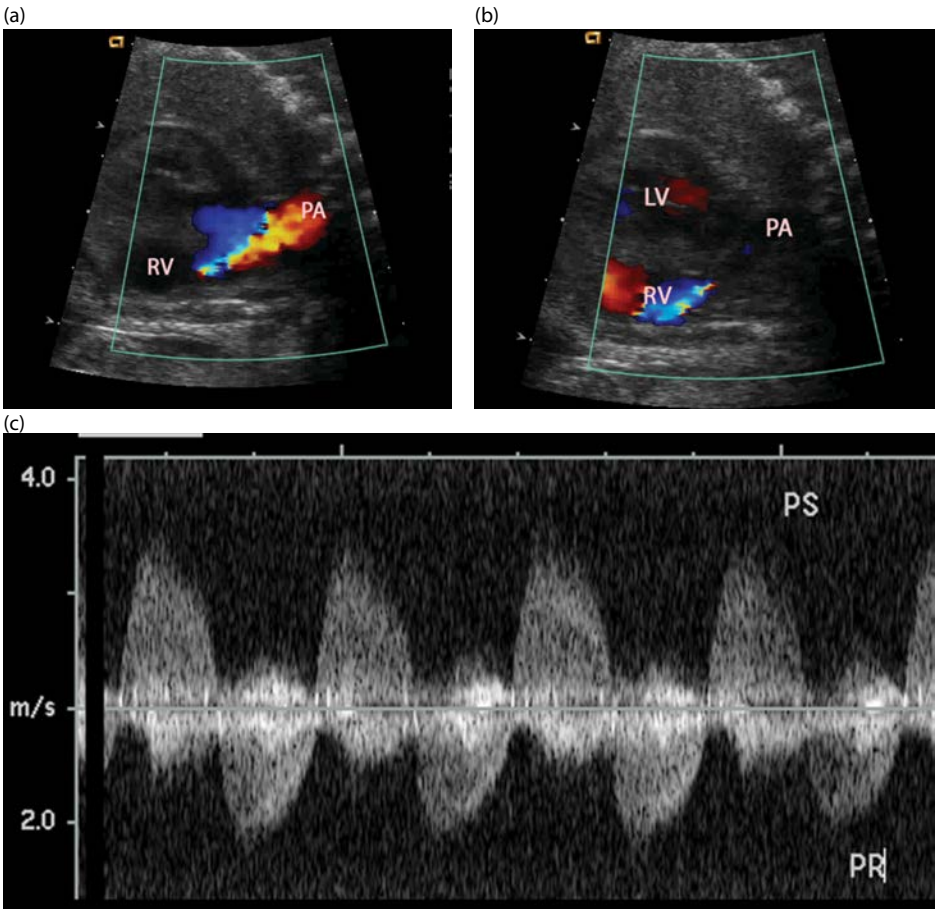


**Figure 43.4**
Fetal tetralogy of Fallot with absent pulmonary valve (PV): (a) systolic forward and (b) diastolic regurgitation, and (c) Doppler of the PV flow pattern.

ablation of the vascular communications.[30] Regardless of the etiology, thickening of the fetal ventricles could restrict the cardiac reserve before or after birth. Because cardiac hypertrophy can occur rapidly but takes weeks or months to resolve, its identification is an important marker of a cardiovascular system at risk. Abnormalities of diastolic function could be expected and should be excluded by comparing the filling patterns of the ventricles using pulsed Doppler to standardized normal values. One rule of thumb is that the A-wave of the ventricular filling is always greater than the E-wave, and, if it is higher or is indistinguishable, then a detailed cardiac study should be performed. Monophasic filling of the ventricles occurs in severe diastolic dysfunction and with external cardiac compression that is severe. Studies using the myocardial performance index may be useful to reflect an abnormality of systolic and diastolic function, and deserve more research.[31]

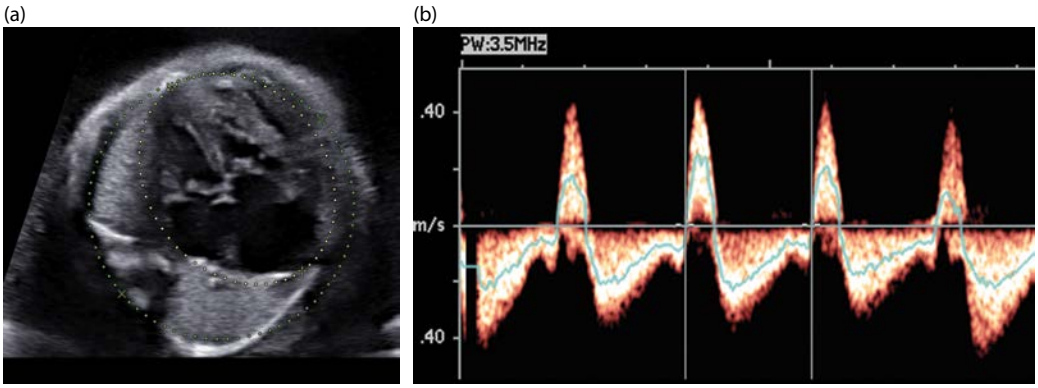


**Figure 43.5**
(a,b) Severe biventricular hypertrophy in the larger recipient twin in twin-twin transfusion syndrome.

For cardiac function,

- RV/LV shortening fraction <0.28, −1 point
- Tricuspid valve regurgitation (holosystolic), −1 point
- Mitral regurgitation, −1 point
- Monophasic ventricular filling, −2 points
- Pulmonary or aortic valve regurgitation, −1 point
- Valve regurgitation dP/dt < 400 mm Hg/s, −2 points
- Ventricular hypertrophy, −1 point

The maximum deduction is 2 points.

## *Arterial Doppler: Redistribution of fetal cardiac output*

It is now well established that the blood velocities measured by Doppler echocardiography in the umbilical artery and in other peripheral vascular beds can be used as an indirect indicator of the relative vascular impedances. Findings of an increased pulsatility index in the umbilical artery (UA) and descending aorta (DAo) and a decreased index in the middle cerebral artery (MCA) are noninvasive signs of redistribution of flow. We calculate the cerebroplacental ratio (CPR) as the ratio of the pulsatility index in the MCA divided by that in the umbilical artery. Throughout pregnancy, this ratio should remain above 1.2. It is important to recognize that a pulsed Doppler finding in one portion of the circulation is affected by changes in the rest of the circulation. For example, if there is significant aortic valvular regurgitation in the fetus, the diastolic reversal in the descending aorta and the increased pulsatility index in the umbilical artery are secondary to this change in the heart and do not reflect peripheral resistance only.

The most common cause of elevated vascular resistance in the fetus is placental dysfunction secondary to vasculopathy leading to asymmetrical growth restriction. This complex pathophysiological state is poorly understood, but there is evidence that there is hypoxemia resulting from placental dysfunction and additional compromise of nutrition severe enough to impair growth. Once the normal pattern of growth is disturbed (usually asymmetrically such that the brain continues growing but the body does not), the fetus is at risk of organ damage from hypoxemic/ischemic injury. The umbilical artery manifests this problem with a loss or reversal of diastolic blood flow (Figure 43.6). There is a redistribution of flow to the brain ("brain sparing") due to reflex vasodilatation of the cerebral vessels. This is manifested by a decrease in the pulsatility

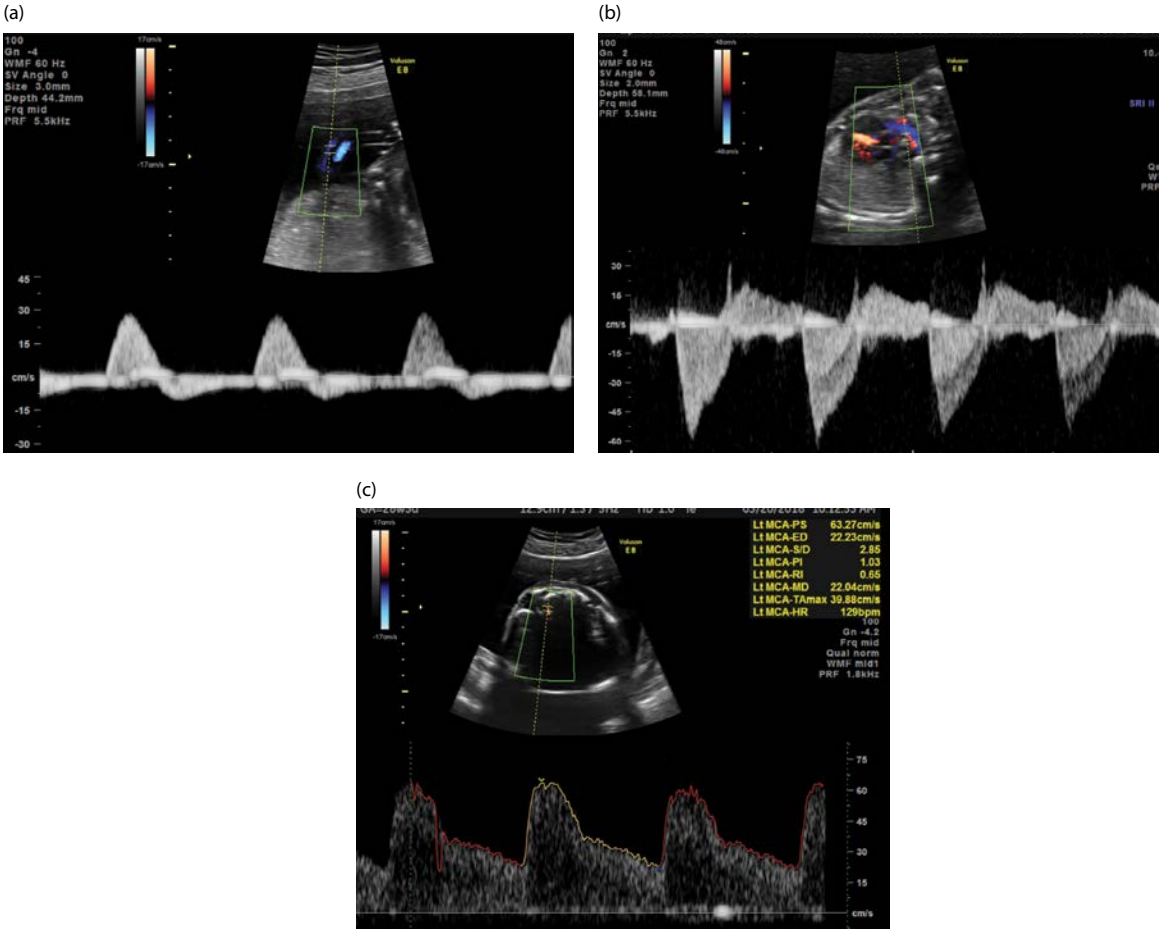


**Figure 43.6**
(a) Umbilical artery in IUGR with diastolic reversal, (b) aortic arch reversal, and (c) middle cerebral artery increased diastolic velocity brain-sparing.

index in the MCA such that diastolic flow is relatively increased (PI less than 2 standard deviations below the mean).[32]

In the fetus with hypoxemia, the peripheral fetal vessels are vasoconstricted, and the larger arteries are suspected to be noncompliant compared to normal fetuses with increased blood pressure.[33] This is a physiological state characterized by increased vascular resistances and, at end stage, decreased cardiac output. Right ventricular enlargement occurs in some cases.

There is evidence that reversal of diastolic flow in the umbilical artery, if confirmed, may be a significant risk factor for abnormal outcomes. Further work is needed in this area. As a sign of fetal heart failure, the vasoconstriction resulting from decreased cardiac output and the compensatory sign of vasodilatation in the brain can be included in the following cardiovascular profile score:

- Absent end-diastolic flow in the umbilical artery + brain sparing (increased MCA diastolic velocity), −1 point
- Reversed end-diastolic flow in the umbilical artery, −2 points

## *Cardiovascular profile score*

The Cardiovascular Profile Score comprises 2 points in each of the five categories used in serial studies to provide a method of uniform physiological assessment (Tables 43.3 and 43.4). By taking a multivariate approach, this type of multifactorial score can combine assessment of direct and indirect markers of cardiovascular function. Initial validation of the Cardiovascular Profile Score in hydrops was shown by Falkensammer et al.[34] Seven fetuses with hydrops, including three with congenital heart disease, had correlation of the Cardiovascular Profile Score with the myocardial performance index (Tei index). RV and LV Tei indexes were assessed in normal fetuses and showed no change with gestational age.

The CVP score aids in the prognosis of fetuses with Ebstein malformation of the TV or TV dysplasia.[35] Hofstaetter et al.[36] measured the Cardiovascular Profile Score in 59 hydrops fetuses. Mortality was 21/59. The average score in those who died pre- or postnatally was 5. The average score in the survivors was 6. The score was evaluated in fetuses with congenital heart disease[37] and in fetal growth restriction[38] in recent studies. Studies in fetal cardiomyopathy have shown the CVP score predictive of outcome in both dilated and hypertrophic types.[39]

# Treatment of fetal heart failure

Treatment of fetal cardiovascular problems can be classified into five of the most common subgroups based on the etiology of congestive heart failure: (1) abnormal peripheral impedances causing redistribution of flow and growth failure, (2) high output due to anemia or arteriovenous fistula, (3) primary or secondary valvular regurgitation, (4) heart failure due to myocardial dysfunction, and (5) tachycardia/bradycardia. Interventions aimed at improving the effective cardiac output are also aimed at prolonging the pregnancy and preventing prematurity and prenatal asphyxia.

The rapidity with which a disease progresses determines the urgency with which treatment should occur. This is due to the fact that the myocardial response to increased wall stress will be either adequate or inadequate depending on the severity and timing and duration of the insult, the coronary perfusion, the nutritional state of the fetus, and the other problems in the pregnancy.

The usual treatment of placental dysfunction is designed to improve the vascular impedance of the placenta and to increase the flow of oxygenated blood to the fetus. With bedrest, improved nutrition, or maternal oxygen, there may be improvement in placental function. Tocolytic medications may relax the placenta and improve its function. Myocardial support for advanced growth restriction has not been proposed, partly because the validation of diagnostic methods is lacking. Studies of ventricular ejection force in growth restriction have shown that both ventricles have decreased ejection force.[17] Advanced heart failure in this setting with severely decreased arterial $PaO_2$ and poor nutrition are manifested by nonspecific signs of increased RV and RA size, atrial reversal in the venous Doppler pattern, and altered forward flow velocities.

Treatment with digoxin for evidence of decreased cardiac output is controversial. Digoxin is known to decrease the catecholamine response to congestive heart failure, and if there is systemic vasoconstriction or diastolic dysfunction in the fetus, then this may improve filling and lower filling pressures. If the afterload is high, then an increase in oxygen consumption could result from increased inotropy without improved myocardial perfusion. Terbutaline appears to have promise as an inotropic and chronotropic agent,[40] but studies of the possible negative effects on the fetal myocardium are needed. At the present time, we use digoxin for fetal cardiac failure due to arrhythmias and high output states such as fistula and anemia.

**Table 43.3** Summary of requirements of Cardiovascular Profile Score

- Cardiac/chest area ratio
- M-mode of right ventricle/left ventricle (RV/LV)
- Doppler of four valves
- Pulsed Doppler of the ductus venosus, cord umbilical vein and artery, and middle cerebral artery

**Table 43.4** Summary of Cardiovascular Profile Score

1. Hydrops: effusion, −1 point; skin edema, −2 points
2. Venous Doppler: atrial reversal: ductus venosus, −1 point; umbilical vein atrial pulsations, −2 points
3. Heart size: C/T area ratio >0.35, −1 point; >0.5 or <0.25, −2 points
4. Cardiac function: RV/LV shortening fraction <0.28, −1 point; tricuspid valve regurgitation (holosystolic), −1 point; mitral regurgitation, −1 point; pulmonary or aortic valve regurgitation, −1 point; valve regurgitation dP/dt < 400 mm Hg/s, −2 points; ventricular hypertrophy, −1 point; monophasic filling, −2 points (maximal deduction is two points for each category)
5. Umbilical artery: absent end-diastolic velocity, −1 point; reversed diastolic velocity, −2 points

The use of relatively low dose digoxin at 0.25 mg by mouth, two times a day in the pregnant woman has low risk, and we consider its use in any fetus with a CVP score of 7/10 or less. In a recent case of acardiac twinning, where the normal fetus was supporting two circulations, digoxin appeared to improve cardiac function and result in a prolonged and successful gestation for the normal twin. In our experience, we consider the use of digoxin for the fetus in sinus rhythm with signs of congestive heart failure with a cardiovascular profile score of 7 or less. We use digoxin 0.25 mg orally two or three times per day based on maternal serum levels and clinical signs. We use a trough level of 1.0–2.0 mg to avoid any maternal side effects.

Laser treatment of the twin-twin communications or cord ligation with acardiac twins can be applied to improve cardiac failure.

With anemia, it is possible to transfuse the fetus via the umbilical vein. The diagnosis of fetal anemia can be made using the middle cerebral artery peak velocity using the data developed by Mari. With anemia, the cardiac output is increased with a reduced oxygen-carrying capacity.

When fetal valvular regurgitation is present on a congenital basis, it could be useful to decrease the afterload of the fetal ventricles as is done in infants with a similar problem. However, medications that reduce the afterload, such as angiotensin-converting enzyme (ACE) inhibitors, are known to be dangerous to the fetus in pregnancy. Reduction of catecholamine levels could have a similar effect, and digoxin could be useful in this situation.

Right heart defects such as Ebstein and tricuspid valve dysplasia have cardiac dilation and tricuspid regurgitation inherently in the diagnosis. If worsening of the cardiac output occurs, pulmonary valve regurgitation may develop, and this is a very poor prognostic sign. Attempts at limiting the resultant "circular shunt" that steal effective cardiac output from the fetus using indomethacin or ibuprofen to constrict the ductus arteriosus and thereby limit the pulmonary valve regurgitation are currently being made, and we have successfully stabilized the circulation in three such fetuses with tricuspid and pulmonary valve regurgitation by constricting the ductus medically.

In pregnancies where the mother has significant levels of anti-Ro and anti-La antibodies, we recommend dexamethasone 4 mg daily if there are signs of valvular regurgitation, heart block, valvulitis, myocardial dysfunction, myocardial echogenicity, or effusion. Early use of this medication may prevent progression of heart block and myocardial injury.

When myocardial dysfunction is seen without obvious reasons, and fetal infection has been excluded, we consider that an inherited form of cardiomyopathy of either the LV or RV can present *in utero*. We use digoxin for these patients as long as there is no sign of ventricular ectopy or tachycardia.

## Fetal cardiac interventions

Several postnatal forms of congenital heart disease may lead to fetal congestive heart failure or irreversible secondary damage to the fetal heart and lungs, for example, right heart obstructive lesions such as tricuspid atresia, critical pulmonary stenosis, or pulmonary atresia with intact ventricular septum with restrictive interatrial shunting, severe atrioventricular valve insufficiency, or premature constriction or occlusion of the foramen ovale associated with left heart obstructions. It was speculated that correcting or improving these anatomical problems *in utero* could prevent heart failure and/or fatal secondary damage.

The first intracardiac fetal interventions were reported in 1991.[41] Two fetuses with critical valvular aortic stenosis underwent an *in utero* attempt at percutaneous valvuloplasty with the goal to prevent irreversible myocardial damage of the LV. In one of these fetuses, the aortic valve could be dilated successfully, but it died postnatally due to persistent left ventricular dysfunction. Due to enormous technical difficulties, poor results (out of 12 human fetuses only one remained alive) and with increasingly better results for stage 1 Norwood palliation, this method was abandoned for several years. More recently, this method has been successfully used again for fetuses with pulmonary atresia with intact septum and signs of heart failure by Tulzer et al. In these fetuses, relief of right ventricular outflow obstruction led to improvement of echocardiographic signs of heart failure. However, as most fetuses with this anatomy do not develop heart failure *in utero* unless there is restrictive interatrial shunting or severe tricuspid regurgitation, this method should be limited to only a small subset. Whether prenatal decompression of small hypertensive RVs is able to establish growth, prevent coronary artery fistulae, and improve the chances of a biventricular repair postnatally has yet to be determined. It also remains unclear whether early dilatation of critical stenotic aortic valves can prevent the development of hypoplastic left heart syndrome without resulting in serious and debilitating left ventricular diastolic dysfunction.

There is evidence that an intact atrial septum in hypoplastic left heart syndrome leads to morphologic changes of the pulmonary vasculature and pulmonary lymphangiectasia.[42] Creating an atrial communication and decompressing the LA should enable normal pulmonary venous drainage and prevent further damage to pulmonary vessels and parenchyma. Such an intervention could improve outcomes in fetal hypoplastic left heart syndrome if the risk for the procedure is low.

To date, many technical problems regarding equipment, imaging, and access have not yet been solved. Clinical indications for therapy have yet to be defined, and there is still a need for more natural history studies regarding *in utero* progression of congenital heart disease and/or congestive heart failure. Therefore, these treatment options should still be considered innovative.

## Conclusions

Fetal cardiac findings must be integrated into the clinical management of the fetus by the perinatologist. The Cardiovascular Profile Score can be used to communicate

between visits and specialists to assess the urgency of abnormalities and the prognosis. Focused centers of excellence in fetal cardiac assessment are needed to investigate and achieve effective fetal treatment. However, fetal diagnosis is only a dream unless providers of ultrasound screening detect abnormalities during otherwise normal gestations. Therefore, each center of excellence in perinatal cardiology must accept the responsibility of education in the surrounding region. A recent publication from a leading fetal cardiology group summarizes the findings and strategy for treatment of fetal congestive heart failure.[43] Good communication between heart screening sites and perinatal cardiology centers will benefit all involved and will allow progress to occur in this new field of cardiology.

## Videos

**Video 43.1** (https://youtu.be/9rw2DdPViJM)
Four-chamber view of a recipient twin with cardiac enlargement, biventricular hypertrophy, and tricuspid valve regurgitation by color Doppler.

**Video 43.2** (https://youtu.be/4dEjoWKoLLk)
Severe pulmonary valve regurgitation is present with tetralogy of Fallot with absent pulmonary valve; however, the open ductus results in diastolic steal from the fetal circulation and hydrops.

**Video 43.3** (https://youtu.be/yfUG7erJ2_U)
Tricuspid valve dysplasia.

**Video 43.4** (https://youtu.be/1sO9rVd-ciA)
Fetus at 27 weeks' gestation with Ebstein malformation of the tricuspid valve and severe regurgitation.

## Appendix

**Table 43A.1** Studies showing use of the Cardiovascular Profile Score in fetal congestive heart failure

| *Group* | *Abnormal Cardiovascular Profile Score* | *Mortality* or early delivery*** |
|---|---|---|
| 1. CHD | 20% < 7 | *87.5% versus 15.2%[37] |
| 2. Hydrops | 60% < 7 | *73.5% versus 26.5%[36] |
| 3. IUGR | 11% < 6 | 100%[38] |
| 4. AVB | *82% < 7 | *100% |
| | **26% | **100%[43] |
| 5. Digoxin | 32% < 5 | 100% (unpublished data) |

*Abbreviations:* AVB, atrioventricular block; CHD, congenital heart disease; IUGR, intrauterine growth restriction.

**Table 43A.2** Cardiovascular Profile Score categories most important in five groups of fetuses diagnosed *in utero*

| *Group* | *Component markers* | *p-Value* |
|---|---|---|
| 1. CHD | Hydrops, cardiomegaly | <0.05 |
| 2. Hydrops | Abnormal venous Doppler | |
| 3. IUGR | Abnormal venous Doppler | <0.001 |
| | Abnormal function | <0.001 |
| | Cardiomegaly | 0.008 |
| 4. LAI–AVB | Hydrops | <0.001 |
| | Cardiomegaly | 0.003 |
| 5. Digoxin | Abnormal DV Doppler | 0.007 |
| | Hydrops | 0.01 |

*Abbreviations:* AVB, atrioventricular block; CHD, congenital heart disease; DV, ductus venosus; IUGR, intrauterine growth restriction; LAI, left atrial isomerism.

## References


1. Huhta JC. *Semin Fetal Neonatal Med* 2005;10:542–52.
2. Kiserud T. *Semin Fetal Neonatal Med* 2005;10:493–503.
3. Angelini A et al. *Br Heart J* 1988;60:221–6.
4. Rudolph AM, Heymann MA. *Am J Obstet Gynecol* 1976;124:183–92.
5. Friedman WF. *Prog Cardiovasc Dis* 1972;15:87–111.
6. Thornburg KL, Morton MJ. *Am J Physiol* 1983;244:H656–63.
7. Johnson P et al. *Am J Obstet Gynecol* 1992;167:1309–13.
8. Westgate J et al. *Lancet* 1992;340:194–8.
9. Manning FA et al. *Am J Obstet Gynecol* 1990;162:918–24; discussion 924–7.
10. Huhta JC. *Ultrasound Obstet Gynecol* 1995;5:145–7.
11. Makikallio K et al. *Am J Obstet Gynecol* 2000;183:726–31.
12. Troughton RW et al. *Lancet* 2000;355:1126–30.
13. Gudmundsson S et al. *Am J Obstet Gynecol* 1991;164:33–7.
14. Chaoui R et al. *Geburtshilfe Frauenheilkd* 1995;55:207–17. [in German]
15. Thornburg KL, Reller MD. *Am J Physiol* 1999;277:R1249–60.
16. Tulzer G et al. *Eur J Pediatr* 1994; 153:151–4.
17. Veille JC et al. *Am J Obstet Gynecol* 1999;180:849–58.
18. Rasanen J et al. *Circulation* 1996;94:1068–73.
19. Tulzer G et al. *Am J Obstet Gynecol* 1991;165:775–8.
20. Respondek ML et al. *Am J Obstet Gynecol* 1994;171:1265–70.
21. Tulzer G et al. *J Matern Fetal Invest* 1991;1:15–8.
22. Sutton MS et al. *Br Heart J* 1991;66:285–9.
23. Rasanen J et al. *Ultrasound Obstet Gynecol* 1997;10:325–32.
24. Tulzer G et al. *J Am Coll Cardiol* 1991;18:532–6.
25. Rizzo G et al. *Ultrasound Obstet Gynecol* 1995;5:247–55.
26. Hecher K et al. *Am J Obstet Gynecol* 1995;173:10–5.
27. Rizzo G et al. *Am J Obstet Gynecol* 1992;166:1271–80.
28. Tulzer G et al. *Ultrasound Obstet Gynecol* 1994;4:279–83.
29. Mahle WT et al. *Ultrasound Obstet Gynecol* 2000;16:620–4.
30. Quintero RA et al. *Ultrasound Obstet Gynecol* 2000;16:230–6.
31. Eidem BW et al. *Echocardiography* 2001;18:9–13.
32. Rizzo G, Arduini D. *Am J Obstet Gynecol* 1991;165:876–82.
33. Stale H et al. *Ultrasound Med Biol* 1991;175:471–8.

34. Falkensammer CB et al. *J Perinat Med* 2001;29:390–8.
35. Freire G et al. *Cardiol Young* 2014;24(6):1049–56.
36. Hofstaetter C et al. *J Matern Fetal Neonatal Med* 2006;19:407–13.
37. Wieczorek A et al. *Int J Ultrasound Obstet Gynecol* 2008;31: 284–8.
38. Mäkikallio K et al. *J Ultrasound Obstet Gynecol* 2008;31:48–54.
39. Weber R et al. *JACC Heart Fail* 2014;2(4):403–11.
40. Sharif DS et al. *J Clin Ultrasound* 1990;18:85–9.
41. Maxwell D et al. *Br Heart J* 1991;65:256–8.
42. Rychik J et al. *J Am Coll Cardiol* 1999;34:554–60.
43. Davey B et al. *Minerva Pediatr* 2012;64(5):471–92.

# 44

# Twin-twin transfusion syndrome: Impact on the cardiovascular system

Jack Rychik

## Introduction

The twin-twin transfusion syndrome (TTTS) is a disorder seen in approximately 20% of monochorionic twin gestations.[1,2] The phenomenon is increasingly recognized as the most important contributor to morbidity and mortality in twin gestations. If left undetected and untreated, the natural history is such that the risk of death in at least one of the twins approaches 90%–100%. Despite the significance of this problem, our understanding of the pathophysiology of the disease and the development of effective treatment strategies is still incomplete and evolving. One can make the argument that TTTS is primarily a circulatory derangement—in essence a failed partnership between the vascular systems of two fetuses sharing the same womb and the same placenta. This failed circulatory arrangement results in serious negative consequences and sets a course for cardiovascular decompensation that is lethal if left unchecked.

In this chapter, we review our current understanding of TTTS from the cardiovascular perspective, propose a score for characterizing the magnitude of cardiovascular perturbation seen in this disease, and discuss some of the questions that continue to challenge investigators and clinical practitioners who deal with this intriguing condition.

## Diagnosis and findings in twin-twin transfusion syndrome

A multiple gestation pregnancy places each of the individual partners at risk. These risks have been known for quite some time. A medieval painting from the Muiderslot castle in Holland *circa* 1617 depicts twin boys, reported to be the children of the mayor of Amsterdam, Jacob Dierkszon De Graeff.[3] In the painting, one twin has a ruddy face and the other an unusually pale white face; these infants likely suffered from TTTS (both died soon after birth).

TTTS is suspected in the presence of monochorionic, diamniotic twins in which there is size discrepancy between the twins of at least 10%–20% and in which there is oligohydramnios in the smaller and polyhydramnios in the larger fetus. Often the degree of oligohydramnios is so severe that the smaller twin appears to be "shrink-wrapped" in its own amniotic sac, with the membrane tightly adherent to it. With the larger twin exhibiting polyhydramnios, the smaller twin is pushed to a corner of the uterus, limiting its mobility—hence, it is commonly referred to as the "stuck twin." Premature labor as a consequence of the polyhydramnios is common. TTTS is to be distinguished from other causes of intertwin size discrepancy, such as intrauterine growth restriction, or the presence of congenital, genetic, or chromosomal anomalies, or infection in the smaller twin.

The impact of TTTS on the outcome of affected twins is considerable.[4] TTTS can result in the demise of the larger or smaller twin,[5] serious neurological insult,[6] and/or cardiovascular abnormalities.[7–10] Death of one twin in a monochorionic system can subsequently lead to the rapid death of the partner twin. A dead twin can act as a vascular low-resistance sink, which through anastomotic intraplacental connections leads to hypotension in the survivor. This "bleed" into the vascular system of the dead fetus can cause either death or neurological damage in the partner twin. The fetal neurological system can be deleteriously impacted in TTTS in a variety of manners, including by the disease process itself, by the death of a cotwin, or as a consequence of premature birth. Studies have demonstrated a high prevalence for morphological abnormalities on brain imaging and an increased prevalence of neurocognitive impairment in survivors. Cardiovascular manifestations with the potential for long-term consequences are common in TTTS and are discussed in the following text.

In order to grade the severity of disease and to allow for rational analysis of treatment strategies and prognosis, Quintero et al. developed a staging system for TTTS.[11] The system is based on a number of variables: presence of polyhydramnios (maximum vertical pocket >8 cm) in the larger twin and oligohydramnios (maximum vertical pocket of <2 cm) in the smaller twin; presence or absence of visualization of a bladder in the smaller twin; presence or absence of critically abnormal Doppler studies defined as absent or reversed diastolic umbilical arterial flow, reverse flow in the ductus venosus, or umbilical venous pulsations; and presence

**Table 44.1** Quintero staging criteria for twin-twin transfusion syndrome (TTTS)

| *Stage* | *Findings* |
|---|---|
| I | Polyhydramnios/oligohydramnios sequence but with visible bladder in smaller twin |
| II | Absent bladder in smaller twin |
| III | Abnormal Doppler studies |
| IV | Hydrops fetalis |
| V | Demise of one or both twins |

or absence of hydrops. The staging system is listed in Table 44.1. Although a number of criticisms of the system have been put forth, by and large the Quintero score has endured as a standard tool used in gauging the magnitude of disease present, and has been extensively applied in clinical trials of various treatment modalities. One limitation of the Quintero staging classification lies in its inability to discriminate between various degrees of cardiovascular derangement, with no consideration given to the absence, presence, or degree of recipient twin cardiomyopathy, as discussed in the following text.

## How and why does twin-twin transfusion syndrome occur?

The name "twin-twin transfusion syndrome" originates from postnatal experience with the disease. Twins born with marked size discrepancy are often identified as having significant differences in hemoglobin, with one manifesting polycythemia and the other anemia. This led to the belief that a simple *in utero* exchange of blood between the twins was the cause of this ailment. Current findings suggest that the pathophysiology is much more complex. Fetal blood sampling commonly demonstrates no significant difference in hemoglobin concentrations between twins with manifestations of TTTS, and hence, a simple intertwin blood "transfusion" is unlikely to be the sole cause.

The current thinking about the primary mechanism of TTTS is that it originates as a placental vasculopathy. In monochorionic twins, placental vascular connections exist between the two circulatory systems of each of the twins (Figure 44.1). These connections consist of arterial-to-arterial (A–A) anastomoses, venovenous (V–V) anastomoses, or arterial-to-venous (A–V) anastomoses.[12] At both A–A and V–V anastomoses, there is an even bidirectional exchange of blood volume between the circulations; however, exchange at A–V anastomoses is unidirectional, based on the pressure gradient. In the balanced state, whatever uneven exchange takes place between twins at A–V anastomoses is counterbalanced by equilibration at the A–A and, less often, V–V anastomoses. TTTS is believed to occur when there is a paucity of adequate A–A connections to allow for equilibration; hence, A–V connections predominate, resulting in a disequilibrium

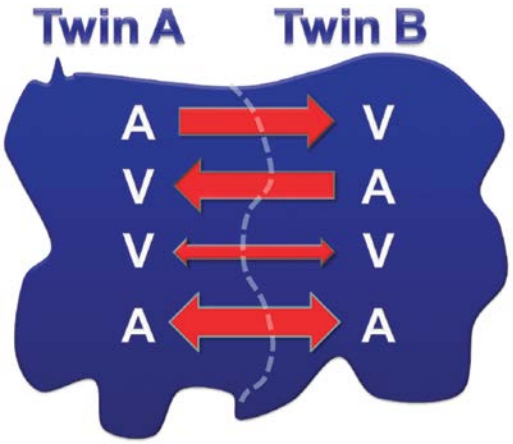


**Figure 44.1**
The possible vascular connections between twins in a monochorionic system. Unidirectional flow occurs between A–V connections, with equilibration of flow occurring at V–V and A–A connections. The hatched line represents the vascular equator between the two fetal circulations. (A, arterial; V, venous.)

of placental flow between the twins.[13] One twin becomes a "donor," while the other is a "recipient" of transplacental blood flow. Ultimately, the donor begins to manifest hypovolemia, and as a consequence oliguria resulting in oligohydramnios, while the recipient manifests hypervolemia and polyhydramnios.

Recent data looking at the renovascular systems of twins in TTTS have shed important light on this complex process.[14] Immunohistochemistry studies have demonstrated the renin-angiotensin system (RAS) to be upregulated in the donor twin. This makes sense, as it is the expected natural response to hypovolemia. The effects of angiotensin II released by the RAS in response to hypovolemia are to increase vasoconstriction and water retention in the donor and thereby promote maintenance of perfusion pressure. Partner recipient twins have been identified as having downregulation of their renin-angiotensin system likely as a consequence of the hypervolemia, yet serum levels of RAS hormones such as renin are similar to those found in the donors. This suggests that RAS hormones found in the recipient are not intrinsically produced but in fact produced by the donor, and delivered to the recipient through vascular connections. Hence, not only does the recipient receive an increase in volume but also an increase in hormonal modulators that are typically released in response to low volume. These agents act as vasoconstrictors within the recipient, resulting in an increase in vascular resistance. In addition, other agents such as brain natriuretic peptide[15] and endothelin,[16] hormonal modulators released in the presence of heart failure, are elevated in the amniotic fluid of recipient twins with hydrops. Hence, there is a double insult that takes place—an increase in *preload* and a paradoxical increase in *afterload*—which, in combination, act deleteriously upon the recipient cardiovascular system and are the cause of the cardiomyopathic changes seen in the recipient in TTTS.

## Impact on the cardiovascular system and echocardiographic findings in twin-twin transfusion syndrome

Important changes take place in the cardiovascular system of fetuses in TTTS, with the potential for a wide spectrum of findings[7–10] (Figure 44.2 through 44.9). The donor heart rarely manifests cardiac abnormalities on echocardiography, as the myocardium deals with a decrease in preload and an increase in afterload quite well. The systolic performance of the donor heart is preserved, with no effect on valvular function. Ventricular cavity size and overall heart size are usually smaller than normal. Since the donor experiences an overall increase in systemic vascular resistance, analysis of placental vascular resistance by Doppler interrogation of the umbilical artery reveals an increase in the pulsatility index. This can be identified qualitatively by observing a low diastolic flow velocity or even absent or reversed flow at end-diastole in the spectral tracing of the umbilical artery. These findings suggest very high placental vascular resistance.

The recipient heart bears the brunt of the disease in TTTS. At first, and at an early stage, one may identify ventricular cavity dilatation and mild ventricular hypertrophy. Mild atrioventricular valve regurgitation, likely as a consequence of cavity dilatation, can be seen. Doppler flow patterns in the umbilical artery and vein are normal, and both systolic and diastolic ventricular performance is preserved. As the disease progresses, ventricular thickening progresses with a consequential effect on ventricular compliance and diastolic function. Of note, it has been observed that it is the right ventricle more so than the left that typically manifests the majority of change in TTTS. As the ventricle hypertrophies, it becomes less compliant, and Doppler parameters of ventricular filling begin to change. The normal twin peaks of inflow into the ventricle relating to passive filling (E-wave) and active atrial filling (A-wave) fuse into a single peak. Ductus venosus flow during atrial contraction diminishes, often becoming absent or reversed in conditions of a very stiff, noncompliant right ventricle. Finally, further

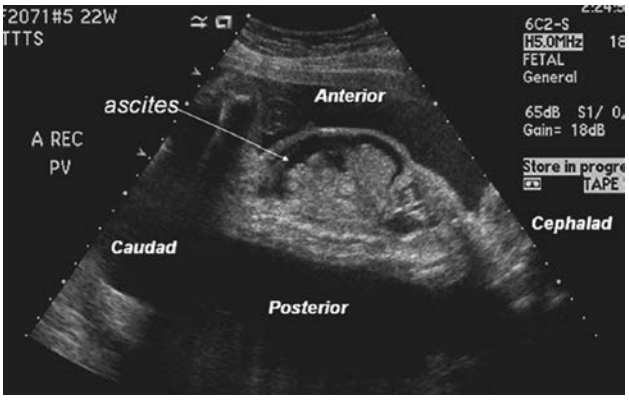


**Figure 44.2**
Ascites in a recipient twin with severe cardiomyopathy.

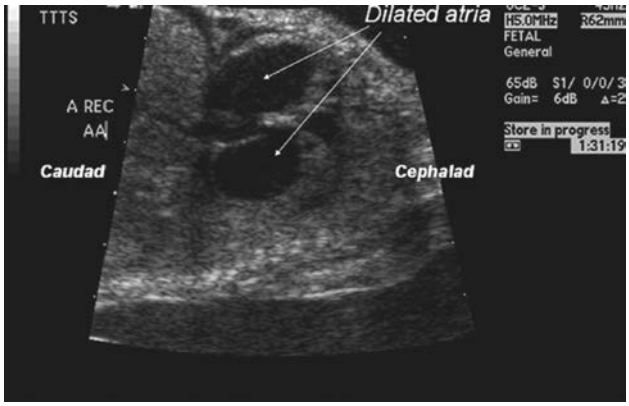


**Figure 44.3**
Dilated atria in a recipient twin with severe cardiomyopathy. The atrial portion of the heart nearly fills the entire diameter of the chest. The atria are enlarged due to the diastolic dysfunction and poor compliance of the ventricles as well as the presence of significant atrioventricular valve regurgitation.

upstream, the finding of pulsations in the umbilical vein can be seen, reflecting a severe degree of impediment to ventricular filling. As diastolic dysfunction progresses, ventricular systolic function is affected as well. Systolic ventricular dysfunction can be observed as a decrease in ventricular shortening fraction and a worsening of atrioventricular valve regurgitation, initially on the right and then progressing to the left side of the heart. Ultimately, severe ventricular dysfunction and severe atrioventricular insufficiency lead to low cardiac output, development of hydrops, and fetal death. Barrea et al. reviewed 28 twin pairs affected by TTTS and found cardiomegaly due to right or left ventricular hypertrophy in 58% of recipient twins.[10] Diastolic dysfunction of both right and left ventricles was present in two-thirds, and right ventricular systolic dysfunction with significant tricuspid regurgitation was seen in one-third. Progression of findings was associated with a higher perinatal mortality.

Right ventricular pressure estimates from the peak velocity of the tricuspid regurgitant jet in the recipient with TTTS will typically demonstrate very high intracavitary values. This finding offers further support to the notion that the recipient twin heart is stressed by the presence of increased vascular resistance and increased afterload. The true blood pressure and ventricular cavity pressure in the human fetus is unknown. However, the typical peak systolic pressure for a newborn premature infant born at 24 weeks' gestation is known to be approximately 30–40 mm Hg. The systolic pressure in the normal fetal heart in series with the low vascular resistance placenta should therefore be perhaps less, but certainly no higher, than this value. We have observed right ventricular pressures as high as 80–90 mm Hg in the absence of any outflow tract obstruction, supporting the notion that an increase in vascular resistance is part of the pathophysiological process resulting in the cardiomyopathy of TTTS seen in the recipient twin.

One fascinating phenomenon seen in TTTS is that of progressive development of right ventricular outflow tract obstruction in select recipient fetuses.[9] This "acquired" right ventricular outflow tract obstruction is phenotypically identical to the

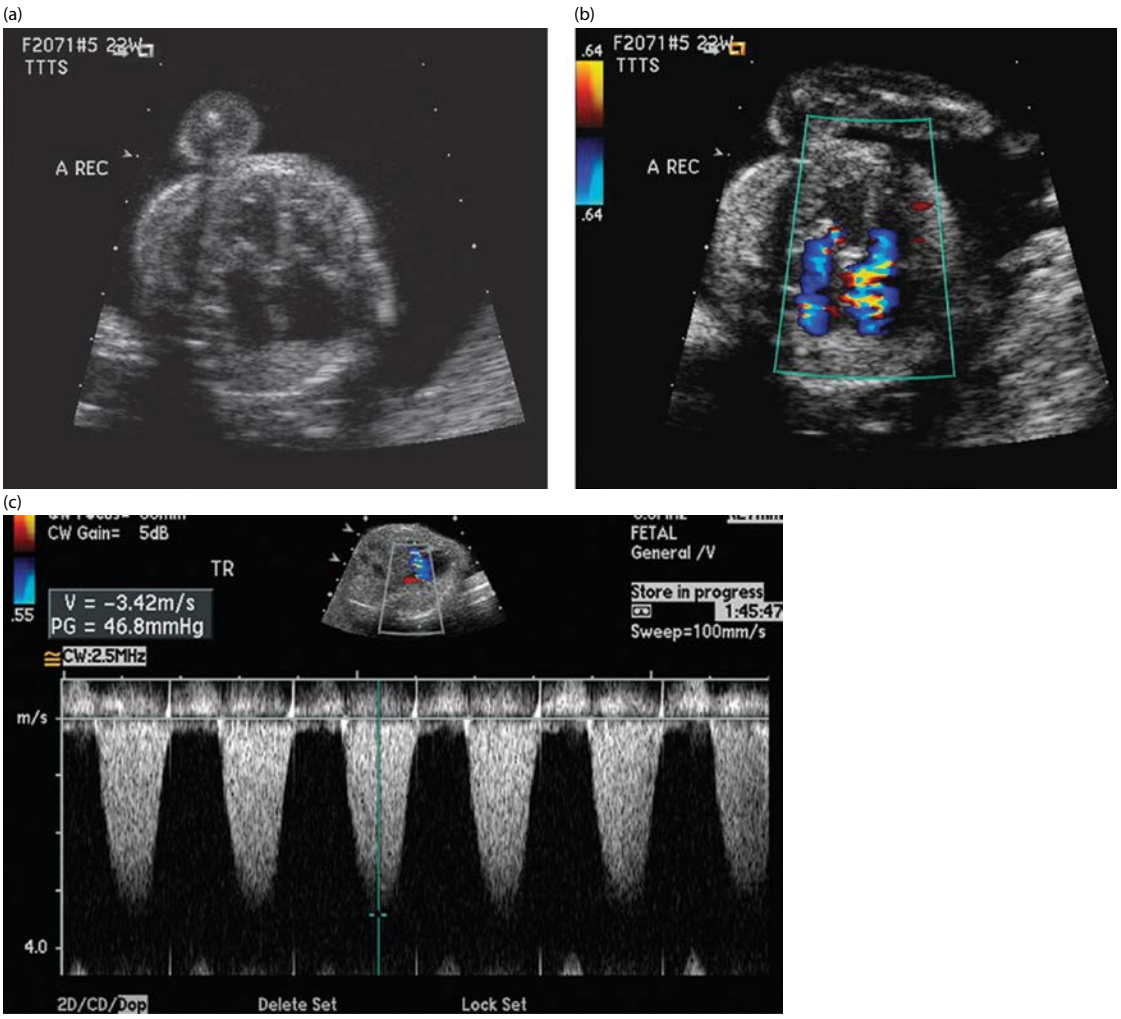


**Figure 44.4**
(a) Four-chamber view of the heart in a recipient twin. Note the heart size which in cross-sectional area exceeds 50% of the chest area. (b) Color Doppler echocardiography demonstrates severe tricuspid and mitral valve regurgitation. (c) The right ventricular pressure estimate from the peak velocity of the spectral Doppler display is elevated at approximately 50 mm Hg. (PG, peak gradient; V, peak velocity.)

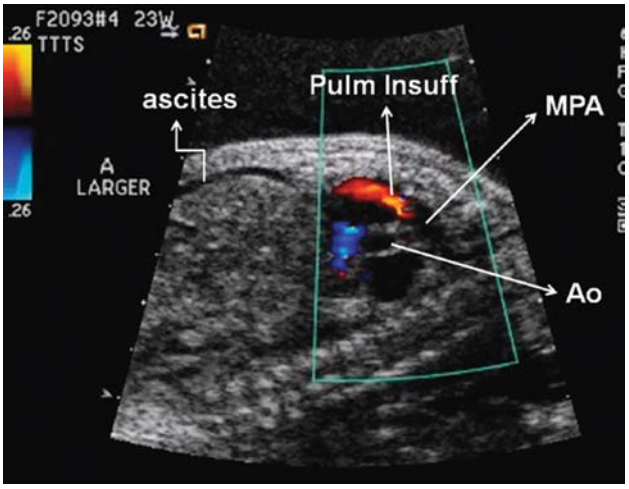


**Figure 44.5**
A significant jet of pulmonary insufficiency in a recipient twin-twin transfusion syndrome fetus. (Ao, aorta; MPA, main pulmonary artery; Pulm Insuff, pulmonary valve insufficiency.)

congenital heart defect of pulmonary atresia or pulmonary stenosis with a hypoplastic, hypertrophied right ventricle. This phenomenon of development of selective right ventricle outflow tract obstruction in otherwise structurally normal hearts begs the question of whether recipient TTTS cardiac changes may offer a clue as to the development of some forms of congenital heart disease. The process of TTTS demonstrates the plasticity of the fetal right ventricle, in that a structurally normal heart is dramatically affected by alterations in extrinsic loading conditions and hormonal modulators, these contributed by the cotwin donor. It is enticing to speculate that perhaps a similar mechanism of hormonal conditions and altered load very early in gestation may be the cause of right-sided obstructive anomalies in the singleton fetus born with these forms of congenital heart disease.[17] This relates to the fundamental mechanisms of formation of congenital heart disease. Alterations in blood flow and other extrinsic variables may potentially lead to the development of "acquired-congenital" heart disease at a period of time following completion of embryological formation of the human heart.

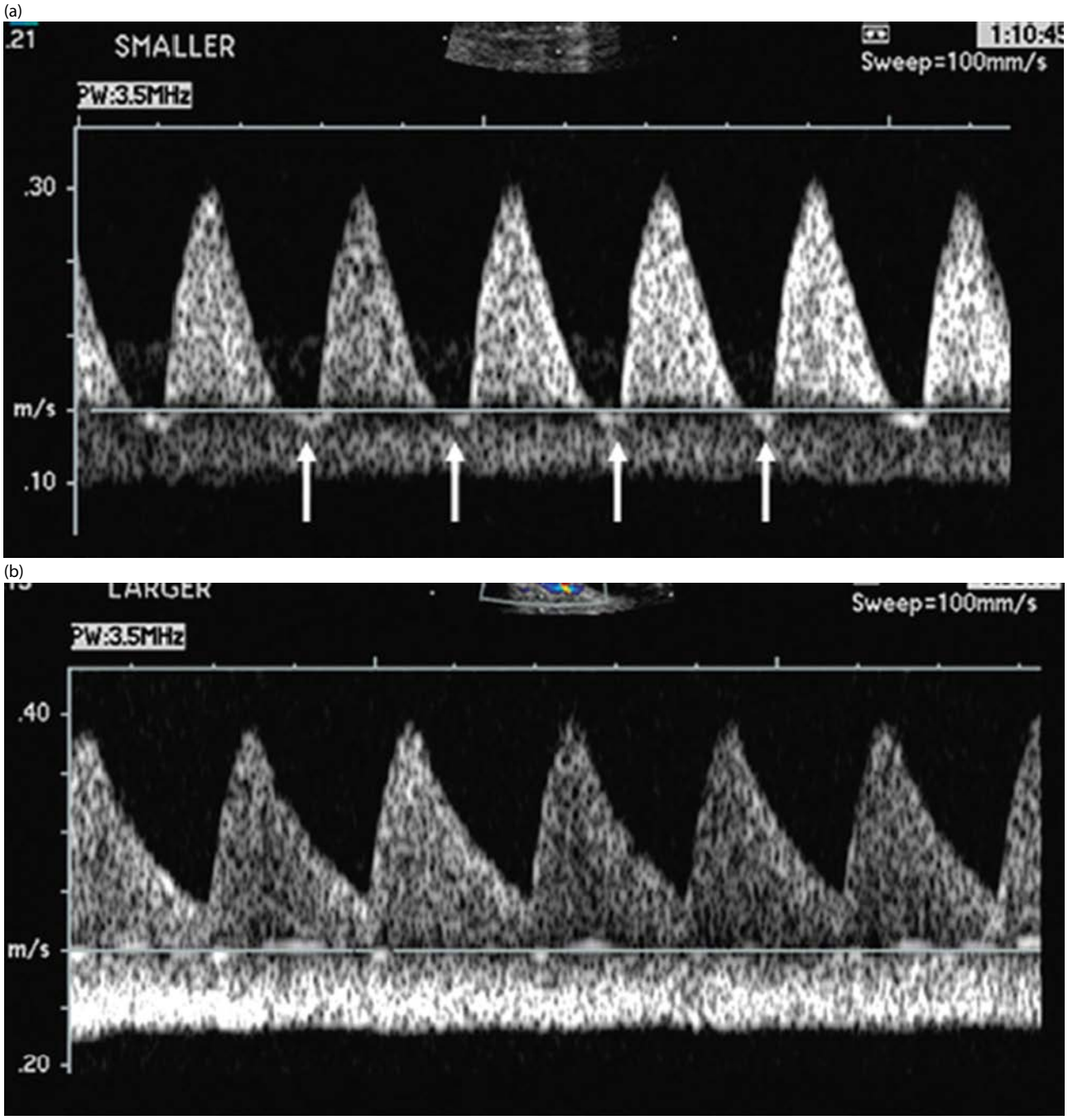


**Figure 44.6**
Doppler sampling in the umbilical cords of a donor twin (a) and a recipient twin (b). Umbilical arterial flow (pulsatile) is above the baseline, while umbilical venous flow is depicted below the baseline. Note the diminution in diastolic velocity in the donor umbilical artery flow as compared to the recipient. The arrows point out reversal of flow in the donor twin (below the baseline) suggesting markedly elevated placental vascular resistance.

## Measures to assess the burden of cardiovascular impairment in twin-twin transfusion syndrome

Gauging the magnitude of cardiovascular derangement in TTTS is important. One such measure of the magnitude of ventricular dysfunction is the myocardial performance index (MPI).[18] The MPI is a ventricular geometry-independent measure of combined systolic and diastolic ventricular performance. By performing Doppler sampling of inflow and outflow across the ventricle, one can measure the time intervals relating to isovolumic contraction, isovolumic relaxation, and ventricular ejection. The MPI is a measure of the ratio of combined isovolumic times to the ejection time. As global systolic and diastolic dysfunction worsens, MPI values

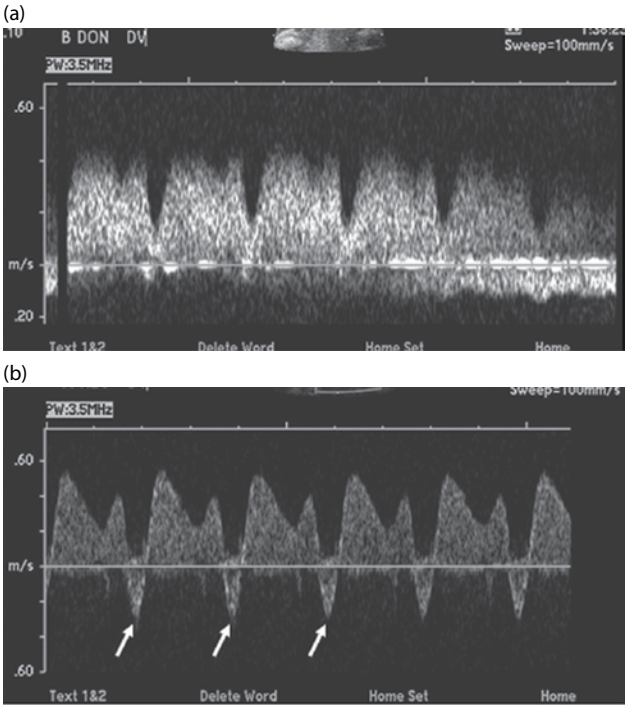


**Figure 44.7**
Doppler sampling in the ductus venosus of a donor twin (a) and recipient twin (b). The donor has a normal Doppler signal with continuous but phasic forward flow in the ductus venosus. The recipient Doppler signal displays reversal of flow with atrial contraction suggesting a poorly compliant, and stiff right ventricle.

increase. Raboisson and colleagues used the MPI to assess the ventricular performance status of recipient and donor twins with TTTS.[19] Recipient twins exhibited higher MPI values relative to their donor partners. The authors also found that ventricular dysfunction in the recipient was so characteristic of TTTS that one could reliably use the MPI to distinguish between TTTS and other causes of twin size discrepancy such as intrauterine growth restriction.

We have been investigating the utility of various Doppler-derived measures of ventricular performance in order to help us improve our understanding of the pathophysiology of TTTS as well as help stratify patients by severity of disease. Szwast et al. applied the MPI, as well as calculated the ventricular ejection force and cardiac output, in 22 twin pairs with TTTS.[20] The ventricular ejection force describes the acceleration of blood across the pulmonary or aortic valve over a specific time interval and is a reflection of systolic ventricular performance derived from Newton's laws. A higher value corresponds to a greater force exerted in ejecting the ventricular volume of blood during systole. The combined right and left ventricle cardiac output (CCO) is a measure of total blood flow through the fetal heart and is indexed to the estimated fetal weight in kilograms. The twin pairs were then compared to 36 age-matched singleton fetuses as normal controls. The findings are listed in Table 44.2. In the donor twins, right ventricle (RV) and left ventricle (LV) MPI values were lower than in the recipient

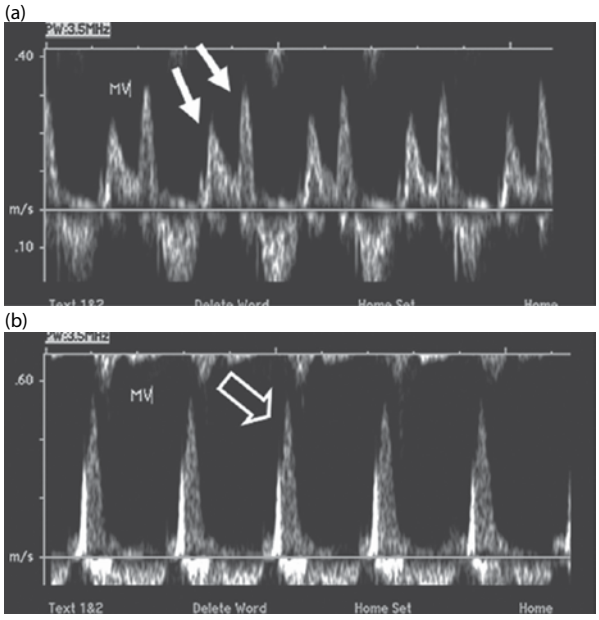


**Figure 44.8**
Doppler interrogation of flow across the mitral valve in a donor twin (a) and a recipient twin (b). The donor twin has a normal "double-peak" inflow pattern (solid arrows) representing flow during passive diastolic filling (first peak) and during atrial contraction (second peak). The recipient twin has a "single peak" inflow pattern (open arrow) suggesting fusion of the diastolic phases into a single phase. This represents a poorly compliant, and stiff ventricle. Note that often tachycardia can cause fusion of the normal double inflow peaks into a single peak; however, as can be seen in this case, the heart rate for the recipient is nearly identical to that of the donor twin.

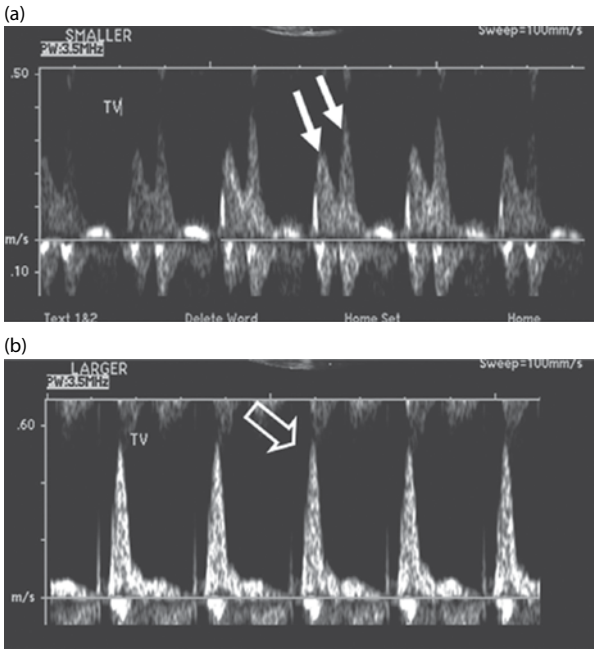


**Figure 44.9**
Doppler interrogation of flow across the tricuspid valve in a donor twin (a) and a recipient twin (b). The donor has a normal "double-peak" pattern (solid arrows), while the recipient has a "single-peak" inflow pattern (open arrow).

**Table 44.2** Results for the twin-donor versus twin-recipient versus normal control are summarized

| *Variable* | *Twin-donor (n = 22)* | *Twin-recipient (n = 22)* | *Normal (n = 36)* | *p1* | *p2* | *p3* |
|---|---|---|---|---|---|---|
| GA (weeks) | 22.3 ± 2.3 | 22.3 ± 2.3 | 22.9 ± 2.0 | 1 | 0.42 | 0.42 |
| Fetal weight (kg) | 0.42 ± 0.22 | 0.56 ± 0.21 | 0.64 ± 0.27 | <0.001 | <0.05 | 0.23 |
| RV MPI | 0.38 ± 0.07 | 0.56 ± 0.09 | 0.42 ± 0.05 | <0.001 | <0.05 | <0.001 |
| LV MPI | 0.35 ± 0.07 | 0.54 ± 0.12 | 0.41 ± 0.05 | <0.001 | <0.05 | <0.001 |
| RV EF (mN) | 2.5 ± 1.5 | 6.1 ± 4.0 | 5.4 ± 3.3 | <0.001 | <0.001 | 0.53 |
| LV EF (mN) | 2.0 ± 1.7 | 5.7 ± 3.2 | 4.6 ± 2.0 | <0.001 | <0.001 | 0.19 |
| CCO (mL/min/kg) | 416 ± 74 | 568 ± 109 | 506 ± 86 | <0.001 | <0.001 | <0.05 |

*Note:* The subgroup of the normal control population with similar gestational age is used for statistical analysis. *p* values are sequentially recorded as *p1,* twin-donor versus twin-recipient; *p2,* twin-donor versus normal; and *p3,* twin-recipient versus normal (From Szwast A et al. *Ultrasound Obstet Gynecol* 2007;30:40–6.[20])

*Abbreviations:* CCO, combined cardiac output; EF, ejection force; GA, gestational age; LV, left ventricle; MPI, myocardial performance index; RV, right ventricle.

twins, and even lower than in normal control fetuses. Donor twins also had diminished RV and LV ejection forces compared to recipient twins, and diminished RV and LV ejection forces compared to normal control fetuses. Donor twins had lower CCO compared to recipient twins as well as compared to normal control fetuses. These findings are consistent with the belief that donor twins are volume depleted but have preserved myocardial function. In contrast, the recipient twins had abnormally elevated RV and LV MPI compared to normal fetuses, although there was no significant difference between LV and RV ejection forces in recipient twins compared to normal fetuses. Finally, recipient twins had elevated CCO compared to their donor counterparts and compared to normal controls. This suggests that in our group of recipient twins, systolic function was still preserved, as ejection forces were increased while diastolic dysfunction was present. Application of these Doppler-derived parameters will help to identify fetuses with diastolic dysfunction, prior to the onset of low cardiac output and hydrops, and may therefore be helpful in grading the magnitude of disease as the twin-twin transfusion process progresses.

An important goal has been to provide a means for quantifying the cardiovascular burden present in TTTS by developing a cardiovascular score that may be used as an adjunct to the more general Quintero classification system. To that end, we have identified cardiovascular features that may be considered in such a score.[21] Table 44.3 lists these features and the values given to the various findings of the Children's Hospital of Philadelphia (CHOP) Cardiovascular Score for TTTS. The CHOP Cardiovascular Score is derived from echocardiographic data of 150 twin pairs referred for TTTS and incorporates features describing ventricular dilatation and hypertrophy, systolic function, valve regurgitation, and diastolic properties as described by Doppler indicators of ventricular compliance in the recipient twin. Umbilical arterial diastolic flow is considered in the donor twin.

While right ventricular outflow tract obstruction is an end result in some cases of recipient cardiomyopathy in TTTS, we have observed situations in which there is reversed-size discrepancy in between the pulmonary artery and the aorta. Whereas the pulmonary artery diameter is normally larger than the aorta by approximately 25%, some recipient fetuses exhibit an equal diameter between the pulmonary artery and aorta, or a pulmonary artery that is smaller than the aorta. We believe that this may reflect the spectrum of the disease, prior to the more severe finding of right ventricle outflow tract obstruction and pulmonary atresia. Altered compliance of the right ventricle can result in increased shunting away from the right side across the foramen ovale to the left ventricle. In such a circumstance, with diminished flow on the right, but increased flow on the left, pulmonary artery growth is inhibited while aortic growth is enhanced. We have therefore included abnormal size discrepancy between the pulmonary artery and aorta in our CHOP Cardiovascular TTTS Score.

The maximum score suggesting the most severe degree of cardiovascular impairment is 20/20. Recently, we have applied this score at the Children's Hospital of Philadelphia in prospectively monitoring all of our fetuses with TTTS. In addition to the score, which is derived from qualitative parameters, we have been routinely measuring MPI values in the recipient and donor twins as a supplemental means of assessing myocardial function. Table 44.4 describes the findings in 150 twin pairs with TTTS with respect to the Doppler-derived measures of umbilical artery pulsatility index, middle cerebral artery index, ductus venosus flow, MPI for right and left ventricles, and the parameters used to calculate the MPI values. It is only through just such a detailed and comprehensive characterization of the recipient and donor twins that one can appropriately gauge the effect of this disease, and the response of the cardiovascular system to various treatment strategies. Quantifying the degree of cardiovascular abnormality in the fetus with TTTS can also potentially be useful as a prognosticator of residual cardiovascular abnormalities after birth. These techniques will require further validation and analysis in a wide variety of cases. Such investigations are currently under way.

**Table 44.3** CHOP Cardiovascular Score for characterizing the severity of cardiovascular perturbation in the twin-twin transfusion syndrome

| *Parameter* | *Finding* | *Numerical score* |
|---|---|---|
| Donor | | |
| Umbilical artery | Normal | 0 |
| | Decreased diastolic flow | 1 |
| Recipient | Absent/reversed diastolic | 2 |
| Ventricular hypertrophy | None | 0 |
| | Present | 1 |
| Cardiac dilatation | None | 0 |
| | Mild | 1 |
| | >Mild | 2 |
| Ventricular dysfunction | None | 0 |
| | Mild | 1 |
| | >Mild | 2 |
| Tricuspid valve regurgitation | None | 0 |
| | Mild | 1 |
| | >Mild | 2 |
| Mitral valve regurgitation | None | 0 |
| | Mild | 1 |
| | >Mild | 2 |
| Tricuspid valve inflow | Double peak | 0 |
| | Single peak | 1 |
| Mitral valve inflow | Double peak | 0 |
| | Single peak | 1 |
| Ductus venosus | All antegrade | 0 |
| | Absent diastolic flow | 1 |
| | Reverse diastolic flow | 2 |
| Umbilical vein | No pulsations | 0 |
| | Pulsations | 1 |
| Right-sided outflow tract | PA > Ao | 0 |
| | PA = Ao | 1 |
| | PA < Ao | 2 |
| | RV outflow obstruction | 3 |
| Pulmonary regurgitation | None | 0 |
| | Present | 1 |
| Maximum total cardiovascular score | | 20 points |

*Source:* Rychik J et al. *Am J Obstet Gynecol* 2007;197:392.e1–8.[21]

*Abbreviations:* Ao, aorta; PA, pulmonary artery; RV, right ventricle.

## Treatment strategies for twin-twin transfusion syndrome

A variety of treatment strategies have been proposed for TTTS. The serial removal of large volumes of amniotic fluid from the recipient—amnioreduction—has been demonstrated to reduce morbidity and mortality.[22] Initially employed as a means of creating comfort for the mother, it soon became apparent that serial amnioreduction exerts a positive effect on fetal outcome as well. This may be related to improved placental circulation following relief of placental compression as well as prevention of preterm labor

**Table 44.4** Quantitative parameters of cardiovascular function evaluated in both the donor and recipient fetuses in 150 twin pairs with TTTS

| | *Donor* | *Recipient* | *p-Value* |
|---|---|---|---|
| Weight (g) | 399 (235) | 527 (285) | <0.0001 |
| UA S-wave peak velocity (cm/s) | 29.2 (8.7) | 41.7 (12.9) | <0.0001 |
| UA D-wave peak velocity (cm/s) | 4.7 (4.3) | 9.7 (4.5) | <0.0001 |
| UA PI | 1.81 (0.8) | 1.46 (0.4) | <0.0001 |
| MCA S-wave peak velocity (cm/s) | 27.3 (8.1) | 26.2 (8) | NS |
| MCA D-wave peak velocity (cm/s) | 5.1 (2.6) | 5.1 (2.1) | NS |
| MCA PI | 1.79 (0.4) | 1.70 (0.4) | NS |
| DV A-wave peak velocity (cm/s) | 18.5 (6.8) | 13.3 (16.7) | <0.01 |
| DV S-wave peak velocity (cm/s) | 51.1 (13) | 53.3 (13.6) | NS |
| DV A/S ratio | 0.38 (0.12) | 0.24 (0.31) | <0.001 |
| TV closure-to-opening time (ms) | 232 (18) | 275 (32) | <0.0001 |
| PA ejection time (ms) | 169 (13) | 169 (21) | NS |
| RV MPI | 0.38 (0.11) | 0.69 (0.47) | <0.0001 |
| MV closure-to-opening time (ms) | 222 (19) | 263 (29) | <0.0001 |
| Ao ejection time (ms) | 166 (15) | 170 (17) | 0.07 |
| LV MPI | 0.34 (0.12) | 0.59 (0.28) | <0.0001 |

*Source:* Rychik J et al. *Am J Obstet Gynecol* 2007;197:392.e1–8.[21]

*Abbreviations:* Ao, aorta; DV, ductus venosus; LV, left ventricle; MCA, middle cerebral artery; MPI, myocardial performance index (Tei index); MV, mitral valve; NS, not significant; PA, pulmonary artery; RV, right ventricle; TV, tricuspid valve; UA, umbilical artery.

by reduction in abdominal/uterine size. Creation of a communication between the donor and recipient amniotic sacs, either intentionally or during amnioreduction procedures, has also been demonstrated to result in improved outcomes. Equilibration of amniotic volumes and pressure between the twins by creating a "microseptostomy" can help; however, these communications commonly seal off, making this only a temporary measure.

Ville and others pioneered the concept of direct interruption of the guilty vascular anastomoses within the placental plate by percutaneous laparoscopic laser techniques.[23–26] Currently, this appears to be the most effective strategy for treating TTTS. In a large randomized trial of endoscopic laser photocoagulation therapy versus serial amnioreduction (The Eurofoetus Consortium Trial), laser therapy was identified as being superior as a first-line treatment at all stages of severity of the disease.[26] As compared to the amnioreduction group, the laser group had a higher likelihood of survival of at least one twin (76% versus 56%), had a lower incidence of periventricular leukomalacia (6% versus 14%), and was more likely to be free of neurological complications at 6 months of age (52% versus 31%). Although laser therapy currently appears to be the more effective strategy, it is not a cure for the disease in all cases, as significant morbidity and mortality in a large number clearly persist despite treatment. Further work needs to be done in determining the appropriate candidates and the optimal timing for laser therapy.

## Questions, speculations, and long-term issues

There are a number of unanswered questions concerning TTTS and the cardiovascular changes that take place. The outcome studies looking at therapeutic effectiveness have focused on perinatal survival and neurological outcome, with little focus on cardiovascular outcome. Which therapeutic interventions are most likely to result in cardiovascular improvement? Barrea and colleagues demonstrated that, despite amnioreduction, cardiovascular changes may persist or even progress.[10] The impact of laser therapy on cardiovascular changes and the ability to prevent progression of right ventricular outflow tract obstruction, cardiac failure, or hydrops have not yet been investigated. It is through the application of descriptive cardiovascular tools such as the CHOP Cardiovascular Score and other quantitative indexes of function that such questions may be addressed.

Intriguing questions remain concerning the pathophysiology of TTTS. Why do some severely affected recipient twins manifest ventricular dysfunction and heart failure, while others develop ventricular hypertrophy and right ventricular outflow tract obstruction? We propose the possibility that perhaps it is not the severity of the disease alone that dictates this phenotype, but that inherent genetic factors may play a role. It is well recognized in the mature postnatal heart that the myocardial response to stressors is, to a degree, under

genetic control.[27] It is therefore plausible to speculate that the fetal myocardial response to a severe increase in preload (volume exchange) and afterload (hormonal modulators) may similarly be under genetic control—for some twin recipients, the response to these stressors is cardiac hypertrophy, decompensation, and failure, while for others it is hypertrophy and development of right ventricular outflow tract obstruction. In fact, the latter may be a positive adaptive response in those that have the ability to muster it, since few fetuses with right ventricle outflow tract obstruction experience fetal demise, unlike the recipients who develop cardiac decompensation and hydrops. Perhaps variables such as angiotensin-converting enzyme genotype or other myocardial genotypes may influence the phenotypic direction that the recipient fetus will take. Angiotensin II can be a potent stimulant of myocardial hypertrophy in the mature heart; however, its direct myocardial effects are under complex genotypic control (i.e., receptor type, density, and so on).[27–30] Might the phenotypic variability seen in the recipient twin in TTTS be a result of a genetically controlled inherent response to elevated levels of angiotensin II? The genetic determinants of myocardial hypertrophy in the fetus are currently unknown but will likely explain this phenomenon.

The long-term implications of cardiovascular disease in the fetus with TTTS are potentially quite significant. The "Barker hypothesis" proposes the concept of fetal origins of adult cardiovascular disease—"programming" of the heart and vascular system takes place during fetal life, setting the risk for the development of later diseases such as hypertension and atherosclerosis.[31] Cheung and colleagues demonstrated the impact of fetal TTTS on vascular dysfunction in infancy.[32] TTTS donor twins at a mean of 9 months of age exhibited diminished arterial distensibility as measured by abnormal pulse-wave velocity examination. Gardiner and colleagues studied 27 twin pairs with TTTS after birth at a mean of 11 months of age, and found that laser therapy altered but did not abolish these vascular abnormalities of arterial distensibility.[33]

Are the survivors of fetal TTTS at risk for significant cardiovascular difficulties as they grow into later childhood and into adulthood? What is the long-term cardiovascular burden of TTTS, and to what degree do these patients carry added risk for cardiovascular disease as they grow into adulthood? These are intriguing questions yet to be answered in large numbers. Certainly, there is great interest as the population of survivors increases as to how they will fare as adults. Thus far, preliminary data would suggest a very good outcome. Matched donor recipient twin pair survivors at a median of 4.5 years of age showed only slight differences in diastolic left ventricular function with lower left ventricular ratio of early and late diastolic filling compared with their donor co-twins.[34] Values, however, were still within the range of normal for singleton age-matched subjects. Of great interest as well are aspects of quality of life for these survivors, with emerging data suggesting a continuing risk of cerebral palsy and neurocognitive deficit.[35] Increasing knowledge of the pathophysiology, with earlier identification and treatment strategies that manage the condition at an earlier point of disease severity may reduce the risk in the future.

## Summary

TTTS is a unique and complex disease process affecting monochorionic/diamniotic twins. The disease is primarily due to a placental vasculopathy with resultant transfer of both volume and hormonal modulators through intraplacental vascular connections from the donor to the recipient twin. Morbidity and mortality remain high despite the development of treatment strategies such as endoscopic laser photocoagulation. Complex changes take place within the cardiovascular system, which contribute substantially to the outcome of this disease. The application of tools to better grade the degree of cardiovascular derangement will help in determining the efficacy of current and to-be-developed treatment strategies. The long-term impact of TTTS on the postnatal and mature adult cardiovascular system, although likely of significance, is yet to be fully understood.

## References


1. Sebire NJ et al. *Br J Obstet Gynaecol* 1997;104:1203–7.
2. Harkness UF, Crombleholme TM. *Semin Perinatol* 2005;29:296–304.
3. Berger HM et al. *Lancet* 2000;356:847–8.
4. Fisk NM, Galea P. *N Engl J Med* 2004;351:182–4.
5. Gonsoulin W et al. *Obstet Gynecol* 1990;75:214–16.
6. Haverkamp F et al. *Eur J Paediatr Neurol* 2001;5:21–7.
7. Zosmer N et al. *Br Heart J* 1994;72:74–9.
8. Simpson LL et al. *Obstet Gynecol* 1998;92:557–62.
9. Lougheed J et al. *J Am Coll Cardiol* 2001;38:1533–8.
10. Barrea C et al. *Am J Obstet Gynecol* 2005;192:892–902.
11. Quintero RA et al. *J Perinatol* 1999;19:550–5.
12. Bajoria R et al. *Am J Obstet Gynecol* 1995;172:856–63.
13. Galea P et al. *Prenat Diagn* 2005;25:777–85.
14. Mahieu-Caputo D et al. *Pediatr Res* 2005;58:685–8.
15. Bajoria R et al. *Am J Obstet Gynecol* 2002;186:121–7.
16. Bajoria R et al. *Hum Reprod* 1999;14:1614–18.
17. Clark, EB et al. *Am J Physiol Heart Circ Physiol* 1989;257:H55–61.
18. Eidem BW et al. *Echocardiography* 2001;18:9–13.
19. Raboisson MJ et al. *Circulation* 2004;110:3043–8.
20. Szwast A et al. *Ultrasound Obstet Gynecol* 2007;30:40–6.
21. Rychik J et al. *Am J Obstet Gynecol* 2007;197:392.e1–8.
22. Mari G et al. *Am J Obstet Gynecol* 2001;185:708–15.
23. Ville Y et al. *N Engl J Med* 1995;332:224–7.
24. De Lia JE et al. *J Perinat Med* 1999;27:61–7.
25. Hecher K et al. *Eur J Obstet Gynecol Reprod Biol* 2000;92:135–9.
26. Senat MV et al. *N Engl J Med* 2004;351:136–44.
27. Lips DJ et al. *Eur Heart J* 2003;24:883–96.
28. Yamazaki T et al. *Am J Cardiol* 1999;83:53H–7H.
29. Sadoshima J, Izumo S. *Circ Res* 1993;73:413–23.
30. Sadoshima J et al. *Cell* 1993;75:977–84.
31. Barker DJ. *Ann Med* 1999;31(suppl 1):3–6.
32. Cheung YF et al. *Lancet* 2000;355:1157–8.
33. Gardiner HM et al. *Circulation* 2003;107:1906–11.
34. Halvorsen CP et al. *Acta Paediatr* 2015;104:252–8.
35. van Klink JM et al. *Twin Res Hum Genet* 2016;19:255–61.

# 45

# Fetal interventions for congenital heart disease

Lindsay R. Freud, Max E. Godfrey, and Wayne Tworetzky

## Introduction

Advances in fetal echocardiography have facilitated our understanding of the natural history of cardiac disease *in utero*. This knowledge, coupled with improvements in interventional obstetric and catheterization techniques, has led to the advent of minimally invasive percutaneous fetal cardiac intervention (FCI). Since the first report of FCI by Maxwell et al. in London in 1991,[1] the field has evolved considerably. The goal is to alter the natural history of fetuses with severe anomalies that lead to significant lifelong morbidity and mortality, i.e., staged univentricular palliation, and/or improve survival in fetuses with lethal anomalies. We will focus on the three most common forms of congenital heart disease for which minimally invasive percutaneous FCI is currently performed: severe aortic stenosis (AS) with evolving hypoplastic left heart syndrome (HLHS), pulmonary atresia with intact ventricular septum (PA/IVS) and evolving hypoplastic right heart syndrome (HRHS), and established HLHS with intact or highly restrictive atrial septum (IAS). Finally, the emerging possibility of maternal hyperoxygenation as a form of fetal therapy is discussed. The maternal aspects of fetal therapy, which are essential to consider, are beyond the scope of this chapter.

## Severe midgestation aortic stenosis with evolving hypoplastic left heart syndrome

The most commonly performed FCI is fetal aortic valvuloplasty for severe midgestation AS with evolving HLHS. Although early surgical survival has improved for infants with HLHS, staged univentricular palliation to a Fontan circulation carries significant lifelong morbidity and mortality.[2–5] A subset of patients with HLHS shares a common pathophysiologic etiology *in utero*; namely, severe AS with left ventricular (LV) dilation and dysfunction. Natural history studies have demonstrated that severe AS in the midgestation fetus initially leads to LV dilation as the ventricle attempts to overcome significant afterload (Figure 45.1). As gestation progresses, the LV becomes dysfunctional, and ultimately growth arrest of left-sided structures ensues.[6–10] By the time of birth, the left side of the heart is incapable of supporting the systemic circulation, resulting in HLHS.

The first attempt at fetal aortic valvuloplasty was reported by Maxwell et al. in 1991.[1] Over the subsequent decade, multiple centers attempted to perform the procedure; however, due to selection of severe cases in the third trimester and technical difficulties, the experience was largely unsuccessful.[11] In 2000, Boston Children's Hospital and Brigham and Women's Hospital embarked on a program to perform fetal aortic valvuloplasty among second-trimester fetuses that met specific physiologic criteria of fetal AS with evolving HLHS. In conjunction with technical modifications to the procedure, greater success was able to be achieved. The experience has since been replicated at other centers worldwide.[12–17]

Mäkikallio and colleagues at Boston Children's Hospital outlined specific pathophysiologic features of fetuses with severe midgestation AS that reliably predict evolution to HLHS. These features include LV systolic dysfunction, retrograde flow in the transverse aortic arch (Figure 45.2), monophasic mitral inflow, and left-to-right flow across the foramen ovale,[18] which have since been validated in a distinct cohort by colleagues in London.[19] The goal of fetal intervention for this disease is to relieve the severe AS that triggers these hemodynamic alterations in the second trimester, thereby avoiding evolution to HLHS and enabling a biventricular circulation postnatally.[20]

### *Patient selection*

When selecting fetal candidates for aortic valvuloplasty, there are two primary considerations:

1. Does the fetus manifest features that are highly predictive of progression to HLHS?
2. Is the left heart salvageable?

With regard to the first consideration, the fetal candidate must not only have evidence of severe valvar AS but also evidence of features that are highly suggestive of evolution to HLHS, as outlined previously. A small subset of patients may have midgestation AS that is not hemodynamically compromising and may achieve a biventricular circulation with postnatal aortic valvuloplasty alone.[21]

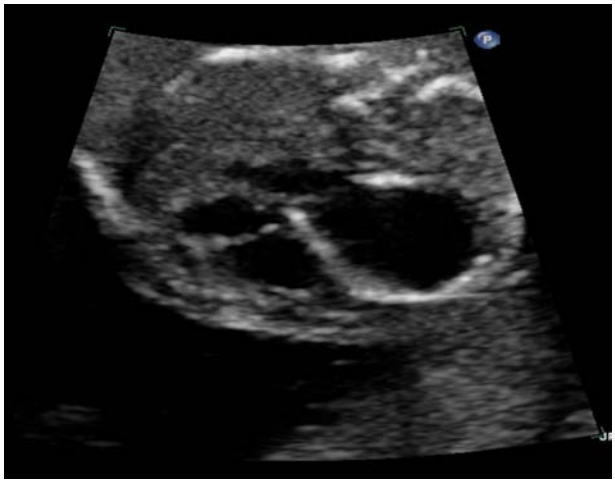

**Figure 45.1**
Four-chamber image demonstrating severe left ventricle dilation as a result of aortic stenosis in a midgestation fetus.

With regard to the second consideration, some fetuses present with disease that is too far advanced, and the LV is not salvageable. For example, if the LV is already hypoplastic at the time of presentation, then recovery is unlikely. Based on fetal aortic valvuloplasty performed in 70 fetuses, McElhinney et al. devised a scoring system to help predict which patients would be likely to have a biventricular circulation postnatally.[22] The scoring system includes LV long-axis z-score greater than 0, LV short-axis z-score greater than 0, aortic annulus z-score greater than −3.5, mitral valve annulus z-score greater than −2, and AS (or mitral regurgitation) maximum systolic gradient ≥20 mm Hg. The presence of four or more of these features had 100% sensitivity and 38% positive predictive value for identifying patients with a biventricular outcome. In addition, certain patients may present with a normal or dilated LV, but extensive scar tissue, or endocardial fibroelastosis (EFE), is present (Figure 45.3). EFE is associated with abnormal LV geometry and more severe diastolic dysfunction, which also limits the salvageability of the LV.[23,24]

Finally, and perhaps most importantly, the mother must be a suitable candidate for FCI. Since the fetus may or may not be of a viable gestational age and carries a significant anomaly, FCI should not be performed unless there is minimal risk to the mother. All mothers should be thoroughly assessed by maternal-fetal medicine specialists prior to offering FCI.

## *Technical aspects of the procedure*

Since the safety of the mother is paramount, we recommend performing FCI in an obstetrical operating room with maternal epidural anesthesia. Once the epidural is placed, the fetal position is determined and, if necessary, the fetus is manipulated into the optimal position. As demonstrated in Figure 45.4, the fetus is ideally positioned such that the left chest is anterior and there is a straightforward pathway from the maternal abdomen to the LV apex and subsequently to the LV outflow tract.[20] Once the fetus is optimally positioned, an intramuscular injection of analgesic (fentanyl), paralytic agent (pancuronium), and atropine are given.

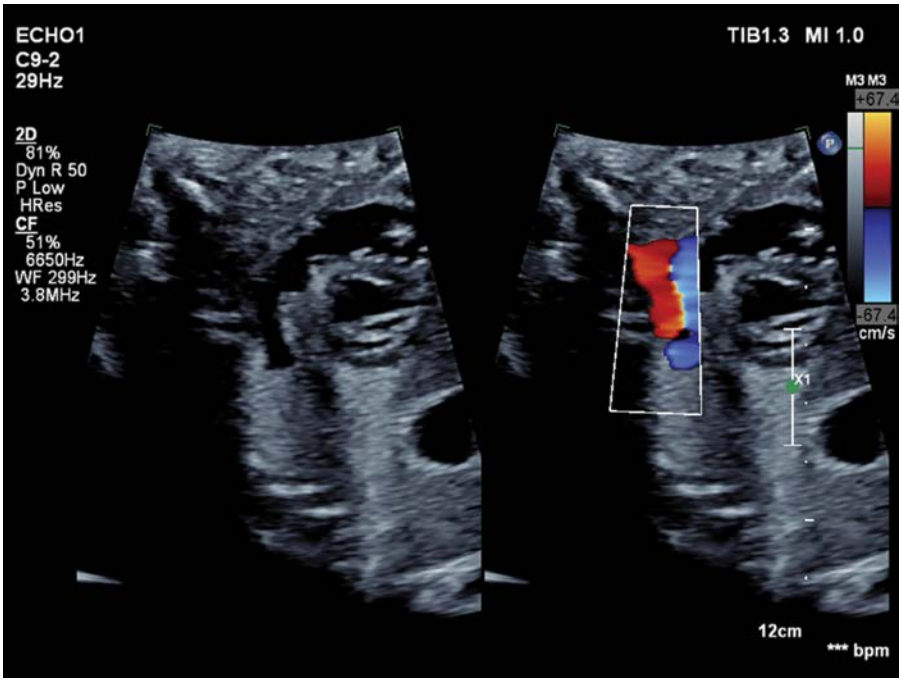


**Figure 45.2**
Sagittal image depicting retrograde flow in the transverse aortic arch in a midgestation fetus with severe aortic stenosis and evolving hypoplastic left heart syndrome.

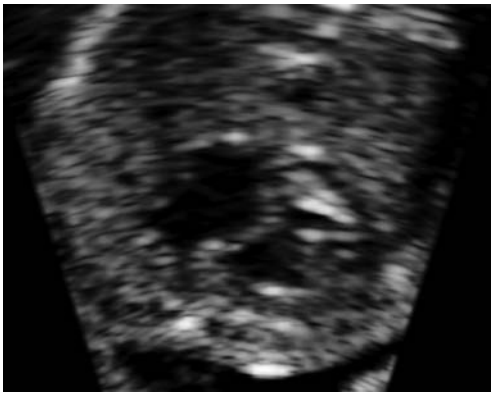

**Figure 45.3**
Example of left ventricle with significant endocardial fibroelastosis, which precluded this fetus from being a candidate for fetal aortic valvuloplasty.

Laparotomy is reserved only for select cases in which optimal fetal positioning is unable to be achieved with external version or imaging is limited.[25] Under ultrasound guidance, a 19-gauge cannula and stylet needle is advanced through the maternal abdomen, uterine wall, and fetal chest wall, and the LV apex is punctured (Figure 45.5; Video 45.1). After stylet removal and evidence of blood return confirming intracardiac cannula position, a 0.014-inch guidewire is manipulated across the LV outflow tract into the ascending aorta. A coronary angioplasty balloon is advanced over the wire, positioned across the aortic valve annulus, and inflated, typically at least two times, to 100%–120% of the size of the aortic annulus (Figure 45.6; Video 45.2).[12,26]

Color Doppler demonstrating a broader jet of antegrade flow across the aortic valve and/or the presence of aortic regurgitation confirms technical success (Video 45.3). After cannula removal, the fetus is monitored for complications in the operating room. The most common complications, which occur in up to 40% of fetuses, are bradycardia, ventricular dysfunction, and hemopericardium.[22] Bradycardia and dysfunction are treated with intracardiac epinephrine and atropine, typically with brisk response.[27] If the hemopericardium is small and hemodynamically insignificant, then no intervention is performed. If the hemopericardium is moderate to large and/or there is associated hemodynamic instability, then pericardiocentesis is performed.

In 2014, Boston Children's Hospital and Brigham and Women's Hospital reported technical success in 77 of the first 100 patients who underwent fetal aortic valvuloplasty.[28] Greater success was noted in the latter half of our experience, as would be expected after an initial learning curve. We also reported an 11% risk of fetal demise. Four of the deaths occurred within 24 hours of the procedure, and two of the deaths were due to premature rupture of membranes leading to delivery of nonviable fetuses. No significant maternal morbidity has been noted.[28,29] Both the risk of fetal demise and the use of laparotomy[25] have substantially decreased with greater experience with FCI.

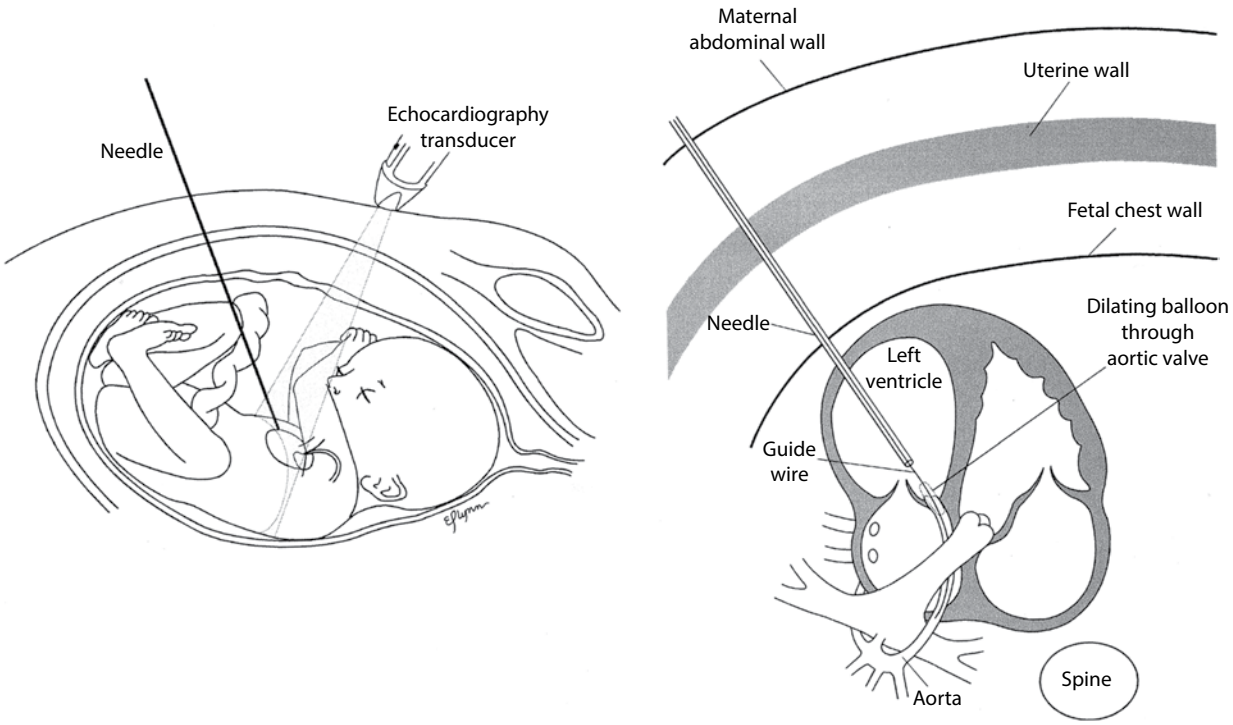


**Figure 45.4**
The ideal fetal position is demonstrated, with the fetal left chest anterior. The cannula has an unobstructed pathway from the maternal abdomen to the left ventricular apex. Once the apex is punctured, the guidewire and coronary angioplasty catheter are positioned for balloon dilation across the aortic valve. (Adapted with permission from Tworetzky W et al. *Circulation* 2004;110(15):2125–31.[20])

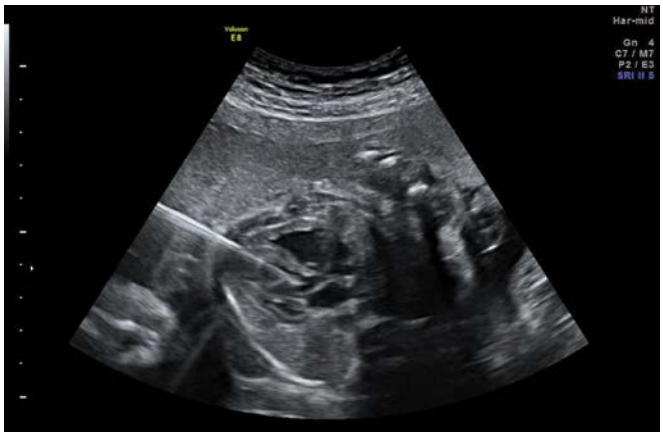

**Figure 45.5**
Needle insertion into the left ventricular apex and aimed toward the left ventricular outflow tract.

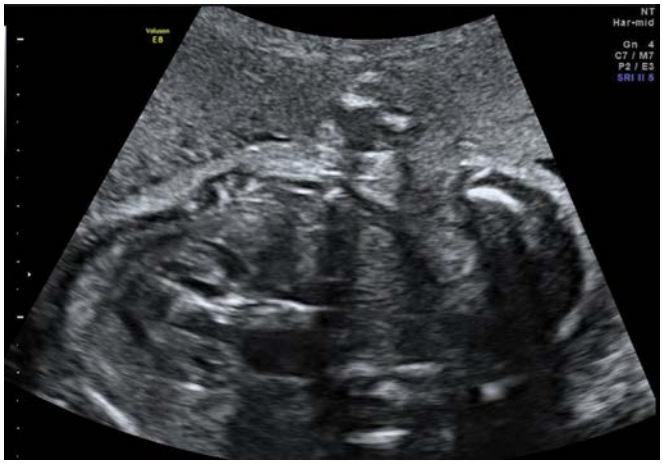

**Figure 45.6**
Balloon positioned across the aortic valve and inflated.

## *Postnatal outcome*

Technically successful FCI for severe AS has been shown to not only alter the hemodynamics[30] and growth of left-sided heart structures *in utero*[22] but also to result in larger left-sided heart structures at the time of birth as depicted in Figure 45.7.[28] Among the technically successful procedures performed at Boston Children's Hospital, 45% resulted in a biventricular outcome postnatally. Compared to patients managed as HLHS, freedom from cardiac death was better among patients with a biventricular circulation at midterm follow-up. However, biventricular patients had substantial cardiac morbidity: nearly all required postnatal cardiac catheterization and/or surgery, with valve replacements commonly performed.[28] This suggests that fetal aortic valvuloplasty may permit a biventricular circulation but often must occur with ongoing LV rehabilitation after birth.

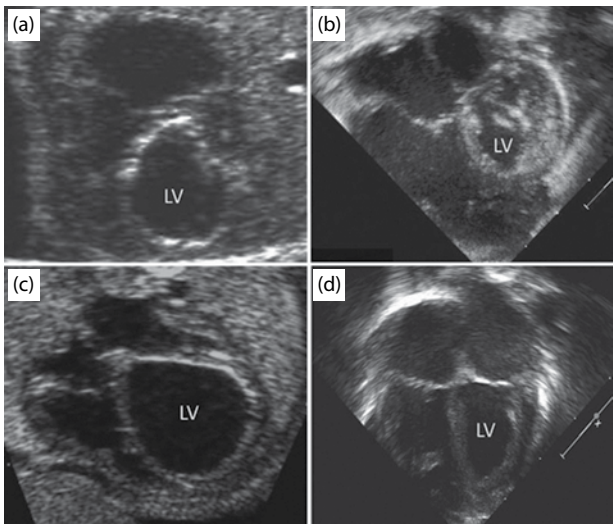


**Figure 45.7**
Four-chamber views of the heart are demonstrated for two patients with the pre-intervention fetal echocardiograms on the left and the postnatal echocardiograms on the right. The patient depicted in the first row (images [a] and [b]) had a technically unsuccessful fetal aortic valvuloplasty and was managed with staged univentricular palliation after birth, whereas the patient in the second row (images [c] and [d]) had a technically successful procedure and a biventricular outcome. LV indicates left ventricle. (Adapted with permission from Freud LR et al. *Circulation* 2014;130(8): 638–45.[28])

# Pulmonary atresia with intact ventricular septum and evolving hypoplastic right heart syndrome

Similar to severe midgestation AS with evolving HLHS, the rationale to perform FCI for PA/IVS and evolving HRHS is to alter the natural history and permit a biventricular outcome after birth. This may be achieved by perforating and dilating the atretic pulmonary valve *in utero* (fetal pulmonary valvuloplasty) to facilitate right heart growth throughout the remainder of gestation. PA/IVS, however, is a more heterogeneous disease than AS with evolving HLHS, and the wide spectrum of management and outcomes is often based on the degree of right ventricular and tricuspid valve hypoplasia.[31,32] For example, fetuses with PA/IVS and severely hypoplastic right ventricles, which may be associated with fibromuscular atresia of the right ventricular outflow and/or a right ventricular-dependent coronary circulation, are not candidates for FCI. As neonates, such patients typically undergo staged univentricular palliation. On the other end of the spectrum are fetuses with only mildly hypoplastic right ventricles in whom postnatal pulmonary valvuloplasty alone is often sufficient to achieve a biventricular circulation.

Fetuses considered for FCI fall in the middle of the spectrum and are often managed with at least one palliative procedure in the neonatal period. These patients are considered to have an intermediate circulation, and whether

a biventricular circulation is ultimately achieved is highly dependent on postnatal management strategy.[33–35] Ideally, FCI would enable such patients to achieve a biventricular circulation in the neonatal period.

## Patient selection

PA/IVS is diagnosed *in utero* by the presence of pulmonary atresia with left to right flow through the ductus arteriosus and right ventricular hypertrophy with elevated right ventricular pressure, which often can be assessed quantitatively by the presence of tricuspid regurgitation. The degree of right ventricular hypoplasia correlates with the z-score of the tricuspid valve, and similar to postnatal studies, the fetal tricuspid valve z-score may predict eventual postnatal outcome.[36–38] FCI is considered for patients with moderate right ventricular hypoplasia who are anticipated to require a palliative procedure in the neonatal period. More specifically, criteria for FCI include the following: (1) membranous atresia of the pulmonary valve with an intact (or highly restrictive) ventricular septum; and (2) tricuspid valve z-score less than –2 with an identifiable but small right ventricle that may be a target for cannula access (Figure 45.8).[39]

## Technical aspects of the procedure

FCI for PA/IVS and evolving HRHS is more challenging due to the complex geometry of the right ventricle as well as the presence of hypertrophy. A 19-gauge cannula is used, and the initial trajectory toward the right ventricular outflow tract is critical as there is less room for repositioning within the right ventricle. The atretic valve is perforated with the stylet or a 22-gauge Chiba needle, and a 0.014-inch guidewire and coronary angioplasty balloon are positioned across the

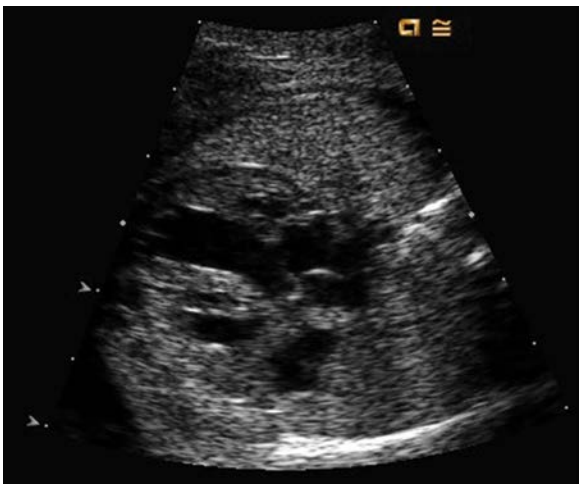

**Figure 45.8**
Example of a fetus with pulmonary atresia with intact ventricular septum and a mild to moderately hypoplastic right ventricle, with marked hypertrophy, that may be a candidate for fetal cardiac intervention.

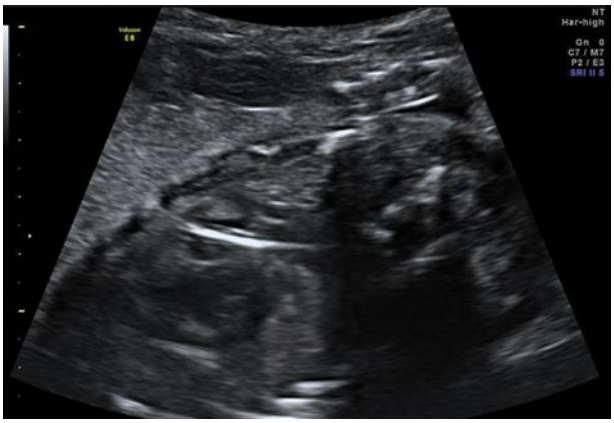

**Figure 45.9**
Balloon positioned across the right ventricular outflow tract in a fetus with pulmonary atresia with intact ventricular septum.

annulus for dilation (Figure 45.9; Video 45.4). Technically successful interventions are characterized by color Doppler imaging demonstrating antegrade flow across the pulmonary valve and pulmonary regurgitation. Complications such as bradycardia, ventricular dysfunction, and hemopericardium may occur, as detailed previously. In 2008, we reported four technically unsuccessful FCI, followed by six technically successful cases at Boston Children's Hospital and Brigham and Women's Hospital. No fetal demises occurred.[39] This experience has also been replicated at other centers worldwide.[16,17,40–42]

## Postnatal outcome

Fetal pulmonary valvuloplasty may alter the natural history of PA/IVS *in utero*, as demonstrated by subsequent right heart growth during gestation. Furthermore, among the five live-born patients with technically successful FCI in our series, four were able to achieve a biventricular circulation with varying degrees of postnatal intervention.[39] Similar to AS with evolving HLHS, FCI for PA/IVS should be viewed as the initial therapy for right ventricular rehabilitation in select patients, which, in conjunction with aggressive postnatal management strategy, may permit a biventricular circulation.

# Hypoplastic left heart syndrome with intact or highly restrictive atrial septum

HLHS with IAS is one of the most lethal forms of congenital heart disease.[43–45] While FCI for severe AS is performed to prevent evolution to HLHS, the rationale for FCI for HLHS with IAS is to improve survival. In this defect, there is established HLHS with minimal or no egress from the left heart. This leads to left atrial and pulmonary venous hypertension with downstream adverse effects on the pulmonary

vasculature and developing lungs.[43] Unlike the newborn, the fetus tolerates this circulation since pulmonary blood flow is low, and oxygenation is not dependent on atrial level shunting. However, at birth, an IAS leads to lack of oxygenated blood from the pulmonary veins entering the systemic circulation, as well as significant pulmonary edema. Cyanosis, acidosis, respiratory failure, and death rapidly ensue.

If HLHS with IAS is diagnosed prenatally, most tertiary care centers proceed with a timed delivery such that the neonate may have a catheter-based or surgical intervention to decompress the left atrium immediately after birth. Despite this postnatal strategy, however, survival remains dismal.[45] Therefore, Boston Children's Hospital and other centers began performing FCI to create an atrial communication *in utero*.[46] The goal of creating an atrial communication *in utero* is (1) to decompress the left atrium and prevent further damage to the pulmonary vasculature and developing lungs; and (2) to enable the patient to be more stable at birth.

## Patient selection

Fetuses with established HLHS and an intact or highly restrictive atrial septum (≤1 mm atrial communication) may be considered for FCI if left atrial hypertension is present and there is concern that the newborn will require an emergent postnatal procedure for left atrial decompression. The degree of atrial septal restriction and left atrial hypertension is assessed by the ratio of forward to reverse flow in the pulmonary veins by pulse wave Doppler evaluation (Figure 45.10).[47–49] Candidacy for this procedure is primarily based on high-risk physiology as opposed to discrete anatomic features; however, fetuses with hypoplastic left atria and exceptionally thick atrial septae may not be candidates for technical reasons.

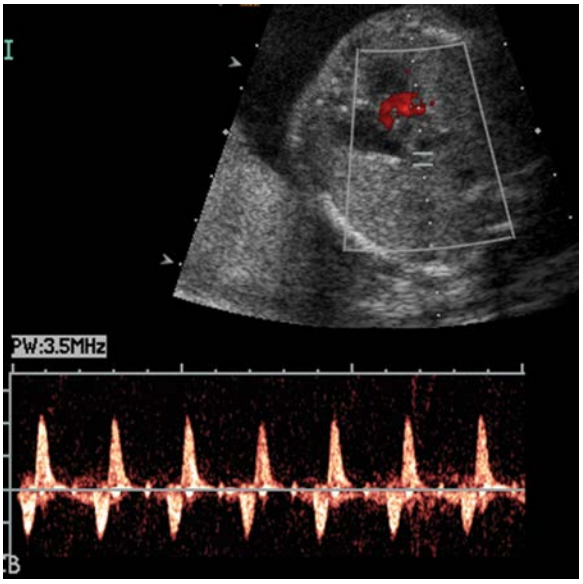


**Figure 45.10**
Pulse wave Doppler of a pulmonary vein in a fetus with hypoplastic left heart syndrome and intact or highly restrictive atrial septum prior to intervention.

## Technical aspects of the procedure

An 18- or 19-gauge cannula is inserted through either the right or left atrium, and the stylet or a 22-gauge Chiba needle is used to puncture the atrial septum. A balloon and/or balloon-mounted stent are inflated across the septum, with the goal of creating an atrial communication ≥3 mm (Video 45.5). Figure 45.11 demonstrates left to right flow across the stent following successful deployment. Bradycardia and ventricular dysfunction are uncommon with atrial access; however, hemopericardium can occur after the cannula is removed. With stent placement, there are additional risks of malposition or embolization.[46,50,51] As of 2008, 19 of 21 procedures were technically successful, and there were two cases of fetal demise, both within 24 hours of the procedure.[50]

## Postnatal outcome

In the series of 19 live-born patients reported from our institution, fetuses with atrial communications ≥3 mm had significantly higher oxygen saturations and a decreased need for emergent left atrial decompression at birth. However, survival following stage 1 surgery was not significantly different as compared to fetuses with smaller atrial communications or unsuccessful FCI. In a recent report from the International Fetal Cardiac Intervention Registry, survival of live-born fetuses was also similar between patients who underwent technically successful FCI versus unsuccessful (or no) FCI.[52] Despite these preliminary results, efforts are still underway given the lethality of this disease.

# Maternal hyperoxygenation and future directions

Beyond percutaneous FCI, another emerging form of fetal therapy is maternal hyperoxygenation. The administration of supplemental oxygen to pregnant mothers was shown to raise the fetal $pO_2$ in the 1950s[53] and was originally proposed as a treatment for intrauterine growth restriction.[54,55] Maternal hyperoxygenation results in vasodilation of the fetal pulmonary vascular bed with increased pulmonary blood flow, particularly later in gestation.[56] Increased fetal $pO_2$ in response to maternal hyperoxygenation, as well as increased pulmonary blood flow, has recently been demonstrated using fetal cardiac magnetic resonance imaging techniques.[57,58] Several groups have investigated the use of maternal hyperoxygenation to increase pulmonary venous return and therefore flow through the mitral valve, aortic valve, and aortic arch in fetuses with hypoplastic left heart structures.[59–61] While the early results are encouraging, this type of therapy might only be applicable in situations of

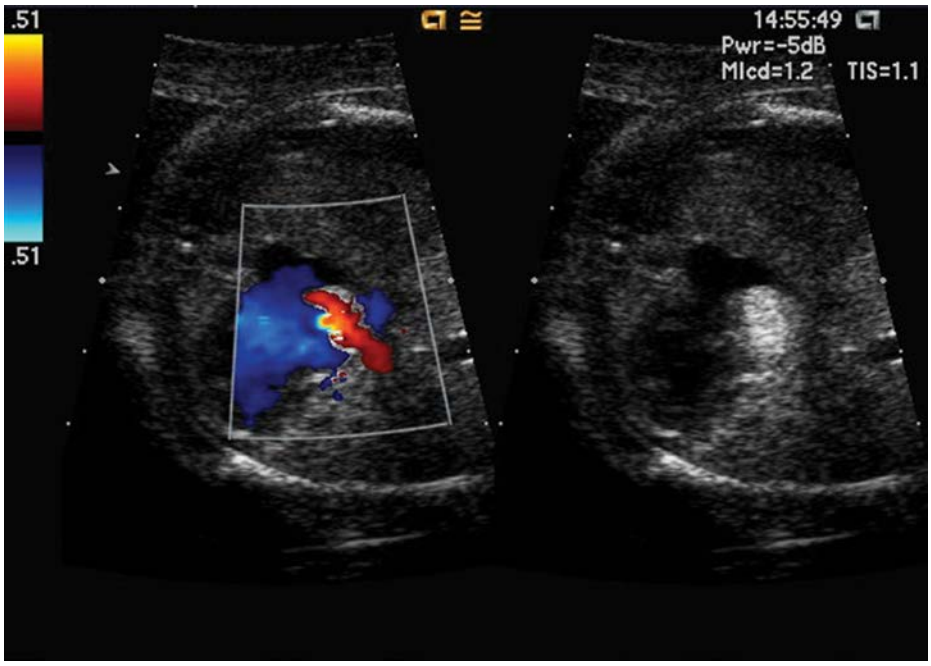


**Figure 45.11**
In this fetus with hypoplastic left heart syndrome and intact or highly restrictive atrial septum, a stent is visualized across the atrial septum with left to right flow.

reduced left ventricular preload, such as premature restriction or closure of the foramen ovale or mildly hypoplastic left heart structures without discrete valvar stenosis or endocardial fibroelastosis. Furthermore, the optimal dose and duration of maternal hyperoxygenation, as well as the potential side effects of chronic oxygen therapy to both the mother and the fetus, have yet to be defined.

Our ability to explore therapies that may benefit the fetal heart depends on our understanding of the *in utero* natural history and risk factors for the most severe forms of disease. As this work evolves, innovative strategies are unfolding. It is an exciting time in our field; however, all strategies should be pursued with the health and safety of the mother paramount.

## Videos

**Video 45.1** (https://youtu.be/GrjUtcuULjo)
Needle insertion into the left ventricular apex and aimed toward the left ventricular outflow tract.

**Video 45.2** (https://youtu.be/j8lZza6YdLQ)
Balloon positioned across the aortic valve and inflated. Balloon positioned across the aortic valve and inflated.

**Video 45.3** (https://youtu.be/TY_D1bL5cq0)
Aortic regurgitation following valvuloplasty, indicating a technically successful procedure.

**Video 45.4** (https://youtu.be/YOnR5xQJMKQ)
Balloon inflated across the right ventricular outflow tract in a fetus with pulmonary atresia with intact ventricular septum.

**Video 45.5** (https://youtu.be/X767fxDV5a4)
Balloon-mounted stent inflated across the atrial septum in a fetus with hypoplastic left heart syndrome and intact or highly restrictive atrial septum.

## References

1. Maxwell D et al. *Br Heart J* 1991;65(5):256–8.
2. Ghanayem NS et al. *J Thorac Cardiovasc Surg* 2012;144(4):896–906.
3. Feinstein JA et al. *J the Am Coll Cardiol* 2012;59(suppl 1):S1–42.
4. Anderson PA et al. *J Am Coll Cardiol* 2008;52(2):85–98.
5. Williams IA et al. *Cardiol Young* 2009;19(4):320–30.
6. Allan LD et al. *Int J Cardiol* 1989;25(3):341–3.
7. Danford DA, Cronican P. *Am Heart J* 1992;123(6):1712–3.
8. Simpson JM, Sharland GK. *Heart* 1997;77(3):205–10.
9. McCaffrey FM, Sherman FS. *Pediatr Cardiol* 1997;18(4):276–81.
10. Hornberger LK et al. *Circulation* 1995;92(6):1531–8.
11. Kohl T et al. *Am J Cardiol* 2000;85(10):1230–3.
12. Arzt W et al. *Ultrasound Obstet Gynecol* 2011;37(6):689–95.
13. Dangel J et al. *Ginekol Pol* 2011;82(8):632–6.
14. Marantz P et al. *Cardiol Young* 2013;23(5):675–81.
15. Gul A et al. *Turk Kardiyol Dern Ars* 2013;41(2):161–5.
16. Pedra SR et al. *Pediatr Cardiol* 2014;35(3):399–405.
17. Jaeggi E et al. *Trends Cardiovasc Med* 2016;26(7):639–46.
18. Makikallio K et al. *Circulation* 2006;113(11):1401–5.
19. Hunter LE et al. *Prenat Diagn* 2015;35(12):1176–81.
20. Tworetzky W et al. *Circulation* 2004;110(15):2125–31.
21. Freud LR et al. *Ultrasound Obstet Gynecol* 2015;45(3):326–32.
22. McElhinney DB et al. *Circulation* 2009;120(15):1482–90.
23. McElhinney DB et al. *Am J Cardiol* 2010;106(12):1792–7.
24. Friedman KG et al. *Am J Cardiol* 2014;114(1):122–7.
25. Wilkins-Haug LE et al. *Ultrasound Obstet Gynecol* 2006;28(1):47–52.

26. Marshall AC et al. *J Pediatr* 2005;147(4):535–9.
27. Mizrahi-Arnaud A et al. *Pediatr Res* 2007;62(3):325–30.
28. Freud LR et al. *Circulation* 2014;130(8):638–45.
29. Wohlmuth C et al. *Ultrasound Obstet Gynecol* 2014;44(5):532–7.
30. Selamet Tierney ES et al. *Ultrasound Obstet Gynecol* 2007;30(5):715–20.
31. Hanley FL et al. *J Thorac Cardiovasc Surg* 1993;105(3):406–23, 24–7; discussion 23–4.
32. Schneider AW et al. *Ann Thorac Surg* 2014;98(5):1680–6.
33. Ashburn DA et al. *J Thorac Cardiovasc Surg* 2004;127(4):1000–7; discussion 7–8.
34. Bryant R3rd et al. *J Thorac Cardiovasc Surg* 2008;136(3):735–42, 42 e1–2.
35. Hasan BS et al. *Catheter Cardiovasc Interv* 2013;81(1):111–8.
36. Peterson RE et al. *J Am Soc Echocardiogr* 2006;19(11):1393–400.
37. Salvin JW et al. *Pediatrics* 2006;118(2):e415–20.
38. Roman KS et al. *Am J Cardiol* 2007;99(5):699–703.
39. Tworetzky W et al. *Pediatrics* 2009;124(3):e510–8.
40. Tulzer G et al. *Lancet* 2002;360(9345):1567–8.
41. Polat T, Danisman N. *Images Paediatr Cardiol* 2012;14(3):6–11.
42. Gomez Montes E et al. *Cardiol Res Pract* 2012;2012:592403.
43. Rychik J et al. *J Am Coll Cardiol* 1999;34(2):554–60.
44. Vlahos AP et al. *Circulation* 2004;109(19):2326–30.
45. Glatz JA et al. *Ann Thorac Surg* 2007;84(5):1633–8.
46. Marshall AC et al. *Circulation* 2004;110(3):253–8.
47. Taketazu M et al. *J Am Coll Cardiol* 2004;43(10):1902–7.
48. Michelfelder E et al. *Circulation* 2005;112(19):2974–9.
49. Divanovic A et al. *J Thorac Cardiovasc Surg* 2011;141(4):988–94.
50. Marshall AC et al. *Prenat Diagn* 2008;28(11):1023–8.
51. Kalish BT et al. *Catheter Cardiovasc Interv* 2014;84(1):77–85.
52. Moon-Grady AJ et al. *J Am Coll Cardiol* 2015;66(4):388–99.
53. Mc CJ. *Obstet Gynecol* 1958;11(6):696–703.
54. Nicolaides KH et al. *Lancet* 1987;1(8539):942–5.
55. Battaglia C et al. *Ultrasound Obstet Gynecol* 1994;4(6):472–5.
56. Rasanen J et al. *Circulation* 1998;97(3):257–62.
57. Porayette P et al. *Prenat Diagn* 2016;36(3):274–81.
58. Borik S et al. *Cardiol Young* 2015;25(6):1214–7.
59. Kohl T. *Pediatr Cardiol* 2010;31(2):250–63.
60. Channing A et al. *Ultrasound Obstet Gynecol* 2015;45(6):664–9.
61. Lara D et al. *Ultrasound Obstet Gynecol* 2016;48(3):365–72.

# 46

# Doppler evaluation in fetal growth restriction

Javier Caradeux and Francesc Figueras

## Identification of small for gestational age

Antenatal detection of babies with defective growth often falls short, missing up to 75% of babies at risk of being small for gestational age (SGA) before delivery.[1] In low-risk pregnancies, the detection rate is worse (~15%).[2] Such poor performance takes a toll, as most instances of avoidable stillbirth and neonatal death are linked to failures in antenatal SGA detection.[3,4]

Current strategies to monitor growth involve symphysis-fundal height determination. However, only 16% of SGA infants are detected this way in low-risk populations.[5] Consequently, most SGA births are full term.[6] Third-trimester ultrasound (US) monitoring of fetal growth is done routinely in some countries, boosting detection rates to 40%–80%.[7,8] A recent well-designed prospective study comparing universal and selective (based on risk factors) third-trimester screening provides evidence that universal screening triples the detection rate of SGA and severe SGA.[9] However, another observational study[10] found that a contingent strategy based on selecting for third-trimester growth assessment the 50% of the population at highest risk as accrued by first- and second-trimester screening yields similar performance as universal screening.

Detecting SGA in advance of delivery has several potential benefits. Detection prompts further investigations, such as umbilical artery Doppler study, which has been shown to reduce stillbirth and increase preterm delivery without increasing neonatal mortality.[11] Detection also alerts clinician and mother to the increased risk involved, enabling deliberations on the optimal timing of delivery. Depending on severity of fetal growth restriction (FGR), the risk of stillbirth may be increased by 5- to 10-fold.[12]

A population-based study in the United States reported a significantly increased risk of stillbirth in pregnancies complicated by SGA when delivered after the 37th week;[13] and another study[14] in the United Kingdom where 92,218 normally formed singletons (including 389 stillbirths) were analyzed found a reduced stillbirth rate (per 1000 births) of 9.7 with antenatal FGR detection, compared to 19.8 when undetected. The impact of timely recognition and delivery of SGA babies is also underscored by the fact that in this study, gestational age in instances of detected versus nondetected SGA differed by only 10 days (270 versus 280 days) but resulted in a 50% lower incidence of stillbirths. Similarly, another large single-center retrospective study by Lindqvist et al.[7] found that fetuses with severe FGR (i.e., weight deviation ≤−22% or approximately less than the third percentile) that went undetected before delivery showed a fourfold increase in risk of adverse fetal outcome. Even in low-risk populations, undetected SGA has been associated with higher rates of hypoxic neonatal morbidity[15] and operative deliveries for nonreassuring fetal status.[16]

## Definition issues

### *Distinction between "fetal growth restriction" and "small for gestational age"*

SGA represent a heterogeneous population that comprises several phenotypes: (1) Those with congenital malformations (including chromosomopathies) or infections are a small proportion; in severe and early onset cases (especially when other markers and/malformations are present), a genetic causation should be suspected. A recent systematic review and meta-analysis found that a genomic chromosomal microarray provides a 4% incremental yield over conventional karyotyping.[17] In those severe cases with early onset or with other markers of infection, ruling out a cytomegalovirus infection seems appropriate. In a setting where malaria is endemic, this should also be considered. Other toxoplasmosis, other infections, rubella, cytomegalovirus infection, and herpes simplex screening are not required in the absence of other markers of infection. (2) Some of the SGA fetuses do not achieved their endowed growth potential mainly due to placental insufficiency. Thus, they could be considered true cases of fetal growth restriction. (3) Finally, a large fraction of the small babies are only constitutionally small (i.e., they have a low growth potential). By convention, these last two groups are normally referred to as FGR versus SGA.

From a clinical point of view, the distinction between FGR versus SGA is relevant because of the correlation with perinatal outcome. Whereas FGR represents a pathological condition

associated with adverse perinatal outcome, SGA merely are the end of the spectrum of healthy babies. While conceptually FGR and SGA are clearly distinct conditions, from a clinical point of view, their differentiation is rather challenging.

## *Distinction between early and late FGR*

Overall during the last decade, two different patterns of clinical presentation, determined primarily by the gestational age of disease onset and the pattern of umbilical artery Doppler, have been more clearly characterized.[18–20] Table 46.1 summarizes the main characteristics of each group.

FGR has a different phenotypic expression, evolution, and outcome when it starts early in gestation. The typical pattern of deterioration progresses from escalating abnormalities in umbilical artery (UA) and venous Doppler parameters to abnormal biophysical parameters. The rate of deterioration of Doppler parameters determines the overall speed of deterioration in early onset FGR, often necessitating preterm delivery. In addition, there is a high association with preeclampsia (PE) and perinatal mortality.[21–23]

In contrast, late-onset FGR is normally associated with less severe placental disease, so that normal or minimally elevated UA Doppler indices are usually observed. Overt cardiovascular adaptation does not extend beyond the cerebral circulation, manifesting as decreased cerebroplacental ratio (CPR). The association between late-onset FGR with PE is minimal in comparison with early onset forms.[22]

A study[24] aimed at setting the optimal cut-off to differentiate early and late forms has shown that a cut-off of 32 weeks at diagnosis or 34 weeks at delivery maximizes differences between early and late-onset FGR, but resulted in substantial overlapping of cases with similar characteristics. Umbilical artery Doppler discriminated better than gestational age between two groups with different timing, natural history, and rate of adverse outcome.

Finally, several studies show that the chief correlate with stillbirth, perinatal complications, and abnormal neurodevelopment is severe smallness (generally birth weight less than the third percentile)[25–30] even in term SGA fetuses without Doppler signs of brain redistribution and normal umbilical and uterine artery Doppler.[26]

Figure 46.1 shows the frequency of FGR and SGA measured by UA Doppler (a) and according to a composite definition including severe smallness, abnormal CPR, and abnormal uterine Doppler (b).

## Current consensus

Gordijn et al.[31] made a major contribution by reaching a consensus definition for early and late FGR (Table 46.2).

Among 45 experts in the field of FGR, there was agreement that before 32 weeks a severely abnormal UA Doppler (defined as an absent/reversed end diastolic flow) or an estimated fetal weight below the third percentile as a stand-alone could be considered as criteria for early FGR. Alternatively, an estimated fetal weight below the 10th percentile plus a pulsatile waveform (above the 95th percentile) in the uterine or UA Doppler also qualifies as early FGR.[31]

There is also substantial agreement to define late FGR after 32 weeks in the presence of an estimated fetal weight below the third percentile or when at least two of the following are met: (1) estimated fetal weight or abdominal circumference below the 10th percentile; (2) a declining fetal growth (defined as when the growth trajectory crosses two quartiles); or (3) an abnormal CPR (less than the fifth percentile).

## Screening strategies

By combining first- or second-trimester uterine Doppler findings with baseline maternal characteristics, detection of early onset growth restriction (needing delivery at <34 weeks) nears acceptable levels.[32] Furthermore, up to 60% of the latter are flagged up by preeclampsia.[33] Unfortunately, growth restriction in late pregnancy is still largely overlooked,[34] while accounting for the largest fraction of adverse perinatal outcomes and stillbirths.[6,12] Detecting late-onset growth restriction, especially severe states, is thus central to third-trimester evaluation.

## Clinical management

The most important prognostic factor in growth restriction is gestational age at delivery.[21,23] The main challenge in

**Table 46.1** Summary of the main differences between early and late-onset forms of fetal growth restriction (FGR)

| *Early onset FGR* | *Late-onset FGR* |
|---|---|
| CHALLENGE: MANAGEMENT | CHALLENGE: DIAGNOSIS |
| Prevalence: ~1% | Prevalence: 3%–5% |
| Severe placental disease: UA Doppler abnormal, high association with PE | Mild placental disease: UA Doppler normal, low association with PE |
| Severe hypoxia ++: systemic CV adaptation | Mild hypoxia: central CV adaptation |
| High mortality and morbidity | Lower mortality (but common cause of late stillbirth) |

*Abbreviations:* CV, cardiovascular; PE, preeclampsia; UA, umbilical artery.

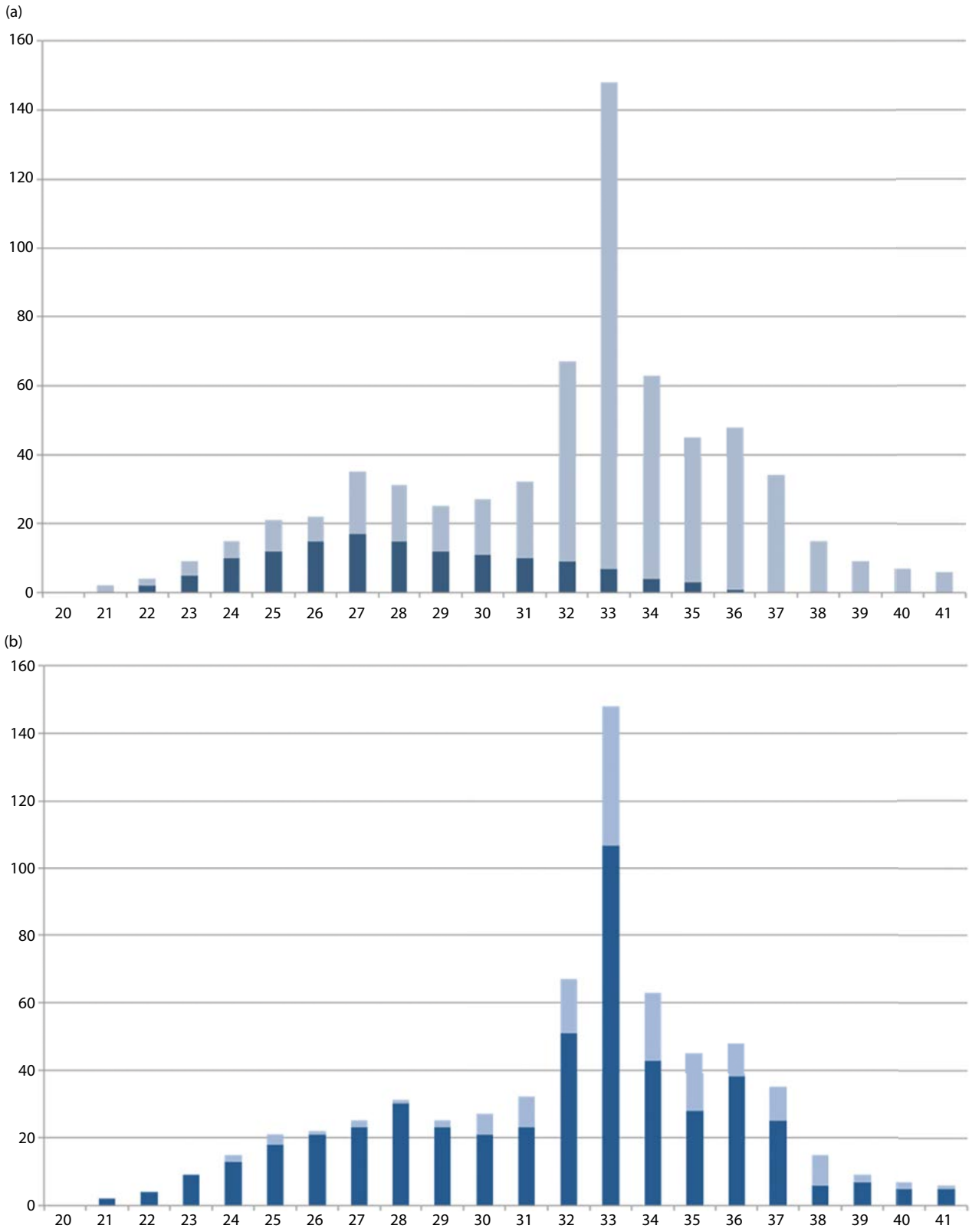


**Figure 46.1**
(a) Frequency distribution of cases with normal (light blue) and abnormal (dark blue) umbilical artery Doppler. (b) Frequency distribution of cases with all normal (light blue) and any abnormal (dark blue) criteria for fetal growth restriction (severe smallness [<3p], abnormal CPR or abnormal uterine artery Doppler).

**Table 46.2** Consensus definition of fetal growth restriction

| *Early fetal growth restriction*<br>*GA <32 weeks* | *Late fetal growth restriction*<br>*GA >32 weeks* |
|---|---|
| AC/EFW <third percentile or UA-AEDV | AC/EFW <third percentile |
| Or: | Or at least two of the following: |
| • AC/EFW <10th percentile combined with<br>• UtA-PI >95th percentile and/or<br>• UA-PI >95th percentile | • AC/EFW <10th percentile<br>• AC/EFW crossing percentiles >2 quartiles on growth percentiles<br>• CPR <FIFTH percentile or UA-PI >95th percentile |

*Abbreviations:* AC, abdominal circumference; AEDV, absent end-diastolic velocity; CPR, cerebroplacental ratio; EFW, estimated fetal weight; GA, gestational age; PI, pulsatility index; UA, umbilical artery; UtA, uterine artery.

management of these pregnancies is timely delivery, where the risk of fetal death has to be weighed against the risk of neonatal mortality and morbidity. Thus, fetuses are not delivered until the risk of dying *in utero* surpasses the risk of adverse perinatal outcome due to prematurity.[35] In cases of early onset growth restriction, placental insufficiency is commonly reflected in the umbilical artery waveform.[24] In extreme cases, this is manifested as absent or reversed end-diastolic velocity associated with critically low umbilical flow before 34 weeks of gestation.

Unlike early onset FGR, late-onset FGR is not associated with a progression of hemodynamic changes, and fetuses only exceptionally display Doppler changes in the umbilical artery or ductus venosus. However, progression to severe fetal deterioration and even fetal death can occur rapidly. This might be explained by reduced tolerance to hypoxia of the term in comparison with the preterm fetus and the more common presence of uterine contractions. Therefore, the strategy in the management of late-onset FGR is essentially based on establishing the distinction between FGR and SGA. Concerning surveillance, a relevant notion is that the status "low risk" versus "high risk," and consequently, the recommended management, can change after an initial diagnosis, and for these reasons, serial measurements of the biometrics and Doppler are recommended. There is evidence from one randomized trial[36] that when compared with monitoring every 2 weeks, twice a week monitoring results in more inductions without any improvement in the perinatal outcomes. Thus, the standard of care for those low-risk SGA would be this latter regime. However, in late-onset FGR, such a definition of "low-risk SGA" could not be reliably trusted on the umbilical Doppler; therefore, some other markers are needed.

# Doppler parameters

## *Umbilical artery Doppler*

There is good evidence that UA Doppler captures well the placental insufficiency that appears early in the pregnancy, and that its use in high-risk pregnancies improves perinatal outcomes, with a 29% reduction in perinatal deaths.[37] Absent or reversed end-diastolic velocities, the end of the spectrum of the abnormalities of the umbilical artery Doppler, have been reported to be present on average 1 week before the acute deterioration.[38] There is an association between reversed end-diastolic flow in the umbilical artery and adverse perinatal outcome (with a sensitivity and specificity of about 60%), which seems to be independent of prematurity.[39] After 30 weeks, the risk of stillbirth of a fetus with isolated reversed end-diastolic velocities in the umbilical artery Doppler overcomes the risks of prematurity[40–42]; therefore, delivery seems justified. There is a sizable body of evidence showing that the umbilical artery does not reliably reflect placental insufficiency and does not predict adverse outcome in late-onset FGR.[18,43] It is intriguing that while most cases of late-onset SGA present signs of placental underperfusion,[44] this is not reflected in UA Doppler. One could speculate that the degree of the extension is what accounts for this finding. Animal[45] and mathematical[46] experimental models of placental vessel obliteration have suggested that UA Doppler becomes abnormal only if an extensive part of the placenta is involved.

Figure 46.2 shows the progression of changes in the umbilical artery.

## *Middle cerebral artery Doppler*

Middle cerebral artery (MCA) informs about the existence of brain vasodilation, a surrogate marker of hypoxia. There is an association between abnormal middle cerebral to uterine artery pulsatility index (MCA-PI) and adverse perinatal and neurological outcome, but it is unclear whether delivering before term could add any benefit. MCA is particularly valuable for the identification[18] and prediction of adverse outcome among[47,48] late-onset FGR, independent of the UA Doppler, which is often normal in these fetuses. Fetuses with abnormal MCA-PI had a sixfold risk of emergency cesarean section for fetal distress when compared with SGA fetuses with normal MCA-PI,[49] which is particularly relevant because labor induction at term is the current standard of care of late-onset FGR.[50,51] Late-FGR neonates with abnormal MCA-PI have poorer neurobehavioral competence at birth and at 2 years of age.[48,52] MCA is considered

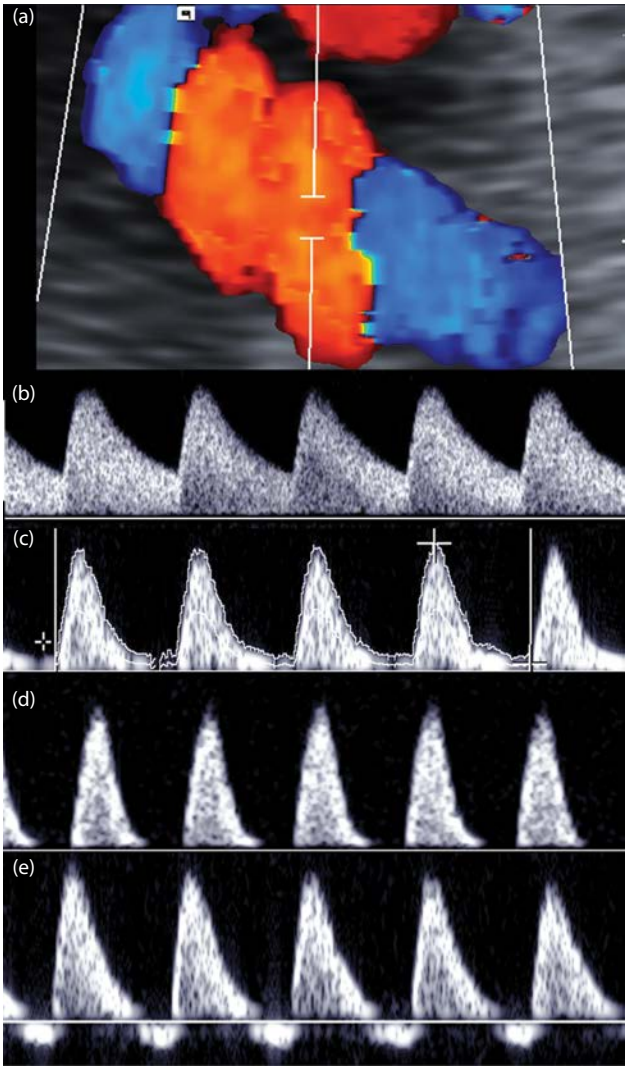


**Figure 46.2**
Site of insonation of the umbilical artery Doppler (a). Progressive waveform patterns with advancing severity: normal UA waveform (b), increased impedance to flow (c), absent end-diastolic flow (d), and reversed end-diastolic flow (e).

a rather late manifestation, with acceptable specificity but low sensitivity.

Figure 46.3 shows the progression of changes in the MCA.

## Cerebroplacental ratio

The CPR, which combines the pulsatility index of the MCA and UA, has been demonstrated to be more sensitive to hypoxia than its individual components,[53] and it correlates better with adverse outcomes.[54,55] Thus, the CPR is already decreased when its individual components suffer mild changes but are still within normal ranges.[53–55] In late-SGA fetuses, abnormal CPR is present before delivery in 20%–25% of the cases,[56] and it is associated with a higher risk of adverse outcome at induction, although to a lesser degree than

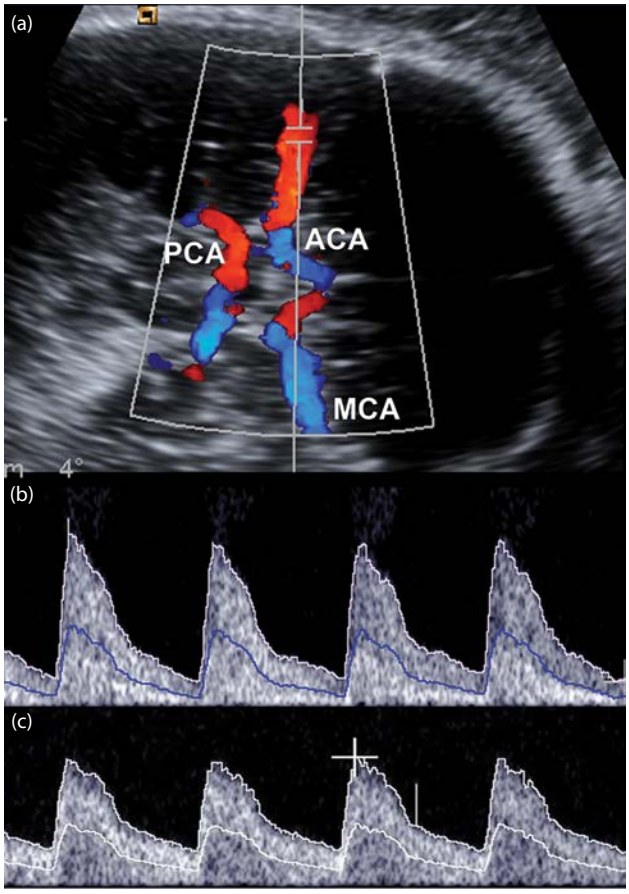


**Figure 46.3**
Color Doppler assessment of the middle cerebral artery at the level of the circle of Willis (a). Normal (b) and abnormal (high-diastolic velocities and decreased pulsatility index) (c) waveforms.

MCA.[49] A systematic review[57] found that in fetuses with SGA born after 32 weeks of gestational age CPR (nine studies) adds value to assessment over MCA (eight studies) in predicting adverse outcomes. Therefore, the CPR could be seen as the primary surveillance tool in late SGA. Several references have been published on CPR, and different cut-offs have been used in the literature.[58]

## Ductus venosus (DV) Doppler

Ductus venosus is the strongest single Doppler parameter to predict the short-term risk of fetal death in early onset FGR. Longitudinal studies have demonstrated that DV flow waveforms become abnormal only in advanced stages of fetal compromise.[19,38,39,59] Absent-reversed velocities during atrial contraction are associated with perinatal mortality independent of the gestational age at delivery,[60] with a risk ranging from 40% to 100% in early onset FGR.[42,61] Thus, this sign is normally considered sufficient to recommend delivery at any gestational age, after completion of steroids. In about 50% of cases, abnormal DV precedes the loss of short-term variability in cCTG,[19] and in about 90% of cases, it is abnormal 48–72

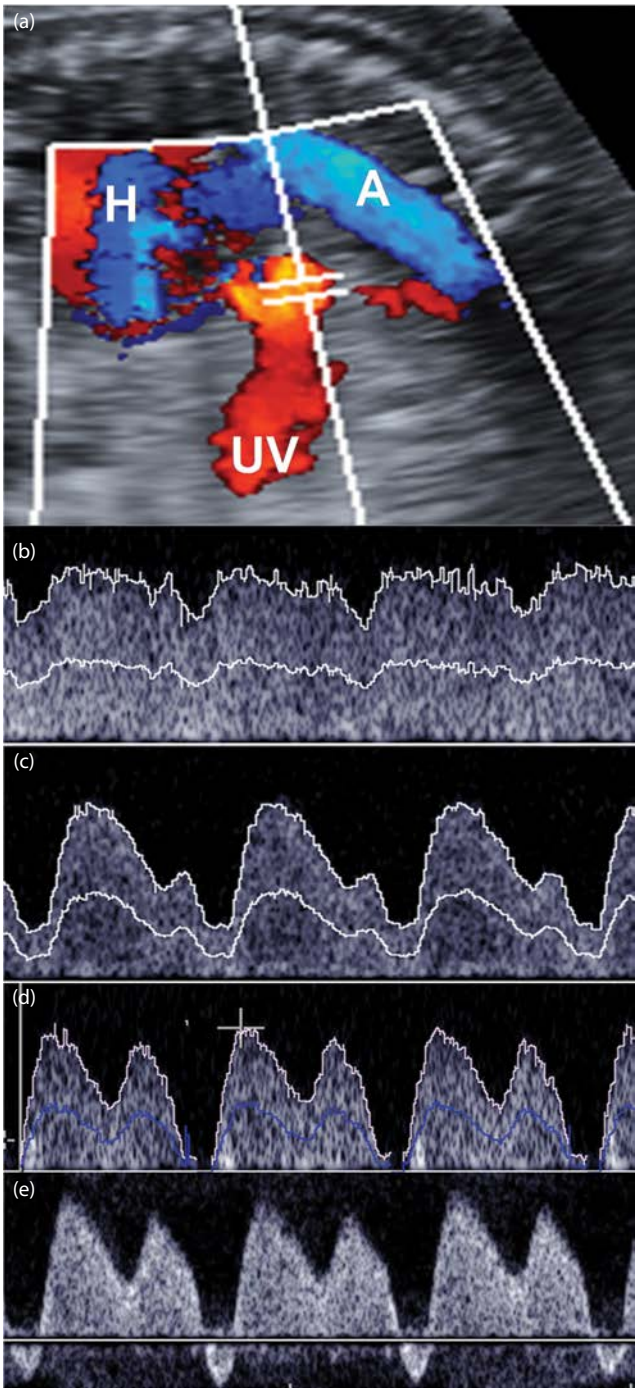


**Figure 46.4**
Site of insonation of the ductus venosus with color Doppler (a). Progressive waveform patterns with advancing severity: normal DV waveform (b), increased impedance to flow (c), absent end-diastolic flow (d), and reversed end-diastolic flow (e). (A, descendent aorta; H, heart; UV, umbilical vein.)

hours before the BPP.[59] Hence, it is considered to provide a better window of opportunity for delivering fetuses in critical conditions at very early gestational ages.

Figure 46.4 shows the progression of changes in the ductus venosus.

## *Uterine artery (UtA) Doppler*

The inclusion of uterine artery (UtA) Doppler in the assessment of early onset FGR has the advantage that it reflects placental insufficiency from the maternal side and that captures the placental insufficiency secondary to pathophysiologic mechanisms other than early defective trophoblastic invasion.[62]

An abnormal UtA Doppler in the assessment of late onset FGR has been associated with an increased risk of adverse perinatal outcomes regardless of fetal size.[63–66] Also, women who demonstrated a *de novo* rise in third-trimester UtA PI are more likely to have an SGA baby and to present significantly higher UA PI, lower MCA PI, and lower CPR.[67]

Figure 46.5 shows the progression of changes in the UtA.

## *Aortic isthmus Doppler*

This vessel reflects the balance between the impedance of the brain and systemic vascular systems.[68,69] Reverse aortic

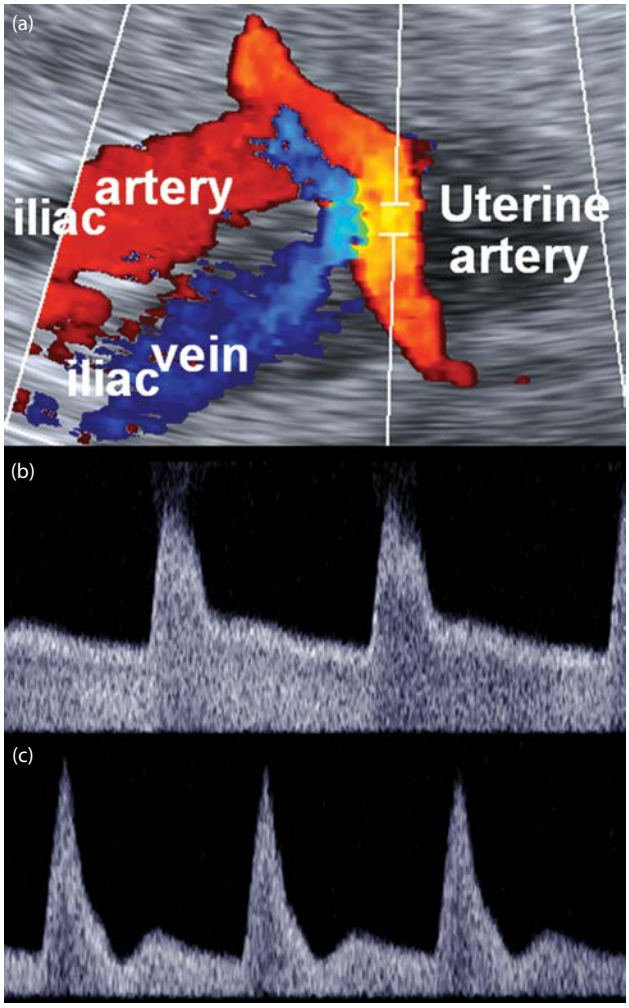


**Figure 46.5**
Site of insonation of the uterine artery with color Doppler at the crossover of the iliac artery (a). Normal (b) and abnormal (increased impedance to flow with early diastolic notching) (c) waveforms.

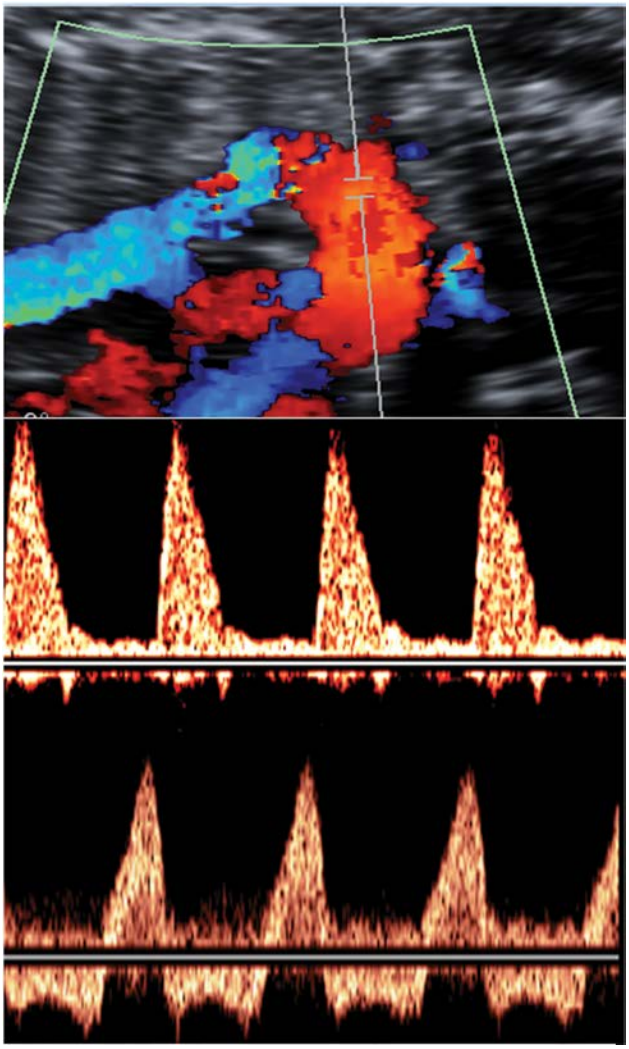

**Figure 46.6**
Color Doppler assessment of the aortic isthmus with normal (upper) and abnormal (reversed end-diastolic velocities) (lower) waveforms.

isthmus (AoI) flow is a sign of advanced deterioration, and a further step in the sequence starting with the UA and MCA Doppler.[70] AoI has an association with both adverse perinatal[70,71] and neurological outcomes.[72] However, longitudinal studies show that the AoI precedes DV abnormalities by 1 week,[70,73,74] and consequently, it is not as good to predict the short-term risk of stillbirth.[42] In contrast, AoI seems to improve the prediction of neurological morbidity.[72] Among early onset FGR with positive DV atrial velocities, a reverse AoI indicated an increased risk of late neonatal neurological injury (57% versus 9.7%).[42] Figure 46.6 shows the progression of changes in the AoI.

## Timing of delivery

No treatment has been demonstrated to be of benefit in growth restriction.[75–79] Thus, assessment of fetal well-being and timely delivery remain as the main management strategies. The best evidence regarding this issue comes from two randomized controlled trials. The first, the GRIT study,[41] was a multicenter randomized controlled trial aimed to compare immediate versus delayed delivery in growth-restricted fetuses below 36 weeks of gestation and demonstrated that early delivery to avoid stillbirth was counterbalanced by neonatal death and neurological sequelae.[40] More recently, the TRUFFLE study[23] aimed to establish the best way to monitor and trigger delivery in early growth restriction. With 503 patients included, the authors concluded that perinatal outcomes are improved if DV measurements are added to CTG-STV in the monitoring of severe early onset FGR.[23,80,81] Moreover, *post hoc* analysis among surviving children showed that the neurological outcomes at 2 years of age were better in those allocated on DV monitoring.[81]

Regarding late-onset FGR, several guidelines recommend delivery at 37–38 weeks.[82,83] This recommendation is based on the results of one randomized equivalence trial (DIGITAT study), which compared the effect of induction of labor or expectant monitoring in women after 37 weeks of gestation with suspected SGA. They found negligible differences in perinatal and neonatal outcomes between induction of labor and expectant monitoring.[50,51] However, their results suggest that if induction is considered, it is reasonable to delay until 38 weeks. Moreover, follow-up at 2 years of age showed no differences in terms of neurodevelopment and neurobehavior between both strategies.[27] While it is seemingly reasonable to offer delivery after 37 weeks in SGA, it should also be acknowledged that further studies differentiating true FGR from other causes of SGA not associated with poor perinatal outcome are required. In the DIGITAT study, all SGA fetuses were managed under a common protocol without any attempt to differentiate between low-risk SGA and high-risk FGR. As discussed, a combination of biometrical and Doppler parameters allows profiling of a subgroup of fetuses that concentrates most instances of adverse outcomes.[84] While delivery of high-risk FGR at 38 weeks is justified, a more expectant management could be offered to low-risk SGA.

An observational study[85] compared a strategy of systematic induction of late SGA at 37 weeks ($n = 138$) with risk stratification and induction indicated by severe smallness, abnormal CPR, or abnormal uterine Doppler velocimetry ($n = 143$). The incidence of neonatal composite adverse outcomes was lower after selective induction (9% versus 22%; $p < 0.01$), as was neonatal admission (13% versus 42%; $p < 0.01$). Furthermore, cesarean section rates (25% versus 40%; $p = 0.06$) were lower after selective induction, suggesting that protocol-based management of SGA babies may improve outcomes and that identification of moderate SGA should not alone prompt delivery.

## References

1. Hepburn M, Rosenberg K. *Br J Obstet Gynaecol* 1986;93(3):212–6.
2. Backe B, Nakling J. *Br J Obstet Gynaecol* 1993;100(8):727–32.

3. Richardus JH et al. *BJOG* 2003;110(2):97–105.
4. Larkin JC et al. *Am J Perinatol* 2017;34(4):409–14.
5. Kean LH, Liu DTY. *J Obstet Gynaecol (Lahore)* 1996;16(2):77–82.
6. Clausson B et al. *Br J Obstet Gynaecol* 1998;105(9):1011–7.
7. Lindqvist PG, Molin J. *Ultrasound Obstet Gynecol* 2005;25(3): 258–64.
8. Souka AP et al. *Ultrasound Obstet Gynecol* 2012;39(5):535–42.
9. Sovio U et al. *Lancet (London, England)* 2015;386(10008): 2089–97.
10. Triunfo S et al. *Ultrasound Obstet Gynecol* 2016;47(1):81–8.
11. Alfirevic Z, Neilson JP. *Am J Obstet Gynecol* 1995;172(5):1379–87.
12. Clausson B et al. *BJOG* 2001;108(8):830–4.
13. Trudell AS et al. *Am J Obstet Gynecol* 2013;208(5):376.e1–7.
14. Gardosi J et al. *BMJ* 2013;346:f108.
15. Chauhan SP et al. *Obstet Gynecol* 2017;130(3):511–9.
16. Policiano C et al. *J Matern Neonatal Med* 2018;31(11):1426–30.
17. Borrell A et al. *Fetal Diagn Ther* September 9, 2017. doi: 10.1159/000479506. [Epub ahead of print]
18. Oros D et al. *Ultrasound Obstet Gynecol* 2011;37(2):191–5.
19. Hecher K et al. *Ultrasound Obstet Gynecol* 2001;18(6):564–70.
20. Turan OM et al. *Ultrasound Obstet Gynecol* 2008;32(2):160–7.
21. Baschat AA et al. *Obstet Gynecol* 2007;109(2, Part 1):253–61.
22. Crovetto F et al. *Prenat Diagn* 2015;35(2):183–91.
23. Lees C et al. *Ultrasound Obstet Gynecol* 2013;42(4):400–8.
24. Savchev S et al. *Fetal Diagn Ther* 2014;36(2):99–105.
25. Moraitis AA et al. *Obstet Gynecol* 2014;124(2, Part 1):274–83.
26. Savchev S et al. *Ultrasound Obstet Gynecol* 2012;39(3):299–303.
27. van Wyk L et al. *Am J Obstet Gynecol* 2012;206(5):406.e1–7.
28. Unterscheider J et al. *Am J Obstet Gynecol* 2013;208(4):290.e1–e6.
29. Mlynarczyk M et al. *Am J Obstet Gynecol* 2017;217(2):198.e1–11.
30. Temming LA et al. *Obstet Gynecol* 2017;130(4):865–9.
31. Gordijn SJ et al. *Ultrasound Obstet Gynecol* 2016;48(3):333–9.
32. Cnossen JS et al. *CMAJ* 2008;178(6):701–11.
33. Crovetto F et al. *Ultrasound Obstet Gynecol* 2014;43(1):34–40.
34. Karagiannis G et al. *Fetal Diagn Ther* 2011;29(2):148–54.
35. Mari G, Hanif F. *Clin Obstet Gynecol* 2007;50(2):497–509.
36. McCowan LM et al. *Am J Obstet Gynecol* 2000;182(1 Pt 1):81–6.
37. Alfirevic Z et al. Alfirevic Z, ed. *Cochrane Database System Reviews* 2010, Jan 20;(1):CD007529.
38. Ferrazzi E et al. *Ultrasound Obstet Gynecol* 2002;19(2):140–6.
39. Cosmi E et al. *Obstet Gynecol* 2005;106(6):1240–5.
40. Thornton JG et al. *Lancet (London, England)* 2004;364(9433): 513–20.
41. GRIT Study Group. *BJOG* 2003;110(1):27–32.
42. Cruz-Lemini M et al. *Fetal Diagn Ther* 2012;32(1–2):116–22.
43. Chang TC et al. *Br J Obstet Gynaecol* 1994;101(5):422–7.
44. Parra-Saavedra M et al. *Ultrasound Obstet Gynecol* 2013;42(2): 189–95.
45. Morrow RJ et al. *Am J Obstet Gynecol* 1989;161(4):1055–60.
46. Thompson RS, Stevens RJ. *Med Biol Eng Comput* 1989;27(3): 269–76.
47. Hershkovitz R et al. *Ultrasound Obstet Gynecol* 2000;15(3): 209–12.
48. Eixarch E et al. *Ultrasound Obstet Gynecol* 2008;32(7):894–9.
49. Cruz-Martínez R et al. *Obstet Gynecol* 2011;117(3):618–26.
50. Boers KE et al. *Am J Obstet Gynecol* 2012;206(4):344.e1–7.
51. Boers KE et al. *BMJ* 2010;341(dec21 1):c7087.
52. Oros D et al. *Ultrasound Obstet Gynecol* 2010;35(4):456–61.
53. Arbeille P et al. *Ultrasound Med Biol* 1995;21(7):861–70.
54. Bahado-Singh RO et al. *Am J Obstet Gynecol* 1999;180(3 Pt 1): 750–6.
55. Gramellini D et al. *Obstet Gynecol* 1992;79(3):416–20.
56. Cruz-Martinez R et al. *Am J Obstet Gynecol* 2010;203(1):42.e1–e6.
57. Schreurs CA et al. *Ultrasound Obstet Gynecol* 2018;51(3):313–22. doi:10.1002/uog.18809.
58. DeVore GR. *Am J Obstet Gynecol* 2015;213(1):5–15.
59. Baschat AA et al. *Ultrasound Obstet Gynecol* 2001;18(6): 571–7.
60. Schwarze A et al. *Ultrasound Obstet Gynecol* 2005;25(6): 573–9.
61. Baschat AA et al. *Ultrasound Obstet Gynecol* 2003;22(3):240–5.
62. Llurba E et al. *Am J Perinatol* 2013;30(6):505–11.
63. Monaghan C et al. *Ultrasound Obstet Gynecol* April 2017. doi:10.1002/uog.17500. [Epub ahead of print]
64. Severi FM et al. *Ultrasound Obstet Gynecol* 2002;19(3):225–8.
65. Ghosh GS, Gudmundsson S. *BJOG* 2009;116(3):424–30.
66. Vergani P et al. *Am J Obstet Gynecol* 2002;187(4):932–6.
67. Binder J et al. *Ultrasound Obstet Gynecol*. June 2017. doi: 10.1002/uog.17564. [Epub ahead of print]
68. Fouron JC et al. *Am J Obstet Gynecol* 1999;181(5 Pt 1):1102–7.
69. Mäkikallio K et al. *Ultrasound Obstet Gynecol* 2003;22(4):351–7.
70. Abdelrazzaq K et al. *Acta Obstet Gynecol Scand* 2013;92(6): 656–61.
71. Del Río M et al. *Ultrasound Obstet Gynecol* 2008;31(1):41–7.
72. Fouron J-C et al. *Am J Obstet Gynecol* 2005;192(2):497–503.
73. Cruz-Martinez R et al. *Ultrasound Obstet Gynecol* 2011;38(4): 400–5.
74. Figueras F et al. *Ultrasound Obstet Gynecol* 2009;33(1):39–43.
75. Gülmezoglu AM, Hofmeyr GJ. *Cochrane Database Syst Rev* 2000;(2):CD000167.
76. Gülmezoglu AM, Hofmeyr GJ. *Cochrane Database Syst Rev* 2001;(4):CD000036.
77. Laurin J, Persson PH. *Acta Obstet Gynecol Scand* 1987;66(5): 407–11.
78. Say L et al. *Cochrane Database Syst Rev* 2003;(1):CD000148.
79. Say L et al. *Cochrane Database Syst Rev* 2003;(1):CD000137.
80. Visser GHA et al. *Ultrasound Obstet Gynecol* 2016;50(3):347–52. doi:10.1002/uog.17361.
81. Ganzevoort W et al. *Ultrasound Obstet Gynecol* 2017;49(6): 769–77.
82. American College of Obstetricians and Gynecologists. *Obstet Gynecol* 2013;121(5):1122–33.
83. RCOG. *Green–top Guide No. 31*; 2013.
84. Figueras F, Gardosi J. *Am J Obstet Gynecol* 2011;204(4):288–300.
85. Veglia M et al. *Ultrasound Obstet Gynecol* June 2017. doi: 10.1002/uog.17544. [Epub ahead of print]

# 47

# Venous flow dynamics: Intrauterine growth restriction and cardiac decompensation

Torvid Kiserud

## Introduction

Doppler examination of venous volume flow was introduced almost 40 years ago[1–3]; it has since provided valuable physiological information but so far not progressed to become a common clinical tool. The assessment of venous pulsations[4–6] has become part of the fetal hemodynamic evaluation. Both the chronic challenge of intrauterine growth restriction (IUGR) due to placental compromise and its final stages with cardiac decompensation are examples of how changes in fetal hemodynamics are reflected in the fetal veins. With reason, we believe that the venous velocity pattern is a more instantaneous indicator for hemodynamic performance than is the umbilical artery velocity pattern. In this chapter, the ductus venosus and umbilical vein are used to illustrate general mechanisms operating in the precordial and peripheral fetal veins, and some distributional patterns of IUGR are discussed.

## Physiological background

We focus on the common clinical problem of IUGR due to placental hemodynamic compromise, but also keep in mind that a variety of other causes of altered growth may be associated with modified circulatory development and hemodynamic responses (e.g., malformations, chromosomal aberrations, metabolic disorders, infections, radiation, teratogens, drugs, smoking, alcohol, and malnutrition).

Although the dimension of the umbilical vein is on average smaller in IUGR than in the appropriately grown fetus and flow is low,[2,7,8] the umbilical venous pressure is maintained within normal ranges.[9] There is an increased incidence of hypoxemia and acidosis in this group of fetuses.[10] Based on the experience of animal studies, such fetuses are expected to have a reduced flow in the inferior compared to the superior vena cava, increased ductus venosus shunting, and reduced pulmonary flow.[11] In line with such experiments, it was actually found that IUGR fetuses had an augmented ductus venosus shunting,[12–15] increased foramen ovale flow, and reduced flow through the fetal lungs,[16] with canceled difference between the left and right cardiac output.[16] In recent studies, this concept has been somewhat modified, as follows.

In the human version of placental compromise, the fraction of combined cardiac output circulating the placenta is reduced and reflected in the degree of abnormal umbilical artery pulsation (Figure 47.1).[17] Normally, the umbilical venous return constitutes 30% of the cardiac output at midgestation, and it reduces to 20% near term. These numbers are lower in growth restriction, particularly when associated with absent or reversed end-diastolic (ARED) velocity

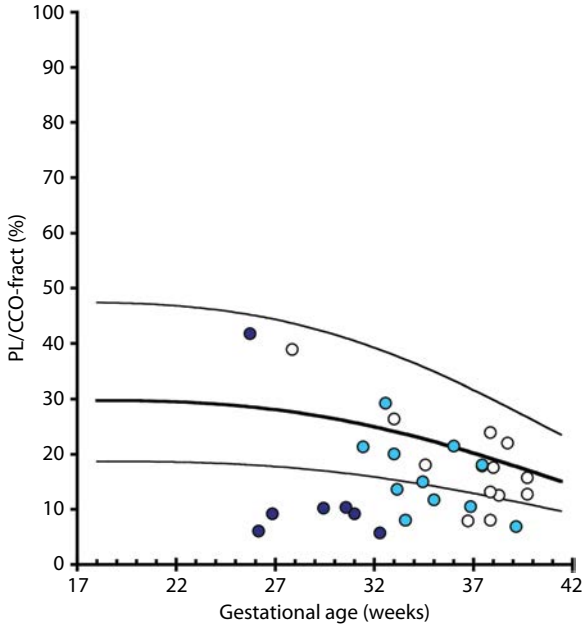


**Figure 47.1**
In normally growing fetuses, one-third of the combined cardiac output (CCO) is directed to the placenta at midgestation. After 32 weeks, the average is one-fifth with the lowest fraction near term. The implication is an increased degree of recirculation of deoxygenated blood within the fetal body near term. In general, growth-restricted fetuses (here $\leq$2.5 percentile: circles) tend to augment this effect as they direct a lower fraction of the CCO to the placenta, particularly those with absent or reversed diastolic flow in the umbilical artery (dark blue). Open circles, normal pulsatility index (PI) in the umbilical artery; light blue, umbilical artery PI $>$ 97.5 percentile. (Reproduced with permission from Kiserud T et al. *Ultrasound Obstet Gynecol* 2006;28:126–36.[17])

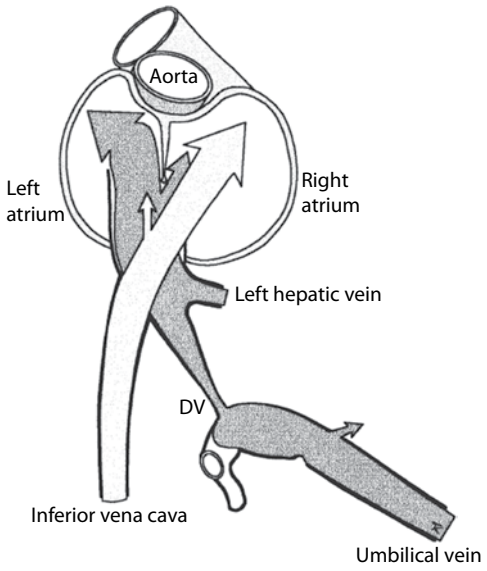


**Figure 47.2**
Distributional mechanism of venous flow at the inferior caval inlet to the heart. Oxygenated umbilical blood is accelerated in the ductus venosus (DV) and directed toward the foramen ovale to enter the left atrium as preferential streaming. Deoxygenated blood in the abdominal portion of the inferior vena cava is predominantly directed to the right atrium. (Reproduced with permission from Kiserud T, Rasmussen S. *Ultrasound Obstet Gynecol* 2001;17:119–24.[133])

in the umbilical artery. For example, in fetuses with ARED, the umbilical venous return is merely 10% or less of the combined cardiac output. This implies that 90% or more recycles within the fetal body, leading to lower oxygen saturation and more demanding oxygen extraction in the fetal tissues.

Directing well-oxygenated blood from the umbilical vein through the ductus venosus to enter the left atrium (via sinistra) is the most prominent mechanism of ensuring oxygenation of the fetal myocardium and brain (Figure 47.2).[18–20] It seems that mild and moderate degrees of compromise induce the well-known pattern of augmenting this pathway (Figure 47.3a,b). However, when deteriorating to extreme degrees of reduced umbilical venous return,[13] the compensatory mechanisms seem to break down, and less is shunted through foramen ovale (Figure 47.3c).[16,17,21]

Subdiaphragmatically, low-oxygenated blood from the portal vein is increasingly blended into the ductus venosus shunt in these fetuses (Figures 47.4 and 47.5).[12,22,23] The foramen ovale is relatively smaller[24] with less blood shunted to the left atrium, where pulmonary venous return fills in more.[16] The right ventricle takes a relatively larger proportion of the combined cardiac output, and there is a net reversed flow in the isthmus of the aorta. It all leads to more recycling within the fetal body.

These fetuses prioritize cardiac and brain circulation, but it is less appreciated that it comes at the expense of the "metabolic brain," i.e., the fetal liver,[15,25] which is an important determinant for differential organ growth of the body,[26,27] fat accretion,[28] and postnatal development[25,29]—i.e., there is a reduced delivery of umbilical blood to the liver.[12,15] Within the liver, however, there is a sparing of the left lobe that continues to receive oxygenated umbilical blood while the right lobe is down-prioritized, increasingly receiving deoxygenated portal blood.[15] Totally, the liver receives less venous blood (umbilical and portal) in this situation, and the portal partial substitution with low-oxygenated blood is graded according to the degree of placental compromise. At its extreme, the right lobe is entirely perfused by portal blood, which may even partially bypass the liver through the left portal branch to reach the umbilical vein and ductus venosus (Figures 47.4b and 47.5). This contributes to keeping up the perfusion pressure both for the ductus venosus and the liver, but also to a further reduced oxygen content of the central circulation.

Hematocrit (and thus viscosity) tends to be higher in IUGR fetuses, compared with normal fetuses,[30] with a higher concentration of cathecolamines,[31] higher concentration of atrial natriuretic peptide,[32] an augmented endothelin-1 response to cordocentesis,[33] and an augmented cortisol response to hypoxemia.[34]

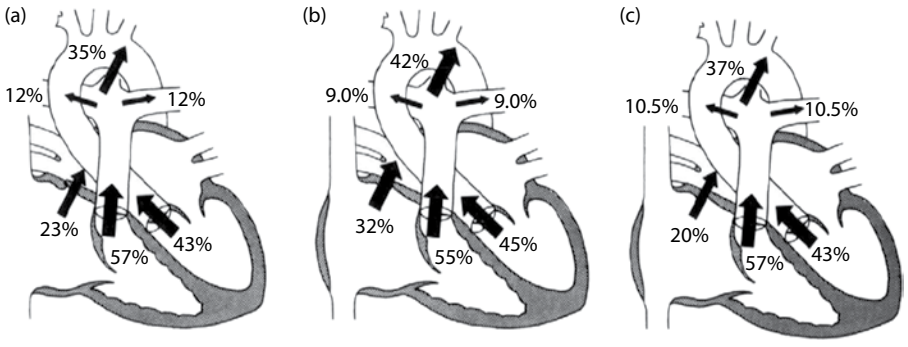


**Figure 47.3**
Blood distribution through the foramen ovale (FO) in control fetuses (a) compared with those having increasing circulatory challenge but still with net antegrade isthmus aortae flow (b), and those with reversed flow (c). Note that the fraction directed through the FO increases with increased challenge (b), but the redistribution breaks down leading to a reduced FO and a correspondingly increased venous return from the lungs at extreme conditions (c). (Reproduced with permission from Mäkikallio K. *Placental Insufficiency and Fetal Heart: Doppler Ultrasonographic and Biochemical Markers of Fetal Cardiac Dysfunction*. University of Oulu; 2002.[132])

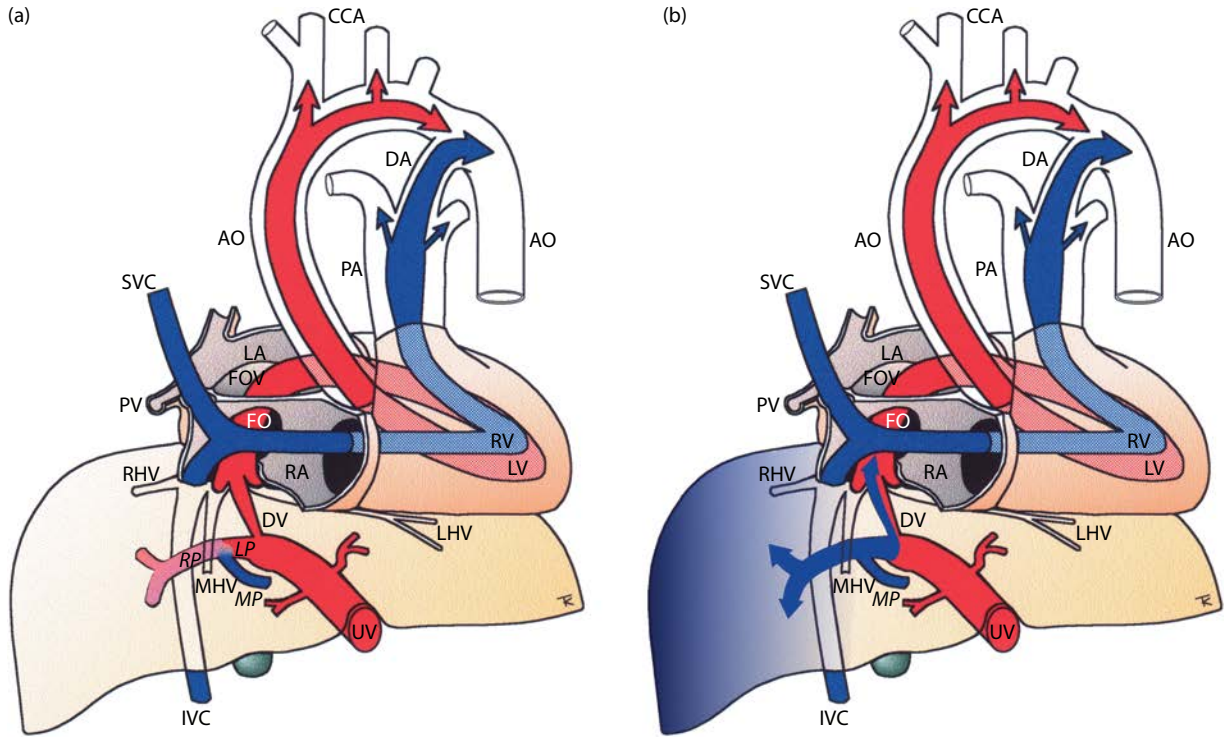


**Figure 47.4**
Umbilical well-oxygenated venous return feeds the liver and the via sinistra pathway (red), while the via dextra pathway carries low-oxygenated blood from the superior and inferior vena cava (SVC and IVC) (blue) (a). When umbilical venous return is insufficient to maintain the pressure needed to perfuse the liver and ductus venosus (DV), low-oxygenated blood from the main portal vein (MP) increasingly covers some of the deficit, and in extreme cases, perfuses the entire right liver and even feeds into the DV (b). (AO, aorta; CCA, common carotid artery; DA, ductus arteriosus; FO, foramen ovale; FOV, foramen ovale valve; LA, left atrium; LHV, left hepatic vein; LPV, left portal vein; LV, left ventricle; MHV, median hepatic vein; PA, pulmonary artery; PV, pulmonary vein; RA, right atrium; RP, right portal vein; RV, right ventricle; UV, umbilical vein.) (Reproduced and modified with permission from Kiserud T et al. *Am J Obstet Gynecol* 2000;182:147–53.[63])

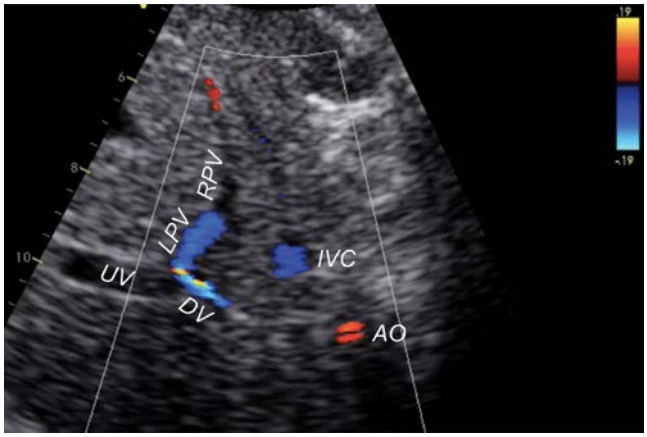


**Figure 47.5**
Rather than feeding well-oxygenated blood antegrade into the left portal vein (LPV) and thus the right liver, the umbilical vein (UV) receives retrograde low-oxygenated blood that is directed into the ductus venosus (DV) in a case complicated with late reduction of UV flow. (AO, aorta; IVC, inferior vena cava; RPV, right portal vein.)

Any increase in hematocrit and viscosity favors a redistribution of umbilical blood from the liver to the ductus venosus, since viscous resistance is higher for the slow (non-Newtonian) flow in the liver vasculature than for the high-velocity (Newtonian) flow in the ductus venosus.[35] Similarly, a reduction in umbilical venous pressure is associated with a relatively higher increase in vascular resistance in the liver than in the ductus venosus, increasing the degree of shunting.[35] Thus, such fluid-dynamic factors govern the basic passive regulation of distribution between the liver and ductus venosus. An active distension of the inlet of the ductus venosus (mediated by nitroxide and prostaglandins) enhances this redistribution, particularly during hypoxemia.[36–40] Interestingly, the distension is not confined to the isthmus (or sphincter) of the ductus venosus alone but to the entire length of the vessel.[32,34,38,40] A more pronounced constrictive response to catecholamines in the portal branches than in the ductus venosus adds to the effect of deviating umbilical blood from the fetal liver.[41]

Experimentally, growth-restricted fetuses have on average a higher heart rate and a lower blood pressure, and in addition, respond with less bradycardia to acute hypoxia, compared to appropriately grown fetuses.[34] Gestational age is

an important determinant. The fetus approaching term has more developed endocrine and neural regulation mechanisms to respond to hypovolemia and hypoxemia by an initial increase in blood pressure and peripheral resistance.[42] During the early weeks of fetal life, dimensions are small, pressures low, and endocrine mechanisms poorly developed. Reduction in maternal $PO_2$ is readily reflected in the amniotic fluid $PO_2$ also before midgestation,[43] but the circulatory responses at this early stage reflect rather direct effects on the heart and vasculature (e.g., bradycardia and reduced flow).[44] Development and maturation of endocrine functions are still incomplete during the second trimester, which is reflected in the responses.[45]

## Determinants of pulsatile flow in veins

Apart from transporting blood toward the heart (Figure 47.2), the fetal veins act as transmission lines for oppositely directed pressure waves.[46–49] The inferior vena cava (IVC), ductus venosus, and umbilical vein form a clinically important transmission line for atrial waves toward the umbilical cord (Figure 47.6). A wave consists of three components—pressure wave, diameter wave, and flow wave—that together obey the requirements of preservation of energy according to the Navier-Stoke equations.[50] The waves transmitted in veins obey the same fluid dynamic laws as in arteries and are modified by several factors. One such factor is the direction of the pressure wave compared with that of the blood velocity.[51] If the direction is the same for both (e.g., umbilical artery and left portal vein), the pressure wave will cause a velocity increment (Figure 47.7).[23] Conversely, with opposite directions of flow and pressure wave, there will be a velocity deflection, which is the rule in precordial veins, e.g., the a-wave in the ductus venosus or umbilical vein (Figures 47.8).[45,49]

Augmented atrial contraction is a documented cause of increased pressure amplitude[52–54] and, thus, pulsatility of the blood velocity. Increased afterload and hypoxic stress lead to increased atrial contraction, mediated by an increased adrenergic drive, a common mechanism in severe IUGR and congestive heart failure.

Other determinants are vessel wall stiffness (e.g., tone) and intravascular pressure.[47] An increased intravascular and transmural pressure in the venous system reduces compliance, increases the speed of the wave, and promotes transport of pulsation further to the periphery. These factors are prominent in congestive heart failure.

However, the most important determinant for wave propagation is described with the phenomenon of wave reflection.[47,48,55] Similar to the reflection and transmission of light at an interface, the pressure wave emitted from the atria is partially reflected and partially transmitted at the junction of veins with different impedance ($Z$), i.e., between the IVC and ductus venosus outlet, and between the ductus venosus inlet and umbilical vein. The degree of reflection at the ductus

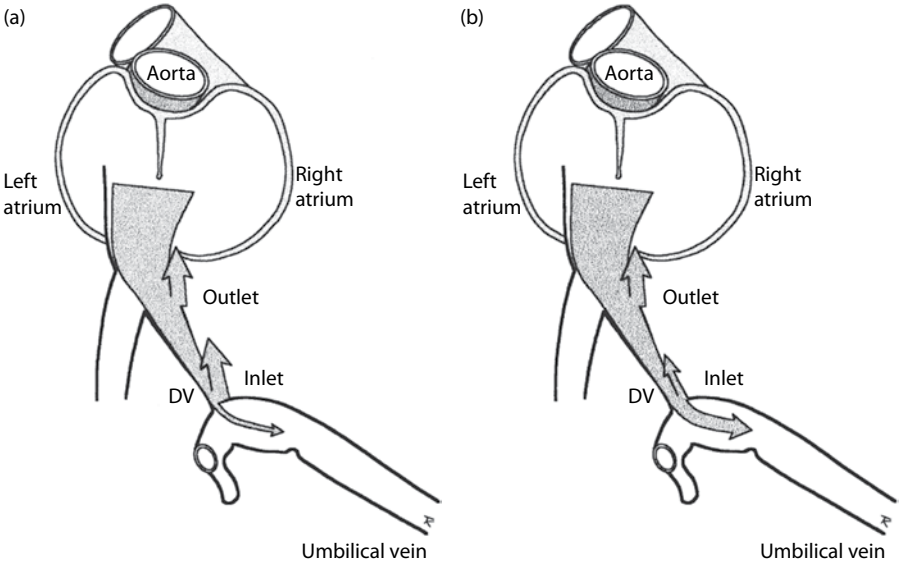


**Figure 47.6**
The pressure wave generated in the atria is emitted into the precordial veins. The inferior vena cava, ductus venosus, and umbilical vein form one clinically important transmission line for this wave. The intensity of the wave traveling down the line is reduced by reflections at each junction. Particularly the junction between the ductus venosus inlet and the umbilical vein represents a large step in impedance (due to the difference in cross section) and causes most of the wave to be reflected, leaving little energy for transmission into the umbilical vein (a). An increase in the diameter of the ductus venosus (e.g., during hypoxemia) reduces the difference in impedance at the junction, leading to reduced wave reflection, increased transmission (b), and subsequently, an increased probability of velocity pulsation in the umbilical vein. (Reproduced with permission from Kiserud T. *J Perinat Med* 2000;28:90–6.[55])

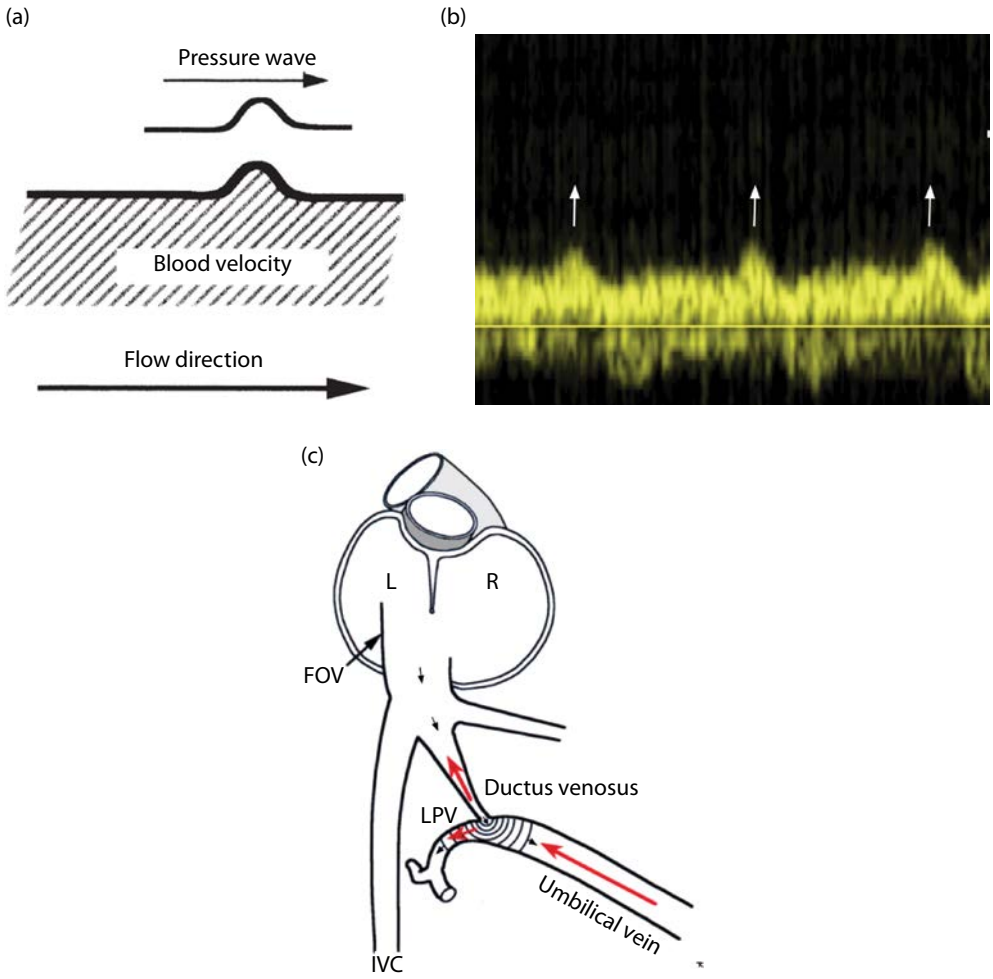


**Figure 47.7**
A pressure wave that travels in the same direction as blood flow causes a blood velocity increment (a). An example is found in the left portal vein (LPV) where the atrial contraction wave (arrows) is a peak in flow velocity because the pressure waves and blood flow travel in the same direction (b). Blood flow (red arrows) in the umbilical vein and ductus venosus travels toward the heart, opposite to the pressure waves (black rings and arrows in [c]). The pressure waves from the atria arrive at the ductus venosus–umbilical vein junction and are transmitted further along the umbilical vein opposite to the blood. The pressure waves also spread along LPV, but here they have the same direction as the blood flow. (FOV, foramen ovale valve; IVC, inferior vena cava; L, left atrium; R, right atrium.) (Reproduced with permission from Kiserud T et al. *Ultrasound Obstet Gynecol* 2003;21:359–64.[23])

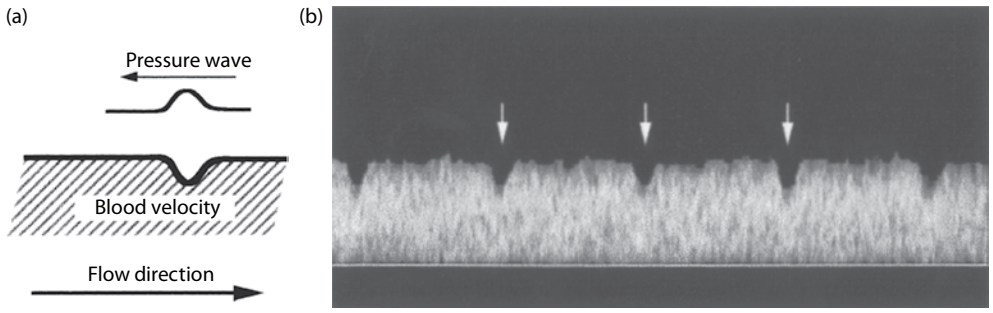


**Figure 47.8**
A pressure wave that travels in the opposite direction to flow causes a corresponding reduction in blood flow velocity (a). The umbilical venous velocity inflection (arrow) due to an augmented atrial contraction represents an example of a pressure wave traveling against the flow direction (b).

venosus–umbilical vein junction, for example, is expressed in the reflection coefficient ($R_C$):

$$R_C = \frac{\text{Reflected wave}}{\text{Incident wave}} = \frac{Z_{UV} - Z_{DV}}{Z_{UV} + Z_{DV}}$$

where $Z_{UV}$ and $Z_{DV}$ represent the impedance of the umbilical vein and the ductus venosus, respectively. The cross section (or diameter) is the main determinant for impedance of the vessel. Normally, the diameter of the umbilical vein is four times larger than that of the isthmus of the ductus venosus (95% prediction limits: 2, 6).[56] It implies a large step in impedance and thus an extensive reflection of waves at the junction between these venous sections, and correspondingly little is transmitted into the umbilical vein (Figure 47.6a). This is the main reason why normally no umbilical venous pulsation is seen during the second half of pregnancy. The other extreme would be that the diameter, and $Z$, were the same above and below the junction, $R_C = 0$, leading to full transmission of the pressure wave and no reflection.

Wall stiffness (and compliance) varies along the transmission line[57] and is associated with differences in impedance. It is therefore a source for wave reflection, but to a much lesser extent compared with the effect of diameter variation alone.

Once any fraction of wave is transmitted across the ductus venosus–umbilical vein junction, the local physical properties of the umbilical vein determine whether this wave appears as visible velocity variation or not.[47,58] A large dimension of the vein allows it to function as a compliant reservoir, which requires a high amount of pulse energy to produce visible changes in blood velocity, and the wave energy is essentially carried forth as a hardly measurable diameter variation and pressure wave, and not by flow velocity wave.[46] However, increased stiffness of the wall (e.g., increased vascular tone), increased intravascular pressure (e.g., congestion), and a small diameter (e.g., early pregnancy)[59] promote transformation of the wave into visible velocity waves in the umbilical vein.[60]

## Umbilical venous flow

Umbilical venous flow, and particularly normalized flow based on estimated fetal weight (mL kg$^{-1}$ min$^{-1}$), was early on suggested as a clinical assessment of growth-restricted fetuses.[2] The concept of assessing umbilical blood flow was based on sound physiological principles, as fetal development depends on 30% of the combined cardiac output circulating the placenta.[17,61] The volume flow can be calculated from the umbilical diameter ($D_{UV}$) and either the time-averaged weighted mean blood velocity[62–64] ($V_{UVwmean}$) or time-averaged maximum velocity[6,64] ($V_{UVmax}$) (Figure 47.9):

$$\pi\left(\frac{D_{UV}}{2}\right)^2 \cdot V_{UVwmean} \quad (47.1)$$

$$\pi\left(\frac{D_{UV}}{2}\right)^2 \cdot 0.5V_{UVmax} \quad (47.2)$$

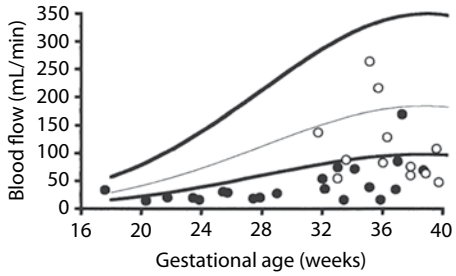


**Figure 47.9**
Umbilical venous flow is generally low in severe growth restriction (estimated fetal weight ≤2.5 percentile), particularly in cases with compromised placental circulation reflected in an increased pulsatility index of the umbilical artery blood velocity (closed circles). Mean (thin rule) and 95% prediction limits (thick rules) are shown. (Reproduced with permission from Kiserud T et al. *Ultrasound Obstet Gynecol* 1994;4:109–14.[6])

Equation 47.1 carries the risk of overestimating flow as the lowest velocities in the vein are lost in the filter, particularly at higher angles of insonation, and is susceptible to interference or incomplete representation of the spatial distribution of the velocities. Method 2 has the disadvantage of assuming that flow is parabolic, which may not always be the case.[65] However, when comparing the two methods in low-risk pregnancies, they produce literally identical results.[64] A more important source of error is the diameter measurement, as this error is expanded by a power of two in calculating flow. This is a likely reason why the method never gained broader acceptance.

Through the years, however, refinements of ultrasound equipment with memory buffer, adjustable focusing, and high-frequency transducers have revived volume flow assessment. Based on repeat measurements of the diameter, the error can be controlled,[66,67] and a new set of reference ranges for human umbilical flow has been established based on both cross-sectional[63,68] and, the usually preferred, longitudinal data.[64,69] At 20 weeks of gestation, the mean flow is 35 mL min$^{-1}$, and at 40 weeks 240 mL min$^{-1}$ in our hands.[63] The corresponding normalized umbilical venous flow drops from 115 to 64 mL kg$^{-1}$ min$^{-1}$ during the same period. These results vary slightly with center and study[64,68–70] and tend to be slightly lower than previously reported, which may in part be due to the fact that many of these studies were based on outer-inner measurements (leading edge) of vessel diameters rather than inner-inner measurements used today.

The method can be advocated for physiological studies, and is a promising method for clinical use, particularly in serial observations (Figure 47.10). Combining the flow measurement with the fetal abdominal circumference rather than with the estimated fetal weight is another suggested improvement of the method.[70]

Applying such methods, it has been shown that the umbilical venous return normally constitutes one-third of the combined cardiac output at midgestation (Figure 47.1),[17] which is in line with previous invasive[71] and noninvasive studies.[72] However, near term, the fraction is normally down to one-fifth,

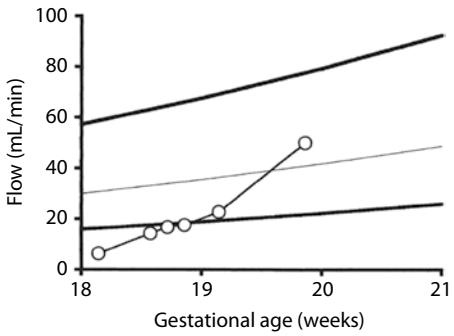


**Figure 47.10**
Serial measurements show how the umbilical venous flow improves in a case of congestive heart failure due to atrial flutter, when the heart rate gradually returns to sinus rhythm and normal myocardial contractility is restored. Mean (thin rule) and 95% prediction limits (thick rules) are shown.

which implies a considerable degree of recirculation within the fetal body.[15] However, the fetuses maintain an unchanged normalized cardiac output of ≈400 mL $min^{-1}$ $kg,^{-1}$ during the entire second half of pregnancy. Although the IUGR fetuses maintain the same normalized cardiac output, they cannot keep up the umbilical circulation correspondingly. The result is a lower fraction of the combined cardiac output returning as oxygenated umbilical venous flow, those with extreme degrees of abnormal umbilical artery pulsatility having the lowest values (Figure 47.1).[17] It seems that this hemodynamic pattern precedes fetal growth impairment.[73]

## Umbilical venous blood velocity

Conventionally, blood velocity (and diameter) is measured distally in the straight portion of the intra-abdominal umbilical vein, but the cord has also been used. The sample volume should include the entire vessel cross section, and the angle of insonation should be zero or close to zero.[3] As a major proportion of severe IUGR fetuses have a fetoplacental circulation with increased impedance, it is of no surprise that these fetuses have reduced umbilical flow reflected in reduced umbilical venous blood velocity.[7,8] Fetuses with signs of intrauterine asphyxia seem to have the lowest velocities.[4,7,8,10] However, umbilical venous velocities in IUGR show a substantial overlap with normal ranges, which makes the method unsuitable for discriminating small fetuses at risk of asphyxia or cases of impaired cardiac performance.

## Pulsatile umbilical venous flow velocity

Since Lingman et al. introduced the pulsatile umbilical venous flow velocity (Figure 47.8b) as a sign of circulatory compromise in fetuses with imminent asphyxia,[4] its simplicity has made it a commonly used clinical marker. Gudmundsson et al. expanded on this concept and showed that hydropic fetuses with congestive heart failure and pulsatile umbilical venous flow had a higher mortality than fetuses without pulsation.[5] Pulsations in the umbilical vein are associated with hypoxemia and impaired acid–base status.[74–76] Pulsation is a normal phenomenon in early pregnancy (<13 weeks)[59] and may also occur in the intra-abdominal portion of the vein in normal late pregnancy,[60,77–79] as mentioned previously, the reason being a small vessel cross section with a low compliance forcing the wave to less diameter pulse and more velocity pulsation to maintain volume and energy transmission.

To make the umbilical venous pulsation a useful diagnostic method, we need to distinguish the pulsations caused by augmented atrial contractions from those caused by other factors.[72] Once fetal respiratory movements are excluded, the blood velocity in the umbilical vein can be regarded as a steady flow, and the two principal rhythmic pressure waves that can influence the velocity come from the atria or the neighboring arterial system. As mentioned previously, the pressure wave of interest (e.g., the a-wave) is emitted from the atria to travel along the transmission line formed by the connecting veins, but in the opposite direction to the flow velocity, the result being a velocity deflection.[49] In contrast, a pressure wave transmitted from the neighboring artery into the vein at the abdominal wall may end up traveling in the same direction as flow, causing a synchronized velocity increment. In most cases, the two sources can be distinguished; the pressure pulse from the artery causes a smooth velocity increment, while the atrial contraction wave is a shorter and sharper velocity deflection (Figure 47.8b).

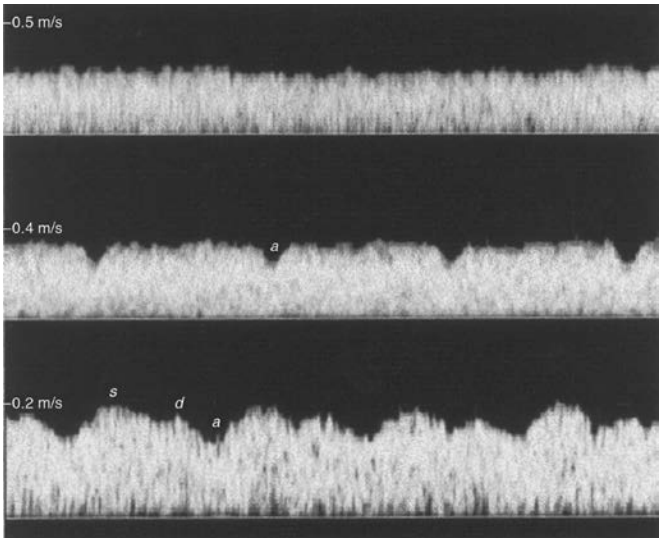


**Figure 47.11**
Umbilical venous flow velocity is generally nonpulsatile during the second half of pregnancy (upper panel). An augmented atrial contraction may lead to a short deflection of the velocity (a) in the umbilical vein (middle panel). A further deterioration (lower panel) causes the entire pressure variation during the cardiac cycle to be reflected in the umbilical venous velocity. (d, passive diastolic filling; s, ventricular systole.)

Factors promoting umbilical venous pulsation of atrial origin are as follows:

- Augmented atrial contraction (increased after- and preload, adrenergic drive, hypoxia)
- Bradycardia (Frank-Starling mechanism on the atria)
- Active distension of the ductus venosus (e.g., hypoxia)
- Increased umbilical venous vascular tone (adrenergic regulation)
- Reduced umbilical compliance (e.g., small dimension in IUGR, venous congestion)
- Low gestational age (i.e., small dimensions of veins)

For such reasons, the impaired cardiac function may change the steady umbilical velocity pattern into a pulsatile pattern, and, with further deterioration, transmit the entire cardiac pressure variation into the umbilical vein velocity pattern (Figure 47.11). However, even a triphasic umbilical venous pulsation may be associated with prolonged intrauterine survival.[80] These signs are more likely to appear in early gestation and in conjunction with a preexisting increased afterload or low heart rate.[6,81]

## Ductus venosus flow

During experimental hypoxia and hypovolemia, an increased fraction of the umbilical blood is shunted through the ductus venosus.[19,82–84] Recent studies have confirmed that this mechanism, first described in animal experiments, also exists in the human fetus, but on a slightly different scale. Under physiological conditions, the fraction of umbilical flow that is shunted through the human ductus venosus is estimated to be 30% at 20 weeks and 20% after 30 weeks,[63,69,85] small fetuses shunting relatively more blood through the ductus venosus than their larger peers.[14,63,86] In growth-restricted fetuses, the effect is augmented and graded according to degree of placental compromise (assessed by umbilical artery pulsation) (Figure 47.12).[13] The earlier in pregnancy it occurs, the larger is the fraction of umbilical blood shunted through the ductus venosus.[13,85] Although repeatedly reproduced in different studies when obeying a strict protocol,[13,20,28,63,69] volume flow assessment in the ductus venosus must be regarded as a rather uncertain undertaking in the evaluation of individual fetuses due to the small dimension of its isthmic portion.[56,66] The technique of repeat measurements and particularly computer power and the development of statistical software give hope for more individualized assessments.

## Ductus venosus blood velocity

The recommended method for recording blood velocity of the ductus venosus uses a large sample volume aligned with the isthmic portion (the inlet) in a near sagittal scan, or an oblique transection of the fetal abdomen.[20,87] The reason for the large sample volume is to ensure recording the maximum velocity. In early pregnancy, the sample volume needs to be restricted in order to discriminate reversed a-wave and the velocities found

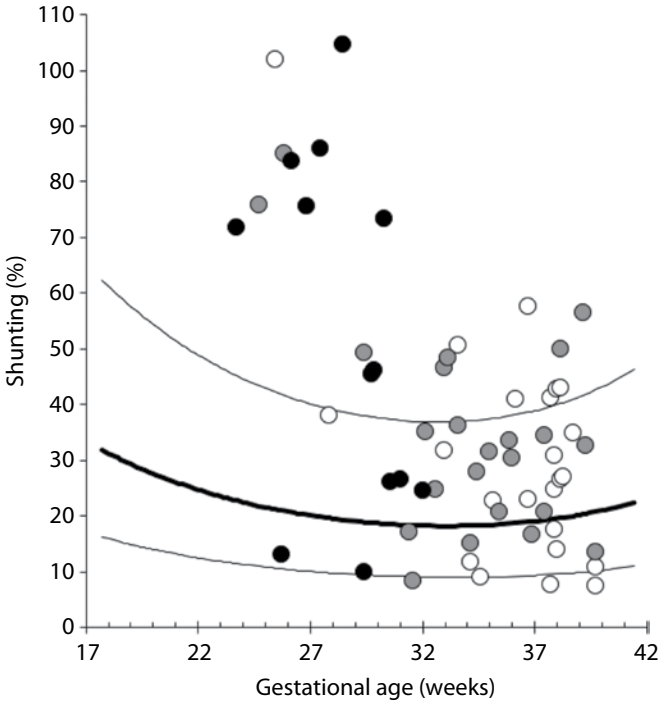


**Figure 47.12**
Ductus venosus shunting (% of umbilical flow) in growth-restricted fetuses (≤2.5 percentile) with varying degrees of placental compromise according to umbilical artery pulsatility index (PI). Open circle, normal PI; gray, PI > 97.5 percentile; black, absent or reversed end-diastolic velocity in the umbilical artery. (Reproduced with permission from Kiserud T et al. *Ultrasound Obstet Gynecol* 2006;28:143–9.[13])

in the umbilical and hepatic veins.[88,89] However, one should be aware that the spatial profile of the low velocities measured during atrial contraction may represent both antegrade and retrograde velocities at the same moment in the isthmic cross section.[90] This is conventionally not sufficiently observed when interpreting early pregnancy results. The blood velocity in the

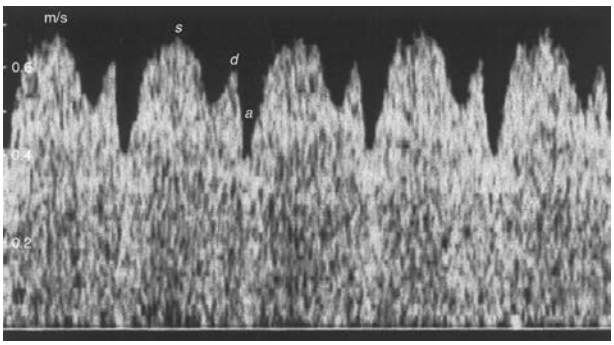


**Figure 47.13**
Normal ductus venosus blood velocity reflecting the various components of the cardiac cycle: ventricular systole (s), passive diastolic filling (d), and the minimum reached during atrial contraction (a). The pulsation is essentially the same as in other precordial veins but superimposed on a higher velocity, which reflects directly the umbilico-caval pressure gradient.

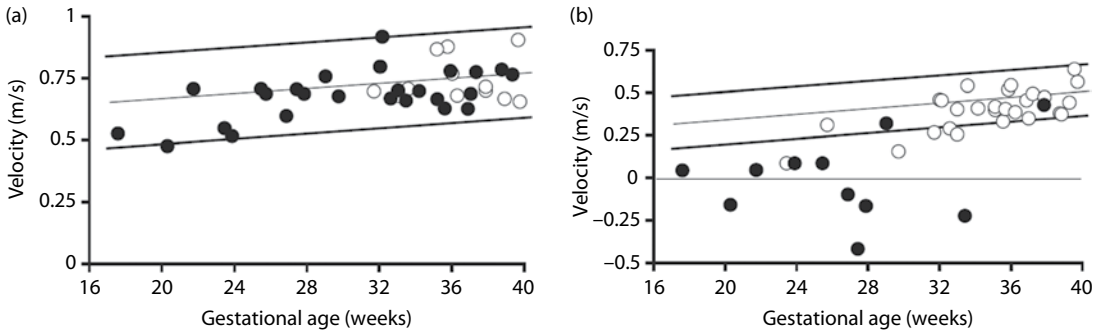


**Figure 47.14**
Severely growth-restricted fetuses manage to maintain peak systolic velocity within normal ranges in the ductus venosus in spite of the compromised placental circulation reflected in the increased pulsatility index of the umbilical artery blood velocity (filled circles in [a]). Circulatory decompensation is reflected in the reduced or negative velocity in the ductus venosus during atrial contraction (b). The sign seems to be more prominent before 32 weeks of gestation and is associated with perinatal death (filled circles in [b]). Mean (thin rule) and 95% prediction limits (thick rules) are shown. (Reproduced with permission from Kiserud T et al. *Ultrasound Obstet Gynecol* 1994;4:109–14.[6])

ductus venosus reflects essentially the same cardiac events as those recorded in other precordial veins (Figure 47.13). However, its direct connection to the umbilical vein combined with its active control makes this a special vessel with an array of possibilities for further exploration.

The cardiac function can be evaluated by determining the absolute velocity at the various phases of the cardiac cycle,[6,20,81,91–94] or by a pulsatile index.[91,92,94,95] As such indices are independent of angle correction, they have gained popularity. Normal ranges are established for several indices.[91,92,94] Zero or reversed velocity during atrial contraction, rather than the pulsatility index, has been advocated and used as a simple clinical sign of affected cardiac function,[81] particularly in early pregnancy.[88,96–98]

In general, the severely growth-restricted fetus manages to maintain systolic blood flow velocity in the ductus venosus within normal ranges in spite of compromised cardiac function (Figure 47.14a).[6] This makes sense as the absolute velocity reflects the pressure gradient driving the ductus flow and the liver perfusion critical for survival and development. However, the a-wave is commonly augmented in precordial veins (including the ductus venosus), reflecting altered cardiac performance (Figures 47.14b and 47.15).[6,20,81,99–104] Increased afterload and preload, and thus increased end-diastolic pressure, may be aggravated by direct effects of hypoxia and increased adrenergic drive, all leading to an augmented atrial contraction and a pronounced deflection during the a-wave in the ductus venosus Doppler recording (Figure 47.16). The amplification of the a-wave is likely to carry the wave further distally in the venous system than is seen in uncompromised fetuses.

An increased venous pressure, increased vascular tone, and active distension of the ductus venosus greatly promote propagation along this transmission line to the umbilical vein. Hypoxemia causes distension of the ductus venosus by itself, thus reducing the difference in cross section (and impedance) between the ductus venosus and the umbilical vein. This results in reduced wave reflection at the junction and an increased wave transmission and umbilical venous pulsation (Figure 47.6).

Advanced cardiac decompensation is characterized by greatly reduced or reversed velocity during the a-wave (Figure 47.16). A reduced velocity in the period between the systolic and diastolic peak probably signifies a further deterioration with hypoxia and acidosis leading to subliminal myocardial distensibility and reduced compliance, i.e., a preterminal state (Figure 47.16).[105,106]

In early pregnancy, a reversed a-wave in the ductus venosus is associated with chromosomal aberrations and cardiac malformations in fetuses with increased nuchal translucency.[88,97,98,107,108] It has been speculated that this may be due to a skewed cardiac function rather than the cardiac decompensation seen in late pregnancy. Second-trimester fetuses

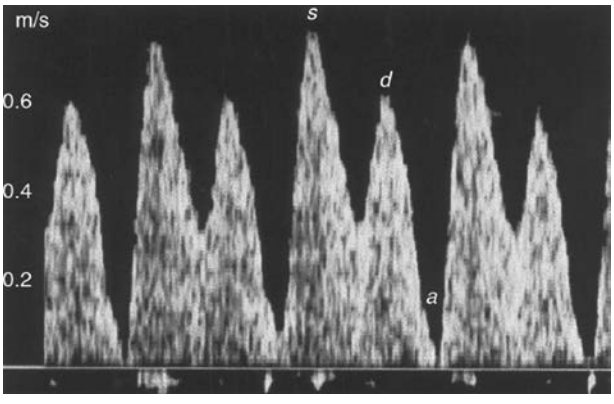


**Figure 47.15**
Impaired cardiac function is commonly seen in severe cases of intrauterine growth restriction as increased pulsatility of the ductus venosus blood velocity, the main reason being reduced blood velocity during an augmented atrial contraction phase (a). Note the early and steep deflection of systolic velocity (s) signifying a reduced myocardial distensibility (compliance) where a beginning hypoxia or acidemia could be the cause. (d, diastolic peak.)

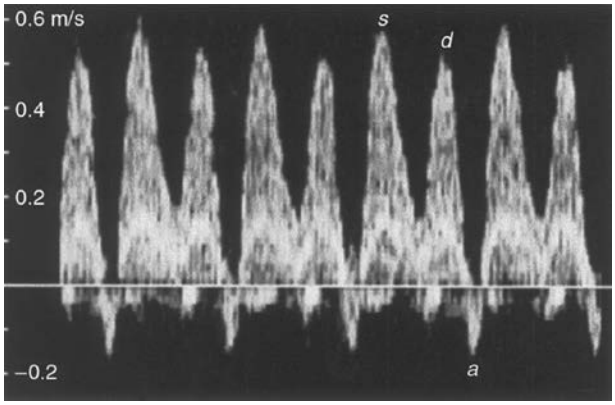


**Figure 47.16**
A further deterioration of cardiac function compared with Figure 47.15 leads to zero or reversed velocity during atrial contraction (a) and an augmented early and steep reduction of the systolic velocity (s) creating a systolic-diastolic dichotomy, probably due to impaired myocardial distensibility during hypoxia and acidosis, commonly observed as preterminal and terminal changes. (d, passive diastolic filling peak.)

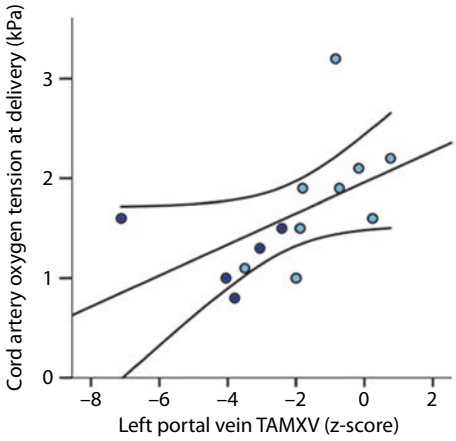


**Figure 47.17**
The left portal vein (the section between the main portal stem and the ductus venosus) is the watershed between the portal and umbilical blood flow. A shift to more portal and less umbilical circulation causes a reduction in left portal venous flow velocity or, in extreme cases, reversed velocity. The graph of z-scores shows the relation between this blood velocity and the $PO_2$ in the umbilical artery at birth in growth-restricted fetuses with normal (light blue) and abnormal umbilical artery pulsatility index (dark blue) with regression line and 95% confidence interval. (Reproduced with permission from Kessler J et al. *Pediatr Res* 2009;66:113–7.[15])

are also more prone to respond with an augmented a-wave than fetuses near term.[6,81] Hypoxemia and other insults tend to have a more direct and pronounced effect on the immature heart,[44,109] while during the third trimester it is essentially the matured endocrine responses and reflexes that modulate hemodynamics,[45] and a reversed a-wave in the ductus venosus is rarely seen (Figure 47.14).

Studies of IUGR fetuses and otherwise compromised pregnancies have shown that fetuses with an increased a-wave, or increased pulsatility, have a higher risk of hypoxemia, acidosis, perinatal morbidity, and demise.[6,75,99,100,110–112] However, as shown in Figure 47.14b, the changes we have described in the ductus venosus velocity pattern tend to be more pronounced in the second trimester and signify a serious prognosis at an age when prematurity in itself carries a high risk of complications and demise.

## Velocimetry of the caval, hepatic, portal, and other fetal veins

As compared to the ductus venosus, the IVC has lower velocities, and a negative a-wave is a normal finding in most of the pregnancy,[92,101,104,113,114] but otherwise essentially the same changes are seen in the decompensating IUGR fetus. Although ductus venosus Doppler velocimetry in the neonatal period represents exciting new possibilities,[115,116] the pediatrician is more acquainted with examination of the IVC and superior vena cava, sometimes making these vessels the preferred ones for measurements also before birth. In the fetus, the velocity measurement is preferably taken in the abdominal portion of the IVC, below the hepatic confluence and ductus venosus outlet, due to the high risk of interference and increased variability at the level of the hepatic confluence.[117] One study has shown that Doppler of the IVC gives a better prediction of hypoxemia and acidosis than does examination of the ductus venosus.[112] This has not been reproduced.[99,100] These vessels may tell different stories, particularly since the ductus venosus is specifically controlled and not connected to a capillary system but directly to the umbilical vein. Second, the abdominal IVC has a lower oxygen saturation and is more actively mobilized than the superior vena cava when $PCO_2$ in the fetus is low.[11,118]

Velocimetry of the hepatic veins is not commonly used, but the method is reproducible since these veins are easily accessed in most positions of the fetus.[92,119,120] Again, the changes seen in the ductus venosus and caval veins during hemodynamic compromise are much the same in the hepatic veins.

The magnitude and direction of blood velocity in the left portal vein have been suggested as additional simple markers of circulatory decompensation.[23,121] The blood velocity is recorded in the left portal branch between the ductus venosus inlet and the junction with the main portal stem. A low or reversed velocity in this section would reflect a down-prioritization of the oxygenation of the right liver lobe, i.e., left liver lobe sparing (Figure 47.4),[15,121] and there seems to be a linear relation between reduced blood velocity in the left portal vein and $PO_2$ in the umbilical artery after birth in the growth-restricted fetus (Figure 47.17).[121]

Intracranial veins have also attracted attention, with studies suggesting that increased pulsation may be used as a marker of circulatory decompensation.[122,123] All of these vessels will transmit and modify waves according to the same mechanisms as have been described here for the ductus venosus and umbilical vein.

## How to use venous Doppler in the evaluation

Venous Doppler is increasingly being used in a battery of Doppler measurements to evaluate the fetal circulation. While the waveform of the umbilical artery commonly reflects long-standing changes in the placental circuit, the reduced pulsatility of the middle cerebral artery is interpreted as a response to impaired placental perfusion. The Doppler recordings of the ductus venosus and umbilical vein reflect instantaneous changes in cardiac function and are commonly added to further differentiate circulatory status and determine time of delivery.[124]

Such a battery has been shown to be useful in describing the sequence of changes that follow a deteriorating placental function before 32 weeks of gestation.[110,111,125] The pattern is less clear after this stage of pregnancy. A recent study has identified groups responding differently with their circulation to growth challenges, including individuals who from an early stage may show venous changes.[126] By adding the Doppler recording of the umbilical vein and ductus venosus, the prediction of fetal acidosis and intrauterine death can be refined,[75] neonatal outcome better predicted,[127] and the group at risk of developing necrotizing enterocolitis better defined.[128] A randomized trial to further specify how to use ductus venosus recording in the management of early onset IUGR, suggests that using it as a monitoring tool could improve neurologic outcomes at 2 years of age.[129]

In order to have a more systematic approach, a "fetal cardiovascular profile score" has been suggested[130,131] and attempted.[119] In short, there is still room for various assessment and monitoring strategies depending on the doctor's experience and physiological insights.

## References


1. Gill RW. *Ultrasound Med Biol* 1979;5:223–35.
2. Gill RW et al. *Ultrasound Med Biol* 1984;10:349–63.
3. Gill RW et al. *Am J Obstet Gynecol* 1981;139:720–5.
4. Lingman G et al. *Biol Neonate* 1986;49:66–73.
5. Gudmundsson S et al. *Am J Obstet Gynecol* 1991;164:33–7.
6. Kiserud T et al. *Ultrasound Obstet Gynecol* 1994;4:109–14.
7. Jouppila P, Kirkinen P. *Br J Obstet Gynaecol* 1984;91:107–10.
8. Laurin J et al. *Obstet Gynecol* 1987;69:895–902.
9. Ville Y et al. *Am J Obstet Gynecol* 1994;170:487–94.
10. Laurin J, Marsal et al. *Br J Obstet Gynaecol* 1987;94:940–8.
11. Rudolph AM. *Circ Res* 1985;57:811–21.
12. Bellotti M et al. *Am J Obstet Gynecol* 2004;190:1347–58.
13. Kiserud T et al. *Ultrasound Obstet Gynecol* 2006;28:143–9.
14. Tchirikov M et al. *Am J Obstet Gynecol* 1998;178:943–9.
15. Kessler J et al. *Pediatr Res* 2009;66:113–7.
16. Mäkikallio K et al. *Ultrasound Obstet Gynecol* 2003;22:351–7.
17. Kiserud T et al. *Ultrasound Obstet Gynecol* 2006;28:126–36.
18. Edelstone DI et al. *Circ Res* 1978;42:426–33.
19. Behrman RE et al. *Am J Obstet Gynecol* 1970;108:956–69.
20. Kiserud T et al. *Lancet* 1991;338:1412–4.
21. Weiner Z et al. *Am J Obstet Gynecol* 1994;170:509–15.
22. Kilavuz O et al. *J Perinat Med* 2003;31:184–7.
23. Kiserud T et al. *Ultrasound Obstet Gynecol* 2003;21:359–64.
24. Kiserud T et al. *Ultrasound Obstet Gynecol* 2004;24:141–6.
25. Godfrey KM et al. *PLOS ONE* 2012;7:e41759.
26. Tchirikov M et al. *Placenta* 2001;22:24–31.
27. Tchirikov M et al. *Placenta* 2002;23:S153–8.
28. Haugen G et al. *Circ Res* 2005;96:12–4.
29. Ikenoue S et al. *Am J Obstet Gynecol* 2017;217:204.e1–04.e8.
30. Jouppila P et al. *Arch Gynecol* 1986;237:191–7.
31. Jones CT, Robinson JS. *J Develop Physiol* 1983;5:77–87.
32. Capponi A et al. *Obstet Gynecol* 1997;89:242–7.
33. Rizzo G et al. *Am J Obstet Gynecol* 1996;175:563–70.
34. Robinson JS et al. *J Develop Physiol* 1983;5:89–100.
35. Kiserud T et al. *Am J Obstet Gynecol* 1997;177:86–90.
36. Coceani F. *Europ J Ped* 1993;152:976–7.
37. Coceani F, Olley PM. *Can J Pharmacol* 1988;66:1129–34.
38. Kiserud T et al. *Am J Physiol Heart Circ Physiol* 2000;279:H1166–71.
39. Momma K et al. *Pediatr Res* 1992;32:386–9.
40. Momma K et al. Pharmacological constriction of the ductus arteriosus and ductus venosus in fetal rats. In: Nora J, Takao A, eds. *Congenital Heart Disease—Causes and Processes*. Mount Kisco: Futura; 1984:313–24.
41. Tchirikov M et al. *J Physiol* 2003;548:519–26.
42. Jensen A, Berger R. Regional distribution of cardiac output. In: Hanson MA, Spencer JAD, Rodeck CH, eds. *Fetus and Neonate Physiology and Clinical Application*. Cambridge: Cambridge University Press; 1993 (vol 1. The circulation):23–74.
43. Jauniaux E et al. *Am J Obstet Gynecol* 2000;182:661–5.
44. Kiserud T et al. *Br J Obstet Gynaecol* 2001;108:359–64.
45. Hanson MA. *Eur J Obstet Gynecol Reprod Biol* 1997;75:55–61.
46. Hellevik LR. *Wave propagation and pressure drop in precordial veins*. MTF-report. Department of Applied Mechanics, Thermodynamics and Fluid Dynamics. Trondheim: Norwegian University of Science and Technology; 1999:181.
47. Hellevik LR et al. *J Biomech* 2000;33:1123–30.
48. Kiserud T. *Eur J Obstet Gynecol Reprod Biol* 1999;84:139–47.
49. Kiserud T. *Fetal Matern Med Rev* 2003;14:57–95.
50. Nichols WW, O'Rourke MF. *McDonald's Blood Flow in Arteries. Theoretical, Experimental and Clinical Principles*. London: Arnold 1998;1–564.
51. Parker KH, Jones CJH. *ASME J Biomech Eng* 1990;112:322–6.
52. Hasaart TH, De Haan J. *J Perinat Med* 1986;14:19–26.
53. Reed KL et al. *Obstet Gynecol* 1996;87:617–20.
54. Reuss ML et al. *Am J Obstet Gynecol* 1983;145:70–6.
55. Kiserud T. *J Perinat Med* 2000;28:90–6.
56. Kiserud T et al. *Ultrasound Med Biol* 1994;20:225–32.
57. Hellevik LR et al. *Heart Vessels* 1998;13:175–80.
58. Nakai Y et al. *Gynecol Obstet Invest* 1997;43:6–7.
59. Rizzo G et al. *Am J Obstet Gynecol* 1992;167:675–7.
60. Skulstad SM et al. *Ultrasound Obstet Gynecol* 2004;23:126–30.
61. Sutton MS et al. *Pediatr Res* 1990;28:383–7.
62. Gill RW, Kossoff G. *Contrib Gynecol Obstet* 1979;6:139–41.
63. Kiserud T et al. *Am J Obstet Gynecol* 2000;182:147–53.
64. Acharya G et al. *Prenat Diagn* 2005;25:99–111.
65. Pennati G et al. *Ultrasound Obstet Gynecol* 2004;23:131–7.
66. Kiserud T, Rasmussen S. *Ultrasound Obstet Gynecol* 1998;11:419–25.
67. Kiserud T et al. *Ultrasound Obstet Gynecol* 1999;13:52–7.
68. Boito S et al. *Ultrasound Obstet Gynecol* 2002;19:344–9.
69. Kessler J et al. *Pediatr Res* 2008;63:315–20.
70. Barbera A et al. *Am J Obstet Gynecol* 1999;181:174–9.
71. Rudolph AM et al. *Pediatr Res* 1971;5:452–65.
72. Sutton MG et al. *Cardiovasc Res* 1991;25:603–8.

73. Rizzo G et al. *Ultrasound Obstet Gynecol* 2008;32:155–9.
74. Baschat AA et al. *Am J Obstet Gynecol* 1999;181:190–5.
75. Baschat AA et al. *Am J Obstet Gynecol* 2004;191:277–84.
76. Rizzo G et al. *Biol Neonate* 1995;68:163–8.
77. Nakai Y et al. *Ultrasound Med Biol* 1995;21:443–6.
78. Nakai Y et al. *Br J Obstet Gynaecol* 1992;99:977–80.
79. Van Splunder IP et al. *Ultrasound Obstet Gynecol* 1994;4:49–53.
80. Baschat AA, Gembruch U. *Ultrasound Obstet Gynecol* 1996;8: 201–5.
81. Kiserud T et al. *J Matern Fetal Invest* 1993;3:15–20.
82. Itskovitz J et al. *Heart Circ Physiol* 1987;252:H100–9.
83. Meyers RL et al. *J Dev Physiol* 1991;15:189–97.
84. Paulick RP et al. *Am J Obstet Gynecol* 1990;163:1357–63.
85. Bellotti M et al. *Am J Physiol Heart Circ Physiol* 2000;279: H1256–63.
86. Emerson DS et al. *J Ultrasound Med* 1991;10:S55.
87. Bhide A et al. *Ultrasound Obstet Gynecol* 2013;41:233–9.
88. Borrell A et al. *Am J Obstet Gynecol* 1998;179:1612–7.
89. Montenegro N et al. *Ultrasound Med Biol* 1997;23:171–6.
90. Leinan PR et al. *Cardiovasc Engineer Technol* 2013;4:257–66.
91. Bahlmann F et al. *Prenat Diagnosis* 2000;20:623–34.
92. Hecher K et al. *Ultrasound Obstet Gynecol* 1994;4:381–90.
93. Huisman TWA et al. *Ultrasound Med Biol* 1992;18:33–7.
94. Kessler J et al. *Ultrasound Obstet Gynecol* 2006;28:890–8.
95. Devore GR, Horenstein J. *Ultrasound Obstet Gynecol* 1993;3: 338–42.
96. Matias A et al. *Ultrasound Obstet Gynecol* 1998;12:380–4.
97. Maiz N et al. *Ultrasound Obstet Gynecol* 2009;33:512–7.
98. Murta CG et al. *Fetal Diagn Ther* 2002;17:308–14.
99. Hecher K et al. *Circulation* 1995;91:129–38.
100. Hecher K et al. *Am J Obstet Gynecol* 1995;173:10–5.
101. Kanzaki T, Chiba Y. *Fetal Diagn Ther* 1990;5:168–74.
102. Nakata M. *J Obstet Gynaecol Res* 1996;22:489–96.
103. Reed KL et al. *Circulation* 1990;81:498–505.
104. Rizzo G et al. *Am J Obstet Gynecol* 1992;166:1271–80.
105. Szunyogh N et al. *Ultrasound Obstet Gynecol* 2006;28:392.
106. Picconi JL et al. *J Ultrasound Med* 2008;27:1283–9.
107. Matias A et al. *Ultrasound Obstet Gynecol* 1999;14:307–10.
108. Matias A, Montenegro N. *Semin Perinatol* 2001;25:32–7.
109. Iwamoto HS et al. *Heart Circ Physiol* 1989;256:H613–20.
110. Ferrazzi E et al. *Ultrasound Obstet Gynecol* 2002;19:140–6.
111. Hecher K et al. *Ultrasound Obstet Gynecol* 2001;18:564–70.
112. Rizzo G et al. *Ultrasound Obstet Gynecol* 1996;7:401–10.
113. Huisman TW et al. *Ultrasound Med Biol* 1993;19:441–5.
114. Huisman TWA et al. *Ultrasound Med Biol* 1991;17:679–82.
115. Fugelseth D et al. *Arch Dis Child Fetal Neonatal Ed* 1999;81: F35–9.
116. Fugelseth D et al. *Arch Dis Child* 1997;77:F131–4.
117. Rizzo G et al. *J Matern Fetal Invest* 1992;2:153–6.
118. Nyberg MK et al. *Ultrasound Obstet Gynecol* 2011;38:658–64.
119. Hofstaetter C et al. *Eur J Ultrasound* 1996;4:153–60.
120. Mari G et al. *Obstet Gynecol* 1995;86:729–33.
121. Kessler J et al. *Ultrasound Obstet Gynecol* 2007;30:757–64.
122. Cheema R et al. *Ultrasound Obstet Gynecol* 2004;24:147–53.
123. Li H et al. *Ultrasound Obstet Gynecol* 2004;24:516–21.
124. Baschat AA. *Early Hum Dev* 2005;81:877–87.
125. Baschat AA et al. *Ultrasound Obstet Gynecol* 2001;18:571–7.
126. Unterscheider J et al. *Am J Obstet Gynecol* 2013;209:539.e1–7.
127. Baschat AA et al. *Obstet Gynecol* 2007;109:253–61.
128. Manogura AC et al. *Am J Obstet Gynecol* 2008;198:638.e1–5.
129. Lees CC et al. *Lancet* 2015;385:2162–72.
130. Huhta JC. *Pediatr Cardiol* 2004;25:274–86.
131. Makikallio K et al. *Ultrasound Obstet Gynecol* 2008;31:48–54.
132. Mäkikallio K. *Placental Insufficiency and Fetal Heart: Doppler Ultrasonographic and Biochemical Markers of Fetal Cardiac Dysfunction*. University of Oulu, Oulu; 2002.
133. Kiserud T, Rasmussen S. *Ultrasound Obstet Gynecol* 2001; 17:119–24.

# 48

# Evaluation of fetal cardiac function: Techniques and implications

Christoph Wohlmuth and Helena M. Gardiner

## Basic principles of cardiac function

### *Introduction*

Assessment of cardiac function forms an integral part of every fetal cardiac evaluation.[1] In the screening echocardiogram, subjective assessment of ventricular contractility in a standard four-chamber view may be sufficient to meet this requirement. Where there is congenital heart disease (CHD), however, detailed assessment of cardiac function is crucial, and in complicated pregnancies such as twin-twin transfusion syndrome (TTTS), twin-reversed arterial perfusion (TRAP), intrauterine growth restriction (IUGR), fetal infection (parvovirus, cytomegalovirus, coxsackievirus, etc.), anemia, lung masses, hydrops, sacrococcygeal teratoma, or placental chorioangiomas, cardiovascular function is an important element in guiding the management of these pregnancies.

### *Ventricular filling*

As blood is returning from the systemic and pulmonary veins, the atria act as a reservoir, and the intra-atrial pressure rises.[2,3] Once atrial pressure exceeds the ventricular end-diastolic pressure, the atrioventricular (AV) valves open, and early ventricular filling occurs. Atrial contraction then completes ventricular filling. From early gestation, early and late ventricular filling can be distinguished as E ("early") and A ("active" or "atrial") waves with pulsed wave Doppler interrogation of the AV valves (Figure 48.1a).[4] In the fetus, the velocity of atrial contraction is higher than the early filling velocity resulting in an E/A ratio less than 1. Both E- and A-velocities increase throughout gestation; however, the E-wave does more than the A-wave, reflecting increasing ventricular compliance toward term.[5–7] Active filling becomes even more important in hemodynamic states where there is reduced filling time, such as physiological high fetal heart rate, or under pathological conditions where the end-diastolic ventricular pressure is increased. Under these conditions, the E/A ratio decreases followed by fusion of the mitral and tricuspid E- and A-waves (Figure 48.1b). With further increases in ventricular end-diastolic pressure and with volume overload, the AV ring stretches, and regurgitation can be detected (Figure 48.1c). Color Doppler can guide placement of the pulsed Doppler sample in the maximum velocity of the regurgitant jet to obtain optimal peak velocities and time duration, and the modified Bernoulli equation can be applied to estimate pressure drop across a valve from its peak regurgitant velocity. The estimate of ventricular pressure is obtained by adding atrial pressure to the value of the pressure gradient (Table 48.1). Different grading systems have been used to describe the severity of AV valve regurgitation utilizing color Doppler signals to assess its extent into the atrial cavity or more reproducible data from the vena contracta width, measured relative to the valvar width and information on peak velocity and duration using pulsed or continuous wave Doppler.[8] Generally, regurgitation is considered important when the jet duration occupies greater than 50% of the cardiac cycle and/or the color jet reaches the back of the atrial wall.

### *Ventricular output*

After the action potential is conducted to the ventricles, ventricular contraction begins, and the AV valves close due to the pressure increase. This time period is referred to as the isovolumic contraction time, where the ventricular pressure is less than the arterial pressure. When the ventricular pressure exceeds the arterial pressure, the semilunar valves open, and the stroke volume is ejected.

Experimental lamb studies have shown that the Frank-Starling mechanism is active in the fetal heart.[9] Thus, stroke volume is determined by preload, myocardial contractility, and afterload. However, the preload reserve is limited, and the heart operates near the upper limit of the Frank-Starling function curve.[10,11] Therefore, heart rate is the most important regulator of cardiac output during fetal life. Stroke volume can be calculated for each ventricle using two-dimensional (2D) and pulsed wave Doppler ultrasound of the semilunar valves, and cardiac output can be calculated by multiplying stroke volume and heart rate (Table 48.1).

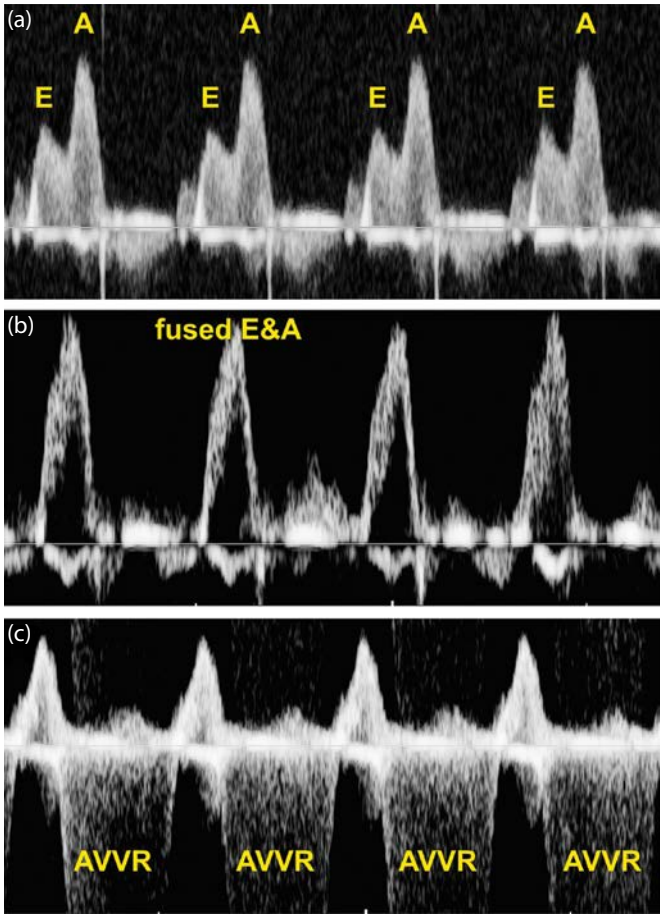


**Figure 48.1**
(a–c) Atrioventricular inflow. (a) Normal biphasic atrioventricular inflow Doppler profile with separate E- and A-waves; (b) fusion of E- and A-waves (monophasic inflow); (c) monophasic inflow and severe atrioventricular valve regurgitation (AVVR).

In the fetus, right heart dominance has been observed with around 60% of combined cardiac output coming from the right ventricle and 40% from the left.[12] Biventricular cardiac output significantly increases from around 40 mL/min at 15 weeks of gestation to 1470 mL/min at 40 weeks. Mean cardiac output normalized to estimated fetal weight does not change with gestation and is estimated to be 429 mL/min/kg with a relatively high standard deviation of 100 mL/min/kg.[12]

While the interoperator variability for outflow Doppler is low provided the angle is kept as close to zero as possible,[13] the valve diameter is very sensitive to variation as measurement errors are potentiated with calculation of the cross-sectional area. Therefore, when cardiac output is assessed longitudinally in conditions such as TRAP, the measurements should be acquired by the same operator.

Other parameters such as ventricular shortening fraction, which can be obtained by placing an M-mode through both ventricles perpendicular to the interventricular septum, and ejection fraction (Table 48.1) play a less important role in fetal cardiac assessment as these measurements are relatively crude and changes are often not noticeable until late in the disease. Therefore, assessment of long-axis function is preferred and is discussed in the section "Long-axis motion."

## *Myocardial performance index*

The myocardial performance index (MPI) was first described for global cardiac assessment in adults by Tei et al.[14] and was therefore originally referred to as the Tei index.[14] It is defined as the ratio of isovolumic contraction and relaxation time over ejection time (Table 48.1). Since the introduction of the MPI in fetal medicine, several gestational age–adjusted reference values have been published with low agreement between these studies, most likely due to heterogeneity in caliper

**Table 48.1** Equations for the calculation of cardiac function parameters

| *Equation* | *Abbreviations and units* |
|---|---|
| Ventricular pressure (mmHg) $= 4^{(a)} + 4 * V_{max^2}$ | $V_{max}$, peak velocity of mitral or tricuspid regurgitant jet (m/s) |
| Stroke volume (mL) $= VTI * \pi * \frac{d^2}{4}$ | VTI, velocity time integral of aortic or pulmonary outflow (cm)<br>d, diameter of aortic or pulmonary valve (cm) |
| Cardiac output (mL / min) $= VTI * \pi * \frac{d^2}{4} * HR$ | VTI, velocity time integral of aortic or pulmonary outflow (cm)<br>d, diameter of aortic or pulmonary valve (cm)<br>HR, heart rate (bpm) |
| Biventricular output (mL / min) $= LCO + RCO$ | LCO, left cardiac output (mL/min)<br>RCO, right cardiac output (mL/min) |
| Shortening fraction (%) $= \frac{EDD - ESD}{EDD}$ | EDD, end-diastolic diameter (mm)<br>ESD, end-systolic diameter (mm) |
| Ejection fraction (%) $= \frac{SV}{EDV}$ | SV, stroke volume (mL)<br>EDV, end-diastolic volume (mL) |
| Myocardial performance index $= \frac{ICT + IRT}{ET}$ | ICT, isovolumic contraction time (ms)<br>IRT, isovolumic relaxation time (ms)<br>ET, ejection time (ms) |

[a] 4 mm Hg are added as an estimate of fetal intra-atrial pressure.

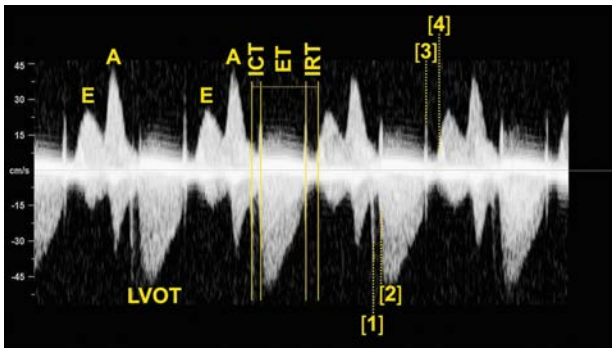


**Figure 48.2**
Myocardial performance index. Calculation of the left modified myocardial performance index (MPI) using valve clicks for the demarcation of time intervals. MPI = (ICT + IRT)/ET. (A, early ventricular filling; E, late ventricular filling; ET, ejection time; ICT, isovolumic contraction time; IRT, isovolumic relaxation time; LVOT, left ventricular outflow tract; MPI, myocardial performance index. [1] mitral valve closure click; [2] aortic valve opening click; [3] aortic valve closure click; [4] mitral valve opening click.)

position and to the use of different ultrasound equipment.[15] An important step toward standardization of MPI measurement was made with the description of the "modified MPI," where opening and closing clicks of both the aortic and mitral valves are used for the demarcation of the time periods.[16,17] To obtain the left modified MPI, a five-chamber view is used, and a 3–4 mm Doppler sample gate is placed on the lateral wall of the ascending aorta close to the mitral valve. The valve clicks are used to determine the intervals (Figure 48.2). More recently, algorithms for automated MPI calculation using the morphology of the waveform to identify the clicks have been suggested.[18] Despite efforts to refine MPI measures, the drawback remains that the "single-strip" approach as shown in Figure 48.2 is only applicable for the left heart, because the tricuspid and pulmonary valves are located in different anatomical planes requiring right MPI estimation from two different locations. This limitation may be overcome by using tissue Doppler imaging as described in the section "Tissue Doppler imaging."

## Long-axis motion

The AV valve annulus moves toward the cardiac apex during ventricular contraction, storing kinetic energy during this motion, and ascends toward the base during relaxation. The outer contours of the ventricles remain relatively unchanged.[19] Annular displacement can be recorded by M-mode echocardiography with high spatial and temporal resolution. Mitral and tricuspid annular plane systolic excursion (MAPSE, TAPSE) are obtained by placing the M-mode cursor at right angles through the AV ring at the base of the heart (Figure 48.3). The parameters reflect the shortening of the myocardium in a longitudinal fashion during ventricular systole and lengthening in diastole.[20] Although not load independent, MAPSE and TAPSE are easy to obtain and

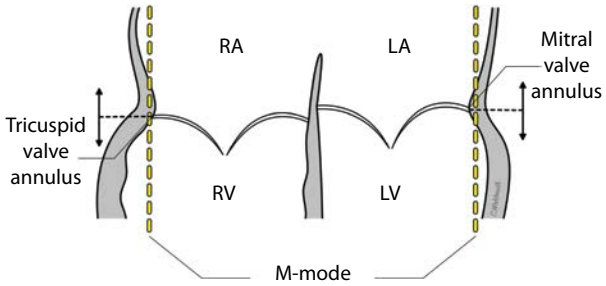


**Figure 48.3**
Mitral and tricuspid annular plane systolic excursion. The M-mode cursor is placed at right angles through the atrioventricular ring at the base of the heart, and the maximal amplitude of systolic excursion is measured. (LA, left atrium; LV, left ventricle; RA, right atrium; RV, right ventricle.)

have a high degree of reproducibility.[21] The amplitude of annular displacement increases with gestation.[20] Therefore, gestational age–adjusted reference ranges should be applied. Throughout gestation, TAPSE is higher than MAPSE,[20] which may be explained by two features: the right heart dominance in fetal life[12] and the different myocardial fiber orientations in the right and left ventricles.[22] Annular displacement is a sensitive marker of cardiac function and has been studied in pathological conditions. In IUGR, both TAPSE and MAPSE are decreased, and TAPSE has been shown to be predictive of postnatal cardiovascular remodeling.[23] In critical aortic stenosis, prompt improvement of MAPSE has been reported after successful fetal valvuloplasty.[24]

The clinical utility of annular displacement is limited when there is suboptimal fetal lie, as parallel alignment of the M-mode sample is critical for a reliable measurement. However, anatomic M-mode allows the offline placement of a virtual M-mode line on digitally stored cine loops of the four-chamber view, and the angle can be manually aligned perpendicular to the AV annulus. It demonstrates good correlation with "natural" M-mode annular excursion, but overestimates TAPSE and MAPSE, on average, by 6% and 5%, respectively.[20,21] As an alternative, acquisition of TAPSE using spatiotemporal image correlation (STIC) has been reported and is described with other three- and four-dimensional (3D/4D) methods later in this chapter.

## Tissue Doppler imaging

Tissue Doppler imaging (TDI) uses the Doppler principle to measure regional contraction and relaxation velocities of the myocardium.[25] Signals of tissue motion have lower velocities and higher amplitudes as compared to the Doppler signals of blood flow.[26] TDI can be acquired by pulsed wave (PW) Doppler, which measures peak myocardial velocities at distinct points, or color mode, which simultaneously acquires multiple pixel velocities superimposed on grayscale 2D images.

Since the cardiac apex remains relatively stationary during the cardiac cycle, PW-TDI of the mitral and tricuspid annulus

give a reasonable approximation of longitudinal cardiac function.[26] Left and right ventricular PW-TDI signals are acquired from a standard four-chamber view with the cardiac apex at 6 or 12 o'clock by placing a Doppler sample on the ventricular myocardium immediately adjacent to the mitral and tricuspid annulus. The ultrasound beam must be kept as parallel to the longitudinal myocardial wall motion as possible, and no angle correction should be applied (Figure 48.4a and b).[24] PW-TDI gives three distinct waveforms: the velocities during early diastole (E′), late diastole with atrial contraction (A′), and systole in the ejection phase (S′), where prime (′) is most commonly used to differentiate TDI velocities from the E- and A-waves of AV blood flow (Figure 48.4c). Sometimes, Ea, Aa, and Sa or Em, Am, and Sm may be found in the literature, where "a" stands for "annulus" and "m" refers to ""myocardial."[26]

The E′ signal reflects the velocity of myocardial relaxation as the annulus ascends during early ventricular filling and therefore goes in the opposite direction to the AV blood flow. In invasive postnatal animal studies, peak E′ velocity had a strong negative association with tau (τ), a parameter reflecting ventricular relaxation. Diastolic dysfunction with abnormal relaxation thus is associated with a decrease in E′ velocity. Only large changes in filling pressure alter E′; therefore, the parameter is less load dependent than the standard Doppler of AV flow.[27] Nagueh et al. suggested a novel annular velocity ratio (E/E′) using peak E from mitral inflow and E′ from the mitral annulus as a means to predict left ventricular filling pressures.[28] A high value of E/E′ has been shown to indicate increased ventricular filling pressure in subsequent adult human catheterization studies.[29]

A′ reflects the upward movement of the annulus during active ventricular filling around atrial contraction. Increased ventricular end-diastolic pressure results in a decrease in A′ velocity. A positive association has been found between atrial pressure and A′ as well as between the atrial relaxation index and A′. Abnormal ventricular relaxation may result in abnormally increased A′ velocities due to the reduced early diastolic filling time and thus higher atrial preload, provided ventricular filling pressures are normal.[27]

Ventricular shortening during ejection is reflected by the S′ velocity. In adults, S′ correlates with ejection fraction and *dP/dt* and is a prognostic indicator of mortality.[30–32] Animal validation studies have shown that S′ is independently determined by afterload and cardiac contractility.[33] Therefore, S′ is an important parameter in conditions with increased fetal cardiac afterload such as IUGR,[34,35] TTTS,[36] and critical aortic stenosis.[24]

Myocardial tissue Doppler-derived parameters have a significant association with gestational age. Normal values derived from regression equations from Comas et al.[37] are shown in Figure 48.5a–l. Generally, right ventricular velocities are higher than the corresponding left ventricular parameters. As with MAPSE and TAPSE (Figure 48.5m–n), this may be explained by right heart predominance during fetal development and differing myocardial fiber orientation in the ventricles.[38]

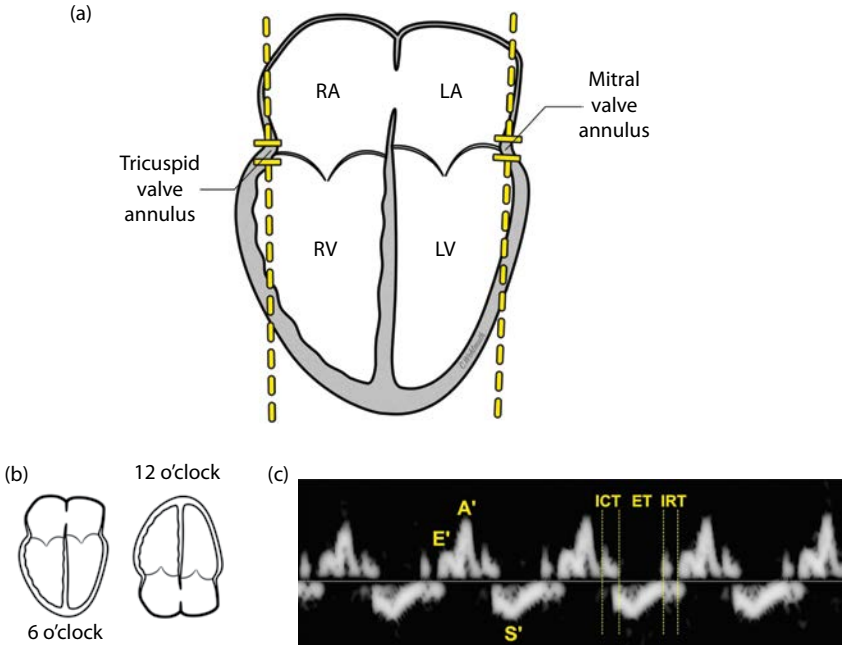


**Figure 48.4**
(a–c) Tissue Doppler imaging (TDI). The pulsed wave Doppler sample is placed at right angles through the atrioventricular ring (a) with the apex of the heart at 6 or 12 o'clock (b). TDI gives three distinct waveforms: E′, A′, and S′. ICT, ET, and IRT can be obtained to calculate myocardial performance index as described. (A′, peak velocity during late ventricular filling; E′, peak velocity during early ventricular filling; ET, ejection time; ICT, isovolumic contraction time; IRT, isovolumic relaxation time; LA, left atrium; LV, left ventricle; RA, right atrium; RV, right ventricle; S′, peak velocity during ventricular systole.)

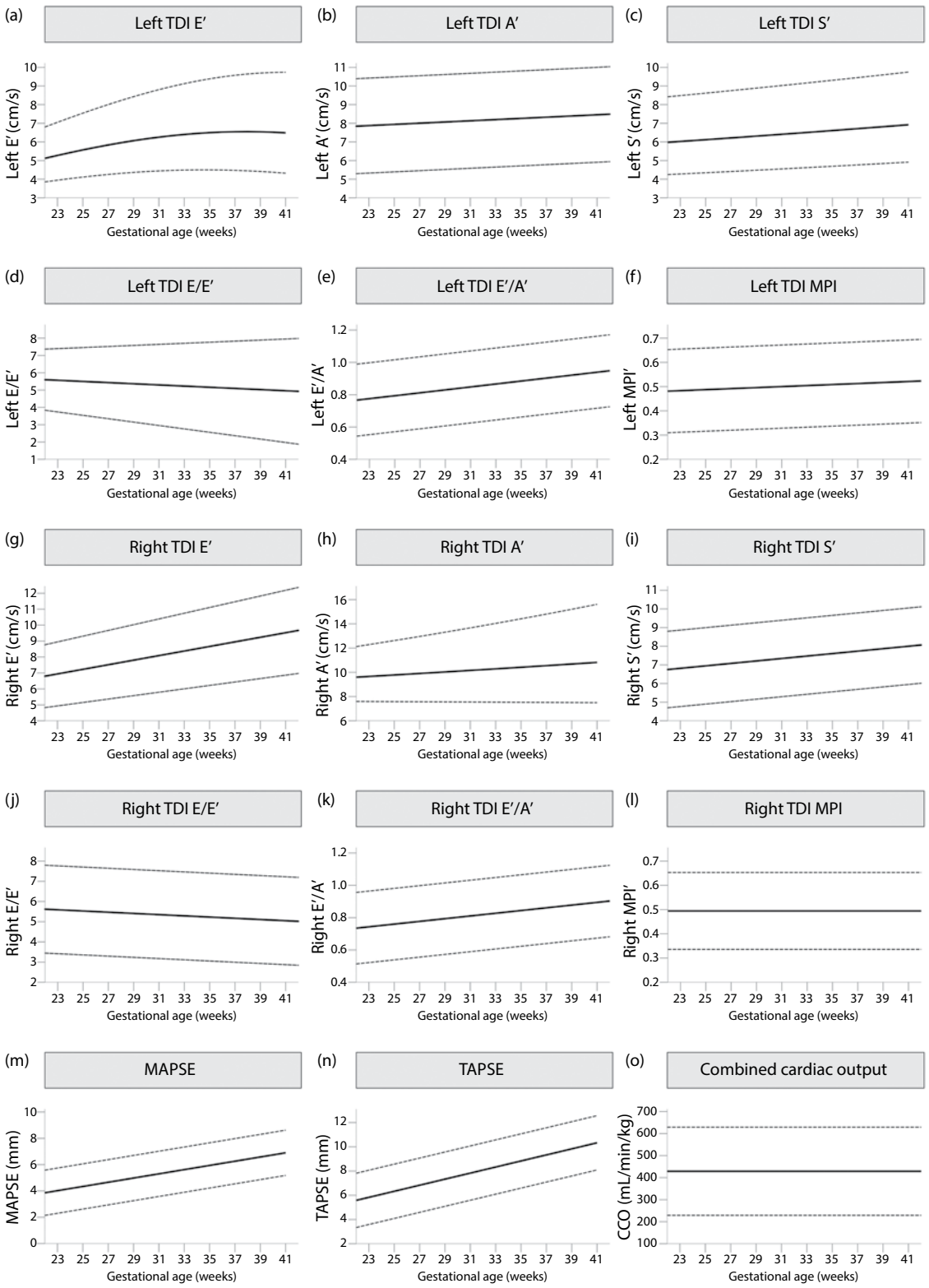


**Figure 48.5**
(a–o) Gestational age–adjusted reference values for long-axis function and cardiac output. Gestational age–adjusted reference values (mean ± 2 SD) for left and right ventricular tissue Doppler-derived parameters (a–l) MAPSE (M) and TAPSE (N) and CCO (O) derived from the regression equations from Comas et al.,[37] Gardiner et al.,[20] and Mielke et al.[12] (A′, peak velocity during late ventricular filling; E′, peak velocity during early ventricular filling; MAPSE; mitral annular peak systolic excursion; MPI, myocardial performance index; S′, peak velocity during ventricular systole; TAPSE, tricuspid annulus peak systolic excursion.)

There are some important limitations to TDI: Most importantly, TDI is an angle-dependent technique and only measures the vector parallel to the ultrasound beam. Furthermore, it measures absolute tissue velocity and thus does not differentiate between active and passive or external motion.[26] With higher heart rate or increasing diastolic dysfunction, fusion of the E′ and A′ waves precludes the differentiation of the waves and calculation of derived parameters (E/E′ and E′/A′).

## *Speckle tracking*

Speckle tracking (also known as vector velocity imaging) is a recent non-Doppler approach to assess fetal cardiac function by measuring myocardial wall deformation. Unlike Doppler techniques, speckle tracking is angle independent and therefore especially appealing for examination of the fetal heart. It provides measurements of displacement, strain, and strain rate using frame-by-frame tracking of bright myocardial speckles (Figure 48.6).[39]

The displacement (or motion) of a point measures the distance a point travels in the scanning plane. Strain is a measure of tissue deformation under applied force and defines the change in position of two points over a set period of time.[40] It is a relative measure (%) and is mathematically described as

$$Strain\ (\varepsilon) = \frac{Final\ length\ (L) - Initial\ length\ (L_0)}{Initial\ length\ (L_0)}$$

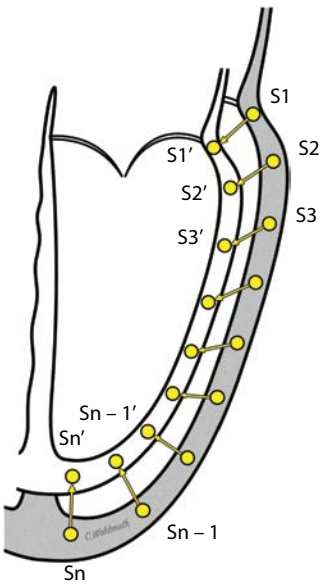


**Figure 48.6**
Speckle tracking: Displacement, strain, and strain rate. Bright myocardial speckles (S1, S2, S3, … Sn − 1, Sn) are tracked frame-by-frame to provide measurements of displacement, strain, and strain rate. Displacement is a measure of the distance a point travels; strain measures the change of the size of a segment; and strain rate quantifies how rapidly the size of a segment is changing.

Negative strain values represent ventricular shortening during systole, and positive values correspond to lengthening during diastole.

Strain rate (or speed of deformation) describes how fast two different points of the myocardium move toward or away from each other and therefore quantifies how rapidly the size of a segment is changing.[40]

### Technique

Speckle tracking can be performed offline on four-chamber or short-axis clips obtained during routine fetal echocardiography. However, frame rate must be optimized by decreasing the acquisition angle and depth as mean and peak velocities are significantly lower with lower frame rates, and automated speckle tracking is more successful in high-frame rate clips.[41] The digitally stored images are exported in DICOM format from the ultrasound machine into a commercially available speckle tracking software. Stored images are not usually satisfactory because of their low frame rate. When speckle tracking analysis was introduced in fetal medicine, the limitation of lacking fetal electrocardiogram tracings was overcome by using dummy spike-signals created from a metronome.[41] Recently, the technique has been refined allowing the use of anatomical M-mode to guide timing in speckle tracking software packages. The left and right ventricular endocardial border is traced manually from the septal aspect of the AV valve annulus over the apex back to the basolateral valve ring. The border between the cavity and the endocardium is tracked automatically in subsequent frames by the software package (Video 48.1).

### Implication

The association between myocardial strain and gestational age is controversial, with some reports describing a decrease in strain during gestation[41–44] and others reporting no change.[45–50] Technical limitations such as the use of stored clips, point strain versus Lagrangian strain measurements, and the users' learning curve most likely explain this controversy. However, speckle tracking is an elegant method to detect subtle alterations in cardiac contractility and has been applied in several cardiac and extracardiac anomalies.

In CHD, a wide distribution of values for strain has been reported with a considerable overlap with normal values for most anatomical lesions. The most significant changes have been observed with left heart obstruction, where left ventricular strain was very low. In Ebstein malformation, right ventricular strain is decreased with preserved left ventricular function.[51]

Changes in cardiac strain have been observed in TTTS, where both pre- and afterload are altered resulting in reduced left and right ventricular strain in recipient twins.[52–54] A decrease in strain has also been observed with gestational diabetes,[55] intrahepatic cholestasis,[56] and fetal anemia.[57]

### Limitation

As observed with angle-dependent methods, the small size of the fetal heart, high fetal heart rate, and fetal movements limit

the application of speckle tracking. The latter may cause out-of-plane movement of the tracked speckles, thereby precluding reliable measurements. Maternal obesity and unfavorable fetal lie may cause shadowing hampering clear endocardial delineation.

## Three- and four-dimensional assessment of cardiac function

STIC is an automated volume acquisition where the array inside the ultrasound transducer acquires one 3D dataset consisting of a very high number of 2D images. The software identifies the rhythmic movement of the heart, derives the heart rate, and reconstructs the volume of one real-time cardiac cycle, played in a cine loop.[58] It thereby adds the fourth dimension of time. Apart from its application in the assessment of cardiac anatomy, STIC offers the possibility to measure 3D volumes at different time points during the cardiac cycle, either manually from multiple serial slices[59] or with specialized algorithms such as Virtual Organ Computer-aided AnaLysis (VOCAL).[60] End-diastolic and end-systolic volumes as well as stroke volume, ejection fraction, and cardiac output can be derived. Gestational age–adjusted reference values have been provided[59–65] and should be used accordingly, as results from different methods are not always interchangeable.[66]

More recently, an M-mode function has been added to STIC allowing measurement of long-axis function and shortening fraction in cases of suboptimal fetal lie.[67] Messing et al. compared TAPSE assessed by conventional M-mode versus STIC ("f-TAPSE') and reported comparable measurements between the two methods, but a higher success rate for f-TAPSE.[68]

Three- and four-dimensional imaging depends on the quality of the initial acquisition plane. Thus, shadowing and fetal movements can preclude suitable volume acquisition. The time-consuming processing of STIC and the training required to perform the analyses further limit its "everyday" application.

## *Cardiac magnetic resonance imaging*

Magnetic resonance imaging (MRI) has become a powerful complementary imaging modality in fetal medicine. With advanced gestational age, it may offer improved imaging compared to ultrasound, because it is not affected by decreasing levels of amniotic fluid or ossification.[69] While MRI assessment of the heart is a potent diagnostic tool after birth, limitations from fetal movements, high heart rates, artifacts, and the lack of echocardiography triggering[70,71] have precluded its clinical implementation in fetal medicine. Potential applications in the assessment of cardiac function include speckle tracking and calculation of ventricular volumes, ejection fraction, and cardiac output. Improved blood flow measurement by (phase contrast) MRI would add significant value to fetal care, as cardiac output calculated from ultrasound is a relatively crude estimate as previously described. Recent advances have improved MRI triggering using cardiotocography devices[72] or self-gating approaches.[73,74] Prsa et al.[75] reported blood flow measurements in 40 late-gestation fetuses using a self-gating technique. They provided preliminary MRI reference values for cardiac output and flow in the great arteries, umbilical vein, and superior vena cava as well as placental blood flow, while also raising some concerns about the accuracy of the technique.[75] Furthermore, it is currently not suitable for studying fetuses at younger gestational age.[75] Recently, successful blood flow measurement by 3.0 T MRI has been reported,[76] and with further improvements in resolution and imaging technique, cardiovascular MRI will complement ultrasound in the assessment of the fetal cardiovascular system.

## *Cardiovascular interaction*

Due to the interplay of the heart and vessels, Doppler evaluation of the fetal arterial and venous system forms an integral part of cardiac assessment, and this is achieved by pulsed wave Doppler ultrasound.

### Umbilical artery

Under physiologic conditions, the impedance in the placental circulation is low, showing forward flow in the umbilical artery (UA) throughout the cardiac cycle[77] (Figure 48.7a). Doppler signals of the UA can be obtained from any segment of the cord; however, there is more end-diastolic flow when measured near the placental than at the abdominal cord insertion site.[78] The placental vascular system expands during pregnancy, and this is reflected in a continuous increase in end-diastolic flow with gestational age.[79,80] Abnormal placentation and placental arterial obliteration increase the vascular resistance and cause a reduction in end-diastolic flow. Absent or reversed end-diastolic flow (AREDF) is associated with IUGR and is an indicator of poor prognosis. However, AREDF may also result from reduced cardiac contractility as seen in some recipients with TTTS.[81,82]

### Ductus venosus

The flow in the DV is pulsatile and provides information on atrial pressure-volume changes throughout the cardiac cycle (Figure 48.7b).[83] During ventricular systole, the AV valve ring descends, allowing rapid filling of the atria. This is reflected by an increase in the DV velocity that peaks at the S-wave. Ventricular relaxation results in a decrease in DV velocity during late systole (v-wave). After the opening of the AV valves, passive ventricular filling occurs, causing a pressure drop in the atria and therefore an acceleration of blood flow in the DV (D-wave).[2,84,85] Finally, atrial contraction augments ventricular filling, and the pulse wave is propagated into the DV in a retrograde fashion (a-wave).[86] Increased end-diastolic pressure due to increased ventricular afterload, systolic or diastolic dysfunction, or volume overload may result in a

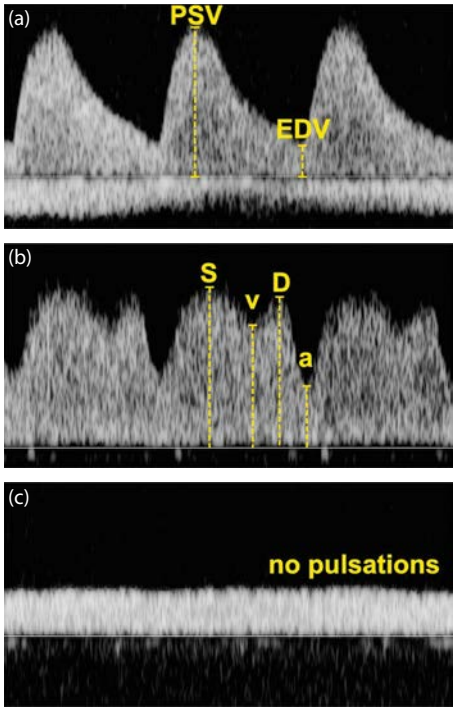


**Figure 48.7**
(a–c) Fetal Doppler. (a) Normal umbilical arterial Doppler waveform with forward flow throughout the cardiac cycle. (EDV, end-diastolic velocity; PSV, peak systolic velocity.) (b) Normal pulsatile flow in the ductus venosus: S reflects rapid atrial filling during early systole (descent of the atrioventricular valve ring); v reflects ventricular relaxation; the opening of the AV valves results in a pressure drop in the atria with an increase in DV velocity (D); and the pulse wave from atrial contraction is propagated into the DV ("a"). (c) Normal nonpulsatile flow in the umbilical vein.

reversal of flow during atrial contraction. Abnormal flow in the DV has been shown to predict fetal death.[87–89] Therefore, assessment of the pulsatile flow in the DV using the pulsatility index for veins (PIV) or qualitatively grading flow during atrial contraction (forward/absent/reverse) has become the standard of clinical practice to predict adverse perinatal outcome in growth restriction and now forms an integral part of the assessment of fetal well-being.[90,91] More recently, new parameters describing altered timing of events have been reported in TTTS. It has been shown that diastolic filling times are shortened in the recipients compared to their donor co-twins, and the extent of relative shortening correlates with disease severity.[92–94]

## Umbilical vein

Under physiologic conditions, pulsations in the umbilical vein (UV) disappear by the end of the first trimester (Figure 48.7c). Fetal hypoxemia as in severe growth restriction results in dilation of the ductus venosus to increase oxygenated blood to the fetal brain. This dilation permits conduction of atrial pressure waves back along its wall resulting in pulsations in the UV.[95] Right heart decompensation or hypervolemia in conditions such as TTTS results in increasing distension of the venous compartment. This reduces the vascular compliance and allows pulsations from atrial contractions to be transmitted into the UV.[83]

## Middle cerebral artery

Under physiologic conditions, the cerebral arteries have high impedance. In the presence of hypoxemia and acidosis, blood is redistributed due to cerebral vasodilation ("brain-sparing effect").[96] This increasing "demand" can lead to reversal of flow at the aortic isthmus and in the transverse arch. Furthermore, an increase in middle cerebral artery (MCA) peak systolic velocity >1.5 MoM is associated with fetal anemia.[97,98] Therefore, assessment of the MCA forms an integral part in the assessment of high-output cardiac conditions.

# Video

**Video 48.1** (https://youtu.be/d1Td9_8KqYE)
Speckle tracking methodology.

# References


1. Carvalho JS et al. *Ultrasound Obstet Gynecol* 2013;41(3):348–59.
2. Wohlmuth C et al. *Pediatr Cardiol* 2015;36(1):96–105.
3. Franzoso FD et al. *Congenit Heart Dis* 2016;11(5):426–36.
4. Mäkikallio K et al. *Heart* 2005;91(3):334–8.
5. Tulzer G et al. *Eur J Pediatr* 1994;153(3):151–4.
6. Reed KL et al. *J Am Coll Cardiol* 1986;8(2):391–5.
7. van Splunder P et al. *Circulation* 1996;94(6):1372–8.
8. Hall SA et al. *Circulation* 1997;95(3):636–42.
9. Kirkpatrick SE et al. *Am J Physiol* 1976;231(2):495–500.
10. Thornburg KL, Morton MJ. *Am J Physiol* 1986;251(5):H961–8.
11. Gilbert RD. *Am J Physiol* 1980;238(1):H80–6.
12. Mielke G, Benda N. *Circulation* 2001;103(12):1662–8.
13. Groenenberg IA et al. *Ultrasound Med Biol* 1991;17(6):583–7.
14. Tei C. *J Cardiol* 1995;26(2):135–6.
15. Maheshwari P et al. *Biomed Res Int* 2015:215910.
16. Hernandez-Andrade E et al. *Ultrasound Obstet Gynecol* 2005;26(3):227–32.
17. Meriki N, Welsh AW. *Fetal Diagn Ther* 2012;31(1):76–80.
18. Welsh AW et al. *Ultrasound Obstet Gynecol* 2016t;48(4):496–503.
19. Acharya G. *Ultrasound Obstet Gynecol* 2013;42(2):125–9.
20. Gardiner HM et al. *Int J Cardiol* 2006;113(1):39–47.
21. Germanakis I et al. *Fetal Diagn Ther* 2012;32(1–2):65–71.
22. Ho SY, Nihoyannopoulos P. *Heart* 2006;92(suppl 1):i2–13.
23. Cruz-Lemini M et al. *Ultrasound Obstet Gynecol* 2013;42(2):175–81.
24. Wohlmuth C et al. *Ultrasound Obstet Gynecol* 2016;47(5):608–15.
25. Isaaz K. *Curr Opin Cardiol* 2002;17(5):431–42.
26. Ho CY, Solomon SD. *Circulation* 2006;113(10):396–9.
27. Nagueh SF et al. *J Am Coll Cardiol* 2001;37(1):278–85.
28. Nagueh SF et al. *Circulation* 1999;99(2):254–61.
29. Ommen SR et al. *Circulation* 2000;102(15):1788–94.
30. Galiuto L et al. *Am J Cardiol* 1998;81(5):609–14.
31. Yamada H et al. *J Am Soc Echocardiogr* 1998;11(5):442–9.
32. Mogelvang R et al. *Circulation* 2009;119(20):2679–85.
33. Uemura K et al. *J Am Soc Echocardiogr* 2011;24(5):582–91.
34. Comas M et al. *Am J Obstet Gynecol* 2010;203(1):45.e1–e7.

35. Larsen LU et al. *Ultrasound Obstet Gynecol* 2009;34(1):62–7.
36. Wohlmuth C et al. *Ultrasound Obstet Gynecol* 2016;48(2):193–9.
37. Comas M et al. *Ultrasound Obstet Gynecol* 2011;37(1):57–64.
38. Watanabe S et al. *Circ J* 2009;73(5):943–7.
39. Sühling M et al. *Circulation* 2004;110(19):3093–9.
40. Bijnens B et al. *Fetal Diagn Ther* 2012;32(1–2):5–16.
41. Matsui H et al. *Ultrasound Obstet Gynecol* 2011;37(2):150–7.
42. Di Salvo G et al. *Eur J Echocardiogr* 2008;9(6):754–6.
43. Willruth AM et al. *Ultrasound Obstet Gynecol* 2011;37(2):143–9.
44. Kapusta L et al. *J Am Soc Echocardiogr* 2013;26(10):1193–200.
45. Perles Z et al. *Am J Cardiol* 2007;99(7):993–6.
46. Ta-Shma A et al. *J Am Soc Echocardiogr* 2008;21(2):146–50.
47. Younoszai AK et al. *J Am Soc Echocardiogr* 2008;21(5):470–4.
48. Peng QH et al. *Prenat Diagn* 2009;29(12):1149–55.
49. Kim SH et al. *Early Hum Dev* 2013;89(9):675–81.
50. Ishii T et al. *J Am Soc Echocardiogr* 2012;25(1):105–11.
51. Germanakis I et al. *Fetal Diagn Ther* 2012;32(1–2):123–30.
52. Taylor-Clarke MC et al. *Am J Obstet Gynecol* 2013;208(6):462.e1–e6.
53. Rychik J et al. *Fetal Diagn Ther* 2012;32(1–2):131–7.
54. Van Mieghem T et al. *J Am Soc Echocardiogr* 2010;23(3):301–8.
55. Wang H et al. *J Matern Fetal Neonatal Med* 2015;28(18):2150–4.
56. Fan X et al. *J Ultrasound Med* 2014;33(7):1171–7.
57. Xiong L et al. *Ultrasound Med Biol* 2010;36(12):2042–7.
58. DeVore GR et al. *Ultrasound Obstet Gynecol* 2003;22(4):380–7.
59. Uittenbogaard LB et al. *Ultrasound Obstet Gynecol* 2009;33(3):272–81.
60. Hamill N et al. *Am J Obstet Gynecol* 2011;205(1):76.e1–e10.
61. Messing B et al. *Ultrasound Obstet Gynecol* 2007;30(2):142–51.
62. Molina FS et al. *Ultrasound Obstet Gynecol* 2008;32(2):181–7.
63. Simioni C et al. *J Matern Fetal Neonatal Med* 2011;24(9):1159–67.
64. Uittenbogaard LB et al. *Ultrasound Obstet Gynecol* 2010;36(3):308–14.
65. Messing B et al. *Ultrasound Obstet Gynecol* 2011;38(2):191–7.
66. Dekoninck P et al. *Fetal Diagn Ther* 2012;32(1–2):72–8.
67. Godfrey ME et al. *Fetal Diagn Ther* 2012;32(1–2):17–21.
68. Messing B et al. *Ultrasound Obstet Gynecol* 2013;42(2):182–8.
69. Pugash D et al. *Eur J Radiol* 2008;68(2):214–26.
70. Manganaro L et al. *J Matern Fetal Neonatal Med* 2013;7058:1–7.
71. Wielandner A et al. *Semin Fetal Neonatal Med* 2013;18(5):286–97.
72. Feinberg DA et al. *Magn Reson Med* 2010;63(2):290–6.
73. Schoennagel BP et al. *MAGMA* 2014;27(3):237–44.
74. Roy CW et al. *Magn Reson Med* 2013;70(6):1598–607.
75. Prsa M et al. *Circ Cardiovasc Imaging* 2014;7(4):663–70.
76. Tsai-Goodman B et al. *J Cardiovasc Magn Reson* 2015;17:30.
77. Fleischer A et al. *Am J Obstet Gynecol* 1985;151(4):502–5.
78. Maulik D et al. *Obstet Gynecol Clin North Am* 1990;17(1):163–86.
79. Giles WB et al. *Br J Obstet Gynaecol* 1985;92(1):31–8.
80. Reuwer PJ et al. *Eur J Obstet Gynecol Reprod Biol* 1984;18(4):199–205.
81. Patel S et al. *J Ultrasound Med* 2015;34(5):843–6.
82. Wohlmuth C et al. *Acta Obstet Gynecol Scand* 2016;95(6):664–71.
83. Kiserud T. *Semin Perinatol* 2001;25(1):11–20.
84. Fujii K et al. *Clin Cardiol* 1994;17(5):258–62.
85. Rossi A et al. *Heart Fail Rev* 2000;5(4):325–31.
86. Schmidt KG et al. *Circulation* 1996;93(4):826–33.
87. Baschat AA et al. *Ultrasound Obstet Gynecol* 2000;16(5):407–13.
88. Baschat AA et al. *Ultrasound Obstet Gynecol* 2003;22(3):240–5.
89. Schwarze A et al. *Ultrasound Obstet Gynecol* 2005;25(6):573–9.
90. Lees C et al. on behalf of the TRUFFLE Group. *Ultrasound Obstet Gynecol* 2013;42(4):400–8.
91. Lees CC et al. for the TRUFFLE study group. Two- *Lancet* 2015;385(9983):2162–72.
92. Bensouda B et al. *Ultrasound Obstet Gynecol* 2007;30(7):983–7.
93. Tachibana D et al. *Ultrasound Obstet Gynecol* 2015;45(5):544–50.
94. Wohlmuth C et al. *Ultrasound Obstet Gynecol* 2016;48(6):744–51.
95. Hellevik LR et al. *Biomech Model Mechanobiol* 2009;8(6):509–17.
96. Kiserud T. *Semin Fetal Neonatal Med* 2005;10(6):493–503.
97. Vyas S et al. *Am J Obstet Gynecol* 1990;162(4):1066–8.
98. Mari G et al. *N Engl J Med* 2000;342(1):9–14.

# 49

# Genetics and cardiac anomalies

Hagit Shani, Pe'er Dar, and Mark I. Evans

## Introduction

As treatments for infectious diseases have dramatically improved over the past century, congenital anomalies have replaced infections as the leading cause of infant mortality in the United States.[1] Congenital heart defects (CHDs) are, in fact, the most common major structural birth defect, affecting 4–8 per 1,000 live births.[2–5] Despite often remarkable progress in clinical care for affected individuals, CHDs remain the leading cause of infant mortality among birth defects.

CHDs are a heterogenous group of anomalies that range from simple small ventricular septal defects to highly complex structural malformations. Accordingly, there is a wide range of developmental mechanisms that lead to these anomalies, such as defects in cell migrations, flow-dependent lesions, defects in the extracellular matrix, and defects in targeted growth. In most cases, however, the etiology remains largely unknown. CHDs have been associated with teratogenic factors (e.g., maternal diabetes mellitus, maternal alcohol abuse, or maternal rubella infection), as well as diverse genetic causes (chromosomal abnormalities or single gene disorders). Yet, the complexity of the clinical picture strongly argues against a simple dysregulation process and typically suggests a multifactorial polygenic origin with elaborate interactions.

Chromosomal and Mendelian malformation syndromes account for approximately 20% of CHDs. In most of these cases, the cardiac anomaly is not isolated but is accompanied by extracardiac anomalies.[6] These carry poorer prognoses with lower likelihood of *in utero* or postnatal survival. Despite strong evidence for familial aggregation, collectively, only 4.2% of heart defect patients had a positive family history in first-degree relatives. Additionally, most CHDs do not follow the traditional Mendelian mode of inheritance. A large Danish cohort study[7] of over 1.7 million people estimated the recurrence risk ratios of CHD among first-degree relatives to be 79.1 for heterotaxia, 11.7 for conotruncal defects, 24.3 for atrioventricular septal defects (AVSDs), 12.9 left ventricular outflow tract obstructions, 48.6 right ventricular outflow tract obstructions, 7.1 isolated atrial septal defects (ASDs), and 3.4 for isolated ventricular septal defects (VSDs).

## Chromosomal abnormalities and congenital heart defects

Van Karnebeek et al.[5] reviewed autosomal anomalies associated with one or more CHDs based on their search in the Human Cytogenetics DataBase: VSD, ASD, tetralogy of Fallot (TOF), pulmonic stenosis (PS), and AVSD were all associated with multiple chromosome loci, suggesting heterogeneity of these types of CHD. Other heart defects were not frequently reported in association with chromosome anomalies. Such include total anomalous pulmonary venous return (TAPVR), cardiomyopathy, cardiac situs inversus (dextrocardia), vascular rings, cardiac tumors, tricuspid stenosis (TS), single ventricle, tricuspid insufficiency (TR), pulmonic insufficiency (PR), and aortic insufficiency (AR).

Moore et al.[8] studied 1,510 cases of CHD who underwent prenatal chromosomal analysis. Forty percent had abnormal cytogenetic results, mostly autosomal trisomies with trisomy 18 (40.9%), trisomy 21 (31.0%), and trisomy 13 (17.1%) being the most prevalent. 45,X was found in 4.4%; 4.8% had triploidy. Structural chromosome abnormalities (balanced inversions or translocations) constituted about 10% of abnormal findings. The del22q11.2 on fluorescent *in situ* hybridization (FISH), was seen in 3% of tested cases.

In live-born, the most common chromosomal aneuploidy (1:691 live births) is trisomy 21, Down syndrome (DS).[1] DS is characterized by well-defined and distinctive phenotypic features including oblique eye fissure, epicanthus, flat nasal bridge, protruding tongue, short, broad hands, clinodactyly of the fifth finger, gap between first and second toes, hypotonia, short stature, and Brushfield spots. More importantly, all patients with DS are moderately to severely intellectually disabled. Many will suffer from hematological malignancies, autoimmune disease, and cardiac malformations.

DS most commonly originates from errors in meiosis I of maternal origin, representing up to 73% of all instances of nondisjunctional trisomy 21; maternal meiosis II errors constitute up to 20% of all cases of nondisjunctional trisomies 21.[9] Both maternal meiosis I and II errors are associated with increased maternal age,[10] probably emanating from reduced recombination rate in meiosis.[11] Trisomy 21 cardiac anomalies are characteristically of a common

AVSD, in which there are both atrial and ventricular septal defects combined with linear insertion (nondifferential insertion) of the A-V valves. Korenberg et al.[12] defined a critical region for AVSD on chromosome 21. Other variants in genes that have been suggested to cause CHD in DS are *COL6A1, COL6A2,* and *CRELD1*.[13,14]

Edwards syndrome, trisomy 18, has an incidence of 1:3,762 live births.[1] Eighty percent of the patients have nondisjunctional trisomy, 10% a mosaic trisomy, and another 10% an unbalanced translocation. Seventy-five percent are females. Typical anomalies include profound neurodevelopmental disabilities, pre- and postnatal growth restriction, dolichocephaly with prominent occiput and small face, dysplastic ears, microcephaly, micro-retrognathia, a prominent calcaneus (rocker bottom feet), and short sternum. Overlapping of the third and fourth fingers by the second and fifth fingers is characteristic. Horseshoe kidney, muscle hypertonia, and joint contractures are common. Only 50% of trisomy 18 babies live longer than 1 week, and only 5%–10% of children survive beyond the first year.[15] CHD is found in almost all patients with trisomy 18, most commonly ASD, VSD, patent ductus arteriosus (PDA), and polyvalvular disease.[16–18] Complex malformations (double-outlet right ventricle [DORV], AVSD, or left-sided obstructive lesion) are present in about 10% of cases.[16]

Patau syndrome, trisomy 13, occurs in 1:7,906 live births.[1] The common features of trisomy 13 include the clinical triad of microphthalmia, cleft lip/palate, and polydactyly. Unbalanced translocation is the cause in 20%. Eighty percent have associated noncyanotic heart defects, mainly ASD, VSD, and PDA. Less frequently, there are complex cardiac defects such as TOF and transposition of the great arteries (TGA). Additional findings include the classic rocker bottom feet and clenched hands, prenatal growth restriction, hypotelorism and ocular defects, and the common central defects: holoprosencephaly, omphalocele, and single umbilical artery.[19,20]

Turner syndrome (TS, monosomy X) occurs in 1:2,000 live births.[21] Maternal nondisjunction accounts for only 20%–30% of TS. There is a relatively variable phenotype, including short stature, ovarian dysgenesis, and infertility. Physical traits include webbed neck, low-set or malrotated ears, ptosis, broad (shield) chest with widely spaced nipples, and skeletal, endocrine, ocular, and renal abnormalities. Average intellectual performance is in the normal range.[22] The most serious clinical aspect of TS is congenital heart disease, particularly aortic valve disease, coarctation of the aorta, and partial APVR.[23] Aortic dilatation and aneurism are less common.[22] Eckhauser et al.[24] reported 167 girls with coarctation of the aorta; 86 patients (51%) had chromosomal studies, and of them 21 (12.6%) were diagnosed with TS. Contrary to TS, the other sex chromosome aneuploidies—Kleinfelter XXY syndrome, XYY, XXX, and XXXX syndromes—are not associated with CHD. However, CHD is frequently seen in higher-order X and Y chromosomal aneuploidies (XXXY, XXXXY, and XXXXX).[25]

## Single gene mutations and CHD

The heart is the first functional organ during embryogenesis. Thousands of genes are expressed in the developmental process.[26] Formation of the heart requires the complex interaction of multiple cells, signaling molecules, transcriptional regulation, and structural proteins to ensure the correct cell migration, differentiation, and function. The process is therefore a complex interplay between genetic variants, epigenetic modifications, and maternal exposure to environmental factors.[27]

Isolating the causal genes for CHD provides opportunities to elucidate disease pathogenesis. Olson et al.[28] reviewed the molecular pathways for genes controlling cardiac embryogenesis. Gene ablation studies performed in experimental animal models shed light on cardiac development and the pathophysiology of cardiac malformation. A different approach includes the investigation of patients with CHD by performing a genome-wide association study through whole genome sequencing (WGS) or through sequencing of the translated code with whole exome sequencing (WES). The pioneering work of Basson et al.[29] and Schott et al.[30] in the late 1990s led to the identification of loss-of-function mutations in *TBX5* and *NKX2-5* genes as causes of Holt-Oram syndrome and ASD, respectively.[31] Hundreds of candidate genes are now being investigated in CHD.

Zaidi et al.[26] analyzed 362 WES of trios (affected proband and both parents) with severe CHD (conotruncal defects, left ventricular obstruction, and heterotaxy). Investigating in 4,169 high heart expression genes, they identified protein-altering mutations in 10% of the cases.

Many mutations found in genes associated with cardiac embryogenesis are unique to a single patient with CHD. However, several are associated with distinct syndromes (Table 49.1). Three of the more common single gene, autosomal dominant disorders associated with CHD are as follows.

*Noonan syndrome* (NS), a RASopathy caused by autosomal dominant mutations in the genes that regulate the RAS-MAPK pathway.[32] The prevalence of NS is estimated to be 1 in 1,000 to 1 in 2,500, but mild cases may be even more common.[33] NS is characterized by learning disability, a typical chest deformity (pectus carinatum and/or excavatum), short stature, and cryptorchidism.[34] Bleeding disorders are common, including thrombocytopenia, platelets disfunction, coagulation factor deficiencies, and Von Willebrand disease.[35] The typical NS CHD consists of PS (50%–60%), ASD (6%–10%), and hypertrophic cardiomyopathy (20%). VSD, peripheral PS, AVSD, AS, mitral valve abnormalities, aortic coarctation, and coronary artery anomalies have also been noted.[36] More than 10 genes in the RAS-MAPK signaling pathway cause Noonan syndrome or closely related conditions. Mutations in the *PTPN11* account for 50% of NS cases, and a genotype phenotype correlation is well described.[36] Prenatal genetic testing is available with sequencing of NS-related genes.

*Alagille syndrome* (ALGS) results from pathogenic mutations in the *JAG1* and *NOTCH2* genes. ALGS is characterized

**Table 49.1** Common syndrome associated with congenital cardiac defects and the chromosomal anomalies/genes involved

| *Syndrome* | *Chromosome* | *Genes* | *Cardiac anomaly* | *Percentage (%) cardiac involvement* |
|---|---|---|---|---|
| **Chromosomal anomalies** | | | | |
| Down syndrome | Trisomy 21 | | AV canal, ASD, VSD | 50% |
| Edward syndrome | Trisomy 18 | | ASD, VSD, PDA, polyvalvular dis. DORV, A-V canal | 90% |
| Patau syndrome | Trisomy 13 | | ASD, VSD, PDA, TGA, TOF | 80% |
| Turner syndrome | Monosomy X | | AV defects, CA, PAPVR, aortic aneurism/dilatation | 50% |
| **Deletion duplication syndromes** | | | | |
| DiGeorge syndrome | 22q11.2 | TBX1, CRKL, and ERK2 | Conotruncal defects; TOF, TA, TGA, IAA | 80% |
| Williams syndrome | 7q11.23 | ELN | SVAS, hypoplasia of the AA, PAS | 70% |
| Cri du chat | 5p15.2 del | | VSD, ASD, PDA | <10% |
| Cat eye syndrome | 22pter->q11 or 22q11 duplication | | TAPVR, LSVC, TOF, VSD | >33% |
| 1p36 deletion syndrome | 1p36 | | ASD, VSD, PDA, bicuspid AV, Ebstein anomaly, cardiomyopathy | 70% |
| 4q deletion | | | VSD, PDA, PAS, TS, ASD, CoA, TOF | |
| 9p deletion | | | VSD, PDA, PS | 30%–50% |
| 11q deletion | 11q24.1 | | VSD, left obstruction defects, TOF | 60% |
| Supernumerary der(22) t(11;22) syndrome | Duplication of 22q10-22q11 and duplication of 11q23-qter on the supernumerary der(22) | | ASD, VSD, TOF, TA, TS, CoA, aberrant subclavian, PLSVC, PDA | 60% |
| **Single gene mutation** | | | | |
| Holt-Oram syndrome | 12q24.21 | *TBX5* | VSD and ostium secundum ASD, conduction defects | 75% |
| Noonan syndrome | 12q24.13, 2p22.1 (for PTPN11 and SOS1) | PTPN11, SOS1, KRAS, NRAS, RAF1, BRAF, SHOC2, *CBL, MAP2K1, RIT1* | PS, ASD, HCM, VSD, peripheral PAS, A-V canal, AS, CoA, MV anomaly, coronary artery anomaly | 50%–80% |
| Alagille | 20P12.2, 1P12 | JAG1, *NOTCH2* | Peripheral PS, PA + MAPCA, ASD, TOF | |
| Ellis-van Creveld | 4p16.2 | EVC, EVC2 | ASD common atrium | 60% |
| Cornelia de Lange | 5p13.2, 8q24.11, 10q25.2, Xp11.22, Xq13.1 | NIPBL, RAD21, SMC3, SMC1A, HDAC8 | Isolated PS, ASD, VSD, supravalvular AS, PDA | 20% |
| Smith-Lemli-Opitz | 11q12-13 | DHCR7 | Endocardial cushion defects HLHS, ASD, VSD, PDA | 50% |
| Marfan | 15q15-21.3 | FBN1 | Dilatation of the ascending aorta | 100% |

*(Continued)*

**Table 49.1 (Continued)** Common syndrome associated with congenital cardiac defects and the chromosomal anomalies/genes involved

| *Syndrome* | *Chromosome* | *Genes* | *Cardiac anomaly* | *Percentage (%) cardiac involvement* |
|---|---|---|---|---|
| CHARGE syndrome | 8q12 | CHD7 | TOF, PDA, DORV, AV canal, ASD, VSD, right side AA | 75%–85% |
| Jacobsen syndrome | 11q24.2-q25 | ETS1 | HLHS, CoA, mitral and aortic valve atresia | 70% |
| Kabuki | 12q13.12, X-linked | KMT2D, KDM6A | CoA, bicuspid AV, MVP, VSD, PS, MS, AS, TOF, single ventricle, DORV, TGA | 50% |
| Costello | 11P15.5 | HRAS | PS, ASD, VSD, HCM | 52% |
| Carpenter syndrome | 6p11.2 | RAB23 | ASD, VSD, PS, TOF, TGA, PDA | 50% |
| Loeys-Dietz syndrome 1 and 2 | 9q22.33, 3p24.1 | TGFBR1, TGFBR2 | Aortic root dilatation and aneurism | |
| Rubinstein-Taybi syndrome | 16P13.3 | CREBBP, EP300 | PDA, ASD, VSD, CoA, PS, BCAV | 30% |

*Abbreviations:* A, artery; AA, aortic arch; AS, aortic stenosis; ASD, atrioseptal defect; AS, aortic stenosis; AV, aortic valve; AV canal, atrioventricular canal; BCAV, bicuspid aortic valve; CoA, coarctation of the aorta; DORV, double-outlet right ventricle; HCM, hypertrophic cardiomyopathy; HLHS, hypoplastic left heart syndrome; IAA B, interrupted aortic arch type B; PA/MAPCA, pulmonic atresia with major aortopulmonary collateral arteries; MV, mitral valve; MVP, mitral valve prolapse; PA, pulmonic atresia; PAPVR, partial anomalous pulmonary venous return; PAS, pulmonary artery stenosis; PDA, patent ductus arteriosus; PLSVC, persistent left superior vena cava; PS, pulmonic stenosis; SVAS, supravalvular aortic stenosis; TA, tricuspid atresia; TS, tricuspid stenosis; TOF, tetralogy of Fallot; TAPVR, total anomalous pulmonary venous return; TGA, transposition of the great arteries; TS, tricuspid atresia/stenosis; TA, truncus arteriosus; VSD, ventrical-septal defect.

by cholestasis with bile duct paucity on liver biopsy; congenital cardiac defects, deep-set eyes; typical facial features; and butterfly vertebrae.[37] Cardiac abnormalities include peripheral PS, pulmonary atresia, ASD, VSD, and TOF.[38] Approximately 95% of patients with ALGS have mutations in *JAG1*, which encode the NOTCH signaling pathway ligand Jagged-1.[39] The remaining patients with ALGS were found to have *NOTCH2* mutations.[40]

Holt-Oram syndrome (HOS) is associated with upper-limb malformations (unilateral, bilateral/symmetric, or asymmetric). Abnormal carpal bone, present in all affected individuals and identified by performing a posterior-anterior hand x-ray,[29] may be the only evidence of disease. CHDs, most commonly ostium secundum ASD and VSD, are present in 75% of affected individuals. Cardiac conduction disease may also be present. Approximately 85% of affected individuals have HOS from a *de novo* pathogenic variant. In the remaining 15% with inherited syndrome, family history of a first-degree relative with a CHD, or cardiac conduction disease may be present.[41]

## Copy number variant changes and CHD

Approximately two-thirds of the entire human genome is composed of DNA repeats, and 5%–10% is classified as copy number variant (CNV). CNV is a phenomenon in which the number of the repeats in the genome varies between individuals and represents one of the main examples of genomic diversion among people. CNVs are the basis of recurrent genomic rearrangements such as deletions, duplications, insertions, inversions, and translocations. The addition of the aCGH technique at the end of the last century allowed the identification of submicroscopic gains (microduplications) or losses (microdeletions) of benign or pathogenic CNVs.

The association of microdeletion and microduplication syndromes with CHD is well-known. The most commonly identified microdeletion syndrome that is associated with major CHD is the 22q11.2 microdeletion syndrome, also known as the DiGeorge syndrome, velo-cardio-facial syndrome, and the Shprintzen syndrome. The 22q11.2 deletion syndrome occurs in 1:2,000 live births[42] and presents with a significant clinical variability. Heart defects are present in over 40%.[43] Additional manifestations include palatal abnormalities (69%), learning difficulties (70%–90%), immune deficiency (77%), hypocalcemia (50%), feeding and swallowing problems (30%), renal anomalies (37%), hearing loss (both conductive and sensorineural), laryngotracheoesophageal anomalies, growth hormone deficiency, autoimmune disorders, seizures (idiopathic or associated with hypocalcemia), central nervous system anomalies, skeletal abnormalities (scoliosis, clubbed feet, polydactyly, and craniosynostosis), ophthalmologic abnormalities (strabismus,

posterior embryotoxon, tortuous retinal vessels, and anophthalmia), enamel hypoplasia, and, rarely, malignancies.[44] Twenty percent develop schizophrenia.

The most common CHD in patients with the 22q11.2 deletion syndrome are the conotruncal anomalies. TOF is seen in 13%–39% of patients; TOF with pulmonary atresia in 2%–10%; TOF, PA, and major aortopulmonary collaterals (MAPCAs) in 25%; truncus arteriosus in 2%–10%; and interrupted aortic arch in 4%–16%.[45–49] Momma concluded that cardiovascular anomalies are present in 80% of neonates with Del22q11.2.[50]

The 22q11.2 segment encompasses four low copy repeat (LCR) regions named LCR22A-D. Eighty-five percent have the common 3Mb deletion that includes all four LCRs, while 15% are diagnosed with atypical or nested deletion (including only one to three of the LCR's regions). The 22q11.2 deletion results in haploinsufficiency of 90 known or predicted genes within the typical 3.0 Mb deletion, including 46 protein-coding genes. Deletion of the TBX1 gene is thought to be responsible for many of the classically associated features. The common 3Mb deletion can be detected by any molecular method that determines the copy number of genomic sequences within the deleted region. The two most utilized methods are FISH and aCGH.[44]

Some laboratories now offer noninvasive screening for Del22q11.2 by analyzing cell free fetal DNA (cffDNA) in maternal blood. Lack of data makes it difficult to determine the cffDNA sensitivity, specificity, and positive and negative predictive values. Lo et al.[51] demonstrated that cffDNA screening by using deep sequencing detected 5/6 cases. Wapner et al.[52] reported a 97.8% detection rate using a SNP-based approach in a study involving a combination of clinical plasma samples and artificial plasma mixtures. The positive predictive value, however, was low (5.3%). These are much lower statistical performance metrics than for disorders such as Down syndrome with positive predictive value reaching 80%–90%.[53,54]

Another common microdeletion syndrome is Williams syndrome (WS), in which 1.5–1.8 million base pairs are deleted in chromosome 7q11.23. WS is found in 1:10,000 live births and is characterized by a distinct "elf-like" facial appearance, developmental delay, friendly personality, and growth and endocrine abnormalities including hypercalcemia.[55] Cardiac and vascular anomalies result from deletion of the elastin gene (*ELN*) leading to supravalvular aortic stenosis (SVAS) in up to 70% of patients, but also hypoplasia of the aortic arch, and PS.[55,56]

Recent data suggest that there is a considerable contribution of the presumably nonpathogenic CNVs to CHD.[57] Children with CHD have a significantly increased burden of large CNVs (>400 kb) than children with autism spectrum disorder. Cooper et al. analyzed over 15,000 cases of developmental delay and over 8,000 controls.[58] In their cohort, uncommon CNVs >400 kb, usually present in less than 1% of the population, were present in 25% of cases with CHD. Soemedi et al.[59] addressed the disease risk associated with the global burden of smaller CNVs (>100 kb) in a population with sporadic nonsyndromic cases. These investigators showed that rare deletions account for 3%–4% of these cases, and that *de novo* CNVs occurred in 5% of the families. Jansen et al.[60] performed a meta-analysis of the use of aCGH in the investigation of CHD when karyotyping and Del22q11.2 FISH analysis were normal. aCGH yielded additional clinically valuable information in 7% of fetal CHD cases. These data were confirmed by others[57] and support the routine use of microarray analysis either prenatally or postnatally in cases of CDH.

## *Nonsyndromic CHD and causative single gene mutations*

All cardiac anomalies can be either nonsyndromic, that is, an isolated anomaly, or part of an association. Examples for nonsyndromic CHD include the isolated bicuspid aortic valve, which is present in 1%–2% of the population. This anomaly can increase the risk of aortic valve stenosis or insufficiency. Mutations in *SMAD6* and *NOTCH1* are associated with bicuspid aortic valve. *NOTCH1* is a signaling transcription factor, and mutations in this gene result in aortic valve anomalies and calcifications.[61] *SMAD6* mutations can lead to Aortic Valve Disease 2 (AOVD2), coarctation of the aorta, and calcification of the aorta.[62]

Isolated ASD is a common CHD (10% of CHD). Mutations in *GATA4, TBX20 MYH5, ACTA1, TLL1, CITED2, GATA6,* and *HAND1* were all associated with the development of ASD as well as with other CHD.[63] Isolated hypoplastic left heart syndrome 1 (HLHS1), another example of nonsyndromic CHD, can result from mutations in the *GJA1* gene, and in *HAND1*, whereas HLHS2 can result from mutations in the *NKX2-5* gene.

# Teratogens and CHD

*Diabetes mellitus*: The association of CHD and maternal diabetes has been recognized for decades and complicates 2.5%–6% of pregnancies of mothers with diabetes mellitus (DM).[64] Congenital malformations associated with diabetic embryopathy are mainly cardiovascular and central nervous system defects (neural tube defects and caudal dysgenesis). Caudal regression syndrome with femoral shortening and sacral agenesis is almost never seen without diabetes. The most common CHDs that are found in diabetic embryopathy include abnormalities of laterality, looping, and conotruncal septation, and they suggest that the maternal metabolic state affects cardiogenesis at a very early stage of the developmental period, prior to 7 weeks of gestation.[64–67] Gabbay-Benziv et al. in their review of pregestational diabetes and birth defects concluded that adequate glycemic control is associated with a reduced risk of congenital anomalies. However, the threshold of HgA1C for pregestational diabetic women is still not known.[66]

*Ethanol*: The teratogenicity of ethanol has been appreciated for centuries. Ethanol affects the central nervous system and

growth, and causes facial and cardiac abnormalities.[68] Fetal alcohol syndrome and the less severe fetal alcohol effects are well-known examples of teratogenicity.[69] Cardiac malformations can be a part of the spectrum. Grewal et al.[70] showed that women who consumed alcohol more often than once a week during the first month of their pregnancy had a 1.5-fold increased risk, relative to nondrinkers, of delivering infants with conotruncal heart defects. A twofold increased risk was observed for d-TGA. An animal model study on quail embryos[71] demonstrated that ethanol-exposed embryos developed smaller AV valves, thin interventricular septae, and thinning of the ventricular wall, as well as anomalies of the aortic valve. Ethanol-exposed embryos also demonstrated abnormal blood flow, a change that might affect cardiac cushion and valve formation.[71]

*Cigarette smoking*: Maternal smoking was previously suggested as a risk factor for CHD in the offspring.[72] Li et al.[73] demonstrated the association between maternal smoke exposure and the occurrence of fetal CHDs. The risk was increased with polymorphisms, benign variations in single nucleotides, in the glutathione S-transferases genes. The products of these genes are responsible for activating and detoxifying xenobiotics, which emphasizes the relationship between environmental factors and genetics in the development of CHDs.

*Valproic acid*: This has been associated with several congenital anomalies including neural tube defects, CHD, and craniofacial (cleft lip), genitourinary, and skeletal defects. The risks are two- to sevenfold higher than other common antiepileptic drugs. Specifically, the risk ratio for CHD was 2.[74] In a review of 70 patients with valproic acid embryopathy, 26% of patients had CHD. These included VSD, AS, PS, and PDA.[75]

*Retinoic acid*: This is the main active metabolic derivative of vitamin A. Proper retinoic acid signaling is required for multiple aspects of vertebrate heart development, in particular, the establishment of the cardiac progenitor fields.[76] Retinoids exert cardiac myocytes differentiation, proliferation, and gene expression through specific receptors.[77] While appropriate levels of retinoic acid are critical for normal heart development in vertebrates, exposure to elevated levels of retinoic acid during embryogenesis can lead to CHD. Animal models demonstrated the development of the following CHD in mice exposed to retinoic acid: TGA (78%), DORV (11%–16%), aortic arch anomalies (24%), and less frequently, TA, TOF, isolated VSD, aortic atresia, mitral atresia, and rudimentary LV.[78]

*HIV therapy*: Highly active antiretroviral therapy (HAART), which usually comprises three drugs, has dramatically reduced the mother-to-child transmission rates of HIV to around 1%–2%, thus changing HIV from a lethal, short-term medical problem into a long-standing chronic illness.[79] Nucleoside and protease inhibitor antiretroviral (ARV) therapy for the treatment of HIV in the first trimester was associated with 2.5% CHD. No specific type of CHD was noted.[80] Since more than 1.2 million people in the United States have HIV,[81] screening for fetal cardiac defects in pregnant women who are treated with antiretroviral medication is critical.

## Genetic approach to a fetus with CHD

Nearly 1% of newborns are diagnosed with a CHD, and approximately one-quarter of those defects are considered critical and require intervention in the first year of life.[82] Therefore, prenatal caregivers should bear in mind the high prevalence of CHD and its association with extracardiac anomalies, syndromes, and chromosomal abnormalities, including CNVs. A thorough medical history may help to identify patients who are at increased risk for fetuses with CHD because of maternal disease, exposure to known cardiac teratogens, infections, and familial history suggestive of a genetic predisposition. The latter includes any familial history of cardiac anomaly in a first- or second-degree relative.

All patients diagnosed with CHD should be referred for genetic counseling, including a three-generation pedigree. Emphasis should be given to family members diagnosed with any CHD (not necessarily the same defect as the patient) as well as to family members with any diagnosis of a syndrome that could be associated with CHD. The discussion should emphasize the multifactorial nature of most CHDs, the fact that CHD can be seen as an isolated anomaly or with association of extracardiac anomalies, or as part of a syndrome, and the different prognoses. For example, Gomez et al. published data on 10,800 women referred for fetal echocardiography, with 995 confirmed cases of CHD, of whom 248 had isolated VSD. There was only one case of a chromosomal anomaly in a patient with perimembranous VSD.[83] Prenatal WES in fetuses with CHD was recently studied.[84] WES was performed in 63 cases on DNA from CVS or amniotic fluid from fetuses with a CHD diagnosed on prenatal ultrasound and who had normal karyotype and aCGH results. The preliminary analysis, limited to genes known to cause CHD, identified mutations in three (5.4%) cases. While the authors concluded that in cases of fetal CHDs with a normal microarray, prenatal WES provides additional clinically relevant genetic information, the American College of Obstetrics and Gynecology and the Society of Fetal Maternal Medicine[85] stated that the routine use of WES for prenatal diagnosis is not recommended.

As previously stated, we believe that amniocentesis or CVS for aCGH should be offered routinely to all patients with a cardiac anomaly. It is our practice to also offer FISH for chromosomes 21, 18, 13 X, and Y in all cases diagnosed with any fetal anomaly. In our view, the availability of the result within 24–48 hours in the setting of known fetal anomaly is sufficient for patients to start making their plans for this pregnancy. For patients who continue the pregnancy in the setting of abnormal karyotype, prenatal diagnosis allows a more informed decision on labor management and on immediate postnatal intervention.

## Cell free fetal DNA and CHD

Cell free fetal DNA (cffDNA), also known as noninvasive prenatal screening (NIPS), is based on the detection of

DNA segments that originate in the syncytiotrophoblast in maternal peripheral circulation.[86] While in most cases the placenta and the fetus share the same genetics, about 1% of placentae have confined placental mosaicism (CPM), or two or more cell lines, one normal and one or more abnormal.[87] Screening for fetal chromosomal abnormalities (currently available for chromosomes 21, 18, 13 X, and Y) is commercially available either through massive or targeted parallel sequencing to identify increase in one of the targeted chromosome (without differentiating fetal and maternal cell free DNA) or through a single nucleotide polymorphism (SNP) that relies on the identification of maternal and fetal allele distributions.

Since it became commercially available in late 2011, the use of cffDNA as a screening test has shown dramatically increased use, and there has been a concomitant decrease in diagnostic procedures performed. We are concerned that the use of NIPS will significantly lower the detection of serious chromosomal anomalies, particularly for younger women. In this age group, the DS incidence is 10× lower than the rate of submicroscopic chromosomal anomalies that could be detected with aCGH on CVS or amniocentesis.[88]

Several commercial companies now offer screening for a limited number of microdeletions and microduplication syndromes through cffDNA. The number and type of syndromes included in the test, and the performance characteristics for the detection of those syndromes differ. Some of the microdeletion syndromes currently available for testing with NIPS are the common deletion syndromes: 22q11.2 (DiGeorge), 1p36, distal 5p (cri du chat), and Prader-Willi/Angelman. NIPS sensitivity is a function of the fetal fraction, read depth, and size of the fetal CNV.[51]

Patients with incidental positive cffDNA results for Del22q11.2 who decline amniocentesis should have a thorough ultrasonographic evaluation of the fetal heart (fetal echocardiogram), lips, and palate for the detection of cleft lip/palate, thymus for thymic hypoplasia,[89] and longitudinal assessment of fetal growth. When a cardiac anomaly is diagnosed prenatally, Benachi et al.[90] and Evans et al.[88] have suggested that noninvasive testing should not be offered. We completely agree, as there are only two possibilities in this circumstance. Either the NIPS is abnormal, in which case a diagnostic test is required to confirm, or it is normal in which case a diagnostic procedure is still required to find out what, if anything, is really going on. Thus, all that is accomplished without wasting 1–2 weeks and needlessly spending close to $1,000.

Finally, a concern exists in the fact that the cffDNA represents placental genetic milieu and not fetal status. The presence of confined placental mosaicism (CPM) accounts for at least 3.6% of high-risk calls in the study by Dar et al.[91] If the ultrasound findings are not consistent with the CVS results, a follow-up test by amniocentesis should be the standard practice to elucidate the proper diagnosis and prevent termination of a normal pregnancy.

## Genetic therapy for prenatally diagnosed CHD

Deciphering the genetic causes of CHD creates the potential for future targeted alteration of DNA sequence *in vivo* to correct the inherited mutation. In the last decade, the alteration of specific DNA sequences has been and continues to be extensively investigated.[92–94] Urnov et al.[95] first introduced the use of zinc finger proteins engineered for the recognition of a unique chromosomal site, and creation of specific sequence alterations. This system, designed against an X-linked severe combined immune deficiency (SCID) mutation in the IL2Rγ gene, yielded more than 18% gene-modified human cells.[95] A new, exciting method of genome editing is derived from an adaptive immune system known as CRISPR (Clustered Regulatory Interspaced Short Palindromic Repeats) that bacteria and archaea use as a means to protect themselves against foreign invasive elements.[96] CRISPR relies on an enzyme called Cas9 that uses a guide RNA molecule to hone in on its target DNA, and then edits the DNA to disrupt genes or insert desired sequences.[97] Other systems were developed for gene editing, including different nuclease-based,[98–100] adenovirus based,[101] and recently protein RNA-based systems.[102,103]

Although approved for human trial in several countries, including the United Kingdom, ethical and technical issues still significantly limit the clinical use of CRISPR for manipulation of the genetic code. In the future, gene therapy for human disease and for CHD may be possible through preimplantation genetic diagnosis, before the fetal heart is being formed or for the remodeling and self-correction of the fetal heart once it is being malformed early in pregnancy.

## More information

More complete discussion of some topics is well beyond the scope or space limitations of this chapter. For ongoing updates, the reader is referred to the Online Mendelian Inheritance in Man (http://www.ncbi.nlm.nih.gov/omim/). For updates on the diagnostic clinical mutations and deletion/duplication studies available, the reader is referred to Gene Test Registry (http://www.ncbi.nlm.nih.gov/gtr/).

## References


1. National Vital Statistics Reports, Birth Defects [Internet]. [cited 02/29/2016]. Available from: http://www.cdc.gov/ncbddd/birthdefects/data.html.
2. Wren C et al. *Heart* 2000;83(4):414–9.
3. Ferencz C, Boughman JA. *Cardiol Clin* 1993;11(4):557–67.
4. Hoffman JI, Kaplan S. *J Am Coll Cardiol* 2002;39(12):1890–900.
5. van Karnebeek CD, Hennekam RC. *Am J Med Genet* 1999;84(2):158–66.
6. Burn J et al. *Lancet* 1998;351(9099):311–6.
7. Oyen N et al. *Circulation* 2009;120(4):295–301.

8. Moore JW et al. *Am J Obstet Gynecol* 2004;191(6):2068–73.
9. Antonarakis SE. *Trends Genet* 1993;9(4):142–8.
10. Antonarakis SE et al. *Am J Hum Genet* 1992;50(3):544–50.
11. Warren AC et al. *Science* 1987;237(4815):652–4.
12. Korenberg JR et al. *Am J Hum Genet* 1990;47(2):236–46.
13. Ackerman C et al. *Am J Hum Genet* 2012;91(4):646–59.
14. Maslen CL et al. *Am J Med Genet Part A* 2006;140(22):2501–5.
15. Cereda A, Carey JC. *Orphanet J Rare Dis* 2012;7:81.
16. Carey JC. Trisomy 18 and Trisomy 13 syndromes. In: *Management of Genetic Syndromes*. 3rd ed. Cassidy SB, Allanson JE., eds. New York, NY: Wiley; 2010.
17. Musewe NN et al. *J Am Coll Cardiol* 1990;15(3):673–7.
18. Kaneko Y et al. *Am J Med Genet Part A* 2008;146A(11):1372–80.
19. Baty BJ et al. *Am J Med Genet* 1994;49(2):175–88.
20. Baty BJ et al. *Am J Med Genet* 1994;49(2):189–94.
21. Castelo-Branco C. *Maturitas* 2014;79(4):471–5.
22. Gravholt CH. *Nat Clin Pract Endocrinol Metab* 2005;1(1):41–52.
23. Bondy CA. *Congenit Heart Dis* 2008;3(1):2–15.
24. Eckhauser A et al. *J Pediatr* 2015;167(5):1062–6.
25. Jones KL et al. *Smith's Recognizable Patterns of Human Malformation*. 7th ed. Philadelphia PA: Elsevier; 2013.
26. Zaidi S et al. *Nature* 2013;498(7453):220–3.
27. Li M et al. *Ann Hum Genet* 2016;80(1):20–31.
28. Olson EN, Srivastava D. *Science* 1996;272(5262):671–6.
29. Basson CT et al. *Nat Genet* 1997;15(1):30–5.
30. Schott JJ et al. *Science* 1998;281(5373):108–11.
31. Marian AJ. *Circ Res* 2014;115(10):821–3.
32. Yaoita M et al. *Hum Genet* 2016;135(2):209–22.
33. Mendez HM, Opitz JM. *Am J Med Genet* 1985;21(3):493–506.
34. Turner AM. *J Paediatr Child Health* 2014;50(10):E14–20.
35. Briggs BJ, Dickerman JD. *Pediatr Blood Cancer* 2012;58(2):167–72.
36. Roberts AE et al. *Lancet* 2013;381(9863):333–42.
37. Spinner NB et al. Alagille syndrome. In: *GeneReviews*; 2009. Seattle, WA: University of Washington. Available from: http://www.ncbi.nlm.nih.gov/books/NBK1273/.
38. Vajro P et al. *Clin Res Hepatol Gastroenterol* 2012;36(3):275–7.
39. Li L et al. *Nat Genet* 1997;16(3):243–51.
40. McDaniell R et al. *Am J Hum Genet* 2006;79(1):169–73.
41. McDermott DA et al. Holt-Oram syndrome. In: *GeneReviews*; 2004 [updated October 8, 2015]. Seattle, WA: University of Washington. Available from: http://www.ncbi.nlm.nih.gov/books/NBK1111/.
42. Botto LD et al. *Pediatrics* 2003;112(1 Pt 1):101–7.
43. Goldmuntz E et al. *J Am Coll Cardiol* 1998;32(2):492–8.
44. McDonald-McGinn DM et al. 22q11.2 deletion syndrome. In: *GeneReviews*; 1999. Seattle, WA: University of Washington. Available from: http://www.ncbi.nlm.nih.gov/books/NBK1523/.
45. Ryan AK et al. *J Med Genet* 1997;34(10):798–804.
46. Park IS et al. *Int J Cardiol* 2007;114(2):230–5.
47. McDonald-McGinn DM et al. *Genet Couns* 1999;10(1):11–24.
48. Oskarsdottir S et al. *Eur J Pediatr* 2005;164(3):146–53.
49. Matsuoka R et al. *Hum Genet* 1998;103(1):70–80.
50. Momma K. *Am J Cardiol* 2010;105(11):1617–24.
51. Lo KK et al. *Am J Hum Genet* 2016;98(1):34–44.
52. Wapner RJ et al. *Am J Obstet Gynecol* 2015;212(3):332e1–9.
53. Gil MM et al. *Fetal Diagn Ther* 2014;35(3):156–73.
54. Dugoff L et al. *Prenat Diagn* 2017;37(1):53–60.
55. Pober BR. *N Engl J Med* 2010;362(3):239–52.
56. Gray JC, 3rd et al. *J Cardiovasc Comput Tomogr* 2013;7(6):400–7.
57. Glessner JT et al. *Circ Res* 2014;115(10):884–96.
58. Cooper GM et al. *Nat Genet* 2011;43(9):838–46.
59. Soemedi R et al. *Am J Hum Genet* 2012;91(3):489–501.
60. Jansen FA et al. *Ultrasound Obstet Gynecol* 2015;45(1):27–35.
61. McBride KL et al. *Hum Mol Genet* 2008;17(18):2886–93.
62. Tan HL et al. *Hum Mutat* 2012;33(4):720–7.
63. Freeze SL et al. *J Genet Couns* 2016;25(6):1171–8.
64. Lisowski LA et al. *Herz* 2010;35(1):19–26.
65. Kitzmiller JL et al. *JAMA* 1991;265(6):731–6.
66. Ferencz C et al. *Teratology* 1990;41(3):319–26.
67. Gabbay-Benziv R et al. *World J Diabetes* 2015;6(3):481–8.
68. Clarren SK, Smith DW. *Lamp* 1978;35(10):4–7.
69. Hagan JF J et al. *Pediatrics* 2016;138(4):1–17.
70. Grewal J et al. *Birth Defects Res A Clin Mol Teratol* 2008;82(7):519–26.
71. Karunamuni G et al. *Am J Physiol Heart Circ Physiol* 2014;306(3):H414–21.
72. Hackshaw A et al. *Hum Reprod Update* 2011;17(5):589–604.
73. Li X et al. *Sci Rep* 2015;5:14915.
74. Tanoshima M et al. *Clin Pharmacol Ther* 2015;98(4):417–41.
75. Kozma C. *Am J Med Genet* 2001;98(2):168–75.
76. D'Aniello E, Waxman JS. *Dev Dyn* 2015;244(3):513–23.
77. Pan J, Baker KM. *Vitam Horm* 2007;75:257–83.
78. Yasui H et al. *Circulation* 1995;91(9):2478–86.
79. Siegfried N et al. *Cochrane Database Syst Rev* 2011;(7):CD003510. doi:10.1002/14651858.CD003510.pub3.
80. Watts DH et al. *J Perinat Med* 2011;39(2):163–70.
81. CDC. Available from: http://www.cdc.gov/nchhstp/newsroom/docs/factsheets/hiv-data-trends-fact-sheet-508.pdf.
82. Olney RS et al. *Semin Perinatol* 2015;39(3):230–7.
83. Gomez O et al. *Ultrasound Obstet Gynecol* 2014;43(1):65–71.
84. Al-Kouatly HB et al. *J Obstet Gynaecol* 2016;214(1):71–2.
85. Committee Opinion No.682. *Obstet Gynecol* 2016;128(6):e262–8.
86. Lo YM et al. *Lancet* 1997;350(9076):485–7.
87. Choi H et al. *Prenat Diagn* 2013;33(2):198–200.
88. Evans MI et al. *Am J Obstet Gynecol* 2016;215(3):298–305.
89. Chaoui R et al. *Ultrasound Obstet Gynecol* 2002;20(6):546–52.
90. Benachi A et al. *Obstet Gynecol* 2015;125(6):1330–7.
91. Dar P et al. *Am J Obstet Gynecol* 2015;213(4):595–6.
92. Jurica MS, Stoddard BL. *Cell Mol Life Sci* 1999;55(10):1304–26.
93. Bibikova M et al. *Science* 2003;300(5620):764.
94. Porteus MH, Baltimore D. *Science* 2003;300(5620):763.
95. Urnov FD et al. *Nature* 2005;435(7042):646–51.
96. Damian M, Porteus MH. *Mol Ther* 2013;21(4):720–2.
97. Ledford H. *Nature* 2015;522(7554):20–4.
98. Miller JC et al. *Nat Biotechnol* 2011;29(2):143–8.
99. Stoddard BL. *Structure* 2011;19(1):7–15.
100. Aiba Y et al. *Chem Soc Rev* 2011;40(12):5657–68.
101. Hendrie PC et al. *J Virol* 2003;77(24):13136–45.
102. Cong L et al. *Science* 2013;339(6121):819–23.
103. Mali P et al. *Science* 2013;339(6121):823–6.

# 50

# Cardiac defects in chromosomally abnormal fetuses

Ritu Mogra and Jon Hyett

## Introduction

Chromosomal abnormalities are associated with high rates of perinatal death and infant morbidity. Similarly, cardiac abnormalities are the most common form of severe congenital abnormality, resulting in stillbirth, and neonatal and childhood death, and are a major cause of childhood morbidity. It is therefore not surprising that the detection of chromosomal abnormalities and of congenital heart defects form two key areas of screening in prenatal diagnosis and that there is significant interaction between the two. Approximately 50% of infants with trisomy 21 are affected by congenital heart disease, and the prevalence is even higher in other, more lethal chromosomal abnormalities. Similarly, a high proportion of fetuses with structural cardiac defects have an underlying chromosomal abnormality.

This chapter reviews the associations that have been described between structural cardiac defects and various chromosomal abnormalities. Prenatal detection rates for cardiac defects in low-risk populations are recognized as being relatively poor, and this chapter also reviews some first-trimester screening tools for aneuploidy that demonstrate cardiac function and may also be useful markers for congenital heart disease in euploid fetuses. Some progress has recently been made in identifying the underlying genetic anomalies associated with cardiac defects specific to chromosomal abnormality, which is also discussed.

## Etiology of congenital heart defects and associations with chromosomal abnormality

Cardiogenesis is a complex process, and the etiology of cardiac abnormality is not completely understood. Epidemiological studies suggest that genetic factors play a specific role in congenital heart defects (CHDs). Known genetic causes include large chromosome abnormalities, single gene disorders, and submicroscopic chromosome abnormalities, otherwise described as copy number variants (CNVs). Chromosomal and Mendelian syndromes account for approximately 20% of CHD.[1–3] Mendelian inheritance patterns have established the role of genes in the etiology of CHD, such as *ZIC3* (heterotaxy), *NOTCH1* (aortic stenosis and bicuspid aortic valve), *NKX2.6* (common arterial trunk), *MYH11* (patent ductus arteriosus), *JAG1* (tetralogy of Fallot), and *MYH6, NKX2.5*, *ACTC1*, and *GATA4* (atrial septal defect).[4–8] The genetic mechanisms underlying sporadic CHDs, which account for the remaining 80%, are poorly understood. Even for sporadic cases, there is evidence from epidemiological studies that there is an increased risk of CHD recurrence of 2%–5% in siblings and offspring, indicating the potential role of common genes and/or the environment.[9,10] The recurrence risk varies according to the type of abnormality in the index case. Aortic valve anomalies and artioventircular septal defects (AVSDs) have recurrence risks (9%–11%) much greater than tetralogy of Fallot (2.4%).[11–14] The maternal methylene tetrahydrofolate reductase variant 677CT and 677TT genotypes are associated with three- and sixfold increases in CHD risk to their children.[15] One randomized controlled trial showed a significant reduction in CHD (OR = 0.6) with periconceptional folate.[16] Meta-analysis of both observational case control studies and randomized or cohort controlled trials has also demonstrated the significant decrease in CHDs following the use of multivitamins containing folic acid.[17] These studies show how genetic and environmental influences can interact in the multifactorial pathogenesis of CHD. Environmental factors, such as maternal diabetes and obesity, can disrupt buffering mechanisms and increase the risk of CHD in offspring.[18,19]

Another interesting observation is that recurrent lesions frequently do not resemble the index lesion.[20] Mutations in certain genes may result in pleiotropic and variable cardiovascular malformations in humans.[21–24] Concordance with parental diagnosis is higher for lesions, such as atrial septal defect (ASD; 68%) and ventricular septal defect (VSD; 45%). The variability in phenotype resulting from a single gene mutation can be explained, in part, by variation in genetic background and also environmental or epigenetic mechanisms.[25–28]

The recurrence risk of CHD increases if a first-degree relative (parent or sibling) is affected. The risk ranges from 1% to 4% if one sibling is affected and is three times higher if two siblings are affected. Approximately 3% of patients with CHD have an identifiable single gene defect.[29] These conditions are often also associated with noncardiac malformations,

examples being Alagille, Holt-Oram, Noonan, and Williams syndromes.[30–31]

One of the main problems in assessment of the association between cardiac defects and chromosomal abnormality is the fact that chromosomal abnormalities have significant rates of intrauterine lethality, and consequently, the prevalence and type of cardiac defects seen within a population will vary markedly depending on the stage of ascertainment. The prevalence of CHD in stillborn fetuses is 10 times higher (21–63/1,000) than that seen in infancy and childhood.[32–38] Most of these studies only included stillbirths >20 weeks' gestation—not those occurring earlier—and may in fact still underestimate the total prevalence of cardiac defects.[39] The types of cardiac lesions most commonly reported in these stillbirth series were ventricular septal defects and complex lesions; death is most likely to have occurred due to the associated chromosomal abnormality rather than the cardiac defect, *per se*.[40] As obstetric sonography skills have improved, routine screening for both chromosomal abnormality and CHD has had a significant impact on the prevalence of live-born CHD. More than 90% of women who have a fetus affected by chromosomal abnormality and 45% of women who have a fetus affected by a cardiac defect opt to terminate the pregnancy.[41]

Table 50.1 summarizes studies describing an association between CHD and chromosomal abnormality.[42–52] Most of the studies are retrospective and based on regional databases/birth registries. The prevalence of CHD varies significantly from 2.9/1,000 to 13/1,000. Differences in prevalence may result from ascertainment bias, different diagnostic criteria, and variable inclusion of minor cardiac lesions. The prevalence of chromosomal abnormality also varies, from 9% to 44%. Postnatal series demonstrate a lower association (9%–14%)

**Table 50.1** Prevalence of chromosomal abnormalities in reported series of congenital heart defects

| *Study* | *Design* | *Population* | *Cases of CHD/total population* | *Prevalence* | *Percentage (%) of chromosomal abnormality* |
|---|---|---|---|---|---|
| Stoll et al.[42] | Retrospective<br>Hospital-based birth defect registry | LB, SB >26 weeks | 801/105,374 | 7.6/1,000 | 11.3 |
| Kidd et al.[43] | Retrospective<br>Hospital-based birth defect registry | LB | 1,479/343,521 | 4.3/1,000 | 9.5 |
| Hafner et al.[44] | Prospective<br>Regional prenatal database | LB | 87/6,541 | 13.0/1,000 | 25.0 |
| Grech and Gatt[45] | Retrospective<br>Hospital-based birth defect registry | LB | 231/26,117 | 8.8/1,000 | 9.0 |
| Harris et al.[46] | Retrospective<br>Population-based birth defects registry | LB, SB >28 weeks | 12,932/4,420,000 | 2.9/1,000 | 18.0 |
| [a]Bosi et al.[47] | Retrospective<br>Population-based birth defects registry | LB, SB >28 weeks | 2,442/480,793 | 5.0/1,000 | 9.1 |
| Calzolari et al.[48] | Retrospective<br>Population-based birth defects registry | LB | 1,549/330,017 | 4.7/1,000 | 9.8 |
| Dadvand et al.[49] | Retrospective<br>Population-based birth defects registry | LB, SB >20 weeks, ToPs >20 weeks | 5,715/665,377 | 8.6/1,000 | 11.6 |
| McBrien et al.[50] | Retrospective<br>Regional perinatal database | LB, SB >22 weeks | 272/89,566 | 3.0/1,000 | 23.5 |
| Tuuli et al.[51] | Retrospective<br>Regional perinatal database | LB | 404/62,111 | 6.5/1,000 | 44.0 |
| [a]Hartman et al.[52] | Retrospective<br>Population-based birth defects registry | LB, SB >20 weeks | 4,430/560,759 | 7.9/1,000 | 12.3 |
| Total | | | 30,342/7,090,176 | 4.3/1,000 | 16.6 |

*Abbreviations:* LB, live birth; SB, stillbirth; ToP, termination of pregnancy.

[a] Included cases with 22q11 deletion.

with chromosomal abnormality than antenatal series (22%–44%). Lethal trisomies, such as trisomies 13 and 18, are more prevalent in the antenatal rather than the postnatal groups. It is also important to note that ascertainment of chromosomal diagnoses is sometimes incomplete; not all studies included analysis for del22q11, and some limited this to specific cardiac conditions (e.g., conotruncal abnormalities).

The most common chromosomal abnormalities seen after the first trimester of pregnancy are trisomies 21, 18, 13, and Turner syndrome (45X). CHD affects 40%–50% of trisomy 21 fetuses, almost 100% of trisomy 18 and 13 fetuses, and 20%–50% of fetuses affected by Turner syndrome.[53–56] Although almost any cardiac malformation can occur with these aneuploidies, certain anatomic lesions are more common; trisomy 21 is strongly associated with atrioventricular septal defects (AVSDs) and Turner syndrome with coarctation of the aorta.[55,56] The patterns of structural malformation, including the type of cardiac defects, seen in these conditions are well described, allowing the sonologist to form an opinion of the likely association based on the cardiac anomaly and the presence of extracardiac abnormalities.

Taking the other perspective, the CHDs most likely associated with chromosomal abnormality are AVSD (50%–60%), interrupted aortic arch (Type B; 69%), double-outlet right ventricle (33%), partial anomalous pulmonary venous return (33%), and truncus arteriosus (33%). CHDs that are least likely to have had a chromosomal abnormality diagnosed include heterotaxy (2%), Ebstein anomaly (3%), pulmonary valve stenosis (3%), and transposition of great arteries (a few case reports).[52]

Many clinicians have recently moved away from traditional cytogenetic evaluation to use a molecular approach (CGH array) for genomic evaluation. The increased resolution of this technique identifies more submicroscopic chromosomal anomalies and will likely impact our understanding of the prevalence and association of chromosomal abnormalities in CHD.[57] Thienpont et al. reported a 17% prevalence of submicroscopic chromosomal anomalies that had not previously been detected in a selected group of 60 adults with CHD and apparently normal cytogenetic karyotype.[58] A systematic review of 13 studies including 1,131 cases of CHD reported that aCGH identified chromosomal anomalies in an additional 7% (95% confidence interval [CI]; 5.3–8.6) of cases compared to cytogenetic plus 22q11 fluorescent *in situ* hybridization (FISH) analysis.[59]

The recognized associations between these chromosomal abnormalities and cardiac defects are listed in Table 50.2.

## Cardiac defects associated with trisomy 21

Trisomy 21 is the most common chromosomal abnormality with potential live birth prevalence of 1 in 700.[60] The pathogenesis of the cardiac malformations associated with Down syndrome remains uncertain, although researchers have hypothesized that they are related to dosage-sensitive genes on chromosome 21. Consistent variations in gene expression have, however, not yet been described.[61]

One common screening test for Down syndrome involves measurement of fetal nuchal translucency (NT) thickness at 11–13 weeks' gestation. There appears to be a bimodal distribution of NT. In euploid populations, 95% of fetuses are in the lower cohort with only 5% of fetuses having a higher NT. In contrast, in trisomy 21, while 15% of fetuses are in the lower distribution, 85% are distributed around a mean NT value of 3.4 mm.[62]

Increased NT is also associated with structural cardiac anomalies, in both euploid and aneuploidy populations.[63,64] Pathological studies have shown that fetuses that are defined as having trisomy 21 on the basis of NT screening are more likely to have a cardiac abnormality, and the prevalence of anomalies increased with NT thickness.[65] Another study that focused on the prevalence of cardiac defects in a series of 417 women who continued the pregnancy beyond 12 weeks confirmed that approximately one-third of these infants have a cardiac defect, the most common being an AVSD. The association between NT thickness and prevalence of CHD was not apparent in this clinical (rather than pathological) series.[66]

The association between trisomy 21 and septal defects was first reported in a postmortem series of infants by Evans.[67] There are now several published cohorts involving prenatal and stillborn findings as well as echocardiographic and surgical findings in live-born infants (Table 50.3).[66,68–86] These series, including a total of 66,925 infants affected by trisomy 21, report a 44% (33%–65%) prevalence of cardiac defects, with AVSD being the most common finding, reported in 32% (9%–59%) of cases. VSDs may be more common in Asian communities, although variations in prevalence/type of CHD may merely reflect methodological differences in source of ascertainment, inclusion, or exclusions of stillbirths and terminations of pregnancy and diagnostic criteria used for detection of cardiac anomalies. An improvement in the resolution of diagnostic ultrasound may have also contributed to the higher prevalence of VSDs reported in the most recent studies.

AVSDs are relatively rare in euploid populations (birth prevalence of 0.83/10,000 live births), and up to 70% of these lesions are associated with trisomy 21.[87] Trisomies 18 and 13 have also been reported in fetuses with AVSD.[88–90] Langford et al. reviewed a series of 125 fetuses diagnosed with an AVSD prenatally and calculated the relative risk for chromosomal abnormality when other variables, such as maternal and gestational age, were taken into account.[91] They found that the presence of an AVSD increased the risk for trisomy 21 by 107 (95% CI 87–127) times, making this the strongest marker for trisomy 21 that has been described. The genomic associations with AVSD are complex, multifactorial, and not clearly understood.[92,93] It has been suggested that poor maternal folic acid supplementation is associated with a high prevalence of septal defects within a trisomy 21 cohort, and disruption of the folate pathway may contribute to the development of AVSD in these infants.[94]

**Table 50.2** Types of congenital heart defects associated with common chromosomal abnormalities/genetic syndromes

| *Chromosomal abnormality or genetic syndrome* | *Genetic etiology* | *Prevalence of congenital heart defect (%)* | *Common cardiac anomalies* | *Increased nuchal translucency (% >4.5 mm)* | *Other structural anomalies that can be detected with ultrasound prenatally* |
|---|---|---|---|---|---|
| Down syndrome | Trisomy 21 | 40–50 | Atrioventricular septal defect, ventricular septal defect, atrial septal defect, tetralogy of Fallot | 50 | Renal anomalies, mild ventriculomegaly, short femur |
| Edwards syndrome | Trisomy 18 | 90–100 | VSD, outlet malaligned; polyvalvular dysplasia | 75 | Central nervous system (CNS) defect, micrognathia, cleft lip/palate, congenital diaphragmatic hernia, omphalocele, renal anomalies, megacystis, clenched hands, rocker bottom feet, talipes, intrauterine growth restriction |
| Patau syndrome | Trisomy 13 | 90–100 | Ventricular septal defect | 60 | Holoprosencephaly, other CNS anomalies, cleft lip and palate, proboscis, cystic renal dysplasia, bladder exstrophy, polydactyl |
| Turner syndrome | 45X | 25–45 | Coarctation of aorta, hypoplastic left heart syndrome, bicuspid aortic valve, aortic stenosis | 90 | Pleural effusion, short femur, renal anomalies |
| DiGeorge syndrome | Del22q11 (TBX1) | 70–75 | Tetralogy of Fallot, interrupted aortic arch, truncus arteriosus, aortic arch anomalies | Few case reports | Absent/hypoplastic thymus, cleft palate, renal anomalies, intrauterine growth restriction |
| Noonan syndrome | RAS-MAPK pathway | 70–80 | Pulmonary stenosis, hypertrophic cardiomyopathy, atrial septal defect | 36–40 | Pleural effusion, hydrops fetalis, renal anomalies, short femur |
| Williams syndrome | 7q11.23 (ELN) | 75–80 | Supravalvular, aortic stenosis, peripheral pulmonary stenosis | Case reports | Renal anomalies, dysmorphism |
| Alagille syndrome | JAG1, NOTCH2 | 90 | Tetralogy of Fallot, pulmonary stenosis, peripheral pulmonary stenosis | Case reports | Hemivertebrae, intrauterine growth restriction, dysmorphism |
| Kabuki syndrome | KMT2D, KDM6A | 30–55 | Coarctation of aorta, aortic stenosis, hypoplastic left heart syndrome, atrial septal defect | Case reports | Cleft palate, vertebral anomalies, renal anomalies, dysmorphism |

**Table 50.3** Prevalence of various congenital heart defects in Down syndrome fetuses

| Author | Population included | Number of T 21 cases | Cases with CHD (%) | Type of CHD (%) | | | | | | | | |
|---|---|---|---|---|---|---|---|---|---|---|---|---|
| | | | | AVSD | ASD | VSD | ASD VSD | TOF | COA | TGA | PDA | Others |
| Rowe and Uchida[68] | LB | 40 | 40 | 36 | 9 | 33 | | 1 | | | 10 | 11 |
| Martin et al.[69] | LB | 137 | 47 | 49 | 14 | 22 | | 3 | | | | 12 |
| Stoll et al.[70] | LB, SB, ToP | 139 | 45 | 42 | | 29 | | 3 | 5 | | 5 | 16 |
| Tubman et al.[71] | LB | 81 | 42 | 38 | 21 | 15 | | | | | 18 | 8 |
| Khoury and Erickson[72] | LB, SB | 532 | 33 | 42 | 15 | 14 | | | | | 29 | |
| Pradat[73] | LB, SB | 167 | | 59 | | | 32 | | 4 | | | 5 |
| Wells et al.[74] | LB | 118 | 48 | 39 | 29 | 31 | | 8 | 4 | | 6 | 14 |
| Freeman et al.[75] | LB | 227 | 44 | 45 | 26 | 35 | | 4 | | | 7 | 1 |
| Vida et al.[76] | LB | 349 | 54 | 9 | 13 | 27 | | | | 0.5 | 29 | |
| Bermudez et al.[77] | LB | 1,207 | 50 | 15 | 42 | 13 | 15 | 2 | | | 7 | 1 |
| Cleves et al.[78] | LB | 43,463 | 36 | 23 | 48 | 29 | | 5 | 2 | 1 | | |
| Nisli et al.[79] | LB | 1,042 | 39 | 34 | 18 | 16 | | 0.5 | | 0.5 | 4 | |
| Elmagrpy et al.[80] | LB | 1,193 | 45 | 23 | 65 | 14 | | 2 | 1 | | 5 | |
| Irving and Chaudhari[81] | LB | 821 | 42 | 37 | 15 | 31 | | 5 | | | 4 | 2 |
| Mogra et al.[66] | LB, SB, ToP | 487 | 34 | 24 | | 1.4 | | 3 | 1 | | | |
| Rankin et al.[82] | LB, SB | 1,103 | 32 | 44 | 15 | 32 | | 5 | 3 | | | |
| Tan et al.[83] | LB | 588 | 65 | 16 | 23 | 39 | | 5 | 0.3 | | 34 | 8 |
| Morris et al.[84] | LB, SB, ToP | 14,109 | 44 | 20 | 26 | 21 | | 2 | 1 | 3 | | |
| Kim et al.[85] | LB | 394 | 57 | 9 | 30 | 16 | | 2 | 2 | 0.3 | 17 | |
| Stoll et al.[86] | LB, SB, ToP | 728 | 44 | 30 | 25 | 22 | | 3 | 5 | | | 9 |
| Total | | 66,925 | 44 | 32 | 21 | 23 | 23 | 3 | 3 | 1 | 13 | 8 |

*Abbreviations:* ASD, atrial septal defect; AVSD, atrioventricular septal defect; COA, coarctation of aorta; LB, live birth; PDA, patent ductus arteriosus; SB, stillbirth; TGA, transposition of great arteries; TOF, tetralogy of Fallot; ToP, termination of pregnancy; VSD, ventricular septal defect.

VSDs, secundum ASDs, and persistent arterial ducts (PDAs) are other common pathologies seen in trisomy 21, while outflow tract abnormalities, particularly transposition of great arteries, coarctation of aorta, and truncus arteriosus are rare. While some VSDs are large and therefore detectable prenatally, ASDs and PDAs are not detectable in the fetus. VSDs seen in trisomy 21 fetuses are typically perimembranous, in the inlet portion of the septum. If these are isolated anomalies (1.4% prevalence in the Mogra series),[66] they are difficult to detect during routine obstetric ultrasound. Karyotyping on the basis of cardiac findings produces interesting results: Palidini et al. showed that 9/21 (43%) AVSDs had trisomy 21, while 0/39 (0%) of VSDs had this chromosomal abnormality.[95,96]

## Trisomy 18

Trisomy 18 is the second most common chromosomal abnormality.[97] There is a high degree of spontaneous fetal loss ranging from 72% to 87%.[98,99] The most striking first-trimester sonographic finding of this condition is the increased NT thickness that is significantly increased and usually associated with subcutaneous edema and multiple structural malformations. Nearly 75% of fetuses with trisomy 18 have an NT measurement of greater than 4.5 mm in the first trimester.[100] Congenital heart disease occurs in more than 90% of these fetuses.[101] In one series of 3,151 pregnancies undergoing first-trimester (NT) screening followed by detailed echocardiography for those with NT $>$ 3 mm at 16 weeks' gestation, all five cases of trisomy 18 had increased NT and a cardiac defect—in comparison to only two of the nine cases of trisomy 21 having both features.[102]

Edward (1960) first described an association between trisomy 18 and cardiac defects, recognizing an association with VSDs and a patent ductus arteriosus. Subsequent postmortem series and echocardiographic studies of live-born infants have described polyvalvular disease in almost all fetuses with trisomy 18.[103–107] In a largest autopsy series, including 41 trisomy 18 fetuses, a VSD was reported in all cases.[108] The most frequent type of VSD was an outlet malalignment type. Polyvalvular disease was present in 93% of cases. A more complex malformation (double-outlet right ventricle, endocardial cushion defect, or a left-sided obstructive lesion)

was present in about 10% of cases. In this series, it appeared that 9/41 (22%) cases had abnormalities, which would not be detectable echocardiographically prenatally, such as a persistent arterial duct, an ASD, or a small VSD.

A second series that reported postmortem findings of 23 trisomy 18 fetuses identified through first-trimester screening also demonstrated cardiac abnormalities in all cases.[109] In this series, the most common defect was a VSD (in 19/23 [83%] cases). Once again, there was a very high prevalence of valvular abnormalities (in 19/23 [83%] cases).

Prenatal series often report a lower prevalence of cardiac anomalies (47%–84%), although detection rates are significantly higher if the cardiac evaluation is performed later in the pregnancy.[110–116] DeVore demonstrated the importance of formal cardiac evaluation during prenatal screening; if the heart is examined properly at the 20-week anomaly scan, the overall prenatal detection rate for trisomy 18 increases from 77% to 97%.[117] In prenatal series, the most common cardiac anomaly identified was a ventricular septal defect (not polyvalvular disease). The largest prenatal series of 162 affected fetuses, many of whom had an early echo (<16 weeks) performed by an experienced fetal cardiologist after recognition of increased NT, reported that 73% had an identifiable cardiac defect.[118] This compared to a series of 55 fetuses that were examined immediately after identifying increased NT (i.e., at 12 weeks), where only 4% were reported to have a cardiac defect.[119] A third trisomy 18 prenatal series ($n = 123$) reported ultrasound findings at 22 weeks defined 95% prevalence of cardiac disease.[120]

While valvular dysplasia is commonly described in pathological series, it is rarely reported in prenatal series. It is more likely to be noted as an additional finding in later gestations, although, interestingly, functional anomalies such as tricuspid regurgitation are reported in 33%–55% of trisomy 18 fetuses and may reflect valvular dysplasia.[118] If a VSD is identified, particularly a malaligned outlet defect, then more detailed evaluation to look for evidence of valvular abnormalities may help identify a cohort of fetuses that have trisomy 18.

## Trisomy 13

Trisomy 13 is relatively rare, being the associated chromosomal anomaly in only 6/129 (4.7%) cases of congenital heart disease reported by Tennstedt et al. and in 5/355 (1.4%) cases reported by Palidini et al., compared to 15% of cases associated with trisomy 21 in each of these series.[121,122] Given the small number of cases reported in most series, it is difficult to define the pattern of cardiac abnormalities seen with this chromosomal abnormality. There are, however, some pathological data: In one series of 12 trisomy 13 fetuses, cardiovascular malformations were identified in all cases. The leading finding was an infundibular VSD, frequently combined with dextroposition of the aorta and abnormalities of the semilunar valves.[123] The findings were similar in a second pathological series of 15 trisomy 13 fetuses, diagnosed through an NT screening program.[110] Once again, cardiac defects were identified in all cases; the most common defects were AVSDs or VSDs, and there were also a variety of valvular defects, including agenesis of the pulmonary valve that was not observed in other common trisomies. The great arteries were also abnormal in all cases. In three cases, there was a truncus arteriosus—also a finding unique to trisomy 13. While these pathological series give some insight into the spectrum of cardiac disease in trisomy 13, it is, once again, important to remember the potential impact of intrauterine lethality on the pattern and percent of malformations that would be expected at later gestations.

The reported frequencies of prenatally detected CHD in fetuses with trisomy 13 in the second and third trimesters have varied from 29% to 70%.[124–129] In these series, the most common CHDs include VSDs, malaligned VSDs, and anomalous pulmonary venous return. Atrial septal defects and a patent ductus arteriosus have also been reported postnatally.[130]

One series of 28 trisomy 13 fetuses reported that CNS and facial anomalies were more common than cardiac abnormalities—the opposite of the situation seen in trisomy 18.[131] In contrast to trisomy 21, the intracardiac defect seen in trisomy 13 is often a component of a more complex cardiac anomaly, and abnormalities of the outflow tracts and great arteries are significant features.

## Del 22q11.2 (DiGeorge syndrome)

The prevalence of the 22q11.2 microdeletion has been variously estimated at 1 in 1,000 to 1 in 4,000 pregnancies; although there are no data that have tested a large unselected population using comprehensive molecular-based tools.[132,133] Consequently, del22q11 is the second most common chromosomal abnormality reported in live-born infants that have cardiac defects. Over 180 different anomalies have been described as being associated with del22q11, common clinical phenotypes include DiGeorge, velocardiofacial, and CATCH-22 (cardiac defects, abnormal facies, thymic hypoplasia, cleft palate, and hypocalcemia, associated with 22q11 deletion) syndromes. The diverse range of anomalies and variable penetrance make counseling about likely long-term outcomes very difficult. Immediate postnatal complications include profound hypocalcaemia that, if not recognized, can cause long-term neurodevelopmental injury and immunodeficiency that can complicate cross-match for transfusion (for surgery).[134] Consequently, early recognition through prenatal diagnosis may have a direct impact on long-term clinical outcomes.

Up to 75% of infants that have del22q11 have a cardiac defect. In the largest series, including 23 European centers, 409 (75%) of 545 patients with del22q11 deletion had a major cardiac defect.[135] Several other single center studies have reported that major cardiac abnormalities are present in 70%–85% of affected patients.[136–139] CHDs associated with del22q11 are mostly of the conotruncal type and/or defects of the aortic arch. The most common reported defect is tetralogy of Fallot (TOF) with pulmonary atresia (26%), interruption of the aortic arch (16%), and truncus arteriosus (13%)

also being common findings. The risk of DiGeorge syndrome with, for example, an isolated right-sided aortic arch, has been reported between 4% and 24%; but again, the data are skewed by patient ascertainment.[140–142] If a deletion is identified, it may be of variable size, but phenotypic variability does not appear to be related to the precise genomic deletion.

Surprisingly, while increased NT has been reported in some fetuses with del22q11, there does not seem to be as clear an association as there is with other chromosomal abnormalities. In three studies, including 75 and 80 cases with NT > 3 mm and 146 with NT > 3.5 mm that had FISH for del22q111, no cases of this anomaly were reported.[143–145]

A review of prenatal and postnatal series of infants that have congenital heart disease and have had a conventional karyotype including FISH for del22q11 (Table 50.4) shows a 6% prevalence of this defect.[146–155] Individual reported prevalence ranged from 3%–21%; mainly due to variation in selection criteria for karyotyping. Studies including all cardiac defects defined a lower prevalence than those that included only conotruncal cardiac defects. The prevalence of del22q11 may be greater than 50% in three specific conditions: tetralogy of Fallot with pulmonary atresia where there are major aortopulmonary collateral arteries, tetralogy of Fallot with absent pulmonary valve or interrupted aortic arch type B. Similarly, the prevalence of this karyotypic abnormality increases with any cardiac abnormality that includes a right-sided aortic arch, aberrant right subclavian artery, or infundibular septal defect.

It is also worth noting that some cardiac defects are rarely reported to be associated with del22q11. This includes tricuspid atresia, double-outlet right ventricle, left atrial isomerism, total anomalous pulmonary venous return, aortic valve stenosis, and hypoplastic left heart.[137]

## Turner syndrome

Turner syndrome is a common sex chromosome abnormality where the fetal karyotype is 45X. This is a highly lethal chromosomal abnormality in the prenatal period, and only a minority survive to term, with a live birth prevalence of 1 in 2,500. Most long-term survivors are actually mosaic rather than having a pure 45X lineage.[156] For example, in one study of 53 cases, 47 were diagnosed on the basis of first-trimester NT, 51 died or were terminated due to the severity of the cardiac abnormality, and only two, with normal cardiac anatomy, were born live.[157]

**Table 50.4** Prevalence of various congenital heart defects in infants affected by del22q11

| *Study* | *Population and prevalence of 22q11 (%) in series* | *Type of CHD with 22q11deletion (%)* | | | | | | | |
|---|---|---|---|---|---|---|---|---|---|
| | | *TOF* | *TOF with PA* | *TOF APVS* | *PA with VSD* | *IAA* | *TA* | *VSD* | *Others* |
| [a]Goldmuntz et al.[146] | Postnatal 18 | 16 | | | | 50 | 34 | 33 | 4 |
| Marino et al.[147] | Postnatal 12 | 26 | | | 27 | 9 | 11 | 17 | 13 |
| Manji et al.[148] | Prenatal 11 | 20 | | | | | 60 | 20 | |
| [a]Boudjemline et al.[149] | Prenatal 21 | 14 | | 37 | 21 | 45 | 31 | | 12 |
| [a]Volpe et al.[150] | Prenatal 20 | 14 | 20 | 28 | | 60 | 43 | | 11 |
| Moore et al.[151] | Prenatal 3 | 29 | | | | | 6 | 35 | 43 |
| Bretelle et al.[152] | Prenatal 5 | 25 | | | 25 | 12 | 12 | 12 | 12 |
| Lee et al.[153] | Prenatal 5 | 45 | 24 | 3 | | 19 | 2 | 9 | 24 |
| [a]Khositseth et al.[154] | Postnatal 15 | 11 | | | 4 | 11 | 22 | 11 | |
| Agergaard et al.[155] | Postnatal 2 | 32 | | | 3 | 17 | 11 | 32 | |
| Total | – 6% | 22 | 4 | 7 | 8 | 22 | 23 | 17 | 12 |

*Abbreviations:* APVS, absent pulmonary valve syndrome; IAA, interrupted aortic arch; PA, pulmonary atresia; TA, truncus arteriosus; TOF, tetralogy of Fallot; VSD, ventricular septal defect.

[a] Included only conotruncal malformation.

From a phenotypic perspective, almost all 45X fetuses have increased NT (with measures >3.5 mm) in the first trimester, which develops into septated cystic hygroma by 20 weeks' gestation.[100] This anomaly is associated with a failure in development of lymphatic channels draining the head and neck to the internal jugular vein.[158] A triad of features—45X karyotype with a "webbed neck" and coarctation of the aorta—is well recognized.[159] It has been postulated that fetal lymphedema contributes to the cardiovascular defects in Turner syndrome as distended lymphatic sacs impair venous return and/or compress the developing outflow tract. Other typical cardiac anomalies include left heart hypoplasia, aortic hypoplasia, and interruption of the aortic arch. In two small pathological series of 45X fetuses terminated after diagnosis at 12–14 weeks' gestation, tubular hypoplasia of the aortic arch was described consistent with the postnatal finding of coarctation of the aorta.[65,160] A bicuspid aortic valve is also a common finding in those fetuses that have this form of coarctation.

In postnatal (likely mosaic) infants, the reported prevalence of cardiac defect varies from 23% to 50% (Table 50.5), including abnormalities of the aortic valve (predominant bicuspid) in 21% (range: 12%–39%) and coarctation of the aorta in 11% (range 4%–16%) of infants.[161–167] The prevalence of congenital heart disease varies between series depending on age at presentation and the type of investigations used to define the presence of an abnormality. Postnatal studies using computed tomography or magnetic resonance imaging have higher detection rates of cardiac abnormalities than studies using echocardiography. The prevalence of bicuspid aortic valve, coarctation of aorta, or partial anomalous pulmonary venous drainage, lesions that are not typically detected prenatally, are 140, 100, and 320 times increased, respectively, compared to karyotypically normal infants.

## Other chromosomal abnormalities

In the last few years, prenatal karyotyping has moved from cytogenetic to molecular array based testing. This allows detection of a whole range of microduplications and microdeletions that were previously difficult to see using standard cytogenetic techniques. As a consequence, we have a better appreciation of the range of microdeletions and duplications that are represented in fetuses that have a cardiac abnormality and of the overall prevalence of these abnormalities.

A review of prenatal studies shows that functionally relevant CNVs ascertained as microdeletions and microduplications are reported in 3% and 20% of CHDs depending on inclusion of syndromic and nonsyndromic cardiac malformations.[168–172] Both deletions and duplications are commonly pathogenic, and to date there are over 40 clinically delineated deletion and duplication syndromes specifically associated with CHD.[173] The prevalence of microchromosomal abnormalities appears to be particularly high for fetuses that have a VSD (mainly perimembranous) with an extracardiac malformation, that have conotruncal (TOF, interrupted arch) or left ventricular outflow tract malformations.[174–176] Interestingly, cardiac anomalies that have not traditionally been associated with chromosomal abnormality, such as transposition of the great arteries and heterotaxy, have been reported to be affected by microchromosomal anomalies.[177] The range of microchromosomal anomalies associated with CHD is highly heterogenous[178]; there does, therefore, appear to be good evidence to support universal prenatal karyotyping (with a microarray) for all fetuses that are recognized as having a structural cardiac abnormality.

A few examples of well-characterized syndromes with CHD caused by CNVs include Williams syndrome (del 7q11.23), Smith-Magenis syndrome (del 17p11.2), and Kleefstra syndrome (del 9q34.3).[179] The characterization of small chromosomal anomalies has improved our understanding of underling etiologies and likely recurrence of disease; for example, Williams syndrome, which is associated with supravalvular aortic stenosis and/or peripheral pulmonary stenosis, was recognized as being "autosomal dominant" prior to the identification of the 7q11.23 microdeletion. Similarly, recognition that Smith-Magenis syndrome (SMS) is associated with del 17p11.2 leads to an improved understanding of the etiology of septal defects and tetralogy of Fallot (seen in SMS) being associated with deletion of the retinoic acid–induced 1 (RAI1) gene. CHDs such as septal defects and TOF are present in about one-third of individuals with SMS.[180]

The potentially most valuable role of recognizing CNVs associated with CHD lies in our ability to use the diagnosis of the cardiac defect to define risk of other phenotypic characteristics such as autism (dup16p13.11) or other neurodevelopmental disorders (del 1q21.1, del 1p36, dup 15q11.2–13, and dup 22q11.2).[181]

Other chromosomal aberrations that have clear associations with specific cardiac defects include tetrasomy 22p (30% prevalence of cardiac defects; frequently total anomalous pulmonary venous drainage), tetrasomy 12p (Pallister-Killian syndrome; 25% prevalence of cardiac defects, predominantly ventricular septal defects), and del 4p (Wolf-Hirschhorn syndrome; 30% prevalence of cardiac defects, predominantly septal defects).[182]

## Single gene disorders

Other genetic syndromes associated with single gene mutations are not defined through extended microarray-based karyotyping. Examples that have strong associations with cardiac abnormalities include Noonan, Alagille, Kabuki, and Sotos syndromes. Single gene defects underlie 3%–5% of all cases of CHD. These will traditionally only be identified if the clinician recognizes the potential for a specific diagnosis (and if an established pathway for molecular testing exists), but more cases may be identified in the future if prenatal testing extends to include exome sequencing.[173]

Noonan syndrome (NS) is the most common single gene disorder associated with CHDs, presenting with pulmonary stenosis with dysplastic leaflets, hypertrophic cardiomyopathy,

**Table 50.5** Prevalence of cardiac defects in postnatal series of individuals with Turner syndrome (45X)

| | | | | | *Type of cardiac defect (%)* | | | | | |
|---|---|---|---|---|---|---|---|---|---|---|
| *Study* | *N* | *Karyotype (% Mosaic)* | *Age* | *Method of investigation* | *Bicuspid aortic valve* | *Coarctation of the aorta* | *Partial anomalous pulmonary venous drainage* | *Left superior vena cava* | *Elongated transverse arch of aorta* | *Other* |
| Gotzsche et al.[161] | 179 | 58% 45X | 6 months–46 years | Echocardiography | 14 | 10 | 1 | | | 26 |
| Mazzanti and Cacciari[162] | 594 | 54% 45X | 1 month–24 years | Echocardiography | 12 | 7 | 5 | | | 23 |
| Prandstraller et al.[163] | 136 | 50% 45X | 1 month–20 years | Echocardiography, angiography | | 4 | 3 | | | 22 |
| Volkl et al.[164] | 117 | 55% 45X | 3 months–43 years | Echocardiography, cardiac catheterization | 18 | 18 | 5 | | | 30 |
| Bondy[165] | 250 | 70% 45X | | Echocardiography, magnetic resonance imaging, computed tomography | 30 | 12 | 13 | 13 | 49 | 50 |
| Kim et al.[166] | 51 | 47% 45X | 6 months–36 years | Echocardiography, magnetic resonance imaging | 39 | 16 | 16 | | 31 | |
| [a]Lee et al.[167] | 20 | 40% 45X | 13–22 years | Computed tomography scan | 15 | | 20 | | | |
| Total | 1,347 | | | | 21 | 11 | 9 | 13 | 40 | 55 |

[a] Included only asymptomatic patients.

and atrial septal defects. The estimated prevalence of this syndrome is 1:1,000–2,500, although the prevalence of the disease and of cardiac disease within affected cases is impacted by the previous requirement of a cardiac defect to make a clinical diagnosis. NS is inherited in an autosomal dominant manner; however, many individuals with NS have a *de novo* pathogenic variant.[183] Prendiville et al. reported an 81% prevalence of cardiac defects in a cohort of 293 patients including valvular pulmonary stenosis (57%), atrial septal defect (32%), and hypertrophic cardiomyopathy (16%).[184] Marino et al., who reported a series of 136 patients, described associations with AVSD (15%), coarctation of the aorta (9%), and mitral valve abnormalities (6%), which had not been defined in other series.[185] Interestingly, the pattern of AVSD described in Noonan syndrome, typically partial with subaortic stenosis, is different from that observed in Down syndrome (complete/without obstruction of the left ventricular outflow tract).

One large retrospective series of 47 patients with confirmed molecular diagnosis of Noonan syndrome described the prenatal features of this entity.[186] Increased NT or cystic hygroma was present in 36%, and other structural ultrasound abnormalities were identified in 25% of cases including hydrothorax (11%) and CHD (8%); postnatally 50% of the series were reported to have CHDs.[187] Extracardiac anomalies were also an important marker for disease in a second series that reported an association with polyhydramnios, cystic hygroma, pleural effusion, hydrops fetalis, renal anomalies, and short femur, but only demonstrated a cardiac abnormality prenatally in 27% cases.[188] Failure to diagnose Noonan cardiac abnormalities prenatally may relate to the fact that many (pulmonary stenosis and hypertrophic cardiomyopathy) tend to become more significant with advancing gestation and are not necessarily recognizable before the third trimester or birth.[189–192]

## Ultrasound markers of chromosomal abnormality and/or cardiac defects

Although tertiary centers have been shown to offer highly sensitive and specific prenatal ultrasound screening for cardiac defects, routine assessment of the four-chamber view and outflow tracts at the 20-week morphology scan have been shown to be less successful as a screening tool.[193–197] In order to improve the antenatal detection of cardiac defects, it may be helpful to consider the role of other morphological abnormalities seen during screening for chromosomal abnormalities that are easier to identify but are recognized as having an association with cardiac defects.

The assessment of NT thickness has been shown to be a very effective method for screening for Down syndrome, and it forms the basis of universal screening programs in many countries.[198–199] The fact that increased NT also has a strong association with cardiac defects means that this can potentially also be used to screen for cardiac defects (Figure 50.1).

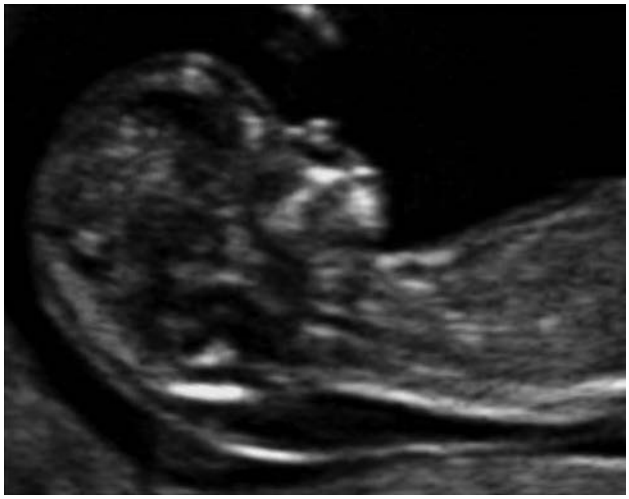

**Figure 50.1**
A midsagittal section of a 12-week fetus showing increased nuchal translucency.

This was first reviewed in a retrospective series of 29,154 pregnancies primarily screened for chromosomal abnormality at 11–14 weeks of pregnancy.[200] In this series, 56% (95% CI 42–70%) of the fetuses later found to have a cardiac defect (by postmortem, fetal echocardiography, or postnatal examination) had increased NT, suggesting that this tool was a more powerful marker in screening a low-risk population than the traditional technique of assessing the four-chamber view and outflow tracts at 20 weeks.

The trend for an association between increased NT and major cardiac defects has been consistent in nine (two retrospective and seven prospective) other studies.[201–208] These included a total of 129,340 pregnancies with 298 cardiac defects; 29% had increased NT, and the prevalence of cardiac defects varied from 0.2% (NT $<$ 2.5 mm) to 0.8% (NT 2.5–3.5 mm) and 4.9% (NT $>$ 3.5 mm). A normal NT is associated with a reduction in risk of a major cardiac abnormality (negative likelihood ratio = 6.5). An NT between the 95th and 99th percentiles is associated with a modest increase in risk (positive likelihood ratio = 3.4) with sensitivity of 12% and specificity of 96% in detecting a major cardiac defect. Screening efficacy improves using an NT cut-off of the 99th percentile, with sensitivity and specificity of 17% and 99%, respectively, and a positive likelihood ratio of 23. While NT screening does not replace formal ultrasound evaluation of the heart at 20 weeks' gestation, it is a useful adjunct for population-based screening. Those identified as at high risk can be offered first-trimester echocardiography, which has, in specialist hands, been shown to have high sensitivity and specificity for the detection of cardiac anomalies.[209–211]

Molecular studies in first-trimester fetuses suggest that the myocardium of fetuses with increased NT and chromosomal abnormality have some cardiac dysfunction.[212] This leads to the investigation of other potential markers of hemodynamic imbalance, and although no significant change in the myocardial performance index of fetuses with increased NT could be demonstrated, there does appear to be an association with

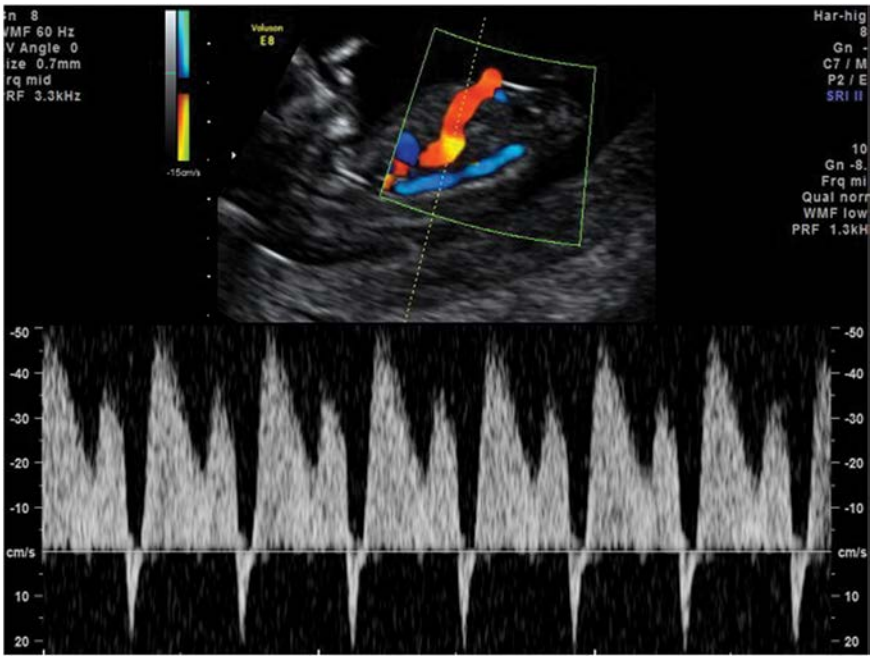


**Figure 50.2**
Doppler sampling shows reversal of the A-wave in the ductus venosus flow of this 12-week fetus.

abnormal flow through the ductus venosus.[213] In a series of 515 pregnancies having cytogenetic testing at 11–14 weeks' gestation, 80% of cases with chromosomal abnormality were also found to have an abnormal ductus venosus, defined by absent or reversed flow in the A-wave (Figure 50.2). The specificity of this test appears to be very high (approximately 99%), and in 7/17 (41%) euploid fetuses in this series that had increased NT and an abnormal ductus venosus waveform, a major cardiac defect was found at a later date.[214] This has been supported by several other datasets, which have suggested that measurement of ductal flow in terms of the pulsatility for veins (PVIV) is more reliable, and that inclusion of this tool in first-trimester testing improves the sensitivity and specificity of screening for chromosomal abnormality and is a powerful marker for euploid fetuses that have major cardiac defects.[215] Combining data from 10 studies shows that the addition of ductus venosus analysis increases the sensitivity of screening (compared to NT alone) for cardiac defects to 70% with 89% specificity.[208,215–223] These findings were supported by another study where NT and ductus venosus were routinely assessed in an unselected population of 12,799 singleton pregnancies. This found that combining NT and ductus venosus assessment improved detection of cardiac defects when compared to using either screening tool alone, with 47% detection for a low (2.7%) false-positive rate.[224]

Another cardiac marker of blood flow, tricuspid regurgitation, has also recently been reported as being associated with both chromosomal abnormalities and cardiac defects, although this, too, seems to be an association limited to early gestations.[225] Tricuspid regurgitation was typically assessed by transabdominal scan, using pulsed wave Doppler. A sample gate of 3 mm was positioned across the tricuspid valve in an apical four-chamber view such that the angle of insonation was less than 20° (Figure 50.3). Valvular flow was assessed three times, and tricuspid regurgitation defined as flow toward the atrium for at least half of systole with a velocity greater than 60 cm/s.[226] In a population of fetuses referred for detailed echocardiography at 11–14 weeks, after the identification of increased NT (>4 mm), tricuspid regurgitation was seen in 27% of cases. Some 83% of these were subsequently found to have a chromosomal abnormality, most commonly trisomy 21, although all types of karyotypic anomaly were seen.[226] A second larger prospective study found tricuspid regurgitation in 4.4% of chromosomally normal fetuses, 67.5% of fetuses affected by trisomy 21, and 33% of fetuses affected by trisomy 18.[227] A third study performed by the same group, again involving a selected population with a high prevalence of increased NT, chromosomal abnormalities, and cardiac defects, defined tricuspid regurgitation more stringently, with flow greater than 80 cm/s.[228] In this study, tricuspid flow was successfully examined in 96.8% cases, and tricuspid regurgitation was found in 8.5% of chromosomally normal fetuses and 65.1% of those with trisomy 21. Further analysis of the euploid population found that tricuspid regurgitation was present in 46.9% of those cases that had a structural cardiac defect and in only 5.6% of euploid fetuses with no cardiac defect. Positive likelihood ratios describing the associations between tricuspid regurgitation and trisomy 21 or isolated cardiac defects were calculated, being 7.7 and 8.4, respectively. The authors have noted an association with crown-rump length and NT thickness, and more precise likelihood ratios can be generated based on these parameters.

The effectiveness of a combination of NT, ductus venosus, and tricuspid flow assessments has been assessed in a large unselected population of 40,000 pregnancies.[208] This

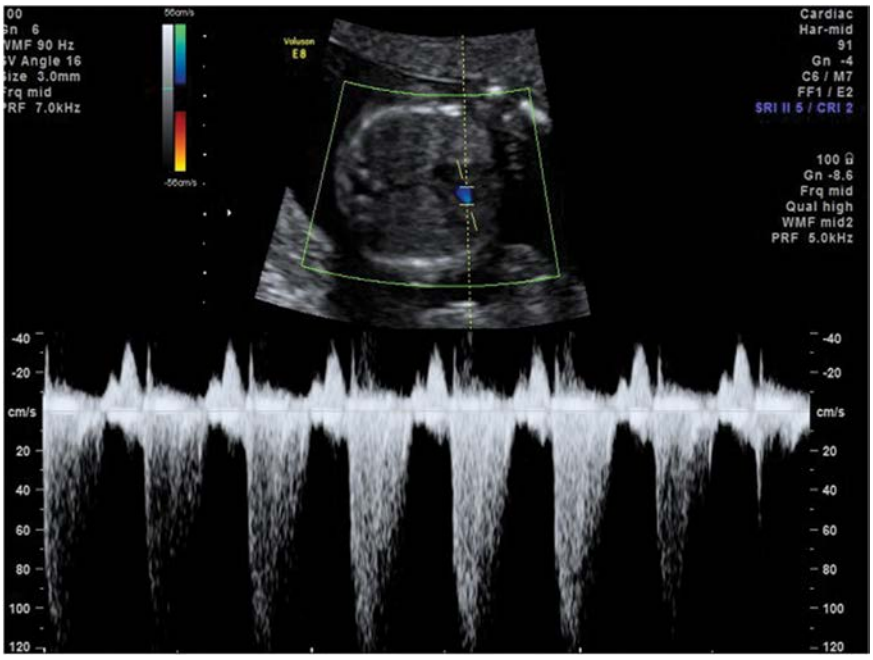


**Figure 50.3**
Doppler sampling across the tricuspid valve (seen in axial section) demonstrates tricuspid regurgitation.

population included 85 fetuses with major cardiac defects. Increased fetal NT (>95th percentile), reversed A-wave in the ductus venosus, or tricuspid regurgitation was reported in 35.3%, 32.9%, and 28.2% of cases, respectively. If any one of these markers was considered to place the pregnancy in a high-risk group, then 57.6% of cardiac defects would have been detected for a false-positive rate of 8%. It appears that this combination of markers is effective in predicting the majority of major cardiac defects at 12 weeks' gestation. Algorithms are now available to describe an individual's risk of having a fetus affected by a major cardiac abnormality in the same way as we have been applying algorithms predicting risk for chromosomal abnormality.[229]

Other authors are investigating simpler methods of screening for cardiac disease at 11–14 weeks' gestation, specifically by making a formal assessment of the cardiac axis, measuring the angle between the anteroposterior dimension of the thorax and the long axis (interventricular septum) of the heart. In a case control study, 74.1% of fetuses that had a cardiac defect had a cardiac axis greater than 1.97 standard deviations from the norm (44.5° + 7.4°), with a screen positive rate of 5%.[230] It will be interesting to see whether this data can be reproduced prospectively and whether there is any value in combining this with NT or the other hemodynamic markers.

## Conclusion

The strong association between cardiac defects and chromosomal abnormality initially recognized in populations of infants and neonates is even stronger in fetal life. The recent improvement of resolution seen in molecular karyotyping has demonstrated additional associations that had not previously been recognized. As a consequence, karyotyping should be offered to all fetuses that have a heart defect, not just those with patterns of abnormality seen with more traditional karyotypic anomalies.

First-trimester screening, with NT, provides a means of screening for heart abnormalities at 11–13$^{+6}$ weeks of pregnancy. This screening tool is more effective when combined with assessment of hemodynamic markers such as ductus venosus flow or tricuspid regurgitation. These tests are associated with both chromosomal abnormality and the presence of structural cardiac defects. First-trimester screening should be seen as an adjunct to formal prenatal assessment of cardiac structures, traditionally done at the time of the 18- to 20-week anomaly scan. This screening test is best structured to look at the four-chamber view and outflow tracts. These structures can also be examined in the first trimester, although a higher level of sonographic expertise is likely needed to use this as a screening test at 11–13$^{+6}$ weeks.

## References

1. Ferencz C et al. *J Am Coll Cardiol* 1989;14:756–63.
2. Ferencz C, Boughman JA. *Cardiol Clin* 1993;11:557–67.
3. Gebbia M et al. *Nat Genet* 1997;17:305–8.
4. Megarbane A et al. *Eur J Hum Genet* 2000;8:704–8.
5. Garg V et al. *Nature* 2005;437:270–4.
6. Schott JJ et al. *Science* 1998;281:108–11.
7. Heathcote K et al. *Hum Mol Genet* 2005;14:585–93.
8. Ching YH et al. *Nat Genet* 2005;37:423–8.
9. Caputo S et al. *Eur Heart J* 2005;26:2179–84.
10. Burn J et al. *Lancet* 1998;351:311–6.
11. Drenthen W et al. *Eur Heart J* 2005;26:2581–7.
12. Sanchez-Cascos A. *Eur J Cardiol* 1978;7:197–210.

13. Emanuel R et al. *Br Heart J* 1983;49:144–7.
14. Huntington K et al. *J Am Coll Cardiol* 1997;30:1809–12.
15. Van Beynum IM et al. *Eur Heart J* 2006;27:981–7.
16. Czeizel AE et al. *Birth Defects Res A Clin Mol Teratol* 2004;70: 853–61.
17. Goh YI et al. *J Obstet Gynaecol Can* 2006;28:680–9.
18. Loffredo CA et al. *Teratology* 2001;64:98–106.
19. Hartman JLT et al. *Science* 2001;291:1001–4.
20. Benson DW et al. *J Clin Invest* 1999;104:1567–73.
21. Goldmuntz E et al. *Circulation* 2001;104:2565–8.
22. Bamford RN et al. *Nat Genet* 2000;26:365–9.
23. Sperling S et al. *Hum Mutat* 2005;26:575–82.
24. Robinson SW et al. *Am J Hum Genet* 2003;72:1047–52.
25. Dennis NR, Warren J. *J Med Genet* 1981;18:8–16.
26. Rose V et al. *J Am Coll Cardiol* 1985;6:376–82.
27. Gill HK et al. *J Am Coll Cardiol* 2003;42:923–9.
28. Ferencz C et al. *J Am Coll Cardiol* 1989;14:756–63.
29. Øyen N et al. *Circulation* 2009;120:295–301.
30. Calcagni G et al. *Eur J Pediatr* 2007;166:111–6.
31. Botto LD, Correa A. *Prog Ped Cardiol* 2003;18:111–21.
32. Boldt T et al. *Scand Cardiovasc J* 2002;36:73–9.
33. Samanek M et al. *Int J Cardiol* 1985;8:235–50.
34. Mitchell SC et al. *Circulation* 1971;43:323–32.
35. Bound JP, Logan WF. *Br Heart J* 1977;39:445–50.
36. Feldt RH et al. *Mayo Clin Proc* 1971;46:794–9.
37. Richards MR et al. *Pediatrics* 1955;15:12–32.
38. Ruiz A et al. *J Matern Fetal Neonatal Med* 2016;29:3271–5.
39. Poland BJ, Lowry RB. *Am J Obstet Gynecol* 1974;118:322–6.
40. Clawson BJ. *J Lancet* 1944;64:1134–6.
41. Germanakis I, Sifakis S. *Pediatr Cardiol* 2006;27:465–72.
42. Stoll C et al. *Eur J Epidemiol* 1989;5:382–91.
43. Kidd SA et al. *J Paediatr Child Health* 1993;29:344–9.
44. Hafner E et al. *Prenat Diagn* 1998;18:808–15.
45. Grech V, Gatt M. *Int J Cardiol* 1998;68:151–6.
46. Harris JA et al. *Pediatr Cardiol* 2003;24:222–35.
47. Bosi G et al. *J Pediatr* 2003;142:690–8.
48. Calzolari E et al. *Eur J Epidemiol* 2003;18:773–80.
49. Dadvand P et al. *Paediatr Perinat Epidemiol* 2009;23:58–65.
50. McBrien A et al. *J Matern Fetal Neonatal Med* 2009;22:101–5.
51. Tuuli MG et al. *Am J Obstet Gynecol* 2009;201:390.e1–5.
52. Hartman RJ et al. *Pediatr Cardiol* 2011;32:1147–57.
53. Trevisan P et al. *Arq Bras Cardiol* 2013;101:495–501.
54. Antonarakis SE et al. *Nat Rev Genet* 2004;5:725–38.
55. Bondy CA. *Horm Res* 2009;71(suppl 1):52–6.
56. Pont SJ et al. *Am J Med Genet A* 2006;140:1749–56.
57. Pollex, RL, Hegele RA. *Circulation* 2007;115:3130–8.
58. Thienpont B et al. *Eur Heart J* 2007;28:2778–84.
59. Jansen FA et al. *Ultrasound Obstet Gynecol* 2015;45:27–35.
60. Irving C et al. *Eur J Hum Genet* 2008;16:1336–40.
61. Sailani MR et al. *Genome Res* 2013;23:1410–21.
62. Wright D et al. *Ultrasound Obstet Gynecol* 2008;31:376–83.
63. Hyett JA et al. *Ultrasound Obstet Gynecol* 1997;10:242–6.
64. Atzei A et al. *Ultrasound Obstet Gynecol* 2005;26:154–7.
65. Hyett J et al. *Am J Med Genet* 1997;69:207–16.
66. Mogra R et al. *Ultrasound Obstet Gynecol* 2011;38:320–4.
67. Evans PR. *Br Heart J* 1950;12:258–62.
68. Rowe RD, Uchida IA. *Am J Med* 1961;31:726–35.
69. Martin GR et al. *Pediatr Res* 1989;25:77A.
70. Stoll C et al. *Ann Genet* 1998;41:44–51.
71. Tubman TRJ et al. *BMJ* 1991;302:1425–7.
72. Khoury MJ, Erickson JD. *Am J Epidemiol* 1992;136:1457–64.
73. Pradat P. *J Epidemiol Community Health* 1992;46:211–5.
74. Wells GL et al. *South Med J* 1994;87:724–7.
75. Freeman SB et al. *Am J Med Genet* 1998;80:213–7.
76. Vida VL et al. *Cardiol Young* 2005;15:286–90.
77. Bermudez BE et al. *Sao Paulo Med J* 2015;133:521–4.
78. Cleves MA et al. *Birth Defects Res A Clin Mol Teratol* 2007;79:657–63.
79. Nisli K et al. *Acta Cardiol* 2008;63:585–9.
80. Elmagrpy Z et al. *Cardiovasc J Afr* 2011;22:306–9.
81. Irving CA, Chaudhari MP. *Arch Dis Child* 2012;97:326–30.
82. Rankin J et al. *Pediatrics* 2012;129:1373–81.
83. Tan M et al. *J Paediatr Child Health* 2013;49:223–7.
84. Morris JK et al. *Am J Med Genet A* 2014;164A:2979–86.
85. Kim MA et al. *J Korean Med Sci* 2014;29:1544–9.
86. Stoll C et al. *Eur J Med Genet* 2015;58:674–80.
87. Freeman SB et al. *Genet Med* 2008;10:173–80.
88. Fesslova V et al. *Cardiol Young* 2002;12:18–26.
89. Huggon IC et al. *J Am Coll Cardiol* 2000;36:593–601.
90. Ashok M et al. *Indian Pediatr* 2003;40:659–64.
91. Langford K et al. *Prenat Diagn* 2005;25:137–9.
92. Ramachandran D et al. *G3 (Bethesda)* 2015;5:1961–71.
93. Ramachandran D et al. *Genet Med* 2015;17:554–60.
94. Locke AE et al. *Genet Epidemiol* 2010;34:613–23.
95. Paladini D et al. *Ultrasound Obstet Gynecol* 2000;15:104–8.
96. Paladini D et al. *Obstet Gynecol* 1993;81:679–82.
97. Cereda A, Carey JC. *Orphanet J Rare Dis* 2012;7:81.
98. Morris JK, Savva GM. *Am J Med Genet* 2008;146A:827–32.
99. Won RH et al. *Prenat Diagn* 2005;25:608–11.
100. Kagan KO et al. *Obstet Gynecol* 2006;107:6–10.
101. Musewe NN et al. *J Am Coll Cardiol* 1990;15:673–77.
102. Cheng PJ et al. *Prenat Diagn* 2003;23:248–51.
103. Bruns DA, Martinez A. *Am J Med Genet A* 2016;170A:337–43.
104. Matsuoka R et al. *Am J Med Genet* 1983;14:657–68.
105. Roberts W et al. *Clin Anat* 2016;29:628–32.
106. Springett A et al. *Am J Med Genet A* 2015;167A:3062–9.
107. Pont SJ et al. *Am J Med Genet A* 2006;140:1749–56.
108. Van Praagh S et al. *J Am Coll Cardiol* 1989;13:1586–97.
109. Hyett JA et al. *Fetal Diagn Therapy* 1995;10:381–6.
110. Kroes I et al. *Facts Views Vis ObGyn*. 2014;6:245–9.
111. Papp C et al. *J Clin Ultrasound* 2007;35:68–72.
112. Yeo L et al. *J Ultrasound Med* 2003;22:581–90.
113. Watson WJ et al. *J Ultrasound Med* 2008;27:1033–8.
114. Nyberg DA et al. *J Ultrasound Med* 1993;12:103–13.
115. Bronsteen R et al. *J Ultrasound Med* 2004;23:233–40.
116. Yang JH et al. *Prenat Diagn* 2005;25:119–22.
117. DeVore GR. *J Ultrasound Med* 2000;19:565–76.
118. Moyano D et al. Fetal echocardiography in trisomy 18. *Arch Dis Child Fetal Neonatal Ed* 2005;90:F520–2.
119. Sepulveda W et al. *Prenat Diagn* 2010;30:256–9.
120. Nagase H et al. *Congenit Anom (Kyoto)* 2016;56:35–40.
121. Paladini D et al. *Prenat Diagn* 2002;22:545–52.
122. Tennstedt C et al. *Heart* 1999;82:34–9.
123. Moerman P et al. *Hum Genet* 1988;80:349–56.
124. Watson WJ et al. *J Ultrasound Med* 2007;26:1209–14.
125. Tongsong T et al. *Int J Gynaecol Obstet* 2002;76:143–8.
126. Papageorghiou AT et al. *Am J Obstet Gynecol* 2006;194:397–401.
127. Chen CP, Chien SC. *J Med Ultrasound* 2007;15:58–66.
128. Chen CP. *Taiwan J Obstet Gynecol* 2010;49:3–12.
129. Lehman CD et al. *Radiology* 1995;194:217–22.
130. Lin HY et al. *Pediatr Int* 2007;49:380–6.
131. Papp C et al. *J Ultrasound Med* 2006;25:429–35.
132. Grati FR et al. *Prenat Diagn* 2015;35:801–9.
133. Scambler PJ. *Hum Mol Genet* 2000;9:2421–6.

134. Kobrynski LJ, Sullivan KE. *Lancet* 2007;370:1443–52.
135. Ryan AK et al. *J Med Genet* 1997;34:798–804.
136. McDonald-McGinn DM, Sullivan KE. *Nat Rev Dis Primers* 2015;1:15071.
137. Momma K. 2010. *Am J Cardiol*. 105:1617–24.
138. Kobrynski LJ, Sullivan KE. *Lancet* 2007;370:1443–52.
139. Carotti A et al. *Dev Disabil Res Rev* 2008;14:35–42.
140. McElhinney DB et al. *J Am Coll Cardiol* 2001;37:2114–9.
141. Zidere V et al. *Ultrasound Obstet Gynecol* 2006;28:876–81.
142. Razon Y et al. *J Am Soc Echocardiogr* 2014;27:1352–8.
143. Donnenfeld AE et al. *Am J Obstet Gynecol* 2006;194:508–11.
144. Lautrup CK et al. *Acta Obstet Gynecol Scand* 2008;87:1252–5.
145. Hollis B et al. *Ultrasound Obstet Gynecol* 2001;18:32–4.
146. Goldmuntz E et al. *J Am Coll Cardiol* 1988;32:492–8.
147. Marino B et al. *Genet Med* 2001;3:45–8.
148. Manji S et al. *Genet Med* 2001;3:65–6.
149. Boudjemline Y et al. *J Pediatr* 2001;138:520–4.
150. Volpe P et al. *Prenat Diagn* 2003;23:752–7.
151. Moore JW et al. *Am J Obstet Gynecol* 2004;191:2068–73.
152. Bretelle F et al. *Eur J Med Genet* 2010;53:367–70.
153. Lee MY et al. *Obstet Gynecol Sci* 2014;57:11–6.
154. Khositseth A et al. *Pediatr Cardiol* 2005;26:570–3.
155. Agergaard P et al. *Am J Med Genet A* 2012;158A:498–508.
156. Saenger P. *N Engl J Med* 1996;335:1749–54.
157. Surerus E et al. 2003. *Ultrasound Obstet Gynecol* 22:264–7.
158. Chervenak FA et al. *N Engl J Med* 1983;309:822–5.
159. Clark EB. 1984. *Teratology* 29:355–61.
160. Miyabara S et al. *Am J Med Genet* 1997;68:135–41.
161. Gotzsche CO et al. *Arch Dis Child* 1994;71:433–6.
162. Mazzanti L, Cacciari E. *J Pediatr* 1998;133:688–92.
163. Prandstraller D et al. *Pediatr Cardiol* 1999;20:108–12.
164. Völkl TM et al. *Clin Cardiol* 2005;28:88–92.
165. Bondy CA. *Congenit Heart Dis* 2008;3:2–15.
166. Kim HK et al. *Am J Roentgenol* 2011;196:454–60.
167. Lee SH et al. *J Korean Med Sci* 2013;28:1169–73.
168. Yan Y et al. *Ultrasound Obstet Gynecol* 2014;43:404–12.
169. Lee CN et al. *BJOG* 2012;119:614–25.
170. Shaffer LG et al. *Prenat Diagn* 2012;32:986–95.
171. Breckpot J et al. *J Pediatr* 2010;156:810–7.
172. Derwińska K et al. *Med Wieku Rozwoj* 2012;16:175–82.
173. Lalani SR, Belmont JW. 2014. *Eur J Med Genet* 57:402–13.
174. Greenway SC et al. *Nat Genet* 2009;41:931–5.
175. Iascone M et al. *Clin Genet* 2012;81:542–54.
176. Hitz MP et al. *PLOS Genet* 2012;8:e1002903.
177. Fakhro KA et al. *Proc Natl Acad Sci USA* 2011;108:2915–20.
178. Helm BM, Freeze SL. *Front Cardiovasc Med* 2016;3:19.
179. Azamian M, Lalani SR. *Mol Syndromol* 2016;7:51–61.
180. Vieira GH et al. *Eur J Hum Genet* 2012;20:148–54.
181. Warburton D. *Hum Genet* 2014;133:1353–9.
182. Reynolds JF et al. *Am J Med Genet* 1987;27:257–74.
183. van der Burgt I. *Orphanet J Rare Dis* 2007;2:4.
184. Prendiville TW et al. *Arch Dis Child* 2014;99:629–34.
185. Marino B(1), Digilio MC, Toscano A. *J Pediatr* 1999; 135:703–6.
186. Baldassarre G et al. *Prenat Diagn* 2011;31:949–54.
187. Nisbet DL et al. *Prenat Diagn* 1999;19:642–7.
188. Menashe M et al. *Ultrasound Obstet Gynecol* 2002;19:51–5.
189. Myers A et al. *Am J Med Genet A* 2014;164A:2814–21.
190. Gaudineau A et al. *Prenat Diagn* 2013;33:238–41.
191. Colquitt JL, Noonan JA. *Congenit Heart Dis* 2014;9:144–50.
192. Burch M et al. *J Am Coll Cardiol* 1993;22:1189–92.
193. Grandjean H et al. *Am J Obstet Gynecol* 1999;181:446–54.
194. Wong SF et al. *Ultrasound Obstet Gynecol* 2003;21:19–25.
195. Chew C et al. *Ultrasound Obstet Gynecol* 2007;29:619–24.
196. Copel JA et al. *Am J Obstet Gynecol* 1987;157:648–55.
197. Stümpflen I et al. *Lancet* 1996;348:854–7.
198. Nicolaides KH et al. *Br Med J* 1992;304:867–9.
199. Snijders RJM et al. *Lancet* 1998;352:343–6.
200. Hyett J et al. *BMJ* 1999;318:81–5.
201. Mavrides E et al. *Ultrasound Obstet Gynecol* 2001;17:106–10.
202. Michailidis GD, Economides DL. *Ultrasound Obstet Gynecol* 2001;17:102–5.
203. Hafner E et al. *Prenat Diagn* 2003;23:985–9.
204. Bahado-Singh RO et al. *Am J Obstet Gynecol* 2005;192:1357–61.
205. Bruns RF et al. *Arq Bras Cardiol* 2006;87:272–9.
206. Westin M et al. *Ultrasound Obstet Gynecol* 2006;27:632–9.
207. Muller MA et al. *Prenat Diagn* 2007;27:164–9.
208. Chelemen T et al. *Fetal Diagn Ther* 2011;29:127–34.
209. Rasiah SV et al. *Ultrasound Obstet Gynecol* 2006;28:110–6.
210. Rustico MA et al. *Ultrasound Obstet Gynecol* 2000;16:614–9.
211. Zidere V et al. *Ultrasound Obstet Gynecol* 2013;42:679–86.
212. Hyett JA et al. *Obstet Gynecol* 1996;87:506–10.
213. Huggon IC et al. *Ultrasound Obstet Gynecol* 2004;24:390–8.
214. Matias A, Montenegro N. *Semin Perinatol* 2001;25:32–7.
215. Timmerman E et al. *Ultrasound Obstet Gynecol* 2010;36:668–75.
216. Matias A et al. *Ultrasound Obstet Gynecol* 1999;14:307–10.
217. Bilardo CM et al. *Ultrasound Obstet Gynecol* 2001;17:288–94.
218. Murta CM et al. *Fetal Diagn Ther* 2002;17:308–14.
219. Zoppi MA et al. *Fetal Diagn Ther* 2002;17:52–7.
220. Favre R et al. *Ultrasound Obstet Gynecol* 2003;21:239–43.
221. Haak MC et al. *Am J Obstet Gynecol* 2003;188:727–33.
222. Toyama JM et al. *Ultrasound Obstet Gynecol* 2004;23;341–5.
223. Maiz N et al. *Ultrasound Obstet Gynecol* 2008;31:256–60.
224. Borrell A et al. *Ultrasound Obstet Gynecol* 2013;42:51–7.
225. Gembruch U, Smrcek JM. *Ultrasound Obstet Gynecol* 1997;9:374–82.
226. Huggon IC et al. *Heart* 2003;89:1071–3.
227. Falcon O et al. *Ultrasound Obstet Gynecol* 2006;27:609–12.
228. Faiola S et al. *Ultrasound Obstet Gynecol* 2005;26:22–7.
229. Pereira S et al. *Obstet Gynecol* 2011;117:1384–91.
230. Sinkovskaya ES et al. *Obstet Gynecol* 2015;125:453–60.

# 51

# Associated anomalies in congenital heart disease

Christoph Berg, Ulrich Gembruch, and Annegret Geipel

## Introduction

Extracardiac malformations are present in 20% of infants with congenital heart defects.[1] In prenatal series, the percentage is considerably higher, owing to the fraction of fetuses with major cardiac anomalies or chromosomal anomalies that either die *in utero* or undergo termination of pregnancy and therefore are not represented in postnatal series. A further bias leading to an increased rate of associated extracardiac malformations in prenatal cardiac series is due to the fact that the detection of a major extracardiac anomaly often prompts fetal echocardiography and therefore enhances the detection rate of cardiac defects in the subset of fetuses with extracardiac anomalies.

In a prospective trial in a nonselected population, Tegnander et al. reported extracardiac anomalies in 65% of fetuses diagnosed with major cardiac malformations (47% in combination with chromosomal anomalies).[2] However, if also less severe cardiac defects are taken into account, the incidence is considerable lower. In a preceding study incorporating critical as well as noncritical cardiac malformations, the same group reported rates of extracardiac anomalies and chromosomal defects of 26% and 9%, respectively.[3] Series from referral centers for fetal echocardiography are reporting rates of extracardiac malformations in their cohorts ranging from 29% to 37%, with percentages of chromosomal anomalies ranging from 18% to 26%, respectively.[4,5]

Complex and critical cardiac defects have a clear association with extracardiac anomalies and/or abnormal karyotype (Table 51.1), and these have a significantly worse outcome.[2,3,6] Furthermore, a cardiac defect is more likely to be recognized if an extracardiac anomaly and/or an abnormal karyotype is present.[2,3] In this context, increased nuchal translucency has evolved to be the most important extracardiac anomaly leading to the diagnosis of a cardiac defect.[7]

Therefore, the prenatal detection of a cardiac defect has to prompt a meticulous examination of the extracardiac anatomy, and *vice versa*, a detailed cardiac scan should follow the detection of any extracardiac malformation (Table 51.2). As some cardiac defects are clearly associated with extracardiac anomalies and/or aneuploidies while others are not, a profound knowledge of the pattern of associated conditions will enable the examiner, on the one hand, to perform a targeted sonography of the fetal anatomy and, on the other hand, to avoid invasive procedures unlikely to reveal an abnormal karyotype. Song et al. analyzed 383 fetuses with major structural cardiac defects.[204] The highest incidence of extracardiac abnormalities (>25%) included heterotaxy, single left ventricle and tricuspid atresia, hypoplastic left heart syndrome, and tetralogy of Fallot. Ninety-four of 334 (28.1%) fetuses tested had chromosomal abnormalities. The most common chromosomal abnormalities were trisomies 21 (43.6%), 18 (19.1%), and 13 (9.6%); monosomy X (7.4%); and 22q11.2 deletion (7.4%). This chapter aims to assist the examiner in two respects: What anomalies are most likely to be associated in the presence of a specific cardiac defect? What cardiac defects have to be taken into consideration when isolated or combined extracardiac anomalies are detected?

## Specific cardiac defects and their association with extracardiac malformations

### *Atrioventricular septal defect*

Atrioventricular septal defect (AVSD) is one of the most frequently diagnosed cardiac defects in the fetal period.[5,9,10] It is found as an isolated cardiac defect or as part of complex heart lesions and is frequently associated with chromosomal anomalies, ambiguities of the situs, extracardiac malformations, and nonkaryotypic syndromes.[11–14]

The prognosis of AVSD strongly depends on the associated conditions as well as the additional cardiac and extracardiac malformations. These parameters that ultimately form the basis for parental counseling differ largely between prenatal and postnatal series, with more severe cases in prenatal cohorts.[14] Furthermore, the associated conditions and therefore also the extracardiac anomalies reported in prenatal AVSD series depend on the referral base of the reporting centers.

Tegnander et al., who analyzed 30,149 fetuses in an unselected population, found 17/21 (80.9%) cases with AVSD to be associated with chromosomal anomalies (14 with trisomy 21, one with trisomy 18, and two others), and only 2/21 (9.5%) had complex cardiac malformations.[2]

**Table 51.1** Frequency of extracardiac and chromosomal anomalies in single types of congenital heart disease in an Italian multicenter study covering 847 fetuses with prenatally diagnosed congenital heart disease

| *Type of congenital heart disease* | *Extracardiac anomalies (%)* | *Chromosomal anomalies (%)* |
|---|---|---|
| Atrioventricular defect | 13.8 | 47.1 |
| Univentricular defect | 17.8 | 6.7 |
| Hypoplastic left heart syndrome | 10.9 | 4.2 |
| Tricuspid atresia | 34.3 | 8.6 |
| Tetralogy of Fallot | 25.0 | 26.7 |
| Double-outlet right ventricle | 19.3 | 45.2 |
| Truncus arteriosus communis | 21.4 | 28.6 |
| Transposition of great arteries | 25.6 | 2.6 |
| Corrected transposition of great arteries | 5.6 | 0.0 |
| Ebstein/dysplasia of tricuspid valve | 6.2 | 6.2 |
| Ventricular septal defect | 37.1 | 37.2 |
| Atrial septal defect ostium secundum | 16.1 | 3.2 |
| Aortic coarctation | 12.5 | 20.8 |
| Aortic stenosis | 13.0 | 17.4 |
| Pulmonary stenosis | 25.9 | 3.7 |
| Dilated cardiomyopathy | 28.6 | 0.0 |
| Myocarditis | 0.0 | 0.0 |
| Hypertrophic cardiomyopathy | 57.6 | 0.0 |
| Tumors | 6.2 | 12.5 |

*Source:* Modified after Fesslova V et al. *Heart* 1999;82:594–9.[5]

Conversely, in a representative study of 246 fetuses with AVSD from a tertiary referral center for fetal echocardiography, we found only 52% of fetuses with abnormal karyotype (31% trisomy 21, 13% trisomy 18, 3% trisomy 13, 5% others) and 29% with heterotaxy syndromes.[192] In this study, complex cardiac malformations were present in 44% of cases. This spectrum is comparable to that reported in previous prenatal AVSD series from tertiary referral centers,[11–15] with higher incidences of complex cardiac malformations and lower incidences of aneuploidies than seen in unselected prenatal populations.[2]

AVSD with a normal karyotype is strongly associated with more complex cardiac malformations and unbalanced ventricular morphology, particularly in heterotaxy syndromes. In contrast, fetuses with chromosomal anomalies are strongly associated with the balanced and isolated type of AVSD, namely, those with trisomy 21.[11–15] Therefore, a balanced AVSD without additional intracardiac malformations is most likely to be associated with the extracardiac anomalies occurring in trisomies 21, 18, and 13, while the unbalanced complex type of AVSD with additional intracardiac malformations is most likely to be associated with anomalies of the situs and the concomitant extracardiac malformations typical for heterotaxy syndromes.

In prenatal AVSD series, isolated extracardiac anomalies and nonkaryotypic syndromes are reported to be present in 13%–26%.[14,16,192] Isolated extracardiac malformations may affect all organ systems and include, among others, hydrocephaly, cleft lip/palate, meningocele, diaphragmatic hernia, tracheoesophageal fistula, omphalocele, duodenal atresia, polycystic kidneys, and anomalies of the extremities.[14,16,192]

Multiple extracardiac malformations are most frequently associated with VACTERL (vertebral anomalies, anal atresia, cardiac defect, tracheoesophageal fistula, renal and limb abnormalities) and CHARGE (coloboma of the eye, heart defects, atresia of the choanae, retardation of growth and/or development, genital and/or urinary abnormalities, ear abnormalities) associations, less frequently with Ellis–van Creveld syndrome, Cornelia de Lange syndrome, and Smith-Lemli-Opitz syndrome, among others.[14–17,192]

Details on the extracardiac anomalies associated with the above-named conditions are provided later in this chapter.

## Ventricular septal defect

Ventricular septal defects (VSDs) are the most frequently diagnosed cardiac defects in the first year of life.[1] Basically, they comprise muscular and perimembranous (inlet and outlet) defects, although a great variety of classification systems exist.[1,18] The rates of associated intra- and extracardiac anomalies depend on the localization as well as the size of the defect. In the prenatal period, VSDs are less frequently diagnosed than in the postnatal period, and in prenatal series the subset

**Table 51.2** Extracardiac malformations frequently associated with cardiac anomalies

| |
|---|
| **Central nervous system (2%–15%)** |
| Hydrocephalus |
| Microcephalus |
| Agenesis of the corpus callosum |
| Encephalocele |
| Dandy-Walker malformation |
| Neural tube defect |
| **Mediastinum (10%–40%)** |
| Diaphragmatic hernia |
| Tracheoesophageal fistula (VACTERL association) |
| **Gastrointestinal (12%–22%)** |
| Esophageal atresia |
| Duodenal atresia |
| Abnormal situs visceralis |
| Anorectal anomalies |
| **Abdominal wall (14%–30%)** |
| Omphalocele |
| Ectopia cordis |
| **Genitourinary (5%–40%)** |
| Hydronephrosis |
| Renal agenesis |
| Renal dysplasia |
| Horseshoe kidney |
| **Vascular (5%–10%)** |
| Single umbilical artery |
| Persistent right umbilical vein |
| Agenesis of ductus venosus |

*Source:* Copel JA et al. *Am J Obstet Gynecol* 1986;154:1121–32.[8]

of cases with associated anomalies is overrepresented.[18,19] The reason for this discrepancy is that a considerable part of the VSD cannot be detected in the four-chamber view, and therefore escapes the basic cardiac scan if the outflow tract is not examined and if the attention of the examiner is not attracted by the presence of extracardiac anomalies.

Furthermore, color Doppler sonography is often required for the diagnosis of small VSDs.

In their nonselected prospective cohort, Tegnander et al. reported 279 VSDs that were diagnosed in the prenatal or postnatal period.[2] Isolated muscular VSDs were present in 62%, small perimembranous VSDs (isolated or in association with minor cardiac defects) in 24%, large VSDs in 3%, and 11% occurred in association with conotruncal anomalies. Isolated muscular defects were associated with aneuploidies and extracardiac malformations in 1.2% and 4.4%, respectively. In small perimembranous defects, aneuploidies and extracardiac malformations were present in 23.5% and 8.8%, respectively. None of the muscular VSDs and only 13% of the isolated perimembranous defects were detected prenatally. All of the detected perimembranous VSDs were associated with aneuploidies. Associated aneuploidies and extracardiac malformations were present in 44% and 22% of the fetuses with large VSDs, and in 30% and 23% of the fetuses with conotruncal anomalies, respectively. In these two groups, the prenatal detection rate reached 52%; again, mainly those fetuses with associated aneuploidies or extracardiac malformations were diagnosed prenatally.

Paladini et al. reported aneuploidies and extracardiac malformations in 47% and 33%, respectively, in their series of 68 isolated VSDs.[18] The aneuploidies included trisomy 18 (21%), trisomy 21 (19%), and trisomy 13 (3%). Although the high rate of associated conditions in this study is certainly biased by the referral base, a distinct association between the site of the defect and the karyotype could be demonstrated: 69% of the fetuses with trisomy 18 had a malalignment VSD, while 82% of the fetuses with trisomy 21 had a perimembranous posterior defect of the inlet.[18] In a recent series of 171 VSD diagnosed in a period of 10 years, Mosimann et al. demonstrated that the risk of aneuploidy is low in cases with normal nuchal translucency and absence of extracardiac anomalies.[202] In fetuses with normal nuchal translucency and no other anomalies, they did not identify any karyotypic abnormality among 33 fetuses that were karyotyped. Conversely, 63 of 108 fetuses (58.3%) with VSDs and other sonographic abnormalities had an underlying karyotypic abnormality or syndromic diagnosis. There was a higher rate of aneuploidy in the group with a perimembranous VSD (69/118 [58.5%]) than in the group with a muscular defect (10/53 [18.9%]).

The extracardiac malformations in isolated VSD with normal karyotype may affect all organ systems. In their study of 146 fetuses with VSD detectable only by color Doppler, Axt-Fliedner et al. reported 18 (12%) euploid fetuses with extracardiac anomalies. Most frequent were anomalies of the central nervous system, neural tube defects, abdominal wall defects, and skeletal anomalies. Multiple malformations were present in four fetuses.[19] Respondek et al., who studied 100 consecutive fetuses with cardiac defects, reported five euploid fetuses with extracardiac anomalies among 12 fetuses with isolated VSD. The diagnoses included hydrocephaly ($n = 2$), gastroschisis, polycystic kidneys, and diaphragmatic hernia.[16]

## Conotruncal anomalies

Conotruncal anomalies comprise common arterial trunk, transposition of the great arteries (atrioventricular concordance with ventriculoarterial discordance), and tetralogy of Fallot. When the group of conotruncal defects is expanded to outflow tract defects, double-outlet right ventricle is added to the group.[20] The concept of grouping these cardiac defects originates from a presumed common etiology: an early failure or delay of the circular outflow tract in attaining an elliptical configuration, and a resulting disturbance of the cushions that form semilunar valves and the conotruncal septum.[21]

However, from an epidemiological point of view, it is doubtful that they represent equivalent malformations.[20] This is emphasized by the different spectrum of associated malformations within this group of cardiac defects. In their review of 12,932 live births and stillbirths with congenital heart defects from three registries, Harris et al. found tetralogy of Fallot, double-outlet right ventricle (DORV), and common truncus to be significantly associated with extracardiac malformations, while transposition of the great arteries was inversely correlated with extracardiac anomalies. Furthermore, DORV did not cluster with any of the three other conotruncal anomalies. The only common feature of the conotruncal anomalies was their occurrence in Patau syndrome.[20] Apparently, the conotruncal defects and the outflow tract defects are rather heterogeneous from an epidemiologic point of view, and it is doubtful that they should be grouped together.[20] In particular, dextrotransposition of the great arteries (atrioventricular concordance with ventriculoarterial discordance) as well as levotransposition (atrioventricular discordance with ventriculoarterial discordance) is most likely to result from looping anomalies, is rarely associated with aneuploidies and extracardiac malformations, and should therefore be considered separately.

## Tetralogy of Fallot

Extracardiac anomalies are present in 28%–30% of infants born with tetralogy of Fallot (TOF).[22] In prenatal collectives, the subset of fetuses with associated conditions is considerably larger. A recent study from a tertiary referral center in 129 prenatally diagnosed TOF reported 55 (43%) cases with aneuploidies (33% trisomy 21, 16% trisomy 18, 16% trisomy 13, 27% 22q11 microdeletions, and 7% miscellaneous).[23] Extracardiac anomalies occurred in 65 (50%) cases and in 22/37 (59%) cases in which chromosomal abnormalities had been excluded. Similar results are reported from other tertiary referral centers.[199] The associated defects vary in type and severity, and include talipes, tracheoesophageal fistula, cleft lip, abdominal wall defects, ventriculomegaly, single umbilical artery, and renal anomalies.[23] In their study of 61 fetuses with conotruncal anomalies, Tometzki et al., found 6/18 (33%) cases with TOF to be associated with extracardiac malformations and two (11%) with aneuploidies.[24] The extracardiac malformations in euploid fetuses included omphalocele, diaphragmatic hernia ($n = 2$), renal agenesis, and pentalogy of Cantrell. In a nonselected prenatal collective, 5/7 (71%) fetuses with TOF had extracardiac anomalies, three of them in combination with aneuploidies.[2]

While the two variants of TOF—pulmonary atresia with VSD and TOF with absent pulmonary valve syndrome—have a spectrum and incidences of associated aneuploidies and extracardiac malformations similar to the classic type of TOF, they differ largely concerning the association with microdeletion 22q11.

Vesel et al. reported 40% chromosomal anomalies and 19% extracardiac malformations in their series of 27 fetuses with pulmonary atresia and VSD.[25] Among 40 fetuses with TOF and absent pulmonary valve syndrome, we found 45% chromosomal anomalies and 8% extracardiac malformations.[196] Furthermore, monosomy 22q11 is found in 14% of classic TOF, 21% of pulmonary atresia with VSD (40% in the presence of major aortopulmonary collateral arteries), and up to 37% of tetralogy of Fallot with absent pulmonary valve syndrome.[26–28]

As there is no specific extracardiac malformation associated with tetralogy of Fallot and its variants, a thorough search of the fetal anatomy is mandatory upon detection. Karyotyping has to be considered, especially in the presence of multiple anomalies, as well as a search for 22q11 microdeletions.

## Double-outlet right ventricle

DORV is a rare anomaly with a high degree of complexity and variation. It is frequently associated with additional intracardiac malformations, extracardiac malformations, anomalies of the situs, and aneuploidies. The reported rates of aneuploidies as well as extracardiac malformations vary considerably. In a series of 19 fetuses diagnosed with DORV, Kim et al. reported 21% chromosomal anomalies and 36% heterotaxy syndromes.[29] In another series of 22 cases with DORV, 14% were associated with aneuploidies and another 14% with major extracardiac malformations in euploid fetuses.[24] These results were largely confirmed in recent studies.[204] In their multicenter series of 847 fetuses with cardiac malformations, Fesslowa et al. reported 45% chromosomal anomalies and 19% extracardiac malformations among the 31 cases of DORV.[5] The most frequently diagnosed aneuploidies were trisomy 18 (26%), trisomy 13 (13%), and trisomy 21 (10%). The associated extracardiac anomalies frequently reported in euploid fetuses with DORV include Dandy-Walker anomaly, hydrocephalus, absence of corpus callosum, diaphragmatic hernia, and the anomalies commonly associated with VACTERL association and heterotaxy syndromes.[6,16,24]

## Common arterial trunk

Common arterial trunk is frequently associated with aneuploidies and extracardiac anomalies. Fesslova et al. reported 29% aneuploidies and 21% extracardiac malformations among 14 cases with common arterial trunk in their series.[5] Likewise, Tometzki et al. found 33% aneuploidies and another 33% with extracardiac anomalies in their cohort.[24] Microdeletions of chromosome 22q11 are present in one-third of the cases,[27] namely, those with associated anomalies of the aortic arch (e.g., right aortic arch and interrupted aortic arch) and its branches (e.g., aberrant right subclavian artery).[30] The leading aneuploidies in common arterial trunk are trisomy 13 and trisomy 18.[5,24,30] The extracardiac anomalies in euploid fetuses include anophthalmos, hydrocephalus, duodenal atresia, imperforate anus, and those occurring in CHARGE association.[4,30,31]

## Hypoplastic left heart syndrome

Hypoplastic left heart syndrome (HLHS) is not a single entity but is rather a spectrum of congenital heart malformations characterized by severe hypoplasia of the left ventricle and left ventricular outflow tract. In "classical" HLHS, the aortic valve is atretic, with either atresia or severe hypoplasia of the mitral valve. In some instances, the term has been applied to other lesions including critical aortic stenosis with severe hypoplasia of the left ventricle, unbalanced AVSD, and severe coarctation of the aorta.[32] Hence, it is not surprising that the reported rates of associated conditions vary widely in published series. In the series of 382 fetuses with major congenital heart defects published by Song et al.,[204] the importance of a meticulous differentiation of the underlying conditions of a small left ventricle has been emphasized: the incidence of extracardiac anomalies (including chromosomal anomalies) in coarctation of the aorta, hypoplastic left heart syndrome, and aortic stenosis was 56%, 37%, and 17%, respectively. In "classical" HLHS, the incidence of karyotypic anomalies is 4%–10%.[10,33,34] Allan et al. reported two cases of trisomy 18 and one case of monosomy X in their series of 30 fetuses with HLHS, resulting in an incidence of aneuploidies of 10%. Two fetuses had extracardiac anomalies (7%)—a tracheoesophageal fistula and multiple small bowel atresias, respectively.[34] Brackley et al. found similar incidences among their 87 fetuses.[35] Seven had chromosomal anomalies (8%), including two cases of trisomy 13, one case of monosomy X, and four structural chromosomal anomalies. The 6/80 (7%) extracardiac anomalies in euploid fetuses included renal hypoplasia, agenesis of corpus callosum, Dandy-Walker variant, omphalocele, hemivertebrae, and tracheoesophageal fistula.[35]

## Tricuspid atresia

Tricuspid atresia is highly associated with additional cardiac anomalies and less frequently with other conditions. Aneuploidies and extracardiac anomalies have been reported in 2%–9% and 19%–34%, respectively.[5,10,20,36] In a series of 65 fetuses, we found five (8%) chromosomal anomalies (two with trisomy 13, one with trisomy 18, and two with partial tetrasomy 22q11), two cases had a VACTERL association, one case had unilateral renal agenesis, one case had hypospadia, one case had unilateral clubfoot and hydrothorax, one case had megazystis, and one case had agenesis of DV.[193]

## Anomalies of the aortic arch

### Right and double aortic arch

Anomalies of the aortic arch that concern the vessel course and/or its branching pattern include right aortic arch (RAA) with mirror-image branching; RAA with aberrant left subclavian or innominate artery; double aortic arch (DAA); circumflex retroesophageal aortic arch; or left aortic arch with an aberrant right subclavian artery.[37]

Depending on the type of anomaly, important associated conditions are intra- and extracardiac malformations, postnatal tracheal or esophageal compression, left subclavian steal syndrome due to constriction of the aberrant artery, and chromosomal anomalies, namely, microdeletion of the DiGeorge critical region of chromosome 22q11.[38–44]

The risk of concomitant congenital heart disease is over 90% with the mirror-image branching type and only 10% with the RAA and aberrant left subclavian artery. Double aortic arch usually occurs as an isolated finding.[44,45]

The most common association is tetralogy of Fallot where the incidence of RAA (usually the mirror-image branching pattern) ranges from 13% to 35%.[42,46,47] Other frequent associations are pulmonary atresia with VSD, and truncus arteriosus with incidences of RAA of 31%–36% and 15%–36%, respectively.[42,46]

In our own series of 71 cases with RAA, 28 (39%) had extracardiac anomalies.[44] Of these, 68% were abnormalities of the situs in heterotaxy syndromes and 18% were associated with microdeletion 22q11. The latter included hydramnios, esophageal atresia, cleft lip/palate, spina bifida, and clubbed feet.

### Coarctation of the aorta

Coarctation accounts for 7.1%–8.3% of CHD in fetal series and is significantly associated with chromosomal and extracardiac anomalies.[4,5,9] Paladini et al. reported 29% chrosomosomal anomalies and 18% major extracardiac anomalies in their series of 68 fetuses.[48] The most frequent diagnoses among the 20 fetuses with chromosomal aberrations were monosomy X (35%), trisomy 21 (15%), trisomy 18 (15%), trisomy 13 (15%), and microdeletion 22q11 (5%). The extracardiac anomalies in euploid fetuses included agenesis of the corpus collosum, encephalocele, esophageal atresia, anorectal atresia, bilateral renal agenesis, pyelectasis, polycystic kidney, hypospadia, club-foot, eye and ear anomalies, osteogenesis imperfecta, thanatophoric dwarfism, Ellis–van Creveld syndrome, Cornelia de Lange syndrome, Roberts syndrome, and Jeune syndrome.[48] Likewise, in the series of Song et al.,[204] aortic arch obstruction was associated with chromosomal and extracardiac anomalies in 37% and 53%, respectively. The leading extracardiac anomalies in euploid fetuses were skeletal (18%), urogenital (18%), and respiratory (12%).

### Interrupted aortic arch

Interrupted aortic arch is a rare, severe form of congenital heart disease; it can be subdivided into three groups according to the site of interruption: type A, interruption distal to the left subclavian artery; type B, interruption between the left carotid and left subclavian arteries; and type C, interruption between the innominate artery and the left carotid artery.[30] Type A is rarely associated with 22q11 deletion,[49,50] whereas type B is associated with 22q11 deletion and other extracardiac features in 50%–80% of cases (only part of them detectable at prenatal ultrasound),[51,52] often in the context of

specific syndromes, namely, DiGeorge syndrome or velocardiofacial syndrome; type C is by far the least common form of interrupted aortic arch, accounting for fewer than 5% of cases.

Among nine fetuses with interrupted aortic arch detected prenatally, Volpe et al. reported six with type B and three with type A. Five had a microdeletion 22q11 (four type B cases and an unusual association with one type A case). All cases were *de novo*. None of the nine cases were associated with extracardiac anomalies.[53] However, in a subsequent study in 141 fetuses with conotruncal anomalies or anomalies of the aortic arch (28 of them with 22q11 microdeletion), the same group reported that the association with 22q11 microdeletions is significantly predicted by the presence of associated ultrasound findings: thymic hypo/aplasia, intrautetine growth restriction (IUGR), and additional aortic arch anomalies.[54] Of the 18 patients with postnatally confirmed interrupted aortic arch in the series of Vogel et al.,[205] 12 (67%) had an identified chromosomal abnormality or syndrome, chromosome 22q11 deletion in 10 patients, Turner syndrome in 1, and VACTERL association in 1.

## Specific cardiac defects less likely to be associated with extracardiac anomalies

While most of the cardiac anomalies are to a certain extent associated with extracardiac anomalies and aneuploidies, this is not true for transposition of the great arteries, left and right outflow tract obstruction with intact ventricular septum, and tricuspid valve dysplasia including Ebstein anomaly.

### *Transposition of the great arteries*

Transposition of the great arteries exists in two distinct variants: atrioventricular concordance with ventriculoarterial discordance (d-TGA) and atrioventricular discordance with ventriculoarterial discordance (congenitally corrected TGA or l-TGA). Both variants are highly associated with additional cardiac malformations but rarely associated with aneuploidies and extracardiac malformations.[6]

Most prenatal series report rates of aneuploidies and extracardiac malformations ranging 0%–7% and 13%–26%, respectively.[4,5,16,24] Fesslova et al. reported one case each of trisomy 21 and trisomy 18 in their series of 39 fetuses with d-TGA.[5] Tometzki et al. reported one case of trisomy 13 among 15 cases of d-TGA.[24] The negative correlation between transposition and an abnormal karyotype is especially true for fetuses with atrioventricular and ventriculoarterial discordancy.[55] The reported extracardiac anomalies in transposition of the great arteries in euploid fetuses include hydrocephalus, diaphragmatic hernia, renal anomalies, and anomalies of the situs associated with heterotaxy syndromes.[24,55]

### *Left ventricular outflow tract obstruction*

In critical aortic stenosis, the incidence of karyotypic abnormalities and extracardiac anomalies is exceedingly low. Two large prenatal series reported no such abnormalities in their cohorts.[10,33] Fesslova et al. reported one case of monosomy X and three cases with extracardiac anomalies among 23 fetuses with aortic stenosis.[5]

### *Right ventricular outflow tract obstruction with intact ventricular septum*

In the presence of an intact ventricular septum, pulmonary atresia and pulmonary stenosis are isolated findings in most cases. Allan et al. reported 5% chromosomal anomalies among their 55 cases.[10] Todros et al. found one case of trisomy 22, one Noonan syndrome, and one case with dysplastic kidneys among their 33 cases, resulting in an incidence of 3% and 6% of aneuploidies and extracardiac anomalies, respectively.[56]

### *Tricuspid dysplasia and Ebstein anomaly*

Although sporadic cases with aneuploidies, namely, Down syndrome, have been reported,[57,58] most cases with tricuspid dysplasia occur as isolated lesions.[59] Sharland et al. reported two cases (5%) with aneuploidy in their series of 38 fetuses with tricuspid dysplasia or Ebstein anomaly.[60] Similar incidences are reported in other large prenatal and neonatal series.[5,10,20] Extracardiac anomalies are reported equally rarely, and include neural tube defects, craniofacial defects, and anomalies of the central nervous system and the limbs.[6,61] In a study on 76 prenatally diagnosed fetuses with Ebstein anomaly, 11 cases (14.5%) were associated with chromosomal anomalies, 7 (9.2%) had nonchromosomal extracardiac anomalies, 3 (3.9%) had a combination of cardiac and extracardiac anomalies, and 2 (2.6%) had nonchromosomal syndromes.[194]

## Specific extracardiac malformations and their association with cardiac defects

### *Head and central nervous system*

Anomalies of the central nervous system are seen in 4% of fetuses indentified to have congenital heart disease.[5] The anomalies most frequently associated with cardiac defects are ventriculomegaly, hydrocephalus, Dandy-Walker malformation,

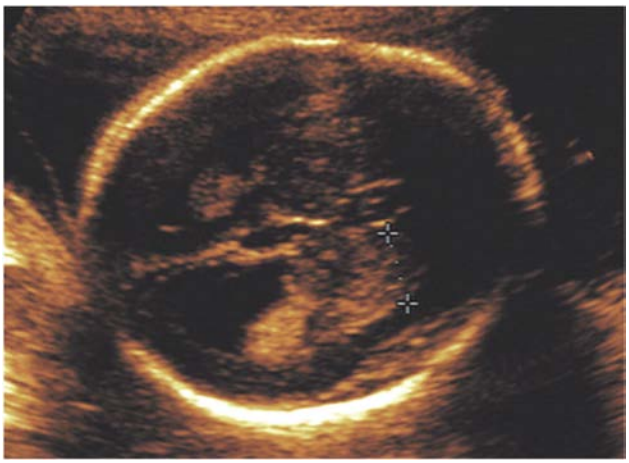

**Figure 51.1**
Mild ventriculomegaly in a fetus with Down syndrome and atrioventricular septal defect.

holoprosencephaly, and agenesis of the corpus callosum, while in neural tube defects (except for encephalocele in Meckel-Gruber syndrome), porencephaly, and hydranencephaly no specific association has been described.[22] Because the etiology of microcephaly is heterogeneous, including chromosomal aberrations, viral infections, and environmental agents (e.g., phenytoin and ethanol), congenital heart disease is often present.[8]

## Ventriculomegaly and hydrocephalus

Identification of isolated mild ventriculomegaly (defined as atrium of the lateral ventricles between 10–15 mm) (Figure 51.1) presents a counseling dilemma because it can represent a normal physiologic variant or can be the epiphenomenon of a heterogeneous group of pathologic processes that include increased intraventricular pressure, primary neuronal loss, and abnormalities of brain development such as those seen with chromosomal anomalies. Mild dilatation of the cerebral ventricles should therefore prompt a careful search for associated anomalies including cardiac defects, whose presence carries a poor prognosis.[62] Among 82 fetuses with mild ventriculomegaly analyzed by Vergani et al.,[62] 34/82 (42%) had associated anomalies, 7/82 (9%) had aneuploidies, and 5/82 (6%) had cardiac defects (one in combination with trisomy 21).

Severe ventriculomegaly (atrium of the lateral ventricles >15 mm) is less frequently associated with aneuploidies and cardiac defects. In the series of Gaglioti et al., 60 fetuses had a ventricular width >15 mm and 116 < 15 mm. All nine cases with aneuploidy and all six cases with cardiac defects (four of them in aneuploidies) occurred in the group <15 mm.[63] Likewise, Breeze et al. found only one case of trisomy 21 and none with associated cardiac defects in their series of 20 fetuses with severe ventriculomegaly.[64]

## Agenesis of the corpus callosum

In fetuses with prenatally diagnosed agenesis of the corpus callosum, about one-third of cases are isolated and two-thirds are complicated by associated structural defects and/or an underlying chromosomal abnormality. In a recent study of 117 cases, 42% had other structural anomalies and 28% had chromosomal aberrations.[65] In a study on 140 fetuses with agenesis of the corpus callosum, 29% (41/140) were isolated and 71% (99/140) were nonisolated cases. Nonisolated forms were associated with additional nonchromosomal cerebral anomalies in 22.2% (22/99), extracerebral nonchromosomal malformations in 40.4% (40/99), aneuploidies in 21.2% (21/99), and syndromes in 16.2% (16/99). All aneuploid fetuses except one showed cerebral or extracerebral malformations.[203] Therefore, the incidence of cardiac defects in complete agenesis of the corpus callosum is high. Among 19 cases of prenatally diagnosed partial agenesis of the corpus callosum, Volpe et al. found five (26%) cases with associated cardiac malformations, three of them in combination with chromosomal anomalies.[66]

## Dandy-Walker malformation

Dandy-Walker malformation (Figure 51.2) is frequently associated with intracranial anomalies, extracranial malformations, and aneuploidies. There seems to be little difference in the spectrum of associated findings between Dandy-Walker malformation and Dandy-Walker variant.[67] Among 99 fetuses with Dandy-Walker malformation (50/99) and Dandy-Walker variant (49/99) in the series of Ecker et al., 85% had associated sonographic anomalies, 49% had cardiac anomalies, and 21% had aneuploidies. Ulm et al. found 46% additional malformations, 18% cardiac anomalies, and 29% aneuploidies in their series of 28 fetuses. Sixty percent of the cardiac defects occurred in aneuploidies.[68] A recent prenatal series of 10 euploid fetuses reported only one case with associated VSD.

## Holoprosencephaly

Holoprosencephaly (Figure 51.3) is causally heterogeneous and is associated with various chromosomal abnormalities, single

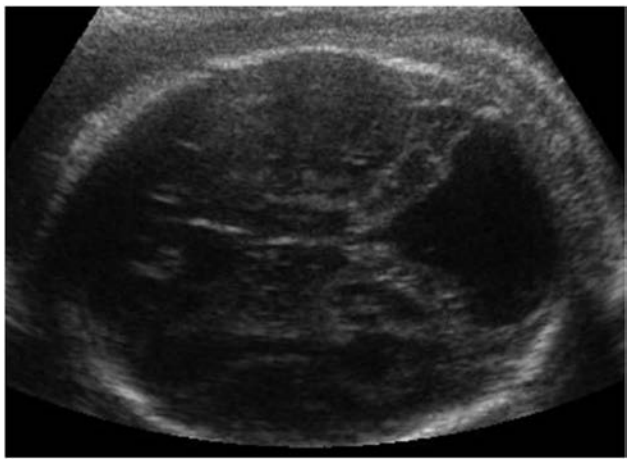

**Figure 51.2**
Dandy-Walker malformation in a fetus with multiple malformations including a large ventricular septal defect.

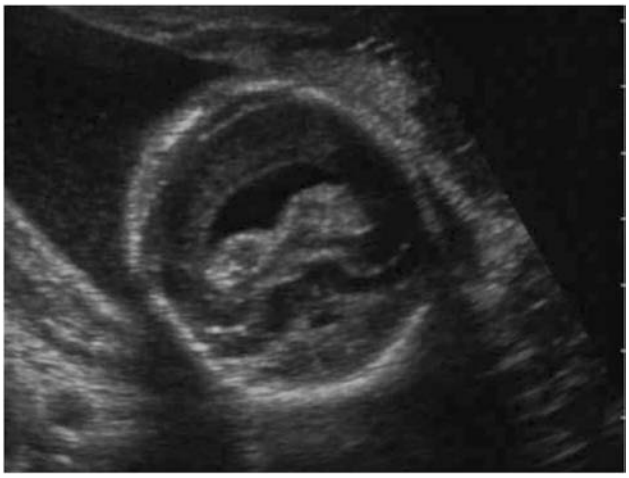

**Figure 51.3**
Alobar holoprosencephaly in a fetus with Patau syndrome and common arterial trunk.

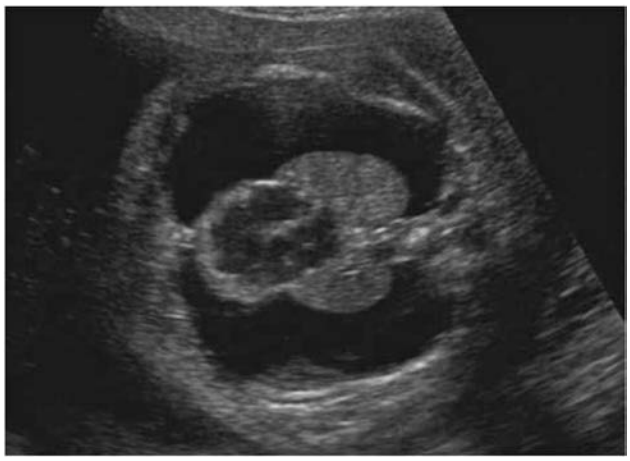

**Figure 51.4**
Bilateral hydrothorax in a fetus with Noonan syndrome and interrupted aortic arch.

gene disorders, teratogens, and maternal diabetes.[69] Cardiac anomalies are frequently detected, particularly in association with trisomy 13 where the incidence of cardiac defects is 90%–94%.[70] In the series of Ong et al., 30/113 (27%) had trisomy 13, 12/113 (11%) had other aneuploidies, 81/113 (72%) had additional malformations, and 24/113 (21%) had cardiac defects.[69]

## *Chest*

Anomalies of the chest likely to be associated with cardiac defects are esophageal atresia, aplasia of the thymus (see 22q11 microdeletion later in this chapter), hydrothorax, and diaphragmatic hernia. Pulmonary sequestration and congenital cystic adenomatoid malformation (CCAM) of the lung are isolated lesions in the vast majority of cases.[71,72] In a study on 41 fetuses with bronchopulmonary sequestration, only one case was associated with a cardiac defect.[200] Similarly, three out of 67 fetuses with CCAM in our recent series had VSDs, one of them in association with trisomy 21.[197]

### Esophageal atresia

Esophageal atresia is found in connection with a number of associations/syndromes, VATER or VACTERL being the most well known (see VACTERL association later in this chapter). Polyhydramnios and a small or invisible fetal stomach are the most common ultrasound findings when esophageal atresia is suspected prenatally.[73] However, these ultrasound findings have a low positive predictive value in diagnosing esophageal obstruction, and the false-positive rate has been high.[74] Conversely, only 20%–44% of affected infants are detected prenatally.[73,75] In a recent series of 48 cases, Brandtberg et al. reported associated anomalies in 79% and an abnormal karyotype in 23%. Cardiac anomalies were present in 21/48 (44%) of the cases and in 10/27 (37%) fetuses with a normal karyotype.[73] Most frequent other anomalies in fetuses with a normal karyotype were urogenital anomalies (48%), imperforate anus (41%), musculoskeletal anomalies (26%), and vertebral anomalies (26%), consistent with the spectrum of malformations seen in VACTERL association.

### Hydrothorax

Pleural effusion may be associated with a number of underlying conditions including nonimmune hydrops, intrathoracic mass, diaphragmatic hernia, trisomy 21, monosomy X, Noonan syndrome, and infection.[76]

Isolated hydrothorax (Figure 51.4) is most often caused by congenital chylothorax, a primary lymphatic abnormality. Associated malformations and aneuploidies are found in about 21%–25% and 4%–7%, respectively, and obviously worsen the outcome.[77,78] Rustico et al. found five (9%) cardiac anomalies among their 53 patients with prenatally diagnosed pleural effusion.[78] Likewise, Waller et al. reported 13 (5%) cardiac defects in their series of 246 fetuses with pleural effusion.[79] In a series of 78 fetuses with hydrothorax undergoing throracoamniotic shunting, 20% had trisomy 21%, 14% had genetic syndromes, and 4% had single cardiac anomalies.[201]

### Diaphragmatic hernia

Congenital diaphragmatic hernia (Figure 51.5) is frequently associated with other major malformations, karyotype anomalies, and syndromes. In a study from 20 registries of congenital malformations, including 187 cases of diaphragmatic hernia, Garne et al. reported 38% associated major malformations, karyotype anomalies, and syndromes. Eleven percent had associated cardiac anomalies.[80] Other authors found 33%–47% fetuses with associated malformations and abnormal karyotype in their series. Cardiac defects were present in 8%–9%.[81,82]

## *Abdomen and abdominal wall*

### Bowel obstruction

The major forms of gastrointestinal abnormality diagnosed prenatally are bowel atresias. Duodenal atresia (Figure 51.6)

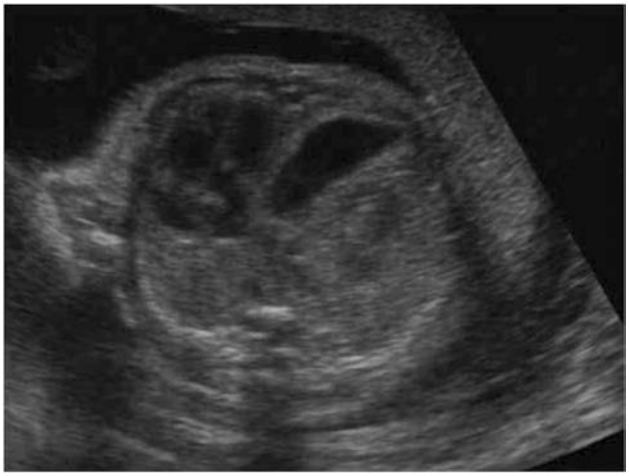

**Figure 51.5**
Dextroposition of the heart and herniated stomach in left-sided diaphragmatic hernia. A perimembranous ventricular septal defect was also present.

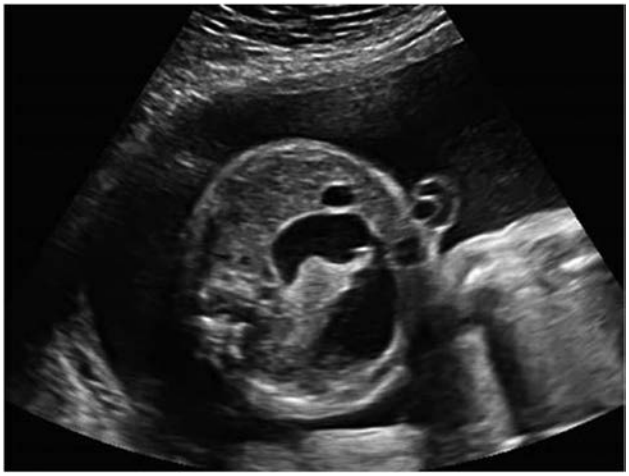

**Figure 51.6**
"Double bubble" sign in a fetus with Down syndrome, duodenal atresia, and atrioventricular septal defect.

is associated with trisomy 21 in 30%–60% of cases; therefore, the incidence of associated cardiac defects in prenatally diagnosed "double bubble" sign is quite high, ranging from 20% to 30%.[8,83] Among 275 cases of duodenal obstruction, Murshed et al. found Down syndrome in 30%, Down syndrome plus cardiac malformation in 14%, cardiac anomalies without Down syndrome in 23%, and other gastrointenstinal disorders in 42%.[84] Among their 10 cases with prenatally diagnosed duodenal atresia, Heydanus et al. reported one case of tetralogy of Fallot and one case of AVSD, both occurring among six cases of trisomy 21.[83]

Cardiac defects are only found in 3%–5% of fetuses diagnosed with jejunal or ileal atresia.[8,85] The affected fetuses mostly become apparent after 24 weeks of pregnancy, with dilated small bowel segments. Heydanus et al. reported one case of cystic fibrosis as the only associated extraintestinal condition among their 11 cases with prenatally diagnosed dilated bowel loops.[83] Likewise, Surana and Puri found only two cardiac defects and two cases with cystic fibrosis among their 59 fetuses with jejunal or ileal atresia.[85]

Anorectal atresia has been rarely recognized as dilated colon in the lower abdomen or as calcified intraluminal meconium at prenatal sonography. However, in these cases, the incidence of additional malformations exceeds 90%, consisting mainly of genitourinary malformations but also of the cardiovascular malformations occurring in VACTERL association.[86]

## *Ventral wall defects*

Fetal abdominal wall defects can be broadly categorized into gastroschisis, omphalocele, limb-body wall complex, cloacal and bladder exstrophy, ectopia cordis, and urachal cyst.[87]

Gastroschisis is isolated in most cases, and is typically not associated with chromosomal abnormalities. In their series of 109 fetuses with abdominal wall defects, Fratelli et al. found associated anomalies in only 2/40 (5%) cases with gastroschisis, while 51/67 (76%) cases with omphalocele were associated with aneuploidies or additional malformations.[88]

Omphalocele has two distinct etiologies: (1) failure of the normal infolding process of the lateral borders of the embryonic disc (folding failure of the caudal borders results in bladder exstrophy and folding failure of the cephalic portion in ectopia cordis); and (2) failure of the normal herniation of small intestine into the umbilical cord to reverse by the 12th week.[8] The former mechanism leads to large omphaloceles containing liver, colon, and other intra-abdominal organs (Figure 51.7), and may be associated with bladder exstrophy or ectopia cordis, and sternal and anterior diaphragmatic defects, while the latter results in omphaloceles containing small bowel only (Figure 51.8). Unsurprisingly, the associated anomalies are different between the two variants.

Fetuses with omphalocele with liver protruding into the sac have lower rates of abnormal karyotypes than fetuses with only the bowel in the sac. The most frequent chromosomal

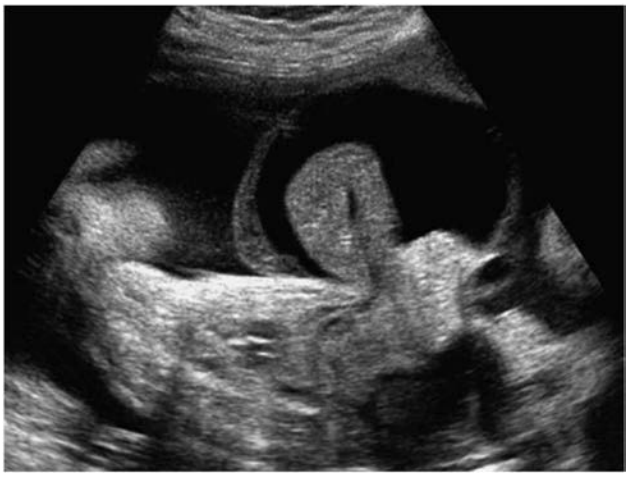

**Figure 51.7**
Large omphalocele containing liver and ascites.

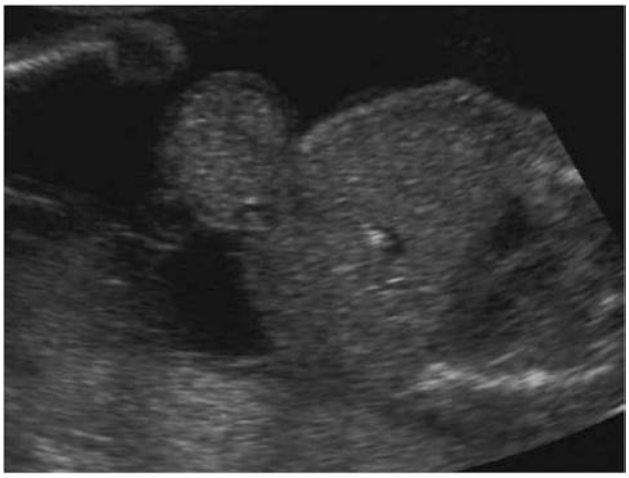

**Figure 51.8**
Small omphalocele containing small bowel only in a fetus with Edwards syndrome and a large perimembranous ventricular septal defect.

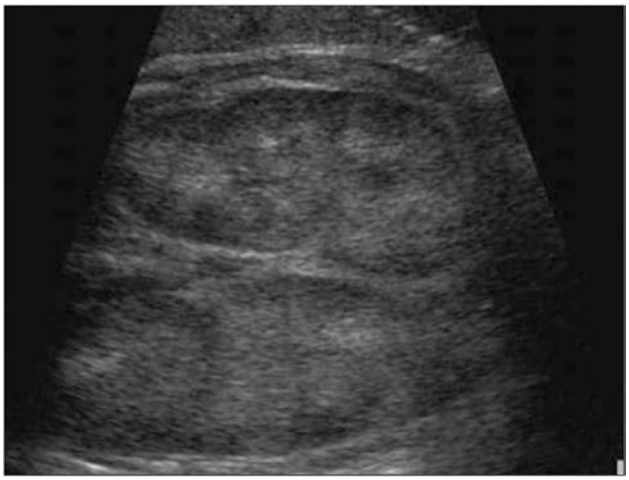

**Figure 51.9**
Large and hyperechogenic kidneys in Meckel-Gruber syndrome.

anomalies associated with omphalocele are trisomy 18 and 13, where cardiac defects are regularly associated.[87,89] Brantberg et al. reported 15 cases with cardiac defects among their cohort of 36 fetuses with omphalocele and a normal karyotype, including two fetuses with Beckwith–Wiedemann syndrome (see nonkaryotypic syndromes later in this chapter) and two with Cantrell pentalogy.[89]

Pentalogy of Cantrell[90] results from a folding failure of the caudal borders of the embryonic disc and features omphalocele, anterior diaphragmatic hernia, sternal cleft, ectopia cordis, and structural cardiac defects. Hornberger et al. reported 7/13 (54%) cases with tetralogy of Fallot and 6/13 (46%) with DORV in their cohort of children with ectopia cordis, most of whom also displayed features of pentalogy of Cantrell.[91]

## *Urogenital*

Cardiac anomalies are present in 8% of children born with genitourinary malformations.[92] The strongest association with cardiac defects has been reported for bilateral renal agenesis, horseshoe kidney, bilateral dysplastic kidneys, obstruction of the pelviureteric junction, and megacystis,[92,93] while unilateral lesions and obstructions of the vesicoureteric junction are less frequently associated with extrarenal anomalies.

Associated anomalies are seen in more than 50% of fetuses with renal agenesis. The major associated anomalies are cardiac defects (25%), the VATER association (27%), digital anomalies (15%), and mullerian anomalies (20%).[94]

Horseshoe kidney is associated with many other anomalies including urogenital, central nervous, gastrointestinal, musculoskeletal, and cardiovascular defects.[95,96] Greenwood et al. reported cardiac defects in 44% of neonates with horseshoe kidneys.[92]

Large "bright," or hyperechogenic, kidneys (Figure 51.9) represent a difficult diagnostic dilemma, particularly in the presence of a normal amout of amniotic fluid, since their underlying etiologies are relatively diverse. The differential diagnosis includes obstruction, autosomal recessive (infantile) polycystic kidney disease, autosomal dominant (adult) polycystic kidney disease, Beckwith–Wiedemann syndrome, Meckel-Gruber syndrome, and trisomy 13.[97] In the latter three, cardiac defects will be frequently present.

Twelve percent of fetuses with obstruction of the pelviureteric junction have other extrarenal abnormalities such as anorectal anomalies, congenital heart disease, VATER association, and esophageal atresia, but no particular pattern exists unless associated with chromosomal abnormality.[98]

Associated anomalies are seen in up to 43% of posterior urethral valves and the resulting megacystis. These include malrotation, anal atresia, the VATER association, and cardiac anomalies.

## *Multiple malformations in aneuploidies and nonkaryotypic syndromes*

### Down syndrome

A number of referral centers with expertise in targeted ultrasound examination report sonographic abnormalities in 60%–90% of second-trimester fetuses with Down syndrome in selected high-risk patients.[99–103]

Sonographic findings are commonly described as structural defects (major abnormalities) or minor abnormalities (markers). A wide variety of ultrasound markers have been associated with fetal Down syndrome during the second trimester.[99,102,104–106] The most frequently reported findings in fetuses with trisomy 21 include thickened nuchal fold, shortened long bones (humerus, femur), hyperechogenic bowel, renal pyelectasis, and intracardiac hyperechogenic foci. More recently, nasal bone hypoplasia, larger iliac wing angle, and shortened fingers have been added to the list of sonographic markers.[107–112] Systematic evaluation of those

multiple markers is commonly referred to as a second-trimester genetic sonogram. As the list of sonographic markers is growing, there is a high chance to identify at least one marker by routine ultrasound.

Congenital malformations associated with Down syndrome are less frequent than with trisomy 18 or trisomy 13 and will be identified in about 20%–30% of fetuses.[99,100,102,103,109,113] Those anomalies include heart defects, fetal hydrops, brachycephaly, ventriculomegaly, Dandy-Walker anomaly, agenesis of the corpus callosum, duodenal atresia, and abnormalities of the fingers, among others. Heart defects represent the most common anomaly, but there is a widely differing detection rate in the second trimester. In a targeted echocardiography study, Paladini et al. reported a 56% incidence of congenital heart disease in fetuses with known Down syndrome, which included VSD (48%), AVSD (44%), tetralogy of Fallot (4%), and coarctation of the aorta (4%). Conversely, 53% of cases with AVSD and normal visceral situs were associated with Down syndrome.[114] DeVore reported cardiac abnormalities in 76% of fetuses with Down syndrome, including structural and functional (tricuspid regurgitation and pericardial effusion) findings.[101]

## Edwards syndrome

Most fetuses with trisomy 18 have multiple abnormalities, and 80%–90% are detected sonographically in centers with expertise.[115–118] The most characteristic syndromal patterns involve the central nervous system, the limbs, and the cardiac system. Typical sonographic findings include choroid plexus cysts, a strawberry-shaped head and cisterna magna abnormalities, clenched fingers, radial defects, and clubbed or rocker bottom feet. They may also have micrognathia, omphalocele, and umbilical cord abnormalities.[115–118]

Pathological series suggest that congenital heart disease is universal in trisomy 18.[70,119,120] However, in prenatal series, the incidence of detected cardiac anomalies varies depending on the gestational age at scanning. Moyano et al. reported 27% sonographically normal hearts in the first trimester and 15% in the second trimester, respectively.[121] The types of cardiac defects seen in trisomy 18 are more varied than those associated with trisomy 21, and some of them might not be detectable at prenatal scan, such as small VSD and atrial septal defects. In Moyano's series, 17% had AVSD, 14% VSD, 13% coarctation of the aorta, 5% tetralogy of Fallot, and 26% no detected anomaly.[121]

Fetal growth restriction is a common finding. The prevalence increases with gestational age from about 30% in the early second trimester to 90% in the third trimester.[115,122] Severe fetal growth restriction in combination with polyhydramnios in a third-trimester fetus should prompt a detailed search for associated malformations, since infants with trisomy 18 do not benefit from altered perinatal management.

## Patau syndrome

Fetuses with trisomy 13 present with a cluster of characteristic sonographic abnormalities. The most frequently observed abnormalities include holoprosencephaly with the associated facial defects (hypotelorism, absent nose, cyclopia, and median clefts), neural tube defects, polydactyly (primarily of the hands), cardiac defects, omphalocele, enlarged polycystic kidneys, and growth restriction.[123,124]

Heart defects are present in up to 94% of fetuses with trisomy 13 in the first trimester. Most common are VSDs and a variety of valvular defects. Tetralogy of Fallot with absent pulmonary valve syndrome and truncus arteriosus are specifically associated with trisomy 13.[70]

The three characteristic features in Meckel-Gruber syndrome—postaxial polydactyly, occipital encephalocele, and polycystic kidneys—overlap with the syndromal pattern in trisomy 13; however, while Meckel-Gruber syndrome tends to present with severe oligohydramnios as early as 16 weeks,[125] the amniotic fluid volume in trisomy 13 may remain unchanged. To reliably distinguish between the two diagnoses, fetal karyotyping is required. This is important despite the lethal condition in both, as Meckel-Gruber syndrome is an autosomal recessive disease with a 25% recurrence risk in affected families.

## Triploidy

The most striking sonographic sign in triploidy (69,XXX; 69,XXY; 69,XYY) in the second trimester is an early onset severe asymmetrical growth restriction. Whereas the head appears appropriate for gestational age, the fetal abdomen and the extremities are growth restricted. Oligohydramnios and placentomegaly are common features, too. Structural fetal defects are observed antenatally in 70%–90%. The central nervous system (ventriculomegaly, Dandy-Walker malformation, and agenesis of the corpus callosum) is commonly affected. Other sonographic abnormalities seen in triploidy include facial dysmorphism (micrognathia), limb anomalies (syndactyly, clinodactyly, and talipes), congenital heart defects, neural tube defects, and renal malformations.[126–129]

In the series of Mittal et al., postmortem examination revealed cardiac defects in 4/20 (20%) fetuses with prenatally diagnosed triploidy (atrial septal defect, VSD, pulmonary stenosis, and common arterial trunk); however, none of these had been detected at sonography.[128]

## Turner syndrome

Clinical features of monosomy X include short stature, webbing of the neck, ovarian dysfunction, and cardiovascular abnormalities. Typical sonographic signs in this syndrome include huge septated cystic hygroma of the neck, increased nuchal translucency, cardiac defects, and renal malformations.[130–133]

A congenital heart defect is found in about 30% of postnatal cases of Turner syndrome. Left-sided obstructive defects predominate, especially bicuspid aortic valve and coarctation of the aorta.[134] There is a higher incidence of structural heart disease diagnosed in those cases that present during fetal life.[130–132] Surerus et al. reported cardiac malformations in 62% (33/53) of fetuses with Turner

syndrome investigated in the first and mid-second trimester. Coarctation of the aorta (45%) and hypoplastic left heart syndrome (13%) were the most common diagnoses. A markedly increased nuchal translucency was frequently associated (47/53).[131]

## Syndromes associated with 22q11 microdeletion

The clinical presentation of monosomy 22q11 includes patients with DiGeorge (DGS), Shprintzen, velocardiofacial (VCFS), and conotruncal anomaly face syndromes. A microdeletion of 22q11 has been shown to be associated with these anomalies in more than 80% of cases.[135,136] Subsequently, the syndromes have been grouped together under the acronym "CATCH-22": cardiac defects, abnormal facies, thymus aplasia or hypoplasia, cleft palate, hypocalcemia, and 22 denoting the deletion on chromosome 22.[137] Recently, it was suggested to abandon the acronym CATCH-22 and instead to use mainly deletion 22q11.

Conotruncal malformations are a major feature of 22q11 microdeletion and are present in 70%–80% of the affected patients.[27,138] The distribution of the various types of conotruncal malformations in neonates with 22qdel is random;[51] nevertheless, various cardiac phenotypes have been proved to be almost as specific for 22qdel as interrupted aortic arch type B or pulmonary atresia with VSD and multiple aortopulmonary collateral arteries.[28,51]

In a series of 261 consecutive fetuses with conotruncal defects and a normal karyotype, 54 (21%) had a 22q11 deletion.[27] Among these, 26% had tetralogy of Fallot, 20% pulmonary atresia with VSD, 19% interrupted aortic arch, 17% common arterial trunk, 11% absent pulmonary valve syndrome, and 7% DORV.

It has been proposed to test all fetuses with conotruncal defects for monosomy 22q11. However, the prevalence of 22q11 deletion has been reported to be fewer than 20% of patients with tetralogy of Fallot, leading to 80% unnecessary tests.[139] In addition, recent postnatal studies have shown that 22q11 deletion is very rare in patients with isolated tetralogy of Fallot.[27,140] Conversely, the vast majority of patients with tetralogy of Fallot and 22q11 deletion exhibit the other phenotypic features of the syndrome, namely, abnormal facial appearance, thymic aplasia or hypoplasia, and neonatal hypocalcemia.[141] In a fetal population, these extracardiac anomalies are difficult to identify. Extracardiac anomalies are also frequent in fetuses with conotruncal defects, but previous studies found no statistical difference between fetuses with and without 22qdel in their series, even for renal anomalies that were present in 30% of the fetuses with 22qdel.[27,142]

In their series of 151 fetuses with tetralogy of Fallot, Boudjemline et al. found increased nuchal translucency (in the first trimester), polyhydramnios, and growth restriction (in late pregnancy) to be more frequent in fetuses with 22q11 deletion as well as pulmonary arterial abnormalities. When these different features were present in the same fetus with tetralogy of Fallot, 22q11 deletion could be predicted with a sensitivity of 88%.[143]

Absence or hypoplasia of the thymus might be a further sonographic target. Chaoui et al. analyzed 149 fetuses with congenital heart disease and normal karyotype. Seventy-six fetuses had conotruncal anomalies and 22q11.2 deletion was present in 10 cases (6.7%), all of which had conotruncal anomalies (13.1%). Thymic hypoplasia or absence was suspected in 11 cases with conotruncal anomaly. Nine of these 11 had the deletion; two cases were false positive. One fetus with a normal-sized thymus had deletion of 22q11.2 (sensitivity 90%, specificity 98.5%, positive predictive value 81.8%, and negative predictive value 99.2%).[144] In a study of Barrea et al. in 16 fetuses with cardiac anomalies at risk for 22q11 deletion, the thymus was absent at prenatal sonography in all six cases with 22q11 deletion and present in all cases without.[145]

There are 763 syndromes listed on the London Dysmorphology Database where cardiac abnormalities can form part of the spectrum, and many of these are very rare.[146] In a recent review, Pajkrt et al. summarized the more common associations with cardiac abnormalities that may be detected prenatally (Table 51.3).

## Thrombocytopenia-absent radius syndrome

Thrombocytopenia-absent radius (TAR) syndrome is a congenital malformation syndrome of unknown inheritance that features bilateral absence of the radii with conservation of the thumbs and thrombocytopenia.[17] Other structural anomalies in TAR syndrome may include an absent ulna and/or humerus in 50%, lower leg involvement in 40%–47%, and renal anomalies in 23%.[147] Greenhalgh et al. reported 34 patients with TAR syndrome of whom five (15%) had cardiac anomalies, including atrial septal defect, VSD, and AVSD.[147]

## Cornelia de Lange syndrome

Cornelia de Lange syndrome is a well-described autosomal dominant multiple malformation syndrome typically involving proportionate small stature, developmental delay, specific facial features, major malformations (particularly the cardiac, gastrointestinal, and musculoskeletal systems), and behavioral abnormalities.[17,148]

Main sonographic features are asymmetrical upper limb defects (27%–58%), distinctive facial features including a long and smooth philtrum and fetal growth restriction (in late pregnancy), which is present in 80%–100% of cases (Figure 51.10).[17,149,150] Long, thick eyelashes may also be apparent on prenatal ultrasound (Figure 51.11). Nonskeletal anomalies include diaphragmatic hernia, nuchal webbing, duodenal atresia, renal dysplasia, cleft palate, and genital anomalies.[150,151] Cardiac anomalies have been reported in 14%–70% of cases, most commonly VSD but also atrial septal defect (ASD), pulmonary stenosis, tetralogy of Fallot, mitral atresia, stenosis or coarctation of the aorta, AVSD, and single ventricle.[17,152,153]

**Table 51.3** Nonkaryotypic syndromes frequently associated with congenital heart defects

| *Cardiac plus* | *Syndrome* | *Most common cardiac anomaly* | *Associated ultrasound features* | *Inheritance* | *Other aids to prenatal diagnosis in "new" cases* |
|---|---|---|---|---|---|
| Radial anomalies | TAR | ASD, VSD, AVSD | Thumbs present, absent ulna or humerus, lower leg involvement, renal anomalies | ?—associated with microdeletion on lq21.1 | Fetal blood sampling for platelet count |
| | Cornelia de Lange | VSD | FGR, microcephaly, abnormal profile, micrognathia, oligodactyly, thumb hypoplasia | AD—most are *de novo* mutations in NIPBL | Low maternal serum PAPP-A |
| | Holt-Oram | ASD | Absent or hypoplastic thumb, or more severe reduction defect of upper limb | AD—mutations in TBX5 | Positive family history and parental examination |
| | VATER association | Tetralogy of Fallot, ASD | Vertebral defects, tracheoesophageal fistula, cleft hard palate, ambiguous genitalia | ? | |
| Skeletal dysplasia | Short rib–polydactyly | Wide variety | Hypoplasia of thorax, short ribs, polydactyly | AR | |
| | Ellis–van Creveld | AVSD, common atrium | Short limbs, short ribs, polydactyly, renal anomalies | AR—mutations in EVC or EVC2 | |
| | Campomelic dysplasia | VSD, ASD, tetralogy of Fallot | Bowing of femur and tibia, talipes, hypoplastic scapulae, 11 pairs of ribs, small chest, micrognathia | AD—*de novo* mutations in SOX9 | |
| Nuchal edema/hydrops | Smith-Lemli-Opitz | AVSD, ASD | Polydactyly, cataracts, two- or three-toe syndactyly, renal anomalies, ambiguous genitalia, FGR | AR—mutations in DHCR7 | Amniotic fluid urinary cholesterol metabolites |
| | Noonan | Left ventricular hypertrophy, pulmonary stenosis | Short femur renal anomalies polyhydramnios | AD—40% have mutations in PTPN11 | Positive family history and parental examination |
| Miscellaneous | Goldenhar | Tetralogy of Fallot, VSD | Vertebral anomalies, renal anomalies | Sporadic | |
| | CHARGE | Conotruncal malformations, tetralogy of Fallot | Microphthalmia, genital anomalies | AD—mostly *de novo* mutations in CHD7 | |
| | Beckwith–Wiedemann | Various | Omphalocele, visceromegaly, macroglossia macrosomia | AD—most are *de novo* mutations | |
| | Meckel-Gruber | VSD | Large echogenic kidneys, polydactyly, encephalocele | AR | |
| | Tuberous sclerosis | Cardiac rhabdomyomas | Occasional renal, intracerebral lesions | AD—mutations in TSC1 or TSC2 | Positive family history parental examination, fetal MRI scan |

*Source:* Modified after Pajkrt E et al. *Prenat Diagn* 2004;24:1104–15.[17]

*Abbreviations:* AD, autosomal dominant; AR, autosomal recessive; ASD, atrial septal defect; AVSD, atrioventricular septal defect; CHARGE, charge association—coloboma, heart anomaly, choanal atresia, retardation, genital and ear anomalies; FGR, fetal growth restriction; MRI, magnetic resonance imaging; PAPP-A, pregnancy-associated plasma protein A; TAR, thrombocytopenia–absent radius syndrome; VSD, ventricular septal defect.

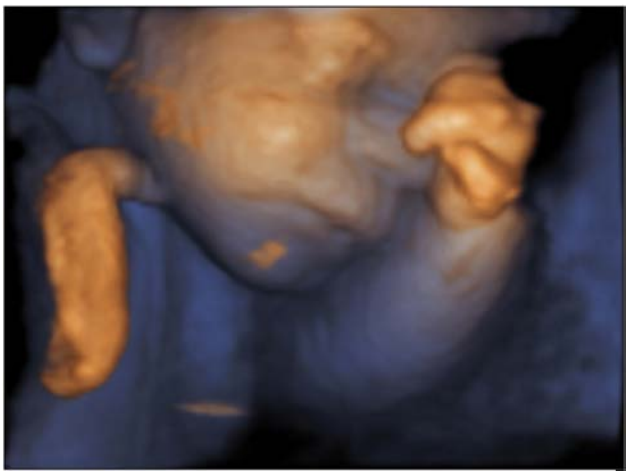

**Figure 51.10**
Limb reduction defect (oligodactyly right hand) and long philtrum in a fetus with Cornelia de Lange syndrome.

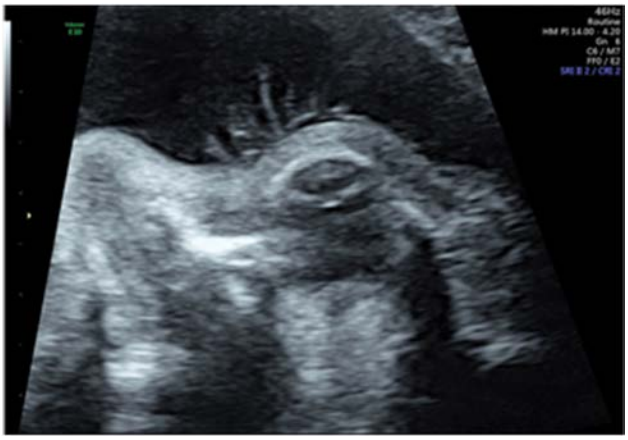

**Figure 51.11**
Long, thick eyelashes in a fetus with Cornelia de Lange syndrome.

## Holt-Oram syndrome

Holt-Oram syndrome is characterized by bilateral upper limb deformities, predominantly involving the radial ray, and congenital heart defects.[17] The characteristic findings are a thumb anomaly and/or radial aplasia. Cardiac anomalies are present in about 90% of patients and most commonly include atrial septal defect, common arterial trunk, mitral valve anomalies, and tetralogy of Fallot.[154]

## VACTERL association

VATER is an acronym for the association of vertebral defects (V), anal atresia (A), tracheoesophageal fistula with esophageal atresia (TE), and radial and renal dysplasia (R). The further observation of cardiac anomalies (C) and limb anomalies (L) expanded the name to VACTERL.[17] Vertebral anomalies and tracheoesophageal defects are present in 60%–65% of patients, anal atresia in 55%–60%, renal and cardiac anomalies in 70%–75%, and limb defects and thoracic anomalies in 35%–45%. Other common findings include ear abnormalities, facial cleft, and genitourinary anomalies.[155–157]

Among 15 cases of VATER association with cardiac defects reported by the Euroscan study group, five had complex cardiac defects, three had tetralogy of Fallot, three had atrial septal defects, two had VSDs, and two had tricuspid atresia.[158]

## Short rib–polydactyly syndromes

Short rib–polydactyly syndromes (Saldino-Noonan syndrome [type I], Majewski syndrome [type II], Verma-Naumoff syndrome [type III], and Beemer-Langer syndrome [type IV]) are lethal skeletal dysplasias inherited in an autosomal recessive fashion. They are characterized by generalized shortening of the long bones, thoracic hypoplasia, short ribs, polydactyly, and multiple visceral anomalies. They should be differentiated from the potentially surviving conditions of Jeune syndrome and Ellis–van Creveld syndrome that also feature shortened long bones/ribs and polydactyly.[17] Although all of these syndromes are associated with cardiac defects, the incidence in each type varies. Diglio et al. reviewed 28 patients with short rib–polydactyly syndromes and reported a wide variety of cardiac anomalies, including transposition of the great arteries (18%), coarctation of the aorta (14%), hypoplastic right or left heart (14%), AVSD (11%), and VSD (11%).[159]

## Ellis–van Creveld syndrome (chondroectodermal dysplasia)

Ellis–van Creveld (ECV) syndrome[160] is a nonlethal, autosomal recessive skeletal dysplasia characterized by short limbs, short ribs, postaxial polydactyly (Figure 51.12), cardiac and

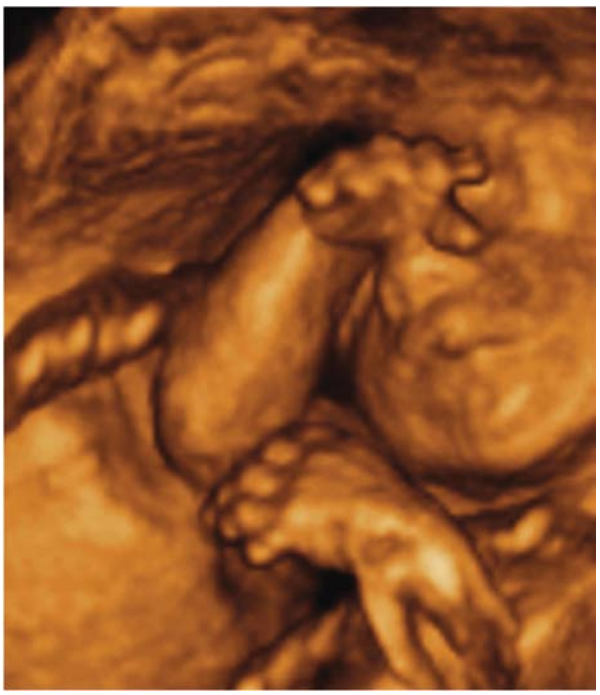

**Figure 51.12**
Bilateral postaxial hexadactyly in a fetus with Ellis–van Creveld syndrome and atrioventricular septal defect.

renal anomalies, and dysplastic nails and teeth. Congenital cardiac defects occur in 60% of affected individuals.[17] In a review of 76 patients with cardiac anomalies and ECV syndrome, 29% had an AVSD, 22% a common atrium, and 18% a combination of both. The remaining cases presented with ASD (11%), VSD (8%), or other defects (11%), including situs inversus.[159]

## Campomelic dysplasia

Campomelic dysplasia is a frequently lethal skeletal disorder caused by a severe defect in cartilage development. It is characterized by anterior bowing of the femur and tibia, a large head, a flat nasal bridge, talipes equinovarus, fan-like toes, and overlying skin dimples. Ambiguous genitalia occur in the majority of patients with an XY karyotype. Most cases are sporadic.[161] A third of the patients have heart malformations, mainly VSD, ASD, and tetralogy of Fallot.[17]

## Smith-Lemli-Opitz syndrome

Smith-Lemli-Opitz syndrome (SLOS)[162] is caused by a disorder of metabolism and features a wide variety of anomalies including postaxial polydactyly, second- and third-toe syndactyly, cataracts, renal anomalies (including cystic kidneys), ambiguous genitalia in males, fetal growth restriction (in late pregnancy), nuchal edema, or hydrops.[17,163] A defect in cholesterol synthesis is now recognized as the cause of SLOS, and leads to hypocholesterolemia with elevated levels of 7-dehydrocholesterol (7-DHC). The high levels of 7-DHC are thought to have teratogenic effects.[164] It is inherited in an autosomal recessive manner.

Almost half of the patients have heart defects, with a strong predominance of AVSD and VSD, and, less often, hypoplastic left heart, teralogy of Fallot, tricuspid atresia, and coarctation of the aorta.[146,163,165]

## Noonan syndrome

Noonan syndrome[166] is a multiple congenital anomaly syndrome comprising typical facial changes and various somatic abnormalities, including short stature, lymphedema, genital anomalies, and cardiac defects (mainly pulmonary stenosis and hypertrophic cardiomyopathy). It is inherited in an autosomal dominant manner.[17] The most common sonographic findings in previous prenatal series were polyhydramnios (58%), cystic hygroma (42%), increased nuchal translucency or fetal hydrops (33%), and cardiac anomalies (29%).[167–169] However, due to the diversity of prenatal presentation, the diagnosis of Noonan syndrome is challenging.

## Goldenhar syndrome (hemifacial microsomia)

Goldenhar syndrome[170] is a sporadic malformation syndrome featuring facial and vertebral anomalies.[17] Facial abnormalities are bilateral, but asymmetrical, and consist of ear deformities, ear dystopia (85%), preauricular or facial tags and/or pits and eye anomalies such as epibulbar dermoids (65%–70%) and upper eye lid colombomas (25%–30%), facial clefting (30%–35%), and hemifacial macrosomia (75%–80%) (Figure 51.13). Vertebral anomalies are present in 70%–75% of cases and affect mainly the cervical and upper thoracic regions.[155,170] Thoracic defects, renal anomalies, and cardiac defects are further features of Goldenhar syndrome.[17]

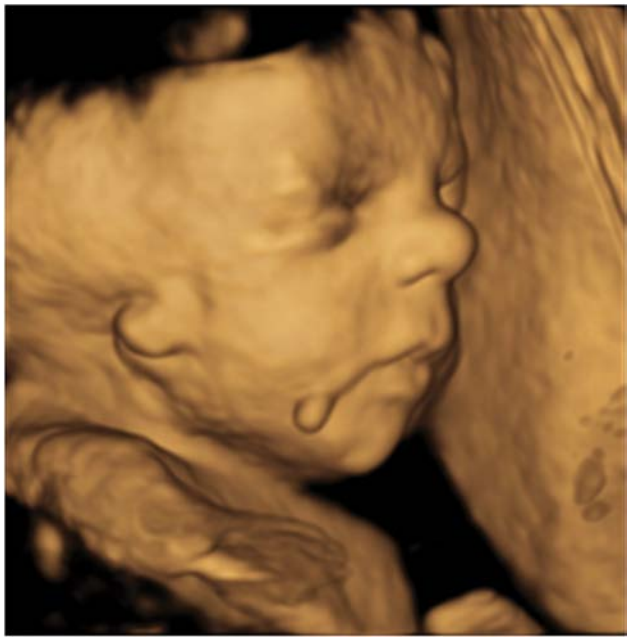

**Figure 51.13**
Ear dystopia and preauricular tags in a fetus with Goldenhar syndrome.

Cardiac defects are present in up to 35% of cases, with tetralogy of Fallot and VSD being most frequent among a wide variety of other cardiac defects.[171]

## CHARGE syndrome

CHARGE[172] is an acronym for coloboma of the eye (C), heart anomaly (H), choanal atresia (A), retardation of mental and somatic development (R), genital anomalies (G), ear abnormalities (E), and/or deafness. Facial palsy, cleft palate, and dysphagia are commonly associated. Cardiac defects of various types occur in CHARGE syndrome with incidences ranging from 50% to 85%,[173,174] and include atrial or VSD, AVSD, tetralogy of Fallot, DORV, and right aortic arch.[174]

## Beckwith–Wiedemann syndrome

Beckwith–Wiedemann syndrome[175] (exomphalos–macroglossia–gigantism syndrome) is sporadic in most cases and features macrosomia, macroglossia, visceromegaly, omphalocele, and a propensity to develop childhood tumors.[176] However, a number of additional other malformations are frequently present, namely, cardiovascular defects. Greenwood et al. reported structural cardiac anomalies in 7/13 (58%) postnatal cases with Beckwith–Wiedemann syndrome. No specific type of cardiac abnormality predominated.[177] In prenatally diagnosed cases, the incidence of cardiac anomalies is considerably lower. In a recent series of 12 prenatally diagnosed cases, none had associated cardiac anomalies.[198]

## Heterotaxy syndromes

Heterotaxy is defined as the abnormal arrangement of viscera across the left-right axis, differing from complete situs solitus and complete situs inversus.[178,179] There are two recognized variants of heterotaxy: left isomerism and right isomerism. Left isomerism is associated with paired left-sided viscera, while right-sided viscera may be absent. In contrast, right isomerism features paired right-sided viscera while left-sided viscera may be absent. Both variants are associated with complex cardiac malformations.

Typical findings in left isomerism are bilateral morphologic left atrial appendages (left atrial isomerism), viscerocardiac heterotaxy (situs ambiguus; with incoherent laterality of heart axis, stomach, portal sinus, or gallbladder), multiple cardiac anomalies (with a predominance of atrioventricular septal defect and right outflow tract obstruction), congenital heart block, bilateral morphologic left (bilobed) lungs with hyparterial bronchi, multiple splenules (polysplenia), intestinal malrotation, and interruption of the inferior vena cava with azygos continuation.[14,180–189]

Typical findings in right isomerism are bilateral morphologic right atrial appendages (right atrial isomerism), viscerocardiac heterotaxy (situs ambiguus; with incoherent laterality of heart axis, stomach, portal sinus, or gallbladder), multiple severe cardiac anomalies (with a predominance of atrioventricular septal defect, right outflow tract obstruction, anomalies of ventriculoarterial connections, and anomalous pulmonary venous return), bilateral morphologic right (trilobed) lungs with eparterial bronchi, an absent spleen (asplenia), and a malpositioned inferior vena cava, which may be anterior or juxtaposed to the aorta.[14,181,182,184–187,190,191]

Among the 165 fetuses diagnosed with heterotaxy syndromes in our centers over a period of 15 years, 91% had major congenital heart defects (89% in left isomerism and 95% in right isomerism). In left isomerism, the most frequently diagnosed cardiac malformations were AVSD (70%), right outflow tract obstruction (38%), and DORV (20%). In right isomerism 60% had an AVSD, 45% right outflow tract obstruction, 36% anomalous pulmonary venous drainage, and 27% each had DORV and transposition of the great arteries.[184,188,191,195]

Extracardiac anomalies that did not involve the spleen were present in 26/165 (15.8%) cases. Fifteen (14.3%) had extracardiac anomalies with significant impact on the postnatal course: one neonate died following repair of an encephalocele, six had successful treatment for various types of intestinal malrotation and/or atresia, and one underwent hiatal hernia repair; the remaining seven had biliary atresia, of which five died and the two survivors are awaiting liver transplantation. The status of the spleen was assessed in 93/105 live-born children and was found to be abnormal in 84/93 (90.3%). There were three cases of lethal sepsis, all associated with asplenia. Of the 38 postnatal deaths, 29 (76.3%) had a cardiac cause, seven (18.4%) had an extracardiac cause, and in two (5.2%) the reason was uncertain.[195]

# References


1. Ferencz C et al. *Am J Epidemiol* 1985;121:31–6.
2. Tegnander E et al. *Ultrasound Obstet Gynecol* 2006;27:252–65.
3. Tegnander E et al. *Ultrasound Obstet Gynecol* 1995;5:372–80.
4. Paladini D et al. *Prenat Diagn* 2002;22:545–52.
5. Fesslova V et al. *Heart* 1999;82:594–9.
6. Pradat P et al. *Pediatr Cardiol* 2003;24:195–221.
7. Carvalho JS et al. *Heart* 2002;88:387–91.
8. Copel JA et al. *Am J Obstet Gynecol* 1986;154:1121–32.
9. Brick DH, Allan LD. *Pediatr Cardiol* 2002;23:449–53.
10. Allan LD et al. *J Am Coll Cardiol* 1994;23:1452–8.
11. Machado MV et al. *Br Heart J* 1988;59:352–5.
12. Allan LD. *Am J Obstet Gynecol* 1999;181:1250–3.
13. Fesslova V et al. *Cardiol Young* 2002;12:18–26.
14. Huggon IC et al. *J Am Coll Cardiol* 2000;36:593–601.
15. Delisle MF et al. *Obstet Gynecol* 1999;94:763–7.
16. Respondek ML et al. *Ultrasound Obstet Gynecol* 1994;4:272–8.
17. Pajkrt E et al. *Prenat Diagn* 2004;24:1104–15.
18. Paladini D et al. *Ultrasound Obstet Gynecol* 2000;16:118–22.
19. Axt-Fliedner R et al. *Ultrasound Obstet Gynecol* 2006;27:266–73.
20. Harris JA et al. *Pediatr Cardiol* 2003;24:222–35.
21. Yu IT, Hutchins GM. *Teratology* 1996;53:31–7.
22. Copel JA et al. *Semin Perinatol* 1993;17:89–105.
23. Poon LC et al. *Ultrasound Obstet Gynecol* 2007;29:625–7.
24. Tometzki AJ et al. *J Am Coll Cardiol* 1999;33:1696–701.
25. Vesel S et al. *Heart* 2006;92:1501–5.
26. Volpe P et al. *Ultrasound Obstet Gynecol* 2004;24:623–8.
27. Boudjemline Y et al. *J Pediatr* 2001;138:520–4.
28. Chessa M et al. *Heart* 1998;79:186–90.
29. Kim N et al. *Prenat Diagn* 2006;26:740–5.
30. Volpe P et al. *Heart* 2003;89:1437–41.
31. Duke C et al. *Am J Cardiol* 2001;88:1379–84.
32. Simpson JM. *Ultrasound Obstet Gynecol* 2000;15:271–8.
33. Raymond FL et al. *Lancet* 1997;350:930.
34. Allan LD et al. *Heart* 1998;79:371–3.
35. Brackley KJ et al. *Lancet* 2000;356:1143–7.
36. Wald RM et al. *Am Heart J* 2007;153:772–8.
37. Yoo SJ et al. *Ultrasound Obstet Gynecol* 2003;22:535–46.
38. Chaoui R et al. *Ultrasound Obstet Gynecol* 2003;22:661–3.
39. Bronshtein M et al. *Am J Cardiol* 1998;81:101–3.
40. Patel CR et al. *J Ultrasound Med* 2006;25:251–7.
41. Rauch R et al. *Eur J Pediatr* 2004;163:642–5.
42. Hastreiter AR et al. *Br Heart J* 1966;28:722–39.
43. Webber SA et al. *J Pediatr* 1996;129:26–32.
44. Berg C et al. *Ultrasound Obstet Gynecol* 2006;28:882–9.
45. Valletta EA et al. *Pediatr Pulmonol* 1997;24:93–105.
46. Glew D, Hartnell GG. *Clin Radiol* 1991;43:305–7.
47. Yoo SJ et al. *Ultrasound Obstet Gynecol* 1999;14:29–37.
48. Paladini D et al. *Heart* 2004;90:1348–9.
49. Lindsay EA et al. *Am J Med Genet* 1995;57:514–22.
50. Takahashi K et al. *Cardiol Young* 1999;9:516–18.
51. Lewin MB et al. *Am J Cardiol* 1997;80:493–7.
52. Rauch A et al. *Am J Med Genet* 1998;78:322–31.
53. Volpe P et al. *Ultrasound Obstet Gynecol* 2002;20:327–31.
54. Volpe P et al. *Prenat Diagn* 2003;23:752–7.
55. Paladini D et al. *Ultrasound Obstet Gynecol* 2006;27:281–5.
56. Todros T et al. *Ultrasound Obstet Gynecol* 2003;21:228–33.
57. Silva SR et al. *Fetal Diagn Ther* 1999;14:149–51.
58. Bauk L et al. *Cardiol Young* 2003;13:370–2.
59. Hornberger LK et al. *J Am Coll Cardiol* 1991;17:167–73.
60. Sharland GK et al. *J Am Coll Cardiol* 1991;17:944–9.

61. Siebert JR et al. *Am J Dis Child* 1989;143:570–2.
62. Vergani P et al. *Am J Obstet Gynecol* 1998;178:218–22.
63. Gaglioti P et al. *Ultrasound Obstet Gynecol* 2005;25:372–7.
64. Breeze AC et al. *Prenat Diagn* 2007;27:124–9.
65. Fratelli N et al. *Prenat Diagn* 2007;27:512–17.
66. Volpe P et al. *Ultrasound Obstet Gynecol* 2006;27:509–16.
67. Ecker JL et al. *Prenat Diagn* 2000;20:328–32.
68. Ulm B et al. *Ultrasound Obstet Gynecol* 1997;10:167–70.
69. Ong S et al. *Prenat Diagn* 2007;27:340–7.
70. Hyett J et al. *Am J Med Genet* 1997;69:207–16.
71. Ierullo AM et al. *Ultrasound Obstet Gynecol* 2005;26:150–3.
72. Adzick NS et al. *Am J Obstet Gynecol* 1998;179:884–9.
73. Brantberg A et al. *Ultrasound Obstet Gynecol* 2007;30:180–7.
74. Stringer MD et al. *J Pediatr Surg* 1995;30:1258–63.
75. Sparey C et al. *Am J Obstet Gynecol* 2000;182:427–31.
76. Goldstein RB. The thorax. In: Nyberg D, McGahan JP, Pretorius D, Pilu G, eds. *Diagnostic Imaging of Fetal Anomalies*. Philadelphia, PA: Lippincott Williams and Wilkins; 2003:381–420.
77. Deurloo KL et al. *Prenat Diagn* 2007;27:893–9.
78. Rustico MA et al. *Prenat Diagn* 2007;27:793–9.
79. Waller K et al. *Genet Med* 2005;7:417–21.
80. Garne E et al. *Ultrasound Obstet Gynecol* 2002;19:329–33.
81. Dommergues M et al. *Am J Obstet Gynecol* 1996;174:1377–81.
82. Geary MP et al. *Ultrasound Obstet Gynecol* 1998;12:107–11.
83. Heydanus R et al. *Prenat Diagn* 1994;14:1035–41.
84. Murshed R et al. *Br J Obstet Gynaecol* 1999;106:1197–9.
85. Surana R, Puri P. *J Pediatr Surg* 1994;29:1250–2.
86. Nyberg D, Neilsen I. Abdomen and gastrointestinal tract. In: Nyberg D, McGahan JP, Pretorius D, Pilu G, eds. *Diagnostic Imaging of Fetal Anomalies*. Philadelphia, PA: Lippincott Williams and Wilkins; 2003:547–603.
87. Gibbin C et al. *Ultrasound Obstet Gynecol* 2003;21:334–7.
88. Fratelli N et al. *Ultrasound Obstet Gynecol* 2007;30:266–70.
89. Brantberg A et al. *Ultrasound Obstet Gynecol* 2005;26:527–37.
90. Cantrell JR et al. *Surg Gynecol Obstet* 1958;107:602–14.
91. Hornberger LK et al. *Circulation* 1996;94:II32–7.
92. Greenwood RD et al. *Clin Pediatr (Phila)* 1976;15:1101–4.
93. Gucer S et al. *Turk J Pediatr* 2005;47:159–66.
94. Newbould MJ et al. *Br J Obstet Gynaecol* 1994;101:598–604.
95. Boatman DL et al. *J Urol* 1972;107:205–7.
96. Kolln CP et al. *J Urol* 1972;107:203–4.
97. Winyard P, Chitty L. *Prenat Diagn* 2001;21:924–35.
98. Bosman G et al. *Ultrasound Med Biol* 1991;17:117–20.
99. Vintzileos AM et al. *Obstet Gynecol* 1997;89:941–4.
100. Nyberg DA et al. *Ultrasound Obstet Gynecol* 1998;12:8–14.
101. DeVore GR. *Ultrasound Obstet Gynecol* 2000;16:133–41.
102. Bromley B et al. *J Ultrasound Med* 2002;21:1087–96.
103. Hobbins JC et al. *J Ultrasound Med* 2003;22:33–8.
104. Vergani P et al. *Prenat Diagn* 2000;20:210–14.
105. Nyberg DA, Souter VL. *J Ultrasound Med* 2001;20:655–74.
106. Hansmann M. *Ultrasound Obstet Gynecol* 2004;23:531–4.
107. Bromley B et al. *J Ultrasound Med* 2002;21:1387–94.
108. Bellini C et al. *Orphanet J Rare Dis* 2006;1:43.
109. Cicero S et al. *Ultrasound Obstet Gynecol* 2003;21:15–8.
110. Massez A et al. *Eur Radiol* 2003;13:2075–81.
111. Vintzileos A et al. *Obstet Gynecol* 2003;101:905–8.
112. Maymon R et al. *Ultrasound Obstet Gynecol* 2004;23:557–60.
113. Rotmensch S et al. *Prenat Diagn* 1997;17:1001–9.
114. Paladini D et al. *Ultrasound Obstet Gynecol* 2000;15:104–8.
115. Shields LE et al. *J Ultrasound Med* 1998;17:327–31.
116. DeVore GR. *J Ultrasound Med* 2000;19:565–76.
117. Tongsong T et al. *J Obstet Gynaecol Res* 2002;28:245–50.
118. Bronsteen R et al. *J Ultrasound Med* 2004;23:233–40.
119. Kinoshita M et al. *Pediatr Pathol* 1989;9:445–57.
120. Moerman P et al. *J Genet Hum* 1982;30:17–38.
121. Moyano D et al. *Arch Dis Child Fetal Neonatal Ed* 2005;90: F520–2.
122. Nyberg DA et al. *J Ultrasound Med* 1993;12:103–13.
123. Tongsong T et al. *Int J Gynaecol Obstet* 2002;76:143–8.
124. Lehman CD et al. *Radiology* 1995;194:217–22.
125. Chaumoitre K et al. *Ultrasound Obstet Gynecol* 2006;28:911–17.
126. Jauniaux E et al. *Obstet Gynecol* 1996;88:983–9.
127. Rijhsinghani A et al. *Obstet Gynecol* 1997;90:884–8.
128. Mittal TK et al. *Prenat Diagn* 1998;18:1253–62.
129. Blaicher W et al. *Ultraschall Med* 2002;23:129–33.
130. Gembruch U et al. *Ultrasound Obstet Gynecol* 1997;10:391–6.
131. Surerus E et al. *Ultrasound Obstet Gynecol* 2003;22:264–7.
132. Bronshtein M et al. *Am J Obstet Gynecol* 2003;188:1016–20.
133. Isaksen CV et al. *Ultrasound Obstet Gynecol* 2000;16:37–45.
134. Saenger P et al. *J Clin Endocrinol Metab* 2001;86:3061–9.
135. Driscoll DA. *Curr Opin Pediatr* 1994;6:702–6.
136. Driscoll DA. *Methods Mol Med* 2006;126:43–55.
137. Wilson DI et al. *J Med Genet* 1993;30:852–6.
138. Ryan AK et al. *J Med Genet* 1997;34:798–804.
139. Maeda J et al. *Am J Med Genet* 2000;92:269–72.
140. Takahashi K et al. *Eur J Pediatr* 1995;154:878–81.
141. Amati F et al. *Hum Genet* 1995;95:479–82.
142. Stewart TL et al. *Teratology* 1999;59:20–2.
143. Boudjemline Y et al. *Prenat Diagn* 2002;22:231–4.
144. Chaoui R et al. *Ultrasound Obstet Gynecol* 2002;20:546–52.
145. Barrea C et al. *Prenat Diagn* 2003;23:9–15.
146. Winter RM, Baraitser M. *The London Dysmorphology Database*. Oxford: Oxford University Press; 2001.
147. Greenhalgh KL et al. *J Med Genet* 2002;39:876–81.
148. Kline AD et al. *Am J Med Genet A* 2007;143:1287–96.
149. Kliewer MA et al. *Am J Med Genet* 1993;47:1035–41.
150. Sekimoto H et al. *Arch Gynecol Obstet* 2000;263:182–4.
151. Aitken DA et al. *Prenat Diagn* 1999;19:706–10.
152. Jackson L et al. *Am J Med Genet* 1993;47:940–6.
153. Mehta AV, Ambalavanan SK. *Am J Med Genet* 1997;71:434–5.
154. Bruneau BG et al. *Dev Biol* 1999;211:100–8.
155. Bergmann C et al. *Am J Med Genet A* 2003;121:151–5.
156. Martinez-Frias ML, Frias JL. *Am J Med Genet* 1999;83:13–6.
157. Weaver DD et al. *Am J Dis Child* 1986;140:225–9.
158. Stoll C, Clementi M. *Ultrasound Obstet Gynecol* 2003;21:543–51.
159. Digilio MC et al. *Am J Med Genet* 1999;84:350–6.
160. Ellis RWB, van Creveld S. *Arch Dis Child* 1940;15:65–84.
161. Promsonthi P, Wattanasirichaigoon D. *Ultrasound Obstet Gynecol* 2006;27:583–5.
162. Smith DW et al. *J Pediatr* 1964;64:210–7.
163. Hyett JA et al. *Am J Med Genet* 1995;58:374–6.
164. Clayton PT. *Arch Dis Child* 1998;78:185–9.
165. Lin AE et al. *Am J Med Genet* 1997;68:270–8.
166. Noonan JA, Ehmke DA. *J Pediatr* 1963;63:468–70.
167. Nisbet DL et al. *Prenat Diagn* 1999;19:642–7.
168. Menashe M et al. *Ultrasound Obstet Gynecol* 2002;19:51–5.
169. Achiron R et al. *Am J Med Genet* 2000;92:159–65.
170. Gorlin RJ et al. *J Pediatr* 1963;63:991–9.
171. Pierpont ME et al. *Pediatr Cardiol* 1982;2:297–302.
172. Hall BD. *J Pediatr* 1979;95:395–8.
173. Tellier AL et al. *Am J Med Genet* 1998;76:402–9.
174. Gilbert-Barness E, Debich-Spicer D. Cardiovascular system defects. In: *Embryo and Fetal Pathology*. Cambridge: Cambridge University Press; 2004:428–69.

175. Wiedemann HR. *J Genet Hum* 1964;13:223–32.
176. Nyberg D et al. Syndromes and multiple anomaly conditions. In: Nyberg D, McGahan JP, Pretorius D, Pilu G, eds. *Diagnostic Imaging of Fetal Anomalies*. Philadelphia, PA: Lippincott Williams and Wilkins; 2003. pp. 133–220.
177. Greenwood RD et al. *Am J Dis Child* 1977;131:293–4.
178. Bowers PN et al. *Semin Perinatol* 1996;20:577–88.
179. Lin AE et al. *Genet Med* 2000;2:157–72.
180. Peoples WM et al. *Pediatr Cardiol* 1983;4:129–37.
181. Van Praagh S et al. *Coeur* 1988;19:484–502.
182. Winer-Muram HT, Tonkin IL. *Radiol Clin North Am* 1989;27: 1147–70.
183. Ho SY et al. *Pediatr Pathol* 1991;11:589–608.
184. Berg C et al. *Ultrasound Obstet Gynecol* 2003;22:451–9.
185. Phoon CK et al. *Am J Cardiol* 1996;77:1083–8.
186. Atkinson DE, Drant S. *Am J Cardiol* 1998;82:1147–9, A10.
187. Lin JH et al. *Am Heart J* 2002;143:1002–8.
188. Berg C et al. *J Ultrasound Med* 2005;24:921–31.
189. Berg C et al. *Ultrasound Obstet Gynecol* 2005;26:4–15.
190. Ivemark BL. *Acta Paediatr Scand* 1955;44(suppl. 104):1–116.
191. Berg C et al. *Ultraschall Med* 2006;27:225–33.
192. Berg C et al. *Ultraschall Med (Stuttgart, Germany: 1980)* 2009;30(1):25–32.
193. Berg C et al. *Ultrasound Obstet Gynecol* 2010;35(2):183–90.
194. Gottschalk I et al. *Ultraschall Med—Eur J Ultrasound* 2016;38(4):427–36.
195. Gottschalk I et al. *Ultrasound Obstet Gynecol* 2015;47(4):443–9.
196. Gottschalk I et al. *Ultrasound Obstet Gynecol* 2017;49(5):637–42.
197. Hellmund A et al. *PLOS ONE* 2016;11(3):e0150474.
198. Kagan KO et al. *Prenat Diagn* 2015;35(4):394–9.
199. Kaguelidou F et al. *Eur Heart J* 2008;29(11):1432–8.
200. Mallmann MR et al. *Ultrasound Obstet Gynecol* 2014;44(4): 441–6.
201. Mallmann MR et al. *Fetal Diagn Ther* 2016;41(1):58–65.
202. Mosimann B et al. *Ultrasound Obstet Gynecol* 2014;44(1):76–81.
203. Rüland AM et al. *Ultraschall Med—Eur J Ultrasound* 2015; 37(6):598–603.
204. Song MS et al. *Ultrasound Obstet Gynecol* 2009;33(5):552–9.
205. Vogel M et al. *Am J Cardiol* 2010;105(5):727–34.

# 52

# Chromosome microarray analysis of the fetal heart

Karina Seidl Nall

Congenital heart disease (CHD) occurs at a conservative incidence of 8 per 1,000 live births[1] and is the single largest cause of infant morbidity and mortality worldwide.[2] When the frequency of structural heart lesions in spontaneous miscarriages and stillbirths is considered, the true incidence of structural heart defects remains underappreciated.[3,4] Genetic etiologies account for approximately 20%–30% of CHD[5] and while individually rare, genetic disorders are in fact collectively common. The World Health Organization (WHO) estimates the global prevalence of all single gene disorders at 10 per 1,000 live births. Approximately 20%–30% of infant death is attributed to a genetic etiology,[6] and by 25 years of age, approximately 5.3% of the population will have a medical diagnosis with a significant genetic component.[7]

When we account for the collective prevalence of genetic disorders, evaluation for genetic risk factors is an important component for comprehensive assessment of the fetus with CHD for multiple reasons: (1) allows the perinatal team to appropriately assess for other organ system involvement including surveillance for evolving fetal manifestations of a molecular disorder; (2) prompts counseling about expected prognosis or anticipated considerations for clinical management; (3) offers clinical evaluation and management of at-risk family members; (4) allows for accurate recurrence risk counseling.[8] As the range of molecular technologies continues to advance, opportunities to evaluate genetic contributions to CHD rapidly expand.

We review the molecular technologies available in the clinician's toolkit for evaluation of genetic etiologies in the fetus with CHD and address considerations for genetic counseling. We kindly direct the reader to Chapter 49 for extended discussion regarding genetic syndromes associated with CHD.

While often overlooked, three-generation pedigree analysis remains a valuable mechanism for assessment of familial CHD as well as evaluation for other familial indicators that may suggest a hereditary syndrome, which is of particular value in syndromic etiologies confounded by reduced penetrance, variable expression, and evolving clinical phenotypes.[8,9]

Conventional metaphase karyotype analysis of cells obtained via amniocentesis or chorionic villus sampling has long been the gold standard for evaluation of the fetal genome, providing genome-wide assessment for whole chromosome aneuploidies and structural genomic changes at a resolution of 5–10 Mb (1 Mb = 1 million base pairs). While advantageous in the setting of a suspected aneuploidy, the accuracy of karyotype analysis is operator dependent and therefore subject to error, particularly in the case of structural chromosome abnormalities in the 5–7 Mb range.[10]

Fluorescence *in situ* hybridization (FISH) technology allows for greater resolution of up to 200 kb of a specific genomic region of interest not amenable to karyotype evaluation by hybridizing biotinylated control DNA probes with fetal metaphase chromosomes to determine whether a deletion or duplication of the targeted genomic region has occurred.[11] FISH is at greatest advantage in the setting of a high degree of clinical suspicion for a specific microdeletion/microduplication syndrome, as FISH does not allow genome-wide assessment.

The development of array-based technology fulfilled the need for comprehensive, whole genome assessment with a resolution of up to 50–100 kb, 100 times greater than metaphase karyotype analysis.[12] Array technology utilizes a microchip-based testing platform that allows high-volume, automated analysis of DNA using labels or probes that bond to specific genomic regions. DNA from a fetal sample is hybridized to a DNA chip or array that contains DNA fragments of known identity/known sequences.

Software allows for evaluation of the fetal genome as compared to the reference DNA, where any difference between fetal DNA and the reference sample is referred to as a copy number variant (CNV). Examples of CNV include deletions and duplications. CNVs are a minimum of 1 kb and found in all humans, described to account for approximately 12% of the human genome.[13] CNV are largely benign variants reflective of the complexity of human diversity; data suggest that humans have an average of 3–7 CNV, representing approximately 540 kb of CNV DNA per person.[14]

Databases of known molecular variants are used to determine the significance of any CNV identified in the fetal sample, including categorization of a variant as pathogenic, benign, or a variant of unknown significance (VOUS).

Two types of microarray commonly used in clinical prenatal testing include comparative genomic hybridization (CGH) and single nucleotide polymorphism (SNP) arrays. While both technologies assess for the presence of CNV, there are some important differences in the genomic variation detected.

Array-based CGH utilizes fluorescently labeled fetal and reference DNA (Figure 52.1), where computer analysis

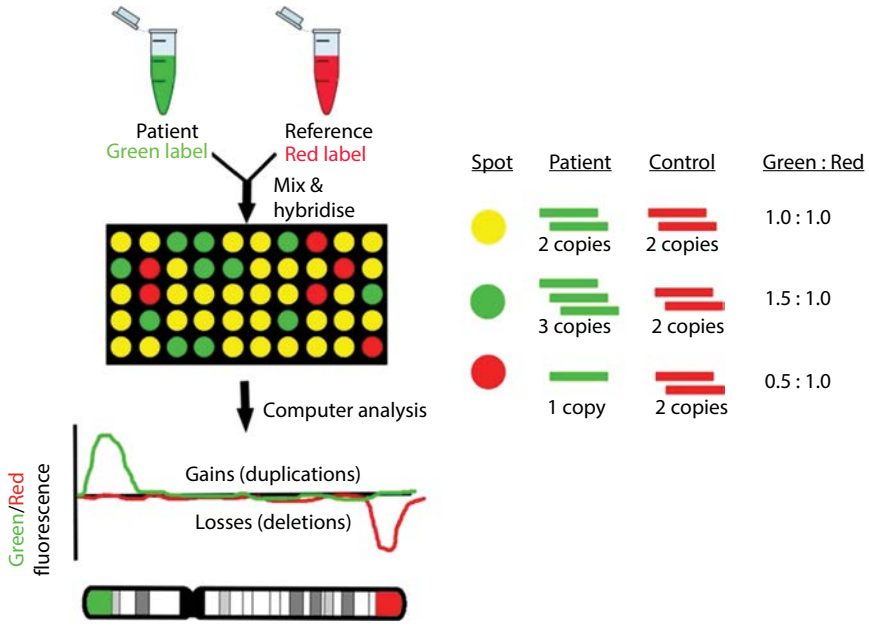


**Figure 52.1**
Comparative genomic hybridisation (CGH) arrays. (From Karampetsou E et al. *J Clin Med* 2014;3(2):663–78, with permission.[66])

compares the relative intensity of fetal versus control DNA on the array chip. While CGH detects copy number variation for deletions or duplications, including aneuploidy, CGH cannot detect fetal triploidy.

By comparison, only fetal DNA is hybridized to a SNP array platform, and the presence or absence of specific known DNA sequence variants is evaluated by signal intensity to provide copy number analysis (Figure 52.2). Unlike CGH, SNP arrays have the ability to detect triploidy, mosaicism, and maternal cell contamination. Extended regions of fetal homozygosity may be identified via SNP array, the presence of which is associated with whole chromosome or segmental uniparental isodisomy (UPD), where both fetal copies of a chromosome are inherited from the same parent. Large genomic regions of homozygosity are additionally seen in pregnancies from a consanguineous relationship, another well-documented contribution to congenital heart disease.[15] As all array technology assesses for the presence of a net gain or loss of genetic material, it is important to note that array cannot assess for the presence of a truly balanced chromosome translocation. While often of limited clinical significance, balanced structural translocations carry important implications to reproductive counseling, namely, an increased risk of future pregnancy with an unbalanced genomic complement.

Array technology was rapidly adopted in clinical practice as initial investigations demonstrated increased diagnostic yield of pathogenic CNV of 10%–25% above karyotype analysis in children with syndromic phenotypes.[16]

Among children with syndromic CHD, defined as CHD with a minimum of one additional significant clinical finding including cognitive delay, other structural birth defects and autism spectrum disorder, microarray analysis demonstrates an incremental yield of 14%–20% above karyotype analysis.[17] Array analysis performed on apparently isolated CHD demonstrates an incremental yield of 3.6%–4.3%[18]; however, may be conservatively interpreted, as cardiac manifestation may be the initial finding of an evolving phenotype. ASHG Consensus Statement recommends CMA as the first-tier molecular evaluation for individuals with cognitive disability, multiple congenital abnormalities, and autism spectrum disorder.[19]

Expanding upon the application of array analysis in the pediatric population, several large studies[20–22] demonstrate array analysis to be equally accurate in identifying aneuploidy and unbalanced structural chromosome arrangements as compared to karyotype evaluation while demonstrating an increased yield of clinically relevant CNV (1.7%–3.6%) as compared to karyotype analysis across all indications for referral of prenatal testing. Increased diagnostic yield is particularly notable in the setting of a fetus with sonographic abnormalities, ranging from 5% to 15% depending on whether single or multiple organ systems are impacted.[23,24]

After exclusion of karyotype abnormalities (>10 Mb) in the fetus with an isolated structural heart lesion, incremental yield of array analysis ranges from 2.5% to 4.6%.[25–26] As previously noted, a structural cardiac lesion may represent the only manifestation in the prenatal period in a presymptomatically syndromic fetus, an important consideration when counseling families. The incremental yield of array analysis is even more pronounced in fetuses with nonisolated CHD and normal karyotype analysis, ranging from 9.3% to 19.3%.[27,28]

Structural heart defects, conotruncal lesions in particular, are a frequent manifestation of 22q11 deletion syndrome, where approximately 75% of diagnoses are associated with CHD. While some may consider FISH prior to array analysis, multiple cases of missed diagnoses of 22q11 deletion syndrome

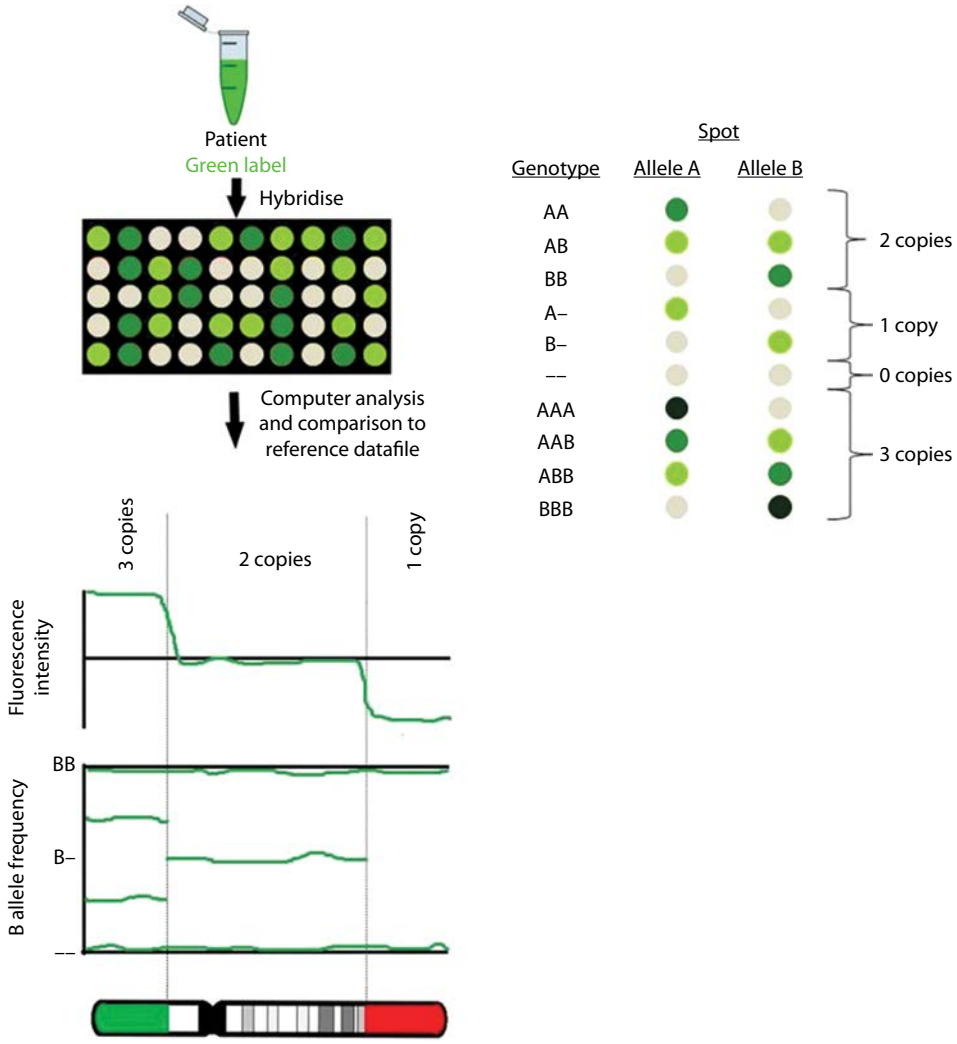


**Figure 52.2**
Single nucleotide polymorphism (SNP) arrays. (From Karampetsou E et al. *J Clin Med* 2014;3(2):663–78, with permission.[66])

have been reported.[29,30] In the setting of normal karyotype analysis and FISH for 22q11 deletion syndrome in a fetus with a structural heart defect, the incremental yield of array analysis is 7%; incremental yield of array increases to 12% when 22q11 deletion syndrome is included in array findings.[31] When categorized by cardiac lesion, array demonstrates incremental diagnostic yield of 18%–34% for conotruncal defects,[32] 33% for septal defects,[33] 4%–10% for tetralogy of Fallot,[34] 10% for left-sided lesions, and 14% for heterotaxy.[35]

Prenatal arrays may be targeted or provide whole genome coverage. Targeted arrays are designed to provide thorough coverage for genomic regions of interest associated with well-defined CNV of clinical significance while minimizing the potential for detecting VOUS. As implied by name, whole genome arrays provide array coverage of the entire genome, increasing detection rate of clinically significant CNV, however, at an increased probability of identifying VOUS. Many whole genome array platforms provide a "backbone" of whole genome coverage at specific spaced intervals in addition to targeting specific genomic regions of interest by increasing coverage in these areas. While the targeted array may be a consideration for a couple concerned about VOUS, whole genome analysis provides superior depth of coverage in the fetus with congenital heart disease. An estimated two-thirds of clinically significant CNV in fetuses with CHD will be missed on a targeted array.[32]

Multiple professional organizations recommend microarray analysis as the first-tier molecular test for prenatal diagnosis of a fetus with structural abnormalities, including congenital heart disease.[36–38]

For the clinician evaluating array results in the fetus or neonate with CHD, suggest assessment of the following array parameters: (1) targeted array versus whole genome array; (2) resolution of the array; and (3) CGH versus SNP array. These details may assist counseling the family regarding results and possible further consideration for molecular studies in the postnatal period, whether higher-resolution array, single gene analysis, or consideration for next-generation sequencing.

Further interrogation of the human genome has been rapidly advanced via the integration of next-generation

sequencing (NGS) technology, which allows the simultaneous investigation of millions of individual fragments of DNA.[39] Bioinformatic analysis pieces together individual DNA fragments by mapping individual reads to a reference genome. As each DNA fragment is sequenced multiple times (multiple "reads"), NGS allows for in-depth interrogation for possible genomic variants as small as a single base pair change within a gene. While Sanger sequencing currently remains the gold standard for gene analysis, emerging data demonstrate that NGS yields superior analysis for genomic variants, faster turnaround times, and decreased cost as compared to the traditional Sanger method[40] (Figure 52.3).

One particular appeal of NGS as an emerging molecular technique is the potential scalability of the technology. While NGS may be used to interrogate the entire genome, it may be tailored to target specific molecular regions of interest including the exome or a small number of specific genes at the individual base pair level.

Furthermore, unlike traditional Sanger sequencing, NGS allows the clinician to investigate the genomic region of interest without bias, which is particularly advantageous for suspected syndromic etiology of unknown cause or in the setting of heterogeneous conditions associated with multiple different genes, such as the case of Noonan syndrome.[41]

Targeted sequencing of specific genomic regions of interest has demonstrated an advantage for advancement of candidate gene investigation.[42,43]

It is a daunting task to sequence and interpret the entire human genome, which contains over 3 billion base pairs. Exons are segments of DNA within a gene that code for protein production, whereas introns are noncoding regions of a gene important for regulation of gene expression. During splicing, introns of the gene are removed, and the remaining exons are translated into protein. The exome describes all protein encoding exons across the human genome. While the exome represents only 1%–2% of genomic DNA, it accounts for approximately 85% of pathogenic mutations,[44] making exome sequencing a preferred NGS technology for clinical application.

Investigations of whole exome sequencing in the undiagnosed, suspected syndromic pediatric population suggest a diagnostic yield of 25%.[45,46] Interpretation of genomic variants is a challenge as exome sequencing identifies upward of 12,000 unique coding variants per exome, of which an estimated 15%–20% are considered rare,[47] further increasing the potential of VOUS.

In the fetus with multiple structural abnormalities where karyotype and microarray have failed to elicit an etiology, early application of exome sequencing has been explored. One pediatric exome study included four samples obtained from products of conception of terminated fetuses, which identified a causative variant in the NIPBL gene, consistent with a diagnosis of Cornelia de Lange syndrome.[45] Another study examined seven specimens from pregnancies resulting in termination or intrauterine fetal demise (IUFD), in which causative pathogenic variants were identified in three samples with an additional likely causative variant identified in a fourth specimen.[48] Carss examined 30 fetal or neonatal specimens with known prenatal ultrasound abnormalities and demonstrated likely causative molecular variants in 3/30 (10%) of samples including variants in FGFR3 (thanatophoric dysplasia type 1), COL2A1 (wide range of collagenopathies), and a 21 kb deletion that involved OFD1, associated with orofaciodigital syndrome 1. An additional 17% (5/30) of the population was remarkable for the identification of possibly causal variants; however, further investigation would be required to assess pathogenicity.[49] As NGS is currently an emerging molecular technology in the clinical arena, we look forward to continued evidence to assess the most appropriate means for NGS integration in the prenatal setting. Notably, the PAGE (Prenatal Assessment of Genome and Exome) Project in the United Kingdom seeks to examine 1,000 fetal samples to explore the utility of exome sequencing as a tool for fetuses with structural abnormalities. Objectives include assessment of the contribution of genetic variation to structural abnormalities, development of genomic assays for improved prenatal diagnosis of fetuses with abnormalities, and establishment of ethical guidelines for implementation of exome sequencing in the prenatal population.[50]

The rapid evolution of molecular diagnostics underscores the importance of comprehensive pre- and posttest counseling. Multiple studies[51–54] specifically emphasized genetic counseling as an integral component of clinical implementation of emerging molecular technologies.

Pretest genetic consultation should provide description of the appropriate molecular technology to be implemented. Families should understand that while array analysis or NGS allows a more in-depth interrogation of the fetal genome as compared to karyotype analysis, no one technology is comprehensive, compared to the analogy of the human genome as a printed instruction manual for human development and function. While a karyotype evaluation is equivalent to assessment of the chapters of the instruction manual, microarray analysis is akin to counting every five pages of the instruction manual, perhaps paying careful attention to certain pages in the book that are more likely to be misnumbered (known genomic regions of susceptibility). Using the instruction manual analogy, a microarray analysis cannot assess for spelling or punctuation errors in the manual (single gene disorders). NGS of the exome may identify spelling errors, but only of specific chapters in the instruction manual.

In the fetus with a CHD, families should understand that in the event of a normal test result, alternate molecular studies may be considered in the prenatal or postnatal period depending on the index of clinical suspicion of an underlying genetic etiology, particularly in the setting of a possible evolving phenotype.

In the setting of an abnormal molecular result consistent with a known pathogenic finding, molecular technologies cannot predict the full range of clinical phenotypes. Using the example of the 22q11 deletion syndrome, molecular technology cannot further assess for the presence of seizure disorders, hearing loss, or cognitive disability associated with the syndrome.

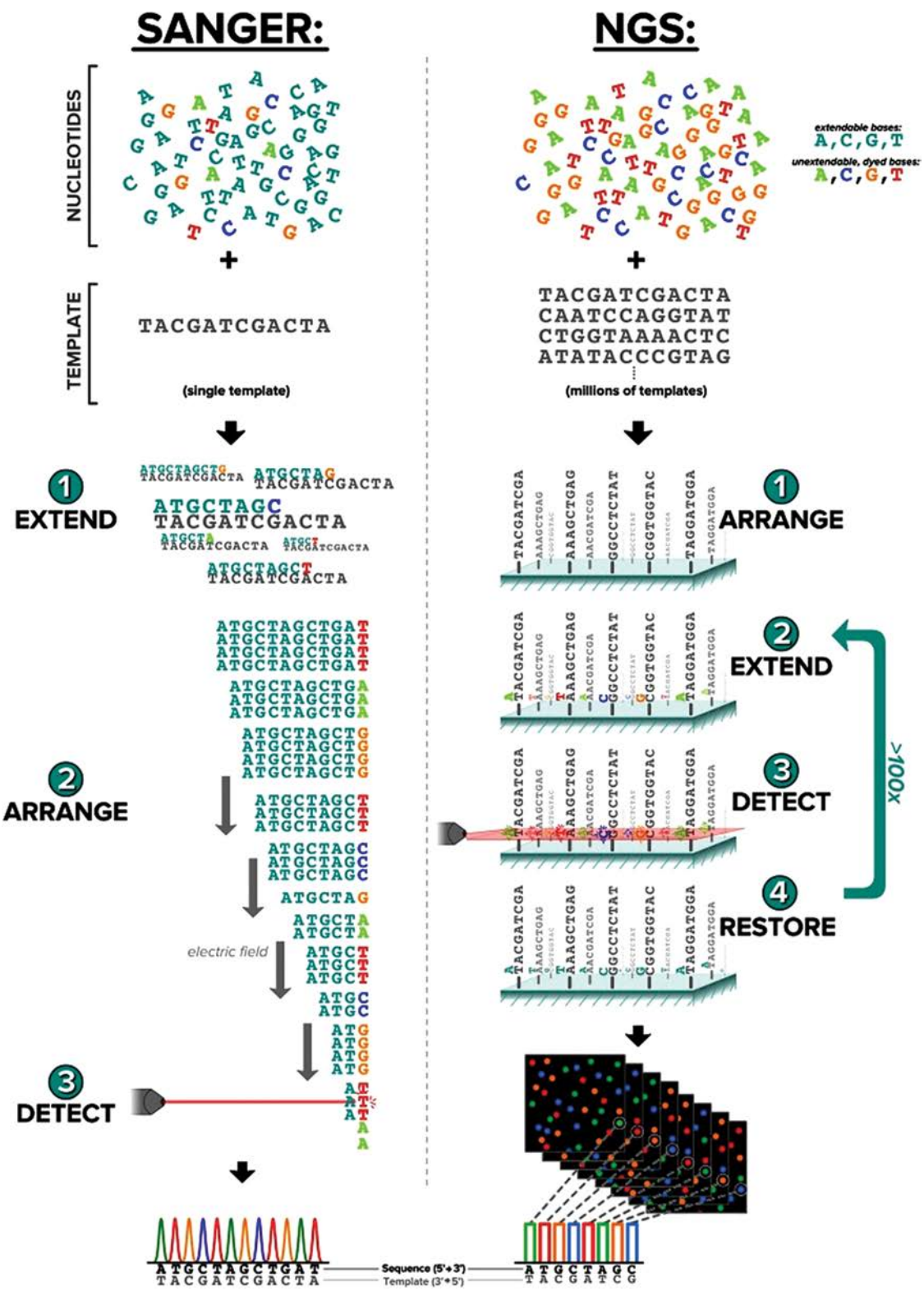


**Figure 52.3**
NGS is a slightly modified, digital, and vastly scaled-up implementation of Sanger sequencing. In both methodologies, a polymerase copies template molecules by incorporating nucleotides from a pool, that is, either partially (Sanger) or entirely (NGS) composed of dyed and unextendable bases. Extension, arrangement, and detection are shared steps in both protocols but occur in different order, with NGS alone having a restoration step that converts bases to the undyed and extendable form. (From Muzzey D et al. *Curr Genet Med Rep* 2015;3(4):158–65, under Creative Commons license.[67])

The possibility of a VOUS should be addressed. VOUS may occur as a *de novo* or as an inherited event. While inheritance of a molecular variant often provides some guidance to the laboratory to assist in interpretation, inheritance alone does not predict clinical significance. An inherited VOUS may be influenced by alternate molecular mechanisms including reduced penetrance, variable clinical expression, mosaicism or molecular imprinting or parent of origin effect. To assist in possible VOUS interpretation, parental samples should be available to the reference laboratory, ideally submitted with the fetal specimen to be on hand at the laboratory as necessary to avoid delays in result reporting and to decrease parental anxiety. While the presence of VOUS undoubtedly is a source of frustration for providers and anxiety for families, this concept is not unique to molecular technology.[55] The prevalence of benign molecular variants further challenges the interpretation of array findings.

A significant limitation to interpretation of VOUS is the incomplete fetal phenotype due to inherent limitations of prenatal ultrasound.[52] Prenatal variant interpretation is further hampered by the absence of large population studies to assess genotype phenotype correlations. No dedicated database of fetal variants is currently available, and there exists very limited information regarding postnatal follow-up of prenatally identified molecular variants. Current interpretation of molecular variants identified in the fetus with CHD relies on studies and case reports of the pediatric population, likely biased toward the severe end of the clinical spectrum as mild phenotypic presentations less likely to be clinically recognized.

Meta-analyses of the utility of prenatal microarray identified the rate of VOUS to be 1.1%–1.4% regardless of the fetal indication for referral and a VOUS rate of 2.1% in fetuses whose referral indication was a structural abnormality. [20,24] A separate meta-analysis of microarray of fetuses with CHD demonstrated a VOUS rate of 3.4%. [31] A VOUS rate of 17% has been reported in prenatal NGS.[49]

Evaluating pathogenicity of VOUS is a dynamic process; continued research is expected to impact the evolution of our understanding to the contributions of CNV in CHD. Further refinement of CNV significance relies on collective contribution to large databases of previously reported variants including Database of Genomic Variation, DECIPHER, and ECARUCA. As evolving molecular techniques become a staple in prenatal diagnosis in the fetus with CHD, continued collaboration between cardiology, perinatology, and genetics is of paramount importance to aid in further definition/classification of molecular variants. In the Wapner[21] study, the initial rate of VOUS was 3.4%; however, as additional information became available over 5 years of study duration, many VOUS were recategorized for a final publication VOUS rate of 1.5%.

The potential for incidental findings unrelated to the structural heart defect should likewise be addressed in pretest counseling, including potential for consanguinity, nonpaternity, carrier status for X-linked or recessive disorders,[55] or adult-onset disorders, which may or may not be actionable (BRCA versus Alzheimer).[56] Some guidance regarding reporting criteria may be derived from the postnatal (ACMG) guidelines; however, no specific prenatal consensus exists.[57]

Pretest counseling should include a discussion of the family's tolerance for uncertainty. Written information regarding the testing technology should be available to all families. Even in the setting of pretest counseling, families may become overwhelmed by the information, such as "toxic" information, particularly when a VOUS is identified.[58]

An integral component of genetic counseling for the fetus with structural heart disease is assessment of recurrence risk to other family members, which is in turn invariably influenced by the underlying etiology of the CHD.

In the setting of a confirmed molecular etiology, recurrence risk is dependent on the specific diagnosis, ranging from low recurrence risk in the setting of whole chromosome aneuploidy to 50% risk of recurrence for a familial diagnosis of a syndromic etiology such as Holt-Oram syndrome. An important counseling caveat is clinical variability and reduced penetrance often associated with syndromic disorders—while the risk of the disorder may be high, the cardiac manifestation may be variable.

We are in the early stages of our collective understanding of human cardiovascular genetics in a rapidly evolving field. While the majority of fetal diagnoses of structural heart defects occur as an isolated finding on ultrasound as a result of polygenic, multifactorial inheritance, advancement of fetal echocardiography and molecular technology continue to refine our understanding of the contributions to congenital heart disease. Specific structural heart lesions demonstrate strong familial clustering in first-degree relatives with eightfold increased risk as compared to the prevalence of the lesion in the general population.[59] The recurrence risk for a discordant structural heart lesion in first-degree relatives is also increased with a risk ratio of 2.68, suggesting that some families carry non-lesion-specific susceptibility to CHD.[60]

Multiple studies estimate the recurrence risk for nonsyndromic, nonchromosomal structural heart lesions ranging 2%–6% in full siblings, with increased risk of 8% in HLHS and coarctation of the aorta.[61,62]

Medical advancements in detection and surgical intervention have contributed to an increase in the prevalence of adults with CHD,[63,64] where for the first time, the number of adults with CHD surpasses the number of minors with CHD, with the greatest increase in the 18- to 40-year demographic. Recurrence risks on the basis of parental lesions is estimated ranging from 3% to 7% for the majority of maternal cardiac lesions, with notable exceptions including AVSD (10%–14%), aortic stenosis (13%–18%), and TOF/d-TGA (<3%).[65] Recurrence risks for paternal congenital heart disease are more uniform at 2%–3%.[61] We continue to explore previously uncharted territory as reproductive fitness of congenital heart lesions continues to improve.

In summary, the appreciation of genetic contributions to CHD is rapidly expanding, particularly as technology allows us to examine the genome with increasing resolution. Molecular diagnosis allows for appropriate counseling of families and offers guidance to the clinician in coordinating care.

Interpretation of possible molecular variants remains a challenge as the genome is not fully understood; however, continued collaboration and cataloging of molecular variants will advance our knowledge base, decreasing the rate of VOUS.

Importance of genetic counseling cannot be underscored, as management of the fetus with CHD is a collaborative approach between maternal fetal medicine, pediatric cardiology, genetics, neonatology, and other pediatric subspecialties.

## References


1. Reller MD et al. *J Pediatr* 2008;153(6):807–13.
2. Cowan JR, Ware SM. *Clin Perinatol* 2015;42:373–93.
3. Hoffman JI, Kaplan S. *J Am Coll of Cardiol* 2002;39(12): 1890–900.
4. Chinn A et al. *Teratology* 1989;40:475–82.
5. Hinton RB et al. *J Cardiovasc Dev Dis* 2015;2(2):76–92.
6. Berry RJ et al. *Public Health Report* 1987;102:171–81.
7. Baird PA et al. *Am J Hum Genet* 1988;42:677–93.
8. Pierpont ME et al. *Circulation* 2007;115:3015–38.
9. Circulation Research. *Circ Res* 2013;112:698–706.
10. Shaffer LG, Lupski JR. *Annu Rev Genet* 2000;34:297–329.
11. Trask BJ. *Trends Genet* 1991;7:149–54.
12. Emanuel BS, Saitta BC. *Nat Rev Genet* 2007;8(11):869–83.
13. Redon R et al. *Nature* 2006;444:444–54.
14. Itsara A et al. *Am J Human Genet* 2009;84:148–61.
15. Shieh JT et al. *Am J Med Genet A* 2012;158A(5):1236–41.
16. Sagoo GS et al. *Genet Med* 2009;11(3):139–46.
17. Thienpont B et al. *Eur Heart J* 2007;28:2778–84.
18. Breckpot J et al. *Cytogenet Genome Res* 2011;135:251–9.
19. Miller D et al. *Am J Hum Genet* 2010;86(5):749–64.
20. Hillman SC et al. *Ultrasound Obstet Gynecol* 2013;41:610–20.
21. Wapner RJ et al. *NEJM* 2012;367:2175–84.
22. Shaffer LG et al. *Prenat Diagn* 2012;32:1–10.
23. Lee CN et al. *BJOG* 2012;119:614–25.
24. Hillman SC et al. *Ultrasound Obstet Gynecol* 2011;37:6–14.
25. Wit MCD et al. *Ultrasound Obstet Gynecol* 2014;43:139–46.
26. Shaffer LG et al. *Prenat Diagn* 2012;32:1–10.
27. Yan Y et al. *Ultrasound Obstet Gynecol* 2014;43:404–12.
28. Mademont-Soler I et al. *Ultrasound Obstet Gynecol* 2013;41: 375–82.
29. Chen M et al. *Ultrasound Obstet Gynecol* 2014;43:396–403.
30. Tyreman M et al. *J Med Genet* 2009;46:531–41.
31. Jansen F et al. *Ultraosound Obstet Gynecol* 2015;45:27–35.
32. Donnelly J et al. *Obstet Gynecol.* 2014 Jul;124(1):83–90.
33. Buckley JR et al. *Congenit Heart Dis* 2015;10(3):E131–8.
34. Greenway SC et al. *Nat Genet* 2009;41(8):931–5.
35. Lander J, Ware S. *Curr Genet Med Rep* 2014;2:168–78.
36. Duncan A et al. *J Obstet Gynaecol Can* 2011;33(12):1256–9.
37. Committee Opinion. *Obstet Gynecol* 2013;122:1374–7.
38. Novelli A et al. *Ultrsound Obstet Gynecol* 2012;39:384–8.
39. Dorn C et al. *Brief Funct Genomics* 2014;13(1):51–65.
40. Shendure J, Ji H. *Nat Biotechnol* 2008;26(10):1135–45.
41. Lepri FR et al. *BMC Med Genet* 2014;15:14.
42. Arrington CB et al. *Circ Cardiovasc Genet* 2012;5:175–82.
43. Tariq M et al. *Genome Biol* 2011;12(9):R91.
44. Stenson PD et al. *Hum Genomics* 2009;4:69–72.
45. Yang Y et al. *NEJM* 2013;369:1502–11.
46. Yang Y et al. *JAMA* 2014;312(18):1870–9.
47. Ng P. *PLOS Genet* 2008;4:e1000160.
48. Alamillo C et al. *Prenat Diagn* 2015;35:1073–8.
49. Carss K et al. *Hum Mol Genet* 2014;23(12):3269–77.
50. Hillman SC et al. *Ultrasound Obstet Gynecol* 2015;45:4–9.
51. Vetro A et al. *Hum Mutat* 2012;33:923–9.
52. Wapner RJ et al. *Prenat Diagn* 2012;32:396–400.
53. Darilek S et al. *Genet Med* 2008;10(1):13–8.
54. McGillivray G et al. *Prenat Diagn* 2012;32:389–5.
55. Westerfield L et al. *J Clin Med.* 2014;3(3):1018–32.
56. Pichert G et al. *J Med Genet* 2011;48(8):535–9.
57. Kearney H et al. *Genet Med* 2011;13(7):680–5.
58. Bernhardt BA et al. *Genet Med* 2013;15(2):139–45.
59. Øyen N et al. *Circulation* 2009;120:295–301.
60. Øyen N et al. *Cir Cardiovasc Genet* 2010;3:122–8.
61. Gill HK et al. *J Am Coll Cardiol* 2003;42(5):923–9.
62. Fesslova V et al. *J Pregnancy* 2011;2011:368067.
63. Marelli AJ et al. *Circulation* 2007;115:163–72.
64. Marelli AJ et al. *Circulation* 2014;130:749–56.
65. Donofrio MT et al. *Circulation* 2014;129(21):2183–242.
66. Karampetsou E et al. *J Clin Med* 2014;3(2):663–78.
67. Muzzey D et al. *Curr Genet Med Rep* 2015;3(4):158–65.

# 53

# Congenital cardiovascular malformations and the fetal and neonatal circulation

Abraham M. Rudolph

## Introduction

Almost 50 years ago, the important role of the change in pulmonary circulation normally occurring after birth in influencing the manifestations of many congenital cardiovascular malformations was recognized.[1] It is now appreciated that changes not only in the pulmonary circulation, but also in other sites in the circulation after birth, may have profound effects on the hemodynamics and clinical manifestations postnatally. In addition, the effects of various congenital cardiovascular lesions on the development of the pulmonary vasculature after birth were documented. The interrelationships between prenatal development of the circulation and the presence of congenital cardiovascular malformations had not previously been appreciated, but with the increasing application of fetal echocardiography, it is now becoming evident that congenital cardiovascular malformations may also have profound effects on normal development of the circulation in the fetus, and the effects may be progressive with intrauterine growth of the fetus. Furthermore, developmental changes in the circulation during fetal life may affect the manner in which cardiovascular malformations present, as well as the time during gestation that the changes become manifest.

This chapter reviews current knowledge regarding interactions between congenital cardiovascular malformations and development of the circulation in the fetus and the interactions during postnatal cardiovascular adaptation. The individual lesions are not discussed in detail, because they are presented in other chapters. Congenital cardiovascular malformations may affect the developing circulation by several mechanisms[2]:

- Altering patterns of blood flow
- Changing volumes of blood flowing through cardiac chambers or great vessels
- Altering levels of oxygen in blood delivered to various fetal organs
- Increasing fetal venous pressure

## Fetal cardiovascular system

### *Alterations in blood flow patterns and volumes*

#### Ventricular development

For several decades, the presence of a small or hypoplastic left or right ventricle at birth has been considered to be related to inadequate volume of blood flow into or out of the chamber during fetal life. This concept was based on the presence of associated aortic or pulmonary valve obstruction, which was thought to limit the volume of blood entering the respective ventricle. In an autopsy study of infants with obstructive vtic left ventricle, Lev et al. noted that the foramen ovale was small, and proposed that the restriction of flow into the left atrium was responsible for the ventricular and aortic anomalies.[3] It is difficult, however, to exclude the possibility that the small foramen was the result of the ventricular and aortic anomalies, rather than their cause.

Postnatally, blood flows serially through the pulmonary and systemic circulations; obstruction to inflow or outflow of either ventricle will thus affect the output of both ventricles. If obstruction is severe, blood supply to the body will be compromised. In the fetus, however, the presence of foramen ovale and ductus arteriosus shunts may permit a normal combined ventricular output to be maintained even if inflow or outflow of either ventricle is severely restricted (see Chapter 8). Thus, with tricuspid or pulmonary valve atresia, venous return is deflected through the foramen ovale to the left atrium and ventricle; blood flow to the lungs is provided from the aorta through the ductus arteriosus. In the presence of mitral or aortic valve obstruction, both pulmonary and systemic venous blood returns to the right atrium and is ejected by the right ventricle into the pulmonary artery; systemic and umbilical arterial blood is provided by flow through the ductus arteriosus. In those congenital malformations with severe obstructions, flow to one ventricle is reduced, while the output of the other ventricle is increased. One functioning

ventricle in the fetus is capable of providing blood flow adequate for normal umbilical and fetal body requirements, as evidenced by normal body growth and absence of hypoxia in many of these fetuses.

To attempt to assess the role of volume of blood flow into or out of the left ventricle on chamber growth, we simulated models of reduced inflow and of obstructed outflow, in fetal lambs at 90–120 days' (0.6–0.8) gestation.[4] Left ventricular inflow was reduced to about one-third of normal by prolonged inflation of a balloon inserted into the left atrial cavity. This resulted in a progressive reduction in the size of the left ventricular cavity, reaching about 50% of normal left ventricular size in about 7 days, and was also associated with a decrease in left ventricular muscle mass.

Outflow obstruction of the left ventricle was accomplished by placing a polyvinyl snare around the ascending aorta, just above the origin of the coronary arteries. It was tightened to achieve a systolic pressure gradient from the left ventricle to the aorta, beyond the obstruction, of about 20 mm Hg. Since the snare does not expand, with growth of the aorta, the obstruction becomes progressively more severe. During the first week, the left ventricular wall became thickened, but within 2–3 weeks, hypoplasia of the left ventricle began to develop, and subsequently, the cavity became almost slit-like (Figure 53.1). These studies are important, because they indicate that in the normal fetus, development of ventricular chamber size is affected by reducing its input or output.

The effects of outflow obstruction of the right ventricle were studied by placing a snare around the main pulmonary trunk in fetal lambs at about 60 days' gestation. As the lamb developed *in utero*, the obstruction of the pulmonary trunk became progressively more severe, simulating pulmonary stenosis. Hemodynamic studies in the lambs, performed about 60 days after the snare was placed around the pulmonary artery, showed that right ventricular systolic pressure was elevated, and right ventricular output was reduced. An increase in left ventricular output achieved almost normal combined ventricular outputs. The right ventricular myocardial mass increased, but the size of the right ventricular cavity varied greatly. In some fetuses, the cavity was almost obliterated and appeared slit-like. In others, the right ventricle was markedly enlarged.

The size of the right ventricle appeared to be related to the competence of the tricuspid valve. When the valve was small, the right ventricular cavity was small, but a large tricuspid orifice was associated with an enlarged right ventricle. The differences in response could be explained by the volume of blood being handled by the ventricle. If the tricuspid valve remained competent, the right ventricular stroke volume was reduced by the outflow obstruction, and the cavity size decreased. However, with tricuspid incompetence, the ventricle ejected a large volume at high pressure, with a large proportion regurgitating into the right atrium; this was associated with enlargement of the right ventricle. This difference in the behavior of the right ventricle to outflow obstruction has been observed in human fetuses with pulmonary atresia, some having markedly hypoplastic right ventricles and others showing marked right ventricular enlargement, sometimes so great as to compromise lung growth in the fetus.[5]

The studies in the lamb fetus provide convincing evidence that interference with flow into or out of a ventricle during fetal development may result in hypoplasia, because the myocardium is normal prior to the introduction of the lesion, and there are no other abnormalities. In human fetuses, several reports have suggested that aortic stenosis may result in a progressive decrease in left ventricular size and may progress to a hypoplastic left heart with advancing gestation.[6,7] If an infant is born with a hypoplastic left ventricle, it may not be capable of providing an output adequate for the needs of the systemic circulation. Survival depends on providing flow to the systemic circulation through the ductus arteriosus from the right ventricle. It has been proposed that it may be possible to avoid severe hypoplasia of the ventricle by relieving the aortic stenosis as early as possible in the fetus by performing balloon angioplasty of the aortic valve. The objective is to promote *in utero* development of the left ventricle so that it will be capable of sustaining an output to provide adequate systemic circulation after birth, a "biventricular circulation." Techniques have been developed to accomplish this by a percutaneous approach from the mother's abdomen. The procedure has now been performed at several centers with a high rate of success, very little risk to the fetus, and minimal risk to the mother. Despite the apparent success in relieving or

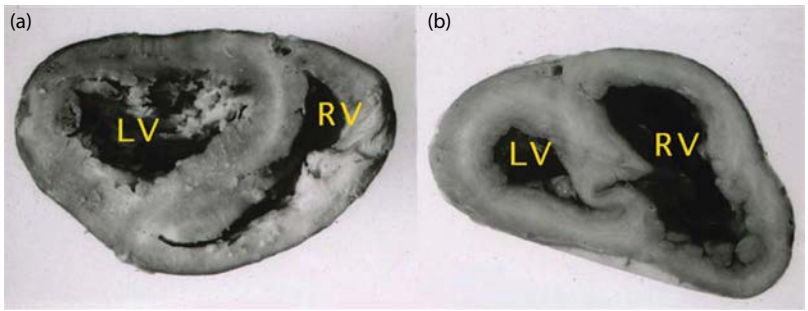


**Figure 53.1**
Sections of fetal hearts midway between apex and atrioventricular sulcus. (a) Normal fetal heart showing left (LV) and right (RV) ventricles. (b) Fetus 10 days after banding ascending aorta to simulate aortic stenosis. Note marked decrease in left ventricular size.

reducing the aortic stenosis in the fetus and avoiding further reduction in ventricular size, until recently there have been relatively few infants in whom the left ventricle has been able to provide an adequate output after an angioplasty *in utero*.[8,9] In a series reported from Boston Children's Hospital in 2006, about one-third of fetuses with successful aortic balloon angioplasty went on to have a biventricular heart after birth.[10] In a more recent study of the results of aortic balloon valvuloplasty performed in 100 fetuses, 88 were live-born. Of these, 38 (43%) established a biventricular circulation after birth.[11] The possibility that some or all of the fetuses who developed a biventricular circulation after birth may have done so with no intervention cannot be excluded. In an attempt to address this concern, the outcomes of 107 fetuses with the diagnosis of aortic stenosis, who were not subjected to valvulotomy *in utero*, were analyzed in a retrospective study.[12] Postnatal procedures were performed in 80 of these patients, and 44 successfully maintained a biventricular circulation. Thus, there was little difference in the number of infants who established a biventricular circulation in the group who had aortic valvulotomy *in utero*, compared with those who had no procedure. There have been ongoing attempts to establish criteria for recommending valvuloplasty in fetuses with the diagnosis of aortic stenosis. Makikallio et al.[10] noted left ventricular growth was much more likely to be affected in fetuses with aortic stenosis that demonstrated retrograde flow in the transverse aortic arch, left-to-right flow across the foramen ovale, monophasic mitral inflow, or significant LV dysfunction. Based on these observations, indications for the performance of valvulotomy in fetuses with aortic stenosis have been developed, but further definition is necessary.[13]

These results of the variable effects of aortic valvulotomy have raised the question of whether abnormal ventricular development is secondary to the abnormal aortic valve, or possibly the primary lesion.[14] Ultrasound observations in fetuses have rarely documented aortic stenosis with normal left ventricular size and function, later progressing to hypoplastic ventricle. In most fetuses observed at about 16–20 weeks' gestation, the left ventricle is large and dysfunctional and has an echodense subintimal layer. The diagnosis of aortic stenosis is considered, and with advancing gestation, the ventricular size is noted to become progressively smaller. It is quite possible that the ventricular muscle is abnormal as a result of exposure to infection or toxin, or as a result of a genetic anomaly. This could interfere with left ventricular output, and the aortic valve anomaly could be the result of the reduced flow. If output is severely reduced, possibly even aortic atresia could develop. It is likely that there are several causes of left ventricular hypoplasia. If the ventricular muscle damage is primary, due to toxic, infectious, or genetic factors, balloon angioplasty of the aortic valve *in utero* is probably contraindicated, because it is not likely to alter the course of the abnormal process. If, however, aortic stenosis is the primary problem, prenatal relief of the obstruction, as early as possible, is likely to improve the prospect of allowing the left ventricle to sustain adequate systemic blood flow after birth. It is thus important to develop techniques that define the cause of the ventricular abnormality.

## Ascending aorta and aortic arch development

Most of the blood ejected by the left ventricle into the ascending aorta is directed to the brain and upper extremities. In fetal lambs, about 33% of combined ventricular output (CVO) is ejected by the left ventricle; about 23%–25% of CVO is distributed to the head and forelimbs, so that only about 10% of CVO passes across the aortic isthmus to the descending aorta (Chapter 8). Although precise measurements of flow across the aortic isthmus in the human fetus are currently not available, it appears that it is similar to that in the lamb. This relatively low blood flow across the aortic isthmus is reflected in the morphology. The ratio of isthmus diameter to ascending aortic diameter in the human fetus is about 0.7, so that the cross-sectional area is about one-half.

In several congenital cardiovascular malformations, the volume of blood flowing into the aorta is altered, and this is associated with an increase or decrease in aortic diameter. Thus, in the fetus with pulmonary atresia with a ventricular septal defect, all the blood from the right and left ventricles is ejected into the ascending aorta, an amount that is at least twice the normal volume; this results in an ascending aorta with a cross-sectional area considerably greater than normal. In contrast, in the fetus with aortic atresia, no blood enters the aorta from the left ventricle; blood passes into the aortic arch and ascending aorta retrograde from the ductus arteriosus, and the ascending aorta conducts only the small amount of blood flowing into the coronary circulation. This results in a hypoplastic ascending aorta with a markedly reduced diameter.

In the fetus with pulmonary atresia and an intact ventricular septum or a small ventricular septal defect, all or most of the blood returning to the heart enters the left atrium and is ejected by the left ventricle into the aorta (Figure 53.2). Thus, as with pulmonary atresia, the ascending aorta is large. However, in the fetus with tricuspid atresia with transposition of the aorta and pulmonary artery, the left ventricle ejects directly into the main pulmonary artery. Blood flow into the ascending aorta is derived from the small right ventricle, which receives blood across a ventricular septal defect (Figure 53.3). As a result of the reduced blood flow into the ascending aorta, it is small. Also, because most of the blood ejected into the aorta is directed to the carotid and subclavian arteries, little crosses the aortic isthmus, which therefore is quite narrow. Flow through the ductus arteriosus compensates for the lack of contribution from the aortic isthmus to the descending aortic flow.

In other malformations, flow into the ascending aorta may be compromised in the fetus by the presence of left ventricular outflow obstruction. This may occur as a result of valvar aortic stenosis, or subvalvar stenosis, as in Taussig-Bing anomaly, and is often associated with aortic arch narrowing and aortic coarctation.

Aortic coarctation is frequently associated with congenital cardiovascular malformations in which left ventricular outflow is reduced; it has been suggested that the low blood flow

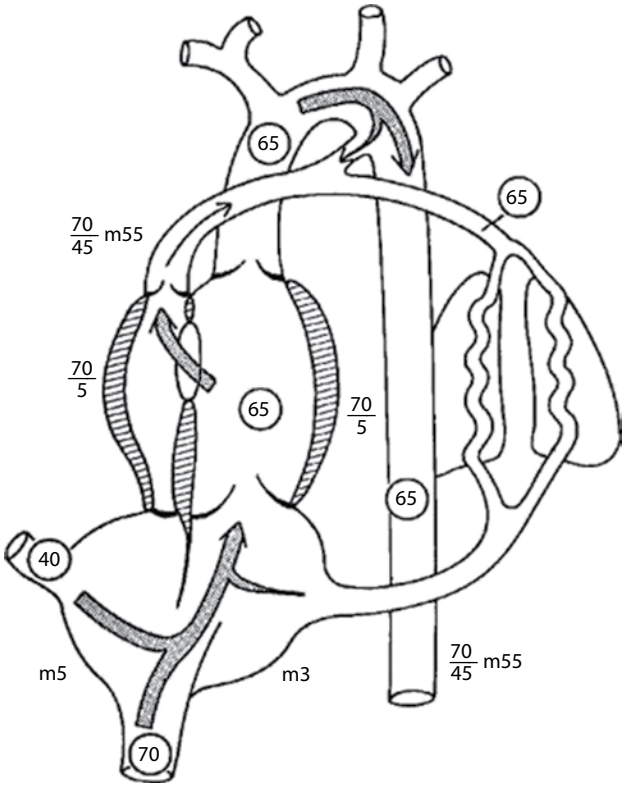


**Figure 53.2**
The heart of a fetus with tricuspid atresia and a small ventricular septal defect. Most of the blood is ejected by the left ventricle. The ascending aorta and aortic arch are large. The pulmonary artery derives blood supply through the ductus arteriosus and is quite small. Pressures and oxygen saturation (in circles) in chambers and great vessels are shown. (m = mean pressure.) (Reproduced with permission from Rudolph AM. *Congenital Diseases of the Heart*. Chichester, UK: Wiley; 2009.[14])

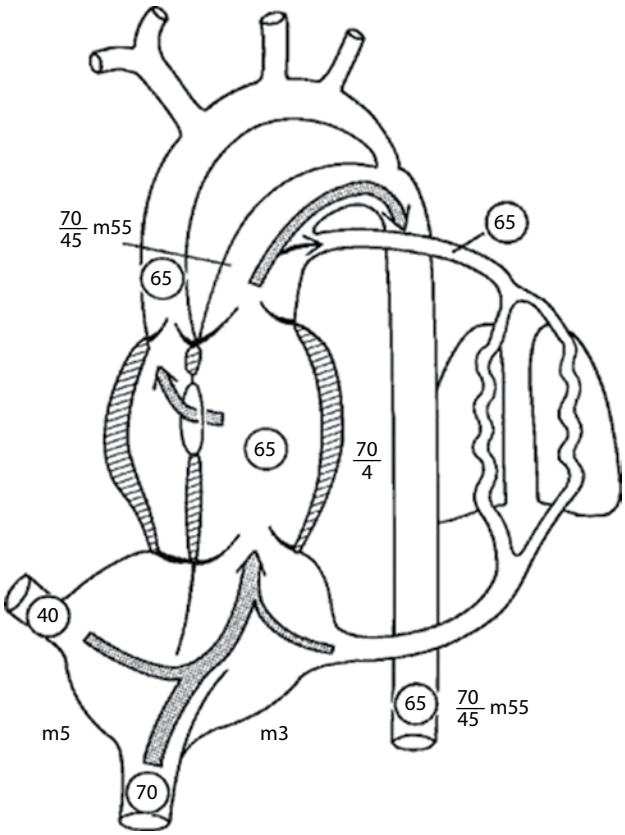


**Figure 53.3**
The heart of a fetus with tricuspid atresia, a small ventricular septal defect, and aortopulmonary transposition. Blood supply to the ascending aorta is decreased, resulting in a narrow ascending and transverse aorta. The ductus arteriosus is large and supplies most of the flow to the descending aorta. Pressures and oxygen saturation (in circles) in chambers and great vessels are shown. (Reproduced with permission from Rudolph AM. *Congenital Diseases of the Heart*. Chichester, UK: Wiley; 2009.[14])

across the isthmus is the cause of the localized aortic narrowing. Coarctation of the aorta is frequently not evident *in utero*, and presents as aortic obstruction postnatally in association with closure of the ductus arteriosus. A shelf projects from the posterolateral wall of the aorta toward the entry of the ductus arteriosus. It has been proposed by Hutchins[15] that the flow through the ductus from the pulmonary artery to the aorta is large and, in association with the low isthmus flow, induces overgrowth at the junction of the aortic isthmus with the descending aorta; this region acts as a branch point. Experimental studies have demonstrated this phenomenon in flow models.

## Ductus arteriosus size and orientation

In the normal fetus, a large proportion of blood ejected by the right ventricle is deflected away from the lung through the ductus arteriosus to the descending aorta. In the fetal lamb, almost 85% of right ventricular output, or slightly more than half of the combined ventricular output, passes through the ductus; in the human fetus, pulmonary blood flow is relatively greater, so 35%–40% of combined ventricular output traverses the ductus arteriosus (see Chapter 6). As a result of the magnitude and direction of flow, the ductus joins the descending aorta with an oblique inferior angle (Figure 53.4). Congenital cardiovascular malformations such as pulmonary atresia or marked right ventricular outflow stenosis, tricuspid atresia, and Ebstein malformation with severe tricuspid insufficiency are associated with reduced or absent flow from the right ventricle into the pulmonary artery. The normal pattern of a large flow from the pulmonary artery through the ductus is replaced by flow from the aorta to the pulmonary artery to provide pulmonary blood flow. Because the volume of flow is less than normal, the ductus arteriosus is usually somewhat narrower. The inferior angle between the aorta and ductus arteriosus varies in these infants. In infants with pulmonary atresia with a ventricular septal defect, the pulmonary arteries are small, and the inferior angle between the ductus and the descending aorta is acute (Figure 53.4). However, in infants with pulmonary atresia with an intact ventricular septum, the pulmonary arteries vary in size. When the right ventricle is fairly well developed with inflow, body, and outflow regions (tripartite), the pulmonary arteries are fairly well developed, and the inferior angle between

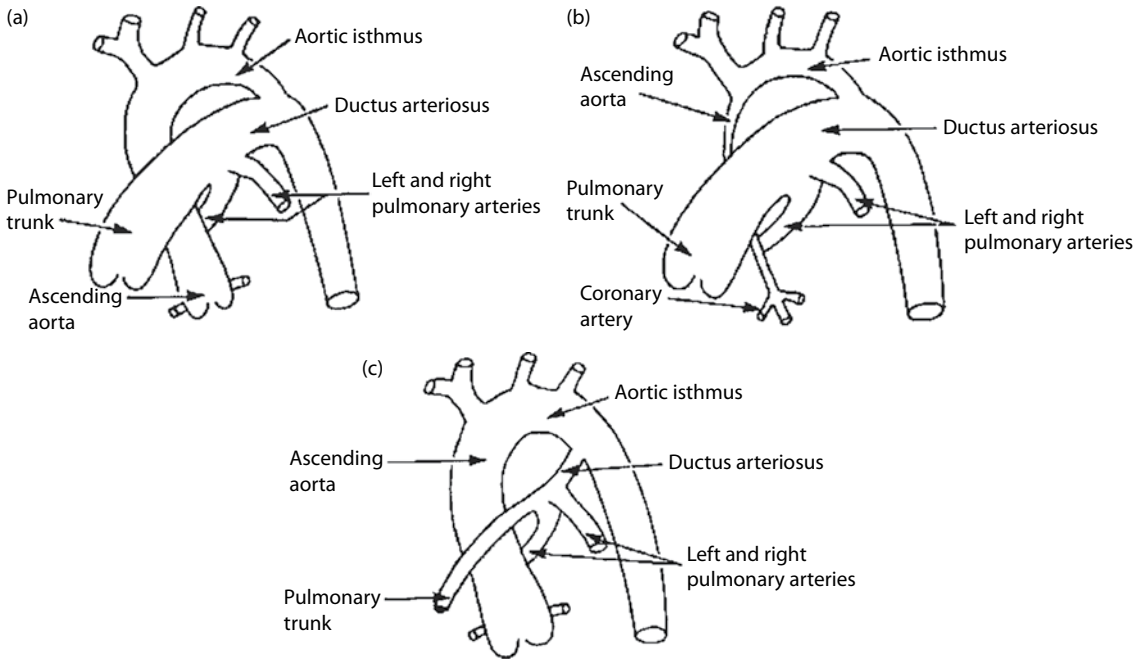


**Figure 53.4**
The pulmonary trunk, ductus arteriosus, and aorta are depicted in the normal fetus (a), a fetus with aortic atresia (b) and a fetus with pulmonary atresia (c). In the normal fetus, a large volume of blood flows from the pulmonary artery through the ductus to the descending aorta. The ductus is large and joins the aorta with an oblique inferior angle. In the fetus with aortic atresia, the total output of the heart is ejected into the pulmonary artery and most passes through the ductus, which is very large and also joins the aorta with an oblique inferior angle. In the fetus with pulmonary atresia, blood flows from the aorta through the ductus to the pulmonary artery. This supplies only the pulmonary circulation. The ductus is small and the junction with the aorta has an acute inferior angle. (Reproduced with permission from Rudolph AM. *Congenital Diseases of the Heart*. Chichester, UK: Wiley; 2009.[14])

the ductus and the aorta is usually obtuse. If the right ventricle is poorly developed (unipartite), the pulmonary arteries are small, and the angle between the ductus and descending aorta is usually acute. This difference can possibly be explained by the time during fetal development that there is interference of flow patterns. When pulmonary atresia is associated with a ventricular septal defect, the atresia is probably present early in development, so that there is no pulmonary arterial to aortic flow through the ductus arteriosus. With pulmonary atresia with intact ventricular septum, the pulmonary valve is open for some time during gestation, and then becomes progressively stenosed and eventually atretic. Flow from the pulmonary artery through the ductus is maintained until the stenosis becomes severe, thus accounting for the normal obtuse angle in those with a well-developed right ventricle.[16,17]

Cardiac lesions causing obstruction on the left side of the heart, such as interrupted aortic arch, aortic atresia, severe aortic or left ventricular outflow stenosis, and mitral atresia, are associated with either markedly reduced or absent blood flow across the aortic isthmus to the descending aorta. Furthermore, ascending as well as descending aortic flow may be derived from flow through the ductus arteriosus from the pulmonary artery. The ductus arteriosus is usually larger than normal in these fetuses, and the inferior angle at the junction of the ductus with the descending aorta is oblique. As mentioned previously, the greater than normal flow across the ductus with a smaller than normal isthmus may create a branch point at the isthmus–descending aorta junction and induce the development of a shelf of aortic coarctation.

## *Effects of obstructive lesions*

The role of obstructive lesions in reducing blood flow in chambers and great vessels is discussed earlier in this chapter. In this section, the possible effects of obstruction on other organ systems are presented.

### Ductus arteriosus obstruction and the pulmonary circulation

In the fetus, pulmonary arterial and aortic pressures are almost identical through most of gestation, but in the last few weeks before birth of the lamb, the pulmonary arterial pressure is slightly higher, presumably because the ductus arteriosus becomes somewhat constricted. Acute compression of the ductus in fetal lambs results in an elevation of pulmonary arterial pressure and a slight fall of aortic pressure. We demonstrated experimentally that compression of the ductus arteriosus in fetal lambs induced an increase in the amount of smooth muscle in fifth-generation pulmonary arterioles, the resistance vessels in the lungs.[18,19] The possibility that this could interfere with the normal fall of pulmonary vascular resistance after birth and cause the clinical syndrome

of persistent pulmonary hypertension in the newborn infant was considered. More recent studies in lambs have confirmed these observations.[20] The possible causes of constriction of the ductus arteriosus *in utero* are not well defined.

As mentioned in Chapter 6, the ductus arteriosus is dilated by prostaglandins. Administration of salicylates or indomethacin to fetal lambs *in utero* resulted in constriction of the ductus with an increase in pulmonary arterial pressure.[21] The association of persistent hypertension of the newborn with ingestion of nonsteroidal anti-inflammatory agents by the mother is now well recognized[22]; this is presumably the result of prolonged pulmonary arterial hypertension in the fetus with resulting increased pulmonary arterial smooth muscle development.

Constriction of the ductus reported in some fetuses with aortopulmonary transposition is discussed in the following text.

## Aortic arch obstruction and cerebral blood flow

In fetuses with hypoplastic left heart and aortic atresia, blood supply to the cerebral circulation cannot be provided from left ventricular output and is derived from retrograde flow across the aortic isthmus and arch from the ductus arteriosus. Studies in fetuses and newborn infants with hypoplastic left heart have demonstrated that head circumference is less than normal[23] and that cerebral development is impaired.[24,25] It has been suggested that this interference with fetal brain development may be the result of decreased oxygen supply to the brain.[26] It has been proposed that this concept is supported by observations of Doppler flow velocity in major cerebral arteries in fetuses with hypoplastic left heart. These have shown that the PI (pulsatility index), which relates maximum systolic velocity and low diastolic velocity to mean velocity, is reduced in cerebral arteries in these fetuses as compared with normal fetuses.[27] A low PI has been interpreted to indicate that the cerebral vascular resistance is decreased, and this is the result of cerebral hypoxia. However, although a decreased PI could be caused by cerebral vasodilation, it could also result from altered circulatory dynamics.

I have proposed that the cerebral developmental disturbances associated with aortic atresia and hypoplastic left ventricle could be the result of interference of blood flow to the brain.[28] Because there is little or no flow in the ascending aorta, blood to the brain is delivered through the circuitous route from the pulmonary artery, through the ductus arteriosus, and then retrograde across the aortic isthmus and aortic arch to the carotid and cerebral arteries. This could well account for the altered Doppler flow pattern in cerebral arteries. Another important factor that may interfere with blood flow to the brain is the frequent presence of coarctation of the aorta either adjacent to the ductus arteriosus, or between the ductus and the aortic isthmus. This has been noted in 75% of infants with hypoplastic left heart.[29]

Although altered hemodynamics have been considered to contribute to the cerebral developmental disturbances, it is possible that whatever genetic or toxic factors may be responsible for the cardiac anomalies could cause the cerebral abnormalities.

## Foramen ovale obstruction

Lev et al. reported the association of narrowing or absence of the foramen ovale with hypoplastic left heart complexes and considered that the lack of flow into the left heart could be the cause of the left-sided hypoplasia.[3] However, the abnormalities in the circulation that would result if left ventricular hypoplasia or aortic or mitral atresia were the primary lesion could well account for the abnormalities of the foramen ovale. Right ventricular output would be increased to maintain combined ventricular output, because left ventricular output is reduced. Pulmonary venous blood returning to the left atrium would not be ejected by the left ventricle and would therefore have to pass through the foramen ovale. Left atrial pressure will be elevated and the atrial septum displaced to the right, promoting closure of the foramen. The increase in left atrial and pulmonary venous pressure has been considered to be the cause of pulmonary lymphangiectasis that may be associated with hypoplastic left heart syndrome and absent foramen ovale.

It is now recognized that the presence of obstructed or absent foramen ovale in infants born with hypoplastic left heart is associated with a high mortality both preoperatively, and following surgical palliation.[30,31] This has stimulated attempts to open the foramen ovale urgently after birth before surgery is performed, if obstruction is identified.[32] More recently, it has been suggested that if foramen ovale obstruction is recognized in the fetus with hypoplastic left heart, attempts should be made to achieve an adequate opening *in utero*.[33] It has been appreciated that echocardiographic evidence of a change in pulmonary venous flow, compatible with interference with forward flow, is useful in detecting the presence of foramen ovale obstruction.[34]

# *Effects of changes in blood oxygen content*

## Increase of pulmonary arterial oxygen saturation

Relatively little consideration has been given to possible effects that alterations in oxygen levels may have on the circulation in the fetus and neonate with congenital cardiovascular malformations. I postulated that in fetuses with aortopulmonary transposition, pulmonary arterial oxygen saturation would be higher, and ascending aortic oxygen saturation lower, than normal.[14,35] It was suggested that this could affect the pulmonary circulation and possibly oxygenation and metabolism of the brain. In echocardiography studies, several fetuses with aortopulmonary transposition were observed to have either a small foramen ovale or a narrowed ductus arteriosus, or both.[36] Jouannic et al. reported that about 4% of infants with transposition had serious difficulty soon after birth, and

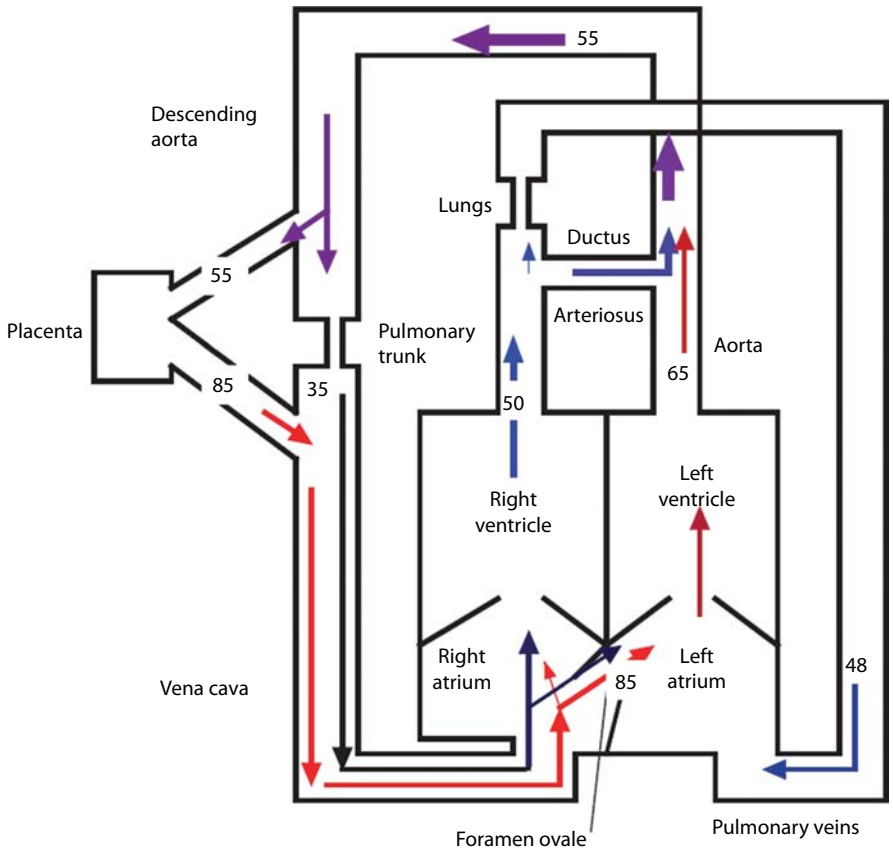


**Figure 53.5**
Circulation in the normal fetal lamb showing patterns of blood flow and oxygen saturations in cardiac chambers and great vessels. Note the higher oxygen saturation in the ascending compared with the descending aorta and low saturation in the pulmonary artery. (Reproduced with permission from Rudolph AM. *Pediatr Res* 2007;61:375–80.[35])

there was a frequent association of early severe hypoxemia with abnormalities of the foramen ovale or ductus arteriosus noted on fetal echocardiography.[37]

These observations could well be explained by higher than normal oxygen saturations in pulmonary arterial blood. In the fetus, well-oxygenated umbilical venous blood passing through the ductus venosus is preferentially directed through the foramen ovale to the left atrium and ventricle. Systemic venous blood from the superior and inferior caval veins preferentially flows through the tricuspid valve to the right ventricle (see Chapter 6). Normally, right ventricular blood with low oxygen saturation is ejected into the pulmonary trunk, and measurements in fetal lambs indicate that the arteries of the lung and the ductus arteriosus are exposed to blood with an oxygen saturation of about 50% and a partial pressure of oxygen ($PO_2$) of about 18 mm Hg (Figure 53.5). Blood ejected by the left ventricle into the ascending aorta has an oxygen saturation of about 65% with a $PO_2$ of about 25 mm Hg. Venous flow patterns in the umbilical vein, ductus venosus, and caval veins appear to be normal in the fetus with aortopulmonary transposition. However, well-oxygenated blood is ejected by the left ventricle into the pulmonary trunk, and thus the pulmonary circulation and the ductus arteriosus are exposed to blood with a higher than normal oxygen saturation and $PO_2$. Based on assumptions that the proportions of combined ventricular output flowing through vessels and shunts are similar to those in normal fetuses, it is estimated that the pulmonary vasculature and ductus arteriosus would be exposed to an oxygen saturation of about 72% and $PO_2$ of about 28 mm Hg (Figure 53.6).

The fetal pulmonary circulation is very sensitive to relatively small changes in $PO_2$. In a study in fetal lambs, in which the ewe inhaled 100% oxygen, an increase in $PO_2$ of 7 mm Hg resulted in a threefold increase of pulmonary blood flow.[38] The lower pulmonary vascular resistance resulting from perfusion with relatively high $PO_2$ in the fetus with transposition will result in an increase of flow through the pulmonary circulation and a reduction of flow through the ductus arteriosus. The increased pulmonary blood flow will result in greater venous return to the left atrium, elevating left atrial pressure; this could deviate the atrial septum to the right and thus tend to reduce foramen ovale size. The reorientation of flow from the pulmonary trunk could also have an effect on the size of the ductus arteriosus, because a smaller volume would flow through it to the descending aorta.

The responsiveness of the pulmonary circulation to oxygen changes with gestational age. In fetal lambs, raising pulmonary arterial $PO_2$ levels produces minimal pulmonary vasodilatation before about 100 days' gestation (term ~150 days); a progressive increase in vasodilator response is

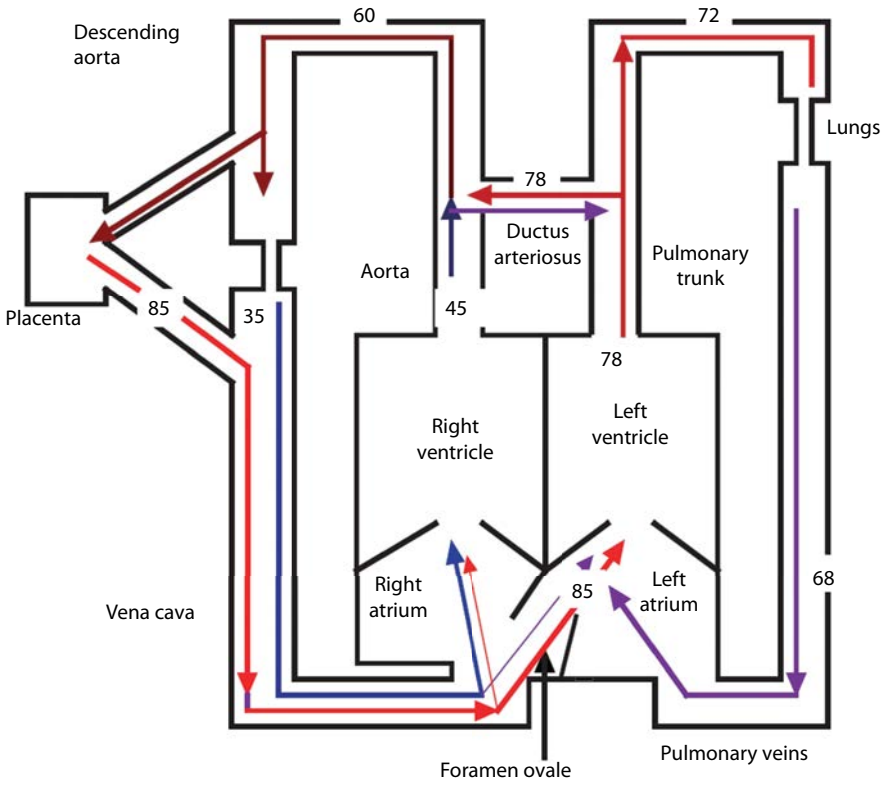


**Figure 53.6**
Circulation in the fetus with aortopulmonary transposition showing patterns of blood flow and oxygen saturations in cardiac chambers and great vessels. Oxygen saturation in the pulmonary artery, which arises from the left ventricle, is very high compared with normal. Saturation in the ascending aorta, which arises from the right ventricle, is relatively low. Data are based on estimates of volumes of blood flow in various vessels. (Reproduced with permission from Rudolph AM. *Pediatr Res* 2007;61:375–80.[35])

observed with increasing gestational age.[39] A similar difference in response with gestational age has been reported in the human. Inhalation of oxygen by the mother did not affect pulmonary blood flow in fetuses of about 25 weeks' gestation, but did increase flow in fetuses beyond 30 weeks' gestation.[40] Based on these observations, the effects of the higher oxygen saturation in pulmonary arterial blood in fetuses with transposition may not be observed until the third trimester.

The higher $PO_2$ in pulmonary arterial blood, in addition to reducing flow through the ductus arteriosus as a result of increased pulmonary blood flow, may have a direct vasoconstrictor effect on the ductus. The response of the ductus to oxygen also increases with advancing gestational age. In lamb fetuses below 90 days' gestation, an increase of $PO_2$ results in minimal constriction of the ductus, but the responsiveness increases with advancing gestation.[41] Constriction of the ductus would tend to enhance diversion of blood into the pulmonary circulation.

It is of interest that constriction of the ductus could provide an explanation for the occurrence of postnatal elevation of pulmonary vascular resistance observed in some infants with transposition with intact ventricular septum.[42]

Constriction of the ductus arteriosus in the fetus elevates pulmonary arterial pressure, and this induces an increase in pulmonary vascular smooth muscle development; this may result in persistent pulmonary hypertension in the newborn infant (see section "Ductus arteriosus obstruction and the pulmonary circulation" of this chapter). This same phenomenon may occur in fetuses with transposition. Whether the increase in pulmonary vascular resistance resulting from pulmonary arterial hypertension is opposed by the increase in pulmonary arterial $PO_2$ in fetuses with aortopulmonary transposition is yet to be resolved.

## Decrease of ascending aortic oxygen saturation

In the normal fetus, oxygen saturation of blood ejected from the left ventricle into the ascending aorta is relatively high—about 65%. This is due to preferential streaming of well-oxygenated umbilical venous blood passing through the ductus venosus, across the foramen ovale into the left atrium (Figure 53.5). In many congenital cardiovascular malformations, all venous blood returning to the heart is mixed almost completely, and blood ejected into the aorta and pulmonary arteries has similar oxygen saturations. Thus, in fetuses with tricuspid or pulmonary atresia with intact ventricular septum, all the venous blood enters the left atrium, whereas with mitral atresia, or aortic atresia with intact ventricular septum, all venous blood mixes in the right atrium. Based on magnitudes of venous return in the lamb fetus, it is estimated that the oxygen saturation of blood delivered to all parts

of the body in the fetuses with complete admixture will be 55%–60%. This represents a small decrease in blood oxygen content delivered to the cerebral and coronary circulations, and, although it may induce some vasodilatation in these organs, the effect is probably minor. These lesions would also result in an increase above normal of oxygen saturation of pulmonary arterial blood, although the effect would not be as marked as with transposition (see previous discussion), but the possibility that pulmonary vascular resistance is lower than normal and the ductus arteriosus is constricted is yet to be determined.

In fetuses with aortopulmonary transposition, the ascending aortic blood oxygen saturation would be reduced considerably, from a normal of ~65%, to about 45% (Figure 53.6). A fall in oxygen saturation of blood perfusing the brain results in cerebral vasodilatation with increased cerebral blood flow.[43] The lower oxygen saturation is not likely to affect brain function and development, because even when oxygen delivery to the brain is decreased acutely, cerebral oxygen consumption is maintained at normal levels.[44]

There is evidence that cerebral blood flow is increased in fetuses with aortopulmonary transposition, because Doppler velocity studies of cerebral arteries have demonstrated a low pulsatility index, suggesting that cerebral vascular resistance is reduced.[45] However, the effect of a prolonged increase in cerebral blood flow on brain development has not been examined. Furthermore, although the increased cerebral flow may permit adequate oxygen consumption in the unstressed fetus with transposition, there may be inadequate reserve to maintain cerebral oxygen consumption at normal levels if hypoxic stress occurs for any reason. The possibility that cerebral development may be affected is suggested by the observation that head circumference is somewhat reduced in infants born with transposition.[23]

The oxygen saturation of blood perfusing the coronary circulation is also reduced in the fetus with transposition. During acute hypoxemia in fetal lambs, coronary blood flow increases markedly, and even with quite severe hypoxemia myocardial oxygen consumption is maintained at normal levels.[46] However, as with the cerebral circulation, no information is available regarding possible deleterious effects of a prolonged increase in coronary blood flow. Also, the ability to maintain oxygen delivery in the event of hypoxic stress is questionable.

# Relationship between congenital cardiovascular malformations and postnatal circulatory adjustments

The changes in the circulation occurring normally after birth are discussed in Chapter 6. The main adjustments that occur are ventilation resulting in a rise in arterial oxygen tension, a fall in pulmonary vascular resistance, constriction of the ductus arteriosus, closure of the foramen ovale, elimination of the umbilical-placental circulation, and closure of the ductus venosus. Blood flow patterns after birth are frequently altered by congenital cardiovascular malformations and may account for the clinical manifestation of these anomalies.

## *Decrease in pulmonary vascular resistance*

### Effect of abnormal communications

Communications between the left and right ventricles, the aorta and pulmonary arteries, and the left and right atria are among the more common congenital cardiac anomalies. The magnitude and time course of changes in pulmonary vascular resistance after birth are important in determining the hemodynamic and clinical manifestations of these lesions after birth.

After birth, the elimination of the relatively low-resistance umbilical-placental circulation, which arises from the aorta, results in an increase in systemic vascular resistance. Ventilation induces a marked fall in pulmonary vascular resistance (Chapter 6). Normally, separation of the left and right sides of the heart is achieved by closure of the ductus arteriosus and foramen ovale, and blood then flows serially through the pulmonary and systemic circulations, as in the adult. With the fall in pulmonary vascular resistance and closure of the ductus arteriosus after birth, pulmonary arterial and right ventricular pressures drop.

A large ventricular septal defect or a large patent ductus arteriosus tends to equalize the pressures in the left and right sides of the heart. With a large patent ductus, both systolic and diastolic pressures in the aorta and pulmonary artery are similar, whereas with a large ventricular septal defect, systolic pressures in the ventricles and great arteries are the same, but diastolic pressure in the pulmonary artery may be lower than that in the aorta. With equal pressures, blood flows through the systemic and pulmonary circulations are determined by the relative resistances of the pulmonary and systemic circulations. As mentioned, systemic vascular resistance increases and pulmonary vascular resistance falls after birth. In the presence of a large communication at the ventricular or aortopulmonary level, blood flows preferentially into the pulmonary circulation, and a left-to-right shunt develops after birth. The blood perfusing the pulmonary circulation includes systemic venous return and the blood shunted from the left to the right side of the heart. The pulmonary/systemic blood flow ratio is commonly used to indicate the magnitude of the blood that is shunted; the higher the ratio, the greater the amount of blood shunted.

The blood shunted left to right reduces the volume of blood ejected by the left ventricle that enters the systemic circulation. Thus, if the pulmonary/systemic blood flow ratio is 2:1, only half the blood ejected by the left ventricle is distributed to the systemic circulation, and if the ratio is 3:1, only one-third of the left ventricular output reaches the systemic circulation. To maintain a systemic blood flow adequate to provide oxygen and nutritional needs, left ventricular output has to be

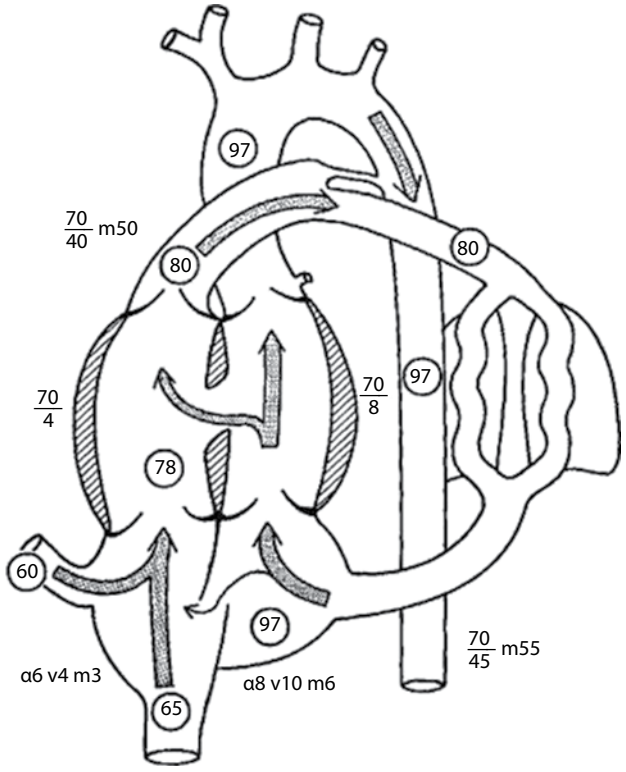


**Figure 53.7**
Circulation in the heart and great vessels of an infant with a large ventricular septal defect in the early neonatal period. Pulmonary vascular resistance has not yet dropped markedly. Oxygen saturations are shown in circles. Note moderate left-to-right shunt with a small increase in left atrial pressure. (Reproduced with permission from Rudolph AM. *Congenital Diseases of the Heart*. Chichester, UK: Wiley; 2009.[14])

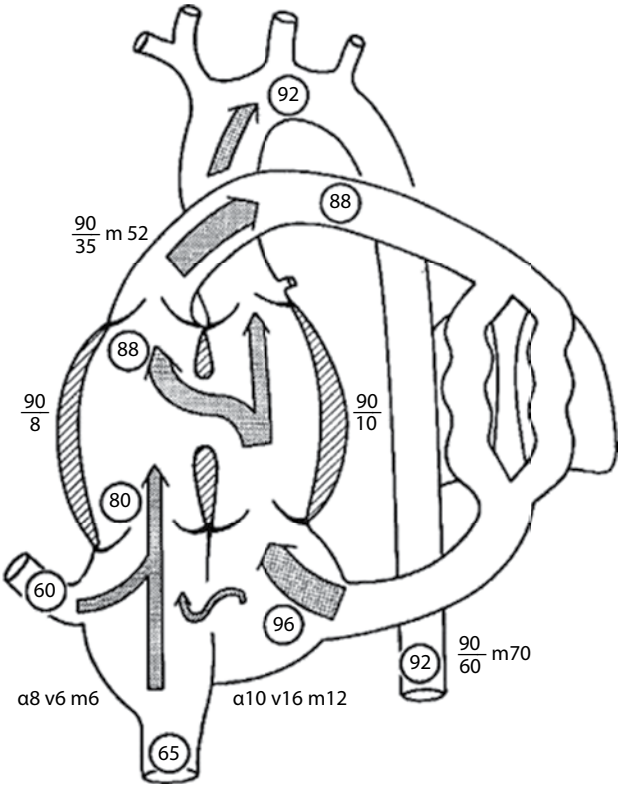


**Figure 53.8**
Circulation in the heart and great vessels of an infant with a large ventricular septal defect after pulmonary vascular resistance has decreased markedly. Oxygen saturations are shown in circles. Note large left-to-right shunt with marked increase in left atrial pressure. Pulmonary arterial systolic pressure is high, but diastolic pressure is lower than in the aorta. (Reproduced with permission from Rudolph AM. *Congenital Diseases of the Heart*. Chichester, UK: Wiley; 2009.[14])

increased. The blood shunted left to right enters the pulmonary circulation and returns through the pulmonary veins to the left atrium, with a resulting increase in left atrial and left ventricular end-diastolic pressures. As discussed in Chapter 6, the heart in the neonate is capable of increasing its output in response to elevated atrial filling pressures.

During the early neonatal period, the decrease in pulmonary vascular resistance is achieved by relaxation of pulmonary vascular smooth muscle, but the fall is limited by the presence of the smooth muscle in the media of the arterioles. Therefore, the magnitude of the left-to-right shunt and increase of left atrial pressure is restricted. The hemodynamic changes associated with a large ventricular septal defect in the early neonatal period are depicted in Figure 53.7.

In the normal infant, pulmonary vascular resistance continues to fall gradually for 6–8 weeks after birth, as the walls of the small pulmonary arteries become thinner as smooth muscle regresses. In the infant with a large left-to-right shunt lesion, pulmonary vascular resistance also continues to fall gradually, resulting in a progressive increase in left-to-right shunt and left atrial pressure (Figure 53.8).

In infants with a large ventricular septal defect or aortopulmonary communication, the fall in pulmonary vascular resistance is somewhat slower, and the levels achieved are not as low as in the normal infant. This is probably the result of the persistence of the high pulmonary arterial pressure after birth.

The progressive increase in the left-to-right shunt results in increasing left atrial pressure, eventually leading to transudation of fluid into the lungs, causing increased respiratory effort. The stress on the left ventricle to markedly increase its output is associated with sympathetic-adrenal and renin-angiotensin stimulation; this is responsible for many of the clinical features of congestive heart failure, such as sweating, fluid retention, increased metabolism, and failure to thrive. Hepatomegaly is a relatively late manifestation. The immediate objectives of treatment are to reduce sodium and fluid retention by diuresis, reduce afterload on the left ventricle by vasodilators, and possibly improve ventricular performance by use of inotropic agents. Following stabilization of the clinical condition, the communication is closed either surgically or, if possible, by an interventional catheterization procedure.

Infants with smaller communications do not present with symptoms in the neonatal period. Small communications do not usually cause symptoms, and pulmonary arterial pressures fall normally after birth. Moderate-sized communications may present with evidence of congestive failure 2–3

months after birth, in association with the fall in pulmonary vascular resistance and increasing shunt.

The postnatal response to a large communication at the atrial level differs from that in ventricular or aortopulmonary communications. Associated with the decrease in pulmonary vascular resistance, pulmonary arterial pressure falls. If the atrial septal defect is large, pressures in the left and right atria will be similar. With equal pressure in the two chambers, flow into the left and right ventricles during ventricular diastole will be determined by their end-systolic volumes and by the compliance of the ventricular walls. During fetal life, the right and left ventricular pressures are equal, and the thickness of the walls is similar; with the same pressure in the atria, flow into each ventricle would be similar, and no significant shunting should occur. However, left-to-right shunting has been observed soon after birth and can be explained by the fall in pulmonary vascular resistance. Ventricular stroke volume is very dependent on afterload, especially in the fetus and neonate (see Chapter 8). The fall in pulmonary vascular resistance results in a decrease in afterload on the right ventricle, and thus right ventricular stroke volume is greater than that of the left. This results in greater emptying and a smaller right ventricular end-systolic volume; thus, a larger volume flows into the right ventricle, and left-to-right shunting across the atrial septum occurs. The progressive fall in pulmonary vascular resistance over 6–8 weeks after birth permits an increasing left-to-right shunt. The decrease in pulmonary arterial and right ventricular pressure is associated with a decrease in right ventricular wall thickness, and the left-to-right shunt is enhanced by the reduction in right ventricular compliance. Most infants with atrial septal defects do not have significant symptoms. The left atrial pressure is not elevated, and thus respiratory symptoms are not evident. The volume overload on the right ventricle increases gradually, and since right ventricular pressure is normal or only modestly increased, it is well tolerated. Occasionally, infants with large atrial septal defects do manifest some evidence of cardiac failure, probably as a result of neurohormonal stimulation.

## Communications in preterm infants

Premature infants with communications between the left and right sides of the heart frequently develop symptoms and signs soon after birth. Although it is not fully understood why this occurs, it could be related to a more rapid and greater decline in pulmonary vascular resistance after birth, inability of the left ventricle to increase its output adequately to maintain systemic blood flow when left-to-right shunt is large, and greater permeability of the pulmonary capillaries to transudation of fluid into the lung tissues and alveoli. As mentioned in Chapter 6, the pulmonary circulation responds poorly to hypoxia in the sheep fetus prior to 90 days' gestation, and the response increases progressively to term.

The preterm infant may therefore have a lower pulmonary vascular resistance at birth and also show a more rapid fall after birth, so that left-to-right shunt develops rapidly. Although left atrial pressure may not be markedly elevated, transudation of fluid into the lung is more likely to occur in the premature infant, because the pulmonary vessels are more permeable. This is further facilitated by the fact that plasma albumin concentrations are low, and this reduces intravascular osmotic pressure.

Preterm infants frequently present with respiratory distress, requiring assisted ventilation due to surfactant deficiency. The presence of a left-to-right shunt lesion may prevent weaning the infant from assisted respiration, because pulmonary fluid accumulation interferes with establishment of normal respiration.

Administration of diuretic agents may improve ventilation, but it may be necessary to close the communication. The most common communication is a patent ductus arteriosus (see text that follows), but ventricular or atrial septal defects, even of relatively small size, may be associated with difficulty in establishing normal respiration in preterm infants.

# *Closure of the ductus arteriosus*

The ductus arteriosus normally constricts after birth, and in the human infant, it is functionally closed within about 15 hours. As previously discussed, during fetal life congenital cardiovascular malformations may affect development of the ductus, and the presence of the ductus may be important in providing blood flow to the pulmonary or systemic circulation if the right or left ventricular outflow is obstructed by a cardiac lesion. The ductus arteriosus may be very important to the survival of infants with various congenital malformations after birth, by providing blood flow to the pulmonary or systemic circulations. Preterm infants frequently have delayed closure of the ductus arteriosus; this may have serious implications for their survival (see the following text).

## Decreased pulmonary blood flow

In the fetus, the lung is not the organ of gas exchange; pulmonary blood flow is relatively low. In the presence of pulmonary atresia or tricuspid atresia with an intact ventricular septum, pulmonary blood flow is supplied through the ductus arteriosus in the fetus. Because the flow is much lower than occurs normally, the ductus is smaller. Postnatally, with the assumption of the function of gas exchange by the lung, pulmonary blood flow has to increase 8- to 10-fold. In the immediate postnatal period, while the ductus is open, pulmonary blood flow may be large enough to provide adequate oxygen uptake to meet metabolic needs. Constriction of the ductus results in a reduction in pulmonary blood flow with a decrease in oxygen uptake in the lungs (Figure 53.9). In these congenital cardiovascular malformations, complete admixture of systemic and pulmonary venous return occurs in the left atrium and ventricle. The oxygen saturation of this mixed blood is determined by the pulmonary/systemic blood flow ratio. The lower the pulmonary blood flow, the lower the arterial oxygen saturation.

Normally, ductus arteriosus closure occurs within 10–15 hours after birth. However, in many infants with pulmonary or tricuspid atresia, the ductus remains patent for a

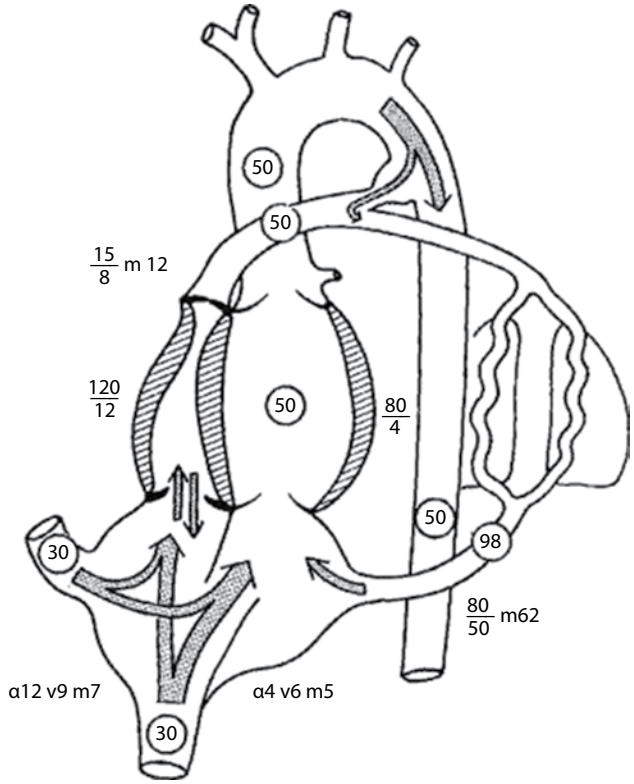


**Figure 53.9**
Pulmonary atresia in a newborn infant, showing that pulmonary blood flow is dependent on patency of the ductus arteriosus. Systemic and pulmonary venous blood mixes in the left atrium and total cardiac output is ejected by the left ventricle. Course of blood flow and oxygen saturations (in circles) are shown. (Reproduced with permission from Rudolph AM. *Congenital Diseases of the Heart*. Chichester, UK: Wiley; 2009.[14])

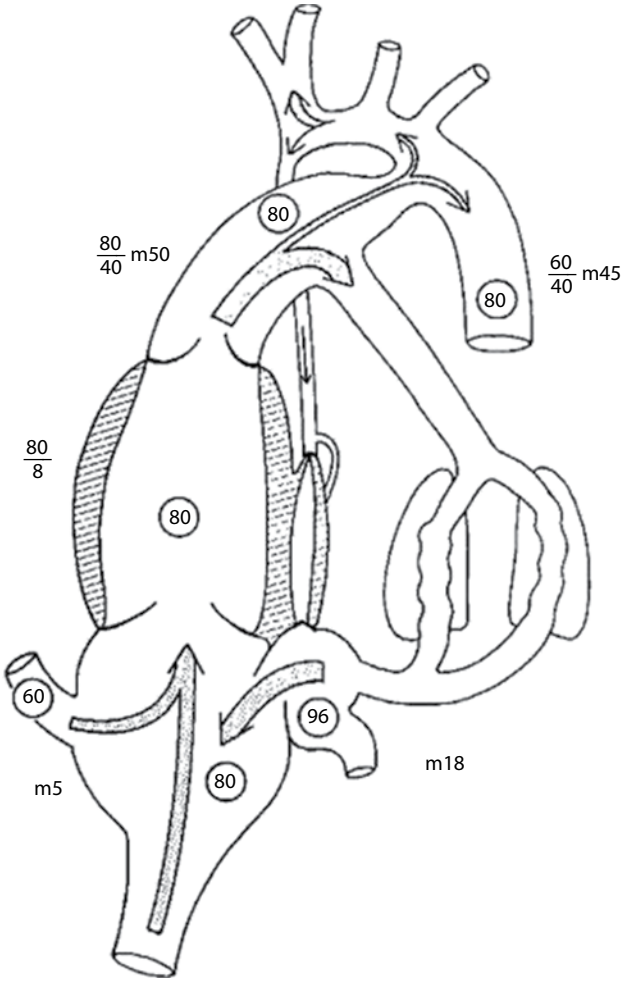


**Figure 53.10**
Course of the circulation and pressures and oxygen saturations (in circles) are shown in a newborn infant with aortic and mitral atresia. Systemic and pulmonary venous blood all returns to the right atrium and is ejected by the right ventricle. Blood flow into the aorta is dependent on patency of the ductus arteriosus. Constriction of the ductus interferes with systemic blood flow. (Reproduced with permission from Rudolph AM. *Congenital Diseases of the Heart*. Chichester, UK: Wiley; 2009.[14])

considerably longer period. It is not known what factors are responsible for the delayed closure. It is possible that the fall in arterial oxygen saturation that occurs when the ductus constricts may then tend to relax it. Possibly, circulating prostaglandin concentrations could remain elevated for longer periods after birth. Prostaglandin is cleared from blood during passage through the pulmonary circulation, and since pulmonary blood flow is low, the postnatal decrease in prostaglandin concentrations may be delayed. When the ductus is constricted, it can usually be opened by infusing prostaglandin E; when it is markedly constricted, the relaxation may be delayed for 15–30 minutes or even more. It is therefore recommended that prostaglandin be infused early, to try to avoid severe constriction.[40]

## Decreased systemic blood flow

In fetuses with aortic atresia, the flow to the systemic circulation, as well as the umbilical-placental circulation, is provided through the ductus arteriosus; it is therefore widely patent in the fetus. After birth, systemic blood flow continues to be dependent on the ductus for flow from the pulmonary artery to the aorta (Figure 53.10). Postnatally, however, flow through the ductus is reduced, because umbilical-placental flow is eliminated. Constriction of the ductus after birth reduces the systemic blood flow, resulting in a decrease in arterial pressure with poor pulse. If flow is greatly reduced, oxygen delivery to the tissues may be inadequate for metabolic needs, and an increase in anaerobic metabolism with lactic acidemia results, even though oxygen saturation is not greatly decreased.

Decreased blood flow to the kidney may result in renal damage.

The ductus arteriosus is necessary to provide systemic blood flow to the lower body in infants with aortic arch interruption; constriction of the ductus results in a reduction of blood flow with inadequate oxygen supply and metabolic acidemia.

In these lesions, as in conditions with ductus-dependent pulmonary blood flow, the ductus arteriosus may remain open for much longer than normal after birth.

In infants with ductus-dependent systemic blood flow, prostaglandin infusion is usually effective in relaxing the ductus, and this may provide adequate flow for tissue requirements and permit planning for a procedure in an infant who has not suffered severe metabolic disturbances. A decision may be made to perform a heart transplant in some infants with aortic atresia, and, to promote survival of the infant until such time as an organ becomes available, a stent has been inserted into the ductus by an interventional catheterization procedure to maintain patency.[47,48]

## Coarctation of the aorta

The presence of an aortic shelf in the region of the entrance to the ductus arteriosus, which narrows the lumen of the descending aorta in the fetus, has been noted in the fetus or neonate soon after birth. However, no evidence of obstruction to flow into the descending aorta may be induced while the ductus is open. Experimental studies in fetal lambs have demonstrated the role of the ductus arteriosus in determining the hemodynamic and clinical manifestations of aortic coarctation. An indentation was created by plicating the aortic wall opposite the entry of the ductus. After recovery from the surgical procedure, pressures were measured in the ascending and descending aorta before and after constriction of the ductus arteriosus. Prior to constriction of the ductus, no pressure difference was noted, but after closure, a considerable pressure gradient developed, indicating restriction of flow into the descending aorta.[49]

Similar observations have been made in infants. It is common for infants with aortic coarctation to have no manifestations in the immediate neonatal period and to have normal pulses in the upper and lower extremities, with equal blood pressures. Within days, or even as long as 8–10 weeks after birth, evidence of aortic coarctation, as manifested by weak pulse and decreased arterial pressures in the lower extremities, becomes manifest. This course can be explained by the behavior of the ductus arteriosus. While the ductus is widely patent, no significant obstruction of the descending aorta is evident (Figure 53.11), but closure of the ductus induces obstruction in the aorta. This results in an increase in ascending aortic pressure, and left ventricular systolic and end-diastolic and left atrial pressures increase (Figure 53.12). The clinical features are those of left ventricular failure such as increased respiratory effort, sweating, and poor perfusion of the peripheral circulation. In some infants, deterioration may occur rapidly as a result of acute onset of aortic obstruction. The ductus arteriosus normally is functionally closed within about 15 hours after birth. The delay in the onset of aortic obstruction in some infants with coarctation could be explained by lack of constriction of the ductus at the aortic end. The ductus usually begins to constrict nearest to the pulmonary arterial attachment, and this progresses to the aortic end. It is not unusual to observe a persistent opening known as the ductus ampulla of the aorta for days or weeks. Closure of this region may result in aortic obstruction.

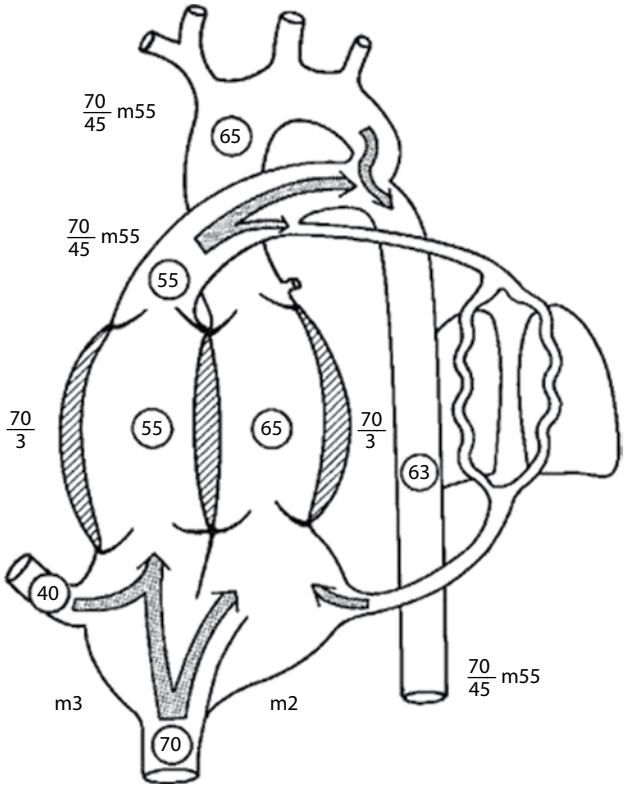


**Figure 53.11**
Circulation in a fetus with an aortic shelf opposite the ductus arteriosus orifice in the aorta. Note that patency of the ductus permits flow with no functional obstruction in the aorta. Course of flow and oxygen saturations (in circles) are shown. (Reproduced with permission from Rudolph AM. *Congenital Diseases of the Heart*. Chichester, UK: Wiley; 2009.[14])

It has been hypothesized that coarctation of the aorta may result from the extension of ductus tissue into the aortic wall, and that when the ductus constricts, this tissue also constricts, thus inducing aortic obstruction. Although this concept cannot be excluded, it does not explain the presence of the aortic shelf noted prenatally.

Use of prostaglandin has been very effective in improving the clinical status of infants with aortic coarctation. Reducing ductus arteriosus constriction decreases the degree of aortic obstruction with improvement of symptoms. The risk of surgery to relieve aortic coarctation in young infants has been greatly improved by using prostaglandin to improve the clinical status prior to the procedure.

## Ductus arteriosus in aortopulmonary transposition

In infants with aortopulmonary transposition, systemic venous blood is ejected into the aorta, and pulmonary venous blood is ejected into the pulmonary artery. If there are no communications, systemic venous blood cannot enter the lungs to be oxygenated, and pulmonary venous blood cannot enter the systemic arterial circulation to provide oxygen to the tissues. In infants who do not have an

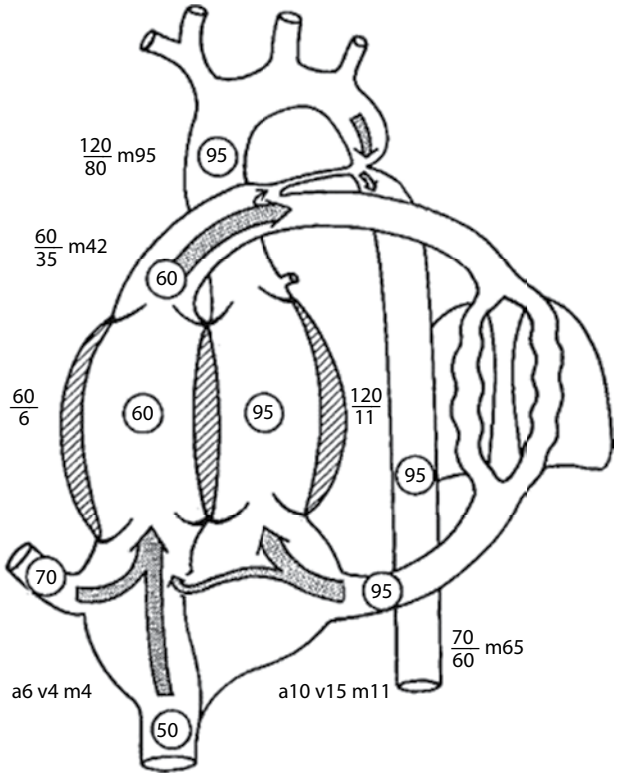


**Figure 53.12**
Circulation in an infant with an aortic shelf showing that constriction of the ductus arteriosus induces obstruction in the descending aorta. Ascending aortic and left ventricular systolic and end-diastolic pressures have increased. Pressures and oxygen saturations (in circles) are shown. (Reproduced with permission from Rudolph AM. *Congenital Diseases of the Heart*. Chichester, UK: Wiley; 2009.[14])

associated ventricular septal defect to allow mixing of the two circulations, survival is dependent on patency of the foramen ovale or the ductus arteriosus, or both. During the early neonatal period, bidirectional shunting of blood may occur through the ductus; blood shunts from the pulmonary artery to the aorta during systole as a result of the kinetic force provided by left ventricular ejection. The short main pulmonary artery and orientation of the ductus arising from the pulmonary artery tend to favor this flow. During diastole, the lower resistance of the pulmonary circulation resulting from ventilation favors flow from the aorta to the pulmonary artery. Shunting from the pulmonary artery to the descending aorta can be recognized by the presence of a higher oxygen saturation or $PO_2$ in blood in the lower extremities than in the right arm. This shunting decreases over a few days as pulmonary vascular resistance falls further, and if the ductus remains patent, shunting occurs only from the aorta to the pulmonary artery. During the early neonatal period, infusion of prostaglandin to maintain patency of the ductus may be helpful in providing bidirectional shunting and thus improve oxygenation in the infant.

### Ductus arteriosus in preterm infants

The high incidence of persistent patency of the ductus arteriosus in premature babies and the possible mechanisms involved are discussed in Chapter 8.

The hemodynamic and clinical manifestations of patent ductus arteriosus in the preterm infant differ in many ways from those in mature infants. Pulmonary vascular resistance falls very rapidly after birth, probably related to immaturity of the pulmonary circulation. This allows the rapid onset of a large left-to-right shunt with increased pulmonary blood flow, placing demands on the left ventricle to increase its output. The pulmonary vascular bed is more permeable to fluids as well as albumin in the preterm infant; this, combined with the relatively low plasma albumin concentration, favors transudation into the lung parenchyma and alveoli. Left ventricular output increases markedly after birth (see Chapter 8), and a left-to-right shunt places an additional burden on the ventricle to increase output. If the shunt is large, the ventricle may not be able to provide an output adequate to maintain flow to systemic tissues. Since left ventricular output is dependent on an adequate filling pressure, an additional factor that could compromise left ventricular output is the presence of incompetence of the foramen ovale. Enlargement of the left atrium due to the enhanced venous return may stretch the foramen and allow a left-to-right shunt. This will limit the ability for left atrial pressure to increase and maintain filling pressure of the ventricle.

The presence of patency of the ductus is recognized clinically by the presence of a murmur in the upper left chest parasternally, and prominent pulse due to the high pulse pressure resulting from diastolic run-off through the shunt. The murmur does not always have the characteristic features of a patent ductus, namely, a continuous murmur, and usually is present only in systole. When the ductus arteriosus is widely patent, no murmur may be audible. These infants often develop respiratory distress due to surfactant deficiency. This is aggravated by the pulmonary edema resulting from the left-to-right shunt. The presence of a patent ductus arteriosus frequently prolongs the need for assisted respiratory support. Inability of the left ventricle to maintain an output that is capable of providing adequate systemic blood flow may result in poor perfusion of many organs and is probably a contributor to the development of necrotizing enterocolitis in some of these infants. The use of prostaglandin synthesis inhibitors to constrict the ductus arteriosus in preterm infants is discussed in Chapter 8.

## Postnatal effects of congenital cardiovascular malformations on pulmonary circulation

The normal changes in the pulmonary circulation after birth are discussed in Chapter 8. In the presence of a large communication between the left and right ventricles or between the aorta and pulmonary artery, pressure in the pulmonary

artery does not fall normally after birth, because the high pressure from the left side is transmitted to the right ventricle and pulmonary artery. The resistance arterioles in the lung retain some degree of vasoconstriction; this is essential to avoid transmission of the high pulmonary arterial pressure into the capillary circulation with resulting fluid transudation and pulmonary edema. The smooth muscle layer of the pulmonary arterioles does not undergo the regression seen normally, and the thicker medial layer in the small pulmonary arteries persists. The mechanisms responsible for the pulmonary arteriolar responses have not been resolved. It has been proposed that pulmonary hypertension affects the smooth muscle through a mechanical effect to prevent regression and to enhance further growth. Recently, however, the possibility that mitogens released from the endothelial or muscle layers may be involved has emerged. During the period that the pulmonary vascular resistance is elevated as a result of the increase in smooth muscle in the media, administration of vasodilators such as tolazoline, prostacyclin, or sildenafil will reduce resistance and increase the left-to-right shunt.

If the communication between the ventricles or great arteries is not closed, progressive changes in the pulmonary circulation are likely to occur. Endothelial proliferation occurs, with thickening of the intima; this may not involve the whole circumference of the vessel. With progressive intimal thickening, the lumen is narrowed. In association with the intimal changes, fibroblast proliferation develops in both the media and the intima. Smooth muscle is gradually replaced, and the lumen becomes quite narrow, With progression of these changes the pulmonary vascular resistance increases and the left-to-right shunt diminishes. When pulmonary vascular resistance approaches levels in the systemic circulation, right-to-left shunting across the communication with cyanosis may occur, first with exercise and later continuously. When these proliferative changes in the pulmonary circulation have occurred, pulmonary vasodilator agents produce almost no response. Closure of the communication at this stage is not likely to result in a significant fall of pulmonary vascular resistance and may be risky, because the high pulmonary vascular resistance may limit venous return to the left ventricle, causing syncope, or may induce right heart failure.

The hypothesis was proposed that the shear on the intima created by high blood flow through constricted arterioles may induce endothelial proliferation. More recently, the role of the release of mitogens or vascular elastase, which promote proliferation of various cell types, is being pursued.

# References


1. Rudolph AM, Nadas AS. *N Engl J Med* 1962;267:968–74.
2. Rudolph AM. *Arch Dis Child Fetal Neonatal Ed* 2010;95:132–6.
3. Lev M et al. *Am Heart J* 1963;65:638–47.
4. Fishman NH et al. *Circulation* 1978;58:354–64.
5. Allan LD et al. *J Am Coll Cardiol* 1986;8:1131–6.
6. Axt-Fliedner R et al. *Ultrasound Obstet Gynecol* 2006;28:106–9.
7. Hornberger LK et al. *Circulation* 1995;92:1531–8.
8. Kohl T et al. *Am J Cardiol* 2000;85:1230–3.
9. Tworetzky W et al. *Circulation* 2004;110:2125–31.
10. Makikallio K et al. *Circulation* 2006;113:1401–5.
11. Freund LR et al. *Circulation* 2014;130:638–45.
12. Gardiner H et al. *Ultrasound Obstet Gynecol* 2016;48(3):373–81.
13. Hunter LE et al. *Prenat Diagn* 2015;35:1178–81.
14. Rudolph AM. *Congenital Diseases of the Heart*. Chichester, UK: Wiley; 2009.
15. Hutchins GM. *Am J Pathol* 1971;63:203–14.
16. Santos MA et al. *Circulation* 1980;62:818–22.
17. Santos MA, Azevedo VM. *Arq Bras Cardiol* 2004;82:420–5.
18. Levin DL et al. *J Pediatr* 1978;92:265–9.
19. Wild LM et al. *Pediatr Res* 1989;25:251–7.
20. Abman SH et al. *J Clin Invest* 1989;83:1849–58.
21. Heymann MA, Rudolph AM. *Circ Res* 1976;38:418–22.
22. Turner GR, Levin DL. *Clin Perinatol* 1984;11:581–9.
23. Manzar S et al. *Saudi Med J* 2005;26:453–6.
24. Hinton RB et al. *Pediatr Res* 2008;64:364–9.
25. Limperopoulos C et al. *Circulation* 2010;121:26–33.
26. Sun L et al. *Circulation* 2015;131:1313–23.
27. Kaltman JR et al. *Ultrasound Obstet Gynecol* 2005;25:32–6.
28. Rudolph AM. *Pediatr Res* 2016;80(2):172–7.
29. Von Rueden TJ et al. *Circulation* 1975;52:951–4.
30. Ikle L et al. *J Pediatr* 2003;142:20–5.
31. Dent CL et al. *J Thorac Cardiovasc Surg* 2006;131:190–7.
32. Vlahos AP et al. *Circulation* 2004;109:2326–33.
33. Marshall AC et al. *Circulation* 2004;110:253–8.
34. Taketazu M et al. *J Am Coll Cardiol* 2004;43:1902–7.
35. Rudolph AM. *Pediatr Res* 2007;61:375–80.
36. Maeno YV et al. *Circulation* 1999;99:1209–14.
37. Jouannic JM et al. *Circulation* 2004;110:1743–6.
38. Konduri GG et al. *Pediatr Res* 1993;33:533–9.
39. Lewis AB et al. *Circ Res* 1976;39:536–41.
40. Rasanen J et al. *Circulation* 1998;97:257–62.
41. McMurphy DM et al. *Pediatr Res* 1972;6:231–8.
42. Dick M2nd et al. *Pediatr Res* 1981;15:1397–401.
43. Cohn HE et al. *Am J Obstet Gynecol* 1974;120:817–24.
44. van Bel F et al. *Biol Neonate* 1995;68:200–10.
45. Jouannic JM et al. *Ultrasound Obstet Gynecol* 2002;20:122–4.
46. Fisher DJ et al. *Am J Physiol* 1982;242:H647–61.
47. Gewillig M et al. *J Am Coll Cardiol* 2004;43:107–12.
48. Chan KC et al. *Catheter Cardiovasc Interv* 2006;68:719–26.
49. Rudolph AM et al. *Am J Cardiol* 1972;30:514–25.

# 54

# Intrapartum evaluation of fetal well-being

Hagai Amsalem, Yoram Sorokin, and Sean C. Blackwell

## Introduction

It has long been known that labor is a risk factor for fetal mortality and for neonatal morbidity and mortality. Through research carried out in the 1950s, 1960s, and early 1970s, obstetricians obtained a better understanding of fetal respiratory physiology and human fetal physiology in response to the labor process. It provided a basis for diagnostic techniques to detect possible fetal well-being and compromise. It was appreciated that clinical management could change fetal conditions. In 1961 Saling introduced intermittent scalp pH measurement as the first technique for direct assessment of fetal well-being during labor.[1] Fetal heart rate (FHR) monitoring technologies were developed in the 1950s and 1960s by Hammacher et al.,[2] Hon and Quilligan,[3] Caldeyro-Barcia,[4] and others. By the late 1960s and early 1970s, equipment for intrapartum fetal evaluation was commercially available. In the 1970s, obstetricians had very optimistic expectations that with intrapartum surveillance (utilizing continuous FHR monitoring and intermittent fetal scalp pH determinations), intrapartum stillbirths and neonatal neurological injuries caused by intrapartum hypoxia could be significantly reduced or eliminated. The hope was that with continuous electronic FHR monitoring, "early asphyxia" will be recognized; through timely obstetrical intervention, asphyxia-induced brain damage, or neonatal death, will be avoided. Continuous electronic fetal monitoring (EFM) was introduced into widespread clinical practice before evidence from randomized clinical trials demonstrated either efficacy or safety. In the 1970s and 1980s, continuous electronic FHR monitoring became routine in most hospitals in the United States and the Western world. During the last 30 years, thousands of articles were written on this topic. Initial retrospective studies evaluated 135,000 patients and showed a more than threefold improvement in the intrapartum fetal death rate for the electronically monitored group versus the control group with intermittent auscultation (IA).[5,6] Many randomized trials were performed comparing the efficacy and safety of routine continuous EFM with IA for intrapartum surveillance. Recently, there has been increasing utilization of central monitoring systems and computerized recognition and interpretation of fetal heart rate patterns.[7–11]

Despite the initial optimism, continuous fetal monitoring during labor has not resulted in reduced adverse neonatal outcome, specifically cerebral palsy rate.[12,13] Moreover, due to the high "false-positive" rate,[14] cardiotocography (CTG) use resulted in an increased incidence of operative delivery for suspected "fetal distress." It has been estimated that 11 cesarean deliveries are needed to prevent one case of hypoxic ischemic encephalopathy.[12,13] During the past two decades, several techniques have been evaluated in an attempt to reduce the high false-positive rate of CTG and the resulting operative delivery rate. Fetal pulse oximetry was first described in 1989.[15] Several randomized control trials (RCTs) were published in the ensuing decades that aimed to evaluate its value in reducing operative delivery rate without increasing fetal adverse outcome, but they showed equivocal results.

Another technique of some promise is the fetal electrocardiogram (ECG). Similar to fetal pulse oximetry, fetal ECG is used as auxiliary to CTG, most often when the tracing is equivocal or "nonreassuring." Valverde et al. conducted an RCT comparing the value of these two techniques as supplements to conventional CTG.[16] Fetal ECG was found to be superior in reducing operative delivery rate and at the same time reducing fetal acidemia.

## Fetal heart rate patterns

Over the past 40 years, many scientific articles were written concerning the definitions of FHR patterns and recommendations for their interpretations. For many years, there was confusion about terminology and definitions used to describe and interpret FHR patterns. In 1997, recommendations for research guidelines for interpretation of fetal heart rate were published.[17] The recommendations resulted from a National Institute of Child Health and Human Development (NICHD) Research Planning Workshop that had the purpose of assessing the research status of this area and publish research recommendations.[17] This consensus report suggested standardized and unambiguous definitions of FHR patterns for the purposes of improving research studies on the reliability and validity of FHR interpretation as well as studies of the relationship between FHR patterns and outcome. Four major parameters of FHR were defined: baseline rate, baseline FHR variability, accelerations, and decelerations (variable, early, late, and prolonged). The most recent American College of Obstetricians and Gynecologists (ACOG) Practice Bulletin 116 published in 2010 was titled "Management of

Intrapartum Fetal Heart Rate Tracings"[18] and includes the NICHD Research Planning Workshop FHR pattern definitions and descriptions.[19]

## Baseline

FHR baseline is the mean FHR over a given 10-minute period (rounded to the nearest 5 beats/minute). The normal range is between 110 and 160 beats/minute. Bradycardia is defined as a decrease in FHR baseline below 110 beats/minute for 10 minutes, or longer. Mild degrees of bradycardia may occur in the second stage of labor and often immediately before birth. The fetus is generally able to tolerate bradycardia by compensating with an increased stroke volume. However, this ability to compensate with increased stroke volume in response to bradycardia breaks down at severe decreases in FHR, below 60 beats/minute. Catastrophic events associated with bradycardia include umbilical cord prolapse, umbilical cord occlusion, uterine rupture, or intrapartum separation of the placenta (abruptio placenta). Congenital heart block due to the presence of anti-Ro and/or anti-La antibodies from maternal collagen vascular disease may be another uncommon cause of persistent bradycardia unrelated to labor.[20] Tachycardia, an FHR baseline >160 beats/minute for 10 minutes or longer, may occur due to maternal pyrexia, medications (ß-sympathomimetics or cocaine), chorioamnionitis, fetal hypoxia, or fetal anemia. Persistent or paroxysmal tachycardia may also be due to an aberrant conduction pathway causing supraventricular tachycardia (SVT).[21] Atrial flutter is a less common cause for fetal tachycardia unrelated to labor. In tachycardia there is increased sympathetic and/or decreased parasympathetic autonomic tone, which is associated with decreased FHR variability. Chronically instrumented fetal sheep exposed to umbilical cord occlusions for 1 minute every 2.5 minutes develop a fall in nadir of FHR decelerations and a rise in interocclusion fetal heart rate, tachycardia, due to increased catecholamine activity.[22,23] Tachycardia, in cases of intrapartum acidemia, does not appear in isolation. If tachycardia is seen with normal FHR variability and no periodic changes, it should be assumed to be due to other causes.

## Variability

Baseline FHR variability is the fluctuation in the baseline FHR of at least two cycles per minute. It represents the balance between sympathetic and parasympathetic systems and is influenced by gestational age. One of the modifications found in the NICHD workshop recommendation is that FHR variability should not be divided into "short-term" and "long-term" components. Variability should be evaluated *in toto*, because in actual practice variability is visually determined as a unit. Hence, the definition of variability is based visually on the amplitude of the complexes.[19] The fluctuations in baseline FHR are visually quantitated as the amplitude of the peak-to-trough in beats per minute. Grades of fluctuations are subdivided into undetectable (no fluctuations), minimal (≤5 beats/minute), moderate (6–25 beats/minute also termed "normal"), and marked (>25 beats/minute). Under normoxemic conditions, cardiac vagal blockade (Atropine) causes an increase in FHR baseline and a decrease in FHR variability. In studies that induced acute mild and moderate fetal hypoxemia, but no acidosis, baseline heart rate did not change significantly with mild hypoxemia but decreased with moderate hypoxemia; FHR variability increased when the fetus became mildly or moderately hypoxemic.[24] The increases in FHR variability during mild and moderate hypoxemia were abolished by atropine. Propranolol (ß-blocker) had no effect on FHR variability in either cases of mild or moderate hypoxemia. It has been demonstrated that the initial response to experimental acute progressive asphyxia typically included an immediate, transient, increase in FHR variability.[25] However, the terminal fetal compromise with profound acidemia and hypotension were accompanied by an increase in FHR variability in some fetuses and a decrease in others.[25]

The importance of FHR variability in evaluating fetal well-being cannot be underestimated, for it is a sensitive predictor of fetal acid-base status.[6,26–28] Several experts believe that with respect to pattern interpretation, there is an overemphasis on the presence of decelerations, and an underappreciation of FHR variability.[5,26–28] Absent variability may be associated with severe fetal acidemia and/or previous fetal central nervous system (CNS) injury. Decreased variability can be caused by fetal acidemia, but also by various medications, among them the commonly used synthetic opiates administered for pain relief during labor. Fetal quiet sleep epochs are associated with the absence of accelerations and decreased variability, but these episodes at term often last approximately 20 minutes and only rarely longer than 60 minutes.[19]

## Accelerations

An FHR acceleration is defined as an abrupt (peak within 30 seconds) increase in FHR above the previously calculated baseline by at least 15 beats/minute that lasts at least 15 seconds, and less than 2 minutes from the onset to return to FHR baseline. The NICHD Research Planning Workshop recommends that before 32 weeks, the criteria for FHR acceleration should be different; the acme must be at least 10 beats/minute over the baseline and lasting at least 10 seconds but less than 2 minutes.[19]

Accelerations are often associated with fetal movements and/or uterine contractions. The presence of FHR accelerations (whether spontaneous or induced) is considered a reassuring sign of fetal well-being and indicates that the fetus is not acidotic (pH < 7.20).[29–31] Intrapartum stimulation tests induce FHR accelerations. They appear to be useful to rule out fetal acidemia in the setting of nonreassuring FHR pattern.[32]

## Decelerations

Deceleration is defined as reduction in the fetal heart rate below previous.[18] There are three basic types of FHR decelerations: late, variable, and early. A late deceleration is a gradual but shallow decrease from the baseline FHR that is associated

with a uterine contraction. The deceleration is delayed in timing with onset, nadir, and recovery of the FHR deceleration occurring after the beginning, peak, and ending of the contraction. Late decelerations are associated with uteroplacental insufficiency and can be divided into two categories.[33–35] A reflex late deceleration is seen with normal FHR variability, thus signifying normal CNS integrity; it occurs due to transient hypoxia associated with uterine contractions; it is caused by a vagal reflex. The second type, a nonreflex late deceleration, is caused by direct myocardial hypoxic depression (or failure), as well as vagal activity; it signifies a risk of "central asphyxia." These are seen with decreased or absent FHR variability and are much more ominous. If late decelerations occur in coordination with more than 50% uterine contractions, they are termed *recurrent*. Most cases of late decelerations reflect reduced fetal reserve rather than myocardial hypoxia or acidosis.[23] Late decelerations are of value in identification of fetuses who are at risk of hypoxia, specifically in cases when they appear with additional findings (e.g., reduced FHR variability).

A variable deceleration is a visually apparent abrupt decrease in FHR below the baseline, of at least more than 15 beats/minute, lasting more than 15 seconds, but less than 2 minutes. These decelerations are termed *variable* because they are variable in shape, depth, duration, and onset relative to uterine contractions. Prior to labor, conditions associated with variable decelerations include decreased amniotic fluid volume, nuchal cord, knotted cord, or a body cord. Variable decelerations are not associated with fetal compromise *per se;* however, during the deceleration there may be transient hypoxemia. Although not caused by uteroplacental insufficiency, if severe, variable decelerations (e.g., FHR decrease to <60 beats per minute, lasting >60 seconds) that become repetitive may lead to fetal hypoxia and acidemia. However, this does not usually occur without noticeable change in other aspects of the FHR pattern, including decreased variability and increased FHR baseline. Most FHR decelerations related to labor are variable.

Variable decelerations are vagally mediated; umbilical cord occlusion, dural stimulation during fetal head compression, increased intracranial pressure, and reduced cerebral perfusion are likely causes of variable FHR decelerations.[23,36] The vagal response may be due to either chemoreceptor or baroreceptor input.[23,36] Cord occlusion mechanism occurs mostly in the first stage of labor[23,36]; other mechanisms occur mostly in the second stage.[23,36] A review summarized our understanding of the pathophysiological mechanisms of fetal responses to hypoxia, reviewed experimental studies in chronically instrumented near-term fetal sheep *in utero*, and described the pathophysiology of intrapartum FHR decelerations.[23] Asphyxia was produced in fetal sheep by repeated complete occlusion of the umbilical cord for 1 minute.[23,37,38] Comparison was performed between two groups of fetuses, concerning the effect of umbilical cord occlusions every 5 minutes, consistent with early labor, and occlusions every 2.5 minutes, consistent with late first-stage and second-stage labor.[23] Once deep decelerations are present, no deceleration pattern is necessarily benign. Fetuses with normal placental reserve had a remarkable ability to adapt to repeated hypoxia; when subjected to deep and brief decelerations, they can compensate fully for surprisingly prolonged intervals before development of profound acidosis and hypotension.[23] The adaptive ability of the term human fetus is illustrated by the consistent finding that neonatal complications and the need for resuscitation are extremely uncommon below an acute base deficit of 10–12 mmol/L.[39] However, even in healthy sheep fetuses, prolonged series of brief variable decelerations, if repeated sufficiently frequently, lead ultimately to severe repeated hypotension and profound metabolic acidosis.[23] Fetuses with preexisting hypoxia are vulnerable even to relatively infrequent periods of additional hypoxia in early labor.[23] Changes in FHR associated with such deterioration, during repeat deep decelerations, develop progressively and surprisingly slow, even during frequent occlusions. When the fetus deteriorates, the sequence of events include increasing amplitude of the deceleration, more rapid rate of initial deceleration, a rising baseline, an initial increase, and then loss of baseline variability, and finally brief overshoot immediately after the deceleration.[23] The authors recommended simplifying terminology, and educating clinicians in the physiological mechanisms of FHR decelerations and the patterns of FHR change that indicate progressive loss of fetal compensation.[23]

Early decelerations are defined as visually apparent gradual decrease in baseline associated with uterine contractions. They are coincident in timing, with the nadir of the deceleration occurring at the same time as the peak of the contraction. They are thought to be due to pressure on the fetal head as it moves down the birth canal. The mechanism is one of reflex, slowing of FHR mediated via the vagus nerve. They are innocuous and are not associated with fetal compromise. The presence of FHR accelerations, normal FHR variability, and cervical dilation of more than 4–5 cm are other features consistent with early decelerations.

## Sinusoidal

A sinusoidal FHR pattern consists of smooth, sine wave–like regular oscillations of the baseline FHR. The pattern lasts at least 10 minutes and has a relatively fixed period of 3–5/minute and an amplitude of 5–15 beats/minute fluctuating above and below the baseline. There is absence of variability or FHR accelerations.[6,18,19,27,40] This pattern is always nonreactive and is strongly associated with poor outcome; the association is with fetal hypoxia, often resulting from severe fetal anemia, as in Rh isoimmunization or fetal-maternal hemorrhage.[41] A derangement of nervous control of the heart, secondary to central or peripheral ischemia, has been hypothesized to result in sinusoidal heart rate. The pattern was also described in some cases of normal infants born without depression or acid-base abnormalities.[42] Such patterns, also called pseudosinusoidal, have been reported following intrapartum administration of the analgesics alphaprodine (Nisentil), butorphanol (Stadol), or meperidine (Demerol), and in association with amnionitis.[6] The pseudosinusoidal pattern has

increased cyclicity and presence of short-term variability; FHR is reactive before and after the episode, and the pattern is benign. True sinusoidal patterns are quite rare and are nonreassuring.

## FHR interpretation and management

Interpretation of tests of intrapartum fetal well-being is performed with the context of the entire obstetrical situation; it should include maternal and fetal factors (i.e., the specific underlying pathology), as well as the course, anticipated duration, and outcome of labor.[6,19,27,43] For instance, the effect of gestational age of the fetus (the difference in fetal CNS maturation at 24 compared to 38 weeks), maternal medical disorder (e.g., hypertension or diabetes), intrinsic fetal pathology (e.g., growth restriction, fetal anemia, fetal infection), and prior results of fetal assessment are several important factors that impact the clinical significance of different FHR patterns.[6,19,27,43] It is obvious that with the number of variables one has to consider, and the often imprecise nature of the information, the medical decision is often difficult.

The obstetrical community has not reached a broad consensus on a standardized approach to assessment and management of most FHR monitoring patterns. Sometimes the interpretation of the pattern is clear. When the FHR pattern is normal and reassuring, no intervention in necessary. In some nonreassuring patterns, the need for intervention is clear. More often, however, the observed pattern is a mixture of reassuring and nonreassuring patterns, and the management is debatable.

Several studies suggest that FHR interpretation is plagued by poor inter- and intra-observer reliability.[44–48] There are several patterns and combination of patterns for which there exists widespread agreement.[19] There is greater agreement in interpretation of FHR tracings if the tracing is reassuring.[49]

A pattern with normal FHR baseline, presence of FHR accelerations, normal (moderate) FHR variability, and absence of FHR decelerations confirms an extremely high predictability of a normally oxygenated fetus with normal acid-base status (Figure 54.1). This is considered a reassuring pattern.[19] When this pattern is obtained, it is nearly always associated with a newborn who is vigorous at birth. Abnormal patterns clearly associated with fetal acidemia are those with absent variability, recurrent late or severe variable decelerations, or sustained bradycardia (see Figure 54.2). These patterns are consistent with hypoxia that is predictive of current or impending fetal asphyxia, so severe that the fetus is at risk for neurological and other fetal damage or death.[19] A fetus with absent FHR variability and severe variable or late decelerations is at significantly high risk to have profound acidosis, and expedited delivery is indicated. A fetus with a prolonged FHR deceleration or bradycardia (e.g., less than 60 bpm) with absent variability is also at significantly increased risk to have acidemia, and expedited delivery is also indicated.

There are many FHR patterns that lie between the reassuring and ominous FHR. These are usually termed *nonreassuring* or *equivocal* FHR. The ACOG practice bulletin based on the NICHD Task Force, termed these FHR traces category

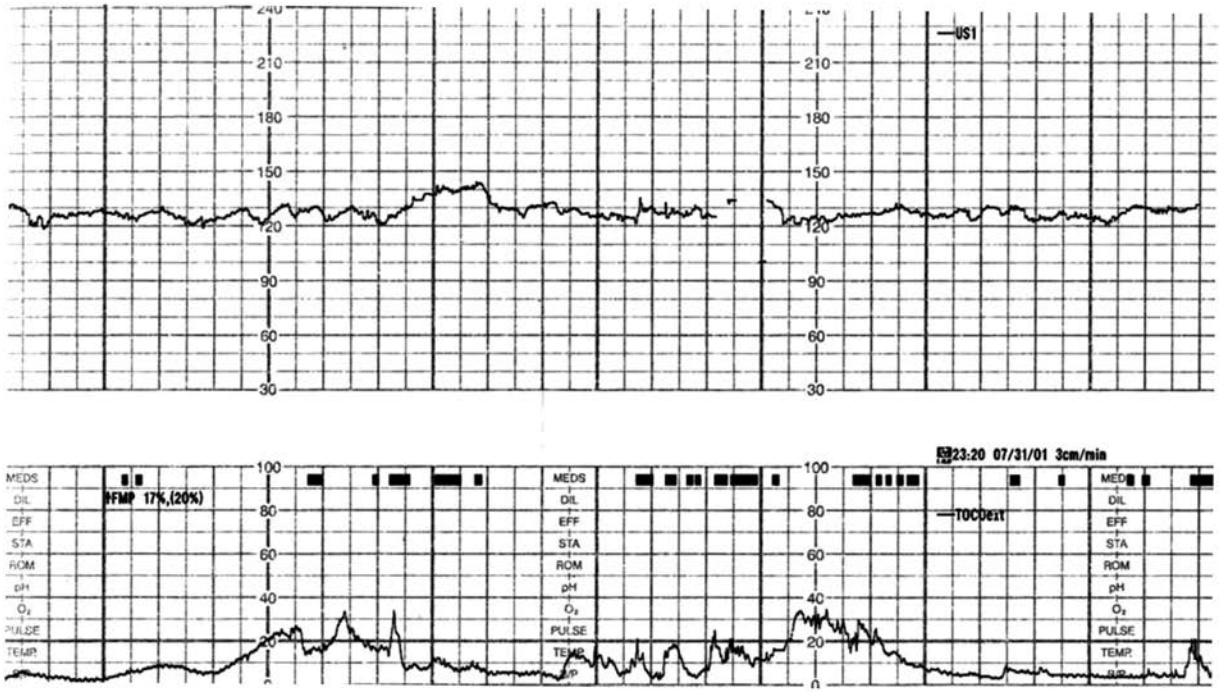


**Figure 54.1**
Normal FHR tracing: normal baseline, spontaneous accelerations, no decelerations, and normal variability.

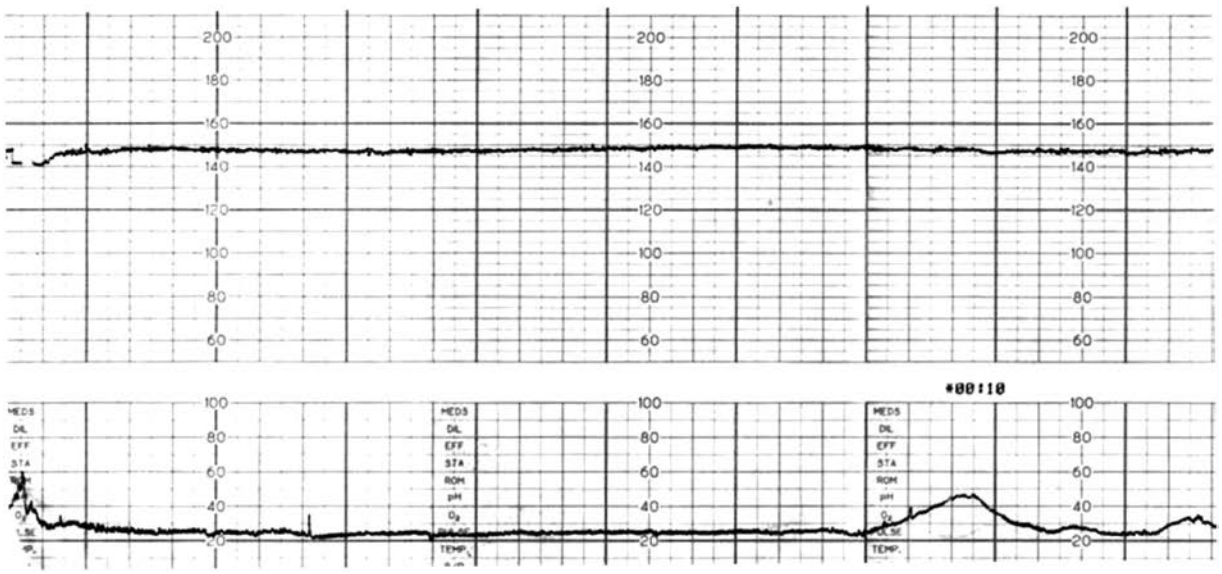


**Figure 54.2**
Abnormal FHR tracing: normal baseline, no accelerations, and decreased variability. Patient presented to hospital complaining of decreased fetal movements, and underwent emergent cesarean delivery after 15 minutes of arrival. The neonate was depressed at birth but had a normal umbilical artery pH. Within 6 hours of life, the neonate began having generalized tonic-clonic seizures. This pattern and case are illustrative of the possibility that the fetus may be neurologically injured prior to labor and recover to a normal acid-base status, but still manifest a significantly abnormal FHR pattern.

II.[19] In intermediate FHR patterns, there is no consensus concerning clinical management. Fetuses have, at various times during labor, patterns, and combinations of patterns, that have some nonreassuring characteristics, e.g., repetitive late decelerations with accelerations and normal variability, variable decelerations with slow return to baseline or late component, absent variability with no decelerations associated with contractions, fetal tachycardia with decreased variability and without decelerations, blunted patterns, and checkmark patterns.[49] Nonreassuring patterns are nonspecific and cannot reliably predict whether a fetus is well oxygenated, depressed, or acidotic. One of the problems with nonreassuring FHR patterns is that factors other than hypoxia, e.g., intrauterine infection, fetal sleep states, congenital abnormality (developmental or acquired), or drugs, may lead to a nonreassuring FHR pattern. Nonreassuring FHR patterns that are associated with hypoxia do not depict the severity of the hypoxia, and it is difficult to predict the progress of the hypoxia if labor continues (see Figure 54.3).

An internal fetal scalp electrode (and/or intrauterine pressure catheter) could be placed when there is technical difficulty using an external monitor, as in morbidly obese women. It is clear that many fetuses with various types of decelerations will not be born with mixed or metabolic acidosis. Clinical observations and retrospective surveys of outcome following monitoring suggest that presence of FHR variability can help

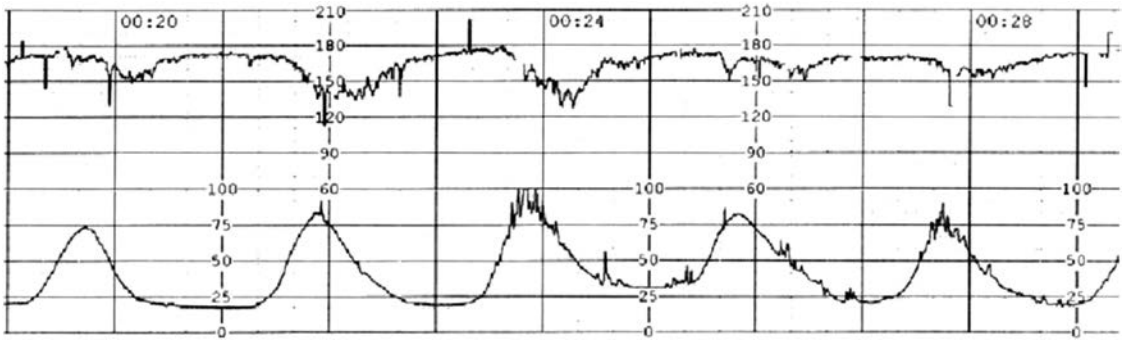


**Figure 54.3**
Abnormal FHR tracing: tachycardia, repetitive late decelerations, and decreased variability. The uterine contraction pattern is consistent with excessive contractions due to recent maternal cocaine use and placental abruption. Approximately 1 hour after this section of the tracing, which did not improve despite resuscitative efforts, a cesarean section was performed for "nonreassuring fetal status remote from delivery." The umbilical artery pH was 7.26, and the neonate had no problems after birth.

in specificity for interpretation of the vigorous well-oxygenated fetus.[2,26,27,50,51] The presence of normal FHR variability is almost invariably associated with a vigorously well-oxygenated neonate at birth (see Figure 54.4).

Moderate levels of FHR variability are a strong indication that the fetus is coping well with labor and is unlikely to have significant acidosis. It has been demonstrated that the most significant intrapartum FHR parameter to predict the development of significant acidemia is the presence of minimal/absent variability for at least 1 hour, as a solitary abnormal finding or in conjunction with late decelerations in the absence of accelerations.[52] A recent review suggests that moderate FHR variability was strongly associated (98%) with an umbilical pH >7.15 or newborn vigor (5 minute Apgar score $\geq$ 7).[53] Undetectable or minimal FHR variability in the presence of late or variable decelerations was the most consistent predictor of newborn acidemia, but the association was only 23%.[53] Despite the reassurance that this single FHR component gives, it is important to remember that FHR variability is a subjective measure, and specifically during the second stage of labor, may be difficult to determine.

Hypoxia usually results in decelerations first. While the type of deceleration usually helps in the understanding of the cause of the hypoxia, the persistence of some decelerations and the duration and depth of variable and prolonged FHR decelerations helps in determination of severity of the hypoxia. However, the evolution of patterns is very important. A pattern of persistence of late decelerations that cannot be reversed, followed by loss of reactivity and loss of variability usually reflect developing acidosis from hypoxia.

Intrapartum management of the FHR deceleration is dependent on the type of deceleration as well as the presence or absence of FHR variability and/or FHR accelerations. However, a fetus with normal FHR variability that has pattern evolution to reduced variability is extremely unlikely to have intrapartum hypoxia unless decelerations precede or are simultaneous with this change. Thus, in this setting, the FHR variability change is most likely due to fetal sleep cycle or medications, and aggressive management may not be warranted.

The fetus generally tolerates decelerations or bradycardias that are not less than 80 beats/minute, because of compensatory interactions that maintain cardiac output. However, at severely reduced heart rates, particularly less than 60 beats/minute, it is likely that cardiac output, and hence umbilical blood flow, cannot be maintained.[36] Correction for the etiology of the deceleration or bradycardia is dependent on the etiology: for repetitive severe variable decelerations due to cord occlusion, maternal positional changes, or intrauterine amnioinfusion may be required although the benefit of these techniques has not been proven by well-conducted trials.[54]

For repetitive late decelerations or bradycardia due to uteroplacental insufficiency, prompt delivery should be considered according to the clinical circumstances. As previously

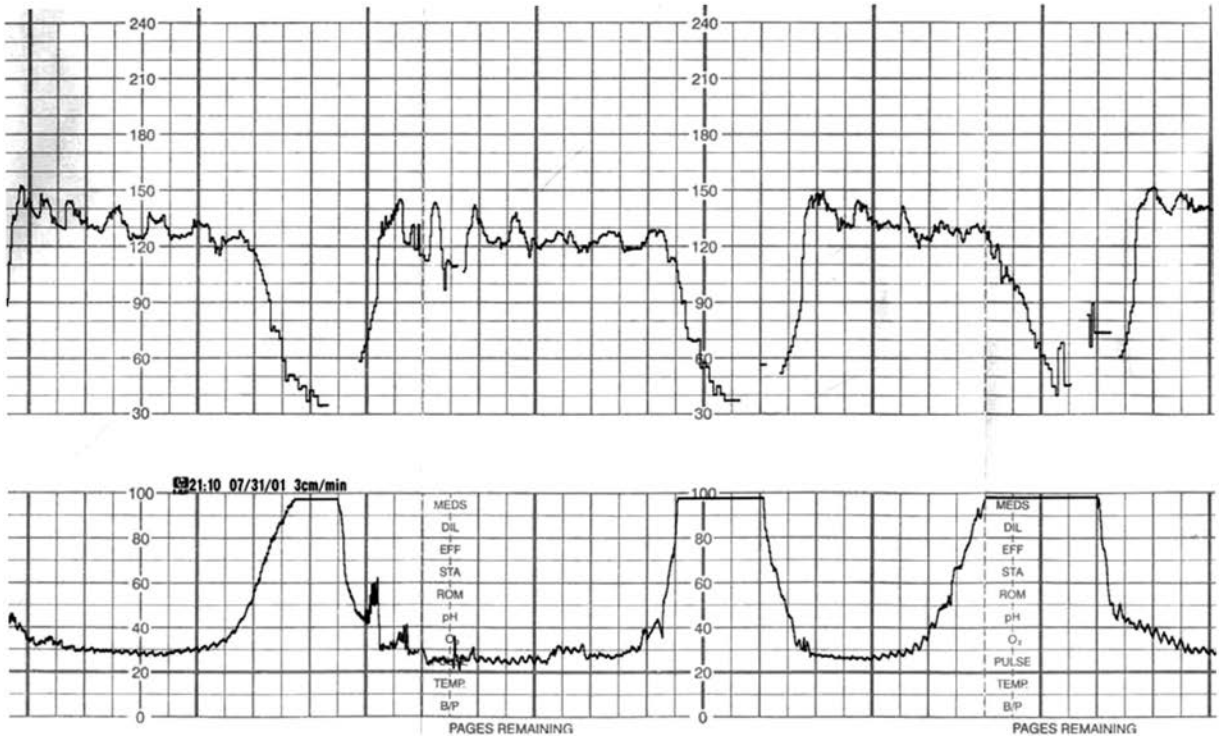


**Figure 54.4**
Abnormal FHR tracing: normal baseline, repetitive severe variable decelerations, and normal variability. Patient had spontaneous vaginal delivery approximately 20 minutes after this section of tracing. Neonate was vigorous at birth with normal Apgar scores and normal umbilical artery pH values. Despite the recurrent severe variable decelerations until delivery, maintenance of normal FHR variability during this time period indicated normal fetal acid-base status and was predictive of the favorable outcome.

mentioned, other insults may occur in labor, e.g., infection, fetal hemorrhage, placental separation, and fetal anemia. All of these may alter fetal physiology and thus impact fetal response to the causes of FHR abnormalities. In addition to hypoxia, any insult, or physiological variant, that causes neurologic depression usually results in decreased FHR variability and elimination of reactivity (see Figure 54.4).

Several professional societies have issued documents on use of EFM that include guidelines for interpretation, assessment, and management.[18,55–57] Current ACOG recommendations include some form of fetal monitoring for all women in labor.[18] Since most clinical trials excluded subjects at high risk for adverse outcomes, the relative safety of IA in such cases is uncertain. The labor of parturients with high-risk conditions (e.g., suspected fetal growth restriction, preeclampsia, and type 1 diabetes) should be monitored continuously.[18] For other patients, the choice of technique (EFM or IA) is based on a variety of factors and is left to the judgment of the woman and her clinician. When EFM is used during labor, in patients without complications, the ACOG recommendation is to review the FHR tracing approximately every 30 minutes in the first stage of labor and every 15 minutes in the second stage. In patients with complications (e.g., fetal growth restriction or preeclampsia) the corresponding frequency is approximately every 15 minutes in the first stage of labor and every 5 minutes during the second stage. There is no comparative data for optimal frequency for IA in the absence of risk factors. One method is to evaluate the FHR at least every 15 minutes in the active phase of the first stage of labor and at least every 5 minutes in the second stage.[18] A 2012 Cochrane Review that included four trials comparing IA to CTG during admission to labor and delivery concluded that the use of CTG during admission was associated with increased risk for cesarean delivery (but not instrumental delivery) but with no reduction in adverse neonatal outcome.[58]

The use of EFM is nearly universal, estimated at 80% in the United States. Intermittent auscultation requires a 1:1 nurse-to-patient ratio. Logistically, it may be difficult to adhere to ACOG guidelines for IA for this reason. A prospective study found that the protocol of IA was successfully completed in only 3% of cases.[59] EFM is easier, cheaper, and provides more data. Economic factors have been suggested as a motivating factor, for hospitals, to use EFM and not IA. Many providers still believe, despite data from randomized trials, that EFM is better than IA, in part because more data are provided with EFM.

A persistently nonreassuring FHR tracing requires evaluation for possible causes,[18] e.g., hypotension, response to medicine or drug, maternal position, cord prolapse, maternal fever, placental abruption, and umbilical cord occlusion. Initial assessment and treatment should include attempts to correct the problem and/or improve fetal oxygenation, e.g., discontinuation or reduction of oxytocin, change in maternal position, treatment with intravenous ephedrine for correction of hypotension secondary to regional anesthesia, and amnioinfusion.[18,60] A Cochrane Database Systematic Review found that there is not enough evidence to support the use of prophylactic oxygen therapy for women in labor, or to evaluate its effectiveness for nonreassuring fetal status.[18,61] Betamimetics or other tocolytic agents (e.g., Nitroglycerin) appear to be able to reduce the number of fetal heart rate abnormalities and perhaps reduce uterine activity. However, there is insufficient evidence to evaluate the use of these agents for suspected fetal distress.[18,62,63] If the nonreassuring pattern is not improved, ancillary tests may be performed, and determination should be made concerning the need for prompt delivery.

## *Ancillary tests to electronic fetal monitoring*

Electronic FHR monitoring has a very high false-positive rate. Several ancillary tests may help to ensure fetal well-being when faced with a nonreassuring FHR tracing. These ancillary tests include fetal scalp stimulation, fetal vibroacoustic stimulation, and fetal scalp pH assessment. The use of scalp puncture, Allis clamp, vibroacoustic and digital stimulation to provoke FHR accelerations, and intermittent fetal scalp blood sampling for pH can help in fetal assessment during labor.[30,32] In at least 50% of patients with nonreassuring patterns, FHR accelerations will be elicited in response to stimulation. The presence of accelerations (spontaneous or induced) correlates with normal fetal pH and reduces the need for further assessment, e.g., fetal scalp sampling for fetal pH assessment. The presence of a response (FHR acceleration) correlates with a normal scalp pH (>7.20). A meta-analysis of 11 studies of 4 techniques of intrapartum fetal stimulation showed that each test was a reliable method to exclude acidosis if accelerations are noted after stimulation.[32] Digital scalp and vibroacoustic stimulation tests are less invasive and preferred.[18] Digital scalp stimulation is the easiest to use routinely, because no device is required, and rupture of membranes is not necessary.

When there is a nonreassuring pattern with lack of FHR acceleration, a fetal stimulation may be performed. When there is an FHR acceleration after stimulation, acidosis is unlikely. If the fetus responds with FHR acceleration but the nonreassuring FHR pattern continues, repeat stimulation testing is necessary. If the fetus does not respond with an FHR acceleration, or the nonreassuring pattern persists, a different method of fetal well-being assessment may be needed.

Fetal scalp blood sampling, for determination of pH, is useful and should be considered when there is a nonreassuring FHR pattern and failure to elicit an FHR acceleration. The use of fetal scalp sampling for fetal scalp pH may result in fewer cesarean deliveries for the indication of nonreassuring fetal status. The use of scalp sampling has decreased, especially in the United States, and it is not available in many hospitals. Fetal scalp sampling has poor sensitivity (35%) and poor positive predictive value (PPV) (9%) for predicting umbilical arterial pH <7, and poor sensitivity (50%) and poor PPV (3%) for identifying newborns with hypoxic-ischemic encephalopathy.[64]

## Fetal pulse oximetry

Fetal pulse oximetry was described for the first time by Gardosi.[15] Following rupture of the membranes and cervical dilatation of at least 2 cm, the intrauterine fetal oxygen sensor is placed against the fetal cheek. It is then connected to an oximetry monitor and a continuous reading is displayed. Often the sensor must be adjusted throughout labor due to fetal positional changes. Fetal oxygen concentrations are examined between contractions; values greater than 30% are considered normal. In 2000, Garite et al.[65] published the results of a multicenter clinical trial that offered some promise for routine use. Eligibility for the trial included term pregnancies in active labor, which developed an abnormal FHR pattern. A total of 1,010 women were randomized to EFM alone or EFM plus continuous fetal pulse oximetry.[65] There was a reduction of more than 50% in the number of cesarean deliveries performed because of nonreassuring fetal status in the EFM plus oximetry group. However, there was no net difference in overall cesarean delivery rates (EFM + fetal oximetry 29% versus EFM alone 26%; $p = 0.49$) because of an increase in cesarean deliveries performed because of dystocia in the oximetry group. In 2006, Bloom et al.[66] published the results of the NICHD Maternal Fetal Medicine Unit (MFMU) Network study of fetal pulse oximetry.[66] Eligibility requirements for the study included nulliparity, gestational age greater than 36 weeks, and active labor. An abnormal FHR was not required for study entry, with a subanalysis performed for those with a nonreassuring pattern. There was no significant difference in the overall rates of cesarean delivery between groups (EFM + fetal oximetry 26.3% and EFM alone 27.5%; $p = 0.31$). The rates of cesarean delivery associated with the separate indications of a nonreassuring fetal heart rate and dystocia were similar between the two groups. This very large study showed that knowledge of the fetal oxygen saturation was not associated with reduction in the rate of cesarean delivery or with improvement in the condition of the newborn.[66] The clinical use of fetal pulse oximetry as an adjunct to electronic fetal monitoring has not been demonstrated. There is insufficient evidence of any benefit, and use of fetal pulse oximetry in clinical practice was not supported by ACOG.[18]

## Fetal ST wave analysis

It is well known that the electrocardiogram (ECG) expression of myocardial ischemia is ST segment alterations. Greene et al.[67] describe changes in the ST waveform of the fetal lamb following induced hypoxia. ST segment elevation preceded fetal demise in chronically compromised lamb fetuses. ST segment elevation was also noted during acute hypoxia and promptly reverted to normal with normoxia.[67]

Fetal ST segment analysis (STAN) is obtained via a spiral electrode attached to the fetal scalp. Similar to fetal pulse oximeter, it can only be applied following rupture of the membranes and at least 2 cm dilatation of the uterine cervix.[68] A Cochrane Review of five randomized trials found that STAN, when used as an adjunct to continuous EFM, gave no significant reduction in the number of neonates with severe metabolic acidosis at birth (umbilical artery pH <7.05 and base deficit >12 mmol/L) or the cesarean section rate. A small although statistically significant reduction in the operative delivery rate was noted (relative risk 0.90%, 95% confidence interval 0.81–0.98).[54]

## FHR interpretation and management: Future directions

One known problem is observer inconsistency in interpretation of the FHR record. A multicenter comparative study of 17 experts and an intelligent computer system in management of labor using EFM, patient information, and fetal blood sampling found the expert system to be indistinguishable from the experts in 50 cases examined, but the intelligent computer system was more consistent.[10] The study demonstrated the potential to improve interpretation of EFM and decrease intervention. Almost 20 years later, Chen-Yu Chen[69] published similar results using a modern computer system and eight expert obstetricians. The computer analysis was in agreement with the visual assessment in most of the CTG parameters analyzed. This work, however, did not specify the advantage in fetal outcome or operative delivery rate of the computerized analysis.

Parer and Ikeda[70] proposed a framework for standardized management of intrapartum FHR patterns. It includes classification of 134 FHR monitor patterns according to available data concerning risk of fetal acidemia and probability of evolution to a more serious pattern as an indicator of urgency of preparation for delivery. Proposed management of the five color-coded categories includes rapidity with which preparation for delivery should be made, based on likelihood of evolution of the FHR pattern to a pattern with a higher risk of acidemia. This preliminary approach was used in two institutions to demonstrate feasibility but was not subjected to appropriate prospective testing.[70]

Education could be of value. A retrospective cohort observational study found that a compulsory fetal monitoring education program in one institution was associated with a significant reduction in the incidence of babies who are born with low Apgar scores and with neonatal hypoxic-ischemic encephalopathy.[71]

## Fetal distress; asphyxia

The term *fetal distress* is often used by professionals in order to describe the clinical situation that includes a concern that the function of the maternal-fetal physiologic unit is altered so that fetal death or serious fetal injury may occur. There is no agreed upon definition of *fetal distress*. The term is imprecise and nonspecific. In fact, the ACOG Committee Opinion recommended that in communication between clinicians caring for the woman and those caring for the neonate, the term *fetal distress* should be replaced by the term *nonreassuring fetal status*. This term should be followed by a further description of the specific FHR findings (e.g., repetitive

variable decelerations, fetal tachycardia, or bradycardia).[72] In the past, the terms *fetal asphyxia* and *birth asphyxia* have also been used. In the Greek origin of the word *asphyxia*, it has the meaning of "pulseless, stopping of the pulse." Asphyxia refers to acidosis resulting from progressive hypoxia *in utero*. The ACOG Committee Opinion also declared that the term *birth asphyxia* is too nonspecific and should not be used.[72] Instead ACOG has advocated more specific language and definitions for criteria required to define an acute intrapartum hypoxic event sufficient to cause cerebral palsy (as modified by the ACOG Task Force on Neonatal Encephalopathy and Cerebral Palsy from the template provided by the International Cerebral Palsy Task Force[72,73]).

Criteria to Define an Acute Intrapartum Hypoxic Event as Sufficient to Cause Cerebral Palsy[72]:

1.1 Essential criteria (must meet all four)
   1. Evidence of a metabolic acidosis in fetal umbilical cord arterial blood obtained at delivery (pH < 7 and base deficit ≥12 mmol/L).
   2. Early onset of severe or moderate neonatal encephalopathy in infants born at 34 or more weeks of gestation.
   3. Cerebral palsy of the spastic quadriplegic or dyskinetic type.
   4. Exclusion of other identifiable etiologies, such as trauma, coagulation disorders, infectious conditions, or genetic disorders.

1.2 Criteria that collectively suggest an intrapartum timing (within close proximity to labor and delivery, e.g., 0–48 hours) but are nonspecific to asphyxia insults.
   1. A sentinel (signal) hypoxic event occurring immediately before or during labor.
   2. A sudden and sustained fetal bradycardia or the absence of fetal heart rate variability in the presence of persistent, late, or variable decelerations, usually after a hypoxic sentinel event when the pattern was previously normal.
   3. Apgar scores of 0–3 beyond 5 minutes.
   4. Onset of multisystem involvement within 72 hours of birth.
   5. Early imaging study showing evidence of acute nonfatal cerebral abnormality.

## Efficacy of FHR monitoring

The move toward evidence-based health care led to increasing utilization of systemic reviews and meta-analyses. Sutton and Abrams[74] reviewed the use of Bayesian methods in meta-analysis and evidence synthesis, and illustrated the main concepts with a meta-analysis examining the evidence relating the effect of electronic FHR monitoring on perinatal mortality.[74]

Virtually all professional organizations believe that some form of monitoring is necessary during labor, although there are no trials comparing either IA or EFM with no monitoring in the control group.[49] The recommendations for FHR assessment during labor are based on protocols used in randomized clinical trials that compared IA and EFM. A recent systematic review of all RCTs comparing the efficacy and safety of routine continuous electronic FHR monitoring during labor with intermittent auscultation (IA) found 13 published randomized controlled trials[12] comprising over 30,000 deliveries in the United States, Europe, and Australia. The authors concluded that the benefits of EFM appear to be primarily in the prevention of early onset neonatal seizures. Long-term implications of neonatal seizures appear to be less serious than once believed. The incidence of abnormal neurological consequences (e.g., cerebral palsy) and perinatal death are not consistently lower among children monitored with electronic methods relative to those monitored with intermittent FHR auscultation. In several trials, EFM was associated with an increased incidence of cesarean delivery and operative vaginal delivery. No significant difference in overall perinatal death rate was found in this comprehensive survey of RCTs despite significant increase in cesarean and instrumental deliveries associated with continuous EFM. Data for subgroups of low-risk, high-risk, and preterm pregnancies and high-quality trials were consistent with the overall results. Access to fetal blood sampling did not influence the difference in neonatal seizures or any other prespecified outcome.

Many institutions use the "labor admission test." It refers to EFM for 20–30 minutes upon admission to labor and delivery for assessment of fetal status and selection of fetuses at increased risk of nonreassuring FHR patterns during labor that might benefit from continuous EFM during labor (as compared to IA). A systemic review of 3 randomized trials and 11 observational studies found no evidence that the labor admission test has benefits in low-risk women.[75] Routine use of the labor admission test leads to higher rates of continuous EFM and intervention, and no reduction in neonatal morbidity.

## Unfulfilled expectations from FHR monitoring?

There were several reasons behind the disappointing story of FHR monitoring and the results of randomized trials.[6,18,27,28,55,57] Expectations were too high. It was assumed that most cases of cerebral palsy are caused by intrapartum asphyxia. In fact, only 10% of cerebral palsy cases are caused by intrapartum asphyxia.[76,77] With a cerebral palsy rate of 2/1,000 infants born at term, FHR monitoring is expected to prevent an event that occurs 1:5,000 (10% of 2/1,000) in term pregnancies. Cerebral palsy has been stable over time.[78] Data are limited in size, but EFM did not result in a reduction in cerebral palsy.[12,13,79] The positive predictive value of nonreassuring FHR patterns to predict cerebral palsy in a singleton newborn at term is 0.14%.[14] A recent review found that although intrapartum EFM abnormalities correlated with umbilical cord base excess, and its use is associated with decreased neonatal seizures, it has no effect on perinatal mortality or pediatric neurologic morbidity.[80]

It is now clear that nomenclature and definitions of FHR patterns used in prior original randomized trials were not

standardized. Interobserver and intraobserver consistency were poor. Due to the low frequency of neonatal death, sample sizes were too low to demonstrate differences in mortality rate. Falsely equating the absence of evidence with evidence of absence should be avoided. Experts have argued that the randomized trials were inadequate because three conditions were not met: establishment of the (1) reliability of FHR interpretation, (2) validity of FHR interpretation, and (3) a causal relationship between FHR patterns and adverse outcome.[28,81] Given the widespread use of EFM in clinical practice, it is extremely unlikely that randomized trial of intrapartum EFM versus IA (or no monitoring) will ever be undertaken. The continued limitations of EFM and the lack of quality data supporting its use serve as a reminder for obstetrics of the hazards of adopting and implementing a new technology without adequately testing it with high-quality research.

# References


1. Saling E. *Arch Gynakol* 1961;197:108–22.
2. Hammacher K et al. *Gynaecologia* 1968;166(4):349–60.
3. Hon EH, Quilligan EJ. *Connecticut Med* 1967;31(11):779–84.
4. Caldeyro-Barcia R et al. Correlation of intrapartum changes in fetal heart rate with fetal blood oxygen and acid-base balance. In: Adamsons K, ed. *Diagnosis and Treatment of Fetal Disorders*. New York, NY: Springer-Verlag; 1968:205.
5. Antenatal diagnosis. *Nat Inst Health Consens Dev Conf Summ* 1979;2:11–5.
6. Freeman RK et al., eds. *Fetal Heart Rate Monitoring*, 3rd ed. Baltimore, MD: Williams and Wilkins; 2003.
7. Strachan BK et al. *BJOG* 2001;108(8):848–52.
8. Ayres-de Campos D et al. *J Matern Fetal Med* 2000;9(5):311–8.
9. Hamilton EF et al. *Am J Obstet Gynecol* 2001;184(4):620–4.
10. Keith RD et al. *Br J Obstet Gynaecol* 1995;102(9):688–700.
11. Agrawal SK et al. *Obstet Gynecol* 2003;102(4):731–8.
12. Alfirevic Z et al. *Cochrane Database Syst Rev* 2013;5:CD006066.
13. Alfirevic Z et al. *Cochrane Database Syst Rev* 2006;3:CD006066.
14. Nelson KB et al. *N Engl J Med* 1996;334(10):613–8.
15. Gardosi J et al. *Lancet* 1989;2(8664):692–3.
16. Valverde M et al. *Eur J Obstet Gynecol Reprod Biol* 2011;159(2):333–7.
17. Electronic fetal heart rate monitoring: Research guidelines for interpretation. *Am J Obstet Gynecol* 1997;177(6):1385–90.
18. ACOG. Practice bulletin no. 116. *Obstet Gynecol* 2010;116(5):1232–40.
19. Macones GA et al. *Obstet Gynecol* 2008;112(3):661–6.
20. Scott JS et al. *N Engl J Med* 1983;309(4):209–12.
21. Maeno Y et al. *J Obstet Gynaecol Res* 2009;35(4):623–9.
22. Bennet L et al. *J Appl Physiol* 2005;99(4):1477–82.
23. Westgate JA et al. *Am J Obstet Gynecol* 2007;197(3):236.e1–11.
24. Yu ZY et al. *Clin Exp Pharmacol Physiol* 1998;25(7-8):577–84.
25. Westgate JA et al. *Br J Obstet Gynaecol* 1999;106(8):774–82.
26. Boehm FH. *Contemporary OB/Gyn* 1977;9:57–61.
27. Parer JT. *Handbook of Fetal Heart Rate Monitoring*, 2nd ed. Philadelphia, PA: Saunders; 1997.
28. Parer JT, King T. *Am J Obstet Gynecol* 2000;182(4):982–7.
29. Tejani N et al. *Obstet Gynecol* 1976;48(4):460–3.
30. Clark SL et al. *Am J Obstet Gynecol* 1982;144(6):706–8.
31. Clark SL et al. *Am J Obstet Gynecol* 1984;148(3):274–7.
32. Skupski DW et al. *Obstet Gynecol* 2002;99(1):129–34.
33. Harris JL et al. *Am J Obstet Gynecol* 1982;144(5):491–6.
34. Martin CB, Jr et al. *Eur J Obstet Gynecol Reprod Biol* 1979;9(6):361–73.
35. Parer JT et al. *Am J Obstet Gynecol* 1980;136(4):478–82.
36. Ball RH, Parer JT. *Am J Obstet Gynecol* 1992;166(6 Pt 1):1683–8; discussion 8–9.
37. de Haan HH et al. *Am J Obstet Gynecol* 1997;176(1 Pt):8–17.
38. De Haan HH et al. *Pediatr Res* 1997;41(1):96–104.
39. Low JA et al. *Am J Obstet Gynecol* 1997;177(6):1391–4.
40. Garite TJ et al. *Am J Obstet Gynecol* 1981;139(2):226–30.
41. Modanlou HD et al. *Obstet Gynecol* 1977;49(5):537–41.
42. Young BK et al. *Am J Obstet Gynecol* 1980;136(5):587–93.
43. Cibils LA. *Am J Obstet Gynecol* 1996;174(4):1382–9.
44. Beaulieu MD et al. *CMAJ* 1982;127(3):214–6.
45. Helfand M et al. *Am J Obstet Gynecol* 1985;151(6):737–44.
46. Nielsen PV et al. *Acta Obstet Gynecol Scand* 1987;66(5):421–4.
47. Peck TM. *Obstet Gynecol* 1980;56(1):13–6.
48. Blix E et al. *BJOG* 2003;110(1):1–5.
49. Freeman RK. *Obstet Gynecol* 2002;100(4):813–26.
50. Krebs HB et al. *Am J Obstet Gynecol* 1979;133(7):762–72.
51. Paul RH et al. *Am J Obstet Gynecol* 1975;123(2):206–10.
52. Williams KP, Galerneau F. *Am J Obstet Gynecol* 2003;188(3):820–3.
53. Parer JT et al. *J Matern Fetal Neonatal Med* 2006;19(5):289–94.
54. Neilson JP. *Cochrane Database Syst Rev* 2015;12:CD000116.
55. Liston R et al. *J Obstet Gynecol Canada* 2002;24(4):342–55.
56. Rooth G et al. *Int J Gynaecol Obstet* 1987;25:159–67.
57. RCOG Clinical Effectiveness Support Unit. *The use of electronic fetal monitoring: The use and interpretation of cardiotocography in intrapartum fetal surveillance*. Evidence-based Clinical Guideline Number 8 London: Royal College of Obstetricians and Gynecologists; 2001.
58. Devane D et al. *Cochrane Database Syst Rev* 2012;2:CD005122.
59. Morrison JC et al. *Am J Obstet Gynecol* 1993;168(1 Pt 1):63–6.
60. Hofmeyr GJ, Lawrie TA. *Cochrane Database Syst Rev* 2012;1:CD000013.
61. Fawole B, Hofmeyr GJ. *Cochrane Database Syst Rev* 2003;4:CD000136.
62. Pullen KM et al. *Am J Obstet Gynecol* 2007;197(4):414 e1–6.
63. Kulier R, Hofmeyr GJ. *Cochrane Database Syst Rev* 2000;2:CD000035.
64. Kruger K et al. *Am J Obstet Gynecol* 1999;181(5 Pt 1):1072–8.
65. Garite TJ et al. *Am J Obstet Gynecol* 2000;183(5):1049–58.
66. Bloom SL et al. *N Engl J Med* 2006;355(21):2195–202.
67. Greene KR et al. *Am J Obstet Gynecol* 1982;144(8):950–8.
68. Amer-Wahlin I et al. *BJOG* 2007;114(10):1191–3.
69. Chen CY et al. *PLOS ONE* 2014;9(12):e112296.
70. Parer JT, Ikeda T. *Am J Obstet Gynecol* 2007;197(1):26 e1–6.
71. Draycott T et al. *BJOG* 2006;113(2):177–82.
72. Committee on Obstetric Practice ACoO, Gynecologists. *Obstet Gynecol* 2005;106(6):1469–70.
73. Hankins GD, Speer M. *Obstet Gynecol* 2003;102(3):628–36.
74. Sutton AJ, Abrams KR. *Stat Methods Med Res* 2001;10(4):277–303.
75. Bix E et al. *BJOG* 2005;112(12):1595–604.
76. Nelson KB. *J Pediatr* 1988;112(4):572–4.
77. Blair E, Stanley FJ. *J Pediatr* 1988;112(4):515–9.
78. Clark SL, Hankins GD. *Am J Obstet Gynecol* 2003;188(3):628–33.
79. Thacker SB et al. *Cochrane Database Syst Rev* 2001;2:CD000063.
80. Graham EM et al. *Obstet Gynecol* 2006;108(3 Pt 1):656–66.
81. Paneth N et al. *Clin Invest Med* 1993;16(2):159–65.

# 55

# Intrapartum and delivery room management of the fetus with congenital heart disease

Mary T. Donofrio and Anita J. Moon-Grady

## Introduction

Advances in prenatal imaging have improved the examination of the fetal heart. Fetal echocardiography is now able to obtain precise details of cardiac structure, function, and blood flow in fetuses with congenital heart disease (CHD) and other anomalies of the cardiovascular system. Serial examination through gestation allows documentation of the evolution of disease *in utero* and identification of those at risk for compromise that may occur either *in utero* or during the transition to a postnatal circulation at delivery. It is now recognized that a fetus may benefit from therapy well before birth, and that care of the pregnant woman must be individualized taking into consideration the condition of both patients, mother, and fetus. Detailed cardiac assessment and the increasing understanding of the fetal and transitional circulation has enabled better prediction of those newborns who will be compromised at birth and therefore facilitates the opportunity for detailed planning to define perinatal management, selecting the fetuses at increased risk for postnatal hemodynamic instability who are likely to require specialized care.[1–5] The prenatal diagnosis and management of severe or critical CHD allows such specialized care to begin in the delivery room, improving outcome in specific high-risk diagnoses[3–5] and potentially reducing the risk of perioperative morbidity,[6–12] including the risk of perioperative neurologic insults.[13] Despite evidence that fetal diagnosis has improved the outcome of some cardiac defects, there are some more critical forms that may still be associated with significant morbidity and mortality caused by hemodynamic instability that occurs after birth, often shortly after separation from the placental circulation.[3] Detailed prenatal assessment including determination of the severity of the defect as well as the anticipated degree of instability and care required at the time of delivery has allowed for disease-specific delivery recommendations to ensure the best care and avoid delays in treatment.[3,4,14] Peripartum and delivery room management of fetuses with CHD require collaboration between obstetric, neonatal, and fetal and pediatric cardiology specialists, including detailed communication and cooperation between the delivery hospital and pediatric tertiary care center.[2,4] This chapter reviews data to support current practice for the intrapartum, perinatal, and delivery room care of infants with a prenatal diagnosis of CHD.

## *In utero* surveillance of the fetus with congenital heart disease

There are limited data regarding benefit of serial *in utero* surveillance of the fetus with CHD, though it may be beneficial in specific instances.[1] Goals of repeat fetal cardiac evaluation may include evaluation for progression of the severity of the lesion *in utero*, including identification of an evolving worse anatomic subtype of the CHD in addition to the potential development of cardiac dysfunction, significant arrhythmias, or restriction or closure of important fetal shunt pathways (i.e., the foramen ovale or ductus arteriosus). Interval monitoring of the fetus may allow for early recognition of fetal compromise, including fetal growth restriction, evidence of abnormal placental function and/or fetal hypoxemia with altered umbilical and/or cerebral Doppler blood flow, or the development of fetal hydrops as a manifestation of fetal congestive heart failure. Findings on serial assessment may require adjustment of the plans for perinatal and delivery management.

### *Cardiotocography and biophysical profile*

Computerized cardiotocography (CTG) and the biophysical profile are tests used to identify fetuses at risk of *in utero* hypoxia and acidosis. These tests are currently used for fetal surveillance during the third trimester in high-risk pregnancies with the goal of identifying fetuses at risk of poor perinatal outcome. Recommendations regarding frequency and timing have been defined for specific obstetric complications such as advanced maternal age, diabetes, hypertension, and previous stillbirth, or specific fetal conditions such as growth restriction and multiple gestations.[15] No guidelines are available that support this testing in fetuses with isolated CHD. Nevertheless, it has been recommended to consider their use

in the CHD population, especially when additional comorbidities exist or the cardiac defect puts the fetus at risk for heart failure or significant arrhythmias.[1]

## Cardiovascular assessment

The cardiovascular profile (CVP) score may be used to assess the degree of cardiovascular compromise in fetuses at risk for heart failure, with or without CHD.[16] The score consists of five parameters: (1) assessment for abnormal fluid collections—edema, effusions, or overt hydrops; (2) heart size in relation to thorax; (3) subjective and objective assessment of cardiac function; (4) venous Doppler evaluation as a surrogate for elevated venous pressure (ductus venosus and umbilical veins flow disturbances); and (5) arterial Doppler interrogation to evaluate for placental dysfunction (umbilical artery flow abnormalities). Each parameter is scored from 0 to 2 with a final score ranging from 0 (worst) to 10 (best) (Table 55.1). The CVP score was validated in a group of fetuses with structurally normal hearts at risk for demise. Fetal death was seen more frequently if the score was less than 7 and showed a decreasing trend on serial assessment. The score has also been evaluated in fetuses with CHD and in fetuses with complete heart block.[17–19] Again, scores less than 7 correlated with a higher risk of perinatal compromise or death. Among the five parameters, the presence of hydrops and severe cardiomegaly, defined as cardiothoracic area ratio greater than 0.5, are most often associated with mortality. In CHD, the presence of hydrops with a CVP less than 7 may represent an indication for urgent delivery and planning for potential immediate postnatal intervention.

# Fetal echocardiography predictors of cardiovascular instability at birth

Most CHD is well tolerated *in utero*, does not present a risk of hemodynamic instability at birth or in the first days of life, and does not require specialized delivery room care.[1,20] However, some severe or critical CHDs have an increased risk of hemodynamic instability after delivery and may require patency of the fetal shunt pathways and/or immediate intervention to maintain stability and improve outcome after separation from the placenta.[1–5] In order to identify the fetuses with CHD at risk of hemodynamic instability at birth, a clear understanding of the normal fetal circulation and the transition to the

**Table 55.1** Cardiovascular profile score

| | *Normal 2 points* | *−1 point* | *−2 points* |
|---|---|---|---|
| Hydrops | None | Ascites or<br>Pleural effusion or<br>Pericardial effusion | Skin edema |
| Venous Doppler<br>(Umbilical vein and<br>ductus venosus) |  <br>UV<br>  <br>DV |  <br>UV<br> 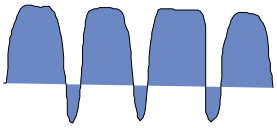 <br>DV |  <br>UV pulsations |
| Heart size<br>(Heart area/chest area) | >0.20 and ≤0.35 | 0.35–0.50 | >0.50 or <0.20 |
| Cardiac function | Normal TV and MV<br>RV/LV FS >0.28<br>Biphasic diastolic filling | Holosystolic TR or<br>RV/LV S.F. < 0.28 | Holosystolic MR or<br>TR dP/dt <400 or<br>Monophasic filling |
| Arterial Doppler<br>(Umbilical artery) | 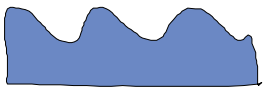 <br>UA | 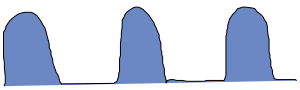 <br>UA (AEDV) | 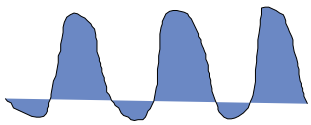 <br>UA (REDV) |

*Source:* Wieczorek A et al. *Ultrasound Obstet Gynecol* 2008;31:285.[87]

*Note:* CVP score is 10 if there are no abnormal signs and reflects two points for each of five categories: hydrops, venous Doppler, heart size, cardiac function, and arterial Doppler.

*Abbreviations:* AEDV, absent end diastolic velocity; *dP/dt*, change in pressure over time of TR jet; DV, ductus venosus; FS, ventricular fractional shortening; LV, left ventricle; MR, mitral valve regurgitation; MV, mitral valve; REDV, reversed end diastolic velocity; RV, right ventricle; TR, tricuspid valve regurgitation; TV, tricuspid valve; UA, umbilical artery; UV, umbilical vein.

extrauterine circulation and how this process is compromised in newborns with a cardiac defect is essential.

## Fetal and transitional circulations

The fetal circulation is a highly efficient system that provides blood to the fetus and the placenta. Fetal shunts allow the more highly oxygenated and nutrient-rich blood from the umbilical vein to be preferentially delivered to the left ventricle, therefore entering the systemic circulation. The remainder of the umbilical vein blood mixes with less-oxygenated blood from the fetal body and passes to the right ventricle, and via the ductus arteriosus is directed into the descending aorta supplying the lower body and the placenta.[21] The fetoplacental circulation is characterized by low resistance, whereas the circulation to the fetal lungs is limited by high resistance. At delivery, multiple important changes occur. Cord clamping interrupts the low-resistance placental circulation, whereas initiation of respiration decreases the pulmonary vascular resistance and increases pulmonary blood flow and ultimately the blood volume returning to the left atrium through the pulmonary veins. Consequently, the left atrial pressure increases, and functional closure of the foramen ovale occurs. With the closure of the ductus venosus and the ductus arteriosus (usually within 12–72 hours),[22] the fetal circulation transitions to the postnatal circulation.[23]

In most CHD, systemic blood flow is maintained *in utero*, and there is no fetal compromise. This includes simple defects as well as more complex lesions in which there is obstruction to pulmonary blood flow given that *in utero* flow to the pulmonary arteries is minimal. Lesions with a functional single ventricle most often require unobstructed atrial flow, and in these instances, patency of the foramen ovale is necessary to maintain an unobstructed circulation. Therefore, in most CHD lesions, even severe forms, the presence of the ductus arteriosus and foramen ovale permits the redistribution of blood flow to maintain cardiac output and adequate oxygen delivery to the fetal body to maintain an adequate fetoplacental circulation. For this reason, as long as cardiac function is good, most CHDs are well tolerated *in utero*,[23] although there is increasing evidence that the altered circulatory pattern may impair systemic oxygenation and nutrient delivery and affect fetal growth and brain development.[24–27]

At delivery, the risk of hemodynamic instability depends on the type of CHD, including whether the circulation is dependent on patency of the ductus arteriosus or foramen ovale and whether there is cardiac dysfunction either from a primary cardiomyopathy, a structural anomaly leading to an excessive pressure or volume load to the heart, or a cardiac rhythm abnormality.

## Protocols for risk assessment of hemodynamic instability at birth

Several postnatal risk stratification protocols for babies diagnosed *in utero* with CHD have been proposed[3–5,14,28] and summarized as part of the American Heart Association Statement on Fetal Cardiology[1] (Table 55.2). The risk of potential compromise at birth is most often determined prenatally by the fetal cardiologist, taking into account the specific CHD as well as patient-specific findings noted on the fetal echocardiogram[1] (Table 55.3). A recent evaluation of the level of care (LOC) risk assessment protocol applied prospectively over an 8-year period to a single-institution patient population was found to be very accurate in predicting postnatal care with a sensitivity ranging from 0.83 to 0.99 for prediction of the level of postnatal care and need for specialized intervention at birth.[4] To simplify, cardiac defects can be divided into three main categories according to the predicted risk of hemodynamic instability at birth: (1) CHD without risk of hemodynamic instability at delivery or in the neonatal period; (2) CHD with minimal risk of hemodynamic instability in the delivery room but need for intervention to stabilize the circulation prior to discharge; and (3) CHD with a high risk of instability in the delivery room.

### CHD without predicted risk of instability in the delivery room or neonatal period

This group includes left-to-right shunt lesions such as ventricular septal defects (VSDs), atrial septal defects, or atrioventricular septal defects, and mild valve abnormalities. Left-to-right shunt lesions most often become hemodynamically unstable weeks after birth when the decrease in the pulmonary vascular resistance causes significant shunting across the defect(s) with excessive pulmonary blood flow.[21] Similarly, infants prenatally diagnosed with a mild isolated valve abnormality and normal cardiac function are usually stable after birth. These conditions do not require specialized care in the delivery room, and babies often can be delivered at the local hospital and be evaluated either in the nursery or as an outpatient.[4,5,14,28,29]

### CHD with minimal risk of instability in the delivery room but requiring postnatal intervention

This group mainly includes cardiac defects that depend on the patency of the ductus arteriosus to maintain the systemic or pulmonary circulation after birth. The ductus arteriosus does not generally close immediately at birth, but after 12–72 hours,[22] and therefore, these babies are not expected to be compromised in the delivery room or immediate perinatal period.[4–5,14,20,28] In these cases, as long as there is adequate perinatal support, babies may be delivered at a location that can institute therapy with prostaglandin E1 for maintenance of ductal patency. After initial stabilization, transport of the newborn to the tertiary care cardiac center for anticipated intervention and/or surgery should be arranged.

#### Ductal-dependent pulmonary flow

The prediction of the need for patency of ductus arteriosus to augment pulmonary flow after birth has been studied, and

**Table 55.2** Predicted level of care and associated delivery recommendations

| *LOC* | *Definition* | *Example CHD* | *Delivery recommendations* | *DR recommendations* |
|---|---|---|---|---|
| P | CHD in which no intervention is planned/palliative care | CHD with severe/fatal chromosome abnormality or multisystem disease | Arrange for family support/ palliative care services; normal delivery at local hospital | |
| 1 | CHD without predicted risk of hemodynamic instability in the DR or first days of life | VSD, AVSD, mild TOF | Arrange cardiology consultation or outpatient evaluation; normal delivery at local hospital | Routine DR care; neonatal evaluation |
| 2 | CHD with minimal risk of hemodynamic instability in DR but requiring postnatal cath/ surgery | Ductal-dependent lesions including HLHS, critical coarctation, severe AS, IAA, PA/IVS, severe TOF | Consider planned induction usually near term; delivery at hospital with neonatologist and accessible cardiology consultation | Neonatologist in DR; routine DR care, initiate PGE if indicated; transport for cath/ surgery |
| 3 | CHD with likely hemodynamic instability in DR requiring immediate specialty care for stabilization | d-TGA with concerning atrial septum primum (note: it is reasonable to consider all d-TGA fetuses without an ASD at risk); uncontrolled arrhythmias<br>CHB with heart failure | Planned induction at 38–39 weeks; consider C/S if necessary to coordinate services; delivery at hospital that can execute rapid care, including necessary stabilizing/lifesaving procedures | Neonatologist and cardiac specialist in DR, including all necessary equipment; plan for intervention as indicated by diagnosis; plan for urgent transport if indicated |
| 4 | CHD with expected hemodynamic instability with placental separation requiring immediate cath/surgery in DR to improve chance of survival | HLHS/severely RFO or IAS<br>d-TGA/severely RFO or IAS and abnormal DA; obstructed TAPVR<br>Ebstein with hydrops; TOF with APV and severe airway obstruction; uncontrolled arrhythmias with hydrops; CHB with low ventricular rate, EFE, or hydrops | C/S in cardiac facility with necessary specialists in the DR usually at 38–39 weeks | Specialized cardiac care team in DR; plan for intervention as indicated by diagnosis; may include cath, surgery, or ECMO |

*Source:* Donofrio MT et al. *Circulation* 2014;129:2183–242.[1]

*Abbreviations:* APV, absent pulmonary valve; AS, aortic stenosis; ASD, atrial septal defect; AVSD, atrioventricular septal defect; CHB, complete heart block; CHD, congenital heart disease; C/S, cesarean section; DA, ductus arteriosus; DR, delivery room; ECMO, extracorporeal membrane oxygenation; EFE, endocardial fibroelastosis; HLHS, hypoplastic left heart syndrome; IAA, interrupted aortic arch; IAS, intact atrial septum; LOC, level of care; PA/IVS, pulmonary atresia/intact ventricular septum; PGE, prostaglandin; RFO, restrictive foramen ovale; TAPVR, total anomalous pulmonary venous return; d-TGA, d-transposition of the great arteries; TOF, tetralogy of Fallot; VSD, ventricular septal defect.

there are criteria available for prediction of postnatal care (Table 55.3). In cases of tetralogy of Fallot (TOF) and double-outlet right ventricle with subaortic VSD and pulmonary obstruction, several echocardiographic findings have been shown to be predictors of ductal-dependent pulmonary flow and/or need for neonatal surgery. Though not as well studied, it is reasonable to assume that other defects with pulmonary outflow tract obstruction, such as critical pulmonary stenosis or atresia and tricuspid valve stenosis or atresia with intact ventricular septum or small VSD will have similar flow alterations in the ductus arteriosus *in utero* that predict a ductal-dependent circulation and need for neonatal surgery. The following findings suggest a ductal dependent pulmonary circulation:

- Reversed orientation of the ductus arteriosus, defined as the angle of junction between the ductus arteriosus and the aorta being less than 90° (Figure 55.1a)[32]
- Reversed flow in the ductus arteriosus, described as flow from the aorta to the pulmonary artery through the ductus arteriosus (Figure 55.1b)[30,31]
- Pulmonary valve z-score less than −3 measured after 16 weeks of gestation (in cases of TOF)[31,33]

Though the pulmonary valve z-score is a sensitive marker, it is not specific. In contrast, flow direction in the ductus arteriosus has both a high sensitivity and specificity to predict postnatal physiology. In a prospective study over an 8-year period,[4] using only reversed (left-to-right) ductal flow to predict postnatal care, fetuses with TOF were evaluated. Of the 47 with straightforward TOF, 30 had normal right-to-left ductal flow and were predicted to be acyanotic (LOC 1; Tables 55.2 and 55.3), and 17 had either bidirectional or reversed ductal flow and were predicted to be cyanotic and likely ductal dependent (LOC 2; Tables 55.2 and 55.3). No babies assigned

**Table 55.3** Current recommendations regarding fetal predictors for delivery planning

| | *Fetal echo finding* | *Delivery recommendation* |
|---|---|---|
| Ductal-dependent lesions | Ductal-dependent pulmonary circulation:<br>• Aorta to pulmonary flow in the DA<br>• Reversed orientation of the DA (inferior angle <90°)<br>Ductal-dependent systemic circulation:<br>• Left to right atrial flow across the foramen ovale | No specialized care in delivery room<br>Initiation of prostaglandin E1 |
| HLHS with RFO or IAS | Pulmonary vein forward to reversed velocity-time integral ratio less than 3<br>Maternal hyperoxygenation in third trimester with no change in fetal branch pulmonary artery pulsatility index | Plan for possible urgent intervention to decompress left atrium (cath-balloon or stent; surgery) |
| d-TGA | Reported FO findings predictive of restriction:<br>• Angle of septum primum less than 30° to the atrial septum<br>• Bowing of septum primum into the left atrium greater than 50%<br>• Lack of normal swinging motion of septum primum<br>• Hypermobile septum primum<br>Note: all fetuses with d-TGA and concerning septum primum should be considered at risk<br>Abnormal DA findings:<br>• Small (low z-score)<br>• Accelerated forward, bidirectional, or reversed diastolic flow | Plan for possible urgent balloon atrial septostomy, on site if possible in the delivery room or ICU; initiation of prostaglandin E1; consider therapy for pulmonary hypertension with abnormal DA flow |
| TOF with APV | Lung finding suggestive of lobar emphysema (fluid trapping) on MRI | Specialized ventilation; consider ECMO |
| Ebstein anomaly | Hydrops fetalis<br>Uncontrolled arrhythmia | Consider early delivery with measures to decrease pulmonary resistance, treat arrhythmias, and support cardiac output |
| TAPVR, obstructed | Decompressing vein below the diaphragm<br>Continuous nonphasic flow in pulmonary vein<br>Accelerated flow in decompressing vein | Consider ECMO |
| Tachyarrhythmias | Rapid heart rate<br>Decreased heart function<br>Pericardial effusion/hydrops fetalis | Consider early delivery if appropriate gestational age; urgent cardioversion or medical therapy in delivery room if possible |
| CHB | Decreasing CVP score (to <7)<br>Very low ventricular rate<br>Decreased heart function/EFE<br>Hydrops fetalis | Consider early delivery; consider medical chronotrope or temporary pacing in delivery room if possible |

*Source:* Donofrio MT et al. *Circulation* 2014;129:2183–242.[1]

*Abbreviations:* CHB, complete heart block; CVP, cardiovascular profile score; DA, ductus arteriosus; ECMO, extracorporeal membrane oxygenation; EFE, endocardial fibroelastosis; FO, foramen ovale; HLHS, hypoplastic left heart syndrome; IAS, intact atrial septum; ICU, intensive care unit; MRI, magnetic resonance imaging; RFO, restrictive foramen ovale; TAPVR, total anomalous pulmonary venous return; d-TGA, d-transposition of the great arteries; TOF with APV, tetralogy of Fallot with absent pulmonary valve.

LOC 1 required transfer for cyanosis. Thirteen of the 17 (76%) assigned LOC 2 were ductal dependent and underwent neonatal repair. Three assigned LOC 2 were transferred to facilitate diagnostic testing, and though cyanotic, did not require prostaglandin E1. Sensitivity was 100%, and specificity was 97% for prediction of ductal-dependent pulmonary flow and subsequent neonatal repair.

### Ductal-dependent systemic flow

In cases of obstruction to the systemic circulation with inadequacy of the left heart to maintain systemic output, the need for prostaglandin E1 infusion to maintain ductal patency to support the systemic circulation can be predicted based on the following:

- Systolic flow reversal in the distal transverse aortic arch, implying perfusion of the aortic arch via the ductus arteriosus (Figure 55.2a and b)[30,34]
- Reversed flow across the foramen ovale, defined as flow directed from the left atrium to the right atrium (Figure 55.3a and b)[30,34]

Though there is no prospective study using these features in isolation to predict ductal-dependent systemic flow at

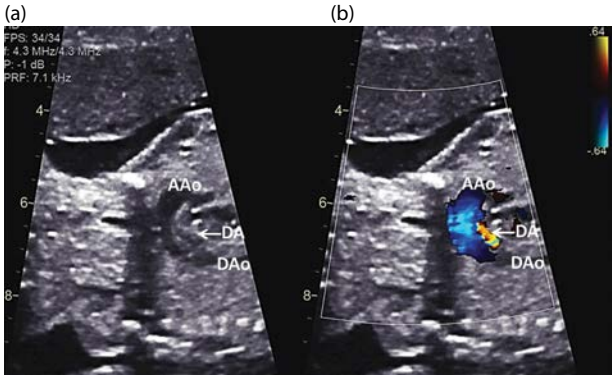


**Figure 55.1**
Fetus with tetralogy of Fallot. (a) Sagittal two-dimensional view of the aortic/ductal arches. (b) Color Doppler shows reversed flow (red) in the ductus arteriosus. (AAo, ascending aorta; DA, ductus arteriosus; DAo, descending aorta.) (Video 55.1)

delivery, it has been shown in fetuses with aortic stenosis that these findings are predictive of progression to hypoplastic left heart syndrome (HLHS).[35]

## CHD with high risk of instability in the delivery room

This group includes cardiac defects that require immediate stabilization after birth with intervention in the immediate perinatal period. Fetuses with these conditions should be delivered at a hospital with neonatology, pediatric cardiology, and cardiovascular surgeons preferably on site, with rapid access to an interventional cardiac catheterization service and/or cardiac surgery. Examples of CHD at risk of deterioration in the delivery room include HLHS with a severely restrictive or closed foramen ovale, d-transposition of the great arteries (d-TGA) with a restrictive foramen ovale, uncontrolled arrhythmias with hemodynamic compromise or hydrops (including both tachy and bradyarrhythmias), TOF with absent pulmonary valve and concern for severe lung disease, airway obstruction, or with hydrops, severe Ebstein anomaly with hydrops, and obstructed total anomalous pulmonary venous return.

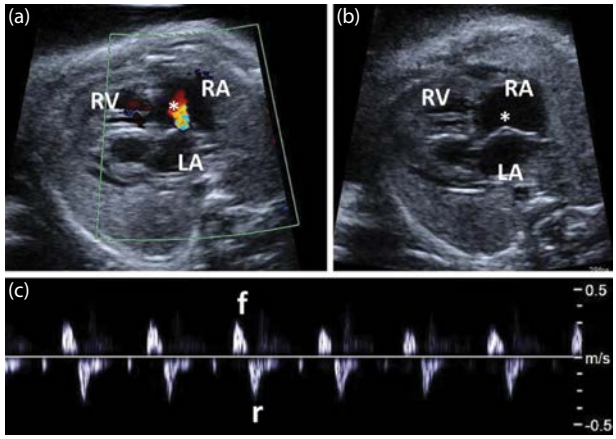


**Figure 55.3**
Fetus with hypoplastic left heart and severely restrictive atrial septum. (a) Axial image with color Doppler showing accelerated left to right flow (red) across the foramen ovale. (b) Axial two-dimensional image of the four-chamber view. (c) Pulmonary vein flow with velocity-time integral forward/reversed flow ratio <3. (f, forward flow; LA, left atrium; r, reversed flow; RA, right atrium; RV, right ventricle. Atrial septum primum noted by asterisk.) (Video 55.3)

### HLHS and a restrictive or closed foramen ovale

Most newborns with HLHS can be stabilized with initiation of prostaglandin E1. Fetuses with HLHS, however, are not only dependent on patency of the ductus arteriosus, but also adequate left-to-right shunting at the atrial septum through the foramen ovale. Foramen ovale restriction or closure has been reported to occur in approximately 6%–20% of fetuses with HLHS.[36–38] Unfortunately, despite good postnatal cardiac care, many of these infants do not survive to undergo the Norwood operation or die in the first 24 hours after surgery.[39] The initial presentation in the delivery room of the infant with HLHS and restrictive or closed foramen ovale immediately after birth may not show the severe hemodynamic abnormality that is present. Unfortunately, without intervention, rapid clinical deterioration usually occurs in the first few hours after delivery. Postnatal delivery room strategies to rapidly create an atrial communication after birth have been used to stabilize newborns with HLHS and restrictive or

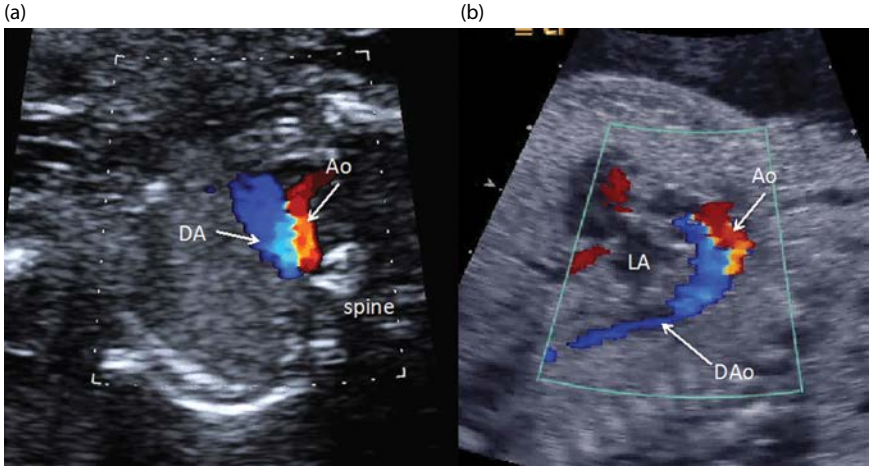


**Figure 55.2**
Fetuses with hypoplastic left heart syndrome. (a) Axial three-vessel-trachea view. (b) Sagittal two-dimensional imaging of the aortic/ductal arches. In both, color Doppler shows reversed flow (red) in the transverse aortic arch. (Ao, aorta; DA, ductus arteriosus; DAo, descending aorta; LA, left atrium.) (Video 55.2a and b.)

closed foramen ovale in an attempt to improve outcomes.[3,5,37] Prenatal selection of this group of fetuses is crucial in order to coordinate the delivery such that an urgent intervention to open the septum can be performed.

Fetal echocardiography allows for assessment of the foramen ovale before delivery in HLHS; however, usual measures assessing the width of the communication is not necessarily predictive of postnatal status.[40] It has been shown that an increased A wave (reversed wave during atrial systole) in the pulmonary veins by pulsed Doppler is useful for determining significant atrial septal restriction in fetuses with HLHS.[41,42] Of the Doppler parameters evaluated, a pulmonary vein Doppler flow forward to reverse velocity time integral ratio (VTIf/VTIr) value of less than five is a fairly sensitive predictor of need for emergent postnatal atrial septectomy. Sensitivity can be increased if a VTIf/VTIr ratio of less than three is used.[7] (Figure 55.3) In a single-center study done prospectively over an 8-year period, using pulmonary vein Doppler in fetuses with HLHS, prediction of postnatal delivery room compromise and need for intervention was excellent.[4] Of 59 with HLHS, 48 had a VTIf/VTIr >5 and an open atrial septum (LOC 2; see Tables 55.2 and 55.3) and 11 had either a VTIf/VTIr <5 and >3 ($n = 3$) or VTIf/VTIr <3 ($n = 8$) and a severely restrictive or closed atrial septum (LOC 3 or 4; Tables 55.2 and 55.3). All assigned LOC 2 did not require intervention, and 10 of 11 (91%) assigned LOC 3 or 4 underwent stabilizing atrial septoplasty. Using the pulmonary vein VTIf/VTIr, sensitivity was 100% and specificity 97% for prediction of need for urgent intervention. Of note, due to the potential for disease progression in HLHS fetuses, serial examination with the final study done late in the third trimester, 1–2 weeks prior to delivery, to assess the pulmonary vein flows as well as changes in RV function is recommended. Finally, assessing fetal pulmonary vasoreactivity using maternal hyperoxygenation in the third trimester has also been used and may be beneficial to assess the need for early postnatal intervention in HLHS.[41] Fetuses found to have less than 10% change in branch pulmonary artery pulsatility were more likely to need urgent intervention. It has been postulated that a finding of abnormally low reactivity may also have long-term clinical implications relating to pulmonary vascular abnormalities, but this has yet to be studied.

In summary, the presence of the following findings in fetuses with HLHS increases the likelihood of need for intervention to open the atrial septum at birth:

- A ratio of forward pulmonary vein flow to reversed flow less than 3 (where the pulmonary vein flow is expressed as velocity-time integral) (Figure 55.3c)[7]
- Lack of vasoreactivity in the fetal branch of the pulmonary artery during the maternal hyperoxygenation testing performed in the third trimester[41]

### d-Transposition of the great arteries

d-TGA is one of the few heart defects that has the potential for higher preoperative morbidity/mortality than postoperative.[12] Differentiating the newborn with d-TGA that will have a nonrestrictive atrial septum from one that will present in the delivery room with hypoxia and acidosis from restriction or closure of the foramen ovale is challenging. Several retrospective studies have suggested that the assessment of anatomic features of the foramen ovale including the position and mobility of septum primum and flow at the ductus arteriosus are useful to predict those that will be compromised at birth.[42,43] It is important to note that foramen ovale flow can vary during gestation and change dramatically at birth.[3,42] It may be that the gradual increase of pulmonary flow during late pregnancy initiates the process of early closure of the foramen ovale.[44] Assessment of the ductus arteriosus may also be useful in predicting postnatal compromise. Retrospective studies have shown the ductus arteriosus to be smaller and have abnormal flow (either reversed or bidirectional) in some fetuses with d-TGA who require postnatal intervention to open the atrial septum.[3,42,43] The single evaluation of the foramen ovale and ductus arteriosus in midgestation may not accurately predict the postnatal course. For this reason, serial echocardiography is often performed in the fetus with the d-TGA with the final study done late in the third trimester 1–2 weeks prior to delivery. This may help to determine which babies with d-TGA will need urgent intervention at delivery or within the first hours of life.

In a prospective study over an 8-year period using the current published criteria, d-TGA fetuses were evaluated with an attempt to predict postnatal course.[4] Of 27 fetuses, 10 were thought to have a foramen ovale with no features suggestive of risk for postnatal restriction (LOC 2; Tables 55.2 and 55.3); seven required balloon septostomy. An abnormal foramen ovale was suggestive of a need for urgent balloon septostomy (LOC 3 or 4; see Tables 55.2 and 55.3) and was found in 17; 15 required balloon septostomy. Of note, four fetuses had both ductal restriction and a concerning foramen ovale; in three, urgent septostomy was performed. Sensitivity for prediction of need for atrial septostomy in d-TGA was 68%, and specificity was 60%. Of note is that after several early cases in which the need for septostomy was not accurately predicted, the protocol was changed such that all patients with d-TGA are now treated as if an immediate cardiac intervention after birth is required.

In fetuses with d-TGA, specific echocardiographic features that have been shown to predict the need for atrial septostomy include the following:

- Atrial septum primum angle of less than 30° to the atrial septum[42]
- Bowing of atrial septum primum into the left atrium greater than 50% (Figure 55.4a and b)[42]
- Lack of normal swinging motion of atrial septum primum[42]
- Hypermobility of atrial septum primum[43]
- Ductus arteriosus restriction or abnormal flow (Figure 55.4c)[42,43]

It is important to note that given the lack of sensitivity of these measures and the potential for significant postnatal morbidity and mortality, it has been recommended by expert consensus that all babies with a prenatal diagnosis of d-TGA

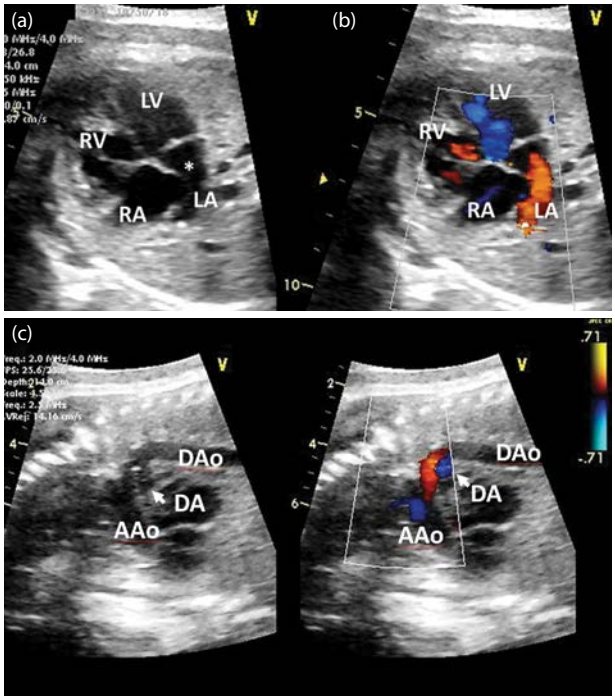


**Figure 55.4**
Fetus with d-transposition of the great arteries and bowing of atrial septum primum. (a) Axial two-dimensional image of four-chamber view. (b) Axial image with color Doppler showing no flow across the foramen ovale. (c) Sagittal two-dimensional and color Doppler of the ductal and aortic arches. Note restriction of the ductus and reversed (blue) flow. (AAo, ascending aorta; DA, ductus arteriosus; DAo, descending aorta; LA, left atrium; LV, left ventricle; RA, right atrium; RV, right ventricle. Atrial septum primum noted by asterisk.) (Video 55.4a–c.)

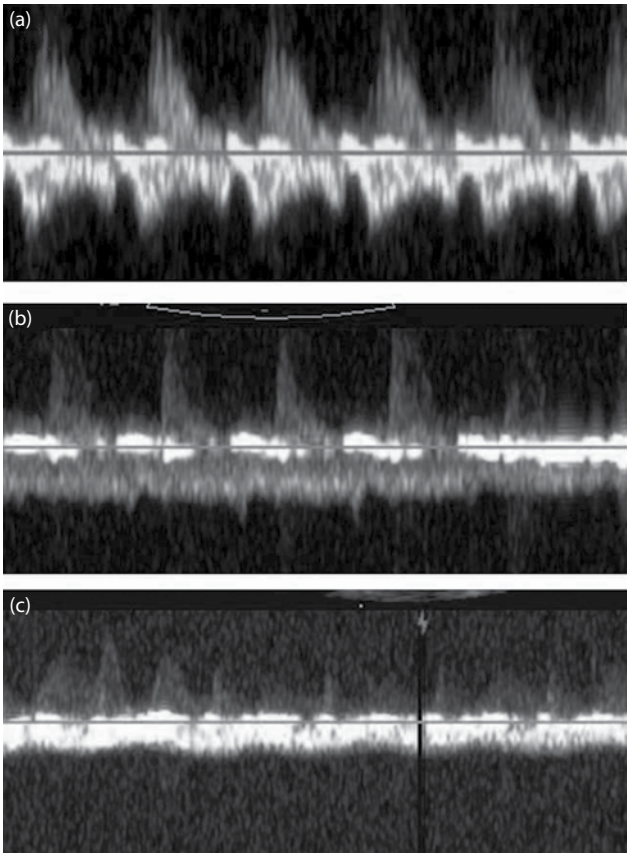


**Figure 55.5**
Pulmonary venous Doppler. (a) Normal. (b) Total anomalous pulmonary venous return, Doppler biphasic with decreased pulsatility, unobstructed pattern. (c) Doppler monophasic, low velocity and continuous, obstructed pattern.

should be treated as if the foramen ovale will close at delivery, and fetuses with this diagnosis should be delivered in a location where there is immediate access to a cardiologist to perform the septostomy if it is needed.[1]

### Obstructed total anomalous pulmonary venous return

Total anomalous pulmonary venous return (TAPVR) with obstruction is a severe CHD with high mortality. In neonates, if the diagnosis is not known, respiratory distress and decompensation may ensue rapidly after delivery.[45] Obstruction occurs in approximately half of TAPVR cases.[45,46] Early detection along with appropriate stabilization and early surgical repair most often result in a good long-term prognosis,[47] but the high morbidity and mortality encountered when not recognized until after birth make prenatal diagnosis of this condition particularly important.[45] The prenatal diagnosis of TAPVR is challenging given that often the four chambers of the heart appear normal, and the pulmonary veins may be difficult to visualize in the fetus. The assessment of pulmonary vein Doppler flow may be beneficial in detecting this potentially very critical heart defect. In a study of 26 patients with a prenatal diagnosis of TAPVR,[45] four were isolated and 22 had heterotaxy syndrome and/or additional cardiac abnormalities. Connections were supracardiac in 18, cardiac in one, and infradiaphragmatic in seven. Lack of a visible connection of the pulmonary veins to the atrium and the presence of a visible venous confluence were the most consistent grayscale findings. Abnormal pulmonary venous pulsed Doppler findings were present in 25 of the 26 fetuses. Flow was monophasic, of low velocity, and nonpulsatile in the presence of severe obstruction of the connecting vertical vein, with all three live-born newborns with this pattern requiring emergency surgery. Maternal hyperoxygenation testing may also be useful for predictive modeling in this population but had not been studied.

In fetuses suspected as having TAPVR, the following suggests obstruction and potential need for urgent cardiac surgery:

- Pulmonary vein flow pattern with continuous nonphasic flow (Figure 55.5c)[45]
- Obstruction of the connecting vertical vein[45]

### Other complex defects with *in utero* heart failure or hydrops

There are limited data available to guide decisions regarding delivery management of complex rare diseases that are at risk of *in utero* or postnatal demise as a result of heart failure, hydrops, or severe airway/lung comorbidity due to

cardiomegaly, such as TOF with absent pulmonary valve and severe Ebstein anomaly. In addition, fetuses with uncontrolled tachyarrhythmias or severe bradyarrhythmias resulting in heart failure or hydrops are also at risk. Because rapid deterioration in the perinatal period can be seen with these defects,[1,48,49] delivery in a setting that affords immediate access to specialized teams including neonatology and pediatric cardiology is suggested if there is any antenatal evidence of fetal compromise including pleural and/or pericardial effusions, hydrops, and/or nonreassuring fetal monitoring.

## *In utero progression of CHD*

Several cardiac lesions have the ability to progress and worsen throughout gestation, necessitating serial follow-up during pregnancy. Changes identified have the potential to modify the delivery plans. For example, in TOF, fetuses may initially have a wide open pulmonary outflow tract and right-to-left ductal flow, suggesting that postnatally the lesion will not be ductal dependent. However, if the pulmonary outflow tract does not grow adequately, these fetuses may progress to have a ductal-dependent lesion requiring prostaglandin E1 infusion after delivery.[31,33] Further study is needed to increase our understanding of what factors are related to CHD progression *in utero*. This is particularly important for the management of fetuses with forms of progressive CHD that are likely to result in CHD at high risk of instability at birth. Progressive restriction at the foramen ovale has been reported to occur in fetuses with both HLHS and with d-TGA.[3] This will impact postnatal care for these fetuses. In addition, fetal CHDs, such as Ebstein anomaly of the tricuspid valve, TOF with absent pulmonary valve, uncontrolled tachyarrhythmias, and complete heart block, have the potential to develop worsening heart failure and hydrops.[49] For some of these fetuses, early delivery may be necessary and specialized care arranged to support the circulation in the postnatal period.[1]

## *Definition of critical CHD in the modern era*

The historical definition of "critical" CHD in pediatric cardiology includes those defects in which the circulation depends on patency of the ductus arteriosus after birth.[50,51] This is understandable given that an infant with an unknown ductal-dependent postnatal circulation will become critically ill once the ductus closes. However, with prenatal diagnosis and initiation of prostaglandin E1 at birth, most cardiac defects are no longer "critical." Clearly, however, there are a small number of fetuses who remain at risk and cannot be stabilized with a prostaglandin E1 infusion alone and require additional intervention or other specialized care in the first hours of life to survive.[3,5,14] With the improved understanding of the fetal and transitional circulation, risk stratification protocols for CHD are now being utilized with some success, though strategies for care continue to err on the side of caution to assure preparedness for unexpected events. As the fetal parameters for evaluating these new "critical" forms of CHD are being perfected, the goal remains to appropriately triage patients, optimize the perinatal and postnatal management (including location, mode, and timing of delivery), and ensure that the necessary level of perinatology and neonatology services and access to cardiology and cardiothoracic surgery care are available.

# Delivery planning for neonates diagnosed *in utero* with CHD

Delivery planning should take into account both the risk of hemodynamic instability at birth as well as the local resources available, including subspecialty services and access to a pediatric cardiac facility.

## *Location of delivery and transportation of the newborn*

Most newborns with CHD do not need specialized care beyond routine neonatal care in the perinatal period, and recommendations can be made to deliver at the local hospital and be followed as outpatients.[1,3–5,14] However, if the presence of a specialized cardiac team after delivery is anticipated, the location of delivery should take into account the special needs of the newborn to maintain stability. Determination of the site of delivery depends on local practice and the proximity of the pediatric cardiac unit. In regions where the number of specialized cardiac centers is limited, strategies to safely plan the delivery and perinatal management of infants prenatally diagnosed with CHD include either creation of a highly specialized neonatal unit or maternal transport with delivery in a facility close to a pediatric cardiac center in those patients determined to be at high risk of hemodynamic instability.[14,29] In order to improve the neonatal outcome of infants with CHD that have hemodynamic instability that occurs after delivery and avoid transportation of potentially unstable newborns, some freestanding children's hospitals have planned deliveries in their facilities to accommodate the highest-risk patients, thus minimizing time to life-saving intervention.[3,52] Variations in strategies for care depend on many factors. For example, an outcome study of HLHS babies in Texas showed that there was improved preoperative survival in newborns delivered close to the pediatric tertiary care medical center.[53] In contrast, in a single-center study in Washington, DC,[4] distance was felt not to be a key factor within the service region, though detailed communication, local on-site education, and well-organized collaboration were in place to assure optimal care for infants determined to require standard care for stabilization prior to transfer (LOC 2; Table 55.2 and 55.3). For those infants thought to have critical CHD with instability in the delivery room (LOC 3 and 4; Tables 55.2 and 55.3),

delivering at the children's hospital or in the adjacent adult hospital with cardiology specialists in the delivery room was arranged.

## Timing of delivery

Recent studies have shown that infants prenatally diagnosed with severe forms of CHD tend to be delivered earlier than neonates in whom the diagnosis of CHD is made after birth[13,54] (Figure 55.6). This finding is particularly worrisome given that otherwise healthy neonates born at 37–38 weeks have an increased risk of worse outcomes compared with those born near or at term.[55] It is important to note that this finding has also been observed in babies with CHD. Studies have shown that babies with CHD have longer postoperative lengths of stay and higher mortality if delivered before 39 weeks.[54,56,57] Therefore, in the absence of fetal or maternal indications for earlier delivery, the potential advantages of an elective delivery of fetuses with CHD early should be carefully considered.

In addition to an increased mortality, there is growing evidence that the decision about timing of delivery of infants with CHD should also consider the potential effect of the gestational age at birth on neurologic outcome. It has been shown that fetuses with severe or critical CHD, such as d-TGA or those with single-ventricle physiology have delays in brain maturation that manifest as alteration of brain growth and neuroaxonal development, particularly of the microstructure of the white matter.[58–61] Postnatal brain magnetic resonance imaging studies suggest that brain development may lag by as much as 5 weeks in term neonates with either d-TGA or HLHS. Given these findings, it has been suggested that planning for the delivery of babies with CHD near or at full term may improve brain development and decrease susceptibility to injury postnatally[60]; however, further studies are needed to establish whether this will translate to improvement in long-term neurologic outcome.

Planning of the delivery of babies with CHD is also affected by the overall risk of preterm birth (occurring in 12.8% of all U.S. births).[62] To date, although there are effective predictors of preterm birth before 34 weeks, such as cervicovaginal fetal fibronectin and cervical length based on ultrasonography evaluations, there is no reliable method to identify the exact timing of the delivery among women with risk factors or symptoms of preterm labor.[63,64] Communication between the obstetrician and the pediatric cardiologist is necessary if spontaneous preterm birth seems likely.

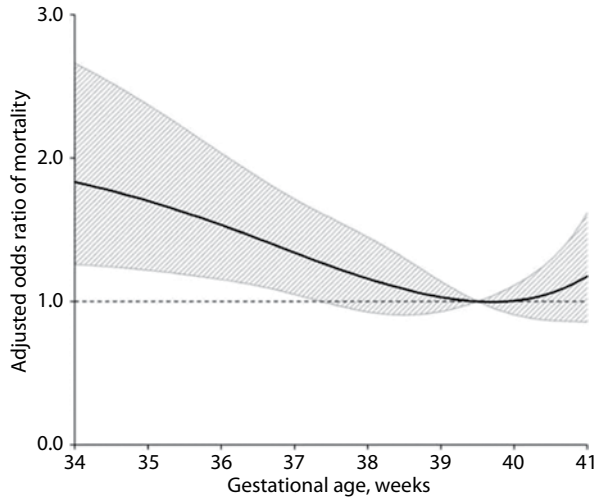


**Figure 55.6**
Representation of data reported to STS database 2010–2011 regarding the relationship between GA at birth and outcomes. Shown are estimated adjusted odds ratios for in-hospital mortality by week of gestational age at birth (reference, 39.5 weeks) and piecewise 95% confidence intervals (shaded area). The data demonstrate a U-shaped relationship with a nadir for adverse results at 39–40 weeks adjusted odds ratio (95% CI) of 1.34 (1.05–1.71; $p = 0.02$). (Reprinted with permission from Costello JM et al. *Circulation* 2014;129(24):2511–7.[57])

## Mode of delivery

Data from retrospective studies show that prenatal diagnosis of a severe CHD, such as HLHS, d-TGA, double-outlet right ventricle, or TOF, increases the likelihood for planned delivery and cesarean section. In fetuses with CHD, the mode of delivery has not been shown to affect the Apgar score, presurgical or postsurgical morbidity including the risk of hemodynamic instability, metabolic acidosis, and end-organ dysfunction, the length of hospitalization, or survival to surgery or discharge.[65,66] Two retrospective studies have concluded that labor is safe for fetuses with CHD in most cases,[67,68] but impact on the long-term functional and neurodevelopmental outcomes is largely unknown.

## Fetal surveillance during labor

The use of CTG to record fetal heart rate and uterine contractile activity has utility during labor to stratify the risk of intrapartum hypoxia and neonatal acidosis,[69,70] but in practice has a low positive predictive value for neonatal hypoxia and acidosis.[71] The introduction of continuous CTG during labor has not been shown to decrease the incidence of cerebral palsy or infant death among low-risk or high-risk pregnancies, but has been associated with a decrease in the incidence of neonatal seizures. Unfortunately, it is also associated with a higher percentage of cesarean and instrumented vaginal deliveries.[71] It has been hypothesized that fetal anomalies involving the central nervous system or the cardiovascular system may alter the fetal heart rate pattern and not correlate with a hypoxic or acidotic state.[72] The few retrospective studies evaluating the use of CTG in labor of fetuses with CHD[67,72,73] have shown that these fetuses show a higher percentage of nonreassuring fetal heart rate tracings, but no characteristic fetal heart rate patterns have been related to specific heart defects. As with normal fetuses, the use of continuous CTG in labor for fetuses with CHD has been associated with an increased rate

of emergent cesarean delivery.[72] In addition, CTG is limited in the assessment of the heart rate in fetuses with significant arrhythmias. To overcome these limitations, the fetal electrocardiogram, performed with scalp electrode, has been proposed in labor to monitor fetuses with a prenatal diagnosis of congenital heart block. Despite encouraging results, data are only available in limited cases, and no studies have been done to determine its routine use in these potentially high-risk fetuses.[74,75]

Other types of fetal surveillance during labor, such as abdominal fetal electrocardiogram, pulse oximetry, and fetal scalp blood sampling for estimation of lactate, may serve as tools to identify those fetuses with nonreassuring CTG fetal heart rate tracings that have hypoxemia and/or acidosis; however, there are no data to support their routine use in fetuses with CHD.[76] Given the lack of data, the CTG remains the main tool for routine surveillance during labor for fetuses with CHD, with the interpretation of the tracings presently based on the classification systems proposed for all pregnancies.[69,70]

# Outcomes of fetuses diagnosed with CHD

Overall, outcomes for infants and children with CHD have improved in recent years; however, there remains controversy as to the impact of prenatal diagnosis on survival. In a recent study[77] of 3,146 infants with isolated CHD, the 1-year survival rate was 77% for prenatally diagnosed versus 96% for those postnatally diagnosed. Comparing 1-year survival rates among those with noncritical CHD alone ($n = 2{,}455$), there was no difference between prenatal and postnatal diagnoses (96% versus 98%, respectively); however, among those with critical CHD, prenatally diagnosed infants actually had a significantly lower survival rate (71% versus 86%, respectively). One theory as to why prenatally diagnosed infants do worse is that they may comprise a more severe spectrum of disease, which may account for the high death rates in population-based studies. In addition, death rates in those diagnosed postnatally may not be accurate unless postmortem data are included of those that died at home or prior to transfer to the tertiary care hospital.

## *Outcome in isolated CHD*

A recent meta-analysis evaluating newborns diagnosed with isolated critical CHD and no other important risk factors, reported findings from eight studies that included outcome data for infants with HLHS, d-TGA, coarctation of the aorta, pulmonary atresia, truncus arteriosus, and/or critical left heart obstruction.[78] Fetuses with other major extracardiac anomalies, genetic diagnoses, low birth weight <2.5 kg, prematurity <35 weeks, neonatal infection, meconium at delivery, HLHS with intact atrial septum, and CHD with no surgical options were excluded. The group of 1,373 patients was studied; 297 (22%) with a prenatal diagnosis. Overall death was 10% in the group with a prenatal diagnosis and 5.6% in those diagnosed postnatally, though those with a prenatal diagnosis were more likely to be high risk and more likely to choose comfort care. Excluding those at high risk, those that received comfort care, and one patient who was prenatally diagnosed with d-TGA that was determined to be incorrectly managed, only 1/221 (0.5%) diagnosed prenatally died versus 31/974 (3.2%) diagnosed postnatally. Though this analysis did not show a decrease in all-cause mortality following a prenatal diagnosis of critical CHD, the results indicated that in patients with comparable anatomy, standard risk, an intent to treat, and optimal postnatal care, those with a prenatal diagnosis of critical CHD were less likely to die prior to planned cardiac surgery (Figure 55.7). Therefore, the role of the fetal cardiologist is not only to make an accurate and precise diagnosis, but to facilitate planning of appropriate delivery room management with coordination of the necessary perinatal care teams.

## *Outcomes of specific high-risk lesions*

The outcome of prenatally diagnosed CHD depends in part on both the nature and the severity of disease. Diagnoses at particular risk of *in utero* or early postnatal demise include heterotaxy syndrome with atrioventricular block, TOF with absent pulmonary valve, and Ebstein anomaly. Those at risk in the delivery room include HLHS with intact atrial septum and d-TGA (Table 55.4).

### Heterotaxy syndrome

In general, mortality of both right atrial isomerism (RAI) and left atrial isomerism (LAI) is high, due to the complexity of the structural defects in a high proportion of patients. In addition, in those with LAI specifically, there is also an

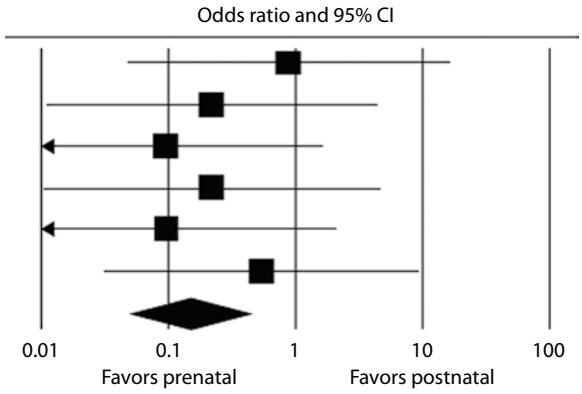


**Figure 55.7**
Meta-analysis of critical congenital heart disease patients with standard risk, planned cardiac surgery, and optimal care: Forest plot of preoperative death for patients with prenatal versus postnatal diagnosis. (Reprinted with permission from Holland BJ et al. *Ultrasound Obstet Gynecol* 2015;45(6):631–8.[78])

**Table 55.4** Reported data for fetal and neonatal outcomes after prenatal diagnosis of congenital heart disease

| *Congenital heart disease (CHD) diagnosis* | *Termination of pregnancy* | *Spontaneous fetal demise* | *Survival* | *Comments* |
|---|---|---|---|---|
| All, with normal birth weight and no other anomalies[78] | – | – | 99.5% postnatal survival to surgical intervention | Meta-analysis |
| All CHD[78]<br>Critical CHD | – | – | 77% 1-year<br>71% 1-year | May be due to high rate of additional comorbidities in the reported cohort |
| Heterotaxy syndrome[79] | 22% | 6%–10% | 72% to live birth<br>53% 5-year (asplenia, following live birth)<br>86% 5-year (polysplenia following live birth) | Atrioventricular block, hydrops correlated with nonsurvival |
| Tetralogy of Fallot[80] | – | – | 85% 6-year | May be partially dependent on 22q11 deletion status and other anomalies |
| Tetralogy of Fallot with absent pulmonary valve[48] | 25%–43% | 7%–15% | As high as 50% after prenatal diagnosis; includes terminations | Case series and review of literature |
| Ebstein anomaly[49] | 6% | 17% | 55% overall perinatal survival | Multicenter |
| Hypoplastic left heart syndrome[7,84] | – | 1%–3% | 70%–75% 1-year, 65% 4-year following live birth | – |

associated risk of complete atrioventricular block causing bradycardia and hydrops. A recent study looked at pregnancy outcomes after a fetal diagnosis of heterotaxy syndrome.[79] Of 154 fetuses evaluated, 61 (40%) had RAI and 93 (60%) had LAI. There were four fetal deaths in the RAI fetuses and five in the LAI fetuses (four had associated bradyarrhythmias). Overall, 72% were live-born, with a significant number of pregnancy interruptions (22%). Bradyarrhythmia was the only predictor of fetal death. In the live-born RAI group, 43% (15 of 35) died, and in the live-born LAI group, 13% (10 of 76) died. Pulmonary vein stenosis and noncardiac anomalies were independent risk factors predictive of postnatal death. The 5-year survival of those born alive was 53% for RAI and 86% for LAI. Though specialized care in the delivery room has been suggested, the prenatal diagnosis of heterotaxy syndrome has not been shown to confer an advantage in these patients.

## Tetralogy of Fallot with absent pulmonary valve

There are several variants of TOF, from those with mild outflow obstruction to those with pulmonary atresia with or without confluent branch pulmonary arteries and major aortopulmonary collateral arteries. For simple TOF with antegrade flow to confluent branch pulmonary arteries, fetal survival is very good, and postnatal postoperative survival is greater than 95%, with approximately an 85% 30-year survival.[80] In contrast, the diagnosis of TOF with absent pulmonary valve has a much worse prognosis, with increased risk for both fetal and neonatal death. A recent review of several case series[48] reported overall survival to more than 1 year of 14%–50%. Termination of pregnancy ranged between 25% and 43%, *in utero* death between 8% and 15%, and neonatal and infant death between 16% and 43%. Death was associated with karyotype abnormality. In addition, although fetal diagnosis has become increasingly more sophisticated in recent years, studies show that current available fetal echocardiographic measurements fail to predict clinical delivery room presentation or outcomes. In one study[81] of multiple anatomic measures made, only hydrops and pulmonary annulus size predicted mortality. This suggests that the pathophysiology resulting in death is not due to the aneurysmal dilation of the pulmonary arteries but may be related to right heart dysfunction.

## Ebstein anomaly of the tricuspid valve and tricuspid valve dysplasia

Tricuspid valve abnormalities in the fetus range from mild displacement of the septal leaflet with mild insufficiency to severe displacement, absent valve coaptation with severe insufficiency, atrialization of the right ventricle, and functional pulmonary atresia. Even with anticipatory care and more novel approaches to postnatal management, some affected fetuses are at very high risk of fetal or neonatal demise. In recent years, however, there have been improvements in outcome likely due to a better understanding of the *in utero* and transitional pathophysiology. In one study, 93% of infants with Ebstein anomaly, including 10 with a fetal diagnosis, survived the neonatal period, largely as a result of limiting ductal patency.[82] A recent multicenter study[49] found early gestational age at diagnosis, pulmonary insufficiency, larger tricuspid annulus diameter, and presence of effusions to be associated with poor outcome; the overall perinatal survival of 55% was low in part due to

inclusion of cases of fetal death (17%) and pregnancy terminations (6%).

## Hypoplastic left heart syndrome

Infants with a prenatal diagnosis of HLHS have in general less preoperative acidosis than those diagnosed after birth, and based on one study may have decreased early mortality to the bidirectional Glenn procedure.[6] In addition, prenatal diagnosis may improve the outcome of those fetuses with HLHS at highest risk by identifying those with a restrictive or intact atrial septum who may benefit from an atrial septostomy either urgently postnatally or *in utero*.[3,7] Early studies showed that prenatal diagnosis improved surgical survival overall in fetuses with HLHS,[6] but more recent studies, perhaps because of improvements in resuscitation and postoperative management resulting in better overall survival after Norwood, have failed to demonstrate a survival advantage.[13,53,83] The overall survival in the current era for HLHS is less than ideal, as even under the best circumstances, only ~70%–75% transplant-free 1-year and 65% 4-year survival are seen in large, multicenter reports.[84] The presence of additional anomalies or karyotype abnormality results in significantly lower survival expectations (with 10-fold higher preoperative mortality and less than 40% 4-year survival).[85,86] Those with a restrictive or closed foramen ovale have been reported to have significantly worse outcome, with survival reported as low as 25%–50%.[36–38]

## d-Transposition of the great arteries

For newborns with d-TGA, patency of fetal shunts, especially at the atrial level, is essential for neonatal survival prior to surgical correction. Surgical survival after arterial switch operation is very high (>95%). Prenatal diagnosis has been shown to improve preoperative status and overall survival in most neonates with d-TGA, presumably due to adequate planning and access to atrial septostomy early after birth. In one study,[12] preoperative survival was 100% in infants with prenatal diagnosis compared to 94% in those diagnosed postnatally. In addition, those diagnosed prenatally were better surgical candidates, with 100% surviving neonatal surgery compared to only 91% operative survival in the postnatally diagnosed group.

# Summary

Prenatal recognition of severe or critical CHD is associated with improvement in preoperative condition and increased survival for select defects. A reduction in morbidity, including neonatal hypoxemia and metabolic acidosis, is clearly gained through advanced knowledge of fetal cardiac disease and preparation for abnormal transition to extrauterine life. Detection of CHD *in utero* allows for delivery planning, especially when the need for urgent postnatal intervention is anticipated based on available predictive models. Perinatal management should be tailored to the specific needs of the mother and fetus, and should include decisions regarding location, timing, and mode of delivery that in general minimize the risk of early or cesarean section delivery. In selected cases, there may be compelling maternal or fetal indications for earlier delivery, including a variety of obstetric indications, such as spontaneous onset of labor, maternal comorbidities, pregnancy complications, or nonreassuring results of fetal testing. Collaboration between obstetric and pediatric cardiology specialty services and careful attention to perinatal management and delivery planning after a prenatal diagnosis of CHD is made can improve the perinatal status of newborns with potential for improvement in both survival and long-term functional and neurodevelopmental outcomes.

# Videos

**Video 55.1** (https://youtu.be/kWvg4Nd5fyU)
Fetus with tetralogy of Fallot. (a) Sagittal two-dimensional view of the aortic/ductal arches. (b) Color Doppler shows reversed flow (red) in the ductus arteriosus.

**Video 55.2a** (https://youtu.be/l68K2mQiAj0)
Fetuses with hypoplastic left heart syndrome. Axial three-vessel-trachea view. Color Doppler shows reversed flow in the transverse aortic arch.

**Video 55.2b** (https://youtu.be/N29lByRtCMk)
Sagittal two-dimensional imaging of the aortic/ductal arches. Color Doppler shows reversed flow (red) in the transverse aortic arch.

**Video 55.3** (https://youtu.be/B7xtjBJDC8o)
Fetus with hypoplastic left heart and severely restrictive atrial septum. (a) Axial image with color Doppler showing accelerated left to right flow (red) across the foramen ovale. (b) Axial two-dimensional image of the four-chamber view.

**Video 55.4a** (https://youtu.be/KCRxyhoIcRs)
Fetus with d-transposition of the great arteries and bowing of atrial septum primum. Axial two-dimensional image of four-chamber view.

**Video 55.4b** (https://youtu.be/YSr8m_P1z5A)
Fetus with d-transposition of the great arteries. Axial image with color Doppler showing minimal bidirectional (blue and red) flow across the foramen ovale.

**Video 55.4c** (https://youtu.be/ZCT28dcmPOE)
Fetus with transposition of the great arteries. Sagittal two-dimensional and color Doppler of the ductal and aortic arches. Note restriction of the ductus and bidirectional with forward (red) and reversed (blue) flow.

# References

1. Donofrio MT et al. *Circulation* 2014;129:2183–242.
2. Brown KL, Sullivan ID. *Heart* 2014;100:359–60.
3. Donofrio MT et al. *Am J Cardiol* 2013;111:737–47.
4. Donofrio MT et al. *J Am Soc Echocardiogr* 2015;28(11):1339–49.
5. Pruetz JD et al. *Prenat Diagn* 2014;34:1127–32.

6. Tworetzky W et al. *Circulation* 2001;103:1269–73.
7. Divanovic A et al. *J Thorac Cardiovasc Surg* 2011;141:988–94.
8. Tzifa A et al. *Arch Dis Child Fetal Neonatal Ed* 2007;92:F199–203.
9. Franklin O et al. *Heart* 2002;87:67–9.
10. Eapen RS et al. *Am J Perinatol* 1998;15:237–42.
11. Kumar RK et al. *Am J Cardiol* 1999;83:1649–53.
12. Bonnet D et al. *Circulation* 1999;99:916–8.
13. Kipps AK et al. *Am J Cardiol* 2011;108:421–7.
14. Berkley EM et al. *Prenat Diagn* 2009;29:654–8.
15. ACOG practice bulletin. *Int J Gynaecol Obstet* 2000;68:175–85.
16. Falkensammer CB et al. *J Perinat Med* 2001;29:390–8.
17. Wieczorek A et al. *Ultrasound Obstet Gynecol* 2008;31:284–8.
18. Huhta JC. *J Perinat Med* 2001;29:381–9.
19. Donofrio MT et al. *J Perinatol* 2004;24:112–7.
20. Johnson BA, Ades A. *Clin Perinatol* 2005;32:921–46.
21. Rudolph AM. The fetal circulation and postnatal adaptation. In: Rudolph AM, ed. *Congenital Diseases of the Heart: Clinical-Physiological Considerations*. Armonk, NY: Futura Publishing; 2001:3–44.
22. Lim MK et al. *Arch Dis Child* 1992;67:1217–8.
23. Friedman AH, Fahey JT. *Semin Perinatol* 1993;17:106–21.
24. Rosenthal GL. *Am J Epidemiol* 1996;143:505–13.
25. Limperopoulos C et al. *Circulation* 2010;121:26–33.
26. Donofrio MT et al. *Curr Opin Pediatr* 2011;23:502–11.
27. Manzar S et al. *Saudi Med J* 2005;26:453–6.
28. Słodki M et al. *J Perinatol* 2016;36(8):575–80.
29. Anagnostou K et al. *Arch Dis Child Fetal Neonatal Ed* 2013;98:F218–21.
30. Berning RA et al. *J Am Coll Cardiol* 1996;27:481–6.
31. Quartermain MD et al. *Ultrasound Obstet Gynecol* 2013;41: 47–53.
32. Hinton R, Michelfelder E. *Am J Cardiol* 2006;97:716–9.
33. Arya B et al. *Pediatr Cardiol* 2014;35:810–6.
34. Makikallio K et al. *Circulation* 2006;113:1401–5.
35. McElhinney DB et al. *Circulation* 2009 13;120:1482–90.
36. Vlahos AP et al. *Circulation* 2004;109:2326–30.
37. Atz AM et al. *Am J Cardiol* 1999;83:1224–8.
38. Rychik J et al. *J Am Coll Cardiol* 1999;34(2):554–60.
39. Cheatham JP. *J Interv Cardiol* 2001;14(3):357–66.
40. Taketazu M et al. *J Am Coll Cardiol* 2004;43(10):1902–7.
41. Szwast A et al. *Circ Cardiovasc Imaging* 2010;3:172–8.
42. Jouannic JM et al. *Circulation* 2004;110:1743–6.
43. Punn R, Silverman NH. *J Am Soc Echocardiogr* 2011;24: 425–30.
44. Donofrio MT et al. *Am J Cardiol* 2004;94(10):1348–51.
45. Ganesan S et al. *J Ultrasound Med* 2014;33(7):1193–207.
46. Karamlou T et al. *Circulation* 2007;115:1591–8.
47. Seale AN et al. *Ultrasound Obstet Gynecol* 2012;40(3):310–8.
48. Wertaschnigg D et al. *Ultrasound Obstet Gynecol* 2013;41(2): 162–7.
49. Freud LR et al. *Circulation* 2015;132:481–9.
50. Chang RK et al. *Arch Pediatr Adolesc Med* 2008;162:969–74.
51. Schultz AH et al. *Pediatrics* 2008;121:751–7.
52. Howell LJ. *Semin Pediatr Surg* 2013;22:3–9.
53. Morris SA et al. *Circulation* 2014;129:285–92.
54. Costello JM et al. *Pediatrics* 2010;126:277–84.
55. Cheng YW et al. *Am J Obstet Gynecol* 2008;199:370.e1–7.
56. Cnota JF et al. *J Pediatr* 2011;159:761–5.
57. Costello JM et al. *Circulation* 2014;129(24):2511–7.
58. Miller SP et al. *N Engl J Med* 2007;357:1928–38.
59. Partridge SC et al. *Ann Neurol* 2006;59:640–51.
60. Licht DJ et al. *J Thorac Cardiovasc Surg* 2009;137:529–36.
61. Clouchoux C et al. *Cereb Cortex* 2013;23:2932–43.
62. Martin JA et al. *Natl Vital Stat Rep* 2009;57:1–104.
63. Honest H et al. *Health Technol Assess* 2009;13:1–627.
64. Lockwood CJ. *N Engl J Med* 2002;346:282–4.
65. Peterson AL et al. *J Pediatr* 2011;159:64–9.
66. Trento LU et al. *Prenat Diagn* 2012;32:1250–5.
67. Walsh CA et al. *J Perinatol* 2014;34:901–5.
68. Reis PM et al. *Am J Obstet Gynecol* 1998;179:1150–4.
69. American College of Obstetricians and Gynecologists. *Obstet Gynecol* 2009;114:192–202.
70. Parer JT et al. *Obstet Gynecol* 2009;114:136–8.
71. Alfirevic Z et al. *Cochrane Database Syst Rev* 2013;(5):CD006066. doi: 10.1002/14651858.CD006066.pub2. Review. Update in: *Cochrane Database Syst Rev*. 2017 Feb 03;2:CD006066.
72. Ueda K et al. *Am J Obstet Gynecol* 2009;201:64.e1–6.
73. Morikawa M et al. *J Obstet Gynaecol Res* 2014;40:424–8.
74. Katz AR et al. *J Adolesc Health Care* 1980;1:152–4.
75. Friedman DM et al. *Am J Perinatol* 1998;15:669–73.
76. East CE et al. *Cochrane Database Syst Rev* 2015;(5):CD006174. doi: 10.1002/14651858.CD006174.pub3.
77. Oster ME et al. *Am J Cardiol* 2014;113:1036–40.
78. Holland BJ et al. *Ultrasound Obstet Gynecol* 2015;45(6): 631–8.
79. Escobar-Diaz MC et al. *Am J Cardiol* 2014;114:612–7.
80. Hirji A et al. *Can J Cardiol* 2010;26:e1–6.
81. Moon-Grady AJ et al. *Am J Cardiol* 2002;89:1280–5.
82. Wald RM et al. *Am J Cardiol* 2005;96:851–6.
83. Atz AM et al. *J Thorac Cardiovasc Surg* 2010;140(6):1245–50.
84. Ohye RG et al. *N Engl J Med* 2010;362(21):1980–92.
85. Bove EL. *Pediatr Cardiol* 1998;19(4):308–15.
86. Tabbutt S et al. *J Thorac Cardiovasc Surg* 2012;144(4):882–95.
87. Wieczorek A et al. *Ultrasound Obstet Gynecol* 2008;31:285.

# 56

# The neonate with congenital heart disease: Medical and interventional management

Alexander Lowenthal, Ulrike Herberg, and Einat Birk

## Introduction

Recent developments in fetal echocardiography steadily enhance the accuracy of the diagnosis of congenital heart disease. Consequently, physicians working in the pre- and postnatal diagnostic fields increasingly encounter the problem of the incorporation of the new perinatal findings in the therapy of complex cardiac defects. Therefore, physicians working in the area of prenatal diagnostics are increasingly confronted with the pre- and postnatal physiology and alternatives for therapy of complex cardiac defects. All of these developments mandate, at all stages, the pediatric cardiologists' close cooperation with the patient's parents, obstetricians, cardiac surgeons, and neonatologists. This chapter deals with the importance of perinatal adaptation of the circulation, and the available choices of drug and interventional therapy of congenital heart diseases. Chapter 57 deals in more detail with the options of neonatal cardiac surgery.

## Transition from fetal to postnatal circulation

The fetal circulation differs uniquely from the postnatal circulation in several ways (Figure 56.1):

- The parallel connection and pressure adaptation of the two circulations
- The high resistance of the undeveloped lung, preventing significant lung perfusion
- The low resistance of the placenta, which supplies oxygen and nutrition
- The bypass of relatively highly oxygenated blood through the ductus venosus and foramen ovale via the left atrium and left ventricle to the heart and the brain
- The bypass of blood from the right ventricle (via the main pulmonary artery) through the ductus arteriosus to the lower body

### *Transition from fetal to postnatal circulation for the healthy fetus*

Transformation of the fetal to the postnatal circulation involves elimination of the umbilical-placental circulation, establishment of the pulmonary circulation, and separation of the pulmonary and systemic circulation by closure of the fetal communications:

1. With the first breath after birth, the lungs of the newborn expand and fill with air. In consequence, the pulmonary vascular resistance decreases 5- to 10-fold, leading to an increase in pulmonary blood flow.
2. The increased pulmonary blood flow increases both filling and pressure of the left atrium. The pressure in the left atrium then exceeds that of the right atrium. The flap of the foramen ovale is pressed against the atrial septum resulting in anatomical closure or reversal of the interatrial shunt (Figure 56.2a).
3. The decrease in the pulmonary vascular resistance initially results in a bidirectional shunt and then, as the resistance further decreases, a dominant left-to-right shunt across the ductus arteriosus prevails. In a complex cascade involving increase in oxygen concentration and changes in levels of circulating mediators, the ductus arteriosus constricts and eventually closes.
4. The systemic vascular resistance increases following closure of the umbilical vessels and loss of the low-resistance vascular system of the placenta.

The two circulations are now connected in series. After further reduction in pulmonary vascular resistance, and functional closure of the foramen ovale and ductus arteriosus, the majority of the right ventricular stroke volume reaches the left ventricle after oxygenation (Figure 56.2b). The left ventricle pumps the oxygenated blood to the entire body, working against a slightly higher resistance than that of the pulmonary circulation. The previously dominant right ventricle pumps into the low-pressure system of the pulmonary circulation. In comparison to the prenatal circulation, the left

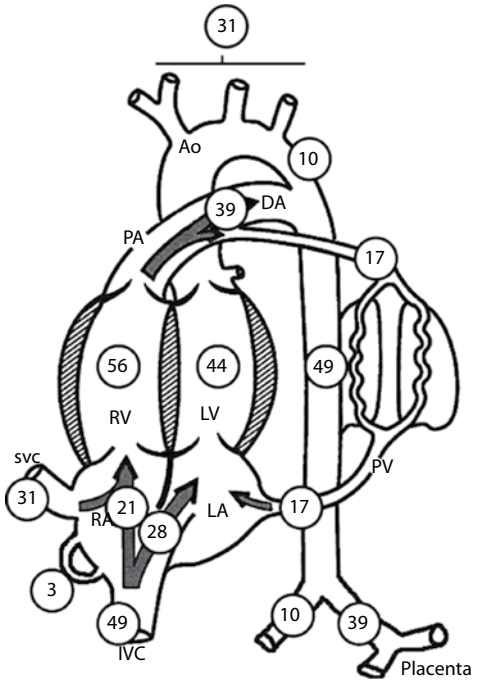


**Figure 56.1**
Percentages of the combined ventricular output in the late gestation human fetus. Right and left ventricle work in parallel, blood is pumped from the right ventricle through the pulmonary trunk to the descending aorta via the ductus arteriosus. The fetal right ventricle ejects about 56% of the combined ventricular output, perfusing the lower body and the placenta. The remaining output is handled by the left ventricle, with most of this blood being directed to the head and the coronary arteries. Antenatally only 10% of the combined ventricular output crosses the isthmus region to the descending aorta. The direction of flow is indicated by arrows. (Ao, aorta; DA, ductus arteriosus; IVC, inferior vena cava; LA, left atrium; LV, left ventricle; PA, pulmonary artery; PV, pulmonary venous return; RA, right atrium; RV, right ventricle; SVC, superior vena cava.) (Adapted from Rudolph AM. *Congenital Diseases of the Heart: Clinical-Physiological Considerations*. 3rd ed. Vols. 1–36. Wiley-Blackwell; 2009:87–147.[1])

ventricle now functions with a higher volume load against an increased pressure and resistance.

Consequently, compensation for pressure or volume load between the two circulatory systems is impossible once the fetal communications are completely closed and the two systems are separated.

The hemodynamic changes during and after birth comprise two phases:

- The immediate postnatal changes during the first few minutes after delivery and establishment of the neonatal circulation over the first 10–15 hours after birth.
- Gradual adaptation to postnatal pressure and resistance conditions during the first 6 weeks of life.

## Establishment of the neonatal circulation

### Closure of the ductus arteriosus

In infants born at term, initial "functional" closure of the ductus occurs within 10–15 hours of birth. The ductus arteriosus narrows gradually during the first 2–7 hours of life. Following clamping of the umbilical cord, a bidirectional shunt via the ductus arteriosus persists for a few hours. With further decrease in the pulmonary vascular resistance, the bidirectional shunt will be replaced by a left-to-right shunt. Contraction and shortening of the ductus arteriosus, migration of smooth muscle cells from the media, and the development of intimal cushions close the mature ductus arteriosus within 3–4 days.[3–5] Classic theories of normal spontaneous ductal closure include a combination of direct smooth muscle contractility in response to the postnatal increase in $PO_2$, reduction in the levels of prostaglandins, and also a decrease in the sensitivity of ductal tissue to the dilating influences of prostaglandins. Rapid histological changes lead to obliteration of the lumen and prevent reopening. These processes result in permanent anatomical occlusion and replacement by a fibrous ligament (ligamentum arteriosum) over the first 2–3 weeks.

The contraction of the ductal tissue causes an anatomical narrowing of the descending part of the aorta in the area of the aortic isthmus. In consequence, aortic isthmus stenosis becomes apparent after complete closure of the arterial duct. Heart defects with duct-dependent pulmonary or systemic perfusion become increasingly symptomatic with progressive ductus constriction (see Chapter 53). The duct will remain open if the normal response at birth is interrupted by changes in the histologic architecture of the ductal tissue, or changes in the oxygen tension at birth. The exact mechanisms causing closure failure in some premature and full-term infants remain unknown.

### Functional closure of the foramen ovale and ductus venosus

The closure of the foramen ovale is functional initially and eventually anatomical; the foramen ovale has been found to be probe patent in up to 20% of adults studied postmortem. The patency of the foramen ovale can be crucial for initial survival and palliation of severe cardiac lesions such as simple transposition of the great arteries or those with single-ventricle physiology. The ductus venosus will be closed in 75% of all cases by the seventh day of life.[6]

### Function of the ventricles

The postnatal demands on the right ventricle are less than in fetal life as the right ventricle supplies blood only to the lower-resistance pulmonary circulation (Figure 56.3). The myocardium of the right ventricle, which has been the dominant ventricle in the fetus, adapts to the falling pulmonary resistance and pressure. However, an increased pressure and volume load due to congenital heart disease can be compensated by the *in utero*–trained right ventricle. Birth is associated with major metabolic requirements: respiratory work and thermoregulation require 50%–60% of the oxygen consumed by the newborn. Thus, oxygen consumption nearly triples at birth. In order to supply the increased oxygen demand, the left ventricular output nearly triples. The left ventricle has to deal abruptly with higher resistance following loss of the placental vascular bed as well as higher volume, because of

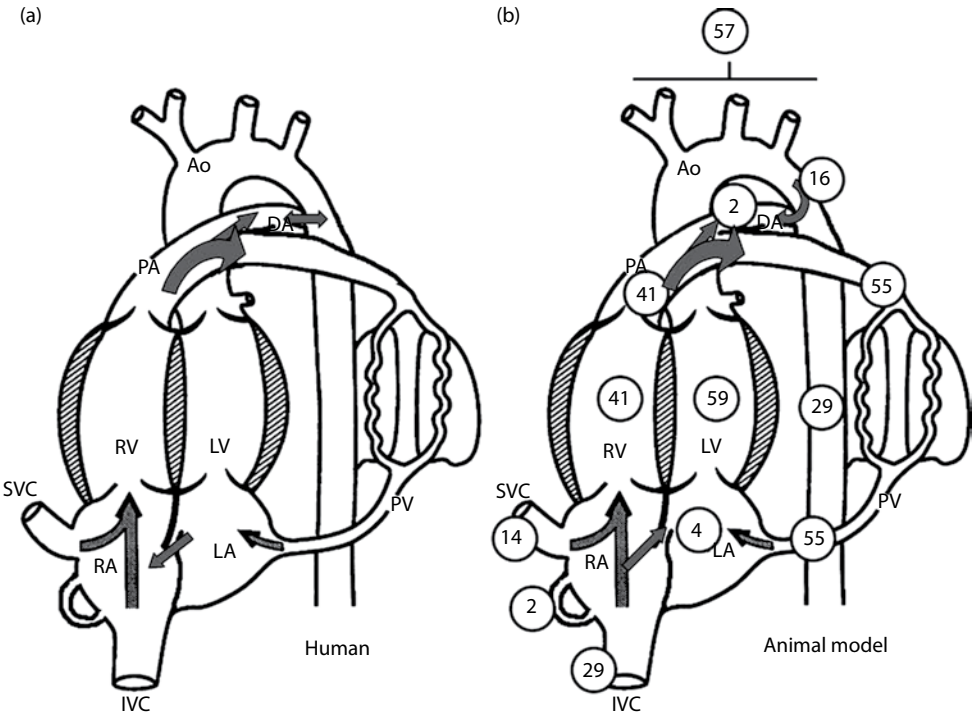


**Figure 56.2**
Transitional circulation. (a) Transitional circulation after birth in the human and (b) in the animal models. Ventilation produces a fall in pulmonary vascular resistance and an increase in pulmonary blood flow, thus reducing the flow across the ductus arteriosus. Left atrial pressure surprasses right atrial pressure, resulting in partial closure of the foramen ovale with a left-to-right shunt. The increased peripheral vascular resistance following umbilical cord occlusion increases the systemic arterial pressure and resistance. (b) The percentages of the combined cardiac output after ventilation with oxygen and umbilical cord occlusion in fetal lambs. The left ventricular output increases from 35% in the fetal lamb to 59% and is slightly higher than that of the right ventricle (41%). The occlusion of the umbilical cord increases the systemic arterial pressure and the left-to-right shunt across the ductus arteriosus. (Adapted from Rudolph AM. In: Moller JH, Hoffmann JIE, eds. *Pediatric Cardiovascular Medicine*. 2nd ed. Vol. 4. Oxford: Wiley-Blackwell; 2012:33–45.[2])

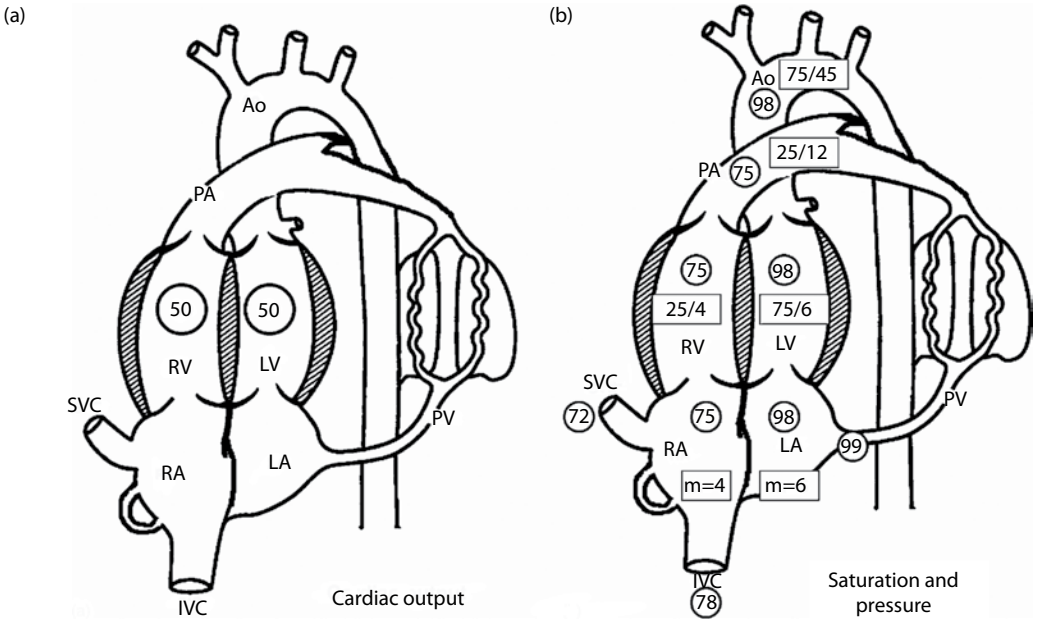


**Figure 56.3**
Serial circulation after closure of fetal communications. (a) In serial circulation, percentages of the total cardiac output are similar in the pulmonary and systemic circulation. (b) Circled figures represent percentages of oxygen saturation; the other numbers represent intracavity pressures for the infant after completed transition. There is no mixing of pulmonary and systemic circulations after closure of fetal shunts.

the increased pulmonary venous return. A further increase in afterload (e.g., due to aortic valve stenosis or coarctation) or preload (e.g., due to an increased volume burden by a large ductus arteriosus or ventricular septal defect) can be tolerated only to a limited extent and may lead to early decompensation. The diastolic function—myocardial relaxation and compliance—also undergoes a maturation process during the first 6 months of life and is especially affected during the first 2 weeks after birth.[7]

Postnatal adaptation of the myocyte to the changing volume and pressure load is complex. Understanding of the differences between fetal left and right ventricular cardiomyocytes is lacking, though clearly divergences in growth trajectories that begin *in utero* set the stage for cardiac function after birth.[8]

### Pulmonary vascular resistance

The pulmonary vascular resistance is mainly determined by the number of peripheral pulmonary vessels and their state of vasoconstriction. This is the cardinal part of the transitional circulation.

The clearance of the alveolar fluid occurs during the first 4–6 hours of life. The pulmonary vascular resistance is reduced by the opening of the alveoli, ventilation with oxygen, loss of vasoconstrictors produced *in utero*, and local vasodilators.[9,10] Pulmonary resistance vessels constrict under the influence of hypoxemia, hypercapnia, or acidosis. Neonatal drug treatment and ventilation make particular use of the pronounced reactivity of the pulmonary vessel bed.

## Adaptation of the pulmonary vascular resistance to postnatal life

The pioneering studies of Rudolph and Heymann made a major contribution to the understanding of the postnatal adaptation of healthy newborns and those with congenital heart defects. Within 24 hours after birth, the pulmonary arterial pressure drops to half the systemic pressure, and after 6 weeks of life it reaches adult values[11,12] (Figure 56.4). The postnatal lung development is anatomically characterized by vascular remodeling, muscular involution, and development of the alveoli.[9,10,16,17]

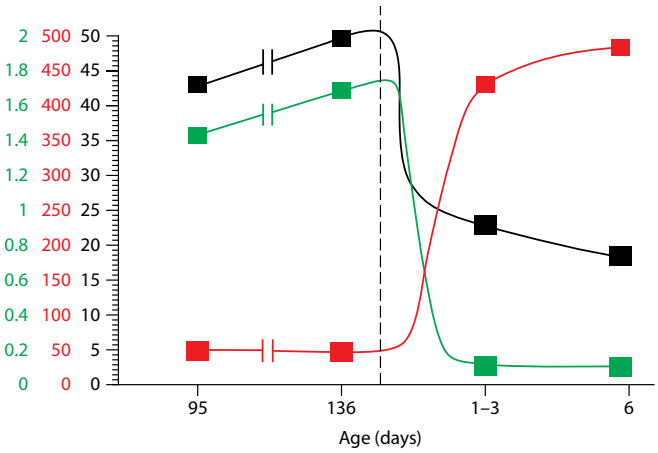


**Figure 56.4**
The changes in pulmonary arterial pressure (black line—torr), blood flow (red line—mL/min/kg), and vascular resistance (green line—mmHg/mL/min/kg) that occur around birth. After the initial rapid decrease in pulmonary vascular resistance and pulmonary arterial blood pressure, there is a slow, progressive decrease, with adult levels being reached after 6 weeks. (Adapted from Fineman JR et al. In: Allen HD, Adams FH, Moss AJ, eds. *Moss and Adams' Heart Disease in Infants, Children, and Adolescents*. 6th ed. Philadelphia, PA: Lippincott Williams and Wilkins; 2001:41–52[13], with data in Morin FC III and Egan E. *J Appl Physiol* 1992;73:213–8[14] and Soifer SJ et al. *J Dev Physiol* 1983;5:237–50.[15])

# *Transition from fetal to postnatal circulation of the fetus with congenital heart disease: Implications of perinatal management*

In the fetus, both ventricles eject into a single vascular bed. As only one ventricle is necessary to maintain the fetal requirements, most fetuses with congenital cardiac malformations grow and develop normally *in utero*. If there is obstruction of an efferent vessel, blood is able to flow via the ductus arteriosus and/or foramen ovale to the neighboring circulatory system.

The point in time of closure of the fetal communications does not differ between the healthy mature newborn and the mature newborn with a congenital heart defect. Thus, major heart defects that are well compensated *in utero* often decompensate during the transition phase from fetal to postnatal circulation. The sequence and timing of transition determine the moment of decompensation and the timing of any therapeutic intervention for the various duct-dependent congenital heart defects.

## Clinical presentation of duct-dependent heart defects

The transition of the circulation and closure of the vital fetal shunts occur at the same times in healthy newborns, and in those with duct-dependent heart defects. This allows for an initial, symptomless postnatal adaptation, but subsequently, symptoms develop as the patent ductus arteriosus constricts (Table 56.1). Chapter 53 deals in detail with the pathophysiology of the perinatal transition in these cases.

Hypoplasia or obstruction of the right or left ventricle and hypoplasia of the aortic arch are the major duct-dependent heart defects. Duct patency is important to maintain adequate circulation in babies with transposition of the great arteries as well. The persistence of fetal communications is essential for supplying adequate perfusion and oxygen delivery.

### Presentation of heart defects with duct-dependent systemic circulation

The hypoplastic left heart syndrome can be used as a perfect example of a duct-dependent systemic circulation. In hypoplastic left heart syndrome, the oxygenated pulmonary venous

**Table 56.1** Clinical presentation of duct-dependent heart disease

| *Early cyanosis* | *Hypotension, acidosis congestive heart failure* | *Hypotension, acidosis >24 hours* |
|---|---|---|
| Duct-dependent pulmonary blood flow | Duct-dependent systemic blood flow | Duct-dependent blood-flow of the lower body |
| Pulmonary atresia | Hypoplastic left heart syndrome | |
| Critical pulmonary stenosis | Critical aortic stenosis | Critical coarctation |
| Severe tetralogy of Fallot | Interrupted aortic arch | |
| Duct-dependent mixing | | |
| Transposition of great arteries | | |

*Note:* Duct-dependent pulmonary flow and inadequate mixing presents as early cyanosis that is unresponsive to oxygen therapy. In duct-dependent systemic blood flow, compromise of systemic perfusion occurs with ductal constriction.

blood reaches the systemic circulation via the foramen ovale and the right ventricle, mixing with the systemic venous blood. The right ventricle pumps both the systemic and the pulmonary venous return into the pulmonary artery, pulmonary arterial branches, and via the ductus arteriosus to the aorta. The aortic arch, the head, and the coronary arteries are perfused in a retrograde fashion with relatively deoxygenated blood (Figure 56.5). The same blood mixture supplies the lower body. Progressive narrowing of the ductus arteriosus, which is the only pathway to the systemic circulation, leads to a fall in the blood pressure and underperfusion of the central and peripheral organs, including the coronary circulation. Tachypnea, hypotension, pronounced acidosis, and moderate cyanosis may lead to the erroneous presumptive diagnosis of neonatal sepsis or metabolic disorder. Progressive ductus arteriosus occlusion leads to progressive decrease in systemic circulation, resulting in acute coronary hypoperfusion, shock, multiorgan failure, and eventually death. Early use of prostaglandin derivatives can prevent ductal occlusion for a limited period of time.

The functionally single right ventricle serves the pulmonary and systemic circulation. The proportion of the ventricular output that goes to the pulmonary or systemic vascular bed is determined by the relative resistance to flow within the two circuits. As the pulmonary resistance continues to drop, more blood preferentially reaches the pulmonary circulation (Qp) than the systemic circulation (Qs). The resulting

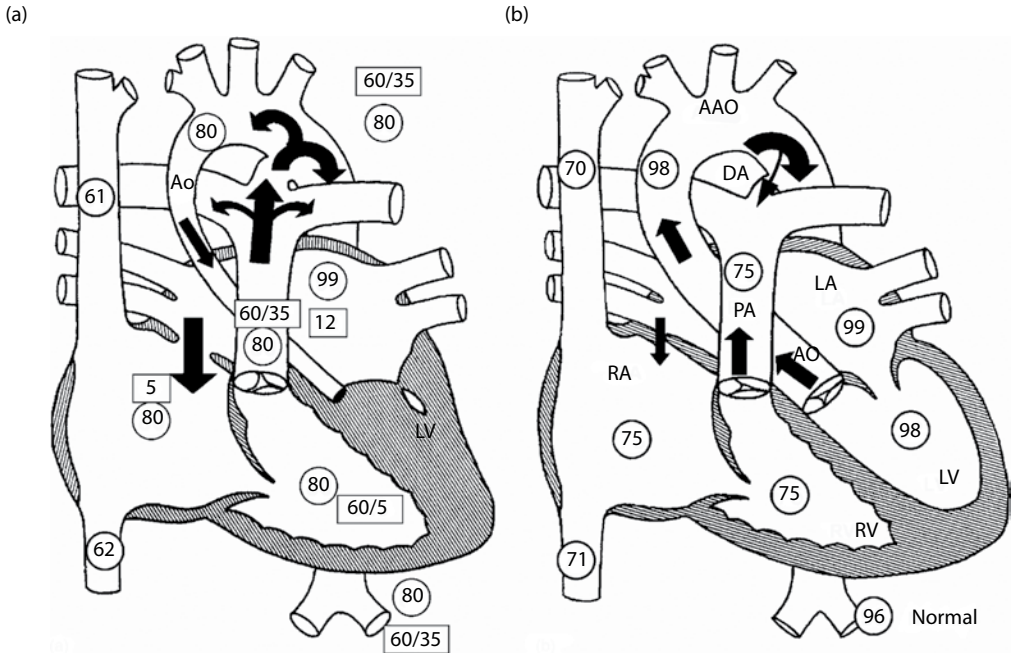


**Figure 56.5**
Circulation in hypoplastic left heart syndrome (HLHS). (a) Blood flow, $O_2$ saturations (circled values), and pressures (values in boxes). (b) A depiction of the blood flow and saturations in the normal neonate. In HLHS, systemic blood flow is served by the right ventricle via the pulmonary artery and ductus arteriosus, with retrograde perfusion of the upper trunk and coronary arteries. Pulmonary venous return enters the right heart through the mildly restrictive foramen ovale. The resultant arterial $O_2$ saturation of 75%–80% represents balanced pulmonary and systemic blood flow (Qp:Qs = 1). (Qp, pulmonary blood flow [L/min]; Qs, systemic blood flow [L/min].) (Adapted from Mullins CE, Mayer DC, eds. *Congenital Heart Disease. A Diagrammatic Atlas*. New York, NY: Alan R Liss; 1988.[18])

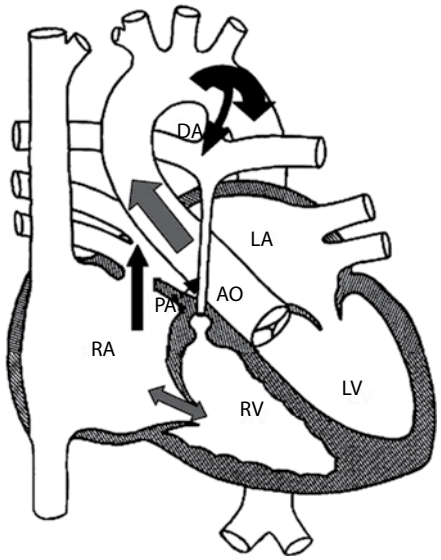


**Figure 56.6**
Circulation in pulmonary atresia with hypoplastic main pulmonary artery. Pulmonary blood flow is served by the left ventricle via the aorta and the ductus arteriosus which has a typical vertical shape. The systemic venous return drains across the open foramen ovale into the left atrium (right-to-left shunt). There is no antegrade flow across the pulmonary valve, and the right ventricle is decompressed by tricuspid regurgitation. (Adapted from Mullins CE, Mayer DC, eds. *Congenital Heart Disease. A Diagrammatic Atlas*. New York, NY: Alan R Liss; 1988.[18])

increased lung perfusion (Qp > Qs) causes a severe volume overload of the right ventricle, which may already suffer from ischemia due to coronary hypoperfusion. Therefore, intensive medical interventions aim to recognize duct-dependent heart defects as early as possible, as well as regulate pulmonary and systemic perfusion.

### Congenital heart defect with duct-dependent pulmonary circulation

Obstructions to pulmonary blood flow such as tricuspid atresia, pulmonary atresia, and heart disease with severe right ventricular dysfunction, such as severe Ebstein malformation, have a duct-dependent pulmonary circulation (Figure 56.6). Clinical signs are progressive cyanosis within a few hours of birth as the patent ductus arteriosus constricts, which does not improve following treatment with oxygen (hyperoxia test).

### Congenital heart disease with duct-dependent mixing

The simple transposition of the great arteries is characterized by parallel arrangement of both circulations: the highly saturated pulmonary venous return reaches the left ventricle and recirculates via the pulmonary artery into the lung; the low saturated systemic venous return reaches the right ventricle, is ejected into the aorta, and recirculates throughout the body. In transposition of the great arteries with an intact ventricular septum, only a small portion of blood is exchanged by mixing between the two circulations (Figure 56.7a). The monitored

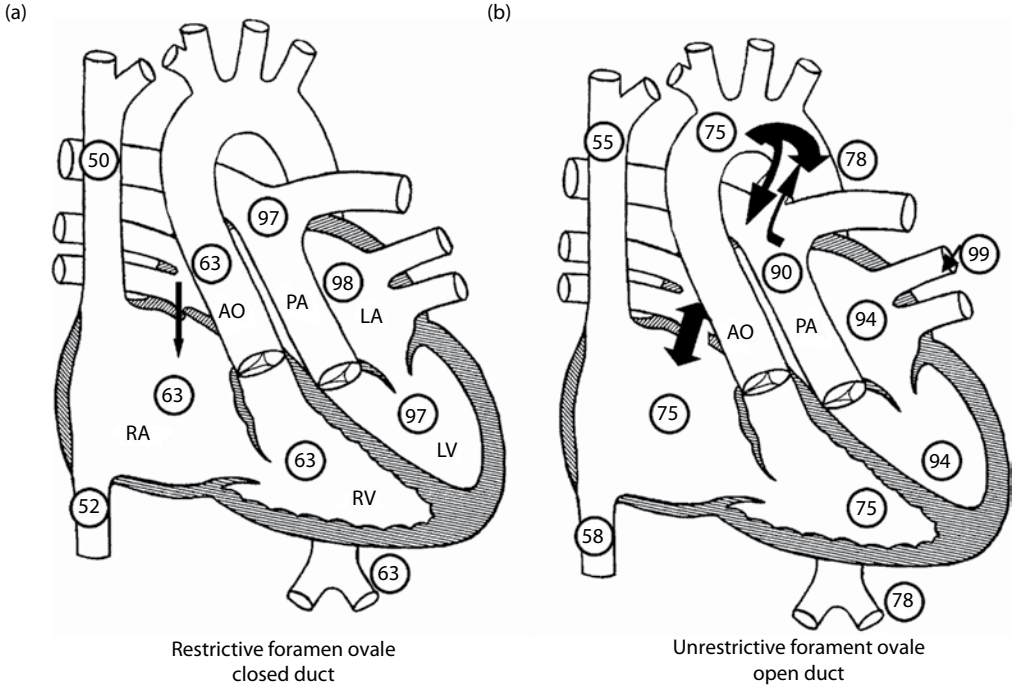


**Figure 56.7**
Circulation in transposition of the great arteries. Parallel connection of the systemic and pulmonary circulation. Arterial $O_2$ saturation reflects mixing between pulmonary and systemic circulations. (a) The ductus arteriosus is already closed; the atrial right-to-left shunt is restrictive and allows minimal mixing. The oxygen saturation of the aorta is similar to the right ventricle, and hence, the neonate appears deeply cyanotic. (b) Opening of the arterial duct by prostaglandin E1 (PGE1) and, most important, of the foramen ovale by balloon-atrial septostomy allows increased mixing and improvement of cyanosis. (Adapted from Mullins CE, Mayer DC, eds. *Congenital Heart Disease. A Diagrammatic Atlas*. New York, NY: Alan R Liss; 1988.[18])

oxygen saturation reflects the magnitude of mixing between the systemic and pulmonary circulation. Although shunting across the patent ductus arteriosus is typically bidirectional, only left-to-right-shunting across the foramen ovale allows highly saturated blood to reach the ascending aorta and through it the coronary circulation as well as head and neck vessels. To a certain extent, an open duct facilitates an exchange between the two circulations; however, the limiting factor is not the size of the ductus, but that of the atrial shunt through the foramen ovale (Figure 56.7b). Enlarging the atrial communication by balloon atrioseptostomy allows an increase in left-to-right shunt across the foramen ovale and significant increase in aortic oxygen saturation.

## Pulmonary hypertension in persistent fetal circulation and total anomalous pulmonary venous return

In persistent pulmonary hypertension, a disturbance of the normal neonatal circulatory transition process is observed. The pulmonary vascular resistance does not drop but instead remains at a high level or even increases. In this situation, the right-to-left shunts at the atrial and ductal levels persist. The reasons for pulmonary hypertension are manifold (meconium aspiration, asphyxia, and hypoplastic lungs) and beyond the scope of this chapter. The therapeutic options to decrease the pulmonary vascular resistance are ventilation with oxygen, hyperventilation, administration of surfactant, nitric oxide, use of vasodilators, and special ventilation regimes, such as high-frequency ventilation or in extreme cases the employment of extracorporeal membrane oxygenation.[12]

Total anomalous pulmonary venous return with obstruction is difficult to distinguish from other causes of persistent pulmonary hypertension. In this lesion, all pulmonary veins drain anomalously into the systemic venous circulation rather than into the left atrium. The systemic perfusion is therefore dependent on the right-to-left shunt via the foramen ovale. The clinical presentation of a neonate with total anomalous pulmonary venous return is typically based on whether the anomalous draining veins are obstructed or not. Infants with obstruction present with severe, sometimes suprasystemic pulmonary hypertension, profound hypoxemia, pulmonary edema, and low cardiac output. Therapy in this condition is an urgent surgical intervention.

A prenatal increase in the pulmonary vascular resistance, as seen in cases of intrauterine constriction of the ductus arteriosus or a restrictive interatrial communication in hypoplastic left heart syndrome,[19] causes hypertrophy of the media of the pulmonary vessels prenatally and severe pulmonary hypertension postnatally.

## Pulmonary hypertension in cardiac shunt defects

All congenital heart defects with large-volume shunts at the ventricular and especially at the great artery level with unrestricted pulmonary blood flow are at an extremely high risk of developing irreversible pulmonary vascular disease during the first year of life. These lesions include common truncus arteriosus, transposition of the great arteries with ventricular septal defect or with persistent ductus arteriosus, single ventricle without pulmonary stenosis, large ventricular septal defect, aortopulmonary window, and large persistent DA (ductus arteriosus).

For most other congenital heart defects, the adaptation from the fetal to the neonatal circulation causes a more gradual increase in the pressure and volume load. These include shunt lesions such as ventricular septal defects, atrioventricular septal defects, and mild valvar stenosis. Chapter 53 deals in more detail with the pathophysiology of these defects.

The presentation of heart failure due to shunt connections depends on the size of the defect, its location, and the rate of the decrease in pulmonary vascular resistance.

For many patients, especially those newborns with trisomy,[20] the reduction in pulmonary resistance is not as rapid or as pronounced as in healthy newborns; in consequence, these babies may develop a less severe degree of heart failure. The normal development of the pulmonary arteries proceeds more slowly. The pulmonary vascular resistance remains three to four times higher than normal but still allows for a significantly increased pulmonary flow (Figure 56.8). For these babies, the excessive pulmonary flow also results in

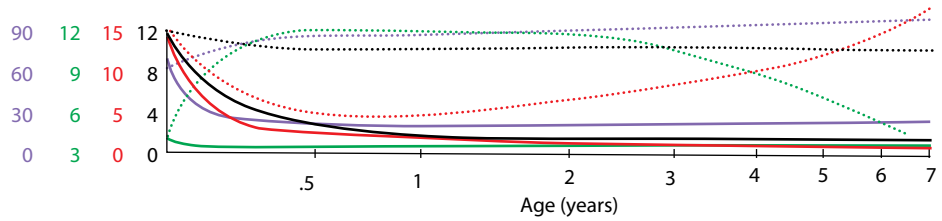


**Figure 56.8**
Postnatal changes in infants with (dotted lines) and without (solid lines) large ventricular septal defects (black—medial muscle as % of vessel diameter). In children with large ventricular septal defect, high pulmonary arterial pressure (blue—mm Hg) persists. The pulmonary vascular resistance falls more slowly after birth and does not reach normal levels. Associated with the fall in pulmonary vascular resistance (red—units/$m^2$), pulmonary blood flow (green—L/min/$m^2$) increases due to left-to-right shunting. After a variable period, the pulmonary vascular resistance begins to increase due to secondary changes of the pulmonary vessels; this is associated with a fall of pulmonary blood flow. (Adapted with permission from Rudolph AM. *Congenital Diseases of the Heart: Clinical-Physiological Considerations*. 3rd ed. Vols. 1–36. Hoboken, NJ: Wiley-Blackwell; 2009:87–147.[1])

reactive changes to the pulmonary vessels. Dysfunction of the endothelium causes a diminished production of vasoconstrictors such as nitric oxide. Increased production of vasoconstrictors leads to vasoconstriction, stimulating the proliferation of smooth muscle cells and fibroblasts and increasing the production of prothrombotic substances. Extended muscularization of the peripheral arteries and decreased diameter of the pulmonary vascular bed is histologically detectable.[9,16] In consequence, the development of pulmonary hypertension is reversible only for a short time. Without timely palliative or corrective intervention, serious pulmonary vessel changes with irreversible pulmonary hypertension (Eisenmenger syndrome) occurs. In this situation, the patient is rendered inoperable. Early corrective measures within the first 3–6 months of life or palliative interventions during the neonatal period, such as pulmonary artery banding, prevent this condition.

Further congenital heart defects that may cause deterioration during the neonatal or infant period are listed in Table 56.2.

### Cardiac malformations without anticipated neonatal problems

In isolated small ventricular septal defects, atrial septal defects, and small ductus arteriosus, there is no need for therapy in the neonatal period. Large atrial communication or partial anomalous pulmonary venous return to the right pump may lead to large left-to-right shunts, yet the neonate is rarely compromised (see Chapter 53).

## Drug or other interventional treatment of congenital heart disease in the neonate

### *Principles of intensive therapy*

The objective is to ensure a balanced circulation with sufficient pulmonary (Qp) and systemic (Qs) blood flow (Table 56.2). In neonates with ductal-dependent heart malformations, the ductus arteriosus patency can be maintained by administration of prostaglandins E1 and E2 (PGE1 and PGE2) for days and sometimes weeks until a more stable solution is provided. If an atrial level shunt is essential, such as in neonates with transposition of the great arteries, balloon atrial septostomy may be performed either bedside with echocardiographic guidance, or in the catheterization laboratory.

The pulmonary vascular resistance that decreases gradually postpartum can also be influenced by medical or ventilatory interventions. Preoperative stabilization and optimal organ perfusion must be established following previous circulatory insufficiency or multiorgan failure. Preoperatively, restored organ function is essential for survival in the pre- and postoperative periods for surgical interventions with or without extracorporeal circulation.

### Opening of the ductus arteriosus with prostaglandins

The effect of PGE1 and PGE2 on ductal tissue is dependent on the dose applied, the age of the newborn, the blood oxygen concentration, and the arterial pH. While a small dose is sufficient in neonates with a patent ductus arteriosus, a significantly higher dose with a correspondingly greater incidence of side effects is necessary in newborns with an obstructed or already closed ductus arteriosus (Table 56.3). Side effects are dose dependent. Additional inspired oxygen should be avoided. Because of the possibility of spontaneous ductal closure even with high-dose prostaglandin therapy, PGE1 treatment should be used only as a short-term palliative measure. Further palliative or corrective interventions should be performed as soon as the patient is in a clinically appropriate state.

### Regulation of pulmonary perfusion

Pulmonary perfusion can be influenced by regulation of pulmonary vascular resistance. High resistance reduces pulmonary perfusion, and low resistance increases pulmonary perfusion. Oxygen supply and hyperventilation (decreased $CO_2$), nitric oxide, prostacyclin, and other vasodilators that reduce pulmonary arterial resistance are used in situations with decreased pulmonary perfusion, for example, in persistent fetal circulation or pulmonary-hypertensive crisis.[22] Hypercapnia, acidosis, and hypoxemia increase pulmonary vasoconstriction (Figure 56.9).

### Balance of pulmonary and systemic perfusion in single-ventricle physiology

In neonates with single-ventricle physiology and duct-dependent pulmonary or systemic flow (e.g., hypoplastic right heart syndrome or hypoplastic left heart syndrome, respectively), the extent of pulmonary (Qp) or systemic (Qs) perfusion depends on the relation between pulmonary vascular resistance and systemic resistance. In case of increased pulmonary resistance, the pulmonary blood flow decreases (lower Qp), and the systemic blood flow increases. In single-ventricle physiology, a balanced ratio of pulmonary to systemic blood flow has to be achieved in order to avoid ventricular overload and dysfunction and yet provide adequate oxygenation. The ideal situation is an equalization of pulmonary and systemic blood flow with $Qp = Qs$. The blood oxygen concentration can therefore be seen as a sensitive marker for the relation of pulmonary to systemic perfusion: when $Qp = Qs$: $SaO_2$ ~75%; $Qp \gg Qs$: $SaO_2 > 85\%$; $Qp \ll Qs$: $SaO_2 < 70\%$ (Figure 56.10). In a balanced situation, the $SaO_2$ is approximately 75%, $PCO_2 \sim 45$ mm Hg, $PO_2 \sim 35$ mm Hg.

If the pulmonary blood flow increases (high Qp), the oxygen saturation increases to the detriment of the systemic circulation (reduced Qs), the single ventricle cannot maintain the needed increased output, and this is then followed by hypotension and reduced organ perfusion. In a balanced situation, the pulmonary blood flow remains high enough to

**Table 56.2** Postnatal physiology and hemodynamics; medical, interventional, and surgical therapy in the neonatal period; and mid- to long-term interventions in various congenital heart defects

| *Congenital heart defect* | *Postnatal physiology* | *Duct dependent* | *Perinatal management* | *Transcatheter intervention in the neonate* | *Surgical intervention in the neonate* | *Interventions and problems in medium- and long-term follow-up* |
|---|---|---|---|---|---|---|
| Critical aortic stenosis | Compromise of systemic perfusion with ductal constriction; low output syndrome, shock | + | PGE<br>Univentricular (staged Norwood-procedures) or biventricular approach? | First choice: interventional balloon valvuloplasty<br>in borderline cases: ductal stenting and bilateral pulmonary banding | Biventricular approach: surgical valvotomy; tunnel subaortic stenosis with hypoplastic aortic valve: Ross-Konno procedure; univentricular: Norwood-Sano procedure; alternative: cardiac transplantation | Restenosis: redilatation, surgical revalvuloplasty; valve regurgitation: Ross procedure, valve replacement |
| Moderate aortic stenosis | Increased left ventricular pressure load | – | Careful follow-up | | | Interventional balloon angioplasty if transaortic gradient >50 mm Hg or symptoms |
| Hypoplastic left heart syndrome | Compromise of systemic perfusion with ductal constriction; low-output syndrome, acidosis; shock | + | Parental counseling; PGE; avoidance of right ventricular volume and pressure overload; therapeutic goal: $O_2$ saturations between 70% and 80%, PCO; 45–50 mm Hg, $PO_2$ 35 mm Hg, balancing of pulmonary and systemic vascular resistance to achieve adequate flow into both vascular beds | Palliative in patients with high surgical risk; stenting of the ductus arteriosus and surgical bilateral banding of the pulmonary arteries | First choice: modified Norwood-Sano procedure or cardiac transplantation | After Norwood procedure: bidirectional cavopulmonary shunt (Glenn shunt), modified [fenestrated] Fontan repair [followed by interventional occlusion of fenestrations]; interventional occlusion of collaterals; balloon dilatation of recoarctation; balloon dilatation of surgical anastomoses, late cardiac transplantation |

(*Continued*)

**Table 56.2 (Continued)** Postnatal physiology and hemodynamics; medical, interventional, and surgical therapy in the neonatal period; and mid- to long-term interventions in various congenital heart defects

| *Congenital heart defect* | *Postnatal physiology* | *Duct dependent* | *Perinatal management* | *Transcatheter intervention in the neonate* | *Surgical intervention in the neonate* | *Interventions and problems in medium- and long-term follow-up* |
|---|---|---|---|---|---|---|
| Hypertrophic (obstructive) cardiomyopathy | Reduced systolic and diastolic ventricular function | – | Beta-blockers, diuretics; exclude metabolic or mitochondrial disease; exclude associated syndromes; examine family members | | | Myotomy-myectomy; transluminal myocardial ablation; dual chamber pacemaker; cardiac transplantation |
| Aortic coarctation | Critical coarctation: ductal-dependent perfusion of the lower limb, hypertension of the upper limb, increased left ventricular pressure load | (+) | PGE in critical coarctation; check for other cardiac malformations | Balloon dilatation in circumscribed stenosis; balloon dilatation and/or stenting in critically ill neonates | First choice: surgical repair: resection and end-to-end repair or subclavian flap | Restenoses: balloon dilatation or stent placement; hypertension |
| Interrupted aortic arch | See critical coarctation | + | PGE | | Surgical repair | Balloon dilatation of restenosis or stent placement |
| Mitral stenosis | Dependent on associated lesions; inflow in the left ventricle is disturbed; decompression of the left atrium across the foramen ovale | (+) | In single-ventricle hemodynamic: PGE and atrial septostomy | Palliative: mitral valve balloon valvotomy (rare) | Supravalvular ring: surgical resection; severe mitral valve stenosis associated with left ventricular hypoplasia: Norwood palliation | |
| D-transposition of the great arteries | Parallel outputs of systemic right and pulmonary left ventricle; $O_2$ saturation dependent on magnitude of mixing between both circulations (foramen ovale, ductus, VSD) | + | PGE<br>Dependent on the $O_2$ saturation (foramen ovale, VSD): balloon atrial septostomy | Balloon atrial septostomy | Arterial switch operation day 7–14 | If arterial switch not possible: staged repair after pulmonary banding, Rastelli repair |
| L-transposition of the great arteries | Dependent on associated lesions (VSD, PS, WPW syndrome) | (+) | | | Classic repairs of associated lesions | Dysfunction of the right systemic ventricle |

| | | | | | | |
|---|---|---|---|---|---|---|
| Double-inlet left (single) ventricle | Hemodynamics dependent on pulmonary stenosis | – | Dependent on associated pulmonary stenosis or subaortic stenosis | Severe pulmonary stenosis: balloon dilatation | Severe pulmonary stenosis: Blalock-Taussig shunt; no pulmonary stenosis: pulmonary banding; severe subaortic stenosis: Damus-Kaye-Stansel | Modified Fontan repair |
| Double-outlet right ventricle without pulmonary stenosis | Pulmonary overflow; congestive heart failure | – | Treatment of heart failure | | Pulmonary banding or early corrective surgery | Surgical: modification dependent on the position of the VSD and associated malformations |
| Double-outlet right ventricle with pulmonary stenosis | See Tetralogy of Fallot | (+) | Associated with severe pulmonary stenosis: PGE | In severe pulmonary stenosis: balloon dilatation | In severe pulmonary stenosis: Blalock-Taussig shunt | Intraventricular tunnel repair/Rastelli procedure |
| Critical pulmonary stenosis/membranous pulmonary atresia | Ductal-dependent pulmonary flow; increased pressure load of the right ventricle; right-to-left shunt across foramen ovale | + | PGE | First choice: balloon dilatation; membranous PA: perforation of membrane and balloon dilatation in cases with well-developed right ventricle and pulmonary arteries, otherwise as palliative procedure in poor surgical patients; ductal stenting | Surgical valvotomy and/or palliation by Blalock-Taussig shunt | Redilatation in restenosis; homograft in severe pulmonary insufficiency or stenosis; 1.5 ventricle repair when RV is hypoplastic |
| Pulmonary atresia with intact ventricular septum | See critical pulmonary stenosis | + | PGE; biventricular or univentricular repair? (dependent on right ventricular morphology, the development of pulmonary arteries, and the presence of right ventricular dependent coronary artery circulation) | | Surgical valvotomy and/or reconstruction of the right ventricular outflow tract and/or palliation by Blalock-Taussig shunt to maintain sufficient pulmonary blood supply | Redilatation in restenosis; homograft in severe pulmonary insufficiency or stenosis; 1.5 ventricle repair or univentricular repair when RV is hypoplastic |

(*Continued*)

**Table 56.2 (Continued)** Postnatal physiology and hemodynamics; medical, interventional, and surgical therapy in the neonatal period; and mid- to long-term interventions in various congenital heart defects

| *Congenital heart defect* | *Postnatal physiology* | *Duct dependent* | *Perinatal management* | *Transcatheter intervention in the neonate* | *Surgical intervention in the neonate* | *Interventions and problems in medium- and long-term follow-up* |
|---|---|---|---|---|---|---|
| Pulmonary stenosis | Increased pressure load of the right ventricle, reduced pulmonary blood flow | – | Careful follow-up | Balloon dilatation if right ventricular pressure 2/3 to left systemic pressure or if symptoms | Rare: surgical valvuloplasty | Redilatation in restenosis; homograft in severe pulmonary insufficiency or stenosis |
| Tetralogy of Fallot | Hemodynamics dependent on severity of right ventricular outflow obstruction and hypoplasia of the pulmonary valve and arteries | (+) | In severe pulmonary stenosis, PGE; beta-blockers to prevent hypoxic spells | Balloon valvotomy in severe pulmonary stenosis (and high surgical risk) | Blalock-Taussig shunt in severe pulmonary stenosis; early repair | Repair: interventional coil, occlusion of main aortopulmonary collaterals; homograft in pulmonary insufficiency, right ventricular dysfunction, ventricular arrhythmia |
| Pulmonary atresia with ventricular septal defect or tetralogy of Fallot with severe pulmonary stenosis and main aortopulmonary collaterals (MAPCAS) | Pulmonary perfusion dependent on ductus arteriosus and main aortopulmonary collaterals | (+) | PGE | Palliative: stenting of the ductus arteriosus or main aortopulmonary collaterals | Palliative: systemico-to-pulmonary artery shunt with or without right ventricular outflow tract reconstruction; early corrective surgery | In case of MAPCAS without central pulmonary arteries: unifocalization; right-ventricular pulmonary artery conduit; interventional coil; occlusion of main aortopulmonary collaterals; right ventricular dysfunction; ventricular arrhythmia |
| Tricuspid atresia | Right-to-left shunt across foramen ovale, hemodynamics dependent on associated lesions | (+) | PGE in TA + PS or TA + PA or TA + transposition + restrictive VSD or coarctation | Atrial septostomy when foramen ovale is restrictive | Blalock-Taussig shunt in ductal-dependent pulmonary perfusion; coarctation repair, pulmonary banding in pulmonary overflow | Modified Fontan repair |

| | | | | | | |
|---|---|---|---|---|---|---|
| Ebstein anomaly | Hemodynamics dependent on right ventricular hypoplasia and tricuspid insufficiency, right-to-left shunt across foramen ovale, arrhythmia (WPW syndrome, first-degree AV block) | (+) | PGE in (functionally) pulmonary atresia; therapy of right heart failure; PGE ductal patency may be detrimental | Balloon dilatation in pulmonary stenosis | | Tricuspid valve reconstruction, valve replacement; 1.5 ventricle repair; modified Fontan repair |
| Atrial septal defect | Right-sided volume loading | – | – | – | – | Interventional or surgical occlusion; atrial septal defect with partial anomalous pulmonary venous connection: surgical repair |
| Total anomalous pulmonary venous return | Right-to-left shunt across foramen ovale permits maintenance of systemic perfusion; pulmonary venous congestion; ductus arteriosus patency provides relief in pulmonary venous obstruction | (+) | PGE in pulmonary venous obstruction (partial bypass of obstructed pulmonary venous return) | Atrial septostomy as palliative procedure before repair | Immediate repair | Residual pulmonary venous obstruction at the anastomotic site: reoperation' proximal pulmonary vein obstruction: dilatation and stent implantation; arrhythmias |
| Ventricular septal defect | Left ventricular volume overloading with falling pulmonary vascular resistance, pulmonary edema, congestive heart failure | – | Anticongestive therapy | – | Pulmonary banding in cases with large communication and left ventricular outflow stenosis or coarctation if primary repair not possible | Repair at the end of first year or earlier depending on communication size; otherwise risk of developing pulmonary vascular obstructive disease; in small VSD no surgical repair |
| Atrioventricular septal defect | Pulmonary vascular resistance and size of atrial and ventricular communication determine clinical presentation | (+) | In rare cases with unbalanced atrioventricular septal defect: single-ventricle physiology<br>Anticongestive therapy | – | – | Early repair at 3–4 months if VSD is large; risk of pulmonary vascular obstructive disease greater in Down syndrome |

(*Continued*)

**Table 56.2 (Continued)** Postnatal physiology and hemodynamics; medical, interventional, and surgical therapy in the neonatal period; and mid- to long-term interventions in various congenital heart defects

| *Congenital heart defect* | *Postnatal physiology* | *Duct dependent* | *Perinatal management* | *Transcatheter intervention in the neonate* | *Surgical intervention in the neonate* | *Interventions and problems in medium- and long-term follow-up* |
|---|---|---|---|---|---|---|
| Persistent ductus arteriosus Botalli | Left ventricular volume overloading with falling pulmonary vascular resistance, pulmonary edema, congestive heart failure | | Avoidance of hypoxemia, acidosis, fluid restriction; treatment by indomethacin or ibuprofen in premature babies | In the neonatal period: interventional occlusion only in large communications after indomethacin failure | Surgical ligation or division in the symptomatic neonate | Age >6–12 months: interventional occlusion |
| Truncus arteriosus communis | Dependent on pulmonary perfusion, mostly pulmonary congestion and ventricular volume | Rare | Anticongestive therapy | | Surgical repair | Reconstruction or replacement of homograft/conduit in homograft insufficiency or stenosis |
| Prenatal or neonatal cardiac failure due to extracardiac shunts<br>a. Twin–twin transfusion<br>b. Aneurysm of vein of Galen, hemangioma, teratoma; pulmonary sequestration | a. Shunt closed after birth: recovery of the (fetal dominant) right ventricle<br>b. Shunt patent after birth: biventricular volume load, pulmonary edema, pulmonary hypertension | – | Anticongestive therapy | Interventional occlusion of shunts | Surgical removal of shunt lesion | |
| Dilated cardiomyopathy | Congestive heart failure | – | Anticongestive therapy; exclude coronary abnormalities (anomalous left coronary artery from pulmonary artery); exclude metabolic and inherited disease; exclude syndromes | Myocardial biopsy | Coronary abnormalities: reconstruction of abnormal origin of coronary artery | Cardiac transplantation |
| Cardiac tumors | Arrhythmia, obstruction | – | Symptomatic | – | – | Surgical removal in obstruction check for tuberous sclerosis in rhabdomyoma |

*Abbreviations:* +, ductal dependent; (+), sometimes ductal dependent; –, not ductal dependent; PGE, prostaglandin E1; PS, pulmonary stenosis; TA, tricuspid atresia; VSD, ventricular septal defect; WPW, Wolff–Parkinson–White.

**Table 56.3** Relevant side effects of prostaglandin treatment

| | |
|---|---|
| Hypotension | Enterocolitis |
| Bradycardia | Tissue fragility |
| Apnea | Temperature elevation |
| Hypoventilation | Hyperexcitability |
| Sepsis | Thrombocytopenia |

*Source:* Adapted from Lucron H et al. *Arch Mal Coeur Vaiss* 2005;98: 524–30.[21]

allow for sufficient oxygenation (for more details, see section "Examples for the management of hypoplastic left heart syndrome" and Figure 56.11).

## Therapy for cardiac insufficiency

Even in healthy neonates, both systolic and diastolic myocardial reserves are limited. Pressure and volume loads are tolerated to a limited extent, so that an additional volume load has to be avoided. The therapeutic measures include drugs to increase contractility, diuretics, angiotensin-converting enzyme inhibitors, volume restriction and ß-blockade, and, in critically ill children, phosphodiesterase inhibitors or catecholamines together with vasodilators.

## Examples for the management of critical congenital heart defects

### Hypoplastic left heart syndrome: Single-ventricle physiology with duct-dependent systemic perfusion

The systemic circulation is supplied by the right ventricle via the ductus arteriosus. Spontaneous closure of the ductus arteriosus results in hypoperfusion of the systemic circulation, hypotension, shock, and death.

Intensive therapy includes maintenance of patency or reopening of the ductus arteriosus, optimization of right ventricular function, and regulation of pulmonary perfusion. In children with prenatally diagnosed hypoplastic left heart syndrome, low-dose prostaglandin E1 can be used immediately postpartum, so avoiding the complication of apnea seen with PGE1. If possible, mechanical ventilation should be avoided.

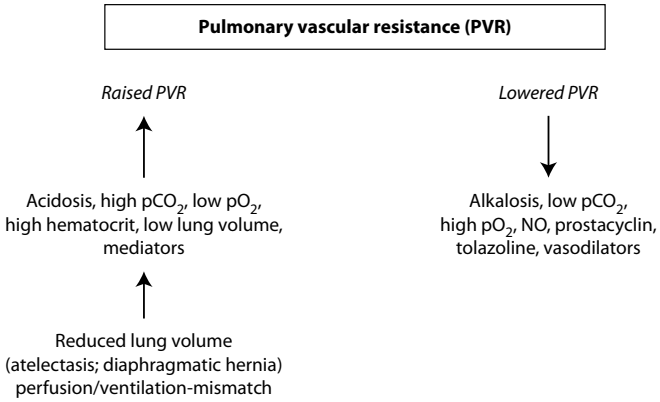


**Figure 56.9**
Factors and therapeutic options increasing (↑) or decreasing (↓) pulmonary vascular resistance.

With the physiological reduction of pulmonary vascular resistance, the pulmonary flow (Qp) increases. Since the ventricular output is limited, the systemic flow (Qs) and perfusion are reduced (Qp > Qs) (Figure 56.10b). To increase the systemic blood flow, the pulmonary blood flow has to be restricted by raising the pulmonary vascular resistance, and lowering the systemic resistance by vasodilators. The pulmonary vascular resistance can be increased by pulmonary vasoconstriction, which (Figure 56.9) can be achieved by avoidance of oxygen therapy, or, in the case of ventilation, by hypoventilation (Figure 56.11). The therapeutic goal is an equilibrium between pulmonary and systemic perfusion (Qp = Qs), which corresponds to an oxygen saturation of about 70%–80% (Figure 56.10a). In a balanced situation, the $SaO_2$ is approximately 75%, $PCO_2$ ~45 mm Hg, $PO_2$ ~35\ mm Hg. Higher oxygen saturations indicate an excessive pulmonary overflow with a risk of additional volume overload of the right ventricle, and are therefore undesirable. Oxygen saturations under 70% indicate pulmonary hypoperfusion (Qp < Qs) caused by increased pulmonary vascular resistance or atelectasis.

A further decisive parameter for the relation of pulmonary to systemic perfusion is the size of the atrial shunt, which can be somewhat restrictive.[23] The rare cases with a significantly restrictive foramen ovale and severe hypoxemia carry a worse prognosis.

If hypoplastic left heart syndrome is diagnosed after ductal narrowing, the intensive care physician is often confronted with low output syndrome and an ischemic right ventricle leading to shock-induced multiorgan failure. It would seem that those prenatally diagnosed with hypoplastic left heart syndrome would have better outcomes,[20–22] but in some later studies there was no survival-to-discharge advantage among the prenatally diagnosed patients.[24,25]

Risk factors for an unfavorable outcome following the Norwood procedure are prematurity, low birth weight (<2.5 kg), and complex lesions.[26,27] Some centers perform a hybrid-type procedure as the first-step palliation for these high-risk patients. This includes interventional stent implantation in the arterial duct with or without atrial septostomy, combined with surgical bilateral pulmonary banding.[28] This alleviates the need for cardiopulmonary bypass in the neonatal period. Whether this strategy is superior in these high-risk patients is unclear.[29]

### Pulmonary atresia: Duct-dependent pulmonary circulation

Pulmonary circulation in pulmonary atresia is provided by the left ventricle and aorta via the patent ductus arteriosus (Figure 56.6). Spontaneous ductal narrowing results in pulmonary hypoperfusion and hypoxemia.

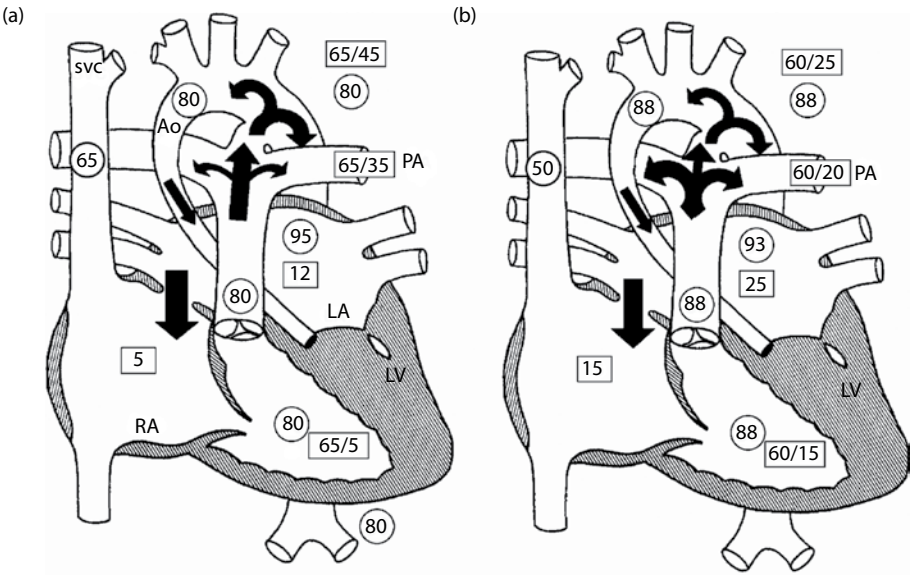


'Ideal' preoperative physiology: Qp/Qs ~1

The 'low PVR' physiology: Qp/Qs ~4

**Figure 56.10**
Preoperative physiology in hypoplastic left heart syndrome. $O_2$ saturations (circles) and intracavity pressures. (a) Ideal preoperative physiology (Qp = Qs). The resultant $O_2$ saturation of 75%–80% represents balanced pulmonary and systemic blood flow (Qp: Qs = 1). (b) Falling pulmonary vascular resistance (PVR) resulting in increased pulmonary perfusion (Qp), decreased systemic perfusion (Qs), and systemic hypotension (Qp ≫ Qs). The relation of Qp and Qs is calculated by: Qp:Qs = [$SO_2$ (aorta)—$SO_2$ (SVC)]: [$SO_2$ (pulmonary vein)–$SO_2$ (pulmonary artery)].

Intensive therapy includes maintenance of patency or reopening of the ductus arteriosus, optimization of left ventricular function, and regulation of pulmonary perfusion.

In neonates with prenatally diagnosed pulmonary atresia, PGE1 is necessary to keep the ductus arteriosus open. Increased pulmonary vascular resistance found in instances with hypoplastic pulmonary vascular beds may be reduced by administration of oxygen or hyperventilation. If necessary, systemic pressure can be enhanced by treatment with catecholamines. Surgery (systemic-to-pulmonary shunt or right ventricular outflow repair) or interventional perforation and balloon dilatation of the pulmonary valve can be performed once stability is achieved.

Severe Ebstein malformation may present in the fetus with functional pulmonary atresia, right ventricular myocardial disease, and duct-dependent pulmonary circulation. Such neonates will present with cyanosis and hypotension. Enlargement of the right-sided cardiac structures and dilatation of the right atrium result in lung hypoplasia and left ventricular dysfunction. The therapeutic goal is to reduce pulmonary vascular resistance by adequate oxygenation and, if necessary, by adding inhaled nitric oxide. Maintaining ductal patency may be deleterious in some of these patients, and in some patients ductal closure has actually improved hemodynamic stability[30] by lowering pulmonary vascular resistance and allowing the failing small right ventricle to produce antegrade flow to the lungs. Following the physiologic fall of pulmonary vascular resistance during postnatal transition, right ventricular pressure and volume load are reduced, and the right ventricle becomes capable of adequately serving the pulmonary circulation after a few days. If antegrade flow across the pulmonary artery is established, the neonate can be gradually weaned off prostaglandins and ventilation without the need for further interventions.

### Transposition of the great arteries without ventricular septal defect: Shunt-dependent mixing

The pulmonary and systemic circulations operate in parallel (Figure 56.7). The systemic $O_2$ saturation is dependent on the

| | | |
|---|---|---|
| Pathophysiology: | Pulmonary vascular resistance (PVR)⇓<br>Pulmonary blood flow (Qp)⇑ | Pulmonary vascular resistance (PVR)⇑<br>Pulmonary blood flow (Qp)⇓ |
| | ↓ | ↓ |
| Clinical signs: | $SaO_2$ >85%<br>Blood pressure (mean) <40 mmHg<br>Oliguria/anuria | $SaO_2$ >70%<br>Blood pressure normal |
| | ↓ | ↓ |
| Therapy: | pH⇓<br>$PCO_2$⇑ | pH⇑<br>$PCO_2$⇓<br>($PO_2$)⇑<br>Inhaled nitric oxide<br>Prostacyclin |

**Figure 56.11**
Therapeutic algorithms for neonates with ductal-dependent systemic flow.

magnitude of mixing between both circulations. Restrictive foramen ovale leads to severe hypoxemia.

Intensive therapy includes maintenance of patency or reopening of the ductus arteriosus and creation of an unrestricted interatrial shunt by balloon atrioseptostomy.

In the neonate without a ventricular septal defect and with a restrictive foramen ovale, the ductus arteriosus is kept open by PGE1, and balloon atrioseptostomy is performed as soon as possible. If good mixing can be achieved at the atrial level, further treatment with PGE1 to maintain ductal patency may not be necessary. In transposition of the great vessels, the left ventricle ejects into the pulmonary circulation via the pulmonary artery. As a result of the physiological reduction in the pulmonary vascular resistance, the left ventricular myocardial mass is subsequently reduced over time. Therefore, the anatomic correction has to be performed by an arterial switch in the first 2–3 weeks after birth to ensure a sufficiently developed and trained left ventricle.

The importance of early intervention is pointed out in the study of Bonnet et al.,[31] which compares the outcomes of neonates with transposition diagnosed prenatally versus postnatally. The clinical condition at arrival in the neonatal intensive care unit, including metabolic acidosis and multiorgan failure, was significantly worse in the postnatally diagnosed group. Prenatal diagnosis of transposition of the great arteries reduced postoperative mortality (0/68 neonates diagnosed prenatally versus 15/250 [6%] neonates diagnosed postnatally) and morbidity. In contrast, Escobar et al.[32] concluded that the mortality rate was not statistically significantly different between prenatally and postnatally diagnosed patients. The rider, however, is that there were significant preoperative differences with regard to earlier balloon atrioseptostomy and fewer neonates that required mechanical ventilation. Further research is required to ascertain whether prenatal diagnosis confers long-term benefits.

# *Established interventional procedures and therapy*

Interventional catheter procedures in neonates may function as life-saving palliative procedures, as well as supplementing or even replacing open surgical interventions.

## Balloon atrioseptostomy

### Principle

Transcutaneous balloon atrioseptostomy, introduced by Rashkind and Miller in 1966, is still the standard procedure for dilatation of the interatrial communication. The therapeutic goal is to achieve admixture of blood from both circulations and atrial decompression.[33]

### Indications

The primary indication is transposition of the great arteries with a restrictive foramen ovale causing severe cyanosis. In hypoplastic left heart syndrome, a restrictive atrial septum confers a dire prognosis and needs prompt left atrial decompression. Other indications are rare.

### Methods

Under ultrasound guidance or fluoroscopy, an uninflated balloon catheter is advanced via the right atrium and foramen ovale into the left atrium. The catheter can be introduced via umbilical vein or femoral vein; both accesses are used depending on operator preference and patient size. Following balloon inflation with fluid or diluted contrast material, the septum is torn by jerking back the catheter (Figure 56.12; Video 56.1). A successful balloon atrioseptostomy should result in an increased saturation (about 10% increase) or decreased interatrial gradient to approximately 3 mm Hg.

Owing to a thick atrial septum and in other cardiac pathologies such as hypoplastic left heart syndrome, a perforation by radiofrequency wire or a blade atrioseptostomy with or without stent placement may be required.[34]

### Results

In more than 85% of patients with transposition of the great arteries, balloon atrioseptostomy is successful; only in isolated cases is a repeat septostomy necessary.

### Complications

This intervention is of low risk with a mortality of 0.7%. The relevant risks are blood loss, perforation, arrhythmia, and thromboembolism with subsequent cerebral infarction.

Some reports link embolic brain injury to balloon atrioseptostomy[35,36] although this has been refuted by others.[37,38]

## Balloon dilatation of valves and blood vessels

### Principle

The principle is transmission of a controlled radial force on the restricted tissue by a balloon inflated to dilated rigidity. The mechanism of luminal enlargement by balloon dilatation may be complicated by tearing of the intima and media. This may lead to dissection of the intima and/or media and the subsequent development of an aneurysm. Such mishaps have to be avoided by appropriate selection of balloon diameter, inflation pressure, balloon length, and compliance.

### Method

The measurement of the annulus or vessel diameter is precisely defined by echocardiography prior to the procedure and during angiography by means of a calibrated marker-catheter. A balloon catheter with a specific final diameter is chosen. Via a guidewire, the uninflated dilatation balloon is advanced to the stenotic vessel or valve. Dilatation is performed by filling the balloon with a contrast–water mixture. At the most narrow position of the valve or vessel, the balloon is inflated under low pressure. By the stenotic vascular segment, a waist is formed, which should disappear when the balloon is maximally inflated. This procedure may need to

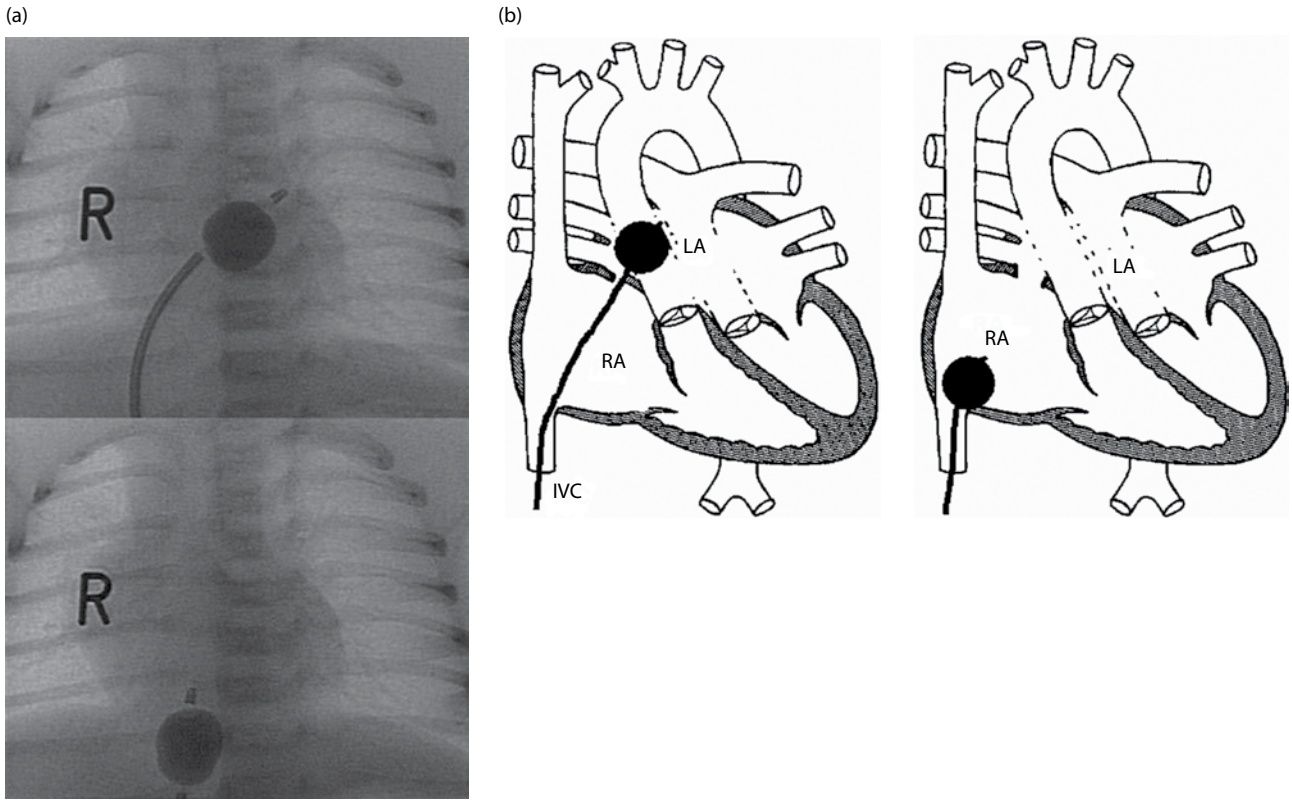


**Figure 56.12**
Balloon atrial septostomy. The balloon-tipped catheter is advanced through the patent foramen ovale to the left atrium, where it is inflated with diluted contrast (a). The balloon is jerked back to the right atrium to tear the septum (Video 56.1). (b) Posterior-anterior projection. (LA, left atrium; RA, right atrium.)

be repeated several times to optimize dilatation. After dilatation, angiography and measurement of the pressure gradients across the dilated segment are repeated.

### Risks

The risks include valvar insufficiency, aneurysm formation, vascular dissection, or perforation. Repeated future dilatation of valves and vessels is possible. Femoral vessel access is the site of first choice for neonates, but in the first 3–4 days after birth—if not yet occluded—the umbilical vein or artery can also be used for access.

## Balloon dilatation of the pulmonary valve in neonates

### Indications

Interventional balloon dilatation of the pulmonary valve is the treatment of choice in neonates with critical and severe pulmonary valve stenosis. It is also used as a palliative procedure in cases of membranous pulmonary atresia with an intact ventricular septum and tetralogy of Fallot.

### Method

In neonates with critical pulmonary stenosis, balloon dilatation is performed while PGE1 maintains patency of the ductus arteriosus (Figure 56.13). Sequential balloon dilatation with a balloon diameter measuring up to 125% of the size of the annulus is recommended to achieve maximal relief of pulmonary stenosis, so causing as little as possible pulmonary regurgitation. In patients with membranous pulmonary atresia, perforation of the obstructive membrane with a wire or, in isolated cases, with radiofrequency catheter, is also possible. Following successful balloon dilatation, prostaglandin infusion can be withdrawn gradually if the restricted right ventricle allows sufficient antegrade flow to support the pulmonary circulation.

### Results

Even in cases of critical pulmonary valve stenosis, the success rate for dilatation is 88%–95% and is defined by acute reduction of the gradient across the abnormal valve to $\leq$30 mm Hg.[39,40] In the neonatal period, the mortality rate is 3.7%–8%,[41] with total mortality for this procedure across the entire pediatric population being 0.4%.

In long-term follow-up, redilation is necessary in 6%. The freedom of reintervention after 1, 2, and 8 years is 90%, 84%, and 84%, respectively. Significant pulmonary insufficiency occurs in 9%.[39] Conversely, the mortality rate following surgery is 25%, with a reintervention rate of 25%.[42] In patients with a dysplastic pulmonary valve, only limited success is achieved.

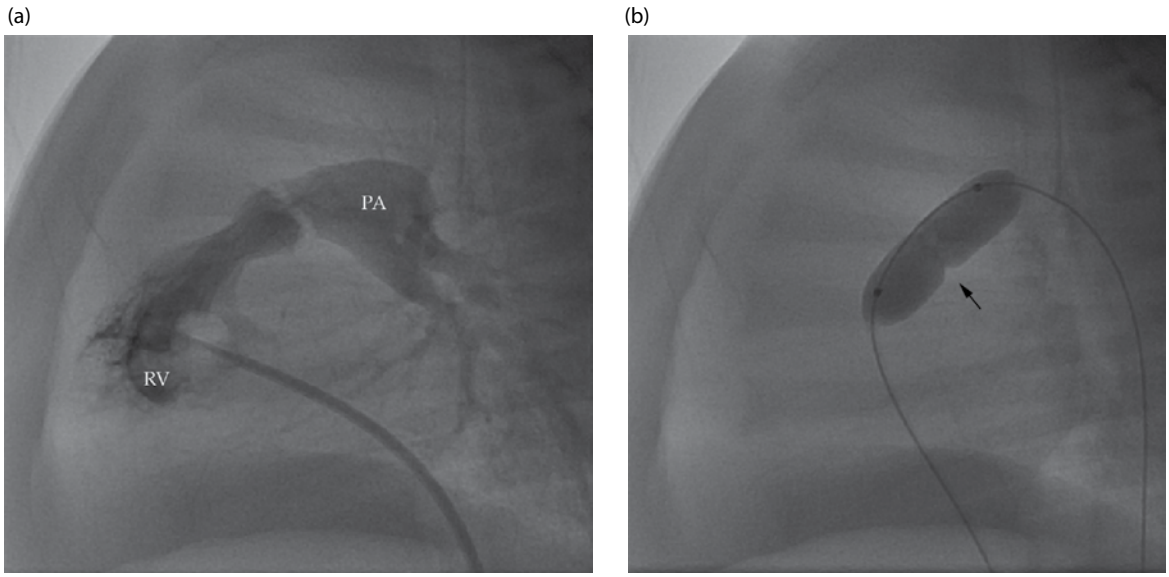


**Figure 56.13**

Interventional balloon dilatation of the pulmonary valve. Right ventricular angiograms-lateral projection before dilation (a) (Video 56.2) in a neonate with pulmonary stenosis. Arrows indicate the site of pulmonary stenosis. (b) The waist (arrow) of the balloon catheter produced by the stenotic valve (Video 56.3).

In pulmonary atresia, valve perforation and dilatation are used to increase antegrade pulmonary blood flow, stimulate right ventricular growth, and allow eventual biventricular surgical repair.[43] The results of pulmonary valvuloplasty depend on right ventricular morphology and volume, tricuspid valve morphology, and diameter of the pulmonary annulus.[40] In cases of refractory cyanosis, additional pulmonary blood flow is achieved by interventional ductal stenting or a Blalock-Taussig-Thomas shunt and/or a right ventricular outflow tract enlargement (6% in the literature[39]).

In patients with tetralogy of Fallot, dilatation of the stenotic pulmonary valve[44] or stent implantation[45] have been performed when early correction was thought to be impossible.

### Conclusion

In preterm newborns and neonates, interventional balloon dilatation is the treatment of first choice for pulmonary valve stenosis.

## Balloon aortic valvuloplasty

### Indication

Neonatal aortic valvar stenosis is challenging to treat because of the varied morphology of the valve, the association with hypoplasia of other left heart structures, and the presence of left ventricular systolic dysfunction or endomyocardial fibroelastosis (Figure 56.14). In contrast to critical pulmonary valve stenosis, dilatation of critical aortic valve stenosis is significantly more difficult in newborns and is therefore associated with higher rates of morbidity and mortality. Neonates with critical aortic valve stenosis are severely ill, deteriorate easily, and present as emergency cases. Without intervention, most will die within weeks. As aortic stenosis is already apparent *in utero*, these newborns may present with fibroelastosis of the left ventricle, reduced systolic and diastolic left ventricular function, and in some cases, severe mitral insufficiency. Prior to the intervention, one must ascertain whether the left-sided structures (i.e., left ventricular volume, mitral morphology, and diameter) are sufficient to support a biventricular circulation.[46] In patients with a very small left ventricle and a small aortic and mitral annulus, a univentricular correction by staged Norwood procedures or cardiac transplantation may be preferred.[46,47]

### Method

These critically ill neonates have duct-dependent systemic perfusion and often need inotropic support. Crossing the aortic valve can be either retrograde from the femoral artery or antegrade via the intra-atrial communication. Transvalvar pressure gradients in critical duct-dependent aortic stenosis may not be directly proportional to the severity of the disease, as the left ventricular function may be compromised, and the systemic perfusion is provided by the right ventricle via the ductus. It is paramount to avoid causing poorly tolerated aortic insufficiency by using a low-profile balloon measuring up to 90% of the annulus diameter. The postinterventional mortality rate depends on left ventricular function, the degree of mitral insufficiency, and the development of pulmonary hypertension.

### Results

As the procedure evolves and patient selection criteria improve, the mortality rates have decreased to 11%–13%,

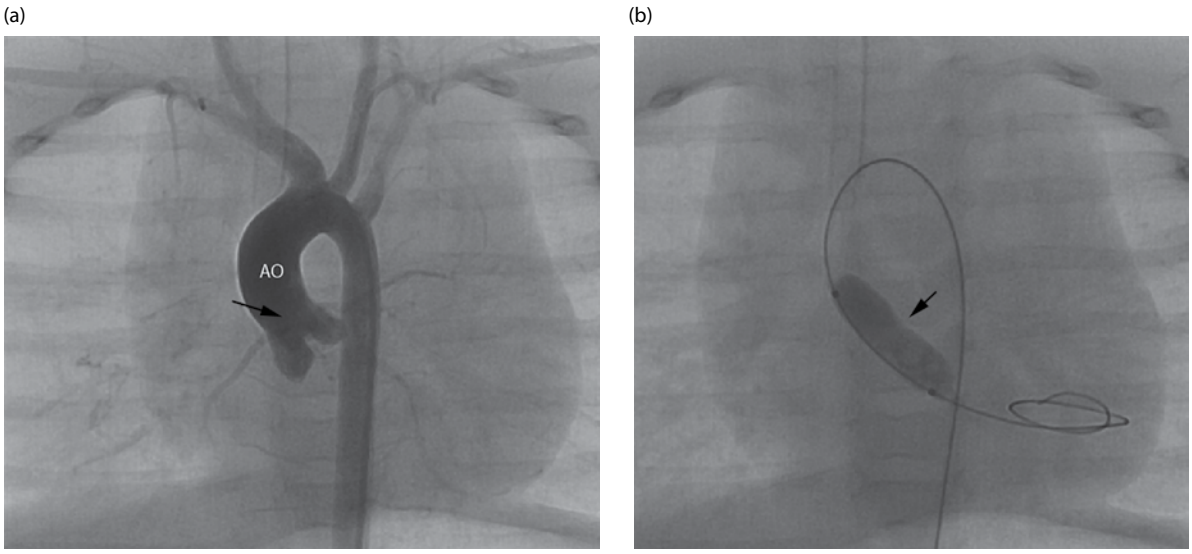


**Figure 56.14**
Interventional balloon dilatation of a critical aortic stenosis in a neonate. A ventriculogram is not usually performed as ventricular function is determined by pre-catheterization echocardiogram. The retrograde aortogram (a) (Video 56.4) shows the doming dysplastic aortic valve (arrow) prior to dilation with a very small aperture. (b) (Video 56.5) The waist (arrow) of the balloon catheter produced by the stenotic valve.

with a 10%–20% surgical mortality in this era. More recent series have reported an early mortality rate of 6%–8% with acute procedural mortality of 2%.[48–50] The mortality rate is much higher for critical aortic valve stenosis associated with malformations, such as mitral stenosis, aortic arch hypoplasia, hypoplastic aortic annulus, hypoplastic left ventricle, and duct-dependent circulation (the mortality rate of duct-dependent circulations is 38% in contrast to 5% for duct-independent circulations).[50,51]

Vascular complications occur, especially following access via the femoral artery. Therefore, the umbilical artery, axillary access carotid artery, or the femoral vein with an antegrade approach can be used as alternative vascular access points.[52] Risk factors associated with the need for earlier reintervention (interventional or surgical) include residual gradient above 35 mm Hg, preprocedural left ventricular dysfunction, and the presence of left ventricular endomyocardial fibroelastosis.[48,50,51,53] The rate of reintervention is 50%–60% after 5 years,[48,51,54] the freedom of intervention is 64% after 8 years,[44] and event-free survival is 34.2% after 10 years, and 27.4% after 15 years.[44] Following balloon dilatation, 6%–15% of patients develop significant aortic insufficiency.[49,54]

### Conclusion

Interventional valvuloplasty of critical aortic valve stenosis is a high-risk procedure with significant morbidity and mortality. It is still not clear whether the transcatheter option is superior to surgical valvotomy.[55] Ongoing evaluation of outcomes and development of criteria for patient selection for balloon valvuloplasty is important in order to provide the best outcomes for these patients.

## Balloon dilatation of aortic coarctation

Clinical presentation of the neonate with coarctation ranges between subtle symptoms such as systemic hypertension in the upper extremities, diminished lower extremity pulses, to congestive heart failure and circulatory collapse when the ductus closes.

The role of balloon angioplasty for native coarctation in neonates remains limited due to higher incidence of early restenosis, need for multiple interventions, potential serious vascular injury and limb ischemia, and incidence of aneurysm formation, when compared with surgical treatment for the same diagnosis and patient population.[56–60] Follow-up data comparing both groups up to 3 years postintervention are consistent with improved arch growth in neonates receiving surgical intervention.[56] Thus, most often a primary balloon angioplasty procedure is recommended only under special circumstances and as palliative treatment for neonatal coarctation of the aorta.

## *Balloon dilatation of other blood vessels*

Native or postoperative pulmonary artery stenosis, stenotic branch pulmonary arteries, or surgical shunts such as the modified Blalock-Taussig anastomosis can also be successfully dilated in neonates. If restenosis occurs and redilation is necessary, intravascular stents can be inserted successfully.

In older children, balloon dilatation is a suitable procedure for vascular stenosis of femoral arteries, renal arteries, systemic veins, collaterals, and surgically placed shunts.

## Intravascular stents

Vascular stenosis can be dilated by balloon angioplasty, but, owing to elastic "recoil" of the vascular wall, stenosis may recur shortly after dilatation. Intravascular stents are inserted to avoid the intrinsic "recoil" of the vascular wall, so that long-term success can be achieved.

### Indication

The placement of intravascular stents is problematic in neonates due to its inability to allow future growth. It is limited by vessel size and the future need to either dilate or remove the stent. Placement may be performed in the ductus arteriosus in those with duct-dependent malformations. Indications in older children are myriad, including pulmonary artery stenosis, peripheral pulmonary artery stenosis, aortic coarctation, stenosis of surgically placed shunts and conduits (baffle after atrial switch operation), systemic veins, major aortopulmonary collateral arteries, and coronary stenosis after Kawasaki syndrome.[61,62] Valvar stents are already in use as percutaneous valve replacements.[63] Stents are also used to maintain the patency of atrial defects and fenestrations, which serve as communications between the venous and systemic circulations.

### Procedure

Stents are placed on a dilatation balloon catheter and are advanced to the stenosis in a long sheet over a guidewire (Figure 56.15). The balloon is inflated to expand the stent, which remains in position after the balloon catheter is removed. Future availability of biodegradable stents will obviate the need for surgical removal once placed in a small vessel and is likely to allow subsequent growth of the stented vessel.

## Ductal stenting

A ductal stent is implanted in congenital defects with either ductal-dependent pulmonary or systemic blood flow (Figure 56.15).[64] Neonates with hypoplastic left heart syndrome

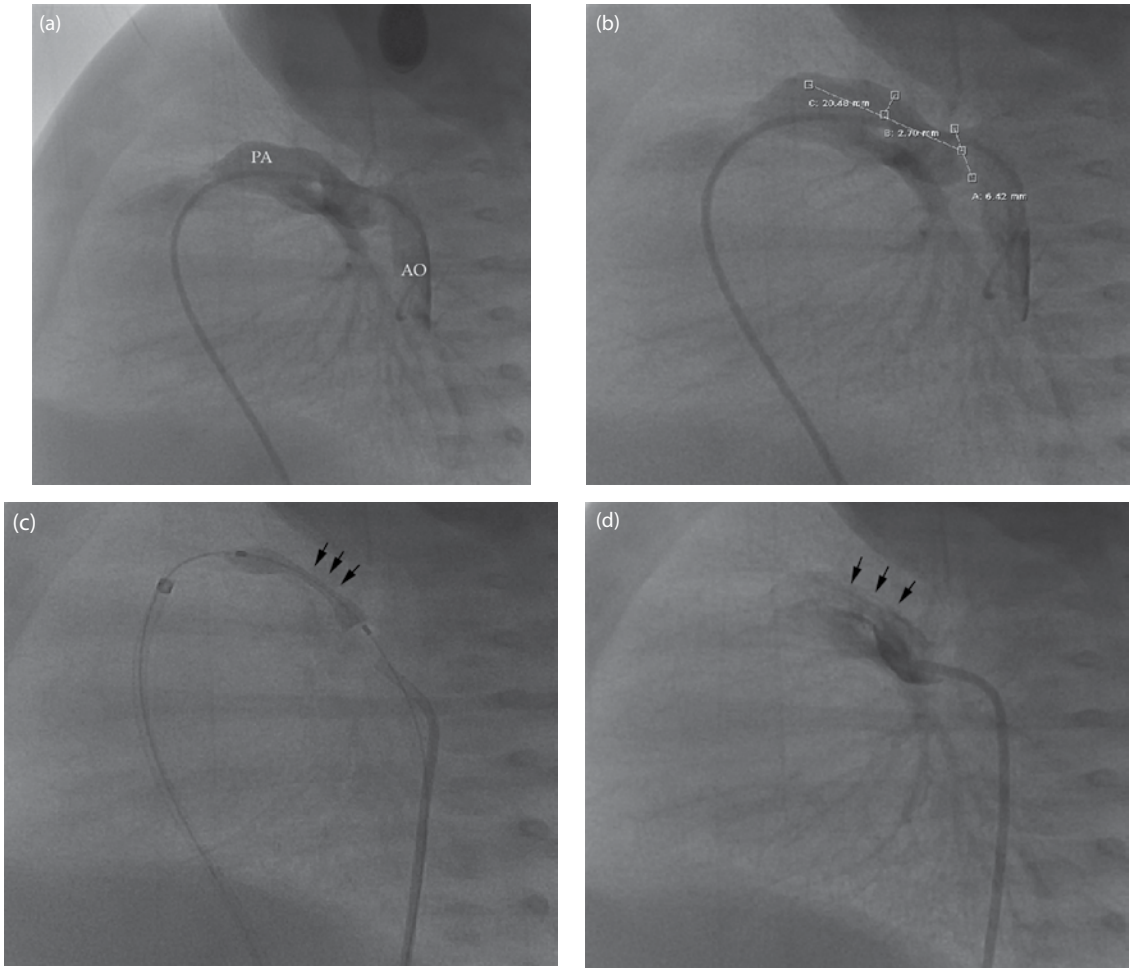


**Figure 56.15**
Stenting of the ductus arteriosus. This procedure was performed on a patient with critical pulmonary stenosis and a small right ventricle, i.e., ductal-dependent pulmonary blood flow. (a) The pigtail catheter enters the ductus arteriosus via the pulmonary artery. The angiography of the ducts shows the duct-dependent perfusion of the pulmonary artery. (b) Measurement of the duct is performed for optimal stent match. (c) The unexpanded stent, mounted on a balloon catheter, is positioned in the ductus arteriosus (dilation of the stent can be seen both in the anteroposterior and lateral projection in Video 56.6 and in Video 56.7, respectively. (d) After removal of the balloon catheter, a repeat angiography is performed showing optimal position of the stent in the lateral projection.

awaiting cardiac transplantation, with prematurity, low birth weight, or not suitable for Norwood palliation can be treated by interventional ductal stenting in association with surgical bilateral banding of the pulmonary artery.[26–29,65,66]

In duct-dependent pulmonary circulation, stents can be placed as an alternative for a surgical aortopulmonary shunt, but the implantation can be technically demanding owing to complicated ductal anatomy.[67,68]

### Risks and complications

Critical limitations are in-stent stenosis and relative stenosis during childhood growth. Neo-intimal proliferation and thrombosis may lead to stent stenosis or occlusion. Stents with intimal proliferation and relative stenosis due to childhood growth can be expanded by redilatation in the short to medium term; long-term results are not yet available.

With improved characteristics of stents, maintaining ductal patency by percutaneous stent implantation offers a safe and feasible means of palliation in neonates and young infants.

## Interventional occlusion of cardiac defects and connecting vessels

### Interventional occlusion of persistent ductus arteriosus

In the neonatal period, persistent ductus arteriosus (PDA) occlusion, if needed, is usually done surgically. Significant hemodynamic PDA at any time, or persistence of smaller PDA for longer than 6–12 months, is an indication for interventional occlusion.

The occlusion rate of all devices is close to 95% in the pediatric population. The risks are embolization, the presence of a residual shunt, and device-induced left pulmonary artery stenosis or coarctation of the aorta. These occur rarely, mostly in low body weight patients with a large PDA requiring a large device.[69] Implantations can even be performed in neonates and small infants as the catheters and devices become smaller, but this is still regarded to be a high-risk procedure, while surgical closure is still the safer routine in preterm and term neonates.[70]

Interventional treatment of symptomatic arteriovenous malformations, such as vein of Galen malformation, hepatic hemangioma, pulmonary sequestration, or aortopulmonary collaterals in neonates is performed successfully with coils, balloons, or vascular plugs.[71]

## Atrial septal defects

Closure of atrial septal defects (ASDs) of the secundum type without anomalous pulmonary venous return is rarely indicated in the first year of life and is even less likely in the neonatal period.

## Ventricular septal defects

Ventricular septal defect device closure is still limited to selected cases, mainly of multiple muscular defects that cannot be safely reached by the surgeon. The main reason for the failure of transcatheter perimembranous VSD closure is the high (6%) incidence of complete heart block. It most probably should be reserved for muscular defects only.[72,73]

# *Drug or interventional treatment of arrhythmia*

Prenatal drug therapy of fetal tachyarrhythmia is usually effective though sometimes difficult and may lead to severe cardiac insufficiency and hydrops fetalis. In contrast, tachycardias in newborns usually have a good prognosis. Although there is approximately 50% incidence of recurrence of supraventricular tachycardia and atrial flutter in the neonatal period,[74] in the first year of life, spontaneous remission can be expected in 30%–90%, in particular, for paroxysmal tachycardia.[75,76]

Postnatally, the initial diagnostic tool is the conventional electrocardiogram (ECG). Once the diagnosis of a tachyarrhythmia is established, treatment may be commenced. If the neonate is hemodynamically unstable, cardioversion should be promptly performed. If the diagnosis remains in question, there are several diagnostic possibilities. Accessory pathways are seen in Wolff–Parkinson–White syndrome—which constitutes over 70% of all supraventricular neonatal tachycardias; atrioventricular node-reentry tachycardia (10%–12% of all supraventricular neonatal tachycardias) are the most frequent in the first year of life.[77] These reentry tachycardias use the atrioventricular node as a pathway and can be interrupted by rapid intravenous administration of adenosine, which blocks the atrioventricular node for a few seconds.[78] Adenosine also facilitates the differentiation between atrial reentry tachycardia, atrial flutter, and ectopic atrial tachycardia, as well as ventricular tachycardia. In the latter, no effect is seen, and in atrial flutter or atrial ectopic tachycardia, the adenosine-induced atrioventricular block allows detection of the atrial focus on ECG.

If the diagnosis is atrial flutter, low-energy cardioversion usually terminates the arrhythmia. Transesophageal overdrive pacing can also be utilized in select tachycardias, such as junctional ectopic tachycardia.

Owing to the limited systolic and diastolic myocardial reserve in the newborn, high-frequency (usually >220 beats/minute) and long-lasting tachycardias are poorly tolerated. Repeat occurrences of supraventricular tachycardias make drug treatment in neonates difficult, and sometimes require multiple drug combinations. Bearing in mind the frequent spontaneous remission of paroxysmal supraventricular tachycardia, drug treatment can be terminated at the end of the first year of life. Data regarding freedom from recurrence of untreated supraventricular tachycardia are limited and may be in the range of 25%–60%. Above all, ectopic atrial and multifocal atrial tachycardias are difficult to manage and may lead to secondary cardiomyopathy.

In the rare case of persistent drug-resistant tachycardia, interventional radiofrequency catheterization may provide conclusive therapy, particularly in cases with accessory pathways. Radiofrequency ablation may be performed as rescue

therapy in newborns and as causative therapy in infants with refractory tachycardia, albeit with complications mainly due to the large bore of the catheters.[79,80] The probability of spontaneous pathway degeneration together with the limitations of vascular access, and possible interventional complications, in neonates, have to be carefully weighed against multiple drug treatment. Ablation should be reserved only for the patient with drug-resistant refractory tachycardia. However, after the first year of life, radiofrequency ablation is a sensible alternative to several years of drug treatment.[80] Absence of recurrence is dependent on the underlying mechanism. The serious complications are complete heart block, cardiac perforation, and cerebrovascular accident.

Ventricular tachycardia (VT) if not complicated by structural heart disease or long QT syndrome (LQTS) is a rarity in neonates with a high tendency of spontaneous remission in 89%.[81]

LQTS is a familial disease characterized by prolonged and abnormal repolarization, associated with a high risk of ventricular arrhythmias and sudden death.[82] Hallmarks are the prolongation of corrected QT (QTc) intervals and the occurrence of torsade de points. In congenital LQTS, bradycardia secondary to 2:1 AV block may be the initial clue to diagnosis. Serial ECGs should be obtained, because the QTc value can vary. Furthermore, screening ECGs from other family members are indicated. Diagnosis, risk assessment, and management are increasingly being guided by gene-specific diagnoses.[82] Beta-blocking medications, cardiac pacing as adjuvant therapy in bradycardia, and implantable cardioverter defibrillator improve survival in LQTS patients. The outcomes of congenital LQTS resulting in bradycardia due to a 2:1 AV block are improving.[83]

Congenital complete atrioventricular block (CHB), may require a temporary pacemaker. Current American College of Cardiology/American Heart Association (AHA) guidelines recommend permanent pacing for CHB in children for the following class 1 indications: (1) symptomatic bradycardia, ventricular dysfunction, or low cardiac output; (2) wide-complex QRS escape rhythm; and (3) infants with ventricular rate less than 55 bpm or with congenital heart disease and a ventricular rate less than 70 bpm.[84] The neonatal survival rate of isolated congenital CHB has been reported to be as high as 95%. Most patients with isolated congenital CHB require permanent pacing during childhood and most commonly during the first month of life.[85,86]

In neonates and infants, transcutaneous pacing is needed in those that are hemodynamically unstable until a permanent epicardial pacemaker may be surgically implanted. This is possible even in the smallest of children.

## Conclusion

As a result of the continuous improvement of prenatal diagnosis, cardiac defects and rhythm disorders can be detected earlier and with a higher sensitivity. The cooperation of obstetricians working in the field of prenatal diagnosis and pediatric cardiologists is extremely important for the care of the fetus suffering from cardiac disease. Counseling and support of the parents after diagnosis, planning and monitoring of intrauterine treatment, as well as planning of delivery, are ensured by obstetricians in cooperation with pediatric cardiologists, neonatologists, and cardiac surgeons. Postpartum, further treatment in specialized centers with the possibilities of interventional and surgical therapy enables interdisciplinary care of the newborn with congenital heart disease.

## Videos

**Video 56.1** (https://youtu.be/ZtLG0-aI64s)
Balloon atrial septostomy

**Video 56.2** (https://youtu.be/DE8XYgaeDJw)
Pulmonary valve stenosis pre-dilation

**Video 56.3** (https://youtu.be/9S3ij7Zn8YI)
Balloon inflated across pulmonary valve

**Video 56.4** (https://youtu.be/tXXE3aGrJhU)
Aortic valve stenosis pre-dilation

**Video 56.5** (https://youtu.be/4EnU0QNIYXg)
Balloon inflated across aortic valve

**Video 56.6** (https://youtu.be/_n8LoWxrl7A)
Balloon dilatation of PDA stent AP projection

**Video 56.7** (https://youtu.be/-o1gs8Cecis)
Balloon dilatation of PDA stent lateral projection

## References


1. Rudolph AM. *Congenital Diseases of the Heart: Clinical-Physiological Considerations*. 3rd ed. Vols. 1–36. Wiley-Blackwell; 2009:87–147.
2. Rudolph AM. Developmental physiology of the circulation. In: Moller JH, Hoffmann JIE, eds. *Pediatric Cardiovascular Medicine*. 2nd ed. Vol. 4. Oxford: Wiley-Blackwell; 2012:33–45.
3. Lim MK et al. *Arch Dis Child* 1992;67:1217–8.
4. Shiraishi H, Yanagisawa M. *Pediatr Cardiol* 1991;12:201–5.
5. Anilkumar M. *Cardiol Clin* 2013;31(3):417–30.
6. Fugelseth D et al. *Arch Dis Child Fetal Neonatal Ed* 1997;77:131–4.
7. Kozak-Barany A et al. *Early Hum Dev* 2000;57:49–59.
8. Jonker SS, Louey S. *J Endocrinol* 2016;228(1):R1–18.
9. Levy M et al. *Pediatr Res* 2005;57:21R–5R.
10. Gao Y, Raj JU. *Physiol Rev* 2010;90(4):1291–335.
11. Rudolph AM. *Circulation* 1970;41:343–59.
12. Jain A, McNamara PJ. *Semin Fetal Neonatal Med* 2015;20(4):262–71.
13. Fineman JR et al. Fetal and postnatal circulations: Pulmonary and persistent pulmonary hypertension of the newborn. In: Allen HD, Adams FH, Moss AJ, eds. *Moss and Adams' Heart Disease in Infants, Children, and Adolescents*. 6th ed. Philadelphia, PA: Lippincott Williams and Wilkins; 2001:41–52.

14. Morin FCIII, Egan E. *J Appl Physiol* 1992;73:213–8.
15. Soifer SJ et al. *J Dev Physiol* 1983;5:237–50.
16. Rabinovitch M, Hopper RK. Pathophysiology of pulmonary hypertension. In: Allen HD, Shaddy RE, Penny DJ et al. eds. *Moss and Adams' Heart Disease in Infants, Children, and Adolescents: Including the Fetus and Young Adult*. 9th ed. Philadelphia, PA: Lippincott Williams and Wilkins; 2016:1483–518.
17. Steinhorn RH, Fineman JR. *Artif Organs* 1999;22:970–4.
18. Mullins CE, Mayer DC, eds. *Congenital Heart Disease. A Diagrammatic Atlas*. New York, NY: Alan R Liss; 1988.
19. Lowenthal A et al. *Prenat Diagn* 2012;32(5):485–90.
20. Tworetzky W et al. *Circulation* 2001;103:1269–73.
21. Lucron H et al. *Arch Mal Coeur Vaiss* 2005;98:524–30.
22. Andropoulos DB et al. Cardiovascular intensive care. In: Allen HD, Shaddy RE, Penny DJ et al. eds. *Moss and Adams' Heart Disease in Infants, Children, and Adolescents: Including the Fetus and Young Adult*. 9th ed. Philadelphia, PA: Lippincott Williams and Wilkins; 2016:665–714.
23. Tweddell JS et al. Hypoplastic left heart syndrome. In: Allen HD, Shaddy RE, Penny DJ et al. eds. *Moss and Adams' Heart Disease in Infants, Children, and Adolescents: Including the Fetus and Young Adult*. 9th ed. Philadelphia, PA: Lippincott Williams and Wilkins; 2016:1125–62.
24. Kipps AK et al. *Am J Cardiol* 2011;108(3):421–7.
25. Oster ME et al. *Am J Cardiol* 2014;113(6):1036–40.
26. Artrip JH et al. *Ann Thorac Surg* 2006;82:1252–7.
27. Venugopal PS et al. *J Thorac Cardiovasc Surg* 2010;139:1211–5.
28. Galantowicz M et al. *Ann Thorac Surg* 2008;85:2063–70, discussion 2070–1.
29. Harada Y. *Gen Thorac Cardiovasc Surg* 2014;62(6):334–41.
30. Wald RM et al. *Am J Cardiol* 2005;96(6):851–6.
31. Bonnet D et al. *Circulation* 1999;99:916–8.
32. Escobar-Diaz MC et al. *Ultrasound Obstet Gynecol* 2015;45(6):678–82.
33. Rashkind WJ, Miller WW. *J Am Med Assoc* 1966:991–2.
34. Park SC et al. *Cathet Cardiovasc Diagn* 1975;1:195–201.
35. McQuillen PS et al. *Circulation* 2006;113:280–5.
36. Mukherjee D et al. *Cardiol Young* 2010;20:373–80.
37. Polito A et al. *Cardiol Young* 2012;22:1–7.
38. Petit CJ et al. *Circulation* 2009;119:709–16.
39. Tabatabaei H et al. *J Am Coll Cardiol* 1996;27:473–8.
40. Gournay V et al. *J Am Coll Cardiol* 1995;26:1725–31.
41. Lee ML et al. *Yonsei Med J* 2008;49(3):416–21.
42. Hanley FL et al. *J Am Coll Cardiol* 1993;22:183–92.
43. Humpl T et al. *Circulation* 2003;108:826–32.
44. Arnold R. *Cardiol Young* 1999;9:4–5.
45. Castleberry CD et al. *Pediatr Cardiol* 2014;35(3):423–30.
46. Colan SD et al. *J Am Coll Cardiol* 2006;47:1858–65.
47. Lofland GK et al. *J Thorac Cardiovasc Surg* 2001;121:10–27.
48. McCrindle BW et al. *Circulation* 2001;104(suppl 1):I152–8.
49. Egito ES et al. *J Am Coll Cardiol* 1997;29:442–7.
50. Hawkins JA et al. *Ann Thorac Surg* 1998;65:1758–62.
51. Gaynor JW et al. *Ann Thorac Surg* 1995;60:122–5.
52. Schranz D, Michel-Behnke I. *Ann Pediatr Cardiol* 2008;1(2):126–30.
53. Brown DW et al. *J Am Coll Cardiol* 2010;56:1740–9.
54. McElhinney DB et al. *Circulation* 2005;111:451–8.
55. Siddiqui J et al. *J Am Coll Cardiol* 2013;62:2134–40.
56. Fiore AC et al. *Ann Thorac Surg* 2005;80:1659–64.
57. Dilawar M et al. *Pediatr Cardiol* 2009;30:404–8.
58. Früh S et al. *Eur J Cardiothorac Surg* 2011;39:898–904.
59. Rodés-Cabau J et al. *Am Heart J* 2007;154:186–92.
60. Cowley CG et al. *Circulation* 2005;111:3453–6.
61. Okubo M, Benson LN. *Curr Opin Cardiol* 2001;26:84–91.
62. Peters B et al. *Ann Pediatr Cardiol* 2009;2(1):3–23.
63. Jalal Z et al. *Arch Cardiovasc Dis* 2014;107(11):635–42.
64. Udink Ten Cate FE et al. *Catheter Cardiovasc Interv* 2013;82(3):E233–43.
65. Akintürk H et al. *Pediatr Cardiol* 2007;28(2):79–87.
66. Ohye RG et al. *Circulation* 2016;134(17):1265–79.
67. Santoro G et al. *Catheter Cardiovasc Interv* 2015;86(2):249–57.
68. Alwi M et al. *J Am Coll Cardiol* 2004;44:438–45.
69. Baruteau AE et al. *Arch Cardiovasc Dis* 2014;107(2):122–32.
70. Dimas VV et al. *JACC Cardiovasc Interv* 2010;3:1295–9.
71. Heran MK, Burrill J. *Can Assoc Radiol J* 2012;63(3 suppl):S59–73.
72. Butera G et al. *J Am Coll Cardiol* 2007;50(12):1189–95.
73. Walsh MA et al. *Heart* 2006;92(9):1295–7.
74. Jaeggi E, Öhman A. *Clin Perinatol* 2016;43(1):99–112.
75. Deal BJ et al. *J Am Coll Cardiol* 1985;5:130–5.
76. Perry JC, Garson A Jr. *J Am Coll Cardiol* 1990;16:1215–20.
77. Weindling SN et al. *Am Heart J* 1996;131:66–72.
78. Paul T, Pfammatter JP. *Pediatr Cardiol* 1997;18:118–26.
79. Asakai H, Kirsh JA. *Expert Rev Cardiovasc Ther* 2015;13(3):333–40.
80. Van Hare GF et al. *J Cardiovasc Electrophysiol* 2004;15:759–70.
81. Pfammater JP, Paul T. *J Am Coll Cardiol* 1999;33:2067–72.
82. Behere SP et al. *Curr Opin Pediatr* 2014;26(6):727–33.
83. Aziz PF et al. *Heart Rhythm* 2010;7(6):781–5.
84. Epstein AE et al. *J Am Coll Cardiol* 2008;51(21):e1–62.
85. Lopes LM et al. *Circulation* 2008;118(12):1268–75.
86. Jaeggi ET et al. *J Am Coll Cardiol* 2002;39(1):130–7.

# 57

# Infants with congenital heart disease in the first year of life

Andrew J. Parry and Frank L. Hanley

## Introduction

For every 10,000 live births, 23 children have congenital heart disease that requires surgery before the age of 1 year. These children fall into two categories: those who require surgery within the first year of life, and those who, philosophically, we consider would do better if complete correction were performed during this time (Table 57.1).

For those who require surgery during the first year of life, a second decision must be made as to what treatment is most appropriate: palliative or corrective. For patients with "single-ventricle" anatomy, there is little choice; in cyanotic neonates and those who are duct dependent, pulmonary blood flow must be secured by means of a systemic-to-pulmonary arterial shunt, usually a modified Blalock-Taussig shunt, whereas in those neonates with an unprotected pulmonary vascular bed, a pulmonary artery band is required.

The group of patients with two-ventricle anatomy, however, may be approached in two different ways: initial palliation or primary complete repair. Studies have shown that establishing normal intracardiac hemodynamics as early as can be safely achieved maximizes the opportunity for optimal cardiac and pulmonary development and results in the best outcome for all organ systems. We must therefore define what the phrases "as can be safely achieved" and "appropriate lesions" mean.

Miniaturization of extracorporeal perfusion equipment and improvements in optics over the past decade allow us now to operate safely on children of 1500 g or more, although smaller children have been treated successfully in specialized units. With these very small infants, the greatest risk is often during the postoperative period when the insult to the child of a period of extracorporeal circulation, and problems primarily related to physical size, may be overwhelming. Physical size is therefore a major determinant of what can be safely achieved. In some units, great expertise has been developed in caring for these very small infants, which has led to a significant reduction in perioperative mortality. However, not all units have adopted this course and therefore perform initial palliation. In these units, the definition of "as can be safely achieved" means correcting children significantly later.

Taking this to an extreme, there is evidence that it is possible to reduce serious cardiac abnormalities postnatally by intervening in the fetus. Secondary cardiac development is dependent on hemodynamic forces rather than on genetic programming, and what may initially be a relatively simple lesion, such as valvar stenosis, may cause a major secondary problem, ventricular hypoplasia, which requires a single-ventricle circulation. Intervening early in fetal life to normalize the hemodynamics may stimulate ventricular growth to the extent that a single-ventricle circulation is avoided. This possibility is considered later.

The other key consideration is the question: What constitutes an "appropriate lesion"? There is a small group of patients that we believe is better managed by delaying complete correction until later, either because no benefit can be demonstrated for operating during the first year of life (such as most children with an atrial septal defect) or because a complete repair in a small individual is more likely to cause significant long-term problems than if the child were initially palliated (such as a child with transposition of the great arteries and pulmonary atresia). While opinions vary as to which operations should be included within this group, there is general acceptance that, despite the advances in pediatric cardiac surgical techniques, there remains a role for palliation even in the modern age.

Currently, for many lesions, treatment pathways are well worked out, and approaches are similar between various units. This discussion therefore focuses primarily on the current areas of contention, although reference will be made to the treatment of the more well-established lesions.

## Essential lesions

### *Inadequate systemic blood flow*

#### Aortic stenosis

Aortic stenosis is part of a spectrum that, in its most severe form, results in complete atresia of the outflow tract. Following resuscitation, there are two key issues: First, is the child best served by a single- or two-ventricle repair? And second, which form of two-ventricle intervention is most appropriate?

Resuscitation is similar regardless of the ultimate adequacy of the left ventricle. The child is treated like a child with

**Table 57.1** Congenital cardiac lesions appropriate for intervention during the first year of life

| |
|---|
| **Essential to intervene** |
| Inadequate systemic blood flow |
| Mitral stenosis |
| Critical aortic stenosis |
| Interrupted aortic arch |
| Coarctation of the aorta |
| Hypoplastic left heart syndrome |
| Inadequate pulmonary blood flow |
| Pulmonary atresia with ventricular septal defect |
| Pulmonary atresia with intact ventricular septum |
| Tricuspid atresia |
| Severe tetralogy of Fallot |
| Excessive pulmonary blood flow |
| Arterial level shunts |
| Truncus arteriosus |
| Aortopulmonary window |
| Persistent ductus arteriosus |
| Ventricular level shunts |
| Atrial-level shunts |
| Inadequate intracardiac mixing |
| Transposition of the great arteries |
| Pulmonary venous obstruction |
| Vascular abnormalities |
| Vascular rings |
| Anomalous origin of the coronary arteries |
| **Preferable to intervene** |
| Tetralogy of Fallot |

single-ventricle anatomy by maintaining the ductus arteriosus; coronary perfusion is achieved by retrograde flow down the ascending aorta if stenosis is severe. So long as the atrial septal defect is unrestrictive, this will allow enough time for more definitive treatment to be planned, though this should not be delayed, as left ventricular function may continue to deteriorate during this time.

### Single- or two-ventricle palliation?

Predicting those who will tolerate a two-ventricle repair is of paramount importance. Risk factors for poor outcome have variously been shown to be low ejection fraction, the presence of endocardial fibroelastosis, high left ventricular end-diastolic pressure, elevated mean pulmonary artery pressure, and low left ventricular volume.[1] However, the most widely adopted approach weighs four factors to determine the adequacy of left ventricular structures (body surface area [BSA], indexed aortic valve annulus [iANNULUS], ratio of long axis of the left ventricle to long-axis dimension of the heart [LAR], and grade 2 or 3 endocardial fibroelastosis [EndoF]) by the following equation:

$$\begin{aligned} DS = {} & 10.98(BSA) + 0.56(iANNULUS) \\ & + 5.89(LAR) - 0.79(EndoF) - 6.78 \end{aligned}$$

This has been found to be predictive of death after a two-ventricle repair accurately in 90% of patients if the score is less than −0.65.[2]

Others have found that this and previous scores have no predictive value.[3] This is particularly true in patients with aortic arch obstruction, in whom relieving the outflow tract obstruction and providing adequate preload by closing intracardiac shunts has been found to allow adequate growth of the left ventricle within a short period.[4,5] Failure in these series was always due to the presence of mitral stenosis.

In some children with critical aortic stenosis who, by other criteria, should ideally undergo a single-ventricle repair, aortic arch reconstruction as for the Norwood stage I repair, a Ross-Konno left ventricular outflow tract (LVOT) reconstruction, and an aggressive, total left ventricular resection of endomyocardial fibroelastosis may permit a two-ventricle repair. Experience with this approach remains, on the whole, the subject of case reports, but it may prove appropriate in the management of children with borderline left ventricles but with severe endocardial fibroelastosis.[6,7]

### What form of two-ventricle palliation?

When the left ventricle is considered to be of adequate size to support a two-ventricle circulation, the type of palliation needs to be decided on. This is either by balloon valvuloplasty or open surgical valvotomy. Which approach is adopted primarily depends on unit philosophy, but comparison of outcome is difficult, as aortic stenosis is frequently associated with other cardiac lesions (such as Shone complex or mitral stenosis). The primary success rate of balloon valvuloplasty is 97%–100%[8,9] with a 6%–21% early mortality[8,10] usually in children with other severe abnormalities or small, non-apex-forming left ventricles, but 4%–43% develop early, significant aortic regurgitation.[11,12] Freedom from reintervention is 54%–59%, and freedom from aortic valve replacement is 75%–79% at 10 years[12,13]; children with a duct-dependent circulation have a higher mortality (38% as opposed to 5% for non-duct-dependent children).

For surgical aortic commissurotomy, early mortality for infants is 4%–6%[14,15] with 10-year survival of 91.2%.[14,16] Freedom from reintervention is 67%–78% at 10 years, with 10%–17% requiring aortic valve replacement. Results for surgical valvotomy in patients with trileaflet valves are significantly better than for those with bicuspid or unicuspid valves, 10-year freedom from intervention being 92% versus 33% and freedom from aortic valve replacement 100% versus 57%, respectively.

Various authors have compared surgical and interventional approaches and many conclude that surgery is better; in one series of 158 patients, 10-year freedom from reintervention was 72% for surgery compared to 53% for balloon valvuloplasty, and 80% versus 75% for freedom from aortic valve replacement.[17] However, comparing compatible groups is difficult, and the choice of initial palliation often depends more on local bias. However, many of these patients return for further intervention, and the question arises as to whether there is not a more definitive treatment that can be offered. While repeat balloon valvuloplasty or surgical valvotomy is possible, the Ross-Konno aortoventriculoplasty may be a more definitive treatment. Operative risk is low,[1,18] and it

allows excellent relief of left ventricular outflow tract obstruction. While there will be the inevitable requirement for pulmonary homograft replacement with growth, encouraging early experience with this procedure obliges us to consider its adoption when primary palliation fails.

## Hypoplastic left heart syndrome

The management of hypoplastic left heart syndrome (HLHS) starts prenatally, as awareness of the diagnosis allows the child to be safely stabilized at birth; it has been shown that prenatal diagnosis is associated with an improved stage I survival. Except when there is pulmonary venous obstruction (including restriction of the interatrial communication), when surgery should be immediate, time should be allowed for the pulmonary vascular resistance to fall somewhat before surgery is undertaken. Surgical palliation is either by the "Norwood" route or primary cardiac transplantation. Classically, the Norwood procedure was performed with a Blalock-Taussig shunt providing pulmonary blood flow,[19] though many now use a right ventricular to pulmonary artery conduit (Sano shunt[20]) instead. The relative benefits of these approaches remain disputed; overall survival for conventional surgery is currently 86%–92%. Comparing conventional surgery to primary cardiac transplantation, data show that similar results can be achieved with either strategy in units with adequate activity,[21] though some units report 100% survival for a hybrid approach of short-term interventional palliation followed by transplantation.[22] However, availability of organs for transplantation remains the limiting factor.

Palliation of children with HLHS using interventional catheter techniques is being performed, either to stabilize patients awaiting primary transplantation or to delay the need for the stage I Norwood procedure until the child is more robust. This involves stenting the ductus arteriosus, banding the branch pulmonary arteries, and achieving an unrestrictive interatrial communication. Originally attempted in 1997[23] with poor results, there has recently been a revival in interest with significantly improved results. When performed in centers with extensive experience, the results are on par with surgery[24–26]; it should be noted that the crude data appear poorer, but many centers reserve a hybrid approach for higher-risk individuals with significant comorbidities (low birth weight, gut ischemia, cerebral bleeds, etc.). The hybrid approach also has the advantage of allowing easy transference between single- and two-ventricle circulations if the initial assessment suggests that the left ventricle is of borderline size. However, the second-stage procedure following initial hybrid palliation is a *tour de force*.

## Mitral stenosis

At the severe end of the spectrum, mitral stenosis is managed as for HLHS. In milder forms, when assessment concludes that mitral valve size is adequate for a two-ventricle repair, the options are balloon valvuloplasty or surgical repair. Which treatment is better is uncertain, as balloon valvuloplasty is infrequently used; in the only series comparing these two approaches, 2-year survival was similar for the two groups (80% versus 85%, respectively), although the surgical patients fared worse.[27] Surgery carries an operative risk of between 0% and 2.2%,[28,29] although mitral stenosis is rarely an isolated lesion, and the other abnormalities are optimally addressed at the same time. Long-term survival and freedom from reintervention at 10 years are 70%–100%[29,30] and 50%–79%,[29,31] respectively, with 2.2%–9% requiring mitral valve replacement.[29,30]

## Interrupted aortic arch

Although interrupted aortic arch is rarely a surgical emergency, there should not be undue delay in the definitive treatment of this lesion as lower body perfusion is precariously dependent on ductal patency. Therefore, after resuscitation using prostaglandin to maintain the arterial duct, surgical repair should be undertaken. Historically a two-stage approach (initial aortic arch reconstruction with pulmonary artery banding and later ventricular septal defect [VSD] closure) was used, though now the consensus tends toward a single-stage approach, though in extremely small neonates or those with associated major comorbidities, a staged approach (either surgical or hybrid) is appropriate. For a single-stage approach, early mortality is 0%–12% and late mortality 20%–25%,[32,33] even in small, premature infants, compared to 8%–37% and 4%–26%,[32,34,35] respectively, for the two-stage approach, though it should be emphasized that these results pertain to different surgical eras. Despite good early results, however, freedom from reintervention at 5 years is only 55%–62% predominantly for arch reobstruction (treated by surgery or balloon aortoplasty) and one-third for LVOT obstruction. When left ventricular outflow tract obstruction is also noted at presentation, the surgical risk is significantly higher, with 42% early and 50% late mortality.[32] There is, however, little agreement on what constitutes an adequate left ventricular outflow tract, with indexed cross-sectional area and absolute aortic annulus size being proposed.

Current surgical practice is to repair the arch using an end-to-side anastomosis, having excised all ductal tissue, though an augmented subclavian/carotid flap may be useful particularly in complex interrupted aortic arch (such as with truncus arteriosus).[36] The use of foreign materials is debated; some claim avoidance of foreign materials minimizes later interventions, while others, following extensive experience with the Norwood procedure, achieve excellent results modifying this technique.[37] Associated subaortic narrowing should be addressed at the first operation and the VSD closed. When LVOT obstruction is severe but left ventricular size is adequate, repair can be performed with a Damus-Kaye-Stansel pulmonary artery/aortic anastomosis with closure of the VSD to the pulmonary artery. The repair is completed using a conduit between the right ventricle and pulmonary artery. Using a selective management of the LVOT at primary operation, a reduction in requirement for LVOT reoperation has been demonstrated.[38]

## Coarctation of the aorta (infantile type)

Infantile aortic coarctation is associated with persistence of the ductus arteriosus, aortic arch hypoplasia, and the presence of other intracardiac defects. If the coarctation is unsuspected, the infant may present in extremis with low cardiac output and severe metabolic acidosis. Stabilization can usually be achieved in neonates by starting an infusion of prostaglandin E1 (PGE1), which may both reopen the ductus arteriosus and relax the "ductal sling" of contractile cells that strangle the aortic isthmus. While this temporizing measure usually allows recovery from the effects of hypoperfusion, this is an unstable circulation, and any benefit derived will be short-lived; definitive treatment should therefore not be imprudently delayed.

The optimal definitive management of native aortic coarctation remains controversial. Balloon aortoplasty of native aortic coarctation has shown a 91%–100% primary success rate.[39,40] However, for children aged less than 1 year, the recurrence rate is 50%–83%,[40,41] though many of these can undergo successful redilatation. However, for recoarctation following primary surgical repair, balloon aortoplasty is now the treatment of choice, with an 88%–91% success rate.

Historically, surgery has been the mainstay of treatment; patch aortoplasty, subclavian flap aortoplasty, and coarctation resection with end-to-end anastomosis have been used. The first of these has a high recurrence rate (50%) and is therefore no longer used.[42] Of the other two, rigorous analysis of early and late mortality has not demonstrated any advantage of either technique (3%–8.6% and 4% versus 0%–5% and 4%–5%, respectively[43–47]); mortality in most series is due to associated cardiac defects. Further, medium-term recurrence rate is identical with the two techniques (6% and 3.6%–4.3%, respectively). Younger age at the time of initial repair is a risk factor for recurrence, and a rate of 11%–44% has been reported for low birth weight infants[48,49]; however, the risk of maintaining these neonates on prostaglandin infusions until they have grown is high, and delaying surgical intervention cannot be reasonably advocated.

# *Inadequate pulmonary blood flow*

Initial management of patients with inadequate pulmonary blood flow involves PGE1 infusion to maintain ductal patency. Thereafter, when the child has been stabilized, more definitive intervention can be undertaken using a surgical shunt or stenting the ductus arteriosus.

## Pulmonary atresia with ventricular septal defect

This lesion is considered by some to be an extreme form of tetralogy of Fallot, and management of children with confluent, good-sized pulmonary arteries is directed by similar considerations as for other forms of tetralogy (see later text). Consequently, in many units, complete correction is performed in the neonatal period even in premature neonates as small as 1400 g, with excellent results.[50] In other units, where the prevailing philosophy advocates initial palliation, a Blalock-Taussig shunt is performed.

In some patients, the pulmonary arteries are severely hypoplastic or absent, and the patient may have major aortopulmonary collateral arteries. The management of these children is more controversial. When all lung segments are supplied by the hypoplastic pulmonary arteries, it is necessary to promote growth of these vessels as early as possible by performing a central aortopulmonary artery shunt (the diminutive branch pulmonary arteries should be avoided, as the risk of vessel stenosis and occlusion is high), reconstructing the right ventricular outflow tract directly (when there is short segment pulmonary atresia), or creating an aortopulmonary window by anastomosing the main pulmonary artery directly to the aorta. Using such techniques, full correction may later be achieved in up to 100% of patients[51]; small collateral vessels may later be coiled by interventional catheter techniques.

For children in whom pulmonary blood flow is primarily dependent on major aortopulmonary collateral arteries rather than native pulmonary arteries, afferent conduits to the lungs must be constructed from the collaterals, a process known as "unifocalization." While correction may be performed in stages, with each lung being unifocalized to a shunt before the intracardiac repair and central reconstruction of the pulmonary arteries is undertaken, this approach produces extremely varied results, with 21%–86% of patients subsequently achieving complete repair,[52,53] with a mortality rate of 11%–14%.[52,54]

The alternative approach is to establish a normal circulation as early as feasible using only native tissue by performing complete unifocalization at the same procedure as undertaking intracardiac repair. This maximizes the opportunity for adequate vessel growth and can be achieved in up to 90% of patients[55] with an early mortality of 3%–10.6%.[56,57] Some of the early deaths are due to low cardiac output state owing to the distal pulmonary vascular bed being too underdeveloped to allow biventricular repair, and as experience has increased, it has been shown that on occasion staged repairs may still be most appropriate. In our experience, 80% of patients have been able to undergo complete primary repair, while 20% require the VSD to be left open initially. However, owing to poorly developed collateral vessels, some patients still require staged unifocalizations through thoracotomies. Overall, the probability of complete repair is 88% with a 3-year survival of 94%.[57] In survivors, reinterventions are frequently required to dilate or stent anastomoses and coil collaterals.[55]

## Pulmonary atresia with intact interventricular septum

Atresia of the pulmonary valve causes secondary problems, which determine what treatment can be offered. These problems are right heart hypoplasia and coronary sinusoids.

When the atresia is long-standing, as suggested from the "flow-related theory" of cardiac development (see text that

follows), the absence of output causes a lack of stimulus for right heart growth, and the right ventricle and tricuspid valve become, secondarily, hypoplastic. In the absence of contraindications, and when the tricuspid valve is not too hypoplastic, relieving the right ventricular outflow tract obstruction and promoting right ventricular output may allow later right ventricular growth.

The presence of sinusoids is an independent risk factor for death, with a 1-year survival of 50%–83%[58,59] for those with sinusoids compared to 92%–98% for those without them.[58,60] When the coronary circulation is truly dependent on the right ventricle (i.e., no connection of the coronary artery/arteries to the aorta), palliation along the single-ventricle route regardless of ventricular size is all that is possible, as decompressing the ventricle will lead to myocardial ischemia. However, when the sinusoids simply interconnect with an essentially normal coronary system, ligation of the sinusoidal connections and decompression of the ventricle may be possible.[61] Further, if the fistulae are confined to a single coronary artery territory, decompression may still be feasible if the amount of left ventricular myocardium "at risk" is small.[62] Sinusoids are predominantly confined to those with very small tricuspid annulus to BSA index (z-score), however, and as studies suggest that the main predictor of a two-ventricle repair is the z-score of the tricuspid valve,[63] some centers do not attempt right ventricular decompression in patients with very small tricuspid valves.

Right ventricular decompression may be achieved by surgery or transvascular balloon valvuloplasty with radiofrequency or laser perforation of the valve plate when complete atresia is present. Primary success with balloon valvuloplasty is 75%–90%, with 0%–14% mortality.[64,65] Of survivors, 29%–55% require further balloon dilatation or surgery.[66,67] In comparison, surgery is associated with an 8%–19% mortality and a 65%–100% requirement for further intervention,[65,68] though these patients often represent the worse end of the spectrum. Further, up to 70% of patients undergoing successful right ventricular outflow tract decompression/reconstruction require augmentation of pulmonary blood flow with shunt or persistent ductus arteriosus (PDA) stenting.

The key to long-term success is stimulating adequate growth of the right ventricle both by relieving outflow obstruction and providing adequate preload. It has therefore been argued that a nonrestrictive atrial septal defect is detrimental to the growth of the right ventricle, and some surgeons deliberately control flow across the interatrial septum to promote ventricular growth.[66] However, despite these efforts, the tricuspid valve and right ventricle may still not grow.

Depending on how aggressively a two-ventricle circulation is pursued, survival is 50%–98% at 1 year[60,66] and 67.5%–98% at 6 years.[58,60] The lower survival rate reflects when a philosophy of right ventricular decompression is pursued in all patients, while the higher survival is for a group in whom the final outcome was assumed from the indexed size of the tricuspid valve at the time of presentation. Inevitably, the number of patients achieving a two-ventricle repair is much smaller with the latter approach, 30%[57] as opposed to 61%–90%.[58,68]

### Tricuspid atresia

In the absence of a VSD, primary palliation is as for other forms of inadequate pulmonary blood flow (see previous text). However, in a subgroup of neonates with an associated VSD ventricular septal defect and no right ventricular outflow tract obstruction, or tricuspid atresia and transposition of the great arteries with unrestrictive VSD, the pulmonary circulation needs to be protected from excessive blood flow. Pulmonary artery banding is therefore required in the neonatal period. Later palliation requires a staged single-ventricle approach by which returning systemic blood bypasses the heart and directly enters the pulmonary arteries. While this is completed in childhood, the first stage, the bidirectional cavopulmonary shunt (in which the superior vena cava is attached directly to the pulmonary artery), should be undertaken during the first year of life to prevent the complications of chronic volume loading of the heart, which causes deterioration in cardiac function. Early reduction of volume overload is associated with improved long-term functional status and an increased aerobic exercise capacity.[70] However, due to the physiologically high pulmonary vascular resistance in the neonate, a cavopulmonary shunt cannot be performed too early, and it has been found that performing a cavopulmonary shunt earlier than 1 month of age has a high failure rate and requirement for shunt takedown.[71] Further, young age at the time of performing the cavopulmonary shunt has been shown to be associated with increased length of stay and hospital morbidity.[72] In general, therefore, a bidirectional cavopulmonary shunt should be performed when patients are between 3 and 6 months of age, even if systemic arterial saturations are adequate at this time. Final-stage palliation, the Fontan procedure, may be accomplished either by an intracardiac baffle or an extracardiac tube. It is usually performed when the child is around 12–15 kg in weight but may be required earlier if the child has decreased oxygen saturation measurements, at which time an intracardiac baffle is usually preferred to allow growth.

### Severe tetralogy of Fallot

When infants are severely cyanosed, some intervention is necessary, either palliation or complete correction. There is evidence that long-term function of the heart and other organs is better if complete repair is undertaken early, but the decision on whether to palliate initially or completely repair depends on the philosophy of the unit; the arguments are therefore discussed in more depth in the section "Desirable lesions."

## *Excessive pulmonary blood flow*

Children with abnormal communications between the chambers of the heart or the great vessels develop shunts, with blood flowing from the high-pressure area to the low-pressure area. At birth, when the pulmonary vascular resistance is physiologically high, the shunt is small, but it increases as the pulmonary vascular resistance falls. This leads to volume

loading of the heart and may cause pulmonary vascular disease. The rate of development of pulmonary vascular disease is dependent on the shear stress that the endothelial cells are exposed to, and therefore children with arterial level shunts are at greatest risk.

### Arterial level shunts

These include aortopulmonary window, truncus arteriosus, and persistent ductus arteriosus. Pulmonary endothelial damage occurs within days of birth and may become irreversible within weeks of life. Further, run-off into the lungs may be so great that systemic perfusion is compromised with systemic arterial diastolic pressures so low that cardiac and intestinal perfusion is at risk. Full correction is undertaken in the neonatal period except when other medical issues (such as necrotizing enterocolitis) preclude the use of cardiopulmonary bypass; in such cases, banding of the branch pulmonary arteries may be considered.

PDA, however, is a variable lesion; the shunt may be so large that urgent closure in the neonatal period is essential to permit adequate systemic perfusion, or the duct may partially close so that the lungs are minimally affected. For severely premature infants, it was suggested that any shunt exacerbates chronic lung disease, and therefore, all PDAs should be closed, although this is now contested. Initial medical therapy using nonsteroidal anti-inflammatory agents is used if not contraindicated, while surgery is reserved for those who fail medical treatment. Other children with small shunts may undergo closure later using percutaneous techniques.

### Ventricular-level shunts

Closure of ventricular septal defects is undertaken during the first year of life if the defect is large and there is pulmonary overcirculation. Pulmonary vascular disease develops more slowly than for arterial level shunts as the shear stress is less, though with large defects irreversible changes may occur within months; it has been shown that delay in repair is associated with increased mortality. Initial management is medical, but as the operation is usually relatively straightforward, delay in surgery is difficult to justify. More problematic are children with multiple ventricular septal defects, as the small size of the heart may preclude successful closure of all the defects, and the proportion of septum splinted by the repair may be prohibitive. In these children, pulmonary artery banding may be more advisable, with debanding of the pulmonary artery and direct closure of the remaining defects performed once the child has grown. This has the added advantage that some of the muscular defects may close in the interim. Recently, there have been a number of reports of VSD closure using devices *via* percutaneous and hybrid approaches, a technique that is particularly appealing in patients with multiple VSDs. While many would accept some role for this approach in muscular VSDs, their place in the management of perimembranous defects is debated, particularly due to a perceived high risk of AV nodal block. However, in centers with a large experience, this risk is quoted as being as low as 0%[73] compared with a current risk following surgery of 0%–1.9%,[73–74] though it should be remembered that the average age of those in the device group is significantly greater than for the surgical group.

### Atrial-level shunts

Atrial septal defects only require closure within the first year of life if the child has other problems and it is anticipated that maximizing the efficiency of the cardiovascular system will benefit the child. As 14%–66% of these defects close spontaneously, intervention before the age of 1 year should be considered extraordinary.

## *Inadequate intracardiac mixing*

### Transposition of the great arteries

Treatment of this abnormality is surgical with anatomic correction in the form of the "arterial switch procedure" being the standard approach. However, initial management is medical/interventional, and surgery is often postponed for a few days until the neonate has overcome the insults of birth and the pulmonary vascular resistance has started to fall. Evidently, there has to be mixing of the saturated and desaturated blood. If transposition is associated with a ventricular septal defect, this alone may allow adequate mixing owing to the higher pulmonary blood flow. If the interventricular septum is intact, an interatrial communication is required. A Rashkind balloon atrial septostomy is often required if atrial mixing is inadequate to provide adequate systemic oxygen saturation. Prostaglandin E1 may be necessary also to maintain patency of the ductus arteriosus to drive mixing of saturated pulmonary venous blood at atrial level.

Definitive treatment should be performed before the left ventricle involutes as the PVR falls (usually within 21 days of birth). If a patient presents out of this timescale, an arterial switch procedure may still be possible either by supporting the child postoperatively using extracorporeal membrane oxygenation or by rapid retraining of the left ventricle by placing a band on the pulmonary artery and performing the switch 8–10 days later. The operation involves transecting the ascending aorta and main pulmonary artery and reanastomosing them in the correct orientation; in addition, the first branches of the aorta, the coronary arteries, must be translocated without compromising coronary artery flow. Surgically this may be demanding due to the highly variable coronary artery anatomy associated with this morphology. Though recent reports suggest that coronary anatomy no longer impacts surgical outcome, some coronary variations (particularly intramural left coronary artery) remain challenging.[75,76] Surgical mortality in the current era is 1%–2%.[77]

## *TAPVD/pulmonary venous obstruction*

This lesion remains a surgical emergency even when there is no apparent restriction as obstruction may develop at

any time. Interventional palliation by balloon venoplasty and stenting of the communicating vein achieves little but to delay definitive treatment. Infusing prostaglandin rarely improves the situation (and indeed may exacerbate it), and prolonged obstruction quickly induces structural changes in the pulmonary veins. If the obstruction has been severe *in utero*, the neonate may already have pulmonary lymphangiectasia which is frequently lethal either *in utero* or in early life. Surgery involves anastomosing the venous confluence to the back of the left atrium and can be performed with an overall risk of 5%–10%[78,79] though this risk is much higher (47%) for patients with heterotaxy syndromes and functional single-ventricle circulations.[79]

## *Vascular abnormalities*

### Vascular rings

Vascular rings always require surgery to relieve the obstruction. At surgery the ring is divided, and all associated fibrous tissue dissected off to allow complete relief of obstruction. Classically this has been performed by open thoracotomy, though nowadays an endoscopic approach may be used.[80] Although operative mortality is low, patients are frequently left with tracheobronchomalacia, and this is the most common cause of death[81]; long-term ventilation with or without tracheostomy may be required. Some surgeons excise the compressed airway segment at the time of repair with end-to-end reconstruction, or suspend the malacic segment within a tube of polytetrafluoroethylene, though these are rarely performed. Intraluminal stenting may also be used. Despite the severe early problems, 70%–97% are asymptomatic at long-term follow-up.[82,83]

### Anomalous origin of the coronary arteries from the pulmonary artery

The anomalous coronary artery usually arises from the main pulmonary artery, though origin from the branch pulmonary arteries may also occur. Most frequently, the left coronary artery is anomalous, but anomalous right and single coronary arteries have also been described. Regardless of the apparent severity of left ventricular dysfunction at the time of presentation, after emergency resuscitation, surgery should be undertaken. Presentation is usually in infancy, as coronary steal is not significant until the pulmonary vascular resistance has fallen, though the diagnosis may go unmade until a patient has had a ventricular septal defect (VSD) closed or PDA ligated and the resulting fall in pulmonary artery pressure reveals the diagnosis.

Historically, the origin of the anomalous coronary artery was tied off at the pulmonary artery, but outcomes were poor; nowadays revascularization is performed. Ideally this is achieved by reimplanting the coronary ostium into the aorta, but when this cannot be achieved a Takeuchi procedure (intrapulmonary artery baffling of the coronary ostium to a surgically created aortopulmonary window) may be done. Alternatively, the coronary artery may be grafted using the saphenous vein or prosthetic tubing, or the subclavian artery may be anastomosed to the coronary ostium.

Surgical mortality is currently 0%–2.4% with revascularization[84,85]; mitral regurgitation, which is frequently present, is an independent risk factor for death. It is, however, not recommended that mitral valve repair be undertaken at the primary operation unless the valve is structurally abnormal, as in up to 62% of patients mitral valve function improves with revascularization alone.[86] Postoperative mechanical support is required in up to 36% of patients due to the preoperative insult, yet long-term outcome is excellent, with cardiac function and regional wall motion returning to normal at rest in infants within 7 months.[87] However, myocardial flow reserve is significantly impaired late postoperatively, and patients have long-term impairment of exercise capacity.[88]

## Desirable lesions

Having considered lesions that require intervention during the first year of life, there are some lesions that are better treated by intervention during the first year of life, although this is more a philosophical issue. The lesion par excellence that falls into this category is tetralogy of Fallot. Correcting the circulation in patients with this lesion as early as possible has been shown to minimize the morbidity and mortality associated with the abnormal circulation, and allows other organ systems to develop more normally. For example, patients with tetralogy of Fallot develop fibrosis of the ventricular muscle due to chronic myocardial ischemia from the hypertrophy and cyanosis[89,90] and have malformed lungs due to impaired pulmonary angiogenesis and alveogenesis.[91]

The argument hinges on the risk/benefit ratio of early complete correction; if it can be achieved with no increase in morbidity or mortality compared to initial palliation, there is no advantage to the latter approach. As experience has grown, overall surgical mortality has fallen to 0%–1.3%,[92–94] and the morbidity of early complete repair is no higher than for a two-stage approach. Based on this evidence, many now pursue a policy of complete surgical correction in all patients with tetralogy of Fallot, regardless of age or size, except in a few with severe coexistent medical problems in whom a bypass run is considered high risk. However, subgroup analysis in some series has shown that age less than 30 days is an independent risk factor for death (6.4% versus 1.1%), postoperative extracorporeal membrane oxygenation, and prolonged duration of ventilatory support and hospital stay.[93] In addition, in many series complete repair at a very young age was associated with increased requirement for a transannular patch.[95] The argument has therefore been made that for asymptomatic children, although it is possible to perform complete correction in the neonatal period, this is not necessarily advantageous and delay until later can be justified. When patients are symptomatic, the decision regarding primary intervention is more philosophical and outcomes are similar between approaches; these arguments pertain also to

neonates with duct-dependent variants of tetralogy of Fallot (pulmonary atresia/VSD, etc.).

Palliation, if selected, may be either by Blalock-Taussig shunt or right ventricular outflow tract stenting. Both of these approaches have been reported as promoting growth of small pulmonary arteries prior to complete repair, the latter having the advantage of being possible without a surgical incision. Right ventricular outflow tract stenting is increasing in popularity as the procedural and interstage risk of a Blalock-Taussig shunt is significant.[96] However, this approach removes any chance of preserving the pulmonary valve.

# Fetal cardiac surgery

If it is considered that life begins at conception, cardiac intervention in the first year of life includes the fetal period. Though practiced to a limited extent to date, there is a sound theoretical basis for considering this strategy: to reduce mortality, to improve outcome in survivors, and to reduce damage to surrounding organs.

## *Preventing death*

Prenatal echocardiographic studies have shown that the *in utero* prognosis is much poorer for fetuses with congenital heart disease than had been appreciated previously, with overall mortality rates of 8.6%–18%[97,98] though survival is much poorer for some morphologies such as tetralogy of Fallot, where fetal loss can be as high as 23%. In addition, postnatally, the transition from a fetal to a neonatal circulation is a period of high risk as the two circulations become separated soon after birth (see Chapter 8), and lesions that are not necessarily lethal before birth may become lethal after birth. The risk is highest when cardiac disease is unexpected and the infants are born in centers inexperienced in the delivery and resuscitation of such individuals; overall survival for neonates with cardiac malformations amenable to biventricular repair may be as high as 96% for those diagnosed prenatally, whereas for a similar cohort not diagnosed prenatally survival is 76%.[99]

## *Improving outcome*

Early intrauterine intervention may also improve the outcome for the affected fetus due to an improvement in either gross or ultrastructural cardiac development.

### Improving gross cardiac development

Following the rotation and folding of the cardiac tube and the formation of the cardiac structures, the flow-directed theory of cardiac development hypothesizes that further growth and development of the cardiac chambers and great vessels are primarily directed by the volume and pressure of blood flowing in the heart.[100] Therefore, if inflow to a chamber is restricted, for example by a stenotic valve, there will be inadequate stimulus for that chamber to grow, and it will become hypoplastic. A relatively simple primary lesion (a stenotic valve) may therefore cause such disturbances in intracardiac flow patterns that a far more complex secondary malformation (ventricular hypoplasia) results. Theoretically, if the primary lesion can be identified and adequately relieved early enough during intrauterine development, normal cardiac growth may be reestablished.

Clinical studies support this theory of secondary cardiac development. Patients with tricuspid atresia and normally related great vessels may be divided into two groups depending on the presence or absence of a VSD. In patients without a VSD, the right ventricle and pulmonary valve are severely hypoplastic, and after birth they require a systemic-pulmonary artery shunt to maintain adequate pulmonary blood flow after closure of the ductus arteriosus. In contrast, in the subgroup of patients with a VSD, right ventricular growth may be entirely normal, as may the right ventricular outflow tract, and in these patients a pulmonary artery band may be required to limit pulmonary blood flow. Blood is able to bypass the blockage caused by the tricuspid atresia and access the right ventricle via the VSD. Developmental hemodynamic forces are therefore normalized, and distal right heart structures develop normally. Although both of these hearts have the substrate to develop tricuspid valve stenosis/atresia, normal growth of other right heart structures may be achieved if normal flow patterns can be reestablished.

Similar results have been obtained using animal models. If obstruction to ventricular inflow is produced by inflating a balloon within the left atrial cavity, left ventricular output falls acutely, and within 7 days the chamber size can decrease by up to 50%.[101] There is an associated fall in the left ventricular/right ventricular weight ratio, which is directly proportional to the length of time that the balloon has been in place, suggesting a direct causal effect. This leads to an early form of hypoplastic left heart syndrome. Similarly, obstructing ventricular outflow by banding the ascending aorta and reducing left ventricular output causes left ventricular hyperplasia over the first 10 days. However, over a longer period of time (30–60 days), the left ventricular cavity becomes obliterated, with a decrease in the left ventricular/right ventricular weight ratio. These changes are more pronounced in fetuses with tighter aortic bands.

As well as affecting the size of cardiac chambers, abnormal flow patterns within the heart have been shown to affect the morphogenesis of the cardiac valves. In a novel mutant zebrafish model, failure of looping of the heart has been found to cause defects in transvalvular flow patterns across the AV valves, and this is associated with defects in morphogenesis of these valves.

### Improving ultrastructural cardiac development

Around the time of birth, the ability for cardiac growth by hyperplasia and angiogenesis (as occurs during development)

is lost, and the neonatal heart responds to stress by hypertrophy, with little or no angiogenesis. This results in a very different ultrastructure of the organ. *In utero* intervention may allow normal cardiac ultrastructural development; in structurally normal hearts, the response of the fetal myocardium to experimentally induced left ventricular outflow tract obstruction is one of hyperplasia.[101] In humans, the age at which this switch occurs is unknown. In rats the hyperplastic response is known to be lost within 3–4 days of birth and angiogenesis by 7 weeks, while in sheep the hyperplastic response is lost after 110 days' gestation (term being 150 days).

### Reducing damage to surrounding organs

The development of other intrathoracic structures is dependent on adequate physical space within the chest, and their growth may be compromised if the heart is enlarged. In one study of patients with pulmonary atresia and intact interventricular septum with a dilated ventricle who survived to term, the neonatal mortality was 100% due to an inability to ventilate the infant adequately after birth, owing to severe lung hypoplasia caused by the grossly enlarged heart.[102] This is similar for fetuses with Ebstein anomaly. If the cardiac distension could be prevented early enough, adequate lung growth may be permitted and postnatal survival ensured.

## *Requirements for fetal cardiac intervention*

If fetal cardiac intervention is to be attempted, the lesion for which the intervention is performed must have such a poor outlook with conventional approaches that the increased risk of *in utero* intervention is justified. These will mainly be lesions that result in single-ventricle physiology, chief of which are hypoplastic left heart syndrome, severe forms of Ebstein anomaly, and pulmonary atresia with intact interventricular septum. Second, there must be a simple primary abnormality that can be readily dealt with. Third, the intervention must be simple, quick, and reliable. Finally, diagnosis of the defect must be practical early enough during fetal development to allow time for adequate catch-up growth.

## *Specific issues*

There are three practical issues that confront the fetal cardiac interventionalist: size, tissue structure, and (if open surgery is undertaken) the response of the fetoplacental unit to cardiac bypass.

### Size

The development of miniaturized bypass circuits and oxygenators now allows us to operate on infants weighing as little as 750 g clinically. Experimentally, bypass has been performed on fetuses weighing as little as 500 g. Size is therefore manageable for the time that the diagnosis has been made.

### Tissue structure

Fetal tissues are extremely friable due to the high water content, which is 88% at 18 weeks' gestation, compared to 69% at term and 60% in adulthood.[103,104] Correspondingly, there is a gradual accumulation of collagen: 2.4, 16.8, and 45.7 g/kg, respectively,[105] with a progressive maturation from type I to type III, which has increased cross-linking.[106] These friable tissues may preclude the use of conventional techniques, and the use of laser-assisted tissue welding and laser scalpels is being investigated.

### Fetoplacental unit response to bypass

The greatest obstacle to fetal cardiac surgery is the reaction of the fetoplacental unit to bypass.

In the fetus, the systemic circulation lies in parallel with the placental circulation. Relative changes in the vascular resistances of the two beds will therefore affect the perfusion of the other bed (analogous to a Blalock-Taussig shunt). Initial experiments showed that fetal bypass caused an increase in blood flow to all fetal organs but a decrease to the placenta by 25%–65%.[107,108] This change persisted even after bypass and was caused by an increase in vascular resistance at the level of the cotyledons and umbilical vein.[109] Inevitably this led to respiratory acidosis and hypoxemia, but while systemic perfusion was initially well maintained, the progressive hypoxemia secondarily caused tissue hypoxia and metabolic acidosis (Figure 57.1).

These changes in placental vascular resistance resemble the effects of postnatal cardiopulmonary bypass, which is due to a "whole-body inflammatory response," and it has been demonstrated that there are similarities between the two. Minimizing the inflammatory response by inhibiting eicosanoid metabolism (using indomethacin and corticosteroids) maintains adequate placental blood flow for a period,[110,111] but later a more insidious metabolic acidosis resistant to this pharmacological manipulation develops, again caused by elevation in placental vascular resistance. This is part of the fetal stress response,[112] and blocking it using a high spinal anesthetic, in combination with the other techniques outlined previously, has permitted long-term survival after cardiac bypass in 80% of fetuses experimentally.[113]

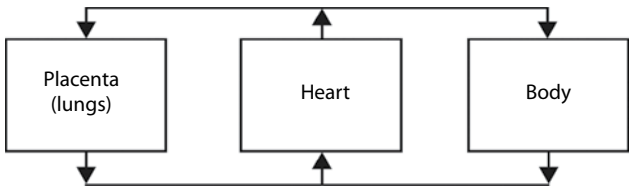


**Figure 57.1**
The balance of fetal cardiac output. Similar to the Blalock-Taussig shunt where the pulmonary and systemic circulations are in parallel, so the placental and systemic circulations are in parallel in the fetus. Relative changes in the impedance of these two circuits will cause dramatic changes in the distribution of the cardiac output in the fetus.

The trigger of the inflammatory and stress responses is unknown; it may be the contact of fetal blood with foreign surfaces, or the hemodilution which accompanies bypass. Both of these issues have been addressed using miniaturized bypass pumps, initially the Hemopump (Johnson & Johnson Interventional Systems, Rancho Cordova, California),[114] and more recently, the Tinypump (custom pump from Tokyo Medical and Dental University).[115] These miniaturized pumps have a priming volume of only 15 mL or 5 mL, respectively (150 mL for a conventional circuit), and also minimize contact surface area. Using these circuits, white cell activation is significantly reduced, and even without pharmacological manipulations, long-term fetal survival has been achieved in 89%.[116]

Other attempts to improve fetal survival following *in utero* bypass have included using pulsatile perfusion[117] and increasing flow rates to above 300 mL/kg/min.[118] However, neither of these studies attempted long-term fetal survival, and their efficacy therefore remains uncertain.

## Intervention or open surgery?

The discussion above has concentrated mainly on issues associated with open cardiac operations, and from the experience to date, it is clear that the fetal stress response is a major factor impacting on the success of open surgery. While efforts to understand the trigger for the stress response and to control its effects are under investigation, using less stressful procedures, such as interventional cardiological techniques, clinical application has already been achieved.

## Clinical experience of interventional techniques

Since as early as 1991, interventional cardiologists have been attempting balloon dilatation of the aortic valve in fetuses with aortic valve stenosis in an attempt to prevent the secondary development of hypoplastic left heart syndrome. In that year, Maxwell published an experience with two fetuses, which underwent three *in utero* aortic balloon valvuloplasties; one fetus died the day after intervention, while the second survived to term but died 5 weeks after birth due to persisting LV dysfunction secondary to subendocardial fibroelastosis.[119]

In the largest experience to date (100 attempted interventions), technical success of fetal aortic valvuloplasty has been reported as being 77% (45% of which achieved biventricular repair) with no maternal deaths or significant complications.[120] Of these fetuses, 88 were live-born, and of these 38 underwent a biventricular repair (three after unsuccessful fetal intervention). Freedom from cardiac death at 5 and 10 years was 96% and 84%, respectively, for those who underwent a two-ventricle repair, though this rose to 100% if children crossing over late from a single ventricle to biventricular palliation were excluded; analyzing outcomes on an intention to treat basis, survival was significantly better in those who underwent a technically successful fetal intervention. However, the requirement for postnatal cardiac intervention is high with all but one of these children requiring further procedures. Forty-two percent required aortic or mitral valve replacement, while 58% underwent mitral and 45% aortic valve repair. Fifty-five percent required endocardial fibroelastosis resection, and balloon valvuloplasty was performed in 90% of patients on the aortic valve and 19% on the mitral valve.

As experience has increased, it has become possible to identify fetuses that are more likely to benefit from fetal aortic balloon valvuloplasty and thereby target intervention on high-risk cases. In one study of fetuses with aortic stenosis, of those that developed hypoplastic left heart syndrome, all had retrograde flow in the transverse aortic arch, while 88% had left-to-right flow across the interatrial septum, 91% had monophasic flow across the mitral valve, and 94% had significant LV dysfunction.[121] Conversely, all fetuses that had antegrade flow in the transverse arch, biphasic flow across the mitral valve, and normal LV function had a biventricular circulation. Further, echocardiographic assessment of the degree of subendocardial fibroelastosis has increased the sensitivity and positive predictive value of this score in predicting patients who will be able to achieve a biventricular outcome. More recently, a scoring system has been developed that is able to discriminate fetuses that will achieve a biventricular circulation with 100% sensitivity and modest predictive value.[122] This model is based on preintervention echocardiographic threshold "z-scores" for LV long-axis dimension, LV short-axis dimension, aortic valve annulus diameter, mitral valve annulus diameter, and a dichotomous LV pressure score.

Similar but more limited experience has been obtained for performing valve perforation and balloon dilatation of the pulmonary valve, primarily because postnatal outcomes for the majority of patients with pulmonary atresia/intact interventricular septum are more favorable than for aortic atresia. Again, fetal intervention on the pulmonary valve has been technically successful in most (71%). Significant growth of the tricuspid valve and right ventricle has been reported, and a number of children that were expected to have a single-ventricle palliation long term have achieved a biventricular repair.[123,124] However, reports are as yet limited, and the impact of this intervention on right ventricular functional development and overall outcome is as yet unclear.

The other situation in which fetal intervention is being performed clinically is in patients who have restriction of their interatrial septum. Such patients may develop hypoplastic left heart syndrome due to inadequate filling of the left ventricle, or severe pulmonary venous hypertension if they have hypoplastic left heart syndrome, but the left atrium is unable to drain freely into the right atrium. A small number of such procedures have been performed with no maternal complications and an 8% fetal loss. Simple ballooning of the interatrial septum has been found to be of limited benefit, and currently, stenting of the interatrial septum is favored. Stent deployment has been successful in 70% of reported cases with immediate reduction in left atrium pressure and

pulmonary vein dilatation; the remaining fetuses underwent static balloon septoplasty with some effect.[125–127] Of those that successfully underwent stent implantation, 8% of stents stenosed prior to birth, and all of these neonates died after birth. Otherwise, there were 11 neonatal deaths (many of which had been stented), and though this mortality appears high (overall 52%), it has been observed that the mortality associated with this condition prior to fetal intervention was poorer (100%). As yet, evidence of long-term survival benefit associated with this fetal intervention is lacking, as all treated fetuses in one study that underwent lung biopsy at the time of further surgery demonstrated muscularization of the pulmonary veins and lymphangiectasia. However, *in utero* stenting of the interatrial septum in such patients may avert immediate postnatal deterioration and allow optimal planning of further intervention.

## Experimental interventional techniques

Various other experimental approaches to fetal intervention have been performed. Percutaneous maternal, transhepatic access to the fetal circulation has been achieved and used to perform simulated balloon dilatation of the pulmonary valve and stenting of the interatrial septum. Success was achieved in 69% of the former experiments, with a fetal loss rate of 8%.[128] In a different approach to fetal intervention, exteriorizing the fetus and performing a left thoracotomy, the circulation was accessed via a transapical approach, and successful delivery of a valved stent into the pulmonary artery was achieved.[129] Finally, in a move toward even less invasive intervention, it has proven possible to consistently pass a guidewire and balloon across the interatrial septum and aortic valve using magnetic navigation equipment in a model of a fetal heart; *in vivo* application is awaited.[130]

## Fetal cardiac pacing

The other area in which fetal cardiac intervention has been used clinically is cardiac pacing. One in 20,000 fetuses develops congenital complete heart block.[131] Of these, 57%–80% have structural heart disease, and this combination is associated with an *in utero* mortality of up to 86%.[132,133] In contrast, in those without severe structural heart disease, the *in utero* mortality is 11%–25%.[133,134] Hemodynamic studies suggest that as the fetal heart can accommodate down to a rate of 40 beats/minute there is no inherent myocardial dysfunction in these fetuses, and that accelerating the cardiac rate by pacing may reverse the cardiac failure.

The aim of intervention is to treat the fetal cardiac failure adequately to allow progression of pregnancy to a safe gestational age, generally 32 weeks. In cases where transplacental or direct intrafetal therapy has failed, there are two options. The first is early delivery and immediate neonatal pacing, accepting the higher risks associated with premature delivery.[135] Initially this may necessitate using temporary epicardial leads if the child is too small for a permanent system. If this is not feasible due to fetal immaturity, fetal cardiac pacing may be undertaken. Experimentally, both epicardial[136] and endocardial[137] approaches have been successfully used both acutely and chronically in fetuses with induced heart block.[136] Further, using conductance catheter techniques, studies have demonstrated normal contractility, a maintained inotropic response, and an intact force-frequency relationship for the paced fetuses,[138] suggesting that the fetal myocardium tolerates pacing as well as the neonatal myocardium. Others have found that there is an optimal pacing rate with cardiac output and systemic blood pressure being maximized at a ventricular rate of 150 bpm.[139]

To date there have been a very small number of clinical cases reported of attempts at *in utero* fetal pacing. Access to the heart has been gained via a variety of routes, transthoracic (with subsequent transmyocardial, intramyocardial, or epicardial electrode placement), transhepatic, or intracaval. In all of these cases, the pacing generator was placed external to the fetus, and although effective pacing was achieved in all cases, capture was lost in many of these hours after the procedure, presumably due to lead dislodgement by fetal movement. To prevent this, a miniaturized epicardial pacing system that lies entirely within the fetal chest has recently been successfully trialed in an experimental model.[140] In other cases, though electrode placement remained secure, the fetus died and was subsequently found to have a bloody pericardial effusion, presumably causing tamponade.[141] However, other reports question whether simply increasing the fetal heart rate is of benefit. In one report, despite achieving and maintaining effective pacing with a demonstrated increase in cardiac output of 150%, the fetus still died.[142] Autopsy showed all the cardiac chambers to be dilated and thin walled, and there was diffuse endocardial fibroelastosis. In addition, there was evidence of chronic liver and renal failure and severe stress involution of the thymus and adrenals; death was attributed to multiorgan failure. Whether this could have been avoided by earlier intervention or whether this is an inevitable part of the disease process and therefore fundamentally untreatable remains to be determined.

Fetal cardiac intervention is in its infancy. Although there are theoretical advantages to this approach, the final proof of its efficacy is awaited. Certainly there are many hurdles that must be overcome, but significant progress has been made over the past 15 years. It is likely that the final proof of whether these achievable interventions positively impact clinical outcomes will be available in the foreseeable future.

# References


1. Hammon JW Jr et al. *Ann Thorac Surg* 1988;45:537–40.
2. Colan SD et al. *J Am Cardiol* 2006;47:1858–65.
3. Eicken A et al. *Catheter Cardiovasc Interv* 2010;76:404–10.
4. Serraf A et al. *J Am Coll Cardiol* 1999;33:827–34.
5. Tani LY et al. *J Thorac Cardiovasc Surg* 1999;118:81–6.
6. Reddy VM et al. *Ann Thorac Surg* 1995;60:S600–3.
7. Aszyk P et al. *Eur J Cardiothorac Surg* 2012;42:687–94.

8. Carminati M et al. *J Interv Cardiol* 1995;8:759–66.
9. Robinson BV et al. *Cardiol Young* 2000;10:225–32.
10. Gatzoulis MA et al. *Arch Dis Child* 1995;73:66–9.
11. Soulatges C et al. *Pediatr Cardiol* 2015;36:1145–52.
12. Fratz S et al. *Circulation* 2008;117:1201–6.
13. Brown DW et al. *J Am Coll Cardiol* 2010;56:1740–9.
14. Bhabra MS et al. *Ann Thorac Surg* 2003;76:1412–6.
15. Miyamoto T et al. *Eur J Cardiothoracic Surg* 2006;30:35–40.
16. Hraska V et al. *Ann Thorac Surg* 2012;94:1519–26.
17. Brown JW et al. *Ann Thorac Surg* 2012;94:146–53.
18. Calhoon JH, Bolton JW. *Ann Thorac Surg* 1995;60(suppl): S597–9.
19. Norwood WI et al. *Am J Cardiol* 1980;45:87–91.
20. Sano S et al. *J Thorac Cardiovasc Surg* 2003;126:504–9.
21. Jacobs ML et al. *J Thorac Cardiovasc Surg* 1998;116:417–31.
22. Miyamoto SD et al. *Pediatr Cardiol* 2009;30:419–25.
23. Gibbs JL et al. *Br Heart J* 1993;69:551–5.
24. Murphy MO et al. *Ann Thorac Surg* 2015;100:2286–90.
25. Malik S et al. *J Thorac Cardiovasc Surg* 2015;150:474–80.
26. Brescia AA et al. *J Thorac Cardiovasc Surg* 2014;147:1777–82.
27. McElhinney DB et al. *Circulation* 2005;112:707–14.
28. Stellin G et al. *J Thorac Cardiovasc Surg* 2010;140:1238–44.
29. Walter EM et al. *Eur J Cardiothorac Surg* 2013;43:473–82.
30. Oppido G et al. *J Thorac Cardiovasc Surg* 2008;135:1313–21.
31. Lee C et al. *Eur J Cardiothorac Surg* 2009;37:267–72.
32. Schreiber C et al. *Ann Thorac Surg* 2000;70:1896–9.
33. Hirooka K, Fraser CD Jr. *Texas Heart Inst J* 1997;24:317–21.
34. Mainwaring RD, Lamberti JJ. *Ann Thorac Surg* 1997;64: 1782–5.
35. Brown JW et al. *Eur J Cardiothorac Surg* 2006;29:666–73.
36. Hakimi M et al. *Ann Thorac Surg* 1997;64:503–7.
37. Morales DL et al. *Ann Thorac Surg* 2006;82:1577–83.
38. Alsoufi B et al. *J Thorac Cardiovasc Surg* 2016;151:412–20.
39. Fletcher SE et al. *J Am Coll Cardiol* 1995;25:730–4.
40. Rothman A et al. *Am J Cardiol* 2010;105:1176–80.
41. Rao PS et al. *J Am Coll Cardiol* 1996;27:462–70.
42. Backer CL et al. *Circulation* 1995;92(suppl 2):132–6.
43. Rajasinghe HA et al. *Ann Thorac Surg* 1996;61:840–4.
44. Cobanoglu A et al. *Eur J Cardiothorac Surg* 1998;14:19–25.
45. Backer CL et al. *Ann Thorac Surg* 1998;66:1365–70.
46. Jahangiri M et al. *J Thorac Cardiovasc Surg* 2000;120:224–9.
47. Kaushal S et al. *Ann Thorac Surg* 2009;88:1932–8.
48. Burch PT et al. *J Thorac Cardiovasc Surg* 2009;138:547–52.
49. Bacha EA et al. *Ann Thorac Surg* 2000;71:1260–4.
50. Reddy VM et al. *Ann Thorac Surg* 1995;60(suppl):S592–6.
51. Kim H et al. *J Thorac Cardiovasc Surg* 2015;149:515–20.
52. Davies B et al. *J Thorac Cardiovasc Surg* 2009;138:1269–75.
53. Tchervenkov CI et al. *J Thorac Cardiovasc Surg* 1997;114:727–35.
54. Iyer KS, Mee RB. *Ann Thorac Surg* 1991;51:65–72.
55. Reddy VM et al. *J Thorac Cardiovasc Surg* 1995;109:832–44.
56. Lofland GK. *Eur J Cardiothorac Surg* 2000;18:480–6.
57. Carrillo SA et al. *Ann Thorac Surg* 2015;100:606–14.
58. Ekman Joelsson BM et al. *Scand Cardiovasc J* 2001;35:192–8.
59. Powell AJ et al. *Am J Cardiol* 2000;86:1272–4.
60. Jahangiri M et al. *J Thorac Cardiovasc Surg* 1999;118:1046–55.
61. Foker JE et al. *J Thorac Cardiovasc Surg* 2008;136:749–56.
62. Giglia TM et al. *Circulation* 1992;86:1516–28.
63. Cleuziou J et al. *Thorac Cardiovasc Surg* 2010;58:339–44.
64. Cho MJ et al. *Congenit Heart Dis* 2013;8:440–9.
65. Alwi M et al. *J Am Coll Cardiol* 2000;35:468–76.
66. Ovaert C et al. *J Thorac Cardiovasc Surg* 1998;115:1055–62.
67. Wang JK et al. *Am J Cardiol* 1999;84:1055–60.
68. Sano S et al. *Ann Thorac Surg* 2000;70:1501–6.
69. Laks H et al. *J Thorac Cardiovasc Surg* 1999;118:1046–52.
70. Adachi I et al. *Am J Cardiol* 2011;107:459–65.
71. Reddy VM et al. *J Am Coll Cardiol* 1997;29:1365–70.
72. Cnota JF et al. *J Thorac Cardiovasc Surg* 2013;145:1288–96.
73. Chern ZY et al. *Ann Thorac Surg* 2014;97:1400–6.
74. Siehr SL et al. *Congenit Heart Dis* 2014;9:211–5.
75. Metton O et al. *Eur J Cardiothorac Surg* 2010;37:1246–53.
76. Pasquali SK et al. *Circulation* 2002;106:2575–80.
77. https://nicor5.nicor.org.uk/CHD/an_paeds.nsf/0/5B3DDC0B57A88C3980257F8E0052CC00?OpenDocument?Benchmark
78. Yong MS et al. *Ann Thorac Surg* 2011;91:1921–7.
79. Kelle AM et al. *J Thorac Cardiovasc Surg* 2010;139:1387–94.
80. Burke RP et al. *J Thorac Cardiovasc Surg* 1995;109:499–507.
81. Chun K et al. *Ann Thorac Surg* 1992;53:597–602.
82. Anand R et al. *Pediatr Cardiol* 1994;15:58–61.
83. Rivilla F et al. *Z Kinderchirurg* 1989;44:199–202.
84. Alexi-Meskishvili V et al. *J Thorac Cardiovasc Surg* 2011;142: 868–74.
85. Naimo PS et al. *Ann Thorac Surg* 2016;101:1842–8.
86. Bakhtiary F et al. *World J Pediatr Congenit Heart Surg* 2011;2: 550–3.
87. Cabrera AG et al. *Ann Thorac Surg* 2015;99:1342–7.
88. Schmitt B et al. *Ann Thorac Surg* 2014;98:1425–36.
89. Kirklin JW et al. *Circulation* 1979;60:373–86.
90. Castañeda AR et al. *J Thorac Cardiovasc Surg* 1977;74:372–81.
91. Kirklin JW et al. *Ann Surg* 1983;198:251–65.
92. Kirsch RE et al. *J Thorac Cardiovasc Surg* 2014;147:713–7.
93. Steiner MB et al. *J Thorac Cardiovasc Surg* 2014;147:1299–305.
94. Tamesberger MI et al. *Ann Thorac Surg* 2008;86:1928–35.
95. Kanter KR et al. *Ann Thorac Surg* 2010;89:858–63.
96. Barron DJ et al. *Eur J Cardiothorac Surg* 2013;44:656–62.
97. Fesslova' V et al. *Heart* 1999;82:594–9.
98. Allan LD et al. *Br Heart J* 1985;54:523–6.
99. Copel JA et al. *Ultrasound Obstet Gynecol* 1997;10:237–41.
100. Rose V, Clark LE. Etiology of congenital heart disease. In: Freedom RM, Benson LN, Smallhorn JF, eds. *Neonatal Heart Disease*. New York, NY: Springer-Verlag; 1992:3–13.
101. Fishman NH et al. *Circulation* 1978;58:354–64.
102. Allan LD et al. *J Am Coll Cardiol* 1986;8:1131–6.
103. Widdowson EM et al. *Clin Sci* 1951;10:113–25.
104. Widdowson EM, Spray CM. *Arch Dis Child* 1951;26:205–14.
105. Hallock GG et al. *Ann Plast Surg* 1988;21:310–5.
106. Lovvorn HN III et al. *J Pediatr Surg* 1999;34:218–23.
107. Richter RC et al. *J Cardiovasc Surg* 1985;26:86.
108. Bradley SM et al. *Am J Physiol* 1992;263:H919–28.
109. Bradley SM et al. *Surg Forum* 1991;72:196–7.
110. Sabik JF et al. *J Thorac Cardiovasc Surg* 1992;103:733–42.
111. Sabik JF et al. *J Thorac Cardiovasc Surg* 1996;111:536–44.
112. Fenton KN et al. *J Thorac Cardiovasc Surg* 1994;107:1416–22.
113. Fenton KN et al. *J Thorac Cardiovasc Surg* 1994;107:1423–7.
114. Reddy VM et al. *Ann Thorac Surg* 1996;62:393–400.
115. Sebastian VA et al. *J Thorac Cardiovasc Surg* 2013;145:1460–4.
116. Reddy VM et al. *J Thorac Cardiovasc Surg* 1996;111:536–44.
117. Champsaur G et al. *Circulation* 1994;90:II47–50.
118. Hawkins JA et al. *Ann Thorac Surg* 1994;57:293–7.
119. Maxwell D et al. *Br Heart J* 1991;65:256–8.
120. Freud LR et al. *Circulation* 2014;130:638–45.
121. Mäkikallio K et al. *Circulation* 2006;113:1401–5.
122. McElhinney DB et al. *Circulation* 2009;120:1482–90.
123. Tulzer G et al. *Lancet* 2002;360:1567–8.
124. Arzt W et al. *Ultrasound Obstet Gynecol* 2003;21:186–8.

125. Kalish BT et al. *Catheter Cardiovasc Interv* 2014;84:77–85.
126. Chaturvedi RR et al. *Int J Cardiol* 2013;168:2029–36.
127. Marshall AC et al. *Prenat Diagn* 2008;28:1023–8.
128. Edwards A et al. *Prenat Diagn* 2015;35:74–80.
129. Weber B et al. *Eur J Cardiothorac Surg* 2012;41:398–403.
130. Nugent AW et al. *J Matern Fetal Neonatal Med* 2013;26: 1778–81.
131. Michaelsson M, Engle MA. Congenital complete heart block: An international study of the natural history. In: Breast YAN, Engle MA, eds. *Cardiovascular Clinics*. Philadelphia, PA: FA Davis; 1972:89–101.
132. Machado MVL et al. *Br Heart J* 1988;60:512–5.
133. Schmidt KG et al. *J Am Coll Cardiol* 1991;17:1360–6.
134. Groves AMM et al. *Heart* 1996;75:190–4.
135. Deloof E et al. *Eur J Pediatr* 1997;156:521–3.
136. Scagliotti D et al. *Pacing Clin Electrophysiol* 1987;10:1253–61.
137. Kikuchi Y et al. *Pacing Clin Electrophysiol* 1995;18:417–23.
138. Liddicoat JR et al. *Circulation* 1997;96:1025–30.
139. Ayustawati et al. *Am J Obstet Gynecol* 2002;186:1052–5.
140. Loeb GE et al. *Ann Biomed Eng* 2013;41:17–27.
141. Assad RS et al. *J Thorac Cardiovasc Surg* 2003;126:300–2.
142. Eghtesady P et al. *J Thorac Cardiovasc Surg* 2011;141:835–7.

# 58

# Neurodevelopment in congenital heart disease: Intrauterine Doppler and fetal and neonatal magnetic resonance imaging

Shabnam Peyvandi and Mary T. Donofrio

## Introduction

With advances in neonatal surgical techniques, survival has improved considerably for patients with congenital heart defects (CHDs). Although there has been a decline in gross neurologic insults in these children, many experience behavioral, emotional, cognitive, and motor impairments, suggesting widespread brain dysfunction. Given these outcomes, recent and ongoing research is focused on the impact of CHD on brain development, brain injury, and neurodevelopmental (ND) outcomes to better understand mechanisms of injury and identify potential therapeutic targets to improve outcome.

This chapter reviews the impact that CHD has on the developing brain of the fetus and infant. Current knowledge on short- and long-term ND outcomes in children with CHD is discussed with a focus on potential etiologies including fetal and neonatal brain development, the risk of preoperative brain injury, and altered fetal cerebral blood flow and intrauterine growth.

## Neurodevelopmental outcome after surgical repair of congenital heart defect

There is an increasing body of literature reporting short- and long-term ND outcomes in patients with various types of CHD. Despite heterogeneity among these reports due to various methodologies for age at follow-up, assessment tools used, and type of cardiac lesion studied, these outcome data have provided us with useful knowledge on ND outcomes and provide the foundation for understanding imaging and clinical data in the fetal and neonatal periods.

### *Short-term neurologic outcomes after surgical repair*

Although the prevalence of overt neurologic dysfunction postoperatively has declined, a small percentage of infants continue to exhibit neurologic abnormalities, including clinical seizures, hypotonia, hypertonia, and asymmetry of tone. Combining several reports, the prevalence of postoperative seizures appears to be 4%–11% and may be detected by continuous electroencephalographic (EEG) monitoring in up to 20% of patients in the immediate postoperative period.[1–6] In addition, there is a higher prevalence of feeding abnormalities (swallow or suck dysfunction) in neonates undergoing cardiac surgery, and this may be an early indicator of abnormal ND later in life.[7]

### *Intermediate- and long-term neurologic outcomes after surgical repair*

Although there have been several reports of ND outcomes in a mixture of CHD types, it is important to recognize that outcomes can vary significantly by cardiac lesion. These outcomes have been studied in two specific high-risk populations: D-transposition of the great arteries (D-TGA) and defects requiring single-ventricle palliation. In patients with D-TGA after an arterial switch operation, the Boston Circulatory Arrest Trial has demonstrated that IQ scores although below the national average, continue to fall within the normal range at 8 and 16 years of age. However, a high percentage of children were judged to have behavioral problems by parents and teachers; 37% required remedial education services, and 10% had repeated a grade.[8–10]

Patients with single-ventricle lesions, in particular, hypoplastic left heart syndrome (HLHS), are at highest risk of worse ND outcomes based on underlying physiology, hemodynamics, and the complexity of surgical repair. These children will undergo a series of palliative surgical procedures typically culminating in a Fontan operation. Various studies have demonstrated that children with HLHS tend to have lower IQs (typically below the general population mean) and problems with visual-motor skills, expressive language, attention, and externalizing behavior.[11–13] In the largest series reported to date, children with HLHS at 12 months of age had a median Mental Development Index of 90 (range 50–129)

and a lower median Psychomotor Development Index of 73 (range 50–117). Risk factors for poor outcome were mainly patient specific and included genetic syndromes, gestational age at delivery, and perioperative stability.[11]

Recent guidelines have recommended repeated surveillance, screening, and evaluation of all children with CHD requiring surgery in the first year of life and appropriate referrals for early intervention.[14] Despite improvements in surgical technique, ND outcomes have not improved significantly over the last decade, suggesting that innate patient-specific risk factors may play a bigger role in ultimate outcome.[15] This also suggests that fetal and preoperative neonatal factors also impact outcome.

## Preoperative neurologic status in congenital heart disease

Much of the early literature is focused on factors related to surgery to explain ND outcomes in these patients. However, an increasing body of literature has demonstrated that these infants are at risk for adverse outcomes before entering the operating room. These findings are likely multifactorial and caused by factors such as hemodynamic alterations, congenital brain abnormalities, and acquired brain injury.

### *Clinical presentation of preoperative brain abnormalities*

Several studies have identified neurobehavioral abnormalities in newborns with CHD prior to their corrective operation. In a series by Limperopoulos, 50% of newborns with critical CHD were found to have neurologic abnormalities including hypotonia, hypertonia, motor asymmetry, jitteriness, absent suck, and seizures.[16,17] The same group described abnormal EEG in 60 infants with CHD. Prior to surgery, 19% had epileptiform activity, and 33% had moderate or diffuse disturbances in background activity. EEG abnormalities were associated with abnormal findings on neurologic examination, and severe abnormalities were predictive of death.[18] Other studies have reported seizures, tone abnormalities, or choreoathetosis in various CHD subtypes.[19]

### *Magnetic resonance imaging evidence of impaired preoperative neurologic status in CHD*

Structural brain malformations in neonates with CHD can be identified in the absence of a defined genetic syndrome. An autopsy study revealed multiple congenital brain anomalies in neonates with HLHS, including microcephaly (brain weight >2 standard deviations below the mean) in 27%, abnormal cortical mantle formation in 27%, and overt central nervous system malformations such as agenesis of the corpus callosum or holoprosencephaly in 10%.[20] Other magnetic resonance imaging (MRI)-based studies have identified other anomalies such as microcephaly, an open operculum, or delayed closure of the opercula.[17,21,22]

In addition to structural abnormalities, there is MRI evidence that brain development is delayed in CHD. Quantitative MRI techniques such as diffusion tensor imaging (DTI) measure the direction and magnitude of water movement and thus microstructural brain development. During normal brain development, the magnitude of water diffusion motion decreases (apparent diffusion coefficient) and regional directionality increases in white matter (fractional anisotropy). Similarly, metabolic brain development can be measured with magnetic resonance spectroscopy (MRS) by measuring major metabolic compounds such as *N*-acetyl aspartate (NAA), choline (Cho), creatine (Cr), and lactate. Using these techniques, Miller et al. discovered that newborns with CHD (D-TGA and single-ventricle lesions) have findings suggesting an immature brain with abnormal DTI (4% higher average diffusivity and 12% lower FA) and MRS (10% lower NAA/Cho).[23] Comparing these findings to those obtained throughout gestation in normal fetuses, newborns with CHD appear approximately 1 month delayed. These observations have been replicated in studies assessing brain development by semiquantitative morphologic scoring, specifically the Brain Total Maturation Score (TMS). In a study by Licht et al., the TMS was significantly lower in 29 neonates with D-TGA and HLHS as compared to a normal population.[24] The group speculated that the immature brain may be more susceptible to injury both *in utero* and in the neonatal period. In another study, Andropoulos showed that newborns with CHD that had low TMS were more likely to have both pre- and postoperative brain injury, and more severe postoperative brain injury.[25]

In addition to developmental abnormalities, acquired brain lesions may be detectable in neonates with CHD before surgery, representing injury due to hemodynamic compromise with or without hypoxia. Much of the ND outcomes have been attributed to clinically silent brain injuries, most commonly focal white matter lesions or strokes identified by sensitive MRI studies. Several large, prospective studies have been performed using pre- and postoperative brain MRI to determine the frequency of acquired brain injury and associated risk factors in newborns with CHD. MRI evidence of preoperative brain injury in the form of white matter injury (periventricular leukomalacia) or stroke has been identified in 28%–39% of newborns with critical CHD, specifically those with single-ventricle lesions and D-TGA.[21,22,26,27]

Risk factors for preoperative brain injury include hypoxemia,[28] the presence of aortic atresia in HLHS,[29,30] hypotension and lower oxygen saturations, and a longer time to surgery.[31] The pattern of brain injury in the form of white matter injury is similar to that observed in premature infants and is thought to be secondary to hypoxic ischemic and inflammatory injury to susceptible immature premyelinating oligodendricytes. Interestingly, another risk factor for preoperative brain injury is a morphologically immature brain or lower TMS,[30] suggesting a similar mechanism of injury

**Table 58.1** MRI evidence of preoperative brain injury in newborns with congenital heart disease

| *Study* | *Sample* | *CHD* | *Findings* | *Risk factors* |
|---|---|---|---|---|
| Mahle et al.[21] | CHD-24 | Mixed | PVL = 16%<br>Infarct = 8%<br>Elevated brain lactate = 53% | N/A |
| Miller et al.[26] | CHD-10<br>Control-5 | TGA | Brain injury (stroke) = 40%<br>Elevated brain lactate = 2.7 × higher than controls | N/A |
| Licht et al.[22] | CHD = 25 | Mixed | PVL = 28% | • Decreased cerebral blood flow<br>• Hypercarbia |
| McQuillen et al.[27] | CHD = 62 | Mixed | WMI = 18%<br>Stroke = 21%<br>IVH = 8% | • Low Apgar score at 5 minutes<br>• BAS |
| Petit et al.[28] | CHD = 26 | TGA | PVL = 38% | • Lower preoperative oxygen saturation<br>• Longer time to surgery |
| Andropoulos et al.[25] | CHD = 68 | Mixed | WMI = 16%<br>Infarct = 18% | • Low total maturation score (brain immaturity) |
| Glass et al.[56] | CHD = 127 | Mixed | WMI = 24% | • Bloodstream infection in TGA subjects |
| Goff et al.[30] | CHD = 57 | HLHS | PVL = 19% | • Male sex<br>• Aortic atresia<br>• Low total maturation score (brain immaturity) |
| Peyvandi et al.[57] | CHD = 153 | Mixed | WMI = 24%<br>Stroke = 20%<br>Hypoxic ischemic = 1% | • Postnatal diagnosis of CHD |

*Abbreviations:* BAS, balloon atrial septostomy; CHD, congenital heart disease; HLHS, hypoplastic left heart syndrome; IVH, intraventricular hemorrhage; PVL, periventricular leukomalacia; TGA, transposition of the great arteries; WMI, white matter injury.

as that seen in premature neonates (Table 58.1). These brain MRI findings in the neonate with CHD even prior to any corrective operations have led to the theory that abnormal brain development and susceptibility to injury begin *in utero*.

## Fetal cardiovascular and cerebral physiology in CHD

Human brain development is a complex process with morphologic events occurring in the first two trimesters, followed by a prolonged period of refinement of connections that occurs in the third trimester and extends into the early postnatal period. Consequently, blood flow to the fetal brain increases and is estimated to be approximately 25% of the combined ventricular output. In the normal fetus, cerebral blood flow is supplied by highly oxygenated blood from the ductus venosus preferentially streaming across the foramen ovale to the left atrium and ventricle (Figure 58.1). Depending on the subtype of CHD, cerebral blood flow and thus oxygen delivery can be impaired (Figure 58.1). In D-TGA, the aorta and pulmonary artery are transposed, and thus, the higher oxygenated blood reaches the pulmonary vasculature as opposed to the aorta. In HLHS, inadequate left heart structures lead to reversal of blood flow in the foramen ovale with mixing of oxygenated and deoxygenated blood in the right ventricle and in cases of aortic atresia, retrograde flow in the ascending aorta. Finally, in tetralogy of Fallot (TOF) or hypoplastic right heart syndrome (HRHS), relatively deoxygenated blood enters the cerebral circulation due to intracardiac mixing.

This altered circulation can lead to flow disturbances that may affect *in utero* growth and brain development. In fact, many large studies have revealed that infants with CHD had abnormal *in utero* somatic growth compared to matched controls. Specifically, those with D-TGA had normal birth weights, but small head circumferences relative to birth weight. Those with HLHS had lower birth weights, length, and a smaller head circumference out of proportion to the weight. Those with TOF had normal proportions, but all somatic growth was less than normal.[32,33]

### *Fetal cerebral blood flow characteristics and compensatory mechanisms*

Cerebral Doppler ultrasound can assess fetal cerebral vascular resistance in the middle cerebral artery (MCA) by calculating

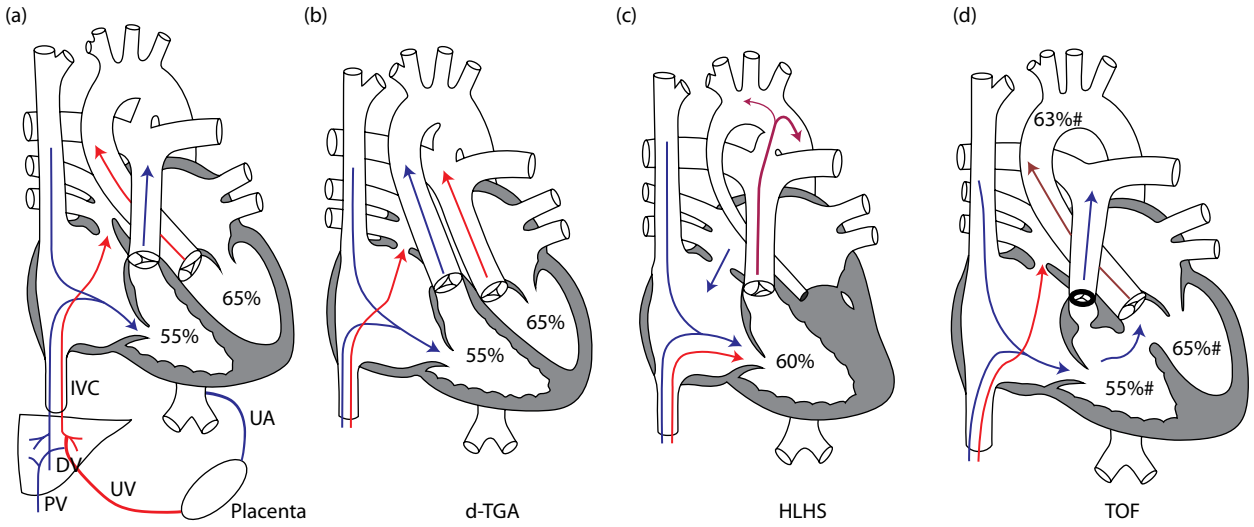


**Figure 58.1**
Normal and altered fetal circulation. (a) Normal fetal blood flow; (b) d-transposition of the great arteries; (c) hypoplastic left heart syndrome; (d) tetralogy of Fallot. Red arrows represent oxygenated blood, and blue arrows represent deoxygenated blood.

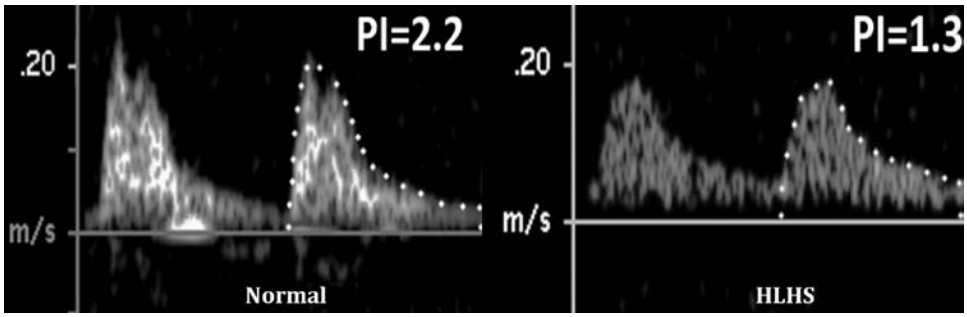


**Figure 58.2**
MCA Doppler patterns in a normal fetus and a fetus with hypoplastic left heart syndrome (HLHS). The pulsatility index (peak systolic velocity–end diastolic velocity/mean velocity) in the HLHS fetus is lower, suggesting decreased impedance in the cerebral vasculature.

the pulsatility index (PI) or resistance index (RI), a measure of vascular resistance in the circulatory bed downstream from the point of Doppler sampling. These indices are calculated by measuring the peak systolic velocity (PSV), end diastolic velocity (EDV), and mean velocity (MV): PI = PSV-EDV/MV; RI = PSV-EDV/PSV (Figure 58.2). Similar calculations can be used to measure placental resistance by calculating the PI or RI in the umbilical artery. Normative indices have been established, and the cerebral to umbilical artery ratio of these indices is more predictive of fetal growth restriction and poor outcome than either index in isolation. Fetuses with placental insufficiency and resultant growth restriction have an elevated resistance in the umbilical artery and lower resistance in the MCA, consistent with the "brain-sparing" effect, which is thought to be an adaptive response to intrauterine hypoxia.[34,35] In normal pregnancies, the cerebral/umbilical resistance or PI ratio is greater than one, whereas in many growth-restricted fetuses, the ratio is less than one and predicts adverse perinatal and neurologic outcome.[36,37] This autoregulatory mechanism is thus paradoxically a harbinger for poor outcome in the setting of fetal growth restriction. A review of the Doppler indices of cerebral blood flow and their implications is presented in Table 58.2.

## *Alterations in cerebral blood flow in fetuses with CHD*

Two major studies have characterized *in utero* blood flow patterns in human fetuses with CHD. Donofrio published a multicenter, prospective study that assessed cerebral blood flow at serial intervals in fetuses with CHD ($n = 36$) as compared to normal controls ($n = 21$).[38] Cerebral artery resistance and cerebral/umbilical resistance ratios were lower for fetuses with CHD compared with controls. In fact, 44% of fetuses with CHD had an abnormal MCA/UA RI compared to only 5% in the control cohort. Interestingly, the percentage of abnormal ratios varied by CHD lesion with fetuses with HLHS and HRHS having the highest percentage of abnormal resistance ratios. Fetuses with TOF and D-TGA were less affected (45% and 25%, respectively). In addition, those with HLHS had the lowest MCA/UA ratio followed by

**Table 58.2** Doppler indices of cerebral blood flow

| *Doppler measure* | *Definition* | *Significance* | *Congenital heart disease* |
|---|---|---|---|
| Middle cerebral artery pulsatility index (MCA PI) | (SV-DV)/MV | Lower value associated with higher mortality and poor neurologic outcome in fetal growth restriction | • Lower in HLHS and higher in right-sided obstructive lesions[39]<br>• Lower in TGA compared to controls[40]<br>• Lower in CHD with intracardiac mixing[41]<br>• Lower in CHD fetuses with CHF[41] |
| Cerebral resistance index (CRI) | (SV-DV)/SV | Lower value associated with fetal growth restriction | • Lower in CHD versus controls[38] |
| Cerebral/umbilical pulsatility ratio | MCA PI/UA PI | Ratio <1 associated with growth restriction and poor outcome | • Increased in CHD[42] |
| Cerebral/umbilical resistance ratio | CRI/URI | Ratio <1 associated with growth restriction and poor outcome | • Lower in CHD versus controls<br>• Lowest in HLHS (58% with ratio <1)[38] |

*Abbreviations:* CHD, congenital heart disease; CHF, congestive heart failure; CRI, cerebral resistance index; DV, diastolic velocity; HLHS, hypoplastic left heart syndrome; MCA PI, middle cerebral artery pulsatility index; MV, mean velocity; SV, systolic velocity; TGA, transposition of the great arteries; UA PI, umbilical artery pulsatility index; URI, umbilical artery resistance index.

D-TGA. Given the anatomical differences between various cardiac lesions, it is not surprising that lesion type affects not only the source of cerebral blood flow but also the degree of deoxygenated blood distributed through the cerebral circulation. The resistance ratio nadir for heart disease fetuses was at 24 weeks' gestation, which is the onset of a critical period in fetal brain development (Figure 58.3). Thus, peak autoregulation of cerebral blood flow in fetuses with CHD occurs during the time of brain development when increased perfusion is needed the most to compensate for cerebral hypoxemia.

In the second largest study to evaluate cerebral blood flow patterns; Kaltman et al. studied MCA PI in fetuses with HLHS ($n = 28$) and right heart obstruction ($n = 14$) compared to controls ($n = 114$).[39] Their study revealed that HLHS fetuses had lower MCA PI, whereas those with right heart obstruction had a higher MCA PI as compared with normal controls. The finding of an increased MCA PI in fetuses with right-sided obstruction may be secondary to cerebral autoregulation to limit excessive flow. In right heart obstruction, antegrade flow from the aorta is unobstructed and perhaps increased from normal. Conversely, in HLHS there is intracardiac mixing with lower oxygen content in the blood delivered to the brain. In addition, perfusion to the brain is likely compromised due to a hypoplastic aortic isthmus with retrograde cerebral circulation. Although cerebral autoregulation appears to be an autoregulatory mechanism to increase cerebral blood flow, the isthmus may restrict the absolute amount of blood that can be delivered to the brain. This may contribute to the higher prevalence of ND abnormalities found in children with HLHS. Several additional studies have investigated cerebral blood flow patterns in the fetus with CHD, all of which have demonstrated similar findings of a lower MCA PI in cardiac lesions with the most intracardiac mixing.[40–42] These studies demonstrate that alterations in the

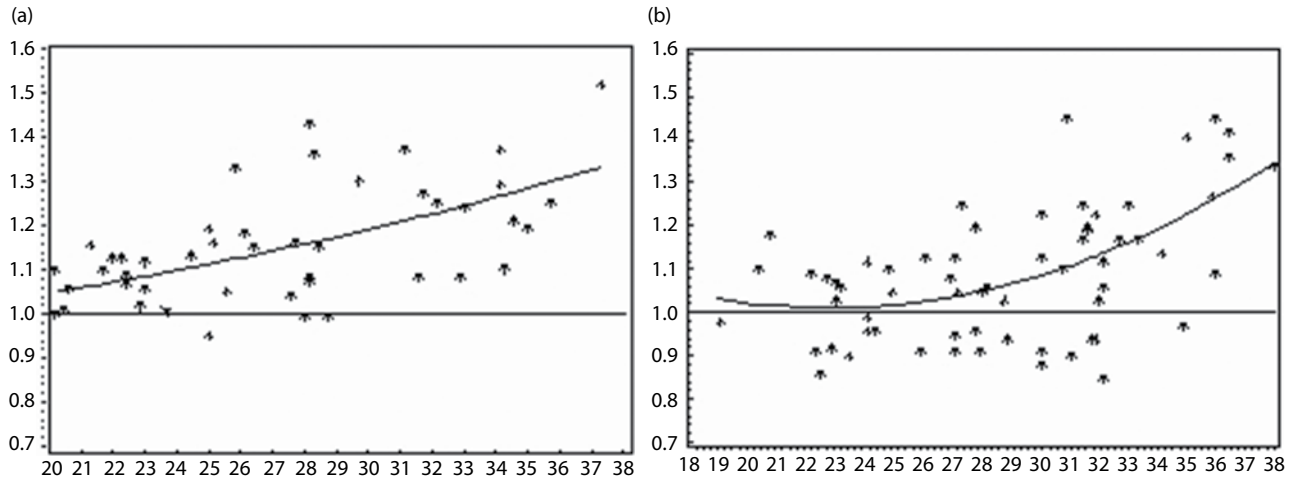


**Figure 58.3**
Cerebral to placental resistance ratio versus gestational age for normal fetuses and fetuses with congenital heart disease (CHD). (a) Normal fetuses; (b) fetuses with congenital heart disease. (CRI, cerebral resistance ratio; URI, umbilical resistance ratio.)

intracardiac circulation caused by specific cardiac defects result in changes in cerebral blood flow characteristics. The mechanism is complex and likely related to altered cerebral blood oxygen content as well as possibly decreased blood flow resulting in overall decreased oxygen delivery.

Cerebral blood flow characteristics have also been shown to predict ND outcomes in fetuses with CHD. A large study conducted by researchers in the Pediatric Heart Network found that in infants with HLHS ($n = 119$), a lower MCA PI *in utero* predicted a better ND outcome at 14 months of age as assessed by the Bayley Scales of Infant Development-II.[43] Specifically, MCA PI z-score was found to correlate negatively with the psychomotor development index (PDI) but was not associated with the mental development index (MDI). In addition, MCA PI z-score remained an independent predictor of PDI at 14 months of age in a multivariable regression model. These findings suggest that the autoregulatory response of cerebral vasodilation in the setting of HLHS may be sufficient and adaptive to a state of chronic hypoxemia. This is in contrast to what is seen in the context of fetal growth restriction, which is largely secondary to placental insufficiency as the primary etiology. Further large prospective studies are needed to understand the predictive utility of cerebral blood flow patterns in fetuses with CHD.

## Fetal structural and developmental abnormalities of the brain in CHD

Technical advances in fetal MRI have made it an important tool in the clinical evaluation of fetuses with suspected cerebral abnormalities. This has extended into the CHD population, and current techniques have revealed structural and developmental abnormalities in the fetal brain.

### *Quantitative assessment of fetal brain development in CHD*

Limperopoulos reported the first *in vivo* MRI brain study in human fetuses with CHD and demonstrated abnormalities in fetal brain growth and development.[44] In this study, 55 fetuses with CHD (gestational age 25–37 weeks) were compared to 50 normal fetuses using three-dimensional volumetric MRI and MRS (Figure 58.4). Measurements included fetal intracranial cavity volume, cerebrospinal fluid volume, total brain volume, cerebral NAA:Cho ratios, and cerebral lactate levels. The results demonstrated a progressive decline in age-adjusted total brain volume and intracranial cavity volume in fetuses with CHD relative to controls. In addition, although NAA:Cho ratios increased over the course of gestation in CHD fetuses, the rate of rise was slower than the control fetuses. On a multivariable analysis, cardiac diagnosis and aortic atresia were independently associated with total brain volume, suggesting that delivery of oxygen and nutrients is influenced by the specific cardiac defect and impacts brain development. Predictors of a lower NAA:Cho ratio included cardiac diagnosis, the absence of antegrade aortic arch flow, and the presence of cerebral lactate. These findings have been replicated in other studies assessing multiple types of CHD[45] and in fetuses with tetralogy of Fallot.[46] In another study using three-dimensional brain MRI, Clouchoux showed that fetuses with HLHS had less gyrification and cortical plate surface area, progressive

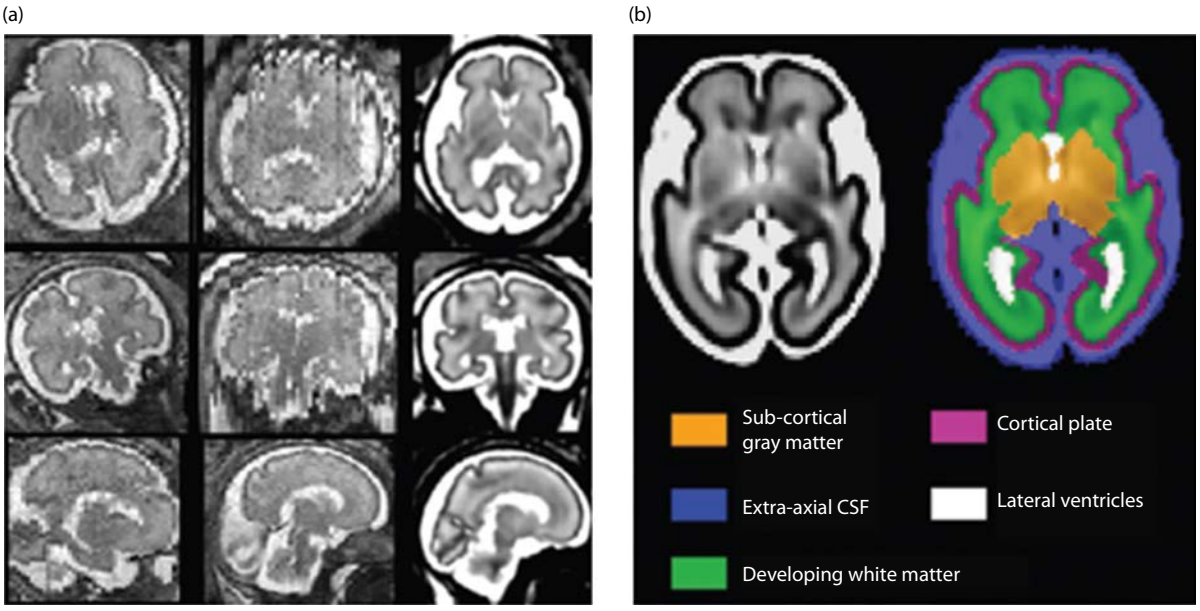


**Figure 58.4**
Three-dimensional manual segmentation of fetal magnetic resonance axial images. (a) The first two columns demonstrate low-resolution volumes for a single fetal brain at 30.1 weeks in the sagittal and axial planes and the third column demonstrates the resulting high-resolution reconstructed volume; (b) axial view of a high-resolution reconstructed fetal brain MR image and the corresponding brain tissue segmentation. (From Clouchoux C et al. *Cereb Cortex* 2012;23(12):2932–43.[47])

third-trimester reduction in cortical white and gray matter volumes, and delayed development of local sulci and gyri compared to normal controls.[47] Abnormal brain findings were seen more often in fetuses with an abnormal cerebral to placental resistance ratio and absent antegrade aortic flow. Finally, a study utilizing DTI in fetuses with CHD found that in three subjects, the DTI measures in the periatrial white matter and thalamus were higher as compared to normal subjects, suggesting brain immaturity.[48] These studies demonstrate the feasibility of performing fetal brain MRI in this population with evidence to suggest that brain immaturity begins *in utero*. The predictive value of these findings for postnatal outcomes such as brain injury and ND outcome remains unknown.

In a recent study, the use of midgestation ultrasound with brain Doppler and biometry was able to predict abnormal brain MRI late in pregnancy. In this single-center study, 58 fetuses with CHD were evaluated.[49] The researchers defined abnormal brain development by a composite score based on the MRI findings, which included: (1) total brain volume less than the 10th percentile, (2) parietoccipital or cingulate fissure depth less than the 10th percentile, or (3) abnormal metabolic profile in the frontal lobe (i.e., NAA:Cho ratio). Based on this model, they found that MCA PI, MCA PI/UA PI ratio and head circumference in midgestation were independent predictors of abnormal brain development near term gestation. A regression analysis suggested that a combination of MCA PI and head circumference z-scores at midgestation were the best predictors of abnormal brain development. A small proportion of subjects in the cohort also underwent neurodevelopmental testing at 4–6 months of age (BSID-III). They found several linear correlations between MDI and PDI scores with MRI measurements of brain development in late gestation including total brain volume, left and right cingulate fissure depth, and frontal NAA:Cho ratio. Although this paper combined several cardiac lesions with varying types of physiology, it suggests that fetal ultrasound measures such as MCA Doppler at the time of diagnosis in the second trimester may be predictive of brain development at birth.

## Structural abnormalities of the fetal brain in CHD

As discussed, structural abnormalities of the brain are seen frequently in the neonate with CHD. However, advanced fetal MRI techniques have enabled the identification of structural brain abnormalities *in utero*. In a study by Brossard-Racine et al., fetal brain MRI detected structural abnormalities in 23% of CHD fetuses (total studied = 144) as compared to 1.5% in normal fetuses.[50] The most common abnormalities included mild unilateral ventriculomegaly and increased extra-axial spaces. The structural brain anomalies were not associated with severity of cardiac lesion and did occur in both cyanotic and acyanotic CHD. Interestingly, four fetuses had evidence of white matter signal hyperintensity, which may represent a precursor to the typical pattern on white matter injury or periventricular leukomalacia seen on postnatal MRI scans in CHD.

The same research group sought to understand the predictive value of structural brain abnormalities in assessing neonatal structural abnormalities and brain injury in the CHD population.[51] Brain abnormalities were found in 16% of the fetal brain MRIs and in 32% of the neonatal MRIs. Structural abnormalities seen on the fetal brain MRI included isolated ventriculomegaly, increased extra-axial spaces, white matter cysts, isolated vermian hypoplasia, and white matter signal hyperintensity on T2-weighted images. On the neonatal brain MRI, acquired injury was seen in 26% of the cases, mostly in the form of white matter injury in the periventricular white matter, the centrum semiovale, and the frontal white matter, as well as nonhemorrhagic parenchymal injury (i.e., focal infarction, diffuse injury, and cysts). Interestingly, of the 33 abnormal neonatal brain MRIs, only nine were preceded by abnormalities on the fetal brain MRI resulting in a high specificity (89%) but low sensitivity (27%) of conventional fetal brain MRI in predicting neonatal findings. In addition, eight subjects had abnormal fetal MRI findings that were not seen on the neonatal MRI. The fetal brain abnormalities that resolved or normalized by the neonatal time period included mild extracerebral space, mild unilateral ventriculomegaly, immature brain appearance, vermis hypoplasia, and single frontal subependymal cyst. This study demonstrates that in addition to prenatal brain immaturity, perinatal and birth-related events contribute and predispose neonates to further cerebral injury after birth.

## Novel fetal magnetic resonance imaging techniques and future directions

The findings from intrauterine Doppler and fetal brain MRI studies suggest that inadequate cerebral oxygen delivery in the fetus may be a cause of the adverse ND abnormalities seen in CHD patients. This has been explored utilizing novel fetal cardiac MRI techniques, which enables measurements of flow and oxygen saturation in fetal blood vessels.[52] By combining fetal brain MRI and cardiovascular magnetic resonance (CMR), Sun et al. found a correlation between fetal cerebral oxygen consumption and brain size (estimated brain weight) among 30 fetuses with CHD in late gestation.[53] There was a direct correlation between estimated brain weight and cerebral oxygen consumption. In addition, there was a modest association between cerebral oxygen delivery and brain size. These findings support the hypotheses generated from the ultrasound and MRI studies suggesting that the hemodynamic alterations that occur *in utero* in fetuses with CHD result in abnormalities in brain development and an increased susceptibility to brain injury. Further exploration is warranted to potentially identify targets and methods of intervention to modify neurodevelopmental outcome in CHD.

## Long-term outcomes and implications for fetal counseling

There are data to support that neurodevelopment remains impaired in teenage years, particularly in those with complex disease such as D-TGA and HLHS. The Boston Circulatory Arrest study revealed that D-TGA patients at 16 years of age continue to exhibit deficits in academic achievement, memory, executive function, visual-spatial skills, attention, and social cognition.[8] Similarly, single-center studies have identified persistent neurodevelopmental abnormalities in adolescents with palliated single-ventricle physiology who undergo the Fontan procedure (i.e., HLHS), including lower IQ and abnormal neuropsychological testing as compared to a normative population.[10] Studies assessing the predictive value of neonatal imaging studies are lacking. However, imaging studies performed on adolescents with Fontan physiology demonstrate an 11-fold increase in structural abnormalities as compared to a normative population.[10] Similarly, a study assessing microstructural brain development in adolescents with D-TGA revealed higher fractional anisotropy in several regions of the brain as compared to controls, indicative of brain immaturity.[54] Longitudinal studies are needed to assess the typical trajectory of brain growth and pattern of injury as these children grow older.

As our knowledge of neurodevelopmental outcomes has increased, this has impacted counseling patterns in the fetal medicine community. Most would agree that for complex CHD requiring a neonatal operation, a discussion should be initiated with the family at the time of fetal diagnosis on short- and long-term neurodevelopmental outcomes, the likely need for continued surveillance, and early intervention. A recent study assessed international prenatal counseling patterns on ND delay in the context of CHD.[55] They found that while most fetal cardiologists and perinatologists were aware of the link between CHD and ND delay, 24% of fetal medicine experts and 12% of fetal/pediatric cardiologists did not counsel families about this association. There was geographic variation with European centers expressing the need for more data to quantify risk factors before incorporating this into their counseling practice. Thus, variability exists in counseling patterns, and further longitudinal studies are needed in prenatally diagnosed subjects with CHD to standardize counseling. It is important to note that the American Heart Association released a statement paper recommending serial neurodevelopmental assessment for at-risk children with CHD.[14] This includes neonates requiring open heart surgery (prior to 30 days of life) and other cyanotic heart lesions such as tetralogy of Fallot that may not require a neonatal operation. In addition, serial evaluation is recommended when CHD is seen in combination with prematurity (<37 weeks), developmental delay recognized in infancy, suspected genetic anomaly, history of mechanical support (extracorporeal membrane oxygenation), heart transplantation, the need for cardiopulmonary resuscitation, prolonged perioperative hospitalization, perioperative seizures, and abnormal neuroimaging.

## Conclusions

Advances in prenatal diagnosis and care and cardiovascular surgical techniques have contributed to the overall increased survival of neonates born with CHD. Given this improvement in survival, greater emphasis is being directed toward improving ND outcomes. More specifically, the study of *in utero* hemodynamics and the effects on cerebral development and susceptibility to injury have identified a potential for optimizing fetal management and intervention strategies to improve outcome.

## References


1. Gaynor JW et al. *J Thorac Cardiovasc Surg* 2005;130(5):1278–86.
2. Gaynor JW et al. *J Thorac Cardiovasc Surg* 2006;131(1):181–9.
3. Newburger JW et al. *N Engl J Med* 1993;329(15):1057–64.
4. Miller G et al. *Arch Pediatr Adolesc Med* 1995;149(7):764–8.
5. Clancy RR et al. *Epilepsia* 2005;46(1):84–90.
6. Ehyai A et al. *JAMA* 1984;252(22):3165–7.
7. Medoff-Cooper B et al. *J Pediatr* 2015;169:154–9.e1.
8. Bellinger DC et al. *Circulation* 2011;124(12):1361–9.
9. Bellinger DC et al. *Cardiol Young* 2009;19(1):86–97.
10. Bellinger DC et al. *J Am Heart Assoc* 2015;4(12):e002302.
11. Newburger JW et al. *Circulation* 2012;125(17):2081–91.
12. Forbess JM et al. *Circulation* 2002;106(12 suppl 1):I95–102.
13. Mahle WT et al. *Pediatr Cardiol* 2012;34(2):327–33.
14. Marino BS et al. *Circulation* 2012;126:1143–72.
15. Gaynor JW et al. *Pediatrics* 2015;135(5):816–25.
16. Limperopoulos C et al. *J Pediatr* 2000;137(5):638–45.
17. Limperopoulos C et al. *Pediatrics* 1999;103(2):402–8.
18. Limperopoulos C et al. *J Child Neurol* 2001;16(7):471–6.
19. Chock VY et al. *J Perinatol* 2006;26(4):237–42.
20. Glauser TA et al. *Pediatrics* 1990;85(6):991–1000.
21. Mahle WT et al. *Circulation* 2002;106(12 suppl 1):I109–14.
22. Licht DJ et al. *J Thorac Cardiovasc Surg* 2004;128(6):841–9.
23. Miller SP et al. *N Engl J Med* 2007;357(19):1928–38.
24. Licht DJ et al. *J Thorac Cardiovasc Surg* 2009;137(3):529–36, discussion 536–7.
25. Andropoulos DB et al. *J Thorac Cardiovasc Surg* 2010;139(3): 543–56.
26. Miller SP et al. *Ann Thorac Surg* 2004;77(5):1698–706.
27. McQuillen PS et al. *Stroke* 2007;38(2 suppl):736–41.
28. Petit CJ et al. *Circulation* 2009;119(5):709–16.
29. Sethi V et al. *Pediatr Res* 2013;73(5):661–7.
30. Goff DA et al. *J Thorac Cardiovasc Surg* 2013;147(4):1312–8.
31. Lynch JM et al. *J Thorac Cardiovasc Surg* 2014;148(5):2181–8.
32. Rosenthal GL et al. *Am J Epidemiol* 1991;133(12):1273–81.
33. Rosenthal GL. *Am J Epidemiol* 1996;143(5):505–13.
34. Mari G, Deter RL. *Am J Obstet Gynecol* 1992;166(4):1262–70.
35. Wladimiroff JW et al. *Obstet Gynecol* 1987;69(5):705–9.
36. Rizzo G et al. *J Ultrasound Med* 1989;8(5):237–40.
37. Gramellini D et al. *Obstet Gynecol* 1992;79(3):416–20.
38. Donofrio MT et al. *Pediatr Cardiol* 2003;24(5): 436–43.
39. Kaltman JR et al. *Ultrasound Obstet Gynecol* 2005;25(1):32–6.

40. Jouannic J-M et al. *Ultrasound Obstet Gynecol* 2002;20(2):122–4.
41. Modena A et al. *Am J Obstet Gynecol* 2006;195(3):706–10.
42. Guorong L et al. *Fetal Diagn Ther* 2009;25(1):167–72.
43. Williams IA et al. *Am Heart J* 2013;165(4):544–50.e1.
44. Limperopoulos C et al. *Circulation* 2010;121(1):26–33.
45. Zeng S et al. *Ultrasound Obstet Gynecol* 2015;46(2):174–81.
46. Schellen C et al. *Am J Obstet Gynecol* 2015;213(3):392.e1–7.
47. Clouchoux C et al. *Cereb Cortex* 2012;23(12):2932–43.
48. Berman JI et al. *Am J Neuroradiol* 2011;32(2):E21–2.
49. Masoller N et al. *Ultrasound Obstet Gynecol* 2016;47(1):65–73.
50. Brossard-Racine M et al. *Am J Neuroradiol* 2014;35(8):1593–9.
51. Brossard-Racine M et al. *Am J Neuroradiol* 2016;37:1–9.
52. Nafisi Al B et al. *J Cardiovasc Magn Reson* 2013;15(1):65.
53. Sun L et al. *Circulation* 2015;131(15):1313–23.
54. Rivkin MJ et al. *J Thorac Cardiovasc Surg* 2013;146(3):543–9.e1.
55. Paladini D et al. *Ultrasound Obstet Gynecol* 2016;47(6):667–71.
56. Glass HC et al. *Cardiol Young* 2011;21(5):562–71.
57. Peyvandi S et al. *JAMA Pediatr* 2016;170(4):e154450.

# 59

# Postnatal neurodevelopment in congenital heart disease: Short- and long-term neurodevelopment and interventions

Hedwig H. Hövels-Gürich and Christopher G. McCusker

## Short- and long-term neurodevelopment

### *Introduction*

The prevalence of congenital heart disease (CHD) is about 1 in every 100 live births, of which about one-third is in critical need of surgical intervention in neonatal or infant age (Figure 59.1).[1] Since the 1980s, advanced diagnostic methods, neonatal cardiopulmonary bypass operations enabling early correction of complex congenital heart defects, and improvements in postoperative care have markedly increased life expectancy. Today, more than 90% of CHD patients survive into adulthood. At the same time, these patients are at significant risk of short- and long-term neurodevelopmental impairment with negative impact on psychosocial and academic performance as well as on quality of life and independence in adulthood.[2–6]

In this chapter, the causes and risk factors for neurodevelopmental disability are discussed, and groups of CHD children who are at high risk are identified. The phenotype of affected children in infant age and throughout childhood and adolescence is described. And, strategies for systematic screening, evaluation, and intervention are suggested.

### *Risk factors for developmental disability*

Since the 1990s, a considerable body of standardized neurodevelopmental evaluations after cardiac surgery in infancy and childhood has given increased evidence that a remarkable number of survivors face significant neurodevelopmental challenges. For a long time, the search for independent risk factors (Figure 59.2) has focused on the perioperative period and *modalities of cardiopulmonary bypass* (CPB). CPB operations to ensure intraoperative vital organ perfusion and oxygen supply with or without circulatory arrest or regional cerebral perfusion bear specific risks. Examples of such risks are embolization, deep hypothermia, flow rate, hemodilution, blood gas management, postoperative hyperthermia, systemic inflammatory reaction, and capillary leak syndrome.[7–11] In recent years, modifications of these factors have been found not to support the effectiveness of the currently used neuroprotective strategies.[12,13] In a recent analysis of more than 1,700 CHD patients from across the world who were born between 1996 and 2009 and had cardiac surgery at age less than 9 months, only modest improvements in the significantly reduced neurodevelopmental outcomes (psychomotor [PDI] and mental developmental index [MDI] of the Bayley Scales of Infant Development-II) at mean age 14 months have been observed over this 14-year period.[14] Moreover, CPB management factors explained only about 1% of the test results' variance, and longer support time was hypothesized to be a surrogate for operative complexity.[15]

However, there is strong evidence that less modifiable innate patient characteristics and socioeconomic environmental factors have an important impact on neurodevelopmental outcomes.[14,16–19] In addition to type and severity of CHD, prematurity, lower birth weight, white race, and genetic or extracardiac anomalies have been identified as predictors of lower PDI, while lower birth weight, male gender, less maternal education, and genetic or extracardiac anomalies were independent risk factors for lower MDI. Significant *postoperative factors*, such as duration of mechanical ventilation, need for extracorporeal membrane oxygenation, or duration of hospital stay, have been found to be associated with perioperative or postoperative complications.[14] In addition, *psychosocial factors,* such as parenting style or maternal mental health, exert significant influence on cognitive outcomes.[20,21]

### *Encephalopathy of CHD and neurodevelopment*

There is evidence that structural and hemodynamic characteristics of different congenital heart defects lead to

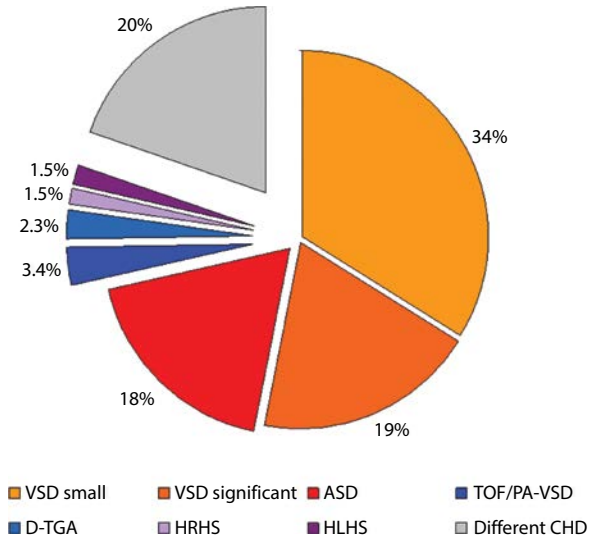


**Figure 59.1**
Spectrum of congenital heart defects among live births in Germany, according to Schwedler et al., 2011.[1] (ASD, atrial septal defect; CHD, congenital heart disease; D-TGA, dextro-transposition of the great arteries; HLHS, hypoplastic left heart syndrome (single right ventricle); HRHS, hypoplastic right heart syndrome (single left ventricle); PA-VSD, tetralogy of Fallot with pulmonary atresia; TOF, tetralogy of Fallot; VSD, ventricular septal defect.)

autoregulation mechanisms in the brain in case of hypoperfusion or hypoxia by vasodilatation of the cerebral arteries with increased diastolic flow and decreased cerebrovascular resistence.[22,23] It has been assumed that prolonged periods of this autoregulation may lead to delayed maturation of the fetal oligodendrocytes, reduced myelinization, and increased vulnerability of the brain.[24–27] However, in fetuses with a single ventricular heart, decreased cerebrovascular resistance has been found to be associated with higher PDI scores at age 14 months.[28,29] It remains unclear whether fetal cerebral blood flow alterations predict neurodevelopmental outcomes later in childhood.

Fetal brain perfusion disturbance is assumed to result in impaired brain growth and maturation with special respect to the white matter. Neuropathological studies indicate that brain disturbance in CHD before neonatal surgery predominantly consists of cerebral white matter injury (WMI), comparable to periventricular leukomalacia (PVL) as observed in preterm infants.[30,31] Magnetic resonance imaging (MRI) studies have suggested the description of *cerebral white matter immaturity*[32–34] and detected a rate of 20%–50% of WMI in newborns prior to surgery, dependent on the severity of the underlying CHD.[35–38] Brain MRI studies have also detected smaller brain volumes, abnormal brain metabolism, and decreases in cortical folding and gyral development in both CHD fetuses[26,39]

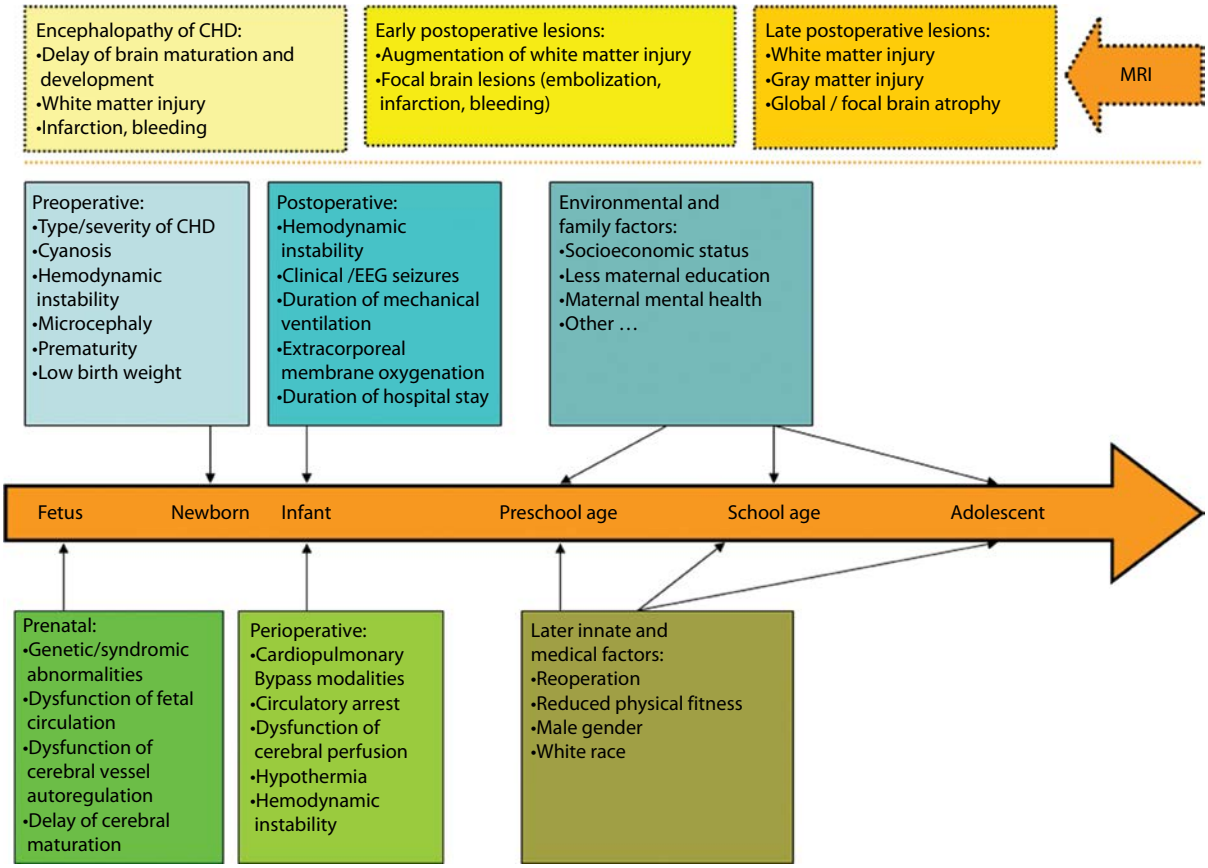


**Figure 59.2**
Time axis of suggested MRI brain lesions and risk factors for neurodevelopment in patients with congenital heart disease from fetal to adolescent age. (Modified after Wernovsky G. *Cardiol Young* 2006;16[suppl 1]:92–104. Review.[52])

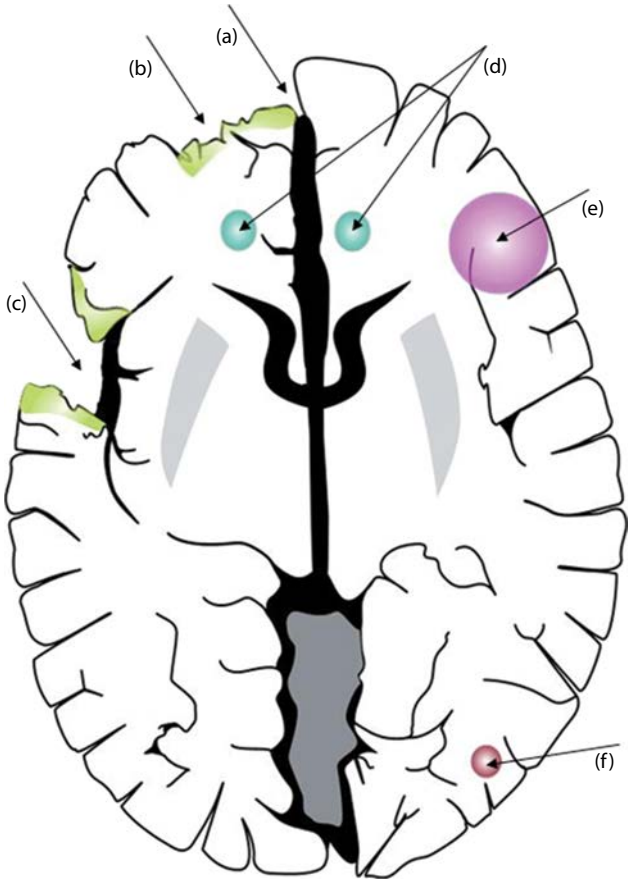


**Figure 59.3**
Schematic brain MRI (horizontal plane) showing macrostructural lesions in mature newborns with congenital heart disease, according to Soul et al., 2009.[91] (a) Extended interhemisphere cleft, (b) reduced brain volume, (c) open operculum insulae, (d) periventricular leukomalacia, (e) focal embolic event, and (f) hemosiderin focus. (Figure taken from Hövels-Gürich HH. *Monatsschr Kinderheilkd* 2012;160:118–28 [Article in German. Abstract in English][4], © Springer-Verlag Berlin Heidelberg, Germany.)

and newborns[40–43] (Figure 59.3). In newborns, studies also found associations with poor behavioral state regulation.[41] Brain maturation has been found to be delayed by 1 month in newborns with transposition of the great arteries or hypoplastic left heart syndrome.[33] Associations between lower brain maturity at birth and increased preoperative and postoperative brain injury[44] as well as neurodevelopmental impairment at age 2 years[37] suggest that *encephalopathy of congenital heart disease*[45,46] may increase the vulnerability of the brain versus hypoxia or ischemia, especially in the setting of the surgical and perioperative management, but also in terms of a longer preoperative period between birth and surgery.[47] After cardiac surgery, more than 50% of the neonates show MRI signs of white matter injury.[35–37] There are also important implications for long-term follow-up studies that link CHD encephalopathy to later neurodevelopmental delay. Brain volumes remain smaller into adolescence and are accompanied by reduced neurodevelopmental outcomes.[48] Recently, MRI macrostructural brain abnormalities[49] (Figure 59.4) as well as regions of

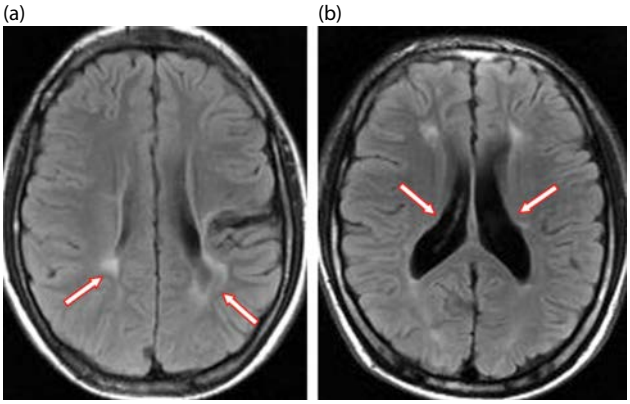


**Figure 59.4**
Brain MRI showing macrostructural abnormalities in young adults 20 years after neonatal arterial switch operation for transposition of the great arteries (T2-weighted axial planes). (a) Focal white matter injury (arrows), (b) intrinsic volume loss with ventricular dilatation (arrows), mild extrinsic volume loss with increased width of sulci, and focal white matter injury. (Figures taken from Heinrichs AK et al. *J Thorac Cardiovasc Surg* 2014;148(5):2190–9,[49] © Elsevier, Philadelphia, PA.)

reduced white matter microstructure[50] in TGA adolescents have been found to be correlated with neurocognitive decline. Diminished white matter microstructure may contribute to cognitive compromise in adolescents who underwent open heart surgery in infancy.

In summary, brain abnormality and immaturity in infants with CHD seem to be a complex disturbance with destructive and developmental elements, similar to the encephalopathy first described in premature infants.[51] Beginning in the fetal period, the encephalopathy of CHD is a major innate risk factor for preoperative, perioperative, and postoperative additional hypoxic or ischemic brain injury and subsequent neurodevelopmental impairment (Figure 59.2).

## *Prevalence of and risk stratification for neurodevelopmental disorder*

In general, children with milder forms of CHD have fewer or milder neurodevelopmental disorders, whereas those with complex forms of CHD have more frequent or more severe disabilities (Figure 59.5).

According to the scientific statement of the American Heart Association,[2,3] children with CHD can be stratified for neurodevelopmental outcomes based on established risk factors. The high-risk patients' group for developmental delay comprises the following:

- Neonates or infants with cyanotic or acyanotic CHD who require open heart surgery
- Children with cyanotic CHD who do not require open heart surgery in infant age
- Any type of CHD in combination with prematurity, developmental delay, suspected genetic abnormality, or syndromes associated with developmental disorder

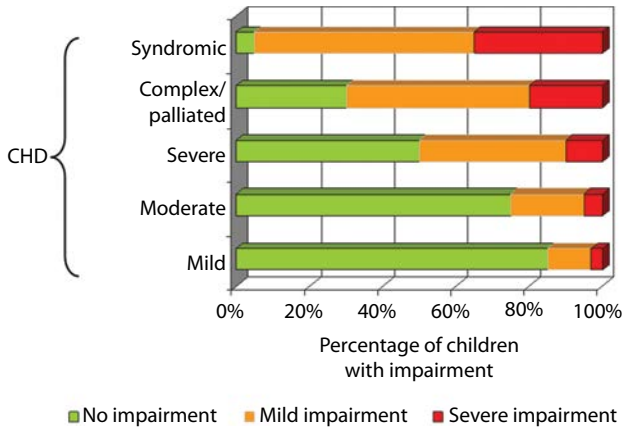


**Figure 59.5**
Neurodevelopmental impairment in school-age children with CHD. Mild CHD: e.g., ASD, VSD; moderate CHD: e.g., TOF: severe CHD: e.g., TGA; complex/palliated CHD: e.g., HRHS, HLHS; syndromic: e.g., Down syndrome, DiGeorge syndrome. (ASD, atrial septal defect; CHD, congenital heart disease; HLHS, hypoplastic left heart syndrome; HRHS, hypoplastic right heart syndrome [single left ventricle]; TGA, transposition of the great arteries [single right ventricle]; TOF, tetralogy of Fallot; VSD, ventricular septal defect.) (Adapted from Wernovsky G. *Cardiol Young* 2006;16(suppl 1):92–104. Review.[52])

**Table 59.1** Neurodevelopmental issues of patients with CHD over the life span

Infancy and early childhood

- Microcephaly
- Muscle tone disorder
- Feeding difficulties
- Delay in achieving early milestones of psychomotor and language development

School age and adolescence

- Dysfunctions of fine and gross motor and coordination skills
- Deficits of sensorimotor skills, organization, memory, attention, speech
- Deficits of academic and school outcomes
- Behavioral and psychosocial problems
- Difficulties in "competence domains"

Adulthood

- Consecutive neurocognitive, psychosocial, and psychiatric problems
- Employment issues
- Consecutive reduced quality of life

- Status after mechanical circulatory support or heart transplantation
- Status after cardiopulmonary resuscitation or prolonged hospitalization
- Children with perioperative seizures related to cardiac surgery
- Children with microcephaly or significant abnormalities in brain MRI

## *The neurodevelopmental phenotype of children with CHD*

Patients with CHD are at risk for neurodevelopmental issues during their life from neonatal age into adulthood (Table 59.1).[2,52,53]

### Short-term neurodevelopmental patterns in infancy and early childhood

A recent meta-analysis comprising 512 neonates with different cardiac lesions has found that the prevalence of brain abnormalities on MRI was between 34% and 49% of CHD neonates without genetic abnormalities in the postnatal, preoperative period. The prevalence of neurodevelopmental disability (low muscle tone and feeding difficulties) was 42%.[38] After open heart surgery, increased brain MRI lesions[35] as well as clinical or electroencephalographic seizures or microcephaly have been detected.

During infancy and early childhood, muscle tone disorder, feeding problems, and delayed achievement of early milestones of psychomotor and language development can emerge. In a longitudinal study on 131 children after neonatal or infant open heart surgery, neurological problems were found in 50% of the children preoperatively, in more than 50% postoperatively, and in about 40% at the age of 20 months. A global neurodevelopmental delay was noticed in about 25% of the cases. These percentages persisted into preschool age, whereas the incidence of cognitive decline was less frequent.[53] In a serial assessment of 99 children with a single- or two-ventricle anatomy, assessed three to six times in the first 3 years of life, 75% showed reduced development (Bayley scales of infant development III). Motor scores were more often affected but showed dynamic improvement, compared to cognitive or language scores that were less often affected.[54] In a recent analysis of more than 1,700 CHD patients evaluated at mean age 14 months, the Bayley scales of infant development II were found significantly lower than normative means, with the psychomotor index again more reduced than the mental index.[14] In the Boston Circulatory Arrest Study in 171 children after neonatal arterial switch operation for transposition of the great arteries, motor skills were significantly reduced at the age of 1 year. In the same study, increased risk of disabilities was reported at age 4 years in several domains, including intelligence quotient, expressive language, visual-motor integration, motor function, and oromotor control.[7,8] In the Single Ventricle Reconstruction Trial for children with hypoplastic left heart syndrome prior to Fontan-type palliation, developmental scores at age 14 months (Bayley-II scales) were significantly reduced, with PDI markedly lower than MDI.[16] At age 3 years, the percentage of delayed scores (Ages and Stages Questionnaire [ASQ]) in several domains ranged from 17% to 35%, with motor scales again markedly reduced. Delay was detected in at least one developmental domain for 51% of the cohort.[55] Within the domain of early cognitive

abilities, perceptual-motor skills have been found markedly disturbed at ages 8 months and 4–5 years, respectively.[20,21]

In summary, early in infancy and childhood, motor deficits like sensorimotor, visual-motor, and speech articulation problems are frequently observed, typical developmental disorders of CHD children, with partial recovery over time questionable.[56,57]

## Midterm neurodevelopmental patterns in school-age children

In later childhood, new domains of neurodevelopmental deficits become apparent: fine and gross motor dysfunctions, often accompanied by academic, behavioral, or psychosocial problems, are challenging symptoms.[58] At school age, more specific developmental measures allow for the detection of deficits in visuomotor function, speech, attention, and social cognition. At the same time, complex problems of integrative and executive functioning emerge.

In a mixed group of 7- to 8-year-old children with CHD, neuropsychological testing showed two developments irrespective of a cyanotic condition: On the one hand, there was some recovery from the perceptual-motor deficits detected in infancy,[21] but on the other hand, moderately reduced sensorimotor skills, attention, narrative memory, and academic performance with increased need for remedial services were observed.[59] School-age children after corrective surgery for tetralogy of Fallot showed a significantly increased risk for developmental delay in the areas of (1) formal intelligence, (2) academic achievement, (3) expressive and receptive language, (4) gross motor function, (5) oral and speech motor control function, (6) executive control of attention, and (7) psychosocial maladjustment. In contrast to this, children after corrective surgery for ventricular septal defect (acyanotic condition) performed with milder impairment, whereas psychological maladjustment was not found to be different between the groups.[11,60–62] Children at age 8 years after neonatal arterial switch operation for TGA are also at risk for disabilities in the domains of intelligence, academic achievement, executive functioning, language, and fine and gross motor skills.[63] In another TGA group, similar patterns of dysfunction emerged, and developmental delay in at least one domain was present in 26% at mean age 5.4 years, but increased to 55% at mean age 10.5 years due to increased recognition of fine and gross motor dysfunctions.[10,64–65] In an additional study, the incidence of motor problems was six times higher than that in the healthy control group.[66] Furthermore, in mixed CHD cohorts, 23% showed reduced emotional, social, and school functioning,[67] and 20% needed remedial academic services, respectively.[53]

In summary, school-age children with CHD develop, even after successful surgical treatment, increased impairment in domains of speech and language, attention, memory, visual-spatial skills, executive functioning, and motor skills, mostly with a mild to moderate degree (after exclusion of children with genetic syndromes), but often associated with deficits in academic and school outcomes and emotional or social problems.

## Long-term neurodevelopmental patterns in adolescents

During adolescence, aspects of executive functioning, psychosocial and behavioral issues as well as quality-of-life outcomes are of increased importance. In a study of 463 adolescents with critical cyanotic CHD (tetralogy of Fallot, transposition of the great arteries, and single ventricle), these adolescents showed nearly two times higher rates of deficits in flexibility, problem solving, or verbally mediated executive functions, than the control group.[68] Social cognition deficits and difficulties in everyday life, including academic progress, have been assessed.[69–71] Even though knowing their deficits significantly improved their resilience, adolescents with corrected transposition of the great arteries showed increased rates of attention deficit hyperactivity disorder and reduced psychosocial functioning,[72] In a large study group of 1,138 CHD children and adolescents aged 8–18 years, health-related quality of life in terms of physical and psychosocial health has been rated significantly lower than in healthy controls and rated similar to patients with other chronic pediatric diseases.[73] However, study results are somewhat contradictory, and caregivers, such as parents and teachers, often rate quality of life less favorable than the patients themselves.[70,74]

A recently detected linking between brain MRI abnormalities and neurodevelopmental disabilities in adolescents should be noted. Abnormal MRI correlated with significantly reduced results in all neuropsychological domains, as did academic achievement, memory, executive functions, visual-spatial skills, attention, and social cognition in patients after correction of tetralogy of Fallot.[75] Distinct regions of impaired white matter microstructure corresponded with a decline in mathematical abilities, attention, executive function, and visual-spatial skills.[50,76] The severity of white matter injury correlated with the grade of neurological impairment, which was observed more often in patients after correction of transposition of the great arteries than the normal population.[49]

In summary, adolescents with CHD remain at increased risk of executive and psychosocial dysfunctions, psychiatric disorders, and reduced quality of life, even if they are aware of their deficits. Concerns emerge with respect to transition into adulthood,[77] where neurocognitive, psychosocial, self-management, and employment issues may be preponderant.

## Specific cardiac defects

A list of selected cardiac defects with current references related to their neurodevelopmental outcomes is provided in Table 59.2.

# Psychosocial interventions: A new focus to improve outcomes

## *The case for psychosocial interventions*

As discussed, there is now compelling evidence to suggest that children with significant congenital heart disease (CHD)

**Table 59.2** Specific CHD lesions and developmental domains at special risk

| *CHD lesion* | *Open heart surgery* | *Developmental domains at risk* | *References* |
|---|---|---|---|
| ASD | Corrective open heart surgery usually not in infant age | Sensorimotor processing, language, attention, social perception | 78,79 |
| VSD | Corrective open heart surgery usually in infant age | Sensorimotor processing, language, attention, gross motor function, academic achievement, psychosocial adjustment | 33–36,77,80 |
| TOF | Corrective open heart surgery in infant age | Sensorimotor processing, language, attention, gross motor function, executive functions, academic achievement, psychosocial adjustment | 33–36,75,81,82 |
| TGA | Corrective open heart surgery in neonatal age (arterial switch operation) | Sensorimotor processing, language, attention, neurology, gross motor function, executive functions, academic achievement, psychosocial adjustment | 7–10,13,49,50,63–65,72,76 |
| HRHS | Palliative open heart surgery (two to three procedures, Fontan principle) in neonatal age, infancy, and early childhood | Sensorimotor processing, language, attention, neurology, gross and fine motor function, general intelligence, executive functions, academic achievement, psychosocial adjustment, quality of life | 83–86 |
| HLHS | Palliative open heart surgery (three procedures, Norwood principle or modifications) in neonatal age, infancy, and early childhood | Sensorimotor processing, language, attention, neurology, gross and fine motor function, general intelligence, executive functions, academic achievement, psychosocial adjustment, quality of life | 16,55,58,87–90 |

*Abbreviations:* ASD, atrial septal defect; CHD, congenital heart disease; HLHS, hypoplastic left heart syndrome (single right ventricle); HRHS, hypoplastic right heart syndrome (single left ventricle); TGA, transposition of the great arteries; TOF, tetralogy of Fallot; VSD, ventricular septal defect.

are at risk for elevated levels of neurodevelopmental deficits and behavior difficulties. Neurodevelopmental and behavior phenotypes have been emerging[92] that suggest features primarily (though not exclusively) related to early psychomotor deficits and later problems with executive functioning, aspects of memory, social cognition, and behavior problems typically related to personal and interpersonal competencies. Evidence was previously outlined for etiological pathways involving neurological concomitants, preoperative hypoxemia, and peri- and postoperative management. Nevertheless, despite advances in neuroprotective and other surgical procedures, and improvements in general medical care, rates of maladjustment in this population have remained stubbornly unchanged when cohorts from the 1980s are compared to those from the mid-1990s onward.[93]

Underlying this has been increasing evidence that family (and especially maternal) factors are often of greater predictive significance for neurodevelopmental and especially behavioral outcomes than medical and surgical factors, *per se*.[20,59,94–96] This relates to psychopathology, but also to outcomes such as levels of activity, exercise, and "illness" behaviors, such as unscheduled medical consultations.[97] Such factors have included maternal mental health, worry, parenting style, and family functioning. Thus, for example, levels of parental distress following the diagnosis of their child with CHD have been shown to predict behavioral adjustment in the child years later,[59,98] and parental levels of anxiety have been shown to compromise the positive impact of exercise intervention with children and adolescents with CHD.[99] Unfortunately, parents of children with CHD are themselves at elevated risk for psychological difficulties,[100,101] thus amplifying the risk for these children. Again, levels of parental maladjustment have not been shown to be reliably associated with the severity of the disease itself, but rather by *perceptions* of the same and their own parenting and coping resources.[101,102] Thus, in considering how to improve quality of life and other psychosocial outcomes for the increasing population of CHD survivors, it is perhaps time to turn our attention toward psychosocial interventions.

## What psychosocial interventions?

Until recently, there have been little or no controlled evaluations of psychosocial interventions for this population. Clinical consensus statements, however, such as those by Marino and his colleagues, have called for neurodevelopmental screening for the at-risk groups and remedial interventions to be put in place where deficits are identified.[2] This follows logically from the evidence base previously discussed in relation to these risks. Others have formulated specific psychological interventions to minimize the adverse emotional impact of repeated and invasive cardiac investigations and surgical interventions on the child.[103] Moreover, given the association between activity and exercise levels and psychosocial adjustment, there have been promising reports that psychologically informed programs can increase levels of exercise in this population.[104–105] As noted previously, however, parental mental health difficulties can actually undermine outcomes in such interventions.[99]

The evidence noted above, for the importance of maternal and family factors for child outcomes, points toward

the importance of working through the family to improve outcomes for the child. Family resource and systems models[106,107] propose that the more able the parents (and in terms of the current evidence base, mostly the mother) are at coping with the stress and distress of having a child with CHD, supporting the child, parenting, and promoting independence in spite of the challenges posed by the disease, the better the child outcomes will be in terms of behavioral and social adjustment. Such a view is not unique to children with CHD and their families, but rather has become an important pillar of pediatric psychology pedagogy and interventions more generally. Law and colleagues, in a recent systematic review of family focused interventions for children with a range of chronic illnesses and disabilities, have noted evidence that such interventions are promising across a number of child and family psychosocial outcome domains.[107]

## The Congenital Heart Disease Intervention Program (CHIP)

The first study to systematically develop and test a new program of psychosocial interventions aimed at families of children with CHD was conducted at the *Royal Belfast Hospital for Sick Children* in Northern Ireland in the early 2000s. CHIP was a secondary prevention program, aimed at bolstering family coping and resilience in order to reduce risk for later adverse neurodevelopmental and behavioral outcomes in the child with CHD. Common to the two arms of the study, which were aimed at key periods of developmental transition for the child and family (the diagnosis in infancy and when the child with CHD was about to start school), was "problem-solving therapy."[108,109] Problem-solving therapy has, in a recent systematic review, been shown to yield the strongest effect size across different types of therapeutic interventions with families of pediatric populations.[107] This trains parents to become active problem solvers in addressing the developmental challenges for the child, and worries within the family, posed by CHD. These challenges varied across the two cohorts. For the parents of infants, challenges related to neurodevelopment, feeding, attachment, and family coping. For the parents of the school-age cohort, concerns related to promoting independence, developing parenting skills, giving information to the child, and establishing safe activity levels. A strength of problem-solving therapy is that it promotes a style of coping that is generalizable to other challenges not specifically focused on in the program or which can emerge at later developmental points.

The content of *CHIP–Infant* and *CHIP–School* are outlined in detail elsewhere.[21,110] In brief, and following training in the problem-solving protocol common to both programs, a number of specific elements were woven, specific to the developmental challenges of that cohort. Thus, in *CHIP–Infant*,[21] key sessions included a narrative intervention related to construction of meaning and emotional processing, together with maternal responsivity training to facilitate feeding, attachment, and neurodevelopmental stimulation. In *CHIP–School*,[110] which was delivered in both group and individual formats, key interventions related to parenting skills to promote independence, a behavior experiment to challenge assumptions about exercise, and training parents to give information to their children about their condition and medical interventions in a way that would facilitate adaptive construction of meaning. Both programs involved psychoeducation supplemented by child-specific (rather than problem-specific) fact sheets, with these being made available to community health and education professionals. Both had parent manuals, and *CHIP–Infant* had a parent DVD where the narratives of "experienced" parents were expounded to help facilitate construction of meaning and emotional processing. Both programs required approximately 8 hours contact time, and both were evaluated in controlled and randomized controlled trials.

Findings from this project were very encouraging. In *CHIP–Infant*, selective gains were found in the intervention, compared to the control group, in relation to maternal anxiety, worry, and adaptive coping skills. Moreover, on the *Bayley Scales of Infant Development–II*,[111] the intervention group infants showed better performance than the control group on the *Mental Development Index* (though not the *Psychomotor Development Index*) at 6-month follow-up. Rates of breastfeeding were also significantly higher.[59] Although attrition rates compromised the study power in a further 7-year follow-up with this sample, there was some evidence (a statistical trend) to suggest that later rates of behavioral adjustment in the intervention group were better than in the control group.[20] In *CHIP–School*, similar benefits were found on both child and family factors.[110] Gains were found in the intervention, compared to the control group, in terms of maternal mental health and impact on family (reduced levels of personal and family strain noted). Although, disappointingly, no statistically significant benefits were found on child adjustment indices at home or at school, trends in the positive directions were noted. Moreover, significant differences were observed in terms of school absenteeism and "sick" behaviors (unscheduled medical consultations with respect to health concerns), with the intervention group showing differentially better outcomes in both domains.

## Concluding remarks

This chapter has focused on the adverse outcomes that children with significant CHD are at risk for with respect to neurodevelopment and psychosocial functioning. It is important to note in these conclusions, however, that in absolute terms, most of this clinical population have good outcomes.[112] The challenges that exacerbate risk may also lead to resilience developing across time, and "posttraumatic growth" can occur.[113] Nevertheless, we have seen in this chapter how neurodevelopmental and psychosocial deficits have now been reliably reported for a significant proportion of these children. Most commonly, these relate to psychomotor, executive functioning, and psychosocial deficits related to personal

and interpersonal competencies. We have seen that while preoperative hypoxemia and surgical management factors are important predictors of outcome, an "encephalopathy of CHD"[45] has been recognized that may underpin risk across the swathe of CHD subtypes. Although the predisposing factors for neurodevelopmental disorders are predominantly innate, and only a few of them are modifiable, research should focus on new approaches for neuroprotection, such as cerebral vascular autoregulation monitoring, new perioperative brain biomarkers, perioperative EEG monitoring, and serial brain MRI with systematic correlation to neurodevelopmental outcomes aiming at improved risk stratification.[3]

However, we have seen how family factors have also been recognized to be of pivotal significance in amplifying or moderating these intrinsic risk factors. This latter recognition raises exciting new directions of travel in interventions to reduce negative outcomes for this population. The evidence of the CHIP program, presented in this chapter, shows that we have now gone beyond consensus statements with respect to what *should* be helpful, toward the development of psychosocial protocols that are offering evidence for potential "first-line" psychosocial treatments. Bolstering the resilience of the family system is key here. Included will be psychological interventions to stimulate neurodevelopment, promote effective feeding and attachment interactions between mother and infant, enhance specific parenting strategies to promote independence and competencies in the child, and attend to emotional processing and construction of meaning for distressed parents.

These interventions should not simply be seen as "icing on the cake" of our medical advances in this area. They will be fundamental to improving the long-term psychosocial legacy of the condition and, in health-care economic terms, to reducing health and social care costs related to disability, educational, and occupational exclusion. Given that evidence is now emerging for the continuation of such difficulties from childhood into adulthood,[114] these costs will be cumulative for a greater number of individuals, and across a greater period of time, than we have previously known. We should, therefore, advance clinical research into the further refinement and extension of these interventions to round the circle of the huge advances we have seen over recent decades in care for this clinical population.

# References


1. Schwedler G et al. *Clin Res Cardiol* 2011;100(12):1111–7.
2. Marino BS et al. *Circulation* 2012;126(9):1143–72.
3. Marino BS. *Curr Opin Pediatr* 2013;25(5):574–84.
4. Hövels-Gürich HH. *Monatsschr Kinderheilkd* 2012;160:118–28. [Article in German. Abstract in English.]
5. Herberg U, Hövels-Gürich H. *Z Geburtshilfe Neonatol* 2012;216(3):132–40. [Article in German. Abstract in English.]
6. Gatzoulis MA. *Nat Clin Pract Cardiovasc Med* 2006;3(1):2–3.
7. Bellinger DC et al. *N Engl J Med* 1995;332(9):549–55.
8. Bellinger DC et al. *Circulation* 1999;100(5):526–32.
9. Bellinger DC et al. *J Thorac Cardiovasc Surg* 2003;126(5):1385–96.
10. Hövels-Gürich HH et al. *J Thorac Cardiovasc Surg* 2002;124(3):448–58.
11. Hövels-Gürich HH et al. *Eur J Paediatr Neurol* 2008;12(5):378–86.
12. Hirsch JC et al. *Ann Thorac Surg* 2012;94(4):1365–73, discussion 1373. Review.
13. Bellinger DC et al. *Circulation* 2011;124(12):1361–9.
14. Gaynor JW et al. *Pediatrics* 2015;135(5):816–25.
15. Gaynor JW et al. *Ann Thorac Surg* 2016;102(3):843–9.
16. Newburger JW et al. Pediatric Heart Network Investigators. *Circulation* 2012;125(17):2081–91.
17. Gaynor JW et al. *J Thorac Cardiovasc Surg* 2007;133(5):1344–53, 1353.e1–3.
18. Gaynor JW et al. *J Thorac Cardiovasc Surg* 2014;148(6):2560–6.
19. Atallah J1 et al. Western Canadian Complex Pediatric Therapies Project Follow-up Group. *J Thorac Cardiovasc Surg* 2007;134(3):772–9.
20. McCusker CG et al. *Arch Dis Child* 2007;92(2):137–41.
21. McCusker CG et al. *Child Care Health Dev* 2010;36(1):110–7.
22. Donofrio MT et al. *Pediatr Cardiol* 2003;4(5):436–43.
23. Kaltman JR et al. *Ultrasound Obstet Gynecol* 2005;25(1):32–6.
24. McQuillen PS et al. *Prog Pediatr Cardiol* 2010;29(2):79–85.
25. Donofrio MT et al. *Curr Opin Pediatr* 2011;23(5):502–11.
26. Limperopoulos C et al. *Circulation* 2010;121(1):26–33.
27. Sanz-Cortés M et al. *Ultrasound Obstet Gynecol* 2010;36(2):159–65.
28. Williams IA et al. *Am Heart J* 2013;165(4):544–50.e1.
29. Hahn E et al. *Ultrasound Obstet Gynecol* 2015;47(4):460–5.
30. Kinney HC et al. *Acta Neuropathol* 2005;110(6):563–78.
31. Hinton RB et al. *Pediatr Res* 2008;64(4):364–9.
32. Miller SP et al. *N Engl J Med* 2007;357(19):1928–38.
33. Licht DJ et al. *J Thorac Cardiovasc Surg* 2009;137(3):529–36, discussion 536–7.
34. Dimitropoulos A et al. *Neurology* 2013;81(3):241–8.
35. Mahle WT et al. *Circulation* 2002;106(12 Suppl. 1):I109–14.
36. Galli KK et al. *J Thorac Cardiovasc Surg* 2004;127(3):692–704.
37. Beca J et al. *Circulation* 2013;127(9):971–9.
38. Khalil A et al. *Ultrasound Obstet Gynecol* 2014;43(1):14–24. Review.
39. Clouchoux C et al. *Cereb Cortex* 2013;23(12):2932–43.
40. Ortinau C et al. *J Pediatr* 2013;163(5):1507–10.
41. Owen M et al. *J Pediatr* 2014;164(5):1121–7.e1.
42. Sethi V et al. *Pediatr Res* 2013;73(5):661–7.
43. von Rhein M et al. Heart and Brain Research Group. *J Pediatr* 2015;167(6):1259–63.e1.
44. Andropoulos DB et al. *J Thorac Cardiovasc Surg* 2010;139(3):543–56.
45. Volpe JJ. *J Pediatr* 2014;164(5):962–5.
46. Gaynor JW. *J Thorac Cardiovasc Surg* 2014;148(5):1790–1.
47. Lynch JM et al. *J Thorac Cardiovasc Surg* 2014;148(5):2181–8.
48. von Rhein M et al. *Brain* 2014;137(Pt 1):268–76.
49. Heinrichs AK et al. *J Thorac Cardiovasc Surg* 2014;148(5):2190–9.
50. Rollins CK et al. *J Pediatr* 2014;165(5):936–44.e1-2.
51. Volpe JJ. *Lancet Neurol* 2009;8(1):110–24. Review.
52. Wernovsky G. *Cardiol Young* 2006;16(suppl. 1):92–104. Review.
53. Majnemer A et al. *Pediatr Neurol* 2009;40(3):197–204.
54. Mussatto KA et al. *Pediatrics* 2014;133(3):e570–7.
55. Goldberg CS et al. Pediatric Heart Network Investigators. *J Pediatr* 2014;165(3):490–6.e8.
56. Snookes SH et al. *Pediatrics* 2010;125(4):e818–27.
57. Anderson V et al. *Brain* 2011;134(Pt 8):2197–221.
58. Shillingford AJ et al. *Pediatrics* 2008;121(4):e759–67.

59. McCusker CG et al. *Cardiol Young* 2013;23(4):507–16.
60. Hövels-Gürich HH et al. *Ann Thorac Surg* 2007;83(4):1425–30.
61. Hövels-Gürich HH et al. *Pediatr Cardiol* 2007;28(5):346–54.
62. Hövels-Gürich HH et al. *Ann Thorac Surg* 2006;81(3):958–66.
63. Bellinger DC et al. *Cardiol Young* 2009;19(1):86–97.
64. Hövels-Gürich HH et al. *J Thorac Cardiovasc Surg* 1997;114(4): 578–85.
65. Hövels-Gürich HH et al. *Arch Dis Child* 2002;87(6):506–10.
66. Holm I et al. *Arch Pediatr Adolesc Med* 2007;161(10):945–50.
67. Uzark K et al. *Pediatrics* 2008;121(5):e1060–7.
68. Cassidy AR et al. *J Int Neuropsychol Soc* 2015;21(1):34–49.
69. Bellinger DC. *Cardiol Young* 2008;18(1):3–9. Review.
70. Bellinger DC, Newburger JW. *Prog Pediatr Cardiol* 2010;29(2): 87–92.
71. Gerstle M et al. Executive functioning and school performance among pediatric survivors of complex congenital heart disease. *J Pediatr* 2016;173:154–9.
72. DeMaso DR et al. *J Pediatr* 2014;165(4):760–6.
73. Mellion K et al. Pediatric Cardiac Quality of Life Inventory Testing Study Consortium. *J Pediatr* 2014;164(4):781–8.e1.
74. Latal B et al. *BMC Pediatr* 2009;9:6.
75. Bellinger DC et al. *Cardiol Young* 2015;25(2):338–47.
76. Rivkin MJ et al. *J Thorac Cardiovasc Surg* 2013;146(3):543–9.e1.
77. Uzark K et al. *J Pediatr* 2015;167(6):1233–8.
78. Sarrechia I et al. *J Pediatr* 2015;166(1):31–8.
79. Sarrechia I et al. *Res Dev Disabil* 2015;45–46:58–68.
80. Matsuzaki T et al. *Pediatr Int* 2010;52(3):420–7.
81. Miatton M et al. *J Thorac Cardiovasc Surg* 2007;133(2):449–55.
82. Neal AE et al. *J Pediatr* 2015;166(1):132–8.
83. Blaufox AD et al. Pediatric Heart Network Investigators. *J Thorac Cardiovasc Surg* 2008;136(1):100–7, 107.e1.
84. Forbess JM et al. *Circulation* 2001;104(12 suppl 1):I127–32.
85. Bellinger DC et al. *J Am Heart Assoc* 2015;4(12):e002302.
86. Uzark K et al. Pediatric Heart Network Investigators. *J Pediatr* 2016;170:166–72.e1.
87. Sarajuuri A et al. *J Pediatr* 2010;157(3):414–20, 420.e1–4.
88. Brosig C et al. *Pediatr Cardiol* 2013;34(7):1597–604.
89. Tabbutt S et al. *Pediatrics* 2008;121(3):476–83.
90. Davidson J et al. *Arch Dis Child* 2015;100(5):449–53.
91. Soul JS et al. *J Thorac Cardiovasc Surg* 2009;138(2):374–81.
92. McCusker CG, Casey FC. *Congenital Heart Disease and Neurodevelopment: Understanding and Improving Outcomes*. London: Elsevier, Academic Press; 2016.
93. Spijkerboer AW et al. *J Pediat Surg* 2008;43:534–9.
94. Karsdorp P et al. *J Ped Psychol* 2007;32(5):527–41.
95. Hövels-Gürich H, McCusker CG. Neurodevelopmental patterns in congenital heart disease across childhood—Longitudinal studies from Europe. In McCusker CG, Casey FC, eds. *Congenital Heart Disease and Neurodevelopment: Understanding and Improving Outcomes*. London: Elsevier, Academic Press; 2016.
96. McCusker CG, Casey FC. Is there a behavioral phenotype for children with congenital heart disease? In McCusker CG, Casey FC, eds. *Congenital Heart Disease and Neurodevelopment: Understanding and Improving Outcomes*. London: Elsevier, Academic Press; in press.
97. Casey FA et al. *Cardiol Young* 2010;20:532–7.
98. Visconti KJ et al. *J Dev Beh Pediatr* 2002;23:314–21.
99. Dulfer K et al. *Pediatr Cardiol* 2015 Jan;36(1):33–40.
100. Doherty N et al. *J Reprod Infant Psychol* 2009;27(4):390–400.
101. Doherty N, Utens E. A family affair. In McCusker CG, Casey FC, eds. *Congenital Heart Disease and Neurodevelopment: Understanding and Improving Outcomes*. London: Elsevier, Academic Press; 2016.
102. Vrijmoet-Wiersma CM et al. *Cardiol Young* 2009;19(6):608–14.
103. LeRoy S et al. *Circulation* 2003;108:2550–64.
104. Morrison ML et al. *Heart* 2013;99:1122–8.
105. Dulfer K et al. *Prev Cardiol* 2014;21:1200–15.
106. Thompson RJ et al. *J Ped Psychol* 1992;17:573–85.
107. Law EF et al. *J Ped Psychol* 2014;39:866–86.
108. D'Zurilla TJ, Nezu AM. *Problem-Solving Therapy: A Social Competence Approach to Clinical Intervention*. 2nd ed. New York, NY: Springer; 1999.
109. Varni JW et al. *J Psychosoc Oncol* 1999;16:41–71.
110. McCusker CG et al. *J Pediatr Psychol* 2012;37:1089–103.
111. Bayley, N. *Bayley Scales of Infant Development*. 2nd ed. San Antonio, TX: The Psychological Corporation, Harcourt Brace & Company; 1993.
112. McCusker CG. Conclusions and future directions for neurodevelopmental research and interventions in congenital heart disease. In McCusker CG, Casey FC, eds. *Congenital Heart Disease and Neurodevelopment: Understanding and Improving Outcomes*. London: Elsevier, Academic Press; 2016.
113. Utens EM et al. *Cardiol Young* 2002;12(6):524–30.
114. Katz D et al. The adult with congenital heart disease. In McCusker CG, Casey FC, eds. *Congenital Heart Disease and Neurodevelopment: Understanding and Improving Outcomes*. London: Elsevier, Academic Press; 2016.

# 60

# Genetic counseling in families with congenital heart defects

Klaus Zerres and Sabine Rudnik-Schöneborn

Congenital heart defects (CHDs) occur in around 1% of births and therefore make up the largest group for which advice is sought, usually regarding the risk for further affected children, but increasingly concerning the offspring of a successfully treated patient. Although around 90% of CHDs are not familial (Table 60.1), it seems increasingly likely that genetic factors are involved in most cases.

The increase of genetic knowledge as well as advances in prenatal echocardiography offer more tools for counseling but require precise information. Among the large amount of literature, the textbook by Nora et al.[1] on cardiovascular disease is still an excellent comprehensive monograph about the subject. Owing to rapidly increasing genetic knowledge, current online information providing details about all aspects of certain conditions is essential. The most important genetic database including relevant references is Online Mendelian Inheritance in Man (http://www.ncbi.nlm.nih.gov/Omim/searchomim.html),[2] based on Victor McKusick's classical catalogs.

## Genetic basis of congenital heart defects

The majority of CHDs do not cluster within families, indicating that monogenic entities are less important in their etiology.

A small but important group of CHDs and most syndromes with CHDs as a major feature follow monogenic modes of inheritance. The major characteristics are shown in Table 60.2.

The vast majority is believed to be "multifactorially" inherited, indicating that the combination of genetic factors as well as often unknown exogenous factors may cause the defect. The genetic predisposition is assumed to be polygenic, with a greater number of relevant genes involved. The essential distinguishing factor from Mendelian disorders is that a single genetic locus cannot be held responsible for the condition, and that it is the result of the additive effect or interaction of a number of genetic loci and of a number of external factors. Due to advances in genomic medicine, there is increasing knowledge about modifier genes, *de novo* mutations, copy number variants, and noncoding mutations in the pathogenesis of CHDs. Despite these advances, the pathogenesis of CHDs is far from understood in the majority of cases, and the practical implications in genetic counseling are still limited. Recent findings in other diseases underline that epigenetic mechanisms might be responsible for gene expression and could also explain transmission to the next generation. Similar observations in CHDs can be expected. The sum of these factors determines a person's liability to be affected with a particular disorder, and the liability should show a more or less "normal" distribution in the population, with most people having an intermediate degree of liability and a smaller number of each end of the distribution curve having unusually low or unusually high liabilities (Figure 60.1).

An important group comprises those who are actually affected, whose liability is above a postulated "threshold" for the disorder. The liability of relatives of a patient with the disorder will be distributed in a similar way to that of the general population, but the curve will be shifted toward a higher liability because of the increased genetic component.

The following practical aspects, which are in contrast to the rules of classical Mendelian modes of inheritance (see Table 60.2) are relevant and are of importance for genetic counseling: (1) increased risk is greatest among closest relatives and decreases rapidly with distance of relationship; (2) the risk of recurrence depends on the incidence of the disorder, with a higher risk in those with more common disease; (3) the risk to offspring is approximately equivalent to the risk for siblings, unless there is evidence of a significant proportion of isolated cases being the result of new dominant mutations; (4) in entities with an unequal sex incidence, the risk is higher for relatives of a patient of the sex in which the condition is less common; (5) the risk may be greater when the disorder is more severe; and (6) the risk is increased when multiple family members are affected.

## Principles of genetic counseling

Owing to the different etiologies of CHDs and the individual reasons for asking for genetic counseling, the possible consequences for families might be completely different. Genetic counseling is in many aspects different from classical medical care in families with a certain disease. As a consequence, specific principles have been formulated.

**Table 60.1** Causes of congenital heart defects

| *Cause* | *Percentage* |
|---|---|
| **Multifactorial** | 70 |
| Genetic | |
| Chromosome abnormalities | 20–25 |
| Monogenic defects | 3–5 |
| Exogenous | |
| Intrauterine infections | 1 |
| Other teratogenic effects | 1 |

**Table 60.2** Modes of inheritance in monogenic disorders

| *Mode of inheritance* | *Characteristics* |
|---|---|
| Autosomal dominant | Usually further first-degree family members are affected. In severe diseases, spontaneous mutations might occur. The clinical picture is often variable (variable expressivity) and sometimes not evident at all (incomplete penetrance). Risk to children depending on the penetrance up to 50%, usually regardless of gender. Often late-onset diseases. Predictive testing in case of known gene and identified mutation possible. In severe disorders, often new mutations occur in a parental germ cell. In this case, parents are unaffected and recurrence risk to siblings is low (but 50% to own children). |
| Autosomal recessive | Mostly single patients, siblings affected, generally no further affected family members in other branches. Both parents are gene carriers (heterozygous). Risk to siblings 25%, risk to children usually low (<1%) except in a case of parental consanguinity. Clinical picture often severe and similar in siblings. Heterozygosity testing in case of known gene defects generally possible. |
| X-linked recessive | Usually only boys/males affected, females only rarely and often milder. If mother is a carrier, recurrence risk to affected brothers is 50%; 50% of sisters are carriers. Risk to children of affected males: none, all daughters are gene carriers. About a third of cases of severe disease represent new mutations in the maternal germline. Genetic testing in a case of known genes is possible. |

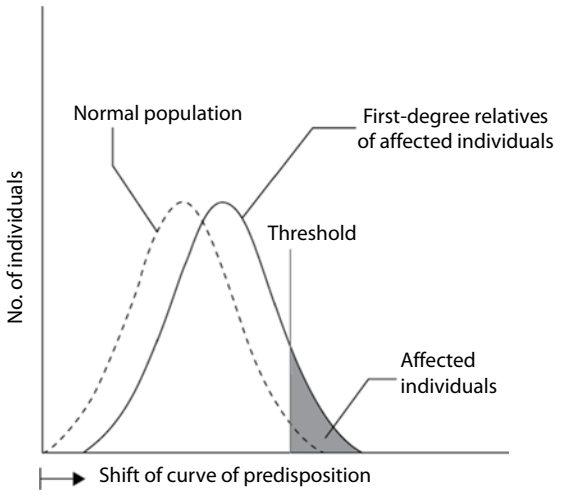


**Figure 60.1**
Model for multifactorial inheritance of CHDs. The liability to the malformation in the general population follows an approximately normal distribution, with individuals exceeding a certain threshold value being affected. First-degree relatives have a similar normal distribution of liability, but the curve is shifted to the right by the increased genetic component. Thus, a greater proportion will exceed the threshold and will be affected.

In 1975 a committee of the American Society of Human Genetics (ASHG) proposed a definition of genetic counseling that was subsequently adopted by the society: "Genetic counseling is a recommendation process which deals with the human problems associated with the occurrence or risk of recurrence of a genetic disorder in a family."

Although the face of genetic counseling has changed continuously since 1975, the basic goals remain as they were then. The following basic principles have been generally accepted:

1. The decision to utilize genetics services should be entirely voluntary. Information should be made available and tests offered when appropriate, but patients and families should have the right to make decisions, particularly about genetic testing and reproduction, unencumbered by pressure or any intimation that a particular course is fiscally or socially irresponsible.
2. Ideally, genetic services, including counseling, diagnosis, and treatment, should be equally available to all who need and choose to use them.
3. A central feature of genetic counseling is a firm belief in the importance of patient education. Typical patient education regarding a particular disorder includes information about (1) the features, natural history, and range of variability of the condition in question; (2) its genetic (or nongenetic) basis; (3) how it can be diagnosed and managed; (4) the chances that it can occur or recur in various family members; (5) the economic, social, and psychological impacts—positive as well as negative—it may have; (6) resources that are available to help families deal with the challenges the disorder presents; and (7) strategies for amelioration or prevention that the family may wish to consider.

4. One of the principal issues regarded by geneticists is that all "relevant information" should be disclosed. Now, however, with the complexity of genetic knowledge and technology, achieving this level of client education is often impracticable. New techniques like microarray analysis or next-generation sequencing might generate findings not related to CHD or those of so far unknown significance. Moreover, full disclosure of all "relevant information" could overwhelm even the most sophisticated patient. It is critical for the counselor to disclose any information relevant to decision-making in ways that the client can interpret and act on.
5. Although the counselor can use clinical judgment in choosing what information is most likely to be important and helpful in a client's adjustment to a diagnosis or in decision-making, it should be presented fairly, not with the purpose of encouraging a particular course of action.

# Molecular genetics and genetic counseling

Recent decades have seen a remarkable expansion and development of molecular genetics. Genetic counseling has been affected profoundly by these molecular advances.

## *Multigene panels*

Although the majority of nonsyndromic cases with CHDs are not monogenic, an increasing number of causative genes have been identified and can be applied as multigene panels in a single diagnostic step. Several diagnostic CHD panels are available.

## *Chromosomal disorders, microdeletions, copy number variants*

CHD is a well-known feature in children with chromosomal disorders. Besides classical chromosomal disorders and an increasing number of microdeletion syndromes (Table 60.3), copy number variants (duplications or deletions) that affect a considerable number of base pairs seem to be of relevance in the etiology of CHDs. While a chromosomal analysis has a resolution of about 5–10 million base pairs (Mb), copy number variants (CNVs) can be detected with a size of more than 250 bp, with some platforms with a higher resolution down to individual genes.

Not only have the advances in molecular genetics resulted in valuable diagnostic tests that allow in an increasing number of cases besides a diagnosis carrier detection, prenatal diagnosis, and preimplantation genetic diagnosis (PGD), where these were previously unreliable or impossible, but also we are gaining insight into the basis of the variability in expression that is characteristic of so many genetic disorders, and which provides some of the most difficult problems of genetic counseling. In addition to difficulties in interpreting molecular changes in several cases, the causal relationship between CNVs and specific CHDs is often unclear and requires caution in genetic counseling.

## *Diseases with localized genes, which have not yet been identified*

After localizing a gene to a specific chromosomal region, the identification of the responsible gene is the next step in research. Since the identification of a gene nowadays often follows within a short period after its localization, the use of indirect genotype analysis has decreasing importance in genetic counseling. Because linkage studies are based on the knowledge of certain haplotypes without knowledge about the responsible mutation itself, this method has major limitations. First, exact clinical diagnosis in an affected family member is necessary. It is a widespread misunderstanding that knowledge of the localization of a gene allows establishment of a diagnosis in a single patient. Linkage studies result in a conclusion about the risk status in persons belonging to a family where specific markers are known to segregate with a disease mutation. Second, genetic heterogeneity of a condition (different genetic entities which usually cannot phenotypically be distinguished in a single person) can lead to misinterpretation. An impressive example is hypertrophic cardiomyopathy, with very many different genes and gene loci. Indirect genotype analysis leads to false results under the assumption of the wrong gene locus. In small families, a certain localization can neither be proven nor excluded. Third, the family has to be informative. Depending on the individual marker constellation, there can be situations where it might not be possible to identify the at-risk haplotype in a family. With the use of multiple flanking and highly polymorphic genetic markers, the majority of families with monogenic CHD with known gene loci are informative, allowing disclosure of the haplotype at risk. In case of a recombination between the analyzed flanking markers, however, a risk estimation can be impossible as well.

## *Conditions with known gene defects*

The situation in conditions where the gene defect is known differs in many aspects from those where only the chromosomal localization of the gene is known. The identification of the responsible mutation usually allows a definite diagnosis of the condition without further investigation or clinical examination.

However, even in diseases where a gene is identified, specific problems can limit the practical application of gene testing:

1. The structure of many genes is complex, and hence, it is often difficult to identify the responsible mutation. In these diseases, DNA mutation analysis is far from being a routine diagnostic method. Unknown mutations and

**Table 60.3** Selected syndromes with congenital heart disease in at least 50% of patients

| *Disorder* | *Main extracardiac features* | *Heart defect* | *Inheritance* |
|---|---|---|---|
| **Microdeletion syndromes** | | | |
| Del22q11 syndrome, DiGeorge syndrome, velocardiofacial syndrome | Short stature, cleft palate, nasal speech, thymus aplasia/hypoplasia, transient hypocalcemia, urogenital anomalies, mild mental retardation, slender fingers | Conotruncal defects, aortic arch anomalies, septal defects | Mostly new deletion of the region 22q11.2, 15%–20% familial |
| Williams syndrome | Short stature, elfin face, mental retardation, renal anomalies, abnormal dentition | SVAS, pulmonary stenosis, stenosis of large vessels | Mostly new deletion of the region 7q11.23 |
| Monosomy 1p36 | Microbrachycephaly, large anterior fontanel, brachydactyly, urogenital anomalies, mental retardation | Septal defects, valvular anomalies, noncompaction cardiomyopathy | Mostly new deletion of the region 1p36 |
| Deletion and duplication 1q21.1 | Developmental delay, microcephaly, cleft lip/palate, and multiple skeletal anomalies represented by malformed phalanges, abnormal acetabula, feet anomalies | Left-sided obstruction, aortic coarctation, bicuspic aortic valve, subaortic stenosis, septal defects, conotrucal anomalies | Mostly micodeletion or reciprocal microduplication 1q21.1 |
| 9q subtelomere deletion syndrome | Microbrachycephaly, arched eyebrows, mental retardation, urogenital anomalies, obesity | Septal defects, artery and valve stenosis, TOF | Mostly new deletion of the region 9q34.3 |
| **Syndromes of known genetic basis, genetic testing possible** | | | |
| Noonan syndrome | Short stature, pterygium colli, sternum deformities, cryptorchidism, facial dysmorphism | Pulmonary stenosis, hypertrophic cardiomyopathy | Heterogeneous, mostly AD new mutations (more than 10 known genes) |
| CFC syndrome/Costello syndrome | C = cardio, F = facio, C = cutaneous manifestations, short stature, sparse hair, skin abnormalities | Pulmonary stenosis, septal defects | See Noonan syndrome |
| Alagille syndrome (arteriohepatic dysplasia) | Liver dysfunction (cholestasis), vertebral arch defects, renal dysfunction, typical face | Right-sided defects, peripheral pulmonary artery stenosis | AD, mostly new mutations (*JAG1* gene) |
| CHARGE syndrome | C = coloboma, H = heart defects, A = choanal atresia, R = mental retardation, G = genital hypoplasia (males), E = ear anomalies, deafness | TOF, PDA, DORV, ASD, VSD | AD, mostly new mutations (*CHD7* gene) |
| Smith-Lemli-Opitz syndrome | Short stature, failure to thrive, microcephaly, syndactyly of two to three toes, postaxial polydactyly, genital abnormalities (males), severe mental retardation | Endocardial cushion defects, hypoplastic left heart, septal defects | AR (biallelic mutations in the *DHCR7* gene) |
| Kartagener syndrome | Bronchiectasis, sinusitis, infertility | Dextrocardia | AR, heterogeneous |
| Holt-Oram syndrome (heart-hand syndrome) | Upper limb defect | Septal defects, conduction defects | AD, heterogeneous (*TBX5* gene) |
| Marfan syndrome | Increased height, arachnodactyly, ectopia lentis, skeletal manifestations, joint laxity, dural ectasia | Aortic dilatation, cardiac valve insufficiency | AD, heterogeneous (*FBN1* gene), neonatal onset cases represent new mutations |
| Kabuki syndrome | Short stature, long palpebral fissures, long, large protruding ears | Variable malformations with altered hemodynamics | Heterogeneous, mutations in *MLL2* gene, deletion of the *KDM6A* gene, most cases are new mutations |
| **Syndrome of unknown etiology** | | | |
| VATER/VACTERL association | V = vertebral anomalies, A = anal atresia, TE = tracheoesophageal fistula, R = radial limb defect/renal anomaly | Septal defects | Unknown, mostly sporadic, axial mesodermal dysplasia |

*Source:* Modified from Jones KL, Smith DW. *Smith's Recognizable Patterns of Human Malformation*. 5th ed. Philadelphia, PA: WB Saunders Company; 2004.[3]

*Abbreviations:* AD, autosomal dominant; AR, autosomal recessive; ASD, atrial septal defect; DORV, double-outlet right ventricle; PDA, patent ductus arteriosus; SVAS, supravalvular aortic stenosis; TOF, tetralogy of Fallot; VSD, ventricular septal defect; XL, X-linked.

among those especially missense changes have often still to be regarded as "changes of unknown significance," until more reliable information is available. With increasing knowledge of genetic variability, observed changes can be classified more safely.

2. Similar to the situation in indirect genotype analysis, the detection of a specific mutation can be impossible in a case of the existence of more than one gene. If a patient turns out to be negative upon mutation analysis of one gene, no diagnostic conclusions can be drawn if there are several gene loci. However, in patients where the mutation has been identified in a specific gene, the diagnosis can be clearly established, and other genetic loci or disease causes can be ruled out. Increasingly applied panel diagnostics with the simultaneous analysis of a greater number of possibly involved genes allows a definite diagnosis in a greater number of cases but might reveal possible causal changes in more than one gene, thus making an interpretation impossible.
3. Another important question that is often forwarded to the medical geneticist is whether the identification of a mutation can predict the individual clinical course. There are diseases where a rough correlation between the type or localization of a mutation and the clinical phenotype exists; in many cases, however, an individual prediction is impossible, since all family members share the same mutation. Although first modifying genes have been identified in CHDs, their knowledge, however, is still of limited value in clinical practice. It is largely unknown which other genetic or nongenetic factors may modify the severity of the disease.

In patients with nonsyndromic CHD, monogenic inheritance is rare. While the diagnosis of a disease-causing mutation does not depend on a clinical phenotype, genetic diagnoses may differ from conventional methods and may have different implications.

## *Prenatal diagnosis*

Prenatal prediction is in most cases limited to severe autosomal recessive or X-linked conditions. There is one exception: a request for prenatal diagnosis in autosomal dominant conditions. This observation can be made in nearly all autosomal dominant diseases (e.g., Huntington's disease, tuberous sclerosis, neurofibromatosis, and breast cancer). One reason might be the fact that always one parent is affected, and that the decision to terminate a pregnancy statistically in 50% of cases is obviously unacceptably high. The question of terminating a pregnancy that is connected with a prenatal diagnosis, when early treatment is not available, is always an important issue that has to be discussed in detail with the parents before they plan the pregnancy.

PGD can only be performed in cases with proven genetic diagnosis in the index patient and the parents. PGD is usually restricted to monogenic conditions or inherited chromosomal translocations.

## *Predictive testing*

The principle is to predict whether a person in a family with a known inherited disease is most likely to be a gene carrier and will develop the disease in the future, although there are no clinical symptoms when tested. Although in many late-onset diseases no prevention is available, the knowledge of a person at risk of being a gene carrier can be of importance. Predictive testing differs from any conventional diagnosis and evaluation of clinical symptoms. Predictive testing has enormous consequences for persons at risk. Different aspects have to be discussed with the individuals who want to undergo predictive testing. Some of the arguments in favor of an early diagnosis are aspects of family planning, therapeutic possibilities, easing the burden of uncertainty, and planning occupation/finance. Insurance and occupational problems are only some of the aspects that have to be discussed intensively.

Predictive testing in children is to be considered only when the diagnosis is of any benefit for the child, for example, in diseases where a specific preclinical therapy is available. In the majority of diseases, this is not the case, and a routine clinical examination is sufficient. As soon as there are clinical signs of the disease, the child can be regarded as a patient and should be taken under medical care. In late-onset diseases, the decision for genetic testing should be made by the individual at risk. There is usually no reason for prenatal prediction of late-onset disease. Predictive testing, however, usually does play only a minor role in families with CHDs.

## *Heterozygosity testing*

In autosomal recessive conditions, heterozygosity testing (identification of healthy gene carrier) is applicable only in families with a known gene mutation or where specific genetic markers are known to segregate with the responsible gene defect.

The situation is different in X-linked diseases where a genotype analysis can identify female carriers for an X-linked condition, which usually has important implications for family planning and possible prenatal diagnosis. The recurrence risk is 50% for males to be affected.

The relevance of being heterozygous for a recessive disorder, which usually has no consequences for the gene carrier, is often misunderstood and needs detailed information before testing. Knowledge of the heterozygous state can be important information for future family planning. Detection of the heterozygosity status in a relative of an affected person is therefore often of limited value, as long as no testing can be applied in a spouse. Prenatal testing in order to evaluate whether the fetus is heterozygous should not usually be performed.

# Genetic counseling before applying genetic testing is essential

According to several guidelines of the various national Societies for Human Genetics and Medical Boards, possible

limitations of DNA analysis and its consequences should be discussed with the family.

## Counseling in families with congenital heart defects

The disclosure of the underlying basis of CHDs is one of the major aims in cardiology. Although around 90% are not obviously familiar, it seems increasingly likely that important genetic factors are involved in most cases, and specific genes and chromosomal regions are starting to be identified. A current update on monogenic defects in human disease and congenital defects is given with the database of Victor McKusick's Inheritance in Man (http://www.ncbi.nlm.nih.gov/Omim/searchomim.html).[2] Thus, the first task in genetic counseling of families is to ensure that a Mendelian lesion has been deemed unlikely, particularly if abnormalities additional to the cardiac lesion are present.

Table 60.3 lists selected syndromes of different etiologies with CHDs in at least 50% of patients. CHDs are also prominent in chromosomal disorders, particularly the autosomal trisomies and microdeletion syndromes (Tables 60.4 and 60.5).

Among the identified environmental causes, rubella is still most important, but CHDs are produced by almost all the less specific teratogens and environmental factors, which should be carefully enquired for, even though it may not be possible to prove cause and effect in an individual case. Lithium is specifically associated with Ebstein anomaly. The offspring of diabetic women also appears to be a high-risk group. Monozygous twinning is itself a risk factor for CHDs, in that twins have an increased risk (around 1.5%).

Genetic advice is most frequently sought for future siblings of an affected child, or sometimes for more distant relatives. However, risks other than for first-degree relatives are low in the absence of multiple cases or an identified Mendelian basis. Information is now becoming available for the offspring of affected individuals, and there is increasing evidence that risks are higher for offspring of affected females than of males. Overall risks are summarized in Table 60.6, but whenever possible, a specific anatomical diagnosis should be used as the basis for risk estimates. When recurrence happens, the defect is the same as previously, in only about half the cases (i.e., clinical concordance). That is, a discordance of the site and severity of heart defects in families with more than one affected individual can be seen in a similar proportion of cases. This is relevant to counseling, because it may mean that a sibling of a proband with a correctable defect may have a fatal or untreatable lesion, or *vice versa*.

The most common discordant lesion in humans is ventricular septal defect (VSD), followed by pulmonary stenosis, aortic stenosis, transposition of the great arteries, and tricuspid atresia.

**Table 60.4** Frequency of heart disease in newborns with selected chromosome abnormalities

| *Chromosomal syndrome* | *Percentage* | *Frequent heart defects* |
|---|---|---|
| Trisomy 18 | 99 | VSD, pulmonary stenosis |
| Trisomy 13 | 90 | VSD, dextrocardia |
| Trisomy 21 | 50 | AV canal, VSD + ASD |
| 4p- (Wolf–Hirschhorn) syndrome | 40 | ASD, VSD |
| 5p- (cri-du-chat) syndrome | 20 | VSD, ASD |
| X0 (Turner syndrome) | 20–30 | SVAS, ASD |
| XXY (Klinefelter syndrome) | 55 | Mitral prolapse |

*Source:* From Nora JJ et al. *Cardiovascular Diseases: Genetics, Epidemiology and Prevention*. New York, NY: Oxford University press; 1991.[1]

*Abbreviations:* ASD, atrial septal defect; AV, atrioventricular; SVAS, supravalvular aortic stenosis; VSD, ventricular septal defect.

**Table 60.5** Frequency of chromosomal aberrations in the presence of a congenital heart defect

| *Heart defect* | *Chromosome aberration (%)* |
|---|---|
| AV canal | 69 |
| VSD + ASD | 32 |
| ASD | 27 |
| VSD | 18 |
| TOF | 10 |
| SVAS | 6 |
| Valve stenosis (aortic or pulmonary) | 4%–5% |
| Hypoplastic left heart | 4 |
| Transposition of great vessels | 0.9 |

*Source:* From Pradat P et al. *Pediatr Cardiol* 2003;24:195–221.[4]

*Abbreviations:* ASD, atrial septal defect; AV, atrioventricular; SVAS, supravalvular aortic stenosis; TOF, tetralogy of Fallot; VSD, ventricular septal defect.

**Table 60.6** Overall risks in congenital heart disease

| *Heart defect* | *Risk (%)* |
|---|---|
| Population incidence | 0.5 |
| Siblings of isolated case | 2–3 |
| Half-siblings or second-degree relative | 1–2 |
| Offspring of isolated case | |
| Father affected | 2–3 |
| Mother affected | 5–6 |
| Two affected siblings or sibling and parent affected | 10 |
| More than two affected first-degree relatives | ~50 |

*Source:* From Harper PS. *Practical Genetic Counselling*. 5th ed. Oxford: Butterworth-Heinemann; 1998.[5]

### Risks to more distant relatives

Data are inadequate, but the excess risk for second-degree relatives of an isolated case of congenital heart disease is certainly under 1%, and it is doubtful whether third-degree relatives have a significantly increased risk. Families with several affected members, none of whom is a first-degree relative, are not infrequently encountered. The possibility of a variable Mendelian form should be seriously considered here. In cases of a chromosomal disorder, a cytogenetic analysis of relatives usually allows individual risks to be specified. CNV in parents of close relatives can be difficult to interpret.

### Multiple cases

Family clusters of CHDs are not uncommon; their occurrence should prompt a careful search for a Mendelian or chromosomal syndrome. After two affected children, the risk of CHDs in future siblings is approximately tripled, regardless of whether the affected individuals have the same heart defect or not. This gives risks ranging from 5% for the rare defects to 10% for a common abnormality, such as ventricular septal defect. A similar risk would be likely for future children where an affected parent has an affected child, although data to confirm this are not yet available. Numbers are insufficient to give individual estimates for specific defects. The occurrence of more distant affected relatives does not increase the risks given in Table 60.6. In exceptional families with more than two affected first-degree relatives, risks are likely to approach 50%.

## Chromosomal disorders, microdeletion syndromes, and copy number variation

CHDs are important manifestations of chromosomal aberrations. The most common lesions are ventricular and atrial septal defects, patent ductus, and pulmonary stenosis. Among fetuses with a prenatally detected CHD and/or intrauterine growth restriction, a chromosomal disorder can be detected in up to 40% of cases.[6] The frequency of CHDs in chromosomal aberrations ranges from near 100% (trisomy 18) to minimal (Table 60.4). While the heart lesion seldom points specifically toward a chromosome abnormality, endocardial cushion defects are frequently seen in Down syndrome, and Turner syndrome is predominantly associated with coarctation of the aorta. A chromosomal disorder normally includes multiple system involvement and is only rarely limited to cardiovascular defects. It is clearly understood that the counseling must relate to the karyotype. Since most chromosome anomalies are nonhereditary, the recurrence risk to siblings is small, if familial translocations or inherited structural defects can be excluded.

A considerable number of conditions are caused by small chromosomal deletions that often escape conventional cytogenetic analysis. By means of fluorescent *in situ* hybridization (FISH) or other molecular cytogenetic methods, many of these small deletions can be made visible and have important implications for genetic counseling. If the same microdeletion can be detected in a parent or a relative, the recurrence risk to a sibling is 50%, with a broad spectrum of phenotypic manifestations in some of these syndromes. CHD is a leading feature in well-known microdeletion syndromes like velocardiofacial syndrome/DiGeorge syndrome and Williams–Beuren syndrome.

### Velocardiofacial syndrome/ DiGeorge syndrome

Patients with velocardiofacial syndrome exhibit a broad spectrum of phenotypic abnormalities. Most important features are short stature, intellectual impairment, velopharyngeal incompetence, and cardiac defects (conotruncal defects, aortic arch anomalies, and septal defects). The condition is autosomal dominantly inherited, with most patients representing new mutations on the basis of a microdeletion of chromosome 22q11. Inherited deletions also occur in about 15%–20% of patients. The corresponding deletions are only rarely visible by conventional cytogenetic analysis.

### Williams–Beuren syndrome

This syndrome is characterized by facial dysmorphism (elfin face), hypercalcemia, CHD (supravalvular aortic stenosis, pulmonary valvular stenosis, peripheral pulmonary artery stenosis, and ventricular and atrial septal defects), and mental retardation. Most affected individuals represent sporadic cases. The syndrome is caused by a small deletion including the elastin gene on chromosome 7q11. A rare mutation in the elastin gene causes isolated supravalvular aortic stenosis and cutis laxa.

Copy number variation can be found in about 5%–10% of cases of nonsyndromic CHD, some CNVs are mapping in chromosomal regions previously known to contain genes pathogenetically related to CHDs (e.g., *JAG1, NOTCH1*), and several were recurrent, with both gain and loss of chromosome 1q21.1 being observed in about 1%.[7] A high prevalence of CNVs in controls up to 4% makes interpretation of CNVs difficult.

## Specific anomalies

In the following, the genetic basis of the most common heart malformations with relevance to prenatal diagnosis is discussed in more detail.

### Atrioventricular septal defects

While the majority are multifactorially inherited (recurrence risk about 2%–3% to first-degree relatives), families following

autosomal dominant inheritance are known. Isolated atrioventricular septal defect (AVSD) exhibits locus heterogeneity. Linkage analysis has established a locus on 1p31–p21 (AVSD1), and deletion mapping has identified a locus on 3p25 (AVSD2), which has been found to be due to mutations in the *CRELD1* gene. AVSD3 is caused by a mutation in the *GJA1* gene, AVSD4 by mutation in the *GATA4* gene, and AVSD5 by mutation in the *GATA6* gene. Somatic mutations in the *HAND1* gene have been identified in tissue samples from patients with AVSDs. AVSD is classically associated with Down syndrome and is seen in other syndromes such as Holt-Oram syndrome and atrial septal defect (ASD) with atrioventricular conduction defects and in rare cases of familial Noonan syndrome. These syndromes are too rare to affect the general recurrence risks but should be considered in patients with extracardiac manifestations. Concordance in siblings and first-degree relatives of patients with ASD is about 50% in combined series.

## Ventricular septal defects

While the majority are multifactorially inherited, families with monogenic VSDs are known, but VSDs are genetically heterogeneous. VSD1 is caused by heterozygous mutation in the *GATA4* gene. Other CHDs caused by mutation in the *GATA4* gene include ASD2, tetralogy of Fallot (TOF), and endocardial cushion defects. VSD2 is caused by mutation in the *CITED2* gene, and VSD3 by mutation in the *NKX2-5* gene. Somatic mutations in the *HAND1* gene have been identified in tissue samples from patients with VSD.

The recurrence risks of 3% to siblings and 2%–9% to offspring apply to severe ventricular septal defects, mostly those in patients requiring surgery. It is doubtful whether the risks are as high for relatives of patients with asymptomatic or transient defects. The risk for offspring seems to be increased in those cases where the mother is affected. The concordance rate with VSD recurring in first-degree relatives varies from 30% to 60%. TOF is the most common discordant lesion, indicating that VSD can be regarded as a *forme fruste* of TOF in these families. TOF can be caused by mutations in the human homolog of rat Jagged-1 (*JAG1*), or in the gene encoding the cardiac-specific homeobox Nkx2.5 (*CSX*). There is also a well-recognized association with 22q11 microdeletion and trisomy 21. Mutations in the *ZFPM2* gene have been identified in sporadic cases of TOF, as have mutations in the *GDF1* gene.

## Hypoplastic left heart syndrome

The overall recurrence risk of about of 3.2% is higher than predicted for multifactorial inheritance alone. Hypoplastic left heart syndrome (HLHS1) can be caused by a mutation in the *GJA1* gene, and HLHS2 by mutation in the *NKX2-5* gene. Somatic mutations in the *HAND1* gene have been identified in tissue samples from patients with HLHS. Only about 25% of recurrences are HLHS, the remaining including a variety of anomalies, VSD, and ASD. There is evidence for a small fraction following autosomal recessive inheritance. In practice, a recessive mode of inheritance should be considered in families with two affected children.

## Endocardial cushion defect

The interpretation of figures for recurrence risks in families with endocardial cushion defects is difficult. The sibling recurrence risk in a larger series of studies is 2.5%. Those of children from affected siblings differ greatly. The offspring risk is given as 14% for children of affected mothers and about 1% for those of affected fathers. Concordance is about 90% in affected families, which is very high.

## Pulmonary stenosis

It is estimated that about 10% of patients with pulmonary stenosis have Noonan syndrome. Pulmonary stenosis can also be found in related diseases such as LEOPARD syndrome or neurofibromatosis. If Noonan syndrome is present in patients with pulmonary stenosis, the risk of Noonan syndrome in offspring is 50%, and the risk for some form of cardiovascular disease is about 25%.

Pulmonary or aortic stenosis generally has a recurrence risk of 2%–5% to first-degree relatives.

# References


1. Nora JJ et al. *Cardiovascular Diseases: Genetics, Epidemiology and Prevention*. New York, NY: Oxford University Press; 1991.
2. McKusick's Online Mendelian Inheritance in Man: http://www.ncbi.nlm.nih.gov/Omim/searchomim.html.
3. Jones KL, Smith DW. *Smith's Recognizable Patterns of Human Malformation*. 5th ed. Philadelphia, PA: WB Saunders Company; 2004.
4. Pradat P et al. *Pediatr Cardiol* 2003;24:195–221.
5. Harper PS. *Practical Genetic Counselling*. 5th ed. Oxford: Butterworth-Heinemann; 1998.
6. Schwanitz G et al. *Ann Genet* 1990;33:79–93.
7. Gelb BD, Chung WK. *Cold Spring Harb Perspect Med* 2014;4: a013953.

# 61

# Cardiac disease in pregnancy

Sabrina D. Phillips and Frank Cetta

## Introduction

Maternal mortality and morbidity remain important health risks for childbearing-aged women. Globally, for women aged 15–49 years, 7.3% of all deaths are related to maternal causes.[1] Hemorrhage, sepsis, hypertensive disorders, and comorbid conditions such as obesity and diabetes mellitus continue to be significant contributors to maternal mortality. But demographic shifts and improved care for women with congenital heart disease have led to an increased influence of cardiovascular disease on maternal morbidity and mortality. Data from the Centers for Disease Control and Prevention in the United States demonstrated that in the surveillance period encompassing 2006–2009, cardiovascular conditions alone accounted for over one-third of all pregnancy-related deaths.[2] Further, assessment of near-miss maternal mortality during pregnancy and childbirth found that the leading intensive care unit admission diagnosis for pregnant and postpartum women was maternal cardiac disease.[3] In another study, 55% of the patients with cardiovascular disease had valvular heart disease, congenital heart disease, Marfan syndrome, or pulmonary hypertension.[4]

## Hemodynamic changes of pregnancy

The hemodynamic changes that occur during pregnancy, delivery, and the postpartum period are significant. Since the early 20th century, attempts have been made to quantify these changes and understand the physiologic mechanisms resulting in this alteration from baseline hemodynamics. In 1932, Grollman reported that cardiac output increased in pregnancy 45%–85% over the nonpregnant state, with the increase occurring rapidly during the first half of pregnancy and peaking by the 32nd week of gestation.[5] Subsequently, cardiac output and other hemodynamic changes have been studied with cardiac catheterization, echocardiography, and thoracic impedance. Most studies agree that cardiac output rises during the first two trimesters, and there is discrepancy regarding cardiac output changes in the third trimester and postpartum period.[6] Some of the discrepancies can be explained by not utilizing the pregnant woman as her own control, and by the position of the patient during testing, thereby altering venous return. It is generally accepted that cardiac output increases in early pregnancy and peaks in the mid-third trimester. A return to baseline cardiac hemodynamics likely does not occur until at least 12 weeks postpartum.[7] The changes in cardiac output are driven by a decrease in systemic vascular resistance, an increase in blood volume, and a slight increase in heart rate. During labor, intravascular volume is increased with uterine contractions leading to increased stroke volume and increased cardiac output.[8] Increased sympathetic tone secondary to pain may further increase cardiac output. Some of these hemodynamic effects of labor may be altered by anesthesia. Immediately after delivery, cardiac output transiently increases secondary to improved venous return and mobilization of extracellular fluid.[9] However, significant blood loss during delivery will result in reduced cardiac output despite these transient changes.

## Maternal risk assessment

These hemodynamic alterations pose a challenge for women with cardiac abnormalities. Ideally, care of a woman with a known cardiac condition begins with preconception counseling to assess current cardiac status, provide risk assessment for maternal and fetal morbidity/mortality, and develop a management strategy for assessment and treatment during pregnancy and delivery. Depending on the cardiac concern, some women may need minimal subspecialty follow-up, but those with a significant disease will need consultation with the following subspecialists: a cardiologist experienced in the care of the pregnant woman, maternal fetal medicine, cardiac/obstetrical anesthesia, neonatology, and genetics. It is appropriate to obtain a screening fetal echocardiogram at 18–22 weeks' gestation in most cases when parental congenital heart disease is present. Delivery in a tertiary care center is recommended for mothers at high risk of cardiac decompensation. To appropriately assess risks of cardiac complications in an individual patient, the hemodynamic changes expected during pregnancy and delivery must be completely understood and applied to that patient's specific cardiac lesion. There are several validated risk assessment models available to assist in estimation of individual risk of a cardiac complication for women with acquired and congenital heart disease.

**Table 61.1** CARPREG predictors of primary cardiac events during pregnancy

1. Prior cardiac event or arrhythmia
2. Baseline NYHA class greater than II or cyanosis
3. Left heart obstruction (aortic valve area <1.5 $cm^2$, mitral valve area <2 $cm^2$, peak left ventricular outflow gradient >30 mm Hg by echocardiography)
4. Reduced systemic ventricular systolic function (ejection fraction <40%)

*Source:* Adapted from Siu SC et al. *Circulation* 2001;104:515–21.[10]

**Table 61.2** ZAHARA predictors of cardiac complications during pregnancy

| | |
|---|---|
| History of arrhythmia | 1.50 points |
| Cardiac medication usage prepregnancy | 1.50 points |
| Baseline NYHA class II or greater | 0.75 points |
| Left heart obstruction (aortic valve area <1 $cm^2$, peak left ventricular outflow gradient >50 mm Hg) | 2.50 points |
| Systemic AV valve regurgitation (moderate/severe) | 0.75 points |
| Pulmonary AV valve regurgitation (moderate/severe) | 0.75 points |
| Mechanical valve prosthesis | 4.25 points |
| Repaired or unrepaired cyanotic heart disease | 1.00 points |

*Source:* Adapted from Drenthen W et al. *Eur Heart J* 2010;31:2124–32.[12]

*Note:* Points for risk calculation (maximum number of points: 13).

**Table 61.3** ZAHARA risk score for cardiac complications during pregnancy

| *Risk score* | *Cardiac complications in percentage (%) of total number of pregnancies* |
|---|---|
| 0–0.50 | 2.9 |
| 0.51–1.50 | 7.5 |
| 1.51–2.50 | 17.5 |
| 2.51–3.50 | 43.1 |
| >3.51 | 70.0 |

*Source:* Adapted from Drenthen W et al. *Eur Heart J* 2010;31:2124–32.[12]

**Table 61.4** Modified WHO classification of maternal cardiovascular risk

| *Risk class* | *Maternal risk during pregnancy* | *Recommended cardiology follow-up during pregnancy* |
|---|---|---|
| I | Maternal mortality risk the same as the general population; maternal morbidity the same to mildly increased | One or two visits |
| II | Maternal mortality risk mildly increased; maternal morbidity moderately increased | Each trimester |
| III | Maternal mortality and morbidity risk significantly higher than general population; Specialized multidisciplinary care required | Monthly or bimonthly |
| IV | Maternal mortality and morbidity risk extremely high; Pregnancy is contraindicated | Monthly or bimonthly if pregnancy is pursued |

*Source:* Regitz-Zagrosek V et al. *Eur Heart J* 2011;32:3147–97.[14]

The CARPREG score[10] was developed after prospectively studying women with both acquired and congenital heart disease. The four predictors of primary cardiac events in this model are shown in Table 61.1. One point is assigned for each predictor, the risk of a cardiac event is predicted at 5%, 27%, and 75% for a pregnancy with 0, 1, or more than 1 point, respectively. This model provides a concise method to estimate risk of cardiovascular events during pregnancy and is very useful in the discussion with patients and referring providers, but may provide a less accurate risk assessment for mothers with congenital heart disease. Subsequent assessment of the CARPREG score in women with congenital heart disease revealed that severe pulmonary valve regurgitation and/or subpulmonary ventricular systolic dysfunction are important additional risk predictors in this patient population.[11] In contrast, the ZAHARA study[12] evaluated the predictors of pregnancy complications only for women with congenital heart disease. It demonstrated additional risk predictors in this cohort that are shown in Table 61.2. The predicted risk of a cardiac complication based on these factors is represented in Table 61.3. In addition, the World Health Organization (WHO) has categorized maternal cardiovascular conditions into four classes, with recommendation on follow-up during pregnancy based on these risk strata (Table 61.4). The WHO classification of specific cardiac conditions is discussed later in this chapter.

## Neonatal risk assessment

Neonatal complications in offspring of mothers with cardiovascular disease are higher than the general population. The most prevalent adverse events include prematurity and growth restriction. Inadequate cardiac output to sustain the pregnancy has been proposed as an overarching mechanism of these complications. A recent prospective study supports this hypothesis, demonstrating that neonatal complications were higher in pregnancies where maternal cardiac output declined as gestation advanced or when third-trimester umbilical artery Doppler flows were abnormal.[13] The independent predictors of neonatal complications in the CARPREG and ZAHARA cohorts include factors that would potentially limit cardiac output and oxygen content delivery to the placental circulation (Table 61.5). Need for maternal

**Table 61.5** Maternal predictors of adverse neonatal outcome

| *CARPREG study* | *ZAHARA study* |
|---|---|
| NYHA class greater than II or cyanosis | Cyanotic heart disease (corrected or uncorrected) |
| Left heart obstruction | Cardiac medication before pregnancy |
| Smoking during pregnancy | Smoking during pregnancy |
| Multiple gestation | Multiple gestation |
| Use of anticoagulants | Mechanical valve prosthesis |

*Source:* Adapted from Siu SC et al. *Circulation* 2001;104:515–21;[10] Drenthen W et al. *Eur Heart J* 2010;31:2124–32.[12]

anticoagulation during pregnancy is also an important risk factor.[10,12]

# Management of valvular heart disease

## *Stenotic lesions*

Semilunar valve stenosis increases ventricular afterload, myocardial oxygen consumption, and wall thickness. Depending on the severity of the stenosis, the ability to augment cardiac output may be limited, diastolic filling pressures may be increased, and endocardial perfusion may be at risk. The hemodynamic changes of pregnancy may not be tolerated well in this situation, but the outcome of pregnancy depends on the symptomatic status and the ventricular function of the mother prior to pregnancy. For these reasons, mothers with aortic valve stenosis or more than mild pulmonary valve stenosis are classified in WHO groups II–III, with severe symptomatic aortic stenosis classified as WHO group IV.[14] The association of ascending aorta enlargement in mothers with bicuspid aortic valves must be integrated into the risk assessment and management plan of these patients, ascending aorta dilatation >45 mm increases the risk of complications during pregnancy.

Medical management of the mother with pulmonary or aortic valve stenosis includes regular assessment of outpatient clinical status. Echocardiography should be performed to follow valve gradient and ascending aorta dimensions. During pregnancy, valve gradients will increase related to increased cardiac output. Valve gradients that do not change or decrease are signs of inability to increase cardiac output. In mothers with limited cardiac output, reduced physical activity should be advised. Signs or symptoms of pulmonary or systemic venous congestion can be treated with judicious use of diuretics, but caution must be exercised to prevent hypotension and placental underperfusion. Mothers who develop significant heart failure symptoms in the setting of severe semilunar valve obstruction should be considered for early delivery if the fetus is viable. Cardiac decompensation prior to 30 weeks' gestation that cannot be managed medically is an indication for valve intervention. Most patients with pulmonary valve stenosis can achieve relief of valve obstruction safely with balloon valvuloplasty. Patients with aortic stenosis should only be considered for balloon valvuloplasty if the valve morphology is appropriate, that is, balloon valvuloplasty should not be performed solely because the patient is pregnant if she would otherwise not be considered a candidate for percutaneous intervention. Aortic valve replacement surgery can be performed safely during pregnancy. Cardiac surgery during pregnancy is discussed in the "Special situations" section. If delivery is indicated for significant cardiac decompensation, cesarean delivery with cardiac anesthesia support is indicated, otherwise most women with aortic or pulmonary valve stenosis can labor and deliver vaginally.

Atrioventricular valve stenosis results in increased atrial pressure and if severe, decreases ventricular preload, reducing cardiac output. The risk of atrial arrhythmias is increased related to atrial stretch. Women with severe mitral stenosis are classified in WHO group IV and lesser degrees of stenosis are considered WHO group II–III.[14] Regular cardiac clinical assessment is indicated. In women who develop symptoms, medical therapy consists of treatment of pulmonary or systemic congestion with diuretics, increasing diastolic filling time with beta-blockers, maintenance of sinus rhythm, and activity restriction. Therapeutic anticoagulation should be considered in patients with heart failure, large atria, or atrial fibrillation.[14] Patients with symptomatic severe mitral stenosis who do not improve with medical therapy should be considered for balloon valvuloplasty if the leaflet characteristics are favorable. Cesarean delivery should be reserved for those women with significant symptoms or pulmonary hypertension despite appropriate utilization of medical and interventional therapies.[14]

## *Regurgitant lesions*

Semilunar valve regurgitation results in an increase in preload, afterload, wall tension, and myocardial oxygen demand. Historically, valve regurgitation was assumed to be well tolerated during pregnancy because of decreased afterload. However, patients with significant regurgitation and ventricular impairment can have hemodynamic compromise during pregnancy. While systemic and pulmonary vascular resistances decrease during pregnancy, preload increases. The ability to tolerate pregnancy in the setting of semilunar valve regurgitation depends on the status of the ventricle prior to pregnancy. Women with severe semilunar valve regurgitation should have regular cardiology assessment during each trimester. Most of these women can deliver vaginally.

Atrioventricular valve regurgitation increases preload but reduces afterload and increases atrial volume. Patients with severe regurgitation can experience heart failure or arrhythmia during pregnancy. Patients with severe atrioventricular valve regurgitation require regular cardiac clinical assessment throughout pregnancy and most can deliver vaginally.

## Valve prostheses

Women with prosthetic valves face a unique set of challenges with pregnancy. While patients with bioprosthetic valves are at lower risk of complications, bioprosthetic valve thrombosis has recently been recognized as an underappreciated cause of structural valve failure.[15] These valves may be vulnerable during the hypercoaguable state of pregnancy. Currently, there is no indication that patients with bioprosthetic valves should have therapeutic anticoagulation or change in management during pregnancy. Many of these patients receive chronic aspirin therapy, and this may be continued during pregnancy. There has been concern, however, that pregnancy leads to more rapid deterioration of bioprosthetic valve function.[16] But several studies have suggested that the rates of structural valve failure are similar in women regardless of pregnancy status.[17–19] The potential for adverse effect on bioprosthetic valve longevity is important in women of childbearing age who will face reoperation in their lifetime.[20]

Women with mechanical valve prostheses are at high risk of maternal and neonatal complications. Recent data from the ROPAC registry showed that women with mechanical heart valves had only a 58% chance of experiencing an uncomplicated pregnancy and live birth.[21] The hypercoagulable state of pregnancy and the alterations in medication protein binding, absorption, and metabolism, add to the potential adverse effects of anticoagulation to the fetus and placenta and make the maintenance of therapeutic anticoagulation a challenge. There is no risk-free therapeutic anticoagulation regimen in pregnancy. Oral vitamin K antagonists cross the placenta and are associated with unpredictable fetal anticoagulation, which can result in fetal intracranial hemorrhage. The fetal international normalized ratio (INR) is not the same as the maternal INR as the fetus has altered protein binding and drug metabolism. Fetal exposure during the first trimester, especially during weeks 6–9, may cause abnormal development of bone and cartilage. These embryopathic changes are mostly manifested as nasal hypoplasia, though more significant neurologic defects have been reported. Warfarin embryopathy may be dose related, a study by Vitale et al. suggested that women taking a dose of warfarin less than 5 mg daily had a markedly lower rate of embryopathy in their offspring.[22] Unfractionated heparin does not cross the placenta, but intravenous administration throughout pregnancy is not feasible, and correct dosing to achieve therapeutic levels with subcutaneous administration is challenging. Long-term use of heparin is also associated with decreased bone density and can result in heparin-induced thrombocytopenia. Low molecular weight heparins do not cross the placenta and are easy to administer, but initial enthusiasm for this method of anticoagulation during pregnancy was tempered when early studies demonstrated increased risk of valve thrombosis. However, the excess thrombosis rate in those reports may be secondary to poor monitoring of anti-Xa levels.[23] At present, the novel direct oral thrombin inhibitors or Factor Xa inhibitors have not been studied rigorously in pregnancy.

The risks and benefits to both mother and fetus must be considered when developing an anticoagulation plan. Options include (1) vitamin K antagonist use throughout most of the pregnancy with discontinuation and use of unfractionated or low molecular weight heparin in the late third trimester to prepare for delivery; (2) discontinuing warfarin and using monitored low molecular weight heparin therapy throughout pregnancy; or (3) monitoring low molecular weight heparin during the first trimester, switching to a vitamin K antagonist after 9–12 weeks with continued use until late in the third trimester, when a switch to intravenous or subcutaneous heparin would be made. A review of the literature by Chan et al. in 2000 demonstrated that maternal risk was lowest with the use of warfarin throughout pregnancy, but this regimen did increase the risks to the fetus.[24] The more contemporary ROPAC data[21] echoed these findings, demonstrating that valve thrombosis in the first trimester was seen only in women utilizing heparin, but fetal loss rate was higher in women who continued vitamin K antagonists throughout the first trimester. The current American College of Cardiology (ACC)/American Heart Association (AHA) guideline recommendations[25] for anticoagulation of mechanical valves during pregnancy are as follows:

*Class I*

1. Therapeutic anticoagulation with frequent monitoring is recommended for all pregnant patients with a mechanical prosthesis (Level of Evidence: B).
2. Warfarin is recommended in pregnant patients with a mechanical prosthesis to achieve a therapeutic international normalized ratio (INR) in the second and third trimesters (Level of Evidence: B).
3. Discontinuation of warfarin with initiation of intravenous UFH (with an activated partial thromboplastin time (aPTT) >2 times control) is recommended before planned vaginal delivery in pregnant patients with a mechanical prosthesis (Level of Evidence: C).

*Class IIa*

1. Continuation of warfarin during the first trimester is reasonable for pregnant patients with a mechanical prosthesis if the dose of warfarin to achieve a therapeutic INR is 5 mg/day or less after full discussion with the patient about risks and benefits (Level of Evidence: B).
2. Dose-adjusted LMWH at least two times per day (with a target anti-Xa level of 0.8–1.2 U/mL, 4–6 hours post-dose) during the first trimester is reasonable for pregnant patients with a mechanical prosthesis if the dose of warfarin is >5 mg/day to achieve a therapeutic INR (Level of Evidence: B).
3. Dose-adjusted continuous intravenous UFH (with an aPTT at least two times control) during the first trimester is reasonable for pregnant patients with a mechanical prosthesis if the dose of warfarin is >5 mg/day to achieve a therapeutic INR (Level of Evidence: B).

*Class IIb*

1. Dose-adjusted LMWH at least two times per day (with a target anti-Xa level of 0.8–1.2 U/mL, 4–6 hours post-dose) during the first trimester may be reasonable for pregnant patients with a mechanical prosthesis if the dose of warfarin is 5 mg/day or less to achieve a therapeutic INR (Level of Evidence: B).
2. Dose-adjusted continuous infusion of UFH (with aPTT at least two times control) during the first trimester may be reasonable for pregnant patients with a mechanical prosthesis if the dose of warfarin is 5 mg/day or less to achieve a therapeutic INR (Level of Evidence: B).

*Class III*

1. LMWH should not be administered to pregnant patients with mechanical prostheses unless anti-Xa levels are monitored 4–6 hours post-dose (Level of Evidence: B).

In all regimens, the monitoring of INR, aPTT, or anti-Xa levels must be done at least weekly to ensure adequate anticoagulation. It has been suggested that measurement of both peak and trough anti-Xa levels, with dose frequency adjusted to every 8 hours if needed, may improve efficacy of the low molecular weight heparin regimen. Postpartum hemorrhage is a concern in women who require anticoagulation, but no data have emerged to direct the optimal time for reinitiation of anticoagulation postdelivery.[26]

# Management of shunt lesions

## *Atrial septal defect and partial anomalous pulmonary venous return*

Patients with atrial septal defect (ASD) or partial anomalous pulmonary venous return (PAPVR) experience volume loading of the right heart chambers and the pulmonary bed. These lesions may not be diagnosed until adulthood, and the hemodynamic changes of pregnancy may unmask the condition. Volume overload of the right heart chambers will produce dilatation and eventual right ventricular dysfunction, but irreversible increase in pulmonary vascular resistance is rare. Some patients will have mild to moderately elevated right heart and pulmonary artery systolic pressures, related to the excess pulmonary blood flow. Pulmonary artery systolic pressure is proportional to the product of pulmonary blood flow (Qp) and pulmonary vascular resistance. Atrial dilatation leaves the patient vulnerable to atrial arrhythmia.

Women with ASD and/or PAPVR can usually complete a pregnancy with minimal difficulty unless there is severe increase in pulmonary vascular resistance. Women with repaired ASD or PAPVR are classified as WHO group I, whereas those with unrepaired defects are considered WHO group II. The risk of pregnancy in women with ASD is low, but there is evidence of increased risk of arrhythmia, preeclampsia, fetal mortality, and fetal growth restriction in mothers with unrepaired ASD, especially if maternal age is greater than 30 years or prior history of arrhythmia.[27] Closure of an ASD during pregnancy is rarely warranted and should only be considered if the mother has significant change in cardiovascular status. Pregnancy is a hypercoagulable state, but therapeutic anticoagulation is not indicated during gestation to prevent paradoxical emboli. Appropriate measures should be undertaken in the postpartum period to prevent venous thrombosis, including prophylactic heparin, early ambulation, and compression stockings.[14] Air filters should be used on all intravenous lines to prevent air emboli. Spontaneous labor and vaginal delivery is preferable in most cases.

## *Ventricular septal defect*

In adulthood, the hemodynamics of unrepaired ventricular septal defects (VSD) generally fall into two categories: small restrictive defects with no significant hemodynamic consequences or large defects with significant elevation in pulmonary vascular resistance (the Eisenmenger syndrome). Pregnancy is contraindicated (WHO group IV) in women with Eisenmenger syndrome. Women with small, restrictive VSD are classified as WHO group II, and those with repaired VSD are classified as WHO group I. There is no indication to alter medical management or to close a small, hemodynamically insignificant VSD during pregnancy, and patients should be allowed to labor spontaneously and deliver vaginally. Most patients should be seen before pregnancy to ensure that there is no hemodynamic compromise. Though the risk of pregnancy is considered low, the ZAHARA investigators demonstrated that women with unrepaired VSD have a higher incidence of preeclampsia compared to the general population (AOR 4.59).[28] Women with repaired VSD were at higher risk of preterm labor (AOR 4.02) and small for gestational age infants (AOR 4.09) when compared to women with unrepaired VSD, this may reflect some degree of cardiac compromise in those women who had VSDs large enough to require surgical intervention.[28]

# Overview of pregnancy and contraception in complex congenital heart disease

In general, the existing literature that describes pregnancy outcomes for women with complex congenital heart disease is scant and in many instances overly optimistic. While it is true that in the current era, few women die during pregnancy and delivery, the more important long-term issue of ventricular preservation after pregnancy has not been assessed. Limited data from reports of patients with d-transposition of the great arteries (d-TGA) after atrial switch or those with single-ventricle/Fontan physiology speculate that progressive ventricular dysfunction and earlier death might be accelerated by pregnancy. In patients with single-ventricle or

systemic right ventricular morphology, one may anticipate a decline in ventricular function during pregnancy. These patients require more frequent follow-up and imaging during pregnancy. Heart failure is the second most common cardiac complication during pregnancy and occurs in at least 10% of all women. Recovery of function in the postpartum period is not necessarily expected or uniform.

Thromboembolic events also occur; however, the frequency of these has not been delineated. Maternal deaths do occur; however, in the current era they are exceedingly rare. All of these issues need to be taken into consideration in women with systemic right ventricle or single-ventricle physiology who are also at higher risk for arrhythmia. Women with baseline systemic ventricular dysfunction may experience irreversible demise during pregnancy. Premature and/or small for gestational age (SGA) newborns are common in pregnancies of woman with complex congenital cardiac disease. Clinicians must remember that two patients are at risk during these pregnancies (mother and child).

## Pregnancy and arrhythmia

Arrhythmias are the most common cardiac event during pregnancy, occurring in at least 16% of women. Normal pregnancy-related changes in the electrocardiogram and heart rhythm are as follows:

- Leftward shift of the QRS axis in the frontal plane
- New-onset arrhythmia
- Sinus tachycardia
- Shortening of the PR and QT intervals
- Small Q and inverted P waves in lead III (abolished by inspiration)
- Increased R waves in leads V1 and V2
- Nonspecific ST-T wave changes, especially in lead III

In women with congenital heart disease, sustained arrhythmia can result in increased risk to the mother and fetus. In 2006, Silversides et al. reported recurrence risks during pregnancy of SVT, atrial fibrillation/flutter, and ventricular tachycardia of 50%, 52%, and 27% respectively.[29] Six women had atrial fibrillation/flutter throughout their entire pregnancy. Adverse fetal events occurred in 20% of these pregnancies and were more common in women who had antepartum arrhythmias. Certain lesions/surgeries predispose women to arrhythmia during pregnancy, namely, d-TGA after atrial switch and after the Fontan operation. In these situations, meticulous surveillance of rhythm issues during and after pregnancy is important.

The outcome for pregnancy in women with atrioventricular (AV) conduction block is varied. Some early studies recommended that all women with AV block undergo pacemaker placement prior to consideration of pregnancy. Opinion on this has become more controversial in recent years. In 2011, Thaman et al. reported good outcomes for women with AV block during pregnancy.[30] In general, AV block in pregnancy was progressive, but not all patients required pacemaker therapy. In those who had pacemaker placement prior to pregnancy, it was well tolerated. Transvenous systems with subclavicular generators generally had fewer issues during pregnancy than epicardial systems with intra-abdominal generators.

There are very few disease-specific recommendations during pregnancy for woman with cardiac channelopathies such as long QT syndrome (LQTS) and Brugada syndrome. Some considerations include management of hyperemesis during pregnancy. If possible, antiemetic agents that are known to be QT prolonging should be avoided. Table 61.6 is a partial list of medicines that should be avoided or used with cardiology consultation in women with LQTS.[31] Pregnancy itself is not considered a proarrhythmic time period for women with channelopathies. However, during the postpartum period, women with LQT2 are at increased risk of an LQT-triggered cardiac event. In general, there is a paucity of data in this field. It seems at this point that the best recommendations are to avoid QT-prolonging medications during pregnancy and in the immediate postpartum period. In the coming decades there will be potential for increased research in this field.[32]

## Pacemakers/implantable cardioverter defibrillators in pregnancy

In general, women with cardiac pacemakers and implantable cardioverter defibrillators (ICDs) tolerate pregnancy well. Vaginal delivery with preexisting pacemaker is low risk and preferred. Pacemakers do not interfere with antepartum or intrapartum external fetal heart rate monitoring. Fetal scalp electrodes may record the pulse from maternal pacemaker, so their data should be interpreted with caution. If cesarean section is necessary, bipolar electrocautery is recommended with short bursts to avoid interference with pacemaker output. Generally, pacemaker and ICD management during noncardiac surgery needs tailoring to patient-specific issues. An electrophysiologist needs to evaluate optimal settings for the pacemaker or defibrillator during cesarian section. Specific management will depend on whether the patient is pacemaker dependent, type of device, and mode of pacing. The most common electrical complication for pacemakers is skin irritation and even ulceration at the site of the generator. This can occur if a generator placed in the chest is not in the subpectoral region. Skin over the generator can be stretched during breast hypertrophy. Generators in the abdomen may have the same erosion issues as skin is stretched during advanced stages of pregnancy.[33]

For women with ICDs, pregnancy is safe. Pregnancy does not increase the risk of major ICD-related complications or result in a high number of ICD discharges. In 1997, Natale et al. reported results for 44 women who had ICDs.[34] Forty-two of these women had abdominal generators, and two had prepectoral devices. During pregnancy, 33 women received

**Table 61.6** Drugs to avoid or obtain cardiology consultation prior to using in patients with prolonged QT interval

| *Drug class* | *Generic name* |
|---|---|
| Anesthetic | Cocaine, Sevoflurane |
| Anti-anginal | Bepridil, Ranolazine |
| Anti-arrhythmic | Amiodarone, Dronadarone, Dofetilide, Disopyramide, Flecainide, Ibutilide, Quinidine, Sotalol |
| Antibiotic | Azithromycin, Ciprofloxacin, Clarithromycin, Erythromycin, Levofloxacin, Trimethoprim-Sulfa |
| Anti-seizure | Fosphenytoin |
| Anti-depressant | Amitriptyline, Citalopram, Imipramine, Nortriptyline, Trazadone, Sertraline |
| Anti-fungal | Fluconazole, Ketoconazole |
| Antihistamine | Diphenhydramine, Terfenadine |
| Anti-hypertensive | Nicardipine |
| Anti-malarial | Chloroquine |
| Anti-mania | Lithium |
| Anti-emesis | Ondansetron |
| Anti-psychotic | Chlorpromazine, Clozapine, Haloperidol, Risperidone, Thioridazine |
| Central nervous stimulants | Amphetamine, Dexmethylphenidate, Methylphenidate |
| Endocrine | Octreotide |
| GI stimulant | Cisapride |
| H2-receptor blocker | Famotidine |
| Immunosuppressant | Tacrolimus |
| Inotropic agents | Dopamine, Dobutamine, Epinephrine, Norepinephrine, Isoproterenol, Phenylephrine |
| Muscle relaxant | Tizanidine |
| Opiate agonists | Methadone |
| Oxytocic | Oxytocin |
| Phosphodiesterase inhibitors | Vardenafil |
| Sedative | Chloral hydrate, Droperidol |
| Uterine relaxant | Ritodrine |
| Vasoconstrictor | Midodrine |

*Source:* Adapted from Fazio G et al. *World J Cardiol* 2013;5:87–93.[31]

*Note:* An updated drug list is available on www.torsades.org.

no ICD therapy, 8 had one shock, and 1 patient had 22 shocks. The fetuses appeared to tolerate ICD discharges without significant issues, since no adverse outcomes were reported. In this study, there was no evidence for abdominal generator skin erosion. The hormonal and autonomic nervous system changes that result in uterine contractions did not precipitate ICD discharges.

Women with arrhythmia may face the need for elective cardioversion during pregnancy. Electrical direct current synchronized cardioversion is safe for mother and fetus. Most antiarrhythmic medications have been used safely in pregnancy. Amiodarone is an exception; it is considered a class D drug and relatively contraindicated since it impacts thyroid function in the fetus/newborn. Beta-blockers are safe, but metoprolol is favored over atenolol due to an association between maternal atenolol use and low birth weight.

# Pregnancy in select congenital cardiac lesions

## *Coarctation of the aorta*

In women with unrepaired coarctation of the aorta, major complications during pregnancy are rare but may be fatal. Pregnancy increases the risk of aortic rupture or dissection both at the coarctation site and the ascending aorta. Also, the coexistence of a bicuspid aortic valve in 40%–70% of these patients complicates pregnancy. During prepregnancy counseling, meticulous evaluation of systemic blood pressure needs to be performed. Women who are normotensive may carry pregnancies to term and pursue repair of coarctation postpartum. In general, a resting upper to lower extremity systolic blood pressure gradient >20 mm Hg or severe exercise-induced hypertension (systolic blood pressure >200 mm Hg) may place the patient at higher risk for cardiovascular complications during pregnancy. If the patient has uncontrolled hypertension prior to pregnancy, intervention for correction of coarctation is indicated.[35]

After successful repair of coarctation of the aorta, many women have uncomplicated pregnancies. But the miscarriage and preeclampsia rates are higher than in the general population. Arrhythmia is rare, but pregnancy-induced hypertension may occur in 11% of patients. During pregnancy, aortic dilation is expected in all women. Women with aortic aneurysms either related to connective tissue disease or coarctation of the aorta may not have resolution of their pregnancy-induced aortic dilation in the postpartum period, necessitating earlier surgical intervention.

In a mouse model of Marfan syndrome, aortic dilation and dissection have been associated with elevated oxytocin levels.[36] Since oxytocin levels peak near the end of pregnancy and are sustained during lactation, some clinicians recommend that women with connective tissue or aortic diseases avoid breastfeeding. This recommendation has not been applied to women with coarctation of the aorta who have ascending aortic aneurysms, but it may be considered if future research substantiates the animal data.

## *Tetralogy of Fallot*

Tetralogy of Fallot (TOF) is the most common cyanotic heart disease. The earliest "repairs" for TOF occurred in

the 1950s, and survival into adulthood has been excellent. Therefore, TOF is the most common lesion among previously cyanotic women who now are considering pregnancy. Pregnancy is not recommended in unrepaired patients with TOF.[37] However, after "reparative" surgery, women with TOF generally tolerate pregnancy well. Long-term issues faced by adults with "repaired" TOF are arrhythmias and progressive right ventricular dilation and dysfunction as a result of chronic pulmonary regurgitation. Many women with TOF had initial palliative systemic to pulmonary artery shunts that may have created branch pulmonary artery abnormalities. Many patients repaired prior to 1990 had transannular patch enlargement of the right ventricular outflow tract, leaving them with free pulmonary regurgitation as a long-term sequela. Maternal complications include arrhythmia in less than 10% and heart failure in less than 5% of patients. The recurrence risk of congenital heart disease in offspring of women with TOF has been reported to be relatively high (6%). In 2004, Veldtman et al. reported the outcomes for 43 women with TOF who had 112 pregnancies.[38] The miscarriage rate was 27% in that cohort. Overall mean birth weight was 3.2 kg. Cardiovascular complications were fairly rare. Included in this cohort were eight women with unrepaired TOF. Unrepaired TOF and important pulmonary artery structural abnormalities were significant independent predictors of low birth weight. Overall, 8.5% of infants were small for gestational age and six of seven infants born to women with unrepaired TOF were SGA. The cesarean section rate in this cohort was lower than the national average of 22%.

In women with the most severe form of TOF (pulmonary atresia/VSD), important hemodynamic concerns that impact candidacy for pregnancy are pulmonary hypertension, severe pulmonary regurgitation (from degeneration of bioprosthetic conduit valves), right ventricular dilation, right ventricular dysfunction, and coexistent left ventricular dysfunction. Vaginal deliveries were preferred for most women with TOF. In a Dutch study from 2005, Meijer et al. reported the results of 29 women who had 63 pregnancies.[39] The miscarriage rate in this cohort was 21%. Obstetrical and cardiac complications occurred in just under 20% of patients. The cesarean section rate was similar to that seen in U.S. studies (28%) but higher than the Dutch general population rate of 6.5%. Chromosomal screening for the 22q11.2 microdeletion is important in women with TOF who are considering pregnancy. Children born to a parent with 22q11.2 microdeletion have a 50% chance of having the deletion with the expected cardiac and noncardiac associations.

Pregnancy is not recommended for women with palliated or unoperated pulmonary valve atresia/VSD. In these patients, the longevity of collateral vessels or surgically created shunts that serve as the sole source of pulmonary perfusion is dubious during and after pregnancy. Progression of cyanosis in patients with palliated TOF or pulmonary atresia/VSD also carries inherent risk of secondary erythrocytosis and paradoxical embolization.

### *Ebstein anomaly*

In 1994, Connolly and Warnes reported the results of pregnancy for 44 women with Ebstein anomaly.[40] These women had a total of 111 pregnancies that resulted in 85 live births (76%). Thirty-three of the 85 (39%) births were preterm. This cohort of women represented a heterogeneous group of operated and unoperated patients. Those who were cyanotic at the time of pregnancy delivered babies with significantly lower mean birth weight when compared to acyanotic women (2.5 kg versus 3.1 kg). The overall incidence of congenital heart disease in offspring of women with Ebstein anomaly was 6%. In this study, there were no maternal deaths and no serious pregnancy-related maternal complications.

A subsequent publication from Mayo Clinic reviewed the entire Ebstein anomaly cohort from 1972 until 2006 and reported 59 unoperated women who had 140 pregnancies prior to surgery.[41] Miscarriage rate in this group was 19%. That study also reported results for women after cardiac surgery for Ebstein anomaly. In this subgroup, 27 women had 62 pregnancies. The miscarriage rate was 33%. No maternal mortality was reported. Although the data were limited, it appeared that women with Ebstein anomaly tolerate pregnancy well.

Given that pregnancy is a state of increased preload, one would speculate that women with severe right ventricular dilation and dysfunction with corresponding severe tricuspid valve regurgitation would be less likely to tolerate pregnancy. However, to date, the pregnancy outcome data for women with Ebstein anomaly are generally good. Risk for arrhythmia is increased during pregnancy. Patients with Ebstein anomaly have a substantial preoperative and postoperative arrhythmia burden. Women with previous history of arrhythmia should be cautioned that arrhythmia may worsen during pregnancy.

### *Transposition of the great arteries*

Several small studies have reported pregnancy results in women with d-TGA. Women with d-TGA who are now in adulthood comprise a diverse patient group. Some of these women had atrial switch operations in childhood (Mustard or Senning operation; Figure 61.1). More recently, the first generation of woman who had an arterial switch operation (ASO) have reached childbearing age. Pregnancy data in the ASO group are very sparse.[42–45]

## Pregnancy after atrial switch (Mustard or Senning operations)

After a Mustard or Senning operation, women face special challenges during pregnancy. Patients who had an atrial switch operation for d-TGA may fail to increase cardiac output with exercise. This can be attributed to impaired contractility, chronotropic incompetence, and baffle stenoses that reduce venous return. The physiologic changes during

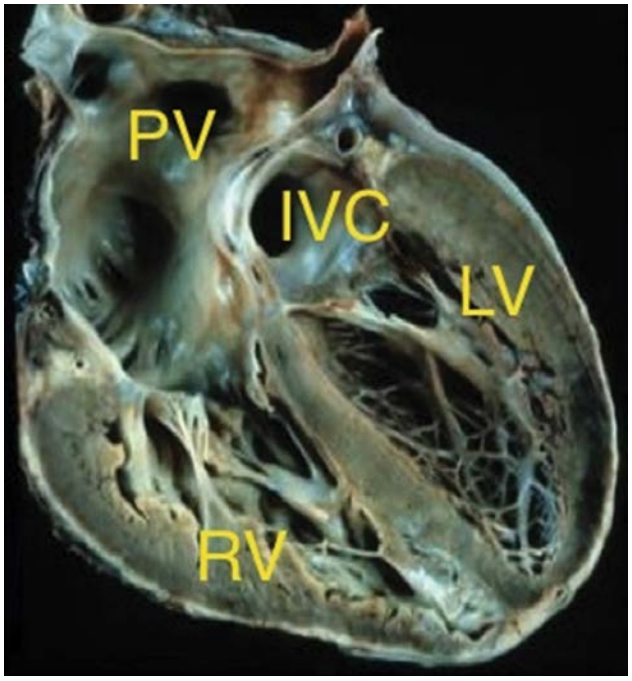


**Figure 61.1**
Gross pathologic specimen cut in a four-chamber projection from an adult with a Mustard operation for d-TGA. The pulmonary venous (PV) pathway is widely patent, and the entrance of the inferior vena caval (IVC) baffle to the native left atrium is shown. Right ventricular (RV) size and wall thickness are increased due to chronic pressure overload of the systemic ventricle. The left ventricle (LV) is smaller and served as the subpulmonary ventricle. (With permission from the William Edwards Collection, Mayo Clinic Foundation.)

pregnancy in some ways are similar to exercise except that they occur over an extended period of time. This may explain why there have been reports of clinical deterioration in women with atrial switch anatomy during and after pregnancy. Pregnancy outcomes in women after atrial switch have generally been good. But these women face unique challenges and possible irreversible right ventricular dysfunction that can occur immediately after pregnancy.

In a study from Montreal, Guedes et al. reported the results of 16 women who completed 28 pregnancies.[42] Right ventricular systolic dysfunction was absent in most women prior to pregnancy. But, during pregnancy, there was progression of right ventricular dysfunction in 25% of this cohort. Three of four women who experienced right ventricular dysfunction during pregnancy never recovered function. Similarly, tricuspid valve regurgitation progressed in these patients. Premature delivery was not common in this case series. Mean gestational age was 38 weeks, and the cesarean section rate was 17%. Mean birth weight of the neonates born to these women was 3.04 kg.

In a study from Utah, Metz et al. reported results of 21 pregnancies in women after atrial switch for d-TGA.[43] The preterm birth rate was 50%. The Utah study highlighted that symptomatic baffle obstruction was present in several women. These women required postpartum intervention. This report emphasized the importance of complete evaluation including advanced imaging of the systemic venous baffles prior to undertaking pregnancy. Significant compromise in venous return due to SVC or IVC baffle obstruction, especially in the volume expanded pregnant state, may cause important symptoms. In 2015, Castaldo et al. reported the results of 34 pregnancies in 21 women after atrial switch operation.[44] Mean follow-up after pregnancy was 100 months. There were no maternal deaths. Progression of tricuspid regurgitation was more common in pregnant women than in nonpregnant controls. The premature birth rate was 38%, and nearly 40% of the babies were SGA.

## Pregnancy after arterial switch

Pregnancy data after arterial switch operation (ASO) are sparse. The combined Boston and Toronto experiences were published in 2010.[46] In that small case series, nine women with d-TGA after ASO had 17 pregnancies. There were 4 miscarriages and 13 full-term births. There were no maternal deaths, but two of the women had cardiac complications. One patient developed postpartum prosthetic mitral valve thrombosis, and another had nonsustained ventricular tachycardia with impaired left ventricular systolic function.

Data regarding women who had an ASO and subsequent pregnancy will be more thoroughly evaluated in the coming decade. Thus far, it seems that evaluation of issues common to these types of patients should be performed in the prepregnancy counseling session. Prior to pregnancy, it is recommended that thorough evaluation of cardiac function be performed with echocardiography. Arrhythmia after ASO is relatively rare, but a baseline electrocardiogram should be obtained. At least 10% of adults after ASO have progressive neo-aortic root dilation and neo-aortic valve regurgitation. In some cases neo-aortic root replacement and/or neo-aortic valve replacement may be necessary. Aortic dilation occurs in normal pregnancies; therefore, imaging the thoracic aorta with magnetic resonance imaging (MRI) or computed tomography (CT) prior would be prudent to obtain a baseline in case there are issues during pregnancy. In addition, prior to pregnancy it is advised that the coronary artery buttons are evaluated with CT or MRI to ensure there are no latent coronary artery ischemia issues. Exercise testing prior to pregnancy in women after ASO provides a relatively simple evaluation of fitness and may uncover rhythm issues.

## Congenitally corrected transposition (L-TGA)

In 2014, a Polish study reported the results of 20 pregnancies in 13 women with congenitally corrected transposition of the great arteries (L-TGA).[47] There were no maternal deaths, and 95% of the pregnancies resulted in a live birth. Two women developed supraventricular tachycardia during pregnancy but required no pharmacological treatment. One patient had

a preterm delivery because of systemic right ventricular dysfunction. There was one case of congenital heart disease in the offspring. These results are similar to those reported by Connolly et al. in 1999 from the Mayo Clinic.[48] In that study, 22 women with congenitally corrected transposition had 60 pregnancies. The live birth rate was 83%. There was only one premature delivery and no maternal mortality. One patient developed congestive heart failure late in the pregnancy because of worsening systemic AV valve regurgitation, and she required valve replacement early postpartum.

Similar to the limited results of pregnancies in women with d-TGA after ASO, pregnancy with a systemic right ventricle in L-TGA may be well tolerated. The results for women with systemic right ventricles (L-TGA and those with d-TGA after atrial switch operation) appear to be better than for women with single-ventricle physiology after Fontan operation. But the long-term fate of the systemic RV is variable. By age 40, more than half of these patients are receiving therapy for congestive heart failure,[48] whether progression of RV dysfunction is influenced by pregnancy remains unknown.

## Pregnancy after Fontan operation

The Fontan operation is used to palliate patients with functional single ventricles wherein caval blood flows directly to the pulmonary arteries. The risk of pregnancy in patients with functional single-ventricle anatomy is not easily assessed, but successful pregnancies have been reported. The cardiac output after Fontan operation is determined by the central venous pressure (CVP), the left atrial pressure (LAP), and the pulmonary vascular resistance (PVR) (cardiac output = [CVP-LAP]/PVR). Patients with Fontan physiology are preload dependent and can have difficultly increasing cardiac output. These patients have an increased incidence of atrial arrhythmias and intracardiac thrombi. Both of these factors impact the ability to complete a successful pregnancy. In a recent French study, 37 women had 59 pregnancies.[50] The miscarriage rate was 27%, lower than other studies that have evaluated pregnancy after Fontan operation. There were 36 live births, and the cardiac complication rate was relatively low, occurring in only 10% of the women.

Data from the North American multicenter registry of 103 pregnancies in women after Fontan demonstrated a 69% live birth rate. The mean gestational age was 34 weeks, and mean birth weight was only 2.2 kg. There were no maternal deaths, but cardiac (33%) and obstetrical (52%) complications were common in these pregnancies. Long-term survival after pregnancy may be adversely affected since during a mean follow-up period of 7.7 years, there were five deaths and two other women required cardiac transplantation.[51]

In a recent publication from the Mayo Clinic, the 10-, 20-, and 30-year survival rates for 1,052 patients after Fontan operation were 74%, 61%, and 43%, respectively.[52] These data describe a cohort of patients who had a Fontan operation between 1973 and 2012. For patients who had surgery after 2001, survival at 10 years from Fontan was 95%. A subset of this large cohort was analyzed for pregnancy outcomes.[53] There were 10 pregnancies prior to the Fontan operation, and none were successful (eight miscarriages and two therapeutic abortions). After the Fontan operation, there were 70 pregnancies; however, the miscarriage rate was high (50%). There were only 29 live births and 6 therapeutic abortions. There were no maternal deaths. During long-term follow-up (>25 years from the Fontan operation), there was one death, and one patient had cardiac transplantation. Preterm deliveries were common (81%). Mean gestational age was 33 weeks, and mean birth weight was only 2.1 kg. There was one neonatal death because of extreme prematurity, and two children were born with congenital heart disease.

The data from the recent North American registry, French multicenter, and Mayo Clinic studies[50,51,53] support the hypothesis that some degree of all complications that occur during pregnancy is a consequence of the fixed low cardiac output that accompanies Fontan circulation. In the Mayo series, there were no viable pregnancies in women who had systemic oxygen saturation less than 90% or an ejection fraction less than 40%. The French study had a similar rate of prematurity (69%) to the Mayo study, but cardiac complications were fairly rare, occurring in only 10% of women. The French Study did highlight that cardiac issues occur postpartum, namely, congestive heart failure and ventricular dysfunction. They reported no arrhythmia or thromboembolic events. The North American multicenter registry had one patient who was successfully resuscitated from a peripartum cardiac arrest.

Anticoagulation during pregnancy for a woman after Fontan has been variable. The optimal approach is not known at this time. In the Mayo Clinic, French, and North American studies, aspirin therapy was common. The French study had a higher rate of low molecular weight heparin and vitamin K antagonist use than the Mayo Clinic or North American cohorts. As North American centers have become more comfortable with the use of low molecular weight heparin and vitamin K antagonists during pregnancy, one may see a change in this practice as it applies to women after Fontan. Table 61.7 is a summary of the French, Mayo Clinic, and North American post-Fontan pregnancy studies.

When evaluating the results of these retrospective studies that evaluated pregnancy outcomes in woman after Fontan, one must factor in the importance of patient selection. Many of these women had rigorous prepregnancy evaluation and thoughtful planning. Despite careful patient selection, miscarriage and preterm birth rates are high for woman after Fontan. The ability to maintain a viable placenta for an entire pregnancy may be the greatest challenge.

## Placental insufficiency in pregnancy after Fontan operation

The Fontan operation creates physiology dependent on preload and elevated filling pressures. Increased central venous pressure in the abdominal organs is a consequence of Fontan

**Table 61.7** Pregnancy outcomes after Fontan

| *Study* | *Number of women* | *Maternal age at pregnancy (yrs)* | *Number of pregnancies* | *Preterm %*<br>*Mean GA*<br>*Mean BW (kg)* | *Maternal deaths* | | *Anticoagulation during pregnancy* | *Ventricular morphology* |
|---|---|---|---|---|---|---|---|---|
| | | | | | *During* | *After* | | |
| *Mayo*<br>Pundi et al. 2016 | 35 | 26 (18–36) | 70 | 81%<br>33 wks<br>(2.1) | 0 | 1 | aspirin – 12<br>LMWH – 3<br>VKA – 0 | LV – 68% |
| *France*<br>Gouton et al. 2015 | 37 | 27 (19–41) | 59 | 69%<br>34 wks<br>(2.0) | 0 | 0 | aspirin – 11<br>LMWH/UFH – 17<br>VKA – 10 | LV – 70% |
| *No. Am.*<br>Cannobio et al. 2013 | 52 | 25 (17–36) | 103 | –<br>34 wks<br>(2.2) | 0 | 5 | aspirin – 52<br>LMWH – 4<br>VKA – 4 | – |
| *ANZ*<br>Zenter et al. 2016 | 20 | 25 (23–32) | 40 | 72%<br>31 wks<br>(1.6) | 0 | 0 | Aspirin – 6<br>LMWH/VKA – 5 | – |

physiology. In addition, patients after Fontan operation have a relatively low cardiac output. They are preload dependent and sometimes have little reserve to increase cardiac output to match physiological needs. The physiology of Fontan flow contributes to many of the long-term issues that these patients encounter, including progressive hepatic fibrosis, cirrhosis, and protein losing enteropathy. The baseline physiology of patients after Fontan operation is important when anticipating pregnancy. Studies evaluating pregnancy outcomes after Fontan identified relatively high obstetrical complication rates (>50%) and high rates of miscarriage, preterm delivery, and low birth weight newborns. In the recent study from the Mayo Clinic, the preterm birth rate for women who had pregnancies after Fontan was 81% .[53] In the recent French study, with a similar number of pregnancies, preterm birth rate was 69% and mean birth weight was 2 kg.[50]

Placental insufficiency may cause oligohydramnios, preeclampsia, miscarriage, or stillbirth. Placental insufficiency is considered the most frequent cause of asymmetric intrauterine growth retardation.[54,55] There is increasing evidence for an association between prepregnancy subclinical cardiac dysfunction and both poor placentation and pregnancy outcome.[56] Melchiorre and colleagues recently reviewed the cardiovascular changes that occur in the maternal heart during pregnancy complicated by preeclampsia.[57] Several geometric and hemodynamic changes occur in the maternal heart due to preeclampsia. Asymmetric septal hypertrophy, left atrial enlargement, right ventricular hypertrophy, and biventricular diastolic dysfunction have been identified in women with preeclampsia. More vigilant recognition and treatment of preeclampsia were advocated to minimize the effect on the maternal heart. When one appreciates these cardiac changes in women with "normal" hearts, it is not surprising that women with single-ventricle physiology and other forms of complex congenital heart disease experience high rates of preeclampsia, poor placentation, and preterm delivery.

Many women after Fontan operation have relatively low arterial oxygen saturation. In the recent Mayo Clinic study, only women who had systemic arterial saturations 90% or greater had successful pregnancies. Hypoxemia is known to cause villous damage in the placenta. In turn, maternal hypoxemia may lead to fetal hypoxemia. This may cause an increase in fetal blood viscosity and increased platelet aggregation, both of which may accelerate placental thrombosis.[54,55] Frequently, the reasons for premature delivery are related to preeclampsia. The deleterious effects of preeclampsia coupled with relatively low cardiac output due to Fontan physiology may ultimately cause placental insufficiency (Figures 61.2a–f and 61.3). More study is required regarding the pathology of the placenta in women after Fontan operation. Perhaps, similar to the liver, the placenta is a site for end-organ damage from Fontan physiology.[58]

Limited data are available for pregnancy results in women after Fontan with liver disease. Portal hypertension is poorly tolerated in pregnancy.[59] Risks of variceal bleeding and hepatic decompensation are increased in women with portal hypertension. In the recent Mayo Clinic study, there were six women with CT or MRI features of cirrhosis who had seven pregnancies. There was only one live birth in this small subgroup. Similarly, pregnancy data are sparse for women with protein losing enteropathy (PLE) after Fontan.[53]

# Special situations

## *Cardiac catheterization during pregnancy*

Cardiac catheterization is only indicated in pregnant women who have hemodynamically important symptoms or when growth of the fetus is adversely affected. Radiation exposure to the fetus is a major concern. Cardiac catheterization, if needed, should be performed after the first trimester. Although external shielding of the pelvis is advocated, some studies have demonstrated that the radiation absorbed by the fetus without shielding was less than 3% higher than those who were shielded.[60] The majority of the total radiation dose is from the posterior/anterior exposure. If possible, cardiac catheterization should be performed with single plane imaging. There are several reports in the literature of cardiac catheterization, electrophysiology, and interventional procedures being performed with echocardiographic guidance, thereby minimizing fluoroscopic exposure.[61]

More recently, percutaneous pulmonary valve replacement has been successfully performed during pregnancy.[62] Radiation exposure to the mother and the fetus was minimized by using single plane fluoroscopy only above the diaphragm, collimating to a minimum field, imaging as close to direct posterior/anterior as possible, and utilizing fluoroscopy frame rates at slow speeds.

## *Cardiopulmonary bypass during surgery*

In the last four decades, approximately 200 cases of pregnant women undergoing cardiopulmonary bypass surgery have been reported. Although controversies exist in the literature regarding details of management, overall results have been good. One of the most important decisions in the surgical and anesthesia management of these patients is deciding on timing of the surgery. Preferably cardiac surgery that occurs in the late second trimester or early third trimester is optimal. Once the neonate has mature lungs, consider elective cesarean section prior to maternal cardiac surgery. Results, not surprisingly, for *elective* cardiac surgery are better than *emergent* cardiac surgery during pregnancy.

In 2011, the Mayo Clinic reported the outcomes of 21 pregnant patients who were considered for cardiac surgery. This cohort came from a review of a surgical database over a 30-year period. Seven patients had elective cesarean section immediately prior to sternotomy. The other 14 patients had cardiopulmonary bypass and subsequent deliveries. There was one early maternal death that occurred 2 days after an

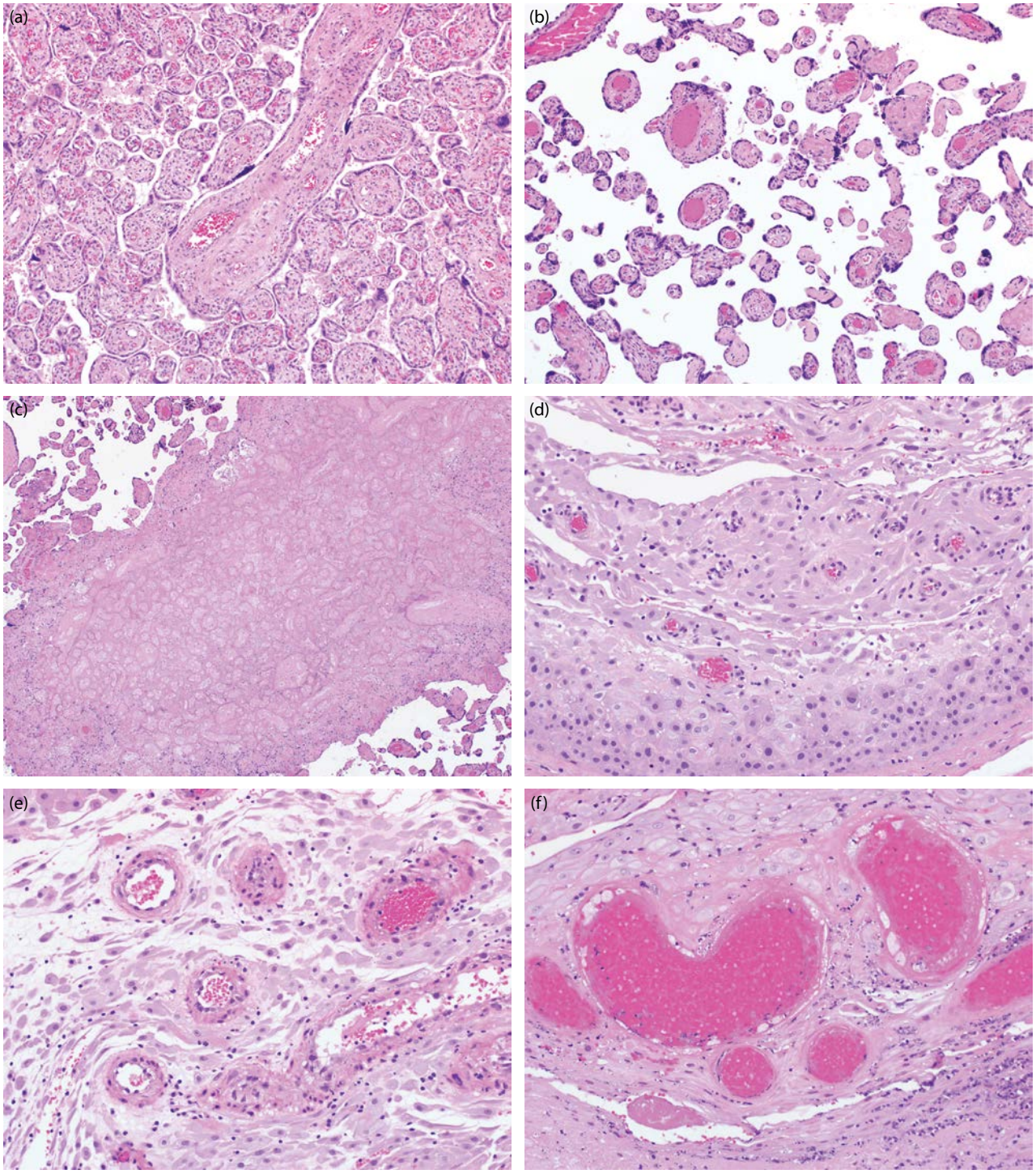


**Figure 61.2**
Hematoxylin and eosin stained sections of placenta and maternal decidua contrasting findings in normal pregnancy and in preeclampsia. (a) 100× magnification. *Normal* mature placental chorionic villi in a term pregnancy. Normal villous size, arborization, and vascularization are present. (b) 100× magnification, shows villous hypoplasia in *preeclampsia*. The chorionic villi are abnormally small with increased syncytial knotting. (c) 40× magnification demonstrates a placental infarct in *preeclampsia*. (d) 200× magnification. *Normal* maternal decidual vessels from a term pregnancy. The spiral arteries are appropriately remodeled by implantation trophoblast, leading to thin vascular walls containing matrix fibrinoid. Normal maternal veins have thin, delicate walls. (e) 200× magnification demonstrates both hypertrophic vasculopathy and incomplete vascular adaptation for pregnancy of a spiral artery in *preeclampsia*. This decidual spiral artery has persistently thickened vascular walls. (f) 200× magnification shows acute atherosis of *preeclampsia*. Injury to the maternal spiral arteries is characterized by fibrinoid necrosis of the vessel wall with associated foamy histiocytes and decidual inflammation. (All specimens courtesy of Sarah Kerr, MD. Anatomic Pathology, Mayo Clinic, Rochester, MN.)

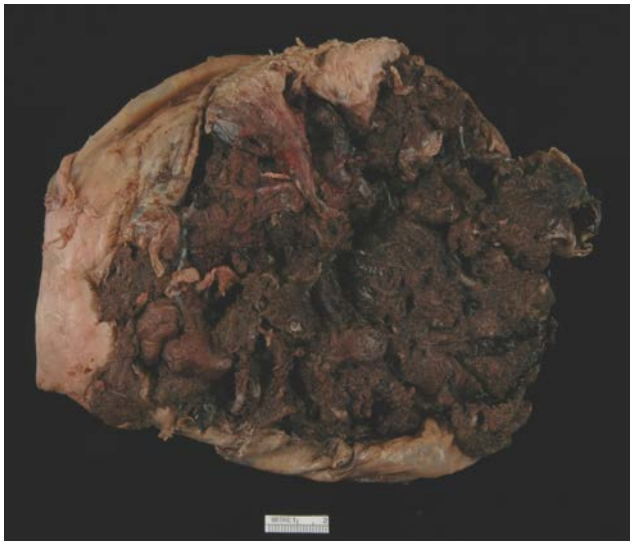

**Figure 61.3**
Gross specimen of the placenta from a 27-year-old woman with preeclampsia who delivered a 850 g newborn at 27 weeks' gestation. The child survived and is doing well. The woman was born with tricuspid atresia and had a Fontan operation in childhood. The specimen demonstrates an intervillous thrombus that measured 11 × 6 × 2 cm and involved 40% of the placental parenchyma. (Image reproduced with permission of Mayo Clinic Foundation.)

emergent mechanical aortic thrombectomy, and there were three late maternal deaths that occurred 2–19 years postoperatively. There were three fetal demises. In that case series, normothermic, nonpulsatile cardiopulmonary bypass was performed using flow rates of greater than 2.4 L/min/m$^2$ and maintaining mean arterial blood pressure greater than 70 mm Hg. In order to maintain this mean arterial blood pressure, pump flow was increased. Vasoconstrictors such as phenylephrine and vasopressin were used sparingly.[63]

Previous reports suggested that maternal mortality associated with cardiopulmonary bypass during pregnancy ranged from 3% to 15%. Fetal loss of 16%–33% has been reported for women who have cardiac surgery during pregnancy.[10] In the modern era, the survival rates for mother and fetus, have improved. Several excellent reviews of cardiac anesthesia for pregnant women are available.[64] Based on numerous case reports, there are no firm data supporting the use of pulsatile versus continuous flow in terms of uteroplacental perfusion and neonatal outcomes. Pulsatile flow has been shown in animal models to improve placental flow and inhibit nitric oxide production. Hypothermia is avoided, because it may increase uterine tone, reduce uterine blood flow, and have deleterious effects on the fetus. To date, there have been no reports of cardiac transplantation during pregnancy. The potential teratogenic effects of drugs utilized during cardiac surgery have been minimal. Fetal monitoring during cardiopulmonary bypass has improved over the years. Continuous fetal assessment of umbilical artery Doppler blood flow may be a useful method that has been described in several cases.[65]

Some studies have demonstrated that pulsatile flow preserves endothelial nitric oxide synthesis and decreases activation of the fetal renin angiotensin pathway resulting in improved blood flow through the placenta. Most authors agree that high pump flows (>2.5 L/min/m$^2$) and mean perfusion pressure greater than 70 mm Hg are necessary to maintain uterine blood flow. Pulsatile flow prevents the drop in placental perfusion and limits a rise in the placental vascular resistance that is observed with nonpulsatile flow. Agreement on normothermic cardiopulmonary bypass appears to be uniform. An important transition occurs when weaning the mother from cardiopulmonary bypass and meticulous attention to blood pressure management is imperative. Despite cardiopulmonary bypass creating a nonphysiological hemodynamic state that can adversely affect both mother and fetus, results of cardiac surgery during pregnancy have generally been good.[66]

## Cardiac myxoma

Myxomas comprise 30%–50% of all benign primary cardiac tumors and are the most common tumors in adults age 30–50 years old. There is a female predominance. These tumors may be detected for the first time during pregnancy. Management strategies need to be individualized to the specific patient. If a myxoma is small, nonmobile, and demonstrates no evidence of valvular obstruction, then conservative management may be prudent. In contrast, if the tumor is large, causing inflow obstruction, or is freely mobile with embolic potential, the hypercoagulable nature of pregnancy makes removal during pregnancy more urgent. John et al. reviewed the literature describing management of atrial myxomas detected during pregnancy.[67] A number of myxomas were surgically excised during pregnancy. No premature deliveries occurred in the cases reported, but all occurred after the first trimester. Avoidance of surgery in the first trimester or early portion of the second trimester is a consistent theme in order to obtain good surgical results in women with pregnancy.

## Pulmonary hypertension

In 2015, a comprehensive summary statement was published from the Pulmonary Vascular Research Institute.[68] This summary statement indicated that despite isolated case reports of successful pregnancies, women with pulmonary hypertension should be counseled to avoid pregnancy. Risks to the mother and fetus are substantial. Permanent contraception should be strongly considered in patients with pulmonary hypertension. In this group, hysteroscopic sterilization was preferred because of lower procedural risks. Laparoscopic tubal ligation or mini-laparotomy may also be utilized. Safety of these methods has been debated, and advances in laparoscopic procedures in recent years may make those more attractive choices. Estrogen-containing contraceptive pills were not recommended because of the increased risk for thromboembolic events and deleterious effects of estrogen

on pulmonary vasculature. Progestin-only pills were recommended. However, it was recognized that progestin-only pills have a relatively high failure rate and complications related to "break-through bleeding." Progestin-only intrauterine devices and implants were acceptable nonpermanent contraceptive measures. Depo-Provera and other injected progestins were relatively contraindicated because of increased risk of thromboembolic events. Barrier and fertility awareness methods were not recommended. Family planning counselors should be involved with these patients on a routine basis.

In patients who are WHO functional Class IV or have evidence of severe right ventricular impairment, prostaglandin therapy was recommended. For those who are functional Class III, inhaled prostaglandins should be considered. Phosphodiesterase-5 inhibitors (sildenafil, tadalafil) are category B drugs in pregnancy and may be considered in patients who are WHO functional Class I or II. Epoprostenol (2–4 ng/kg/min), a naturally occurring prostaglandin and pulmonary vasodilator, is considered category B in pregnancy. A related drug, Iloprost, is considered category C. The currently available endothelial receptor blockers (bosentan, ambrisentan) are considered Category X for pregnancy and contraindicated. At the time of delivery, intravenous prostaglandins may be helpful for those not already treated with this class of medication.

Meticulous monitoring at the time of delivery is important in woman with pulmonary hypertension. Patients should have a central venous catheter placed and an arterial line. Careful management of volume status is imperative. Cardiovascular monitoring with electrocardiography and echocardiography is recommended. However, routine use of a Swan-Ganz catheter is not recommended because of complication risks. Patients with pulmonary hypertension are at greatest risk of death during the peripartum period and for the first 2 months postpartum. Anticoagulation is recommended for patients with pulmonary hypertension. The scheme of low molecular weight heparin and warfarin outlined earlier in this chapter is applicable to patients with pulmonary hypertension. Patients with relatively mild pulmonary hypertension (pulmonary artery systolic pressure <40–50 mm Hg) may tolerate pregnancy fairly well. These patients still require close scrutiny and meticulous follow-up and observation. However, in patients with pulmonary artery systolic pressures greater than 50 mm Hg, termination of pregnancy should be considered due to risk of maternal mortality.

## Contraception in women with congenital heart disease

Some women with congenital heart disease should not consider pregnancy. Traditionally, this recommendation has been applied to the following groups:

1. *Pulmonary hypertension*: pulmonary artery systolic pressures greater than three-quarters systemic
    - Including unrepaired cyanotic disease or Eisenmenger physiology
2. *Ventricular dysfunction:* NYHA Class III or IV symptoms or EF less than 40%
3. *Marfan or connective tissue disease*: aortic root greater than 40–45 mm
4. *Severe obstruction:* valvular, subvalvular, or coarctation

Risks of pregnancy can be additive, and a simple guide to understanding who may be at higher cardiac risk regardless of lesion can be gleaned from the work by Siu et al. previously discussed in this chapter.[10] In addition, Thorne et al. published an excellent review of contraception practices in women with cardiovascular disease based on the WHO risk scheme. Women who fall into WHO Class IV are extremely high risk, and pregnancy is *contraindicated*. Those conditions are similar to the previous list and include the following (adapted from Thorne et al.[69]):

1. Pulmonary arterial hypertension of any cause
2. Severe systemic ventricular dysfunction (NYHA III or IV or EF <30%)
3. History of peripartum cardiomyopathy with any ventricular dysfunction
4. Severe left heart obstruction
5. Marfan syndrome with dilated aorta greater than 40 mm

Women with pulmonary hypertension are at highest risk, and maternal mortality approaches 50%. Pulmonary artery hypertension is defined in the nonpregnant state as elevation of the mean pulmonary artery pressure 25 mm Hg and greater at rest or 30 mm Hg and greater with exercise in the absence of a left-to-right shunt. Mild pulmonary artery hypertension can also be defined as pulmonary artery systolic pressure between 35 and 50 mm Hg.[69]

In women with congenital heart disease and contraindications to pregnancy, the need for a reliable and stable form of contraception is important. Barrier methods, while causing no cardiac issues, are not ideal. Combined hormone contraceptive pills have been used extensively and have high contraceptive efficacy. Skin patches are readily available worldwide and may improve compliance. Progestin-only birth control pills should be utilized in women at risk for thromboembolic events. If estrogen-containing pills are used in high-risk women (e.g., after Fontan), some favor the concomitant use of warfarin therapy. Progestin-only birth control pills have no cardiac contraindications, but menstrual irregularities are frequent, and this negatively impacts compliance. There is no contraindication to the progestin "morning after pill." The failure rate is low, estimated at only 1% if given within 72 hours of unprotected intercourse. Depo-Provera injectable progestin has no cardiac contraindications. Hematoma at the injection site might be problematic for patients on warfarin therapy. Prolonged use of Depo-Provera has been associated with reduction in bone mineral density. However, the bone mineral density rebounds once progestin injections cease. Intrauterine devices (IUDs) with levonorgestrel may be useful for some women. Traditionally, IUDs had been

discouraged in women with Fontan physiology due to potential vasovagal reactions during placement. This may potentiate fatal cardiovascular collapse. More recent experience with IUDs in women with complex congenital heart disease seems more favorable.[53]

Sterilization may be a logical choice for certain women. Laparoscopic sterilization requires insufflation of the abdomen with carbon dioxide and can lead to hemodynamic derangements in those with Fontan physiology or pulmonary vascular disease. Risk of air embolus is a very rare but important complication, especially in those with a residual right-to-left shunt. Some favor a mini-laparotomy with combined spinal and epidural anesthesia.

Laparoscopic techniques have improved over the years, and concerns for their use in women with congenital heart disease may have been overstated. During laparoscopy the main concerns are insufflation of the abdomen with carbon dioxide, positioning of the patient in a head-down position, and the hemodynamic effects of increase intra-abdominal pressures. Several studies have shown that if the intra-abdominal pressure is maintained, at less than 8 $cmH_2O$, no impact on cardiac output occurs. Other studies using intra-abdominal pressures of 10 $cmH_2O$ and 12 $cmH_2O$ did not show a deleterious effect on cardiac output. There have been reports of successful laparoscopic surgery in patients with numerous types of congenital lesions including patients with Fontan physiology, unrepaired pulmonary atresia/VSD and left-sided obstructive lesions. Some studies have suggested that at lower intra-abdominal pressures, cardiac out put may actually be increased. A very rare, but important complication of laparoscopic surgery is carbon dioxide embolism. This may occur if carbon dioxide is directly injected into a vascular structure or if trauma to a vascular structure occurs during surgery, thereby allowing $CO_2$ to leak into the vascular space. In several meta-analyses, the risk of carbon dioxide embolization appears to be approximately 1/100,000 cases. However, when it does occur, it may be fatal, and the reported mortality rate approaches 30%. Transesophageal echocardiography (TEE) is a very sensitive method for detecting intravenous injection of carbon dioxide. Treatment strategies include ventilating the patient with 100% oxygen, aggressive volume expansion, and placing the patient in "Durant" position (steep head down, left lateral decubitus). Hyperbaric oxygen therapy has been reported, but it may not be as successful as reported for air embolization because carbon dioxide is more soluble than air.[70–73]

The Essure sterilization technology is a stent-based system inserted hysteroscopically into the fallopian tubes under sedation and local anesthesia. The Essure failure rate is fairly low.[74] Vasectomy of the partner is a safe method for women with high risk for sterilization procedures.

A recent study from the Mayo Clinic[53] reviewed contraception practices in woman after Fontan operation and noted that 44% of 138 women utilized no form of contraception and 12% used only barrier methods. In this retrospective study, combined hormonal therapy or injectable progestin was used by 8% of women. The partner of 4% of these women had a vasectomy. Only 1% used progestin-only pills. Thromboembolic complications occurred in 8% of woman using contraception, compared to 11% of the women who used no contraception. Interestingly, 7% had IUDs, and there were no complications or reports of endocarditis in these patients. Although IUD use traditionally was discouraged in the Fontan population due to vasovagal episodes at the time of implantation, it seems that the long-term risks of endocarditis may have been overstated.

## Conclusions

Prepregnancy and contraception counseling and education remain essential elements of the current practice of adult congenital heart disease.[75] Care and counseling must be individualized, since we care for a diverse group of patients with a spectrum of cardiac lesions. In many cases, successful pregnancies are anticipated. However, preterm births are common in women with complex disease. The issues surrounding this group of women will only increase as more women with surgically "repaired" disease enter adulthood. In the next decade, research needs to focus on the effects that pregnancy has on ventricular preservation and patient longevity.

## References


1. Lozano R et al. *Lancet* 2013;380:2095–128.
2. Creanga AA et al. *J Women's Health* 2014;23:3–9.
3. Say L et al. *Reprod Health* 2004;1:3.
4. Small MJ et al. *Obstet Gynecol* 2012;119:250–5.
5. Grollman A. *Cardiac Output in Man in Health and Disease*. London: Bailliere, Tindall and Cox; 1932.
6. van Oppen AC et al. *Obstet Gynecol* 1996; 87:310–8.
7. Capeless EL, Clapp JF. *Am J Obstet Gynecol* 1991;165:883–6.
8. Robson SC et al. *Br Med J* 1987;295:1169–72.
9. Ouzounian JG, Elkayam U. *Cardiol Clin* 2012;30:317–29.
10. Siu SC et al. *Circulation* 2001;104:515–21.
11. Khairy P et al. *Circulation* 2006;113:517–24.
12. Drenthen W et al. *Eur Heart J* 2010;31:2124–32.
13. Wald RM et al. *Am Heart J* 2015;4: e002414.
14. Regitz-Zagrosek V et al. *Eur Heart J* 2011;32:3147–97.
15. Pislaru SV et al. *Eur J Cardiothorac Surg* 2015;47:725–32.
16. Badduke BR et al. *J Thorac Cardiovasc Surg* 1991;102:179–86.
17. Avila WS et al. *J Heart Valve Dis* 2002;11:864–9.
18. Salazar E et al. *Am Heart J* 1999;137:714–20.
19. Jamieson WE et al. *Ann Thorac Surg* 1995;60:S282–7.
20. Elkayam U, Bitar F. *J Am Coll Cardiol* 2005;46:403–10.
21. van Hagen IM et al. *Circulation* 2015:132(2):132–42.
22. Vitale N et al. *J Am Coll Cardiol* 1999;33:1637–41.
23. McLintock C et al. *BJOG* 2009;116:1585–92.
24. Chan WS et al. *Arch Intern Med* 2000;160:191–6.
25. Nishimura RA et al. *J Am Coll Cardiol* 2014;63:57–185.
26. Nishimura RA, Warnes CA. *Heart* 2015;101:430–5.
27. Yap SC et al. *BJOG* 2009;116:1593–601.
28. Yap SC et al. *BJOG* 2010;117:683–9.
29. Silversides CK et al. *Am J Cardiol* 2006;97:1206–12.
30. Thaman R et al. *Europace* 2011;13:859–63.
31. Fazio G et al. *World J Cardiol* 2013;5:87–93.

32. Khositseth A et al. *Heart Rhythm* 2004;1:60–4.
33. Grover S et al. *J Obstet Gynecol* 2015;5:60–9.
34. Natale A et al. *Circulation* 1997;96: 2808–12.
35. Agarwal BN et al. *Up to Date* 2016. https://www.uptodate.com/contents/management-of-coarctation-of-the-aorta.
36. Habashi JP et al. *Am Soc Human Gen* 2012:Abstract.
37. Doyle T et al. *Up to Date* 2016, https://www.uptodate.com/contents/management-and-outcome-of-tetralogy-of-fallot.
38. Veldtman GR et al. *J Am Coll Cardiol* 2004;44:174–80.
39. Meijer JM et al. *Heart* 2005;91:801–5.
40. Connolly HM, Warnes CA. *J Am Coll Cardiol* 1994;23:1194.
41. Brown ML et al. *J Am Coll Cardiol* 2008;52:460–6.
42. Guedes A et al. *J Am Coll Cardiol* 2004;44:433–7.
43. Metz TD et al. *Am J Obstet Gynecol* 2011;205:273E1–5.
44. Cataldo S et al. *BJOG* 2016;123(5): 807–13.
45. Canobbio MM et al. *Am J Cardiol* 2006;98:668–72.
46. Tobler D et al. *Am J Cardiol* 2010;106:417–20.
47. Kowalik E et al. *Intl J Gynecol Obstet* 2014;125:154–7.
48. Connolly HM et al. *J Am Coll Cardiol* 1999;33:1692–5.
49. Graham TP et al. *J Am Coll Cardiol* 2000;36:255–61.
50. Gouton M et al. *Intl J Cardiol* 2015;187:84–9.
51. Canobbio MM et al. *J Am Coll Cardiol* 2013;61(10):E427.
52. Pundi KN et al. *J Am Coll Cardiol* 2015;66:1700–10.
53. Pundi KN et al. *Congenit Heart Dis* 2016;11:63–70.
54. Brosens I et al. *BJOG* 1977;84:656–63.
55. Kampman MA et al. *Ultrasound Obstet Gynecol* 2015;46:21–8.
56. Melchiorre K et al. *Circulation* 2014;130: 703–14.
57. Meekins JW et al. *BJOG* 1994;101:669–74.
58. Nitshe JF et al. *Obstet Gynecol Survey* 2009;64:607–14.
59. Aggarwal N et al. *J Clin Exp Hepatol* 2014;4:163–71.
60. Damilakis J et al. *Circulation* 2001;104:893–7.
61. Galal MO et al. *Can J Cardiol* 2015;31:103.e5–7.
62. Ormerod O et al. *Circulation* 2014;129:e373–e75.
63. John AS et al. *Ann Thorac Surg* 2011;91:1191–7.
64. Landau R, Smiley RM. Anesthesia for cardiac surgery in the pregnant patient. In: Estafanous FG, Barash PG, Reves JG, eds. *Cardiac Anesthesia: Principles and Practice*. 2nd ed., Philadelphia, Lippincott Williams and Wilkins, 2001: 895–909.
65. Mishra M et al. *Ann Card Anaesth* 2015;17:46–51.
66. Drenthen W et al. *J Am Coll Cardiol* 2007;49:2303–11.
67. John AS et al. *Int J Cardiol* 2012;155:177–80.
68. Hemnes AR et al. *Pul Circ* 2015;5:435–65.
69. Thorne S et al. *Heart* 2006;92: 1520–5.
70. Sinaha R, Gard R. *J Anesth Clin Pharmacol* 2011;27: 412–3.
71. Koivusalo AM et al. *Surg-Endosc* 2008;22:61–7.
72. McClain CD et al. *Anesth Analg* 2006;103:856–8.
73. Park EY et al. *Yonsei Med J* 2012;53:459–66.
74. Famuyide AO et al. *Mayo Clin Proc* 2008;83:431–8.
75. Stout K. *Heart* 2005;91:713–4.
76. Zenter D et al. *Intl J Cardiol* 2016;208:97–101.

# 62

# Maternal diseases and therapies affecting the fetal cardiovascular system

Waltraut M. Merz and Ulrich Gembruch

## Introduction

The following section deals with infections, noninfectious diseases, drugs, and environmental exposures that exert a teratogenic or fetotoxic effect on the cardiovascular system.

Cardiovascular alterations secondary to known maternal genetic conditions (e.g., pregnancy in women with 22q11 deletion, Marfan syndrome, tuberous sclerosis, or Long Q-T syndrome) are discussed in the respective book chapters.

## Background

Two factors determine the topic's complexity:

1. Morphogenesis of the cardiovascular system is an extremely complex, multistep process under genetic control.[1] More than 300 genes are involved, and many intrinsic and extrinsic factors are responsible for developmental disturbances. It comes, therefore, not as a surprise that cardiovascular malformations (CVMs) constitute the most common major birth defects,[3,4] see Chapter 1.

   Approximately 20%–33% of fetal cardiac malformations (12%–14% of newborn, respectively) are caused by chromosomal abnormalities. Copy number variations (CNVs) may underlie 3%–20% of CVMs, whereas the proportion of single-gene disorders is estimated to be 3%–5%. Epigenetic modifications contribute to some 10% of major cardiovascular malformations. Estimates of the proportion of syndromic CVMs are 20%–30%. Differentiation between isolated and syndromic malformations is difficult; certain features (e.g., developmental delay) may manifest only during the course of development. Heritability of CVMs varies greatly, accounting for 50%–90% in certain types of congenital heart diseases, see Chapters 6,49,50, and 60. For the majority of CVMs (approximately 70%), the causes are unknown and supposedly multifactorial.[1,3,4]

   Difficulties in the disentanglement of genetic causes of CVMs arise, among others, from the following genetic features: (a) dosage sensitivity (abnormal phenotype in the absence of two functional copies of a certain gene); (b) variable penetrance (genetic modifiers interacting with dosage-sensitive genes); (c) phenotypic heterogeneity (varying roles of a particular gene in different stages of development); and (d) locus heterogeneity (different genetic causes of a single phenotype).[1] Genetic variation plays an important role in the sensitivity toward environmentally induced development of malformations.[4]
2. Embryonic and fetal development occurs within the maternal environment, which may be differentiated into external (e.g., maternal temperature, maternal exposition to ambient air pollution) and internal (e.g., maternal or placental polymorphisms in genes involved in detoxification) environments. All of these factors exert an influence on morphology and/or function of the developing cardiovascular system.[5–7] As a consequence, proof of teratogenicity is fraught with difficulty. The number of chemical and physical agents with potential teratogenicity amounts to several thousand. Some 1,500 can produce congenital malformations in animals. Of these, 40 to 180 are definitely teratogenic in humans. Criteria for proof of human teratogenicity are summarized in Table 62.1.[8,9]

Evidence regarding teratogenicity can be obtained by a variety of methods and may be summarized as follows[10,11]: (a) case reports: good for hypothesis generation; association with malformation often by chance, statistical analysis not possible; (b) case series: quality of data may differ; missing controls do not allow for sound statistical analyses, confounding poses a potentially serious problem; (c) pregnancy registries: voluntary; biased unless prospectively recruited; lack of controls; quality of data may be low (particularly relating to exposition timing and dosage); (d) randomized controlled trials: considered unethical; (e) cohort studies, either population based (high numbers required for statistical analysis) or exposition based (limited by recruitment, which may be biased); however, statistical analysis is possible; (f) case-control studies: low risk of bias; unexpected malformations will not be captured; (g) linkage studies: large data; usually collected for a different purpose, quality therefore low; and (h) ecological studies: group analysis of exposition and incident in a defined population section; association difficult to prove; confounding common.

In addition to statistical analyses, the assessment of teratology data relies on the reproducibility of the teratogenic effect, the proof of dose and effect, on animal tests, and on biological plausibility.

**Table 62.1** Criteria for proof of human teratogenicity

1. Proven exposure to agent at critical time(s) in prenatal development (prescriptions, physician's records, dates).
2. Consistent findings by two or more high-quality epidemiologic studies:
   a. Control of confounding factors
   b. Sufficient numbers
   c. Exclusion of positive and negative bias factors
   d. Prospective studies, if possible
   e. Relative risk of six or more (?)
3. Careful delineation of the clinical cases. A specific defect or syndrome, if present, is very helpful.
4. Rare environmental exposure associated with rare defect. Probably three or more cases (examples: oral anticoagulants and nasal hypoplasia, methimazole and scalp defects, and heart block and maternal rheumatic disease).
5. Teratogenicity in experimental animals important but not essential.
6. The association should make biologic sense.
7. Proof in an experimental system that the agent acts in an unaltered state. Important information for prevention.

*Source:* Shepard TH. *Catalog of Teratogenic Agents*. 13th ed. Baltimore, MD: Johns Hopkins University Press; 2010.[8]

*Note:* Items 1, 2, and 3 or 1, 3, and 4 are essential criteria. Items 5, 6, and 7 are helpful but not essential.

In the aftermath of the thalidomide tragedy[12] registries for congenital malformations were initiated in various countries, and international networks were established. They include, for example, the NBDPS (National Birth Defects Prevention Study) in the United States, a prospective national case-control registry, recruiting 1997–2011; the MACDP (Metropolitan Atlanta Congenital Defects Program), a population-based cohort registry, initiated 1967, and ongoing; the Medical Birth Registry of Norway, a nationwide population-based registry; EUROCAT (European Concerted Action on Congenital Anomalies and Twins), founded in 1979, a network for national registries; and the HCCSCA (Hungarian Case-Control Surveillance of Congenital Abnormalities), a population-based case-control registry, recruiting 1980–1996.

Registries for congenital heart defects include the BWIS (Baltimore Washington Infant Study), a population-based case-control study, recruiting 1981–1989[13]; the FRCM, a Finnish population-based case-control registry, recruiting 1982–1983[14]; the Swedish population-based case-control registry, recruiting 1981–1986[15]; and the Milwaukee ecological registry, investigating the association between trichloroethylene exposition and cardiac malformations from 1997 to 1999.[16]

# Maternal conditions, diseases, and therapies causing cardiovascular teratogenicity

The list of potential teratogens not only includes drugs, but also comprises occupational and ambient exposure to hazards; additionally, infections and noninfective diseases may exert teratogenic effects.[2,7,13,14,17–27] The differentiation between the teratogenicity of a certain disease and the medication(s) used for its treatment poses analytical problems (e.g., hypertension and antihypertensive medication, see the following text).

General conditions including maternal or paternal age, prepregnancy weight, reproductive history, parity, and socioeconomic status have been widely investigated.[2,19–21,24,28] Results are conflicting, with either no significance or odds ratios (OR)/relative risks (RR) between 1.1 and 3.5, highlighting the impact of confounding factors. As an example, prenatal detection rates of cardiac malformations inversely correlate with maternal body mass index and may thereby confound the association between obesity and CVM,[29,30] see Figure 62.1a–c.

## *Maternal diseases*

### Rubella

*Rubella* was the first teratogenic virus described.[31] It is a potent teratogen; the congenital rubella syndrome (Gregg syndrome) continues to pose a significant burden of disease/disability.[32,33] Miller et al.,[34] in their prospective study on women infected with rubella at different stages of pregnancy, could establish the gestational age (GA) dependency. Malformations occurred in 100% of cases infected before GA 11; in 35% infected at GA 13–16; and in none after GA 16. CVMs most commonly encountered are atrial and ventricular septal defects (ASD, VSD), pulmonary artery stenosis (PS), and persistent ductus arteriosus (PDA); extracardiac features of Gregg syndrome include microcephaly, cataract, glaucoma, microphthalmia, and hepatosplenomegaly.[35]

### Pregestational diabetes

Recently published data confirm the teratogenic potential of pregestational diabetes. Irrespective of diabetes type (I or II) and medication (insulin or oral antidiabetics), the adjusted relative risk for CVMs amounts to 4 (95%-CI 3.51–4.53).[36–40] All subtypes of malformations seem to occur, with heterotaxies and conotruncal defects (truncus arteriosus communis [TAC], double-outlet right ventricle [DORV]) being the most common.[36] Additionally, Oyen et al. could show a twofold risk in cases with a history of preconception diabetic complications, supporting the hypothesis of the teratogenic effect of hyperglycemia.[36] Increased values of HbA1c indicate poor glycemic control; first-trimester HbA1c may be used to determine the risk of structural cardiac defects.[41] Glucose itself is not a mutagen; a disruption of various signal transduction pathways and oxidative stress may underlie the embryopathic effects of poorly controlled diabetes and explain the variety of additional extracardiac malformations, for example, neural tube defects and caudal regression syndrome.[4,40,42]

### Hypertension

Various analyses challenge the long-held belief of the teratogenic effect of antihypertensive medications; rather, a

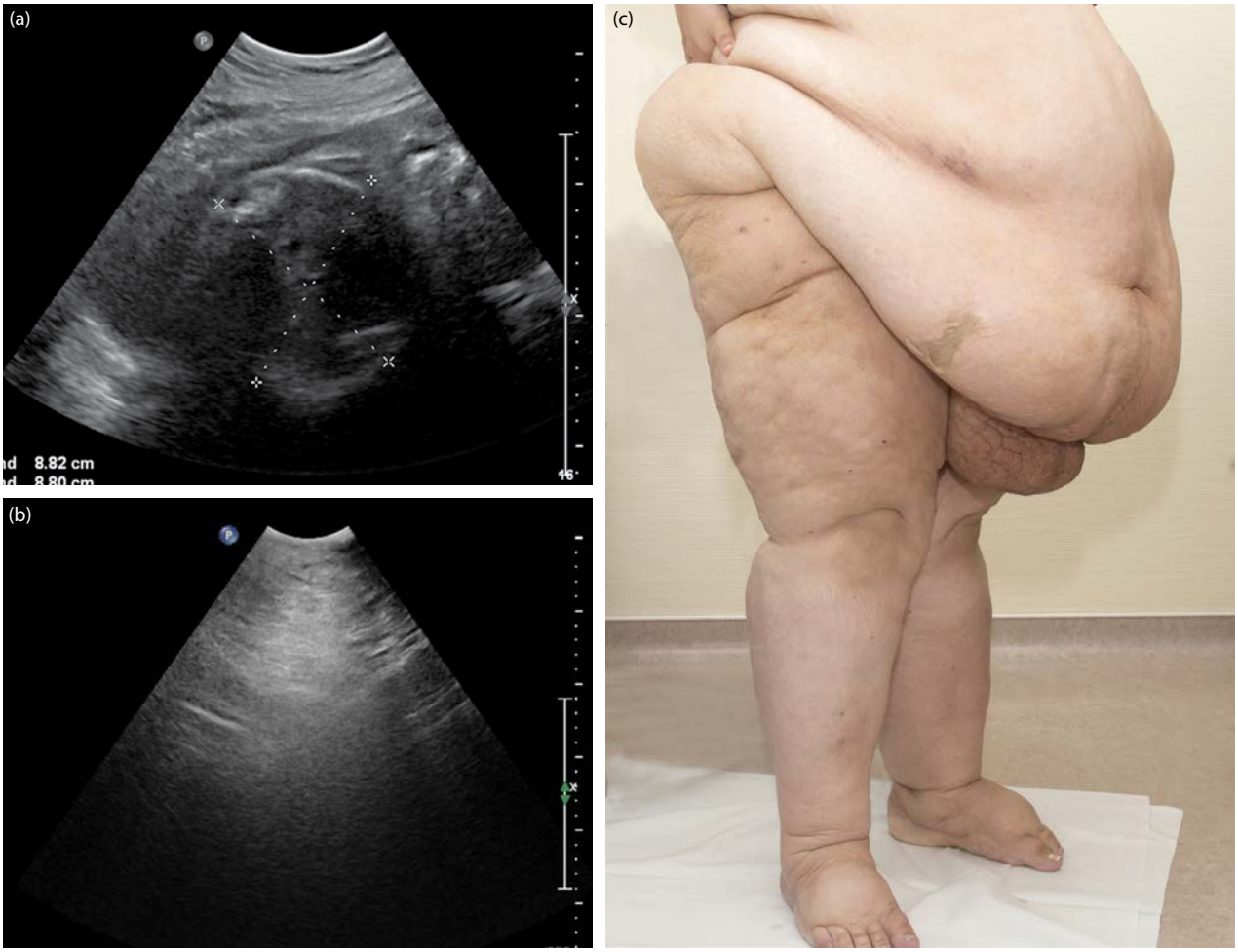


**Figure 62.1**
Confounders in teratology research. Technical limitations confound the association between obesity and congenital malformations. Risk calculations need to include terminations of pregnancy after prenatal diagnosis. Patient with BMI (body mass index): 74 kg/m$^2$. (a) 35 + 6 weeks of gestation. Lateral insonation (from the patient's loin). Transversal plane of the fetal abdomen. (b) 35 + 6 weeks of gestation. Vertical transabdominal insonation (from the patient's abdomen). Maternal adipose tissue precluding any visualization of the fetus. (c) Three days postpartum.

teratogenic effect of hypertension itself has been postulated. Li et al.,[43] for example, report an increased rate of CVMs in untreated hypertension compared to normotensive pregnancies, with no difference between treated and untreated cases. Various other studies show conflicting results, with the overall estimate of hypertension as a teratogen ranging between nonsignificant and OR/RR of 2.8 (five studies, including 17,202 cases and 500,561 controls, as summarized in Patel et al.).[14,16,20,43–47] Further clarification is warranted, particularly as pregnancies in chronic hypertension are on the rise.

## Phenylketonuria

Lenke et al.,[48] in their retrospective case-control series, report a 12%–15% prevalence of structural cardiac defects in pregnancies exposed to increased plasma concentrations of phenylalanine. Extracardiac malformations include microcephaly and developmental delay. In the study by Levy et al.,[49] coarctation of the aorta (CoA), hypoplastic left heart syndrome (HLHS), and tetralogy of Fallot (ToF) were overrepresented; a dose effect seems likely, with a threshold concentration of 900 μM phenylalanine at 8 weeks of gestation. More recent research suggests a lower risk of CVMs in hyperphenylalaninemia.[50]

## Temperature/influenza/febrile illness

The teratogenic effect of hyperthermia was investigated by Edwards and proven by animal experiments.[51,52] The type of defect is related to dose and timing of the insult, and requires an increase of minimum 1.5°C in core temperature (or a rise in body temperature of 2–2.5°C for 1 hour minimum).[53] The central nervous system is most commonly affected, and CVMs may occur. The distinction between maternal temperature, underlying condition (e.g., viral infection), and treatment (medication) as cause for a particular malformation may pose difficulties.[28]

## Environmental exposures

Associations between environmental hazards and CVMs are investigated for occupational and ambient exposure, and through analyses of neighborhoods of hazardous waste sites or industrial facilities. They entail exposition toward air, water, food, and soil pollution. The studies are fraught with methodological difficulties,[25] and levels of significance are generally low, highlighting the multifactorial etiology, for example, for air pollution.[26,54] Electronic databases complement publications[8,13] on the health hazards of the many chemicals found in the environment (e.g., the integrated risk information system [IRIS] of the U.S. Environmental Protection Agency [EPA]).[55] The relevance of environmental exposures and congenital malformations may be substantial; Boyd and Genuis[56] calculated for Canada a yearly number of 128–640 major malformations attributable to adverse environmental exposures. Paternal exposition also has to be taken into consideration.[25,57]

Regarding air pollution, investigations include ozone ($O_3$), particulate matter with less than 10 μm diameter ($PM_{10}$), nitrogen dioxide ($NO_2$), carbon monoxide (CO), and sulfur dioxide ($SO_2$).[25,26,54,58] A possible association between $NO_2$ and CoA has been found in two recently published meta-analyses.[26,54]

Di- and trichloroethylene are solvents that when entering groundwater can persist, accumulate, and cause considerable contamination. In animal experiments, exposure is associated with an increased rate of CVMs. Data on humans are conflicting but do not seem to support a role of di- or trichloroethylene in cardiovascular teratogenicity.[16,27,59]

## Maternal medication

Very rarely, maternal first-trimester drug exposure results in a well-recognizable pattern of malformations. Highly teratogenic medications include, for example, thalidomide, warfarin, phenytoin, isotretinoin, and mycophenolate mofetil. CVMs usually form part of these embryopathies but do not constitute their cardinal feature. Teratogenicity of the vast majority of drugs is difficult to establish (see section Background), the average time for precise risk classification may amount to 27 years.[60] Information on the teratogenic and fetotoxic potential of drugs was previously provided by the U.S. Food and Drug Administration (FDA) five-letter risk system; this was replaced by a new labeling system ("pregnancy and lactation labeling rule") in 2015.[61]

### Angiotensin-converting enzyme inhibitors (ACE-I), angiotensin II receptor blockers (ARB)

The controversies surrounding these two classes of antihypertensives illustrate many aspects of medication in pregnancy. The first reports on reproductive toxicity of ACE-Is date back to 1980.[62] The focus of attention turned toward their toxicity, emerging during the late second and third trimesters. Renal tubular dysplasia, hypocalvaria, postnatal prolonged hypotension, and pulmonary hypoplasia were observed in a high percentage of newborns exposed to ACE-Is/ARBs during pregnancy; additionally, fetal growth restriction (FGR), oligo-/anhydramnios, and PDA were usually present (Figure 62.2a–c). These features constitute a specific pattern, contributing to its early recognition.[63–66] Renal tubular dysplasia, oligohydramnios, and FGR are sequelae of ACE-Is and ARBs on the fetal kidney, induced presumably via hypoperfusion secondary to alterations in the renin-angiotensin-aldosterone system; hypotheses regarding hypocalvaria and PDA vary.

Initial data on teratogenicity were reassuring, even though a high rate of miscarriages was noted after first-trimester use of ACE-Is/ARBs.[66] In 2006, Cooper et al. reported an increased rate of cardiovascular and central nervous system (CNS) malformations after first-trimester exposition to ACE-Is.[67] CVMs included isolated ASD, ASD in complex defects, PDA, and VSD. Since then, a series of investigations and meta-analyses have been published[20,43–47,68–72] with conflicting results. Compared to their toxicity, however, the teratogenic potential of these classes of drugs appears low.

### Antiepileptic medication

In women with epilepsy, the risk for major malformations, including CVMs is twofold increased.[4,15,24,73–75] This may be a direct teratogenic effect; a modifying influence of genetic polymorphisms (e.g., folic acid metabolism) on the development of CVMs; a teratogenic effect of the disease itself; or associated with the number of seizures.

### Lithium

Since animal studies had revealed a high teratogenic potential of lithium (up to 30%–60% malformation rates), the "register of lithium babies" was initiated with introduction into clinical use.[76–78] Early reports suggested a markedly increased risk for CVMs, in particular, for Ebstein anomaly (two affected cases in a group of 118 exposed), and a 400-fold increased risk was calculated for Ebstein anomaly in pregnant women on lithium.[79] Subsequent investigations continue to reveal conflicting data. The magnitude of the effect of lithium on the development of CVMs may not be significant, but also could be sixfold (for CVMs in general) to 30-fold (for Ebstein anomaly) increased[73,80–87] (Figure 62.3a–c).

### Selective serotonin reuptake inhibitors (SSRI)—including serotonin-norepinephrin reuptake inhibitors (SNRI)

The steep rise of SSRI prescriptions to women of reproductive age[88] has resulted in extensive investigations regarding their teratogenicity. In the United States in 2004, 6.4% of pregnancies may have been exposed to SSRIs. Data are conflicting but allow the conclusion of a 1.5- to 2-fold increased risk of CVMs, in particular ASD, VSD, and left ventricular outflow tract (LVOT) obstruction.[73,89–97] Cardiovascular toxicity of

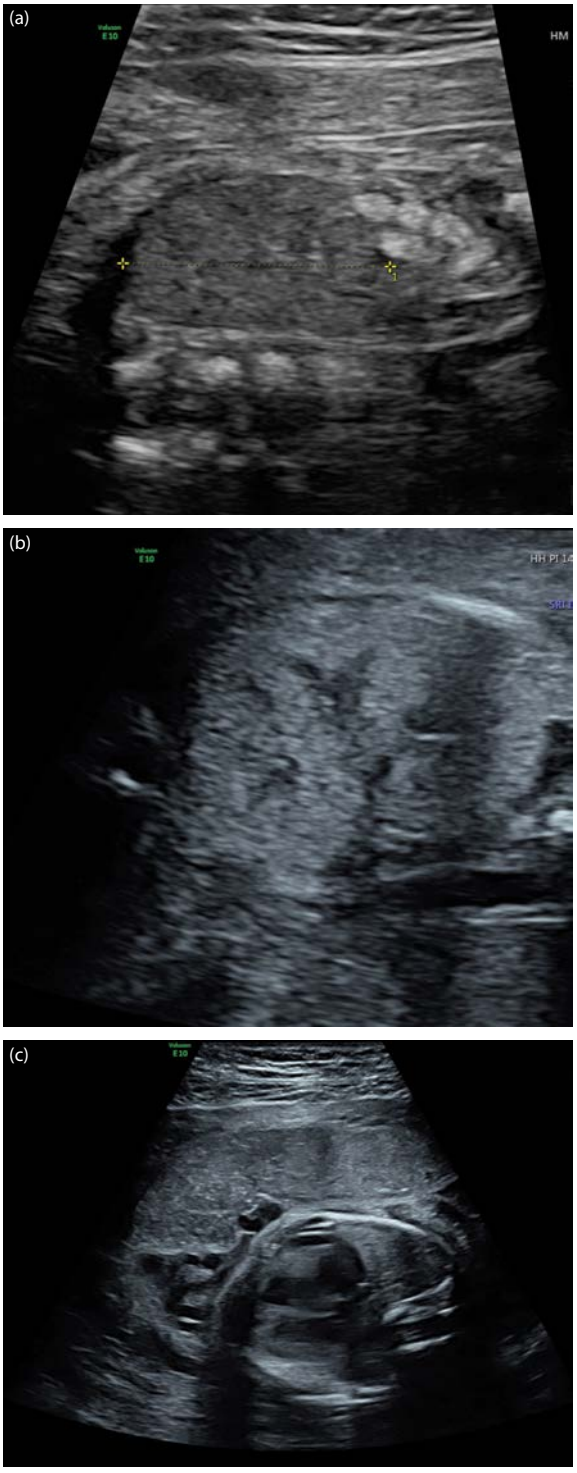


**Figure 62.2**
Toxicity of ACE-Is/ARBs. Patient with dilated cardiomyopathy; ejection fraction 35%. Medication: valsartan 80 mg daily; furosemide 20 mg daily; bisoprolol 10 mg daily; omeprazole 20 mg daily; ASS 100 mg daily. (a) 24 + 4 weeks of gestation. Coronal plane. Normally sized fetal kidney, markedly reduced corticomedullary differentiation. (b) 27 + 0 weeks of gestation. Coronal plane. Normally sized fetal kidney, complete loss of corticomedullary differentiation. (c) 27 + 0 weeks of gestation. Transversal plane. Four-chamber view. Fetal cardiomegaly; biventricular myocardial hypertrophy; severe oligohydramnios.

SSRIs consists of persistent pulmonary hypertension of the newborn (PPHN). SSRI treatment during the second half of pregnancy is associated with an increased risk of PPHN (aOR 1.28–6.1).[98–101]

### Retinoids

Retinoids comprise vitamin A and related compounds. Multivitamin preparations taken during pregnancy may contain vitamin A. Data on the teratogenicity of vitamin A are conflicting,[102–105] as is the required dosage to increase the risk of malformations; intake, however, should not exceed the recommended daily allowance of 8000 IU/d.[106] Isotretinoin, in contrast, is a very potent teratogen (25% rate of major malformations after use during organogenesis) with a well-described pattern of malformations (retinoid embryopathy). This includes CNS, thymic, and craniofacial malformations; cardiovascular defects include conotruncal malformations, transposition of the great arteries (TGA), ToF, DORV, TAC, ASD, and VSD. A disruption of the cranial neural crest cell differentiation and migration is likely to be involved in the pathomechanism.[107]

### Nontherapeutic drug exposure/illicit drugs

Alcohol, cocaine, marijuana, caffeine, and cigarette smoking are among the substances extensively investigated for their teratogenic potential. With respect to CVMs, the data are inconclusive or do not support a major role. Alcohol, for example, is a potent teratogen, and CVMs may occur in fetal alcohol syndrome, but confounding factors interfere heavily.[106,108–110]

## Beyond organogenesis: Maternal conditions, diseases, and therapies affecting the fetal cardiovascular system

After completion of cardiac morphogenesis, the fetus continues to be exposed to the maternal environment. The effects on the fetal cardiovascular system may be direct or indirect.

## *Maternal diseases*

### Pregestational diabetes

The toxic effects of poorly controlled diabetes result in the development of hypertrophic cardiomyopathy and impaired myocardial function, particularly diastolic dysfunction. Interventricular septum thickness and myocardial function measurements as well as tissue-Doppler investigations reveal the negative impact of maternal hyperglycemia.[111,112] Serial investigations of cardiac dimensions point to the development of cardiac hypertrophy even in the presence of good

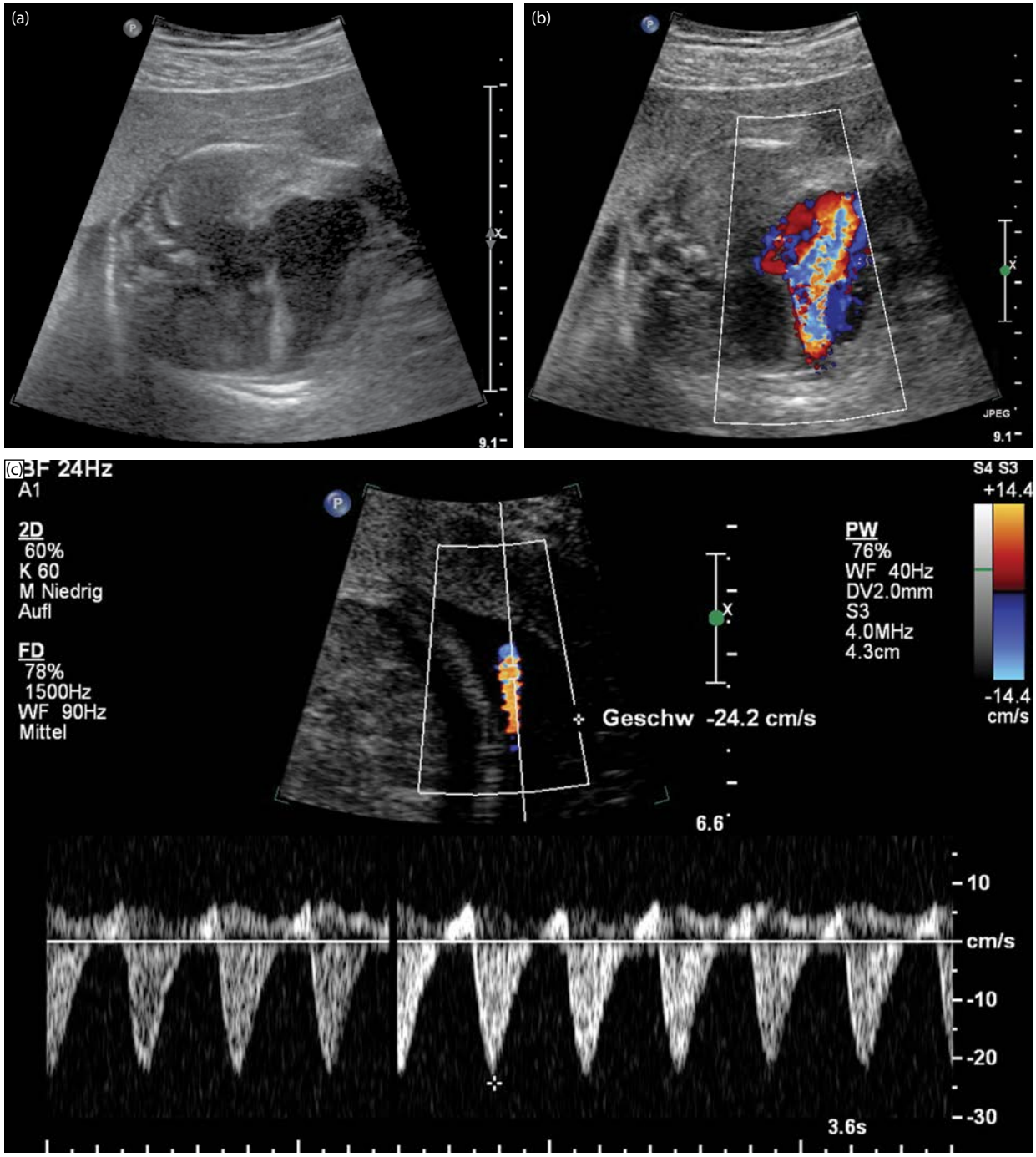


**Figure 62.3**
Teratogenicity of psychiatric medication. Patient with bipolar affective disorder. Medication: lithium 900 mg bd; quetiapine 200 mg daily. (a) 24 + 0 weeks of gestation. Four-chamber view. Ebstein anomaly with apical displacement of septal tricuspid leaflet and functional atrialization of a large part of the right ventricle. (b) 24 + 0 weeks of gestation. Color Doppler imaging. Severe tricuspid insufficiency. (c) 24 + 0 weeks of gestation. Umbilical artery reverse end-diastolic flow indicating circular left-to-right shunt via the arterial duct resulting in critical decrease of the systemic arterial flow due to severe steal effect.

glycemic control.[112,113] Evidence for gestational diabetes is not as obvious, studies struggle with confounding (study group heterogeneity, e.g., obesity, severity of hyperglycemia, etc.).[111,114–119] Data on the association between fetal heart rate and hyperglycemia[120] and diabetic control and cardiac function[121] require further clarification.

## Grave disease

Thyrotropin-receptor antibodies (TRAbs) of Grave disease are class G immunoglobulins and transferred to the fetus in the second half of pregnancy; binding to the fetal TSH receptor may have stimulating or inhibiting effects. Some 0.01% of

pregnancies are complicated by fetal thyrotoxicosis secondary to TRAbs[122]; the risk seems to correlate with antibody levels.[123] Fetal cardiovascular sequelae include tachycardia and cardiomegaly; rarely, hydrops may develop. Fetal thyrotoxicosis as early as at 18 weeks of gestation has been described.[124]

### Systemic lupus erythematosus, Sjögren's syndrome, and other chronic inflammatory, autoimmune (connective tissue) diseases (systemic sclerosis, idiopathic inflammatory myopathy, primary biliary cholangitis, and rheumatoid arthritis)

A feature of these autoimmune diseases is the production of autoantibodies against nuclear ribonucleoproteins, in particular, the 52-kd and 60-kd Ro/SSA and the 48-kd La/SSB, which may cause various degrees of congenital heart block. Frequency of third-degree congenital heart block in the presence of anti-Ro +/− anti-La antibodies is 2%[125] (95%-CI 0.2%–7%,[126]); in case of an affected child, the risk in a subsequent pregnancy is 17%.[127] Endocardial fibroelastosis/dilated cardiomyopathy is another finding in Ro/SSA- or La/SSB-positive pregnancies. Autoantibody production may precede the onset of clinical symptoms in the mother by years. Correlations between autoantibody titers and risk of congenital heart block are difficult to establish because a variety of analytical tests are used in clinical practice.[128] Treatment with hydroxychloroquine may reduce risk for development of complete AV-block.[129] For further details, see Chapter 40: Fetal bradyarrhythmia and the long Q-T syndrome and Chapter 33.

### Rhesus and other blood group system alloimmunizations

Blood group alloimmunization causing fetal anemia results in tissue hypoxia and compensatory hyperdynamic circulation. Myocardial strain increases, and ultimately high cardiac output failure and fetal hydrops may develop.[130,131] For details, see Chapters 42 and 43.

### Parvovirus B-19 infection

Cardiovascular sequelae of maternal parvovirus B-19 infection are twofold. Infection of fetal red blood progenitor cells causes anemia; additionally, infection of the fetal myocardium may occur, further compromising fetal cardiac function. High cardiac output failure and hydrops may develop. For details, see Chapter 42 and 43.

## *Maternal medication*

### Glucocorticoids

Maternal long-term glucocorticoid medication is associated with fetal growth restriction (see text that follows). Fluorinated corticosteroids (dexa- and betamethasone) are characterized by high placental transfer; short-term treatment is indicated in threatened preterm delivery for prevention of respiratory distress syndrome in the newborn. Fetal cardiovascular side effects have been extensively investigated. Fetal heart rate pattern changes have been demonstrated,[132] and transient fetal hypertension may develop.[133,134]

### Antihypertensive medication

All classes of antihypertensive drugs cross the placenta. Fetal side effects include hypotension (methyldopa and labetalol) or bradycardia (labetalol, atenolol, propranolol, and esmolol).[133] For details regarding direct side effects of the various classes of antihypertensive drugs on the fetal cardiovascular system see NICE.[135] Additionally, antihypertensive medication, beta-blockers in particular, may contribute to FGR. For treatment with atenolol, a reduction of the maternal cardiac output has been demonstrated.

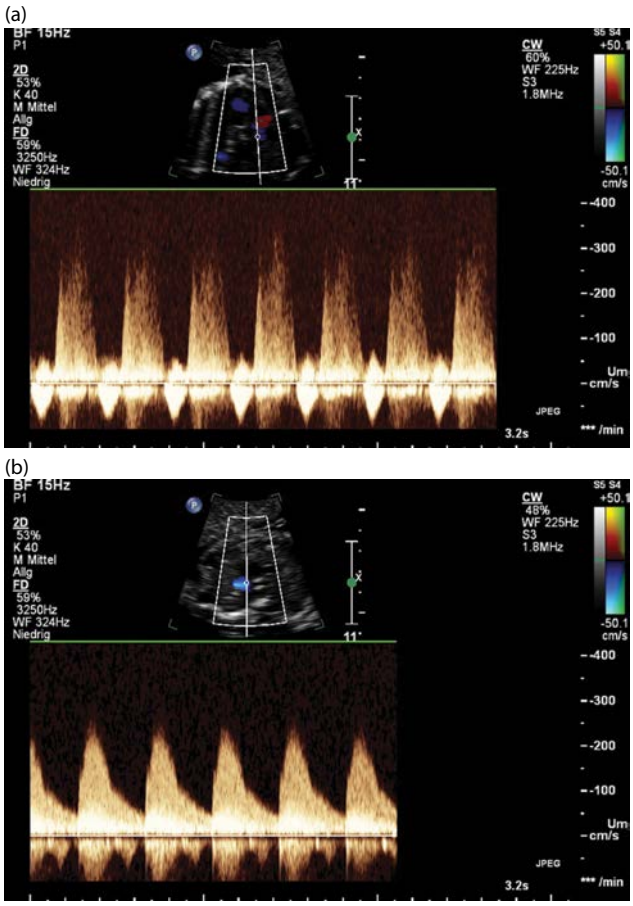


**Figure 62.4**
Fetal ductus arteriosus constriction. (a) 26 + 4 weeks of gestation. Intracardiac Doppler studies. Severe holosystolic tricuspid regurgitation (peak velocity: 4 m/s; pressure gradient across tricuspid valve: 64 mm Hg). (b) 26 + 4 weeks of gestation. Doppler examination in the ductus arteriosus indicating severe ductal constriction. Increased systolic (260 cm/s) and diastolic (55 cm/s) blood flow velocities and markedly reduced pulsatility (pulsatility index: 1.50); loss of end-systolic notching.

Since the uteroplacental perfusion lacks autoregulation, the significantly lower birth weight[136] in normotensive pregnancies after treatment may be a result of the reduced maternal cardiac output with consecutive reduction of the uteroplacental perfusion. Conversely, an inverse correlation between blood pressure and birth weight could be demonstrated in term pregnancies of women with prehypertension.[137]

### Nonsteroidal anti-inflammatory drugs

Constriction or premature closure of the ductus arteriosus after maternal nonsteroidal anti-inflammatory drug (NSAID) ingestion in the third trimester is a well-known side effect,[138–140] see Figure 62.4a,b.

### Beta-2 receptor agonists

Widely used for treatment of preterm labor, data on fetal cardiovascular effects of beta-2 receptor agonists are inconclusive. Gestational age, concomitant medication, and fetal well-being are confounding factors. A rise in the fetal heart rate and redistribution of the fetal cardiac output may occur.[141–146]

## *Indirect effects: Uteroplacental dysfunction secondary to maternal diseases, medication, or other substances*

Conditions or substances causing uteroplacental dysfunction ultimately result in FGR with its associated changes in the fetal cardiovascular function and cardiac remodeling.[147–151] For details, see Chapters 35 and 46.

*Maternal diseases* associated with uteroplacental dysfunction comprise a large spectrum of disorders. These include chronic hypertension, preexisting diabetes, renal diseases, autoimmune disorders, anemia, infections (cytomegalovirus, toxoplasmosis, rubella, varicella, tuberculosis, malaria), and maternal exposure to tobacco or alcohol. Environmental hazards have also been linked to FGR.[152]

A wide range of *medications* may cause uteroplacental dysfunction. These include, among others, cytotoxic agents, immunosuppressives (e.g., ciclosporin, azathioprine, glucocorticoids), antiepileptics, and antihypertensives. However, in pregnant women on treatment for a certain disorder, the mechanism causing FGR may be difficult to ascertain. The underlying disease itself, a direct side effect of the drug on the fetus, or an indirect effect of the drug on the placenta or its perfusion may contribute to the development of FGR in these circumstances (see previous text).

## References


1. Azhar M, Ware SM. *Clin Perinatol* 2016;43(1):39–53.
2. Wilson PD et al. *Am J Epidemiol* 1998;148(5):414–23.
3. Lalani SR, Belmont JW. *Eur J Med Genet* 2014;57(8):402–13.
4. Wlodarczyk BJ et al. *Am J Med Genet C Semin Med Genet* 2011;157C(3):215–26.
5. Dorfman EH et al. *Pharmacogenomics J* 2016;16(4):303–4.
6. Tasnif Y et al. *Clin Pharmacol Ther* 2016;100(1):53–62.
7. Tikkanen J, Heinonen OP. *Teratology* 1991;43(6):591–600.
8. Shepard TH. *Catalog of Teratogenic Agents*. 13rd ed. Baltimore MD: Johns Hopkins University Press; 2010.
9. Shepard TH. *Teratology* 1994;50(2):97–8.
10. Friedman JM. *Am J Med Genet C Semin Med Genet* 2011;157C (3):170–4.
11. Chambers CD. Investigating drug effects in human pregnancy. In: Hansen DK, Abbott BD, eds. *Developmental Toxicology*. 3rd ed. New York, NY: Informa Healthcare; 2009:361–75 (Target organ toxicology series; vol. 27).
12. Lenz W. *Teratology* 1988;38(3):203–15.
13. Ferencz C et al., eds. *Genetic and Environmental Risk Factors of Major Cardiovascular Malformations: The Baltimore-Washington Infant Study: 1981–1989*. Armonk, NY: Futura; 1997.
14. Tikkanen J, Heinonen OP. *Eur J Epidemiol* 1990;6(4):348–56.
15. Pradat P. *Eur J Epidemiol* 1992;8(6):789–96.
16. Yauck JS et al. *Birth Defects Res A Clin Mol Teratol* 2004;70(10): 808–14.
17. Chou H-H et al. *CMAJ* 2016;188(17–18):E438–46.
18. van Gelder MM et al. *Hum Reprod* 2014;29(1):168–83.
19. Donofrio MT et al. *Circulation* 2014;129(21):2183–242.
20. Patel SS, Burns TL. *Pediatr Cardiol* 2013;34(7):1535–55.
21. Liu S et al. *Circulation* 2013;128(6):583–9.
22. Fung A et al. *J Am Heart Assoc* 2013;2(3):e000064.
23. Obican S, Scialli AR. *Am J Med Genet C Semin Med Genet* 2011;157C(3):150–69.
24. Jenkins KJ et al. *Circulation* 2007;115(23):2995–3014.
25. Foster WG et al. *Crit Rev Toxicol* 2017;1:59–84.
26. Vrijheid M et al. *Environ Health Perspect* 2011;119(5):598–606.
27. Bukowski J. *Crit Rev Toxicol* 2014;44(7):581–9.
28. Tikkanen J, Heinonen OP. *Eur J Epidemiol* 1991;7(6):628–35.
29. Cai G-J et al. *Am J Obstet Gynecol* 2014;211(2):91–117.
30. Bertagna F et al. *Prenat Diagn* 2014;34(6):534–7.
31. Gregg NM. *Epidemiol Infect* 1991;107(1):iii–xiv; discussion xiii–xiv.
32. Simons EA et al. *Risk Anal* 2016;36(7):1332–56.
33. Lazar M et al. *EBioMedicine* 2016;3:86–92.
34. Miller E et al. *Lancet* 1982;2(8302):781–4.
35. Yazigi A et al. *J Matern Fetal Neonatal Med* 2017;30(3):274–8.
36. Oyen N et al. *Circulation* 2016;133(23):2243–53.
37. Garne E et al. *Birth Defects Res A Clin Mol Teratol* 2012;94(3): 134–40.
38. Correa A et al. *Am J Obstet Gynecol* 2008;199(3):237.e1–9.
39. Kousseff BG. *Curr Opin Pediatr* 1999;11(4):348–52.
40. Mills JL. *Teratology* 1982;25(3):385–94.
41. Starikov R et al. *Pediatr Cardiol* 2013;34(7):1716–22.
42. Zabihi S, Loeken MR. *Birth Defects Res A Clin Mol Teratol* 2010;88(10):779–90.
43. Li D-K et al. *BMJ* 2011;343:d5931.
44. Czeizel AE, Banhidy F. *Curr Opin Obstet Gynecol* 2011;23(2): 76–81.
45. Caton AR et al. *Hypertension* 2009;54(1):63–70.
46. Moretti ME et al. *Obstet Gynecol Int* 2012;2012:658310.
47. Diav-Citrin O et al. *Reprod Toxicol* 2011;31(4): 540–5.
48. Lenke RR, Levy HL. *N Engl J Med* 1980;303(21):1202–8.
49. Levy HL et al. *Pediatr Res* 2001;49(5):636–42.

50. Prick BW et al. *Am J Clin Nutr* 2012;95(2):374–82.
51. Edwards MJ. *Teratology* 1968;1(2):173–7.
52. Graham JM Jr., *Birth Defects Res A Clin Mol Teratol* 2005; 73(11):857–64.
53. Power GGBAB. Thermoregulation: Perinatal thermal physiology. In: Polin RA, Fox WW, Abman SH, eds. *Fetal and Neonatal Physiology*. Philadelphia: Elsevier Saunders; pp. 615–9. https://federalregister.gov/a/2014-28241 (accessed June 04, 2018).
54. Chen EK-C et al. *Int J Environ Res Public Health* 2014;11(8): 7642–68.
55. Environmental Protection Agency EPA. https://www.epa.gov/iris (accessed June 04, 2018).
56. Boyd DR, Genuis SJ. *Environ Res* 2008;106(2):240–9.
57. Snijder CA et al. *Hum Reprod* 2012;27(5):1510–7.
58. Hwang B-F et al. *Medicine (Baltimore)* 2015;94(44):e1883.
59. Hardin BD et al. *Birth Defects Res A Clin Mol Teratol* 2005;73(12):931–55.
60. Adam MP et al. *Am J Med Genet C Semin Med Genet* 2011;157C (3):175–82.
61. US FDA.
62. Broughton Pipkin F et al. *Lancet* 1980;1(8180):1256.
63. Shotan A et al. *Am J Med* 1994;96(5):451–6.
64. Barr M Jr. *Teratology* 1994;50(6):399–409.
65. Spence SG et al. *Teratology* 1995;51(6):383–97.
66. Centers for Disease Control and Prevention (CDC). *MMWR Morb Mortal Wkly Rep* 1997;46(11):240–2.
67. Cooper WO et al. *N Engl J Med* 2006;354(23):2443–51.
68. Lennestal R et al. *Eur J Clin Pharmacol* 2009;65(6):615–25.
69. Karthikeyan VJ et al. *J Hypertens* 2011;29(2):396–9.
70. Walfisch A et al. *J Obstet Gynaecol* 2011;31(6):465–72.
71. Koren G. *Nat Rev Cardiol* 2011;9(1):7–8.
72. Bullo M et al. *Hypertension* 2012;60(2):444–50.
73. Petersen I et al. *Health Technol Assess* 2016;20(23):1–176.
74. Thomas SV et al. *Pediatr Cardiol* 2008;29(3):604–8.
75. Barrett C, Richens A. *Epilepsy Res* 2003;52(3):147–87.
76. Schou M et al. *Br Med J* 1973;2(5859):135–6.
77. Schou M et al. *Br Med J* 1973;2(5859):137–8.
78. Schou M, Amdisen A. *Br Med J* 1973;2(5859):138.
79. Nora JJ et al. *Lancet* 1974;2(7880):594–5.
80. Weinstein MR, Goldfield M. *Am J Psychiatry* 1975;132(5):529–31.
81. Kallen B, Tandberg A. *Acta Psychiatr Scand* 1983;68(2):134–9.
82. Jacobson SJ et al. *Lancet* 1992;339(8792):530–3.
83. Cohen LS et al. *JAMA* 1994;271(2):146–50.
84. McKnight RF et al. *The Lancet* 2012;379(9817):721–8.
85. Diav-Citrin O et al. *Am J Psychiatry* 2014;171(7):785–94.
86. Bergink V, Kushner SA. *Am J Psychiatry* 2014;171(7):712–5.
87. Moore JA. *Reprod Toxicol* 1995;9(2):175–210.
88. Andrade SE et al. *Am J Obstet Gynecol* 2008;198(2):194.e1–5.
89. Jordan S et al. *PLOS ONE* 2016;11(12):e0165122.
90. Furu K et al. *BMJ* 2015;350:h1798.
91. Reefhuis J et al. *BMJ* 2015;351:h3190.
92. Wemakor A et al. *Eur J Epidemiol* 2015;30(11):1187–98.
93. Huybrechts KF et al. *N Engl J Med* 2014;370(25):2397–407.
94. Jimenez-Solem E et al. *BMJ Open* 2012;2(3):e00148.
95. Wurst KE et al. *Birth Defects Res A Clin Mol Teratol* 2010;88(3): 159–70.
96. FDA. 2005. Available from: URL: http://www.fda.gov/NewsEvents/Newsroom/PressAnnouncements/2005/ucm108527.htm.
97. Chambers CD et al. *N Engl J Med* 1996;335(14):1010–5.
98. Berard A et al. *Br J Clin Pharmacol* 2017;83(5):1126–33.
99. Huybrechts KF et al. *JAMA* 2015;313(21):2142–51.
100. Grigoriadis S et al. *BMJ* 2014;348:f6932.
101. Chambers CD et al. *N Engl J Med* 2006;354(6):579–87.
102. Botto LD et al. *Epidemiology* 2001;12(5):491–6.
103. Shaw GM et al. *Lancet* 1996;347(9005):899–900.
104. Khoury MJ et al. *Lancet* 1996;347(8997):322.
105. Rothman KJ et al. *N Engl J Med* 1995;333(21):1369–73.
106. Pregnancy CoNSD. *Nutrition during Pregnancy: Part I: Weight Gain, Part II: Nutrient Supplements*. Washington, DC: National Academies Press; 1989.
107. Lammer EJ et al. *N Engl J Med* 1985;313(14):837–41.
108. Burd L et al. *Congenit Heart Dis* 2007;2(4):250–5.
109. Yang J et al. *PLOS ONE* 2015;10(6):e0130681.
110. Zhu Y et al. *Birth Defects Res A Clin Mol Teratol* 2015;103(7): 617–29.
111. Kulkarni A et al. *Ultrasound Obstet Gynecol* 2017;49(5):630–6.
112. Pauliks LB. *Expert Rev Cardiovasc Ther* 2015;13(1):67–74.
113. Lisowski LA et al. *Ultrasound Obstet Gynecol* 2003;21(4):365–9.
114. Fouda UM et al. *J Matern Fetal Neonatal Med* 2013;26(6):571–5.
115. Bui YK et al. *J Am Soc Echocardiogr* 2013;26(5):507–14.
116. Figueroa H et al. *Prenat Diagn* 2012;32(10):943–8.
117. Garcia-Flores J et al. *Eur J Obstet Gynecol Reprod Biol* 2011; 154(1):24–6.
118. Gandhi JA et al. *Am J Obstet Gynecol* 1995;173(4):1132–6.
119. Rizzo G et al. *Am J Obstet Gynecol* 1991;164(3):837–43.
120. Costa VN et al. *Eur J Obstet Gynecol Reprod Biol* 2009;143(1): 14–7.
121. Gardiner HM et al. *Heart* 2006;92(8):1125–30.
122. de Groot L et al. *J Clin Endocrinol Metab* 2012;97(8): 2543–65.
123. Peleg D et al. *Obstet Gynecol* 2002;99(6):1040–3.
124. Donnelly MA et al. *Obstet Gynecol* 2015;125(5):1059–62.
125. Brucato A et al. *Arthritis Rheum* 2001;44(8):1832–5.
126. Buyon JP et al. *Arthritis Rheum* 2001;44(8):1723–7.
127. Llanos C et al. *Arthritis Rheum* 2009;60(10):3091–7.
128. Jaeggi E et al. *J Am Coll Cardiol* 2010;55(24):2778–84.
129. Izmirly PM et al. *Ann Rheum Dis* 2010;69(10):1827–30.
130. Merz WM et al. *Pediatr Res* 2012;72(2):174–8.
131. Merz WM et al. *Clin Res Cardiol* 2012;101(2):73–9.
132. Verdurmen KMJ et al. *Obstet Gynecol Surv* 2013;68(12): 811–24.
133. Kent AL, Chaudhari T. *Curr Hypertens Rep* 2013;15(5):426–32.
134. Simchen MJ et al. *Am J Obstet Gynecol* 2004;190(2):296–304.
135. NICE. 2010. Tx RR SS.
136. Easterling TR et al. *Obstet Gynecol* 1999;93(5 Pt 1):725–33.
137. Wikstrom A-K et al. *Hypertension* 2016;67(3):640–6.
138. Majed BH, Khalil RA. *Pharmacol Rev* 2012;64(3):540–82.
139. Gewillig M et al. *Eur Heart J* 2009;30(12):1530–6.
140. Momma K, Takeuchi H. *Prostaglandins* 1983;26(4):631–43.
141. Grzesiak M et al. *Neuro Endocrinol Lett* 2013;34(6):549–52.
142. Grzesiak M et al. *Neuro Endocrinol Lett* 2013;34(6):553–8.
143. Gokay Z et al. *Ultrasound Obstet Gynecol* 2001;18(1):44–6.
144. Kast A, Hermer M. *J Perinat Med* 1993;21(2):97–106.
145. Räsänen J. *Acta Obstet Gynecol Scand* 1990;69(6):487–92.
146. Cheung K, Wladimiroff JW. *Eur J Obstet Gynecol Reprod Biol* 1990;35(2-3):147–51.
147. Demicheva E, Crispi F. *Fetal Diagn Ther* 2014;36(2):143–53.
148. Cruz-Lemini M et al. *Am J Obstet Gynecol* 2014;210(6):552. e1–22.
149. Cruz-Lemini M et al. *Ultrasound Obstet Gynecol* 2016;48(3): 349–56.
150. Crispi F et al. *Am J Obstet Gynecol* 2012;207(2):121.e1–9.
151. Crispi F et al. *Circulation* 2010;121(22):2427–36.
152. Longnecker MP et al. *Lancet* 2001;358(9276):110–4.

Taylor & Francis
Taylor & Francis Group
http://taylorandfrancis.com

# Index